Ex. II - 1

Society of Petroleum Engineers
6200 North Central Expressway
Dallas, Texas 75206

PAPER
NUMBER: SPE6513

VERTILOG® – A DOWN-HOLE CASING INSPECTION SERVICE

BY
JOHN N. HAIRE AND JEARALD D. HEFLIN, MEMBERS SPE-AIME, DRESSER ATLAS

THIS PAPER IS SUBJECT TO CORRECTION

Copyright 1977

American Institute of Mining, Metallurgical, and Petroleum Engineers, Inc.

This paper was prepared for the 1977 47th Annual California Regional Meeting of the Society of Petroleum Engineers of AIME, held in Bakersfield, California, April 13-15, 1977. Permission to copy is restricted to an abstract of not more than 300 words. Illustrations may not be copied. The abstract should contain conspicuous acknowledgement of where and by whom the paper is presented. Publication elsewhere after publication in the JOURNAL OF PETROLEUM TECHNOLOGY or the SOCIETY OF PETROLEUM ENGINEERS JOURNAL is usually granted upon request to the Editor of the appropriate journal, provided agreement to give proper credit is made. Discussion of this paper is invited.

ABSTRACT

In California the shortages and resulting economics of new oil has intensified the search for new sources. With casing and drilling costs increasing, this search has resulted in a renewed interest and re-evaluation of many existing wells.

A knowledge of the condition of the existing casing is necessary for repairs, workovers, and possible developement of additional zones.

The Vertilog is a casing inspection service which is now available to the oil and gas industry to determine the condition of the casing in existing wells. It is a quantitative measurement of corrosive damage, indicating if the metal loss is internal or external, and if it is isolated or circumferential. Holes in the casing can be identified as well as parted casing. This survey in conjunction with other measurements, can be used to detect, monitor, and establish preventive techniques for corrosive problems.

This paper is intended to familiarize the industry with tool specifications, theory of operations, calibrations, applications, interpretation principles, and field examples.

INTRODUCTION

The Vertilog is a downhole casing inspection service. The recordings produced allow identification of damaged intervals and severity of corrosion. Measurements taken determine if corrosion or damage is internal or external and if it is isolated or circumferential.

Due to instrument design, casing inspection covers the full circumference and minor elongation does not effect the reliability of the measurements. Anomalies as small as 1/8" in diameter with as little as 20% penetration of the nominal bodywall of the casing can be detected.

All casing sizes, weights, and grades from 4-1/2" O.D. through 8-5/8" O.D., except 6-5/8" O.D., can be inspected at the present time.

The tools are temperature rated at 250°F and pressure rated at 10,000 PSI.

The logging speed is 125 feet per minute and no special borehole fluids are required for the survey. It is recommended that the casing be scraped just prior to the survey for the most definitive measurements.

PRESENTATION

The data is presented in a standard log format, however, the usual depth scale is 10" per 100 feet of borehole for improved definition. The measurements are presented on a four track log grid as illustrated in Figure 1.

Track one and two are designated as Flux Leakage-1 (FL-1) and Flux Leakage-2 (FL-2) and correspond to the two rings of shoes on the Vertilog instrument. Recorder deflections in these tracks indicate the severity of corrosion that has taken place and also the location of the collars.

The third track is designated the Disciminator Track

with recorder deflections allowing interpretation of whether the damage is internal or external.

The fourth track is referred to as the Average Track. The ratio of the height of the signal recorded by a casing collar (360°) to one within a joint determines if the damage is isolated or circumferential.

Figure 2 is a comparison of an Electrolog recorded on a well in California in 1945 and casing set through the interval and the well completed below. On the right is a Vertilog recorded in 1976 showing the condition of the casing. It shows a correlative of severe damage, with holes in the casing, in the string which is next to the permeable, fluid bearing intervals. It is the condition of the casing, in intervals such as these, which has to be known to enable the engineer to properly evaluate future potentials and cost estimates of the well.

Figure 3 is a section of the log from this well illustrating the magnitude of the outside circumferencial damage and indicating areas where this has resulted in holes in the casing.

This survey has proven to be the most accurate method of locating perforated intervals, determining effectiveness, as well as indicating shot density. This is illustrated in Figure 4.

Well completion equipment is detected with the Vertilog as illustrated in Figure 5 showing scratchers and centralizers.

THEORY OF OPERATION

The Vertilog® instrument is designed for maximum resolution for each size of casing. Because of this a different tool is required for each size of casing. Figure 6 gives tool specifications for the available sizes. The instrument designed to survey 8-5/8" O.D. casing is shown in Figure 7.

A basic block diagram of the Vertilog system incorporating the shoes, electronics, wireline, and recorder is shown in Figure 8.

The downhole instrument consists of six or twelve shoes (depending on size casing being surveyed), an electromagnet and two electronic packages. Figure 9 illustrates the shoe section of the tool. Each shoe has four transducers, two connected to each electronic package. The Flux Leakage (FL) electronic package processes the signal relating to the severity of the corrosion. The Eddy Current (EC) electonic package discriminates between internal and external corrosion.

The two electronic packages relate directly to the two principles used in the Vertilog system.

The magnetic flux leakage detection theory is used in the FL package and eddy current sensing is used in the EC package.

Since the recorded log, the magnetic principles, and electronic packages are all inter-related they will be discussed together.

Flux Leakage

The Flux Leakage electronic package will be discussed first. The signals processed through this package are recorded in tracks one and two on the log.

If a DC current is sent through a coil of wire, a magnetic field will be generated along the axis of the coil. The magnitude of the magnetic field will be determined by the amount of current sent through the coil and the number of turns in the coil of wire.

This magnetic field consistes of lines of force called magnetic flux lines. These magnetic flux lines have two basic properties that the Vertilog system uses.

1. Magnetic flux lines will travel through casing much easier than they will through air or fluids.
2. One magnetic flux line will not cross another flux line.

The Vertilog instrument has a coil of wire in its center. A regulated DC current is sent through the coil of wire. The magnitude of the current is made great enough to saturate the bodywall of the casing with magnetic lines of flux. As long as the bodywall of the casing is consistent then most of the magnetic flux lines will travel through the bodywall of the casing. This is illustrated in Figure 10. When corrosive pits appear, then flux leakage will occur. The amount of flux leakage that occurs will be proportional to the percentage of metal loss in the bodywall of the casing. When a coil of wire is passed through an area of flux leakage a small voltage will be generated.

The magnitude of the voltage will be determined by the design of the coil, the speed of the coil as it passes through the area of flux leakage, and the amount of flux leakage that the coil passes through.

Each shoe on the Vertilog tool has two coils of wire, called transducers, for flux leakage detection. The size of the coils are constant. The logging speed is constant at 125'/min. These conditions make the

recorded signal of the flux leakage proportional to the percentage of metal loss in the bodywall of the casing. A visualization of the magnetic flux lines flowing around a pit in the casing bodywall is illustrated in Figure 11a. The resultant signal as the Vertilog® shoes pass the anomaly is illustrated in Figure 11b, 11c, and 11d.

The FL electronic package is divided into two sections and corresponds to the two rings of shoes on the instrument. The top ring of shoes is recorded in the FL-1 track and the bottom ring of shoes is recorded in the FL-2 track.

Since circumferential corrosion will produce a higher signal than an isolated pit of the same casing bodywall penetration, a method to distinguish between the two is necessary.

All the transducers in the top ring of shoes are connected to the circuit that produces the Average signal. The averaging circuit takes a portion of the signal that is produced by each transducer and adds them. A casing collar will produce a signal equal to 360 degrees in circumference. If we take the height of a signal produced by a casing collar on the average track and divide this height by the number of transducers in the top ring of shoes, then it can be determined what percentage of the signal each transducer contributed. Experimentation has shown that a signal recorded in the Average track that is equal to or greater than the percentage produced by 2½ transducers indicates an anomaly that is circumferential in nature.

The Average Track will also confirm that the Vertilog instrument is functioning properly. Anytime a signal is recorded in Flux leakage track one there should be a corresponding signal in the Average track.

Eddy Current

The amount of Flux leakage detected has been found to be related to the location of the leakage with respect to the transducers. Relative to the Vertilog instrument this means that internal corrosion will produce a greater signal on the log than external corrosion of the same casing bodywall penetration. The causes of internal and external corrosion are different so the interpretation of internal and external corrosion of FL-1 and FL-2 on the log will be different. The Discriminator circuit differentiates between the two--using an eddy current sensing technique.

By varying the amplitude and polarity of a current flowing through a coil of wire, a corresponding variance in the amplitude and polarity of the magnetic field produced by the coil will occur. If an electrical conductor is placed in this varying magnetic field, small varying eddy currents will be in the electrical conductor due to the relative movement of the magnetic field with respect to the electrical conductor. These eddy currents will produce small magnetic fields of their own. The small magnetic fields will have a polarity opposite that of the original field and will resist the original field.

This magnetic "resistance" is reflected back to the coil and causes a small change in amplitude of the current passing through it. The amplitude of the current passing through this eddy current coil is affected by the distance of the coil from the conductor, the electrical conductivity of the conductor, the permeability of the conductor, the design of the coil, the frequency of the current, and the amount of the conductor present. A change in any of these factors will produce a corresponding change in the amplitude of the coil's current.

Each shoe on the Vertilog instrument has two eddy current coils. The two coils are located so that the area of the casing that affects them is also the area that affects the flux leakage transducers.

It has been shown that an increase in the frequency of the current through the eddy current coil will reduce the depth of the metal which affects the amplitude of the current. The frequency of the eddy current used in the Vertilog instrument was selected high enough so that less than .040" of metal on the inside wall of the casing is affecting the eddy current coil. Any change in this metal thickness will cause a change in the amplitude of the current flowing through the coil.

It is this change in the current amplitude that the eddy current electronics sense. This change is recorded on the Discriminator track on the log. If the signal on the Discriminator track has a corresponding signal on FL-1 or FL-2 then the corrosion that has taken place is considered to be internal. If there is no corresponding signal on FL-1 or FL-2 then the signal is interpreted as poor pad contact.

CALIBRATIONS

Rigid calibration standards are required to insure accuracy of measurements.

Prior to logging a well the tool is calibrated. A magnetic signal of a known level is induced into each transducer. Each transducer has its own amplifier located within the instrument. Each amplifier is

adjusted so that the magnetic signal induced in each transducer gives the same response on the log. This calibration procedure is necessary so that all transducers will react identically to the same anomaly.

The standard for the tool calibration is responses observed in casings of known weights with machined defects. Figure 12 shows the Horizontal Tester used to record the measurements. Casing with known defects, 15, 30, 40, 50, 60, 75, 90 percent metal loss, (as shown in Figure 13) is placed on stands at the end of the horizontal tester and the Vertilog® tool is mounted in the tester. The responses of the machined defects are recorded. Then an auxiliary calibrator is used in the field for calibration purposes.

INTERPRETATION

Before an interpretation of the log can be made certain information is helpful if available. This is the size, weight, and grade of the casing being inspected. It is also beneficial to know the size and length of the surface casing and the size and length of any intermediate string of casing that may be present.

Other information that is helpful if available is the location of centralizers, scratches, D-V collars, perforations or any other equipment that would alter the string of casing. This information should be made available to the engineer at the well site. The logging engineer will include this information when the log is submitted for interpretation.

When the log is received for interpretation, each joint of casing is numbered starting at the surface. The depth of the surface casing is marked on the log along with all other available information.

The casing will be inspected on a joint by joint basis. The FL-1 and FL-2 tracks in each joint of casing are examined for indications of the most severe damage. The full joint of casing will be graded from its weakest point. After it has been determined which is the most severe damage the Discriminator is used to determine if the corrosion is internal or external. Next the Average track is checked to determine whether corrosion is isolated or circumferential. The above damages are identified and marked on the log.

A unique advantage with the Vertilog system is that the inner strings or multiple strings can be surveyed for corrosion or other damages. This condition causes a decrease in amplitude of the signal, however, if casing configurations are known it does not cause interpretation problems. This decrease in amplitude is also true for isolated corrosion over circumferential corrosion, and external corrosion over internal corrosion.

After all four tracks have been checked the interpretation is made using charts. Charts relating the flux leakage responses to percentage metal loss are designed for each casing size, weight, and grade. Other parameters such as internal or external, isolated or circumferential corrosion, single or multiple strings are also considered in the interpretation. These charts are derived in the laboratory using machined defects as references and cross-checked with measured damages in recovered casings.

The joint of casing will then be classified either Class One, Class Two, Class Three, or Class Four. This classification will be stamped on the log to indicate the amount of damage. The four classes represent percentage of metal loss in the casing. Class One indicates less than 20% metal loss, Class Two indicates 20% to 40%, Class Three indicates 40% to 60%, and Class Four indicates over 60%. After all joints of casing have been evaluated and recorded, a final report is prepared. Figures 14, 15, and 16 are representative of the three reports included in the interpretation. Figure 14 is a brief casing record as supplied from the well history. The report summarizes the interpretation of the log with the number of joints of each class of percentage of corrosion as illustrated by Figure 15. Any unusual signals or well completion equipment will be noted in the remark section. This report also includes a listing of all joints of casing that show evidence of corrosion exceeding 20% and the type of defect that has taken place. This is illustrated by Figure 16. This interpretation along with the recorded log will give a very complete record of the condition of the casing in the well at the time of the survey.

The Vertilog alone cannot identify the cause or rate of progression of the corrosion. However, if a base log is established on a given well, subsequent inspections will evaluate the rate of progression.

There are other surveys available which may help to evaluate the condition of a given well. Since each logging survey relates to different parameters of the well, a combination of surveys will help develop an understanding of the overall condition of a well.

An Acoustic Cement Bond log will show the areas where the cement is protecting the external surface of the casing. It has been noted that external corrosion usually occurs in uncemented sections.

A Magnelog will indicate different weights of pipe where this information is unavailable. It will also

locate severe damage in casing sizes for which no Vertilog tools are available.

A Casing Potential Profile will help determine the effectiveness of a cathodic protection program. If the well is in its native state, this survey will help determine the area where electro-chemical corrosion might occur.

A Sonan Survey in conjunction with a Differential Termperature survey will help locate casing leaks, and help determine the magnitude and direction of fluid movement outside the casing.

FIELD EXAMPLES

In determining the condition of casing in existing wells many examples have been documented illustrating measurements as indicated with the Vertilog® and defects confirmed after the casing was recovered.

Figures 17 and 18 are illustrations of recorded damage as confirmed with photographs of the recovered casing.

CONCLUSION

The Vertilog can be successfully used to determine the condition of the casing at the time the log is run. The Vertilog is useful in detecting and monitoring casing corrosion. This survey is an improvement of existing methods of casing inspection because of its improved sensitivity and its ability to detect and evaluate smaller anomalies. Also its surveys the complete circumference of the casing. Another advantage is that this service does not require special fluids in the borehole. The Vertilog in conjunction with other measurements will help formulate techniques to solve corrosion problems.

The Vertilog is helpful in resolving questions that might arise concerning perforated intervals or shot density.

REFERENCES

1. Bradshaw, James M. "Vertilog: A Downhole Casing Inspection Service" presented at Corrosion/76, Houston, March 22-26, 1976.

2. Cook, A. D., "Vertilog: A Downhole Inspection Service" Technical Memorandum, Vol. 7, No. 1, March 1976.

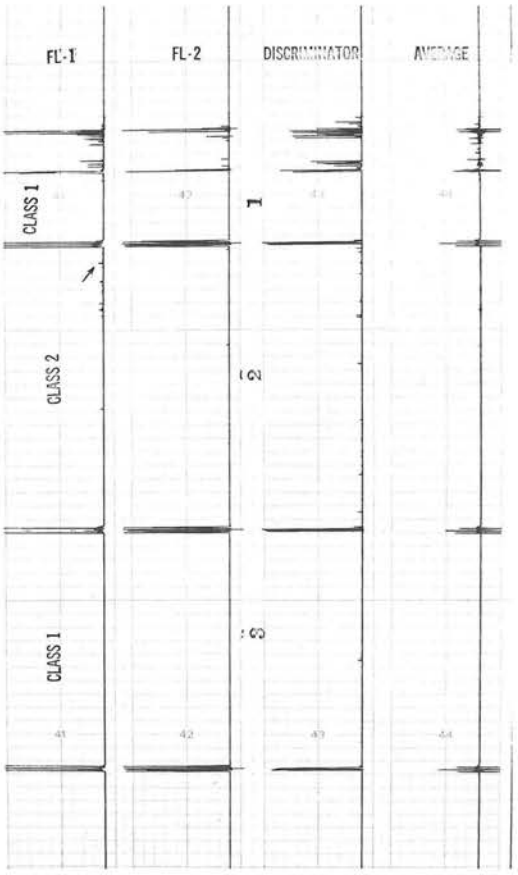

Figure 1 - Standard Vertilog Presentation

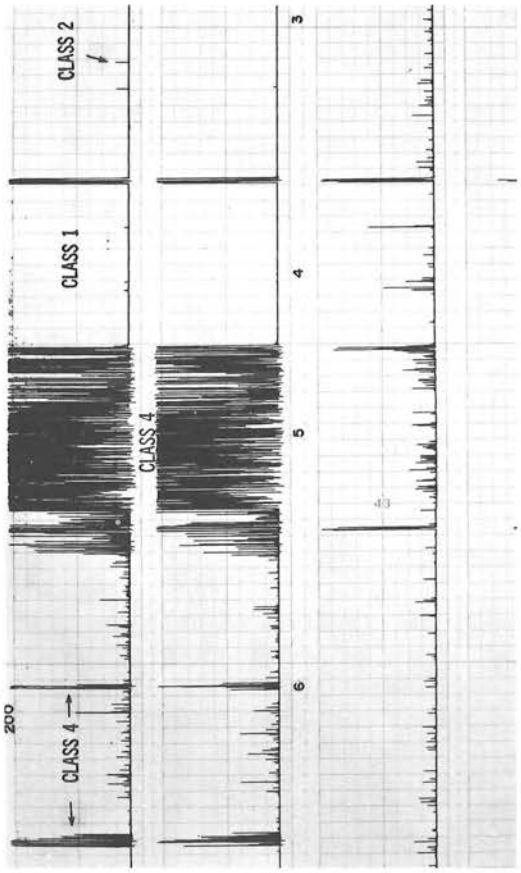

Figure 3 - Severe Casing Damage

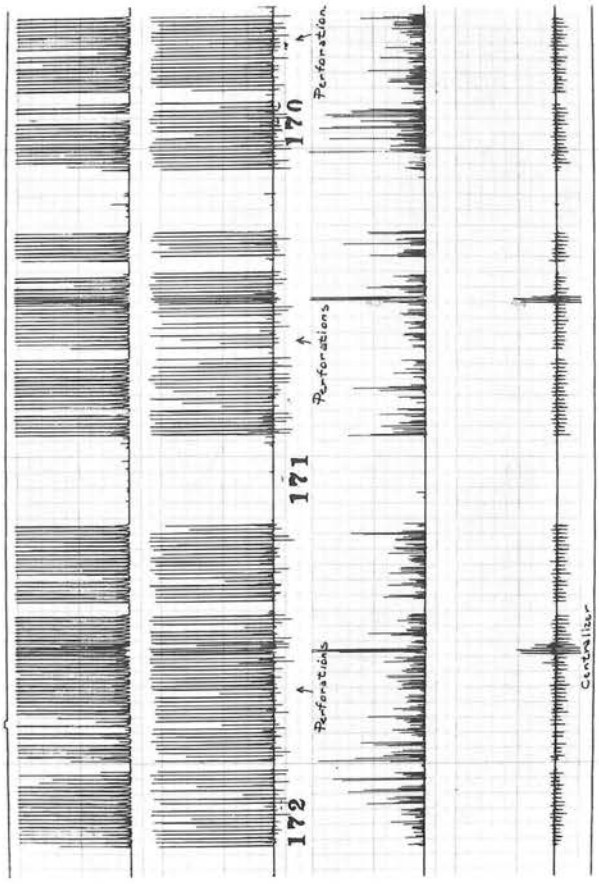

Figure 4 - Perforations As Shown By Vertilog

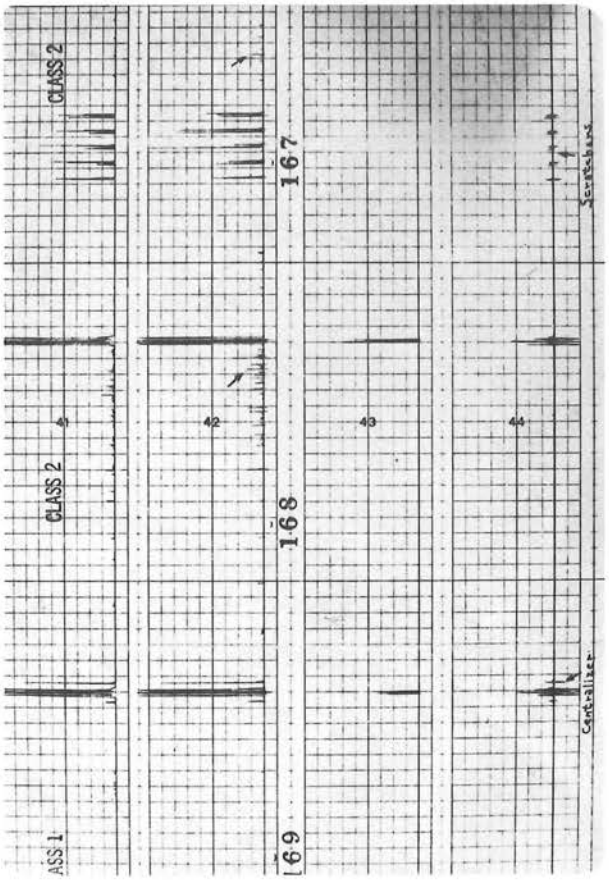

Figure 5 - Well Completion Equipment

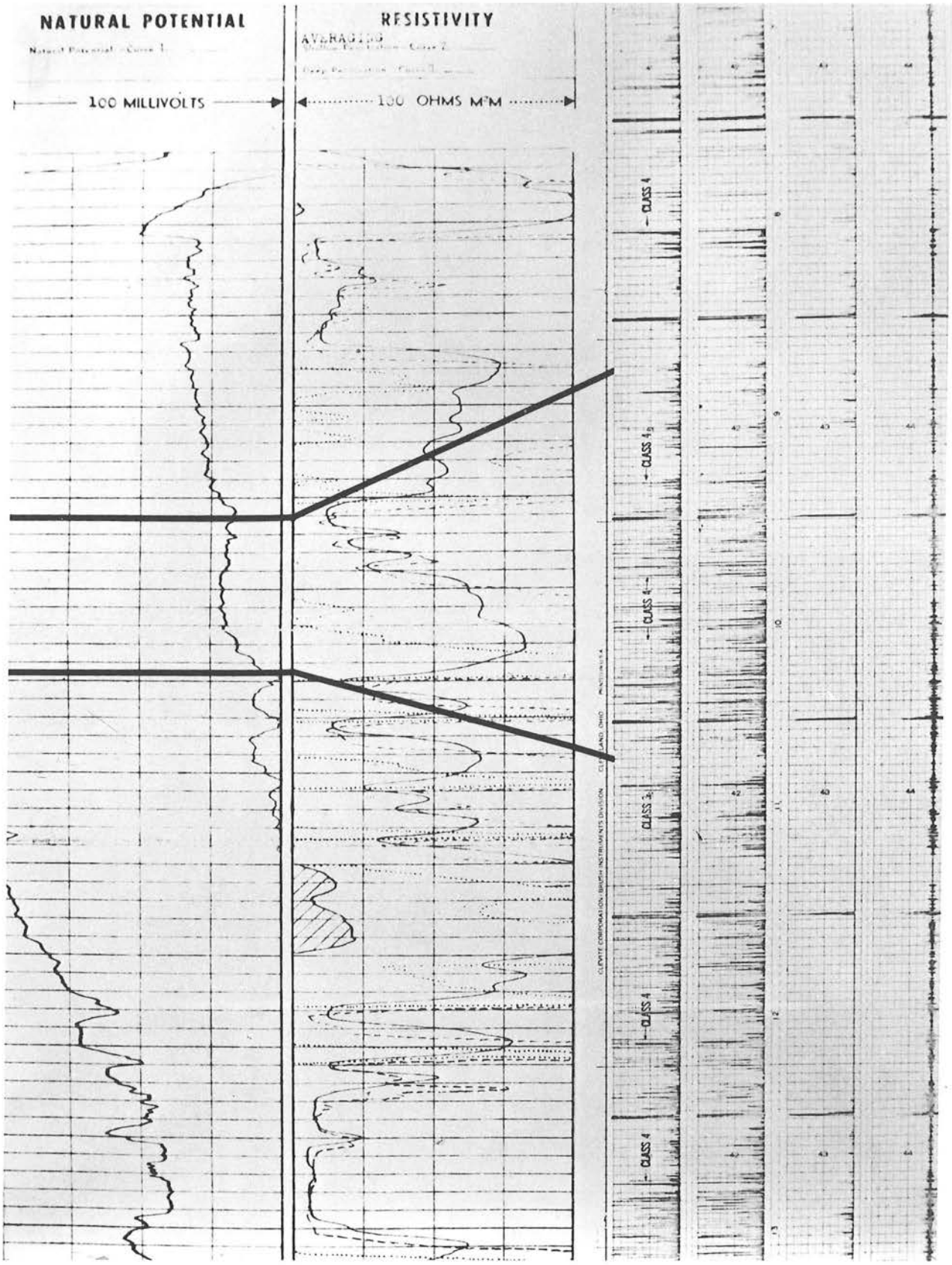

Figure 2 - Electrolog - Vertilog Comparison

Dresser Atlas
VERTILOG-DOWNHOLE CASING INSPECTION

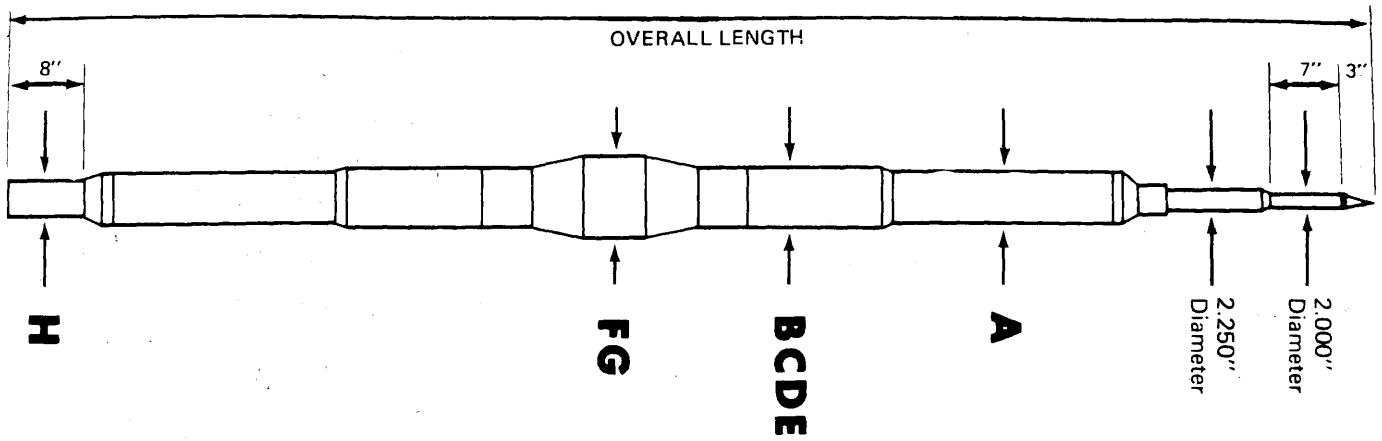

Tool Specifications

	Specifications	4½"Tool	4½"Tool 5"Transducers	5½"Tool	5½,,Tool 5"Transducers	7"Tool	8-5/8"Tool
A	Diameter	3.437	3.437	3.437	3.437	4.875	4.875
B	Diameter	3.625	3.625	4.250	4.250	5.500	7.125
C	#1 Sleeve Diameter	3.875	3.875	4.625	4.625	5.875	7.310
D	#2 Sleeve Diameter						7.500
E	#3 Sleeve Diameter						7.700
F	Minimum Diameter	3.743	3.882	4.447	4.325	5.923	7.358
G	Maximum Diameter	4.954	4.954	5.579	5.579	7.363	8.391
H	Diameter	3.438	3.438	3.438	3.438	3.438	3.438
	Approx. Weight (lbs.)	225	225	260	260	440	650

Overall Length of Tool

	Specifications	4½"Tool	4½"Tool with 5"Transducers	5½"Tool	5½"Tool with 5"Transducers	7"Tool	8-5/8"Tool
	No Sinker Bar	10'-10-7/32"	10'-10-7/32"	10'-10-7/32"	10'-10-7/32"	11'-1-1/32"	11'-1-9/32"
	1 Sinker Bar	13'-10-7/32"	13'-10-7/32"	13'-10-7/32"	13'-10-7/32"	14'-1-1/32"	14'-1-9/32"
	2 Sinker Bar	16'-10-7/32"	16'-10-7/32"	16'-10-7/32"	16'-10-7/32"	17'-1-1/32"	17'-1-9/32"
	3 Sinker Bar	19'-10-7/32"	19'-10-7/32"	19'-10-7/32"	19'-10-7/32"	20'-1-1/32"	20'-1-9/32"

1 Sinker Bar weighs approximately 140 lbs.

Figure 6 - Tool Specifications

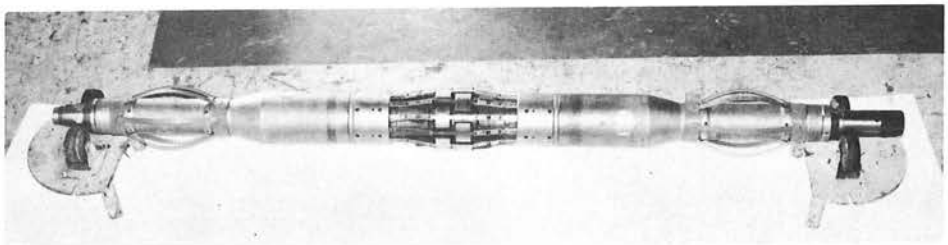

Figure 7 - 8-5/8" O.D. Vertilog Tool

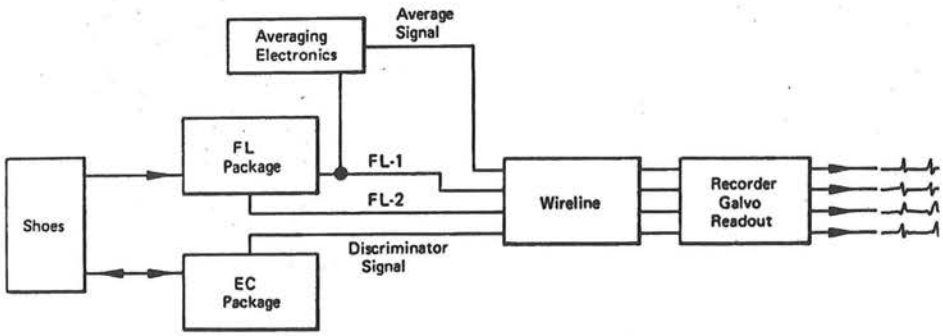

Block diagram of the Vertilog® system.

Figure 8 - Block Diagram of the Vertilog System

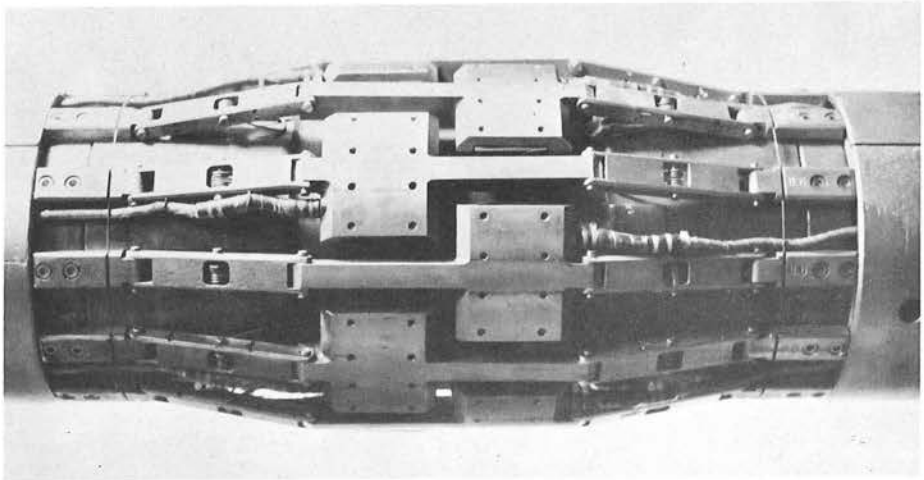

Figure 9 - Shoe Section

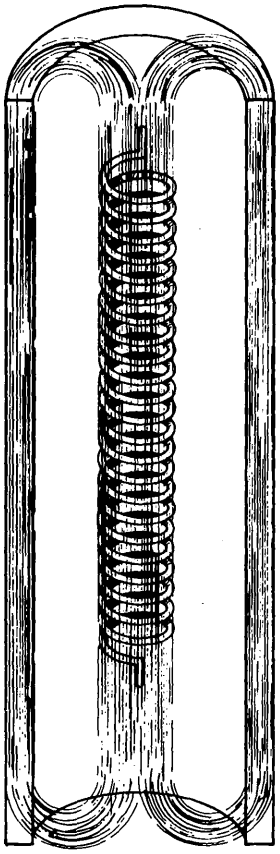

Figure 10 - Flux Lines

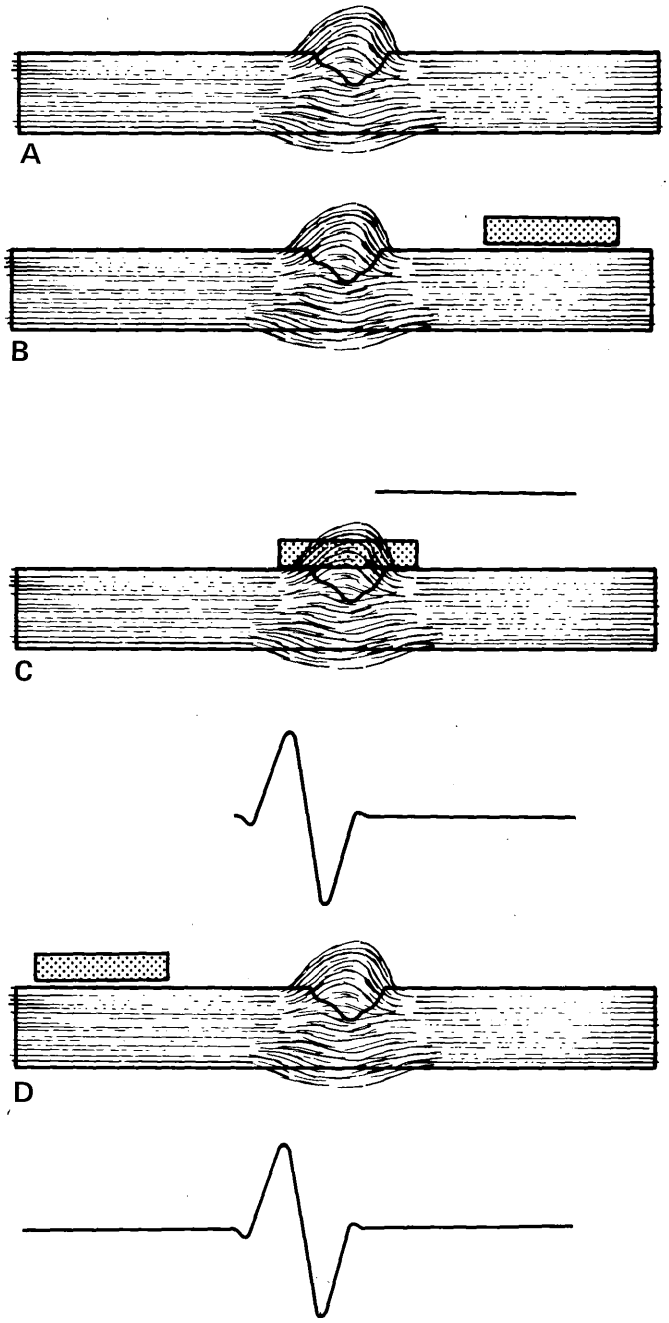

Figure 11 - (A) A Visualization of Magnetic Lines of Flux Flowing Around A Pit In Casing Bodywall, (B) The Signal Produced As A Shoe Approaches The Pit, (C) As It Passes Over The Pit, and (D) As It Leaves The Pit

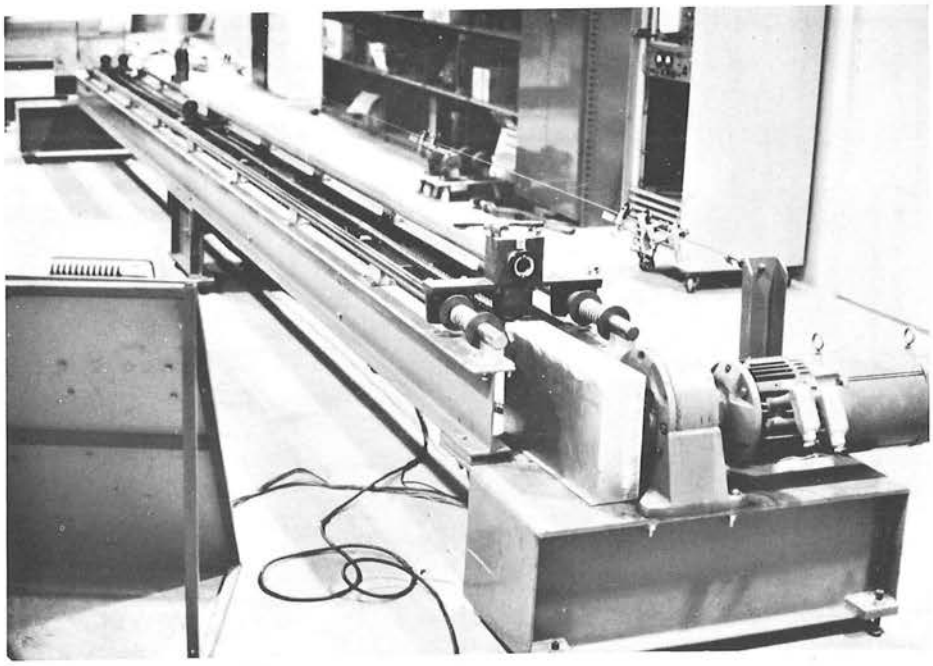

Figure 12 - Horizontal Tester

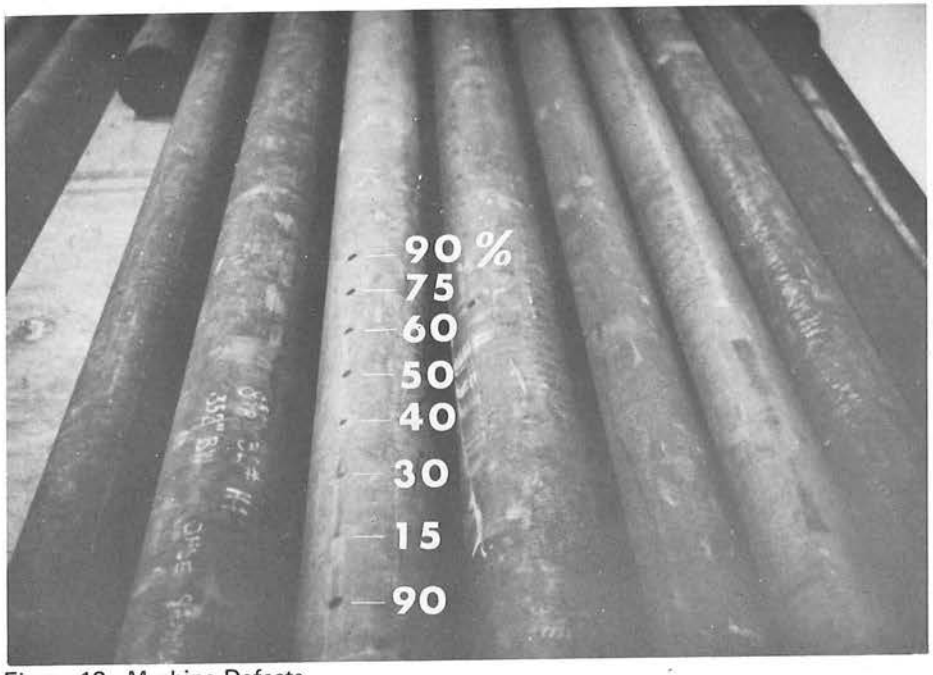

Figure 13 - Machine Defects

VERTILOG®

CUSTOMER	Wildcat Oil Company		DATE 2-14-77
LEASE/WELL NO.	Hope 1		
FIELD	New Hope	COUNTY Kern	STATE California

CASING RECORD

DRESSER ATLAS MEASUREMENTS	CUSTOMER CASING RECORDS
10 3/4" @ 225'	10 3/4" @ 225'
7" @ 1100'	7" @ 1102'

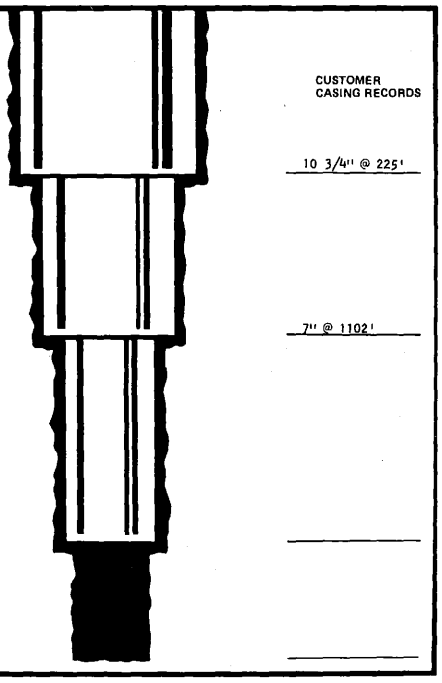

Figure 14 - Casing Record

VERTILOG®

CUSTOMER	Wildcat Oil Company	WORK ORDER NO. 345		DATE 2-14-77	
LEASE/WELL NO.	Hope 1	CUSTOMER ORDER NO. 123			
FIELD	New Hope	COUNTY Kern		STATE California	
CASING O.D. 7"	WEIGHT(S) 26#	NOMINAL WALL THICKNESS .362		GRADE J-55	
TOTAL FOOTAGE INSPECTED 1100'		FROM Surface	TO 1100'		DEPTH

SUBSURFACE CASING INSPECTION REPORT

SUMMARY

20	LENGTHS WERE FOUND TO SHOW NO EVIDENCE OF CORROSION EXCEEDING PERCENT OF THE NOMINAL BODY WALL.	20% CLASS 1
5	LENGTHS WERE FOUND TO SHOW EVIDENCE OF CORROSION EXCEEDING PERCENT BUT LESS THAN 41% PERCENT OF THE NOMINAL BODY WALL.	20% CLASS 2
4	LENGTHS WERE FOUND TO SHOW EVIDENCE OF CORROSION EXCEEDING PERCENT BUT LESS THAN 61% PERCENT OF THE NOMINAL BODY WALL.	40% CLASS 3
1	LENGTHS WERE FOUND TO SHOW EVIDENCE OF CORROSION EXCEEDING PERCENT OF THE NOMINAL BODY WALL.	60% CLASS 4
30	TOTAL LENGTHS	
1100'	TOTAL FOOTAGE	

REFERENCE FOR FOOTAGE MEASURE Surface

LENGTHS ARE NUMBERED FROM Surface

COMMENTS Length #26 and #28 appear to have centralizers located on them, if none present then Class 3 corrosion exists.

SERVICED BY

Figure 15 - Summary

VERTILOG®

CUSTOMER	Wildcat Oil Company	WORK ORDER NO. 345		DATE 2-14-77	
LEASE/WELL NO.	Hope 1	CUSTOMER ORDER NO. 123			
FIELD	New Hope	COUNTY Kern		STATE California	
CASING O.D. 7"	WEIGHT(S) 26#	NOMINAL WALL THICKNESS .362		GRADE J-55	
TOTAL FOOTAGE INSPECTED 1100'		FROM Surface	TO 1100'		DEPTH

SUBSURFACE CASING DEFECT REPORT

LENGTH NO.	TYPE DEFECT	PENETRATION	LENGTH NO.	TYPE DEFECT	PENETRATION
	Inside Surface Pipe				
3	O.D. I.P.	20-40			
5	O.D. I.P.	20-40			
	Outside Surface Pipe				
8	I.D. I.P.	40-60			
9	O.D. C.C.	40-60			
10	O.D. I.P.	20-40			
15	I.D. I.P.	20-40			
18	O.D. I.P.	20-40			
25	O.D. I.P.	40-60			
26	O.D. C.C.	40-60			
29	O.D. I.P.	over 60			

ABBREVIATIONS:
O. D. – OUTSIDE DIAMETER
I. D. – INSIDE DIAMETER
O. S. – OUTSIDE SURFACE PIPE
I. S. – INSIDE SURFACE PIPE
T. L. – THROUGHOUT LENGTH
I. P. – ISOLATED PITTING
C. C. – CIRCUMFERENTIAL CORROSION
M. C. – MINOR CORROSION
S. C. – SEVERE CORROSION

Figure 16 - Casing Defect Report

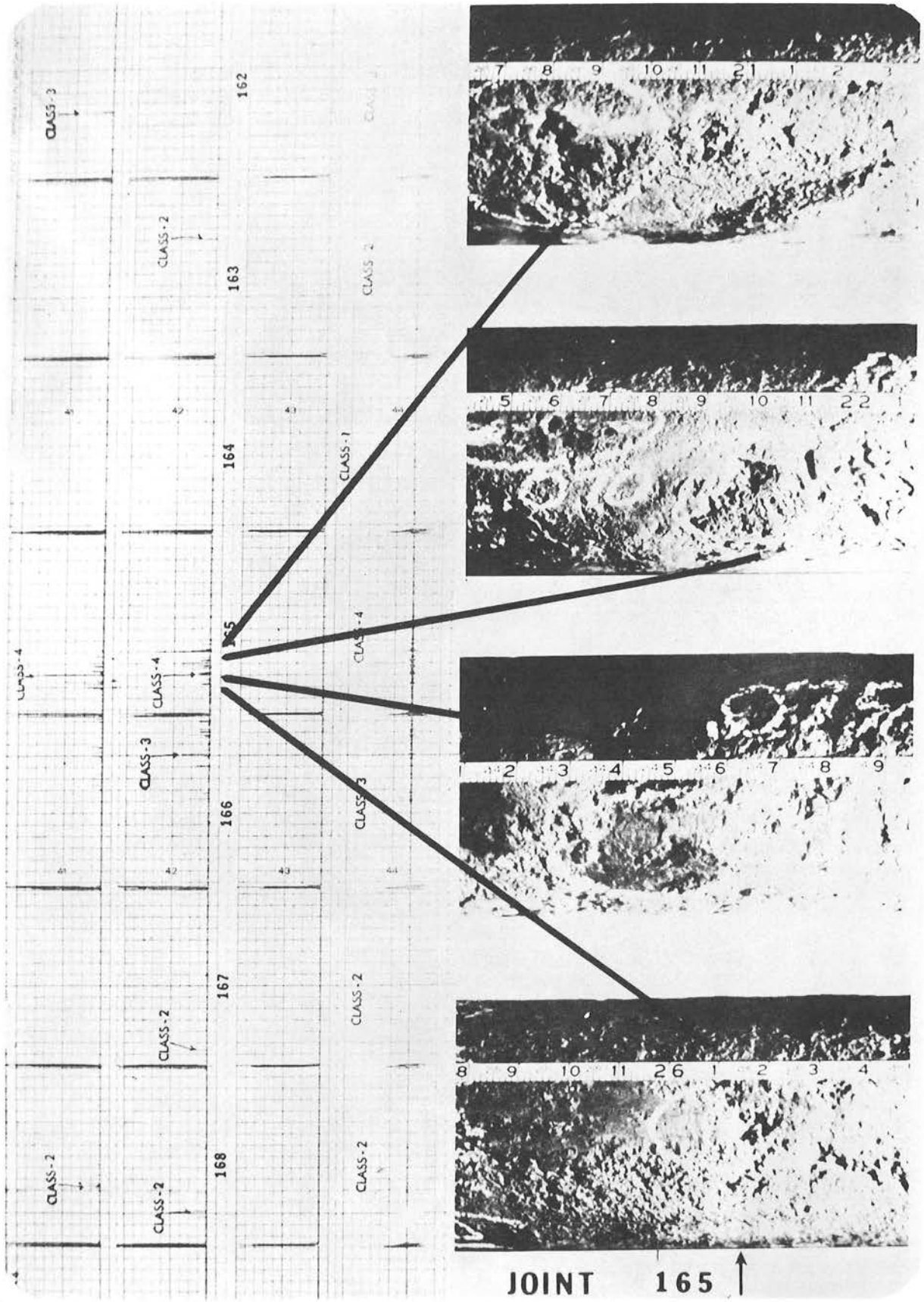

Figure 17 - Vertilog and Recovered Casing Example

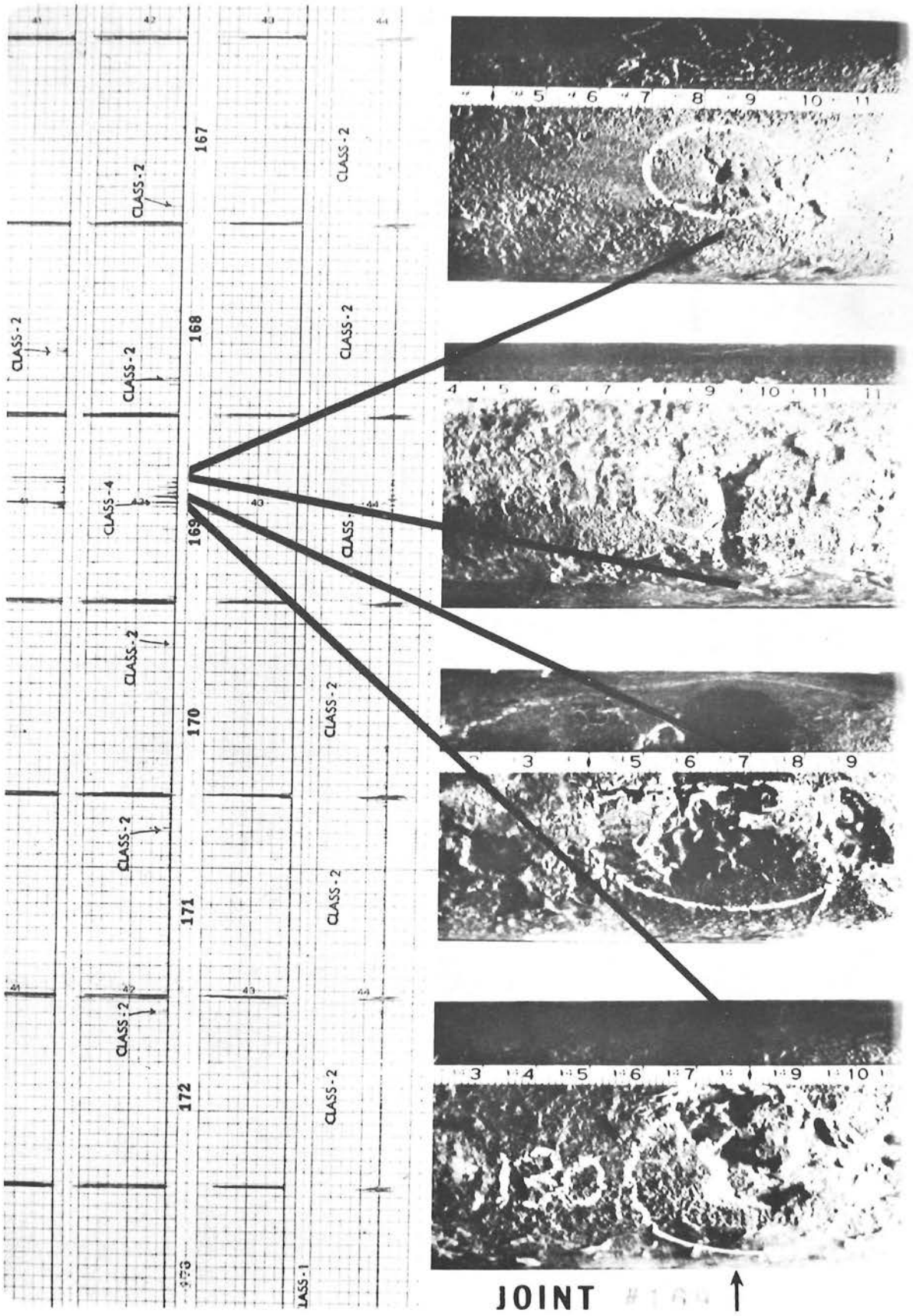

Figure 18 - Vertilog and Recovered Casing Example

Ex. II - 2

Order Reprints | Permission to Copy

Ultrasonic Or MFL Inspection: Which Technology Is Better For You?

by **Hartmut Goedecke, GE Oil & Gas,** United Kingdom

The pipeline operator can make an informed choice as to which inspection technology to use — UT or MFL — in part by using assessment information provided in this article. GE Power Systems, Oil and Gas, PII Pipeline Solutions (PII) has more than 35 years experience in pipeline inspection using high resolution techniques and, as such, offers the industry an authoritative view of both MFL and UT technologies.

Listed here are discussions about several factors ranging from pipeline features and typical defects to operating conditions of a pipeline. The benefits of using each type of technology are outlined. Both ultrasonic (UT) and magnetic (MFL) are good inspection technologies and are available in the full range of popular pipeline diameters.

Both MFL and UT techniques offer benefits for pipeline inspection projects. Taking pipeline features and defect types into account, each technology has its strong points, and the choice of tool depends to a large extent on some knowledge of the type of defects to be encountered. In some cases, operational factors need to be balanced against performance factors. In other cases, cleaning issues in heavily waxed pipelines may make the MFL technique the more robust choice.

Tool Technologies

Depth sizing accuracy. The MFL tool measures magnetic leakage fields. The measured field strength and field extension are dependent on the depth and extension of the defect, but they also depend on other factors such as defect shape, wall thickness, magnetization, magnetic properties, and speed. The algorithms to turn the measured magnetic field into defect dimensions are based on defect-sizing models and experience and must take into account many secondary influences.

Historically, the results of the first-generation MFL tools were not very satisfactory, but BG (British Gas) and then PII developed advanced electronics and analysis algorithms and software which set new standards in the industry. Defect depth sizing now has a typical accuracy of (10 percent of wt with a confidence level of 80 percent. For a typical wt of 8 mm this would be ±0.8 mm.

The ultrasonic technique employed in PII's UT tool is used extensively in all parts of industry. Given smooth steel surfaces, this technology has a depth-sizing accuracy of 0.1 mm. In the pipeline environment, the accuracy very much depends on the surface roughness of the walls measured. The unperturbed spool wall thickness is measured locally with an accuracy of ±0.2 mm, whereas corrosion, which has usually quite rough surfaces, is measured with an average depth accuracy of ±0.5 mm at a confidence level of 95 percent. Up to 22 mm wt this accuracy is independent of wt.

Figure 2 and Figure 3 display the defect detection and sizing capability and accuracy of both tool types. The principal difference is that for MFL the accuracy is given as percent of wt, whereas for UT the numbers are in mm, independent of wt or pipe type.

This means that a performance comparison is dependent on wall thickness. Accuracy for both tools is identical at 5 mm wt, which also happens to be the lower limit of the UT wt inspection range. This means that for all wt >5 mm, UT is the more accurate technology.

Defect surface area. In both technologies data are displayed in graphical form as a multi-trace diagram or "C-Scan". Figure 1 displays the MFL and Ultrasonic data of the same spool piece. This comparison shows how the ultrasonic data relate directly to the defect surface area,

Figure 1: C-Span Comparison

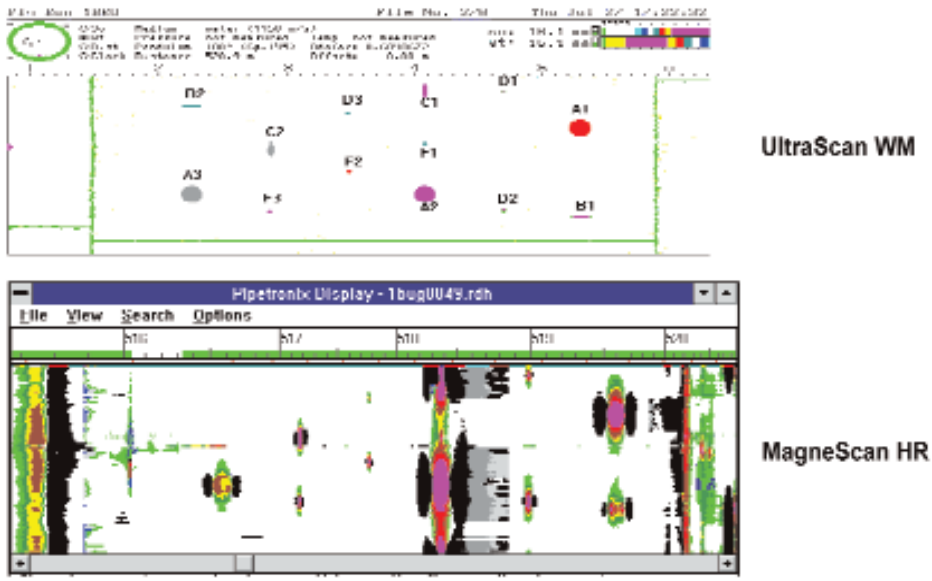

Figure 2: Magnescan - 12-56", **Manual Specification - Pipe Body**

	GENERAL METAL-LOSS @4t * 4t		PITTING @ 2t * 2t		AXIAL GROOVING		CIRCUMFERENTIAL GROOVING	
	SMLS	SW	SMLS	SW	SMLS	SW	SMLS	SW
Depth At Pod=90%	9%Wt	5%WT	13%WT	8%WT	13%WT	8%WT	9%WT	5%WT
Depth Sizing Accuracy At 80% Confidence	10%Wt	+10%WT	10%WT	+10%WT	-15% / +10%WT	-15% / +10%WT	-10% / +15%WT	-10% / +15%WT
Width Sizing Accuracy At 80% Confidence	20mm	+20mm	20mm	+20mm	20mm	+20mm	20mm	+20mm
Length Sizing Accuracy At 80% Confidence	20mm	+20mm	20mm	+10mm	20mm	+20mm	20mm	+20mm

whereas the magnetic data cover a much wider surface area that require a complicated sizing function to enable a prediction of the surface area.

This demonstrates a basic difference in the technologies. For MFL the data analysis has to take many secondary effects including defect shape into account, whereas for ultrasonics the defect dimensions can be deduced directly from the data because they are based on direct wt measurement.

Confidence Level. The confidence level for defect depth sizing is higher for UT at 95 percent vs. 80 percent for the MFL data. This means that in addition to having a higher accuracy, the UT results will be within this accuracy more often.

Figure 3: General Inspection in 5 mm to 22 mm Wall Thickness Pipeline - PII Standard -

	Pitting with diameter 10 mm (all pipe types)	Pitting with diameter 20 mm (all pipe types)		Axial Grooving	Circumferential Grooving	Lamination Fabricated or HIC
Min. Depth at POD = 90%	1.5 mm	1 mm	1 mm	1 mm	1 mm	1 mm
Depth Sizing Accuracy at 95% Confidence	Detection only	0.5 mm	?0.5 mm	0.5 mm	0.5 mm	0.5 mm
Width Sizing Accuracy at 85% Confidence	12 mm	12 mm	12 mm	12 mm	12 mm	12 mm
Length Sizing Accuracy at 85% Confidence	6 mm at 1 m/sec	6 mm at 1 m/sec	6 mm or 1% of length at 1 m/sec	6 mm or 1% of length at 1 m/sec	6 mm at 1 m/sec	6 mm at 1 m/sec or 1% of length

Note: POD = Probability of detection; POI = Probability of identification

Pipeline Features

Next, we should consider the features of a pipeline, inasmuch as MFL and UT technology operate better in different types of pipeline.

Thick wall. To achieve the optimum inspection results with the MFL technology, the pipe wall must be fully saturated with magnetic field. For thicker walls, the magnets need to be stronger and take up more volume. In smaller diameter tools, only magnets up to a certain size can be fitted, which limits the wt capability of these MFL tools.

Typical wt capabilities range from 8 mm for a 6-inch tool to 38 mm for a 42-inch XHR tool. Ultrasonic tools, on the other hand, can inspect wt up to 45 mm, independent of tool diameter. For lines with thick wall, especially in the small diameter range, the UT tool is the right choice.

Thin wall. The direct wall thickness measurement capability of the ultrasonic system now only works for remaining wt values of 2.5 mm and above, and thinner wall can only be measured when the second echo can be detected.

This means that external defects with less than 2.5 mm wt remaining may only be reported as "very deep with remaining wt less than 2.5mm." For internal defects the defect depth can always be measured via the stand off, so this restriction does not apply. Due to this restriction the application of the UT tool for lines with nominal wt below 5 mm is not feasible. For thin-wall pipes with deep external defects, the MFL tool is the right choice.

Diameter variations and dual diameter. Based on their sensor carrier design, the UT tools can cope with relatively large internal diameter variations, such as ±10 to ±15 percent for standard tool designs. For MFL tools, this figure varies from ±5 to ±10 percent.

There are dual-diameter tool designs for both tool technologies that cover large variations in nominal pipe diameter, like 25 percent for UT or 15 to 20 percent for MFL. Although there are several dual-diameter kits for these applications available for MFL tools, the UT tool design still offers the advantage that the dual-diameter capability can be obtained relatively easy as a variation of an existing tool in any diameter, thereby improving the availability and economy for dual-diameter applications.

Stainless steel and cladded pipe. Stainless steel has low magnetic permeability and can therefore not be inspected with MFL technology. In pipelines with stainless steel cladding, the carbon steel wall can be magnetized by the MFL tool, but the cladding causes a sensor liftoff which reduces the signal picked up by the sensor.

For stainless steel and cladded pipelines, the UT technology can be employed without problems, as long as the cladding is firmly bonded to the carbon steel, which is usually the case.

Seamless pipe. Two typical features of seamless pipes are varying general wall thickness and local wall thickness patterns, which are typical for the production process. In the MFL data analysis, the recorded signals are set in relation to the wall thickness of the pipe joint. The fact that this wall thickness is only known as a nominal value within a very wide tolerance band causes the MFL inspection results to be less accurate for seamless pipe than for seam-welded pipe.

Additionally, the local wt patterns cause a background signal level, which tends to hide shallow defects. Consequently, the detection threshold is higher in seamless pipe. The UT tool constantly records the true wall thickness of the pipe. Manufacturing patterns are displayed and easily recognized.

Defects are measured accurately in conjunction with the real local wt. This means that during analysis, the depth can be related to the true wt such that many quite deep defects, which happen to be in a portion of thicker wall, turn out to be harmless, and shallow defects in thinner wall are more dangerous than expected. In these circumstances, UT can be the best-suited technology for seamless pipe.

Special Defects

There are some kinds of defects, which can be detected by one technology but not by the other. On one hand, MFL tools do not see defects which cause no leakage field, and on the other hand, UT tools do not detect defects which are smaller than the ultrasonic beam.

Lamination and blisters. Lamination is a classical case of a defect which cannot be detected by MFL, but which shows up clearly in the UT data. One particular strength of UT is the detection of HIC-related lamination and blistering. MFL tools are capable of indicating sloping lamination penetrating the inner or outer pipe surface.

Very small pittings. Pittings need to be above 20 mm diameter (or above 10 mm for the pitting tool) to be measured reliably with the UT tool. For thin wall pipe with 5 mm wt this relates to a threshold size of 4t (or 2t respectively) (t=wt). The MFL tool, on the other hand, can detect and measure pittings down to 7 mm diameter (or 0.4t for thick wall). This is another reason why MFL tools are particularly suited for thin wall pipe or small diameter pitting.

Channeling corrosion. MFL tools measure mainly the change of magnetic stray flux. This means that for long and shallow defects they see only the beginning and end of the defect and it is difficult to determine the depth correctly. UT tools measure the correct wt of longitudinal channeling corrosion over the entire length. The TranScan TFI tool, a magnetic tool with transverse magnetization, also detects this type of defect very well. This tool will find very narrow channels and longitudinal cracks which are open to the surface.

Cracks in girth welds. MFL tools are capable of detecting radial cracks in the circumferential girth welds. These often arise as manufacturing defects due to poor welding procedures. The UT tool

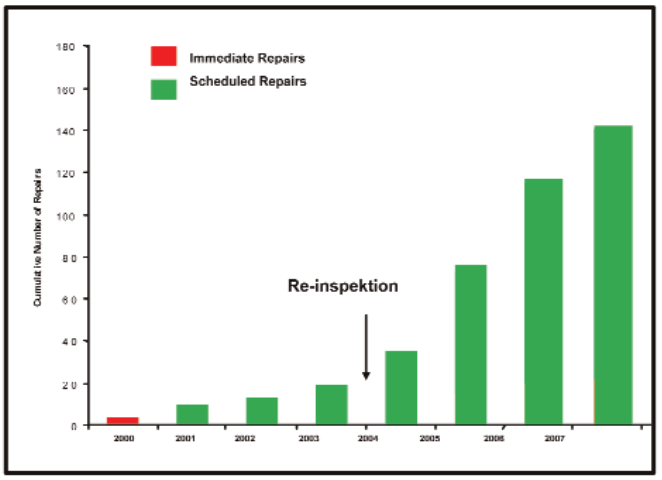

Figure 4

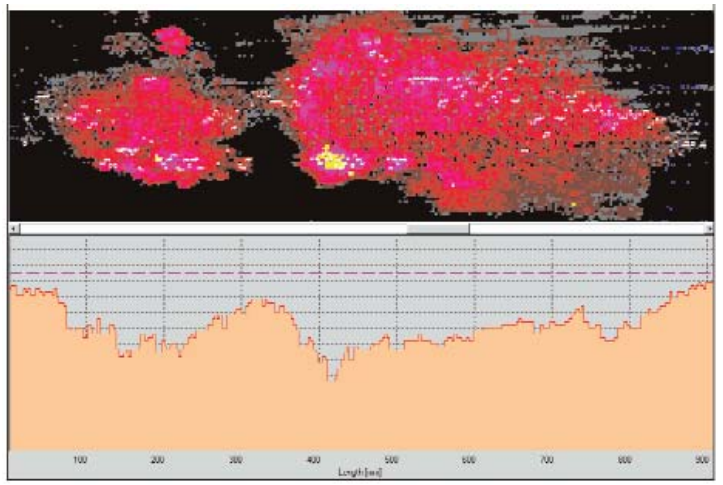

Figure 5

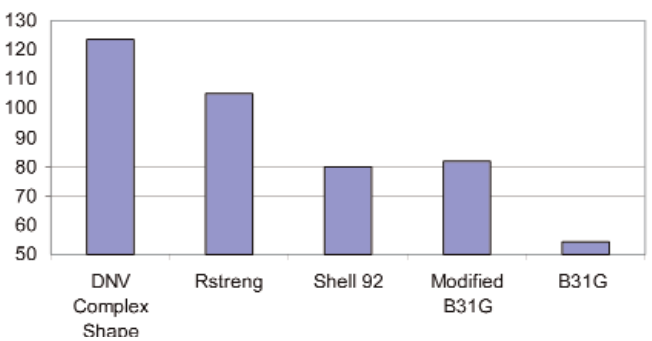

Figure 6

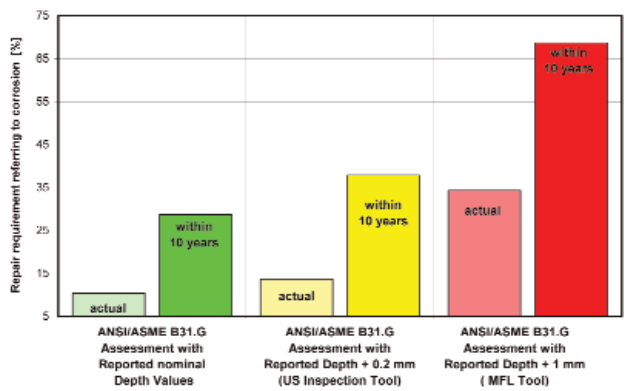

Figure 7: Influence of the degree of accuracy with respect to corrosion depth on actual and long term repair requirement. (BAsis: Inspection results of a corroded pipeline)

cannot see this kind of defect.

Grinding metal loss. Repair grindings sometimes have considerable metal loss associated and should be taken note of. Grindings are difficult to detect or size with MFL because the transitions are smooth, the wt change is very gradual and the grinder can significantly change the magnetic properties of the remaining steel. The UT direct wt measurement is better suited for detecting this type of defect.

Baseline surveys. Inspecting a brand new pipeline with an intelligent tool can be very advantageous for the pipeline owner because any irregularities found can be corrected under the guarantee clause.

Using a UT tool, the spool wt (specially seamless) can be accurately checked and defects like lamination or metal loss, misalignments, repair grindings and others reported. This is also an effective quality check of the manufacturing and construction process.

Small irregularities, which do not affect the structural strength and have passed the hydro test, can be passed over as save during later inspections.

Operating Conditions

The operating conditions within a pipeline are extremely important to find the appropriate type of technology.

Speed. MFL and UT tools operate over different speed ranges.

This range is typically:

- 0.3 to 5 m/sec for MFL, and
- 0.1 to 1 m/sec for UT, with 2 m/sec as an option for some UT sizes.

For gas lines, where the speed is considerably higher than in liquid lines, the MFL tools are again more suitable. Additionally, a bypass speed control unit is available for large diameter MFL tools (>24 inches), thus extending the applicable speed range for that tool type up to 12 m/sec.

Liquid lines operate at 1 to 2 m/sec, with 3 m/sec as exception. Lines are generally slowed down to 1 m/sec for an UT inspection. When this is not possible, a MFL tool should be run. The next generation of UT tools will operate at higher speeds.

The very low speeds of some liquid lines do not present a problem to UT tools, but would at the moment for MFL tools. The next generation of MFL tools will operate at lower speeds.

Pressure. Gas lines operate at pressures

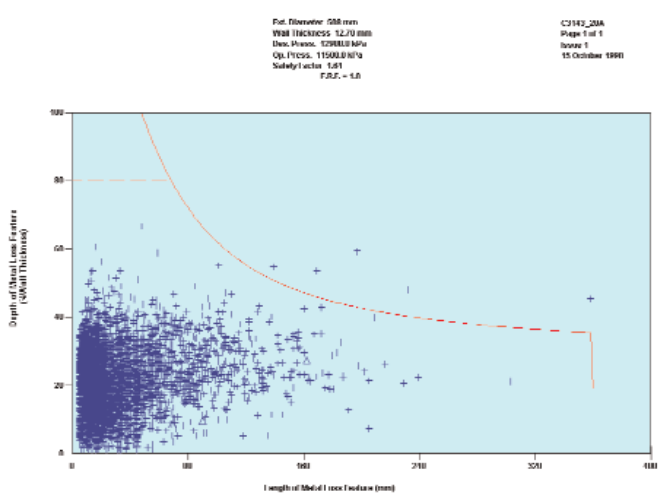

Figure 8

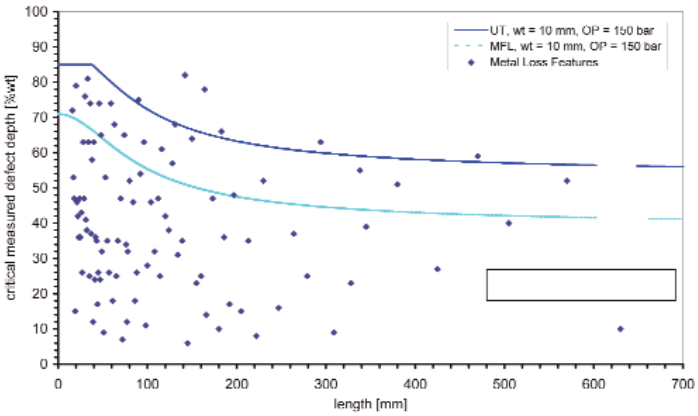

Figure 9

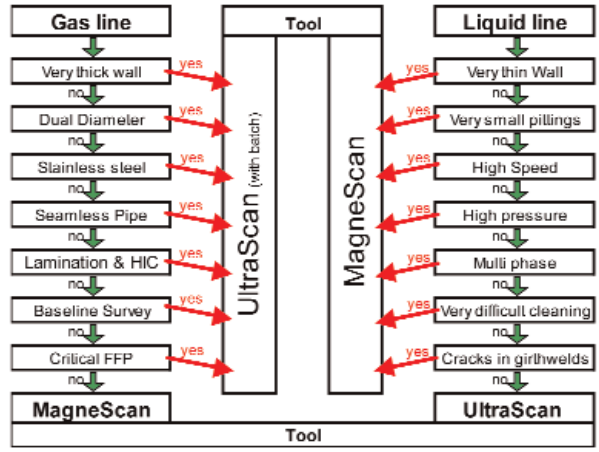

Figure 10: Choosing the right tool.

as high as 200 bar, whereas liquid lines usually are not run above 80 to 100 bar. Consequently, MFL and UT tools are designed for 220 bar and 120 bar respectively. The 120 bar pressure rating of the UT tool may restrict its use in some offshore high pressure gathering lines.

Advanced FFP

Fitness For Purpose (FFP) Calculations. When an inspection shows that a pipeline has areas of corrosion, the next task is to determine the influence of the corrosion on the safe operation of the line. The general aim is to calculate the safe operating pressure for each defect, and then only repair those defects, which are a safety hazard, and continue operating the line with the presence of the harmless defects. Repeat runs after periods of time will provide data to determine the corrosion growth, which can then be used to design repair programs with the least repairs for future years. At the point where annual repair cost takes a sharp rise, it becomes economical to carry out a re-inspection to re-evaluate the remaining corrosion and update the corrosion growth data, Figure 4.

The accuracy and confidence level of the inspection data have an important influence on the economy of the repair and rehabilitation programs.

Assessment codes. The most commonly used code is ANSI/ASME B31 G.

However, this code provides overly conservative answers, and in the case of pipelines with many defects, the number of repairs according to B31 G can be substantial, and it is more economical to use more advanced assessment codes such as RSTRENG or DNV RP F 101, which are less conservative.

Figure 6 provides a comparison of the results: for a given defect (Figure 5) the safe operating pressure according to B31 G is the lowest, whereas the DNV RP F 101 code provides a much higher safe operating pressure. Assuming the line to operate at 110 bar would mean a repair according to the B31 G and RSTRENG codes, but no repair according to the DNV code.

The RSTRENG and DNV codes need more information on the defect than B31 G, the most important being the profile of the defect. The ultrasonic method provides an accurate and detailed profile of the defects. Therefore, UT data are very well- suited for these advanced assessment codes.

Accounting for accuracy and confidence level. Inspection data have tolerances and in order to provide safe FFP calculations these tolerance levels must be taken into account. The magnitude of the tolerance affects the amount of rehabilitation and repair work as shown in Figure 7. The chart shows the immediate repairs and the repairs within the next 10 years, using the nominal depth values as a reference, as shown in the left section of the chart.

The middle and right sections show the repairs required with the tolerances of different tool types taken into account. The best tolerances result in the least repairs, which means money saved in the repair program. In some cases, pipelines have been evaluated with over 1 million corrosion defects. In these cases, statistical methods are used to cope with the wealth of data.

It is customary to display defects in a pressure-sentenced plot, as shown in Figure 8. An acceptance curve, which is generated according to the assessment code used, separates the defects that can be accepted without repair from those that must be repaired at the given operating pressure. The shown chart is based on B31G with nominal defect dimensions entered. To allow for tolerances caused by accuracy and confidence level, one option would be to recalculate all defect dimensions accordingly, which is very tedious.

A better way is to calculate a designated acceptance curve for each set of accuracy and confidence values. DNV RP F 101 includes such a procedure — the acceptance curves for MFL and UT tools are shown in Figure 9 for a pipe with 10 mm wt. The curve corresponding to the tool with the lower accuracy has the lower position on the graph, which means a group of deeper defects, which can be accepted when they are measured by the more accurate tool, cannot be accepted when measured by the lower accuracy tool. Again the data set with the smaller tolerances leads to fewer repairs.

Conclusions

For all defect assessment and growth calculations the tool with the higher depth-sizing accuracy — the UT tool — offers substantial savings to the customer by reducing the number of necessary repairs and stretching repair programs over longer time periods.

The MFL tool, on the other hand, offers big advantages from the operational point of view for surveys in gas lines. Here, the UT tool needs to be run in liquid batches, a process which adds cost to a survey project. The UT tool also generally needs a cleaner line than the MFL tool, which could affect the economy of the inspection project in very difficult-to-clean crude oil pipelines. It is therefore recommended to first consider the MFL tool for all gas lines, and the UT tool for all liquid line projects. ***P&GJ***

REFERENCES

"Assessing the value of advanced internal inspections in pipelines," by Mark Marley, Dave Taberner and Andy Tallin, DNV, NACE conference "Corrosion 2002," paper no. 02076.

"Anwendung stochastischer Modelle zur Beurteilung des Schädigungszustandes von Pipelines" ("Application of stochastic models for the evaluation of the damage condition of pipelines") of by T. Hoffmann and A. Brückner-Foit, University of Kassel, Institut für Werkstofftechnik, DVM report no. 233.

Ex. II - 3

SPE
Society of Petroleum Engineers

SPE 22101

Full-Signature Multiple-Channel Vertilog

G.W. Adams and W.D. Moffat, Atlas Wireline Services

Copyright 1991, Society of Petroleum Engineers, Inc.

This paper was prepared for presentation at the International Arctic Technology Conference held in Anchorage, Alaska, May 29–31, 1991.

This paper was selected for presentation by an SPE Program Committee following review of information contained in an abstract submitted by the author(s). Contents of the paper, as presented, have not been reviewed by the Society of Petroleum Engineers and are subject to correction by the author(s). The material, as presented, does not necessarily reflect any position of the Society of Petroleum Engineers, its officers, or members. Papers presented at SPE meetings are subject to publication review by Editorial Committees of the Society of Petroleum Engineers. Permission to copy is restricted to an abstract of not more than 300 words. Illustrations may not be copied. The abstract should contain conspicuous acknowledgment of where and by whom the paper is presented. Write Publications Manager, SPE, P.O. Box 833836, Richardson, TX 75083-3836 U.S.A. Telex, 730989 SPEDAL.

ABSTRACT

A new version of the Vertilog flux leakage (DC Magnetic Inspection) pipe evaluation tool has been developed. This new system is called the Digital Vertilog (DV). This paper presents an explanation of the DV tool theory, operating system and its working components. The sensor system of the standard Vertilog has been provided with an updated data gathering system in order to increase the information available to the log analyst. This new system transmits true bi-polar representations of each flux leakage sensor and a number of eddy current sensors to the surface recorder. The multiple bi-polar flux leakage (FL) channels allow easier interpretation by contrasting changes due to hardware and corrosion. Some of the features more easily determined include pitting, perforation (including the phase of gun used), scratchers, and centralizers. Log examples generated in the lab and their interpretation will be presented. These examples successfully demonstrate the advantage of recording full signature wave response and accurately differentiating pipe hardware from corrosion.

INTRODUCTION

The Vertilog pipe evaluation tool utilizes flux leakage and eddy current detectors to inspect both the inner and outer wall of the primary pipe string. Previous experimentation[1] prompted the development of a new generation of Vertilog tool. These instruments utilize downhole digital processing to provide a new element to the Vertilog survey. Switched gain circuits controlled at the surface improves the signal response. The downhole digitization of the data allows the recording of each flux leakage channel and a number of eddy current channels. This allows true circumferential inspection of the pipe. The high data rate of the system reproduces the true bi-polar characteristic of the flux leakage signals. This allows easier interpretation between hardware and corrosion. Figure 1 shows a typical casing configuration. Notice that some of the collars of the production string are surrounded by centralizers, which hold the casing centered within the wellbore. Also note that scratchers appear on the outside of some casing joints. These are used to roughen the surface of the wellbore before cementing. The Vertilog survey is recorded while moving upward within the production string. In the earlier Vertilog survey, casing hardware (e.g., scratchers and centralizers) caused responses which are similar to corrosive defect responses. Often casing records must be relied upon for identifying the log responses due to scratchers and centralizers, to insure that these responses are not misinterpreted as casing defects. If the records are accurate, casing hardware responses are not mistakenly interpreted as defects. If the records are inaccurate, casing hardware responses can be interpreted as corrosive defects. The Digital Vertilog survey provides bi-polar data channels. The additional log data permits identification of casing hardware responses without reference to the casing records. From the log data alone, corrosive defect responses can be differentiated from casing hardware responses. Even if the casing records are inaccurate, the additional log data prevents the misinterpretation of casing hardware responses as defect responses.

References and figures at end of paper.

Digital Vertilog System Overview

The Digital Vertilog tool is composed of an electromagnet and sensor assembly housed in the mandrel section and

three electronic sections. There are four different mandrel sizes. The electronics are designed to be used with all four mandrel sizes. Figure 2 shows a Vertilog tool mandrel. The coil of the electromagnet is located under the shoes containing the sensors. The poles of the electromagnet are formed by the electronic housing of the mandrel. On the sensor section shown in Figure 3 two separate rings of shoes are mounted in an overlapping arrangement. This insures certain detection of corrosive defects.

Flux Leakage (FL)

Figure 4 shows a representation of the flux field produced by the tool's electromagnet. A DC current produced uphole is injected into the electromagnet's coil. This produces a static magnetic field in the core, which is coupled to the casing across air gaps at the tool's poles. In the example, flux lines that are not present in the casing have been omitted for clarity. In a section of casing without defects, the field is uniform. Around defects, the field is disturbed and flux lines leak out of the casing wall. The tool's FL coils respond to the flux leakage according to Maxwell's equations:

$$\oint_l E \odot dl = -\int_s \partial\beta/\partial t \odot dS + \oint_l (v \otimes \beta) \odot dl \qquad (1)$$

Removing the fixed reference point and applying Stoke's theorem reduces the above equation to the point relation:

$$\nabla \otimes E = -\partial\beta/\partial t \qquad (2)$$

Thus the amplitude of the coil's output is proportional to the rate of change of the magnetic flux density. Since the vector of the flux is determined by metal gain, or metal loss in the field, the coil's output will also reflect loss or gain. It has been empirically determined that an equation of the form;

$$A_1 * \ln((\nabla \otimes E) * A_2 + 1) \qquad (3)$$

can be used to generate interpretation charts. The values of the "A" factors are empirically determined from data obtained from actual pipe samples.

Eddy Current (EC)

An eddy current system is used to detect changes in the internal wall of the casing being surveyed. Injecting an alternating current into a coil of wire will produce an alternating magnetic flux field around the coil. The coil is then placed parallel to a conducting material (pipe). As a magnetic field expands and collapses, small circulating currents are set up in the material. These currents, eddy or Foucault currents, are set up in a direction which resists the change in the injected flux field. The circulating currents generate their own magnetic fields of opposite polarity to the original field. These opposing fields act as a load on the coil, affecting the amplitude of the current passing through the coil. As the frequency of the AC field increases, the EC losses will increase. As the material moves further away from the coil, the loading effect decreases and the amplitude of the coil current will increase. Measuring the change in the current injected into the coil will give an indication of changes in the internal wall of the casing. As an EC coil passes an internal defect the pit wall moves away from the coil and the amplitude of the injected current increases. As the coil passes the defect, the pit wall moves towards the coil and the current returns to normal. By keeping the frequency of the injected current high, a skin effect is produced where the eddy currents set up in the casing will be present near the inner surface only.

Data Flow

Figure 5 is a block diagram of data flow in the Digital Vertilog. The diagram is broken up into three blocks, two analog circuits and digital circuitry. Each analog circuit processes up to twelve individual FL and EC circuits depending upon the size of the mandrel. Each FL coil in the mandrel is processed separately in a manner that preserves the integrity of the coil's data. Each EC coil in the mandrel is also processed separately. The individual signals are feed into the two switching circuits. This allows an analog to digital converter to access each signal individually, converting each tool signal to a 2's compliment value. The digitized signals are then accessed by a microprocessor. The processor also controls the multiplexer switching and A/D conversion. Due to the amount of data acquired and the high tool speed of the Vertilog, two processors are used to reduce the overhead that communication with the surface telemetry produces. Both of the processor's circuits are housed in a flasked sub. The control processor handles all data acquisition and data processing. The communication processor handles all telemetry operations including data transmission to the CLS (Computerized Logging System). A high speed parallel interface between the processors allows transfer of data and instructions. Each processor has a ROM for programming. The control processor also has RAM for data and supplemental program downloading. The communication processors retains data in its own internal RAM.

Sensor Configuration

Consider a Vertilog tool with six shoes, three in the upper ring and three in the lower ring. Each shoe contains two FL sensors to detect changes of magnetic flux and two EC sensors which respond only to the defects on the inside pipe wall. A vertilog shoe cross section is shown in Figure 6 where the configuration of the FL and EC sense coils arrangement can easily be seen. To ensure that no defect escapes detection, the shoes of the upper ring are in a

staggered, overlapping relationship with the shoes of the lower ring, as shown in Figure 3. The Digital Vertilog is arranged to provide the signals from all twelve or twenty-four of the flux leakage sensors. Channels 1-2, 5-6 and 9-10 display the signals from the flux leakage sensors of the three shoes of the upper ring. Channels 3-4, 7-8 and 11-12 display the signals from the flux leakage sensors of the lower rings. In addition to the twelve bi-polar flux leakage signals, a Digital Vertilog provides twelve or twenty-four EC signals. The EC coil configuration is identical to the FL coil configuration.

Lab Tests

To assure both the reliability and accuracy of the Digital Vertilog, Atlas Wireline Services operates a surface calibration facility[2] at its center in Houston, Texas. This facility is used to record tool response data for calibration charts as well as all experimental data. To develop the test data for the DV survey, two separate joints of test pipe were individually positioned on the calibrator.

Log Examples

With regard to the Digital Vertilog presentation, mass changes effect the signals from the flux leakage sensor as follows:

1) A mass increase causes a positive (left) excursion of the flux leakage signal.

2) A mass decrease causes a negative (right) excursion of the flux leakage signal.

Figure 7 shows a pipe maintained as a calibration reference standard in the surface calibration facility. Typical of a reference standard, the pipe contains a series of machined defects, a regular casing collar and a flush joint collar. In addition, a casing centralizer has been placed around the regular collar and a scratcher has been placed on the pipe 1.25 feet above the flush joint collar.

Figure 8 shows the log response to this pipe. Figure 8A shows the response of the tool to the machined defects. A series of external defects are present on channels one and two. These defects are spaced six inches apart. The defects decrease in size from 90% to 20%. Six inches above the 20% defect is another 90% defect. Three inches above this defect is a 100% defect. The EC response on these two channels is to the 100% defect only. To machine internal defects of varying depths, the pipe wall is drilled through and an internal defect is machined on the opposite wall. Channels four and five respond to the internal defects. These defects exhibit the same pattern as the external defects, with the exclusion of the 100% penetration. Channels ten, eleven and twelve respond to the through holes produced during the machining process. All of the channels discussed exhibit EC response to the internal machining.

Figure 8B shows the response to a regular casing collar surrounded by a casing centralizer. The response to the centralizer shows metal gain just below ninety-six feet and metal loss at ninety-four feet. The response to the collar is characterized by five signatures. At the leading edge of the collar, a large metal gain response is first encountered. A smaller metal loss signature is shown at the edge of the lower casing. Metal gain is encountered at the edge of the upper casing. A large metal loss is encountered at the trailing edge of the collar. The final signature is the EC response to the gap between the two casings. The characteristic responses are present on all channels, showing the circumferential nature of the collar.

The tool's response to a flush joint collar is shown in Section 8C. The characteristic response of a series of three metal gain signatures is evident. The circumferential nature of the collar is also present in the tool's response.

Response to a scratcher is shown in Section 8D. A circumferential metal gain, followed by a circumferential metal loss signature is evident on all of the tool's FL signals.

Figure 9 shows a log response to the same pipe as figure 8. In this example, the casing centralizer has been moved to a location one foot above the scratcher.

The response to a regular collar is shown in Section 9A. The signature of the casing centralizer is not present.

The three sharp metal gain characteristics of a flush joint collar are still evident in Section 9B.

The scratcher's characteristic signature is present in Figure 9C.

The response to an isolated casing centralizer is easily identified in Section 9D. The response is the same as the response to a centralizer around a collar.

Figure 10 shows the log response to general corrosion. This pipe sample was pulled from a well in West Texas. A standard Vertilog survey was run on this well. The survey showed uncorroded pipe from the surface to 5572 feet. From 5572 to 5670, three casing sections were interpreted as class 4 with holes. This pipe sample was the casing section from 5604 to 5637. Visual inspection of the casing sample showed severe general corrosion on the exterior wall with five holes at different locations on the pipe. Details of the log are:

An isolated hole is present on channels one and two, shown in Section 10A.

In Section 10B annular corrosion is present on 66% of the circumference of the pipe. A hole is present on channel ten.

Section 10C shows that general corrosion is present on 33% to 66% of the external wall.

Section 10D shows that annular corrosion is present on 50% of the circumference of the pipe. A large hole is present on channel two through five.

Section 10E shows that severe annular corrosion is present on 100% of the circumference of the pipe, accompanied by a large hole.

Section 10F shows that an isolated hole is present on channels one and two.

Log Presentation

While the Digital Vertilog is ideal for identifying log responses due to corrosive defects, it is preferable to use a Computerized Logging System (CLS) generated log presentation to estimate the penetration of a defect. The generated presentation which accompanies the DV presentation, is shown in Figure 11. The ten chart division of the left hand track are reserved for the flux leakage average response, which is zero at the fifth division and increases simultaneously to the left and right. A 360 degree response is indicated by flux leakage average which covers ten chart divisions. The first five chart divisions of the right hand track are reserved for the eddy current response which is zero at the fifth division and increases to the left. The remaining fifteen chart divisions of the right hand track display the maximum flux leakage response, which is zero at the fifth division and increases to the right. For estimating penetration depth, the generated log is preferred because it offers more resolution than the DV presentation. To estimate the penetration depth of a defect, first determine the number of Vertilog units associated with the maximum flux leakage response, then:

1) Determine the casing O.D., weight and grade.

2) Determine whether the defect is inside or outside (an inside defect is accompanied by an EC response)

3) Is it an isolated pit or general corrosion.

4) Determine whether the defect is inside the surface pipe logging interval. If so, determine the O.D. of the outside casing.

Data charts are available for converting the maximum flux leakage response to a corresponding percent penetration. The value of the percent penetration depends on the condition summarized above. Figure 12 is the chart which is appropriate to the conditions enumerated in 1 - 4. The chart shows the percent penetration which corresponds to the number of Vertilog units of the maximum flux leakage.

CONCLUSION

The ability of the tested Digital Vertilog to transmit the entire signal as seen by the sensor coil provides an opportunity to better understand the condition of casing in a well. Corrosion is readily differentiated from completion equipment like scratchers and centralizers. Collars can be studied; the physical size of the collar and the location of the ends of the two joints of casing that are joined by the collar can be examined. Detailed analysis of the sensor signal itself (signal width, rise time, area, etc.) provides more information regarding the physical parameters of the anomaly. These types of studies which can be done have previously be unavailable in the industry. It has been demonstrated that analyzing the entire sensor signal enhances the ability to interpret anomalies responses in a pipe, whether they are equipment or corrosion.

NOMENCLATURE

$\partial/\partial x$ ≡ partial derivative with respect to x
$\oint_l$ ≡ line integral around a closed curve
$\int_s$ ≡ area integral over a specified surface
$\odot$ ≡ scalar product
$\otimes$ ≡ vector product
∇ ≡ gradient operator
ln ≡ natural logarithm to the base e = 2.718281828...
l ≡ linear displacement in meters
t ≡ time in seconds
S ≡ surface area in meters^2
v ≡ velocity in meters/second
E ≡ electric field strength vector in volts/meter
β ≡ magnetic flux density vector in tesla
%Penetration ≡ depth of a corrosive defect in percent of total nominal wall thickness
A_1 , A_2 ≡ dimensionless correlation coefficients

ACKNOWLEDGEMENT

Cooperation from J. McCarter and Dr. J. Hwang of Atlas Wireline Services, Houston, for supplying data for this project is gratefully acknowledged. The authors also wish to thank the management of AWS Technology department for permission to publish this work.

REFERENCES

1. Mato, S.A., "Multi-Channel Casing Inspection Instrument," presented at Operating Section Distribution/Transmission Conference, May 3-6, 1987, Las Vegas, Nevada.

2. Dresser Atlas, Dresser Industries Inc., "Casing Evaluation Services," 1985.

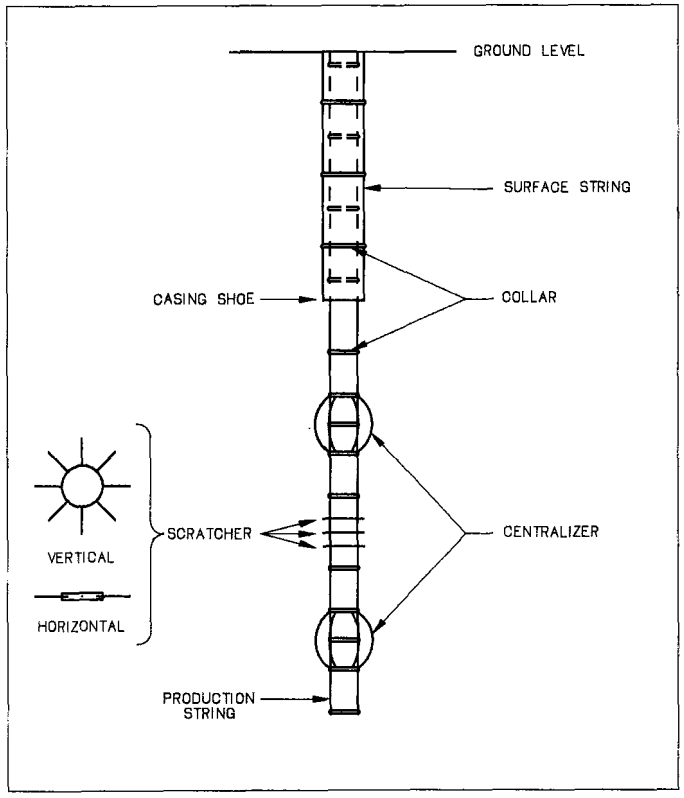

Fig. 1—Typical casing configuration in a well.

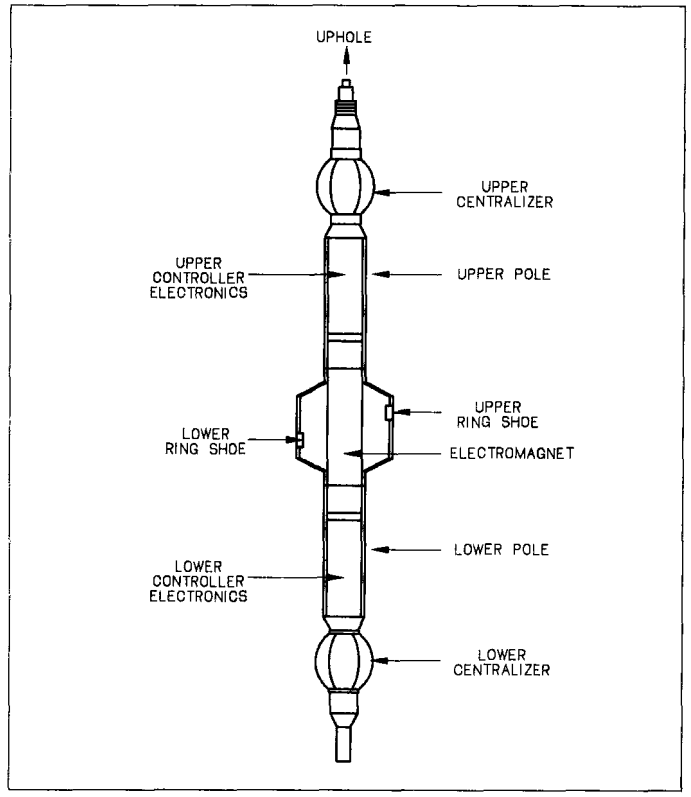

Fig. 2—Vertilog tool mandrel.

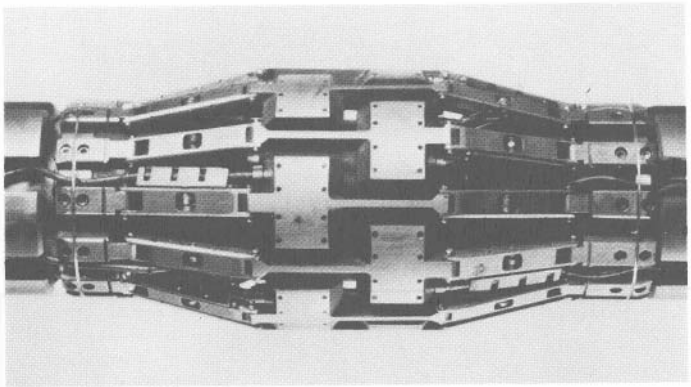

Fig. 3—Vertilog tool sensor section.

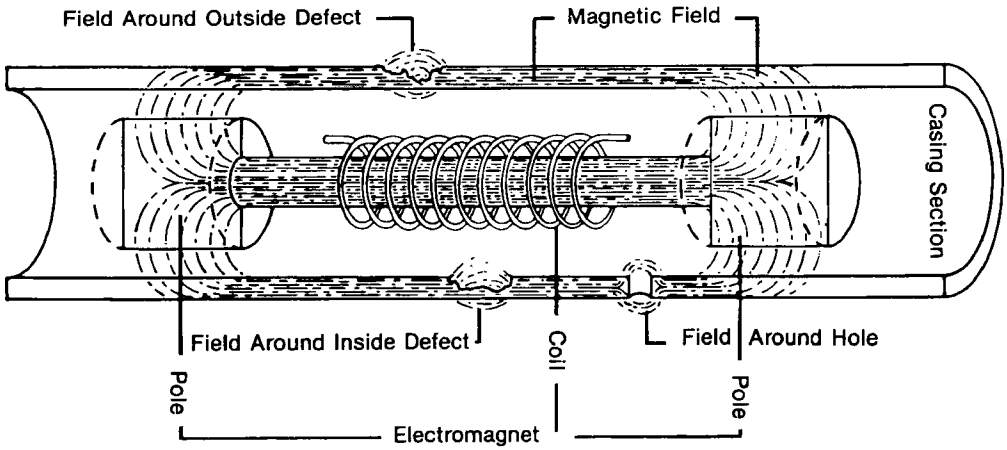

Fig. 4—Vertilog tool flux field.

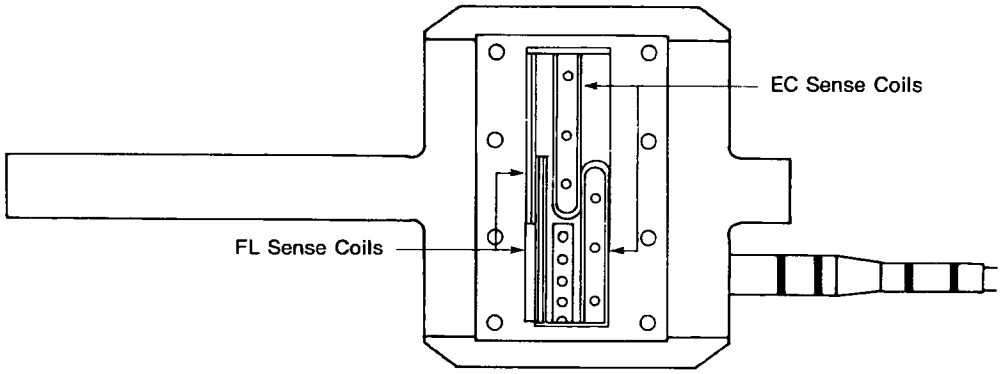

Fig. 5—Vertilog sensor pad.

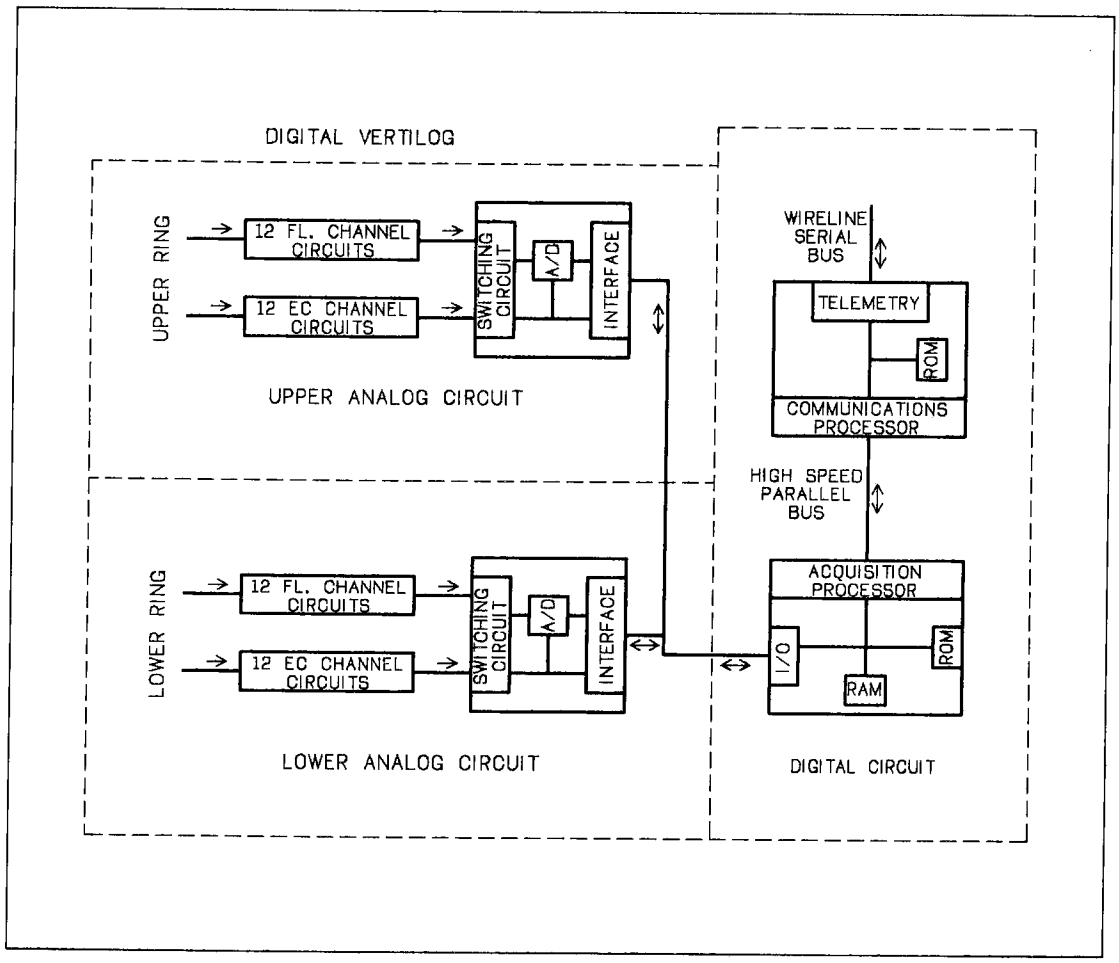

Fig. 6—Block diagram of data flow.

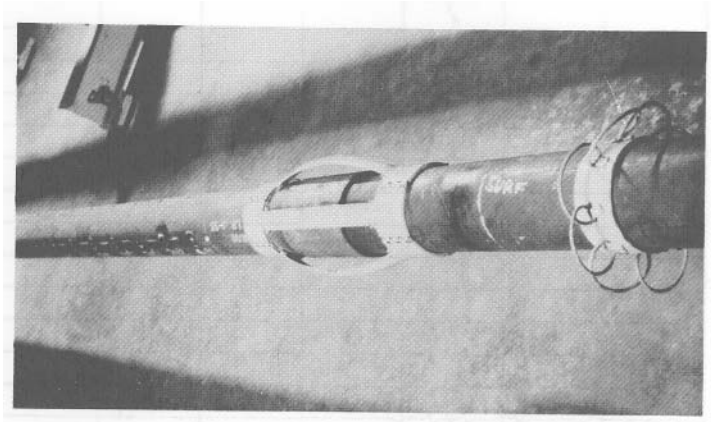

Fig. 7—Test pipe setup.

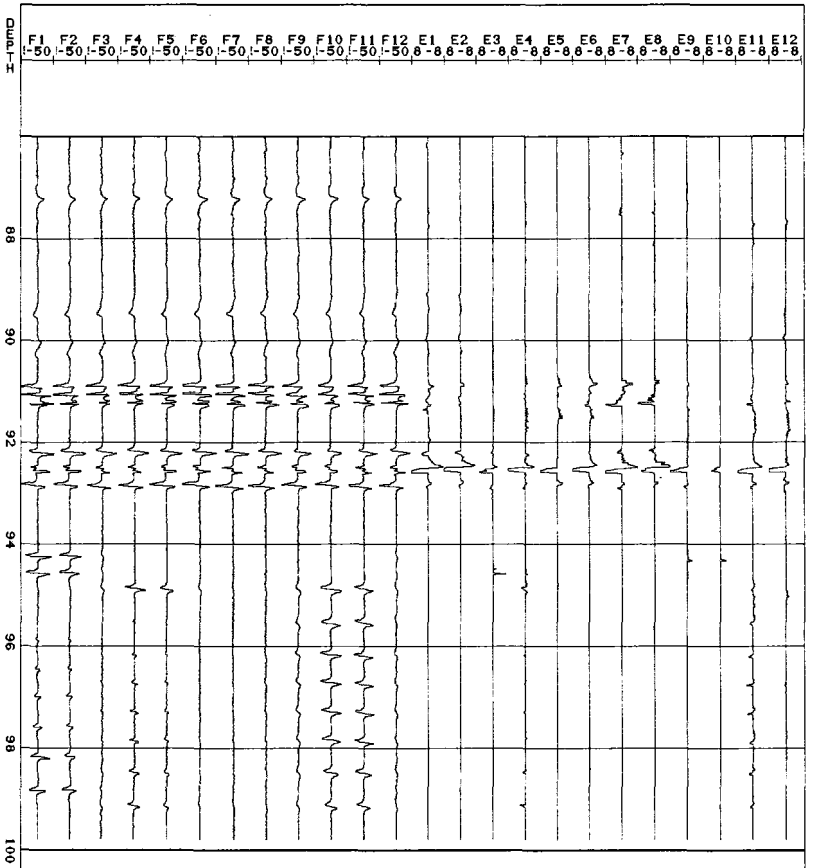

Fig. 9—Log response to test pipe.

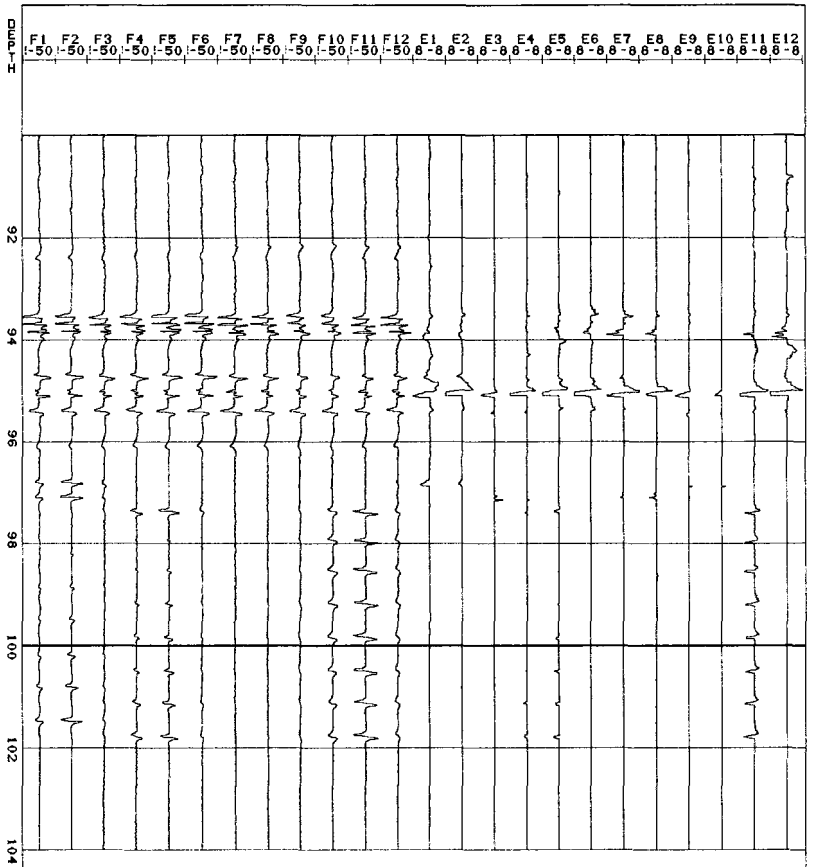

Fig. 8—Log response to test pipe.

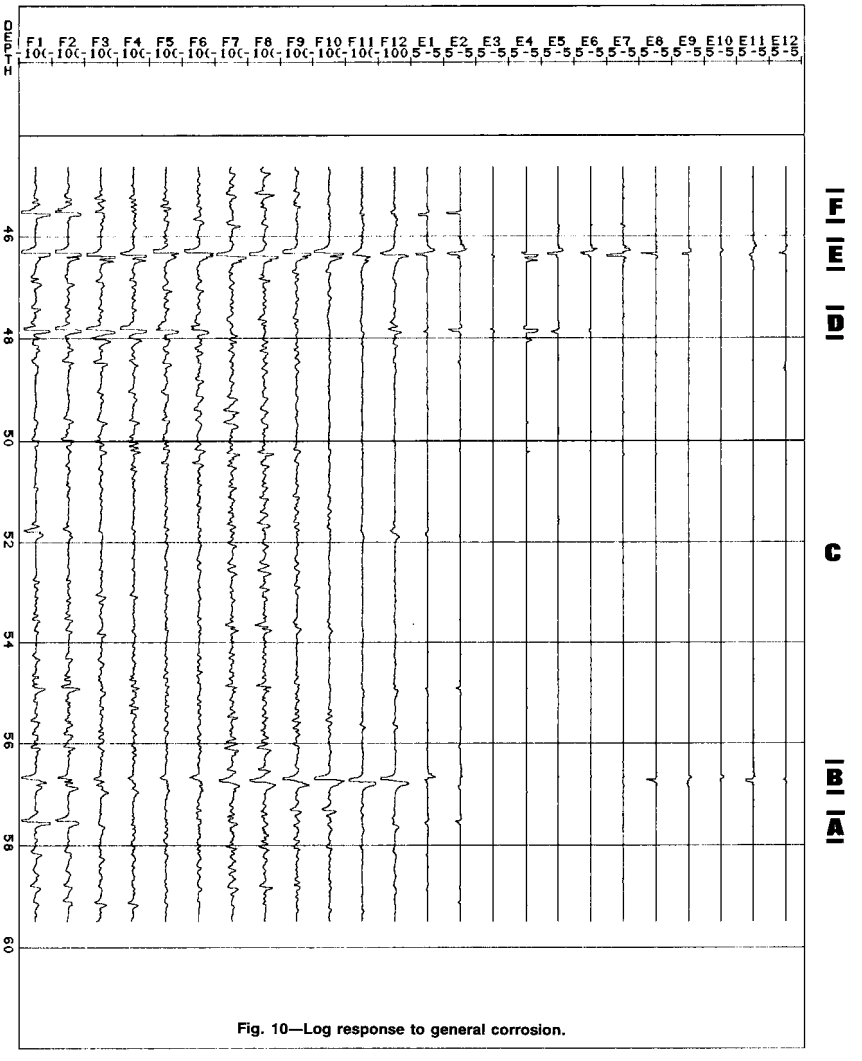

Fig. 10—Log response to general corrosion.

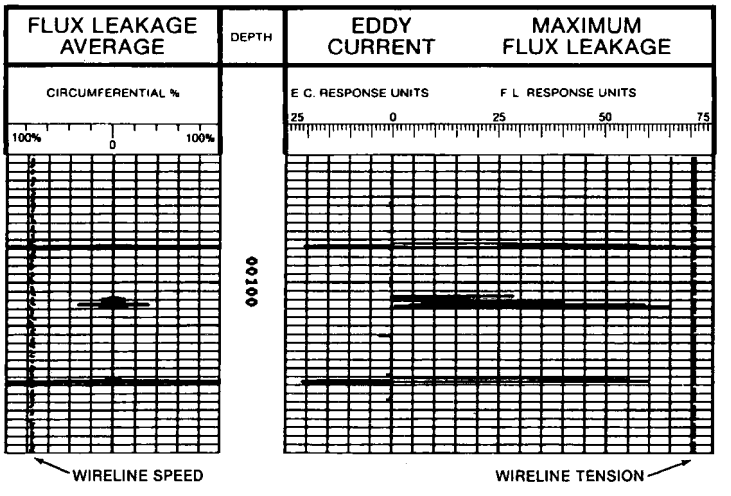

Fig. 11—Standard log presentation.

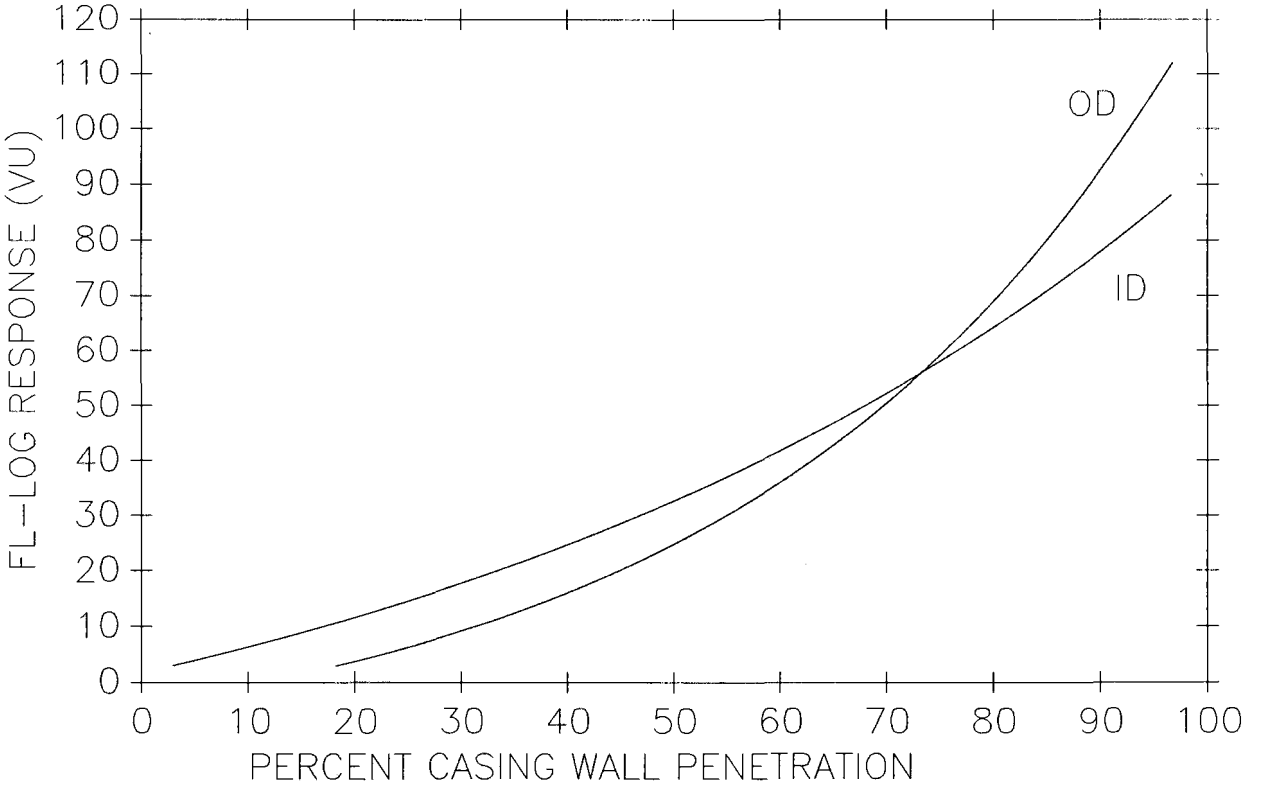

Fig. 12—Vertilog interpretation curves.

Ex. II - 4

VERTILOG®

Western Atlas International
A Litton/Dresser Company

CUSTOMER SOUTHERN CALIFORNIA GAS COMPANY	WORK ORDER NO. 124303	DATE 12-16-88	
LEASE/WELL NO. STANDARD SESNON No. 9	CUSTOMER ORDER NO.		
FIELD ALISO CANYON	COUNTY LOS ANGELES	STATE CALIFORNIA	
CASING O.D. 7"	WEIGHT(S) 23,26,29	NOMINAL WALL THICKNESS	GRADE J-55,N-80
TOTAL FOOTAGE INSPECTED 8553'	FROM SURFACE	TO 8553'	DEPTH

SUBSURFACE CASING DEFECT REPORT

LENGTH NO.	TYPE DEFECT	PENETRATION	LENGTH NO.	TYPE DEFECT	PENETRATION
OUTSIDE 13-3/8" SURFACE CASING					
51	OD IP	21 - 40			
62	OD IP	21 - 40			
64	OD IP	21 - 40			
67	ID IP	21 - 40			
85	ID IP	21 - 40			
91	ID IP	21 - 40			

ABBREVIATIONS:

O.D. – OUTSIDE DIAMETER
I.D. – INSIDE DIAMETER
I.S. – INSIDE SURFACE PIPE
T.L. – THROUGHOUT LENGTH
I.P. – ISOLATED PITTING
C.C. – CIRCUMFERENTIAL CORROSION
G.C. - GENERAL CORROSION

WA-1364-C (10/87)

Ex. II - 5

VERTILOG INTERPRETATION

COMPANY: SOUTHERN CALIFORNIA GAS COMPANY
WELL: I.W. 82
FIELD: ALISO CANYON 11·11·89
CNTY: LOS ANGELES
STATE: CALIFORNIA

wall loss

DEPTH	VERTILOG UNIT	LOCATION & EXTENT	CHART NO. 86J55E	CHART NO. 86P1E	PERCENT AVE
74	20	ID or OD, IP	60 or 52		60 or 52
2148	15	ID, IP	34		34
2166	14	OD, IP	39		39
2251	21	OD, IP	48		48
3962	8	OD or ID, IP	30 or 19		30 or 19
4136	8	OD, IP	30		30
4841	8	OD, IP	30		30
6180	9	OD, IP	31	24	27.5
6682	34	OD, IP	60	53	56.5
6786	10	OD, IP	33	26	29.5
6825	12	OD, IP	36	29	32.5
6867	18	OD, IP or GC	44 or 32	37 or 25	40.5 or 28.5
6891	12	ID, IP	28	15	21.5
6960	8	OD, IP	30	23	26.5
6971	12	OD, IP	36	29	32.5
6976	10	ID, GC	15	6	10.5
7034	10	OD, IP	33	26	29.5
7051	10	OD, IP	33	26	29.5
7078	76	ID, IP	94	87	90.5
7088	64	ID, IP	86	75	80.5
7112	122	ID, GC	83+	72	77.5
7123	16	OD or ID, IP	42 or 36	35 or 20	38.5 or 28
7150	40	ID, GC	42	25	33.5

Ex. II - 6

87-DT-102

Multi-Channel Casing Inspection Instrument

STEPHAN A. MATO, JR., Senior Research Engineer, Atlas Oilfield Services
Western Atlas International, Inc.

ABSTRACT

The present state of the art in casing corrosion analysis is represented by the Vertilog survey. This tool provides accurate information regarding the extent and depth of anomalies in casing in a well. Advances in instrumentation have been made that can increase the ability to define and interpret anomalous responses in this type of downhole measurement. Studies have been performed relative to these advances. An experimental tool that incorporates these advances into its design has been built and commercially run. Independent research by Southwest Research Institute, in studies sponsored by the A.G.A. (PRC Projects PR-15-411 and PR-15-614), has also demonstrated these advances and further demonstrated the "next generation" of technology needed to exploit more fully these advances in defining the complete condition of the casing in a well.

INTRODUCTION

The Atlas Oilfield Services Vertilog® casing inspection tool is designed to evaluate the condition of casing in place in a well. Data that are provided by the tool are used to determine the depth and extent of corrosion or other defects, natural or man-made, in the casing. The tool responds to isolated pitting and general casing body wall losses over small areas. Furthermore, the tool will also respond to completion equipment (centralizers, scratchers, etc.) that are placed within the well; however, it does not respond to gradual changes in the casing body wall, as in drill string wear.

HARDWARE DESCRIPTION

The mechanical assembly (Figure 1) consists of an iron core (A), pole pieces (B), and a sensor assembly (C). The core is made of a soft iron material wound with several layers of wire. A DC current is passed through the wire to generate a large DC magnetic field. The specially designed pole pieces are used to improve the coupling of the magnetic field to the casing. Sensors are placed around the core in two parallel rings (Figure 1-C, upper and lower shoe ring) so that the coverage by one sensor overlaps the coverage of another sensor. This sensor arrangement assures that the entire casing wall is inspected. The sensors are contained in "shoes" that are spring loaded to maintain contact with the casing wall. Two sets of sensors are contained in each shoe, which provide flux leakage or FL and eddy current or EC data (Figure 2). The FL sensors are oriented with

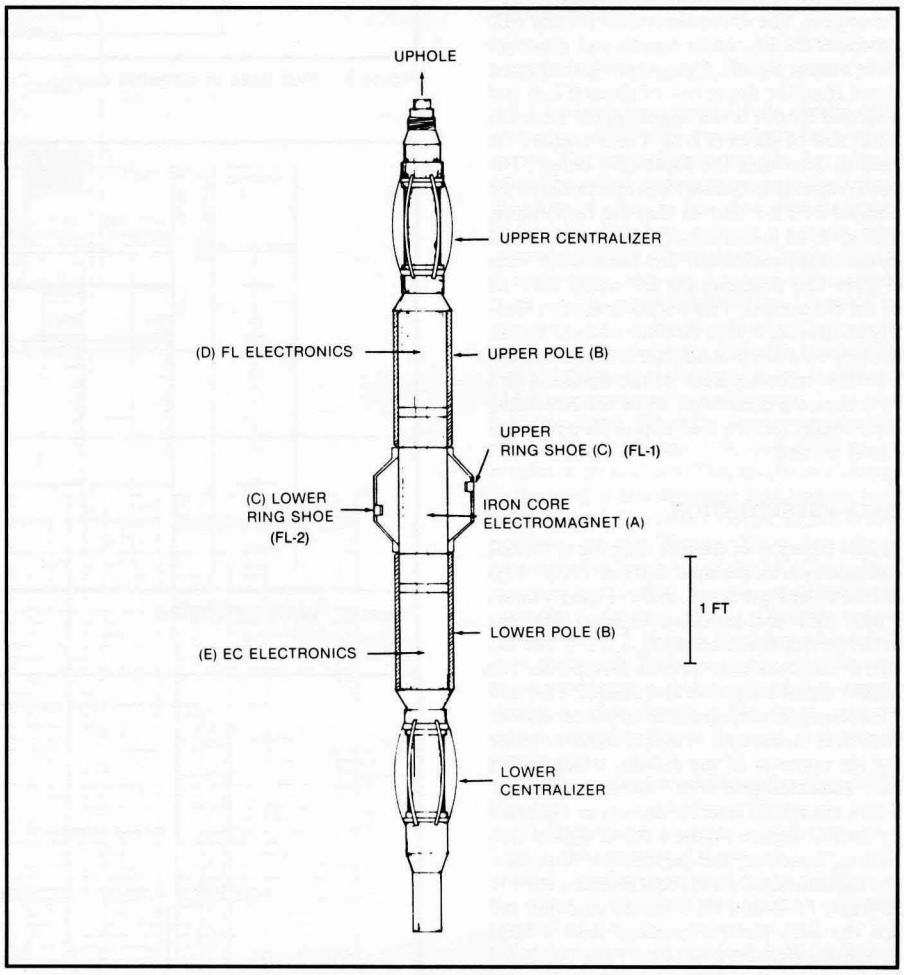

Figure 1. Vertilog mechanical assembly.

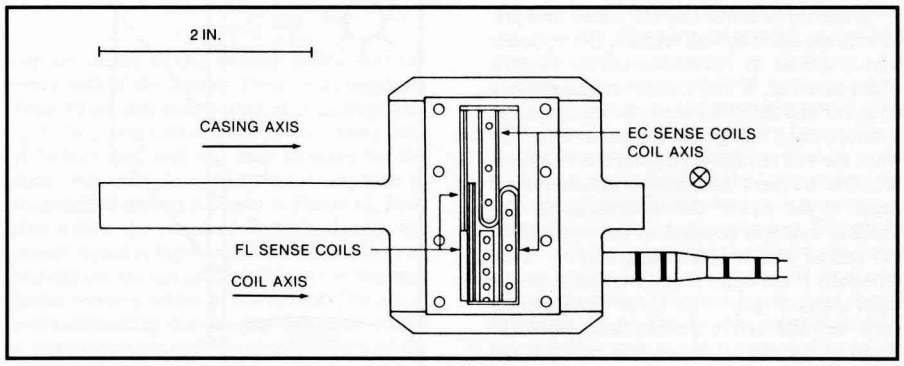

Figure 2. Vertilog shoe.

their axis parallel to the casing axis and used to determine the depth and extent of defects. The EC sensors are oriented with their axis perpendicular to the casing axis and used to determine whether the defects are external or internal. Figure 3 shows a typical joint of casing under the influence of the magnetic field generated by the core. Note the lines of flux that leave the casing at the defect sites. These magnetic field lines are detected by the FL coils and then processed by the subsurface electronics.

Two electronic packages are enclosed in the pole pieces (Figure 1-D and 1-E) to process and transmit the four different signals produced by the sensors. The upper electronics (Figure 1-D) processes the FL sensor signals and generates three output signals. One output is the largest signal from the upper row of shoes (FL-1) and a second output is the largest signal from the lower row of shoes (FL-2). These outputs are used to determine the depth of a defect. The third output (FL-Average) is proportional to the number of FL-1 sensors that are responding. This gives an indication of the circumferential extent of the corrosion. The lower electronics (Figure 1-E) processes the EC signal from all of the EC sensors. This output is used to identify an internal defect. All four of these signals are sent up a seven-conductor wireline cable to a surface recorder. Each of the signals is sent up a separate conductor, while the remaining three conductors are used to provide power and signal ground.

DATA PRESENTATION

Typical examples of the tool response to various conditions in an example well (see Figure 5-A) are shown in Figures 4, 6, and 7. Figure 4 shows typical collar and corrosion response. Note that at the collars, the Average, FL-1, FL-2, and EC signals all have a large amplitude response. The smaller signal amplitude and unequal FL-1 and FL-2 responses correspond to corrosion defects. Also note the absence of an EC signal response for the majority of the defects, which in this case indicates primarily external corrosion. There are several internal defects as indicated by the EC signals. Figure 6 shows typical centralizer, scratcher, and perforation responses. For the centralizers and the scratchers, the FL-Average, FL-1, and FL-2 signals respond, but not the EC. The perforations have a large amplitude signal response on FL-1, FL-2 and EC but only a small response on the Average. Figure 7 shows a response to the end of the surface casing (casing shoe).

It should be noted that the above interpretations are aided by well records. If a response that is similar to a scratcher occurs where it is not expected, it may not be recognized as a scratcher and therefore would be interpreted as a defect. Such interpretations occur primarily when the well records are incomplete or inaccurate. One frequent inaccuracy is the determined depth of the end of the surface casing. The Vertilog tool will respond to the presence of the end of the surface casing (casing shoe), especially if the outer string is offset from the inner string (Figure 5-B). Large signal deflections indicate severe defects, but, when the depth of the end of the surface casing is not known, it cannot be determined if the surface casing shoe is responsible for the observed

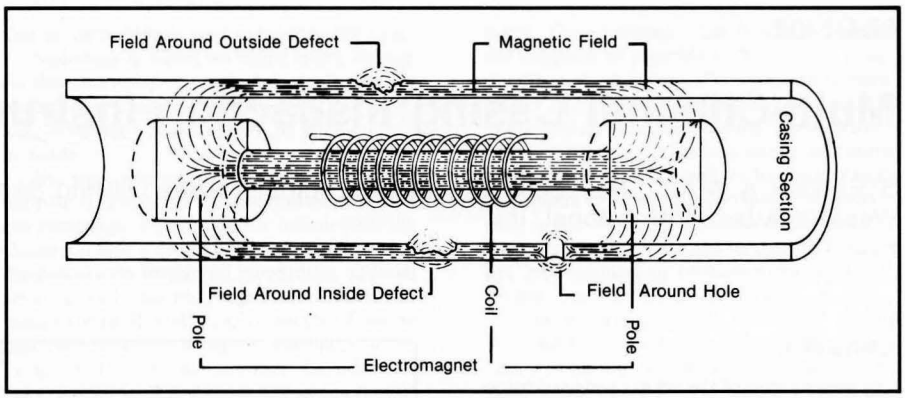

Figure 3. Flux lines in defective casing.

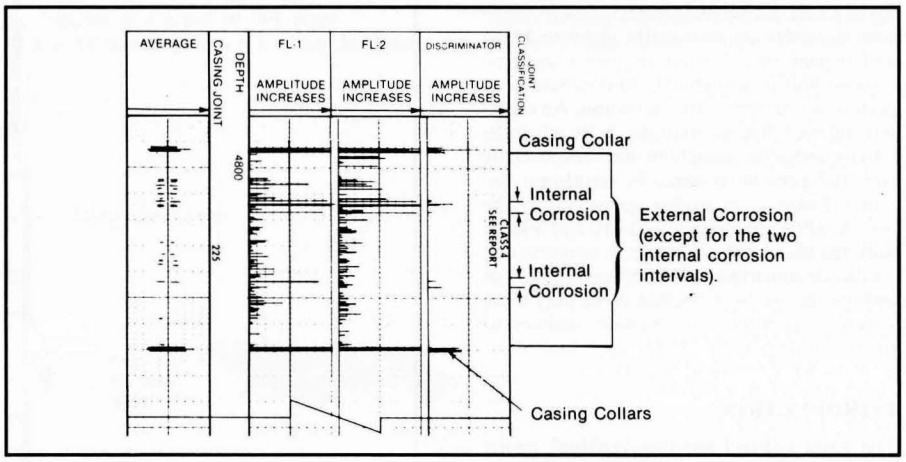

Figure 4. Vertilog examples.

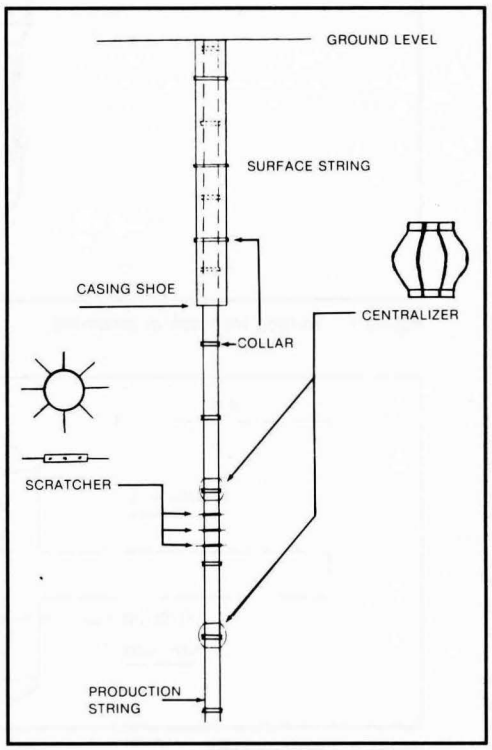

Figure 5A. Typical well.

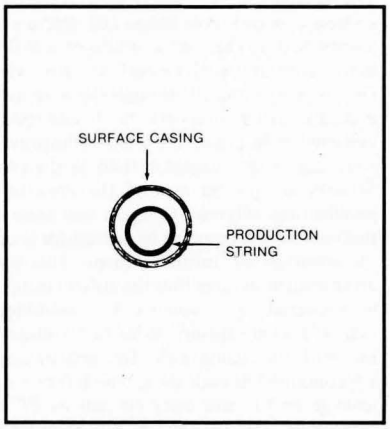

Figure 5B. Offset casing.

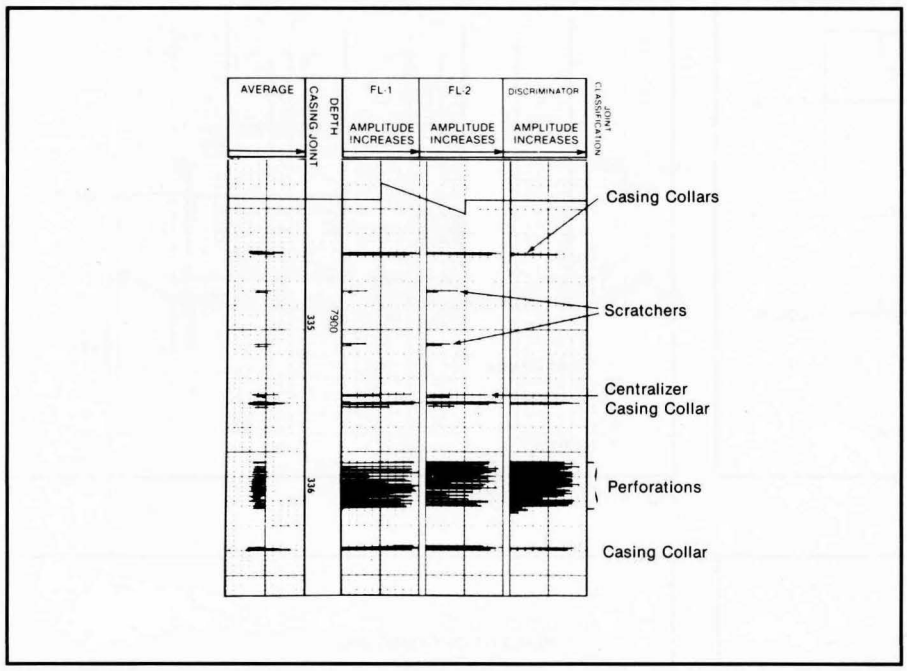

Figure 6. Vertilog examples.

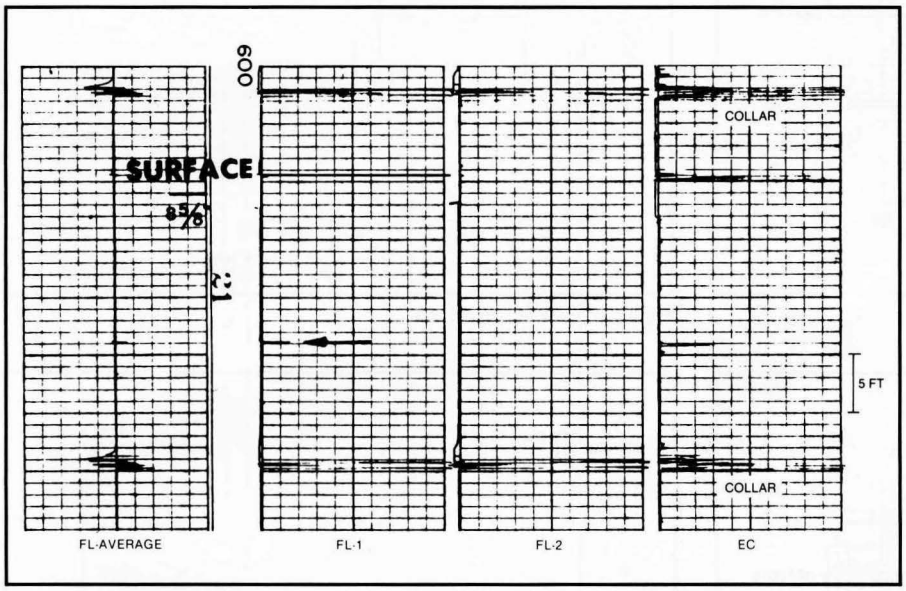

Figure 7. Surface casing response.

response. It must therefore be assumed that the response is due to corrosion. Figures 8, 9, 10, and 11 show examples of typical surface casing shoe responses.

EXPERIMENTAL TOOL

In an effort to improve the identification of anomalous responses from the Vertilog tool, a decision was made to re-examine the information obtained from the tool. The standard mechanical assembly was used in combination with an experimental electronics package. The output from a single sensor, without any signal processing other than amplification and noise reduction, was examined initially. Lab tests were run on casing having defects milled into the body wall of the casing. These defects ranged from 10 percent penetration of the casing wall up to 90 percent penetration of the casing wall. A ¾-inch ball mill was used to make the defects. An example of the sensor response to these milled defects is shown in Figure 12. Note that unlike the standard Vertilog signals, the sensor signal is bipolar. Of immediate interest was the correlation of the width of the response to the physical width of the defect. The initial evaluation of the data implied that there existed a relationship between the defect width and the sensor response width (Figure 13), but further analysis is required in order to clarify the exact nature of the relationship. An examination of the signals from the end of a surface casing was performed next. Tests using only one shoe as before, yielded some very interesting results (Figure 14). As can be seen, the amplitude and form of the surface casing shoe signal is different from the defect signals. It was then decided to transmit the signals from all of the sensors in the 5½-inch tool. The signals were electronically mixed and transmitted to the surface by wireline. At the surface, the signals were separated, and sent to a 12-channel analog recorder. Pitting in the casing was studied first. Later, the response to the surface casing shoe was examined.

FIELD TEST RESULTS

After having logged several wells, certain characteristics of the sensor waveform became apparent. The main observation was that a signal caused by added mass is opposite to that caused by a loss of mass (a fact that was confirmed in the lab). This brings about a unique interpretation method of signals seen by the sensors. A basic sensor response for most casing conditions can be predetermined by knowing its geometry, e.g., a pit (Figure 15). The sensors respond to changes in the magnetic flux leakage field. If the body wall of the casing is constant (A), the sensors would not be expected to generate any signal. When the sensors pass the first edge of the pit (B), the body wall of the casing is reduced (mass loss). This results in a change in the level of the magnetic flux leakage field at the sensor. The sensor output signal is proportional to this change. When the sensor passes the trailing edge of the pit (C), the wall increases (mass gain), causing another change, opposite to the first change. Once the sensor passes the pit, it is again in casing with a constant body wall (D), hence no signal is expected. A sensor output would be expected to appear similar to that shown in Figure 15, and the actual sensor response to a pit is shown in Figure 16.

As the tool approaches a collar (Figure 17), the body wall suddenly increases (A) (mass gain). This causes a decrease of the magnetic field at the sensor and, hence, the sensor generates a signal proportional to the thickness of the collar. Further into the collar, we approach the end of the lower casing joint (B). At this point, it appears to the tool as if the wall is reduced in thickness (mass loss), causing the sensor to generate a signal opposite in amplitude to the first response at the collar. A short distance later, the sensor enters the upper casing joint (C). Since it now appears to the tool that the wall is increased in thickness, the change in the magnetic field causes a corresponding change in the sensor output signal. This signal is the same polarity as the signal received upon entering the collar. Finally, as the tool leaves the collar (D), the body wall of the casing becomes thinner and thus generates a signal proportional to the mass lost. This signal is opposite in polarity to the signal generated as the tool entered the casing. The final output of the sensor will then be like that shown in Figure 17. As can be seen from Figure 18, the actual sensor signal is very similar to the predetermined sensor signal shown in Figure 17.

Other well-completion equipment is detected equally well. Since both scratchers and

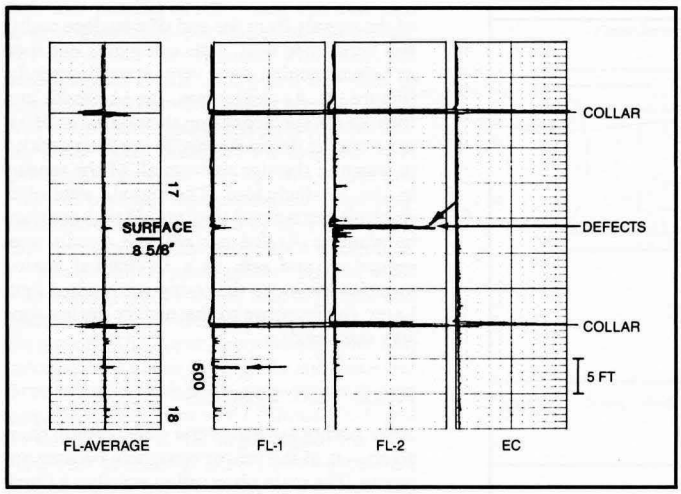

Figure 8. Surface casing response.

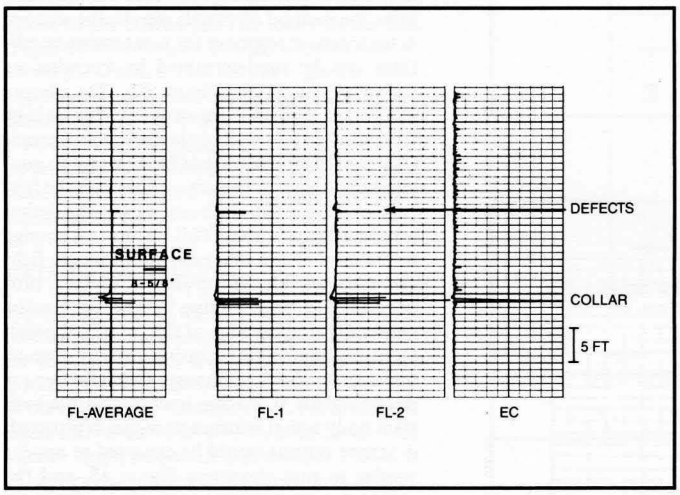

Figure 9. Surface casing response.

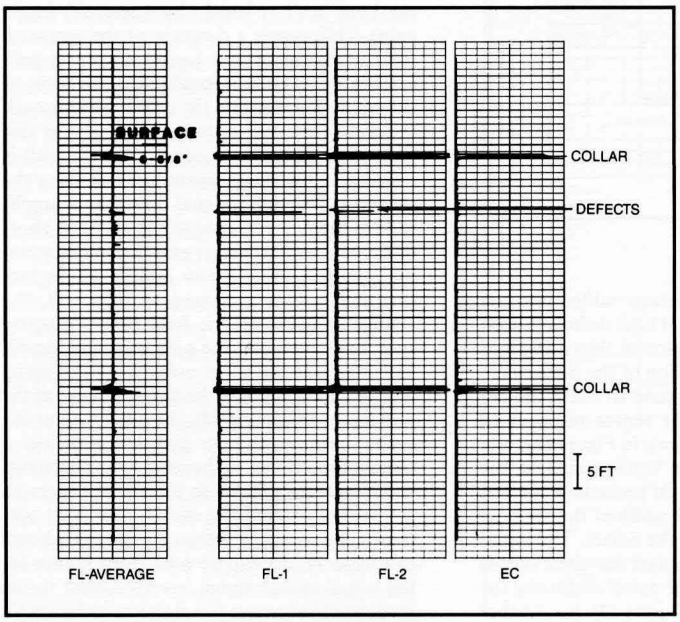

Figure 10. Surface casing response.

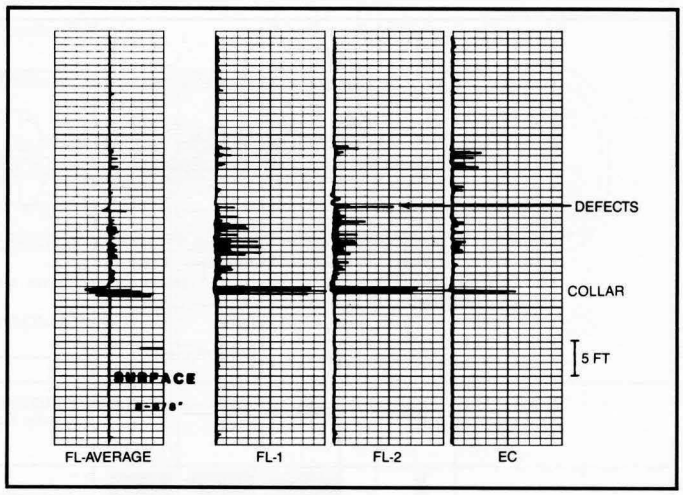

Figure 11. Surface casing response.

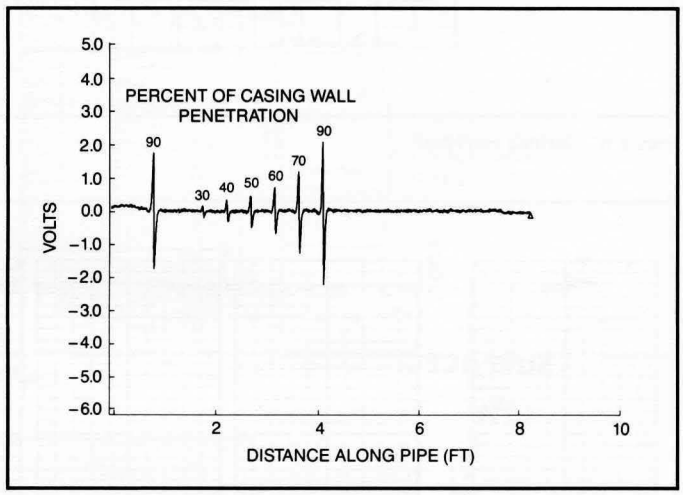

Figure 12. Defect response.

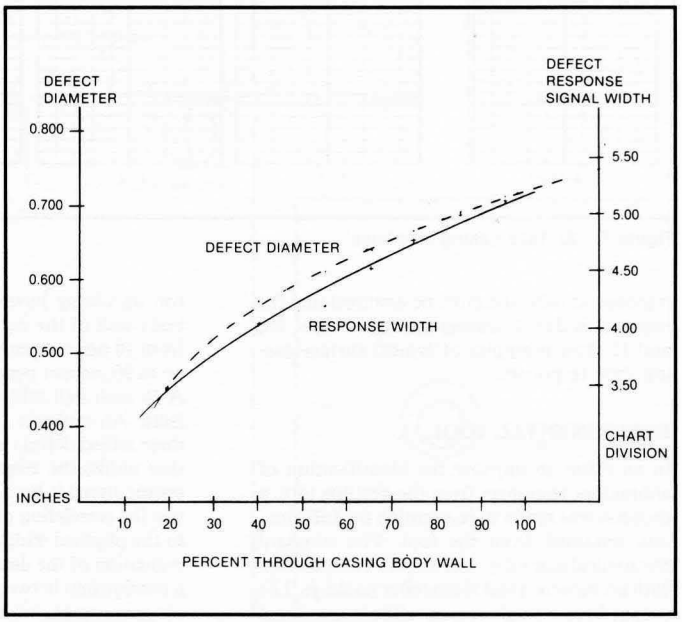

Figure 13. Defect diameter vs. response width.

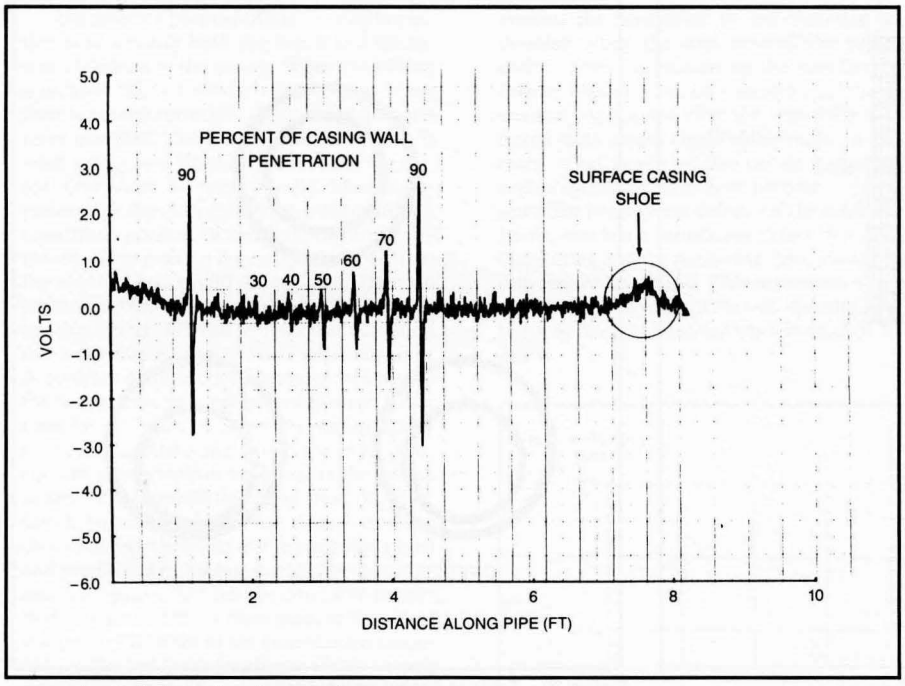

Figure 14. Defects and surface casing response.

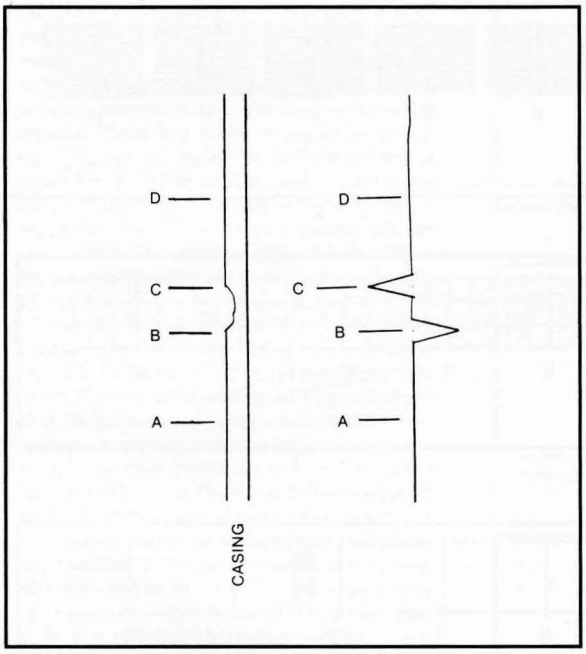

Figure 15. Theoretical isolated pit response.

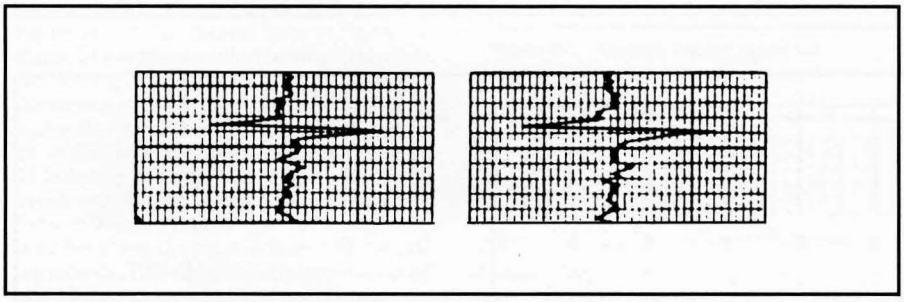

Figure 16. Isolated pit.

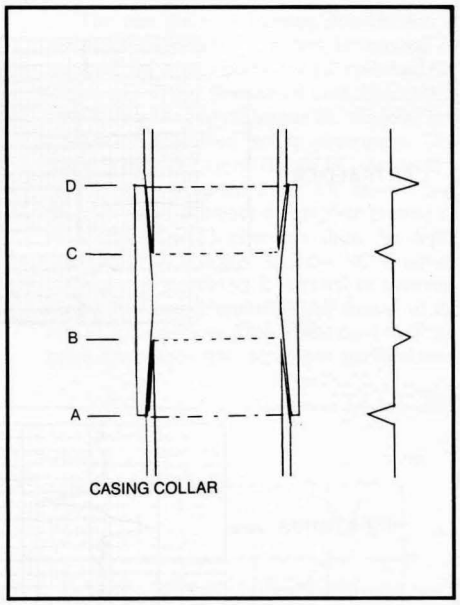

Figure 17. Theoretical casing collar response.

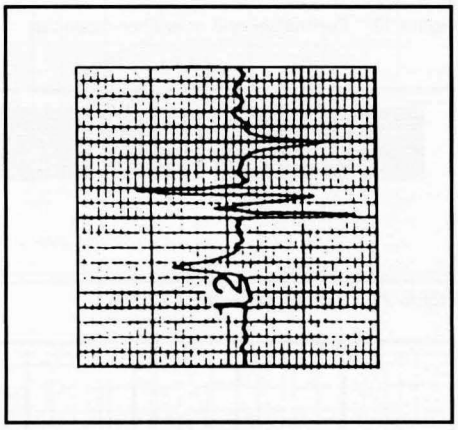

Figure 18. Collar response.

centralizers are placed on the outside of the casing, they, in effect, increase the casing wall at the point that they are attached. They should then appear on the log as a mass gain event (Figure 19). Other completion equipment will appear in a similar way and, if the geometry is known, its characteristic signal should be predictable.

As the tool approaches the second string of casing, the effective wall thickness suddenly appears to increase. If the two strings were concentric, a signal similar in polarity to that of entering the collar would be expected on all channels, only smaller in amplitude. However, since there is not a corresponding "thinning" of the wall, only one signal would be expected. Since the casings are rarely concentric, the possible geometries are centralized, offset, and contact (Figure 20). An example of each of these geometries is shown in Figures 21 to 24. Figure 21 shows the centralized condition, Figure 22 shows the offset condition when the two casings are near to being centralized, Figure 23 shows the offset condition when the two casings are close to contact, and Figure 24 shows contact.

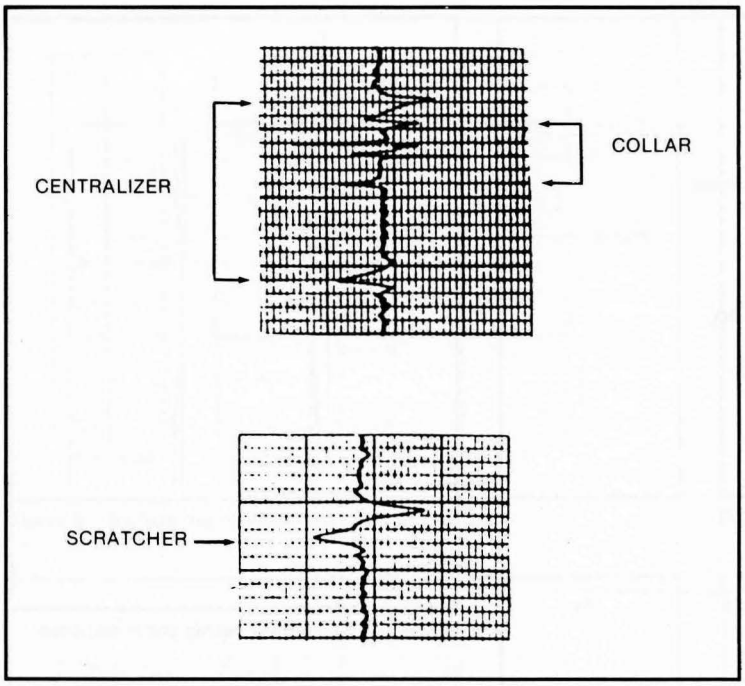

Figure 19. Centralizer and scratcher response.

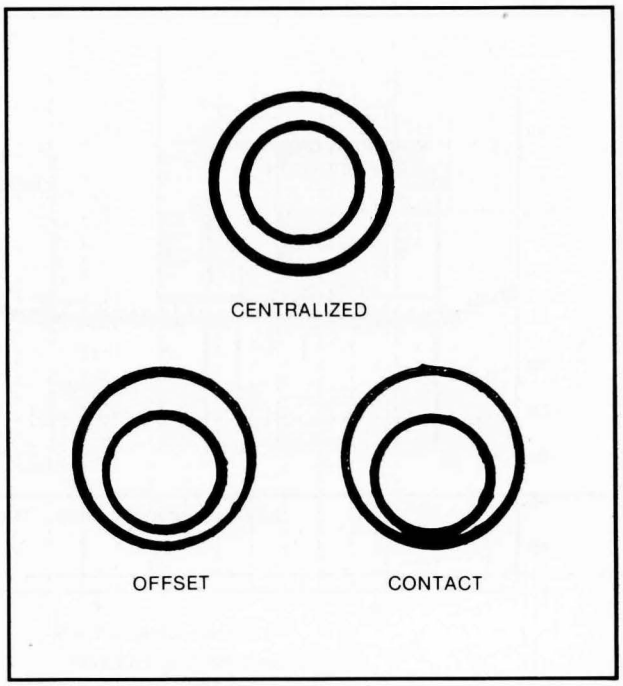

Figure 20. Surface casing geometrics.

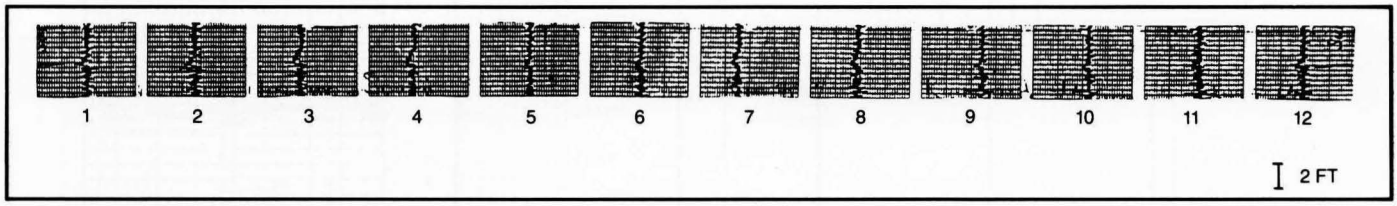

Figure 21. Centralized surface casing.

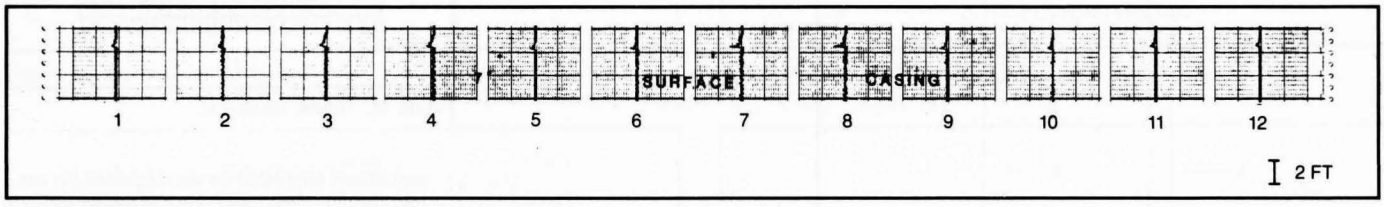

Figure 22. Offset surface casing.

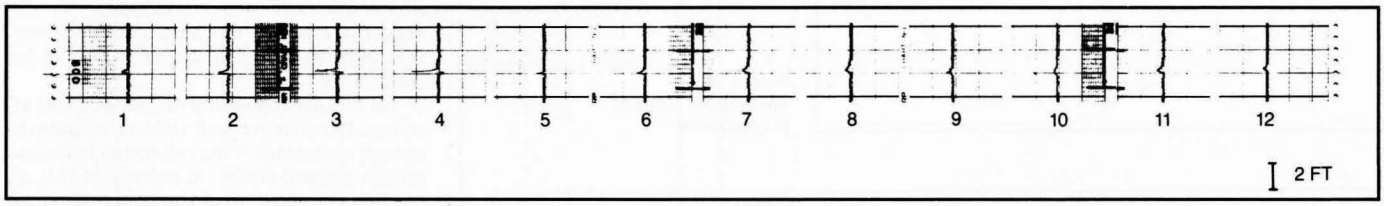

Figure 23. Offset surface casing.

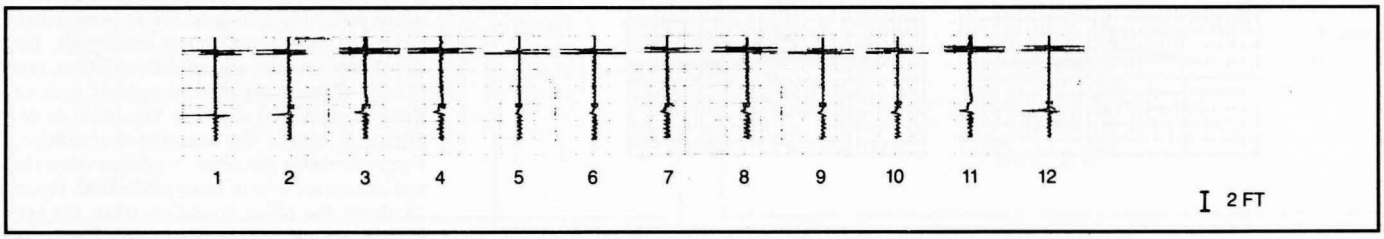

Figure 24. Contact surface casing.

The ultimate purpose of the Vertilog inspection is to identify both the depth and the extent of defects in the casing. When the pitting is isolated, this is a relatively simple task. When there is general corrosion, the situation becomes more complex. The extent of the corrosion is readily discerned from the response of the sensor. One must be more careful when interpreting the depth in general corrosion since a significant portion of the body wall may be missing. This causes a larger signal output from the sensor than would be expected from an isolated defect of a similar size and depth. It becomes more difficult to interpret corrosion that is underneath or just inside the casing shoe. A complex magnetic field pattern occurs with the casing shoe response generally much larger than for pitting. The closer the surface string is to touching the inner string, the more difficult the interpretation becomes. If the pitting is directly underneath the casing shoe, the situation is somewhat simplified, since the casing shoe enhances the effect of the corrosion signal and produces a much larger response than normal. The sensor that sets the corrosion detects both a mass loss and a mass gain, so the signal is bipolar. The ratio of the gained mass amplitude to the lost mass amplitude yields an estimate of the depth of penetration of the pitting. If the pitting is just inside (two inches or less) the surface casing, the signal is attenuated and the corrosion appears to be less than it is in reality. As the pitting gets further into the surface string, the response returns to the expected values for two strings of casing. Figure 25 shows a typical interpretation curve for external (OD) defects. There is a single string curve and a curve for casing inside of 10¾-inch surface pipe. A ratio curve is also used to determine the depth of corrosion that is directly underneath the casing shoe. There is another similar set of curves for internal (ID) defects. There are a series of curves for each weight and grade of casing.

Figures 7, 8, 9, 10, and 11 can now be reevaluated by use of the 12-channel format instead of the standard data format. Figure 26 is the 12-channel equivalent of Figure 7. Note that the surface casing response appears centralized. Secondly, note the large pit approximately one foot below the end of the surface casing. In this case, there is a defect. Figure 27 is the 12-channel equivalent of Figure 8. Once again, note that the surface casing response appears centralized and that there is pitting, although not as severe as the defect in Figure 26. Figure 28 is the 12-channel form of Figure 9. In this instance, the casing appears offset. Notice the pit response just inside the surface casing where the inner string is closest to the surface casing. This corrosion is not severe. Figure 24 is the 12-channel form of Figure 10. Figure 24 was the example of contact, therefore the Vertilog response is due to the presence of the surface casing. If there is corrosion directly under the shoe, then another interpretation curve similar to the curve presented in Figure 25 indicates it is less than 35 percent of the casing wall. Finally, Figure 29 is the 12-channel form of Figure 11. Note that the casing shoe is 20 feet above the point indicated by the casing records. This changes the interpretation of all of the corrosion, since it is now located outside of the surface casing. With the standard system, the sensitivity of the recorder was doubled when the tool entered the surface casing. Severe corrosion on the standard log format becomes minor corrosion on the 12-channel log format after the sensitivity is reduced to its proper single string value. In summary, what began as five casing joints with severe corrosion have now become only one joint that has a severe defect. Of the other four joints, one has a significant defect that needs monitoring and the remaining three joints have only minor corrosion. This represents a considerable cost savings to the well operator. Only one well requires remedial work instead of five wells.

The one piece of missing information is determining whether a defect is internal or external. Up to this point, the EC coils had not been used on the 12-channel tool. Electronics have been added to utilize the EC sensors. Two signals are produced by the electronics. One signal is from the upper ring of EC sensors and one signal is from the lower EC sensor ring. We can now formulate a complete picture of the casing. The FL channels show the depth and shape of a defect and the EC channels determine if the defect is internal or external. Figure 30 shows a "multichannel" format of the sensor information. This is best used to determine the nature (pit, scratcher, perforations,

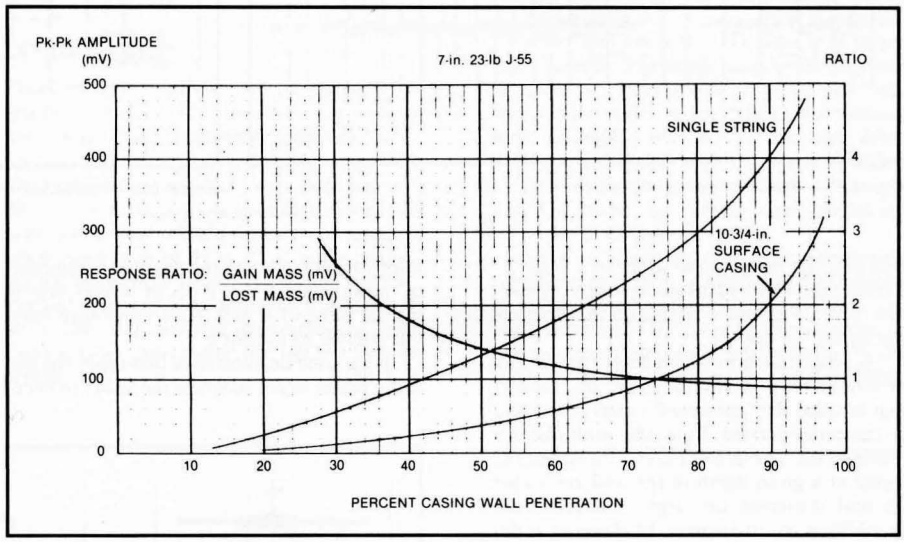

Figure 25. O.D. interpretation curves.

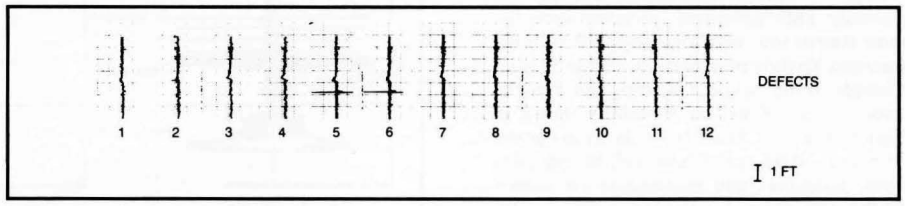

Figure 26. Surface casing response.

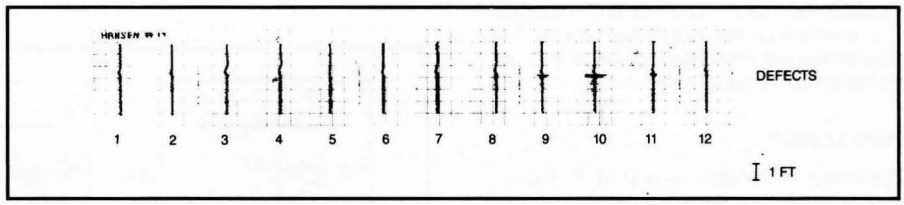

Figure 27. Surface casing response.

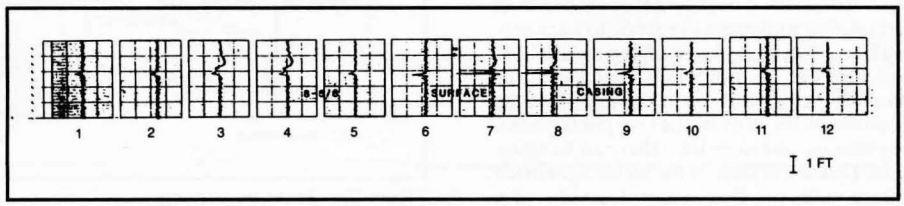

Figure 28. Surface casing response.

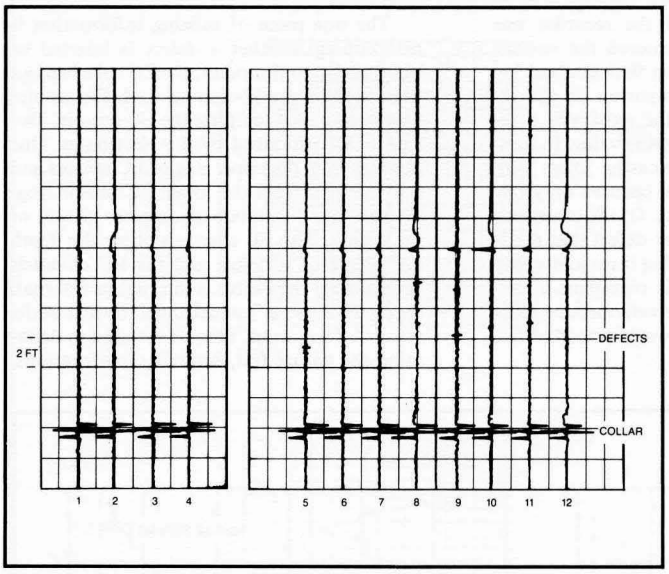

Figure 29. Surface casing response.

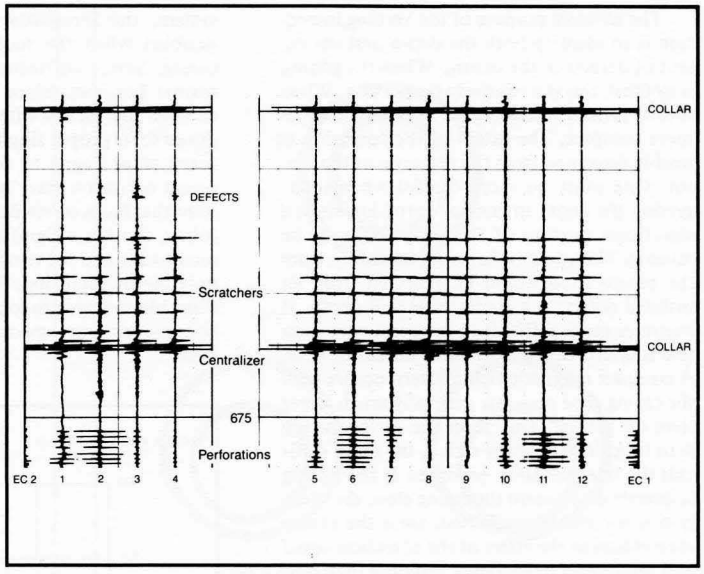

Figure 30. Multi-channel Vertilog.

etc.) and the extent (how wide, how long) of a sensor response. This format does not, however, provide adequate resolution to determine the depths of defects.

A presentation in which defect depths can be interpreted is shown in Figure 31. This format is called the "generated" presentation and is computer-derived from the multichannel presentation. The largest FL and the largest EC signal at a given depth in the well are scaled up and displayed for depth interpretation. In addition, another curve, FL-Average, is derived from the total number of FL channels that are responding at any given instant to give an indication of the circumferential extent of the anomaly. This "generated" presentation is the same format that was originally used with the standard Vertilog presentation. Figure 32 is an example of the standard Vertilog run over the same section of well as previously shown in Figures 30 and 31. Note the similarity in Figures 32 and 31. Also notice how well the perforations, scratchers and centralizers are shown on the multichannel presentation (Figure 30). Comparing the same depth intervals on Figures 30, 31 and 32, the multichannel presentation enhances the interpretation of tool responses to conditions in the well. This type of log presentation and interpretation is unique to the Multichannel Vertilog system.

CONCLUSION

The ability of the experimental Multichannel Vertilog to transmit the entire signal as seen by the sensor coils provides an opportunity to understand better the condition of casing in a well. Corrosion is readily differentiated from completion equipment like scratchers and centralizers. The exact depth of the surface casing shoe can be determined. Collars can be studied; the physical size of the collar and the location of the ends of the two joints of casing that are joined by the collar can be examined. Detailed analysis of the sensor signal itself (signal width, rise time, area, etc.) provides more information regarding the physical parameters of the anomaly. These types of studies, which can be done in a well, have previously been unavailable to industry.

It has been demonstrated that analyzing the entire sensor signal enhances the ability to interpret anomalous responses in a well. Using the experience gained from designing and building the experimental Multichannel Vertilog, an instrument is being designed to transmit information from all of the FL sensors and from all of the EC sensors.

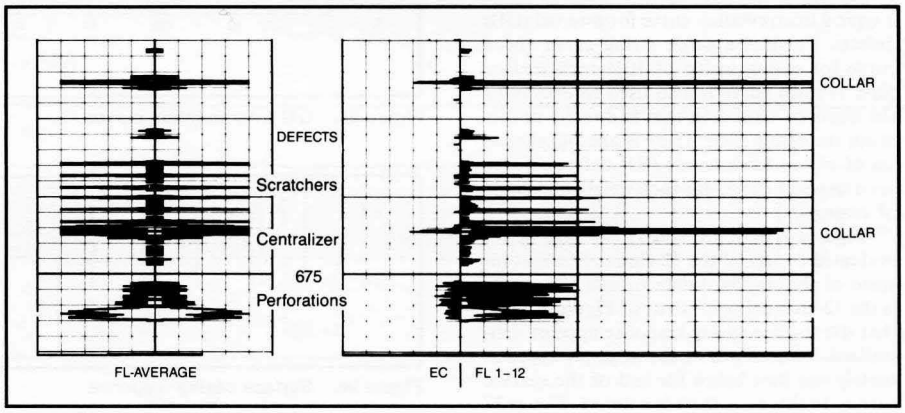

Figure 31. Generated Vertilog.

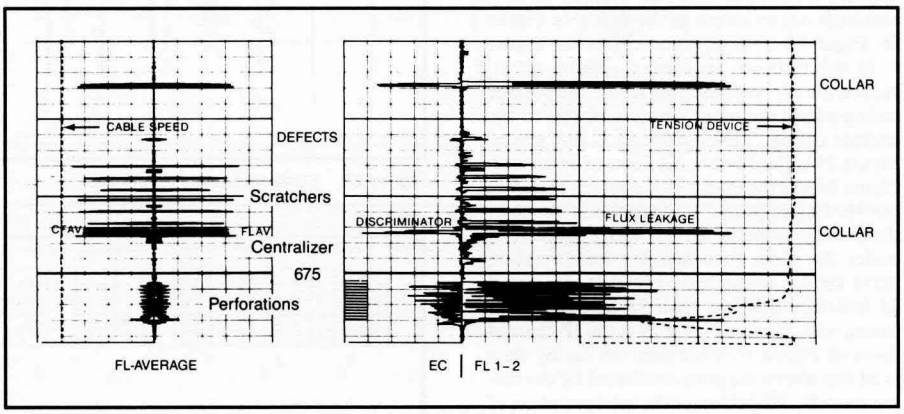

Figure 32. Standard Vertilog.

Ex. II - 7

SPE 81442

North Kuwait Down-hole Corrosion Management Challenge and the Use of New Corrosion Detection Tools to Define the Extent of the Problem

Moudi Fahad Al-Ajmi, SPE, Kuwait Oil Company; Juma K. Attid, SPE, BP; Alex Daye, Baker Atlas

Copyright 2003, Society of Petroleum Engineers Inc.

This paper was prepared for presentation at the SPE 13th Middle East Oil Show & Conference held in Bahrain 5-8 April 2003.

This paper was selected for presentation by an SPE Program Committee following review of information contained in an abstract submitted by the author(s). Contents of the paper, as presented, have not been reviewed by the Society of Petroleum Engineers and are subject to correction by the author(s). The material, as presented, does not necessarily reflect any position of the Society of Petroleum Engineers, its officers, or members. Papers presented at SPE meetings are subject to publication review by Editorial Committees of the Society of Petroleum Engineers. Electronic reproduction, distribution, or storage of any part of this paper for commercial purposes without the written consent of the Society of Petroleum Engineers is prohibited. Permission to reproduce in print is restricted to an abstract of not more than 300 words; illustrations may not be copied. The abstract must contain conspicuous acknowledgment of where and by whom the paper was presented. Write Librarian, SPE, P.O. Box 833836, Richardson, TX 75083-3836, U.S.A., fax 01-972-952-9435.

Abstract

The North Kuwait (NK) Development Plan calls for rapid increase in NK production, mainly through the implementation of waterflooding in NK major reservoirs. The new production profile incorporates increased water production and, based on corrosion prediction models, results in elevated corrosion rates in down-hole completion equipment. This predicted increased corrosion has already become a reality in the past three years. Severe down-hole corrosion in production and injection wells has resulted in tubing and casing failures and severe casing/tubing corrosions. Remediation of these wells has resulted in problematic, high cost workovers, and in one case, the loss of the productive interval and the associated reserves.

To manage current and future corrosion in NK, an extensive corrosion-monitoring program has been implemented to initially identify the extent of corrosion in the current well stock and then to adopt corrosion prevention strategies to mitigate the problem and reduce the associated cost and production impact. The down-hole internal corrosion monitoring effort is one of the first steps in implementing the NK Corrosion Management Plan.

This paper discusses the results of the program to date and describes the diagnostic tools used to effectively monitor the extent of down-hole corrosion in North Kuwait. Different tools such as the caliper, MicroVertiLog tool (MVRT), and surface inspection methods have been utilized to quantify down-hole corrosion. The paper also compares MVRT tool response with caliper and surface inspection data in an effort to ensure down-hole corrosion detection corresponds with results measured at surface. This will allow immediate corrective action to be taken for the completions based on down-hole log results.

Introduction

First commercial oil production from North Kuwait started back in 1955. According to the Kuwait Oil Company (KOC) production database, production of crude oil with watercut in North Kuwait started in the mid 1980's as water-handling facilities became available. However, the water production was in insignificant quantities.

Down-hole corrosion was not a major issue up to late 1990's due to low or no watercut in most of the wells. In addition, the corrosion problem was indirectly managed through the process of converting wet producers to dry production by applying down-hole water shut-off techniques. The water shut-off (mostly carried out by a rig workover operation) was necessary to allow maximum oil production through the then existing facilities with limited water handling capacity. However, lately, with the increasing water production and water handling capacity in North Kuwait, corrosion has become an important issue. With the implementation of the current development plan, which includes waterflooding of several major reservoirs, down-hole corrosion needs to be managed properly to avoid severe production and operating cost impacts. Corrosion in North Kuwait will impact the whole production and processing stream. This paper, however, only discusses the down-hole tubular corrosion issues.

Causes of Down-hole Corrosion In North Kuwait

Although this issue needs to be fully investigated and confirmed, the cause of current down-hole corrosion in North Kuwait fields is suspected to be mostly the CO_2 in the formation water. The dissolved CO_2 in the formation water is assumed to result in the formation of carbonic acid (H_2CO_3), which reacts with metal and causes corrosion. The pH of most of the reservoir waters in North Kuwait is acidic (between 5.5-6.5). In addition, the high salinity of the formation water reduces the formation/presence of the protective film on the tubing wall and exposes the tubing to corrosion. We note a strong correlation between cumulative water production and severity of corrosion in most of the wells. This leads to support the hypothesis of CO_2-induced corrosion. With the implementation of seawater injection in Mauddud, Upper Burgan, and Zubair reservoirs, the cause of future corrosion is expected to include other factors as well.

Completion Metallurgy

All the existing tubing and casing in NK are low alloy carbon steel (N-80, L-80 or J-55). Trials of chrome steel tubing have been suggested in the past but have not yet been implemented.

Logging Tools Used

Briefly are described below the main corrosion logging tools that have been used to record down-hole corrosion in NK wells both in tubing and casing strings. The description of the MVRT tool however is extended, as it is currently the main tool being used to monitor tubing strings for corrosion in NK. It is worth mentioning that tubing visual surface inspection has recently been applied in some wells in NK as well. As for liners, no logs to specifically address liner corrosion have been ran in NK.

1. Casing Corrosion Logging Tools Used

Casing corrosion logs are usually recorded during rig workover operations when the tubing string is pulled out. In North Kuwait, casing is routinely pressure tested, and, unless corrosion is suspected, quite often a casing corrosion log is not acquired. The main logging tools used so far are Ultrasonic Casing Imager (UCI), and Pipe Analysis Tool (PAT). Although not widely used in Kuwait yet, Circumferential Acoustic Scanning Tool (Cast-V) provided by Halliburton is an equivalent sonic imaging tool that could be used for casing corrosion monitoring. The Baker Atlas MVRT tool can also be used to inspect casing, but have not been widely used in North Kuwait for casing corrosion monitoring.

UCI (Ultrasonic Casing Imager)

This tool has been marketed by Schlumberger as the UBI tool to provide borehole images, USI to evaluate cement bond and casing corrosion, and UCI to quantitatively measure both internal and external casing corrosion or damage (for casing diameter ranging mostly between 4 ½ to 13 3/8 in). The sonde includes a rotating transducer subassembly. The transducer is both a transmitter and a receiver transmitting an ultrasonic pulse and receiving the reflected pulse.

The tool is making radius and thickness measurements allowing the depth of the anomaly to be quantified. With 180 focused measurement during each revolution of the ultrasonic sensor, and up to five rotations every inch of travel inside the casing, the UCI tool is claimed to have the resolution and sensitivity needed to measure pits and other anomalies down to diameters as small as 0.3 in. on either the inside or outside surface of the casing. The high resolution of the UCI tool is claimed to be due to the high transducer frequency of 2 MHz. The signal is, however, attenuated by the borehole fluid and therefore best results are obtained when brine, oil, or very light mud are used.

Tool Operation: The tool works in the following way: first echo time gives internal radius measurement. The second echo time gives casing thickness. Internal and external surface echo amplitudes give a qualitative visual image of casing condition. Wellsite presentation is corrected for tool decentralization effects.

The UCI logs have been used in several North Kuwait completions to assess the casing conditions and make well intervention decisions. However, in North Kuwait no efforts have been made to verify the UCI results through pulling the damaged casing out and performing surface inspection.

PAT (Pipe Analysis Tool)

This tool used to be marketed by Schlumberger. However, newer tools such as UCI have replaced it.

Tool Operation: The PAT sonde has two sets of arrays. Each array has six pads, and each pad makes two measurements: the first one is an eddy current measurement where a high-frequency signal induces a flux on the inner wall of the casing. The presence of the inner wall corrosion causes a flux distortion that is measured by the tool. The second measurement is the flux leakage measurement where electromagnets generate a flux in the casing. The presence of inner and/or outer wall corrosion generates flux leakage that is measured by the tool. In NK, several casing strings have been surveyed by this tool in the past.

CAST-V (Circumferential Acoustic Scanning Tool)

This tool marketed by Halliburton, is the equivalent of Schlumberger's UCI tool. CAST-V furnishes borehole images (when operated in image mode) and provides casing inspection and cement evaluation capabilities (when operated in cased-hole mode)[1]. It can cover casing diameters ranging between 5 ½ to 13 3/8 in. When ultrasonic CAST-V operates in cased-hole mode, full circumferential maps of casing thickness and acoustic amplitude are generated. These maps are used to reveal thinned casing as well as to distinguish between cement and fluid in the annular space behind casing.

Tool Operation: CAST-V uses two ultrasonic transducers: a primary and a secondary transducer. The primary transducer is mounted in a rotating scanner head and is in direct contact with borehole fluid. The scanner head rotates continuously about the tool axis, transmitting ultrasonic signals and receiving reflections from the casing or formation. The secondary transducer is secured in a fixed position on the scanner assembly and is in direct contact with the borehole fluid.

This tool is fairly new to Kuwait and has not been used to monitor casing corrosion in North Kuwait as much as UCI.

2. Tubing Corrosion Logging Tools Used

Tubing corrosion monitoring tools were not available in Kuwait Prior to 1998. In early 1998 efforts were made to evaluate the extent of corrosion in down-hole tubular. New tools were brought in Kuwait specifically for this purpose: multi-finger calipers, which can detect internal defects only, and MVRT, built to detect both internal and external corrosion.

Multi-finger Caliper

Historically, mechanical calipers have mostly performed inspection of production tubing. Mechanical arms serve to provide a profile of the tubing inner diameter (ID). Experience has shown however, that mechanical calipers have a number of limitations, including the inability to provide 100% coverage or identify external defects of the tubing. Internal deposits may also adversely affect mechanical calipers and their use may cause preferential caliper track corrosion unless the tubing is inhibited after logging. Results from the caliper

log might prove difficult to repeat due to incomplete coverage/tool rotation.

Due to these limitations, calipers have not been widely used in NK for down-hole tubing inspection. Caliper was mainly used where there were no concerns about the tubing external corrosion. It was also used to validate MVRT response.

Modified versions of mechanical calipers are available now providing better coverage of the tubing ID and better log presentation.

MVRT (Micro VerRtilog Tool)

MVRT tool marketed by Baker Atlas, applies magnetic flux leakage (FL) technology to determine the location, extent and severity of corrosion and other metal loss defect in carbon steel tubular.

MicroVertilog tools employ a permanent magnet circuit designed to produce high levels of magnetic flux within the tubing or casing body wall. Defects, such as internal or external corrosion pitting, cause flux perturbations (leakage) that are detected by a circumferential array of inductive coil (FL) sensors.

The MicroVertilog tools also employ a circumferential array of discriminator (DIS) sensors, each aligned with a corresponding FL sensor that respond to flux anomalies occurring at the tubing inner surface. The combination of FL and DIS data allow the MicroVertilog to differentiate between internal and external features **(Fig. 1-2)**.

The MicroVertilog system produces digital bipolar waveforms, allowing metal gain anomalies (centralizers, down-hole hardware) versus metal loss (corrosion, mill defects) to be determined from the log signatures **(Fig. 3)**.

The MicroVertilog tools are configured such that the FL sensors are all housed within a smooth cylindrical mandrel with dynamic wheeled centralizers located above and below the mandrel. The DIS sensors are conveyed to the tubing ID via spring loaded shoe assemblies to maintain close proximity to the tubing inner wall during logging.

MVRT Applications: The MVRT tool can be used to:

- Detects internal and external tubular corrosion and quantify extent and depth of penetration.
- Monitor corrosion rates over time through the use of successive logging surveys.
- Determine effectiveness of corrosion inhibition program.
- Identify tubing string make-up and location of collars, pups, mandrels valves and crossovers.
- Determine the appropriate timing and scope of workovers and tubing replacement.

Tool Calibration: Calibration of the MVRT is based on observed correlation between defect size in tubular and the amplitude of a signal produced by measurement of the flux leakage field around such defects. To provide the basis for interpretation each size of tool has to be logged in a controlled situation with a variety of artificial and natural defects.

A series of man made defects is created in tubing/casing samples purchased from a typical oil field supply yard consisting of pit depths ranging from 20% to 90% of the pipe wall thickness. Through holes are also produced. Three different diameters are drilled producing a 6:1, 4:1, and 2:1 width to depth ratio. Defects are produced both internal and external. The tools are pulled through the test tubing in a series of runs. Care is taken to maintain a constant logging speed and adequate sampling. The amplitude of the responses to each type of pit is recorded. The responses are plotted on an x-y chart of amplitude versus percent penetration. Curves are fit through the data points for each group and then as a whole. The result is a general best-fit curve to represent the range of defects available. Each size, weight and grade of pipe that has been characterized has a corresponding chart and best-fit curve to represent the tool response to defects. Calibration charts are available for all weights and grades of pipe.

MVRT Log Data Display: The MVRT log data is displayed on a continuous depth versus senors' response format and includes several data tracks. In addition to raw data, maps of internal and external defects and a joint-by-joint classification of logged tubing string into four classes is presented **(Fig. 4)**. If tubing joint has at one or more points (0 –25)% wall loss, it is classified as class 1, (25-50)% class 2, (50 – 75)% class 3 and (75-100)% is class 4. Obviously class 4 includes holes or 100% wall loss. Here the class is determined by the highest wall loss recorded in the joint. One has to use his/her own assessment of how one class 4 joint compares to another one and therefore, a review of the foot-by-foot data becomes necessary. A summary plot showing wall loss versus depth is usually presented in a condensed format in a single page. This is a useful display to review the overall tubing conditions **(Fig. 5)**.

It is worth noting that the tool resolution is within +/- 10% wall loss. It is claimed that MVRT can quantatively measure defects as small as 0.25 in. diameter with only 25% wall loss.

Data Gathered

As of August 2001, in NK, 85 tubing strings have been logged with calipers and MVRT tools as shown in **Fig. 6**. The ramp up of corrosion surveys in NK in year 2000 was partially due to the recording of baseline corrosion surveys in the injectors of the waterflood reservoirs in NK. The baselines were deemed necessary to assist in time-lapse interpretation and corrosion rate determination.

In addition to tubing monitoring logs, over 16 casing corrosion logs have also been recorded in NK wells since 1994 **(Fig. 7)**. In light of the relatively large number of wells in NK, this number of casing corrosion logs is low. It is recommended to obtain more casing corrosion logs to cover casing and liners particularly in the wells that have produced and or producing wet crude through casing. Liners are exposed to production fluids and subject to corrosion. In some oil fields, to prevent liner corrosion, liners/casings below the production packer are completed with corrosion resistant material.

Out of the 85 tubing corrosion logs recorded in NK, nine MVRT logs were recorded in NK Water Flood Pilot project (WFP) eight producers, as MVRT was repeated in one of the producers[2]. 22 baselines MVRT logs were recorded in NK Sea Water Injection (SWI) project injectors. Two caliper logs were recorded in Effluent Water Disposal wells (EWD). The rest of the tubing down-hole corrosion logs were recorded in NK

producers where reservoir pressure is naturally maintained through strong aquifer support. MVRT was also repeated in one of these producers.

Data Analysis

The analysis was done mainly for the tubing strings that have been logged with MVRT. Only a small number of caliper logs were included in the analysis. The reason behind this was that in caliper log display, the tubing wall loss is not classified numerically, while in MVRT data disply, results are displayed in four classes depending on the percentage wall loss of each joint. In addition, a summary chart showing tubing joint wall loss in percent versus depth is presented. This made it easy to use the data. The down-hole corrosion data of the SWI injectors are not included in the analysis. The gathered data was analyzed for the following relationships.

1. Watercut vs. Corrosion Severity

Fig. 8 shows a graph of the stable watercut in the producing string versus tubing wall loss. From the data the following observations can be made:

- There is a general correlation between the stable watercut of the produced fluid from the tubing versus the tubing wall loss. It has been observed that class 3 corrosion (50-75% wall loss) occurs mostly at watercuts above 25%.
- Some of the tubing strings despite having low watercut showed higher corrosion (class 2 to 4) in few joints. However, the reason for this anomaly is believed to be poor quality control of tubing during running completion **(Fig. 9)**. Mixing tubing of different grade and age in a well completion causes down-hole corrosion data interpretation problems and potentially reduces effective life of the completion.
- For the wells that were producing at high watercut but showed relatively lower wall loss (corrosion classes of 1 or 2), the reason was found to be shorter duration of wet production.

2. Depth vs. Corrosion

In about 15 wells a peculiar relationship between depth and corrosion severity was observed. However, it was not a linear depth versus corrosion relationship. The corrosion was observed to start almost abruptly after certain depth. A closer look at these wells revealed that these depths where corrosion abruptly increased correspond to reservoir fluid bubble point pressure in the tubing. It was interpreted that since corrosion in North Kuwait wells in the non-waterflooded reservoirs is mainly due to CO_2 being dissolved in formation water, the bubble point pressure does play a role in changing corrosion pattern in the tubing. Below the bubble point pressure the CO_2 is dissolved in the water, which consequently makes the water more acidic due to the formation of carbonic acid. The acidic water causes more corrosion. Above the bubble point pressure in the tubing, the CO_2 is released and therefore, the water becomes relatively less corrosive **(Fig. 10-11)**.

3. Corrosion Rate Estimate

MVRT was run twice in two tubing strings: WELL-0123 and WELL-0030. **Fig. 12** and **Fig. 13** show depth versus penetration charts for each well with the time lapse logs. In WELL-0123 the time lapse between the two MVRT logs was about seven months. The N-80 3 ½ tubing (which has a tubing wall thickness of about 12.9 mm) shows 31% increase in wall loss/year in one of the corroded intervals. This suggests a corrosion rate of 4 mm/yr in N-80, 3 ½ in. tubing.

The time lapse in WELL-0030 was about 20 months during most of which the well was not flowing. The preliminary investigations in WELL-0030 show that the corrosion rate of N-80, 3 ½ in. tubing is approximately 3 mm/yr. However, if the well had not been shut-in, corrosion rate could have been higher. Overall, these rates of corrosion are alarmingly high but broadly agree with corrosion rates predicted by corrosion models.

MVRT Data Verification

1. MVRT vs. Caliper

Both, MVRT and Caliper have been run in three wells (WELL-0043, -0030, -0102) to provide a comparison between the two tools. Both logs were qualitatively comparable **(Fig. 14)** with the exception of WELL-0043 where the caliper log covered the last four joints of the damaged tubing, which were not covered by the MVRT due to borehole restriction. As mentioned earlier, the MVRT tool measures both internal and external corrosion while the caliper measures only the internal corrosion. Therefore, the corrosion recorded by the caliper is less than corrosion reported by the MVRT tool as shown in Fig. 14.

WELL-0043 was worked over and the retrieved tubing confirmed the observed corrosion on both logs. It is worth mentioning that due to severe corrosion, an expensive and lengthy fishing operation had to be performed to fish the corroded tubing out. **Fig. 15** and **Fig. 16** show caliper log summary chart of depth vs. corrosion data, and a picture of a piece of the pulled out tubing. It is clear that the caliper has correctly identified this badly corroded pipe.

2. MVRT Data vs. Surface Inspection

A detailed comparison of down-hole MVRT data and pulled-out tubing segments of corroded tubing have been carried out in at least one well, namely WELL-0057. The comparisons have validated the results of the MVRT for both internal and external defects. A visual inspection was conducted at site and samples of tubing, packers and completion assembly sent to the corrosion and inspection workshops for detailed examination. The samples have underdone both destructive and nondestructive testing to assess the type and the magnitude of the damage. Wall thickness, chemical composition, and visual inspection records have been made **(Fig. 17-18)**. It is important to note that the rig workover recommendation in this well was solely based on the MVRT log data. The log data proved to have appropriately identified the badly corroded pipe. The decision to pull the tubing out was surely correct. The workover, unlike WELL-

0043 and WELL-0082 (which will be discussed later in the paper), was trouble free and less costly.

The surface inspection study concluded that the damage observed was most severe at the bottom of the tubing as seen on the MVRT log. The tubing joints higher in the string have suffered significantly less damage; this was attributed to the presence of an adherent protective scale. Results again confirm the MVRT data.

Based on observed corrosion data, down-hole corrosion inspection guidelines and tubing inspection/quality control during completion/workovers for NK well completions have been established.

Impact-Economic Cost of Corrosion

Severe down-hole corrosion in production and injection wells, have so far resulted in six tubing and three casing failures and severe casing/tubing corrosions. Remediation of these wells has resulted in problematic, high cost workovers and in one case the loss of the productive interval and the associated reserves. Due to problematic and lengthy workovers, corrosion also impacts the well availability for production. These lengthy workovers cause significant production deferral.

Fig. 19 plots the cost of rig workover and time associated with each rig workover. It is obvious that Well-0043 and Well-0082 (failed completions due to corrosion) stand out in both cost and workover time compared to the normal rig workover cost of other similar completions. In Well-0043, the cost was 3X the normal rig workover cost due to corrosion related fishing/milling jobs. While in Well-0082 it was decided to reduce the rig workover cost by not continuing the fishing operations. This however led to the abandonment of a major producing section of the reservoir. The reserves of the abandoned zone can only be recovered by drilling a new well in the area.

From the experience learned from WELL-0043, which was a casing/tubing producer with both strings producing wet oil for some time, the economics of producing oil through casing versus corrosion risk should be evaluated, particularly if the casing production is expected to become wet.

Conclusions

- Corrosion is already a major issue in NK and will become more significant as water production increases.
- Down-hole corrosion needs to be properly monitored and managed to reduce operating cost and well down time.
- There is a fair correlation between water production and corrosion in NK.
- It has been observed that class 3 corrosion (50-75% wall loss) occurs mostly at watercuts above 25%.
- Corrosion has been seen in fairly low watercuts situations that may be partially related to mixing of tubing of different age and grade while re-completing the well.
- The MVRT results recorded down-hole have been verified against caliper and surface inspection. The comparison has validated MVRT results.
- In North Kuwait, MVRT has been used to monitor down-hole corrosion and make timely decision to pull out completions and avoid costly/problematic rig workover's.
- Through time lapse logging, MVRT has been used to estimate corrosion rate in North Kuwait completions. These estimates broadly agree with corrosion rates predicted by corrosion models.
- Based on observed corrosion data, down-hole corrosion inspection guidelines and tubing inspection/quality control during completion/workovers for North Kuwait well completions have been established.

Recommendations

- Along with monitoring, a comprehensive corrosion management plan such as "North Kuwait Corrosion Management Plan" need to be implemented in North Kuwait to manage corrosion cost and production impact.
- Timely rig workovers, based on down-hole corrosion monitoring data, are recommended to pull tubing before becoming problematic and costly.
- Mixing tubing of different grade and age in a well completion causes down-hole corrosion data interpretation problems and reduces effective life of the completion. It is recommended not to mix tubing of different grade and age.
- Investigating preventive methods including field-testing of corrosion-resistant alloys and chemical treatments need to be carried out as soon as possible to provide input for future material selection.
- Eliminating casing production to reduce the risk of casing corrosion should be considered particularly when the production is expected to become wet.
- It is recommended to obtain casing corrosion logs during rig workovers to cover casings and liners of the wells that have produced wet crude particularly those with casing production. In addition, it is recommended to monitor the liner of wet producers with through tubing calipers.

Acknowledgements

The authors are thankful to the management of Kuwait Oil Company and Ministry of Oil for their permission to publish this work. The authors would, also, like to thank the colleagues who reviewed the paper for their useful comments.

References

1. Graham, W.L., Silva, C.I., Leimkuhler, J.M., de Kock, A. J.: "Cement Evaluation and Casing Inspection With Advanced Ultrasonic Scanning Methods," paper SPE 38651 presented at the 1997 SPE Annual Technical Conference and Exhibition, San Antonio, Texas, Oct. 5-8.
2. Al-Aqeel, Z. A., El-Shourbagi, S. M., and Mousawi, A. Z.: "Corrosion Monitoring in Mauddud Pilot Wells in North Kuwait Oil Fields: Data Analysis, LPR/pH and Downhole ESP Relationships, Problems and Solutions," paper ADIPEC-0955 presented at the 2000 Abu Dhabi International Petroleum Exhibition and Conference, Abu Dhabi, U.A.E., Oct. 15-19.

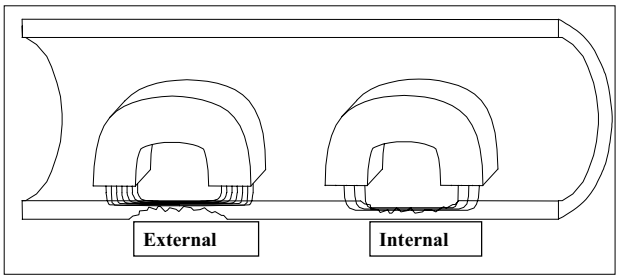

Fig. 1: MVRT measurement theory: Flux Leakage (FL) sensors alone cannot differentiate internal from external defects. To perform this function, Discriminator (DIS) sensors are deployed within a weak magnetic field that is completed through the tubing's inner surface.
External defects do not affect this flux path and therefore cause no DIS response. Internal defects, however, serve to alter the flow of flux in their vicinity, producing a characteristic DIS log response.

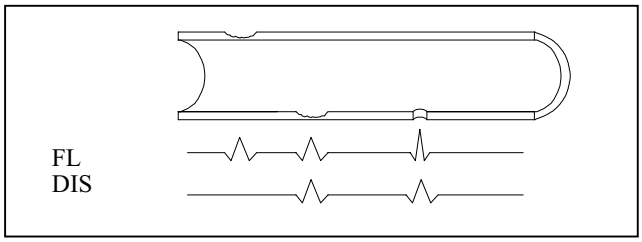

Fig. 2: MVRT tool response: The combination of FL and DIS sensors serves to identify the type and origin of tubular defects. An FL response alone indicates an external feature. An FL response in combination with a DIS response indicates an internal feature.

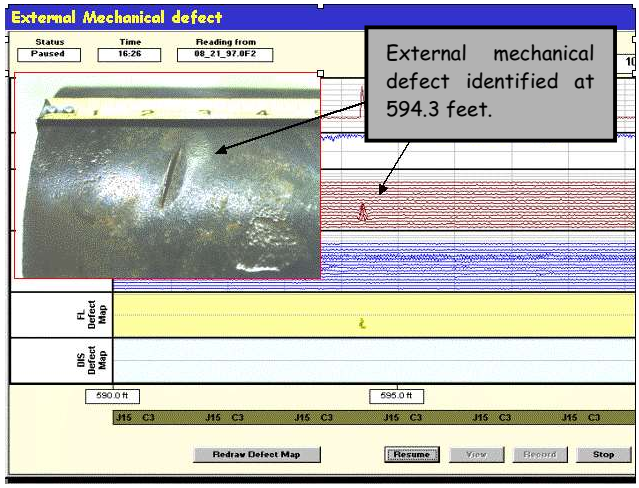

Fig. 3 The MVRT system produces digital bipolar waveforms, allowing metal gain anomalies versus metal loss to be determined from the log signatures.

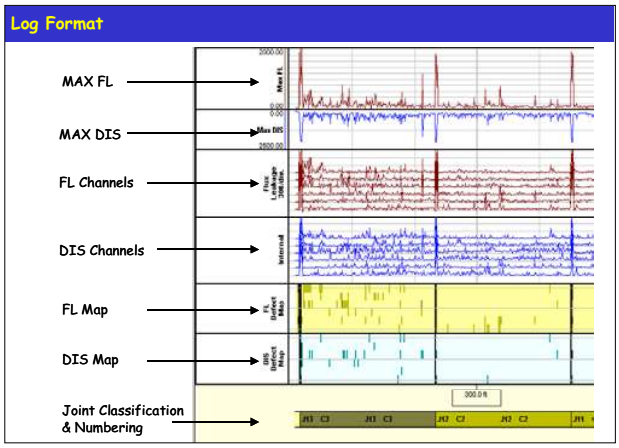

Fig. 4: MVRT log display format showing depth versus senor response, maps of internal and external defects, and a joint-by-joint classification of logged tubing string into four classes.

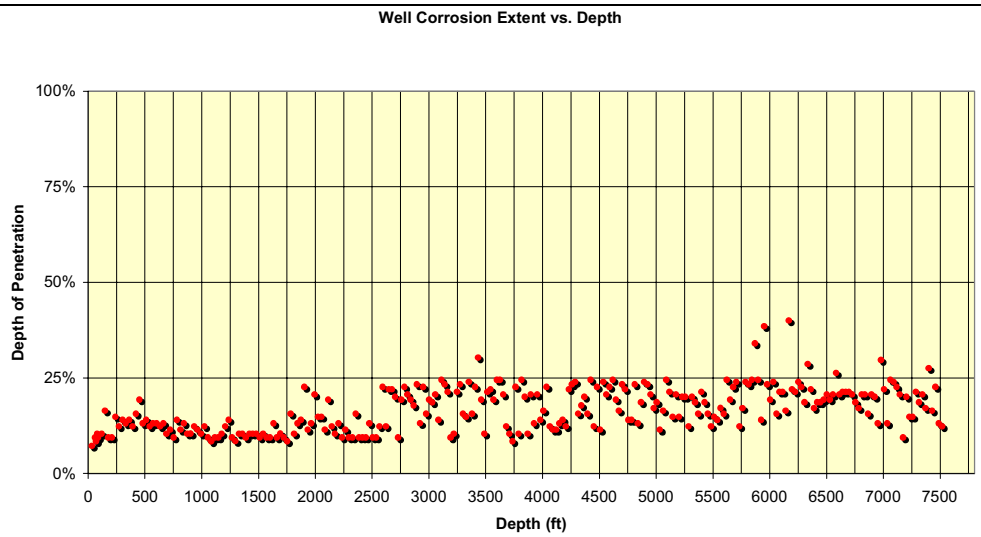

Fig. 5: MVRT log plot of wall loss vs. depth displaying overall tubing string conditions

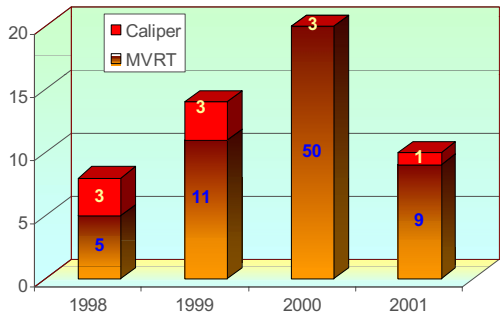

Fig. 6: Number of corrosion logs recorded in North Kuwait wells (tubing strings) vs. time

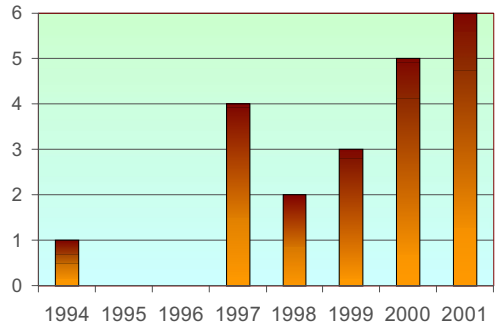

Fig. 7: Number of corrosion logs recorded in North Kuwait wells (casing strings) vs. time

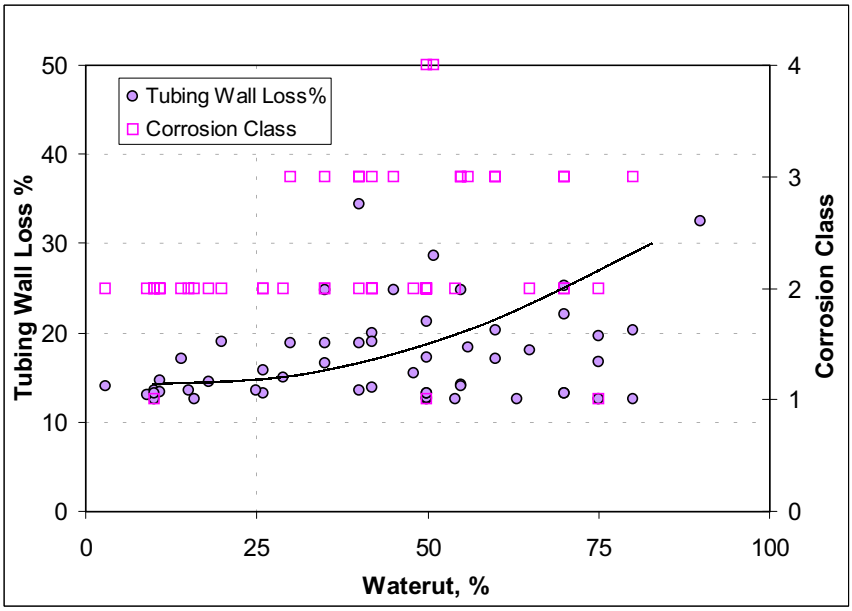

Fig. 8: A plot of stable watercut (%) of the logged tubing string vs. tubing wall loss (%) and the worst class of corrosion observed in the tubing.

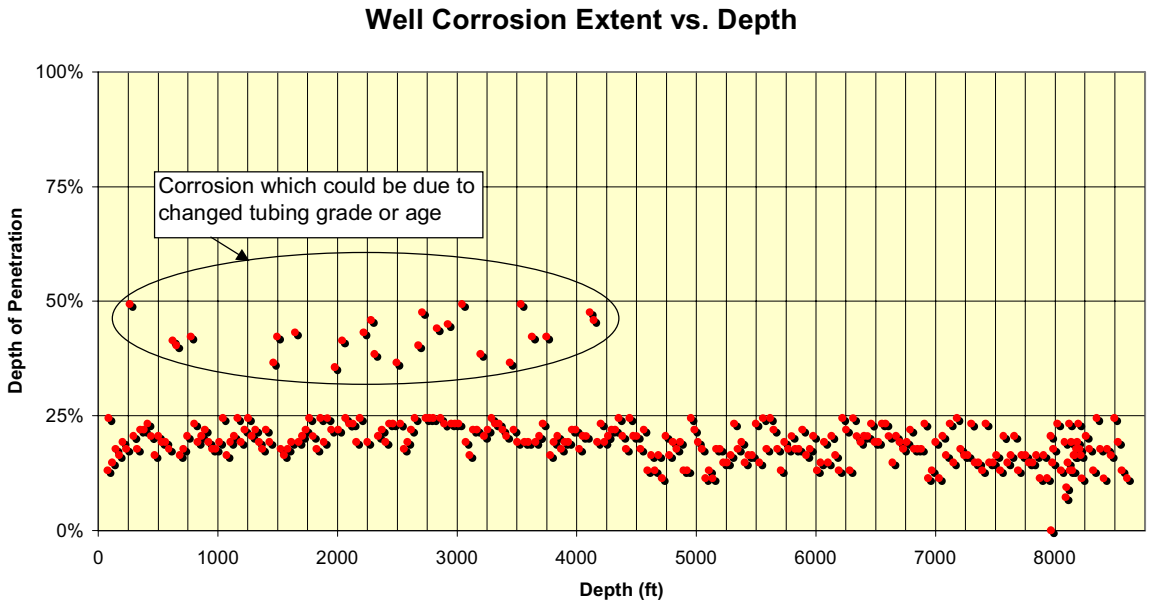

Fig. 9: An example of MVRT log in which the tubing shows corrosion in some joints. This corrosion interpreted by the MVRT could be as a result of completing the tubing with joints of different grade or age.

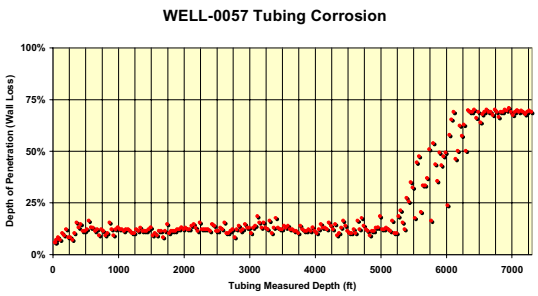

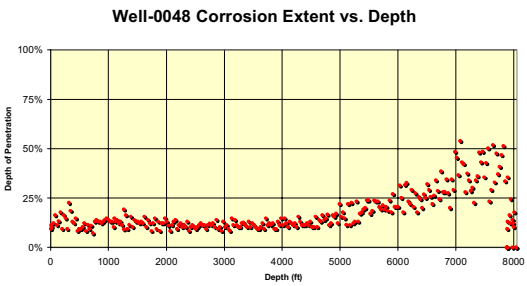

Fig. 10-11: Two examples of wells showing the depth vs. corrosion relationship. See increased corrosion after certain depth.

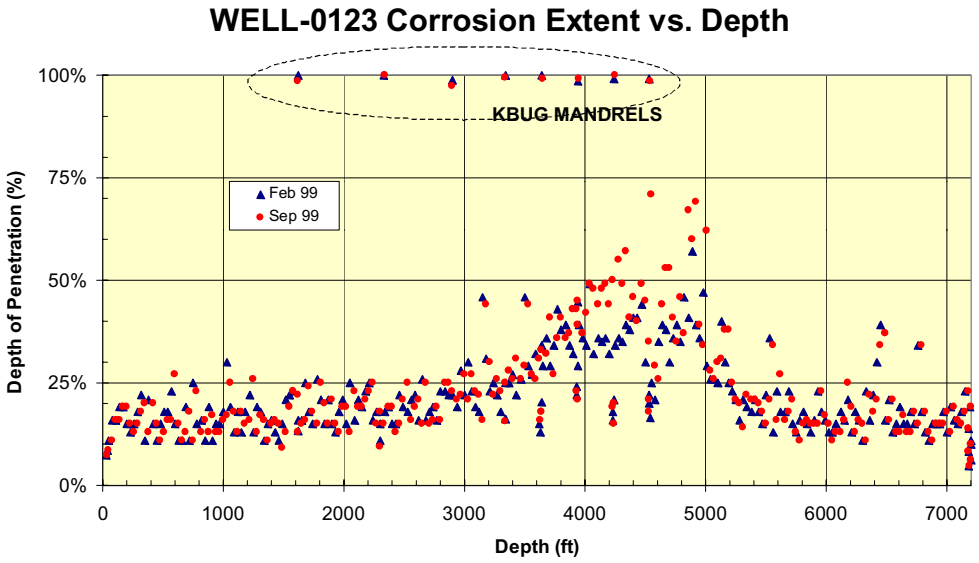

Fig. 12: WELL-0123 tubing penetration chart using time-lapsed corrosion logs

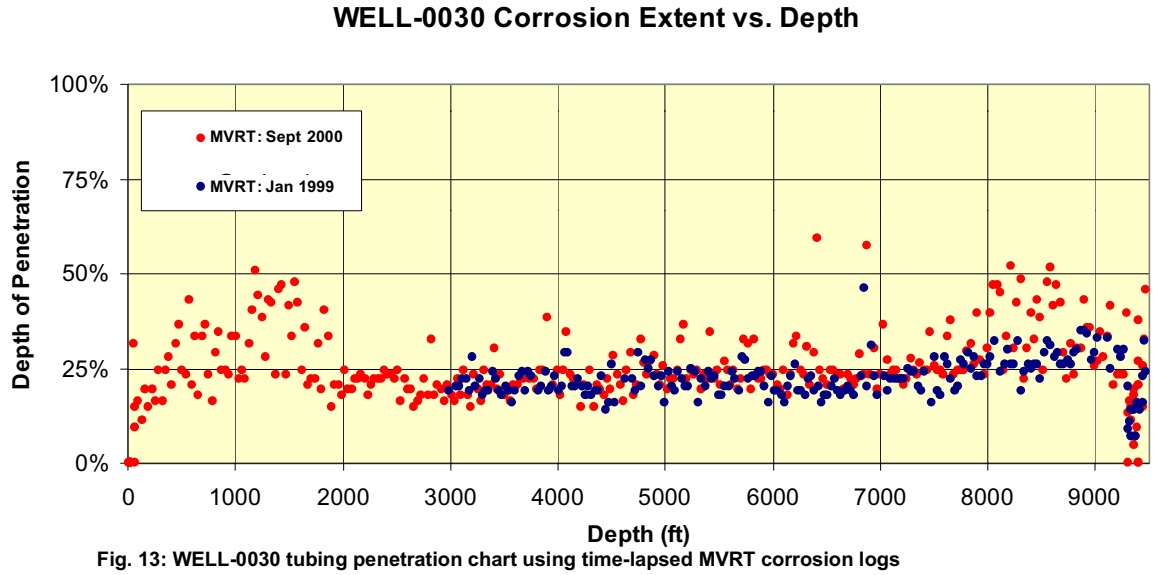

Fig. 13: WELL-0030 tubing penetration chart using time-lapsed MVRT corrosion logs

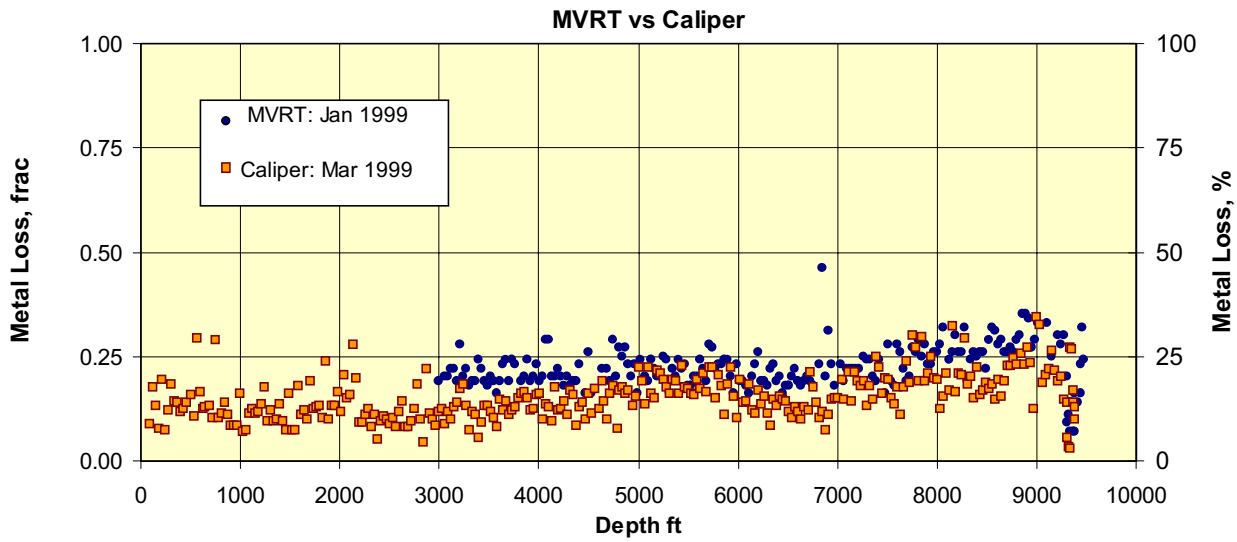

Fig. 14: WELL-0030 tubing penetration chart of the MVRT and caliper corrosion logs. Note that the caliper log is showing less corrosion than the MVRT log. This is because the MVRT tool measures both internal and external corrosion while the caliper measures only the internal corrosion.

Fig. 15: Piece of WELL-0043 pulled out tubing showing severe damage

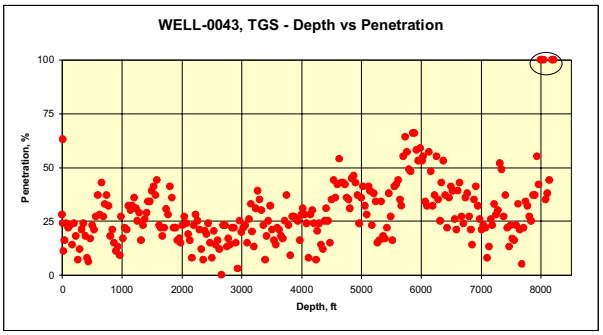

Fig. 16: WELL-0043 tubing penetration chart of the caliper log. Class 4 damage (100% wall loss in this case) is clearly identified by the caliper log

Fig. 17: WELL-0057 Tubing joint pin end

Fig. 18: WELL-0057 Tubing joint box end corroded section

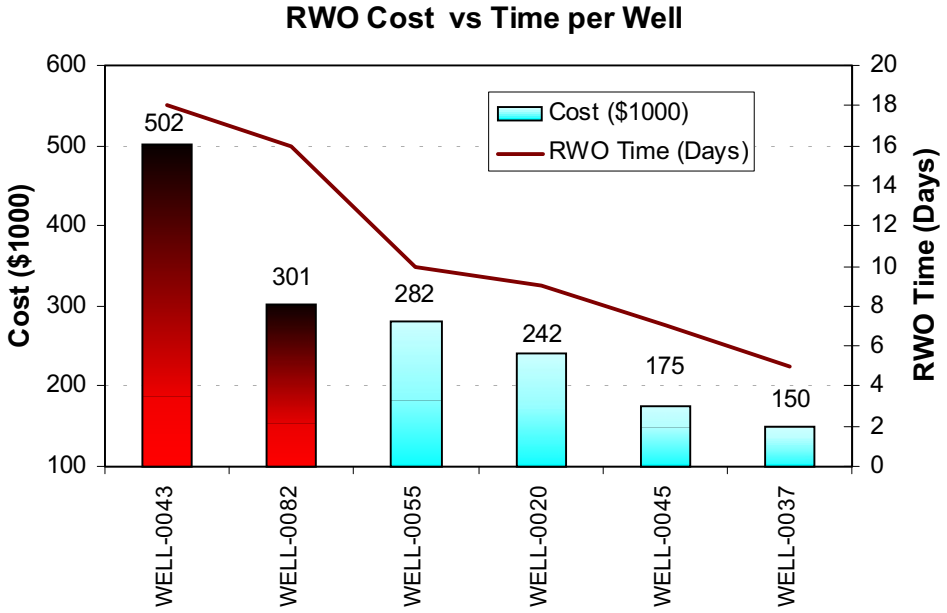

Fig. 19: Rig workover cost and the time associated with each rig workover for WELL-0043 and WELL-0082 compared to the normal rig workover cost of other similar completions.

Ex. II - 8

SPE 84828

The Importance in Developing a Surveillance Logging Quality Assurance and Quality Control Plan

Mark A. Newman, Columbia Gas Transmission

Copyright 2003, Society of Petroleum Engineers Inc.

This paper was prepared for presentation at the SPE Eastern Regional/AAPG Eastern Section Joint Meeting held in Pittsburgh, Pennsylvania, U.S.A., 6–10 September 2003.

This paper was selected for presentation by an SPE Program Committee following review of information contained in an abstract submitted by the author(s). Contents of the paper, as presented, have not been reviewed by the Society of Petroleum Engineers and are subject to correction by the author(s). The material, as presented, does not necessarily reflect any position of the Society of Petroleum Engineers, its officers, or members. Papers presented at SPE meetings are subject to publication review by Editorial Committees of the Society of Petroleum Engineers. Electronic reproduction, distribution, or storage of any part of this paper for commercial purposes without the written consent of the Society of Petroleum Engineers is prohibited. Permission to reproduce in print is restricted to a proposal of not more than 300 words; illustrations may not be copied. The proposal must contain conspicuous acknowledgment of where and by whom the paper was presented. Write Librarian, SPE, P.O. Box 833836, Richardson, TX 75083-3836 U.S.A., fax 01-972-952-9435.

Abstract

A quality assurance and quality control (QA/QC) plan is important to the success of a surveillance logging program. A QA/QC Plan for a surveillance logging program can provide adequate and accurate information in assessing the level of pipe defects reported from casing inspection logs and can be used to record possible trends regarding individual casing inspection tools[1]. Measurements taken from pulled well casing can be used to enhance the analysis of general corrosion in areas of large-diameter pits. Over time the accuracy in estimating depth of penetration in large-diameter corrosion pits can be improved.

Introduction

With increased pressure to control costs and decrease spending, most companies will at some time or another review operating budget practices. For storage operators, a surveillance logging program may represent a significant portion of the operating and maintenance budget. To help control costs for a surveillance logging program, an operator may decide to alter the traditional log sweep or look at more effective ways to obtain the information they require. Altering the traditional log sweep simply means being more selective in choosing what log information the operator requires. A QA/QC plan is another way for an operator to verify information, to effectively manage the data, and to justify operating costs.

Quality Assurance / Quality Control Plan

The main focus of a surveillance logging QA/QC plan is to acquire pipe samples that contain identified defects and to validate the log analysis provided by the vendor. For the purpose of this paper, pipe samples will be compared to magnetic flux leakage casing inspection logs and specifically to that of the MicroVertilog (MVRT). Most comments will apply to all magnetic flux leakage casing inspection logs.

The key objective of a surveillance logging QA/QC plan is to ensure that the data being provided is adequate and accurate. A QA/QC plan can improve confidence in the data being generated, improve the data credibility with a contractor, and improve upon operational, product, or service efficiencies[1]. Information from the QA/QC plan can be used to better assess the level of pipe defects, recognize trends from the casing inspection logs, characterize possible errors in measuring tubular thickness, and monitor tool accuracy and data interpretation.

Casing Inspection Logs

A flux leakage casing inspection log such as the MVRT or Pipe Analysis Log (PAL) uses a computer software program to compare statistical data with the average depth of penetration over a specific area of investigation. Essentially, the software program compares recorded images with fixed images or examples of pipe defects as shown in Figures 1 and 2.

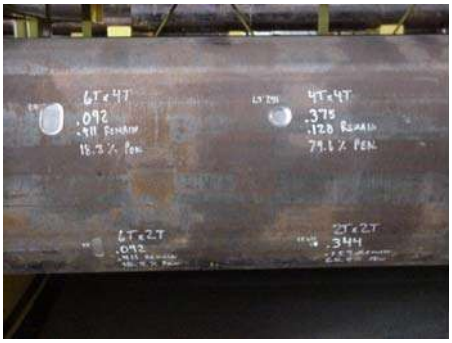

Figure 1 – Manufactured defects used for calibration.

Figure 2 - Manufactured defects used for calibration.

Tool Calibration. Calibration is important to quantifying measurements observed by the tool. Tool calibration is based on observed correlation between known defects in the pipe wall and the amplitude of a signal produced. Defects used for calibration are typically smooth, flat, or round uniform surfaces unlike the surfaces found when corrosion is present. Holes with three different diameters are drilled into the internal and external walls of the pipe, and are intended to represent typical defects found on pipe. The width-to-depth ratios used to drill the defects are typically 6:1, 4:1, and 2:1. The amplitude response for each of the calibrated defects is then plotted on an x-y chart of amplitude versus percent penetration. Curves are then fitted through the data points. The best-fit curve is in the form of $y=ax^b$. Calibration results in a general best-fit curve to represent the range of defects observed in the pipe samples.

To improve the curve fit, data points from corrosion samples can be collected and measured. With sufficient data points a new flux leakage amplitude curve (as shown in Figure 3) can be generated. The new amplitude curve can only be used to verify log analysis from the population that it was collected from. For example, data collected from general corrosion found on 5 ½", 17 ppf, J-55 casing can only be used to verify general corrosion on 5 ½", 17 ppf, J-55 casing.

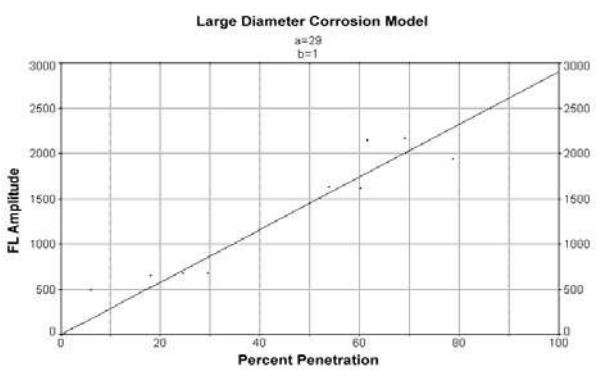

Figure 3 – Flux leakage amplitude curve developed for large-diameter corrosion.

Large-diameter Pit Corrosion. Most vendors would agree that large-diameter pit corrosion typically found in areas of general corrosion are the hardest to estimate and are generally overstated. The following are examples of large-diameter pit corrosion with a length and width greater than 1" and with an average depth of penetration greater than 60%. In each of the following examples the original log data was re-analyzed using a large-diameter pit corrosion model.

Example 1
Well A
Joint # 14
Pipe size – 5.5 in.
Pipe weight and grade – 17 ppf, J-55
Nominal pipe wall – 0.304 in.
Measured pipe wall – 0.304 in.

Log Measurements (Figure 4)
Location – external
Corrosion model - general
Length – 1.7 in.
% penetration – 100%

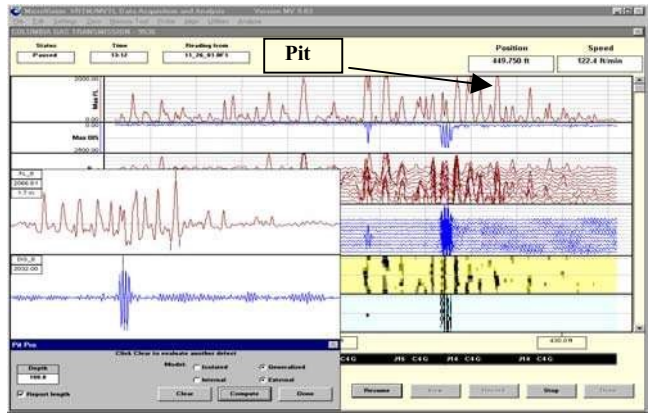

Figure 4 – Snapshot of Example 1 MicroVertilog taken from Pit Pro.

Physical Measurements (Figures 5 and 6)
Defect location – external
Defect depth – 0.21 in.
Defect width – 3.00 in.
Defect length – 1.75 in.
% penetration – 69.1%

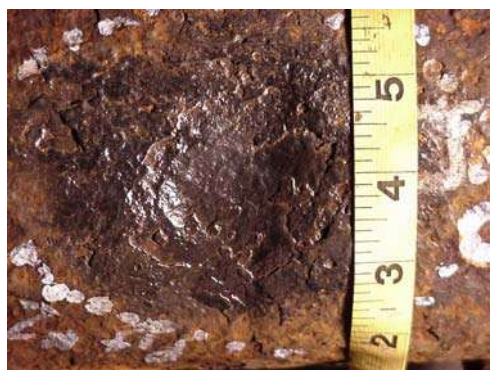

Figure 5 – Digital image showing the defect where Example 1 physical measurements were taken.

Figure 6 - Digital image showing the defect where Example 1 physical measurements were taken.

Comments
Using the preliminary large-diameter corrosion model, the predicted depth of penetration from the MVRT data would be 75.2%.

Example 2
Well B
Joint # 2
Pipe size – 5.5 in.
Pipe weight and grade – 17 ppf, J-55
Nominal pipe wall – 0.304 in.
Measured pipe wall – 0.301 in.

Log Measurements (Figure 7)
Location – external
Corrosion model - general
Length – 0.7 in.
% penetration – 83.5%

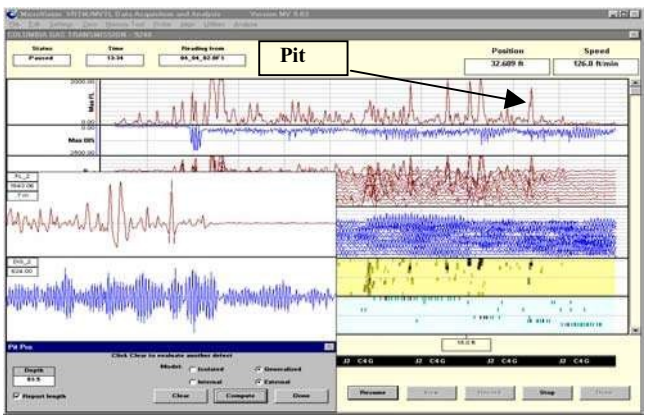

Figure 7 – Snapshot of Example 2 MicroVertilog taken from Pit Pro.

Physical Measurements (Figures 8 and 9)
Defect location – external
Defect depth – 0.162 in.
Defect width – 1.5 in.
Defect length – 1.0 in.
% penetration – 53.8%

Figure 8 - Digital image showing the defect where Example 2 physical measurements were taken.

Figure 9 - Digital image showing the defect where Example 2 physical measurements were taken.

Comments
Using the preliminary large-diameter corrosion model, the predicted depth of penetration from the MVRT data would be 56.6%.

Example 3
Well C
Joint # 7
Pipe size – 5.5 in.
Pipe weight and grade – 17 ppf, J-55
Nominal pipe wall – 0.304 in.
Measured pipe wall – 0.356 in.

Log Measurements (Figure 10)
Location – external
Corrosion model - isolated
Length – 1.4 in.
% penetration – 42.9%

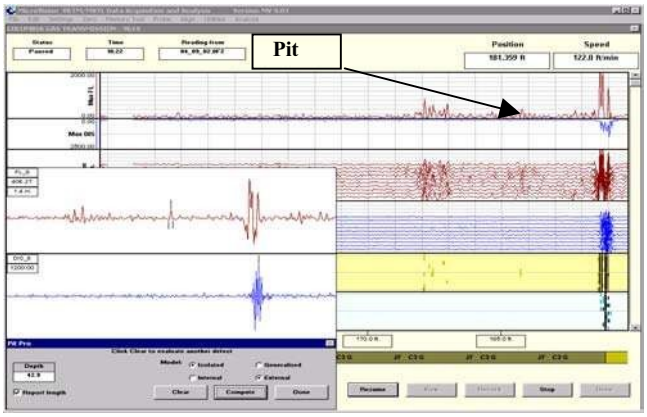

Figure 10 – Snapshot of Example 3 MicroVertilog taken from Pit Pro.

Physical Measurements (Figures 11 and 12)
Defect Location – external
Defect depth – 0.064 in.
Defect width – 1.5 in.
Defect length – 1.5 in.
% penetration – 18.0%

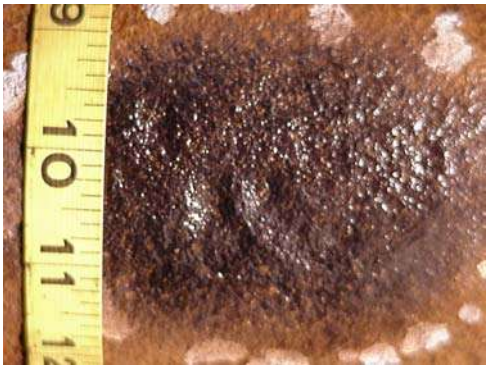

Figure 11 - Digital image showing the defect where Example 3 physical measurements were taken.

Figure 12 - Digital image showing the defect where Example 3 physical measurements were taken.

Comments

Using the preliminary large-diameter corrosion model, the predicted depth of penetration from the MVRT data would be 22.6%.

Example 4

Well D
Joint # 1
Pipe size – 5.5 in.
Pipe weight and grade – 17 ppf, J-55
Nominal pipe wall – 0.304 in.
Measured pipe wall – 0.282 in.

Log Measurements (Figure 13)

Location – external
Corrosion model - isolated
Length – 1.4 in.
% penetration – 44.1%

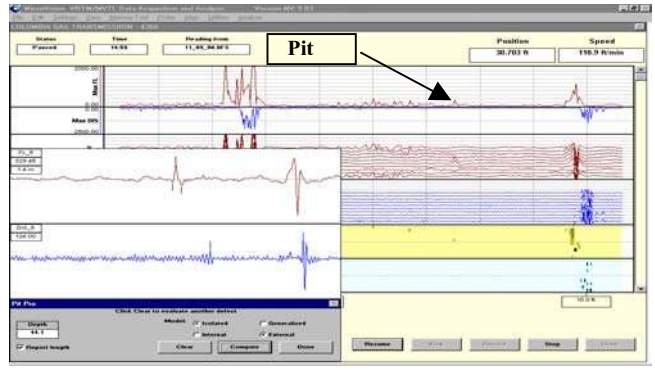

Figure 13 - Snapshot of Example 4 MircoVertilog taken from Pit Pro.

Physical Measurements (Figure 14 and 15)

Defect location – external
Defect depth – 0.07 in.
Defect width – 3.00 in.
Defect length – 2.00 in.
% penetration – 24.5%

Figure 14 - Digital image showing the defect where Example 4 physical measurements were taken.

Figure 15 - Digital image showing the defect where Example 4 physical measurements were taken.

Comments

Using the preliminary large-diameter corrosion model, the predicted depth of penetration from the MVRT data would be 23.9%.

Validation Measurements. Measurements taken from pipe samples with various types of corrosion, pipe defects, and mechanical defects should be used to validate log data. Validation is essential for verifying tool calibration and for monitoring the tool accuracy. Validations similar to the following examples are important and necessary functions for a QA/QC plan.

Example 5
Well B
Joint # 2
Pipe size – 5.5 in.
Pipe weight and grade – 17 ppf, J-55
Nominal pipe wall – 0.304 in.
Measured pipe wall – 0.301in.

Log Measurements (Figure 16)
Location – external
Corrosion model - general
Length – 0.5 in.
% penetration – 43.4%

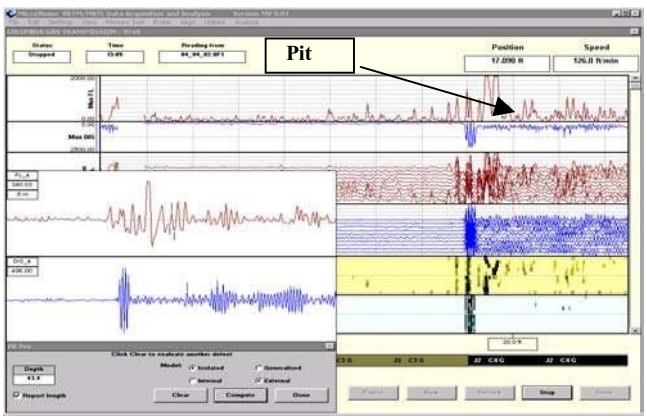

Figure 16 - Snapshot of Example 5 MircoVertilog taken from Pit Pro.

Physical Measurements(Figures 17 and 18)
Defect location – external
Defect depth – 0.135 in.
Defect width – 0.5 in.
Defect length – 0.5 in.
% penetration – 44.9%

Figure 17 - Digital image showing the defect where Example 5 physical measurements were taken.

Figure 18 - Digital image showing the defect where Example 5 physical measurements were taken.

Comments
This defect is an external pit located in close proximity to general corrosion. Notice how the pit is very symmetrical and resembles a calibration pit. Corrosion may have been produced by the presence of hydrogen sulfide.

Example 6
Well C
Joint # 7
Pipe size – 5.5 in.
Pipe weight and grade – 17 ppf, J-55
Nominal pipe wall – 0.304 in.
Measured pipe wall – 0.356in.

Log Measurements (Figure 19)
Location – external
Corrosion model - general
Length – 1.4 in.
% penetration – 33.7%

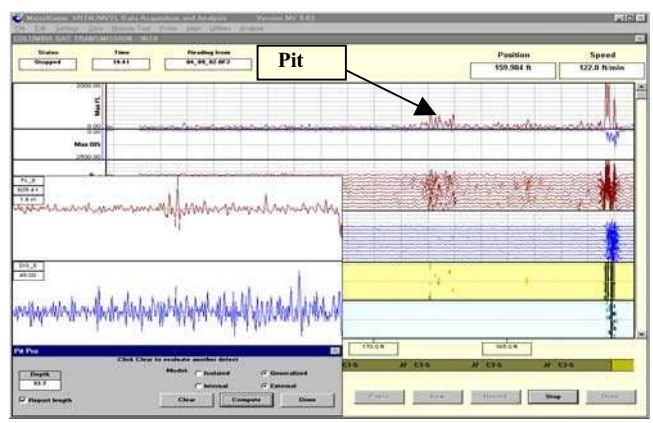

Figure 19 - Snapshot of Example 6 MircoVertilog taken from Pit Pro.

Physical Measurements (Figures 20 and 21)
Defect location – external
Defect depth – 0.092 in.
Defect width – 1.0 in.
Defect length – 1.5 in.
% penetration – 25.8%

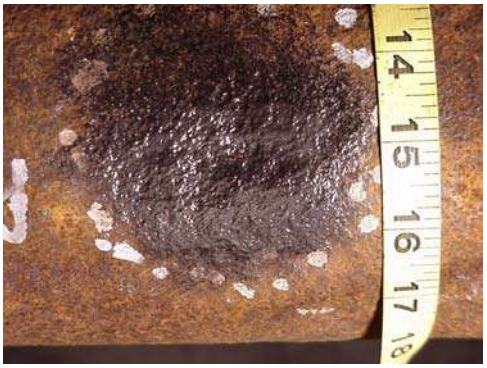

Figure 20 - Digital image showing the defect where Example 6 physical measurements were taken.

Figure 21 - Digital image showing the defect where Example 6 physical measurements were taken.

Comments

This defect is an external pit located in a one-foot section of pipe with generalized corrosion.

Example 7

Well A
Joint # 27
Pipe size – 5.5 in.
Pipe weight and grade – 17 ppf, J-55
Nominal pipe wall – 0.304 in.
Measured pipe wall – 0.311 in.

Log Measurements (Figure 22)

Location – internal
Corrosion model - isolated
Length – 0.4 in.
% penetration – 98.5%

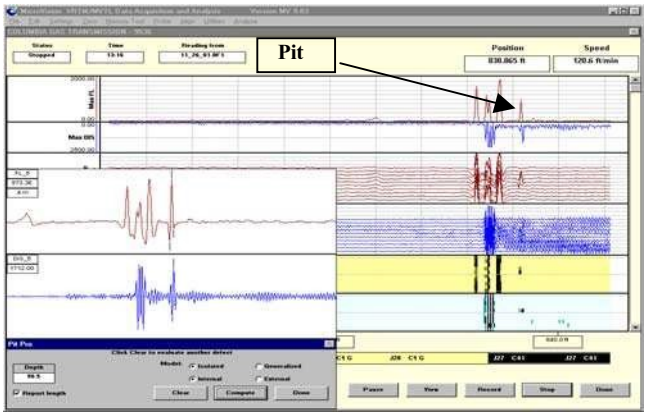

Figure 22 - Snapshot of Example 7 MicroVertilog taken from Pit Pro.

Physical Measurements (Figures 23, 24 and 25)

Defect location – internal
Defect depth – 0.09 in.
Defect width – 2.5 in.
Defect length – 0.25 in.
% penetration – 29.0%

Figure 23 - Digital image showing the defect where Example 7 physical measurements were taken.

Figure 24 - Digital image showing the defect where Example 7 physical measurements were taken.

Figure 25 - Digital image showing the defect where Example 7 physical measurements were taken.

Comments
This defect is a mechanical anomaly with a very deep, transverse pit that has a steep undercut shelf. Note the discriminator activity on the MVRT corresponds to an internal surface groove that is associated with severe laminations.

Example 8
Well E
Joint # 1
Pipe size – 5.5 in.
Pipe weight and grade – 17 ppf, J-55
Nominal pipe wall – 0.304 in.
Measured pipe wall – 0.309 in.
Log Measurements (Figure 26)
Location – external
Corrosion model - isolated
Length – 0.5 in.
% penetration – 56.1%

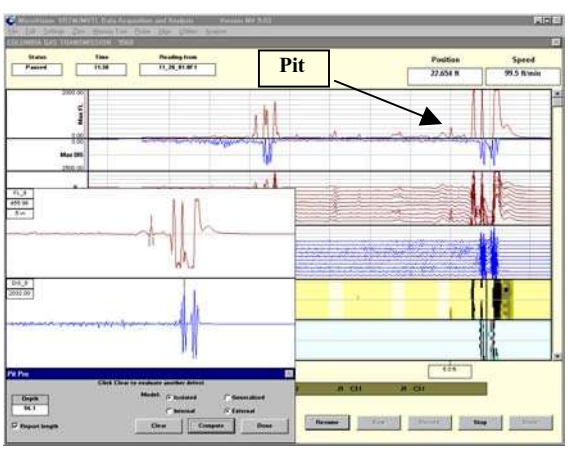

Figure 26 - Snapshot of Example 8 MicroVertilog taken from Pit Pro.

Physical Measurements (Figure 27)
Defect location – external
Defect depth – 0.017 in.
Defect width – 3.0 in.
Defect length – 0.25 in.
% penetration – 5.5%

Figure 27 - Digital image showing the defect where Example 8 physical measurements were taken.

Comments
This defect is a sharp-edged mechanical defect along the axis of the pipe. The proximity to the collar suggests that this is a tong mark.

Example 9
Well E
Joint # 12
Pipe size – 5.5 in.
Pipe weight and grade – 17 ppf, J-55
Nominal pipe wall – 0.304 in.
Measured pipe wall – 0.310 in.

Log Measurements (Figure 28)
Location – external
Corrosion model - general
Length – 0.5 in.
% penetration – 19.2%

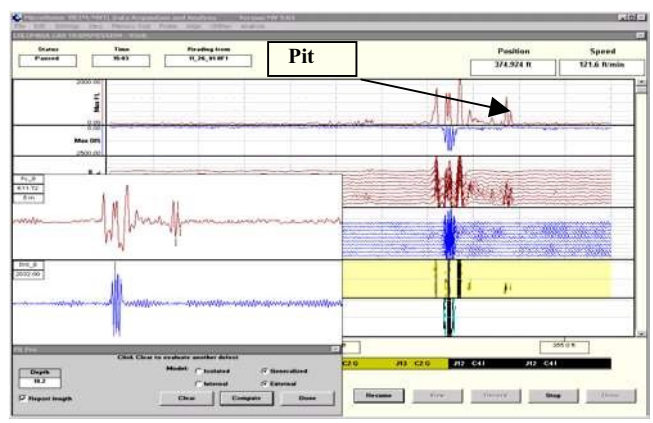

Figure 28 - Snapshot of Example 9 MicroVertilog taken from Pit Pro.

Physical Measurements (Figure 29)
Defect location – external
Defect depth – 0.032 in.
Defect width – 4.0 in.
Defect length – 0.38 in.
% penetration – 10.3%

Figure 29 - Digital image showing the defect where Example 9 physical measurements were taken.

Comments

This defect is a mechanical anomaly located 1.5' above the pin end of a joint. The original damage to the pipe is believed to be due to tongs or slips. Notice how corrosion appears to be forming around the damage area.

Conclusion

Developing a quality assurance and quality control plan is important to the success of a surveillance logging program. Information collected from pipe samples is critical for verifying the log analysis. As data reliability improves, an operator can better determine areas of concern and adjust the log frequency. Eventually, an operator can use the plan information to justify operating costs.

A QA/QC plan tends to enforce the need to collect and validate data in order to verify the reliability of the analysis of casing inspection logs. Due to the statistical nature of the log analysis, the operator can only improve the accuracy and reliability of the log information by comparing actual field measurements with log measurements. In some cases, an operator can greatly improve the log data by populating data points used to generate the amplitude curve. Collecting pipe samples is by far the most important component of a QA/QC plan.

As demonstrated by the examples provided in this paper, data reliability will eventually improve. An operator will develop a comfort level in accepting the information provided by a magnetic flux leakage casing inspection log, and begin to focus more attention on areas of known corrosion and can better determine the log frequency required to monitor well conditions.

It may be years before the actual benefits of the plan are apparent. One major reason is that most operators will need to start from the beginning, possibly ignoring previous data, in an effort to build a new, more dependable database. While past log data may be beneficial, data validation and corrections may not be possible. Over the life of the plan, an operator is sure to develop additional justification for surveillance logging operating costs.

Acknowledgements

The author of this paper would like to extend his appreciation to Columbia Gas Transmission for permission to publish this paper. All figures presented in this paper were provided by Bill Rubin, of Baker Atlas as part of Columbia's ongoing Quality Assurance and Quality Control Program.

References

1. "Fundamentals of Developing a Surveillance Logging Quality Assurance and Quality Control Plan", SPE 78714, 2002 Eastern Regional Meeting, Lexington, KY (October 2002), 1

Ex. II - 9

SPE-175871-MS

Magnetic Flux Leakage (MFL) Technology Provides the Industry's Most Precise Pipe Integrity and Corrosion Evaluation, Accurately Characterizing Casing and Tubing Strength. Technology Overview and Case History

Wael El Sherbeny,PhD Ivo Nuic, Gasser Hasan,Abba Abdesslam, and Tharwat HassanePh.D. , Baker Hughes

Copyright 2015, Society of Petroleum Engineers

This paper was prepared for presentation at the SPE North Africa Technical Conference and Exhibition held in Cairo, Egypt, 14–16 September 2015.

This paper was selected for presentation by an SPE program committee following review of information contained in an abstract submitted by the author(s). Contents of the paper have not been reviewed by the Society of Petroleum Engineers and are subject to correction by the author(s). The material does not necessarily reflect any position of the Society of Petroleum Engineers, its officers, or members. Electronic reproduction, distribution, or storage of any part of this paper without the written consent of the Society of Petroleum Engineers is prohibited. Permission to reproduce in print is restricted to an abstract of not more than 300 words; illustrations may not be copied. The abstract must contain conspicuous acknowledgment of SPE copyright.

Abstract

The Magnetic Flux Leakage (MFL) Technique is the most commonly used technique to inspect large diameter transmission pipelines. A typical MFL inspection system uses permanent magnets to apply an axially oriented magnetic field to the ferromagnetic pipe material. The magnetic field is perturbed by a metal-loss region (usually caused by corrosion) to produce flux leakage outside the pipe, which can be measured by field sensors.

The magnetization system in an MFL inspection system should ideally produce a magnetic field that is strong enough to cause a measurable amount of magnetic flux to leak from the pipe material at metal-loss regions, uniform from inside to the outside surface of the wall thickness so that the measured signal is more linearly related to metal-loss depth, and consistent in magnitude along the length of a pipe so that flux leakage measurements can be compared at different locations during an inspection run.

In general, the field strength most strongly affects detection of metal loss defects while characterization of defect geometry requires a field that is strong, uniform, and consistent.

Improvements in the downhole hardware also provide more flexible and efficient data acquisition, reducing operating time while improving data accuracy and operational safety. In conventional magnetic flux leakage (MFL) tools, the flux leakage sensors are coils; in the "high-resolution" tool, the coil is replaced by multiple "Hall Effect" sensors.

The HR Vertilog service uses MFL measurements to identify and quantify internal and external corrosion defects. The overlapping arrays of flux-leakage sensors and discriminator sensors offer full circumferential inspection of the tubing or casing string. This process differentiates between metal-loss (corrosion) and metal-gain (hardware) Features, and distinguishes between general corrosion and isolated pitting. Paper represents technology overview and field cases history

Corrosion, corrosion root-causes and corrosion inhibitors

Corrosion is the destruction of metal through electrochemical action between metal and its environment. About 75 to 85 percent of drillpipe loss can be attributed to corrosion. Other areas affected by corrosion include pump parts, bits, and casings. Factors affecting corrosion include:

- Temperature. Corrosion rates can double with every 55° increase in temperature.
- Velocity. The higher the mud velocity, the higher the rate of corrosion due to film erosion (oxide, oil, amine, etc.).
- Solids. Abrasive solids remove protective films and cause increased corrosive attack.
- Metallurgical factors. Mill scale and heat treatment of pipe can cause localized corrosion.
- Corrosive agents. Corrosive agents such as oxygen carbon dioxide and hydrogen sulfide can increase stress cracking corrosion and lead to pipe failure.

The corrosion that occurs because of these various factors falls into four categories:

- Uniform corrosion results in an even corrosion pattern over surfaces.
- Localized corrosion results in a mesa-like corrosion pattern over surfaces.
- Pitting is a highly localized corrosion that results in the deep penetration of surfaces.
- Mechanical damage dislocates or completely removes surfaces.

Drilling-fluid corrosive agents

Corrosive agents found in drilling fluids include:

- Oxygen (O2)
- Hydrogen sulfide (H2S)
- Carbon dioxide (CO2)
- Bacteria
- Dissolved salts (Zn+, Br−, etc.)
- Mineral scale (CaSo4, FeCO3

Oxygen

Oxygen causes a major portion of corrosion damage to drilling equipment. Oxygen removes protective films such hydrogen; this action causes accelerated corrosion and increased pitting under deposits. The four primary sources of oxygen are:

- Water additions
- Actions of mixing and solids control equipment
- Aerated drilling fluids
- The atmosphere

Water additions

Water added to a drilling fluid during normal drilling operations can contain dissolved oxygen. Very small concentrations of oxygen (<1 ppm) can cause severe corrosion by setting up differential aeration cells that can show preferential attack with pitting under barriers or deposits. The primary corrosion by-product of low oxygen concentrations is magnetite. The products recommended for the removal of dissolved oxygen are called oxygen scavengers

Actions of mixing and solids control equipment

Mixing and solids-control equipment can cause aeration of the drilling fluid during drilling operations. For example, aeration occurs as mud falls through the shaker screen or when hopper or mud guns are discharged above the surface of the mud in the pits. To reduce the amount of oxygen injected into drilling fluid by mixing and solids-control equipment, follow these guidelines.

- Use a premix tank to mix mud when possible.
- Maintain the minimum mud volume.

- Operate mud-mixing pumps, especially the hopper, only when mixing mud.
- Keep the packing tight on centrifugal pumps.
- Keep the mud in the suction pit deep enough to keep the mud pump from pulling in air.
- Keep discharge below the mud surface when moving mud from the reserve pit.
- Ensure guns discharge below the mud surface.
- Ensure the degasser and desander discharges are below the mud surface.

The products recommended for treating drilling fluid containing oxygen because of mixing and solids-control equipment are called oxygen scavengers.

Aerated drilling fluids

Aerated drilling (foam and mist drilling) fluids require the use of passivating (oxidizing) inhibitors to combat corrosion due to oxygen. The product recommended for inhibiting oxygen in aerated drilling fluids is BARACOR 700.

Atmosphere

The atmosphere is another source of oxygen. The main by-product of atmospheric corrosion is iron oxide rust. To prevent atmospheric corrosion, wash the pipe free of all salts and mud products and then spray or dip the pipe in an atmospheric corrosion inhibitor. The product recommended for inhibiting atmospheric corrosion is BARAFILM.

Hydrogen sulfide

Hydrogen sulfide can enter the mud system from:

- Formation fluids containing hydrogen sulfide
- Bacterial action on sulfur compounds in drilling mud
- Thermal degradation of sulfur-containing drilling-fluid additives
- Chemical reactions with tool-joint thread lubricants containing sulfur

The corrosion process, bacterial action, and thermal degradation of organic additives can generate hydrogen sulfide in drilling fluids. Hydrogen sulfide is very soluble in water. Dissolved hydrogen sulfide behaves as a weak acid and causes pitting. Another problem with hydrogen sulfide is that some of the hydrogen ions at the cathodic areas may enter the steel instead of evolving from the surface as a gas. This process can result in hydrogen blistering in low-strength steels. Both the hydrogen and sulfide components of hydrogen sulfide can bring about drillstring failures.

Hydrogen sulfide corrosion is mitigated by increasing the pH to above 9.5 and by using sulfide scavengers and film-forming inhibitors. The products recommended for combating corrosion due to hydrogen sulfide are called H2S scavengers

Note: Hydrogen sulfide and carbon dioxide are often encountered in the same geologic formation; therefore, design treatments to deal with both contaminants simultaneously.

Treatment

$$\frac{682 \text{ x } P_m}{SG\ brine} = mg/l\ H_2S$$

$$mg/l\ H_2S \text{ x } 0.00602 = Kg/\ m^3\ ZnCO_3$$

Carbon dioxide

Carbon dioxide is found in natural gas in trace-element and major-element quantities. When combined with water, carbon dioxide forms carbonic acid and decreases the water's pH, which increases the water's corrosivity. While carbon dioxide is not as corrosive as oxygen, it can cause pitting. A large drop in pH, combined with a negative test for hydrogen sulfide, is an indication that CO2 has contaminated the mud.

Maintaining the correct pH is the primary treatment for carbon dioxide contamination. Either lime or caustic soda can be used to maintain pH, although, lime is preferred. The following table provides the reactions for each of these treatments.

Treatment	Reaction
Caustic soda	2 NaOH+CO2→2H2O+Na2CO3
Lime	Ca(OH)2+CO2+H2O→2H2O+CaCO2

Treatment with caustic soda produces sodium carbonate, which is soluble and can create mud problems. Treatment with lime, on the other hand, produces an insoluble calcium-carbonate precipitate and water.

Note: To maintain pH in water-based muds, use BARACOR 95 instead of a lime. BARACOR 95 is a liquid amine compound that serves as a carbon-dioxide scavenger. This treatment is particularly useful with a polymeric system that may be pH-sensitive. However, keep in mind that it does not treat for hydrogen sulfide.

In addition to maintaining pH, use a filming amine inhibitor to mitigate corrosion caused by carbon dioxide. The product recommended for mitigating corrosion is BARAFILM.

Note: Hydrogen sulfide and carbon dioxide are often encountered in the same geologic formation; therefore, design treatments to deal with both contaminants simultaneously.

Bacteria

Microorganisms can cause fermentation of organic mud additives, changing viscosity and lowering pH. A sour odor and gas are other indicators that bacteria are present. Degradation of mud additives can result in increased maintenance costs.

The by-products of bacteria are carbon dioxide and hydrogen sulfide. The presence of bacteria is determined by the phenol-red test. Microbiocides are used to control bacteria in drilling environments. The products recommended for controlling bacteria are:

ALDACIDE G
Isothiazotone-based biocide powder

Dissolved salts

Dissolved salts increase corrosion by decreasing the electrical resistance of drilling fluids and increasing the solubility of corrosion by-products. These by-products can cause a film to form on the surface of the metal.

Mineral scale

Mineral scale deposits set up conditions for local corrosion-cell activity. The continuous addition of scale inhibitor can control the formation of scale deposits. The product recommended for inhibiting the formation of scale deposits is Scale-inhibitors

Brine fluids

The corrosivity of a brine fluid depends on its type. Brines fall into two categories: monovalent and divalent.

Monovalent brines

Monovalent brines contain salts that have monovalent cations; such as salts include sodium chloride, potassium chloride, potassium bromide, and sodium bromide. Potassium bromide and sodium bromide are especially effective in calcium-sensitive formations and in formation where carbon dioxide gas might react with calcium brines to create a calcium-carbonate precipitate. Monovalent brines generally show low corrosivity, even at temperatures exceeding 400F (204C).

Divalent brines

Divalent brines contain salts that have divalent cations; such as calcium chloride, calcium bromide, and zinc bromide. A divalent brine might consist of single salt or a blend of salts, depending on the required brine density and crystallization point. The corrosiveness of these brines depends on their density and chemical composition. Laboratory data show that the addition of calcium chloride lowers the rate of corrosion, while the addition of zinc bromide rapidly increases the rate of corrosion.

Corrosive agents

When working with brine based fluids, the two corrosive agents to monitor are oxygen and hydrogen sulfide.

Oxygen

The oxygen content of fluids is difficult to determine, and most engineers in the field do not have access to the proper equipment. Because the dissolved oxygen content varies as conditions change, it is difficult to select a set feed rate of an oxygen scavenger to remove a known concentration of oxygen.

Laboratory tests show that the oxygen content of calcium chloride, calcium bromide, and zinc bromide brines is very low. The solubility of gases in a liquid is directly related to the total dissolved-solids concentration of that liquid. The higher the dissolved-solids content, the lower the solubility of gases in the liquid. The following table lists oxygen concentrations measured in stock brine at room temperature.

Brine	Oxygen concentration, ppm
11.6 lb/gal $CaCl_2$	0.1 to 0.2
14.2 lb/gal $CaBr_2$	0.05 to 0.1
19.2 lb/gal $Ca/ZnBr_2$	0.4 to 0.6

Note: In a well at elevated temperatures, the oxygen content should be much lower.

Some products used as oxygen scavengers contain sulfides that react with the dissolved oxygen in fluids to form sulfates, eliminating the corrosive effects of the dissolved oxygen. Calcium brines should not be treated with oxygen scavengers containing sulfides because chemicals could precipitate calcium scale and cause problems. In a packer-fluid application where there is a static system with no aeration of the fluid, the dissolved oxygen content is so low that an oxygen scavenger usually is not required.

Hydrogen sulfide

In solids-enhanced systems, the most often used hydrogen-sulfide scavenger is zinc carbonate. The zinc reacts with the soluble sulfide ions to form zinc sulfide, which is insoluble and precipitates as an

unreactive compound. In solids-free systems, soluble zinc bromide salt serves the same function and absorbs the hydrogen sulfide.

In operations where hydrogen-sulfide contamination is expected, offset the hydrogen sulfide's acidic nature by maintaining a proper pH in the brine, as outlined in the following table.

Brine	Recommended pH		Treatment
Nonzinc	7.0	7.0	Caustic soda or lime
Calcium	7.0 – 10.5	7.0 to 10.5	Caustic soda or lime
Zinc	3.0 – 5.0	3.0 to 5.0	Lime

Technology Overview

The Digital Vertilog™ service (DVRT™) uses DC flux leakage measurements to determine the depth of penetration of casing defects in the primary casing string, providing rapid 360° pipe inspection. The DVRT service helps operators monitor—when deployed for periodic surveys—the progress of corrosion within tubulars. This information is invaluable when considering remediation or well abandonment.

12 or 24 separate channels are sampled up to 32 times per foot to provide a complete circumferential survey of corrosion extent. The waveforms of these channels are preserved during logging in order to discriminate between actual corrosion and well completion equipment. Two additional channels of eddy current measurements are provided. These channels are used to determine whether flux leakage activity is occurring on the inner or outer surface of the casing.

Applications

Performs rapid 360° pipe inspection
Detects corrosion and evaluates its extent
Determines the effectiveness of cathodic protection and corrosion inhibitors
Confirms location of leaks and perforations
Assists determining the financial value of casing when considering well abandonment

Benefits

Ensures continuous production with accurate evaluation of remaining strength of casing and tubing
Delivers survey information via high logging speeds, reducing rig time

Features

Available in 4½- to 22-in. tubular sizes
Detects centralization of primary casing string at the bottom of the next casing string
Checks casing string makeup and joint lengths; locates well completion equipment
Overlapping sensor arrays insure complete coverage inside and out
Combination of FL and DIS sensors differentiate internal and external defects during interpretation

Tool series	2938	2939
Casing range and weight	4½ in. (9.5ppf) to 5 in. (24.1 ppf)	5 in. (11.5ppf) to 6⅝ in. (32 ppf)
Instrument length	18 ft (5.49 mt)	18 ft (5.49 mt)
Instrument weight	382 lb (173.64 Kg)	405 lb (184.09 Kg)
Logging speed	125 ft/min (40 M/min)	125 ft/min (40 M/min)
Maximum pressure	12,000 psi (82.7 Mpa)	15,000 psi (103.4 Mpa)
Maximum temperature	280°F (138°C)	280° F (138°C)

Digital Vertilog Service

Tool series	2940	2941
Casing range and weight	6⅝ in. (20 ppf)	8⅝ in. (40 ppf) to 22 in.
Instrument length	18 ft (5.49 mt)	18 ft (5.49 mt)
Instrument weight	625 lb (284.09 Kg)	838 lb (380.91 Kg)
Logging speed	125 ft/min (40 M/min)	125 ft/min (40 M/min)
Maximum pressure	15,000 psi (103.4 Mpa)	15,000 psi (103.4 Mpa)
Maximum temperature	280°F (138°C)	280°F (138°C)

Tool series specifications

HRVRT – Success

- 1200+ Operational jobs per year worldwide
- 95% Market Share in gas wells in USL
- 345°F Maximum DH Temperature for HRVRT job till date
- Service covering range from 4 ½” to 9 5/8”
- Global approval by more than 70 NOC/IOC
- Wireline, Tractor and CT Conveyance jobs conducted

Measurements theory or Physics behind the technology

- A permanent magnet circuit is completed through the tubing, producing a very high magnetic flux density within the tubing body wall.

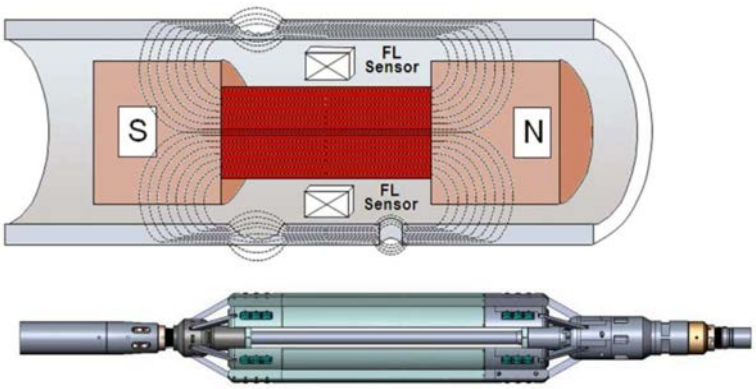

FL sensors alone cannot differentiate internal from external defects. To perform this function, Discriminator (DIS) sensors are deployed within a weak magnetic field that is completed through the tubing's inner surface.

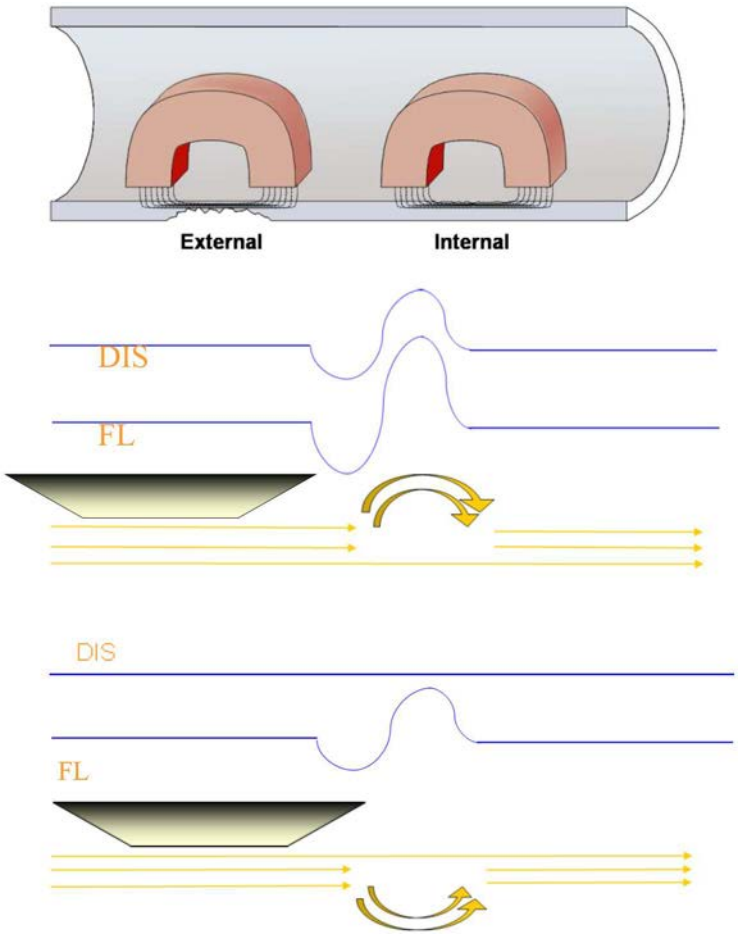

How do we get such a high resolution?

Increased circumferential and axial resolution

Highest number of sensors
144 FL, 48 DIS in 4 ½″ tool
144 FL, 48 DIS in 5″ – 5 ½″ tool
288 FL, 96 DIS in 7″ – 9 ⅝″ tool
Smaller sensors (1 ¼″ coil to. 25″ Hall Sensors)

Multi-axial Sensors

Results in better defect description

Quantifiable defect description

Field verifiable calibration
Increased accuracy for length, width and depth of penetration determination
Results in better input into burst pressure calculations
Data base output for long term data storage and integration into other data systems

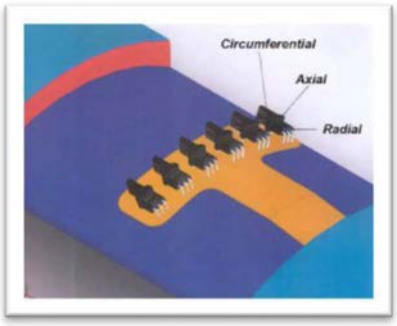

Uses tri-axial sensors at 10 samples/foot providing defect geometry and depth of penetration
100% coverage
192 sensors in 4½- and 5½-in. tools
384 sensors in 7- to 9⅝-in. tools

High-resolution report provides executive summary, feature list, hardware reports, histograms, feature type, and quantifiable LxWxD with burst pressure calculations for each feature

Case Histories

Case I

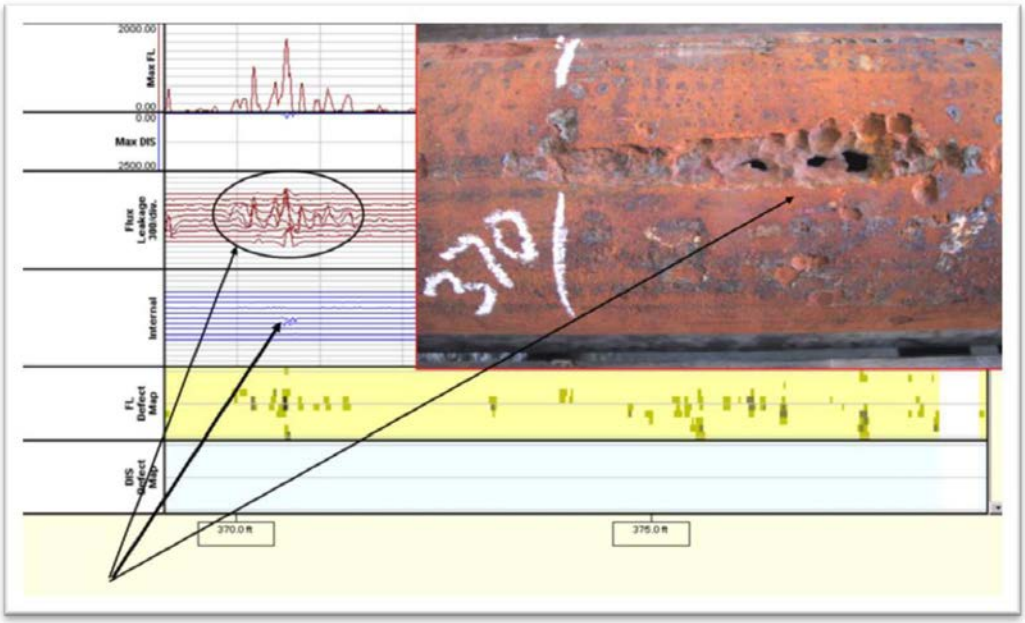

Several external pits interconnected, observe the response of discriminator

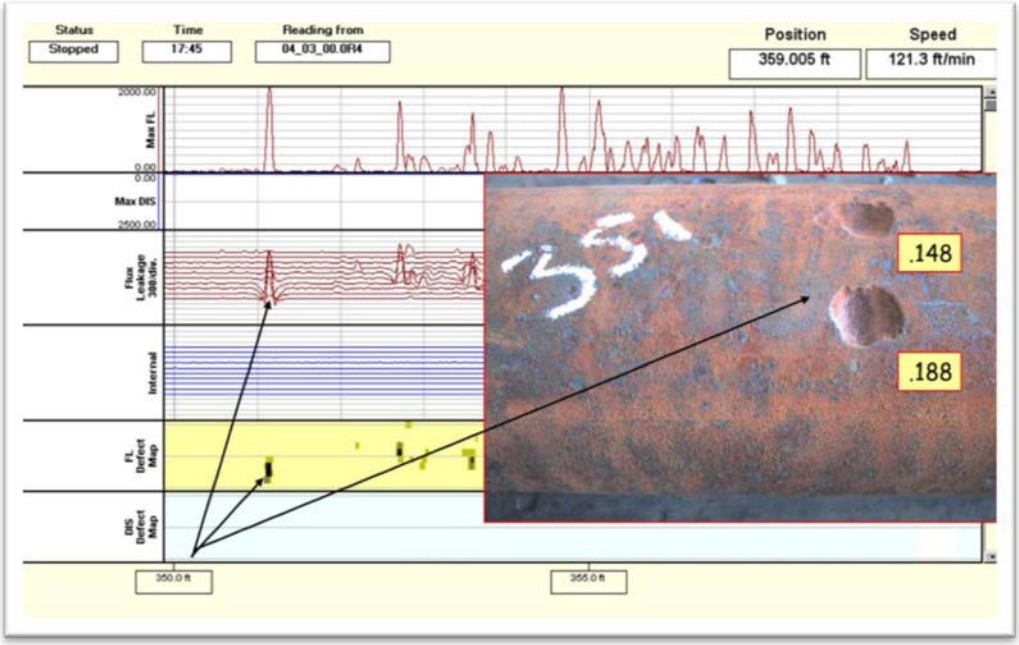

Two external pits

Case II

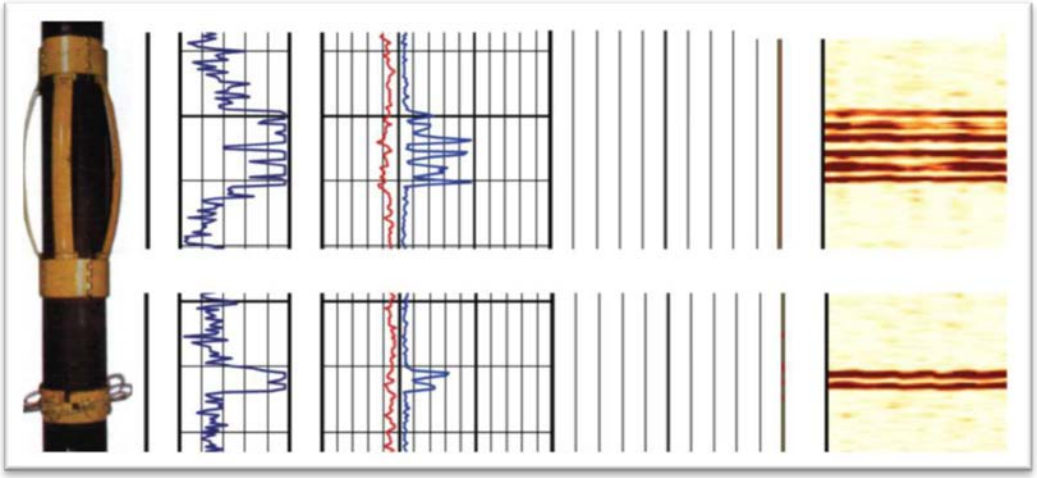

Accessories log example

Case III

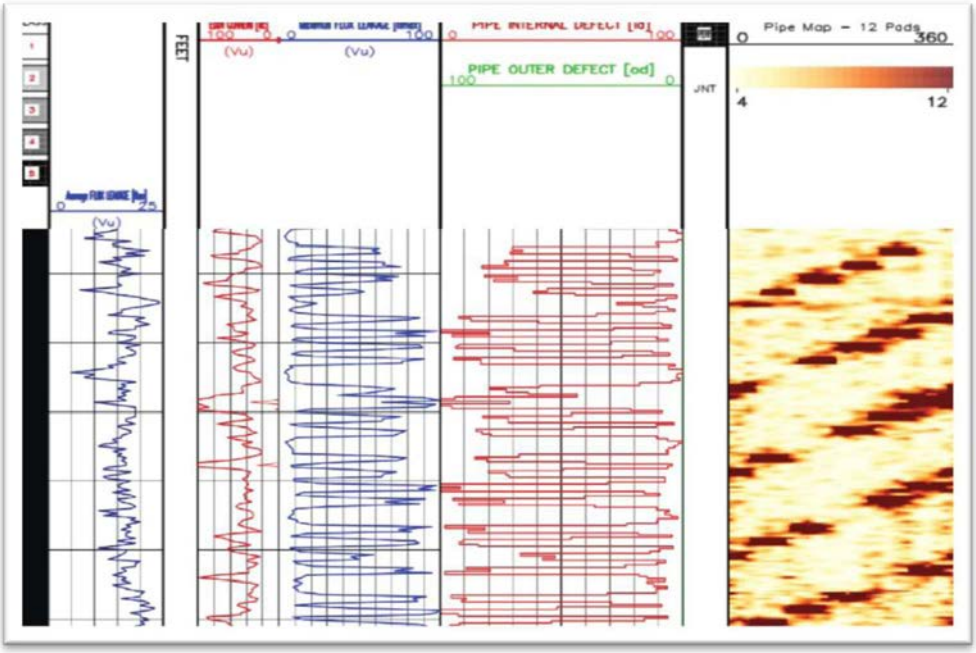

Perforating log example

Case IV – Algerian Case History

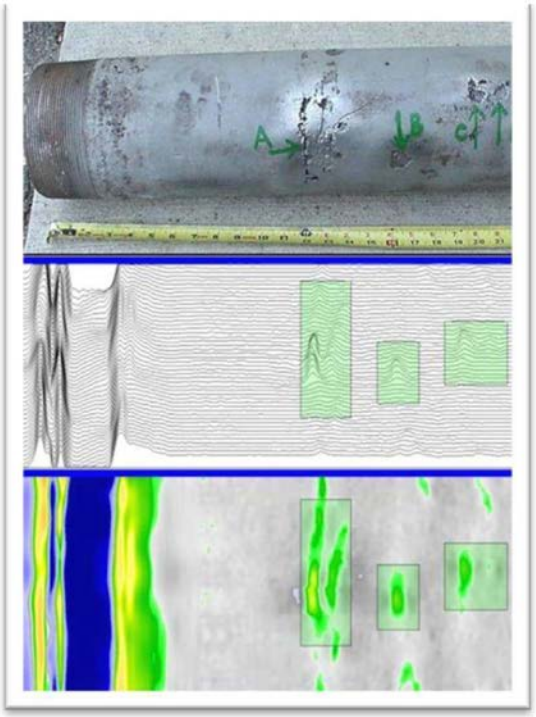

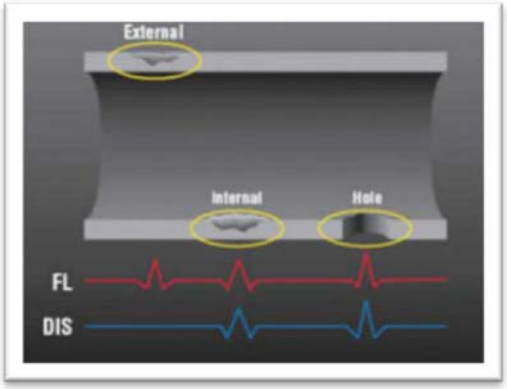

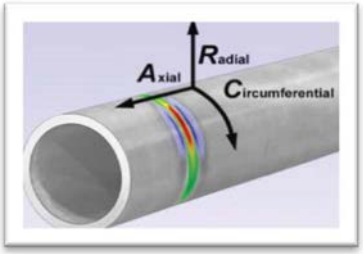

The HRVRT service performs an inspection over the radial, axial, and circumferential axes.

Typical flux leakage (FL) and discriminator (DIS) – sensor response to common defects—the FL sensors respond to internal and external anomalies, while the DIS sensors respond to internal anomalies only.

An operator working in the southeastern part of the Saharan platform in Algeria strongly suspected that major corrosion damage in the casing of an old well would complicate plans to restore production. When logging operations performed by another service company failed to find any defects or anomalies, the operator contacted Baker Hughes to get a second opinion.

Working at the wellsite, a Baker Hughes geoscientist used the HRVRT™ high-resolution vertilog service to quickly and accurately quantify the extent and penetration depth of corrosion defects.

The HRVRT service also evaluated the burst pressure of tubulars to help manage the well integrity risk. Based on this data, the operator was able to reduce production downtime by cutting the pipe and pulling it to the surface to replace the defective casing section instead of performing a time-consuming and more

expensive remediation. As a result, the operator now plans to use the HRVRT service on future wells in its recovery program.

Benefits

- Quickly and accurately assessed damage to casing of well scheduled to go back into production
- Prevented production downtime by allowing operator to plan intervention instead of remediation

Background and challenges

Southeastern Saharan platform in Algeria. Review state of the casing in an old well after logging operations by another service company failed to discover any defects or anomalies.

Baker Hughes solution and results

Used HRVRT service to quickly and accurately identify and quantify the extent and penetration depth of corrosion defects in tubulars.

Evaluated burst pressure to manage well integrity risk. Success of the operation has led operator to use the HRVRT service for other wells in the recovery program

Case V – ME Region Case History

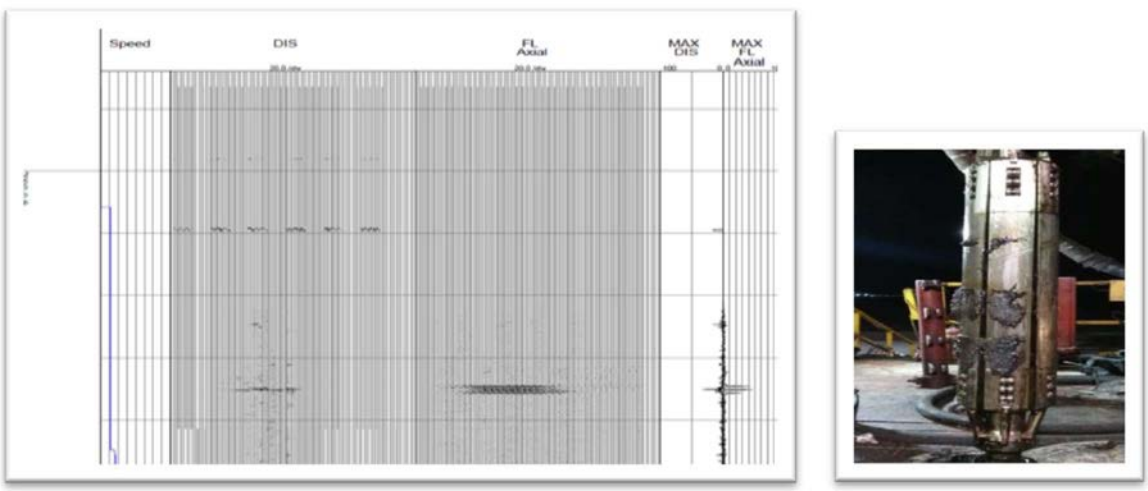

HR Vertilog – Magnetic Flux Leakage Inspection

HVRT run on 7″ Liner showed no corrosion and was able to identify all the perforations. The client was questioning the HVRT results because of the metal debris collected by the magnet. The client compared our data with a competitor corrosion tool and it showed exactly the same results; it means no corrosion then he did not change the perforation plan. Metal debris collected by magnets meant for 7″ liner could have easily been collected from the 9 5/8″ section (even though it's not centralized in the larger casing)

Metal debris could be corrosion from the 9 5/8″ section which has fallen lower into the 7″ section.

Conclusion and Summary

MFL has a lot of advantages for the industry as it is consider the highest resolution corrosion identification in the industry, pit resolution. Quantifiable defect description and it is the widest coverage range of casing ID.

MFL is the Fastest logging speed in the industry, up to 200 ft/min, with flexibility of variable logging speed.

Advanced analysis from three axes of magnetic flux leakage data feature based reporting Control lines orientation capability, ControlView Memory acquisition capability. Magnetic flux leakage "MFL" tolerant for BHT up to 350 F. information from MFL, could be utilized as a guidance regarding not only the adequate corrosion inhibitors, brine and drilling fluids to be utilized in the future wells in the same fields, but also gives a visibility regarding proper corrosion inhibitors additives for injected waters.

Acknowledgement

Sincere thanks are extended to Baker Hughes for the permission to present this paper. Thanks are also extended to the Baker Hughes field personnel for their efforts in executing this wireline Technology Geoscience team involved in processing and interpretation.

About the Author

Wael El Sherbeny, is currently Business Development Manager – RDS. Wael holds BSc. In Geology, MSc. in Wellbore instability, clay mineralogy and formation pressures for Gulf of Suez and Red Sea Miocene age rocks, Cairo University, accredited from Texas Tech. University, Department of Petroleum Engineering, Houston, Texas. PhD in drilling fluids, reservoir damage and chemical remediation and geomechanics "sand production prediction", Mediterranean sea, Tertiary age, Ain Shams University, Cairo, Egypt. Wael is an SPE & SPWLA member and worked along MEAP and Africa regions. Wael has more than 20 years in oil industry in technical and managerial positions; covering mud logging, Petrophysics, drilling & completion fluids, chemical stimulation and reservoir damage, and recently Geoscience, Geology "borehole imaging and mineralogy, geomechanics with Baker Hughes. Wael is an author and co-author for almost 37 published papers covering many aspects in drilling and G & G application and production technology. Wael is a technical steering committee member for SPE, NATC, North Africa technology exhibition and conference.

Tharwat Hassane, is currently Geoscience manager for Qatar – RDS. Tharwat holds BSc. In petroleum engineering and PhD in reservoir engineering from Heriot Watt University UK. Tharwat is also working as a petrophysical advisor and has more than 20 years oil industry in technical and managerial positions

Gasser Hassan is a Petroleum Engineering Advisor with more than 10 years of experience in the industry, currently he is the Geoscience country lead of Baker Hughes in Saudi Arabia. His experience includes reservoir engineering & formation evaluation and he has worked in various locations in the middle east Gasser holds a Bsc. degree in petroleum engineering from Cairo University

Ex. II - 10

Specifications and requirements for in-line inspection of pipelines

Version 2016

PIPELINE
OPERATORS FORUM

Contents

1 Introduction ... 3

2 Definitions and abbreviations ... 4

2.1 General ... 4

2.2 Definitions ... 4

2.3 Abbreviations ... 9

2.4 Parameters and interaction of anomalies ... 11

2.4.1 Metal loss ... 11

2.4.2 Dent ... 13

2.4.3 Gouge ... 14

2.4.4 Ovality ... 14

2.4.5 Buckle ... 14

2.4.6 Ripple/Wrinkle ... 15

2.4.7 Roof topping/peaking ... 16

2.4.8 Crack and crack-like ... 16

2.4.9 Crack colonies ... 17

2.5 Nomenclature of features ... 17

2.6 Anomaly assessment ... 18

2.6.1 Interaction rules ... 18

2.6.2 Indication of anomaly severity (ERF) ... 18

2.7 Resolution of measurement parameters ... 19

3 Health and safety ... 20

3.1 ATEX ... 20

3.2 IECEx ... 21

4 Tool specifications ... 22

4.1 Introduction ... 22

4.2 Tool data sheets ... 22

4.3 Tool class history ... 22

4.4 Tool performance specification ... 23

4.4.1 General ... 23

4.4.2 Basis of performance ... 24

4.4.3 Exclusions and limitations ... 24

4.4.4 Access to supporting performance information ... 25

4.5 Tool performance verification ... 25

4.6 Changes to tool specification or performance specification sheets 25
5 Personnel qualification 26
6 ILI preparation and contracting 27
6.1 ILI preparation 27
6.2 Contracting 27
7 Reporting 28
7.1 Operations report 28
7.2 Preliminary report 29
7.3 Final report 30
7.3.1 Pipe tally 30
7.3.2 List of anomalies, clusters, data loss and other lists 30
7.3.3 List of components 31
7.3.4 Summary and statistical data 31
7.3.5 Performance 33
7.3.6 Dig sheet 33
7.3.7 Software and signal 33
7.3.8 Anomaly ranking method for ERF 34
7.3.9 Detection of markers 34
7.3.10 Personnel qualification 34
7.4 Raw data report 34
7.5 Multiple run comparisons report 34
7.6 Experience report 35
7.7 Additional reporting 35
8 References 36
Appendix 1: ILI companies that provided comments to the draft version of these specifications 37
Appendix 2: Guideline to clients for defining specific details of the POF specifications 38
Appendix 3: Report structure, terminology and acronyms 42
Appendix 4: Detailed tool data sheet requirements 44
Appendix 5: Tool technology performance specifications 47
Appendix 6: Typical example of Pipe tally* 53
Appendix 7: Typical example List of anomalies* 54
Appendix 8: Typical example List of clusters* 55
Appendix 9: Typical example Run comparison overview* 56

1 Introduction

This document specifies the advised operational and reporting requirements for tools to be used for geometric measurement, mapping, metal loss, crack or other anomaly detection during their passage through pipelines. The tools may pass through the pipeline driven by the flow of a medium or may be towed by a vehicle or cable. The tools may be automatic and self-contained or may be operated from outside the pipeline via a data and power link.

This document has been reviewed and approved by the Pipeline Operator Forum (POF). It is stated however, that neither any of the member companies of the POF nor their representatives can be held responsible for the fitness for purpose, completeness, accuracy and/or application of this document.

A draft version of this document has been sent for comments to in-line-inspection Contractors as listed in Appendix 1. The POF like to thank the Contractors for their constructive feedback.

This document is intended to serve as a generic in-line-inspection specification and therefore cannot cover all pipeline or pipeline operator specific issues. POF members and other users of this specification are therefore free to add or change requirements that should be based on their specific pipeline situation. To support the pipeline operator in specifying/detailing optional items in this document, a guideline with a short description of these items is given in Appendix 2.

Comments on this specification and proposals for updates may be submitted to the Administrator at specifications@pipelineoperators.org with the form which is available on the POF website (www.pipelineoperators.org).

2 Definitions and abbreviations

2.1 General

During the update of this specification, reference to standards such as API 1163 [1] and PDAM[1] [2] have been reviewed and some terminology has been aligned. However, if referenced standards are in conflict with this (POF) specification, this specification prevails.

If the word "shall" is used in this document it indicates a requirement.

If the word "should" is used in this document it indicates a recommendation.

2.2 Definitions

Anomaly/feature definitions are provided in such manner that the ILI vendor can identify them accurately, e.g. general reporting like metal loss and deformation is not sufficiently detailed.

For the purpose of this document, the following definitions apply:

Above Ground Marker:	A device, on the outside of and close to a pipeline, that detects and records the passage of an ILI tool or transmits a signal that is detected and recorded by the tool. Reference magnets can be applied to serve identical purposes.
Anomaly:	An indication, detected by in-line inspection, of an irregularity or deviation from the norm in pipe material, weld material or coating, which may or may not be an actual flaw.
Arc strike [2]:	Localised point(s) of surface melting caused by arcing between a welding electrode or ground and the pipe surface. The defect formed is a surface depression which may be associated with a local increase in hardness.
Blister [2]:	A raised spot on the surface of the pipe caused by expansion of gas in a cavity within the pipe wall.
Buckle [2]:	A local geometric instability causing ovalisation and flattening of the pipe as a result of excessive bending or compression with possibly abrupt changes in the local curvature, which may or may not result in a loss of containment. *Note: Buckle to be defined in detail for reporting as Global, Local or Propagation, see below.*
Buckle arrestor:	A device or element in the pipeline with high wall thickness that will act to stop the advance of a propagating buckle.
Buckle, global or Global buckle [2]:	A Global Buckle will typically involve several pipe joints. It can be horizontal or vertical.
Buckle, local or Local buckle [2]:	A Local Buckle is a mode causing gross deformation of the pipe cross section, also known as pipe wall buckling. Collapse,

[1] PDAM is only used as a reference for definitions

	localised wall wrinkling and kinking are examples of local buckling.
Buckle, propagation or Propagating Buckle [2]:	A Propagating Buckle is the result of a dynamic process whereby a local buckle propagates along the length of the pipeline. A propagating buckle cannot initiate unless a local buckle has occurred.
Casing:	A type of feature consisting of a larger diameter pipe placed concentrically around the pipeline, usually in high stress areas such as road crossings or otherwise protecting the pipe from mechanical damage.
Certainty:	The probability that the characteristics of a reported anomaly are within the stated tolerances.
Characteristic [1]:	A physical descriptor of a pipeline e.g. grade, wall thickness, manufacturing process or type, size, shape of an anomaly.
Client [1]:	An organisation that owns and/or operates the pipeline facilities.
Cluster:	Two or more adjacent anomalies in the wall of a pipeline or component of a pipeline that may interact to weaken the pipeline more than either would individually.
Colony [3]:	A grouping of stress corrosion cracks (cluster) occurring in groups of a few to thousands of cracks within a relative confined area.
Combined features:	Features that appear at the same location but at different (inner and outer) surfaces.
Component [1]:	Any physical part of the pipeline, other than line pipe, including but not limited to valve, weld, tee, flange, fitting, tap, branch connection, outlet, support, anchor, above ground marker, anode, repair, additional metal and wall thickness change.
Contractor [1]:	Any organisation providing ILI services to Clients.
Corrosion:	An (electro)-chemical reaction causing loss of metal.
Corrosion Resistant Alloy (CRA):	An alloy with increased corrosion resistance which may contain metals such as: chrome, cobalt, nickel, iron, titanium, molybdenum.
Corrosion related to CRA:	Corrosion between carbon steel and CRA affecting the interface.
Crack:	A planar, two-dimensional anomaly feature with a high length to width ratio, a sharp root radius and a possible displacement (surface opening) < 0.1 mm of the fracture surfaces.

Crack-like	An anomaly feature similar to a crack with some volume and a displacement (surface opening) between 0.1 and 1.0 mm of the fracture surfaces but that might not have a sharp root radius.
Debris:	Extraneous material in a pipeline.
Deformation:	A plastic change in shape in the steel pipeline. *Note: Deformations are to be reported as e.g. bend, dent, ripple/wrinkle, buckle or ovality, see below.*
Dent:	A local plastic or elastic deformation of the pipe wall resulting in a change of the internal diameter caused by an external force. *Note: Dents to be defined in more detail for reporting as Kinked, Plain or Complex*
Dent, Complex	A dent which causes a smooth change in curvature of the pipe wall that contains an anomaly (such as e.g. gouge, corrosion loss, crack) and/or is associated with an adjacent girth, spiral or seam weld.
Dent, Kinked [2]:	Dent with an abrupt change in the curvature of the pipe wall if any radius of curvature in the dent is ≤ 5 times the wall thickness. This type of dent might also be associated with wall thickness reduction or crack.
Dent, Plain [2]:	A dent which causes a smooth change in curvature of the pipe wall that contains no wall thickness reduction (such as gouge, crack, corrosion) and is not associated with an adjacent girth, spiral or seam weld.
Detection threshold:	Minimum detectable feature dimension at a certain certainty.
Feature:	Component or anomaly in a pipeline detected by in-line inspection.
Geodetic Datum	3D coordinate system. *Note: the World Geodetic System (WGS84) is commonly used, but others include ETRF89, NAD83, NAD27, RGF93 and more.*
Gouge:	A surface damage with elongated grooves or cavities caused by mechanically displaced or removed material from the pipe wall by interference with a foreign object.
Grinding:	Wall thickness reduction by removal of material by hand filing or power disk grinding.
Heat affected zone (HAZ):	The area around a weld where the metallurgy of the metal is altered by the rise in temperature caused by the welding process, but this is distinct from the weld itself. For the purpose of this specification it is considered to be within 2t with a minimum of 20mm.

In-Line Inspection (ILI):	Inspection of a pipeline from the interior of the pipe using an In-Line Inspection tool.
In-Line Inspection (ILI) tool:	Device or vehicle, also known as an intelligent or smart pig that uses a non-destructive testing technique to inspect the pipeline from the inside.
Interaction of anomalies:	Two or more adjacent anomalies in the wall of a pipeline or component of a pipeline that may interact to weaken the pipeline more than either would individually.
Joint:	Single section (also pipe spool) of pipe that is circumferentially welded to form a pipeline.
Lamination [2]:	Internal metal wall separation creating layers generally orientated parallel to the pipe wall.
Lap:	A flap of metal that has been rolled or otherwise worked against the surface of the metal but is not fixed, usually with a trapped residue of oxide or scale beneath it.
Mapping:	Recording of the 3D pipeline route using the inertial navigation system of the ILI tool.
Maximum allowable operating pressure [2]:	The maximum allowable operating pressure (MAOP) is a pressure less than or equal to the design pressure and represents the maximum allowed pressure during normal operation.
Metal loss [2]:	Any volumetric pipe anomaly in which metal has been removed. *Note: Metal loss to be reported as e.g. corrosion, gouging, grinding or mill anomaly*.
Measurement threshold:	The minimum dimension(s) of a feature to make sizing possible.
Mill anomaly:	An anomaly that arises during manufacture of a pipe joint or component. *Note: Mill anomalies to be reported as e.g. lap, sliver, lamination, non-metallic inclusion, grinding roll mark or arc strike*.
Ovality [2]:	Out-of-roundness of the pipe joint, defined in terms of the difference between the maximum and minimum internal diameter of the pipe joint.
Pinhole:	Localized corrosion with surface dimensions smaller than 1t or 10 mm whichever is greater in length and width direction.
Pipeline:	A system of joints and other components used for the transportation of products. A pipeline extends from launcher tool trap to receiver tool trap, including the tool traps, or, if no tool trap is fitted, to the first isolation valve within the

	plant boundaries or a more inward valve if so nominated and designed to a pipeline design code.
Pitting:	Localized corrosion of a metal surface that is confined to small areas and takes the form of cavities called pits, but are larger than pinholes. *Note: The dimensions of pitting are defined in detail further in this document.*
Probability of Detection:	The probability of detection is the probability that a specified feature will be detected by the ILI tool. *Note: The level of probability to be used is defined in detail further in this document.*
Probability of Identification:	The probability that a detected anomaly or feature will be correctly identified.
Processed raw data:	Data gathered from ILI tool sensors and passed through one or several filtering algorithms e.g. corrected for odometer slippage.
Raw data:	Unprocessed data from all sensors attached to the respective inspection tool during a pipeline inspection.
Reference magnet:	A permanent magnet placed on the pipeline with known location and/or coordinates used to correlate the inspection data. See also Above Ground Marker.
Reporting threshold:	A parameter, which defines whether or not an anomaly will be reported.
Ripple/Wrinkle:	A smooth local plastic, mainly circumferential orientated, deformation on the out and/or inside wall of the pipe caused by bending stresses. For a wrinkle, the peak-to-valley distance is greater than a ripple.
Roll mark [2]:	Markings on the pipe surface resulting from the plate or pipe rolling process used for spirally or longitudinally seam welded pipe.
Roof topping/peaking [2]:	Incorrect forming of the plate edges into the pipe curvature during fabrication, resulting in meeting of the edges as a triangular apex with the seam weld projecting beyond the circular contour of the pipe, also called peaking or angular misalignment.
Sizing accuracy:	Sizing accuracy is given by the interval with which a fixed percentage of features will be sized. This fixed percentage is stated as the certainty level.
Sliver [2]:	A thin elongated piece of metal rolled into the surface of the pipe, often metallurgically attached at one end. Sometimes reported as lap or lamination.

Strain	Geometrical, non-dimensional measure of deformation representing the relative displacement between particles in a material body.
Trap, launcher/receiver:	An ancillary item of pipeline equipment, with associated pipe work and valves, for introducing an ILI tool into a pipeline (launcher trap) or removing an ILI tool from a pipeline (receiver trap).
Wall thickness, Measured:	The average of measured, un-corroded wall thickness values that is representative for a whole pipe joint/component.
Wall thickness, Nominal:	The wall thickness required by the specification for the manufacture of the pipe.
Wall thickness, Reference:	The actual undiminished wall thickness surrounding a feature, used as reference for the determination of the feature depth.
Weld:	The area where joining has been realised by welding. This is distinct from the heat-affected zone, but is located within it.
Weld anomaly:	Anomaly in the body or the heat affected zone of a weld.
Weld affected area:	Area on both sides of a weld where ILI measurements are affected by the geometry of the weld. See also "Heat affected zone".

2.3 Abbreviations

For the purpose of this document, the following acronyms apply:

A	A geometrical parameter used to specify the dimension class of metal loss anomalies detected by in-line inspection of a pipeline and further defined in Figure 2.1 of this document.
AGM	Above Ground Marker
CRA	Corrosion Resistant Alloy
d	Depth of metal loss
E	End point of anomaly
EC	Eddy Current
EMAT	Electro Magnetic Acoustic Transducer
ERF	Estimated Repair Factor
GIS	Geographic Information System
GNSS	Global Navigation Satellite System
GPS	Global Positioning System
h	Height or depth of Wrinkle/Ripple/Dent or Roof topping
HAZ	Heat Affected Zone

ILI	In-Line Inspection
IMU	Inertial Mapping Unit
ID	Internal pipe Diameter
l	Length of anomaly/feature dimension in the axial direction and length of cracks in any direction
MAOP	Maximum Allowable Operating Pressure
MOP	Maximum Operating Pressure
MFL	Magnetic Flux Leakage
NDE/NDT	Non-Destructive Examination/Non-Destructive Testing
OD	Outer pipe Diameter
PDAM	Pipeline Defect Assessment Manual
POD	Probability Of Detection
POI	Probability Of Identification
P_{safe}	Safe operation pressure as per calculated defect assessment method
R	Internal pipe Radius
S	Start point of anomaly
SCC	Stress Corrosion Cracking
t	Wall thickness
UT	Ultrasonic Testing
w	Width of anomaly/feature in the circumferential direction and opening dimension for crack-like features
WGS 84	World Geodetic System 1984

2.4 Parameters and interaction of anomalies

2.4.1 Metal loss

The parameters of anomalies are length "l", width "w" and depth "d". The starting point, S, and the dimension of an anomaly are defined as illustrated in *Figure 2.1* looking in the ILI run direction. Start and end points are diagonally in a rectangle enclosing the anomaly. The depth represents the deepest point reported within the rectangle.

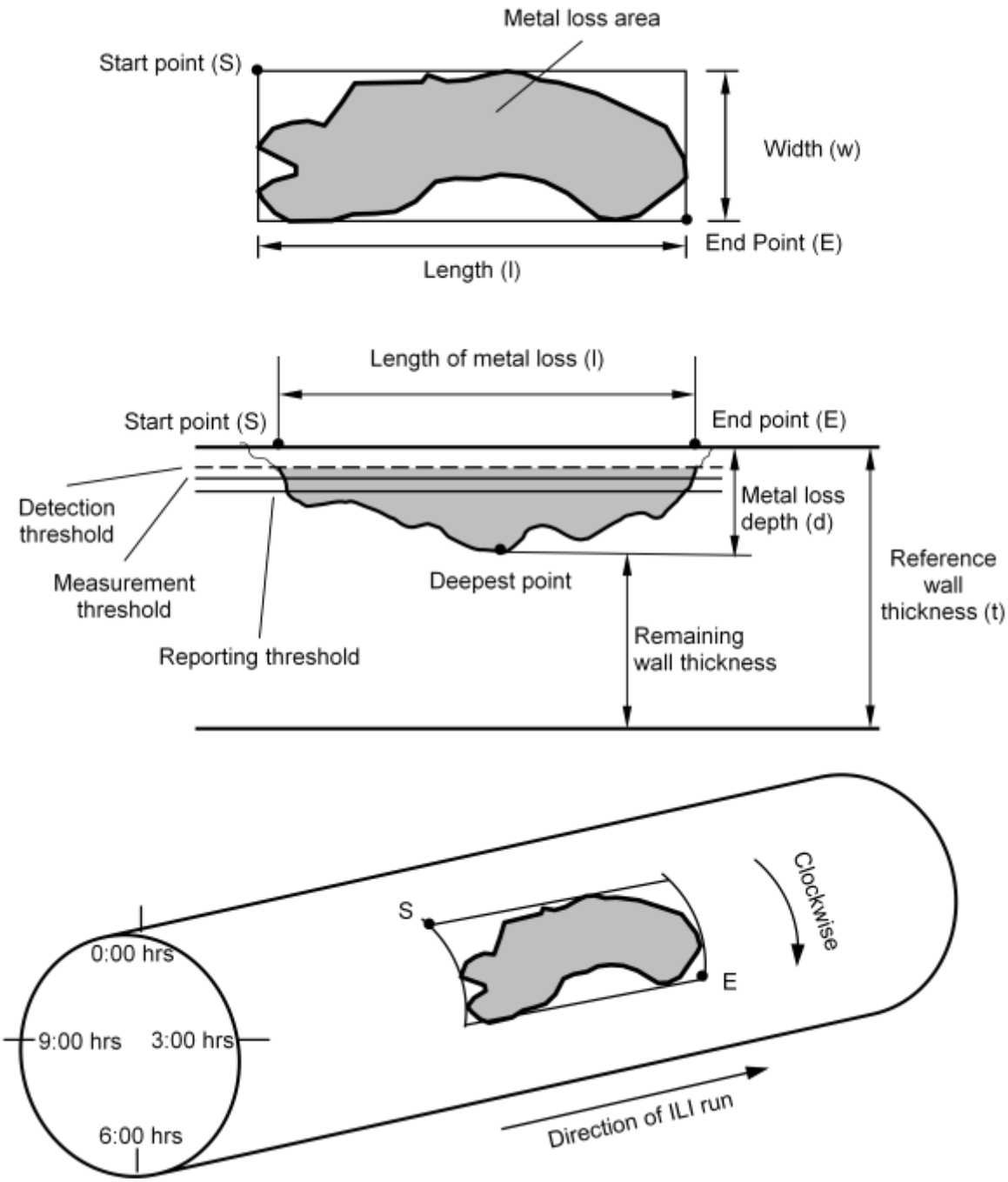

Figure 2.1: Illustration of parameters describing location and dimension of metal loss feature.

The start position of the anomaly has a lower clock position than the end position. Anomalies crossing the 0:00 o'clock position have a higher clock position at the start. Full circumferential anomalies are reported with S at 0:00 o'clock. *Note: highest clock position shall be 11:59.*

Metal loss anomaly classification

The measurement capabilities of non-destructive examination techniques, in particular the MFL technique, depend on the geometry of the metal loss anomalies. Metal loss anomaly classes have been defined as shown in Figure 2.2 for anomaly reporting purposes. In addition it allows for a proper specification of the measurement capabilities of MFL ILI tools.

Each anomaly class permits a large range of shapes. Within that shape a reference point/size is defined at which the POD for MFL tools is specified, see Table 2.1. An even distribution of length, width and depth shall be assumed for each anomaly dimension class to derive a statistical measurement performance on sizing accuracy.

Table 2.1: Definition of anomaly dimension class and MFL POD reference point/size

Anomaly dimension class	Definition	Reference point/size for the POD in terms of l x w
General:	{[w ≥ 3A] and [l ≥ 3A]}	4A x 4A
Pitting:	{([1A ≤ w < 6A] and [1A ≤ l < 6A] and [0.5 < l/w < 2]) and not ([w ≥ 3A] and [l ≥ 3A])}	2A x 2A
Axial grooving:	{[1A ≤ w < 3A] and [l/w ≥ 2]}	4A x 2A
Circumferential grooving:	{[l/w ≤ 0.5] and [1A ≤ l < 3A]}	2A x 4A
Pinhole:	{[0 mm < w < 1A] and [0 mm < l < 1A}	Minimum dimensions to be further defined by Contractor, see table A3-2
Axial slotting*:	{[0 mm < w < 1A] and [l ≥ 1A]}	2A x ½A
Circumferential slotting*:	{[w ≥ 1A] and [0 mm < l < 1A]}	½A x 2A

* Anomalies with a width < 1mm are defined as crack of crack-like which might or might not be metal loss

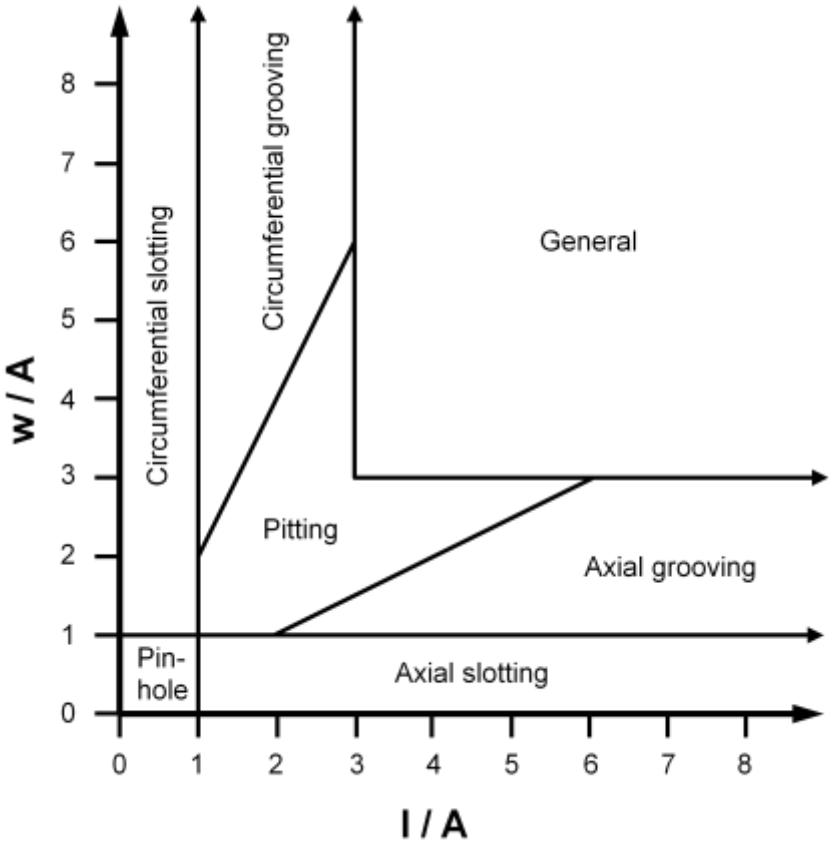

The geometrical parameter A is linked to the NDE methods in the following manner:

- If t < 10 mm then A = 10 mm
- If t ≥ 10 mm then A = t

Figure 2.2: Graphical presentation of surface dimensions of metal loss anomalies per dimension class.

2.4.2 Dent

A dent is defined by its type (Kinked, Plain, Smooth), maximum depth (h), width and length, as shown in Figure 2.3. If requested, the maximum strain based on a methodology agreed between Client and Contractor. If the dent results in an ovality of the pipe then a more detailed description and evaluation is required.

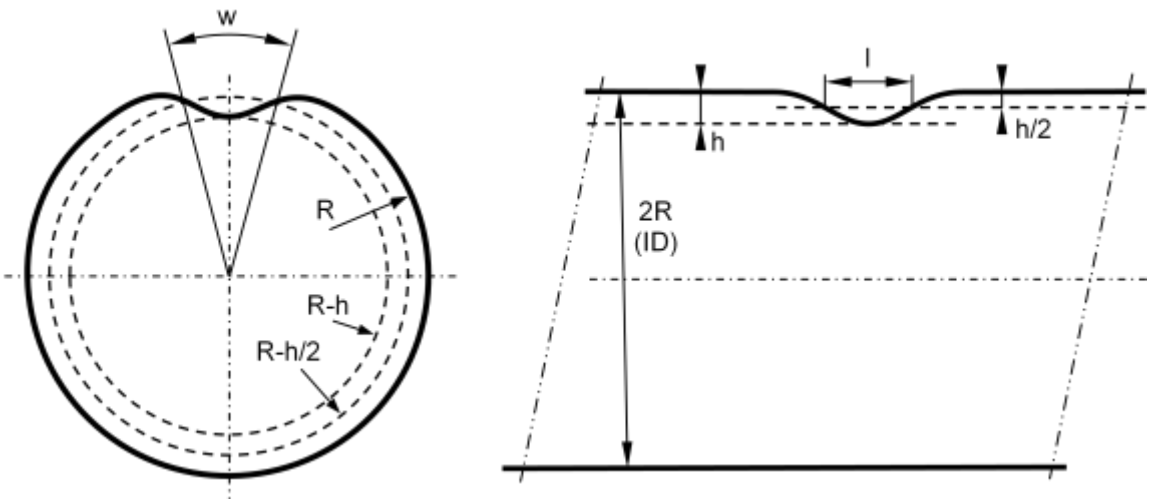

Figure 2.3: Measurement of dent.

The dent is defined as a percentage of the OD where h is measured from either the inside or outside of the pipe:

$$\frac{h}{OD} * 100\%$$

2.4.3 Gouge

As a gouge can take various forms, a schematic drawing is not available. Gouge anomaly dimensions are defined by the rectangle as shown in Figure 2.1, but the Contractor shall classify them as gouges with the angle related to the pipe axis reported as well. If a gouge is associated with a dent, then it shall be reported as a "Smooth or Kinked Dent with Gouge" with separate dimensions of the gouge and dent.

2.4.4 Ovality

Ovality is specified by ID_{max} and ID_{min} as shown in Figure 2.4

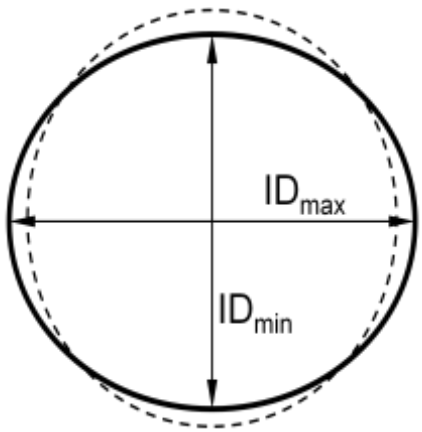

Figure 2.4: Measurement of ovality at one point over distance.

The ovality is defined as the ratio given in the equation below:

$$\frac{ID_{max} - ID_{min}}{\left[\frac{ID_{max}+ID_{min}}{2}\right]}$$

The ovality reported at the joint is based on a statistical approach of the measurements along the joint. It can be the mean ovality or any percentile (90th is common) or the maximum measured, which is to be detailed by the Client in the contract. If not specified otherwise, the maximum shall be reported. *Note: Reporting of ovality dimensions depends on the used formula (code) and it is therefore required that the formula applied is stated in the report.*

2.4.5 Buckle

As a buckle can take various forms, a schematic drawing is not available.

2.4.6 Ripple/Wrinkle

A ripple/wrinkle is specified by its height and length as shown in Figure 2.5Figure 2.5, Figure 2.6 and Figure 2.7. The maximum values shall be reported and, if requested, also the maximum strain based on a methodology agreed between Client and Contractor.

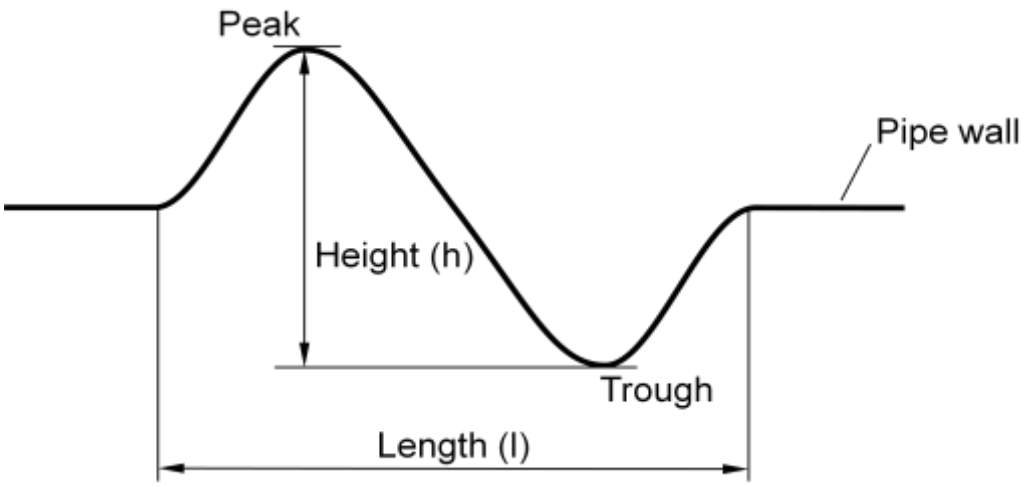

Figure 2.5: Measurement of ripple / wrinkle.

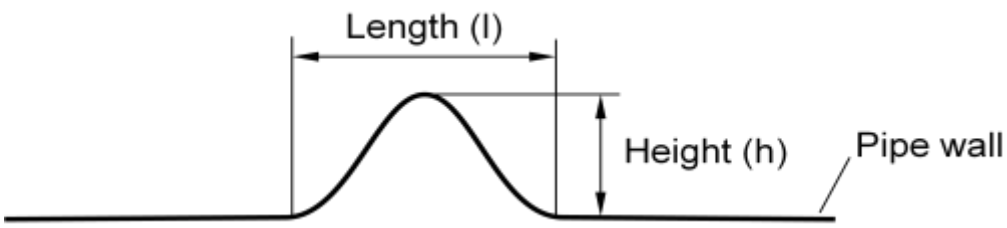

Figure 2.6: Measurement of single ripple/wrinkle.

A ripple/wrinkle is defined by its length (l) and maximum height (h).

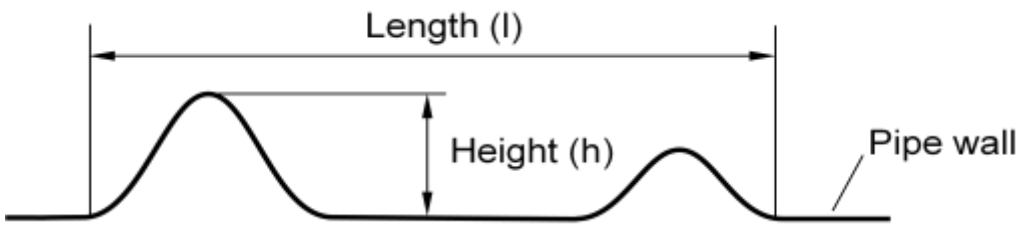

Figure 2.7: Measurement of multiple ripple / wrinkle.

Multiple ripples/wrinkles are defined by the total length (l) and maximum height (h).

2.4.7 Roof topping/peaking

Roof topping/peaking is specified by the angle 2Θ and height (h), see Figure 2.8.

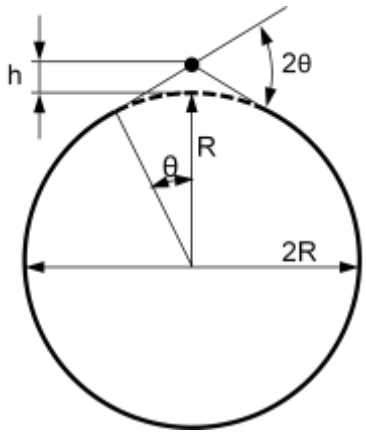

Figure 2.8: Measurement of peaking/roof topping.

Roof topping/peaking is defined by its height h in mm and angle 2Θ in degrees (°).

2.4.8 Crack and crack-like

A crack or crack-like feature is specified by the length (l, from tip S to tip E), depth (d) and orientation (angle α) to the pipeline axis, see Figure 2.9.

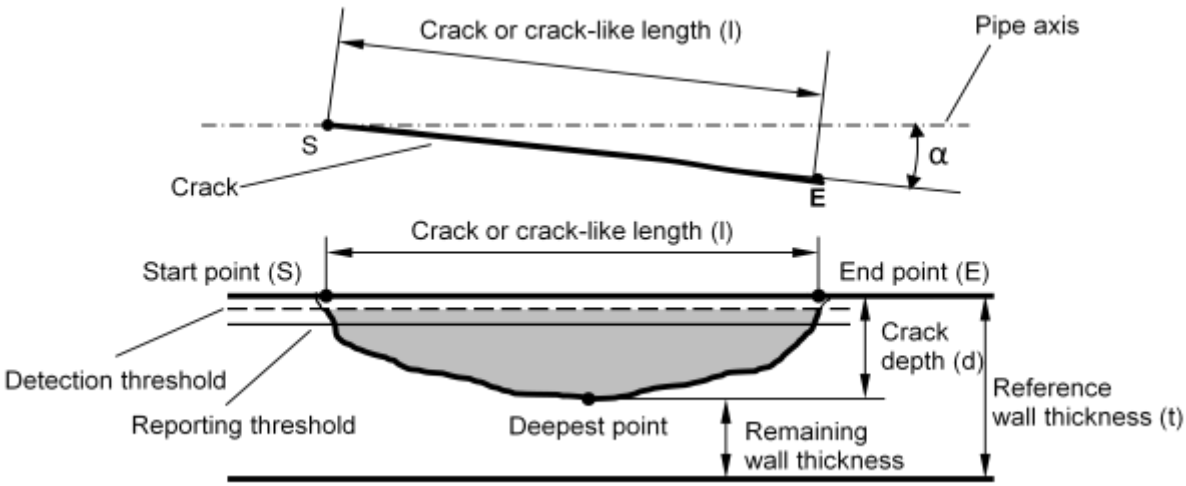

Figure 2.9: Illustration (top view and cross section) of parameters describing location and dimension of crack and crack-like features.

Planar, two-dimensional and elongated pipeline features mechanically splitting the pipe wall into two parts and oriented primarily perpendicular to the pipe surface are referred to as cracks or crack-like anomalies depending on the driving cracking mechanism.

Cracks are typically oriented either axially in the pipe body, or in the longitudinal, spiral, or circumferential weld areas and welds. Independent from the nature of the cracking mechanism, cracks in pipelines are observed as single or colonies.

The parameters of single crack and crack-like anomalies are length "l" and depth "d". Due to its planar, two-dimensional nature a crack or crack-like anomaly shows no width but may show a crack opening depending on the geometry and nature of the crack.

Cracks are regarded to have an opening at the surface < 0.1 mm, crack like defects to have an opening at the surface of 0.1 mm to 1.0 mm.

The capabilities of non-destructive examination techniques to detect, classify and size crack and crack-like anomalies strongly depend on the technology itself and its implementation on the inspection tool. In contrast to metal loss anomalies, no anomaly classes exist for cracks and crack-like anomalies. The Contractor shall provide the tool performance specifications in accordance to section 4.4 and table A5-4 with special emphasis on:

- The POD at 90% as a function of the anomaly dimensions.
- Details on the basis of the performance shall be clearly presented with regards to artificial and/or natural features.

2.4.9 Crack colonies

A crack colony is specified by the length (l), width (w), see Figure 2.10 and depth of the deepest single crack in the colony (see Figure 2.9).

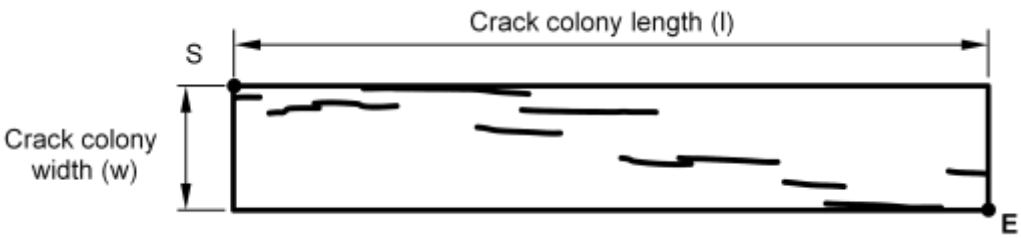

Figure 2.10: Illustration (top view) of parameters describing location and dimensions of crack colonies.

Colonies of cracks can be formed as a result of corrosion (e.g. SCC) and cracks in such a colony might interact depending on their dimensions, separation and density. Interaction rules are applicable for assessment, see 2.6.1.

2.5 Nomenclature of features

Features can be divided into component features and anomaly features.

Features shall be identified in accordance with Appendix 3: Report structure, terminology and abbreviations: Column Feature type.

The type of features shall be further identified in accordance with Appendix 3: Report structure, terminology and abbreviations: Column Feature identification.

2.6 Anomaly assessment

2.6.1 Interaction rules

Clustering of anomalies will be required if defects can interact and thereby pose a greater risk to the pipeline than individually assessed. The applicable assessment method shall define the interaction rules and clustering requirement.

If not specified otherwise by the Client, the latest version of ASME B31G [11] should be used for assessment and interaction rules of metal loss. Possible alternative methods include, but are not limited to:

- API 579/ASME FFS (general, including metal loss and cracking) [9]
- Modified ASME B31 G, (metal loss) [11]
- BS 7910 (general, including metal loss and cracking) [10]
- DNV RP-F101 (metal loss) [12]
- Kastner (only circumferential features) [8]
- CEPA Recommended Practices for Managing Near-neutral pH Stress Corrosion Cracking (only SCC) [3]
- Pipeline Defect Assessment Manual (PDAM) [2].

2.6.2 Indication of anomaly severity (ERF)

To allow the Client to rank the indications of anomalies in the pipeline on the basis of a first pass screening of severity, the Estimated Repair Factor (ERF) can be used. It is noted that for significantly ranked defects a more sophisticated assessment may then be applied.

The ERF is defined as:

$$ERF = MAOP/P_{safe}$$

P_{safe} is the safe working pressure as calculated by the latest version of an appropriate anomaly assessment method as agreed between Client and Contractor. P_{safe} shall be calculated using specific information of the pipeline segment such as the measured wall thickness and appropriate design factor for the area class.

If not specified otherwise by the Client, the latest version of ASME B31G [11] should be used for metal loss features. For possible alternative assessment methods (but not limited to) see section 2.6.1.

Note: The calculation of ERF has been updated from previous versions of this POF specification by replacing MOP with the MAOP. Whereas MOP could be applied as a temporary process restriction, MAOP implies the maximum pressure that could be introduced to the pipeline both at the time of the calculation and for any future operations.

2.7 Resolution of measurement parameters

A list of definitions with resolution and associated units to be used is presented in Table 2.2.

Table 2.2: List of definitions with minimum resolution and associated units to be used.

Definition	SI/metric units	Alternative units
Log distances	0.001 m	0.01 ft
Feature length and width	1 mm	0.01 inch
Feature depth	0.1 mm or 1%	0.01”or 1%
Reference t	0.1 mm or 1%	0.01” or 1%
Orientation	0.5° or 1 minute	1 minute
ERF	0.01	0.01
Magnetic field strength (H)	0.1 kA/m	1 Oe (Oersted)
Magnetic flux density (B)	0.1 T (Tesla)	10^3 G (Gauss)
Axial sampling distance	0.1 mm	0.01 inch
Circumferential sensor spacing	0.1 mm	0.01 inch
Tool speed	0.1 m/s	0.1 ft/sec
Temperature	1 °C	1 °F
Pressure	0.01 MPa/0.1 bar	1 psi
Global Position Coordinates[1)]	0.01 m	10^{-8} ° (Decimal degree)

1) Unless specified otherwise, WGS84 shall be used as the coordinate system

3 Health and safety

Care for health and safety is essential during any stage of any activity. As ILI of pipelines typically involves working with pressurized components and potentially explosive, flammable or hazardous atmosphere, adequate procedures must be in place to prevent any harm to personnel, environment or equipment. It is the responsibility of both Client and Contractor to agree on health and safety requirements and procedures and to check if latest and most stringent versions of (local) HSE requirements are met.

ILI operations require a pipeline to be opened and an inspection tool to be loaded/unloaded whereby explosive environments might occur. Special measures to prevent unsafe situations during ILI activities shall be taken.

Regulations have been developed to prevent accidents due to explosive environments. Examples of these regulations are the ATEX guidelines (ATmosphères EXplosive) which is mandatory for activities in the European Union or the IECEx system (*International Electro technical Commission: IEC System for Certification to Standards relating to equipment for use in Explosive Atmospheres*).

Implementation of ATEX, IECEx or an equivalent directive might be mandatory on the basis of national, local legislation or Client policy and if required shall be employed for ILI operations in addition to already applicable standards and procedures.

For use of non-electrical equipment in potentially explosives atmospheres, EN 13463 or an equivalent standard can be applicable.

For use of electrical equipment in potentially explosives atmospheres, EN-IEC 60079-xx (-10, -14, -17) or an equivalent standard can be applicable.

3.1 ATEX

ATEX zone 1 is considered to be applicable for ILI operations. The Client shall specify if ATEX certification is required and if so, the following two directives shall be followed:

- ATEX 114[2], Directive 2014/34/EU of the European Parliament and of the Council of 26 February 2014 on the harmonization of the laws of the Member States relating to equipment and protective systems intended for use in potentially explosive atmospheres.

  For ILI activities in the oil and gas industry it is considered that, unless specific measures are taken, zone 1 (areas with occasional dangerous explosive atmosphere caused by gas, vapour or mist) is typically applicable. Unless the Client specifies otherwise, the ATEX certified ILI tool shall comply with:
  - Group II: Equipment intended for use in explosive atmospheres other than mines
  - Category 2: High protection level for use in zone 1
  - Minimum temperature class T3: Surface temperature of equipment < 200°C (depending on the medium, another temperature class might be required e.g. T4 (<135°C).

  Note: This directive implies that the Contractor has to assess all potential explosion risks of its equipment and has to design the equipment to this directive.

- ATEX 153[2], Organizational requirements for health & safety protection of industrial workers at risk from potentially explosive atmospheres.

[2] Latest or superseding versions of the relevant codes shall be used

ATEX 153 gives organizational and operational requirements for activities in potentially explosive environments. Client and Contractor are to define the operating procedures and work instructions to assure safe work environment. Client is in lead and stays responsible. The operating procedures are considered outside the scope of this document.

Note: This directive requires that the Client assess the zoning of the launch/receive trap workspace through risk assessment and that Client is responsible for ensuring that all equipment introduced into these zones is compliant and QA certified against ATEX 114.

In addition to the ATEX requirements, which are only valid for atmospheric conditions, the Client shall specify, whether the contractor shall ensure safe operation of ILI equipment under explosive conditions for pressures > .11 MPa during receiving and launching of tools.

3.2 IECEx

The IECEx is an alternative code for certification of ILI equipment with equal area of application as ATEX 114, but not further discussed in this specification.

4 Tool specifications

4.1 Introduction

Tool specifications are important for the Client to clearly understand the capabilities and limitations of an ILI tool before selection and use. The purpose of this section is to present a consistent approach for presenting tool specifications and agreed tool specifications shall be part of the contract between Client and Contractor, as further described in chapter 6. Tool specifications typically consist of the combination of tool data sheets and tool performance specification:

- Tool data sheets cover the physical dimensions of the tool and operating conditions the tool can work in
- Performance specifications describe the inspection capabilities and limitations of the inspection technology applied. Tool performance follows the general requirements of API 1163 supported by Contractor quality systems.

The Client should clearly define the goals and objectives of an ILI before tool selection can take place. A key aspect in this process is a proper identification of pipeline threats and anticipated degradation mechanisms. The expected type, size, location and orientation of anomalies are important inputs to tool selection. In many cases tool selection requires a deeper understanding and details of specific tools which can best be obtained in a discussion between Client and Contractor. Factors that may influence tool performance, such as level of cleanliness and pipeline operating conditions need to be considered as well.

Prior to an in-line inspection the following should be in place:

- The Client to communicate the goal and objectives of the ILI to the Contractor
- Tool selection to be discussed and agreed between Client and Contractor
- Contractor to confirm that tool selection is appropriate given the goals and objectives of the ILI.

4.2 Tool data sheets

Tool data sheets provide information to allow Client to understand the limitations of service and suitability for use in pipeline system. Typically separate tool data sheets exist for each diameter and inspection technology combination.

They shall clearly present:

- Tool identification
- Tool specifications
- Safety
- Operating conditions/parameters
- Pipeline restrictions
- Launcher and Receiver trap details.

Detailed tool data sheet requirements are included in Appendix 4.

4.3 Tool class history

In order to achieve a high probability of first run success (Ref. POF document "Guidance on achieving ILI First Run Success" [5]), it is important that the Client clearly understands the operating history of

the tool class and its level of operational testing. Before the ILI contract is confirmed and unless otherwise agreed, Client may request any or all of the following information:

- Technology readiness of tool class hardware for operating conditions using the following grades:
  1. Newly designed component with limited testing
  2. Limited field operation (< 20 runs or < 500 km distance)
  3. Multiple uses with clear history of components and subsequent changes
- Provide a unique tool reference number and applicable data sheet.

Design changes to tool components or modules that may affect level of readiness shall be clearly communicated to Client both at time of placing order and for any subsequent change made by Contractor.

4.4 Tool performance specification

Tool performance specifications shall define the ability of the ILI system to detect, locate, identify, and size pipeline features, components and anomalies. It is typically linked to the inspection technology applied in the tool (e.g. UT, MFL, EC, EMAT or mapping).

4.4.1 General

Tool performance specifications shall comply with requirements given in API 1163 [1], chapter 6. The following general requirements are given for tool performance specifications:

- The Probability Of Detection, POD (a), is the probability that a feature with size a will be detected by the ILI tool. Two feature sizes are frequently extracted from the POD information: $a_{90/50}$ (a_{90}) is the feature size at which the average POD is 90% and $a_{90/95}$ is the feature size at which the lower 95% confidence limit of the POD is 90%, see also Figure 4.1. In the tool performance specification it shall be clearly specified what POD value is given. It is recommended to specify the $POD_{90/95}$ value
- The Probability of Identification, POI, is the probability that a feature is correctly identified by the ILI tool. The type or types of anomalies, components, and characteristics that are to be detected, identified, and sized by the ILI system shall be clearly indicated. Identification of each feature type shall be reported as specified in Appendix 5, Table A5-1
- The measurement specifications for detection and sizing of the various anomalies and pipeline location shall be reported as specified in Appendix 5, Tables A5-2 to A5-8 where they apply. The Client might request to complete the alternative Table A5-3a in favour of Tables A5-2 and A5-3
- Performance specification shall clearly state the level of analysis that is required to support the level of specification
- Where a higher level of performance is based on more detailed analysis, the additional performance level and commercial basis for additional analysis shall be clearly stated and agreed by Client and Contractor
- If different technologies (e.g. MFL, UT, EC or EMAT) are combined into one tool, then the specifications shall be provided as if the technologies were applied in a separate tool and additionally a table with the specifications of the multi-technology tool shall be provided.

The performance specification shall define and document the essential variables. In general two types of essential variables should be considered for ILI tool performance: i) pipeline design and

operational characteristics, ii) inspection tool design and physical characteristics. More detailed requirements on the essential variables are to be included in the performance specifications as listed in Appendix 5.

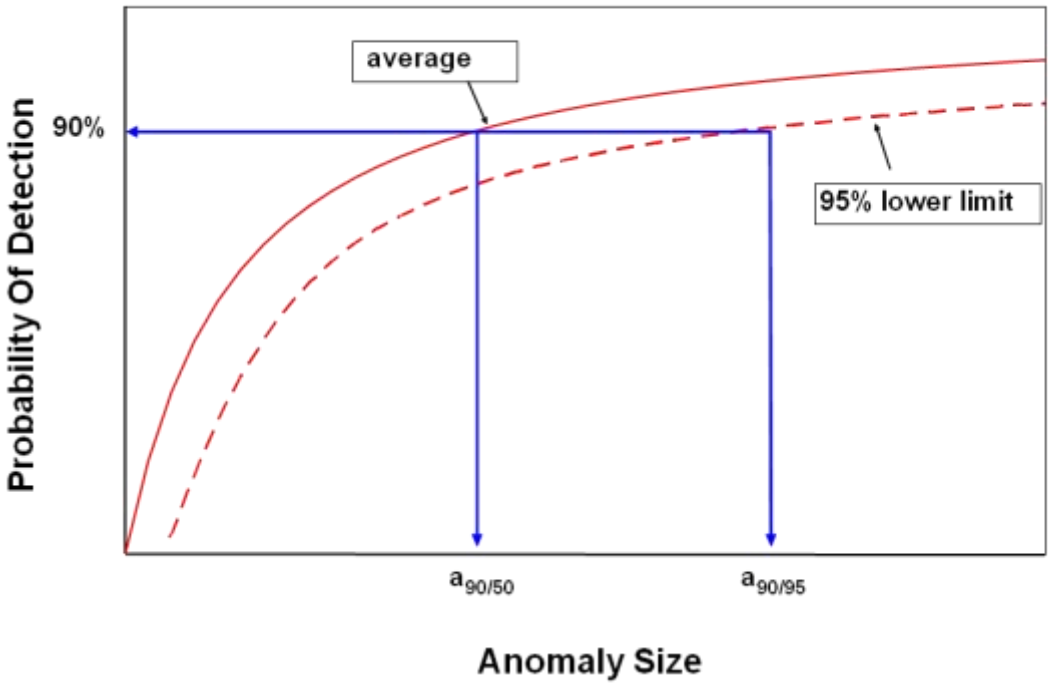

Figure 4.1: Typical example of the average and lower limit POD curve as function of anomaly size with indication of the definitions of $a_{90/50}$ (a_{90}) and $a_{90/95}$

4.4.2 Basis of performance

The basis on which performance specification is made shall be clearly stated for each feature type using the following:

- Modelling only
- Limited pull through tests and modelling (where effects of essential variables have not been fully tested by pull through runs and features used are predominantly manufactured)
- Extensive pull through tests covering range of speed and wall thickness using a combination of manufactured and natural features
- Limited field verification with less than 20 operational runs
- Extensive field verification results reviewed on an annual basis.

Where multiple methods are used, the Contractor shall clarify what has been used. Details of manufactured and/or natural features shall be clearly presented.

4.4.3 Exclusions and limitations

Physical and operational factors or conditions that limit the detection thresholds, PODs, POIs, and sizing accuracies shall be identified in the performance specification. It shall be clearly stated what the acceptable limits are for, but not limited to, e.g. tool speed and pipe wall thickness, see also Appendix 5.

4.4.4 Access to supporting performance information

Contractor shall provide access to information in support of stated tool performance specification on request of Client.

The ILI tool testing information of the contractor shall be auditable and contain information regarding the calibration procedure and latest calibration record of the tool. The procedure should give insight in, but not limited to: used calibration features, line pipe material, wall thickness and manufacturing process, tool velocity, date and frequency of calibration. For magnetic tools the calibration information will include the tool speed and the measured magnetic field strength value with the position where it was measured. In addition the Contractor shall supply a definition of which sizing model and revision was used.

How and where the information is to be provided is to be agreed between Contractor and Client. It is the responsibility of the Contractor to check that the tool and the calibration methods are valid and adapted to the Client's objectives.

4.5 Tool performance verification

A Client may choose to verify tool performance through formal testing or field verification.

In case formal testing is carried out, the report should at least contain the following information:

- Details of runs and essential variables tested
- Details of features
- Comparison of stated performance with actual reported features.

Regarding field verification more guidance can be found in POF document "Guidance on Field Verification Procedures for In-Line-Inspection" and API 1163 [1] (chapter 8 and Annex C). In case field verification is performed the following requirements apply:

- To ensure meaningful data is collected from the field, Client should facilitate access for Contractor to verify field measurement
- Client shall provide Contractor with field verification data (dig data)
- Contractor shall use field verification data to confirm tool performance.

4.6 Changes to tool specification or performance specification sheets

Changes to tool and performance specifications shall be tracked in Contractor Quality Assurance system. Each revision shall have date and issue number.

Where a change could affect earlier pipeline integrity assessment, Client shall be notified of change and potential implications. This typically applies when performance specification for certain features is reduced based on new information or additional testing. Any requirement for reassessment of features as a result of change shall be agreed between Client and Contractor.

5 Personnel qualification

The personnel operating the ILI systems and the personnel handling, analyzing and reporting the inspection results shall be qualified and certified according to ANSI/ASNT-ILI-PQ-2005 (reapproved 2010) [4] or later version/superseding document.

Unless the Client specifies otherwise, key personnel shall meet the following minimum qualifications, ref. ANSI/ASNT-ILI-PQ-2005 [4]:

- Team leader during ILI field activities: Level II Tool Operator for the applicable technology
- Data analysis and reporting Lead: Level II Data Analyst for the applicable technology
- Review of final Client report: Level III Data Analyst for the applicable technology. The review should include (but not limited to) e.g. a quality check of data analysis and reported results.

An overview of personnel qualifications that will be deployed for the ILI tool run, data analysis and final report review shall be submitted to the Client. The personnel qualifications shall be auditable.

6 ILI preparation and contracting

6.1 ILI preparation

The POF document “Guidance on achieving ILI First Run Success” [4] stresses the importance of the preparation and contracting phases to meet all the objectives of the inspection. The preparation phase is described in length in this document, which includes some check lists in Appendix B.

6.2 Contracting

This POF document is intended to serve as a generic ILI specification where details and deviations for ILI runs still need to be defined to serve Client's specific issues. Such details and deviations (Appendix 2 provides guidance), should be agreed between Client and Contractor and stated in the ILI contract.

The contract between the Client and the Contractor shall, as a minimum include the following items:

- Organization: The organization shall be defined between Client and Contractor, in terms of human and materials resources, communication, schedule of the operations, run conditions, procedures, roles and responsibilities, actions in the event of an emergency etc. The POF document "In-Line-Inspection Check Lists" [6] provides guidance
- Specific details: Details and deviations from the POF document "Specifications and requirements for in-line inspection of pipelines" (this document, if applicable)
- Run preparation: The Client should supply the Contractor with details of the pipeline(s) to be inspected. The POF document "ILI Pipeline Questionnaire" [7] provides guidance
- Operations: The operations shall be defined in terms of pipeline technical data, tool specifications, characteristics and performances, criteria for cleaning and run validation
- Results: The results shall be reported as per chapter 7. If requested by the Client, a revised version of the final report shall be issued in case of proven discrepancies between reported information and verifications.

The requirements herein may be changed at Client’s request. Some points may depend on the configuration of the network to be inspected, the Contractor, the technology used, the internal (Client) policies and practices and local regulations.

It can be considered that, for specific applications, specifications and/or defect geometries, dedicated tool calibration can be performed (e.g. with spare project pipes), followed by a modified interpretation/sizing model.

7 Reporting

Reporting is an essential part of the inspection process and depending on the time and information required by the Client, various types of reports can be issued, see below. If the Contractor finds an anomaly during the inspection and/or evaluation of the ILI data which could be an immediate threat to the integrity of the pipeline, he has the duty to report this to the Client without delay.

If not agreed otherwise between Client and Contractor, reporting is based on at least two separate documents:

- Operations report
- Final report.

In addition to the above mentioned reports, one or more of the following reports can be requested and agreed between Client and Contractor:

- Preliminary report
- Raw data report
- Multiple run comparison report
- Additional reporting.

All documents and all lists (e.g. pipe tally, list of anomalies, etc.) will contain the following general information:

- Identification of the Contractor and Client
- Identification of the pipeline
- Product
- Outside or nominal diameter
- Length
- Construction year
- ILI technology/technologies
- Inspection date/Reference.

7.1 Operations report

The operations report should summarize important operational information such that the Client is informed on the success of the inspection and quality of data collected and should include information on run preparation, running of tool, run quality including pipeline cleanliness to verify if targets are achieved. If data quality is not as required for a successful pipeline feature evaluation, a re-run (if possible) can be considered. This report follows good practices regarding ILI activities as described in the POF document "Guidance on achieving ILI First Run Success" [5].

The operations report shall be sent in electronic form to the Client before demobilization of the tool and ultimately within 2 days of the ILI run, unless agreed otherwise. The demobilization of tool and crew shall be agreed between Client and Contractor based on the operations report results using the criteria below.

The operations report shall contain, unless agreed otherwise:

- Any reported safety observation (e.g. near miss)
- A description of the operations (cleaning, gauging, dummy tool run, ILI tool run) including run conditions

- Used tool(s) identification (serial number) with tool(s) data sheet and calibration
- AGM statistics (if applicable)
- Cleaning results and comparison to criteria
- Gauging/dummy tool run results and comparison to criteria
- Details of ILI run(s):
  - Time and date of tool launching and receiving
  - Travelling time
  - Min/max tool velocity, and tool velocity plot over the length of the pipeline
  - Min/max pressure
  - For MFL tools: min/max magnetization level, and a plot of the magnetic field strength in kA/m over the length of the pipeline measured at the inner surface of the pipe
  - Condition of tool(s) after receipt e.g. damaged sensors
  - Data loss statistics from faulty sensors and in case of UT echo loss statistics
  - Data recording and quality within contract specifications
- The suitability of the recorded data to allow a successful evaluation.

,The formulation for acceptable data loss shall be, unless specified otherwise:

- Continuous loss of data less or equal to 0.5 % of pipeline length
- Discontinuous loss of data less or equal to 3% of pipeline length
- Continuous loss of data from less than 4 adjacent sensors or 25 mm circumference (whichever is smallest).
- The criteria apply to each section of the pipeline i.e. each diameter, wall thickness and pipe manufacturing process.
- If data loss exceeds one of the criteria above, this shall be discussed between Client and Contractor to reveal the cause and decide on follow-up actions which might be:
  - A re-run of the tool
  - Check if the data loss has an effect on anomaly detection and sizing capability of the ILI tool.

The tool operational data statement shall indicate whether the tool has performed according to specifications and shall detail all locations of data loss and where the measurement specifications are not met. When the specifications are not met (e.g. due to speed excursions, sensor/data loss), the number and total length of the sections shall be reported with possible changes of accuracies and certainties of the reported results.

7.2 Preliminary report

A preliminary report is a list of features, including by their dig sheets. The reporting format is as per the list of anomalies in the final report. The preliminary report shall be delivered if requested by the Client or if the Contractor finds an anomaly (or anomalies) during the analysis of the ILI data which might be (are) an integrity threat to the pipeline.

The preliminary report aims at summarizing the most important features (individual and clustered) based on Client criteria as defined in the contract, in order to guarantee a safe pipeline operation. Unless agreed otherwise, typical reporting should include:

- Features with an ERF ≥ 0.8
- Metal loss features ≥ 50%

- Dents, Wrinkles/Buckles ≥5%
- Cracks with depth ≥ 4.0 mm.

Actual data quality shall be confirmed in terms of:

- Reporting threshold
- Method of analysis
- POD, POI, Sizing accuracy.

The preliminary report shall be sent in electronic form to the Client within 4 weeks of the ILI run, unless agreed otherwise.

7.3 Final report

Standard criteria for the final report are given in this chapter, but can be changed if agreed between Client and Contractor.

The final inspection report (hard and electronic copy) of either a single or combined ILI tool run shall contain the information as described in this chapter and be submitted within 8 weeks of the ILI run, unless agreed otherwise.

The reporting thresholds shall (if not specified otherwise) be:

- For MFL tools: Metal loss with a depth ≥ 10% t for welded pipe and ≥15% for SMLS pipe
- For UT and other tools: Metal loss with a depth ≥ 1.0 mm
- Cracks with a length ≥ 25 mm
- Dents, ripples/wrinkles with a height/depth ≥ 1% ID
- Ovalities ≥ 5% ID.

7.3.1 Pipe tally

The pipe tally shall be a listing of all pipeline component features and anomaly features and should be reported in accordance with a typical report structure as given in Appendix 6 (including terminology, see Appendix 3 "Feature identification"). The Client can specify the pipe tally to specific requirements, e.g. add or delete specific columns.

The pipe tally shall be compatible with standard files such as CSV, ODS or another agreed format.

7.3.2 List of anomalies, clusters, data loss and other lists

Unless specified otherwise by the Client, the following lists shall be provided:

- List of anomalies:
  The list of anomalies shall contain the anomalies which are clustered if required by the interaction rules (according to chapter 2.6.1), with dimensions above the reporting threshold at POD=90% or above a reporting threshold as specified by the Client (including terminology, see Appendix 3). For a typical example see Appendix 7. *Note: if no defect interaction rule is applied, then this list can be waived in favour of the "List of individual anomalies", see below.*
- List of clusters:
  The list of clusters (according to chapter 2.6.1) shall contain the clusters and the individual anomalies that are part of the cluster. It shall be clearly indicated what anomalies form a certain cluster. For a typical example see Appendix 8.
- List of individual anomalies:

The list of individual (all) anomalies shall be a listing of all anomalies without applying a defect interaction rule and with dimensions above the detection threshold at POD=90% or above a reporting threshold as specified by the Client.

- List of data loss:
  The list of data loss shall be a listing of all locations with data loss indicating the cause of data loss. *(Note:* as *data loss might be caused by e.g. a dent or debris whereby an anomaly can be missed such a location shall be carefully checked).*
- Other lists:
  If requested by the client a list with specific, to be indicated, items.

On the Client's request also the location of the deepest point in the metal loss area or clustered area shall be reported.

Unidentified/unknown features with strong signal shall be reported as "unknown" with, in commentary, an indication of the signal level.

The list of anomalies shall be compatible with standard files such as CSV, ODS or another agreed format.

7.3.3 List of components

The list of components shall be a listing of all feature types as listed in Appendix 3, except welds and anomalies. The list of components shall contain the same fields as the pipe tally.

The list of components shall be compatible with standard files such as CSV, ODS or another agreed format.

7.3.4 Summary and statistical data

The summary and statistical information as stated below should be agreed between Client and Contractor.

7.3.4.1 Metal loss

If a metal loss tool was run, the summary report for metal loss shall contain a listing of:

- Total number of anomalies
- Number of internal anomalies
- Number of external anomalies
- Number of anomalies for each metal loss anomaly class
- Number of anomalies per depth range of 10% (lower limit included)
- If applicable, number of anomalies per ERF range of 0.1, starting from 0.6 (lower limit included).

The following plots shall be provided:

- If applicable, sentenced plot including ERF=1 curve of anomaly length against metal-loss feature depth showing all anomalies for each representative wall thickness
- Orientation plot of all anomalies over the full pipeline length
- Orientation plot of all internal anomalies over the full pipeline length
- Orientation plot of all external anomalies over the full pipeline length
- Orientation plot of all anomalies as function of relative distance to the closest girth weld.

7.3.4.2 Cracks, crack-like and crack colonies

If a crack detection tool was run, the summary report for cracks, crack-like and crack colonies shall contain a listing of:

- Total number of anomalies per type and orientation to pipe axis
- Number of internal anomalies per type and orientation to pipe axis
- Number of external anomalies per type and orientation to pipe axis
- Number of anomalies per type per depth range of 2 mm and orientation to pipe axis (lower limit included).

The following plots shall be provided:

- Number of anomalies over the pipeline length
- Circumferentially orientated anomalies as function of relative distance to the closest girth weld
- Longitudinally orientated anomalies as a function of relative distance to the seam weld over the pipeline length.

7.3.4.3 Local and global geometry features

If a geometry tool was run, the summary report of geometry tool shall contain a listing of:

- Total number of dents, ripples/wrinkles, buckles
- Total number of ovalities
- Total number of joints with ovality
- Total number of other localized deformation/geometry anomalies
- Number of dents, ripples/wrinkles, buckles per depth range of 1%
- Number of ovalities per ratio range of 1%
- Number of joints with ovality per ratio range of 1%
- Orientation plot of all dents, ripples/wrinkles, buckles over the pipeline length
- Orientation plot of all ovalities over the pipeline length.

7.3.4.4 Other types of features (e.g. illegal taps)

If a tool capable of detecting other feature types was run, on request of the Client, the summary report for these features shall contain a listing of:

- Total number of features per type
- Number of internal features per type
- Number of external features per type
- Number of features per type per depth range of 10% (lower limit included).

The following plots shall be provided:

- Number of features over the pipeline length
- Orientation plot of all anomalies as function of relative distance to the closest girth weld
- Relative distance plot of all anomalies to the seam weld over the pipeline length.

The lists and plots as defined above can be completed at Client's request.

7.3.5 Performance

The final report shall contain:

- Completed tables A3-1 to A3-8 as per the Contract
- Completed tables A3-1 to A3-8 with actual run performance data depending on run conditions, tool functioning, pipeline cleanliness, etc.

Actual performance data must be given for each pipeline section where it is constant. These sections will be clearly identified.

7.3.6 Dig sheet

The purpose of the dig sheet is to provide the Client with all the information useful to carry out the field verification of a chosen feature.

Unless agreed otherwise, dig sheets shall be included in the final report.

Dig sheets shall contain the following information:

- Length of pipe joint and (when present) orientation of longitudinal or spiral seam at start and end of every joint
- Length and longitudinal or spiral seam orientation of the 3 upstream and 3 downstream neighbouring pipe joints
- Log distance of anomaly
- Wall thickness of the pipe joints (up to the 3 upstream and 3 downstream joints)
- Log distance of closest features like magnet markers, fixtures, steel casings, tees, valves, etc.
- Distance of upstream girth weld to nearest, second and third upstream marker
- Distance of upstream girth weld to nearest, second and third downstream marker
- Distance of anomaly to upstream girth weld
- Distance of anomaly to downstream girth weld
- Orientation of anomaly
- Geographical coordinates of an anomaly if a mapping unit was applied, including the Geodetic Datum Standard used. Unless specified otherwise, WGS84 shall be used
- Anomaly description and dimensions
- Internal/external/mid-wall indication.

7.3.7 Software and signal

In addition to the hard copy (if applicable), a user friendly software package shall be provided to enable review and assessment of the data collected by the inspection tool.

This software shall enable the Client to carry out the following tasks:

- Viewing of signal for each tool which was run, with possibility to modify gain, scale, etc.
- Preparing dig sheet for each anomaly (including dents, combined features, etc.)
- Plotting graphs and histograms
- Computing ERF (input data, models)
- Accessing detailed profile data for dents.

7.3.8 Anomaly ranking method for ERF

If requested by the Client, the Estimated Repair Factor for anomalies shall be reported on the basis of the assessment method indicated in Chapter 2.6.2 and input data shall be clearly stated in the final report.

ERF shall be reported for each individual feature. When clustering is applied, specific ERF for clusters shall be provided by the Contractor.

7.3.9 Detection of markers

AGMs or permanent markers that have been positively identified during the ILI run shall be indicated in the pipe tally. In addition, in the final inspection report the total number of installed AGMs and the number of identified AGMs shall be reported.

7.3.10 Personnel qualification

An overview of key personnel qualification level that has been deployed for the ILI tool run, data analysis, reporting and final report review shall be reported.

7.4 Raw data report

On request of the Client the raw data or processed raw data from an ILI run or a specific pipeline section shall be provided. The format of the data depends on the type of tool applied and is to be agreed between Client and Contractor and shall be defined in the inspection contract.

7.5 Multiple run comparisons report

If requested by the Client, anomaly data from two or more successive ILI runs carried out on the same pipeline, shall be compared individually and clustered. Aim is to detect discrepancies between reported anomalies of successive runs like new or missed features, corrosion growth, etc.

The run comparison report shall contain a table with matching and non-matching features per joint and include the results of these matching in terms of location, sizing and evolution. For a typical example see Appendix 9.

If the same Contractor is chosen for two successive inspection runs, the Client may request:

- A signal to signal comparison analysis between the two inspections
- A 2nd report based on the raw data of the previous inspection, but processed with the new algorithm.

The final run comparison report shall include the "Final report" (section 7.3) requirements and in addition:

- A comparison in terms of quality, velocity, performance and accuracy (tool rotation, velocity, acceleration, behaviour anomalies, magnetization level, …)
- A comparison of used tools (performance, characteristics, number, type and distance between sensors, acquisition frequency, environment, magnetization, …)
- A comparison of analysis and reporting parameters (e.g. but not limited to algorithms, thresholds, assessment code, interacting rules, …)

7.6 Experience report

The experience report summarizes the operation. Good practices as well as possible improvements are reported. Special attention is paid to

- Project planning
- Interaction between interfaces
- Logistics on site
- Coordination with other operations
- Data quality
- Dig up results

The report will contribute to improved future operations.

7.7 Additional reporting

On request of the client an additional report might be requested including separate reports for each technology used in combination runs, Integrity assessment reports, etc.

8 References

1. Anon, “In-Line Inspection Systems Qualification”, API 1163, American Petroleum Institute, 2nd Ed., April 2013.
2. Cosham, A. and Hopkin, P., “Pipeline Defect Assessment Manual (PDAM)”, A Joint Industry Project, Penspen, 2013.
3. Anon, “Recommended Practices For Managing Near-Neutral Ph Stress Corrosion Cracking” 3rd Ed., Canadian Energy Pipeline Association (CEPA), May 2015.
4. Anon, “In-line Inspection Personnel Qualification and Certification” ANSI/ASNT-ILI-PQ-2005, American Society for Nondestructive Testing. 2010.
5. Anon, “Guidance on Achieving ILI First Run Success”, Pipeline Operators Forum, December 2012.
6. Anon, “In-line Inspection Check Lists”, Pipeline Operators Forum, December 2012.
7. Anon, “ILI Pipeline Questionnaire”, Pipeline Operators Forum, December 2012.
8. Kastner, W., Rohrich, E., Schmitt, W. and Steinbuch, R., “Critical Crack Sizes in Ductile Piping”, Int. J. Press. Ves. Piping 9 (3) 197–219, 1981.
9. Anon, “Fitness-For-Service”, API 579-1/ASME FFS-1, American Petroleum Institute, 2016.
10. Anon, “Guide to Methods for Assessing the Acceptability of Flaws in Metallic Structures”, BS 7910, British Standards Institution, 2013.
11. Anon, “Manual for Determining the Remaining Strength of Corroded Pipelines”, ASME B31G, American Society for Mechanical Engineers, 2012.
12. Anon, “Corroded Pipelines”, DNV-RP-F101, Det Norske Veritas, January 2015.

Appendix 1: ILI companies that provided comments to the draft version of these specifications

COMPANY	COUNTRY	WEBSITE
3P Services	Germany	www.3p-services.com
A. Hak Industrial Services	Netherlands	www.a-hak-is.com
Baker Hughes	USA	www.bakerhughes.com
General Electric (PII)	USA	www.geoilandgas.com/pii
NDT Global	Ireland	http://www.ndt-global.com
Pipe Survey International	Netherlands	www.pipesurveyinternational.com
PipeWay	Brazil	www.pipeway.com
Rosen	Switzerland	www.rosen-group.com
T.D. Williamson	USA	www.tdwilliamson.com
Quest Integrity	USA	www.questintegrity.com

Appendix 2: Guideline to clients for defining specific details of the POF specifications

Introduction

The POF document "Specifications and requirements for in-line inspection of pipelines" gives an outline of advised specifications for In-line-inspection (ILI) of pipelines. The Client should adapt certain specifications to reflect Client's specific requirements. For certain aspects of the inspection and/or reporting requirements, some options and default values are already considered, but the document gives the opportunity to define specific items. This guideline is intended to support the Client by listing the considered optional items in the specifications based on the expected integrity threats of the pipeline to be inspected. The items should be defined prior to sending the specifications to the ILI company and agreement of the contract.

In addition, in this guideline also some notes and advised specifications are given (*printed in Italic*), like the minimum requirements that are regarded essential for a successful ILI run.

Chapter 2.4.2 - Dent

The Client should agree with Contractor the methodology if strain based assessment is required and of minimum planar size accuracies of dents expected to be reported for technology selection.

Chapter 2.4.4 - Ovality

Default reporting is the maximum ovality measured. If another value shall be reported, this is to be indicated.

Chapter 2.4.6 - Ripple/Wrinkle

Maximum values shall be reported. If additionally also the maximum strain should be reported, the methodology shall be agreed between Client and Contractor.

Chapter 2.6.1- Interaction rules

ASME B31G methodology is specified as the default assessment method, but another methodology can be specified and agreed if required.

Chapter 2.6.2- Indication of anomaly severity (ERF)

The ASME B31G methodology is specified as the default assessment method for the ERF calculation, but another methodology can be specified if required.

Chapter 2.7 Resolution of measurement parameters

The Client shall specify if SI, metric or alternative units shall be used.

Chapter 2.7 – Coordinates for mapping work.

It is important for the client to specify the final coordinates required from the mapping data. Considerations will include using the latest geodetic system to ensure 'future proofing' of data, but also to ensure the data will match any existing mapping system used (which may in fact not be the latest system).

Chapter 0 - Health and Safety

Health and safety requirements to be agreed between Client and Contractor, including Client' policy on ATEX, IECEx or equivalent directive.

Chapter 3.1 – ATEX
Client shall specify if ATEX certification is required and if so, assess the zone classification.
Client shall specify, whether the Contractor shall ensure safe operation of ILI equipment under explosive conditions for pressures > .11 MPa during receiving and launching of tools.

Chapter 4.3
Client may request for information on tool readiness.

Chapter 4.4.1 - General
Client may request to complete the alternative table A5-3a in favour of tables A5-2 and A5-3.
If a higher level of performance is based on more detailed analysis, the additional performance level and commercial basis shall be agreed.

Chapter 4.4.4 Access to supporting performance information
If access on information in support of stated tool performance specification is requested, details on how and where shall to be agreed.

Chapter 4.6 - Changes to tool specification or performance specification sheets
Any requirement for reassessment of features as a result of tool specification changes shall be agreed (if required).

Chapter 0 - Personnel qualification
Default requirements for qualifications of key personnel are given but can be specified otherwise by the Client.

Chapter 6.2 - Contracting
Various contracting details should be specified.

Chapter 0 - Reporting
Two reports are indicated as standard (default). Additional reporting should be requested and agreed.

Chapter 7.1 - Operations report
Default time for reporting is within 2 days. Change of reporting time should be agreed.
Default content report is listed, modifications to be agreed.
Default values for acceptable data loss are given, modifications to be agreed.

Chapter 7.2 - Preliminary report
Default time for reporting is within 4 weeks. Change of reporting time should be agreed.
Default content report is listed, modifications to be agreed.
Typical reporting criteria are given, modifications to be agreed.

Chapter 7.3 - Final report
Default time for reporting is within 8 weeks. Change of reporting time should be agreed.
Default content report is listed, modifications to be agreed.
Default reporting thresholds are listed, modifications to be agreed.

In chapter 7.3.1 to 7.3.10 typical reporting options are listed and should be used as default.
Modifications to be agreed.

Chapter 7.4 - RAW data report
If requested by Client, the raw data or processed raw data shall be provided by agreement.

Chapter 7.5- Multiple run comparisons report
If requested by Client, anomaly data from two or more runs shall be compared. A typical reporting structure is given, modifications to be agreed.

Chapter 7.6- Additional reporting
Any additional desired reporting should be requested and agreed upon by Client and Contractor.

Appendix 5 - Tool technology performance specifications
It is requested that the ILI company provides information on anomaly detection and sizing and other measurement capabilities of their tool. Below some typical values that can support the Client in his review of the proposed specifications.

POD of detected anomalies
The POD of a tool is normally taken at 90% and is based on anomalies with reference dimensions as given in the tables of appendix 5.

The typical minimal detectable depth of a high resolution MFL tool for general corrosion is 10% t and for pitting defects it is 15% t both with a POD of 90%. For seamless pipes and other category defects other values can apply.

The typical minimal detectable defect depth of a UT tool is 1 to 1.5 mm with a POD of 90%.

Depth, length and width sizing accuracies
The accuracy depends on the anomaly dimension class:
Typical for (high resolution) MFL tools: depth 10-15% t, length and width accuracy 10-20 mm
Typical for UT tools: depth 0.3 – 0.5 mm, length and width accuracy 10 mm
For anomaly depth, length and width sizing accuracy, the typical certainty level is 80%.

Accuracy of distance and orientation (clock position) of features:
Typical accuracy of distance to/from marker: 0.25% of distance
Typical accuracy of distance to closest weld: 0.15 m
Typical accuracy of circumferential position: 10°.

Certainty and accuracy of sizing deformations by geometry tool:
The certainties and accuracies of reported dents and ovalities shall be defined.
Typical certainties and accuracies are:
Ovalities: ID reduction, accuracy 1% of pipeline ID with certainty = 90%
Length, accuracy 10% of pipeline ID with certainty = 90%.
Dents: Depth, accuracy 1% of pipeline ID with certainty = 90%
Length, accuracy 10% pipeline ID with certainty = 90%
Width, accuracy 10% pipeline ID with certainty = 90%.

Mapping: The accuracy of mapping is dependent on a variety of factors. Some of the main ones include the quality/technology of the IMU, the accelerometers, the odometer, the AGM's clock matching that of the inspection tool, the AGM's and also spacing of the accuracy with which the position of AGM is determined. Manufacturers and service providers will have varying technologies that provide varying accuracies.

It is generally thought that the accuracy of an IMU varies over distance travel, but the accuracy degrades over time, so it is important to consider the speed of the product in the pipe during the mapping inspection run. It is therefore important to specify maximum and minimum flow rates during mapping surveys.

AGM's are used to correct the IMU's 'drift' over time (and hence distance). The closer the AGM spacing, the more accurate the final coordinates will be. Many mapping runs use a 1 mile or 2 kilometre spacing, but for very or extremely high accuracy work 1 kilometre or even 500m spacing can be used.

AGM's should not be placed where the pipe is too deep for the inspection tool to be detected by the AGM.

Below are some reference documents that relate to magnetic properties for MFL inspection:

- *In "Magnetisation as a key parameter of magnetic flux leakage pigs for pipeline inspection" by H.J.M. Jansen, P.B.J. van de Camp and M. Geerdink (Insight Vol. 36, September 1994) it is concluded that MFL pigs are least sensitive to error sources (e.g. residual stresses, pressure, remnant magnetization) if the magnetic induction in the pipe wall > 1.8T. The magnetic field strength required to obtain such an induced magnetisation level depends on the type of material, wall thickness, pig speed etc.*
- *NACE International Publication 35100: "In-Line Non-destructive Inspection of Pipelines gives the following typical specifications for high-resolution MFL tools:*
  Minimum magnetic field strength: 10 to 12 kA/m (3 to 3.7 kA/ft)
  Minimum magnetic flux density: 1.7 T.

<u>Mapping tool specifications</u>

Geographical locations shall be reported in GPS coordinates by default, but another method can be specified if required.

Appendix 3: Report structure, terminology and acronyms

Column title	Unit	Prescribed terminology	Acronym	Explanatory note
Log distance	m	-		Starting point: trap valve
Abs up weld dist.	m	-		Absolute distance to upstream weld
L joint	m	-		Joint length to downstream weld
Feature type	-	- Above Ground Marker	AGM	
		- Additional metal/material	ADME	Further identified below
		- Anode	ANOD	
		- Anomaly	ANOM	Further identified below
		- Buckle arrestor begin/-end	BUAB/BUAE	
		- Casing begin/-end	CASB/CASE	
		- Change in wall thickness	CHWT	
		- CP connection	CPCO	
		- External support	ESUP	
		- Ground anchor	ANCH	
		- Off take	OFFT	
		- Other	OTHE	
		- Pipeline fixture	PFIX	
		- Reference magnet	MGNT	
		- Repair	REPA	Further identified below
		- Tee	TEE	
		- Valve	VALV	
		- Weld	WELD	Further identified below
Feature identification	-	Additional metal/material:		
		- Debris	DEBR	
		- Touching metal to metal	TMTM	
		- Other	OTHE	
		Anomaly:		
		- Arc strike	ARCS	
		- Artificial defect	ARTD	
		- Blister	BLIS	
		- Buckle Global	BUCG	
		- Buckle Local	BUCL	
		- Buckle Propagation	BUCP	
		- Corrosion	CORR	
		- Corrosion cluster	COCL	
		- Corrosion related to CRA	COCR	
		- Crack	CRAC	
		- Crack cluster	CRCL	
		- Dent complex	DENC	
		- Dent kinked	DENK	
		- Dent plain	DENP	
		- Gouge	GOUG	
		- Gouge cluster	GOCL	
		- Grinding	GRIN	
		- Girth weld crack	GWCR	
		- Girth weld anomaly	GWAN	
		- Longitudinal weld crack	LWCR	
		- Longitudinal weld anomaly	LWAN	
		- Mill anomaly Grinding	MGRI	
		- Mill anomaly Lamination	MLAM	
		- Mill anomaly Lap	MLAP	
		- Mill anomaly Non-Metallic Inclusion	MNOI	

		- Mill anomaly cluster - Ovality - Ripple/Wrinkle - Roof Topping - SCC - Spiral weld crack - Spiral weld anomaly <u>Repair:</u> - Welded sleeve begin/-end - Composite sleeve begin/-end - Weld deposit begin/-end - Coating begin/-end - Crack arrestor begin/end - Other begin/-end <u>Weld:</u> - - Bend begin/-end - Change in diameter - Change in wall thickness - Adjacent tapering - Longitudinal seam - Spiral seam - Not identifiable seam - Seamless	MACL OVAL RIWR ROTP SCC SWCR SWAN WSLB/WSLE CSLB/CSLE WDPB/WDPE COTB/COTE CRAB/CRAE OTHB/OTHE BENB/BENE CHDI CHWT ADTA LOSE SPSE NISE SMLS	No abbreviation for all welds different from welds below Applicable for: Pipe – pipe unequal WT
Feature class		- Axial Grooving - Axial Slotting - Circumferential Grooving - Circumferential Slotting - General - Pinhole - Pitting	AXGR AXSL CIGR CISL GENE PINH PITT	See Fig. 2.2 See Fig. 2.2 See Fig. 2.2 See Fig. 2.2 See Fig. 2.2 See Fig. 2.2 See Fig. 2.2
Clock position	h: min			See Fig. 2.1
Nominal t	mm			Nominal wall thickness of every joint
Reference t	mm			The actual not diminished wall thickness surrounding a feature
Length	mm			Anomaly length in axial direction
Width	mm			Anomaly width in circumferential direction
d (peak)	% or mm			If MFL: depth in % of ref t or nominal t*. If other technology in mm from ref t or nominal t*. *if ref. t is not available
d (mean)	% or mm			
Surface location		- Internal - External - Mid wall - Not applicable	INT EXT MID N/A	Location of anomaly on the pipeline: internal, external, mid wall or Not Applicable
ERF				
Comments	-	-		-

Appendix 4: Detailed tool data sheet requirements

Provide where appropriate following data.

Tool identification:

Tool type and model number
Unique reference number and date

Tool specifications:

Total Length:
Weight:
Number of Modules:
Maximum inspection range:
Maximum inspection time:
Inspection duration constraints: length of pipeline that can be inspected in one run due to e.g. wear of components, data storage limits or battery life:
Wall thickness range for full specification at minimum speed:
Wall thickness range for full specification at maximum speed:
Speed control range (if available):
Number and type of primary sensors:
Number and type of secondary (e.g. ID/OD) sensors:
Number of calliper/geometry sensors (if applicable):
Nominal circumferential centre to centre distance of primary sensors:
Longitudinal sampling distance: (specify values for either time or distance based):
Feature Location Accuracy - Axial
Feature Location Accuracy - Circumferential
Optimum tool speed Range:
One- or bi-directional design:

MFL specific:

- Direction of magnetization (axial/circumferential, helical) and polarity of magnetic field
- Required minimal magnetic field strength H in kA/m at the inner surface of the pipe to meet the given POD and sizing accuracy
- Type of magnet: (brushes, flaps, wear plates, wear knobs, wheels, ...).

Maximum circumferential secondary sensor spacing (i.e. circumferential centre to centre distance).

UT specific:

- Dimensions of UT transducers and diameter of crystal
- Frequency of UT signal
- Stand-off distance of UT transducers
- Diameter of UT beam at the inner pipe surface and outer pipe surface. The diameter of sound beam is defined by the diameter where the sound beam pressure is 6dB below the pressure at the centre of the beam
- Maximum tolerable attenuation in liquid and metal to receive sufficient response.

UT crack detection (in addition to UT specific)

- Angle of UT signal in steel
- Direction of angle of UT signal relative to pipe axis (longitudinal direction is 0°, circumferential is 90°).

Phased Array UT (in addition to UT crack detection)

- Number and dimensions of active elements within each transducer
- Range of angles of UT signal that can be generated in pipe wall.

EMAT UT:

- Type, mode and frequency of ultrasonic signal generated.

Safety:

ATEX and/or IECEx certification:
Type of batteries:
Magnetization hazard alert:
Pressurized containers alert:

Operating Parameters:

Maximum Operating Pressure:
Minimum Operating Pressure:
Temperature range:
Speed range for full performance specification:
Acceptable (proven) pipeline media (e.g. H2S, saline water, chemicals):
Excluded pipeline media:

Pipeline Parameters:

Maximum nominal bore:
Minimal nominal bore:
Minimum pipeline bend radius:
Minimal internal diameter in bend:
Maximum diameter barred:
Maximum diameter unbarred:
Minimum full bore adjacent tees:
Minimum full bore adjacent tees - Centreline separation:
Gauge plate diameter:
Back to Back bend capability:

Valves

Minimum ball valve bore:
Minimum gate valve bore:
Maximum void length:
Maximum Local Restriction:

Launcher and Receiver trap details

Launch and receive requirements including handling for vertical and horizontal traps:
Please provide a drawing with dimensions or complete the table below.

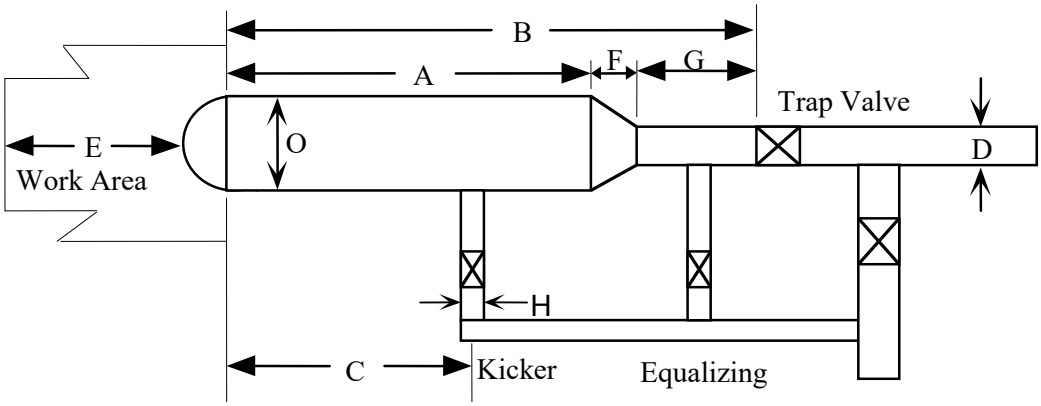

Trap Details		Launcher Dimensions (mm)	Receiver Dimensions (mm)
8.1.1 A	Closure to reducer		
B	Closure to trap valve		
C	Closure to bridle CL		
D	Pipeline internal diameter		
O	Overbore internal diameter		
E	Axial clearance		
F	Reducer length		
G	Reducer to valve		
H	Bridle		

Appendix 5: Tool technology performance specifications

Tool technology performance specifications shall define the ability of the ILI system to detect, locate, identify, and size pipeline features, components and anomalies. It is typically linked to the inspection technology applied in the tool e.g. High resolution MFL, standard MFL, Ultrasonic pitting detection tool, Ultrasonic wall thickness measuring tool etc.

The tool performance specifications as listed in this appendix shall be given. The influence of the operating or pipeline variables on the performance specifications shall be clearly indicated via e.g. correction factors or additional tables.

Essential variables that might influence the specifications and possibly require additional specifications are e.g. (but not limited to) listed below:

General specifications:

- Tool inspection technology
- Tool speed range
- Maximum axial sampling interval
- Maximum circumferential primary sensor spacing (i.e. circumferential centre to centre distance)
- Influence of line pipe manufacturing process (e.g. SAW, HFW, Seamless, etc)
- Influence of the location of the anomaly with respect to girth weld and/or seam weld; i.e. the ability to detect and size anomalies in and near weld and HAZ
- Influence of curvature of the pipeline, i.e. minimal bend radius.

MFL specific:

- Direction of magnetisation (axial/circumferential/ spiral) and polarity of magnetic field
- Required minimal magnetic field strength H in kA/m at the inner surface of the pipe to meet the given POD and sizing accuracy
- Maximum circumferential secondary sensor spacing (i.e. circumferential centre to centre distance).

UT specific:

- Dimensions of UT transducers and diameter of crystal
- Frequency of UT signal
- Stand-off distance of UT transducers
- Diameter of UT beam at the inner pipe surface and outer pipe surface. The diameter of sound beam to be defined by the dimension where the sound beam pressure is 6dB below the pressure in the centre of the beam.
- Maximum tolerable attenuation in liquid and metal to receive sufficient response.

UT crack detection (in addition to UT specific)

- Angle of UT signal in steel
- Direction of angle of UT signal relative to pipe axis (longitudinal direction is 0°, circumferential is 90°).

Phased Array UT (in addition to UT crack detection)

- Number and dimensions of active elements within each transducer
- Range of angles of UT signal that is generated in pipe wall.

EMAT UT:

- Type, mode and frequency of ultrasonic signal generated.

Table A5-1: Identification of features

Feature	Yes POI>90%	No POI<50%	May be 50%<=POI<=90%
Int./ext./mid wall discrimination			
Additional metal/material:			
- debris, magnetic			
- debris, non-magnetic			
- touching metal to metal			
- Other			
Anode			
Anomaly:			
- arc strike			
- artificial defect			
- blister			
- buckle global			
- buckle local			
- buckle propagation			
- corrosion			
- corrosion cluster			
- corrosion related to CRA			
- crack			
- crack cluster			
- dent kinked			
- dent plain			
- dent smooth			
- gouge			
- gouge cluster			
- grinding			
- girth weld crack			
- girth weld anomaly			
- longitudinal weld crack			
- longitudinal weld anomaly			
- mill anomaly - grinding			
- mill anomaly lamination			
- mill anomaly lap			

- mill anomaly non-metallic inclusion			
- mill anomaly cluster			
- ovality			
- ripple/wrinkle			
- SCC			
- spalling			
- spiral weld crack			
- spiral weld anomaly			
Eccentric pipeline casing			
Change in wall thickness			
CP connection/anode			
External support			
Ground anchor			
Off take			
Pipeline fixture			
Reference magnet			
Repair:			
- welded sleeve begin/end			
- composite sleeve begin/end			
- weld deposit begin/end			
- coating begin/end			
- crack arrestor begin/end			
Tee			
Valve			
Weld:			
- bend			
- diameter change			
- wall thickness change (pipe/pipe connection)			
- adjacent tapering			
- longitudinal weld			
- spiral weld			
- not identifiable seam			
- seamless			

Table A5-2: MFL detection and sizing accuracy for metal loss anomalies

	General metal-loss	Pitting	Axial grooving	Circumf. grooving	Pinhole	Axial slotting	Circumf. Slotting
Depth at POD=90%					N/A see below		
Depth sizing accuracy at 90% certainty							
Width sizing accuracy at 90% certainty							
Length sizing accuracy at 90% certainty							
Minimum pinhole diameter at POD=90% if depth=50%t						n.a.	
Minimum pinhole diameter at POD=90% if depth=20%t						n.a.	

Table A5-3: Metal loss detection and sizing accuracy for technologies other than MFL.

Detection but no sizing at POD=90%	Minimum diameter	
	Minimum depth	
Detection and sizing at POD=90%	Minimum diameter	
	Minimum depth	
Depth sizing accuracy at 90% certainty		
Length sizing accuracy at 90% certainty		
Width accuracy at 90% certainty		
Accuracy of wall thickness measurement at 90% certainty		

Table A5-3a: Detection and sizing of internal and external metal loss, regardless of technology. One table for each wall thickness must be filled out. Note: this table might be requested by the Client as an alternative for tables A5-2 and A5-3.

Wall Thickness xx-xx mm, POD/POI =90%							
Technique	Speed interval for stated detection limit and accuracy, m/s	Minimum defect size, Internal			Minimum defect size, External		
		Depth, mm	Length, mm	Width, mm	Depth, mm	Length, mm	Width, mm
Technique 1							
Technique 2							
Resulting tool performance							

Table A5-4: Detection and sizing accuracy for cracks or crack-like anomalies.

	Axial crack Pipe body/weld	Axial crack colony Pipe body	Circumferential crack Pipe body/weld	Spiral crack Pipe body/weld
Depth at POD=90% of crack with L=25 mm				
Minimum crack opening (mm)				
Depth sizing accuracy at 90% certainty				
Length sizing accuracy at 90% certainty				
Orientation limits (in degrees) for detectability				

Table A5-5: Detection and sizing accuracy for dents, ovalities, ripples/wrinkles, buckles

	Dent	Ovality
Height/Depth POD=90%		n.a.
Height/Depth sizing accuracy at 90% certainty		n.a.
Width sizing accuracy at 90% certainty		n.a.
Length sizing accuracy at 90% certainty		
Ovality at POD=90%	n.a.	

Table A5-6: Detection and sizing accuracy in 90˚ bends.

Minimal bend radius for detection of metal loss anomalies as given in Table A5-2, A5-3, A5-3a	OD*
Minimal bend radius for sizing accuracy for metal loss anomalies as given in Table A5-2, A5-3, A5-3a	OD*
Minimal bend radius for detection of crack or crack-like anomalies as given in Table A5-4	OD*
Minimal bend radius for sizing accuracy of crack or crack-like anomalies as given in Table A5-4	OD*

* If the bend radius in the pipeline is smaller than given in the table, then applicable specifications for that bend radius shall additionally be provided in the form of Tables A5-2, A5-3, A5-3a or A5-4.

Table A5-7: Location accuracy of features.

Accuracy of distance to upstream girth weld at 90% certainty	
Accuracy of distance from trap valve at 90% certainty	
Accuracy of circumferential position at 90% certainty	

Table A5-8: Mapping tool accuracy and horizontal and vertical accuracy of pipeline location as function of marker distance and certainty.

Accelerometer accuracy (micro g)		
Gyroscope accuracy (°/h)		
Horizontal accuracy (m) at 90% certainty	Vertical accuracy (m) at 90% certainty	Marker distance (m) (add rows to table if required)
0.5	0.5	
1.0	1.0	
2.0	2.0	

The values to be entered in this table depend on the accuracy of the individual company's technology and their way of operating their system as a whole. It is generally thought that the accuracy of an IMU varies over distance travelled, but the accuracy degrades over time, so it is important to consider the speed of the product in the pipe during the mapping inspection run. It is therefore important to specify, in consultation with the Contractor, the maximum and minimum flow rates during mapping surveys as well as spacing of AGMs. Very slow rates will reduce accuracy.

AGM's are used to correct the IMU's 'drift' over time (and hence distance). The closer the AGM spacing, the more accurate the final coordinates will be. Many 'standard' mapping runs use a 1 mile or 2 kilometre spacing, but for very or extremely high accuracy work 1 kilometre or even 500m spacing can be used.

Appendix 6: Typical example of Pipe tally*

Log distance [m]	GPS coordinates			Feature type and ID			Reference joint						Joint global geometry		Feature location on joint			Anomly sizing and further information									Reference table for performance	Comments
																		Deformations			Cracks and metal losses							
	latitude	longitude	altitude [m]	Feature type	Feature identification	Comment / Cluster ID	Girth weld Nr	Joint manufacturing type	Joint / component length [m]	Internal diameter [mm]	Nominal thickness [mm]	Measured/reference thickness [mm]	Ovality [%]	Bend Y/N	Abs. Dist. to upstream weld [m]	Clock position seam weld / anomaly	Surface location	Inward/outward	Depth / height [%.D or mm]	Size (length x width) [mm]	Mean depth [%.t or mm]	Max. depth [%.t or mm]	Length [mm]	Width [mm]	Anomaly dimension classification	ERF (metal losses)		
-1.136				Weld			10	Seamless	2.272	508	14	14.2																
0				Valve		Starting point: City									1.136													
1.136				Weld	Change wall thickness		20	Seamless	8.001	508	12	12.3	0.8														A3-5	
9.137				Weld			30	Long seam	12.001	508	12	12.1	0.4			8:04											A3-5	
21.138				Weld	Change wall thickness	Adjacent tapering	40	Spiral seam	12.001	508	8	8.4	0.2			4:42											A3-5	
23.139				Anomaly	Corrosion	Abnormal signal						8.4			2.001	10:32	Ext				18%	25%	126	42	GENE	Not calculated	A3-2	
30.143				Above ground marker	Marker	AGM 1									9.005													
33.141				Weld			50	Long seam	11.003	508	8	8.3	1.2			7:26											A3-5	
35.001				Anomaly	Dent, Kinked	Mechanical damage						8.3			12.860	0:22	Ext	Inw	2.7%	45x78	12%	21%	31	67	GENE	Not calculated	A3-2	
35.801				Anomaly	Gouge Cluster	GOCL-01						8.3			2.800	0:10	Ext				8%	15%	38	20	AXGR	Not calculated	A3-2	
44.144				Weld	Bend begin	Adjacent tapering	60	Long seam	2.004	508	12	12.2	0.9	Y		1:38												Installation S-449
44.999				Anomly	Corrosion Cluster	COCL-01						12.1		Y	0.855	8:36	Ext				32%	32%	42	25	PITT	Not calculated	A3-2	
46.148				Weld	Bend end	Adjacent tapering	70	Long seam	11.145	508	8	8.4	0.8			11:10												Installation S-449
47.151				Anomaly	Mill anomaly Cluster	MACL-01						8.4			1.003	8:53	Int				17%	36%	159	120	GENE	Not calculated	A3-2	
57.293				Weld			80	Long seam	10.999	508	8	8.5	0.9			7:12											A3-5	

* Columns can be added or deleted, e.g. depending on the ILI tool technology/technologies applied and/or on request of the Client.

Appendix 7: Typical example List of anomalies*

Log distance [m]	GPS coordinates			Feature type and ID			Reference joint						Joint global geometry		Feature location on joint			Anomaly sizing and further information									Reference table for performance	Comments
																		Deformations			Cracks and metal losses							
	latitude	longitude	altitude [m]	Feature type	Feature identification	Comment / Cluster ID	Girth weld Nr	Joint manufacturing type	Joint / component length [m]	Internal diameter [mm]	Nominal thickness [mm]	Measured/reference thickness [mm]	Ovality [%]	Bend Y/N	Abs. Dist. to upstream weld [m]	Clock position seam / anomaly	Surface location	Inward/outward	Depth / height [%.D or mm]	Size (length x width) [mm]	Mean depth [%.t or mm]	Max. depth [%.t or mm]	Length [mm]	Width [mm]	Anomaly dimension classification	ERF (metal losses)		
23.139				Anomaly	Corrosion	Abnormal signal						8.4			2.001	10:32	Ext				18%	25%	126	42	GENE	Not calculated	A3-2	
35.001				Anomaly	Dent, Kinked	Mechanical damage						8.3			12.860	0:22	Ext	Inw	2.7%	45x78	12%	21%	31	67	GENE	Not calculated	A3-2	
35.801				Anomaly	Gouge Cluster	GOCL-01						8.3			2.800	0:10	Ext				8%	15%	38	20	AXGR	Not calculated	A3-2	
44.999				Anomaly	Corrosion Cluster	COCL-01						12.1		Y	0.855	8:36	Ext				32%	32%	42	25	PITT	Not calculated	A3-2	
47.151				Anomaly	Mill anomaly Cluster	MACL-01						8.4			1.003	8:53	Int				17%	36%	159	120	GENE	Not calculated	A3-2	

* Columns can be added or deleted, e.g. depending on the ILI tool technology/technologies applied and/or on request of the Client.

Appendix 8: Typical example List of clusters*

Log distance [m]	GPS coordinates			Feature type and ID			Reference joint						Joint gobal geometry		Feature location on joint			Anomly sizing and further information									Reference table for performance	Comments
																		Deformations			Cracks and metal losses							
	latitude	longitude	altitude [m]	Feature type	Feature identification	Comment / Cluster ID	Girth weld Nr	Joint manufacturing type	Joint / component length [m]	Diameter [mm]	Nominal thickness [mm]	Measured/reference thickness [mm]	Ovality [%]	Bend Y/N	Abs. Dist. to upstream weld [m]	Clock position seam / anomaly	Surface location	Inward/Outward	Depth / height [%.D or mm]	Size (lenght x width) [mm]	Mean depth [%.t or mm]	Max. depth [%.t or mm]	Length [mm]	Width [mm]	Anomaly dimension classification	ERF (metal losses)		
35.801				Anomaly	Gouge Cluster	GOCL-01						8,3			2.8	0:10	Ext				8%	15%	38	20	AXGR	Not calculated	A3-2	
35.801					Gouge	GOCL-01.01						8.3			2.8	0:10	Ext				7%	12%	30	11	AXGR	Not calculated	A3-2	24° angle
35.811					Gouge	GOCL_01.02						8.3			2.8	0:14	Ext				5%	15%	28	12	AXGR	Not calculated	A3-2	35° angle
44.999				Anomly	Corrosion Cluster	COCL-01						12.1			0.855	8:36	Ext				32%	32%	42	25	PITT	Not calculated	A3-2	
44.999					Corrosion	COCL-01-01						12.1			0.855	8:36	Ext				24%	24%	12	12	PITT	Not calculated	A3-2	
45.015					Coprrosion	COCL-01-02						12.1			0.871	8:43	Ext				36%	36%	26	20	PITT	Not calculated	A3-2	
47.151				Anomaly	Mill anomaly Cluster	MACL-01						8.4			1.003	8:53	Int				17%	36%	159	120	GENE	Not calculated	A3-2	
47.151					Grinding	MACL-01-01						8.4			1.003	9:16	Int				14%	36%	64	70	GENE	Not calculated	A3-2	
47.221					Non- metallic inclusion	MACL-01-02						8.4			1.073	9:42	Int				12%	12%	10	12	PITT	Not calculated	A3-2	
47.232					Lamination	MACL-01-03						8.4			1.084	8:53	Mid				11%	24%	78	55	GENE	Not calculated	A3-2	

* Columns can be added or deleted, e.g. depending on the ILI tool technology/technologies applied and/or on request of the Client.

Appendix 9: Typical example Run comparison overview*

DATA RUN 1 (yyyy-mm-dd)															DATA RUN 2 (yyyy-mm-dd)															Difference				Comment
Log distance [m]	Latitude	Longitude	Altitude	Girth weld number	Joint / component length [m]	Wall thickness [mm]	Abs. dist. feature to upstream weld [m]	Feature	Clock position	Length [mm]	Width [mm]	Depth %	Int / Ext	...	Log distance [m]	Latitude	Longitude	Altitude	Girth weld number	Joint / component length [m]	Wall thickness [mm]	Abs. dist. feature to upstream weld [m]	Feature	Clock position	Length [mm]	Width [mm]	Depth %	Int / Ext	...	Δ Length [mm]	Δ Width [mm]	Δ Depth %	...	
10,250.250				7500	14.651	10.0		weld							10,250.000				7500	14.811	10.5		weld											Weld matched
10,256.630						10.0		corrosion	6:00	35	40	12	Int		10,257.000								corrosion	5:42	120	80	18	Int		85	40	6		Corrosion matched
															10,262.650								corrosion	4:12	15	10	5	Int						New corrosion
10,263.305						10.0		grinding	11:04	120	80	8	Ext		10,263.500								corrosion	11:00	140	90	12	Ext		20	10	4		Identification correction: grinding to corrosion
10,264.910				7510	15.100	10.0		weld							10,264.818				7510	15.080	10.5		weld											Weld matched
10,280.008				7520	15.000	10.0		weld							10,279.898				7520	3.110	10.5		weld											Weld matched
															10,283.000				7522	7.000	12.5		weld											New weld
															10,290.064				7524	4.905	10.5		weld											New weld
10,294.800				7530	14.805	10.0		weld							10,294.900				7530	14.805	10.5		weld											Weld matched

* Columns can be added or deleted, e.g. depending on the ILI tool technology/technologies applied and/or on request of the Client.

Ex. II - 11

Casing Mechanical Integrity Tests Utilizing Wireline Ultrasonic Imaging Logs

Jerry Rushing

Schlumberger Well Services
Signal Hill, CA 90806

Keywords

Ultrasonic, logs, logging, mechanical integrity, corrosion

ABSTRACT

The UltraSonic Imager Tool (USIT) is a wireline conveyed logging tool used for cement and casing evaluation. The tool and acquisition system utilize color imaging to present the measurements obtained from a rotating ultrasonic transducer, which gives 360° coverage at high resolution. For mechanical integrity tests, the most important measurements are casing internal radius and casing thickness. A presentation of the cement bonding to the casing is also derived from its measurement. Based on these measurements and the radial color maps generated from them, interpretations are made as to the metal loss and general condition of the casing.

Since the Bureau of Land Management started requesting that mechanical integrity tests be performed, geothermal operators have utilized the USI tool to help them evaluate and optimize their operations. Currently, one operator is using titanium casing in hopes of extending the well life. Also, types of latex based foam cements are being used to cement the newer casing strings. A study is currently ongoing through a consultant and Sandia Laboratories to examine the USI measurement and parameters in these new environments. Various examples illustrate typical log results of heavy internal scaling, corrosion, mechanical wear, and cement bonding. Examples will also show the changes in the wellbore environment over time and the effect of "clean out" jobs on internal scale. Recovered casing is shown to validate the log results.

Introduction

Geothermal operators are using the USI tool for various purposes in evaluation of their casing. The bulk of the evaluation is performed in geothermal injection wells. The Bureau of Land Management started in 1994 requesting that injection wells older than 3 years old have a mechanical integrity test of their casing performed every other year. Acceptable techniques were conventional packer pressure tests and/or wireline logging. The most common failure in the Holtville area is from shallow external corrosion. Because of this fact and the fact that the BLM criteria was based on remediating casing with 25% or greater metal loss, the conventional packer pressure tests did not make sense as they did not provide the information and accuracy needed to make these decisions.

The technique of utilizing the USI wireline technology has allowed for evaluations and interpretations to be made conveniently and cost effectively for a monitoring program of the casing condition. The accuracy and repeatability of the device gives confidence in the interpreted results. Approximately 30 geothermal wells are logged each year in the geothermal areas of Southern California. A discussion of the tool measurement and following field examples show how the tool is utilized in the ongoing monitoring of casing mechanical integrity.

Principle of Measurement

The ultrasonic transducer of the USI serves as both the transmitter and receiver of acoustic energy. A short pulse of acoustic energy is emitted and received as multiple echoes from the casing and cement. These multiple echoes create a resonance in the casing relative to its thickness. The presence of cement bonded to the casing is detected as dampening of the resonance.

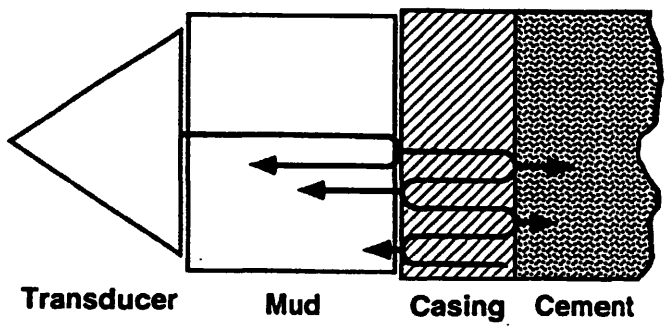

Figure 1. USI principle of measurement.

Table 1: Acoustic properties of materials.

Material	Density (kg.m-3)	Acoustic Velocity (m.s.-1)	Acoustic Impedance (MRayl)
Air (1-100 bar)	1.3 - 130	330	0.0004 - 0.04
Water	1000	1500	1.5
Drilling fluids	1000 - 2000	1300 - 1800	1.5 – 3.0
Cement slurries	1000 - 2000	1500 – 1800	1.8 – 3.0
Cement (Litefil)	1400	2200 - 2600	3.1 – 3.6
Cement (class G)	1900	2700 - 3700	5.0 – 7.0
Limestone	2700	5500	17
Steel	7800	5900	46

The transducer subs are appropriately sized to position the transducer one to two inches from the casing wall. The largest reflection of the acoustic energy pulse is from the internal casing interface, with a small fraction of the signal entering the casing. This smaller fraction resonates with energy lost back to the wellbore fluid at each reflection. (See Figure 1, previous page).

An analysis of the echoes yields four measurements:

1. Echo amplitude – an indicator of casing condition
2. Internal radius – calculated from the travel time of the echo.
3. Casing thickness – calculated from the resonance frequency.
4. Acoustic impedance – calculated from the dampening of the resonance.

The acoustic impedance is the basis for cement evaluation. In a homogeneous medium, the acoustic impedance Z is equal to the product of the density ρ and acoustic velocity v:$Z = \rho v$. Acoustic impedance is expressed in units of Mrayl. Table 1 lists acoustic properties of some materials encountered.

In order to accurately measure internal diameter and thickness of the casing, and to determine the cement bonding from impedance, the USI needs to measure the velocity and acoustic impedance of the wellbore fluid. Fluid density changes and temperature affects the fluid velocity and impedance measurements.

The tool has a separate operating mode to only measure the wellbore fluid properties (see Figure 2).

- In the fluid properties mode, the transducer faces inward towards a target plate. The plate properties are known and therefore the properties of the fluid between the transducer and the plate can be measured.
- In the logging position, the transducer faces outward towards the casing wall.

The fluid properties mode is used when logging while running into the well. These values obtained are then input at the appropriate depth as the tool is logged up in the logging mode.

Because this is a geothermal environment, the temperature limitations of 350° F have to be considered prior to logging. Simply injecting water can usually cool the injection wells. However, the scaling problem that exists is some areas are not that easily overcome. Internal scaling will create an environment in which accurate data cannot be obtained. Acid cleanouts and scale blasting techniques are employed to sufficiently clean these problem wells.

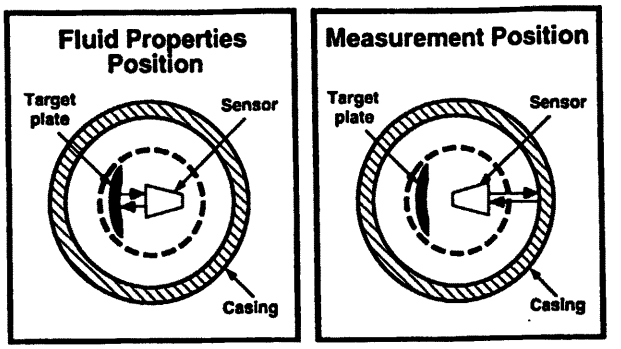

Figure 2. Rotating sub operating positions

Field Examples

Each of the following log examples emphasizes the point that color images and logs are critical to the interpretations as they are difficult to view and understand in black and white.

Field Example #1 Corrosion

This example clearly shows the value and effectiveness of the corrosion monitoring program utilizing the Ultrasonic Imager. Shown in Figures 3 and 4 are two of the three USIT logs, which were run on the same well. This well has been logged three times at two-year intervals as required by the BLM for the monitoring of casing integrity. The area of focus is the upper section of the 13 3/8" just below where the tool enters the well head master valve. The first log (not

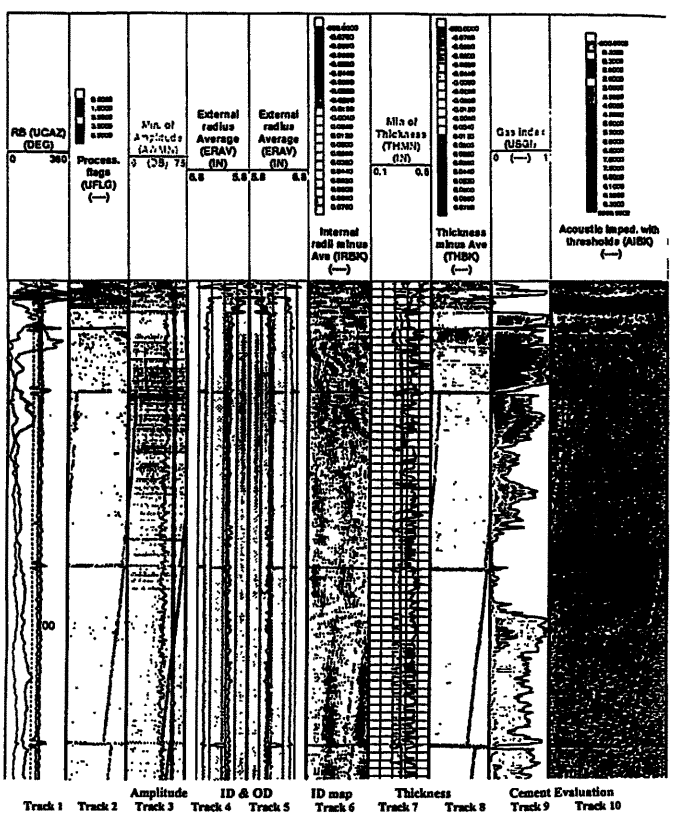

Figure 3. Log 1 with minor corrosion.

shown here) showed no evidence of corrosion. The second log, Figure 3, recorded two years later shows a small patch of external corrosion at a log-measured depth of 24'-29' with approximately 20% metal loss. The third log, Figure 4, recorded two years later shows the external corrosion is now extending downfrom 24' -55' with approximately 30% metal loss. The corrosion is most easily recognized in the thickness map display, which is Track 6 of the log display. It shows up as the darker areas in the black and white copy. The corrosion appears to be predominately on one side of the pipe. Figures 5 and 6 are photos of the casing that was excavated which confirms the log response and the severity of external corrosion.

Example #2 Cement Analysis

In the last few years, there has been the introduction of running titanium casing and latex based foam cements in a few wells. Although the USIT was not initially characterized for these materials, new parameters and processing have been developed to accurately analyze both the cement bond and the casing thickness. Figures 7 and 8 (overleaf) are two logs created from the same acquired raw data. Figure 7 is the original log using parameters for titanium casing and the micro-debonding processing to identify the foam and latex cement. The micro-debonding processing uses logic that says if it doesn't see "normal" cement or water filled space, it then compares each measurement with the one above, below, left and right of it. If the fluid type is water or drilling fluid, these measurements are consistent with each other. When the software

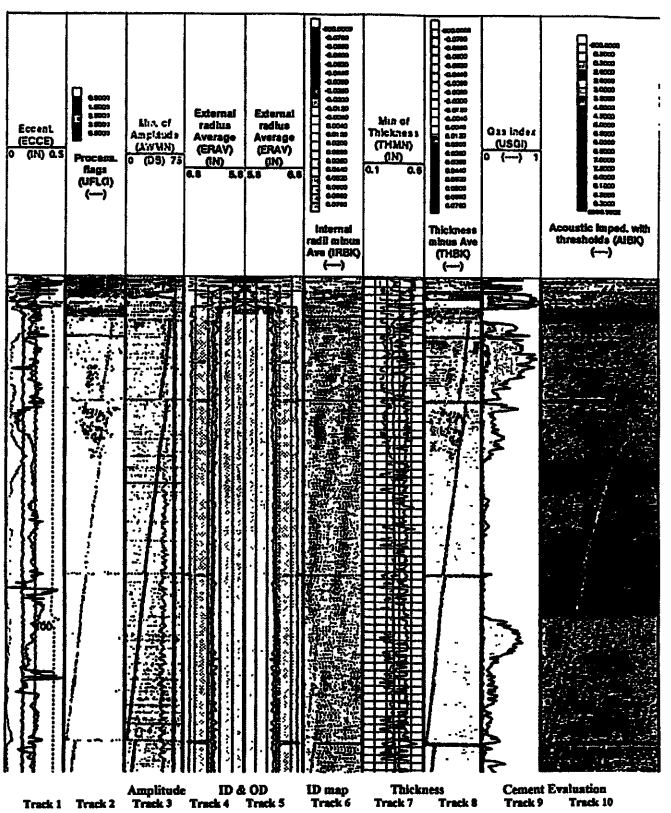

Figure 4. Log 2 with increased corrosion.

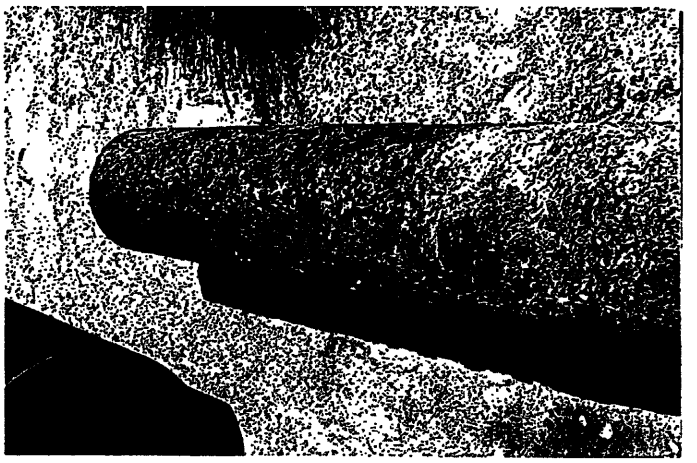

Figure 5. Excavated casing confirming external corrosion.

Figure 6. Close up of external corosion.

recognizes differences in the surrounding measurements it codes it as such. This should incorporate gas or mud contaminated cements, and the foam and latex cements. In Figure 7, the thickness measurement is accurate and the cement is recognized and interpreted with the new processing. Figure 8 is the same log data played with parameters for steel casing and standard USIT processing for the cement evaluation. The output for thickness is now too high and the area where we were seeing cement is now being classified as gas and many processing error flags are present in Track 2. A current review and study is underway with a consultant and Sandia Laboratories to analyze the parameters used by the USIT for various cement types in both steel and titanium.

Example #3 Drill Wear

Figures 9, 10 and 11 are part of an example which shows a case of drill wear. Figure 9 is of the USIT log taken from the well. The wear extends for almost 50'. The fact that the defect shows up as an increase in the ID in Track 6 and a loss of metal thickness in Track 8 indicates that it is internal wear of the pipe. The amplitude map is Track 3 also clearly shows the wear groove. Figure 10 is photo of the recovered casing. Figure 11 is a cross sectional plot taken from the depth of the wear with

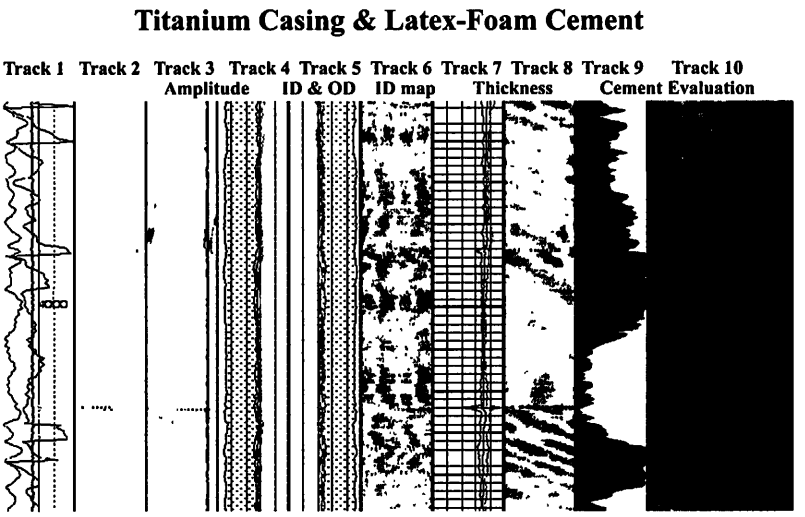

Figure 7. Correct settings for titanium and latex-foam cement.

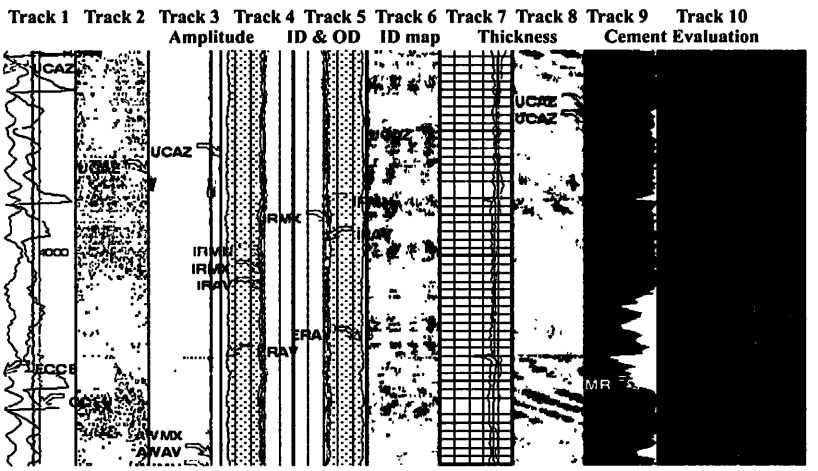

Figure 8. Log replayed with standard settings for steel & neat cement.

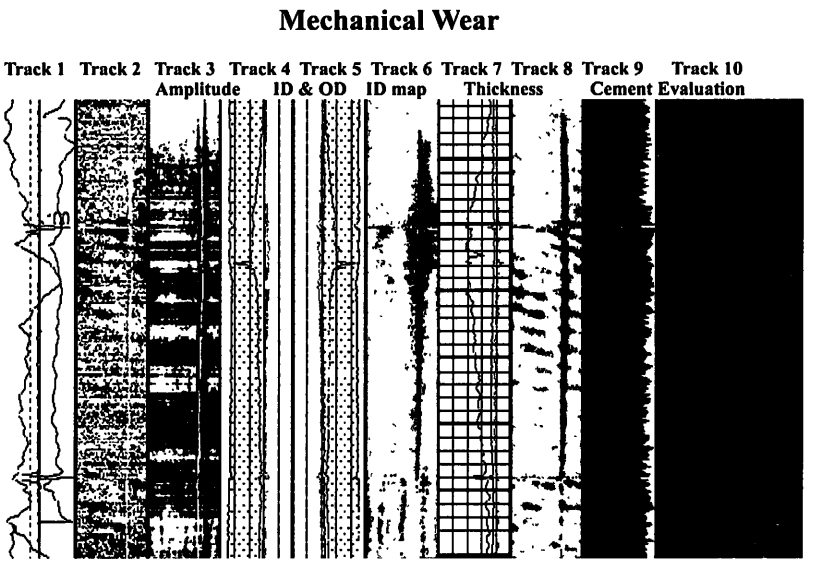

Figure 9. Mechanical wear evident.

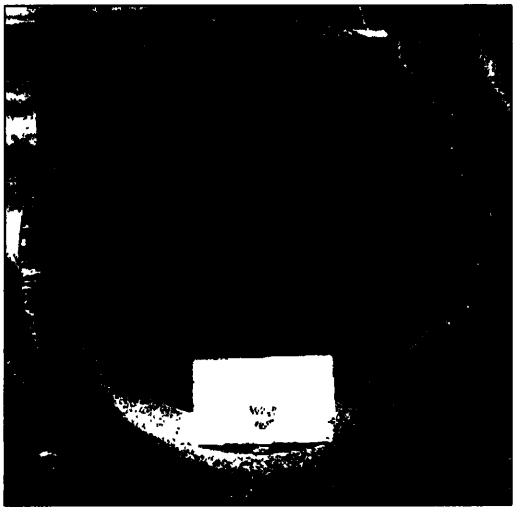

Figure 10. Excavated casing.

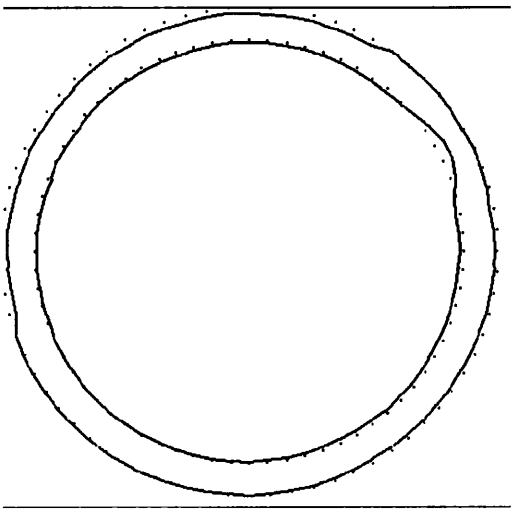

Figure 11. Plot from USIT log.

the USIT. Notice the casing OD is still round but the ID and thus the thickness change on the worn side. The thickness measurement of the USIT is accurate from 0.27" to 0.59". In this case, the excavated casing was actually thinner than the 0.27" USIT measurement that is represented on the log and the cross section plot.

Example #4 Internal Scaling

This is a log example of internal scaling and subsequent cleaning. Some areas in the geothermal areas in Southern California have a problem with a soft internal scale. This soft scale is identifiable by the dark impedance and by "grooves" in Track 3. These "grooves" are impressions made in the internal scale by the centralizing arms on the USI tool. Figures 12 and 13 are two logs recorded

from the same well at different times. Figure 12 shows the presence of a heavy build-up of soft internal scale. The grooves left by our centralizing arms are slightly visible in Track 3 of the log by the lighter vertical stripes against the darker scale. Figure 13 shows the casing condition after an acid clean-out was performed. For some reason, the clean-out was very effective down to 622'. This log comparison is an outstanding example of how the scale affects the log response. Prior to the clean-out, the minimum and maximum internal diameter measurements and the minimum and maximum thickness measurements are very erratic. This makes the data unreliable for a detailed and accurate interpretation. The average thickness measurement is still accurate. After the clean-out, the measurements above the depth of 622' are of very good quality. The interpretation of the data can be made accurately and confidently.

Conclusion

The USI tool is being used by the geothermal operators to monitor casing conditions as required by the Bureau of Land Management.

1. The USI has been proven to be effective in identifying external corrosion and been verified by excavations done by geothermal operators. External corrosion near the surface is the most prevalent in the Holtville area.
2. Current software processes are being qualified to provide accurate measurements in newer environments of titanium casing and latex based foam cements.
3. The accuracy of the internal radius and thickness measurement from the USI tool makes it a very effective tool for evaluating mechanical wear and to base wellbore decision on.
4. The USI has been useful in long term monitoring of corrosion, scale increase, and the effectiveness of clean out jobs. Heavy buildup of soft internal scale is problematic is certain areas and makes it very difficult to get a reliable interpretation of the casing and cement condition.
5. Color imaging and 360° coverage of the USI presentation are critical to the interpretation of casing condition.

Acknowledgments

Thanks to the geothermal operators their assistance in obtaining photos and information and for the permission to publish the logs and well information.

References

Hayman, A. J. Hutin, R. and Wright, P.V.: "High-Resolution Cementation and Corrosion Imaging by Ultrasound" Paper KK presented at the 1991 SPWLA Symposium, Midland, Texas, June 17-19.

Woods, Terry: "Ultrasonic Logging in Cased Boreholes for Corrosion Evaluation."

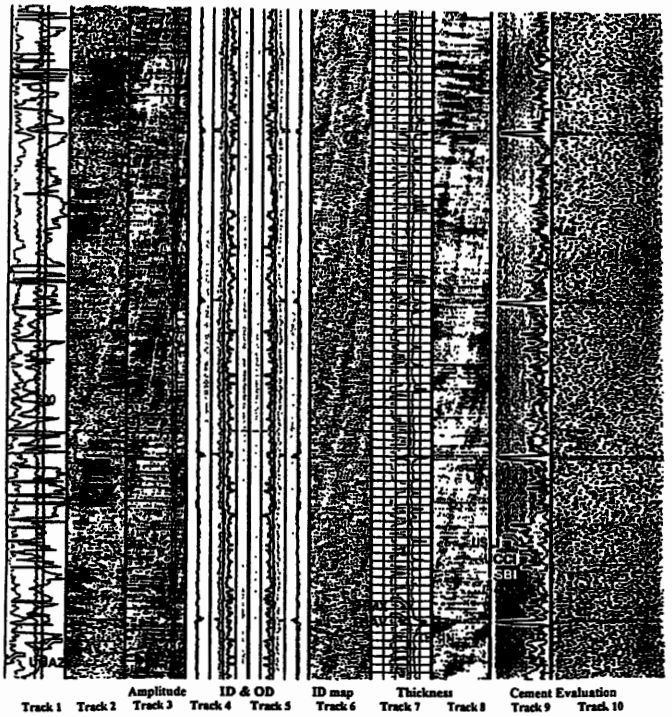

Figure 12. Log with heavy internal scale.

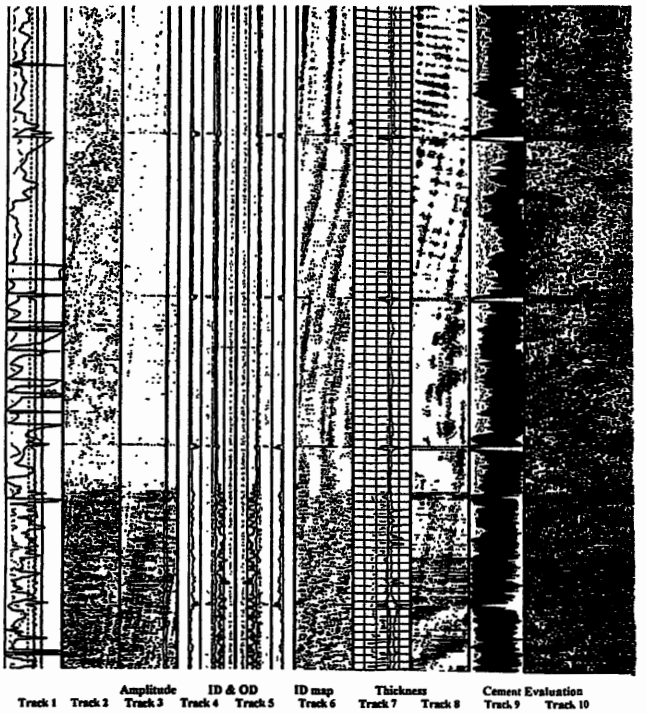

Figure 13. Same log as Figure 12 after acid clean out.

Ex. II - 12

IADC/SPE-180679-MS

Well Side-Track Optimization Using Electromagnetic and Ultrasonic Measurements Across Dual Strings for Well Integrity Assurance

Dhari M. Al-Saadi, Yousef A. Yateem, Shaikhah S. Omani, and Mohammad B. Al-Ajmi, Kuwait Oil Company; Mohamed AlMahdy and Yosra Abugreen, Schlumberger

Copyright 2016, IADC/SPE Asia Pacific Drilling Technology Conference

This paper was prepared for presentation at the IADC/SPE Asia Pacific Drilling Technology Conference held in Singapore, 22–24 August 2016.

This paper was selected for presentation by an IADC/SPE program committee following review of information contained in an abstract submitted by the author(s). Contents of the paper have not been reviewed by the International Association of Drilling Contractors or the Society of Petroleum Engineers and are subject to correction by the author(s). The material does not necessarily reflect any position of the International Association of Drilling Contractors or the Society of Petroleum Engineers, its officers, or members. Electronic reproduction, distribution, or storage of any part of this paper without the written consent of the International Association of Drilling Contractors or the Society of Petroleum Engineers is prohibited. Permission to reproduce in print is restricted to an abstract of not more than 300 words; illustrations may not be copied. The abstract must contain conspicuous acknowledgment of IADC/SPE copyright.

Abstract

This paper describes the application of a combined answer from Electromagnetic and Ultrasonic imaging measurements to assess the well integrity prior to well side track and Whip-Stock setting. This solution was applied in a very old well in Raudhatain field in Kuwait that was completed since 1959.

To optimize the cut depth for the side track across the single string, it was essential to identify an accurate depth of the external casing shoe, in addition to evaluation of both internal and external casings integrity and the cement bond quality for zonal isolation assurance. Data was acquired in September 2015 where the Electromagnetic log along with Ultrasonic images have been utilized with the advantage to provide answer in sections completed with dual strings for well integrity assessment.

The log results could detect the external casing shoe at the depth 7170-ft, presented good pipe integrity for the internal casing, and indicated good pipe condition with minor metal loss in the external casing across the double strings interval. The measured outer casing shoe was found 21-ft deeper than the theoretical from the old well sketch data, hence the depth of the well side track and Whip-Stock setting were optimized accordingly.

Failing to confirm the actual depth of the external casing shoe could have unintentionally led into drilling the side track across the double casing section resulting in undesirable workover operations and rig cost. Drilling a side track in dual pipe completed interval would also result-in damaging the outer casing and high remedial cost that cannot be predicted.

The operator ″Kuwait Oil Company″ has achieved their objective to side-track the well across single casing string without taking any risk and avoiding any implications through wireline technology and solutions.

INTRODUCTION

The Electromagnetic and Ultrasonic imaging measurements were acquired on Spetember 2015 in a very old well in Raudhatain field in Kuwait that was completed since 1959 and there was no enough information on accurate well completion sketch, cement or drilling mud data. The well is subject for cased hole side track drilling after evaluating the pipe and cement integrity.

The main objective was to assess the well integrity and optimize the cut depth prior to side track and Whip-Stock setting in the subject well by identifying an accurate depth of the external casing shoe of 9 5/8-in casing.

Electromagnatic measurements is planned to provide the pipe thickness across single and double casings interval that will confirm the outer casing shoe depth of 9 5/8-in and assess the casing integrity for both 7-in and 9 5/8-in pipes.

Ultrasonic measurement is planned in order to identify casing corrosion and loss of integrity, in addition to evaluate the cement to casing bond quality behind 7-in casing. Sonic measurement was also recorded to evaluate cement bond quality across the single casing section.

Following is a technical introduction on each acquisition technique implemented for this case study prior the discussion of results.

ELECTROMAGNATIC (EM) MEASUREMENT

"The EM casing inspection tool measures both internal and external corrosion. Its slim 2 1/8-in. diameter allows a deployment through tubing to quantitatively evaluate casing below the packer and in multiple casing strings or casing behind tubing by estimating the scale deposits and physical damage such as splits, holes, and partially collapsed sections.

This tool combines four types of EM measurements to assess tubular integrity:

- *EM metal thickness (ethick), an estimate of the average tubular metal thickness, using long-spacing low-frequency measurements for 2 7/8-in. through 13 3/8-in. casing outside diameter (OD)*
- *High-resolution image of total metal thickness, using low-frequency measurements on 18 radial arms for casings up to 9 5/8-in. OD*
- *High-resolution internal-defect image, using high-frequency measurements on 18 radial arms for casings up to 9 5/8-in. OD*
- *Casing inner diameter (ID), using closely spaced, high-frequency measurements"* (Taken from SPE 149069, Page 2, by Thilo Michael Brill et al).

EM inspection tool provides measurements to evaluate and identify corrosion in casing and tubing. The tool uses nondestructive induction methods to detect metal loss, pits, and holes, and it utilizes both Remote Field Eddy Current (RFEC) and High Frequency-Near Field Eddy Current (HF-NFEC) techniques. Refer to Figure 1.

The main applications and features of this techaniqe are:

1. Quantitative thickness evaluation of single casing
2. Qualitative thickness evaluation of multiple casing
3. Thickness image with discrimination in single casing
4. Pinpoint damage by depth and azimuth
5. Thru-tubing measurements
6. Operable in any down-hole fluid

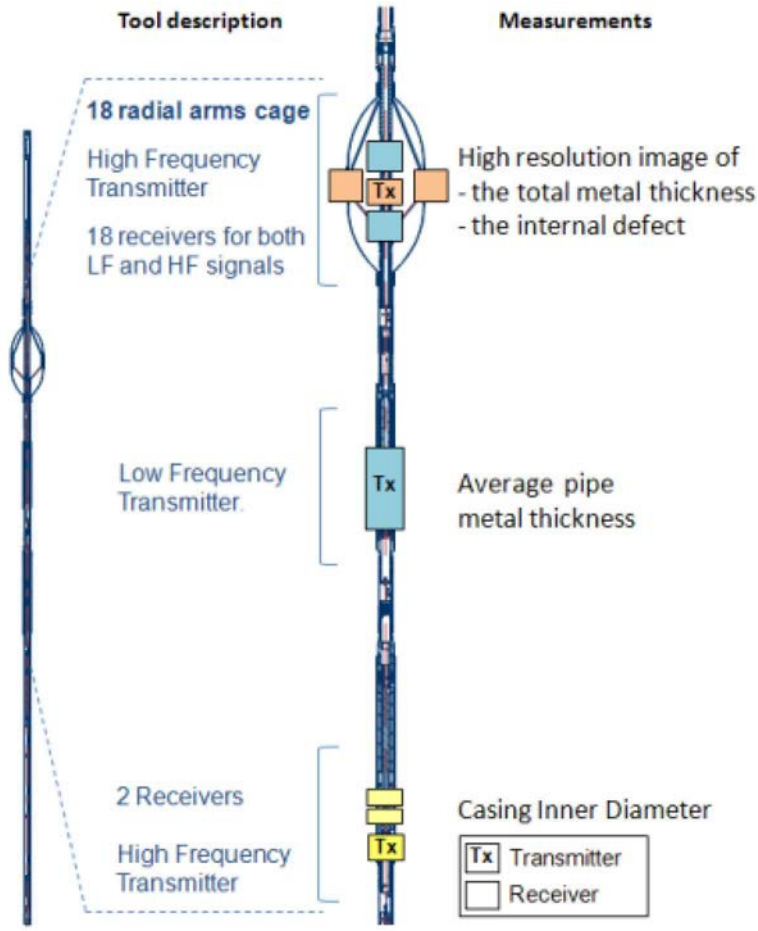

Figure 1—EM casing Inspection Tool (Taken from SPE 149069, Page 8, by Thilo Michael Brill et al.).

ULTRASONIC MEASUREMENT

The Ultrasonic imaging tool has a single rotating transducer that rotates at high speed (7+ rev/sec), and operates at high frequencies of between 200 and 700 kHz depending on casing thickness. This technique evaluates both casing integrity and cement bond around the entire circumference of the casing at a resolution of 1.2 inches across each depth. The ultrasonic signal processing will yield four measurements of the casing thickness, pipe internal radius, inner wall smoothness (from the initial echo amplitude and time), and the acoustic impedance of materials in the annulus (from the signal resonance decay). Refer to Figure 2.

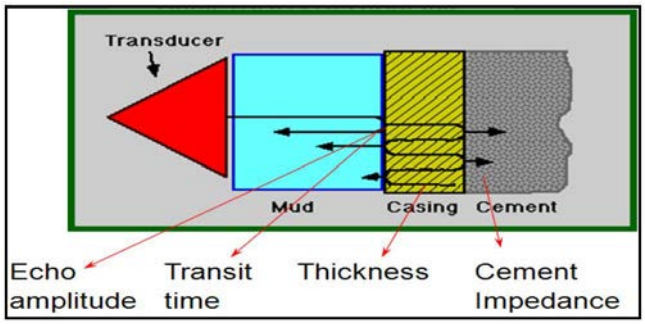

Figure 2—Ultrasonic tool principle of measurement

The acoustic impedance of any material is the product of its density by the sound velocity through it (Z=density x acoustic velocity). Z is usually expressed in MRayl (106 $kg.m^{-2}\cdot s^{-1}$). Empirical cutoffs or thresholds are used to determine solids, liquid, or gas. The default value of the threshold between liquid and solid is 2.6 MRayls, and between liquid and gas is 0.3 MRayls, as illustrated in Figure 3.

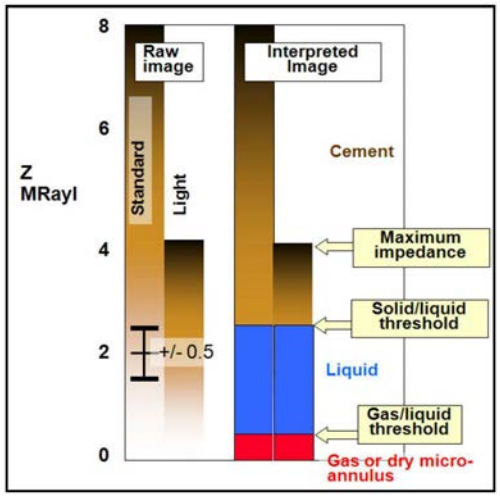

Figure 3—Empirical threshold of measured acoustic impedance to discriminate solid-liquid-gas

SONIC MEASUREMENT

The ″CBL″ or cement bond log has been around since the 1960's. It is based on the principle that a signal transmitted through a casing unsupported by cement will ring strongly and attenuate slowly while that same signal will ring weakly and attenuate quickly when transmitted through a casing well supported by cement.

This measurement is omni-directional, responding to the average of contributions from around the circumference of the casing, and is made at a relatively low frequency of ~ 20 kHz at a transmitter-to-receiver spacing of 1 to 3 feet. The measurement is normally accompanied by a variable density log (VDL) that is made at a longer transmitter-to-receiver spacing of 5 feet (Figure 4). This VDL may yield an indication of cement bond to the formation.

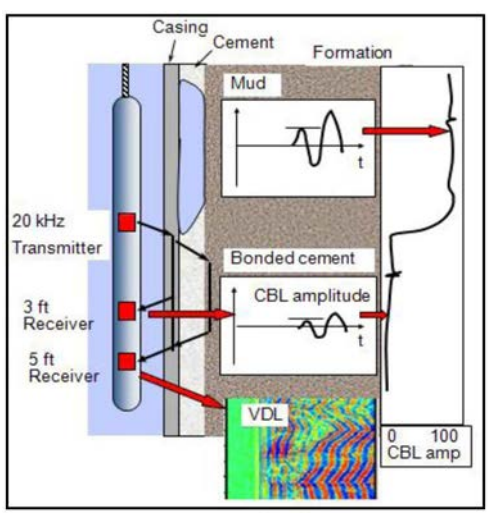

Figure 4—Sonic tool principle of operation

The CBL measurement has some strengths that have allowed it to stand the test of time. It is still used today for cement evaluation, either independently or in combination with an ultrasonic measurement. The measurement responds well to solidity, works well in most fluids, is unaffected by internal casing condition and provides an indication of cement-formation bond. Latest generation tools also include mapping features that can indicate broad channels.

The CBL is sensitive to fast formation, and extremely sensitive to both eccentering and liquid microannulus. The omni-directional nature of the measurement and the low frequency at which it is taken also render the CBL ineffective in identifying channels or contaminated cements.

CBL/VDL tool is not designed to work in dual completion environment, in which the received signal will be affected by all casing resonance, hence cannot be interpreted to provide cement bond evaluation across multiple strings.

CASE STUDY

The well was completed with 7-in, 26 ppf casing from surface till 8645.5 ft and the outer 9 5/8-in, 43.5 ppf that was reported to be set from 5729.3 ft to 7149 ft as per the old well sketch. To inspect the 9 5/-in casing condition with the 7-in casing in place, the Electromagnetic Imaging Tool was used in combination with the ultrasonic to achieve this objective. The logging interval extends from 6500 ft to 7500 ft.

The Electormagnatic data, using its deep reading Low Frequency Remote Field Eddy Current measurement (RFEC), is able to provide a reliable ″Total″ wall thickness indicator in inches. Note that the EMIT reads an average pipe thickness and has no azimuthal resolution. The double casing string (7-in and 9 5/8-in) extending above 7170 ft. The outer casing thickness is then computed by subtracting the inner casing pseudo thickness from the total thickness.

The percentages of average metal loss are computed based on the fraction of measured minimum and average thickness of each joint, with reference to nominal casing wall thickness.

ACQUISITION RESULTS

The log analysis was divided in two sections as following:

1. Single casing string (i.e. 7-in casing section extending from 7500 ft to 7170 ft). Log results show that casing is in overall good condition. The average metal loss calculated translates to less than 5% across this section suggesting no severe anomaly or casing damage.
   Overall it shows a reasonable consistency with the USIT findings from both inner radii and thickness readings.
2. Double casing string (i.e. 7-in × 9 5/8-in casing section extending from 7170 ft to 6500 ft). The total thickness of (7-in and 9 5/8-in) casings, as measured by EMIT, shows that both pipes are in good condition except for the possibility of some minor metal loss in the outer casing between depths 6527-6584 ft and 6851-6869.5 ft where thickness is reading slightly lower values than total nominal casing thickness.
   The percentages of metal loss are computed based on the fraction of measured minimum and average thickness of each joint, with reference to nominal casing wall thickness.

Refer to Figure 5 for the Statistical Analysis for Single & Double Casing Strings from EMIT.

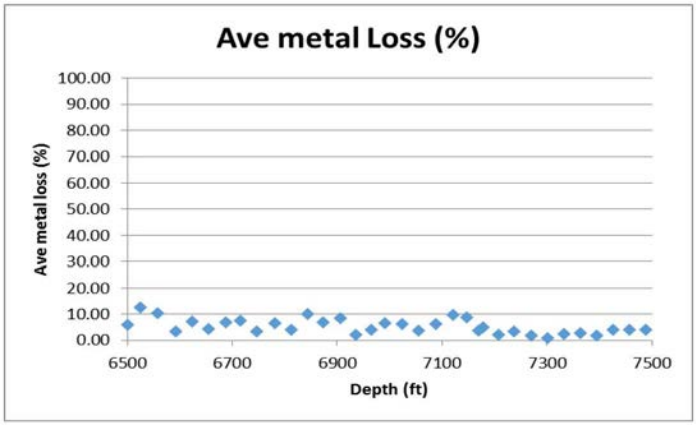

Figure 5—EMIT estimated average metal loss%

Electromagnatic measurements could detect the presence of 9.625-in casing shoe at 7170 ft that was also suggested from the Ultrasonic log. Comnined answer from sonic and ultrasonic indocated fair presence of cement in the annulus across the single and double strings. Refer to Figure 6.

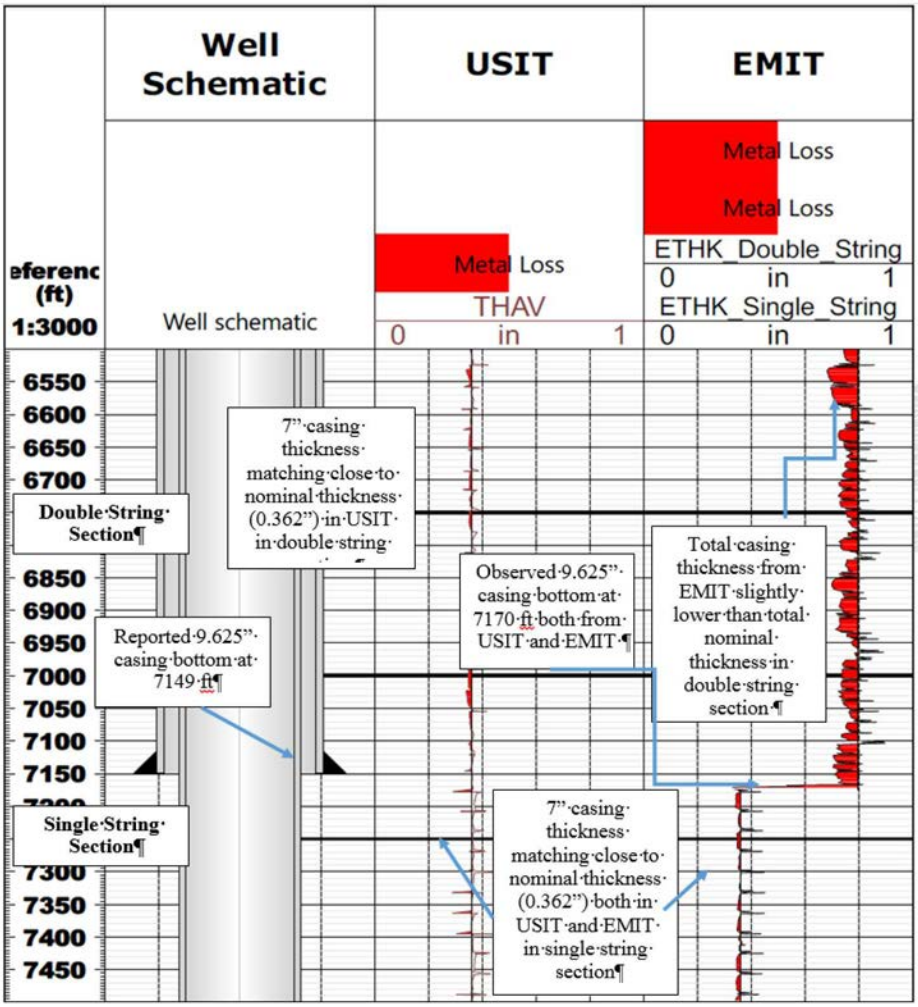

Figure 6—Casing evaluation summary

CONCLUSION

Ultrasonic and sonic measurements could present fair cement presence in the annulus behind the 7-in casing in single and double strings with good pipe integrity. Electromagnetic log analysis indicated both strings of 7-in and 9 5/8-in casings in good condition with no serious metal loss and detected the outer casing shoe depth at 7170 ft.

The measured outer casing shoe was found 21-ft deeper than the theoretical as reported in the old well sketch data, hence the depth of the well side track and Whip-Stock setting were optimized accordingly.

Failing to confirm the actual depth of the external casing shoe could have unintentionally led into drilling the side track across the double casing section resulting in undesirable workover operations and rig cost. Drilling a side track in dual pipe completed interval would also result-in damaging the outer casing and high remedial cost that cannot be predicted.

The operator ″Kuwait Oil Company″ has achieved their objective to side-track the well across single casing string without taking any risk and avoiding any implications through WL provided technology and solutions.

REFERENCES

Quantitative Corrosion Assessment with an EM Casing Inspection Tool, SPE 149069, 2011, Thilo Michael Brill, Jean-Luc Le Calvez, SPE, Cindy Demichel, Edward Nichols, and Fernando Zapata Bermudez, Schlumberger

Identification and Qualification of Shale Annular Barriers Using Wireline Logs During Plug and Abandonment Operations, SPE/IADC 119321, 2009, Thilo Michael Brill, Jean-Luc Le Calvez, SPE, Cindy Demichel, Edward Nichols, and Fernando Zapata Bermudez, Schlumberger

Improved critical work over decisions through the integration of flexural attenuation and Pseudo annulus thickness measurements, INTERGAS-VI, 2011, Mohamed Radi, Mohamed Farouk, Helmy Fahmy, Radi El-Nasher, and Maged Morris, Gupco, Yosra Abugren, Enas Thabet, Mohamed Hamdy, and Maria Vazquez, Schlumberger

Ex. II - 13

SPE 156052

An Integrated Approach to Well Integrity Evaluation via Reliability Assessment of Well Integrity Tools and Methods: Results from Dukhan Field, Qatar

Sanjay K Singh, Herry Subekti, Mona Al-Asmakh, Layth Al-Samarraie, Qatar Petroleum

Copyright 2012, Society of Petroleum Engineers

This paper was prepared for presentation at the SPE International Production and Operations Conference and Exhibition held in Doha Qatar, 14–16 May 2012.

This paper was selected for presentation by an SPE program committee following review of information contained in an abstract submitted by the author(s). Contents of the paper have not been reviewed by the Society of Petroleum Engineers and are subject to correction by the author(s). The material does not necessarily reflect any position of the Society of Petroleum Engineers, its officers, or members. Electronic reproduction, distribution, or storage of any part of this paper without the written consent of the Society of Petroleum Engineers is prohibited. Permission to reproduce in print is restricted to an abstract of not more than 300 words; illustrations may not be copied. The abstract must contain conspicuous acknowledgment of SPE copyright.

Abstract

Qatar Petroleum's super-giant Dukhan field located onshore Qatar has a mature inventory of hundreds of wells. Managing integrity of such mature well inventory to avoid unplanned downtime has been no less crucial than any other activity to maximizing production and injection. This involves costly wellwork decisions for integrity control and repair, which rely heavily on data obtained from a well integrity monitoring program. Well integrity monitoring program ranges from using basic methods to state-of-the-art downhole monitoring tools. Their applications are almost always associated with limitations that impose uncertainty in well integrity evaluation. This paper presents an integrated approach Qatar Petroleum used to address this issue. This approach consisted of performing reliability assessment of the entire array of available tools and methods against given well conditions with a matrix of assessment criteria. This matrix enabled selection of a fit-for-purpose set of tools and methods with clear understanding of their strengths and limitations. Techniques of correlation, bracketing and elimination were then applied to analyze the outputs obtained from using the selected set of tools and methods. The approach allowed detecting well integrity problems and determining their severity with minimal uncertainty. The paper focuses on intricacies of the approach, and how its implementation results in a sound well integrity evaluation. It also presents field examples that demonstrate efficacy of the approach in supporting costly wellwork decisions for restoring well integrity. Successfully restoring the well integrity unlocked revenue potential, made quick payout of the wellwork costs and extended the field life.

Introduction

Dukhan field is located onshore Qatar approximately 80 km to west of Doha, the capital of the state of Qatar. The field has a mature inventory of a large number of wells. Qatar Petroleum (QP) manages integrity of such wells via its established well integrity monitoring and remedial wellwork programs. Data obtained from the monitoring program are used for integrity evaluation that in turn leads to deciding the requirement and type of wellwork for integrity control and repair. Majority of the wellwork decisions are cost-intensive and a sound integrity evaluation is key to their success.

One of the most popular definitions of well integrity, as provided in NORSOK D-010, is "application of technical, operational and organizational solutions to reduce risk of uncontrolled release of formation fluids throughout the life cycle of a well". Application of the solutions mentioned in this definition basically aim at preventing, detecting and repairing integrity problems. QP's well integrity monitoring program focuses on preventing and detecting a wide range of potential integrity problems that can occur in surface and downhole components of a well. An array of techniques involving basic methods to state-of-the-art downhole tools is used. Each of the methods and tools has its own strengths as well as limitations. Limitations of methods and tools have the potential of imposing uncertainty in well integrity evaluation. An integrated approach has been developed to address this issue. Subsequent sections of this paper discuss intricacies of this approach and present some field examples to show how implementation of the approach resulted in sound well integrity evaluation.

The Approach

The approach consists of the following steps:

1. Setting reliability matrices for methods and tools
2. Prognosticating the range of possible well integrity problems
3. Using the reliability matrices for selection of a fit-for-purpose set of tools and methods

4. Evaluating outputs with correlation, elimination and bracketing techniques
5. Identifying well integrity problems

1. Setting reliability matrices for methods and tools

Reliability matrices have been set up separately for surface methods and downhole tools in investigating various well integrity elements. Surface methods comprise wellhead pressure monitoring, fluid sampling & pressure testing. Downhole tools include a range of logging tools used for wellbore and behind-casing inspection. Well integrity elements range from wellhead or near surface to downhole and behind casing elements. Table-1 and 2 present reliability matrices summarizing reliability of each of the methods and tools as 'good', 'fair' or 'poor' in investigating the well integrity elements. An elaboration on how the reliabilities were defined is given below.

Surface Methods

Wellhead Pressure Monitoring & Produced Fluid Sampling

Fluctuations in wellhead pressure coupled with abrupt change in well rate may be indicative of downhole casing and tubing/ packer leak. Continuous analysis of wellhead pressure data to identify such anomaly helps in early detection of downhole leaks and taking a suitable action to prevent charging of shallow aquifers with either hydrocarbons or injected water.

Wellhead produced fluid sampling with well test data forms an important input to the above analysis. For example, if the water-cut and GOR haven't changed and there is sudden drop or significant fluctuation in wellhead pressure, it could be a strong indication of downhole leak that need confirmation by running appropriate downhole tools.

However, it is recognized that in several cases, downhole casing & tubing/ packer leaks may not present any noticeable anomaly in wellhead pressure and fluid. Hence reliability of wellhead pressure monitoring & fluid sampling in determining downhole leak is considered '**fair to poor'**.

Annuli Pressure Monitoring & Effluent Sampling

Procedures for drilling and completing wells are designed such that no pressure should be seen on any one of the annuli during the well's operation phase. The exceptions are wells on gaslift, where pressure in annulus between tubing and production casing is due to lift gas pressure or the wells without packer. Thermal expansion of tubing, casing or packer fluid when the well is first placed on production may also cause pressures to build up in one or more of the annuli; however these pressures should not recur once they are bled off and the well is in normal production mode.

Pressure in cemented annuli between two casings develops due to one or more of the following factors:

- Cement channelling
- Incomplete cement circulation
- Casing leak(s)
- Leak through wellhead seal(s)

Pressure in annulus between tubing and production/ injection casing develops due to one or more of the following factors:

- Production/ injection casing leak
- Tubing or packer leak(s)
- Tubing bonnet and hanger pack-off leak

There are multiple factors as mentioned above that can cause annuli pressures. Hence reliability of annuli pressure monitoring and effluent sampling is considered **'fair'** in determining presence of either or a combination of such factors, but '**poor'** in finding which one of these factors is the unique cause.

Pressure Testing of Wellhead Seals

Pressure testing of wellhead seals is a direct and conclusive method to ascertain wellhead seals integrity with '**good**' reliability.

Pressure Testing of Tubing & Production/ Injection Casing

Successful pressure testing of tubing (with plug installed at bottom of the tubing string and dummies in gas lift mandrels, if any) & production/ injection casing establishes integrity of wellhead seals, production/ injection casing and packer. If during successful pressure testing of tubing string, no pressure is seen on tubing – casing annulus, integrity of tubing string is also established. However an unsuccessful pressure test could be due to integrity failure of any or a combination of these components or a leak through the tubing plug or gas lift mandrel. Hence reliability of pressure testing in determining casing, tubing or packer integrity is considered **'fair'**.

Annuli Pressure Testing

Annuli pressure testing consists of:

- Testing the annuli between casings in a recommended sequence
- Analyzing results to diagnose the cause of annuli leak
- Identifying the need for remedial cement top-up or securing well for further action such as workover or abandonment.

Annuli pressure test are performed after pressure testing of wellhead seals has ruled out wellhead communication. An unsuccessful annuli pressure test without having performed pressure testing of wellhead seals could be due to either wellhead communication or cemented annulus or both. Hence reliability of annuli pressure testing in determining wellhead seal integrity is considered **'fair'.**

Annuli pressure test is effective in determining whether a cemented annulus isolates downhole pressure zones (hydrocarbon or aquifer) from surface. However, it is inconclusive in detecting cement channels or voids that might be present in the annulus causing isolation failure between two zones. This is because presence of a cement bridge could mask such channels or voids from surface. Hence reliability of annuli pressure testing in determining wellhead seal integrity is considered **'fair to poor'**.

Surface Casing & Casing Head Inspection

Near surface external corrosion (i.e. corrosion on casing head housing and portion of surface casing just below ground) is caused by cyclic or consistent ingress of oxygenated surface water or moisture in the annular space between the conductor pipe and surface casing. The retained oxygenated water in the annulus leaches out chemical salts from the cement and at elevated well operating temperatures (around 120 deg F) creates low resistance electrolyte resulting in an extremely corrosive environment. Additionally, the cement micro annulus that emanates behind the surface casing tends to retain small amount of water which also cause slow but steady development of near-surface corrosion on the surface casing.

Downhole Tools

Temperature & Flowmeter Logs

Static temperature profiling is the primary means to finding downhole casing leaks and static temperature surveys usually are required first after a well's initial completion or re-completion to generate a base temperature profile. Thereafter, it is needed at pre-determined intervals and results are compared with base temperature profile to detect any anomaly.

Casing leak & resultant cross-flow via wellbore is detected easily and with **'good'** reliability from the anomalies detected on the static temperature profile. Flowmeter surveys are normally required to confirm a downhole casing leak (detected from temperature survey or otherwise) and quantify the cross-flow rate. It should be conducted based on a specific requirement (such as indicated by static temperature anomaly) and after considering downhole completion to decide whether or not it will provide any useful result.

Temperature anomalies could also be due to fluid movement through cement channels behind casing and their analysis should be done in correlation with other information such as quality of cementation, stratigraphic and petrophysical information. Some cases of fluid flow through cement channels behind casing may not be convincingly detected by temperature anomalies particularly when the cross-sectional area of the channel compared to the wellbore is very small. In such cases, running a noise or ultrasonic log can supplement temperature anomalies to detect behind-casing flow. Hence, reliability of temperature logs in detecting cross-flow behind production/ injection casing is just about **'fair'**.

Multi-fingered Calipers

Multi-fingered callipers are well-established tools to evaluate production / injection casing internal corrosion with **'good'** reliability. They provide no data about external corrosion though and are affected by scale build-up on inner wall of the casing.

Ultrasonic Pipe Imaging Tool

Ultrasonic pipe imaging tools yield excellent pipe thickness information with superior azimuthal resolution in a single casing. Pipe thickness coupled with internal radii measurements makes reliability of this tool '**fair**' in determining internal and external corrosion of Production/ Injection casing. However, they are unable to operate in gas wells, through tight restrictions and their measurements can be disrupted by pipe roughness and excessive corrosion.

Electromagnetic Pipe Imaging Tool™

Electromagnetic pipe imaging tools measure gross metal thickness around it and hence are able to examine both internal & external corrosion in multiple casing strings. Correlating their measurements with ultrasonic measurement of single casing thickness helps determine whether outer casings are corroded. These tools provide electromagnetic flux leakage based measurements and therefore are good at measuring sudden thickness changes rather than constant or gradual variation of thickness over a whole section of pipe. It can operate in any fluid and has excellent vertical resolution. Azimuthal resolution is not as high as that of ultrasonic measurements and small holes can go unnoticed. Hence reliability of electromagnetic imaging tools in determining corrosion of multiple casing strings is considered **'fair'**.

Downhole Camera

Downhole camera requires the wellbore to be filled with clean fluid or gas for detecting internal corrosion and hence, its reliability is considered **'fair'**.

Cement Bond Log

Cement Bong Log (CBL) with Variable Density Log (VDL) gives an overall idea about cement to casing & cement to formation bond. Lack of azimuthal coverage renders reliability of this tool to be **'fair'** in determining production/ injection casing cement isolation.

Ultrasonic Cement Imaging Tool

Ultrasonic cement imaging tool provides azimuthal image of cement around the casing and a detailed map of solid cement, liquid & gas filled annuli/ voids and micro-debonded cement. Its reliability in determining production/ injection casing cement isolation is considered **'good'**.

2. Prognosticating the range of possible well integrity problems

Review of well construction and operation history and previous experiences enables predicting possible well integrity problems. For example, an incomplete cement circulation during cementing could point towards such problems as the presence of cement micro-annuli, casing external corrosion, casing leak and zonal cross-flow. A previously recorded onset of corrosion in a downhole tubular with no mitigation undertaken over a time lapse could point towards the integrity failure of the downhole tubular. In addition, if experience in some other well(s) recorded failure of wellhead similar of similar material & type, then wellhead seal failure in the well being evaluated is also likely.

3. Using reliability matrices

Relating the prognosticated range of integrity problems to reliability matrices enables selecting a fit-for-purpose set of methods & tools for integrity evaluation. The matrices provide a technical basis for making such selection reasonable and avoiding running a tool which could add to the cost with little value. For example, temperature log's reliability in detecting zonal cross-flow via wellbore is **'good'**. Hence, if static temperature profile establishes such cross-flow in a well, running downhole camera will add little value to enhancing the reliability of this finding. Flowmeter however can be considered to determine the cross-flow rate, if required.

4. Evaluating outputs with correlation, elimination and bracketing techniques

Correlation, bracketing and elimination are mathematical techniques that are implicitly applied during qualitative assessment of outputs received from the applied set of methods and tools for well integrity evaluation.

Correlation means comparing and analyzing well integrity data obtained from more than one method or tool to determine similar, dissimilar or overlapping problem areas they relate to. Elimination is finding the data that relate to an overlapping problem area. Bracketing implies extracting dissimilar or non-overlapping problem areas and determining their uncertainty-band. Application of these techniques enables focused assessment of problem areas while making best use of outputs from the applied methods and tools.

5. Identifying well integrity problems

Systematic application of the above steps enables identifying well integrity problem(s) with reasonable confidence. This helps determine type of repair wellwork required to resolve the problem. Prioritization of repair wellwork is done based on relative severity of integrity problem(s). QP uses a comprehensive technique to assess problem severity and consequential impact. Discussion on such technique is beyond the scope of this paper, and will be presented in a separate paper in future.

Field Examples

Typical well construction design in Dukhan field consists of 13-3/8" surface casing, 9-5/8" intermediate casing & 7" production casing. All casing strings are cemented up to surface through either single or dual stage primary cementing jobs. Examples below show how the approach discussed above was applied in the field for well integrity evaluation.

Well No. 1 (Oil Producer)

Prognosticating the range of possible well integrity problems

Primary cementation of 13-3/8" was incomplete because of losses into highly porous shallow aquifer. The 7" and 9-5/8" casings were cemented successfully. The 13-3/8" and 9-5/8" casings in the well covered the porous shallow aquifer, which is also corrosive. The well was completed as a perforated oil producer and continued oil production for a period of over 20 years. Towards the end of this period, the well started showing a sustained annulus pressure in 7" x 9-5/8" casing annulus.

Based on the above information, the following possible well integrity problems were prognosticated initially for evaluation:

- Loss of wellhead seal integrity
- Zonal cross-flow via wellbore or behind 7" production casing
- Loss of cement integrity in 7" x 9-5/8" casing annulus
- External corrosion of casings due to possible contact with corrosive aquifers

Using the reliability matrices for selection of a fit-for-purpose set of tools and methods

For determining wellhead seal integrity, the method of pressure testing of wellhead seals has **'good'** reliability based on reliability matrix and hence, was used. It showed wellhead communication. Rigless attempts to eliminate wellhead communication were unsuccessful.

For investigating the possibility of zonal cross-flow via wellbore, temperature log has **'good'** reliability based on reliability matrix. It also has **'fair'** reliability in investigating zonal cross-flow behind 7" production casing. Results of static temperature log run in the well ruled out the possibility of zonal cross-flow via wellbore. It however presented some anomaly across 1600-1800 ft (Figure-1), which could not be conclusively interpreted because of unavailability of base-line static temperature profile.

For checking cement integrity in 7” x 9-5/8” casing annulus, the method of annuli pressure testing has ‘**fair/poor’** reliability. 7” casing could not be pressure tested due to packerless completion. Pressure testing 7” x 9-5/8” casing annulus without successful pressure testing of 7” casing integrity has the risk of creating wellbore – annulus communication. Hence, annuli pressure testing was not performed.

Failure of rigless attempts to eliminate wellhead communication as well as presence of anomaly on temperature log necessitated to workover the well. It was decided to investigate casing and cement integrity during the workover.

Ultrasonic pipe imaging tool and electromagnetic pipe imaging tool have **‘fair’** reliability for investigating production casing corrosion and outer casings corrosion respectively. It was decided to run both tools in the well after pulling out completion string during the workover. Moreover, it was decided to run ultrasonic cement imaging tool for investigating cement integrity in 7” x 9-5/8” casing annulus since this tool has **‘good’** reliability for such purpose.

Outputs were evaluated with correlation, elimination and bracketing techniques to reach conclusions.

Evaluating outputs with correlation, elimination and bracketing techniques

Output of electromagnetic imaging tool showed a section of anomaly across 210 – 250 ft (Figure-2). The gross thickness measured by this tool was correlated with the thickness measured by ultrasonic imaging tool over this section. Output of ultrasonic imaging tool showed 7” casing thickness around 0.3” with no significant metal loss. Output of electromagnetic imaging tool showed remaining gross thickness of 3 casings (7”, 9-5/8” & 13-3/8”) around 0.7” against the original of around 1.0”.

Similar or overlapping data between the two measurements was the thickness of 7” casing i.e. 0.3”. Eliminating this thickness from the gross thickness bracketed the remaining thickness of outer 2 casings (9-5/8” and 13-3/8”) at around 0.4” over the section of anomaly. Uncertainty-band of this bracket ranged from a remaining thickness 0.2” of each casing to 0.4” of either casing.

This uncertainty-band was further analyzed and resolved as following:

- 7” casing didn’t show any sign of internal corrosion. Hence, the entire metal loss could be attributed to external corrosion caused by corrosive aquifer.
- Corrosive aquifer acts first on outermost 13-3/8” casing. Hence, external corrosion on 9-5/8” casing cannot start unless 13-3/8” remaining thickness reduces to zero. This implies that since the remaining thickness of outer 2 casings (0.4”) is more than the thickness of 13-3/8” casing (0.35”), 9-5/8” casing didn’t suffer from metal loss.

Identifying well integrity problems

Application of the above techniques established the integrity of 7” & 9-5/8” casings across corrosive aquifer and confirmed that the entire metal loss took place on 13-3/8” casing. Anomaly seen on static temperature log across 1600 – 1800 ft (Figure 1) was examined with output of ultrasonic pipe & cement imaging tools and no casing and cement integrity problem was detected (Figure-3).This helped salvaging and completing the well for production.

Well No. 2 (Water Injector)

Prognosticating the range of possible well integrity problems

9-5/8” casing was cemented in 2 stages with incomplete cementation in 1st stage because of downhole problem. 7” casing was cemented in 2 stages with complete & successful cementation in both stages. Incompletely cemented section of 9-5/8” casing in the well covered a corrosive aquifer.

Based on the above information, the following possible well integrity problems were prognosticated initially for evaluation:

- Loss of cement integrity in 9-5/8” x 13-3/8” casing annulus
- External corrosion of casings due to possible contact with corrosive aquifer

Using the reliability matrices for selection of a fit-for-purpose set of tools and methods

For checking cement integrity in 9-5/8” x 13-3/8” casing annulus, the method of annuli pressure testing has **‘fair/poor’** reliability based on reliability matrix. Hence, even though pressure testing of this annulus was successful, it didn’t conclusively establish the cement integrity.

Workover of the well for reservoir management reason was used as an opportunity to investigate external corrosion of casings and cement integrity in 7” x 9-5/8” casing annulus. Ultrasonic pipe imaging tool and electromagnetic pipe imaging tool have **‘fair’** reliability for investigating injection casing corrosion and outer casings corrosion respectively. It was decided to run both tools in the well after pulling out completion string during the workover. Moreover, it was decided to run ultrasonic cement imaging tool for investigating cement integrity since this tool has **‘good’** reliability for such purpose.

Evaluating outputs with correlation, elimination and bracketing techniques

Output of electromagnetic imaging tool showed a section of anomaly across 3510 – 3530 ft (Figure-4). The gross thickness measured by this tool was correlated with the thickness measured by ultrasonic imaging tool over this section.

Output of ultrasonic imaging tool showed minor external corrosion in 7” casing with remaining thickness of 0.25” against original thickness of 0.3”. Output of electromagnetic imaging tool showed remaining gross thickness of 3 casings (7”, 9-5/8” & 13-3/8”) around 0.25” against the original of around 1.0”.

Similar or overlapping data between the two measurements was the thickness of 7” casing i.e. 0.25”. Eliminating this thickness from the gross thickness bracketed the remaining thickness of outer 2 casings (9-5/8” and 13-3/8”) to zero. This showed majority of the metal loss tool place in the outer 2 casings and they lost their integrity while 7” casing still retained most of its metal thickness.

Identifying well integrity problems

Application of the above techniques established the integrity of 7” casing. Output of ultrasonic cement imaging tool confirmed cement integrity (Figure-5).

Based on above evaluation, 5” casing was run and cemented inside 7” casing to enhance casing barrier against corrosive aquifer and salvage the well for injection.

Conclusions

Well integrity evaluation is an inexact science, reasonably matured yet imperfect. Several methods and tools have been in use with their relative strengths and limitations. The integrated approach used for well integrity evaluation includes selecting a fit-for-purpose set of methods and tools via reliability matrices and analyzing their outputs with correlation, bracketing and elimination techniques. The approach allowed detecting well integrity problems with increased confidence and supported costly wellwork decisions to restore well integrity. Successfully restoring the well integrity unlocked revenue potential, made quick payout of the wellwork costs and extended the field life.

Acknowledgements

The authors like to thank Qatar Petroleum management for permission to publish this paper.

References

1. Fanoiki, J.B.: ‘Sustaining Surface Casing Integrity in a Saline Environment’, paper SPE 77244 presented at IADC/SPE Drilling Conference, Jakarta, Indonesia, September 0-11, 2002.
2. Corneliussen, K. *et al*.: ‘Well Integrity Management System (WIMS) – A Systematic Way of Describing the Actual and Historical Integrity Status of Operational Wells’, paper SPE 110347 presented at SPE Drilling Annual Technical Conference and Exhibition, Anaheim, California, U.S.A., November 11-14, 2007.
3. Julian, J. Y. *et al*.: ‘Detecting Ultra-small Leaks with Ultrasonic Leak Detection – Case Histories From the North Slope, Alaska’, paper SPE 108906 presented at International Oil Conference and Exhibition, Veracruz, Mexico, June 27-30, 2007.

Tables

Table – 1: Reliability Matrix for Surface Methods

Integrity Element	Reliability (Good / Fair / Poor)					
	Wellhead Pressure Monitoring & Produced Fluid Sampling	**Annuli Pressure Monitoring & Effluent Sampling**	**Pressure Testing of Wellhead Seals**	**Pressure Testing of Tubing & Production/ Injection Casing**	**Annuli Pressure Testing**	**Surface Casing & Casinghead Inspection**
Wellhead seal Integrity	---	Fair/ Poor	Good	---	Fair	---
Near surface external corrosion of surface casing	---	---	---	---	---	Good
Production/ injection casing integrity	Fair/ Poor	Fair/ Poor	---	Fair	---	---
Tubing/ packer integrity	Fair/ Poor	Fair/ Poor	---	Fair	---	
Annuli cement integrity	---	Fair/ Poor	---	---	Fair/ Poor	---

Table – 2: Reliability Matrix for Downhole Tools/ Techniques

Integrity Element	Reliability (Good / Fair / Poor)						
	Temperature & Flowmeter Log	**Multi-fingered Calipers**	**Ultrasonic Pipe Imaging Tool**	**Electro-magnetic Pipe Imaging Tool**	**Downhole Camera**	**Cement Bond Log**	**Ultrasonic Cement Imaging Tool**
Zonal cross-flow via wellbore	Good	---	---	---	Fair	---	---
Zonal cross-flow behind production/ injection casing	Fair	---	---	---	---	---	---
Production/ Injection casing internal corrosion	---	Good	Fair	---	Fair	---	---
Production/ Injection casing external corrosion	---	---	Fair	Fair	---	---	---
Outer casings corrosion	---	---	---		---	---	---
Production/ Injection casing cement integrity	---	---	---	---	---	Fair	Good
Outer casings cement integrity	---	---	---	---	---	---	---

Figures

Figure-1: Well No.1 – Output of Temparature Log

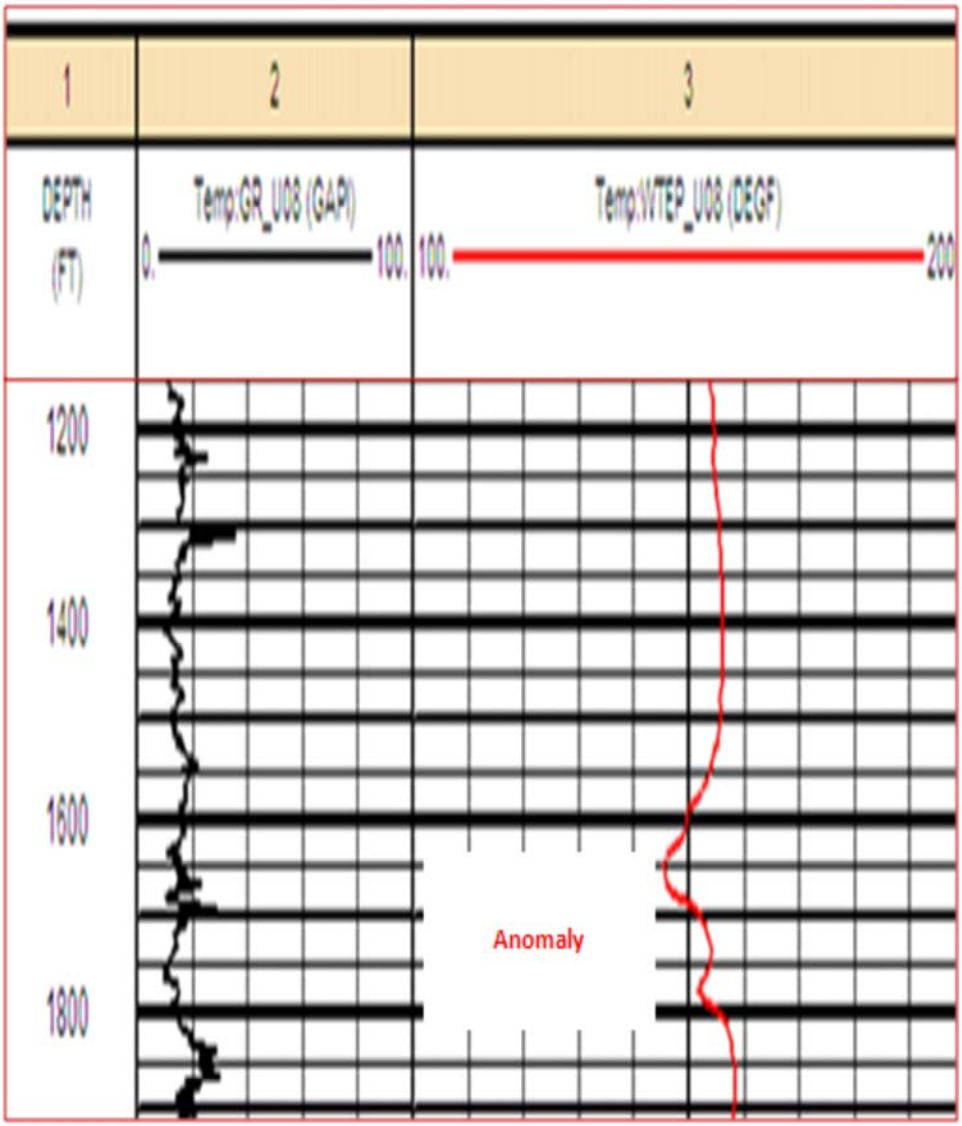

Figure-2: Well No.1 – Output of Ultrasonic & Electromagnetic Pipe Imaging Tools

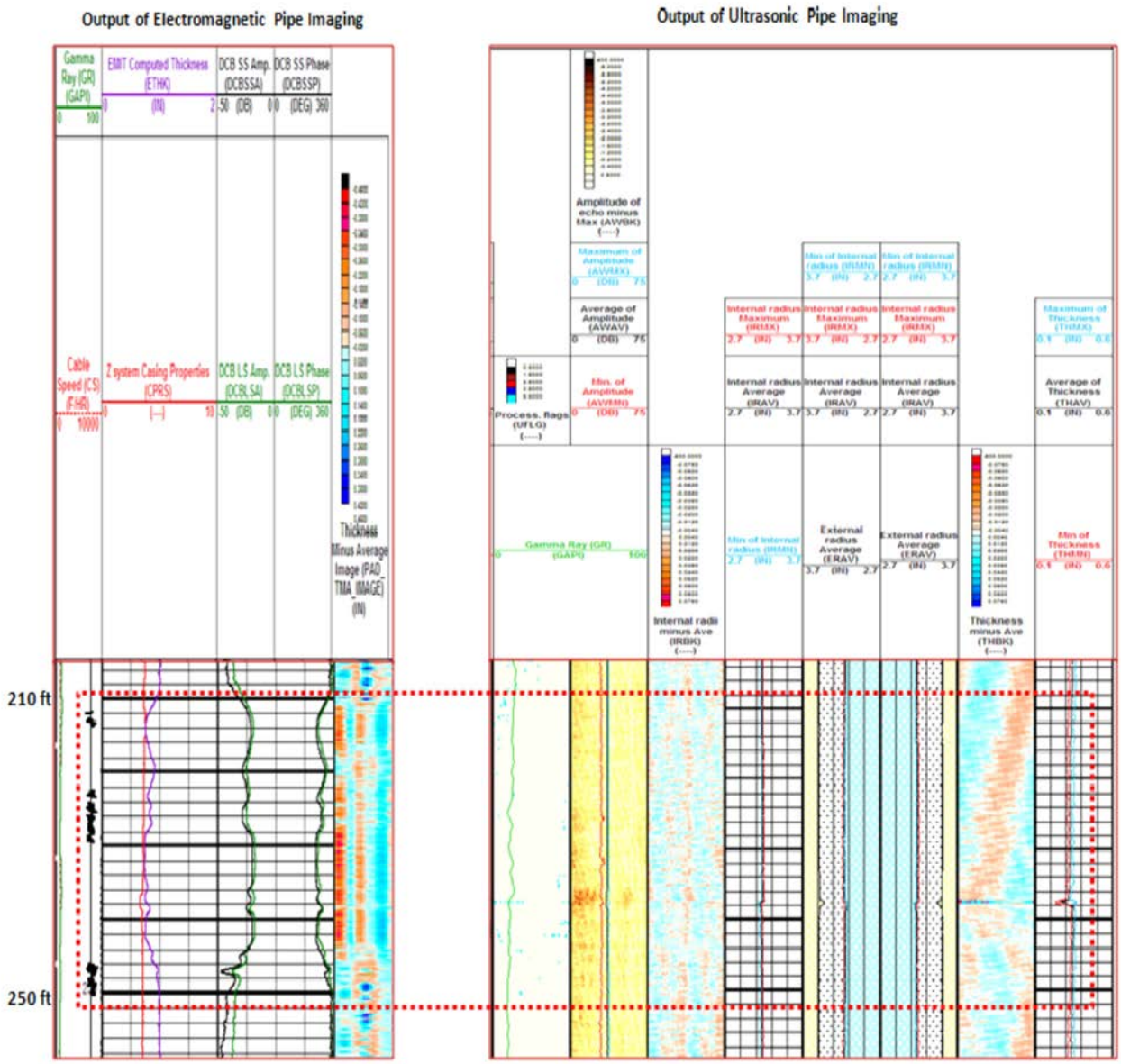

Figure-3: Well No.1 – Output of Ultrasonic Pipe & Cement Imaging Tools

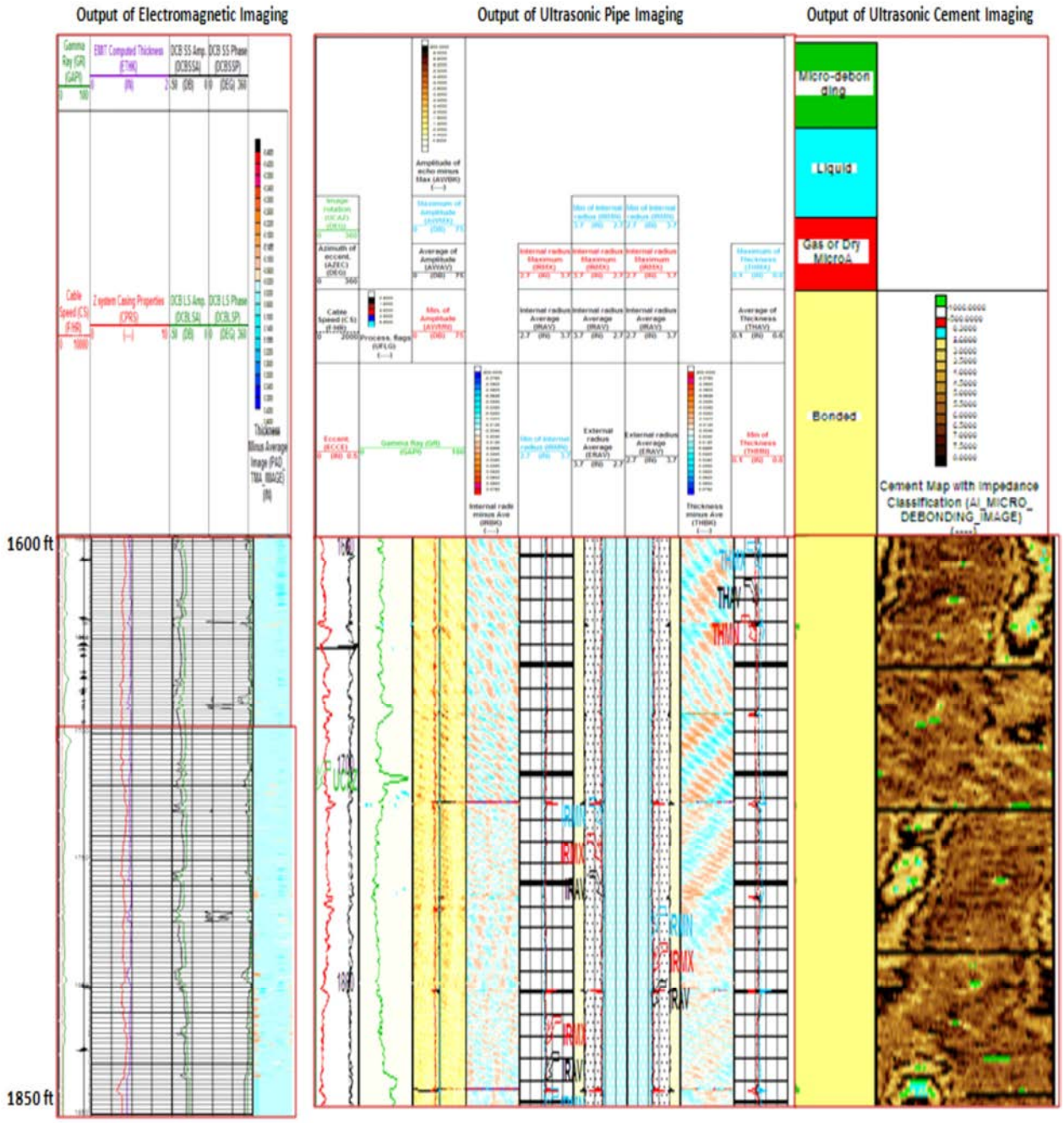

Figure-4: Well No.2 – Output of Ultrasonic & Electromagnetic Pipe Imaging Tools

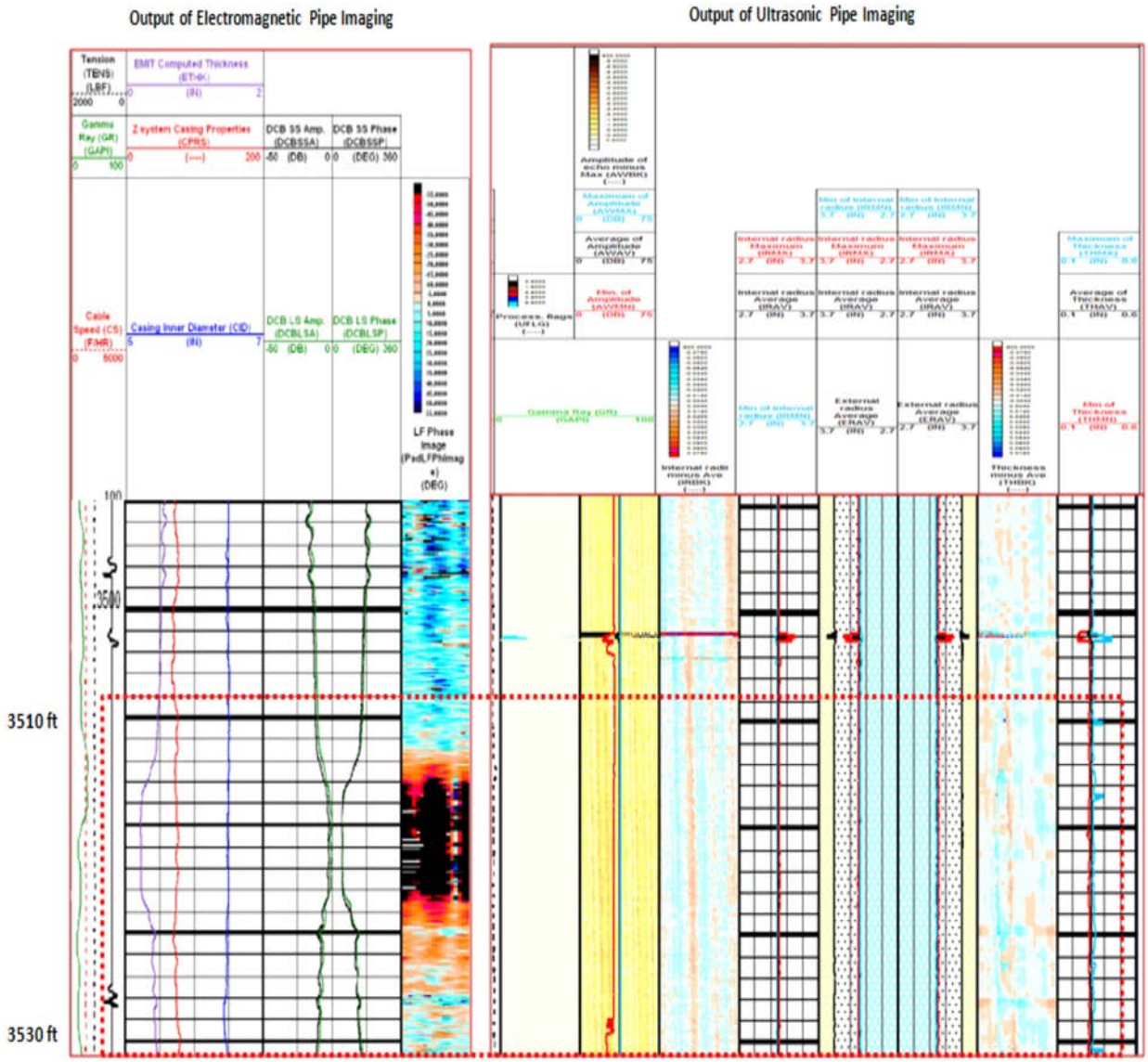

Figure-5: Well No.2 – Output of Ultrasonic Cement Imaging Tools

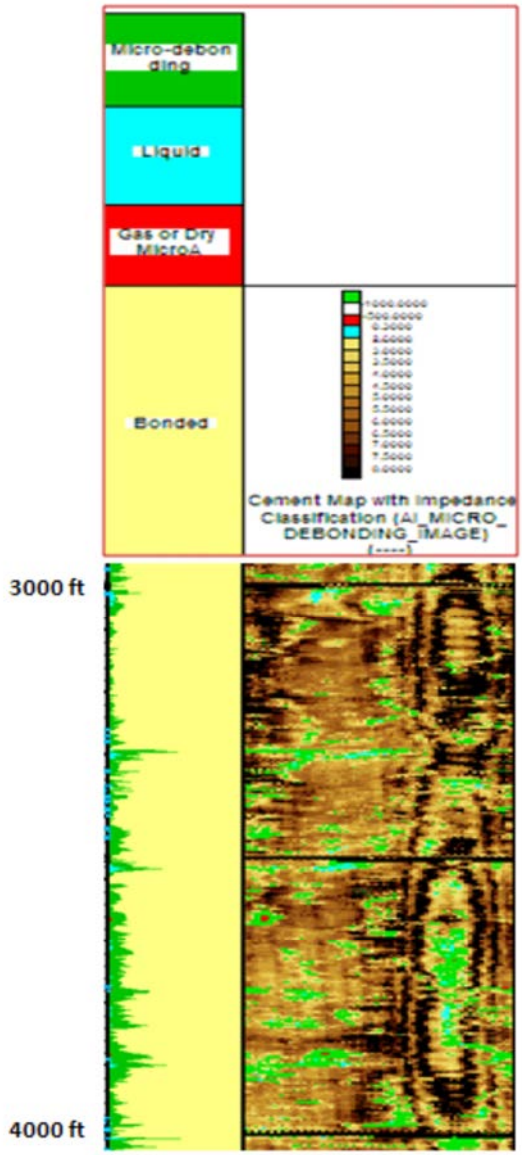

Ex. II - 14

VERTILOG®

Western Atlas International
A Litton/Dresser Company

CUSTOMER	SOUTHERN CALIFORNIA GAS CO.	WORK ORDER NO.	124303	DATE	12-16-88
LEASE/WELL NO.	STANDARD SESNON No. 9	CUSTOMER ORDER NO.			
FIELD	ALISO CANYON	COUNTY	LOS ANGELES	STATE	CALIFORNIA
CASING O.D.	7"	WEIGHT(S)	23,26,29	NOMINAL WALL THICKNESS	GRADE J-55, N-80
TOTAL FOOTAGE INSPECTED	8553'	FROM	SURFACE	TO 8553'	DEPTH

SUBSURFACE CASING INSPECTION REPORT

SUMMARY

198 LENGTHS WERE FOUND TO SHOW NO EVIDENCE OF CORROSION EXCEEDING 20 PERCENT OF THE NOMINAL BODY WALL. CLASS 1

6 LENGTHS WERE FOUND TO SHOW EVIDENCE OF CORROSION EXCEEDING 20 PERCENT BUT LESS THAN PERCENT OF THE NOMINAL BODY WALL. CLASS 2

0 LENGTHS WERE FOUND TO SHOW EVIDENCE OF CORROSION EXCEEDING 40 PERCENT BUT LESS THAN PERCENT OF THE NOMINAL BODY WALL. CLASS 3

0 LENGTHS WERE FOUND TO SHOW EVIDENCE OF CORROSION EXCEEDING 60 PERCENT OF THE NOMINAL BODY WALL. CLASS 4

204 TOTAL LENGTHS

8553' TOTAL FOOTAGE

REFERENCE FOR FOOTAGE MEASURE: GROUND LEVEL +6.92'

LENGTHS ARE NUMBERED FROM: SURFACE

COMMENTS

SERVICED BY

WA-1363 (10/87)

VERTILOG®

Western Atlas International
A Litton/Dresser Company

CUSTOMER SOUTHERN CALIFORNIA GAS COMPANY	WORK ORDER NO. 124303	DATE 12-16-88	
LEASE/WELL NO. STANDARD SESNON No. 9	CUSTOMER ORDER NO.		
FIELD ALISO CANYON	COUNTY LOS ANGELES	STATE CALIFORNIA	
CASING O.D. 7"	WEIGHT(S) 23,26,29	NOMINAL WALL THICKNESS	GRADE J-55,N-80
TOTAL FOOTAGE INSPECTED 8553'	FROM SURFACE	TO 8553'	DEPTH

SUBSURFACE CASING DEFECT REPORT

LENGTH NO.	TYPE DEFECT	PENETRATION	LENGTH NO.	TYPE DEFECT	PENETRATION
OUTSIDE 13-3/8" SURFACE CASING					
51	OD IP	21 - 40			
62	OD IP	21 - 40			
64	OD IP	21 - 40			
67	ID IP	21 - 40			
85	ID IP	21 - 40			
91	ID IP	21 - 40			

ABBREVIATIONS:

O.D. – OUTSIDE DIAMETER
I.D. – INSIDE DIAMETER
I.S. – INSIDE SURFACE PIPE
T.L. – THROUGHOUT LENGTH
I.P. – ISOLATED PITTING
C.C. – CIRCUMFERENTIAL CORROSION
G.C. - GENERAL CORROSION

WA-1364-C (10/87)

Ex. II - 15

Due to the large file size, please view document DOGGR_03700762_Vertilog_12-16-1988 at the below publicly available website. The native file of this document is available upon request.

(https://secure.conservation.ca.gov/WellRecord/037/03700762/tifs/03700762_Vertilog_12-16-1988.tif) (accessed March 20, 2020)

HR Vertilog

Magnetic Flux Leakage Inspection

Advanced Analysis

Company	Southern California Gas Company
Well	Standard Sesnon 9
Field	Aliso Canyon
County	Los Angeles
State	California
Location:	

Section 28	Township 3N	Range 16W	

Date	Sep. 6, 2018
Service Order	US142360J
Recorded by	Josh Farris
Witnessed by	Tom McMahon
API Serial No.	040370076200

Permanent Datum:	DF	Elevation: 2842.630 ft.		Depth	8580.000
Log Measured From:	DF	6.920 ft. above Perm. Datum		Btm. Log Interval	8580.000
Drilling Measured From:	DF	6.920 ft. above Perm. Datum		Top Log Interval	0.000
				Fluid Type	KCL

Casing Data

Size	Weight	Grade	From	To	Length
7 inch	23.0 lb/ft	J55	0'	3777'	3777.0
7 inch	23.0 lb/ft	N-80	3777'	5463'	1686.0
7 inch	26.0 lb/ft	N-80	5463'	7093'	1630.0
7 inch	29.0 lb/ft	N-80	7093'	8625'	1532.0
5 inch	17.93 lb/ft	N-80	8599'	8859'	260.0

Software Version 7.6.1.4

Equipment Data

Run	Trip	Tool Type	Tool Series	Serial Number	Position
1	1	HRVRT MFL	4997	PB13150203	LOWER
1	1	HRVRT MFL	4997	PB12116589	UPPER
1	1	HRVRT TELEM	4993	265	

Calibration Data

Calibration File Name	4997-7-001-PB12116589-U.CAL

Date of Calibration	08/04/2016 15:08
Calibration Identifier	64583794-BD8B-4D61-AD05-9F80BA6D56F5
Tool Number	4997-00
Calibrator Number	4997-7-001
Calibrator Size	(7 In - 178 mm)
Calibration Source File	20160804_144043_MEM.MVL
Calibration Software Rev	Microvision 32-bit 7.3.4.0
Comment	RMA1273

Calibration Data

Calibration File Name	4997-7-001-PB13150203-U.CAL
Date of Calibration	08/01/2014 09:59
Calibration Identifier	7D517C26-6B34-4D7B-9646-D03C51CFEE9F
Tool Number	4997-00
Calibrator Number	4997-7-001
Calibrator Size	(7 In - 178 mm)
Calibration Source File	20140801_092608_MEM.MVL
Calibration Software Rev	Microvision 32-bit 7.3.4.0
Comment	New PO 4506516300

Baker Hughes, a GE company, LLC and its affiliates BHGE provides this information on an as is basis for general information purposes and believes it to be accurate as of the date of publication. BHGE does not make any representation as to the accuracy or completeness of the information and makes no warranties of any kind, specific, implied or oral, to the fullest extent permissible by law, including those of merchantability and fitness for a particular purpose or use. BHGE hereby disclaims any and all liability for any direct, indirect, consequential or special damages, claims for lost profits, or third party claims arising from the use of the information, whether a claim is asserted in contract, tort, or otherwise. The BHGE logo is a trademark of Baker Hughes, a GE company, LLC. GE and the GE monogram are trademarks of General Electric Company used under trademark license.
Copyright 2018 Baker Hughes, a GE company, LLC All rights reserved.

Remarks

Interpretation

The HRVRT data was correlated to the SLB GRN log dated 9-7-2018.

The following external hardware was detected and excluded from analysis:

```
  13.98 ft   Hardware - External CSG Head Response
 593.91 ft   Hardware - Bottom of 13.375" External Casing
8571.84 ft   Float Collar
```

Seamless pipe noise was detected in several joints. See Joint #22 as example.

Joint Interpretation Summary

Joint	From	To	Length	Class	Max Depth	Position	ID/OD
1	12.24	38.53	26.29	Class 1	-	-	-

2	38.53	74.18	35.65	Class 1	-	-	-
3	74.18	115.79	41.61	Class 1	-	-	-
4	115.79	157.65	41.86	Class 1	-	-	-
5	157.65	199.80	42.15	Class 1	-	-	-
6	199.80	241.77	41.97	Class 1	-	-	-
7	241.77	284.16	42.39	Class 1	-	-	-
8	284.16	326.19	42.03	Class 1	-	-	-
9	326.19	368.28	42.09	Class 1	-	-	-
10	368.28	410.35	42.07	Class 1	-	-	-
11	410.35	453.02	42.67	Class 1	-	-	-
12	453.02	494.83	41.81	Class 1	-	-	-
13	494.83	535.98	41.15	Class 1	-	-	-
14	535.98	578.15	42.17	Class 1	-	-	-
15	578.15	619.29	41.14	Class 1	-	-	-
16	619.29	660.47	41.18	Class 1	-	-	-
17	660.47	702.80	42.33	Class 1	-	-	-
18	702.80	744.70	41.90	Class 1	-	-	-
19	744.70	784.93	40.23	Class 1	16.0%	773.01	OD
20	784.93	826.75	41.82	Class 1	-	-	-
21	826.75	869.01	42.26	Class 1	-	-	-
22	869.01	911.47	42.46	Class 1	-	-	-
23	911.47	953.31	41.84	Class 1	-	-	-
24	953.31	995.20	41.89	Class 1	-	-	-
25	995.20	1037.22	42.02	Class 1	-	-	-
26	1037.22	1078.98	41.76	Class 1	-	-	-
27	1078.98	1121.36	42.38	Class 1	-	-	-
28	1121.36	1158.13	36.77	Class 1	-	-	-
29	1158.13	1200.42	42.29	Class 1	-	-	-
30	1200.42	1243.55	43.13	Class 1	-	-	-
31	1243.55	1285.51	41.96	Class 1	-	-	-
32	1285.51	1325.94	40.43	Class 1	-	-	-
33	1325.94	1368.28	42.34	Class 1	-	-	-
34	1368.28	1410.38	42.10	Class 1	-	-	-
35	1410.38	1451.62	41.24	Class 1	-	-	-
36	1451.62	1493.16	41.54	Class 1	-	-	-
37	1493.16	1535.70	42.54	Class 1	-	-	-
38	1535.70	1578.16	42.46	Class 1	-	-	-
39	1578.16	1619.86	41.70	Class 1	-	-	-
40	1619.86	1662.39	42.53	Class 1	-	-	-
41	1662.39	1704.09	41.70	Class 1	-	-	-
42	1704.09	1741.16	37.07	Class 1	-	-	-
43	1741.16	1781.97	40.81	Class 1	-	-	-
44	1781.97	1822.61	40.64	Class 1	-	-	-
45	1822.61	1865.02	42.41	Class 1	-	-	-
46	1865.02	1905.07	40.05	Class 1	-	-	-
47	1905.07	1945.86	40.79	Class 1	-	-	-
48	1945.86	1987.40	41.54	Class 1	-	-	-
49	1987.40	2028.80	41.40	Class 1	-	-	-
50	2028.80	2070.51	41.71	Class 1	-	-	-
51	2070.51	2113.28	42.77	Class 1	-	-	-
52	2113.28	2154.65	41.37	Class 1	-	-	-
53	2154.65	2197.03	42.38	Class 1	-	-	-
54	2197.03	2239.08	42.05	Class 1	-	-	-
55	2239.08	2275.74	36.66	Class 1	-	-	-
56	2275.74	2317.66	41.92	Class 1	-	-	-
57	2317.66	2357.88	40.22	Class 1	-	-	-
58	2357.88	2399.62	41.74	Class 1	-	-	-
59	2399.62	2442.99	43.37	Class 1	-	-	-
60	2442.99	2485.08	42.09	Class 1	-	-	-
61	2485.08	2525.60	40.52	Class 1	-	-	-
62	2525.60	2567.40	41.80	Class 1	-	-	-
63	2567.40	2606.93	39.53	Class 1	-	-	-
64	2606.93	2648.93	42.00	Class 1			

64	2606.93	2648.93	42.00	Class 1	-	-	-
65	2648.93	2690.98	42.05	Class 1	-	-	-
66	2690.98	2733.14	42.16	Class 1	-	-	-
67	2733.14	2773.16	40.02	Class 1	-	-	-
68	2773.16	2814.96	41.80	Class 1	-	-	-
69	2814.96	2856.26	41.30	Class 1	-	-	-
70	2856.26	2899.36	43.10	Class 1	-	-	-
71	2899.36	2936.78	37.42	Class 1	-	-	-
72	2936.78	2978.76	41.98	Class 1	-	-	-
73	2978.76	3020.71	41.95	Class 1	-	-	-
74	3020.71	3063.24	42.53	Class 1	-	-	-
75	3063.24	3105.60	42.36	Class 1	-	-	-
76	3105.60	3147.28	41.68	Class 1	-	-	-
77	3147.28	3188.93	41.65	Class 1	-	-	-
78	3188.93	3227.81	38.88	Class 1	-	-	-
79	3227.81	3269.52	41.71	Class 1	-	-	-
80	3269.52	3311.18	41.66	Class 1	-	-	-
81	3311.18	3353.08	41.90	Class 1	-	-	-
82	3353.08	3394.55	41.47	Class 1	-	-	-
83	3394.55	3436.81	42.26	Class 1	-	-	-
84	3436.81	3479.00	42.19	Class 1	-	-	-
85	3479.00	3520.14	41.14	Class 1	-	-	-
86	3520.14	3562.81	42.67	Class 1	-	-	-
87	3562.81	3598.36	35.55	Class 1	-	-	-
88	3598.36	3640.95	42.59	Class 1	-	-	-
89	3640.95	3683.71	42.76	Class 1	-	-	-
90	3683.71	3726.33	42.62	Class 1	-	-	-
91	3726.33	3768.12	41.79	Class 1	-	-	-
92	3768.12	3810.20	42.08	Class 1	-	-	-
93	3810.20	3852.86	42.66	Class 1	-	-	-
94	3852.86	3895.41	42.55	Class 1	15.0%	3874.13	OD
95	3895.41	3937.52	42.11	Class 1	-	-	-
96	3937.52	3980.90	43.38	Class 1	-	-	-
97	3980.90	4023.22	42.32	Class 1	-	-	-
98	4023.22	4065.65	42.43	Class 1	-	-	-
99	4065.65	4106.87	41.22	Class 1	-	-	-
100	4106.87	4148.24	41.37	Class 1	-	-	-
101	4148.24	4190.33	42.09	Class 1	-	-	-
102	4190.33	4232.66	42.33	Class 1	-	-	-
103	4232.66	4275.03	42.37	Class 1	-	-	-
104	4275.03	4315.13	40.10	Class 1	-	-	-
105	4315.13	4357.87	42.74	Class 1	-	-	-
106	4357.87	4398.67	40.80	Class 1	-	-	-
107	4398.67	4442.62	43.95	Class 1	-	-	-
108	4442.62	4485.49	42.87	Class 1	-	-	-
109	4485.49	4527.42	41.93	Class 1	-	-	-
110	4527.42	4569.22	41.80	Class 1	15.0%	4530.65	ID
111	4569.22	4610.04	40.82	Class 1	-	-	-
112	4610.04	4652.91	42.87	Class 1	-	-	-
113	4652.91	4695.45	42.54	Class 1	-	-	-
114	4695.45	4738.08	42.63	Class 1	-	-	-
115	4738.08	4780.42	42.34	Class 1	-	-	-
116	4780.42	4822.80	42.38	Class 1	-	-	-
117	4822.80	4865.13	42.33	Class 1	-	-	-
118	4865.13	4906.93	41.80	Class 1	-	-	-
119	4906.93	4948.57	41.64	Class 1	18.0%	4932.25	ID
120	4948.57	4991.13	42.56	Class 1	-	-	-
121	4991.13	5033.11	41.98	Class 1	-	-	-
122	5033.11	5075.90	42.79	Class 1	-	-	-
123	5075.90	5118.18	42.28	Class 1	-	-	-
124	5118.18	5161.13	42.95	Class 1	-	-	-
125	5161.13	5203.23	42.10	Class 1	-	-	-
126	5203.23	5245.17	41.94	Class 1	-	-	-

127	5245.17	5287.55	42.38	Class 1	-	-	-
128	5287.55	5326.64	39.09	Class 1	-	-	-
129	5326.64	5369.45	42.81	Class 1	-	-	-
130	5369.45	5411.86	42.41	Class 1	-	-	-
131	5411.86	5454.90	43.04	Class 1	-	-	-
132	5454.90	5496.15	41.25	Class 1	-	-	-
133	5496.15	5538.08	41.93	Class 1	-	-	-
134	5538.08	5581.39	43.31	Class 1	-	-	-
135	5581.39	5624.07	42.68	Class 1	-	-	-
136	5624.07	5667.96	43.89	Class 1	-	-	-
137	5667.96	5710.53	42.57	Class 1	-	-	-
138	5710.53	5753.63	43.10	Class 1	-	-	-
139	5753.63	5795.90	42.27	Class 1	-	-	-
140	5795.90	5838.95	43.05	Class 1	-	-	-
141	5838.95	5880.33	41.38	Class 1	-	-	-
142	5880.33	5923.96	43.63	Class 1	-	-	-
143	5923.96	5967.00	43.04	Class 1	-	-	-
144	5967.00	6010.17	43.17	Class 1	-	-	-
145	6010.17	6053.92	43.75	Class 1	-	-	-
146	6053.92	6095.40	41.48	Class 1	-	-	-
147	6095.40	6138.92	43.52	Class 1	-	-	-
148	6138.92	6181.79	42.87	Class 1	-	-	-
149	6181.79	6223.50	41.71	Class 1	-	-	-
150	6223.50	6266.53	43.03	Class 1	-	-	-
151	6266.53	6309.87	43.34	Class 1	-	-	-
152	6309.87	6352.97	43.10	Class 1	-	-	-
153	6352.97	6396.53	43.56	Class 1	-	-	-
154	6396.53	6439.50	42.97	Class 1	-	-	-
155	6439.50	6482.51	43.01	Class 1	-	-	-
156	6482.51	6525.42	42.91	Class 1	-	-	-
157	6525.42	6568.19	42.77	Class 1	-	-	-
158	6568.19	6611.15	42.96	Class 1	-	-	-
159	6611.15	6654.77	43.62	Class 1	-	-	-
160	6654.77	6698.79	44.02	Class 1	-	-	-
161	6698.79	6742.52	43.73	Class 1	-	-	-
162	6742.52	6784.53	42.01	Class 1	-	-	-
163	6784.53	6826.07	41.54	Class 1	-	-	-
164	6826.07	6869.30	43.23	Class 1	-	-	-
165	6869.30	6912.74	43.44	Class 1	-	-	-
166	6912.74	6956.22	43.48	Class 1	-	-	-
167	6956.22	6999.59	43.37	Class 1	-	-	-
168	6999.59	7043.24	43.65	Class 1	-	-	-
169	7043.24	7086.75	43.51	Class 1	-	-	-
170	7086.75	7129.73	42.98	Class 1	-	-	-
171	7129.73	7172.46	42.73	Class 1	-	-	-
172	7172.46	7214.81	42.35	Class 1	-	-	-
173	7214.81	7257.58	42.77	Class 1	-	-	-
174	7257.58	7299.71	42.13	Class 1	-	-	-
175	7299.71	7341.70	41.99	Class 1	16.0%	7315.51	ID
176	7341.70	7385.13	43.43	Class 1	-	-	-
177	7385.13	7427.08	41.95	Class 1	-	-	-
178	7427.08	7470.85	43.77	Class 1	-	-	-
179	7470.85	7513.45	42.60	Class 1	-	-	-
180	7513.45	7556.89	43.44	Class 1	-	-	-
181	7556.89	7599.71	42.82	Class 1	-	-	-
182	7599.71	7642.37	42.66	Class 1	-	-	-
183	7642.37	7685.12	42.75	Class 1	-	-	-
184	7685.12	7727.80	42.68	Class 1	-	-	-
185	7727.80	7770.52	42.72	Class 1	-	-	-
186	7770.52	7813.28	42.76	Class 1	-	-	-
187	7813.28	7855.44	42.16	Class 1	-	-	-
188	7855.44	7897.42	41.98	Class 1	-	-	-

189	7897.42	7940.80	43.38	Class	1	-	-	-
190	7940.80	7982.98	42.18	Class	1	-	-	-
191	7982.98	8020.03	37.05	Class	1	-	-	-
192	8020.03	8062.36	42.33	Class	1	-	-	-
193	8062.36	8104.78	42.42	Class	1	-	-	-
194	8104.78	8147.35	42.57	Class	1	-	-	-
195	8147.35	8190.89	43.54	Class	1	-	-	-
196	8190.89	8233.86	42.97	Class	1	-	-	-
197	8233.86	8277.47	43.61	Class	1	-	-	-
198	8277.47	8319.86	42.39	Class	1	-	-	-
199	8319.86	8362.54	42.68	Class	1	-	-	-
200	8362.54	8404.99	42.45	Class	1	-	-	-
201	8404.99	8447.21	42.22	Class	1	-	-	-
202	8447.21	8486.46	39.25	Class	1	-	-	-
203	8486.46	8528.95	42.49	Class	2	23.0%	8522.45	ID
204	8528.95	8571.84	42.89	Class	4	81.0%	8543.19	ID
205	8571.84	8581.63	9.79	Class	1	-	-	-

Southern California Gas Company Standard Sesnon 9

File 20180906_15093B_RSP_0_0_0_0_0.mvl

MAIN LOG (5"/100')

Class 1	Class 2	Class 3	Class 4
0 - 20%	20 - 40%	40 - 60%	60 - 100%

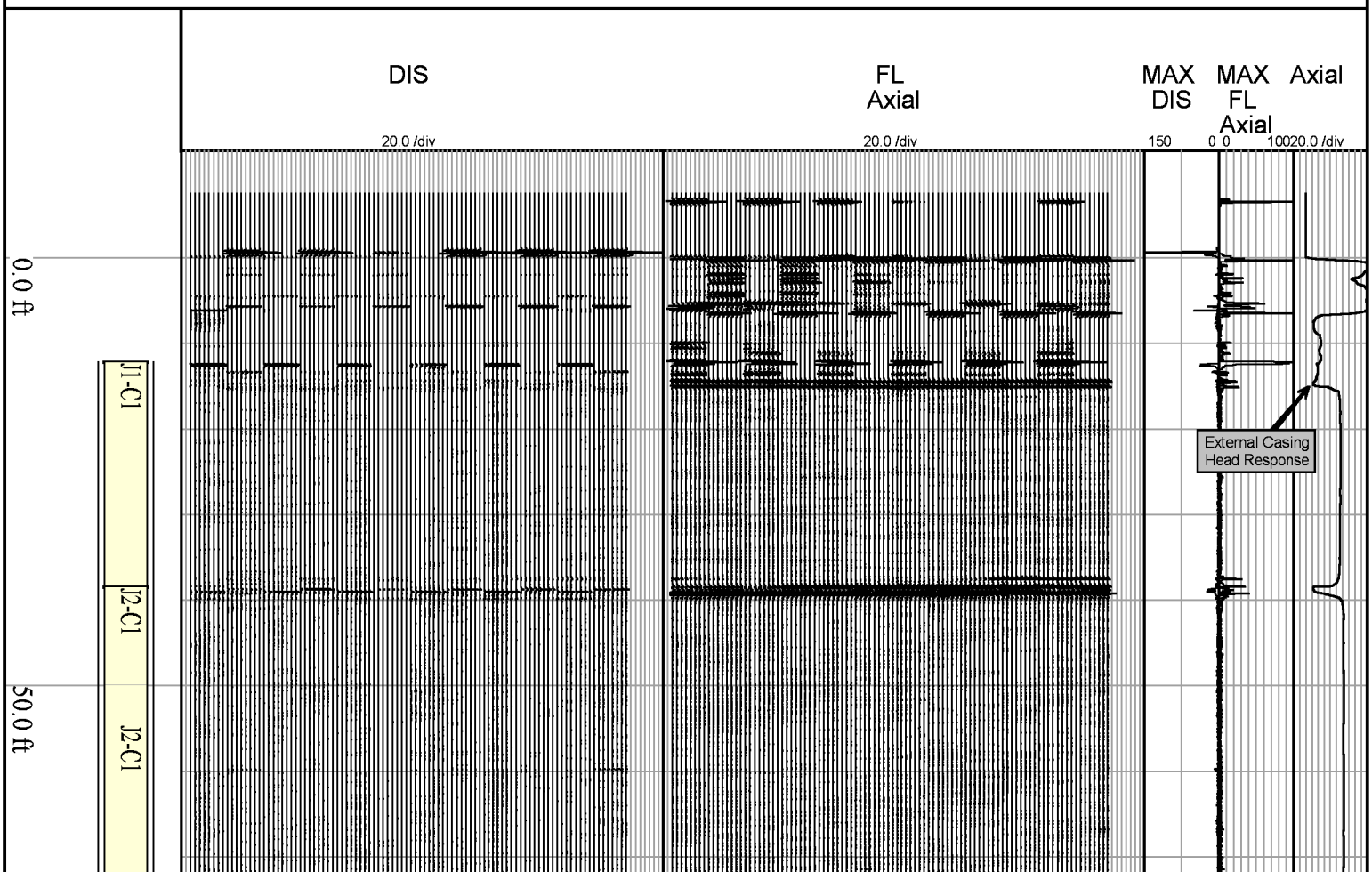

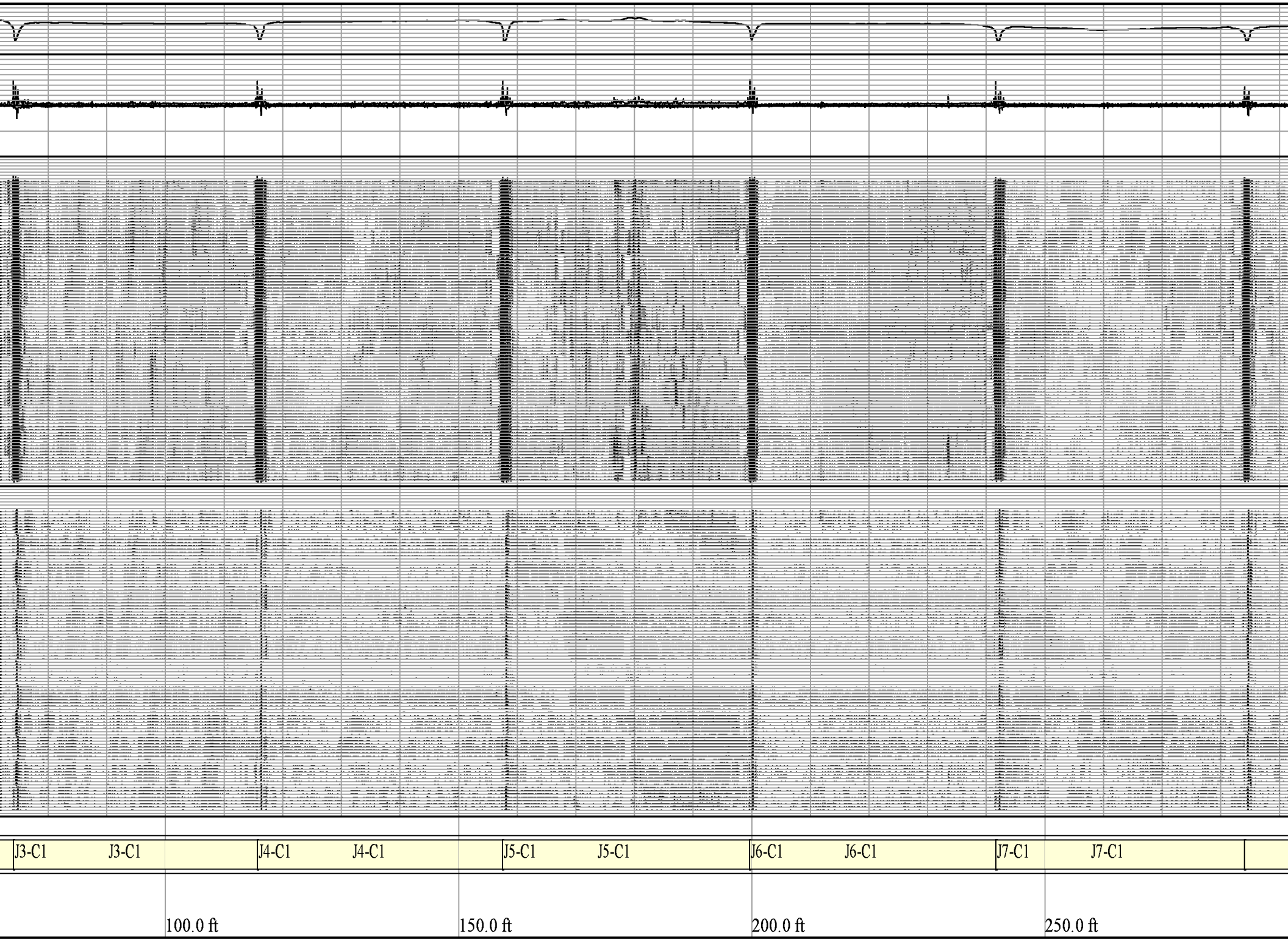
J3-C1
J3-C1
J4-C1
J4-C1
J5-C1
J5-C1
J6-C1
J6-C1
J7-C1
J7-C1
100.0 ft
150.0 ft
200.0 ft
250.0 ft

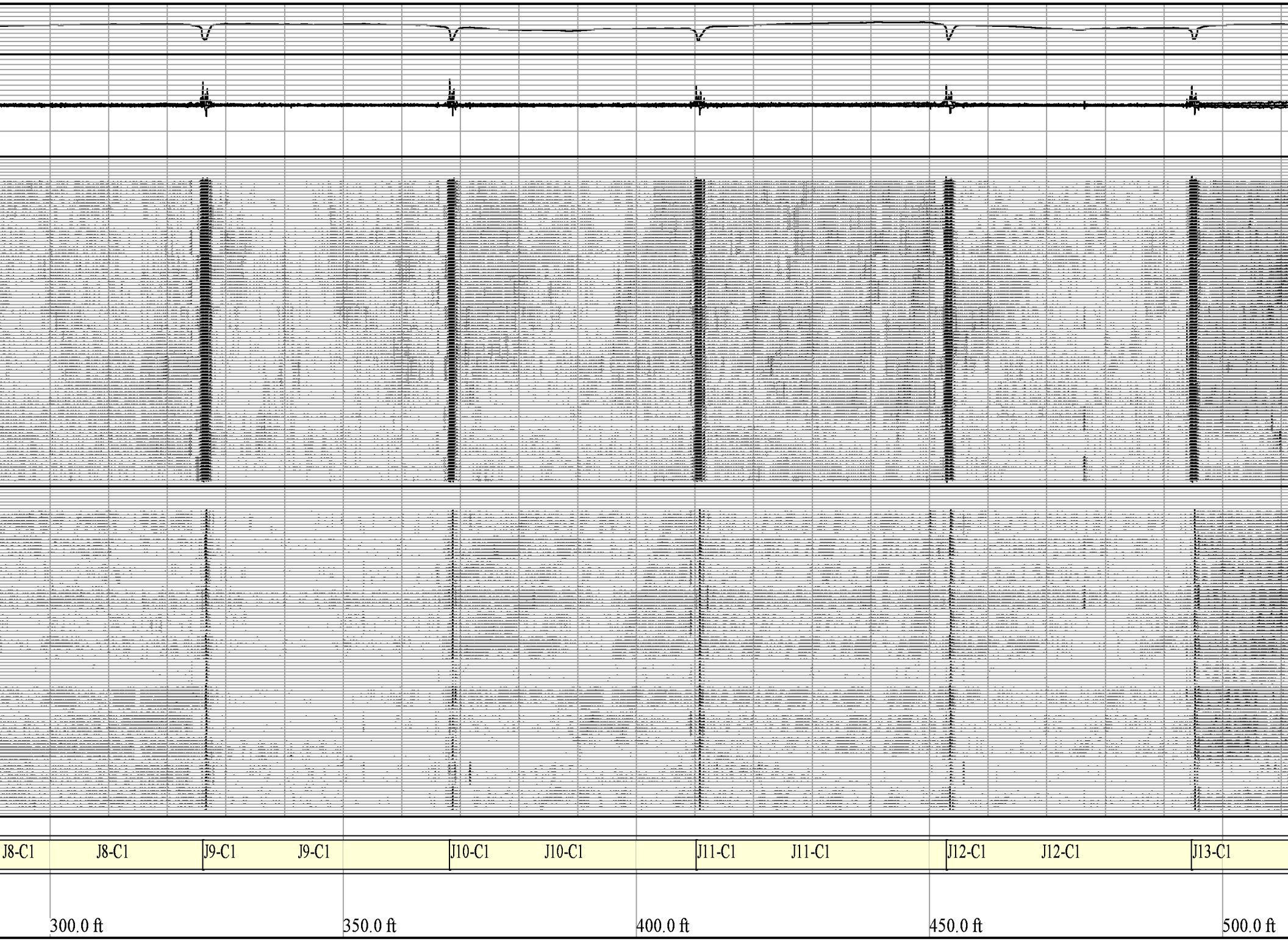
J8-C1
J8-C1
J9-C1
J9-C1
J10-C1
J10-C1
J11-C1
J11-C1
J12-C1
J12-C1
J13-C1
300.0 ft
350.0 ft
400.0 ft
450.0 ft
500.0 ft

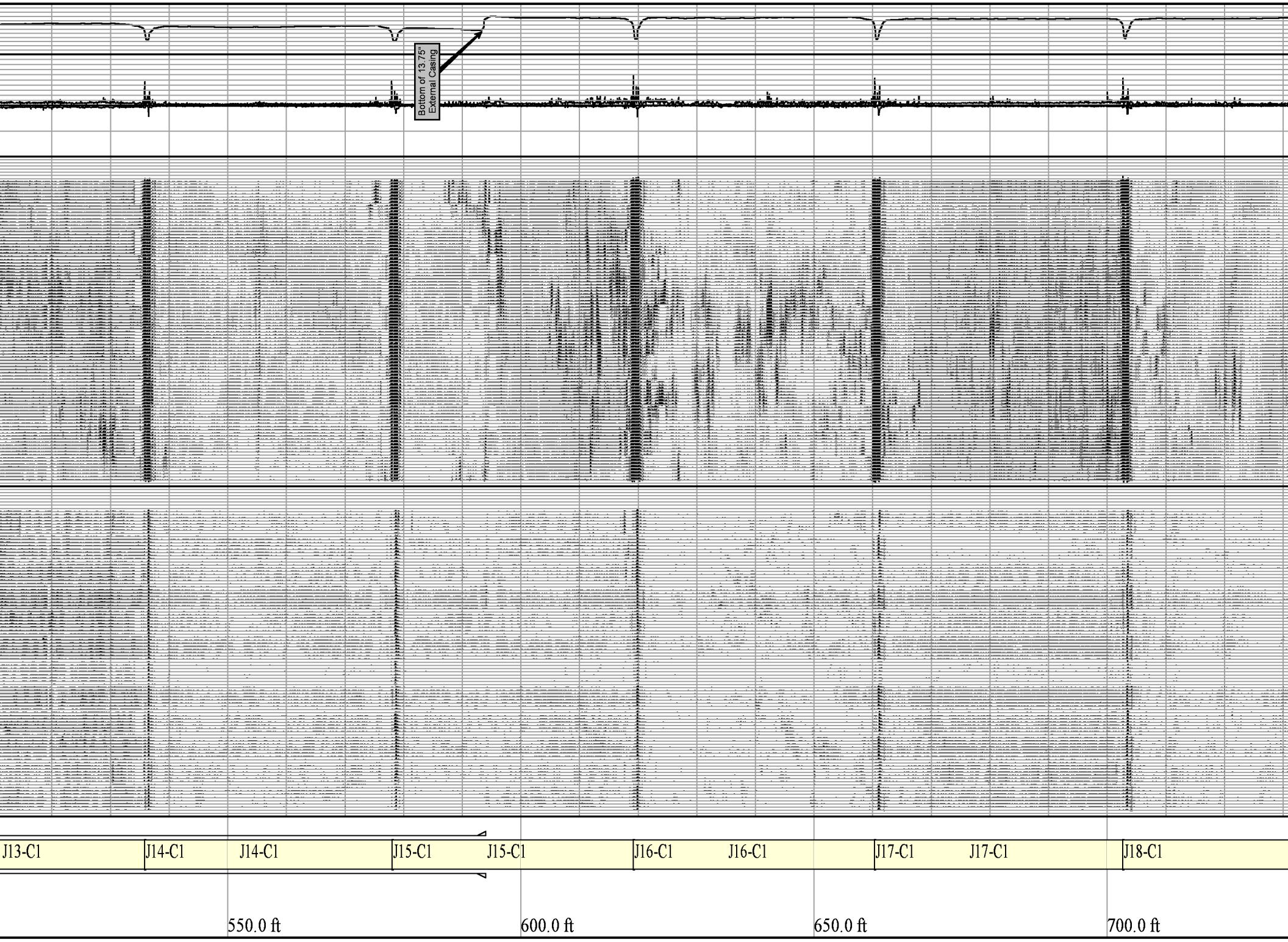
Bottom of 13.75" External Casing
J13-C1
J14-C1
J14-C1
J15-C1
J15-C1
J16-C1
J16-C1
J17-C1
J17-C1
J18-C1
550.0 ft
600.0 ft
650.0 ft
700.0 ft

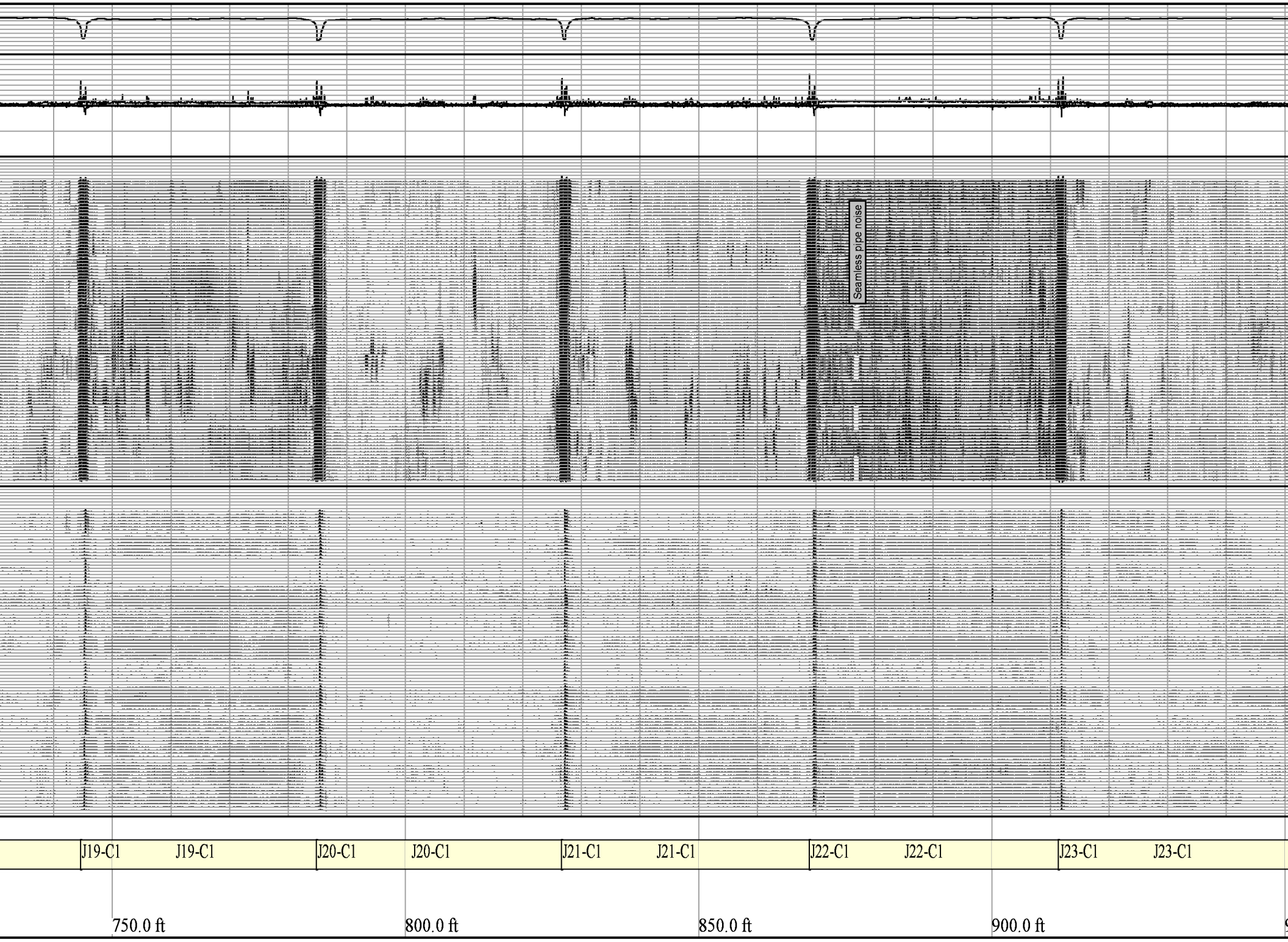
Seamless pipe noise
J19-C1
J19-C1
J20-C1
J20-C1
J21-C1
J21-C1
J22-C1
J22-C1
J23-C1
J23-C1
750.0 ft
800.0 ft
850.0 ft
900.0 ft

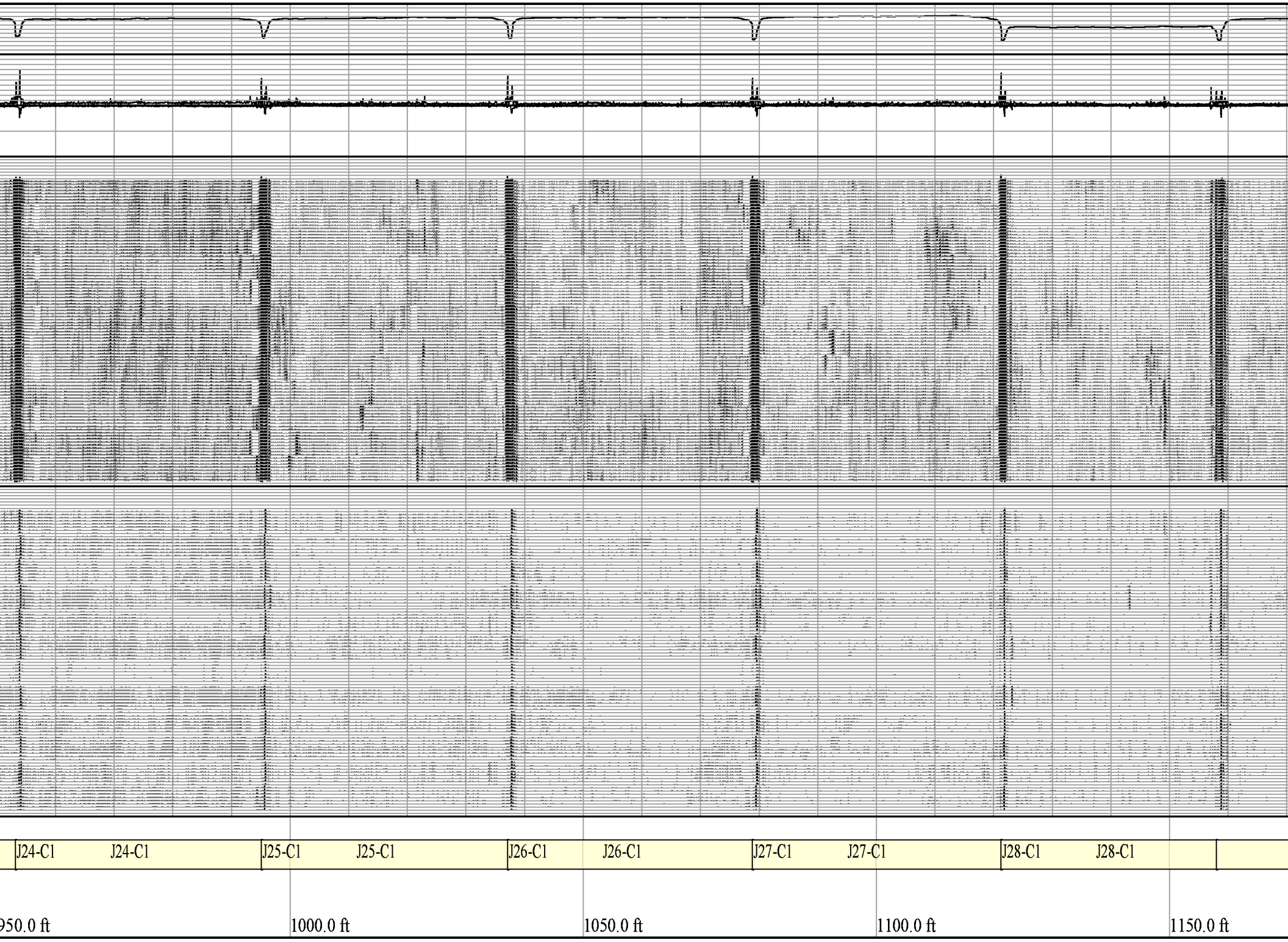
J24-C1
J24-C1
J25-C1
J25-C1
J26-C1
J26-C1
J27-C1
J27-C1
J28-C1
J28-C1
950.0 ft
1000.0 ft
1050.0 ft
1100.0 ft
1150.0 ft

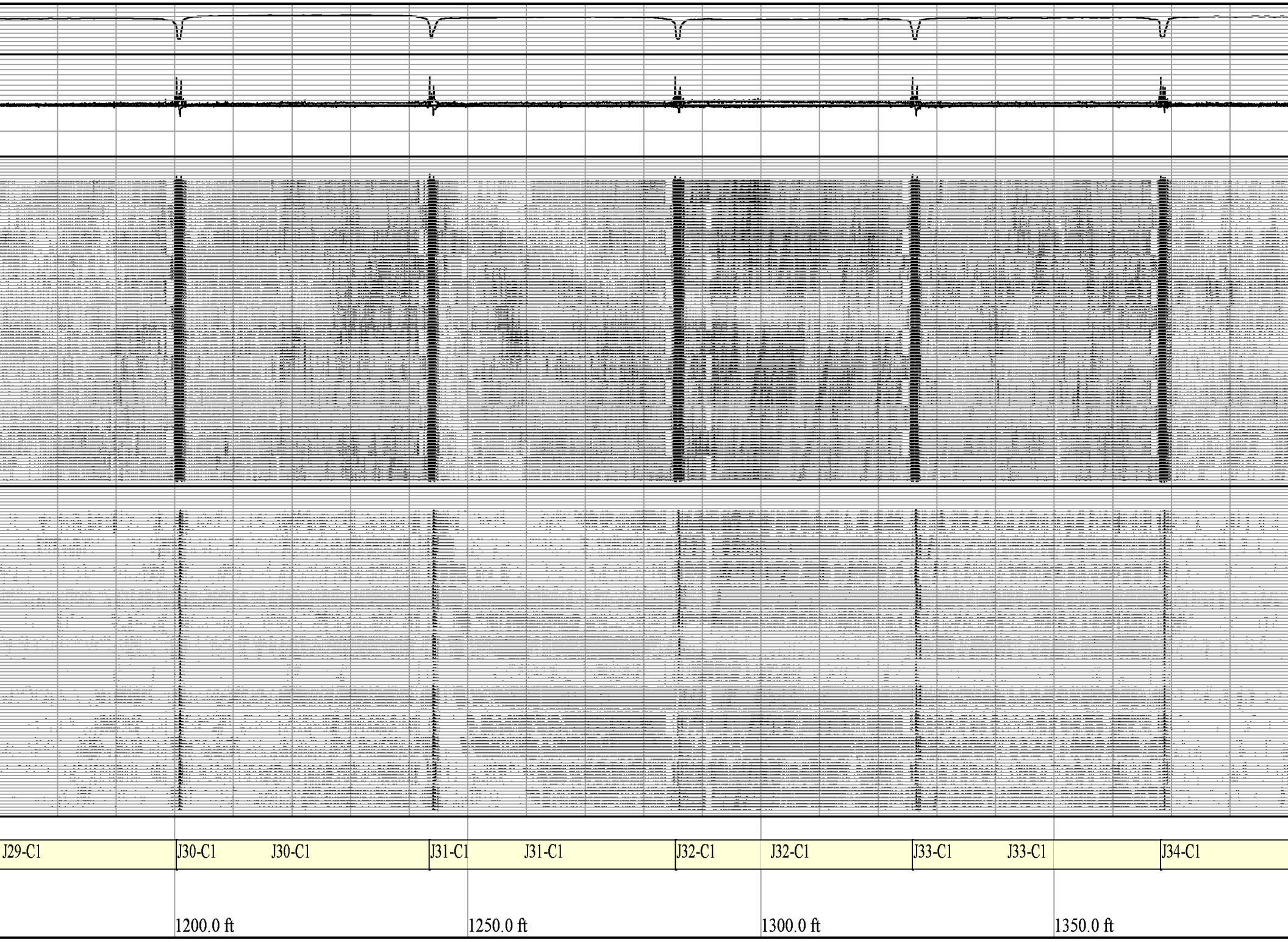
J29-C1
J30-C1
J30-C1
J31-C1
J31-C1
J32-C1
J32-C1
J33-C1
J33-C1
J34-C1
1200.0 ft
1250.0 ft
1300.0 ft
1350.0 ft

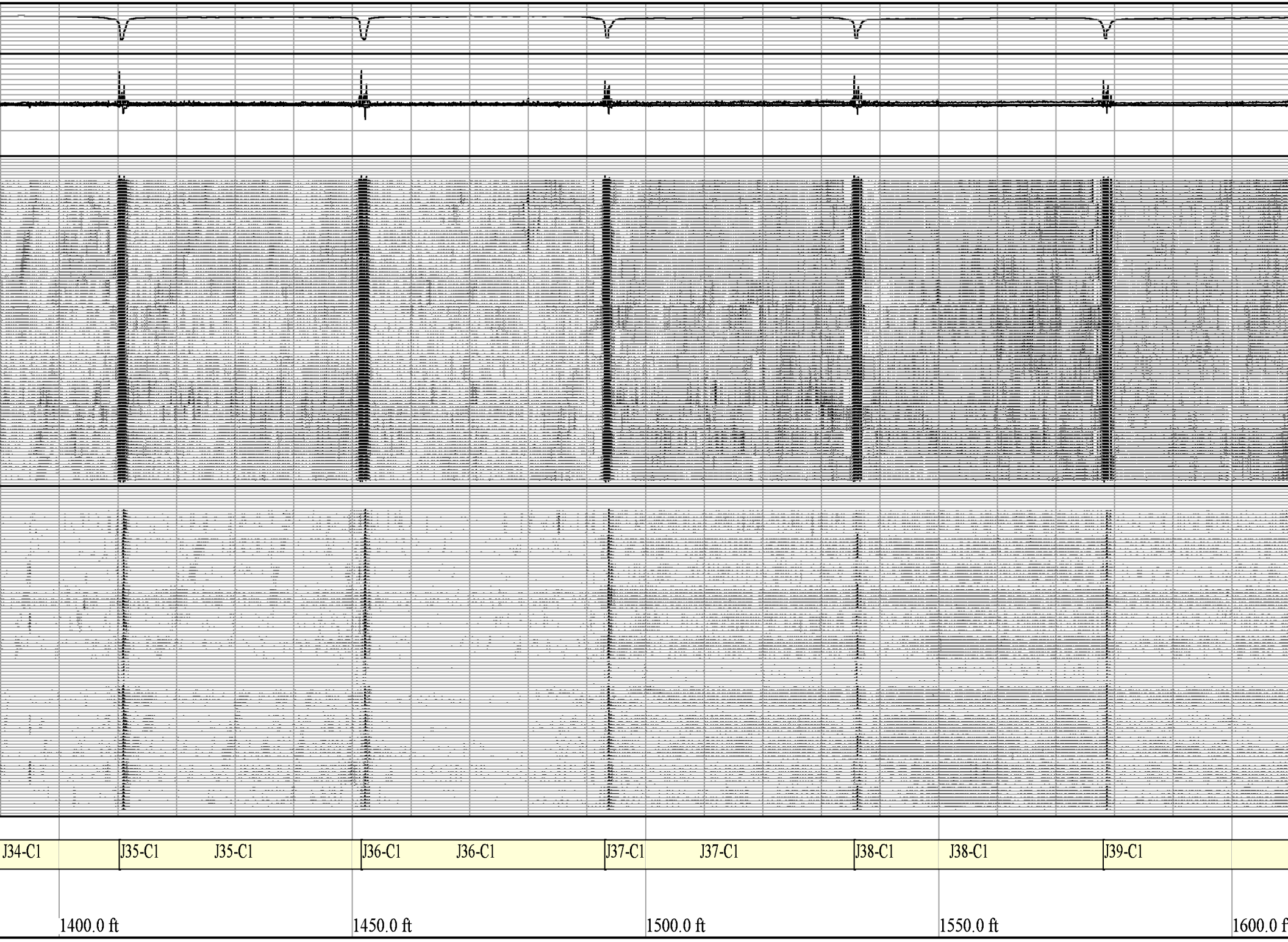
J34-C1
J35-C1
J35-C1
J36-C1
J36-C1
J37-C1
J37-C1
J38-C1
J38-C1
J39-C1
1400.0 ft
1450.0 ft
1500.0 ft
1550.0 ft
1600.0 f

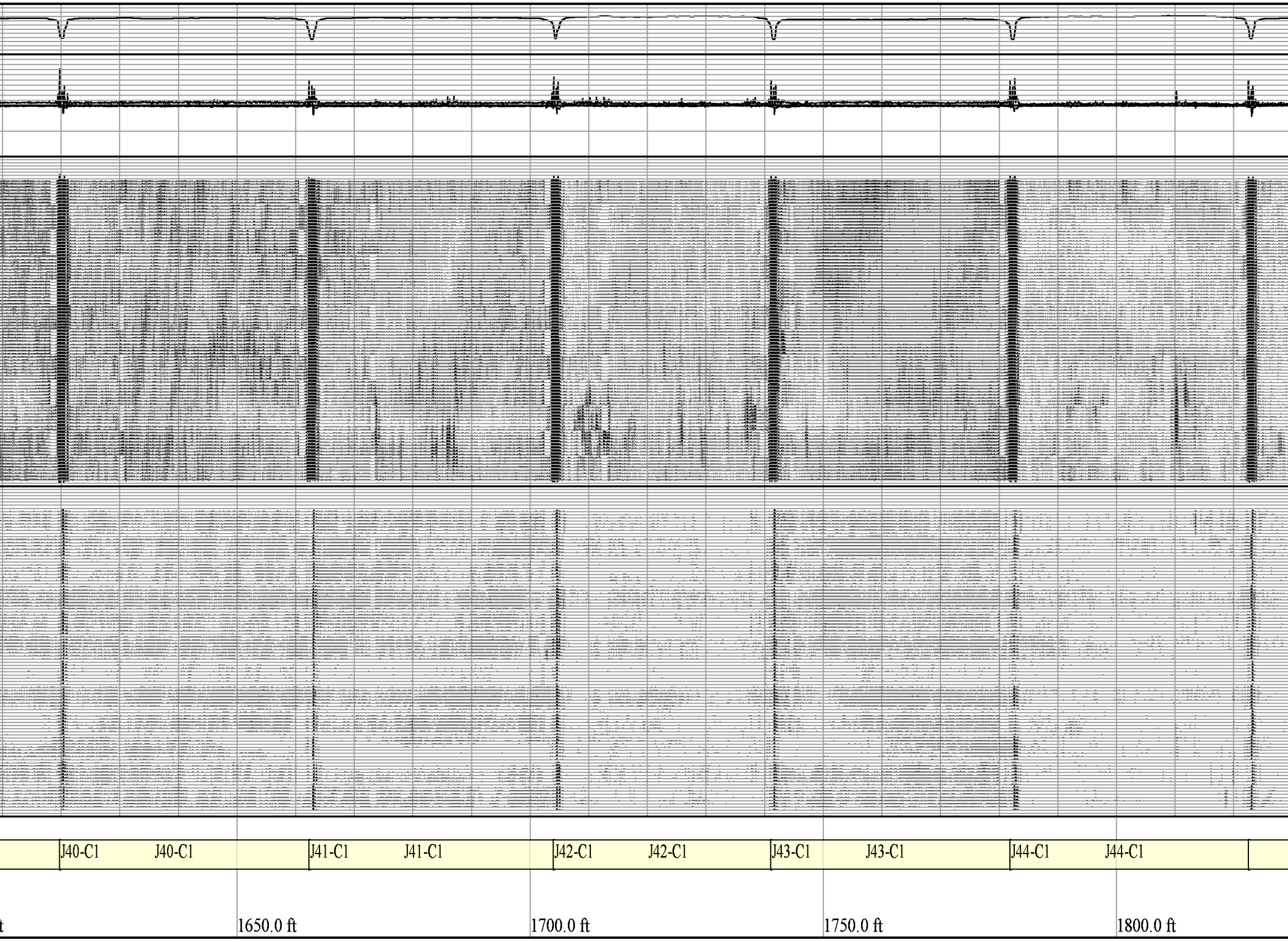
J40-C1
J40-C1
J41-C1
J41-C1
J42-C1
J42-C1
J43-C1
J43-C1
J44-C1
J44-C1
t
1650.0 ft
1700.0 ft
1750.0 ft
1800.0 ft

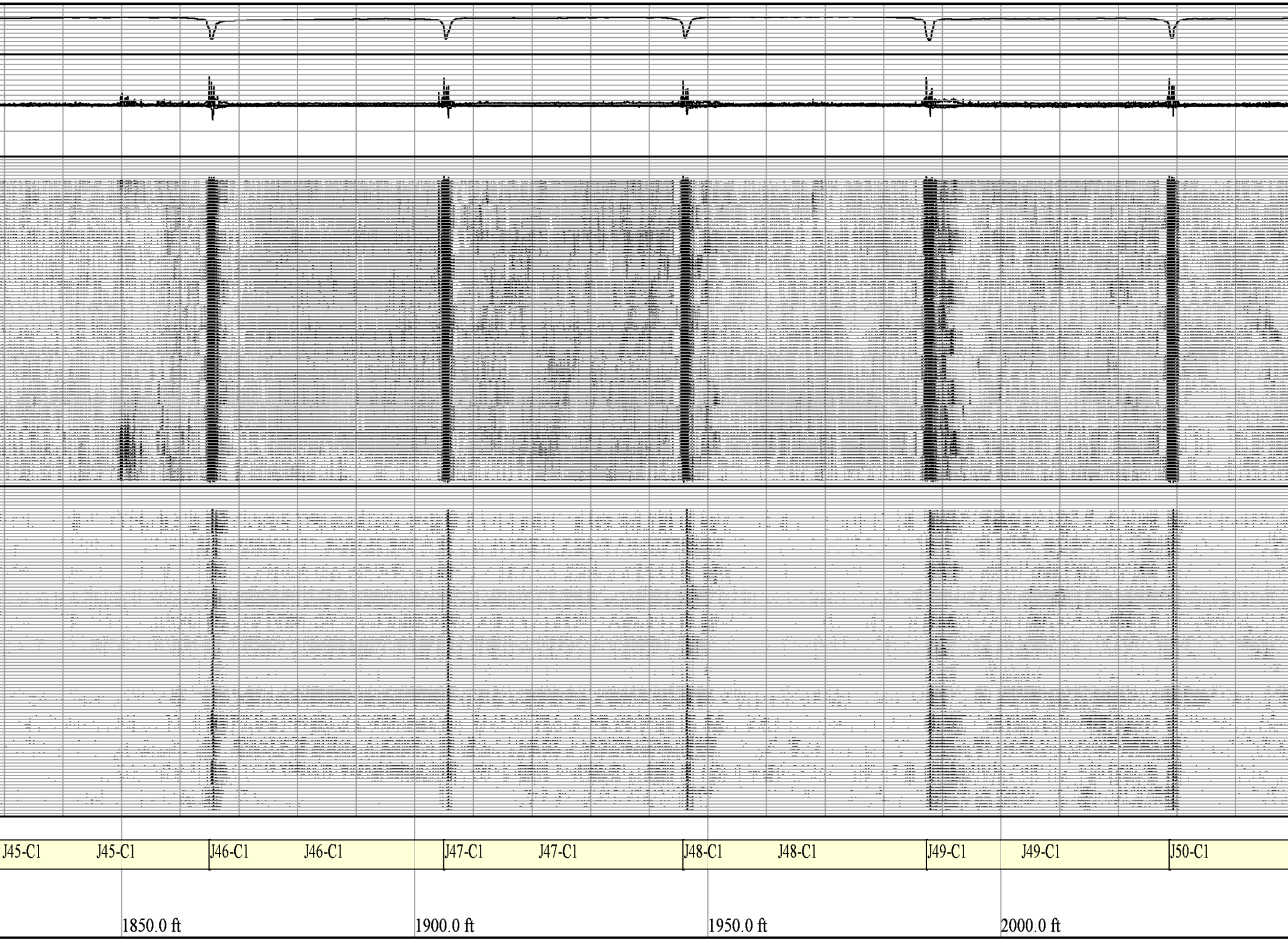
J45-C1
J45-C1
J46-C1
J46-C1
J47-C1
J47-C1
J48-C1
J48-C1
J49-C1
J49-C1
J50-C1
1850.0 ft
1900.0 ft
1950.0 ft
2000.0 ft

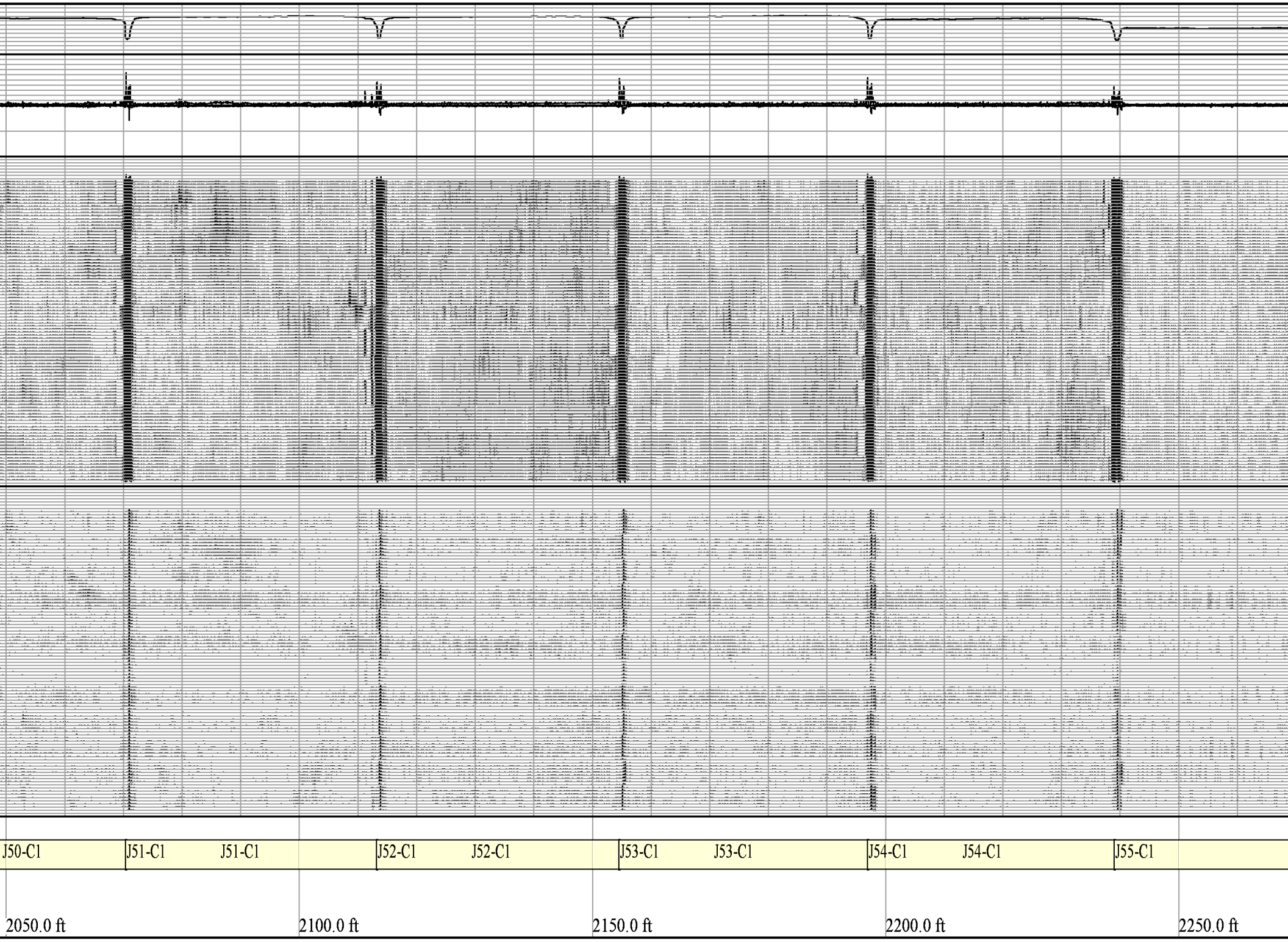
J50-C1
J51-C1
J51-C1
J52-C1
J52-C1
J53-C1
J53-C1
J54-C1
J54-C1
J55-C1
2050.0 ft
2100.0 ft
2150.0 ft
2200.0 ft
2250.0 ft

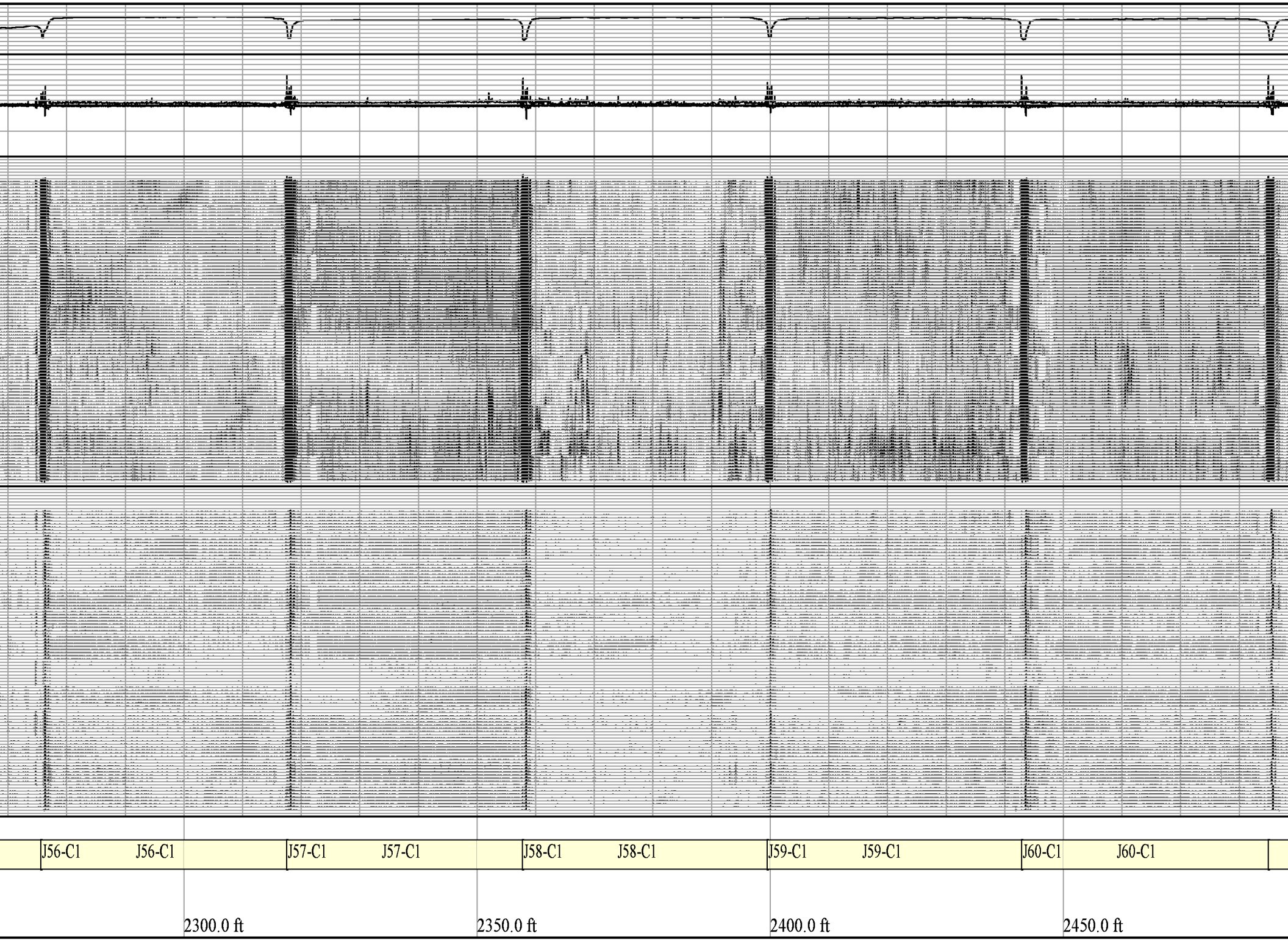
J56-C1
J56-C1
J57-C1
J57-C1
J58-C1
J58-C1
J59-C1
J59-C1
J60-C1
J60-C1
2300.0 ft
2350.0 ft
2400.0 ft
2450.0 ft

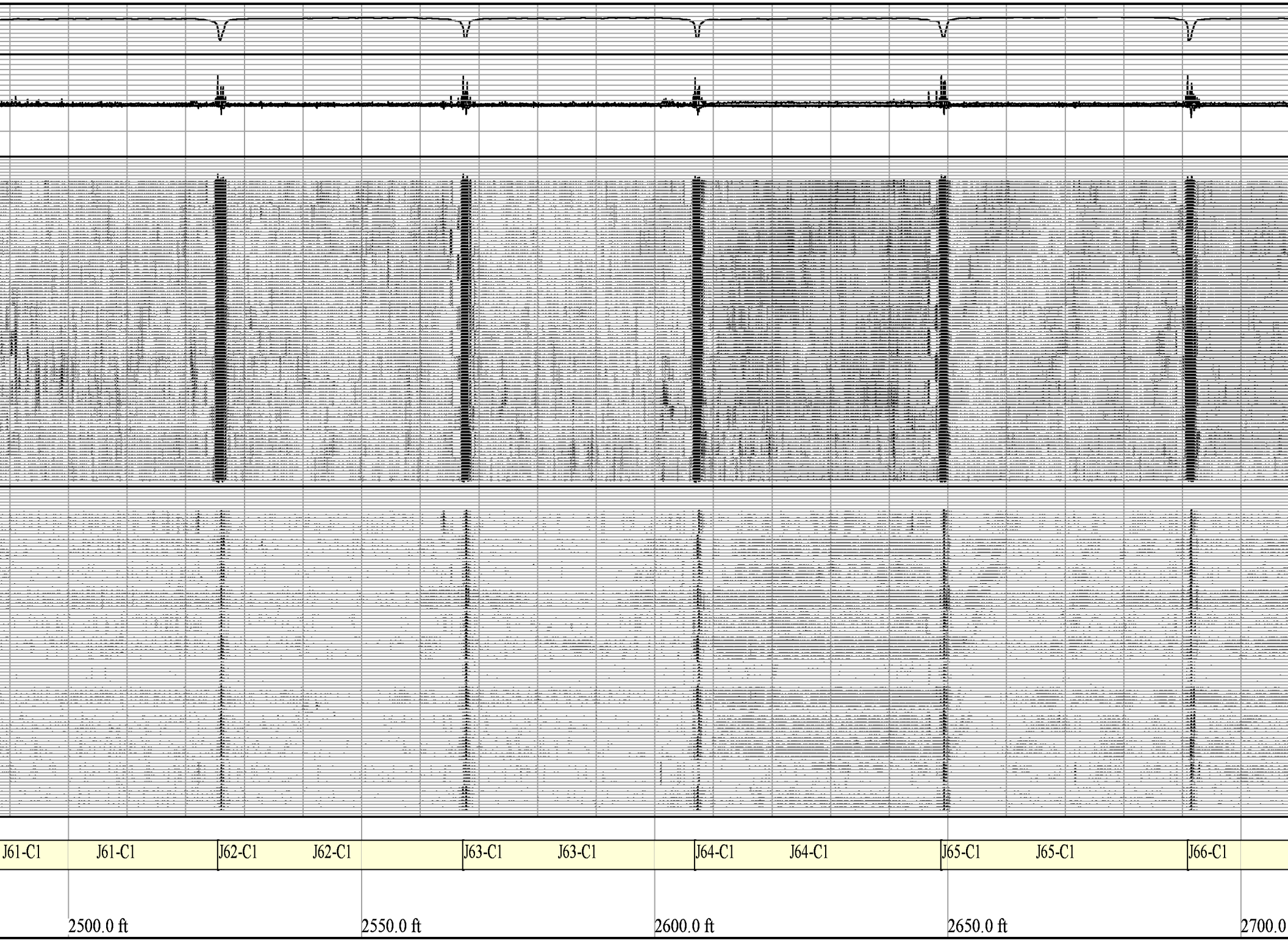
J61-C1
J61-C1
J62-C1
J62-C1
J63-C1
J63-C1
J64-C1
J64-C1
J65-C1
J65-C1
J66-C1
2500.0 ft
2550.0 ft
2600.0 ft
2650.0 ft
2700.0

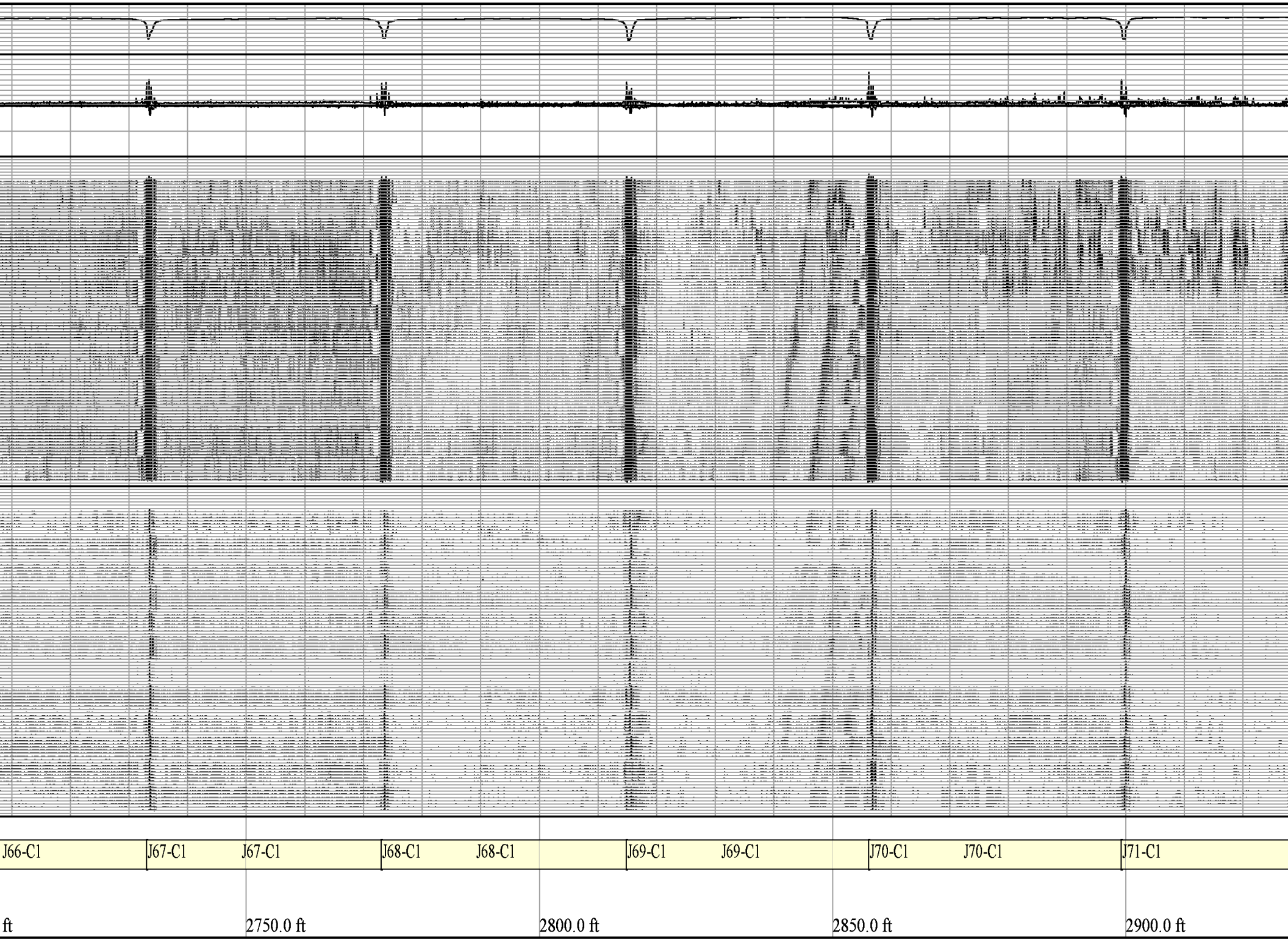
J66-C1
J67-C1
J67-C1
J68-C1
J68-C1
J69-C1
J69-C1
J70-C1
J70-C1
J71-C1
ft
2750.0 ft
2800.0 ft
2850.0 ft
2900.0 ft

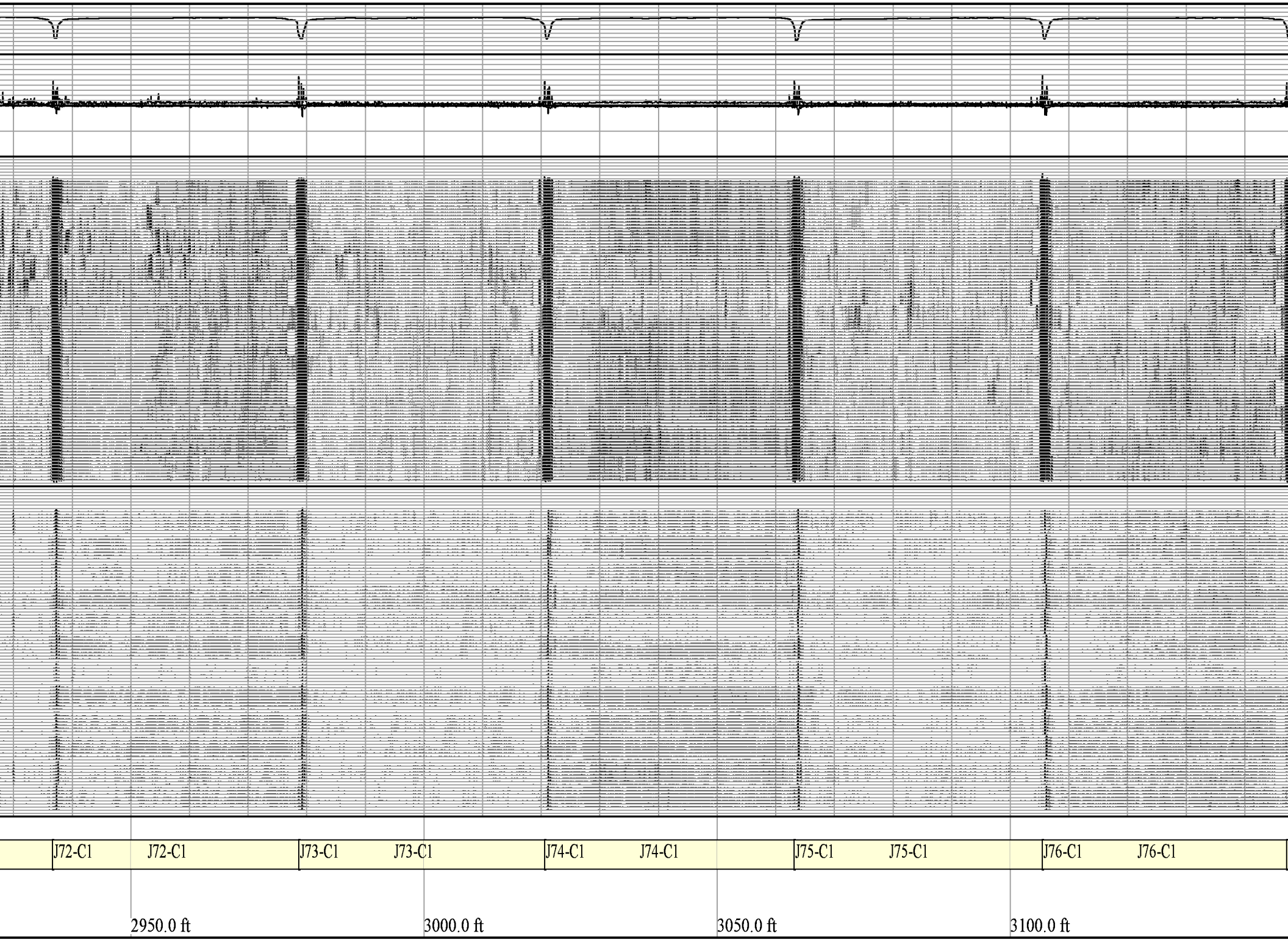
J72-C1
J72-C1
J73-C1
J73-C1
J74-C1
J74-C1
J75-C1
J75-C1
J76-C1
J76-C1
2950.0 ft
3000.0 ft
3050.0 ft
3100.0 ft

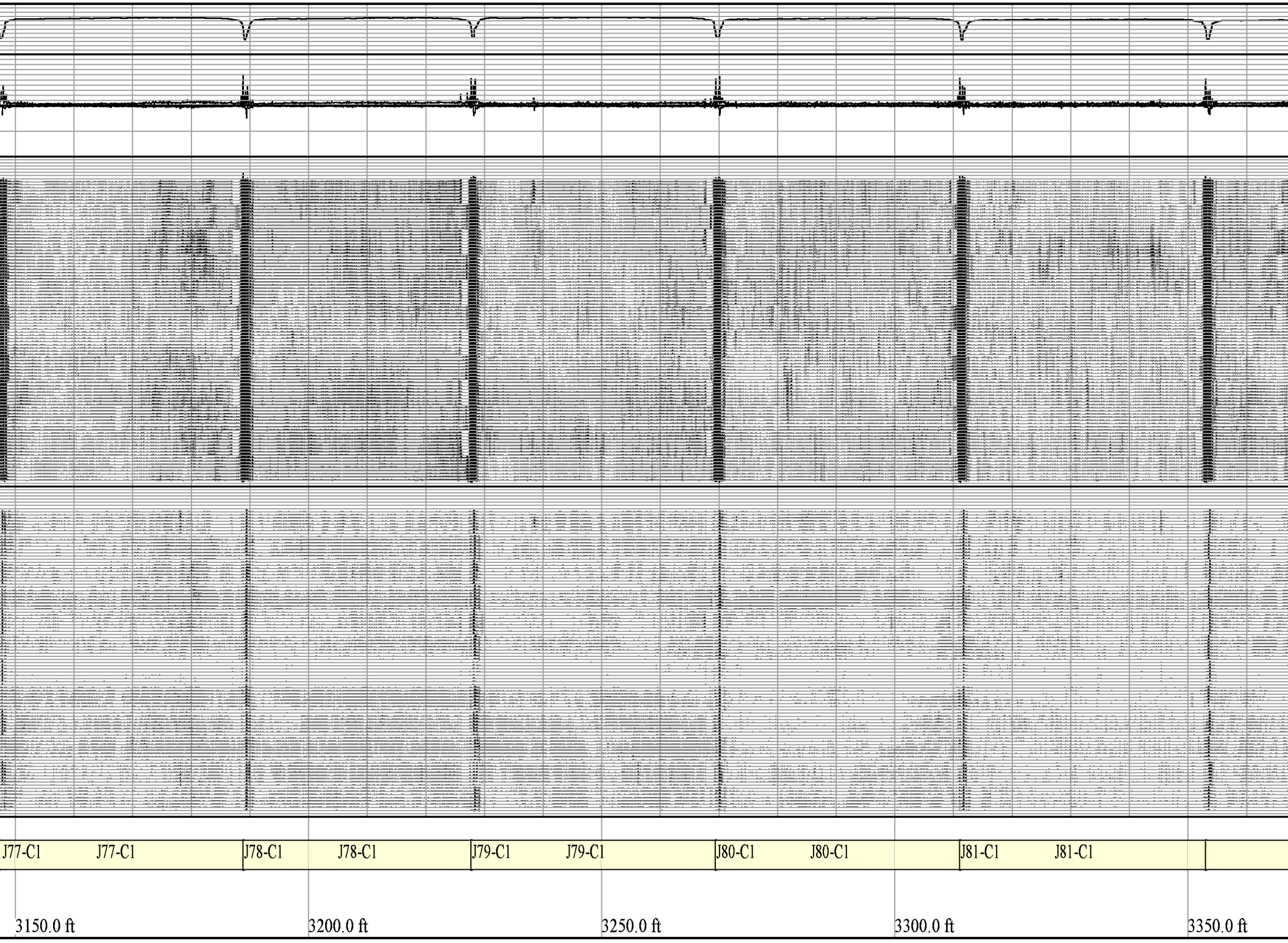
J77-C1
J77-C1
J78-C1
J78-C1
J79-C1
J79-C1
J80-C1
J80-C1
J81-C1
J81-C1
3150.0 ft
3200.0 ft
3250.0 ft
3300.0 ft
3350.0 ft

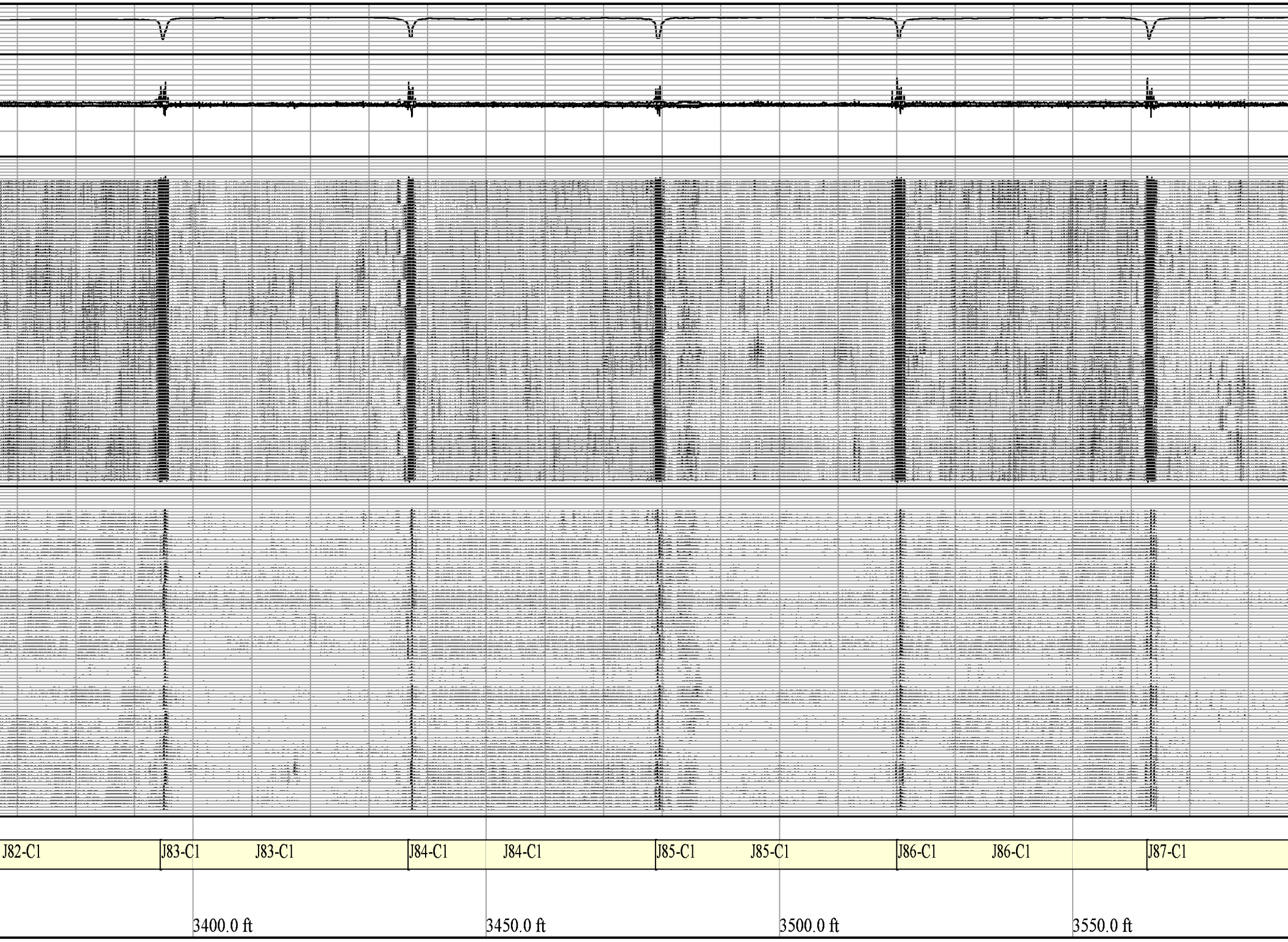
J82-C1
J83-C1
J83-C1
J84-C1
J84-C1
J85-C1
J85-C1
J86-C1
J86-C1
J87-C1
3400.0 ft
3450.0 ft
3500.0 ft
3550.0 ft

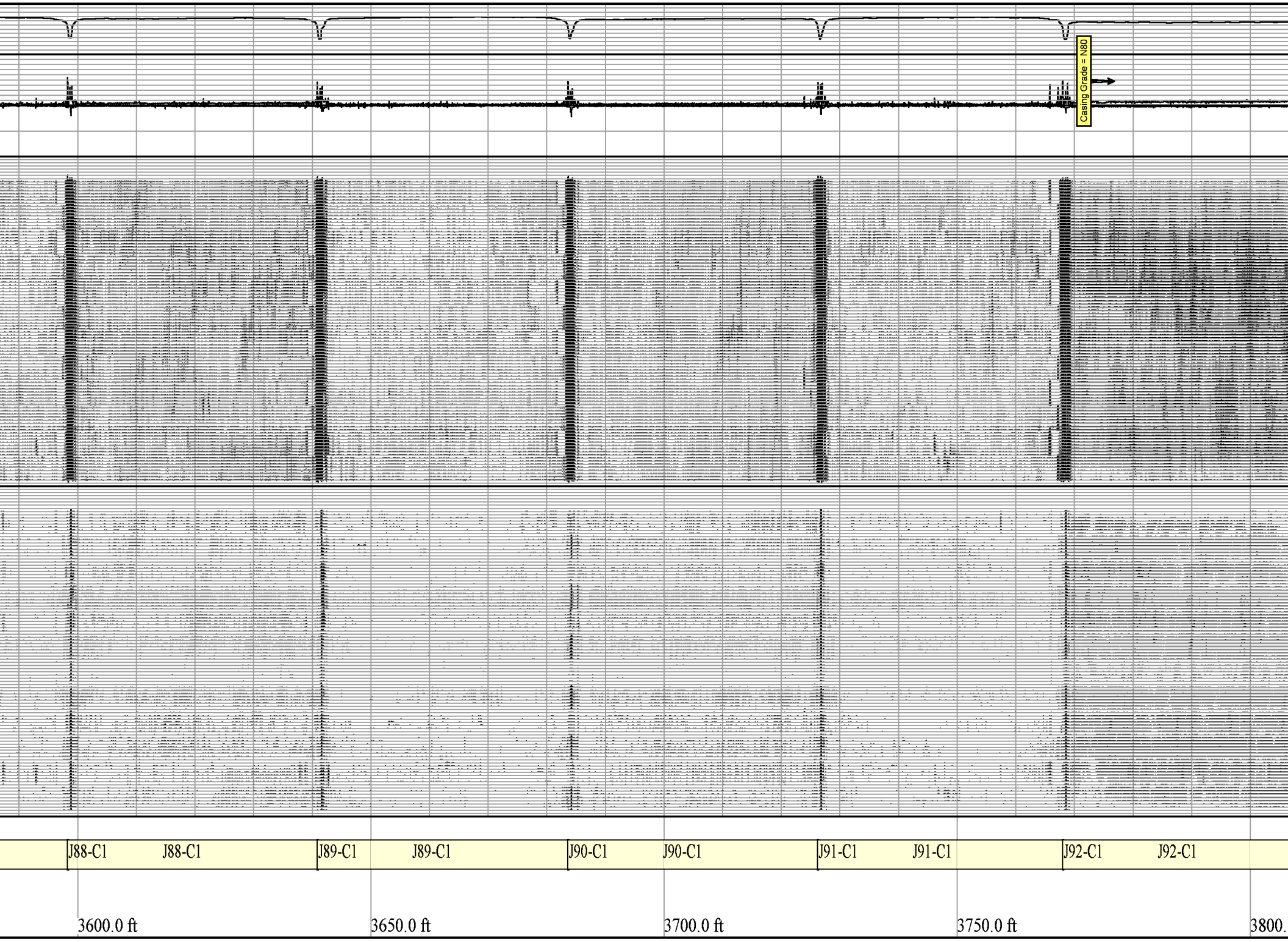
Casing Grade = N80
J88-C1
J88-C1
J89-C1
J89-C1
J90-C1
J90-C1
J91-C1
J91-C1
J92-C1
J92-C1
3600.0 ft
3650.0 ft
3700.0 ft
3750.0 ft
3800.

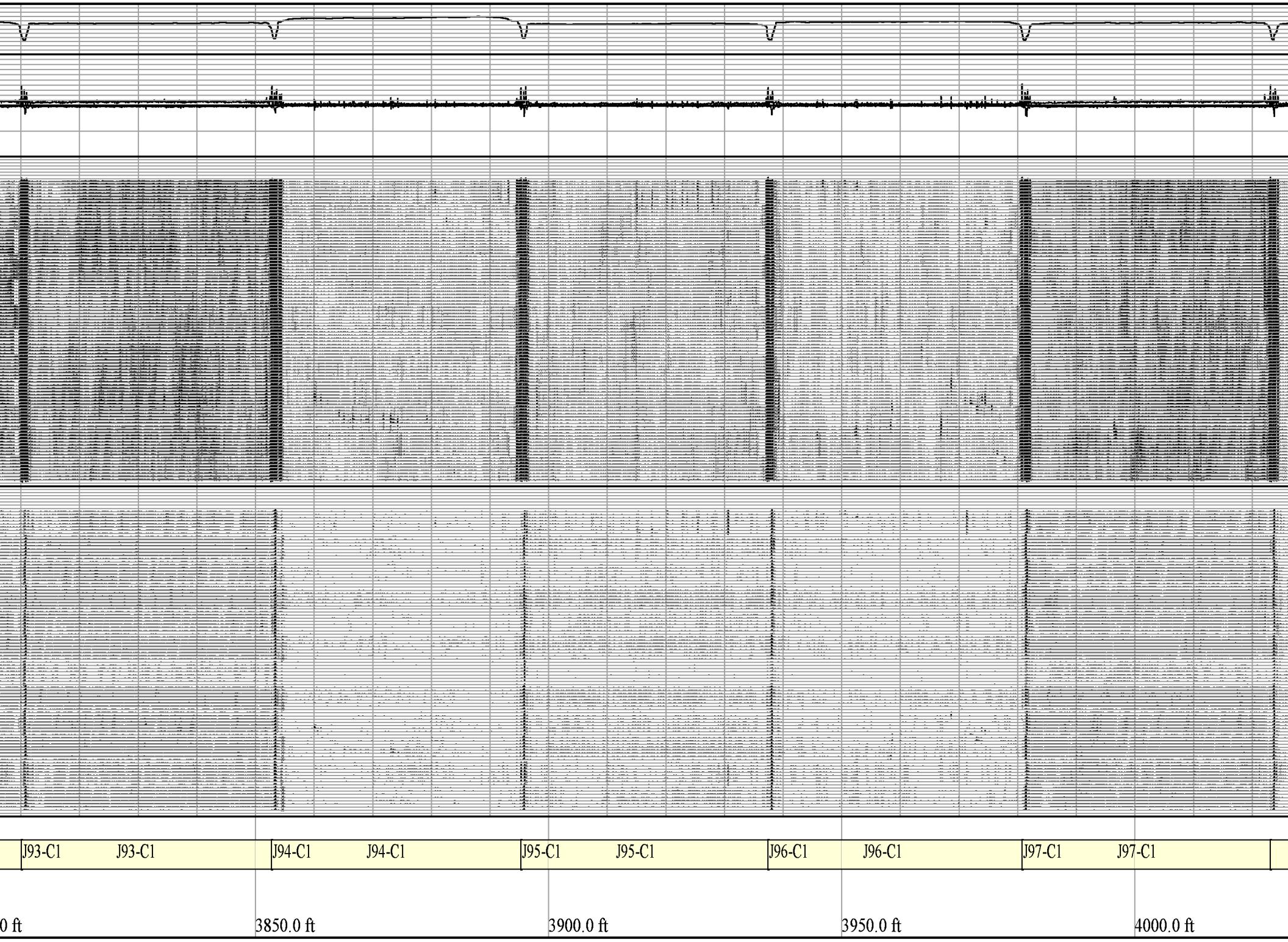
J93-C1
J93-C1
J94-C1
J94-C1
J95-C1
J95-C1
J96-C1
J96-C1
J97-C1
J97-C1
0 ft
3850.0 ft
3900.0 ft
3950.0 ft
4000.0 ft

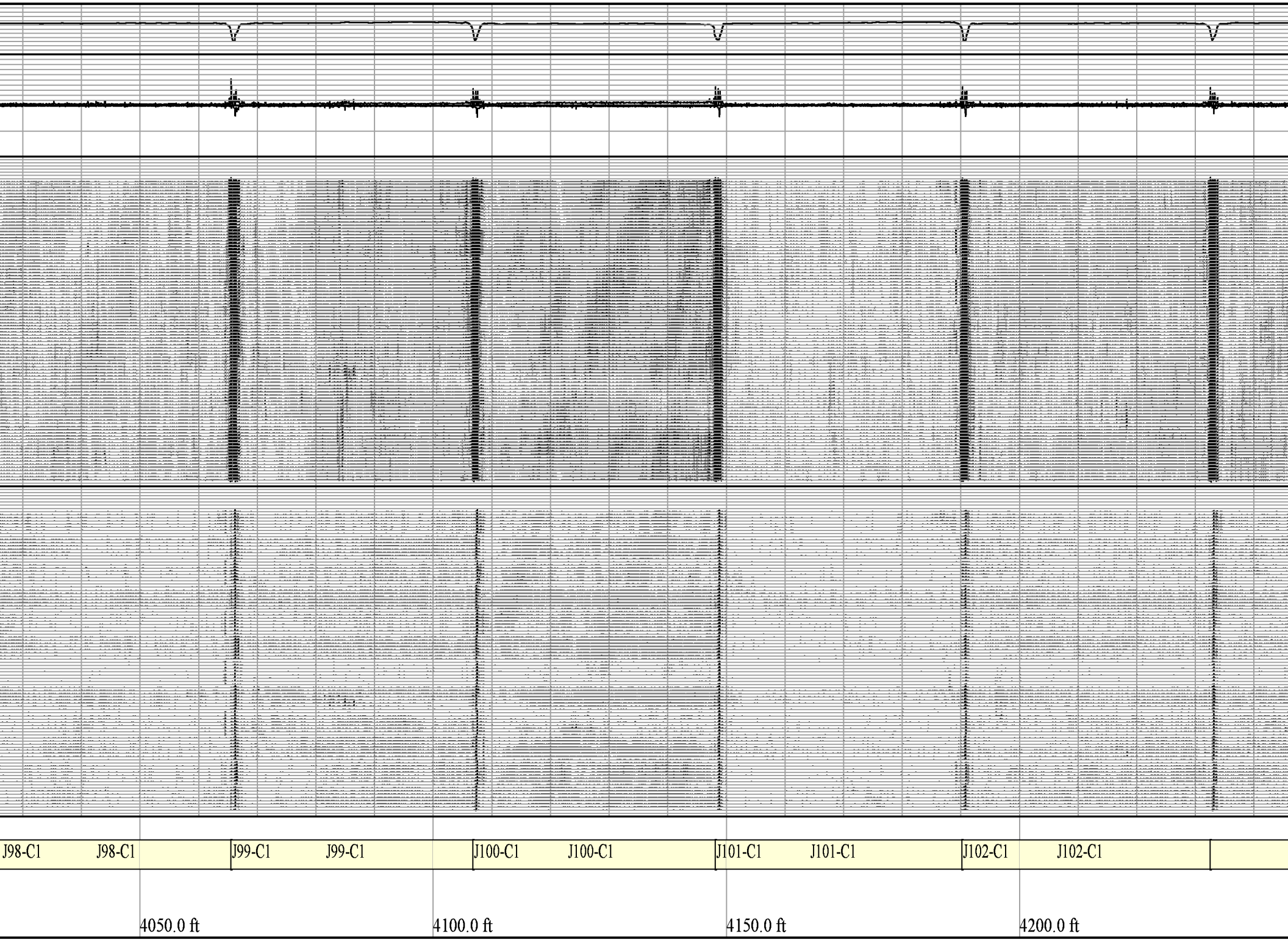
J98-C1
J98-C1
J99-C1
J99-C1
J100-C1
J100-C1
J101-C1
J101-C1
J102-C1
J102-C1
4050.0 ft
4100.0 ft
4150.0 ft
4200.0 ft

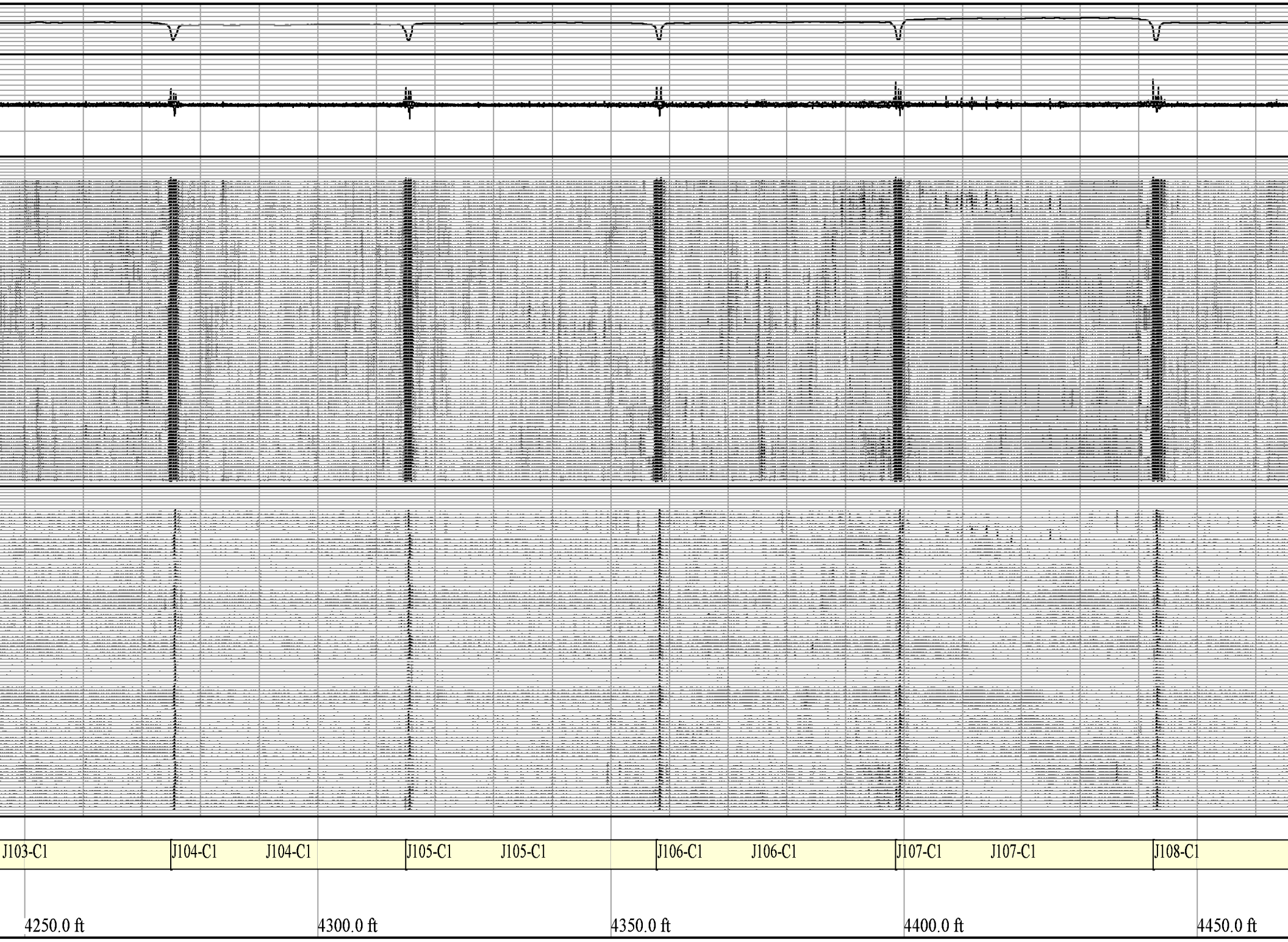
J103-C1
J104-C1
J104-C1
J105-C1
J105-C1
J106-C1
J106-C1
J107-C1
J107-C1
J108-C1
4250.0 ft
4300.0 ft
4350.0 ft
4400.0 ft
4450.0 ft

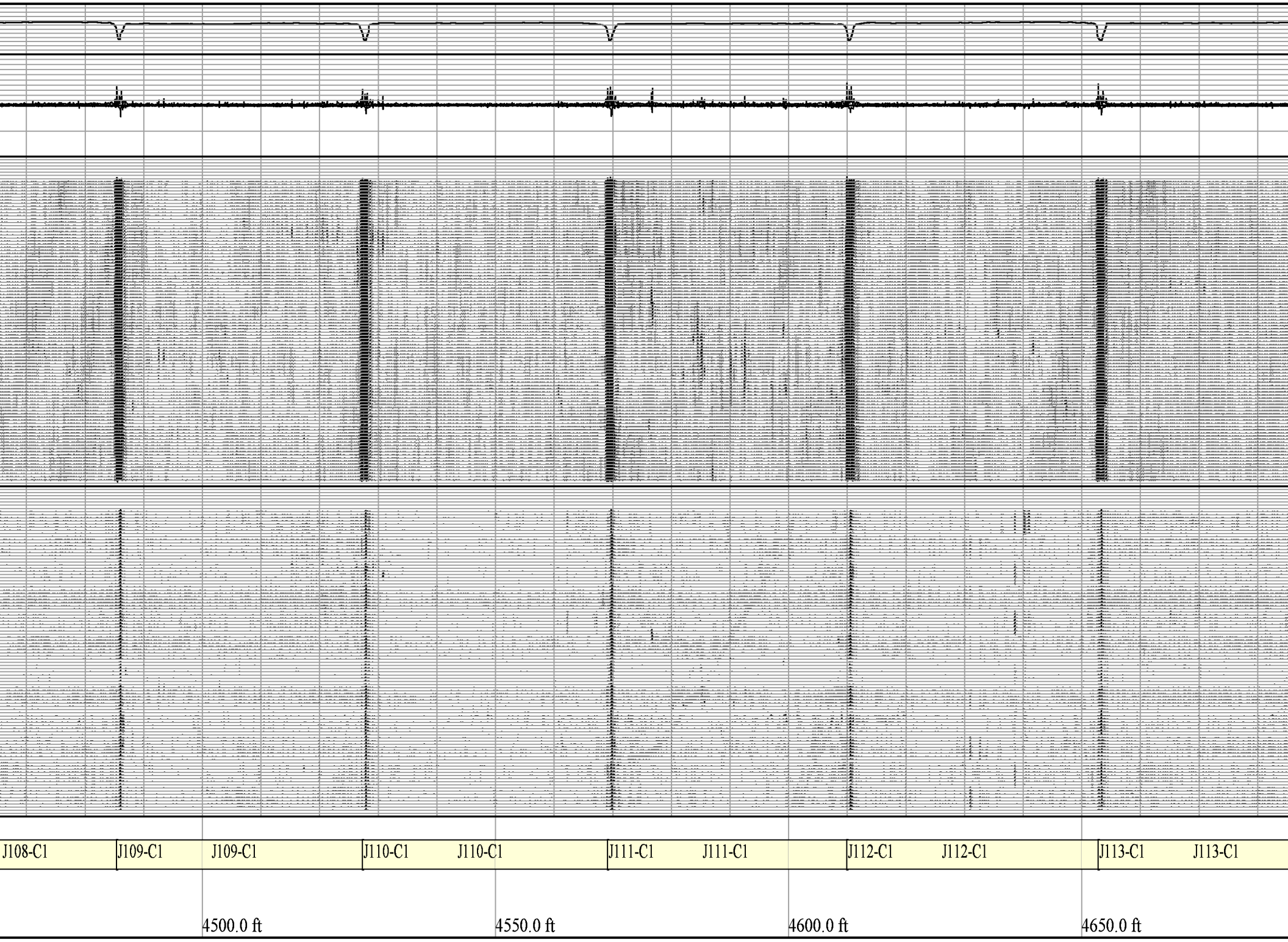
J108-C1
J109-C1
J109-C1
J110-C1
J110-C1
J111-C1
J111-C1
J112-C1
J112-C1
J113-C1
J113-C1
4500.0 ft
4550.0 ft
4600.0 ft
4650.0 ft

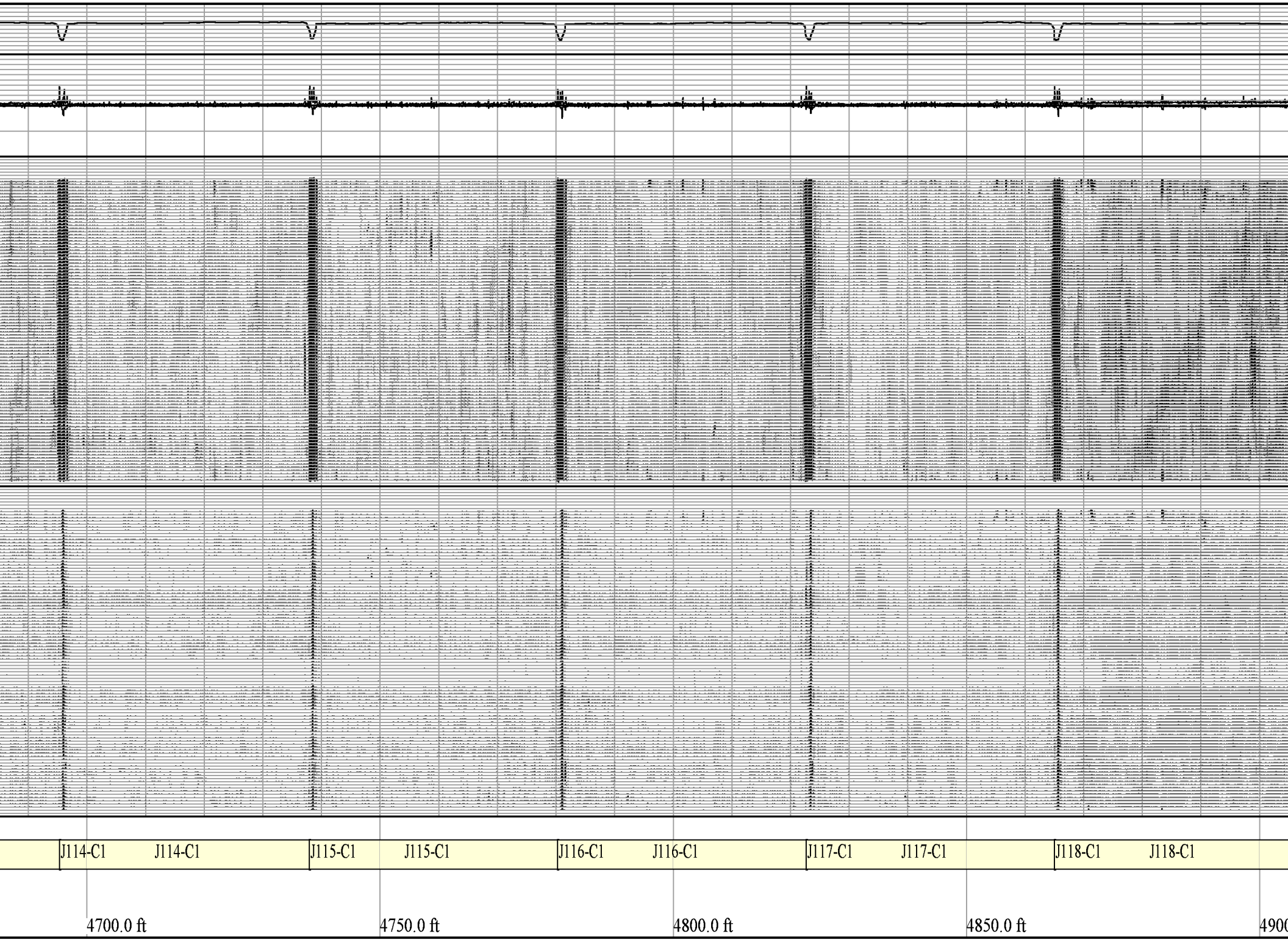
J114-C1
J114-C1
J115-C1
J115-C1
J116-C1
J116-C1
J117-C1
J117-C1
J118-C1
J118-C1
4700.0 ft
4750.0 ft
4800.0 ft
4850.0 ft
4900

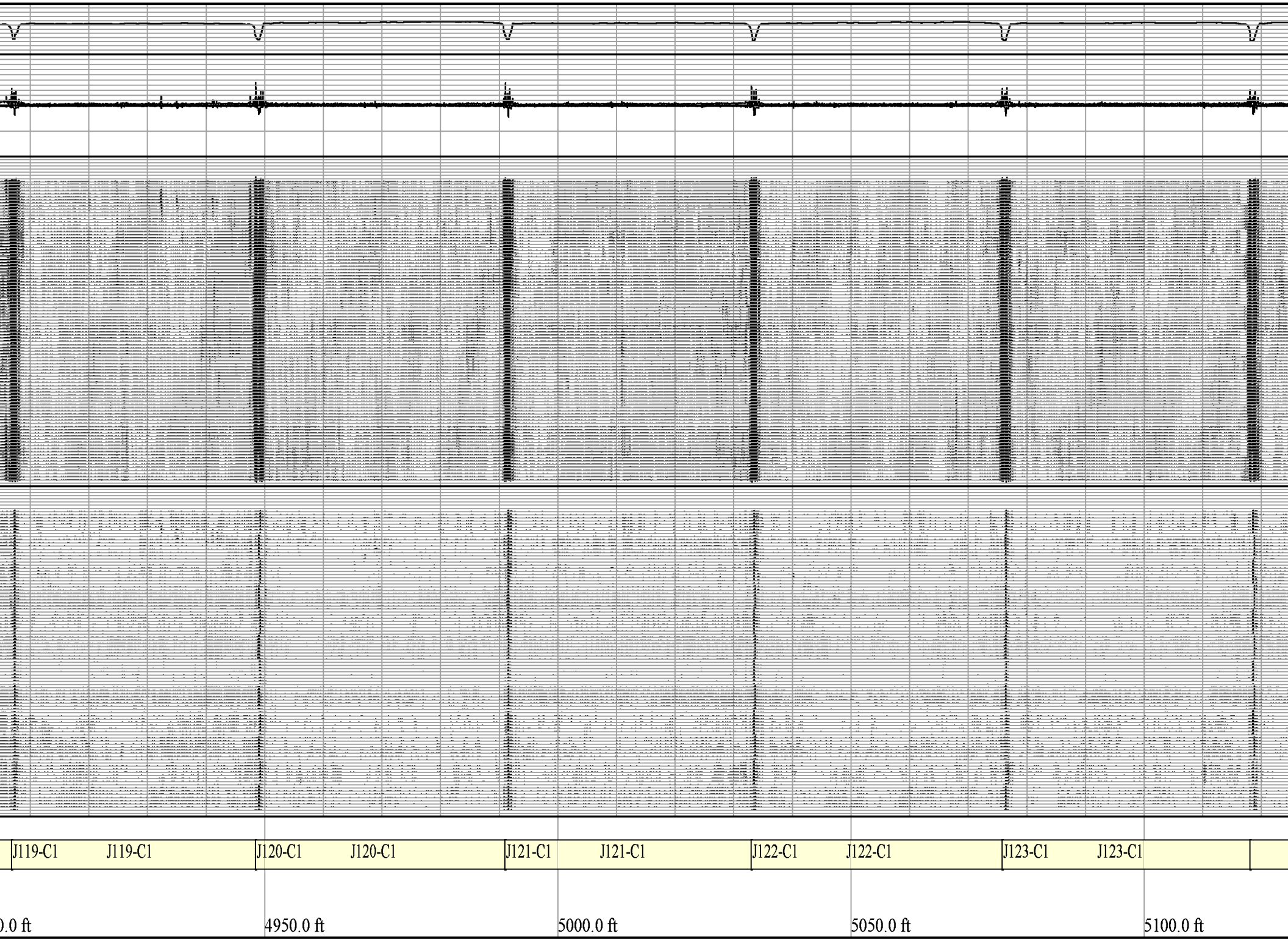
J119-C1
J119-C1
J120-C1
J120-C1
J121-C1
J121-C1
J122-C1
J122-C1
J123-C1
J123-C1
0.0 ft
4950.0 ft
5000.0 ft
5050.0 ft
5100.0 ft

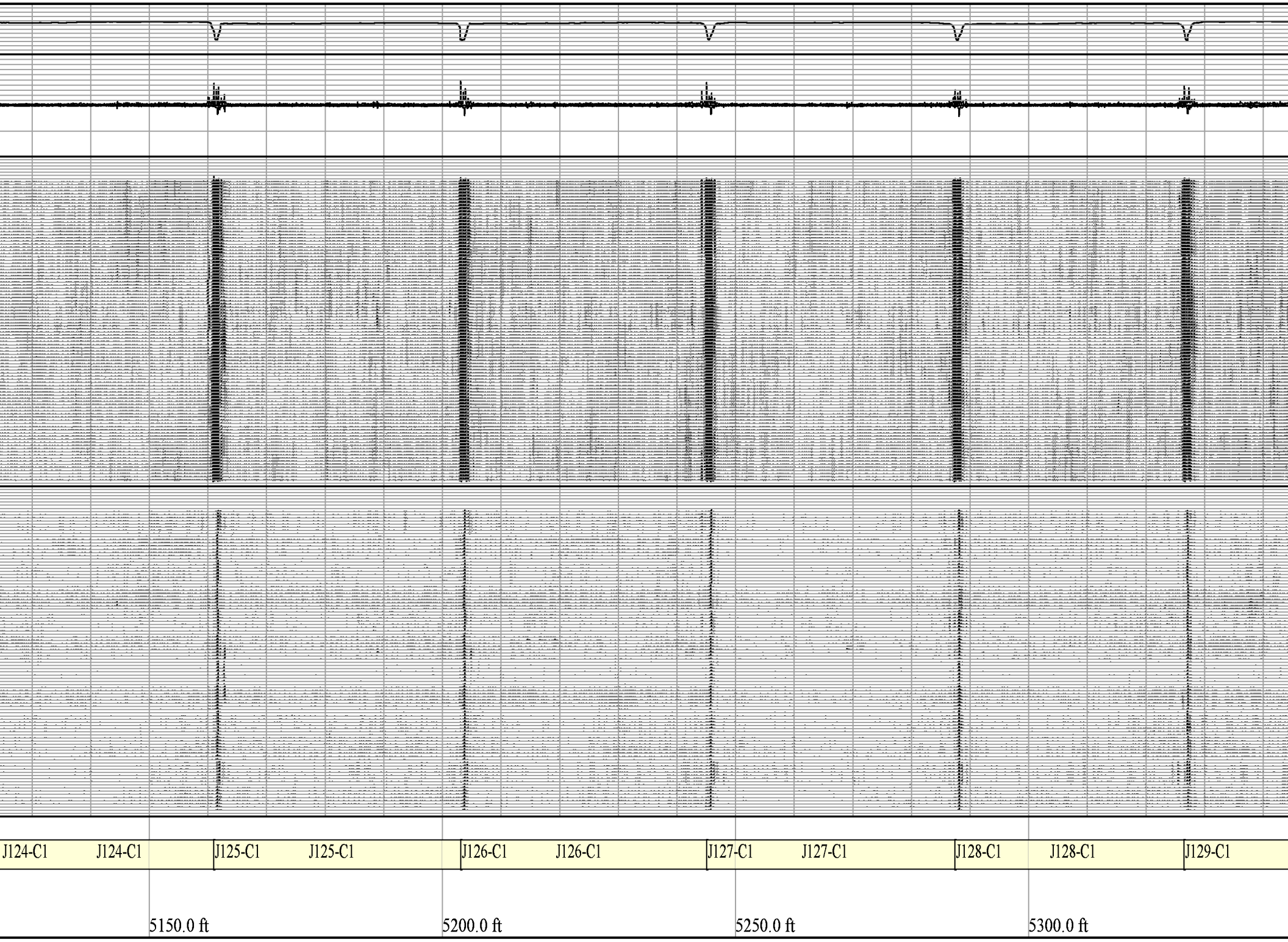
J124-C1
J124-C1
J125-C1
J125-C1
J126-C1
J126-C1
J127-C1
J127-C1
J128-C1
J128-C1
J129-C1
5150.0 ft
5200.0 ft
5250.0 ft
5300.0 ft

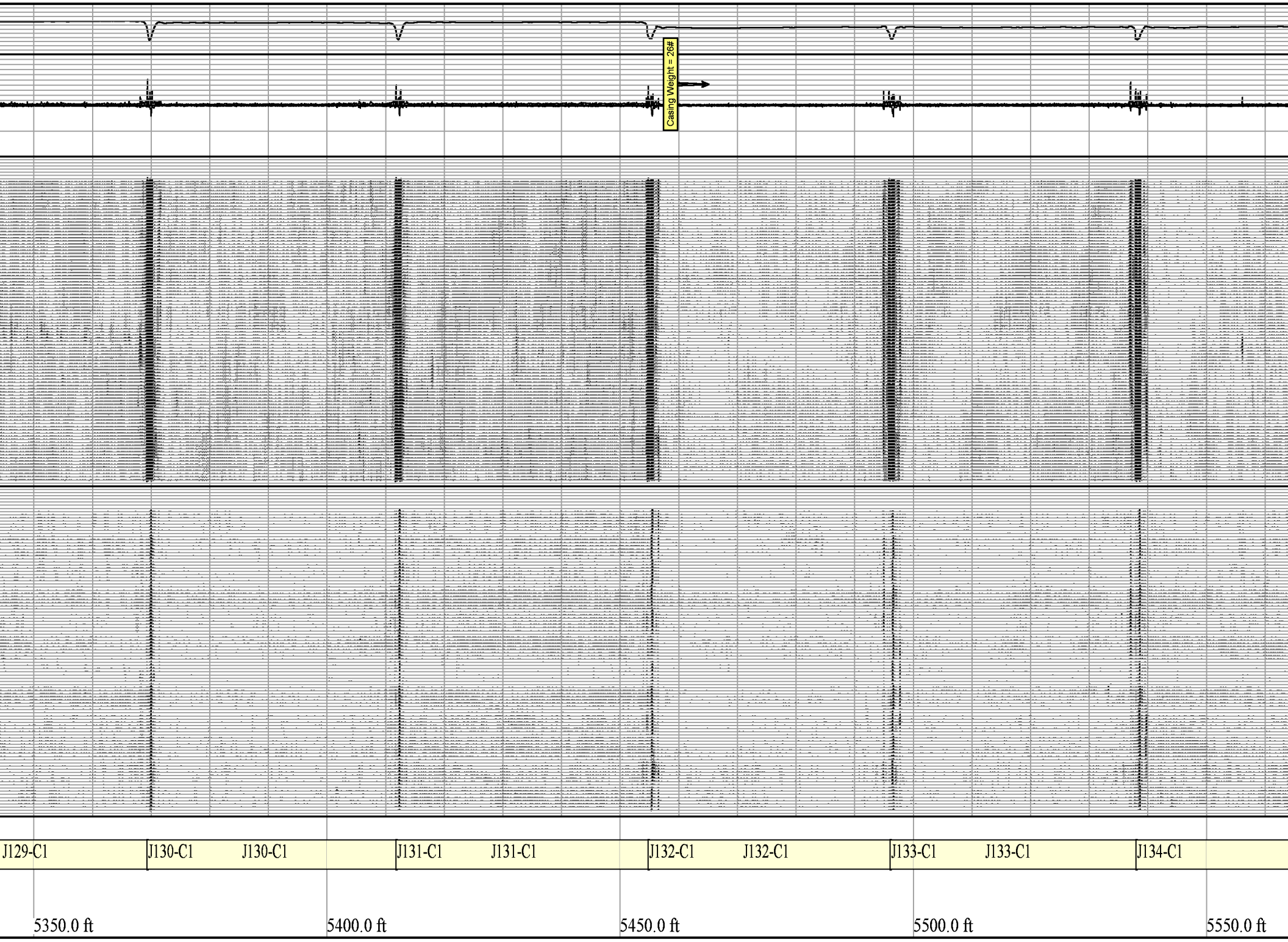
Casing Weight = 26#
J129-C1
J130-C1
J130-C1
J131-C1
J131-C1
J132-C1
J132-C1
J133-C1
J133-C1
J134-C1
5350.0 ft
5400.0 ft
5450.0 ft
5500.0 ft
5550.0 ft

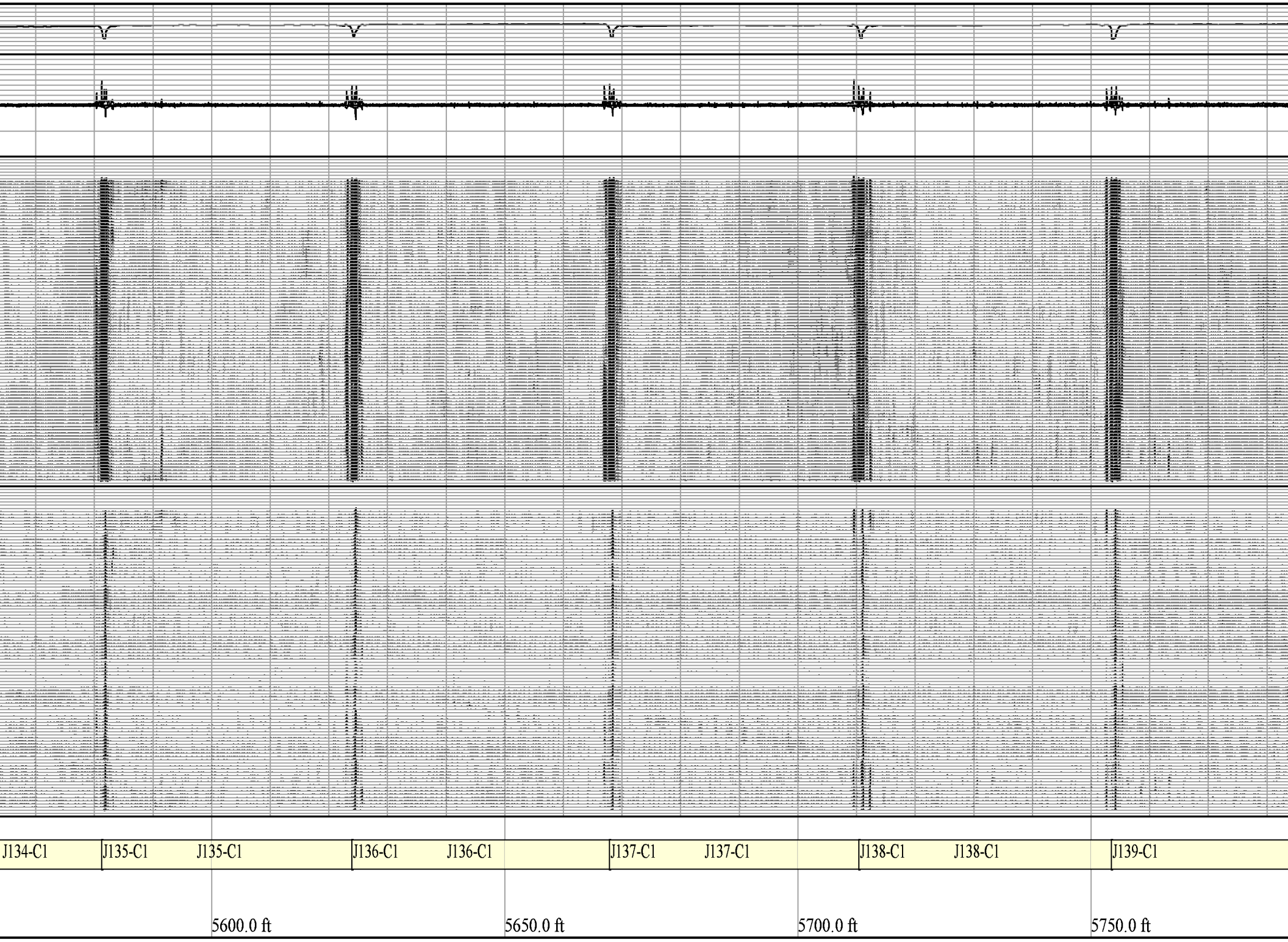
J134-C1
J135-C1
J135-C1
J136-C1
J136-C1
J137-C1
J137-C1
J138-C1
J138-C1
J139-C1
5600.0 ft
5650.0 ft
5700.0 ft
5750.0 ft

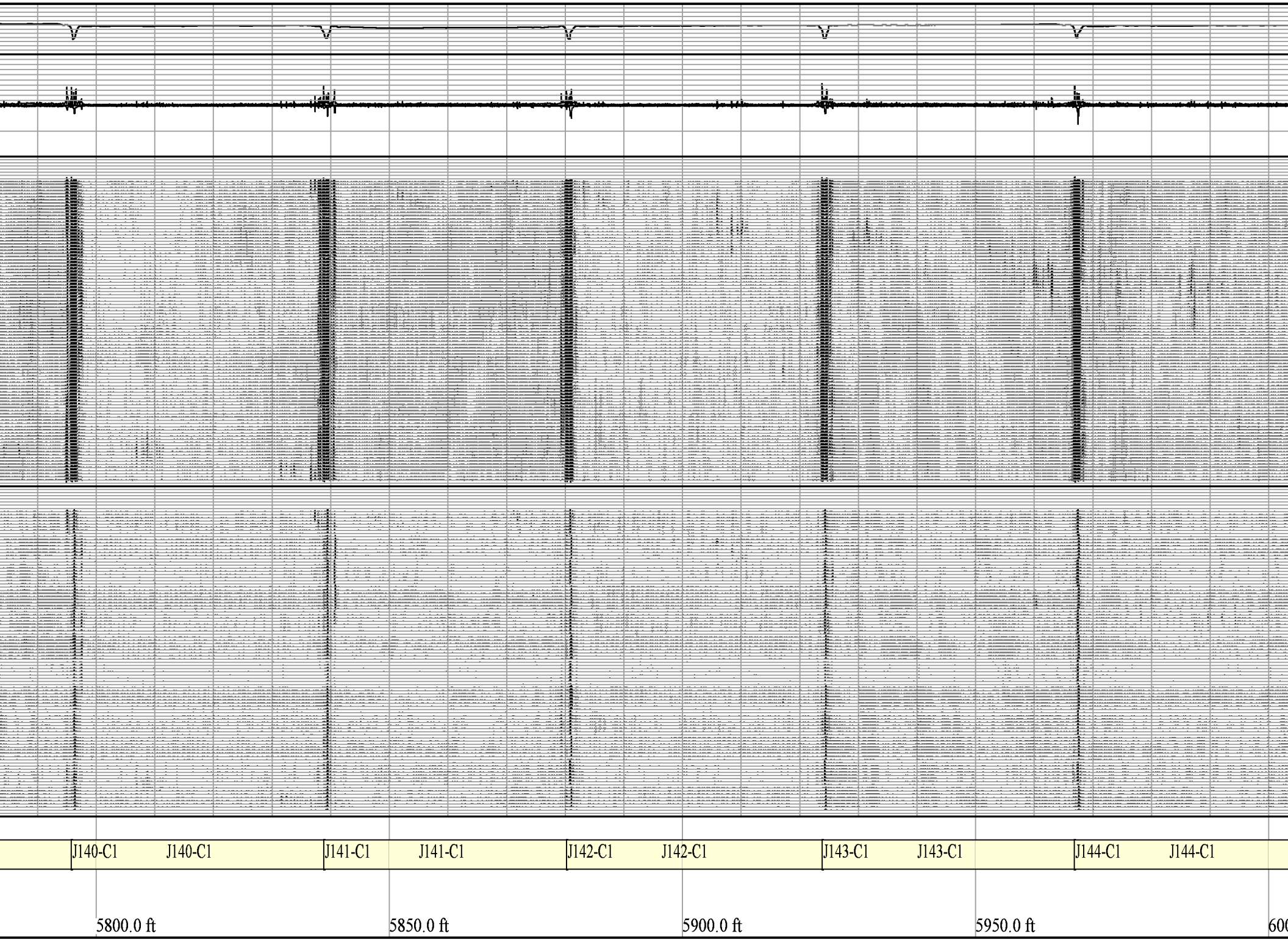
J140-C1
J140-C1
J141-C1
J141-C1
J142-C1
J142-C1
J143-C1
J143-C1
J144-C1
J144-C1
5800.0 ft
5850.0 ft
5900.0 ft
5950.0 ft
600

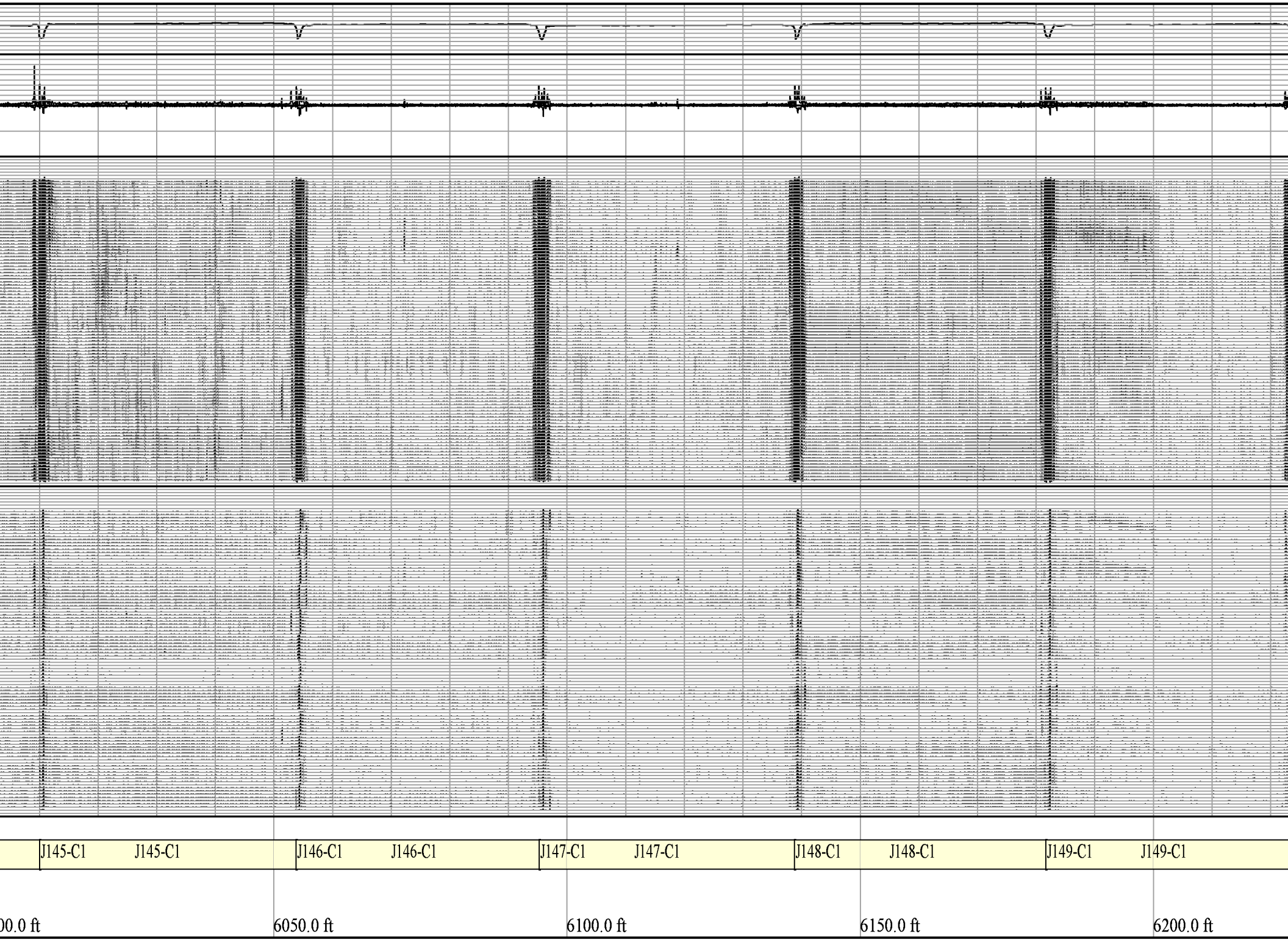
J145-C1
J145-C1
J146-C1
J146-C1
J147-C1
J147-C1
J148-C1
J148-C1
J149-C1
J149-C1
00.0 ft
6050.0 ft
6100.0 ft
6150.0 ft
6200.0 ft

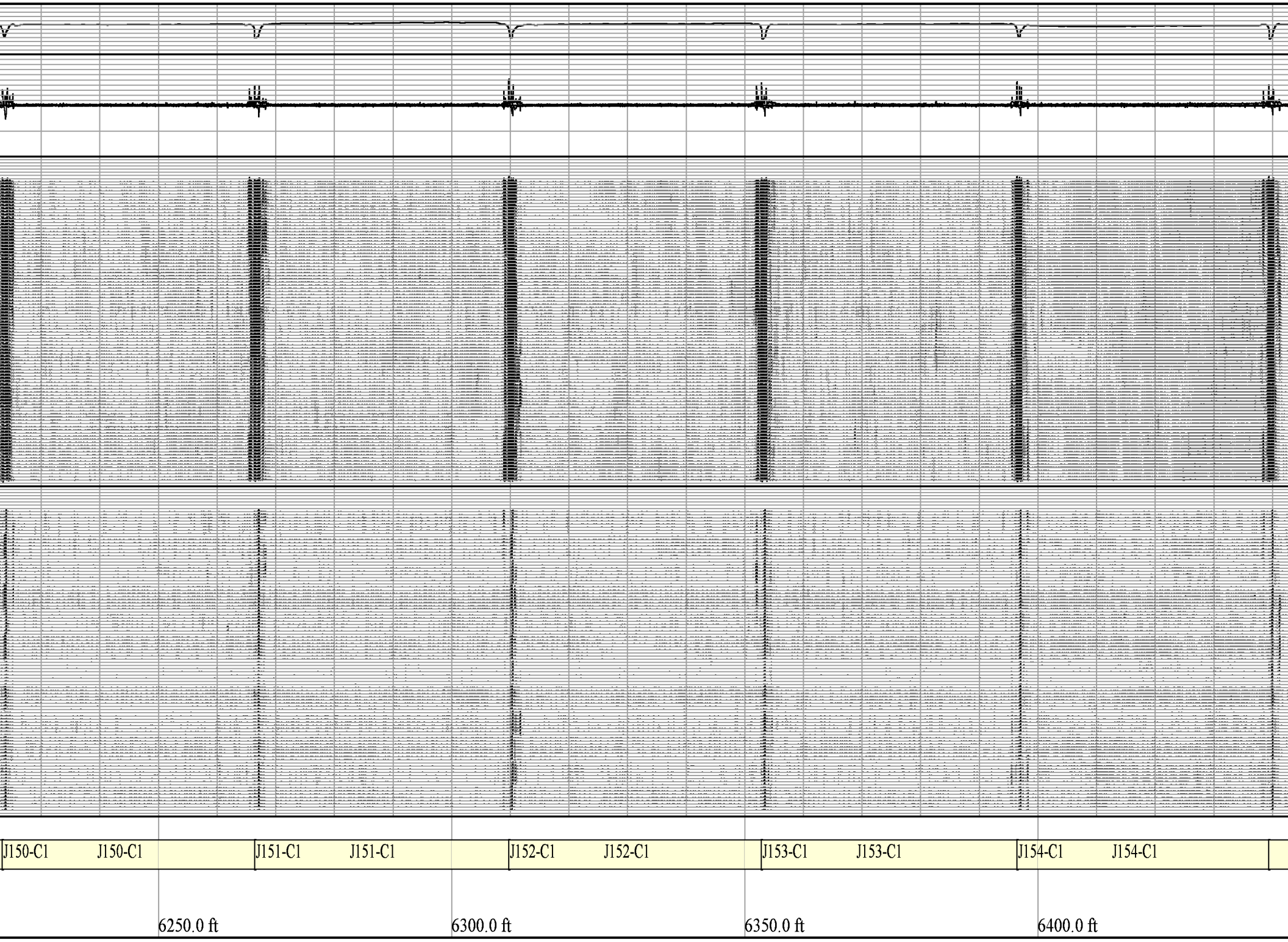
J150-C1
J150-C1
J151-C1
J151-C1
J152-C1
J152-C1
J153-C1
J153-C1
J154-C1
J154-C1
6250.0 ft
6300.0 ft
6350.0 ft
6400.0 ft

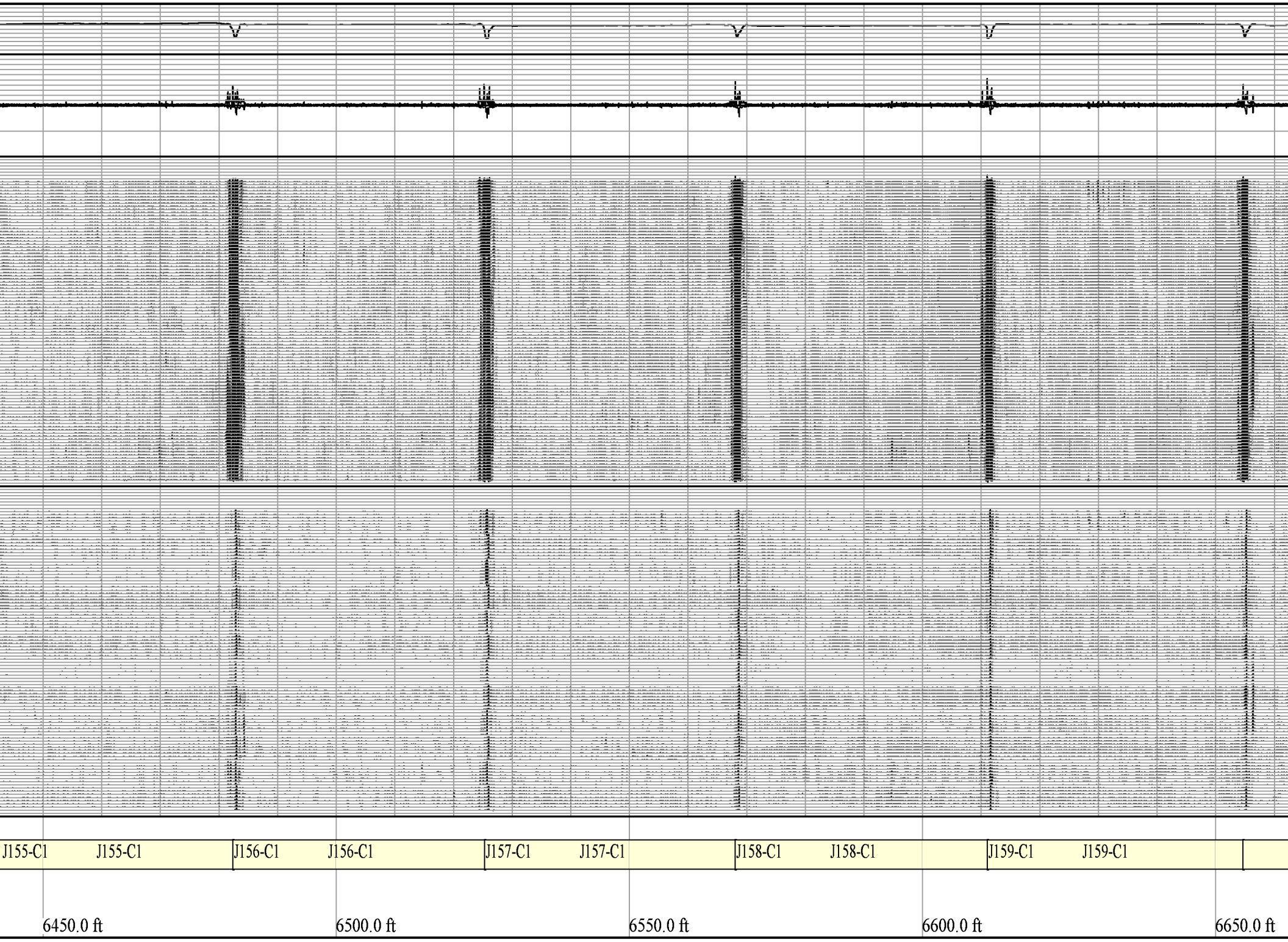
J155-C1
J155-C1
J156-C1
J156-C1
J157-C1
J157-C1
J158-C1
J158-C1
J159-C1
J159-C1
6450.0 ft
6500.0 ft
6550.0 ft
6600.0 ft
6650.0 ft

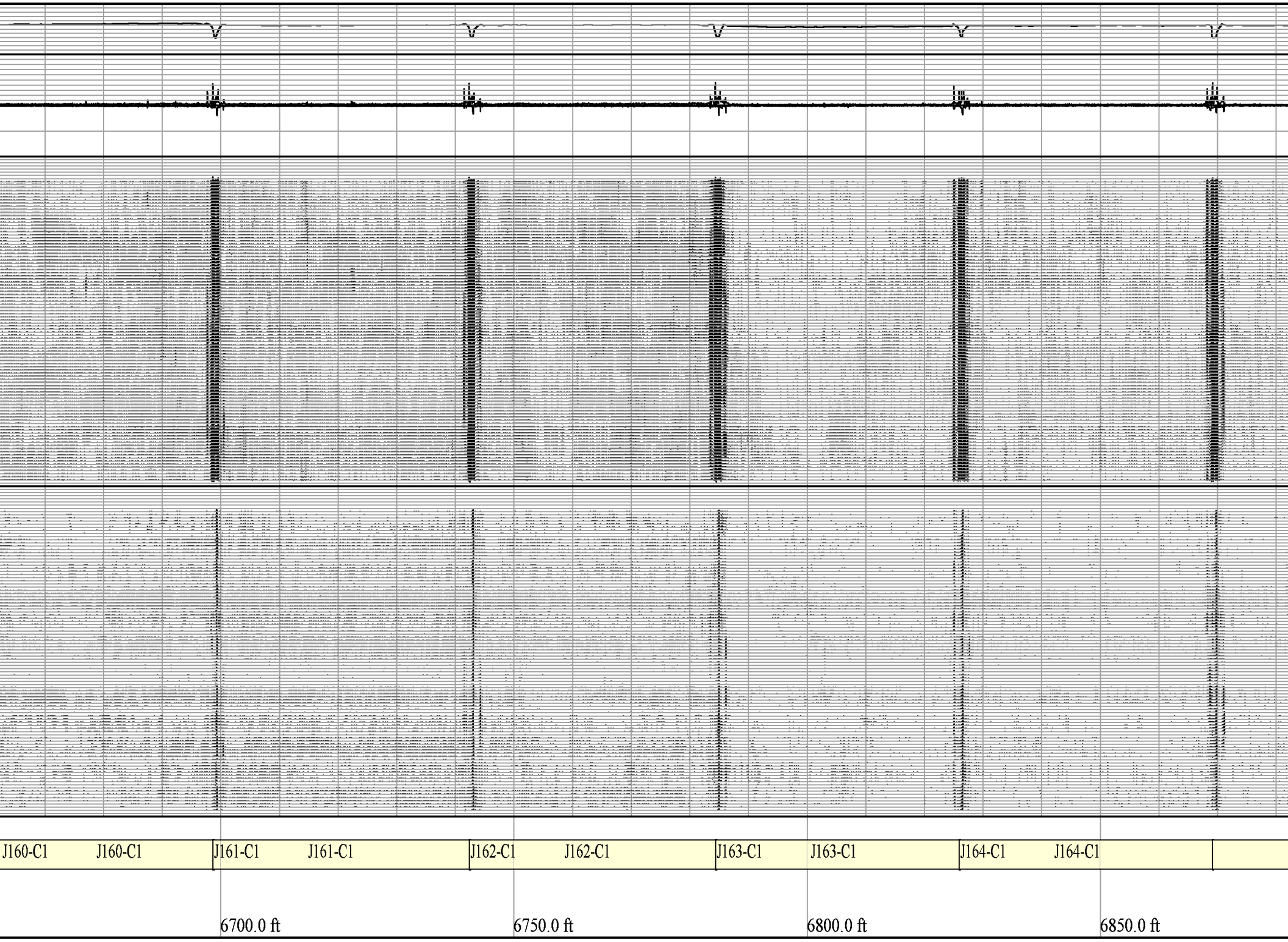
J160-C1
J160-C1
J161-C1
J161-C1
J162-C1
J162-C1
J163-C1
J163-C1
J164-C1
J164-C1
6700.0 ft
6750.0 ft
6800.0 ft
6850.0 ft

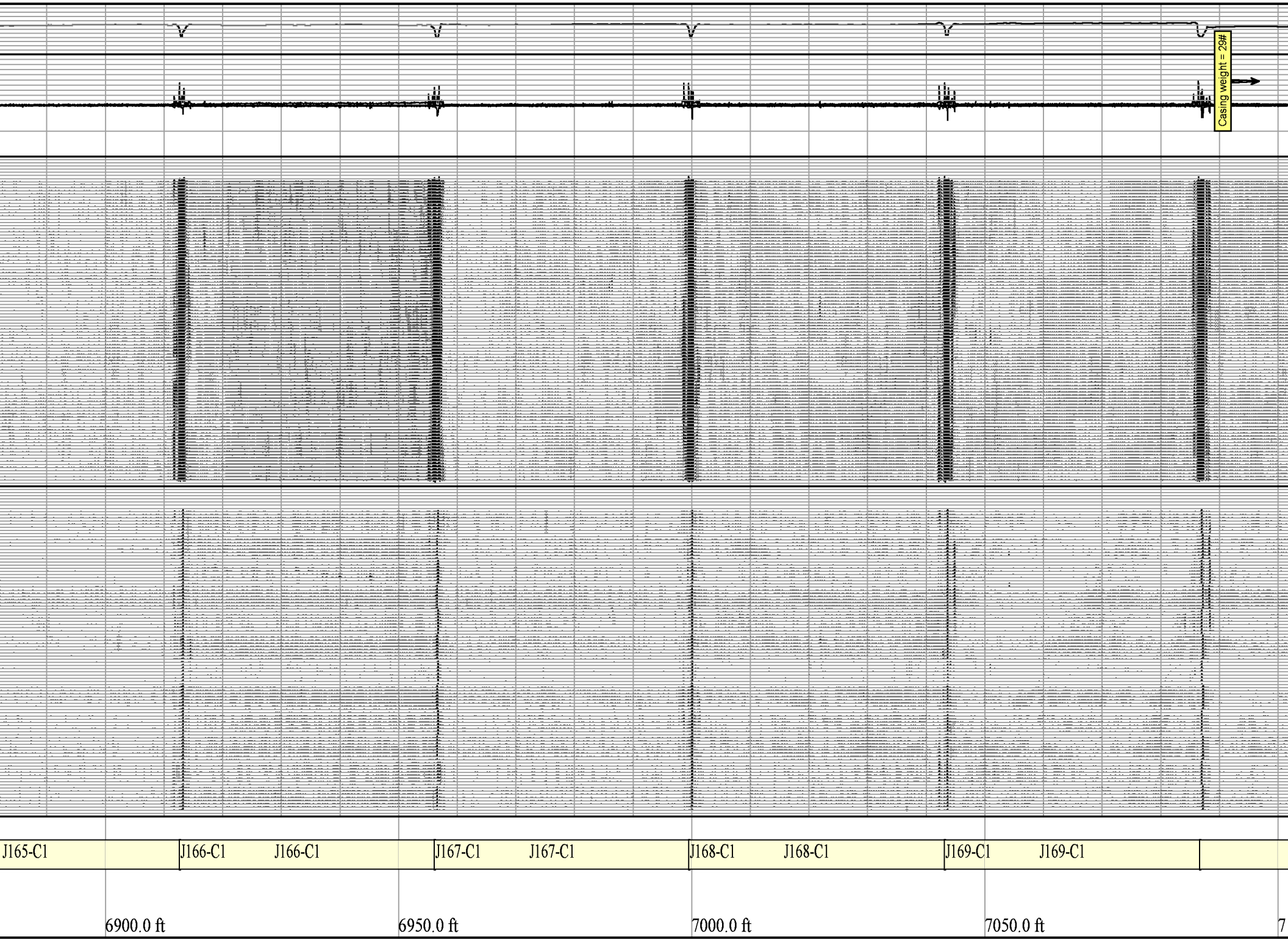
Casing weight = 29#
J165-C1
J166-C1
J166-C1
J167-C1
J167-C1
J168-C1
J168-C1
J169-C1
J169-C1
6900.0 ft
6950.0 ft
7000.0 ft
7050.0 ft

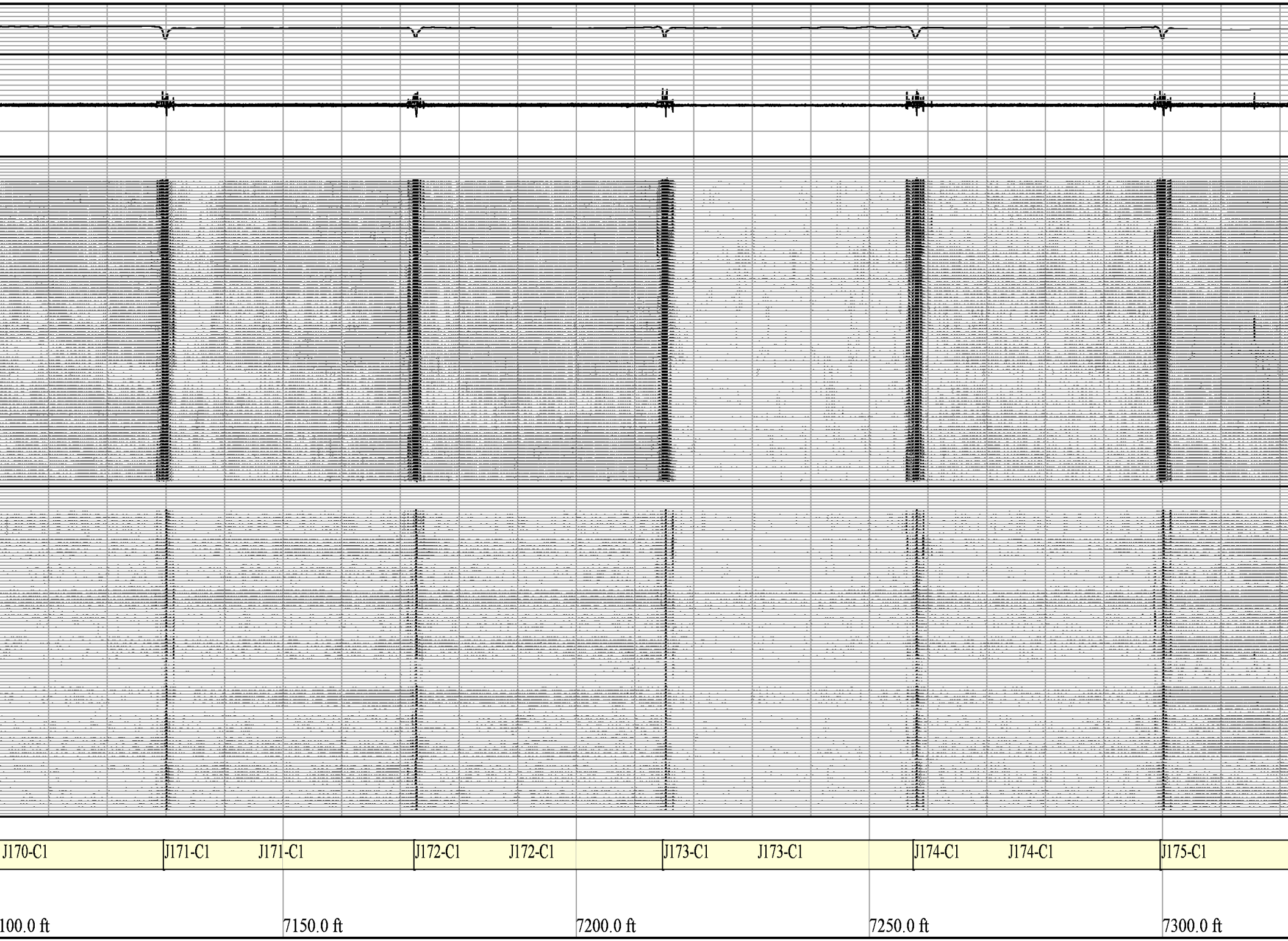
J170-C1
J171-C1
J171-C1
J172-C1
J172-C1
J173-C1
J173-C1
J174-C1
J174-C1
J175-C1
100.0 ft
7150.0 ft
7200.0 ft
7250.0 ft
7300.0 ft

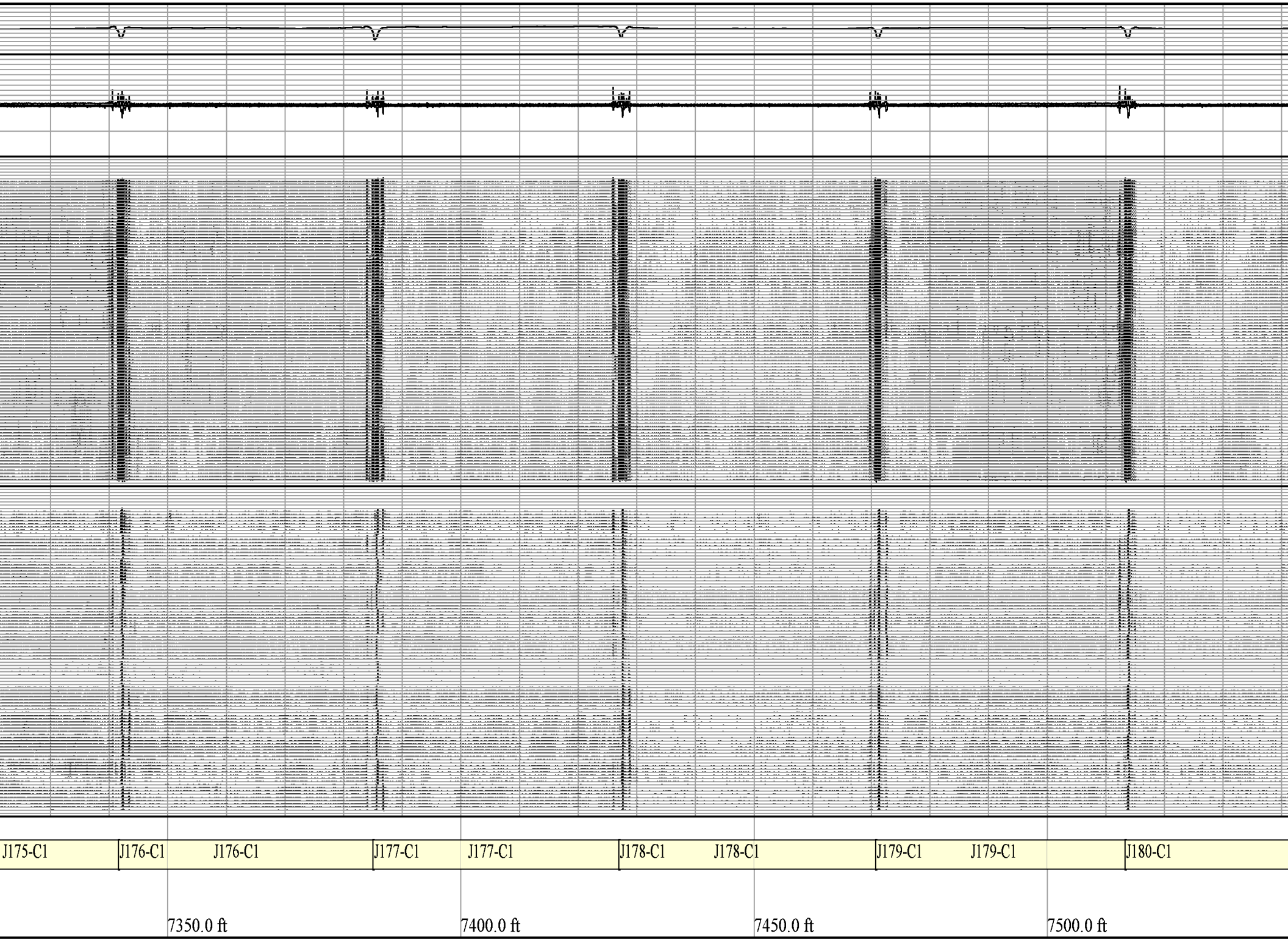
J175-C1
J176-C1
J176-C1
J177-C1
J177-C1
J178-C1
J178-C1
J179-C1
J179-C1
J180-C1
7350.0 ft
7400.0 ft
7450.0 ft
7500.0 ft

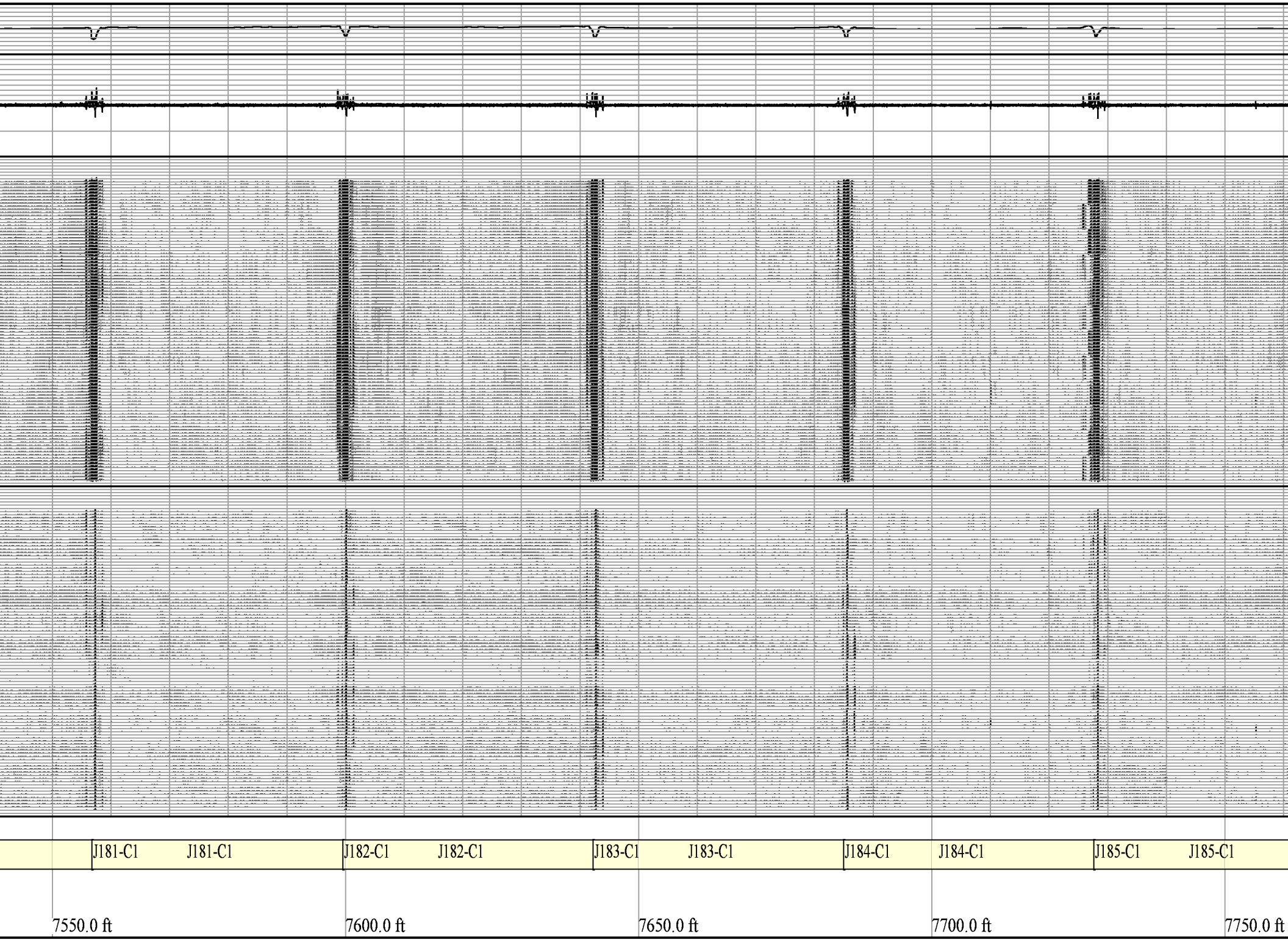
J181-C1
J181-C1
J182-C1
J182-C1
J183-C1
J183-C1
J184-C1
J184-C1
J185-C1
J185-C1
7550.0 ft
7600.0 ft
7650.0 ft
7700.0 ft
7750.0 ft

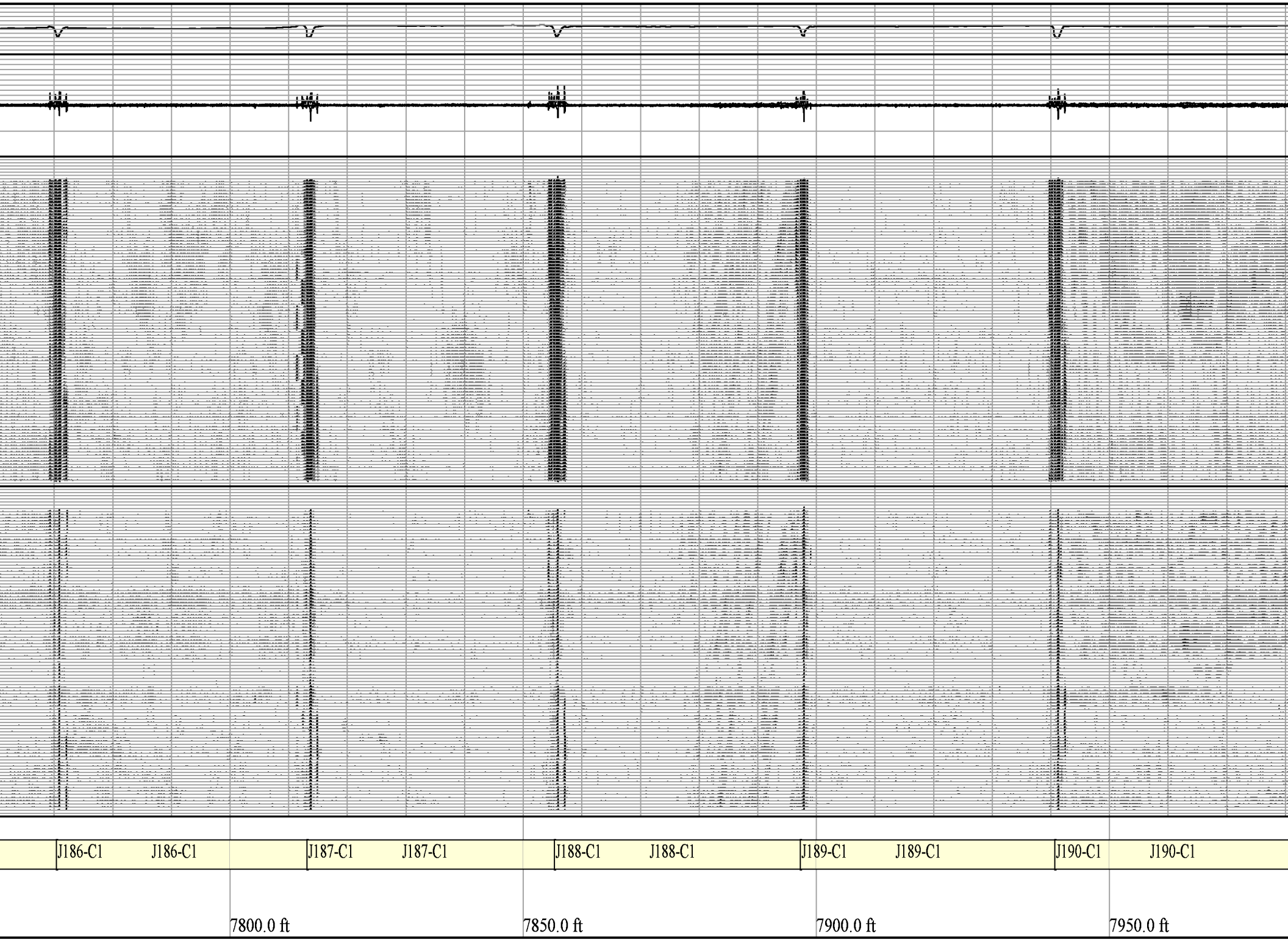
J186-C1
J186-C1
J187-C1
J187-C1
J188-C1
J188-C1
J189-C1
J189-C1
J190-C1
J190-C1
7800.0 ft
7850.0 ft
7900.0 ft
7950.0 ft

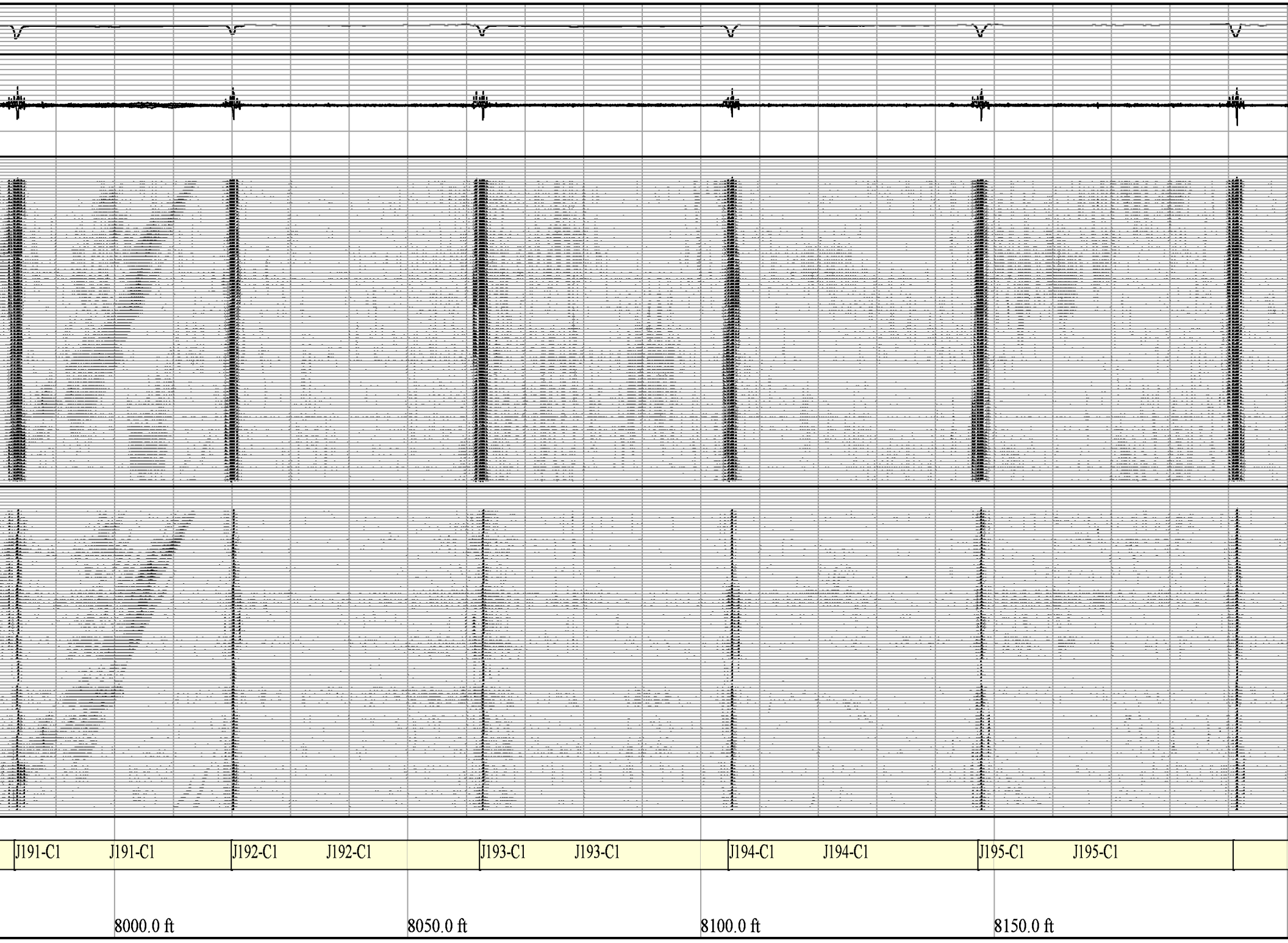
J191-C1
J191-C1
J192-C1
J192-C1
J193-C1
J193-C1
J194-C1
J194-C1
J195-C1
J195-C1
8000.0 ft
8050.0 ft
8100.0 ft
8150.0 ft

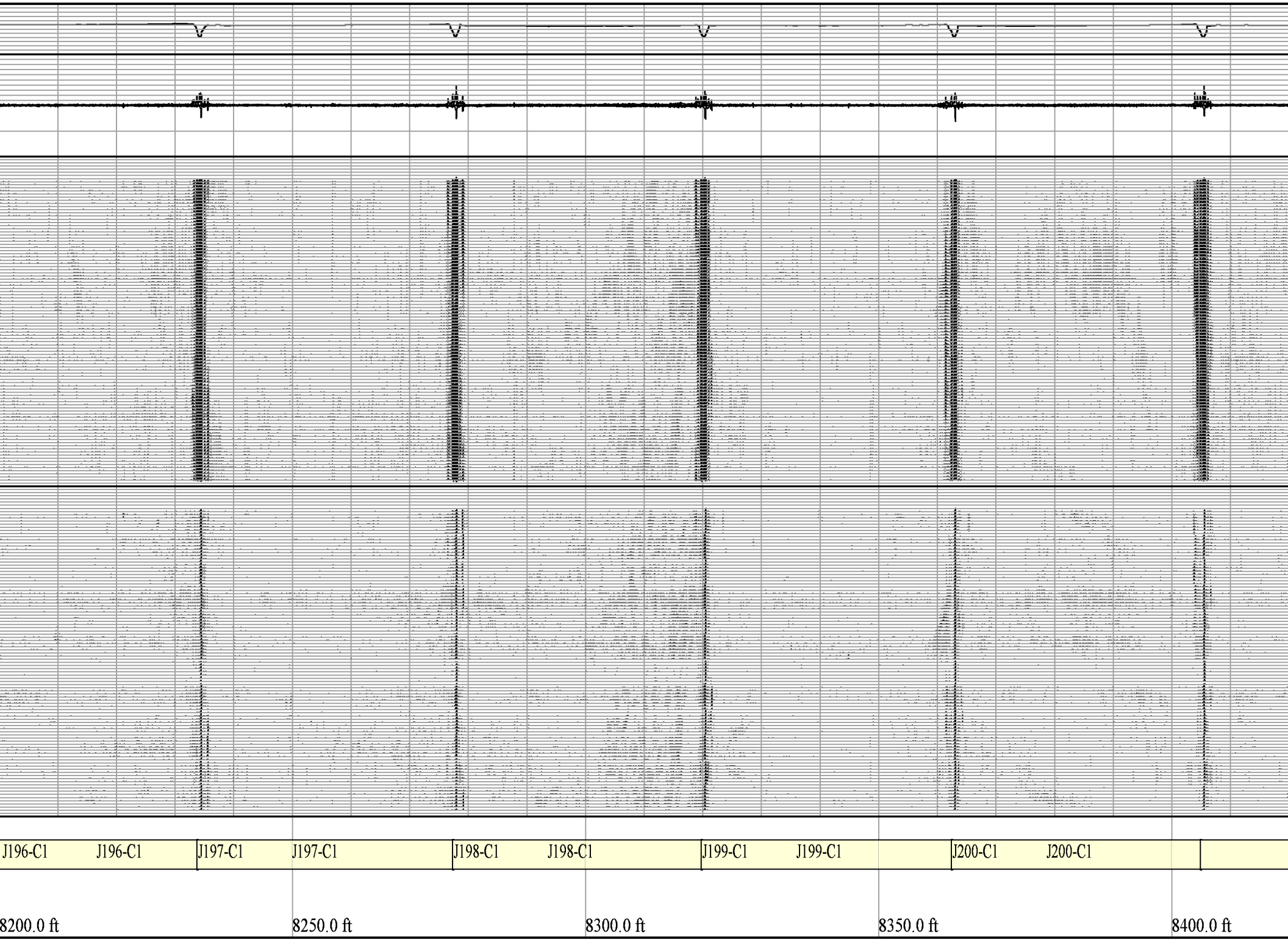
J196-C1
J196-C1
J197-C1
J197-C1
J198-C1
J198-C1
J199-C1
J199-C1
J200-C1
J200-C1
8200.0 ft
8250.0 ft
8300.0 ft
8350.0 ft
8400.0 ft

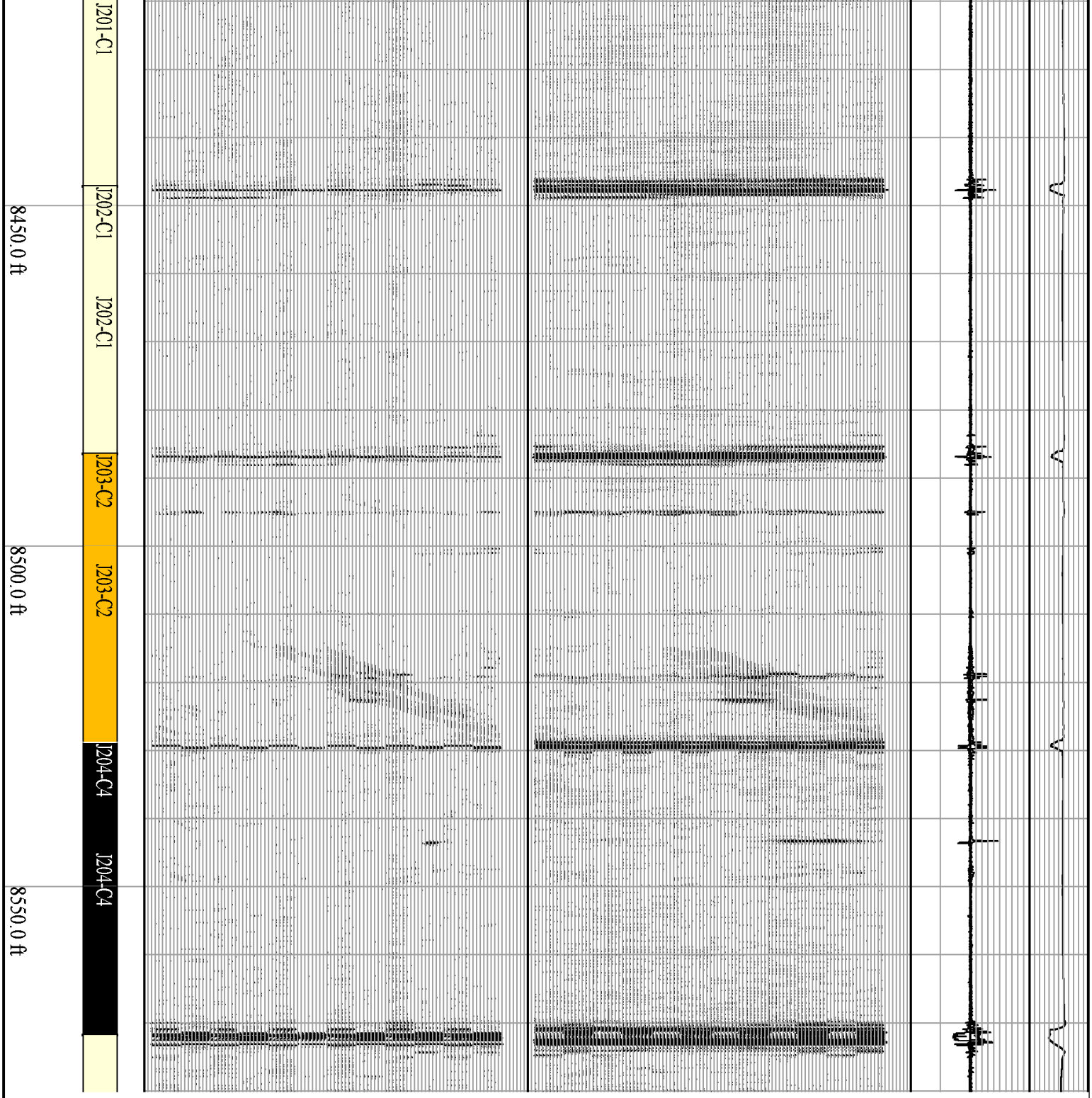

Southern California Gas Company Standard Sesnon 9

File 20180906_15093B_RSP_0_0_0_0_0.mvl

Joint Summary

Southern California Gas Company
Aliso Canyon
Standard Sesnon 9

Identifier	Start Log Depth	Joint Length	Diameter	Wall Thickness	Weight	Max ML Depth	Max ML Position	Min Burst Pressure	Joint Depth Class
	ft	ft	in	in	lb/ft	%	ft	psi	
JT-1	12.24	26.29	7.000	0.317	23.0	0			1
JT-2	38.53	35.65	7.000	0.317	23.0	0			1

JT-3	74.18	41.61	7.000	0.317	23.0	0			1
JT-4	115.79	41.86	7.000	0.317	23.0	0			1
JT-5	157.65	42.15	7.000	0.317	23.0	0			1
JT-6	199.80	41.97	7.000	0.317	23.0	0			1
JT-7	241.77	42.39	7.000	0.317	23.0	0			1
JT-8	284.16	42.03	7.000	0.317	23.0	0			1
JT-9	326.19	42.09	7.000	0.317	23.0	0			1
JT-10	368.28	42.07	7.000	0.317	23.0	0			1
JT-11	410.35	42.67	7.000	0.317	23.0	0			1
JT-12	453.02	41.82	7.000	0.317	23.0	0			1
JT-13	494.83	41.15	7.000	0.317	23.0	0			1
JT-14	535.98	42.17	7.000	0.317	23.0	0			1
JT-15	578.15	41.13	7.000	0.317	23.0	0			1
JT-16	619.29	41.18	7.000	0.317	23.0	0			1
JT-17	660.47	42.33	7.000	0.317	23.0	0			1
JT-18	702.80	41.90	7.000	0.317	23.0	0			1
JT-19	744.70	40.24	7.000	0.317	23.0	16	773.01	5348	1
JT-20	784.93	41.82	7.000	0.317	23.0	0			1
JT-21	826.75	42.25	7.000	0.317	23.0	0			1
JT-22	869.01	42.46	7.000	0.317	23.0	0			1
JT-23	911.47	41.85	7.000	0.317	23.0	0			1
JT-24	953.31	41.89	7.000	0.317	23.0	0			1
JT-25	995.20	42.01	7.000	0.317	23.0	0			1
JT-26	1037.22	41.76	7.000	0.317	23.0	0			1
JT-27	1078.98	42.38	7.000	0.317	23.0	0			1
JT-28	1121.36	36.77	7.000	0.317	23.0	0			1
JT-29	1158.13	42.30	7.000	0.317	23.0	0			1
JT-30	1200.42	43.12	7.000	0.317	23.0	0			1
JT-31	1243.55	41.96	7.000	0.317	23.0	0			1
JT-32	1285.51	40.43	7.000	0.317	23.0	0			1
JT-33	1325.94	42.34	7.000	0.317	23.0	0			1
JT-34	1368.28	42.10	7.000	0.317	23.0	0			1
JT-35	1410.38	41.24	7.000	0.317	23.0	0			1
JT-36	1451.62	41.54	7.000	0.317	23.0	0			1
JT-37	1493.16	42.53	7.000	0.317	23.0	0			1
JT-38	1535.70	42.46	7.000	0.317	23.0	0			1
JT-39	1578.16	41.70	7.000	0.317	23.0	0			1
JT-40	1619.86	42.52	7.000	0.317	23.0	0			1
JT-41	1662.39	41.70	7.000	0.317	23.0	0			1
JT-42	1704.09	37.07	7.000	0.317	23.0	0			1
JT-43	1741.16	40.80	7.000	0.317	23.0	0			1
JT-44	1781.97	40.64	7.000	0.317	23.0	0			1
JT-45	1822.61	42.41	7.000	0.317	23.0	0			1
JT-46	1865.02	40.05	7.000	0.317	23.0	0			1
JT-47	1905.07	40.79	7.000	0.317	23.0	0			1
JT-48	1945.86	41.54	7.000	0.317	23.0	0			1
JT-49	1987.40	41.40	7.000	0.317	23.0	0			1
JT-50	2028.80	41.70	7.000	0.317	23.0	0			1
JT-51	2070.51	42.77	7.000	0.317	23.0	0			1
JT-52	2113.28	41.37	7.000	0.317	23.0	0			1
JT-53	2154.65	42.37	7.000	0.317	23.0	0			1
JT-54	2197.03	42.05	7.000	0.317	23.0	0			1
JT-55	2239.08	36.66	7.000	0.317	23.0	0			1
JT-56	2275.74	41.92	7.000	0.317	23.0	0			1
JT-57	2317.66	40.22	7.000	0.317	23.0	0			1
JT-58	2357.88	41.74	7.000	0.317	23.0	0			1
JT-59	2399.62	43.37	7.000	0.317	23.0	0			1
JT-60	2442.99	42.09	7.000	0.317	23.0	0			1
JT-61	2485.08	40.52	7.000	0.317	23.0	0			1
JT-62	2525.60	41.80	7.000	0.317	23.0	0			1
JT-63	2567.40	39.52	7.000	0.317	23.0	0			1
JT-64	2606.93	42.01	7.000	0.317	23.0	0			1
JT-65	2648.93	42.04	7.000	0.317	23.0	0			1
JT-66	2690.98	42.16	7.000	0.317	23.0	0			1
JT-67	2733.14	40.02	7.000	0.317	23.0	0			1
JT-68	2773.16	41.80	7.000	0.317	23.0	0			1
JT-69	2814.96	41.30	7.000	0.317	23.0	0			1
JT-70	2856.26	43.10	7.000	0.317	23.0	0			1
JT-71	2899.36	37.42	7.000	0.317	23.0	0			1
JT-72	2936.78	41.98	7.000	0.317	23.0	0			1
JT-73	2978.76	41.95	7.000	0.317	23.0	0			1
JT-74	3020.71	42.52	7.000	0.317	23.0	0			1
JT-75	3063.24	42.36	7.000	0.317	23.0	0			1
JT-76	3105.60	41.68	7.000	0.317	23.0	0			1
JT-77	3147.28	41.65	7.000	0.317	23.0	0			1
JT-78	3188.93	38.88	7.000	0.317	23.0	0			1
JT-79	3227.81	41.71	7.000	0.317	23.0	0			1
JT-80	3269.52	41.66	7.000	0.317	23.0	0			1
JT-81	3311.18	41.90	7.000	0.317	23.0	0			1
JT-82	3353.08	41.47	7.000	0.317	23.0	0			1
JT-83	3394.55	42.27	7.000	0.317	23.0	0			1

JT-84	3436.81	42.18	7.000	0.317	23.0	0			1
JT-85	3479.00	41.15	7.000	0.317	23.0	0			1
JT-86	3520.14	42.67	7.000	0.317	23.0	0			1
JT-87	3562.81	35.55	7.000	0.317	23.0	0			1
JT-88	3598.36	42.59	7.000	0.317	23.0	0			1
JT-89	3640.95	42.76	7.000	0.317	23.0	0			1
JT-90	3683.71	42.62	7.000	0.317	23.0	0			1
JT-91	3726.33	41.79	7.000	0.317	23.0	0			1
JT-92	3768.12	42.08	7.000	0.317	23.0	0			1
JT-93	3810.20	42.67	7.000	0.317	23.0	0			1
JT-94	3852.86	42.55	7.000	0.317	23.0	15	3874.13	7890	1
JT-95	3895.41	42.11	7.000	0.317	23.0	0			1
JT-96	3937.52	43.39	7.000	0.317	23.0	0			1
JT-97	3980.90	42.31	7.000	0.317	23.0	0			1
JT-98	4023.22	42.44	7.000	0.317	23.0	0			1
JT-99	4065.65	41.22	7.000	0.317	23.0	0			1
JT-100	4106.87	41.37	7.000	0.317	23.0	0			1
JT-101	4148.24	42.09	7.000	0.317	23.0	0			1
JT-102	4190.33	42.32	7.000	0.317	23.0	0			1
JT-103	4232.66	42.37	7.000	0.317	23.0	0			1
JT-104	4275.03	40.10	7.000	0.317	23.0	0			1
JT-105	4315.13	42.74	7.000	0.317	23.0	0			1
JT-106	4357.87	40.80	7.000	0.317	23.0	0			1
JT-107	4398.67	43.95	7.000	0.317	23.0	0			1
JT-108	4442.62	42.87	7.000	0.317	23.0	0			1
JT-109	4485.49	41.93	7.000	0.317	23.0	0			1
JT-110	4527.42	41.80	7.000	0.317	23.0	15	4530.65	7909	1
JT-111	4569.22	40.82	7.000	0.317	23.0	0			1
JT-112	4610.04	42.87	7.000	0.317	23.0	0			1
JT-113	4652.91	42.53	7.000	0.317	23.0	0			1
JT-114	4695.45	42.64	7.000	0.317	23.0	0			1
JT-115	4738.08	42.34	7.000	0.317	23.0	0			1
JT-116	4780.42	42.38	7.000	0.317	23.0	0			1
JT-117	4822.80	42.33	7.000	0.317	23.0	0			1
JT-118	4865.13	41.80	7.000	0.317	23.0	0			1
JT-119	4906.93	41.64	7.000	0.317	23.0	18	4932.25	7840	1
JT-120	4948.57	42.55	7.000	0.317	23.0	0			1
JT-121	4991.13	41.99	7.000	0.317	23.0	0			1
JT-122	5033.11	42.79	7.000	0.317	23.0	0			1
JT-123	5075.90	42.27	7.000	0.317	23.0	0			1
JT-124	5118.18	42.95	7.000	0.317	23.0	0			1
JT-125	5161.13	42.10	7.000	0.317	23.0	0			1
JT-126	5203.23	41.94	7.000	0.317	23.0	0			1
JT-127	5245.17	42.37	7.000	0.317	23.0	0			1
JT-128	5287.55	39.09	7.000	0.317	23.0	0			1
JT-129	5326.64	42.81	7.000	0.317	23.0	0			1
JT-130	5369.45	42.41	7.000	0.317	23.0	0			1
JT-131	5411.86	43.04	7.000	0.317	23.0	0			1
JT-132	5454.90	41.25	7.000	0.362	26.0	0			1
JT-133	5496.15	41.93	7.000	0.362	26.0	0			1
JT-134	5538.08	43.31	7.000	0.362	26.0	0			1
JT-135	5581.39	42.68	7.000	0.362	26.0	0			1
JT-136	5624.07	43.89	7.000	0.362	26.0	0			1
JT-137	5667.96	42.57	7.000	0.362	26.0	0			1
JT-138	5710.53	43.10	7.000	0.362	26.0	0			1
JT-139	5753.63	42.27	7.000	0.362	26.0	0			1
JT-140	5795.90	43.05	7.000	0.362	26.0	0			1
JT-141	5838.95	41.37	7.000	0.362	26.0	0			1
JT-142	5880.33	43.63	7.000	0.362	26.0	0			1
JT-143	5923.96	43.04	7.000	0.362	26.0	0			1
JT-144	5967.00	43.17	7.000	0.362	26.0	0			1
JT-145	6010.17	43.75	7.000	0.362	26.0	0			1
JT-146	6053.92	41.47	7.000	0.362	26.0	0			1
JT-147	6095.40	43.52	7.000	0.362	26.0	0			1
JT-148	6138.92	42.87	7.000	0.362	26.0	0			1
JT-149	6181.79	41.71	7.000	0.362	26.0	0			1
JT-150	6223.50	43.02	7.000	0.362	26.0	0			1
JT-151	6266.53	43.35	7.000	0.362	26.0	0			1
JT-152	6309.87	43.10	7.000	0.362	26.0	0			1
JT-153	6352.97	43.56	7.000	0.362	26.0	0			1
JT-154	6396.53	42.97	7.000	0.362	26.0	0			1
JT-155	6439.50	43.02	7.000	0.362	26.0	0			1
JT-156	6482.51	42.90	7.000	0.362	26.0	0			1
JT-157	6525.42	42.77	7.000	0.362	26.0	0			1
JT-158	6568.19	42.96	7.000	0.362	26.0	0			1
JT-159	6611.15	43.62	7.000	0.362	26.0	0			1
JT-160	6654.77	44.02	7.000	0.362	26.0	0			1
JT-161	6698.79	43.73	7.000	0.362	26.0	0			1
JT-162	6742.52	42.00	7.000	0.362	26.0	0			1
JT-163	6784.53	41.54	7.000	0.362	26.0	0			1

JT-164	6826.07	43.23	7.000	0.362	26.0	0			1
JT-165	6869.30	43.44	7.000	0.362	26.0	0			1
JT-166	6912.74	43.48	7.000	0.362	26.0	0			1
JT-167	6956.22	43.37	7.000	0.362	26.0	0			1
JT-168	6999.59	43.65	7.000	0.362	26.0	0			1
JT-169	7043.24	43.51	7.000	0.362	26.0	0			1
JT-170	7086.75	42.98	7.000	0.408	29.0	0			1
JT-171	7129.73	42.72	7.000	0.408	29.0	0			1
JT-172	7172.46	42.35	7.000	0.408	29.0	0			1
JT-173	7214.81	42.77	7.000	0.408	29.0	0			1
JT-174	7257.58	42.13	7.000	0.408	29.0	0			1
JT-175	7299.71	41.99	7.000	0.408	29.0	16	7315.51	10212	1
JT-176	7341.70	43.43	7.000	0.408	29.0	0			1
JT-177	7385.13	41.95	7.000	0.408	29.0	0			1
JT-178	7427.08	43.77	7.000	0.408	29.0	0			1
JT-179	7470.85	42.60	7.000	0.408	29.0	0			1
JT-180	7513.45	43.44	7.000	0.408	29.0	0			1
JT-181	7556.89	42.82	7.000	0.408	29.0	0			1
JT-182	7599.71	42.66	7.000	0.408	29.0	0			1
JT-183	7642.37	42.76	7.000	0.408	29.0	0			1
JT-184	7685.12	42.67	7.000	0.408	29.0	0			1
JT-185	7727.80	42.73	7.000	0.408	29.0	0			1
JT-186	7770.52	42.75	7.000	0.408	29.0	0			1
JT-187	7813.28	42.17	7.000	0.408	29.0	0			1
JT-188	7855.44	41.97	7.000	0.408	29.0	0			1
JT-189	7897.42	43.39	7.000	0.408	29.0	0			1
JT-190	7940.80	42.17	7.000	0.408	29.0	0			1
JT-191	7982.98	37.05	7.000	0.408	29.0	0			1
JT-192	8020.03	42.33	7.000	0.408	29.0	0			1
JT-193	8062.36	42.42	7.000	0.408	29.0	0			1
JT-194	8104.78	42.57	7.000	0.408	29.0	0			1
JT-195	8147.35	43.54	7.000	0.408	29.0	0			1
JT-196	8190.89	42.97	7.000	0.408	29.0	0			1
JT-197	8233.86	43.61	7.000	0.408	29.0	0			1
JT-198	8277.47	42.39	7.000	0.408	29.0	0			1
JT-199	8319.86	42.68	7.000	0.408	29.0	0			1
JT-200	8362.54	42.45	7.000	0.408	29.0	0			1
JT-201	8404.99	42.22	7.000	0.408	29.0	0			1
JT-202	8447.21	39.25	7.000	0.408	29.0	0			1
JT-203	8486.46	42.50	7.000	0.408	29.0	23	8522.45	10092	2
JT-204	8528.95	42.89	7.000	0.408	29.0	81	8543.19	0	4
JT-205	8571.84	9.79	7.000	0.408	29.0	0			1

Schlumberger

Company: Southern California Gas Company

Well: Standard Sesnon 9

Field: Aliso Canyon

County: Los Angeles State: California

County: Los Angeles
Field: Aliso Canyon
Location: 1389.74' S & 5254.80' W From Station 84
Well: Standard Sesnon 9
Company: Southern California Gas Company

Ultrasonic Imager

Gamma Ray - CCL

7" 23, 26, 29# casing

Location:			
1389.74' S & 5254.80' W From Station 84		Elev.: K.B.	
		G.L.	2835.71 ft
		D.F.	2842.63 ft
Permanent Datum:	Ground Level	Elev.:	2835.71 f
Log Measured From:	Drill Floor	6.92 ft	above Perm.Datum
Drilling Measured From:	Drill Floor		

API Serial No.	Section:	Township:	Range:
0403700762	28	3N	16W

Logging Date		07-Sep-2018	
Run Number		One	
Depth Driller		8599.00 ft	
Schlumberger Depth		8592.00 ft	
Bottom Log Interval		8588.00 ft	
Top Log Interval		14.00 ft	
Casing Fluid Type		Water	
Salinity			
Density		8.5 lbm/gal	
Fluid Level		0.00 ft	
BIT/CASING/TUBING STRING			
Bit Size		6.00 in	
From		8625.00 ft	
To		8859.00 ft	
Casing/Tubing Size		7 in	
Weight		29 lbm/ft	
Grade		N80	
From		7088.00 ft	
To		8625.00 ft	
Max Recorded Temperatures			
Logger on Bottom	Time	07-Sep-2018 10:35:00	
Unit Number	Location:	3079 Ventura Ca	
Recorded By		John Lopez	
Witnessed By		Mr Tom MacMahon	

Disclaimer

THE USE OF AND RELIANCE UPON THIS RECORDED-DATA BY THE HEREIN NAMED COMPANY (AND ANY OF ITS AFFILIATES, PARTNERS, REPRESENTATIVES, AGENTS, CONSULTANTS AND EMPLOYEES) IS SUBJECT TO THE TERMS AND CONDITIONS AGREED UPON BETWEEN SCHLUMBERGER AND THE COMPANY, INCLUDING: (a) RESTRICTIONS ON USE OF THE RECORDED-DATA; (b) DISCLAIMERS AND WAIVERS OF WARRANTIES AND REPRESENTATIONS REGARDING COMPANY'S USE AND RELIANCE UPON THE RECORDED-DATA; AND (c) CUSTOMER'S FULL AND SOLE RESPONSIBILITY FOR ANY INFERENCE DRAWN OR DECISION MADE IN CONNECTION WITH THE USE OF THIS RECORDED-DATA.

Contents

1. Header
2. Disclaimer
3. Contents
4. Well Sketch
5. Borehole Size/Casing/Tubing Record
6. Remarks and Equipment Summary
7. Job Event Summary
8. USI Fluid Properties Measurement
9. Composite 1 Main Pass 5 in = 100 ft
   9.1 Integration Summary
   9.2 Software Version
   9.3 Composite Summary
   9.4 Log (LBV1_USI-VDL (DSLT) Cement 7inch)
   9.5 Parameter Listing
10. Composite 1 Main Pass 5 IN = 100 FT
   10.1 Integration Summary
   10.2 Composite Summary
   12.2 Composite Summary
   12.3 Log (LBV1_USI Corrosion 5inch)
13. Composite 1 USI Compressed Goodwin
   13.1 Integration Summary
   13.2 Composite Summary
   13.3 Log (Import of USI Goodwin)
14. One Hi res Corrosion 10 in = 100 ft
   14.1 Integration Summary
   14.2 Composite Summary
   14.3 Log (LBV1_USI Corrosion 5inch)
15. One Hi res Corrosion 10 in = 100 ft
   15.1 Integration Summary
   15.2 Composite Summary
   15.3 Log (LBV1_USI Corrosion 5inch)
16. XYZ (USI Fluid Acoustic Slowness vs Depth)
17. XYZ (USI Theoretical Acoustic impedance of mud vs Depth)

10.3 Log (LBV1_USI Composite 7inch)
11. Composite 1 Cement Log 2 IN = 100 FT
11.1 Integration Summary
11.2 Composite Summary
11.3 Log (LBV1_USI Cement 7inch)
12. Composite 1 Corrosion 5 in = 100 ft
12.1 Integration Summary
18. USI Fluid Properties Measurement
19. Tail

Well Sketch

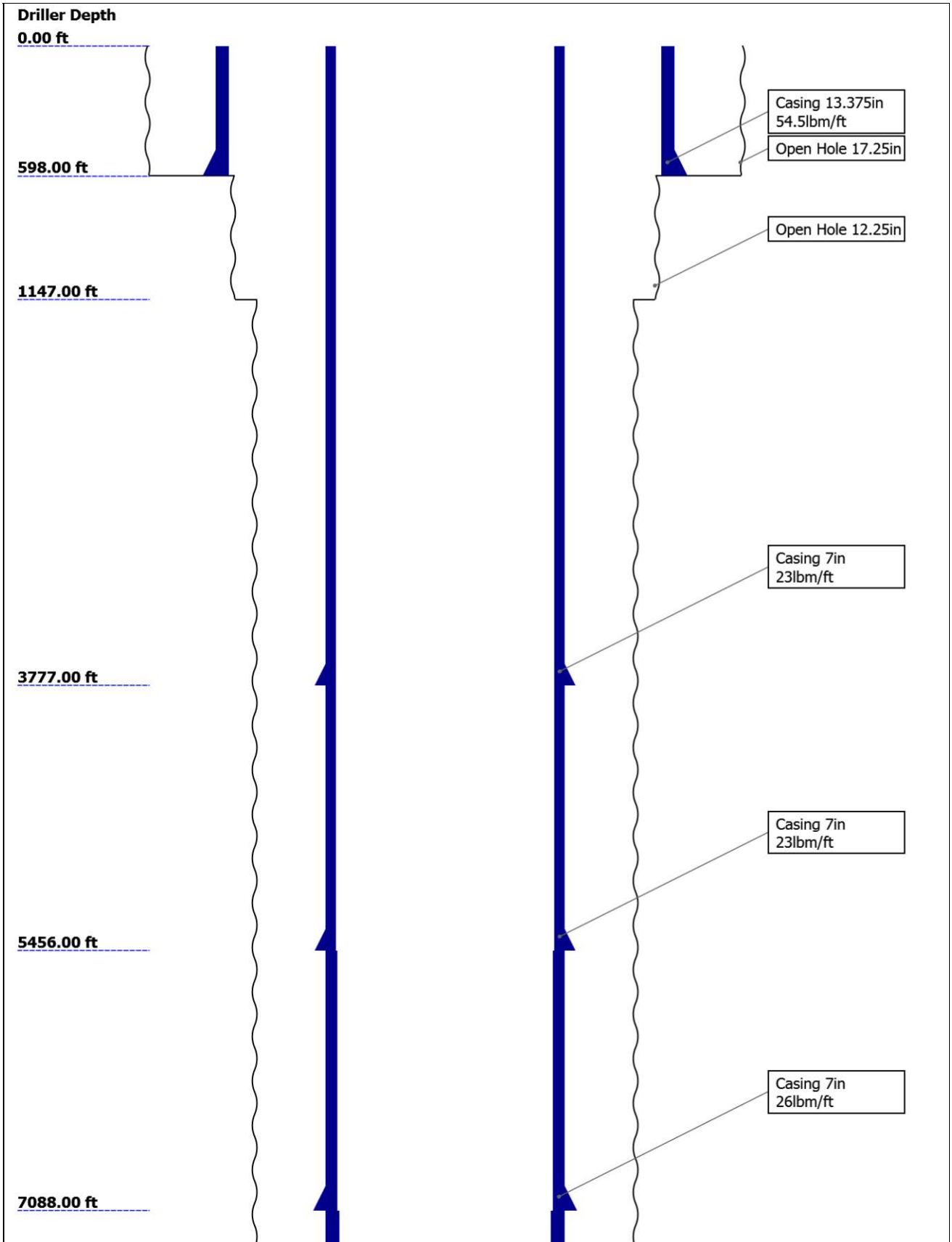

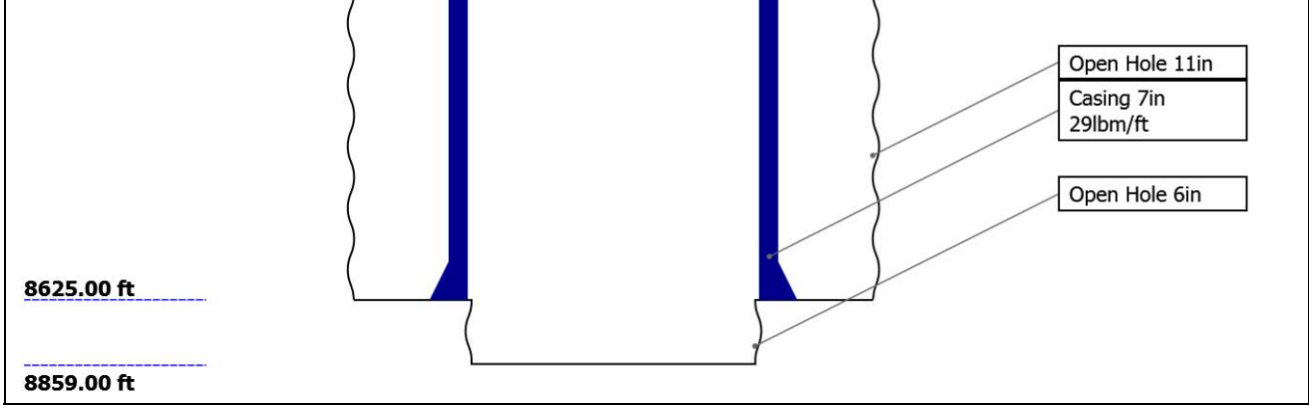

Borehole Size/Casing/Tubing Record

Bit						
Bit Size (in)	17.25	12.25	11	6		
Top Driller (ft)	0	598	1147	8625		
Top Logger (ft)	0	598	1147	8625		
Bottom Driller (ft)	598	1147	8625	8859		
Bottom Logger (ft)	598	1147	8625	8859		
Casing						
Size (in)	13.375	7	7	7	7	
Weight (lbm/ft)	54.5	23	23	26	29	
Inner Diameter (in)	12.615	6.366	6.366	6.276	6.184	
Grade	J55	J55	N80	N80	N80	
Top Driller (ft)	0	0	3777	5456	7088	
Top Logger (ft)	0	0	3777	5456	7088	
Bottom Driller (ft)	598	3777	5456	7088	8625	
Bottom Logger (ft)	598	3777	5456	7088	8625	

Remarks and Equipment Summary

One: Toolstring

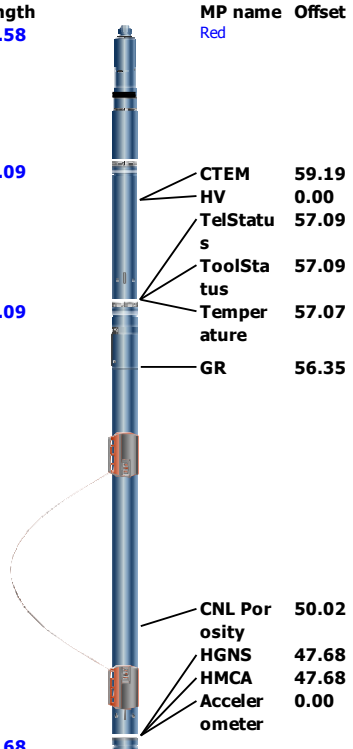

One: Remarks

Rig: Ensign 343
Toolstring ran as per toolsketch.
Two centralizers on USIS and two CME-Y used to centralize ultrasonic tool.
Correlated to Schlumberger resistivity Log dated 1-17-47
No pressure run on repeat pass, 1000 PSI pressure run on main pass
USIT run for cement and corrosion
USIT run at 10 deg 1.5 inch standard res 2800 FPH, Anomolies repeated at 10 Deg 0.6 inch res at 1200 FPH
CNL run eccentered
Crew: Coupart, Allen
Thank You For Choosing Schlumberger
5 inch Liner top at 8599 ft, logged from Liner top to surface
Anomolies noted at 2560 to 2570 ft and from 1628 to 1630 ft, appear to be caused by tool eccentering. Repeated in Hi-Res

Speed correction applied to Logs

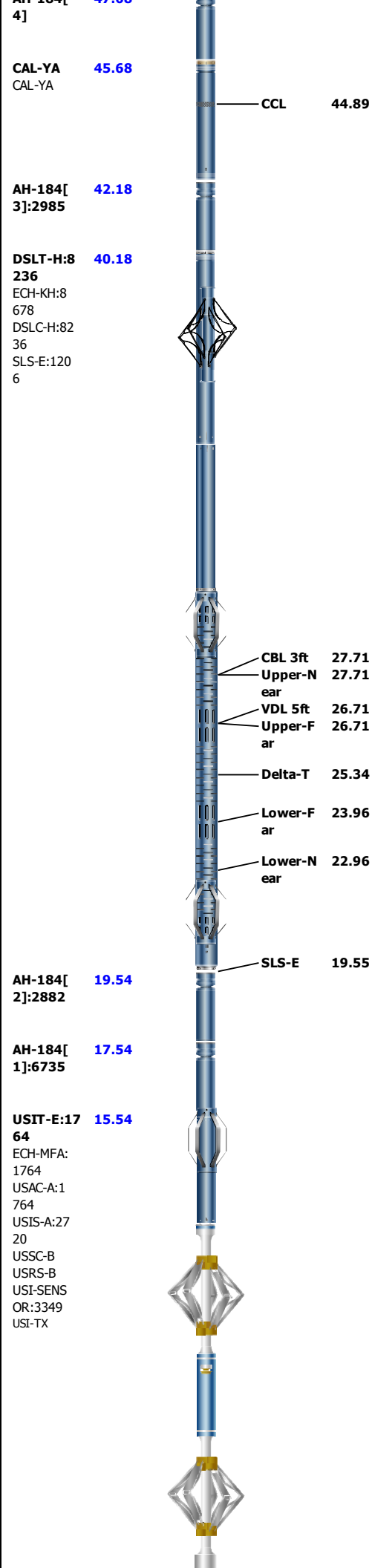

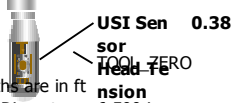

Lengths are in ft
Maximum Outer Diameter = 6.500 in
Line: Sensor Location, Value: Gating Offset
All measurements are relative to TOOL_ZERO

Job Event Summary

Event	Time	Duration	Interval	Remark
Log[2]:Down	Sep-07-2018 08:08	01:15:54	436.1 - 8598.16 ft	FPM
Log[5]:Up	Sep-07-2018 09:40	00:07:43	8593.13 - 8282.49 ft	Repeat No pressure
Log[6]:Up	Sep-07-2018 09:51	04:01:06	8592.71 - 93.36 ft	Main 1000 Psi Pressure applied
Log[7]:Up	Sep-07-2018 14:11	00:11:18	2659.49 - 2491.49 ft	Hi-Res 1
Log[8]:Up	Sep-07-2018 14:26	00:14:03	1758.38 - 1551.52 ft	Hi Res 2
Log[9]:Up	Sep-07-2018 14:46	00:13:24	318.32 - 11.43 ft	Surface data

USIT - Fluid Properties Measurement

Run Name	Pass Name	Start Depth(ft)	Stop Depth(ft)
Run 1	Log[2]:Down	436.1	8598.16

Fluid Velocity = "Automatic".
CFVL equals DFSL channel

Start Depth(ft)	Stop Depth(ft)	Start Value(us/ft)	End Value(us/ft)

Mud Impedance = "Theoretical".
CZMD uses theoretical results.
MUD_N_THE=1.00
DFD=1.02g/cm3(8.50lbm/gal)

Start Depth(ft)	Stop Depth(ft)	Start Value(Mrayl)	End Value(Mrayl)

Composite 1

Main Pass 5 in = 100 ft

Software Version

Acquisition System	Version
Maxwell 2018 SP1	8.1.99839.3100
Application Patch	Wireline_Hotfix-Mandatory-2018SP1_8.1.102865

Computation	Description	Version
CEVAL	Sonic Cement Evaluation Computation Ensemble provides common Parameters and Channels	8.1.99839.3100
Cementation	Cementation Computation Application	8.1.99839.3100

Tool Elements	Description	Software Version	Firmware Version
HGNS-H	HILT Gamma-Ray and Neutron Sonde, 150 degC	8.1.99839.3100	2.0
SLS-E	Sonic Logging Sonde E supports 3'-5'BHC DT and CBL/VDL	8.1.99839.3100	4.0
USI-SENSOR	USIT Transducer Element	1.2.111	DSP: v2.99

Composite Summary

Run Name	Pass Objective	Direction	Top	Bottom	Start	Stop	DSC Mode	Depth Shift	Include Parallel Data
One	Log[6]:Up	Up	93.36 ft	8592.71 ft	07-Sep-2018 9:51:23 AM	07-Sep-2018 1:52:30 PM	ON	8.00 ft	No
One	Log[9]:Up	Up	11.43 ft	318.32 ft	07-Sep-2018 2:46:40 PM	07-Sep-2018 3:00:05 PM	ON	9.00 ft	No

All depths are referenced to toolstring zero

Log

Company:Southern California Gas Company Well:Standard Sesnon 9
Composite 1:S003

Description: USI VDL Cement Format: Log (LBV1_USI-VDL (DSLT) Cement 7inch) Index Scale: 5 in per 100 ft Index Unit: ft Index Type: Measured Depth
Creation Date: 07-Sep-2018 22:55:36

TIME_1900 - Time Marked every 60.00 (s)

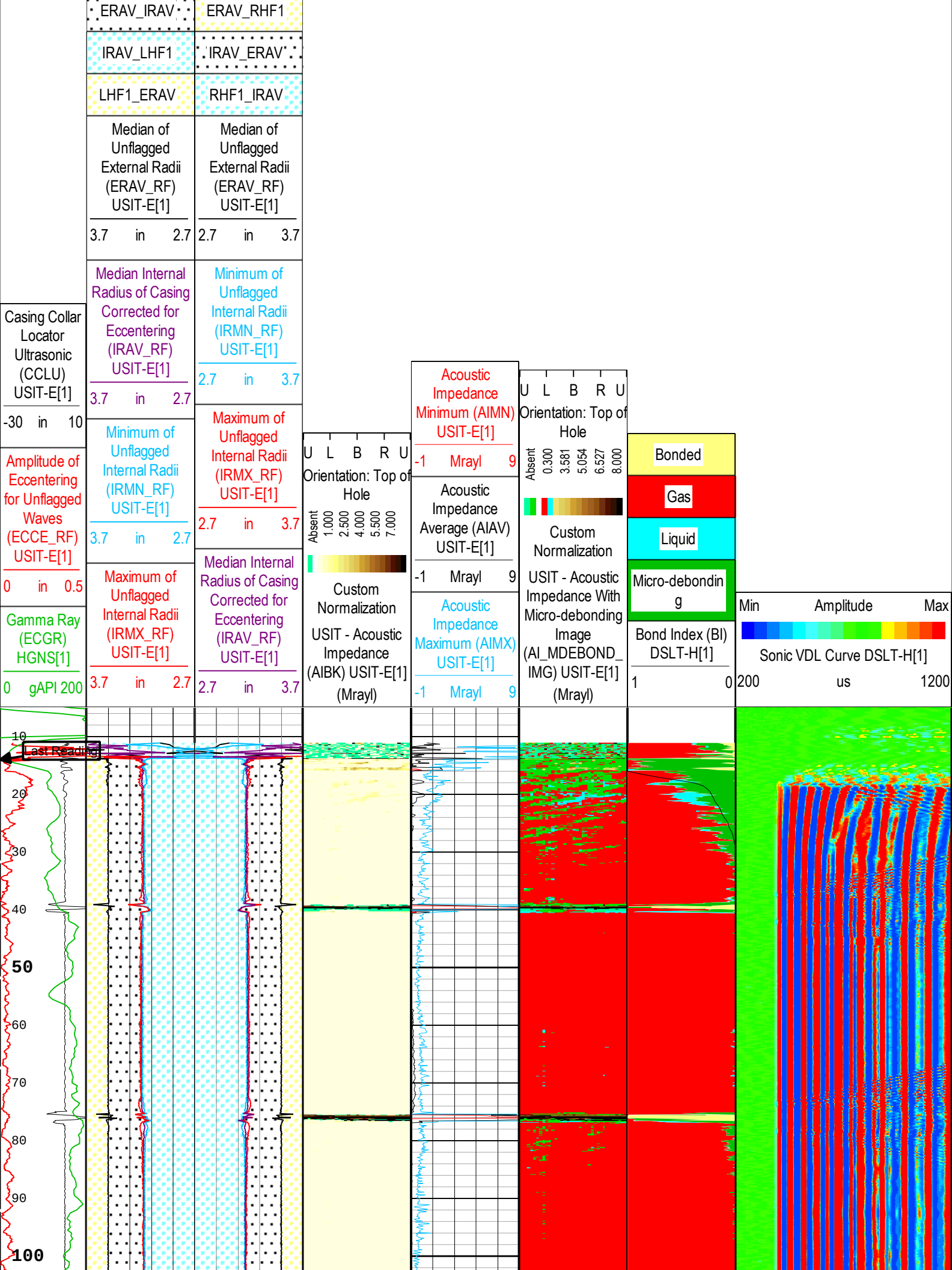
ERAV_IRAV
ERAV_RHF1
IRAV_LHF1
IRAV_ERAV
LHF1_ERAV
RHF1_IRAV
Median of Unflagged External Radii (ERAV_RF) USIT-E[1]
3.7 in 2.7
Median of Unflagged External Radii (ERAV_RF) USIT-E[1]
2.7 in 3.7
Casing Collar Locator Ultrasonic (CCLU) USIT-E[1]
-30 in 10
Median Internal Radius of Casing Corrected for Eccentering (IRAV_RF) USIT-E[1]
3.7 in 2.7
Minimum of Unflagged Internal Radii (IRMN_RF) USIT-E[1]
2.7 in 3.7
Amplitude of Eccentering for Unflagged Waves (ECCE_RF) USIT-E[1]
0 in 0.5
Minimum of Unflagged Internal Radii (IRMN_RF) USIT-E[1]
3.7 in 2.7
Maximum of Unflagged Internal Radii (IRMX_RF) USIT-E[1]
2.7 in 3.7
Gamma Ray (ECGR) HGNS[1]
0 gAPI 200
Maximum of Unflagged Internal Radii (IRMX_RF) USIT-E[1]
3.7 in 2.7
Median Internal Radius of Casing Corrected for Eccentering (IRAV_RF) USIT-E[1]
2.7 in 3.7
U L B R U
Orientation: Top of Hole
Absent 1.000 2.500 4.000 5.500 7.000
Custom Normalization
USIT - Acoustic Impedance (AIBK) USIT-E[1] (Mrayl)
Acoustic Impedance Minimum (AIMN) USIT-E[1]
-1 Mrayl 9
Acoustic Impedance Average (AIAV) USIT-E[1]
-1 Mrayl 9
Acoustic Impedance Maximum (AIMX) USIT-E[1]
-1 Mrayl 9
U L B R U
Orientation: Top of Hole
Absent 0.300 3.581 5.054 6.527 8.000
Custom Normalization
USIT - Acoustic Impedance With Micro-debonding Image (AI_MDEBOND_IMG) USIT-E[1] (Mrayl)
Bonded
Gas
Liquid
Micro-debonding
Bond Index (BI) DSLT-H[1]
1 0
Min Amplitude Max
Sonic VDL Curve DSLT-H[1]
200 us 1200
Last Reading
10
20
30
40
50
60
70
80
90
100

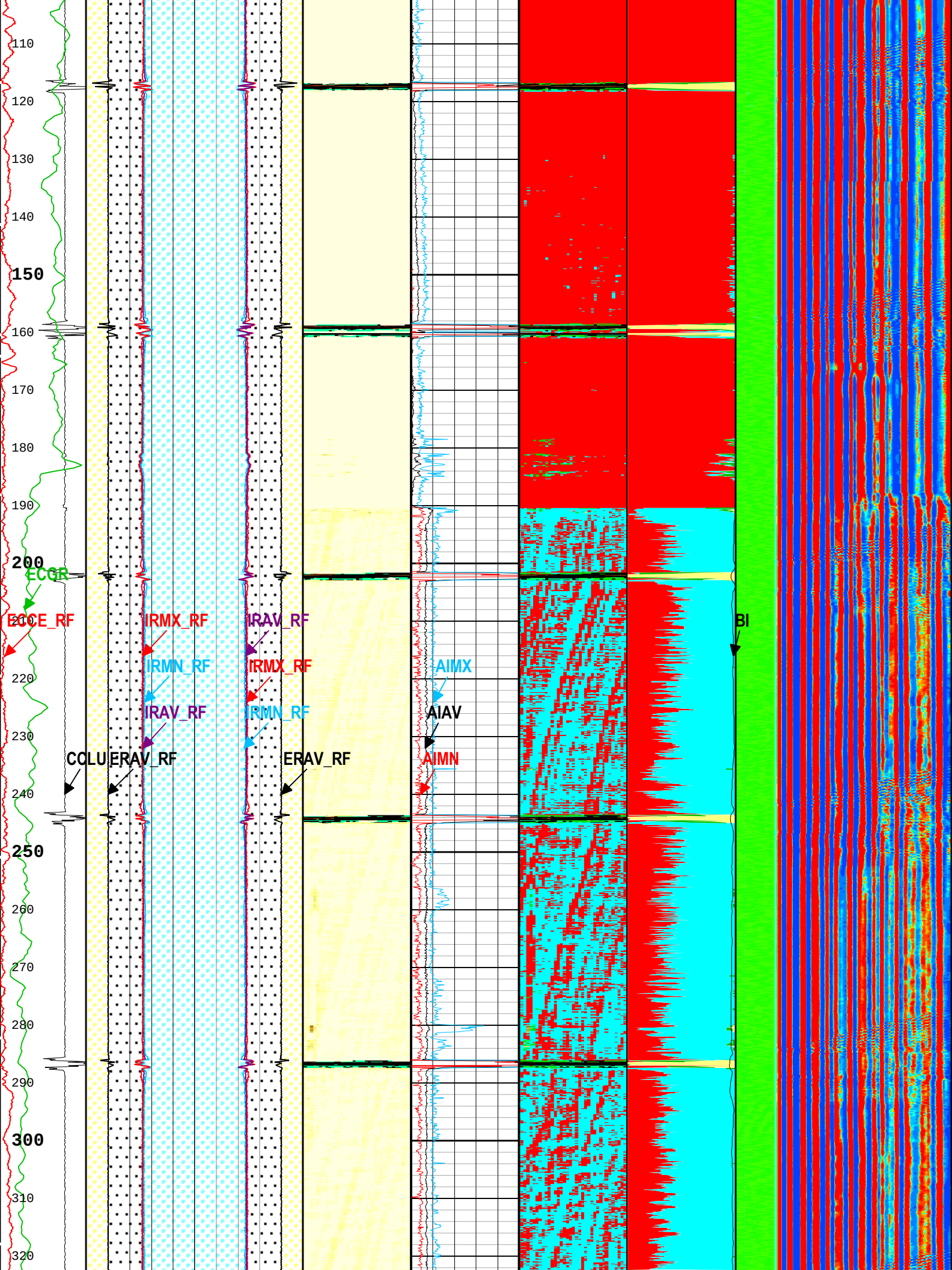
110
120
130
140
150
160
170
180
190
200
210
220
230
240
250
260
270
280
290
300
310
320
ECGR
ECCE_RF
IRMX_RF
IRAV_RF
IRMN_RF
IRMX_RF
IRAV_RF
IRMN_RF
AIMX
AIAV
AIMN
BI
COLU
ERAV_RF
ERAV_RF

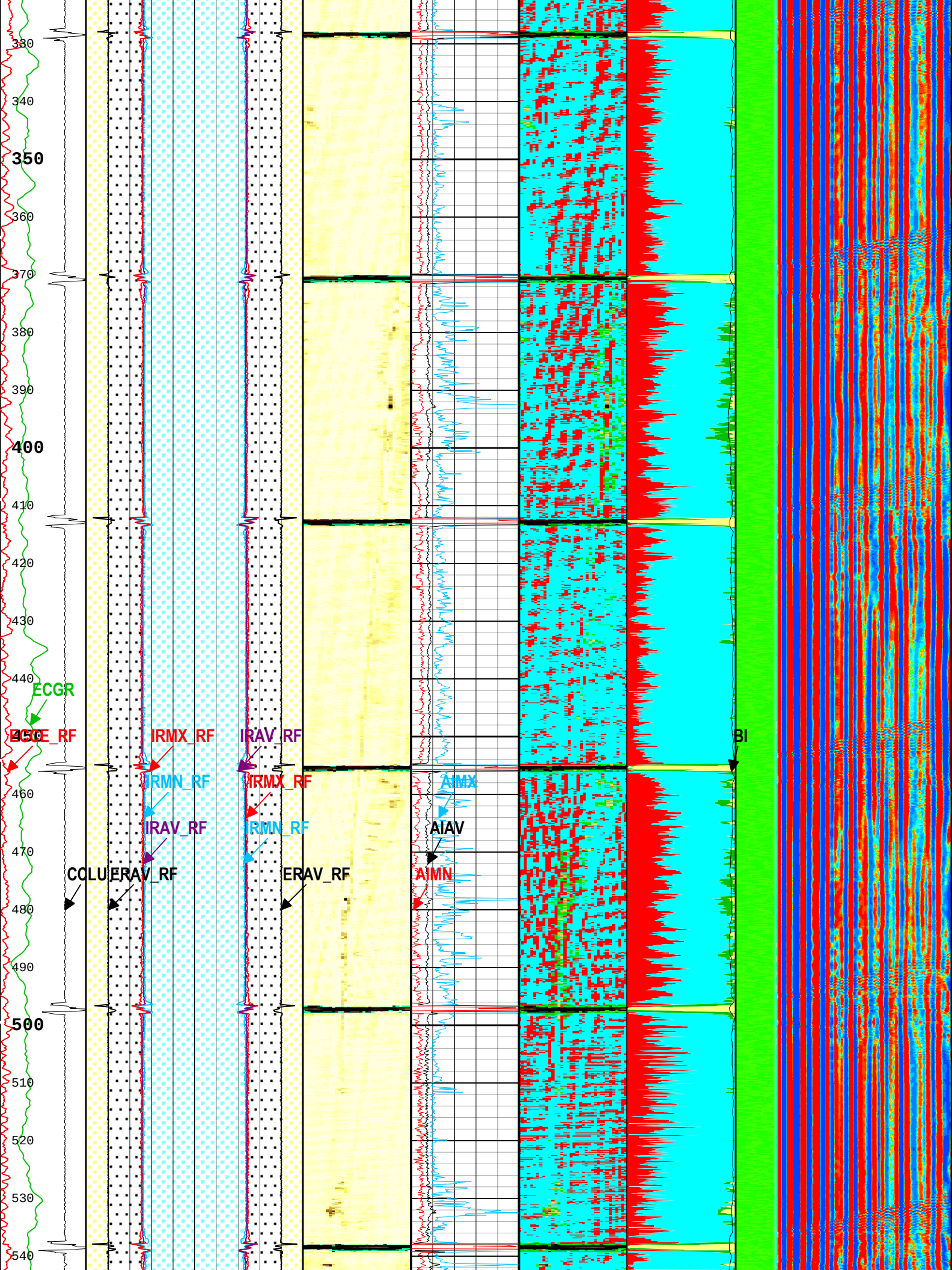
330
340
350
360
370
380
390
400
410
420
430
440
450
460
470
480
490
500
510
520
530
540
ECGR
ECGE_RF
IRMX_RF
IRAV_RF
IRMN_RF
IRMX_RF
IRAV_RF
IRMN_RF
AIMX
AIAV
AIMN
COLU
ERAV_RF
ERAV_RF
BI

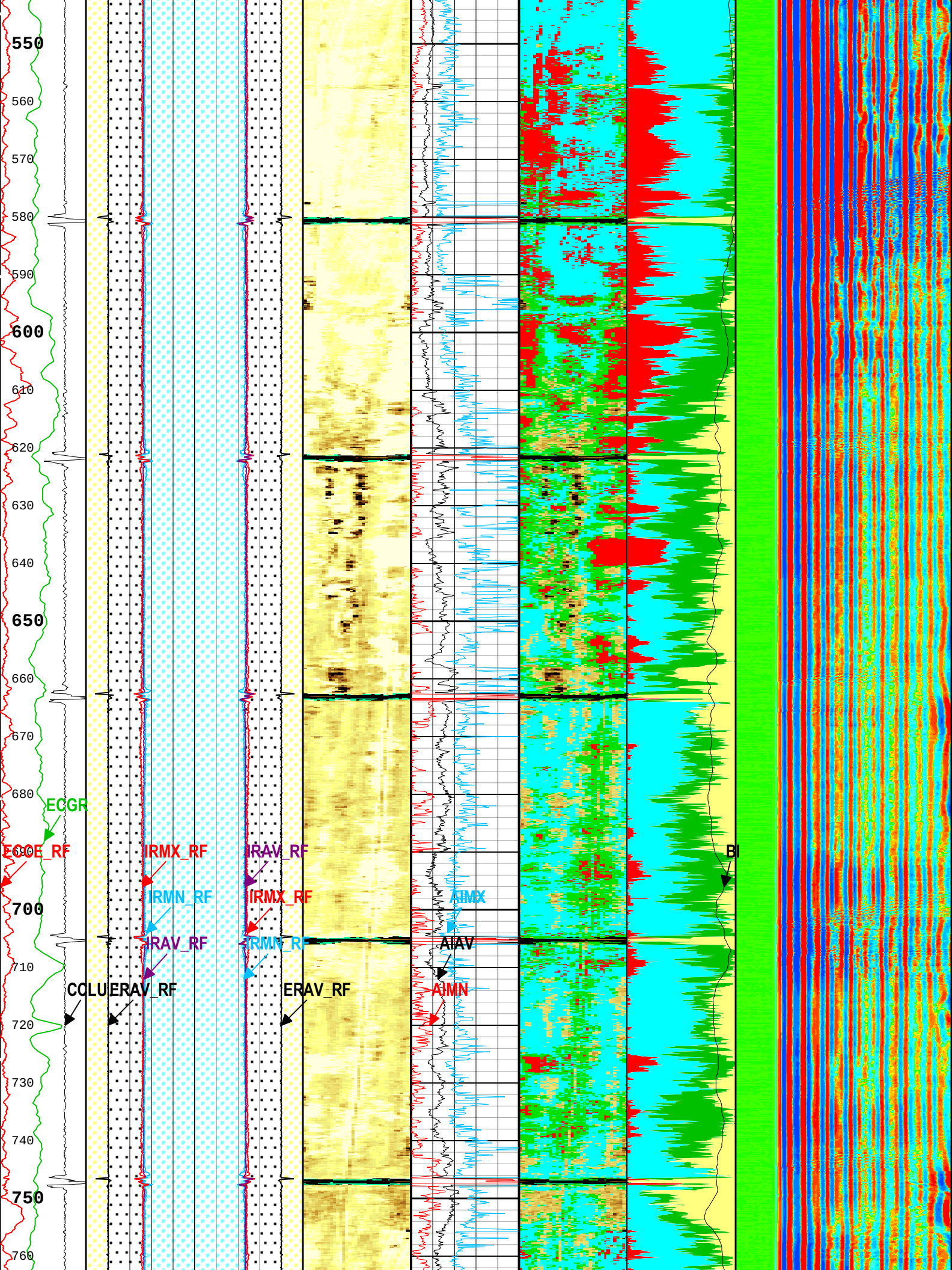
550
560
570
580
590
600
610
620
630
640
650
660
670
680
690
700
710
720
730
740
750
760
ECGR
ECCE_RF
IRMX_RF
IRAV_RF
IRMN_RF
IRMX_RF
IRAV_RF
IRMN_RF
COLU
ERAV_RF
ERAV_RF
AIMX
AIAV
AIMN
BI

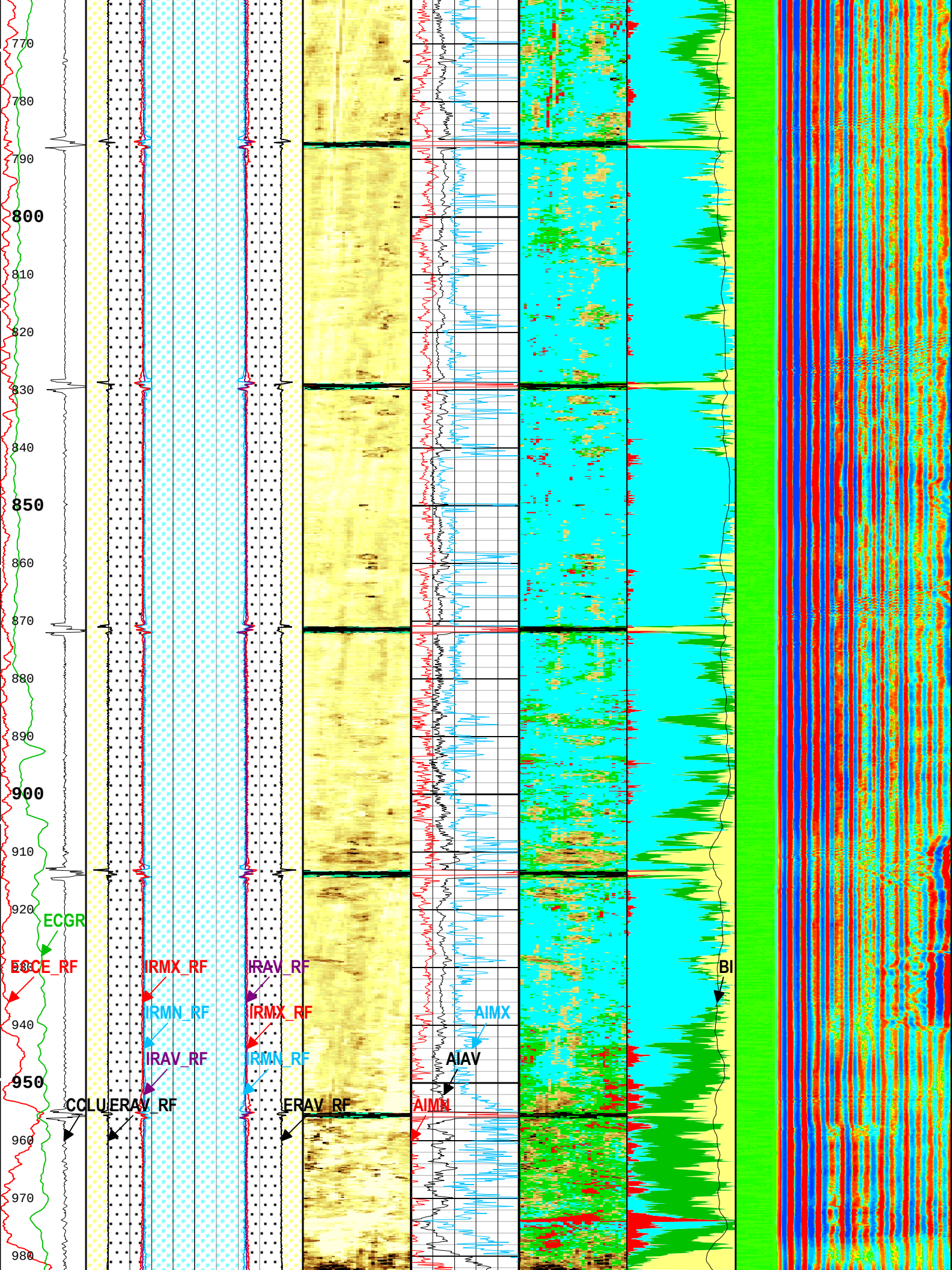
770
780
790
800
810
820
830
840
850
860
870
880
890
900
910
920
930
940
950
960
970
980
ECGR
ECCE_RF
IRMX_RF
IRMN_RF
IRAV_RF
IRAV_RF
IRMX_RF
IRMN_RF
ERAV_RF
ERAV_RF
CCLU
AIMX
AIAV
AIMN
BI

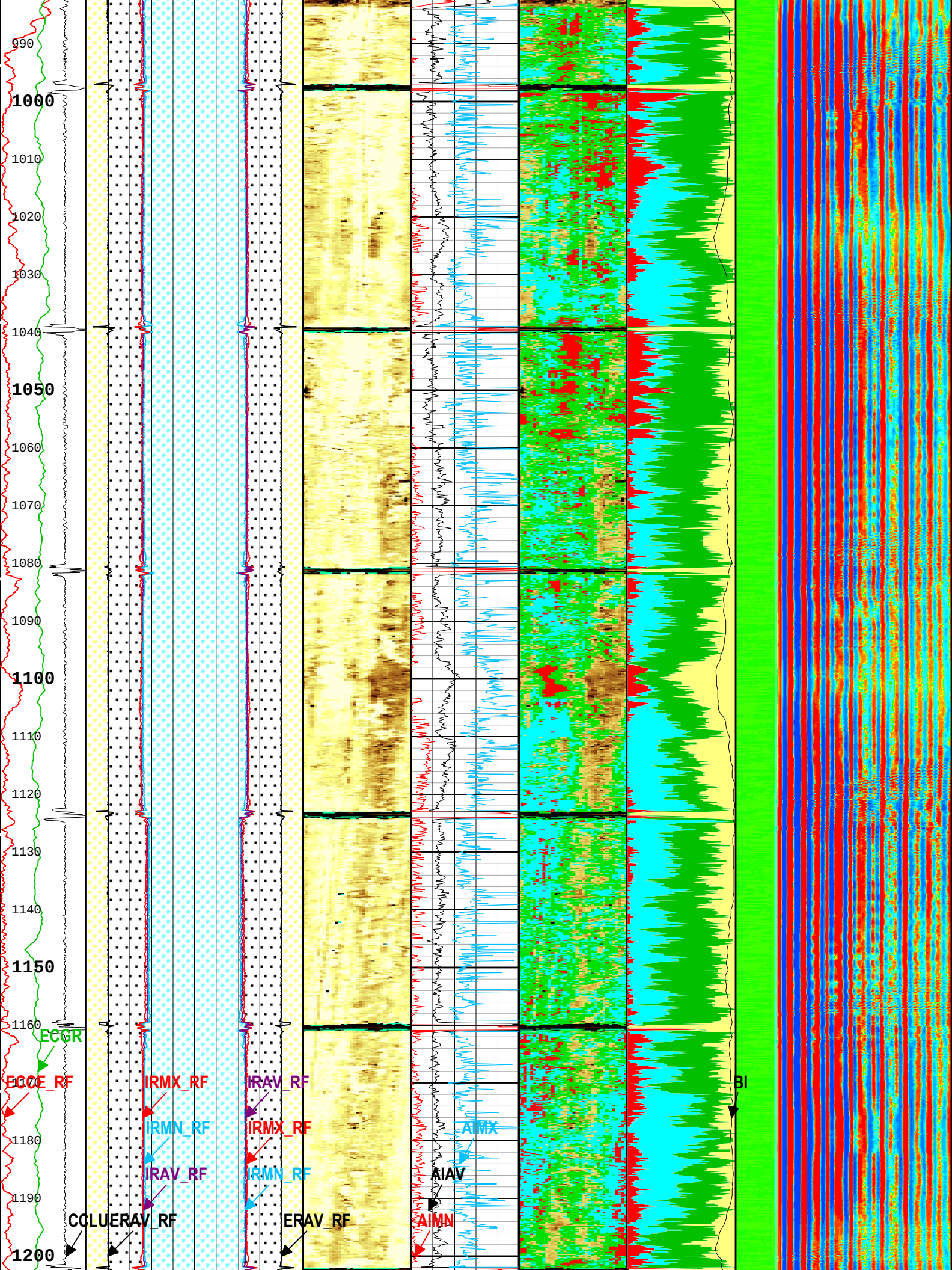
990
1000
1010
1020
1030
1040
1050
1060
1070
1080
1090
1100
1110
1120
1130
1140
1150
1160
1170
1180
1190
1200
ECGR
ECCE_RF
IRMX_RF
IRAV_RF
IRMN_RF
IRMX_RF
IRAV_RF
IRMN_RF
AIMX
AIAV
AIMN
BI
CCLU
ERAV_RF
ERAV_RF

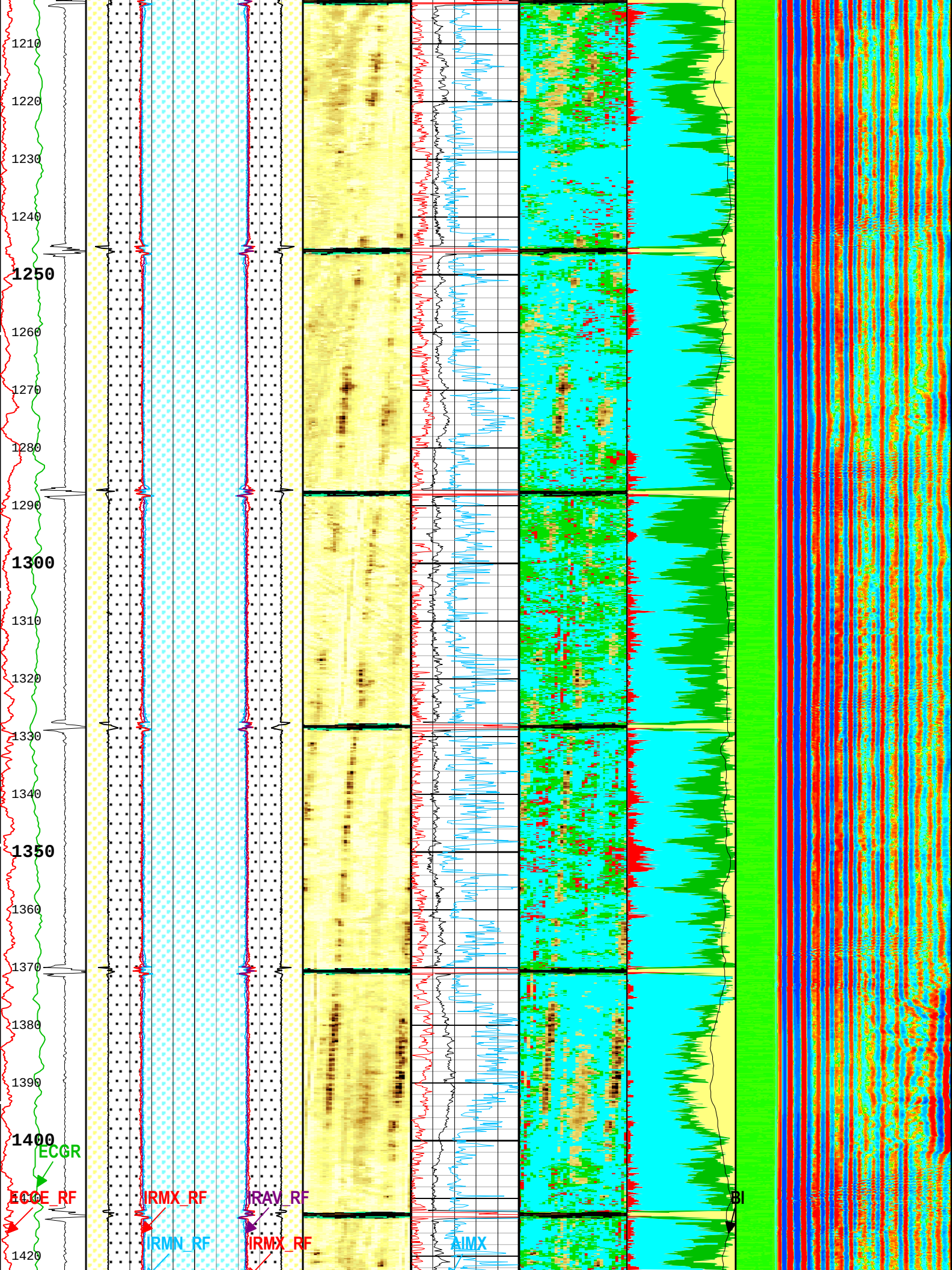
1210
1220
1230
1240
1250
1260
1270
1280
1290
1300
1310
1320
1330
1340
1350
1360
1370
1380
1390
1400
1420
ECGR
ECCE_RF
IRMX_RF
IRAV_RF
IRMN_RF
IRMX_RF
AIMX
BI

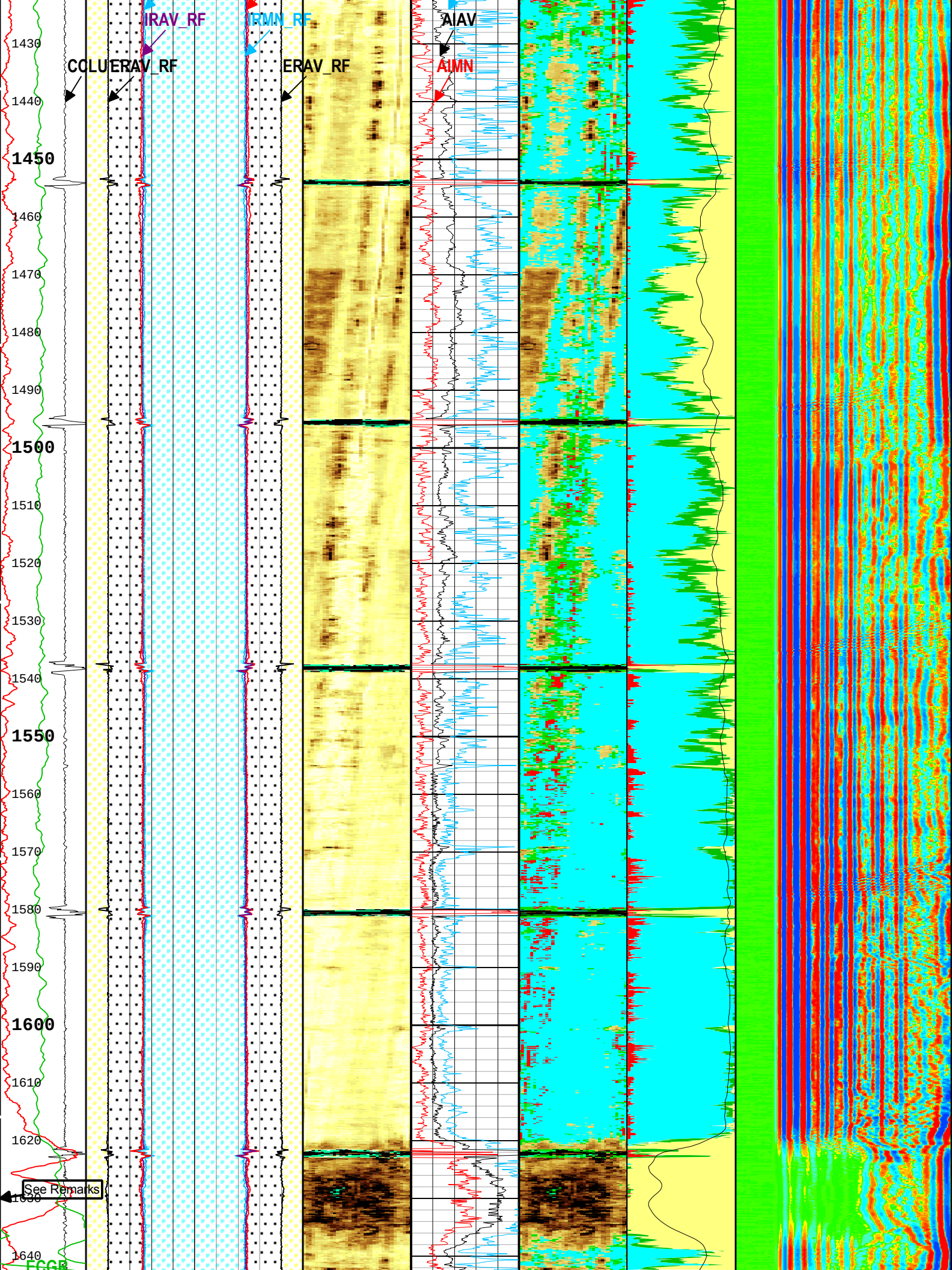
IRAV_RF
IRMN_RF
AIAV
COLU
ERAV_RF
ERAV_RF
AIMN
1430
1440
1450
1460
1470
1480
1490
1500
1510
1520
1530
1540
1550
1560
1570
1580
1590
1600
1610
1620
See Remarks
1630
1640
FCGR

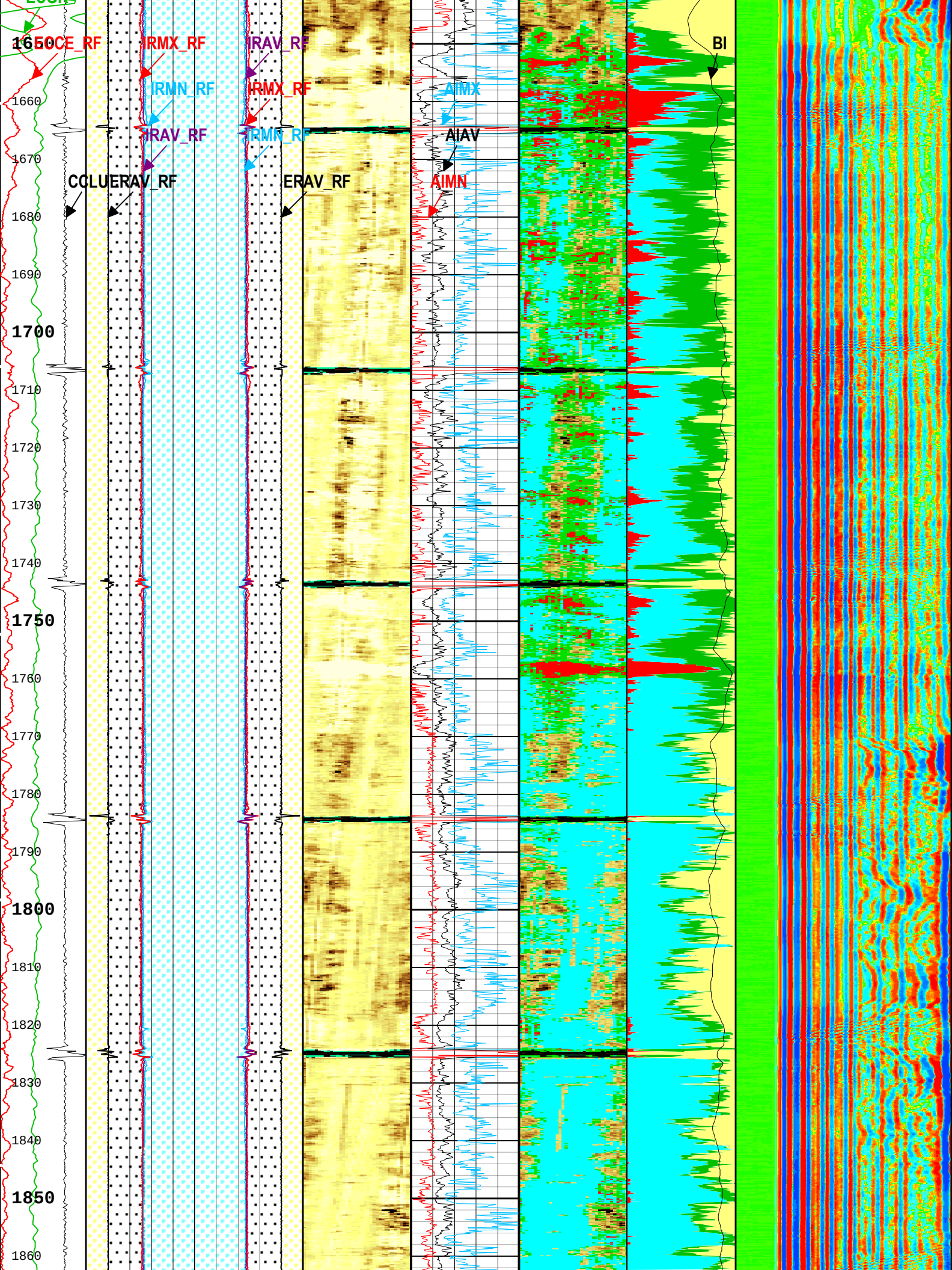
CCLUE
CE_RF
IRMX_RF
IRAV_RF
IRMN_RF
IRMX_RF
IRAV_RF
IRMN_RF
CCLUE
RAV_RF
ERAV_RF
AIMX
AIAV
AIMN
BI
1650
1660
1670
1680
1690
1700
1710
1720
1730
1740
1750
1760
1770
1780
1790
1800
1810
1820
1830
1840
1850
1860

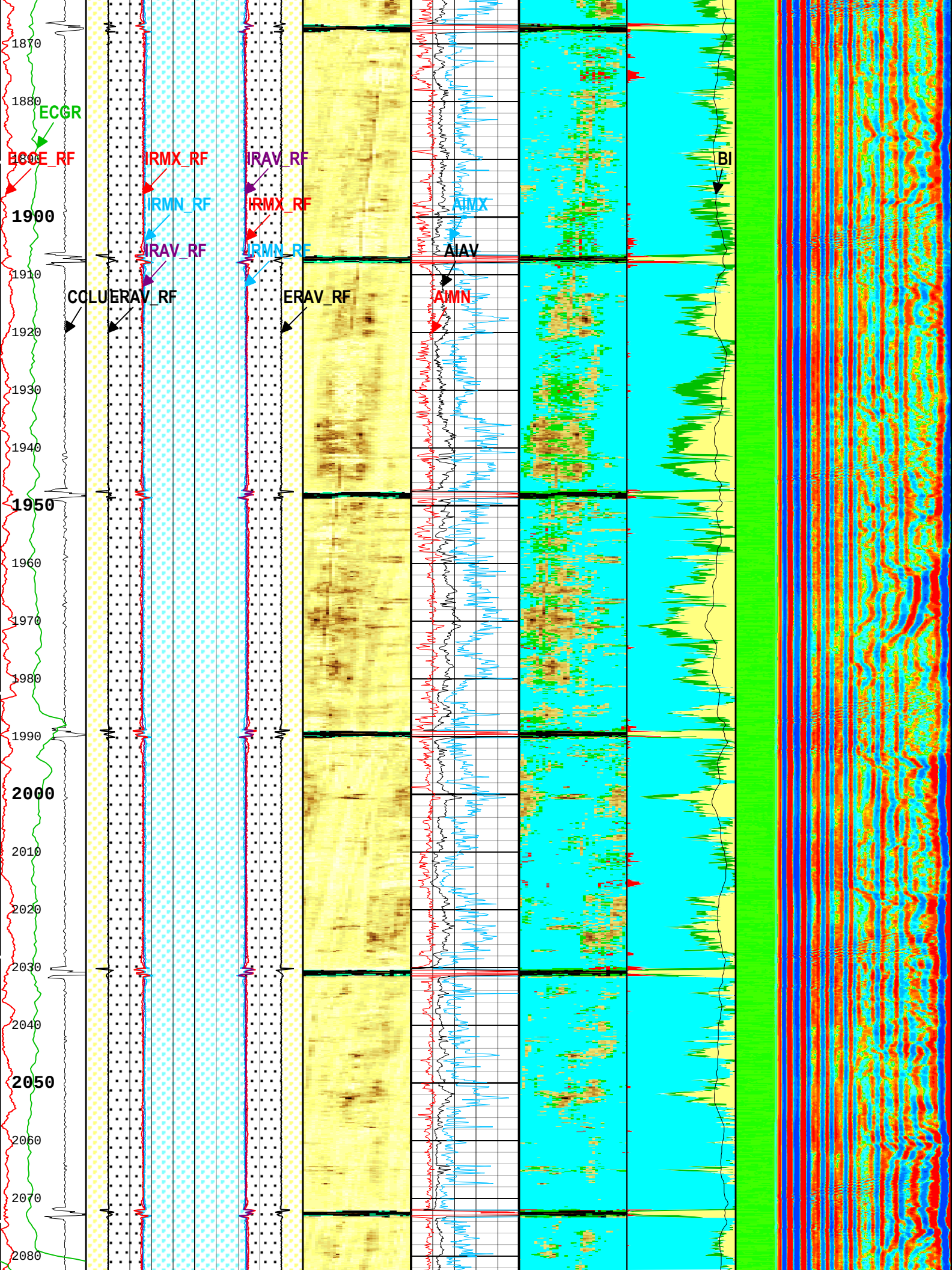
1870
1880
ECGR
ECOE_RF
IRMX_RF
IRAV_RF
BI
1900
IRMN_RF
IRMX_RF
AIMX
IRAV_RF
IRMN_RF
AIAV
1910
COLU
ERAV_RF
ERAV_RF
AIMN
1920
1930
1940
1950
1960
1970
1980
1990
2000
2010
2020
2030
2040
2050
2060
2070
2080

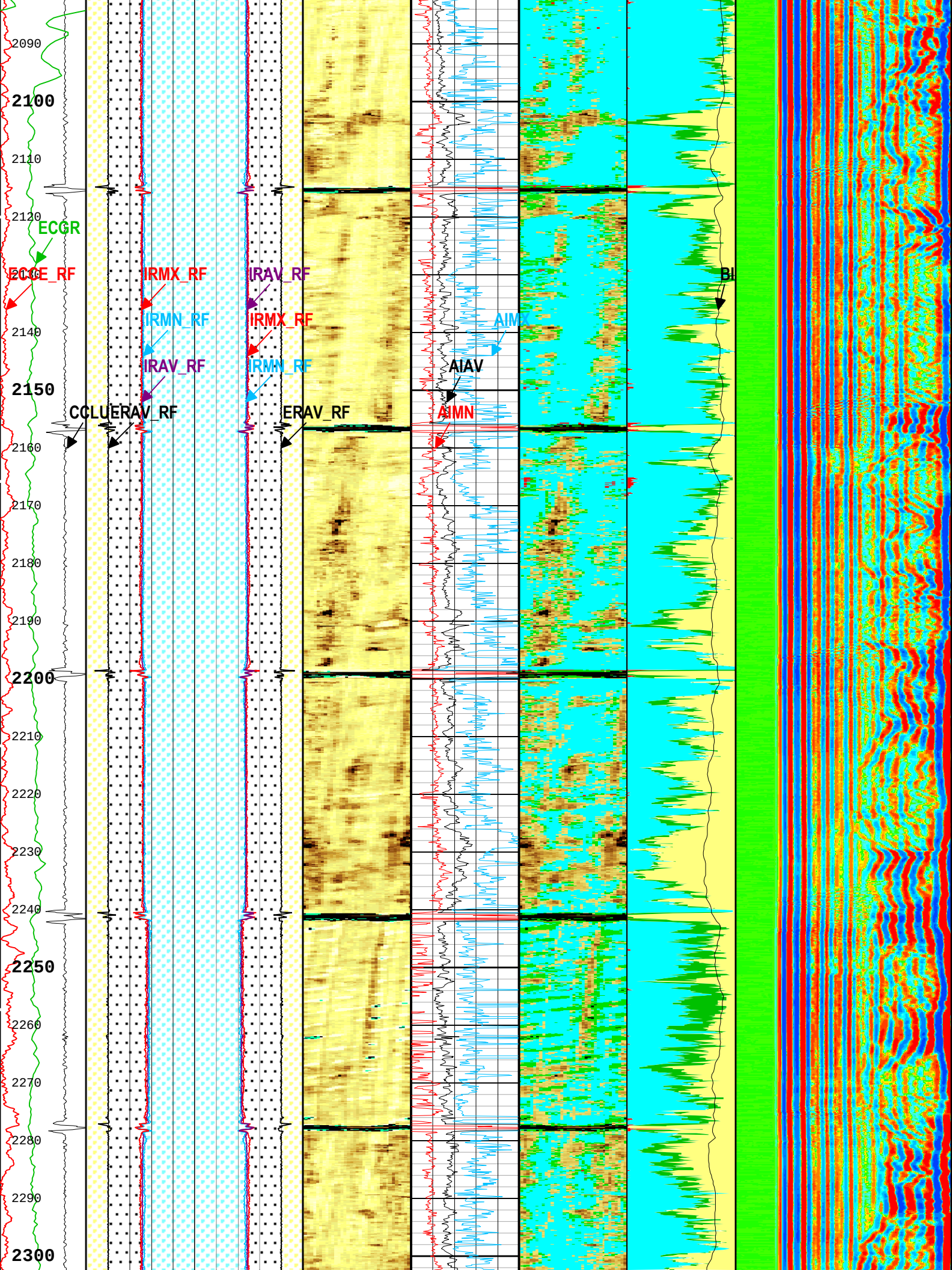
2090
2100
2110
2120
ECGR
ECCE_RF
IRMX_RF
IRAV_RF
IRMN_RF
IRMX_RF
IRAV_RF
IRMN_RF
BI
AIMX
AIAV
AIMN
2140
2150
CCLU
ERAV_RF
ERAV_RF
2160
2170
2180
2190
2200
2210
2220
2230
2240
2250
2260
2270
2280
2290
2300

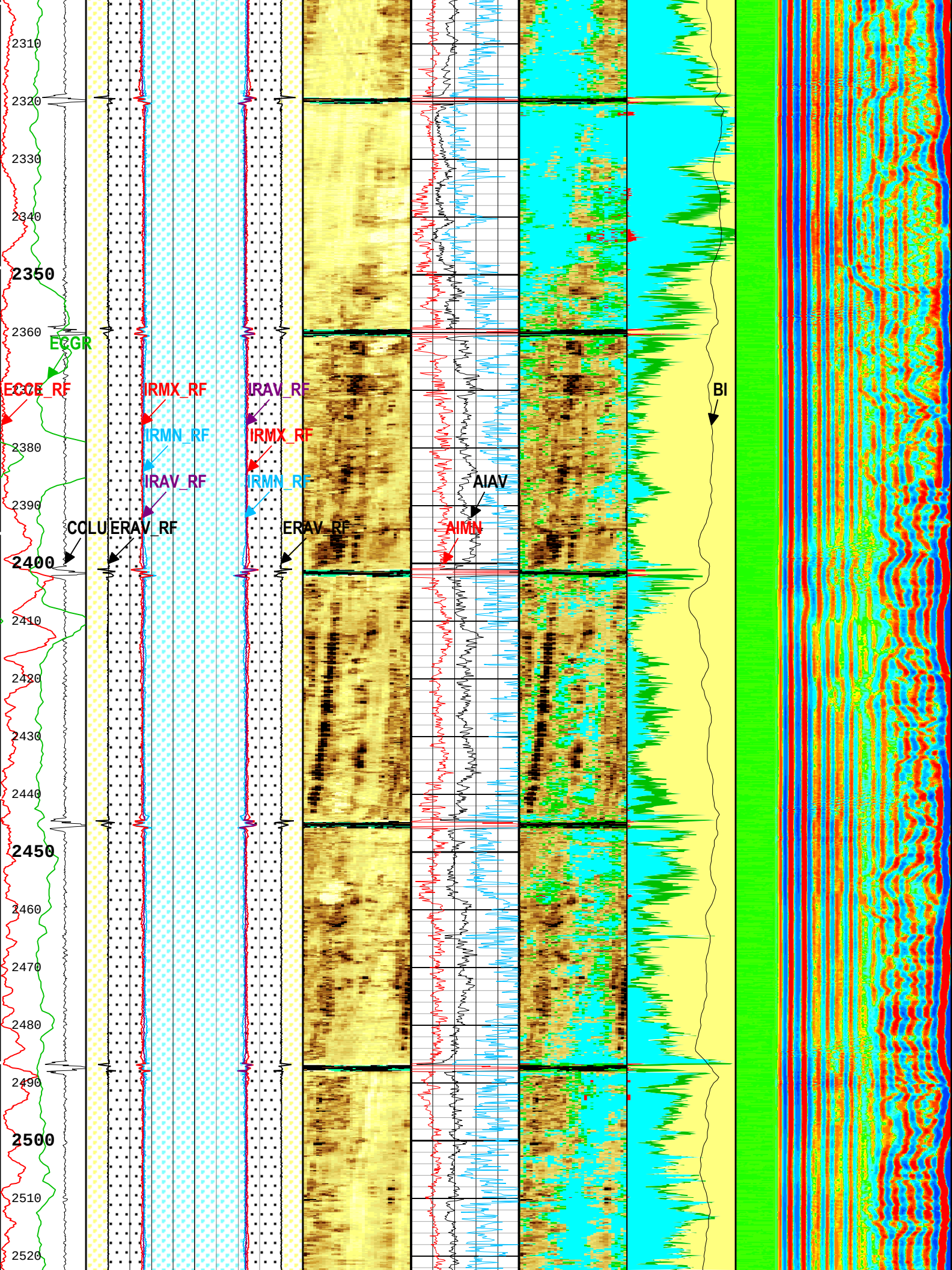
2310
2320
2330
2340
2350
2360
2370
2380
2390
2400
2410
2420
2430
2440
2450
2460
2470
2480
2490
2500
2510
2520
ECGR
ECCE_RF
IRMX_RF
IRAV_RF
IRMN_RF
IRMX_RF
IRAV_RF
IRMN_RF
COLU
ERAV_RF
ERAV_RF
AIAV
AIMN
BI

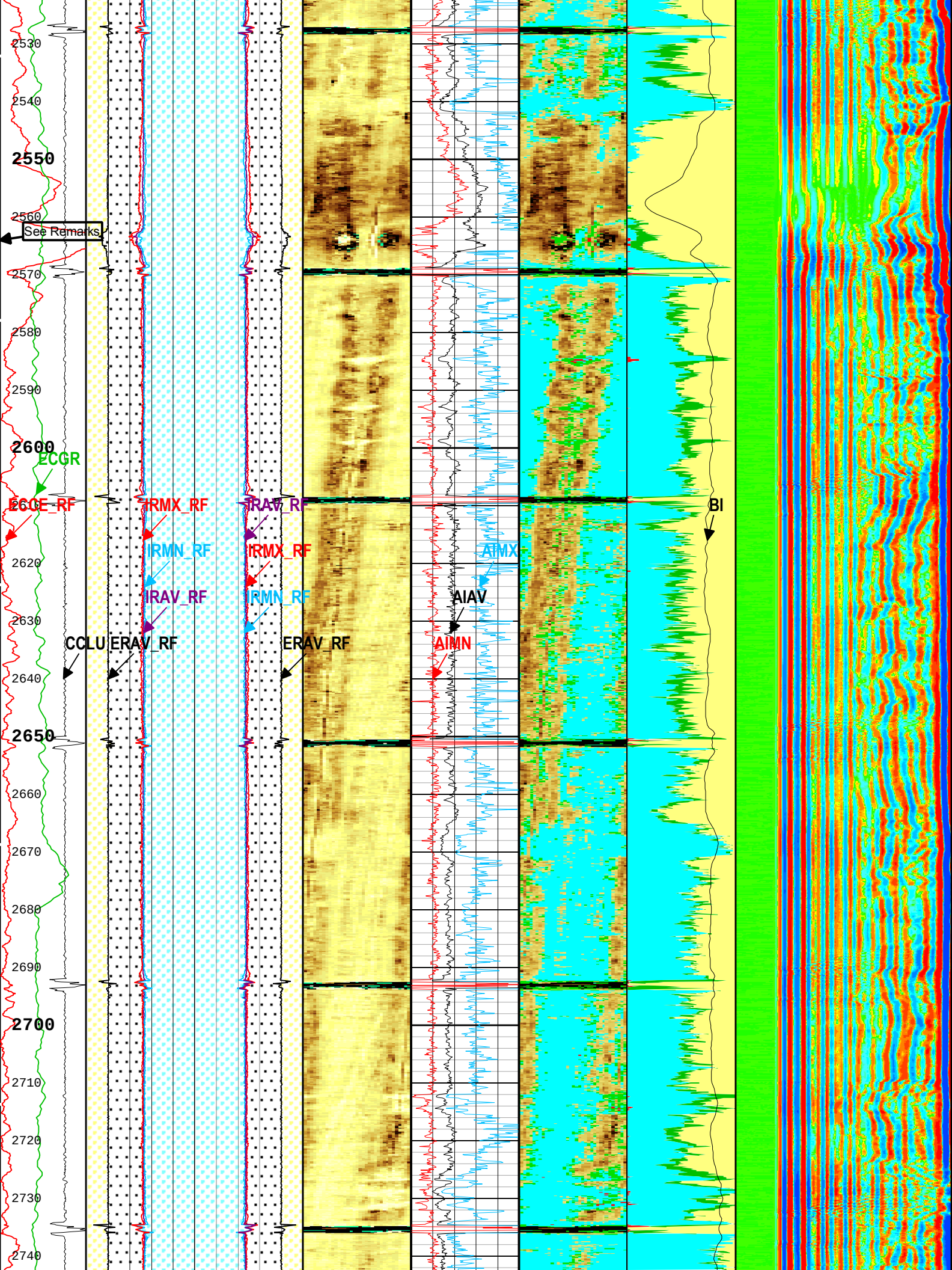
2530
2540
2550
2560
See Remarks
2570
2580
2590
2600
ECGR
ECCE_RF
IRMX_RF
IRAV_RF
IRMN_RF
IRMX_RF
IRAV_RF
IRMN_RF
AIMX
AIAV
AIMN
BI
2620
2630
CCLU
ERAV_RF
ERAV_RF
2640
2650
2660
2670
2680
2690
2700
2710
2720
2730
2740

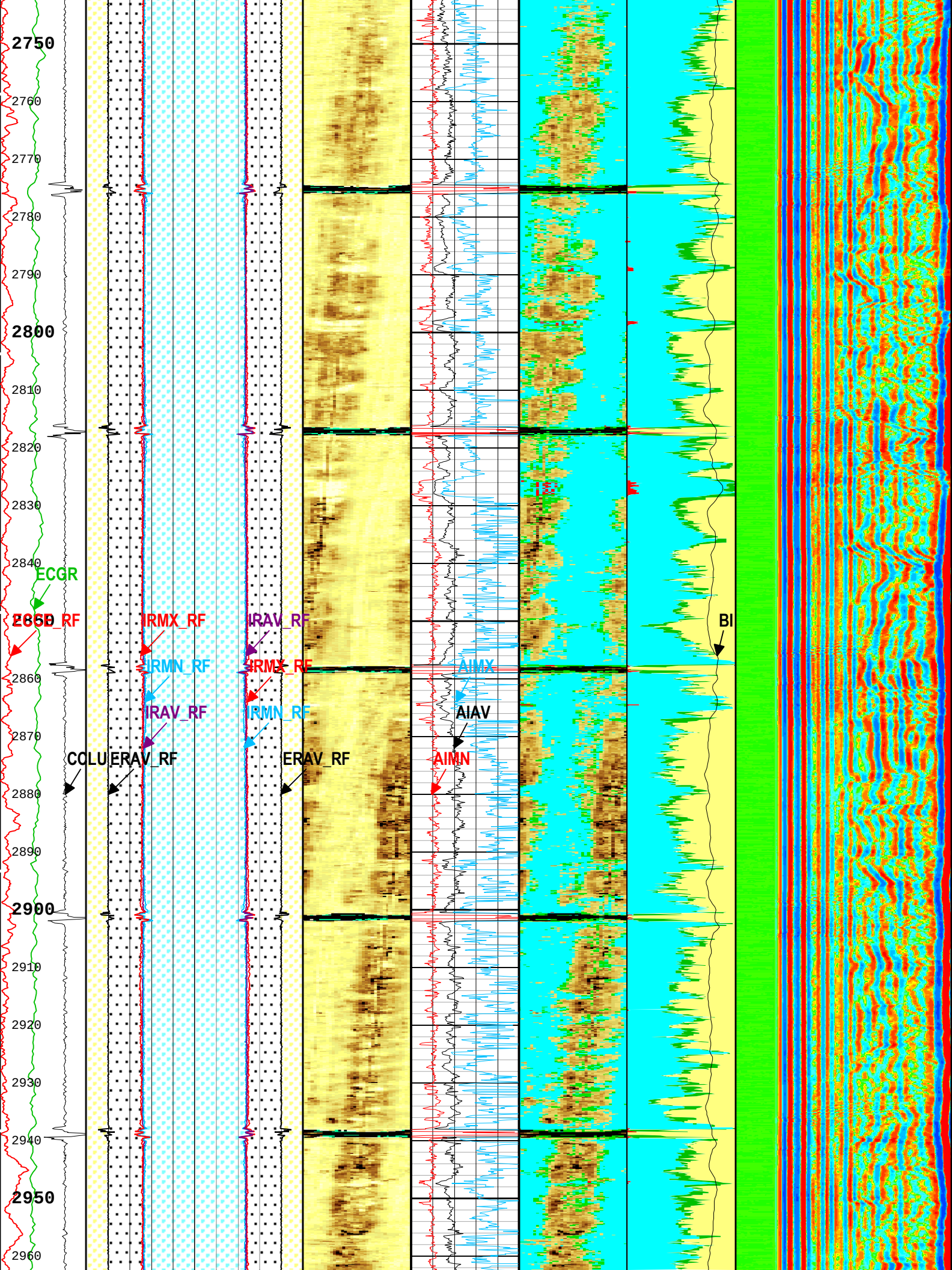
2750
2760
2770
2780
2790
2800
2810
2820
2830
2840
ECGR
2860
2870
2880
2890
2900
2910
2920
2930
2940
2950
2960
IRMX_RF
IRMN_RF
IRAV_RF
IRAV_RF
IRMX_RF
IRMN_RF
AIMX
AIAV
AIMN
BI
COLU
ERAV_RF
ERAV_RF

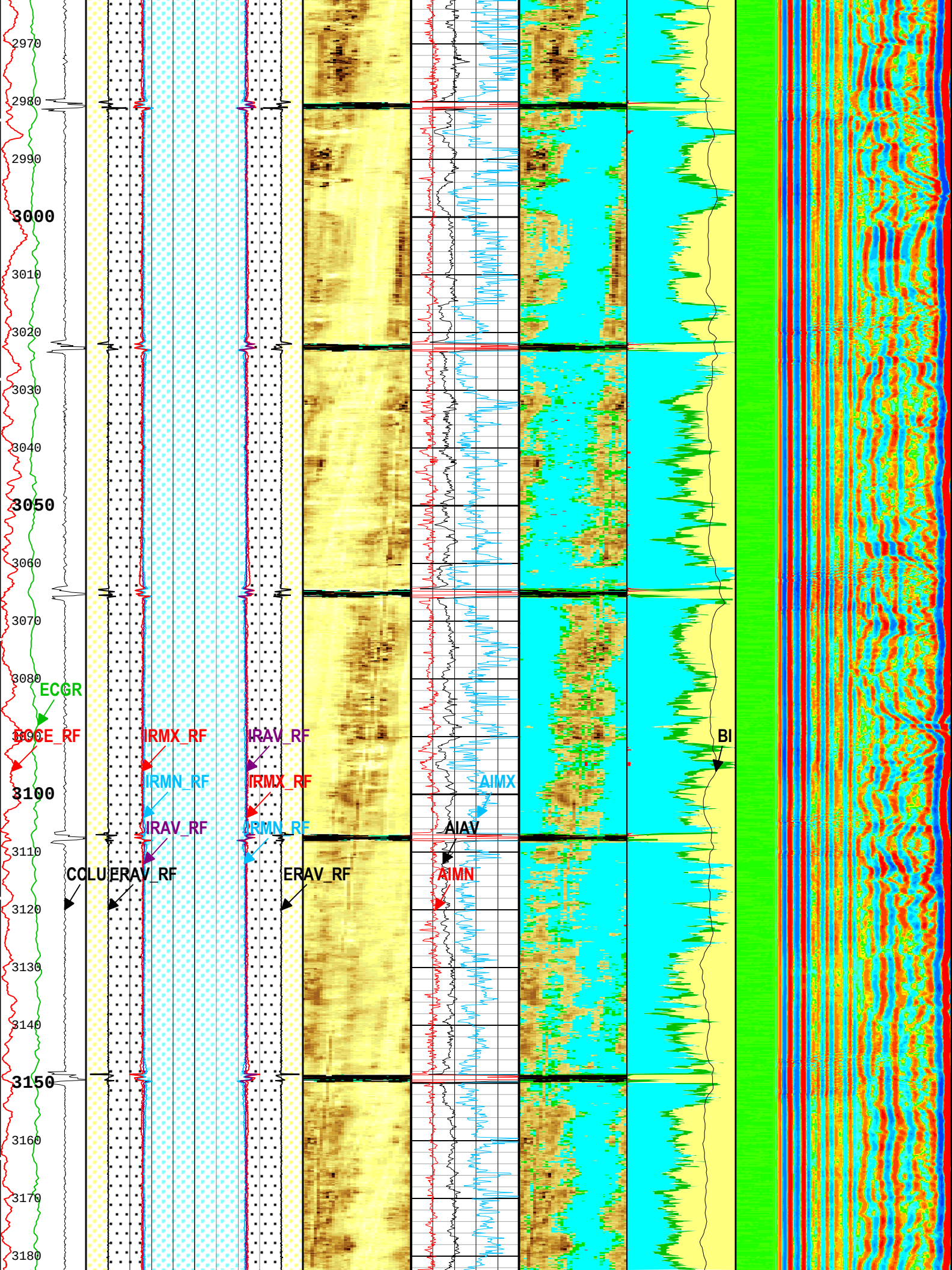
2970
2980
2990
3000
3010
3020
3030
3040
3050
3060
3070
3080
ECGR
3090
3100
3110
3120
3130
3140
3150
3160
3170
3180
IRMX_RF
IRAV_RF
IRMN_RF
IRMX_RF
IRAV_RF
IRMN_RF
AIMX
AIAV
AIMN
BI
CCLU
ERAV_RF
ERAV_RF

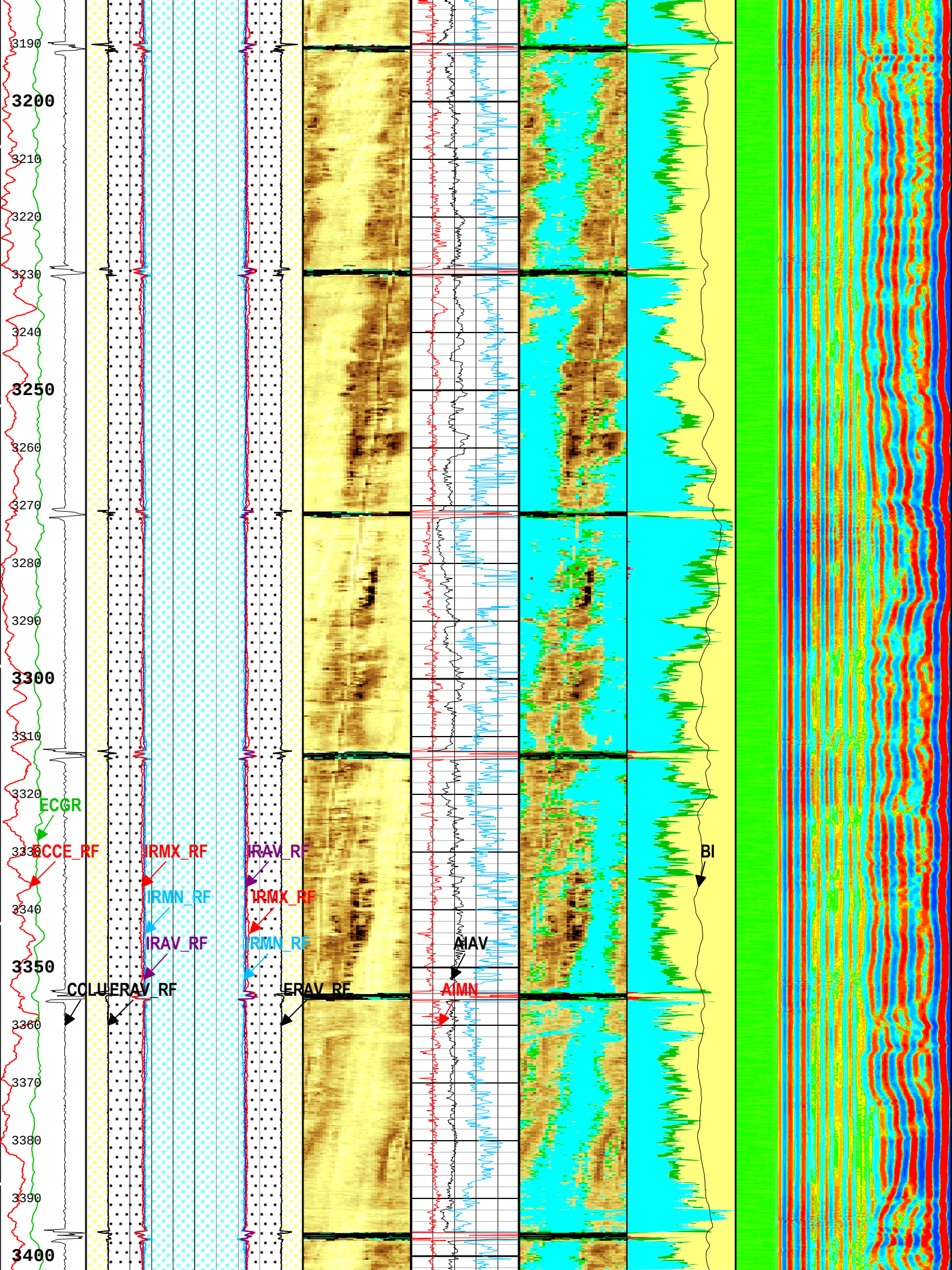
3190
3200
3210
3220
3230
3240
3250
3260
3270
3280
3290
3300
3310
3320
3330
3340
3350
3360
3370
3380
3390
3400
ECGR
ECCE_RF
IRMX_RF
IRAV_RF
IRMN_RF
IRMX_RF
IRAV_RF
IRMN_RF
COLU
ERAV_RF
ERAV_RF
AIAV
AIMN
BI

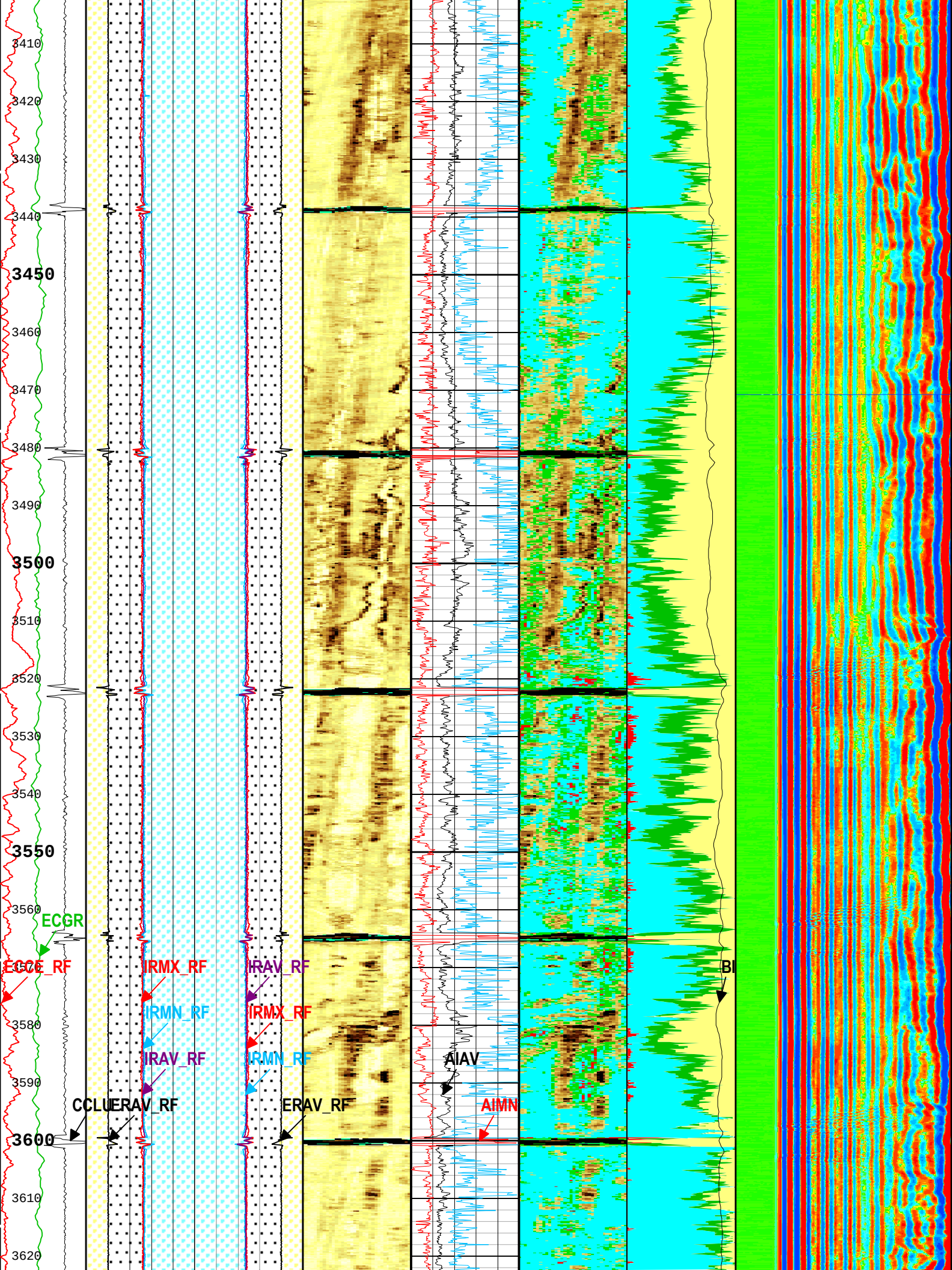
3410
3420
3430
3440
3450
3460
3470
3480
3490
3500
3510
3520
3530
3540
3550
3560
3580
3590
3600
3610
3620
ECGR
ECCE_RF
IRMX_RF
IRAV_RF
IRMN_RF
IRMX_RF
IRAV_RF
IRMN_RF
CCLU
ERAV_RF
ERAV_RF
AIAV
AIMN
BI

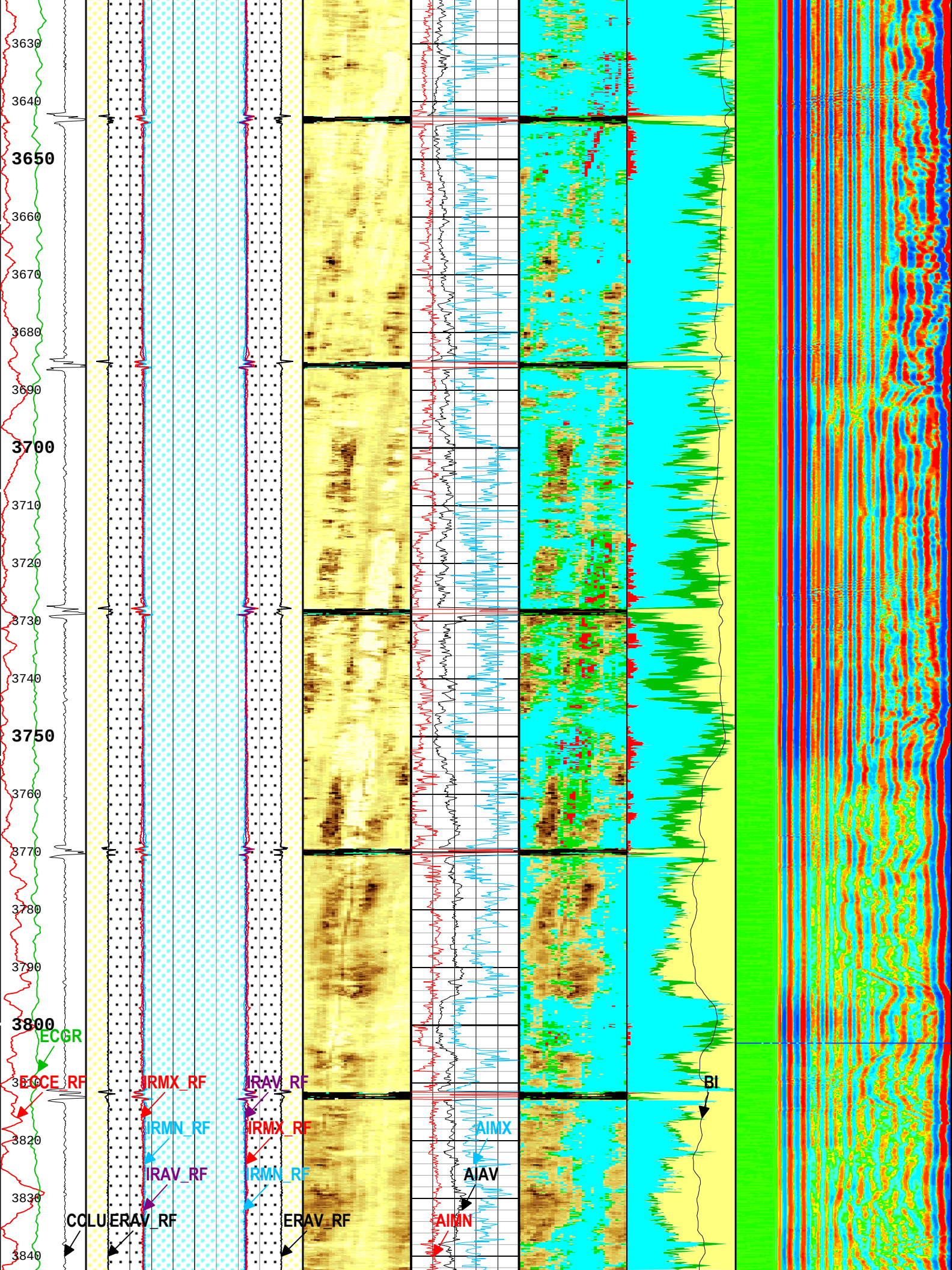
3630
3640
3650
3660
3670
3680
3690
3700
3710
3720
3730
3740
3750
3760
3770
3780
3790
3800
3820
3830
3840
ECGR
ECCE_RF
IRMX_RF
IRAV_RF
IRMN_RF
IRMX_RF
IRAV_RF
IRMN_RF
AIMX
AIAV
AIMN
BI
CCLU
ERAV_RF
ERAV_RF

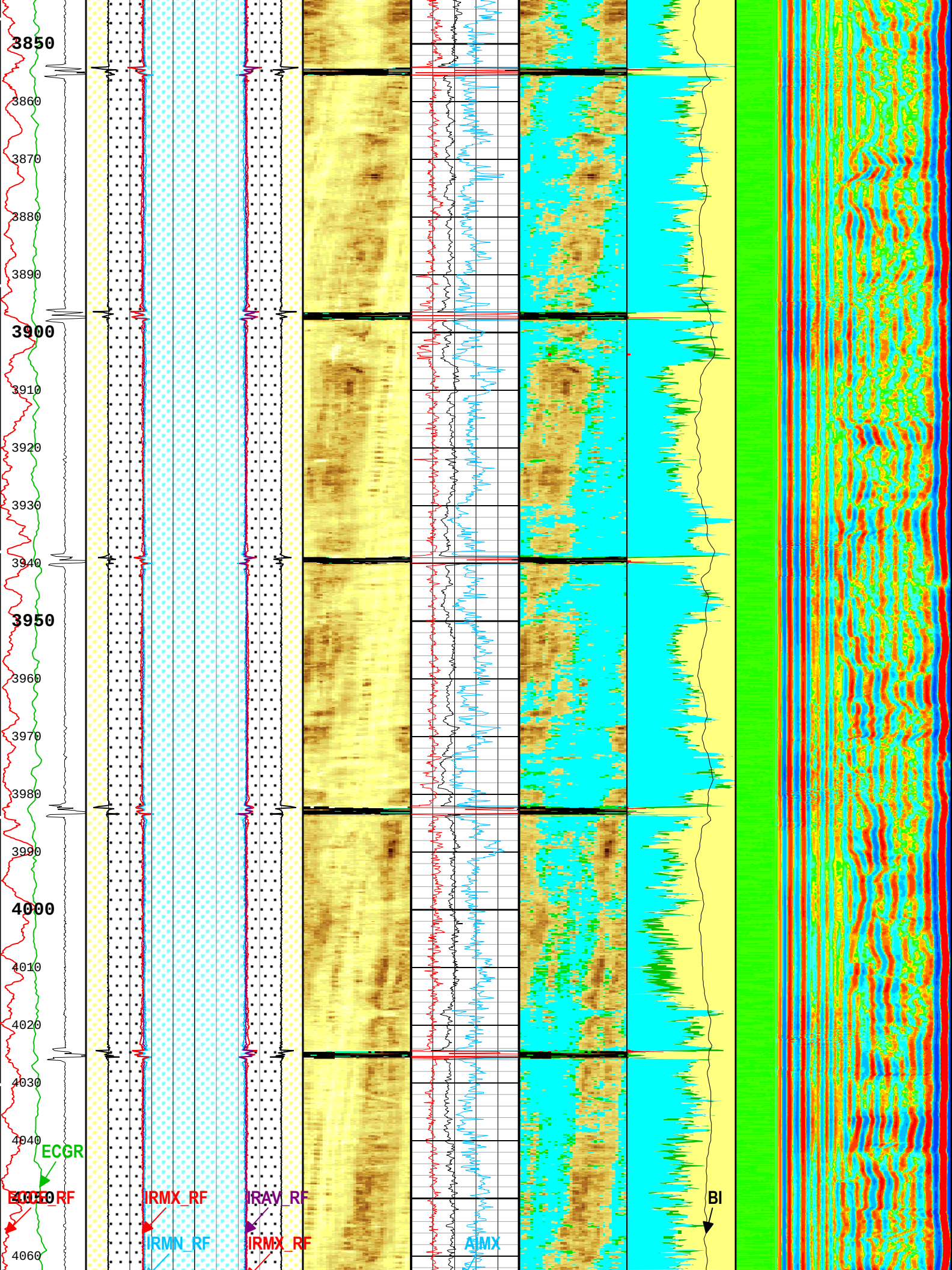
3850
3860
3870
3880
3890
3900
3910
3920
3930
3940
3950
3960
3970
3980
3990
4000
4010
4020
4030
4040
4050
4060
ECGR
IRMX_RF
IRAV_RF
IRMN_RF
IRMX_RF
AIMX
BI

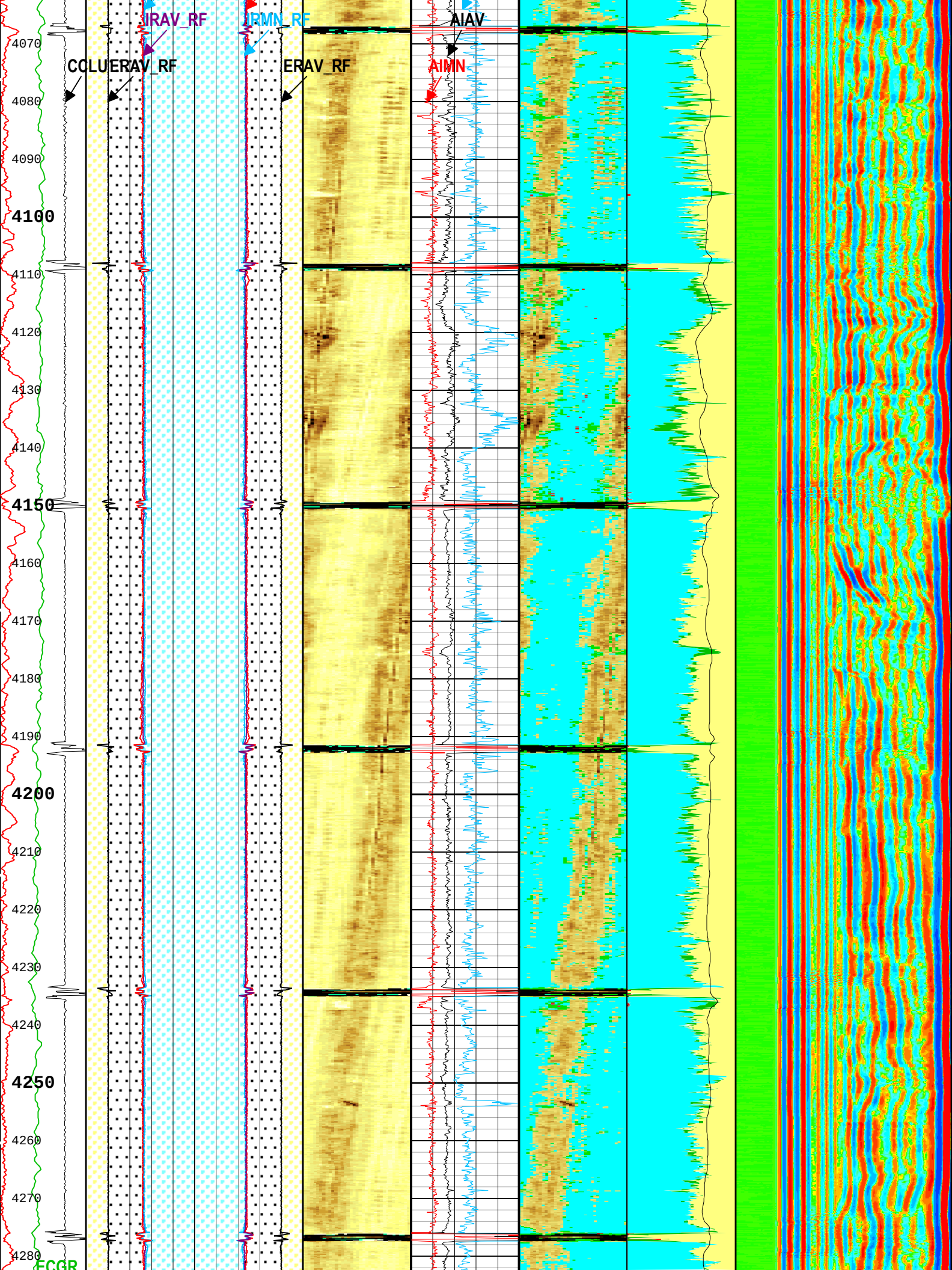
IRAV_RF
IRMN_RF
AIAV
COLU
ERAV_RF
ERAV_RF
AIMN
4070
4080
4090
4100
4110
4120
4130
4140
4150
4160
4170
4180
4190
4200
4210
4220
4230
4240
4250
4260
4270
4280
ECGR

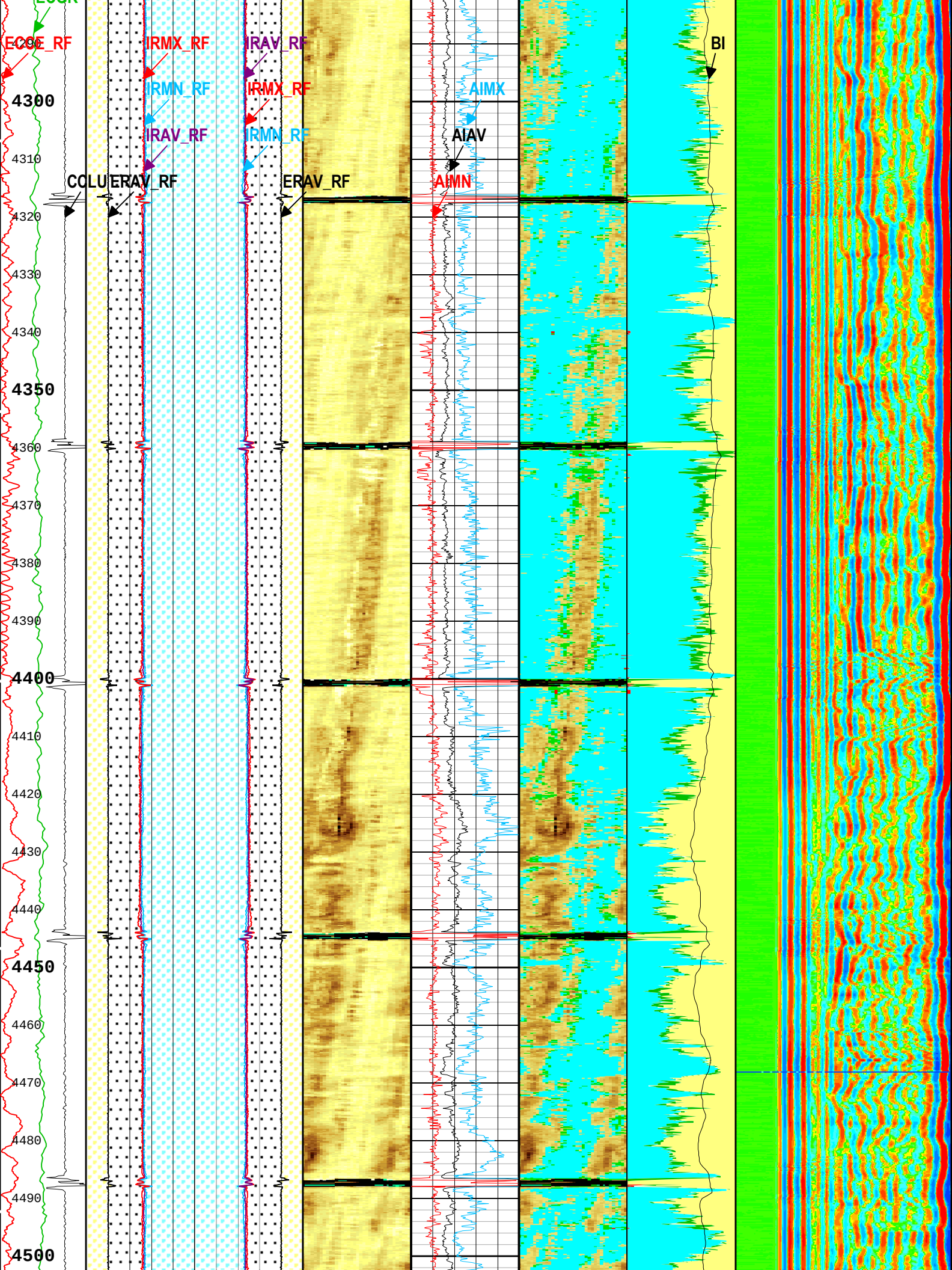
ECOE_RF
IRMX_RF
IRAV_RF
IRMN_RF
IRMX_RF
IRAV_RF
IRMN_RF
AIMX
AIAV
AIMN
BI
COLU
ERAV_RF
ERAV_RF
4300
4310
4320
4330
4340
4350
4360
4370
4380
4390
4400
4410
4420
4430
4440
4450
4460
4470
4480
4490
4500

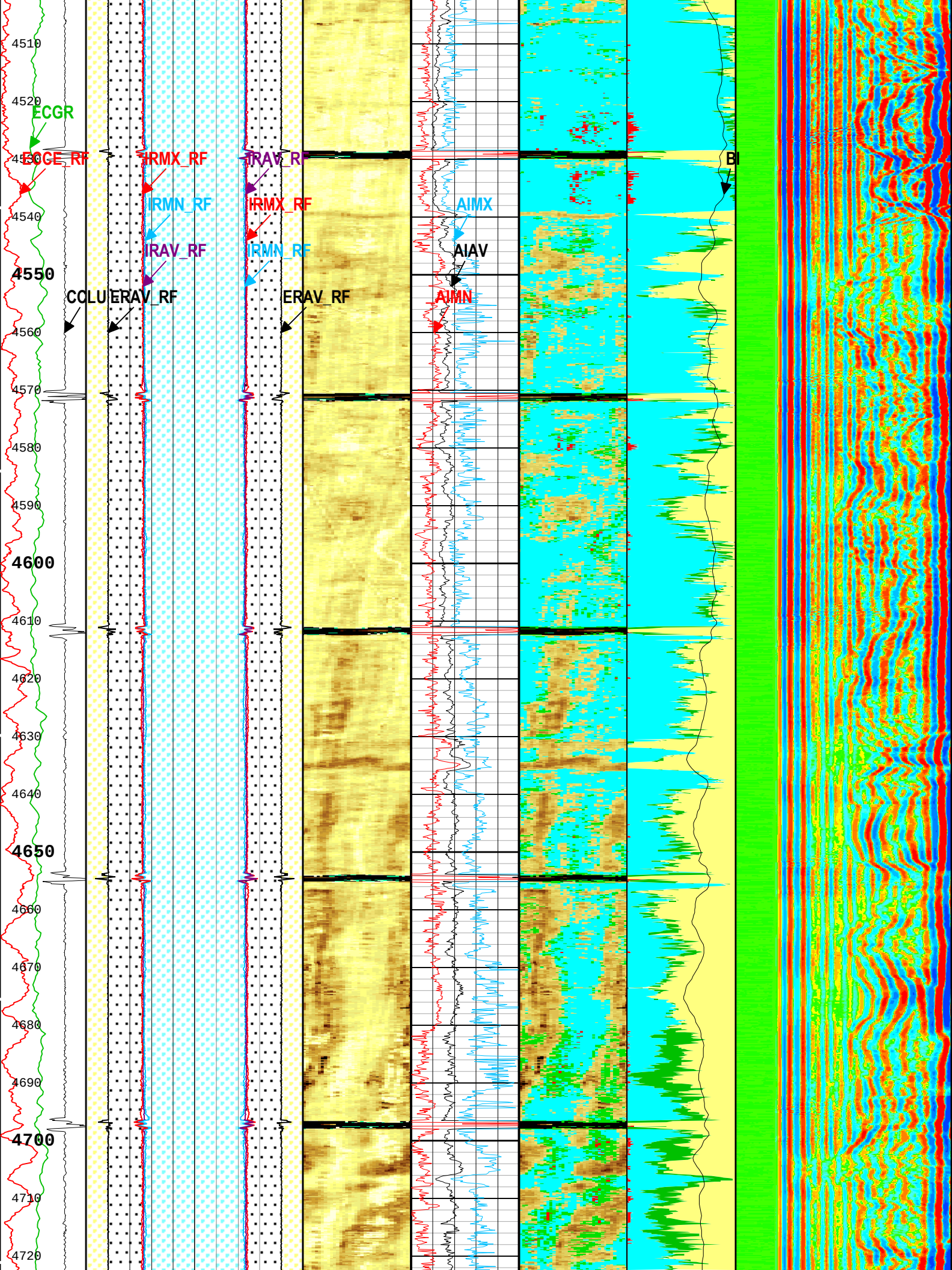
4510
4520
ECGR
4530
CGE_RF
IRMX_RF
IRAV_RF
IRMN_RF
IRMX_RF
AIMX
4540
IRAV_RF
IRMN_RF
AIAV
4550
COLU
ERAV_RF
ERAV_RF
AIMN
BI
4560
4570
4580
4590
4600
4610
4620
4630
4640
4650
4660
4670
4680
4690
4700
4710
4720

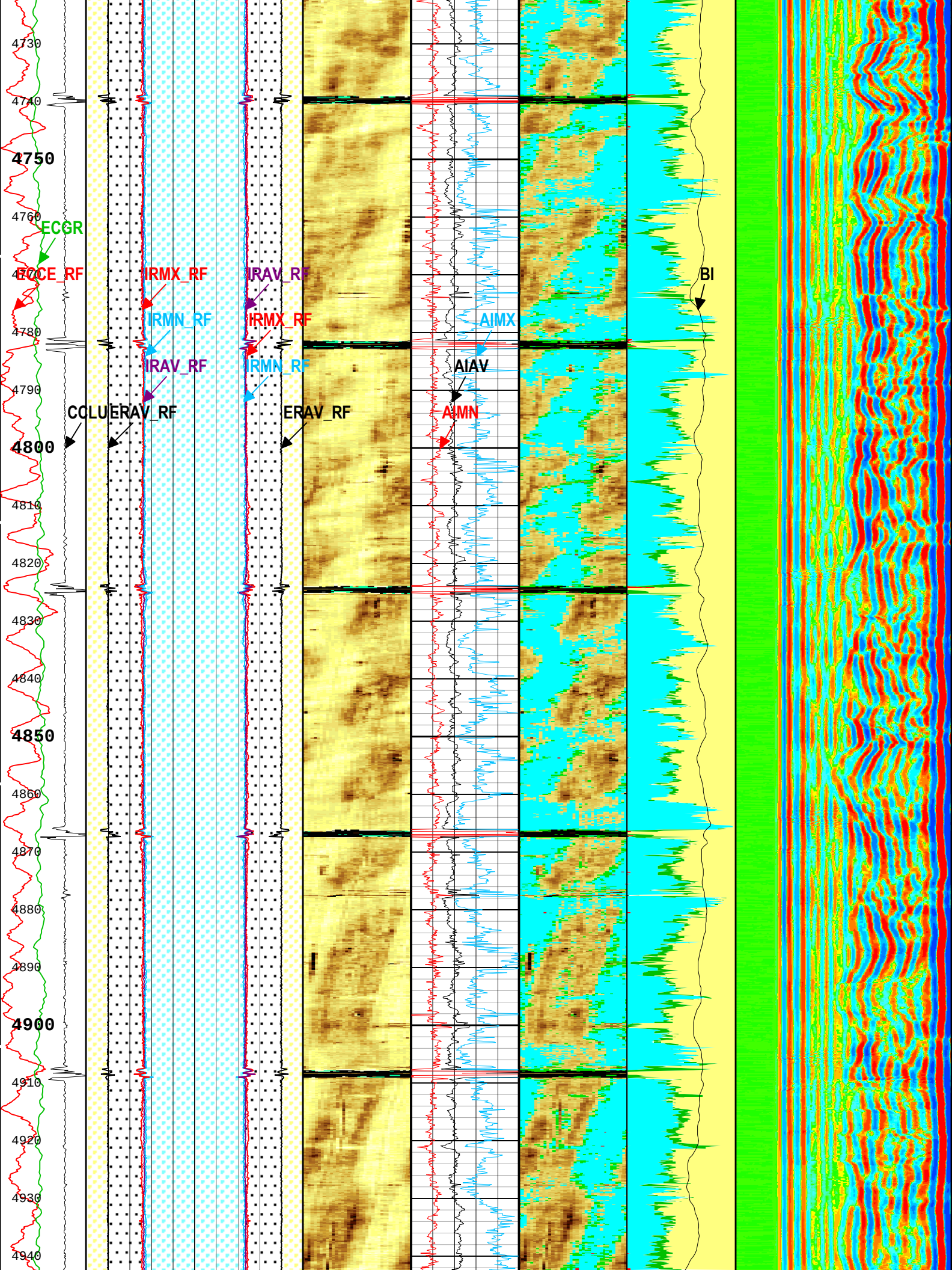
4730
4740
4750
4760
ECGR
ECCE_RF
IRMX_RF
IRAV_RF
IRMN_RF
IRMX_RF
IRAV_RF
IRMN_RF
BI
AIMX
AIAV
AIMN
4780
4790
COLU
ERAV_RF
ERAV_RF
4800
4810
4820
4830
4840
4850
4860
4870
4880
4890
4900
4910
4920
4930
4940

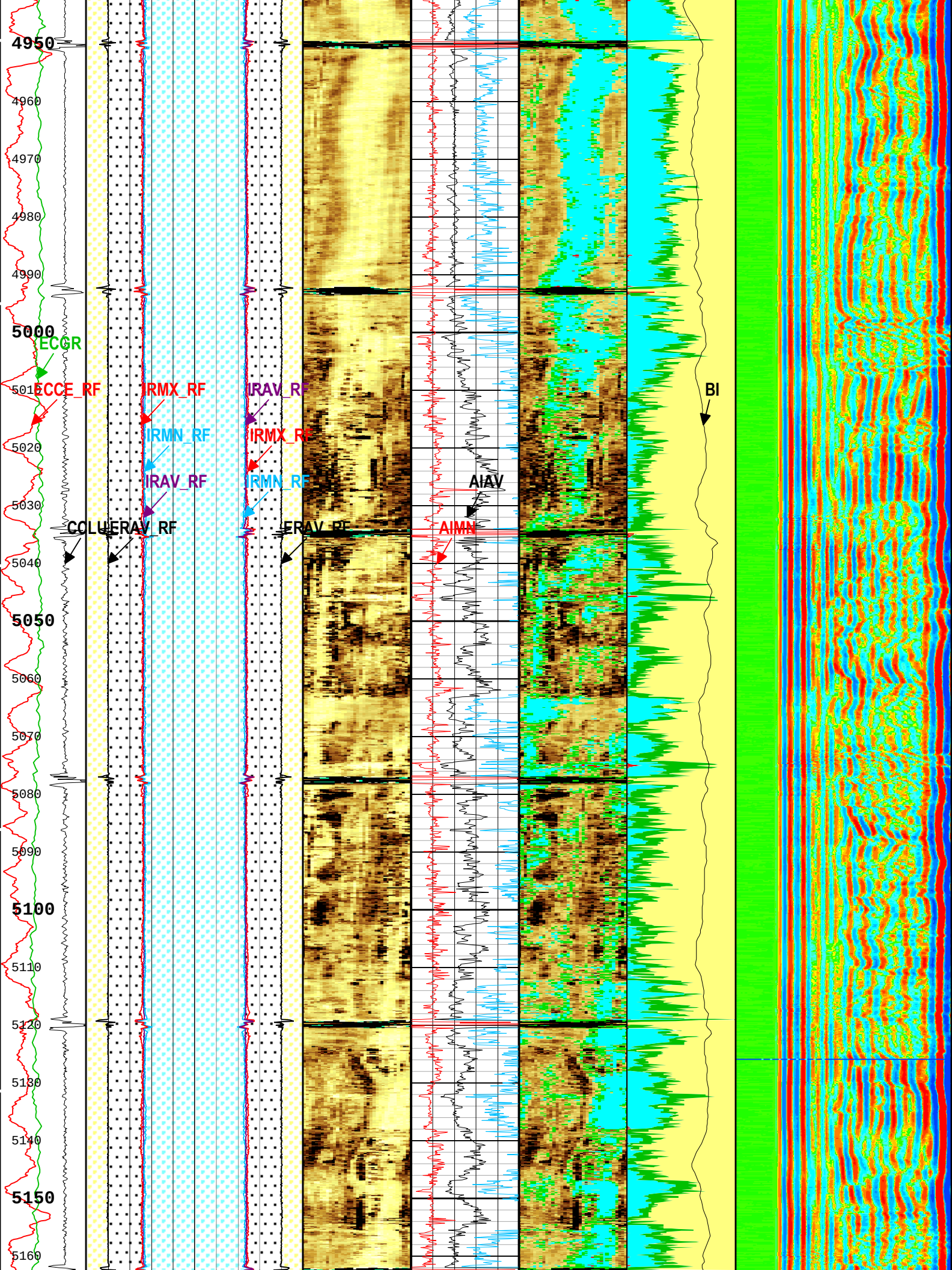
4950
4960
4970
4980
4990
5000
ECGR
ECCE_RF
IRMX_RF
IRAV_RF
IRMN_RF
IRMX_RF
IRAV_RF
IRMN_RF
BI
AIAV
AIMN
COLU
ERAV_RF
ERAV_RF
5010
5020
5030
5040
5050
5060
5070
5080
5090
5100
5110
5120
5130
5140
5150
5160

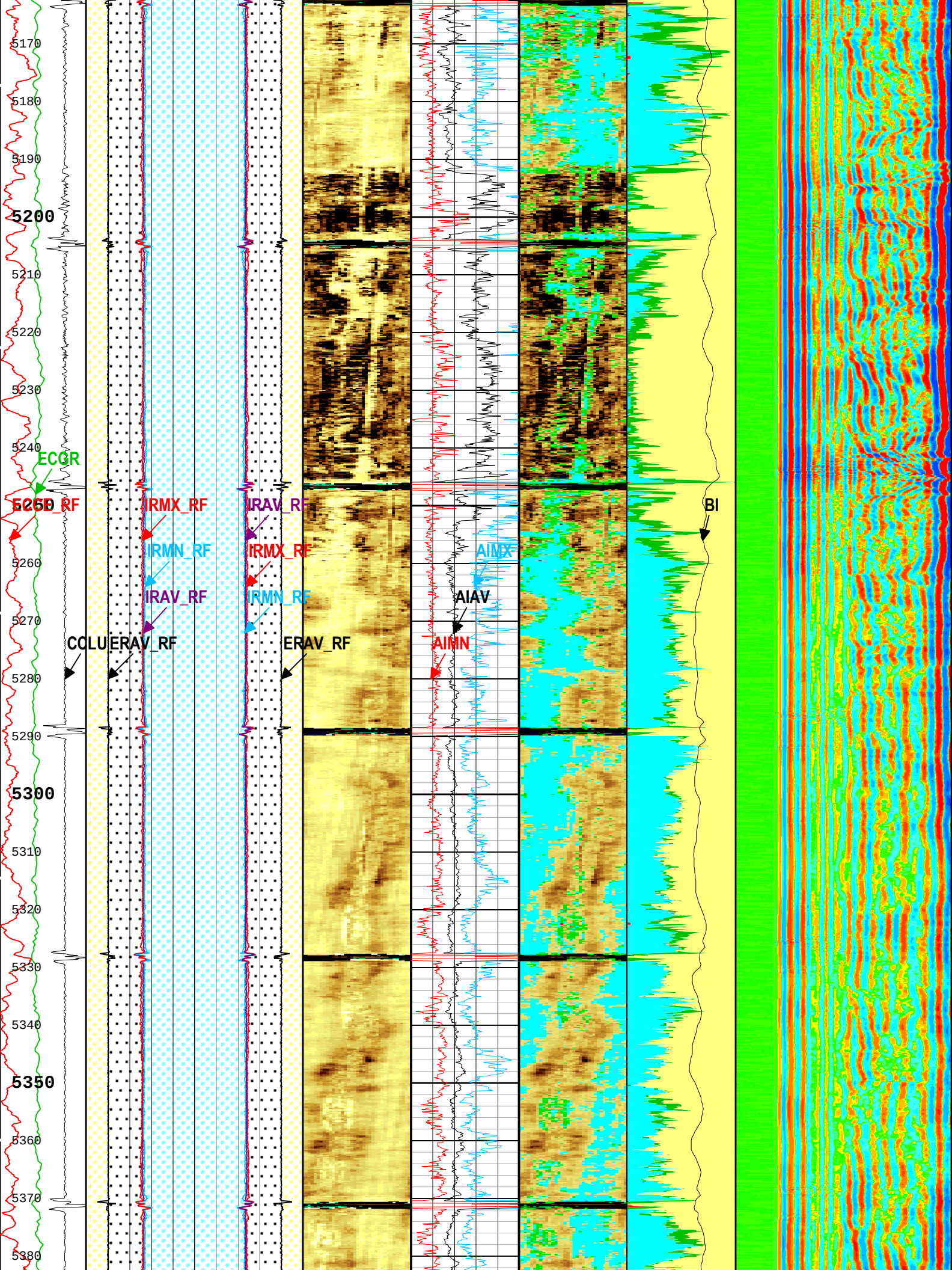
5170
5180
5190
5200
5210
5220
5230
5240
ECGR
5250
IRMX_RF
IRAV_RF
IRMX_RF
IRMN_RF
IRMX_RF
AIMX
5260
IRAV_RF
IRMN_RF
AIAV
5270
COLU
ERAV_RF
ERAV_RF
AIMN
BI
5280
5290
5300
5310
5320
5330
5340
5350
5360
5370
5380

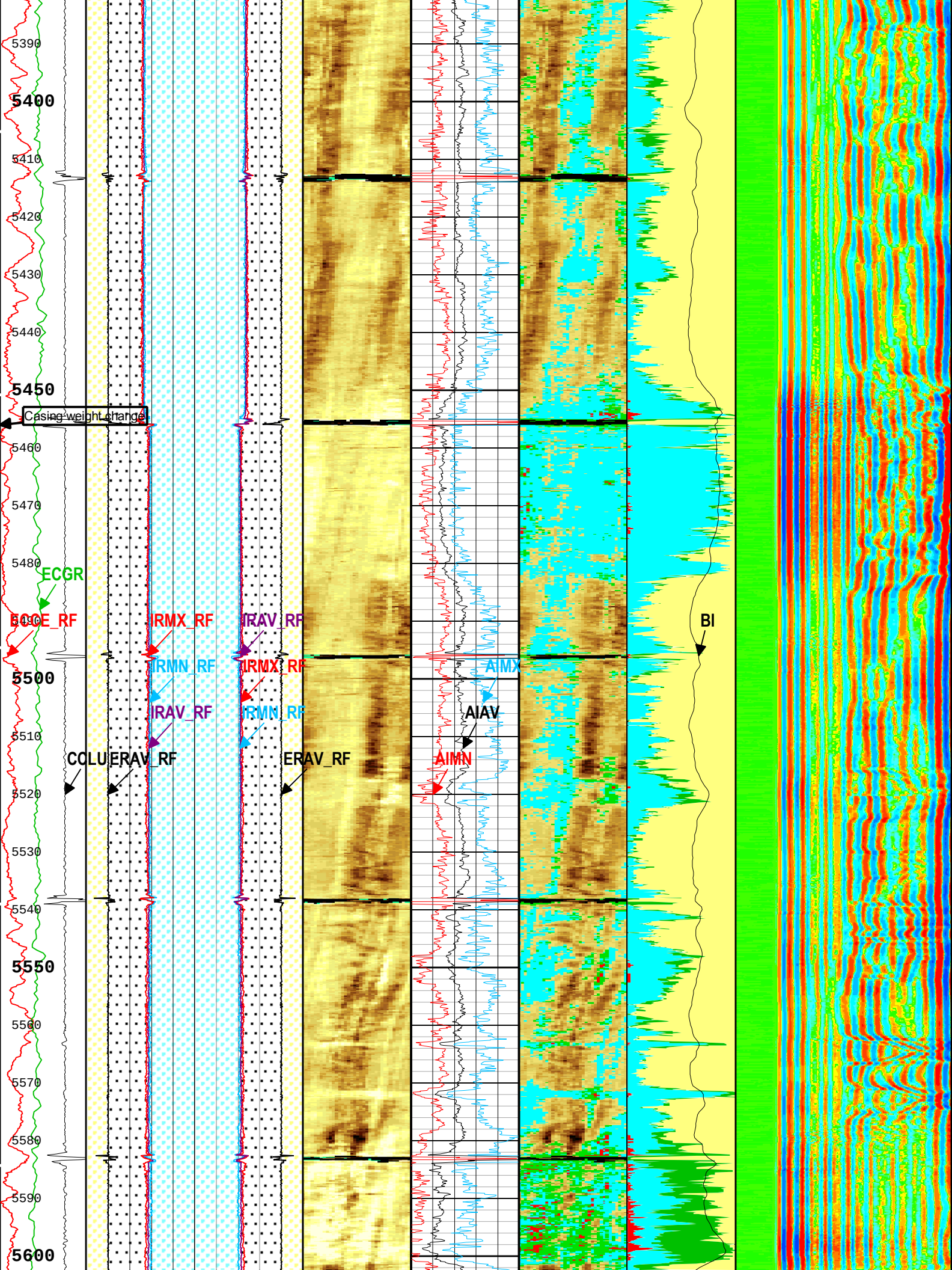
5390
5400
5410
5420
5430
5440
5450
Casing weight change
5460
5470
5480
ECGR
ECCE_RF
IRMX_RF
IRAV_RF
IRMN_RF
IRMX_RF
5500
IRAV_RF
IRMN_RF
AIMX
AIAV
5510
COLU
ERAV_RF
ERAV_RF
AIMN
5520
5530
5540
5550
5560
5570
5580
5590
5600
BI

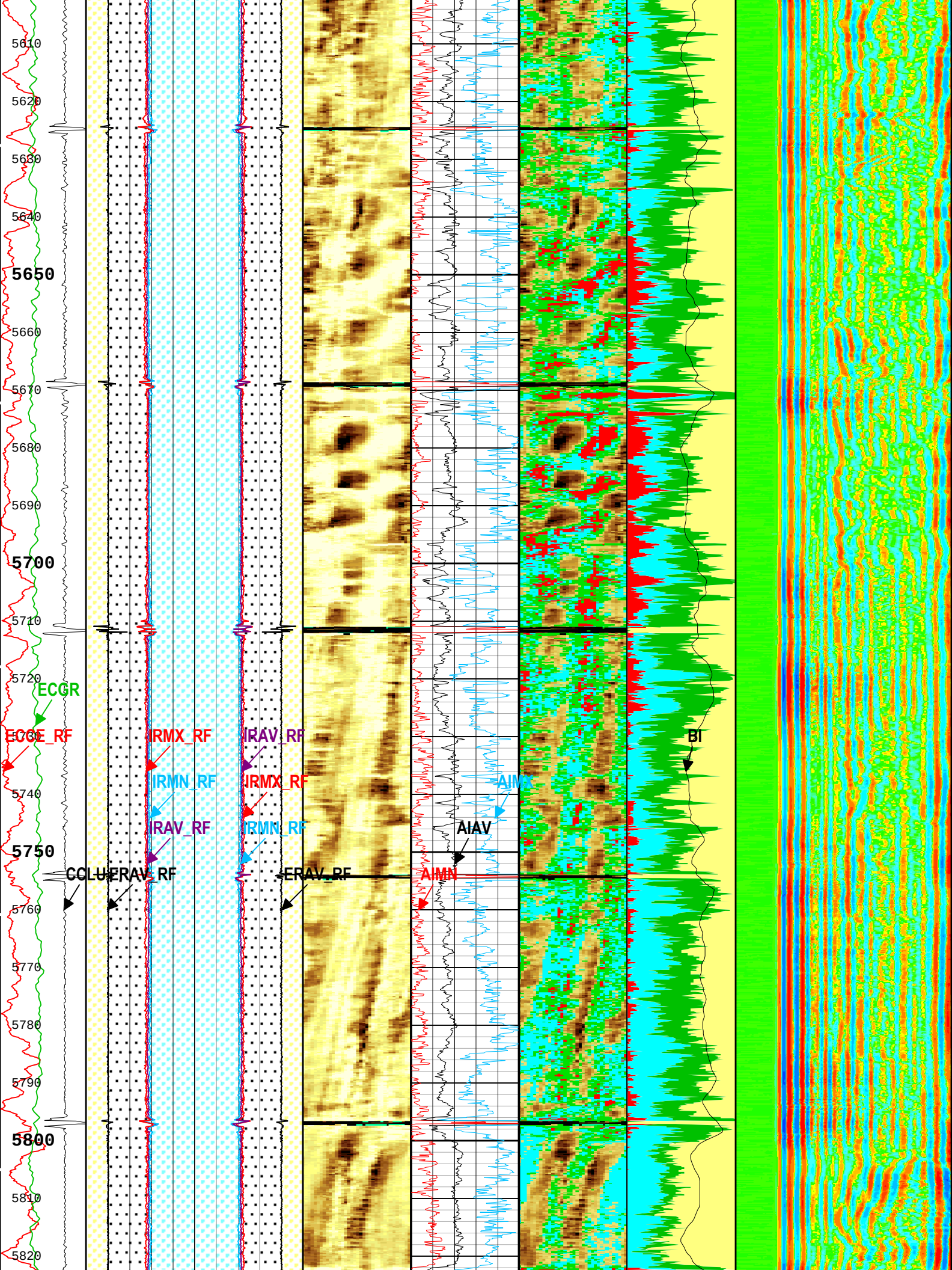
5610
5620
5630
5640
5650
5660
5670
5680
5690
5700
5710
5720
ECGR
ECGE_RF
IRMX_RF
IRAV_RF
IRMN_RF
IRMX_RF
IRAV_RF
IRMN_RF
BI
AIMX
AIAV
5740
5750
CCLU
ERAV_RF
ERAV_RF
AIMN
5760
5770
5780
5790
5800
5810
5820

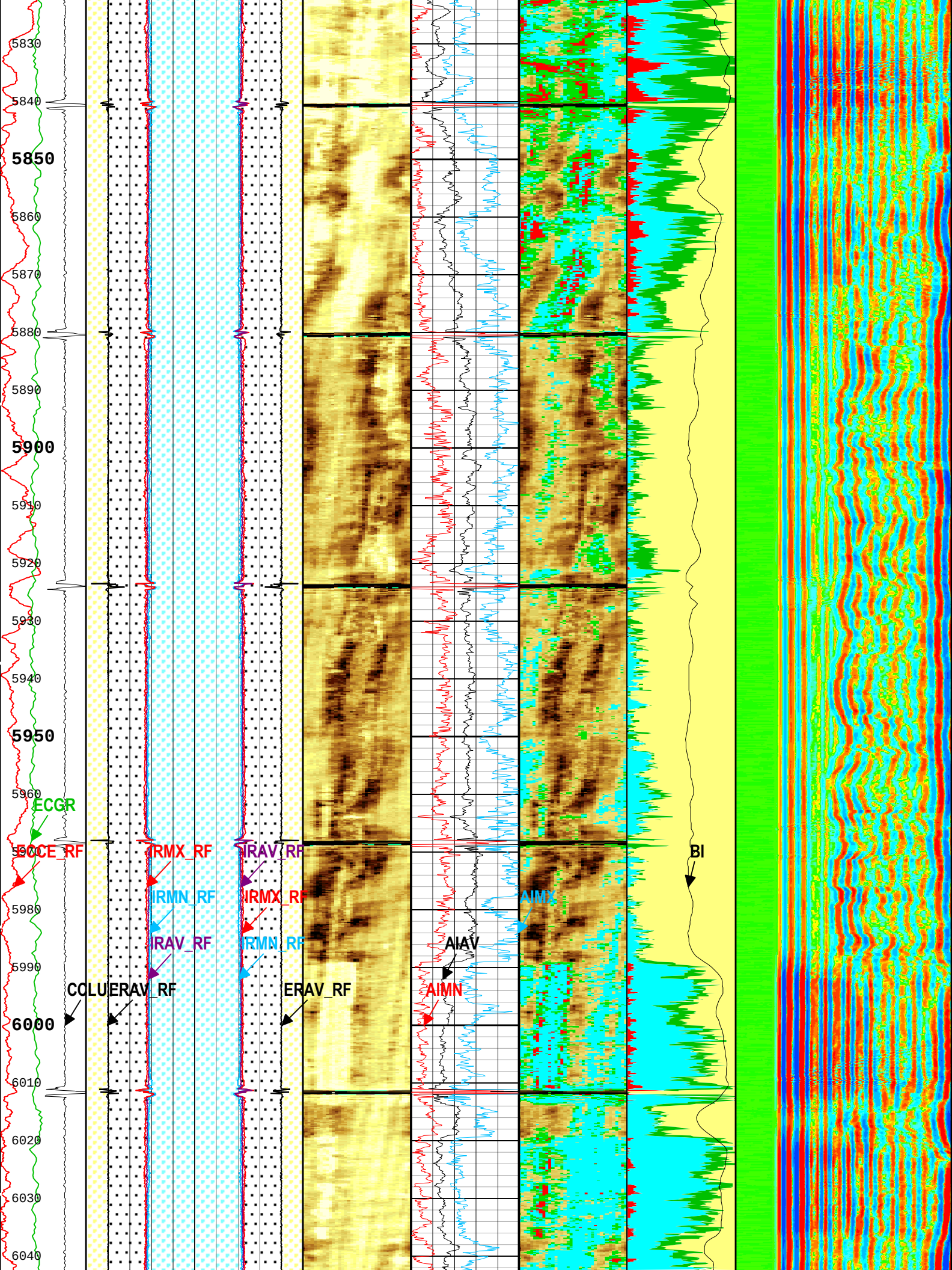
5830
5840
5850
5860
5870
5880
5890
5900
5910
5920
5930
5940
5950
5960
5970
5980
5990
6000
6010
6020
6030
6040
ECGR
ECCE_RF
IRMX_RF
IRAV_RF
IRMN_RF
IRMX_RF
IRAV_RF
IRMN_RF
COLU
ERAV_RF
ERAV_RF
AIAV
AIMN
AIMX
BI

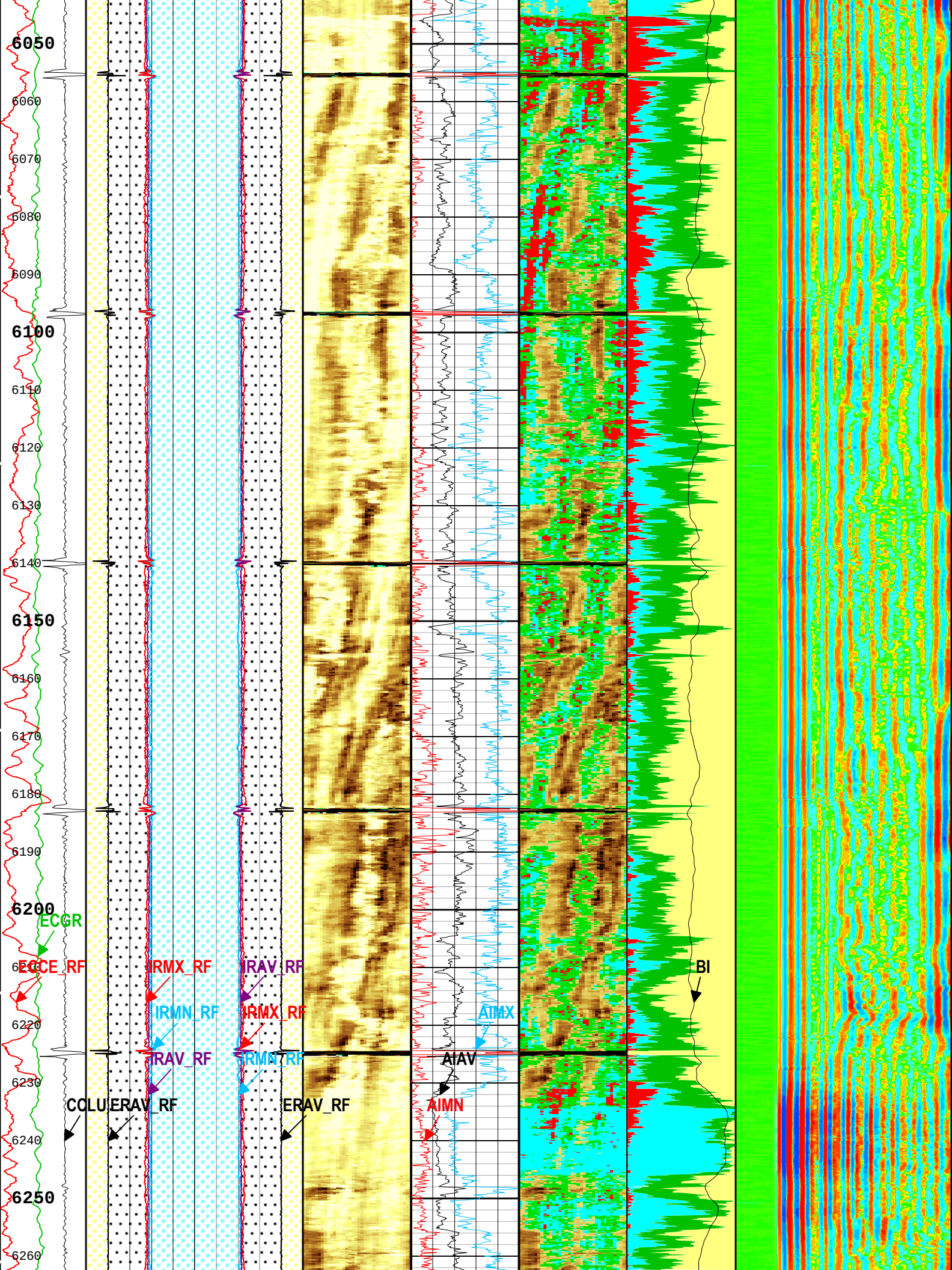
6050
6060
6070
6080
6090
6100
6110
6120
6130
6140
6150
6160
6170
6180
6190
6200
ECGR
ECCE_RF
IRMX_RF
IRAV_RF
IRMN_RF
IRMX_RF
IRAV_RF
IRMN_RF
AIMX
AIAV
AIMN
BI
COLU
ERAV_RF
ERAV_RF
6220
6230
6240
6250
6260

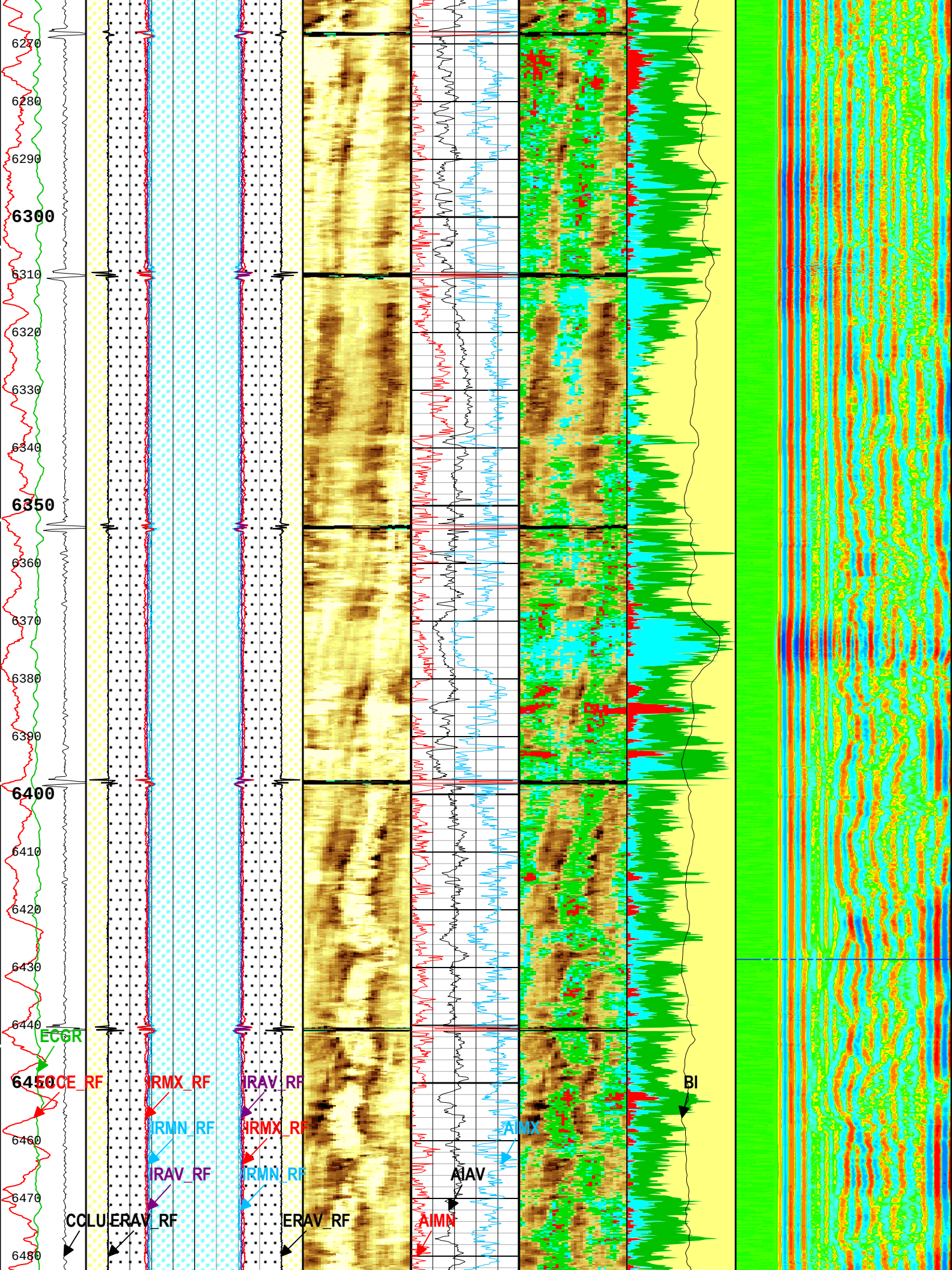
6270
6280
6290
6300
6310
6320
6330
6340
6350
6360
6370
6380
6390
6400
6410
6420
6430
6440
6450
6460
6470
6480
ECGR
CCLU
ERAV_RF
IRMX_RF
IRMN_RF
IRAV_RF
HRAV_RF
HRMX_RF
HRMN_RF
ERAV_RF
AIMX
AIAV
AIMN
BI

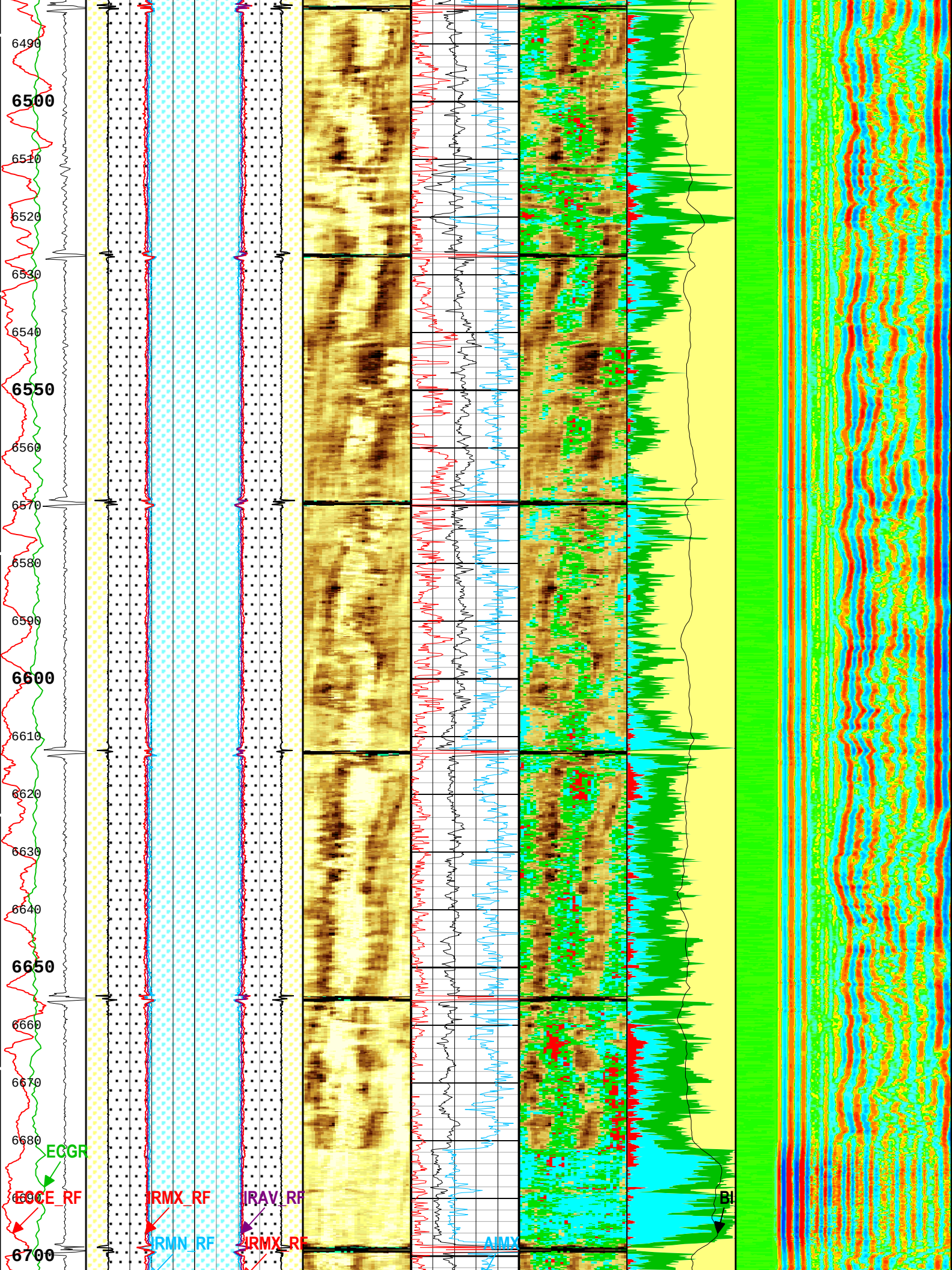
6490
6500
6510
6520
6530
6540
6550
6560
6570
6580
6590
6600
6610
6620
6630
6640
6650
6660
6670
6680
6690
6700
ECGR
ECCE_RF
IRMX_RF
IRAV_RF
IRMN_RF
IRMX_RF
AIMX
BI

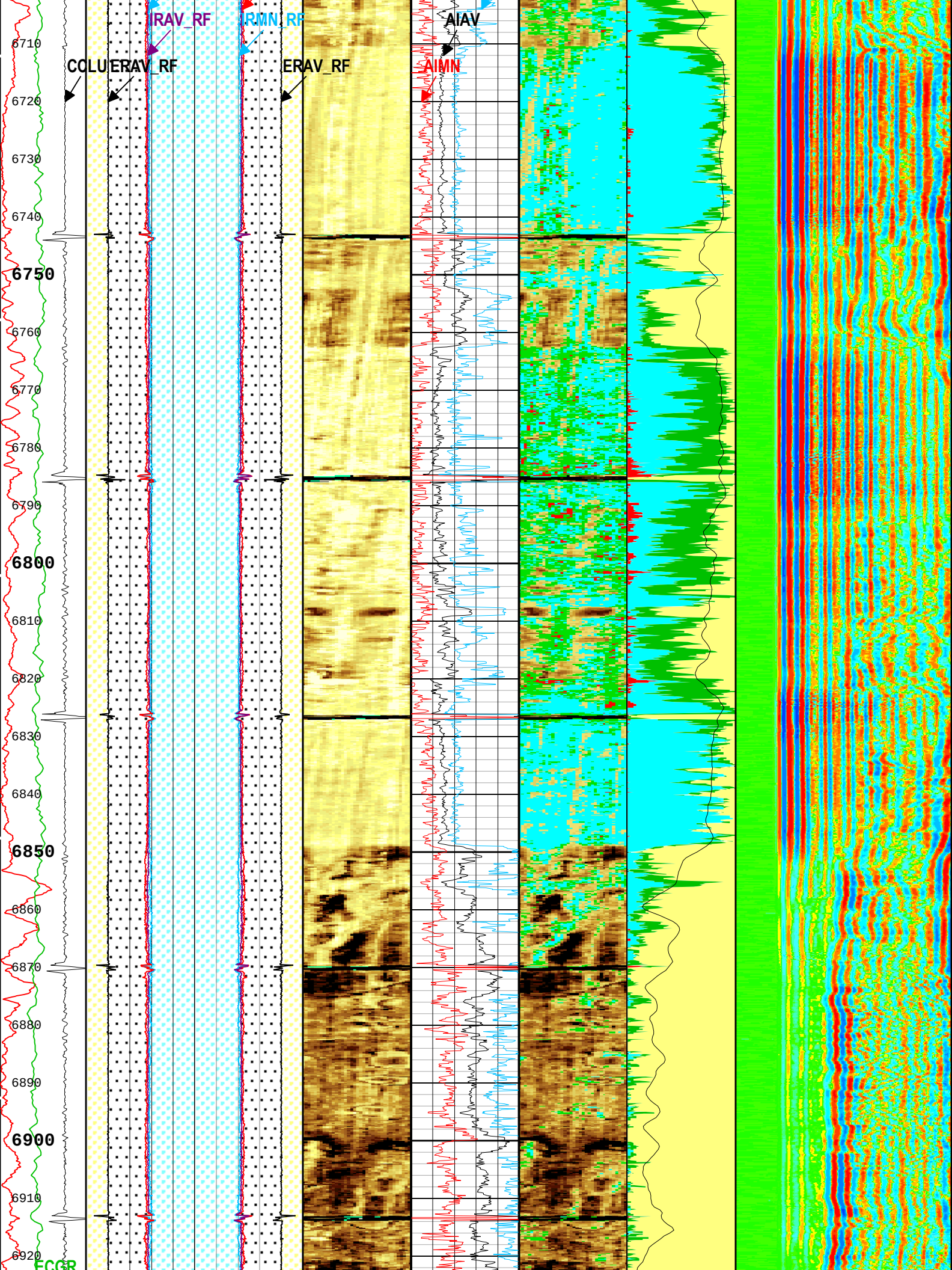
IRAV_RF
IRMN_RF
AIAV
COLU
ERAV_RF
ERAV_RF
AIMN
6710
6720
6730
6740
6750
6760
6770
6780
6790
6800
6810
6820
6830
6840
6850
6860
6870
6880
6890
6900
6910
6920
ECGR

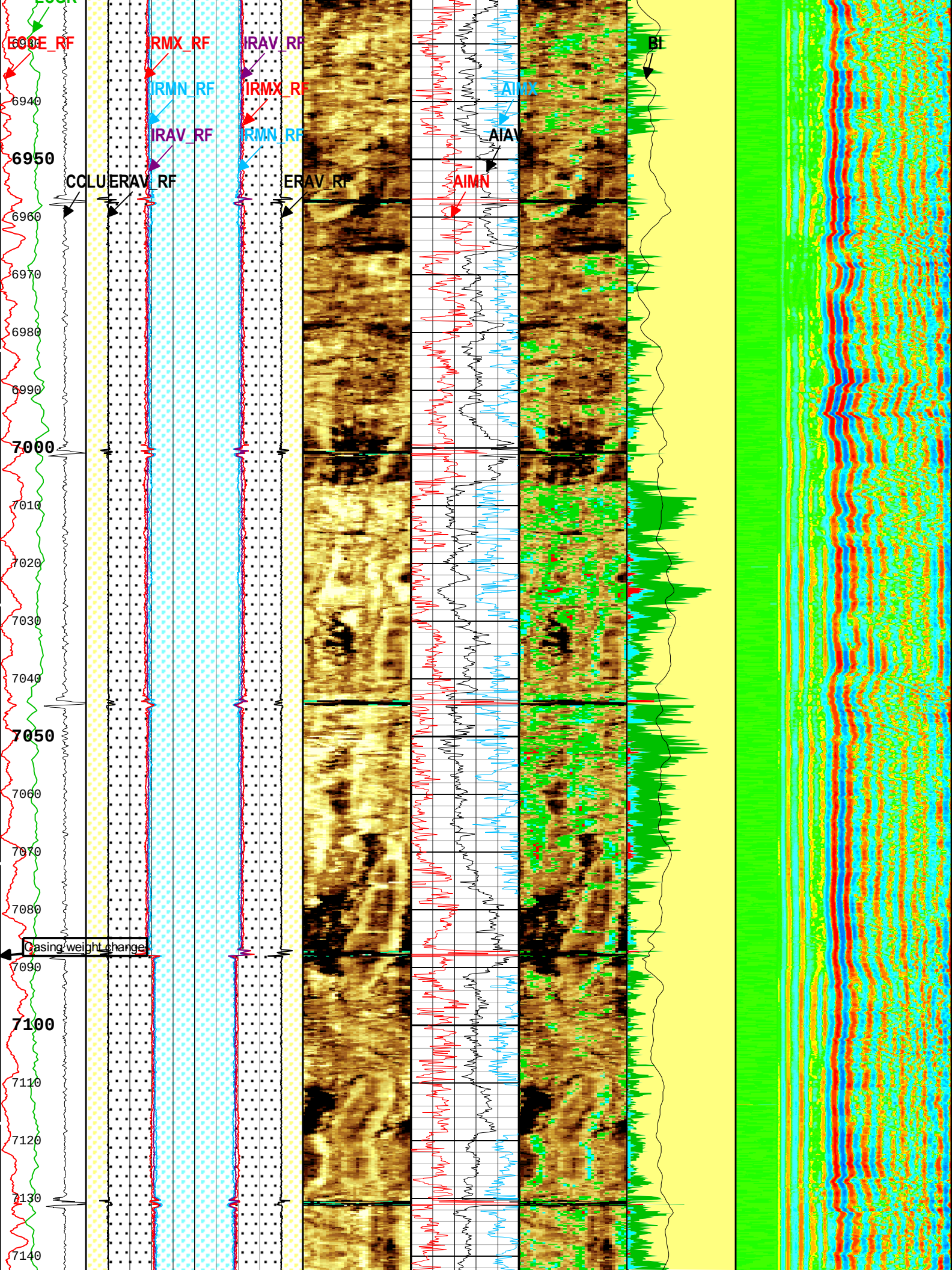
ECOE_RF
IRMX_RF
IRAV_RF
IRMN_RF
IRMX_RF
IRAV_RF
IRMN_RF
BI
AIMX
AIAV
AIMN
CCLU
ERAV_RF
ERAV_RF
Casing weight change
6930
6940
6950
6960
6970
6980
6990
7000
7010
7020
7030
7040
7050
7060
7070
7080
7090
7100
7110
7120
7130
7140

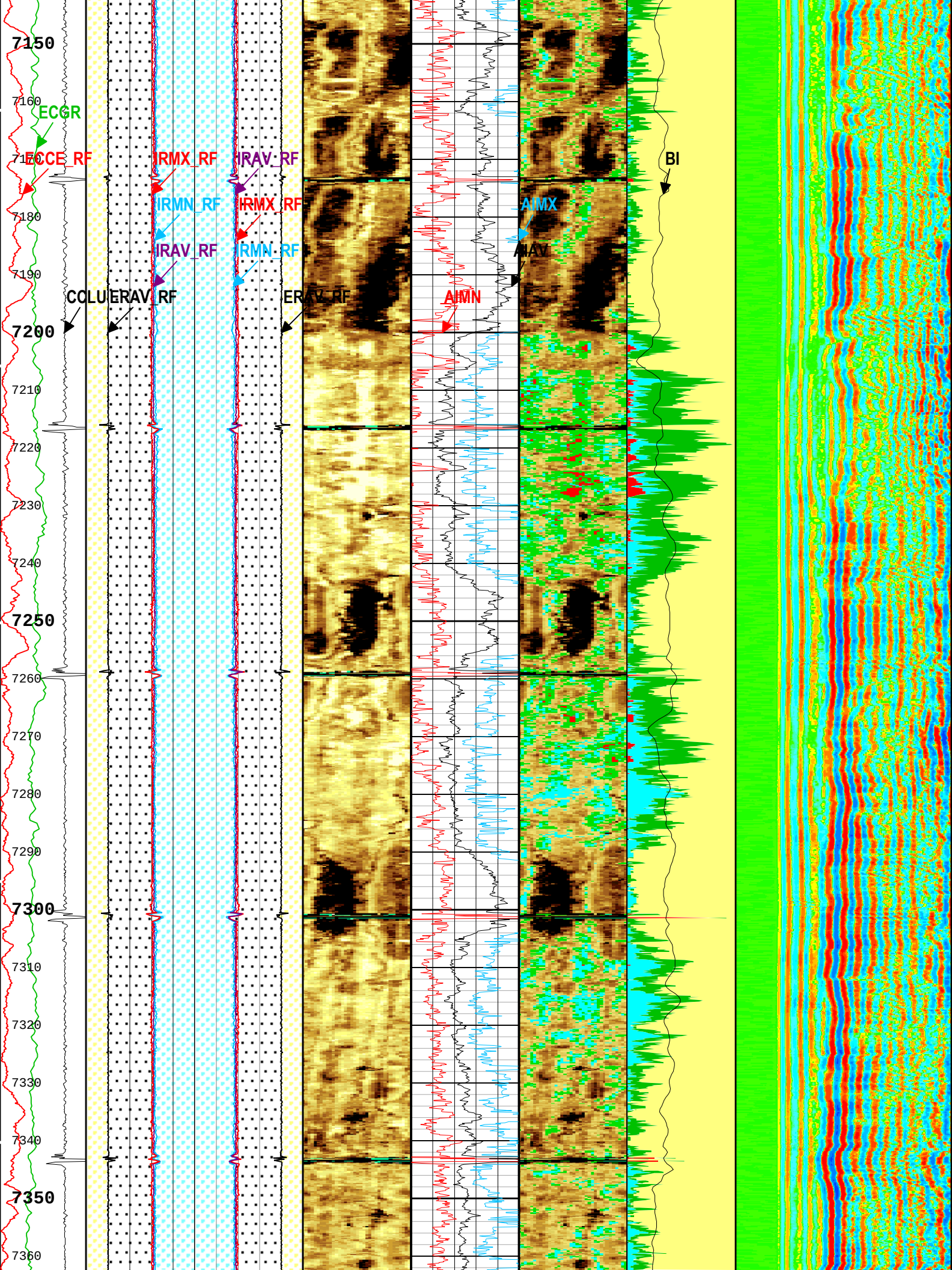
7150
7160
ECGR
ECCE_RF
IRMX_RF
IRAV_RF
BI
7180
IRMN_RF
IRMX_RF
AIMX
IRAV_RF
IRMN_RF
AIAV
7190
COLU
ERAV_RF
ERAV_RF
AIMN
7200
7210
7220
7230
7240
7250
7260
7270
7280
7290
7300
7310
7320
7330
7340
7350
7360

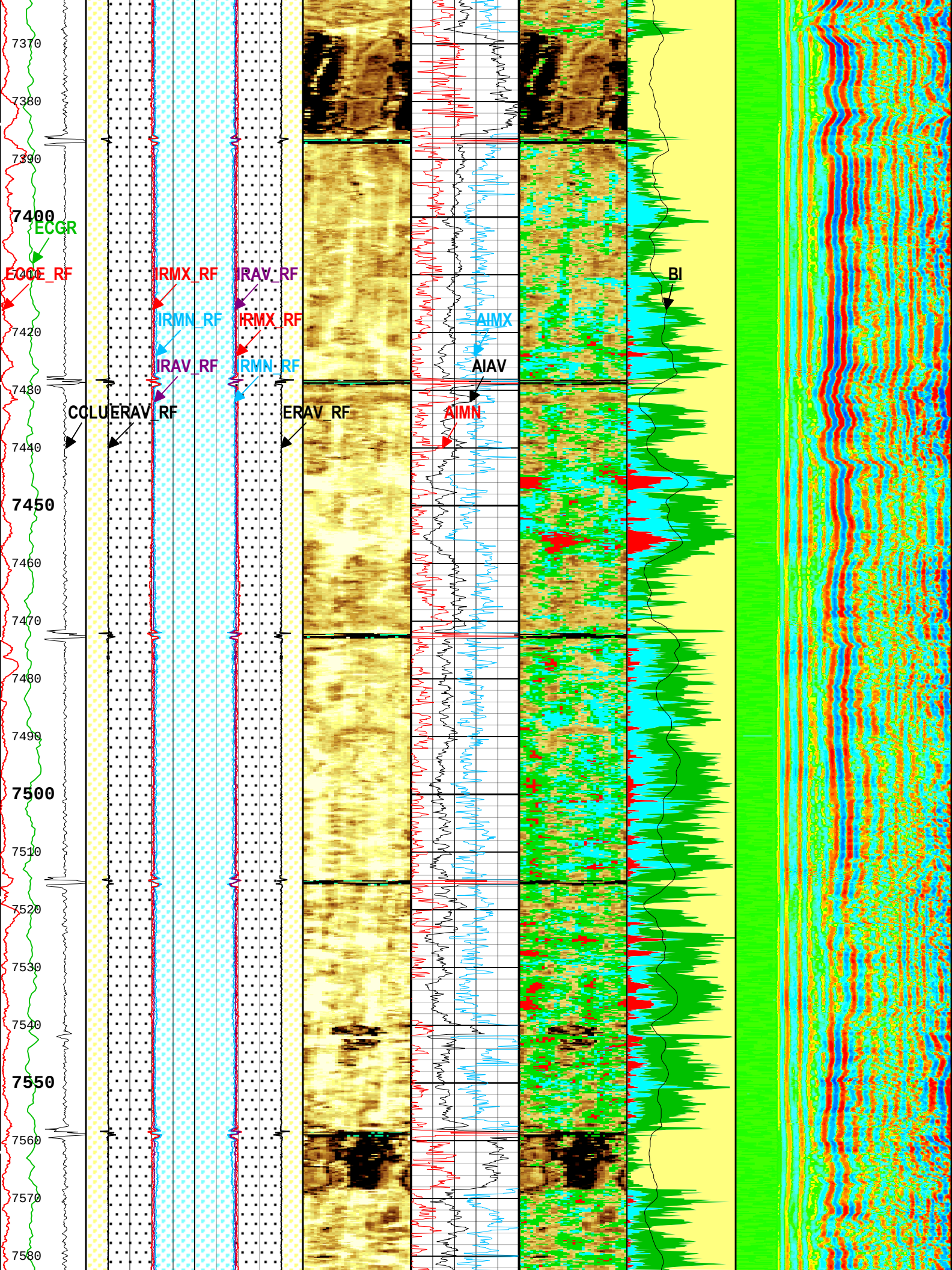
7370
7380
7390
7400
ECGR
ECCE_RF
IRMX_RF
IRAV_RF
IRMN_RF
IRMX_RF
IRAV_RF
IRMN_RF
BI
AIMX
AIAV
AIMN
7420
7480
CCLU
ERAV_RF
ERAV_RF
7440
7450
7460
7470
7480
7490
7500
7510
7520
7530
7540
7550
7560
7570
7580

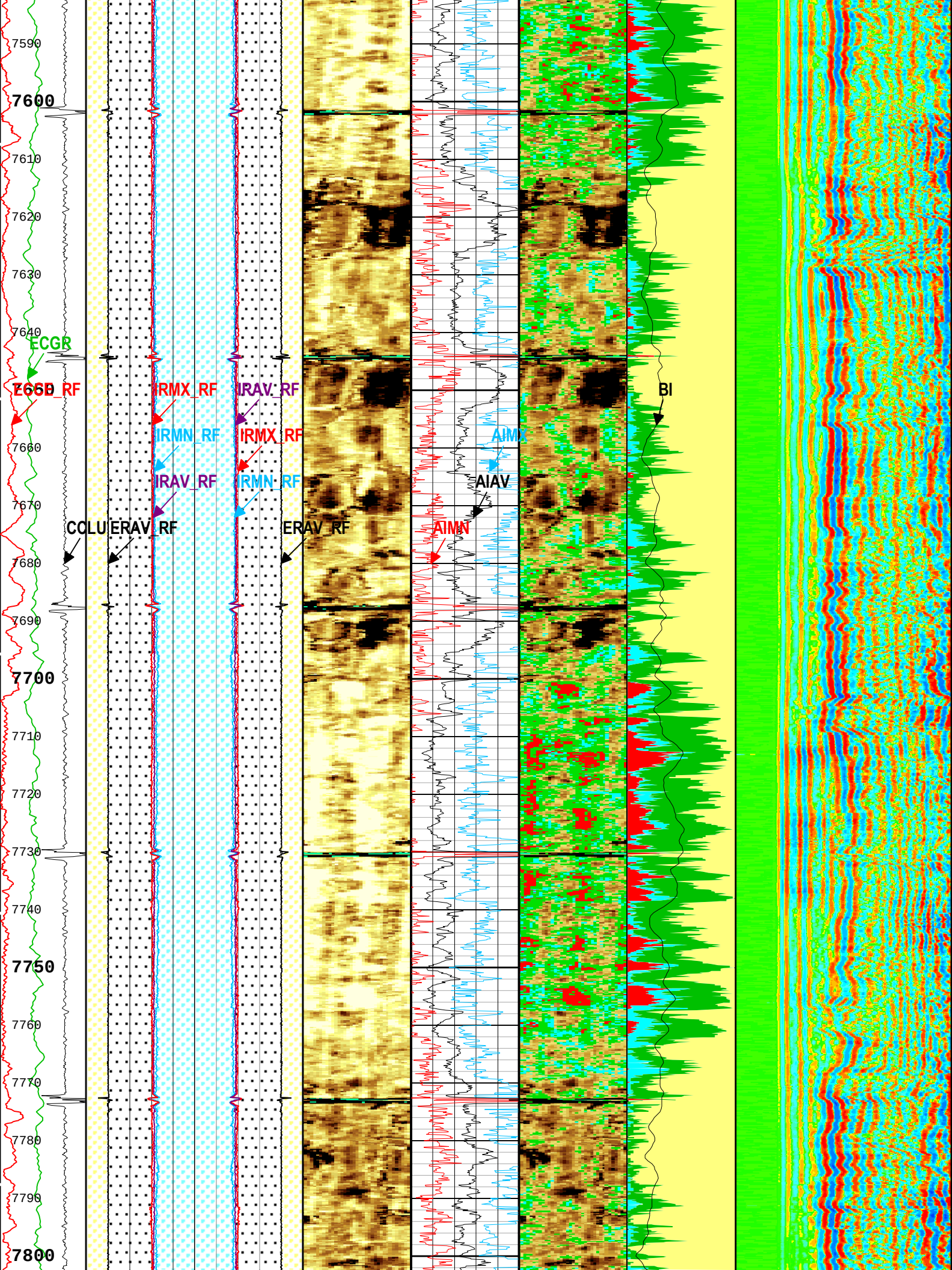
7590
7600
7610
7620
7630
7640
ECGR
7660
7670
7680
7690
7700
7710
7720
7730
7740
7750
7760
7770
7780
7790
7800
IRMX_RF
IRAV_RF
IRMN_RF
IRMX_RF
IRAV_RF
IRMN_RF
CCLU
ERAV_RF
ERAV_RF
AIMX
AIAV
AIMN
BI

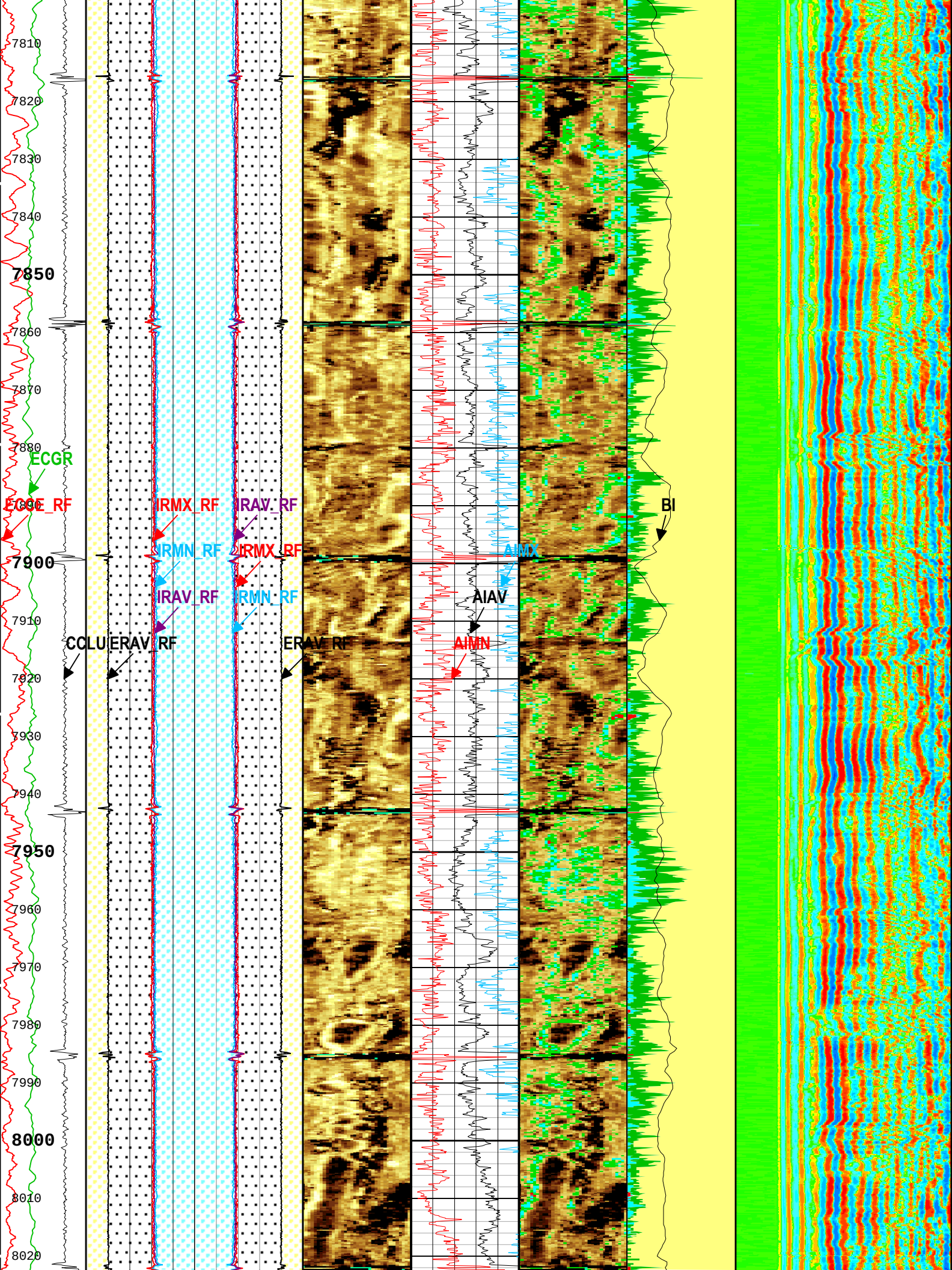
7810
7820
7830
7840
7850
7860
7870
7880
ECGR
ECCE_RF
IRMX_RF
IRAV_RF
IRMN_RF
IRMX_RF
IRAV_RF
IRMN_RF
BI
AIMX
AIAV
AIMN
7900
7910
CCLU
ERAV_RF
ERAV_RF
7920
7930
7940
7950
7960
7970
7980
7990
8000
8010
8020

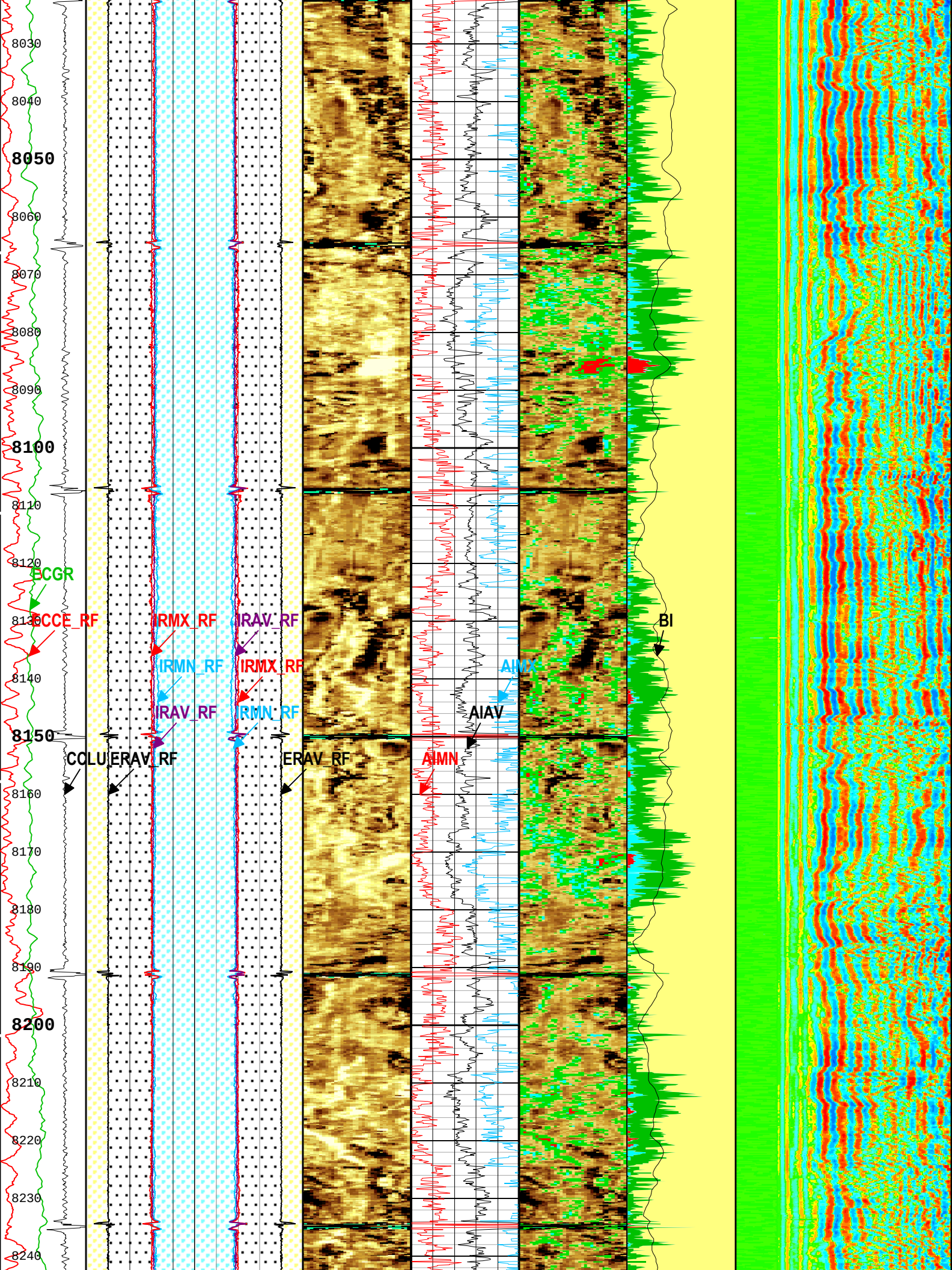
8030
8040
8050
8060
8070
8080
8090
8100
8110
8120
8130
8140
8150
8160
8170
8180
8190
8200
8210
8220
8230
8240
ECGR
ECCE_RF
IRMX_RF
IRAV_RF
IRMN_RF
IRMX_RF
IRAV_RF
IRMN_RF
AIMX
AIAV
AIMN
BI
COLU
ERAV_RF
ERAV_RF

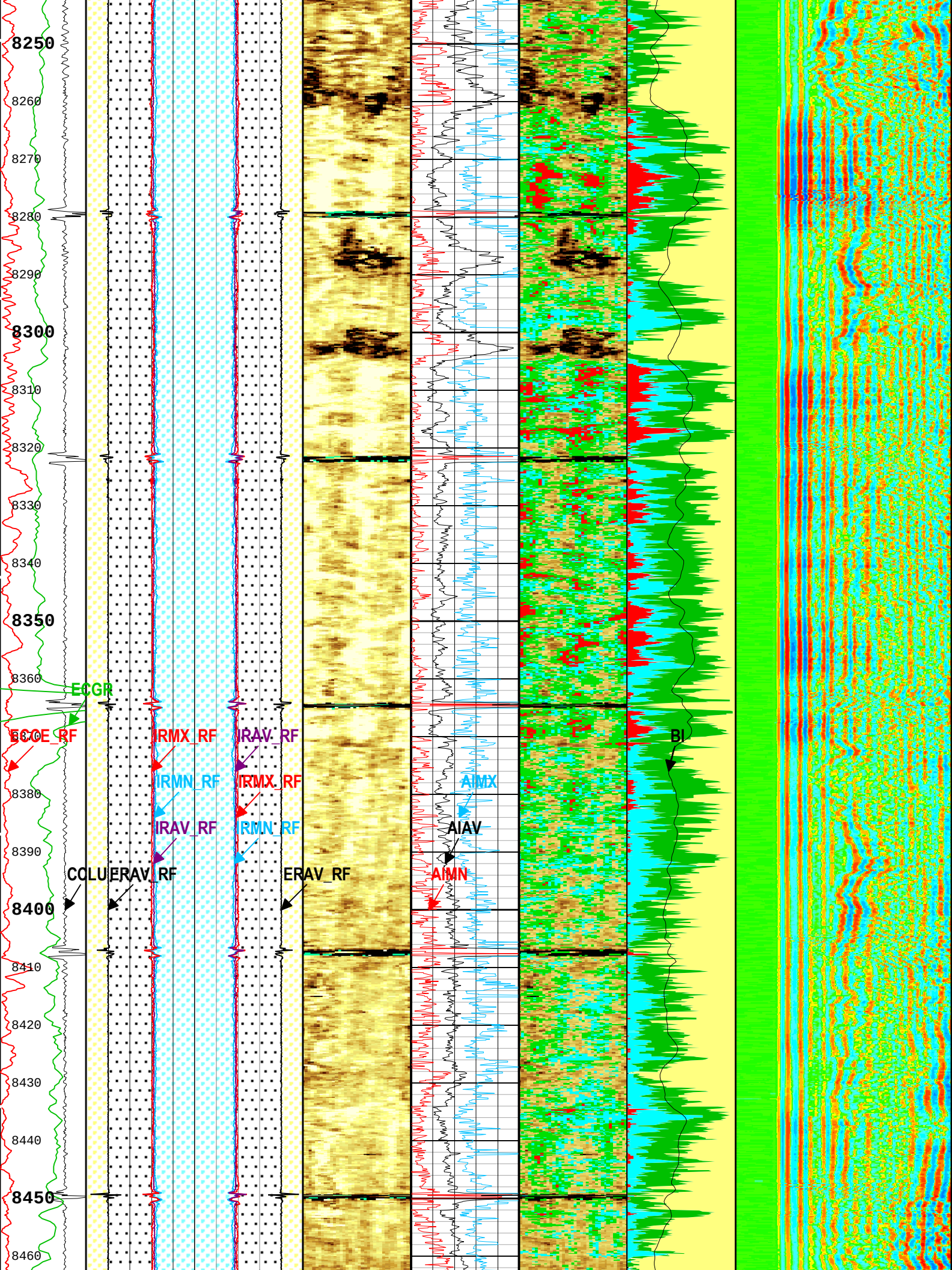
8250
8260
8270
8280
8290
8300
8310
8320
8330
8340
8350
8360
8370
8380
8390
8400
8410
8420
8430
8440
8450
8460
ECGR
ECCE_RF
IRMX_RF
IRAV_RF
IRMN_RF
IRMX_RF
IRAV_RF
IRMN_RF
COLU
ERAV_RF
ERAV_RF
AIMX
AIAV
AIMN
BI

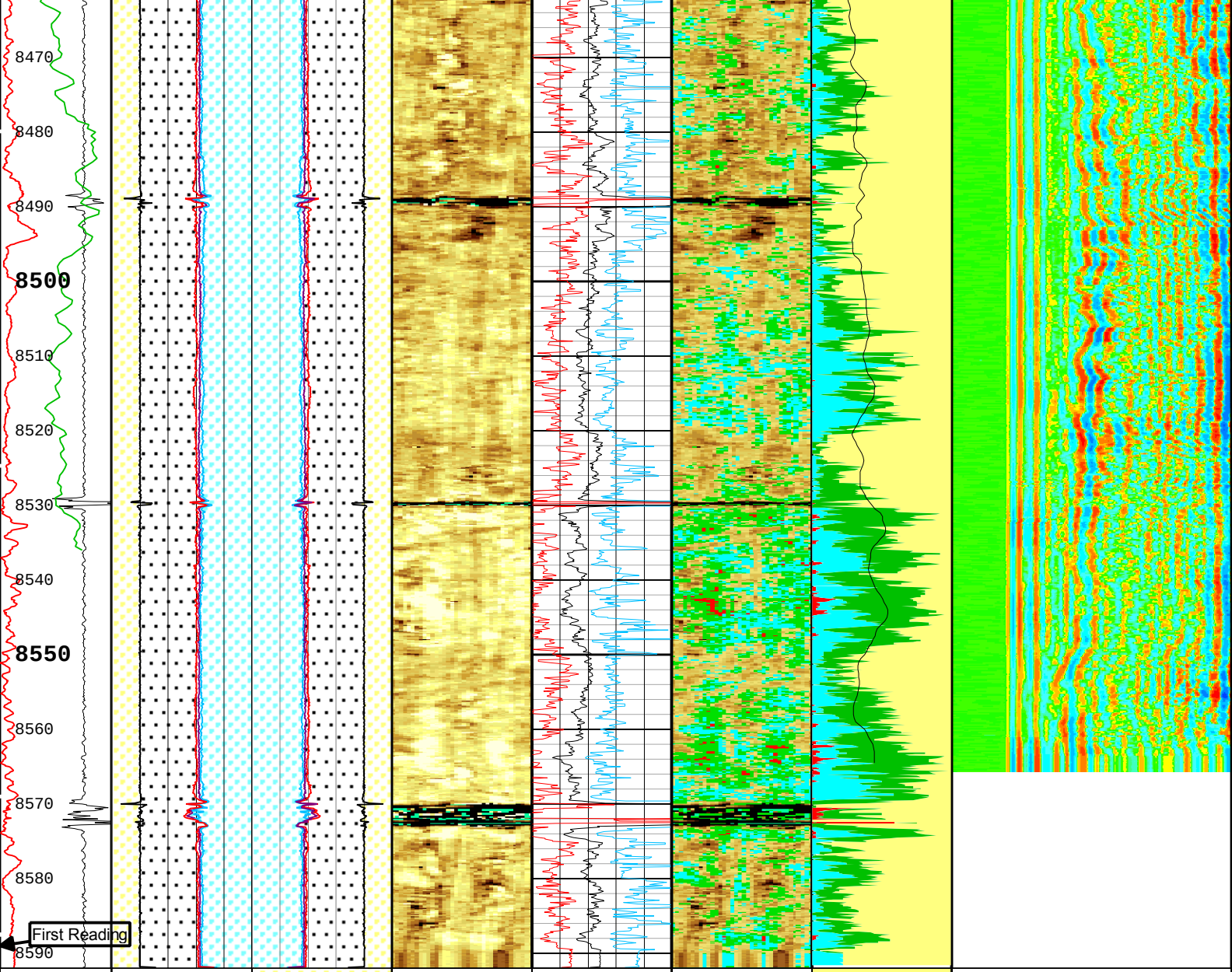
8470
8480
8490
8500
8510
8520
8530
8540
8550
8560
8570
8580
8590
First Reading
Casing Collar Locator Ultrasonic (CCLU) USIT-E[1]
-30 in 10
Amplitude of Eccentering for Unflagged Waves (ECCE_RF) USIT-E[1]
0 in 0.5
Gamma Ray (ECGR) HGNS[1]
0 gAPI 200
ERAV_IRAV
IRAV_LHF1
LHF1_ERAV
Median of Unflagged External Radii (ERAV_RF) USIT-E[1]
3.7 in 2.7
Median Internal Radius of Casing Corrected for Eccentering (IRAV_RF) USIT-E[1]
3.7 in 2.7
Minimum of Unflagged Internal Radii (IRMN_RF) USIT-E[1]
ERAV_RHF1
IRAV_ERAV
RHF1_IRAV
Median of Unflagged External Radii (ERAV_RF) USIT-E[1]
2.7 in 3.7
Minimum of Unflagged Internal Radii (IRMN_RF) USIT-E[1]
2.7 in 3.7
Maximum of Unflagged Internal Radii (IRMX_RF) USIT-E[1]
Absent 1.000 2.500 4.000 5.500 7.000
Custom Normalization
USIT - Acoustic Impedance (AIBK) USIT-E[1] (Mrayl)
Orientation: Top of Hole
U L B R U
Acoustic Impedance Minimum (AIMN) USIT-E[1]
-1 Mrayl 9
Acoustic Impedance Average (AIAV) USIT-E[1]
-1 Mrayl 9
Acoustic Impedance Maximum (AIMX) USIT-E[1]
-1 Mrayl 9
Absent 0.300 3.581 5.054 6.527 8.000
Custom Normalization
USIT - Acoustic Impedance With Micro-debonding Image (AI_MDEBOND_IMG) USIT-E[1] (Mrayl)
Orientation: Top of Hole
U L B R U
Bonded
Gas
Liquid
Micro-debonding
Bond Index (BI) DSLT-H[1]
1 0
Min Amplitude Max
Sonic VDL Curve DSLT-H[1]
200 us 1200

USIT-E[1] 3.7 in 2.7	2.7 in 3.7
Maximum of Unflagged Internal Radii (IRMX_RF) USIT-E[1] 3.7 in 2.7	Median Internal Radius of Casing Corrected for Eccentering (IRAV_RF) USIT-E[1] 2.7 in 3.7

TIME_1900 - Time Marked every 60.00 (s)

Description: USI VDL Cement Format: Log (LBV1_USI-VDL (DSLT) Cement 7inch) Index Scale: 5 in per 100 ft Index Unit: ft Index Type: Measured Depth
Creation Date: 07-Sep-2018 22:55:36

Channel Processing Parameters

One: Parameters

Parameter	Description	Tool	Value	Unit
AMSG	Auxiliary Minimum Sliding Gate	DSLT-H	140	us
ISSBAR	Barite Mud Presence Flag	Borehole	No	
BERJ	Bad Echo Rejection	USIT-E	On	
BHS	Borehole Status (Open or Cased Hole)	Borehole	Cased	
BILI	Bond Index Level for Zone Isolation	DSLT-H	0.8	
BS	Bit Size	WLSESSION	Depth Zoned	in
CASING_PRATIO	Casing Poisson Ratio	USIT-E	Standard Poisson Ratio	
CBLG	CBL Gate Width	DSLT-H	45	us
CBLO	Casing Bottom (Logger)	WLSESSION	8625	ft
CBRA	CBL LQC Reference Amplitude in Free Pipe	DSLT-H	Depth Zoned	mV
CDEN	Cement Density	HGNS-H	2	g/cm3
CMCF	CBL Cement Type Compensation Factor	DSLT-H	1	
CMTY(U-USIT_CEMT)	Cement Type	USIT-E	Regular Cement	
THNO	Nominal Casing Thickness - Zoned along logger depths	WLSESSION	Depth Zoned	in
DETE	Delta-T Detection	DSLT-H	E1	
DFD	Drilling Fluid Density	Borehole	8.5	lbm/gal
DFT_CATEGORY	Drilling Fluid Type	Borehole	Water	
DTMD	Borehole Fluid Slowness	Borehole	206	us/ft
FCF	CBL Fluid Compensation Factor	DSLT-H	1	
FDII	FPM Data Interpolation Interval	USIT-E	0	ft
GCSE_DOWN_PASS	Generalized Caliper Selection for WL Log Down Passes	Borehole	BS(RT)	
GCSE_UP_PASS	Generalized Caliper Selection for WL Log Up Passes	Borehole	BS(RT)	
GOBO_CURR	Good Bond in Arbitrary Cement	DSLT-H	Depth Zoned	mV
GR_MULTIPLIER	Gamma Ray Multiplier	HGNS-H	1	
HEMA	Hematite Presence Flag	Borehole	No	
ICE_PROCESS	ICE Processing	USIT-E	Yes	
IMAR	Image Rotation	USIT-E	RB	
MAHTR	Manual High Threshold Reference for first arrival detection	DSLT-H	120	
MATT_CURR	Maximum Attenuation in Arbitrary Cement	DSLT-H	Depth Zoned	dB/ft
MCI	Minimum Cemented Interval for Isolation	DSLT-H	Depth Zoned	ft
MEAS_WLEN	Tcube Processing Window Length in Measurement Mode	USIT-E	Depth Zoned	us
MNHTR	Minimum High Threshold Reference for first arrival detection	DSLT-H	100	
MSA	Minimum Sonic Amplitude	DSLT-H	Depth Zoned	mV
MSA_CURR	Minimum Sonic Amplitude in Arbitrary Cement	DSLT-H	Depth Zoned	mV
MUD_N_THE	Theoretical Mud Normalization Factor	USIT-E	1	
NMSG	Near Minimum Sliding Gate	DSLT-H	280	us

NMXG	Near Maximum Sliding Gate	DSLT-H	950	us
NUMP	Number of Detection Passes	DSLT-H	2	
OPLEV	USIT Remove Flagged Data Level	USIT-E	OPT2	
RCOD	Reference Calibrator Outer Diameter	USIT-E	7	in
RCSO	Reference Calibrator Standoff	USIT-E	1.181	in
RCTH	Reference Calibrator Thickness	USIT-E	0.295	in
SDNV	Number of Vertical Samples used for Micro-debonding Computation	USIT-E	5	
SDTHOR	Acoustic Impedance STD Horizontal Threshold for Micro-debonding	USIT-E	0.5	Mrayl
SDTVER	Acoustic Impedance STD Vertical Threshold for Micro-debonding	USIT-E	0.3	Mrayl
SFAF	Sonic Formation Attenuation Factor	DSLT-H	3.25	dB/ft
SGAD	Sliding Gate Status	DSLT-H	Off	
SGCL	Sliding Gate Closing Delta-T	DSLT-H	130	us/ft
SGCW	Sliding Gate Closing Width	DSLT-H	25	us
SGDT	Sliding Gate Delta-T	DSLT-H	57	us/ft
SGW	Sliding Gate Width	DSLT-H	110	us
SLEV	Signal Level for AGC	DSLT-H	5000	mV
SOCN	Standoff Distance	HGNS-H	0.125	in
SOCO	Standoff Correction Option	HGNS-H	No	
THDH	Maximum Search Thickness (percentage of nominal)	USIT-E	130	%
THDL	Minimum Search Thickness (percentage of nominal)	USIT-E	70	%
HISC	Tool Position: Centered or Eccentered	HGNS-H	Eccentered	
U-USIT_DFSZ	Drilling Fluid Specific Acoustic Impedance	USIT-E	0.1	Mrayl
USI_FVEL_SEL	USI Fluid Velocity Selection	USIT-E	Automatic	
USI_RPLUS	Ultrasonic R+ Processing	USIT-E	No	
USI_ZMUD_SEL	USI Mud Impedance Selection	USIT-E	Theoretical	
THDP	Thickness Detection Policy	USIT-E	Fundamental	
VCAS	Ultrasonic Transversal Velocity in Casing	USIT-E	51.4	us/ft
VDLG	VDL Manual Gain	DSLT-H	5	
ZCAS	Acoustic Impedance of Casing	USIT-E	46.25	Mrayl
ZCMT	Acoustic Impedance of Cement	DSLT-H	6.8	Mrayl
ZCMT_NEAT	Acoustic Impedance of Cement in Neat Cement	DSLT-H	6.8	Mrayl
ZINI	Initial Estimate of Cement Impedance	USIT-E	-1	Mrayl
ZMUD	Acoustic Impedance of Mud	Borehole	1.48	Mrayl
ZTCM	Acoustic Impedance Threshold for Cement	USIT-E	2.6	Mrayl
ZTGS	Acoustic Impedance Threshold for Gas	USIT-E	0.3	Mrayl

OneDepth Zoned Parameters

Parameter	Value	Start (ft)	Stop (ft)
BS	17.25	5	598
BS	12.25	598	1147
BS	11	1147	8592
CBRA	62	5	7088
CBRA	63	7088	8592
THNO	0.317	5	5456
THNO	0.362	5456	7088
THNO	0.408	7088	8592
GOBO_CURR	1.87	5	5456
GOBO_CURR	2.87	5456	7088
GOBO_CURR	4.08	7088	8592
MATT_CURR	13.39	5	5456

MATT_CURR	13.59	5	5456
MATT_CURR	11.82	5456	7088
MATT_CURR	10.59	7088	8592
MCI	21.68	5	598
MCI	10	598	8592
MEAS_WLEN	19.62	5	5456
MEAS_WLEN	22.5	5456	7088
MEAS_WLEN	25.48	7088	8592
MSA	0.78	5	5456
MSA	1.33	5456	7088
MSA	2.06	7088	8592
MSA_CURR	0.78	5	5456
MSA_CURR	1.33	5456	7088
MSA_CURR	2.06	7088	8592

All depth are actual.

Tool Control Parameters

One: Parameters

Parameter	Description	Tool	Value	Unit
AGMN	Minimum Gain of Cartridge	USIT-E	-12	dB
AGMX	Maximum Gain of Cartridge	USIT-E	Time Zoned	dB
DDEL	Digitizing Delay	DSLT-H	0	us
U-USIT_DDT5	USIC Downhole Decimation for T5 only	USIT-E	0_NONE	
DOT(DOS)	Distance between Opposite Transducer Faces	USIT-E	2.874	in
MODE	DSLT Acquisition Mode	DSLT-H	CBL	
RATE	DSLT Firing Rate	DSLT-H	15 Hz	
DTFS	DSLT Telemetry Frame Size	DSLT-H	536	
DWCO	Digitizer Word Count	DSLT-H	250	
EMXV	EMEX Voltage	USIT-E	Time Zoned	V
HRES	Horizontal Resolution	USIT-E	10 deg	
ICE2_ACQ	Ultrasonic ICE2 Acquisition	USIT-E	No	
MOTOR_PROTECT	Motor Protection	USIT-E	Off	
SDTH	Switch Down Threshold	DSLT-H	20000	
SGAI	Selectable Acquisition Gain	DSLT-H	x1	
SUTH	Switch Up Threshold	DSLT-H	1000	
UACLV_PERM	Ultrasonic ACLV Permanent	USIT-E	Yes	
ULOG	Logging Objective	USIT-E	MEASUREMENT	
USFR	Ultrasonic Sampling Frequency	USIT-E	500000	Hz
UPAT	USIT Emission Pattern	USIT-E	Pattern 500 KHz	
UWKM	USIT Working Mode	USIT-E	Uncompressed 10 deg at 1.5 in LF	
USSP	Ultrasonic Service	USIT-E	USI	
VRES	Vertical Resolution	USIT-E	1.5 in	
WINB	Window Begin Time	USIT-E	Time Zoned	us
WINE	Window End Time	USIT-E	Time Zoned	us
WMOD	Waveform Firing Mode	DSLT-H	Full	

OneTime Zoned Parameters

Pass Log[6]:Up

Parameter	Value	Start Time	Stop Time	Start Depth (ft)	Stop Depth (ft)
AGMX	18	07-Sep-2018 09:51:23	07-Sep-2018 13:15:19	8592.38	1601.14
AGMX	25	07-Sep-2018 13:15:19	07-Sep-2018 13:52:30	1601.14	100.00

AGMX	25	07-Sep-2018 13:15:19	07-Sep-2018 13:52:30	1601.14	160.38
EMXV	45	07-Sep-2018 09:51:23	07-Sep-2018 13:15:38	8592.38	1587.43
EMXV	55	07-Sep-2018 13:15:38	07-Sep-2018 13:52:30	1587.43	160.38
WINB	32.8	07-Sep-2018 09:51:29	07-Sep-2018 13:52:30	8592.38	160.38
WINE	80.19	07-Sep-2018 09:51:23	07-Sep-2018 12:58:06	8592.38	2390.05
WINE	83.19	07-Sep-2018 12:58:06	07-Sep-2018 13:52:30	2390.05	160.38

Pass Log[9]:Up

AGMX	25	07-Sep-2018 14:53:13	07-Sep-2018 15:00:05	160.38	11.51
EMXV	55	07-Sep-2018 14:53:13	07-Sep-2018 15:00:05	160.38	11.51
WINB	36.82	07-Sep-2018 14:53:13	07-Sep-2018 15:00:05	160.38	11.51
WINE	76.82	07-Sep-2018 14:53:13	07-Sep-2018 15:00:05	160.38	11.51

All depth are at tool zero.

Composite 1

Main Pass 5 IN = 100 FT

Composite Summary

Run Name	Pass Objective	Direction	Top	Bottom	Start	Stop	DSC Mode	Depth Shift	Include Parallel Data
One	Log[6]:Up	Up	93.36 ft	8592.71 ft	07-Sep-2018 9:51:23 AM	07-Sep-2018 1:52:30 PM	ON	8.00 ft	No
One	Log[9]:Up	Up	11.43 ft	318.32 ft	07-Sep-2018 2:46:40 PM	07-Sep-2018 3:00:05 PM	ON	9.00 ft	No

All depths are referenced to toolstring zero

Log

Company:Southern California Gas Company Well:Standard Sesnon 9

Composite 1:S003

Description: USI Composite Format: Log (LBV1_USI Composite 7inch) Index Scale: 5 in per 100 ft Index Unit: ft Index Type: Measured Depth Creation Date: 07-Sep-2018 22:55:55

TIME_1900 - Time Marked every 60.00 (s)

USIT Processing Flags (UFLG[0]) USIT-E[1]

1 - UFLG 1 Value within [0.0 - 1.5] - :

2 - UFLG 2 Value within [1.5 - 2.5] - :

3 - UFLG 3 Value within [2.5 - 3.5] - :

4 - UFLG 4 UFLG 5 UFLG 6 Value within [3.5 - 6.5] - :

5 - UFLG 7 UFLG 8 UFLG 9 Value within [6.5 - 10] - :

- UTIM Error
- Pulse Origin Not Detected
- WINLEN Error
- Casing Thickness Error
- Loop Processing Error

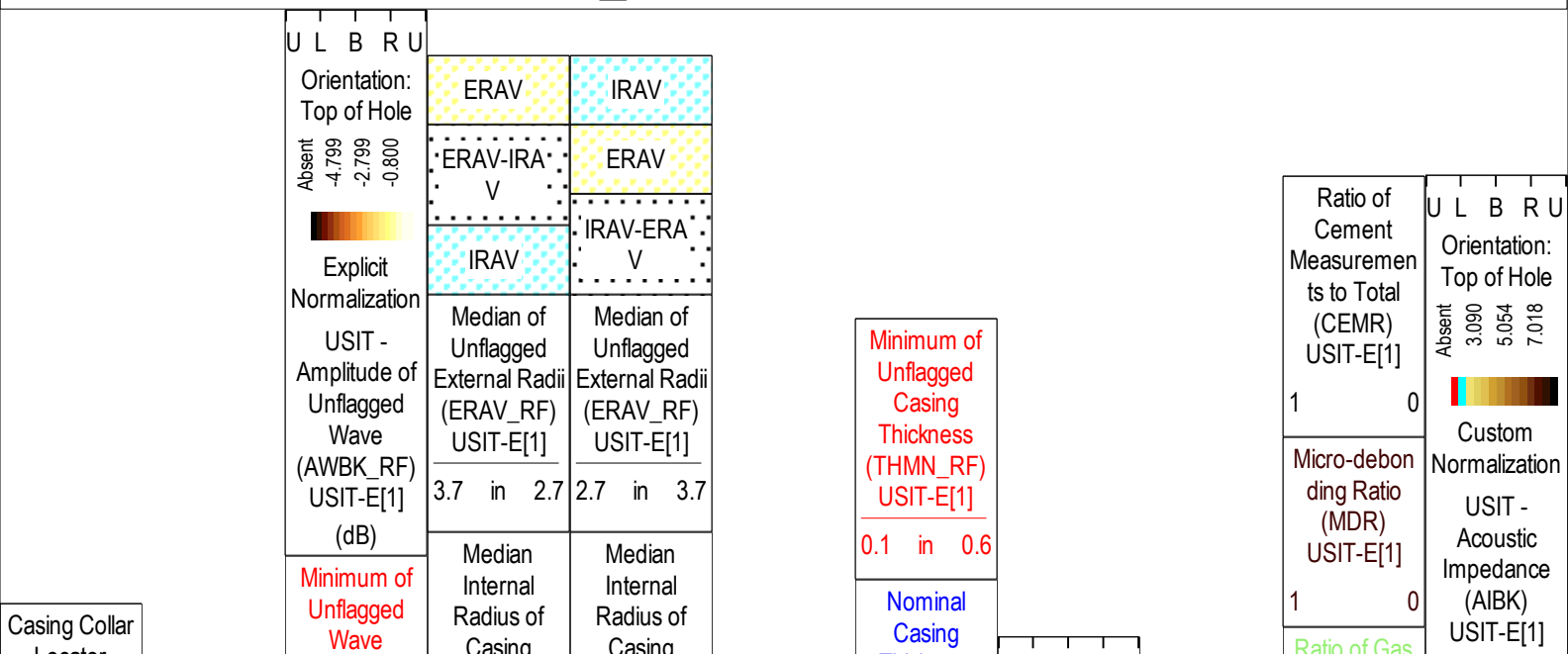

Locator Ultrasonic (CCLU) USIT-E[1]
-30 in 10

Amplitude of Eccentering for Unflagged Waves (ECCE_RF) USIT-E[1]
0 in 0.5

Motor Revolution Speed (RSAV) USIT-E[1]
6 c/s 8

U L B R U
Orientation: Top of Hole
Absent 1.500 3.500
Explicit Normalization
USIT - USIT Processing Flags (UFLG) USIT-E[1]

USIT Processing Flags (UFLG[0]) USIT-E[1]
1 5

Amplitude (AWMN_RF) USIT-E[1]
0 dB 75

Average of Unflagged Wave Amplitude (AWAV_RF) USIT-E[1]
0 dB 75

Maximum of Unflagged Wave Amplitude (AWMX_RF) USIT-E[1]
0 dB 75

Casing Corrected for Eccentering (IRAV_RF) USIT-E[1]
3.7 in 2.7

Maximum of Unflagged Internal Radii (IRMX_RF) USIT-E[1]
3.7 in 2.7

Minimum of Unflagged Internal Radii (IRMN_RF) USIT-E[1]
3.7 in 2.7

Casing Corrected for Eccentering (IRAV_RF) USIT-E[1]
2.7 in 3.7

Maximum of Unflagged Internal Radii (IRMX_RF) USIT-E[1]
2.7 in 3.7

Minimum of Unflagged Internal Radii (IRMN_RF) USIT-E[1]
2.7 in 3.7

U L B R U
Orientation: Top of Hole
Absent -0.051 -0.012 0.028 0.068
Explicit Normalization
USIT - Unflagged Internal Radii minus Median Internal Radius (IRBKM_RF) USIT-E[1] (in)

Thickness (THNO) USIT-E[1]
0.1 in 0.6

Median of Unflagged Casing Thickness (THAV_RF) USIT-E[1]
0.1 in 0.6

Maximum of Unflagged Casing Thickness (THMX_RF) USIT-E[1]
0.1 in 0.6

U L B R U
Orientation: Top of Hole
Absent -0.051 -0.012 0.028 0.068
Explicit Normalization
USIT - Unflagged Casing Thickness minus Median of Unflagged Casing Thickness (THBKM_RF) USIT-E[1] (in)

U L B R U
Orientation: Top of Hole
Absent 1.500 3.500 5.500 7.500
Custom Normalization
USIT - Acoustic Impedance (AIBK) USIT-E[1] (Mrayl)

Ratio of Gas Measurements to Total (GASR) USIT-E[1]
1 0

Bonded
Gas
Liquid
Micro-debonding

Bond Index (BI) DSLT-H[1]
1 0

(Mrayl)
U L B R U
Orientation: Top of Hole
Absent 2.599 4.563 6.527
Custom Normalization
USIT - Acoustic Impedance With Micro-debonding Image (AI_MDEBOND_IMG) USIT-E[1] (Mrayl)

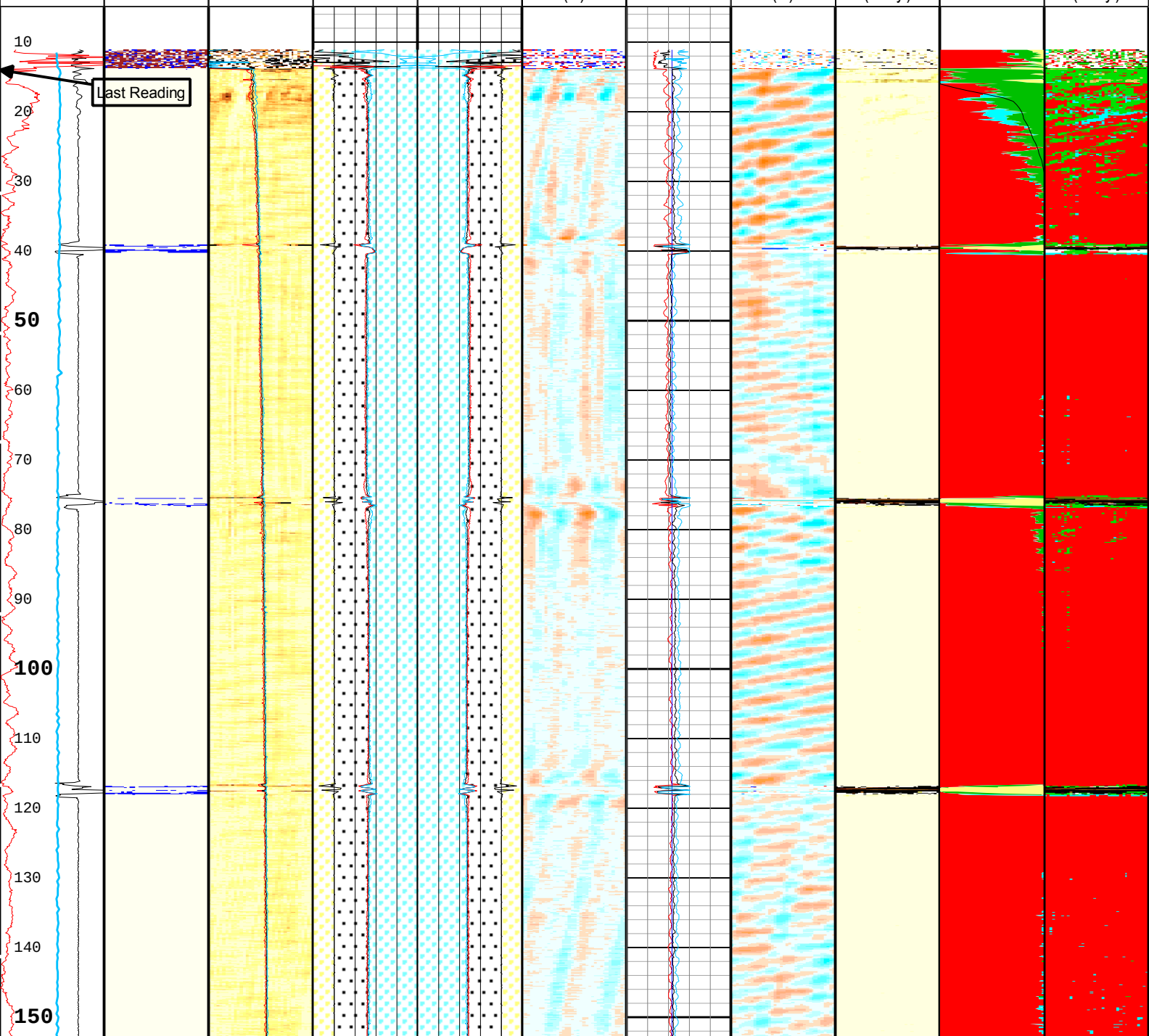

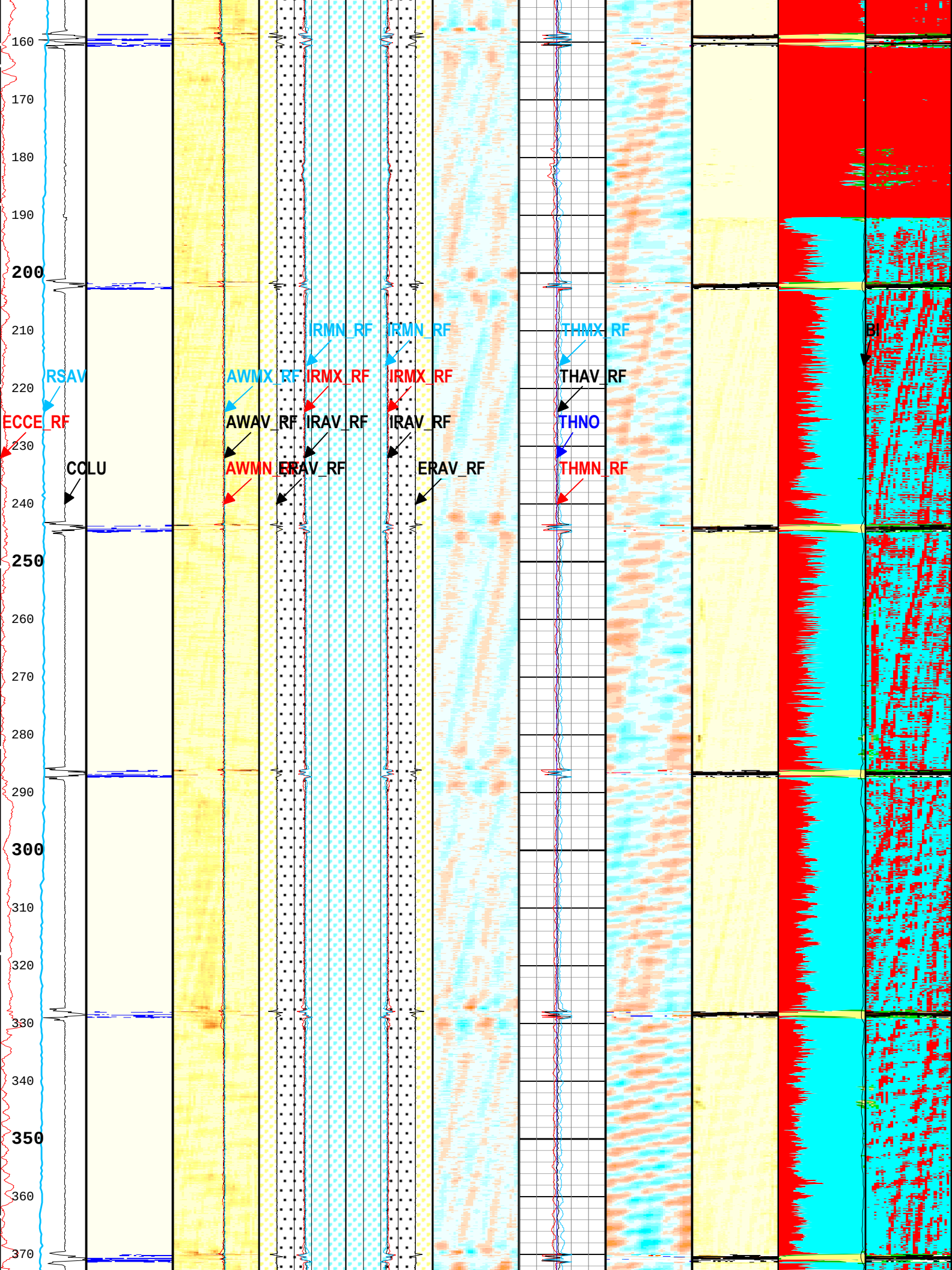
160
170
180
190
200
210
220
230
240
250
260
270
280
290
300
310
320
330
340
350
360
370
RSAV
ECCE_RF
COLU
AWMX_RF
AWAV_RF
AWMN_RF
IRMN_RF
IRMX_RF
IRAV_RF
ERAV_RF
IRMN_RF
IRMX_RF
IRAV_RF
ERAV_RF
THMX_RF
THAV_RF
THNO
THMN_RF
BI

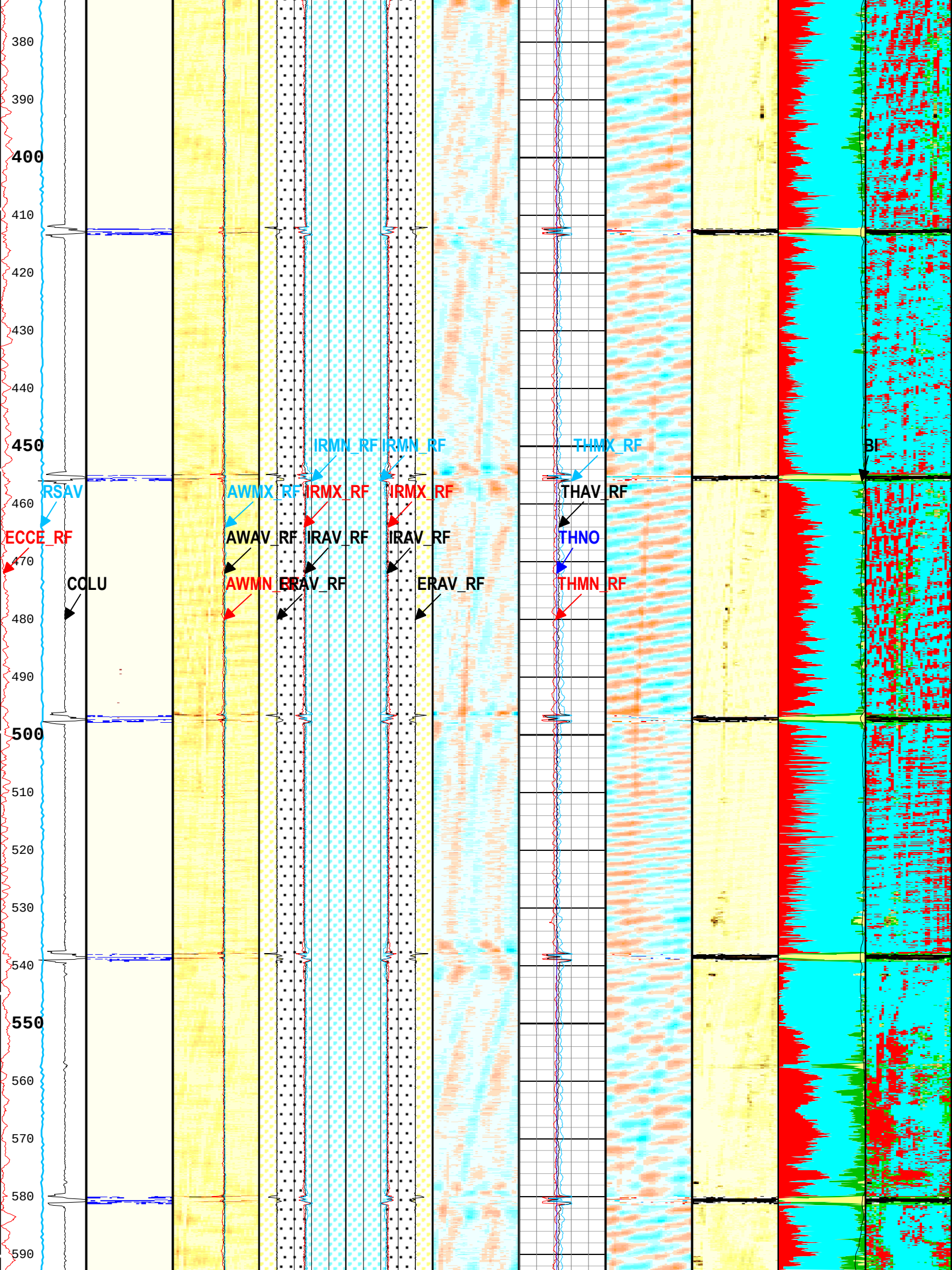
380
390
400
410
420
430
440
450
460
470
480
490
500
510
520
530
540
550
560
570
580
590
RSAV
ECCE_RF
COLU
AWMX_RF
AWAV_RF
AWMN_RF
IRMN_RF
IRMX_RF
IRAV_RF
ERAV_RF
IRMN_RF
IRMX_RF
IRAV_RF
ERAV_RF
THMX_RF
THAV_RF
THNO
THMN_RF
BI

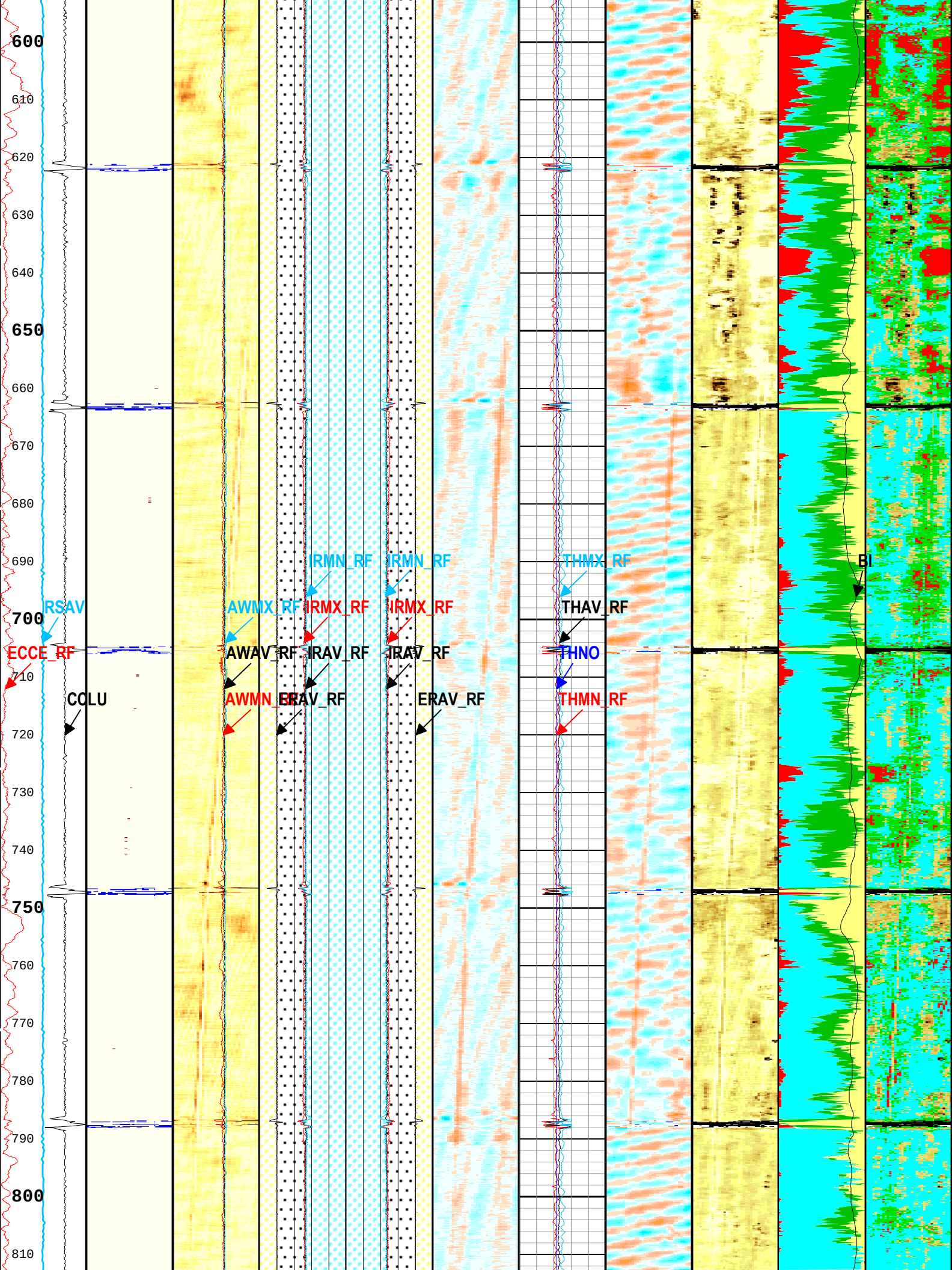
600
610
620
630
640
650
660
670
680
690
700
710
720
730
740
750
760
770
780
790
800
810
RSAV
ECCE_RF
COLU
AWMX_RF
AWAV_RF
AWMN_RF
IRMN_RF
IRMX_RF
IRAV_RF
ERAV_RF
IRMN_RF
IRMX_RF
IRAV_RF
ERAV_RF
THMX_RF
THAV_RF
THNO
THMN_RF
BI

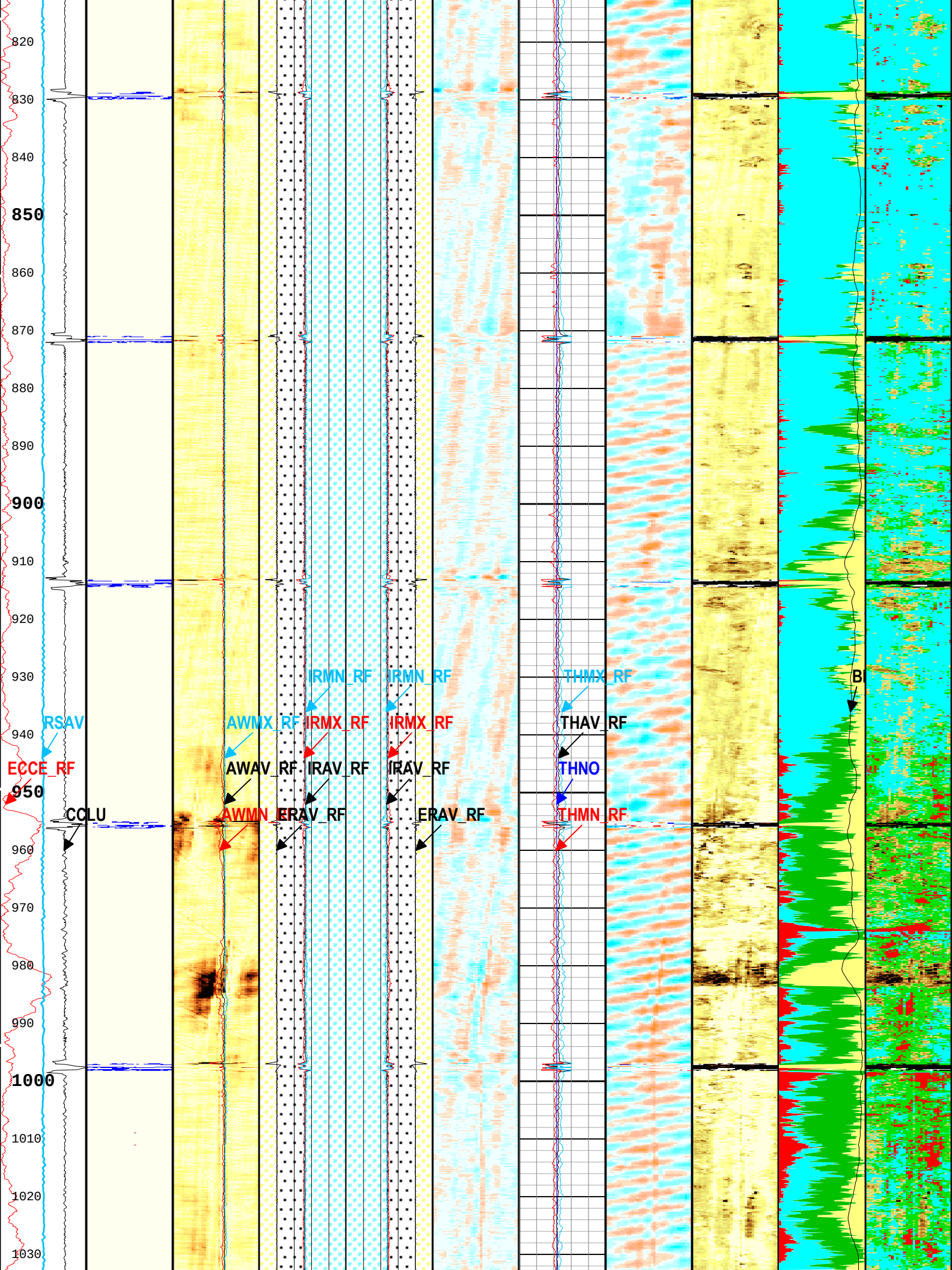
820
830
840
850
860
870
880
890
900
910
920
930
940
950
960
970
980
990
1000
1010
1020
1030
RSAV
ECCE_RF
CCLU
AWMX_RF
AWAV_RF
AWMN_RF
IRMN_RF
IRMX_RF
IRAV_RF
ERAV_RF
IRMN_RF
IRMX_RF
IRAV_RF
ERAV_RF
THMX_RF
THAV_RF
THNO
THMN_RF
BI

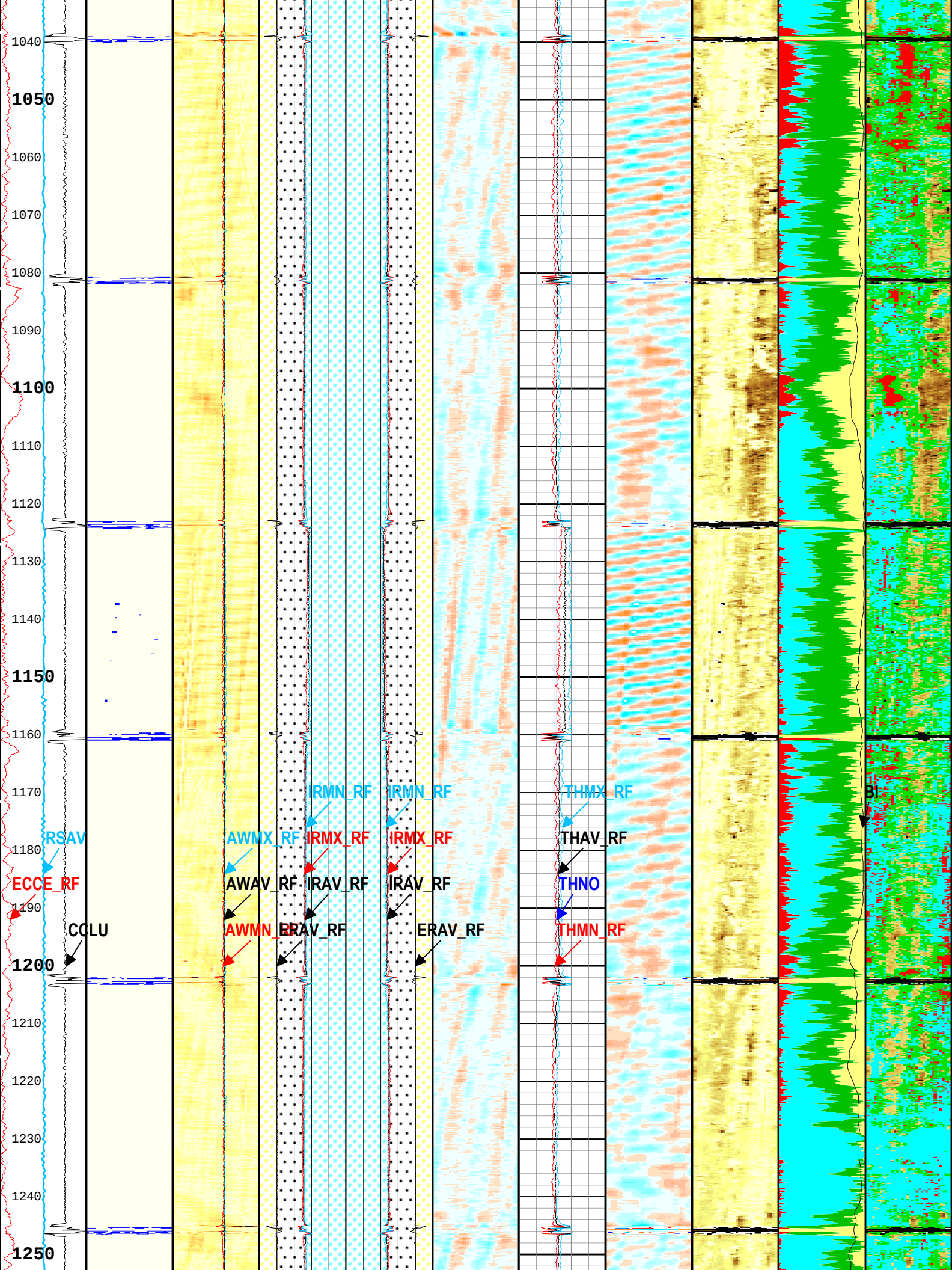
1040
1050
1060
1070
1080
1090
1100
1110
1120
1130
1140
1150
1160
1170
1180
1190
1200
1210
1220
1230
1240
1250
RSAV
ECCE_RF
CCLU
AWMX_RF
AWAV_RF
AWMN_RF
IRMN_RF
IRMX_RF
IRAV_RF
ERAV_RF
IRMN_RF
IRMX_RF
IRAV_RF
ERAV_RF
THMX_RF
THAV_RF
THNO
THMN_RF
BI

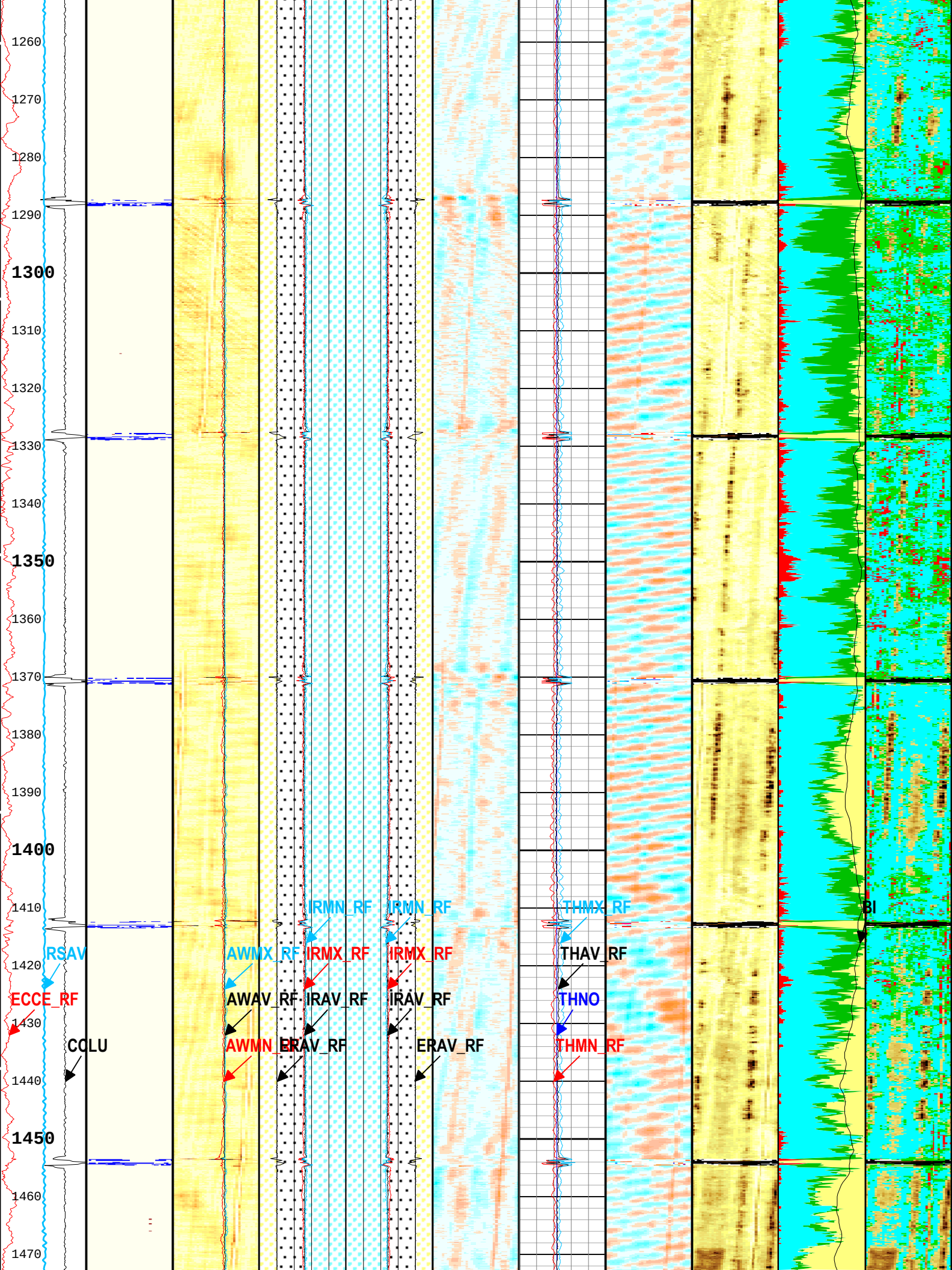
1260
1270
1280
1290
1300
1310
1320
1330
1340
1350
1360
1370
1380
1390
1400
1410
1420
1430
1440
1450
1460
1470
RSAV
ECCE_RF
COLU
AWMX_RF
AWAV_RF
AWMN_RF
IRMN_RF
IRMX_RF
IRAV_RF
ERAV_RF
IRMN_RF
IRMX_RF
IRAV_RF
ERAV_RF
THMX_RF
THAV_RF
THNO
THMN_RF
BI

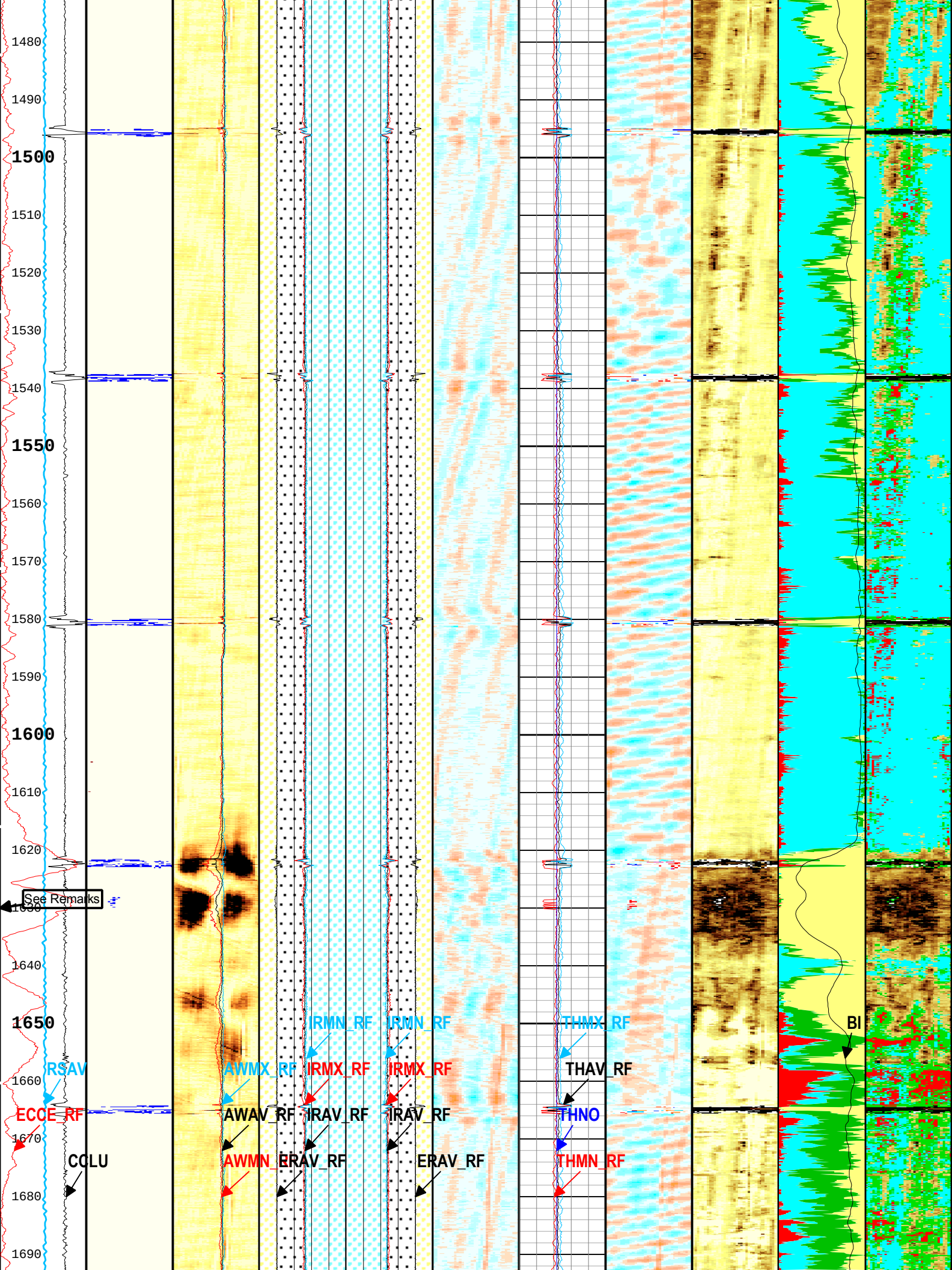
1480
1490
1500
1510
1520
1530
1540
1550
1560
1570
1580
1590
1600
1610
1620
See Remarks
1630
1640
1650
1660
1670
1680
1690
RSAV
ECCE_RF
CCLU
AWMX_RF
AWAV_RF
AWMN_RF
IRMN_RF
IRMX_RF
IRAV_RF
ERAV_RF
IRMN_RF
IRMX_RF
IRAV_RF
ERAV_RF
THMX_RF
THAV_RF
THNO
THMN_RF
BI

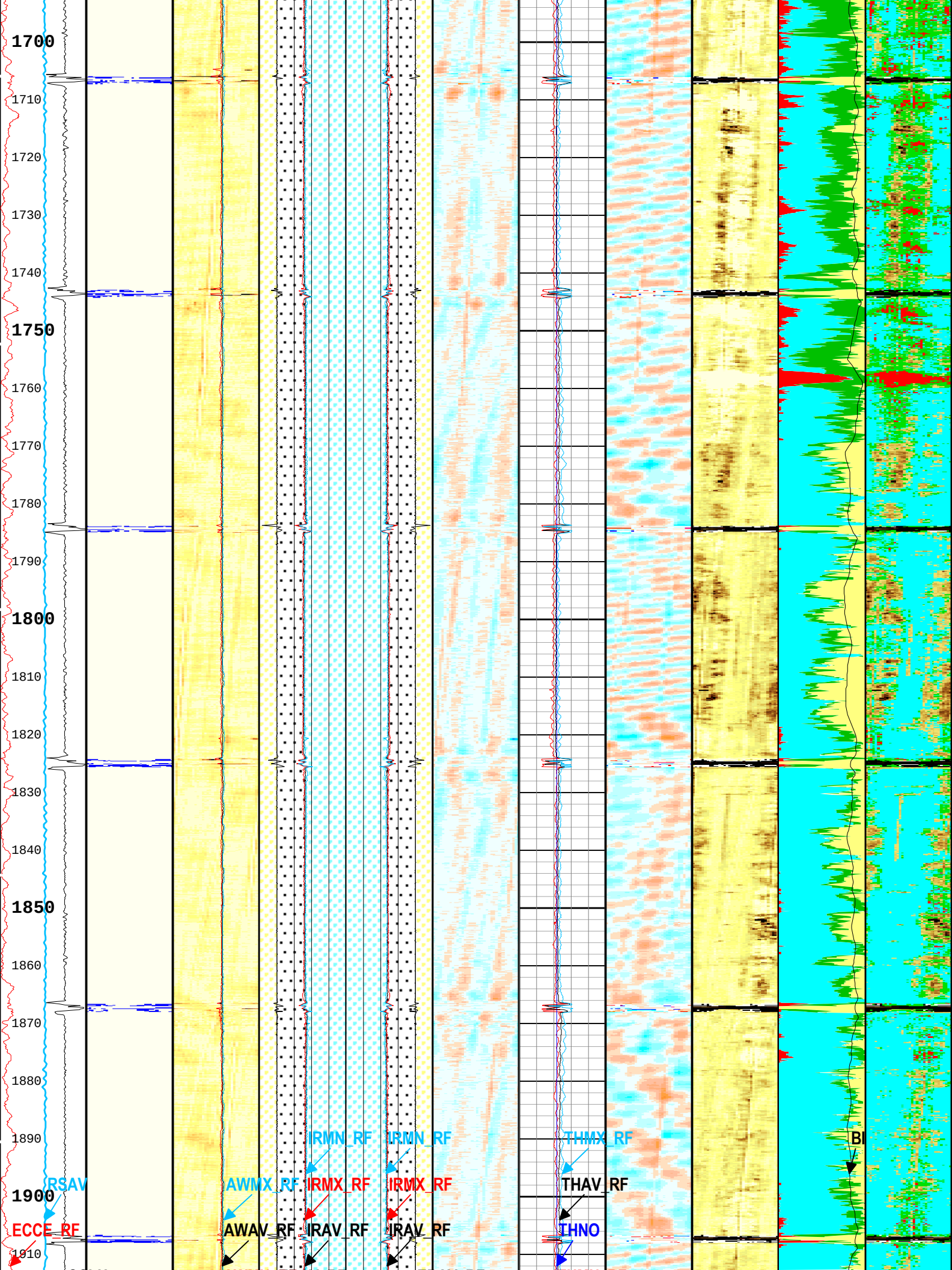
1700
1710
1720
1730
1740
1750
1760
1770
1780
1790
1800
1810
1820
1830
1840
1850
1860
1870
1880
1890
1900
1910
RSAV
ECCE_RF
AWMX_RF
AWAV_RF
IRMN_RF
IRMX_RF
IRAV_RF
IRMN_RF
IRMX_RF
IRAV_RF
THMX_RF
THAV_RF
THNO
BI

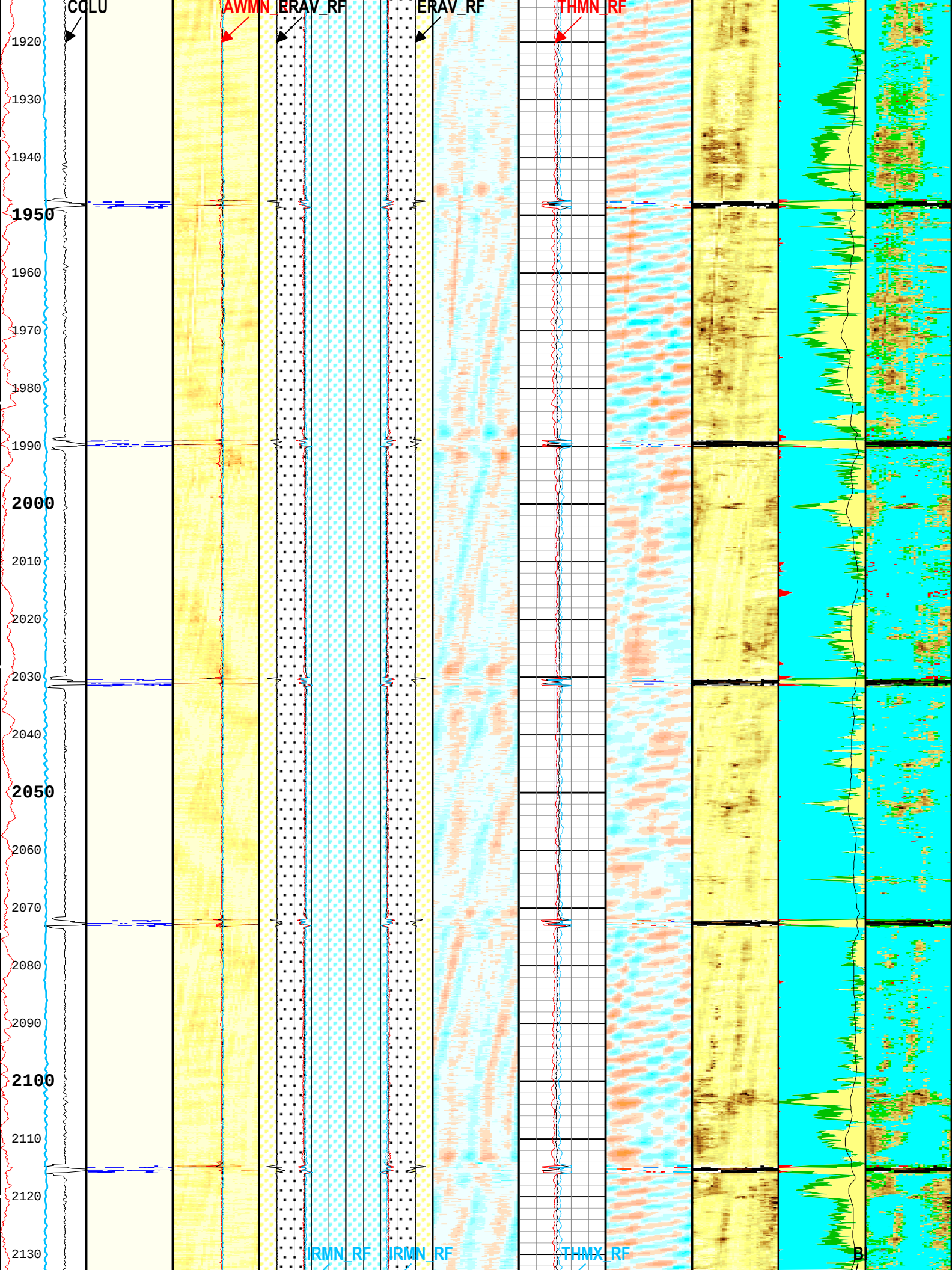
COLU
AWMN_RF
ERAV_RF
ERAV_RF
THMN_RF
1920
1930
1940
1950
1960
1970
1980
1990
2000
2010
2020
2030
2040
2050
2060
2070
2080
2090
2100
2110
2120
2130
IRMN_RF
IRMN_RF
THMX_RF
B

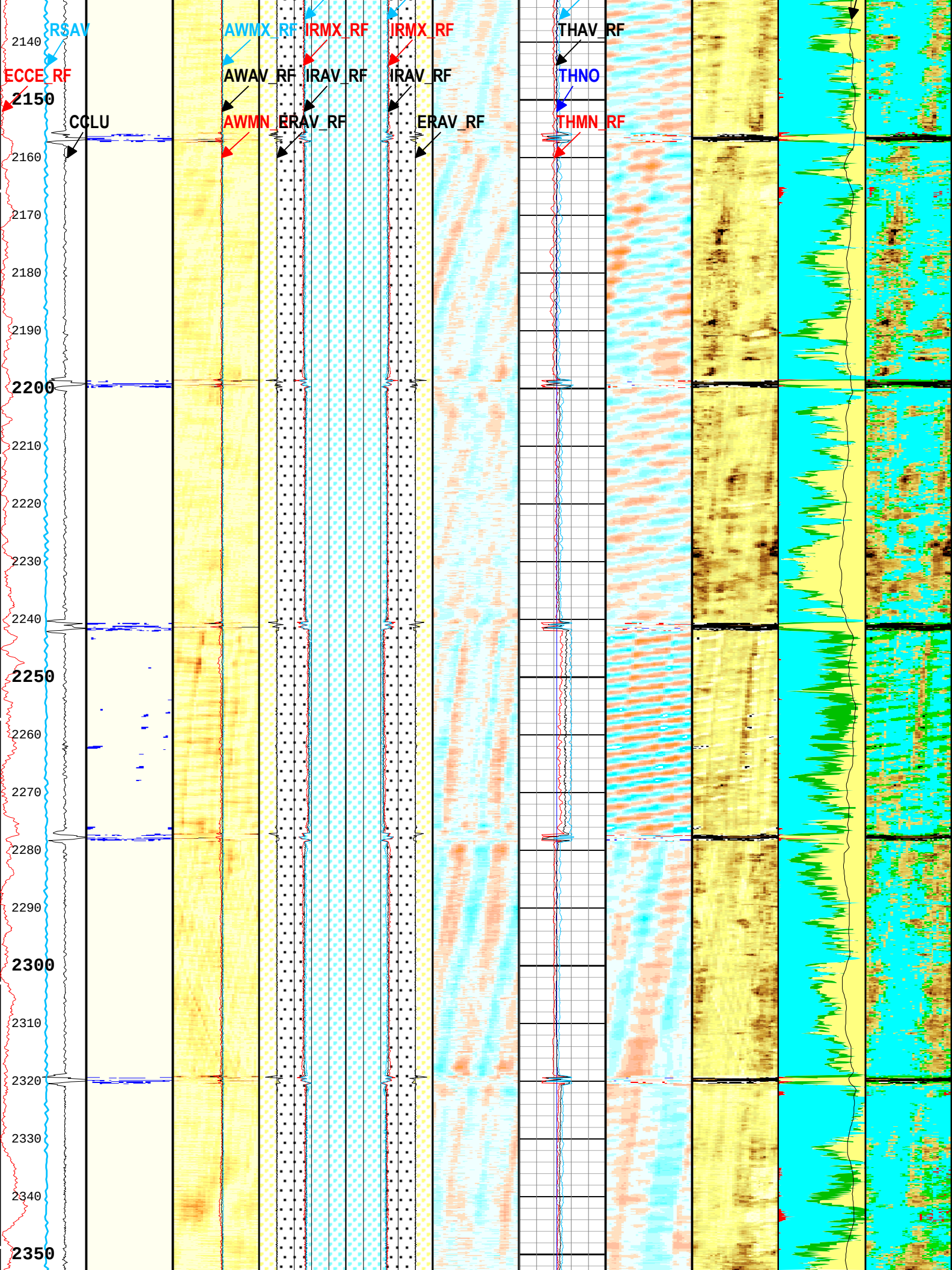
RSAV
ECCE_RF
CCLU
AWMX_RF
AWAV_RF
AWMN_RF
IRMX_RF
IRAV_RF
ERAV_RF
IRMX_RF
IRAV_RF
ERAV_RF
THAV_RF
THNO
THMN_RF
2140
2150
2160
2170
2180
2190
2200
2210
2220
2230
2240
2250
2260
2270
2280
2290
2300
2310
2320
2330
2340
2350

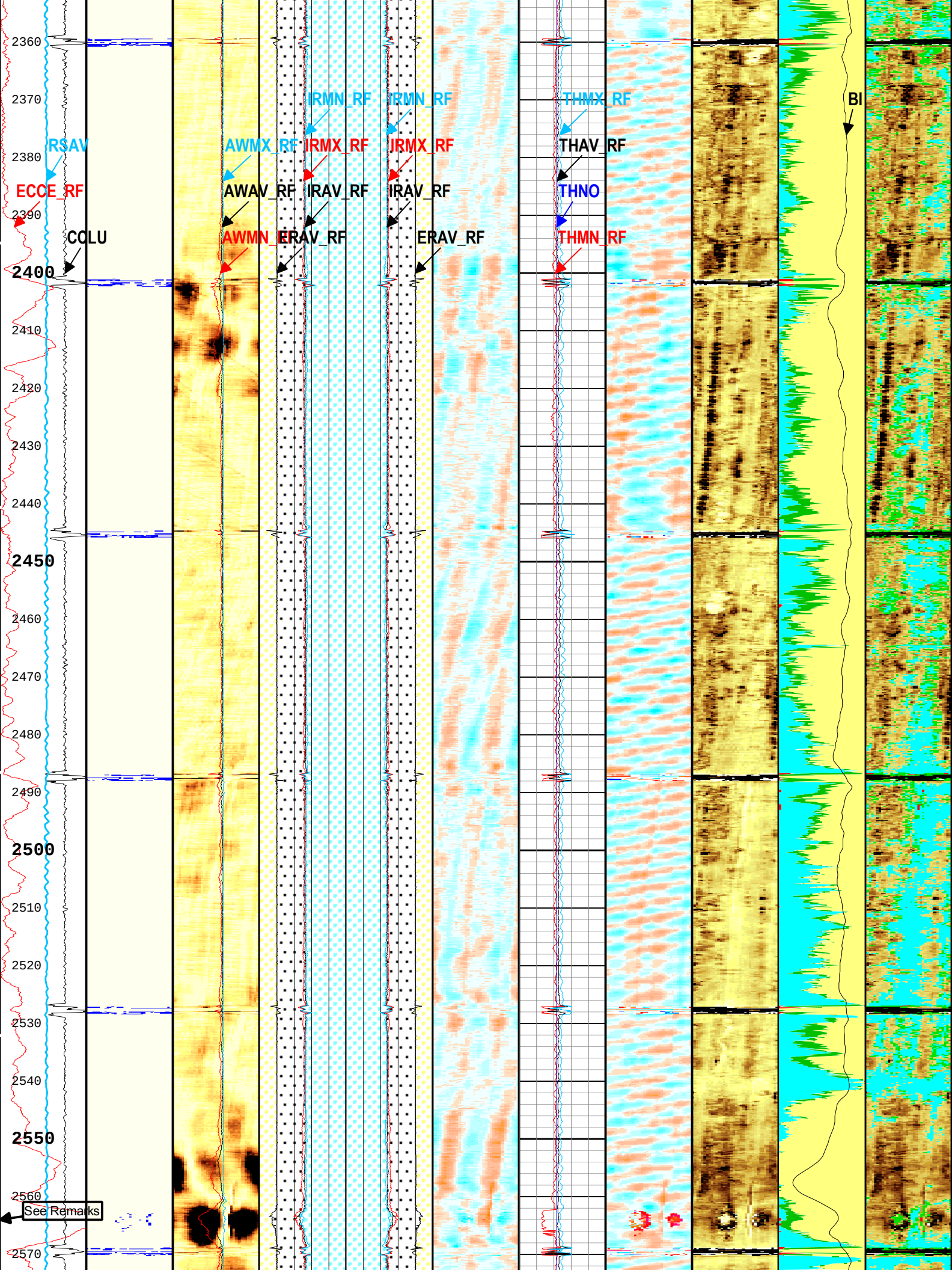
2360
2370
2380
2390
2400
2410
2420
2430
2440
2450
2460
2470
2480
2490
2500
2510
2520
2530
2540
2550
2560
2570
RSAV
ECCE_RF
COLU
AWMX_RF
AWAV_RF
AWMN_RF
IRMN_RF
IRMX_RF
IRAV_RF
ERAV_RF
IRMN_RF
IRMX_RF
IRAV_RF
ERAV_RF
THMX_RF
THAV_RF
THNO
THMN_RF
BI
See Remarks

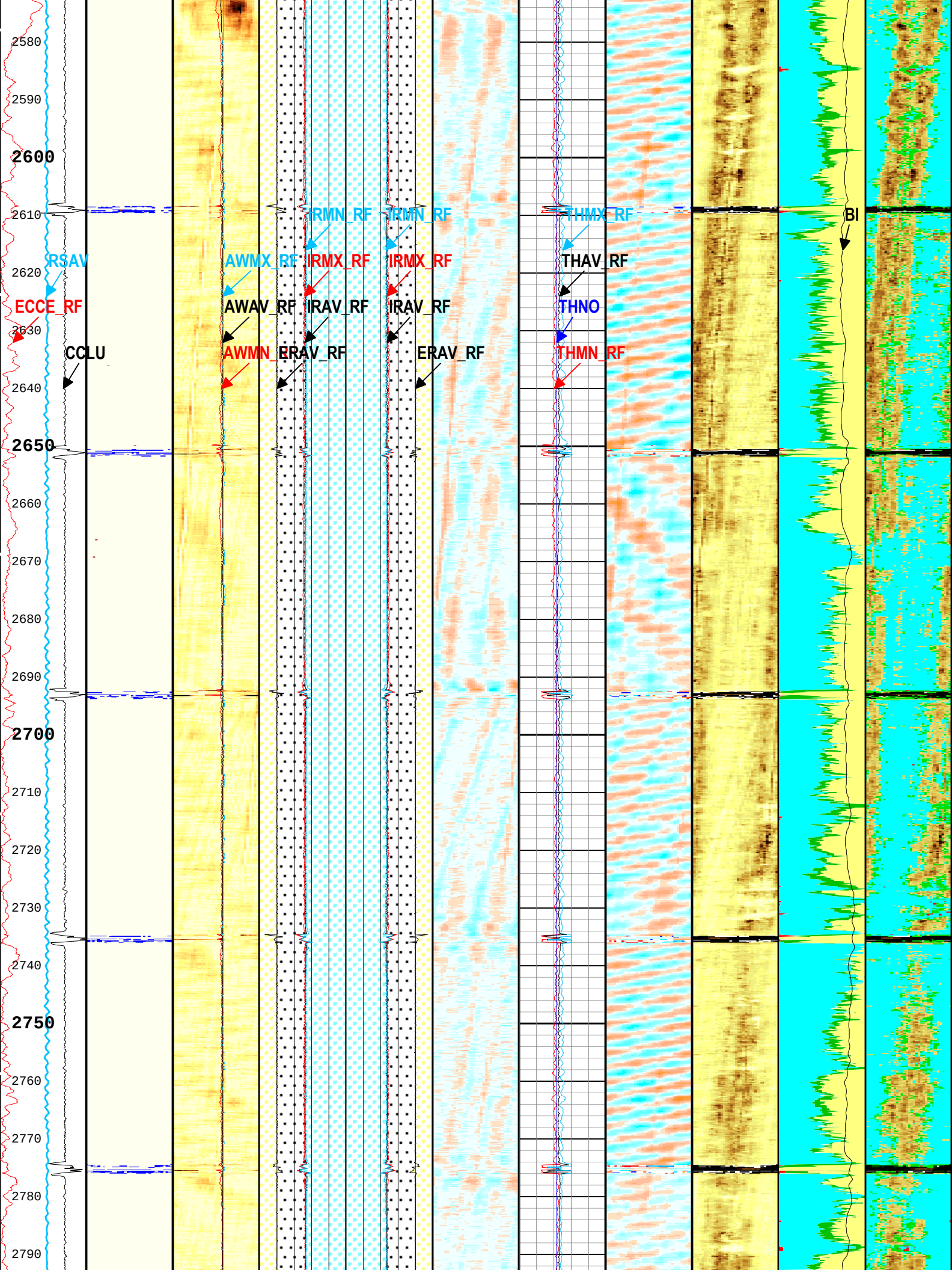
2580
2590
2600
2610
2620
2630
2640
2650
2660
2670
2680
2690
2700
2710
2720
2730
2740
2750
2760
2770
2780
2790
RSAV
ECCE_RF
CCLU
AWMX_RF
AWAV_RF
AWMN_RF
IRMN_RF
IRMX_RF
IRAV_RF
ERAV_RF
IRMN_RF
IRMX_RF
IRAV_RF
ERAV_RF
THMX_RF
THAV_RF
THNO
THMN_RF
BI

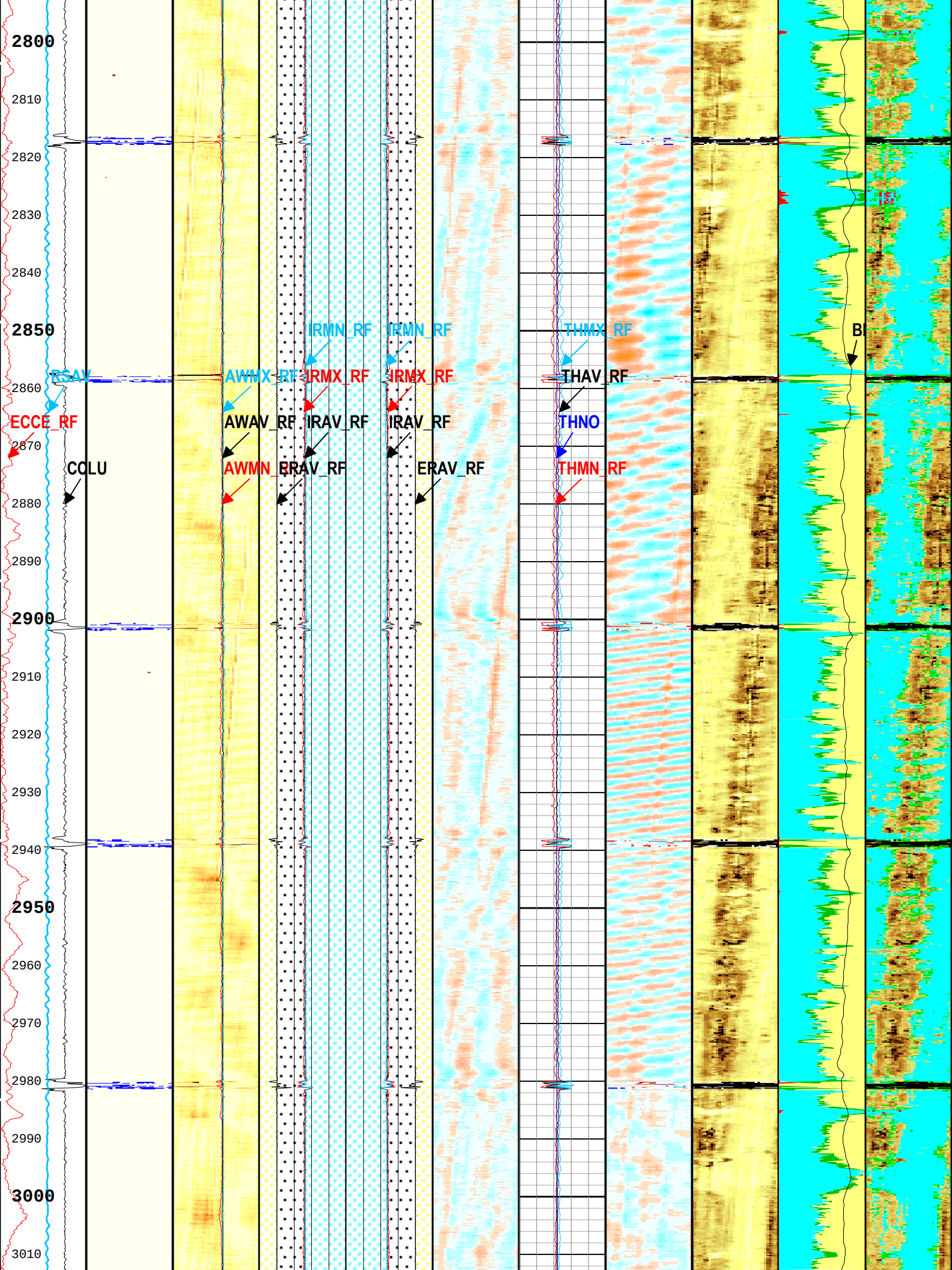
2800
2810
2820
2830
2840
2850
2860
2870
2880
2890
2900
2910
2920
2930
2940
2950
2960
2970
2980
2990
3000
3010
RSAV
ECCE_RF
COLU
AWMX_RF
AWAV_RF
AWMN_RF
IRMN_RF
IRMX_RF
IRAV_RF
ERAV_RF
IRMN_RF
IRMX_RF
IRAV_RF
ERAV_RF
THMX_RF
THAV_RF
THNO
THMN_RF
BI

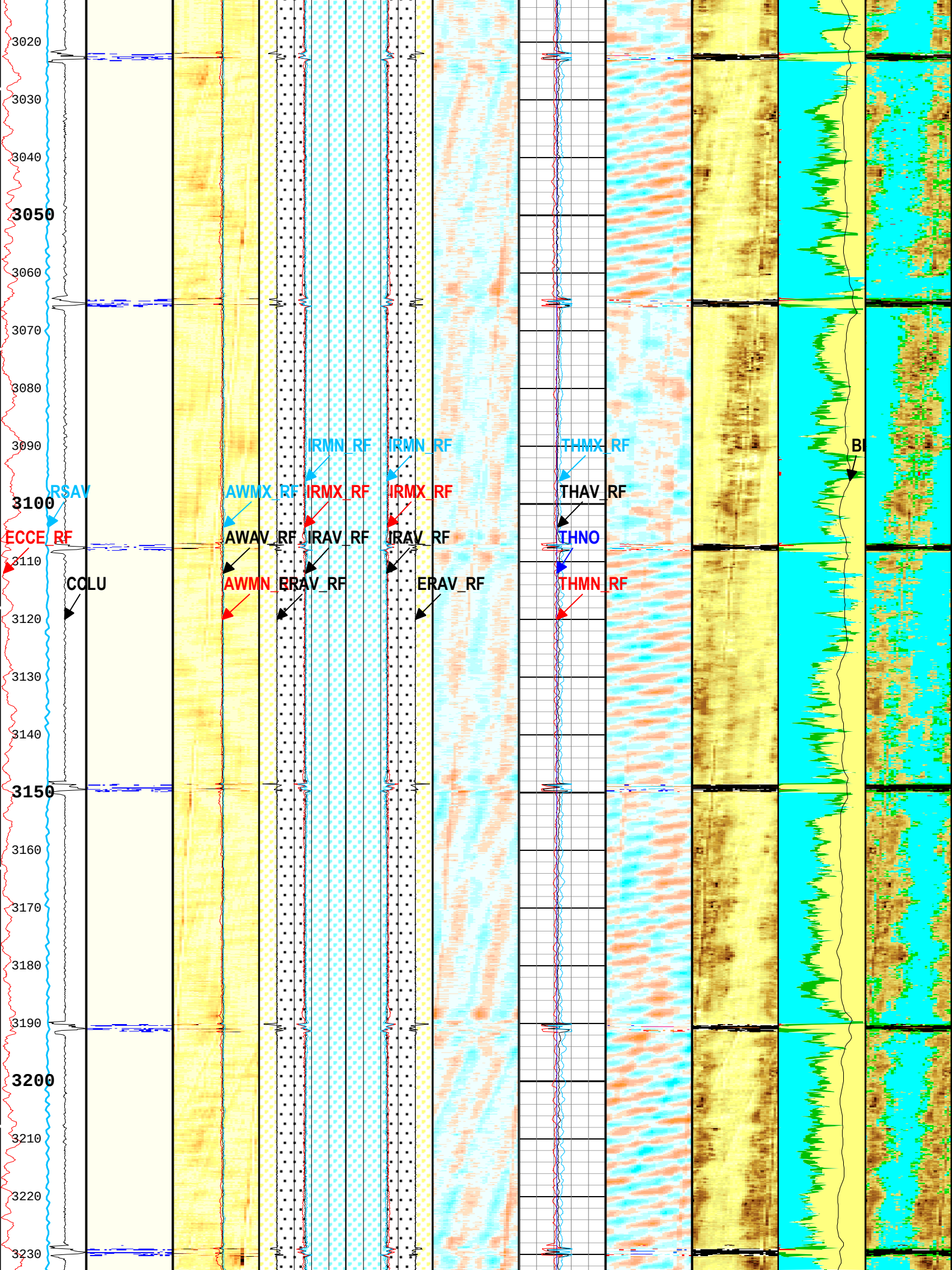
3020
3030
3040
3050
3060
3070
3080
3090
3100
3110
3120
3130
3140
3150
3160
3170
3180
3190
3200
3210
3220
3230
RSAV
ECCE_RF
CCLU
AWMX_RF
AWAV_RF
AWMN_RF
IRMN_RF
IRMX_RF
IRAV_RF
ERAV_RF
IRMN_RF
IRMX_RF
IRAV_RF
ERAV_RF
THMX_RF
THAV_RF
THNO
THMN_RF

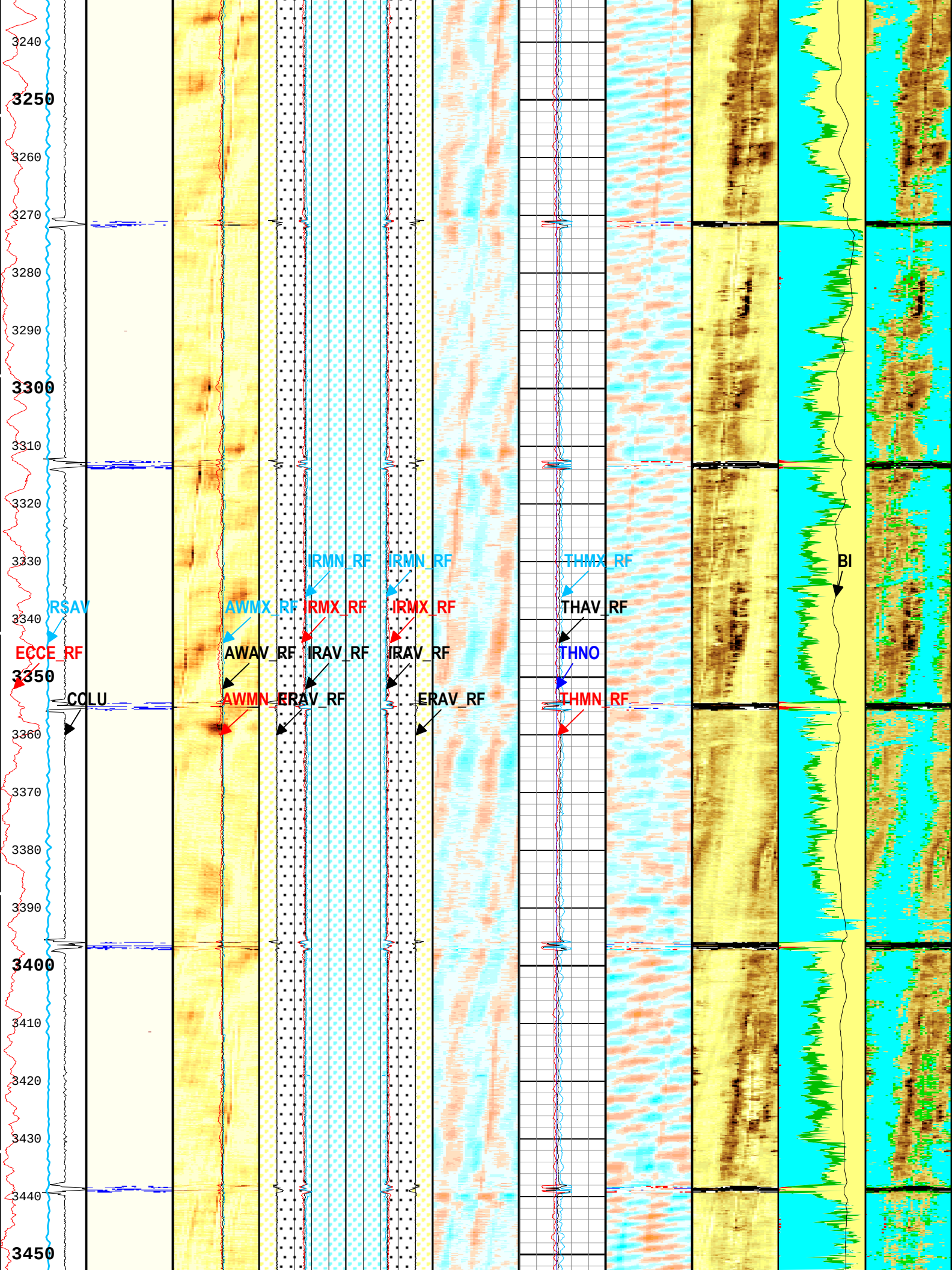
3240
3250
3260
3270
3280
3290
3300
3310
3320
3330
3340
3350
3360
3370
3380
3390
3400
3410
3420
3430
3440
3450
RSAV
ECCE_RF
COLU
AWMX_RF
AWAV_RF
AWMN_RF
IRMN_RF
IRMX_RF
IRAV_RF
ERAV_RF
IRMN_RF
IRMX_RF
IRAV_RF
ERAV_RF
THMX_RF
THAV_RF
THNO
THMN_RF
BI

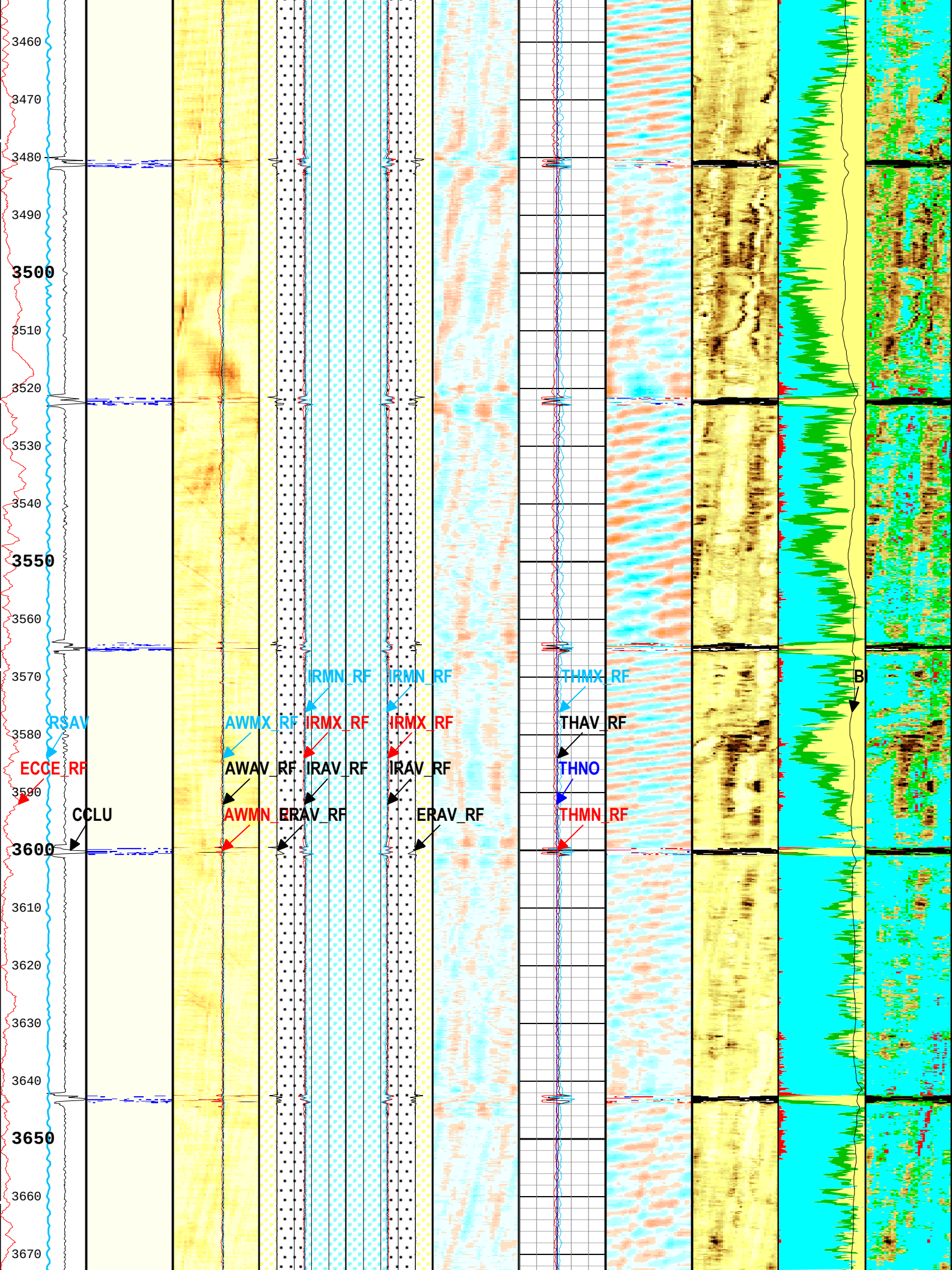
3460
3470
3480
3490
3500
3510
3520
3530
3540
3550
3560
3570
3580
3590
3600
3610
3620
3630
3640
3650
3660
3670
RSAV
ECCE_RF
CCLU
AWMX_RF
AWAV_RF
AWMN_RF
IRMN_RF
IRMX_RF
IRAV_RF
ERAV_RF
IRMN_RF
IRMX_RF
IRAV_RF
ERAV_RF
THMX_RF
THAV_RF
THNO
THMN_RF
BI

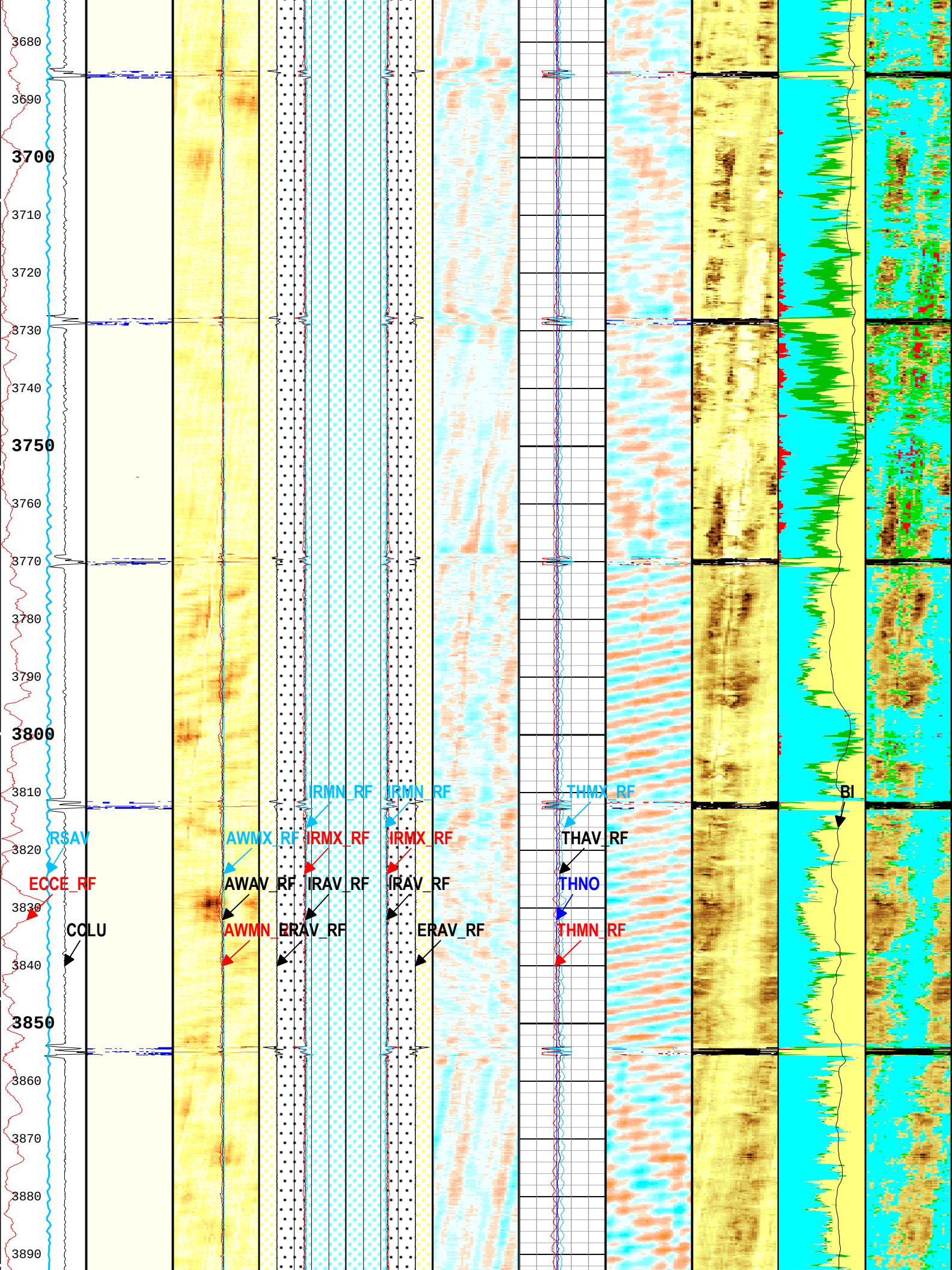
3680
3690
3700
3710
3720
3730
3740
3750
3760
3770
3780
3790
3800
3810
3820
3830
3840
3850
3860
3870
3880
3890
RSAV
ECCE_RF
COLU
AWMX_RF
AWAV_RF
AWMN_RF
IRMN_RF
IRMX_RF
IRAV_RF
ERAV_RF
IRMN_RF
IRMX_RF
IRAV_RF
ERAV_RF
THMX_RF
THAV_RF
THNO
THMN_RF
BI

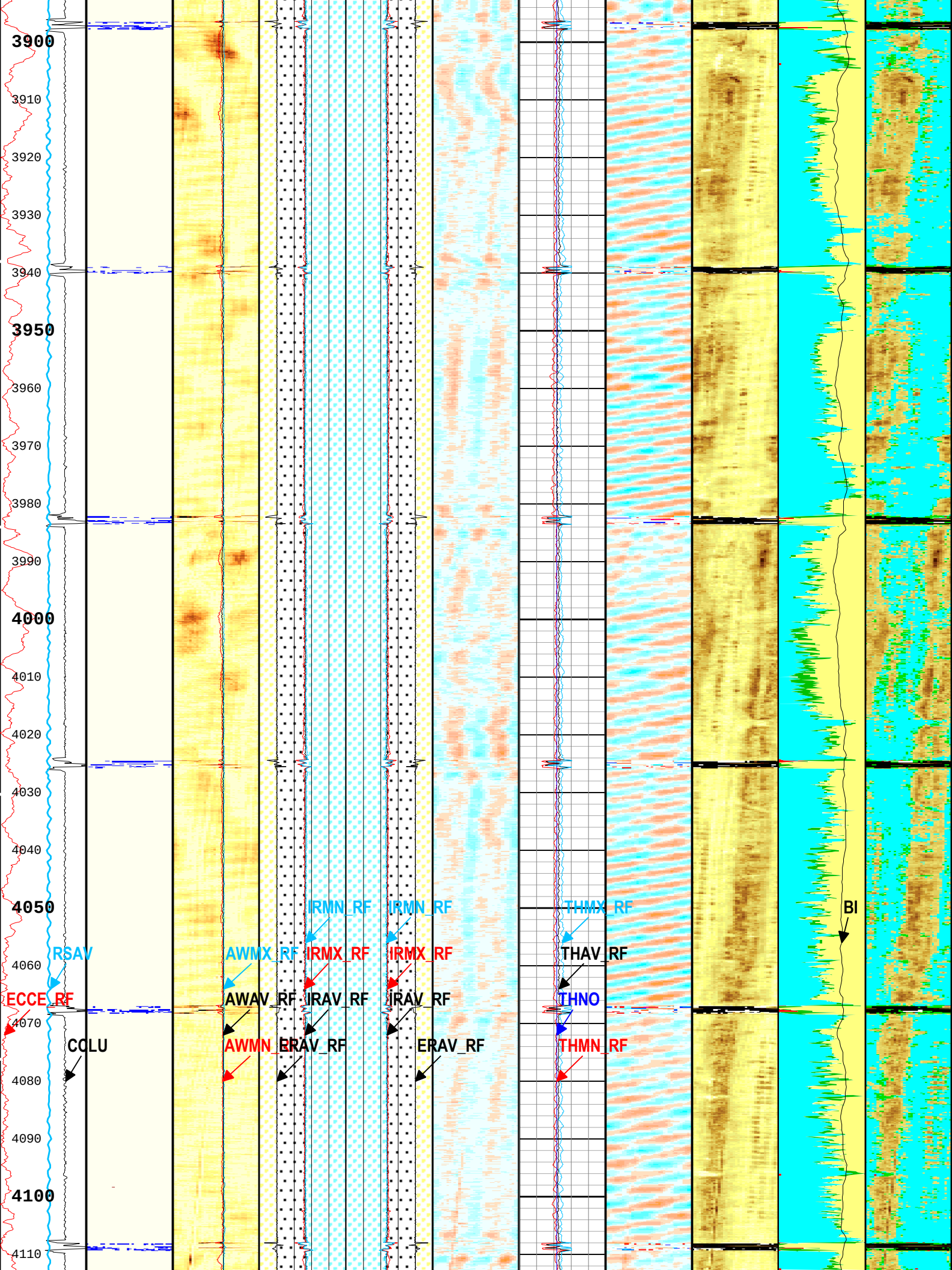
3900
3910
3920
3930
3940
3950
3960
3970
3980
3990
4000
4010
4020
4030
4040
4050
4060
4070
4080
4090
4100
4110
RSAV
ECCE_RF
COLU
AWMX_RF
AWAV_RF
AWMN_RF
IRMN_RF
IRMX_RF
IRAV_RF
ERAV_RF
IRMN_RF
IRMX_RF
IRAV_RF
ERAV_RF
THMX_RF
THAV_RF
THNO
THMN_RF
BI

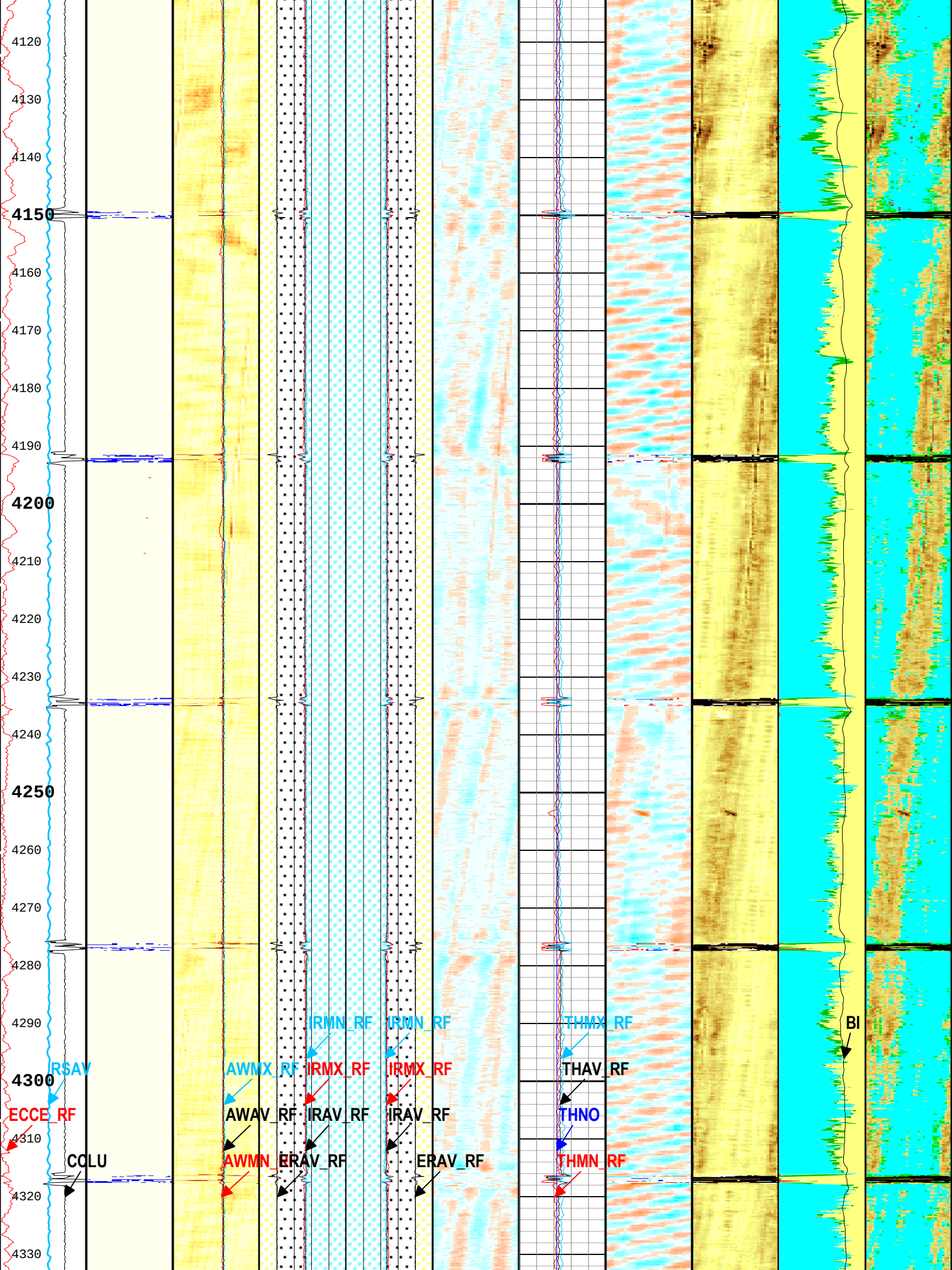
4120
4130
4140
4150
4160
4170
4180
4190
4200
4210
4220
4230
4240
4250
4260
4270
4280
4290
4300
4310
4320
4330
RSAV
ECCE_RF
COLU
AWMX_RF
AWAV_RF
AWMN_RF
IRMN_RF
IRMX_RF
IRAV_RF
ERAV_RF
IRMN_RF
IRMX_RF
IRAV_RF
ERAV_RF
THMX_RF
THAV_RF
THNO
THMN_RF
BI

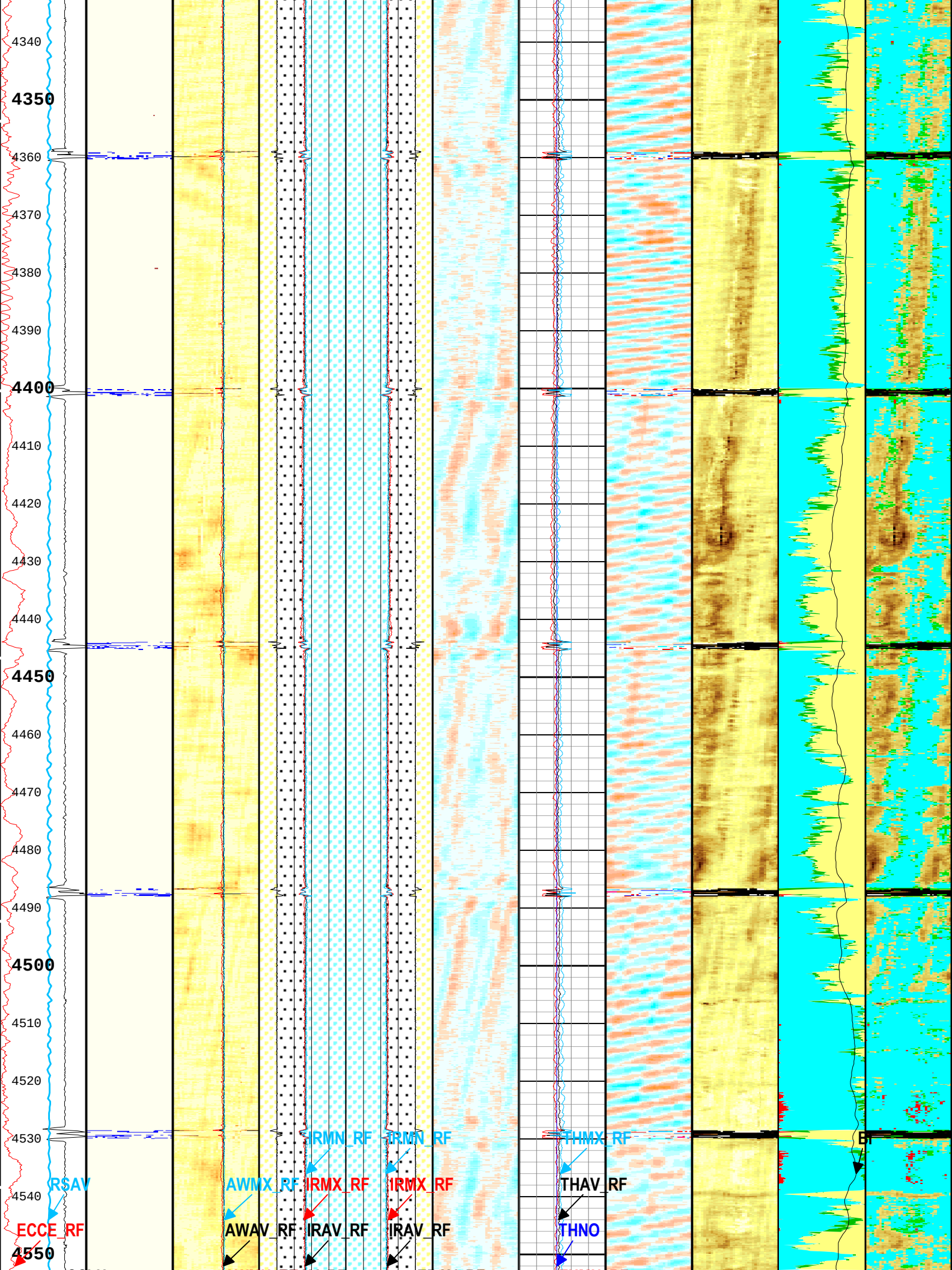
4340
4350
4360
4370
4380
4390
4400
4410
4420
4430
4440
4450
4460
4470
4480
4490
4500
4510
4520
4530
4540
4550
RSAV
ECCE_RF
AWMX_RF
AWAV_RF
IRMN_RF
IRMX_RF
IRAV_RF
IRMN_RF
IRMX_RF
IRAV_RF
THMX_RF
THAV_RF
THNO
BI

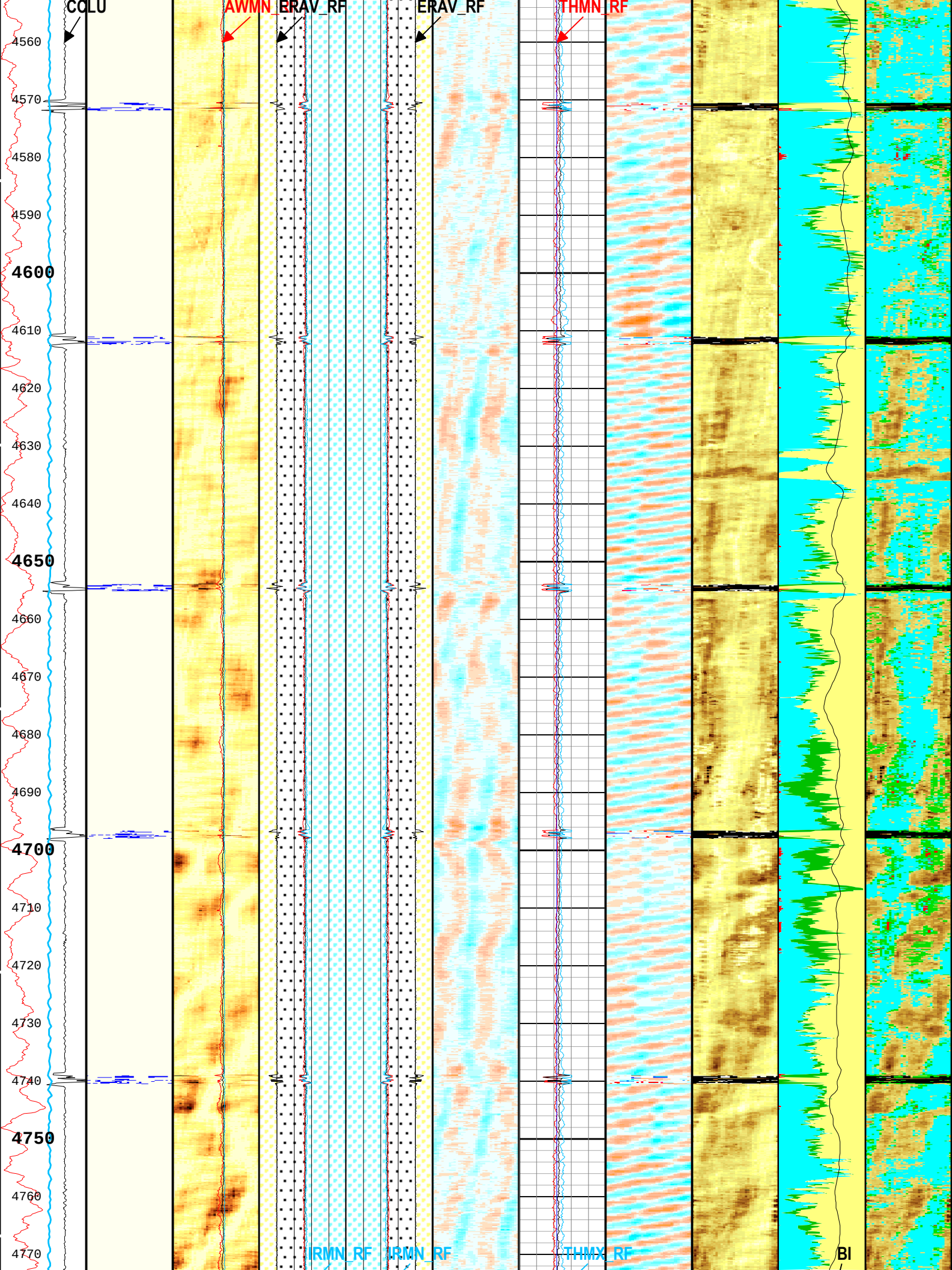
COLU
AWMN_RF
ERAV_RF
ERAV_RF
THMN_RF
4560
4570
4580
4590
4600
4610
4620
4630
4640
4650
4660
4670
4680
4690
4700
4710
4720
4730
4740
4750
4760
4770
IRMN_RF
IRMN_RF
THMX_RF
BI

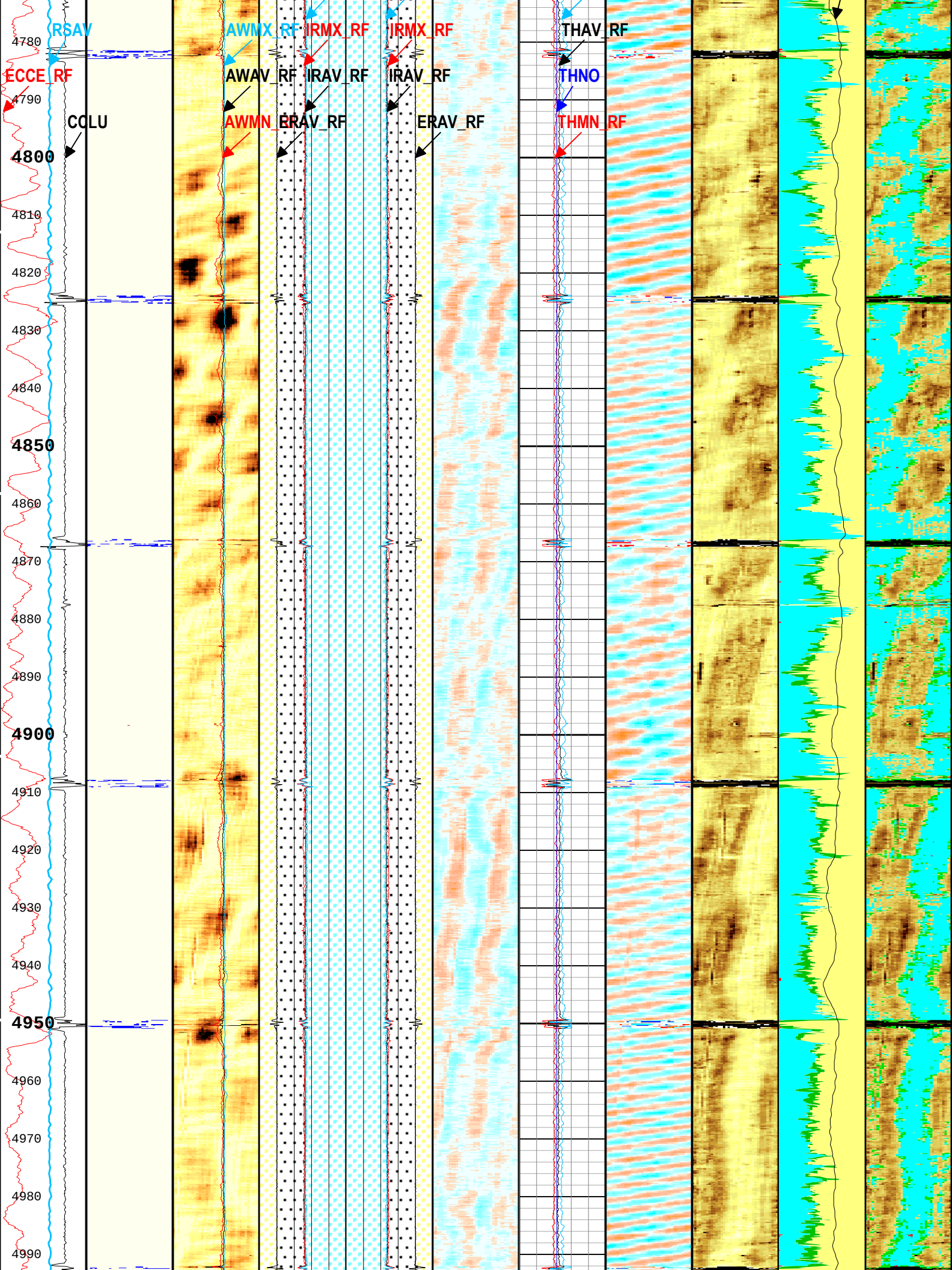
RSAV
ECCE_RF
COLU
AWMX_RF
AWAV_RF
AWMN_RF
IRMX_RF
IRAV_RF
ERAV_RF
IRMX_RF
IRAV_RF
ERAV_RF
THAV_RF
THNO
THMN_RF
4780
4790
4800
4810
4820
4830
4840
4850
4860
4870
4880
4890
4900
4910
4920
4930
4940
4950
4960
4970
4980
4990

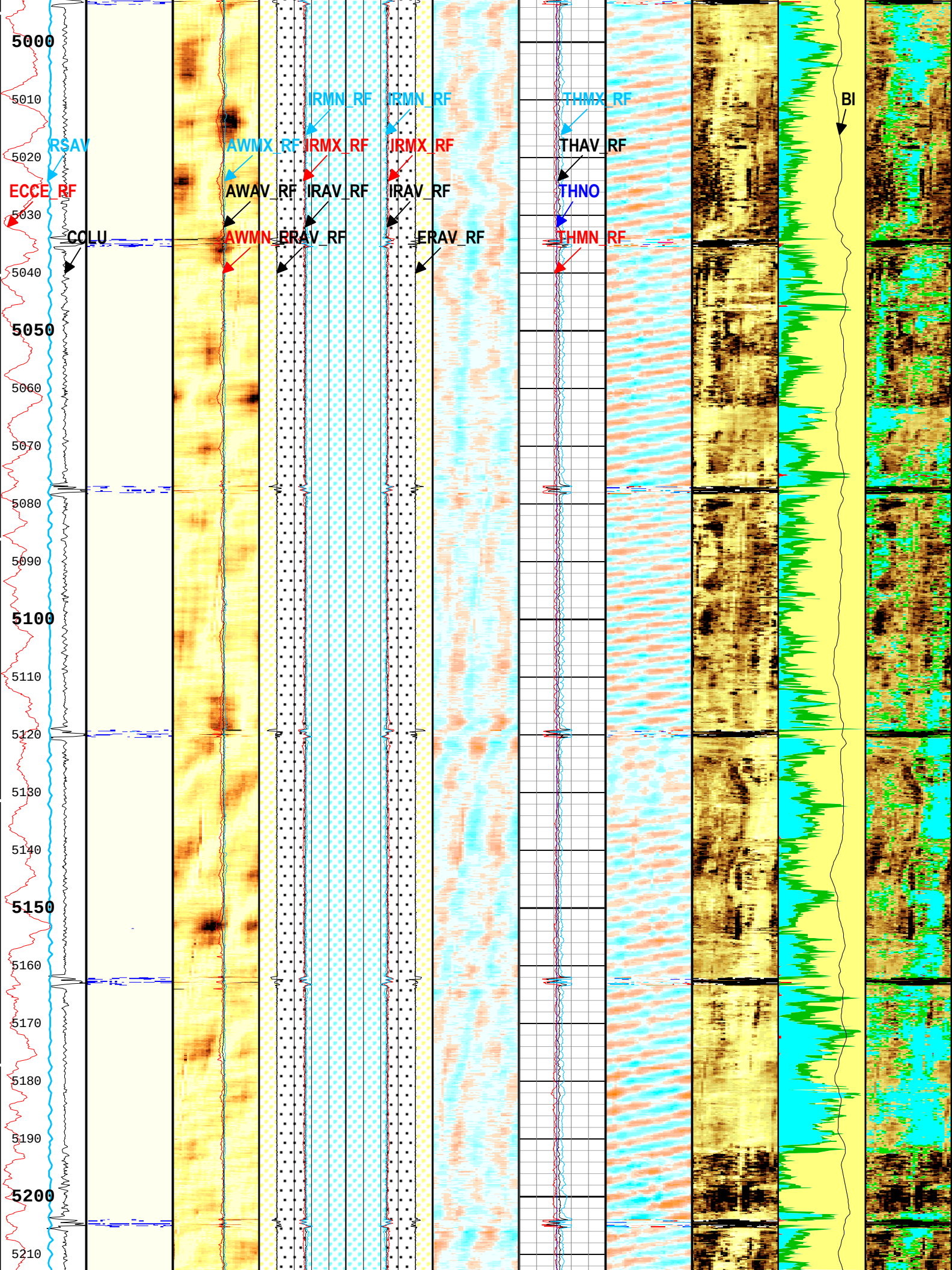
5000
5010
5020
5030
5040
5050
5060
5070
5080
5090
5100
5110
5120
5130
5140
5150
5160
5170
5180
5190
5200
5210
RSAV
ECCE_RF
COLU
AWMX_RF
AWAV_RF
AWMN_RF
IRMN_RF
IRMX_RF
IRAV_RF
ERAV_RF
IRMN_RF
IRMX_RF
IRAV_RF
ERAV_RF
THMX_RF
THAV_RF
THNO
THMN_RF
BI

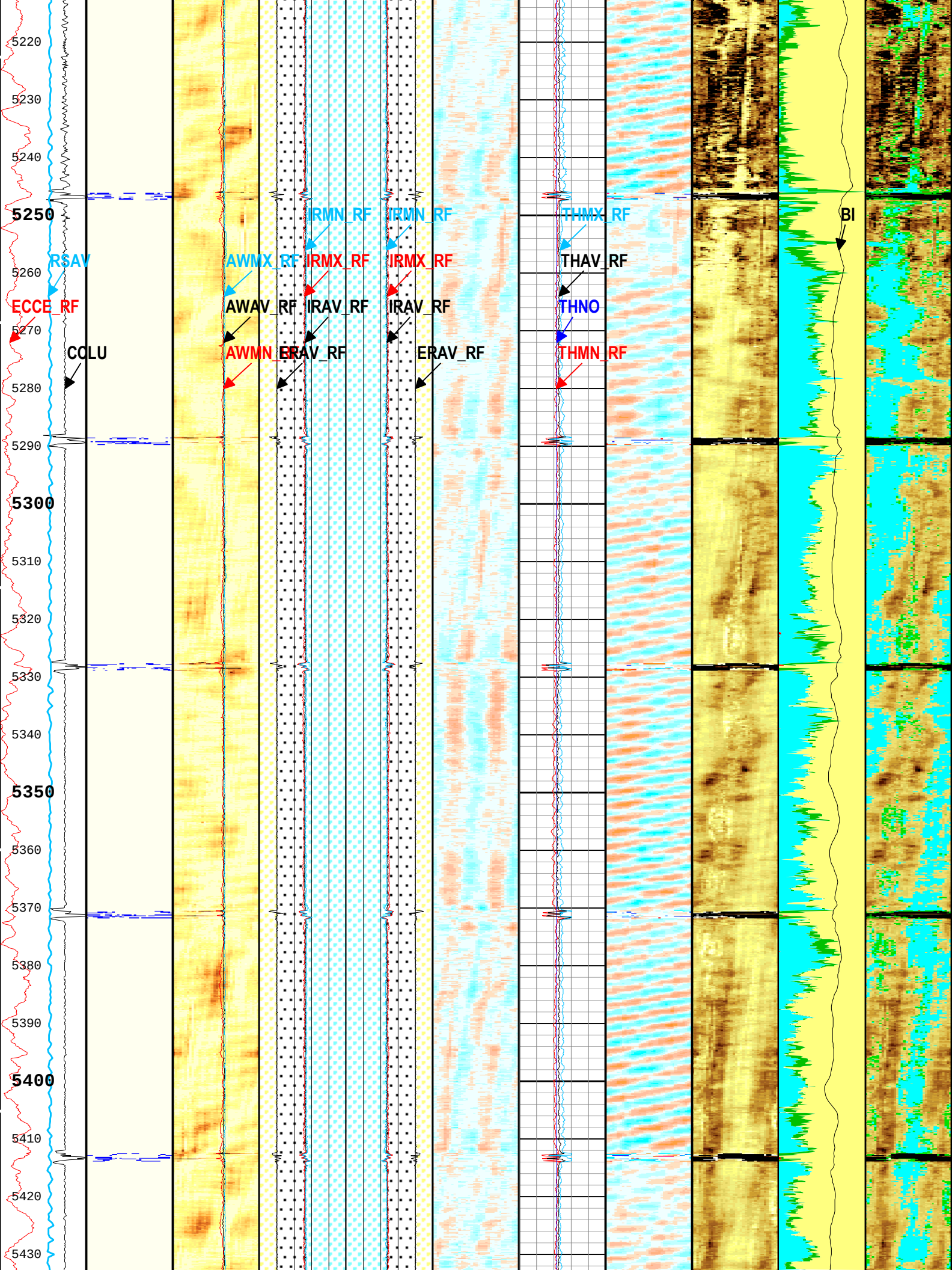
5220
5230
5240
5250
5260
5270
5280
5290
5300
5310
5320
5330
5340
5350
5360
5370
5380
5390
5400
5410
5420
5430
RSAV
ECCE_RF
COLU
AWMX_RF
AWAV_RF
AWMN_RF
IRMN_RF
IRMX_RF
IRAV_RF
ERAV_RF
IRMN_RF
IRMX_RF
IRAV_RF
ERAV_RF
THMX_RF
THAV_RF
THNO
THMN_RF
BI

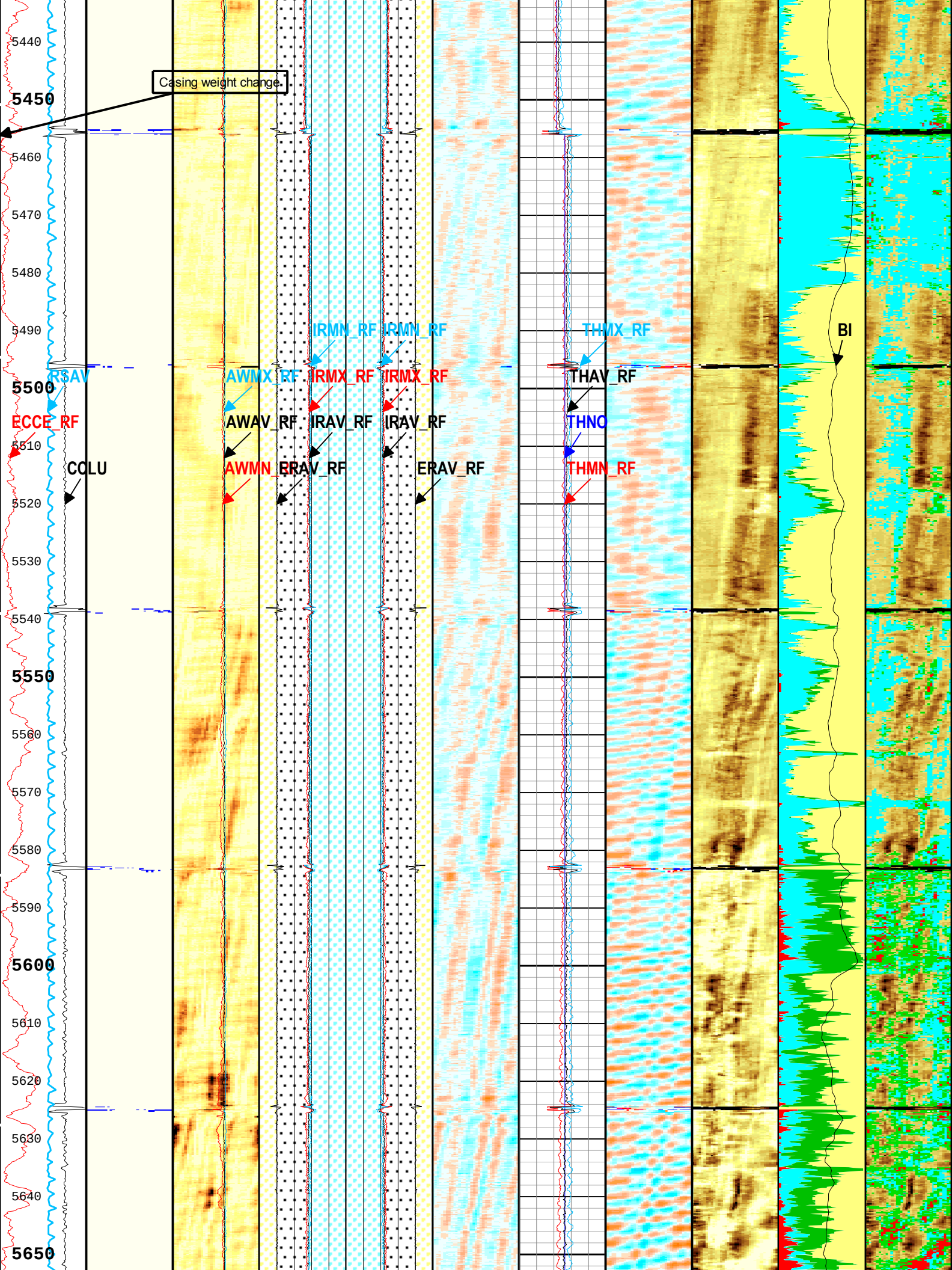
Casing weight change
5440
5450
5460
5470
5480
5490
5500
5510
5520
5530
5540
5550
5560
5570
5580
5590
5600
5610
5620
5630
5640
5650
RSAV
ECCE_RF
COLU
AWMX_RF
AWAV_RF
AWMN_RF
IRMN_RF
IRMX_RF
IRAV_RF
ERAV_RF
IRMN_RF
IRMX_RF
IRAV_RF
ERAV_RF
THMX_RF
THAV_RF
THNO
THMN_RF
BI

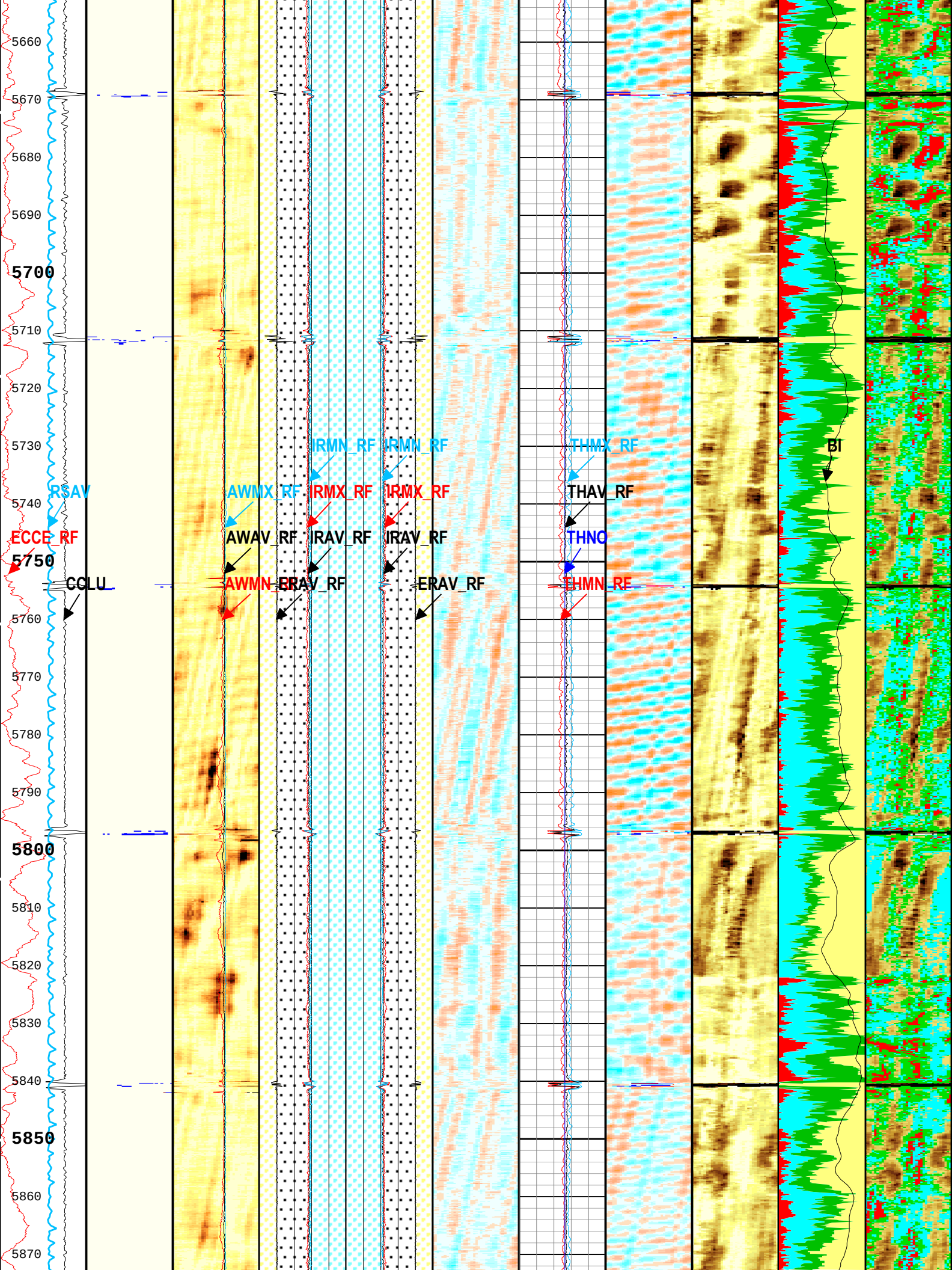
5660
5670
5680
5690
5700
5710
5720
5730
5740
5750
5760
5770
5780
5790
5800
5810
5820
5830
5840
5850
5860
5870
RSAV
ECCE_RF
CCLU
IRMN_RF
IRMN_RF
AWMX_RF
IRMX_RF
IRMX_RF
AWAV_RF
IRAV_RF
IRAV_RF
AWMN_RF
IRAV_RF
ERAV_RF
THMX_RF
THAV_RF
THNO
THMN_RF
BI

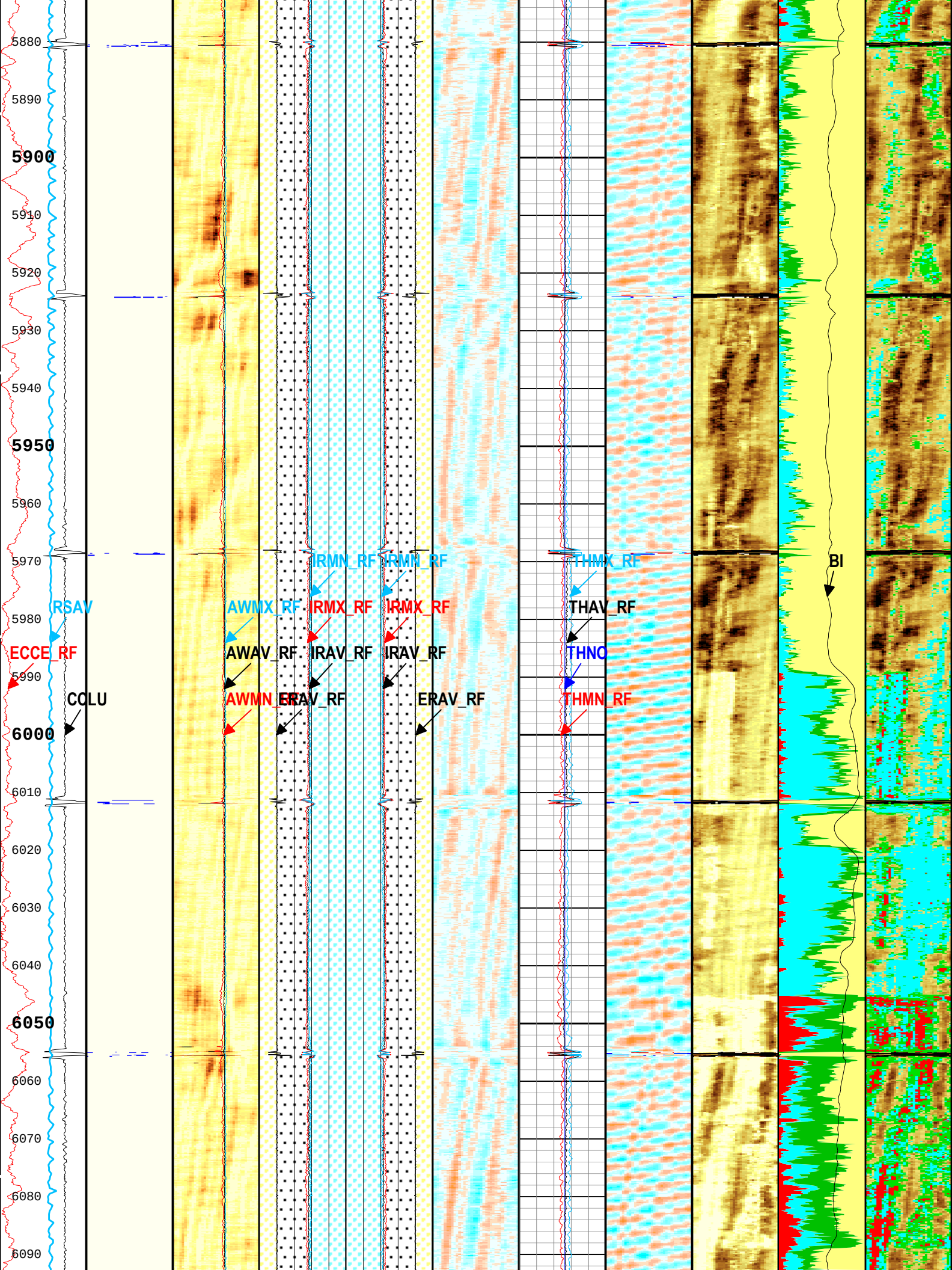
5880
5890
5900
5910
5920
5930
5940
5950
5960
5970
5980
5990
6000
6010
6020
6030
6040
6050
6060
6070
6080
6090
RSAV
ECCE_RF
COLU
AWMX_RF
AWAV_RF
AWMN_RF
IRMN_RF
IRMX_RF
IRAV_RF
ERAV_RF
IRMN_RF
IRMX_RF
IRAV_RF
ERAV_RF
THMX_RF
THAV_RF
THNO
THMN_RF
BI

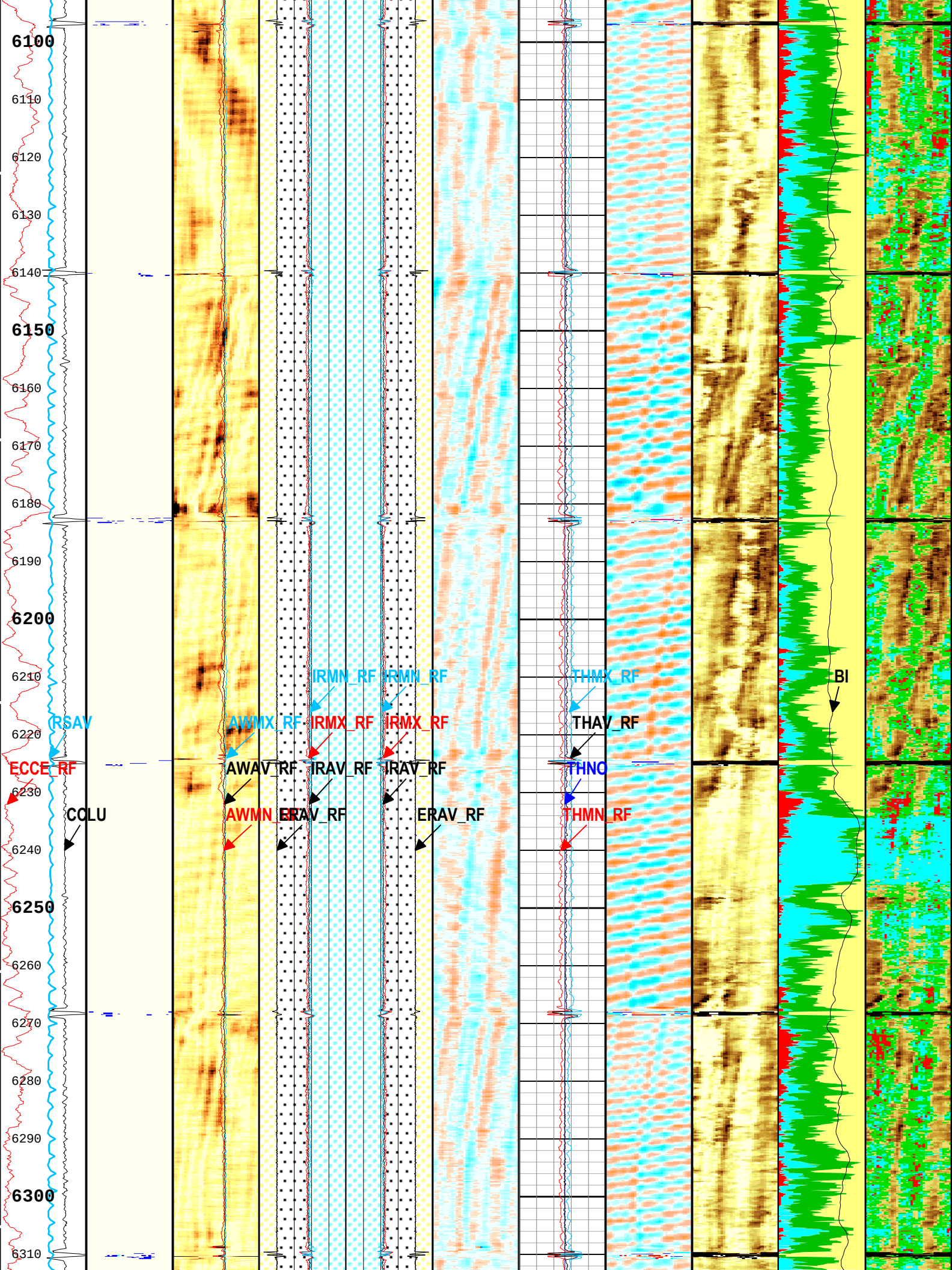
6100
6110
6120
6130
6140
6150
6160
6170
6180
6190
6200
6210
6220
6230
6240
6250
6260
6270
6280
6290
6300
6310
RSAV
ECCE_RF
COLU
AWMX_RF
AWAV_RF
AWMN_RF
IRMN_RF
IRMX_RF
IRAV_RF
ERAV_RF
IRMN_RF
IRMX_RF
IRAV_RF
ERAV_RF
THMX_RF
THAV_RF
THNO
THMN_RF
BI

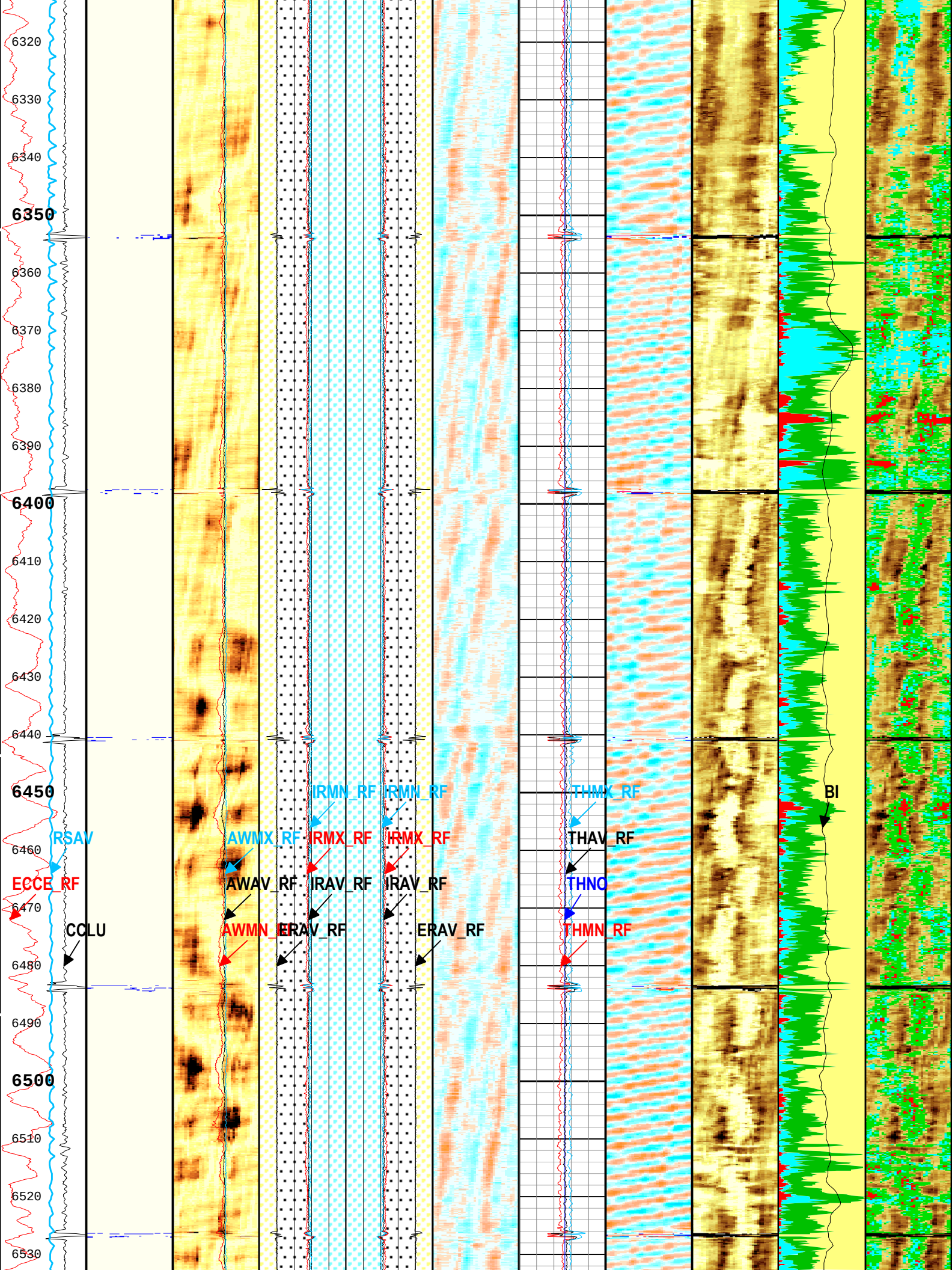
6320
6330
6340
6350
6360
6370
6380
6390
6400
6410
6420
6430
6440
6450
6460
6470
6480
6490
6500
6510
6520
6530
RSAV
ECCE_RF
CCLU
AWMX_RF
AWAV_RF
AWMN_RF
IRMN_RF
IRMX_RF
IRAV_RF
ERAV_RF
IRMN_RF
IRMX_RF
IRAV_RF
ERAV_RF
THMX_RF
THAV_RF
THNO
THMN_RF
BI

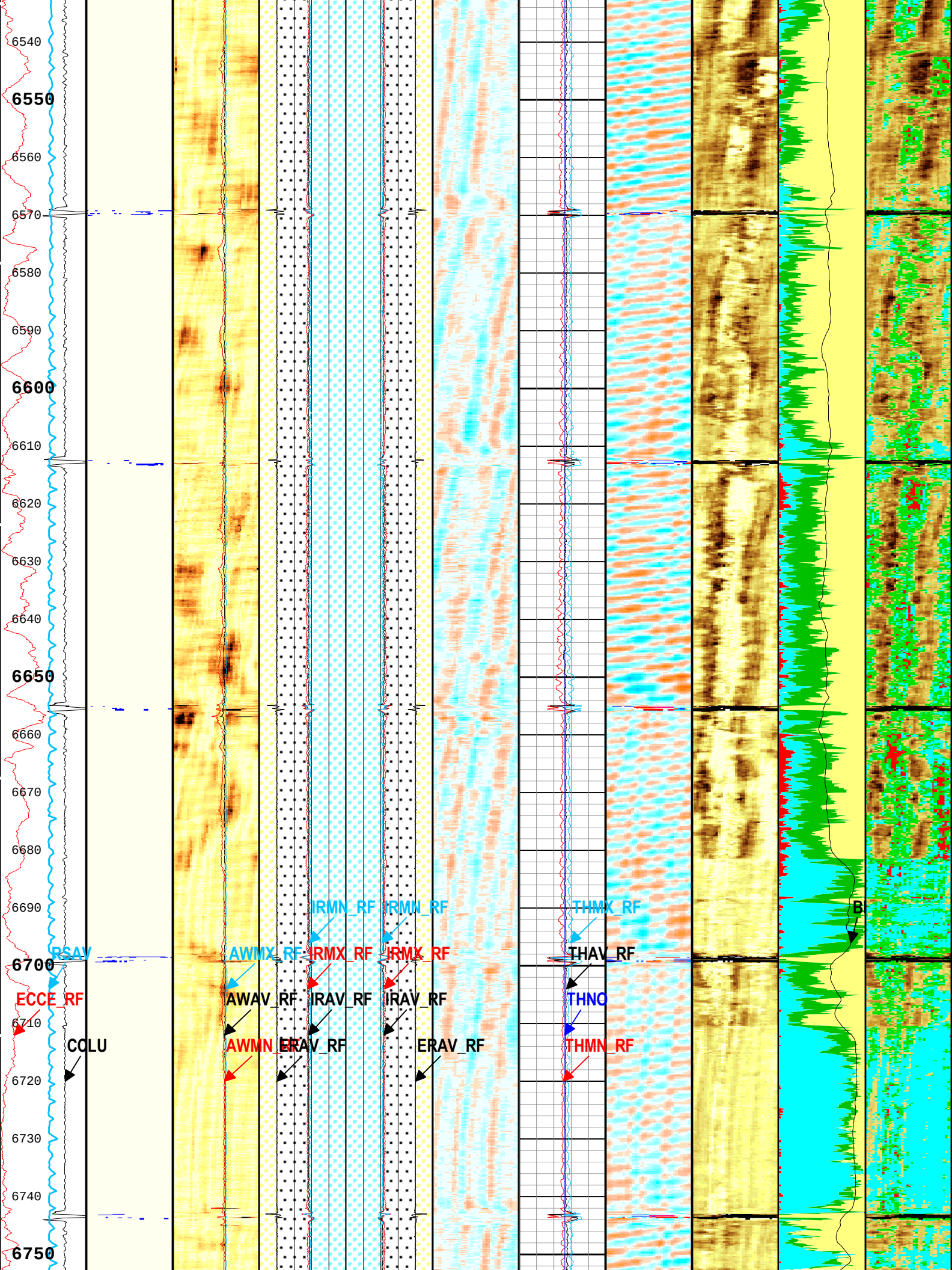
6540
6550
6560
6570
6580
6590
6600
6610
6620
6630
6640
6650
6660
6670
6680
6690
6700
6710
6720
6730
6740
6750
IRMN_RF
IRMN_RF
THMX_RF
B
RSAV
AWMX_RF
IRMX_RF
IRMX_RF
THAV_RF
ECCE_RF
AWAV_RF
IRAV_RF
IRAV_RF
THNO
COLU
AWMN_RF
ERAV_RF
ERAV_RF
THMN_RF

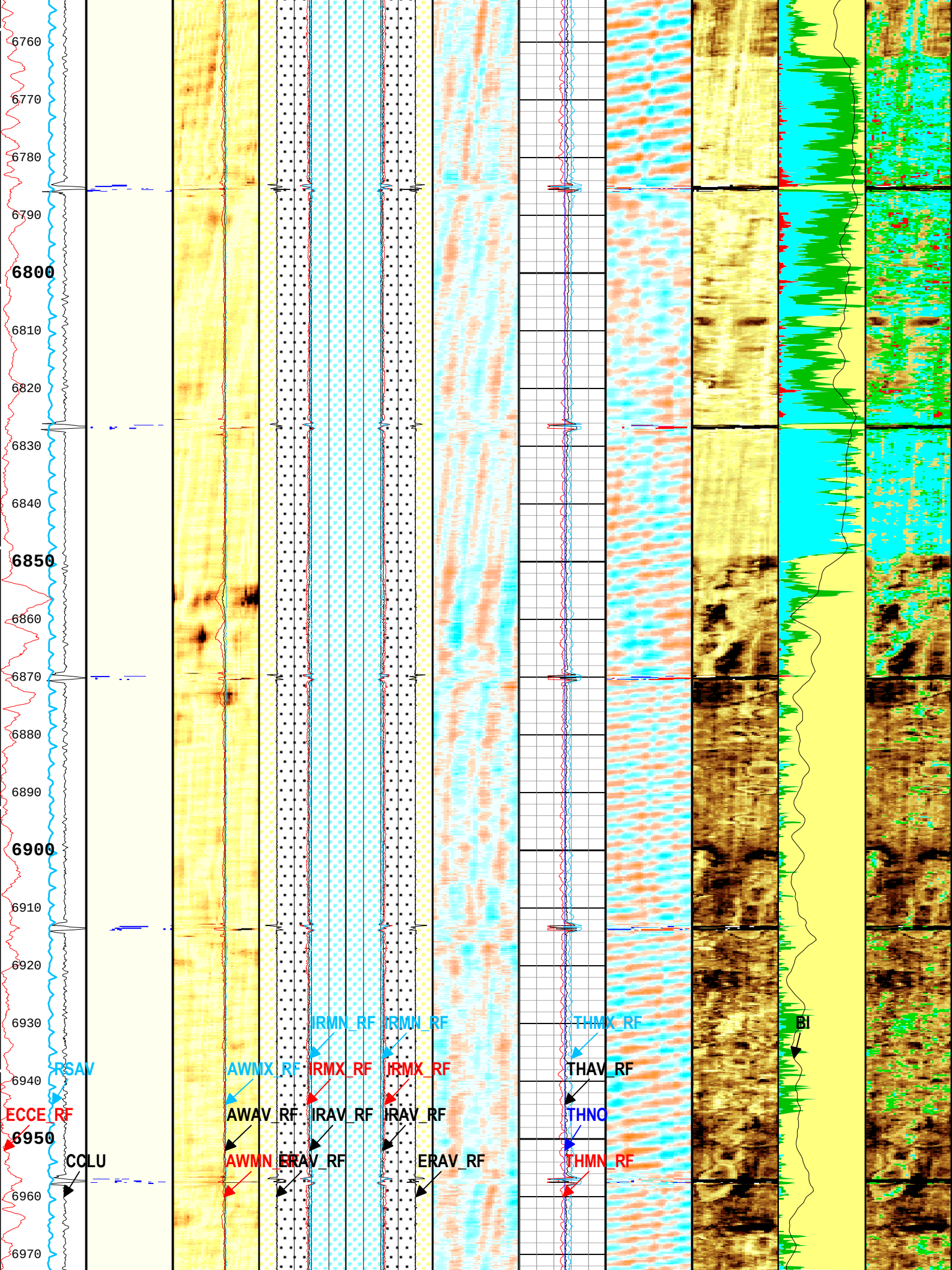
6760
6770
6780
6790
6800
6810
6820
6830
6840
6850
6860
6870
6880
6890
6900
6910
6920
6930
6940
6950
6960
6970
RSAV
ECCE_RF
CCLU
AWMX_RF
AWAV_RF
AWMN
IRMN_RF
IRMX_RF
IRAV_RF
ERAV_RF
IRMN_RF
IRMX_RF
IRAV_RF
ERAV_RF
THMX_RF
THAV_RF
THNO
THMN_RF
BI

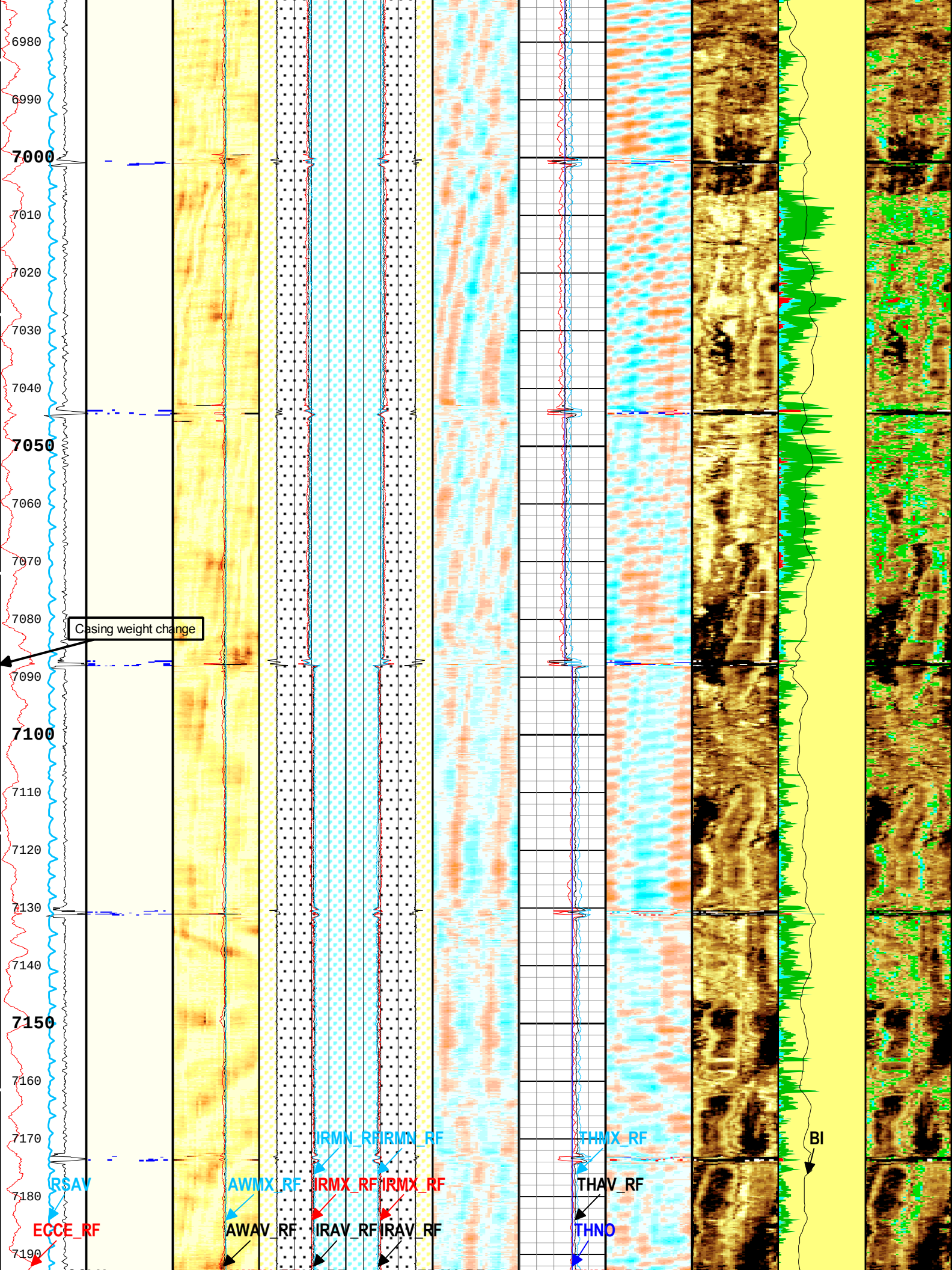
6980
6990
7000
7010
7020
7030
7040
7050
7060
7070
7080
7090
7100
7110
7120
7130
7140
7150
7160
7170
7180
7190
Casing weight change
RSAV
ECCE_RF
AWMX_RF
AWAV_RF
IRMN_RF
IRMX_RF
IRAV_RF
IRMN_RF
IRMX_RF
IRAV_RF
THMX_RF
THAV_RF
THNO
BI

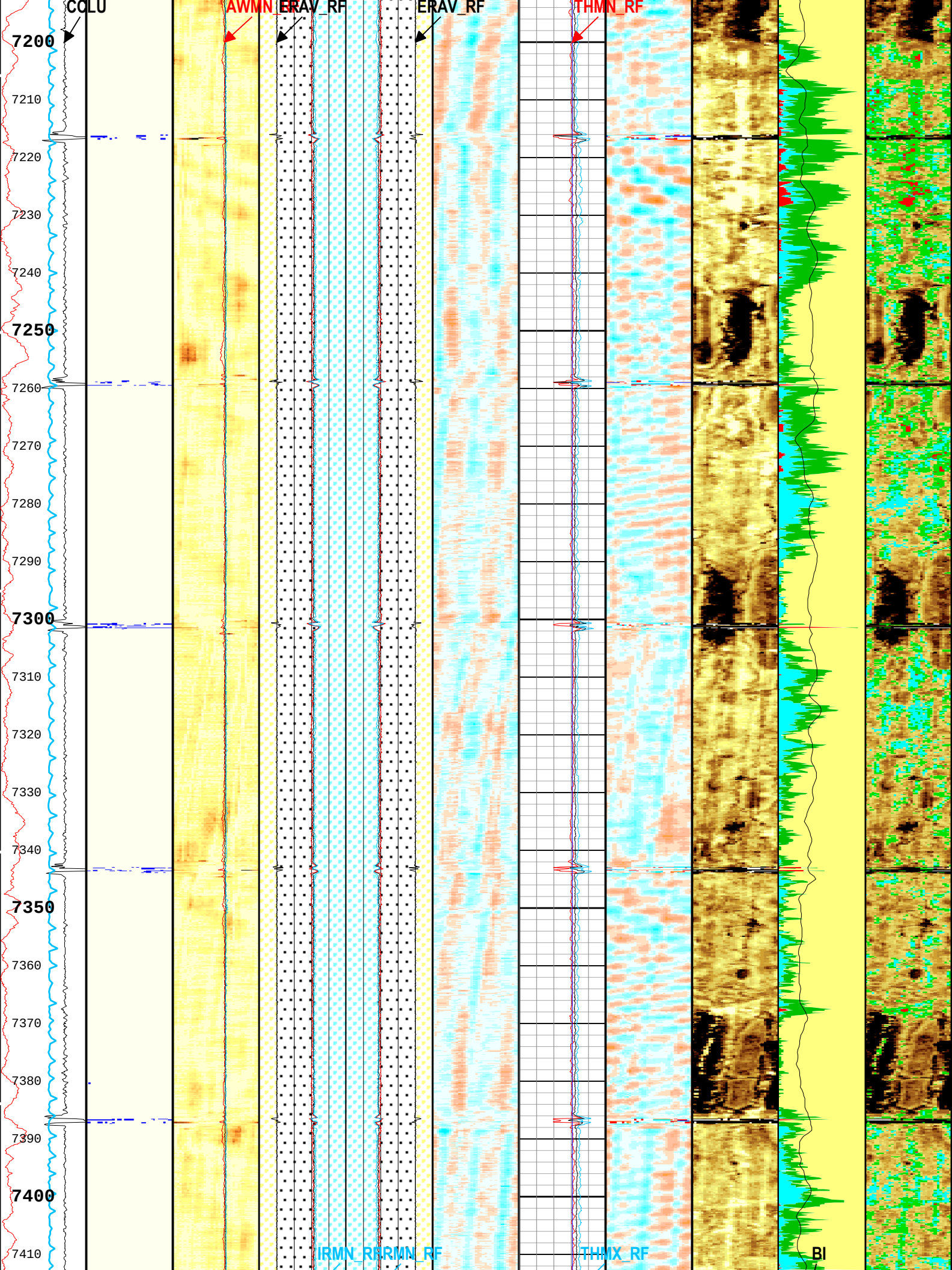
COLU
AWMN_ERAV_RF
ERAV_RF
THMN_RF
7200
7210
7220
7230
7240
7250
7260
7270
7280
7290
7300
7310
7320
7330
7340
7350
7360
7370
7380
7390
7400
7410
IRMN_RF
RMN_RF
THMX_RF
BI

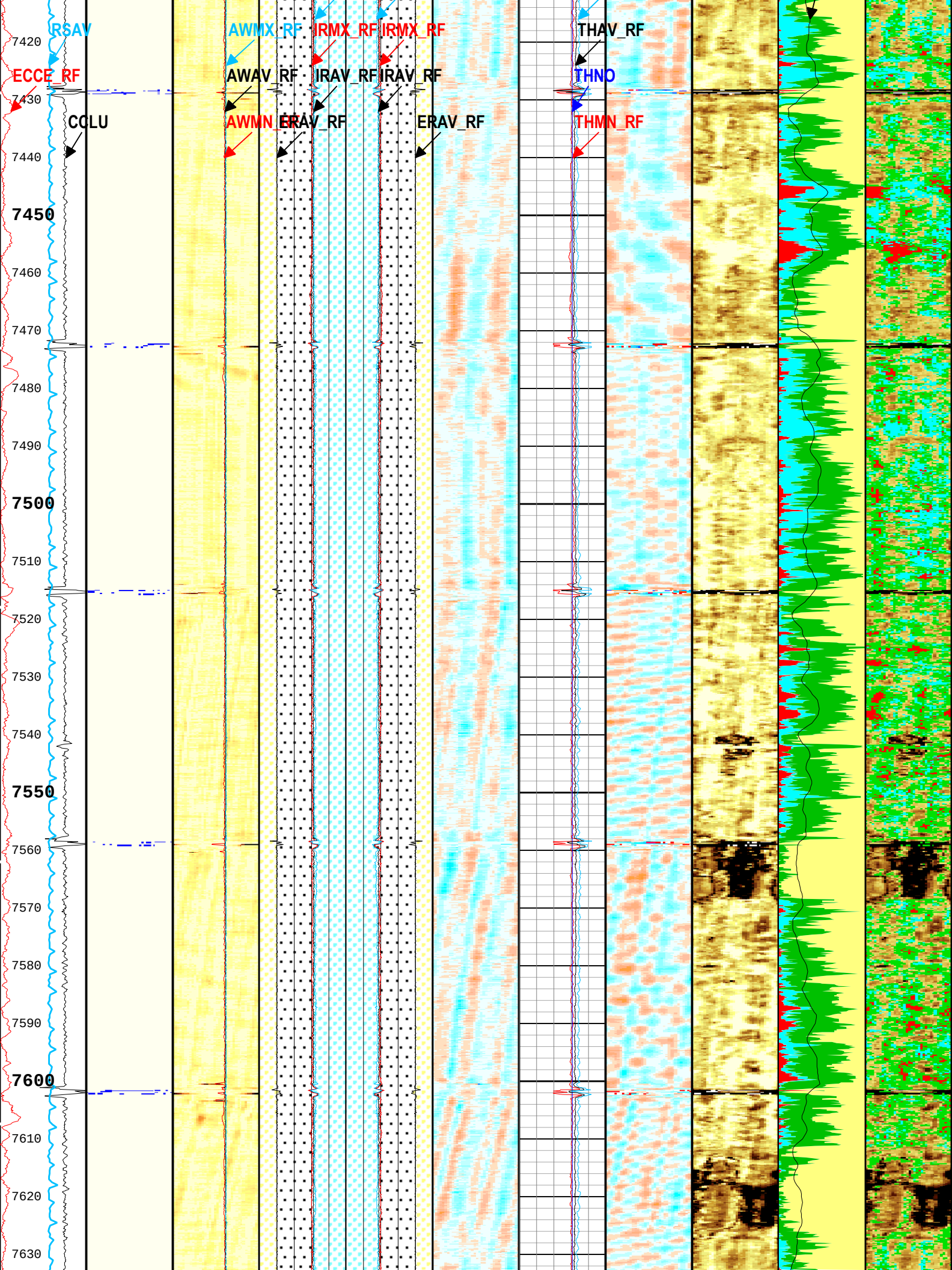
RSAV
ECCE_RF
CCLU
AWMX_RF
AWAV_RF
AWMN_RF
IRMX_RF
IRAV_RF
ERAV_RF
IRMX_RF
IRAV_RF
ERAV_RF
THAV_RF
THNO
THMN_RF
7420
7430
7440
7450
7460
7470
7480
7490
7500
7510
7520
7530
7540
7550
7560
7570
7580
7590
7600
7610
7620
7630

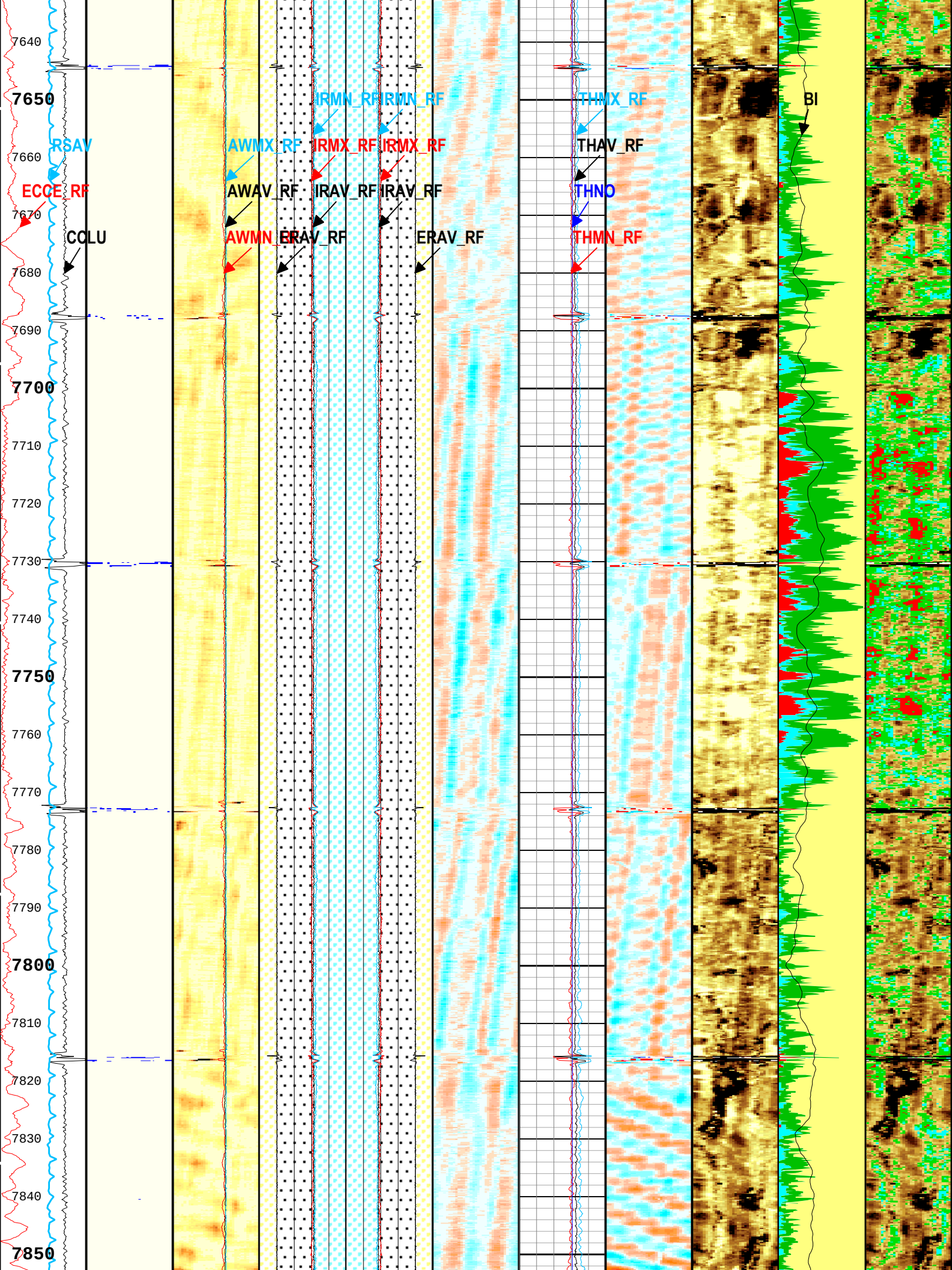
7640
7650
7660
7670
7680
7690
7700
7710
7720
7730
7740
7750
7760
7770
7780
7790
7800
7810
7820
7830
7840
7850
RSAV
ECCE_RF
COLU
AWMX_RF
AWAV_RF
AWMN_RF
IRMN_RF
IRMX_RF
IRAV_RF
ERAV_RF
IRMN_RF
IRMX_RF
IRAV_RF
ERAV_RF
THMX_RF
THAV_RF
THNO
THMN_RF
BI

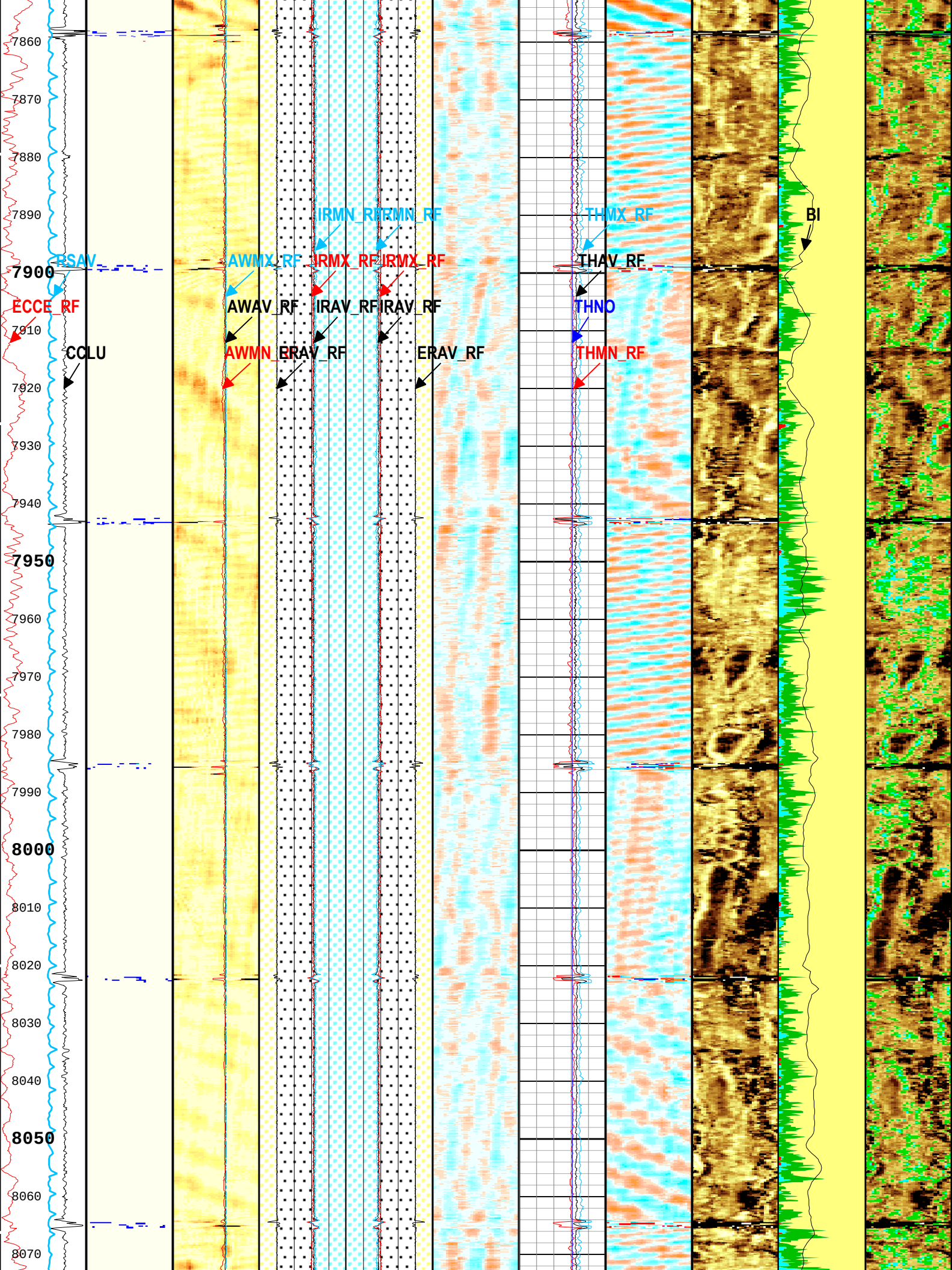
7860
7870
7880
7890
7900
7910
7920
7930
7940
7950
7960
7970
7980
7990
8000
8010
8020
8030
8040
8050
8060
8070
RSAV
ECCE_RF
CCLU
AWMX_RF
AWAV_RF
AWMN_RF
IRMN_RF
IRMX_RF
IRAV_RF
ERAV_RF
THMX_RF
THAV_RF
THNO
THMN_RF
BI

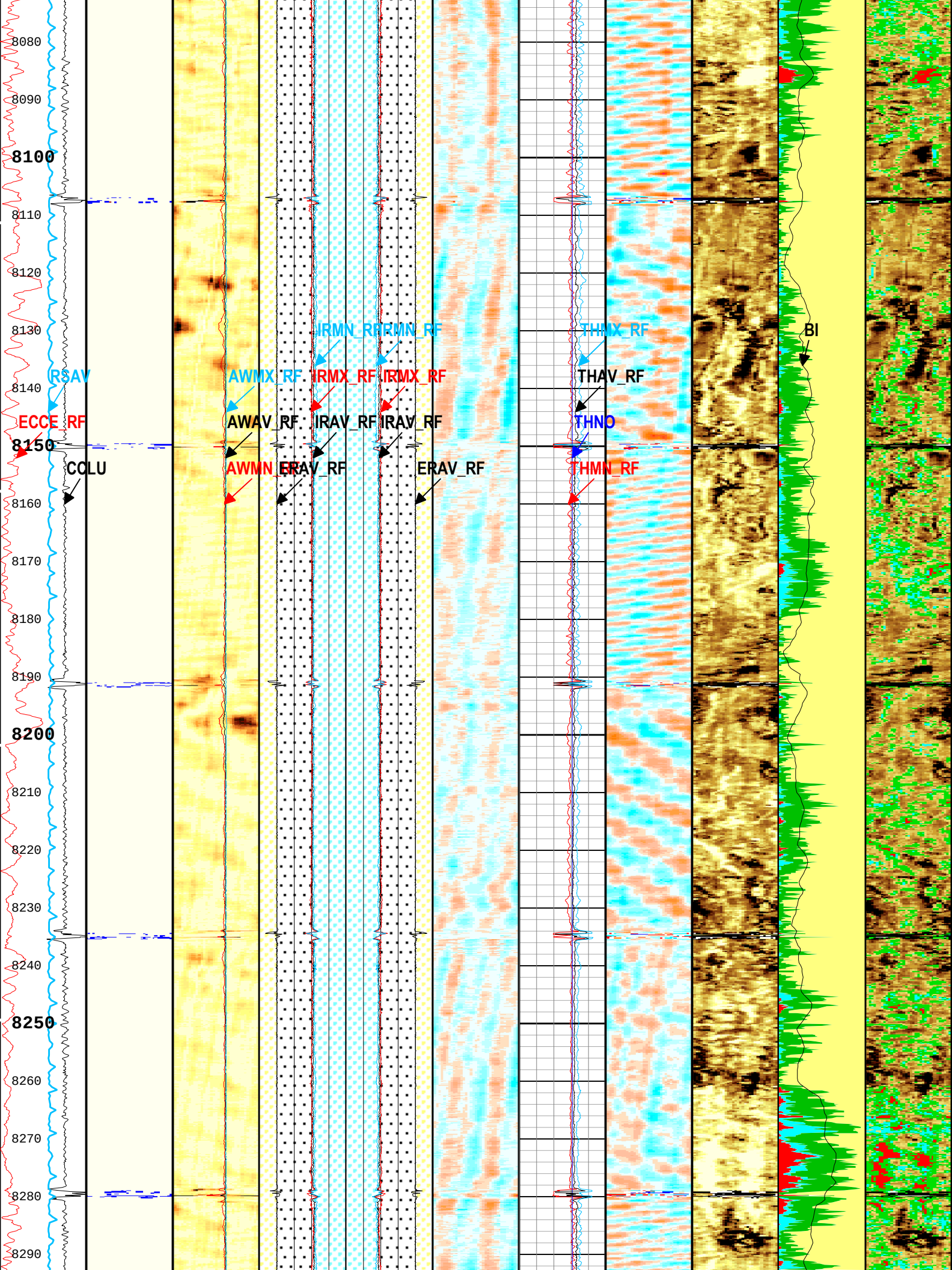
8080
8090
8100
8110
8120
8130
8140
8150
8160
8170
8180
8190
8200
8210
8220
8230
8240
8250
8260
8270
8280
8290
RSAV
ECCE_RF
COLU
AWMX_RF
AWAV_RF
AWMN_RF
IRMN_RF
IRMX_RF
IRAV_RF
ERAV_RF
IRMN_RF
IRMX_RF
IRAV_RF
ERAV_RF
THMX_RF
THAV_RF
THNO
THMN_RF
BI

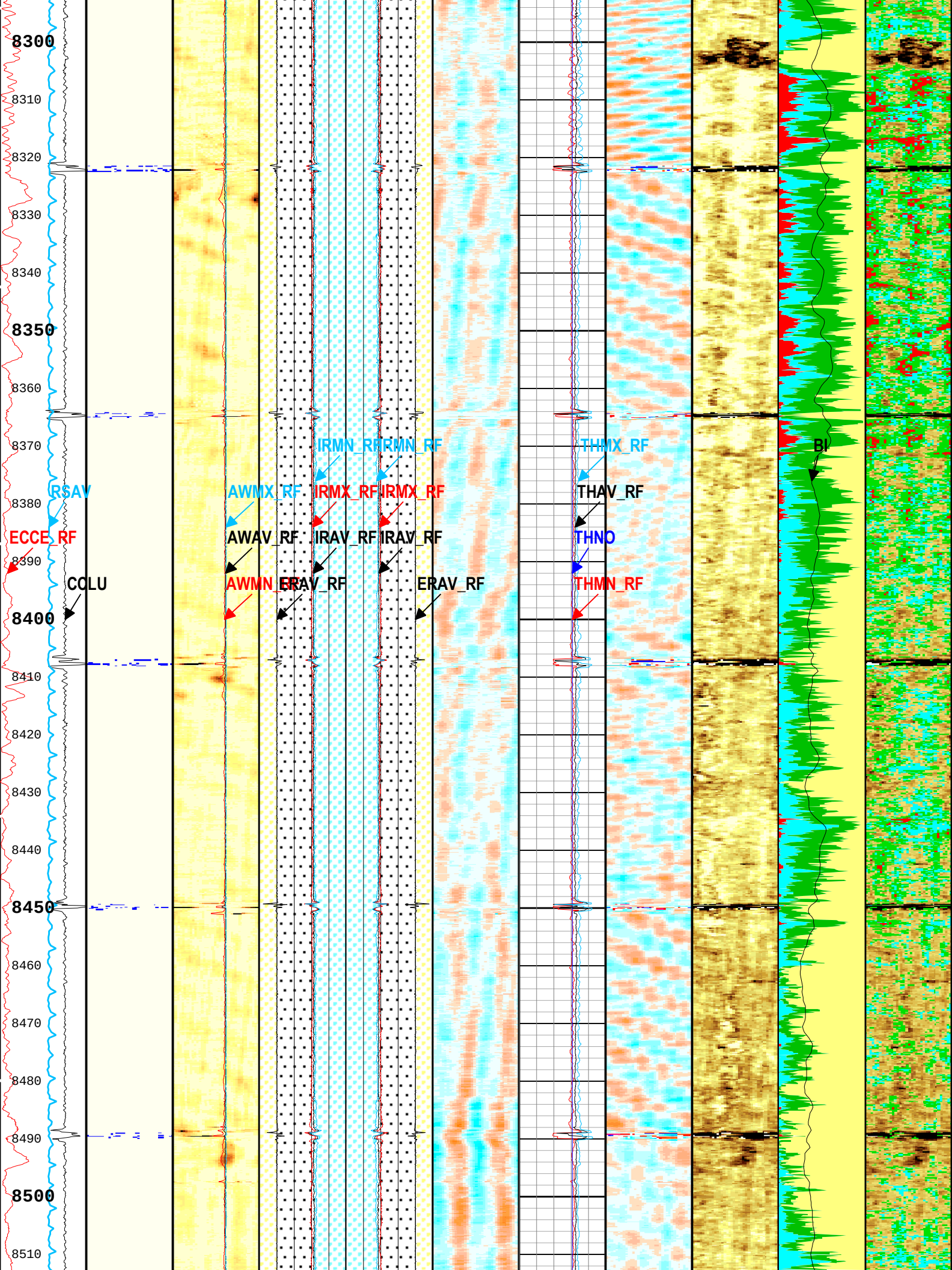
8300
8310
8320
8330
8340
8350
8360
8370
8380
8390
8400
8410
8420
8430
8440
8450
8460
8470
8480
8490
8500
8510
RSAV
ECCE_RF
COLU
AWMX_RF
AWAV_RF
AWMN_RF
IRMN_RF
IRMX_RF
IRAV_RF
ERAV_RF
IRMN_RF
IRMX_RF
IRAV_RF
ERAV_RF
THMX_RF
THAV_RF
THNO
THMN_RF
BI

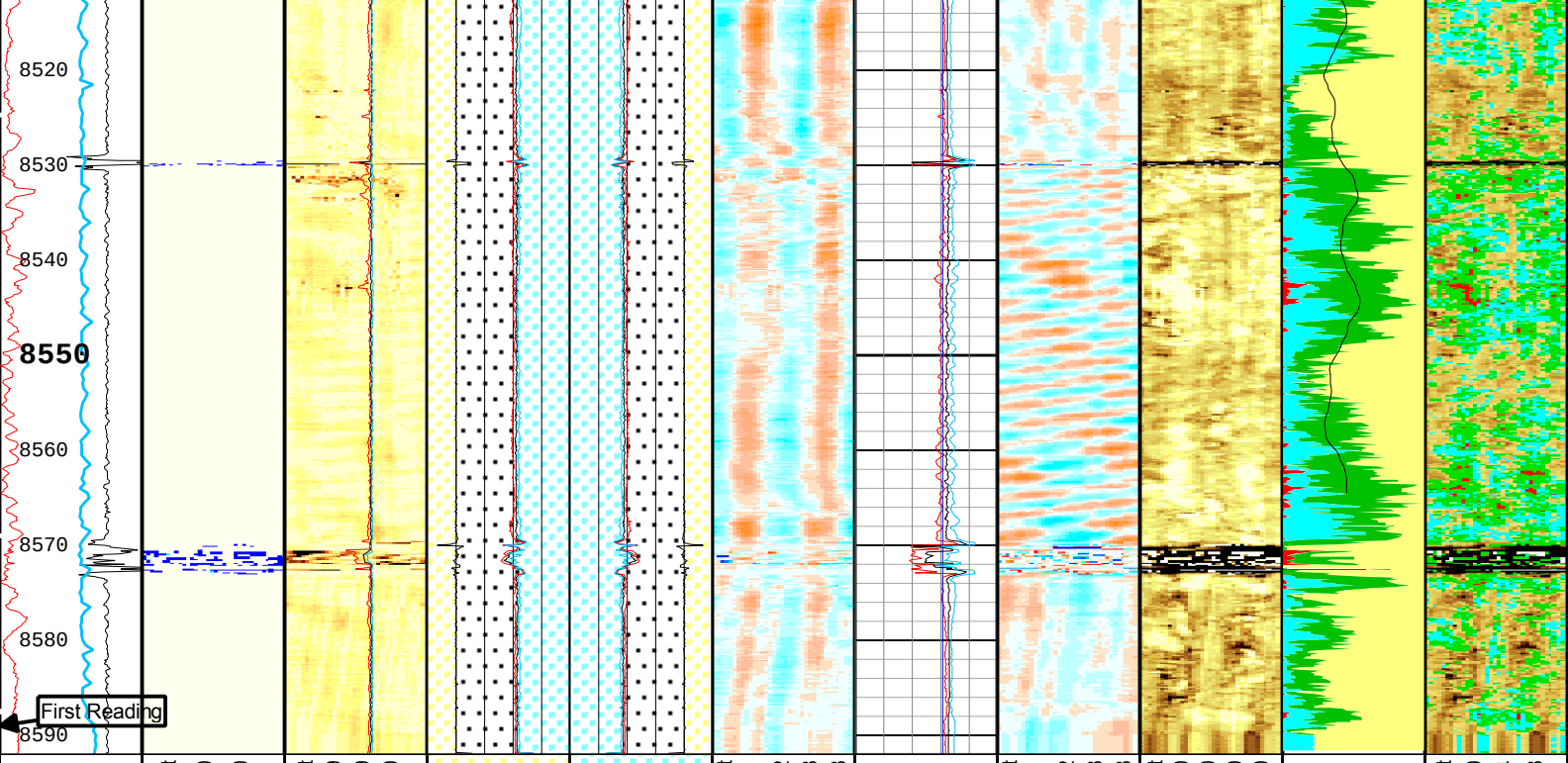

Casing Collar Locator Ultrasonic (CCLU) USIT-E[1]
-30 in 10

Amplitude of Eccentering for Unflagged Waves (ECCE_RF) USIT-E[1]
0 in 0.5

Motor Revolution Speed (RSAV) USIT-E[1]
6 c/s 8

Absent 1.500 3.500
Explicit Normalization
USIT - USIT Processing Flags (UFLG) USIT-E[1]
Orientation: Top of Hole
U L B R U

USIT Processing Flags (UFLG[0]) USIT-E[1]
1 5

Absent -4.799 -2.799 -0.800
Explicit Normalization
USIT - Amplitude of Unflagged Wave (AWBK_RF) USIT-E[1]
(dB)
Orientation: Top of Hole
U L B R U

Minimum of Unflagged Wave Amplitude (AWMN_RF) USIT-E[1]
0 dB 75

Average of Unflagged Wave Amplitude (AWAV_RF) USIT-E[1]
0 dB 75

Maximum of Unflagged Wave Amplitude (AWMX_RF) USIT-E[1]
0 dB 75

ERAV
ERAV-IRAV
IRAV

Median of Unflagged External Radii (ERAV_RF) USIT-E[1]
3.7 in 2.7

Median Internal Radius of Casing Corrected for Eccentering (IRAV_RF) USIT-E[1]
3.7 in 2.7

Maximum of Unflagged Internal Radii (IRMX_RF) USIT-E[1]
3.7 in 2.7

Minimum of Unflagged Internal Radii (IRMN_RF) USIT-E[1]
3.7 in 2.7

IRAV
ERAV
IRAV-ERAV

Median of Unflagged External Radii (ERAV_RF) USIT-E[1]
2.7 in 3.7

Median Internal Radius of Casing Corrected for Eccentering (IRAV_RF) USIT-E[1]
2.7 in 3.7

Maximum of Unflagged Internal Radii (IRMX_RF) USIT-E[1]
2.7 in 3.7

Minimum of Unflagged Internal Radii (IRMN_RF) USIT-E[1]
2.7 in 3.7

Absent -0.051 -0.012 0.028 0.068
Explicit Normalization
USIT - Unflagged Internal Radii minus Median Internal Radius (IRBKM_RF) USIT-E[1]
(in)
Orientation: Top of Hole
U L B R U

Minimum of Unflagged Casing Thickness (THMN_RF) USIT-E[1]
0.1 in 0.6

Nominal Casing Thickness (THNO) USIT-E[1]
0.1 in 0.6

Median of Unflagged Casing Thickness (THAV_RF) USIT-E[1]
0.1 in 0.6

Maximum of Unflagged Casing Thickness (THMX_RF) USIT-E[1]
0.1 in 0.6

Absent -0.051 -0.012 0.028 0.068
Explicit Normalization
USIT - Unflagged Casing Thickness minus Median of Unflagged Casing Thickness (THBKM_RF) USIT-E[1]
(in)
Orientation: Top of Hole
U L B R U

Absent 1.500 3.500 5.500 7.500
Custom Normalization
USIT - Acoustic Impedance (AIBK) USIT-E[1]
(Mrayl)
Orientation: Top of Hole
U L B R U

Ratio of Cement Measurements to Total (CEMR) USIT-E[1]
1 0

Micro-debonding Ratio (MDR) USIT-E[1]
1 0

Ratio of Gas Measurements to Total (GASR) USIT-E[1]
1 0

Bonded
Gas
Liquid
Micro-debonding

Bond Index (BI) DSLT-H[1]
1 0

Absent 3.090 5.054 7.018
Custom Normalization
USIT - Acoustic Impedance (AIBK) USIT-E[1]
(Mrayl)
Orientation: Top of Hole
U L B R U

Absent 2.599 4.563 6.527
Custom Normalization
USIT - Acoustic Impedance With Micro-debonding Image (AI_MDEBOND_IMG) USIT-E[1]
(Mrayl)
Orientation: Top of Hole
U L B R U

USIT Processing Flags (UFLG[0]) USIT-E[1]

1 - UFLG 1 Value within [0.0 - 1.5] - :	UTIM Error
2 - UFLG 2 Value within [1.5 - 2.5] - :	Pulse Origin Not Detected
3 - UFLG 3 Value within [2.5 - 3.5] - :	WINLEN Error
4 - UFLG 4 UFLG 5 UFLG 6 Value within [3.5 - 6.5] - :	Casing Thickness Error
5 - UFLG 7 UFLG 8 UFLG 9 Value within [6.5 - 10] - :	Loop Processing Error

TIME_1900 - Time Marked every 60.00 (s)

Description: USI Composite Format: Log (LBV1_USI Composite 7inch) Index Scale: 5 in per 100 ft Index Unit: ft Index Type: Measured Depth Creation Date: 07-Sep-2018 22:55:55

Composite 1

Cement Log 2 IN = 100 FT

Composite Summary

Run Name	Pass Objective	Direction	Top	Bottom	Start	Stop	DSC Mode	Depth Shift	Include Parallel Data
One	Log[6]:Up	Up	93.36 ft	8592.71 ft	07-Sep-2018 9:51:23 AM	07-Sep-2018 1:52:30 PM	ON	8.00 ft	No
One	Log[9]:Up	Up	11.43 ft	318.32 ft	07-Sep-2018 2:46:40 PM	07-Sep-2018 3:00:05 PM	ON	9.00 ft	No

All depths are referenced to toolstring zero

Log

Company:Southern California Gas Company Well:Standard Sesnon 9

Composite 1:S003

Description: USI Cement Format: Log (LBV1_USI Cement 7inch) Index Scale: 2 in per 100 ft Index Unit: ft Index Type: Measured Depth Creation Date: 07-Sep-2018 22:56:20

TIME_1900 - Time Marked every 60.00 (s)

ERAV_IRAV | ERAV_RHF1

IRAV_LHF1 | IRAV_ERAV

LHF1_ERAV | RHF1_IRAV

Median of Unflagged External Radii (ERAV_RF) USIT-E[1]
3.7 in 2.7

Median of Unflagged External Radii (ERAV_RF) USIT-E[1]
2.7 in 3.7

Median Internal Radius of Casing Corrected for Eccentering (IRAV_RF) USIT-E[1]
3.7 in 2.7

Median Internal Radius of Casing Corrected for Eccentering (IRAV_RF) USIT-E[1]
2.7 in 3.7

Minimum of Unflagged Internal Radii (IRMN_RF) USIT-E[1]
3.7 in 2.7

Minimum of Unflagged Internal Radii (IRMN_RF) USIT-E[1]
2.7 in 3.7

Maximum of Unflagged Internal Radii (IRMX_RF) USIT-E[1]

Maximum of Unflagged Internal Radii (IRMX_RF) USIT-E[1]

Casing Collar Locator Ultrasonic (CCLU) USIT-E[1]
-30 in 10

Gamma Ray (ECGR) HGNS[1]
0 gAPI 150

Amplitude of Eccentering for Unflagged Waves (ECCE_RF) USIT-E[1]

U L B R U
Orientation: Top of Hole
Absent 0.500 1.500 2.500 3.500 4.500 5.500 6.500 7.500
Custom Normalization
USIT - Acoustic Impedance With

Acoustic Impedance Minimum (AIMN) USIT-E[1]
-1 Mrayl 9

Acoustic Impedance Average (AIAV) USIT-E[1]
-1 Mrayl 9

Acoustic Impedance Maximum (AIMX)

Bonded

Gas

Liquid

U L B R U
Orientation: Top of Hole
Absent -500.000 2.599 3.581 4.563 5.545 6.527 7.509
Custom Normalization
USIT - Acoustic Impedance With Micro-debonding Image

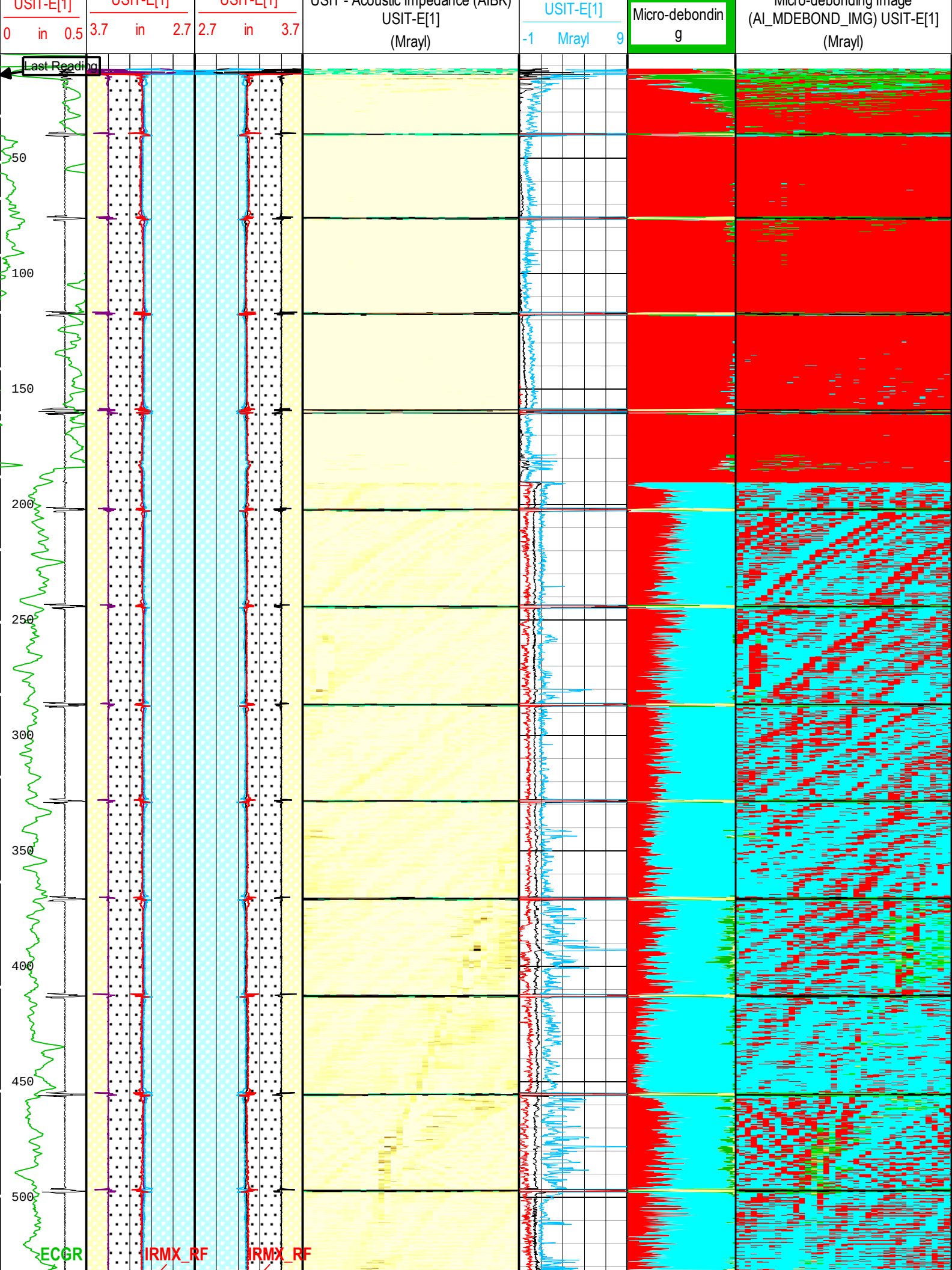
USIT-E[1]
0 in 0.5
USIT-E[1]
3.7 in 2.7
USIT-E[1]
2.7 in 3.7
USIT - Acoustic Impedance (AIBK) USIT-E[1] (Mrayl)
USIT-E[1]
-1 Mrayl 9
Micro-debonding
Micro-debonding Image (AI_MDEBOND_IMG) USIT-E[1] (Mrayl)
Last Reading
50
100
150
200
250
300
350
400
450
500
ECGR
IRMX_RF
IRMX_RF

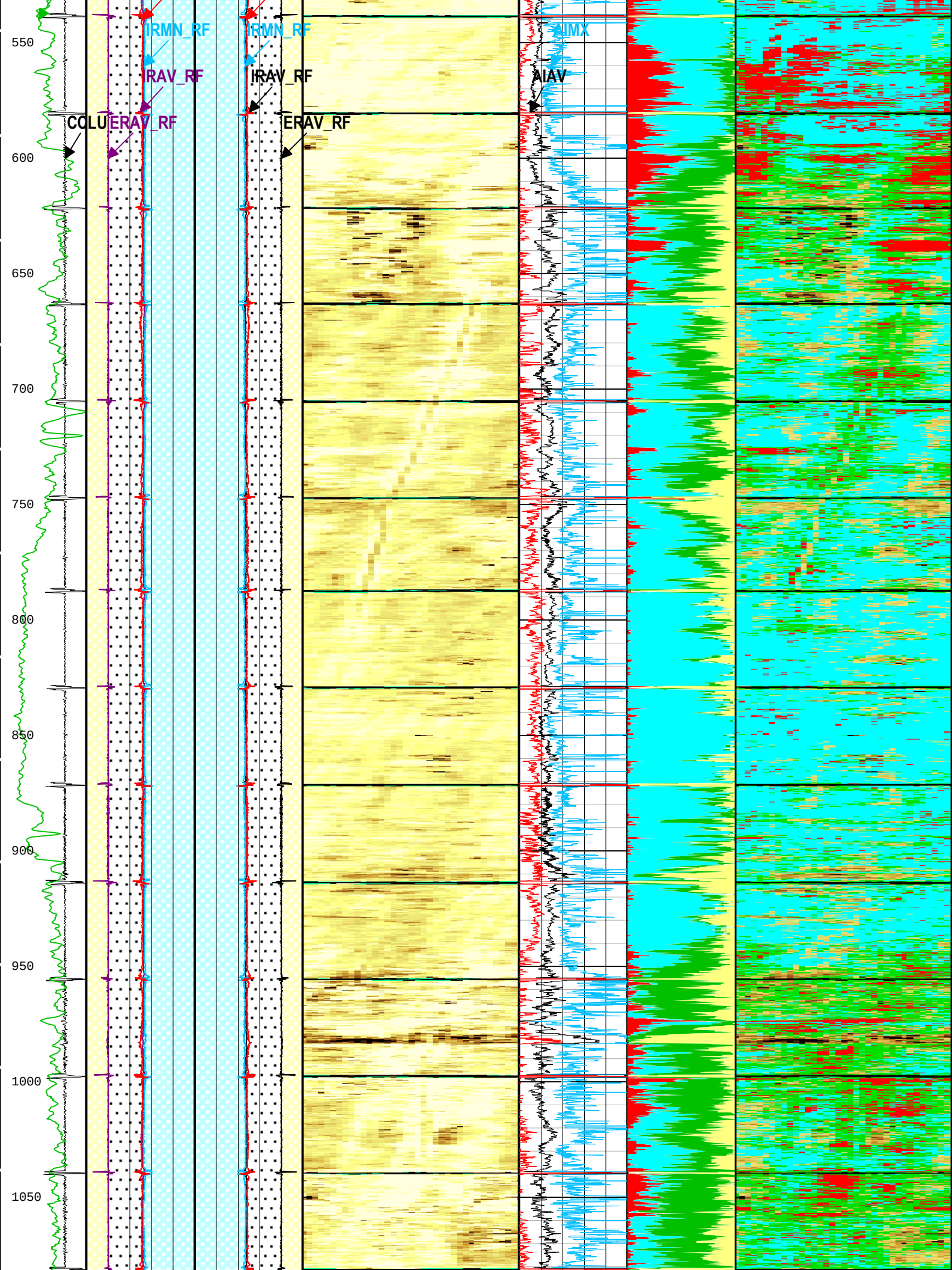
IRMN_RF
IRMN_RF
AIMX
IRAV_RF
IRAV_RF
AIAV
COLU
ERAV_RF
ERAV_RF
550
600
650
700
750
800
850
900
950
1000
1050

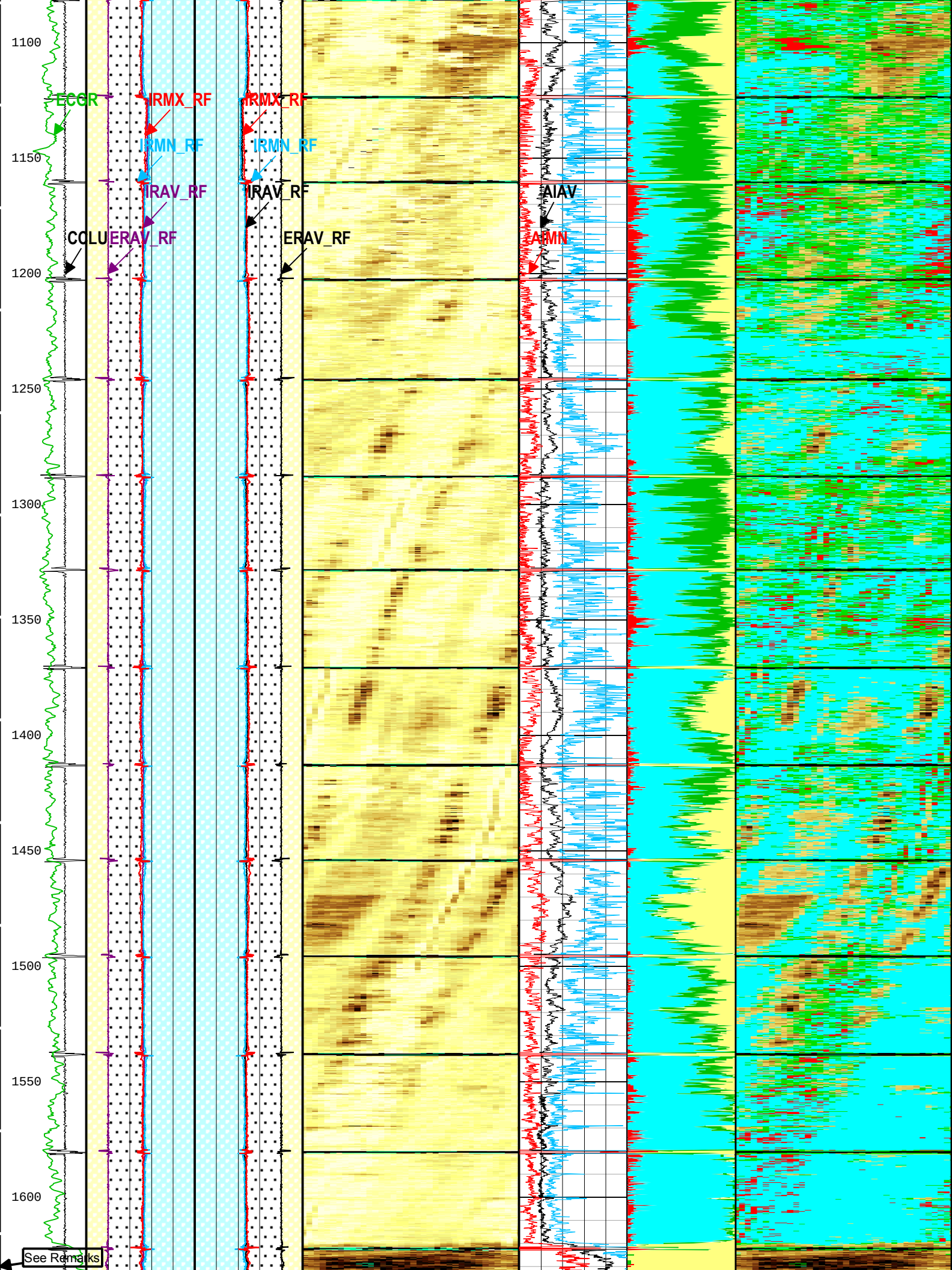
1100
1150
1200
1250
1300
1350
1400
1450
1500
1550
1600
ECGR
IRMX_RF
IRMN_RF
IRAV_RF
COLU
ERAV_RF
IRMX_RF
IRMN_RF
IRAV_RF
ERAV_RF
AIAV
AIMN
See Remarks

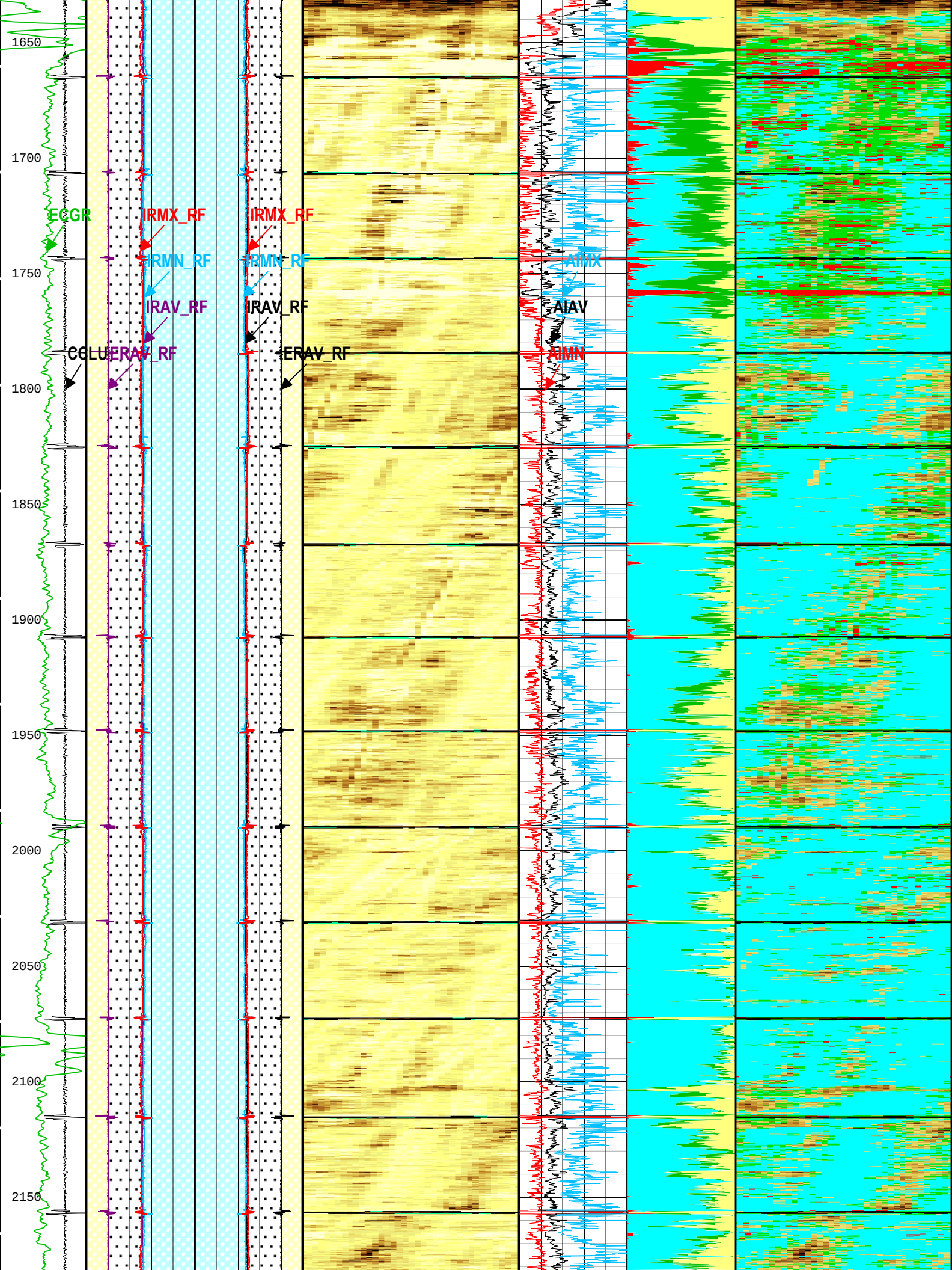
1650
1700
1750
1800
1850
1900
1950
2000
2050
2100
2150
ECGR
IRMX_RF
IRMN_RF
IRAV_RF
CCLU
ERAV_RF
IRMX_RF
IRMN_RF
IRAV_RF
ERAV_RF
AIMX
AIAV
AIMN

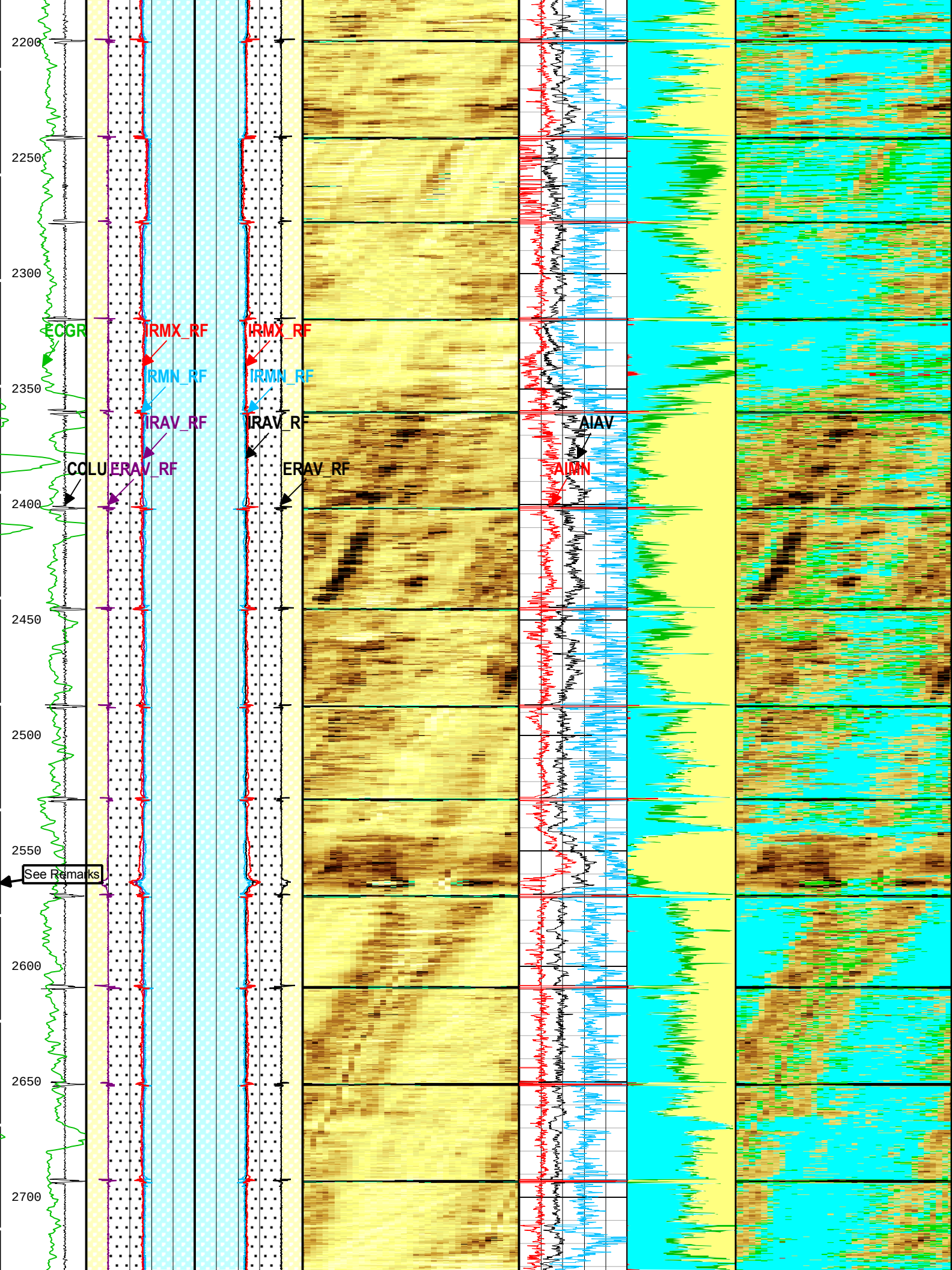
2200
2250
2300
2350
2400
2450
2500
2550
2600
2650
2700
ECGR
IRMX_RF
IRMN_RF
IRAV_RF
COLU
ERAV_RF
IRMX_RF
IRMN_RF
IRAV_RF
ERAV_RF
AIAV
AIMN
See Remarks

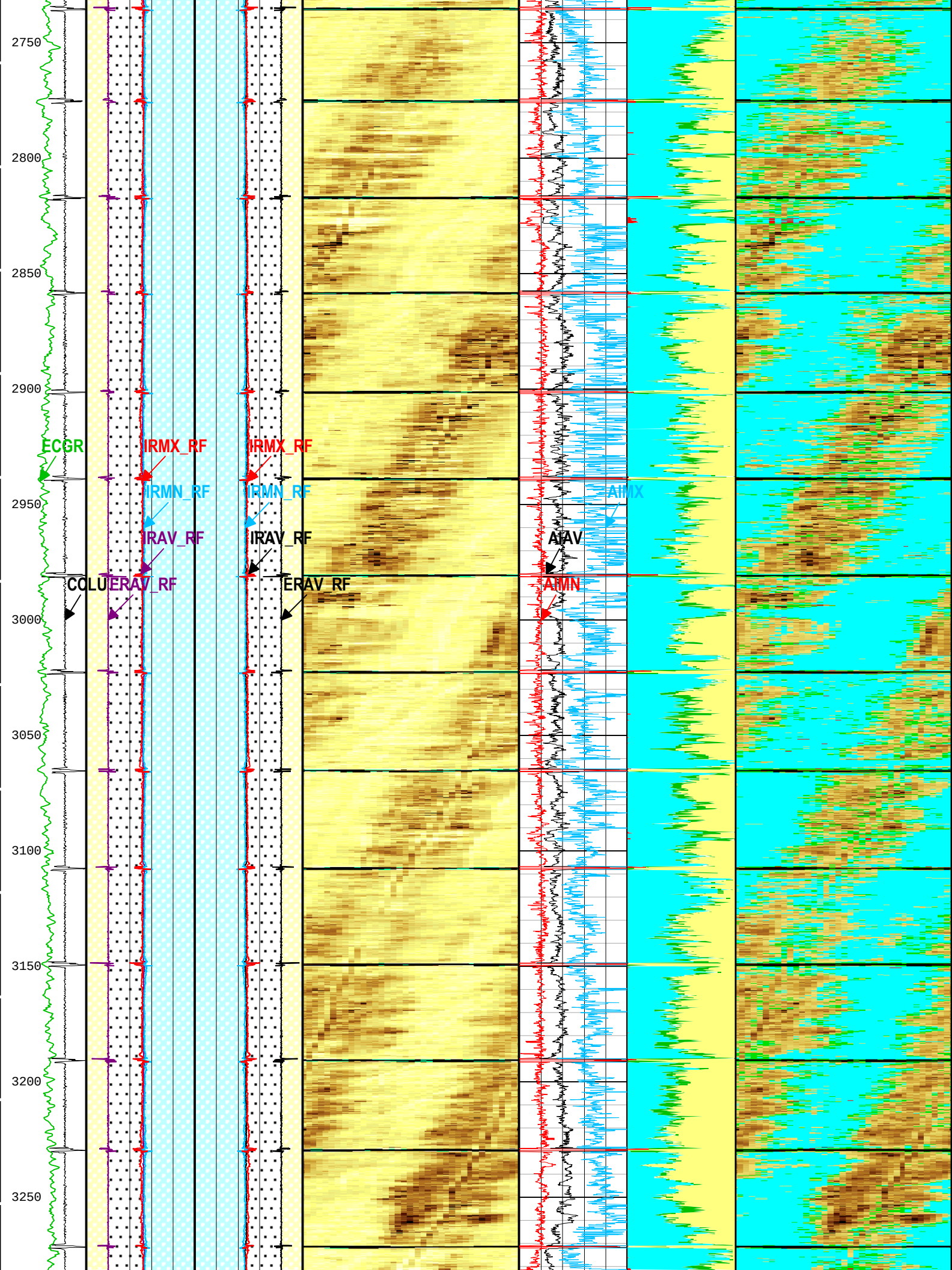
2750
2800
2850
2900
2950
3000
3050
3100
3150
3200
3250
ECGR
IRMX_RF
IRMN_RF
IRAV_RF
COLU
ERAV_RF
IRMX_RF
IRMN_RF
IRAV_RF
ERAV_RF
AIMX
AIAV
AIMN

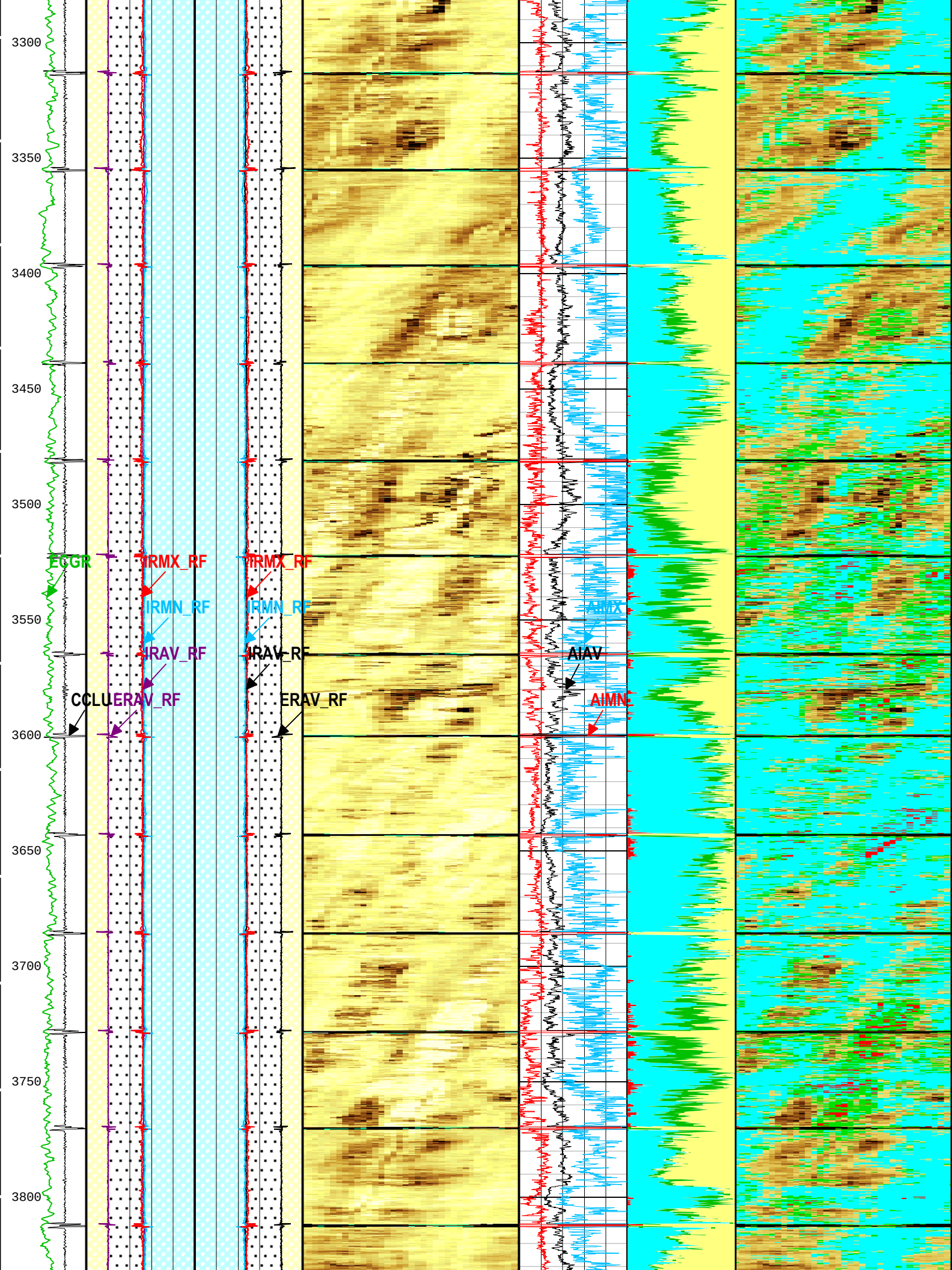
3300
3350
3400
3450
3500
3550
3600
3650
3700
3750
3800
ECGR
IRMX_RF
IRMN_RF
IRAV_RF
CCLU
ERAV_RF
IRMX_RF
IRMN_RF
IRAV_RF
ERAV_RF
AIMX
AIAV
AIMN

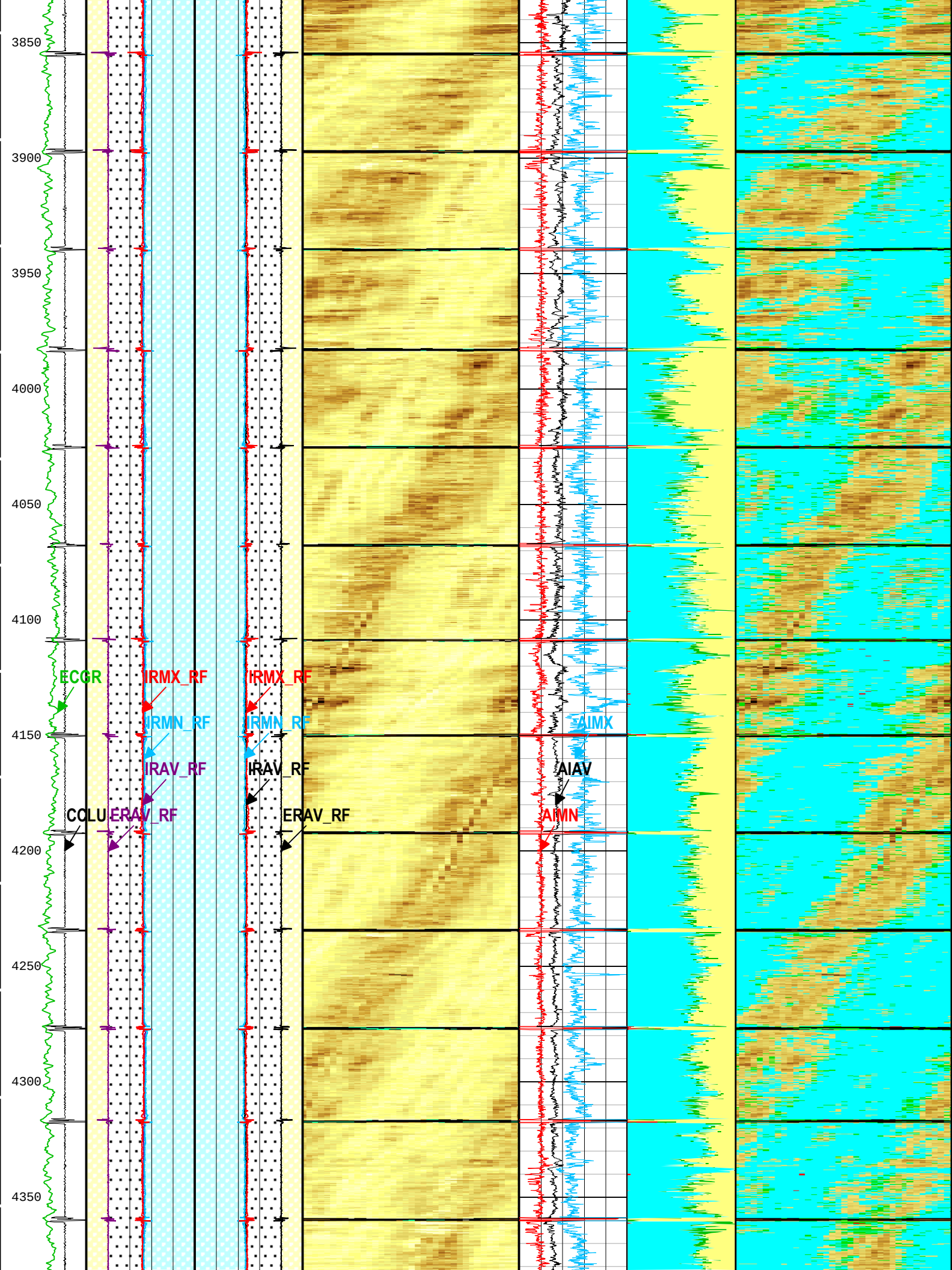
3850
3900
3950
4000
4050
4100
4150
4200
4250
4300
4350
ECGR
IRMX_RF
IRMN_RF
IRAV_RF
COLU
ERAV_RF
IRMX_RF
IRMN_RF
IRAV_RF
ERAV_RF
AIMX
AIAV
AIMN

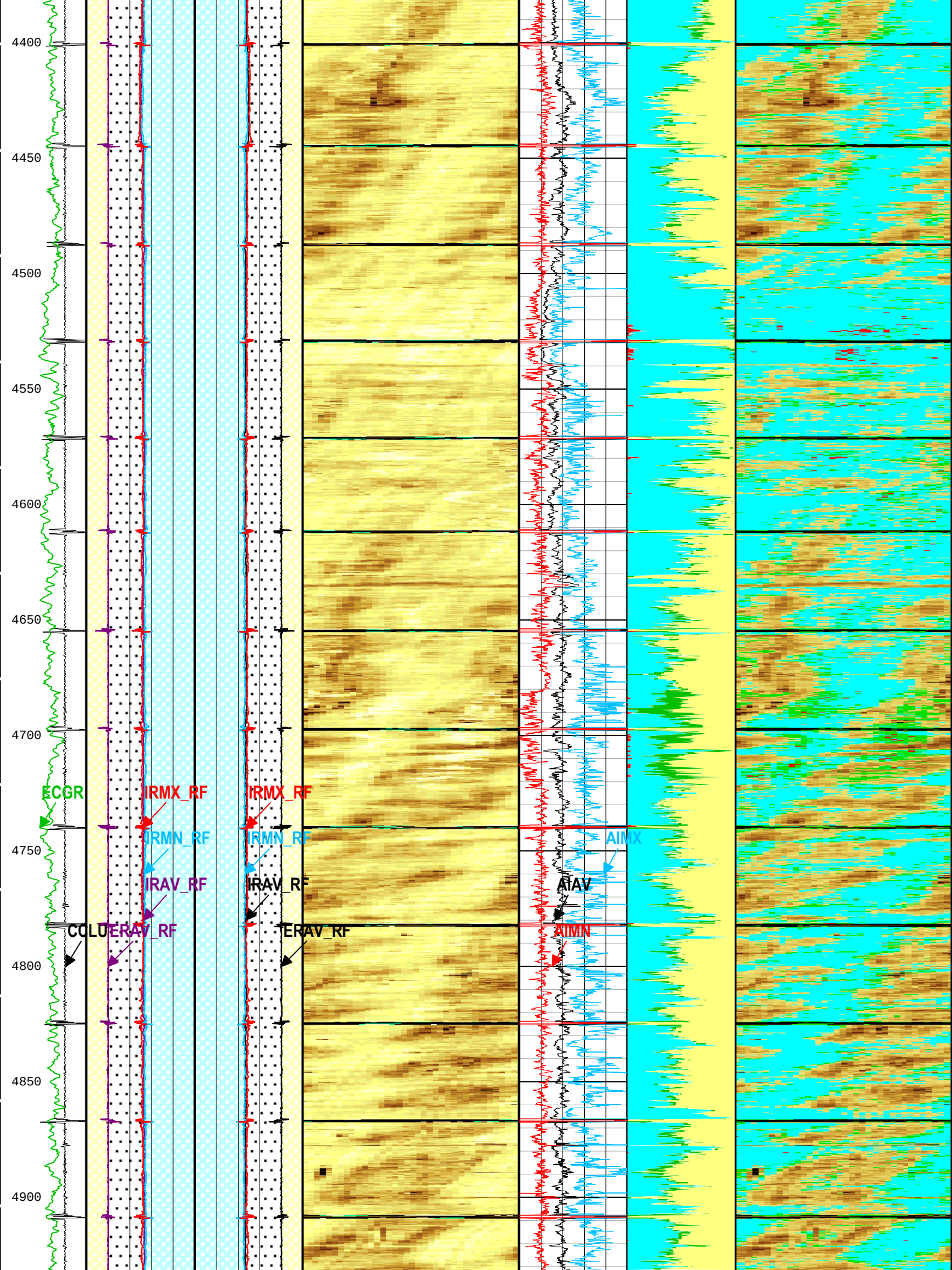
4400
4450
4500
4550
4600
4650
4700
4750
4800
4850
4900
ECGR
IRMX_RF
IRMN_RF
IRAV_RF
COLU
ERAV_RF
IRMX_RF
IRMN_RF
IRAV_RF
ERAV_RF
AIMX
AIAV
AIMN

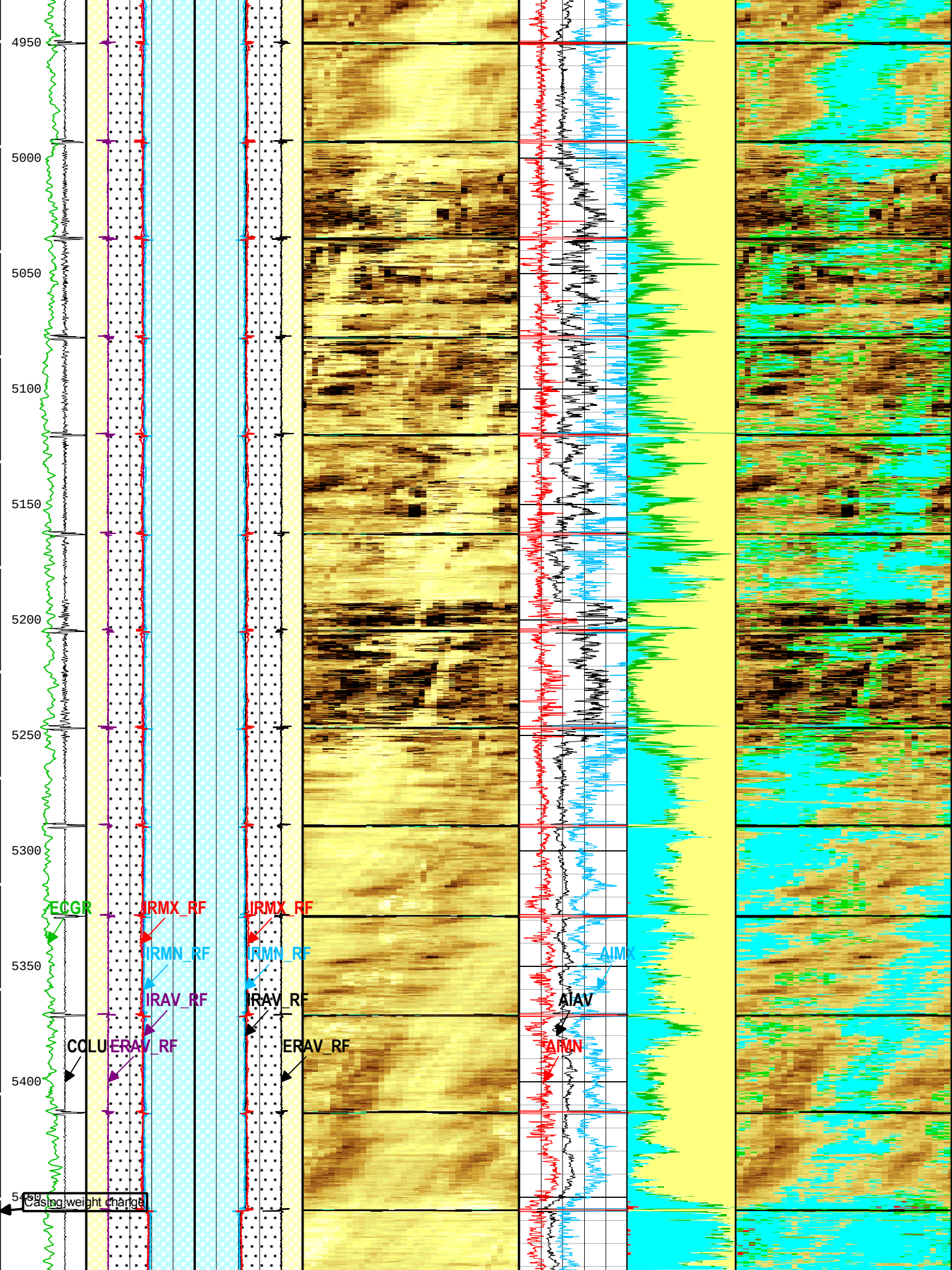
4950
5000
5050
5100
5150
5200
5250
5300
5350
5400
5450
ECGR
IRMX_RF
IRMN_RF
IRAV_RF
COLU
ERAV_RF
IRMX_RF
IRMN_RF
IRAV_RF
ERAV_RF
AIMX
AIAV
ARMN
Casing weight change

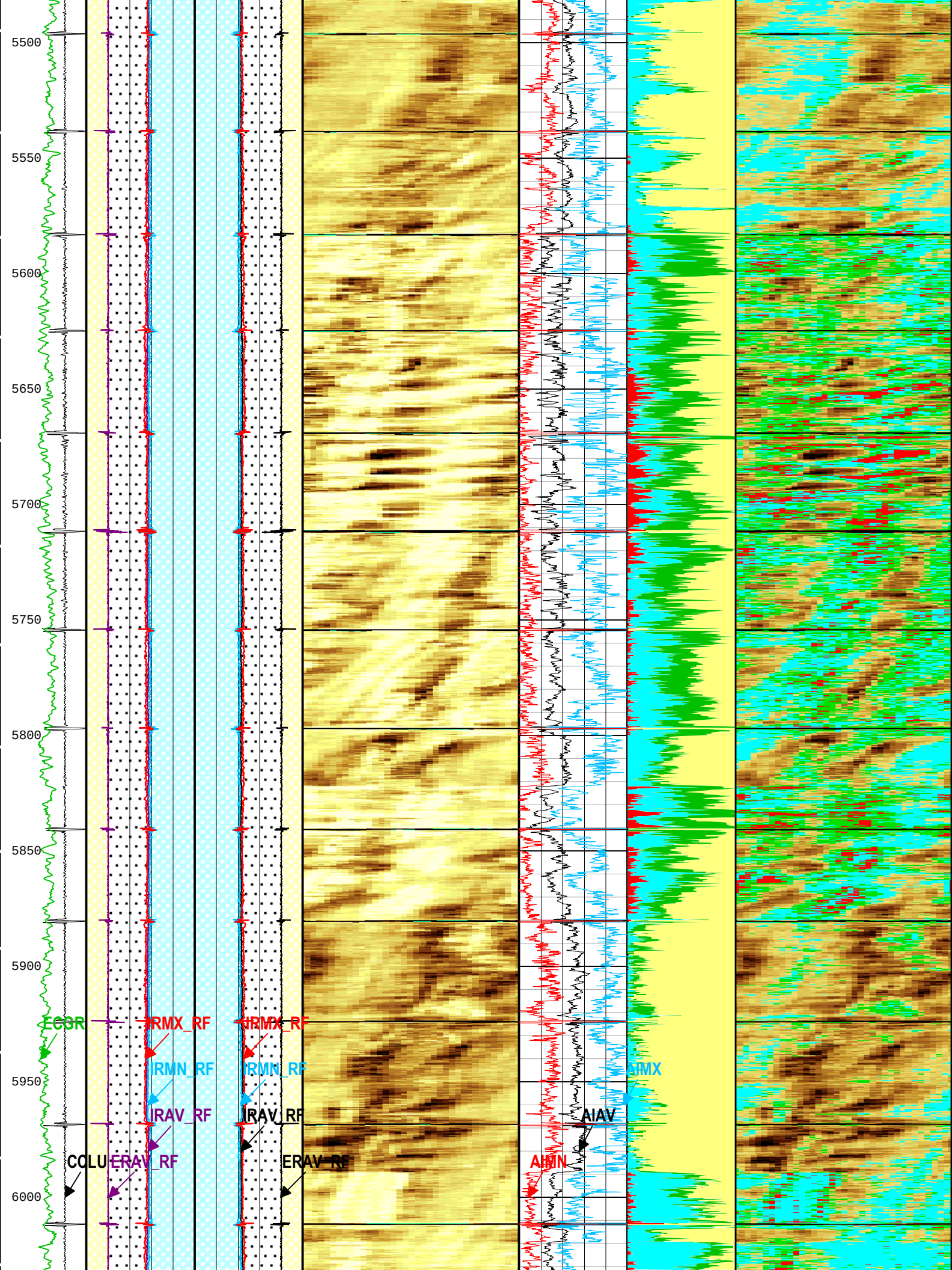
5500
5550
5600
5650
5700
5750
5800
5850
5900
5950
6000
ECGR
IRMX_RF
IRMX_RF
IRMN_RF
IRMN_RF
IRAV_RF
IRAV_RF
COLU
ERAV_RF
ERAV_RF
AIMX
AIAV
AIMN

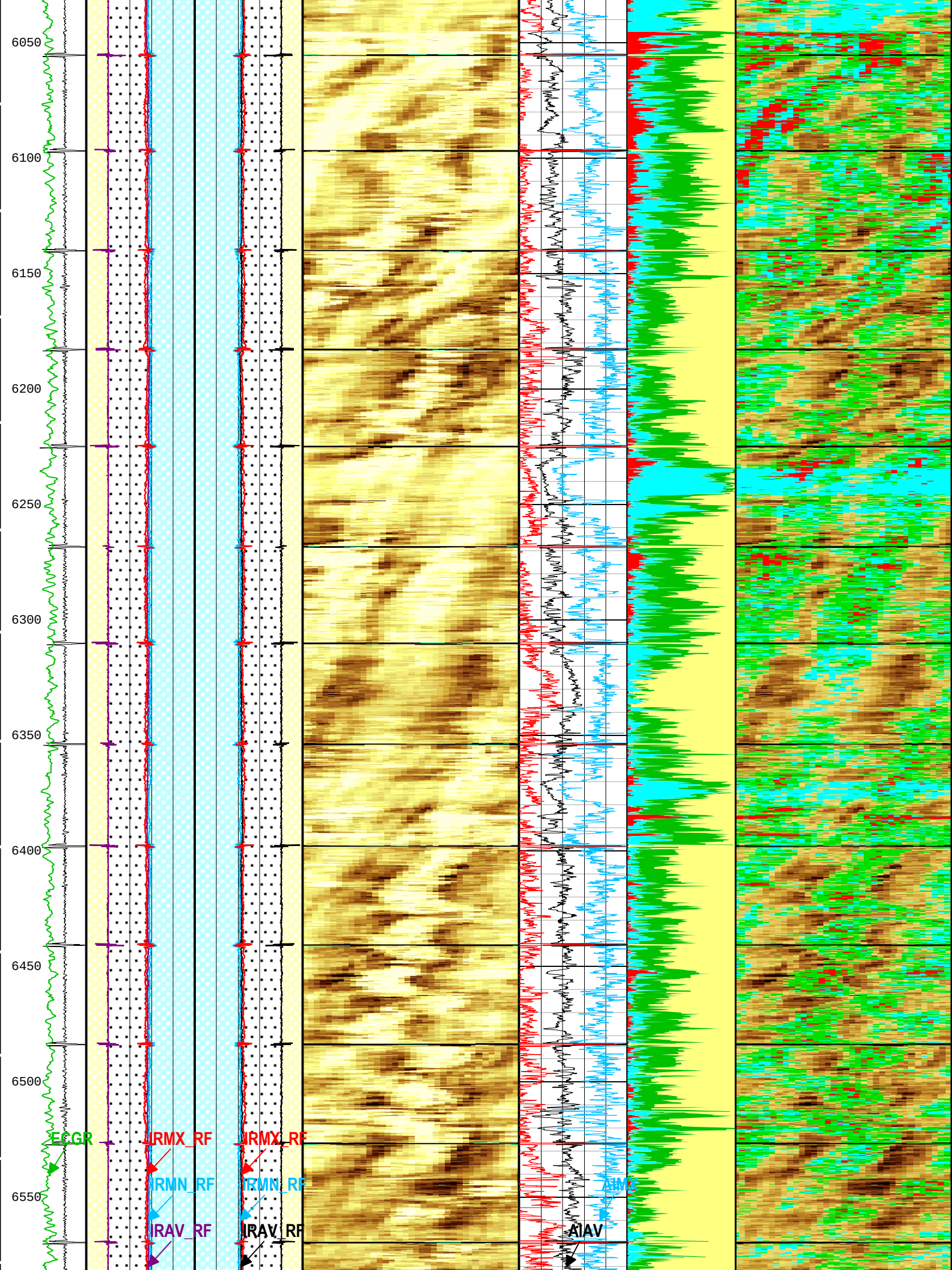
6050
6100
6150
6200
6250
6300
6350
6400
6450
6500
6550
ECGR
IRMX_RF
IRMX_RF
IRMN_RF
IRMN_RF
IRAV_RF
IRAV_RF
AIAV

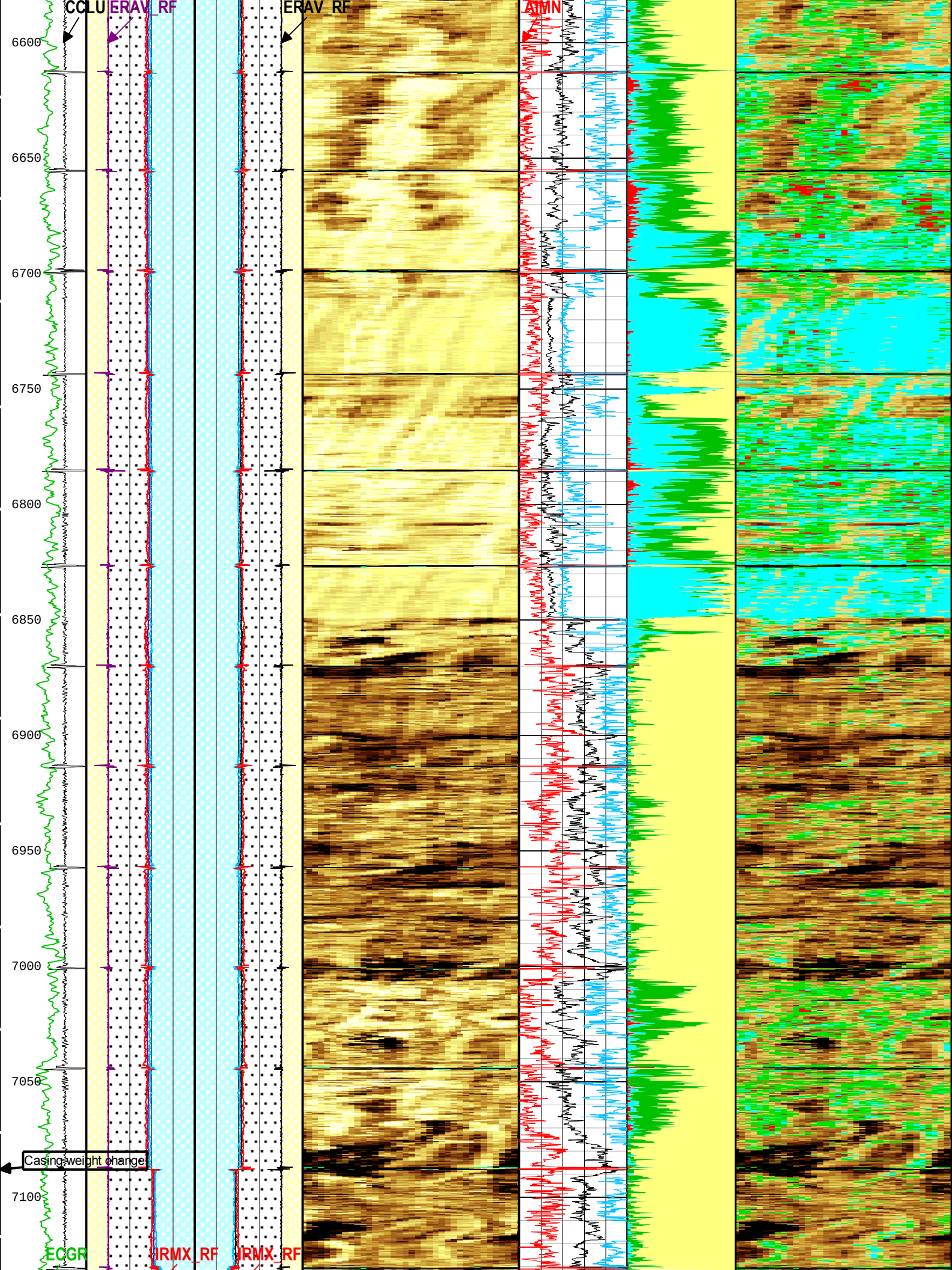
CCLU
ERAV_RF
ERAV_RF
AMN
6600
6650
6700
6750
6800
6850
6900
6950
7000
7050
Casing weight change
7100
ECGR
HRMX_RF
HRMX_RF

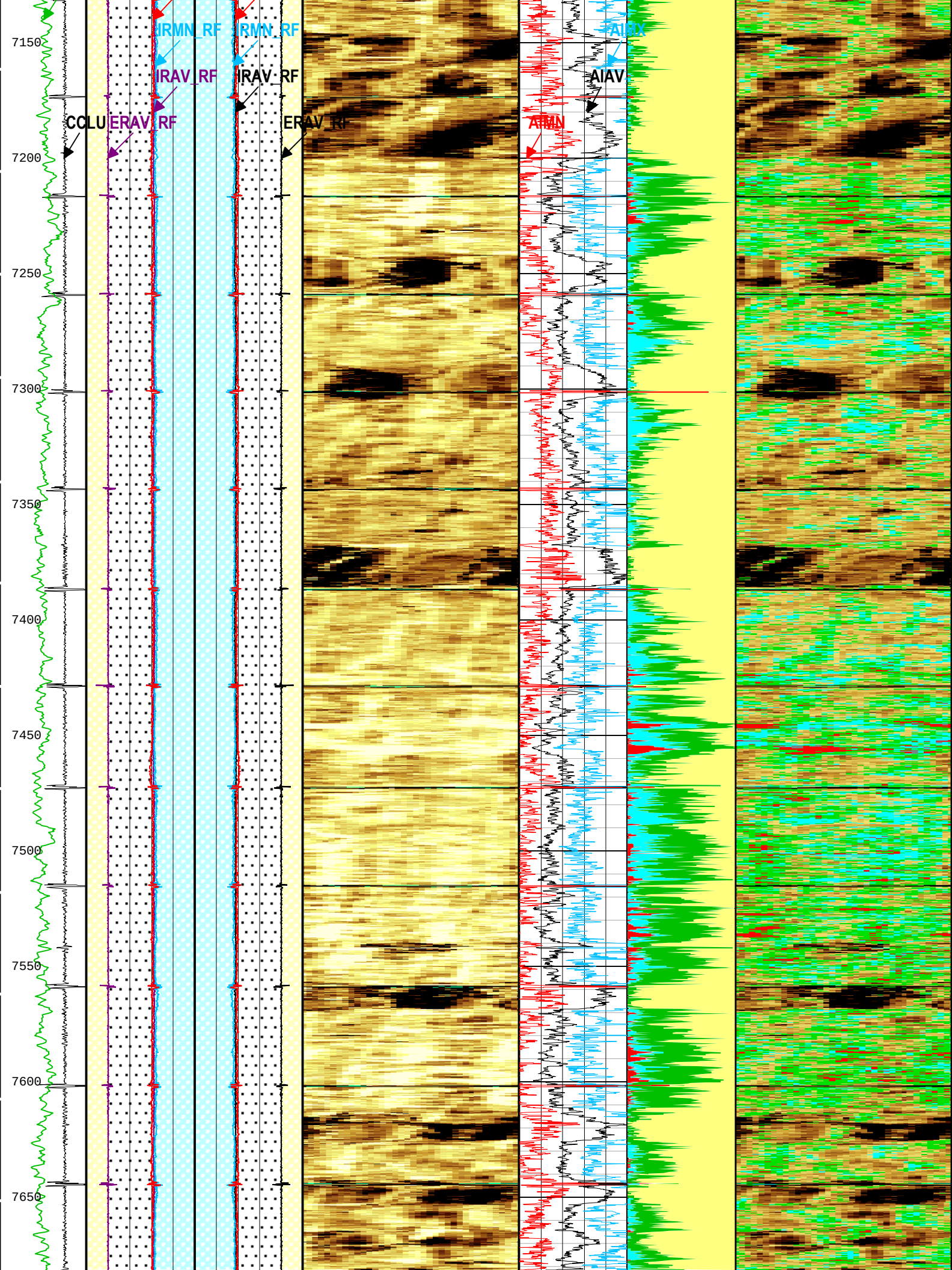
IRMN_RF
IRMN_RF
IRAV_RF
IRAV_RF
CCLU
ERAV_RF
ERAV_RF
AIAV
AIMN
7150
7200
7250
7300
7350
7400
7450
7500
7550
7600
7650

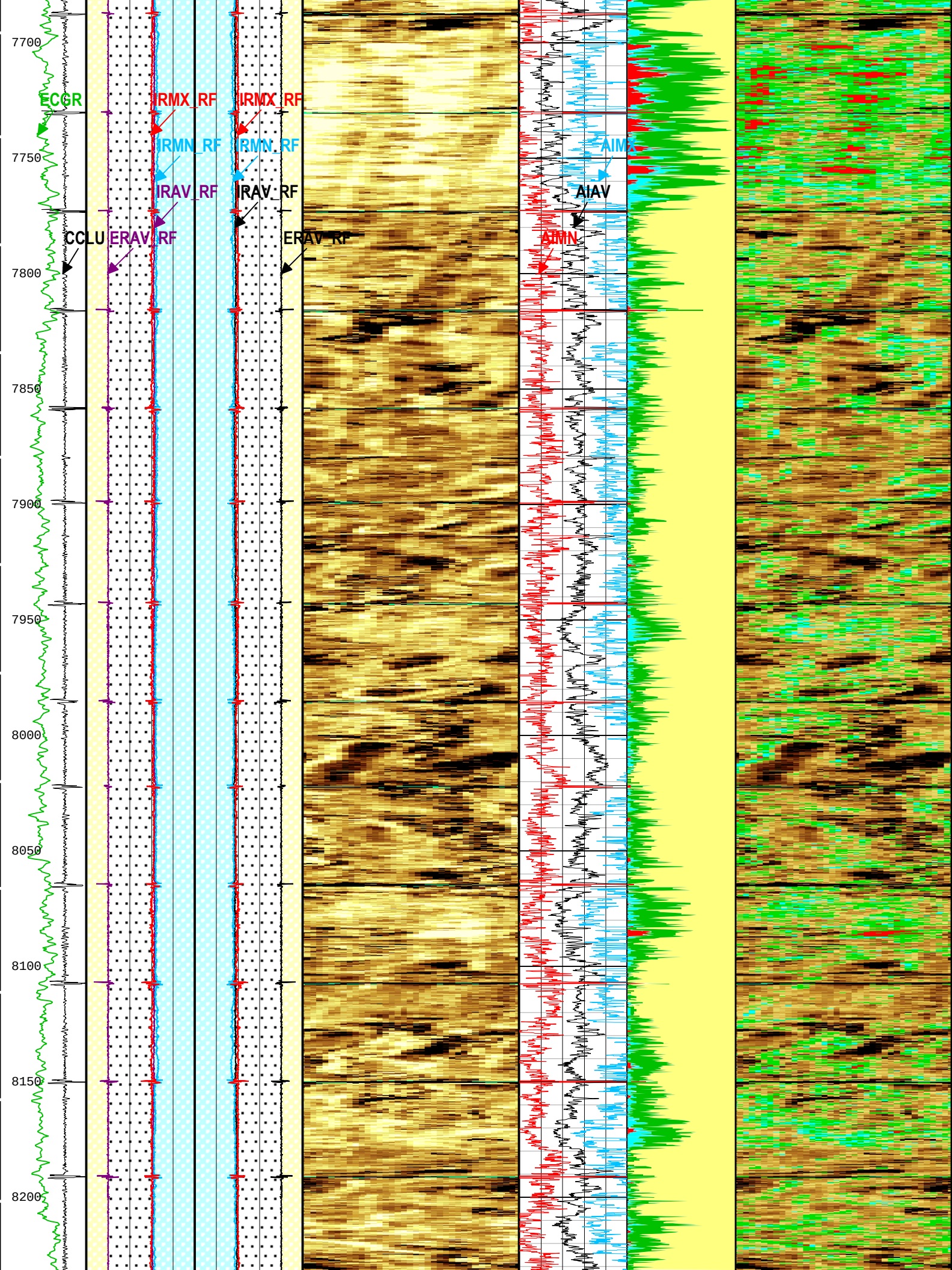
7700
7750
7800
7850
7900
7950
8000
8050
8100
8150
8200
ECGR
IRMX_RF
IRMN_RF
IRAV_RF
CCLU
ERAV_RF
IRMX_RF
IRMN_RF
IRAV_RF
ERAV_RF
AIMX
AIAV
AIMN

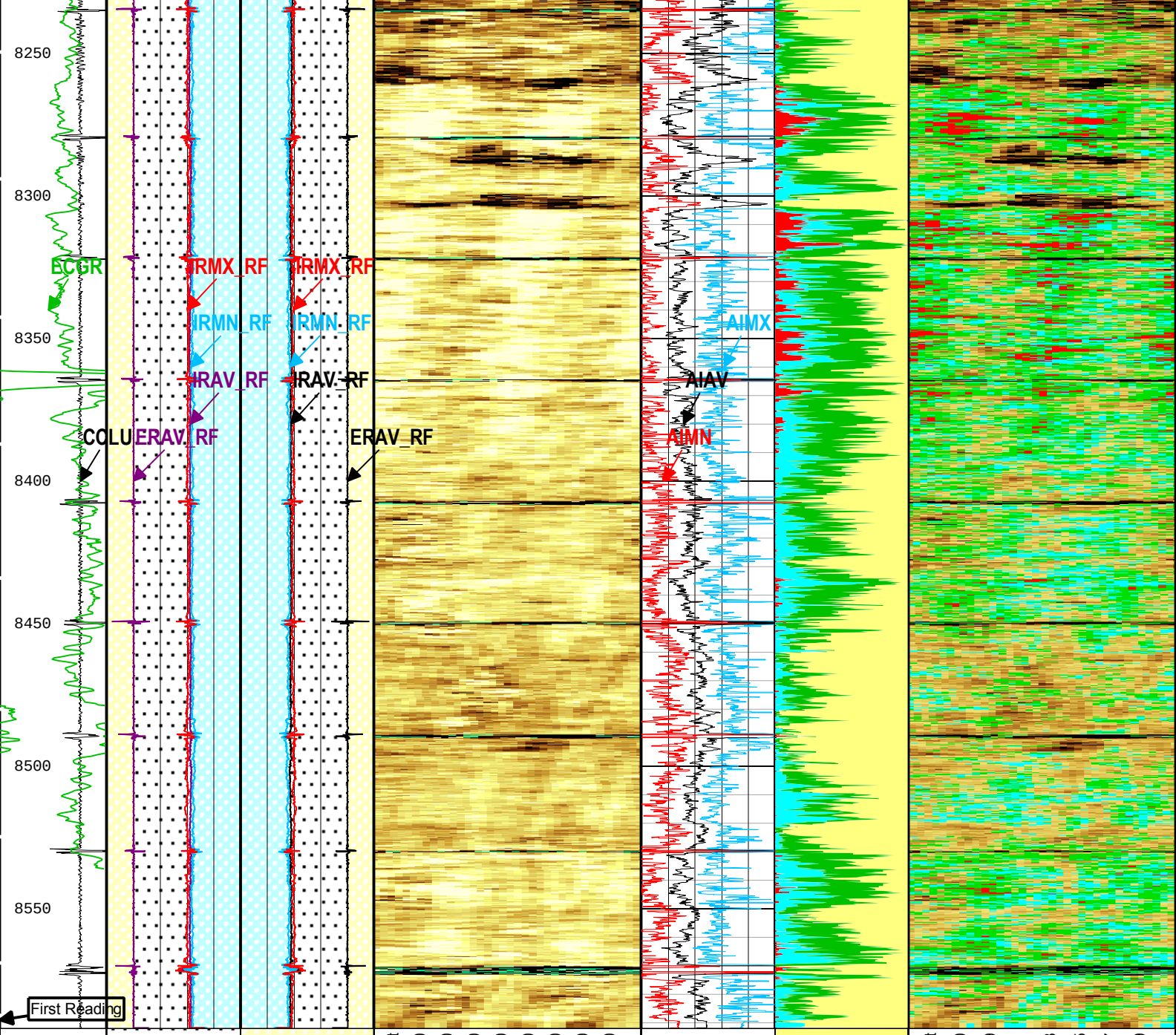

Casing Collar Locator Ultrasonic (CCLU) USIT-E[1]

-30 in 10

Gamma Ray (ECGR) HGNS[1]

0 gAPI 150

Amplitude of Eccentering for Unflagged Waves (ECCE_RF) USIT-E[1]

0 in 0.5

ERAV_IRAV

IRAV_LHF1

LHF1_ERAV

Median of Unflagged External Radii (ERAV_RF) USIT-E[1]

3.7 in 2.7

Median Internal Radius of Casing Corrected for Eccentering (IRAV_RF) USIT-E[1]

3.7 in 2.7

ERAV_RHF1

IRAV_ERAV

RHF1_IRAV

Median of Unflagged External Radii (ERAV_RF) USIT-E[1]

2.7 in 3.7

Median Internal Radius of Casing Corrected for Eccentering (IRAV_RF) USIT-E[1]

2.7 in 3.7

Absent 0.500 1.500 2.500 3.500 4.500 5.500 6.500 7.500

Custom Normalization

USIT - Acoustic Impedance (AIBK) USIT-E[1] (Mrayl)

Orientation: Top of Hole

U L B R U

Acoustic Impedance Minimum (AIMN) USIT-E[1]

-1 Mrayl 9

Acoustic Impedance Average (AIAV) USIT-E[1]

-1 Mrayl 9

Acoustic Impedance Maximum (AIMX) USIT-E[1]

-1 Mrayl 9

Bonded

Gas

Liquid

Micro-debonding

Absent -500.000 2.599 3.581 4.563 5.545 6.527 7.509

Custom Normalization

USIT - Acoustic Impedance With Micro-debonding Image (AI_MDEBOND_IMG) USIT-E[1] (Mrayl)

Orientation: Top of Hole

U L B R U

Minimum of Unflagged Internal Radii (IRMN_RF) USIT-E[1]	Minimum of Unflagged Internal Radii (IRMN_RF) USIT-E[1]
3.7 in 2.7	2.7 in 3.7
Maximum of Unflagged Internal Radii (IRMX_RF) USIT-E[1]	Maximum of Unflagged Internal Radii (IRMX_RF) USIT-E[1]
3.7 in 2.7	2.7 in 3.7

TIME_1900 - Time Marked every 60.00 (s)

Description: USI Cement Format: Log (LBV1_USI Cement 7inch) Index Scale: 2 in per 100 ft Index Unit: ft Index Type: Measured Depth Creation Date: 07-Sep-2018 22:56:20

Composite 1

Corrosion 5 in = 100 ft

Composite Summary

Run Name	Pass Objective	Direction	Top	Bottom	Start	Stop	DSC Mode	Depth Shift	Include Parallel Data
One	Log[6]:Up	Up	93.36 ft	8592.71 ft	07-Sep-2018 9:51:23 AM	07-Sep-2018 1:52:30 PM	ON	8.00 ft	No
One	Log[9]:Up	Up	11.43 ft	318.32 ft	07-Sep-2018 2:46:40 PM	07-Sep-2018 3:00:05 PM	ON	9.00 ft	No

All depths are referenced to toolstring zero

Log

Company:Southern California Gas Company Well:Standard Sesnon 9 Composite 1:S003

Description: USI Composite Format: Log (LBV1_USI Corrosion 5inch) Index Scale: 5 in per 100 ft Index Unit: ft Index Type: Measured Depth Creation Date: 07-Sep-2018 22:56:36

TIME_1900 - Time Marked every 60.00 (s)

USIT Processing Flags (UFLG[0]) USIT-E[1]

1 - UFLG 1 Value within [0.0 - 1.5] - :
2 - UFLG 2 Value within [1.5 - 2.5] - :
3 - UFLG 3 Value within [2.5 - 3.5] - :
4 - UFLG 4 UFLG 5 UFLG 6 Value within [3.5 - 6.5] - :
5 - UFLG 7 UFLG 8 UFLG 9 Value within [6.5 - 10] - :

- UTIM Error
- Pulse Origin Not Detected
- WINLEN Error
- Casing Thickness Error
- Loop Processing Error

U L B R U
Orientation: Top of Hole

Absent -5.200 -3.600 -2.000 -0.400

Explicit Normalization

USIT - Amplitude of Unflagged Wave (AWBK_RF) USIT-E[1] (dB)

ERAV	IRAV
ERAV-IRAV	ERAV
IRAV	IRAV-ERAV

Median of Unflagged External Radii (ERAV_RF) USIT-E[1]	Median of Unflagged External Radii (ERAV_RF) USIT-E[1]
3.7 in 2.7	2.7 in 3.7
Median Internal Radius of Casing Corrected for Eccentering	Median Internal Radius of Casing Corrected for Eccentering

Minimum of Unflagged Casing Thickness (THMN_RF) USIT-E[1]

0.1 in 0.6

Nominal Casing Thickness (THNO) USIT-E[1]

Minimum of Unflagged Wave Amplitude

Casing Collar Locator Ultrasonic

U L B R U
Orientation: Top

Ultrasonic (CCLU) USIT-E[1]
-30 in 10

Amplitude of Eccentering for Unflagged Waves (ECCE_RF) USIT-E[1]
0 in 0.5

Motor Revolution Speed (RSAV) USIT-E[1]
6 c/s 8

U L B R U
Orientation: Top of Hole
Absent 1.500 3.500
Explicit Normalization
USIT - USIT Processing Flags (UFLG) USIT-E[1]

USIT Processing Flags (UFLG[0]) USIT-E[1]
1 5

(AWMN_RF) USIT-E[1]
0 dB 75

Average of Unflagged Wave Amplitude (AWAV_RF) USIT-E[1]
0 dB 75

Maximum of Unflagged Wave Amplitude (AWMX_RF) USIT-E[1]
0 dB 75

U L B R U
Orientation: Top of Hole
Absent -0.059 -0.028 0.004 0.035 0.068
Explicit Normalization
USIT - Unflagged Internal Radii minus Median Internal Radius (IRBKM_RF) USIT-E[1] (in)

Internal Radius Averaged Value (IRAV) USIT-E[1]
2.7 in 3.7

Internal Radius Maximum Value (IRMX) USIT-E[1]
2.7 in 3.7

Internal Radius Minimum Value (IRMN) USIT-E[1]
2.7 in 3.7

(IRAV_RF) USIT-E[1]
3.7 in 2.7

Maximum of Unflagged Internal Radii (IRMX_RF) USIT-E[1]
3.7 in 2.7

Minimum of Unflagged Internal Radii (IRMN_RF) USIT-E[1]
3.7 in 2.7

(IRAV_RF) USIT-E[1]
2.7 in 3.7

Maximum of Unflagged Internal Radii (IRMX_RF) USIT-E[1]
2.7 in 3.7

Minimum of Unflagged Internal Radii (IRMN_RF) USIT-E[1]
2.7 in 3.7

Orientation: Top of Hole
Absent -0.059 -0.028 0.004 0.035 0.068
Explicit Normalization
USIT - Unflagged Casing Thickness minus Median of Unflagged Casing Thickness (THBKM_RF) USIT-E[1] (in)

USIT-E[1]
0.1 in 0.6

Median of Unflagged Casing Thickness (THAV_RF) USIT-E[1]
0.1 in 0.6

Maximum of Unflagged Casing Thickness (THMX_RF) USIT-E[1]
0.1 in 0.6

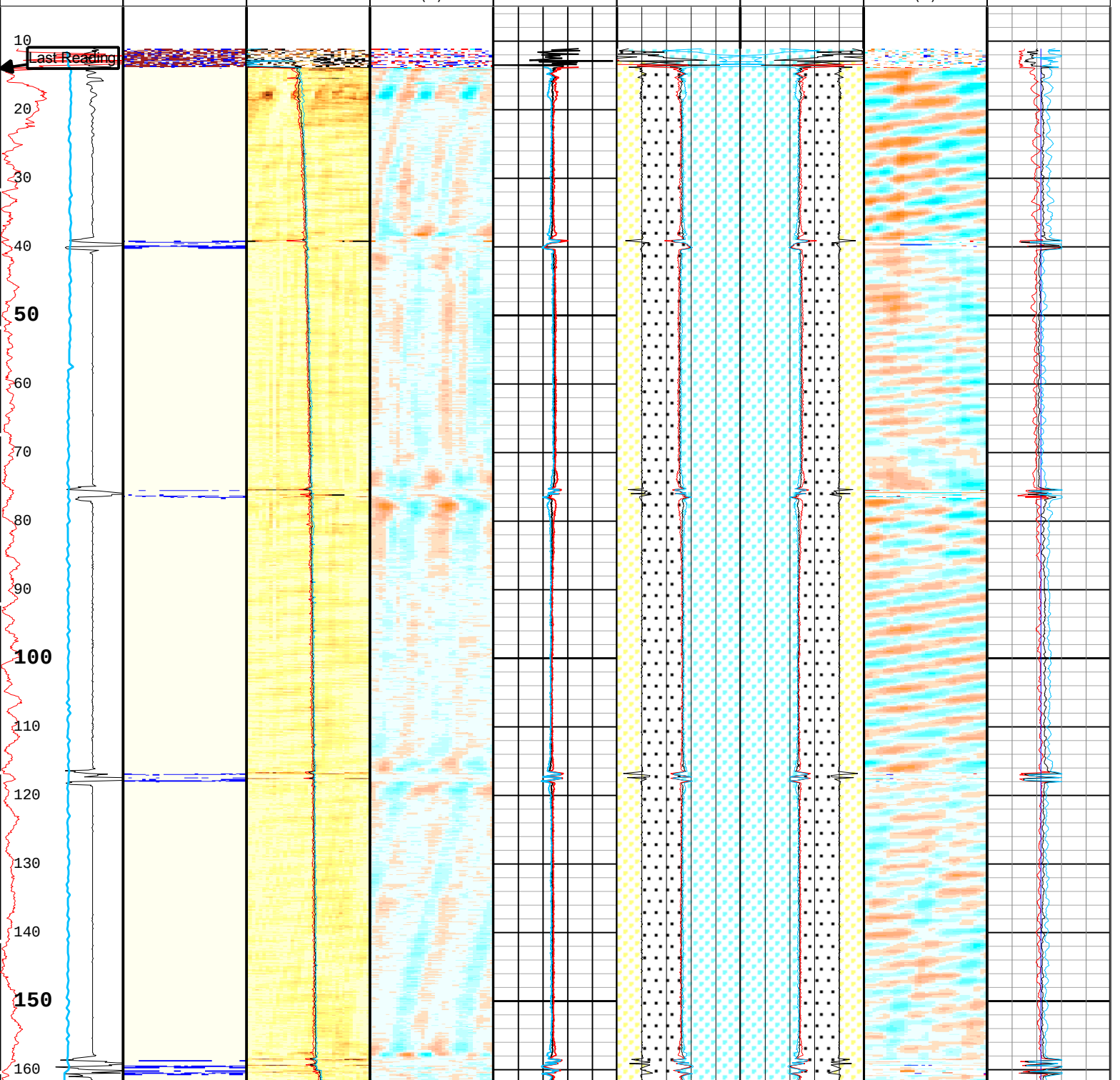

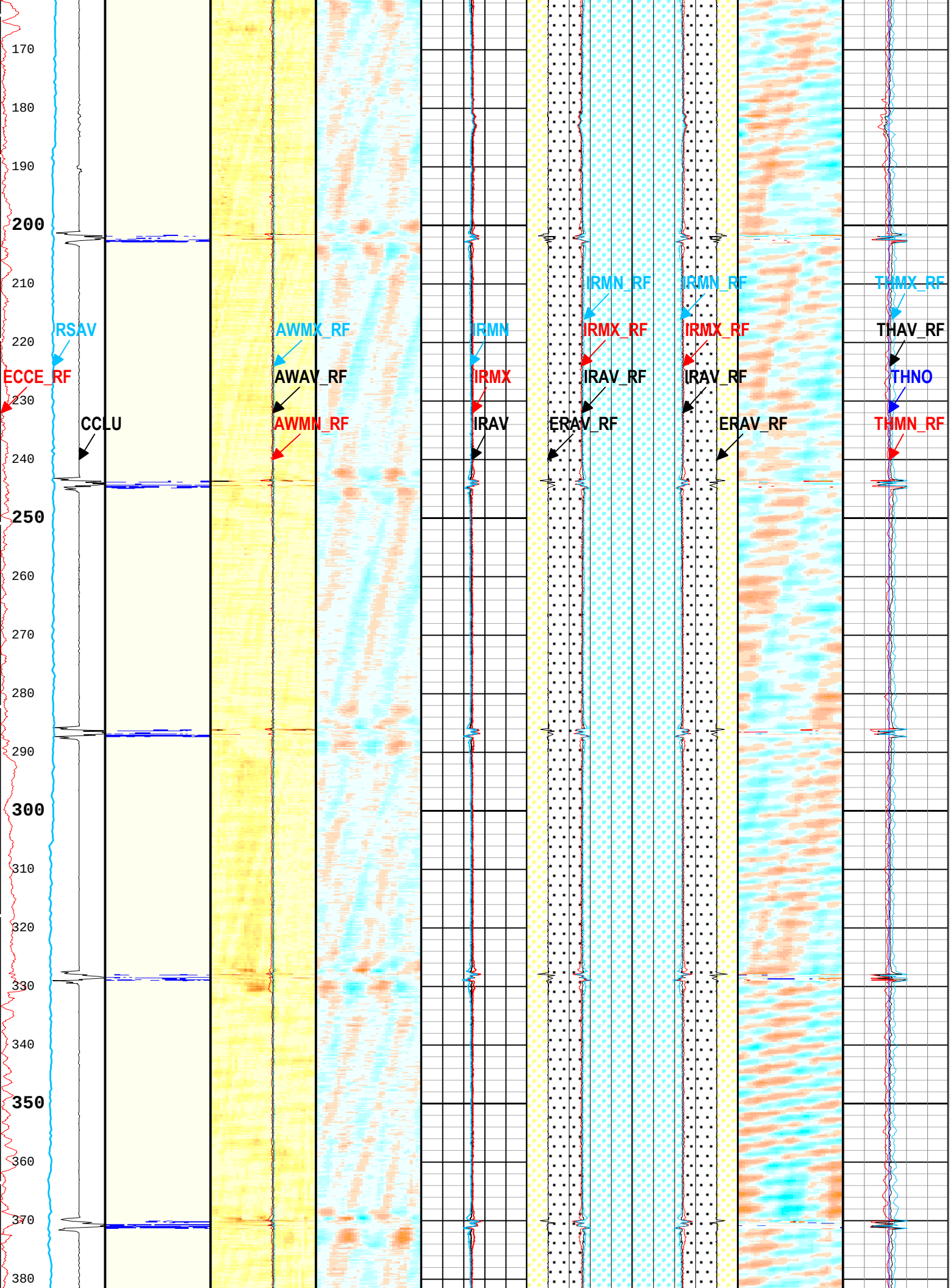
170
180
190
200
210
220
230
240
250
260
270
280
290
300
310
320
330
340
350
360
370
380
RSAV
ECCE_RF
CCLU
AWMX_RF
AWAV_RF
AWMN_RF
IRMN
IRMX
IRAV
IRMN_RF
IRMX_RF
IRAV_RF
ERAV_RF
IRMN_RF
IRMX_RF
IRAV_RF
ERAV_RF
THMX_RF
THAV_RF
THNO
THMN_RF

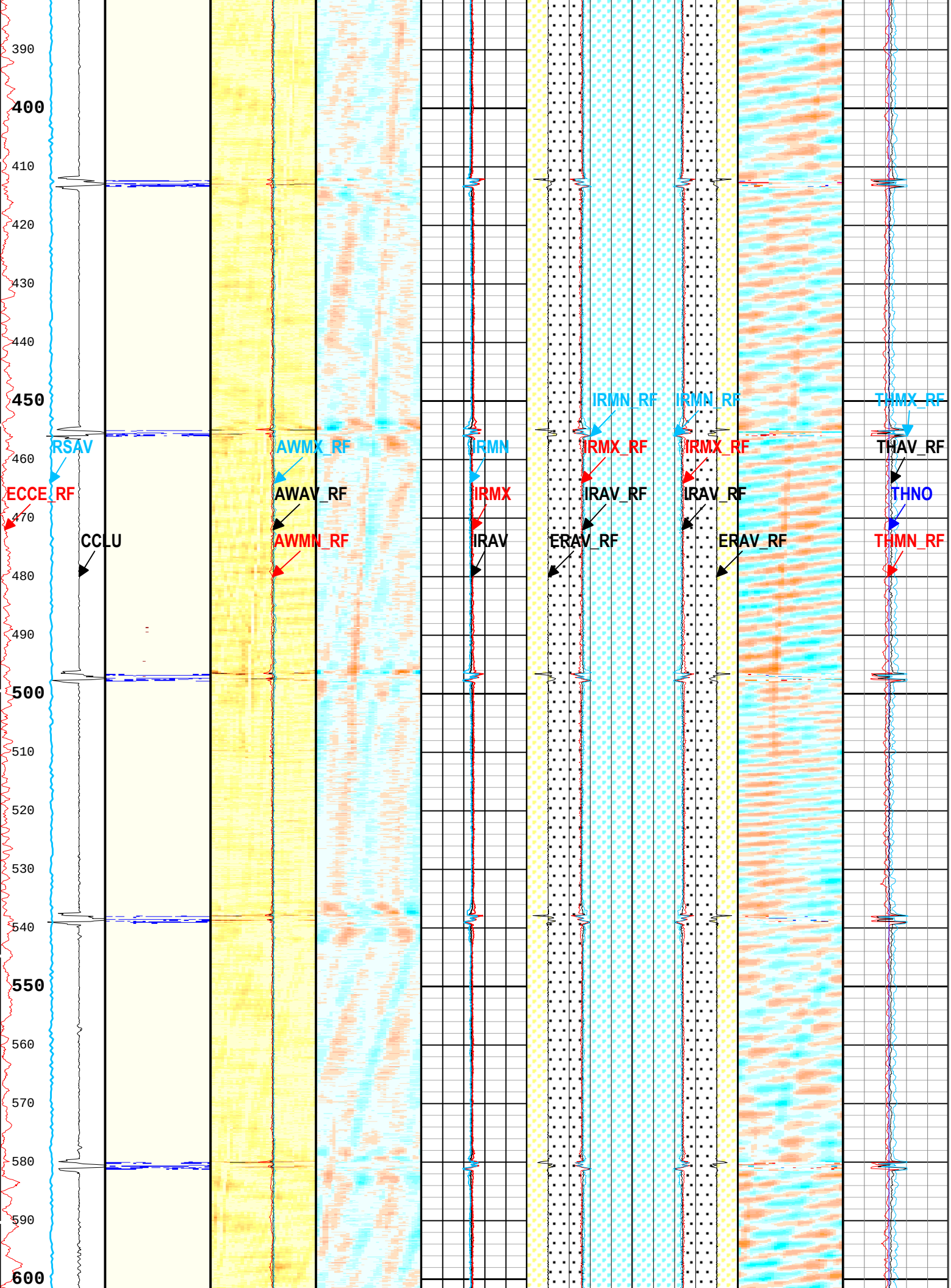
390
400
410
420
430
440
450
460
470
480
490
500
510
520
530
540
550
560
570
580
590
600
RSAV
ECCE_RF
CCLU
AWMX_RF
AWAV_RF
AWMN_RF
IRMN
IRMX
IRAV
IRMN_RF
IRMX_RF
IRAV_RF
ERAV_RF
IRMN_RF
IRMX_RF
IRAV_RF
ERAV_RF
THMX_RF
THAV_RF
THNO
THMN_RF

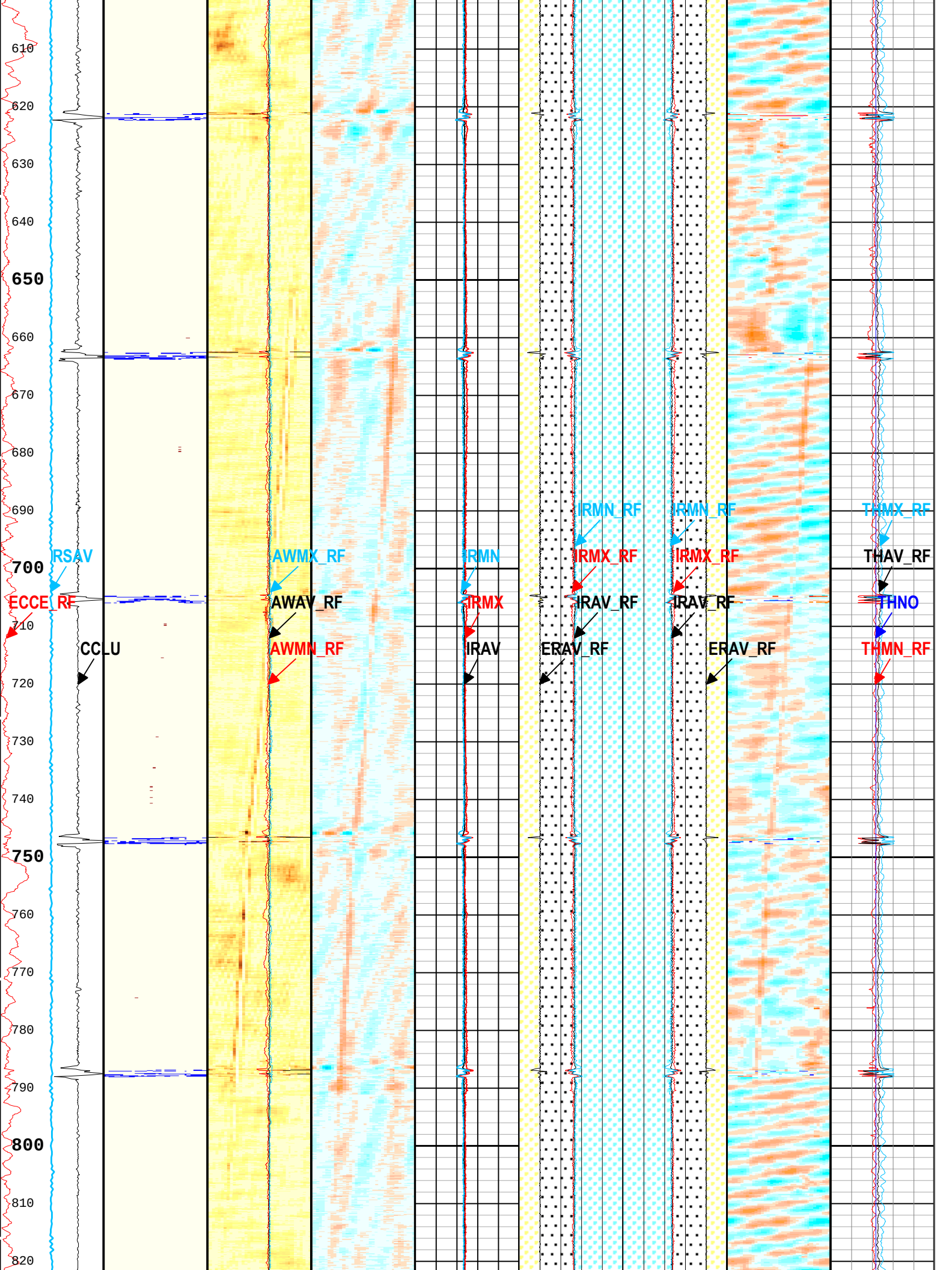
610
620
630
640
650
660
670
680
690
700
710
720
730
740
750
760
770
780
790
800
810
820
RSAV
ECCE_RF
CCLU
AWMX_RF
AWAV_RF
AWMN_RF
IRMN
IRMX
IRAV
IRMN_RF
IRMX_RF
IRAV_RF
ERAV_RF
IRMN_RF
IRMX_RF
IRAV_RF
ERAV_RF
THMX_RF
THAV_RF
THNO
THMN_RF

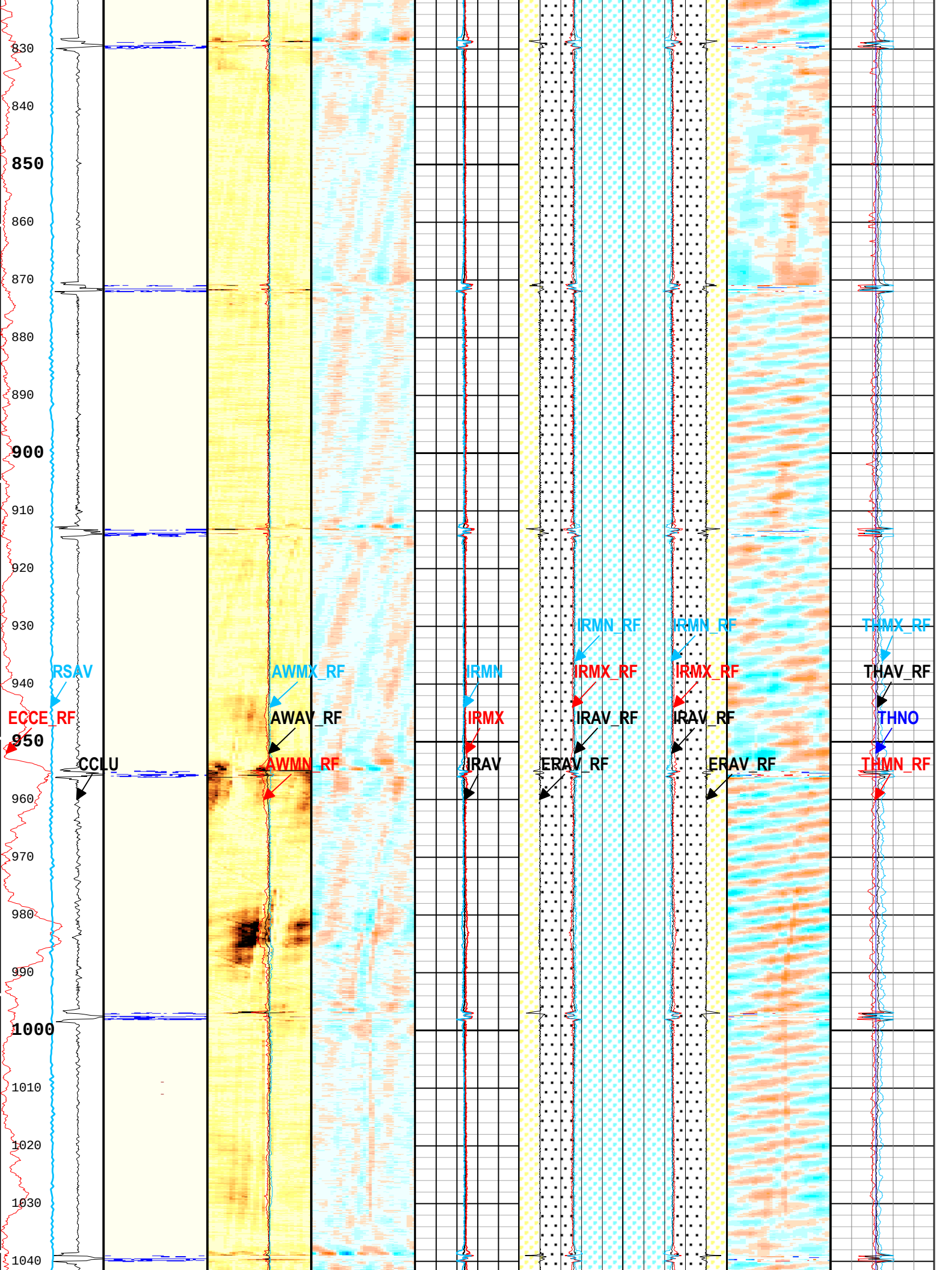
830
840
850
860
870
880
890
900
910
920
930
940
950
960
970
980
990
1000
1010
1020
1030
1040
RSAV
ECCE_RF
CCLU
AWMX_RF
AWAV_RF
AWMN_RF
IRMN
IRMX
IRAV
IRMN_RF
IRMX_RF
IRAV_RF
ERAV_RF
IRMN_RF
IRMX_RF
IRAV_RF
ERAV_RF
THMX_RF
THAV_RF
THNO
THMN_RF

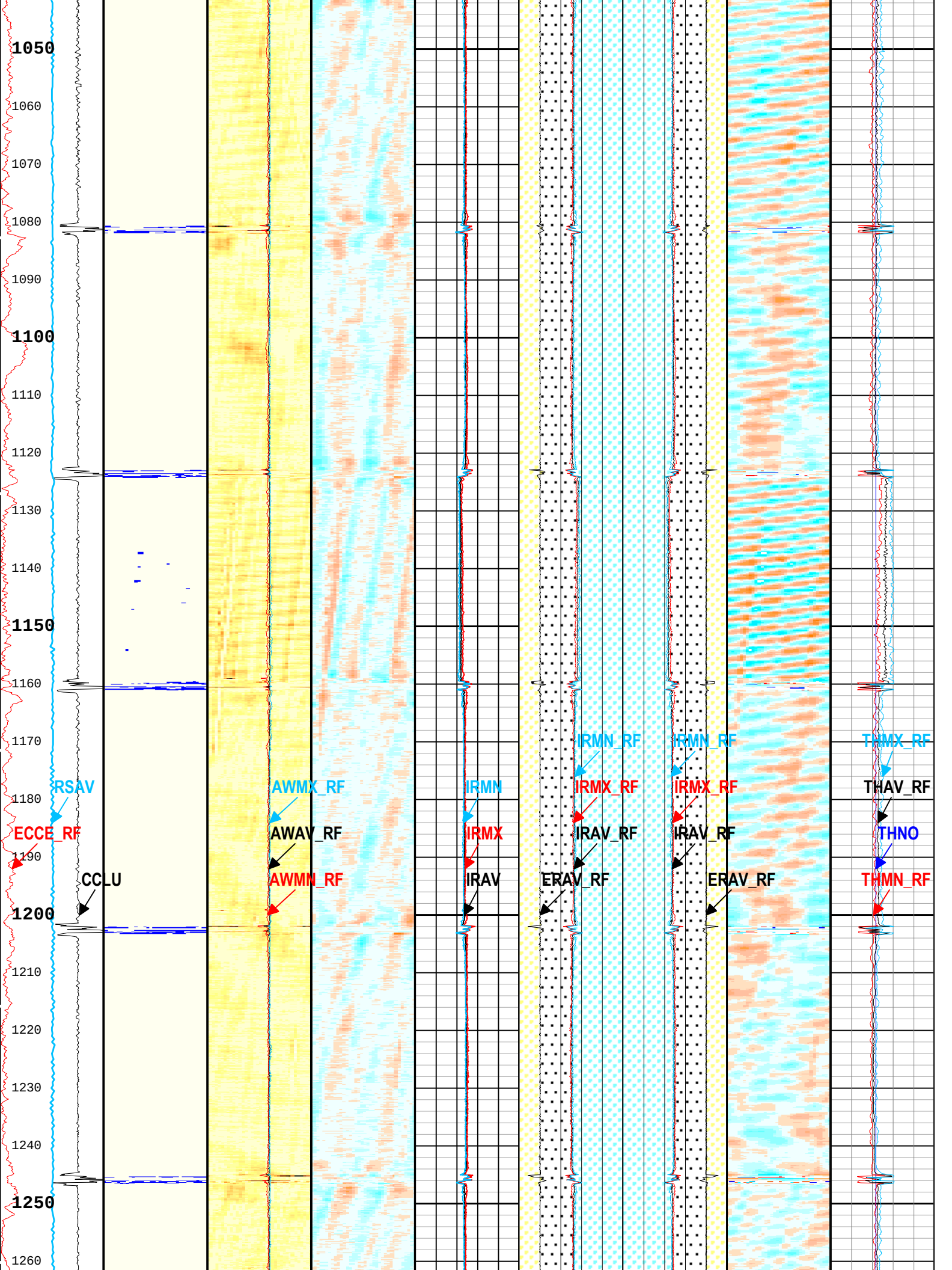
1050
1060
1070
1080
1090
1100
1110
1120
1130
1140
1150
1160
1170
1180
1190
1200
1210
1220
1230
1240
1250
1260
RSAV
ECCE_RF
CCLU
AWMX_RF
AWAV_RF
AWMN_RF
IRMN
IRMX
IRAV
IRMN_RF
IRMX_RF
IRAV_RF
ERAV_RF
IRMN_RF
IRMX_RF
IRAV_RF
ERAV_RF
THMX_RF
THAV_RF
THNO
THMN_RF

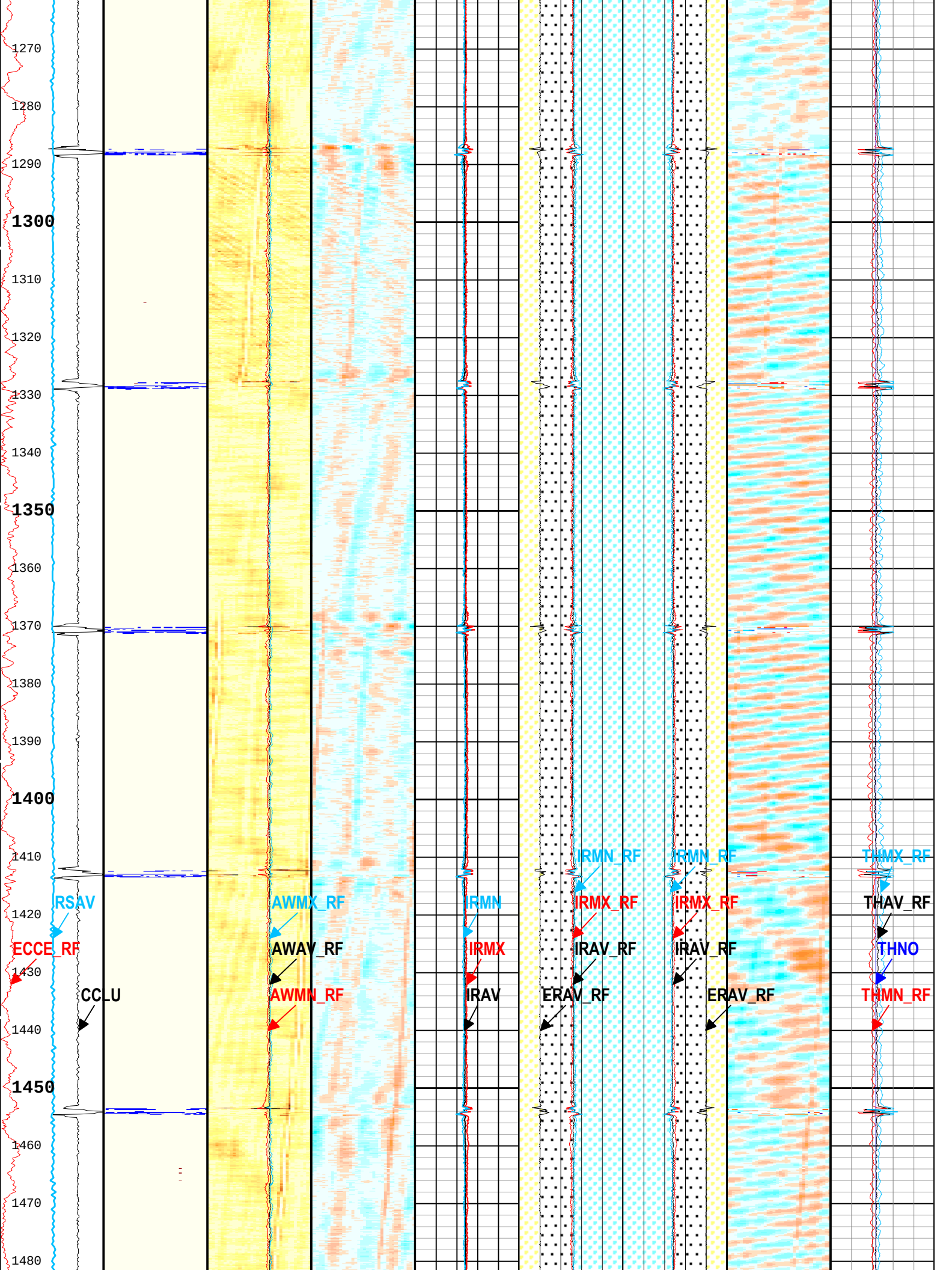
1270
1280
1290
1300
1310
1320
1330
1340
1350
1360
1370
1380
1390
1400
1410
1420
1430
1440
1450
1460
1470
1480
RSAV
ECCE_RF
CC_U
AWMX_RF
AWAV_RF
AWMN_RF
IRMN
IRMX
IRAV
IRMN_RF
IRMX_RF
IRAV_RF
ERAV_RF
IRMN_RF
IRMX_RF
IRAV_RF
ERAV_RF
THMX_RF
THAV_RF
THNO
THMN_RF

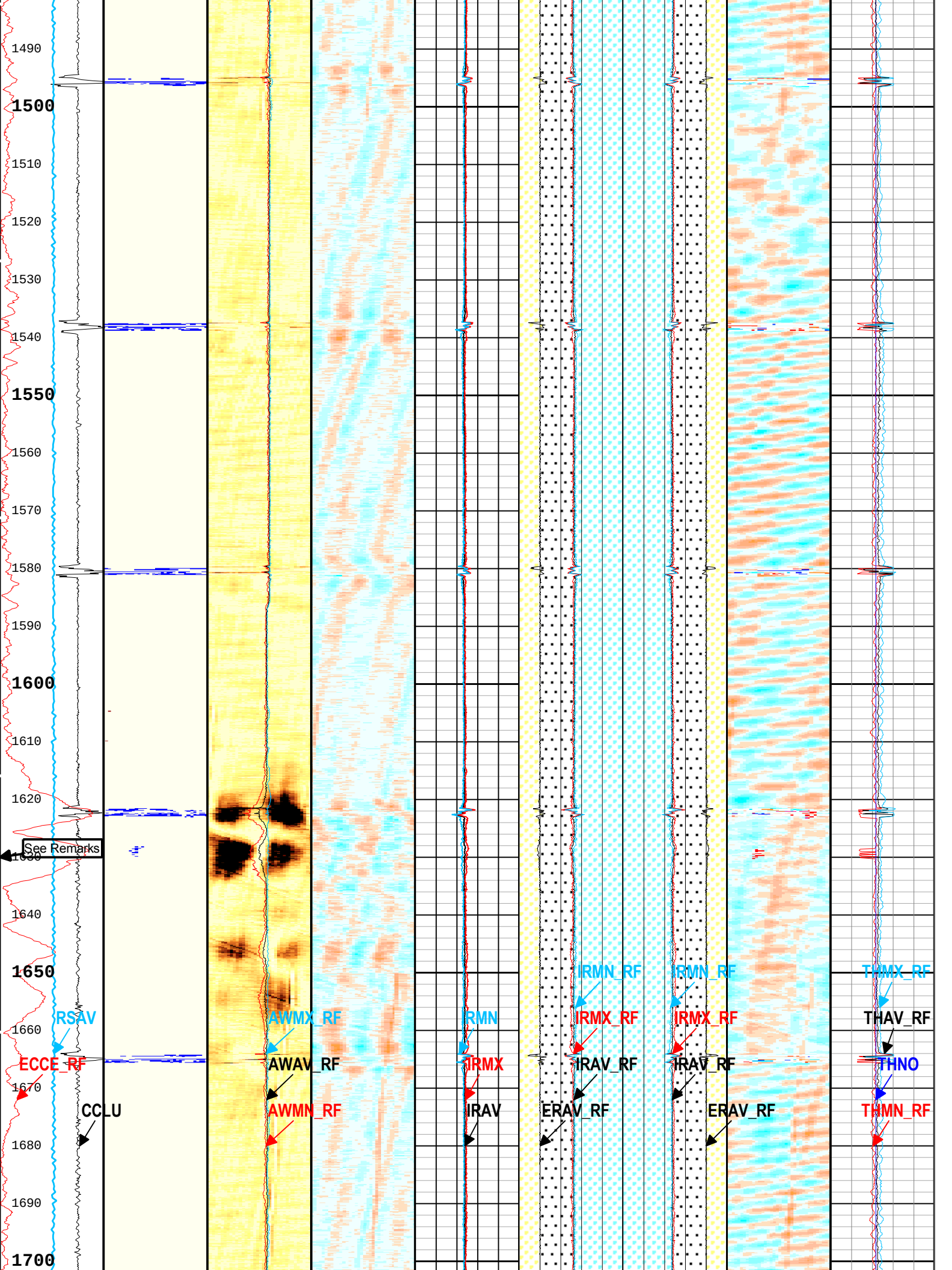
1490
1500
1510
1520
1530
1540
1550
1560
1570
1580
1590
1600
1610
1620
See Remarks
1630
1640
1650
1660
1670
1680
1690
1700
RSAV
ECCE_RF
CCLU
AWMX_RF
AWAV_RF
AWMN_RF
RMN
IRMX
IRAV
IRMN_RF
IRMX_RF
IRAV_RF
ERAV_RF
RMN_RF
IRMX_RF
IRAV_RF
ERAV_RF
THMX_RF
THAV_RF
THNO
THMN_RF

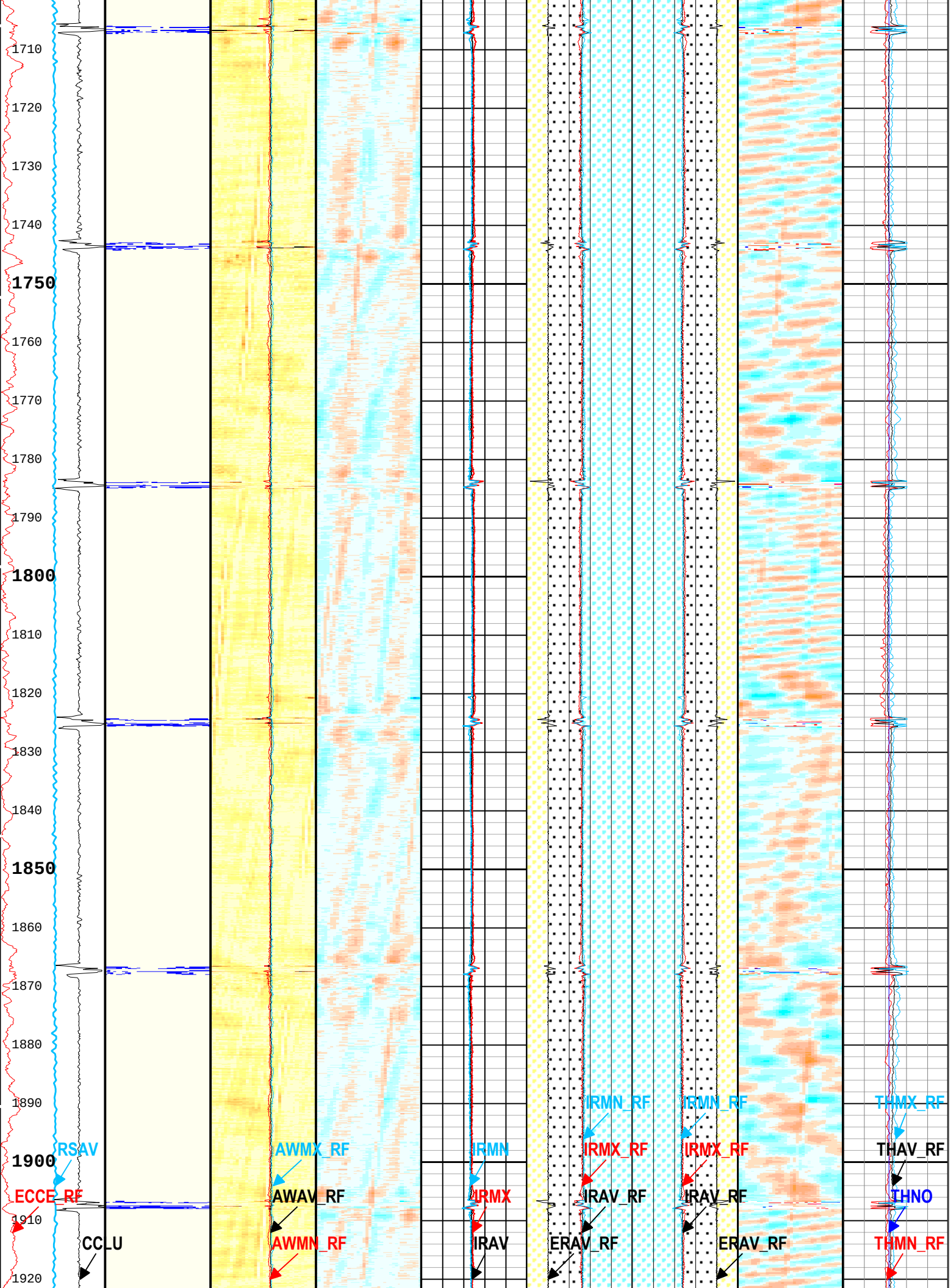
1710
1720
1730
1740
1750
1760
1770
1780
1790
1800
1810
1820
1830
1840
1850
1860
1870
1880
1890
1900
1910
1920
RSAV
ECCE_RF
CC_U
AWMX_RF
AWAV_RF
AWMN_RF
IRMN
IRMX
IRAV
IRMN_RF
IRMX_RF
IRAV_RF
ERAV_RF
IRMN_RF
IRMX_RF
IRAV_RF
ERAV_RF
THMX_RF
THAV_RF
THNO
THMN_RF

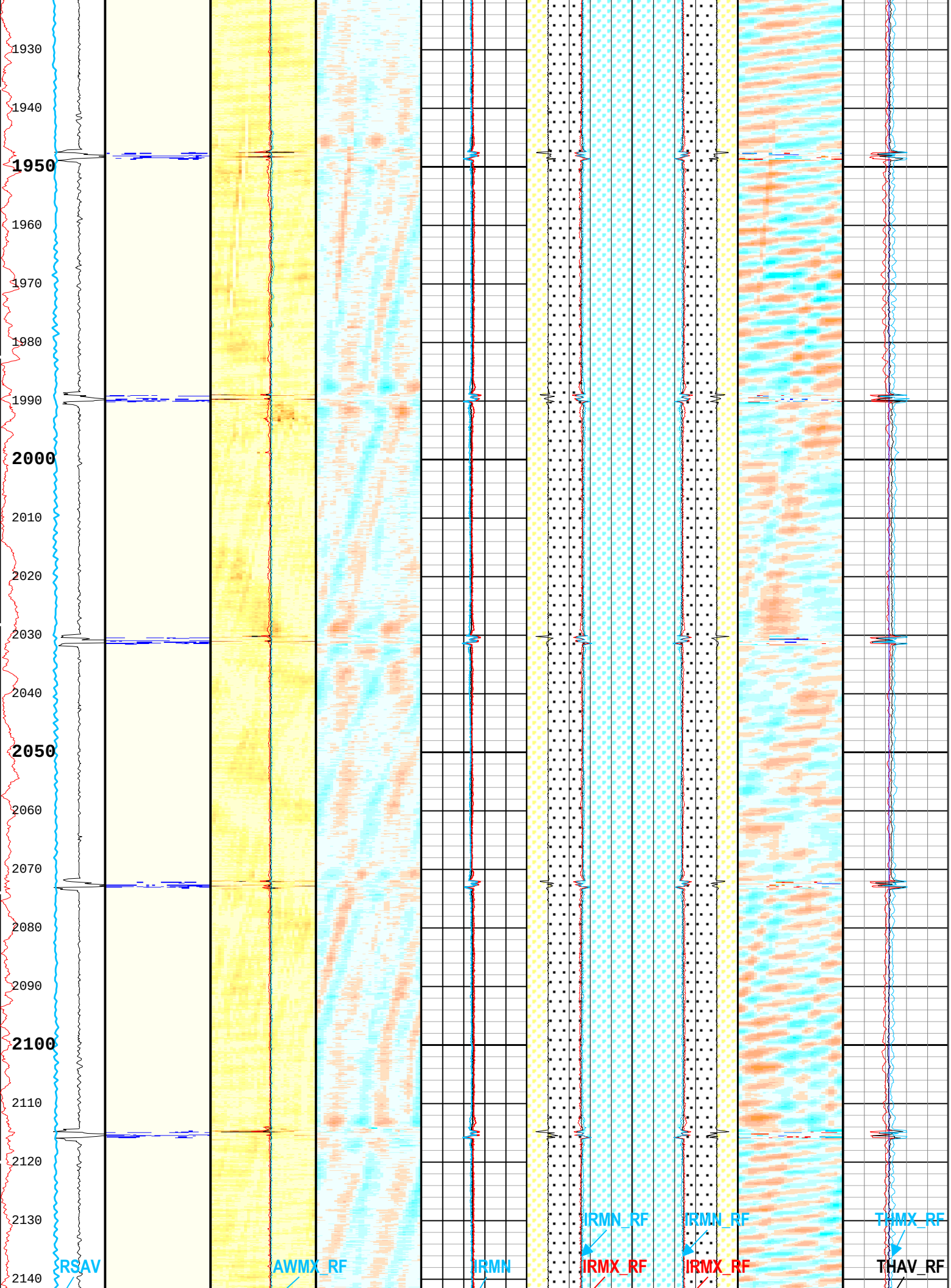
1930
1940
1950
1960
1970
1980
1990
2000
2010
2020
2030
2040
2050
2060
2070
2080
2090
2100
2110
2120
2130
2140
RSAV
AWMX_RF
IRMN
IRMN_RF
IRMX_RF
IRMN_RF
IRMX_RF
THMX_RF
THAV_RF

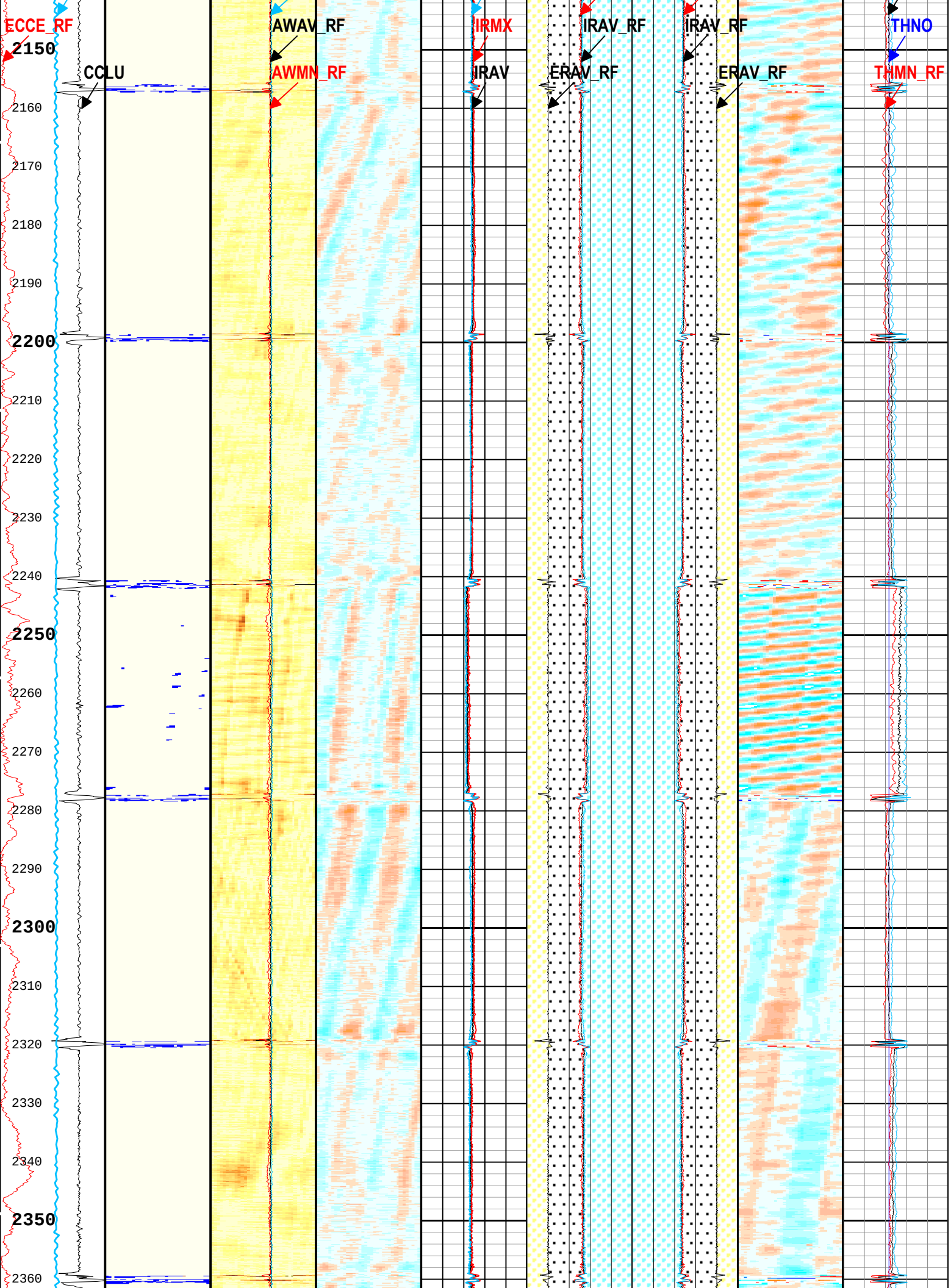
ECCE_RF
CCLU
AWAV_RF
AWMN_RF
IRMX
IRAV
IRAV_RF
ERAV_RF
IRAV_RF
ERAV_RF
THNO
THMN_RF
2150
2160
2170
2180
2190
2200
2210
2220
2230
2240
2250
2260
2270
2280
2290
2300
2310
2320
2330
2340
2350
2360

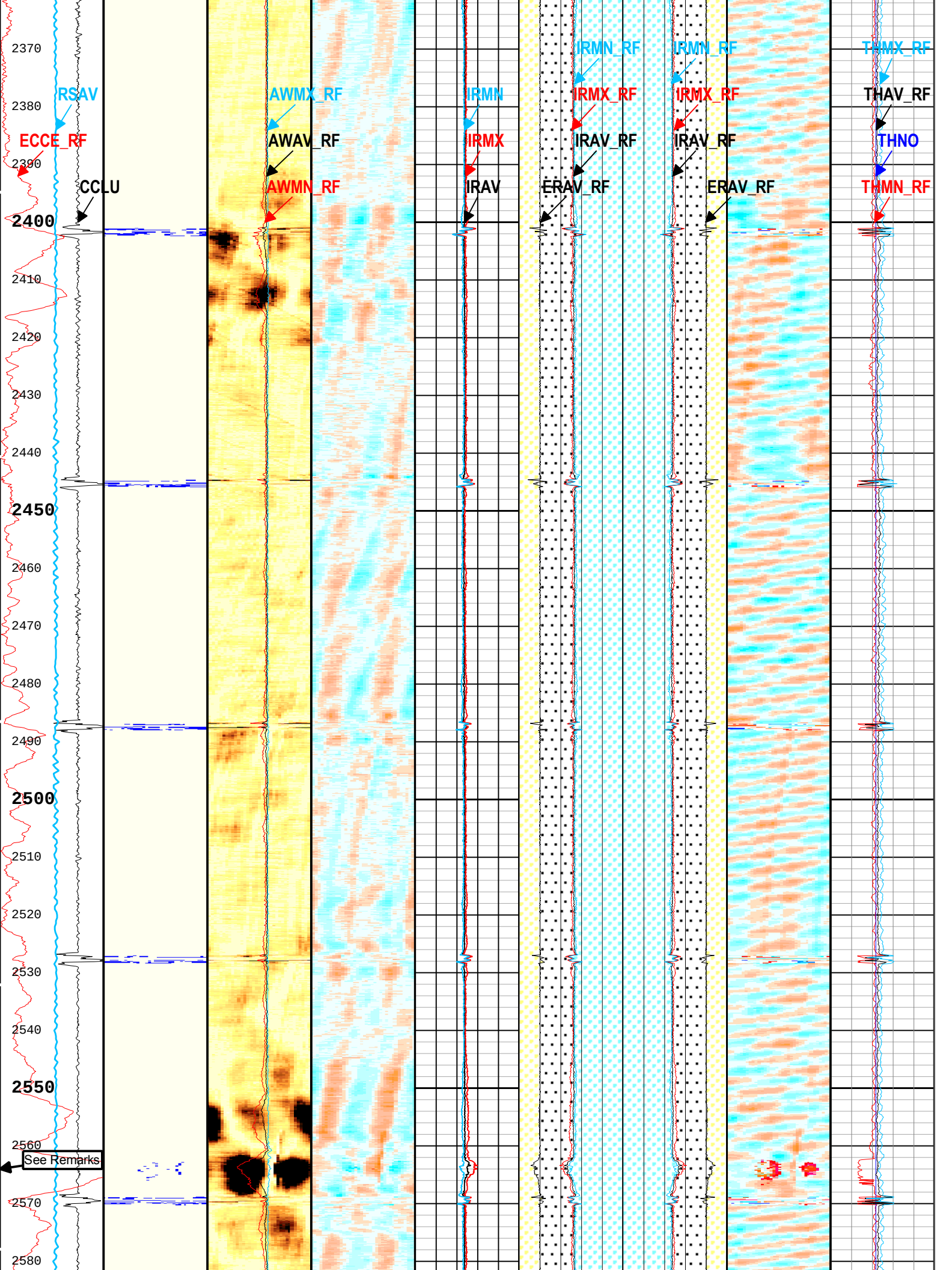
RSAV
ECCE_RF
CCLU
AWMX_RF
AWAV_RF
AWMN_RF
IRMN
IRMX
IRAV
IRMN_RF
IRMX_RF
IRAV_RF
ERAV_RF
IRMN_RF
IRMX_RF
IRAV_RF
ERAV_RF
THMX_RF
THAV_RF
THNO
THMN_RF
See Remarks
2370
2380
2390
2400
2410
2420
2430
2440
2450
2460
2470
2480
2490
2500
2510
2520
2530
2540
2550
2560
2570
2580

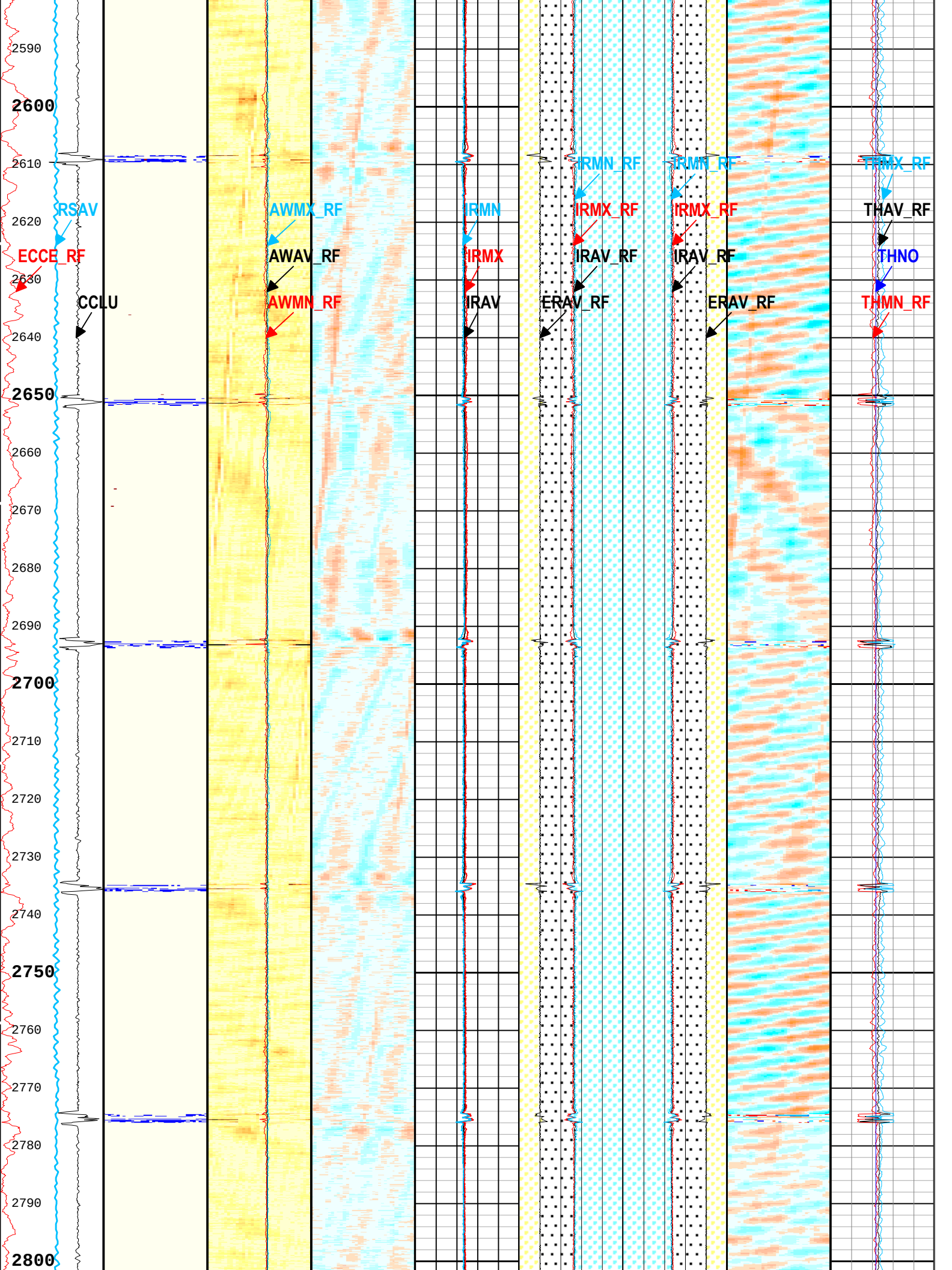
2590
2600
2610
2620
2630
2640
2650
2660
2670
2680
2690
2700
2710
2720
2730
2740
2750
2760
2770
2780
2790
2800
RSAV
ECCE_RF
CCLU
AWMX_RF
AWAV_RF
AWMN_RF
IRMN
IRMX
IRAV
IRMN_RF
IRMX_RF
IRAV_RF
ERAV_RF
IRMN_RF
IRMX_RF
IRAV_RF
ERAV_RF
THMX_RF
THAV_RF
THNO
THMN_RF

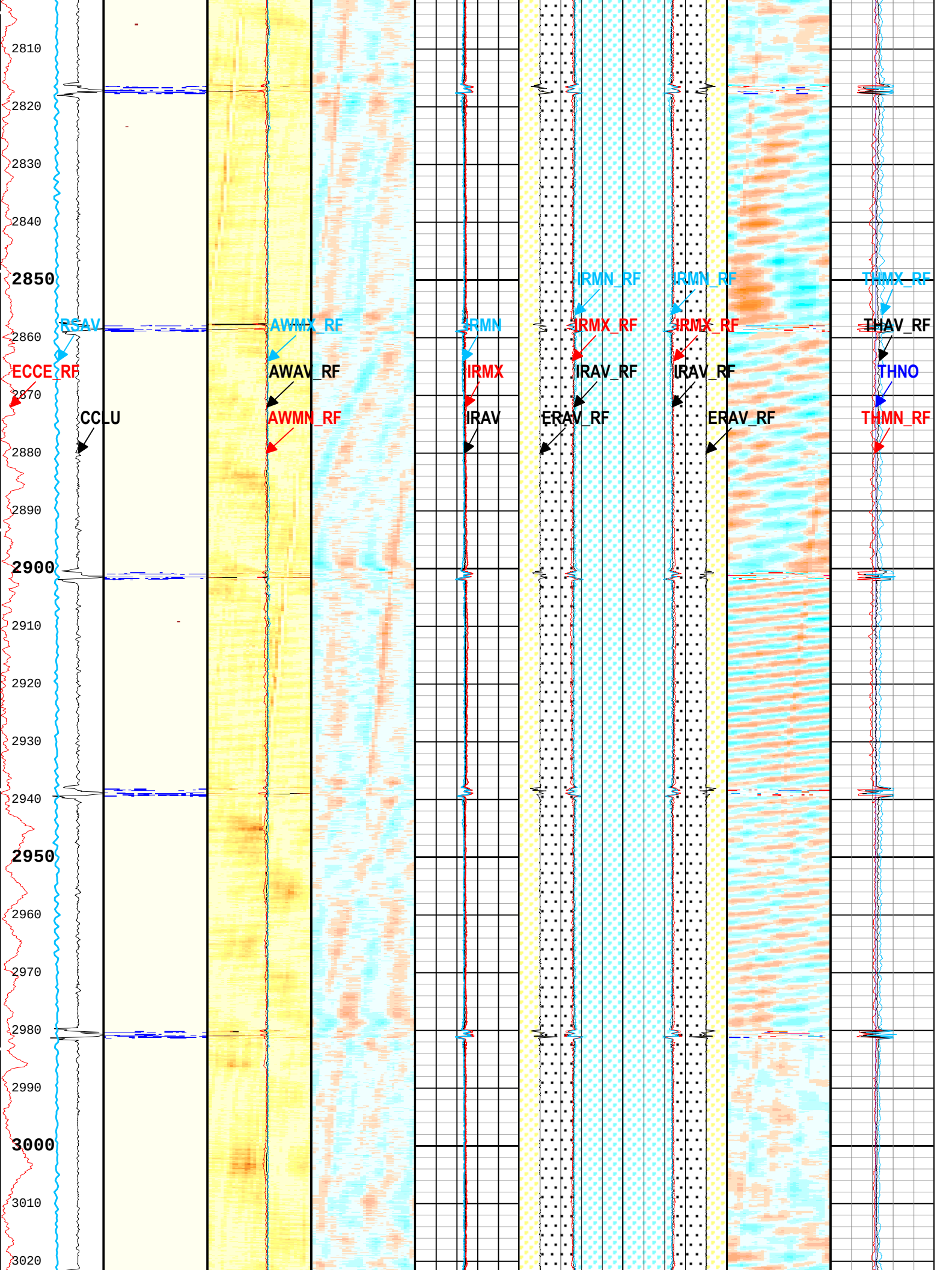
2810
2820
2830
2840
2850
2860
2870
2880
2890
2900
2910
2920
2930
2940
2950
2960
2970
2980
2990
3000
3010
3020
RSAV
ECCE_RF
CCLU
AWMX_RF
AWAV_RF
AWMN_RF
IRMN
IRMX
IRAV
IRMN_RF
IRMX_RF
IRAV_RF
ERAV_RF
IRMN_RF
IRMX_RF
IRAV_RF
ERAV_RF
THMX_RF
THAV_RF
THNO
THMN_RF

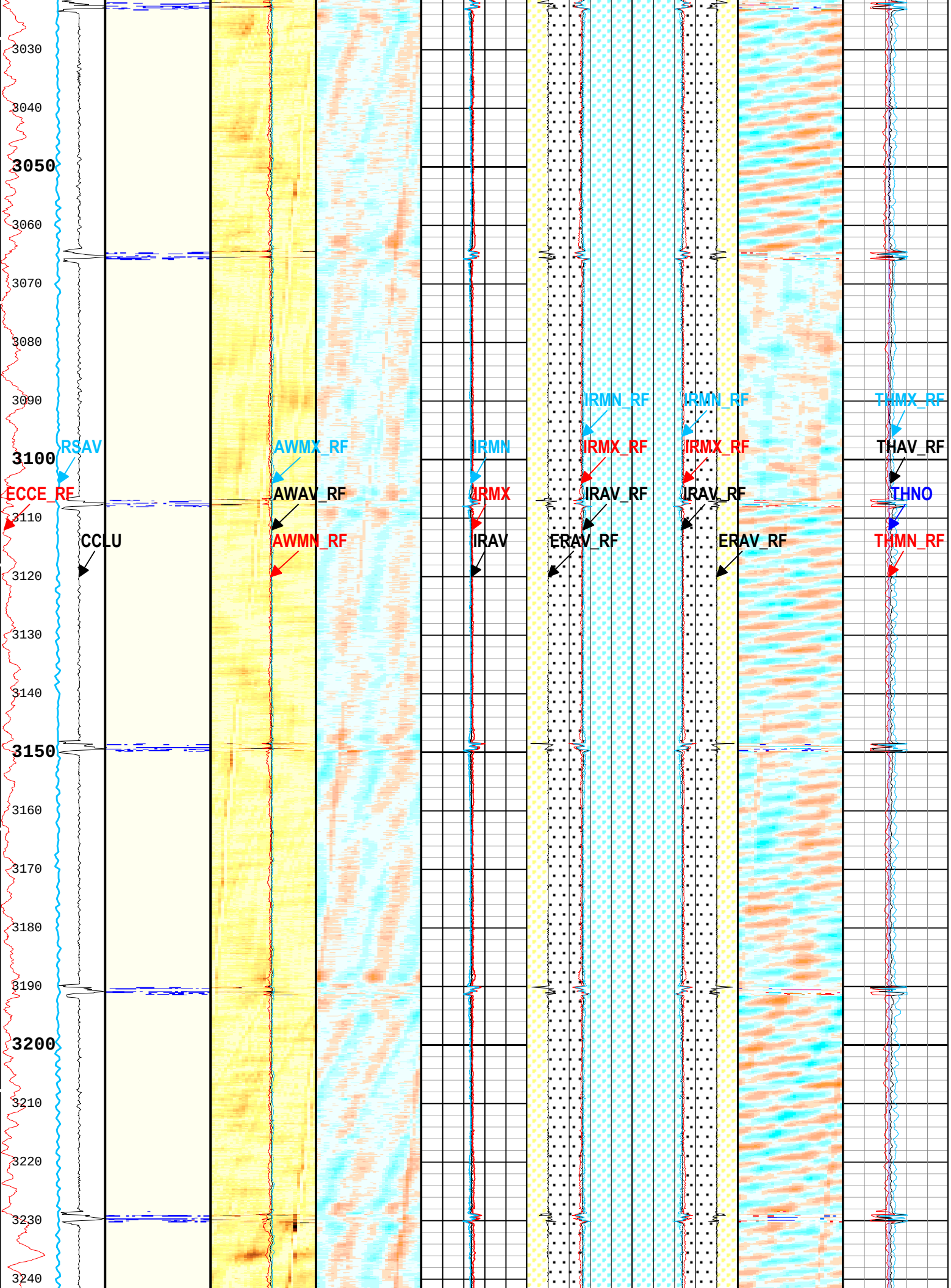
3030
3040
3050
3060
3070
3080
3090
3100
3110
3120
3130
3140
3150
3160
3170
3180
3190
3200
3210
3220
3230
3240
RSAV
ECCE_RF
CCLU
AWMX_RF
AWAV_RF
AWMN_RF
IRMN
IRMX
IRAV
IRMN_RF
IRMX_RF
IRAV_RF
ERAV_RF
IRMN_RF
IRMX_RF
IRAV_RF
ERAV_RF
THMX_RF
THAV_RF
THNO
THMN_RF

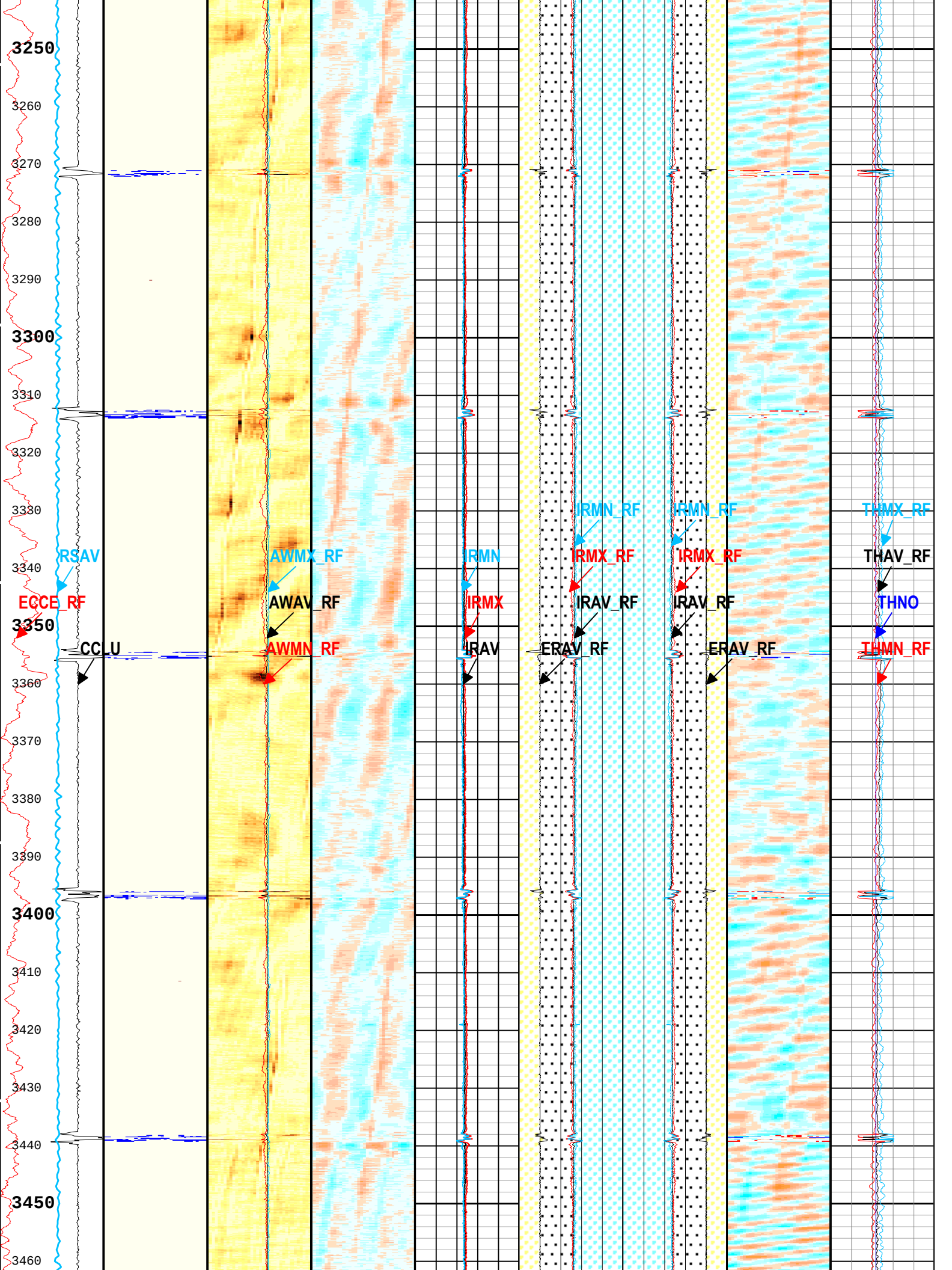
3250
3260
3270
3280
3290
3300
3310
3320
3330
3340
3350
3360
3370
3380
3390
3400
3410
3420
3430
3440
3450
3460
RSAV
ECCE_RF
CCLU
AWMX_RF
AWAV_RF
AWMN_RF
IRMN
IRMX
IRAV
IRMN_RF
IRMX_RF
IRAV_RF
ERAV_RF
IRMN_RF
IRMX_RF
IRAV_RF
ERAV_RF
THMX_RF
THAV_RF
THNO
THMN_RF

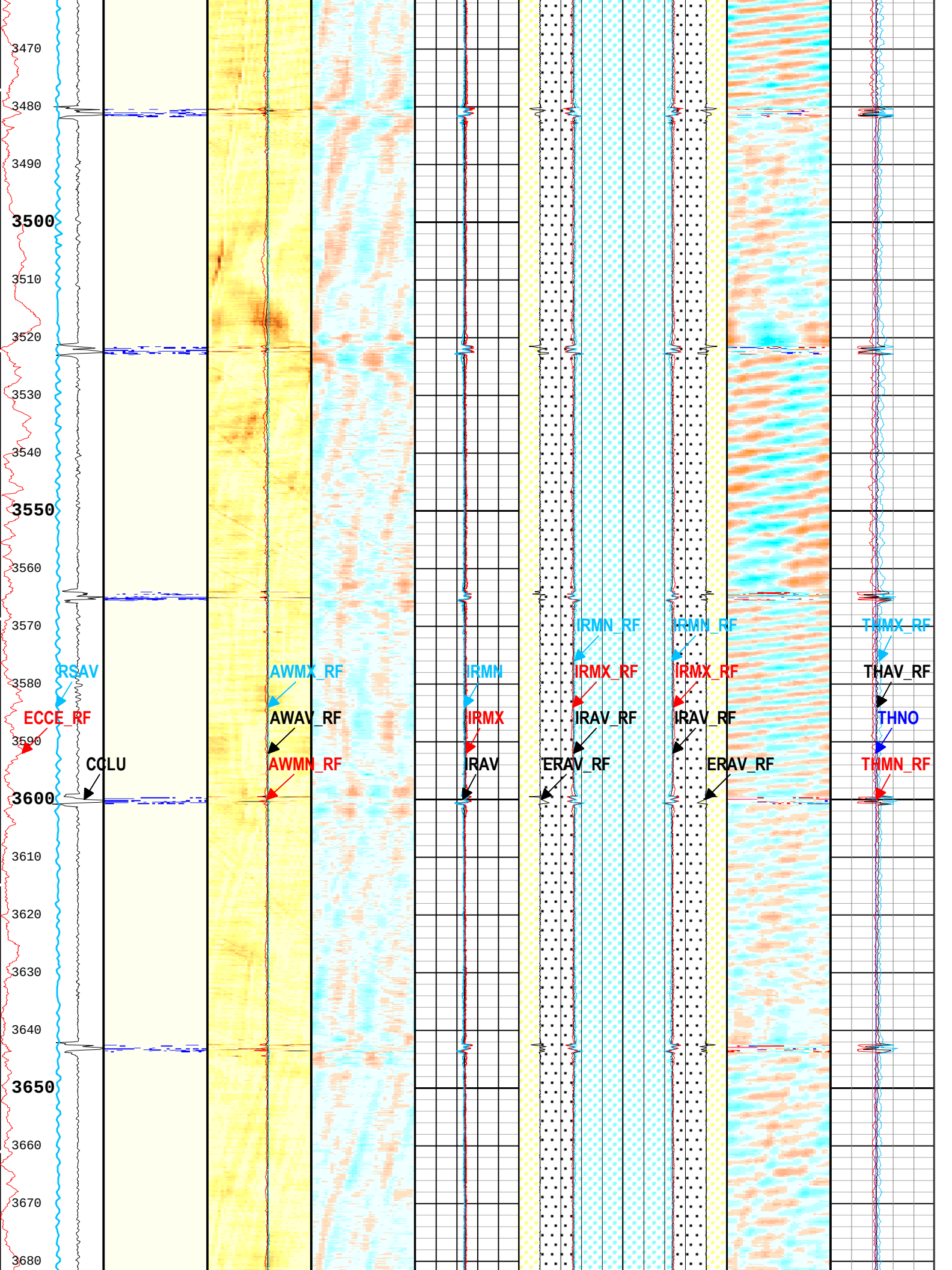
3470
3480
3490
3500
3510
3520
3530
3540
3550
3560
3570
3580
3590
3600
3610
3620
3630
3640
3650
3660
3670
3680
RSAV
ECCE_RF
CCLU
AWMX_RF
AWAV_RF
AWMN_RF
IRMN
IRMX
IRAV
IRMN_RF
IRMX_RF
IRAV_RF
ERAV_RF
IRMN_RF
IRMX_RF
IRAV_RF
ERAV_RF
THMX_RF
THAV_RF
THNO
THMN_RF

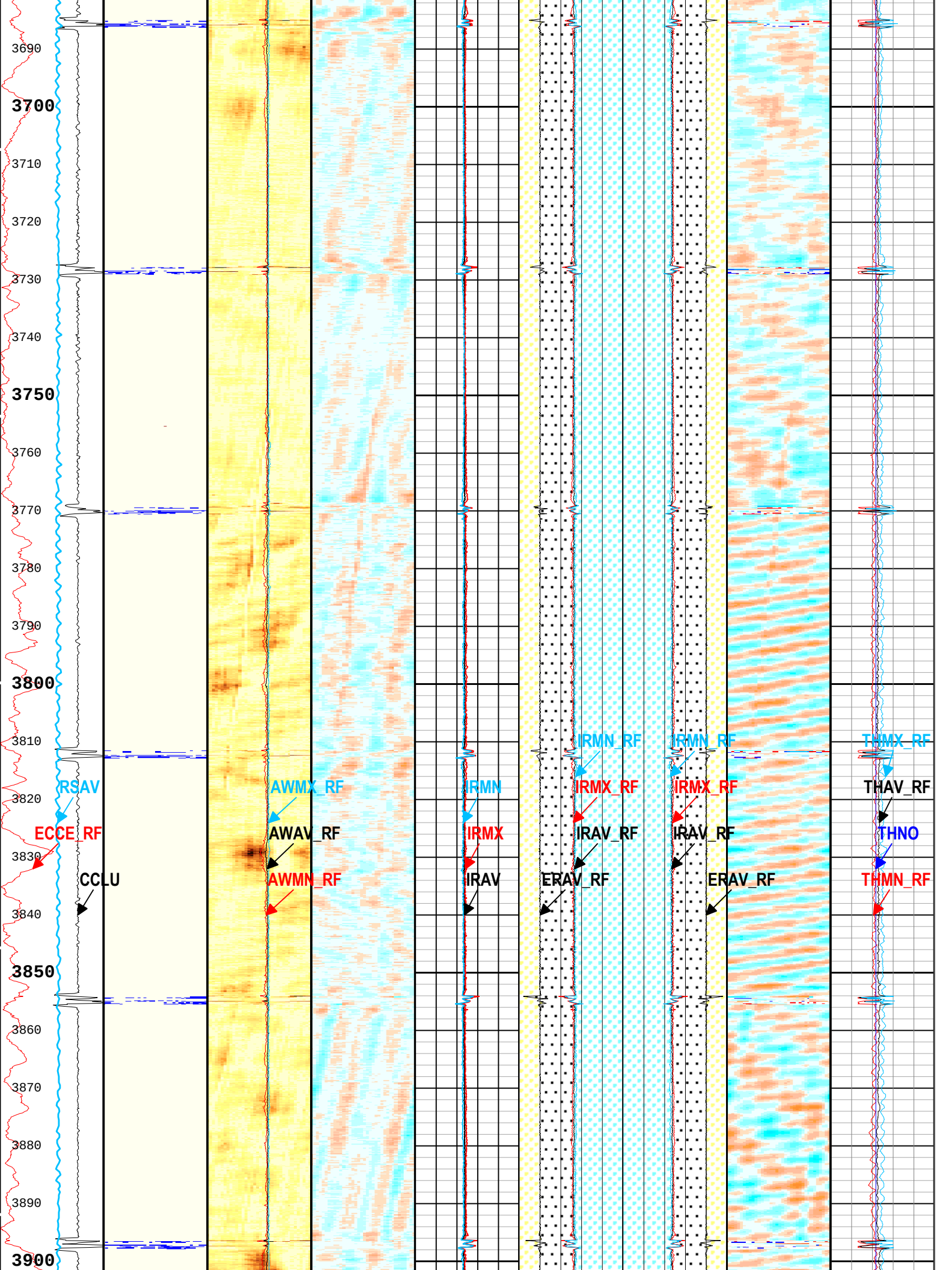
3690
3700
3710
3720
3730
3740
3750
3760
3770
3780
3790
3800
3810
3820
3830
3840
3850
3860
3870
3880
3890
3900
RSAV
ECCE_RF
CCLU
AWMX_RF
AWAV_RF
AWMN_RF
IRMN
IRMX
IRAV
IRMN_RF
IRMX_RF
IRAV_RF
ERAV_RF
IRMN_RF
IRMX_RF
IRAV_RF
ERAV_RF
THMX_RF
THAV_RF
THNO
THMN_RF

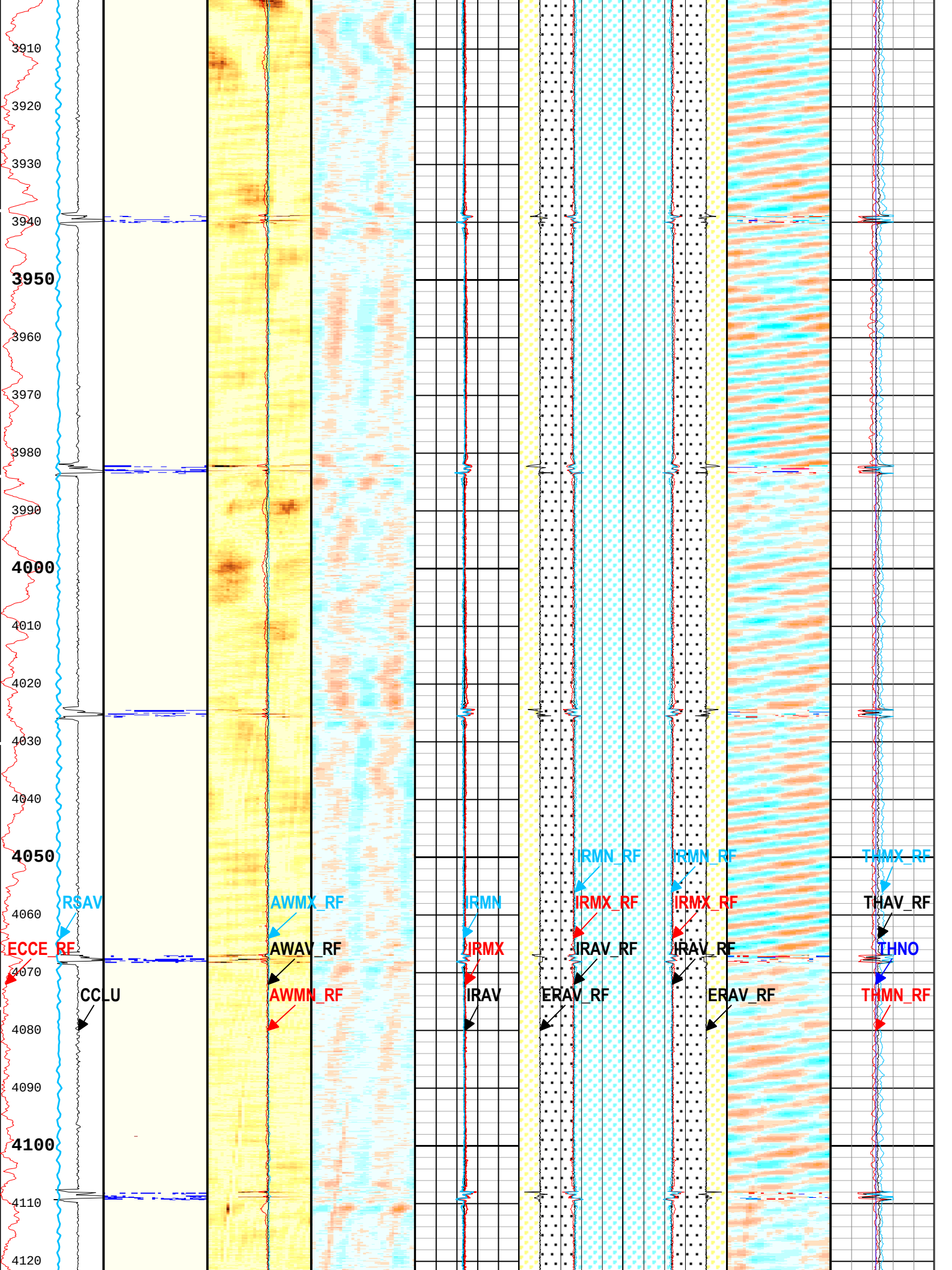
3910
3920
3930
3940
3950
3960
3970
3980
3990
4000
4010
4020
4030
4040
4050
4060
4070
4080
4090
4100
4110
4120
RSAV
ECCE_RF
CCLU
AWMX_RF
AWAV_RF
AWMN_RF
IRMN
IRMX
IRAV
IRMN_RF
IRMX_RF
IRAV_RF
ERAV_RF
IRMN_RF
IRMX_RF
IRAV_RF
ERAV_RF
THMX_RF
THAV_RF
THNO
THMN_RF

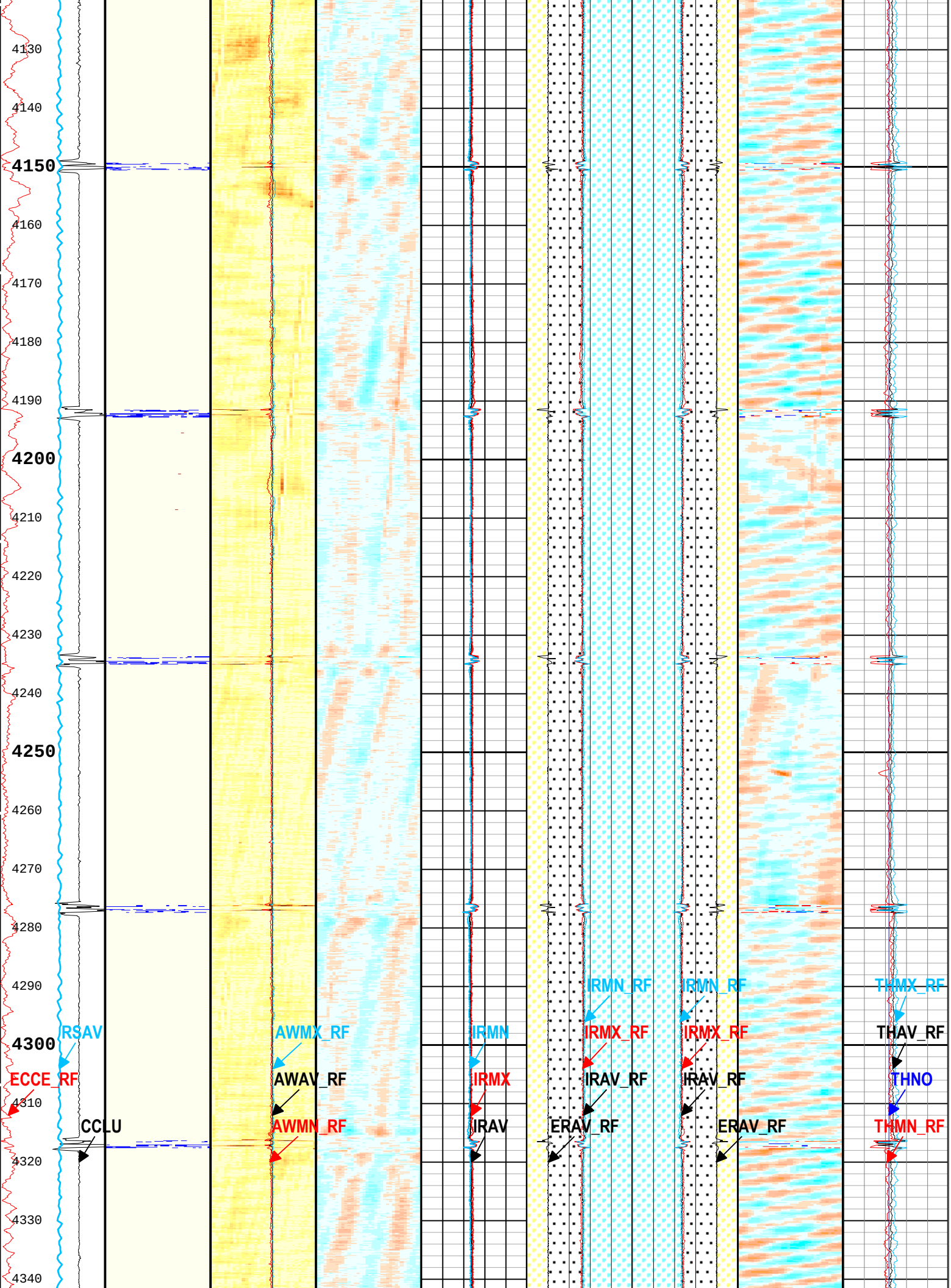
4130
4140
4150
4160
4170
4180
4190
4200
4210
4220
4230
4240
4250
4260
4270
4280
4290
4300
4310
4320
4330
4340
IRSAV
ECCE_RF
CCLU
AWMX_RF
AWAV_RF
AWMN_RF
IRMN
IRMX
IRAV
IRMN_RF
IRMX_RF
IRAV_RF
ERAV_RF
IRMN_RF
IRMX_RF
IRAV_RF
ERAV_RF
THMX_RF
THAV_RF
THNO
THMN_RF

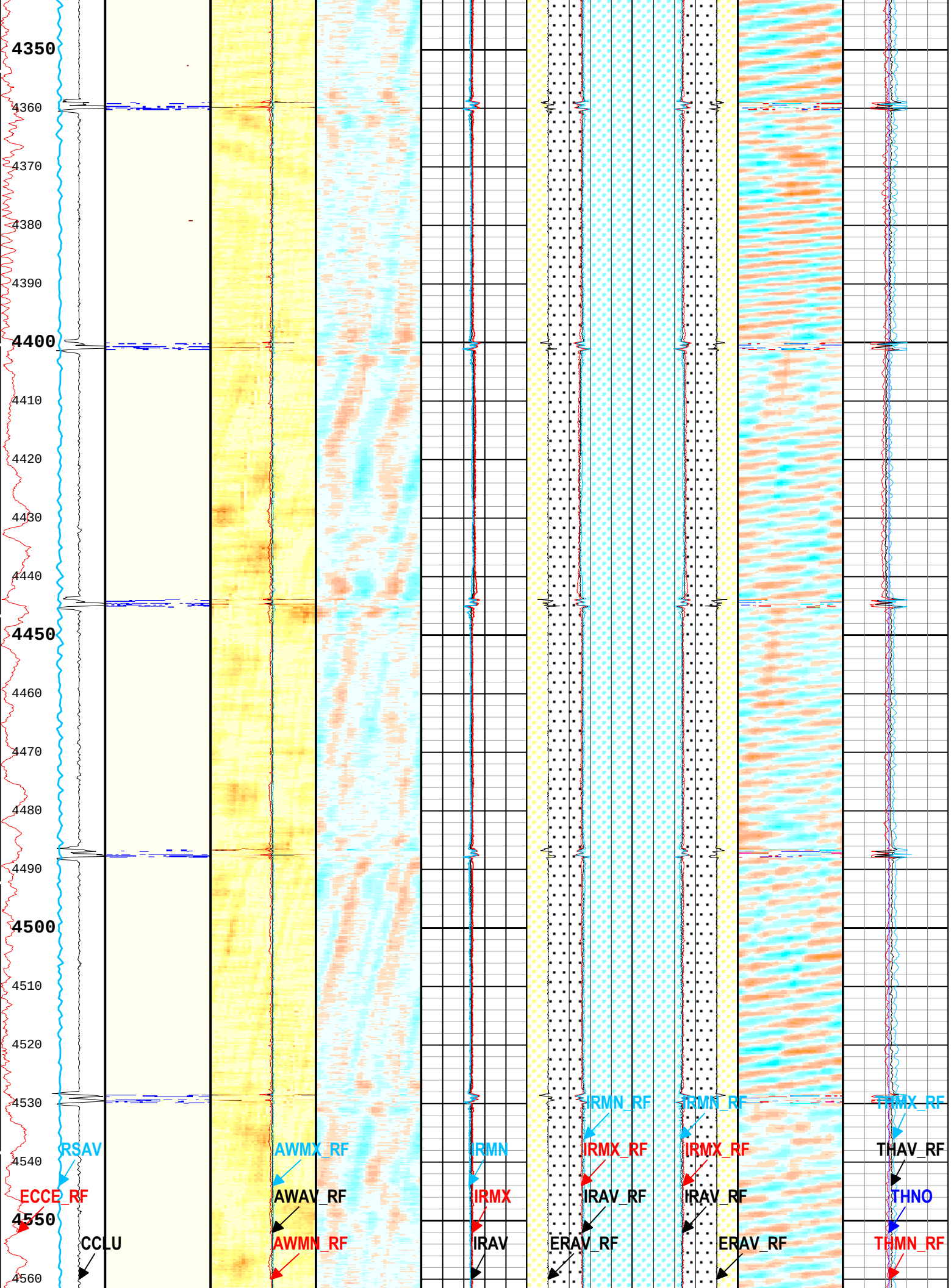
4350
4360
4370
4380
4390
4400
4410
4420
4430
4440
4450
4460
4470
4480
4490
4500
4510
4520
4530
4540
4550
4560
RSAV
ECCE_RF
CCLU
AWMX_RF
AWAV_RF
AWMN_RF
IRMN
IRMX
IRAV
IRMN_RF
IRMX_RF
IRAV_RF
ERAV_RF
IRMN_RF
IRMX_RF
IRAV_RF
ERAV_RF
THMX_RF
THAV_RF
THNO
THMN_RF

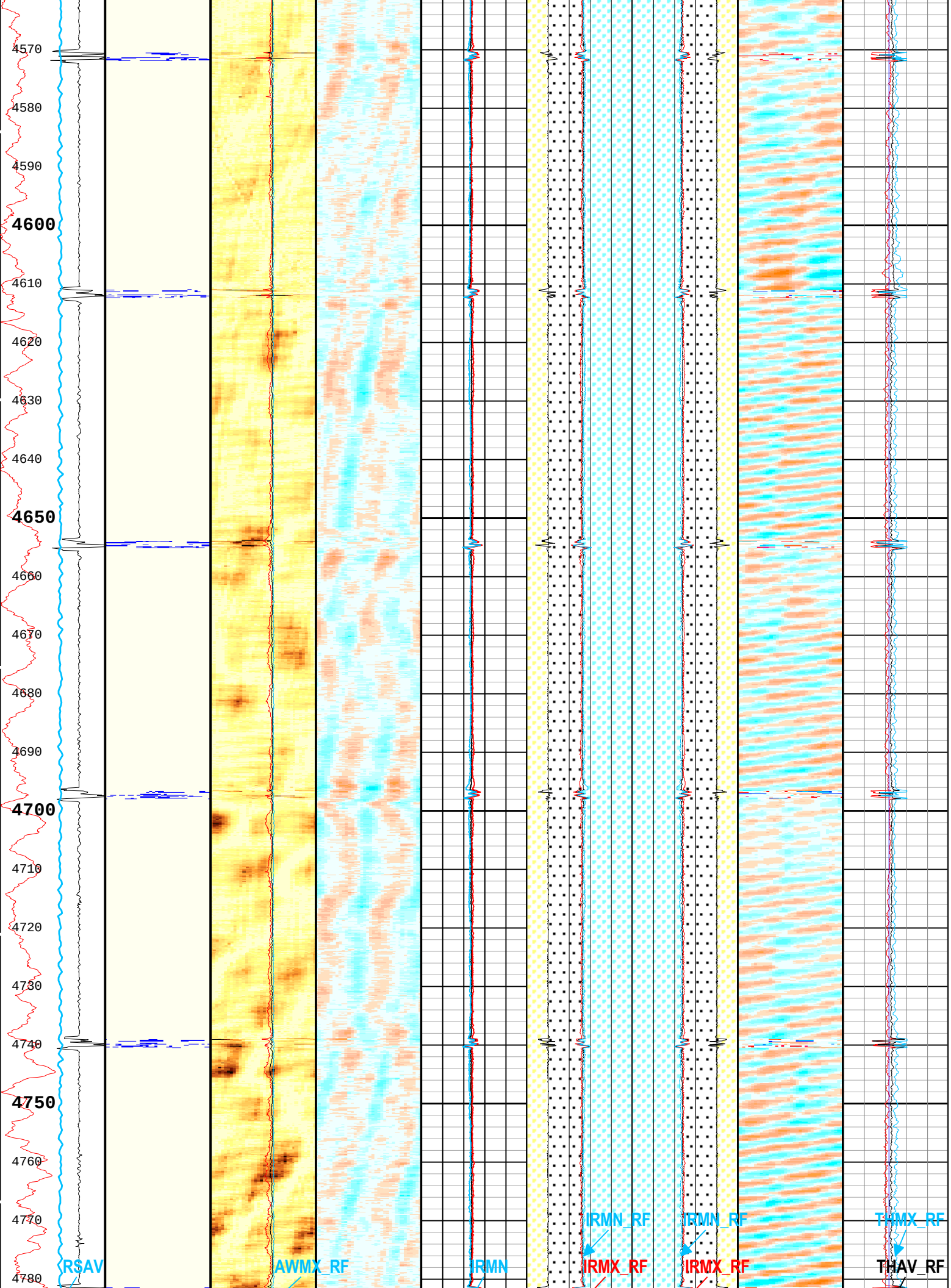
4570
4580
4590
4600
4610
4620
4630
4640
4650
4660
4670
4680
4690
4700
4710
4720
4730
4740
4750
4760
4770
4780
RSAV
AWMX_RF
IRMN
IRMN_RF
IRMX_RF
IRMN_RF
IRMX_RF
THMX_RF
THAV_RF

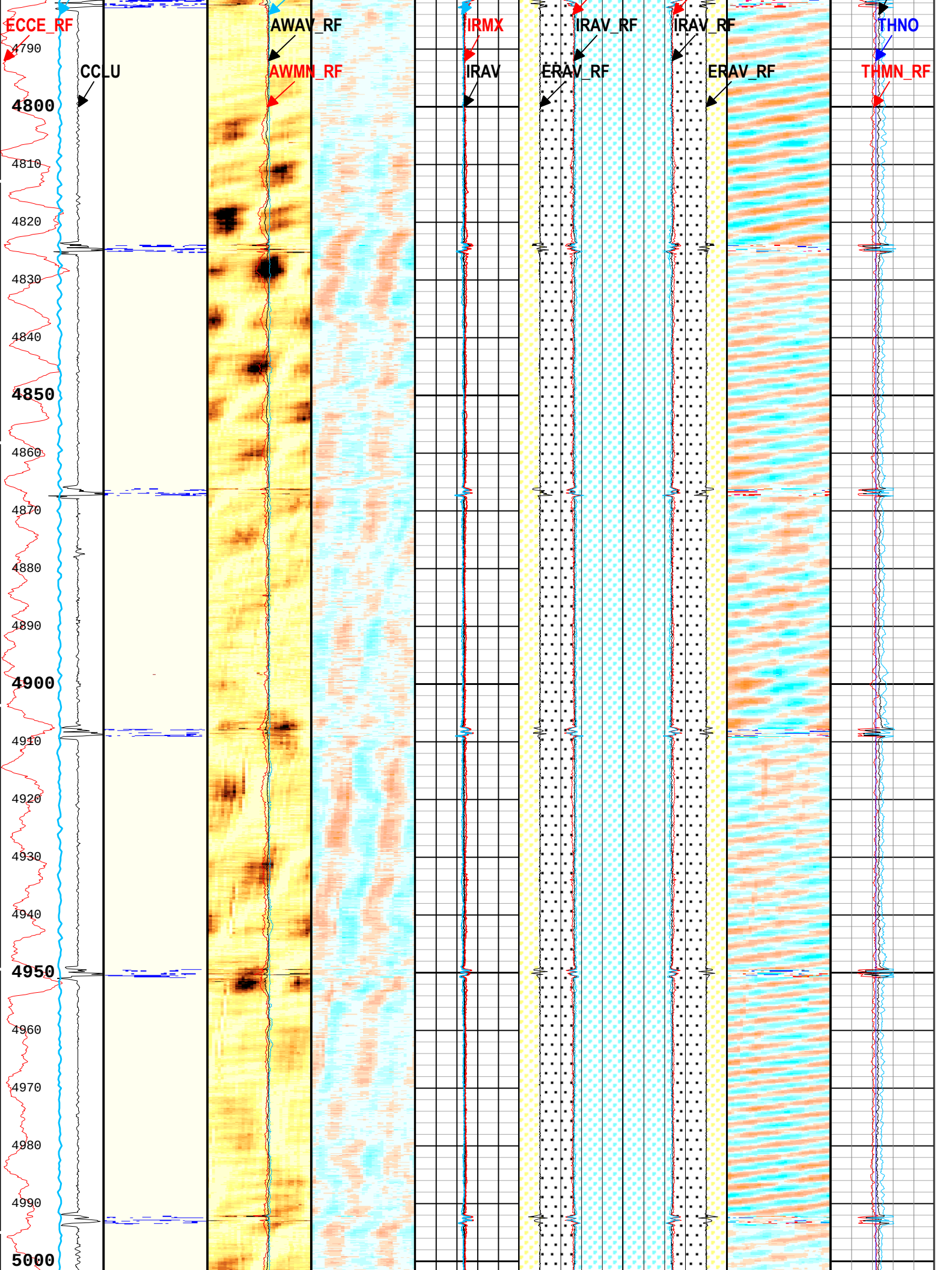
ECCE_RF
CCLU
AWAV_RF
AWMN_RF
IRMX
IRAV
IRAV_RF
ERAV_RF
IRAV_RF
ERAV_RF
THNO
THMN_RF
4790
4800
4810
4820
4830
4840
4850
4860
4870
4880
4890
4900
4910
4920
4930
4940
4950
4960
4970
4980
4990
5000

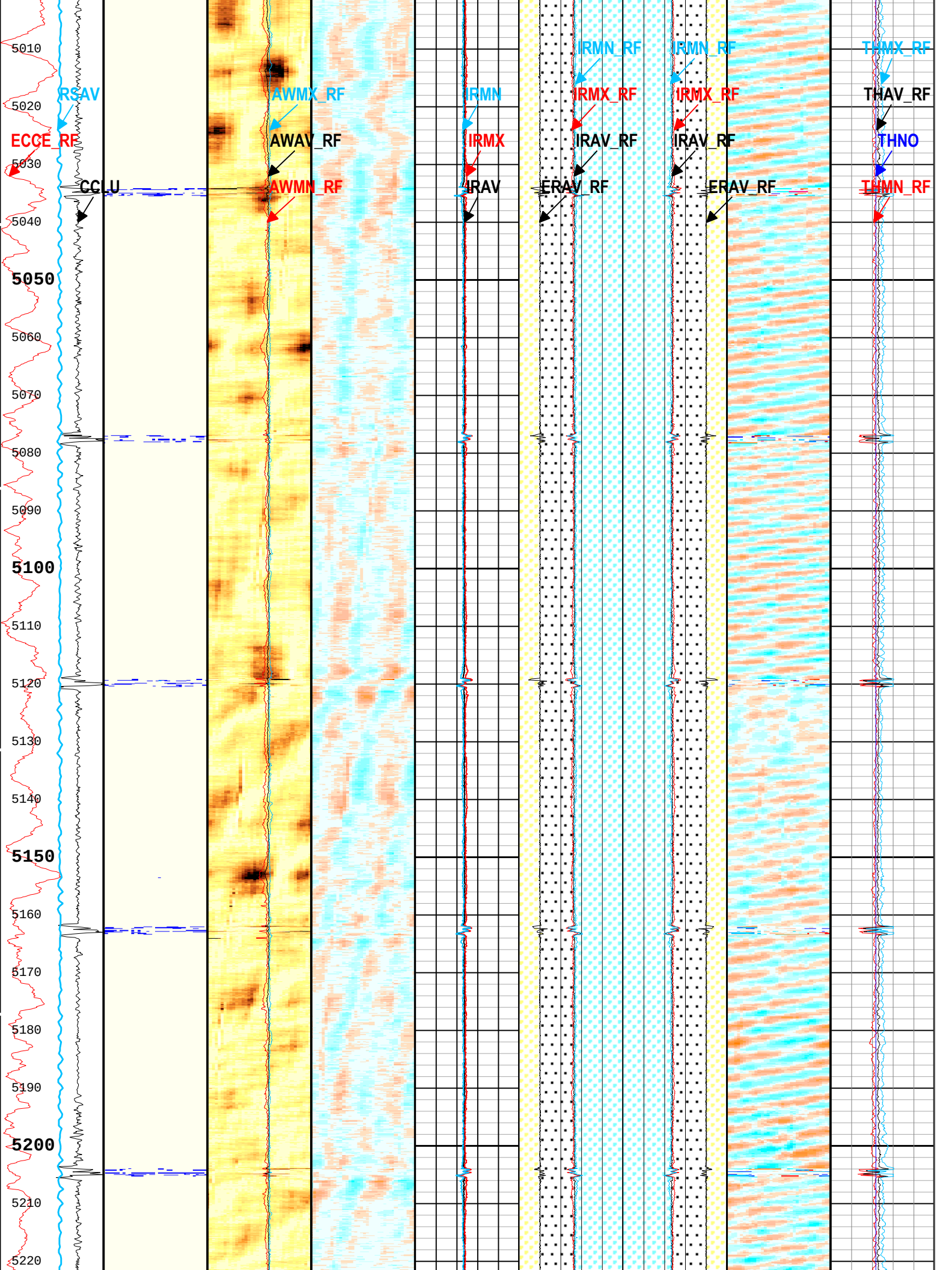
5010
5020
5030
5040
5050
5060
5070
5080
5090
5100
5110
5120
5130
5140
5150
5160
5170
5180
5190
5200
5210
5220
RSAV
ECCE_RF
CCLU
AWMX_RF
AWAV_RF
AWMN_RF
IRMN
IRMX
IRAV
IRMN_RF
IRMX_RF
IRAV_RF
ERAV_RF
IRMN_RF
IRMX_RF
IRAV_RF
ERAV_RF
THMX_RF
THAV_RF
THNO
THMN_RF

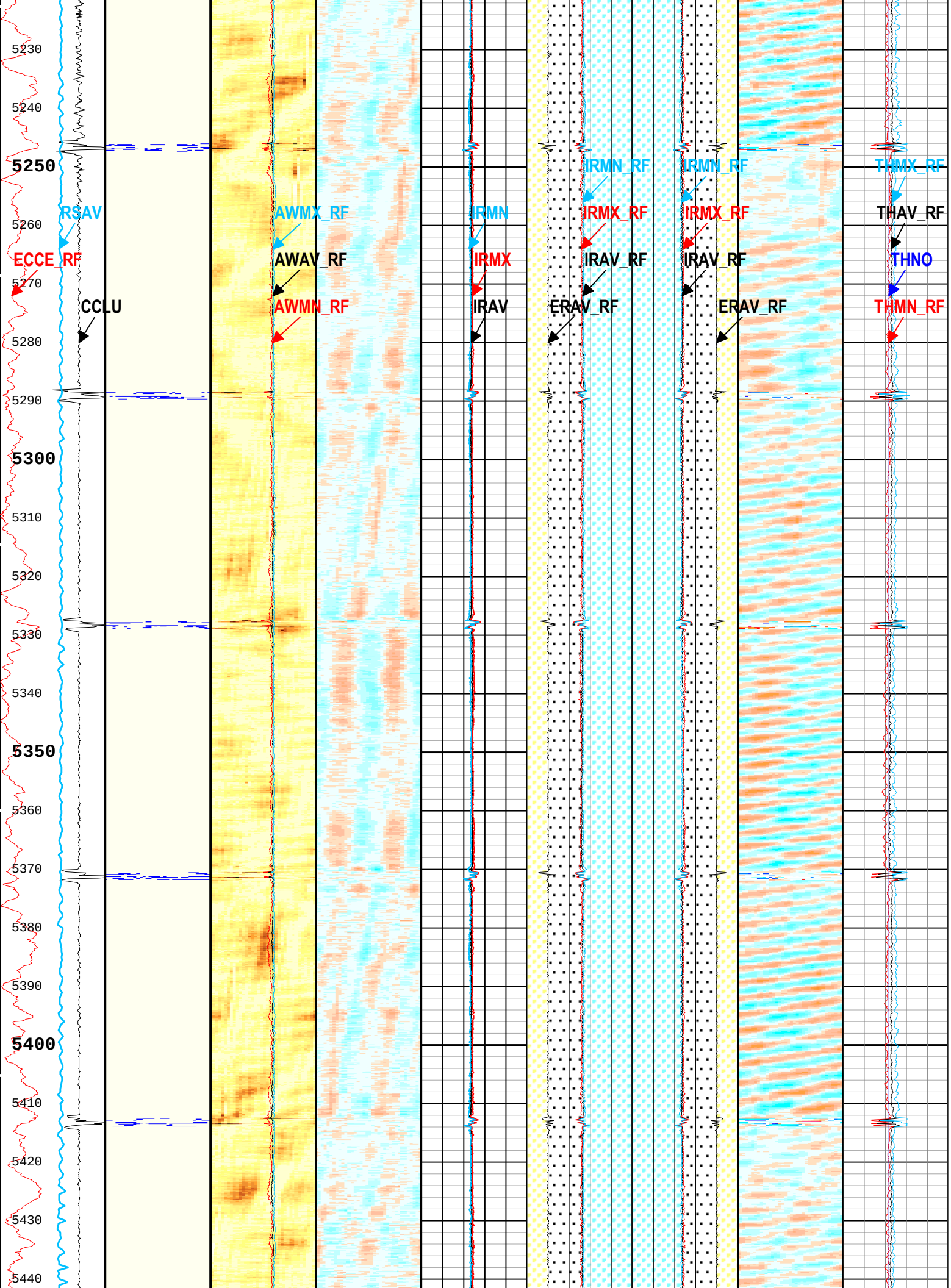
5230
5240
5250
5260
5270
5280
5290
5300
5310
5320
5330
5340
5350
5360
5370
5380
5390
5400
5410
5420
5430
5440
RSAV
ECCE_RF
CCLU
AWMX_RF
AWAV_RF
AWMN_RF
IRMN
IRMX
IRAV
IRMN_RF
IRMX_RF
IRAV_RF
ERAV_RF
IRMN_RF
IRMX_RF
IRAV_RF
ERAV_RF
THMX_RF
THAV_RF
THNO
THMN_RF

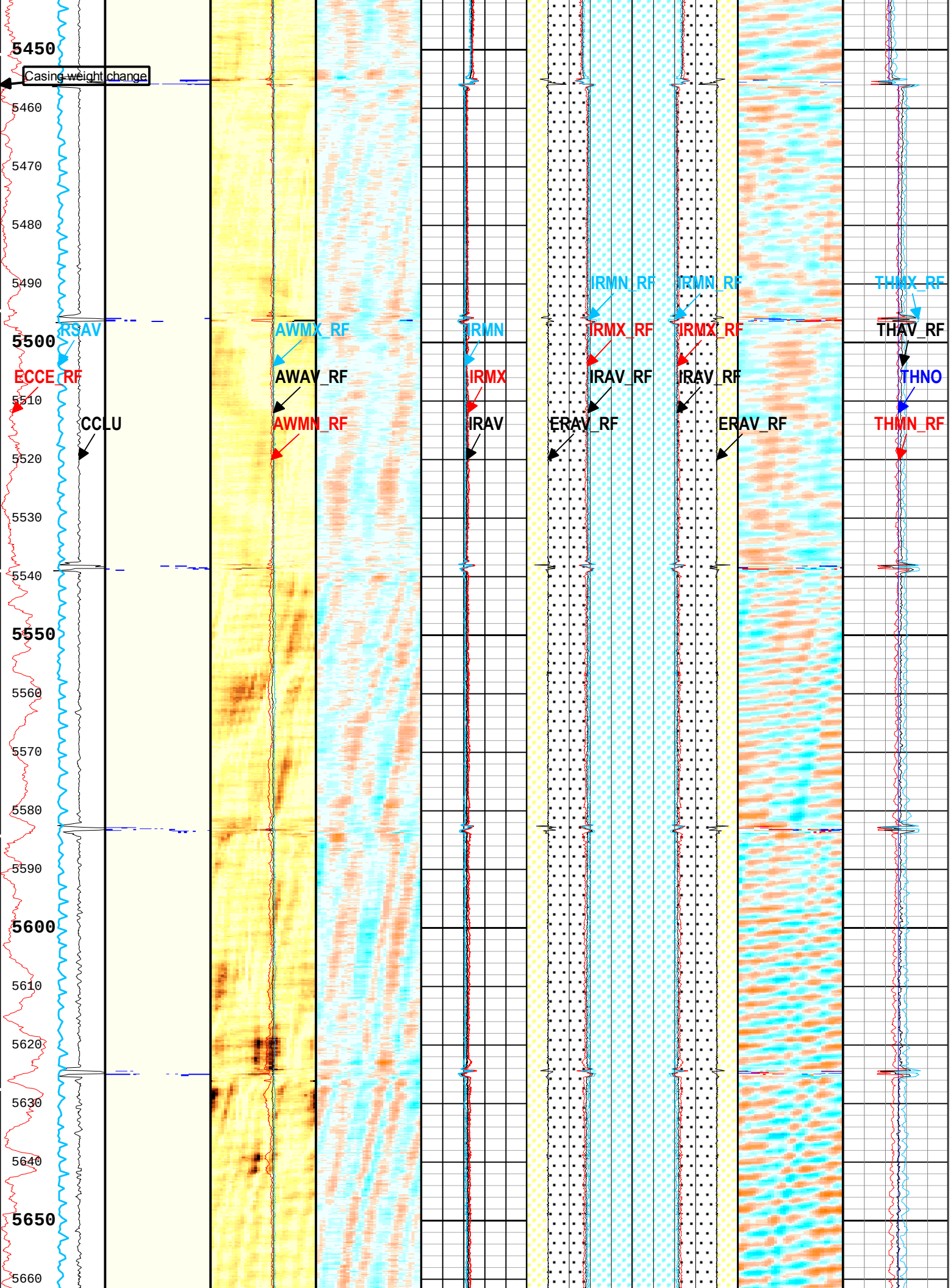
5450
Casing weight change
5460
5470
5480
5490
5500
5510
5520
5530
5540
5550
5560
5570
5580
5590
5600
5610
5620
5630
5640
5650
5660
RSAV
ECCE_RF
CCLU
AWMX_RF
AWAV_RF
AWMN_RF
IRMN
IRMX
IRAV
IRMN_RF
IRMX_RF
IRAV_RF
ERAV_RF
IRMN_RF
IRMX_RF
IRAV_RF
ERAV_RF
THMX_RF
THAV_RF
THNO
THMN_RF

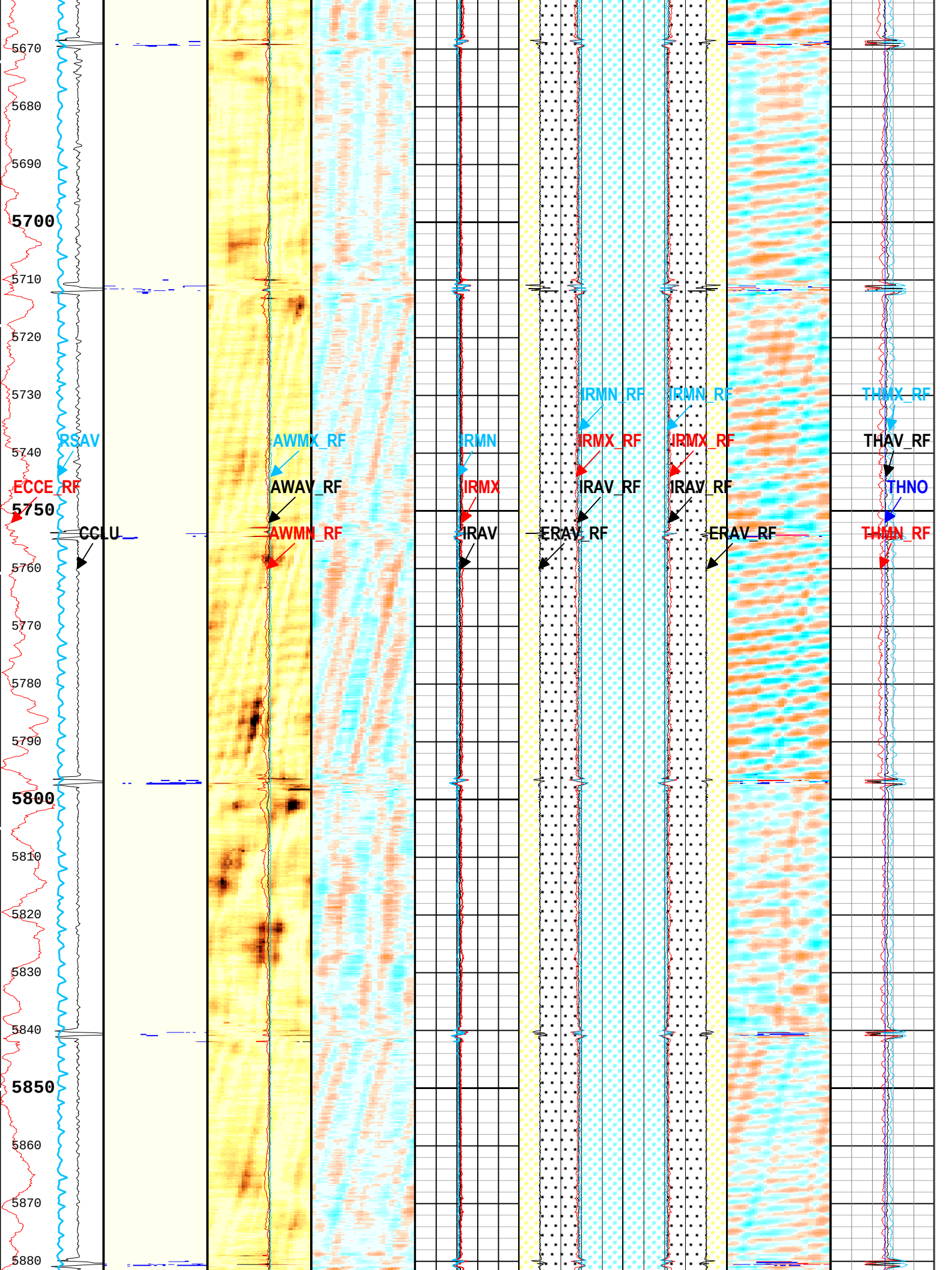
5670
5680
5690
5700
5710
5720
5730
5740
5750
5760
5770
5780
5790
5800
5810
5820
5830
5840
5850
5860
5870
5880
RSAV
ECCE_RF
CCLU
AWMX_RF
AWAV_RF
AWMN_RF
IRMN
IRMX
IRAV
IRMN_RF
IRMX_RF
IRAV_RF
ERAV_RF
IRMN_RF
IRMX_RF
IRAV_RF
ERAV_RF
THMX_RF
THAV_RF
THNO
THMN_RF

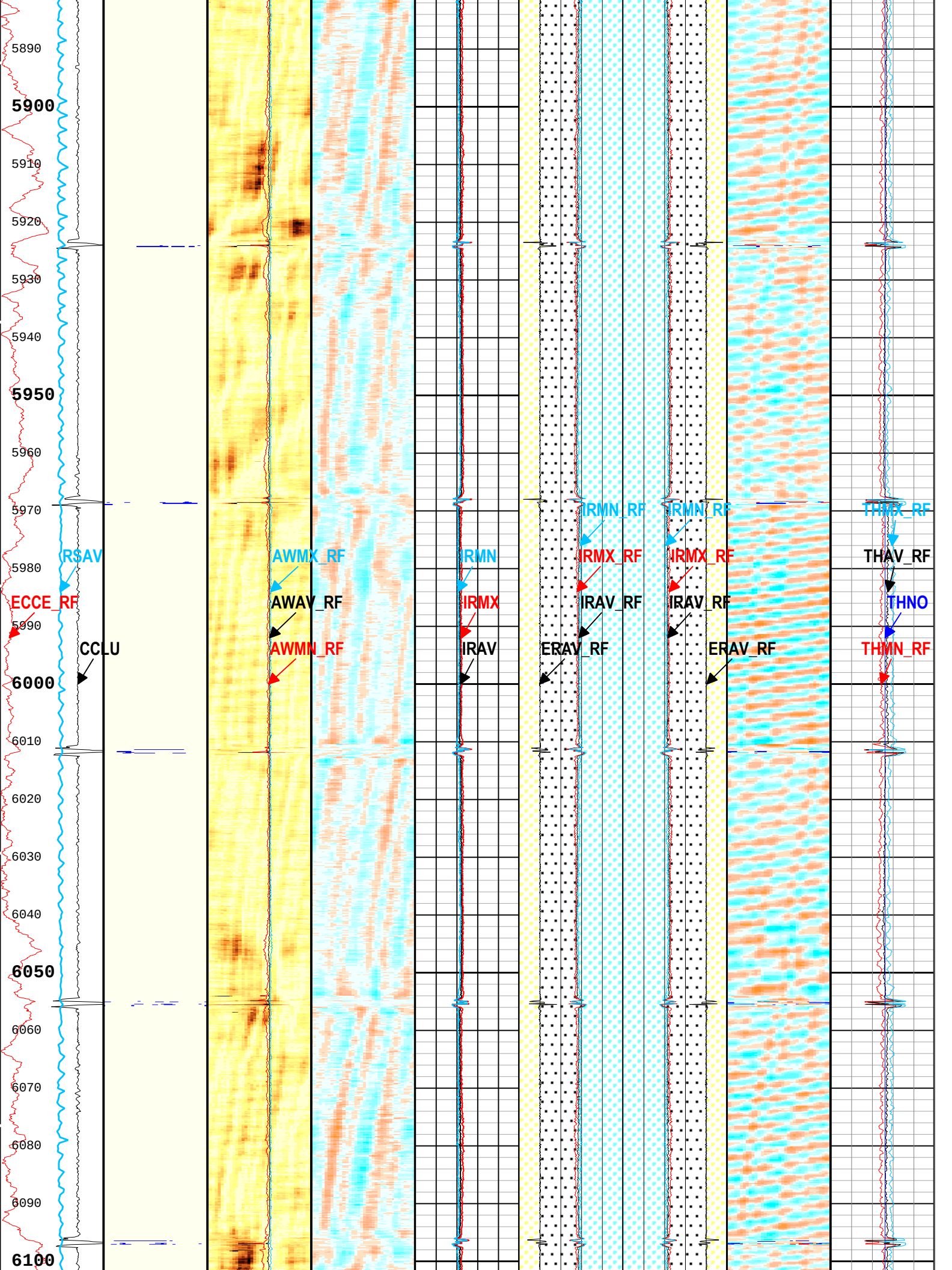
5890
5900
5910
5920
5930
5940
5950
5960
5970
5980
5990
6000
6010
6020
6030
6040
6050
6060
6070
6080
6090
6100
RSAV
ECCE_RF
CCLU
AWMX_RF
AWAV_RF
AWMN_RF
IRMN
IRMX
IRAV
IRMN_RF
IRMX_RF
IRAV_RF
ERAV_RF
IRMN_RF
IRMX_RF
IRAV_RF
ERAV_RF
THMX_RF
THAV_RF
THNO
THMN_RF

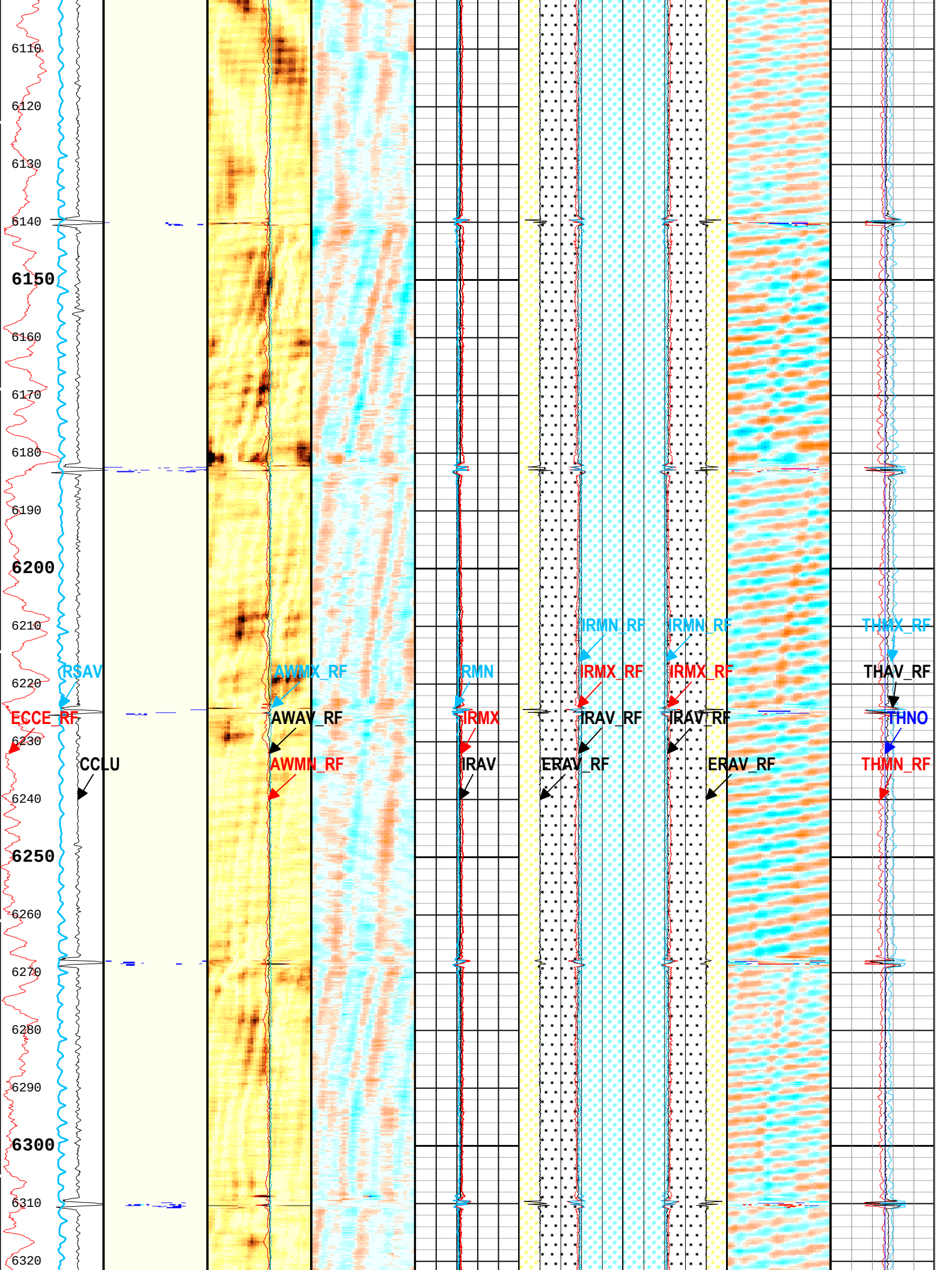
6110
6120
6130
6140
6150
6160
6170
6180
6190
6200
6210
6220
6230
6240
6250
6260
6270
6280
6290
6300
6310
6320
RSAV
ECCE_RF
CCLU
AWMX_RF
AWAV_RF
AWMN_RF
IRMN
IRMX
IRAV
IRMN_RF
IRMX_RF
IRAV_RF
ERAV_RF
IRMN_RF
IRMX_RF
IRAV_RF
ERAV_RF
THMX_RF
THAV_RF
THNO
THMN_RF

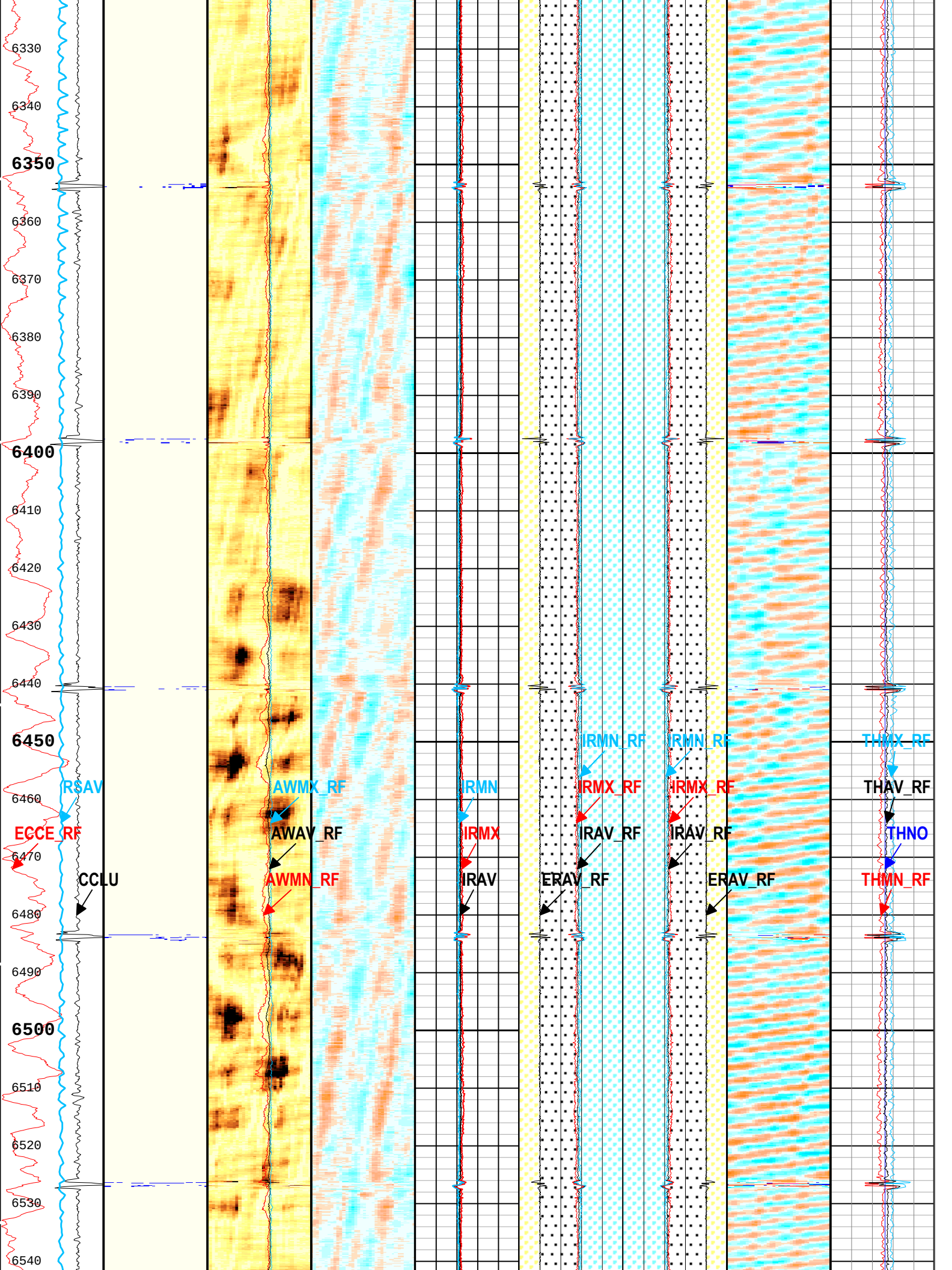
6330
6340
6350
6360
6370
6380
6390
6400
6410
6420
6430
6440
6450
6460
6470
6480
6490
6500
6510
6520
6530
6540
RSAV
ECCE_RF
CCLU
AWMX_RF
AWAV_RF
AWMN_RF
IRMN
IRMX
IRAV
IRMN_RF
IRMX_RF
IRAV_RF
ERAV_RF
IRMN_RF
IRMX_RF
IRAV_RF
ERAV_RF
THMX_RF
THAV_RF
THNO
THMN_RF

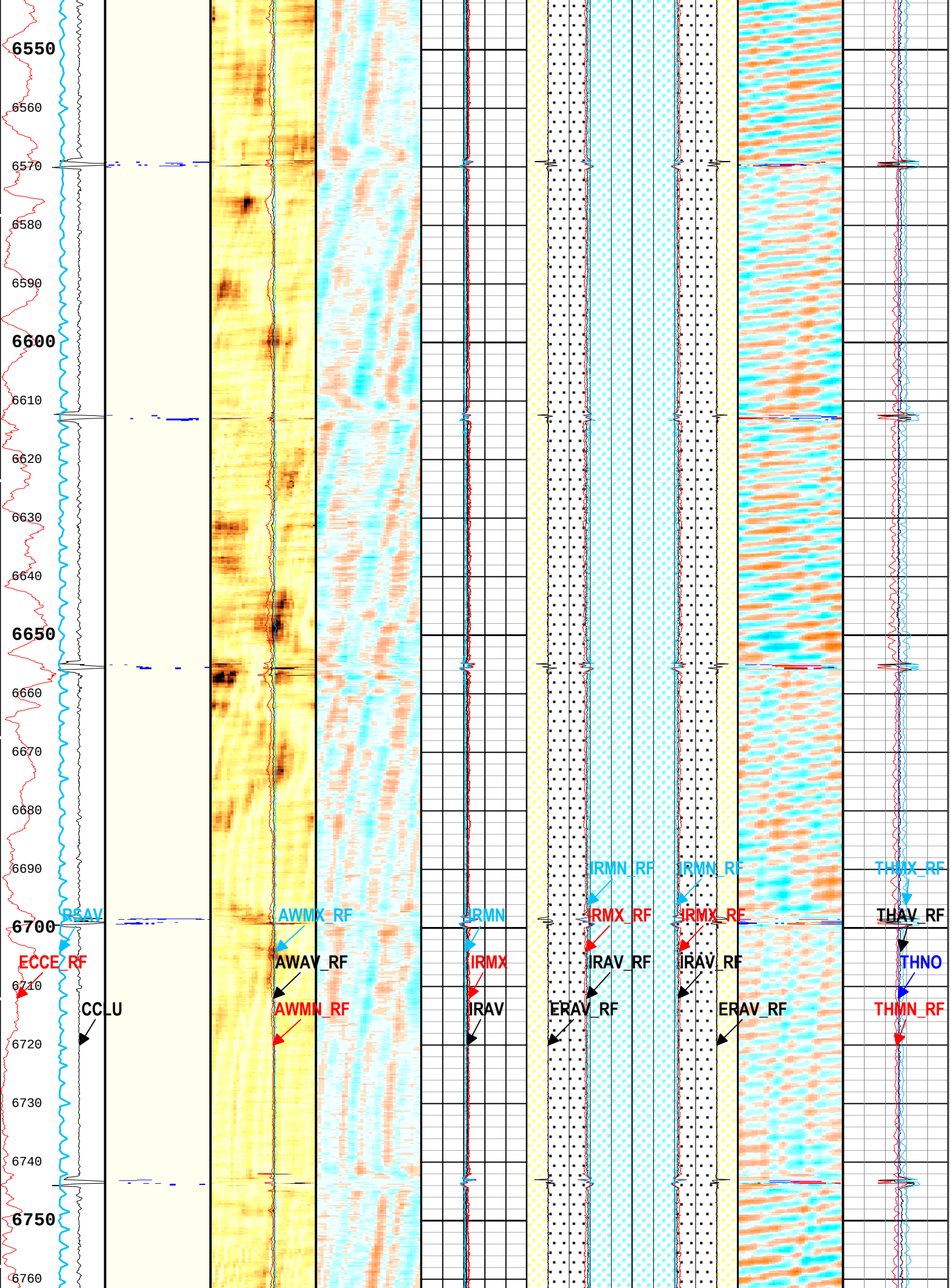
6550
6560
6570
6580
6590
6600
6610
6620
6630
6640
6650
6660
6670
6680
6690
6700
6710
6720
6730
6740
6750
6760
RSAV
ECCE_RF
CCLU
AWMX_RF
AWAV_RF
AWMN_RF
IRMN
IRMX
IRAV
IRMN_RF
IRMX_RF
IRAV_RF
ERAV_RF
IRMN_RF
IRMX_RF
IRAV_RF
ERAV_RF
THMX_RF
THAV_RF
THNO
THMN_RF

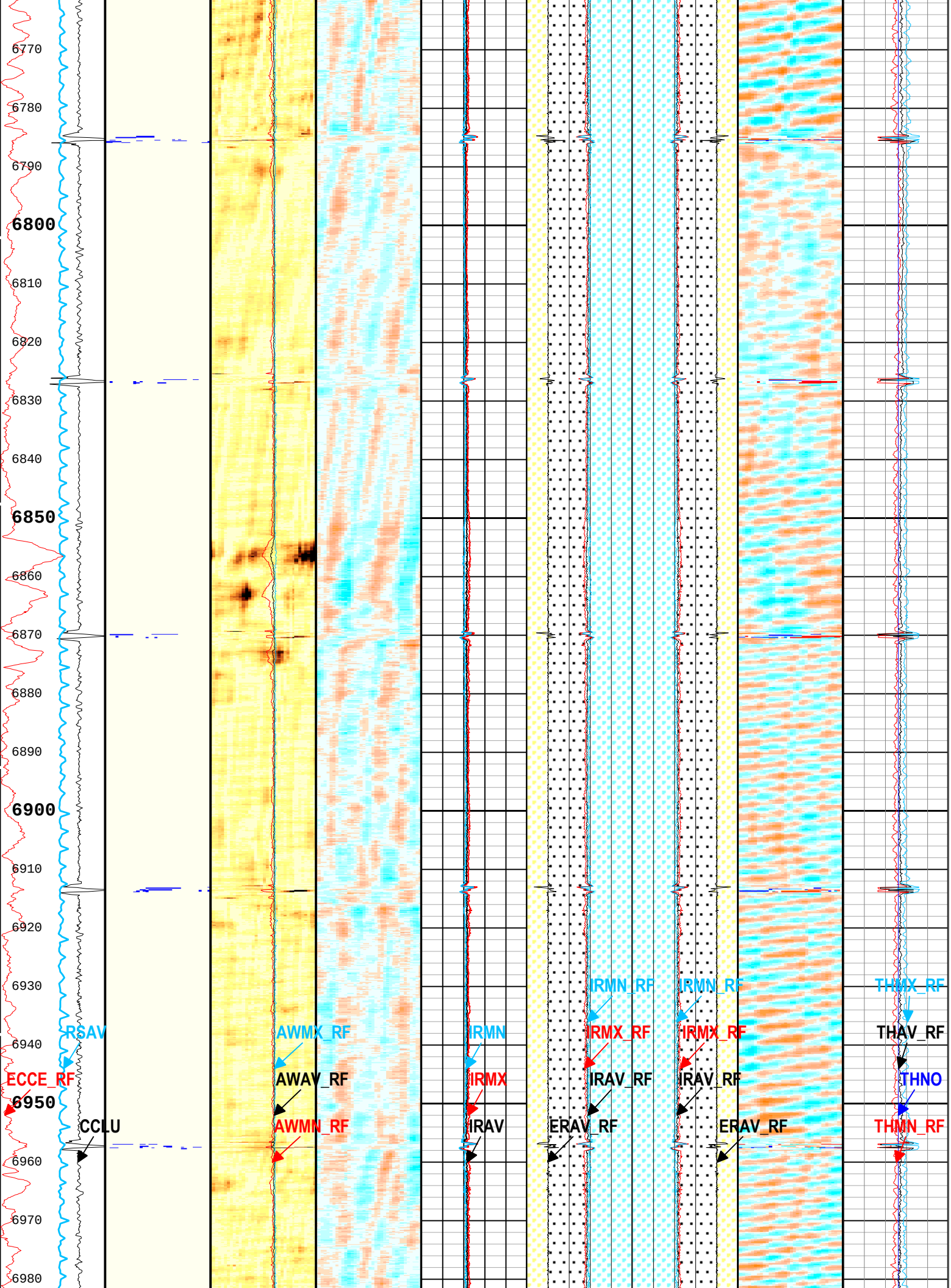
6770
6780
6790
6800
6810
6820
6830
6840
6850
6860
6870
6880
6890
6900
6910
6920
6930
6940
6950
6960
6970
6980
RSAV
ECCE_RF
CCLU
AWMX_RF
AWAV_RF
AWMN_RF
IRMN
IRMX
IRAV
IRMN_RF
IRMX_RF
IRAV_RF
ERAV_RF
IRMN_RF
IRMX_RF
IRAV_RF
ERAV_RF
THMX_RF
THAV_RF
THNO
THMN_RF

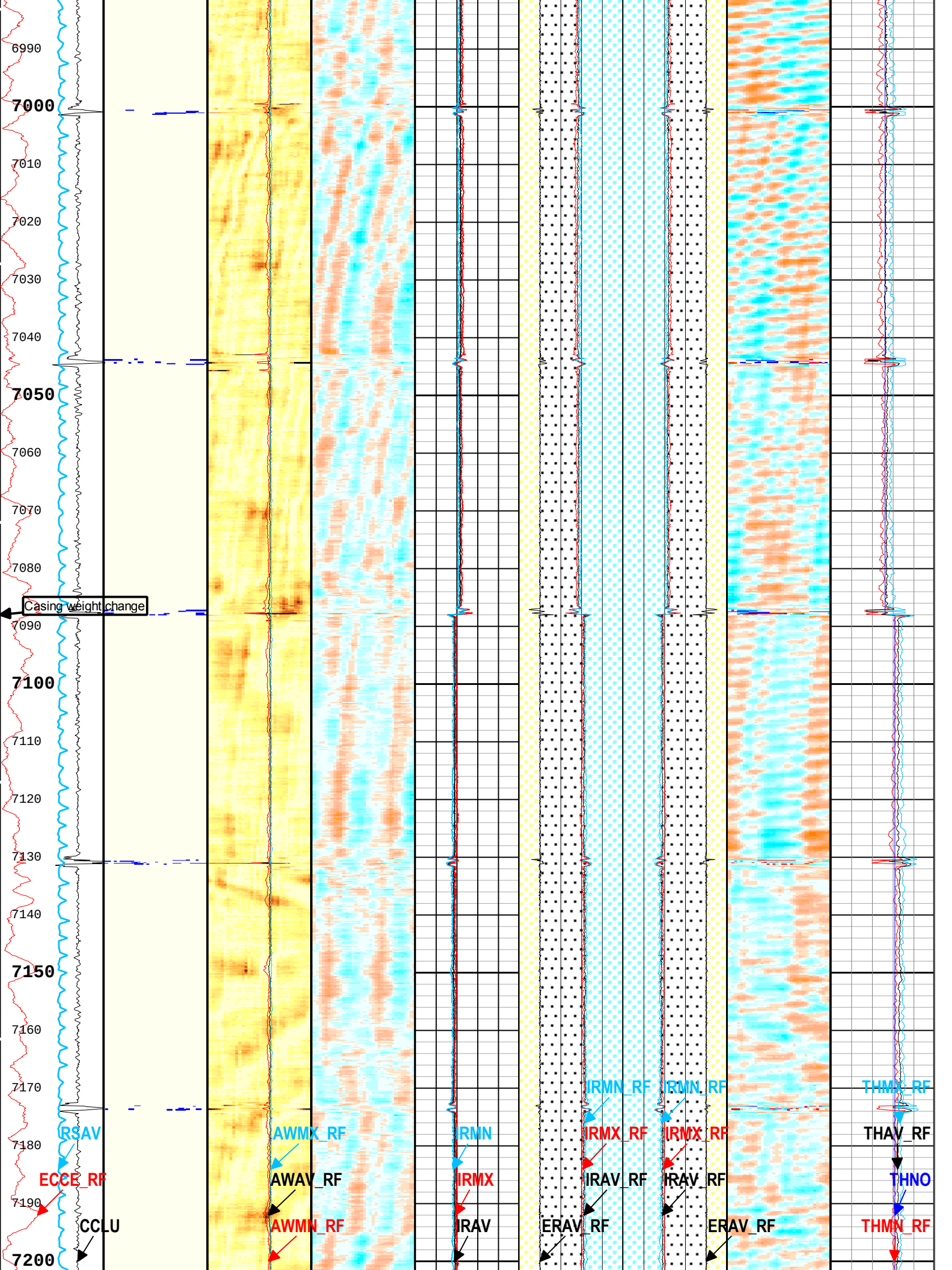
6990
7000
7010
7020
7030
7040
7050
7060
7070
7080
Casing weight change
7090
7100
7110
7120
7130
7140
7150
7160
7170
7180
7190
7200
RSAV
ECCE_RF
CCLU
AWMX_RF
AWAV_RF
AWMN_RF
IRMN
IRMX
IRAV
IRMN_RF
IRMX_RF
IRAV_RF
ERAV_RF
IRMN_RF
IRMX_RF
IRAV_RF
ERAV_RF
THMX_RF
THAV_RF
THNO
THMN_RF

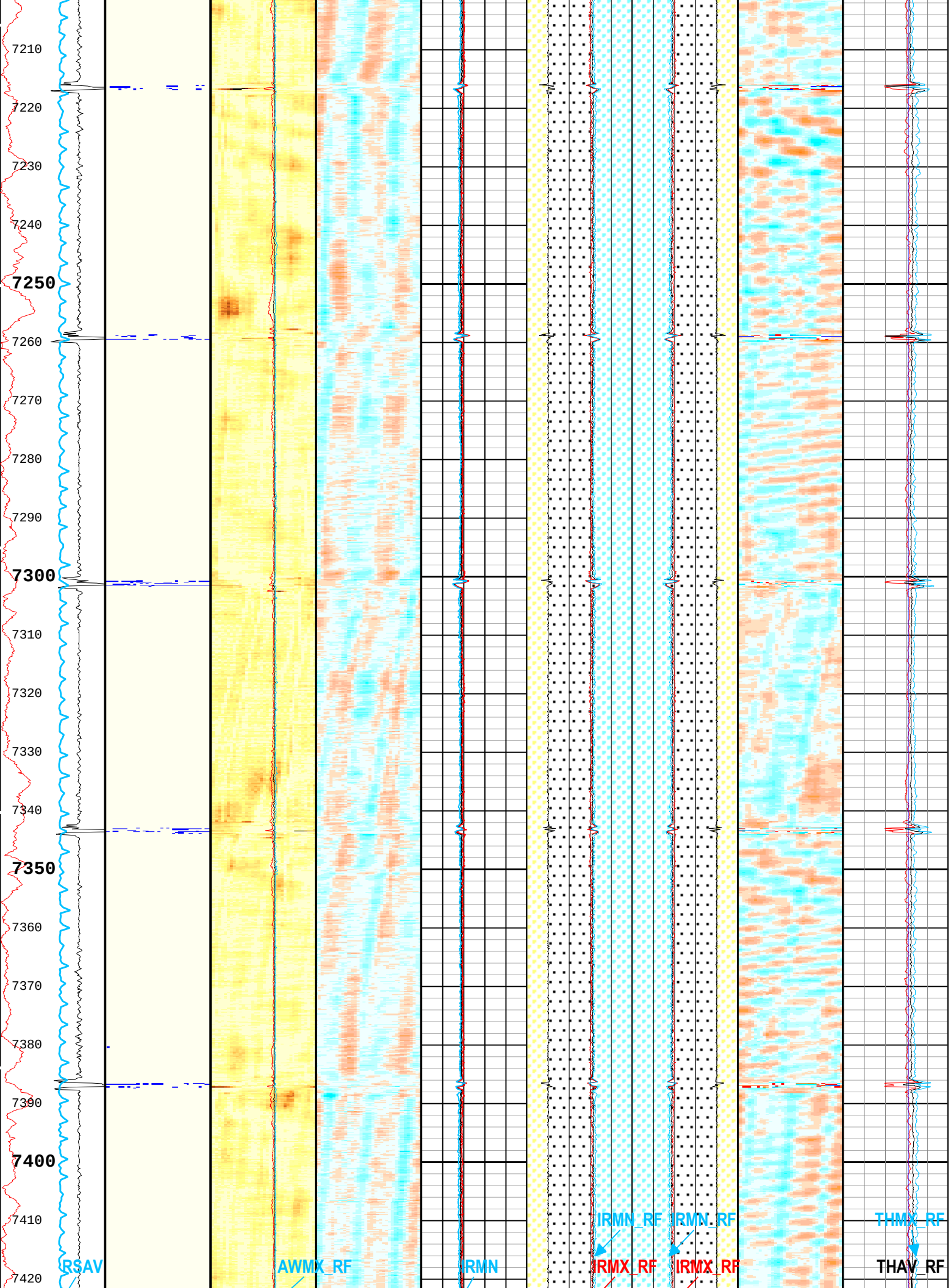
7210
7220
7230
7240
7250
7260
7270
7280
7290
7300
7310
7320
7330
7340
7350
7360
7370
7380
7390
7400
7410
7420
RSAV
AWMX_RF
IRMN
IRMN_RF
IRMX_RF
IRMN_RF
IRMX_RF
THMX_RF
THAV_RF

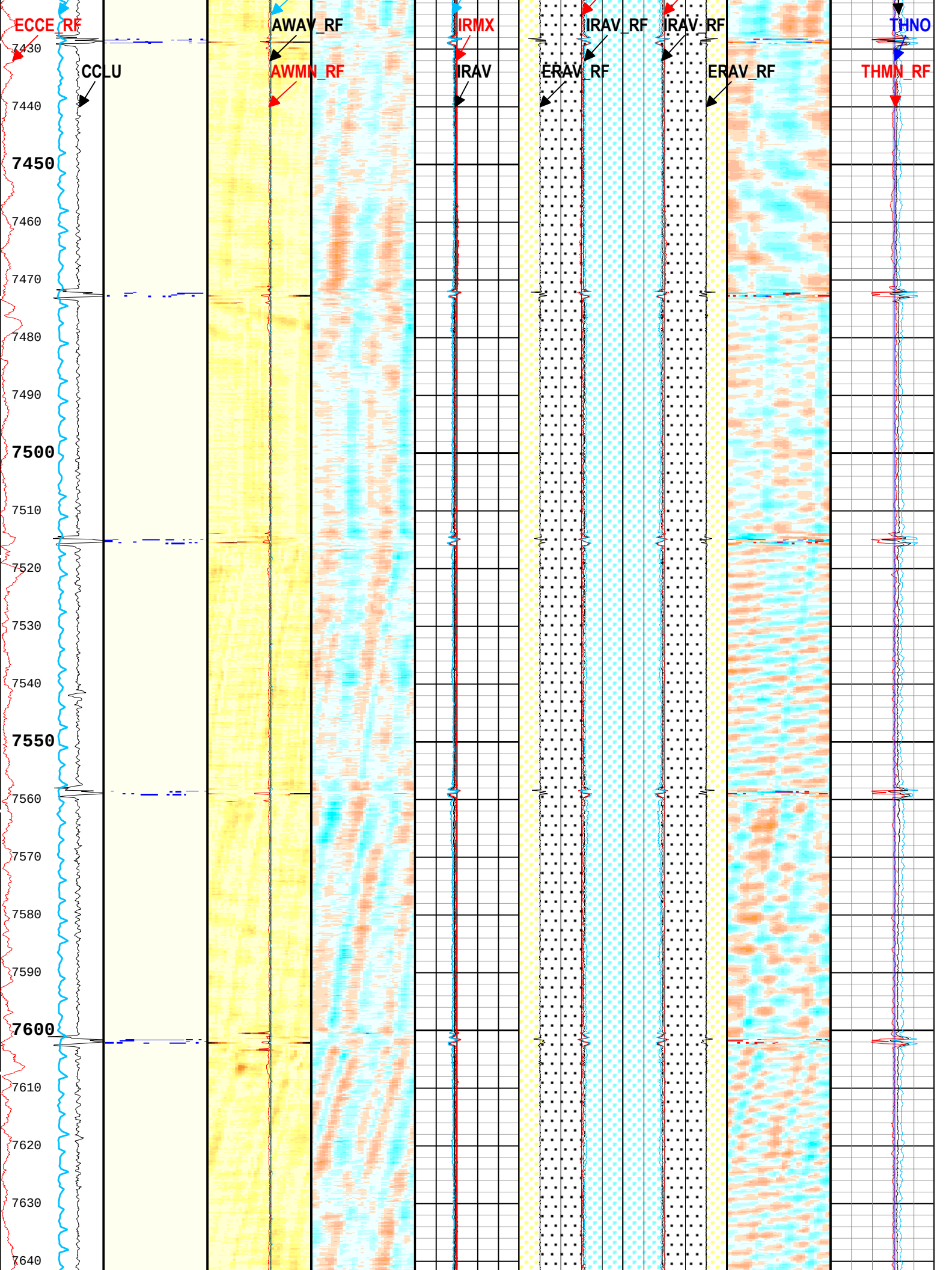
ECCE_RF
CCLU
AWAV_RF
AWMN_RF
IRMX
IRAV
IRAV_RF
ERAV_RF
IRAV_RF
ERAV_RF
THNO
THMN_RF
7430
7440
7450
7460
7470
7480
7490
7500
7510
7520
7530
7540
7550
7560
7570
7580
7590
7600
7610
7620
7630
7640

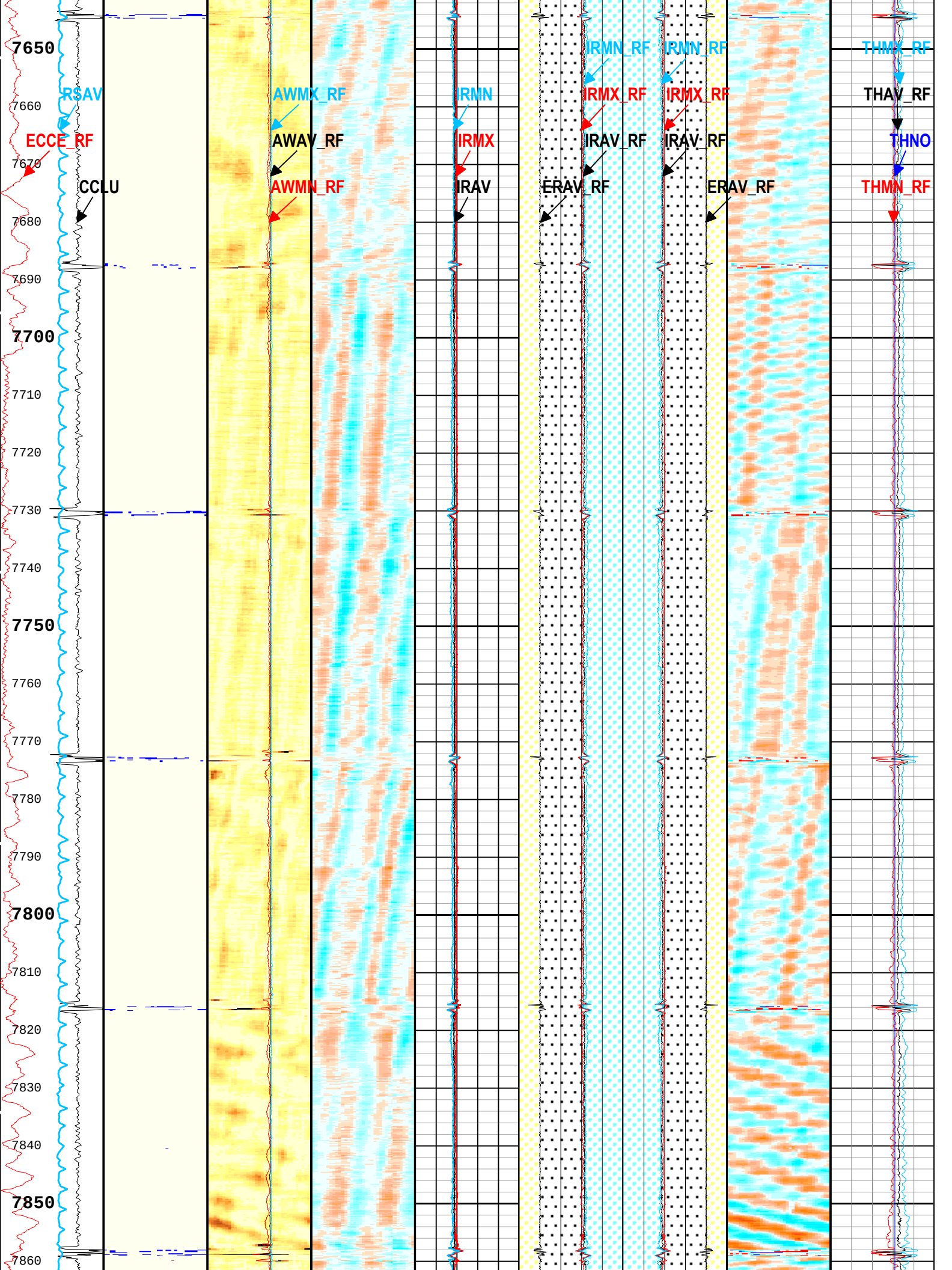
7650
7660
7670
7680
7690
7700
7710
7720
7730
7740
7750
7760
7770
7780
7790
7800
7810
7820
7830
7840
7850
7860
RSAV
ECCE_RF
CCLU
AWMX_RF
AWAV_RF
AWMN_RF
IRMN
IRMX
IRAV
IRMN_RF
IRMX_RF
IRAV_RF
ERAV_RF
IRMN_RF
IRMX_RF
IRAV_RF
ERAV_RF
THMX_RF
THAV_RF
THNO
THMN_RF

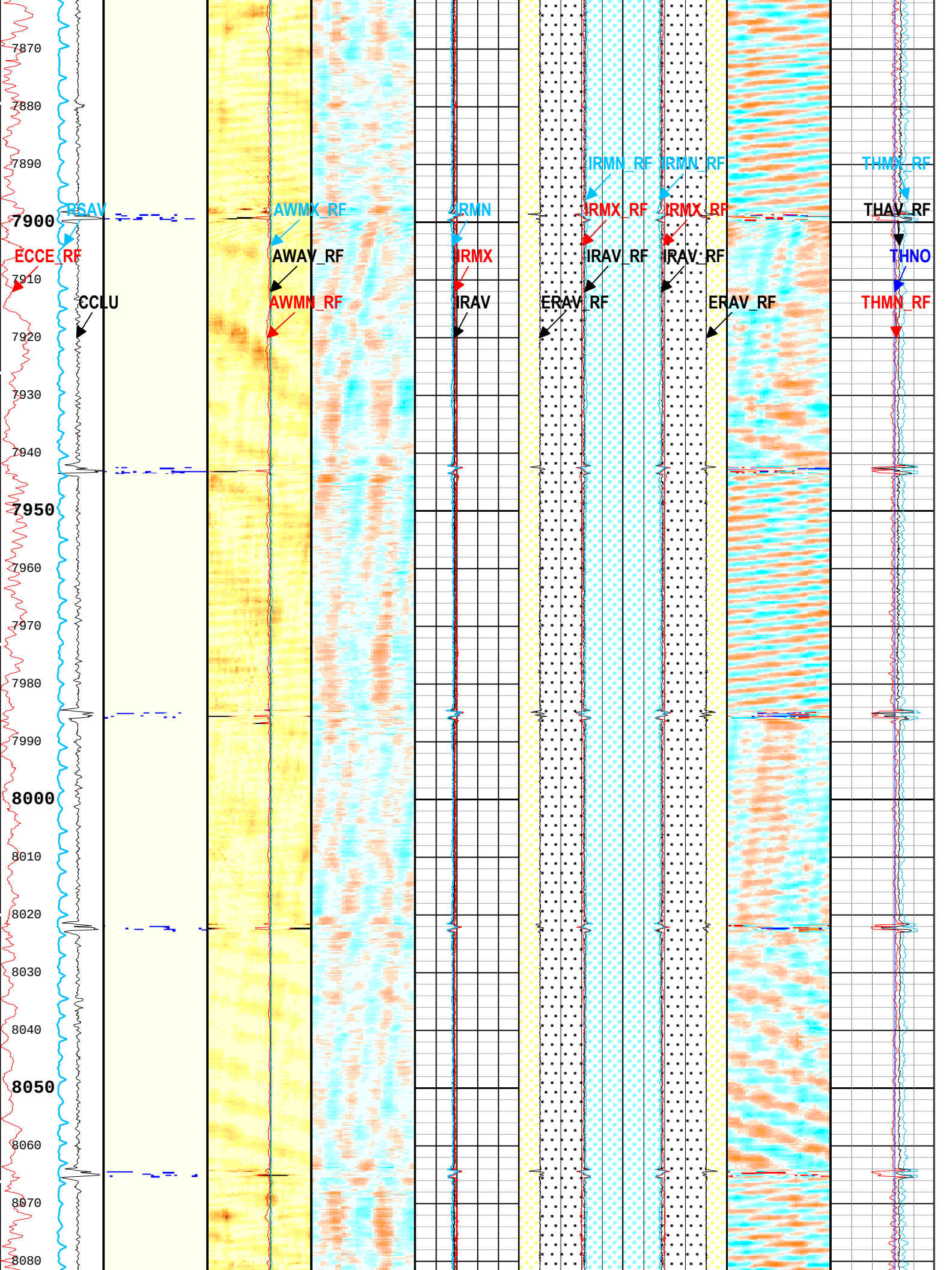
7870
7880
7890
7900
7910
7920
7930
7940
7950
7960
7970
7980
7990
8000
8010
8020
8030
8040
8050
8060
8070
8080
RSAV
ECCE_RF
CCLU
AWMX_RF
AWAV_RF
AWMN_RF
IRMN
IRMX
IRAV
IRMN_RF
IRMX_RF
IRAV_RF
ERAV_RF
IRMN_RF
IRMX_RF
IRAV_RF
ERAV_RF
THMX_RF
THAV_RF
THNO
THMN_RF

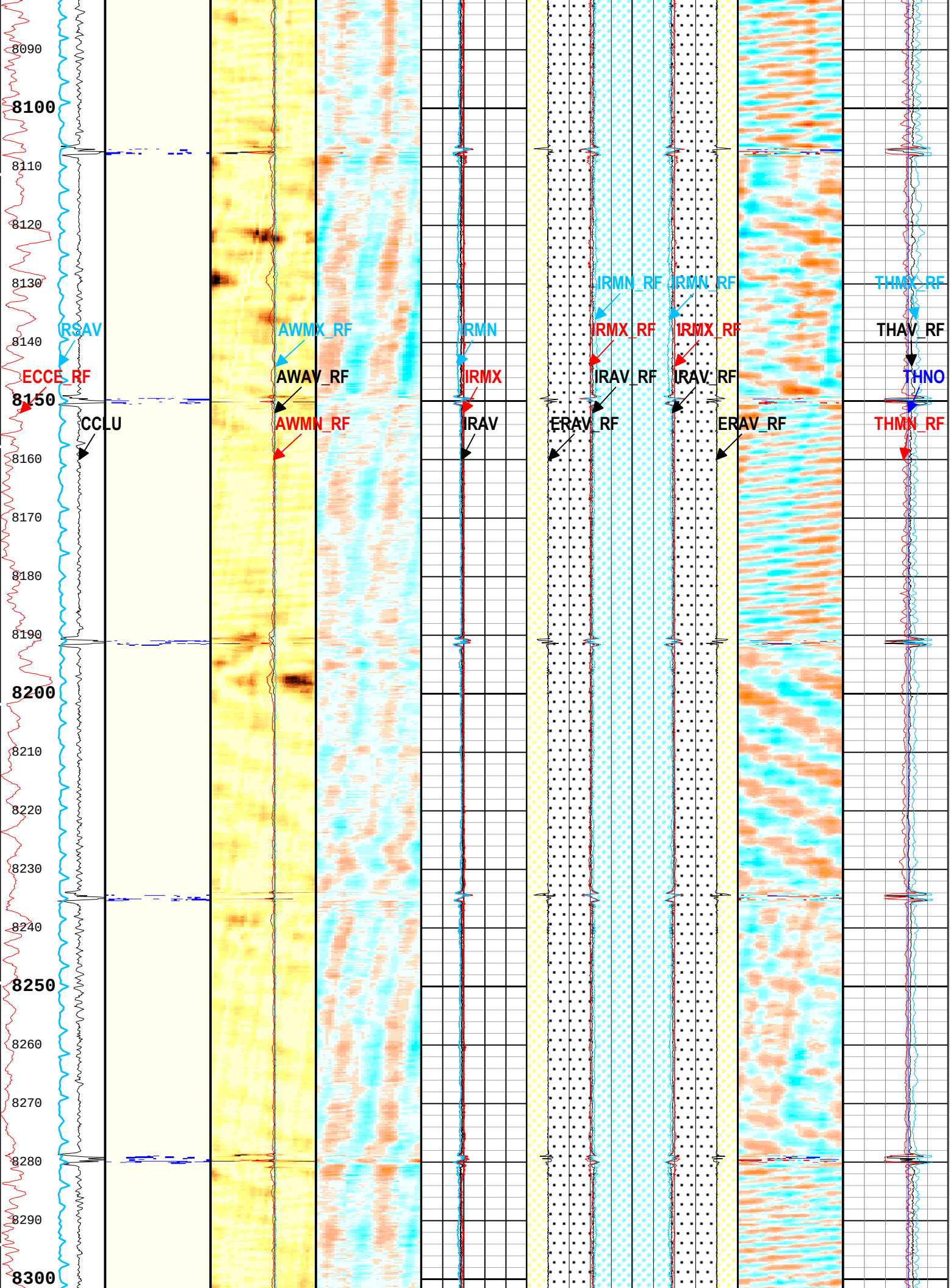
8090
8100
8110
8120
8130
8140
8150
8160
8170
8180
8190
8200
8210
8220
8230
8240
8250
8260
8270
8280
8290
8300
RSAV
ECCE_RF
CCLU
AWMX_RF
AWAV_RF
AWMN_RF
IRMN
IRMX
IRAV
IRMN_RF
IRMX_RF
IRAV_RF
ERAV_RF
IRMN_RF
IRMX_RF
IRAV_RF
ERAV_RF
THMX_RF
THAV_RF
THNO
THMN_RF

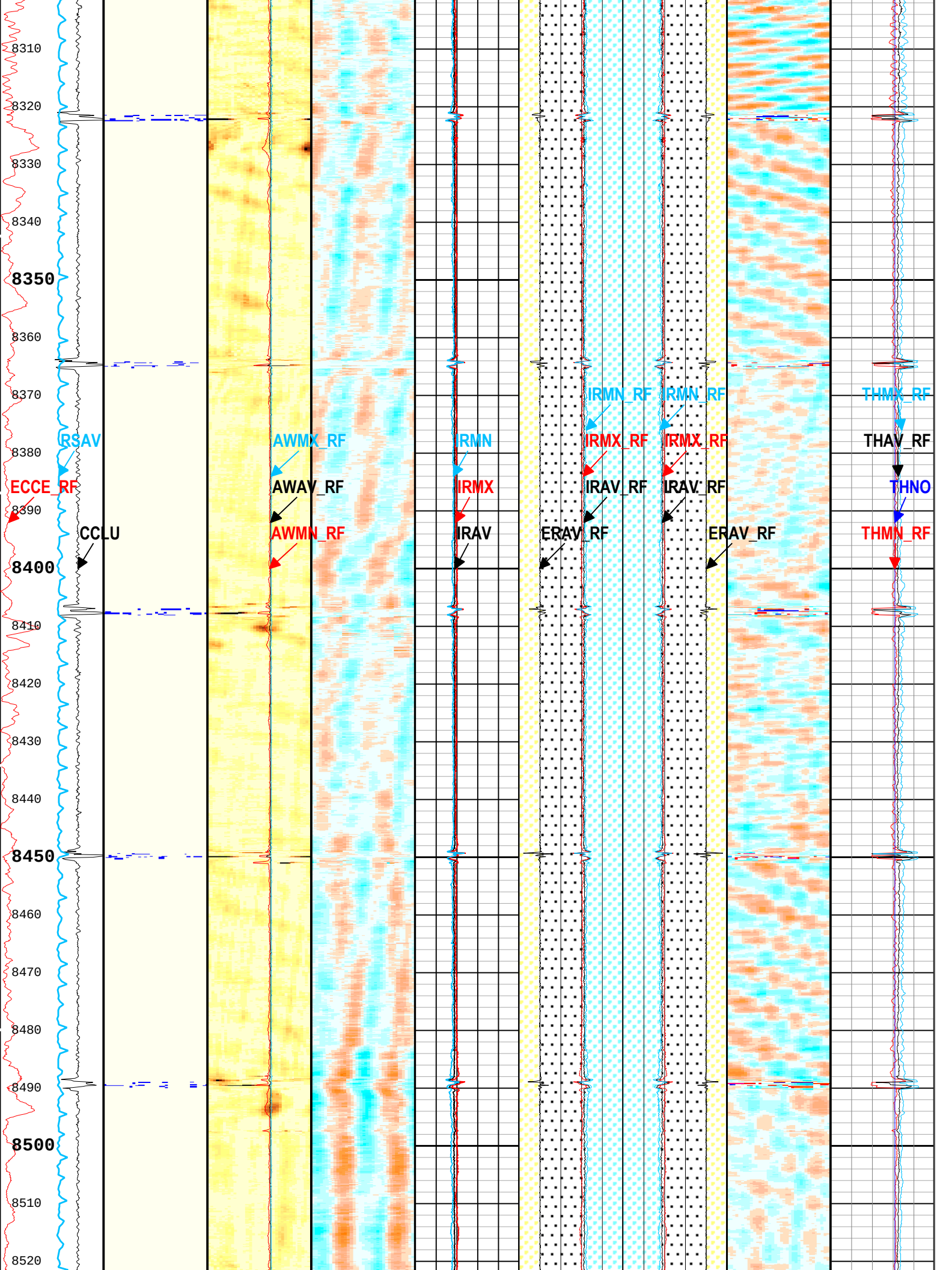
8310
8320
8330
8340
8350
8360
8370
8380
8390
8400
8410
8420
8430
8440
8450
8460
8470
8480
8490
8500
8510
8520
RSAV
ECCE_RF
CCLU
AWMX_RF
AWAV_RF
AWMN_RF
IRMN
IRMX
IRAV
IRMN_RF
IRMX_RF
IRAV_RF
ERAV_RF
RMN_RF
IRMX_RF
IRAV_RF
ERAV_RF
THMX_RF
THAV_RF
THNO
THMN_RF

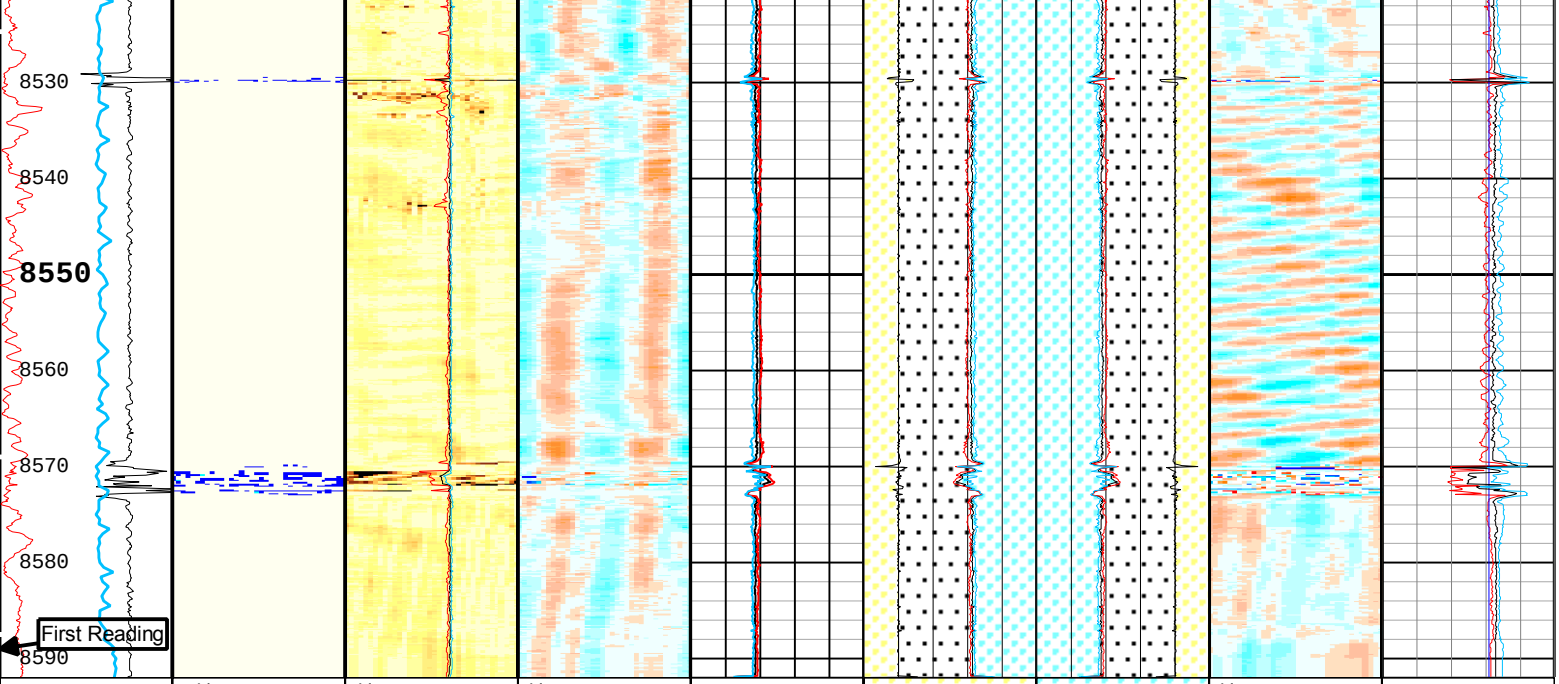

Casing Collar Locator Ultrasonic (CCLU) USIT-E[1]
-30 in 10

Amplitude of Eccentering for Unflagged Waves (ECCE_RF) USIT-E[1]
0 in 0.5

Motor Revolution Speed (RSAV) USIT-E[1]
6 c/s 8

Absent 1.500 3.500
Explicit Normalization
USIT - USIT Processing Flags (UFLG) USIT-E[1]
Orientation: Top of Hole
U L B R U

USIT Processing Flags (UFLG[0]) USIT-E[1]
1 5

Absent -5.200 -3.600 -2.000 -0.400
Explicit Normalization
USIT - Amplitude of Unflagged Wave (AWBK_RF) USIT-E[1]
(dB)
Orientation: Top of Hole
U L B R U

Minimum of Unflagged Wave Amplitude (AWMN_RF) USIT-E[1]
0 dB 75

Average of Unflagged Wave Amplitude (AWAV_RF) USIT-E[1]
0 dB 75

Maximum of Unflagged Wave Amplitude (AWMX_RF) USIT-E[1]
0 dB 75

Absent -0.059 -0.028 0.004 0.035 0.068
Explicit Normalization
USIT - Unflagged Internal Radii minus Median Internal Radius (IRBKM_RF) USIT-E[1]
(in)
Orientation: Top of Hole
U L B R U

Internal Radius Averaged Value (IRAV) USIT-E[1]
2.7 in 3.7

Internal Radius Maximum Value (IRMX) USIT-E[1]
2.7 in 3.7

Internal Radius Minimum Value (IRMN) USIT-E[1]
2.7 in 3.7

ERAV | IRAV
ERAV-IRAV | ERAV
IRAV | IRAV-ERAV

Median of Unflagged External Radii (ERAV_RF) USIT-E[1]
3.7 in 2.7

Median of Unflagged External Radii (ERAV_RF) USIT-E[1]
2.7 in 3.7

Median Internal Radius of Casing Corrected for Eccentering (IRAV_RF) USIT-E[1]
3.7 in 2.7

Median Internal Radius of Casing Corrected for Eccentering (IRAV_RF) USIT-E[1]
2.7 in 3.7

Maximum of Unflagged Internal Radii (IRMX_RF) USIT-E[1]
3.7 in 2.7

Maximum of Unflagged Internal Radii (IRMX_RF) USIT-E[1]
2.7 in 3.7

Minimum of Unflagged Internal Radii (IRMN_RF) USIT-E[1]
3.7 in 2.7

Minimum of Unflagged Internal Radii (IRMN_RF) USIT-E[1]
2.7 in 3.7

Absent -0.059 -0.028 0.004 0.035 0.068
Explicit Normalization
USIT - Unflagged Casing Thickness minus Median of Unflagged Casing Thickness (THBKM_RF) USIT-E[1]
(in)
Orientation: Top of Hole
U L B R U

Minimum of Unflagged Casing Thickness (THMN_RF) USIT-E[1]
0.1 in 0.6

Nominal Casing Thickness (THNO) USIT-E[1]
0.1 in 0.6

Median of Unflagged Casing Thickness (THAV_RF) USIT-E[1]
0.1 in 0.6

Maximum of Unflagged Casing Thickness (THMX_RF) USIT-E[1]
0.1 in 0.6

USIT Processing Flags (UFLG[0]) USIT-E[1]

1 - UFLG 1 Value within [0.0 - 1.5] - :
2 - UFLG 2 Value within [1.5 - 2.5] - :
3 - UFLG 3 Value within [2.5 - 3.5] - :
4 - UFLG 4 - UFLG 5 - UFLG 6 Value within [3.5 - 6.5] - :

UTIM Error
Pulse Origin Not Detected
WINLEN Error
Casing Thickness Error

4 - UFLG 4 UFLG 5 UFLG 6 Value within [3.5 - 6.5] - : Casing Thickness Error

5 - UFLG 7 UFLG 8 UFLG 9 Value within [6.5 - 10] - : Loop Processing Error

TIME_1900 - Time Marked every 60.00 (s)

Description: USI Composite Format: Log (LBV1_USI Corrosion 5inch) Index Scale: 5 in per 100 ft Index Unit: ft Index Type: Measured Depth Creation Date: 07-Sep-2018 22:56:36

Composite 1

USI Compressed Goodwin

Composite Summary

Run Name	Pass Objective	Direction	Top	Bottom	Start	Stop	DSC Mode	Depth Shift	Include Parallel Data
One	Log[6]:Up	Up	93.36 ft	8592.71 ft	07-Sep-2018 9:51:23 AM	07-Sep-2018 1:52:30 PM	ON	8.00 ft	No
One	Log[9]:Up	Up	11.43 ft	318.32 ft	07-Sep-2018 2:46:40 PM	07-Sep-2018 3:00:05 PM	ON	9.00 ft	No

All depths are referenced to toolstring zero

Log

Company:Southern California Gas Company Well:Standard Sesnon 9

Composite 1:S003

Description: USI Goodwin Format: Log (Import of USI Goodwin) Index Scale: 0.1 in per 100 ft Index Unit: ft Index Type: Measured Depth Creation Date: 07-Sep-2018 22:56:58

TIME_1900 - Time Marked every 60.00 (s)

Minimum Acoustic Impedance 1 (MIN_AI1) USIT-E[1]	Minimum Acoustic Impedance 3 (MIN_AI3) USIT-E[1]	Minimum Acoustic Impedance 5 (MIN_AI5) USIT-E[1]	Minimum Acoustic Impedance 7 (MIN_AI7) USIT-E[1]
0 Mrayl 10	0 Mrayl 10	0 Mrayl 10	0 Mrayl 10
Maximum Acoustic Impedance 1 (MAX_AI1) USIT-E[1]	Maximum Acoustic Impedance 3 (MAX_AI3) USIT-E[1]	Maximum Acoustic Impedance 5 (MAX_AI5) USIT-E[1]	Maximum Acoustic Impedance 7 (MAX_AI7) USIT-E[1]
0 Mrayl 10	0 Mrayl 10	0 Mrayl 10	0 Mrayl 10
Average Acoustic Impedance 1 (AV_AI1) USIT-E[1]	Average Acoustic Impedance 3 (AV_AI3) USIT-E[1]	Average Acoustic Impedance 5 (AV_AI5) USIT-E[1]	Average Acoustic Impedance 7 (AV_AI7) USIT-E[1]
0 Mrayl 10	0 Mrayl 10	0 Mrayl 10	0 Mrayl 10

Minimum Acoustic Impedance 2 (MIN_AI2) USIT-E[1]	Minimum Acoustic Impedance 4 (MIN_AI4) USIT-E[1]	Minimum Acoustic Impedance 6 (MIN_AI6) USIT-E[1]	Minimum Acoustic Impedance 8 (MIN_AI8) USIT-E[1]	Minimum Acoustic Impedance 9 (MIN_AI9) USIT-E[1]	Acoustic Impedance Minimum (AIMN) USIT-E[1]
0 Mrayl 10	0 Mrayl 10	0 Mrayl 10	0 Mrayl 10	0 Mrayl 10	-1 Mrayl 9
Maximum Acoustic Impedance 2 (MAX_AI2) USIT-E[1]	Maximum Acoustic Impedance 4 (MAX_AI4) USIT-E[1]	Maximum Acoustic Impedance 6 (MAX_AI6) USIT-E[1]	Maximum Acoustic Impedance 8 (MAX_AI8) USIT-E[1]	Maximum Acoustic Impedance 9 (MAX_AI9) USIT-E[1]	Acoustic Impedance Maximum (AIMX) USIT-E[1]
0 Mrayl 10	0 Mrayl 10	0 Mrayl 10	0 Mrayl 10	0 Mrayl 10	-1 Mrayl 9
Average Acoustic Impedance 2	Average Acoustic Impedance 4	Average Acoustic Impedance 6	Average Acoustic Impedance 8	Average Acoustic Impedance 9	Acoustic Impedance Average

GR

0 gAPI 150

Motor Revolution Speed (RSAV) USIT-E[1]

6 c/s 8

Amplitude of

U L B R U

Orientation: Top of Hole

Absent 1.500 3.500 5.500 7.500

Custom Normalization

USIT -

U L B R U

Orientation: Top of Hole

-1000.000 3.090 5.054 7.018

Custom Normalization

USIT - Acoustic Impedance With Micro-debonding Image

Bonded

Micro-Debonding

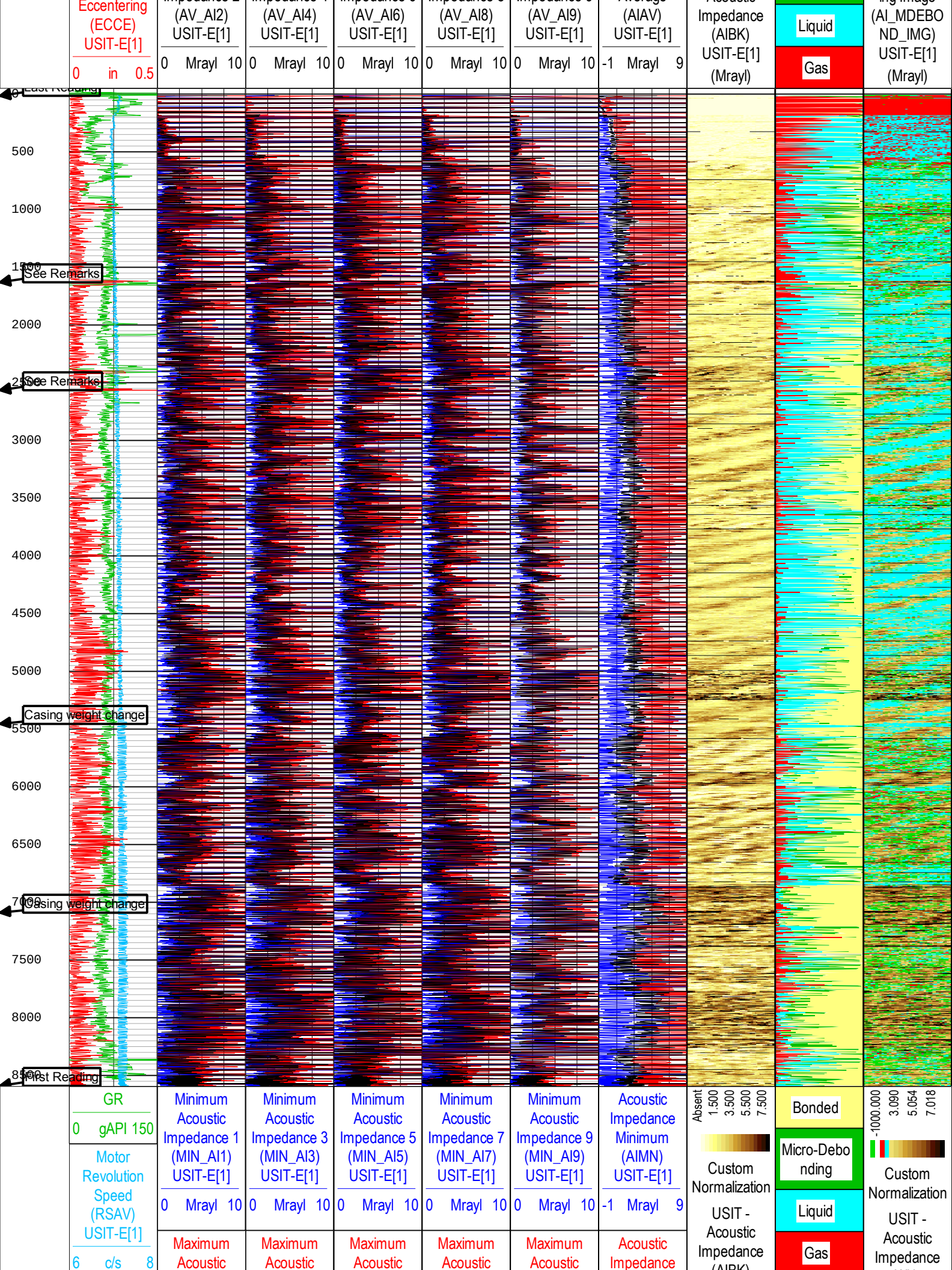
Eccentering (ECCE) USIT-E[1]
0 in 0.5
Impedance 2 (AV_AI2) USIT-E[1]
0 Mrayl 10
Impedance 4 (AV_AI4) USIT-E[1]
0 Mrayl 10
Impedance 6 (AV_AI6) USIT-E[1]
0 Mrayl 10
Impedance 8 (AV_AI8) USIT-E[1]
0 Mrayl 10
Impedance 9 (AV_AI9) USIT-E[1]
0 Mrayl 10
Average (AIAV) USIT-E[1]
-1 Mrayl 9
Impedance (AIBK) USIT-E[1] (Mrayl)
Liquid
Gas
(AI_MDEBOND_IMG) USIT-E[1] (Mrayl)
Last Reading
See Remarks
See Remarks
Casing weight change
Casing weight change
First Reading
0
500
1000
1500
2000
2500
3000
3500
4000
4500
5000
5500
6000
6500
7000
7500
8000
8500
GR
0 gAPI 150
Motor Revolution Speed (RSAV) USIT-E[1]
6 c/s 8
Minimum Acoustic Impedance 1 (MIN_AI1) USIT-E[1]
0 Mrayl 10
Minimum Acoustic Impedance 3 (MIN_AI3) USIT-E[1]
0 Mrayl 10
Minimum Acoustic Impedance 5 (MIN_AI5) USIT-E[1]
0 Mrayl 10
Minimum Acoustic Impedance 7 (MIN_AI7) USIT-E[1]
0 Mrayl 10
Minimum Acoustic Impedance 9 (MIN_AI9) USIT-E[1]
0 Mrayl 10
Acoustic Impedance Minimum (AIMN) USIT-E[1]
-1 Mrayl 9
Maximum Acoustic
Maximum Acoustic
Maximum Acoustic
Maximum Acoustic
Maximum Acoustic
Acoustic Impedance
Absent
1.500
3.500
5.500
7.500
Custom Normalization
USIT - Acoustic Impedance (AIBK)
Bonded
Micro-Debonding
Liquid
Gas
-1000.000
3.090
5.054
7.018
Custom Normalization
USIT - Acoustic Impedance

Amplitude of Eccentering (ECCE) USIT-E[1]	Impedance 1 (MAX_AI1) USIT-E[1]	Impedance 3 (MAX_AI3) USIT-E[1]	Impedance 5 (MAX_AI5) USIT-E[1]	Impedance 7 (MAX_AI7) USIT-E[1]	Impedance 9 (MAX_AI9) USIT-E[1]	Maximum (AIMX) USIT-E[1]
0 in 0.5	0 Mrayl 10	0 Mrayl 10	0 Mrayl 10	0 Mrayl 10	0 Mrayl 10	-1 Mrayl 9
	Average Acoustic Impedance 1 (AV_AI1) USIT-E[1]	Average Acoustic Impedance 3 (AV_AI3) USIT-E[1]	Average Acoustic Impedance 5 (AV_AI5) USIT-E[1]	Average Acoustic Impedance 7 (AV_AI7) USIT-E[1]	Average Acoustic Impedance 9 (AV_AI9) USIT-E[1]	Acoustic Impedance Average (AIAV) USIT-E[1]
	0 Mrayl 10	0 Mrayl 10	0 Mrayl 10	0 Mrayl 10	0 Mrayl 10	-1 Mrayl 9
	Minimum Acoustic Impedance 2 (MIN_AI2) USIT-E[1]	Minimum Acoustic Impedance 4 (MIN_AI4) USIT-E[1]	Minimum Acoustic Impedance 6 (MIN_AI6) USIT-E[1]	Minimum Acoustic Impedance 8 (MIN_AI8) USIT-E[1]		
	0 Mrayl 10	0 Mrayl 10	0 Mrayl 10	0 Mrayl 10		
	Maximum Acoustic Impedance 2 (MAX_AI2) USIT-E[1]	Maximum Acoustic Impedance 4 (MAX_AI4) USIT-E[1]	Maximum Acoustic Impedance 6 (MAX_AI6) USIT-E[1]	Maximum Acoustic Impedance 8 (MAX_AI8) USIT-E[1]		
	0 Mrayl 10	0 Mrayl 10	0 Mrayl 10	0 Mrayl 10		
	Average Acoustic Impedance 2 (AV_AI2) USIT-E[1]	Average Acoustic Impedance 4 (AV_AI4) USIT-E[1]	Average Acoustic Impedance 6 (AV_AI6) USIT-E[1]	Average Acoustic Impedance 8 (AV_AI8) USIT-E[1]		
	0 Mrayl 10	0 Mrayl 10	0 Mrayl 10	0 Mrayl 10		

(AIBK) USIT-E[1] (Mrayl) Orientation: Top of Hole U L B R U

With Micro-debonding Image (AI_MDEBOND_IMG) USIT-E[1] (Mrayl) Orientation: Top of Hole U L B R U

TIME_1900 - Time Marked every 60.00 (s)

Description: USI Goodwin Format: Log (Import of USI Goodwin) Index Scale: 0.1 in per 100 ft Index Unit: ft Index Type: Measured Depth Creation Date: 07-Sep-2018 22:56:58

One

Hi res Corrosion 10 in = 100 ft

Pass Summary

Run Name	Pass Objective	Direction	Top	Bottom	Start	Stop	DSC Mode	Depth Shift	Include Parallel Data
One	Log[8]:Up	Up	1551.52 ft	1758.38 ft	07-Sep-2018 2:26:31 PM	07-Sep-2018 2:40:35 PM	ON	9.00 ft	No

All depths are referenced to toolstring zero

Log

Company:Southern California Gas Company Well:Standard Sesnon 9

One: Log[8]:Up:S003

Description: USI Composite Format: Log (LBV1_USI Corrosion 5inch) Index Scale: 10 in per 100 ft Index Unit: ft Index Type: Measured Depth Creation Date: 07-Sep-2018 22:57:01

TIME_1900 - Time Marked every 60.00 (s)

USIT Processing Flags (UFLG[0]) USIT-E

1 - UFLG 1 Value within [0.0 - 1.5] - :

2 - UFLG 2 Value within [1.5 - 2.5] - :

3 - UFLG 3 Value within [2.5 - 3.5] - :

4 - UFLG 4 UFLG 5 UFLG 6 Value within [3.5 - 6.5] - :

5 - UFLG 7 UFLG 8 UFLG 9 Value within [6.5 - 10] - :

- UTIM Error
- Pulse Origin Not Detected
- WINLEN Error
- Casing Thickness Error
- Loop Processing Error

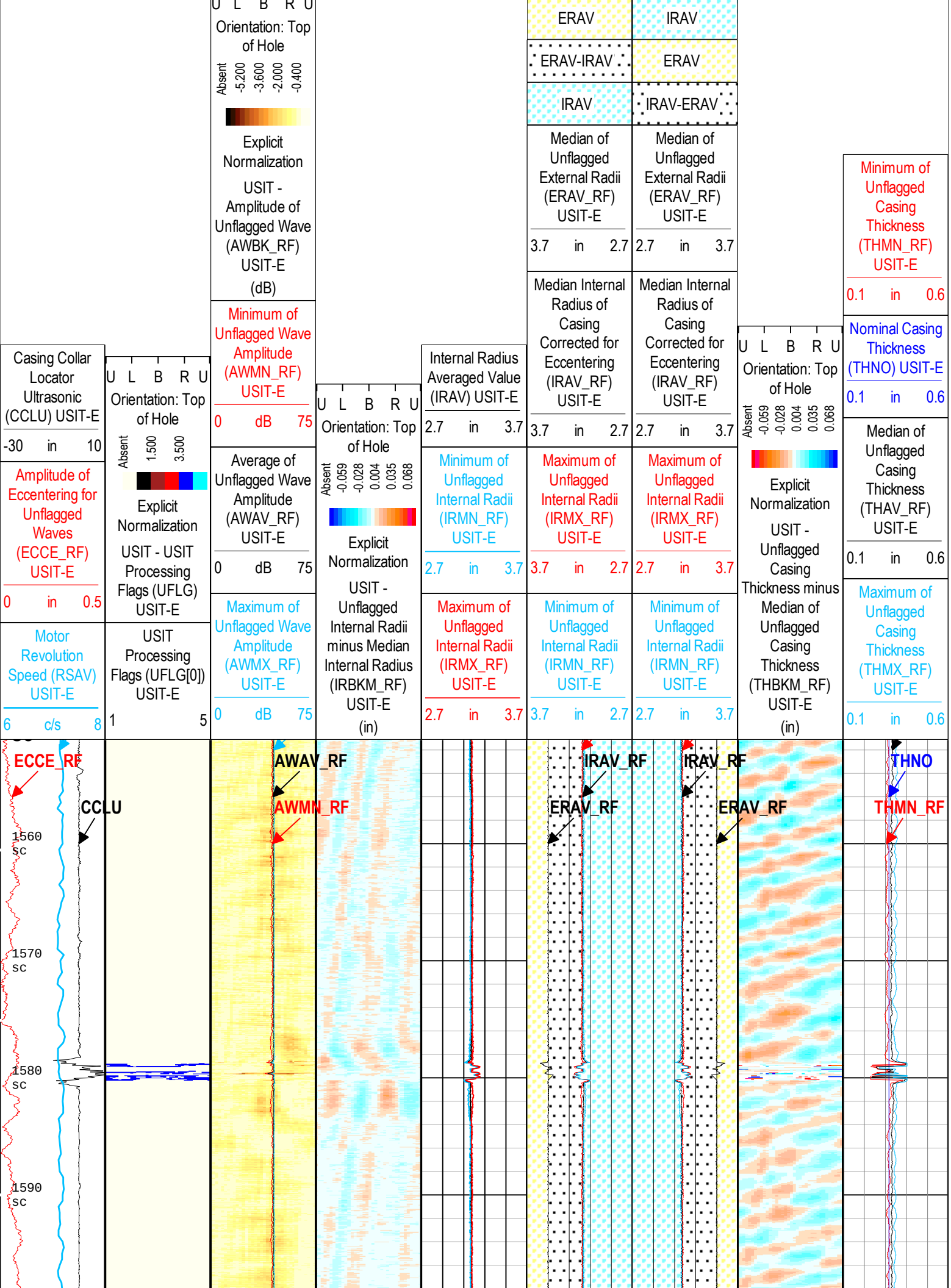
Casing Collar Locator Ultrasonic (CCLU) USIT-E
-30 in 10
Amplitude of Eccentering for Unflagged Waves (ECCE_RF) USIT-E
0 in 0.5
Motor Revolution Speed (RSAV) USIT-E
6 c/s 8
U L B R U
Orientation: Top of Hole
Absent 1.500 3.500
Explicit Normalization
USIT - USIT Processing Flags (UFLG) USIT-E
USIT Processing Flags (UFLG[0]) USIT-E
1 5
U L B R U
Orientation: Top of Hole
Absent -5.200 -3.600 -2.000 -0.400
Explicit Normalization
USIT - Amplitude of Unflagged Wave (AWBK_RF) USIT-E
(dB)
Minimum of Unflagged Wave Amplitude (AWMN_RF) USIT-E
0 dB 75
Average of Unflagged Wave Amplitude (AWAV_RF) USIT-E
0 dB 75
Maximum of Unflagged Wave Amplitude (AWMX_RF) USIT-E
0 dB 75
U L B R U
Orientation: Top of Hole
Absent -0.059 -0.028 0.004 0.035 0.068
Explicit Normalization
USIT - Unflagged Internal Radii minus Median Internal Radius (IRBKM_RF) USIT-E
(in)
Internal Radius Averaged Value (IRAV) USIT-E
2.7 in 3.7
Minimum of Unflagged Internal Radii (IRMN_RF) USIT-E
2.7 in 3.7
Maximum of Unflagged Internal Radii (IRMX_RF) USIT-E
2.7 in 3.7
ERAV
ERAV-IRAV
IRAV
Median of Unflagged External Radii (ERAV_RF) USIT-E
3.7 in 2.7
Median Internal Radius of Casing Corrected for Eccentering (IRAV_RF) USIT-E
3.7 in 2.7
Maximum of Unflagged Internal Radii (IRMX_RF) USIT-E
3.7 in 2.7
Minimum of Unflagged Internal Radii (IRMN_RF) USIT-E
3.7 in 2.7
IRAV
ERAV
IRAV-ERAV
Median of Unflagged External Radii (ERAV_RF) USIT-E
2.7 in 3.7
Median Internal Radius of Casing Corrected for Eccentering (IRAV_RF) USIT-E
2.7 in 3.7
Maximum of Unflagged Internal Radii (IRMX_RF) USIT-E
2.7 in 3.7
Minimum of Unflagged Internal Radii (IRMN_RF) USIT-E
2.7 in 3.7
U L B R U
Orientation: Top of Hole
Absent -0.059 -0.028 0.004 0.035 0.068
Explicit Normalization
USIT - Unflagged Casing Thickness minus Median of Unflagged Casing Thickness (THBKM_RF) USIT-E
(in)
Minimum of Unflagged Casing Thickness (THMN_RF) USIT-E
0.1 in 0.6
Nominal Casing Thickness (THNO) USIT-E
0.1 in 0.6
Median of Unflagged Casing Thickness (THAV_RF) USIT-E
0.1 in 0.6
Maximum of Unflagged Casing Thickness (THMX_RF) USIT-E
0.1 in 0.6
ECCE_RF
CCLU
AWAV_RF
AWMN_RF
IRAV_RF
ERAV_RF
IRAV_RF
ERAV_RF
THNO
THMN_RF
1560 sc
1570 sc
1580 sc
1590 sc

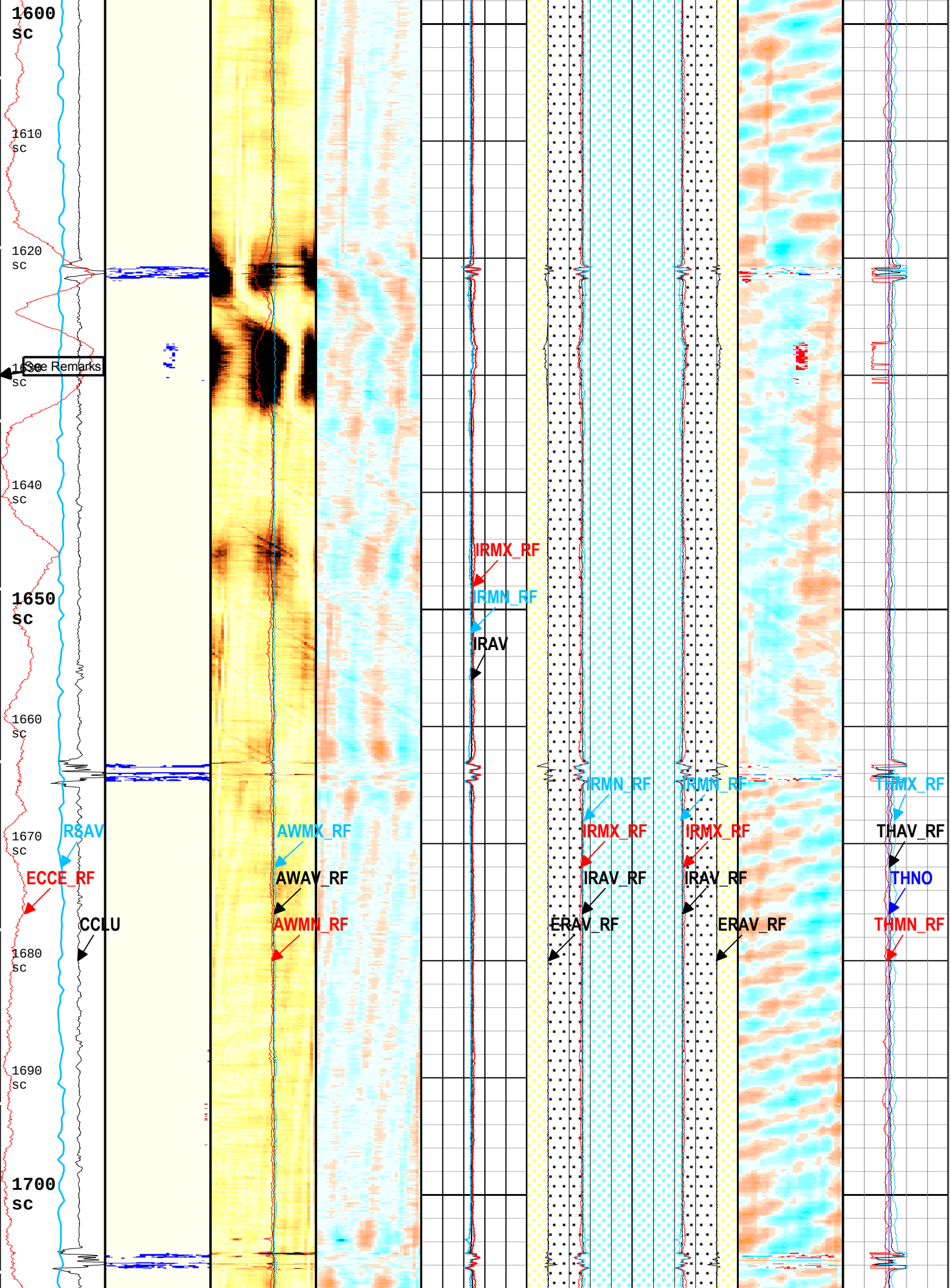
1600 sc
1610 sc
1620 sc
See Remarks
1630 sc
1640 sc
1650 sc
1660 sc
1670 sc
1680 sc
1690 sc
1700 sc
IRMX_RF
IRMN_RF
IRAV
R8AV
ECCE_RF
CCLU
AWMX_RF
AWAV_RF
AWMN_RF
IRMN_RF
IRMX_RF
IRAV_RF
ERAV_RF
IRMN_RF
IRMX_RF
IRAV_RF
ERAV_RF
THMX_RF
THAV_RF
THNO
THMN_RF

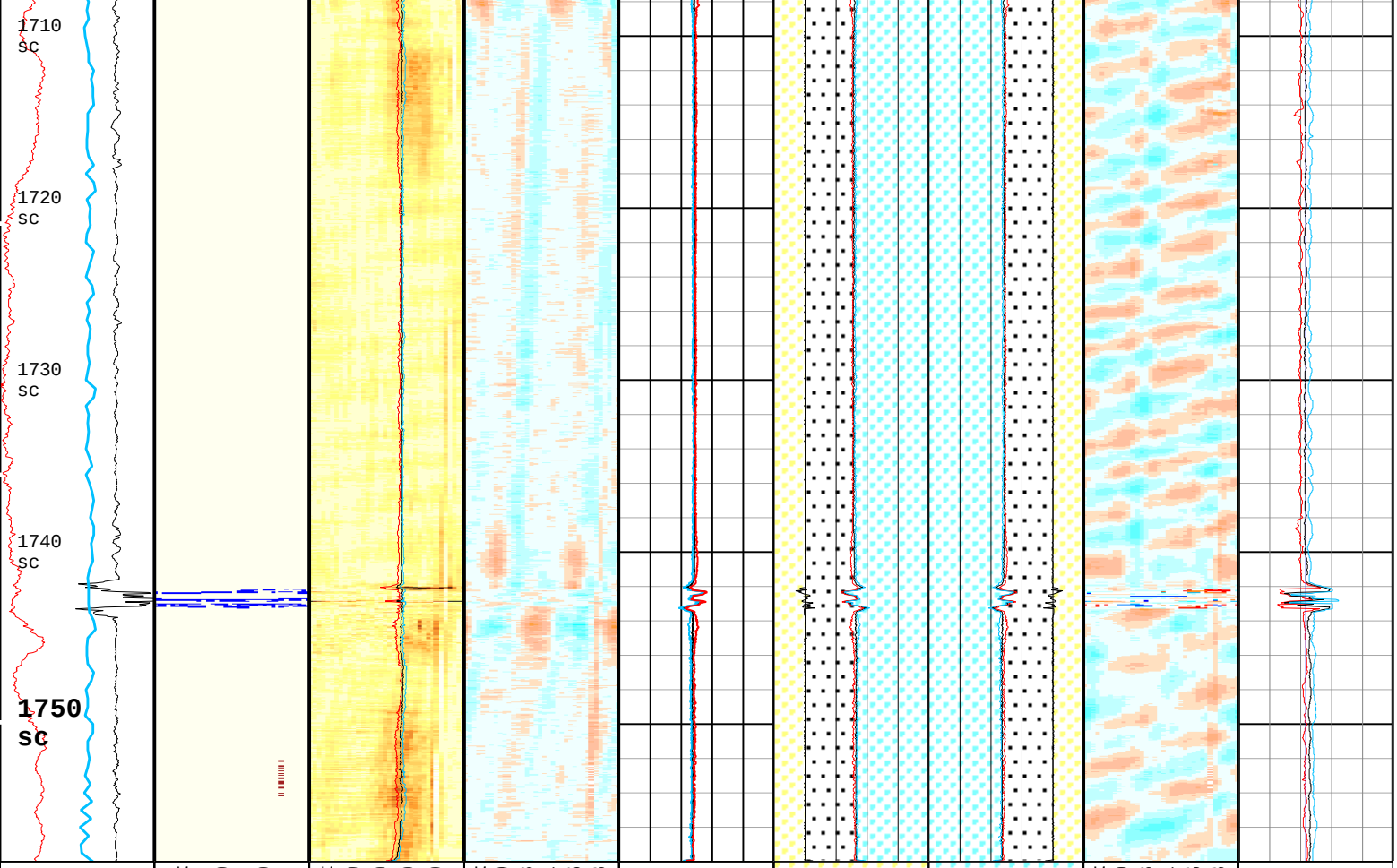

Casing Collar Locator Ultrasonic (CCLU) USIT-E
-30 in 10

Amplitude of Eccentering for Unflagged Waves (ECCE_RF) USIT-E
0 in 0.5

Motor Revolution Speed (RSAV) USIT-E
6 c/s 8

Absent 1.500 3.500
Explicit Normalization
USIT - USIT Processing Flags (UFLG) USIT-E
Orientation: Top of Hole
U L B R U

USIT Processing Flags (UFLG[0]) USIT-E
1 5

Absent -5.200 -3.600 -2.000 -0.400
Explicit Normalization
USIT - Amplitude of Unflagged Wave (AWBK_RF) USIT-E
(dB)
Orientation: Top of Hole
U L B R U

Minimum of Unflagged Wave Amplitude (AWMN_RF) USIT-E
0 dB 75

Average of Unflagged Wave Amplitude (AWAV_RF) USIT-E
0 dB 75

Maximum of Unflagged Wave Amplitude (AWMX_RF) USIT-E

Absent -0.059 -0.028 0.004 0.035 0.068
Explicit Normalization
USIT - Unflagged Internal Radii minus Median Internal Radius (IRBKM_RF) USIT-E
(in)
Orientation: Top of Hole
U L B R U

Internal Radius Averaged Value (IRAV) USIT-E
2.7 in 3.7

Minimum of Unflagged Internal Radii (IRMN_RF) USIT-E
2.7 in 3.7

Maximum of Unflagged Internal Radii (IRMX_RF) USIT-E
2.7 in 3.7

ERAV | IRAV
ERAV-IRAV | ERAV
IRAV | IRAV-ERAV

Median of Unflagged External Radii (ERAV_RF) USIT-E
3.7 in 2.7 | 2.7 in 3.7

Median Internal Radius of Casing Corrected for Eccentering (IRAV_RF) USIT-E
3.7 in 2.7 | 2.7 in 3.7

Maximum of Unflagged Internal Radii (IRMX_RF) USIT-E
3.7 in 2.7 | 2.7 in 3.7

Minimum of Unflagged Internal Radii (IRMN_RF) USIT-E | Minimum of Unflagged Internal Radii (IRMN_RF) USIT-E

Absent -0.059 -0.028 0.004 0.035 0.068
Explicit Normalization
USIT - Unflagged Casing Thickness minus Median of Unflagged Casing Thickness (THBKM_RF) USIT-E
(in)
Orientation: Top of Hole
U L B R U

Minimum of Unflagged Casing Thickness (THMN_RF) USIT-E
0.1 in 0.6

Nominal Casing Thickness (THNO) USIT-E
0.1 in 0.6

Median of Unflagged Casing Thickness (THAV_RF) USIT-E
0.1 in 0.6

Maximum of Unflagged Casing Thickness (THMX_RF) USIT-E
0.1 in 0.6

USIT-E

0 dB 75

3.7 in 2.7 | 2.7 in 3.7

USIT Processing Flags (UFLG[0]) USIT-E

1 - UFLG 1 Value within [0.0 - 1.5] - :
2 - UFLG 2 Value within [1.5 - 2.5] - :
3 - UFLG 3 Value within [2.5 - 3.5] - :
4 - UFLG 4 UFLG 5 UFLG 6 Value within [3.5 - 6.5] - :
5 - UFLG 7 UFLG 8 UFLG 9 Value within [6.5 - 10] - :

- UTIM Error
- Pulse Origin Not Detected
- WINLEN Error
- Casing Thickness Error
- Loop Processing Error

TIME_1900 - Time Marked every 60.00 (s)

Description: USI Composite Format: Log (LBV1_USI Corrosion 5inch) Index Scale: 10 in per 100 ft Index Unit: ft Index Type: Measured Depth
Creation Date: 07-Sep-2018 22:57:01

One

Hi res Corrosion 10 in = 100 ft

Pass Summary

Run Name	Pass Objective	Direction	Top	Bottom	Start	Stop	DSC Mode	Depth Shift	Include Parallel Data
One	Log[7]:Up	Up	2491.49 ft	2659.49 ft	07-Sep-2018 2:11:27 PM	07-Sep-2018 2:22:46 PM	ON	9.00 ft	No

All depths are referenced to toolstring zero

Log

Company:Southern California Gas Company Well:Standard Sesnon 9

One: Log[7]:Up:S003

Description: USI Composite Format: Log (LBV1_USI Corrosion 5inch) Index Scale: 10 in per 100 ft Index Unit: ft Index Type: Measured Depth
Creation Date: 07-Sep-2018 22:57:05

TIME_1900 - Time Marked every 60.00 (s)

USIT Processing Flags (UFLG[0]) USIT-E

1 - UFLG 1 Value within [0.0 - 1.5] - :
2 - UFLG 2 Value within [1.5 - 2.5] - :
3 - UFLG 3 Value within [2.5 - 3.5] - :
4 - UFLG 4 UFLG 5 UFLG 6 Value within [3.5 - 6.5] - :
5 - UFLG 7 UFLG 8 UFLG 9 Value within [6.5 - 10] - :

- UTIM Error
- Pulse Origin Not Detected
- WINLEN Error
- Casing Thickness Error
- Loop Processing Error

U L B R U
Orientation: Top of Hole
Absent -5.200 -3.600 -2.000 -0.400
Explicit Normalization
USIT - Amplitude of Unflagged Wave (AWBK_RF) USIT-E (dB)

Minimum of Unflagged Wave Amplitude (AWMN_RF) USIT-E
0 dB 75

ERAV | IRAV
ERAV-IRAV | ERAV
IRAV | IRAV-ERAV

Median of Unflagged External Radii (ERAV_RF) USIT-E
3.7 in 2.7

Median of Unflagged External Radii (ERAV_RF) USIT-E
2.7 in 3.7

Minimum of Unflagged Casing Thickness (THMN_RF) USIT-E
0.1 in 0.6

Casing Collar Locator Ultrasonic (CCLU) USIT-E
-30 in 10

U L B R U
Orientation: Top of Hole
Absent 1.500 3.500

U L B R U
Orientation: Top of Hole
Absent -0.059 -0.028 0.004 0.035 0.068

Internal Radius Averaged Value (IRAV) USIT-E
2.7 in 3.7

Median Internal Radius of Casing Corrected for Eccentering (IRAV_RF) USIT-E
3.7 in 2.7

Median Internal Radius of Casing Corrected for Eccentering (IRAV_RF) USIT-E
2.7 in 3.7

Nominal Casing Thickness (THNO) USIT-E
0.1 in 0.6

Average of

Minimum of

Maximum of

Maximum of

Median of Unflagged Casing

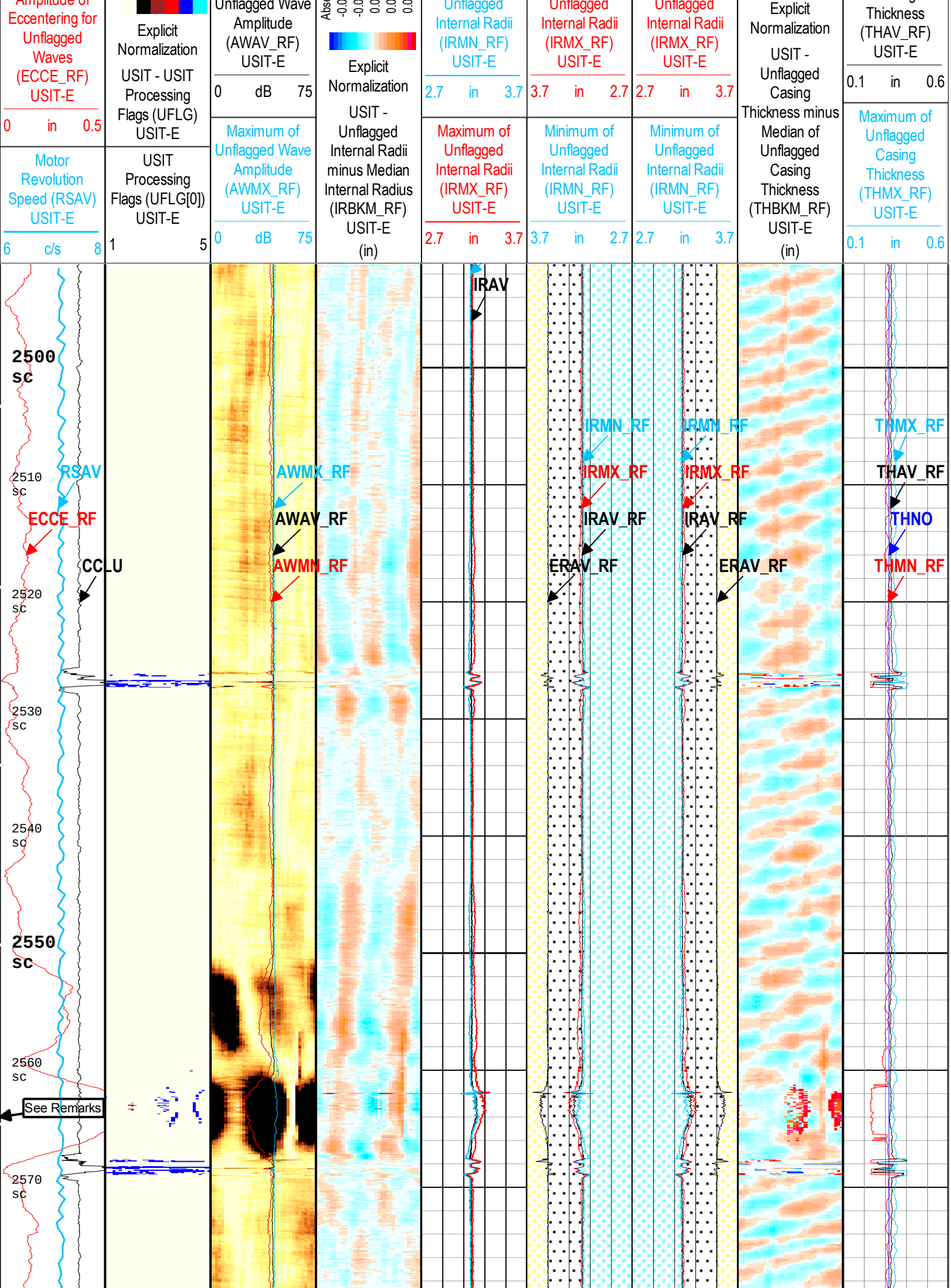
Amplitude of Eccentering for Unflagged Waves (ECCE_RF) USIT-E
0 in 0.5
Motor Revolution Speed (RSAV) USIT-E
6 c/s 8
Explicit Normalization
USIT - USIT Processing Flags (UFLG) USIT-E
USIT Processing Flags (UFLG[0]) USIT-E
1 5
Unflagged Wave Amplitude (AWAV_RF) USIT-E
0 dB 75
Maximum of Unflagged Wave Amplitude (AWMX_RF) USIT-E
0 dB 75
Explicit Normalization
USIT - Unflagged Internal Radii minus Median Internal Radius (IRBKM_RF) USIT-E
(in)
Unflagged Internal Radii (IRMN_RF) USIT-E
2.7 in 3.7
Maximum of Unflagged Internal Radii (IRMX_RF) USIT-E
2.7 in 3.7
Unflagged Internal Radii (IRMX_RF) USIT-E
3.7 in 2.7
Minimum of Unflagged Internal Radii (IRMN_RF) USIT-E
3.7 in 2.7
Unflagged Internal Radii (IRMX_RF) USIT-E
2.7 in 3.7
Minimum of Unflagged Internal Radii (IRMN_RF) USIT-E
2.7 in 3.7
Explicit Normalization
USIT - Unflagged Casing Thickness minus Median of Unflagged Casing Thickness (THBKM_RF) USIT-E
(in)
Thickness (THAV_RF) USIT-E
0.1 in 0.6
Maximum of Unflagged Casing Thickness (THMX_RF) USIT-E
0.1 in 0.6
2500 sc
2510 sc
2520 sc
2530 sc
2540 sc
2550 sc
2560 sc
2570 sc
RSAV
ECCE_RF
CCLU
See Remarks
AWMX_RF
AWAV_RF
AWMN_RF
IRAV
IRMN_RF
IRMX_RF
IRAV_RF
ERAV_RF
THMX_RF
THAV_RF
THNO
THMN_RF

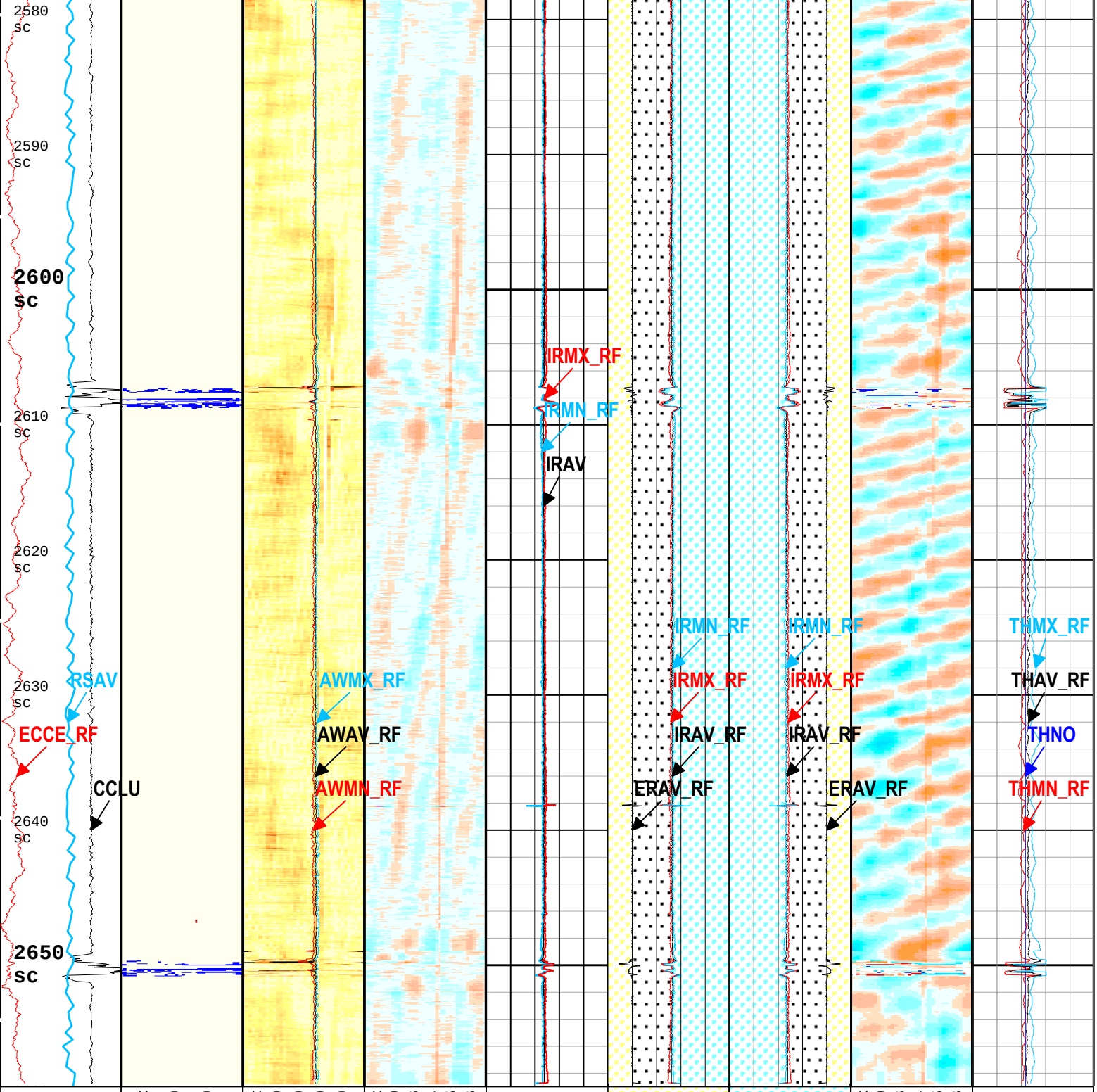

Casing Collar Locator Ultrasonic (CCLU) USIT-E

-30 in 10

Amplitude of Eccentering for Unflagged Waves (ECCE_RF) USIT-E

0 in 0.5

Motor Revolution Speed (RSAV) USIT-E

Absent 1.500 3.500

Explicit Normalization

USIT - USIT Processing Flags (UFLG) USIT-E

Orientation: Top of Hole

U L B R U

USIT Processing Flags (UFLG[0]) USIT-E

Absent -5.200 -3.600 -2.000 -0.400

Explicit Normalization

USIT - Amplitude of Unflagged Wave (AWBK_RF) USIT-E

(dB)

Orientation: Top of Hole

U L B R U

Minimum of

Absent -0.059 -0.028 0.004 0.035 0.068

Explicit Normalization

USIT - Unflagged Internal Radii minus Median Internal Radius (IRBKM_RF) USIT-E

(in)

Orientation: Top of Hole

U L B R U

Internal Radius Averaged Value (IRAV) USIT-E

2.7 in 3.7

Minimum of Unflagged Internal Radii (IRMN_RF) USIT-E

2.7 in 3.7

Maximum of Unflagged Internal Radii (IRMX_RF) USIT-E

ERAV

ERAV-IRAV

IRAV

Median of Unflagged External Radii (ERAV_RF) USIT-E

3.7 in 2.7

Median Internal Radius of Casing

IRAV

ERAV

IRAV-ERAV

Median of Unflagged External Radii (ERAV_RF) USIT-E

2.7 in 3.7

Median Internal Radius of Casing

Absent -0.059 -0.028 0.004 0.035 0.068

Explicit Normalization

USIT - Unflagged Casing Thickness minus Median of Unflagged Casing Thickness (THBKM_RF) USIT-E

(in)

Minimum of Unflagged Casing Thickness (THMN_RF) USIT-E

0.1 in 0.6

Nominal Casing Thickness (THNO) USIT-E

0.1 in 0.6

Median of Unflagged Casing Thickness

USIT-E
6 c/s 8

1 5

Unflagged Wave Amplitude (AWMN_RF) USIT-E
0 dB 75

Average of Unflagged Wave Amplitude (AWAV_RF) USIT-E
0 dB 75

Maximum of Unflagged Wave Amplitude (AWMX_RF) USIT-E
0 dB 75

2.7 in 3.7

Corrected for Eccentering (IRAV_RF) USIT-E
3.7 in 2.7

Corrected for Eccentering (IRAV_RF) USIT-E
2.7 in 3.7

Maximum of Unflagged Internal Radii (IRMX_RF) USIT-E
3.7 in 2.7

Maximum of Unflagged Internal Radii (IRMX_RF) USIT-E
2.7 in 3.7

Minimum of Unflagged Internal Radii (IRMN_RF) USIT-E
3.7 in 2.7

Minimum of Unflagged Internal Radii (IRMN_RF) USIT-E
2.7 in 3.7

Orientation: Top of Hole
U L B R U

(THAV_RF) USIT-E
0.1 in 0.6

Maximum of Unflagged Casing Thickness (THMX_RF) USIT-E
0.1 in 0.6

USIT Processing Flags (UFLG[0]) USIT-E

1 - UFLG 1 Value within [0.0 - 1.5] - :
2 - UFLG 2 Value within [1.5 - 2.5] - :
3 - UFLG 3 Value within [2.5 - 3.5] - :
4 - UFLG 4 UFLG 5 UFLG 6 Value within [3.5 - 6.5] - :
5 - UFLG 7 UFLG 8 UFLG 9 Value within [6.5 - 10] - :

UTIM Error
Pulse Origin Not Detected
WINLEN Error
Casing Thickness Error
Loop Processing Error

TIME_1900 - Time Marked every 60.00 (s)

Description: USI Composite Format: Log (LBV1_USI Corrosion 5inch) Index Scale: 10 in per 100 ft Index Unit: ft Index Type: Measured Depth
Creation Date: 07-Sep-2018 22:57:05

XYZ

Company:Southern California Gas Company Well:Standard Sesnon 9
One: Log[2]:Down:S003

Fluid Acoustic Slowness vs Depth

2D Cross Plot

Index Range: From 436.00 to 8597.50 ft

DEPTH-DFSL (DFSL : Data Not Found)
DEPTH-CFVL (CFVL : Data Not Found)
DEPTH-FVEM

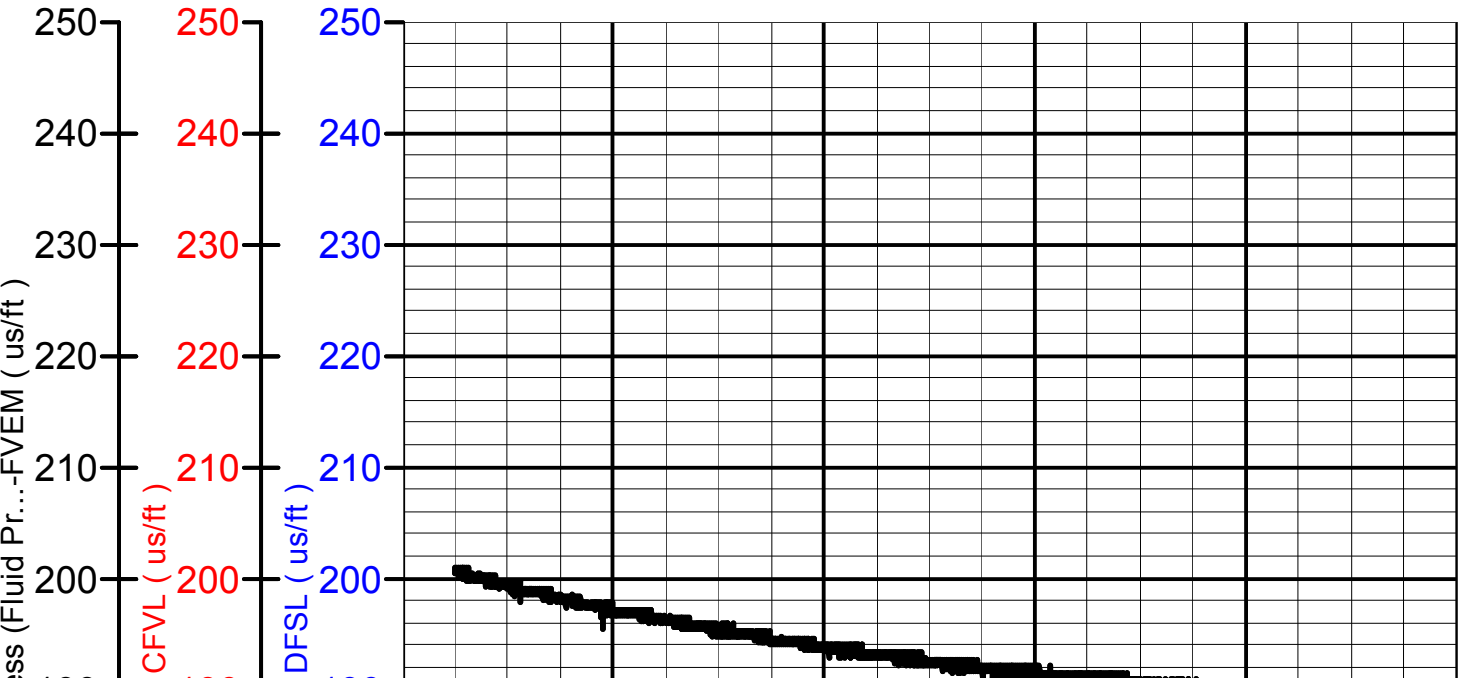

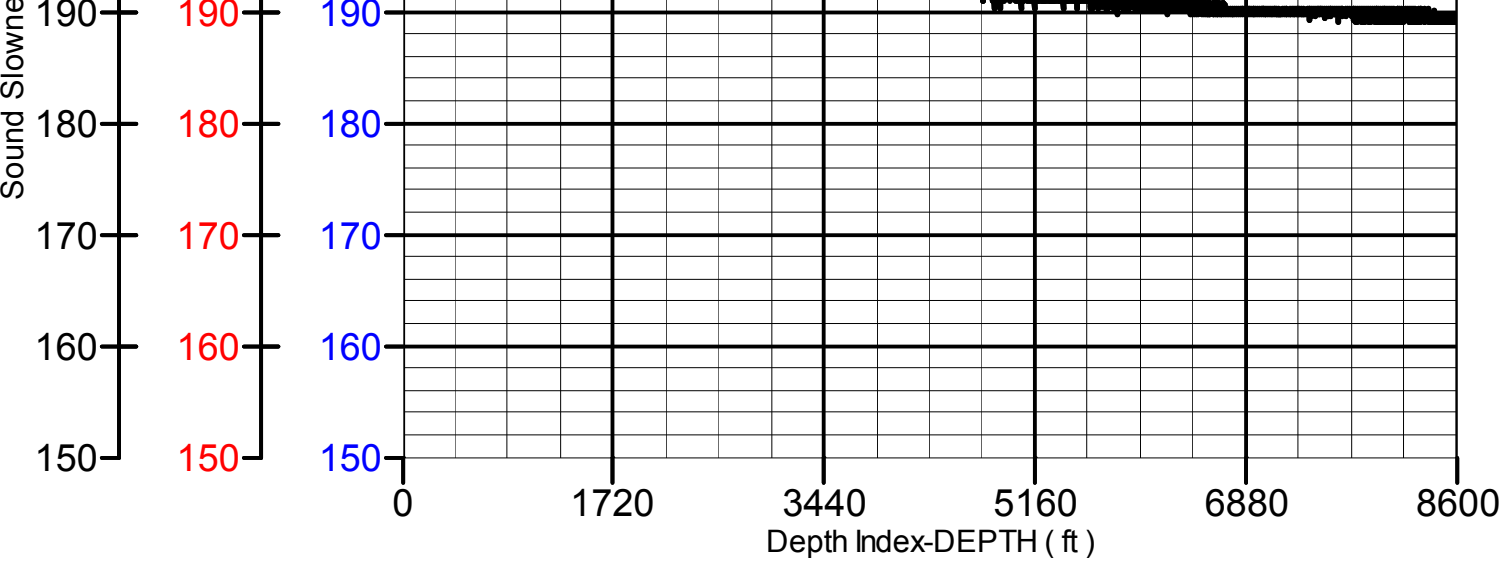

XYZ

Company:Southern California Gas Company Well:Standard Sesnon 9
One: Log[2]:Down:S003

Theoretical Acoustic Impedance of Mud vs Depth

2D Cross Plot

Index Range: From 436.00 to 8597.50 ft

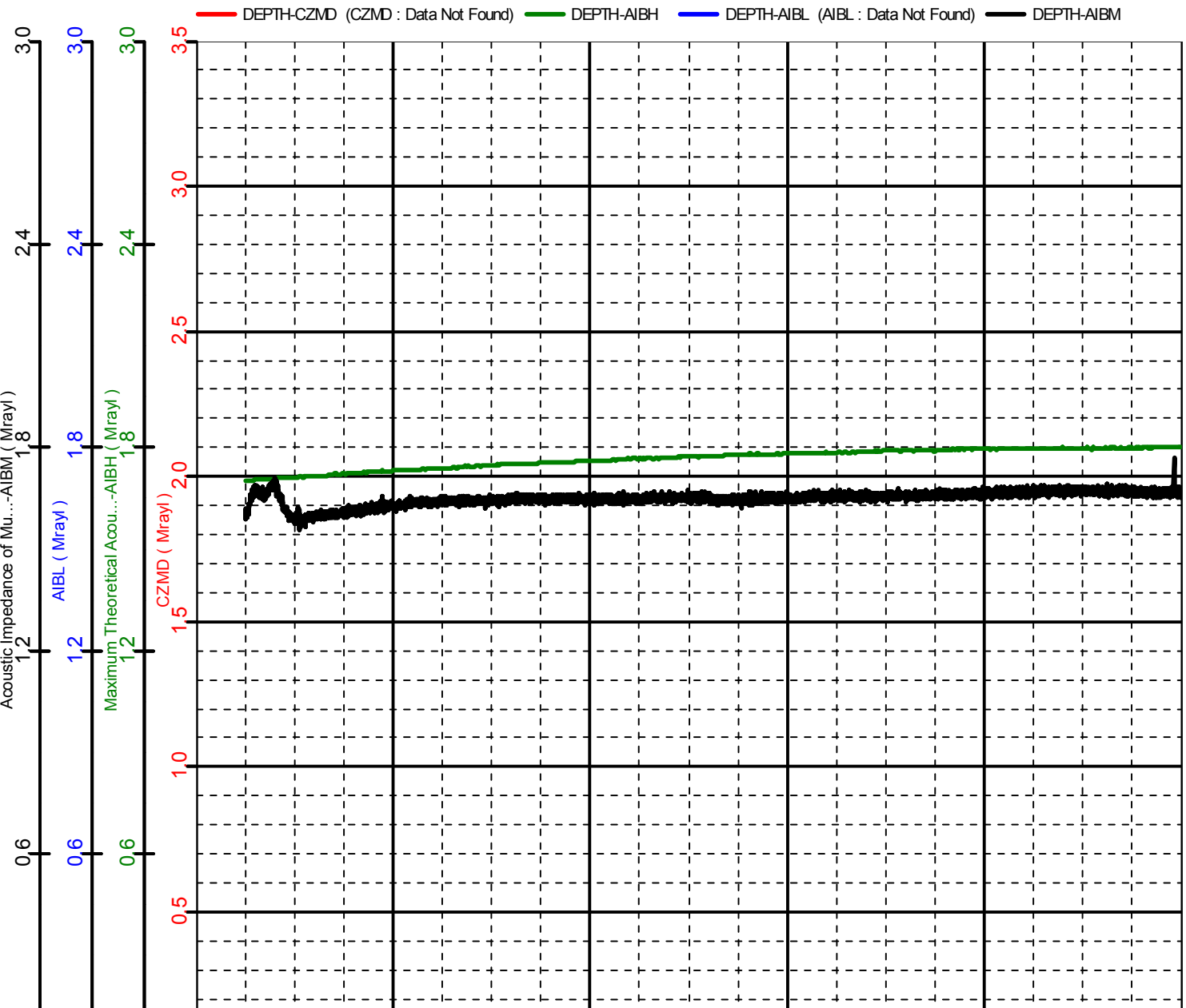

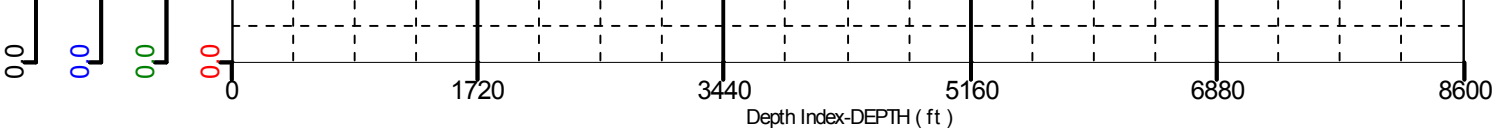

USIT - Fluid Properties Measurement

Run Name	Pass Name	Start Depth(ft)	Stop Depth(ft)
Run 1	Log[2]:Down	436.1	8598.16

Fluid Velocity = "Automatic".
CFVL equals DFSL channel

Start Depth(ft)	Stop Depth(ft)	Start Value(us/ft)	End Value(us/ft)

Mud Impedance = "Theoretical".
CZMD uses theoretical results.
MUD_N_THE=1.00
DFD=1.02g/cm3(8.50lbm/gal)

Start Depth(ft)	Stop Depth(ft)	Start Value(Mrayl)	End Value(Mrayl)

Company: Southern California Gas Company

Schlumberger

Well: Standard Sesnon 9

Field: Aliso Canyon

County: Los Angeles

State: California

Ultrasonic Imager

Ultrasonic Imager

Gamma Ray - CCL

7" 23, 26, 29# casing

Ex. II - 16

Ex. II - 16

Ex. II - 17

HR Vertilog

Magnetic Flux Leakage Inspection

Advanced Analysis

Company	Southern California Gas Company
Well	Porter 46
Field	Aliso Canyon
County	Los Angeles
State	California

Location:
1425'S And 3225'W From Station 84

Section 28	Township 3N	Range 16W	

Date	Aug. 17, 2017
Service Order	126679
Recorded by	J Burge
Witnessed by	G Ross
API Serial No.	04-037-00733-00

Permanent Datum:	GL	Elevation: 2254.850 ft.		Depth	7918.000
Log Measured From:	DF	6.920 ft. above Perm. Datum		Btm. Log Interval	7590.000
Drilling Measured From:	DF	6.920 ft. above Perm. Datum		Top Log Interval	0.000
				Fluid Type	KCL

Casing Data

Size	Weight	Grade	From	To	Length
7 inch	23.0 lb/ft	J-55	0	3381'	3381.0
7 inch	23.0 lb/ft	N-80	3381'	5166'	1785.0
7 inch	26.0 lb/ft	N-80	5166'	6717'	1551.0
7 inch	29.0 lb/ft	N-80	6717'	7710'	993.0
13.375 inch	54.5 lb/ft	J-55	0	533'	533.0

Software Version 7.4.0.1

Equipment Data

Run	Trip	Tool Type	Tool Series	Serial Number	Position
1	1	HRVRT MFL	4997	PB11988737	LOWER
1	1	HRVRT MFL	4997	QB11988736	UPPER
1	1	HRVRT TELEM	4993	10360727	

Calibration Data

Calibration File Name	4997-7-001-PB11988737-U.CAL

Date of Calibration	03/31/2017 15:36
Calibration Identifier	9CC09EF0-FC22-4FC5-BC58-63EBD50C7056
Tool Number	4997-00
Calibrator Number	4997-7-001
Calibrator Size	(7 In - 178 mm)
Calibration Source File	20170331_150812_MEM.MVL
Calibration Software Rev	Microvision 32-bit 7.3.4.0
Comment	RMA1529

Calibration Data

Calibration File Name	4997-7-001-QB11988736-L.CAL
Date of Calibration	03/31/2017 15:36
Calibration Identifier	9CC09EF0-FC22-4FC5-BC58-63EBD50C7056
Tool Number	4997-00
Calibrator Number	4997-7-001
Calibrator Size	(7 In - 178 mm)
Calibration Source File	20170331_150812_MEM.MVL
Calibration Software Rev	Microvision 32-bit 7.3.4.0
Comment	RMA1529

In making interpretations of logs our employees will give customer the benefit of their best judgment. But since all interpretations are opinions based on inferences from electrical or other measurements, we cannot, and we do not guarantee the accuracy or correctness of any interpretation. We shall not be liable or responsible for any loss, cost, damages, or expenses whatsoever incurred or sustained by the customer resulting from any interpretation made by any of our employees.

Interpretation

HRVRT analysis was depth correlated to SLB GR-CCL logged 16 August 2017.

```
  19.16 ft   Hardware - Possible Girth Weld
  19.57 ft   Hardware - External casing head response.
 538.35 ft   Hardware - Bottom of 13.375" external casing
1540.48 ft   Anomaly - Mechanical/Manufacturing Artifacts,
    Possible Dent or hard spot
2634.29 ft   Anomaly - Mechanical/Manufacturing Artifacts,
    possible Dent or hard spot
3375.55 ft   Anomaly - Mechanical/Manufacturing Artifacts,
    Possible Dent or hard spot
```

The collar identified as anomalous has an apparent metal loss feature at the edges of the makeup region and accurate metal loss cannot be qualified. It is recommended that this anomalous connection is continued to be monitored in future surveys.

Reviewing the data stick and pull of the tool in the up pass and down pass was observed throughout the surveyed interval, more prominent over the bottom . This misalignment was normalized as best as possible to correct for the acceleration changes of the tool and the analysis over this interval was done by analyzing the feature with the best alignment as well as we could.

Internal circumferential features with metal loss signature can be seen in some joints. These features appear to be mechanical

be seen in some joints. These features appear to be mechanical or manufacturing in nature and fall below the 15 % threshold value for classification. These features were also evident in the MAC survey. See examples Joint # 16 at 687' and 691' and joint # 24 at 1002'.

Joint Interpretation Summary

Joint	From	To	Length	Class	Max Depth	Position	ID/OD
1	18.16	58.96	40.80	Class 1	-	-	-
2	58.96	103.09	44.13	Class 1	-	-	-
3	103.09	147.10	44.01	Class 1	-	-	-
4	147.10	188.45	41.35	Class 1	-	-	-
5	188.45	232.31	43.86	Class 1	-	-	-
6	232.31	275.52	43.21	Class 1	-	-	-
7	275.52	318.11	42.59	Class 1	-	-	-
8	318.11	362.00	43.89	Class 1	-	-	-
9	362.00	405.07	43.07	Class 1	-	-	-
10	405.07	447.32	42.25	Class 1	-	-	-
11	447.32	488.33	41.01	Class 1	-	-	-
12	488.33	530.72	42.39	Class 1	-	-	-
13	530.72	573.43	42.71	Class 1	-	-	-
14	573.43	614.91	41.48	Class 1	-	-	-
15	614.91	657.65	42.74	Class 1	-	-	-
16	657.65	701.31	43.66	Class 1	-	-	-
17	701.31	743.52	42.21	Class 1	-	-	-
18	743.52	785.87	42.35	Class 1	-	-	-
19	785.87	827.85	41.98	Class 1	-	-	-
20	827.85	868.62	40.77	Class 1	-	-	-
21	868.62	910.76	42.14	Class 1	-	-	-
22	910.76	953.75	42.99	Class 1	-	-	-
23	953.75	995.71	41.96	Class 1	-	-	-
24	995.71	1039.14	43.43	Class 1	16.0%	999.61	OD
25	1039.14	1082.27	43.13	Class 1	-	-	-
26	1082.27	1124.04	41.77	Class 1	-	-	-
27	1124.04	1166.93	42.89	Class 1	-	-	-
28	1166.93	1209.82	42.89	Class 1	-	-	-
29	1209.82	1252.44	42.62	Class 1	-	-	-
30	1252.44	1295.36	42.92	Class 1	-	-	-
31	1295.36	1339.49	44.13	Class 1	-	-	-
32	1339.49	1382.58	43.09	Class 1	-	-	-
33	1382.58	1426.36	43.78	Class 1	-	-	-
34	1426.36	1470.54	44.18	Class 1	-	-	-
35	1470.54	1511.98	41.44	Class 1	-	-	-
36	1511.98	1555.07	43.09	Class 1	-	-	-
37	1555.07	1598.21	43.14	Class 1	-	-	-
38	1598.21	1640.49	42.28	Class 1	-	-	-
39	1640.49	1683.76	43.27	Class 1	-	-	-
40	1683.76	1726.06	42.30	Class 1	-	-	-
41	1726.06	1767.63	41.57	Class 1	-	-	-
42	1767.63	1810.55	42.92	Class 1	-	-	-
43	1810.55	1853.57	43.02	Class 1	-	-	-
44	1853.57	1895.92	42.35	Class 1	-	-	-
45	1895.92	1938.04	42.12	Class 1	-	-	-
46	1938.04	1980.44	42.40	Class 1	-	-	-
47	1980.44	2021.38	40.94	Class 1	-	-	-
48	2021.38	2063.99	42.61	Class 1	-	-	-

49	2063.99	2106.47	42.48	Class 1	-	-	-
50	2106.47	2149.38	42.91	Class 1	-	-	-
51	2149.38	2192.63	43.25	Class 1	-	-	-
52	2192.63	2235.81	43.18	Class 1	-	-	-
53	2235.81	2279.22	43.41	Class 1	-	-	-
54	2279.22	2321.22	42.00	Class 1	-	-	-
55	2321.22	2363.70	42.48	Class 1	-	-	-
56	2363.70	2406.27	42.57	Class 1	-	-	-
57	2406.27	2448.57	42.30	Class 1	-	-	-
58	2448.57	2491.17	42.60	Class 1	-	-	-
59	2491.17	2534.55	43.38	Class 1	-	-	-
60	2534.55	2576.91	42.36	Class 1	-	-	-
61	2576.91	2619.31	42.40	Class 1	-	-	-
62	2619.31	2662.08	42.77	Class 1	-	-	-
63	2662.08	2703.14	41.06	Class 1	-	-	-
64	2703.14	2746.81	43.67	Class 1	-	-	-
65	2746.81	2790.59	43.78	Class 1	-	-	-
66	2790.59	2833.45	42.86	Class 1	-	-	-
67	2833.45	2876.02	42.57	Class 1	-	-	-
68	2876.02	2919.28	43.26	Class 1	-	-	-
69	2919.28	2962.11	42.83	Class 1	-	-	-
70	2962.11	3004.41	42.30	Class 1	-	-	-
71	3004.41	3046.20	41.79	Class 1	-	-	-
72	3046.20	3088.68	42.48	Class 1	-	-	-
73	3088.68	3130.79	42.11	Class 1	-	-	-
74	3130.79	3174.09	43.30	Class 1	-	-	-
75	3174.09	3216.76	42.67	Class 1	-	-	-
76	3216.76	3260.23	43.47	Class 1	16.0%	3236.75	OD
77	3260.23	3303.70	43.47	Class 1	-	-	-
78	3303.70	3345.28	41.58	Class 1	-	-	-
79	3345.28	3388.38	43.10	Class 1	-	-	-
80	3388.38	3426.07	37.69	Class 1	-	-	-
81	3426.07	3469.60	43.53	Class 1	-	-	-
82	3469.60	3512.63	43.03	Class 1	-	-	-
83	3512.63	3551.44	38.81	Class 1	-	-	-
84	3551.44	3594.09	42.65	Class 1	-	-	-
85	3594.09	3636.63	42.54	Class 1	-	-	-
86	3636.63	3679.92	43.29	Class 1	-	-	-
87	3679.92	3724.03	44.11	Class 1	-	-	-
88	3724.03	3767.16	43.13	Class 1	-	-	-
89	3767.16	3808.89	41.73	Class 1	-	-	-
90	3808.89	3851.70	42.81	Class 1	-	-	-
91	3851.70	3895.43	43.73	Class 1	-	-	-
92	3895.43	3937.93	42.50	Class 1	-	-	-
93	3937.93	3981.08	43.15	Class 1	-	-	-
94	3981.08	4023.77	42.69	Class 1	-	-	-
95	4023.77	4067.72	43.95	Class 1	-	-	-
96	4067.72	4107.51	39.79	Class 1	-	-	-
97	4107.51	4150.92	43.41	Class 1	-	-	-
98	4150.92	4194.12	43.20	Class 1	-	-	-
99	4194.12	4237.62	43.50	Class 1	-	-	-
100	4237.62	4280.10	42.48	Class 1	-	-	-
101	4280.10	4322.96	42.86	Class 1	-	-	-
102	4322.96	4365.35	42.39	Class 1	-	-	-
103	4365.35	4405.10	39.75	Class 1	-	-	-
104	4405.10	4448.27	43.17	Class 1	-	-	-
105	4448.27	4490.65	42.38	Class 1	-	-	-
106	4490.65	4532.30	41.65	Class 1	-	-	-
107	4532.30	4576.49	44.19	Class 1	-	-	-
108	4576.49	4620.10	43.61	Class 1	-	-	-
109	4620.10	4662.07	41.97	Class 1	-	-	-
110	4662.07	4705.49	43.42	Class 1	-	-	-
111	4705.49	4747.17	41.68	Class 1			

111	4705.49	4747.17	41.68	Class 1	-	-	-
112	4747.17	4787.60	40.43	Class 1	-	-	-
113	4787.60	4831.10	43.50	Class 1	-	-	-
114	4831.10	4873.87	42.77	Class 1	-	-	-
115	4873.87	4915.58	41.71	Class 1	-	-	-
116	4915.58	4958.47	42.89	Class 1	-	-	-
117	4958.47	5002.13	43.66	Class 1	-	-	-
118	5002.13	5044.79	42.66	Class 1	-	-	-
119	5044.79	5087.29	42.50	Class 1	-	-	-
120	5087.29	5130.78	43.49	Class 1	-	-	-
121	5130.78	5173.22	42.44	Class 1	-	-	-
122	5173.22	5216.59	43.37	Class 1	-	-	-
123	5216.59	5259.87	43.28	Class 1	-	-	-
124	5259.87	5302.71	42.84	Class 1	-	-	-
125	5302.71	5345.89	43.18	Class 1	-	-	-
126	5345.89	5389.34	43.45	Class 1	-	-	-
127	5389.34	5432.22	42.88	Class 1	-	-	-
128	5432.22	5469.94	37.72	Class 1	18.0%	5468.43	ID
129	5469.94	5513.20	43.26	Class 1	-	-	-
130	5513.20	5555.33	42.13	Class 1	-	-	-
131	5555.33	5599.60	44.27	Class 1	-	-	-
132	5599.60	5642.30	42.70	Class 1	-	-	-
133	5642.30	5686.44	44.14	Class 1	-	-	-
134	5686.44	5730.13	43.69	Class 1	-	-	-
135	5730.13	5773.64	43.51	Class 1	-	-	-
136	5773.64	5816.41	42.77	Class 1	-	-	-
137	5816.41	5860.91	44.50	Class 1	-	-	-
138	5860.91	5903.37	42.46	Class 1	-	-	-
139	5903.37	5946.54	43.17	Class 1	-	-	-
140	5946.54	5990.14	43.60	Class 1	-	-	-
141	5990.14	6034.21	44.07	Class 1	-	-	-
142	6034.21	6074.82	40.61	Class 1	-	-	-
143	6074.82	6118.34	43.52	Class 1	-	-	-
144	6118.34	6160.38	42.04	Class 1	-	-	-
145	6160.38	6202.84	42.46	Class 1	-	-	-
146	6202.84	6245.38	42.54	Class 1	-	-	-
147	6245.38	6287.77	42.39	Class 1	-	-	-
148	6287.77	6330.87	43.10	Class 1	-	-	-
149	6330.87	6374.72	43.85	Class 1	-	-	-
150	6374.72	6418.54	43.82	Class 1	-	-	-
151	6418.54	6462.42	43.88	Class 1	-	-	-
152	6462.42	6505.98	43.56	Class 1	-	-	-
153	6505.98	6549.54	43.56	Class 1	-	-	-
154	6549.54	6593.07	43.53	Class 1	-	-	-
155	6593.07	6635.22	42.15	Class 1	-	-	-
156	6635.22	6679.34	44.12	Class 1	-	-	-
157	6679.34	6721.57	42.23	Class 1	-	-	-
158	6721.57	6765.35	43.78	Class 1	-	-	-
159	6765.35	6809.04	43.69	Class 1	-	-	-
160	6809.04	6852.56	43.52	Class 1	-	-	-
161	6852.56	6895.10	42.54	Class 1	-	-	-
162	6895.10	6936.56	41.46	Class 1	-	-	-
163	6936.56	6980.78	44.22	Class 1	-	-	-
164	6980.78	7022.56	41.78	Class 1	-	-	-
165	7022.56	7066.04	43.48	Class 1	-	-	-
166	7066.04	7109.98	43.94	Class 1	-	-	-
167	7109.98	7152.84	42.86	Class 1	-	-	-
168	7152.84	7196.85	44.01	Class 1	-	-	-
169	7196.85	7239.50	42.65	Class 1	-	-	-
170	7239.50	7283.50	44.00	Class 1	-	-	-
171	7283.50	7327.65	44.15	Class 1	-	-	-
172	7327.65	7364.94	37.29	Class 1	-	-	-
173	7364.94	7407.87	42.93	Class 1	-	-	-

174	7407.87	7449.54	41.67	Class 1	-	-	-
175	7449.54	7493.24	43.70	Class 1	-	-	-
176	7493.24	7536.44	43.20	Class 1	-	-	-
177	7536.44	7579.91	43.47	Class 1	-	-	-
178	7579.91	7584.18	4.27	Class 1	-	-	-

Southern California Gas Company Porter 46

File 20170817_16334B_RSP_0_0_0_0_0_0.mvl

MAIN LOG
5" / 100'

Class 1	Class 2	Class 3	Class 4
0 - 20%	20 - 40%	40 - 60%	60 - 100%

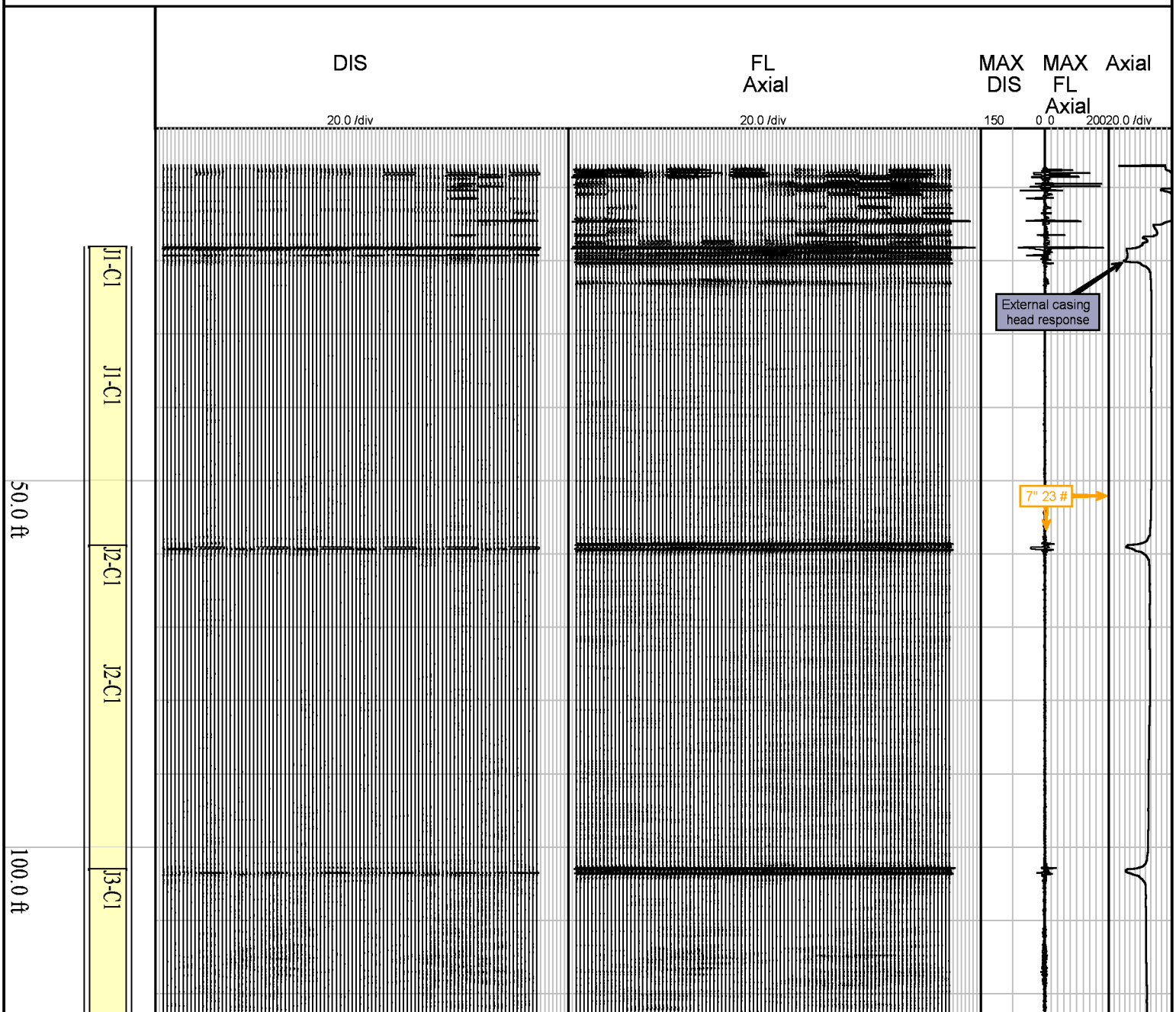

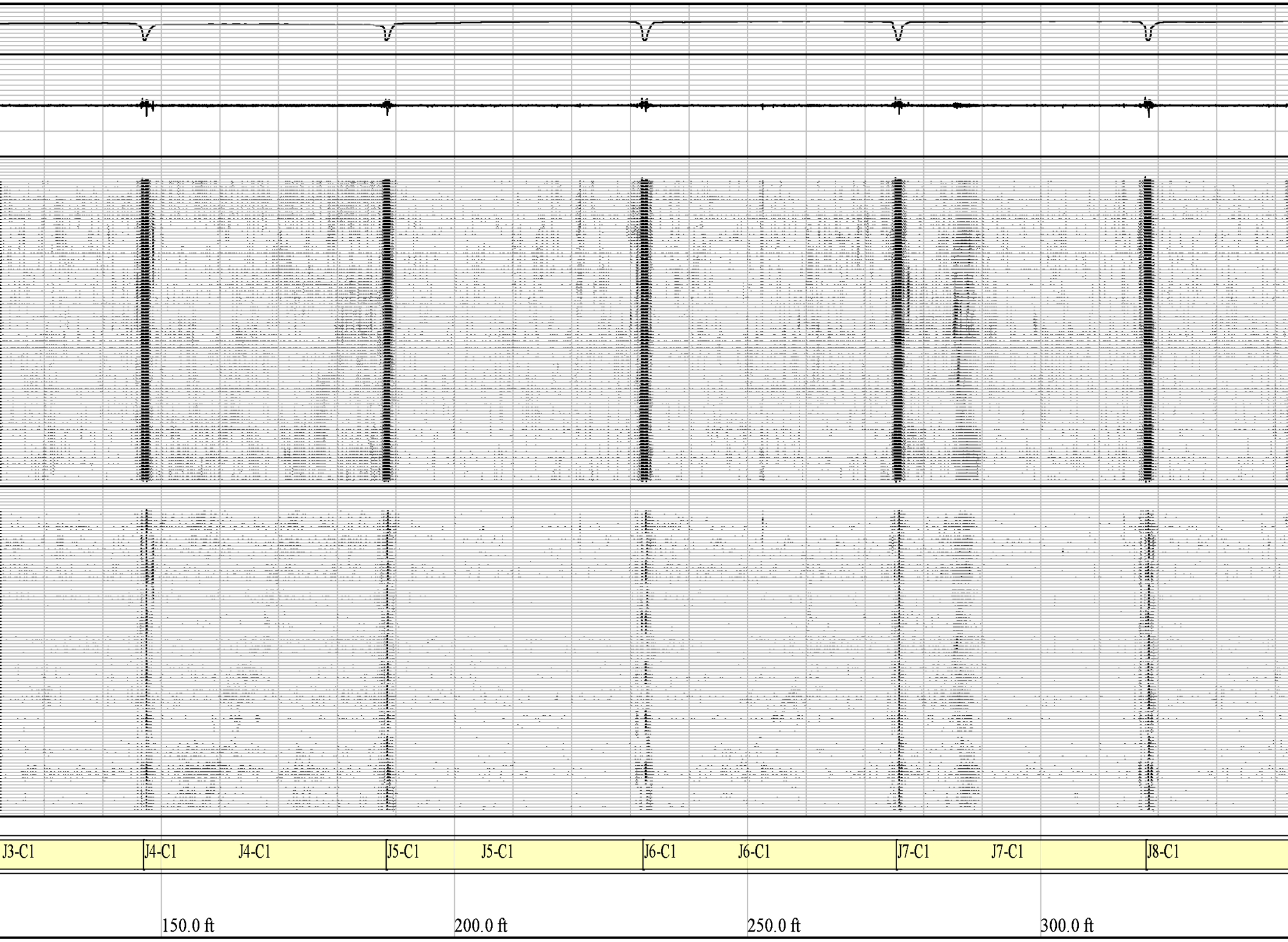
J3-C1
J4-C1
J4-C1
J5-C1
J5-C1
J6-C1
J6-C1
J7-C1
J7-C1
J8-C1
150.0 ft
200.0 ft
250.0 ft
300.0 ft

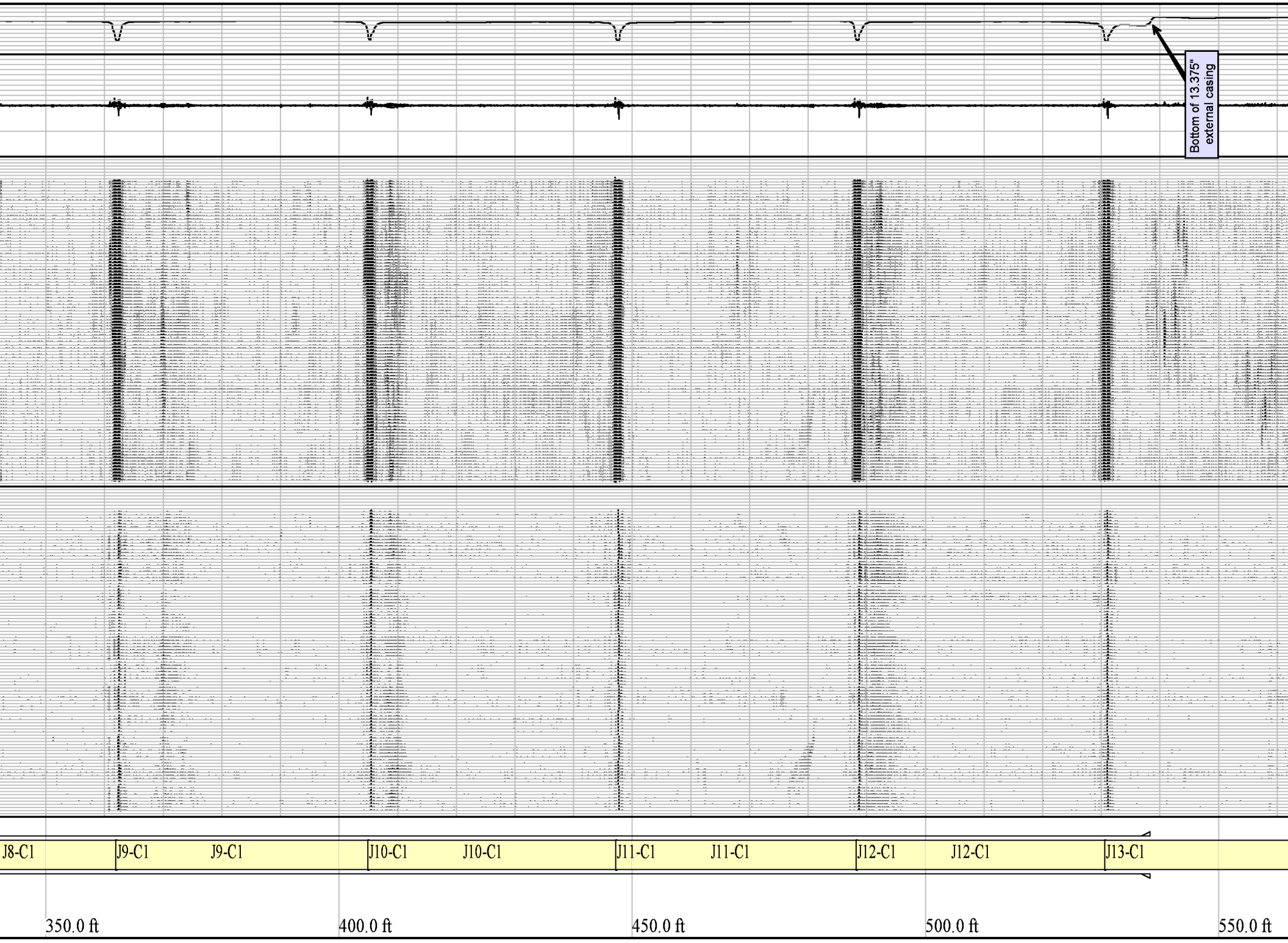
Bottom of 13.375" external casing
J8-C1
J9-C1
J9-C1
J10-C1
J10-C1
J11-C1
J11-C1
J12-C1
J12-C1
J13-C1
350.0 ft
400.0 ft
450.0 ft
500.0 ft
550.0 ft

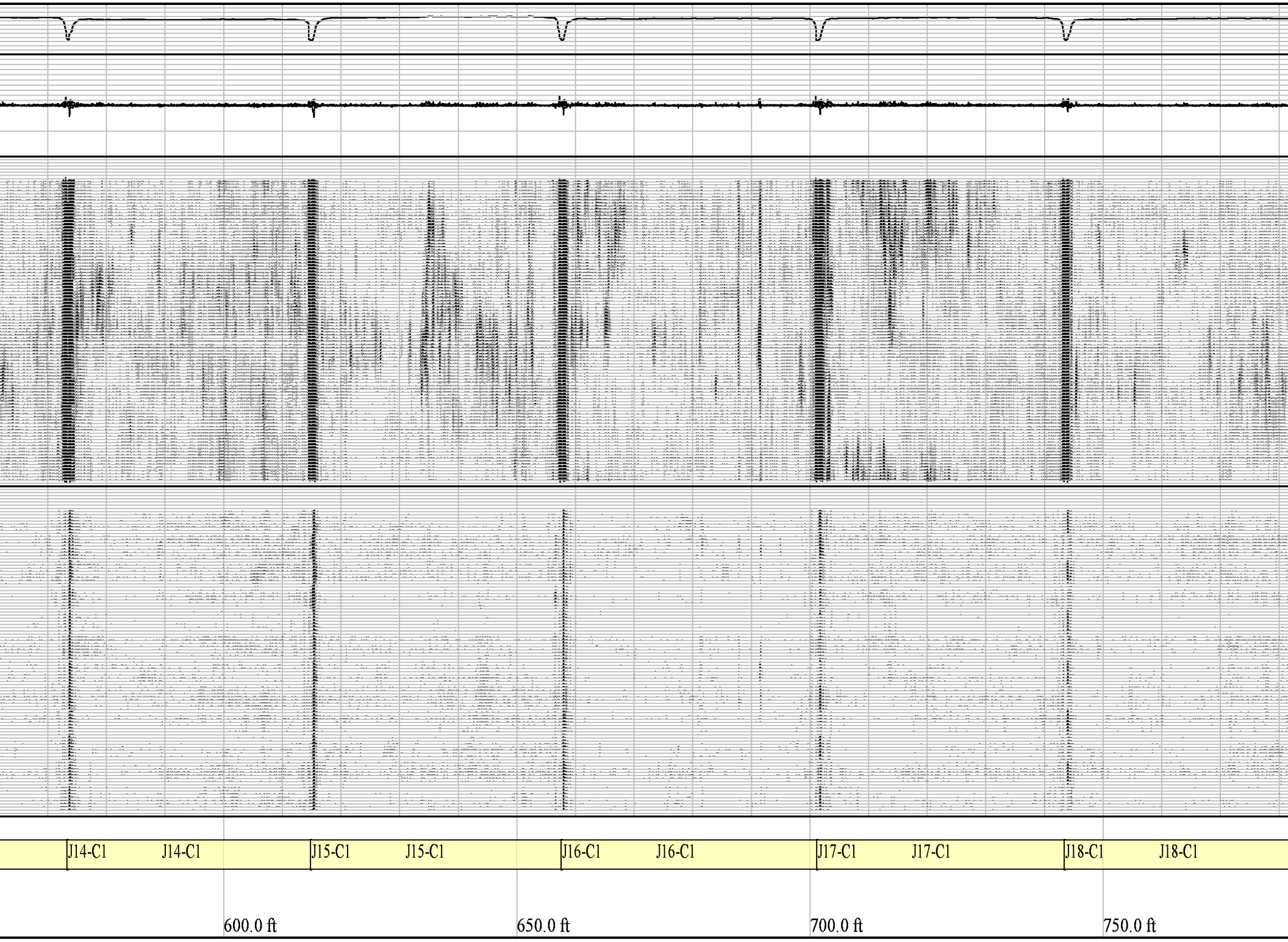
J14-C1
J14-C1
J15-C1
J15-C1
J16-C1
J16-C1
J17-C1
J17-C1
J18-C1
J18-C1
600.0 ft
650.0 ft
700.0 ft
750.0 ft

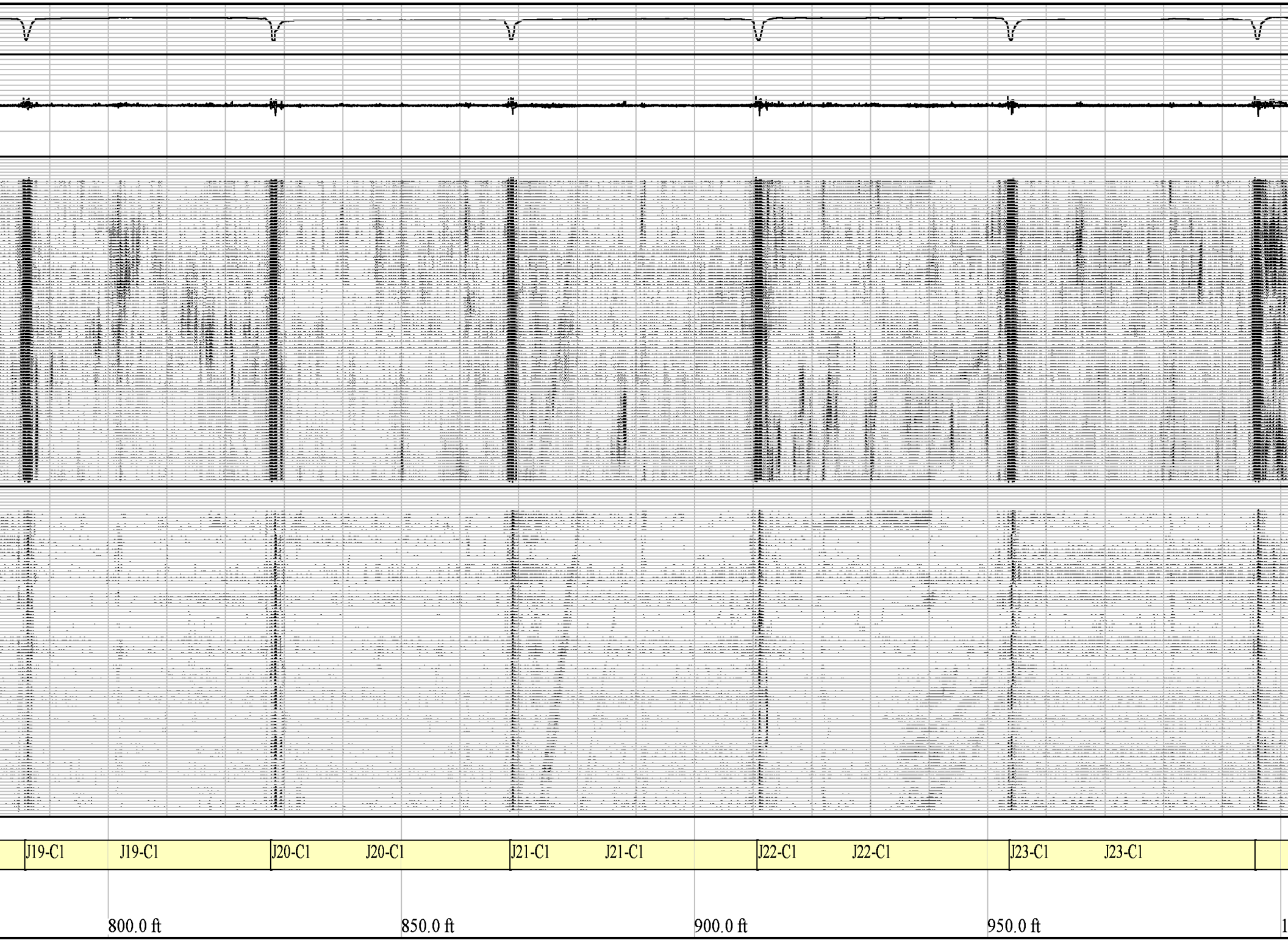
J19-C1
J19-C1
J20-C1
J20-C1
J21-C1
J21-C1
J22-C1
J22-C1
J23-C1
J23-C1
800.0 ft
850.0 ft
900.0 ft
950.0 ft

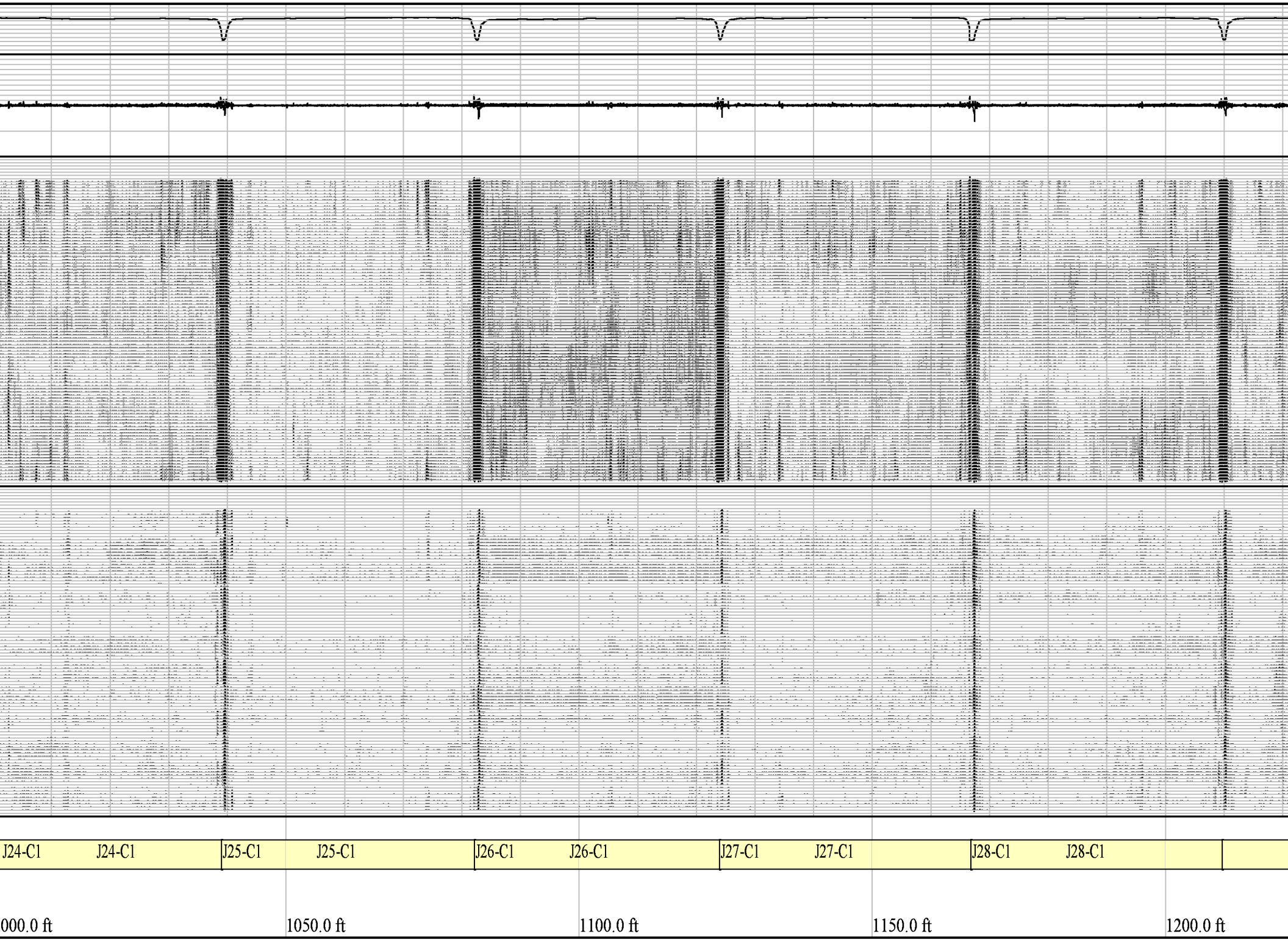
J24-C1
J24-C1
J25-C1
J25-C1
J26-C1
J26-C1
J27-C1
J27-C1
J28-C1
J28-C1
000.0 ft
1050.0 ft
1100.0 ft
1150.0 ft
1200.0 ft

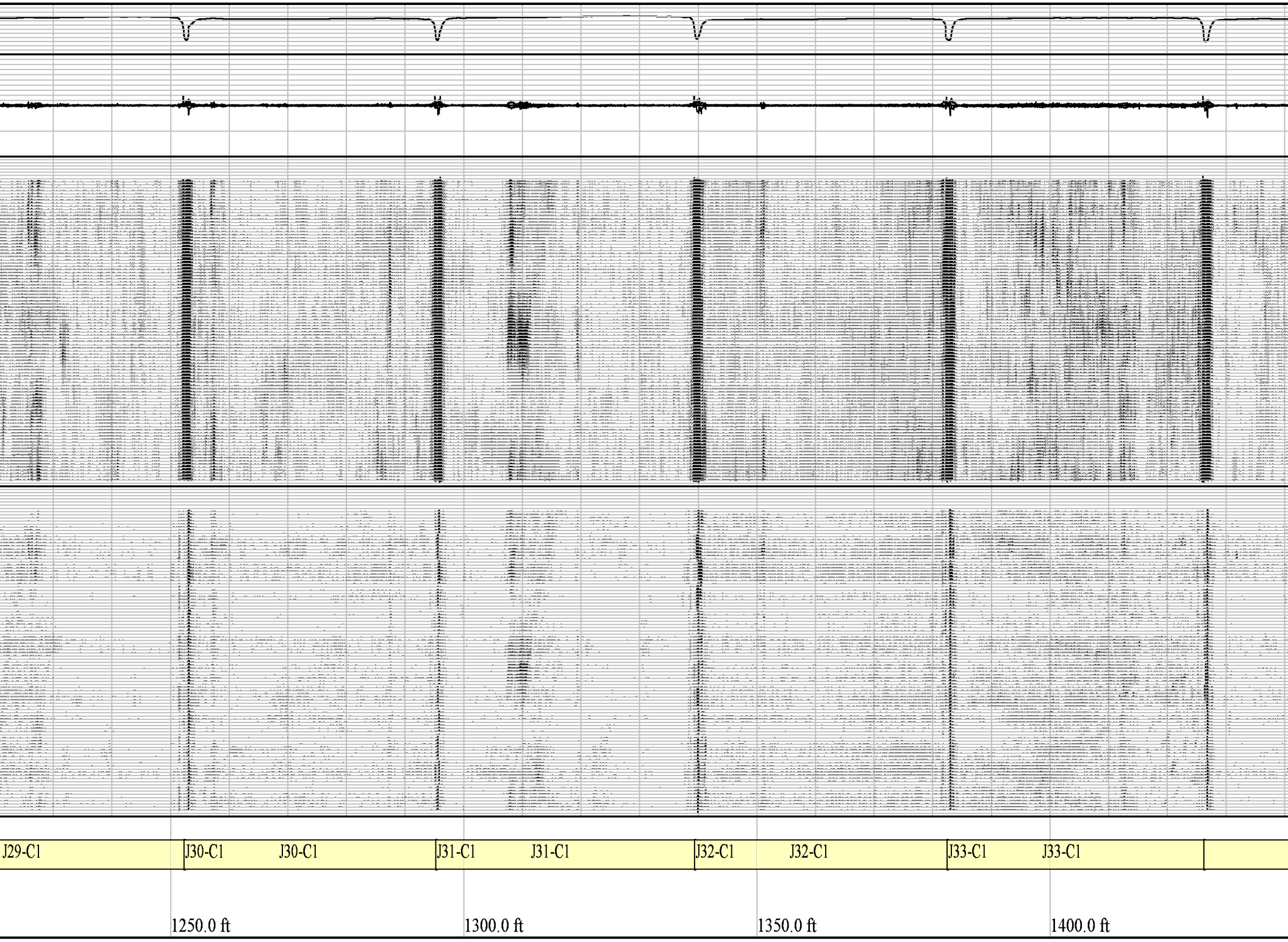
J29-C1
J30-C1
J30-C1
J31-C1
J31-C1
J32-C1
J32-C1
J33-C1
J33-C1
1250.0 ft
1300.0 ft
1350.0 ft
1400.0 ft

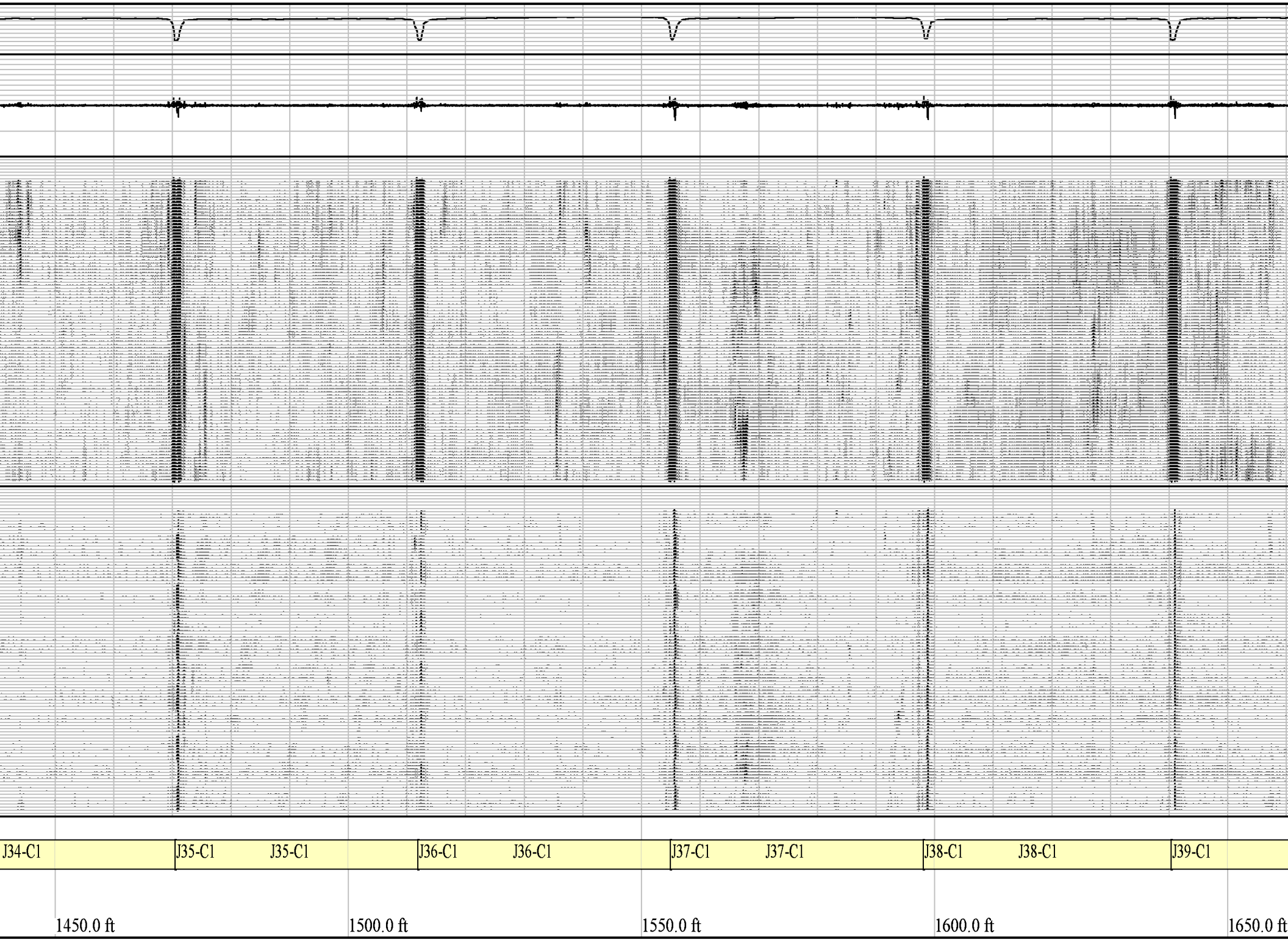
J34-C1
J35-C1
J35-C1
J36-C1
J36-C1
J37-C1
J37-C1
J38-C1
J38-C1
J39-C1
1450.0 ft
1500.0 ft
1550.0 ft
1600.0 ft
1650.0 ft

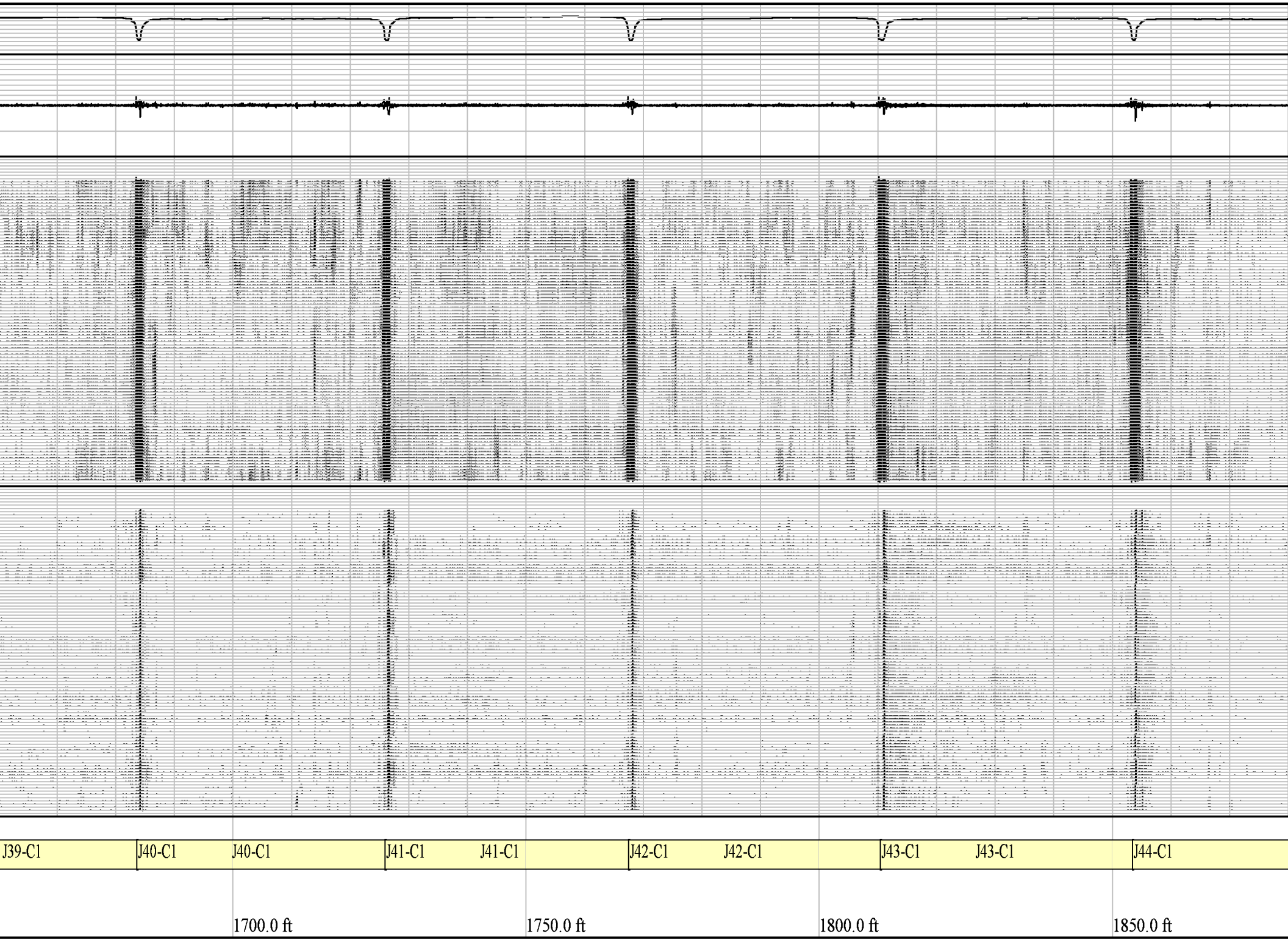
J39-C1
J40-C1
J40-C1
J41-C1
J41-C1
J42-C1
J42-C1
J43-C1
J43-C1
J44-C1
1700.0 ft
1750.0 ft
1800.0 ft
1850.0 ft

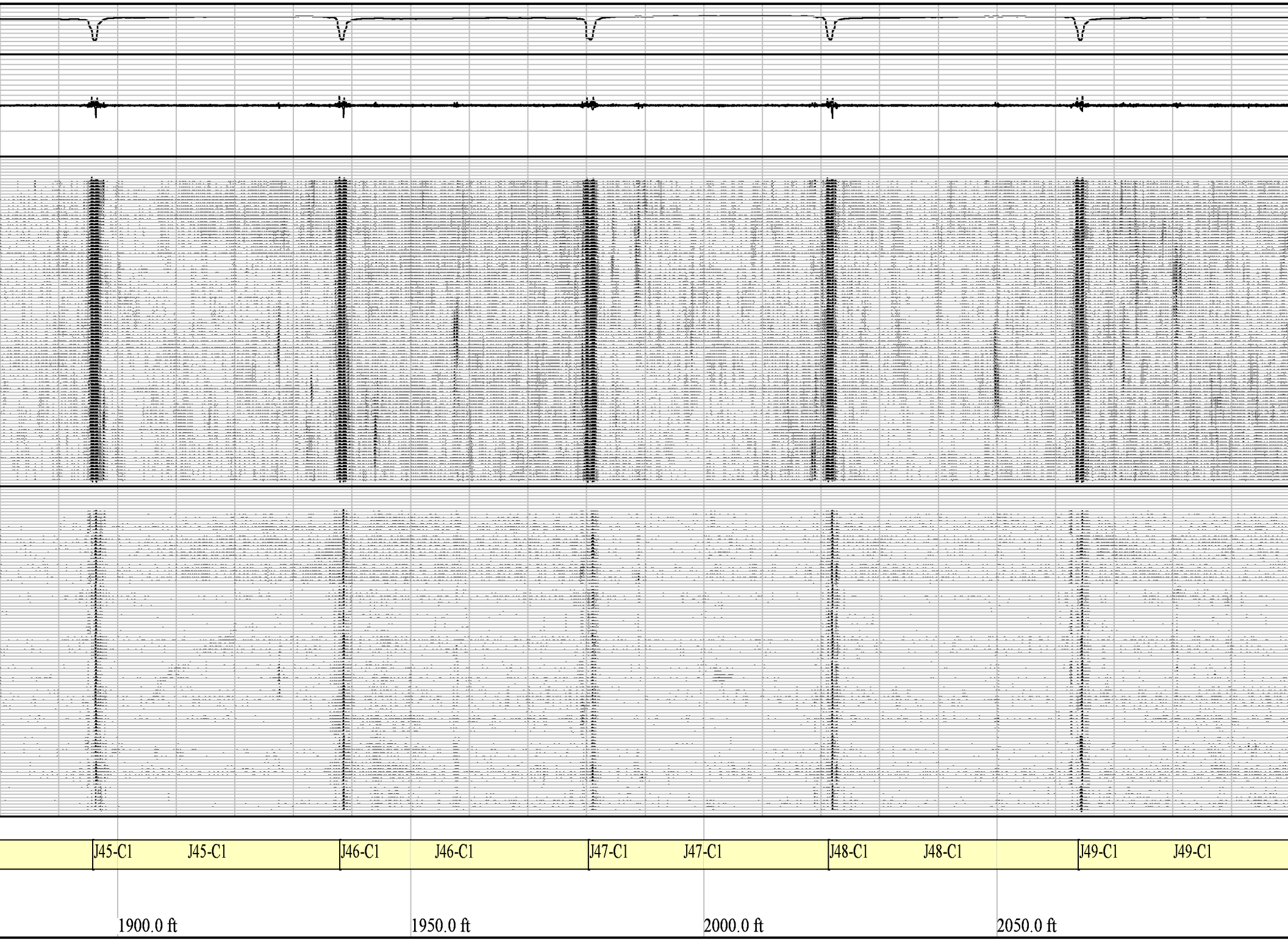
J45-C1
J45-C1
J46-C1
J46-C1
J47-C1
J47-C1
J48-C1
J48-C1
J49-C1
J49-C1
1900.0 ft
1950.0 ft
2000.0 ft
2050.0 ft

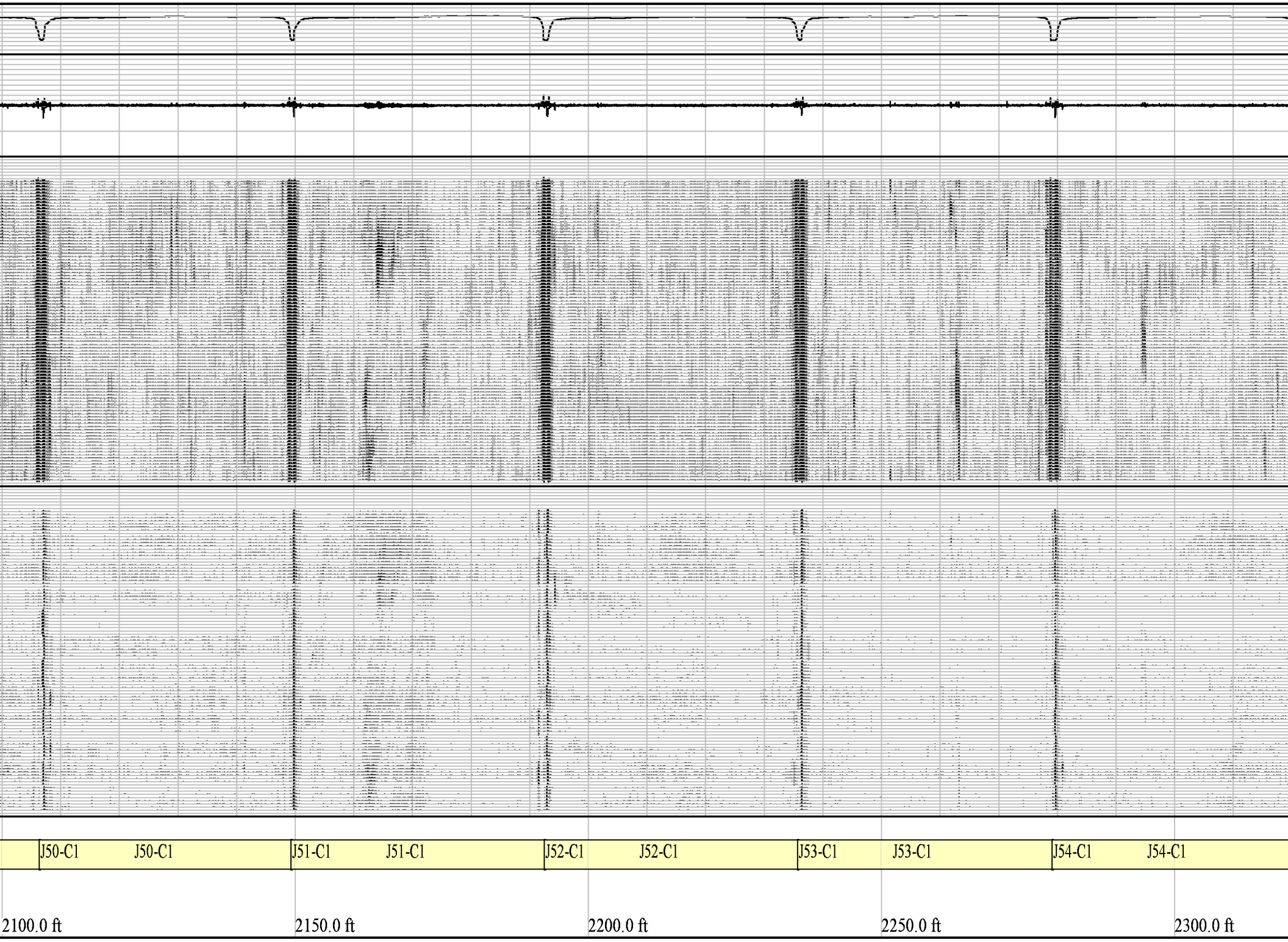
J50-C1
J50-C1
J51-C1
J51-C1
J52-C1
J52-C1
J53-C1
J53-C1
J54-C1
J54-C1
2100.0 ft
2150.0 ft
2200.0 ft
2250.0 ft
2300.0 ft

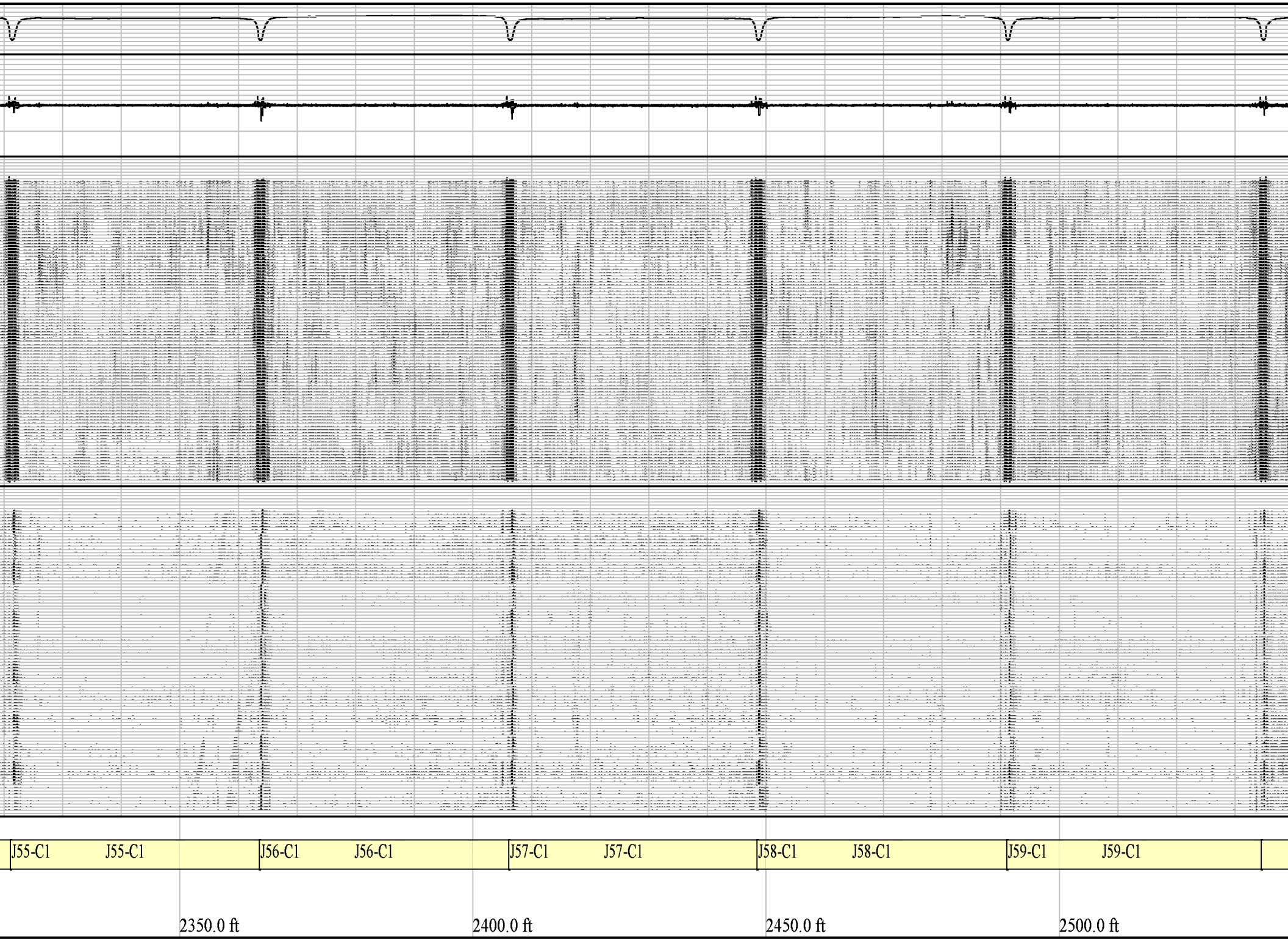
J55-C1
J55-C1
J56-C1
J56-C1
J57-C1
J57-C1
J58-C1
J58-C1
J59-C1
J59-C1
2350.0 ft
2400.0 ft
2450.0 ft
2500.0 ft

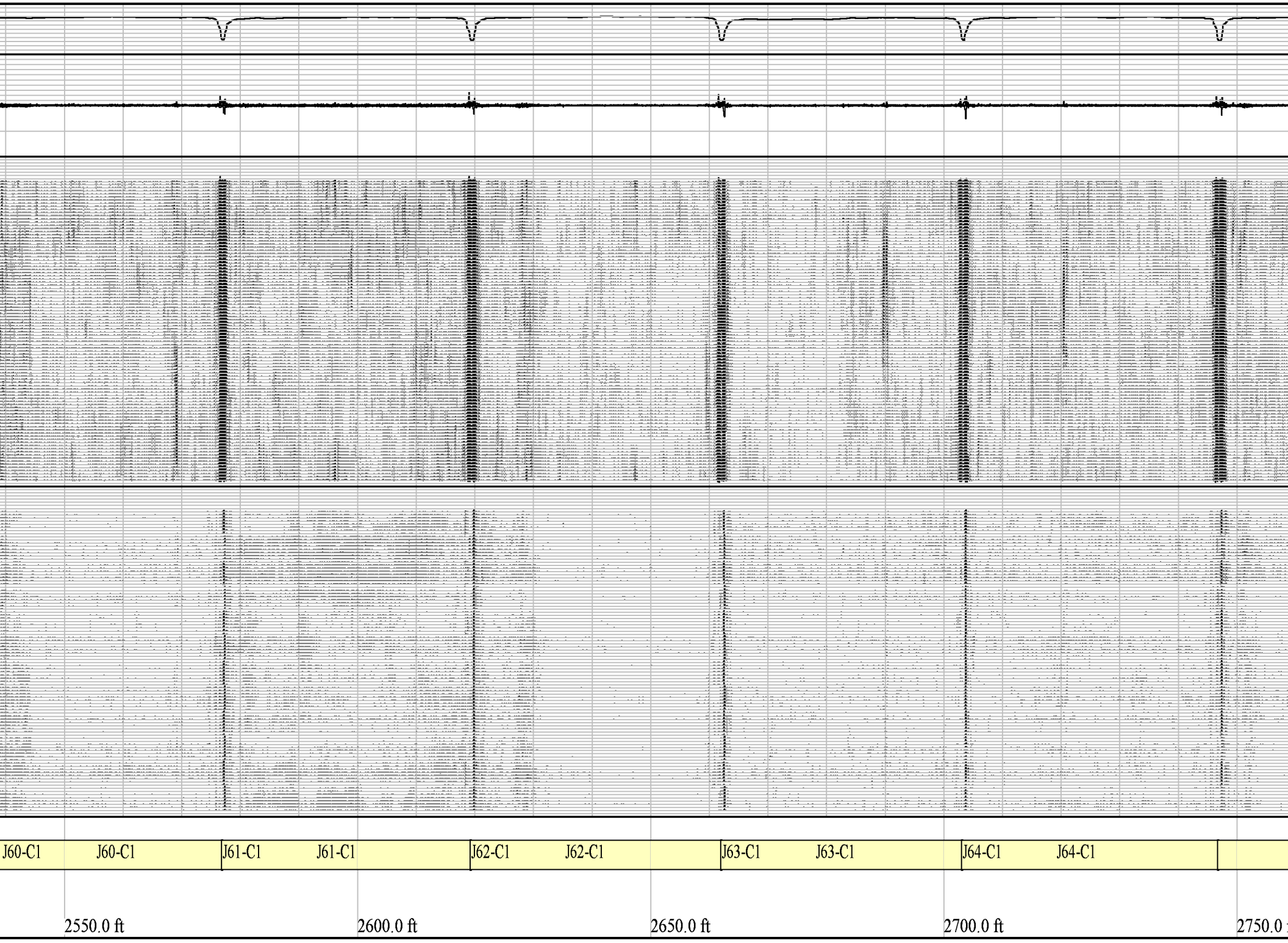
J60-C1
J60-C1
J61-C1
J61-C1
J62-C1
J62-C1
J63-C1
J63-C1
J64-C1
J64-C1
2550.0 ft
2600.0 ft
2650.0 ft
2700.0 ft
2750.0

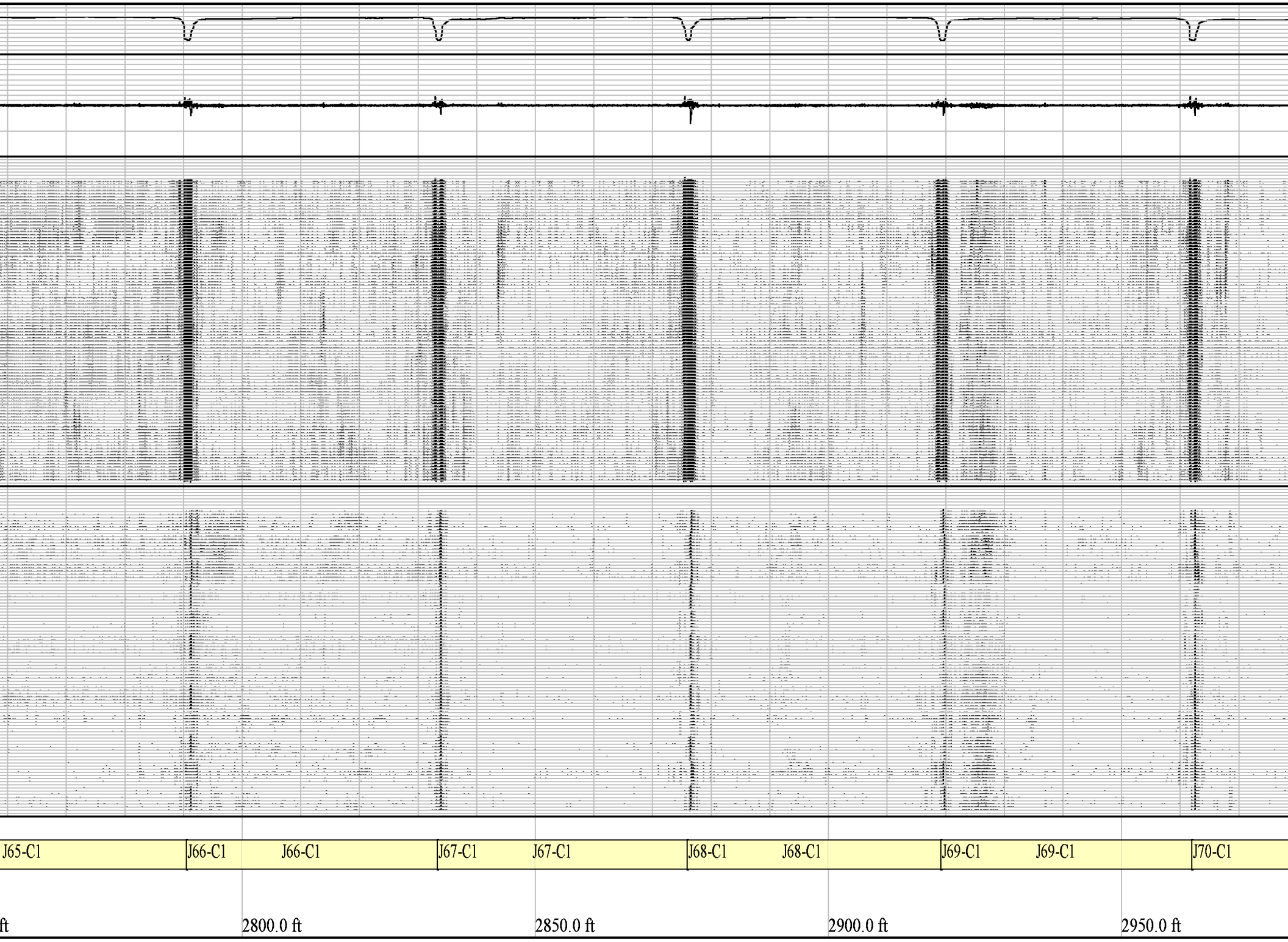
J65-C1
J66-C1
J66-C1
J67-C1
J67-C1
J68-C1
J68-C1
J69-C1
J69-C1
J70-C1
ft
2800.0 ft
2850.0 ft
2900.0 ft
2950.0 ft

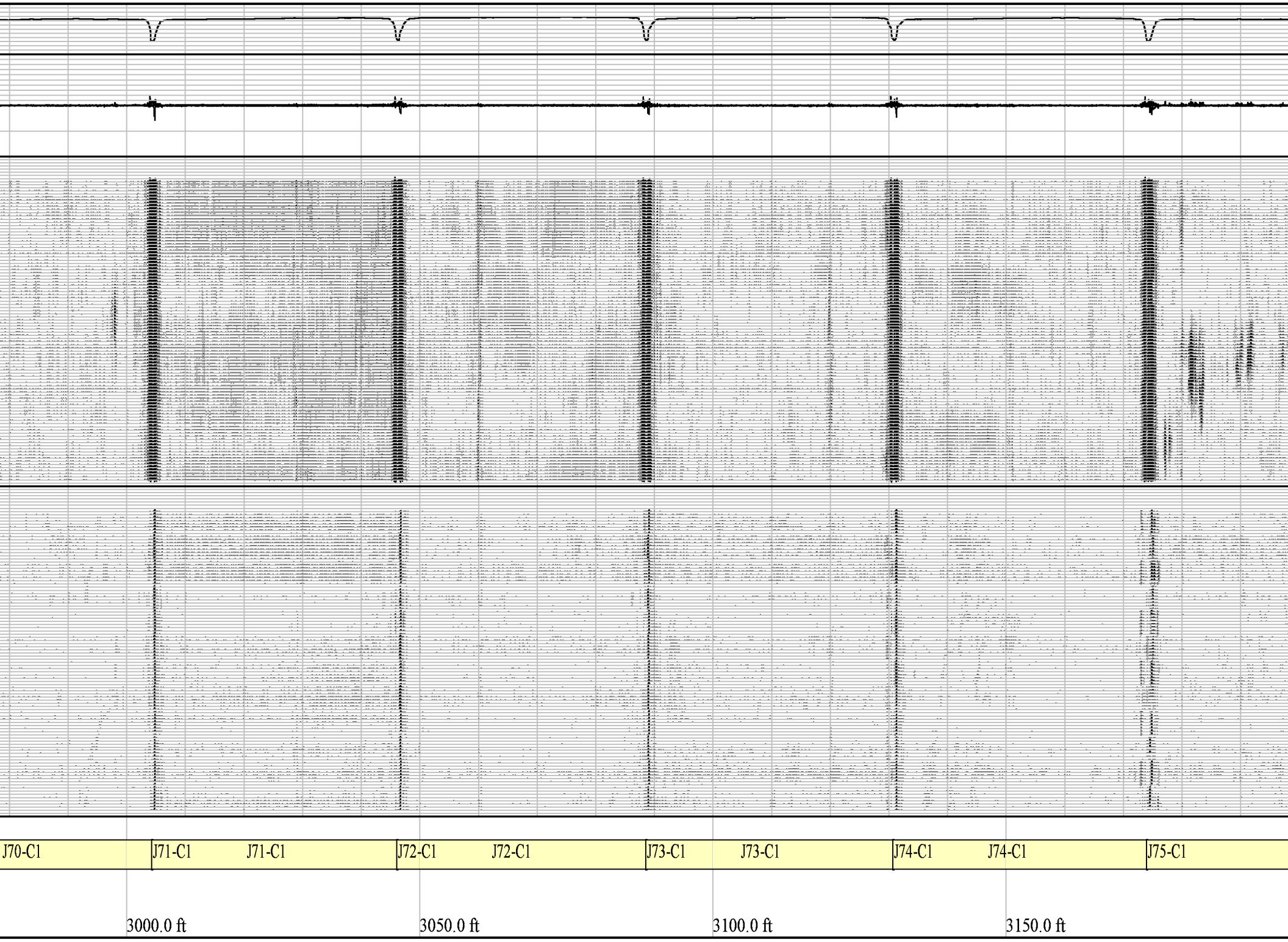
J70-C1
J71-C1
J71-C1
J72-C1
J72-C1
J73-C1
J73-C1
J74-C1
J74-C1
J75-C1
3000.0 ft
3050.0 ft
3100.0 ft
3150.0 ft

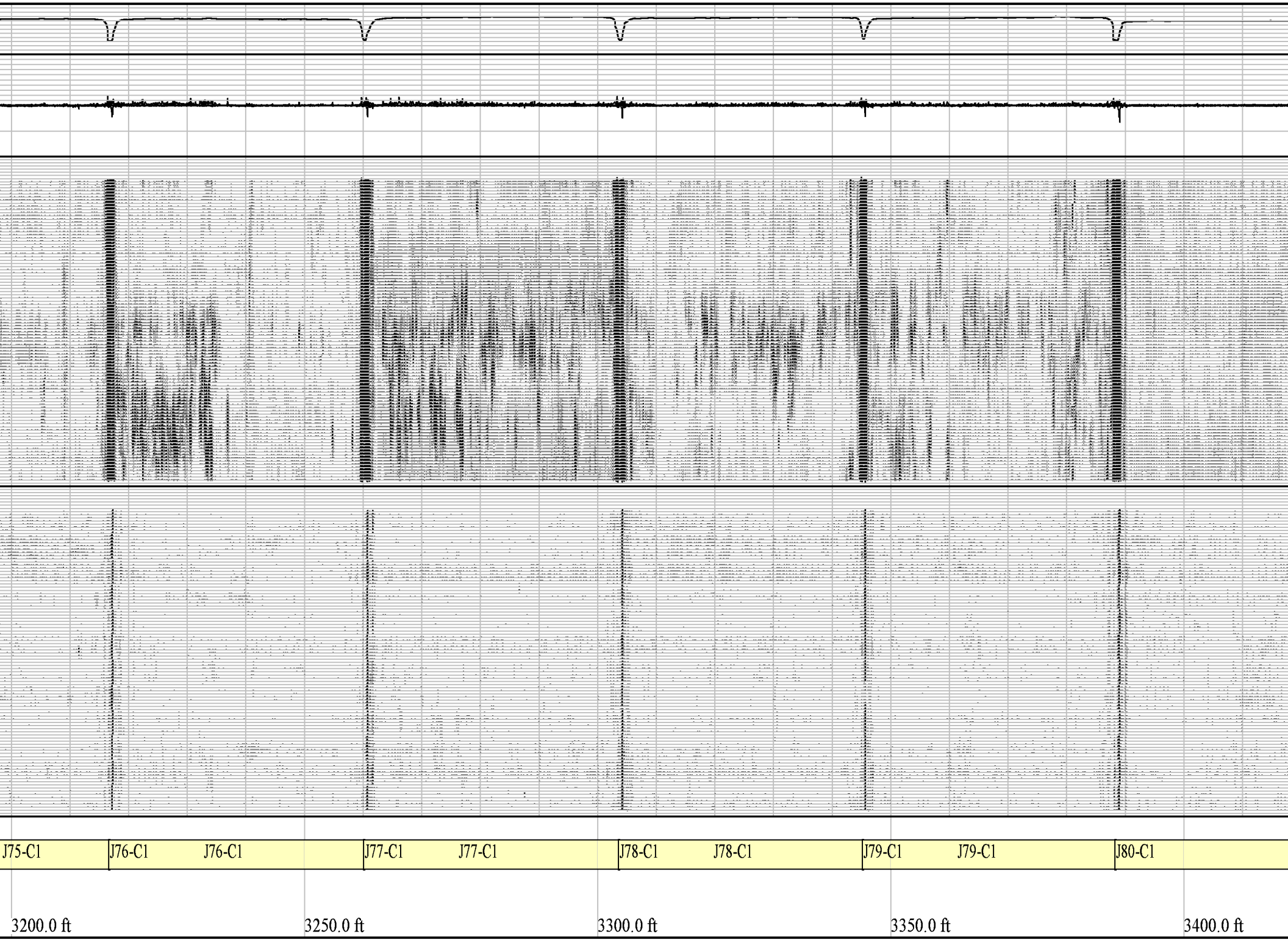
J75-C1
J76-C1
J76-C1
J77-C1
J77-C1
J78-C1
J78-C1
J79-C1
J79-C1
J80-C1
3200.0 ft
3250.0 ft
3300.0 ft
3350.0 ft
3400.0 ft

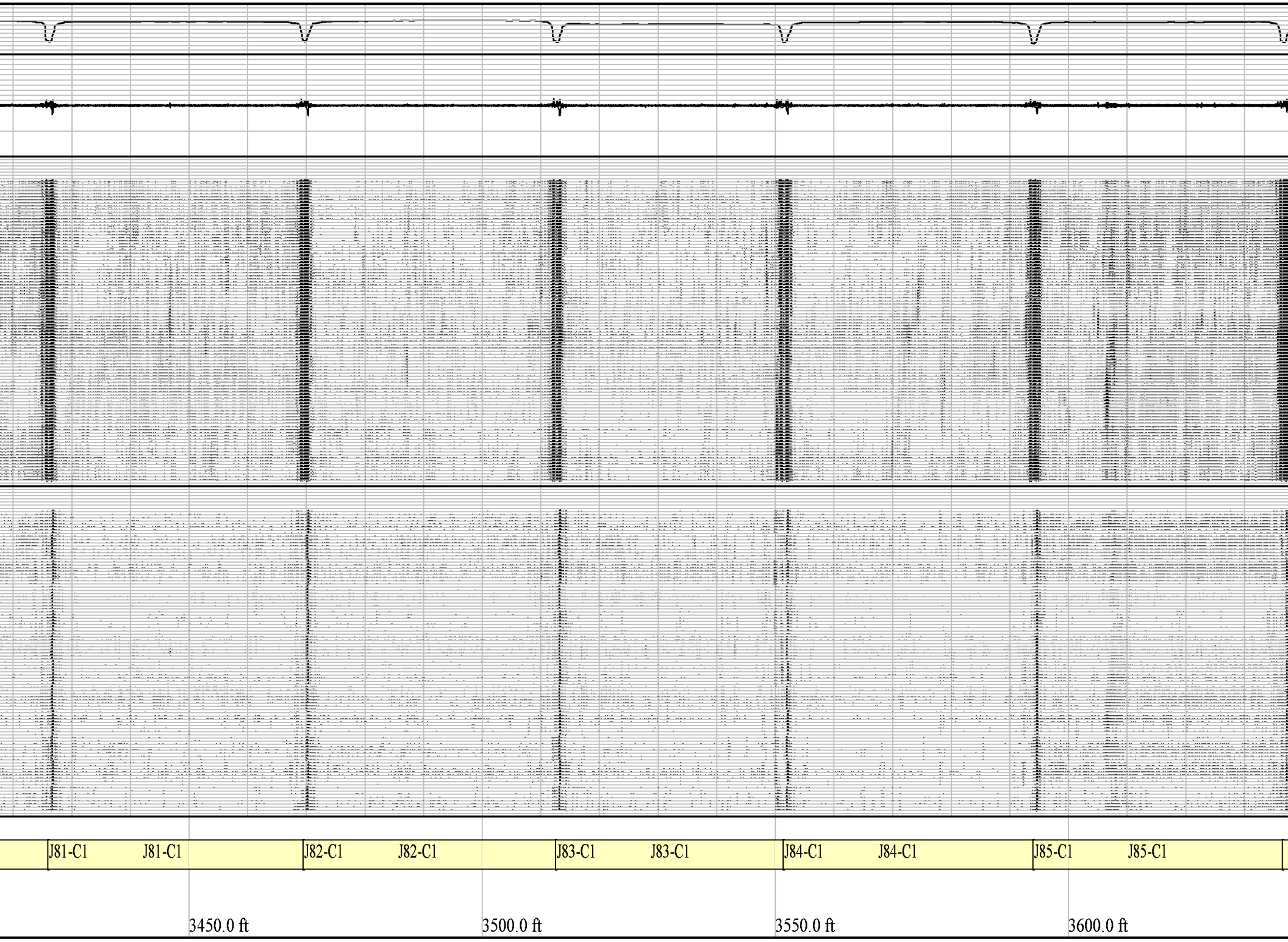
J81-C1
J81-C1
J82-C1
J82-C1
J83-C1
J83-C1
J84-C1
J84-C1
J85-C1
J85-C1
3450.0 ft
3500.0 ft
3550.0 ft
3600.0 ft

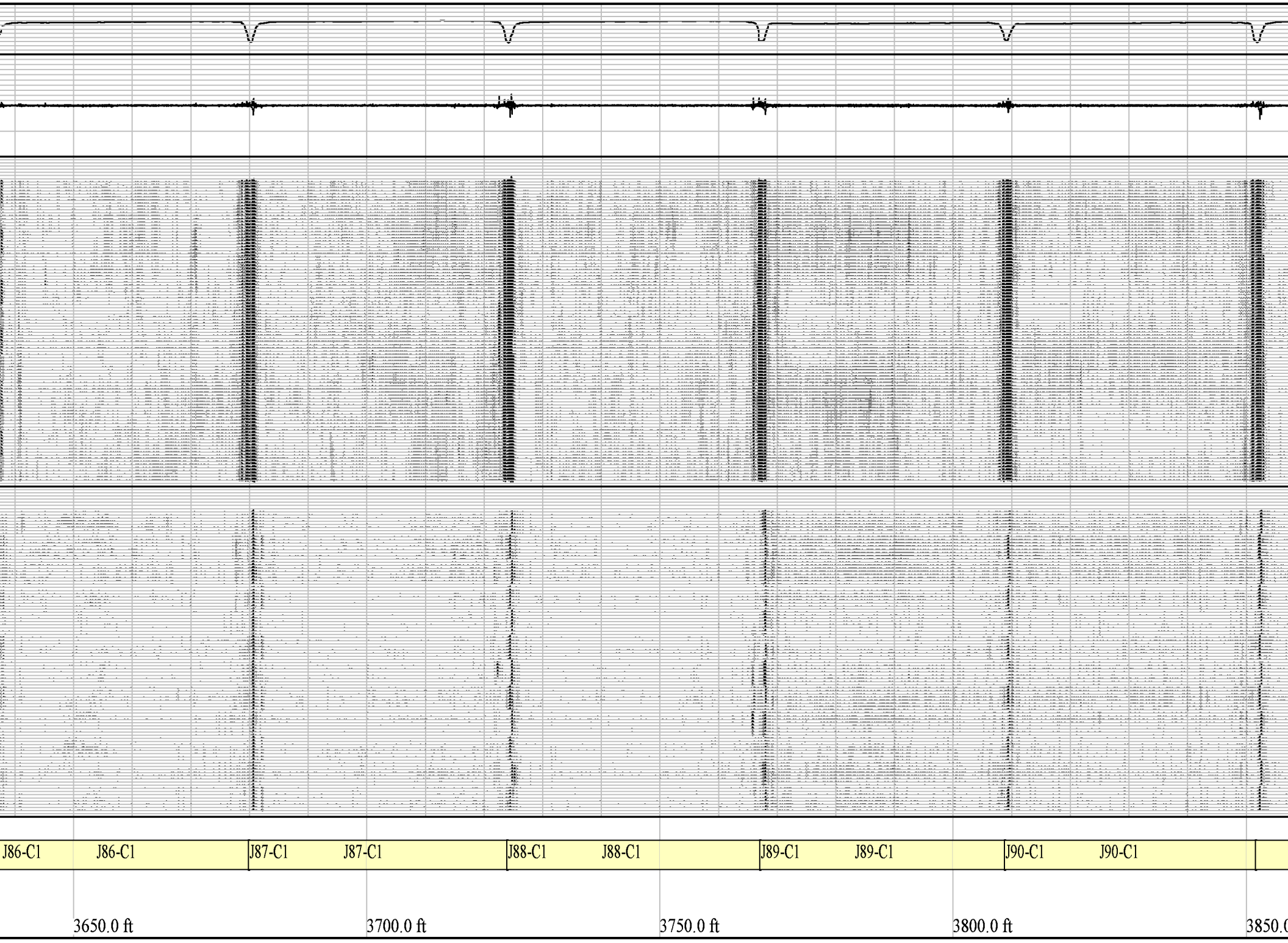
J86-C1
J86-C1
J87-C1
J87-C1
J88-C1
J88-C1
J89-C1
J89-C1
J90-C1
J90-C1
3650.0 ft
3700.0 ft
3750.0 ft
3800.0 ft

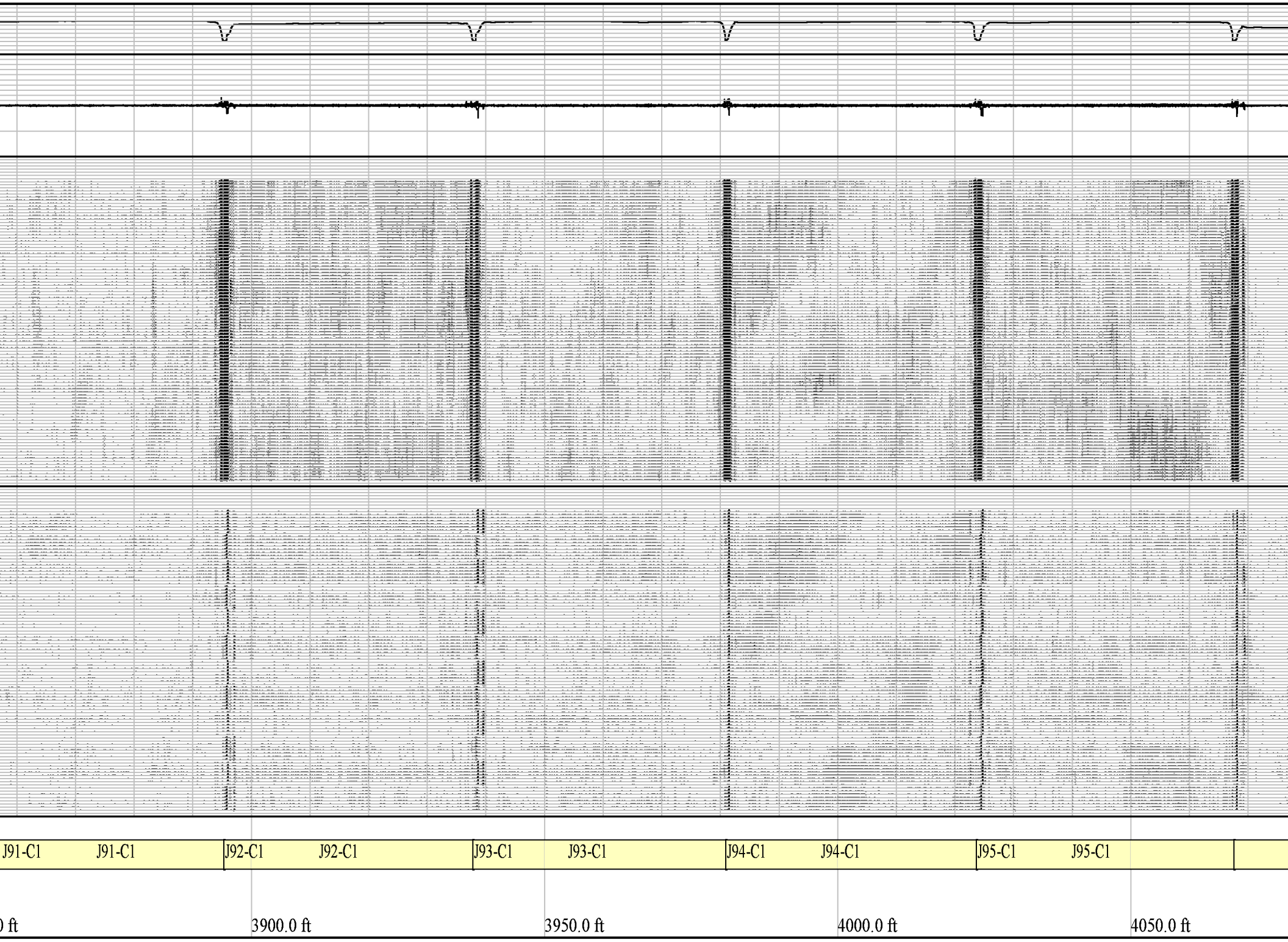
J91-C1
J91-C1
J92-C1
J92-C1
J93-C1
J93-C1
J94-C1
J94-C1
J95-C1
J95-C1
0 ft
3900.0 ft
3950.0 ft
4000.0 ft
4050.0 ft

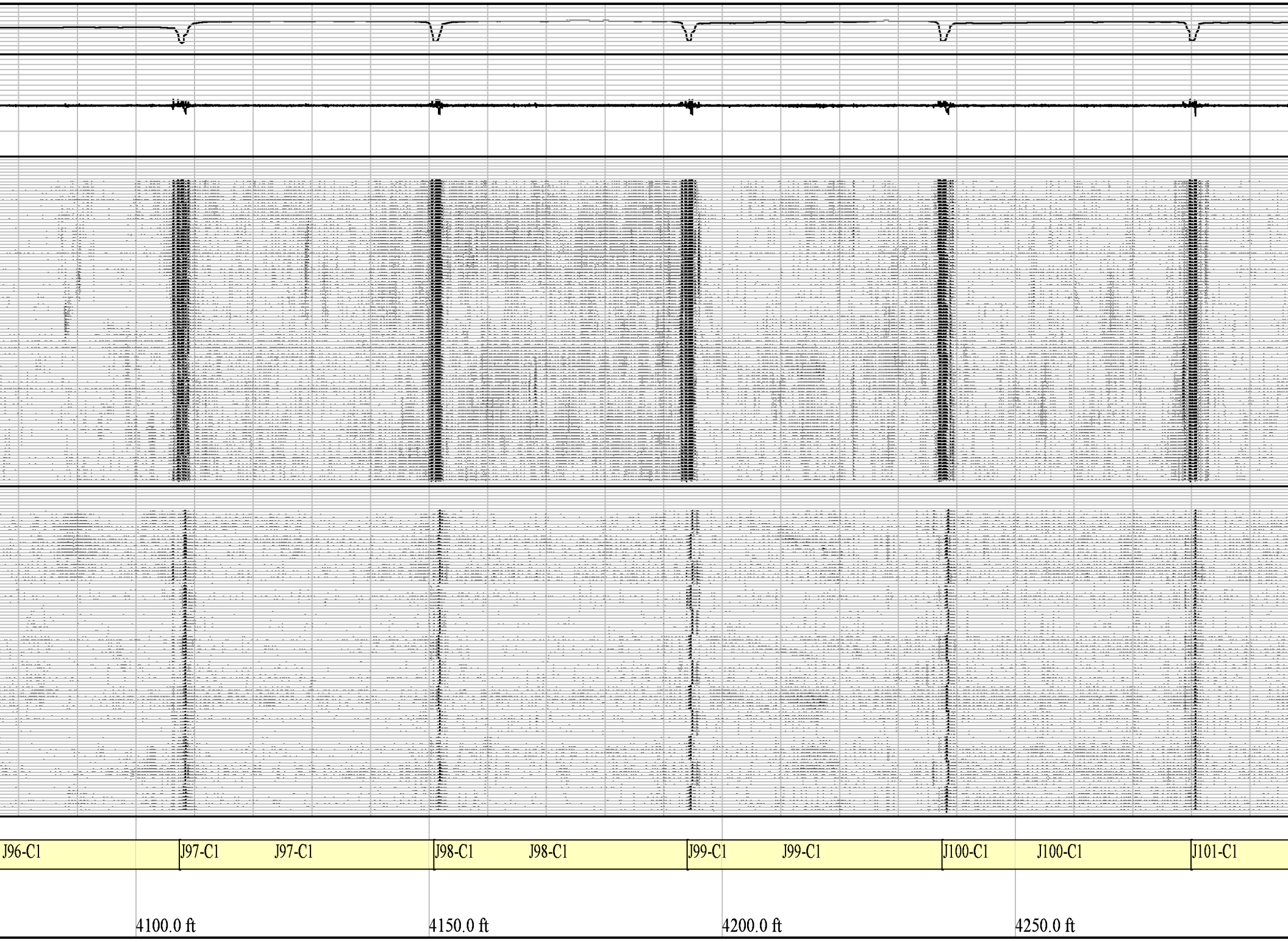
J96-C1
J97-C1
J97-C1
J98-C1
J98-C1
J99-C1
J99-C1
J100-C1
J100-C1
J101-C1
4100.0 ft
4150.0 ft
4200.0 ft
4250.0 ft

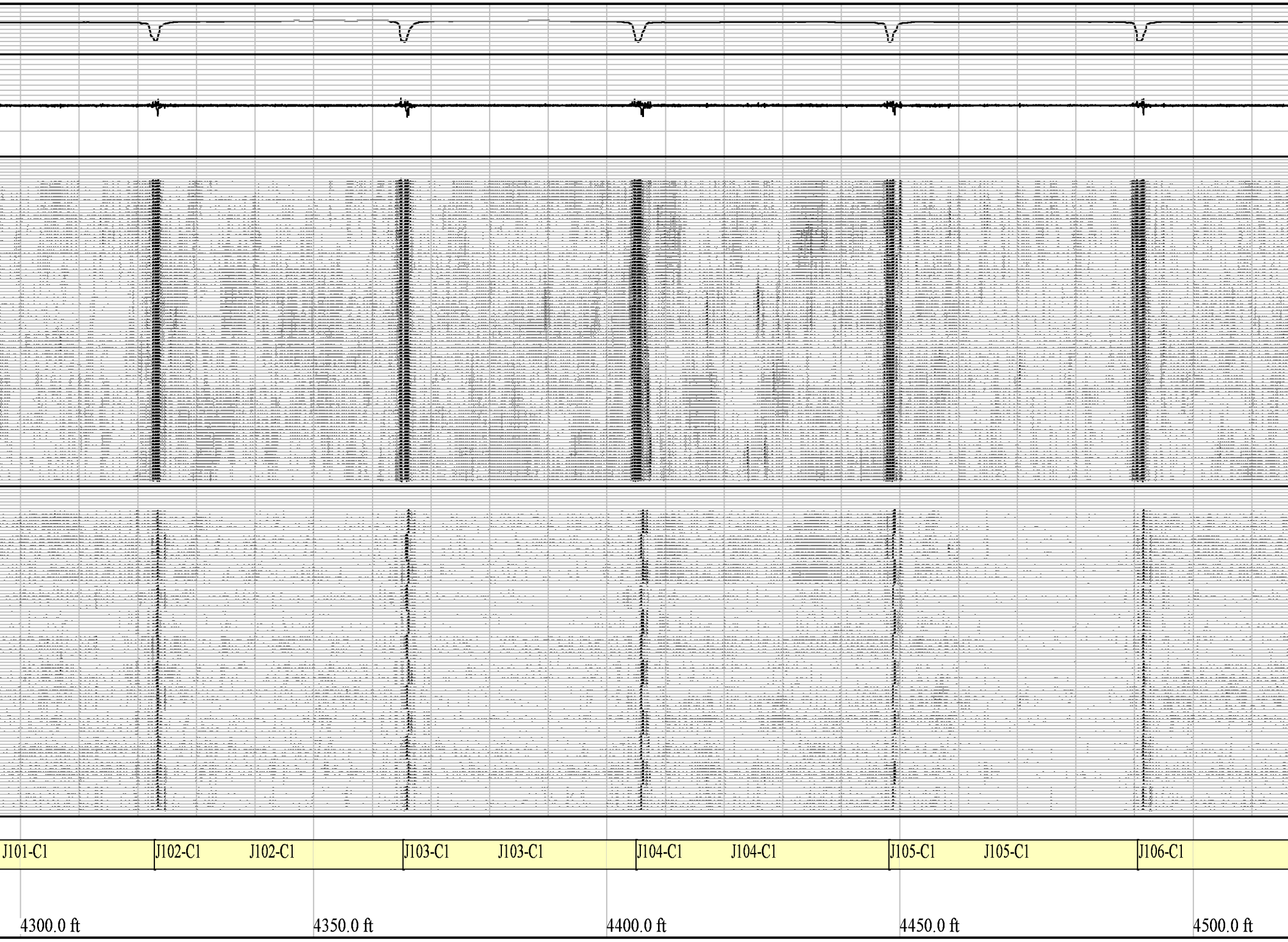
J101-C1
J102-C1
J102-C1
J103-C1
J103-C1
J104-C1
J104-C1
J105-C1
J105-C1
J106-C1
4300.0 ft
4350.0 ft
4400.0 ft
4450.0 ft
4500.0 ft

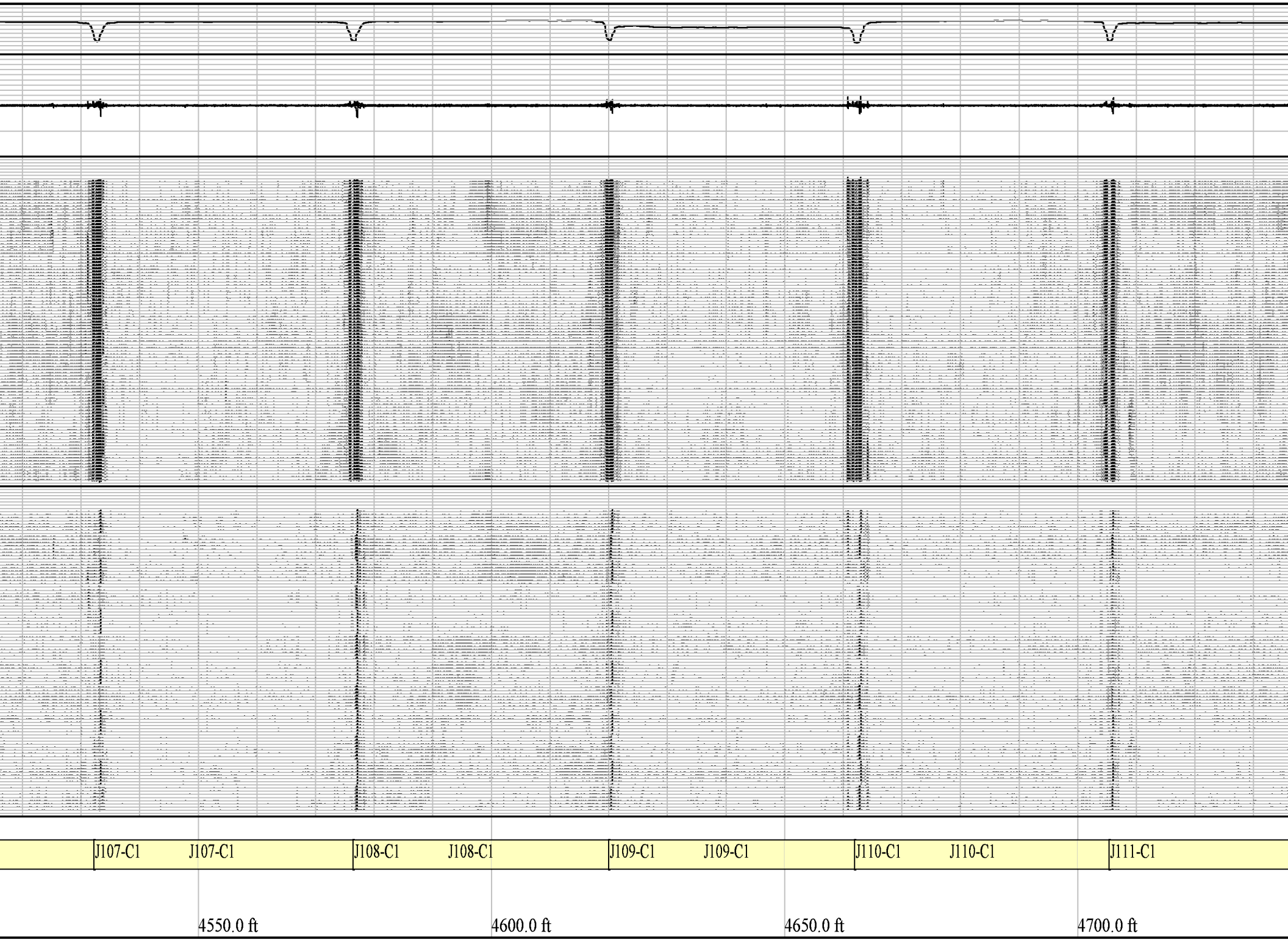
J107-C1
J107-C1
J108-C1
J108-C1
J109-C1
J109-C1
J110-C1
J110-C1
J111-C1
4550.0 ft
4600.0 ft
4650.0 ft
4700.0 ft

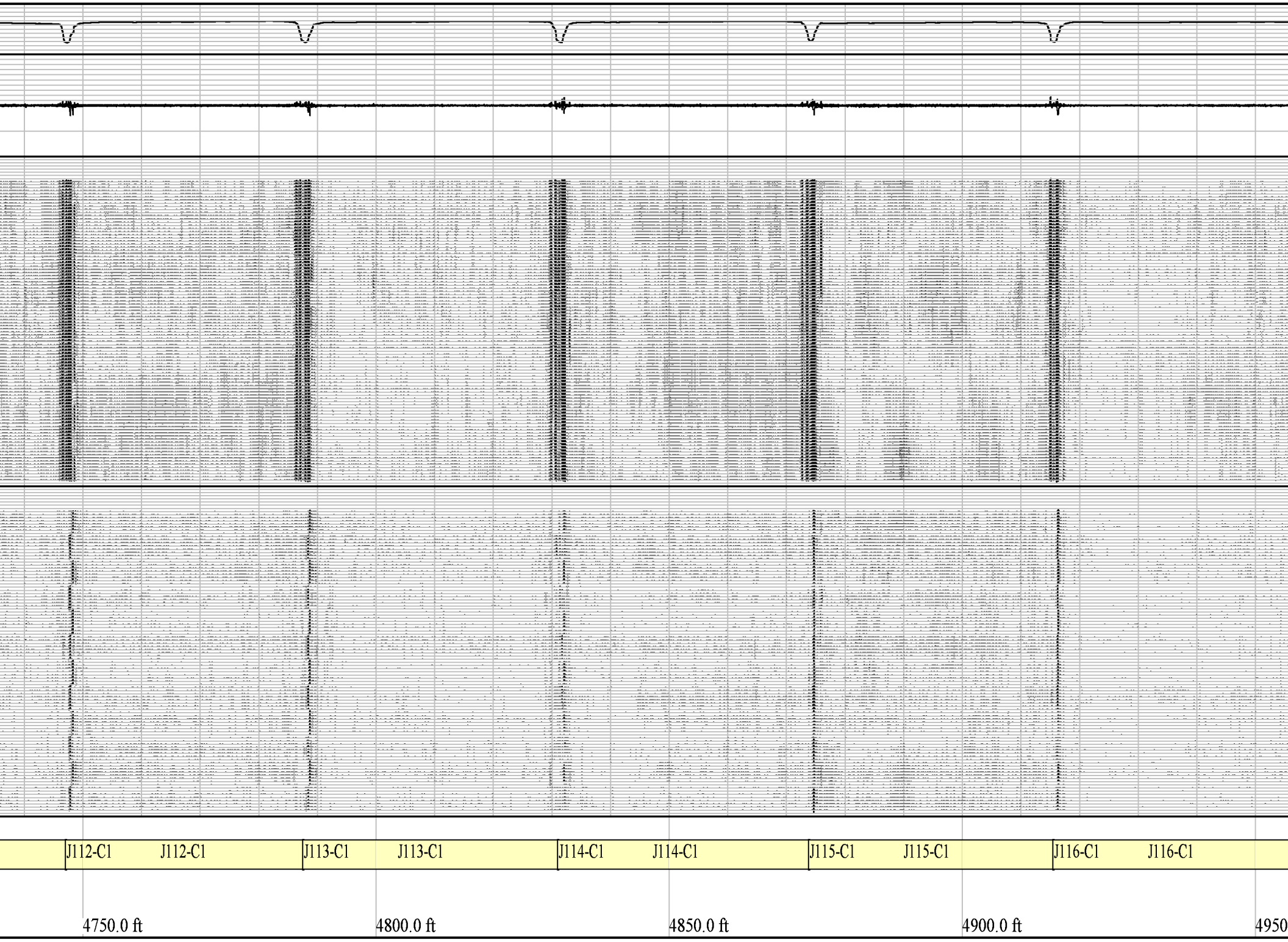
J112-C1
J112-C1
J113-C1
J113-C1
J114-C1
J114-C1
J115-C1
J115-C1
J116-C1
J116-C1
4750.0 ft
4800.0 ft
4850.0 ft
4900.0 ft
4950

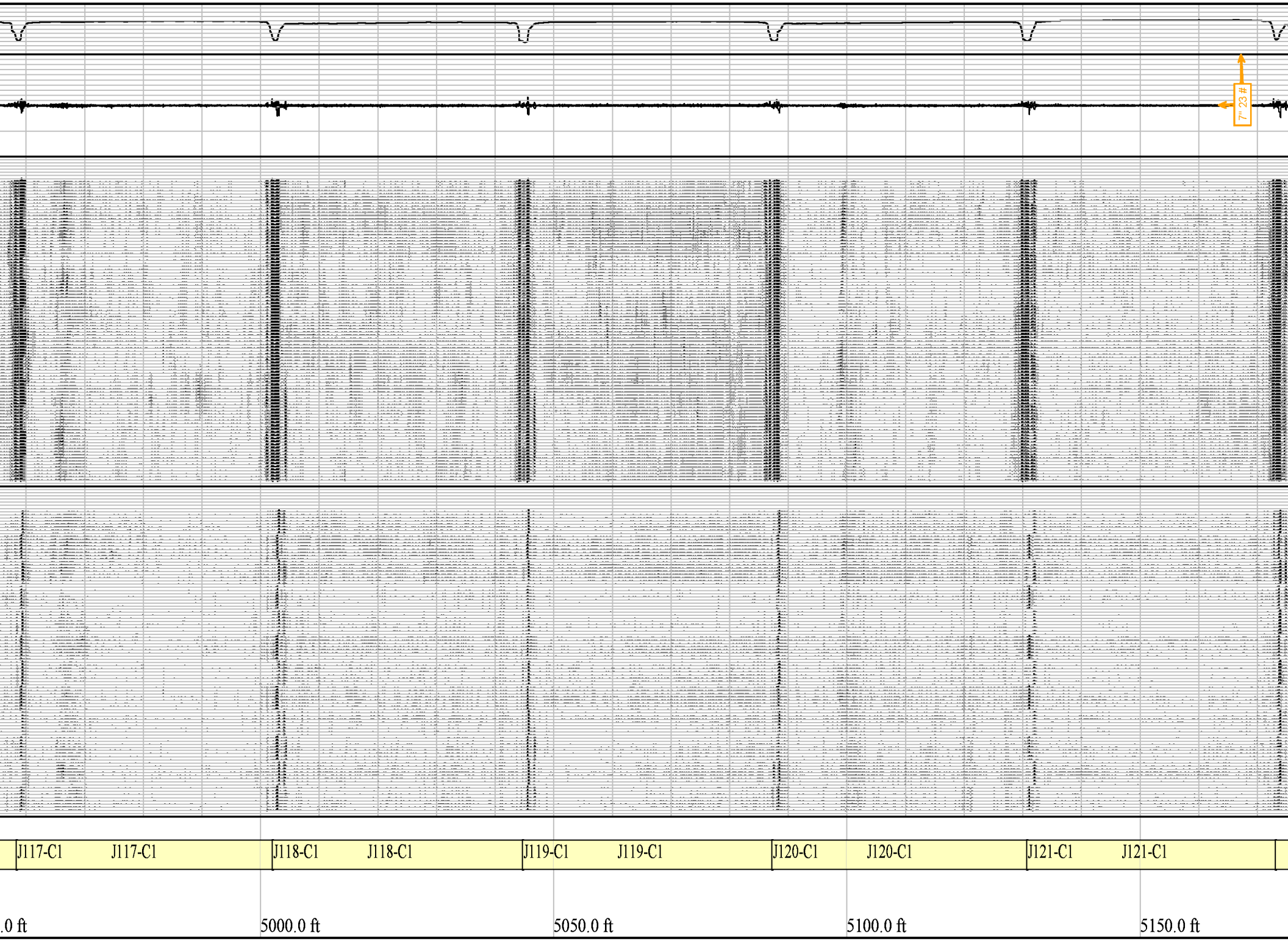
7" 23 #
J117-C1
J117-C1
J118-C1
J118-C1
J119-C1
J119-C1
J120-C1
J120-C1
J121-C1
J121-C1
.0 ft
5000.0 ft
5050.0 ft
5100.0 ft
5150.0 ft

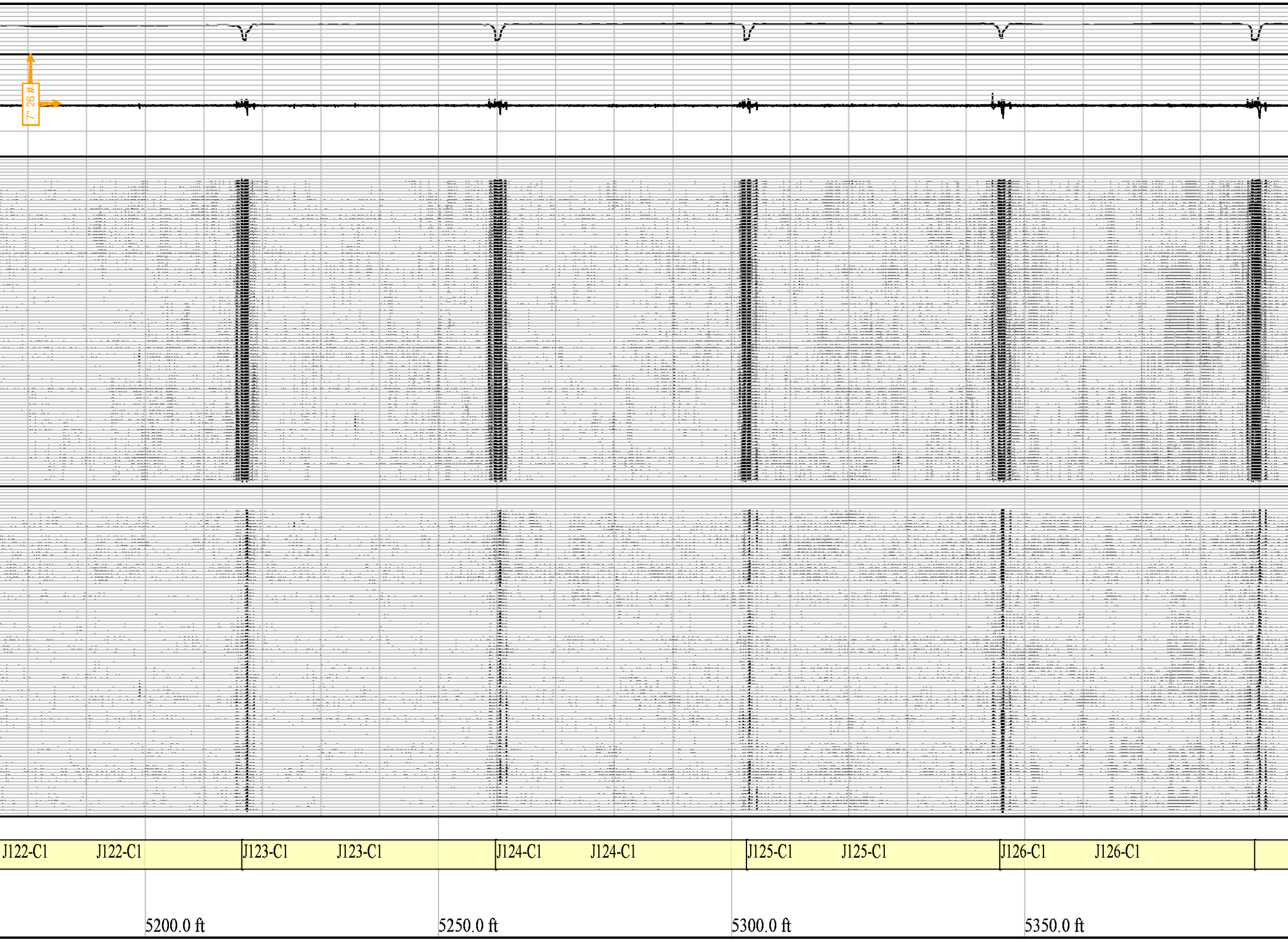
7" 29 #
J122-C1
J122-C1
J123-C1
J123-C1
J124-C1
J124-C1
J125-C1
J125-C1
J126-C1
J126-C1
5200.0 ft
5250.0 ft
5300.0 ft
5350.0 ft

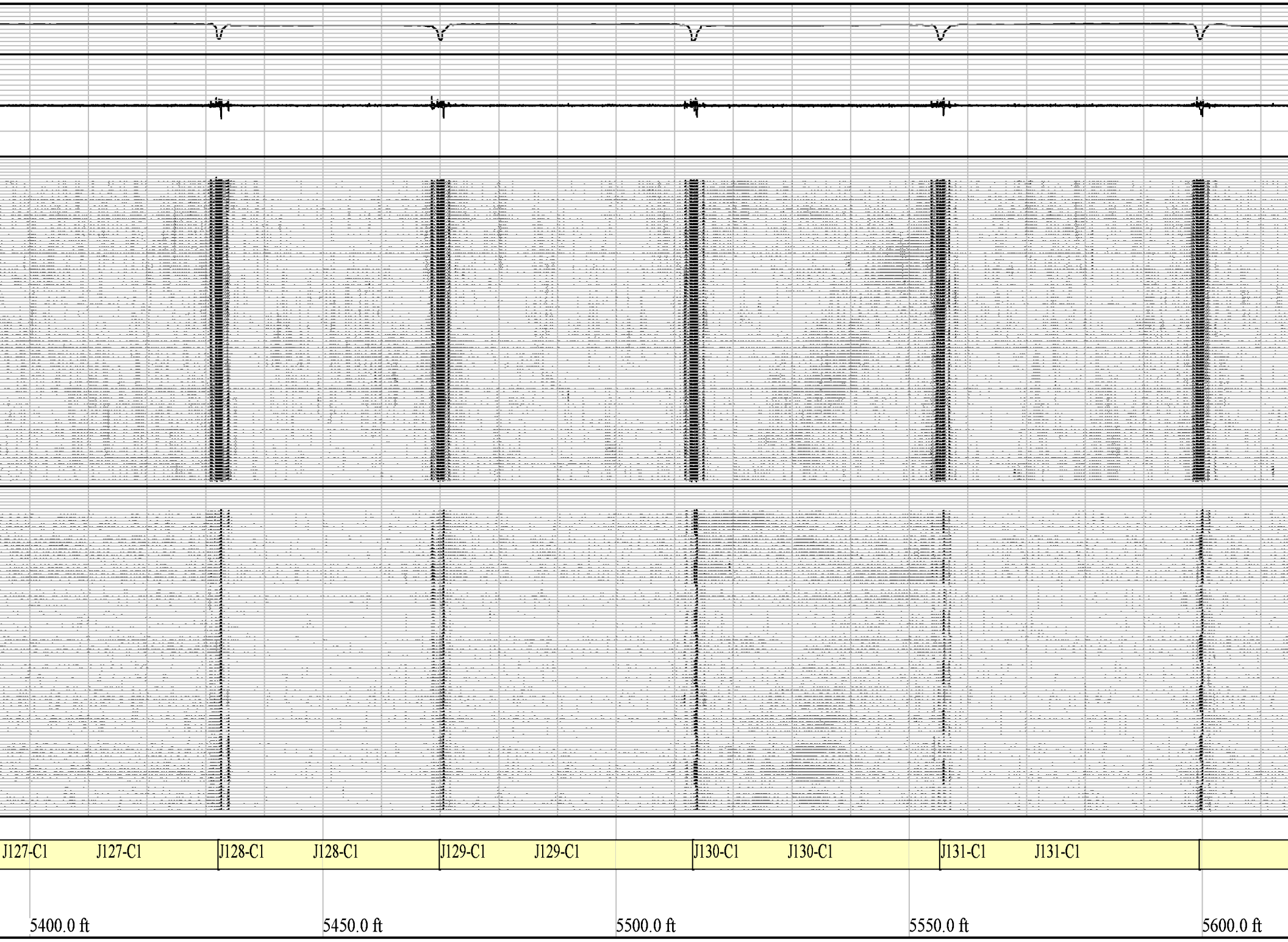
J127-C1
J127-C1
J128-C1
J128-C1
J129-C1
J129-C1
J130-C1
J130-C1
J131-C1
J131-C1
5400.0 ft
5450.0 ft
5500.0 ft
5550.0 ft
5600.0 ft

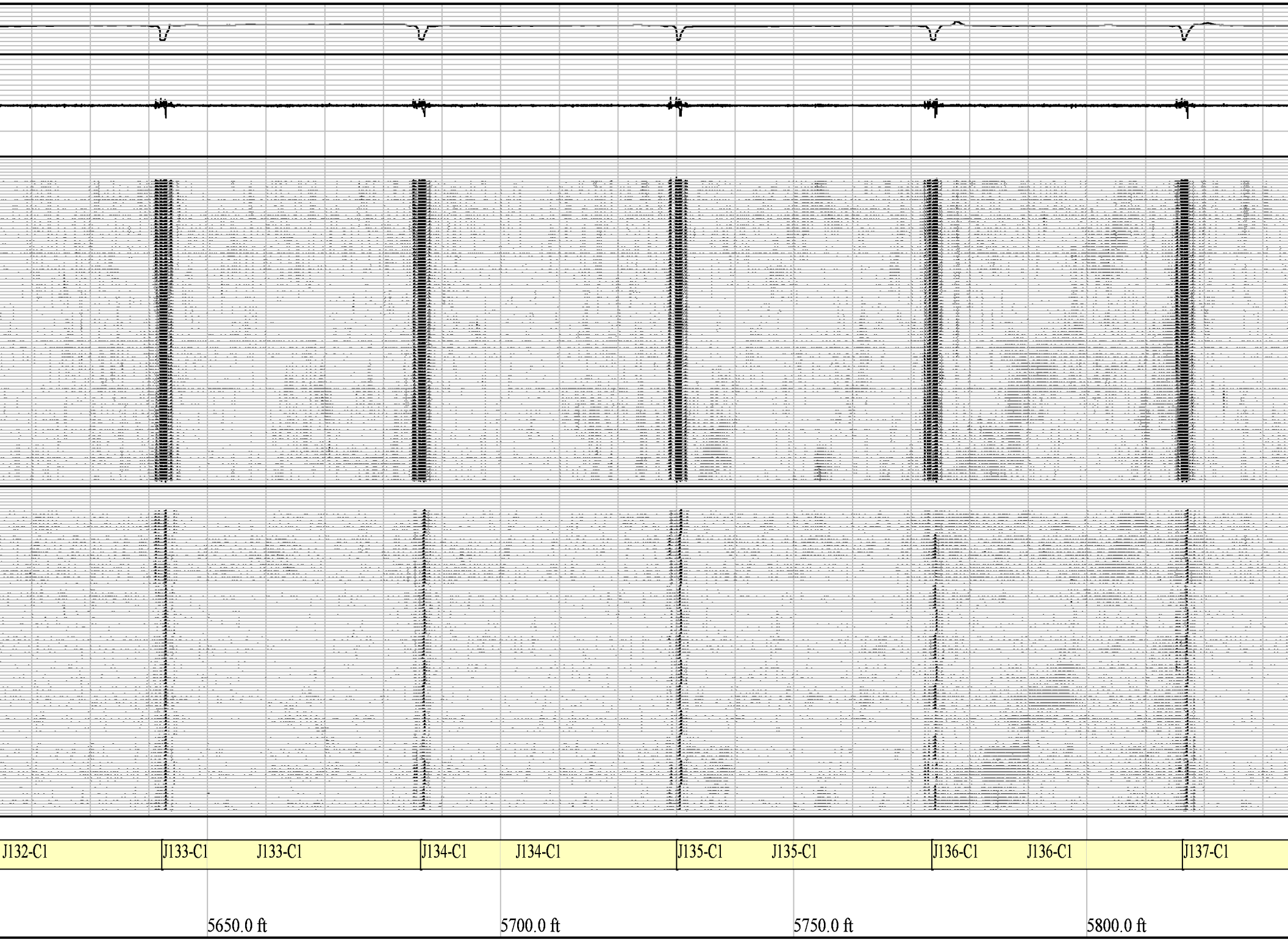
J132-C1
J133-C1
J133-C1
J134-C1
J134-C1
J135-C1
J135-C1
J136-C1
J136-C1
J137-C1
5650.0 ft
5700.0 ft
5750.0 ft
5800.0 ft

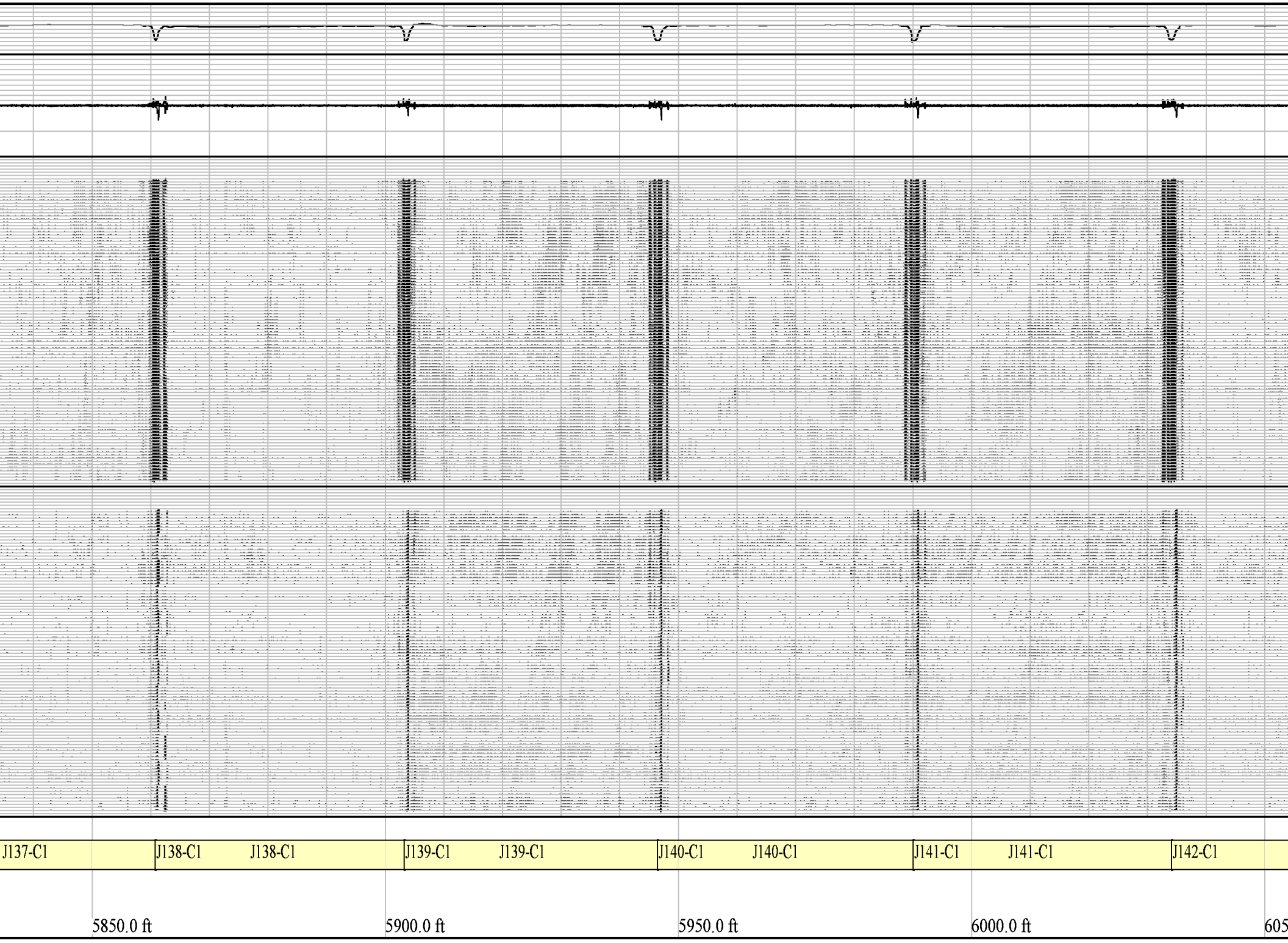
J137-C1
J138-C1
J138-C1
J139-C1
J139-C1
J140-C1
J140-C1
J141-C1
J141-C1
J142-C1
5850.0 ft
5900.0 ft
5950.0 ft
6000.0 ft
605

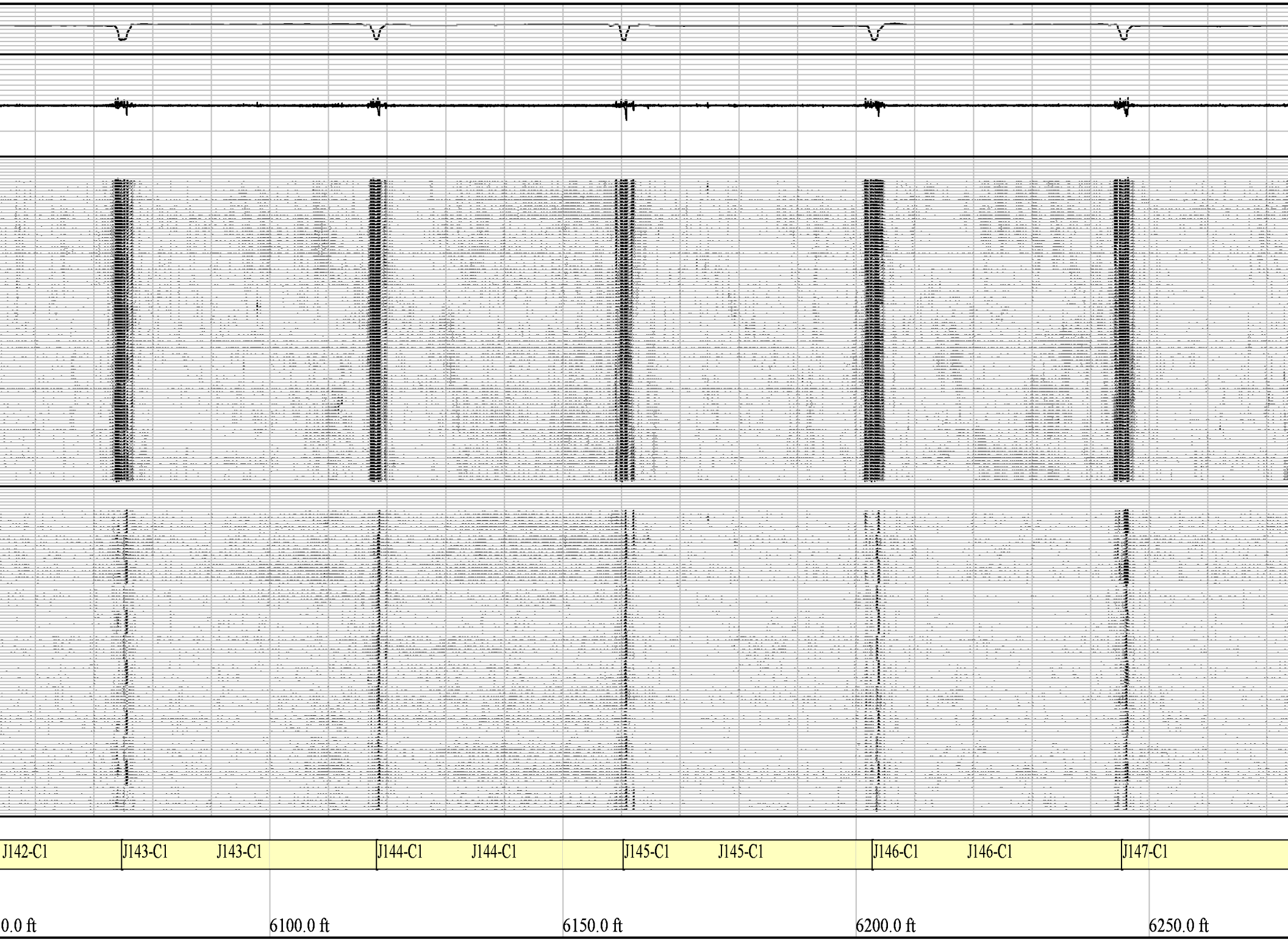
J142-C1
J143-C1
J143-C1
J144-C1
J144-C1
J145-C1
J145-C1
J146-C1
J146-C1
J147-C1
0.0 ft
6100.0 ft
6150.0 ft
6200.0 ft
6250.0 ft

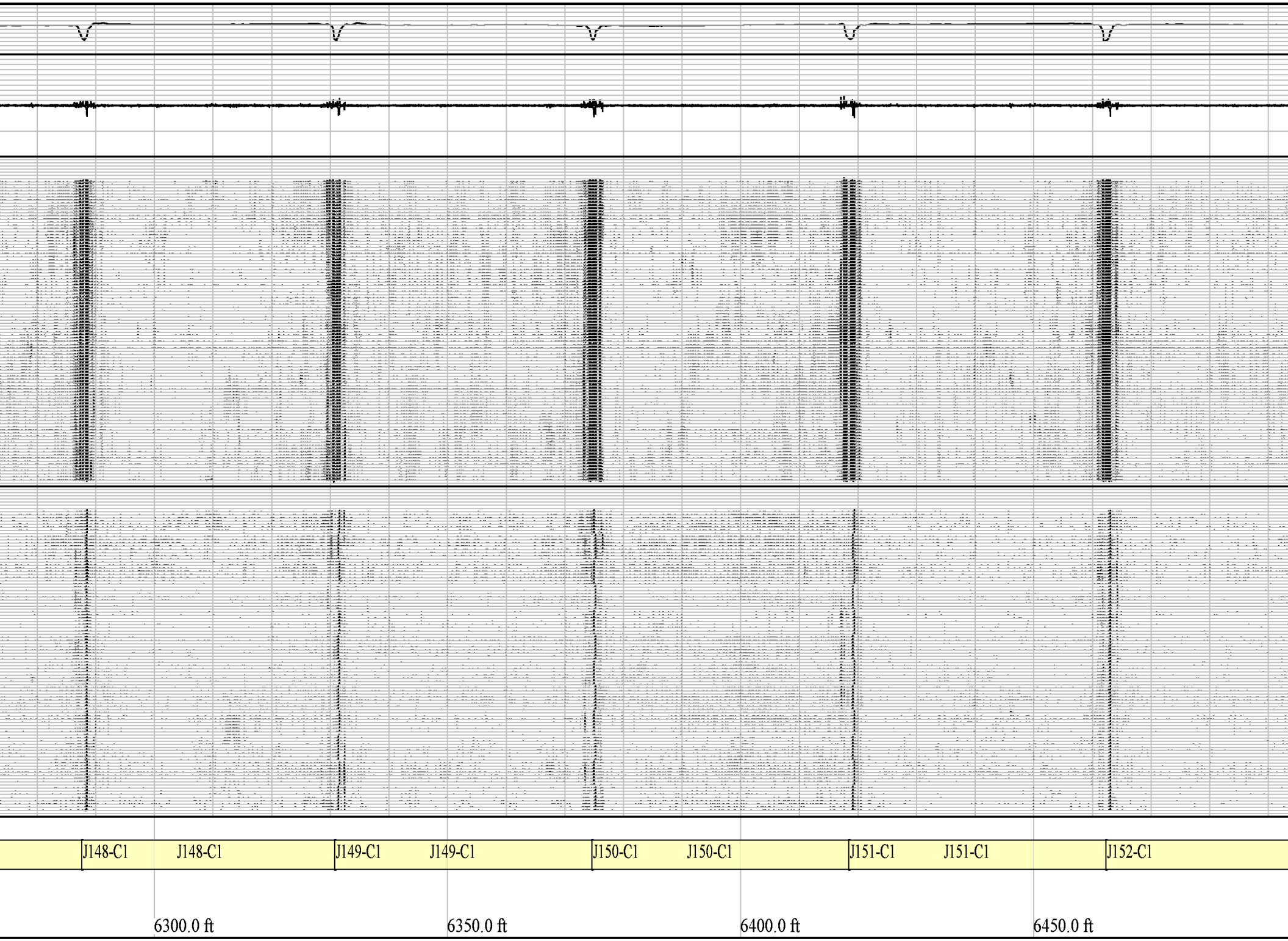
J148-C1
J148-C1
J149-C1
J149-C1
J150-C1
J150-C1
J151-C1
J151-C1
J152-C1
6300.0 ft
6350.0 ft
6400.0 ft
6450.0 ft

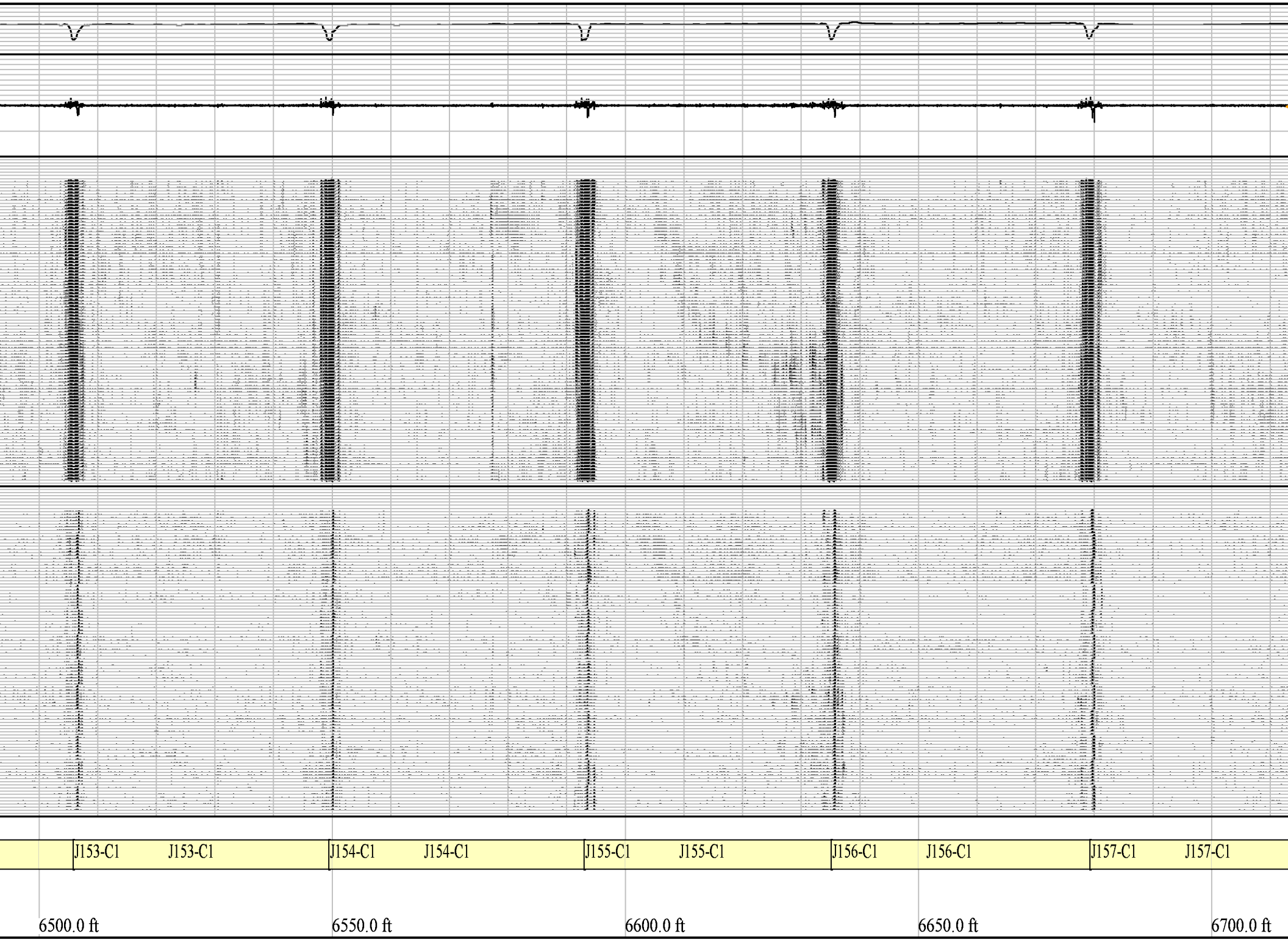
J153-C1
J153-C1
J154-C1
J154-C1
J155-C1
J155-C1
J156-C1
J156-C1
J157-C1
J157-C1
6500.0 ft
6550.0 ft
6600.0 ft
6650.0 ft
6700.0 ft

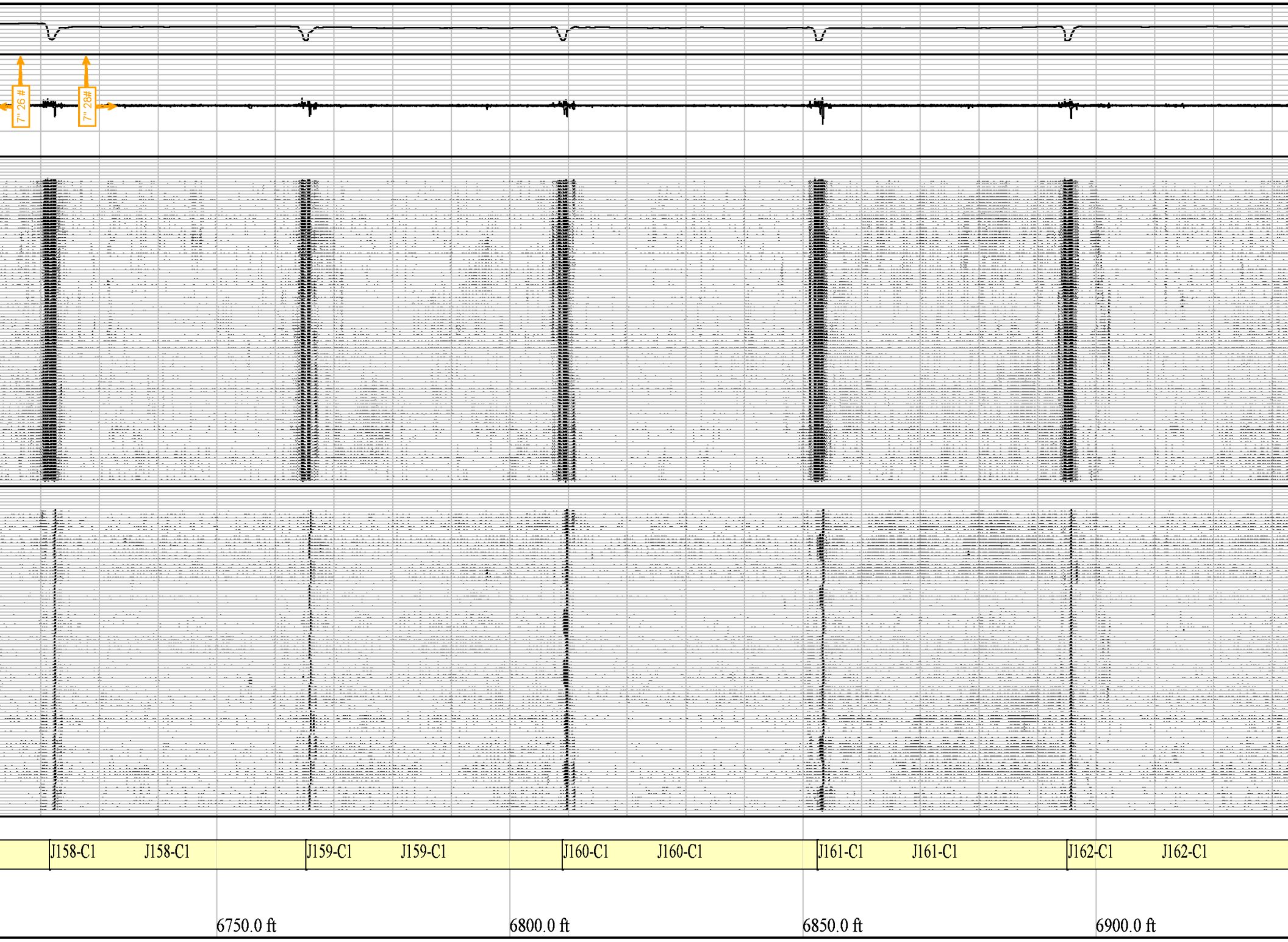
7" 26 #
7" 28#
J158-C1
J158-C1
J159-C1
J159-C1
J160-C1
J160-C1
J161-C1
J161-C1
J162-C1
J162-C1
6750.0 ft
6800.0 ft
6850.0 ft
6900.0 ft

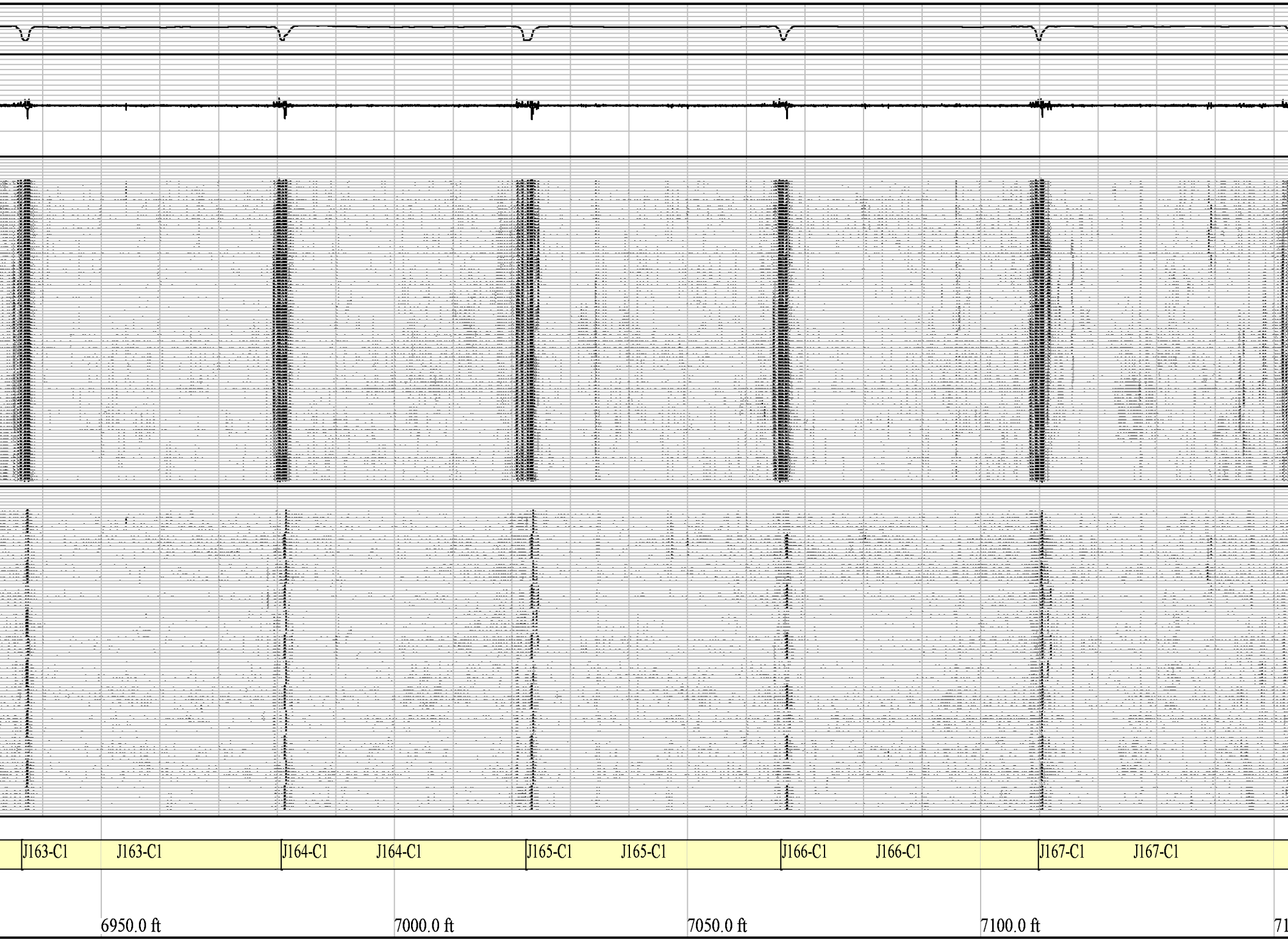
J163-C1
J163-C1
J164-C1
J164-C1
J165-C1
J165-C1
J166-C1
J166-C1
J167-C1
J167-C1
6950.0 ft
7000.0 ft
7050.0 ft
7100.0 ft

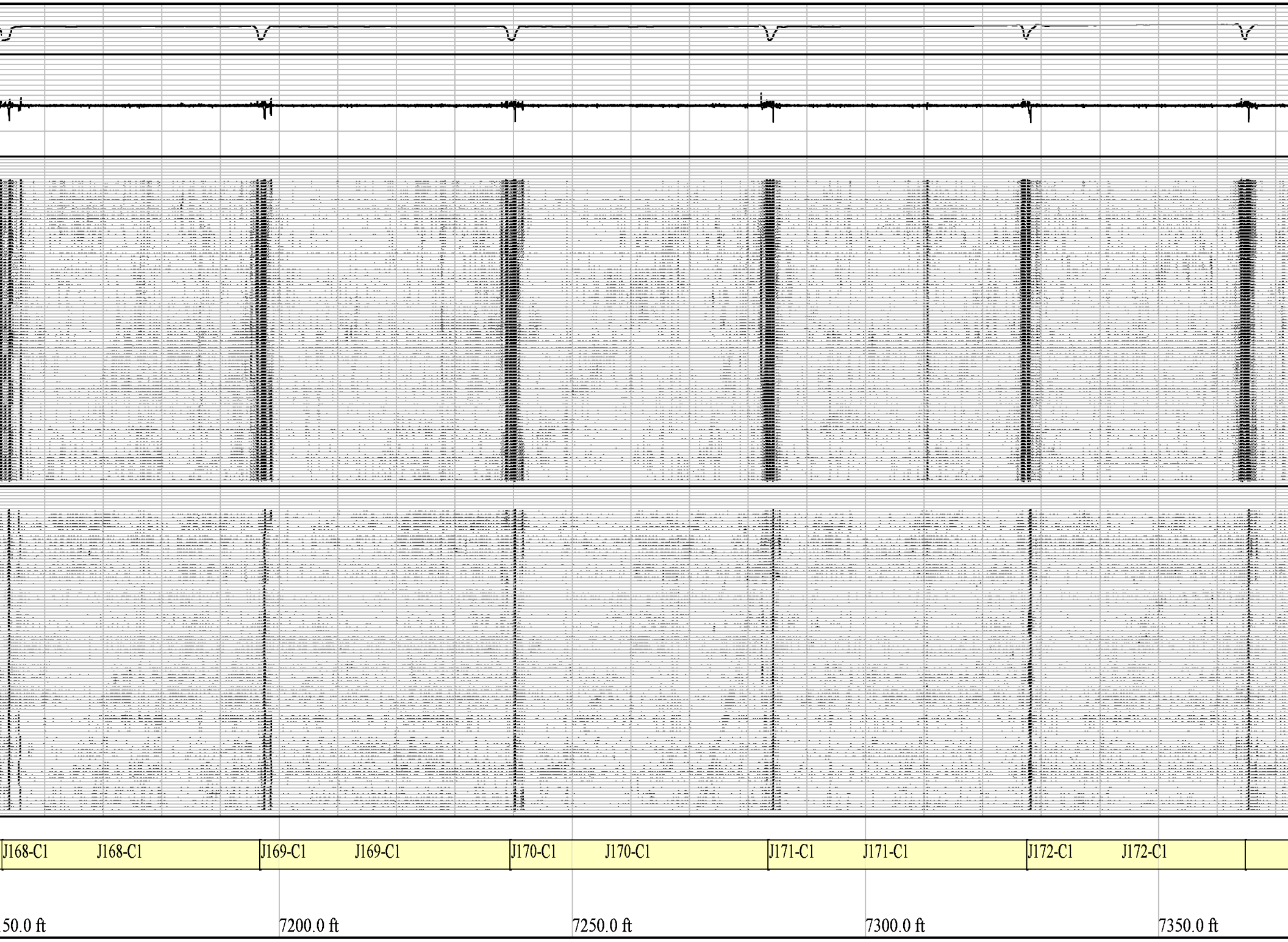
J168-C1
J168-C1
J169-C1
J169-C1
J170-C1
J170-C1
J171-C1
J171-C1
J172-C1
J172-C1
50.0 ft
7200.0 ft
7250.0 ft
7300.0 ft
7350.0 ft

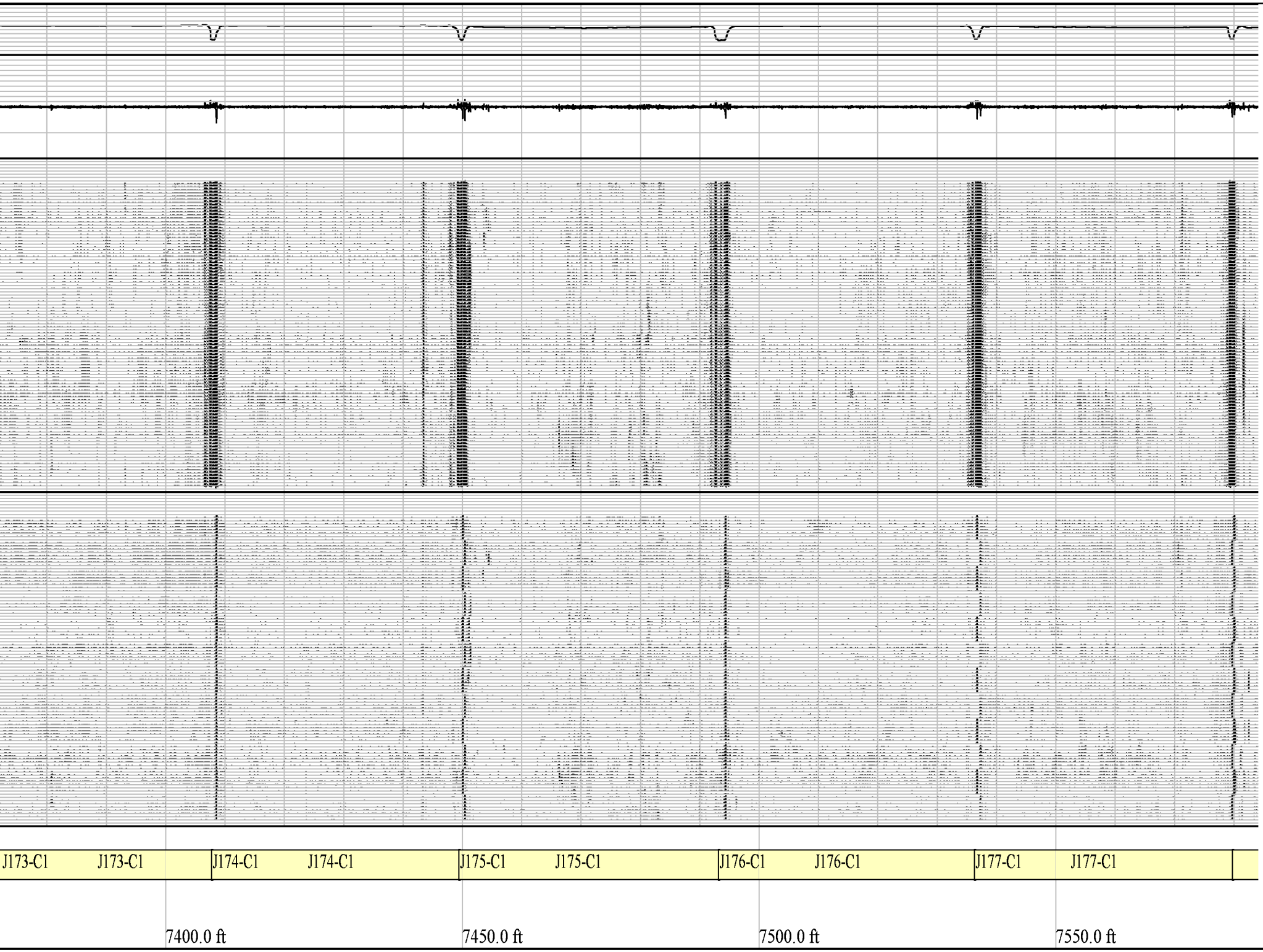
J173-C1
J173-C1
J174-C1
J174-C1
J175-C1
J175-C1
J176-C1
J176-C1
J177-C1
J177-C1
7400.0 ft
7450.0 ft
7500.0 ft
7550.0 ft

Joint Summary

Southern California Gas Company
Aliso Canyon
Porter 46

Identifier	Start Log Depth	Joint Length	Diameter	Wall Thickness	Weight	Max ML Depth	Max ML Position	Min Burst Pressure	Joint Depth Class
	ft	ft	in	in	lb/ft	%	ft	psi	
JT-1	18.16	40.80	7.000	0.317	23	0			1
JT-2	58.96	44.13	7.000	0.317	23	0			1
JT-3	103.09	44.02	7.000	0.317	23	0			1
JT-4	147.10	41.35	7.000	0.317	23	0			1
JT-5	188.45	43.86	7.000	0.317	23	0			1
JT-6	232.31	43.22	7.000	0.317	23	0			1
JT-7	275.52	42.58	7.000	0.317	23	0			1
JT-8	318.11	43.89	7.000	0.317	23	0			1
JT-9	362.00	43.07	7.000	0.317	23	0			1
JT-10	405.07	42.25	7.000	0.317	23	0			1
JT-11	447.32	41.01	7.000	0.317	23	0			1
JT-12	488.33	42.39	7.000	0.317	23	0			1
JT-13	530.72	42.70	7.000	0.317	23	0			1
JT-14	573.43	41.48	7.000	0.317	23	0			1
JT-15	614.91	42.74	7.000	0.317	23	0			1
JT-16	657.65	43.66	7.000	0.317	23	0			1
JT-17	701.31	42.21	7.000	0.317	23	0			1
JT-18	743.52	42.35	7.000	0.317	23	0			1
JT-19	785.87	41.99	7.000	0.317	23	0			1
JT-20	827.85	40.77	7.000	0.317	23	0			1
JT-21	868.62	42.14	7.000	0.317	23	0			1
JT-22	910.76	42.99	7.000	0.317	23	0			1
JT-23	953.75	41.95	7.000	0.317	23	0			1
JT-24	995.71	43.44	7.000	0.317	23	16	999.61	5705	1
JT-25	1039.14	43.13	7.000	0.317	23	0			1
JT-26	1082.27	41.77	7.000	0.317	23	0			1
JT-27	1124.04	42.88	7.000	0.317	23	0			1
JT-28	1166.93	42.89	7.000	0.317	23	0			1
JT-29	1209.82	42.63	7.000	0.317	23	0			1
JT-30	1252.44	42.91	7.000	0.317	23	0			1
JT-31	1295.36	44.13	7.000	0.317	23	0			1
JT-32	1339.49	43.09	7.000	0.317	23	0			1
JT-33	1382.58	43.78	7.000	0.317	23	0			1
JT-34	1426.36	44.18	7.000	0.317	23	0			1
JT-35	1470.54	41.44	7.000	0.317	23	0			1
JT-36	1511.98	43.10	7.000	0.317	23	0			1
JT-37	1555.07	43.14	7.000	0.317	23	0			1
JT-38	1598.21	42.28	7.000	0.317	23	0			1
JT-39	1640.49	43.27	7.000	0.317	23	0			1
JT-40	1683.76	42.31	7.000	0.317	23	0			1
JT-41	1726.06	41.56	7.000	0.317	23	0			1
JT-42	1767.63	42.92	7.000	0.317	23	0			1
JT-43	1810.55	43.02	7.000	0.317	23	0			1
JT-44	1853.57	42.35	7.000	0.317	23	0			1
JT-45	1895.92	42.12	7.000	0.317	23	0			1
JT-46	1938.04	42.40	7.000	0.317	23	0			1
JT-47	1980.44	40.94	7.000	0.317	23	0			1
JT-48	2021.38	42.62	7.000	0.317	23	0			1
JT-49	2063.99	42.47	7.000	0.317	23	0			1
JT-50	2106.47	42.91	7.000	0.317	23	0			1
JT-51	2149.38	43.25	7.000	0.317	23	0			1
JT-52	2192.63	43.18	7.000	0.317	23	0			1
JT-53	2235.81	43.40	7.000	0.317	23	0			1
JT-54	2279.22	42.00	7.000	0.317	23	0			1
JT-55	2321.22	42.48	7.000	0.317	23	0			1
JT-56	2363.70	42.57	7.000	0.317	23	0			1
JT-57	2406.27	42.30	7.000	0.317	23	0			1
JT-58	2448.57	42.59	7.000	0.317	23	0			1
JT-59	2491.17	43.38	7.000	0.317	23	0			1
JT-60	2534.55	42.36	7.000	0.317	23	0			1
JT-61	2576.91	42.40	7.000	0.317	23	0			1
JT-62	2619.31	42.77	7.000	0.317	23	0			1
JT-63	2662.08	41.07	7.000	0.317	23	0			1

JT-64	2703.14	43.66	7.000	0.317	23	0			1
JT-65	2746.81	43.79	7.000	0.317	23	0			1
JT-66	2790.59	42.85	7.000	0.317	23	0			1
JT-67	2833.45	42.57	7.000	0.317	23	0			1
JT-68	2876.02	43.26	7.000	0.317	23	0			1
JT-69	2919.28	42.83	7.000	0.317	23	0			1
JT-70	2962.11	42.30	7.000	0.317	23	0			1
JT-71	3004.41	41.79	7.000	0.317	23	0			1
JT-72	3046.20	42.48	7.000	0.317	23	0			1
JT-73	3088.68	42.11	7.000	0.317	23	0			1
JT-74	3130.79	43.30	7.000	0.317	23	0			1
JT-75	3174.09	42.66	7.000	0.317	23	0			1
JT-76	3216.76	43.47	7.000	0.317	23	16	3236.75	5722	1
JT-77	3260.23	43.47	7.000	0.317	23	0			1
JT-78	3303.70	41.58	7.000	0.317	23	0			1
JT-79	3345.28	43.11	7.000	0.317	23	0			1
JT-80	3388.38	37.68	7.000	0.317	23	0			1
JT-81	3426.07	43.54	7.000	0.317	23	0			1
JT-82	3469.60	43.02	7.000	0.317	23	0			1
JT-83	3512.63	38.81	7.000	0.317	23	0			1
JT-84	3551.44	42.65	7.000	0.317	23	0			1
JT-85	3594.09	42.54	7.000	0.317	23	0			1
JT-86	3636.63	43.29	7.000	0.317	23	0			1
JT-87	3679.92	44.10	7.000	0.317	23	0			1
JT-88	3724.03	43.13	7.000	0.317	23	0			1
JT-89	3767.16	41.73	7.000	0.317	23	0			1
JT-90	3808.89	42.80	7.000	0.317	23	0			1
JT-91	3851.70	43.73	7.000	0.317	23	0			1
JT-92	3895.43	42.51	7.000	0.317	23	0			1
JT-93	3937.93	43.15	7.000	0.317	23	0			1
JT-94	3981.08	42.69	7.000	0.317	23	0			1
JT-95	4023.77	43.95	7.000	0.317	23	0			1
JT-96	4067.72	39.78	7.000	0.317	23	0			1
JT-97	4107.51	43.41	7.000	0.317	23	0			1
JT-98	4150.92	43.20	7.000	0.317	23	0			1
JT-99	4194.12	43.50	7.000	0.317	23	0			1
JT-100	4237.62	42.48	7.000	0.317	23	0			1
JT-101	4280.10	42.86	7.000	0.317	23	0			1
JT-102	4322.96	42.39	7.000	0.317	23	0			1
JT-103	4365.35	39.74	7.000	0.317	23	0			1
JT-104	4405.10	43.17	7.000	0.317	23	0			1
JT-105	4448.27	42.38	7.000	0.317	23	0			1
JT-106	4490.65	41.66	7.000	0.317	23	0			1
JT-107	4532.30	44.19	7.000	0.317	23	0			1
JT-108	4576.49	43.60	7.000	0.317	23	0			1
JT-109	4620.10	41.97	7.000	0.317	23	0			1
JT-110	4662.07	43.42	7.000	0.317	23	0			1
JT-111	4705.49	41.68	7.000	0.317	23	0			1
JT-112	4747.17	40.43	7.000	0.317	23	0			1
JT-113	4787.60	43.49	7.000	0.317	23	0			1
JT-114	4831.10	42.77	7.000	0.317	23	0			1
JT-115	4873.87	41.71	7.000	0.317	23	0			1
JT-116	4915.58	42.89	7.000	0.317	23	0			1
JT-117	4958.47	43.66	7.000	0.317	23	0			1
JT-118	5002.13	42.66	7.000	0.317	23	0			1
JT-119	5044.79	42.51	7.000	0.317	23	0			1
JT-120	5087.29	43.49	7.000	0.317	23	0			1
JT-121	5130.78	42.43	7.000	0.317	23	0			1
JT-122	5173.22	43.37	7.000	0.362	26	0			1
JT-123	5216.59	43.28	7.000	0.362	26	0			1
JT-124	5259.87	42.84	7.000	0.362	26	0			1
JT-125	5302.71	43.18	7.000	0.362	26	0			1
JT-126	5345.89	43.45	7.000	0.362	26	0			1
JT-127	5389.34	42.88	7.000	0.362	26	0			1
JT-128	5432.22	37.72	7.000	0.362	26	18	5468.43	9047	1
JT-129	5469.94	43.27	7.000	0.362	26	0			1
JT-130	5513.20	42.13	7.000	0.362	26	0			1
JT-131	5555.33	44.27	7.000	0.362	26	0			1
JT-132	5599.60	42.69	7.000	0.362	26	0			1
JT-133	5642.30	44.14	7.000	0.362	26	0			1
JT-134	5686.44	43.69	7.000	0.362	26	0			1
JT-135	5730.13	43.51	7.000	0.362	26	0			1
JT-136	5773.64	42.77	7.000	0.362	26	0			1
JT-137	5816.41	44.50	7.000	0.362	26	0			1
JT-138	5860.91	42.46	7.000	0.362	26	0			1
JT-139	5903.37	43.17	7.000	0.362	26	0			1
JT-140	5946.54	43.61	7.000	0.362	26	0			1
JT-141	5990.14	44.07	7.000	0.362	26	0			1
JT-142	6034.21	40.61	7.000	0.362	26	0			1
JT-143	6074.82	43.53	7.000	0.362	26	0			1

JT-143	6074.82	43.52	7.000	0.362	26	0	1
JT-144	6118.34	42.04	7.000	0.362	26	0	1
JT-145	6160.38	42.47	7.000	0.362	26	0	1
JT-146	6202.84	42.53	7.000	0.362	26	0	1
JT-147	6245.38	42.39	7.000	0.362	26	0	1
JT-148	6287.77	43.10	7.000	0.362	26	0	1
JT-149	6330.87	43.85	7.000	0.362	26	0	1
JT-150	6374.72	43.83	7.000	0.362	26	0	1
JT-151	6418.54	43.88	7.000	0.362	26	0	1
JT-152	6462.42	43.55	7.000	0.362	26	0	1
JT-153	6505.98	43.56	7.000	0.362	26	0	1
JT-154	6549.54	43.53	7.000	0.362	26	0	1
JT-155	6593.07	42.16	7.000	0.362	26	0	1
JT-156	6635.22	44.12	7.000	0.362	26	0	1
JT-157	6679.34	42.23	7.000	0.362	26	0	1
JT-158	6721.57	43.78	7.000	0.408	29	0	1
JT-159	6765.35	43.69	7.000	0.408	29	0	1
JT-160	6809.04	43.52	7.000	0.408	29	0	1
JT-161	6852.56	42.54	7.000	0.408	29	0	1
JT-162	6895.10	41.46	7.000	0.408	29	0	1
JT-163	6936.56	44.21	7.000	0.408	29	0	1
JT-164	6980.78	41.79	7.000	0.408	29	0	1
JT-165	7022.56	43.47	7.000	0.408	29	0	1
JT-166	7066.04	43.95	7.000	0.408	29	0	1
JT-167	7109.98	42.86	7.000	0.408	29	0	1
JT-168	7152.84	44.01	7.000	0.408	29	0	1
JT-169	7196.85	42.65	7.000	0.408	29	0	1
JT-170	7239.50	43.99	7.000	0.408	29	0	1
JT-171	7283.50	44.15	7.000	0.408	29	0	1
JT-172	7327.65	37.29	7.000	0.408	29	0	1
JT-173	7364.94	42.94	7.000	0.408	29	0	1
JT-174	7407.87	41.67	7.000	0.408	29	0	1
JT-175	7449.54	43.70	7.000	0.408	29	0	1
JT-176	7493.24	43.20	7.000	0.408	29	0	1
JT-177	7536.44	43.47	7.000	0.408	29	0	1
JT-178	7579.91	4.28	7.000	0.408	29	0	1

Inspection Date: 08-17-2017
Report Date: 08-19-2017

Ex. II - 18

Hello Jovy,

I talked to Bruce about your email. Please submit the critical elements that will be in your Supplement NOI, especial the details on where the shoe of the 5 ½" inner string. The Supplement notice should be submitted ASAP.

Dave

From: Kroh, Jovy E [mailto:JKroh@semprautilities.com]
Sent: Friday, August 25, 2017 9:08 AM
To: Ortiz, David@DOC <David.Ortiz@conservation.ca.gov>
Cc: McMahon, Thomas D. <TMcMahon@semprautilities.com>; Iguaz, Jose <JIguaz@semprautilities.com>; Charleston, Anthony <ACharleston@semprautilities.com>
Subject: Porter 46 Proposed squeeze plan
Importance: High

Hello David,
After reviewing the P46 log results at length, we have elected to run a 5.5" inner string and cement it to 2706'.
The rig is currently pulling the test packer and will be ready to begin perf and squeezing on Monday morning.
Below is our squeeze plan to abandon critical zones behind the 7" casing. Please let me know if you approve.
I will follow up with a Supplementary notice shortly.

MP @ 7446': Squeeze
LDA @ 6895': Squeeze
MDA @ 6718': Squeeze
UDA1 @ 5955': Squeeze
UP @ 5220': Squeeze
A1 @ 3974': Squeeze
PGS @ 2906': Squeeze

Thanks,
Jovy

Jovy Kroh
Southern California Gas Company
Sr. Gas Storage Field Engineer
Direct: 818-725-1119
Cell: 937-239-0279

This email originated outside of Sempra Energy. Be cautious of attachments, web links, or requests for information.

Ex. II - 19

VERTILOG®

Dresser Atlas DRESSER

CUSTOMER	SOUTHERN CALIFORNIA GAS COMPANY	DATE	10-19-88
WELL	PORTER No. 46	SERVICE ORDER NO.	124301
FIELD	ALISO CANYON	COUNTY LOS ANGELES STATE	CALIFORNIA
CASING SIZE	7" WEIGHT(S) 23#, 26# & 29# GRADE J-55, N-80	NOMINAL WALL THICKNESS	
TOTAL FOOTAGE INSPECTED	7660' FROM SURFACE TO 7660'	DEPTH	

SJ

SUBSURFACE CASING INSPECTION REPORT

SUMMARY

169	LENGTHS WERE FOUND TO SHOW NO EVIDENCE OF CORROSION EXCEEDING PERCENT OF THE NOMINAL BODY WALL.	20 CLASS 1
10	LENGTHS WERE FOUND TO SHOW EVIDENCE OF CORROSION EXCEEDING PERCENT BUT LESS THAN 41 PERCENT OF THE NOMINAL BODY WALL.	20 CLASS 2
0	LENGTHS WERE FOUND TO SHOW EVIDENCE OF CORROSION EXCEEDING PERCENT BUT LESS THAN 61 PERCENT OF THE NOMINAL BODY WALL.	40 CLASS 3
0	LENGTHS WERE FOUND TO SHOW EVIDENCE OF CORROSION EXCEEDING PERCENT OF THE NOMINAL BODY WALL.	60 CLASS 4
179	TOTAL LENGTHS	
7660'	TOTAL FOOTAGE	

REFERENCE FOR FOOTAGE MEASURE: GROUND LEVEL + 11'

LENGTHS ARE NUMBERED FROM: SURFACE

COMMENTS: NOISE ON FL 12 BETWEEN 6150' - 6200' IS DUE TO ELECTRONICS NOT CORROSION, FL 1 AND FL 2 WERE OBSERVED DURING LOG AND NOISE WAS IDENTIFIED.

CHART 7J6F
CHART 7N1E

SERVICED BY

DA-1363-C (08/82)

VERTILOG®

Western Atlas International
A Litton/Dresser Company

CUSTOMER	SOUTHERN CALIFORNIA GAS CO.	WORK ORDER NO. 124301	DATE 10-19-88
LEASE/WELL NO.	PORTER No. 46	CUSTOMER ORDER NO.	
FIELD	ALISO CANYON	COUNTY LOS ANGELES	STATE CALIFORNIA
CASING O.D. 7"	WEIGHT(S) 23, 26, 29#	NOMINAL WALL THICKNESS	GRADE J-55, N-80
TOTAL FOOTAGE INSPECTED	7660'	FROM SURFACE	TO 7660' DEPTH

SUBSURFACE CASING DEFECT REPORT

LENGTH NO.	TYPE DEFECT	PENETRATION	LENGTH NO.	TYPE DEFECT	PENETRATION
INSIDE 13-3/8" SURFACE CASING					
1	OD IP	21 - 40			
2	OD IP	21 - 40			
3	OD IP	21 - 40			
5	OD IP	21 - 40			
6	OD IP	21 - 40			
7	OD IP	21 - 40			
8	OD IP	21 - 40			
9	OD IP	21 - 40			
12	OD IP	21 - 40			
OUTSIDE 13-3/8" SURFACE CASING					
178	OD IP	21 - 40			

ABBREVIATIONS:

O.D. – OUTSIDE DIAMETER
I.D. – INSIDE DIAMETER
I.S. – INSIDE SURFACE PIPE
T.L. – THROUGHOUT LENGTH
I.P. – ISOLATED PITTING
C.C. – CIRCUMFERENTIAL CORROSION

WA-1364-C (10/87)

Ex. II - 20

Due to the large file sizes, please view documents DOGGR_03700733_Vertilog_10-19-1988 and DOGGR_03700733_USIT-GR-CCL_8-16-2017 at the below publicly available websites. The native files of these documents are available upon request.

(https://secure.conservation.ca.gov/WellRecord/037/03700733/tifs/03700733_Vertilog_10-19-1988.tif) (accessed March 20, 2020)

(https://secure.conservation.ca.gov/WellRecord/037/03700733/03700733_USIT-GR-CCL_8-16-2017.tif) (accessed March 20, 2020)

Ex. II - 21

Schlumberger

Company: Southern California Gas Company

Well: Fernando Fee 35B

Field: Aliso Canyon

County: Los Angeles State: California

Ultrasonic Imager

Gamma Ray - CCL

8 5/8" 36# casing

County: Los Angeles
Field: Aliso Canyon
Location:
Well: Fernando Fee 35B
Company: Southern California Gas Company

Location:			
		Elev.: K.B.	1689.00 ft
		G.L.	1674.00 ft
		D.F.	
Permanent Datum:	Ground Level	Elev.:	1674.00 f
Log Measured From:	Kelly Bushing	15.00 ft	above Perm.Datum
Drilling Measured From:	Kelly Bushing		

API Serial No.	Section:	Township:	Range:
040372145800	34	3N	16W

Logging Date	01-Jun-2017		
Run Number	One		
Depth Driller	7333.00 ft		
Schlumberger Depth	7044.00 ft		
Bottom Log Interval	7044.00 ft		
Top Log Interval	15.00 ft		
Casing Fluid Type	Water		
Salinity			
Density	8.9 lbm/gal		
Fluid Level	15.00 ft		
BIT/CASING/TUBING STRING			
Bit Size	15.00 in		
From	7229.00 ft		
To	7335.00 ft		
Casing/Tubing Size	5 in		
Weight	18 lbm/ft		
Grade	N80		
From	7100.00 ft		
To	7331.00 ft		
Max Recorded Temperatures	173 degF		
Logger on Bottom Time	01-Jun-2017	13:27:00	
Unit Number Location:	3080	Ventura	
Recorded By	Omar Reid		
Witnessed By	Jeff Sandoval		

Disclaimer

THE USE OF AND RELIANCE UPON THIS RECORDED-DATA BY THE HEREIN NAMED COMPANY (AND ANY OF ITS AFFILIATES, PARTNERS, REPRESENTATIVES, AGENTS, CONSULTANTS AND EMPLOYEES) IS SUBJECT TO THE TERMS AND CONDITIONS AGREED UPON BETWEEN SCHLUMBERGER AND THE COMPANY, INCLUDING: (a) RESTRICTIONS ON USE OF THE RECORDED-DATA; (b) DISCLAIMERS AND WAIVERS OF WARRANTIES AND REPRESENTATIONS REGARDING COMPANY'S USE AND RELIANCE UPON THE RECORDED-DATA; AND (c) CUSTOMER'S FULL AND SOLE RESPONSIBILITY FOR ANY INFERENCE DRAWN OR DECISION MADE IN CONNECTION WITH THE USE OF THIS RECORDED-DATA.

Contents

1. Header
2. Disclaimer
3. Contents
4. Well Sketch
5. Borehole Size/Casing/Tubing Record
6. Remarks and Equipment Summary
7. USI Fluid Properties Measurement
8. One USIT VDL Main Pass 5 in = 100 ft
   8.1 Integration Summary
   8.2 Software Version
   8.3 Composite Summary
   8.4 Log (LBV1_USI-VDL (DSLT) Cement 7inch)
   8.5 Parameter Listing
9. One USIT Composite 5" = 100'
   9.1 Integration Summary
   9.2 Software Version
   9.3 Composite Summary
   11.5 Parameter Listing
12. One USI Compressed Goodwin 1" = 100'
   12.1 Integration Summary
   12.2 Composite Summary
   12.3 Log (Import of USI Goodwin)
13. XYZ (USI Fluid Acoustic Slowness vs Depth)
14. XYZ (USI Theoretical Acoustic impedance of mud vs Depth)
15. One USIT CORROSION 10" = 100'
   15.1 Integration Summary
   15.2 Software Version
   15.3 Composite Summary
   15.4 Log (LBV1_USI Corrosion 9.625inch)
   15.5 Parameter Listing
16. One USIT CORROSION 10" = 100'
   16.1 Integration Summary
   16.2 Software Version

9.4 Log (USI Composite_7inch)
9.5 Parameter Listing
10. One USIT Cement Log 2 IN = 100 FT
10.1 Integration Summary
10.2 Composite Summary
10.3 Log (LBV1_USI Cement 7inch)
11. One USIT CORROSION 5" = 100'
11.1 Integration Summary
11.2 Software Version
11.3 Composite Summary
11.4 Log (LBV1_USI Corrosion 9.625inch)
16.3 Composite Summary
16.4 Log (LBV1_USI Corrosion 9.625inch)
16.5 Parameter Listing
17. One USIT CORROSION 10" = 100'
17.1 Integration Summary
17.2 Software Version
17.3 Composite Summary
17.4 Log (LBV1_USI Corrosion 9.625inch)
17.5 Parameter Listing
18. Tail

Well Sketch

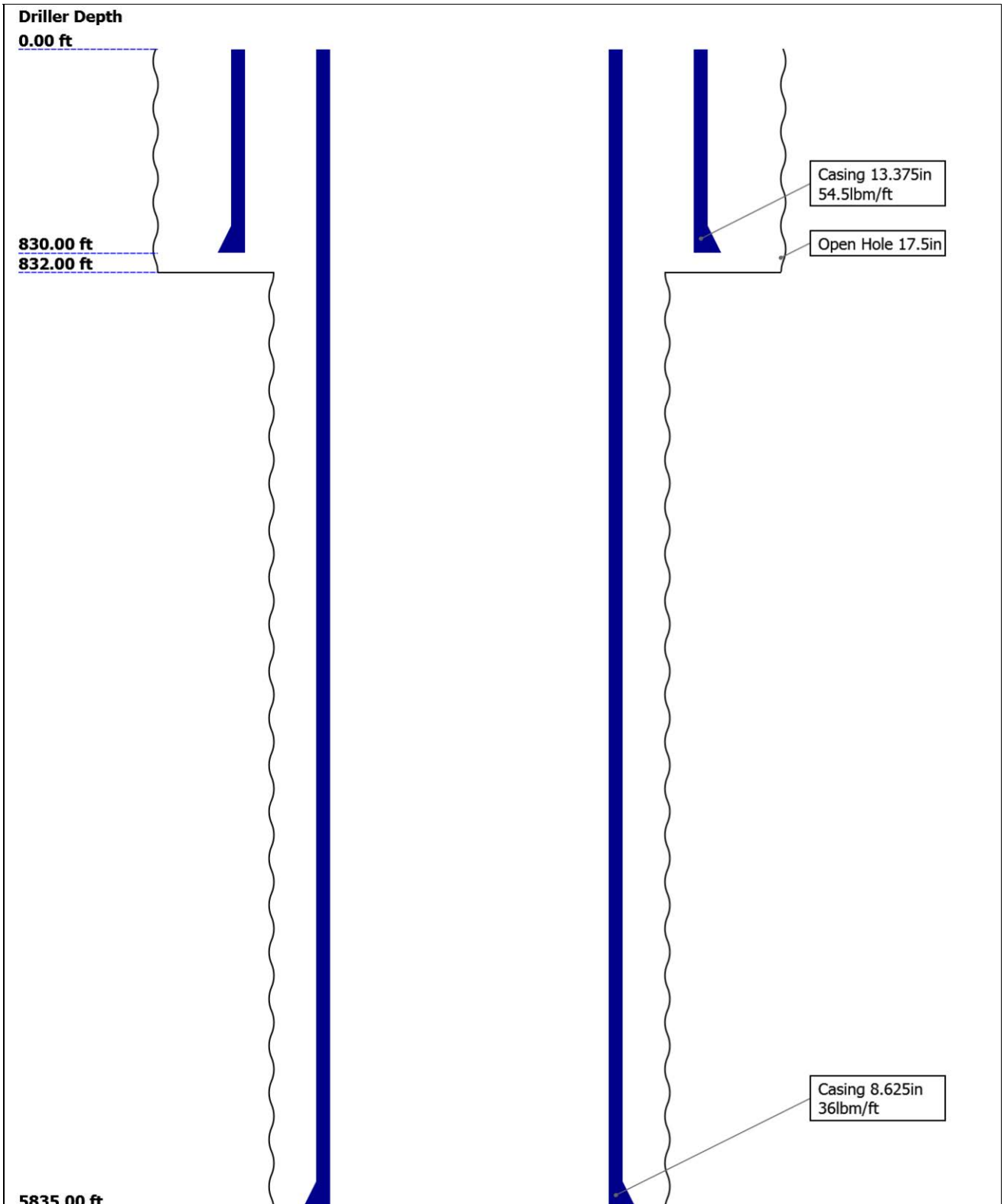

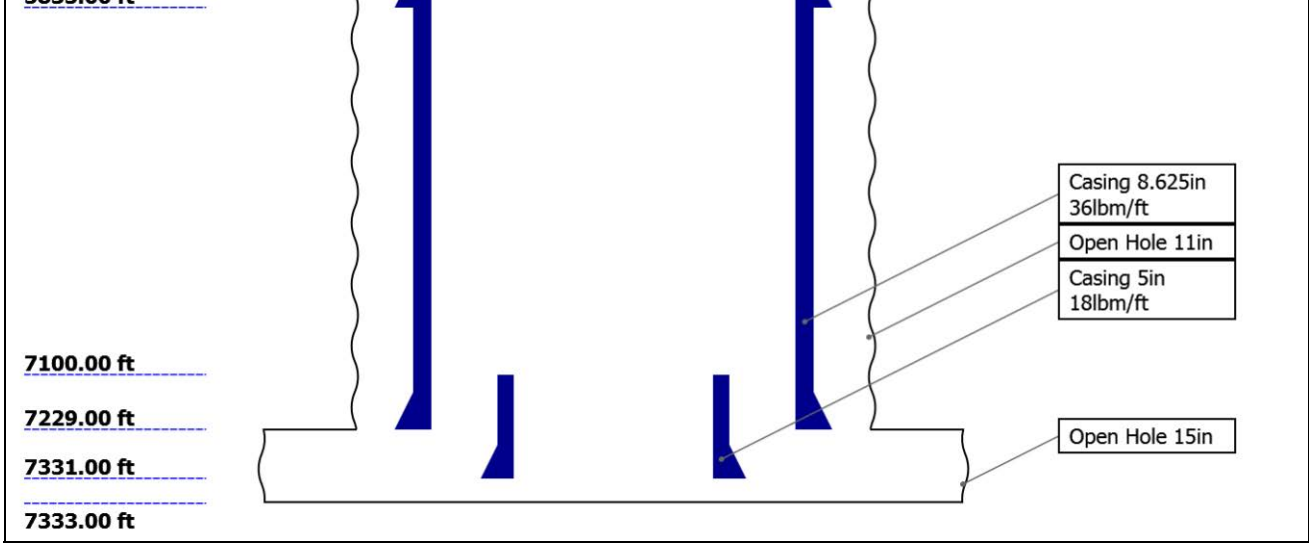

Borehole Size/Casing/Tubing Record

Bit						
Bit Size (in)	17.5	11	15			
Top Driller (ft)	0	832	7229			
Top Logger (ft)	0	832	7229			
Bottom Driller (ft)	832	7229	7333			
Bottom Logger (ft)	832	7229	7335			
Casing						
Size (in)	13.375	8.625	8.625	5		
Weight (lbm/ft)	54.5	36	36	18		
Inner Diameter (in)	12.615	7.825	7.825	4.276		
Grade	K55	K55	N80	N80		
Top Driller (ft)	0	0	5835	7100		
Top Logger (ft)	0	0	5835	7100		
Bottom Driller (ft)	830	5835	7229	7331		
Bottom Logger (ft)	830	5835	7229	7331		

Remarks and Equipment Summary

One: Toolstring

Equip name	Length	MP name	Offset
LEH-QT:2867	**57.51**	Red	
LEH-QT:2867			
DTC-H	**54.59**	**CTEM**	**53.69**
ECH-KC		**HV**	**0.00**
DTC-H		**TelStatus**	**51.59**
		ToolStatus	**51.59**
HGNS-H:4177	**51.59**	**Temperature**	**51.57**
HGNH:4819		**GR**	**50.85**
NPV-N			
NSR-F:1546			
HGNS-H:4177			
HACCZ-H:7642			
HMCA-H			
		CNL Por	**44.52**

One: Remarks

Correlated to Schlumberger Induction Electrical log
Dated: 9-17-1974
USIT logged at 10 deg 1.5" resolution at 2800 ft/hr High Res passes logged at 10deg .6" at 1200 ft/hr
USIT ran for cement and corrosion
Top of sand on the plug 7072
Rig Ensign 341
Free pipe = 55 mv
Crew: J.Marinez / M.Salazar
Thank you for using Schlumberger!

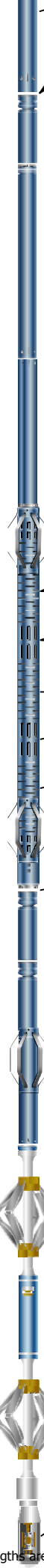

		CNL Porosity	44.32
		HMCA	42.18
		HGNS	42.18
		Accelerometer	0.00
AH-184[3]:2985	42.18		
DSLT-H:8236 ECH-KH:8678 DSLC-H:8236 SLS-E:1206	40.18		
		CBL 3ft	27.71
		Upper-Near	27.71
		VDL 5ft	26.71
		Upper-Far	26.71
		Delta-T	25.34
		Lower-Far	23.96
		Lower-Near	22.96
		SLS-E	19.55
AH-184[2]:2882	19.54		
AH-184[1]:6735	17.54		
USIT-E:1764 ECH-MFA:1764 USAC-A:1764 USIS-A:2720 USSC-B USRS-B USI-SENSOR:3349	15.54		
		USI Sensor	0.38
		Head Tension	

TOOL ZERO

Lengths are in ft

Maximum Outer Diameter = 6.500 in

Line: Sensor Location, Value: Gating Offset
All measurements are relative to TOOL_ZERO

One

USIT VDL Main Pass 5 in = 100 ft

Software Version

Acquisition System	Version
Maxwell 2017 SP1	7.1.82245.3100

Computation	Description	Version
CEVAL	Sonic Cement Evaluation Computation Ensemble provides common Parameters and Channels	7.1.82245.3100
Cementation	Cementation Computation Application	7.1.82245.3100

SoftwareVersion_Tool	SoftwareVersion_Run Version	SoftwareVersion_Build Version
WAFE-SEC	Synergy SV451EC version 9.10	Synergy SV451EC version 9.10
WAFE-FEC	Synergy SV451EC version 9.10	Synergy SV451EC version 9.10
WAFE-TMDI	Synergy SV451EC version 46.19	Synergy SV451EC version 46.19

Tool Elements	Description	Software Version	Firmware Version
HGNS-H	HILT Gamma-Ray and Neutron Sonde, 150 degC	7.1.82245.3100	2.0
SLS-E	Sonic Logging Sonde E supports 3'-5'BHC DT and CBL/VDL	7.1.82245.3100	
USI-SENSOR	USIT Transducer Element	7.1.82245.3100	DSP: v1.82

Pass Summary

Run Name	Pass Objective	Direction	Top	Bottom	Start	Stop	DSC Mode	Depth Shift	Include Parallel Data
One	Log[4]:Up	Up	4.12 ft	7044.38 ft	02-Jun-2017 1:27:12 AM	02-Jun-2017 4:20:07 AM	ON	4.20 ft	Yes

All depths are referenced to toolstring zero

Log

Company:Southern California Gas Company Well:Fernando Fee 35B

One: Log[4]:Up:S011

Description: USI VDL Cement Format: Log (LBV1_USI-VDL (DSLT) Cement 7inch) Index Scale: 5 in per 100 ft Index Unit: ft Index Type: Measured Depth
Creation Date: 17-Jul-2017 14:11:00

TIME_1900 - Time Marked every 60.00 (s)

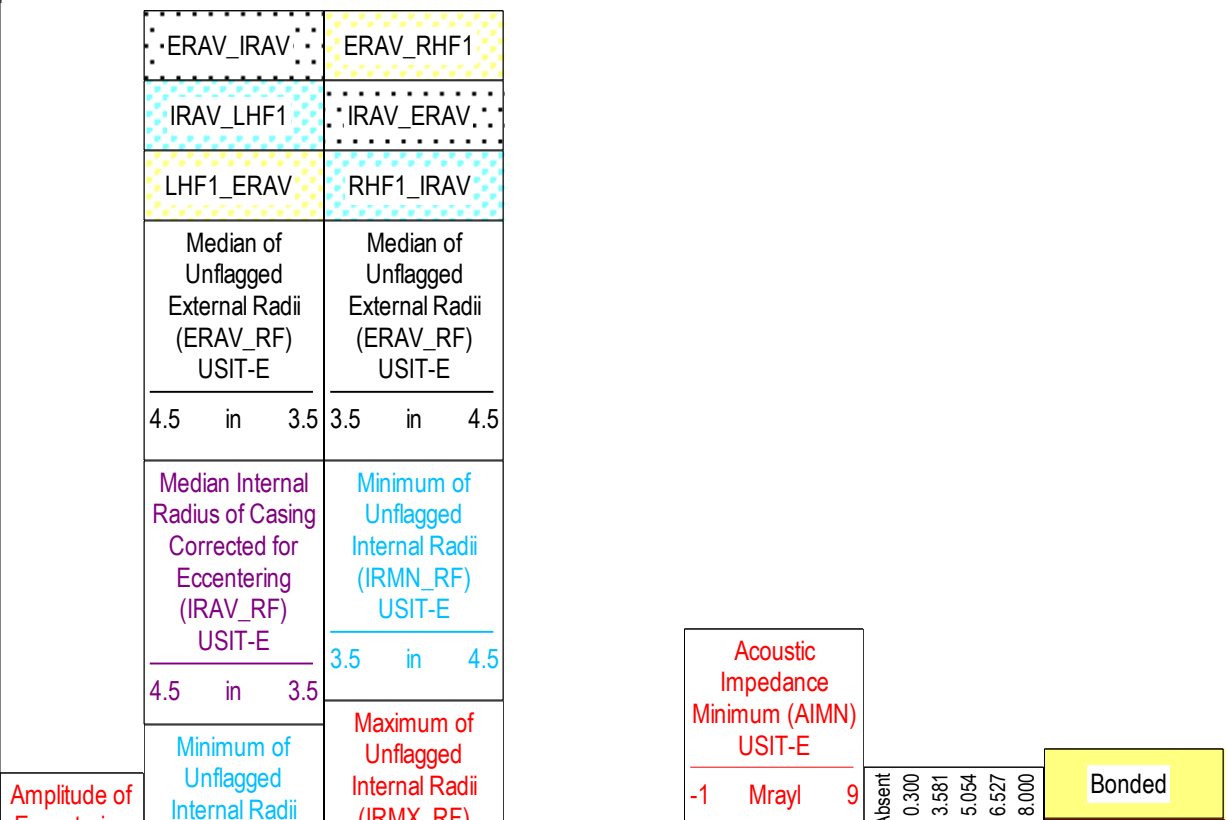

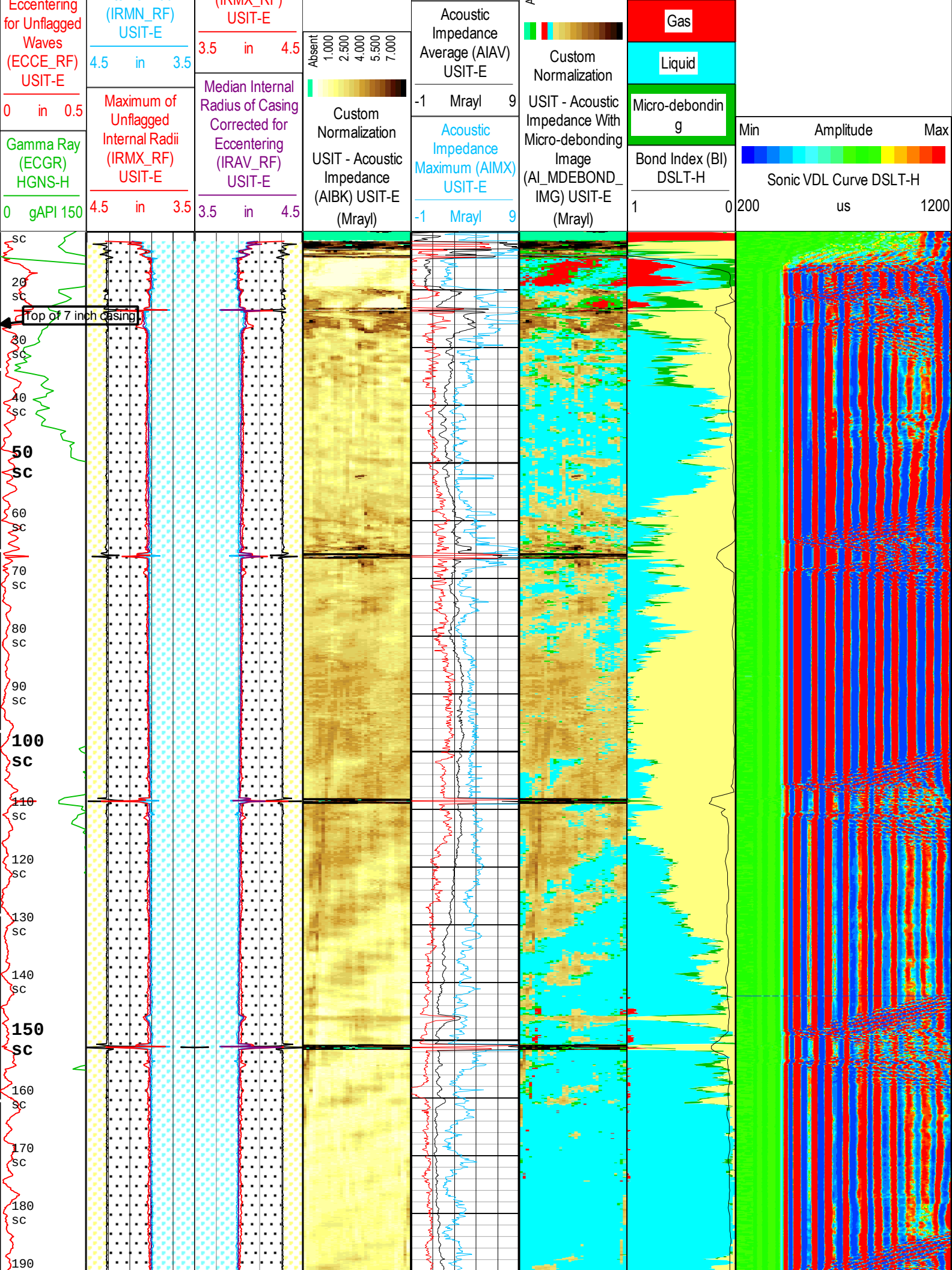
Eccentering for Unflagged Waves (ECCE_RF) USIT-E
0 in 0.5
Gamma Ray (ECGR) HGNS-H
0 gAPI 150
(IRMN_RF) USIT-E
4.5 in 3.5
Maximum of Unflagged Internal Radii (IRMX_RF) USIT-E
4.5 in 3.5
(IRMX_RF) USIT-E
3.5 in 4.5
Median Internal Radius of Casing Corrected for Eccentering (IRAV_RF) USIT-E
3.5 in 4.5
Absent
1.000
2.500
4.000
5.500
7.000
Custom Normalization
USIT - Acoustic Impedance (AIBK) USIT-E (Mrayl)
Acoustic Impedance Average (AIAV) USIT-E
-1 Mrayl 9
Acoustic Impedance Maximum (AIMX) USIT-E
-1 Mrayl 9
Custom Normalization
USIT - Acoustic Impedance With Micro-debonding Image (AI_MDEBOND_IMG) USIT-E (Mrayl)
Gas
Liquid
Micro-debonding
Bond Index (BI) DSLT-H
1 0
Min Amplitude Max
Sonic VDL Curve DSLT-H
200 us 1200
Top of 7 inch Casing
20 sc
30 sc
40 sc
50 sc
60 sc
70 sc
80 sc
90 sc
100 sc
110 sc
120 sc
130 sc
140 sc
150 sc
160 sc
170 sc
180 sc
190

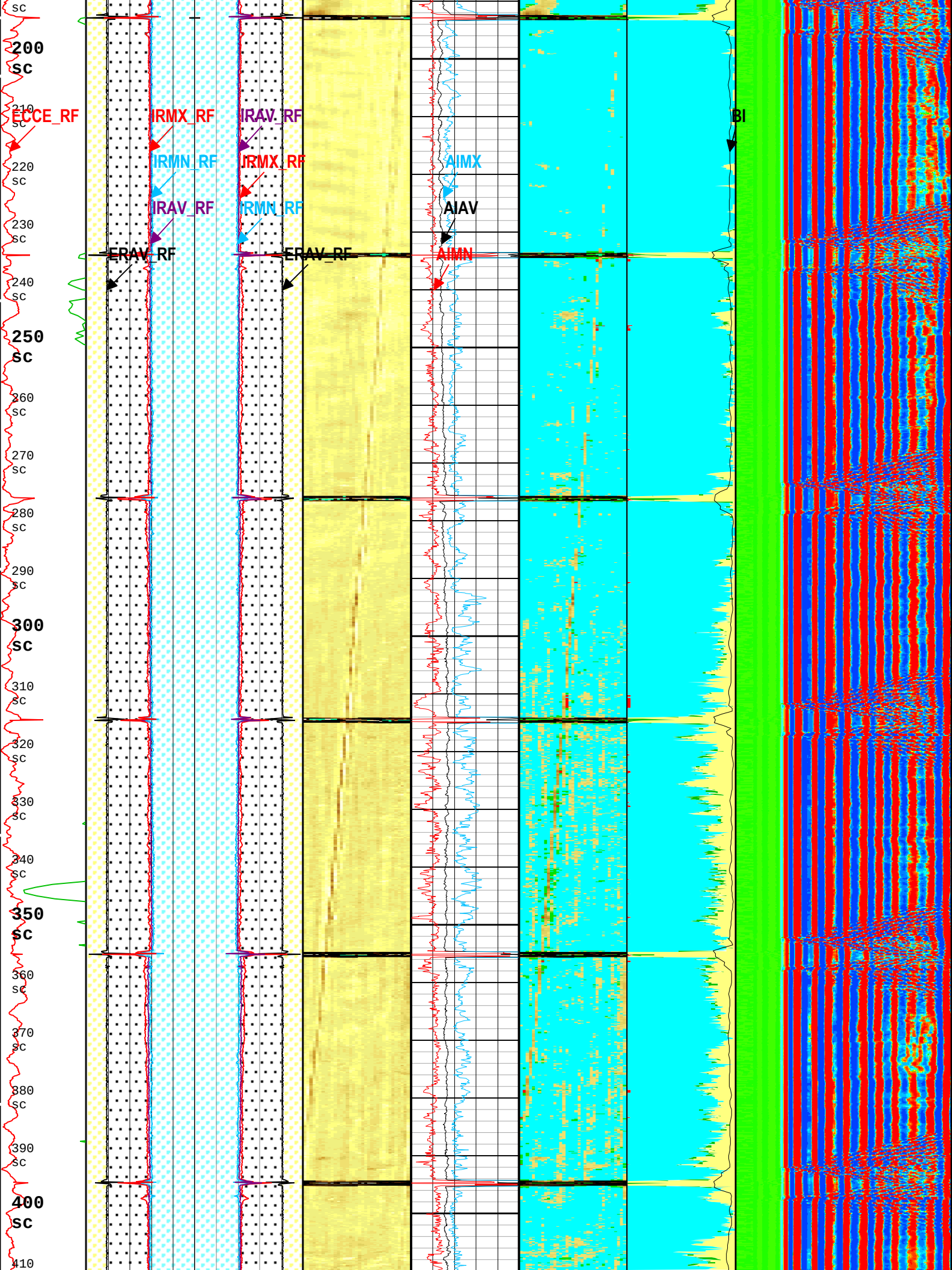
200 sc
210 sc
220 sc
230 sc
240 sc
250 sc
260 sc
270 sc
280 sc
290 sc
300 sc
310 sc
320 sc
330 sc
340 sc
350 sc
360 sc
370 sc
380 sc
390 sc
400 sc
410
ECCE_RF
IRMX_RF
IRAV_RF
IRMN_RF
IRMX_RF
IRAV_RF
IRMN_RF
ERAV_RF
ERAV_RF
AIMX
AIAV
AIMN
BI

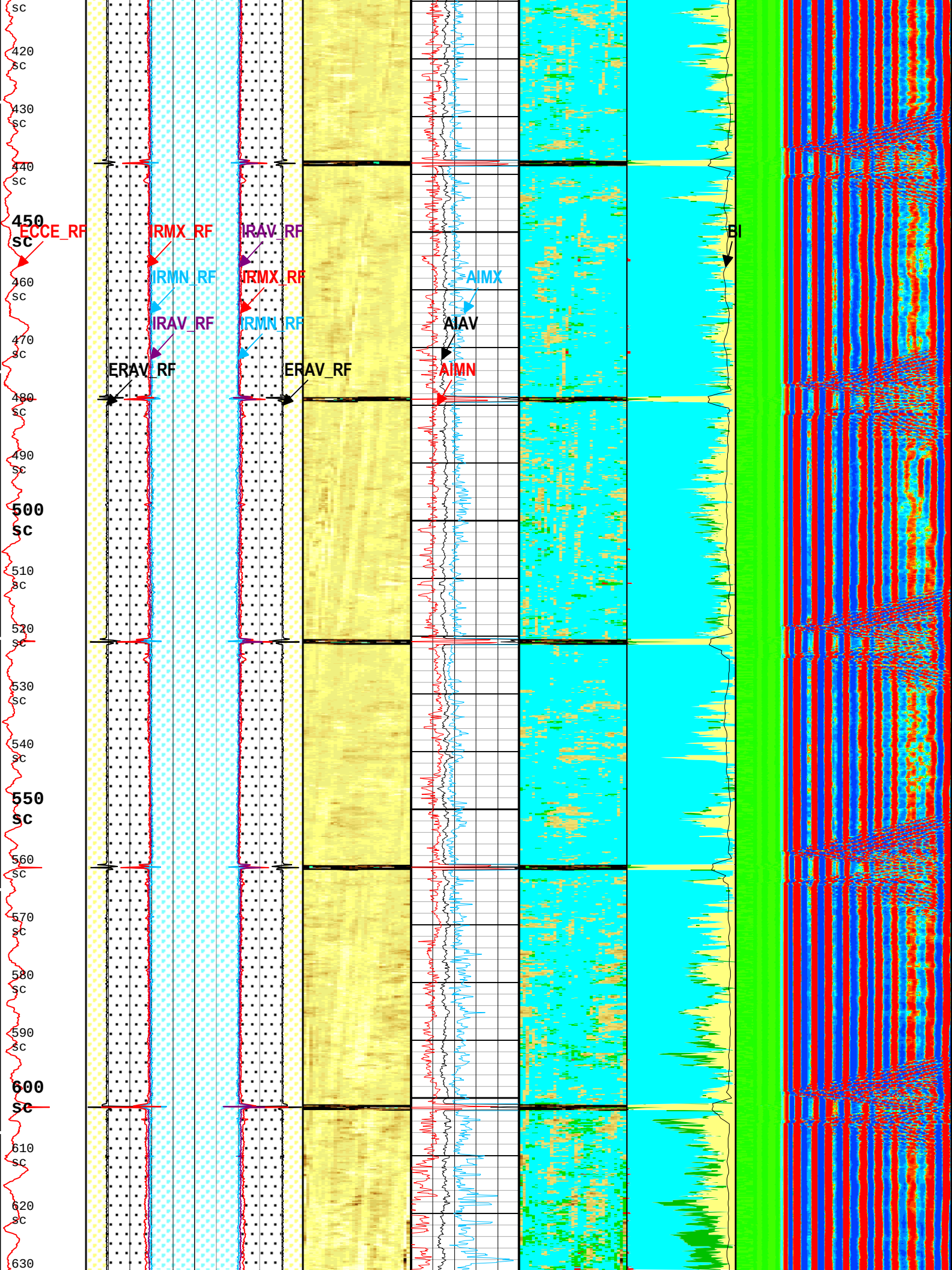
420
430
440
450
460
470
480
490
500
510
520
530
540
550
560
570
580
590
600
610
620
630
ECCE_RF
IRMX_RF
IRAV_RF
IRMN_RF
IRMX_RF
IRAV_RF
IRMN_RF
ERAV_RF
ERAV_RF
AIMX
AIAV
AIMN
BI

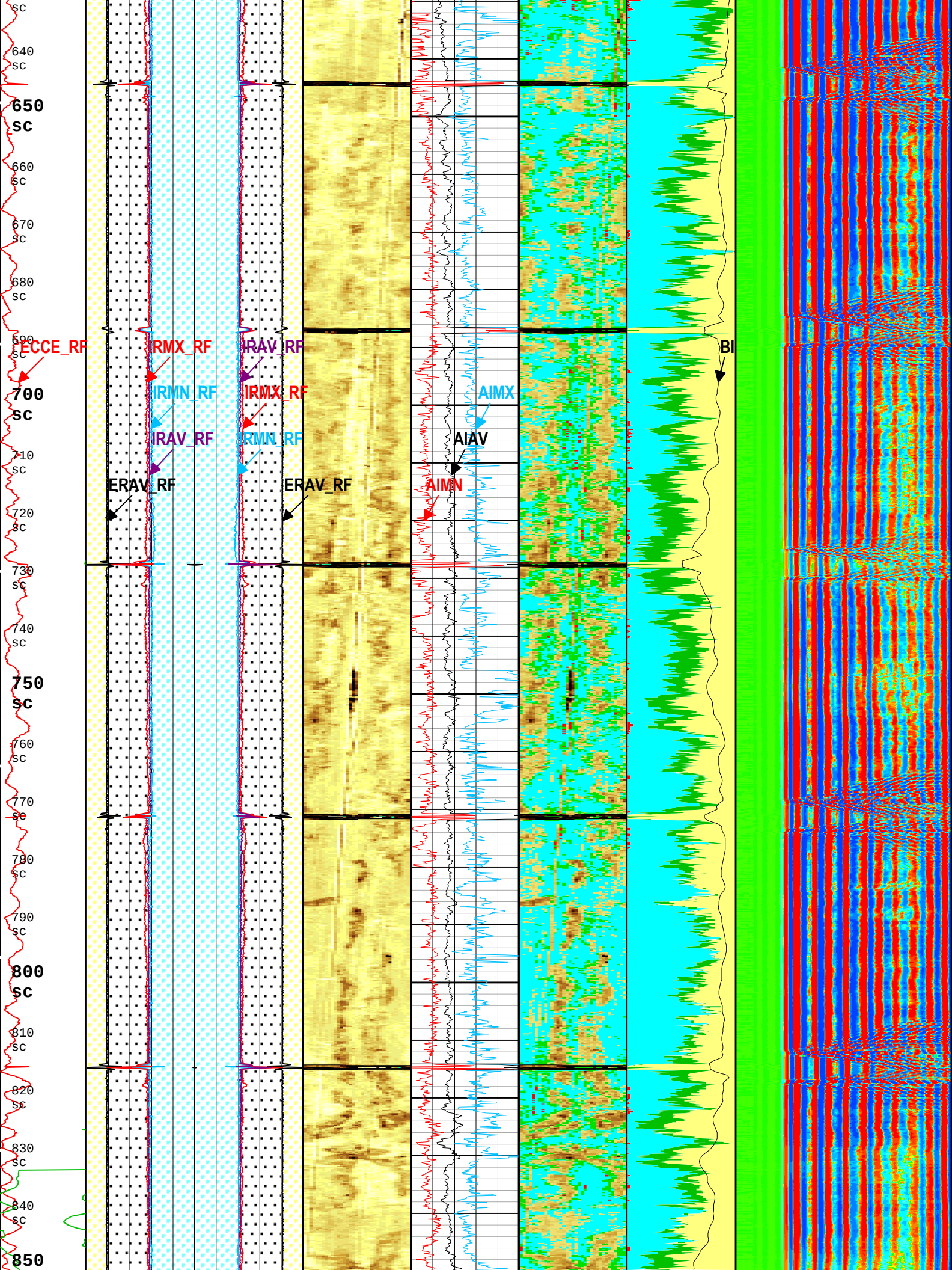
640 sc
650 sc
660 sc
670 sc
680 sc
690 sc
700 sc
710 sc
720 sc
730 sc
740 sc
750 sc
760 sc
770 sc
780 sc
790 sc
800 sc
810 sc
820 sc
830 sc
840 sc
850
ECCE_RF
IRMX_RF
IRAV_RF
IRMN_RF
IRMX_RF
IRAV_RF
IRMN_RF
ERAV_RF
ERAV_RF
AIMX
AIAV
AIMN
BI

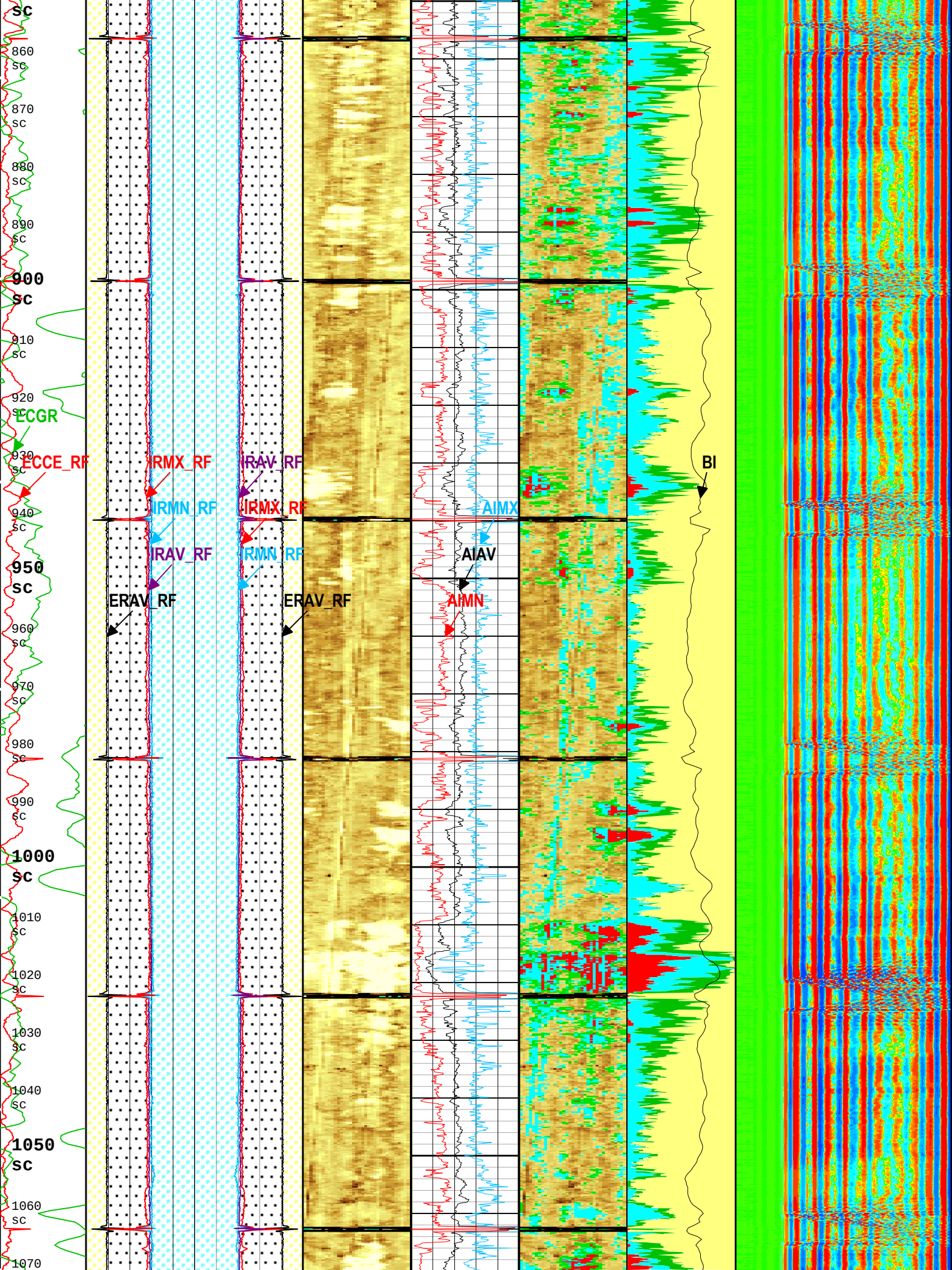
SC
860
870
880
890
900
910
920
930
940
950
960
970
980
990
1000
1010
1020
1030
1040
1050
1060
1070
ECGR
ECCE_RF
IRMX_RF
IRAV_RF
IRMN_RF
IRMX_RF
IRAV_RF
IRMN_RF
ERAV_RF
ERAV_RF
AIMX
AIAV
AIMN
BI

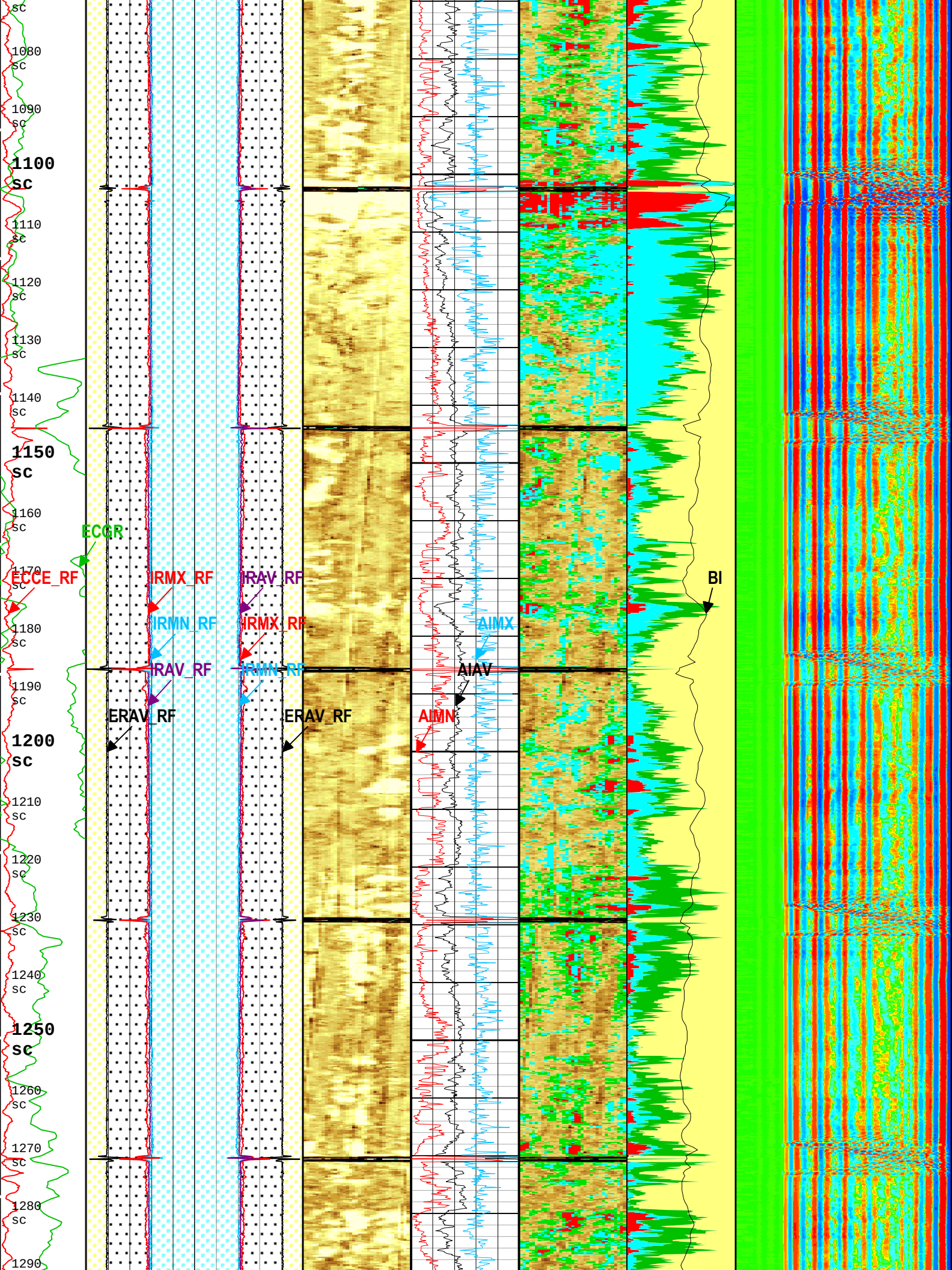
1080 sc
1090 sc
1100 sc
1110 sc
1120 sc
1130 sc
1140 sc
1150 sc
1160 sc
ECGR
1170 sc
ECCE_RF
IRMX_RF
IRAV_RF
BI
1180 sc
IRMN_RF
IRMX_RF
AIMX
IRAV_RF
IRMN_RF
AIAV
1190 sc
ERAV_RF
ERAV_RF
AIMN
1200 sc
1210 sc
1220 sc
1230 sc
1240 sc
1250 sc
1260 sc
1270 sc
1280 sc
1290

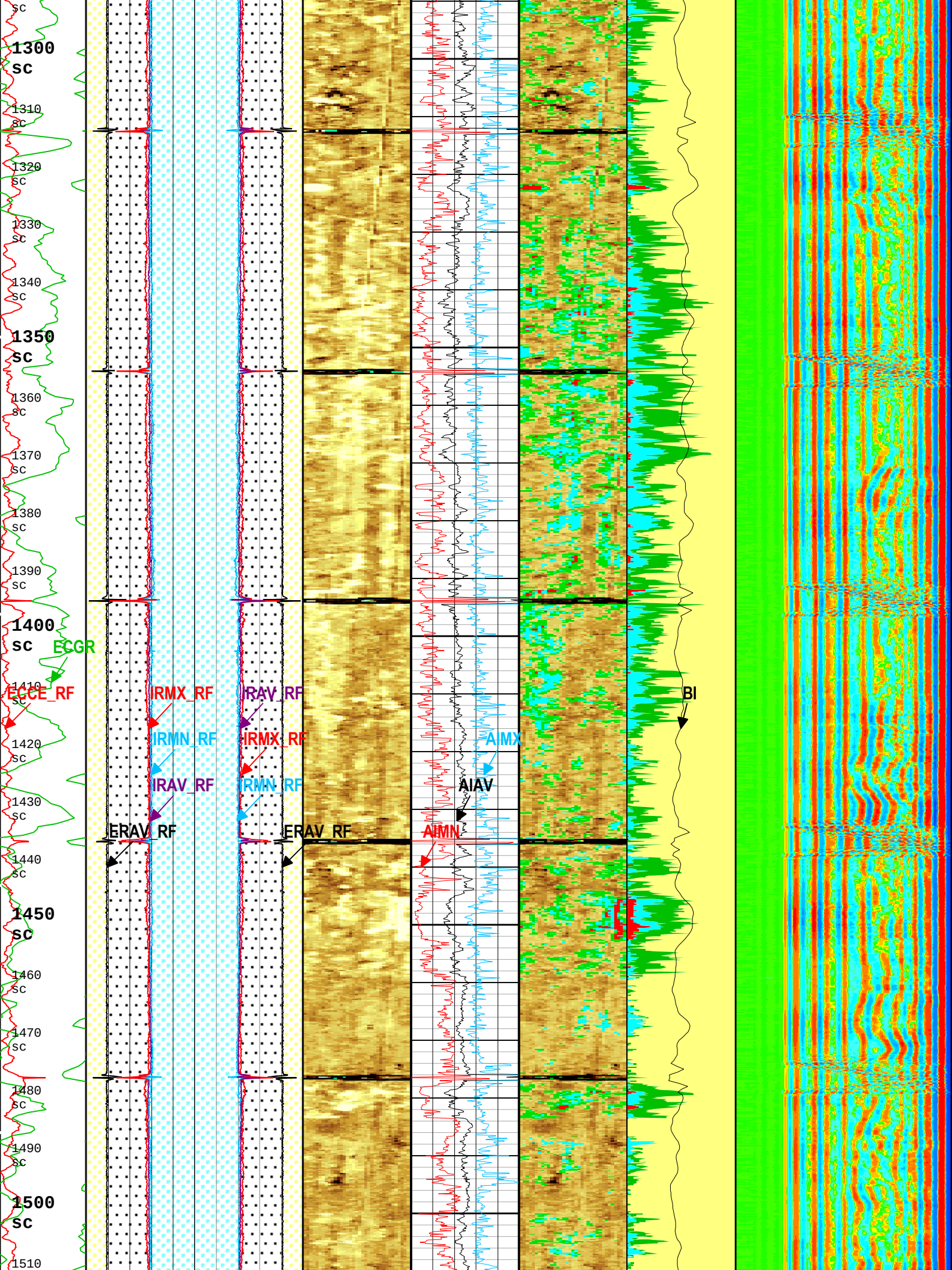
1300 sc
1310 sc
1320 sc
1330 sc
1340 sc
1350 sc
1360 sc
1370 sc
1380 sc
1390 sc
1400 sc
ECGR
ECCE_RF
1410 sc
1420 sc
1430 sc
1440 sc
1450 sc
1460 sc
1470 sc
1480 sc
1490 sc
1500 sc
1510
IRMX_RF
IRMN_RF
IRAV_RF
ERAV_RF
IRAV_RF
IRMX_RF
IRMN_RF
ERAV_RF
AIMX
AIAV
AIMN
BI

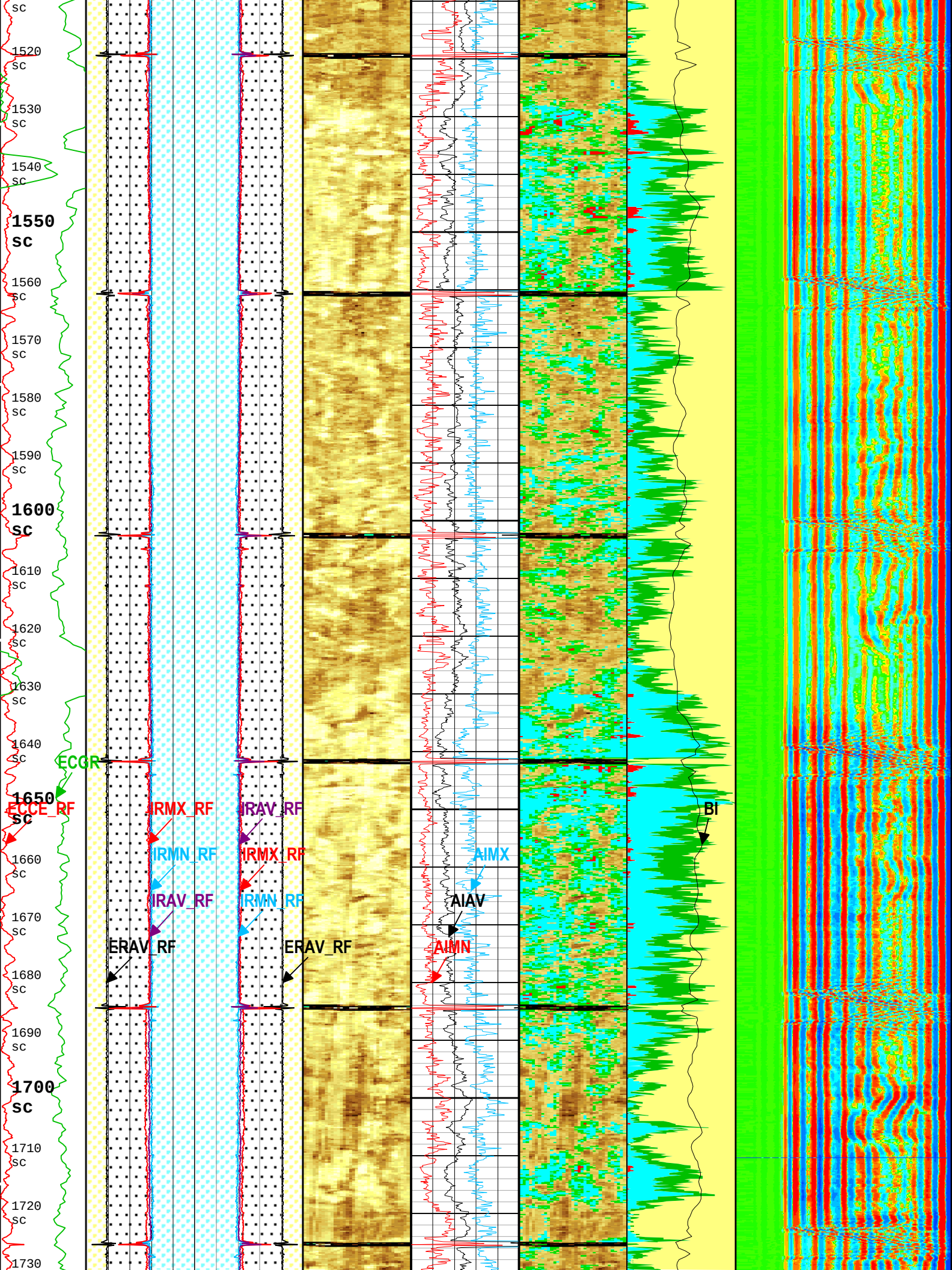
1520 sc
1530 sc
1540 sc
1550 sc
1560 sc
1570 sc
1580 sc
1590 sc
1600 sc
1610 sc
1620 sc
1630 sc
1640 sc
ECGR
1650 sc
ECCE_RF
IRMX_RF
IRAV_RF
BI
1660 sc
IRMN_RF
IRMX_RF
AIMX
IRAV_RF
IRMN_RF
AIAV
1670 sc
ERAV_RF
ERAV_RF
AIMN
1680 sc
1690 sc
1700 sc
1710 sc
1720 sc
1730

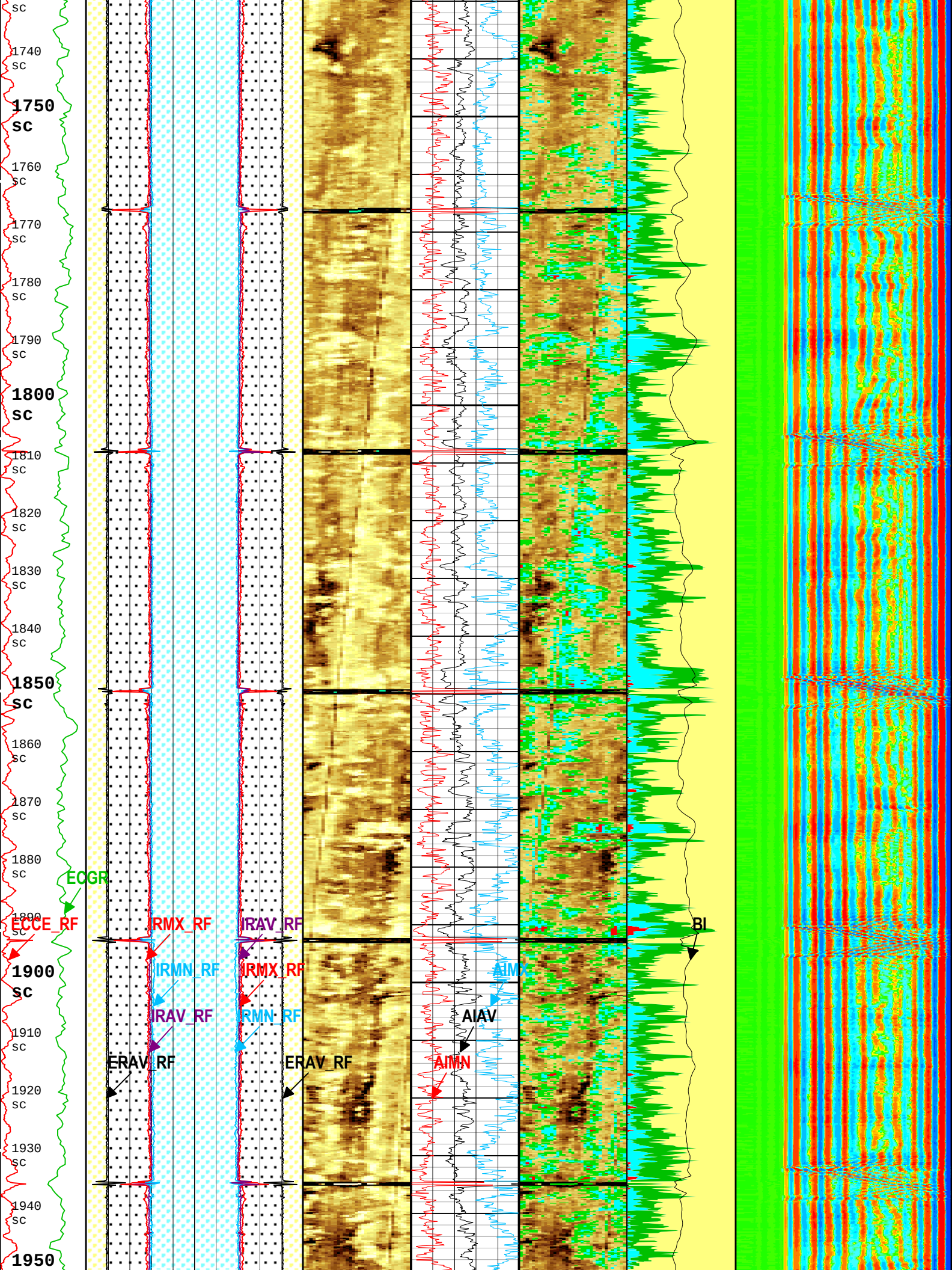
1740 sc
1750 sc
1760 sc
1770 sc
1780 sc
1790 sc
1800 sc
1810 sc
1820 sc
1830 sc
1840 sc
1850 sc
1860 sc
1870 sc
1880 sc
1890 sc
1900 sc
1910 sc
1920 sc
1930 sc
1940 sc
1950
ECGR
ECCE_RF
IRMX_RF
IRAV_RF
IRMN_RF
IRMX_RF
IRAV_RF
IRMN_RF
ERAV_RF
ERAV_RF
AIMX
AIAV
AIMN
BI

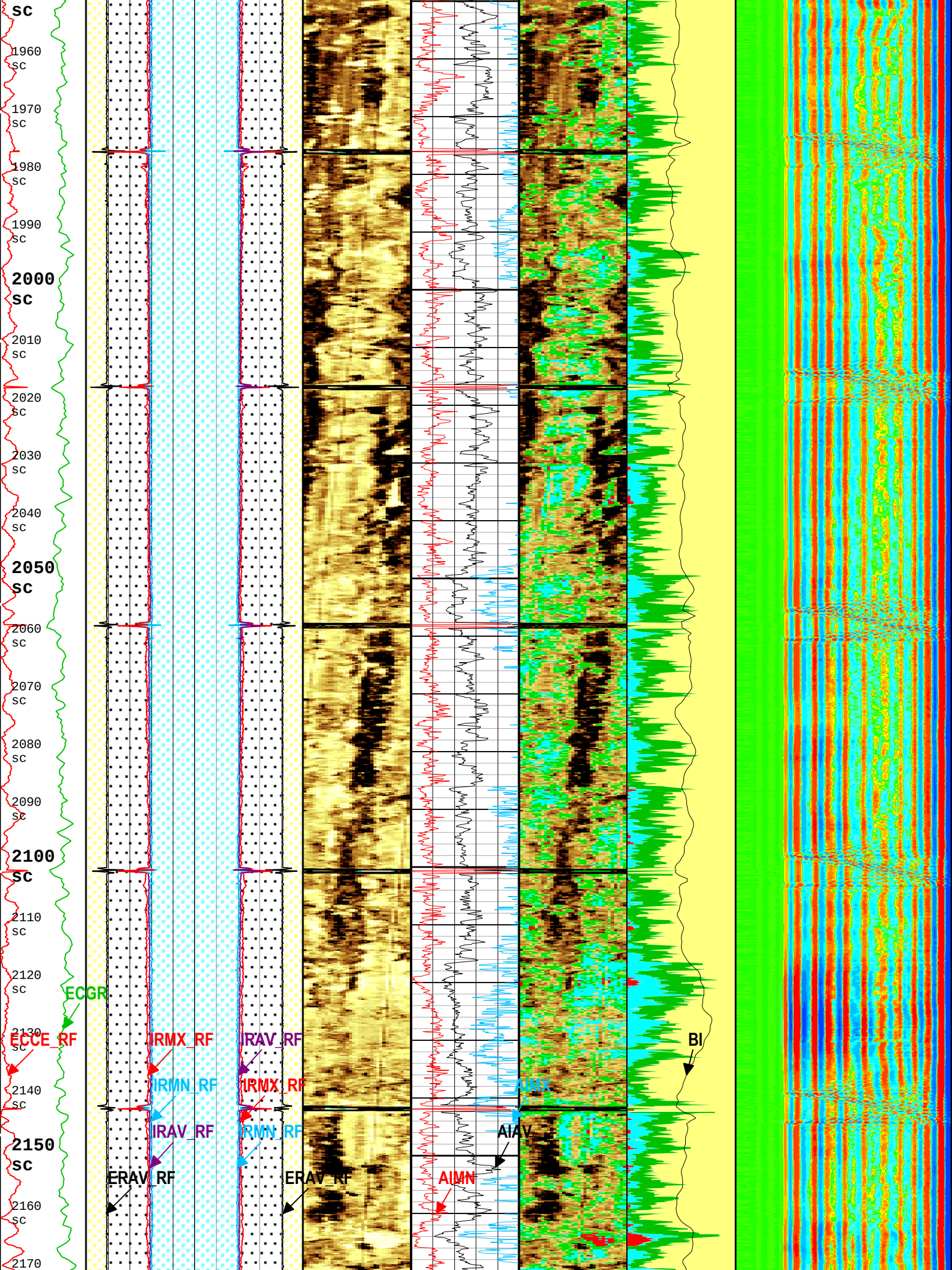
sc
1960 sc
1970 sc
1980 sc
1990 sc
2000 sc
2010 sc
2020 sc
2030 sc
2040 sc
2050 sc
2060 sc
2070 sc
2080 sc
2090 sc
2100 sc
2110 sc
2120 sc
2130 sc
2140 sc
2150 sc
2160 sc
2170
ECGR
ECCE_RF
IRMX_RF
IRAV_RF
IRMN_RF
IRMX_RF
IRAV_RF
IRMN_RF
ERAV_RF
ERAV_RF
AIMX
AIAV
AIMN
BI

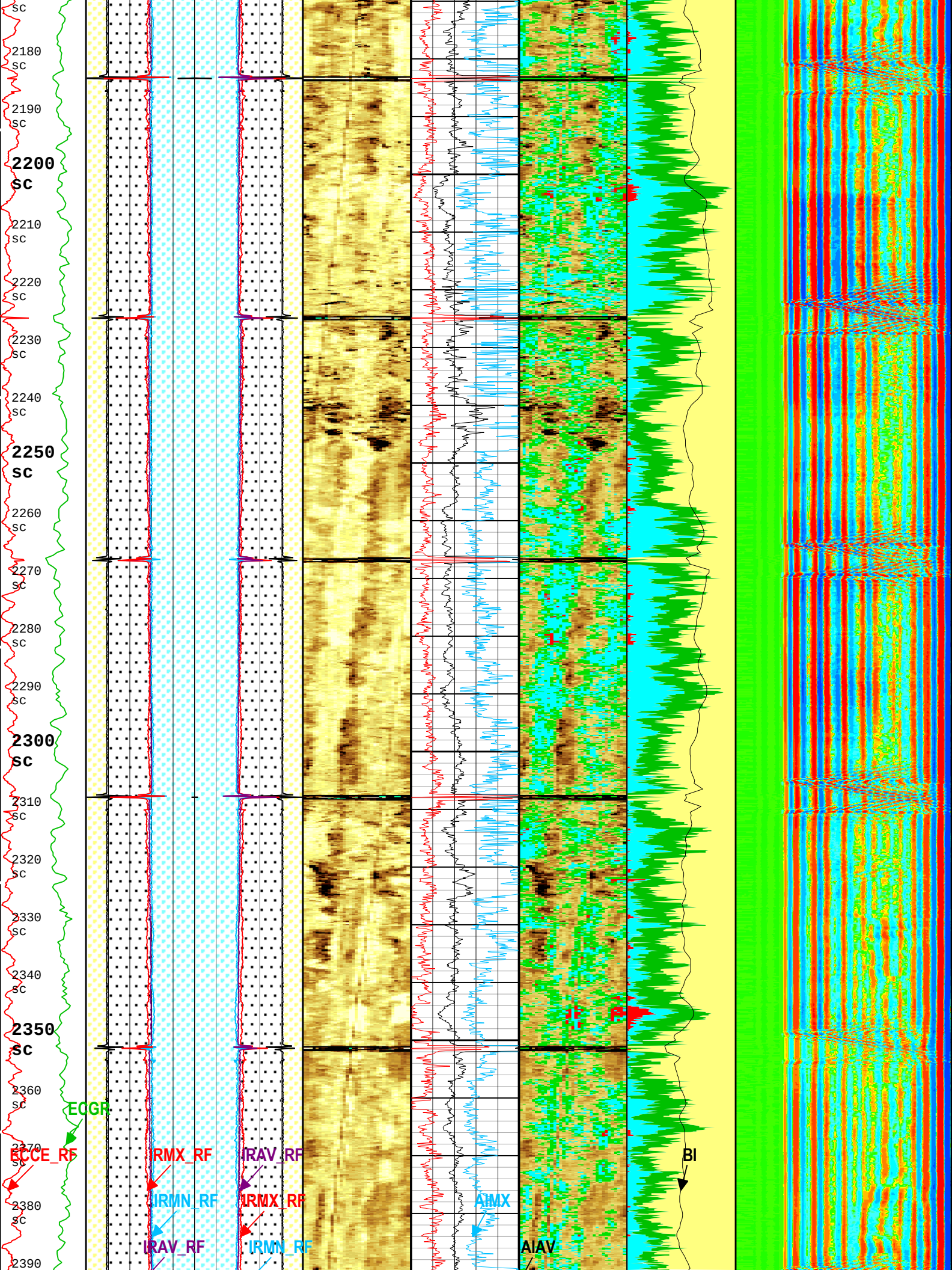
2180 sc
2190 sc
2200 sc
2210 sc
2220 sc
2230 sc
2240 sc
2250 sc
2260 sc
2270 sc
2280 sc
2290 sc
2300 sc
2310 sc
2320 sc
2330 sc
2340 sc
2350 sc
2360 sc
2370 sc
2380 sc
2390
ECGR
ECCE_RF
RMX_RF
IRAV_RF
IRMN_RF
IRMX_RF
IRAV_RF
IRMN_RF
AIMX
AIAV
BI

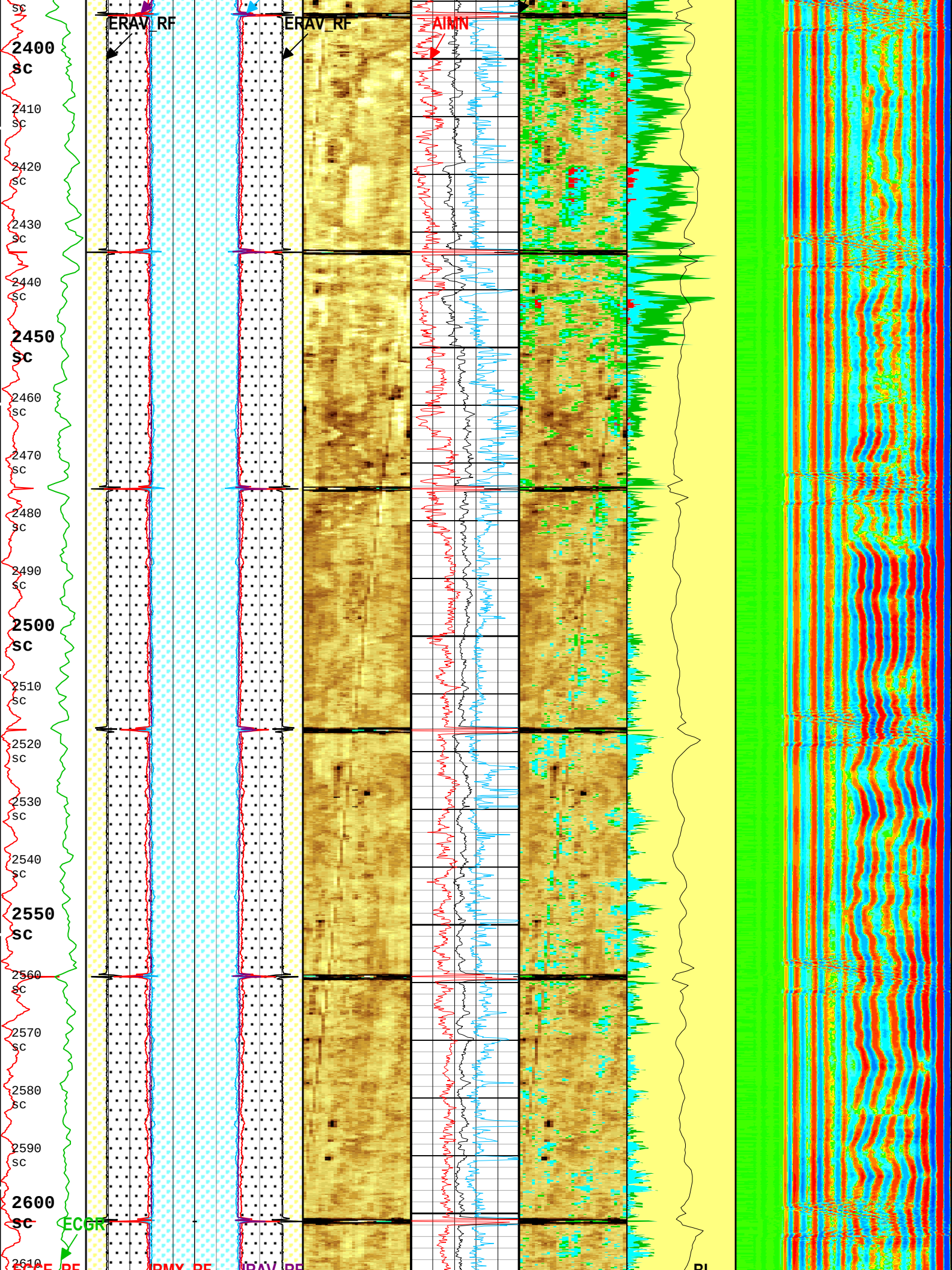
ERAV_RF
ERAV_RF
AIMN
2400 sc
2410 sc
2420 sc
2430 sc
2440 sc
2450 sc
2460 sc
2470 sc
2480 sc
2490 sc
2500 sc
2510 sc
2520 sc
2530 sc
2540 sc
2550 sc
2560 sc
2570 sc
2580 sc
2590 sc
2600 sc
ECGR
2610
RMX_RF
RAV_RF

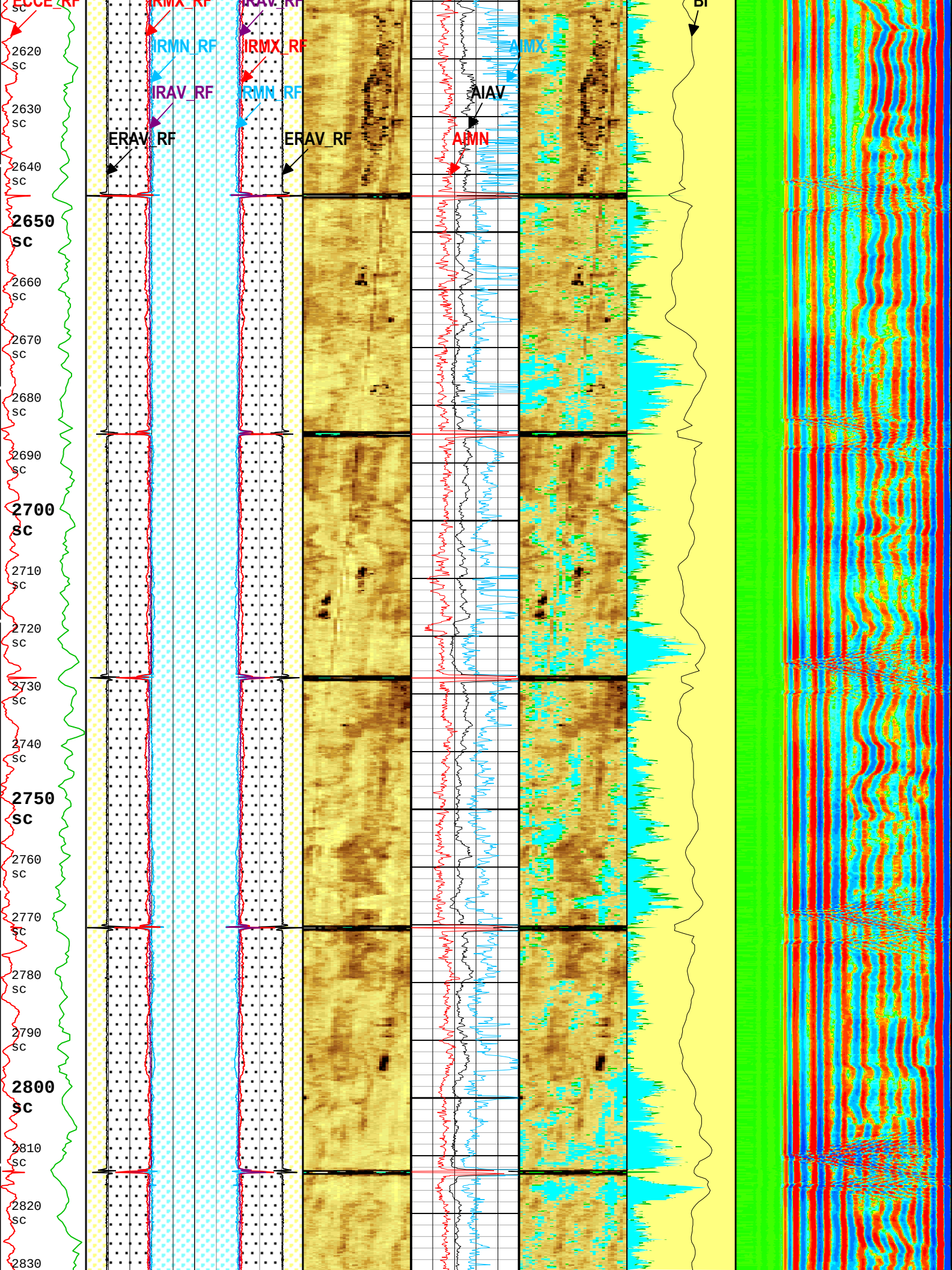
ECCE_RF
IRMX_RF
IRMN_RF
IRAV_RF
ERAV_RF
IRAV_RF
IRMX_RF
IRMN_RF
ERAV_RF
AIMX
AIAV
AIMN
BI
2620 sc
2630 sc
2640 sc
2650 sc
2660 sc
2670 sc
2680 sc
2690 sc
2700 sc
2710 sc
2720 sc
2730 sc
2740 sc
2750 sc
2760 sc
2770 sc
2780 sc
2790 sc
2800 sc
2810 sc
2820 sc
2830

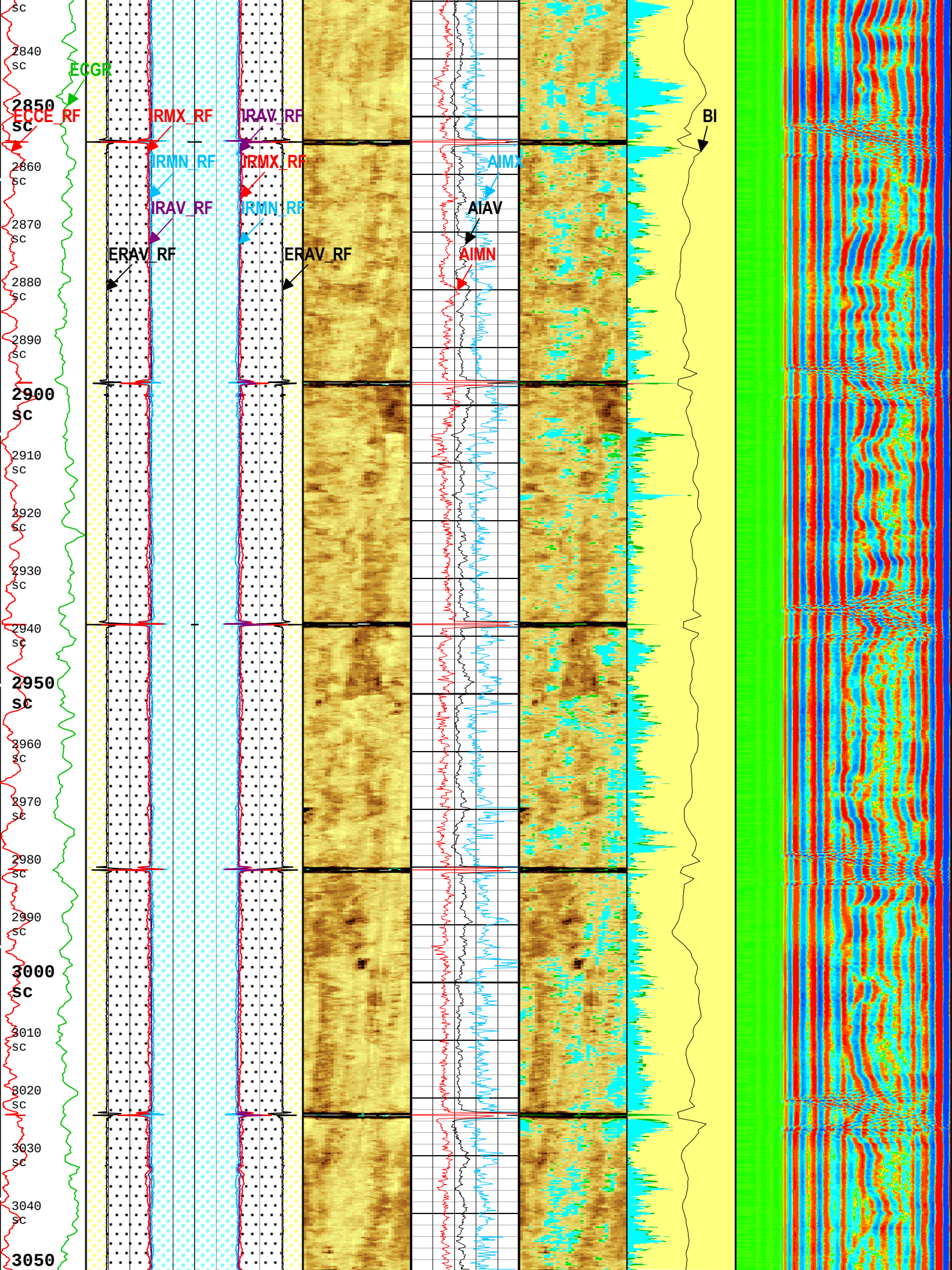
ECGR
ECCE_RF
IRMX_RF
IRAV_RF
IRMN_RF
IRMX_RF
IRAV_RF
IRMN_RF
ERAV_RF
ERAV_RF
AIMX
AIAV
AIMN
BI
2840 sc
2850 sc
2860 sc
2870 sc
2880 sc
2890 sc
2900 sc
2910 sc
2920 sc
2930 sc
2940 sc
2950 sc
2960 sc
2970 sc
2980 sc
2990 sc
3000 sc
3010 sc
3020 sc
3030 sc
3040 sc
3050

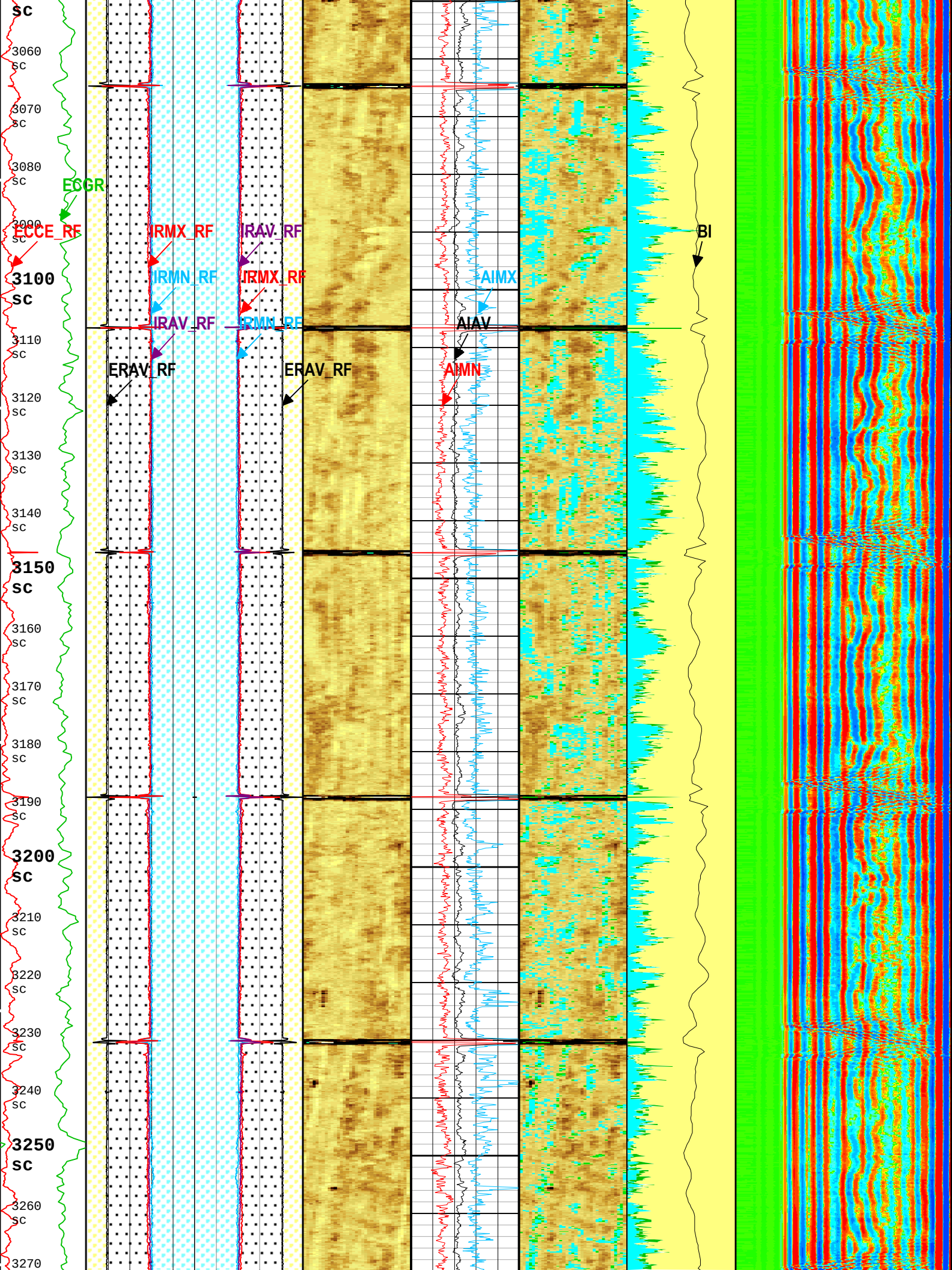
sc
3060
sc
3070
sc
3080
sc
ECGR
3090
sc
ECCE_RF
IRMX_RF
IRAV_RF
BI
3100
sc
IRMN_RF
IRMX_RF
AIMX
IRAV_RF
IRMN_RF
AIAV
3110
sc
ERAV_RF
ERAV_RF
AIMN
3120
sc
3130
sc
3140
sc
3150
sc
3160
sc
3170
sc
3180
sc
3190
sc
3200
sc
3210
sc
3220
sc
3230
sc
3240
sc
3250
sc
3260
sc
3270

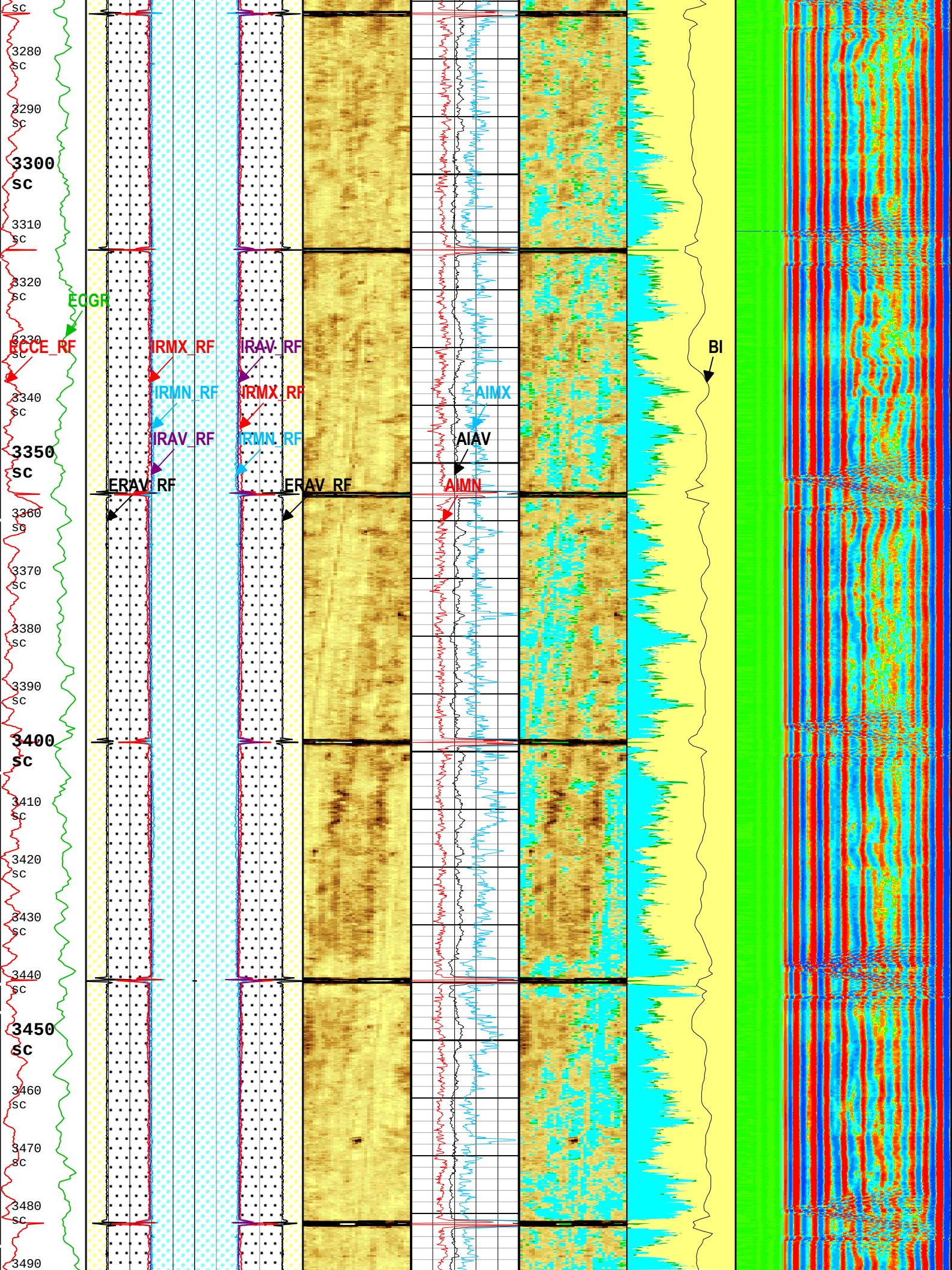
3280 SC
3290 SC
3300 SC
3310 SC
3320 SC
3330 SC
3340 SC
3350 SC
3360 SC
3370 SC
3380 SC
3390 SC
3400 SC
3410 SC
3420 SC
3430 SC
3440 SC
3450 SC
3460 SC
3470 SC
3480 SC
3490
ECGR
ECCE_RF
IRMX_RF
IRAV_RF
IRMN_RF
IRMX_RF
IRAV_RF
IRMN_RF
ERAV_RF
ERAV_RF
AIMX
AIAV
AIMN
BI

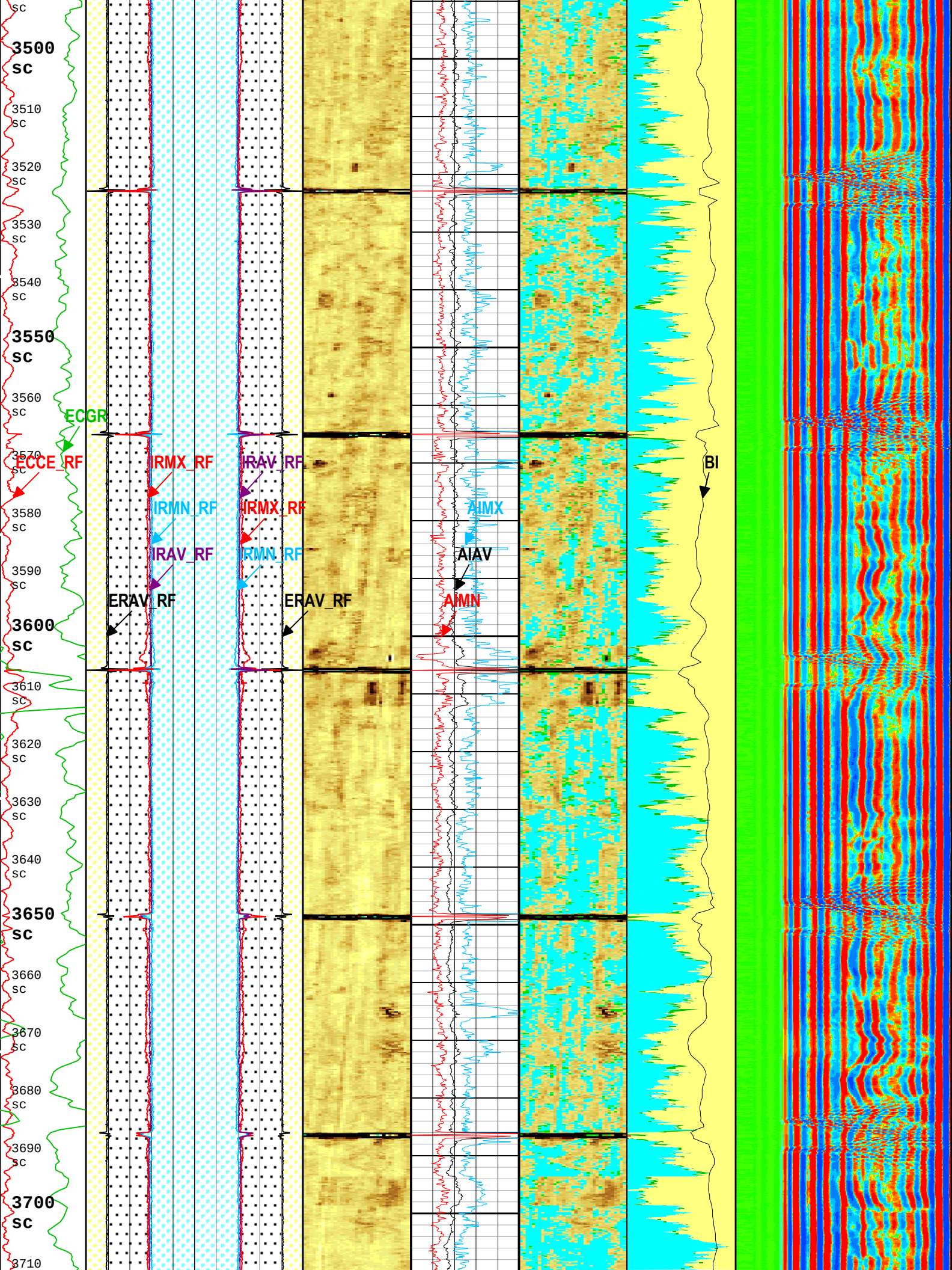
3500 sc
3510 sc
3520 sc
3530 sc
3540 sc
3550 sc
3560 sc
3570 sc
3580 sc
3590 sc
3600 sc
3610 sc
3620 sc
3630 sc
3640 sc
3650 sc
3660 sc
3670 sc
3680 sc
3690 sc
3700 sc
3710
ECGR
ECCE_RF
IRMX_RF
IRMN_RF
IRAV_RF
ERAV_RF
IRAV_RF
IRMX_RF
IRMN_RF
ERAV_RF
AIMX
AIAV
AIMN
BI

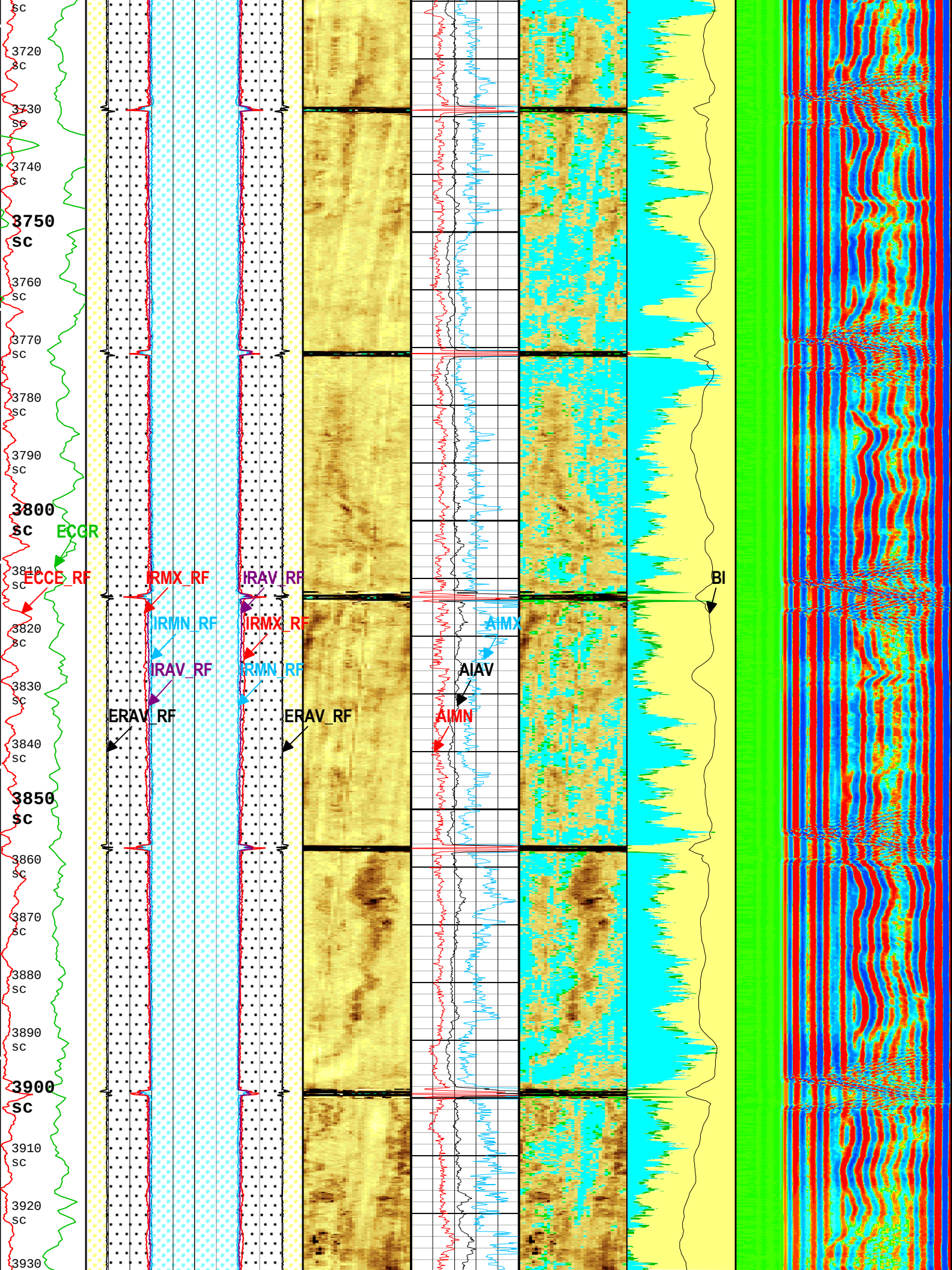
3720 sc
3730 sc
3740 sc
3750 sc
3760 sc
3770 sc
3780 sc
3790 sc
3800 sc
ECGR
3810 sc
ECCE_RF
IRMX_RF
IRAV_RF
BI
3820 sc
IRMN_RF
IRMX_RF
AIMX
3830 sc
IRAV_RF
IRMN_RF
AIAV
ERAV_RF
ERAV_RF
AIMN
3840 sc
3850 sc
3860 sc
3870 sc
3880 sc
3890 sc
3900 sc
3910 sc
3920 sc
3930

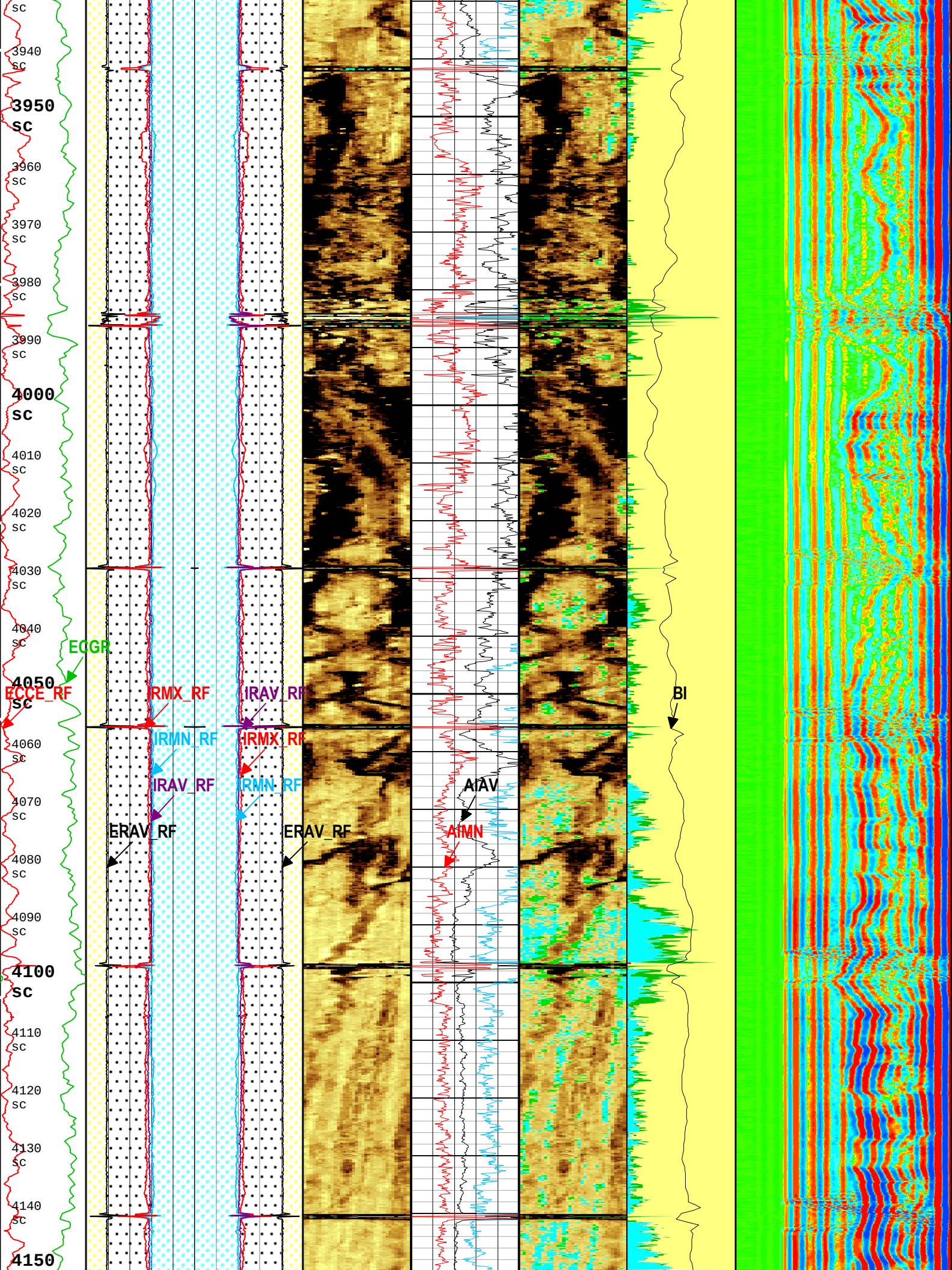
3940 sc
3950 sc
3960 sc
3970 sc
3980 sc
3990 sc
4000 sc
4010 sc
4020 sc
4030 sc
4040 sc
ECGR
4050 sc
ECCE_RF
IRMX_RF
IRAV_RF
IRMN_RF
IRMX_RF
IRAV_RF
IRMN_RF
ERAV_RF
ERAV_RF
AIAV
AIMN
BI
4060 sc
4070 sc
4080 sc
4090 sc
4100 sc
4110 sc
4120 sc
4130 sc
4140 sc
4150

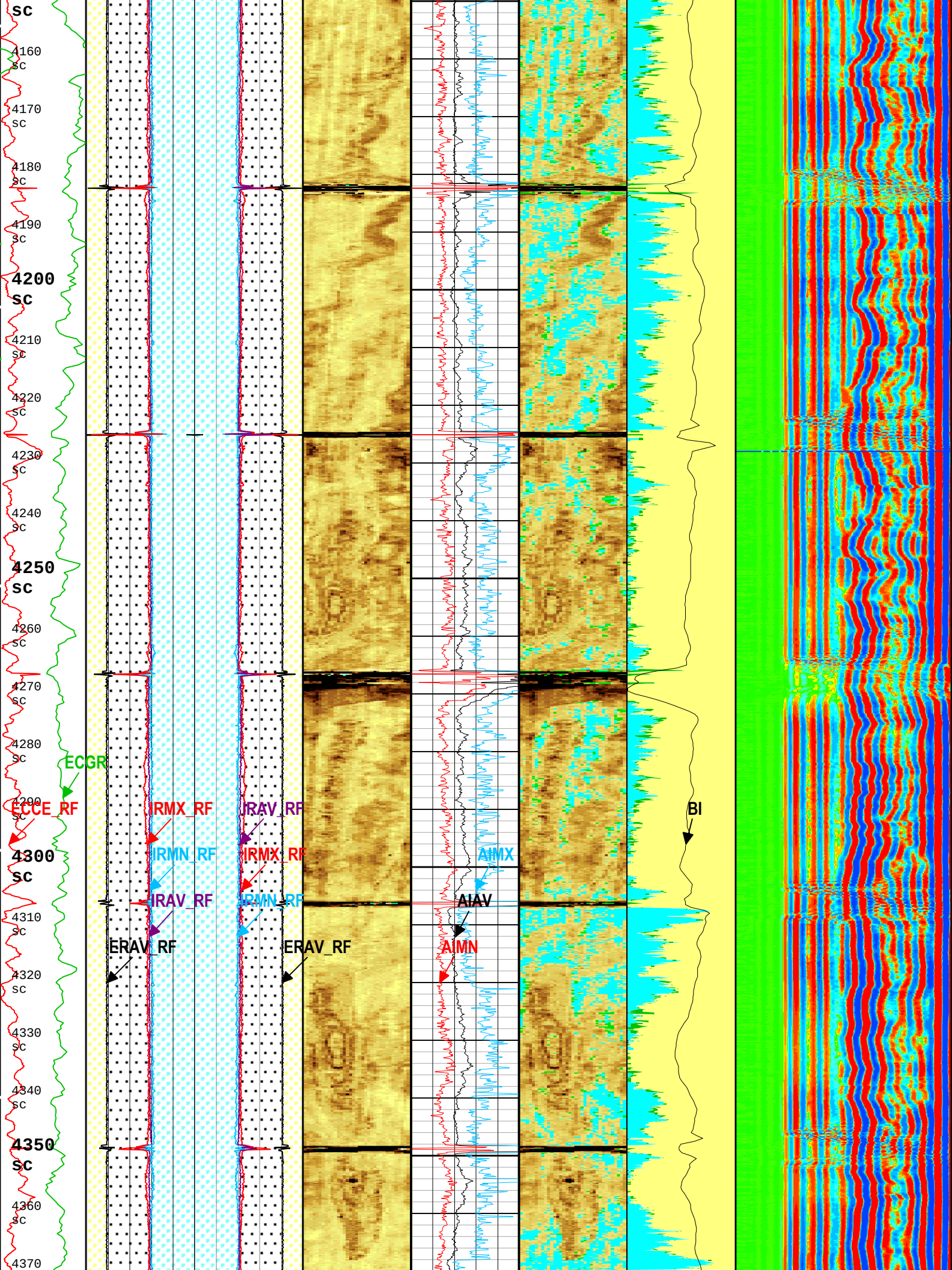
4160
4170
4180
4190
4200
4210
4220
4230
4240
4250
4260
4270
4280
4290
4300
4310
4320
4330
4340
4350
4360
4370
ECGR
ECCE_RF
IRMX_RF
IRAV_RF
IRMN_RF
IRMX_RF
IRAV_RF
IRMN_RF
ERAV_RF
ERAV_RF
AIMX
AIAV
AIMN
BI

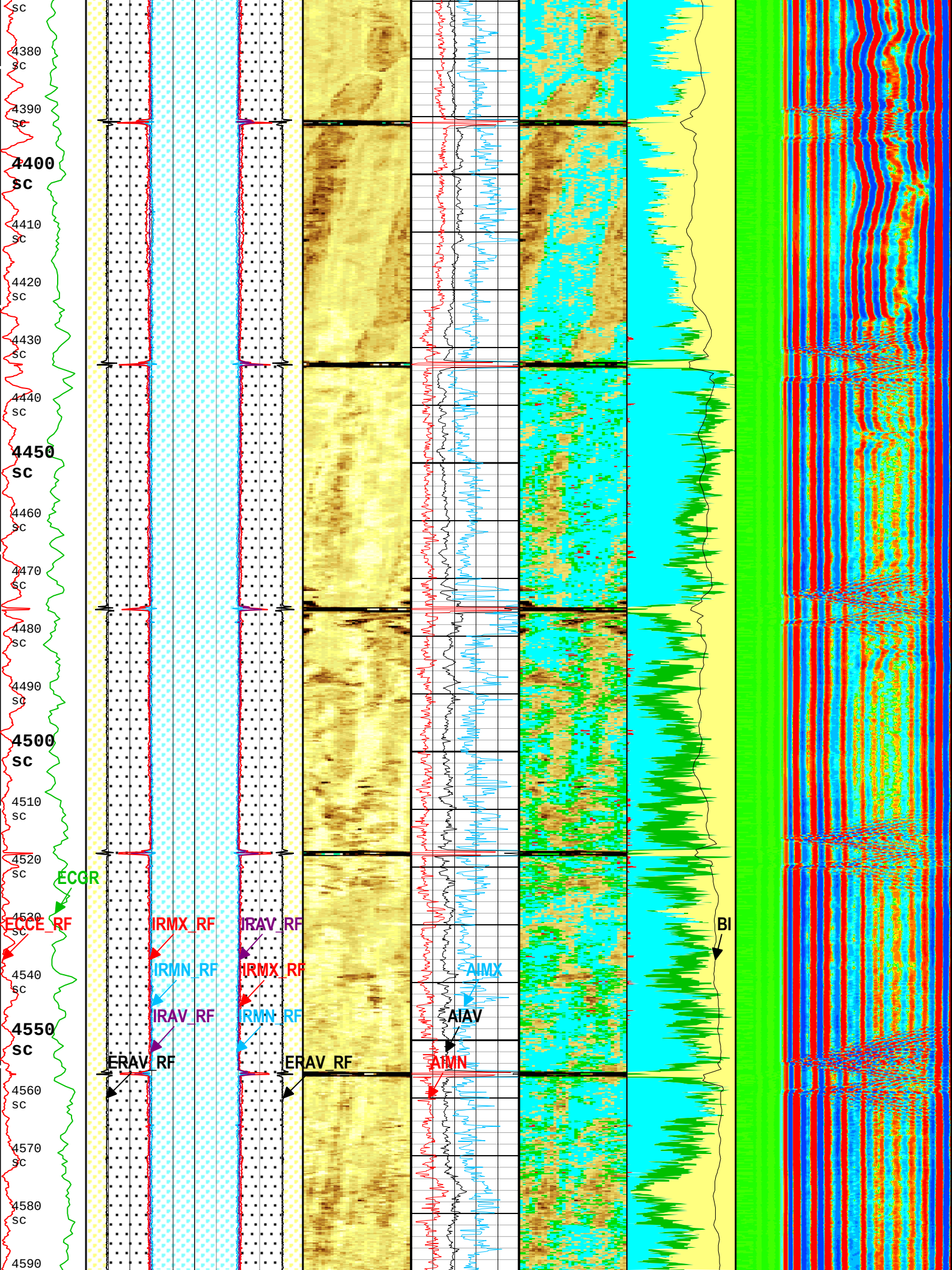
4380 sc
4390 sc
4400 sc
4410 sc
4420 sc
4430 sc
4440 sc
4450 sc
4460 sc
4470 sc
4480 sc
4490 sc
4500 sc
4510 sc
4520 sc
4530 sc
4540 sc
4550 sc
4560 sc
4570 sc
4580 sc
4590
ECGR
ECCE_RF
IRMX_RF
IRAV_RF
IRMN_RF
IRMX_RF
IRAV_RF
IRMN_RF
ERAV_RF
ERAV_RF
AIMX
AIAV
AIMN
BI

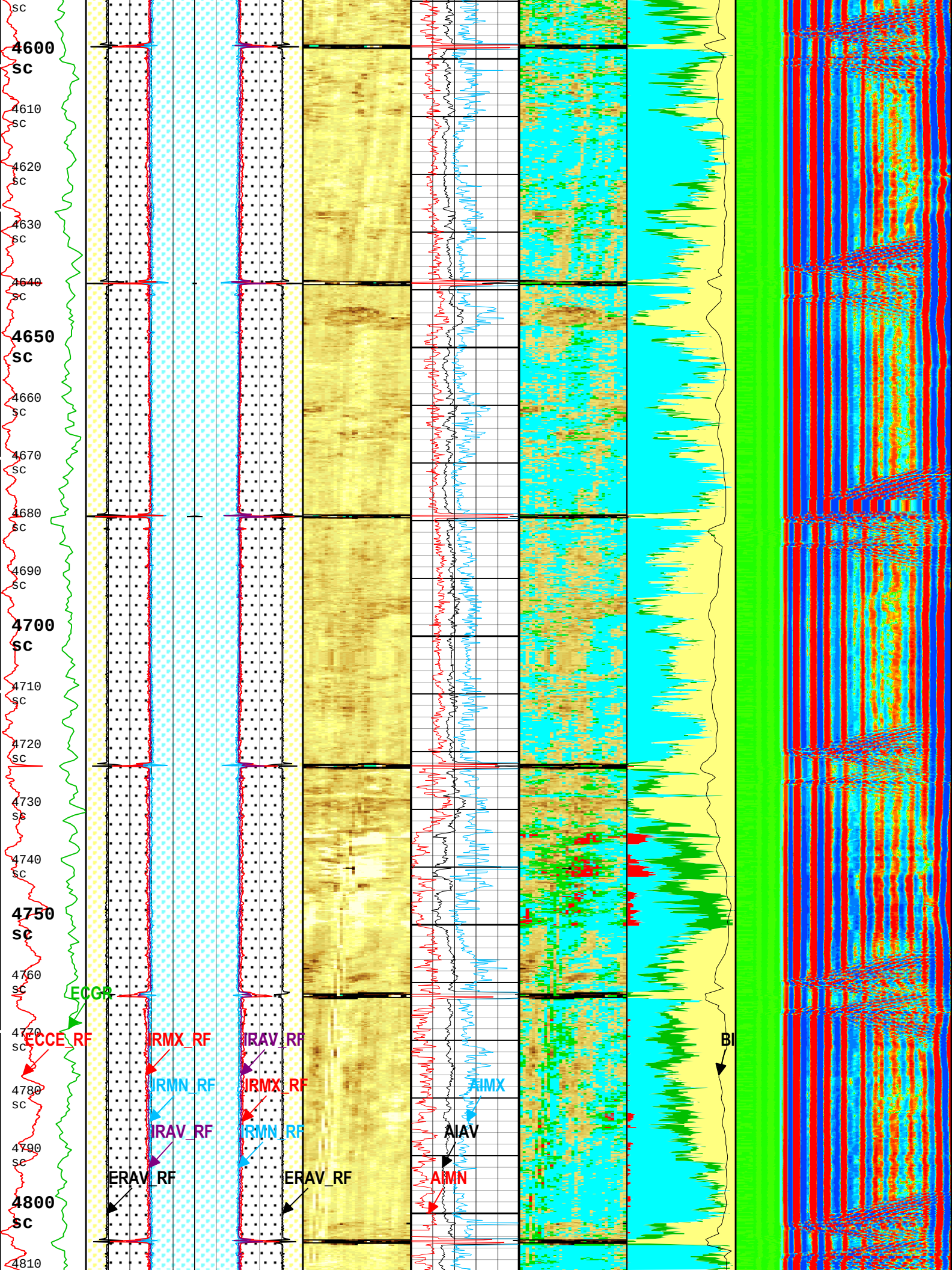
4600
sc
4610
sc
4620
sc
4630
sc
4640
sc
4650
sc
4660
sc
4670
sc
4680
sc
4690
sc
4700
sc
4710
sc
4720
sc
4730
sc
4740
sc
4750
sc
4760
sc
4770
sc
4780
sc
4790
sc
4800
sc
4810
ECGR
ECCE_RF
IRMX_RF
IRAV_RF
IRMN_RF
IRMX_RF
IRAV_RF
IRMN_RF
ERAV_RF
ERAV_RF
AIMX
AIAV
AIMN
BI

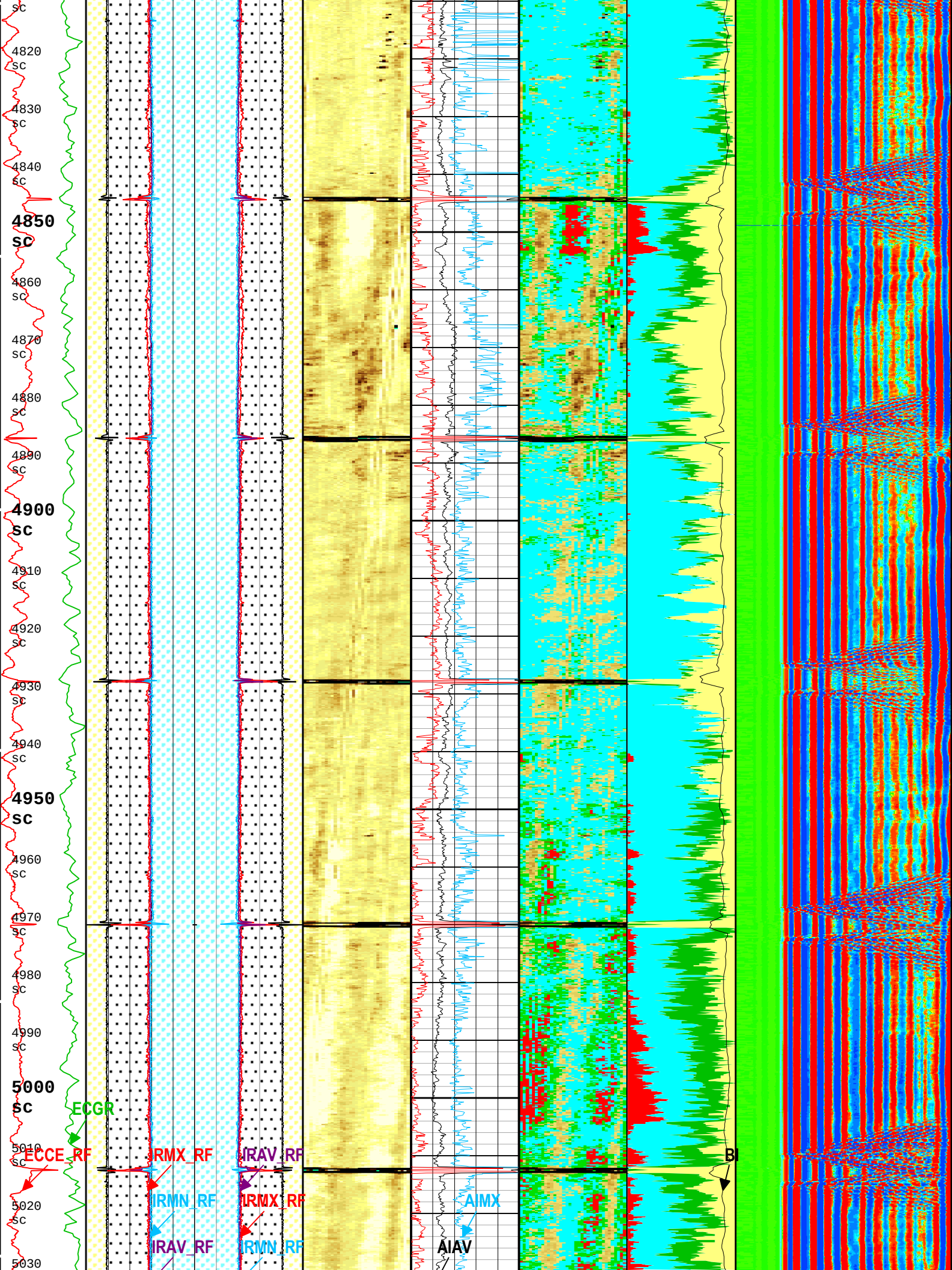
4820 SC
4830 SC
4840 SC
4850 SC
4860 SC
4870 SC
4880 SC
4890 SC
4900 SC
4910 SC
4920 SC
4930 SC
4940 SC
4950 SC
4960 SC
4970 SC
4980 SC
4990 SC
5000 SC
5010 SC
5020 SC
5030
ECGR
ECCE_RF
IRMX_RF
IRAV_RF
IRMN_RF
IRMX_RF
IRAV_RF
IRMN_RF
AIMX
AIAV
BI

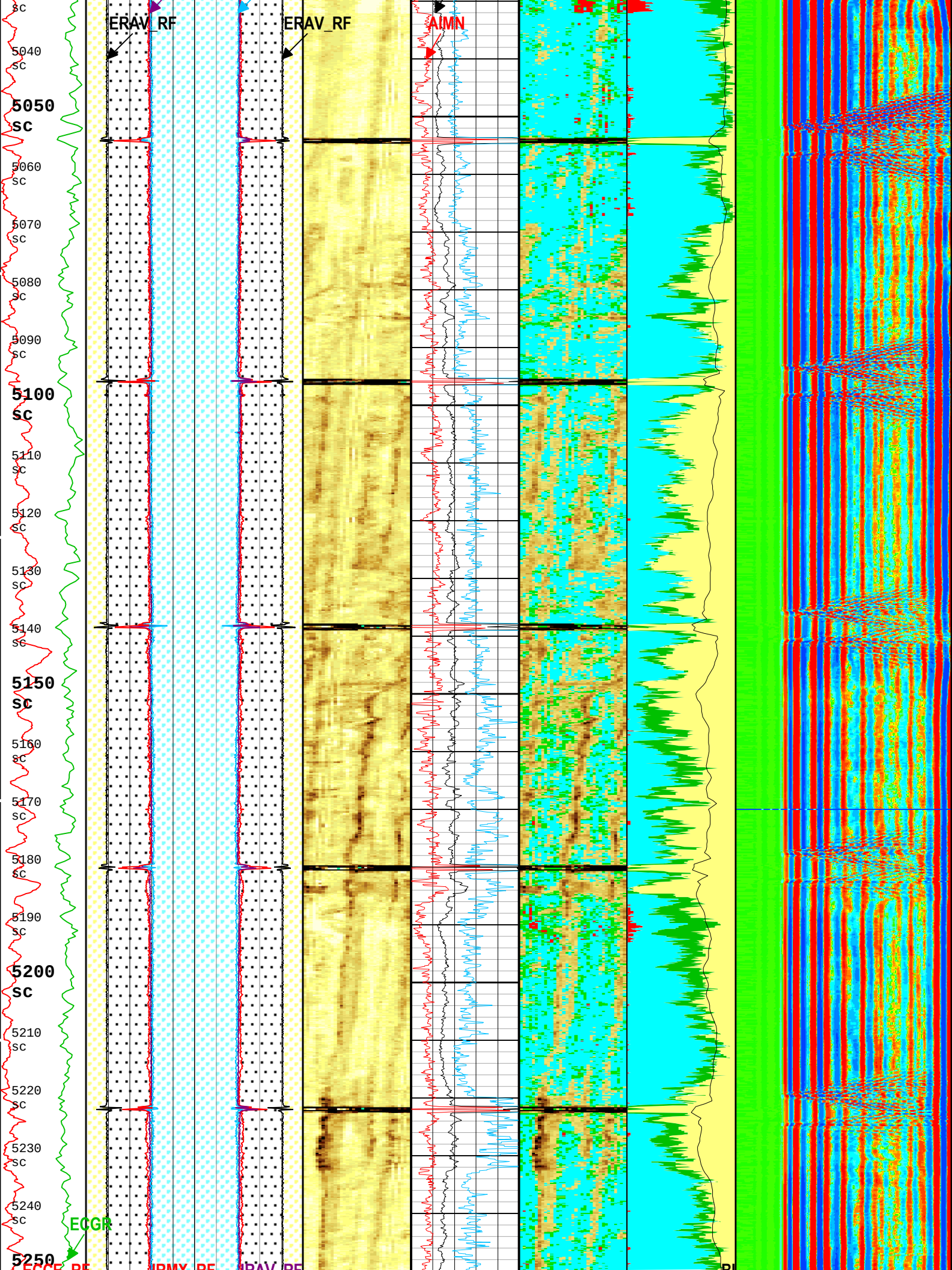
ERAV_RF
ERAV_RF
AIMN
5040
SC
5050
SC
5060
SC
5070
SC
5080
SC
5090
SC
5100
SC
5110
SC
5120
SC
5130
SC
5140
SC
5150
SC
5160
SC
5170
SC
5180
SC
5190
SC
5200
SC
5210
SC
5220
SC
5230
SC
5240
SC
ECGR
5250

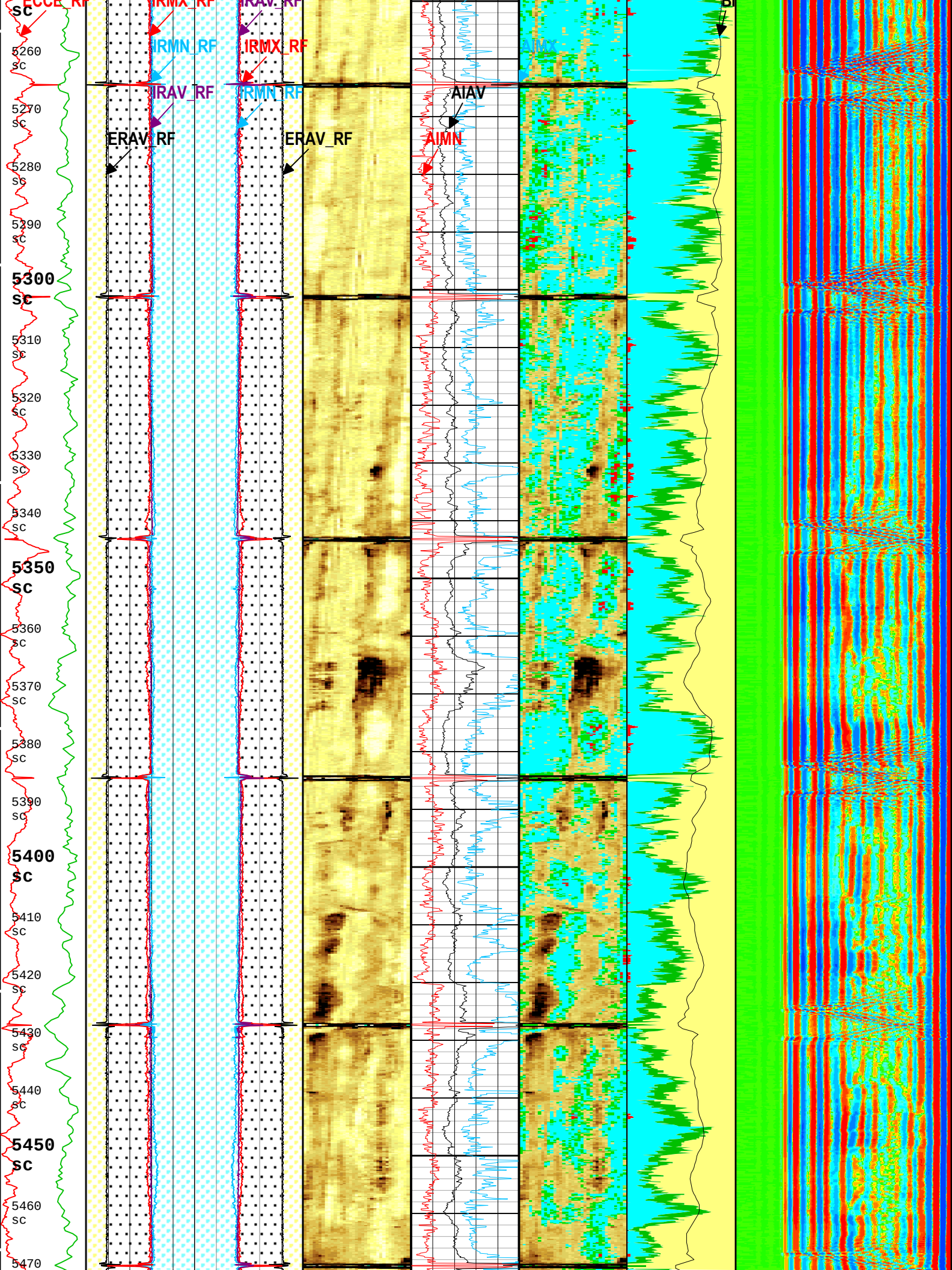
ECCE_RF
IRMX_RF
IRAV_RF
IRMN_RF
IRMX_RF
IRAV_RF
IRMN_RF
ERAV_RF
ERAV_RF
AIAV
AIMN
AIMX
5260 sc
5270 sc
5280 sc
5290 sc
5300 sc
5310 sc
5320 sc
5330 sc
5340 sc
5350 sc
5360 sc
5370 sc
5380 sc
5390 sc
5400 sc
5410 sc
5420 sc
5430 sc
5440 sc
5450 sc
5460 sc
5470

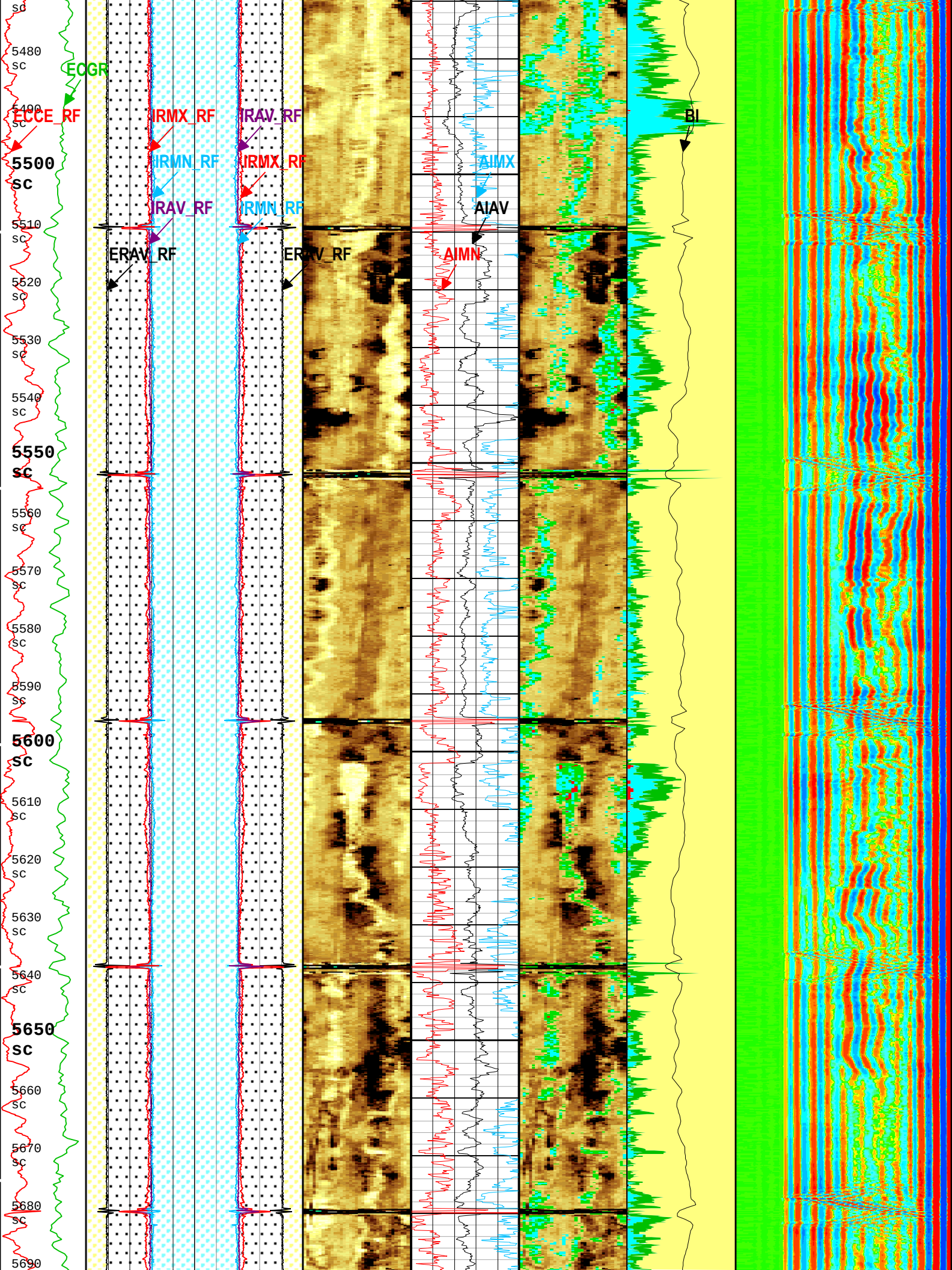
5480 sc
ECGR
5490 sc
ECCE_RF
IRMX_RF
IRAV_RF
BI
5500 sc
IRMN_RF
IRMX_RF
AIMX
IRAV_RF
IRMN_RF
AIAV
5510 sc
ERAV_RF
ERAV_RF
AIMN
5520 sc
5530 sc
5540 sc
5550 sc
5560 sc
5570 sc
5580 sc
5590 sc
5600 sc
5610 sc
5620 sc
5630 sc
5640 sc
5650 sc
5660 sc
5670 sc
5680 sc
5690

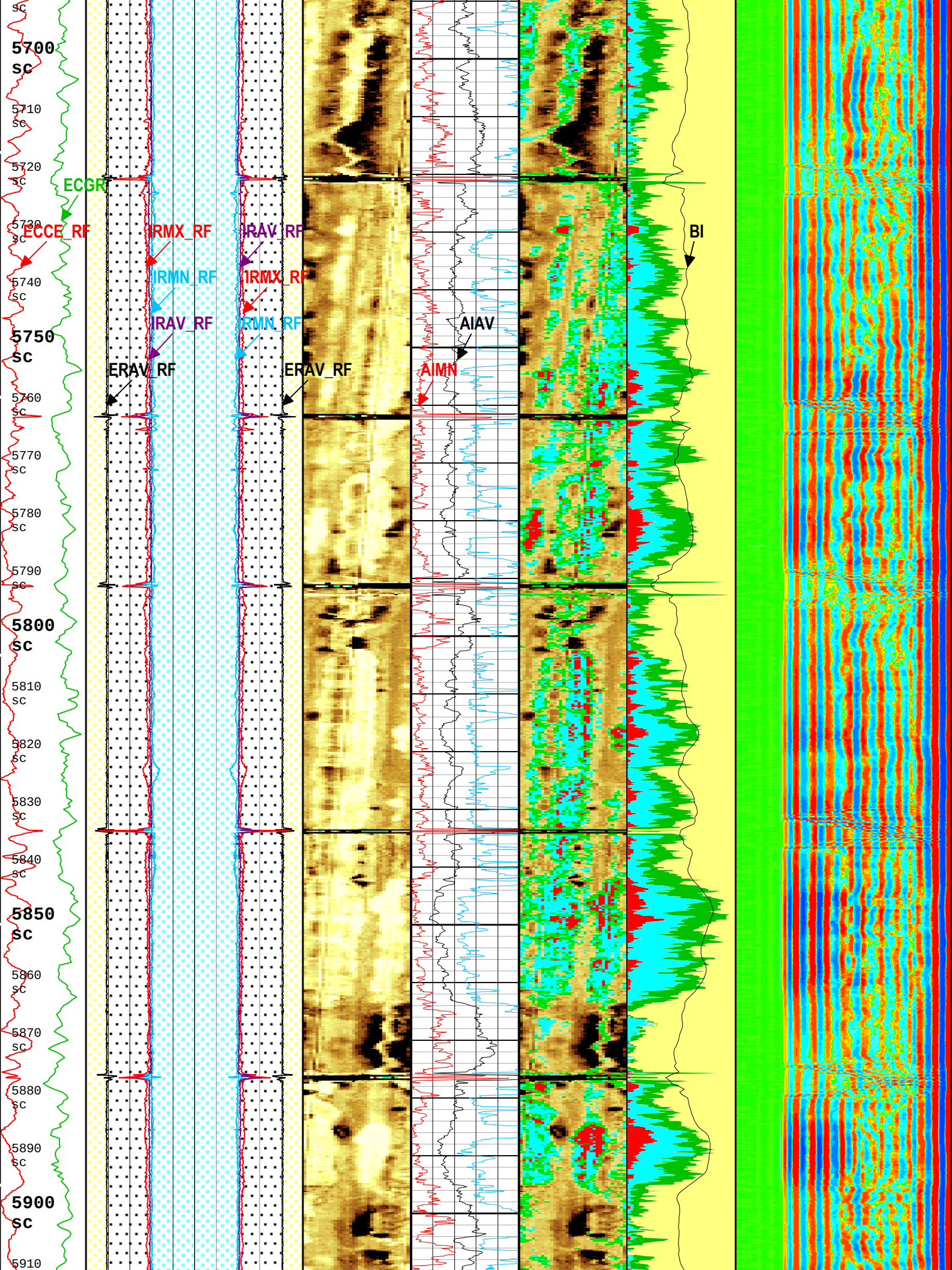
5700 SC
5710 SC
5720 SC
5730 SC
5740 SC
5750 SC
5760 SC
5770 SC
5780 SC
5790 SC
5800 SC
5810 SC
5820 SC
5830 SC
5840 SC
5850 SC
5860 SC
5870 SC
5880 SC
5890 SC
5900 SC
5910
ECGR
ECCE_RF
IRMX_RF
IRMN_RF
IRAV_RF
ERAV_RF
IRAV_RF
IRMX_RF
IRMN_RF
ERAV_RF
AIAV
AIMN
BI

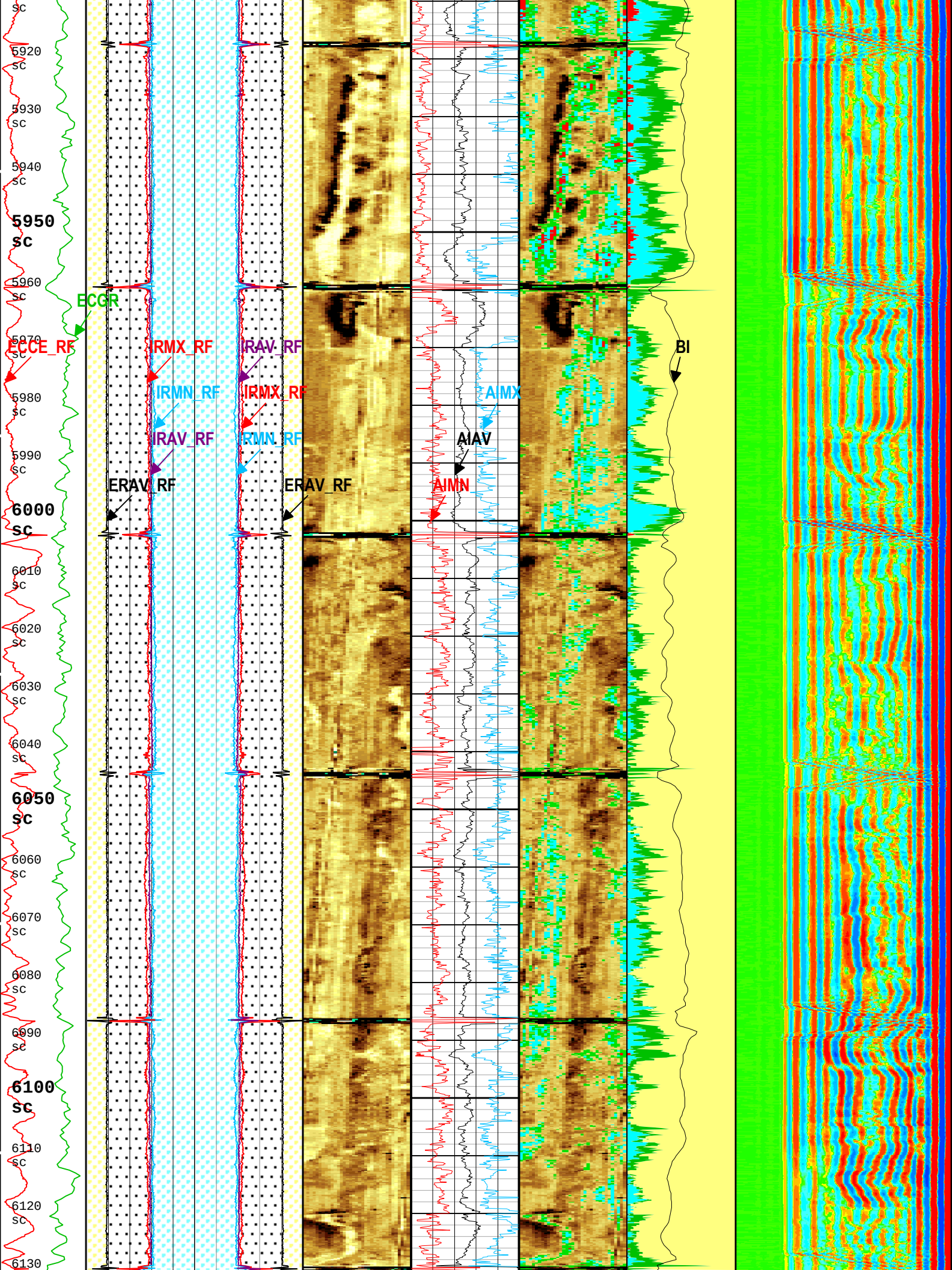
5920 sc
5930 sc
5940 sc
5950 sc
5960 sc
5970 sc
5980 sc
5990 sc
6000 sc
6010 sc
6020 sc
6030 sc
6040 sc
6050 sc
6060 sc
6070 sc
6080 sc
6090 sc
6100 sc
6110 sc
6120 sc
6130
ECGR
ECCE_RF
IRMX_RF
IRMN_RF
IRAV_RF
ERAV_RF
IRAV_RF
IRMX_RF
IRMN_RF
ERAV_RF
AIMX
AIAV
AIMN
BI

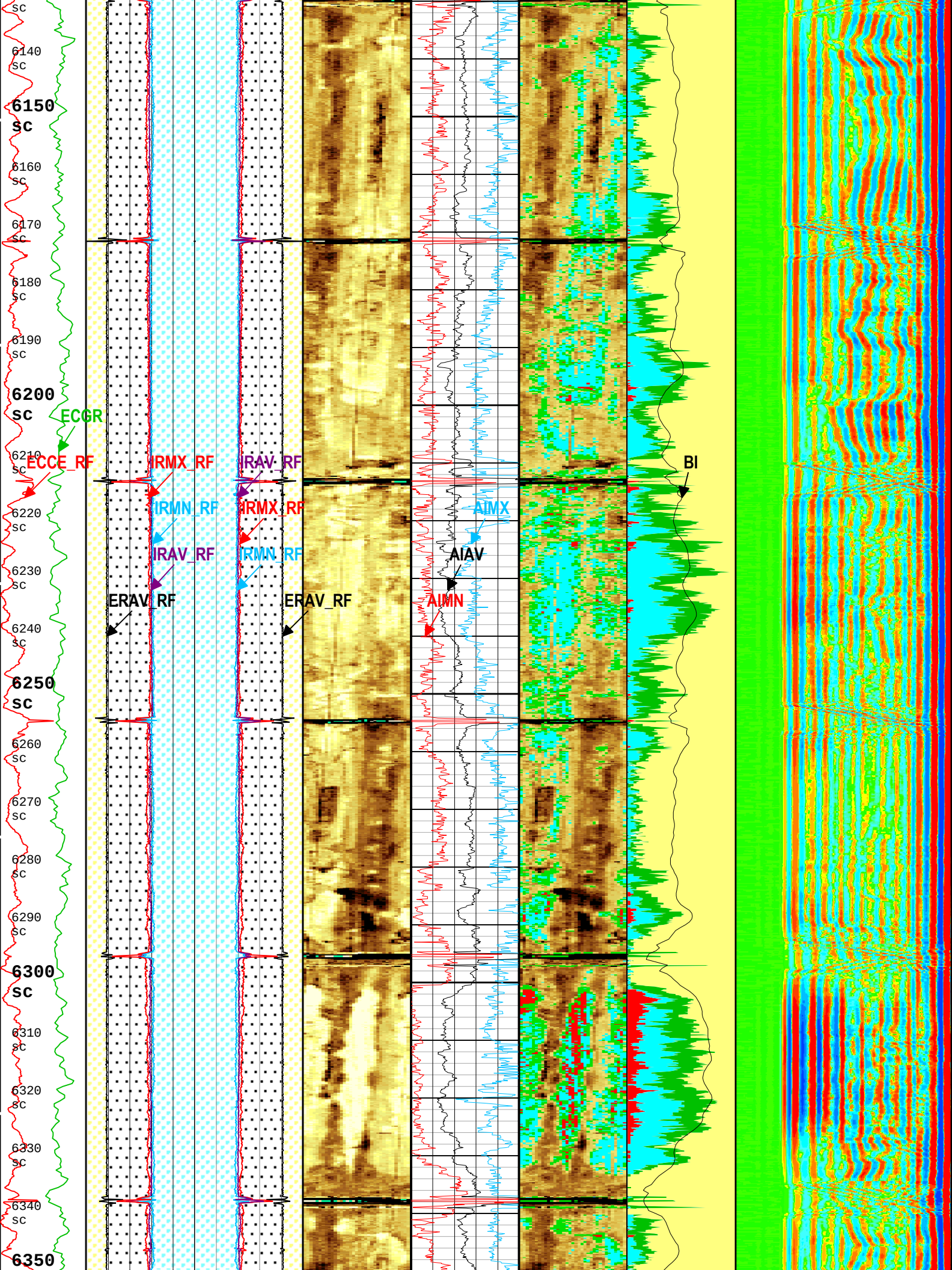
6140 sc
6150 sc
6160 sc
6170 sc
6180 sc
6190 sc
6200 sc
ECGR
6210 sc
ECCE_RF
IRMX_RF
IRAV_RF
BI
6220 sc
IRMN_RF
IRMX_RF
AIMX
6230 sc
IRAV_RF
IRMN_RF
AIAV
ERAV_RF
ERAV_RF
AIMN
6240 sc
6250 sc
6260 sc
6270 sc
6280 sc
6290 sc
6300 sc
6310 sc
6320 sc
6330 sc
6340 sc
6350

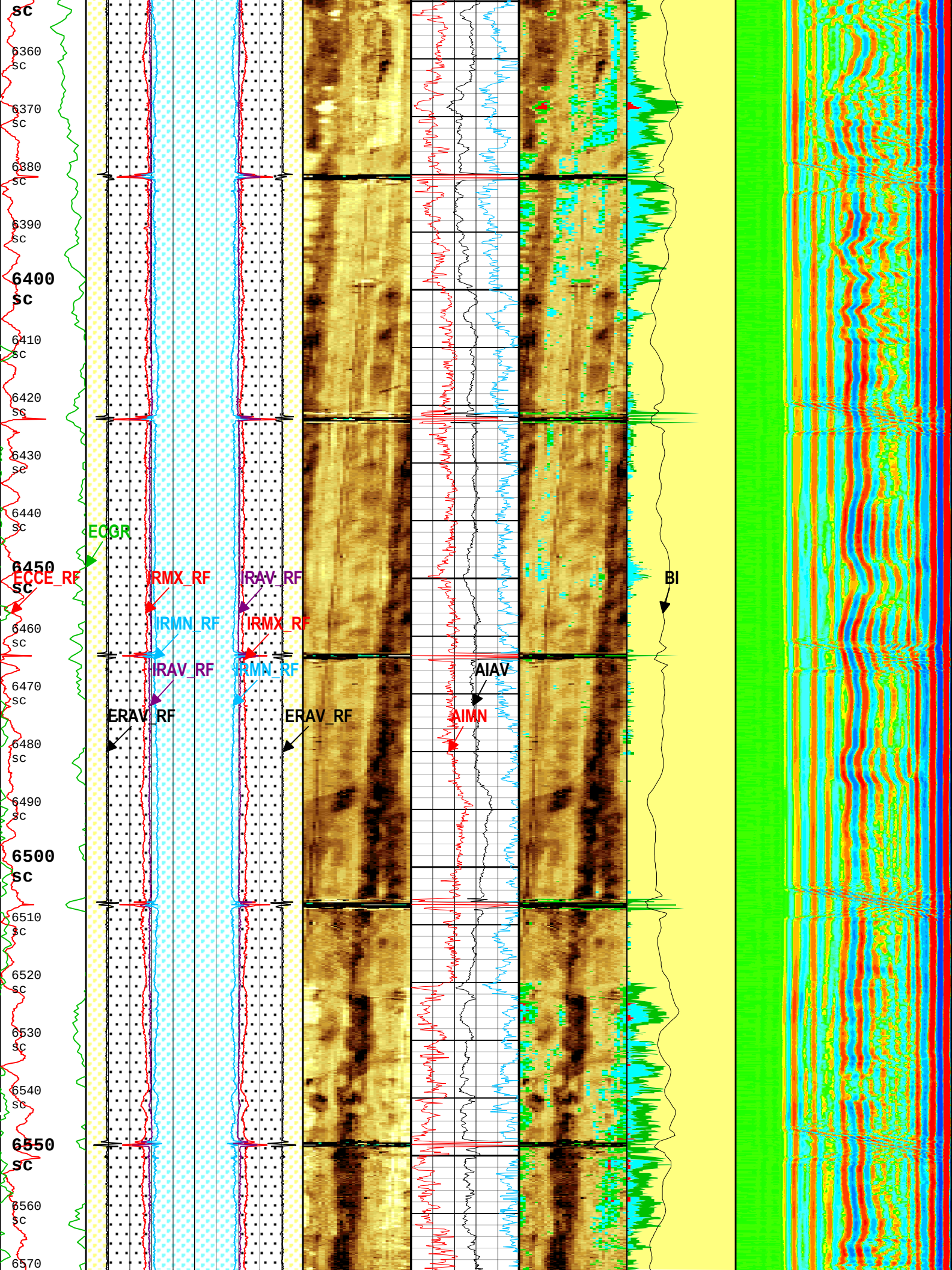
6360
6370
6380
6390
6400
6410
6420
6430
6440
6450
6460
6470
6480
6490
6500
6510
6520
6530
6540
6550
6560
6570
ECGR
ECCE_RF
IRMX_RF
IRAV_RF
IRMN_RF
IRMX_RF
IRAV_RF
IRMN_RF
ERAV_RF
ERAV_RF
AIAV
AIMN
BI

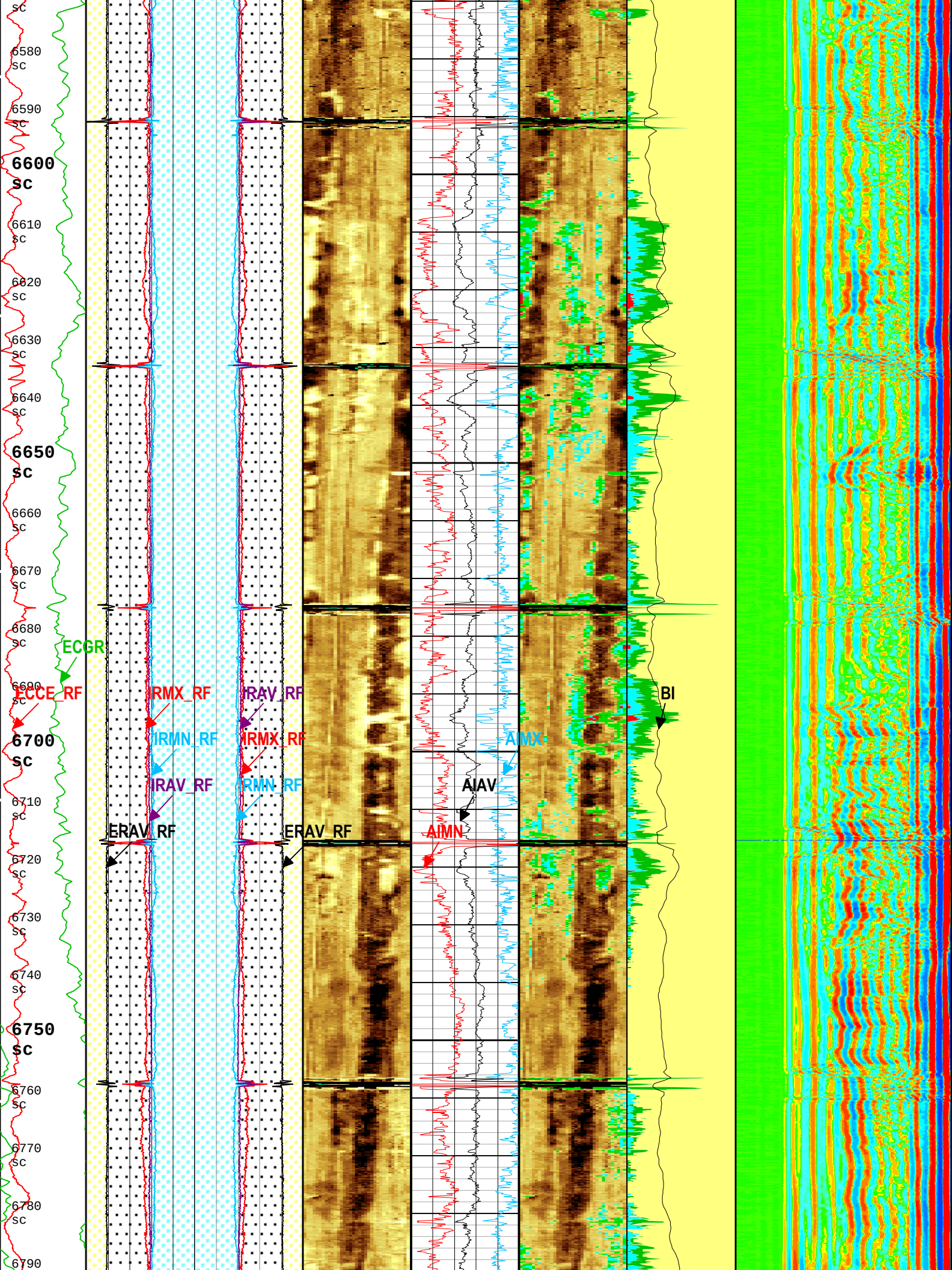
6580 sc
6590 sc
6600 sc
6610 sc
6620 sc
6630 sc
6640 sc
6650 sc
6660 sc
6670 sc
6680 sc
6690 sc
6700 sc
6710 sc
6720 sc
6730 sc
6740 sc
6750 sc
6760 sc
6770 sc
6780 sc
6790
ECGR
ECCE_RF
RMX_RF
IRAV_RF
IRMN_RF
IRMX_RF
IRAV_RF
IRMN_RF
ERAV_RF
ERAV_RF
AIAV
AIMN
BI

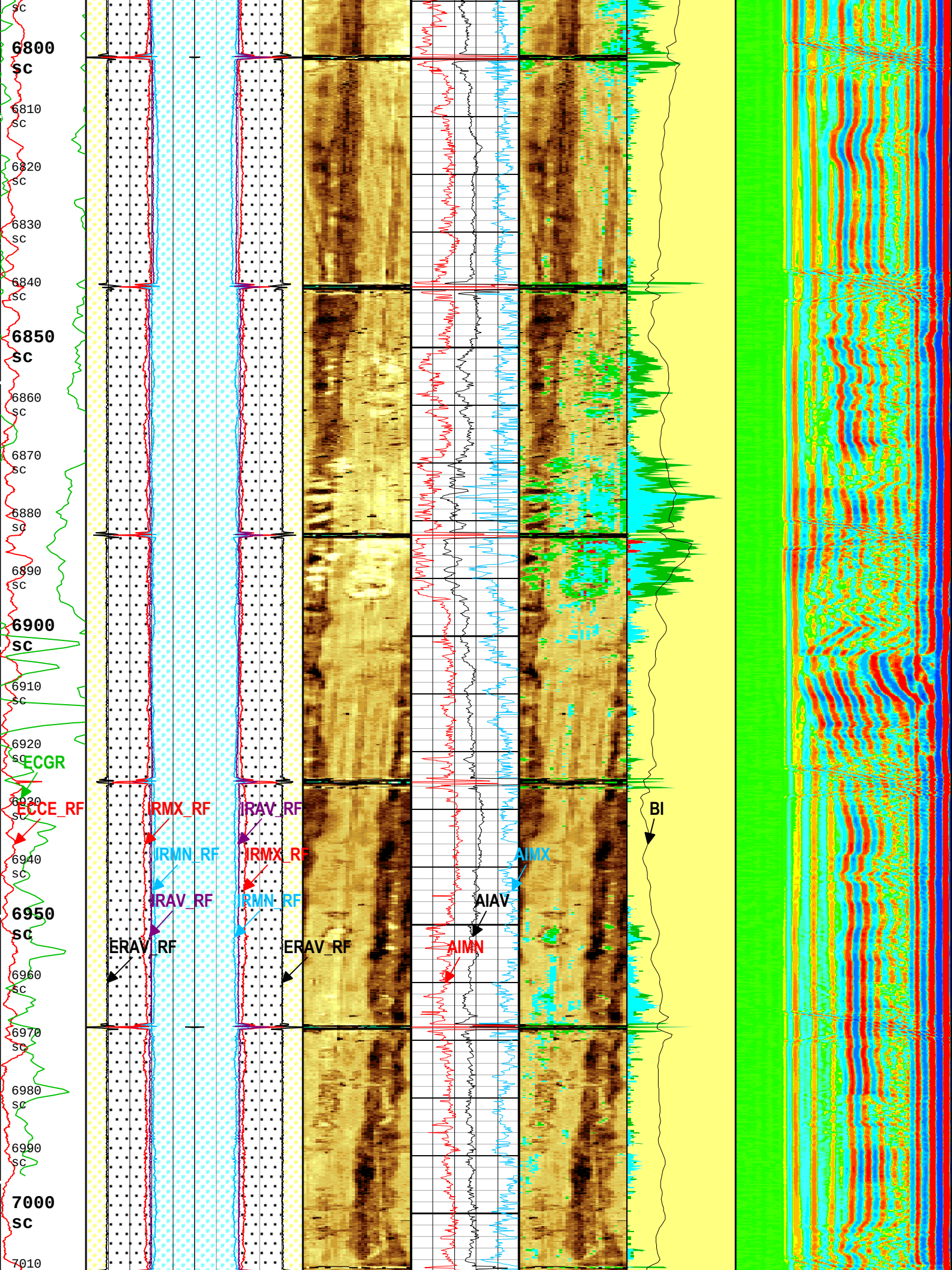
6800 sc
6810 sc
6820 sc
6830 sc
6840 sc
6850 sc
6860 sc
6870 sc
6880 sc
6890 sc
6900 sc
6910 sc
6920 sc
ECGR
6930 sc
ECCE_RF
IRMX_RF
IRAV_RF
BI
6940 sc
IRMN_RF
IRMX_RF
AIMX
IRAV_RF
IRMN_RF
AIAV
6950 sc
ERAV_RF
ERAV_RF
AIMN
6960 sc
6970 sc
6980 sc
6990 sc
7000 sc
7010

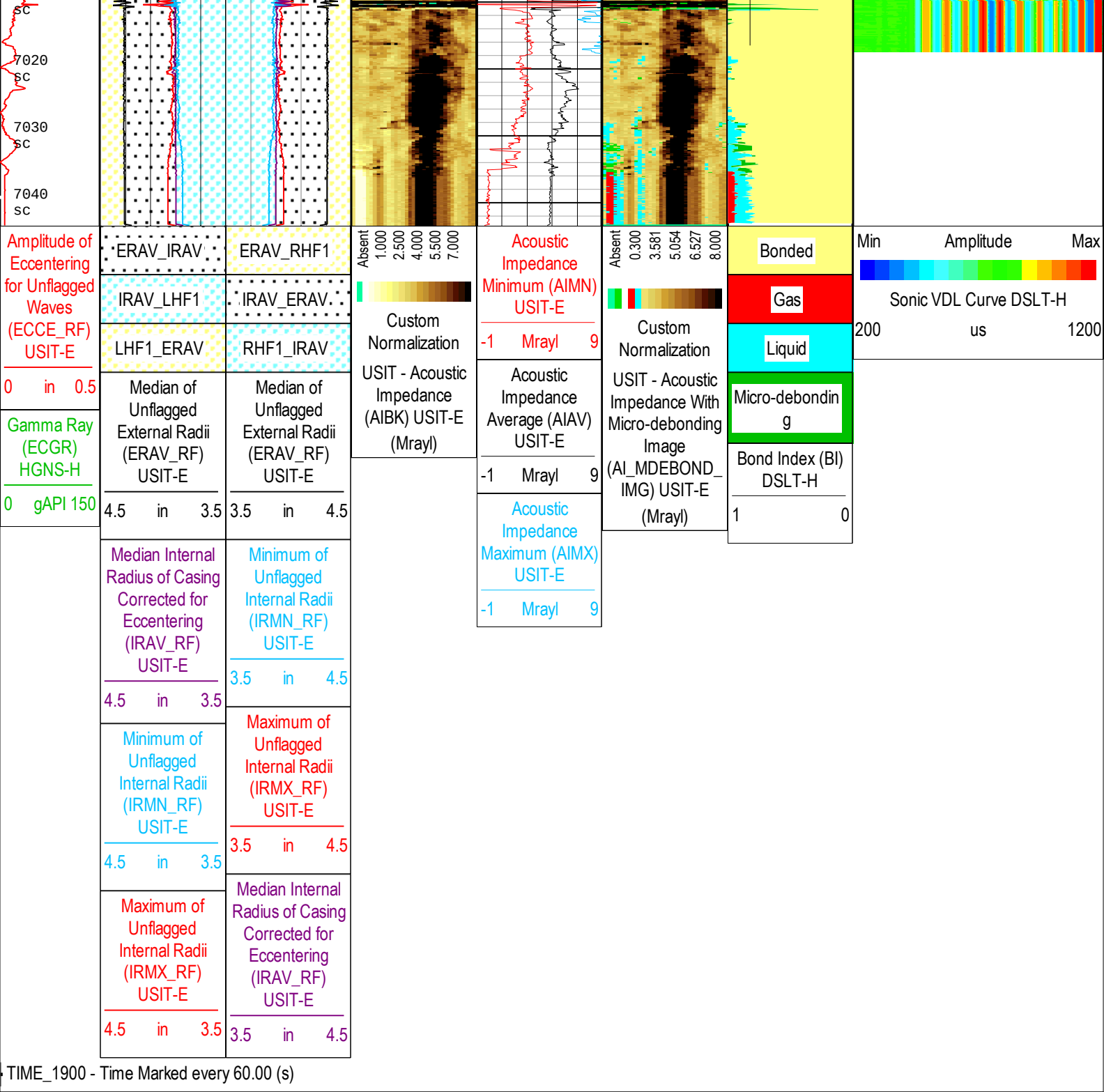

Description: USI VDL Cement Format: Log (LBV1_USI-VDL (DSLT) Cement 7inch) Index Scale: 5 in per 100 ft Index Unit: ft Index Type: Measured Depth
Creation Date: 17-Jul-2017 14:11:00

Channel Processing Parameters

One: Parameters

Parameter	Description	Tool	Value	Unit
AMSG	Auxiliary Minimum Sliding Gate	DSLT-H	140	us
ISSBAR	Barite Mud Presence Flag	Borehole	No	
BERJ	Bad Echo Rejection	USIT-E	On	
BHS	Borehole Status (Open or Cased Hole)	Borehole	Cased	
BILI	Bond Index Level for Zone Isolation	DSLT-H	0.8	
BS	Bit Size	WLSESSION	Depth Zoned	in
CASING_PRATIO	Casing Poisson Ratio	USIT-E	Standard Poisson Ratio	
CBLG	CBL Gate Width	DSLT-H	45	us

CBLG	CBL Gate Width	DSLT-H	45	us
CBLO	Casing Bottom (Logger)	WLSESSION	7331	ft
CBRA	CBL LQC Reference Amplitude in Free Pipe	DSLT-H	55	mV
CDEN	Cement Density	HGNS-H	2.65	g/cm3
CMCF	CBL Cement Type Compensation Factor	DSLT-H	1	
CMTY(U-USIT_CEMT)	Cement Type	USIT-E	Regular Cement	
THNO	Nominal Casing Thickness - Zoned along logger depths	WLSESSION	0.4	in
DETE	Delta-T Detection	DSLT-H	E1	
DFD	Drilling Fluid Density	Borehole	8.9	lbm/gal
DFT_CATEGORY	Drilling Fluid Type	Borehole	Water	
DTMD	Borehole Fluid Slowness	Borehole	193	us/ft
FCF	CBL Fluid Compensation Factor	DSLT-H	0.89	
FDII	FPM Data Interpolation Interval	USIT-E	0	ft
GCSE_DOWN_PASS	Generalized Caliper Selection for WL Log Down Passes	Borehole	BS	
GCSE_UP_PASS	Generalized Caliper Selection for WL Log Up Passes	Borehole	BS	
GOBO_CURR	Good Bond in Arbitrary Cement	DSLT-H	3.39	mV
GR_MULTIPLIER	Gamma Ray Multiplier	HGNS-H	1	
HEMA	Hematite Presence Flag	Borehole	No	
ICE_PROCESS	ICE Processing	USIT-E	Yes	
IMAR	Image Rotation	USIT-E	Off	
MAHTR	Manual High Threshold Reference for first arrival detection	DSLT-H	120	
MATT_CURR	Maximum Attenuation in Arbitrary Cement	DSLT-H	10.78	dB/ft
MCI	Minimum Cemented Interval for Isolation	DSLT-H	Depth Zoned	ft
MEAS_WLEN	Tcube Processing Window Length in Measurement Mode	USIT-E	24.96	us
MNHTR	Minimum High Threshold Reference for first arrival detection	DSLT-H	100	
MSA	Minimum Sonic Amplitude	DSLT-H	1.69	mV
MSA_CURR	Minimum Sonic Amplitude in Arbitrary Cement	DSLT-H	1.69	mV
MUD_N_FRP	Free Pipe Mud Normalization Factor	USIT-E	1.06	
MUD_N_THE	Theoretical Mud Normalization Factor	USIT-E	1	
NMSG	Near Minimum Sliding Gate	DSLT-H	310	us
NMXG	Near Maximum Sliding Gate	DSLT-H	950	us
NUMP	Number of Detection Passes	DSLT-H	2	
OPLEV	USIT Remove Flagged Data Level	USIT-E	OPT2	
RCOD	Reference Calibrator Outer Diameter	USIT-E	7	in
RCSO	Reference Calibrator Standoff	USIT-E	1.181	in
RCTH	Reference Calibrator Thickness	USIT-E	0.295	in
SDNV	Number of Vertical Samples used for Micro-debonding Computation	USIT-E	5	
SDTHOR	Acoustic Impedance STD Horizontal Threshold for Micro-debonding	USIT-E	0.5	Mrayl
SDTVER	Acoustic Impedance STD Vertical Threshold for Micro-debonding	USIT-E	0.3	Mrayl
SFAF	Sonic Formation Attenuation Factor	DSLT-H	3.25	dB/ft
SGAD	Sliding Gate Status	DSLT-H	Off	
SGCL	Sliding Gate Closing Delta-T	DSLT-H	130	us/ft
SGCW	Sliding Gate Closing Width	DSLT-H	25	us
SGDT	Sliding Gate Delta-T	DSLT-H	57	us/ft
SGW	Sliding Gate Width	DSLT-H	110	us
SLEV	Signal Level for AGC	DSLT-H	5000	mV
SOCN	Standoff Distance	HGNS-H	0.125	in
SOCO	Standoff Correction Option	HGNS-H	No	
TCUB	T^3 Processing Level	USIT-E	Loop	
THDH	Maximum Search Thickness (percentage of nominal)	USIT-E	130	%

THDL	Minimum Search Thickness (percentage of nominal)	USIT-E	65	%
HISC	Tool Position: Centered or Eccentered	HGNS-H	Centered	
U-USIT_DFSZ	Drilling Fluid Specific Acoustic Impedance	USIT-E	0	Mrayl
UFGDE	Fiberglass Density	USIT-E	1.95	g/cm3
UFGPS	Fiberglass Processing Selection	USIT-E	No	
UFGVL	Fiberglass Velocity	USIT-E	9678.48	ft/s
USI_FSOD	USIT USI Fluid Slowness Fits Casing Outer Diameter	USIT-E	0_OFF	
USI_FVEL_SEL	USI Fluid Velocity Selection	USIT-E	Automatic	
USI_ZMUD_SEL	USI Mud Impedance Selection	USIT-E	FreePipe Norm.	
THDP	Thickness Detection Policy	USIT-E	Fundamental	
VCAS	Ultrasonic Transversal Velocity in Casing	USIT-E	51.4	us/ft
VDLG	VDL Manual Gain	DSLT-H	5	
ZCAS	Acoustic Impedance of Casing	USIT-E	46.25	Mrayl
ZCMT	Acoustic Impedance of Cement	DSLT-H	6.8	Mrayl
ZCMT_NEAT	Acoustic Impedance of Cement in Neat Cement	DSLT-H	6.8	Mrayl
ZINI	Initial Estimate of Cement Impedance	USIT-E	-1	Mrayl
ZMUD	Acoustic Impedance of Mud	Borehole	1.68	Mrayl
ZTCM	Acoustic Impedance Threshold for Cement	USIT-E	2.6	Mrayl
ZTGS	Acoustic Impedance Threshold for Gas	USIT-E	0.3	Mrayl

Depth Zone Parameters

Parameter	Value	Start (ft)	Stop (ft)
BS	17.5	10	832
BS	11	832	7043.5
MCI	21.68	10	830
MCI	12.98	830	7043.5

All depth are actual.

Tool Control Parameters

One: Parameters

Parameter	Description	Tool	Value	Unit
AGMN	Minimum Gain of Cartridge	USIT-E	-12	dB
AGMX	Maximum Gain of Cartridge	USIT-E	48	dB
DDEL	Digitizing Delay	DSLT-H	0	us
U-USIT_DDT5	USIC Downhole Decimation for T5 only	USIT-E	0_NONE	
DOT(DOS)	Distance between Opposite Transducer Faces	USIT-E	2.874	in
MODE	DSLT Acquisition Mode	DSLT-H	CBL	
RATE	DSLT Firing Rate	DSLT-H	15 Hz	
DTFS	DSLT Telemetry Frame Size	DSLT-H	536	
DWCO	Digitizer Word Count	DSLT-H	250	
EMXV	EMEX Voltage	USIT-E	80	V
HRES	Horizontal Resolution	USIT-E	10 deg	
MOTOR_PROTECT	Motor Protection	USIT-E	On	
SDTH	Switch Down Threshold	DSLT-H	20000	
SGAI	Selectable Acquisition Gain	DSLT-H	x1	
SUTH	Switch Up Threshold	DSLT-H	1000	
TMUC	Type of Mud	USIT-E	BRI	
UACLV_PERM	Ultrasonic ACLV Permanent	USIT-E	No	
ULOG	Logging Objective	USIT-E	MEASUREMENT	
UMFR	Modulation Frequency	USIT-E	333333	Hz
USFR	Ultrasonic Sampling Frequency	USIT-E	500000	Hz

USFR	Ultrasonic Sampling Frequency	USIT-E	500000	Hz
UPAT	USIT Emission Pattern	USIT-E	Pattern 500 KHz	
UWKM	USIT Working Mode	USIT-E	Uncompressed 10 deg at 1.5 in LF	
USIT_DEPTHLOG	Starting Depth Log for Ultrasonics	USIT-E	7030	ft
USSP	Ultrasonic Service	USIT-E	USI	
VRES	Vertical Resolution	USIT-E	1.5 in	
WINB	Window Begin Time	USIT-E	59.63	us
WINE	Window End Time	USIT-E	99.63	us
WMOD	Waveform Firing Mode	DSLT-H	Full	

One

USIT Composite 5" = 100'

Software Version

Acquisition System	Version
Maxwell 2017 SP1	7.1.82245.3100

Pass Summary

Run Name	Pass Objective	Direction	Top	Bottom	Start	Stop	DSC Mode	Depth Shift	Include Parallel Data
One	Log[4]:Up	Up	4.12 ft	7044.38 ft	02-Jun-2017 1:27:12 AM	02-Jun-2017 4:20:07 AM	ON	4.20 ft	Yes

All depths are referenced to toolstring zero

Log

Company:Southern California Gas Company Well:Fernando Fee 35B

One: Log[4]:Up:S011

Description: USI Composite Format: Log (USI Composite_7inch) Index Scale: 5 in per 100 ft Index Unit: ft Index Type: Measured Depth Creation Date: 17-Jul-2017 14:11:12

USIT Processing Flags (UFLG[0]) USIT-E

1 - UFLG 1 Value within [0.0 - 1.5] - :
2 - UFLG 2 Value within [1.5 - 2.44] - :
3 - UFLG 2 Value within [2.44 - 2.5] - :
4 - UFLG 3 Value within [2.5 - 3.5] - :
5 - UFLG 4 UFLG 5 UFLG 6 Value within [3.5 - 6.5] - :
6 - UFLG 7 UFLG 8 UFLG 9 Value within [6.5 - 10] - :

- UTIM Error
- Pulse Origin Not Detected
- Spiky Waveform
- WINLEN Error
- Casing Thickness Error
- Loop Processing Error

TIME_1900 - Time Marked every 60.00 (s)

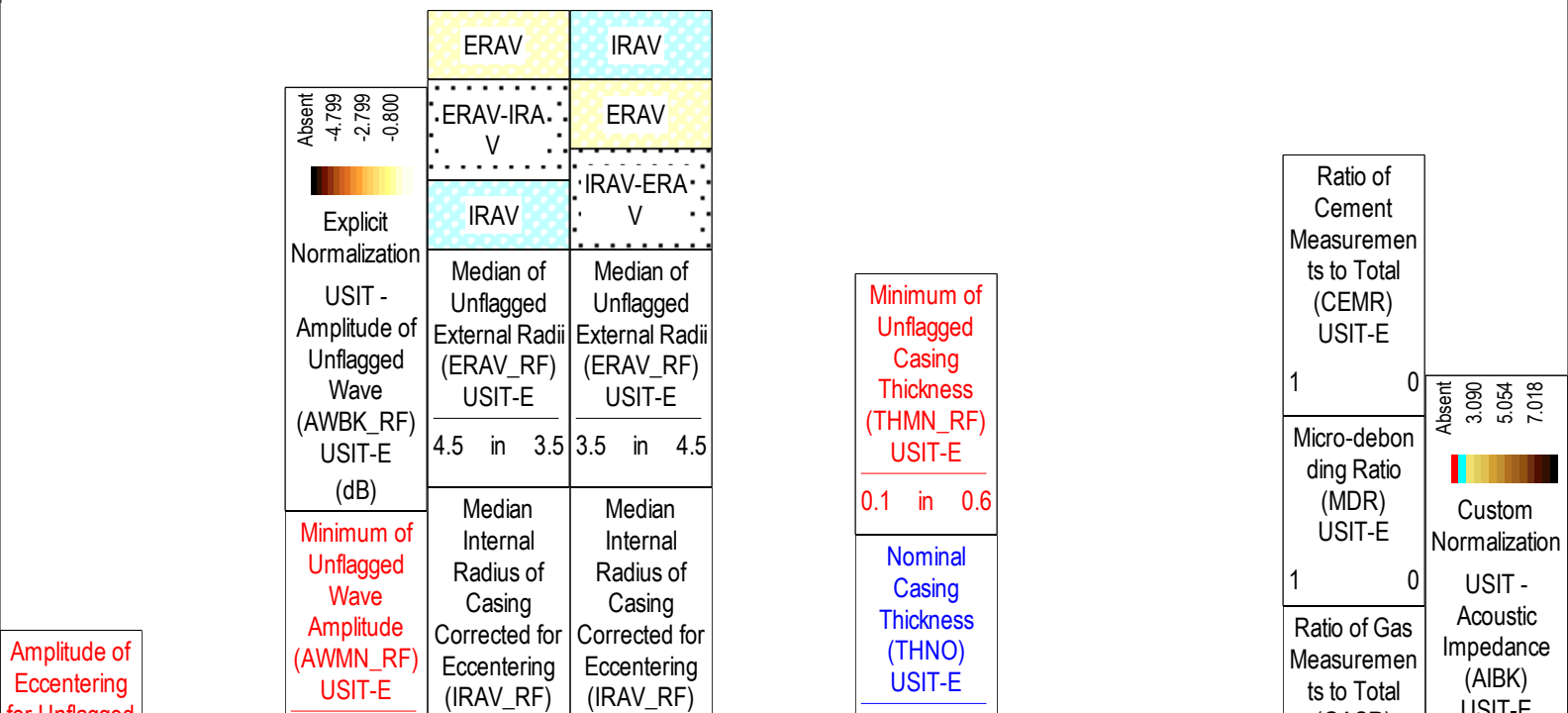

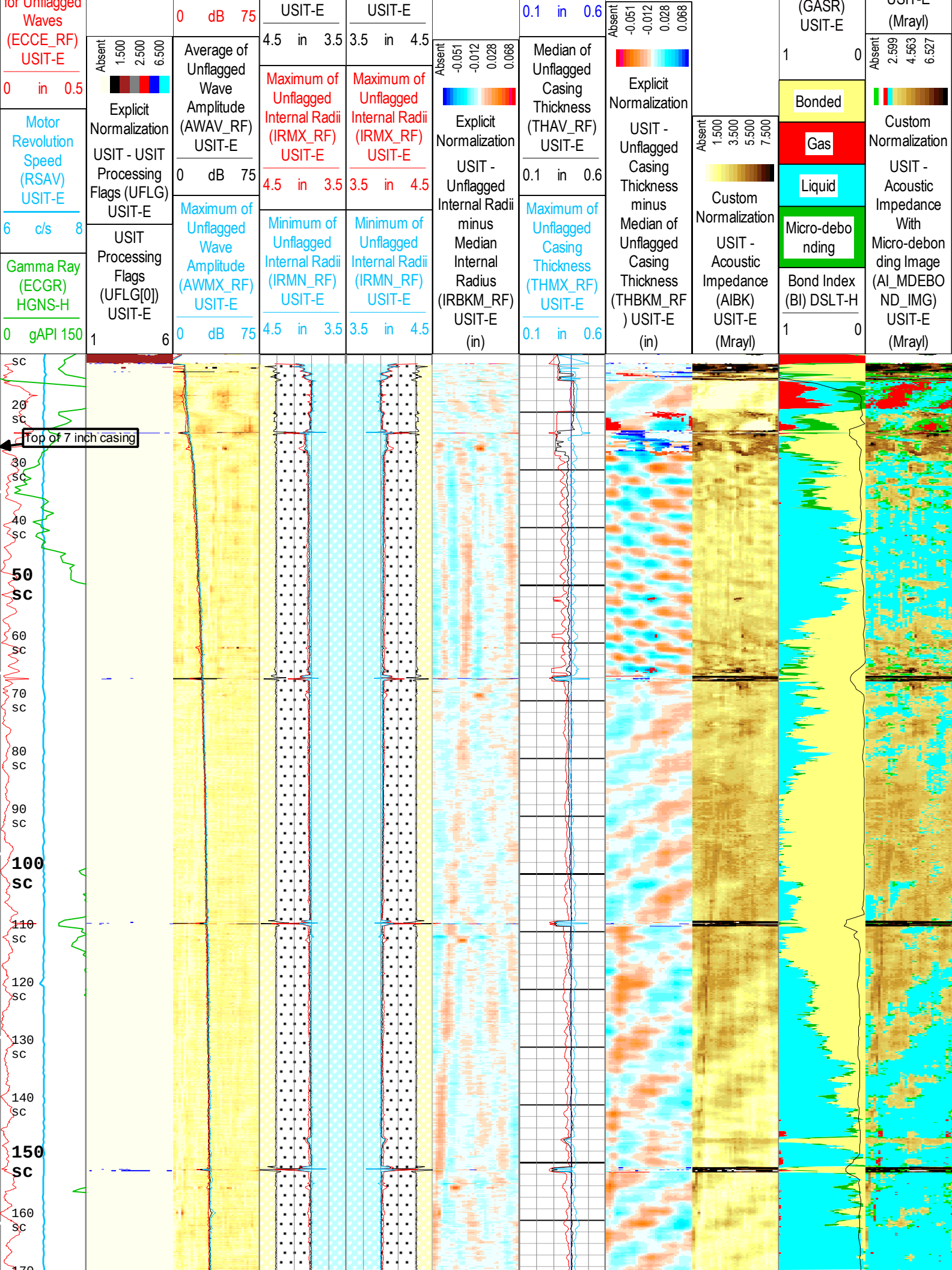
for Unflagged Waves (ECCE_RF) USIT-E
0 in 0.5
Motor Revolution Speed (RSAV) USIT-E
6 c/s 8
Gamma Ray (ECGR) HGNS-H
0 gAPI 150
Absent 1.500 2.500 6.500
Explicit Normalization
USIT - USIT Processing Flags (UFLG) USIT-E
USIT Processing Flags (UFLG[0]) USIT-E
1 6
0 dB 75
Average of Unflagged Wave Amplitude (AWAV_RF) USIT-E
0 dB 75
Maximum of Unflagged Wave Amplitude (AWMX_RF) USIT-E
0 dB 75
USIT-E
4.5 in 3.5
Maximum of Unflagged Internal Radii (IRMX_RF) USIT-E
4.5 in 3.5
Minimum of Unflagged Internal Radii (IRMN_RF) USIT-E
4.5 in 3.5
USIT-E
3.5 in 4.5
Maximum of Unflagged Internal Radii (IRMX_RF) USIT-E
3.5 in 4.5
Minimum of Unflagged Internal Radii (IRMN_RF) USIT-E
3.5 in 4.5
Absent -0.051 -0.012 0.028 0.068
Explicit Normalization
USIT - Unflagged Internal Radii minus Median Internal Radius (IRBKM_RF) USIT-E (in)
0.1 in 0.6
Median of Unflagged Casing Thickness (THAV_RF) USIT-E
0.1 in 0.6
Maximum of Unflagged Casing Thickness (THMX_RF) USIT-E
0.1 in 0.6
Absent -0.051 -0.012 0.028 0.068
Explicit Normalization
USIT - Unflagged Casing Thickness minus Median of Unflagged Casing Thickness (THBKM_RF) USIT-E (in)
Absent 1.500 3.500 5.500 7.500
Custom Normalization
USIT - Acoustic Impedance (AIBK) USIT-E (Mrayl)
(GASR) USIT-E
1 0
Bonded
Gas
Liquid
Micro-debonding
Bond Index (BI) DSLT-H
1 0
(Mrayl)
Absent 2.599 4.563 6.527
Custom Normalization
USIT - Acoustic Impedance With Micro-debonding Image (AI_MDEBOND_IMG) USIT-E (Mrayl)
Top of 7 inch casing
20 sc
30 sc
40 sc
50 sc
60 sc
70 sc
80 sc
90 sc
100 sc
110 sc
120 sc
130 sc
140 sc
150 sc
160 sc

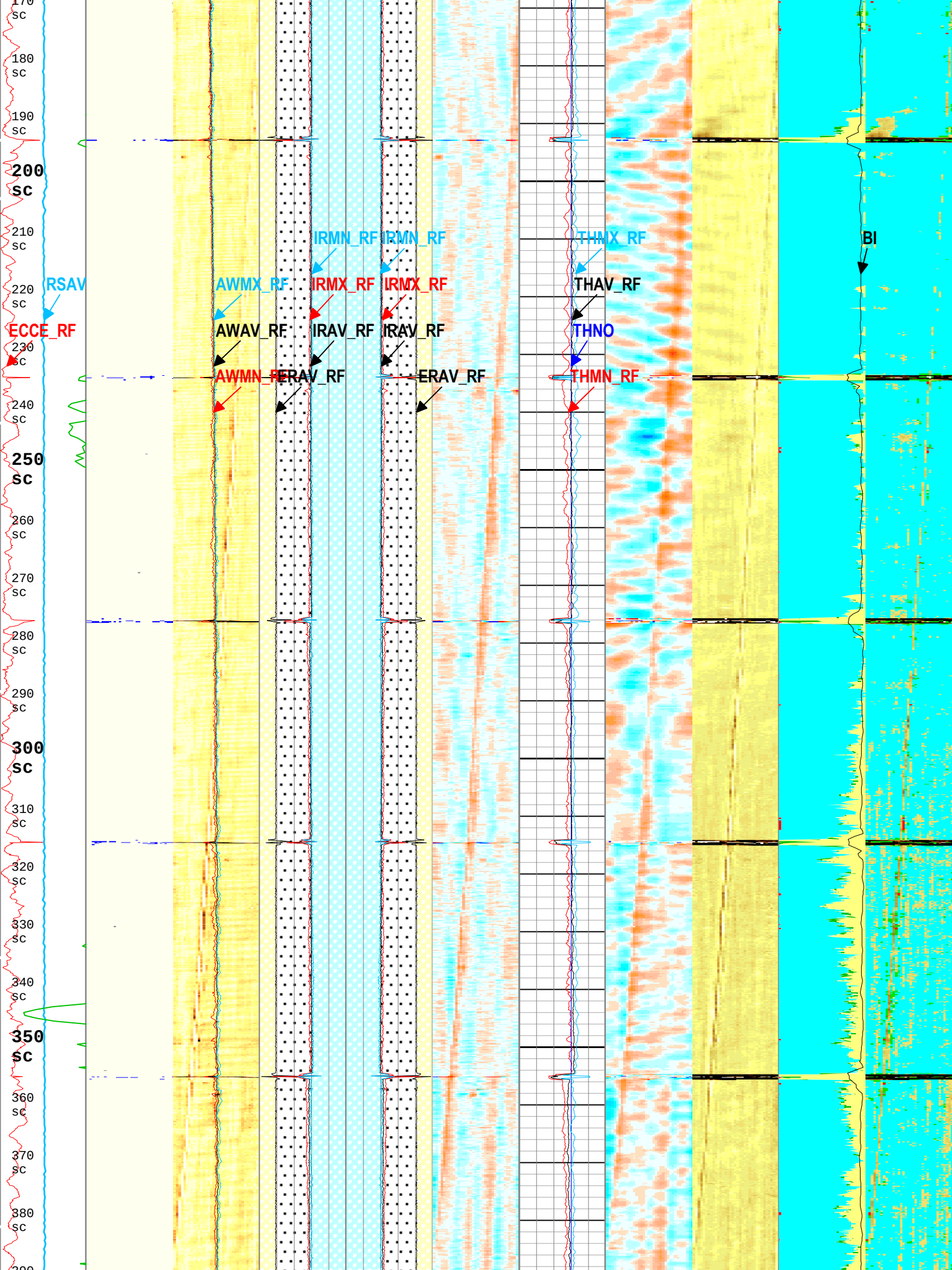
170 sc
180 sc
190 sc
200 sc
210 sc
220 sc
230 sc
240 sc
250 sc
260 sc
270 sc
280 sc
290 sc
300 sc
310 sc
320 sc
330 sc
340 sc
350 sc
360 sc
370 sc
380 sc
RSAV
ECCE_RF
AWMX_RF
AWAV_RF
AWMN_RF
IRMN_RF
IRMX_RF
IRAV_RF
ERAV_RF
IRMN_RF
IRMX_RF
IRAV_RF
ERAV_RF
THMX_RF
THAV_RF
THNO
THMN_RF
BI

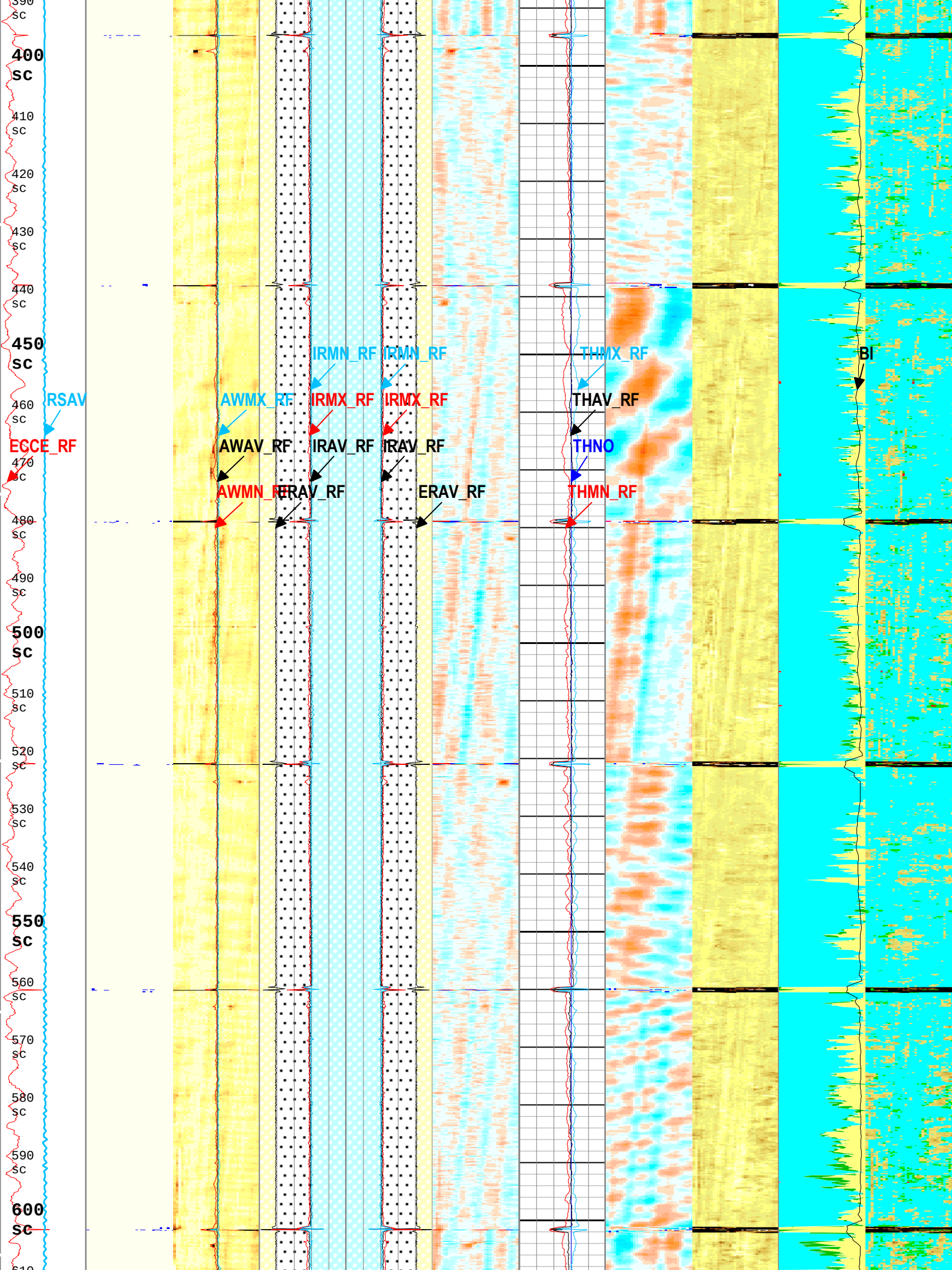
390 sc
400 sc
410 sc
420 sc
430 sc
440 sc
450 sc
460 sc
470 sc
480 sc
490 sc
500 sc
510 sc
520 sc
530 sc
540 sc
550 sc
560 sc
570 sc
580 sc
590 sc
600 sc
RSAV
ECCE_RF
AWMX_RF
AWAV_RF
AWMN_RF
IRMN_RF
IRMX_RF
IRAV_RF
ERAV_RF
IRMN_RF
IRMX_RF
IRAV_RF
ERAV_RF
THMX_RF
THAV_RF
THNO
THMN_RF
BI

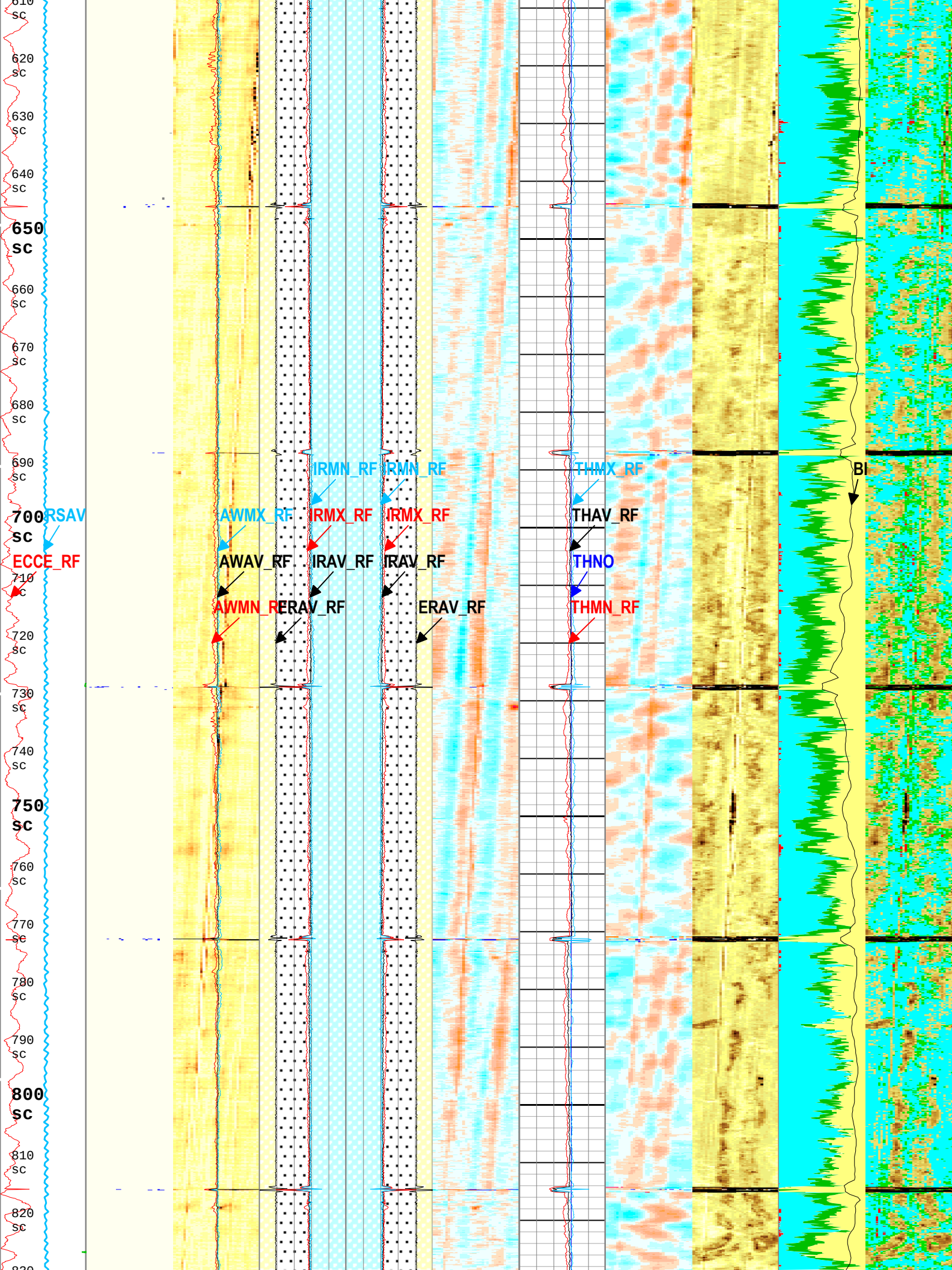
610 sc
620 sc
630 sc
640 sc
650 sc
660 sc
670 sc
680 sc
690 sc
700 sc
710 sc
720 sc
730 sc
740 sc
750 sc
760 sc
770 sc
780 sc
790 sc
800 sc
810 sc
820 sc
RSAV
ECCE_RF
AWMX_RF
AWAV_RF
AWMN_RF
IRMN_RF
IRMX_RF
IRAV_RF
ERAV_RF
IRMN_RF
IRMX_RF
IRAV_RF
ERAV_RF
THMX_RF
THAV_RF
THNO
THMN_RF
BI

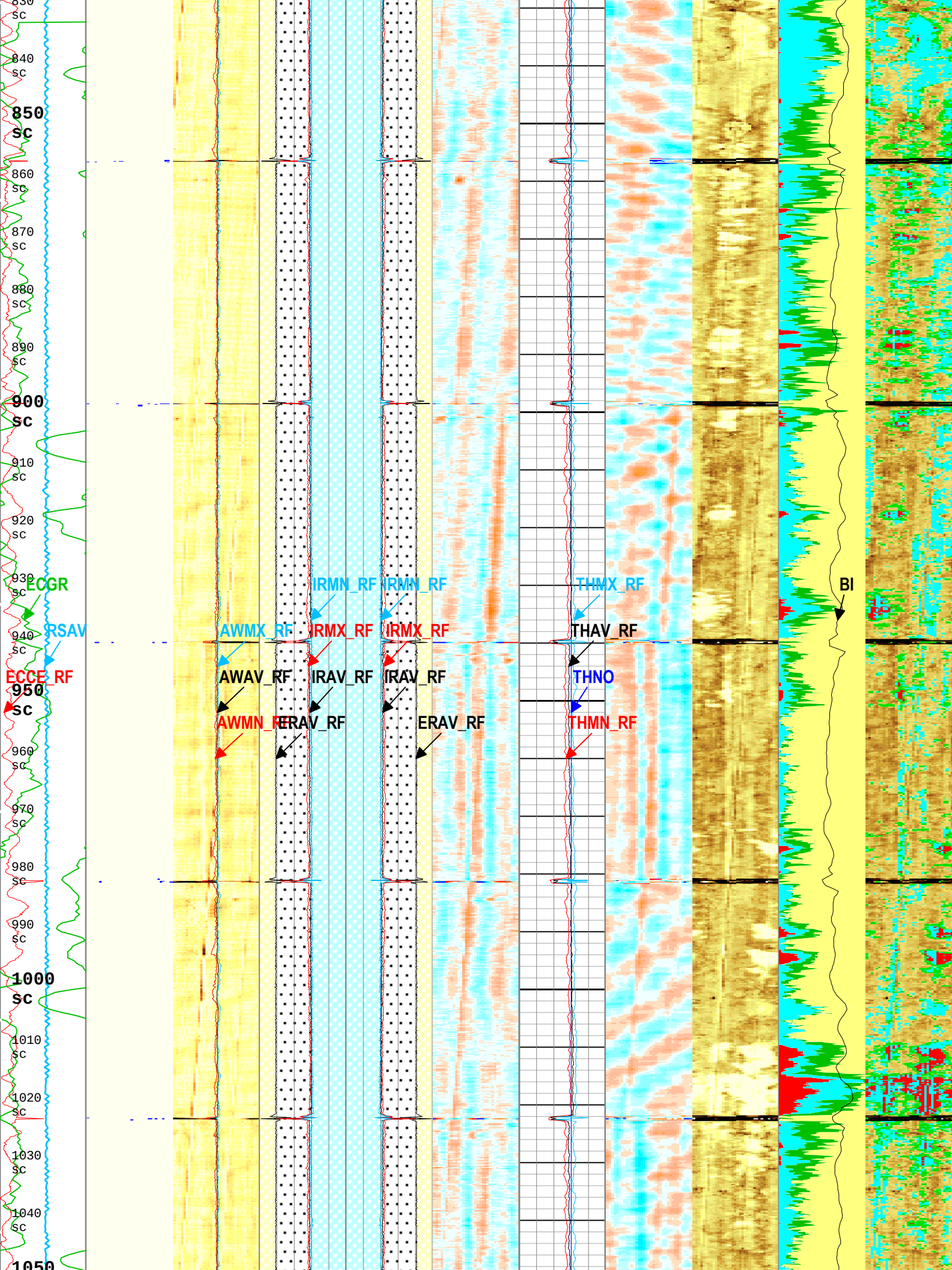
830 SC
840 SC
850 SC
860 SC
870 SC
880 SC
890 SC
900 SC
910 SC
920 SC
930 SC
940 SC
950 SC
960 SC
970 SC
980 SC
990 SC
1000 SC
1010 SC
1020 SC
1030 SC
1040 SC
1050
ECGR
RSAV
ECCE_RF
IRMN_RF
IRMN_RF
AWMX_RF
IRMX_RF
IRMX_RF
AWAV_RF
IRAV_RF
IRAV_RF
AWMN_RF
ERAV_RF
ERAV_RF
THMX_RF
THAV_RF
THNO
THMN_RF
BI

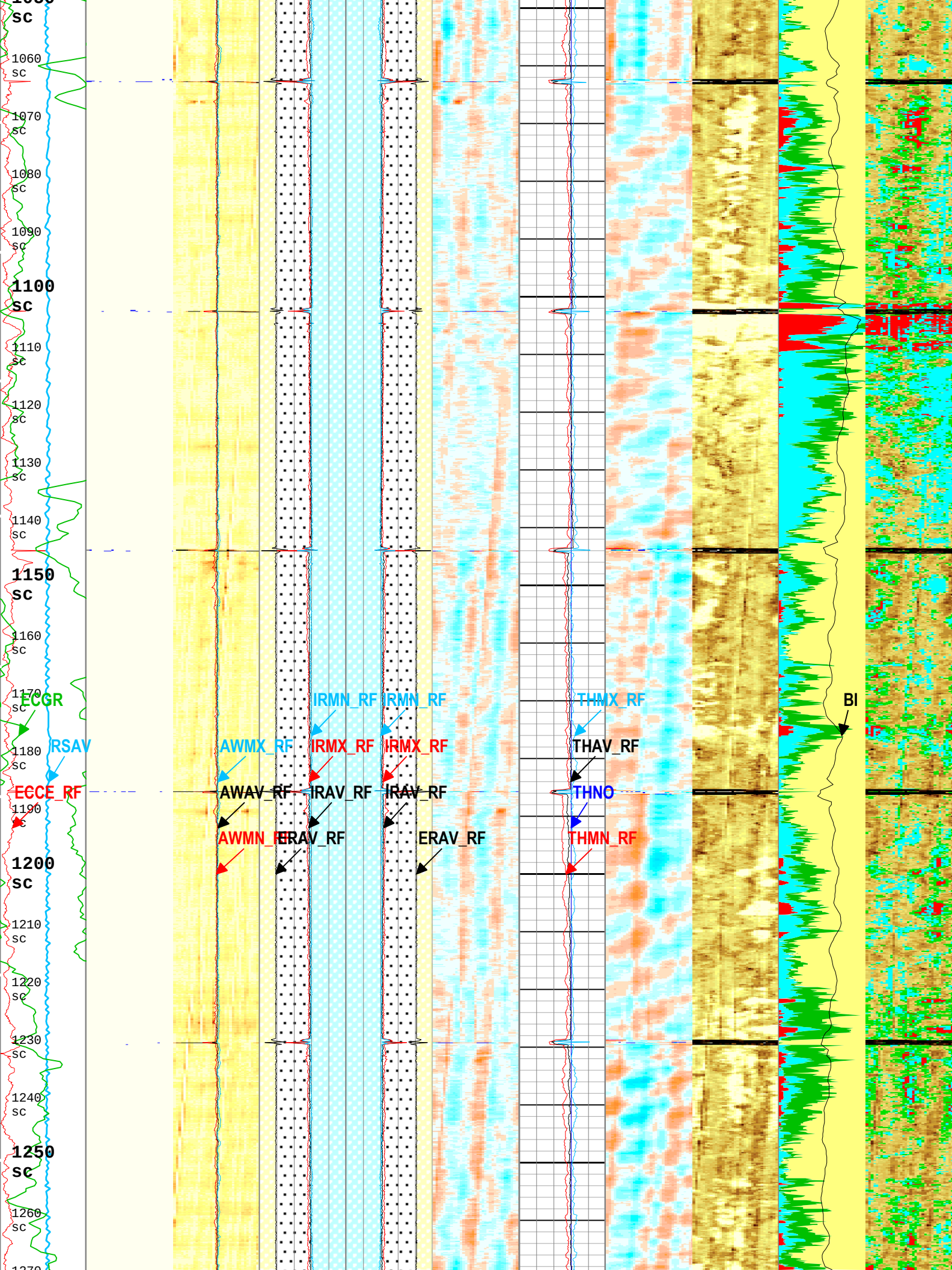
1060 sc
1070 sc
1080 sc
1090 sc
1100 sc
1110 sc
1120 sc
1130 sc
1140 sc
1150 sc
1160 sc
1170 sc
1180 sc
1190 sc
1200 sc
1210 sc
1220 sc
1230 sc
1240 sc
1250 sc
1260 sc
ECGR
RSAV
ECCE_RF
IRMN_RF
IRMN_RF
AWMX_RF
IRMX_RF
IRMX_RF
AWAV_RF
IRAV_RF
IRAV_RF
AWMN_RF
ERAV_RF
ERAV_RF
THMX_RF
THAV_RF
THNO
THMN_RF
BI

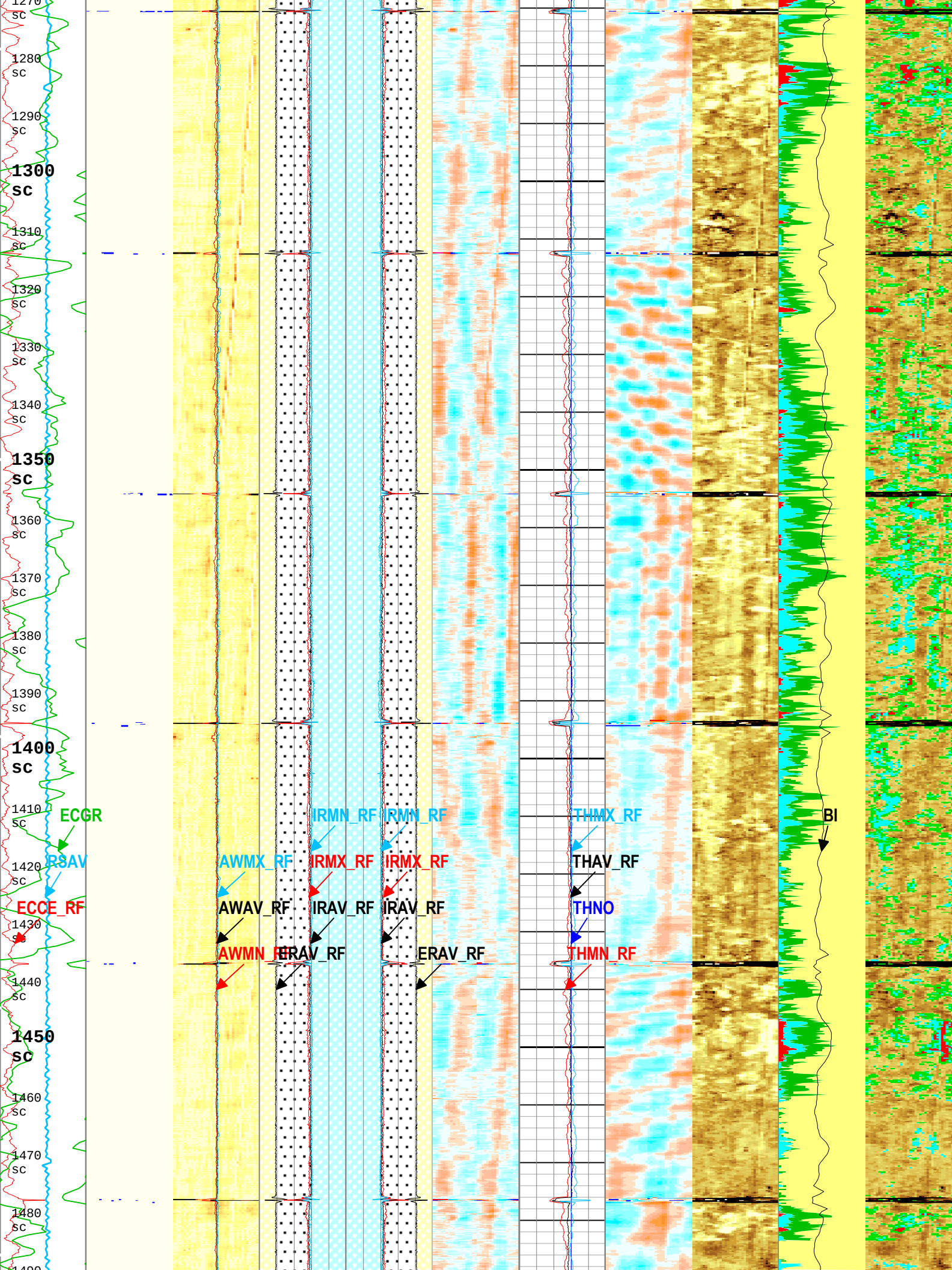
1270 sc
1280 sc
1290 sc
1300 sc
1310 sc
1320 sc
1330 sc
1340 sc
1350 sc
1360 sc
1370 sc
1380 sc
1390 sc
1400 sc
1410 sc
1420 sc
1430 sc
1440 sc
1450 sc
1460 sc
1470 sc
1480 sc
ECGR
RSAV
ECCE_RF
IRMN_RF
IRMN_RF
AWMX_RF
IRMX_RF
IRMX_RF
AWAV_RF
IRAV_RF
IRAV_RF
AWMN_RF
ERAV_RF
ERAV_RF
THMX_RF
THAV_RF
THNO
THMN_RF
BI

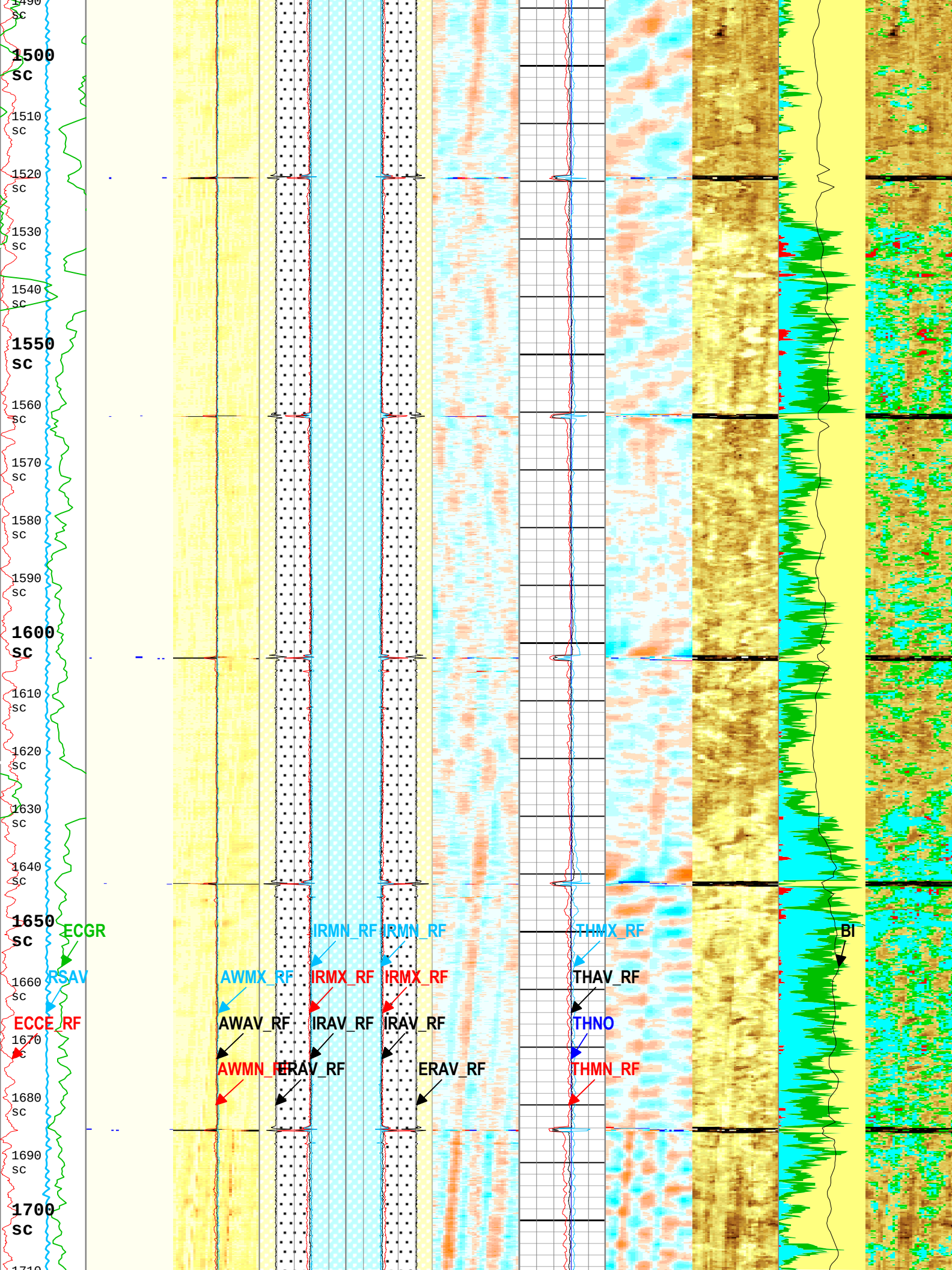
1500 sc
1510 sc
1520 sc
1530 sc
1540 sc
1550 sc
1560 sc
1570 sc
1580 sc
1590 sc
1600 sc
1610 sc
1620 sc
1630 sc
1640 sc
1650 sc
1660 sc
1670 sc
1680 sc
1690 sc
1700 sc
ECGR
RSAV
ECCE_RF
IRMN_RF
IRMN_RF
AWMX_RF
IRMX_RF
IRMX_RF
AWAV_RF
IRAV_RF
IRAV_RF
AWMN_RF
ERAV_RF
ERAV_RF
THMX_RF
THAV_RF
THNO
THMN_RF
BI

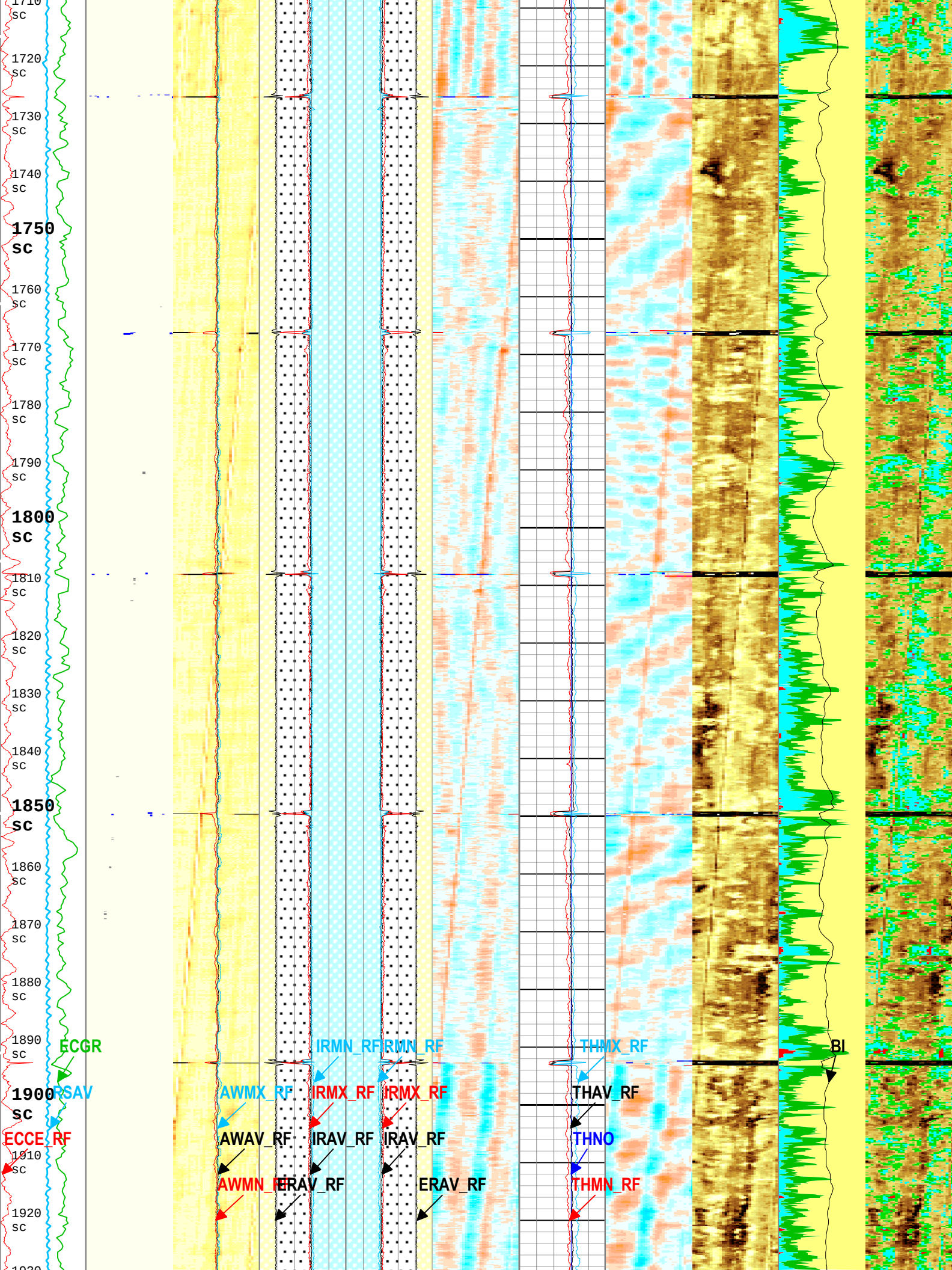
1710 sc
1720 sc
1730 sc
1740 sc
1750 sc
1760 sc
1770 sc
1780 sc
1790 sc
1800 sc
1810 sc
1820 sc
1830 sc
1840 sc
1850 sc
1860 sc
1870 sc
1880 sc
1890 sc
1900 sc
1910 sc
1920 sc
ECGR
RSAV
ECCE_RF
AWMX_RF
AWAV_RF
AWMN_RF
IRMN_RF
IRMX_RF
IRAV_RF
ERAV_RF
IRMN_RF
IRMX_RF
IRAV_RF
ERAV_RF
THMX_RF
THAV_RF
THNO
THMN_RF
BI

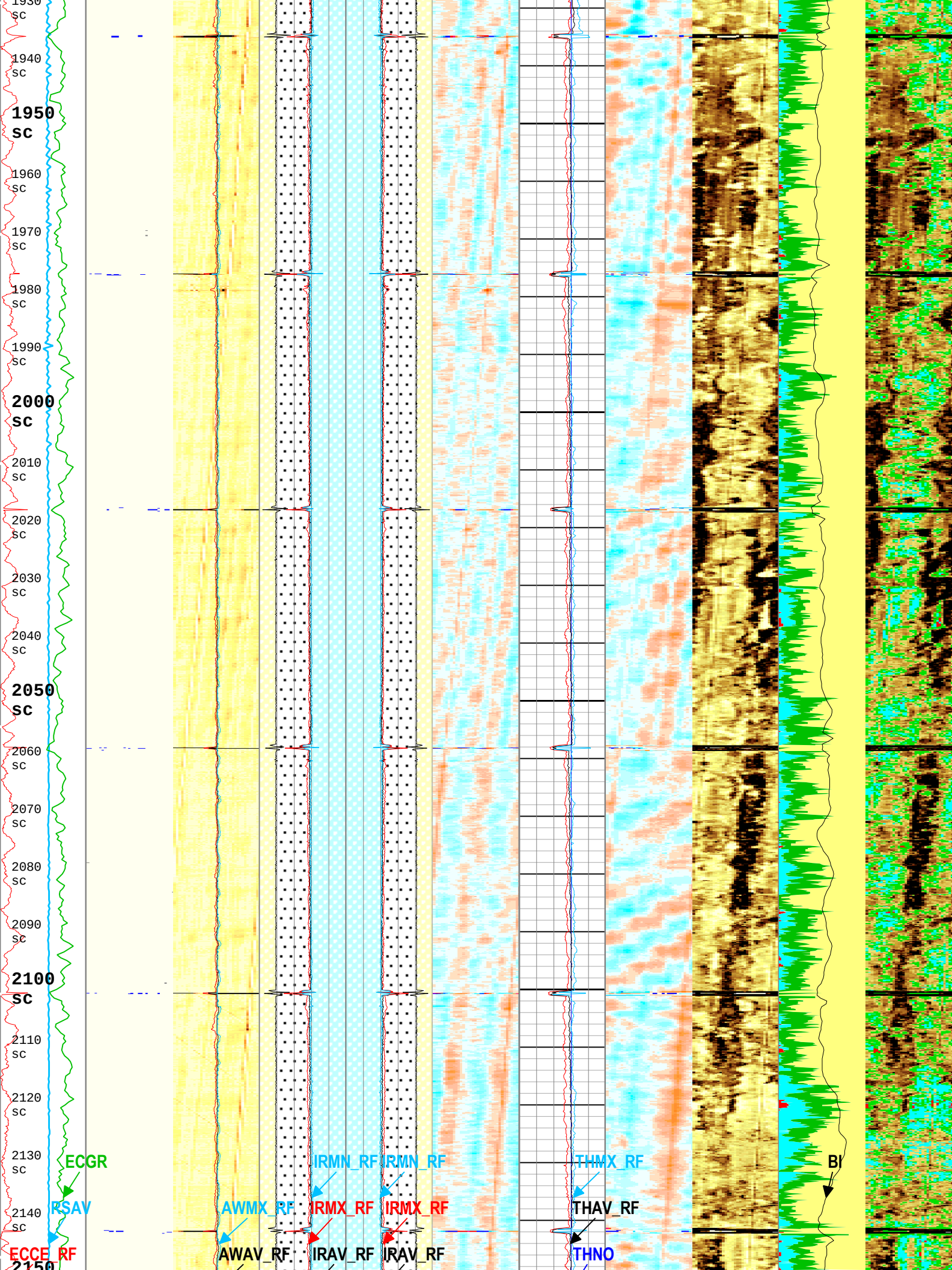
1930 sc
1940 sc
1950 sc
1960 sc
1970 sc
1980 sc
1990 sc
2000 sc
2010 sc
2020 sc
2030 sc
2040 sc
2050 sc
2060 sc
2070 sc
2080 sc
2090 sc
2100 sc
2110 sc
2120 sc
2130 sc
2140 sc
2150
ECGR
RSAV
ECCE_RF
AWMX_RF
AWAV_RF
IRMN_RF
IRMX_RF
IRAV_RF
IRMN_RF
IRMX_RF
IRAV_RF
THMX_RF
THAV_RF
THNO
BI

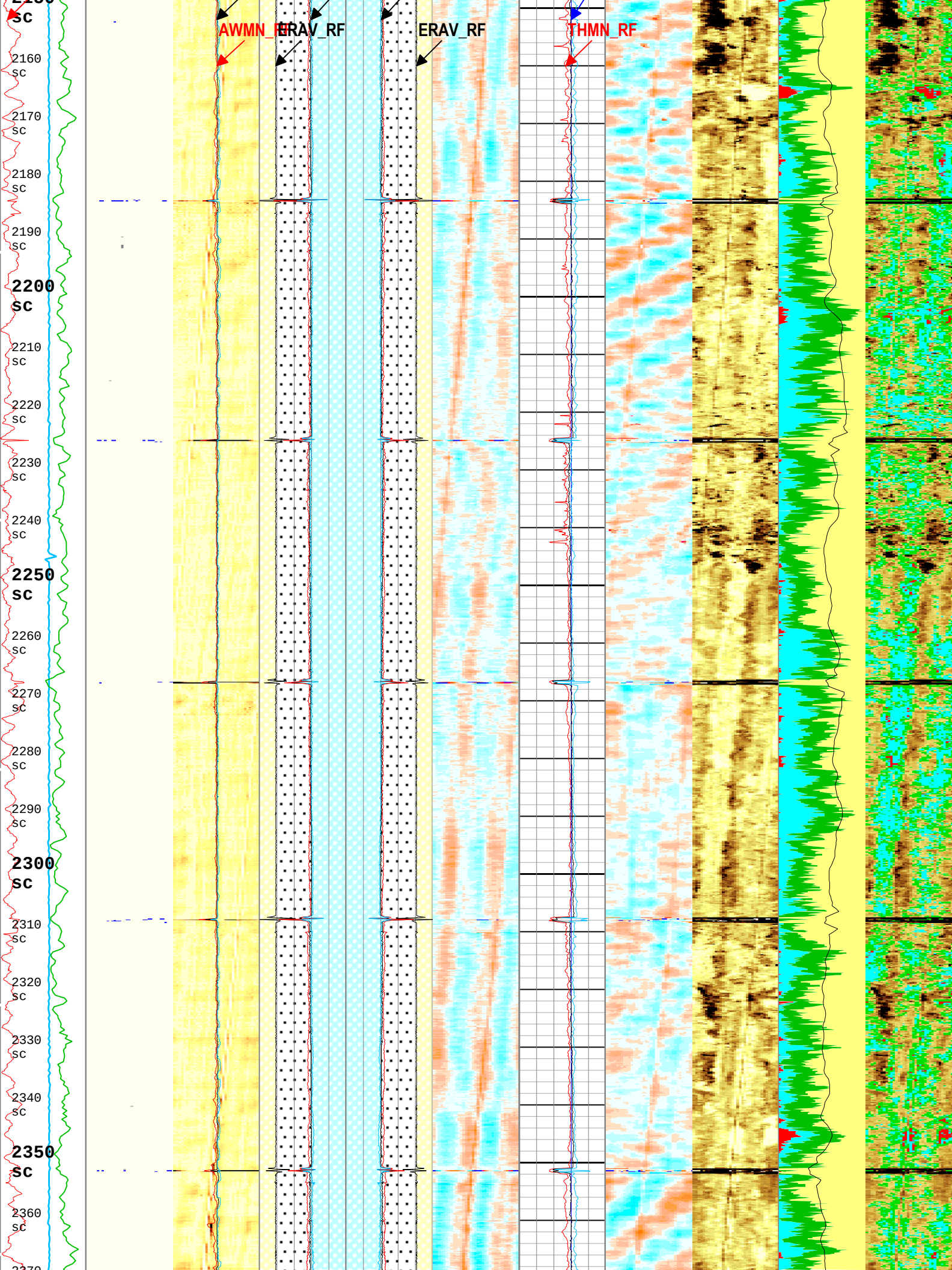
AWMN_RF
ERAV_RF
ERAV_RF
THMN_RF
2160 sc
2170 sc
2180 sc
2190 sc
2200 sc
2210 sc
2220 sc
2230 sc
2240 sc
2250 sc
2260 sc
2270 sc
2280 sc
2290 sc
2300 sc
2310 sc
2320 sc
2330 sc
2340 sc
2350 sc
2360 sc

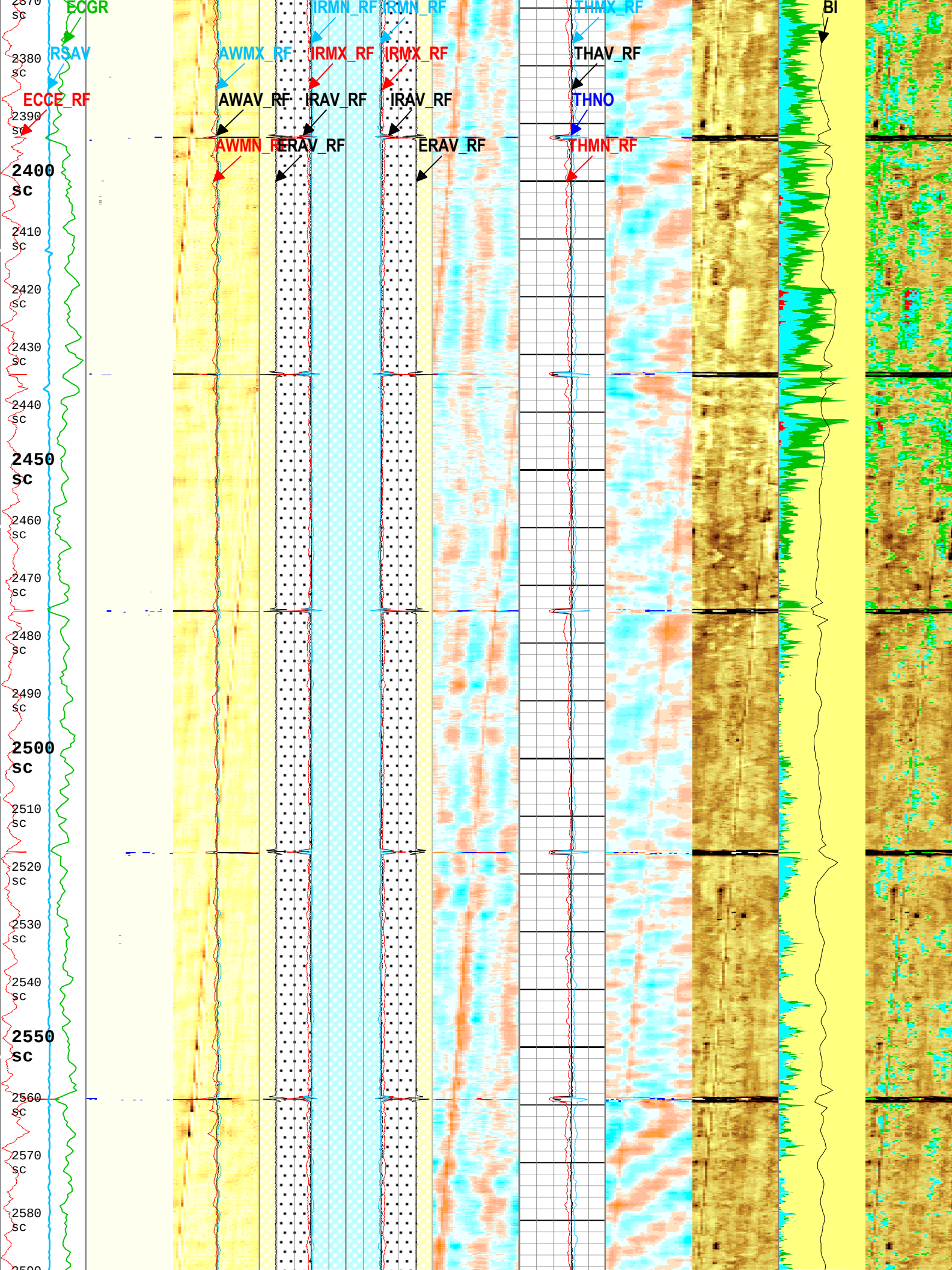
ECGR
RSAV
ECCE_RF
IRMN_RF
IRMN_RF
AWMX_RF
IRMX_RF
IRMX_RF
AWAV_RF
IRAV_RF
IRAV_RF
AWMN_RF
ERAV_RF
ERAV_RF
THMX_RF
THAV_RF
THNO
THMN_RF
BI
2370 SC
2380 SC
2390 SC
2400 SC
2410 SC
2420 SC
2430 SC
2440 SC
2450 SC
2460 SC
2470 SC
2480 SC
2490 SC
2500 SC
2510 SC
2520 SC
2530 SC
2540 SC
2550 SC
2560 SC
2570 SC
2580 SC

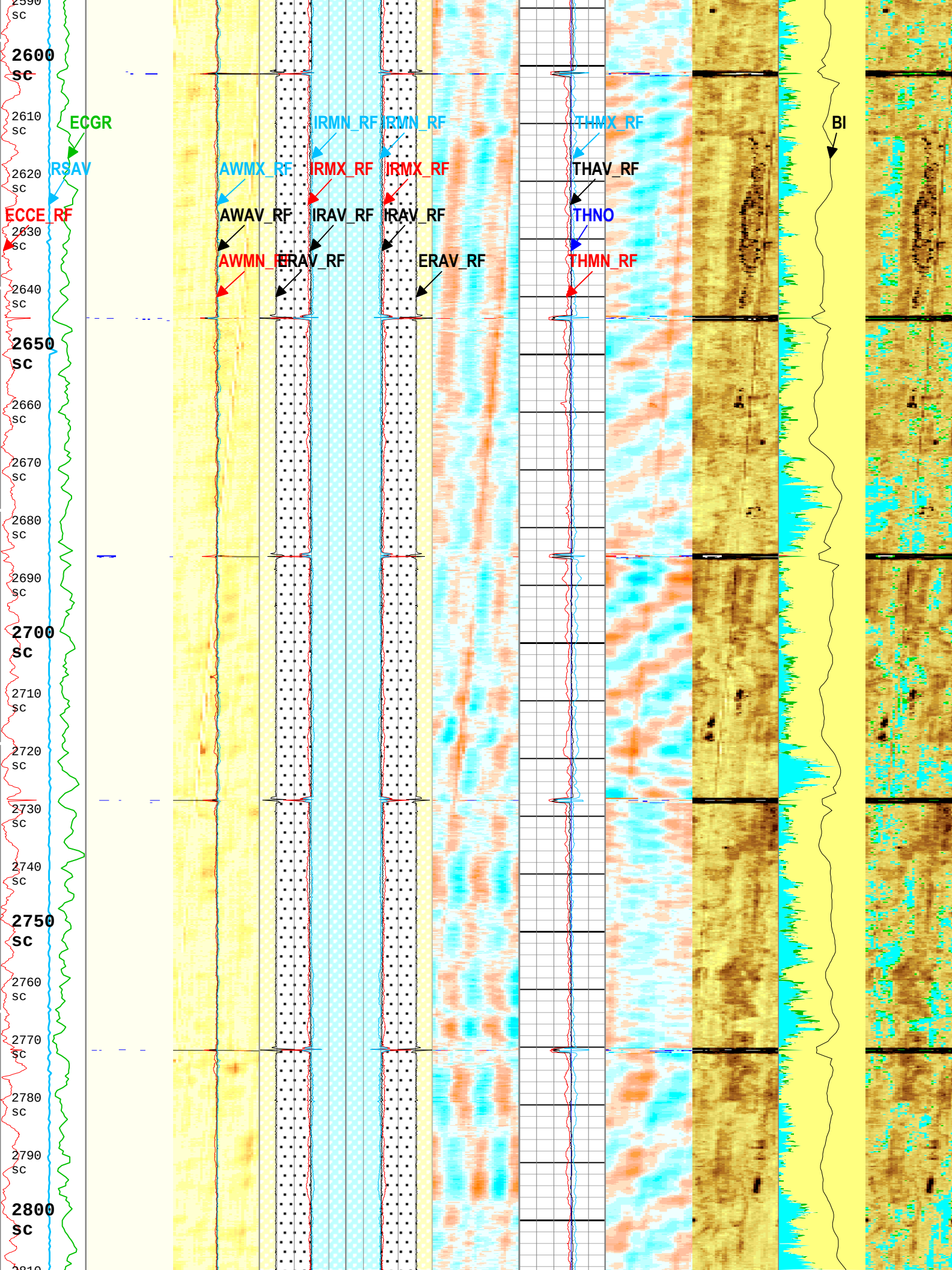
2590 sc
2600 sc
2610 sc
2620 sc
2630 sc
2640 sc
2650 sc
2660 sc
2670 sc
2680 sc
2690 sc
2700 sc
2710 sc
2720 sc
2730 sc
2740 sc
2750 sc
2760 sc
2770 sc
2780 sc
2790 sc
2800 sc
ECGR
RSAV
ECCE_RF
IRMN_RF
IRMN_RF
THMX_RF
BI
AWMX_RF
IRMX_RF
IRMX_RF
THAV_RF
AWAV_RF
IRAV_RF
IRAV_RF
THNO
AWMN_RF
ERAV_RF
ERAV_RF
THMN_RF

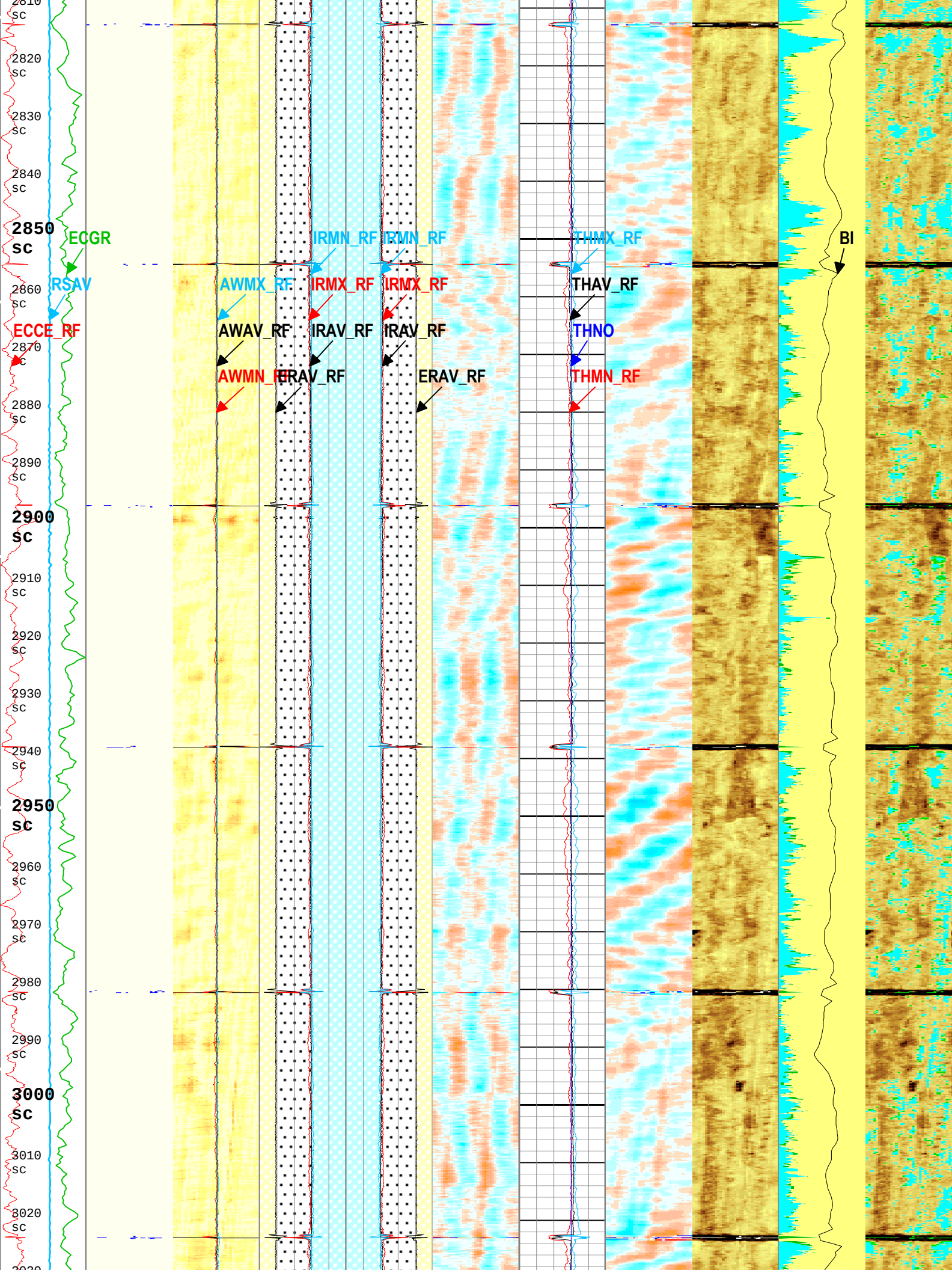
2810 sc
2820 sc
2830 sc
2840 sc
2850 sc
2860 sc
2870 sc
2880 sc
2890 sc
2900 sc
2910 sc
2920 sc
2930 sc
2940 sc
2950 sc
2960 sc
2970 sc
2980 sc
2990 sc
3000 sc
3010 sc
3020 sc
ECGR
RSAV
ECCE_RF
IRMN_RF
IRMN_RF
THMX_RF
BI
AWMX_RF
IRMX_RF
IRMX_RF
THAV_RF
AWAV_RF
IRAV_RF
IRAV_RF
THNO
AWMN_RF
ERAV_RF
ERAV_RF
THMN_RF

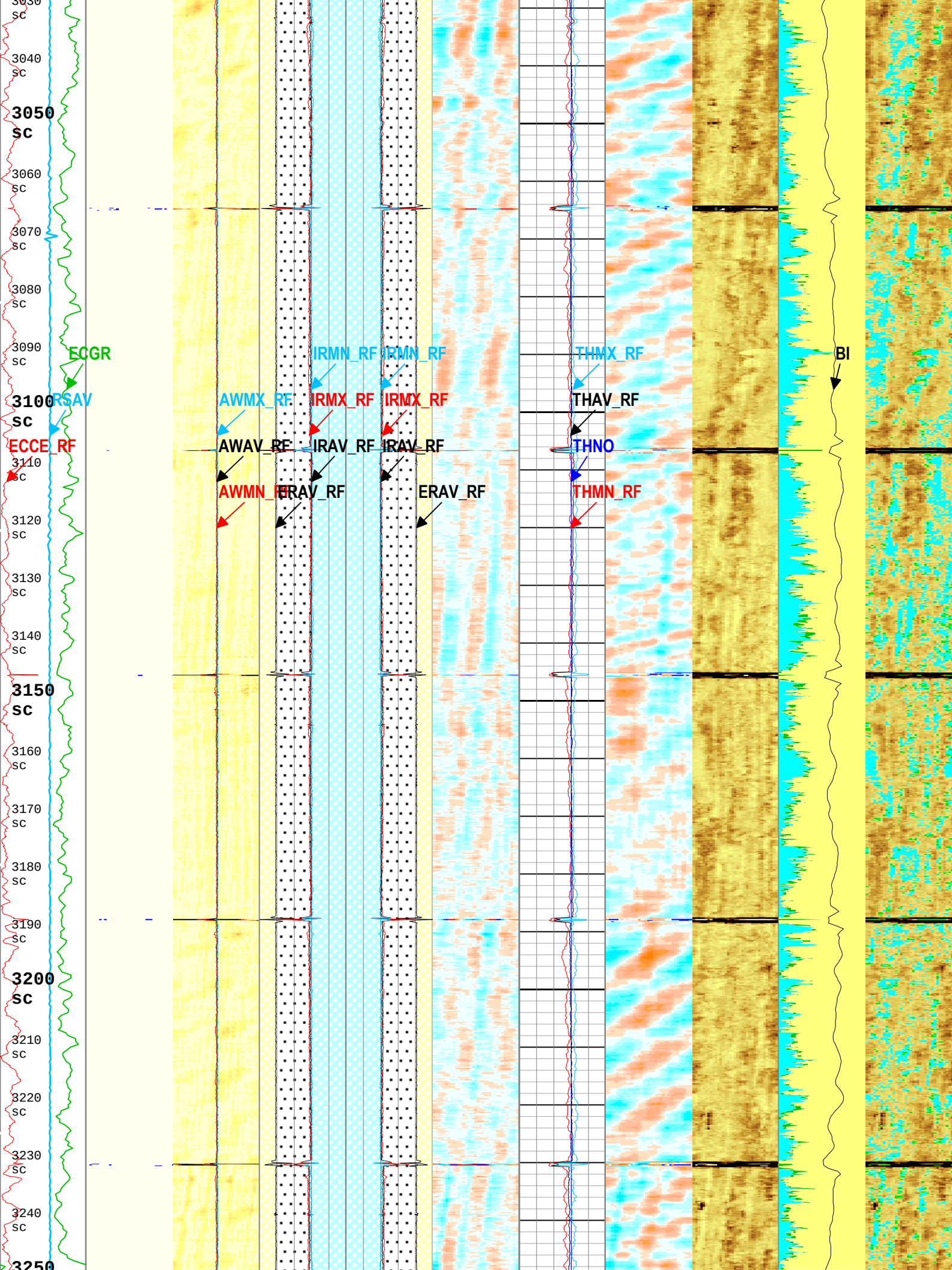
3030 sc
3040 sc
3050 sc
3060 sc
3070 sc
3080 sc
3090 sc
3100 sc
3110 sc
3120 sc
3130 sc
3140 sc
3150 sc
3160 sc
3170 sc
3180 sc
3190 sc
3200 sc
3210 sc
3220 sc
3230 sc
3240 sc
3250
ECGR
RSAV
ECCE_RF
IRMN_RF
IRMN_RF
AWMX_RF
IRMX_RF
IRMX_RF
AWAV_RF
IRAV_RF
IRAV_RF
AWMN_RF
ERAV_RF
ERAV_RF
THMX_RF
THAV_RF
THNO
THMN_RF
BI

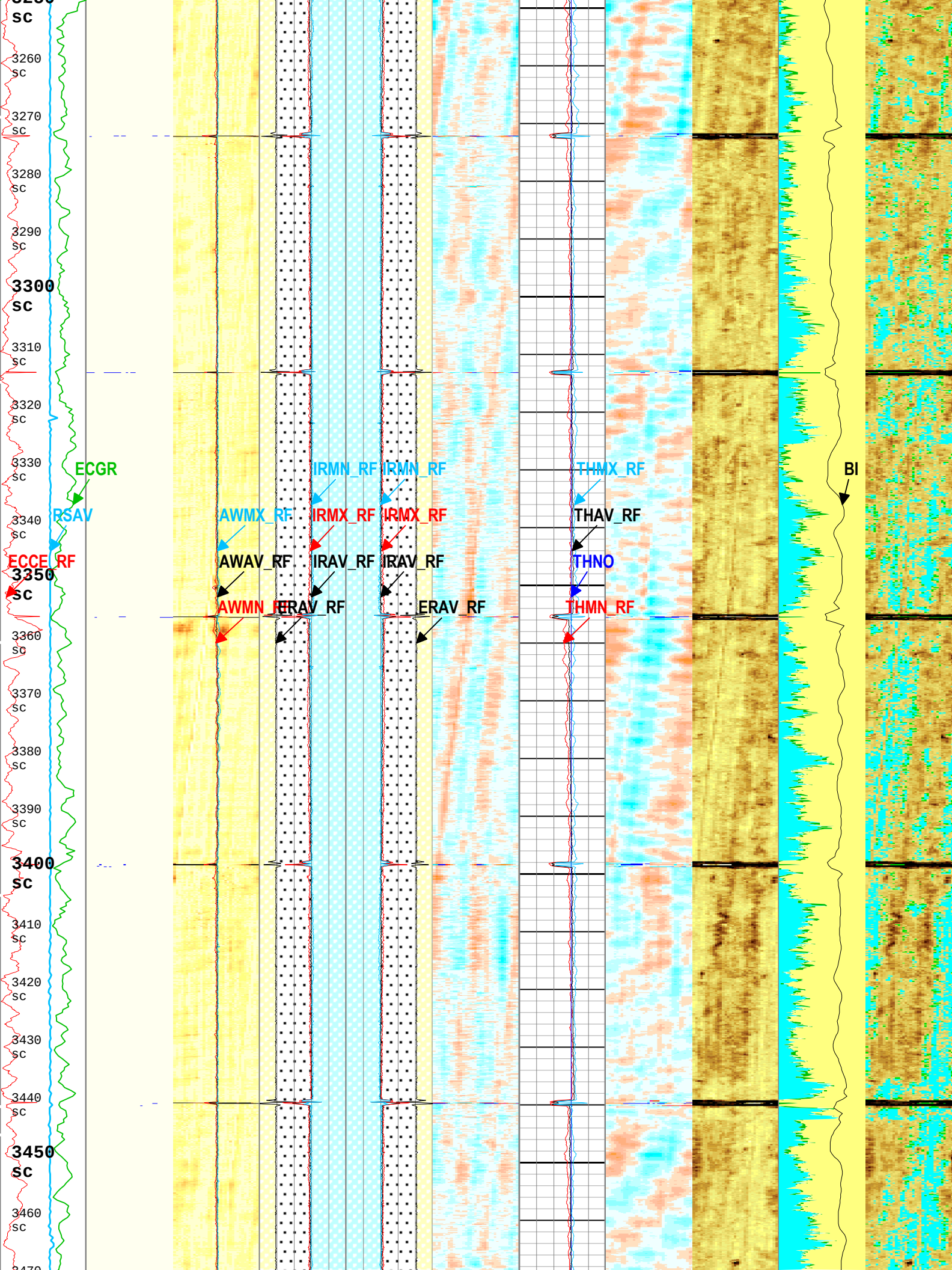
3250 sc
3260 sc
3270 sc
3280 sc
3290 sc
3300 sc
3310 sc
3320 sc
3330 sc
3340 sc
3350 sc
3360 sc
3370 sc
3380 sc
3390 sc
3400 sc
3410 sc
3420 sc
3430 sc
3440 sc
3450 sc
3460 sc
ECGR
RSAV
ECCE_RF
AWMX_RF
AWAV_RF
AWMN_RF
IRMN_RF
IRMX_RF
IRAV_RF
ERAV_RF
IRMN_RF
IRMX_RF
IRAV_RF
ERAV_RF
THMX_RF
THAV_RF
THNO
THMN_RF
BI

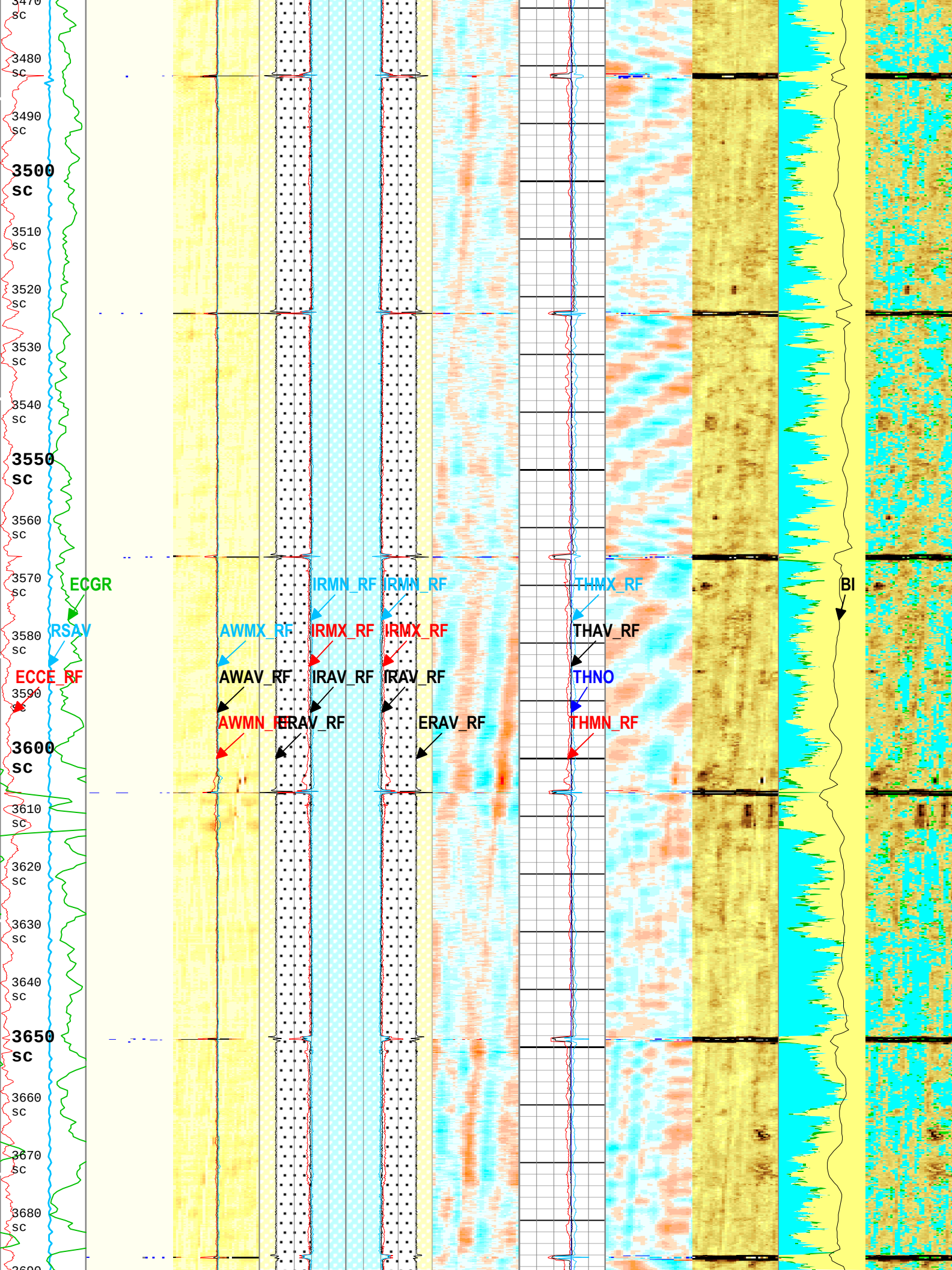
3470 sc
3480 sc
3490 sc
3500 sc
3510 sc
3520 sc
3530 sc
3540 sc
3550 sc
3560 sc
3570 sc
3580 sc
3590 sc
3600 sc
3610 sc
3620 sc
3630 sc
3640 sc
3650 sc
3660 sc
3670 sc
3680 sc
ECGR
RSAV
ECCE_RF
AWMX_RF
AWAV_RF
AWMN_RF
IRMN_RF
IRMX_RF
IRAV_RF
ERAV_RF
IRMN_RF
IRMX_RF
IRAV_RF
ERAV_RF
THMX_RF
THAV_RF
THNO
THMN_RF
BI

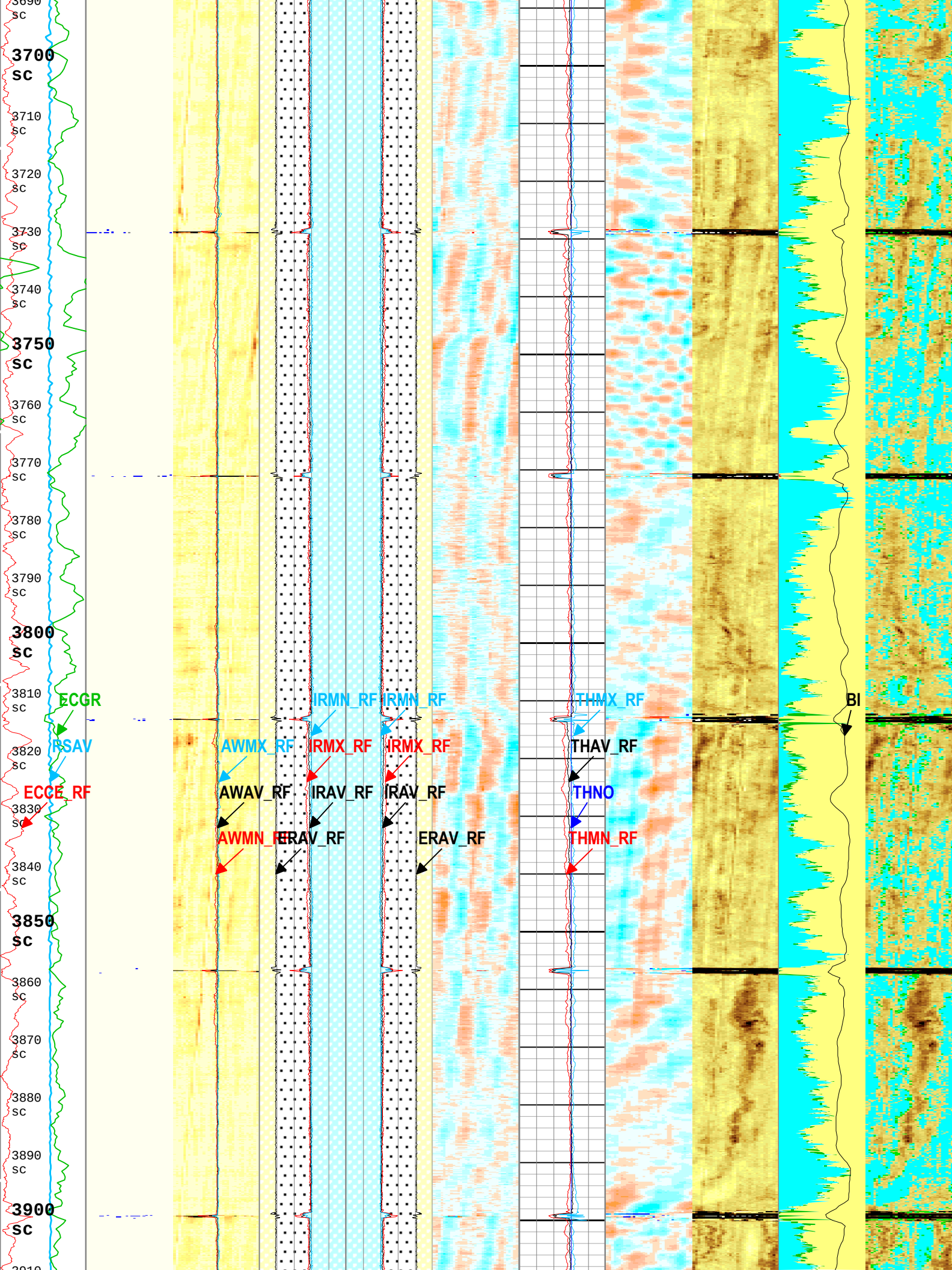
3690 sc
3700 sc
3710 sc
3720 sc
3730 sc
3740 sc
3750 sc
3760 sc
3770 sc
3780 sc
3790 sc
3800 sc
3810 sc
3820 sc
3830 sc
3840 sc
3850 sc
3860 sc
3870 sc
3880 sc
3890 sc
3900 sc
ECGR
RSAV
ECCE_RF
IRMN_RF
IRMN_RF
AWMX_RF
IRMX_RF
IRMX_RF
AWAV_RF
IRAV_RF
IRAV_RF
AWMN_RF
ERAV_RF
ERAV_RF
THMX_RF
THAV_RF
THNO
THMN_RF
BI

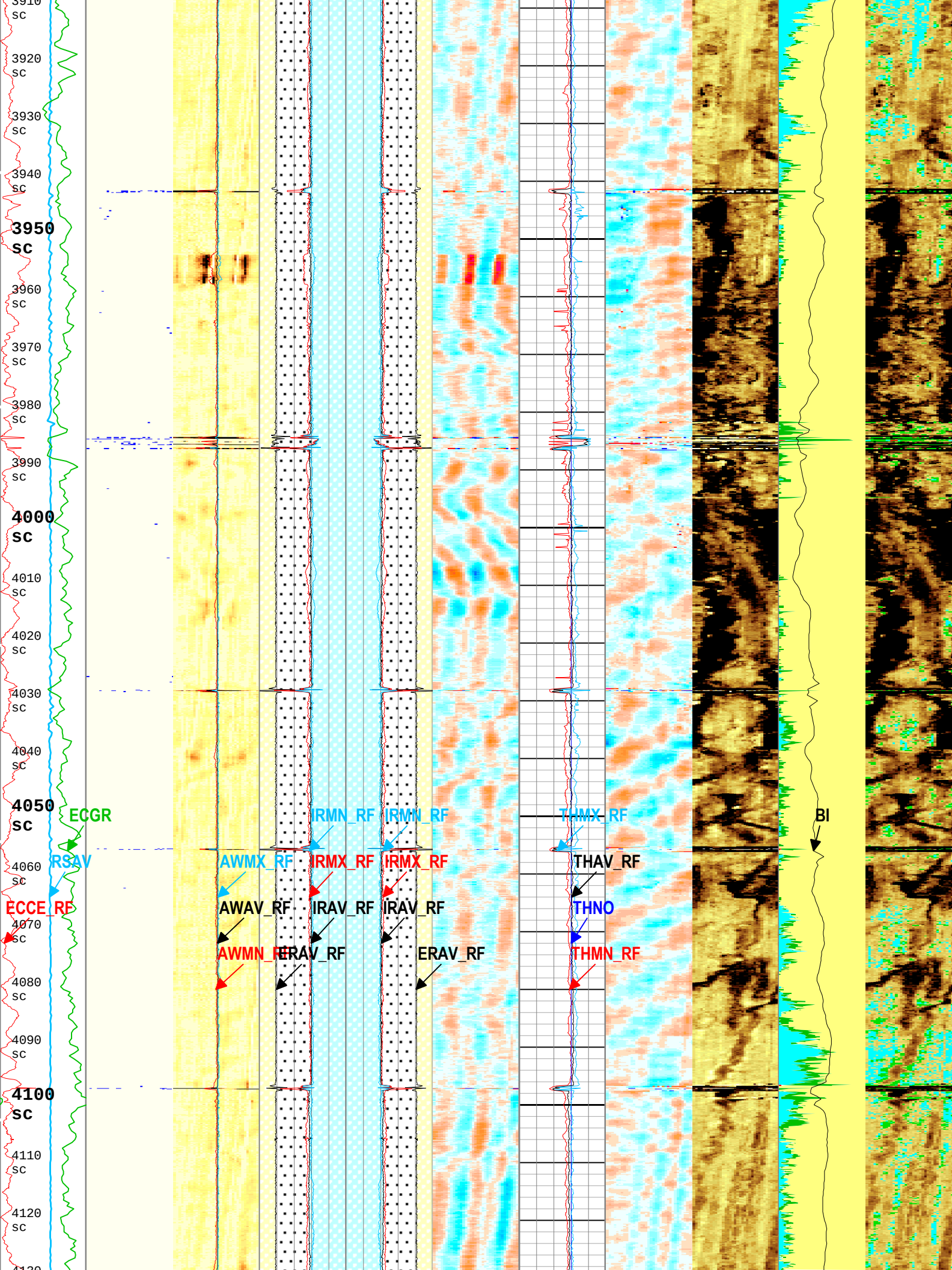
3910 sc
3920 sc
3930 sc
3940 sc
3950 sc
3960 sc
3970 sc
3980 sc
3990 sc
4000 sc
4010 sc
4020 sc
4030 sc
4040 sc
4050 sc
4060 sc
4070 sc
4080 sc
4090 sc
4100 sc
4110 sc
4120 sc
ECGR
RSAV
ECCE_RF
IRMN_RF
IRMN_RF
AWMX_RF
IRMX_RF
IRMX_RF
AWAV_RF
IRAV_RF
IRAV_RF
AWMN_RF
ERAV_RF
ERAV_RF
THMX_RF
THAV_RF
THNO
THMN_RF
BI

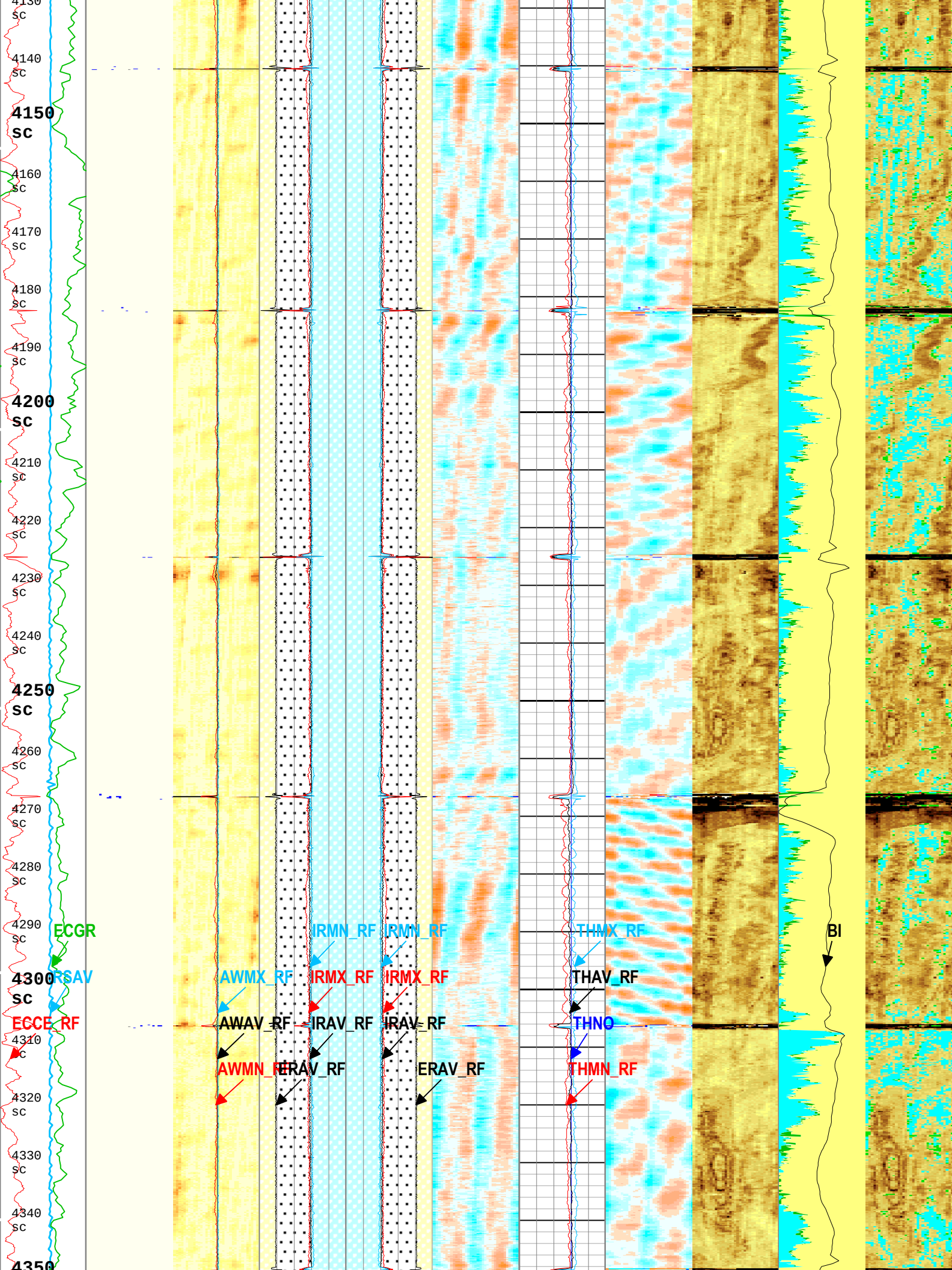
4130 sc
4140 sc
4150 sc
4160 sc
4170 sc
4180 sc
4190 sc
4200 sc
4210 sc
4220 sc
4230 sc
4240 sc
4250 sc
4260 sc
4270 sc
4280 sc
4290 sc
4300 sc
4310 sc
4320 sc
4330 sc
4340 sc
4350
ECGR
RSAV
ECCE_RF
IRMN_RF
IRMN_RF
AWMX_RF
IRMX_RF
IRMX_RF
AWAV_RF
IRAV_RF
IRAV_RF
AWMN_RF
ERAV_RF
ERAV_RF
THMX_RF
THAV_RF
THNO
THMN_RF
BI

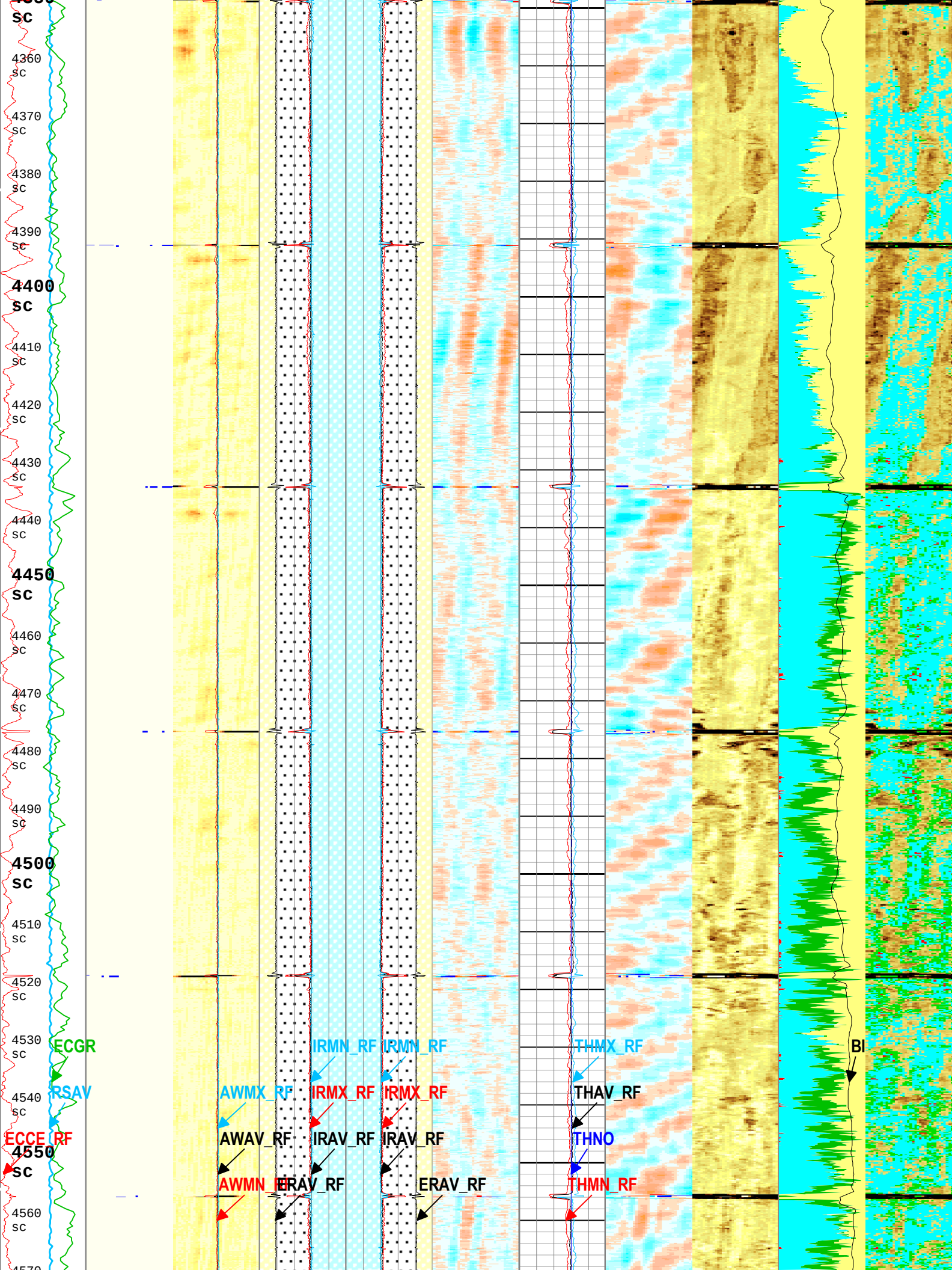
4360 sc
4370 sc
4380 sc
4390 sc
4400 sc
4410 sc
4420 sc
4430 sc
4440 sc
4450 sc
4460 sc
4470 sc
4480 sc
4490 sc
4500 sc
4510 sc
4520 sc
4530 sc
4540 sc
4550 sc
4560 sc
ECGR
RSAV
ECCE_RF
IRMN_RF
IRMN_RF
AWMX_RF
IRMX_RF
IRMX_RF
AWAV_RF
IRAV_RF
IRAV_RF
AWMN_RF
ERAV_RF
ERAV_RF
THMX_RF
THAV_RF
THNO
THMN_RF
BI

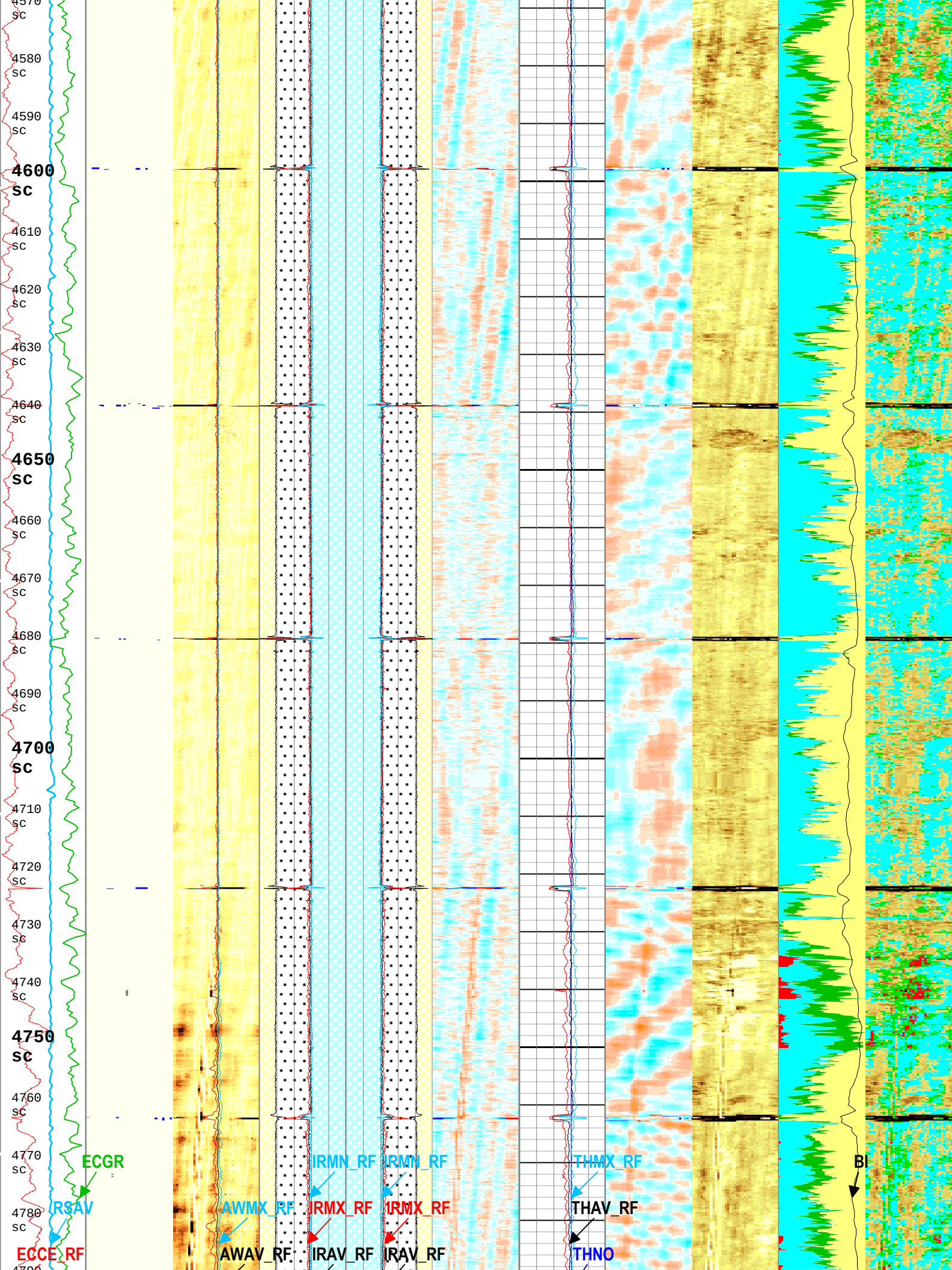
4570 sc
4580 sc
4590 sc
4600 sc
4610 sc
4620 sc
4630 sc
4640 sc
4650 sc
4660 sc
4670 sc
4680 sc
4690 sc
4700 sc
4710 sc
4720 sc
4730 sc
4740 sc
4750 sc
4760 sc
4770 sc
4780 sc
ECGR
RSAV
ECCE_RF
AWMX_RF
AWAV_RF
IRMN_RF
IRMX_RF
IRAV_RF
IRMN_RF
IRMX_RF
IRAV_RF
THMX_RF
THAV_RF
THNO
BI

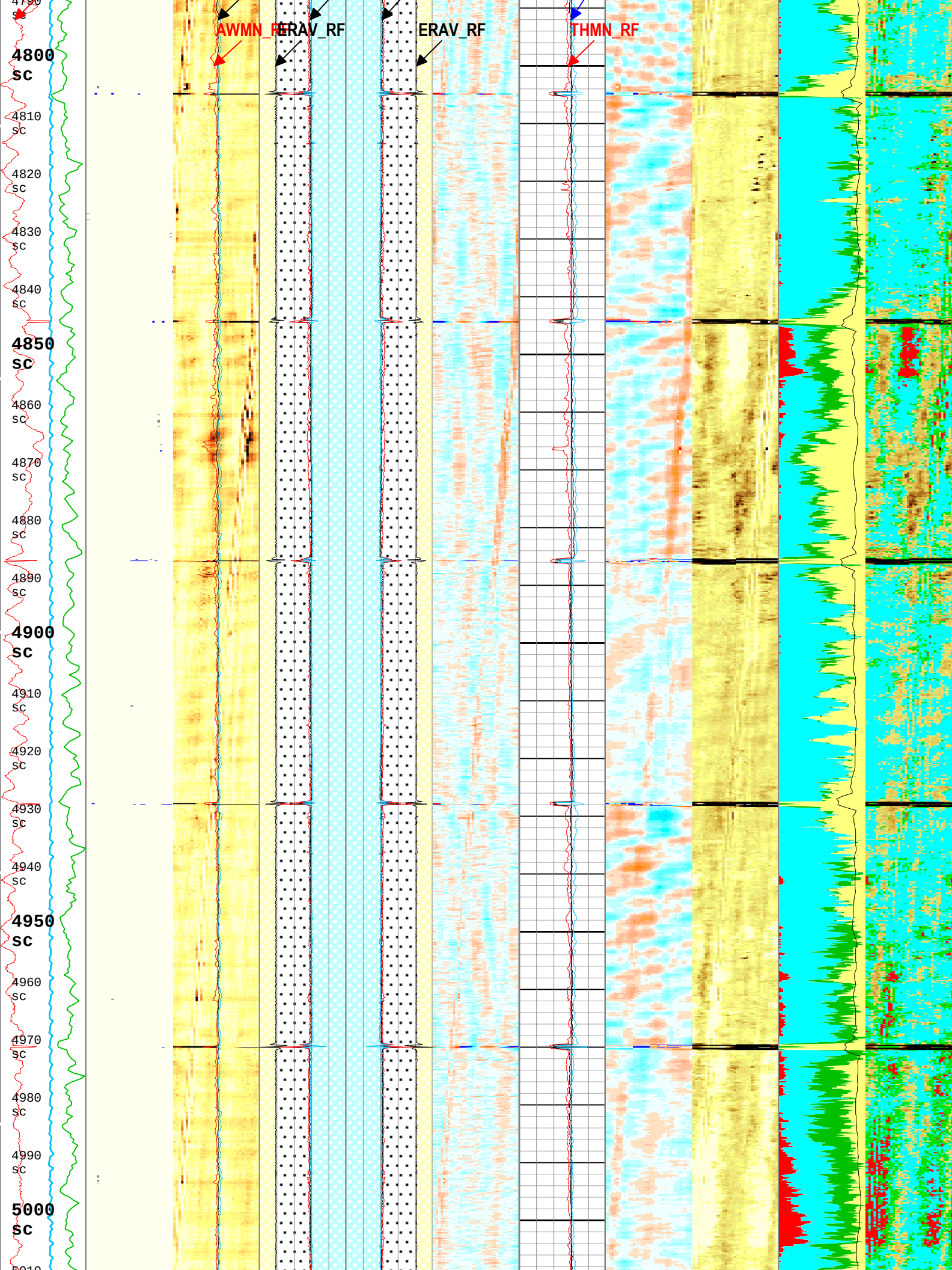
AWMN_RF
ERAV_RF
ERAV_RF
THMN_RF
4800 sc
4810 sc
4820 sc
4830 sc
4840 sc
4850 sc
4860 sc
4870 sc
4880 sc
4890 sc
4900 sc
4910 sc
4920 sc
4930 sc
4940 sc
4950 sc
4960 sc
4970 sc
4980 sc
4990 sc
5000 sc

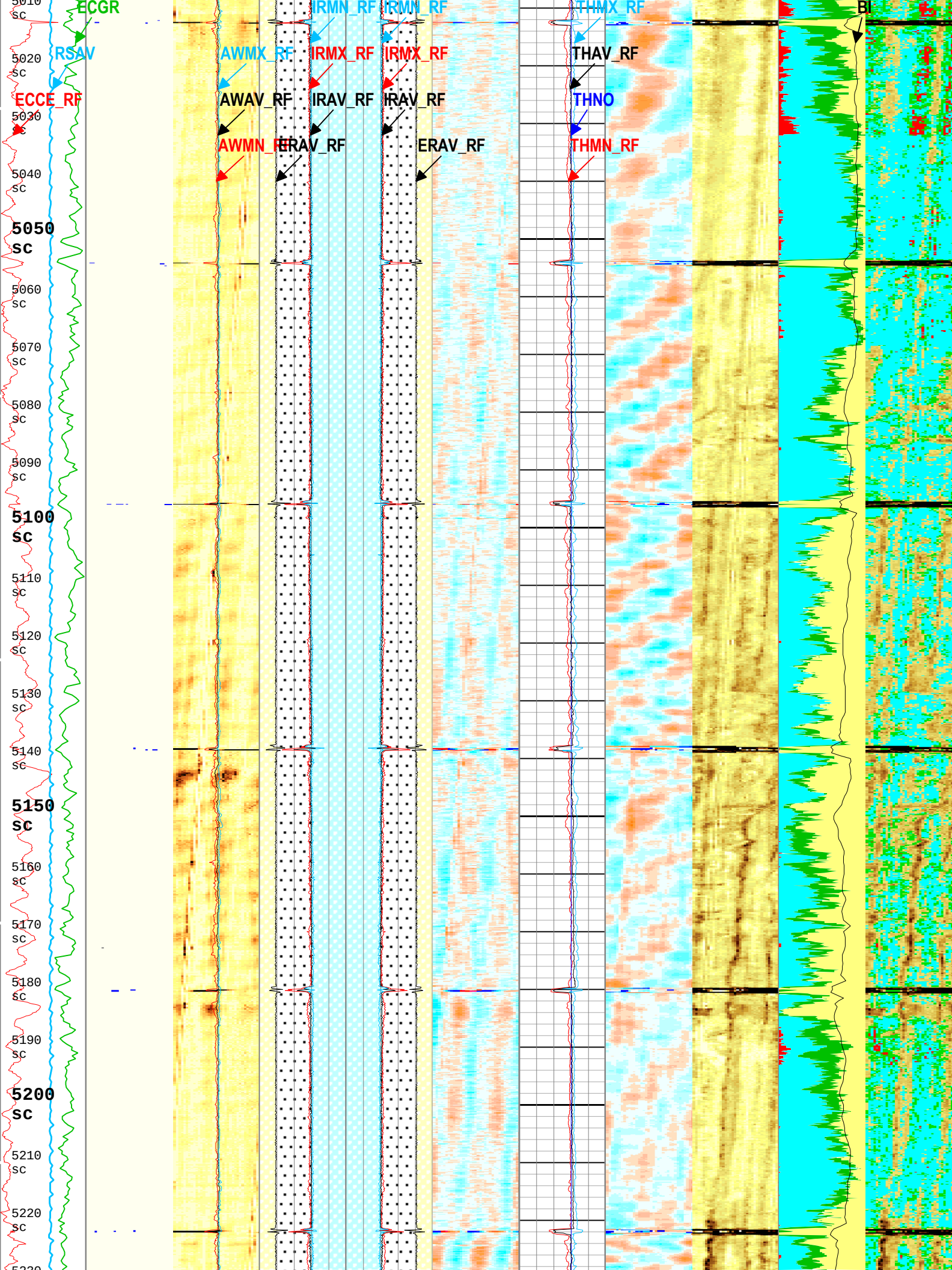
ECGR
RSAV
ECCE_RF
AWMX_RF
AWAV_RF
AWMN_RF
IRMN_RF
IRMX_RF
IRAV_RF
ERAV_RF
IRMN_RF
IRMX_RF
IRAV_RF
ERAV_RF
THMX_RF
THAV_RF
THNO
THMN_RF
BI
5010 sc
5020 sc
5030 sc
5040 sc
5050 sc
5060 sc
5070 sc
5080 sc
5090 sc
5100 sc
5110 sc
5120 sc
5130 sc
5140 sc
5150 sc
5160 sc
5170 sc
5180 sc
5190 sc
5200 sc
5210 sc
5220 sc

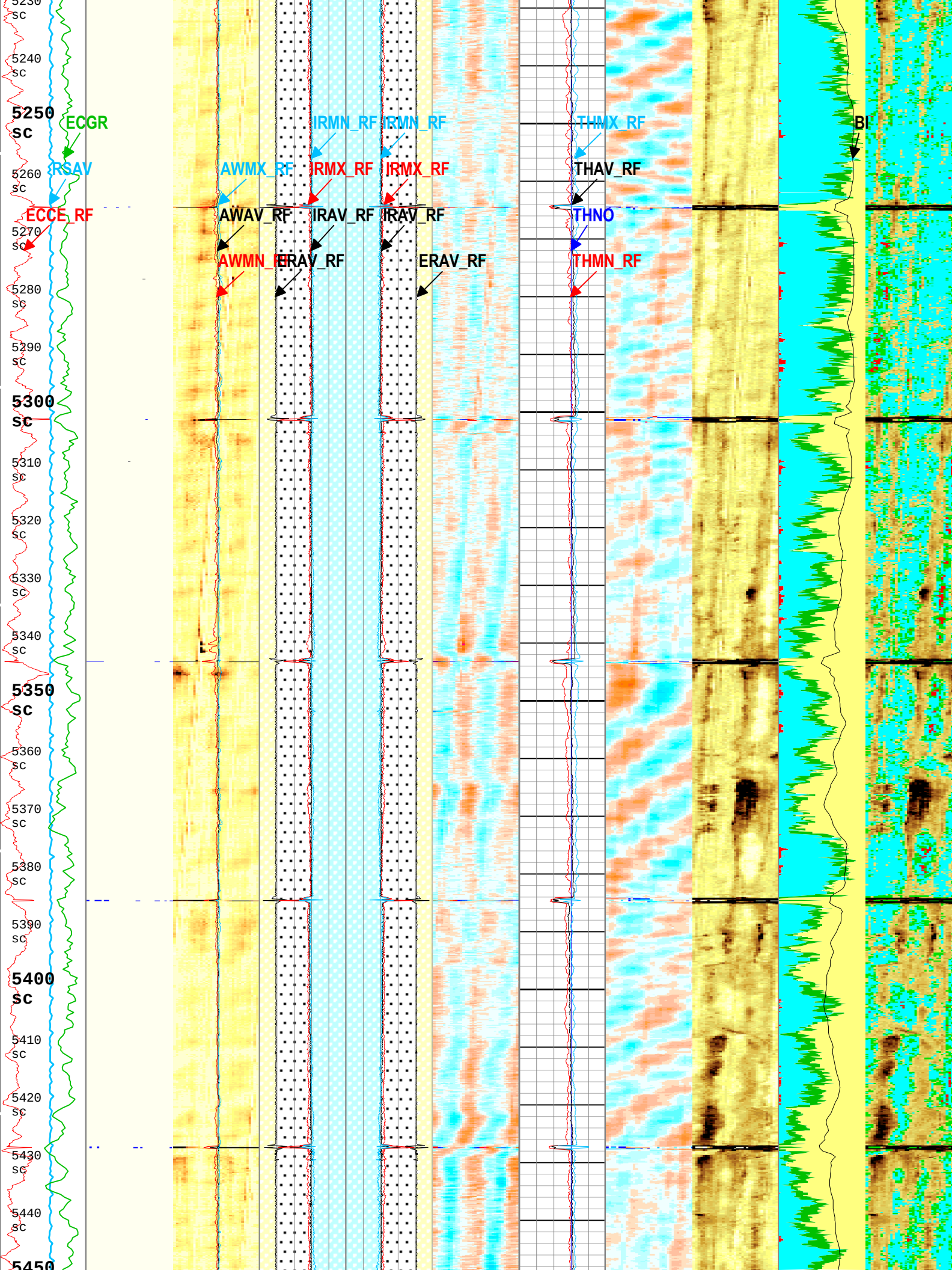
5230 sc
5240 sc
5250 sc
5260 sc
5270 sc
5280 sc
5290 sc
5300 sc
5310 sc
5320 sc
5330 sc
5340 sc
5350 sc
5360 sc
5370 sc
5380 sc
5390 sc
5400 sc
5410 sc
5420 sc
5430 sc
5440 sc
5450
ECGR
RSAV
ECCE_RF
IRMN_RF
IRMN_RF
AWMX_RF
IRMX_RF
IRMX_RF
AWAV_RF
IRAV_RF
IRAV_RF
AWMN_RF
ERAV_RF
ERAV_RF
THMX_RF
THAV_RF
THNO
THMN_RF
BI

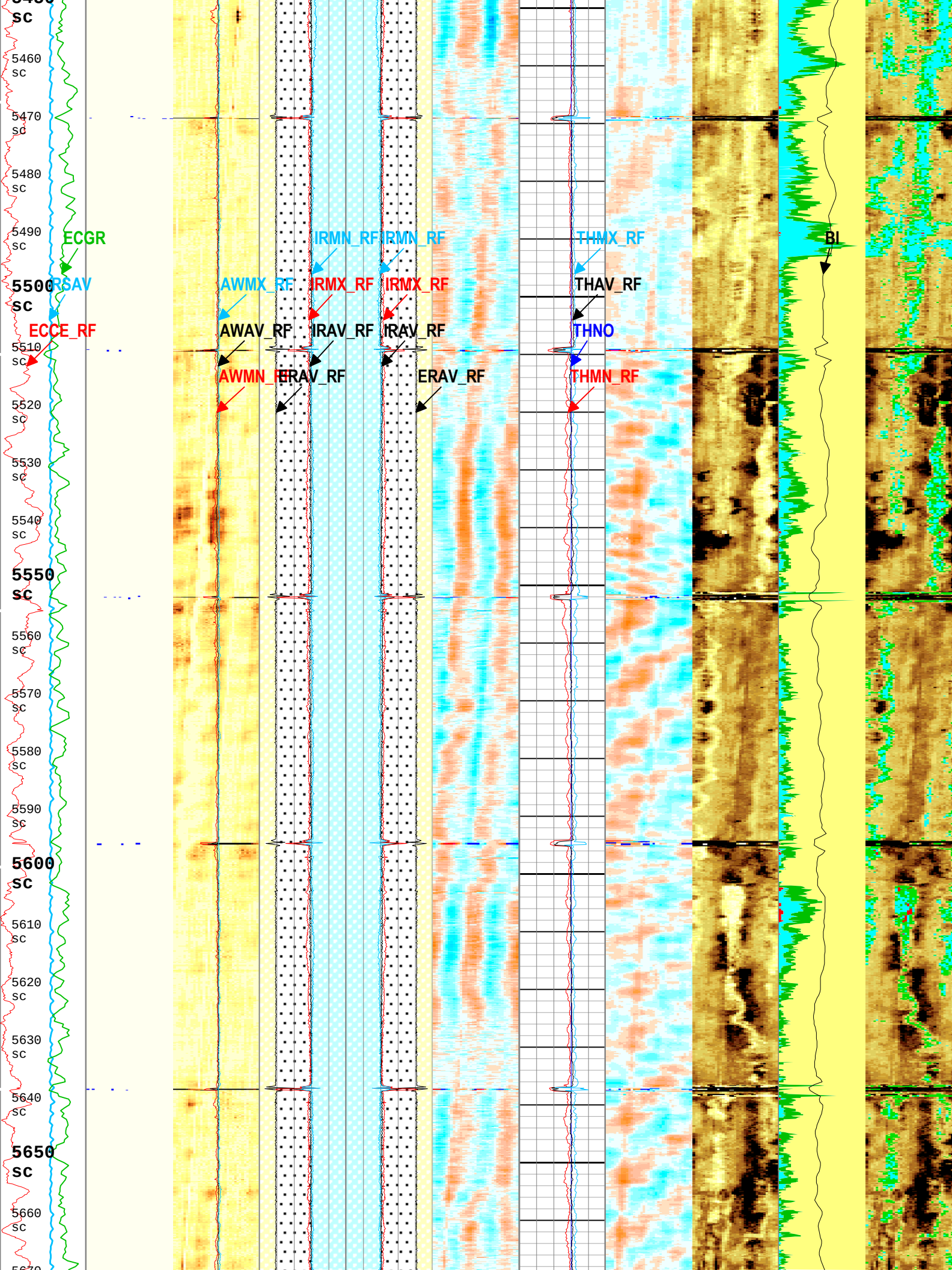
5460 sc
5470 sc
5480 sc
5490 sc
5500 sc
5510 sc
5520 sc
5530 sc
5540 sc
5550 sc
5560 sc
5570 sc
5580 sc
5590 sc
5600 sc
5610 sc
5620 sc
5630 sc
5640 sc
5650 sc
5660 sc
ECGR
RSAV
ECCE_RF
IRMN_RF
IRMN_RF
AWMX_RF
IRMX_RF
IRMX_RF
AWAV_RF
IRAV_RF
IRAV_RF
AWMN_RF
ERAV_RF
ERAV_RF
THMX_RF
THAV_RF
THNO
THMN_RF
BI

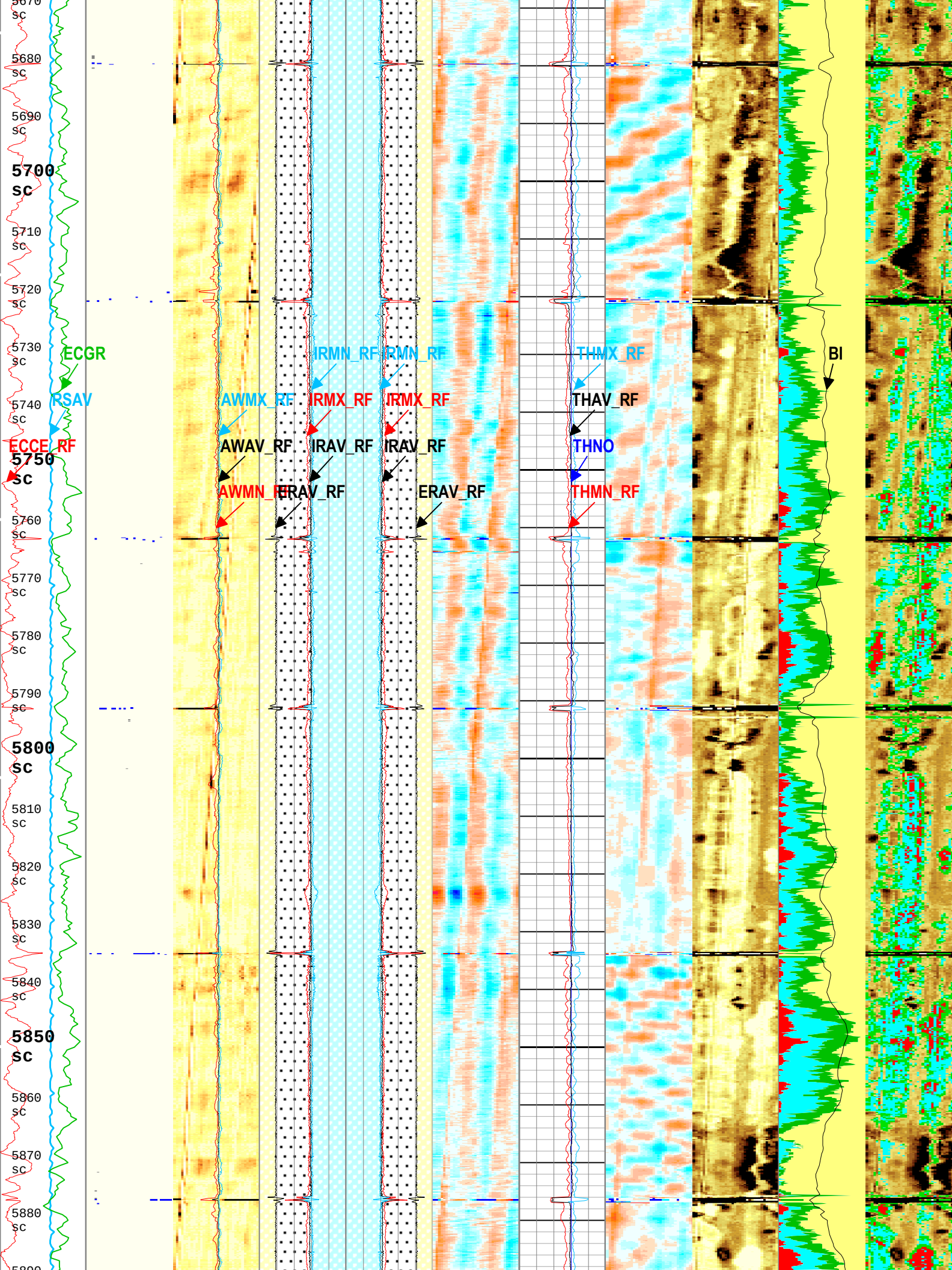
5670 sc
5680 sc
5690 sc
5700 sc
5710 sc
5720 sc
5730 sc
5740 sc
5750 sc
5760 sc
5770 sc
5780 sc
5790 sc
5800 sc
5810 sc
5820 sc
5830 sc
5840 sc
5850 sc
5860 sc
5870 sc
5880 sc
ECGR
RSAV
ECCE_RF
IRMN_RF
IRMN_RF
THMX_RF
BI
AWMX_RF
IRMX_RF
IRMX_RF
THAV_RF
AWAV_RF
IRAV_RF
IRAV_RF
THNO
AWMN_RF
ERAV_RF
ERAV_RF
THMN_RF

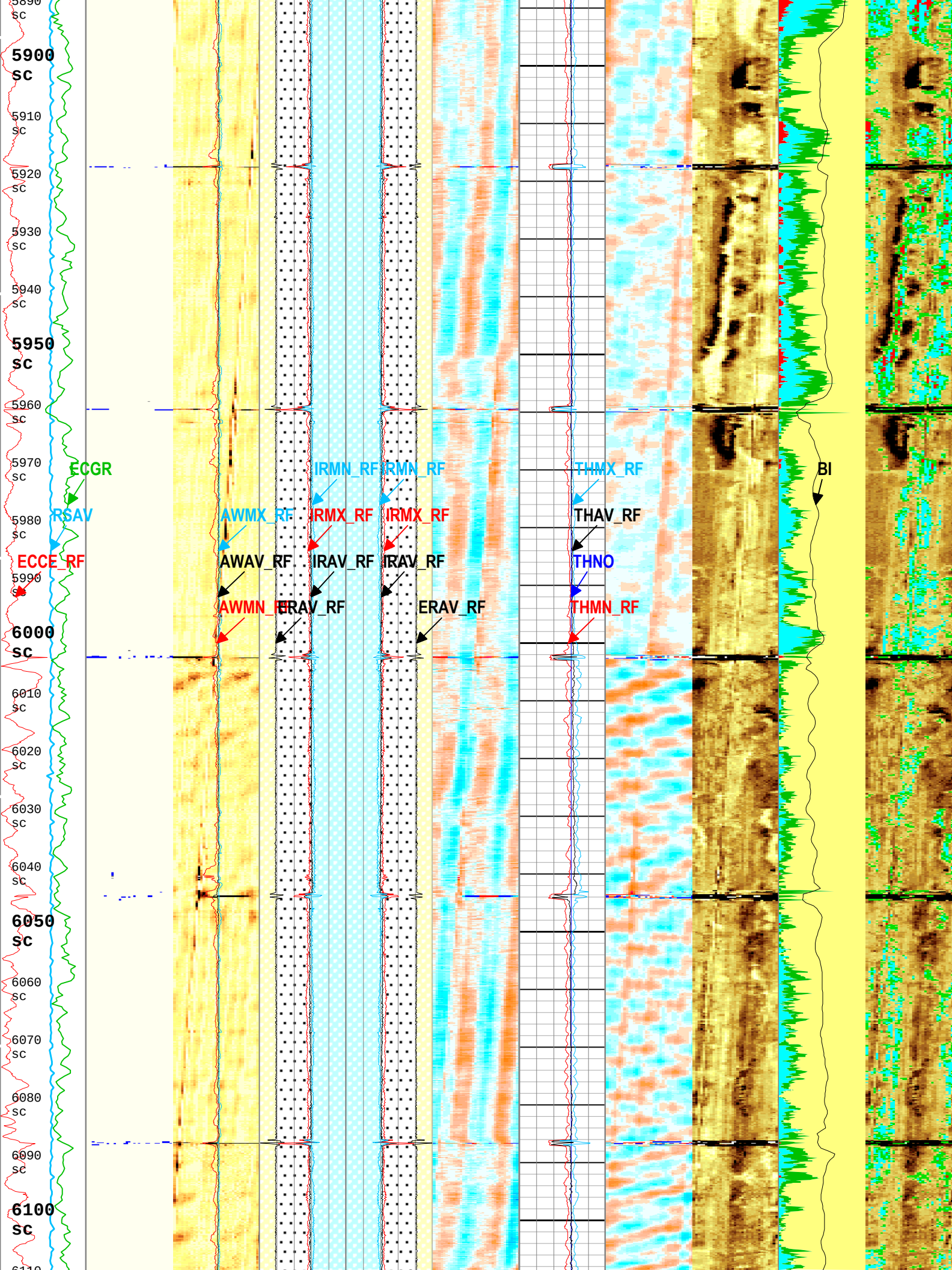
5900 sc
5910 sc
5920 sc
5930 sc
5940 sc
5950 sc
5960 sc
5970 sc
5980 sc
5990 sc
6000 sc
6010 sc
6020 sc
6030 sc
6040 sc
6050 sc
6060 sc
6070 sc
6080 sc
6090 sc
6100 sc
ECGR
RSAV
ECCE_RF
AWMX_RF
AWAV_RF
AWMN_RF
IRMN_RF
IRMX_RF
IRAV_RF
ERAV_RF
IRMN_RF
IRMX_RF
IRAV_RF
ERAV_RF
THMX_RF
THAV_RF
THNO
THMN_RF
BI

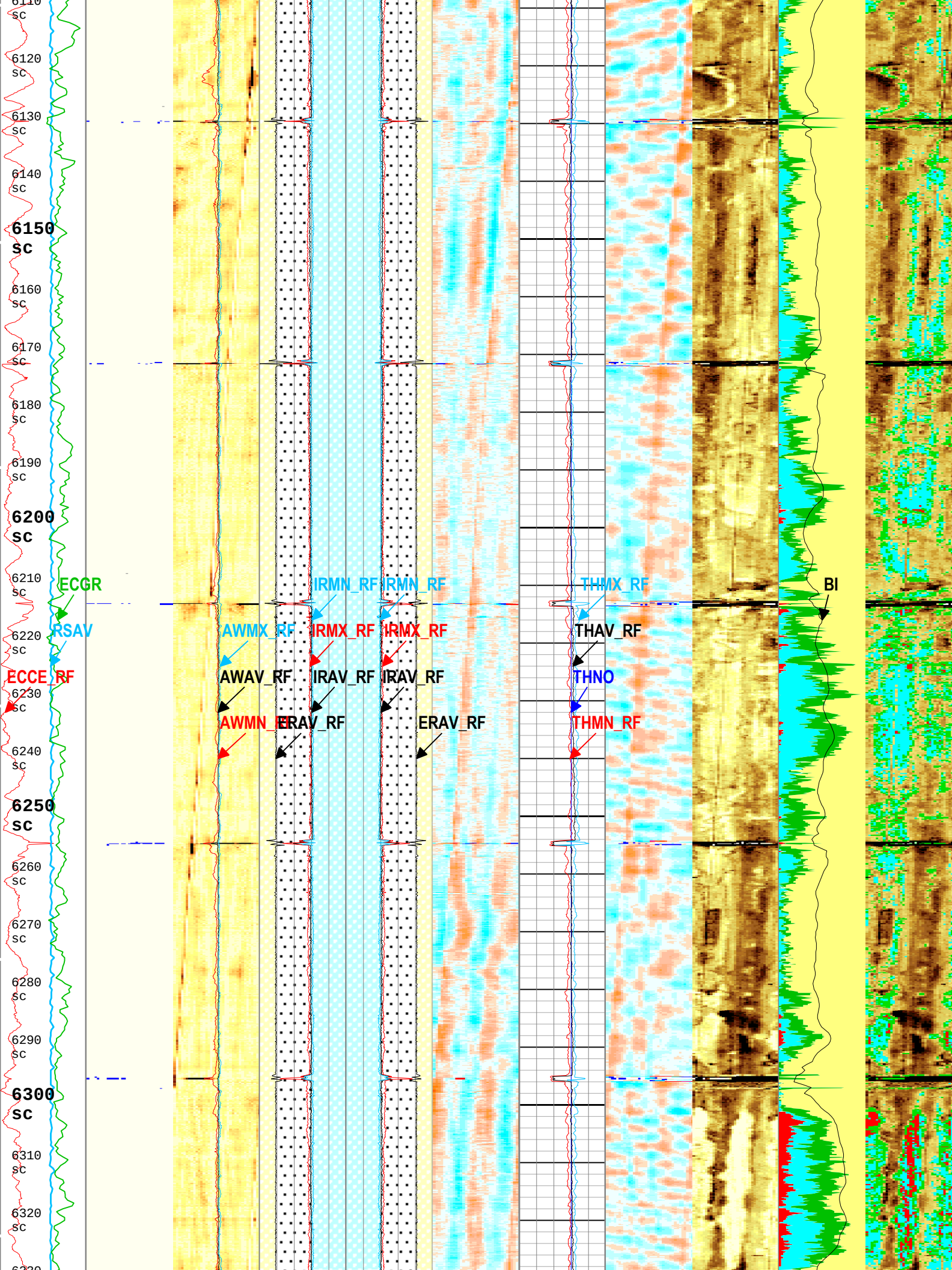
6110 sc
6120 sc
6130 sc
6140 sc
6150 sc
6160 sc
6170 sc
6180 sc
6190 sc
6200 sc
6210 sc
6220 sc
6230 sc
6240 sc
6250 sc
6260 sc
6270 sc
6280 sc
6290 sc
6300 sc
6310 sc
6320 sc
ECGR
RSAV
ECCE_RF
IRMN_RF
IRMN_RF
AWMX_RF
IRMX_RF
IRMX_RF
AWAV_RF
IRAV_RF
IRAV_RF
AWMN_RF
ERAV_RF
ERAV_RF
THMX_RF
THAV_RF
THNO
THMN_RF
BI

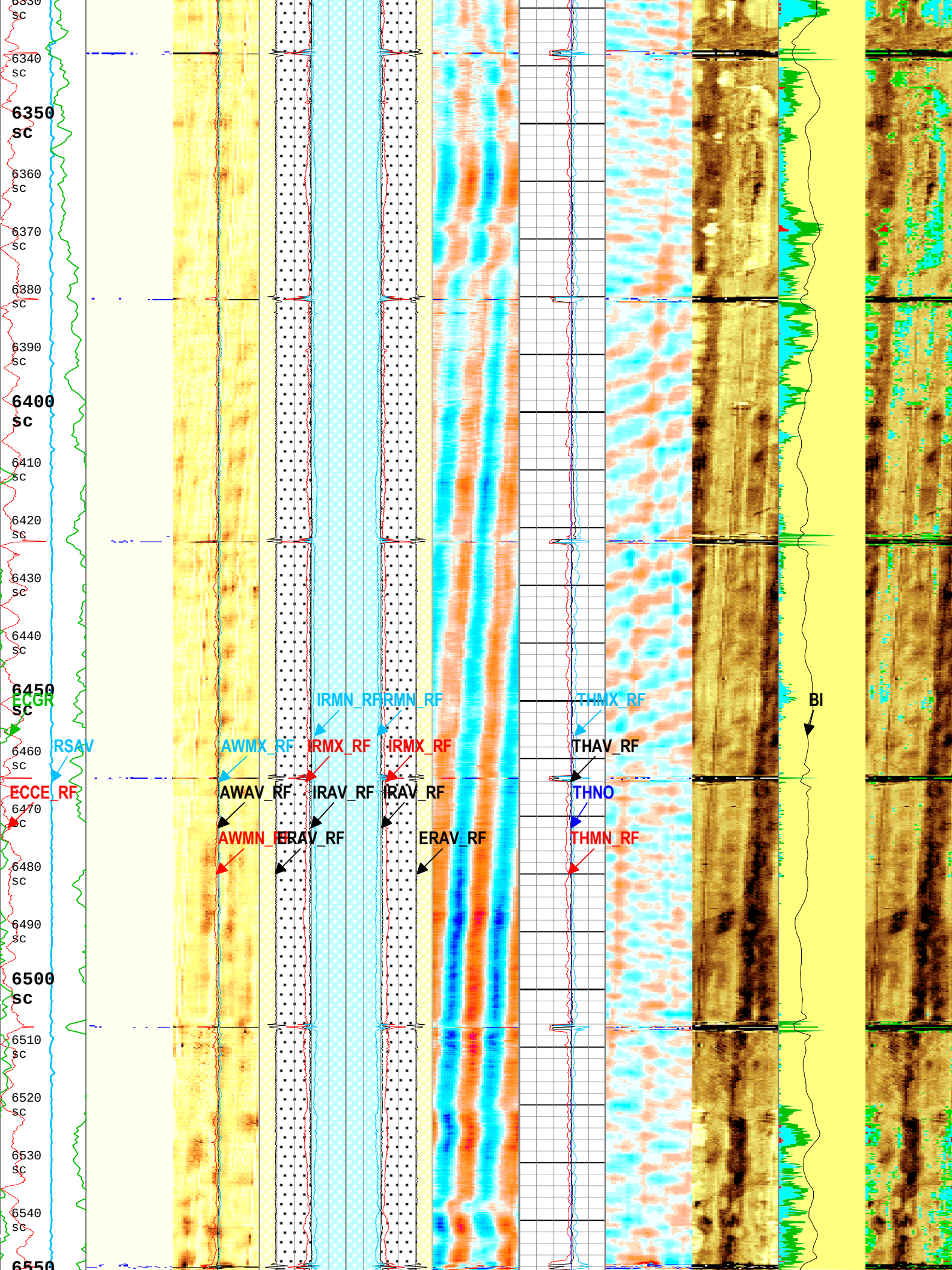
6330 sc
6340 sc
6350 sc
6360 sc
6370 sc
6380 sc
6390 sc
6400 sc
6410 sc
6420 sc
6430 sc
6440 sc
6450 sc
6460 sc
6470 sc
6480 sc
6490 sc
6500 sc
6510 sc
6520 sc
6530 sc
6540 sc
6550
ECGR
RSAV
ECCE_RF
IRMN_RF
IRMN_RF
AWMX_RF
IRMX_RF
IRMX_RF
AWAV_RF
IRAV_RF
IRAV_RF
AWMN_RF
ERAV_RF
ERAV_RF
THMX_RF
THAV_RF
THNO
THMN_RF
BI

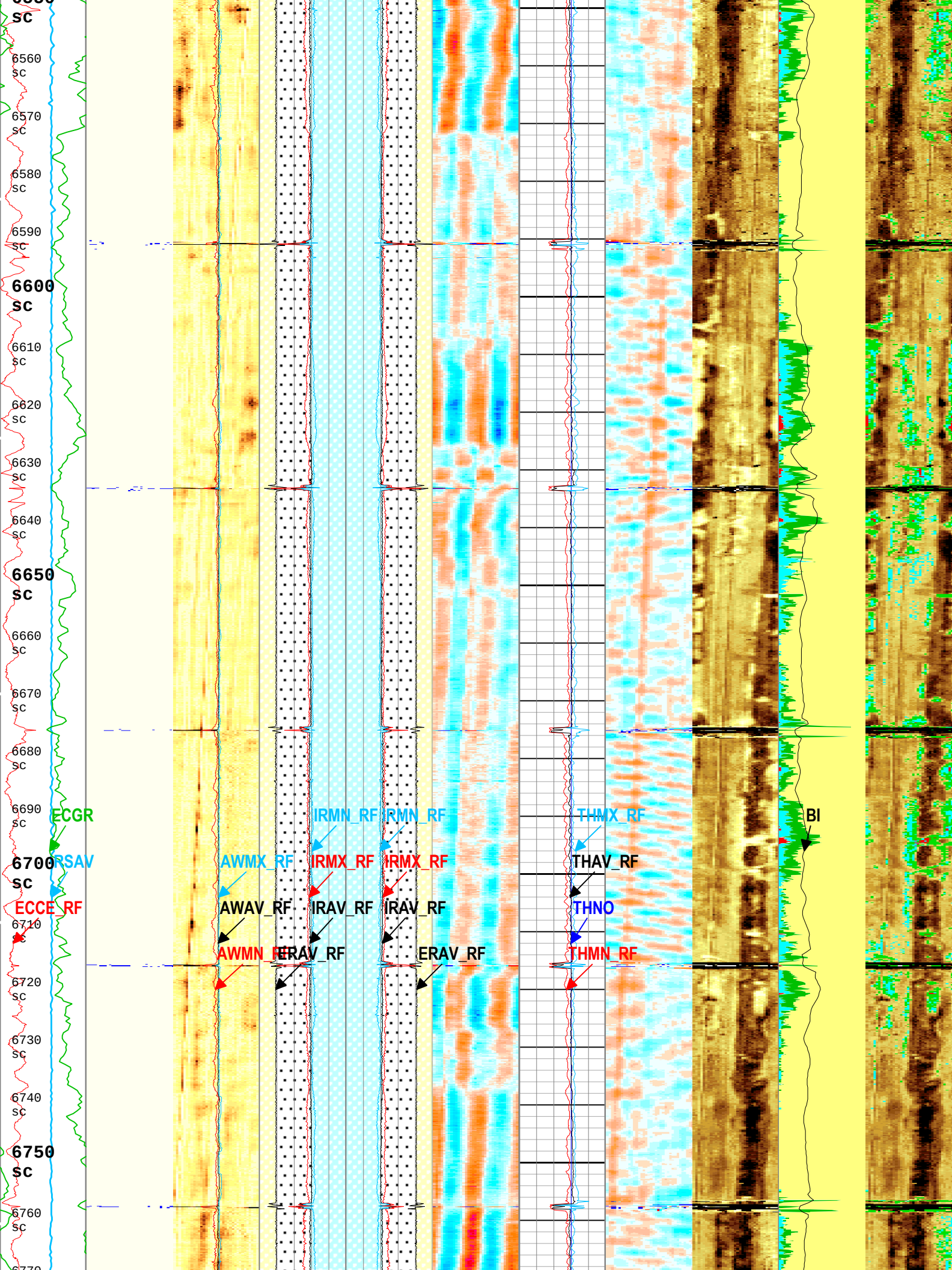
6560 sc
6570 sc
6580 sc
6590 sc
6600 sc
6610 sc
6620 sc
6630 sc
6640 sc
6650 sc
6660 sc
6670 sc
6680 sc
6690 sc
6700 sc
6710 sc
6720 sc
6730 sc
6740 sc
6750 sc
6760 sc
ECGR
RSAV
ECCE_RF
IRMN_RF
IRMN_RF
AWMX_RF
IRMX_RF
IRMX_RF
AWAV_RF
IRAV_RF
IRAV_RF
AWMN_RF
ERAV_RF
ERAV_RF
THMX_RF
THAV_RF
THNO
THMN_RF
BI

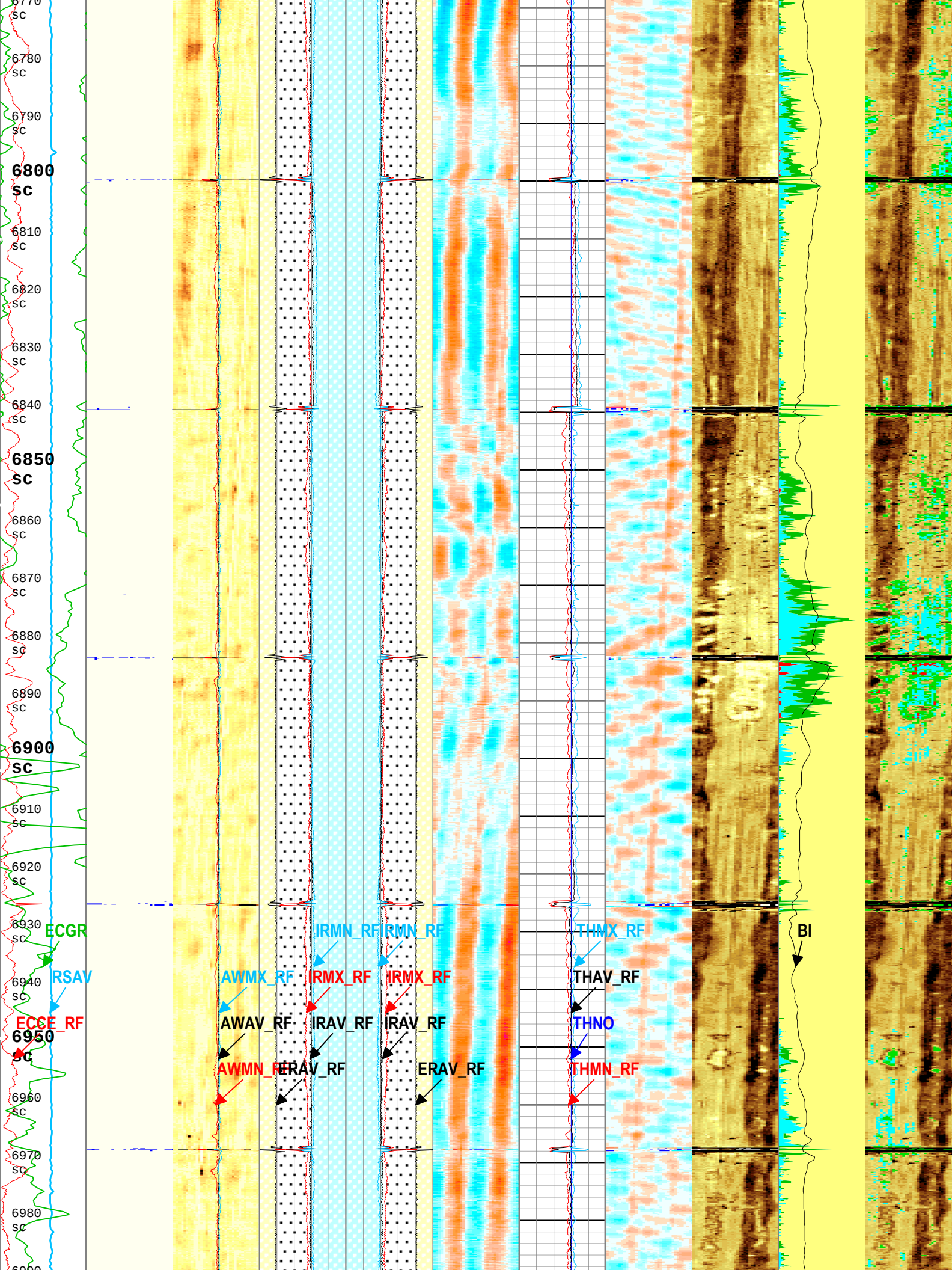
6770 sc
6780 sc
6790 sc
6800 sc
6810 sc
6820 sc
6830 sc
6840 sc
6850 sc
6860 sc
6870 sc
6880 sc
6890 sc
6900 sc
6910 sc
6920 sc
6930 sc
6940 sc
6950 sc
6960 sc
6970 sc
6980 sc
ECGR
RSAV
ECCE_RF
IRMN_RF
IRMN_RF
AWMX_RF
IRMX_RF
IRMX_RF
AWAV_RF
IRAV_RF
IRAV_RF
AWMN_RF
ERAV_RF
ERAV_RF
THMX_RF
THAV_RF
THNO
THMN_RF
BI

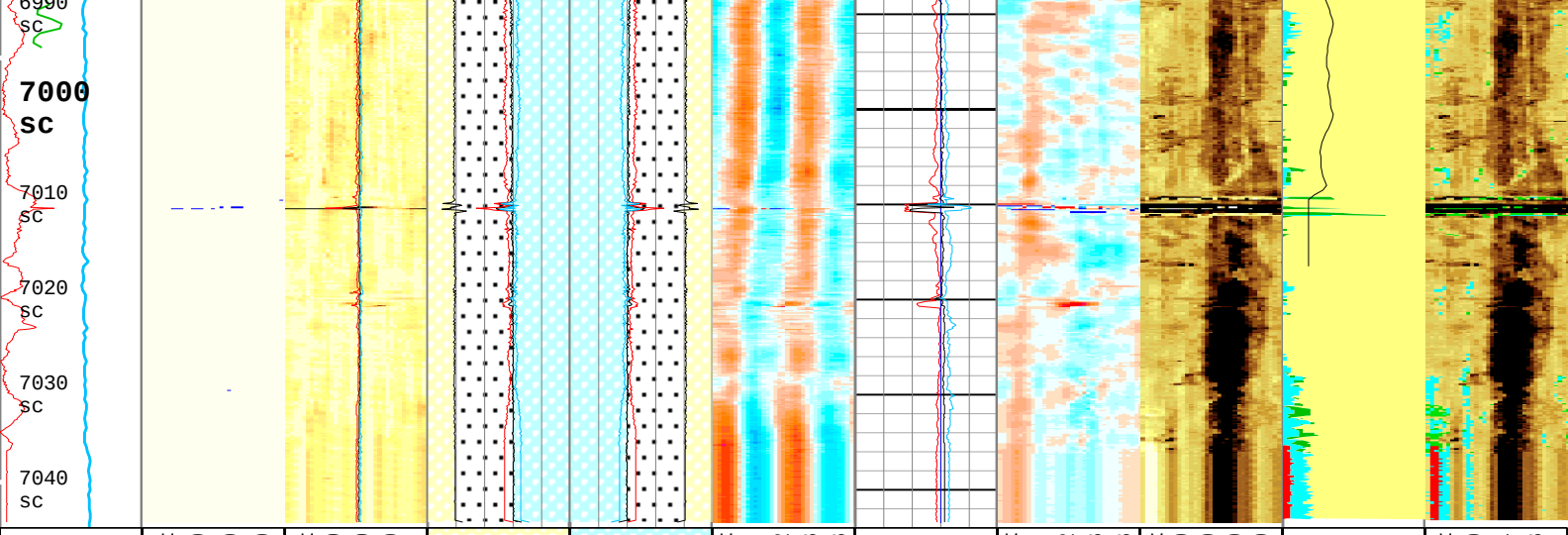

Amplitude of Eccentering for Unflagged Waves (ECCE_RF) USIT-E
0 in 0.5

Motor Revolution Speed (RSAV) USIT-E
6 c/s 8

Gamma Ray (ECGR) HGNS-H
0 gAPI 150

Absent 1.500 2.500 6.500
Explicit Normalization
USIT - USIT Processing Flags (UFLG) USIT-E

USIT Processing Flags (UFLG[0]) USIT-E
1 6

Absent -4.799 -2.799 -0.800
Explicit Normalization
USIT - Amplitude of Unflagged Wave (AWBK_RF) USIT-E (dB)

Minimum of Unflagged Wave Amplitude (AWMN_RF) USIT-E
0 dB 75

Average of Unflagged Wave Amplitude (AWAV_RF) USIT-E
0 dB 75

Maximum of Unflagged Wave Amplitude (AWMX_RF) USIT-E
0 dB 75

ERAV
ERAV-IRAV
IRAV

Median of Unflagged External Radii (ERAV_RF) USIT-E
4.5 in 3.5

Median Internal Radius of Casing Corrected for Eccentering (IRAV_RF) USIT-E
4.5 in 3.5

Maximum of Unflagged Internal Radii (IRMX_RF) USIT-E
4.5 in 3.5

Minimum of Unflagged Internal Radii (IRMN_RF) USIT-E
4.5 in 3.5

IRAV
ERAV
IRAV-ERAV

Median of Unflagged External Radii (ERAV_RF) USIT-E
3.5 in 4.5

Median Internal Radius of Casing Corrected for Eccentering (IRAV_RF) USIT-E
3.5 in 4.5

Maximum of Unflagged Internal Radii (IRMX_RF) USIT-E
3.5 in 4.5

Minimum of Unflagged Internal Radii (IRMN_RF) USIT-E
3.5 in 4.5

Absent -0.051 -0.012 0.028 0.068
Explicit Normalization
USIT - Unflagged Internal Radii minus Median Internal Radius (IRBKM_RF) USIT-E (in)

Minimum of Unflagged Casing Thickness (THMN_RF) USIT-E
0.1 in 0.6

Nominal Casing Thickness (THNO) USIT-E
0.1 in 0.6

Median of Unflagged Casing Thickness (THAV_RF) USIT-E
0.1 in 0.6

Maximum of Unflagged Casing Thickness (THMX_RF) USIT-E
0.1 in 0.6

Absent -0.051 -0.012 0.028 0.068
Explicit Normalization
USIT - Unflagged Casing Thickness minus Median of Unflagged Casing Thickness (THBKM_RF) USIT-E (in)

Absent 1.500 3.500 5.500 7.500
Custom Normalization
USIT - Acoustic Impedance (AIBK) USIT-E (Mrayl)

Ratio of Cement Measurements to Total (CEMR) USIT-E
1 0

Micro-debonding Ratio (MDR) USIT-E
1 0

Ratio of Gas Measurements to Total (GASR) USIT-E
1 0

Bonded
Gas
Liquid
Micro-debonding

Bond Index (BI) DSLT-H
1 0

Absent 3.090 5.054 7.018
Custom Normalization
USIT - Acoustic Impedance (AIBK) USIT-E (Mrayl)

Absent 2.599 4.563 6.527
Custom Normalization
USIT - Acoustic Impedance With Micro-debonding Image (AI_MDEBOND_IMG) USIT-E (Mrayl)

TIME_1900 - Time Marked every 60.00 (s)

USIT Processing Flags (UFLG[0]) USIT-E

1 - UFLG 1 Value within [0.0 - 1.5] - :
2 - UFLG 2 Value within [1.5 - 2.44] - :
3 - UFLG 2 Value within [2.44 - 2.5] - :
4 - UFLG 3 Value within [2.5 - 3.5] - :
5 - UFLG 4 - UFLG 5 - UFLG 6 Value within [2.5 - 6.5] - :

UTIM Error
Pulse Origin Not Detected
Spiky Waveform
WINLEN Error
Casing Thickness Error

5 - UFLG 4 UFLG 5 UFLG 6 Value within [3.5 - 6.5] - : Casing Thickness Error

6 - UFLG 7 UFLG 8 UFLG 9 Value within [6.5 - 10] - : Loop Processing Error

Description: USI Composite Format: Log (USI Composite_7inch) Index Scale: 5 in per 100 ft Index Unit: ft Index Type: Measured Depth Creation Date: 17-Jul-2017 14:11:12

Channel Processing Parameters

One: Parameters

Parameter	Description	Tool	Value	Unit
ISSBAR	Barite Mud Presence Flag	Borehole	No	
BHS	Borehole Status (Open or Cased Hole)	Borehole	Cased	
BS	Bit Size	WLSESSION	Depth Zoned	in
CBLO	Casing Bottom (Logger)	WLSESSION	7331	ft
CBRA	CBL LQC Reference Amplitude in Free Pipe	DSLT-H	55	mV
CDEN	Cement Density	HGNS-H	2.65	g/cm3
CMTY(U-USIT_CEMT)	Cement Type	USIT-E	Regular Cement	
THNO	Nominal Casing Thickness - Zoned along logger depths	WLSESSION	0.4	in
CYSTLGR	Casing Yield Strength - Zoned along logger depths	WLSESSION	Depth Zoned	psi
DETE	Delta-T Detection	DSLT-H	E1	
DFD	Drilling Fluid Density	Borehole	8.9	lbm/gal
DFT_CATEGORY	Drilling Fluid Type	Borehole	Water	
DTMD	Borehole Fluid Slowness	Borehole	193	us/ft
FCF	CBL Fluid Compensation Factor	DSLT-H	0.89	
FDII	FPM Data Interpolation Interval	USIT-E	0	ft
GCSE_DOWN_PASS	Generalized Caliper Selection for WL Log Down Passes	Borehole	BS	
GCSE_UP_PASS	Generalized Caliper Selection for WL Log Up Passes	Borehole	BS	
GOBO_CURR	Good Bond in Arbitrary Cement	DSLT-H	3.39	mV
HEMA	Hematite Presence Flag	Borehole	No	
ICE_PROCESS	ICE Processing	USIT-E	Yes	
IMAR	Image Rotation	USIT-E	Off	
MAHTR	Manual High Threshold Reference for first arrival detection	DSLT-H	120	
MATT_CURR	Maximum Attenuation in Arbitrary Cement	DSLT-H	10.78	dB/ft
MCI	Minimum Cemented Interval for Isolation	DSLT-H	Depth Zoned	ft
MEAS_WLEN	Tcube Processing Window Length in Measurement Mode	USIT-E	24.96	us
MNHTR	Minimum High Threshold Reference for first arrival detection	DSLT-H	100	
MSA	Minimum Sonic Amplitude	DSLT-H	1.69	mV
MSA_CURR	Minimum Sonic Amplitude in Arbitrary Cement	DSLT-H	1.69	mV
MUD_N_FRP	Free Pipe Mud Normalization Factor	USIT-E	1.06	
NMSG	Near Minimum Sliding Gate	DSLT-H	310	us
SGAD	Sliding Gate Status	DSLT-H	Off	
SGDT	Sliding Gate Delta-T	DSLT-H	57	us/ft
THDH	Maximum Search Thickness (percentage of nominal)	USIT-E	130	%
THDL	Minimum Search Thickness (percentage of nominal)	USIT-E	65	%
HISC	Tool Position: Centered or Eccentered	HGNS-H	Centered	
U-USIT_DFSZ	Drilling Fluid Specific Acoustic Impedance	USIT-E	0	Mrayl
UFGDE	Fiberglass Density	USIT-E	1.95	g/cm3
UFGPS	Fiberglass Processing Selection	USIT-E	No	
UFGVL	Fiberglass Velocity	USIT-E	9678.48	ft/s
USI_FSOD	USIT USI Fluid Slowness Fits Casing Outer Diameter	USIT-E	0_OFF	
USI_FVEL_SEL	USI Fluid Velocity Selection	USIT-E	Automatic	
USI_ZMUD_SEL	USI Mud Impedance Selection	USIT-E	FreePipe Norm.	
ZMUD	Acoustic Impedance of Mud	Borehole	1.68	Mrayl

ZTCM	Acoustic Impedance Threshold for Cement	USIT-E	2.6	Mrayl
ZTGS	Acoustic Impedance Threshold for Gas	USIT-E	0.3	Mrayl

Depth Zone Parameters

Parameter	Value	Start (ft)	Stop (ft)
BS	17.5	10	832
BS	11	832	7044
CYSTLGR	55000	10	5835
CYSTLGR	80000	5835	7044
MCI	21.68	10	830
MCI	12.98	830	7044

All depth are actual.

Tool Control Parameters

One: Parameters

Parameter	Description	Tool	Value	Unit
AGMN	Minimum Gain of Cartridge	USIT-E	-12	dB
AGMX	Maximum Gain of Cartridge	USIT-E	48	dB
U-USIT_DDT5	USIC Downhole Decimation for T5 only	USIT-E	0_NONE	
MODE	DSLT Acquisition Mode	DSLT-H	CBL	
RATE	DSLT Firing Rate	DSLT-H	15 Hz	
DTFS	DSLT Telemetry Frame Size	DSLT-H	536	
EMXV	EMEX Voltage	USIT-E	80	V
HRES	Horizontal Resolution	USIT-E	10 deg	
TMUC	Type of Mud	USIT-E	BRI	
ULOG	Logging Objective	USIT-E	MEASUREMENT	
UMFR	Modulation Frequency	USIT-E	333333	Hz
USFR	Ultrasonic Sampling Frequency	USIT-E	500000	Hz
UPAT	USIT Emission Pattern	USIT-E	Pattern 500 KHz	
UWKM	USIT Working Mode	USIT-E	Uncompressed 10 deg at 1.5 in LF	
USIT_DEPTHLOG	Starting Depth Log for Ultrasonics	USIT-E	7030	ft
VRES	Vertical Resolution	USIT-E	1.5 in	
WINB	Window Begin Time	USIT-E	59.63	us
WINE	Window End Time	USIT-E	99.63	us

One

USIT Cement Log 2 IN = 100 FT

Pass Summary

Run Name	Pass Objective	Direction	Top	Bottom	Start	Stop	DSC Mode	Depth Shift	Include Parallel Data
One	Log[4]:Up	Up	4.12 ft	7044.38 ft	02-Jun-2017 1:27:12 AM	02-Jun-2017 4:20:07 AM	ON	4.20 ft	Yes

All depths are referenced to toolstring zero

Log

Company:Southern California Gas Company Well:Fernando Fee 35B

One: Log[4]:Up:S011

Description: USI Cement Format: Log (LBV1_USI Cement 7inch) Index Scale: 2 in per 100 ft Index Unit: ft Index Type: Measured Depth Creation Date: 17-Jul-2017 14:11:28

TIME_1900 - Time Marked every 60.00 (s)

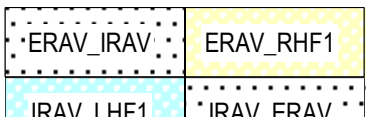

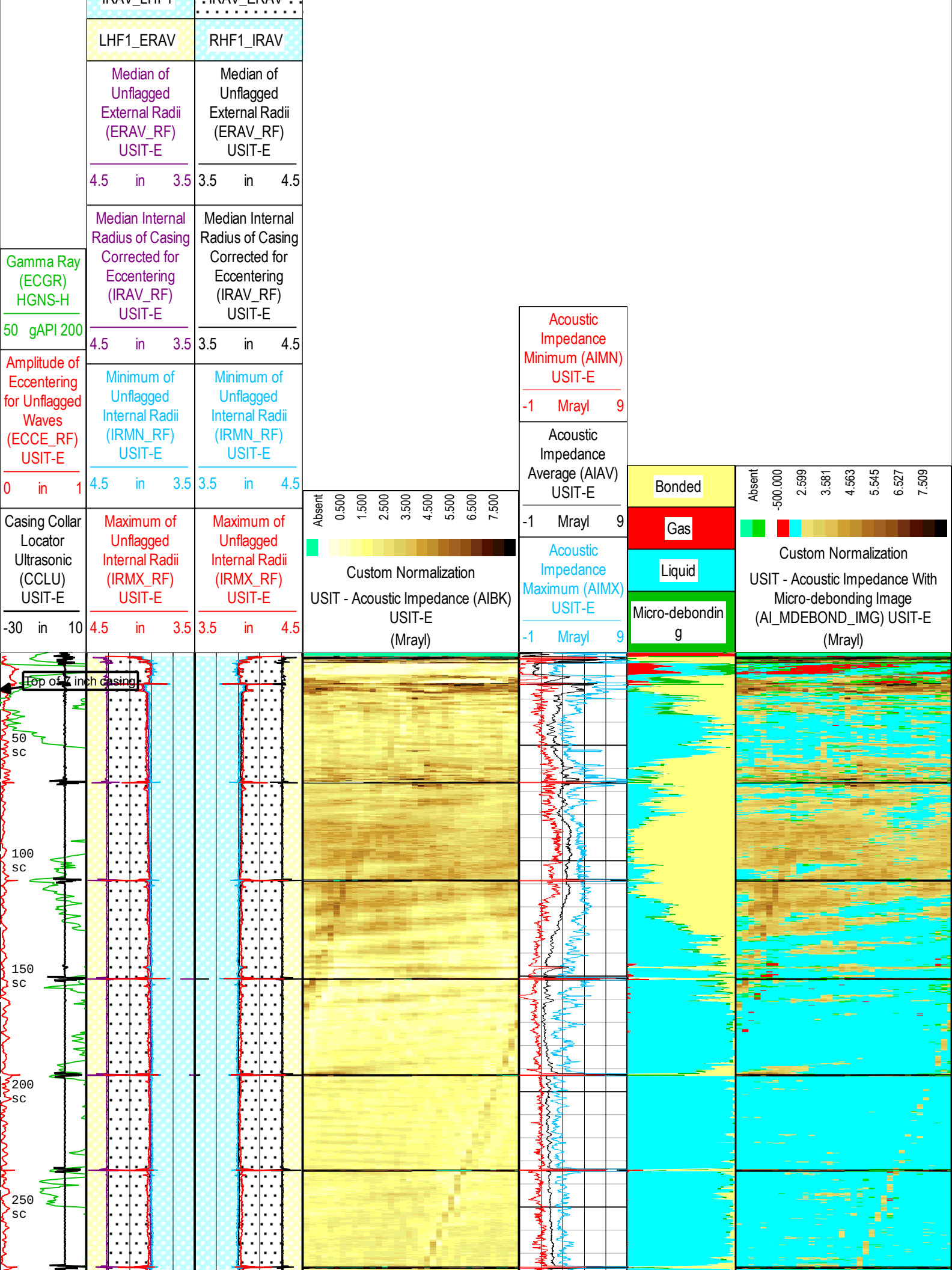
LHF1_ERAV
RHF1_IRAV
Median of Unflagged External Radii (ERAV_RF) USIT-E
4.5 in 3.5
3.5 in 4.5
Median Internal Radius of Casing Corrected for Eccentering (IRAV_RF) USIT-E
4.5 in 3.5
3.5 in 4.5
Gamma Ray (ECGR) HGNS-H
50 gAPI 200
Amplitude of Eccentering for Unflagged Waves (ECCE_RF) USIT-E
0 in 1
Minimum of Unflagged Internal Radii (IRMN_RF) USIT-E
4.5 in 3.5
3.5 in 4.5
Casing Collar Locator Ultrasonic (CCLU) USIT-E
-30 in 10
Maximum of Unflagged Internal Radii (IRMX_RF) USIT-E
4.5 in 3.5
3.5 in 4.5
Top of 7 inch casing
50 sc
100 sc
150 sc
200 sc
250 sc
Absent
0.500
1.500
2.500
3.500
4.500
5.500
6.500
7.500
Custom Normalization
USIT - Acoustic Impedance (AIBK) USIT-E (Mrayl)
Acoustic Impedance Minimum (AIMN) USIT-E
-1 Mrayl 9
Acoustic Impedance Average (AIAV) USIT-E
-1 Mrayl 9
Acoustic Impedance Maximum (AIMX) USIT-E
-1 Mrayl 9
Bonded
Gas
Liquid
Micro-debonding
Absent
-500.000
2.599
3.581
4.563
5.545
6.527
7.509
Custom Normalization
USIT - Acoustic Impedance With Micro-debonding Image (AI_MDEBOND_IMG) USIT-E (Mrayl)

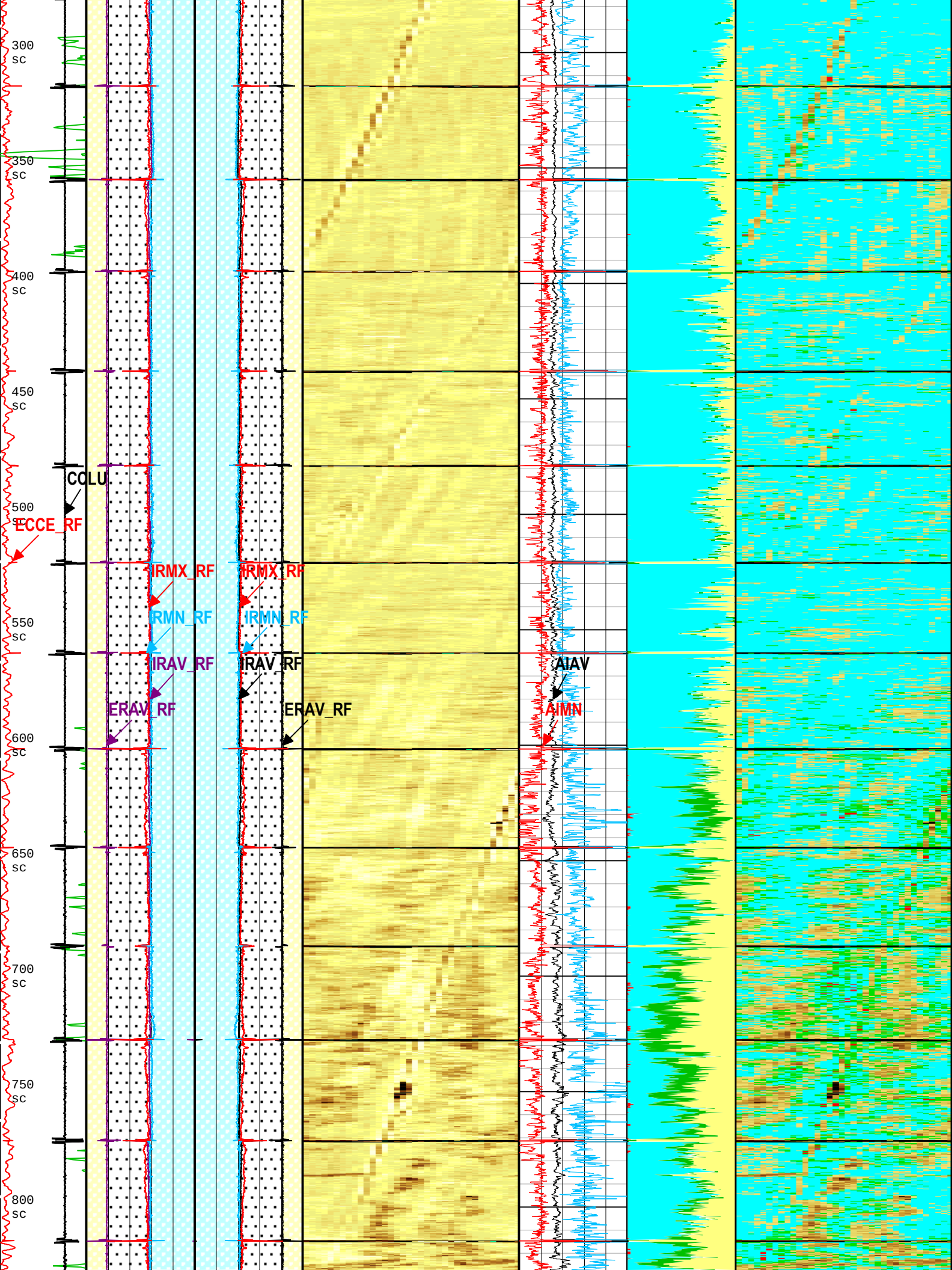
300 sc
350 sc
400 sc
450 sc
500 sc
550 sc
600 sc
650 sc
700 sc
750 sc
800 sc
COLU
ECCE_RF
IRMX_RF
IRMX_RF
IRMN_RF
IRMN_RF
IRAV_RF
IRAV_RF
ERAV_RF
ERAV_RF
AIAV
AIMN

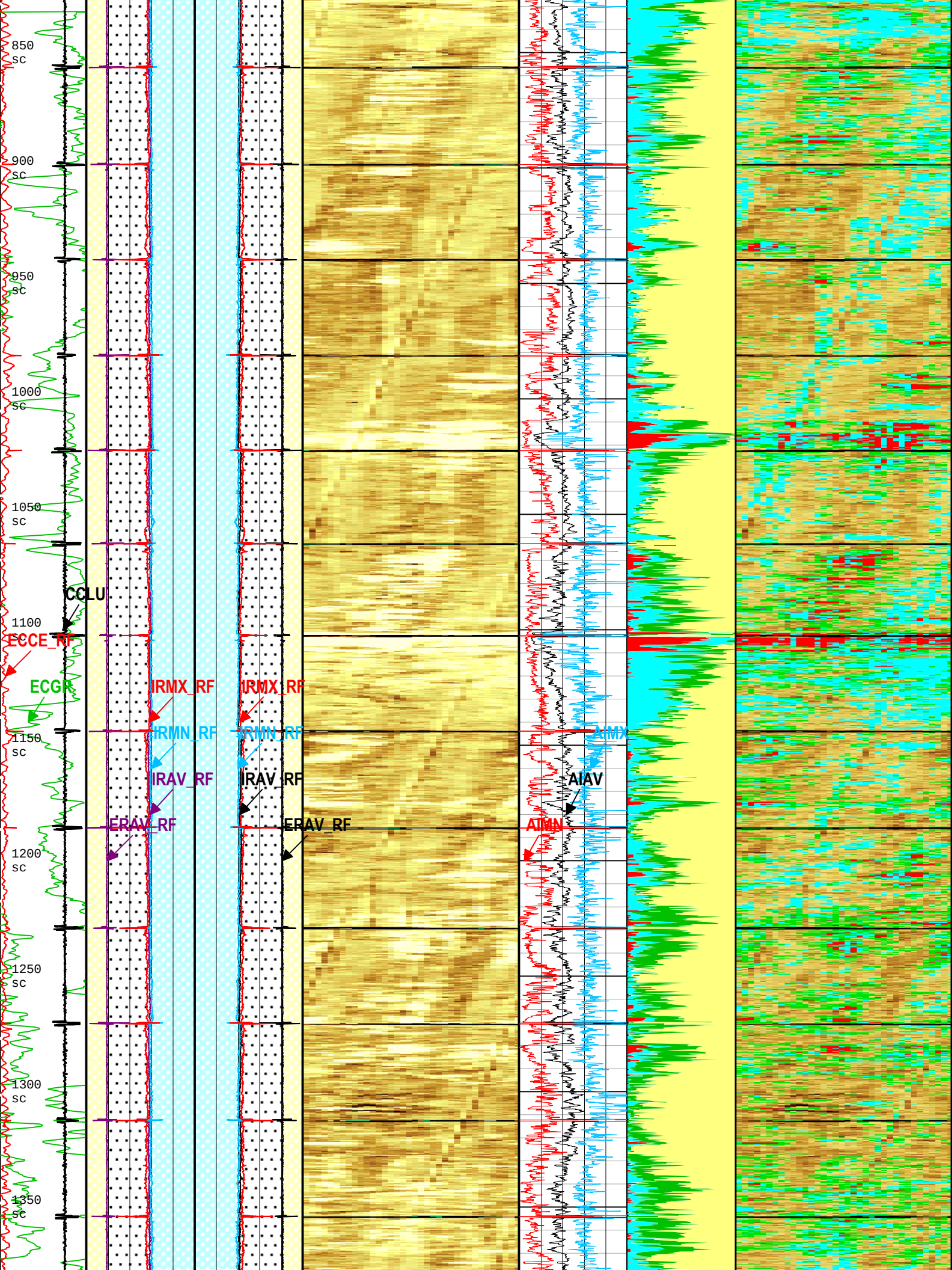
850
sc
900
sc
950
sc
1000
sc
1050
sc
CCLU
1100
ECCE_RF
ECGR
IRMX_RF
IRMX_RF
IRMN_RF
IRMN_RF
1150
sc
AIMX
IRAV_RF
IRAV_RF
AIAV
ERAV_RF
ERAV_RF
AIMN
1200
sc
1250
sc
1300
sc
1350
sc

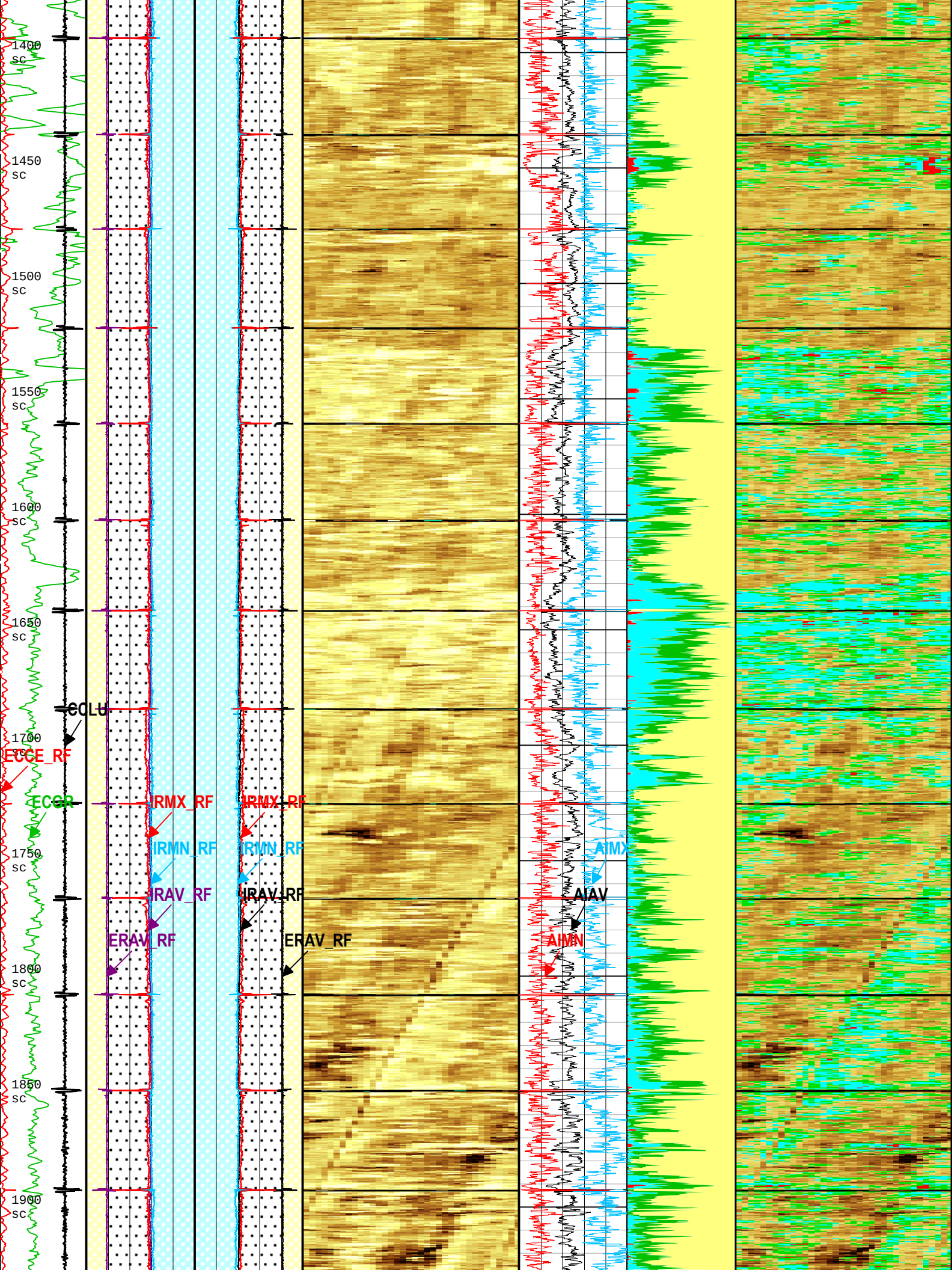
1400 sc
1450 sc
1500 sc
1550 sc
1600 sc
1650 sc
1700 sc
1750 sc
1800 sc
1850 sc
1900 sc
COLU
ECCE_RF
ECGR
IRMX_RF
IRMX_RF
IRMN_RF
IRMN_RF
IRAV_RF
IRAV_RF
ERAV_RF
ERAV_RF
AIMX
AIAV
AIMN

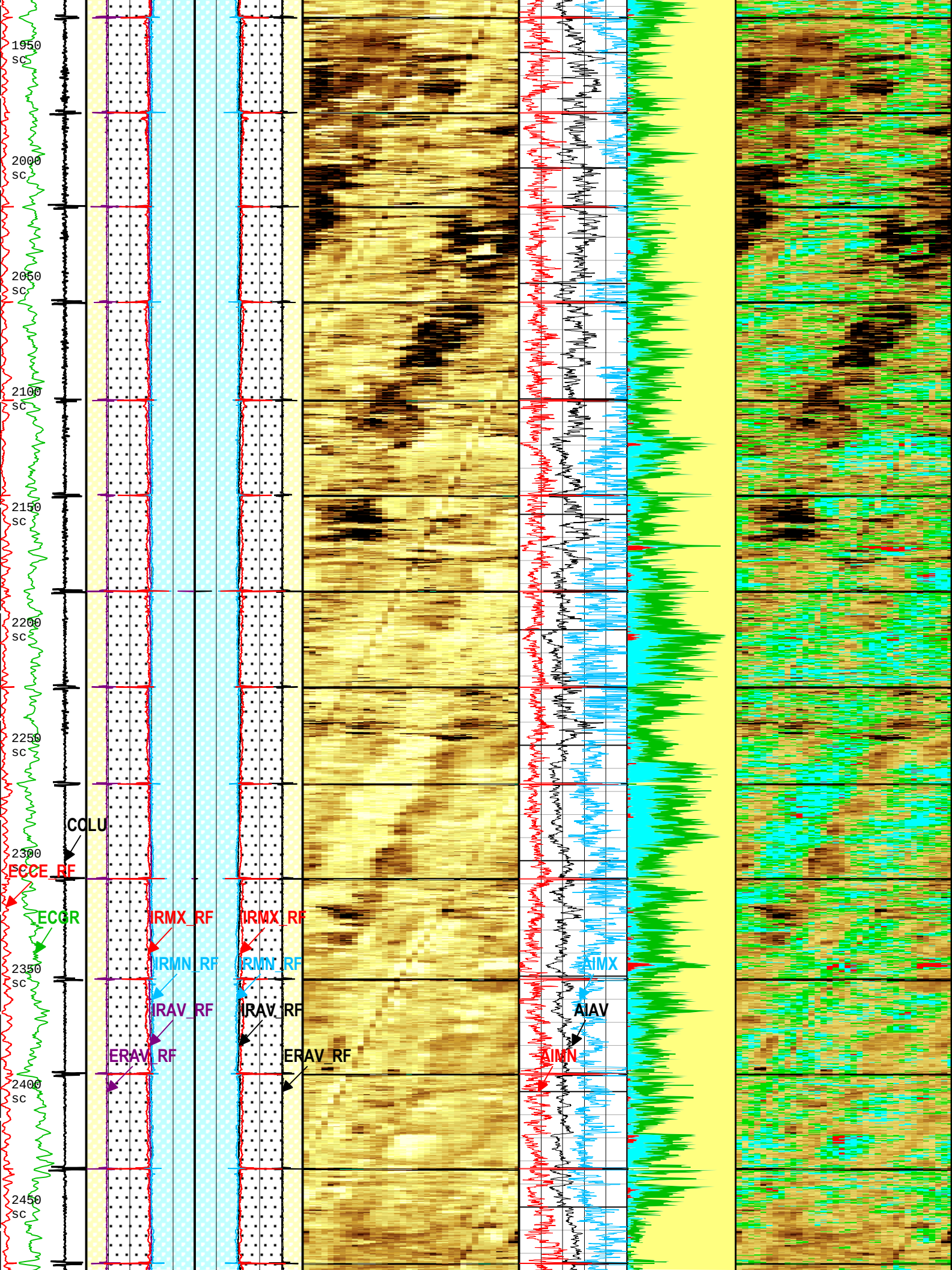
1950
sc
2000
sc
2050
sc
2100
sc
2150
sc
2200
sc
2250
sc
COLU
2300
ECCE_RF
ECGR
IRMX_RF
IRMX_RF
IRMN_RF
IRMN_RF
2350
sc
AIMX
IRAV_RF
IRAV_RF
AIAV
ERAV_RF
ERAV_RF
AIMN
2400
sc
2450
sc

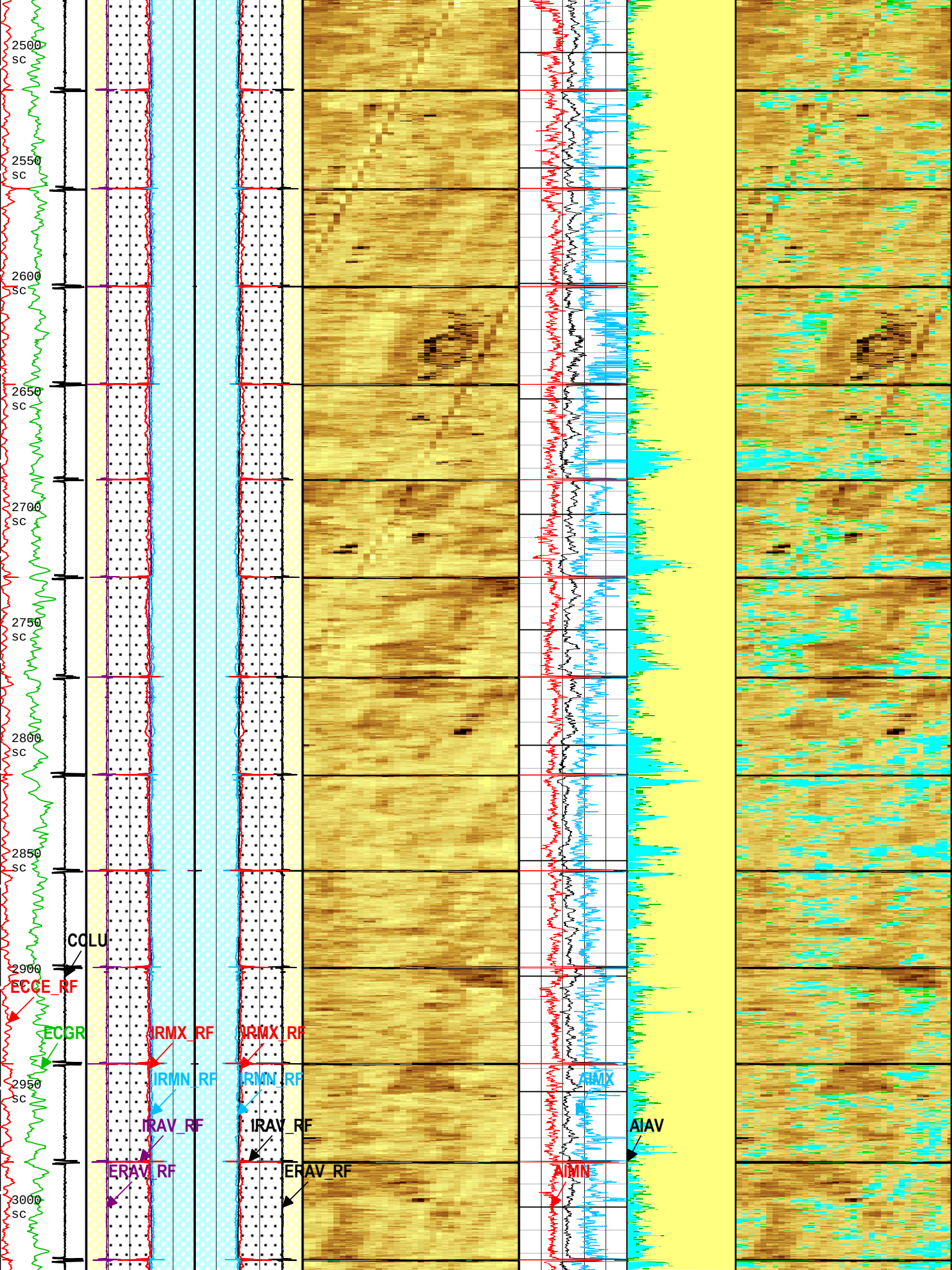
2500 sc
2550 sc
2600 sc
2650 sc
2700 sc
2750 sc
2800 sc
2850 sc
2900 sc
2950 sc
3000 sc
COLU
ECCE_RF
ECGR
IRMX_RF
IRMX_RF
IRMN_RF
IRMN_RF
IRAV_RF
IRAV_RF
ERAV_RF
ERAV_RF
AIMX
AIAV
AIMN

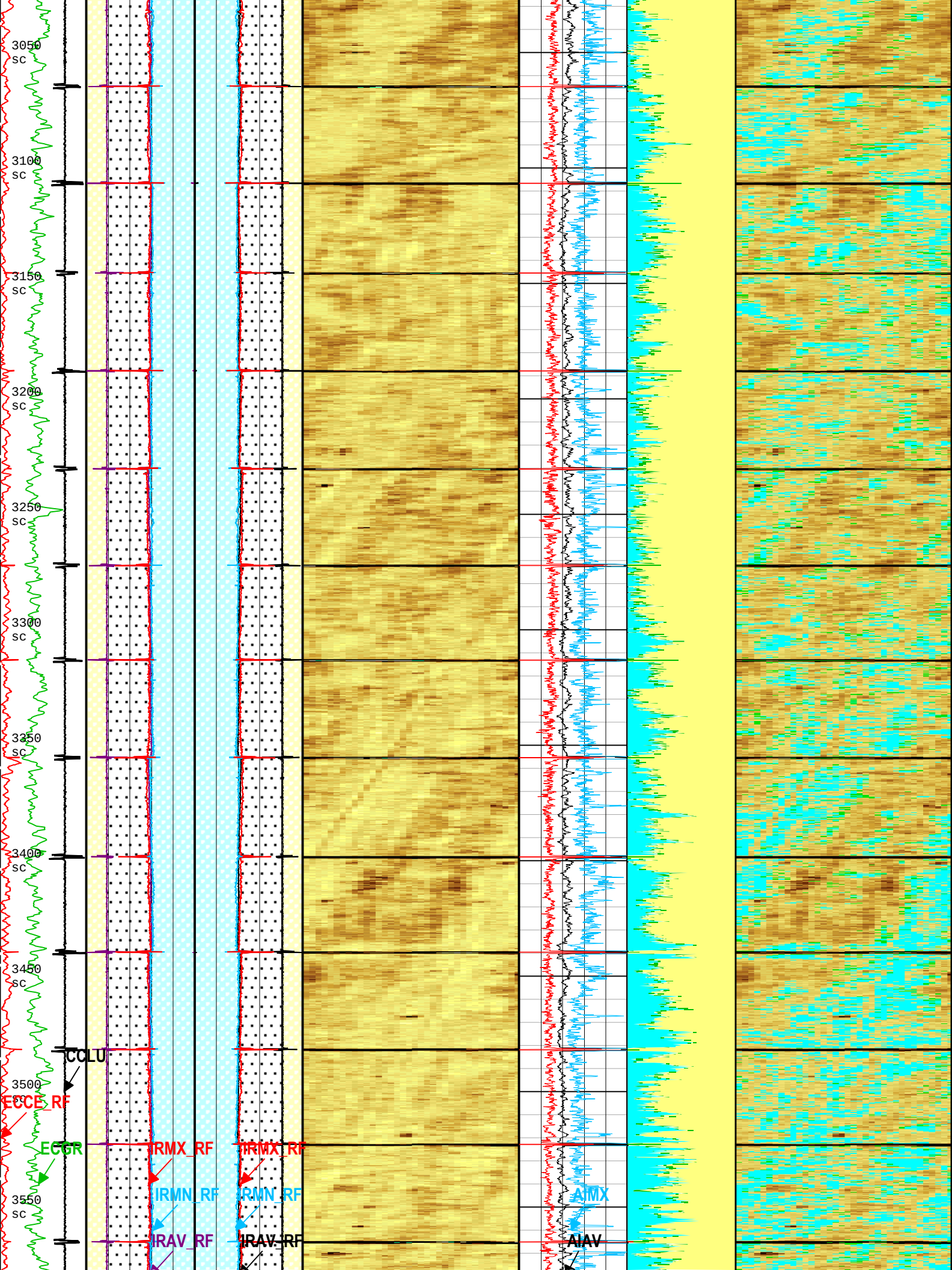
3050
sc
3100
sc
3150
sc
3200
sc
3250
sc
3300
sc
3350
sc
3400
sc
3450
sc
CCLU
3500
ECCE_RF
ECGR
IRMX_RF
IRMX_RF
IRMN_RF
IRMN_RF
AIMX
3550
sc
IRAV_RF
IRAV_RF
AIAV

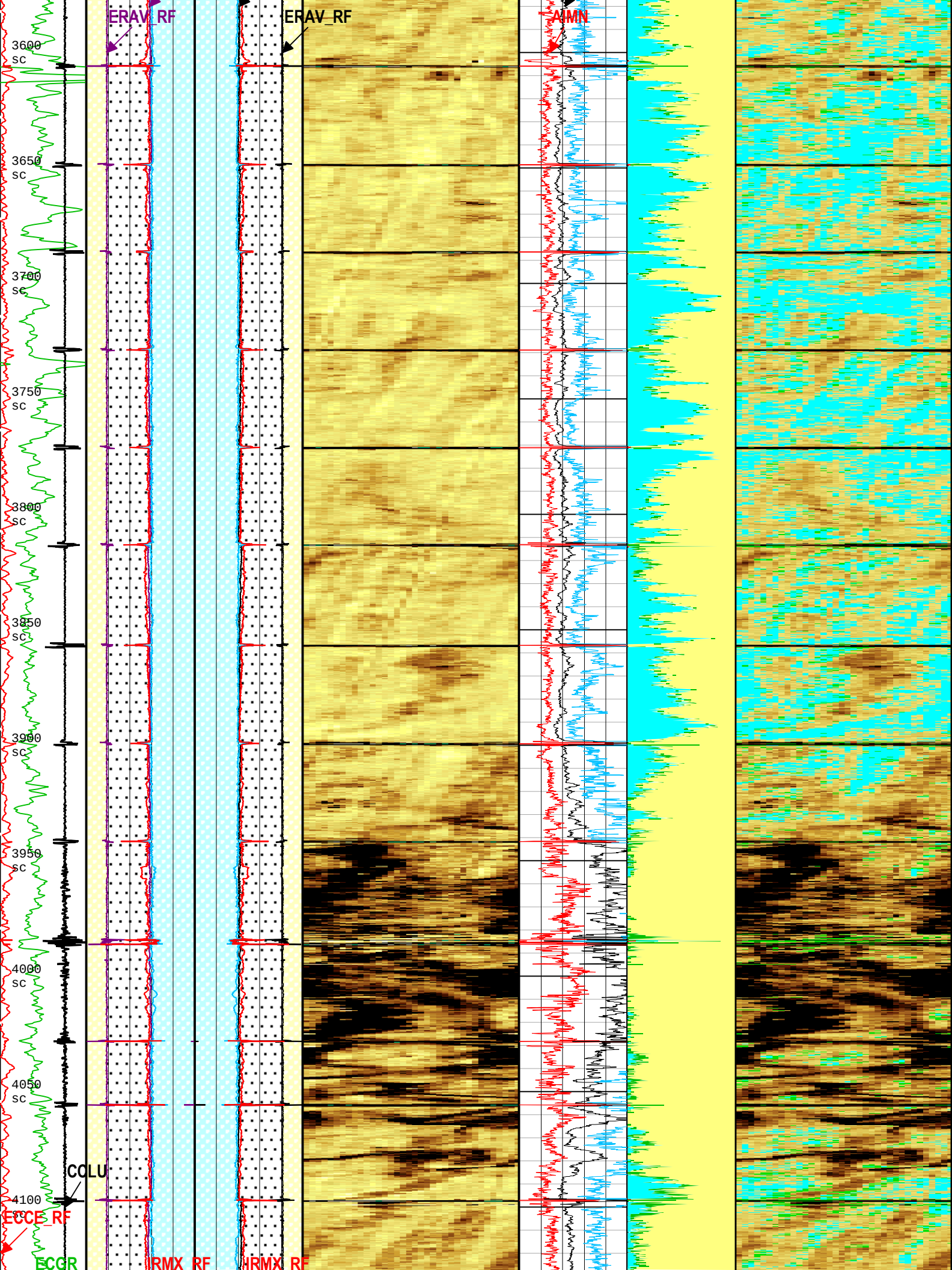
ERAV_RF
ERAV_RF
AMN
3600
sc
3650
sc
3700
sc
3750
sc
3800
sc
3850
sc
3900
sc
3950
sc
4000
sc
4050
sc
COLU
4100
sc
ECCE_RF
ECGR
RMX_RF
HRMX_RF

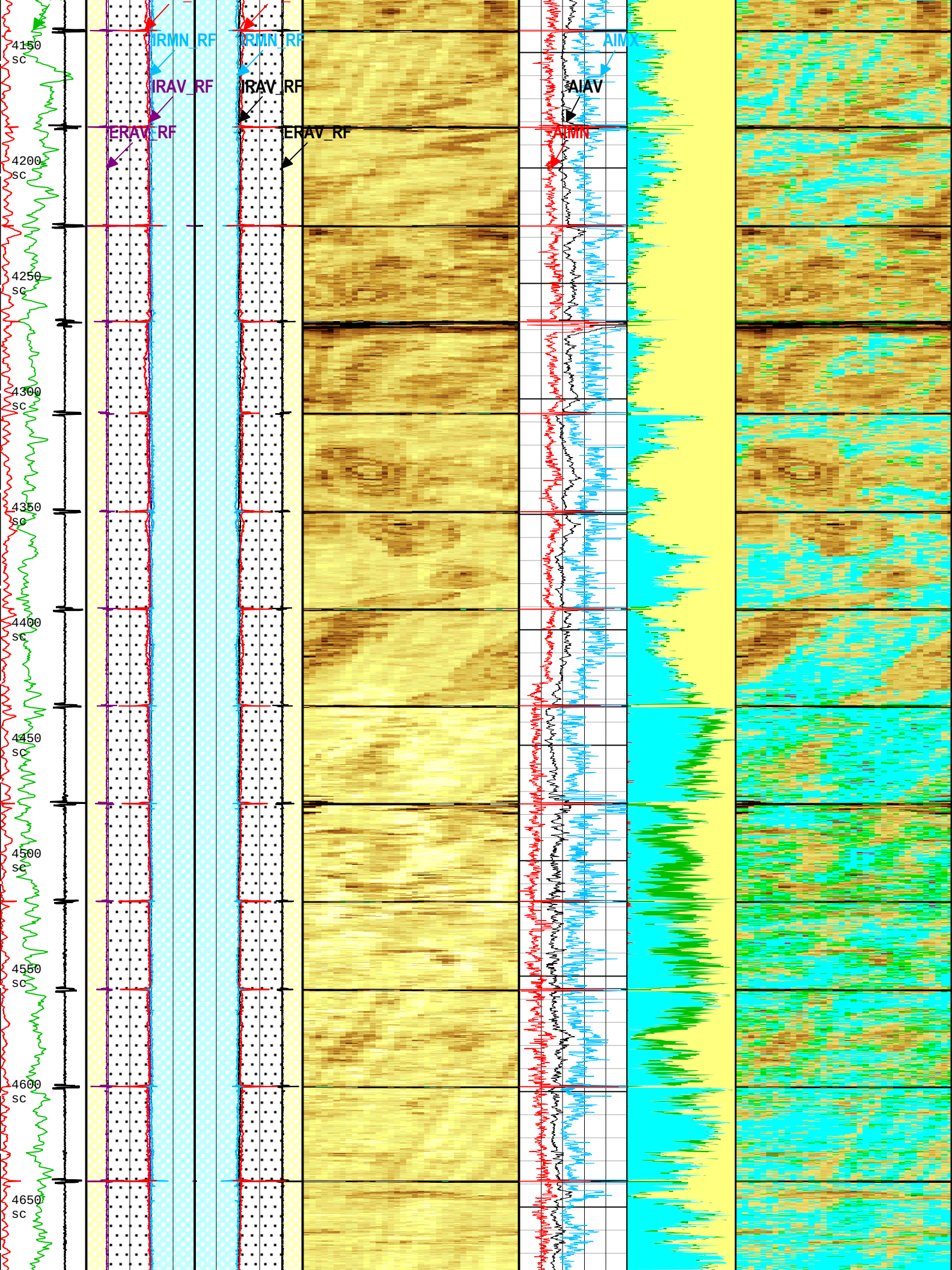
IRMN_RF
IRMN_RF
AIMX
IRAV_RF
IRAV_RF
AIAV
ERAV_RF
ERAV_RF
AIMN
4150 sc
4200 sc
4250 sc
4300 sc
4350 sc
4400 sc
4450 sc
4500 sc
4550 sc
4600 sc
4650 sc

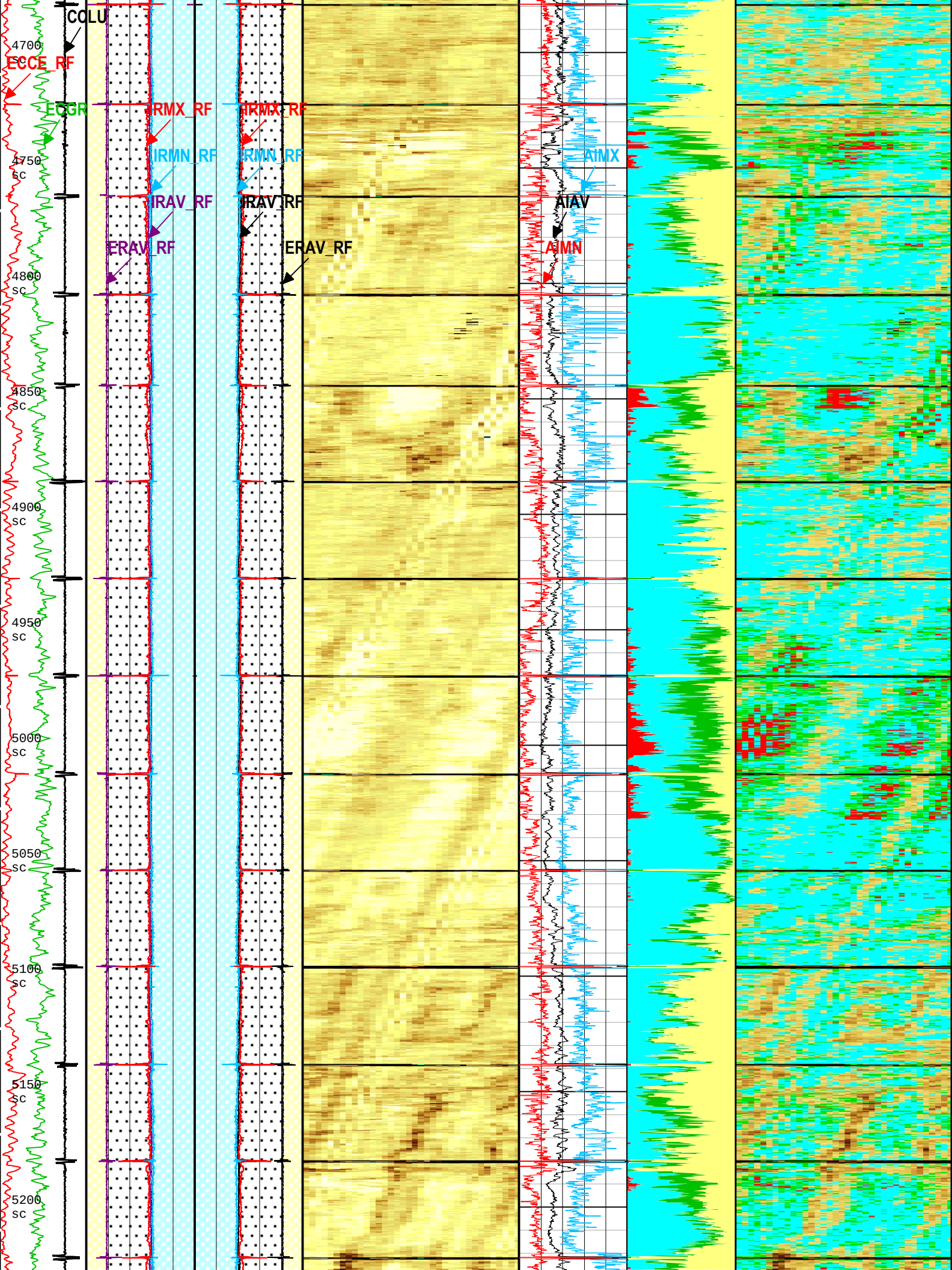
COLU
4700
ECCE_RF
ECGR
IRMX_RF
IRMX_RF
IRMN_RF
IRMN_RF
AIMX
4750
sc
IRAV_RF
IRAV_RF
AIAV
ERAV_RF
ERAV_RF
AIMN
4800
sc
4850
sc
4900
sc
4950
sc
5000
sc
5050
sc
5100
sc
5150
sc
5200
sc

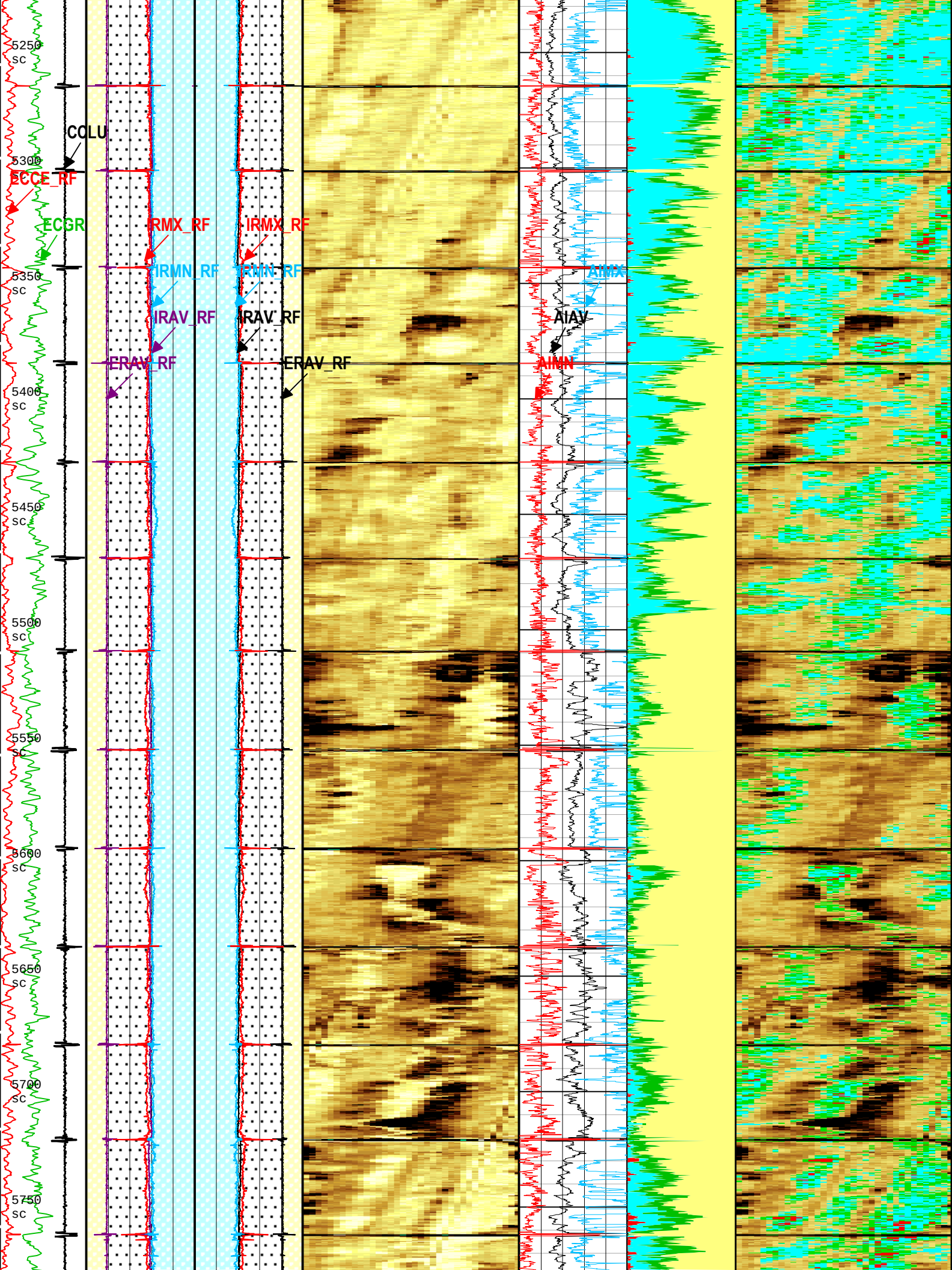
5250
sc
COLU
5300
ECCE_RF
ECGR
RMX_RF
IRMX_RF
IRMN_RF
IRMN_RF
5350
sc
AIMX
IRAV_RF
IRAV_RF
AIAV
ERAV_RF
ERAV_RF
AIMN
5400
sc
5450
sc
5500
sc
5550
sc
5600
sc
5650
sc
5700
sc
5750
sc

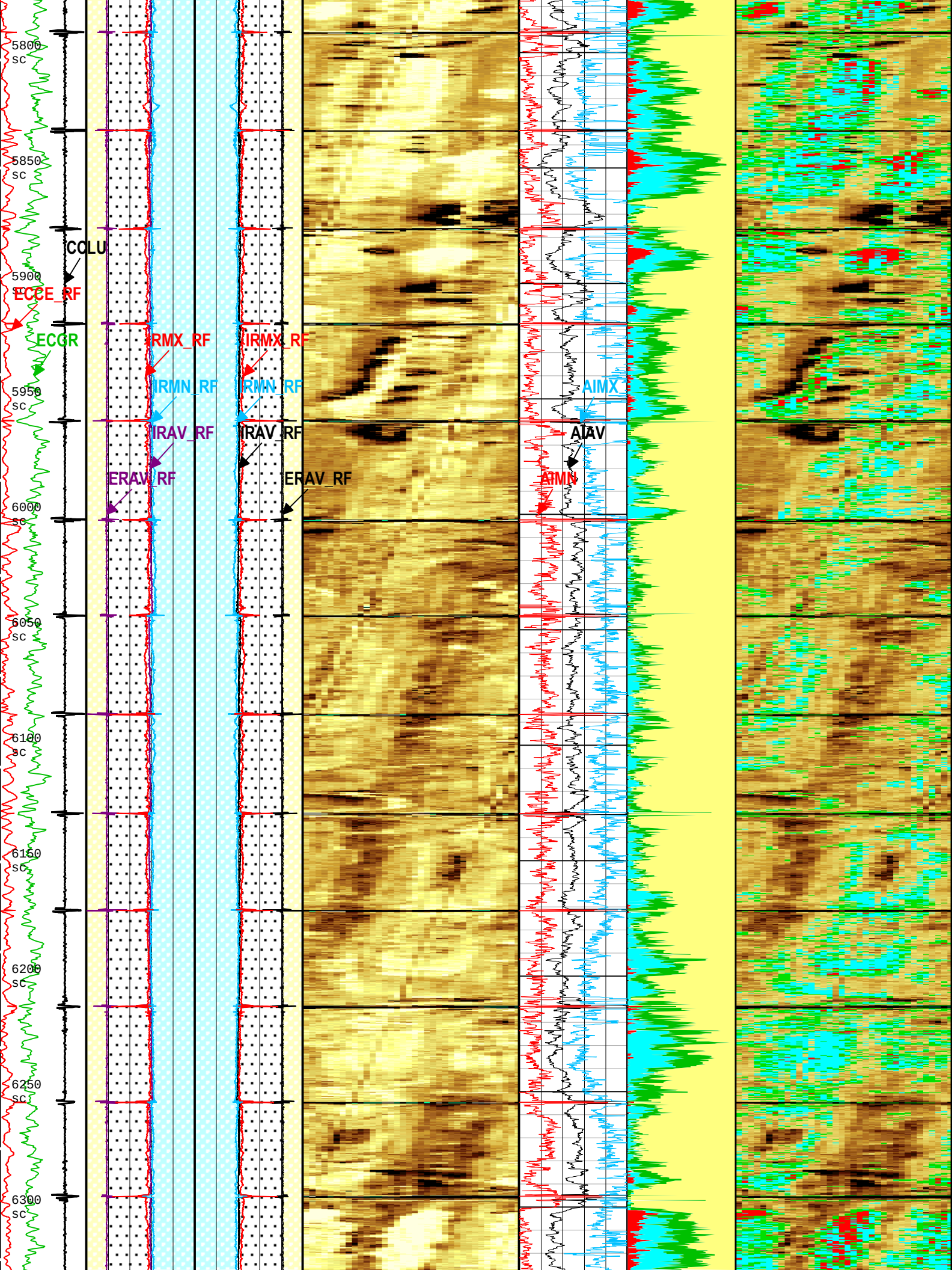
5800
sc
5850
sc
COLU
5900
sc
ECCE_RF
ECGR
IRMX_RF
IRMX_RF
5950
sc
IRMN_RF
IRMN_RF
AIMX
IRAV_RF
IRAV_RF
AIAV
ERAV_RF
ERAV_RF
AIMN
6000
sc
6050
sc
6100
sc
6150
sc
6200
sc
6250
sc
6300
sc

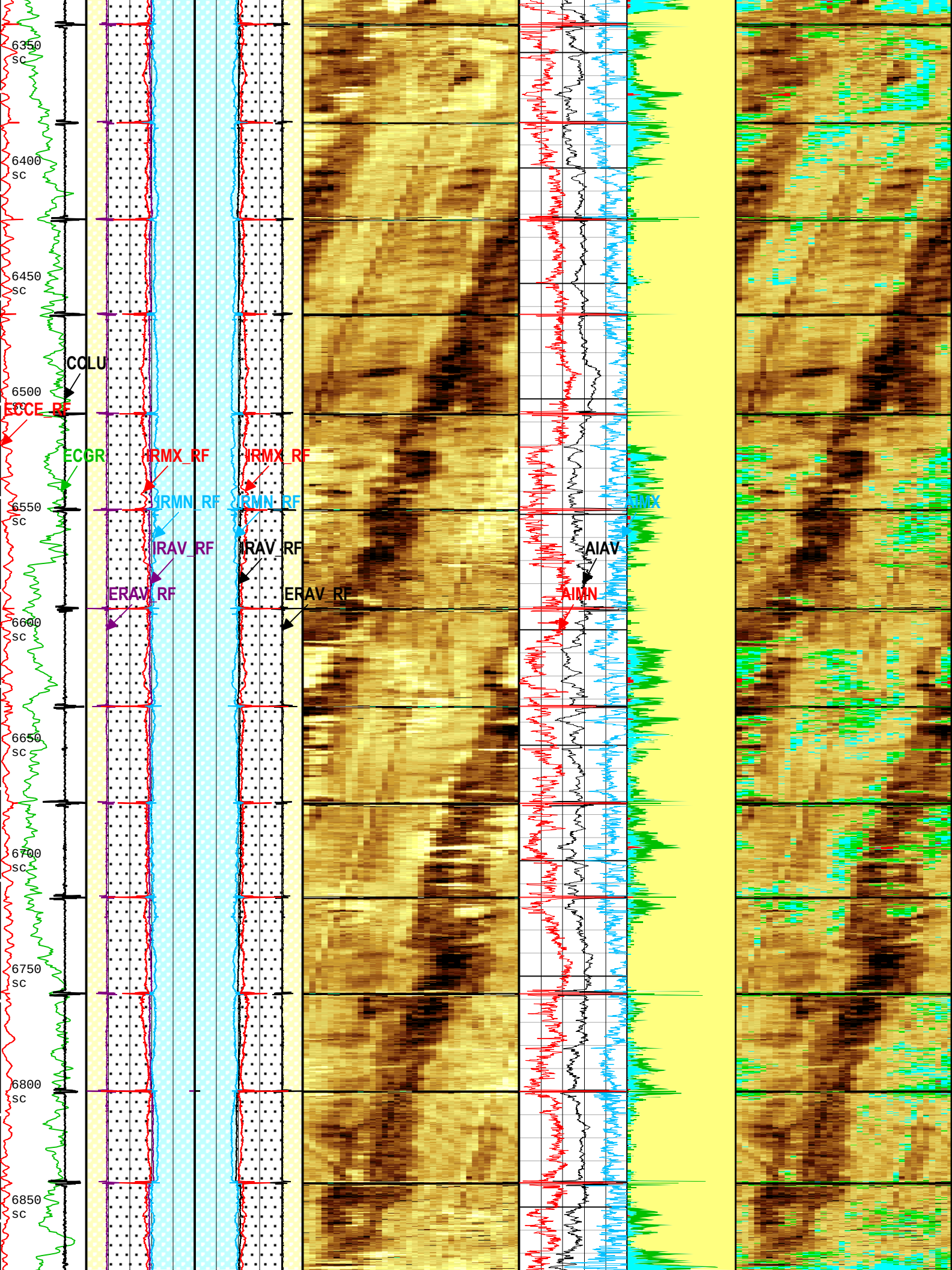
6350 sc
6400 sc
6450 sc
COLU
6500 sc
ECCE_RF
ECGR
IRMX_RF
IRMX_RF
IRMN_RF
IRMN_RF
6550 sc
AIMX
IRAV_RF
IRAV_RF
AIAV
ERAV_RF
ERAV_RF
AIMN
6600 sc
6650 sc
6700 sc
6750 sc
6800 sc
6850 sc

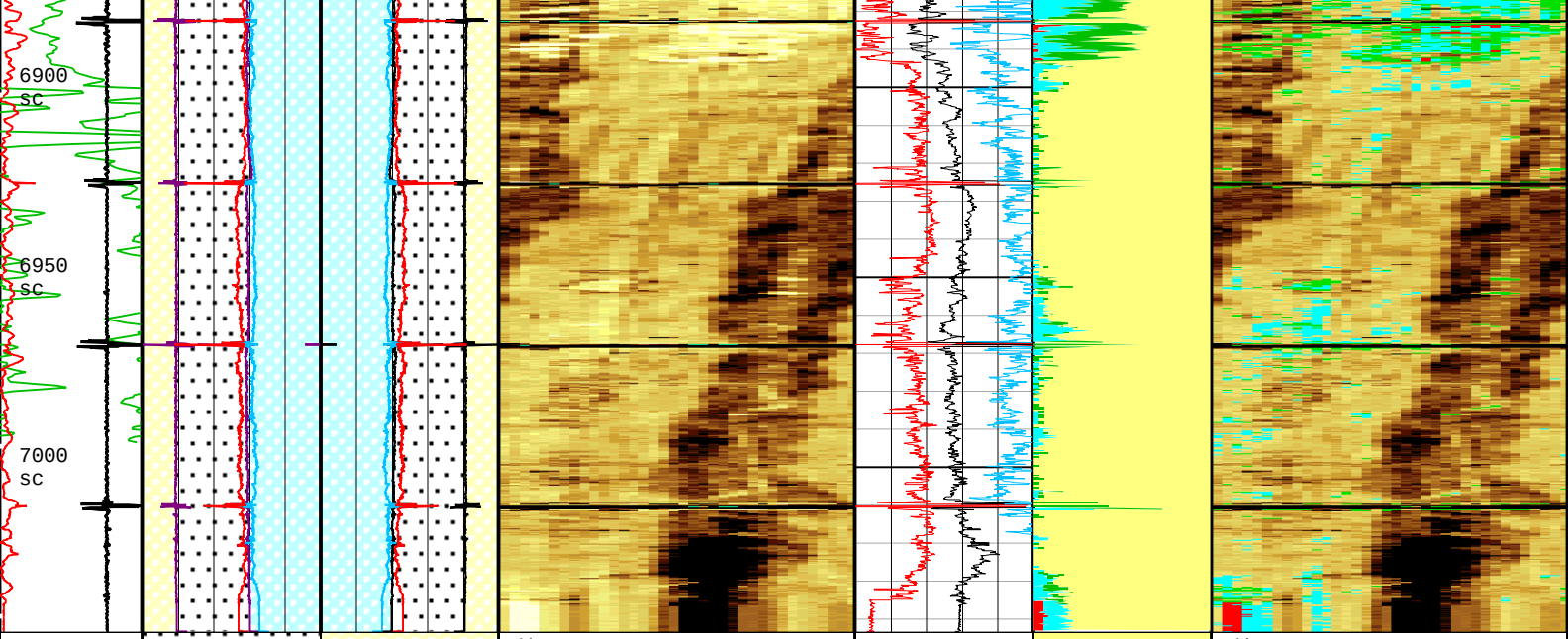

Gamma Ray (ECGR) HGNS-H
50 gAPI 200

Amplitude of Eccentering for Unflagged Waves (ECCE_RF) USIT-E
0 in 1

Casing Collar Locator Ultrasonic (CCLU) USIT-E
-30 in 10

ERAV_IRAV

IRAV_LHF1

LHF1_ERAV

ERAV_RHF1

IRAV_ERAV

RHF1_IRAV

Median of Unflagged External Radii (ERAV_RF) USIT-E
4.5 in 3.5

Median of Unflagged External Radii (ERAV_RF) USIT-E
3.5 in 4.5

Median Internal Radius of Casing Corrected for Eccentering (IRAV_RF) USIT-E
4.5 in 3.5

Median Internal Radius of Casing Corrected for Eccentering (IRAV_RF) USIT-E
3.5 in 4.5

Minimum of Unflagged Internal Radii (IRMN_RF) USIT-E
4.5 in 3.5

Minimum of Unflagged Internal Radii (IRMN_RF) USIT-E
3.5 in 4.5

Maximum of Unflagged Internal Radii (IRMX_RF) USIT-E
4.5 in 3.5

Maximum of Unflagged Internal Radii (IRMX_RF) USIT-E
3.5 in 4.5

Custom Normalization
USIT - Acoustic Impedance (AIBK) USIT-E
(Mrayl)

Acoustic Impedance Minimum (AIMN) USIT-E
-1 Mrayl 9

Acoustic Impedance Average (AIAV) USIT-E
-1 Mrayl 9

Acoustic Impedance Maximum (AIMX) USIT-E
-1 Mrayl 9

Bonded

Gas

Liquid

Micro-debonding

Custom Normalization
USIT - Acoustic Impedance With Micro-debonding Image (AI_MDEBOND_IMG) USIT-E
(Mrayl)

TIME_1900 - Time Marked every 60.00 (s)

Description: USI Cement Format: Log (LBV1_USI Cement 7inch) Index Scale: 2 in per 100 ft Index Unit: ft Index Type: Measured Depth Creation Date: 17-Jul-2017 14:11:28

One

USIT CORROSION 5" = 100'

Software Version

Acquisition System	Version
Maxwell 2017 SP1	7.1.82245.3100

Pass Summary

Run Name	Pass Objective	Direction	Top	Bottom	Start	Stop	DSC Mode	Depth Shift	Include Parallel Data
One	Log[4]:Up	Up	4.12 ft	7044.38 ft	02-Jun-2017 1:27:12 AM	02-Jun-2017 4:20:07 AM	ON	4.20 ft	Yes

All depths are referenced to toolstring zero

Log

Company:Southern California Gas Company Well:Fernando Fee 35B

One: Log[4]:Up:S011

Description: USI Composite Format: Log (LBV1_USI Corrosion 9.625inch) Index Scale: 5 in per 100 ft Index Unit: ft Index Type: Measured Depth
Creation Date: 17-Jul-2017 14:11:36

TIME_1900 - Time Marked every 60.00 (s)

USIT Processing Flags (UFLG[0]) USIT-E

1 - UFLG 1 Value within [0.0 - 1.5] - :
2 - UFLG 2 Value within [1.5 - 2.5] - :
3 - UFLG 3 Value within [2.5 - 3.5] - :
4 - UFLG 4 UFLG 5 UFLG 6 Value within [3.5 - 6.5] - :
5 - UFLG 7 UFLG 8 UFLG 9 Value within [6.5 - 10] - :

- UTIM Error
- Pulse Origin Not Detected
- WINLEN Error
- Casing Thickness Error
- Loop Processing Error

Amplitude of Eccentering for Unflagged Waves (ECCE_RF) USIT-E
0 in 0.5

Motor Revolution Speed (RSAV) USIT-E
6 c/s 8

Gamma Ray (EHGR) HGNS-H
50 gAPI 200

Absent 1.500 3.500
Explicit Normalization
USIT - USIT Processing Flags (UFLG) USIT-E

USIT Processing Flags (UFLG[0]) USIT-E
1 5

Absent -5.200 -3.600 -2.000 -0.400
Explicit Normalization
USIT - Amplitude of Unflagged Wave (AWBK_RF) USIT-E
(dB)

Minimum of Unflagged Wave Amplitude (AWMN_RF) USIT-E
0 dB 75

Average of Unflagged Wave Amplitude (AWAV_RF) USIT-E
0 dB 75

Maximum of Unflagged Wave Amplitude (AWMX_RF) USIT-E
0 dB 75

Absent -0.059 -0.028 0.004 0.035 0.068
Explicit Normalization
USIT - Unflagged Internal Radii minus Median Internal Radius (IRBKM_RF) USIT-E
(in)

Internal Radius Averaged Value (IRAV) USIT-E
3.5 in 4.5

Internal Radius Maximum Value (IRMX) USIT-E
3.5 in 4.5

Internal Radius Minimum Value (IRMN) USIT-E
3.5 in 4.5

ERAV | IRAV
ERAV-IRAV | ERAV
IRAV | IRAV-ERAV

Median of Unflagged External Radii (ERAV_RF) USIT-E
4.5 in 3.5

Median of Unflagged External Radii (ERAV_RF) USIT-E
3.5 in 4.5

Median Internal Radius of Casing Corrected for Eccentering (IRAV_RF) USIT-E
4.5 in 3.5

Median Internal Radius of Casing Corrected for Eccentering (IRAV_RF) USIT-E
3.5 in 4.5

Maximum of Unflagged Internal Radii (IRMX_RF) USIT-E
4.5 in 3.5

Maximum of Unflagged Internal Radii (IRMX_RF) USIT-E
3.5 in 4.5

Minimum of Unflagged Internal Radii (IRMN_RF) USIT-E
4.5 in 3.5

Minimum of Unflagged Internal Radii (IRMN_RF) USIT-E
3.5 in 4.5

Absent -0.059 -0.028 0.004 0.035 0.068
Explicit Normalization
USIT - Unflagged Casing Thickness minus Median of Unflagged Casing Thickness (THBKM_RF) USIT-E
(in)

Minimum of Unflagged Casing Thickness (THMN_RF) USIT-E
0.1 in 0.6

Nominal Casing Thickness (THNO) USIT-E
0.1 in 0.6

Median of Unflagged Casing Thickness (THAV_RF) USIT-E
0.1 in 0.6

Maximum of Unflagged Casing Thickness (THMX_RF) USIT-E
0.1 in 0.6

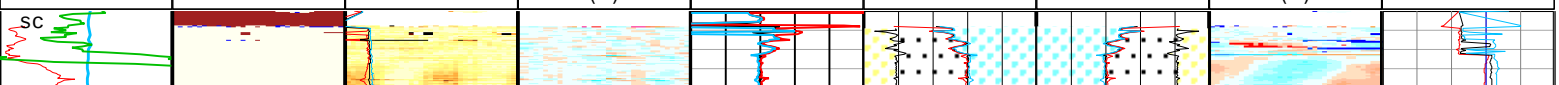

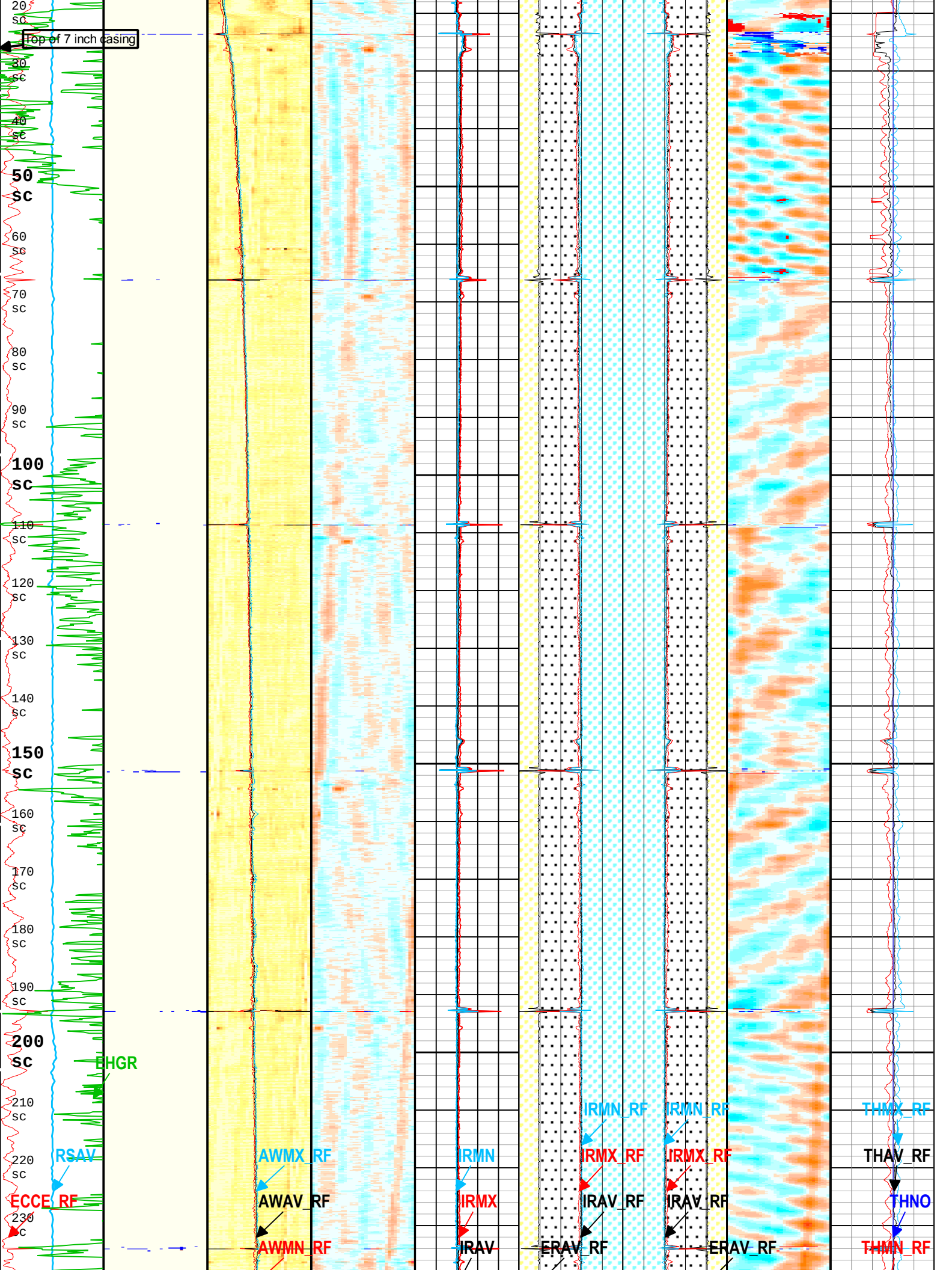
Top of 7 inch casing
20 sc
30 sc
40 sc
50 sc
60 sc
70 sc
80 sc
90 sc
100 sc
110 sc
120 sc
130 sc
140 sc
150 sc
160 sc
170 sc
180 sc
190 sc
200 sc
210 sc
220 sc
230 sc
EHGR
RSAV
ECCE_RF
AWMX_RF
AWAV_RF
AWMN_RF
IRMN
IRMX
IRAV
IRMN_RF
IRMX_RF
IRAV_RF
ERAV_RF
IRMN_RF
IRMX_RF
IRAV_RF
ERAV_RF
THMX_RF
THAV_RF
THNO
THMN_RF

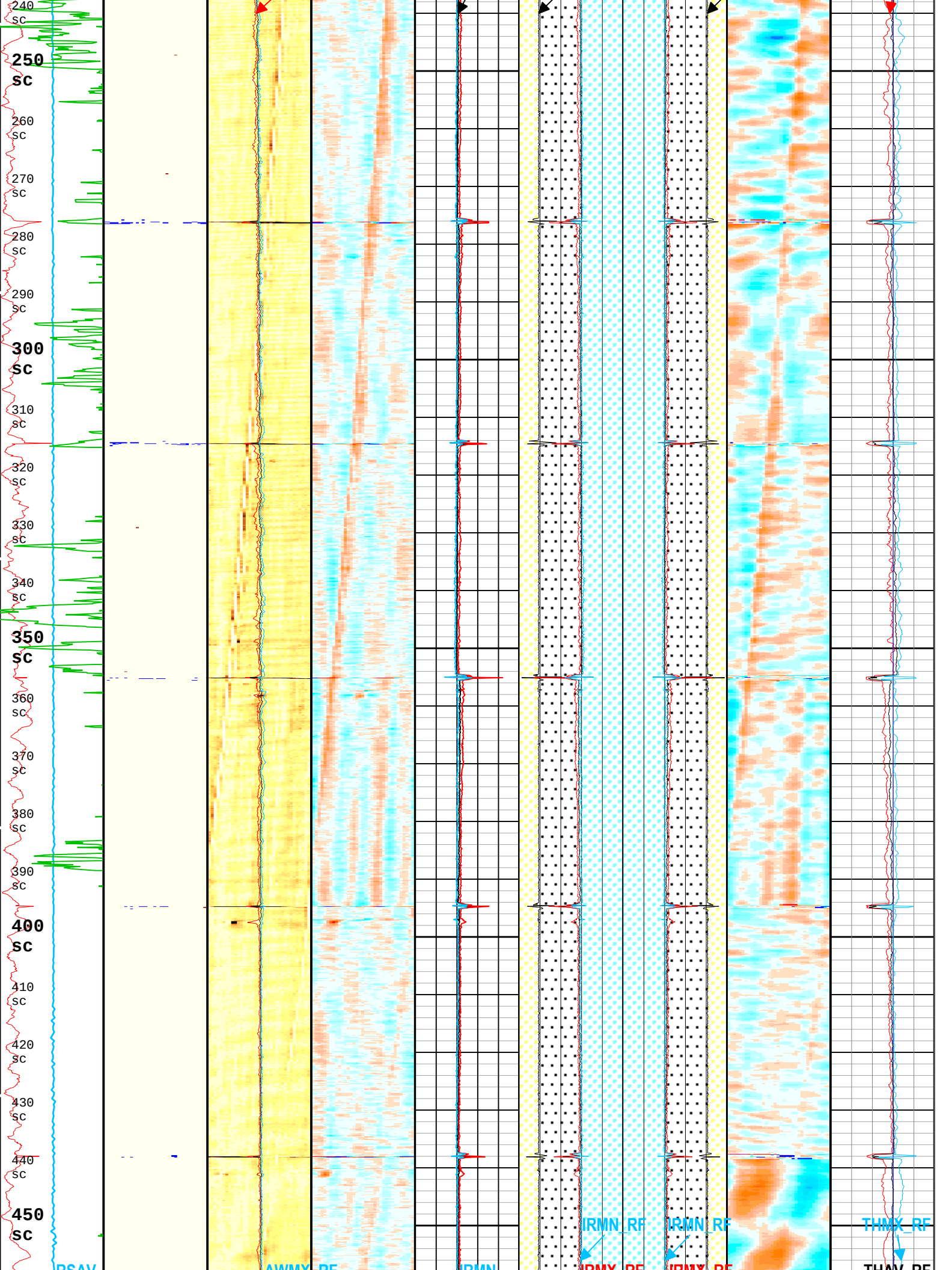
240 sc
250 sc
260 sc
270 sc
280 sc
290 sc
300 sc
310 sc
320 sc
330 sc
340 sc
350 sc
360 sc
370 sc
380 sc
390 sc
400 sc
410 sc
420 sc
430 sc
440 sc
450 sc
RSAV
AWMX_RF
IRMN
IRMN_RF
IRMX_RF
IRMN_RF
IRMX_RF
THMX_RF
THMX_RF

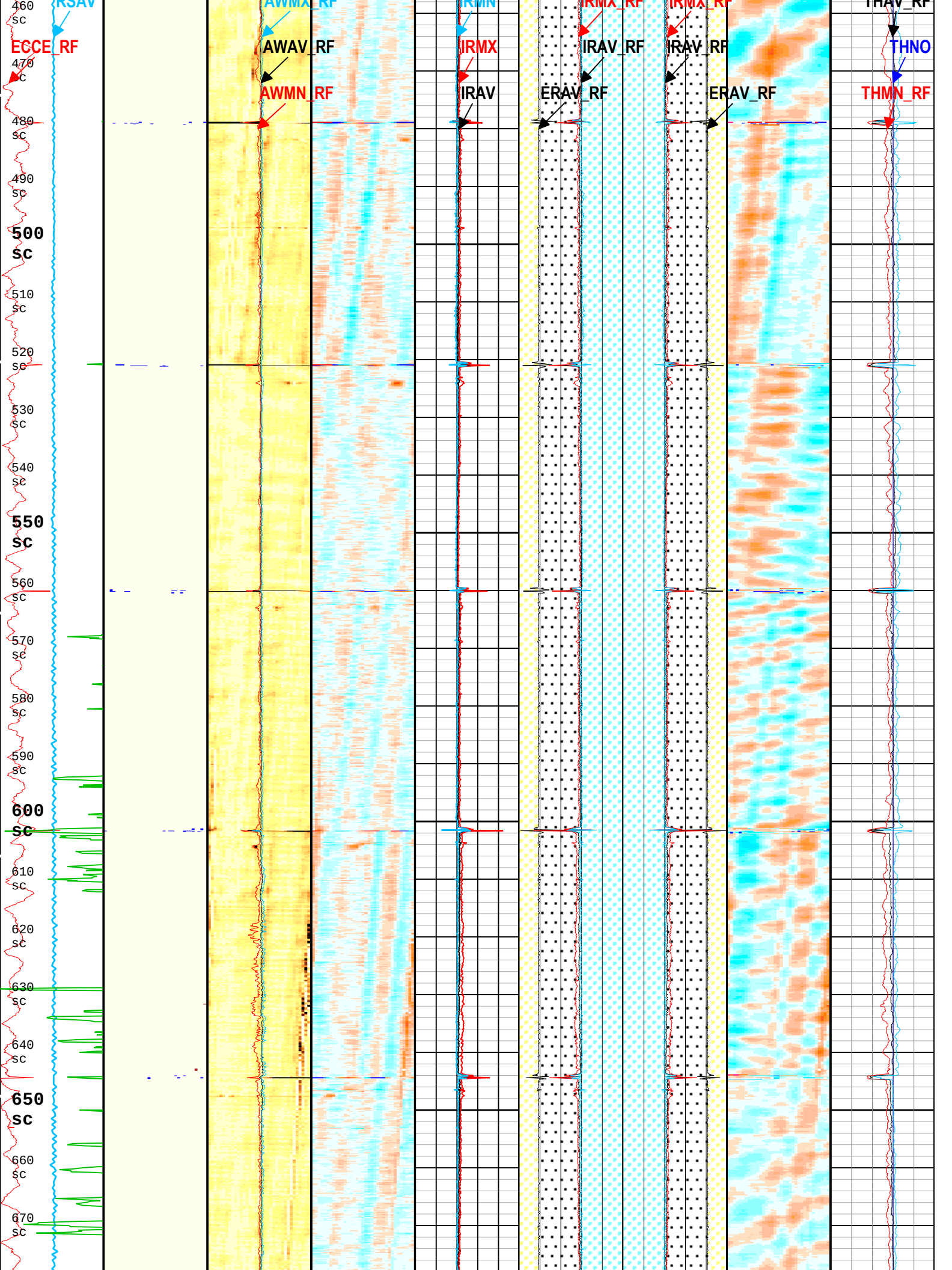
RSAV
ECCE_RF
AWMX_RF
AWAV_RF
AWMN_RF
IRMN
IRMX
IRAV
IRMX_RF
IRAV_RF
ERAV_RF
IRMX_RF
IRAV_RF
ERAV_RF
THAV_RF
THNO
THMN_RF
460 sc
470 sc
480 sc
490 sc
500 sc
510 sc
520 sc
530 sc
540 sc
550 sc
560 sc
570 sc
580 sc
590 sc
600 sc
610 sc
620 sc
630 sc
640 sc
650 sc
660 sc
670 sc

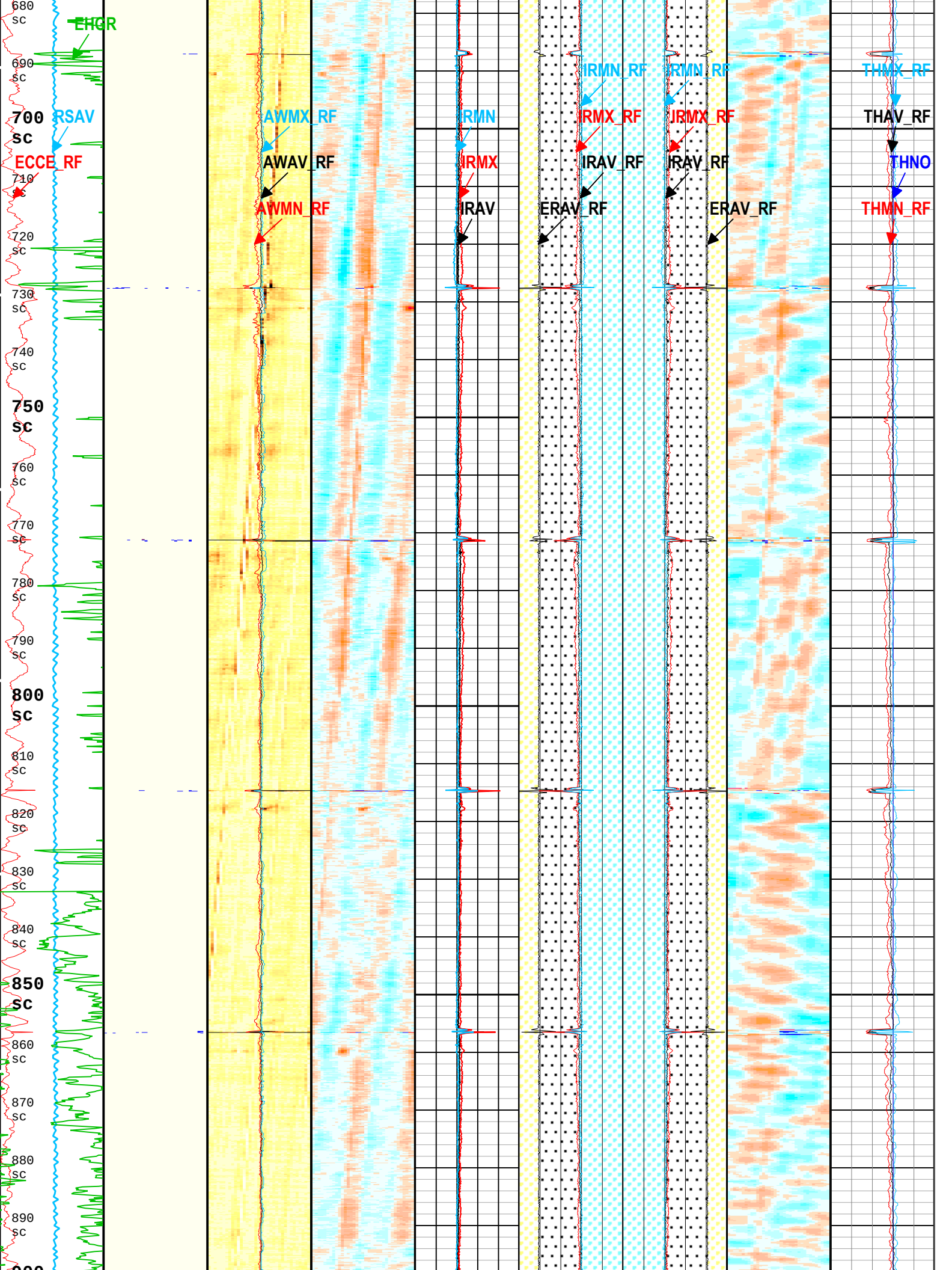
680 sc
690 sc
700 sc
710 sc
720 sc
730 sc
740 sc
750 sc
760 sc
770 sc
780 sc
790 sc
800 sc
810 sc
820 sc
830 sc
840 sc
850 sc
860 sc
870 sc
880 sc
890 sc
EHGR
RSAV
ECCE_RF
AWMX_RF
AWAV_RF
AWMN_RF
IRMN
IRMX
IRAV
IRMN_RF
IRMX_RF
IRAV_RF
ERAV_RF
IRMN_RF
IRMX_RF
IRAV_RF
ERAV_RF
THMX_RF
THAV_RF
THNO
THMN_RF

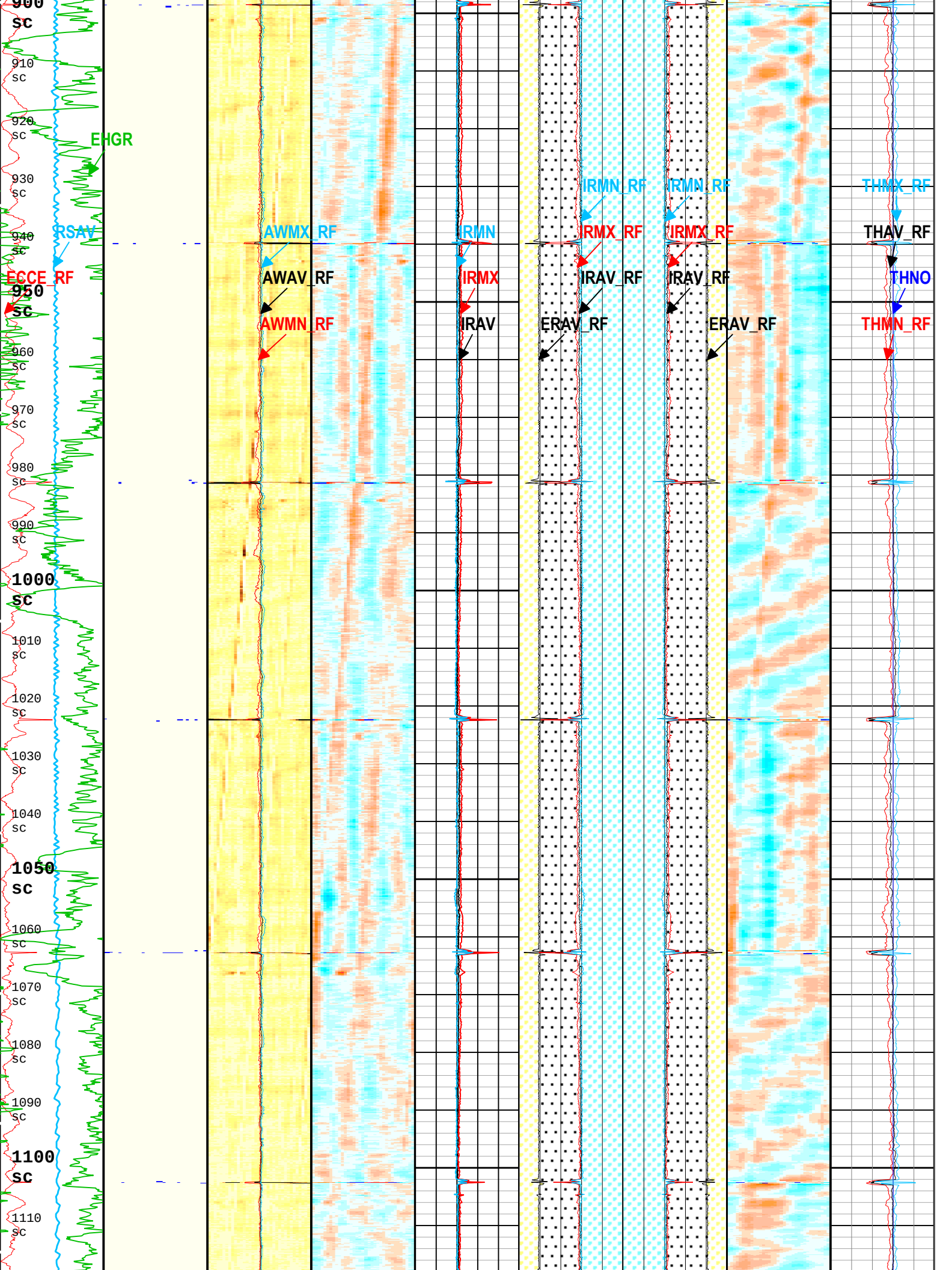
900 sc
910 sc
920 sc
930 sc
940 sc
950 sc
960 sc
970 sc
980 sc
990 sc
1000 sc
1010 sc
1020 sc
1030 sc
1040 sc
1050 sc
1060 sc
1070 sc
1080 sc
1090 sc
1100 sc
1110 sc
EHGR
RSAV
ECCE_RF
AWMX_RF
AWAV_RF
AWMN_RF
IRMN
IRMX
IRAV
IRMN_RF
IRMX_RF
IRAV_RF
ERAV_RF
IRMN_RF
IRMX_RF
IRAV_RF
ERAV_RF
THMX_RF
THAV_RF
THNO
THMN_RF

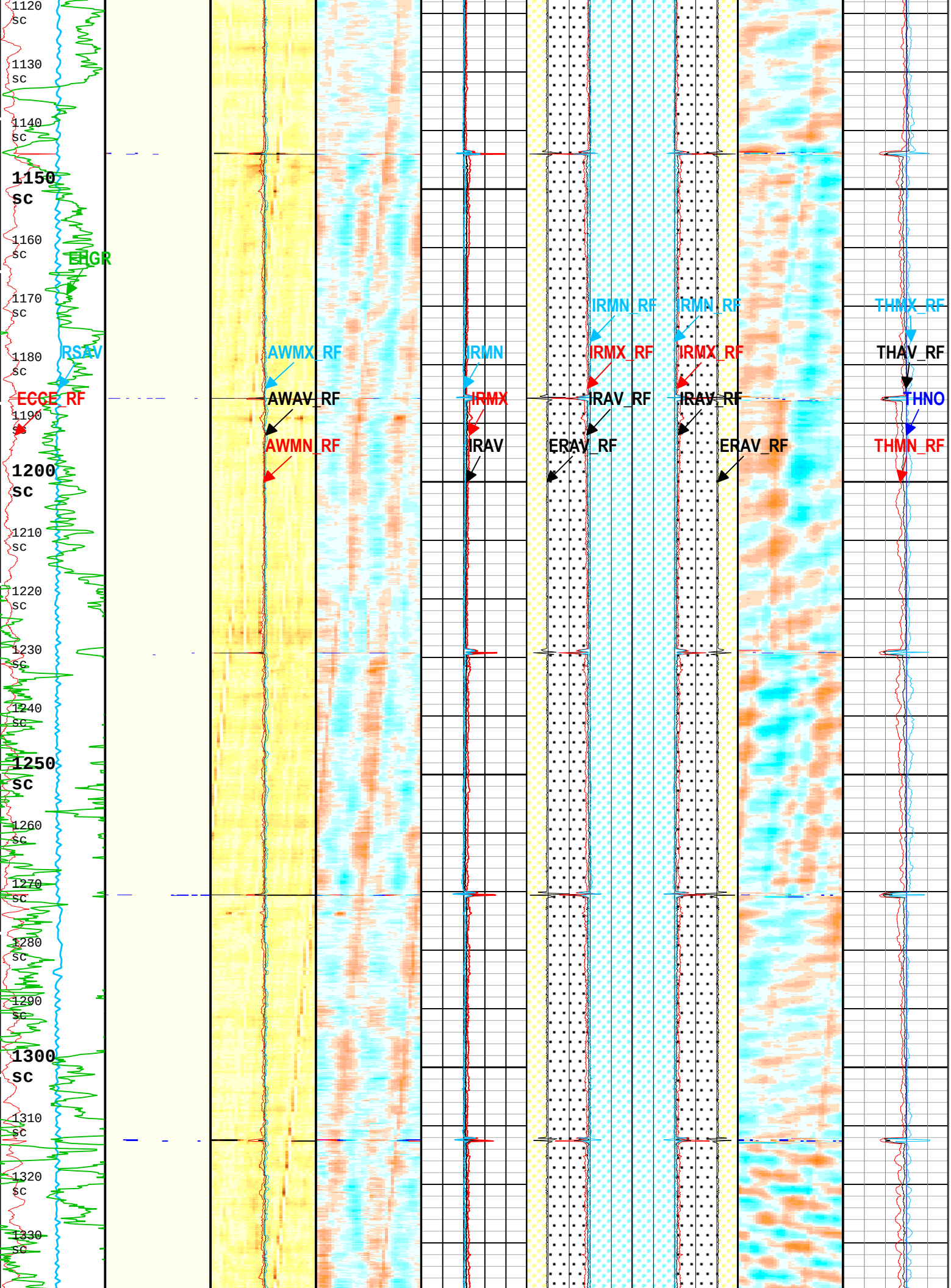
1120 sc
1130 sc
1140 sc
1150 sc
1160 sc
1170 sc
1180 sc
1190 sc
1200 sc
1210 sc
1220 sc
1230 sc
1240 sc
1250 sc
1260 sc
1270 sc
1280 sc
1290 sc
1300 sc
1310 sc
1320 sc
1330 sc
EHGR
RSAV
ECGE_RF
AWMX_RF
AWAV_RF
AWMN_RF
IRMN
IRMX
IRAV
IRMN_RF
IRMX_RF
IRAV_RF
ERAV_RF
IRMN_RF
IRMX_RF
IRAV_RF
ERAV_RF
THMX_RF
THAV_RF
THNO
THMN_RF

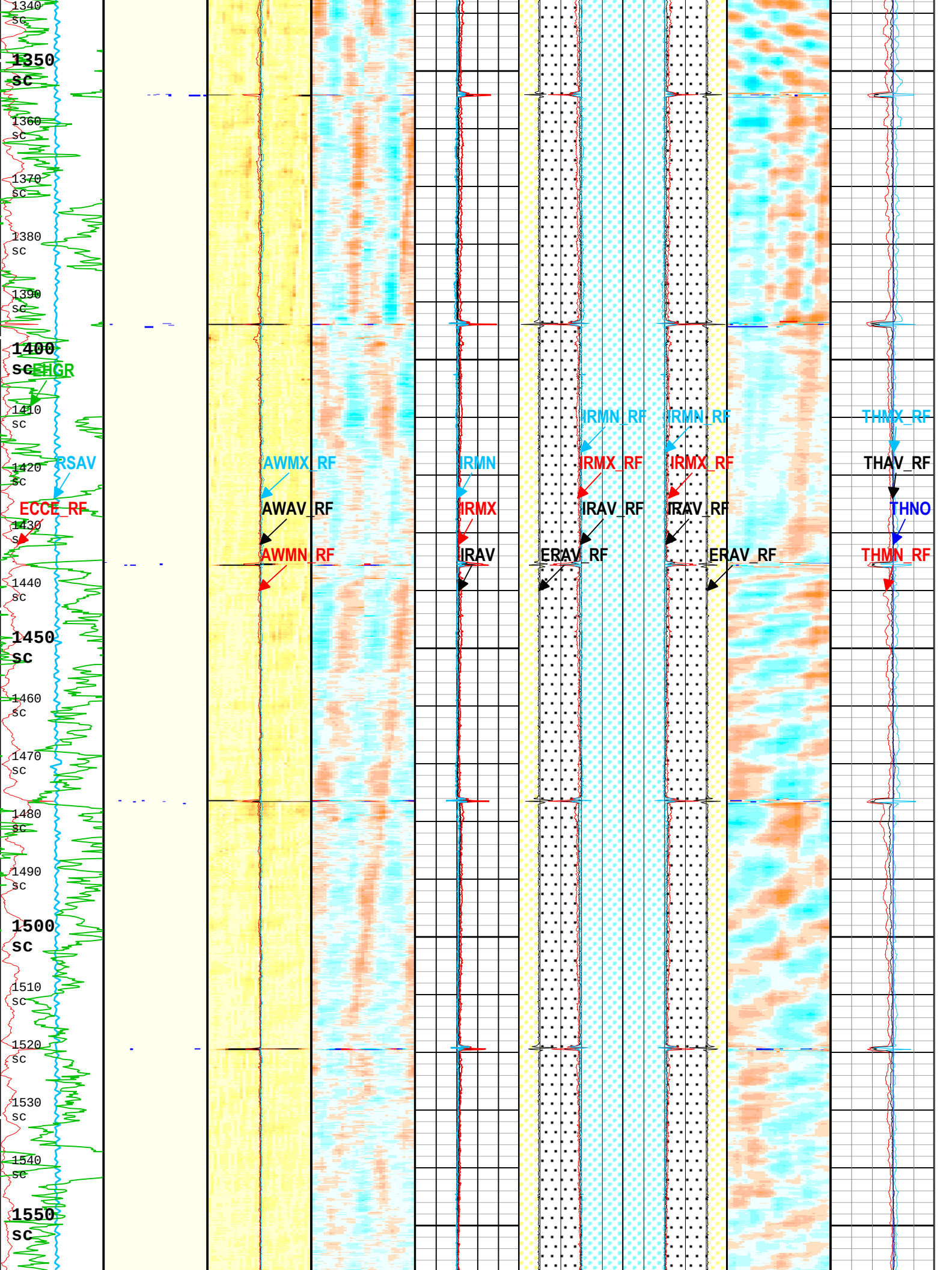
1340 sc
1350 sc
1360 sc
1370 sc
1380 sc
1390 sc
1400 sc
EHGR
1410 sc
RSAV
1420 sc
ECCE_RF
1430 sc
1440 sc
1450 sc
1460 sc
1470 sc
1480 sc
1490 sc
1500 sc
1510 sc
1520 sc
1530 sc
1540 sc
1550 sc
AWMX_RF
AWAV_RF
AWMN_RF
IRMN
IRMX
IRAV
IRMN_RF
IRMX_RF
IRAV_RF
ERAV_RF
IRMN_RF
IRMX_RF
IRAV_RF
ERAV_RF
THMX_RF
THAV_RF
THNO
THMN_RF

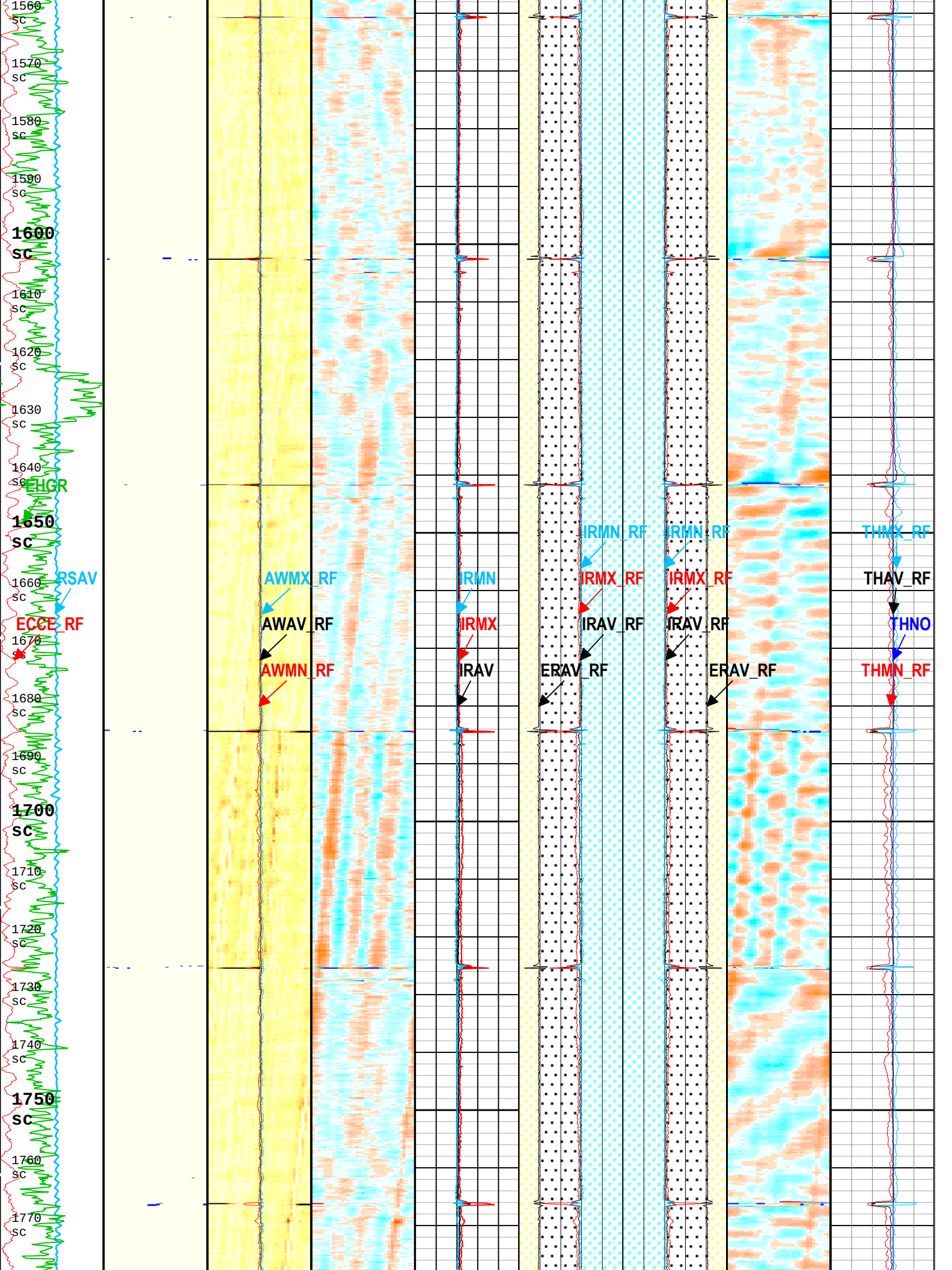
1560 sc
1570 sc
1580 sc
1590 sc
1600 sc
1610 sc
1620 sc
1630 sc
1640 sc
LHGR
1650 sc
RSAV
1660 sc
ECCE_RF
1670 sc
1680 sc
1690 sc
1700 sc
1710 sc
1720 sc
1730 sc
1740 sc
1750 sc
1760 sc
1770 sc
AWMX_RF
AWAV_RF
AWMN_RF
IRMN
IRMX
IRAV
IRMN_RF
IRMX_RF
IRAV_RF
ERAV_RF
IRMN_RF
IRMX_RF
IRAV_RF
ERAV_RF
THMX_RF
THAV_RF
THNO
THMN_RF

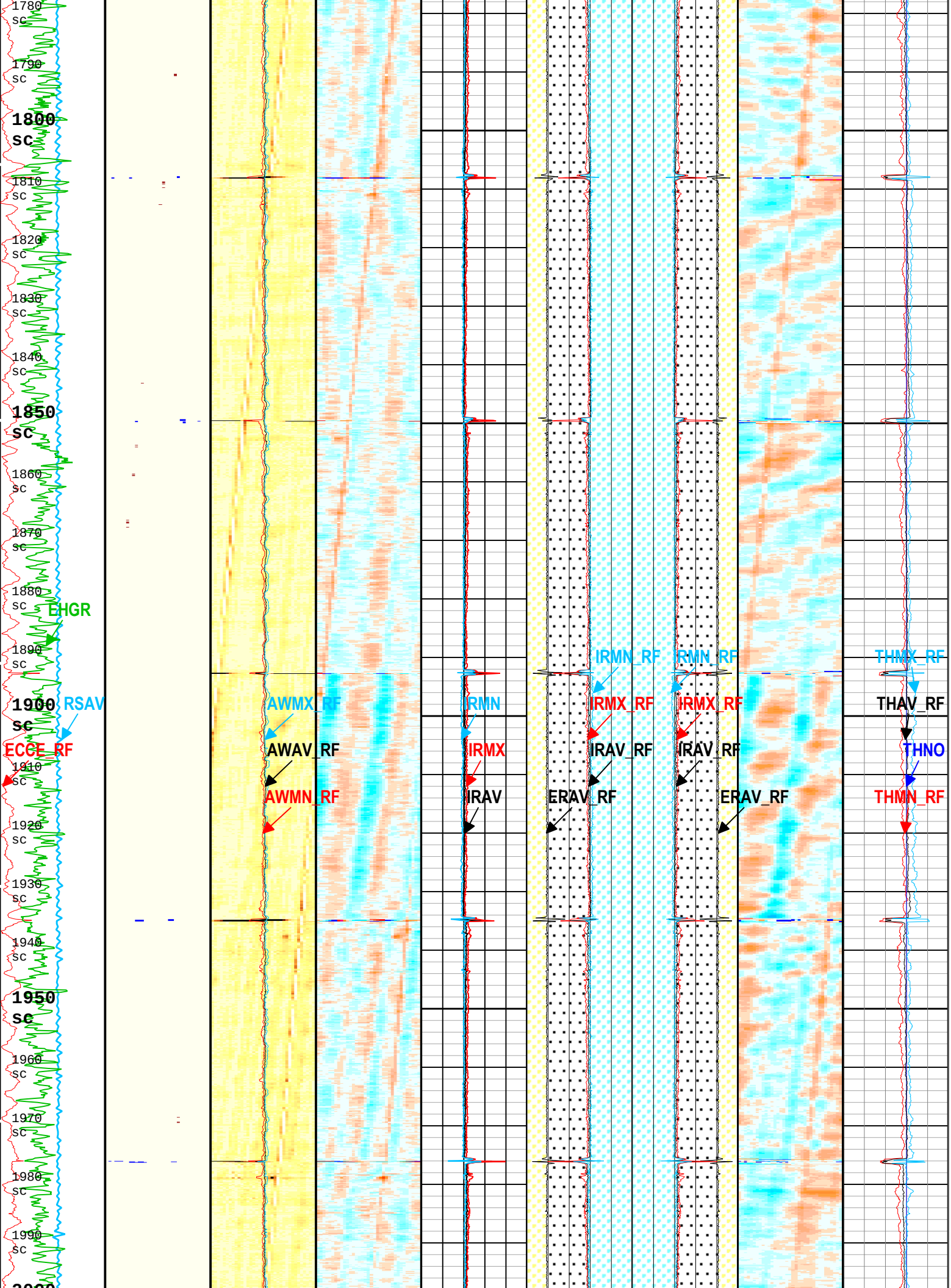
1780 sc
1790 sc
1800 sc
1810 sc
1820 sc
1830 sc
1840 sc
1850 sc
1860 sc
1870 sc
1880 sc
EHGR
1890 sc
1900 sc
RSAV
ECCE_RF
1910 sc
1920 sc
1930 sc
1940 sc
1950 sc
1960 sc
1970 sc
1980 sc
1990 sc
AWMX_RF
AWAV_RF
AWMN_RF
IRMN
IRMX
IRAV
IRMN_RF
IRMX_RF
IRAV_RF
ERAV_RF
RMN_RF
IRMX_RF
IRAV_RF
ERAV_RF
THMX_RF
THAV_RF
THNO
THMN_RF

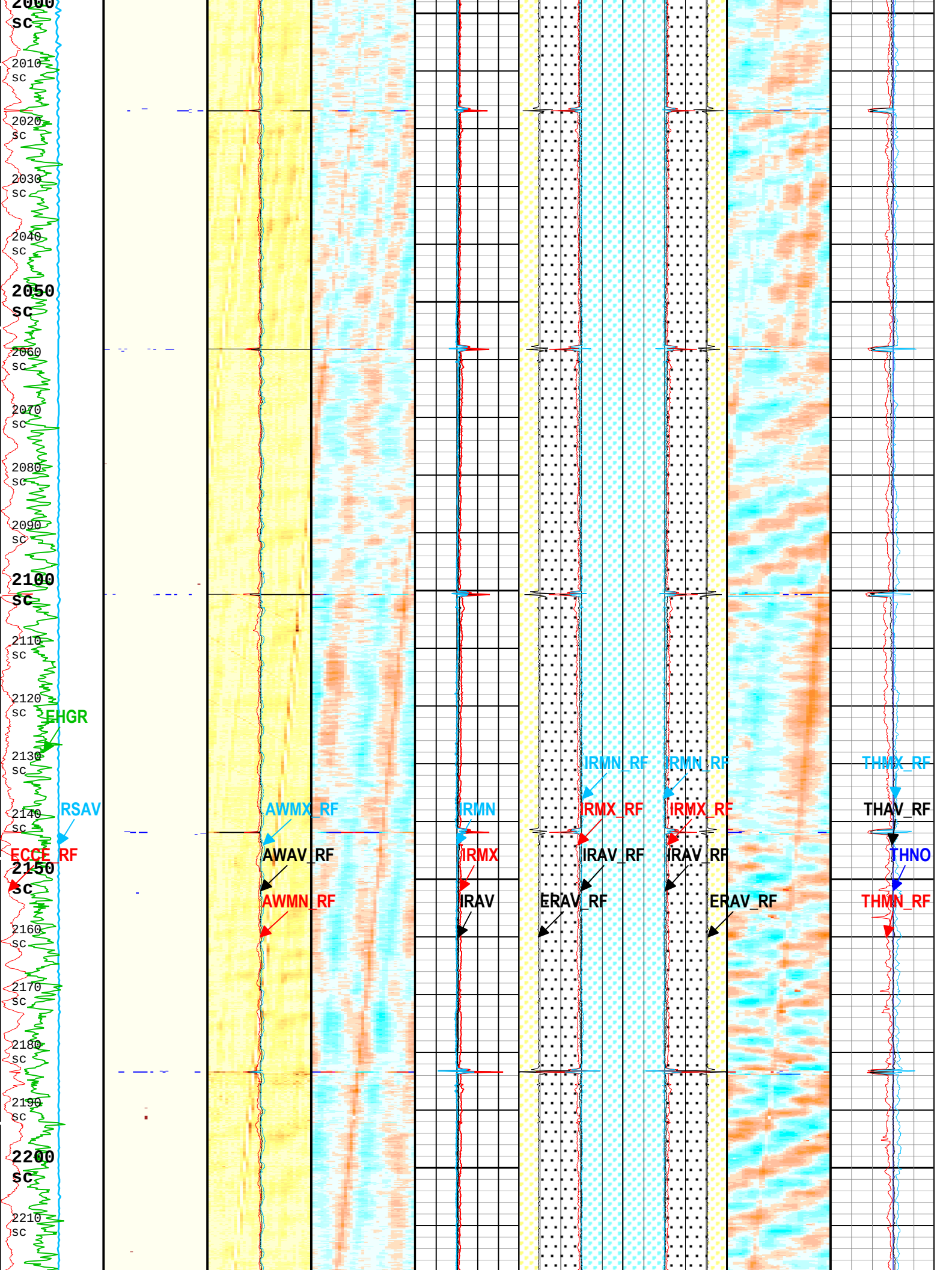
2000 SC
2010 SC
2020 SC
2030 SC
2040 SC
2050 SC
2060 SC
2070 SC
2080 SC
2090 SC
2100 SC
2110 SC
2120 SC
2130 SC
2140 SC
2150 SC
2160 SC
2170 SC
2180 SC
2190 SC
2200 SC
2210 SC
EHGR
RSAV
ECCE_RF
AWMX_RF
AWAV_RF
AWMN_RF
IRMN
IRMX
IRAV
IRMN_RF
IRMX_RF
IRAV_RF
ERAV_RF
IRMN_RF
IRMX_RF
IRAV_RF
ERAV_RF
THMX_RF
THAV_RF
THNO
THMN_RF

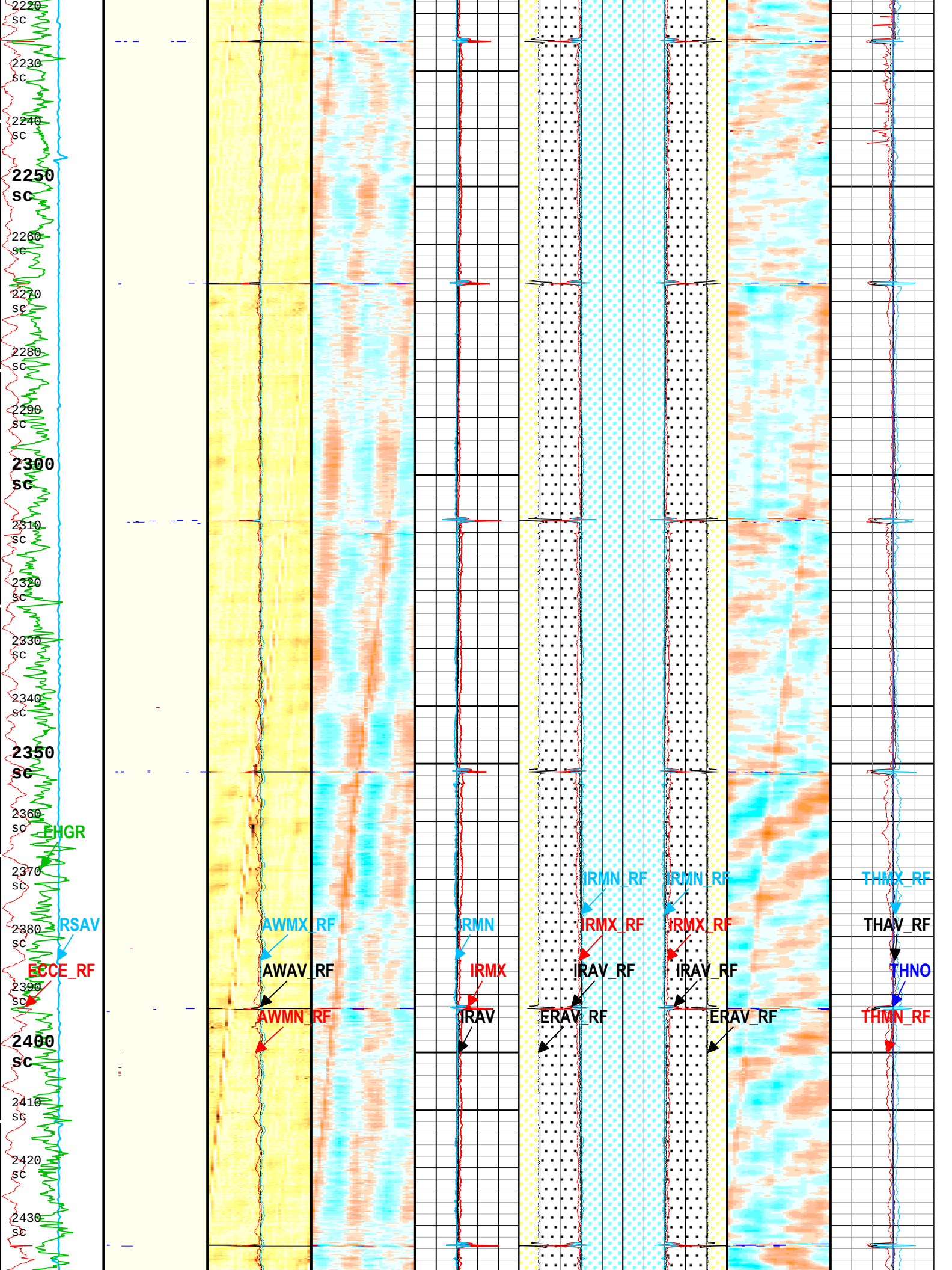
2220 sc
2230 sc
2240 sc
2250 sc
2260 sc
2270 sc
2280 sc
2290 sc
2300 sc
2310 sc
2320 sc
2330 sc
2340 sc
2350 sc
2360 sc
EHGR
2370 sc
RSAV
2380 sc
ECCE_RF
2390 sc
2400 sc
2410 sc
2420 sc
2430 sc
AWMX_RF
AWAV_RF
AWMN_RF
IRMN
IRMX
IRAV
IRMN_RF
IRMX_RF
IRAV_RF
ERAV_RF
IRMN_RF
IRMX_RF
IRAV_RF
ERAV_RF
THMX_RF
THAV_RF
THNO
THMN_RF

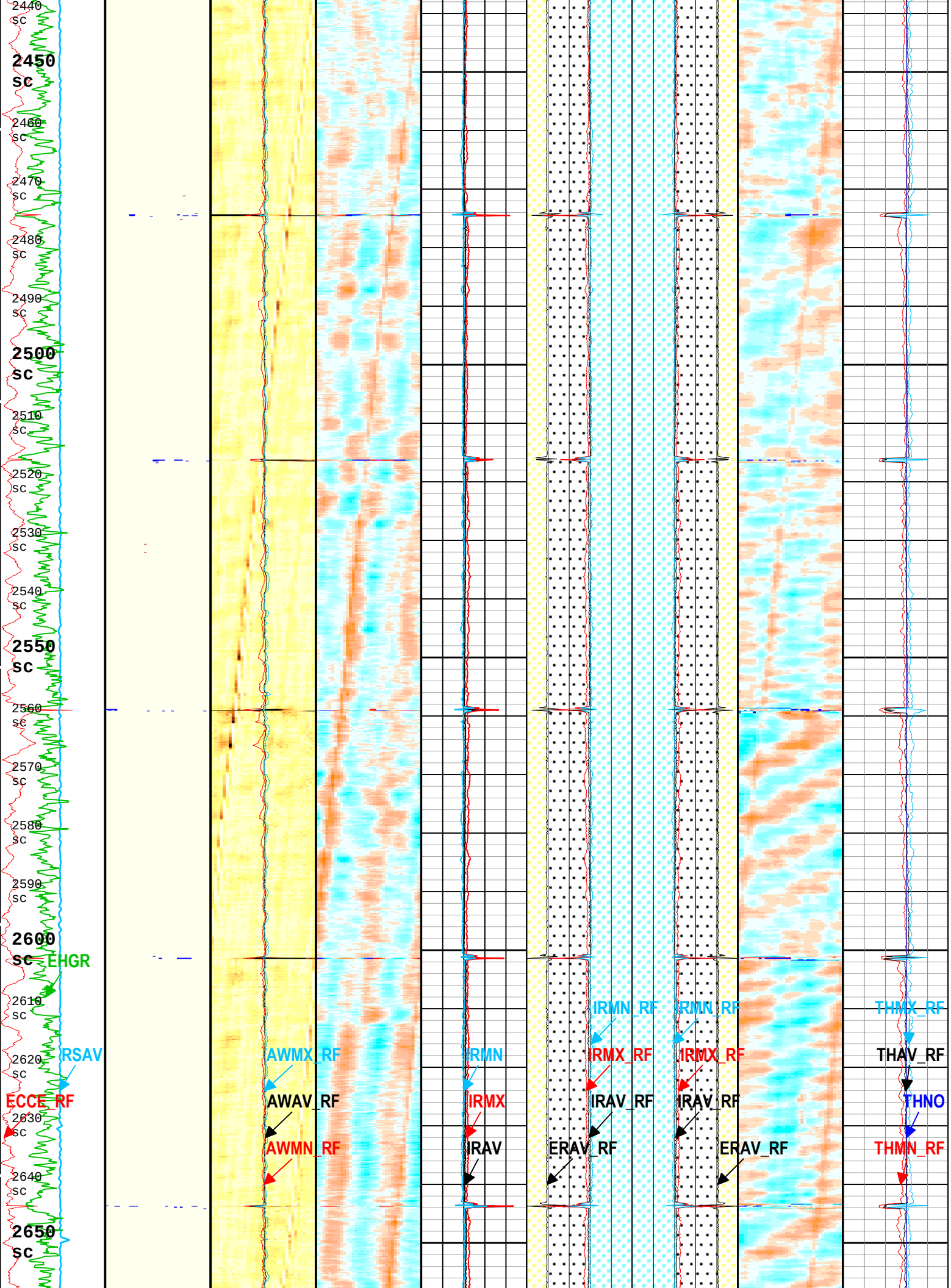
2440 sc
2450 sc
2460 sc
2470 sc
2480 sc
2490 sc
2500 sc
2510 sc
2520 sc
2530 sc
2540 sc
2550 sc
2560 sc
2570 sc
2580 sc
2590 sc
2600 sc
2610 sc
2620 sc
2630 sc
2640 sc
2650 sc
EHGR
RSAV
ECCE_RF
AWMX_RF
AWAV_RF
AWMN_RF
IRMN
IRMX
IRAV
IRMN_RF
RMX_RF
IRAV_RF
ERAV_RF
IRMN_RF
IRMX_RF
IRAV_RF
ERAV_RF
THMX_RF
THAV_RF
THNO
THMN_RF

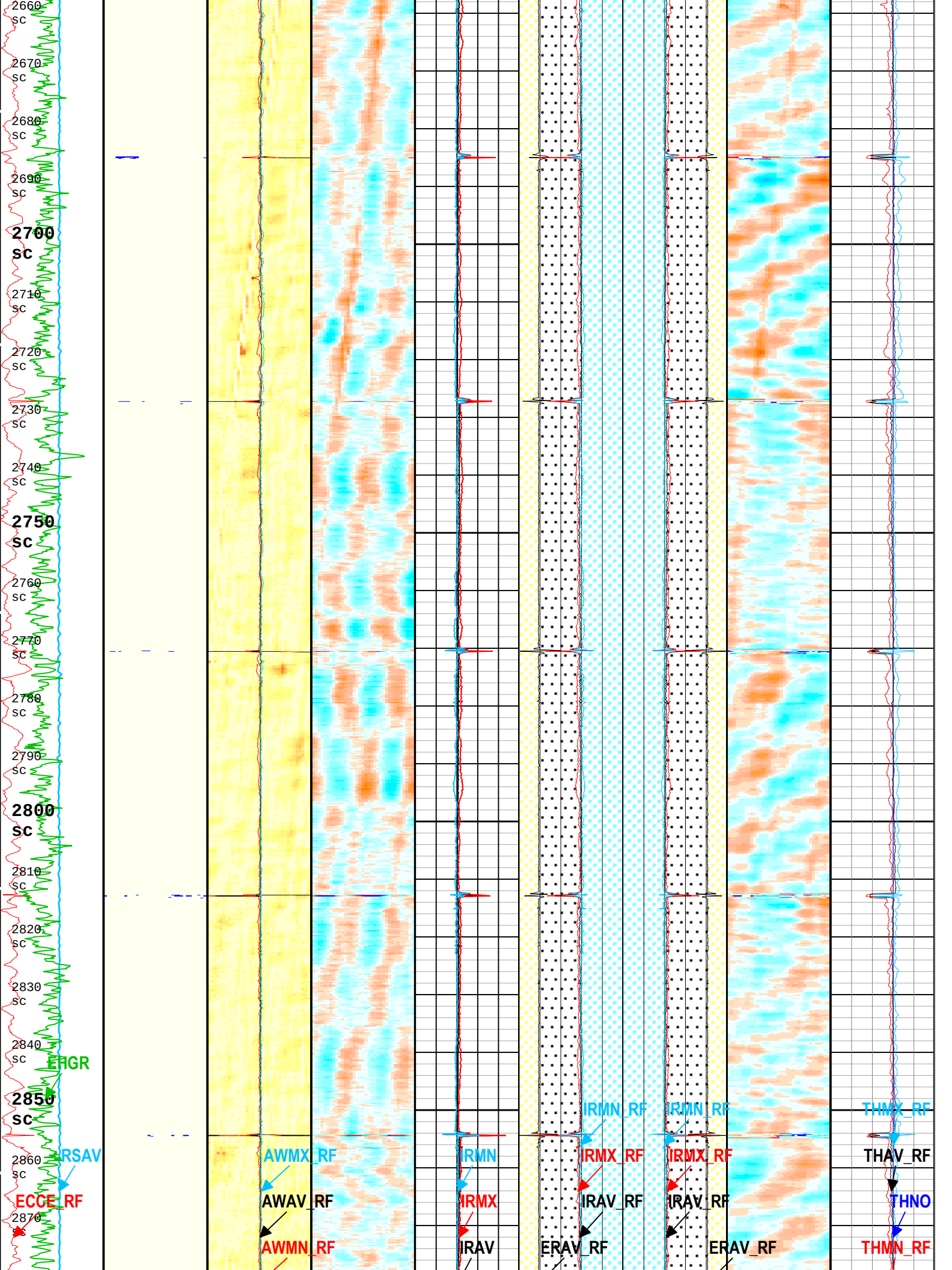
2660 sc
2670 sc
2680 sc
2690 sc
2700 sc
2710 sc
2720 sc
2730 sc
2740 sc
2750 sc
2760 sc
2770 sc
2780 sc
2790 sc
2800 sc
2810 sc
2820 sc
2830 sc
2840 sc
EHGR
2850 sc
RSAV
2860 sc
ECCE_RF
2870 sc
AWMX_RF
AWAV_RF
AWMN_RF
IRMN
IRMX
IRAV
IRMN_RF
IRMX_RF
IRAV_RF
ERAV_RF
IRMN_RF
IRMX_RF
IRAV_RF
ERAV_RF
THMX_RF
THAV_RF
THNO
THMN_RF

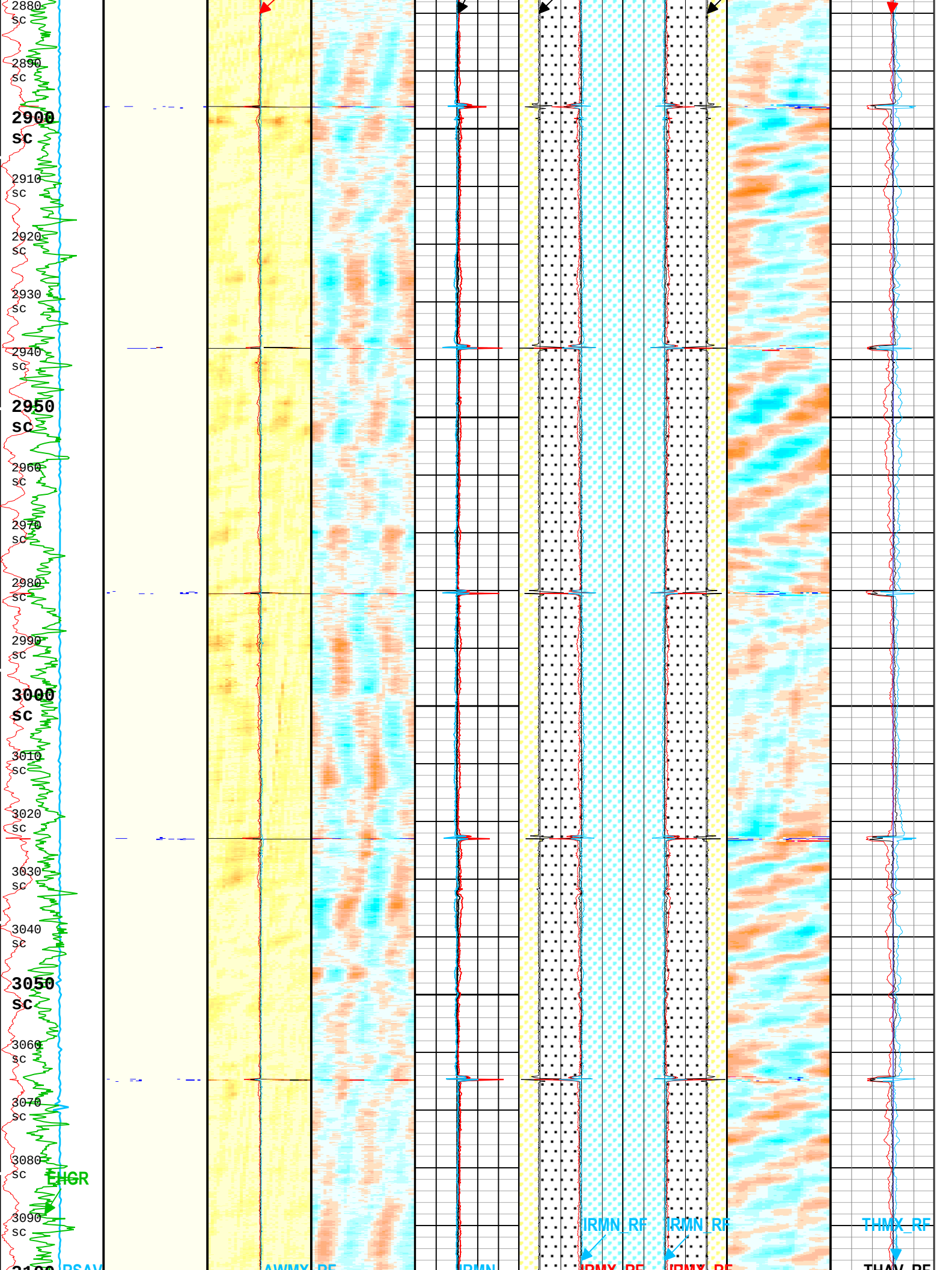
2880 sc
2890 sc
2900 sc
2910 sc
2920 sc
2930 sc
2940 sc
2950 sc
2960 sc
2970 sc
2980 sc
2990 sc
3000 sc
3010 sc
3020 sc
3030 sc
3040 sc
3050 sc
3060 sc
3070 sc
3080 sc
3090 sc
THGR
IRMN_RF
IRMN_RF
THMX_RF

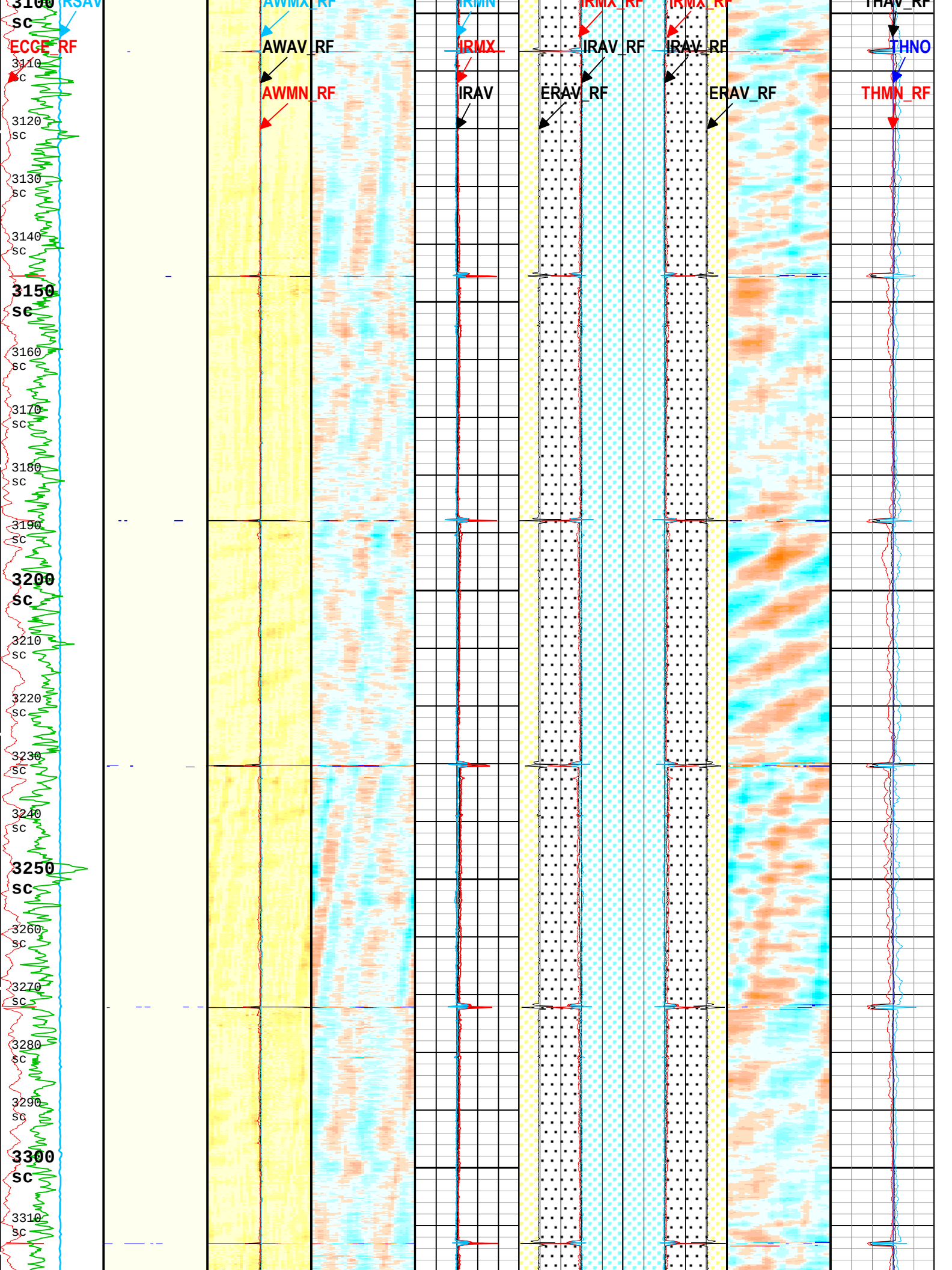
RSAV
ECGE_RF
AWMX_RF
AWAV_RF
AWMN_RF
IRMN
IRMX
IRAV
IRMX_RF
IRAV_RF
ERAV_RF
IRMX_RF
IRAV_RF
ERAV_RF
THAV_RF
THNO
THMN_RF
3100 sc
3110 sc
3120 sc
3130 sc
3140 sc
3150 sc
3160 sc
3170 sc
3180 sc
3190 sc
3200 sc
3210 sc
3220 sc
3230 sc
3240 sc
3250 sc
3260 sc
3270 sc
3280 sc
3290 sc
3300 sc
3310 sc

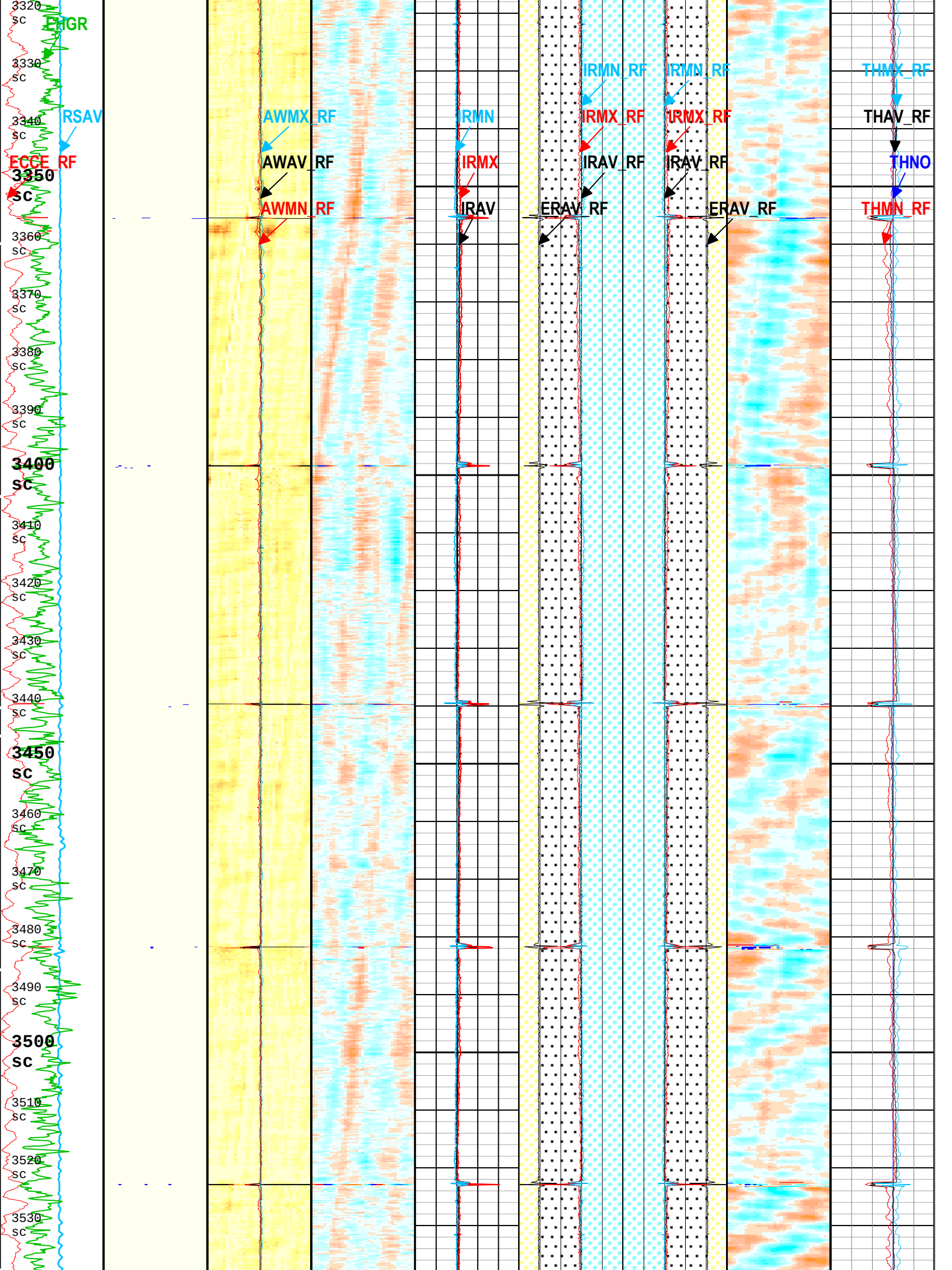
EHGR
RSAV
ECCE_RF
AWMX_RF
AWAV_RF
AWMN_RF
IRMN
IRMX
IRAV
IRMN_RF
IRMX_RF
IRAV_RF
ERAV_RF
IRMN_RF
IRMX_RF
IRAV_RF
ERAV_RF
THMX_RF
THAV_RF
THNO
THMN_RF
3320 sc
3330 sc
3340 sc
3350 sc
3360 sc
3370 sc
3380 sc
3390 sc
3400 sc
3410 sc
3420 sc
3430 sc
3440 sc
3450 sc
3460 sc
3470 sc
3480 sc
3490 sc
3500 sc
3510 sc
3520 sc
3530 sc

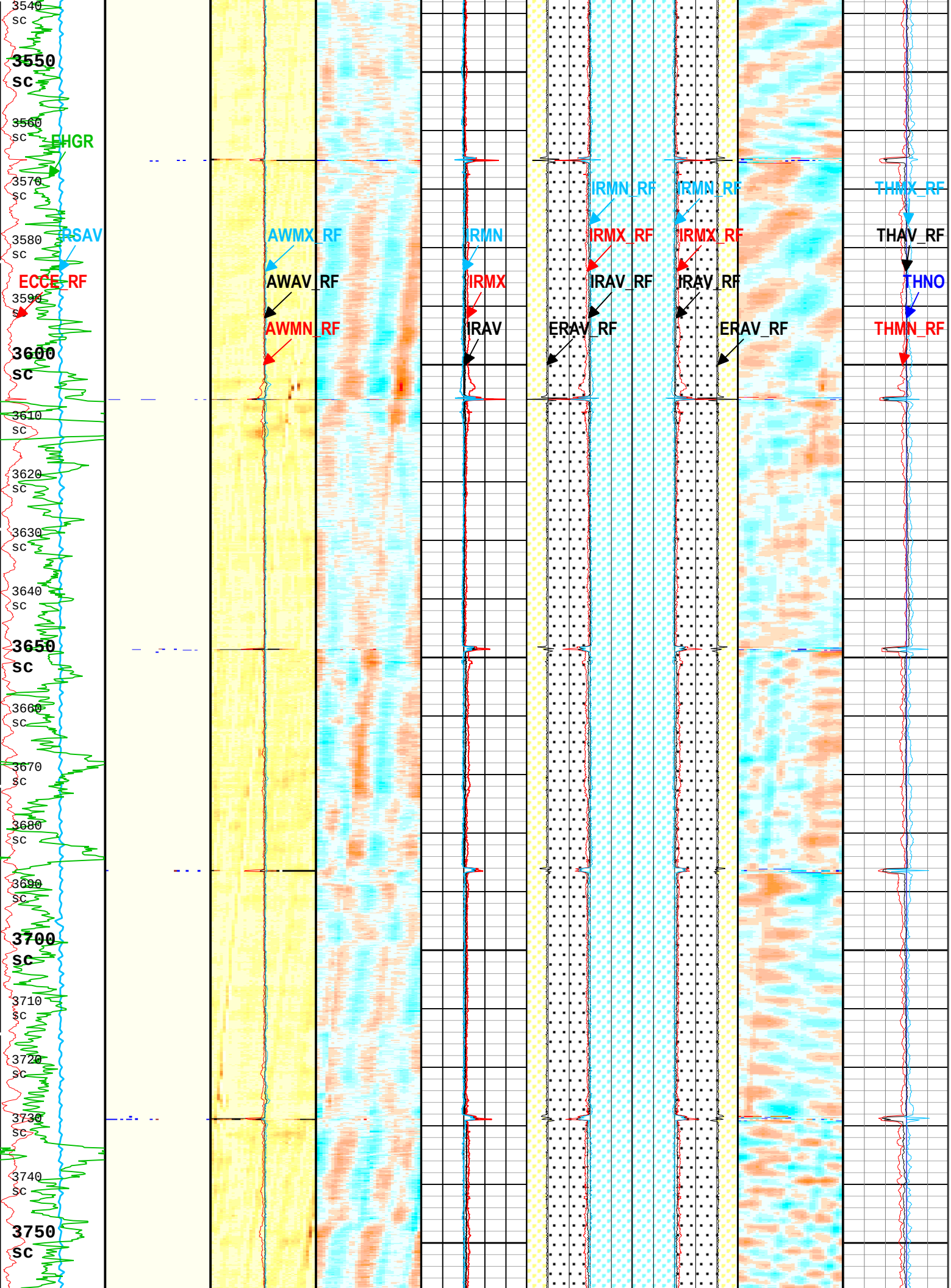
3540 sc
3550 sc
3560 sc
EHGR
3570 sc
3580 sc
IRSAV
ECCE_RF
3590 sc
3600 sc
3610 sc
3620 sc
3630 sc
3640 sc
3650 sc
3660 sc
3670 sc
3680 sc
3690 sc
3700 sc
3710 sc
3720 sc
3730 sc
3740 sc
3750 sc
AWMX_RF
AWAV_RF
AWMN_RF
IRMN
IRMX
IRAV
IRMN_RF
IRMX_RF
IRAV_RF
ERAV_RF
IRMN_RF
IRMX_RF
IRAV_RF
ERAV_RF
THMX_RF
THAV_RF
THNO
THMN_RF

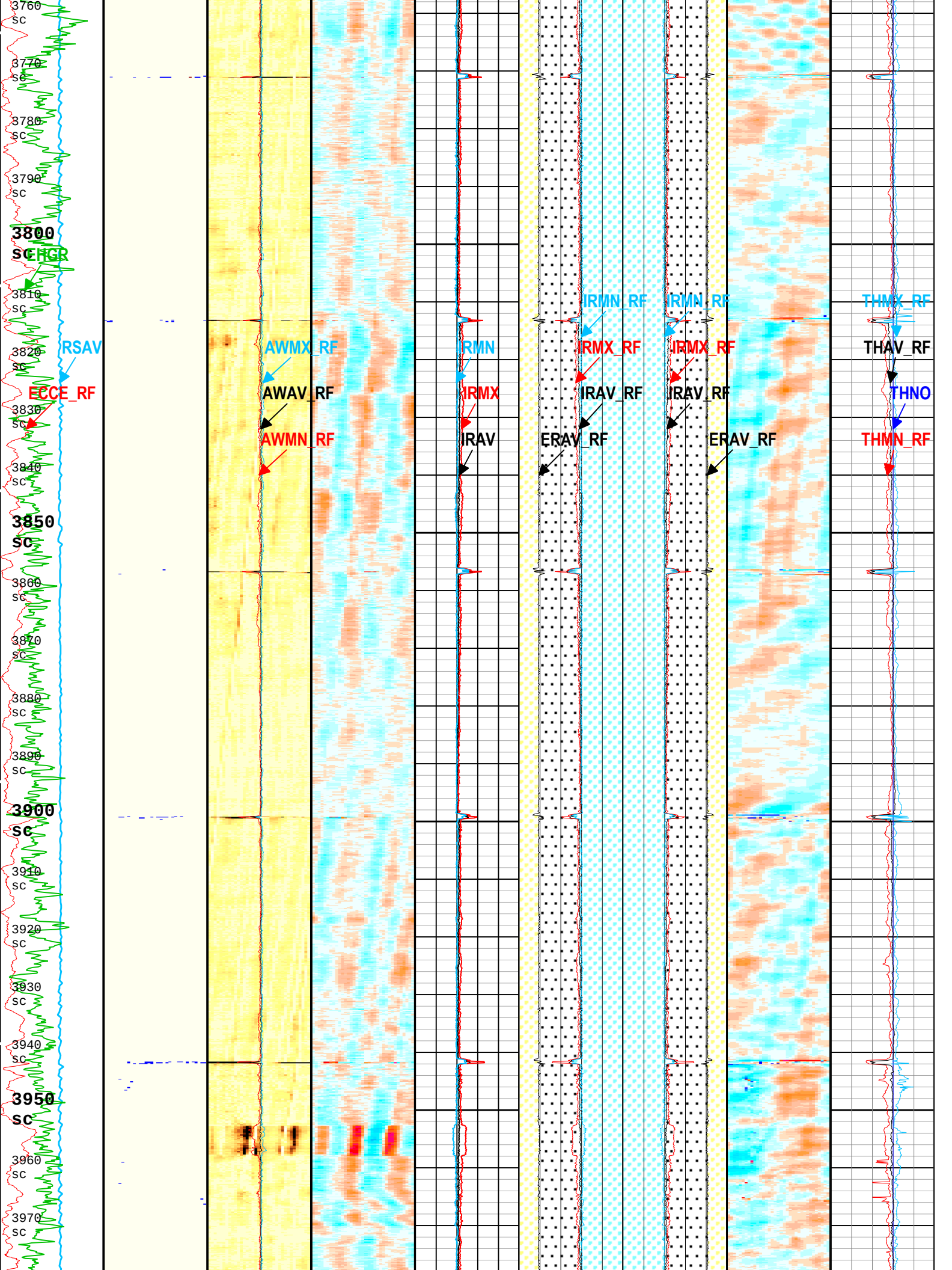
3760 sc
3770 sc
3780 sc
3790 sc
3800 sc
HGR
3810 sc
RSAV
3820 sc
ECCE_RF
3830 sc
3840 sc
3850 sc
3860 sc
3870 sc
3880 sc
3890 sc
3900 sc
3910 sc
3920 sc
3930 sc
3940 sc
3950 sc
3960 sc
3970 sc
AWMX_RF
AWAV_RF
AWMN_RF
IRMN
IRMX
IRAV
IRMN_RF
IRMX_RF
IRAV_RF
ERAV_RF
IRMN_RF
IRMX_RF
IRAV_RF
ERAV_RF
THMX_RF
THAV_RF
THNO
THMN_RF

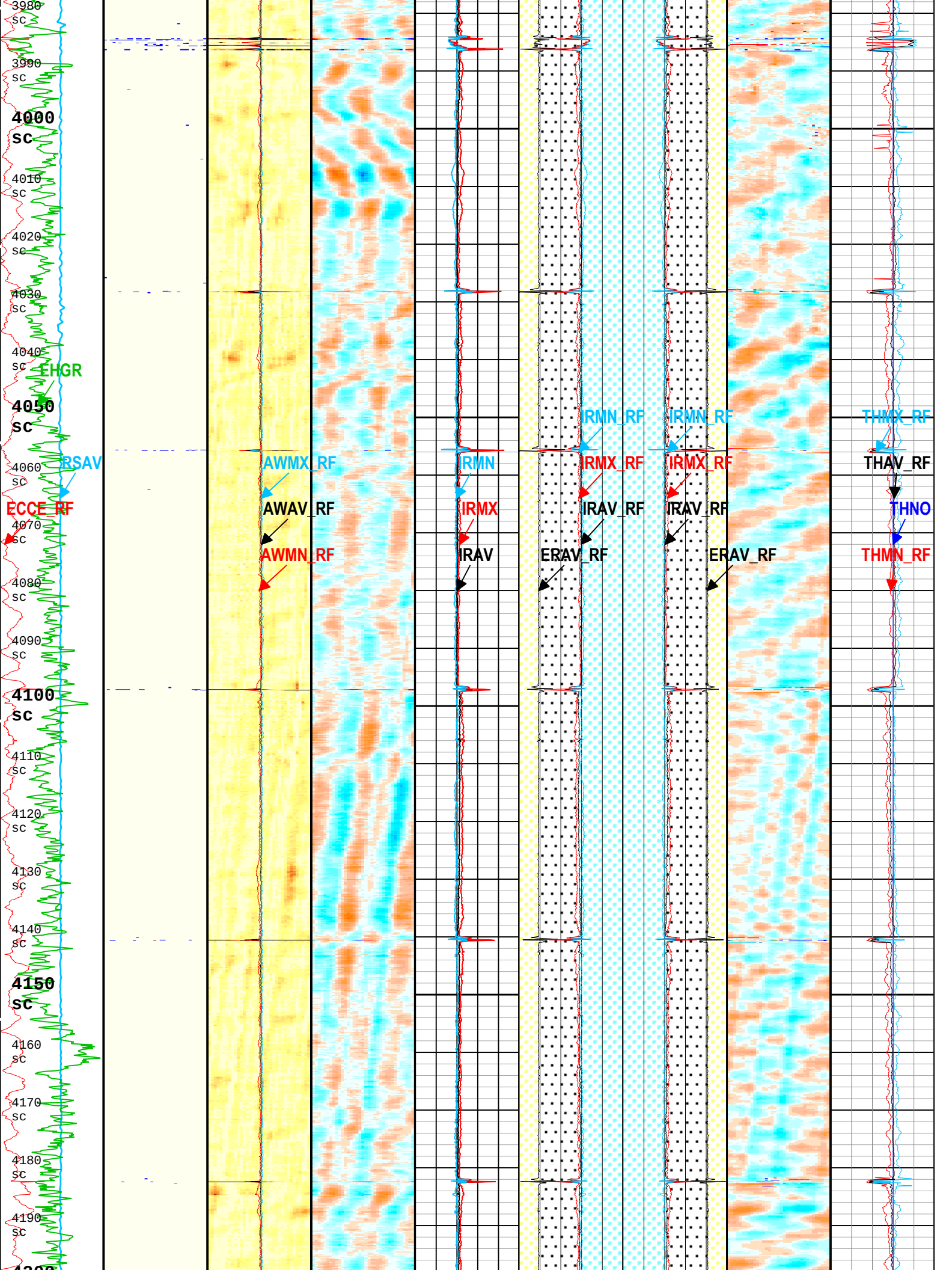
3980 sc
3990 sc
4000 sc
4010 sc
4020 sc
4030 sc
4040 sc
EHGR
4050 sc
4060 sc
RSAV
ECCE_RF
4070 sc
4080 sc
4090 sc
4100 sc
4110 sc
4120 sc
4130 sc
4140 sc
4150 sc
4160 sc
4170 sc
4180 sc
4190 sc
AWMX_RF
AWAV_RF
AWMN_RF
IRMN
IRMX
IRAV
IRMN_RF
IRMX_RF
IRAV_RF
ERAV_RF
IRMN_RF
IRMX_RF
IRAV_RF
ERAV_RF
THMX_RF
THAV_RF
THNO
THMN_RF

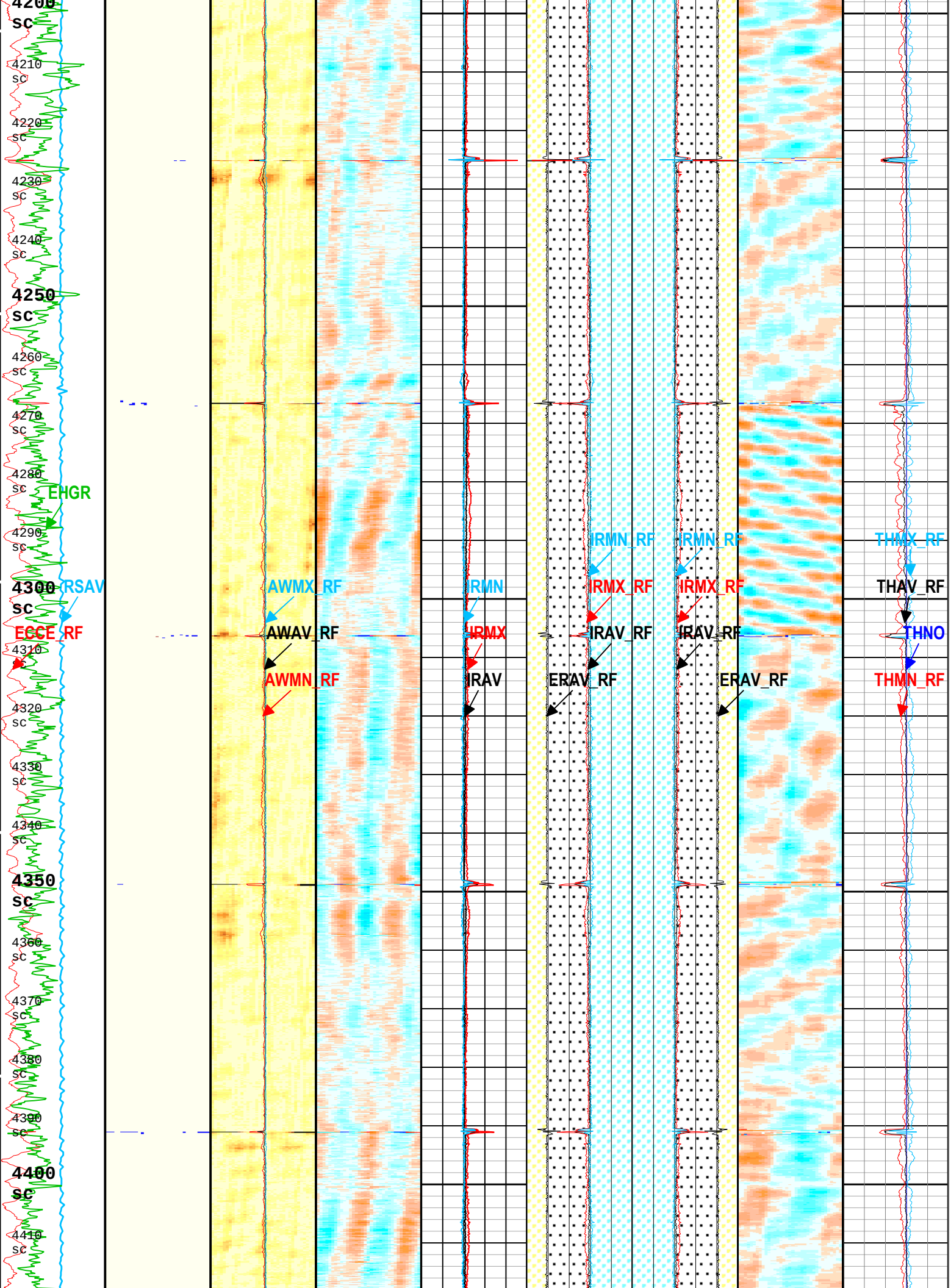
4200
sc
4210
sc
4220
sc
4230
sc
4240
sc
4250
sc
4260
sc
4270
sc
4280
sc
EHGR
4290
sc
4300
sc
RSAV
ECCE_RF
4310
sc
4320
sc
4330
sc
4340
sc
4350
sc
4360
sc
4370
sc
4380
sc
4390
sc
4400
sc
4410
sc
AWMX_RF
AWAV_RF
AWMN_RF
IRMN
IRMX
IRAV
IRMN_RF
IRMX_RF
IRAV_RF
ERAV_RF
IRMN_RF
IRMX_RF
IRAV_RF
ERAV_RF
THMX_RF
THAV_RF
THNO
THMN_RF

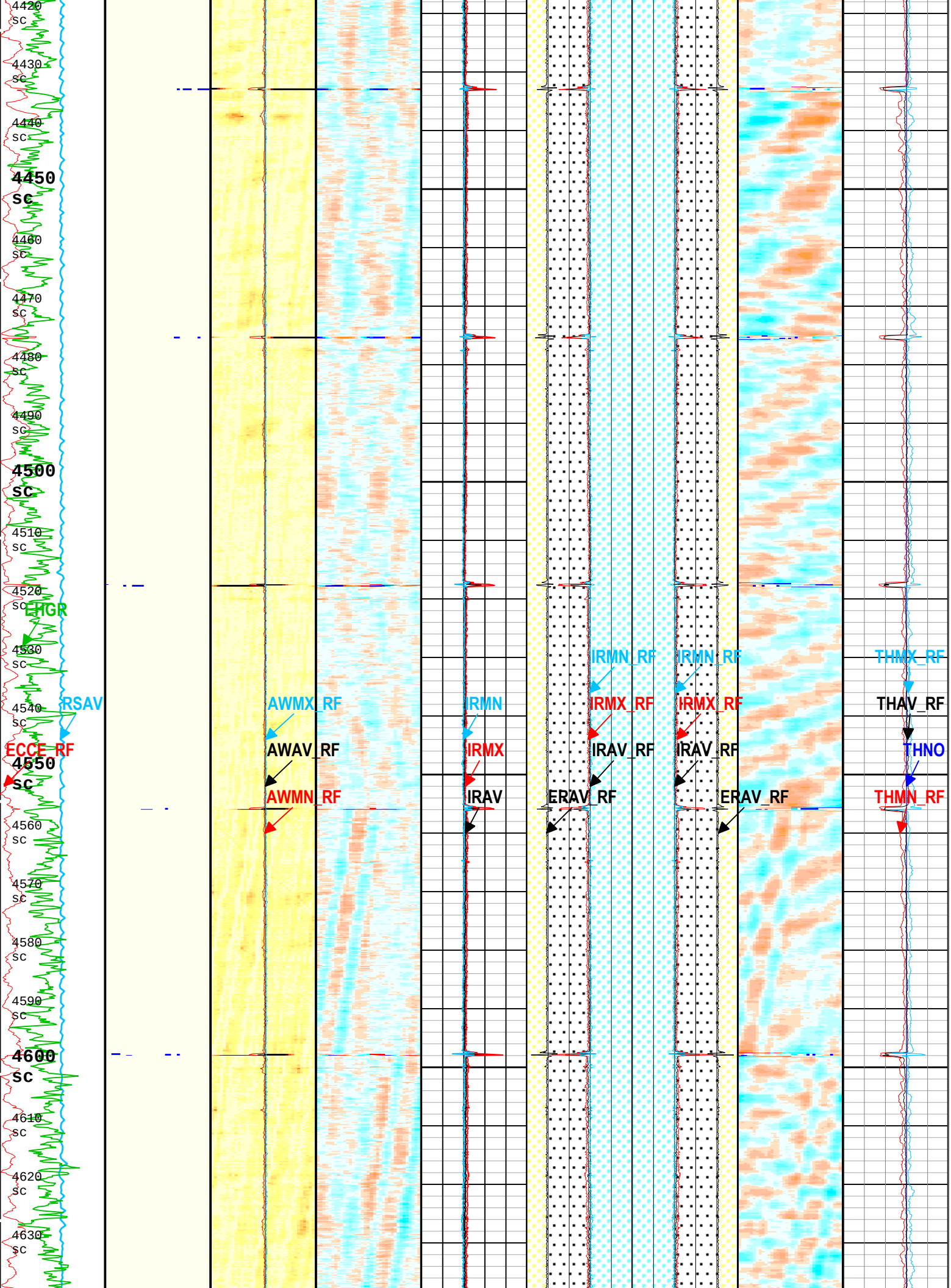
4420 sc
4430 sc
4440 sc
4450 sc
4460 sc
4470 sc
4480 sc
4490 sc
4500 sc
4510 sc
4520 sc
LHGR
4530 sc
RSAV
4540 sc
ECCE_RF
4550 sc
4560 sc
4570 sc
4580 sc
4590 sc
4600 sc
4610 sc
4620 sc
4630 sc
AWMX_RF
AWAV_RF
AWMN_RF
IRMN
IRMX
IRAV
IRMN_RF
IRMX_RF
IRAV_RF
ERAV_RF
IRMN_RF
IRMX_RF
IRAV_RF
ERAV_RF
THMX_RF
THAV_RF
THNO
THMN_RF

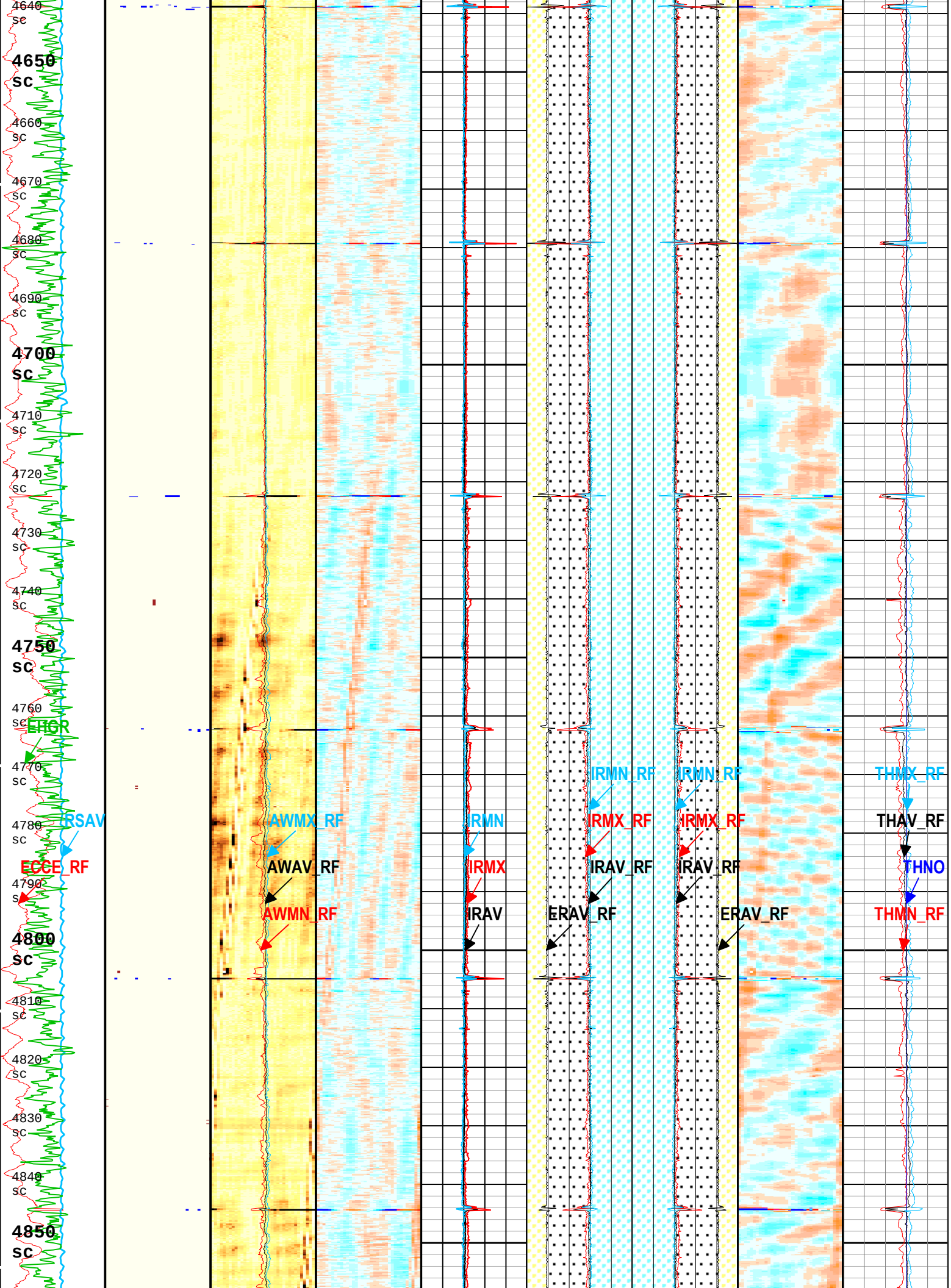
4640 sc
4650 sc
4660 sc
4670 sc
4680 sc
4690 sc
4700 sc
4710 sc
4720 sc
4730 sc
4740 sc
4750 sc
4760 sc
ETIOR
4770 sc
IRSAV
4780 sc
ECCE_RF
4790 sc
4800 sc
4810 sc
4820 sc
4830 sc
4840 sc
4850 sc
AWMX_RF
AWAV_RF
AWMN_RF
IRMN
IRMX
IRAV
IRMN_RF
IRMX_RF
IRAV_RF
ERAV_RF
IRMN_RF
IRMX_RF
IRAV_RF
ERAV_RF
THMX_RF
THAV_RF
THNO
THMN_RF

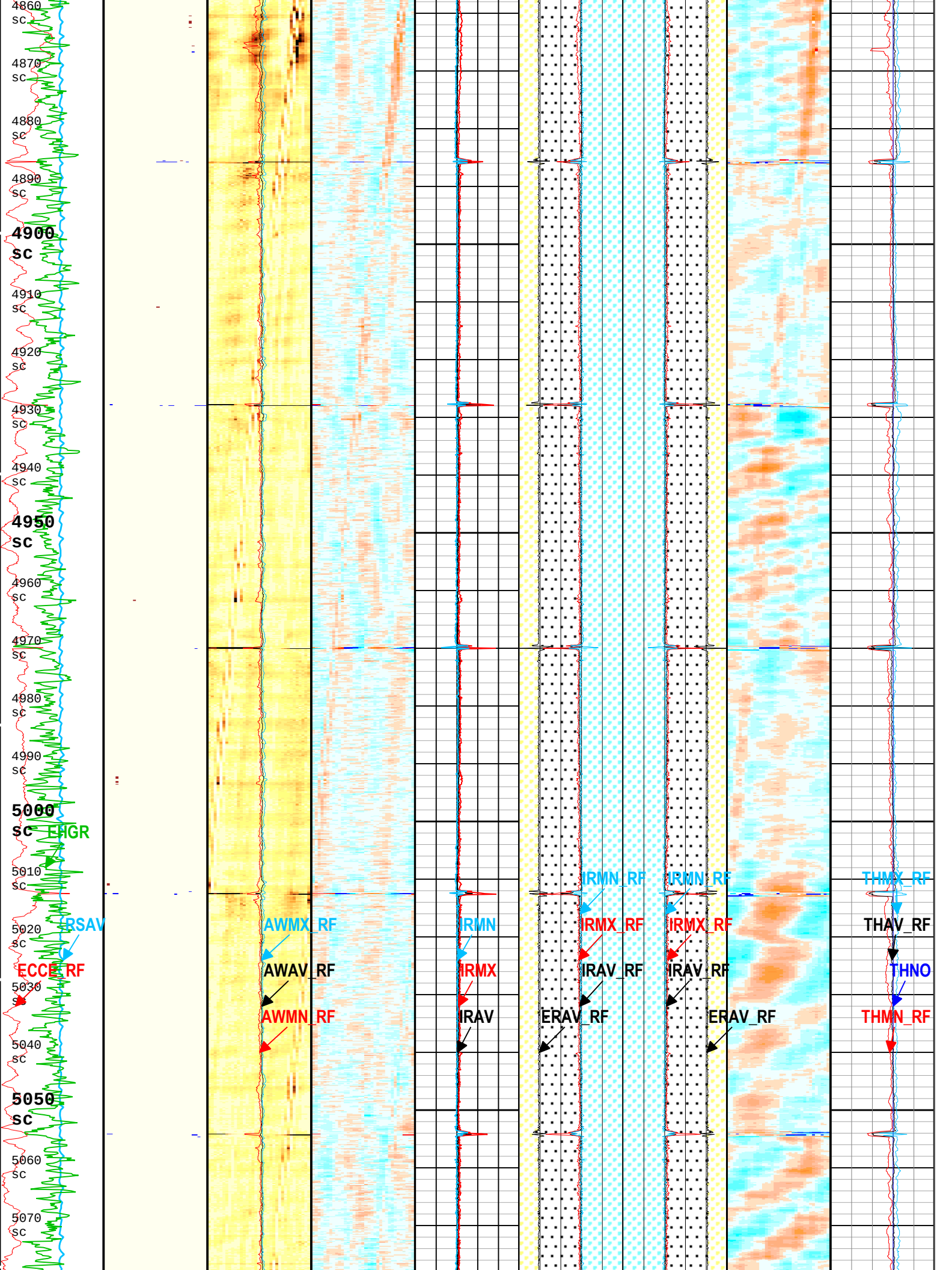
4860 sc
4870 sc
4880 sc
4890 sc
4900 sc
4910 sc
4920 sc
4930 sc
4940 sc
4950 sc
4960 sc
4970 sc
4980 sc
4990 sc
5000 sc
5010 sc
5020 sc
5030 sc
5040 sc
5050 sc
5060 sc
5070 sc
THGR
RSAV
ECCE_RF
AWMX_RF
AWAV_RF
AWMN_RF
IRMN
IRMX
IRAV
IRMN_RF
IRMX_RF
IRAV_RF
ERAV_RF
IRMN_RF
IRMX_RF
IRAV_RF
ERAV_RF
THMX_RF
THAV_RF
THNO
THMN_RF

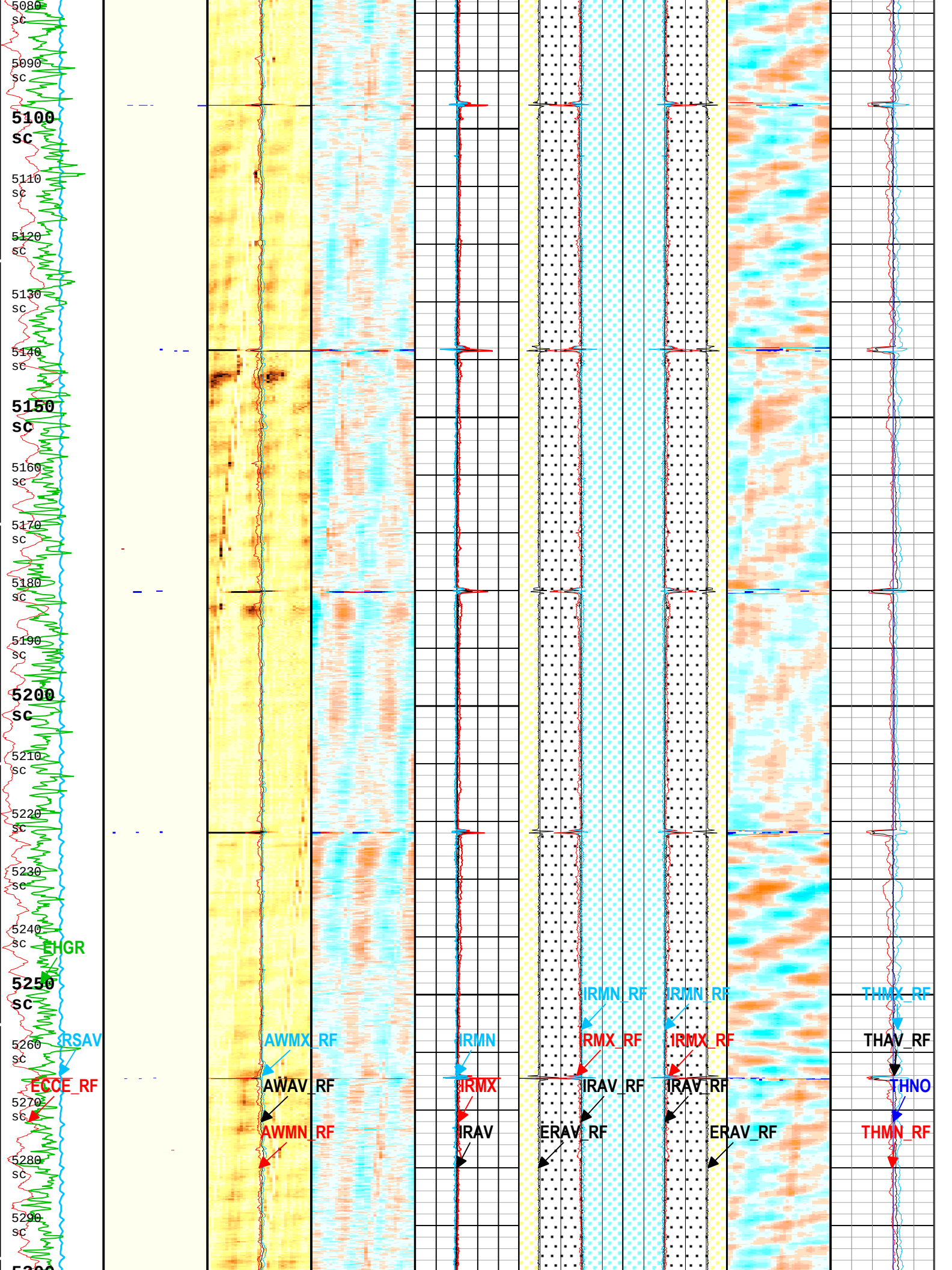
5080 sc
5090 sc
5100 sc
5110 sc
5120 sc
5130 sc
5140 sc
5150 sc
5160 sc
5170 sc
5180 sc
5190 sc
5200 sc
5210 sc
5220 sc
5230 sc
5240 sc
EHGR
5250 sc
5260 sc
RSAV
ECCE_RF
5270 sc
5280 sc
5290 sc
AWMX_RF
AWAV_RF
AWMN_RF
IRMN
IRMX
IRAV
IRMN_RF
IRMX_RF
IRAV_RF
ERAV_RF
IRMN_RF
IRMX_RF
IRAV_RF
ERAV_RF
THMX_RF
THAV_RF
THNO
THMN_RF

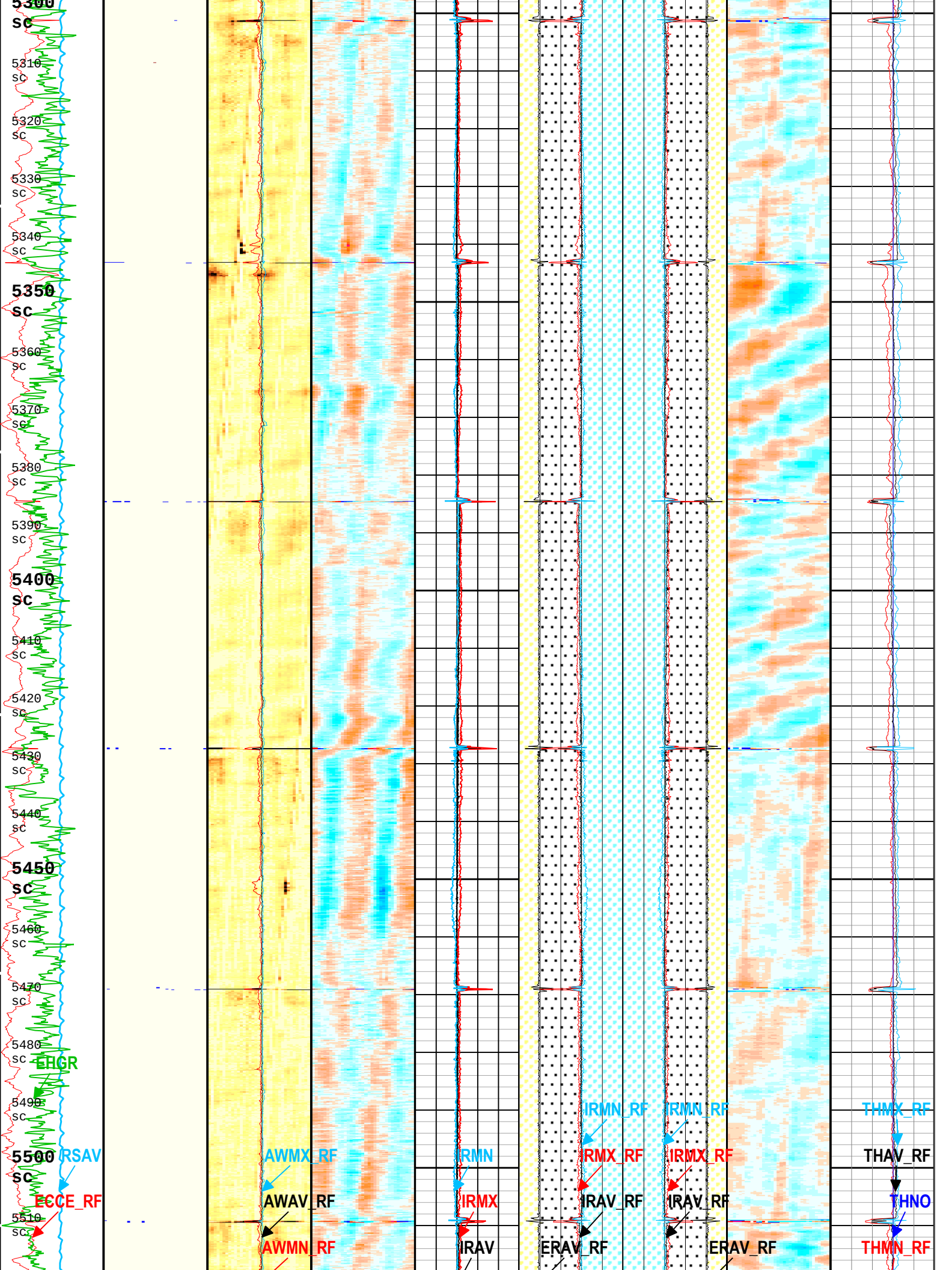
5300 sc
5310 sc
5320 sc
5330 sc
5340 sc
5350 sc
5360 sc
5370 sc
5380 sc
5390 sc
5400 sc
5410 sc
5420 sc
5430 sc
5440 sc
5450 sc
5460 sc
5470 sc
5480 sc
5490 sc
5500 sc
5510 sc
THGR
RSAV
ECCE_RF
AWMX_RF
AWAV_RF
AWMN_RF
IRMN
IRMX
IRAV
IRMN_RF
IRMX_RF
IRAV_RF
ERAV_RF
IRMN_RF
IRMX_RF
IRAV_RF
ERAV_RF
THMX_RF
THAV_RF
THNO
THMN_RF

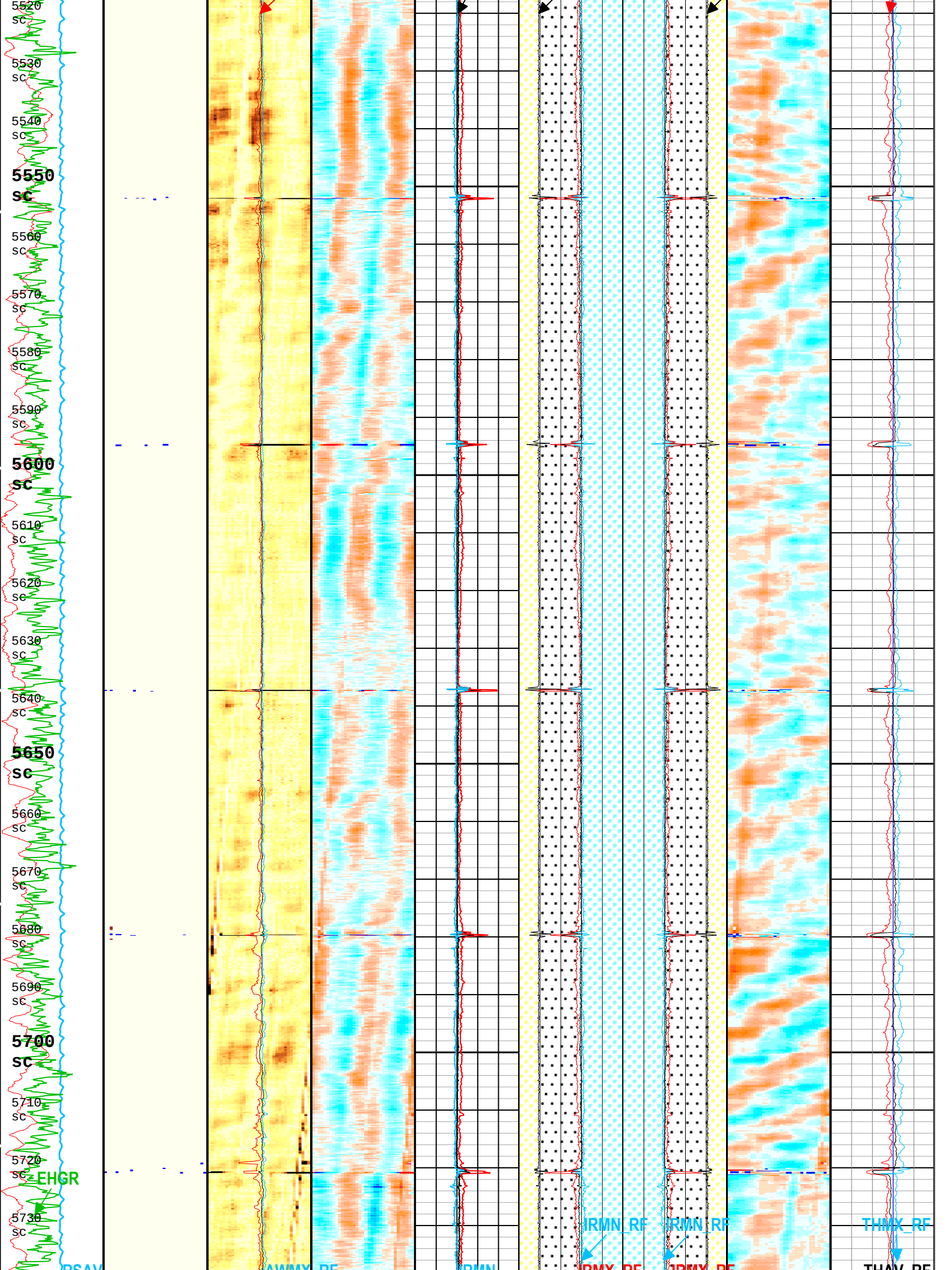
5520 sc
5530 sc
5540 sc
5550 sc
5560 sc
5570 sc
5580 sc
5590 sc
5600 sc
5610 sc
5620 sc
5630 sc
5640 sc
5650 sc
5660 sc
5670 sc
5680 sc
5690 sc
5700 sc
5710 sc
5720 sc
5730 sc
EHGR
RSAV
AWMX_RF
RMN
IRMN_RF
IRMN_RF
IRMX_RF
IRMX_RF
THMX_RF
THAV_RF

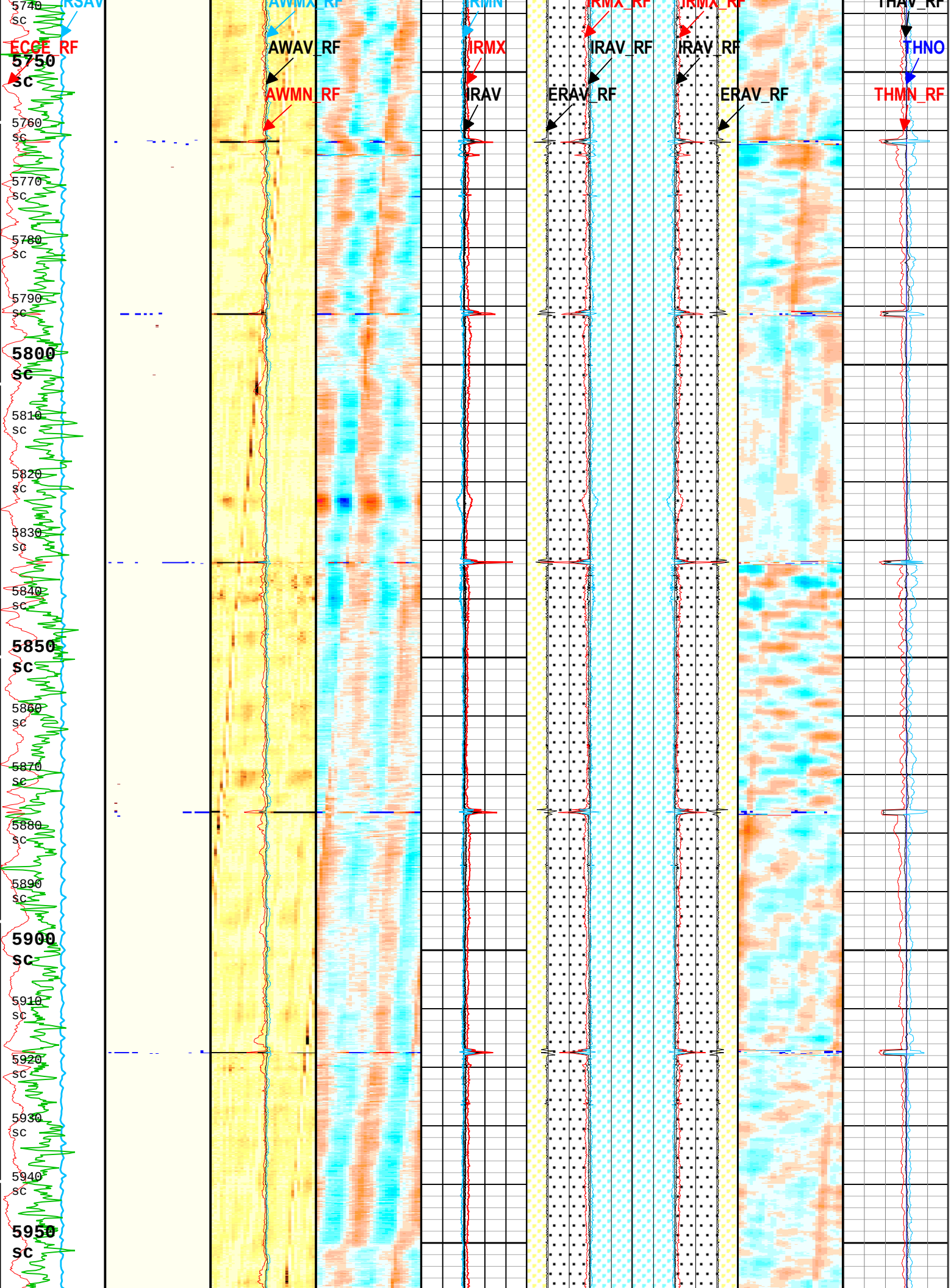
IRSAV
ECGE_RF
AWMX_RF
AWAV_RF
AWMN_RF
IRMN
IRMX
IRAV
IRMX_RF
IRAV_RF
ERAV_RF
IRMX_RF
IRAV_RF
ERAV_RF
THAV_RF
THNO
THMN_RF
5740 sc
5750 sc
5760 sc
5770 sc
5780 sc
5790 sc
5800 sc
5810 sc
5820 sc
5830 sc
5840 sc
5850 sc
5860 sc
5870 sc
5880 sc
5890 sc
5900 sc
5910 sc
5920 sc
5930 sc
5940 sc
5950 sc

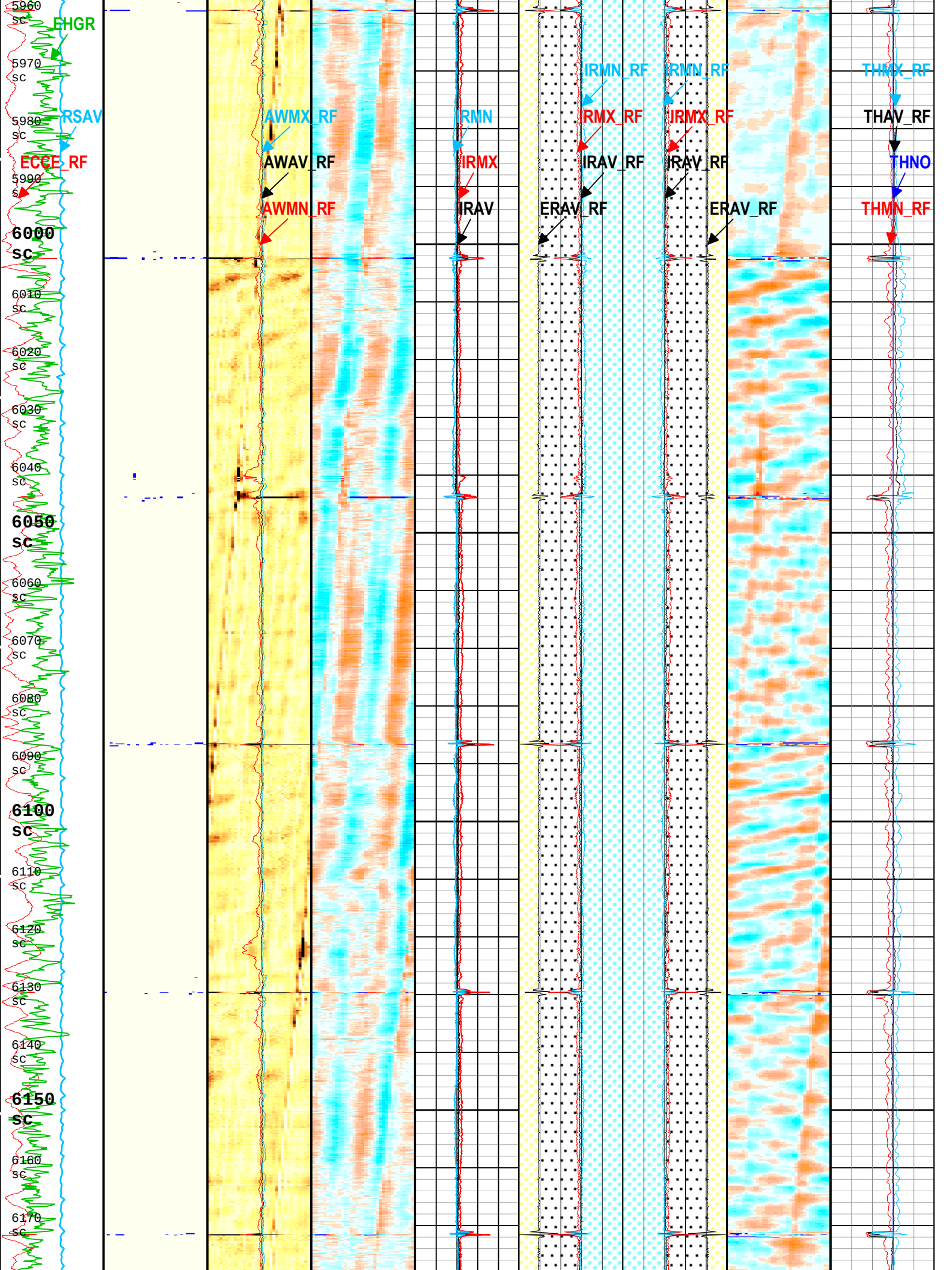
5960 sc
EHGR
5970 sc
RSAV
5980 sc
ECCE_RF
5990 sc
6000 sc
6010 sc
6020 sc
6030 sc
6040 sc
6050 sc
6060 sc
6070 sc
6080 sc
6090 sc
6100 sc
6110 sc
6120 sc
6130 sc
6140 sc
6150 sc
6160 sc
6170 sc
AWMX_RF
AWAV_RF
AWMN_RF
IRMN
IRMX
IRAV
IRMN_RF
RMX_RF
IRAV_RF
ERAV_RF
IRMN_RF
IRMX_RF
IRAV_RF
ERAV_RF
THMX_RF
THAV_RF
THNO
THMN_RF

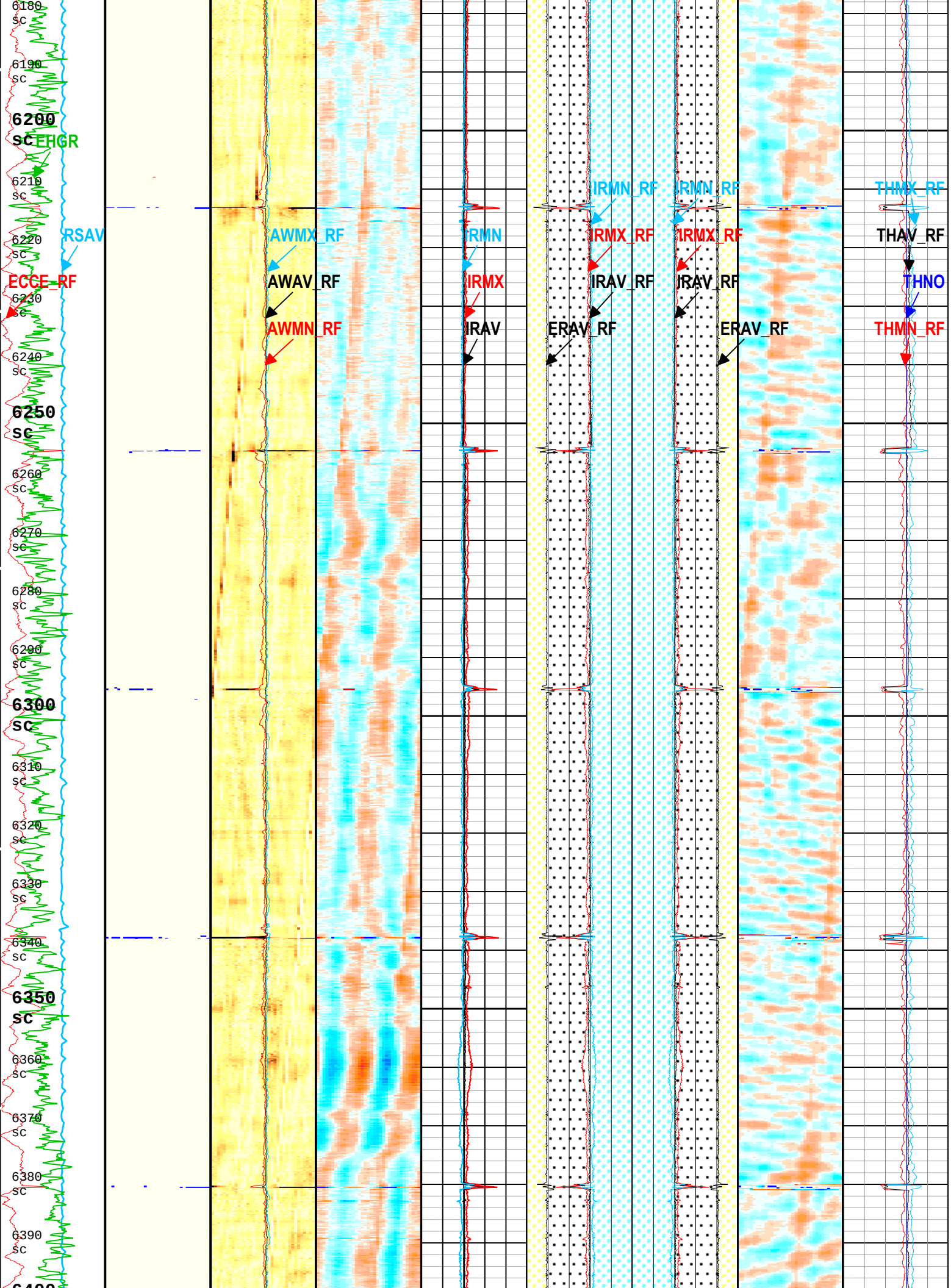
6180 sc
6190 sc
6200 sc
EHGR
6210 sc
6220 sc
RSAV
ECCE_RF
6230 sc
6240 sc
6250 sc
6260 sc
6270 sc
6280 sc
6290 sc
6300 sc
6310 sc
6320 sc
6330 sc
6340 sc
6350 sc
6360 sc
6370 sc
6380 sc
6390 sc
AWMX_RF
AWAV_RF
AWMN_RF
IRMN
IRMX
IRAV
IRMN_RF
IRMX_RF
IRAV_RF
ERAV_RF
IRMN_RF
IRMX_RF
IRAV_RF
ERAV_RF
THMX_RF
THAV_RF
THNO
THMN_RF

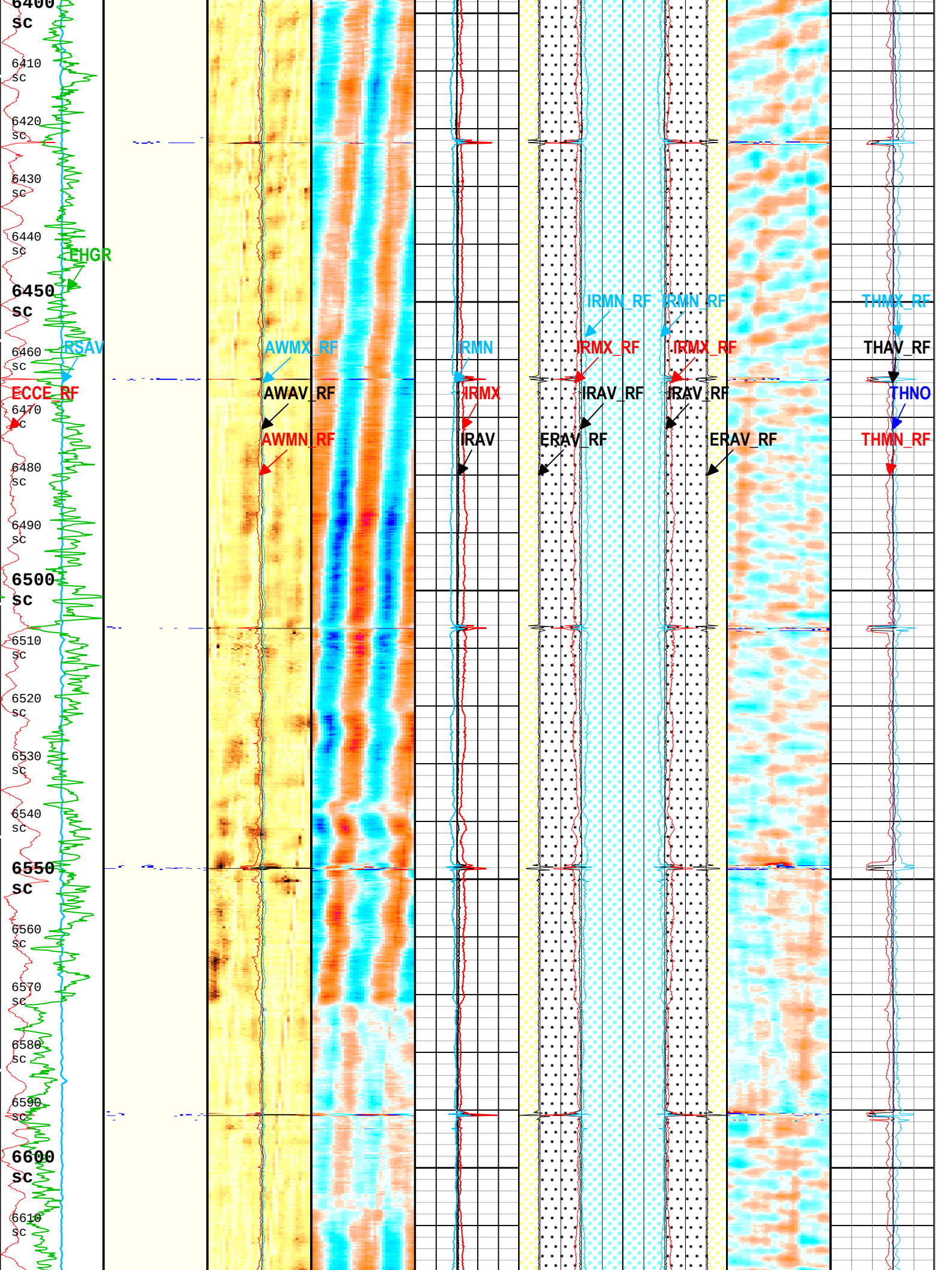
6400 sc
6410 sc
6420 sc
6430 sc
6440 sc
EHGR
6450 sc
RSAV
6460 sc
ECCE_RF
6470 sc
6480 sc
6490 sc
6500 sc
6510 sc
6520 sc
6530 sc
6540 sc
6550 sc
6560 sc
6570 sc
6580 sc
6590 sc
6600 sc
6610 sc
AWMX_RF
AWAV_RF
AWMN_RF
IRMN
IRMX
IRAV
IRMN_RF
IRMX_RF
IRAV_RF
ERAV_RF
IRMN_RF
IRMX_RF
IRAV_RF
ERAV_RF
THMX_RF
THAV_RF
THNO
THMN_RF

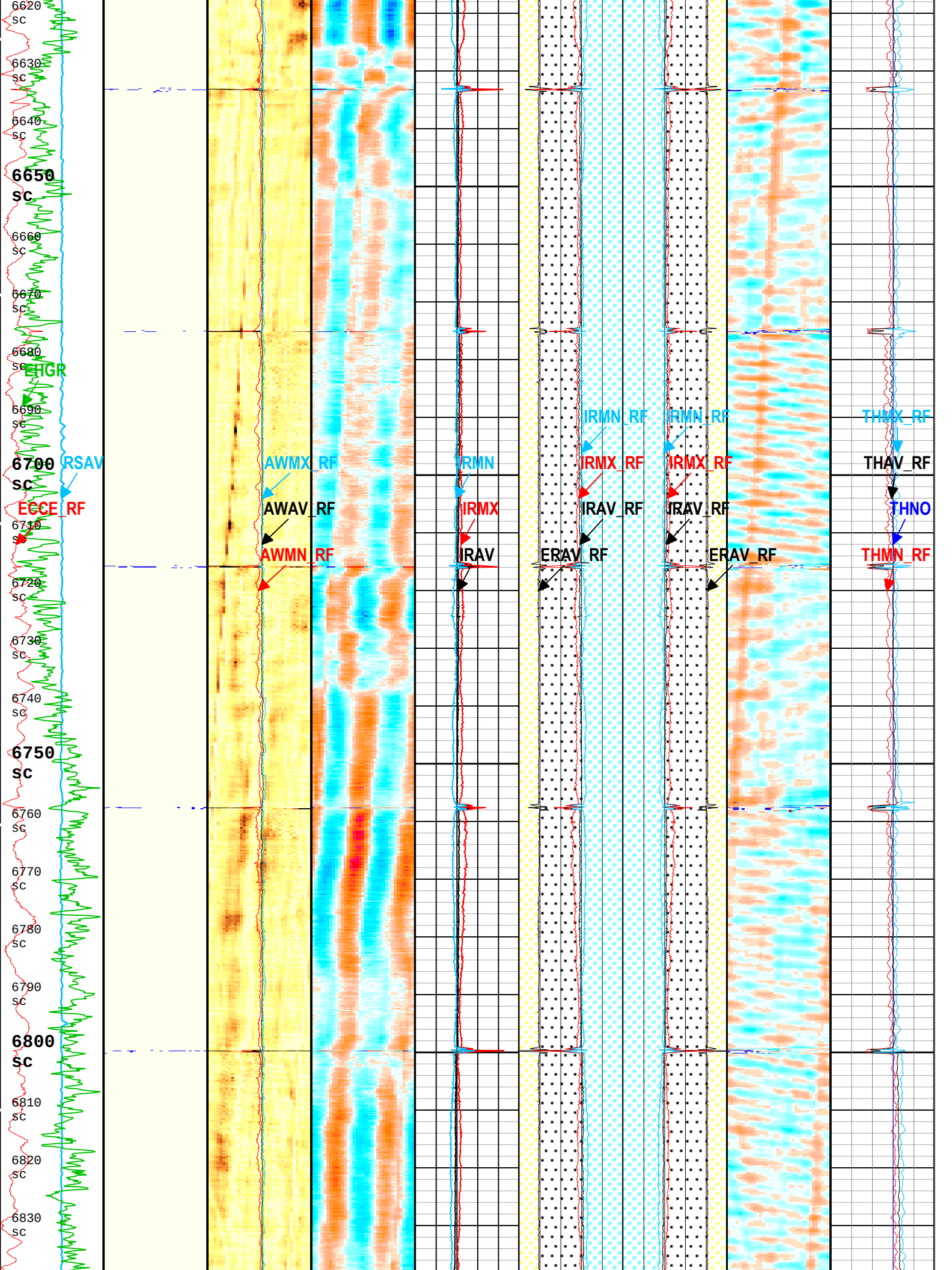
6620 sc
6630 sc
6640 sc
6650 sc
6660 sc
6670 sc
6680 sc
EHGR
6690 sc
6700 sc
RSAV
ECCE_RF
6710 sc
6720 sc
6730 sc
6740 sc
6750 sc
6760 sc
6770 sc
6780 sc
6790 sc
6800 sc
6810 sc
6820 sc
6830 sc
AWMX_RF
AWAV_RF
AWMN_RF
IRMN
IRMX
IRAV
IRMN_RF
IRMX_RF
IRAV_RF
ERAV_RF
IRMN_RF
IRMX_RF
IRAV_RF
ERAV_RF
THMX_RF
THAV_RF
THNO
THMN_RF

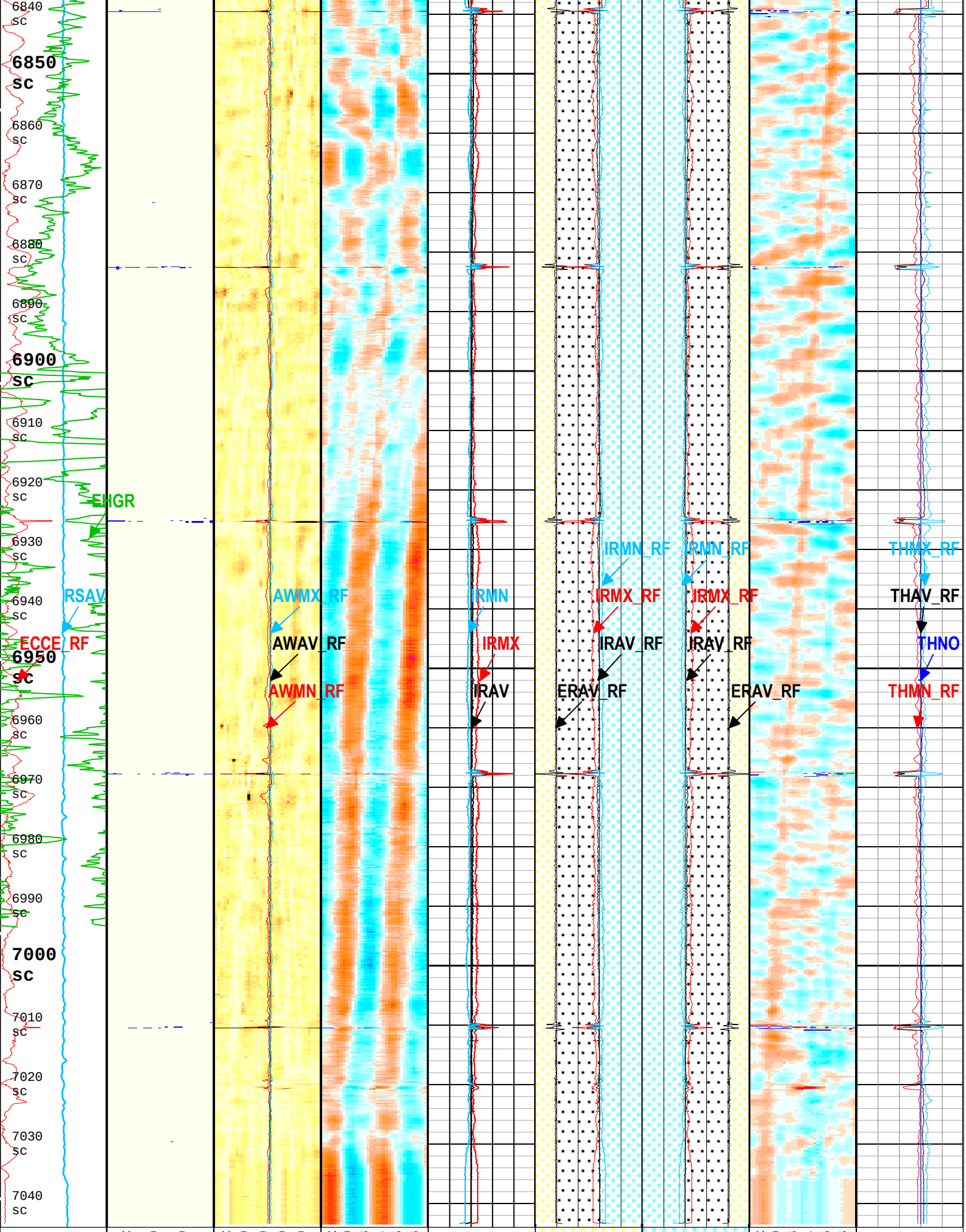
6840 sc
6850 sc
6860 sc
6870 sc
6880 sc
6890 sc
6900 sc
6910 sc
6920 sc
6930 sc
6940 sc
6950 sc
6960 sc
6970 sc
6980 sc
6990 sc
7000 sc
7010 sc
7020 sc
7030 sc
7040 sc
EHGR
RSAV
ECCE_RF
AWMX_RF
AWAV_RF
AWMN_RF
IRMN
IRMX
IRAV
IRMN_RF
IRMX_RF
IRAV_RF
ERAV_RF
IRMN_RF
IRMX_RF
IRAV_RF
ERAV_RF
THMX_RF
THAV_RF
THNO
THMN_RF
Amplitude of Eccentering for Unflagged Waves
Absent 1.500 3.500
Explicit
Absent -5.200 -3.600 -2.000 -0.400
Absent -0.059 -0.028 0.004 0.035 0.068
Internal Radius Averaged Value (IRAV) USIT-E
ERAV
ERAV-IRAV
IRAV
ERAV
Absent -0.059 -0.028 0.004 0.035 0.068
Minimum of Unflagged Casing Thickness

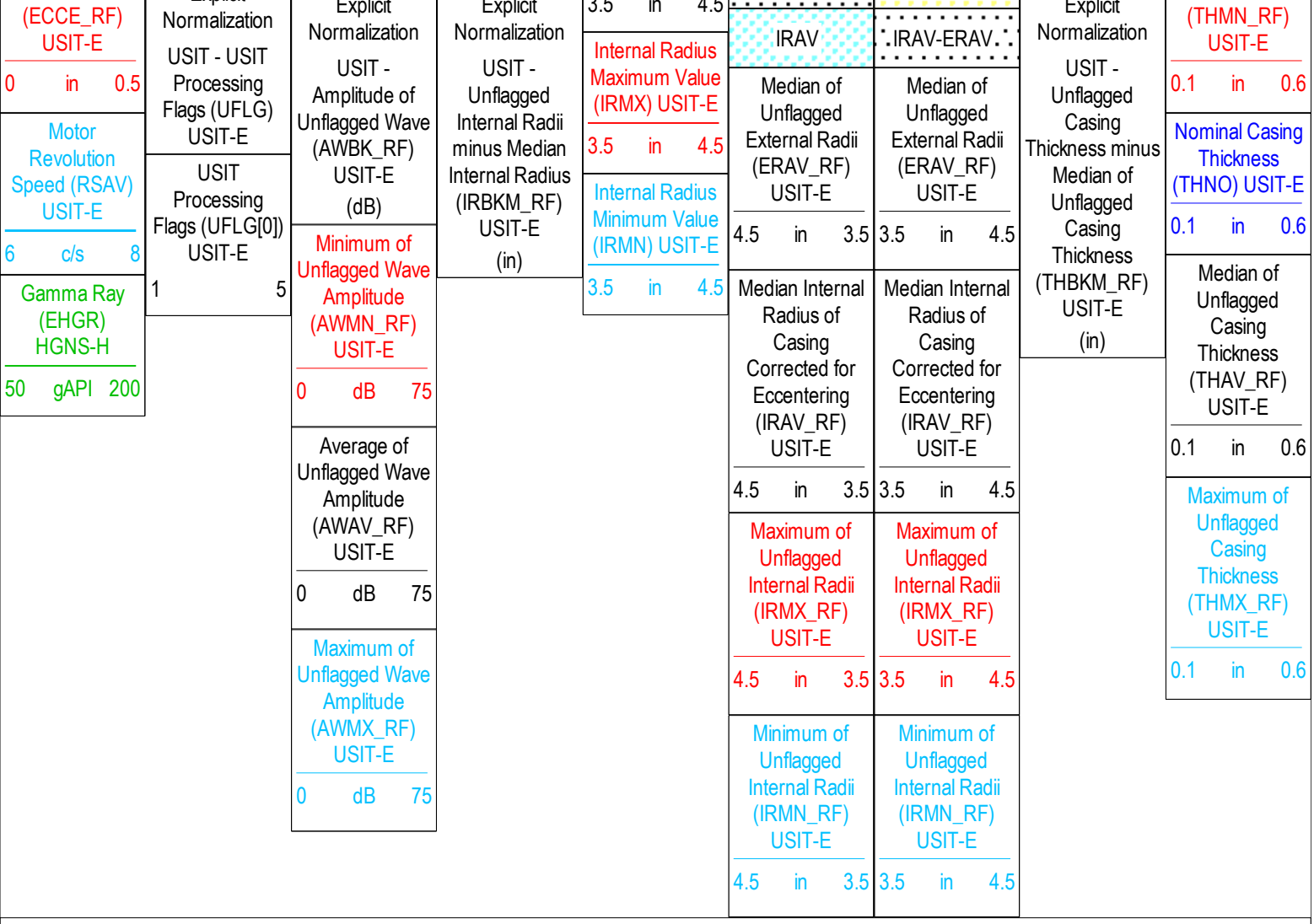

Channel Processing Parameters

One: Parameters

Parameter	Description	Tool	Value	Unit
ISSBAR	Barite Mud Presence Flag	Borehole	No	
BHS	Borehole Status (Open or Cased Hole)	Borehole	Cased	
BS	Bit Size	WLSESSION	Depth Zoned	in
CBLO	Casing Bottom (Logger)	WLSESSION	7331	ft
CDEN	Cement Density	HGNS-H	2.65	g/cm3
CMTY(U-USIT_CEMT)	Cement Type	USIT-E	Regular Cement	
THNO	Nominal Casing Thickness - Zoned along logger depths	WLSESSION	0.4	in
CYSTLGR	Casing Yield Strength - Zoned along logger depths	WLSESSION	Depth Zoned	psi
DFD	Drilling Fluid Density	Borehole	8.9	lbm/gal
DFT_CATEGORY	Drilling Fluid Type	Borehole	Water	
DTMD	Borehole Fluid Slowness	Borehole	193	us/ft
EDII	EDM Data Interpolation Interval	USIT-E	0	ft

FDII	FPM Data Interpolation Interval	USIT-E	0	ft
GCSE_DOWN_PASS	Generalized Caliper Selection for WL Log Down Passes	Borehole	BS	
GCSE_UP_PASS	Generalized Caliper Selection for WL Log Up Passes	Borehole	BS	
HEMA	Hematite Presence Flag	Borehole	No	
ICE_PROCESS	ICE Processing	USIT-E	Yes	
IMAR	Image Rotation	USIT-E	Off	
MEAS_WLEN	Tcube Processing Window Length in Measurement Mode	USIT-E	24.96	us
MUD_N_FRP	Free Pipe Mud Normalization Factor	USIT-E	1.06	
THDH	Maximum Search Thickness (percentage of nominal)	USIT-E	130	%
THDL	Minimum Search Thickness (percentage of nominal)	USIT-E	65	%
HISC	Tool Position: Centered or Eccentered	HGNS-H	Centered	
U-USIT_DFSZ	Drilling Fluid Specific Acoustic Impedance	USIT-E	0	Mrayl
UFGDE	Fiberglass Density	USIT-E	1.95	g/cm3
UFGPS	Fiberglass Processing Selection	USIT-E	No	
UFGVL	Fiberglass Velocity	USIT-E	9678.48	ft/s
USI_FSOD	USIT USI Fluid Slowness Fits Casing Outer Diameter	USIT-E	0_OFF	
USI_FVEL_SEL	USI Fluid Velocity Selection	USIT-E	Automatic	
USI_ZMUD_SEL	USI Mud Impedance Selection	USIT-E	FreePipe Norm.	
ZMUD	Acoustic Impedance of Mud	Borehole	1.68	Mrayl
ZTCM	Acoustic Impedance Threshold for Cement	USIT-E	2.6	Mrayl
ZTGS	Acoustic Impedance Threshold for Gas	USIT-E	0.3	Mrayl

Depth Zone Parameters

Parameter	Value	Start (ft)	Stop (ft)
BS	17.5	10	832
BS	11	832	7044
CYSTLGR	55000	10	5835
CYSTLGR	80000	5835	7044

All depth are actual.

Tool Control Parameters

One: Parameters

Parameter	Description	Tool	Value	Unit
AGMN	Minimum Gain of Cartridge	USIT-E	-12	dB
AGMX	Maximum Gain of Cartridge	USIT-E	48	dB
U-USIT_DDT5	USIC Downhole Decimation for T5 only	USIT-E	0_NONE	
EMXV	EMEX Voltage	USIT-E	80	V
HRES	Horizontal Resolution	USIT-E	10 deg	
TMUC	Type of Mud	USIT-E	BRI	
ULOG	Logging Objective	USIT-E	MEASUREMENT	
UMFR	Modulation Frequency	USIT-E	333333	Hz
USFR	Ultrasonic Sampling Frequency	USIT-E	500000	Hz
UPAT	USIT Emission Pattern	USIT-E	Pattern 500 KHz	
UWKM	USIT Working Mode	USIT-E	Uncompressed 10 deg at 1.5 in LF	
USIT_DEPTHLOG	Starting Depth Log for Ultrasonics	USIT-E	7030	ft
VRES	Vertical Resolution	USIT-E	1.5 in	
WINB	Window Begin Time	USIT-E	59.63	us
WINE	Window End Time	USIT-E	99.63	us

One

USI Compressed Goodwin 1" = 100'

Pass Summary

Run Name	Pass Objective	Direction	Top	Bottom	Start	Stop	DSC Mode	Depth Shift	Include Parallel Data
One	Log[4]:Up	Up	4.12 ft	7044.38 ft	02-Jun-2017 1:27:12 AM	02-Jun-2017 4:20:07 AM	ON	4.20 ft	Yes

All depths are referenced to toolstring zero

Log

Company:Southern California Gas Company Well:Fernando Fee 35B

One: Log[4]:Up:S011

Description: USI Goodwin Format: Log (Import of USI Goodwin) Index Scale: 1 in per 100 ft Index Unit: ft Index Type: Measured Depth Creation Date: 17-Jul-2017 14:11:47

TIME_1900 - Time Marked every 60.00 (s)

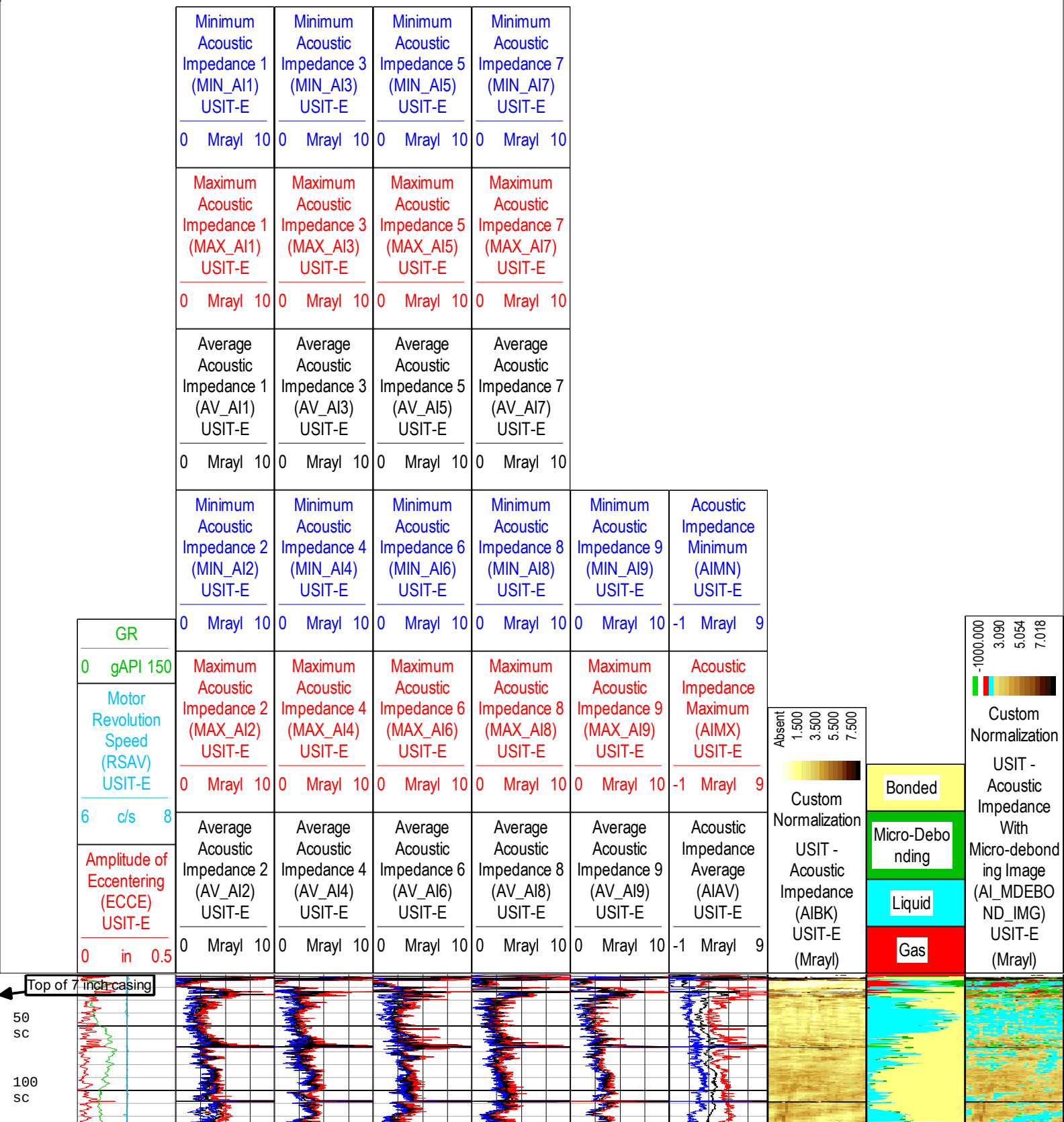

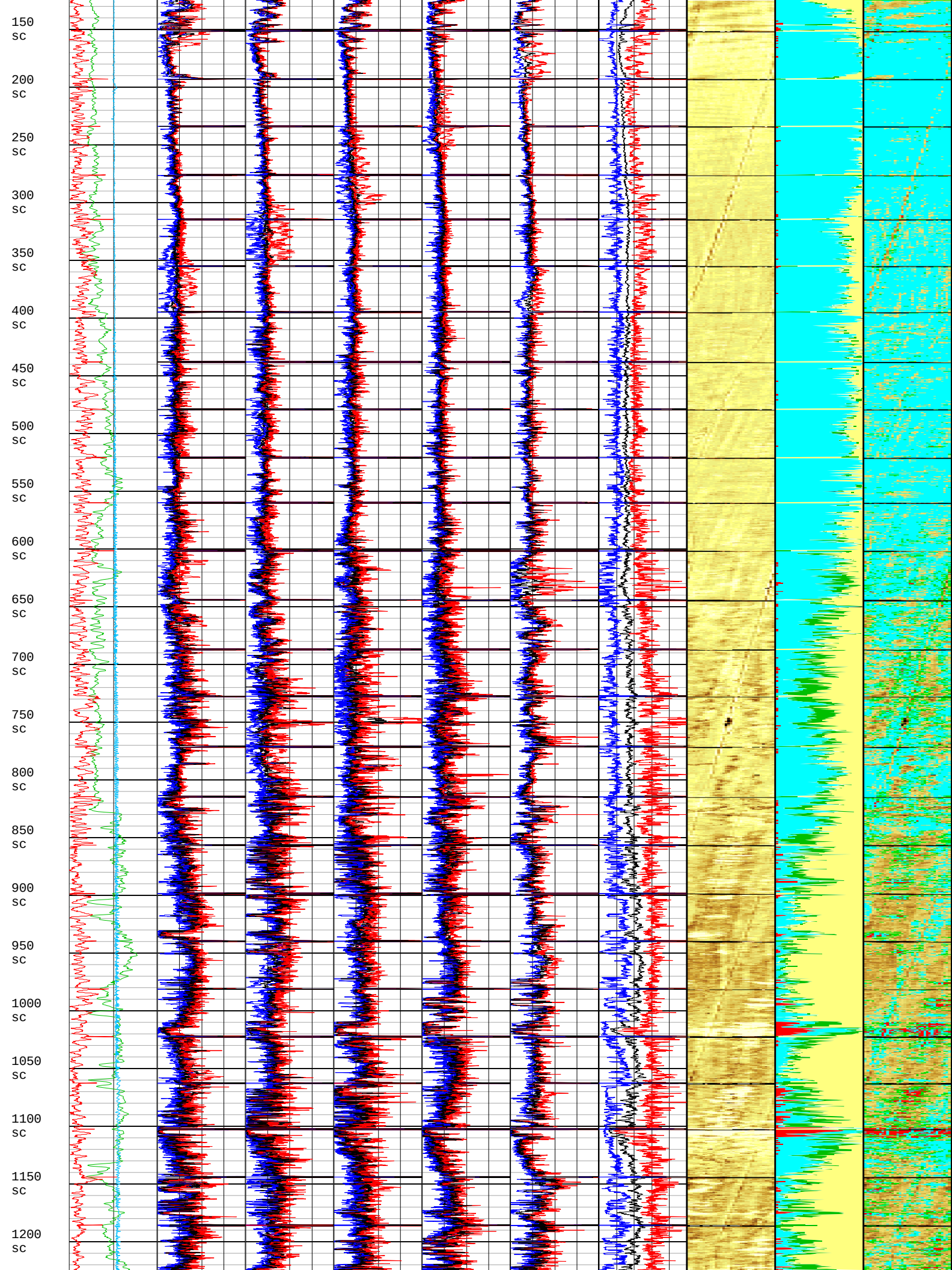
150
sc
200
sc
250
sc
300
sc
350
sc
400
sc
450
sc
500
sc
550
sc
600
sc
650
sc
700
sc
750
sc
800
sc
850
sc
900
sc
950
sc
1000
sc
1050
sc
1100
sc
1150
sc
1200
sc

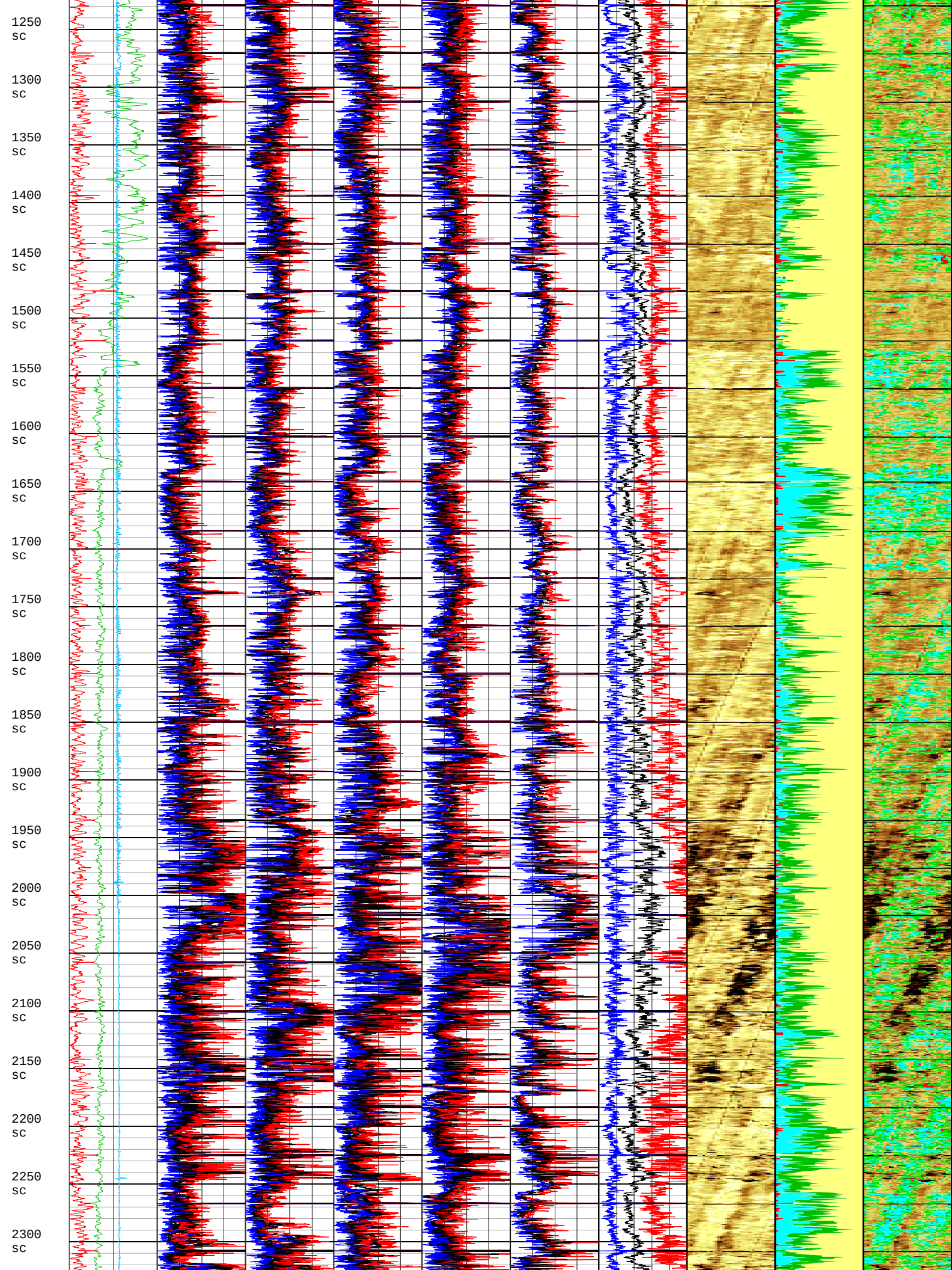
1250
sc
1300
sc
1350
sc
1400
sc
1450
sc
1500
sc
1550
sc
1600
sc
1650
sc
1700
sc
1750
sc
1800
sc
1850
sc
1900
sc
1950
sc
2000
sc
2050
sc
2100
sc
2150
sc
2200
sc
2250
sc
2300
sc

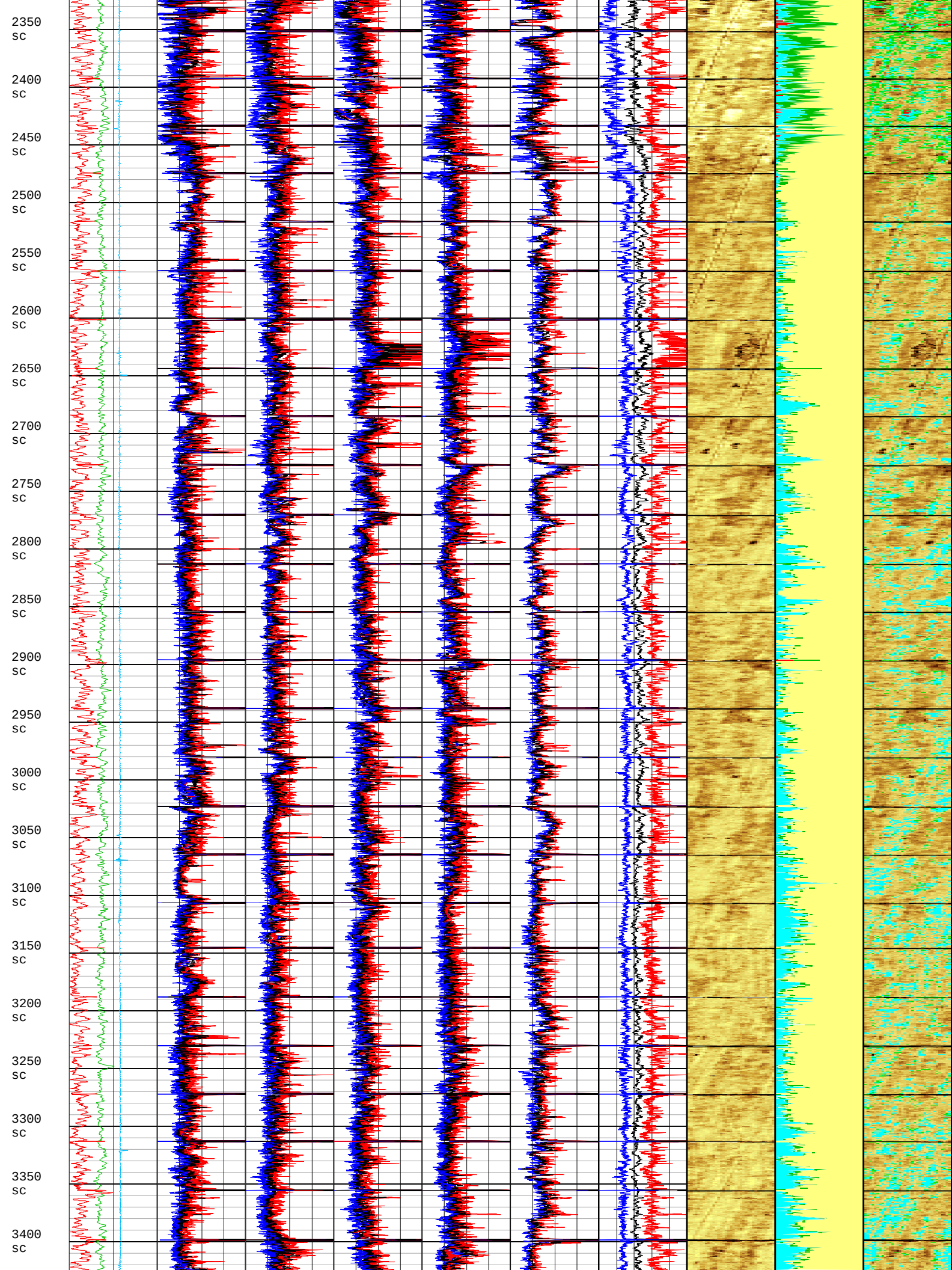
2350
sc
2400
sc
2450
sc
2500
sc
2550
sc
2600
sc
2650
sc
2700
sc
2750
sc
2800
sc
2850
sc
2900
sc
2950
sc
3000
sc
3050
sc
3100
sc
3150
sc
3200
sc
3250
sc
3300
sc
3350
sc
3400
sc

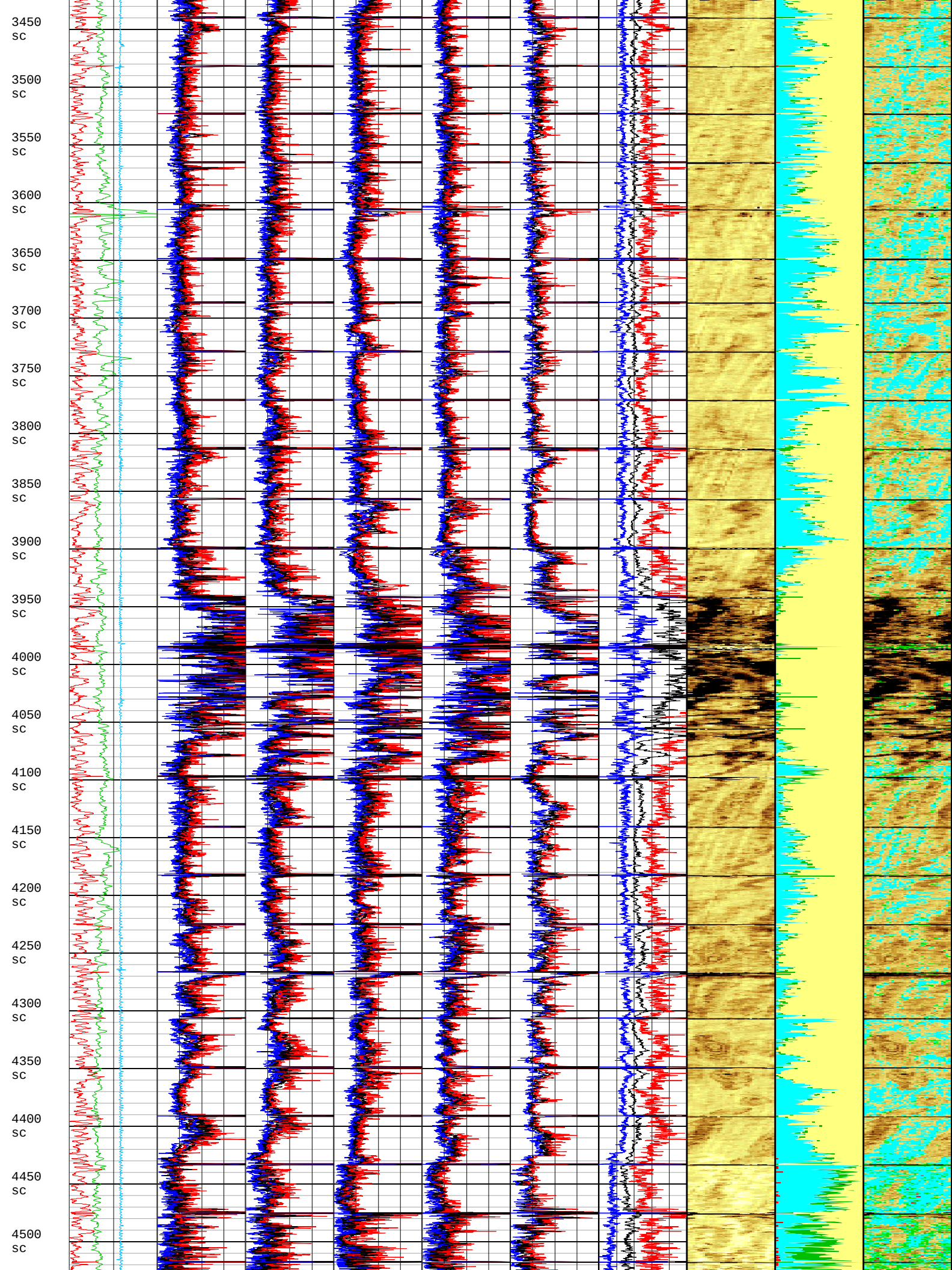
3450
sc
3500
sc
3550
sc
3600
sc
3650
sc
3700
sc
3750
sc
3800
sc
3850
sc
3900
sc
3950
sc
4000
sc
4050
sc
4100
sc
4150
sc
4200
sc
4250
sc
4300
sc
4350
sc
4400
sc
4450
sc
4500
sc

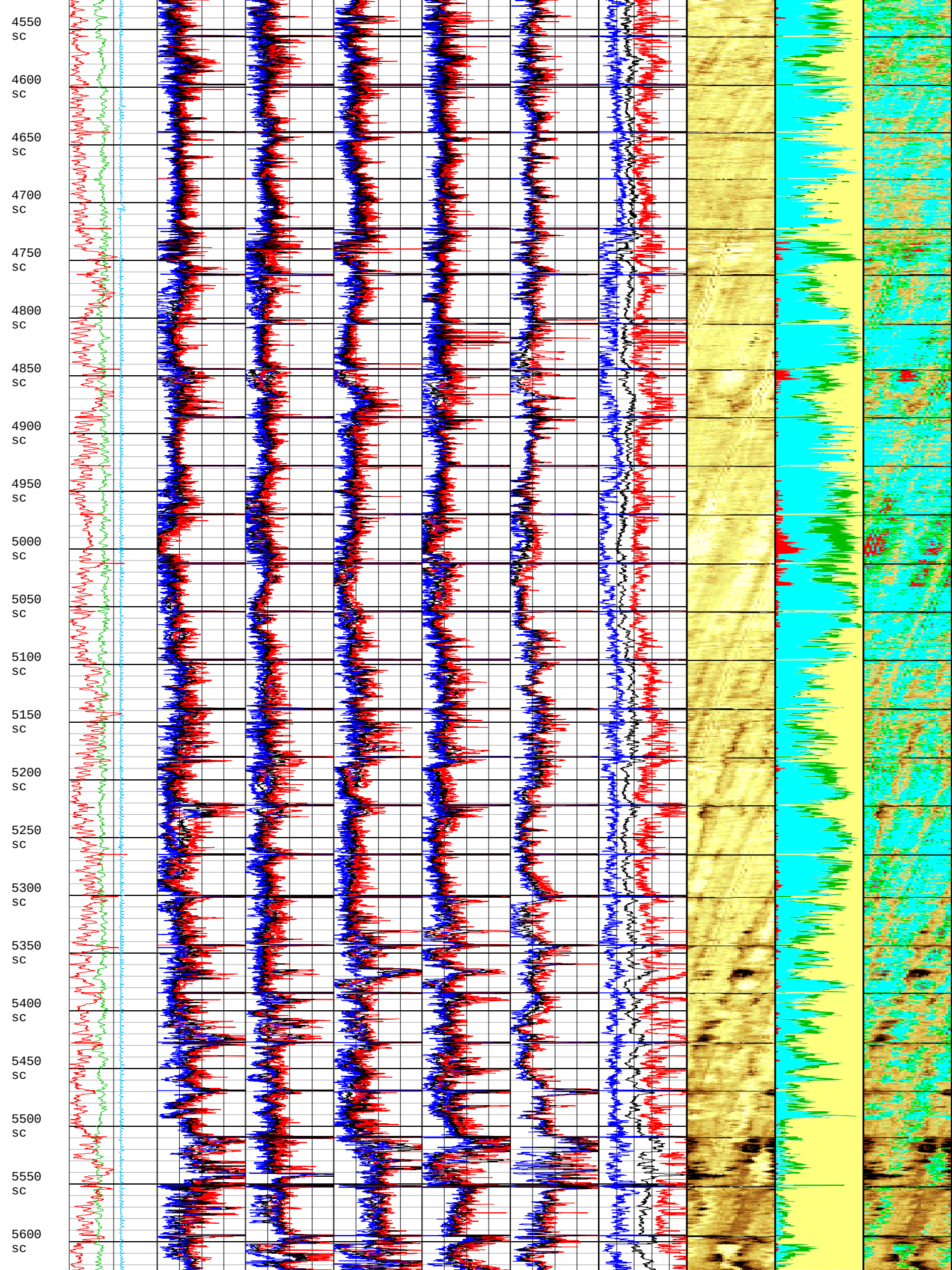
4550
sc
4600
sc
4650
sc
4700
sc
4750
sc
4800
sc
4850
sc
4900
sc
4950
sc
5000
sc
5050
sc
5100
sc
5150
sc
5200
sc
5250
sc
5300
sc
5350
sc
5400
sc
5450
sc
5500
sc
5550
sc
5600
sc

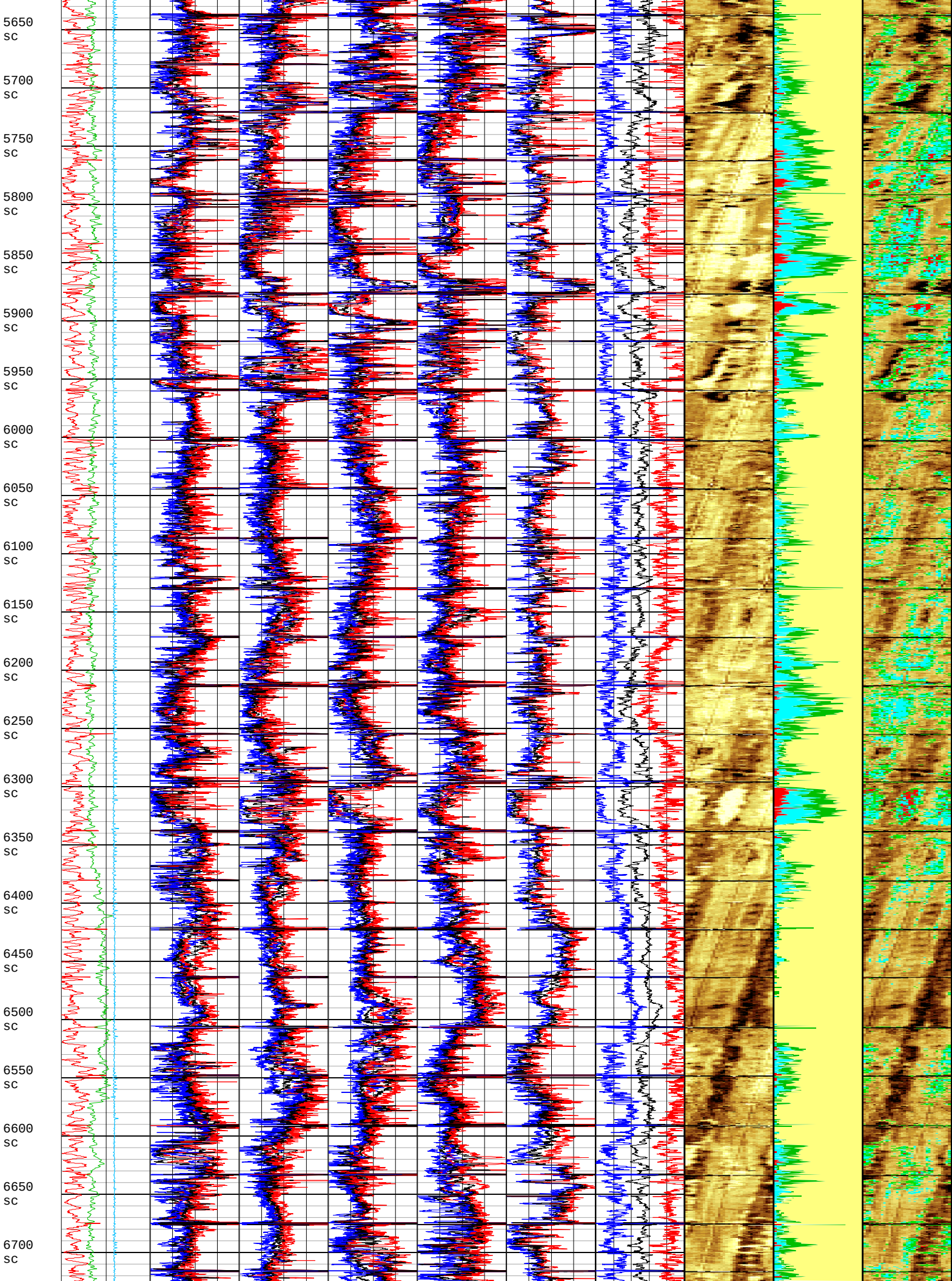
5650
sc
5700
sc
5750
sc
5800
sc
5850
sc
5900
sc
5950
sc
6000
sc
6050
sc
6100
sc
6150
sc
6200
sc
6250
sc
6300
sc
6350
sc
6400
sc
6450
sc
6500
sc
6550
sc
6600
sc
6650
sc
6700
sc

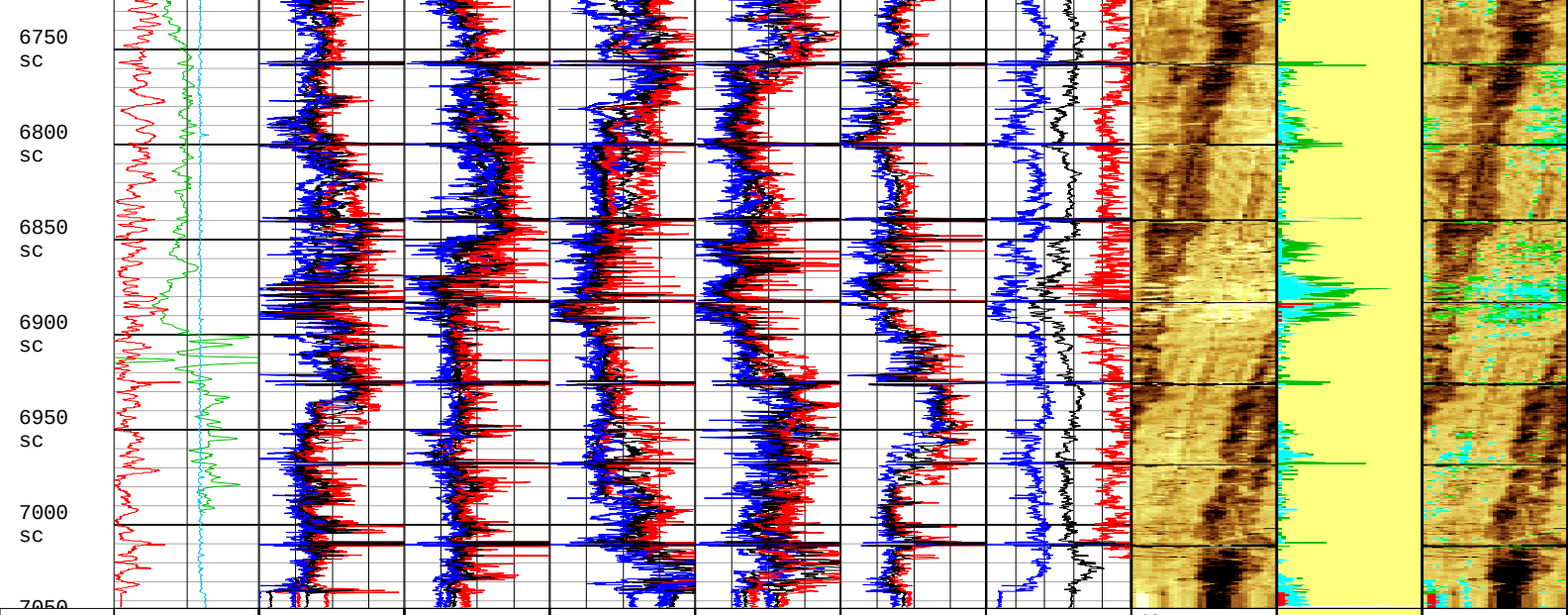

GR 0 gAPI 150	Minimum Acoustic Impedance 1 (MIN_AI1) USIT-E 0 Mrayl 10	Minimum Acoustic Impedance 3 (MIN_AI3) USIT-E 0 Mrayl 10	Minimum Acoustic Impedance 5 (MIN_AI5) USIT-E 0 Mrayl 10	Minimum Acoustic Impedance 7 (MIN_AI7) USIT-E 0 Mrayl 10	Minimum Acoustic Impedance 9 (MIN_AI9) USIT-E 0 Mrayl 10	Acoustic Impedance Minimum (AIMN) USIT-E -1 Mrayl 9
Motor Revolution Speed (RSAV) USIT-E 6 c/s 8	Maximum Acoustic Impedance 1 (MAX_AI1) USIT-E 0 Mrayl 10	Maximum Acoustic Impedance 3 (MAX_AI3) USIT-E 0 Mrayl 10	Maximum Acoustic Impedance 5 (MAX_AI5) USIT-E 0 Mrayl 10	Maximum Acoustic Impedance 7 (MAX_AI7) USIT-E 0 Mrayl 10	Maximum Acoustic Impedance 9 (MAX_AI9) USIT-E 0 Mrayl 10	Acoustic Impedance Maximum (AIMX) USIT-E -1 Mrayl 9
Amplitude of Eccentering (ECCE) USIT-E 0 in 0.5	Average Acoustic Impedance 1 (AV_AI1) USIT-E 0 Mrayl 10	Average Acoustic Impedance 3 (AV_AI3) USIT-E 0 Mrayl 10	Average Acoustic Impedance 5 (AV_AI5) USIT-E 0 Mrayl 10	Average Acoustic Impedance 7 (AV_AI7) USIT-E 0 Mrayl 10	Average Acoustic Impedance 9 (AV_AI9) USIT-E 0 Mrayl 10	Acoustic Impedance Average (AIAV) USIT-E -1 Mrayl 9
	Minimum Acoustic Impedance 2 (MIN_AI2) USIT-E 0 Mrayl 10	Minimum Acoustic Impedance 4 (MIN_AI4) USIT-E 0 Mrayl 10	Minimum Acoustic Impedance 6 (MIN_AI6) USIT-E 0 Mrayl 10	Minimum Acoustic Impedance 8 (MIN_AI8) USIT-E 0 Mrayl 10		
	Maximum Acoustic Impedance 2 (MAX_AI2) USIT-E 0 Mrayl 10	Maximum Acoustic Impedance 4 (MAX_AI4) USIT-E 0 Mrayl 10	Maximum Acoustic Impedance 6 (MAX_AI6) USIT-E 0 Mrayl 10	Maximum Acoustic Impedance 8 (MAX_AI8) USIT-E 0 Mrayl 10		
	Average Acoustic Impedance 2 (AV_AI2) USIT-E 0 Mrayl 10	Average Acoustic Impedance 4 (AV_AI4) USIT-E 0 Mrayl 10	Average Acoustic Impedance 6 (AV_AI6) USIT-E 0 Mrayl 10	Average Acoustic Impedance 8 (AV_AI8) USIT-E 0 Mrayl 10		

TIME_1900 - Time Marked every 60.00 (s)

Description: USI Goodwin Format: Log (Import of USI Goodwin) Index Scale: 1 in per 100 ft Index Unit: ft Index Type: Measured Depth Creation Date: 17-Jul-2017 14:11:47

XYZ

Company:Southern California Gas Company Well:Fernando Fee 35B
One: Log[4]:Up:S011

Fluid Acoustic Slowness vs Depth

2D Cross Plot

Index Range: From 7044.50 to 3.75 ft

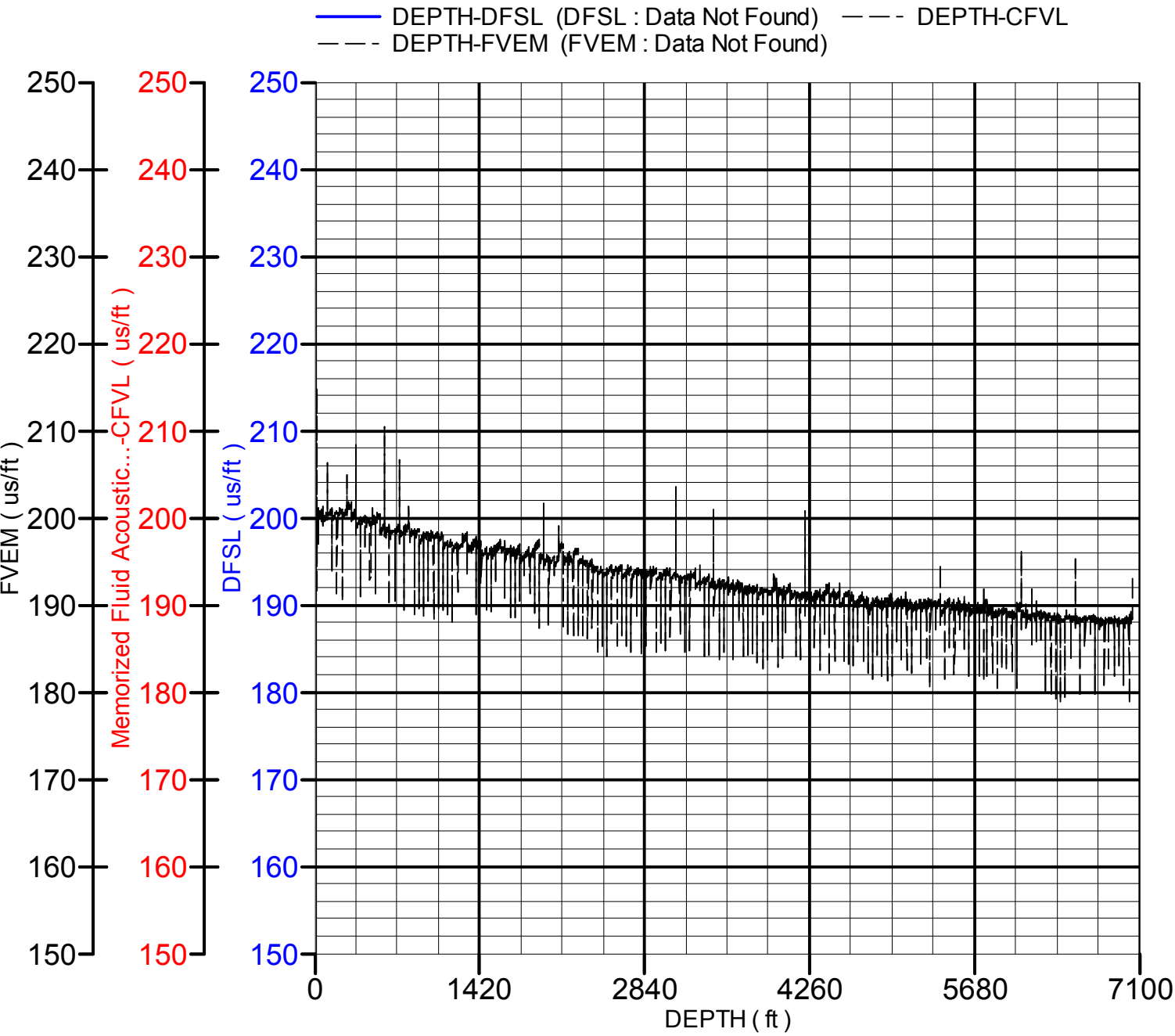

XYZ

Company:Southern California Gas Company Well:Fernando Fee 35B
One: Log[4]:Up:S011

Theoretical Acoustic Impedance of Mud vs Depth

2D Cross Plot

Index Range: From 7044.50 to 3.75 ft

DEPTH-CZMD
DEPTH-AIBH (AIBH : Data Not Found)

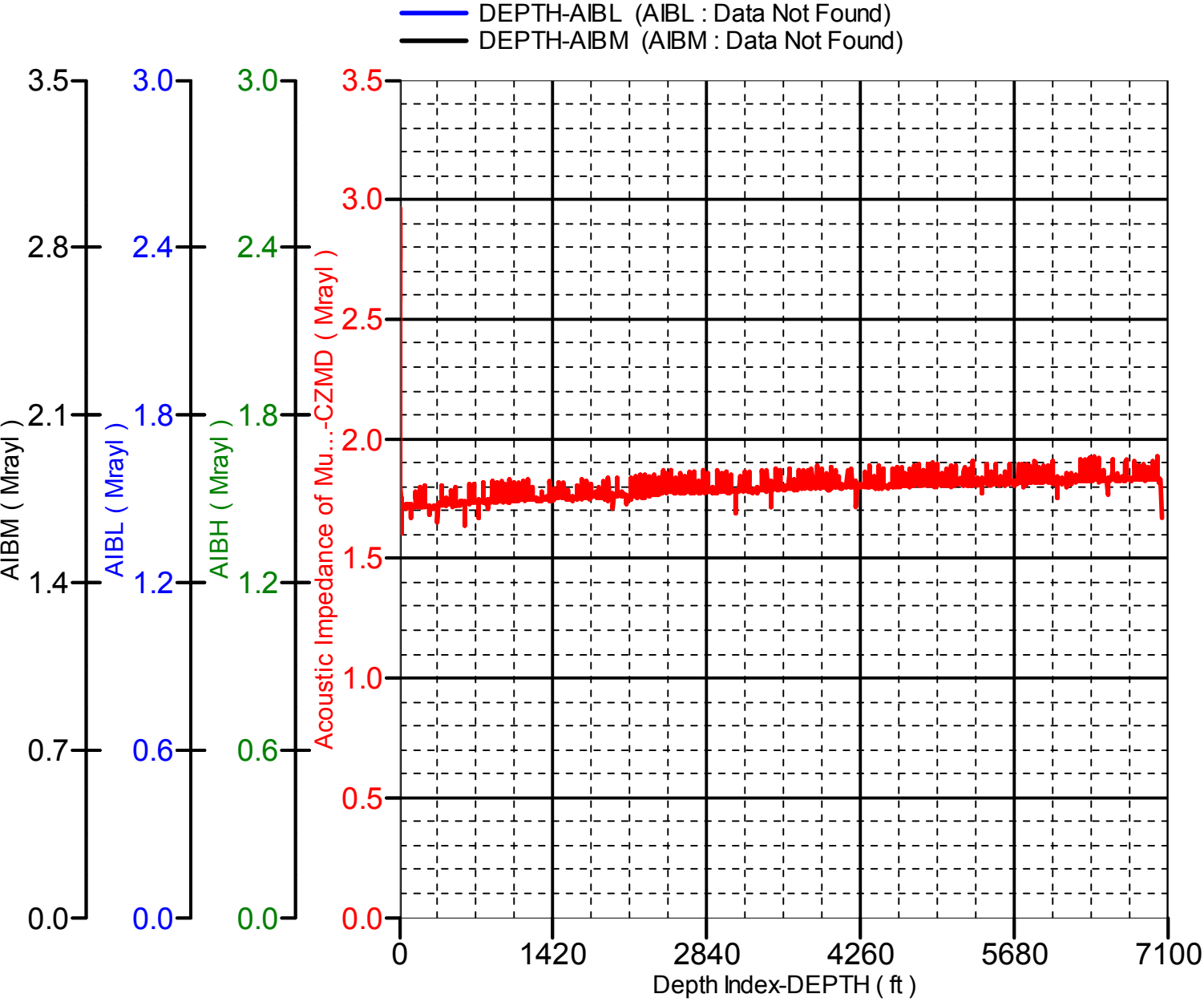

One

USIT CORROSION 10" = 100'

Software Version

Acquisition System	Version
Maxwell 2017 SP1	7.1.82245.3100

Pass Summary

Run Name	Pass Objective	Direction	Top	Bottom	Start	Stop	DSC Mode	Depth Shift	Include Parallel Data
One	Log[8]:Up	Up	3873.88 ft	4368.53 ft	02-Jun-2017 9:19:48 PM	02-Jun-2017 9:47:05 PM	ON	2.00 ft	Yes

All depths are referenced to toolstring zero

Log

Company:Southern California Gas Company Well:Fernando Fee 35B

One: Log[8]:Up:S011

Description: USI Composite Format: Log (LBV1_USI Corrosion 9.625inch) Index Scale: 10 in per 100 ft Index Unit: ft Index Type: Measured Depth
Creation Date: 17-Jul-2017 14:11:55

TIME_1900 - Time Marked every 60.00 (s)

USIT Processing Flags (UFLG[0]) USIT-E

1 - UFLG 1 Value within [0.0 - 1.5] - : UTIM Error

2 - UFLG 2 Value within [1.5 - 2.5] - :
3 - UFLG 3 Value within [2.5 - 3.5] - :
4 - UFLG 4 UFLG 5 UFLG 6 Value within [3.5 - 6.5] - :
5 - UFLG 7 UFLG 8 UFLG 9 Value within [6.5 - 10] - :

Pulse Origin Not Detected
WINLEN Error
Casing Thickness Error
Loop Processing Error

Amplitude of Eccentering for Unflagged Waves (ECCE_RF) USIT-E
0 in 0.5

Motor Revolution Speed (RSAV) USIT-E
6 c/s 8

Gamma Ray (EHGR) HGNS-H
50 gAPI 200

Absent 1.500 3.500
Explicit Normalization
USIT - USIT Processing Flags (UFLG) USIT-E

USIT Processing Flags (UFLG[0]) USIT-E
1 5

Absent -5.200 -3.600 -2.000 -0.400
Explicit Normalization
USIT - Amplitude of Unflagged Wave (AWBK_RF) USIT-E (dB)

Minimum of Unflagged Wave Amplitude (AWMN_RF) USIT-E
0 dB 75

Average of Unflagged Wave Amplitude (AWAV_RF) USIT-E
0 dB 75

Maximum of Unflagged Wave Amplitude (AWMX_RF) USIT-E
0 dB 75

Absent -0.059 -0.028 0.004 0.035 0.068
Explicit Normalization
USIT - Unflagged Internal Radii minus Median Internal Radius (IRBKM_RF) USIT-E (in)

Internal Radius Averaged Value (IRAV) USIT-E
3.5 in 4.5

Minimum of Unflagged Internal Radii (IRMN_RF) USIT-E
3.5 in 4.5

Maximum of Unflagged Internal Radii (IRMX_RF) USIT-E
3.5 in 4.5

ERAV
ERAV-IRAV
IRAV

Median of Unflagged External Radii (ERAV_RF) USIT-E
4.5 in 3.5

Median Internal Radius of Casing Corrected for Eccentering (IRAV_RF) USIT-E
4.5 in 3.5

Maximum of Unflagged Internal Radii (IRMX_RF) USIT-E
4.5 in 3.5

Minimum of Unflagged Internal Radii (IRMN_RF) USIT-E
4.5 in 3.5

IRAV
ERAV
IRAV-ERAV

Median of Unflagged External Radii (ERAV_RF) USIT-E
3.5 in 4.5

Median Internal Radius of Casing Corrected for Eccentering (IRAV_RF) USIT-E
3.5 in 4.5

Maximum of Unflagged Internal Radii (IRMX_RF) USIT-E
3.5 in 4.5

Minimum of Unflagged Internal Radii (IRMN_RF) USIT-E
3.5 in 4.5

Absent -0.059 -0.028 0.004 0.035 0.068
Explicit Normalization
USIT - Unflagged Casing Thickness minus Median of Unflagged Casing Thickness (THBKM_RF) USIT-E (in)

Minimum of Unflagged Casing Thickness (THMN_RF) USIT-E
0.1 in 0.6

Nominal Casing Thickness (THNO) USIT-E
0.1 in 0.6

Median of Unflagged Casing Thickness (THAV_RF) USIT-E
0.1 in 0.6

Maximum of Unflagged Casing Thickness (THMX_RF) USIT-E
0.1 in 0.6

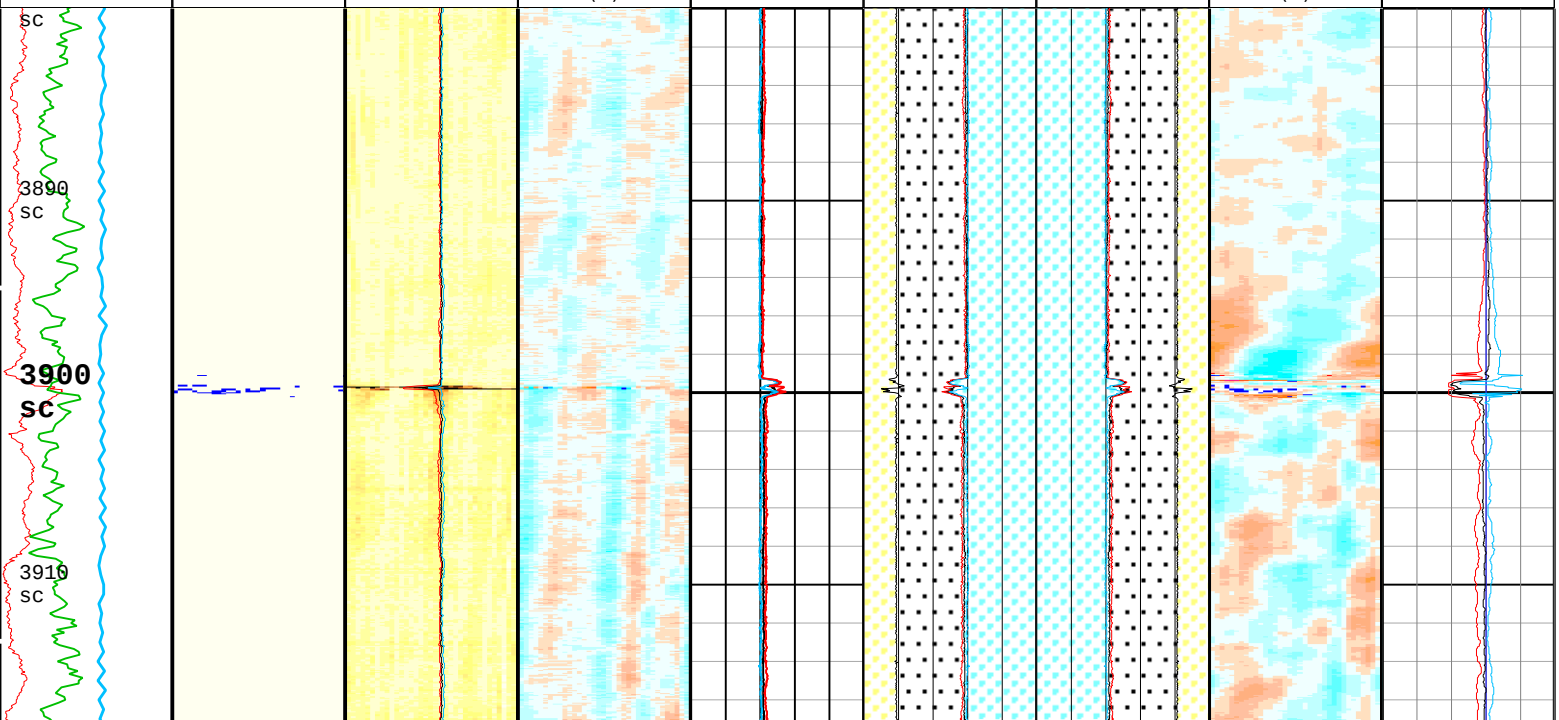

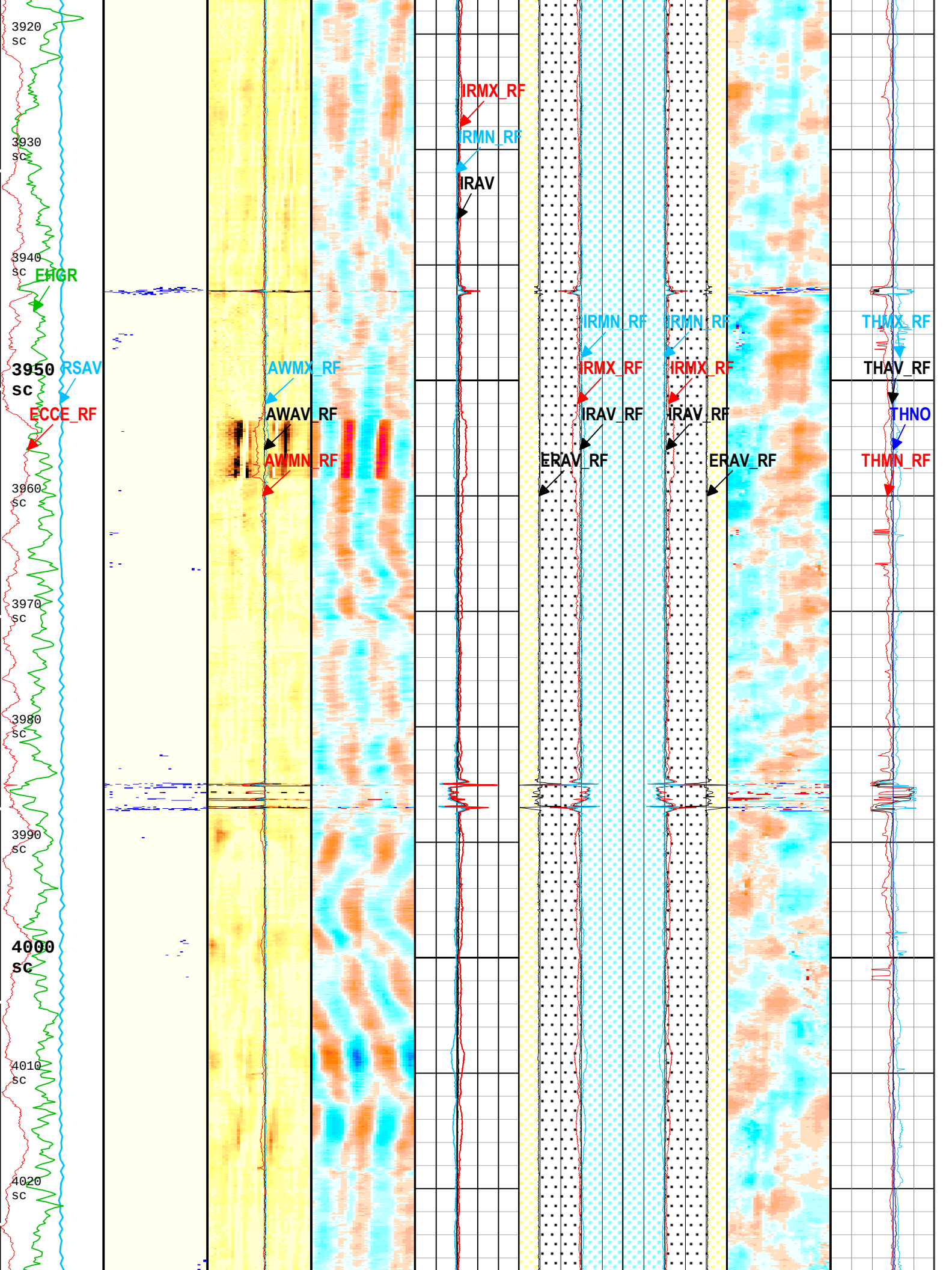
3920 sc
3930 sc
3940 sc
3950 sc
3960 sc
3970 sc
3980 sc
3990 sc
4000 sc
4010 sc
4020 sc
EHGR
RSAV
ECCE_RF
AWMX_RF
AWAV_RF
AWMN_RF
IRMX_RF
IRMN_RF
IRAV
IRMN_RF
IRMX_RF
IRAV_RF
ERAV_RF
IRMN_RF
IRMX_RF
IRAV_RF
ERAV_RF
THMX_RF
THAV_RF
THNO
THMN_RF

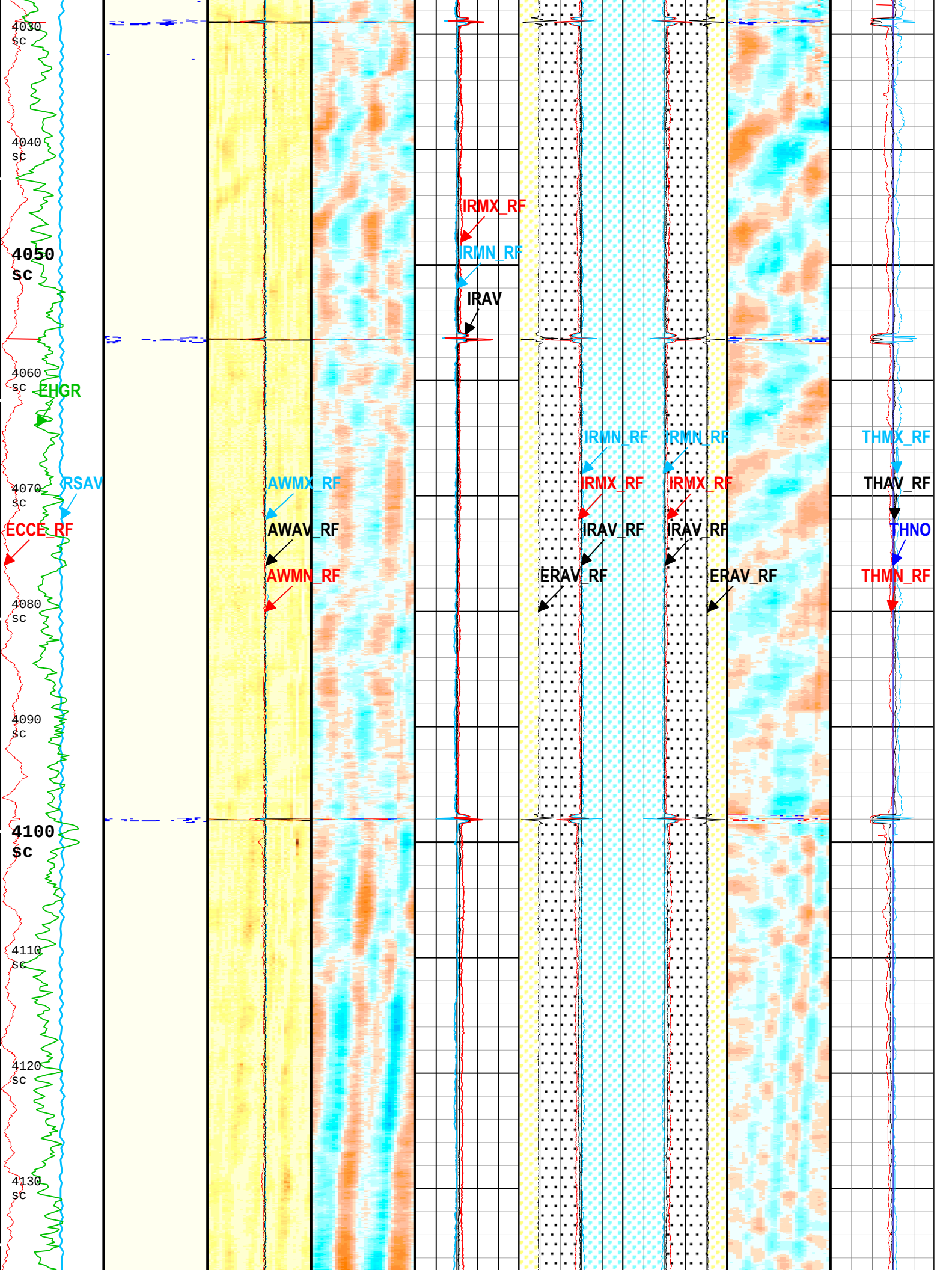
4030 sc
4040 sc
4050 sc
4060 sc
4070 sc
4080 sc
4090 sc
4100 sc
4110 sc
4120 sc
4130 sc
ZHGR
RSAV
ECCE_RF
AWMX_RF
AWAV_RF
AWMN_RF
IRMX_RF
IRMN_RF
IRAV
IRMN_RF
IRMX_RF
IRAV_RF
ERAV_RF
IRMN_RF
IRMX_RF
IRAV_RF
ERAV_RF
THMX_RF
THAV_RF
THNO
THMN_RF

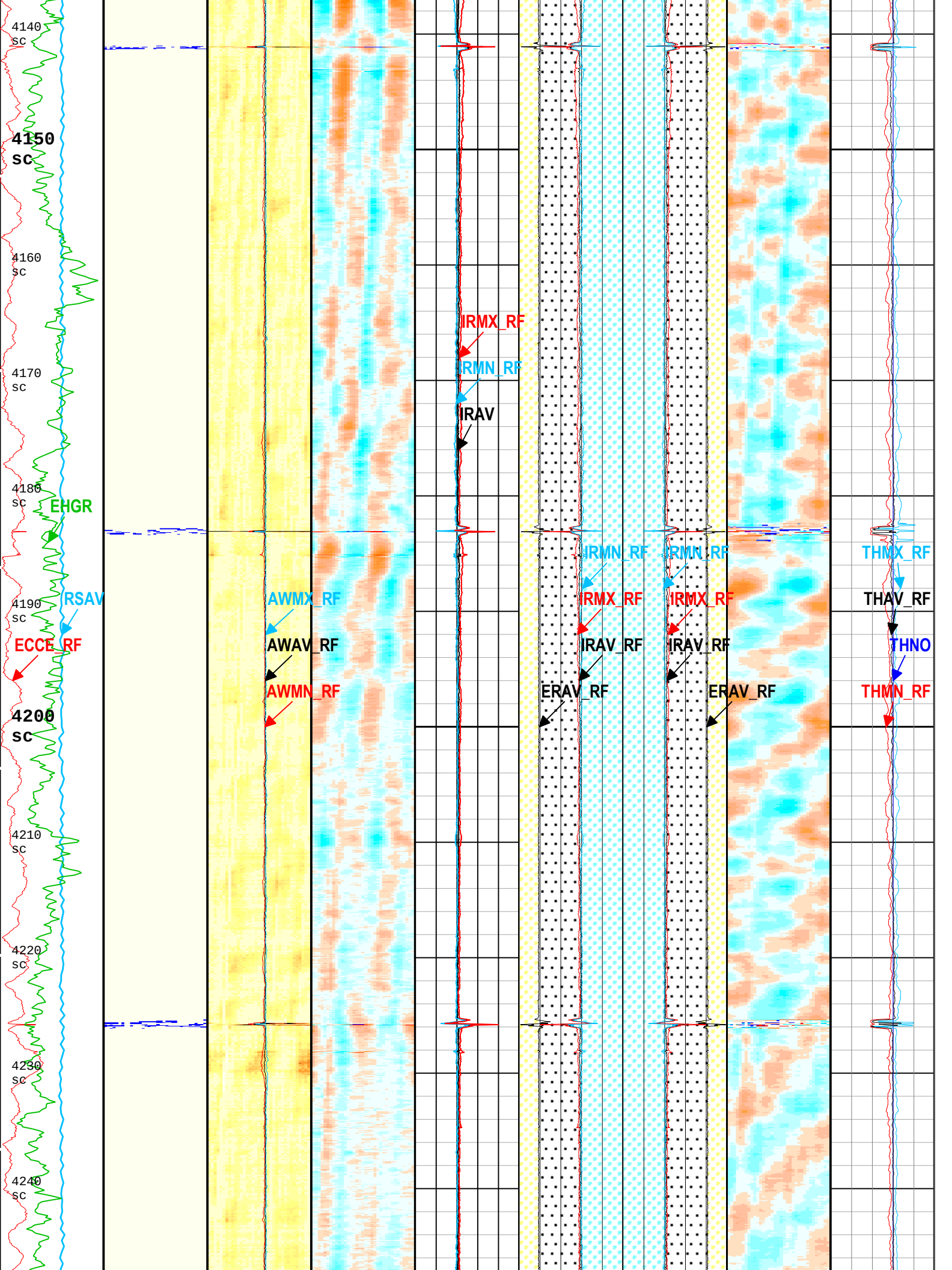
4140 sc
4150 sc
4160 sc
4170 sc
4180 sc
4190 sc
4200 sc
4210 sc
4220 sc
4230 sc
4240 sc
EHGR
RSAV
ECCE_RF
AWMX_RF
AWAV_RF
AWMN_RF
IRMX_RF
IRMN_RF
IRAV
IRMN_RF
IRMX_RF
IRAV_RF
ERAV_RF
IRMN_RF
IRMX_RF
IRAV_RF
ERAV_RF
THMX_RF
THAV_RF
THNO
THMN_RF

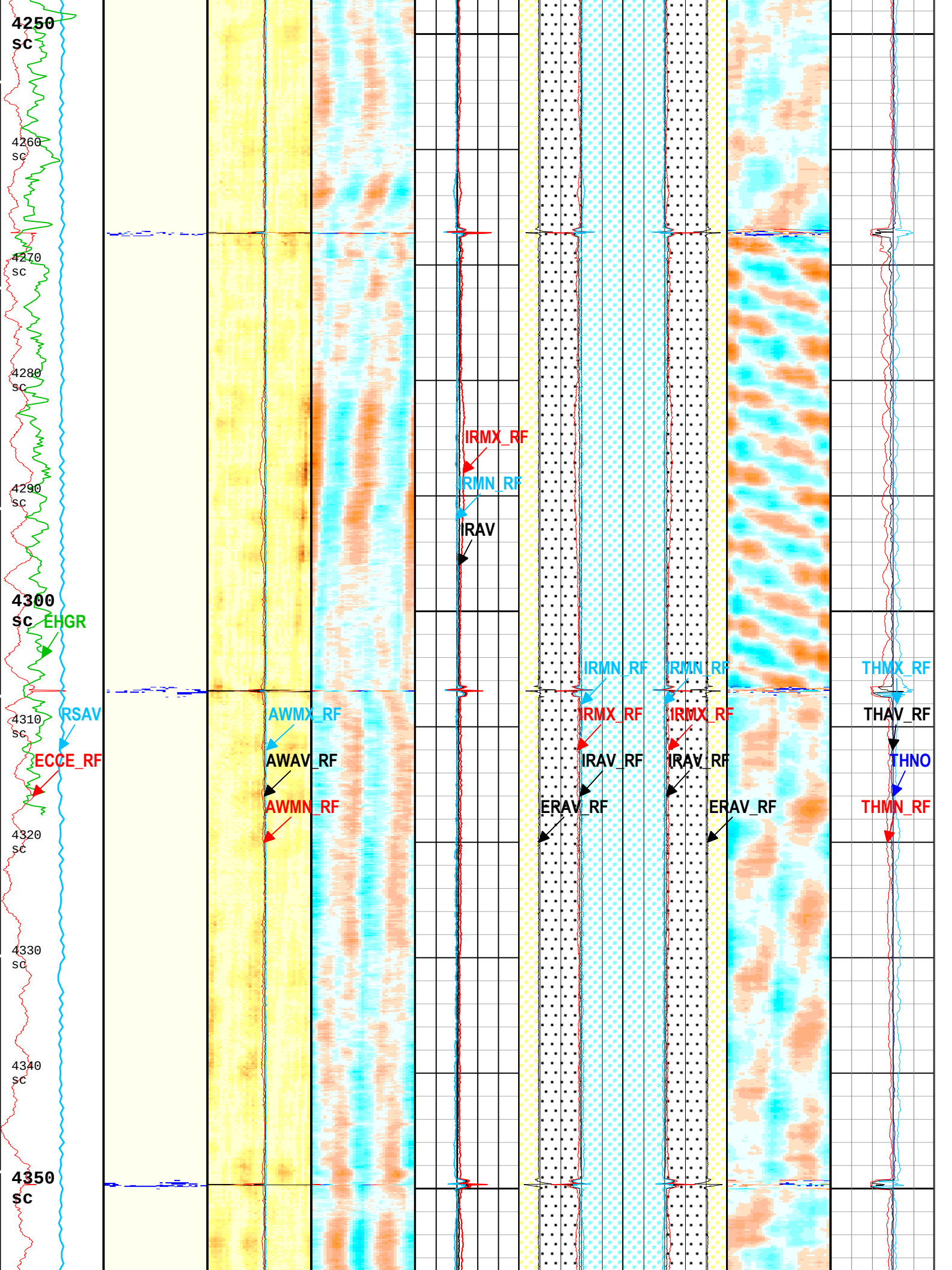
4250
sc
4260
sc
4270
sc
4280
sc
4290
sc
4300
sc
EHGR
RSAV
ECCE_RF
4310
sc
4320
sc
4330
sc
4340
sc
4350
sc
AWMX_RF
AWAV_RF
AWMN_RF
IRMX_RF
IRMN_RF
IRAV
IRMN_RF
IRMX_RF
IRAV_RF
ERAV_RF
IRMN_RF
IRMX_RF
IRAV_RF
ERAV_RF
THMX_RF
THAV_RF
THNO
THMN_RF

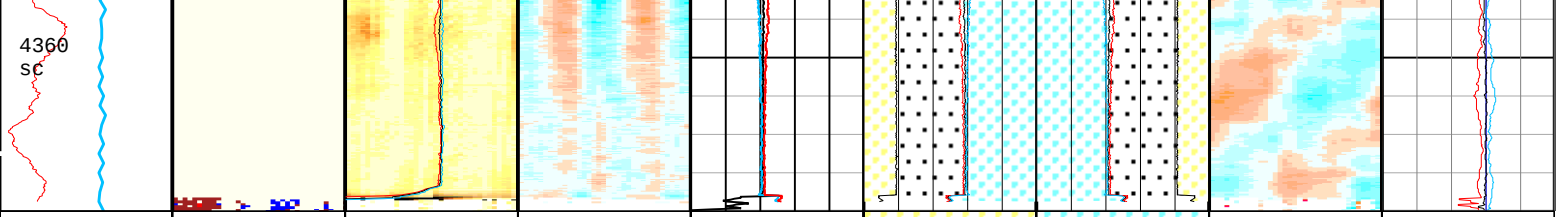

Amplitude of Eccentering for Unflagged Waves (ECCE_RF) USIT-E
0 in 0.5

Motor Revolution Speed (RSAV) USIT-E
6 c/s 8

Gamma Ray (EHGR) HGNS-H
50 gAPI 200

Absent 1.500 3.500
Explicit Normalization
USIT - USIT Processing Flags (UFLG) USIT-E

USIT Processing Flags (UFLG[0]) USIT-E
1 5

Absent -5.200 -3.600 -2.000 -0.400
Explicit Normalization
USIT - Amplitude of Unflagged Wave (AWBK_RF) USIT-E
(dB)

Minimum of Unflagged Wave Amplitude (AWMN_RF) USIT-E
0 dB 75

Average of Unflagged Wave Amplitude (AWAV_RF) USIT-E
0 dB 75

Maximum of Unflagged Wave Amplitude (AWMX_RF) USIT-E
0 dB 75

Absent -0.059 -0.028 0.004 0.035 0.068
Explicit Normalization
USIT - Unflagged Internal Radii minus Median Internal Radius (IRBKM_RF) USIT-E
(in)

Internal Radius Averaged Value (IRAV) USIT-E
3.5 in 4.5

Minimum of Unflagged Internal Radii (IRMN_RF) USIT-E
3.5 in 4.5

Maximum of Unflagged Internal Radii (IRMX_RF) USIT-E
3.5 in 4.5

ERAV
ERAV-IRAV
IRAV

Median of Unflagged External Radii (ERAV_RF) USIT-E
4.5 in 3.5

Median Internal Radius of Casing Corrected for Eccentering (IRAV_RF) USIT-E
4.5 in 3.5

Maximum of Unflagged Internal Radii (IRMX_RF) USIT-E
4.5 in 3.5

Minimum of Unflagged Internal Radii (IRMN_RF) USIT-E
4.5 in 3.5

IRAV
ERAV
IRAV-ERAV

Median of Unflagged External Radii (ERAV_RF) USIT-E
3.5 in 4.5

Median Internal Radius of Casing Corrected for Eccentering (IRAV_RF) USIT-E
3.5 in 4.5

Maximum of Unflagged Internal Radii (IRMX_RF) USIT-E
3.5 in 4.5

Minimum of Unflagged Internal Radii (IRMN_RF) USIT-E
3.5 in 4.5

Absent -0.059 -0.028 0.004 0.035 0.068
Explicit Normalization
USIT - Unflagged Casing Thickness minus Median of Unflagged Casing Thickness (THBKM_RF) USIT-E
(in)

Minimum of Unflagged Casing Thickness (THMN_RF) USIT-E
0.1 in 0.6

Nominal Casing Thickness (THNO) USIT-E
0.1 in 0.6

Median of Unflagged Casing Thickness (THAV_RF) USIT-E
0.1 in 0.6

Maximum of Unflagged Casing Thickness (THMX_RF) USIT-E
0.1 in 0.6

USIT Processing Flags (UFLG[0]) USIT-E

1 - UFLG 1 Value within [0.0 - 1.5] - :
2 - UFLG 2 Value within [1.5 - 2.5] - :
3 - UFLG 3 Value within [2.5 - 3.5] - :
4 - UFLG 4 UFLG 5 UFLG 6 Value within [3.5 - 6.5] - :
5 - UFLG 7 UFLG 8 UFLG 9 Value within [6.5 - 10] - :

- UTIM Error
- Pulse Origin Not Detected
- WINLEN Error
- Casing Thickness Error
- Loop Processing Error

TIME_1900 - Time Marked every 60.00 (s)

Description: USI Composite Format: Log (LBV1_USI Corrosion 9.625inch) Index Scale: 10 in per 100 ft Index Unit: ft Index Type: Measured Depth
Creation Date: 17-Jul-2017 14:11:55

Channel Processing Parameters

One: Parameters

Parameter	Description	Tool	Value	Unit
ISSBAR	Barite Mud Presence Flag	Borehole	No	
BHS	Borehole Status (Open or Cased Hole)	Borehole	Cased	
BS	Bit Size	WLSESSION	11	in

CBLO	Casing Bottom (Logger)	WLSESSION	7331	ft
CDEN	Cement Density	HGNS-H	2.65	g/cm3
CMTY(U-USIT_CEMT)	Cement Type	USIT-E	Regular Cement	
THNO	Nominal Casing Thickness - Zoned along logger depths	WLSESSION	0.4	in
CYSTLGR	Casing Yield Strength - Zoned along logger depths	WLSESSION	55000	psi
DFD	Drilling Fluid Density	Borehole	8.9	lbm/gal
DFT_CATEGORY	Drilling Fluid Type	Borehole	Water	
DTMD	Borehole Fluid Slowness	Borehole	193	us/ft
FDII	FPM Data Interpolation Interval	USIT-E	0	ft
GCSE_DOWN_PASS	Generalized Caliper Selection for WL Log Down Passes	Borehole	BS	
GCSE_UP_PASS	Generalized Caliper Selection for WL Log Up Passes	Borehole	BS	
HEMA	Hematite Presence Flag	Borehole	No	
ICE_PROCESS	ICE Processing	USIT-E	Yes	
IMAR	Image Rotation	USIT-E	Off	
MEAS_WLEN	Tcube Processing Window Length in Measurement Mode	USIT-E	24.96	us
MUD_N_FRP	Free Pipe Mud Normalization Factor	USIT-E	1.06	
THDH	Maximum Search Thickness (percentage of nominal)	USIT-E	130	%
THDL	Minimum Search Thickness (percentage of nominal)	USIT-E	70	%
HISC	Tool Position: Centered or Eccentered	HGNS-H	Centered	
U-USIT_DFSZ	Drilling Fluid Specific Acoustic Impedance	USIT-E	0	Mrayl
UFGDE	Fiberglass Density	USIT-E	1.95	g/cm3
UFGPS	Fiberglass Processing Selection	USIT-E	No	
UFGVL	Fiberglass Velocity	USIT-E	9678.48	ft/s
USI_FSOD	USIT USI Fluid Slowness Fits Casing Outer Diameter	USIT-E	0_OFF	
USI_FVEL_SEL	USI Fluid Velocity Selection	USIT-E	Automatic	
USI_ZMUD_SEL	USI Mud Impedance Selection	USIT-E	FreePipe Norm.	
ZMUD	Acoustic Impedance of Mud	Borehole	1.68	Mrayl
ZTCM	Acoustic Impedance Threshold for Cement	USIT-E	2.6	Mrayl
ZTGS	Acoustic Impedance Threshold for Gas	USIT-E	0.3	Mrayl

Tool Control Parameters

One: Parameters

Parameter	Description	Tool	Value	Unit
AGMN	Minimum Gain of Cartridge	USIT-E	-12	dB
AGMX	Maximum Gain of Cartridge	USIT-E	48	dB
U-USIT_DDT5	USIC Downhole Decimation for T5 only	USIT-E	0_NONE	
EMXV	EMEX Voltage	USIT-E	120	V
HRES	Horizontal Resolution	USIT-E	10 deg	
TMUC	Type of Mud	USIT-E	BRI	
ULOG	Logging Objective	USIT-E	MEASUREMENT	
UMFR	Modulation Frequency	USIT-E	333333	Hz
USFR	Ultrasonic Sampling Frequency	USIT-E	500000	Hz
UPAT	USIT Emission Pattern	USIT-E	Pattern 500 KHz	
UWKM	USIT Working Mode	USIT-E	Uncompressed 10 deg at 0.6 in LF	
USIT_DEPTHLOG	Starting Depth Log for Ultrasonics	USIT-E	7030	ft
VRES	Vertical Resolution	USIT-E	0.6 in	
WINB	Window Begin Time	USIT-E	59.63	us
WINE	Window End Time	USIT-E	99.63	us

One

USIT CORROSION 10" = 100'

Software Version

Acquisition System	Version
Maxwell 2017 SP1	7.1.82245.3100

Pass Summary

Run Name	Pass Objective	Direction	Top	Bottom	Start	Stop	DSC Mode	Depth Shift	Include Parallel Data
One	Log[7]:Up	Up	4689.11 ft	4946.23 ft	02-Jun-2017 9:02:58 PM	02-Jun-2017 9:18:10 PM	ON	2.00 ft	Yes

All depths are referenced to toolstring zero

Log

Company:Southern California Gas Company Well:Fernando Fee 35B

One: Log[7]:Up:S011

Description: USI Composite Format: Log (LBV1_USI Corrosion 9.625inch) Index Scale: 10 in per 100 ft Index Unit: ft Index Type: Measured Depth
Creation Date: 17-Jul-2017 14:12:00

TIME_1900 - Time Marked every 60.00 (s)

USIT Processing Flags (UFLG[0]) USIT-E

1 - UFLG 1 Value within [0.0 - 1.5] - :
2 - UFLG 2 Value within [1.5 - 2.5] - :
3 - UFLG 3 Value within [2.5 - 3.5] - :
4 - UFLG 4 UFLG 5 UFLG 6 Value within [3.5 - 6.5] - :
5 - UFLG 7 UFLG 8 UFLG 9 Value within [6.5 - 10] - :

- UTIM Error
- Pulse Origin Not Detected
- WINLEN Error
- Casing Thickness Error
- Loop Processing Error

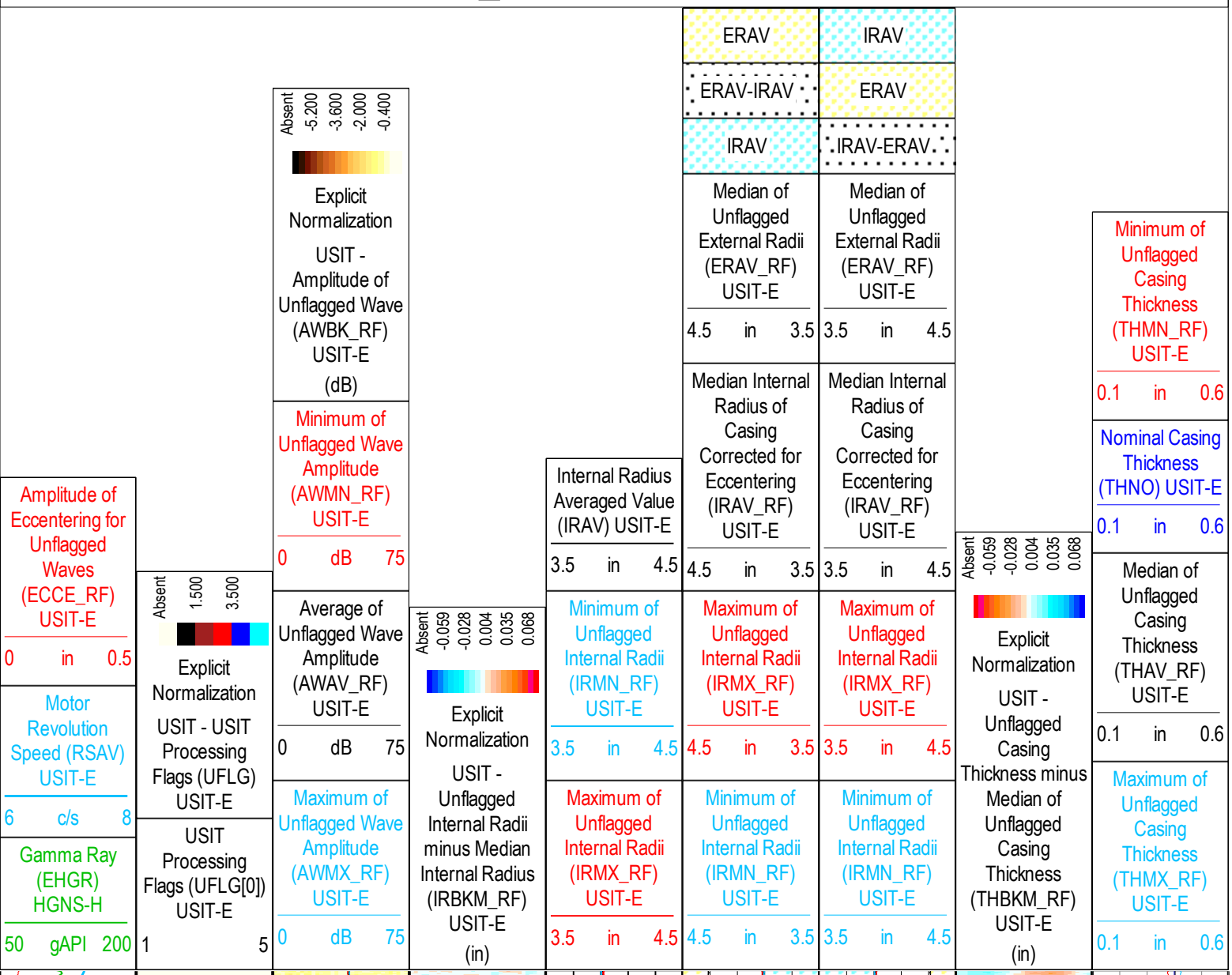

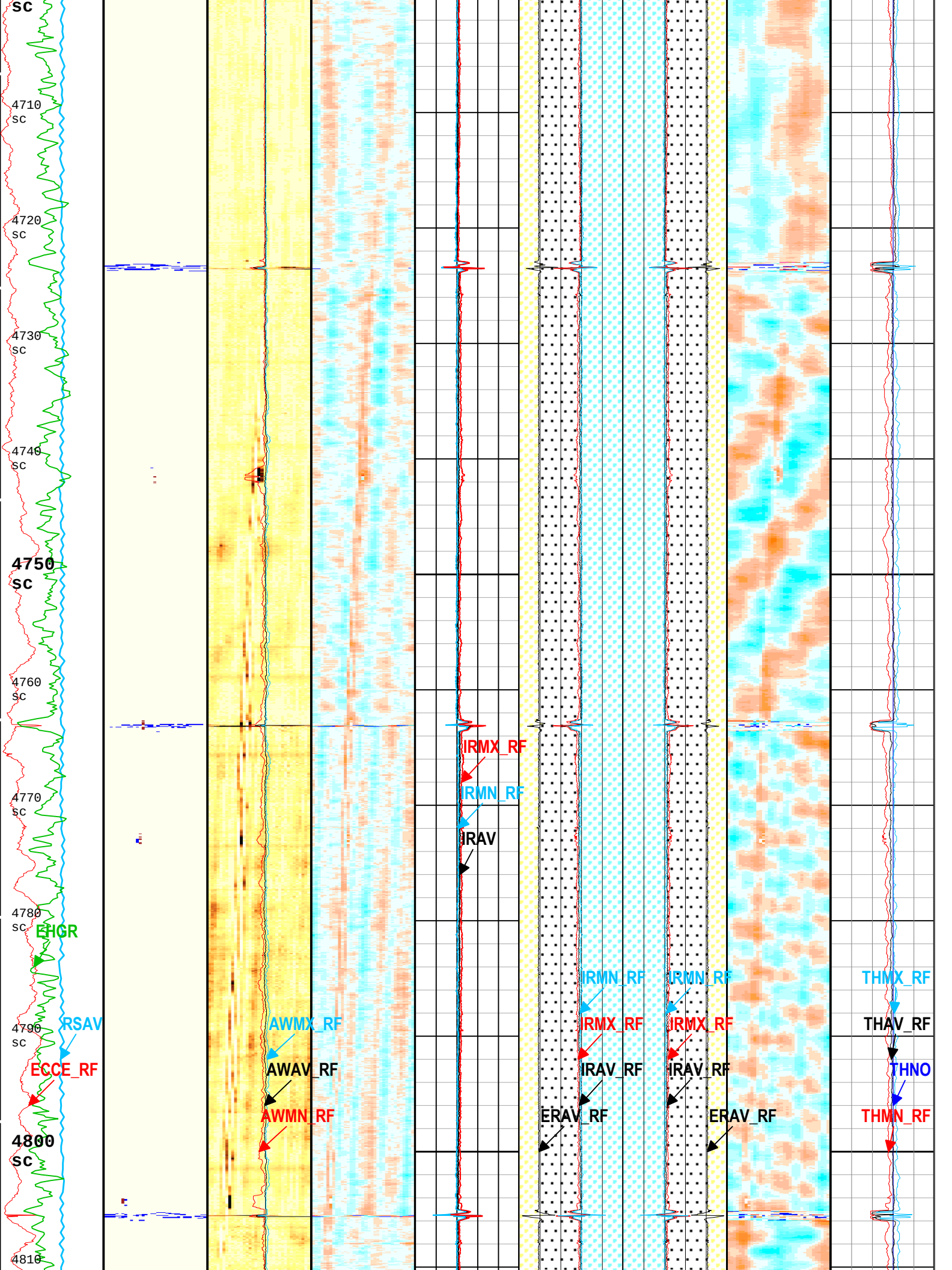
sc
4710
sc
4720
sc
4730
sc
4740
sc
4750
sc
4760
sc
4770
sc
4780
sc
4790
sc
4800
sc
4810
EHGR
RSAV
ECCE_RF
AWMX_RF
AWAV_RF
AWMN_RF
IRMX_RF
IRMN_RF
IRAV
IRMN_RF
IRMX_RF
IRAV_RF
ERAV_RF
IRMN_RF
IRMX_RF
IRAV_RF
ERAV_RF
THMX_RF
THAV_RF
THNO
THMN_RF

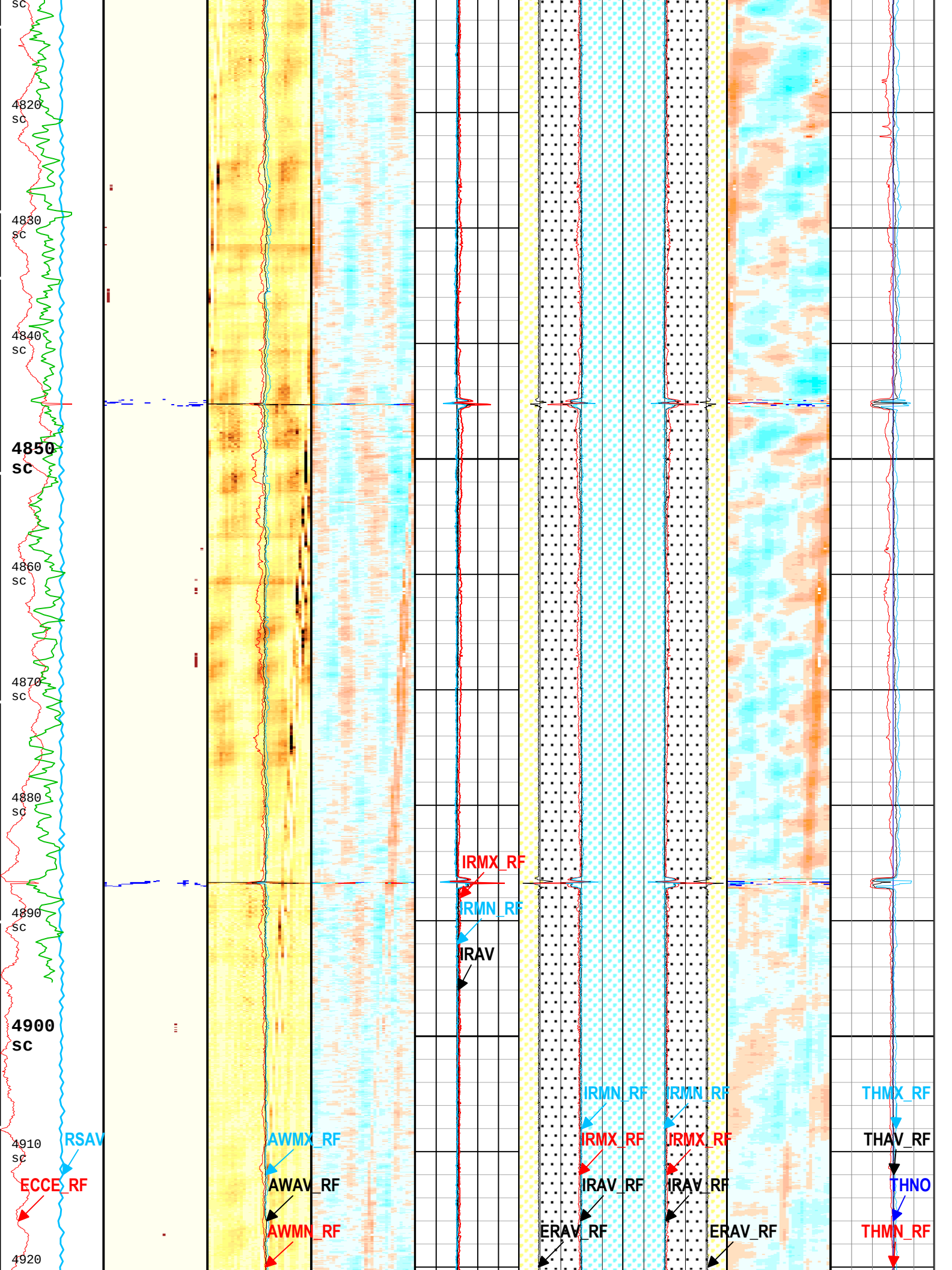
4820 sc
4830 sc
4840 sc
4850 sc
4860 sc
4870 sc
4880 sc
4890 sc
4900 sc
4910 sc
4920
RSAV
ECCE_RF
AWMX_RF
AWAV_RF
AWMN_RF
IRMX_RF
IRMN_RF
IRAV
IRMN_RF
IRMX_RF
IRAV_RF
ERAV_RF
IRMN_RF
IRMX_RF
IRAV_RF
ERAV_RF
THMX_RF
THAV_RF
THNO
THMN_RF

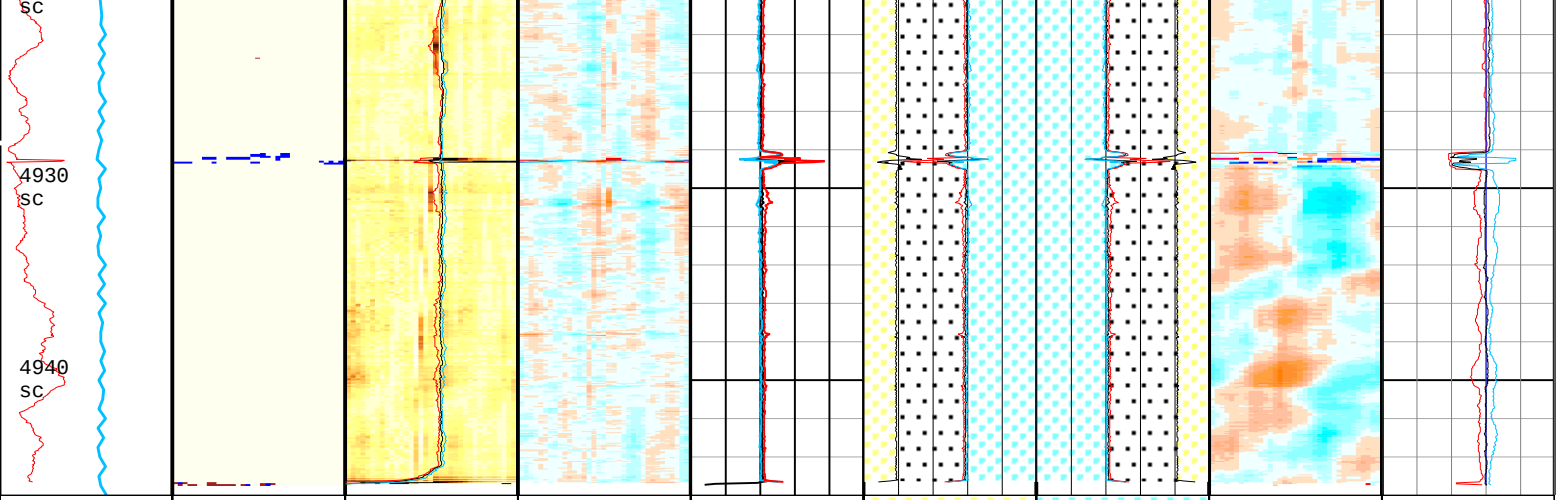

Amplitude of Eccentering for Unflagged Waves (ECCE_RF) USIT-E
0 in 0.5

Motor Revolution Speed (RSAV) USIT-E
6 c/s 8

Gamma Ray (EHGR) HGNS-H
50 gAPI 200

Absent 1.500 3.500
Explicit Normalization
USIT - USIT Processing Flags (UFLG) USIT-E

USIT Processing Flags (UFLG[0]) USIT-E
1 5

Absent -5.200 -3.600 -2.000 -0.400
Explicit Normalization
USIT - Amplitude of Unflagged Wave (AWBK_RF) USIT-E
(dB)

Minimum of Unflagged Wave Amplitude (AWMN_RF) USIT-E
0 dB 75

Average of Unflagged Wave Amplitude (AWAV_RF) USIT-E
0 dB 75

Maximum of Unflagged Wave Amplitude (AWMX_RF) USIT-E
0 dB 75

Absent -0.059 -0.028 0.004 0.035 0.068
Explicit Normalization
USIT - Unflagged Internal Radii minus Median Internal Radius (IRBKM_RF) USIT-E
(in)

Internal Radius Averaged Value (IRAV) USIT-E
3.5 in 4.5

Minimum of Unflagged Internal Radii (IRMN_RF) USIT-E
3.5 in 4.5

Maximum of Unflagged Internal Radii (IRMX_RF) USIT-E
3.5 in 4.5

ERAV
ERAV-IRAV
IRAV

Median of Unflagged External Radii (ERAV_RF) USIT-E
4.5 in 3.5

Median Internal Radius of Casing Corrected for Eccentering (IRAV_RF) USIT-E
4.5 in 3.5

Maximum of Unflagged Internal Radii (IRMX_RF) USIT-E
4.5 in 3.5

Minimum of Unflagged Internal Radii (IRMN_RF) USIT-E
4.5 in 3.5

IRAV
ERAV
IRAV-ERAV

Median of Unflagged External Radii (ERAV_RF) USIT-E
3.5 in 4.5

Median Internal Radius of Casing Corrected for Eccentering (IRAV_RF) USIT-E
3.5 in 4.5

Maximum of Unflagged Internal Radii (IRMX_RF) USIT-E
3.5 in 4.5

Minimum of Unflagged Internal Radii (IRMN_RF) USIT-E
3.5 in 4.5

Absent -0.059 -0.028 0.004 0.035 0.068
Explicit Normalization
USIT - Unflagged Casing Thickness minus Median of Unflagged Casing Thickness (THBKM_RF) USIT-E
(in)

Minimum of Unflagged Casing Thickness (THMN_RF) USIT-E
0.1 in 0.6

Nominal Casing Thickness (THNO) USIT-E
0.1 in 0.6

Median of Unflagged Casing Thickness (THAV_RF) USIT-E
0.1 in 0.6

Maximum of Unflagged Casing Thickness (THMX_RF) USIT-E
0.1 in 0.6

USIT Processing Flags (UFLG[0]) USIT-E

1 - UFLG 1 Value within [0.0 - 1.5] - :
2 - UFLG 2 Value within [1.5 - 2.5] - :
3 - UFLG 3 Value within [2.5 - 3.5] - :
4 - UFLG 4 UFLG 5 UFLG 6 Value within [3.5 - 6.5] - :
5 - UFLG 7 UFLG 8 UFLG 9 Value within [6.5 - 10] - :

- UTIM Error
- Pulse Origin Not Detected
- WINLEN Error
- Casing Thickness Error
- Loop Processing Error

TIME_1900 - Time Marked every 60.00 (s)

Description: USI Composite Format: Log (LBV1_USI Corrosion 9.625inch) Index Scale: 10 in per 100 ft Index Unit: ft Index Type: Measured Depth
Creation Date: 17-Jul-2017 14:12:00

Channel Processing Parameters

One: Parameters

Parameter	Description	Tool	Value	Unit
ISSBAR	Barite Mud Presence Flag	Borehole	No	
BHS	Borehole Status (Open or Cased Hole)	Borehole	Cased	
BS	Bit Size	WLSESSION	11	in
CBLO	Casing Bottom (Logger)	WLSESSION	7331	ft
CDEN	Cement Density	HGNS-H	2.65	g/cm3
CMTY(U-USIT_CEMT)	Cement Type	USIT-E	Regular Cement	
THNO	Nominal Casing Thickness - Zoned along logger depths	WLSESSION	0.4	in
CYSTLGR	Casing Yield Strength - Zoned along logger depths	WLSESSION	55000	psi
DFD	Drilling Fluid Density	Borehole	8.9	lbm/gal
DFT_CATEGORY	Drilling Fluid Type	Borehole	Water	
DTMD	Borehole Fluid Slowness	Borehole	193	us/ft
FDII	FPM Data Interpolation Interval	USIT-E	0	ft
GCSE_DOWN_PASS	Generalized Caliper Selection for WL Log Down Passes	Borehole	BS	
GCSE_UP_PASS	Generalized Caliper Selection for WL Log Up Passes	Borehole	BS	
HEMA	Hematite Presence Flag	Borehole	No	
ICE_PROCESS	ICE Processing	USIT-E	Yes	
IMAR	Image Rotation	USIT-E	Off	
MEAS_WLEN	Tcube Processing Window Length in Measurement Mode	USIT-E	24.96	us
MUD_N_FRP	Free Pipe Mud Normalization Factor	USIT-E	1.06	
THDH	Maximum Search Thickness (percentage of nominal)	USIT-E	130	%
THDL	Minimum Search Thickness (percentage of nominal)	USIT-E	70	%
HISC	Tool Position: Centered or Eccentered	HGNS-H	Centered	
U-USIT_DFSZ	Drilling Fluid Specific Acoustic Impedance	USIT-E	0	Mrayl
UFGDE	Fiberglass Density	USIT-E	1.95	g/cm3
UFGPS	Fiberglass Processing Selection	USIT-E	No	
UFGVL	Fiberglass Velocity	USIT-E	9678.48	ft/s
USI_FSOD	USIT USI Fluid Slowness Fits Casing Outer Diameter	USIT-E	0_OFF	
USI_FVEL_SEL	USI Fluid Velocity Selection	USIT-E	Automatic	
USI_ZMUD_SEL	USI Mud Impedance Selection	USIT-E	FreePipe Norm.	
ZMUD	Acoustic Impedance of Mud	Borehole	1.68	Mrayl
ZTCM	Acoustic Impedance Threshold for Cement	USIT-E	2.6	Mrayl
ZTGS	Acoustic Impedance Threshold for Gas	USIT-E	0.3	Mrayl

Tool Control Parameters

One: Parameters

Parameter	Description	Tool	Value	Unit
AGMN	Minimum Gain of Cartridge	USIT-E	-12	dB
AGMX	Maximum Gain of Cartridge	USIT-E	48	dB
U-USIT_DDT5	USIC Downhole Decimation for T5 only	USIT-E	0_NONE	
EMXV	EMEX Voltage	USIT-E	120	V
HRES	Horizontal Resolution	USIT-E	10 deg	
TMUC	Type of Mud	USIT-E	BRI	
ULOG	Logging Objective	USIT-E	MEASUREMENT	
UMFR	Modulation Frequency	USIT-E	333333	Hz
USFR	Ultrasonic Sampling Frequency	USIT-E	500000	Hz
UPAT	USIT Emission Pattern	USIT-E	Pattern 500 KHz	
UWKM	USIT Working Mode	USIT-E	Uncompressed 10 deg at 0.6	

			in LF	
USIT_DEPTHLOG	Starting Depth Log for Ultrasonics	USIT-E	7030	ft
VRES	Vertical Resolution	USIT-E	0.6 in	
WINB	Window Begin Time	USIT-E	59.63	us
WINE	Window End Time	USIT-E	99.63	us

One

USIT CORROSION 10" = 100'

Software Version

Acquisition System	Version
Maxwell 2017 SP1	7.1.82245.3100

Pass Summary

Run Name	Pass Objective	Direction	Top	Bottom	Start	Stop	DSC Mode	Depth Shift	Include Parallel Data
One	Log[6]:Up	Up	5305.38 ft	5812.78 ft	02-Jun-2017 8:32:42 PM	02-Jun-2017 9:01:04 PM	ON	2.00 ft	Yes

All depths are referenced to toolstring zero

Log

Company:Southern California Gas Company Well:Fernando Fee 35B

One: Log[6]:Up:S011

Description: USI Composite Format: Log (LBV1_USI Corrosion 9.625inch) Index Scale: 10 in per 100 ft Index Unit: ft Index Type: Measured Depth
Creation Date: 17-Jul-2017 14:12:04

TIME_1900 - Time Marked every 60.00 (s)

USIT Processing Flags (UFLG[0]) USIT-E

1 - UFLG 1 Value within [0.0 - 1.5] - :	UTIM Error
2 - UFLG 2 Value within [1.5 - 2.5] - :	Pulse Origin Not Detected
3 - UFLG 3 Value within [2.5 - 3.5] - :	WINLEN Error
4 - UFLG 4 UFLG 5 UFLG 6 Value within [3.5 - 6.5] - :	Casing Thickness Error
5 - UFLG 7 UFLG 8 UFLG 9 Value within [6.5 - 10] - :	Loop Processing Error

Amplitude of Eccentering for Unflagged Waves (ECCE_RF) USIT-E
0 in 0.5

Motor Revolution Speed (RSAV)

Absent 1.500 3.500
Explicit Normalization
USIT - USIT Processing

Absent -5.200 -3.600 -2.000 -0.400
Explicit Normalization
USIT - Amplitude of Unflagged Wave (AWBK_RF) USIT-E
(dB)

Minimum of Unflagged Wave Amplitude (AWMN_RF) USIT-E
0 dB 75

Average of Unflagged Wave Amplitude (AWAV_RF) USIT-E
0 dB 75

Absent -0.059 -0.028 0.004 0.035 0.068
Explicit Normalization

Internal Radius Averaged Value (IRAV) USIT-E
3.5 in 4.5

Minimum of Unflagged Internal Radii (IRMN_RF) USIT-E
3.5 in 4.5

ERAV | IRAV
ERAV-IRAV | ERAV
IRAV | IRAV-ERAV

Median of Unflagged External Radii (ERAV_RF) USIT-E
4.5 in 3.5

Median of Unflagged External Radii (ERAV_RF) USIT-E
3.5 in 4.5

Median Internal Radius of Casing Corrected for Eccentering (IRAV_RF) USIT-E
4.5 in 3.5

Median Internal Radius of Casing Corrected for Eccentering (IRAV_RF) USIT-E
3.5 in 4.5

Maximum of Unflagged Internal Radii (IRMX_RF) USIT-E
4.5 in 3.5

Maximum of Unflagged Internal Radii (IRMX_RF) USIT-E
3.5 in 4.5

Absent -0.059 -0.028 0.004 0.035 0.068
Explicit Normalization
USIT - Unflagged Casing

Minimum of Unflagged Casing Thickness (THMN_RF) USIT-E
0.1 in 0.6

Nominal Casing Thickness (THNO) USIT-E
0.1 in 0.6

Median of Unflagged Casing Thickness (THAV_RF) USIT-E
0.1 in 0.6

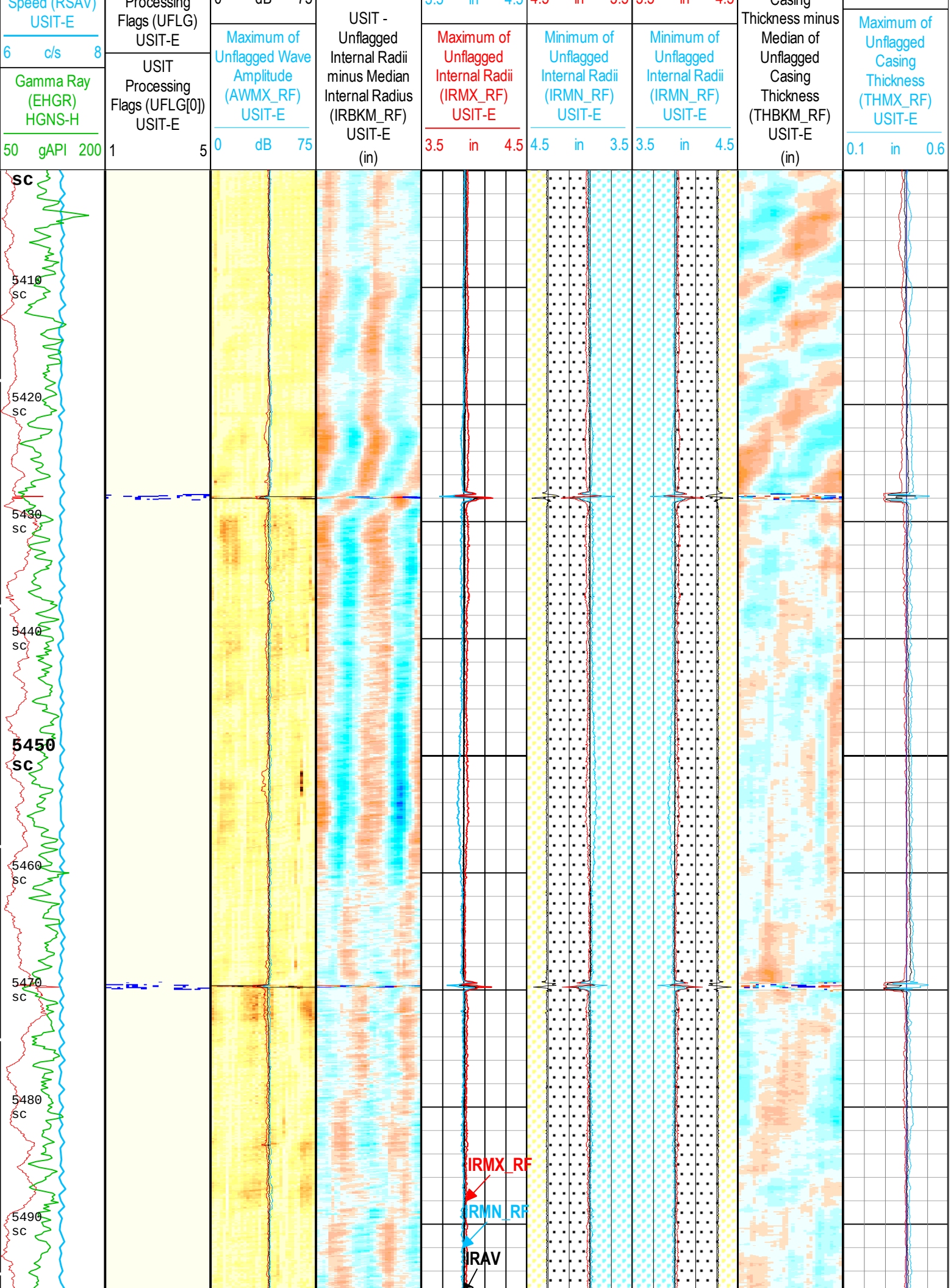
Speed (RSAV) USIT-E
6 c/s 8
Gamma Ray (EHGR) HGNS-H
50 gAPI 200
Processing Flags (UFLG) USIT-E
USIT Processing Flags (UFLG[0]) USIT-E
1 5
Maximum of Unflagged Wave Amplitude (AWMX_RF) USIT-E
0 dB 75
USIT - Unflagged Internal Radii minus Median Internal Radius (IRBKM_RF) USIT-E
(in)
Maximum of Unflagged Internal Radii (IRMX_RF) USIT-E
3.5 in 4.5
Minimum of Unflagged Internal Radii (IRMN_RF) USIT-E
4.5 in 3.5
Minimum of Unflagged Internal Radii (IRMN_RF) USIT-E
3.5 in 4.5
Casing Thickness minus Median of Unflagged Casing Thickness (THBKM_RF) USIT-E
(in)
Maximum of Unflagged Casing Thickness (THMX_RF) USIT-E
0.1 in 0.6
sc
5410 sc
5420 sc
5430 sc
5440 sc
5450 sc
5460 sc
5470 sc
5480 sc
5490 sc
IRMX_RF
IRMN_RF
IRAV

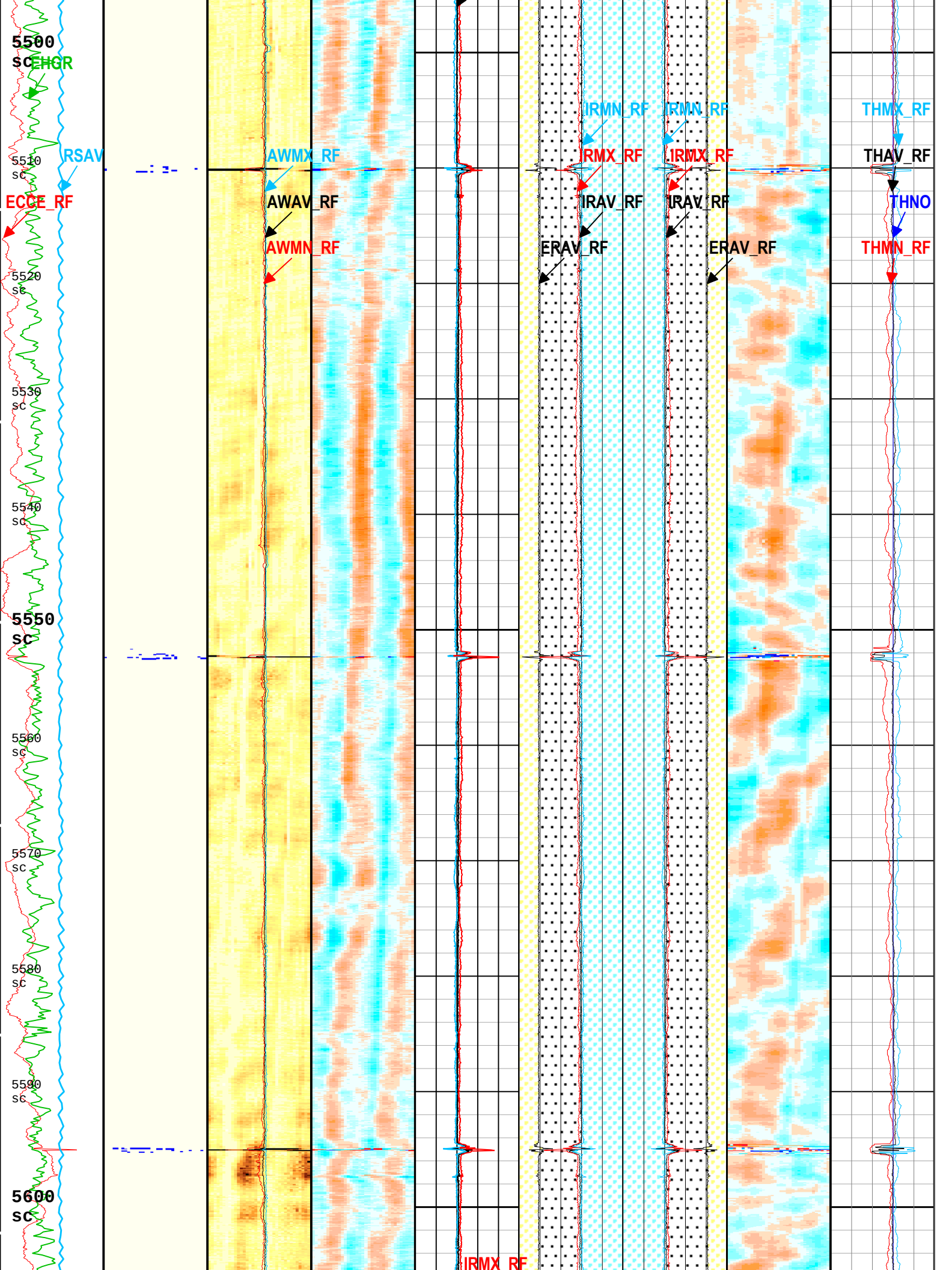
5500
SC
EHGR
RSAV
ECCE_RF
5510
SC
AWMX_RF
AWAV_RF
AWMN_RF
5520
SC
5530
SC
5540
SC
5550
SC
5560
SC
5570
SC
5580
SC
5590
SC
5600
SC
IRMN_RF
IRMX_RF
IRAV_RF
ERAV_RF
IRMN_RF
IRMX_RF
IRAV_RF
ERAV_RF
THMX_RF
THAV_RF
THNO
THMN_RF
IRMX_RF

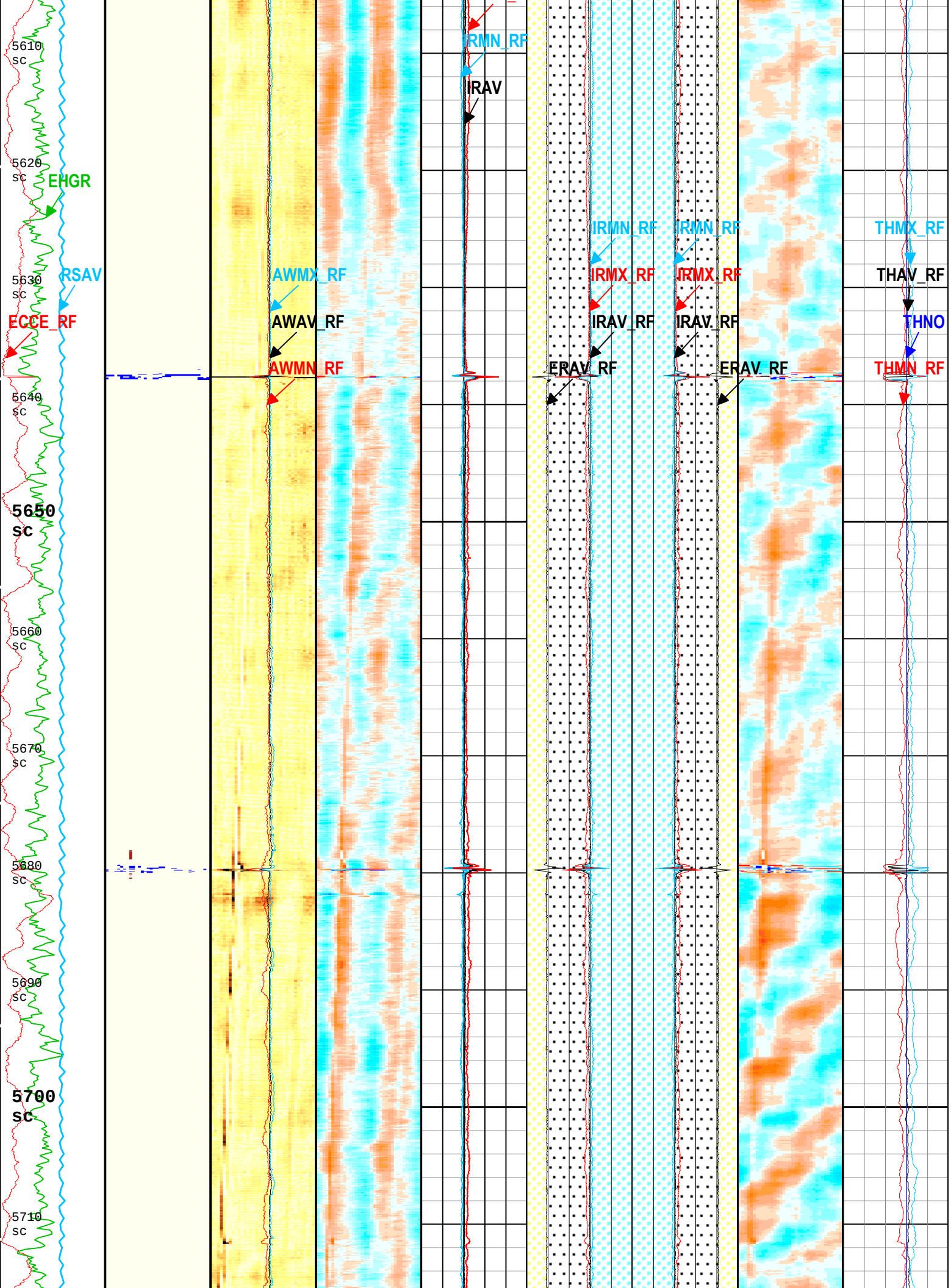
5610 sc
5620 sc
5630 sc
5640 sc
5650 sc
5660 sc
5670 sc
5680 sc
5690 sc
5700 sc
5710 sc
EHGR
RSAV
ECCE_RF
AWMX_RF
AWAV_RF
AWMN_RF
IRMN_RF
IRAV
IRMN_RF
IRMX_RF
IRAV_RF
ERAV_RF
IRMN_RF
IRMX_RF
IRAV_RF
ERAV_RF
THMX_RF
THAV_RF
THNO
THMN_RF

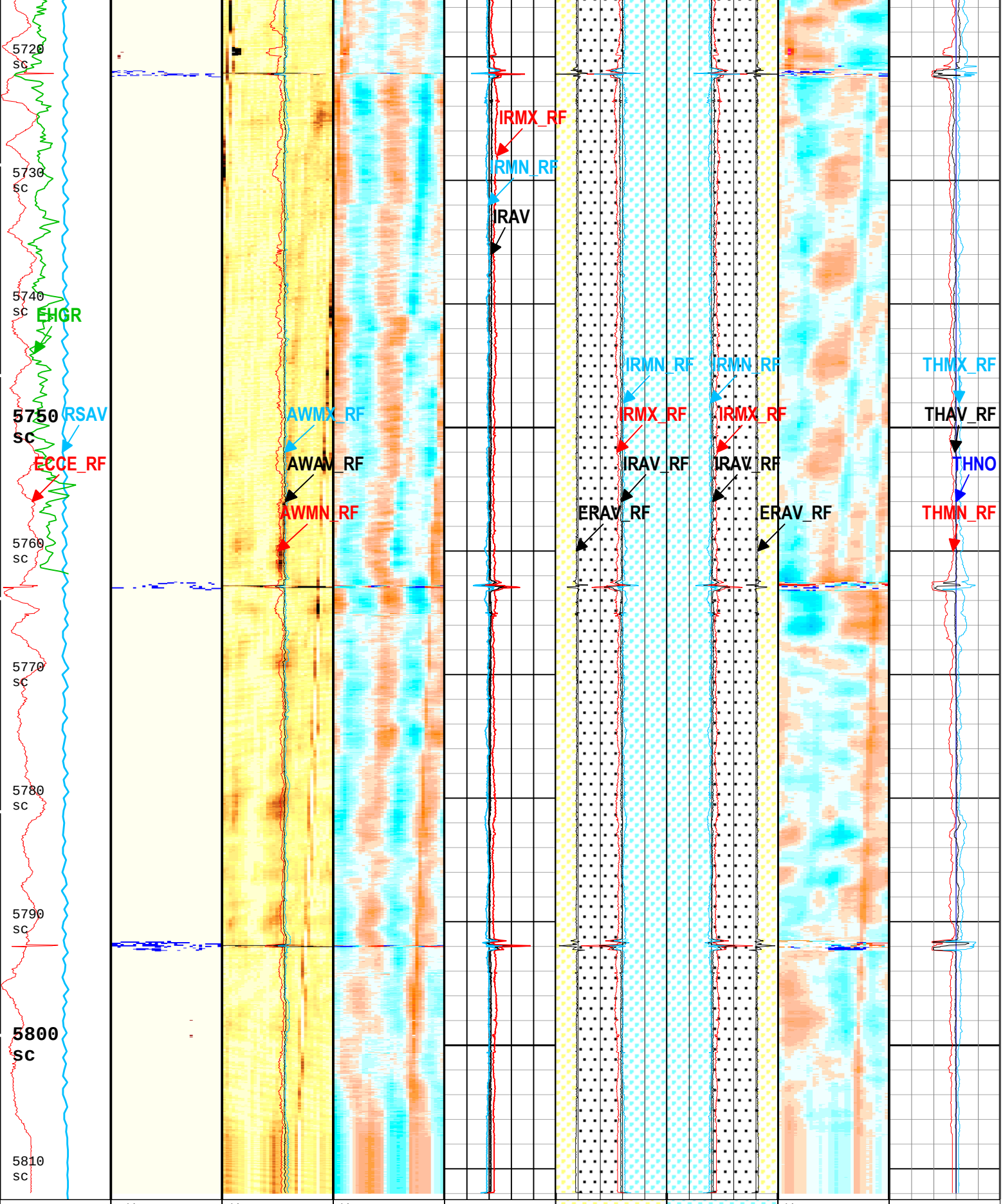
5720 sc
5730 sc
5740 sc
5750 sc
5760 sc
5770 sc
5780 sc
5790 sc
5800 sc
5810 sc
EHGR
RSAV
ECCE_RF
AWMX_RF
AWAV_RF
AWMN_RF
IRMX_RF
IRMN_RF
IRAV
IRMN_RF
IRMX_RF
IRAV_RF
ERAV_RF
IRMN_RF
IRMX_RF
IRAV_RF
ERAV_RF
THMX_RF
THAV_RF
THNO
THMN_RF
Amplitude of Eccentering for Unflagged Waves (ECCE_RF) USIT-E
0 in 0.5
Absent 1.500 3.500
Explicit Normalization
USIT - USIT Processing
Absent -5.200 -3.600 -2.000 -0.400
Explicit Normalization
USIT - Amplitude of
Absent -0.059 -0.028 0.004 0.035 0.068
Explicit Normalization
USIT - Unflagged
Internal Radius Averaged Value (IRAV) USIT-E
3.5 in 4.5
Minimum of Unflagged
ERAV
ERAV-IRAV
IRAV
Median of
IRAV
ERAV
IRAV-ERAV
Median of
Absent -0.059 -0.028 0.004 0.035 0.068
Explicit Normalization
USIT - Unflagged
Minimum of Unflagged Casing Thickness (THMN_RF) USIT-E
0.1 in 0.6

Motor Revolution Speed (RSAV) USIT-E
6 c/s 8

Gamma Ray (EHGR) HGNS-H
50 gAPI 200

Flags (UFLG) USIT-E

USIT Processing Flags (UFLG[0]) USIT-E
1 5

Unflagged Wave (AWBK_RF) USIT-E (dB)

Minimum of Unflagged Wave Amplitude (AWMN_RF) USIT-E
0 dB 75

Average of Unflagged Wave Amplitude (AWAV_RF) USIT-E
0 dB 75

Maximum of Unflagged Wave Amplitude (AWMX_RF) USIT-E
0 dB 75

Internal Radii minus Median Internal Radius (IRBKM_RF) USIT-E (in)

Internal Radii (IRMN_RF) USIT-E
3.5 in 4.5

Maximum of Unflagged Internal Radii (IRMX_RF) USIT-E
3.5 in 4.5

Unflagged External Radii (ERAV_RF) USIT-E
4.5 in 3.5

Median Internal Radius of Casing Corrected for Eccentering (IRAV_RF) USIT-E
4.5 in 3.5

Maximum of Unflagged Internal Radii (IRMX_RF) USIT-E
4.5 in 3.5

Minimum of Unflagged Internal Radii (IRMN_RF) USIT-E
4.5 in 3.5

Unflagged External Radii (ERAV_RF) USIT-E
3.5 in 4.5

Median Internal Radius of Casing Corrected for Eccentering (IRAV_RF) USIT-E
3.5 in 4.5

Maximum of Unflagged Internal Radii (IRMX_RF) USIT-E
3.5 in 4.5

Minimum of Unflagged Internal Radii (IRMN_RF) USIT-E
3.5 in 4.5

Unflagged Casing Thickness minus Median of Unflagged Casing Thickness (THBKM_RF) USIT-E (in)

Nominal Casing Thickness (THNO) USIT-E
0.1 in 0.6

Median of Unflagged Casing Thickness (THAV_RF) USIT-E
0.1 in 0.6

Maximum of Unflagged Casing Thickness (THMX_RF) USIT-E
0.1 in 0.6

USIT Processing Flags (UFLG[0]) USIT-E

1 - UFLG 1 Value within [0.0 - 1.5] - :
2 - UFLG 2 Value within [1.5 - 2.5] - :
3 - UFLG 3 Value within [2.5 - 3.5] - :
4 - UFLG 4 UFLG 5 UFLG 6 Value within [3.5 - 6.5] - :
5 - UFLG 7 UFLG 8 UFLG 9 Value within [6.5 - 10] - :

- UTIM Error
- Pulse Origin Not Detected
- WINLEN Error
- Casing Thickness Error
- Loop Processing Error

TIME_1900 - Time Marked every 60.00 (s)

Description: USI Composite Format: Log (LBV1_USI Corrosion 9.625inch) Index Scale: 10 in per 100 ft Index Unit: ft Index Type: Measured Depth
Creation Date: 17-Jul-2017 14:12:04

Channel Processing Parameters

One: Parameters

Parameter	Description	Tool	Value	Unit
ISSBAR	Barite Mud Presence Flag	Borehole	No	
BHS	Borehole Status (Open or Cased Hole)	Borehole	Cased	
BS	Bit Size	WLSESSION	11	in
CBLO	Casing Bottom (Logger)	WLSESSION	7331	ft
CDEN	Cement Density	HGNS-H	2.65	g/cm3
CMTY(U-USIT_CEMT)	Cement Type	USIT-E	Regular Cement	
THNO	Nominal Casing Thickness - Zoned along logger depths	WLSESSION	0.4	in
CYSTLGR	Casing Yield Strength - Zoned along logger depths	WLSESSION	55000	psi
DFD	Drilling Fluid Density	Borehole	8.9	lbm/gal
DFT_CATEGORY	Drilling Fluid Type	Borehole	Water	
DTMD	Borehole Fluid Slowness	Borehole	193	us/ft
FDII	FPM Data Interpolation Interval	USIT-E	0	ft
GCSE_DOWN_PASS	Generalized Caliper Selection for WL Log Down Passes	Borehole	BS	
GCSE_UP_PASS	Generalized Caliper Selection for WL Log Up Passes	Borehole	BS	

HEMA	Hematite Presence Flag	Borehole	No	
ICE_PROCESS	ICE Processing	USIT-E	Yes	
IMAR	Image Rotation	USIT-E	Off	
MEAS_WLEN	Tcube Processing Window Length in Measurement Mode	USIT-E	24.96	us
MUD_N_FRP	Free Pipe Mud Normalization Factor	USIT-E	1.06	
THDH	Maximum Search Thickness (percentage of nominal)	USIT-E	130	%
THDL	Minimum Search Thickness (percentage of nominal)	USIT-E	70	%
HISC	Tool Position: Centered or Eccentered	HGNS-H	Centered	
U-USIT_DFSZ	Drilling Fluid Specific Acoustic Impedance	USIT-E	0	Mrayl
UFGDE	Fiberglass Density	USIT-E	1.95	g/cm3
UFGPS	Fiberglass Processing Selection	USIT-E	No	
UFGVL	Fiberglass Velocity	USIT-E	9678.48	ft/s
USI_FSOD	USIT USI Fluid Slowness Fits Casing Outer Diameter	USIT-E	0_OFF	
USI_FVEL_SEL	USI Fluid Velocity Selection	USIT-E	Automatic	
USI_ZMUD_SEL	USI Mud Impedance Selection	USIT-E	FreePipe Norm.	
ZMUD	Acoustic Impedance of Mud	Borehole	1.68	Mrayl
ZTCM	Acoustic Impedance Threshold for Cement	USIT-E	2.6	Mrayl
ZTGS	Acoustic Impedance Threshold for Gas	USIT-E	0.3	Mrayl

Tool Control Parameters

One: Parameters

Parameter	Description	Tool	Value	Unit
AGMN	Minimum Gain of Cartridge	USIT-E	-12	dB
AGMX	Maximum Gain of Cartridge	USIT-E	48	dB
U-USIT_DDT5	USIC Downhole Decimation for T5 only	USIT-E	0_NONE	
EMXV	EMEX Voltage	USIT-E	120	V
HRES	Horizontal Resolution	USIT-E	10 deg	
TMUC	Type of Mud	USIT-E	BRI	
ULOG	Logging Objective	USIT-E	MEASUREMENT	
UMFR	Modulation Frequency	USIT-E	333333	Hz
USFR	Ultrasonic Sampling Frequency	USIT-E	500000	Hz
UPAT	USIT Emission Pattern	USIT-E	Pattern 500 KHz	
UWKM	USIT Working Mode	USIT-E	Uncompressed 10 deg at 0.6 in LF	
USIT_DEPTHLOG	Starting Depth Log for Ultrasonics	USIT-E	7030	ft
VRES	Vertical Resolution	USIT-E	0.6 in	
WINB	Window Begin Time	USIT-E	59.63	us
WINE	Window End Time	USIT-E	99.63	us

Company:	Southern California Gas Company
Well:	Fernando Fee 35B
Field:	Aliso Canyon
County:	Los Angeles
State:	California

Schlumberger

Ultrasonic Imager

Gamma Ray - CCL

8 5/8" 36# casing

Company Southern California Gas Company
Well Name Fernando Fee 35B
Log Date 01-Jun-2017

Joint No	Joint_Top	Joint_Len	CWEI_Joi	YIELD_Joint	IRAV_Join	IRMN_Joi	IRMN_Joi	IRMX_Joi	IRMX_Joi
	ft	ft	lbf/ft	psi	in	in	ft	in	ft
1	14.621	8.978	36.000	55000.000	3.904	3.846	18.371	3.952	17.121
2	23.599	42.511	36.000	55000.000	3.932	3.899	60.724	4.006	26.099
3	66.109	42.516	36.000	55000.000	3.924	3.895	104.984	3.967	69.109
4	108.625	42.625	36.000	55000.000	3.916	3.875	110.875	3.975	146.000
5	151.250	41.625	36.000	55000.000	3.907	3.872	153.625	3.962	154.250
6	192.875	41.125	36.000	55000.000	3.908	3.883	229.250	3.952	195.625
7	234.000	42.250	36.000	55000.000	3.910	3.869	236.375	3.970	236.250
8	276.250	38.375	36.000	55000.000	3.915	3.879	282.250	3.961	278.500
9	314.625	40.500	36.000	55000.000	3.903	3.871	350.625	3.941	336.125
10	355.125	39.625	36.000	55000.000	3.924	3.889	357.250	3.976	358.000
11	394.750	43.375	36.000	55000.000	3.917	3.869	397.000	3.987	397.375
12	438.125	40.875	36.000	55000.000	3.913	3.884	473.375	3.970	441.000
13	479.000	42.000	36.000	55000.000	3.915	3.872	512.375	3.972	497.250
14	521.000	39.125	36.000	55000.000	3.910	3.879	556.375	3.970	524.125
15	560.125	41.500	36.000	55000.000	3.916	3.880	568.625	3.958	563.000
16	601.625	42.750	36.000	55000.000	3.922	3.879	610.125	3.995	603.750
17	644.375	42.750	36.000	55000.000	3.918	3.871	646.500	3.978	646.750
18	687.125	40.500	36.000	55000.000	3.918	3.862	723.250	3.964	724.625
19	727.625	43.750	36.000	55000.000	3.915	3.880	731.125	3.989	731.125
20	771.375	43.375	36.000	55000.000	3.927	3.889	786.875	3.977	775.500
21	814.750	41.750	36.000	55000.000	3.922	3.884	855.250	3.976	817.750
22	856.500	42.000	36.000	55000.000	3.919	3.886	858.750	3.971	859.750
23	898.500	41.375	36.000	55000.000	3.917	3.879	900.875	3.962	901.000
24	939.875	41.500	36.000	55000.000	3.922	3.881	942.000	3.966	943.000
25	981.375	41.000	36.000	55000.000	3.907	3.878	1016.000	3.952	986.250
26	1022.375	40.375	36.000	55000.000	3.921	3.873	1053.000	3.965	1031.000
27	1062.750	39.750	36.000	55000.000	3.912	3.878	1066.250	3.980	1066.125
28	1102.500	41.500	36.000	55000.000	3.912	3.872	1104.625	3.964	1104.750
29	1144.000	41.750	36.000	55000.000	3.923	3.891	1181.125	3.967	1145.125
30	1185.750	43.500	36.000	55000.000	3.923	3.892	1220.875	3.985	1189.000
31	1229.250	41.375	36.000	55000.000	3.919	3.880	1268.125	3.968	1232.125
32	1270.625	41.875	36.000	55000.000	3.922	3.885	1303.750	3.972	1273.750
33	1312.500	41.625	36.000	55000.000	3.923	3.887	1351.625	3.966	1332.000
34	1354.125	39.750	36.000	55000.000	3.915	3.865	1386.875	3.966	1362.875
35	1393.875	41.750	36.000	55000.000	3.917	3.865	1402.625	3.966	1397.125
36	1435.625	40.875	36.000	55000.000	3.914	3.886	1471.250	3.961	1447.125
37	1476.500	42.875	36.000	55000.000	3.924	3.896	1512.375	3.969	1479.500
38	1519.375	41.375	36.000	55000.000	3.915	3.885	1544.625	3.953	1522.625
39	1560.750	41.875	36.000	55000.000	3.912	3.875	1594.375	3.949	1563.125
40	1602.625	39.125	36.000	55000.000	3.911	3.873	1604.875	3.989	1604.875
41	1641.750	42.625	36.000	55000.000	3.912	3.857	1644.000	3.958	1650.500
42	1684.375	41.000	36.000	55000.000	3.919	3.865	1686.625	3.974	1686.750
43	1725.375	40.875	36.000	55000.000	3.915	3.870	1727.625	3.957	1734.000
44	1766.250	41.875	36.000	55000.000	3.919	3.884	1806.500	3.979	1769.125
45	1808.125	41.500	36.000	55000.000	3.905	3.873	1816.750	3.957	1810.875
46	1849.625	43.125	36.000	55000.000	3.914	3.887	1890.875	3.969	1851.750
47	1892.750	42.250	36.000	55000.000	3.907	3.865	1926.250	3.956	1896.125
48	1935.000	41.125	36.000	55000.000	3.917	3.877	1943.375	3.972	1937.500
49	1976.125	40.750	36.000	55000.000	3.923	3.896	2012.625	3.990	1978.750
50	2016.875	41.375	36.000	55000.000	3.916	3.886	2053.375	3.957	2020.375
51	2058.250	42.500	36.000	55000.000	3.919	3.884	2060.375	3.968	2061.250
52	2100.750	41.125	36.000	55000.000	3.917	3.879	2117.875	3.972	2103.250
53	2141.875	41.500	36.000	55000.000	3.913	3.880	2174.250	3.954	2144.125
54	2183.375	41.500	36.000	55000.000	3.909	3.877	2185.750	3.964	2186.375
55	2224.875	42.000	36.000	55000.000	3.920	3.890	2255.375	3.962	2227.875
56	2266.875	41.000	36.000	55000.000	3.907	3.877	2295.375	3.940	2270.000
57	2307.875	43.500	36.000	55000.000	3.911	3.872	2343.500	3.967	2310.125

THAV_Joi	THMN_Joi	THMN_Joi	IDMN_Joi	IDMN_Joi	PENMX_R	PENMX_J	BURSTMN	COLLAPS	COLLAPS
in	in	ft	in	ft	%	%	psi	psi	psi
0.418	0.388	22.496	7.726	18.371	9.931	2.910	4953.008	3226.124	2690.559
0.383	0.324	29.849	7.802	60.724	23.425	18.954	4134.536	2134.440	1907.545
0.389	0.353	75.734	7.792	106.734	13.611	11.636	4507.828	2560.462	2409.807
0.396	0.340	146.125	7.755	110.875	15.556	15.052	4333.562	2332.416	2306.859
0.405	0.348	154.125	7.765	153.625	12.449	12.909	4442.897	2463.374	2498.485
0.405	0.348	229.625	7.773	227.625	9.860	13.109	4432.675	2448.089	2695.946
0.402	0.345	235.250	7.768	236.375	14.466	13.738	4400.619	2400.156	2362.156
0.398	0.363	277.250	7.777	292.000	12.079	9.288	4627.625	2739.592	2526.661
0.409	0.369	327.125	7.751	350.625	7.163	7.799	4703.574	2853.154	2901.682
0.388	0.348	364.500	7.782	357.250	15.776	13.101	4433.133	2448.774	2295.710
0.395	0.366	402.375	7.755	397.000	18.660	8.610	4662.195	2791.282	2149.344
0.400	0.342	467.000	7.777	473.125	14.271	14.387	4367.516	2366.189	2372.055
0.398	0.355	487.625	7.754	512.375	14.760	11.182	4530.998	2595.108	2347.229
0.403	0.354	525.500	7.772	556.375	14.298	11.553	4512.076	2566.814	2370.694
0.397	0.363	563.500	7.787	568.625	11.253	9.273	4628.379	2740.719	2589.687
0.391	0.339	631.875	7.773	603.625	20.527	15.227	4324.629	2323.530	2054.618
0.394	0.363	646.500	7.743	646.500	16.287	9.282	4627.923	2740.036	2269.786
0.395	0.359	688.875	7.747	723.250	12.829	10.347	4573.579	2658.777	2469.487
0.397	0.353	731.500	7.768	768.500	19.102	11.772	4500.898	2550.101	2126.896
0.386	0.354	776.375	7.790	786.875	16.125	11.623	4508.491	2561.455	2278.004
0.391	0.352	818.750	7.780	855.250	15.936	12.041	4487.164	2529.564	2287.565
0.394	0.358	863.125	7.780	858.750	14.728	10.461	4567.776	2650.101	2348.877
0.396	0.354	901.375	7.776	900.875	12.266	11.598	4509.803	2563.416	2512.412
0.391	0.356	962.375	7.774	942.000	13.397	10.990	4540.788	2609.746	2426.184
0.405	0.362	985.000	7.764	999.500	9.778	9.391	4622.366	2731.727	2702.212
0.391	0.345	1056.500	7.761	1053.000	13.226	13.781	4398.416	2396.927	2439.210
0.400	0.366	1064.000	7.776	1097.750	16.914	8.437	4671.048	2804.519	2237.939
0.401	0.365	1106.375	7.771	1104.625	12.865	8.772	4653.932	2778.927	2466.772
0.389	0.349	1148.750	7.787	1157.625	13.560	12.716	4452.750	2478.107	2413.731
0.389	0.345	1193.750	7.798	1214.625	18.013	13.712	4401.924	2402.107	2182.189
0.394	0.345	1236.000	7.767	1268.625	13.965	13.647	4405.239	2407.066	2387.617
0.391	0.354	1274.750	7.775	1303.750	14.884	11.484	4515.602	2572.087	2340.956
0.389	0.343	1315.875	7.782	1351.625	13.463	14.252	4374.389	2373.026	2421.156
0.398	0.354	1358.875	7.751	1386.875	13.342	11.395	4520.149	2578.886	2430.340
0.395	0.370	1395.250	7.752	1402.625	13.433	7.558	4715.861	2871.527	2423.411
0.398	0.353	1440.500	7.776	1471.750	12.124	11.786	4500.167	2549.008	2523.296
0.389	0.337	1480.250	7.795	1512.375	14.060	15.743	4298.312	2297.351	2382.750
0.398	0.363	1524.625	7.781	1544.625	10.105	9.240	4630.097	2743.287	2677.310
0.401	0.369	1561.750	7.767	1595.125	9.074	7.715	4707.888	2859.605	2755.880
0.402	0.362	1640.250	7.757	1604.750	19.066	9.464	4618.643	2726.161	2128.765
0.400	0.360	1646.250	7.719	1644.000	11.262	10.007	4590.934	2684.728	2588.991
0.393	0.349	1691.875	7.758	1686.625	15.315	12.812	4447.872	2470.813	2319.094
0.397	0.349	1727.250	7.767	1727.625	11.038	12.837	4446.568	2468.863	2606.100
0.393	0.353	1780.125	7.777	1803.750	16.554	11.652	4507.018	2559.252	2256.232
0.407	0.374	1841.000	7.755	1816.750	11.103	6.425	4773.691	2957.999	2601.162
0.399	0.355	1856.125	7.780	1851.875	14.003	11.198	4530.177	2593.880	2385.648
0.405	0.366	1912.500	7.744	1899.000	10.806	8.471	4669.296	2801.900	2623.786
0.396	0.356	1939.750	7.760	1943.375	14.990	10.893	4545.772	2617.199	2335.572
0.390	0.346	1981.250	7.801	2009.625	19.487	13.605	4407.415	2410.318	2107.389
0.396	0.360	2038.625	7.775	2053.375	11.139	9.958	4593.466	2688.514	2598.375
0.393	0.357	2061.000	7.779	2060.375	13.898	10.687	4556.272	2632.899	2390.975
0.395	0.351	2110.000	7.768	2128.375	14.803	12.173	4480.458	2519.536	2345.060
0.399	0.329	2151.875	7.766	2174.250	10.356	17.692	4198.900	2198.464	2658.132
0.403	0.343	2195.250	7.769	2200.000	12.952	14.251	4374.461	2373.098	2460.111
0.393	0.346	2231.750	7.780	2255.375	12.355	13.452	4415.219	2421.988	2505.628
0.405	0.370	2272.000	7.759	2295.375	6.803	7.573	4715.137	2870.445	2929.117
0.402	0.363	2310.500	7.750	2343.500	13.667	9.218	4631.216	2744.961	2405.552

IDMN_Col	IRMX_Coll	MAOP	Delta_MAOP_Barlow
in	in	psi	psi
7.731	4.013	3625.000	1328.008
7.460	4.215	3625.000	509.536
7.787	4.184	3625.000	882.828
7.675	4.339	3625.000	708.562
7.457	4.356	3625.000	817.897
7.629	4.326	3625.000	807.675
7.698	4.304	3625.000	775.619
7.685	4.205	3625.000	1002.625
7.669	4.189	3625.000	1078.574
7.572	4.346	3625.000	808.133
7.721	4.212	3625.000	1037.195
7.802	4.170	3625.000	742.516
7.685	4.147	3625.000	905.998
7.746	4.215	3625.000	887.076
7.781	4.194	3625.000	1003.379
7.511	4.344	3625.000	699.629
7.799	4.214	3625.000	1002.923
7.774	4.050	3625.000	948.579
7.578	4.309	3625.000	875.898
7.762	4.172	3625.000	883.491
7.671	4.319	3625.000	862.164
7.699	4.273	3625.000	942.776
7.783	4.227	3625.000	884.803
7.794	4.232	3625.000	915.788
7.592	4.237	3625.000	997.366
7.664	4.285	3625.000	773.416
7.722	4.307	3625.000	1046.048
7.776	4.166	3625.000	1028.932
7.667	4.295	3625.000	827.750
7.663	4.265	3625.000	776.924
7.819	4.214	3625.000	780.239
7.591	4.204	3625.000	890.602
7.722	4.181	3625.000	749.389
7.797	4.230	3625.000	895.149
7.660	4.283	3625.000	1090.861
7.801	4.207	3625.000	875.167
7.719	4.214	3625.000	673.312
7.680	4.179	3625.000	1005.097
7.786	4.192	3625.000	1082.888
7.751	4.207	3625.000	993.643
7.735	4.266	3625.000	965.934
7.668	4.260	3625.000	822.872
7.785	4.206	3625.000	821.568
7.786	4.259	3625.000	882.018
7.777	4.208	3625.000	1148.691
7.779	4.203	3625.000	905.177
7.738	4.242	3625.000	1044.296
7.652	4.189	3625.000	920.772
7.628	4.294	3625.000	782.415
7.766	4.194	3625.000	968.466
7.777	4.213	3625.000	931.272
7.702	4.218	3625.000	855.458
7.787	4.212	3625.000	573.900
7.429	4.342	3625.000	749.461
7.721	4.229	3625.000	790.219
7.772	4.215	3625.000	1090.137
7.518	4.330	3625.000	1006.216

58	2351.375	41.000	36.000	55000.000	3.910	3.862	2353.500	3.976	2353.375
59	2392.375	41.125	36.000	55000.000	3.913	3.879	2427.500	3.952	2412.625
60	2433.500	41.000	36.000	55000.000	3.906	3.865	2464.250	3.943	2435.625
61	2474.500	41.750	36.000	55000.000	3.911	3.874	2487.125	3.952	2487.375
62	2516.250	42.750	36.000	55000.000	3.912	3.867	2545.125	3.965	2536.250
63	2559.000	42.375	36.000	55000.000	3.910	3.869	2584.625	3.963	2584.500
64	2601.375	42.375	36.000	55000.000	3.915	3.874	2636.625	3.953	2617.625
65	2643.750	41.250	36.000	55000.000	3.916	3.883	2659.750	3.964	2646.250
66	2685.000	42.250	36.000	55000.000	3.908	3.868	2716.125	3.951	2709.625
67	2727.250	43.250	36.000	55000.000	3.918	3.869	2766.250	3.963	2740.625
68	2770.500	42.375	36.000	55000.000	3.910	3.861	2779.375	3.960	2794.500
69	2812.875	41.500	36.000	55000.000	3.912	3.867	2815.125	3.952	2821.625
70	2854.375	41.875	36.000	55000.000	3.914	3.874	2892.125	3.956	2856.375
71	2896.250	41.750	36.000	55000.000	3.913	3.870	2926.250	3.969	2898.250
72	2938.000	42.500	36.000	55000.000	3.911	3.873	2969.875	3.945	2946.625
73	2980.500	42.500	36.000	55000.000	3.903	3.869	3004.875	3.943	2989.250
74	3023.000	41.750	36.000	55000.000	3.910	3.873	3034.125	3.956	3031.750
75	3064.750	41.875	36.000	55000.000	3.914	3.887	3094.875	3.947	3067.125
76	3106.625	38.875	36.000	55000.000	3.902	3.875	3109.000	3.929	3143.000
77	3145.500	42.375	36.000	55000.000	3.910	3.875	3154.250	3.946	3154.125
78	3187.875	42.500	36.000	55000.000	3.913	3.877	3190.375	3.950	3190.250
79	3230.375	41.875	36.000	55000.000	3.919	3.877	3254.000	3.970	3232.500
80	3272.250	40.875	36.000	55000.000	3.910	3.873	3280.875	3.946	3274.375
81	3313.125	42.250	36.000	55000.000	3.905	3.862	3321.875	3.941	3351.875
82	3355.375	43.000	36.000	55000.000	3.917	3.880	3364.125	3.954	3357.750
83	3398.375	41.375	36.000	55000.000	3.903	3.872	3434.625	3.946	3400.625
84	3439.750	42.000	36.000	55000.000	3.915	3.888	3467.625	3.944	3450.875
85	3481.750	41.125	36.000	55000.000	3.903	3.874	3518.500	3.951	3490.625
86	3522.875	42.250	36.000	55000.000	3.908	3.871	3531.625	3.938	3531.500
87	3565.125	40.750	36.000	55000.000	3.914	3.863	3604.625	4.007	3604.000
88	3605.875	42.750	36.000	55000.000	3.907	3.864	3608.125	3.980	3608.125
89	3648.625	37.500	36.000	55000.000	3.915	3.877	3650.875	3.981	3651.000
90	3686.125	42.750	36.000	55000.000	3.917	3.879	3727.125	3.952	3725.750
91	3728.875	42.250	36.000	55000.000	3.922	3.880	3762.250	3.966	3748.750
92	3771.125	42.125	36.000	55000.000	3.912	3.876	3807.625	3.946	3785.250
93	3813.250	43.500	36.000	55000.000	3.922	3.880	3844.000	3.969	3825.125
94	3856.750	42.625	36.000	55000.000	3.912	3.888	3884.250	3.945	3859.125
95	3899.375	42.375	36.000	55000.000	3.916	3.888	3935.250	3.950	3916.625
96	3941.750	43.715	36.000	55000.000	3.916	3.860	3954.625	3.995	3956.625
97	3985.466	42.785	36.000	55000.000	3.910	3.843	4007.341	3.968	4007.466
98	4028.250	27.702	36.000	55000.000	3.914	3.877	4036.750	3.957	4036.500
99	4055.952	41.173	36.000	55000.000	3.904	3.874	4080.702	3.933	4068.827
100	4097.125	43.375	36.000	55000.000	3.923	3.870	4136.000	3.967	4105.000
101	4140.500	41.875	36.000	55000.000	3.917	3.876	4174.500	3.971	4142.250
102	4182.375	42.750	36.000	55000.000	3.915	3.868	4184.250	3.980	4184.125
103	4225.125	41.500	36.000	55000.000	3.910	3.869	4262.625	3.949	4227.125
104	4266.625	39.750	36.000	55000.000	3.923	3.888	4291.125	3.973	4282.250
105	4306.375	42.375	36.000	55000.000	3.913	3.868	4345.250	3.944	4317.000
106	4348.750	42.375	36.000	55000.000	3.912	3.875	4353.625	3.958	4353.250
107	4391.125	41.875	36.000	55000.000	3.913	3.869	4406.500	3.959	4406.500
108	4433.000	42.375	36.000	55000.000	3.915	3.886	4467.750	3.952	4437.125
109	4475.375	42.250	36.000	55000.000	3.910	3.866	4477.625	3.951	4477.375
110	4517.625	38.250	36.000	55000.000	3.911	3.880	4548.250	3.951	4520.000
111	4555.875	42.000	36.000	55000.000	3.913	3.877	4564.750	3.951	4565.000
112	4597.875	41.000	36.000	55000.000	3.916	3.876	4625.750	3.962	4599.875
113	4638.875	40.375	36.000	55000.000	3.910	3.870	4640.875	3.959	4640.750
114	4679.250	43.250	36.000	55000.000	3.911	3.875	4681.500	3.970	4681.375
115	4722.500	39.875	36.000	55000.000	3.915	3.876	4724.750	3.969	4740.750
116	4762.375	42.500	36.000	55000.000	3.922	3.885	4802.750	3.973	4764.625
117	4804.875	39.500	36.000	55000.000	3.906	3.854	4813.375	3.957	4813.500
118	4844.375	41.375	36.000	55000.000	3.907	3.876	4879.000	3.958	4852.500
119	4885.750	42.125	36.000	55000.000	3.911	3.884	4922.125	3.959	4887.875

0.403	0.345	2362.125	7.733	2353.500	15.836	13.738	4400.613	2400.147	2292.643
0.399	0.361	2397.250	7.763	2427.500	9.980	9.668	4608.235	2710.598	2686.844
0.407	0.363	2436.875	7.731	2435.750	7.690	9.219	4631.142	2744.850	2861.513
0.401	0.354	2478.125	7.764	2514.125	9.970	11.454	4517.111	2574.344	2687.549
0.400	0.364	2534.375	7.755	2557.125	13.039	8.908	4647.031	2768.609	2453.464
0.403	0.362	2565.375	7.763	2577.875	12.606	9.414	4621.187	2729.964	2486.528
0.397	0.355	2603.125	7.751	2636.625	10.136	11.244	4527.854	2590.408	2674.886
0.397	0.339	2658.500	7.774	2678.625	12.755	15.209	4325.586	2324.482	2475.120
0.405	0.346	2688.875	7.745	2717.000	9.746	13.510	4412.256	2417.557	2704.676
0.395	0.363	2734.875	7.744	2766.250	12.714	9.352	4624.357	2734.705	2478.257
0.403	0.361	2778.250	7.736	2779.375	11.785	9.805	4601.234	2700.130	2549.158
0.400	0.357	2814.500	7.742	2815.125	9.819	10.711	4555.029	2631.041	2699.125
0.399	0.355	2859.375	7.751	2892.125	10.869	11.282	4525.926	2587.525	2618.981
0.400	0.351	2899.250	7.743	2926.750	14.078	12.353	4471.275	2505.807	2381.855
0.401	0.352	2947.500	7.764	2969.875	8.206	11.917	4493.502	2539.041	2822.111
0.409	0.379	3021.750	7.743	3004.875	7.566	5.249	4833.695	3047.721	2870.947
0.403	0.361	3024.000	7.753	3034.125	10.960	9.633	4610.026	2713.277	2612.061
0.398	0.357	3075.250	7.776	3094.875	8.580	10.855	4547.677	2620.048	2793.595
0.410	0.384	3130.000	7.758	3108.875	4.090	4.087	4892.969	3136.351	3136.076
0.403	0.366	3148.375	7.753	3154.250	8.449	8.544	4665.587	2796.355	2803.566
0.400	0.345	3194.375	7.775	3190.375	9.471	13.771	4398.948	2397.658	2725.609
0.393	0.354	3243.375	7.778	3239.000	14.356	11.499	4514.859	2570.975	2367.776
0.402	0.372	3276.125	7.772	3280.875	8.299	7.106	4738.916	2906.001	2815.005
0.408	0.376	3320.500	7.738	3321.875	7.129	6.025	4794.105	2988.523	2904.279
0.395	0.349	3362.875	7.776	3389.125	10.454	12.655	4455.850	2482.741	2650.680
0.409	0.375	3401.125	7.750	3414.625	8.369	6.356	4777.198	2963.242	2809.713
0.397	0.360	3448.375	7.782	3474.500	7.920	9.910	4595.904	2692.159	2843.935
0.409	0.372	3484.375	7.757	3518.750	9.633	7.079	4740.334	2908.122	2713.301
0.405	0.365	3528.375	7.763	3549.250	6.332	8.730	4656.090	2782.154	2965.040
0.398	0.358	3569.500	7.742	3604.500	23.566	10.553	4563.076	2643.073	1900.413
0.406	0.375	3616.375	7.759	3608.125	16.920	6.250	4782.628	2971.362	2237.616
0.397	0.363	3649.625	7.763	3650.875	17.228	9.271	4628.510	2740.914	2221.990
0.395	0.355	3689.375	7.766	3727.625	9.812	11.175	4531.366	2595.658	2699.606
0.391	0.355	3732.875	7.773	3762.250	13.315	11.291	4525.468	2586.839	2432.377
0.400	0.369	3778.250	7.764	3806.125	8.472	7.794	4703.863	2853.587	2801.865
0.390	0.344	3825.125	7.782	3845.875	14.057	14.067	4383.847	2382.435	2382.926
0.401	0.366	3865.625	7.780	3884.250	8.221	8.597	4662.855	2792.269	2820.975
0.397	0.352	3924.375	7.781	3939.750	9.276	11.950	4491.845	2536.563	2740.494
0.396	0.327	3981.500	7.758	3980.625	20.607	18.140	4176.028	2175.713	2050.520
0.402	0.347	3993.591	7.687	4007.341	13.764	13.293	4423.321	2434.103	2398.159
0.398	0.355	4034.250	7.760	4036.750	11.070	11.203	4529.943	2593.531	2603.631
0.408	0.367	4062.327	7.755	4095.952	5.091	8.291	4678.465	2815.610	3059.729
0.390	0.348	4098.375	7.746	4136.125	13.522	12.950	4440.809	2460.251	2416.604
0.396	0.358	4147.625	7.765	4174.750	14.545	10.538	4563.858	2644.242	2358.157
0.397	0.350	4186.625	7.748	4184.125	16.995	12.601	4458.626	2486.894	2233.844
0.403	0.367	4232.250	7.743	4262.625	9.044	8.135	4686.471	2827.581	2758.213
0.389	0.336	4267.750	7.788	4290.000	15.250	15.945	4287.999	2287.093	2322.388
0.399	0.362	4316.125	7.751	4345.250	7.977	9.446	4619.568	2727.544	2839.607
0.401	0.368	4361.250	7.763	4353.625	11.370	8.085	4688.972	2831.321	2580.812
0.400	0.357	4395.375	7.741	4406.500	11.577	10.627	4559.336	2637.481	2564.975
0.398	0.352	4438.250	7.776	4463.000	9.798	11.959	4491.357	2535.834	2700.679
0.403	0.374	4496.250	7.741	4477.625	9.589	6.496	4770.069	2952.583	2716.661
0.401	0.376	4525.500	7.773	4548.250	9.607	5.975	4796.633	2992.303	2715.297
0.399	0.366	4559.250	7.772	4564.750	9.667	8.503	4667.663	2799.458	2710.709
0.397	0.360	4604.875	7.764	4627.750	12.383	9.954	4593.662	2688.807	2503.518
0.402	0.369	4652.000	7.761	4640.875	11.577	7.676	4709.877	2862.580	2564.994
0.401	0.370	4686.125	7.761	4687.750	14.474	7.504	4718.614	2875.644	2361.784
0.398	0.352	4746.375	7.761	4724.750	14.058	12.091	4484.612	2525.748	2382.863
0.391	0.349	4763.625	7.774	4802.750	15.164	12.692	4453.987	2479.957	2326.740
0.406	0.340	4821.500	7.737	4813.375	11.129	14.933	4339.633	2338.454	2599.171
0.406	0.356	4860.500	7.757	4879.000	11.264	10.909	4544.917	2615.921	2588.868
0.402	0.380	4910.625	7.775	4925.500	11.674	4.997	4846.510	3066.882	2557.564

7.716	4.181	3625.000	775.613
7.674	4.249	3625.000	983.235
7.654	4.305	3625.000	1006.142
7.707	4.337	3625.000	892.111
7.775	4.179	3625.000	1022.031
7.677	4.231	3625.000	996.187
7.742	4.283	3625.000	902.854
7.649	4.371	3625.000	700.586
7.788	4.270	3625.000	787.256
7.769	4.237	3625.000	999.357
7.573	4.245	3625.000	976.234
7.783	4.225	3625.000	930.029
7.535	4.370	3625.000	900.926
7.742	4.184	3625.000	846.275
7.527	4.341	3625.000	868.502
7.528	4.308	3625.000	1208.695
7.690	4.216	3625.000	985.026
7.594	4.348	3625.000	922.677
7.551	4.363	3625.000	1267.969
7.718	4.283	3625.000	1040.587
7.569	4.282	3625.000	773.948
7.630	4.218	3625.000	889.859
7.743	4.238	3625.000	1113.916
7.711	4.294	3625.000	1169.105
7.639	4.208	3625.000	830.850
7.782	4.215	3625.000	1152.198
7.561	4.208	3625.000	970.904
7.675	4.242	3625.000	1115.334
7.681	4.310	3625.000	1031.090
7.781	4.234	3625.000	938.076
7.642	4.296	3625.000	1157.628
7.785	4.149	3625.000	1003.510
7.776	4.082	3625.000	906.366
7.770	4.168	3625.000	900.468
7.795	4.139	3625.000	1078.863
7.793	4.148	3625.000	758.847
7.800	4.136	3625.000	1037.855
7.789	4.093	3625.000	866.845
7.803	4.116	3625.000	551.028
7.640	4.201	3625.000	798.321
7.669	4.157	3625.000	904.943
7.732	4.200	3625.000	1053.465
7.770	4.084	3625.000	815.809
7.795	4.146	3625.000	938.858
7.702	4.120	3625.000	833.626
7.666	4.143	3625.000	1061.471
7.684	4.155	3625.000	662.999
7.723	4.078	3625.000	994.568
7.767	4.109	3625.000	1063.972
7.750	4.187	3625.000	934.336
7.778	4.210	3625.000	866.357
7.802	4.199	3625.000	1145.069
7.748	4.195	3625.000	1171.633
7.782	4.189	3625.000	1042.663
7.708	4.272	3625.000	968.662
7.545	4.327	3625.000	1084.877
7.528	4.398	3625.000	1093.614
7.711	4.260	3625.000	859.612
7.803	4.181	3625.000	828.987
7.697	4.282	3625.000	714.633
7.715	4.153	3625.000	919.917
7.775	4.149	3625.000	1221.510

120	4927.875	42.125	36.000	55000.000	3.910	3.879	4968.250	3.952	4930.250
121	4970.000	42.500	36.000	55000.000	3.915	3.883	4972.125	3.953	4992.625
122	5012.500	41.750	36.000	55000.000	3.914	3.879	5052.875	3.950	5014.500
123	5054.250	41.625	36.000	55000.000	3.908	3.872	5081.375	3.946	5056.625
124	5095.875	42.625	36.000	55000.000	3.912	3.872	5104.750	3.961	5098.250
125	5138.500	41.750	36.000	55000.000	3.903	3.864	5161.000	3.951	5140.625
126	5180.250	41.750	36.000	55000.000	3.906	3.870	5183.250	3.948	5182.375
127	5222.000	42.500	36.000	55000.000	3.910	3.874	5226.625	3.956	5224.250
128	5264.500	36.750	36.000	55000.000	3.897	3.857	5273.125	3.942	5278.125
129	5301.250	42.000	36.000	55000.000	3.904	3.859	5338.625	3.958	5340.250
130	5343.250	41.375	36.000	55000.000	3.907	3.864	5351.750	3.950	5365.375
131	5384.625	42.750	36.000	55000.000	3.918	3.867	5422.125	3.955	5425.875
132	5427.375	41.750	36.000	55000.000	3.903	3.839	5453.375	3.963	5429.375
133	5469.125	40.125	36.000	55000.000	3.906	3.859	5500.750	3.949	5499.500
134	5509.250	42.875	36.000	55000.000	3.912	3.857	5533.625	3.966	5529.875
135	5552.125	42.625	36.000	55000.000	3.912	3.869	5580.750	3.963	5554.250
136	5594.750	42.500	36.000	55000.000	3.911	3.864	5597.000	3.978	5597.125
137	5637.250	42.500	36.000	55000.000	3.909	3.869	5675.625	3.958	5678.125
138	5679.750	41.125	36.000	55000.000	3.907	3.846	5682.000	3.976	5687.875
139	5720.875	41.125	36.000	55000.000	3.918	3.835	5723.250	3.983	5722.750
140	5762.000	29.375	36.000	55000.000	3.910	3.847	5764.250	3.973	5771.000
141	5791.375	42.375	36.000	55000.000	3.912	3.829	5823.125	3.982	5823.000
142	5833.750	42.750	36.000	80000.000	3.912	3.857	5838.000	3.962	5840.125
143	5876.500	41.000	36.000	80000.000	3.915	3.864	5885.500	3.967	5881.000
144	5917.500	42.000	36.000	80000.000	3.913	3.869	5941.875	3.970	5919.625
145	5959.500	43.125	36.000	80000.000	3.909	3.859	5981.750	3.965	5962.250
146	6002.625	40.875	36.000	80000.000	3.899	3.848	6040.250	3.981	6040.375
147	6043.500	43.125	36.000	80000.000	3.916	3.862	6067.500	3.972	6061.375
148	6086.625	43.000	36.000	80000.000	3.911	3.858	6103.500	3.961	6095.625
149	6129.625	42.000	36.000	80000.000	3.915	3.871	6149.125	3.958	6154.000
150	6171.625	41.500	36.000	80000.000	3.915	3.888	6209.750	3.954	6180.500
151	6213.125	41.625	36.000	80000.000	3.899	3.856	6215.375	3.961	6215.500
152	6254.750	40.750	36.000	80000.000	3.910	3.868	6290.375	3.960	6263.250
153	6295.500	42.375	36.000	80000.000	3.906	3.864	6317.125	3.958	6304.375
154	6337.875	42.500	36.000	80000.000	3.909	3.840	6361.875	3.982	6359.750
155	6380.375	42.000	36.000	80000.000	3.903	3.833	6413.625	3.965	6389.375
156	6422.375	41.000	36.000	80000.000	3.909	3.849	6459.750	3.969	6429.250
157	6463.375	43.066	36.000	80000.000	3.914	3.833	6504.000	4.002	6486.875
158	6506.441	41.562	36.000	80000.000	3.910	3.829	6540.566	3.995	6510.066
159	6548.003	42.872	36.000	80000.000	3.915	3.841	6550.378	3.992	6554.878
160	6590.875	42.375	36.000	80000.000	3.911	3.842	6619.625	3.980	6619.375
161	6633.250	41.875	36.000	80000.000	3.912	3.862	6641.625	3.969	6639.625
162	6675.125	40.750	36.000	80000.000	3.919	3.871	6708.500	3.961	6683.875
163	6715.875	41.750	36.000	80000.000	3.910	3.838	6724.375	3.973	6724.500
164	6757.625	42.125	36.000	80000.000	3.914	3.848	6764.000	4.001	6761.750
165	6799.750	39.750	36.000	80000.000	3.885	3.832	6814.375	3.949	6813.875
166	6839.500	43.000	36.000	80000.000	3.918	3.865	6853.875	3.978	6854.000
167	6882.500	42.750	36.000	80000.000	3.905	3.863	6923.875	3.948	6919.000
168	6925.250	42.500	36.000	80000.000	3.913	3.856	6955.500	3.990	6952.000
169	6967.750	42.750	36.000	80000.000	3.913	3.846	6999.875	3.978	6972.750
170	7010.500	32.750	36.000	80000.000	3.903	3.838	7035.000	3.973	7020.500

0.402	0.358	4939.000	7.766	4930.375	9.822	10.534	4564.063	2644.549	2698.852
0.397	0.369	4978.750	7.770	5009.250	10.211	7.793	4703.892	2853.629	2669.157
0.398	0.357	5015.000	7.764	5052.875	9.398	10.719	4554.621	2630.431	2731.188
0.404	0.366	5060.375	7.756	5092.250	8.266	8.429	4671.472	2805.154	2817.569
0.400	0.358	5101.875	7.759	5104.750	12.006	10.455	4568.091	2650.571	2532.290
0.410	0.366	5151.500	7.737	5161.000	9.569	8.569	4664.306	2794.439	2718.193
0.406	0.375	5183.250	7.752	5182.625	8.974	6.309	4779.585	2966.811	2763.537
0.402	0.350	5231.250	7.753	5226.625	10.778	12.421	4467.782	2500.583	2625.946
0.415	0.368	5267.250	7.735	5298.125	7.387	7.926	4697.120	2843.503	2884.637
0.408	0.370	5303.125	7.730	5340.750	11.478	7.493	4719.213	2876.540	2572.555
0.405	0.347	5347.250	7.741	5367.625	9.406	13.150	4430.618	2445.014	2730.628
0.394	0.361	5405.875	7.740	5422.125	10.517	9.691	4607.089	2708.885	2645.838
0.410	0.381	5433.250	7.692	5453.375	12.683	4.687	4862.353	3090.571	2480.630
0.406	0.383	5477.000	7.729	5500.750	9.079	4.141	4890.218	3132.238	2755.539
0.401	0.358	5541.750	7.730	5540.375	13.491	10.433	4569.192	2652.218	2418.987
0.400	0.348	5556.500	7.748	5587.875	12.617	12.958	4440.426	2459.678	2485.691
0.401	0.367	5604.625	7.742	5612.250	16.478	8.273	4679.410	2817.023	2260.092
0.404	0.345	5678.625	7.754	5665.000	11.350	13.658	4404.682	2406.232	2582.298
0.405	0.344	5719.125	7.720	5682.000	15.858	13.987	4387.929	2386.495	2291.554
0.395	0.365	5728.125	7.708	5723.250	17.529	8.737	4655.732	2781.619	2206.713
0.403	0.352	5764.375	7.719	5781.875	15.090	11.901	4494.347	2540.305	2330.509
0.401	0.371	5801.375	7.684	5823.125	17.254	7.306	4728.723	2890.760	2220.702
0.400	0.355	5837.250	7.716	5838.000	12.737	11.649	6588.665	3108.409	3027.413
0.397	0.340	5879.375	7.748	5885.500	14.055	15.536	6298.788	2818.890	2929.219
0.400	0.373	5936.125	7.741	5941.875	14.709	7.196	6920.743	3440.079	2880.539
0.403	0.356	6001.375	7.742	5961.750	13.481	11.512	6598.933	3118.665	2971.948
0.414	0.352	6040.000	7.708	6040.250	17.627	12.370	6534.909	3054.720	2663.204
0.397	0.358	6048.875	7.735	6067.500	15.249	10.909	6643.864	3163.540	2840.323
0.401	0.358	6093.500	7.739	6103.750	12.452	10.867	6647.003	3166.676	3048.643
0.397	0.354	6135.875	7.759	6149.125	11.834	11.874	6571.934	3091.699	3094.637
0.398	0.353	6172.875	7.788	6210.750	10.878	12.143	6551.835	3071.625	3165.827
0.414	0.366	6215.875	7.726	6215.375	12.686	8.867	6796.145	3315.634	3031.155
0.402	0.361	6256.500	7.748	6285.000	12.364	10.127	6702.149	3221.754	3055.145
0.406	0.365	6296.625	7.734	6331.500	11.779	9.186	6772.333	3291.851	3098.749
0.403	0.369	6376.875	7.692	6361.875	17.828	8.320	6836.914	3356.353	2648.207
0.410	0.368	6405.500	7.675	6418.625	13.525	8.486	6824.541	3343.995	2968.724
0.404	0.363	6430.375	7.703	6459.750	14.536	9.811	6725.734	3245.309	2893.389
0.399	0.365	6481.750	7.672	6504.000	22.711	9.291	6764.546	3284.074	2284.470
0.402	0.363	6509.566	7.677	6507.691	21.111	9.613	6740.509	3260.067	2403.665
0.397	0.359	6572.753	7.720	6570.503	20.350	10.695	6659.827	3179.484	2460.357
0.402	0.364	6593.250	7.692	6618.625	17.376	9.501	6748.838	3268.385	2681.867
0.400	0.362	6637.375	7.737	6641.625	14.601	9.918	6717.777	3237.363	2888.548
0.393	0.351	6680.500	7.751	6708.500	12.661	12.661	6513.191	3033.029	3033.076
0.403	0.360	6719.125	7.689	6724.375	15.601	10.367	6684.274	3203.901	2814.058
0.399	0.369	6761.500	7.702	6764.000	22.425	8.298	6838.572	3358.009	2305.789
0.427	0.390	6828.625	7.674	6820.750	9.470	3.027	7231.638	3810.400	3270.705
0.395	0.347	6843.875	7.746	6856.125	16.911	13.669	6438.026	2957.957	2716.526
0.408	0.370	6890.875	7.728	6923.875	9.254	7.949	6864.638	3384.043	3286.820
0.400	0.358	6926.250	7.715	6955.500	19.741	10.843	6648.780	3168.450	2505.720
0.400	0.360	7007.500	7.712	6999.875	16.776	10.407	6681.329	3200.959	2726.545
0.409	0.316	7020.375	7.691	7035.000	15.508	21.442	5858.379	2379.023	2820.975

7.712	4.258	3625.000	939.063
7.630	4.270	3625.000	1078.892
7.784	4.275	3625.000	929.621
7.768	4.193	3625.000	1046.472
7.654	4.198	3625.000	943.091
7.614	4.243	3625.000	1039.306
7.749	4.199	3625.000	1154.585
7.724	4.167	3625.000	842.782
7.544	4.321	3625.000	1072.120
7.666	4.246	3625.000	1094.213
7.747	4.207	3625.000	805.618
7.671	4.274	3625.000	982.089
7.716	4.281	3625.000	1237.353
7.732	4.246	3625.000	1265.218
7.644	4.178	3625.000	944.192
7.671	4.255	3625.000	815.426
7.692	4.189	3625.000	1054.410
7.606	4.286	3625.000	779.682
7.751	4.200	3625.000	762.929
7.768	4.220	3625.000	1030.732
7.750	4.176	3625.000	869.347
7.740	4.203	3625.000	1103.723
7.741	4.364	3625.000	2963.665
7.781	4.216	3625.000	2673.788
7.783	4.180	3625.000	3295.743
7.784	4.254	3625.000	2973.933
7.726	4.158	3625.000	2909.909
7.717	4.098	3625.000	3018.864
7.637	4.258	3625.000	3022.003
7.749	4.219	3625.000	2946.934
7.673	4.222	3625.000	2926.835
7.709	4.241	3625.000	3171.145
7.744	4.223	3625.000	3077.149
7.765	4.219	3625.000	3147.333
7.722	4.232	3625.000	3211.914
7.742	4.216	3625.000	3199.541
7.731	4.241	3625.000	3100.734
7.715	4.175	3625.000	3139.546
7.692	4.185	3625.000	3115.509
7.681	4.182	3625.000	3034.827
7.761	4.290	3625.000	3123.838
7.643	4.344	3625.000	3092.777
7.779	4.180	3625.000	2888.191
7.734	4.287	3625.000	3059.274
7.754	4.178	3625.000	3213.572
7.708	4.357	3625.000	3606.638
7.659	4.192	3625.000	2813.026
7.720	4.257	3625.000	3239.638
7.720	4.232	3625.000	3023.780
7.712	4.303	3625.000	3056.329
7.729	4.155	3625.000	2233.379

HR Vertilog

Magnetic Flux Leakage Inspection

Advanced Analysis

Company	Southern California Gas Company
Well	Fernando Fee 35B
Field	Aliso Canyon
County	Los Angeles
State	California

Location:
146' S & 659' E
From Station 84 3

Section 34	Township 3N	Range 16W	

Date	Jul. 14, 2016
Service Order	US108271
Recorded by	B. Deal
Witnessed by	T. McMahon
API Serial No.	04-037-21458

Permanent Datum:	G.L.	Elevation:	1674.000 ft.	Depth	7331.000
Log Measured From:	K.B.	15.000	ft. above Perm. Datum	Btm. Log Interval	7049.900
Drilling Measured From:	K.B.	15.000	ft. above Perm. Datum	Top Log Interval	14.610
				Fluid Type	KCL

Casing Data

Size	Weight	Grade	From	To	Length
8 5/8 inch	36.0 lb/ft	K-55	Surface	5835	5835.0
8 5/8 inch	36.0 lb/ft	N-80	5835	7229	1394.0
13 3/8 inch	54.5 lb/ft	K-55	Surface	830	830.0
5 inch liner	18.0 lb/ft	N-80	7100	7331	231.0

Software Version 6.0.0.0

Equipment Data

Run	Trip	Tool Type	Tool Series	Serial Number	Position
1	1	HRVRT MFL	4997	PA10409830	LOWER
1	1	HRVRT MFL	4997	QA10409822	UPPER
1	1	HRVRT TELEM	4993	EA10360726	

Calibration Data

Calibration File Name	4997-8-001-PA10409822-U.CAL
Date of Calibration	06/16/2016 16:01

Calibration Identifier	A00C9D82-DCC8-4973-8454-0F98E8079F2F
Tool Number	4997-00
Calibrator Number	4997-8-001
Calibrator Size	(8-5/8 In - 219 mm)
Calibration Source File	20160616_141623_MEM.MVL
Calibration Software Rev	Microvision 32-bit 7.3.4.0
Comment	RMA1333

Calibration Data

Calibration File Name	4997-8-001-QA10409830-L.CAL
Date of Calibration	06/16/2016 16:01
Calibration Identifier	A00C9D82-DCC8-4973-8454-0F98E8079F2F
Tool Number	4997-00
Calibrator Number	4997-8-001
Calibrator Size	(8-5/8 In - 219 mm)
Calibration Source File	20160616_141623_MEM.MVL
Calibration Software Rev	Microvision 32-bit 7.3.4.0
Comment	RMA1333

In making interpretations of logs our employees will give customer the benefit of their best judgment. But since all interpretations are opinions based on inferences from electrical or other measurements, we cannot, and we do not guarantee the accuracy or correctness of any interpretation. We shall not be liable or responsible for any loss, cost, damages, or expenses whatsoever incurred or sustained by the customer resulting from any interpretation made by any of our employees.

Interpretation

HRVRT analysis was depth correlated Welex Micro-Seismogram logged 14 Sep 1974.

The top joint (JT-1), joint 98 (JT-98) and joint 140 (JT-140) are shorter joints.

15.54 ft	Hardware -External Casing Head Response.
829.00 ft	Hardware - Bottom of 13 3/8" External Casing.
3815.45 ft	Hardware - Multiple Centralizers can be seen throughout the logged interval, see the Feature List for a complete centralizer listing.
3984.60 ft	Hardware - Centralizer - not over collar.
3987.46 ft	Hardware - Stage Collar.

Interpretation was zoned for variable casing weights and grades.

5837.43 ft	Collar - 8 5/8" Casing Grade change; K-55 36 lb/ft above and N-80 36 lb/ft below.

Joint Interpretation Summary

Joint	From	To	Length	Class	Max Depth	Position	Type	ID/OD
1	14.61	25.12	10.51	Class 1	-	-	-	-
2	25.12	67.28	42.16	Class 1	-	-	-	-
3	67.28	110.17	42.89	Class 1	-	-	-	-
4	110.17	151.93	41.76	Class 1	-	-	-	-

5	151.93	193.57	41.64	Class	1	-	-	-	-
6	193.57	234.71	41.14	Class	1	-	-	-	-
7	234.71	276.80	42.09	Class	1	-	-	-	-
8	276.80	315.29	38.49	Class	1	-	-	-	-
9	315.29	355.91	40.62	Class	1	-	-	-	-
10	355.91	395.64	39.73	Class	1	-	-	-	-
11	395.64	438.85	43.21	Class	1	-	-	-	-
12	438.85	479.85	41.00	Class	1	-	-	-	-
13	479.85	521.86	42.01	Class	1	-	-	-	-
14	521.86	560.94	39.08	Class	1	-	-	-	-
15	560.94	602.52	41.58	Class	1	-	-	-	-
16	602.52	645.30	42.78	Class	1	-	-	-	-
17	645.30	688.07	42.77	Class	1	-	-	-	-
18	688.07	728.53	40.46	Class	1	-	-	-	-
19	728.53	772.22	43.69	Class	1	-	-	-	-
20	772.22	815.55	43.33	Class	1	-	-	-	-
21	815.55	857.39	41.84	Class	1	-	-	-	-
22	857.39	899.51	42.12	Class	1	-	-	-	-
23	899.51	940.76	41.25	Class	1	-	-	-	-
24	940.76	982.16	41.40	Class	1	-	-	-	-
25	982.16	1023.29	41.13	Class	1	-	-	-	-
26	1023.29	1063.82	40.53	Class	1	-	-	-	-
27	1063.82	1103.66	39.84	Class	1	-	-	-	-
28	1103.66	1145.25	41.59	Class	1	-	-	-	-
29	1145.25	1187.29	42.04	Class	1	-	-	-	-
30	1187.29	1230.74	43.45	Class	1	-	-	-	-
31	1230.74	1272.31	41.57	Class	1	-	-	-	-
32	1272.31	1314.21	41.90	Class	1	-	-	-	-
33	1314.21	1355.91	41.70	Class	1	-	-	-	-
34	1355.91	1395.67	39.76	Class	1	-	-	-	-
35	1395.67	1437.23	41.56	Class	1	-	-	-	-
36	1437.23	1478.61	41.38	Class	1	-	-	-	-
37	1478.61	1521.61	43.00	Class	1	-	-	-	-
38	1521.61	1562.81	41.20	Class	1	-	-	-	-
39	1562.81	1604.69	41.88	Class	1	-	-	-	-
40	1604.69	1643.71	39.02	Class	1	-	-	-	-
41	1643.71	1686.42	42.71	Class	1	-	-	-	-
42	1686.42	1727.46	41.04	Class	1	-	-	-	-
43	1727.46	1768.46	41.00	Class	1	-	-	-	-
44	1768.46	1810.38	41.92	Class	1	-	-	-	-
45	1810.38	1852.05	41.67	Class	1	-	-	-	-
46	1852.05	1895.18	43.13	Class	1	-	-	-	-
47	1895.18	1937.08	41.90	Class	1	-	-	-	-
48	1937.08	1978.19	41.11	Class	1	-	-	-	-
49	1978.19	2019.05	40.86	Class	1	-	-	-	-
50	2019.05	2060.44	41.39	Class	1	-	-	-	-
51	2060.44	2103.07	42.63	Class	1	-	-	-	-
52	2103.07	2144.14	41.07	Class	1	-	-	-	-
53	2144.14	2185.84	41.70	Class	1	17.0%	2158.84	ISO	OD
54	2185.84	2227.23	41.39	Class	1	19.0%	2197.13	ISO	OD
55	2227.23	2269.24	42.01	Class	2	21.0%	2242.62	ISO	OD
56	2269.24	2310.32	41.08	Class	1	-	-	-	-
57	2310.32	2353.87	43.55	Class	1	15.0%	2318.22	ISO	OD
58	2353.87	2394.92	41.05	Class	1	-	-	-	-
59	2394.92	2435.92	41.00	Class	1	-	-	-	-
60	2435.92	2477.11	41.19	Class	1	-	-	-	-
61	2477.11	2518.93	41.82	Class	1	-	-	-	-
62	2518.93	2561.61	42.68	Class	1	-	-	-	-
63	2561.61	2603.89	42.28	Class	1	-	-	-	-
64	2603.89	2646.18	42.29	Class	1	15.0%	2635.20	ISO	OD
65	2646.18	2687.38	41.20	Class	1	-	-	-	-
66	2687.38	2729.58	42.20	Class	1	-	-	-	-
67	2729.58	2772.88	43.30	Class	1	-	-	-	-
68	2772.88	2815.07	42.19	Class	1				

68	2772.88	2815.07	42.19	Class 1	-	-	-	-
69	2815.07	2856.73	41.66	Class 1	-	-	-	-
70	2856.73	2898.44	41.71	Class 1	-	-	-	-
71	2898.44	2940.32	41.88	Class 1	-	-	-	-
72	2940.32	2982.83	42.51	Class 1	-	-	-	-
73	2982.83	3025.48	42.65	Class 1	-	-	-	-
74	3025.48	3067.05	41.57	Class 1	-	-	-	-
75	3067.05	3109.08	42.03	Class 1	-	-	-	-
76	3109.08	3148.06	38.98	Class 1	-	-	-	-
77	3148.06	3190.40	42.34	Class 1	-	-	-	-
78	3190.40	3232.71	42.31	Class 1	-	-	-	-
79	3232.71	3274.56	41.85	Class 1	-	-	-	-
80	3274.56	3315.65	41.09	Class 1	-	-	-	-
81	3315.65	3357.77	42.12	Class 1	-	-	-	-
82	3357.77	3400.67	42.90	Class 1	-	-	-	-
83	3400.67	3441.93	41.26	Class 1	-	-	-	-
84	3441.93	3484.33	42.40	Class 1	-	-	-	-
85	3484.33	3525.30	40.97	Class 1	-	-	-	-
86	3525.30	3567.46	42.16	Class 1	-	-	-	-
87	3567.46	3608.34	40.88	Class 1	-	-	-	-
88	3608.34	3651.02	42.68	Class 1	-	-	-	-
89	3651.02	3688.89	37.87	Class 1	-	-	-	-
90	3688.89	3731.09	42.20	Class 1	-	-	-	-
91	3731.09	3773.37	42.28	Class 1	-	-	-	-
92	3773.37	3815.47	42.10	Class 1	-	-	-	-
93	3815.47	3859.01	43.54	Class 1	-	-	-	-
94	3859.01	3901.84	42.83	Class 1	-	-	-	-
95	3901.84	3944.10	42.26	Class 1	-	-	-	-
96	3944.10	3988.27	44.17	Class 1	15.0%	3979.22	ISO	OD
97	3988.27	4031.12	42.85	Class 1	-	-	-	-
98	4031.12	4058.52	27.40	Class 1	-	-	-	-
99	4058.52	4100.02	41.50	Class 1	-	-	-	-
100	4100.02	4143.26	43.24	Class 1	-	-	-	-
101	4143.26	4185.14	41.88	Class 1	-	-	-	-
102	4185.14	4227.73	42.59	Class 1	-	-	-	-
103	4227.73	4269.40	41.67	Class 1	-	-	-	-
104	4269.40	4309.08	39.68	Class 1	-	-	-	-
105	4309.08	4351.98	42.90	Class 1	-	-	-	-
106	4351.98	4394.38	42.40	Class 1	-	-	-	-
107	4394.38	4435.99	41.61	Class 1	-	-	-	-
108	4435.99	4478.39	42.40	Class 1	-	-	-	-
109	4478.39	4520.91	42.52	Class 1	-	-	-	-
110	4520.91	4559.26	38.35	Class 1	-	-	-	-
111	4559.26	4600.54	41.28	Class 1	-	-	-	-
112	4600.54	4642.04	41.50	Class 1	-	-	-	-
113	4642.04	4683.11	41.07	Class 1	-	-	-	-
114	4683.11	4725.33	42.22	Class 1	-	-	-	-
115	4725.33	4765.11	39.78	Class 1	-	-	-	-
116	4765.11	4807.61	42.50	Class 1	-	-	-	-
117	4807.61	4847.01	39.40	Class 1	-	-	-	-
118	4847.01	4888.72	41.71	Class 1	-	-	-	-
119	4888.72	4930.53	41.81	Class 1	-	-	-	-
120	4930.53	4972.76	42.23	Class 1	-	-	-	-
121	4972.76	5015.40	42.64	Class 1	-	-	-	-
122	5015.40	5057.06	41.66	Class 1	-	-	-	-
123	5057.06	5098.89	41.83	Class 1	-	-	-	-
124	5098.89	5141.31	42.42	Class 1	-	-	-	-
125	5141.31	5183.34	42.03	Class 1	-	-	-	-
126	5183.34	5225.15	41.81	Class 1	-	-	-	-
127	5225.15	5267.72	42.57	Class 1	-	-	-	-
128	5267.72	5304.53	36.81	Class 1	-	-	-	-
129	5304.53	5346.26	41.73	Class 1	-	-	-	-
130	5346.26	5387.93	41.67	Class 1	-	-	-	-
131	5387.93	5430.38	42.45	Class 1	-	-	-	-

132	5430.38	5472.58	42.20	Class	1	-	-	-	-
133	5472.58	5512.88	40.30	Class	1	-	-	-	-
134	5512.88	5555.31	42.43	Class	1	-	-	-	-
135	5555.31	5598.00	42.69	Class	1	-	-	-	-
136	5598.00	5640.52	42.52	Class	1	-	-	-	-
137	5640.52	5682.91	42.39	Class	1	-	-	-	-
138	5682.91	5724.06	41.15	Class	1	-	-	-	-
139	5724.06	5765.91	41.85	Class	1	-	-	-	-
140	5765.91	5795.27	29.36	Class	1	-	-	-	-
141	5795.27	5837.43	42.16	Class	1	-	-	-	-
142	5837.43	5880.12	42.69	Class	1	-	-	-	-
143	5880.12	5921.23	41.11	Class	1	-	-	-	-
144	5921.23	5963.62	42.39	Class	1	-	-	-	-
145	5963.62	6005.59	41.97	Class	1	-	-	-	-
146	6005.59	6047.57	41.98	Class	1	-	-	-	-
147	6047.57	6090.23	42.66	Class	1	-	-	-	-
148	6090.23	6132.68	42.45	Class	1	-	-	-	-
149	6132.68	6175.52	42.84	Class	1	-	-	-	-
150	6175.52	6216.65	41.13	Class	1	-	-	-	-
151	6216.65	6258.56	41.91	Class	1	-	-	-	-
152	6258.56	6299.19	40.63	Class	1	-	-	-	-
153	6299.19	6341.27	42.08	Class	1	-	-	-	-
154	6341.27	6384.11	42.84	Class	1	-	-	-	-
155	6384.11	6426.29	42.18	Class	1	-	-	-	-
156	6426.29	6467.76	41.47	Class	1	-	-	-	-
157	6467.76	6510.25	42.49	Class	1	-	-	-	-
158	6510.25	6552.00	41.75	Class	1	-	-	-	-
159	6552.00	6594.93	42.93	Class	1	-	-	-	-
160	6594.93	6637.29	42.36	Class	1	-	-	-	-
161	6637.29	6679.41	42.12	Class	1	-	-	-	-
162	6679.41	6720.36	40.95	Class	1	-	-	-	-
163	6720.36	6762.91	42.55	Class	1	-	-	-	-
164	6762.91	6805.15	42.24	Class	1	-	-	-	-
165	6805.15	6844.56	39.41	Class	1	-	-	-	-
166	6844.56	6887.15	42.59	Class	1	17.0%	6867.55	ISO	ID
167	6887.15	6929.61	42.46	Class	2	26.0%	6907.94	ISO	ID
168	6929.61	6972.45	42.84	Class	1	18.0%	6969.86	ISO	ID
169	6972.45	7015.17	42.72	Class	1	-	-	-	-
170	7015.17	7049.90	34.73	Class	1	18.0%	7025.67	ISO	ID

Southern California Gas Company Fernando Fee 35B

File 20160714_081635_RSP_0_0_0_0_0.mvl

Main Log
5" / 100'

Class 1	Class 2	Class 3	Class 4
0 - 20%	20 - 40%	40 - 60%	60 - 100%

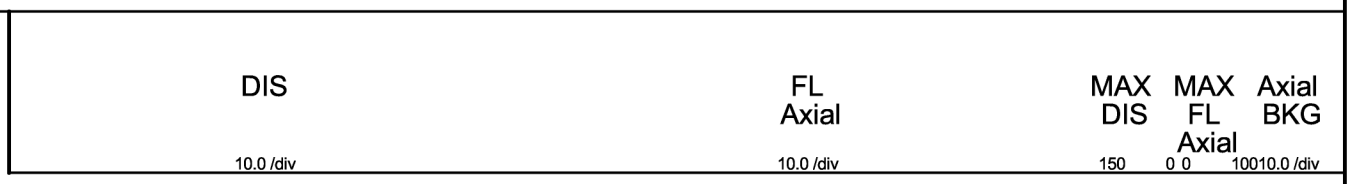

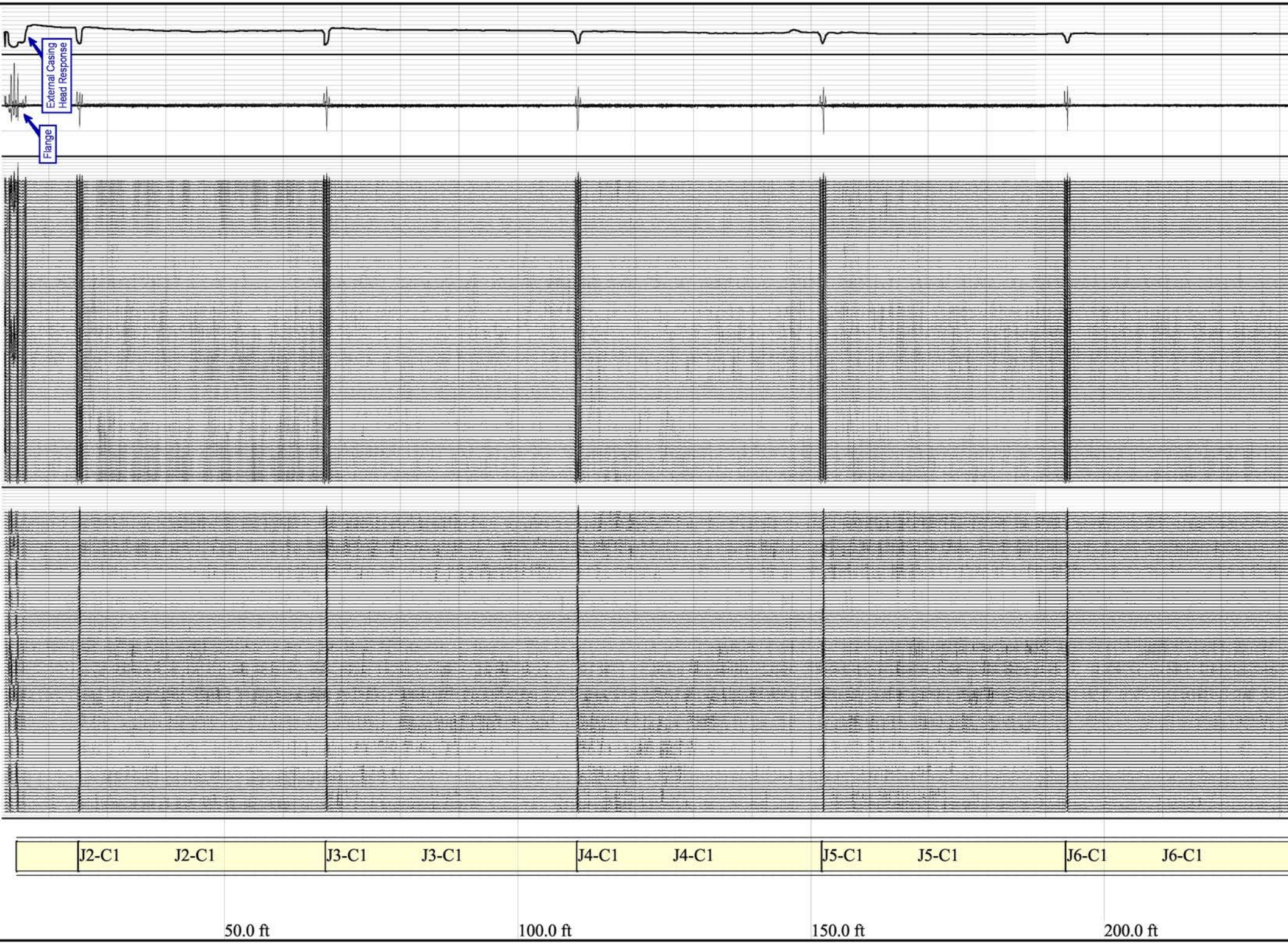
External Casing Head Response
Flange
J2-C1
J2-C1
J3-C1
J3-C1
J4-C1
J4-C1
J5-C1
J5-C1
J6-C1
J6-C1
50.0 ft
100.0 ft
150.0 ft
200.0 ft

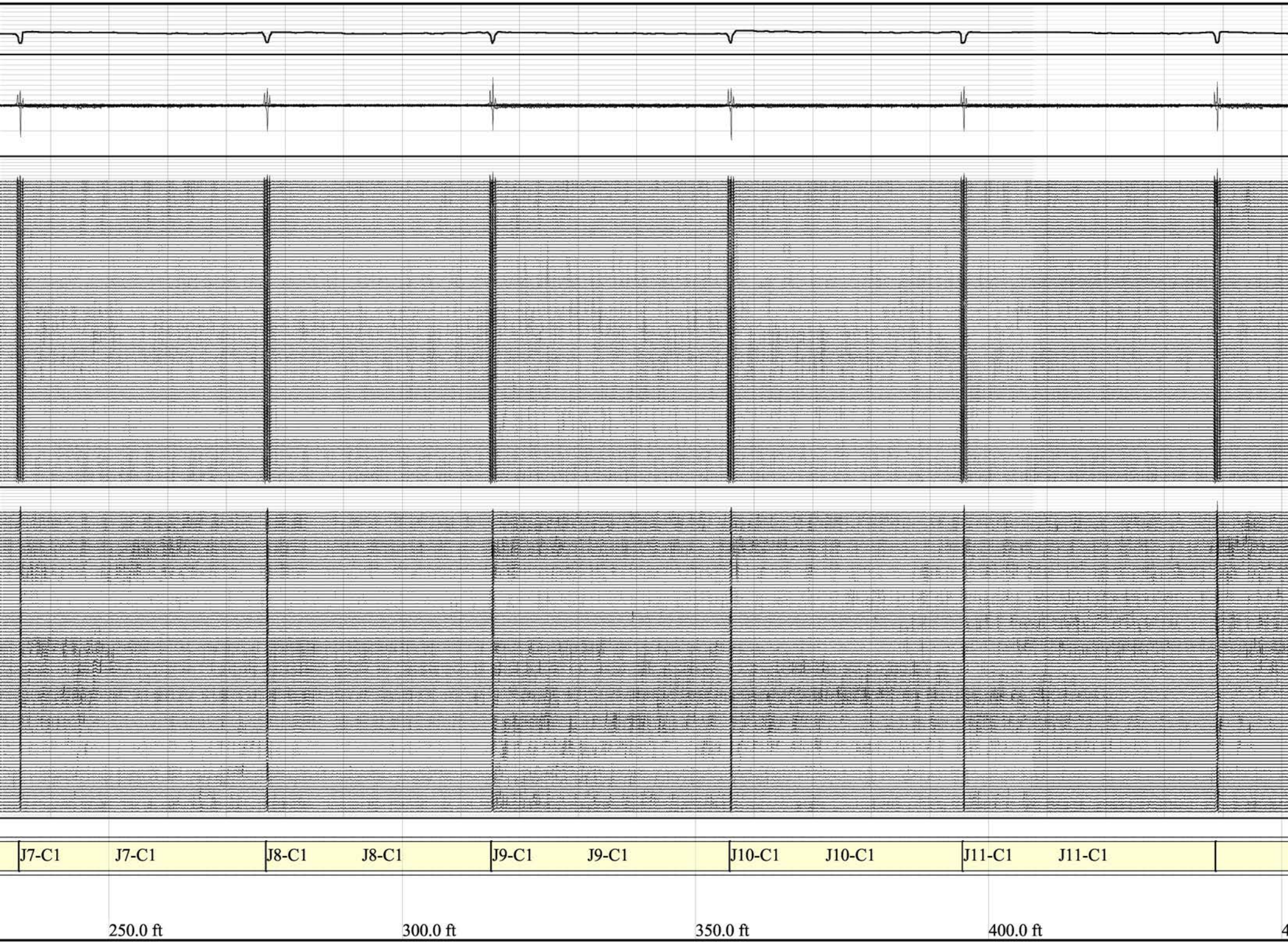
J7-C1
J7-C1
J8-C1
J8-C1
J9-C1
J9-C1
J10-C1
J10-C1
J11-C1
J11-C1
250.0 ft
300.0 ft
350.0 ft
400.0 ft

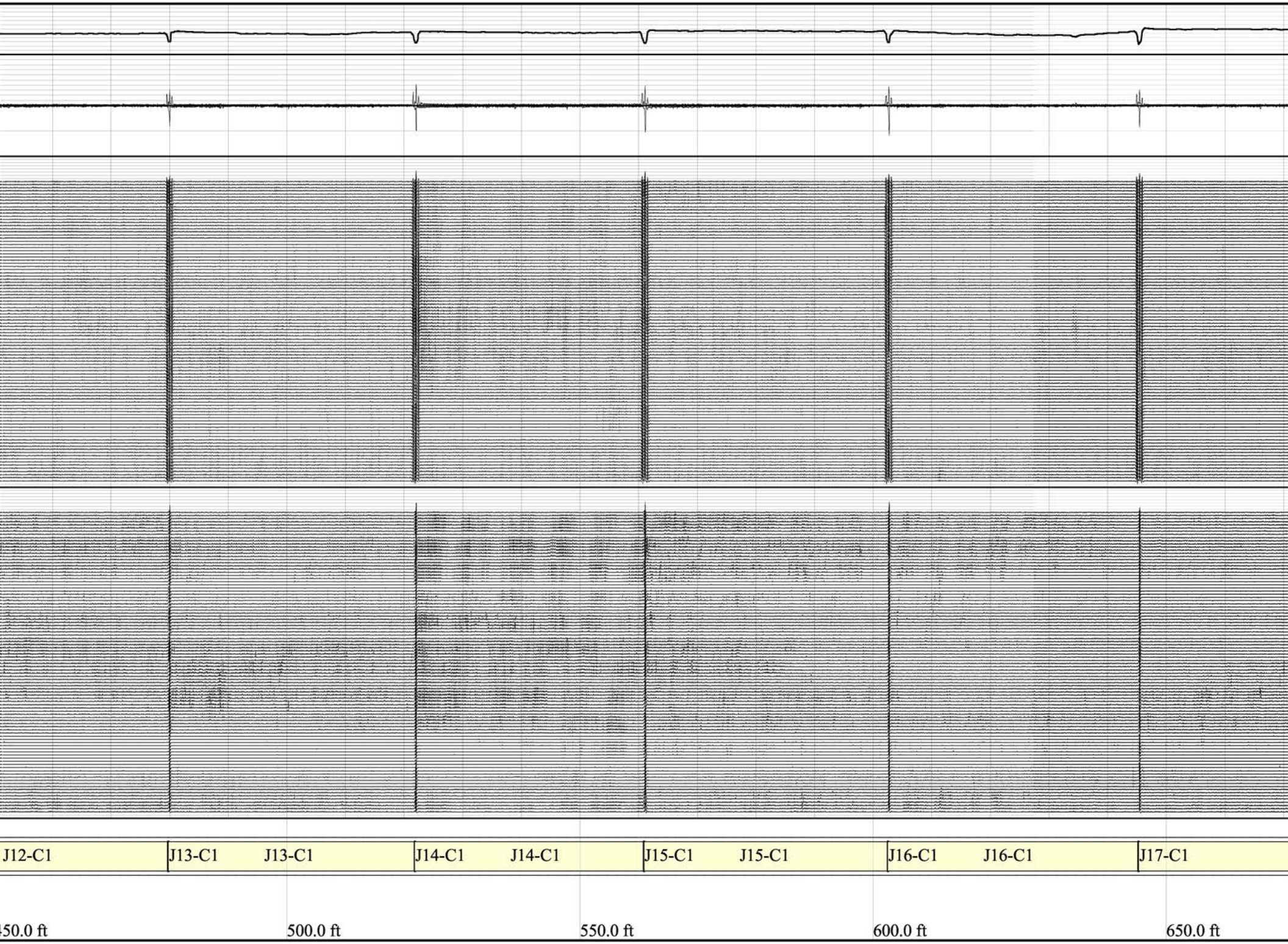
J12-C1
J13-C1
J13-C1
J14-C1
J14-C1
J15-C1
J15-C1
J16-C1
J16-C1
J17-C1
450.0 ft
500.0 ft
550.0 ft
600.0 ft
650.0 ft

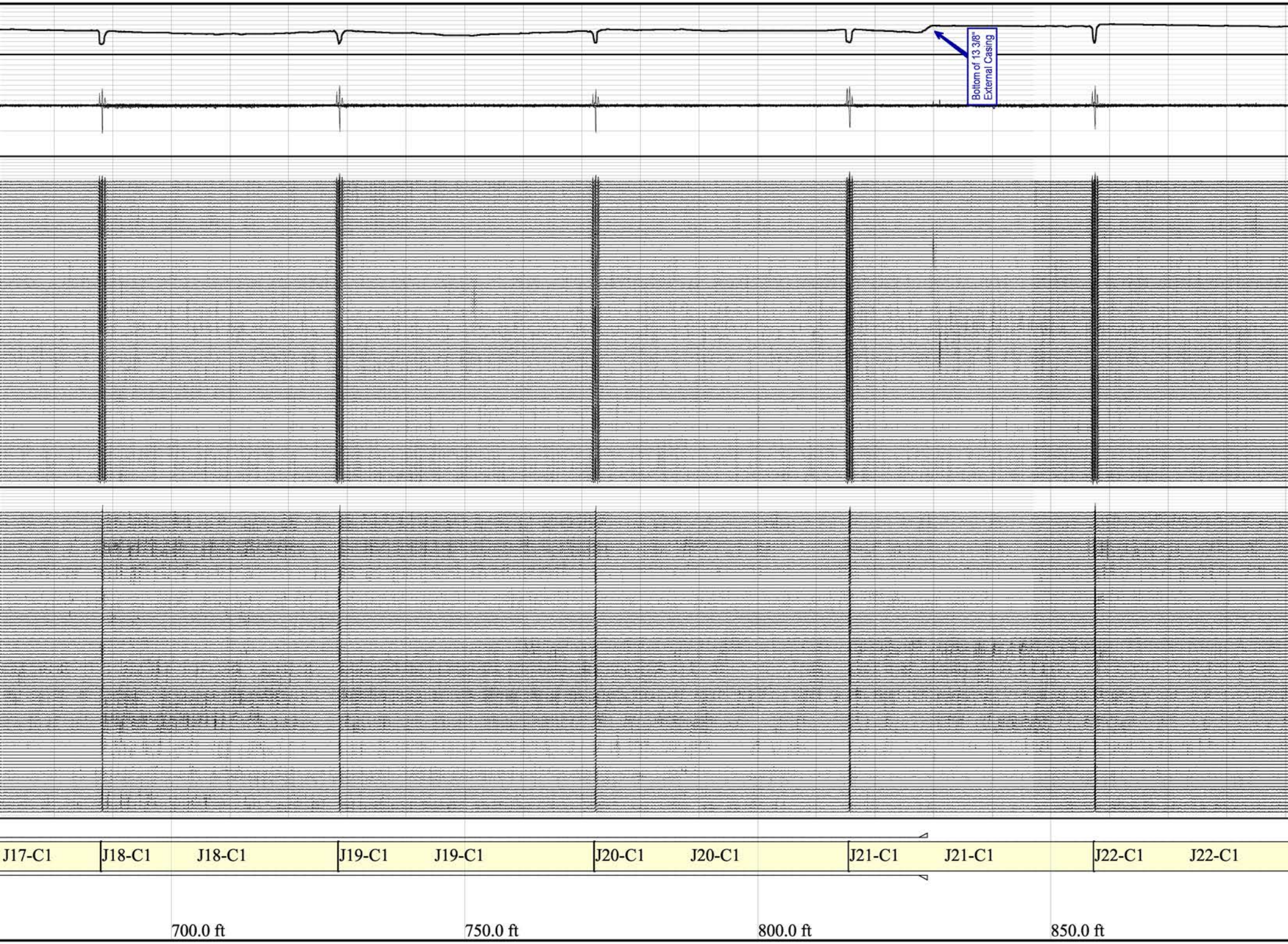
Bottom of 13 3/8" External Casing
J17-C1
J18-C1
J18-C1
J19-C1
J19-C1
J20-C1
J20-C1
J21-C1
J21-C1
J22-C1
J22-C1
700.0 ft
750.0 ft
800.0 ft
850.0 ft

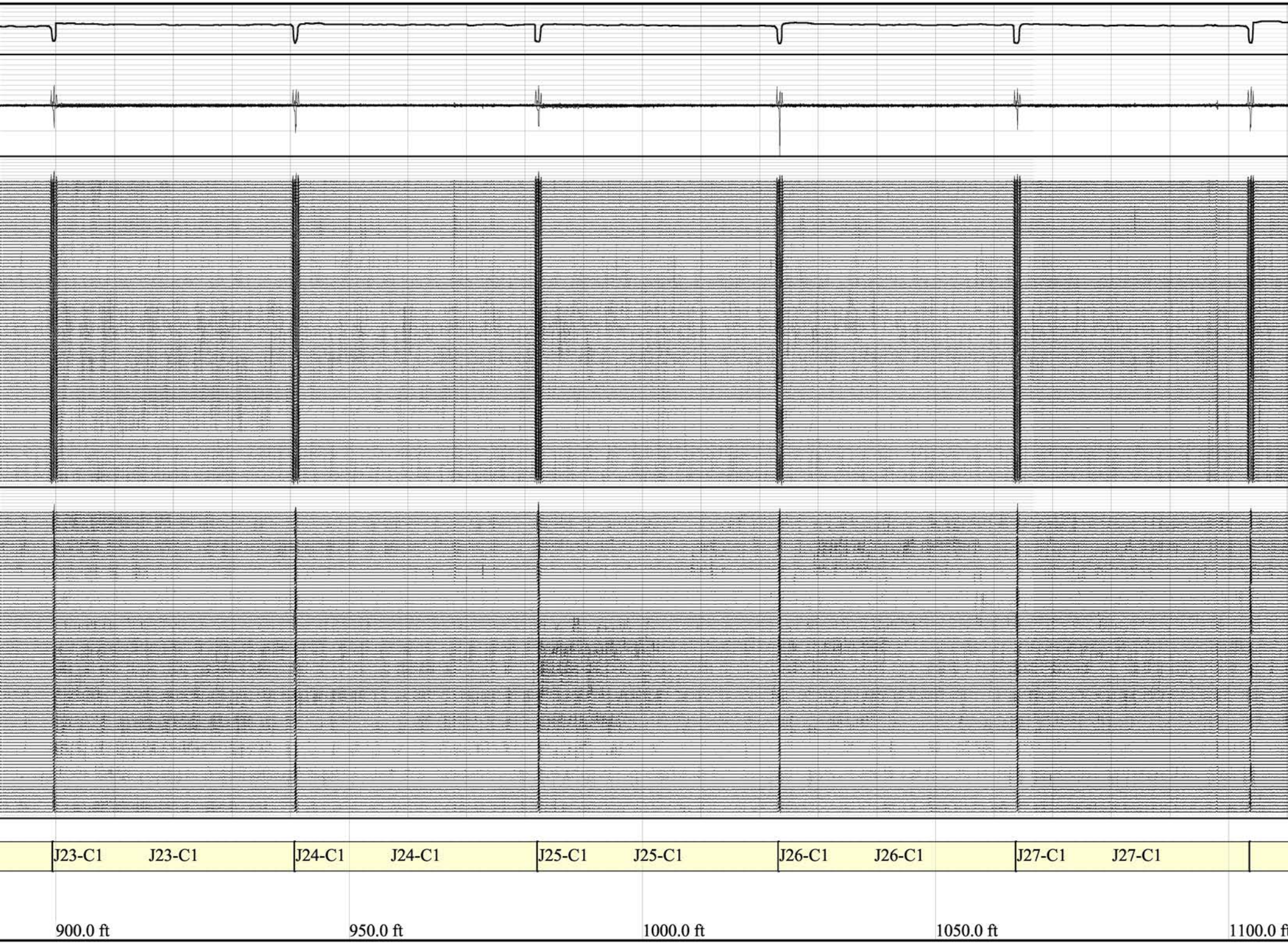
J23-C1
J23-C1
J24-C1
J24-C1
J25-C1
J25-C1
J26-C1
J26-C1
J27-C1
J27-C1
900.0 ft
950.0 ft
1000.0 ft
1050.0 ft
1100.0 f

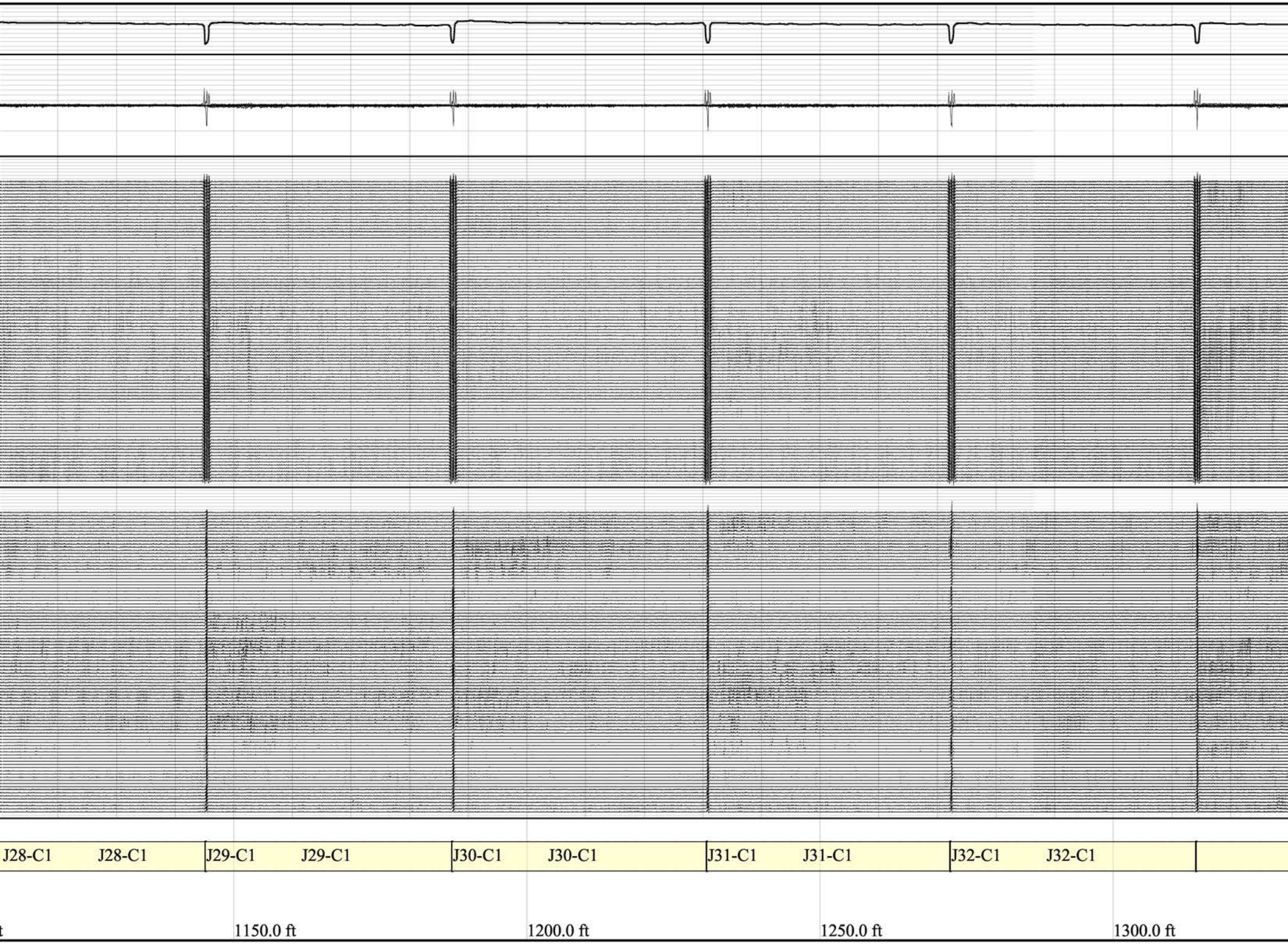
J28-C1
J28-C1
J29-C1
J29-C1
J30-C1
J30-C1
J31-C1
J31-C1
J32-C1
J32-C1
t
1150.0 ft
1200.0 ft
1250.0 ft
1300.0 ft

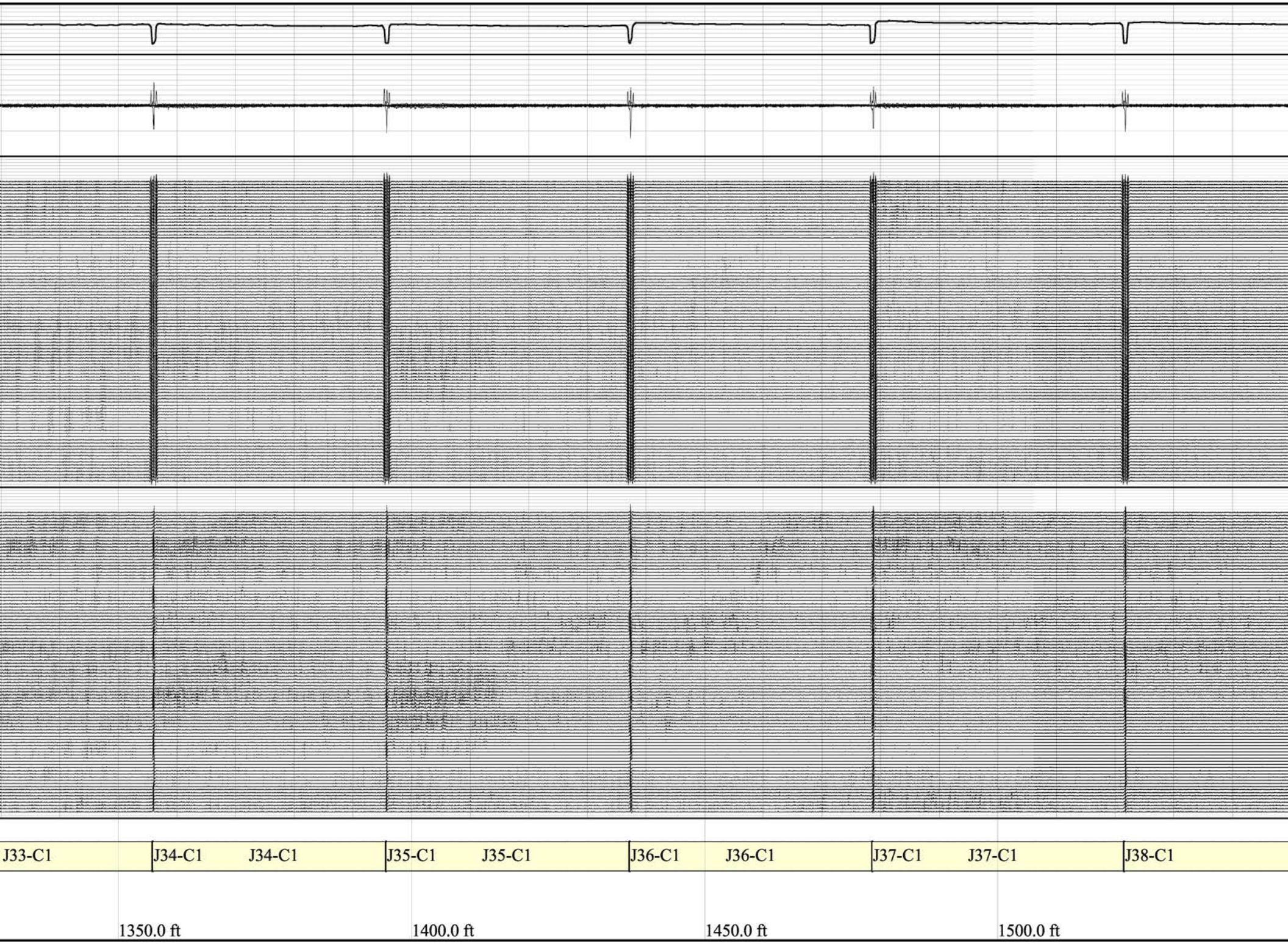
J33-C1
J34-C1
J34-C1
J35-C1
J35-C1
J36-C1
J36-C1
J37-C1
J37-C1
J38-C1
1350.0 ft
1400.0 ft
1450.0 ft
1500.0 ft

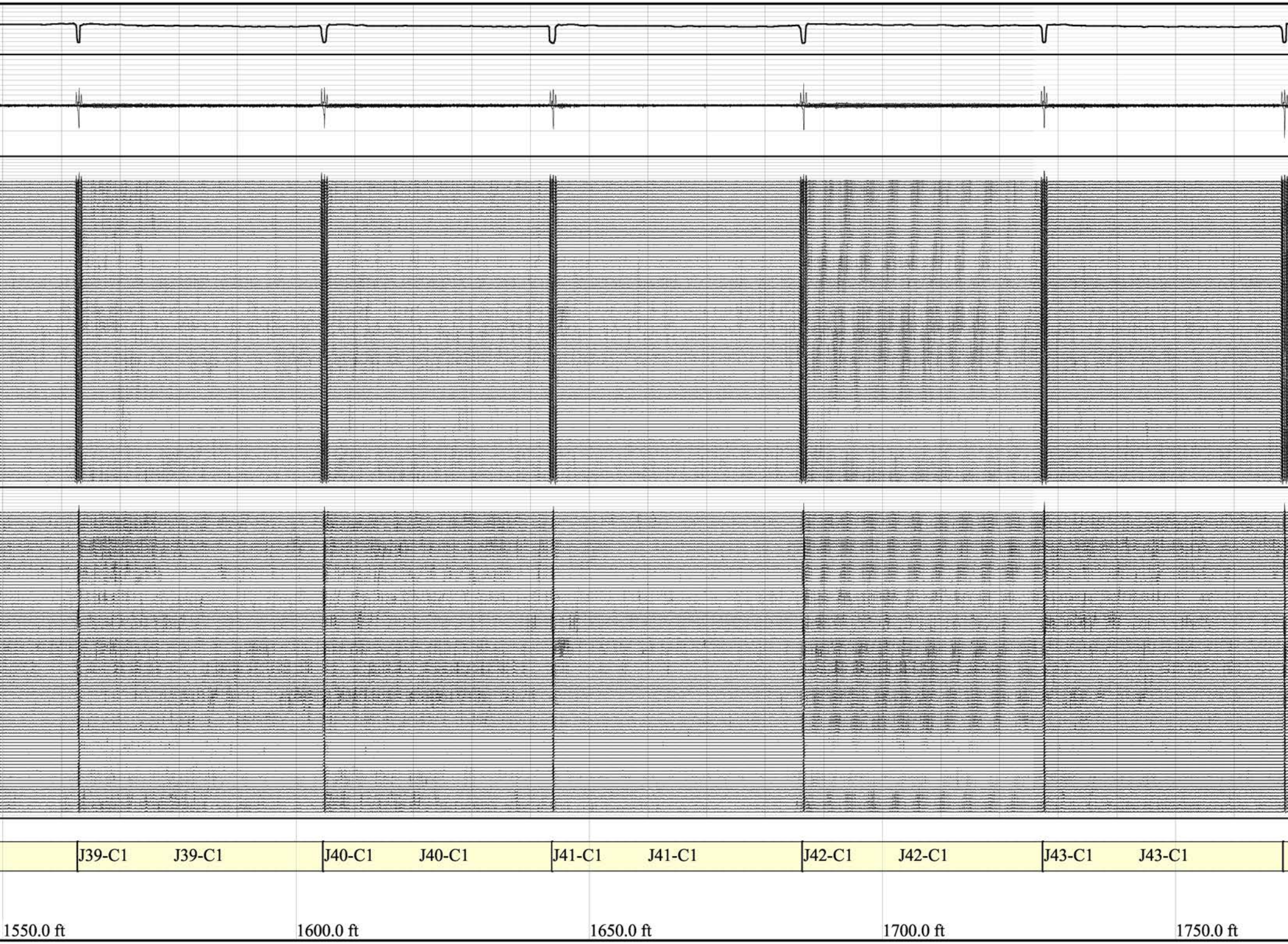
J39-C1
J39-C1
J40-C1
J40-C1
J41-C1
J41-C1
J42-C1
J42-C1
J43-C1
J43-C1
1550.0 ft
1600.0 ft
1650.0 ft
1700.0 ft
1750.0 ft

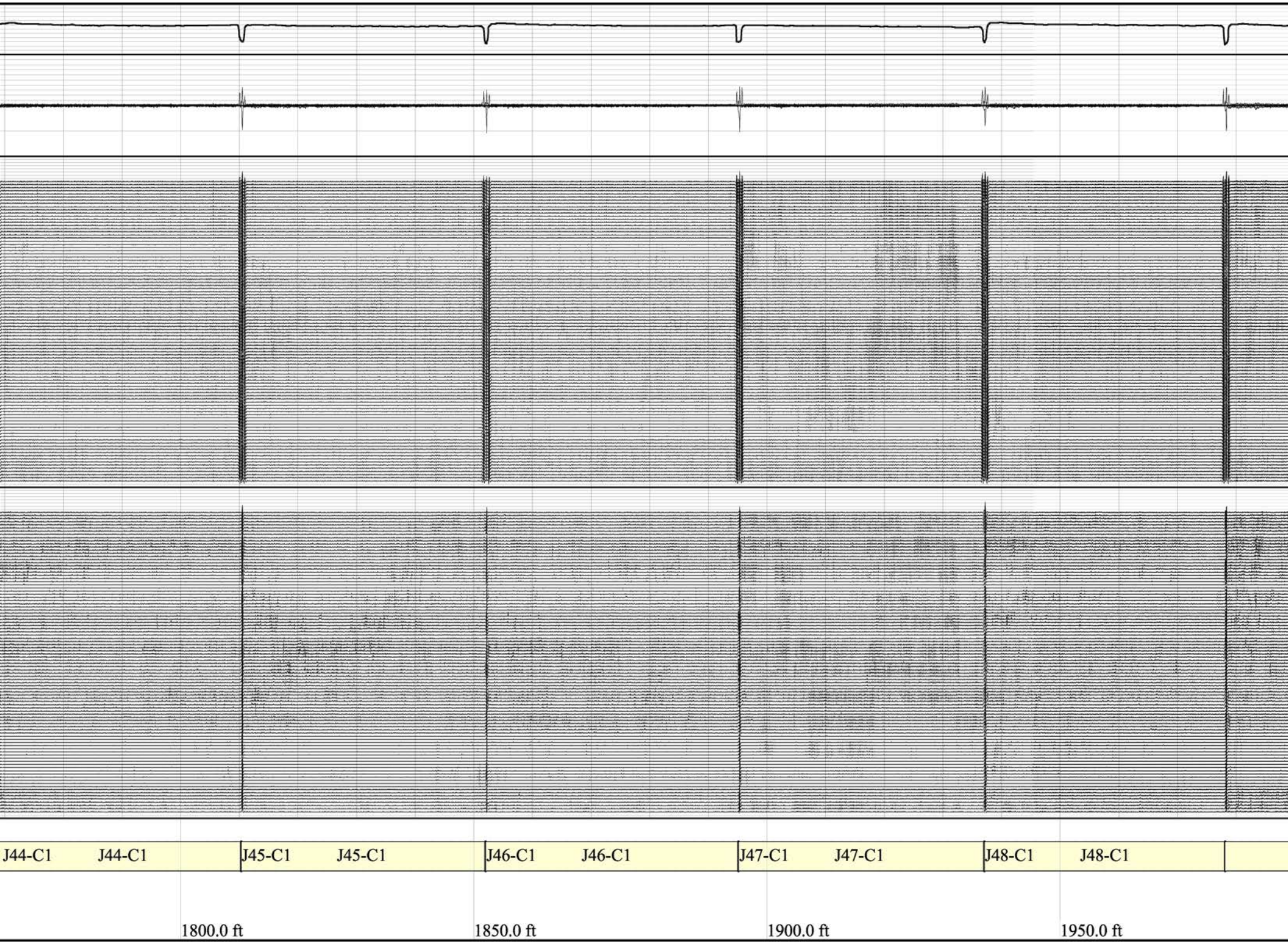
J44-C1
J44-C1
J45-C1
J45-C1
J46-C1
J46-C1
J47-C1
J47-C1
J48-C1
J48-C1
1800.0 ft
1850.0 ft
1900.0 ft
1950.0 ft

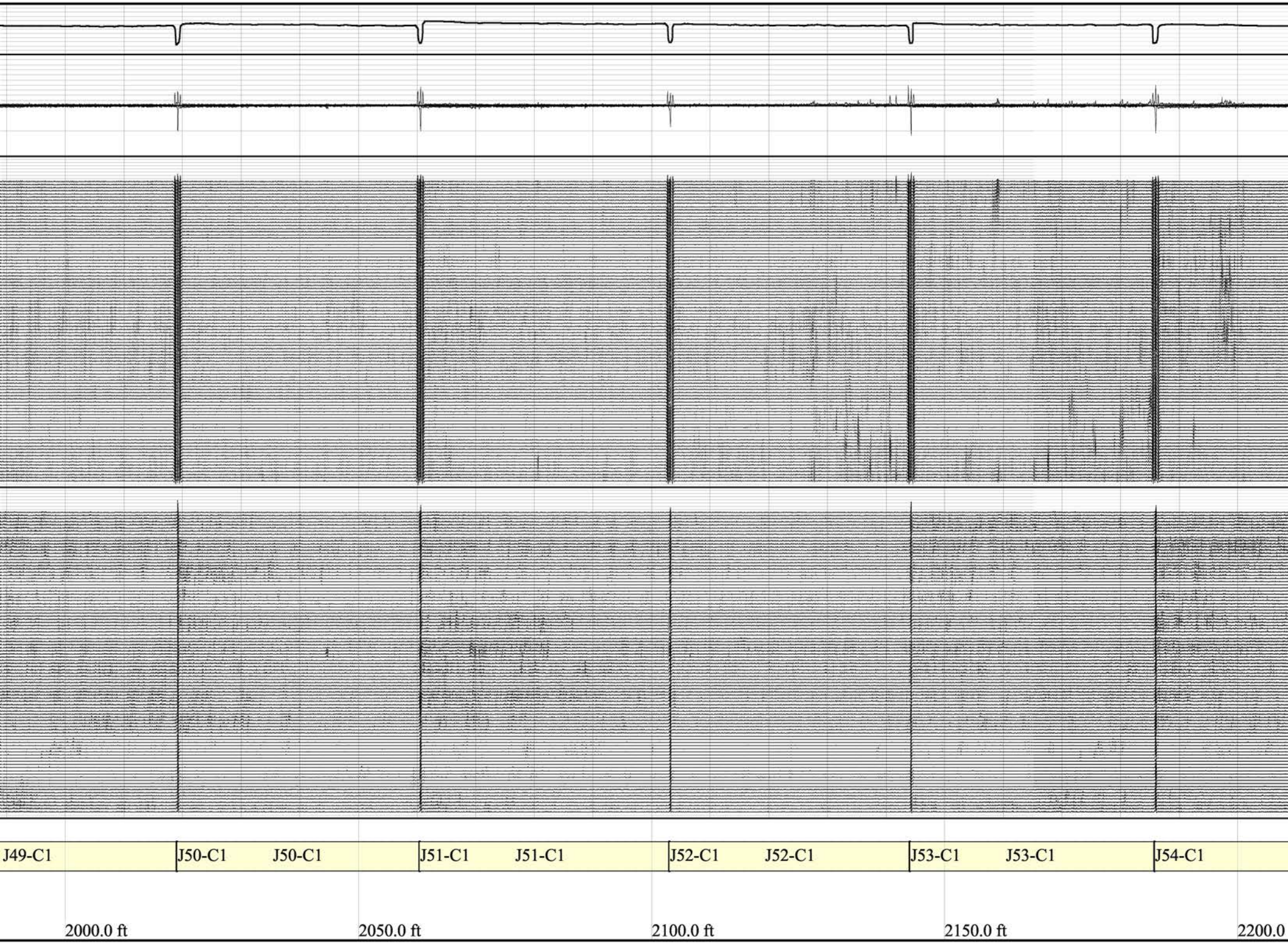
J49-C1
J50-C1
J50-C1
J51-C1
J51-C1
J52-C1
J52-C1
J53-C1
J53-C1
J54-C1
2000.0 ft
2050.0 ft
2100.0 ft
2150.0 ft
2200.0

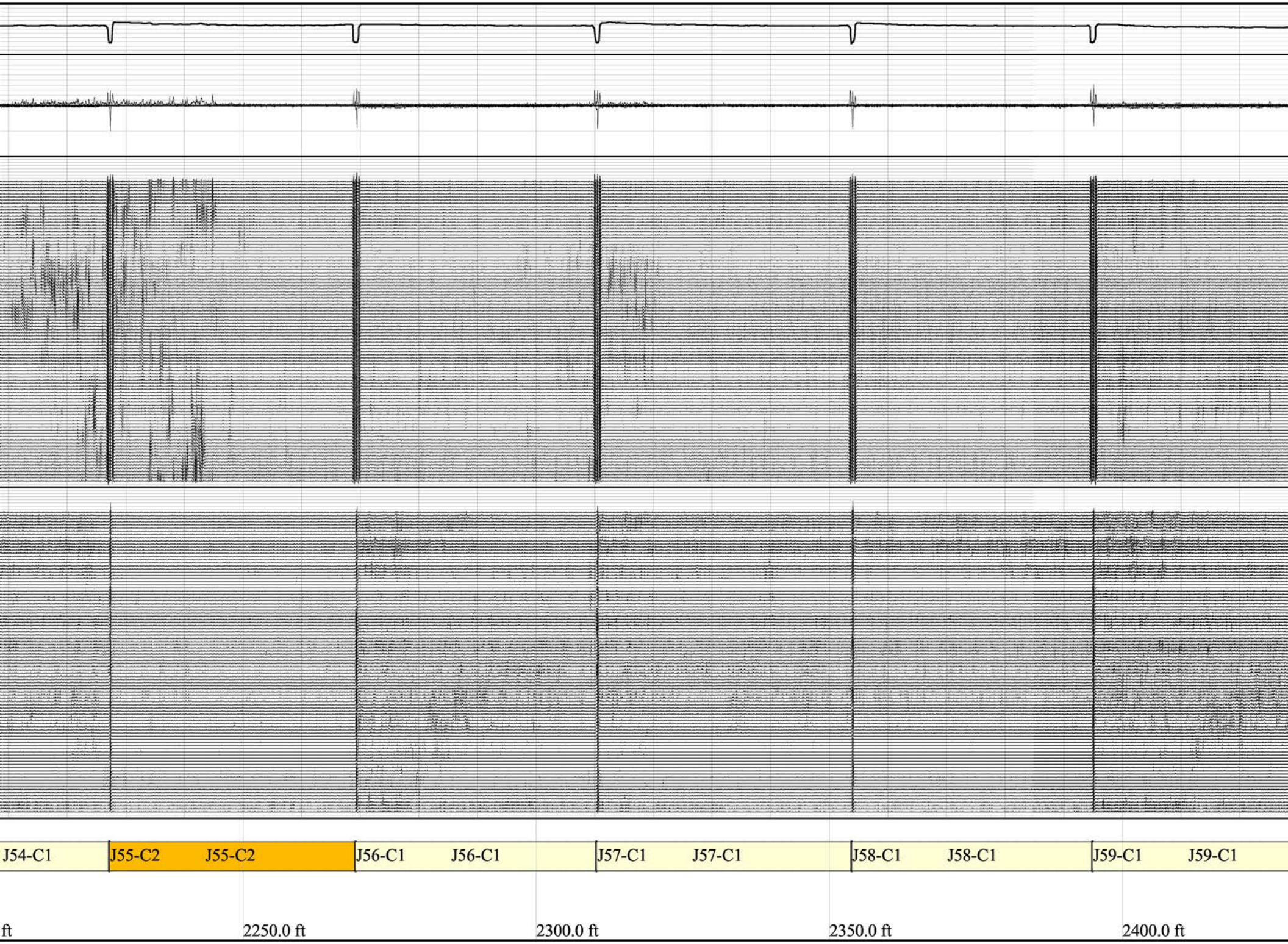
J54-C1
J55-C2
J55-C2
J56-C1
J56-C1
J57-C1
J57-C1
J58-C1
J58-C1
J59-C1
J59-C1
ft
2250.0 ft
2300.0 ft
2350.0 ft
2400.0 ft

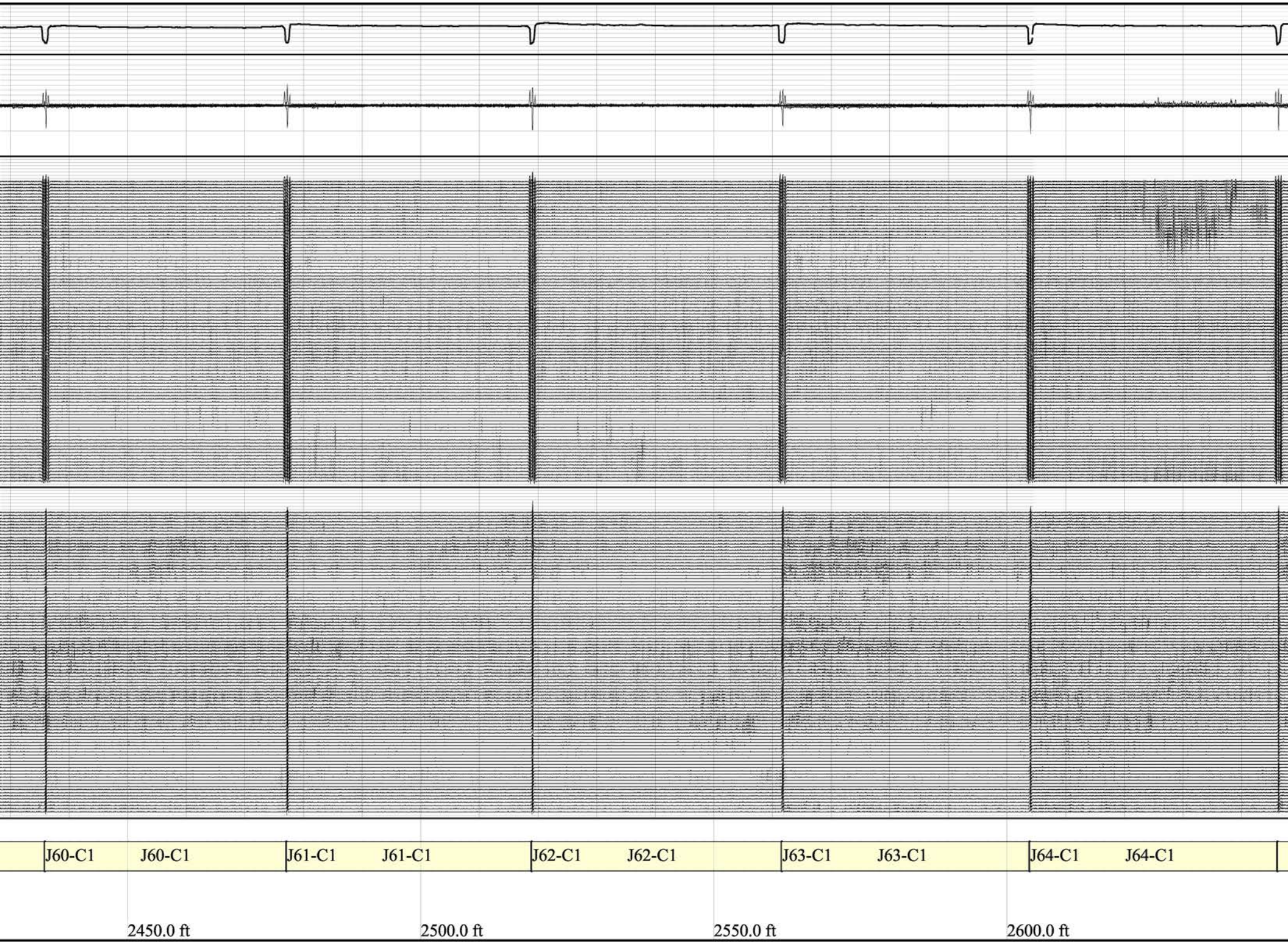
J60-C1
J60-C1
J61-C1
J61-C1
J62-C1
J62-C1
J63-C1
J63-C1
J64-C1
J64-C1
2450.0 ft
2500.0 ft
2550.0 ft
2600.0 ft

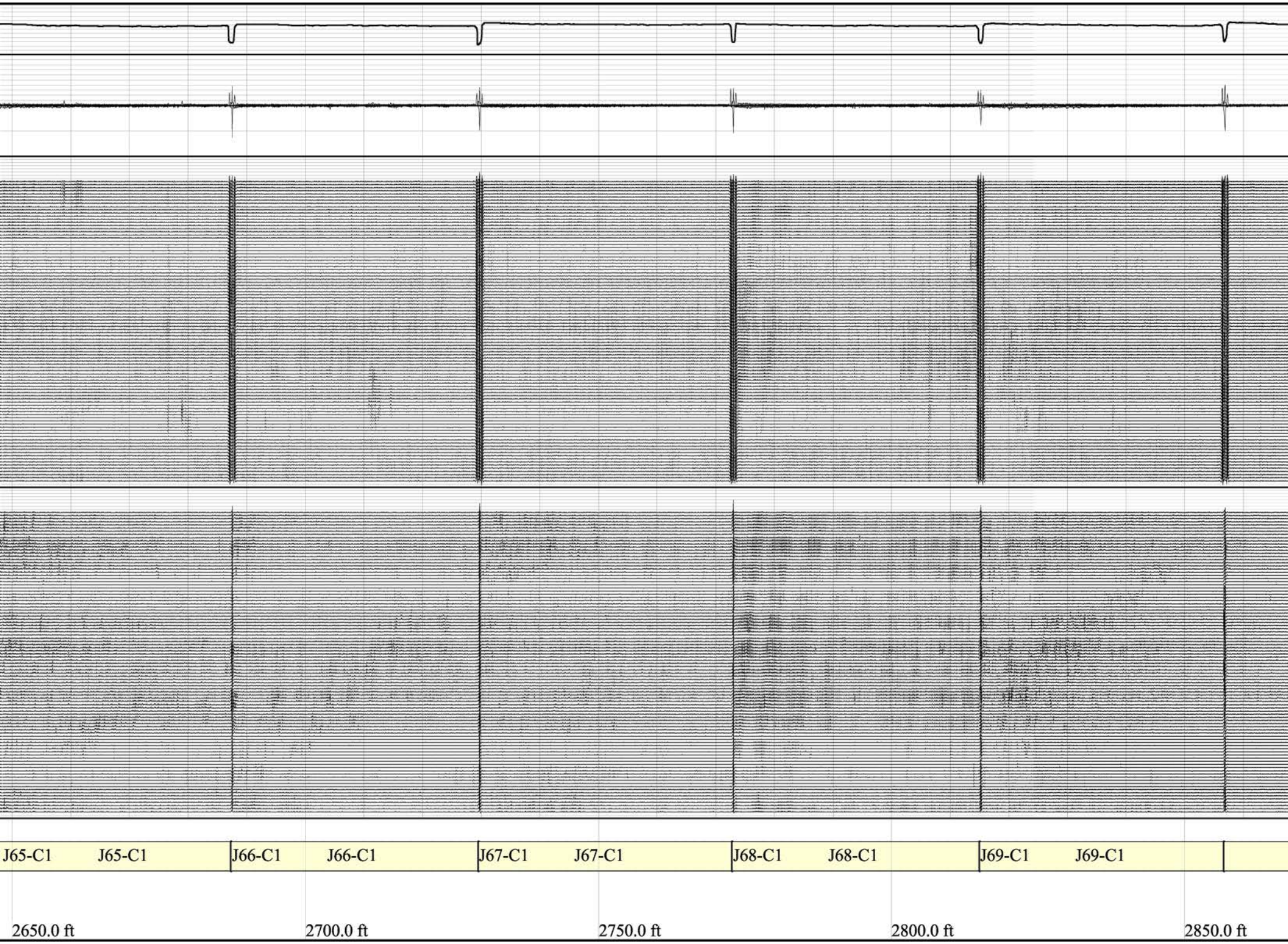
J65-C1
J65-C1
J66-C1
J66-C1
J67-C1
J67-C1
J68-C1
J68-C1
J69-C1
J69-C1
2650.0 ft
2700.0 ft
2750.0 ft
2800.0 ft
2850.0 ft

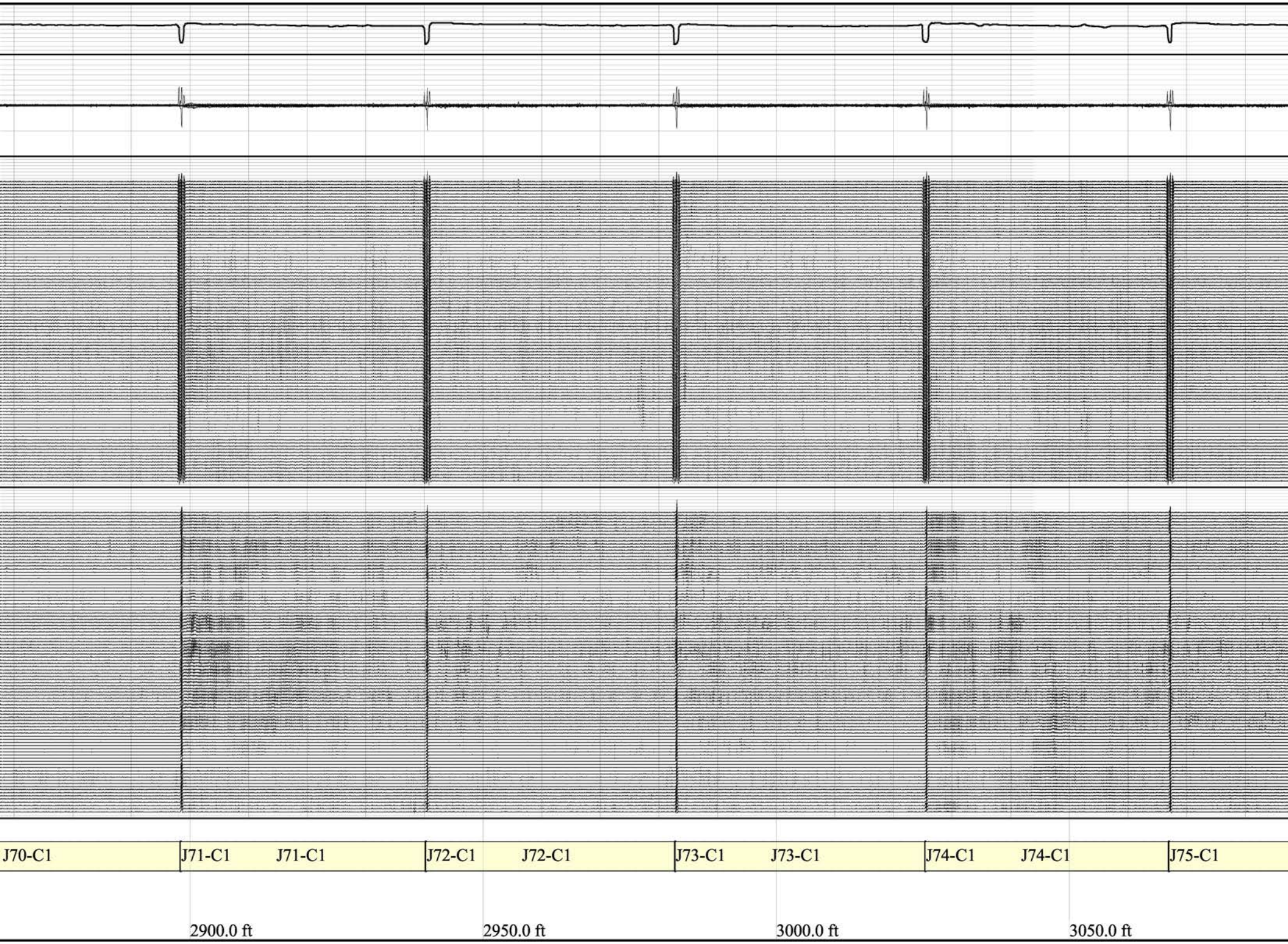
J70-C1
J71-C1
J71-C1
J72-C1
J72-C1
J73-C1
J73-C1
J74-C1
J74-C1
J75-C1
2900.0 ft
2950.0 ft
3000.0 ft
3050.0 ft

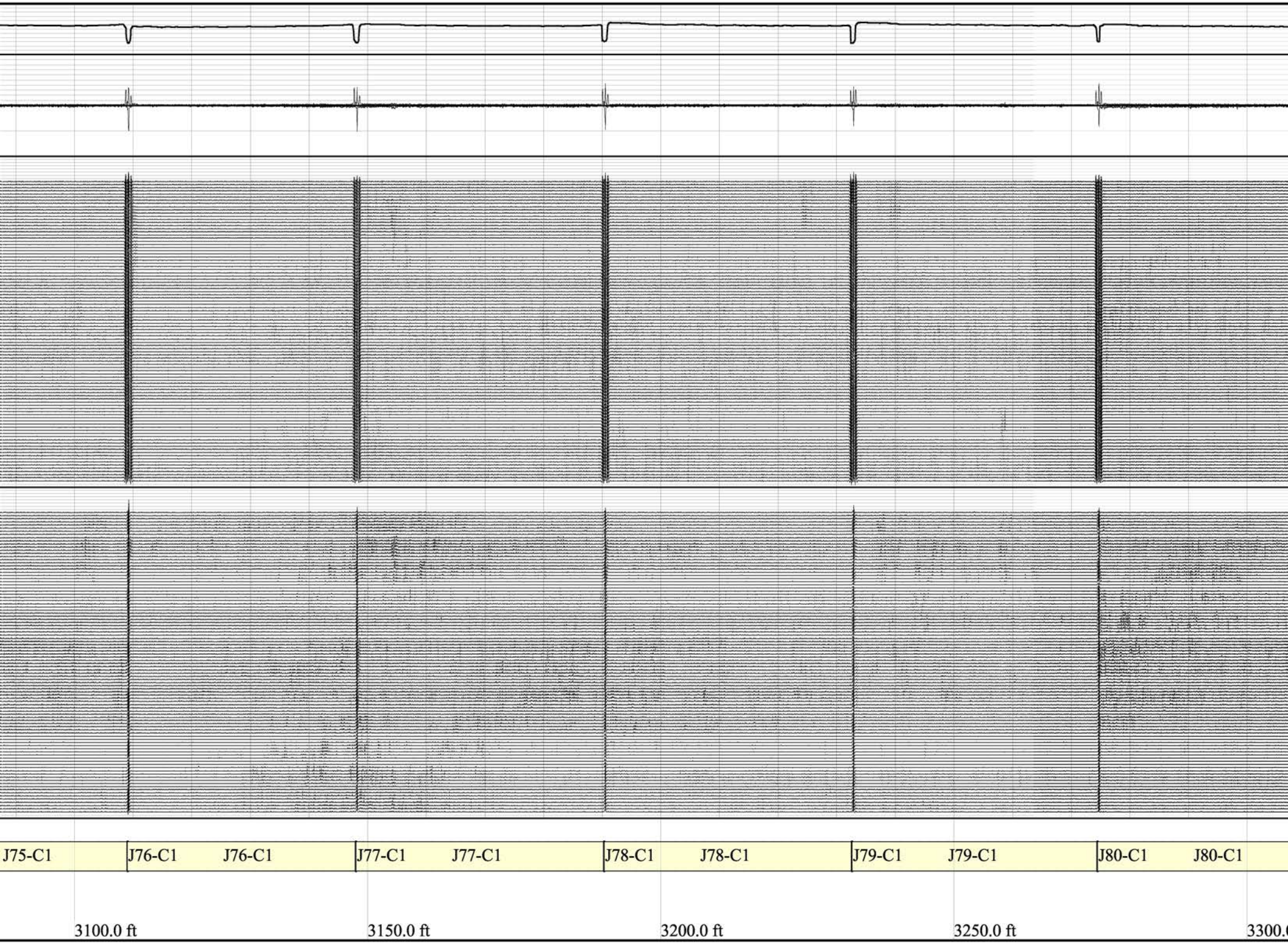
J75-C1
J76-C1
J76-C1
J77-C1
J77-C1
J78-C1
J78-C1
J79-C1
J79-C1
J80-C1
J80-C1
3100.0 ft
3150.0 ft
3200.0 ft
3250.0 ft

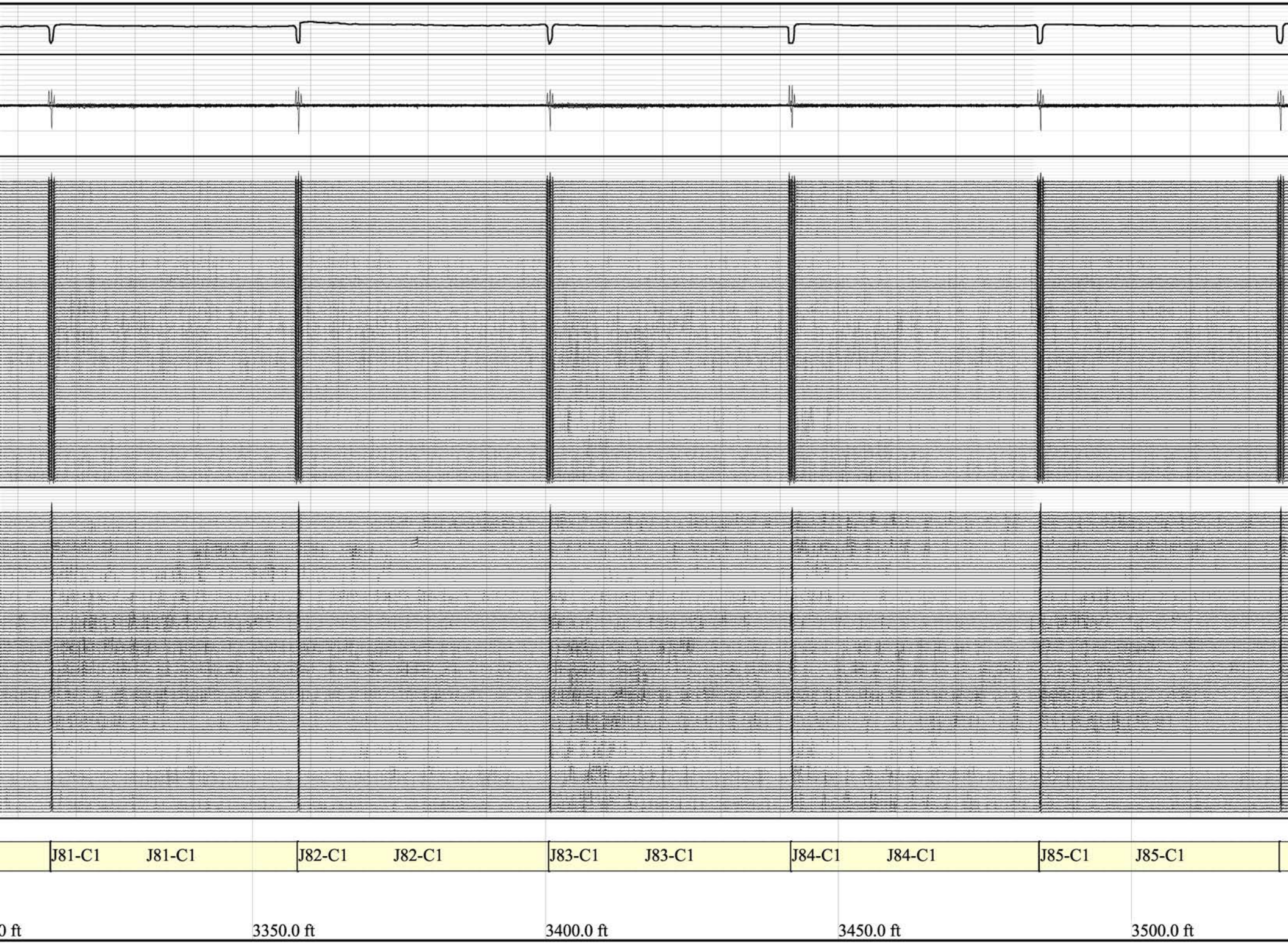
J81-C1
J81-C1
J82-C1
J82-C1
J83-C1
J83-C1
J84-C1
J84-C1
J85-C1
J85-C1
0 ft
3350.0 ft
3400.0 ft
3450.0 ft
3500.0 ft

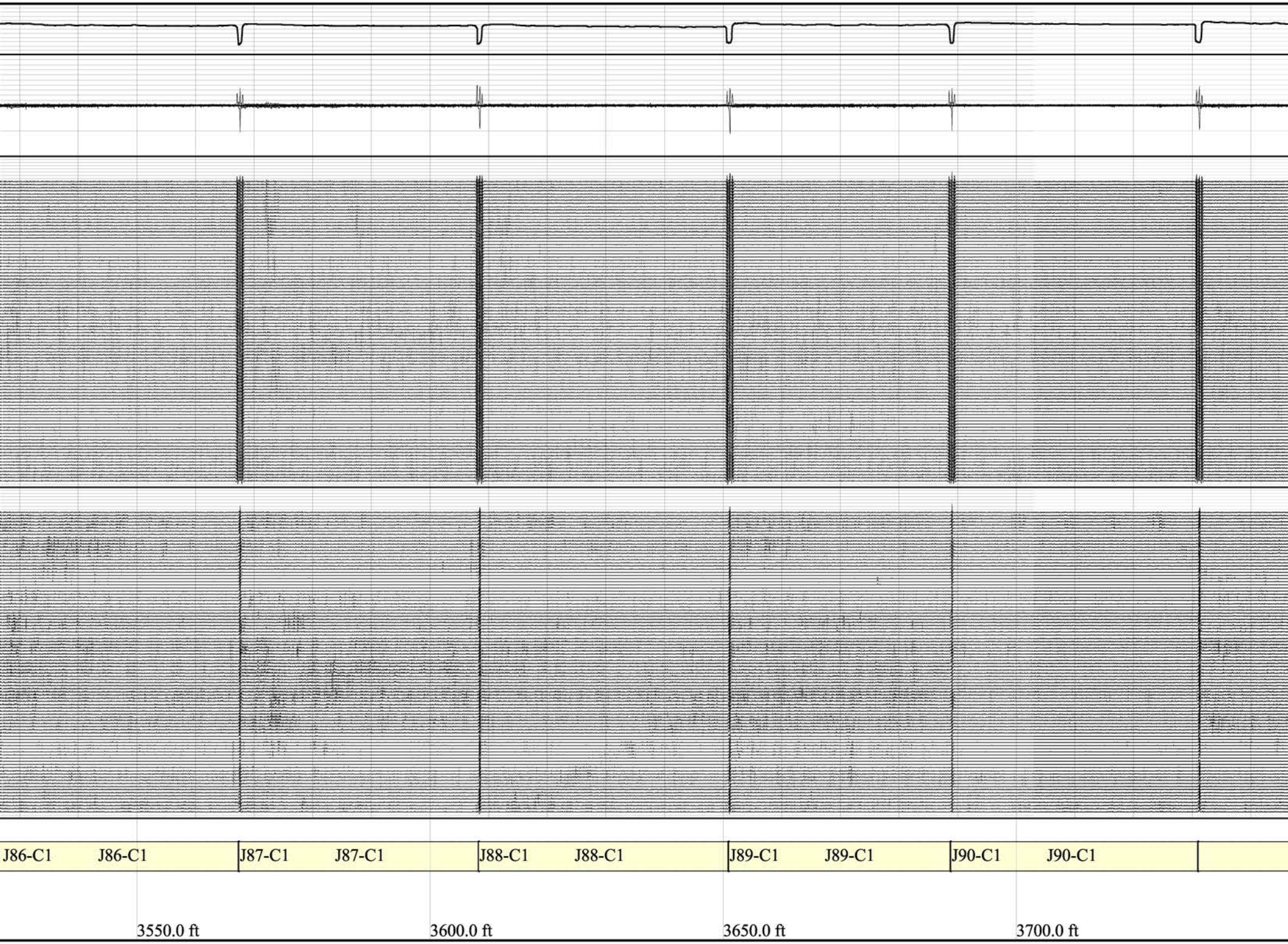
J86-C1
J86-C1
J87-C1
J87-C1
J88-C1
J88-C1
J89-C1
J89-C1
J90-C1
J90-C1
3550.0 ft
3600.0 ft
3650.0 ft
3700.0 ft

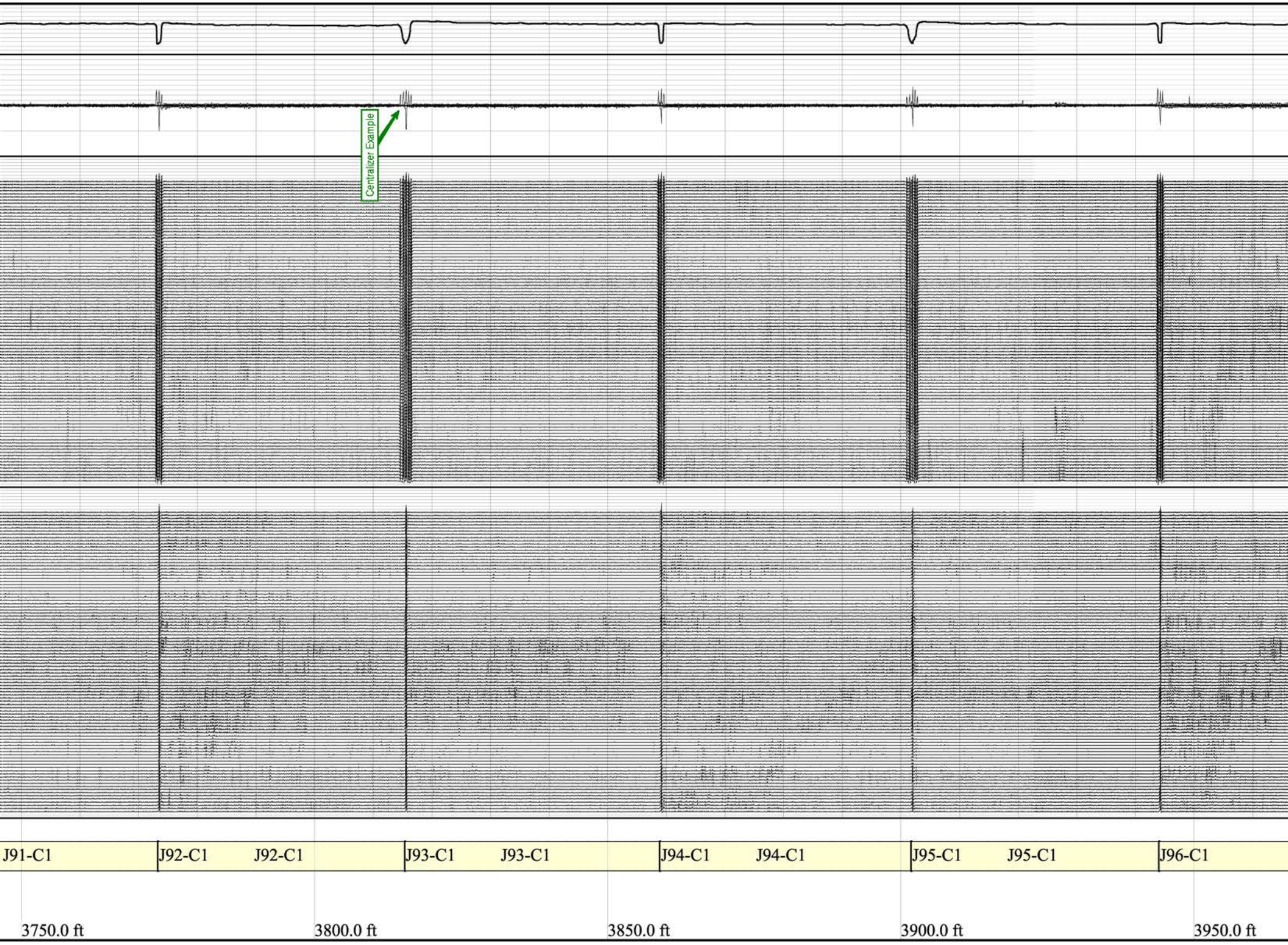
Centralizer Example
J91-C1
J92-C1
J92-C1
J93-C1
J93-C1
J94-C1
J94-C1
J95-C1
J95-C1
J96-C1
3750.0 ft
3800.0 ft
3850.0 ft
3900.0 ft
3950.0 ft

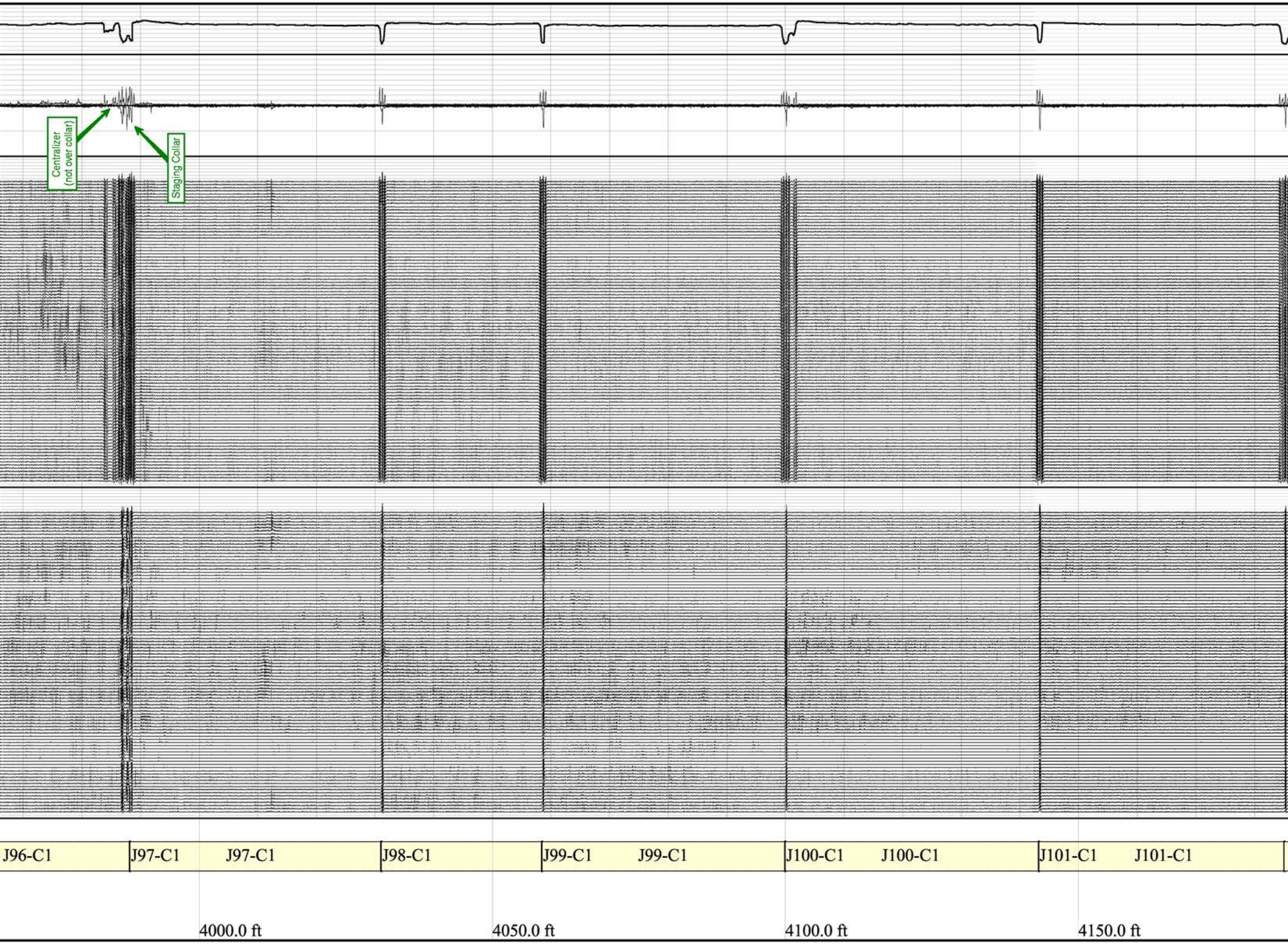
Centralizer
(not over collar)
Staging Collar
J96-C1
J97-C1
J97-C1
J98-C1
J99-C1
J99-C1
J100-C1
J100-C1
J101-C1
J101-C1
4000.0 ft
4050.0 ft
4100.0 ft
4150.0 ft

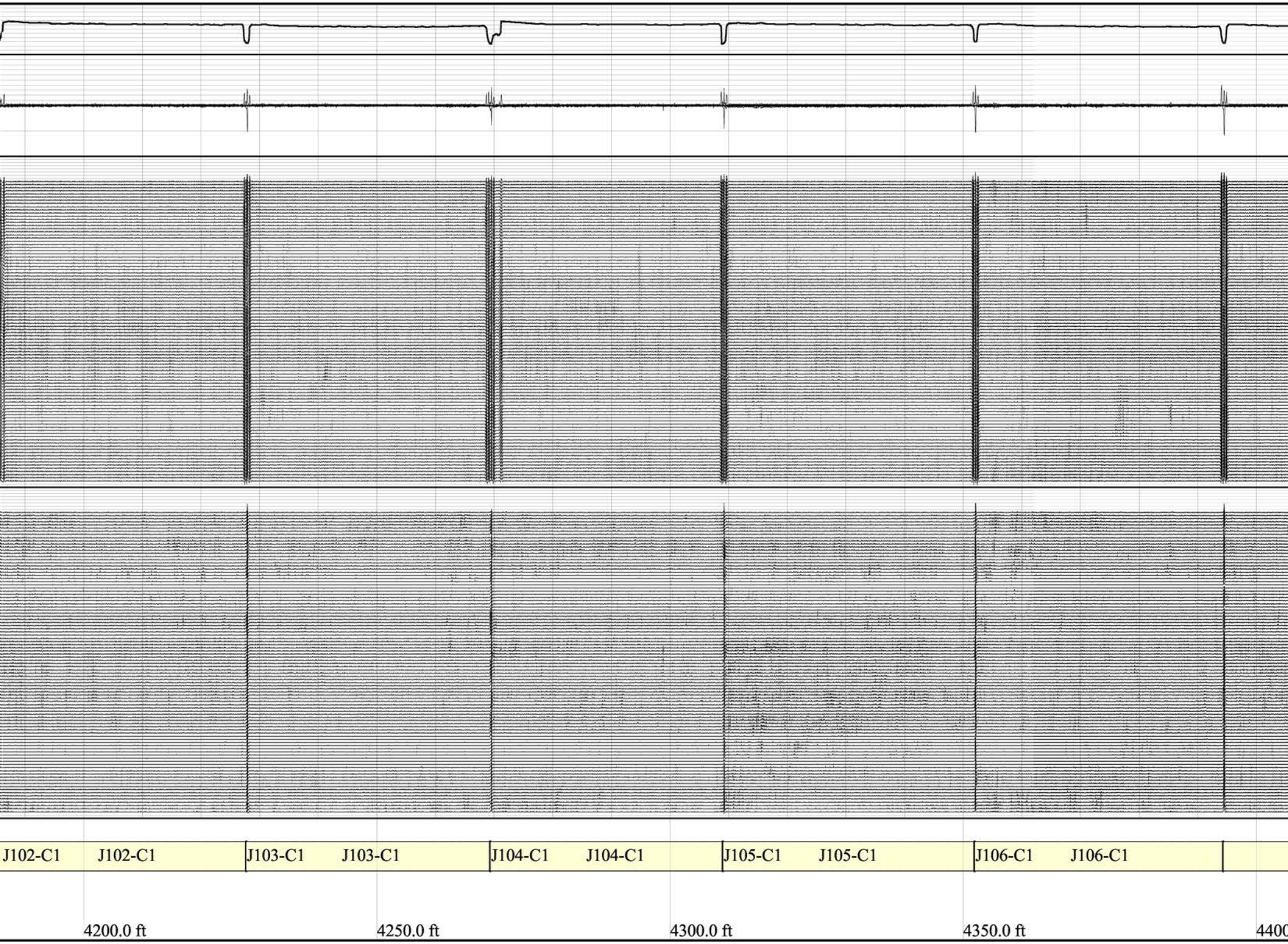
J102-C1
J102-C1
J103-C1
J103-C1
J104-C1
J104-C1
J105-C1
J105-C1
J106-C1
J106-C1
4200.0 ft
4250.0 ft
4300.0 ft
4350.0 ft
4400

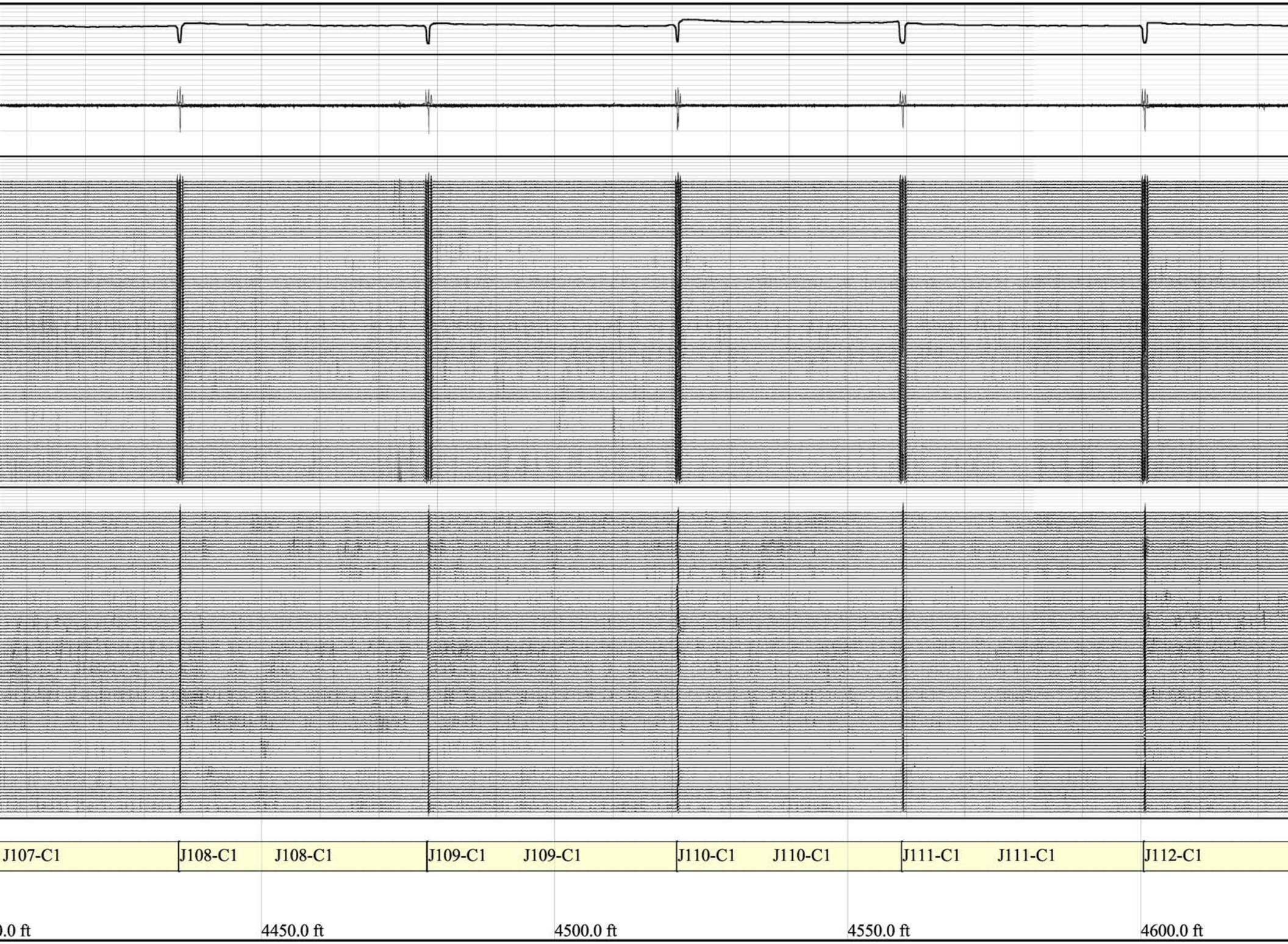
J107-C1
J108-C1
J108-C1
J109-C1
J109-C1
J110-C1
J110-C1
J111-C1
J111-C1
J112-C1
.0 ft
4450.0 ft
4500.0 ft
4550.0 ft
4600.0 ft

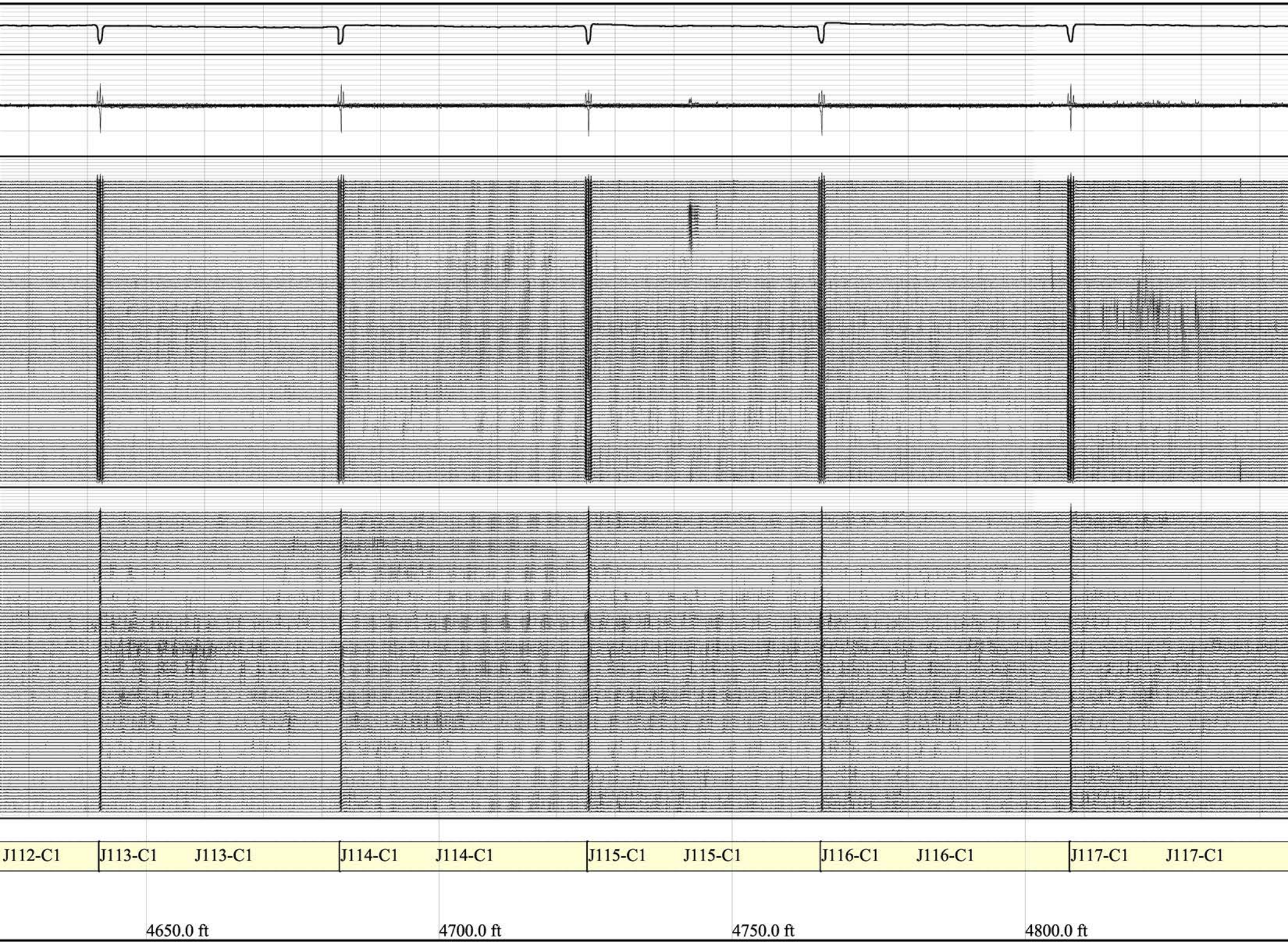
J112-C1
J113-C1
J113-C1
J114-C1
J114-C1
J115-C1
J115-C1
J116-C1
J116-C1
J117-C1
J117-C1
4650.0 ft
4700.0 ft
4750.0 ft
4800.0 ft

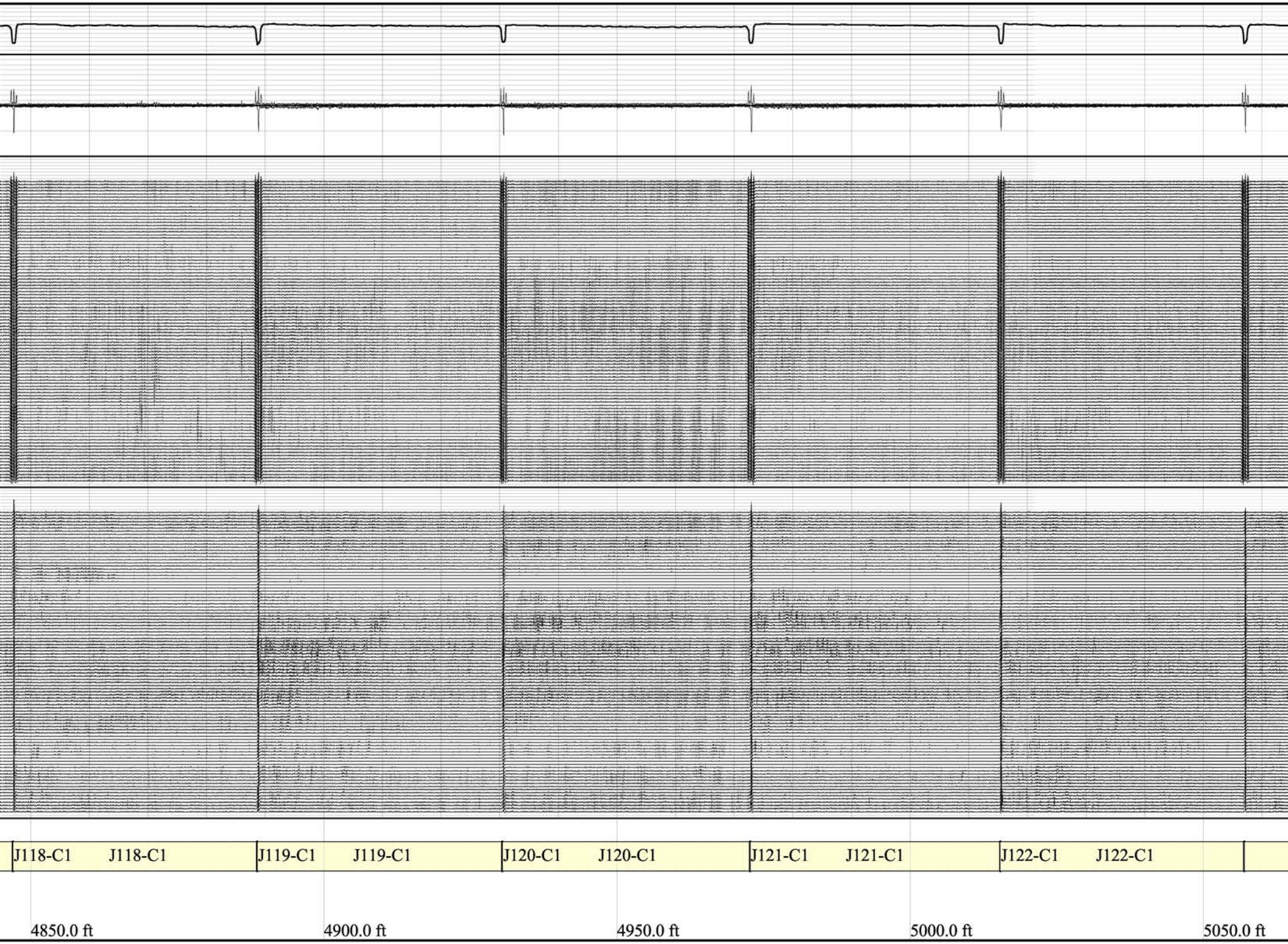
J118-C1
J118-C1
J119-C1
J119-C1
J120-C1
J120-C1
J121-C1
J121-C1
J122-C1
J122-C1
4850.0 ft
4900.0 ft
4950.0 ft
5000.0 ft
5050.0 ft

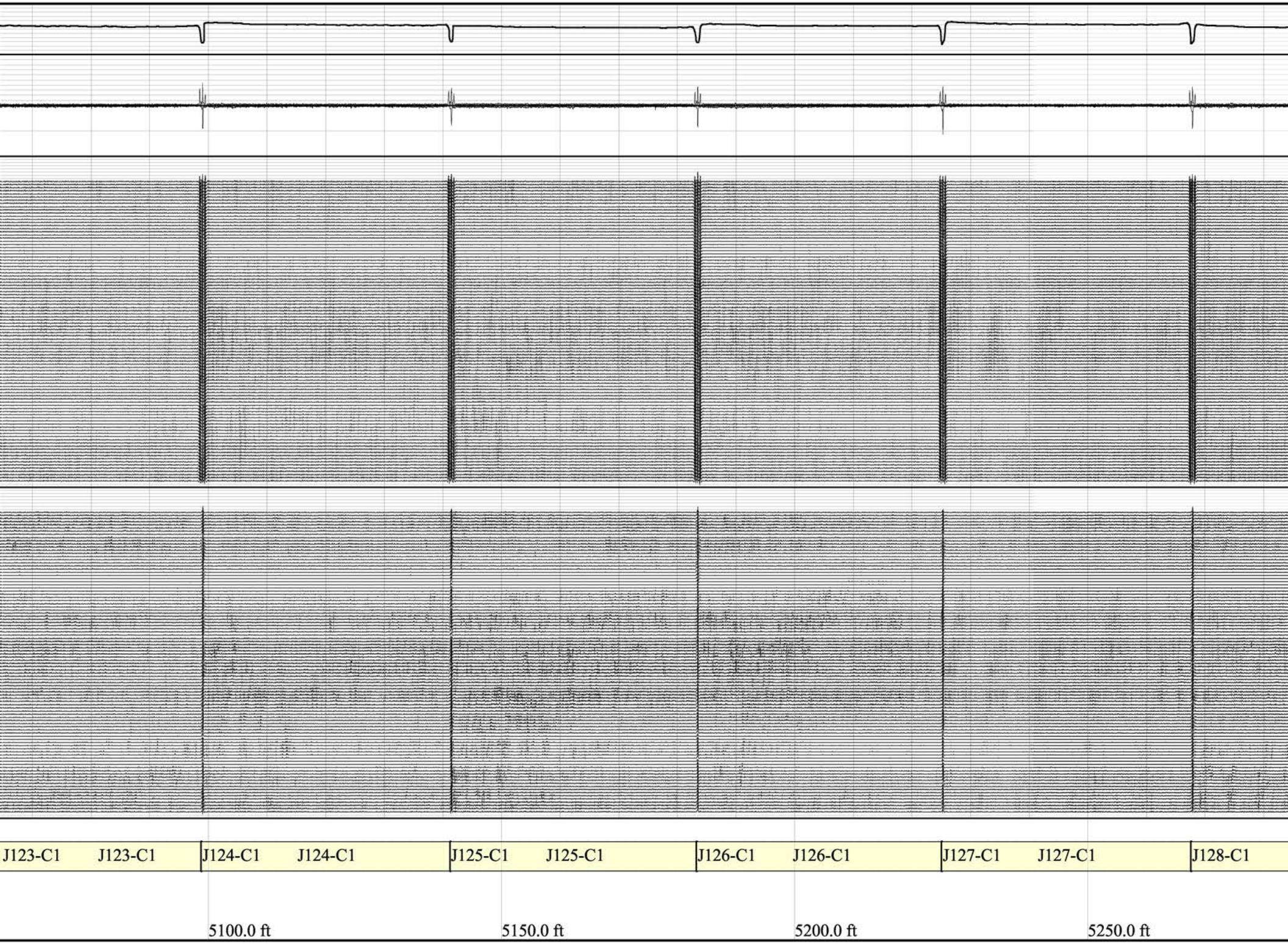
J123-C1
J123-C1
J124-C1
J124-C1
J125-C1
J125-C1
J126-C1
J126-C1
J127-C1
J127-C1
J128-C1
5100.0 ft
5150.0 ft
5200.0 ft
5250.0 ft

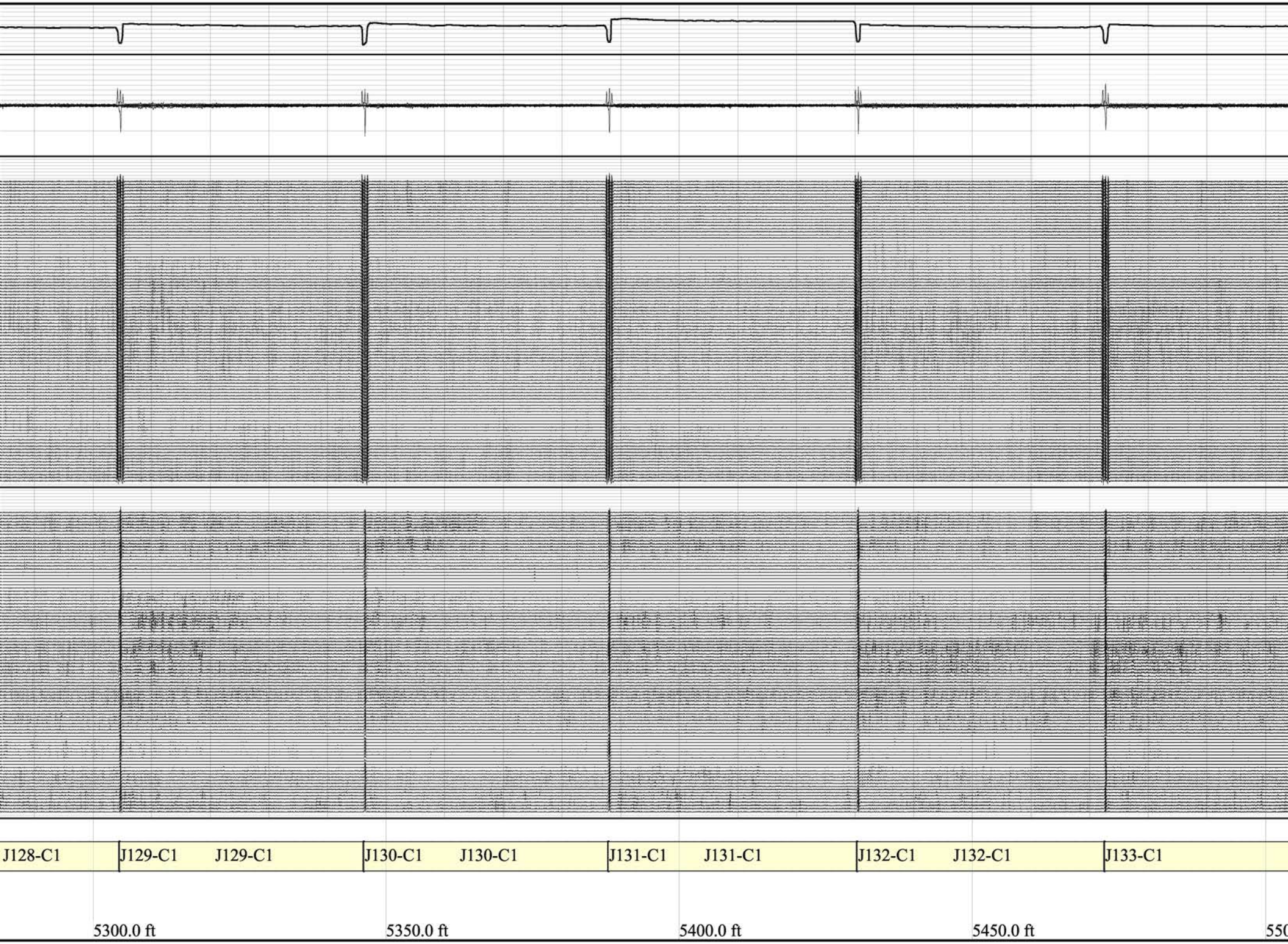
J128-C1
J129-C1
J129-C1
J130-C1
J130-C1
J131-C1
J131-C1
J132-C1
J132-C1
J133-C1
5300.0 ft
5350.0 ft
5400.0 ft
5450.0 ft

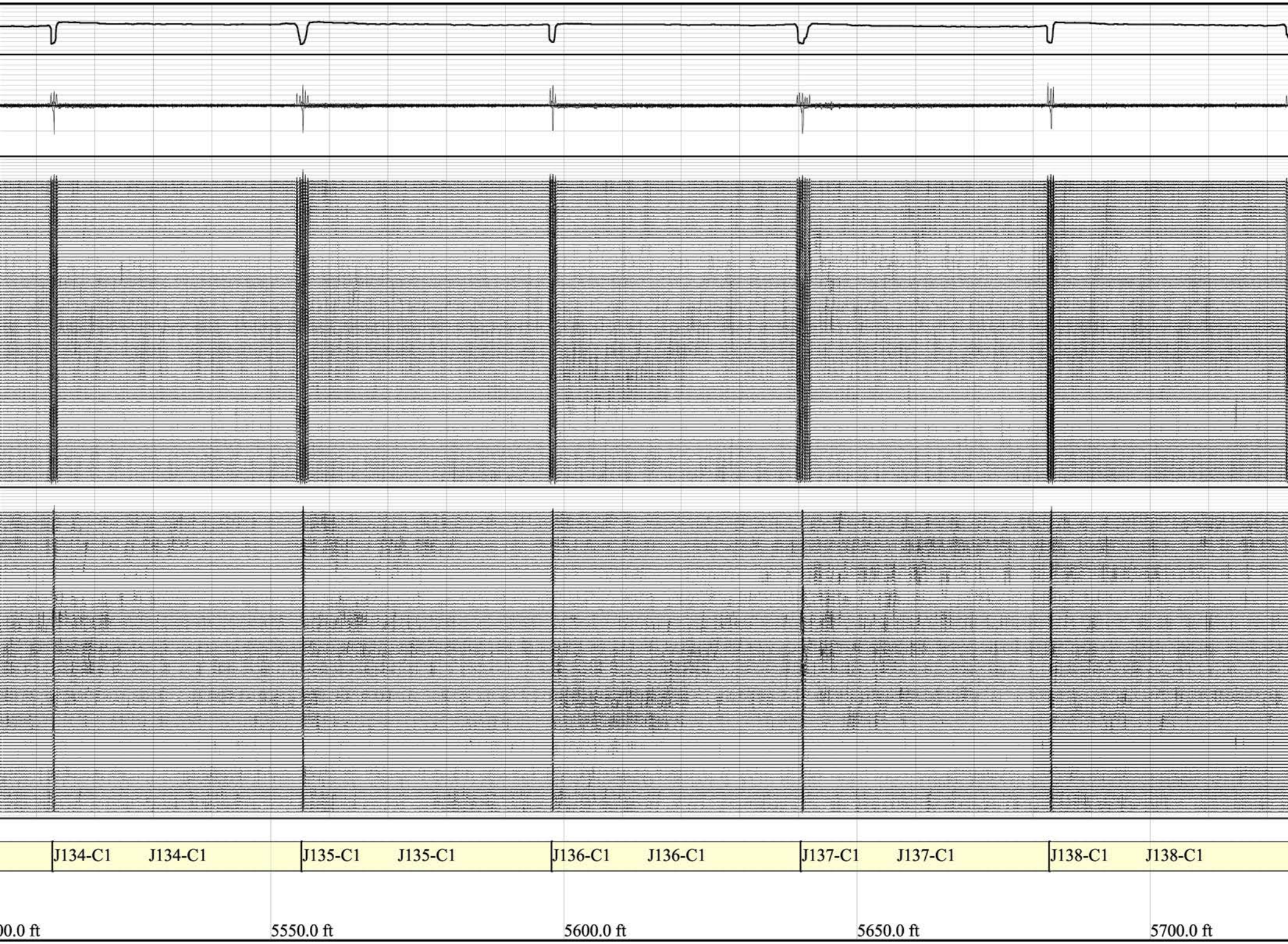
J134-C1 J134-C1
J135-C1 J135-C1
J136-C1 J136-C1
J137-C1 J137-C1
J138-C1 J138-C1
00.0 ft
5550.0 ft
5600.0 ft
5650.0 ft
5700.0 ft

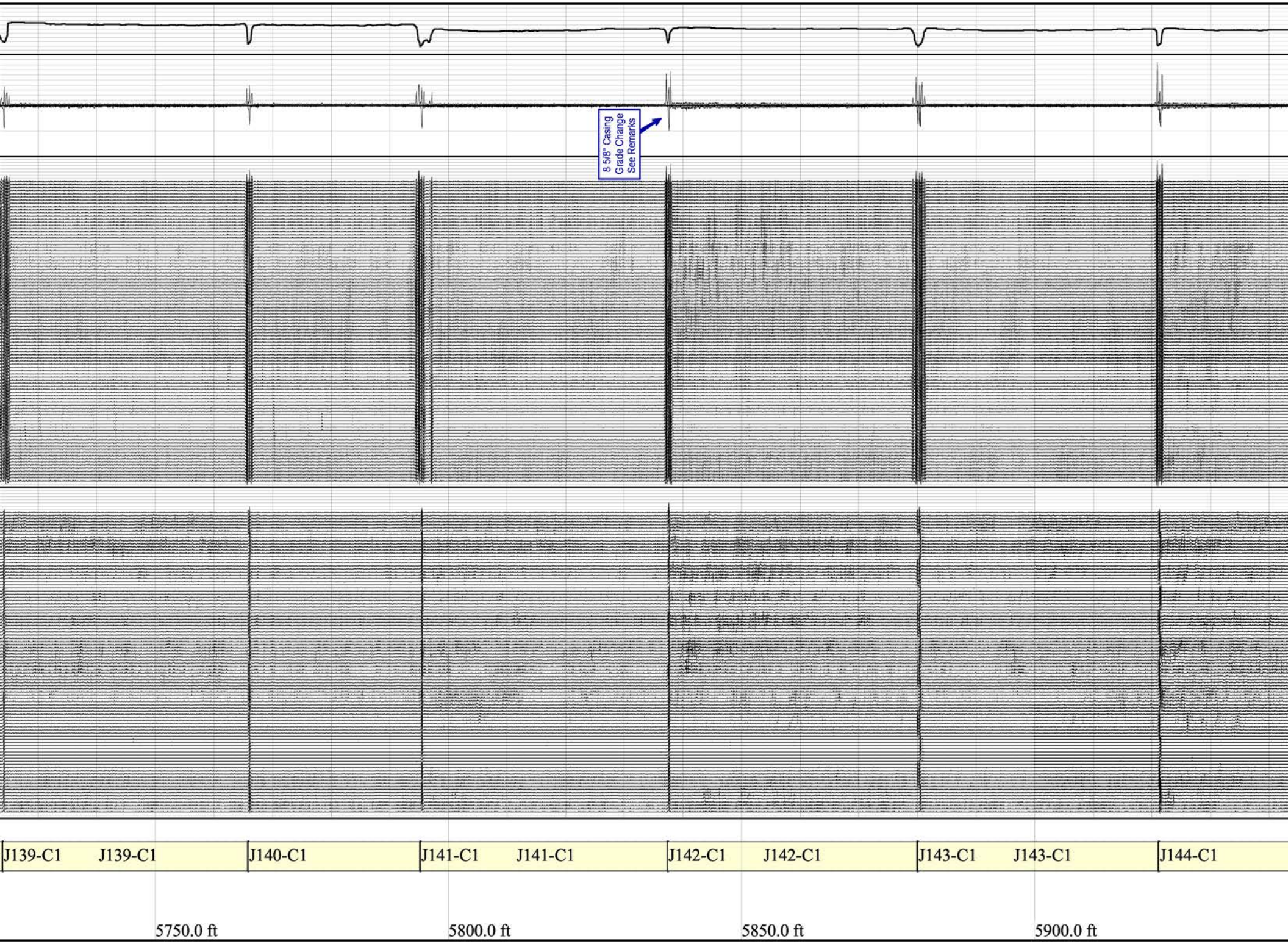
8 5/8" Casing
Grade Change
See Remarks
J139-C1
J139-C1
J140-C1
J141-C1
J141-C1
J142-C1
J142-C1
J143-C1
J143-C1
J144-C1
5750.0 ft
5800.0 ft
5850.0 ft
5900.0 ft

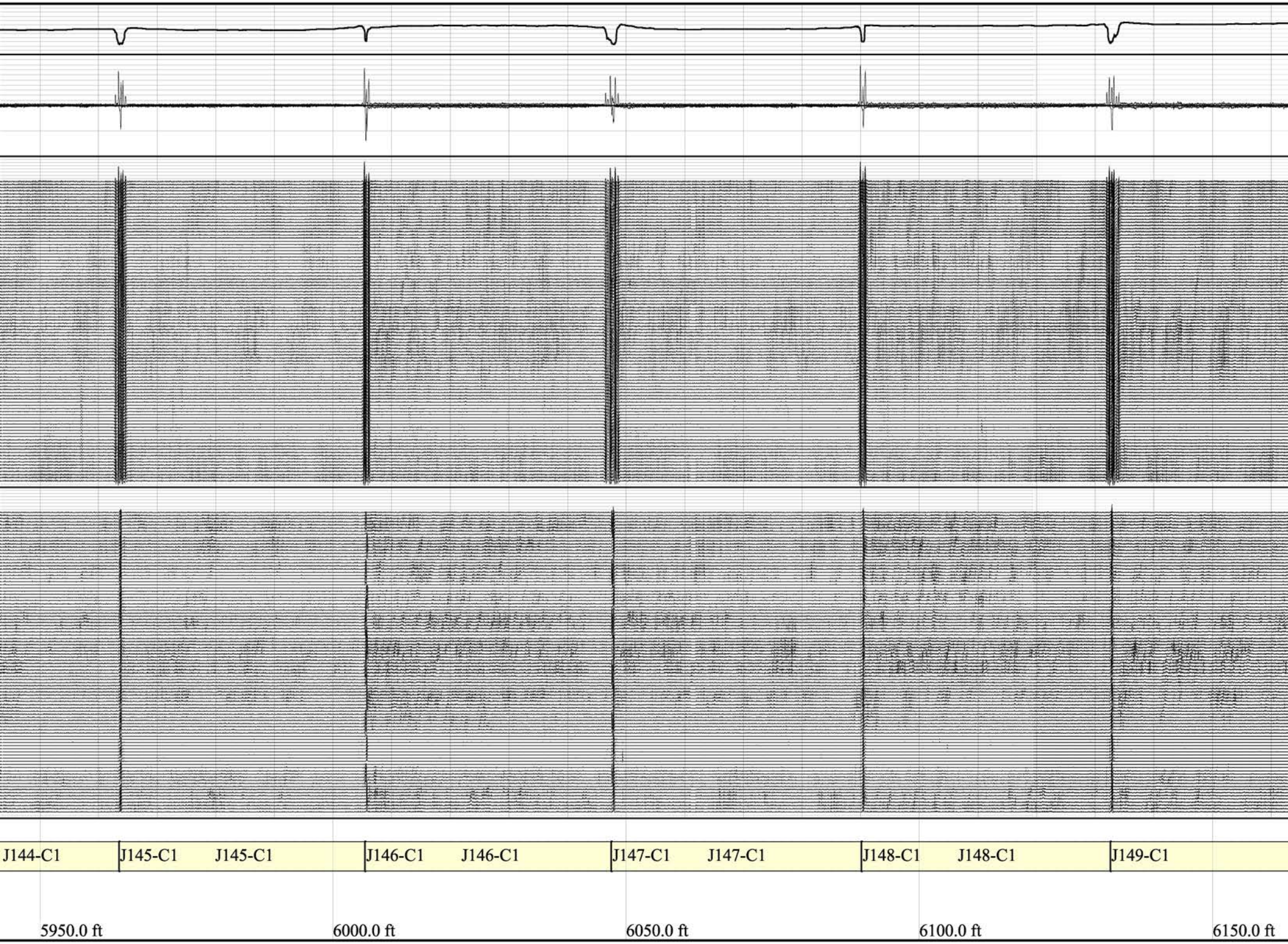
J144-C1
J145-C1
J145-C1
J146-C1
J146-C1
J147-C1
J147-C1
J148-C1
J148-C1
J149-C1
5950.0 ft
6000.0 ft
6050.0 ft
6100.0 ft
6150.0 ft

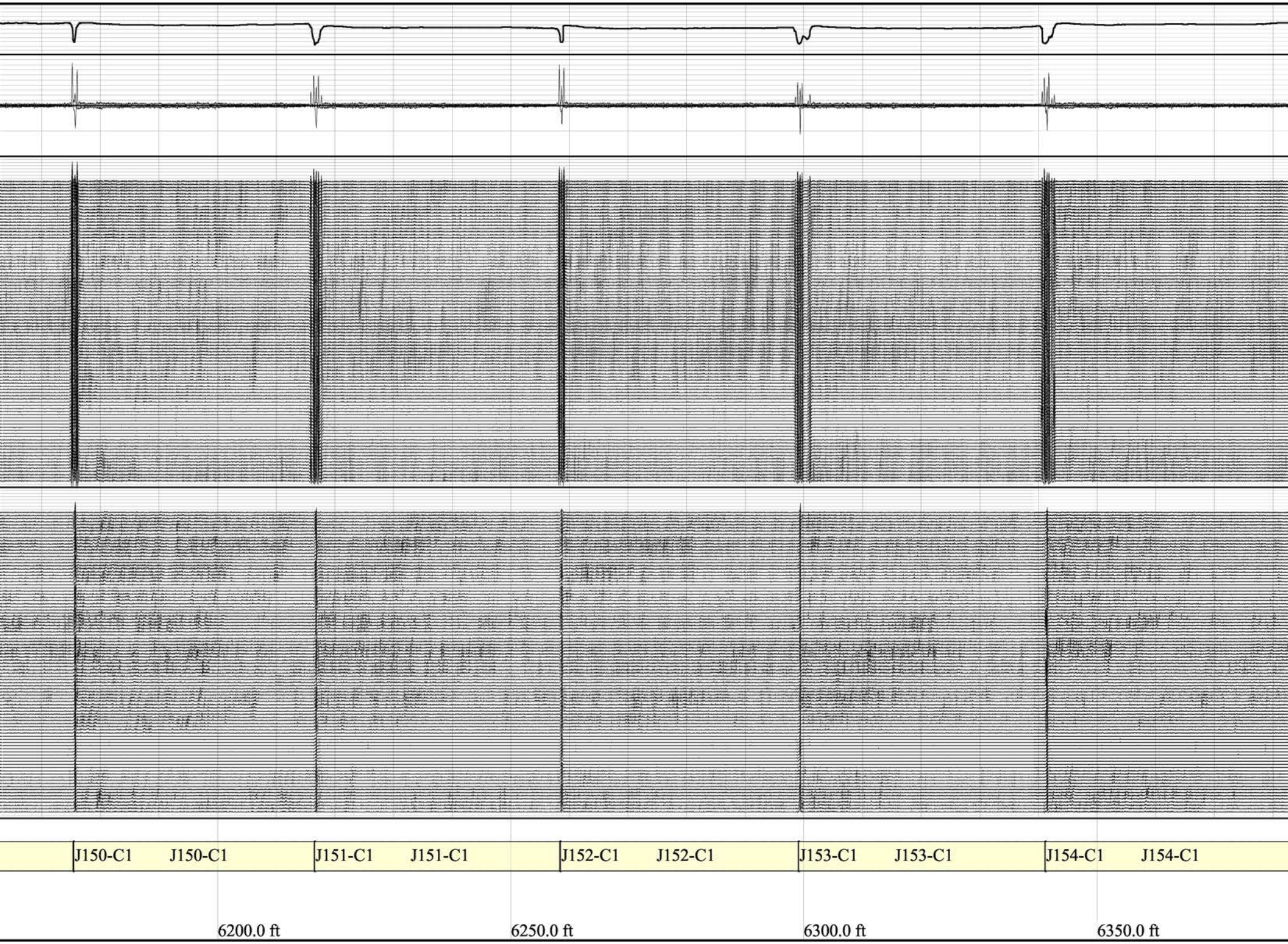
J150-C1
J150-C1
J151-C1
J151-C1
J152-C1
J152-C1
J153-C1
J153-C1
J154-C1
J154-C1
6200.0 ft
6250.0 ft
6300.0 ft
6350.0 ft

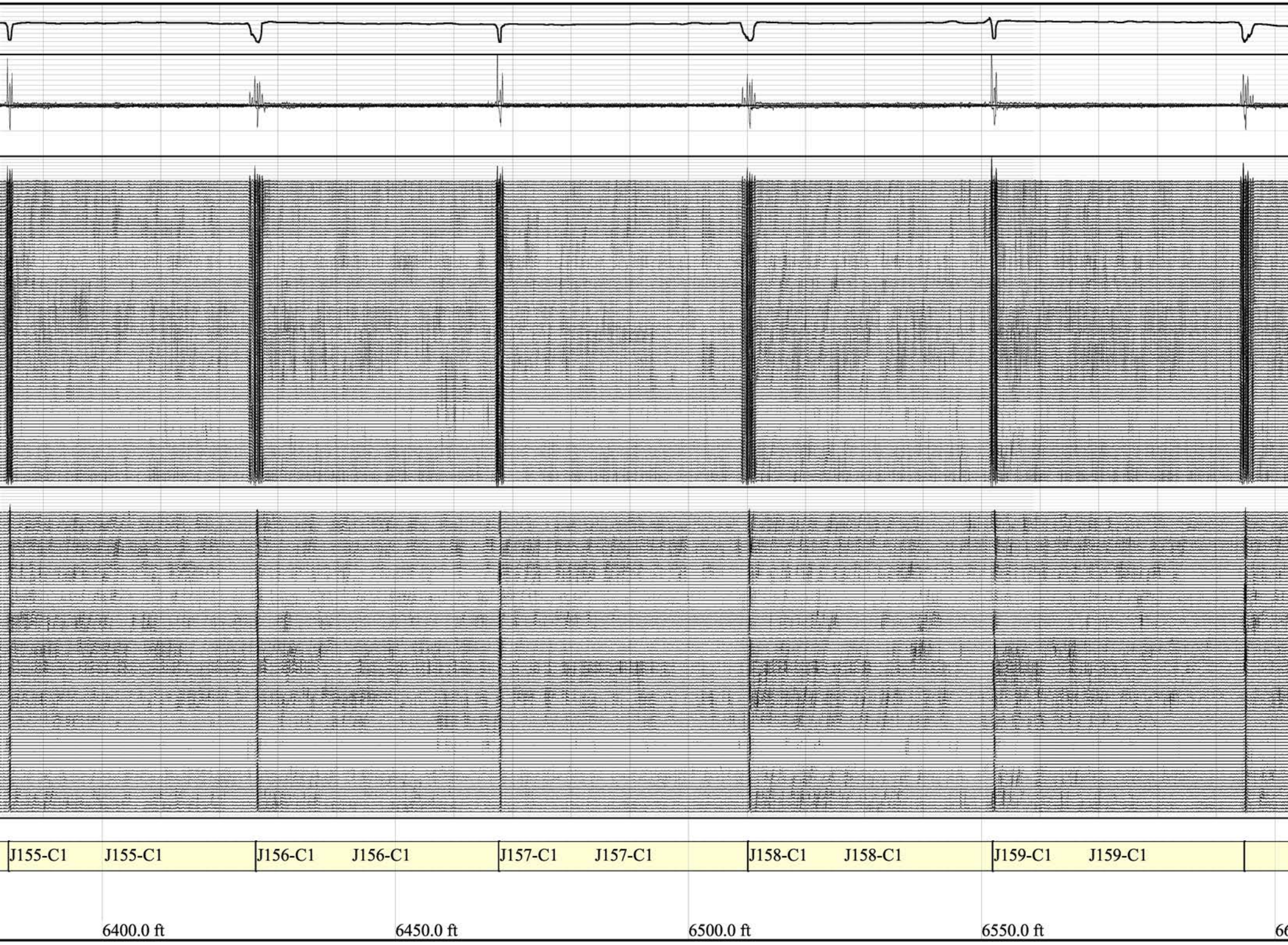
J155-C1
J155-C1
J156-C1
J156-C1
J157-C1
J157-C1
J158-C1
J158-C1
J159-C1
J159-C1
6400.0 ft
6450.0 ft
6500.0 ft
6550.0 ft

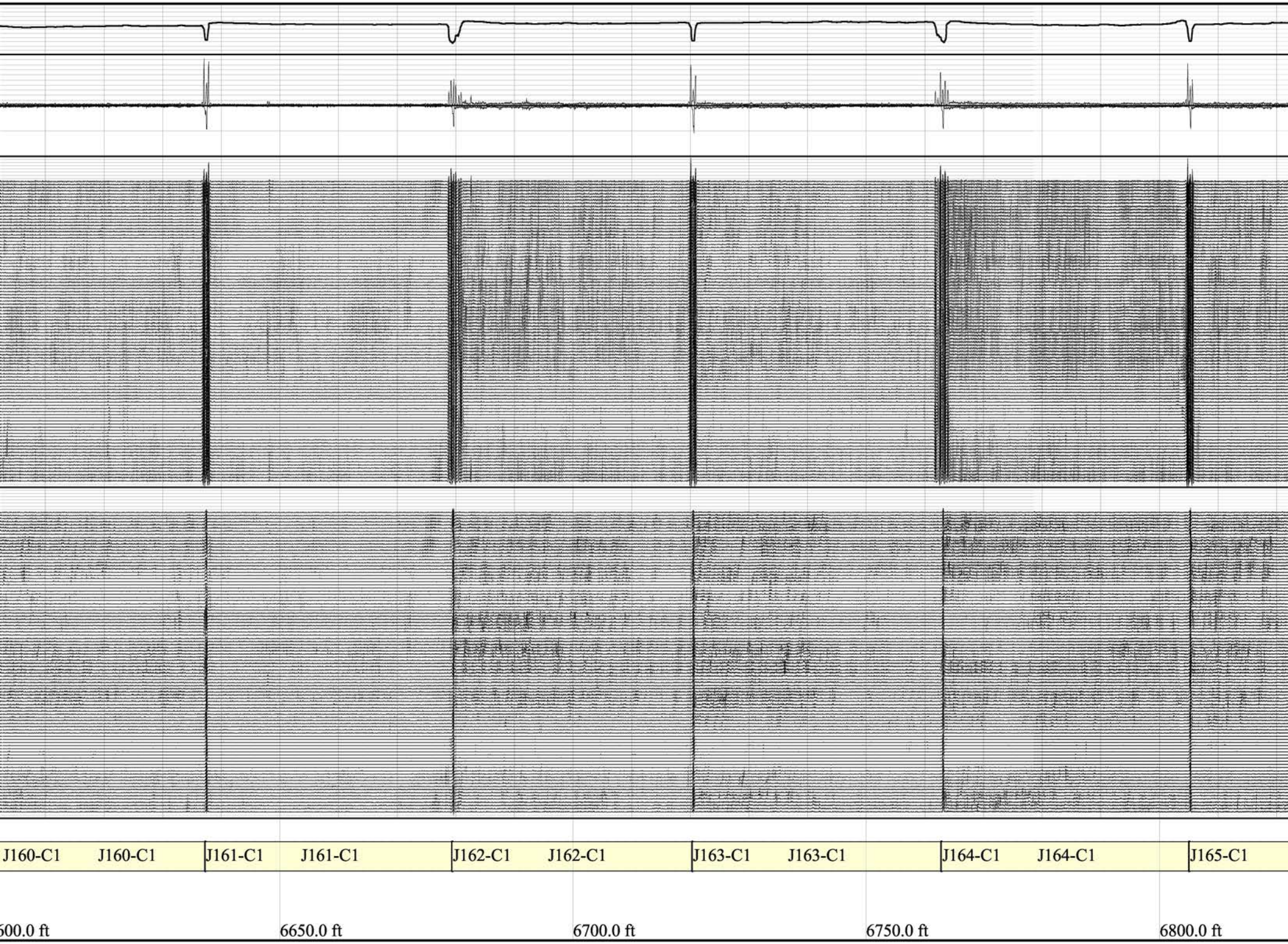
J160-C1
J160-C1
J161-C1
J161-C1
J162-C1
J162-C1
J163-C1
J163-C1
J164-C1
J164-C1
J165-C1
600.0 ft
6650.0 ft
6700.0 ft
6750.0 ft
6800.0 ft

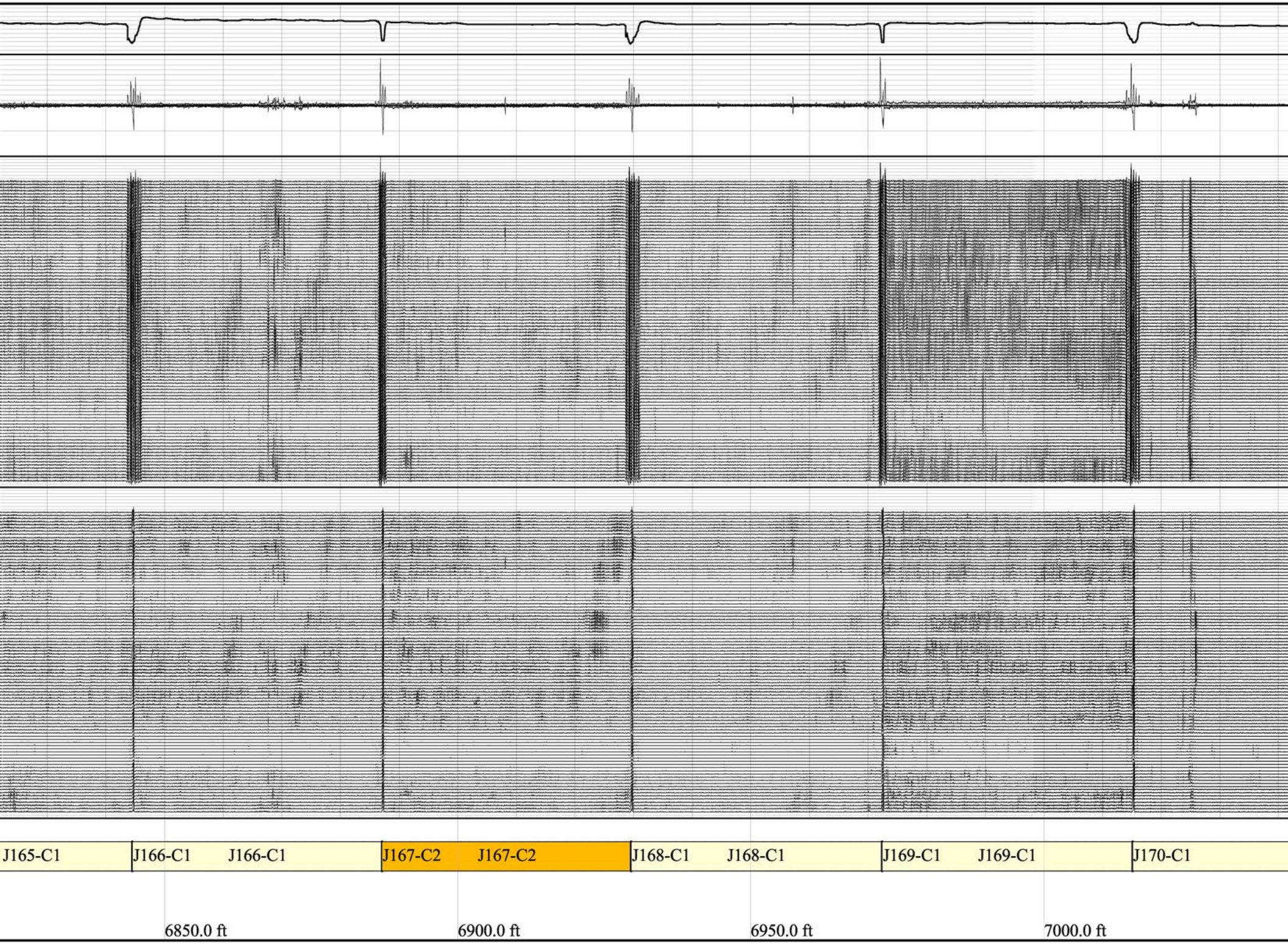
J165-C1
J166-C1
J166-C1
J167-C2
J167-C2
J168-C1
J168-C1
J169-C1
J169-C1
J170-C1
6850.0 ft
6900.0 ft
6950.0 ft
7000.0 ft

Southern California Gas Company Fernando Fee 35B
File 20160714_081635_RSP_0_0_0_0_0.mvl

Joint Summary

Southern California Gas Company
Aliso Canyon
Fernando Fee 35B

Identifier	Start Log Depth	Joint Length	Diameter	Wall Thickness	Weight	Max ML Depth	Max ML Position	Min Burst Pressure	Joint Depth Class
	ft	ft	in	in	lb/ft	%	ft	psi	
JT-1	14.61	10.51	8.625	0.400	36.0	0			1
JT-2	25.12	42.16	8.625	0.400	36.0	0			1
JT-3	67.28	42.89	8.625	0.400	36.0	0			1
JT-4	110.17	41.77	8.625	0.400	36.0	0			1
JT-5	151.93	41.64	8.625	0.400	36.0	0			1
JT-6	193.57	41.14	8.625	0.400	36.0	0			1
JT-7	234.71	42.09	8.625	0.400	36.0	0			1
JT-8	276.80	38.49	8.625	0.400	36.0	0			1
JT-9	315.29	40.62	8.625	0.400	36.0	0			1
JT-10	355.91	39.73	8.625	0.400	36.0	0			1
JT-11	395.64	43.21	8.625	0.400	36.0	0			1
JT-12	438.85	41.00	8.625	0.400	36.0	0			1
JT-13	479.85	42.02	8.625	0.400	36.0	0			1
JT-14	521.86	39.07	8.625	0.400	36.0	0			1
JT-15	560.94	41.58	8.625	0.400	36.0	0			1
JT-16	602.52	42.78	8.625	0.400	36.0	0			1
JT-17	645.30	42.77	8.625	0.400	36.0	0			1
JT-18	688.07	40.45	8.625	0.400	36.0	0			1
JT-19	728.53	43.69	8.625	0.400	36.0	0			1
JT-20	772.22	43.33	8.625	0.400	36.0	0			1
JT-21	815.55	41.84	8.625	0.400	36.0	0			1
JT-22	857.39	42.12	8.625	0.400	36.0	0			1
JT-23	899.51	41.25	8.625	0.400	36.0	0			1
JT-24	940.76	41.40	8.625	0.400	36.0	0			1
JT-25	982.16	41.13	8.625	0.400	36.0	0			1
JT-26	1023.29	40.52	8.625	0.400	36.0	0			1
JT-27	1063.82	39.84	8.625	0.400	36.0	0			1
JT-28	1103.66	41.60	8.625	0.400	36.0	0			1
JT-29	1145.25	42.04	8.625	0.400	36.0	0			1
JT-30	1187.29	43.45	8.625	0.400	36.0	0			1
JT-31	1230.74	41.56	8.625	0.400	36.0	0			1
JT-32	1272.31	41.90	8.625	0.400	36.0	0			1
JT-33	1314.21	41.71	8.625	0.400	36.0	0			1
JT-34	1355.91	39.76	8.625	0.400	36.0	0			1
JT-35	1395.67	41.56	8.625	0.400	36.0	0			1
JT-36	1437.23	41.37	8.625	0.400	36.0	0			1
JT-37	1478.61	43.00	8.625	0.400	36.0	0			1
JT-38	1521.61	41.20	8.625	0.400	36.0	0			1
JT-39	1562.81	41.88	8.625	0.400	36.0	0			1
JT-40	1604.69	39.01	8.625	0.400	36.0	0			1
JT-41	1643.71	42.71	8.625	0.400	36.0	0			1
JT-42	1686.42	41.05	8.625	0.400	36.0	0			1
JT-43	1727.46	41.00	8.625	0.400	36.0	0			1
JT-44	1768.46	41.92	8.625	0.400	36.0	0			1
JT-45	1810.38	41.67	8.625	0.400	36.0	0			1
JT-46	1852.05	43.13	8.625	0.400	36.0	0			1
JT-47	1895.18	41.90	8.625	0.400	36.0	0			1
JT-48	1937.08	41.11	8.625	0.400	36.0	0			1
JT-49	1978.19	40.85	8.625	0.400	36.0	0			1
JT-50	2019.05	41.40	8.625	0.400	36.0	0			1
JT-51	2060.44	42.63	8.625	0.400	36.0	0			1
JT-52	2103.07	41.07	8.625	0.400	36.0	0			1
JT-53	2144.14	41.70	8.625	0.400	36.0	17	2158.88	5787	1
JT-54	2185.84	41.39	8.625	0.400	36.0	19	2197.13	5838	1
JT-55	2227.23	42.01	8.625	0.400	36.0	21	2242.62	5788	2
JT-56	2269.24	41.08	8.625	0.400	36.0	0			1
JT-57	2310.32	43.55	8.625	0.400	36.0	15	2318.22	5978	1
JT-58	2353.87	41.05	8.625	0.400	36.0	0			1

JT-59	2394.92	41.00	8.625	0.400	36.0	0			1
JT-60	2435.92	41.18	8.625	0.400	36.0	0			1
JT-61	2477.11	41.82	8.625	0.400	36.0	0			1
JT-62	2518.93	42.68	8.625	0.400	36.0	0			1
JT-63	2561.61	42.28	8.625	0.400	36.0	0			1
JT-64	2603.89	42.29	8.625	0.400	36.0	15	2635.20	5978	1
JT-65	2646.18	41.20	8.625	0.400	36.0	0			1
JT-66	2687.38	42.20	8.625	0.400	36.0	0			1
JT-67	2729.58	43.29	8.625	0.400	36.0	0			1
JT-68	2772.88	42.19	8.625	0.400	36.0	0			1
JT-69	2815.07	41.66	8.625	0.400	36.0	0			1
JT-70	2856.73	41.71	8.625	0.400	36.0	0			1
JT-71	2898.44	41.88	8.625	0.400	36.0	0			1
JT-72	2940.32	42.52	8.625	0.400	36.0	0			1
JT-73	2982.83	42.65	8.625	0.400	36.0	0			1
JT-74	3025.48	41.57	8.625	0.400	36.0	0			1
JT-75	3067.05	42.03	8.625	0.400	36.0	0			1
JT-76	3109.08	38.97	8.625	0.400	36.0	0			1
JT-77	3148.06	42.35	8.625	0.400	36.0	0			1
JT-78	3190.40	42.31	8.625	0.400	36.0	0			1
JT-79	3232.71	41.85	8.625	0.400	36.0	0			1
JT-80	3274.56	41.09	8.625	0.400	36.0	0			1
JT-81	3315.65	42.12	8.625	0.400	36.0	0			1
JT-82	3357.77	42.90	8.625	0.400	36.0	0			1
JT-83	3400.67	41.26	8.625	0.400	36.0	0			1
JT-84	3441.93	42.40	8.625	0.400	36.0	0			1
JT-85	3484.33	40.97	8.625	0.400	36.0	0			1
JT-86	3525.30	42.16	8.625	0.400	36.0	0			1
JT-87	3567.46	40.87	8.625	0.400	36.0	0			1
JT-88	3608.34	42.68	8.625	0.400	36.0	0			1
JT-89	3651.02	37.87	8.625	0.400	36.0	0			1
JT-90	3688.89	42.20	8.625	0.400	36.0	0			1
JT-91	3731.09	42.27	8.625	0.400	36.0	0			1
JT-92	3773.37	42.10	8.625	0.400	36.0	0			1
JT-93	3815.47	43.54	8.625	0.400	36.0	0			1
JT-94	3859.01	42.83	8.625	0.400	36.0	0			1
JT-95	3901.84	42.26	8.625	0.400	36.0	0			1
JT-96	3944.10	44.17	8.625	0.400	36.0	15	3979.22	5989	1
JT-97	3988.27	42.85	8.625	0.400	36.0	0			1
JT-98	4031.12	27.40	8.625	0.400	36.0	0			1
JT-99	4058.52	41.50	8.625	0.400	36.0	0			1
JT-100	4100.02	43.24	8.625	0.400	36.0	0			1
JT-101	4143.26	41.88	8.625	0.400	36.0	0			1
JT-102	4185.14	42.59	8.625	0.400	36.0	0			1
JT-103	4227.73	41.66	8.625	0.400	36.0	0			1
JT-104	4269.40	39.68	8.625	0.400	36.0	0			1
JT-105	4309.08	42.90	8.625	0.400	36.0	0			1
JT-106	4351.98	42.40	8.625	0.400	36.0	0			1
JT-107	4394.38	41.61	8.625	0.400	36.0	0			1
JT-108	4435.99	42.40	8.625	0.400	36.0	0			1
JT-109	4478.39	42.52	8.625	0.400	36.0	0			1
JT-110	4520.91	38.35	8.625	0.400	36.0	0			1
JT-111	4559.26	41.28	8.625	0.400	36.0	0			1
JT-112	4600.54	41.50	8.625	0.400	36.0	0			1
JT-113	4642.04	41.07	8.625	0.400	36.0	0			1
JT-114	4683.11	42.22	8.625	0.400	36.0	0			1
JT-115	4725.33	39.77	8.625	0.400	36.0	0			1
JT-116	4765.11	42.50	8.625	0.400	36.0	0			1
JT-117	4807.61	39.40	8.625	0.400	36.0	0			1
JT-118	4847.01	41.71	8.625	0.400	36.0	0			1
JT-119	4888.72	41.81	8.625	0.400	36.0	0			1
JT-120	4930.53	42.23	8.625	0.400	36.0	0			1
JT-121	4972.76	42.64	8.625	0.400	36.0	0			1
JT-122	5015.40	41.66	8.625	0.400	36.0	0			1
JT-123	5057.06	41.83	8.625	0.400	36.0	0			1
JT-124	5098.89	42.42	8.625	0.400	36.0	0			1
JT-125	5141.31	42.03	8.625	0.400	36.0	0			1
JT-126	5183.34	41.80	8.625	0.400	36.0	0			1
JT-127	5225.15	42.57	8.625	0.400	36.0	0			1
JT-128	5267.72	36.81	8.625	0.400	36.0	0			1
JT-129	5304.53	41.72	8.625	0.400	36.0	0			1
JT-130	5346.26	41.68	8.625	0.400	36.0	0			1
JT-131	5387.93	42.44	8.625	0.400	36.0	0			1
JT-132	5430.38	42.20	8.625	0.400	36.0	0			1
JT-133	5472.58	40.30	8.625	0.400	36.0	0			1
JT-134	5512.88	42.43	8.625	0.400	36.0	0			1
JT-135	5555.31	42.69	8.625	0.400	36.0	0			1
JT-136	5598.00	42.52	8.625	0.400	36.0	0			1
JT-137	5640.52	42.39	8.625	0.400	36.0	0			1
JT-138	5682.91	41.15	8.625	0.400	36.0	0			1
JT-139	5724.06	41.85	8.625	0.400	36.0	0			1
JT-140	5765.91	29.37	8.625	0.400	36.0	0			1
JT-141	5795.27	42.16	8.625	0.400	36.0	0			1
JT-142	5837.43	42.69	8.625	0.400	36.0	0			1
JT-143	5880.12	41.11	8.625	0.400	36.0	0			1

JT-143	5880.12	41.11	8.625	0.400	36.0	0			1
JT-144	5921.23	42.39	8.625	0.400	36.0	0			1
JT-145	5963.62	41.97	8.625	0.400	36.0	0			1
JT-146	6005.59	41.98	8.625	0.400	36.0	0			1
JT-147	6047.57	42.67	8.625	0.400	36.0	0			1
JT-148	6090.23	42.45	8.625	0.400	36.0	0			1
JT-149	6132.68	42.84	8.625	0.400	36.0	0			1
JT-150	6175.52	41.13	8.625	0.400	36.0	0			1
JT-151	6216.65	41.91	8.625	0.400	36.0	0			1
JT-152	6258.56	40.63	8.625	0.400	36.0	0			1
JT-153	6299.19	42.08	8.625	0.400	36.0	0			1
JT-154	6341.27	42.84	8.625	0.400	36.0	0			1
JT-155	6384.11	42.18	8.625	0.400	36.0	0			1
JT-156	6426.29	41.48	8.625	0.400	36.0	0			1
JT-157	6467.76	42.48	8.625	0.400	36.0	0			1
JT-158	6510.25	41.75	8.625	0.400	36.0	0			1
JT-159	6552.00	42.93	8.625	0.400	36.0	0			1
JT-160	6594.93	42.36	8.625	0.400	36.0	0			1
JT-161	6637.29	42.11	8.625	0.400	36.0	0			1
JT-162	6679.41	40.95	8.625	0.400	36.0	0			1
JT-163	6720.36	42.55	8.625	0.400	36.0	0			1
JT-164	6762.91	42.24	8.625	0.400	36.0	0			1
JT-165	6805.15	39.41	8.625	0.400	36.0	0			1
JT-166	6844.56	42.59	8.625	0.400	36.0	17	6867.50	8283	1
JT-167	6887.15	42.46	8.625	0.400	36.0	26	6907.94	8290	2
JT-168	6929.61	42.84	8.625	0.400	36.0	18	6969.86	8228	1
JT-169	6972.45	42.72	8.625	0.400	36.0	0			1
JT-170	7015.17	34.73	8.625	0.400	36.0	18	7025.67	8132	1

Inspection Date: 07-14-2016
Report Date: 07-18-2016

Southern California Gas Company
Aliso Canyon
Fernando Fee 35B

Log Depth	Dist UHC	Joint Length	Identifier	Class	Description	Surface Indication	Length	Width	Depth	Dim Class	P Safe Barlow	ERF Barlow	P Safe Mod B31G	ERF Mod B31G	P Safe Effective Area	ERF Effective Area	NWT	Comment	115% MAOP	Delta MAOP (Barlow)
ft	ft	ft					in	in	%		psi		psi		psi		in		psi	psi
14.61		10.51		Begin External Casing													0.400		3625	
14.61		10.51	C-1	Appurtenance	Flange												0.400		3625	
15.54	0.94	10.51	H-1-1	Hardware	Other												0.400	External Casing Head Response.	3625	
25.12	10.51	42.16	C-2	Collar													0.400		3625	
67.28	42.16	42.89	C-3	Collar													0.400		3625	
110.17	42.89	41.77	C-4	Collar													0.400		3625	
146.88	36.71	41.77	MO-4-1	Metal Object	External Casing Collar												0.400		3625	
151.93	41.77	41.64	C-5	Collar													0.400		3625	
193.57	41.64	41.64	C-6	Collar													0.400		3625	
234.71	41.14	42.09	C-7	Collar													0.400		3625	
276.80	42.09	38.49	C-8	Collar													0.400		3625	
315.29	38.49	40.62	C-9	Collar													0.400		3625	
355.91	40.62	39.73	C-10	Collar													0.400		3625	
395.64	39.73	43.21	C-11	Collar													0.400		3625	
438.85	43.21	41.00	C-12	Collar													0.400		3625	
479.85	41.00	42.02	C-13	Collar													0.400		3625	
521.86	42.02	39.07	C-14	Collar													0.400		3625	
560.94	39.07	41.58	C-15	Collar													0.400		3625	
602.52	41.58	42.78	C-16	Collar													0.400		3625	
645.30	42.78	42.77	C-17	Collar													0.400		3625	
688.07	42.77	40.45	C-18	Collar													0.400		3625	
728.53	40.45	43.69	C-19	Collar													0.400		3625	
772.22	43.69	43.33	C-20	Collar													0.400		3625	
815.55	43.33	41.84	C-21	Collar													0.400		3625	
829.00	13.45	41.84		End External Casing													0.400		3625	
829.00	13.45	41.84	H-21-1	Hardware	Bottom Of External Casing												0.400	Bottom of 13 3/8 External Casing.	3625	
857.39	41.84	42.12	C-22	Collar													0.400		3625	
899.51	42.12	41.25	C-23	Collar													0.400		3625	
940.76	41.25	41.40	C-24	Collar													0.400		3625	
982.16	41.40	41.13	C-25	Collar													0.400		3625	
1023.29	41.13	40.52	C-26	Collar													0.400		3625	
1063.82	40.52	39.84	C-27	Collar													0.400		3625	
1103.66	39.84	41.60	C-28	Collar													0.400		3625	
1145.25	41.60	42.04	C-29	Collar													0.400		3625	
1187.29	42.04	43.45	C-30	Collar													0.400		3625	
1230.74	43.45	41.56	C-31	Collar													0.400		3625	
1272.31	41.56	41.90	C-32	Collar													0.400		3625	
1314.21	41.90	41.71	C-33	Collar													0.400		3625	
1355.91	41.71	39.76	C-34	Collar													0.400		3625	
1395.67	39.76	41.56	C-35	Collar													0.400		3625	
1437.23	41.56	41.37	C-36	Collar													0.400		3625	
1478.61	41.37	43.00	C-37	Collar													0.400		3625	
1521.61	43.00	41.20	C-38	Collar													0.400		3625	
1562.81	41.20	41.88	C-39	Collar													0.400		3625	
1604.69	41.88	39.01	C-40	Collar													0.400		3625	
1643.71	39.01	42.71	C-41	Collar													0.400		3625	
1686.42	42.71	41.05	C-42	Collar													0.400		3625	
1727.46	41.05	41.00	C-43	Collar													0.400		3625	
1768.46	41.00	41.92	C-44	Collar													0.400		3625	
1810.38	41.92	41.67	C-45	Collar													0.400		3625	
1852.05	41.67	43.13	C-46	Collar													0.400		3625	
1895.18	43.13	41.90	C-47	Collar													0.400		3625	
1937.08	41.90	41.11	C-48	Collar													0.400		3625	
1978.19	41.11	40.85	C-49	Collar													0.400		3625	
2019.05	40.85	41.40	C-50	Collar													0.400		3625	
2060.44	41.40	42.63	C-51	Collar													0.400		3625	
2103.07	42.63	41.07	C-52	Collar													0.400		3625	
2144.14	41.07	41.70	C-53	Collar													0.400		3625	
2158.84	14.70	41.70	MLCB-53-1	Metal Loss Call Box		External	1.1	1.1	17	PITT	4227	0.858	5926	0.612			0.400		3625	602
2158.88	14.74	41.70	MLC-53-1	Metal Loss Cluster		External	2.0	1.7	17	GENE	4227	0.858	5787	0.626	5753	0.630	0.400		3625	602
2158.93	14.79	41.70	MLCB-53-2	Metal Loss Call Box		External	0.8	1.4	16	PITT	4262	0.850	5973	0.607			0.400		3625	637
2167.49	23.35	41.70	MLCB-53-3	Metal Loss Call Box		External	0.8	1.4	15	PITT	4327	0.838	5978	0.606			0.400		3625	702
2185.84	41.70	41.39	C-54	Collar													0.400		3625	
2197.13	11.29	41.39	MLCB-54-1	Metal Loss Call Box		External	0.8	1.1	19	PITT	4130	0.878	5962	0.608			0.400		3625	505
2198.03	12.20	41.39	MLCB-54-2	Metal Loss Call Box		External	1.1	1.2	16	PITT	4307	0.842	5937	0.611			0.400		3625	682
2198.48	12.65	41.39	MLCB-54-3	Metal Loss Call Box		External	0.8	1.0	15	PITT	4336	0.836	5978	0.606			0.400		3625	711
2212.61	26.77	41.39	MLCB-54-4	Metal Loss Call Box		External	1.7	1.1	18	PITT	4201	0.863	5838	0.621			0.400		3625	576
2212.83	27.00	41.39	MLCB-54-5	Metal Loss Call Box		External	1.1	1.3	15	PITT	4336	0.836	5940	0.610			0.400		3625	711

Southern California Gas Company
Aliso Canyon
Fernando Fee 35B

Log Depth	Dist UHC	Joint Length	Identifier	Class	Description	Surface Indication	Length	Width	Depth	Dim Class	P Safe Barlow	ERF Barlow	P Safe Mod B31G	ERF Mod B31G	P Safe Effective Area	ERF Effective Area	NWT	Comment	115% MAOP	Delta MAOP (Barlow)
ft	ft	ft					in	in	%		psi		psi		psi		in		psi	psi
2224.49	38.65	41.39	MLCB-54-6	Metal Loss Call Box		External	1.9	1.9	15	GENE	4336	0.836	5840	0.621			0.400		3625	711
2227.23	41.39	42.01	C-55	Collar													0.400		3625	
2235.88	8.65	42.01	MLCB-55-1	Metal Loss Call Box		External	2.2	1.1	16	AXGR	4310	0.841	5788	0.626			0.400		3625	685
2241.37	14.14	42.01	MLCB-55-2	Metal Loss Call Box		External	1.1	1.2	16	PITT	4287	0.846	5939	0.610			0.400		3625	662
2242.62	15.39	42.01	MLCB-55-3	Metal Loss Call Box		External	0.7	1.0	21	PITT	4033	0.899	5979	0.606			0.400		3625	408
2242.94	15.71	42.01	MLCB-55-4	Metal Loss Call Box		External	1.6	1.4	15	GENE	4336	0.836	5885	0.616			0.400		3625	711
2269.24	42.01	41.08	C-56	Collar													0.400		3625	
2310.32	41.08	43.55	C-57	Collar													0.400		3625	
2318.22	7.90	43.55	MLCB-57-1	Metal Loss Call Box		External	0.8	0.7	15	PITT	4336	0.836	5978	0.606			0.400		3625	711
2353.87	43.55	41.05	C-58	Collar													0.400		3625	
2394.92	41.05	41.00	C-59	Collar													0.400		3625	
2435.92	41.00	41.18	C-60	Collar													0.400		3625	
2477.11	41.18	41.82	C-61	Collar													0.400		3625	
2518.93	41.82	42.68	C-62	Collar													0.400		3625	
2561.61	42.68	42.28	C-63	Collar													0.400		3625	
2603.89	42.28	42.29	C-64	Collar													0.400		3625	
2635.20	31.31	42.29	MLCB-64-1	Metal Loss Call Box		External	0.8	1.1	15	PITT	4336	0.836	5978	0.606			0.400		3625	711
2646.18	42.29	41.20	C-65	Collar													0.400		3625	
2687.38	41.20	42.20	C-66	Collar													0.400		3625	
2729.58	42.20	43.29	C-67	Collar													0.400		3625	
2772.88	43.29	42.19	C-68	Collar													0.400		3625	
2815.07	42.19	41.66	C-69	Collar													0.400		3625	
2856.73	41.66	41.71	C-70	Collar													0.400		3625	
2898.44	41.71	41.88	C-71	Collar													0.400		3625	
2940.32	41.88	42.52	C-72	Collar													0.400		3625	
2982.83	42.52	42.65	C-73	Collar													0.400		3625	
3025.48	42.65	41.57	C-74	Collar													0.400		3625	
3067.05	41.57	42.03	C-75	Collar													0.400		3625	
3109.08	42.03	38.97	C-76	Collar													0.400		3625	
3148.06	38.97	42.35	C-77	Collar													0.400		3625	
3190.40	42.35	42.31	C-78	Collar													0.400		3625	
3232.71	42.31	41.85	C-79	Collar													0.400		3625	
3274.56	41.85	41.09	C-80	Collar													0.400		3625	
3315.65	41.09	42.12	C-81	Collar													0.400		3625	
3357.77	42.12	42.90	C-82	Collar													0.400		3625	
3400.67	42.90	41.26	C-83	Collar													0.400		3625	
3441.93	41.26	42.40	C-84	Collar													0.400		3625	
3484.33	42.40	40.97	C-85	Collar													0.400		3625	
3525.30	40.97	42.16	C-86	Collar													0.400		3625	
3567.46	42.16	40.87	C-87	Collar													0.400		3625	
3608.34	40.87	42.68	C-88	Collar													0.400		3625	
3651.02	42.68	37.87	C-89	Collar													0.400		3625	
3688.89	37.87	42.20	C-90	Collar													0.400		3625	
3731.09	42.20	42.27	C-91	Collar													0.400		3625	
3773.37	42.27	42.10	C-92	Collar													0.400		3625	
3815.45	42.09	42.10	H-92-1	Hardware	Centralizer												0.400		3625	
3815.47	42.10	43.54	C-93	Collar													0.400		3625	
3859.01	43.54	42.83	C-94	Collar													0.400		3625	
3901.80	42.80	42.83	H-94-1	Hardware	Centralizer												0.400		3625	
3901.84	42.83	42.26	C-95	Collar													0.400		3625	
3944.10	42.26	44.17	C-96	Collar													0.400		3625	
3979.22	35.12	44.17	MLCB-96-1	Metal Loss Call Box		External	0.7	1.6	15	CIGR	4336	0.836	5989	0.605			0.400		3625	711
3984.60	40.50	44.17	H-96-1	Hardware	Centralizer												0.400		3625	
3987.46	43.36	44.17	H-96-2	Hardware	DV Tool												0.400	Stage Collar	3625	
3988.27	44.17	44.17	C-97	Collar													0.400		3625	
4031.12	42.85	27.40	C-98	Collar													0.400		3625	
4058.52	27.40	41.50	C-99	Collar													0.400		3625	
4100.02	41.50	43.24	C-100	Collar													0.400		3625	
4100.40	0.38	43.24	H-100-1	Hardware	Centralizer												0.400		3625	
4143.26	43.24	41.88	C-101	Collar													0.400		3625	
4185.14	41.88	42.59	C-102	Collar													0.400		3625	
4185.22	0.07	42.59	H-102-1	Hardware	Centralizer												0.400		3625	
4227.73	42.59	41.66	C-103	Collar													0.400		3625	
4269.40	41.66	39.68	C-104	Collar													0.400		3625	
4269.83	0.44	39.68	H-104-1	Hardware	Centralizer												0.400		3625	
4309.08	39.68	42.90	C-105	Collar													0.400		3625	
4351.98	42.90	42.40	C-106	Collar													0.400		3625	
4394.38	42.40	41.61	C-107	Collar													0.400		3625	
4435.99	41.61	42.40	C-108	Collar													0.400		3625	
4478.39	42.40	42.52	C-109	Collar													0.400		3625	

Southern California Gas Company
Aliso Canyon
Fernando Fee 35B

Log Depth	Dist UHC	Joint Length	Identifier	Class	Description	Surface Indication	Length	Width	Depth	Dim Class	P Safe Barlow	ERF Barlow	P Safe Mod B31G	ERF Mod B31G	P Safe Effective Area	ERF Effective Area	NWT	Comment	115% MAOP	Delta MAOP (Barlow)
ft	ft	ft					in	in	%		psi		psi		psi		in		psi	psi
4520.91	42.52	38.35	C-110	Collar													0.400		3625	
4559.26	38.35	41.28	C-111	Collar													0.400		3625	
4600.54	41.28	41.50	C-112	Collar													0.400		3625	
4642.04	41.50	41.07	C-113	Collar													0.400		3625	
4683.11	41.07	42.22	C-114	Collar													0.400		3625	
4725.33	42.22	39.77	C-115	Collar													0.400		3625	
4765.11	39.77	42.50	C-116	Collar													0.400		3625	
4807.61	42.50	39.40	C-117	Collar													0.400		3625	
4847.01	39.40	41.71	C-118	Collar													0.400		3625	
4888.72	41.71	41.81	C-119	Collar													0.400		3625	
4930.53	41.81	42.23	C-120	Collar													0.400		3625	
4972.76	42.23	42.64	C-121	Collar													0.400		3625	
5015.40	42.64	41.66	C-122	Collar													0.400		3625	
5057.06	41.66	41.83	C-123	Collar													0.400		3625	
5098.89	41.83	42.42	C-124	Collar													0.400		3625	
5141.31	42.42	42.03	C-125	Collar													0.400		3625	
5183.34	42.03	41.80	C-126	Collar													0.400		3625	
5225.15	41.80	42.57	C-127	Collar													0.400		3625	
5267.72	42.57	36.81	C-128	Collar													0.400		3625	
5304.53	36.81	41.72	C-129	Collar													0.400		3625	
5346.26	41.72	41.68	C-130	Collar													0.400		3625	
5387.93	41.68	42.44	C-131	Collar													0.400		3625	
5430.38	42.44	42.20	C-132	Collar													0.400		3625	
5472.58	42.20	40.30	C-133	Collar													0.400		3625	
5512.88	40.30	42.43	C-134	Collar													0.400		3625	
5555.28	42.41	42.43	H-134-1	Hardware	Centralizer												0.400		3625	
5555.31	42.43	42.69	C-135	Collar													0.400		3625	
5598.00	42.69	42.52	C-136	Collar													0.400		3625	
5640.52	42.52	42.52	C-137	Collar													0.400		3625	
5640.72	0.20	42.39	H-137-1	Hardware	Centralizer												0.400		3625	
5682.91	42.39	41.15	C-138	Collar													0.400		3625	
5724.01	41.10	41.15	H-138-1	Hardware	Centralizer												0.400		3625	
5724.06	41.15	41.15	C-139	Collar													0.400		3625	
5765.91	41.85	29.37	C-140	Collar													0.400		3625	
5795.27	29.37	42.16	C-141	Collar													0.400		3625	
5795.72	0.45	42.16	H-141-1	Hardware	Centralizer												0.400		3625	
5837.43	42.16	42.69	C-142	Collar													0.400	8 5/8" Casing Grade change, K-55 36 lb/ft above and N-80 36 lb/ft below.	3625	
5880.06	42.63	42.69	H-142-1	Hardware	Centralizer												0.400		3625	
5880.12	42.69	41.11	C-143	Collar													0.400		3625	
5921.23	41.11	42.39	C-144	Collar													0.400		3625	
5963.62	42.39	42.39	C-145	Collar													0.400		3625	
5963.65	0.03	41.97	H-145-1	Hardware	Centralizer												0.400		3625	
6005.59	41.97	41.98	C-146	Collar													0.400		3625	
6047.38	41.79	41.98	H-146-1	Hardware	Centralizer												0.400		3625	
6047.57	41.98	41.98	C-147	Collar													0.400		3625	
6090.23	42.67	42.45	C-148	Collar													0.400		3625	
6132.68	42.45	42.45	C-149	Collar													0.400		3625	
6132.89	0.21	42.84	H-149-1	Hardware	Centralizer												0.400		3625	
6175.52	42.84	41.13	C-150	Collar													0.400		3625	
6216.65	41.13	41.13	C-151	Collar													0.400		3625	
6216.67	0.03	41.91	H-151-1	Hardware	Centralizer												0.400		3625	
6258.56	41.91	40.63	C-152	Collar													0.400		3625	
6299.19	40.63	40.63	C-153	Collar													0.400		3625	
6299.68	0.50	42.08	H-153-1	Hardware	Centralizer												0.400		3625	
6341.27	42.08	42.08	C-154	Collar													0.400		3625	
6341.53	0.26	42.84	H-154-1	Hardware	Centralizer												0.400		3625	
6384.11	42.84	42.18	C-155	Collar													0.400		3625	
6426.16	42.05	42.18	H-155-1	Hardware	Centralizer												0.400		3625	
6426.29	42.18	41.48	C-156	Collar													0.400		3625	
6467.76	41.48	42.48	C-157	Collar													0.400		3625	
6510.17	42.41	42.48	H-157-1	Hardware	Centralizer												0.400		3625	
6510.25	42.48	42.48	C-158	Collar													0.400		3625	
6552.00	41.75	42.93	C-159	Collar													0.400		3625	
6594.93	42.93	42.93	C-160	Collar													0.400		3625	
6595.09	0.16	42.36	H-160-1	Hardware	Centralizer												0.400		3625	
6637.29	42.36	42.11	C-161	Collar													0.400		3625	
6679.41	42.11	42.11	C-162	Collar													0.400		3625	
6679.70	0.30	40.95	H-162-1	Hardware	Centralizer												0.400		3625	

Southern California Gas Company
Aliso Canyon
Fernando Fee 35B

Log Depth	Dist UHC	Joint Length	Identifier	Class	Description	Surface Indication	Length	Width	Depth	Dim Class	P Safe Barlow	ERF Barlow	P Safe Mod B31G	ERF Mod B31G	P Safe Effective Area	ERF Effective Area	NWT	Comment	115% MAOP	Delta MAOP (Barlow)
ft	ft	ft					in	in	%		psi		psi		psi		in		psi	psi
6720.36	40.95	42.55	C-163	Collar													0.400		3625	
6762.79	42.43	42.55	H-163-1	Hardware	Centralizer												0.400		3625	
6762.91	42.55	42.24	C-164	Collar													0.400		3625	
6805.15	42.24	39.41	C-165	Collar													0.400		3625	
6844.56	39.41	42.59	C-166	Collar													0.400		3625	
6844.64	0.08	42.59	H-166-1	Hardware	Centralizer												0.400		3625	
6867.50	22.94	42.59	MLCB-166-1	Metal Loss Call Box		Internal	0.7	1.4	17	PITT	6143	0.590	8283	0.438			0.400		3625	2518
6887.15	42.59	42.46	C-167	Collar													0.400		3625	
6907.94	20.79	42.46	MLCB-167-1	Metal Loss Call Box		Internal	0.5	0.6	26	PITT	5455	0.664	8290	0.437			0.400		3625	1830
6929.61	42.46	42.84	C-168	Collar													0.400		3625	
6929.68	0.07	42.84	H-168-1	Hardware	Centralizer												0.400		3625	
6969.86	40.25	42.84	MLCB-168-1	Metal Loss Call Box		Internal	1.0	0.9	18	PITT	6080	0.596	8228	0.441			0.400		3625	2455
6972.45	42.84	42.72	C-169	Collar													0.400		3625	
7014.92	42.47	42.72	H-169-1	Hardware	Centralizer												0.400		3625	
7015.17	42.72	34.73	C-170	Collar													0.400		3625	
7024.83	9.65	34.73	MLCB-170-1	Metal Loss Call Box		Internal	1.6	6.5	16	GENE	6233	0.582	8132	0.446			0.400		3625	2608
7025.67	10.50	34.73	MLCB-170-2	Metal Loss Call Box		Internal	1.4	3.9	18	GENE	6085	0.596	8150	0.445			0.400		3625	2460
7049.90	34.73		C-171	Interpretation Boundary															3625	

Inspection Date: 07-14-2016
Report Date: 07-18-2016

Ex. II - 22

Schlumberger

Company: Southern California Gas Company

Well: Frew 4

Field: Aliso Canyon

County: Los Angeles State: California

Ultrasonic Imager

Gamma Ray - CCL

7" casing

County:	Los Angeles
Field:	Aliso Canyon
Location:	
Well:	Frew 4
Company:	Southern California Gas Company

Location:

		Elev.: K.B.	2428.00 ft
		G.L.	2419.75 ft
		D.F.	
Permanent Datum:	Ground Level	Elev.:	2419.75 f
Log Measured From:	Kelly Bushing	8.25 ft	above Perm.Datum
Drilling Measured From:	Kelly Bushing		

API Serial No.	Section:	Township:	Range:
04-037-00667-00	29	3N	16W

Logging Date		19-Oct-2016	
Run Number		Two	
Depth Driller		8176.00 ft	
Schlumberger Depth		8176.00 ft	
Bottom Log Interval		8168.00 ft	
Top Log Interval		7.00 ft	
Casing Fluid Type		KCl Brine with Polymer	
Salinity			
Density		9 lbm/gal	
Fluid Level		8.00 ft	
BIT/CASING/TUBING STRING			
Bit Size		11.00 in	
From		7421.00 ft	
To		8300.00 ft	
Casing/Tubing Size		7 in	
Weight		26 lbm/ft	
Grade		N80	
From		6774.00 ft	
To		8280.00 ft	
Max Recorded Temperatures			
Logger on Bottom	Time	20-Oct-2016 09:51:00	
Unit Number	Location:	3189 Ventura	
Recorded By		I. Kartawidjaja	
Witnessed By		Mr. Tom McMahon	

Disclaimer

THE USE OF AND RELIANCE UPON THIS RECORDED-DATA BY THE HEREIN NAMED COMPANY (AND ANY OF ITS AFFILIATES, PARTNERS, REPRESENTATIVES, AGENTS, CONSULTANTS AND EMPLOYEES) IS SUBJECT TO THE TERMS AND CONDITIONS AGREED UPON BETWEEN SCHLUMBERGER AND THE COMPANY, INCLUDING: (a) RESTRICTIONS ON USE OF THE RECORDED-DATA; (b) DISCLAIMERS AND WAIVERS OF WARRANTIES AND REPRESENTATIONS REGARDING COMPANY'S USE AND RELIANCE UPON THE RECORDED-DATA; AND (c) CUSTOMER'S FULL AND SOLE RESPONSIBILITY FOR ANY INFERENCE DRAWN OR DECISION MADE IN CONNECTION WITH THE USE OF THIS RECORDED-DATA.

Contents

1. Header
2. Disclaimer
3. Contents
4. Well Sketch
5. Borehole Size/Casing/Tubing Record
6. Remarks and Equipment Summary
7. Job Event Summary
8. USI Fluid Properties Measurement
9. Composite 1 Main Pass 5 in = 100 ft
   9.1 Integration Summary
   9.2 Software Version
   9.3 Composite Summary
   9.4 Log (LBV1_USI-VDL (DSLT) Cement 7inch)
   9.5 Parameter Listing
10. Composite 1 Main Pass 5 IN = 100 FT
   10.1 Integration Summary
   10.2 Composite Summary
   12.2 Composite Summary
   12.3 Log (LBV1_USI Corrosion 7inch)
13. Composite 1 USI Compressed Goodwin
   13.1 Integration Summary
   13.2 Composite Summary
   13.3 Log (Import of USI Goodwin)
14. XYZ (USI Fluid Acoustic Slowness vs Depth)
15. XYZ (USI Theoretical Acoustic impedance of mud vs Depth)
16. Tail

10.3 Log (LBV1_USI Composite 7inch)
11. Two Cement Log 2 IN = 100 FT
11.1 Integration Summary
11.2 Composite Summary
11.3 Log (LBV1_USI Cement 7inch)
12. Composite 1 Corrosion 5 in = 100 ft
12.1 Integration Summary

Well Sketch

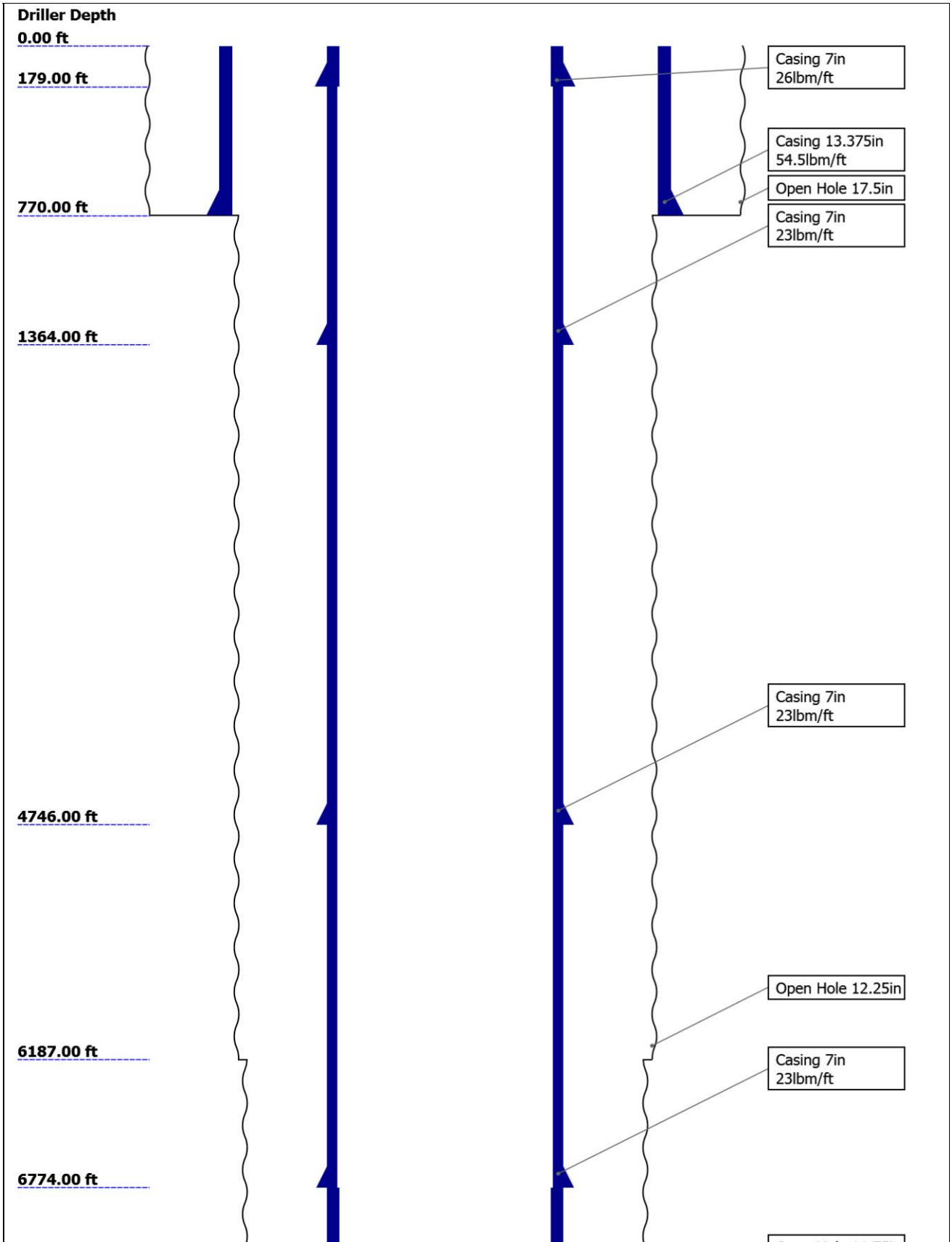

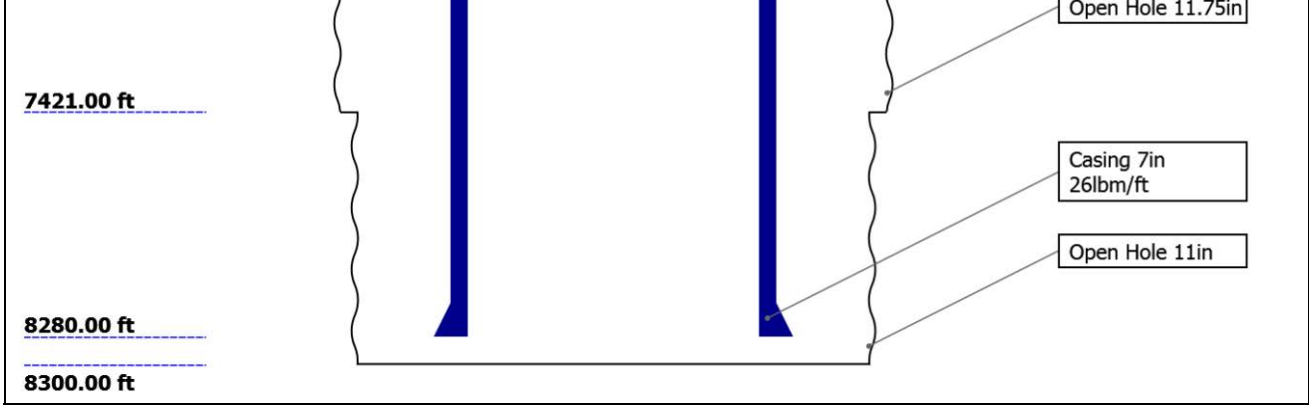

Borehole Size/Casing/Tubing Record

Bit						
Bit Size (in)	17.5	12.25	11.75	11		
Top Driller (ft)	0	770	6187	7421		
Top Logger (ft)	0	770	6187	7421		
Bottom Driller (ft)	770	6187	7421	8300		
Bottom Logger (ft)	770	6187	7421	8300		
Casing						
Size (in)	13.375	7	7	7	7	7
Weight (lbm/ft)	54.5	26	23	23	23	26
Inner Diameter (in)	12.615	6.276	6.366	6.366	6.366	6.276
Grade	J55	N80	N80	J55	N80	N80
Top Driller (ft)	0	0	179	1364	4746	6774
Top Logger (ft)	0	0	179	1364	4746	6774
Bottom Driller (ft)	770	179	1364	4746	6774	8280
Bottom Logger (ft)	770	179	1364	4746	6774	8280

Remarks and Equipment Summary

Two: Toolstring

Equip name	Length	MP name	Offset
LEH-QT:2867 LEH-QT:2867	**57.51**	Red	
DTC-H ECH-KC DTC-H	**54.59**	**CTEM** **HV** **TelStatus** **ToolStatus**	**53.69** **0.00** **51.59** **51.59**
HGNS-H:3923 HGNH:4819 NPV-N NSR-F:1303 HMCA-H HGNS-H:3923 HACCZ-H:4177	**51.59**	**Temperature** **GR** **CNL Porosity** **HGNS** **HMCA** **Accelerometer**	**51.57** **50.85** **44.52** **42.18** **42.18** **0.00**
AH-184[	**42.18**		

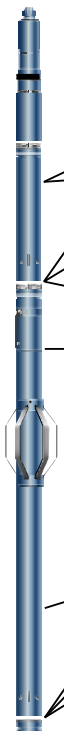

Two: Remarks

Depth correlated to Neutron Lifetime Log dated 4-19-74. Tied-in to Neutron curves between 7700-8100 ft

USIT logged at 10 deg 1.5 inch, speed 3200 fph. No hi-res repeat recorded as requested by client.

Main pass recorded with 0 psi surface pressure. Repeat pass recorded with 1000 psi from TD to ~6900 ft.

Logged from above top of sand at ~8168 ft to surface.

Rig: Ensign 334

Toolstring ran as per toolsketch.

Two centralizers on USIS and two CME-Y used to centralize ultrasonic tool.

Thank you for choosing Schlumberger!

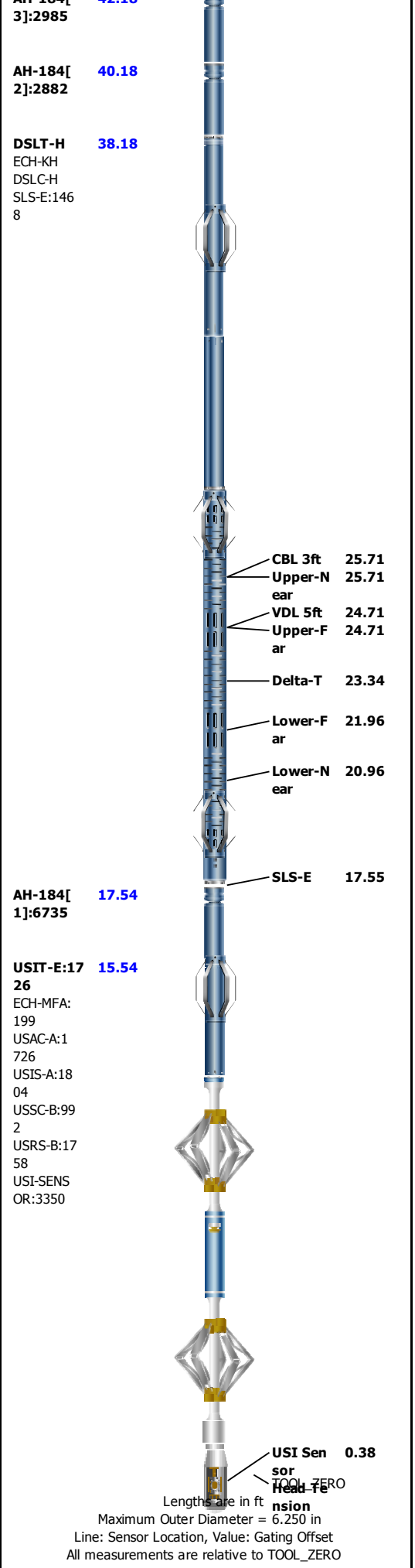

Job Event Summary

Event	Time	Duration	Interval	Remark

Event	Time	Duration	Interval	Remark
Log[1]:Down	Oct-19-2016 13:19	01:54:44	185.28 - 8127.82 ft	Fluid Properties Measurement
Log[6]:Up	Oct-19-2016 14:46	00:24:25	8162.42 - 6845.38 ft	Repeat Pass 1000 PSI
Log[9]:Up	Oct-20-2016 09:51	00:29:01	8170.38 - 6638.82 ft	Main Pass #1 0 PSI
Log[11]:Up	Oct-20-2016 10:24	02:09:06	6736.16 - 35.34 ft	Main Pass #2 0 PSI
Log[14]:Up	Oct-20-2016 12:53	00:04:58	153.18 - 3.59 ft	Main Pass #3 0 PSI

USIT - Fluid Properties Measurement

Run Name	Pass Name	Start Depth(ft)	Stop Depth(ft)
Run 1	Log[11]:Up	6737.51	36.69

Fluid Velocity = "Automatic".
CFVL equals DFSL channel

Start Depth(ft)	Stop Depth(ft)	Start Value(us/ft)	End Value(us/ft)

Mud Impedance = "FreePipe Norm.".
Free Pipe normalization zone is : 120.75m(396.17ft) to 129.39m(424.50ft)
MUD_N_FRP = 1.10
DFD = 1.08g/cm3(9.00lbm/gal)
CZMD median computed in free pipe normalization interval = 1.80 MRayl

Start Depth(ft)	Stop Depth(ft)	Start Value(Mrayl)	End Value(Mrayl)

Composite 1

Main Pass 5 in = 100 ft

Software Version

Acquisition System	Version
Maxwell 2016 SP1	6.1.58882.3100
Application Patch	Wireline_Hotfix-Perfo-2016SP1_6.1.63773

Computation	Description	Version
CEVAL	Sonic Cement Evaluation Computation Ensemble provides common Parameters and Channels	6.1.58882.3100
Cementation	Cementation Computation Application	6.1.58882.3100

SoftwareVersion_Tool	SoftwareVersion_Run Version	SoftwareVersion_Build Version
WAFE-SEC	Synergy SV451EC version 9.10	Synergy SV451EC version 9.10
WAFE-FEC	Synergy SV451EC version 9.10	Synergy SV451EC version 9.10
WAFE-TMDI	Synergy SV451EC version 46.19	Synergy SV451EC version 46.19

Tool Elements	Description	Software Version	Firmware Version
HGNS-H	HILT Gamma-Ray and Neutron Sonde, 150 degC	6.1.58882.3100	2.0
SLS-E	Sonic Logging Sonde E supports 3'-5'BHC DT and CBL/VDL	6.1.58882.3100	4.0
USI-SENSOR	USIT Transducer Element	6.1.58882.3100	DSP: v1.82

Composite Summary

Run Name	Pass Objective	Direction	Top	Bottom	Start	Stop	DSC Mode	Depth Shift	Include Parallel Data
Two	Log[9]:Up	Up	6640.29 ft	8171.85 ft	20-Oct-2016 9:51:39 AM	20-Oct-2016 10:20:40 AM	ON	1.47 ft	No
Two	Log[11]:Up	Up	36.69 ft	6737.51 ft	20-Oct-2016 10:24:53 AM	20-Oct-2016 12:34:00 PM	ON	1.35 ft	No
Two	Log[14]:Up	Up	5.56 ft	155.15 ft	20-Oct-2016 12:53:24 PM	20-Oct-2016 12:58:23 PM	ON	1.96 ft	No

All depths are referenced to toolstring zero

Log

Company:Southern California Gas Company Well:Frew 4
Composite 1:S008

Description: USI VDL Cement Format: Log (LBV1_USI-VDL (DSLT) Cement 7inch) Index Scale: 5 in per 100 ft Index Unit: ft Index Type: Measured Depth
Creation Date: 20-Oct-2016 14:28:02

TIME_1900 - Time Marked every 60.00 (s)

ERAV_IRAV ERAV_RHF1

IRAV_LHF1

IRAV_ERAV

LHF1_ERAV

RHF1_IRAV

Median of Unflagged External Radii (ERAV_RF) USIT-E[1]

3.7 in 2.7

Median of Unflagged External Radii (ERAV_RF) USIT-E[1]

2.7 in 3.7

Median Internal Radius of Casing Corrected for Eccentering (IRAV_RF) USIT-E[1]

3.7 in 2.7

Minimum of Unflagged Internal Radii (IRMN_RF) USIT-E[1]

2.7 in 3.7

Minimum of Unflagged Internal Radii (IRMN_RF) USIT-E[1]

3.7 in 2.7

Maximum of Unflagged Internal Radii (IRMX_RF) USIT-E[1]

2.7 in 3.7

Amplitude of Eccentering for Unflagged Waves (ECCE_RF) USIT-E[1]

0 in 0.5

Maximum of Unflagged Internal Radii (IRMX_RF) USIT-E[1]

3.7 in 2.7

Median Internal Radius of Casing Corrected for Eccentering (IRAV_RF) USIT-E[1]

2.7 in 3.7

Absent 1.000 2.500 4.000 5.500 7.000

Custom Normalization

USIT - Acoustic Impedance (AIBK) USIT-E[1] (Mrayl)

Acoustic Impedance Minimum (AIMN) USIT-E[1]

-1 Mrayl 9

Acoustic Impedance Average (AIAV) USIT-E[1]

-1 Mrayl 9

Acoustic Impedance Maximum (AIMX) USIT-E[1]

-1 Mrayl 9

Absent 0.300 3.581 5.054 6.527 8.000

Custom Normalization

USIT - Acoustic Impedance With Micro-debonding Image (AI_MDEBOND_IMG) USIT-E[1] (Mrayl)

Bonded

Gas

Liquid

Micro-debonding

Bond Index (BI) DSLT-H[1]

1 0

Min Amplitude Max

Sonic VDL Curve DSLT-H[1]

200 us 1200

Gamma Ray (ECGR) HGNS[1]

0 gAPI 150

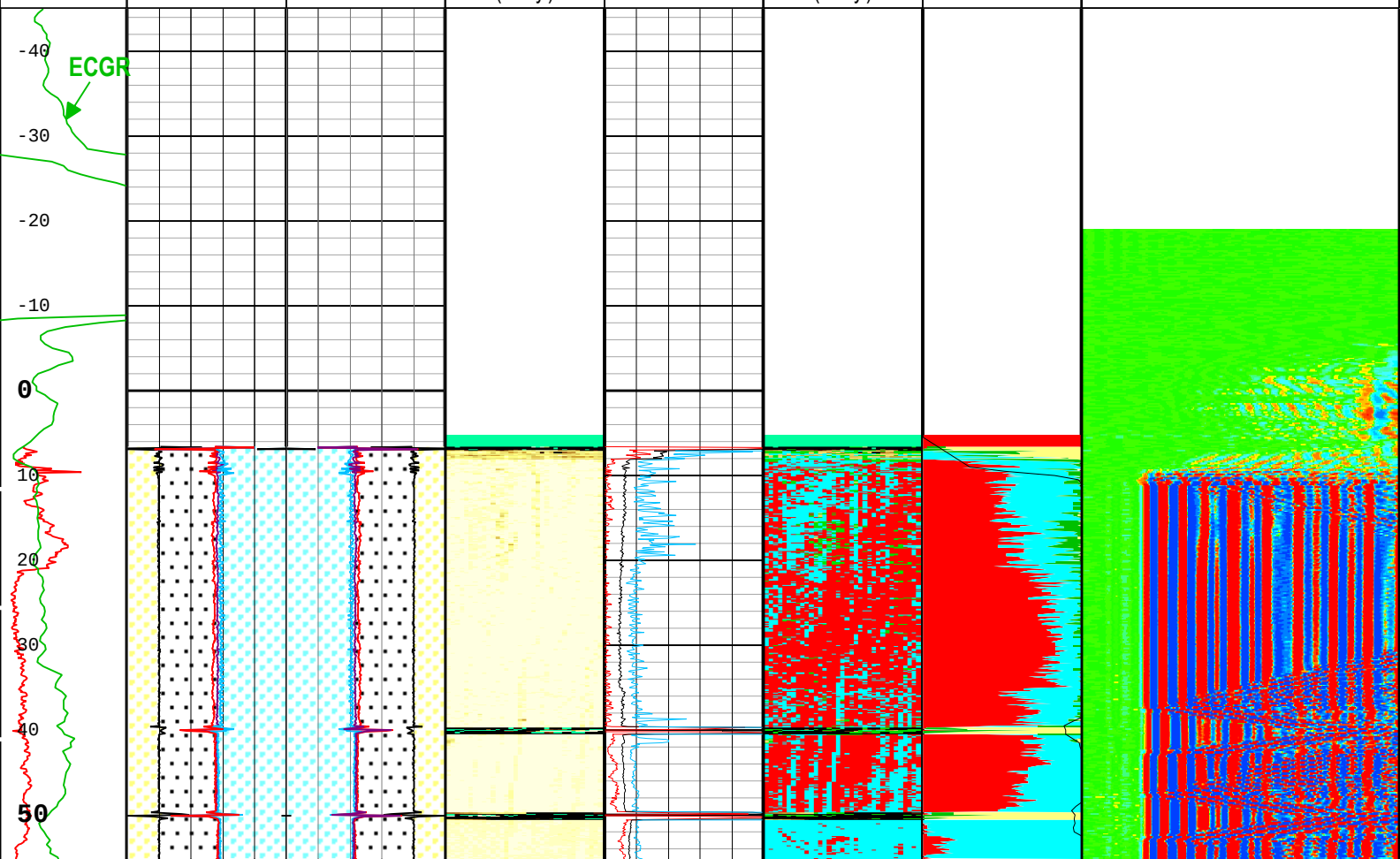

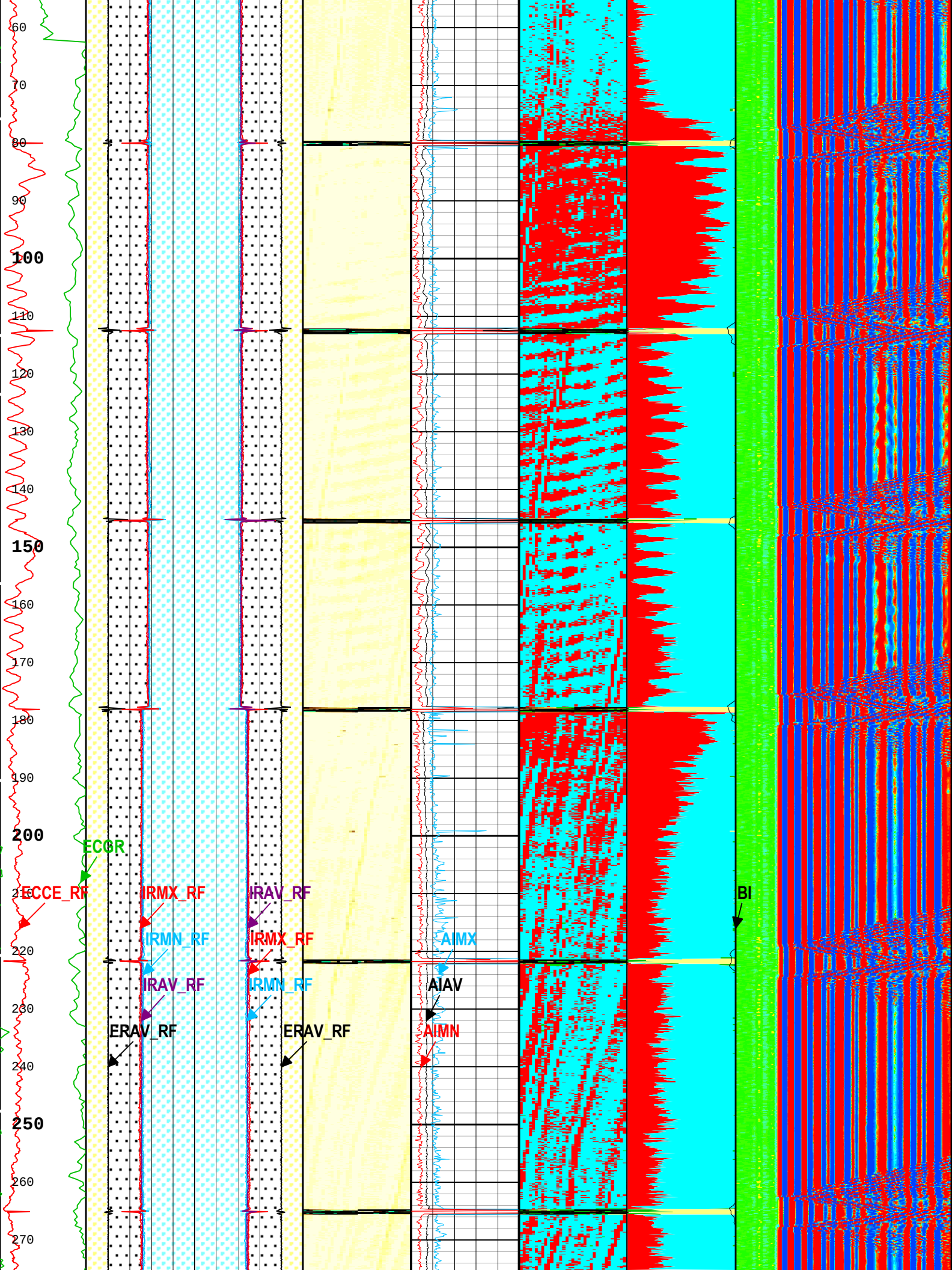
60
70
80
90
100
110
120
130
140
150
160
170
180
190
200
210
220
230
240
250
260
270
ECGR
ECCE_RF
IRMX_RF
IRAV_RF
IRMN_RF
IRMX_RF
IRAV_RF
IRMN_RF
ERAV_RF
ERAV_RF
AIMX
AIAV
AIMN
BI

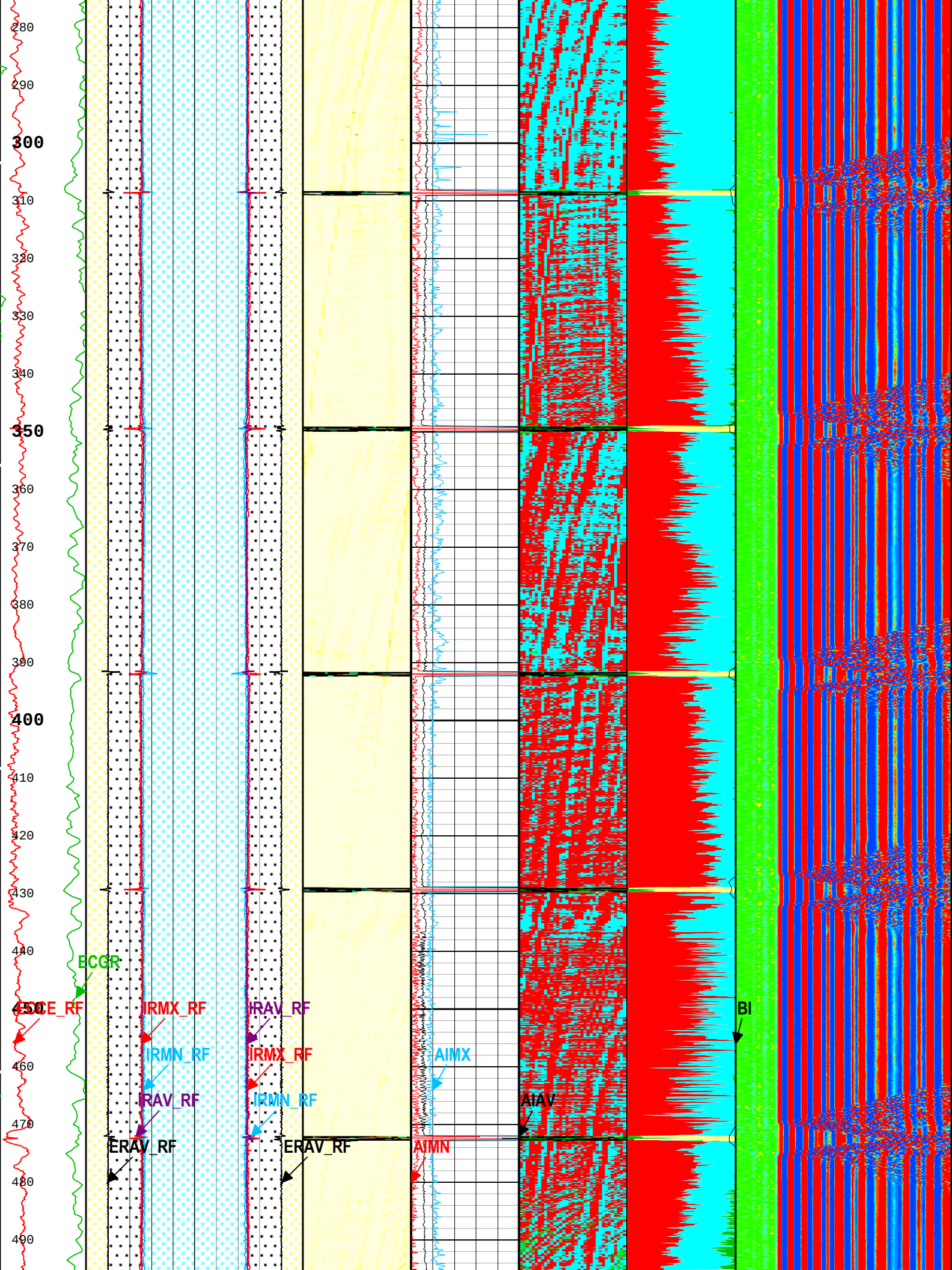
280
290
300
310
320
330
340
350
360
370
380
390
400
410
420
430
440
450
460
470
480
490
ECGR
ECCE_RF
IRMX_RF
IRAV_RF
IRMN_RF
IRMX_RF
IRAV_RF
IRMN_RF
ERAV_RF
ERAV_RF
AIMX
AIMN
AIAV
BI

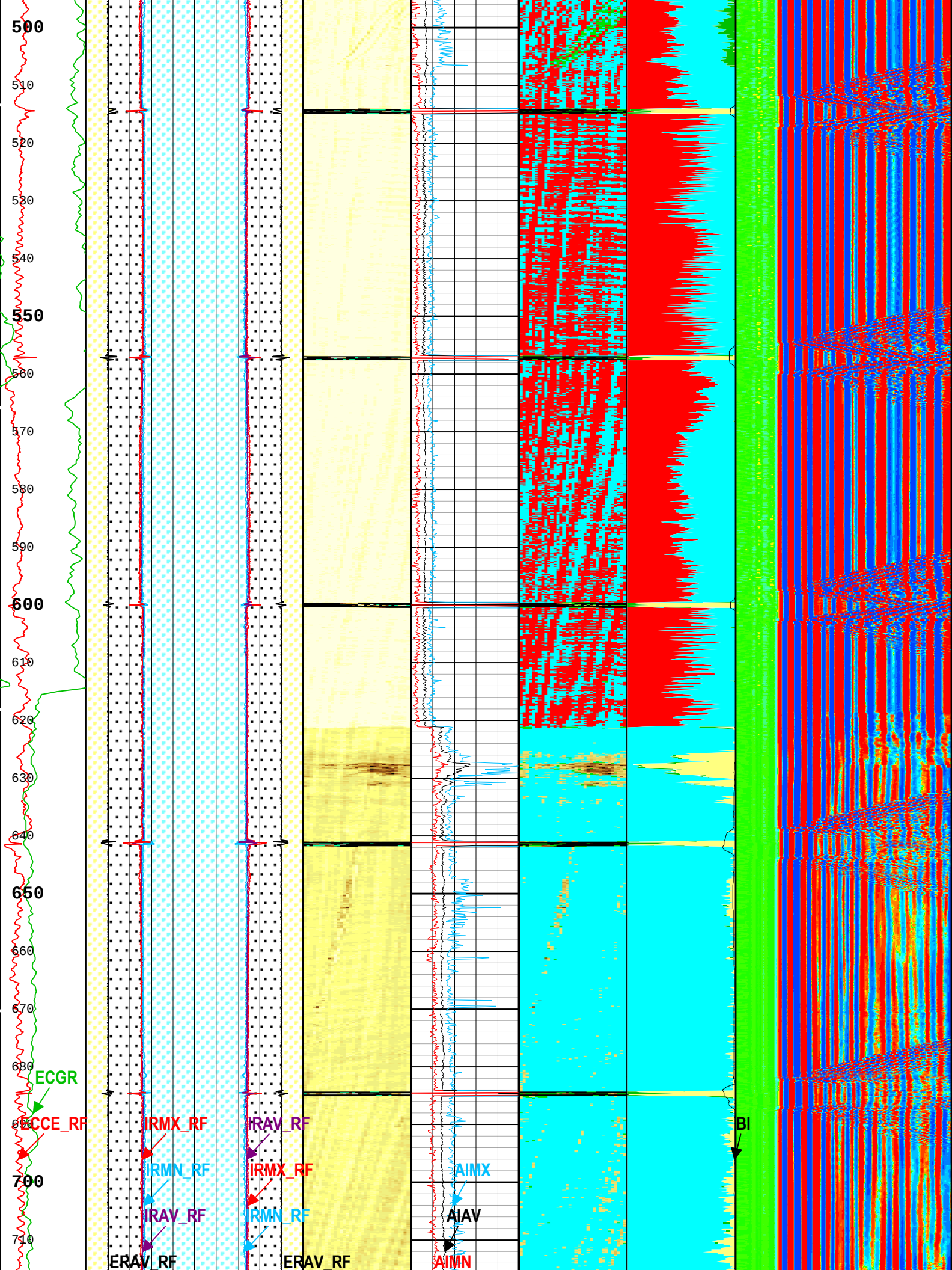
500
510
520
530
540
550
560
570
580
590
600
610
620
630
640
650
660
670
680
690
700
710
ECGR
CCE_RF
IRMX_RF
IRMN_RF
IRAV_RF
ERAV_RF
IRAV_RF
IRMX_RF
IRMN_RF
ERAV_RF
AIMX
AIAV
AIMN
BI

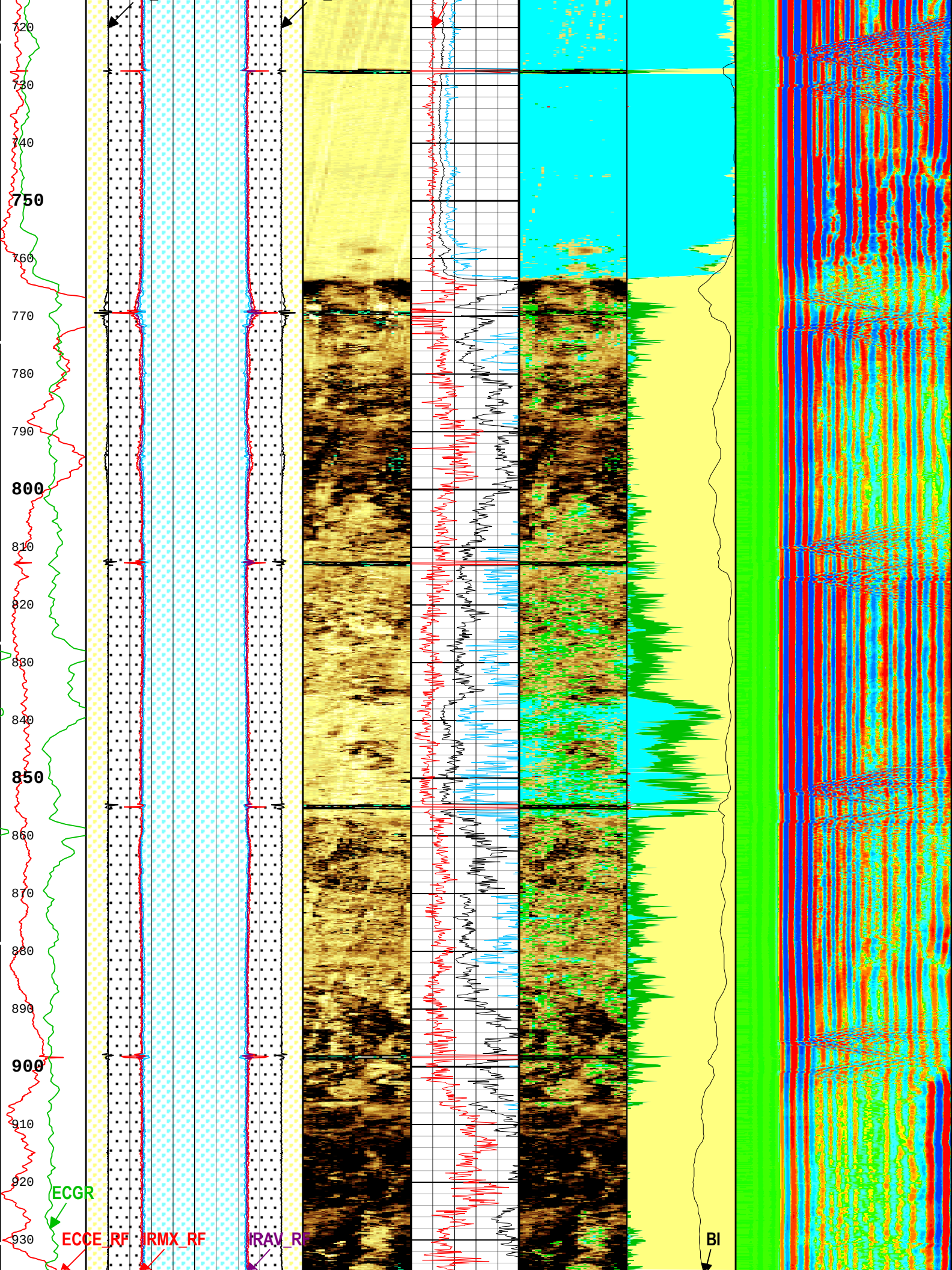
720
730
740
750
760
770
780
790
800
810
820
830
840
850
860
870
880
890
900
910
920
930
ECGR
ECCE_RF
IRMX_RF
IRAV_RF
BI

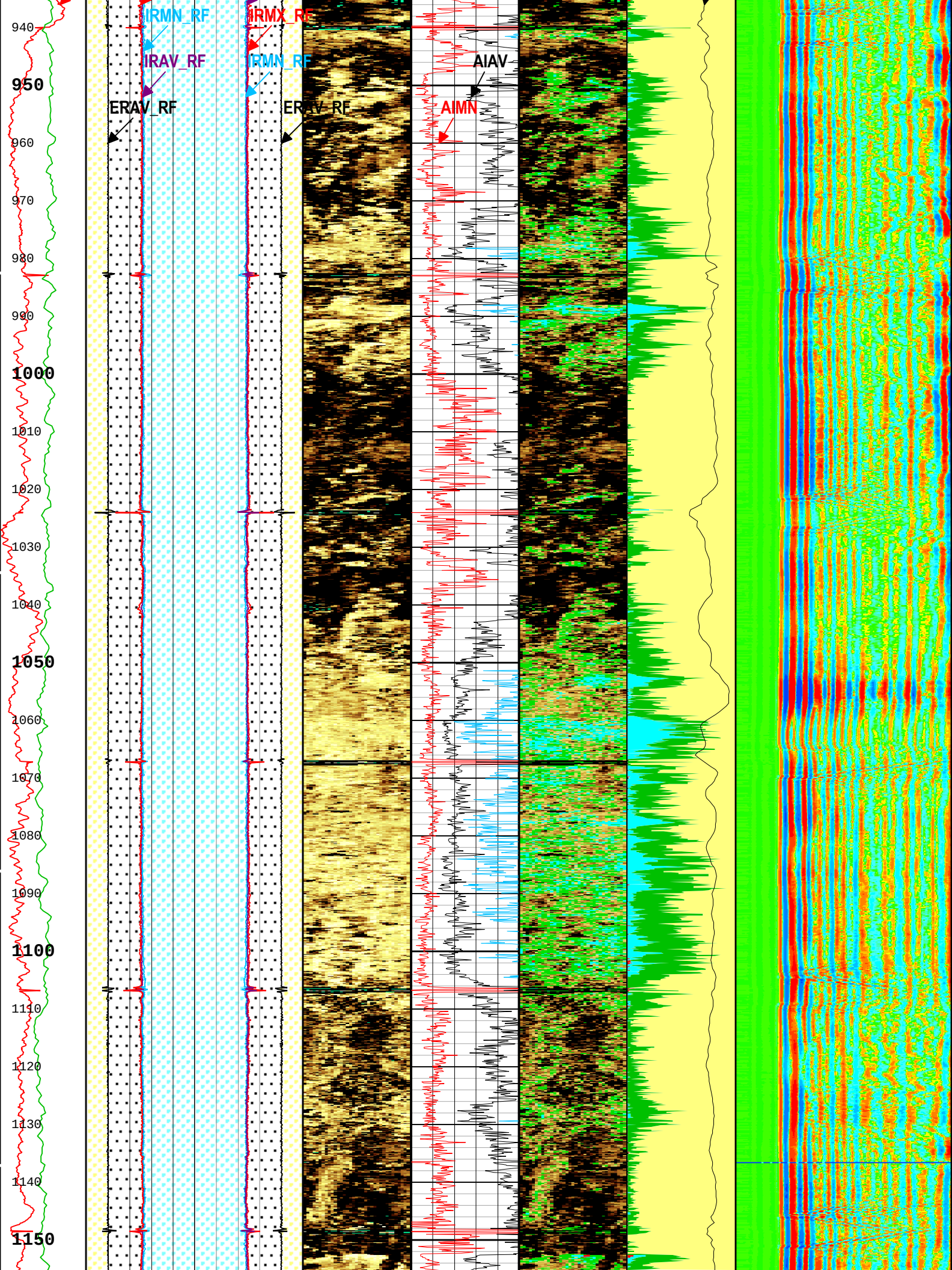
IRMN_RF
IRMX_RF
IRAV_RF
IRMN_RF
AIAV
ERAV_RF
ERAV_RF
AIMN
940
950
960
970
980
990
1000
1010
1020
1030
1040
1050
1060
1070
1080
1090
1100
1110
1120
1130
1140
1150

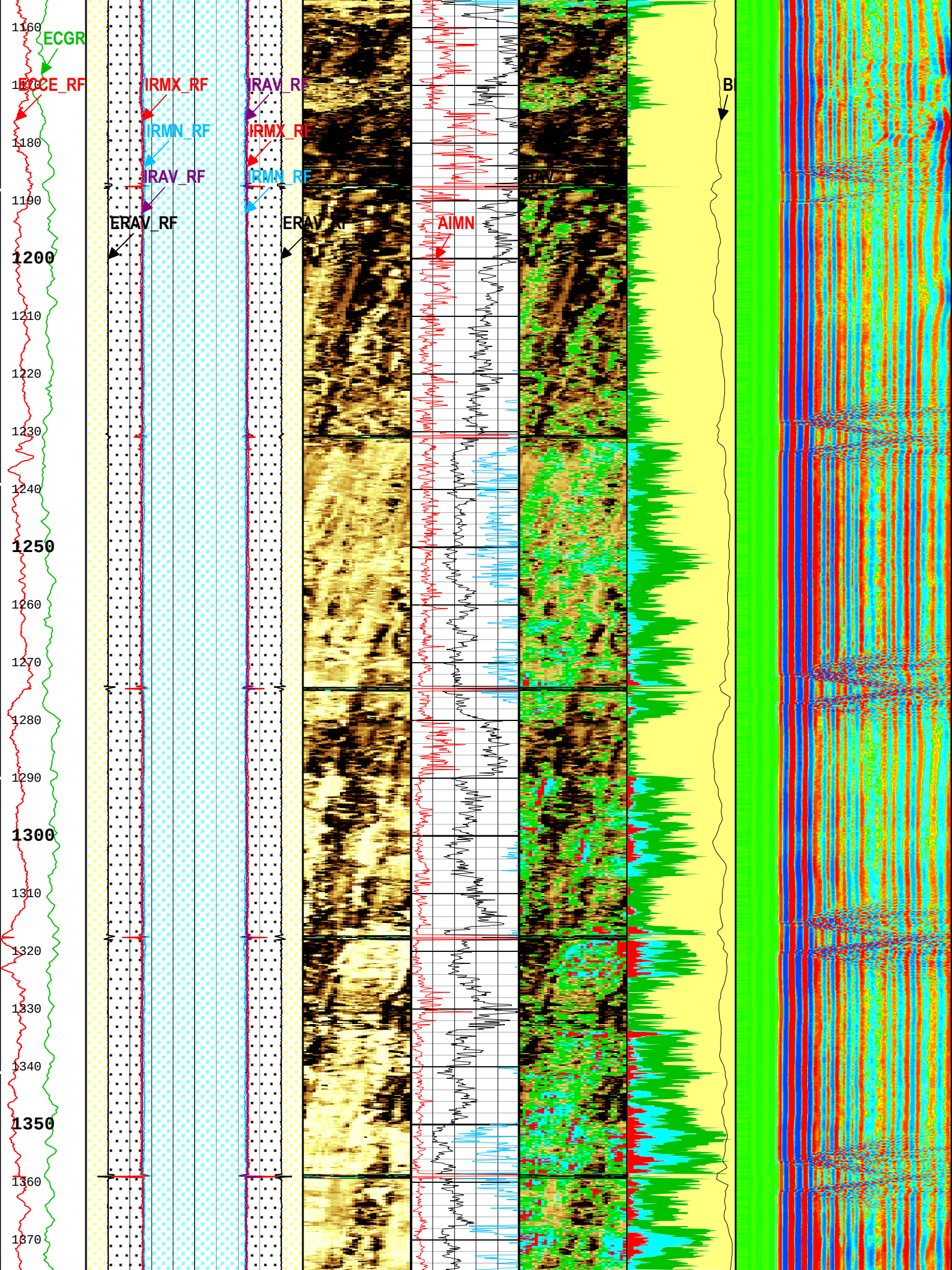
ECGR
ECCE_RF
IRMX_RF
IRAV_RF
IRMN_RF
IRMX_RF
IRAV_RF
IRMN_RF
ERAV_RF
ERAV_RF
AIMN
B
1160
1180
1200
1210
1220
1230
1240
1250
1260
1270
1280
1290
1300
1310
1320
1330
1340
1350
1360
1370

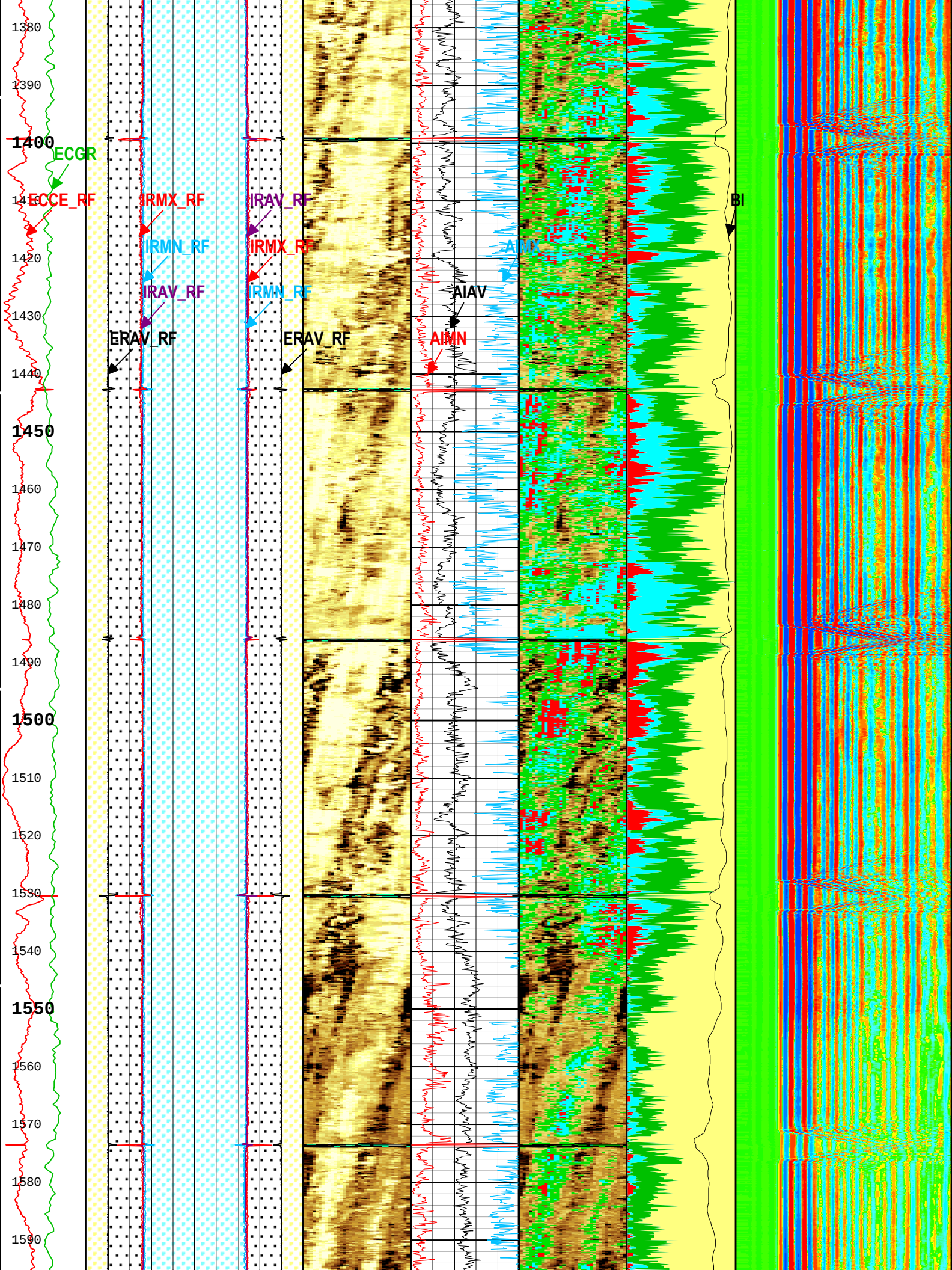
1380
1390
1400
ECGR
ECCE_RF
IRMX_RF
IRAV_RF
IRMN_RF
IRMX_RF
IRAV_RF
IRMN_RF
AIMN
AIAV
AIMN
ERAV_RF
ERAV_RF
BI
1420
1430
1440
1450
1460
1470
1480
1490
1500
1510
1520
1530
1540
1550
1560
1570
1580
1590

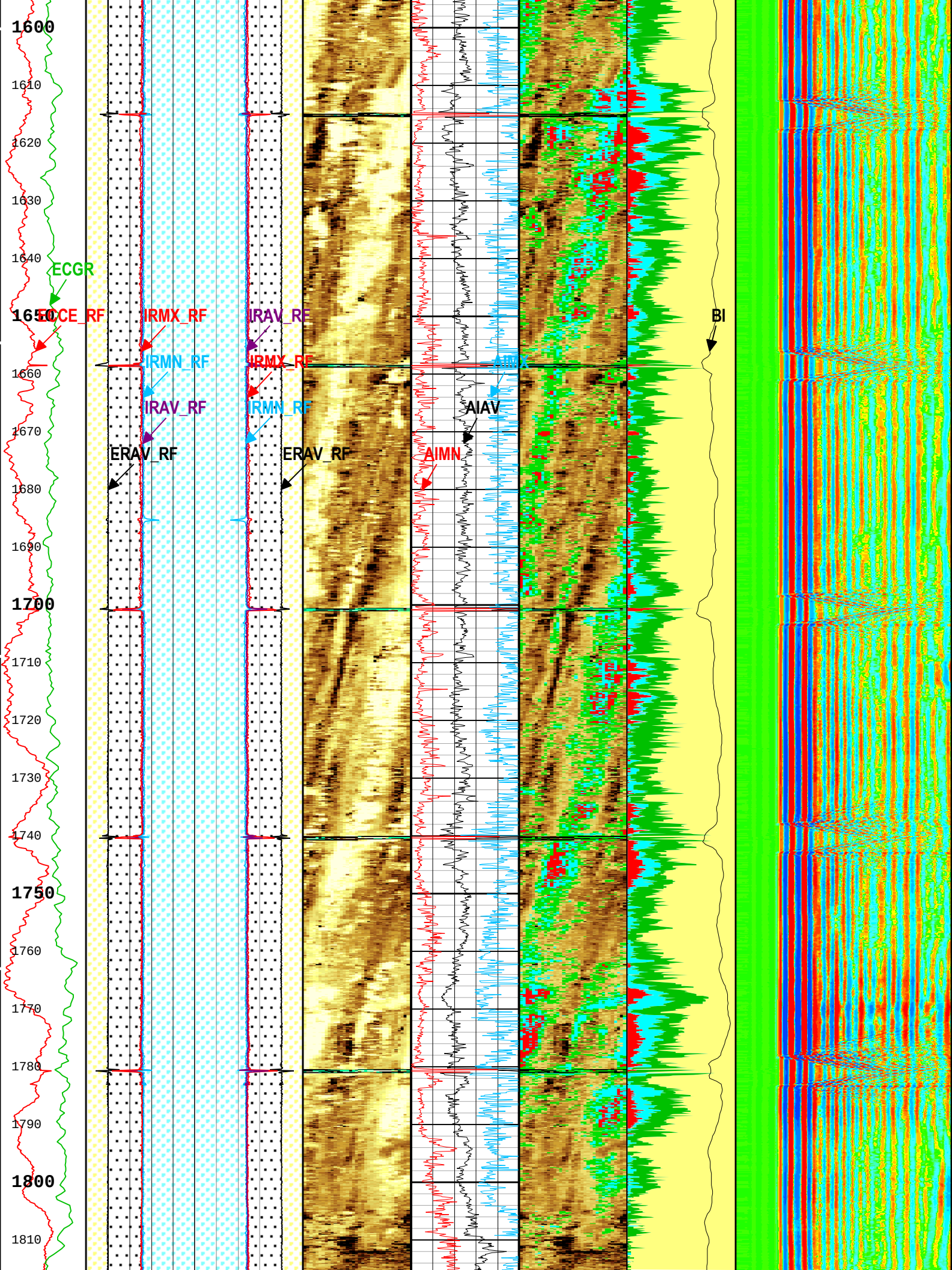
1600
1610
1620
1630
1640
1650
1660
1670
1680
1690
1700
1710
1720
1730
1740
1750
1760
1770
1780
1790
1800
1810
ECGR
CE_RF
IRMX_RF
IRAV_RF
IRMN_RF
IRMX_RF
IRAV_RF
IRMN_RF
ERAV_RF
ERAV_RF
AIMX
AIAV
AIMN
BI

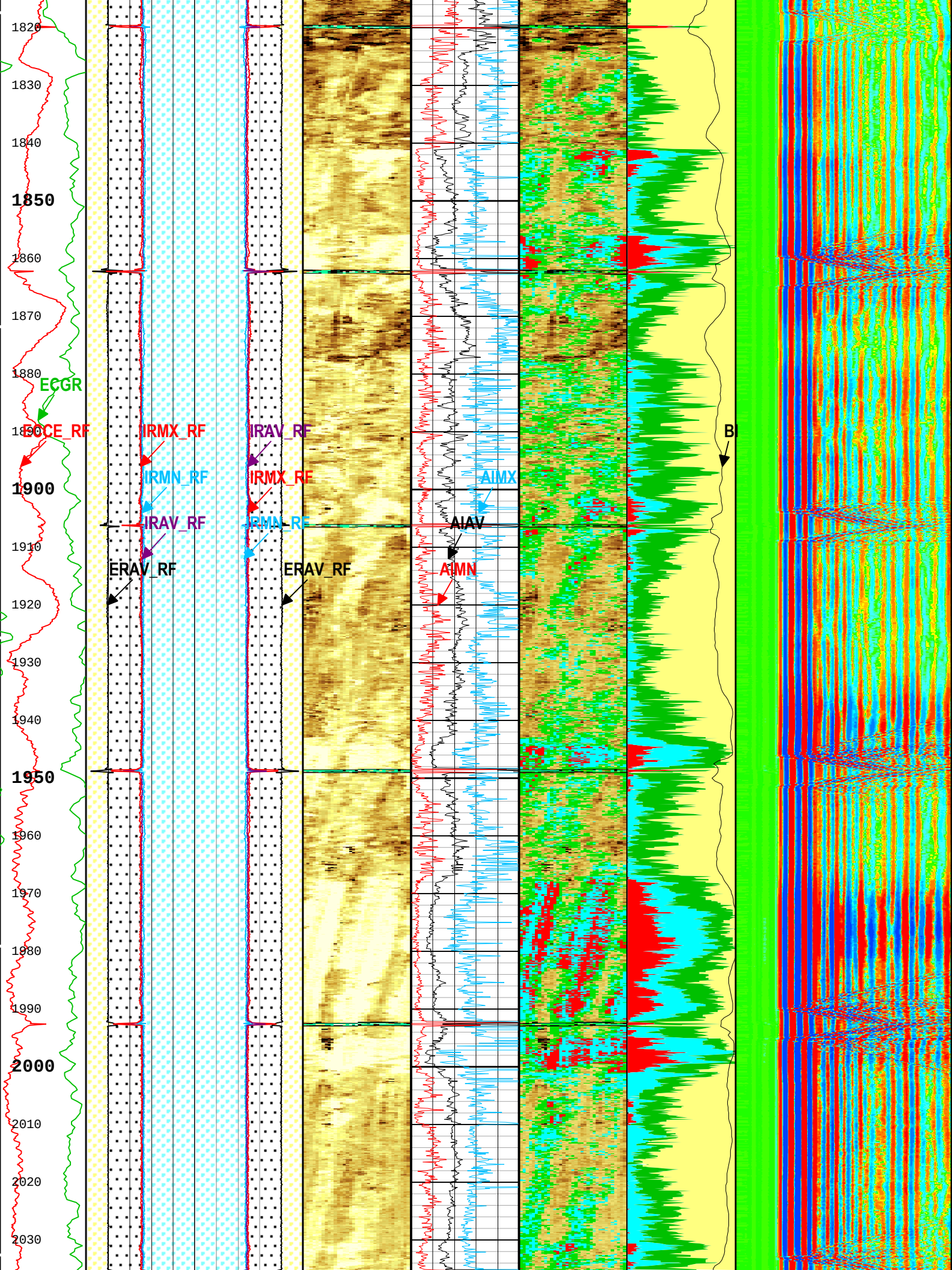
1820
1830
1840
1850
1860
1870
1880
1890
1900
1910
1920
1930
1940
1950
1960
1970
1980
1990
2000
2010
2020
2030
ECGR
ECCE_RF
IRMX_RF
IRMN_RF
IRAV_RF
ERAV_RF
IRAV_RF
IRMX_RF
IRMN_RF
ERAV_RF
AIMX
AIAV
AIMN
B

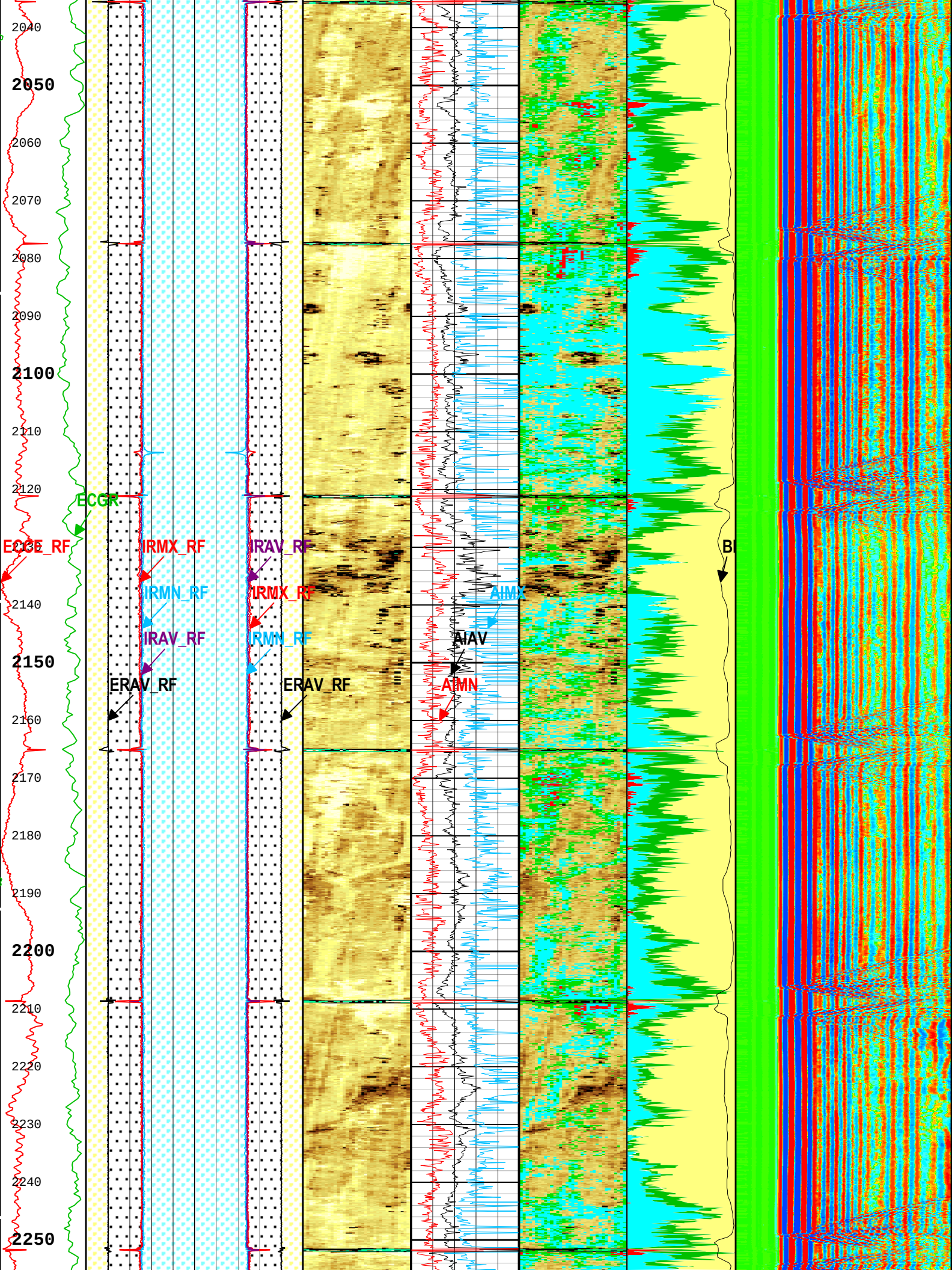
2040
2050
2060
2070
2080
2090
2100
2110
2120
2140
2150
2160
2170
2180
2190
2200
2210
2220
2230
2240
2250
ECGR
ECGE_RF
IRMX_RF
IRMN_RF
IRAV_RF
ERAV_RF
IRAV_RF
IRMX_RF
IRMN_RF
ERAV_RF
AIMX
AIAV
AIMN
BI

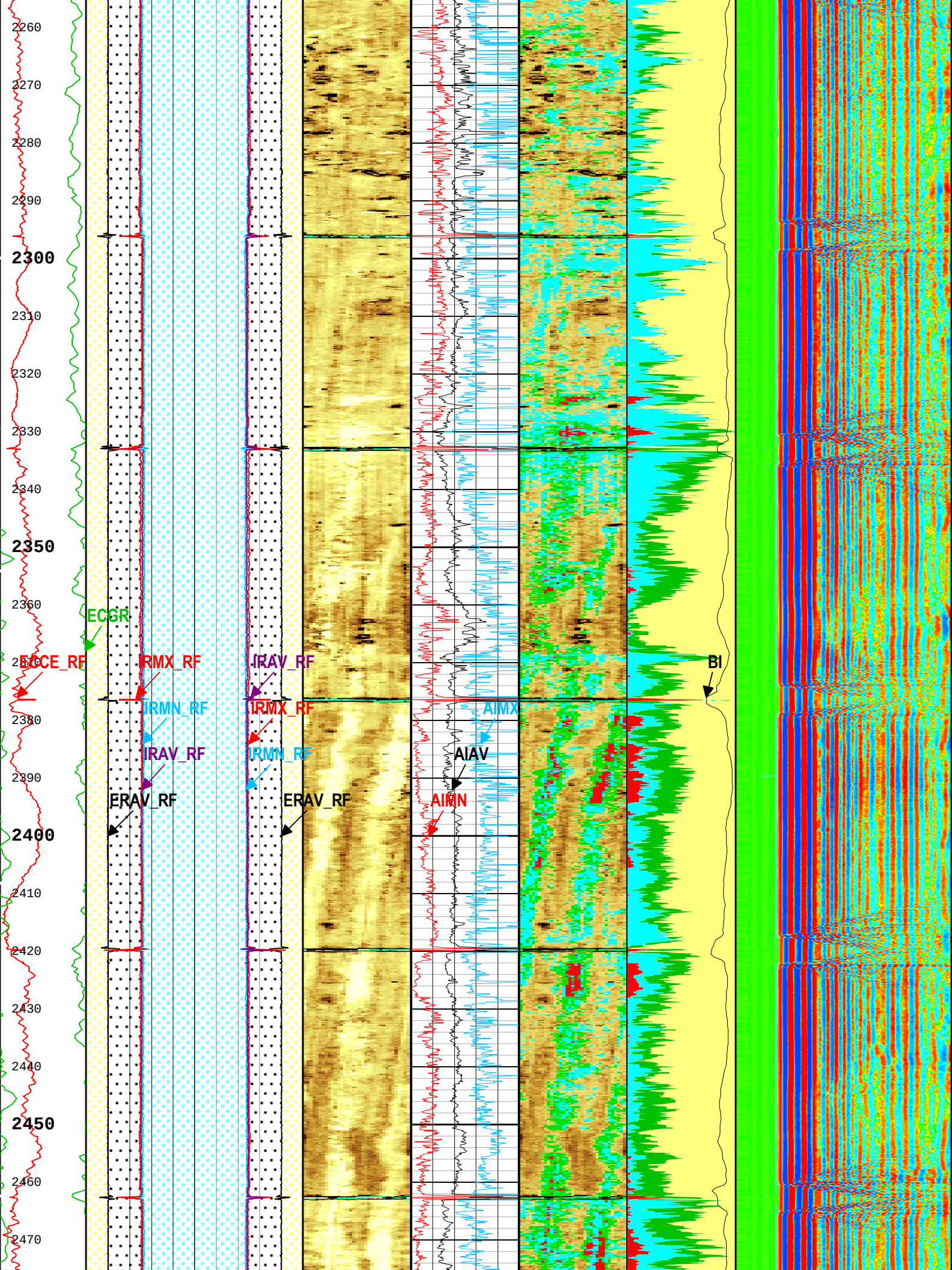
2260
2270
2280
2290
2300
2310
2320
2330
2340
2350
2360
2370
2380
2390
2400
2410
2420
2430
2440
2450
2460
2470
ECGR
ECCE_RF
IRMX_RF
IRAV_RF
IRMN_RF
IRAV_RF
ERAV_RF
IRAV_RF
IRMX_RF
IRMN_RF
ERAV_RF
AIMX
AIAV
AIMN
BI

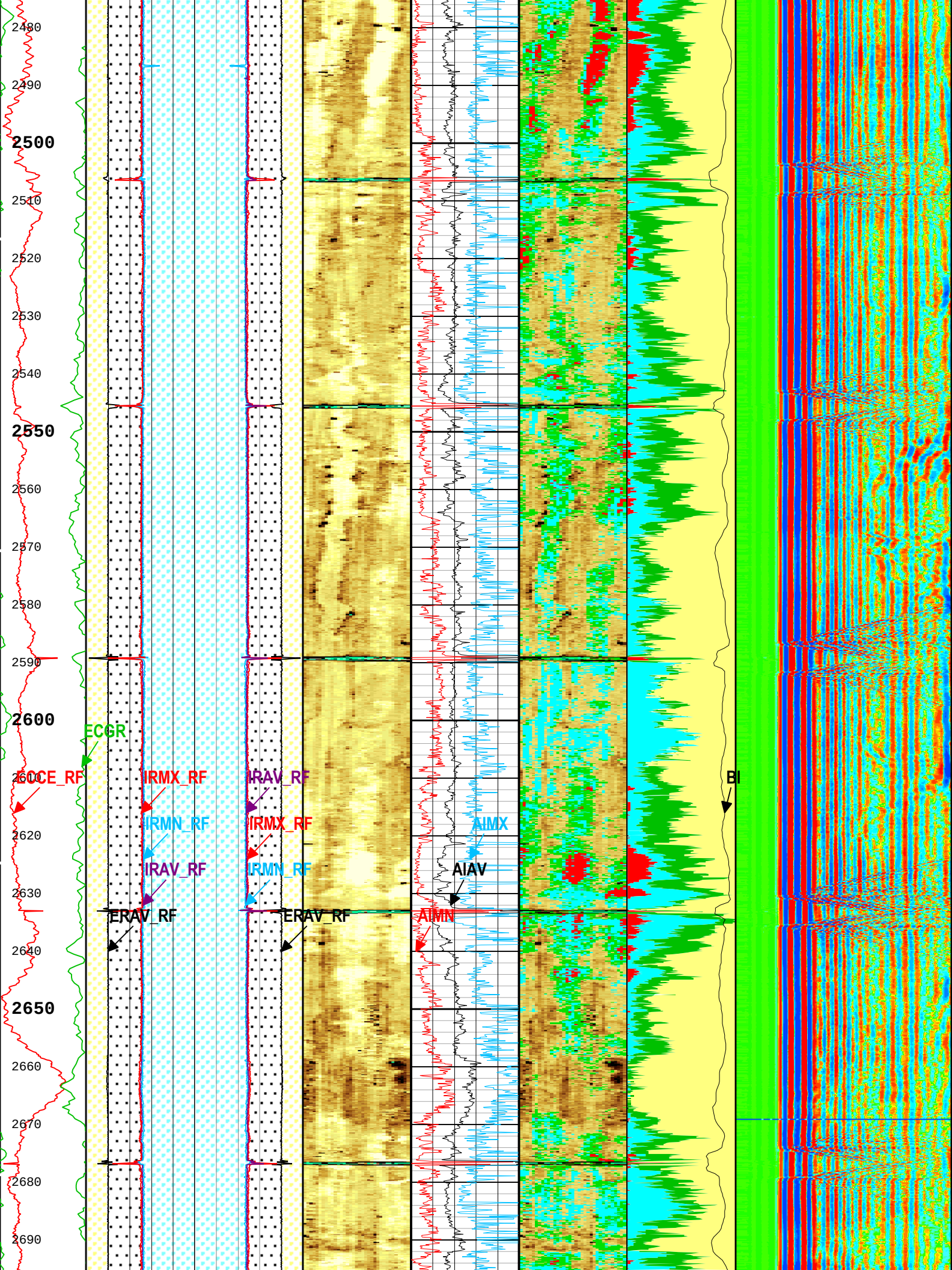
2480
2490
2500
2510
2520
2530
2540
2550
2560
2570
2580
2590
2600
2610
2620
2630
2640
2650
2660
2670
2680
2690
ECGR
ECCE_RF
IRMX_RF
IRMN_RF
IRAV_RF
ERAV_RF
IRAV_RF
IRMX_RF
IRMN_RF
ERAV_RF
AIMX
AIAV
AIMN
BI

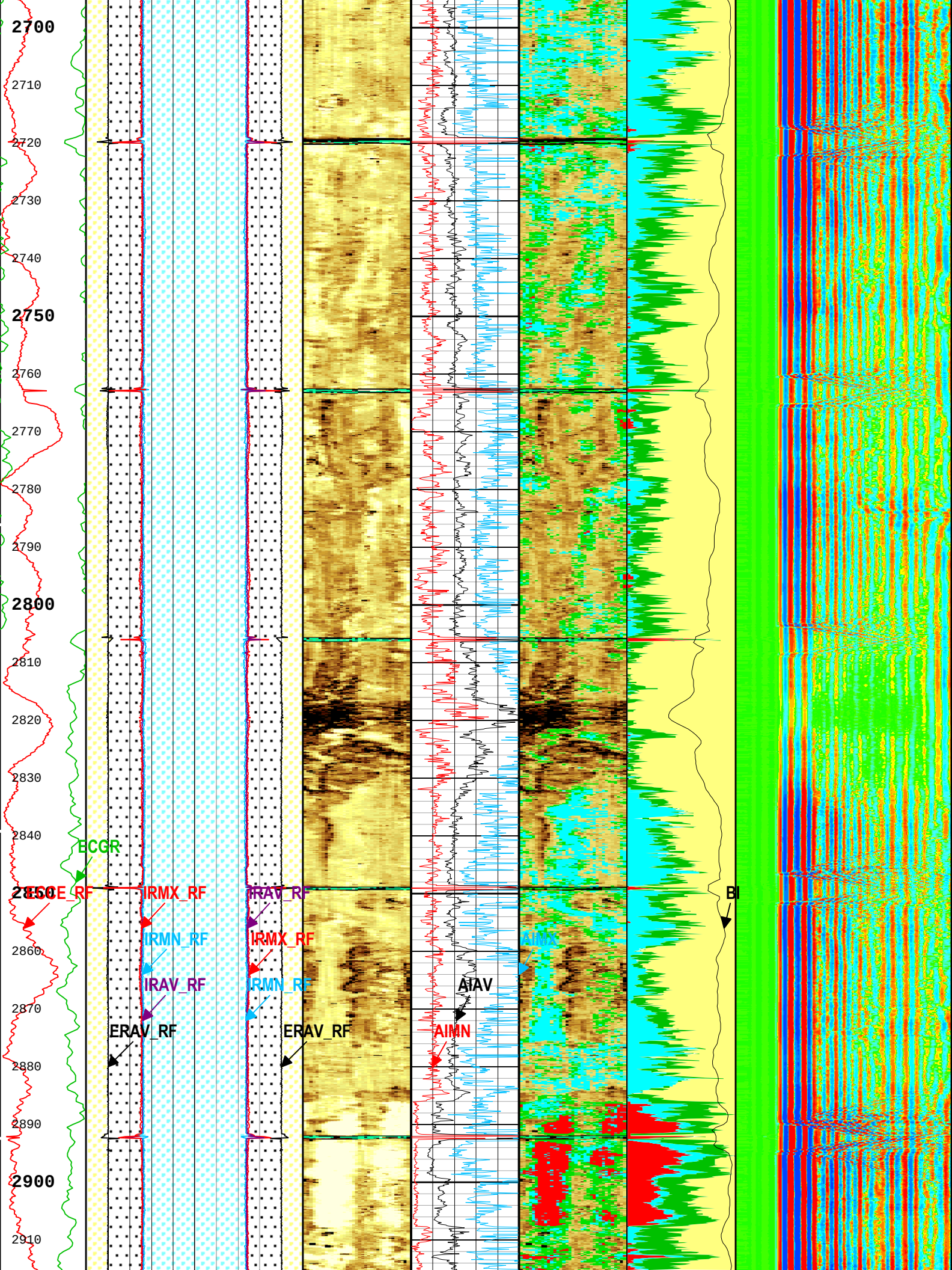
2700
2710
2720
2730
2740
2750
2760
2770
2780
2790
2800
2810
2820
2830
2840
2850
2860
2870
2880
2890
2900
2910
ECGR
IRMX_RF
IRMN_RF
IRAV_RF
ERAV_RF
IRAV_RF
IRMX_RF
IRMN_RF
ERAV_RF
AIMX
AIAV
AIMN
BI

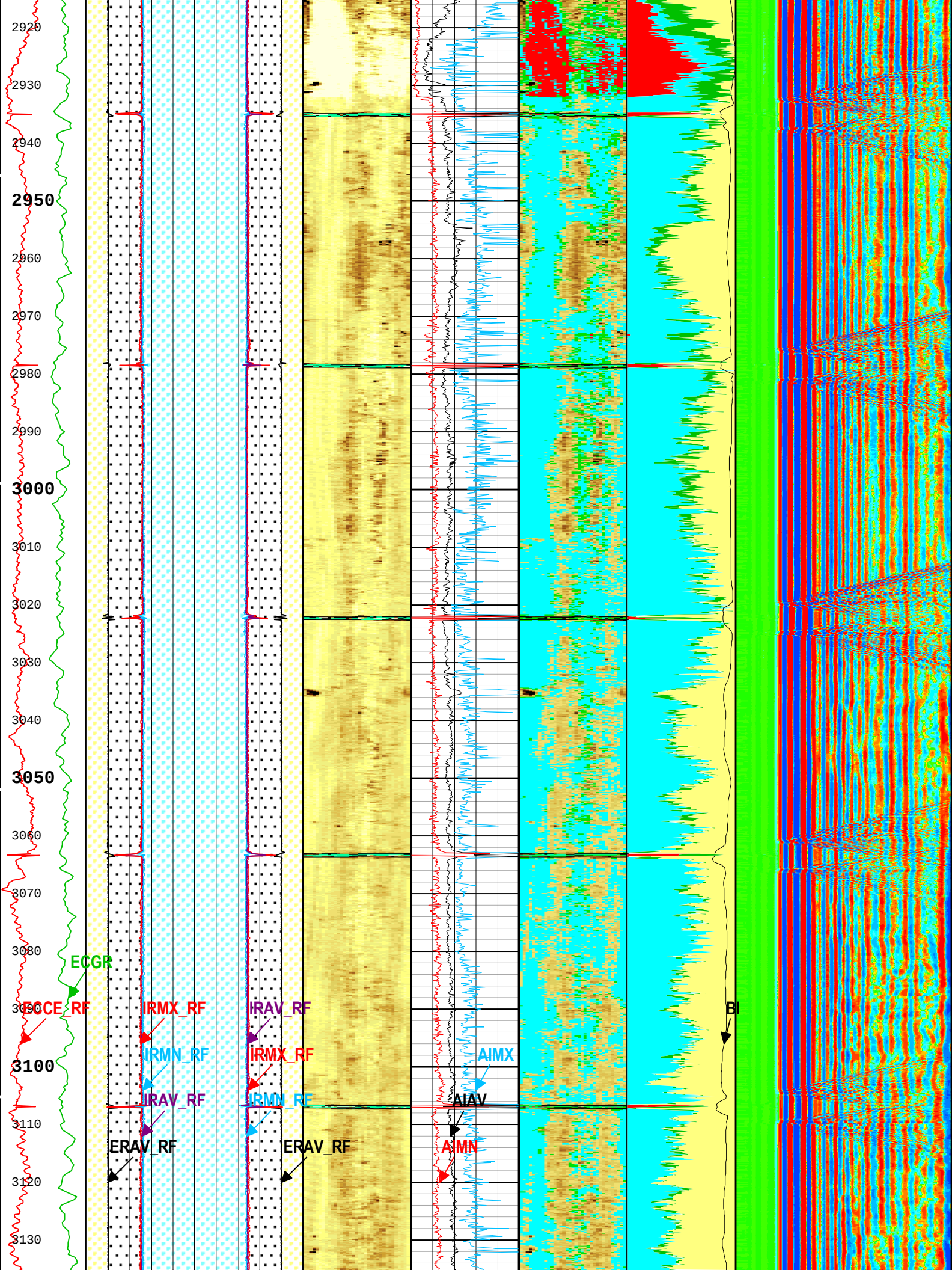
2920
2930
2940
2950
2960
2970
2980
2990
3000
3010
3020
3030
3040
3050
3060
3070
3080
3090
3100
3110
3120
3130
ECGR
ECCE_RF
IRMX_RF
IRMN_RF
IRAV_RF
ERAV_RF
IRAV_RF
IRMX_RF
IRMN_RF
ERAV_RF
AIMX
AIAV
AIMN
BI

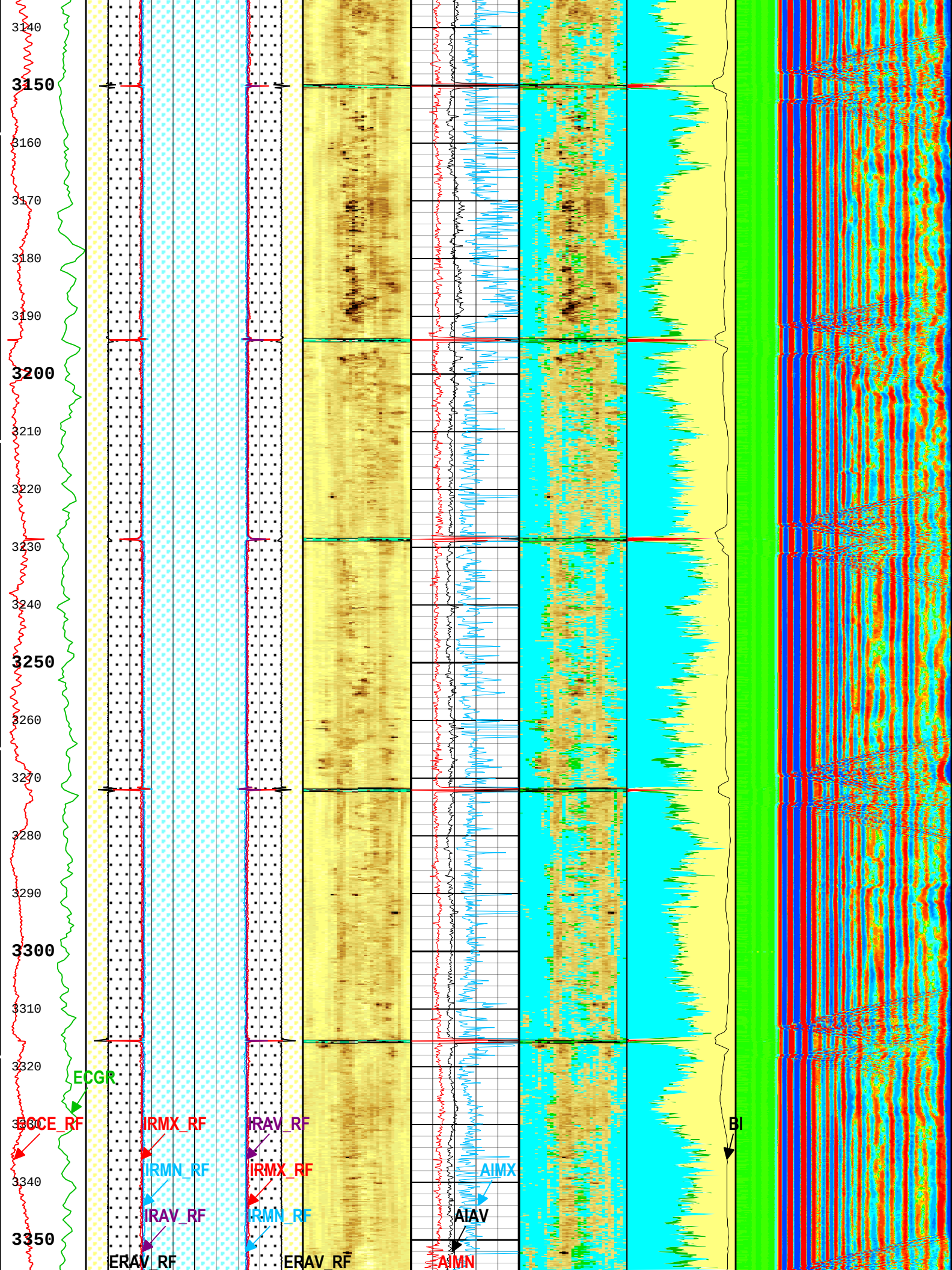
3140
3150
3160
3170
3180
3190
3200
3210
3220
3230
3240
3250
3260
3270
3280
3290
3300
3310
3320
3330
3340
3350
ECGR
CCE_RF
IRMX_RF
IRMN_RF
IRAV_RF
ERAV_RF
IRAV_RF
IRMX_RF
IRMN_RF
ERAV_RF
AIMX
AIAV
AIMN
BI

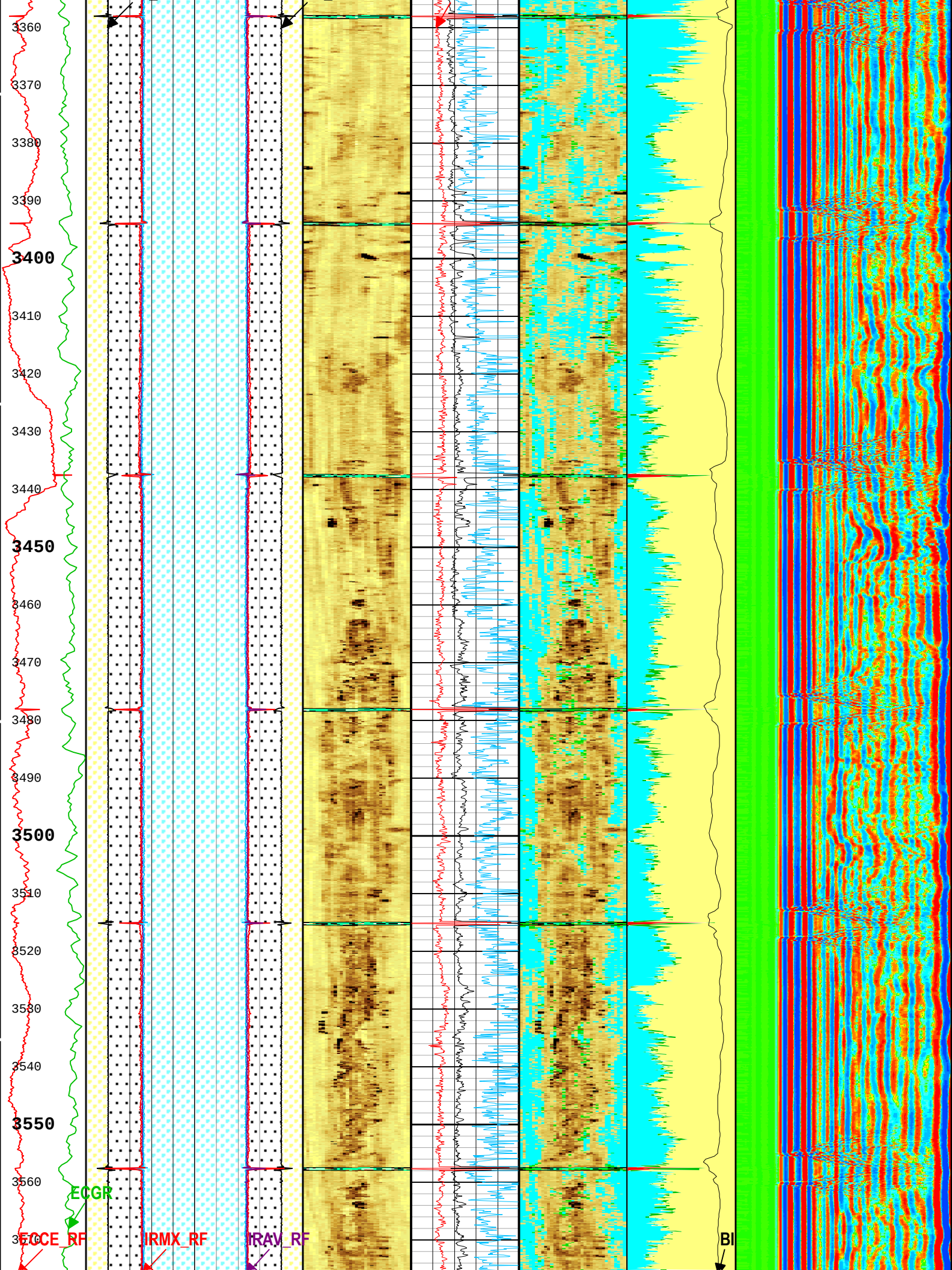
3360
3370
3380
3390
3400
3410
3420
3430
3440
3450
3460
3470
3480
3490
3500
3510
3520
3530
3540
3550
3560
ECGR
ECCE_RF
IRMX_RF
IRAV_RF
BI

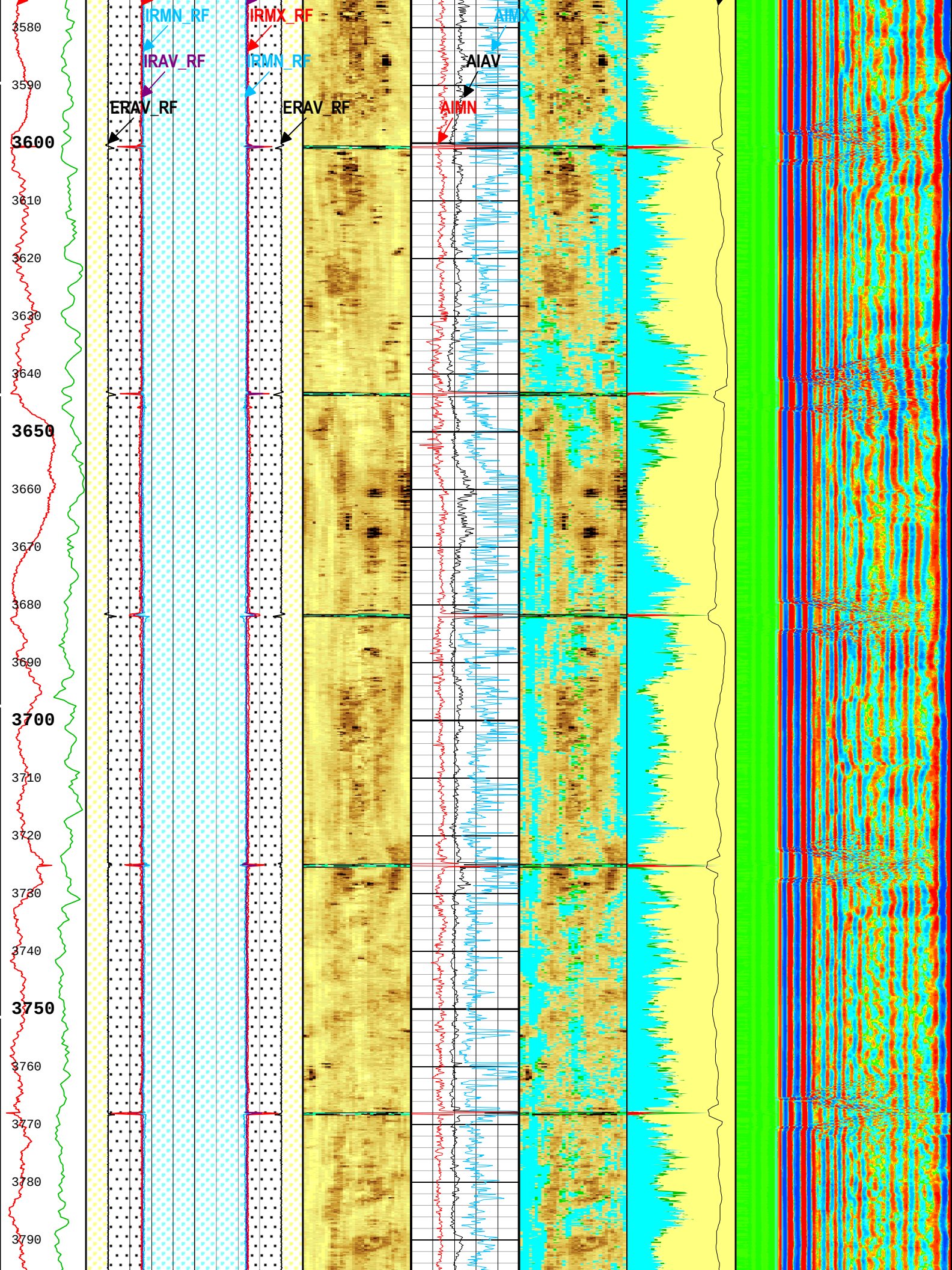
IRMN_RF
IRMX_RF
AIMX
IRAV_RF
IRMN_RF
AIAV
ERAV_RF
ERAV_RF
AIMN
3580
3590
3600
3610
3620
3630
3640
3650
3660
3670
3680
3690
3700
3710
3720
3730
3740
3750
3760
3770
3780
3790

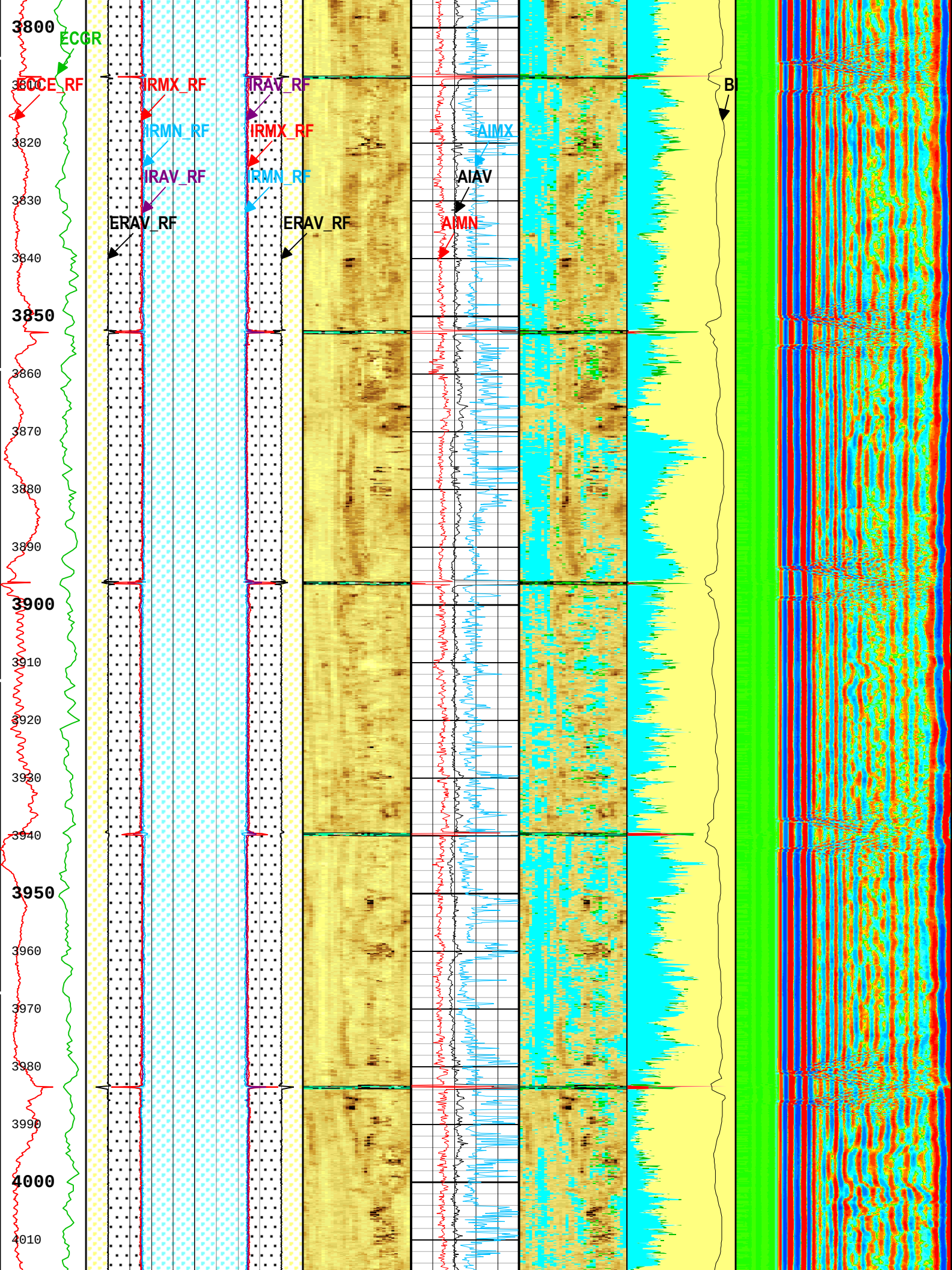
3800
ECGR
ECCE_RF
IRMX_RF
IRAV_RF
IRMN_RF
IRMX_RF
IRAV_RF
IRMN_RF
AIMX
AIAV
AIMN
ERAV_RF
ERAV_RF
B
3820
3830
3840
3850
3860
3870
3880
3890
3900
3910
3920
3930
3940
3950
3960
3970
3980
3990
4000
4010

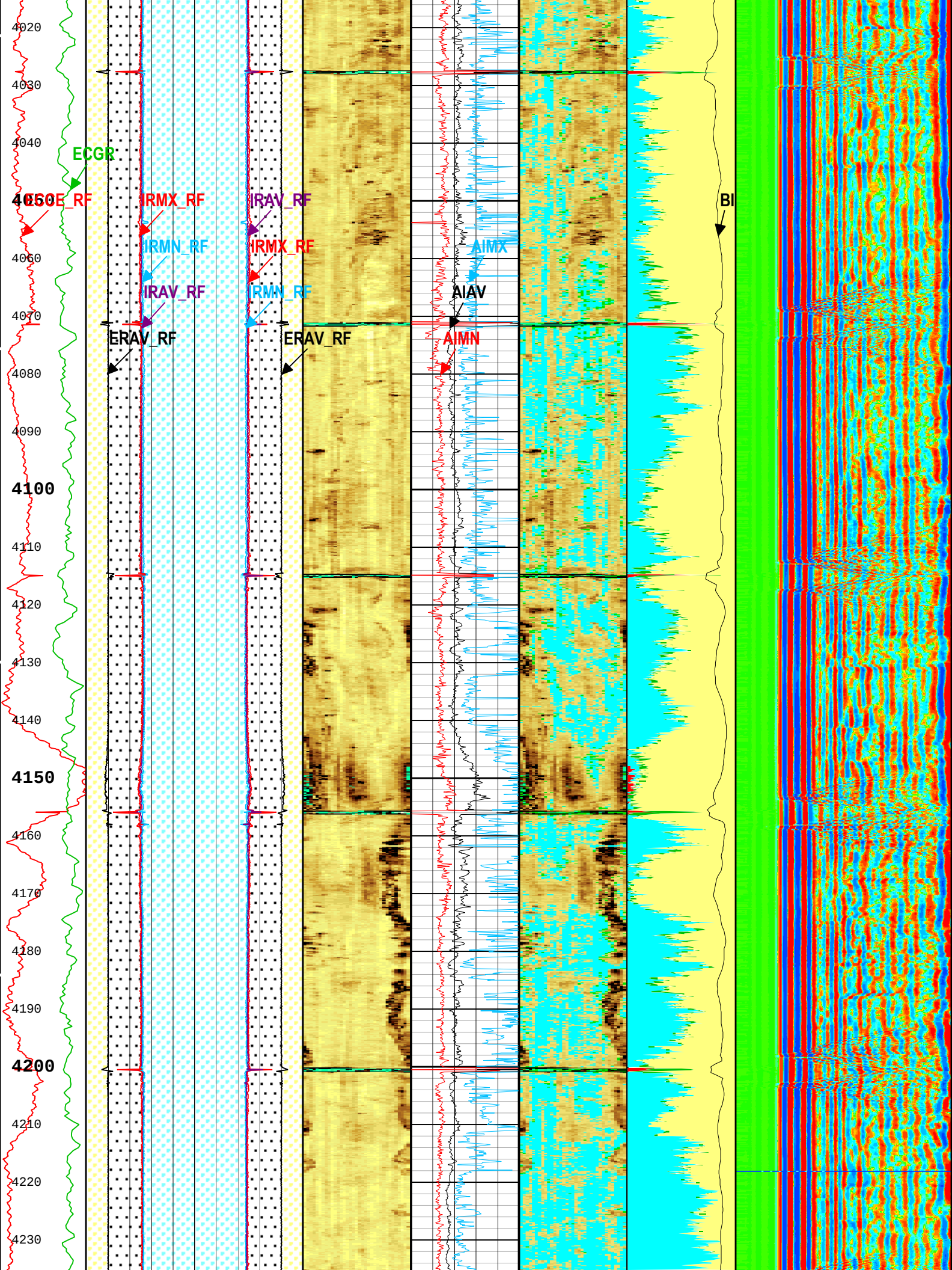
4020
4030
4040
ECGR
4050
ECDE_RF
IRMX_RF
IRAV_RF
IRMN_RF
IRMX_RF
IRAV_RF
IRMN_RF
AIMX
AIAV
AIMN
BI
4060
4070
ERAV_RF
ERAV_RF
4080
4090
4100
4110
4120
4130
4140
4150
4160
4170
4180
4190
4200
4210
4220
4230

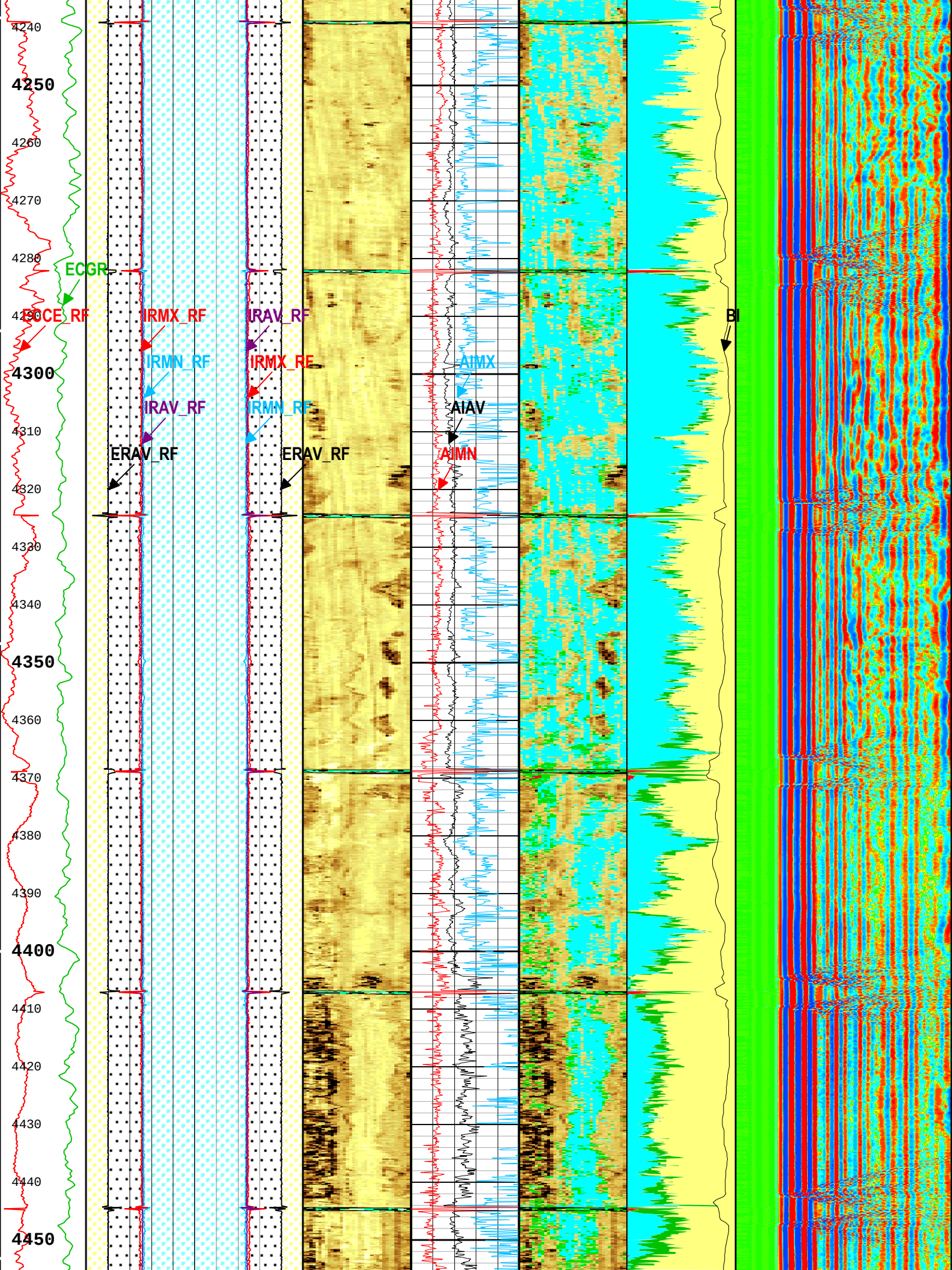
4240
4250
4260
4270
4280
4290
4300
4310
4320
4330
4340
4350
4360
4370
4380
4390
4400
4410
4420
4430
4440
4450
ECGR
ECE_RF
IRMX_RF
IRMN_RF
IRAV_RF
ERAV_RF
IRAV_RF
IRMX_RF
IRMN_RF
ERAV_RF
AIMX
AIAV
AIMN
BI

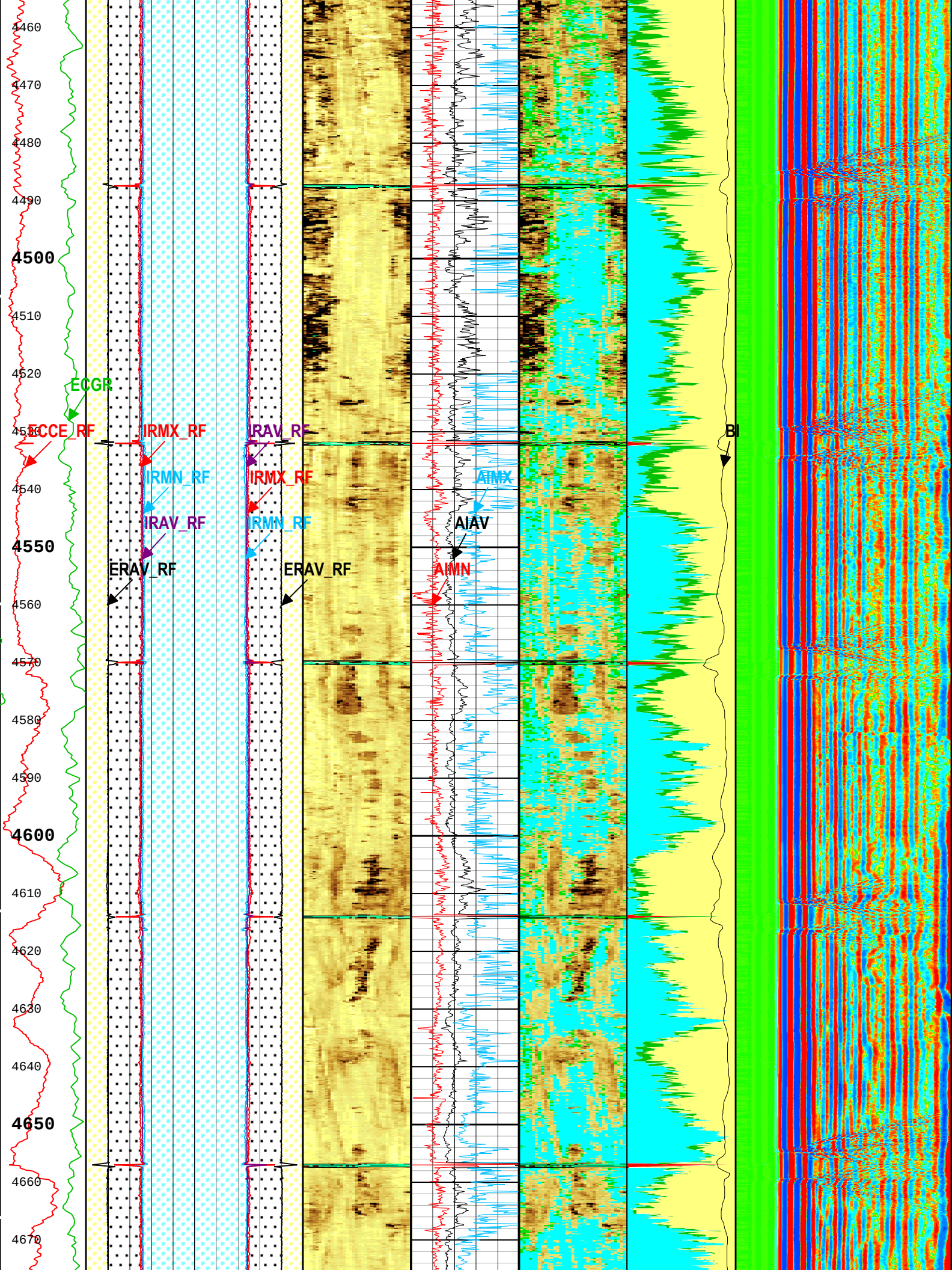
4460
4470
4480
4490
4500
4510
4520
4530
4540
4550
4560
4570
4580
4590
4600
4610
4620
4630
4640
4650
4660
4670
ECGR
ECCE_RF
IRMX_RF
IRAV_RF
IRMN_RF
IRMX_RF
IRAV_RF
IRMN_RF
ERAV_RF
ERAV_RF
AIMX
AIAV
AIMN
BI

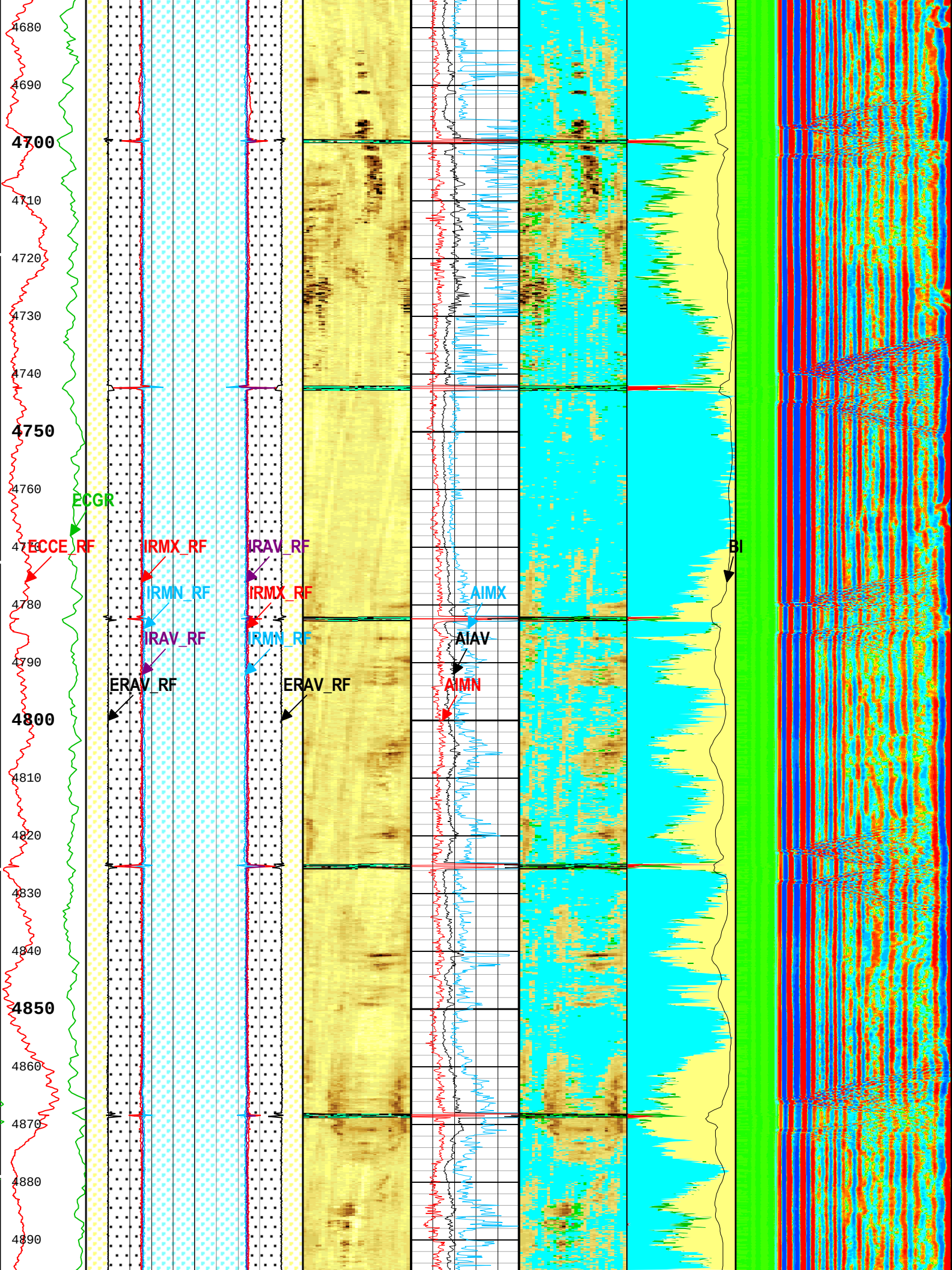
4680
4690
4700
4710
4720
4730
4740
4750
4760
4770
4780
4790
4800
4810
4820
4830
4840
4850
4860
4870
4880
4890
ECGR
ECCE_RF
IRMX_RF
IRAV_RF
IRMN_RF
IRMX_RF
IRAV_RF
IRMN_RF
ERAV_RF
ERAV_RF
AIMX
AIAV
AIMN
BI

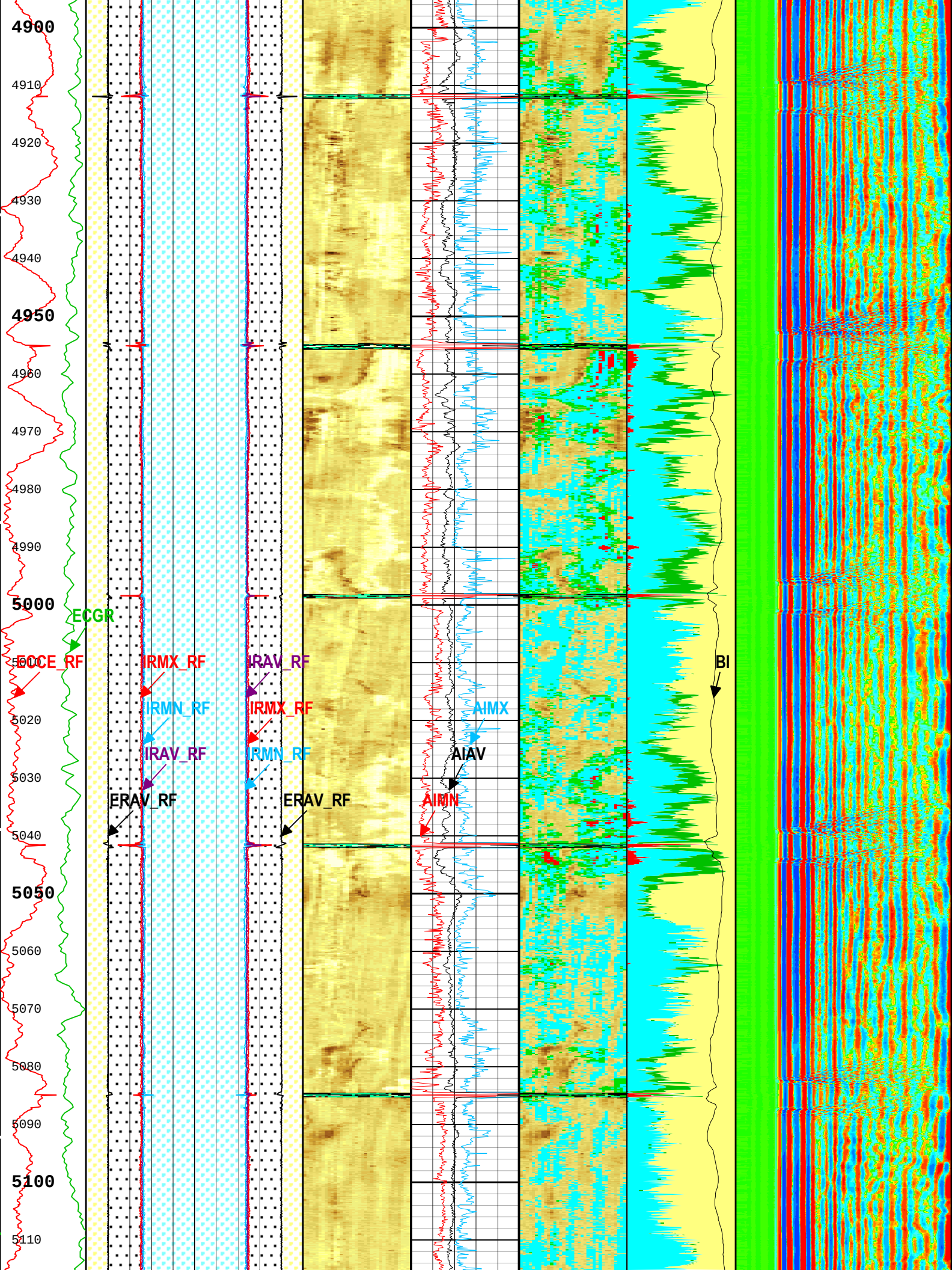
4900
4910
4920
4930
4940
4950
4960
4970
4980
4990
5000
5010
5020
5030
5040
5050
5060
5070
5080
5090
5100
5110
ECGR
ECCE_RF
IRMX_RF
IRAV_RF
IRMN_RF
IRMX_RF
IRAV_RF
IRMN_RF
ERAV_RF
ERAV_RF
AIMX
AIAV
AIMN
BI

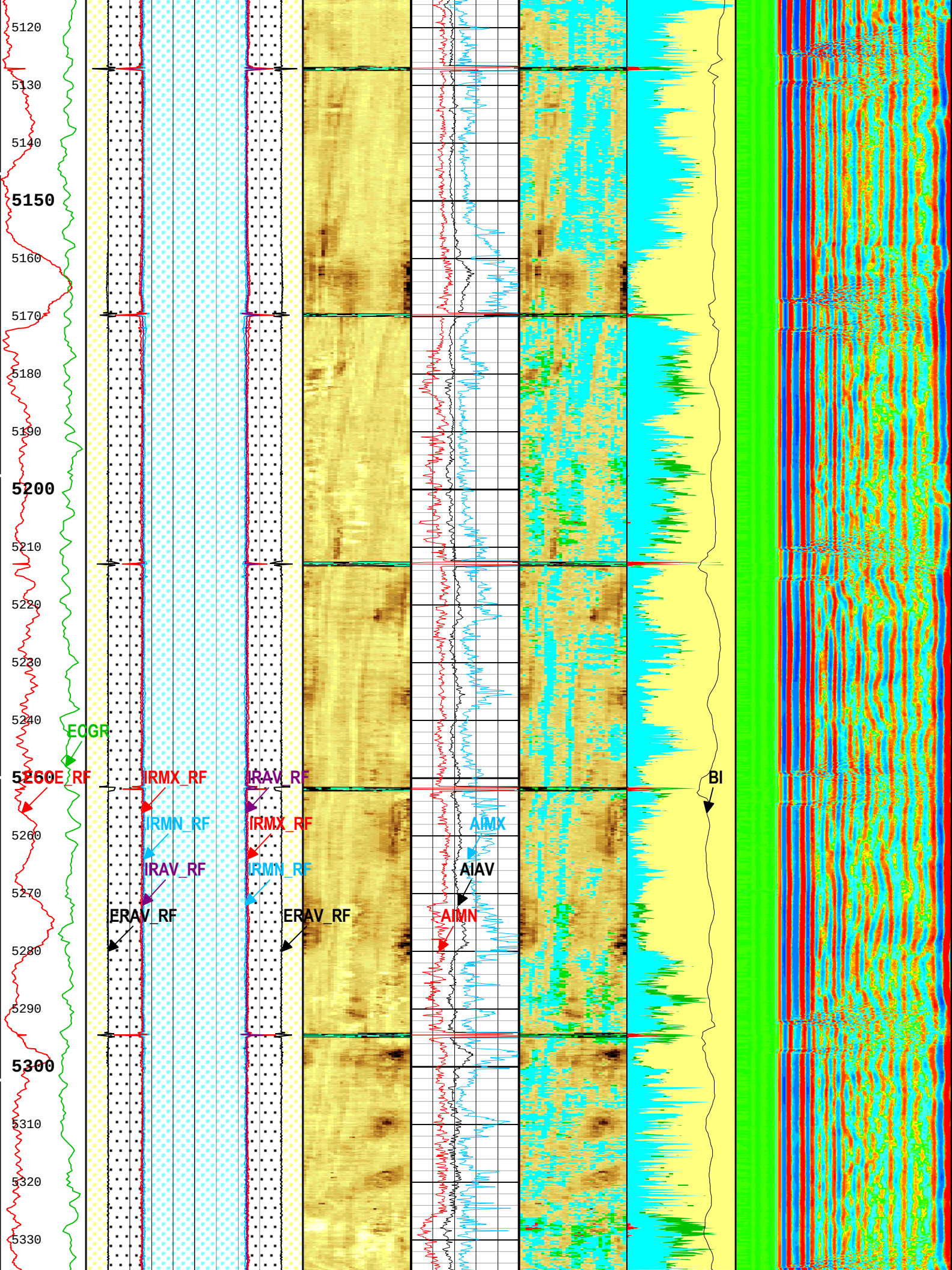
5120
5130
5140
5150
5160
5170
5180
5190
5200
5210
5220
5230
5240
5250
5260
5270
5280
5290
5300
5310
5320
5330
ECGR
ERAV_RF
IRMX_RF
IRMN_RF
IRAV_RF
ERAV_RF
IRAV_RF
IRMX_RF
IRMN_RF
ERAV_RF
AIMX
AIAV
AIMN
BI

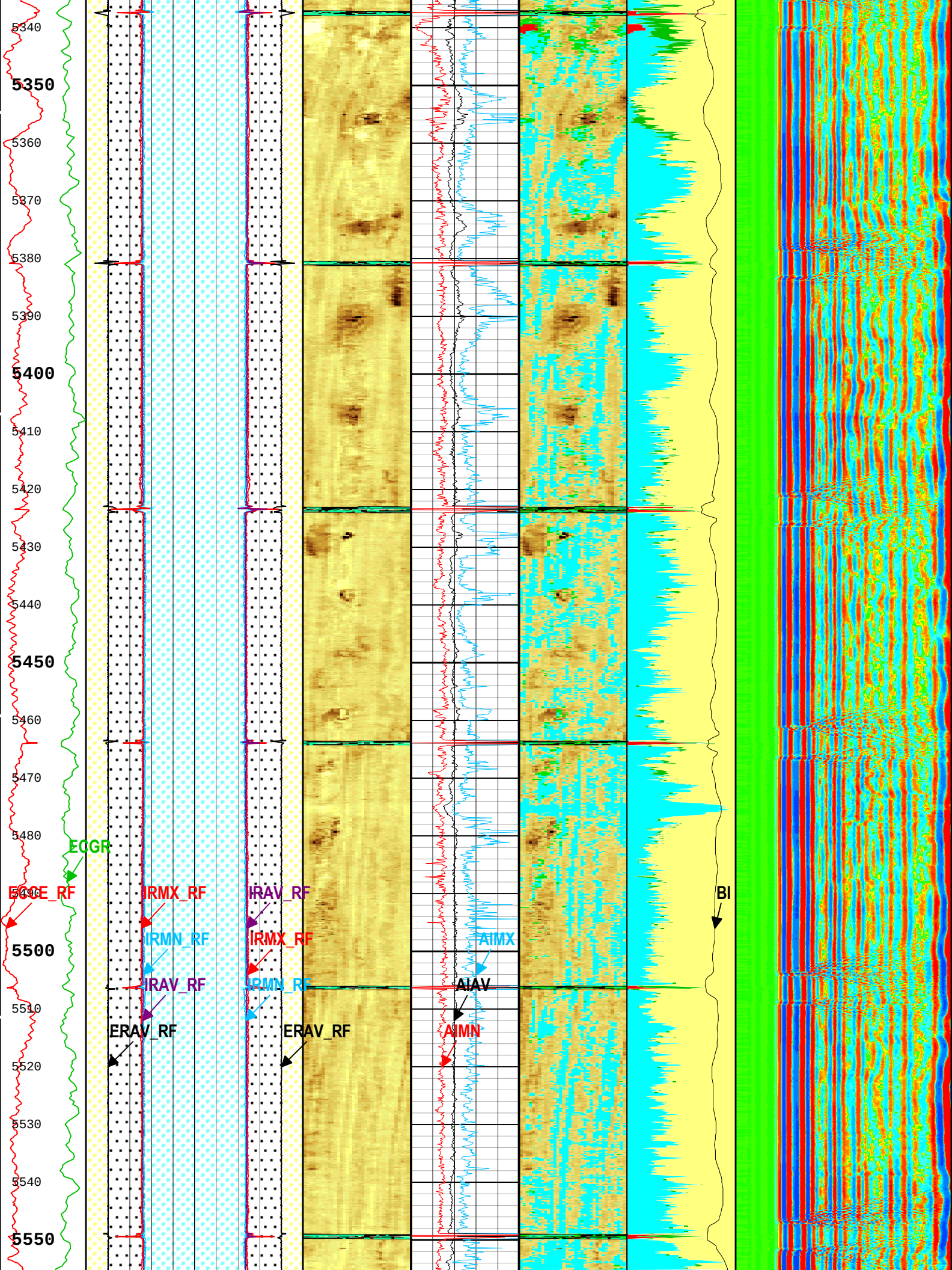
5340
5350
5360
5370
5380
5390
5400
5410
5420
5430
5440
5450
5460
5470
5480
5500
5510
5520
5530
5540
5550
ECGR
ECCE_RF
IRMX_RF
IRAV_RF
IRMN_RF
IRMX_RF
IRAV_RF
IRMN_RF
ERAV_RF
ERAV_RF
AIMX
AIAV
AIMN
BI

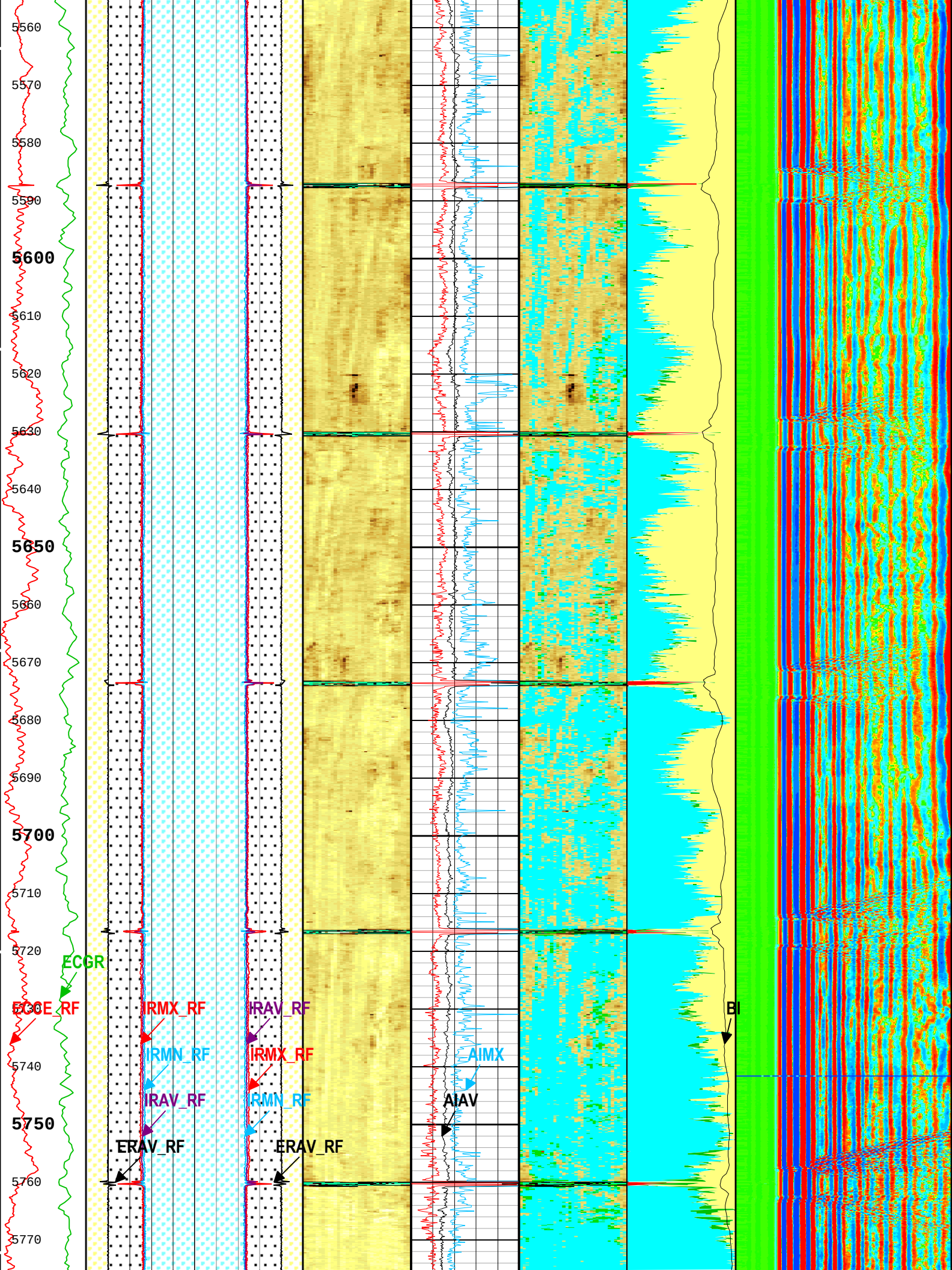
5560
5570
5580
5590
5600
5610
5620
5630
5640
5650
5660
5670
5680
5690
5700
5710
5720
5730
5740
5750
5760
5770
ECGR
ECCE_RF
IRMX_RF
IRMN_RF
IRAV_RF
ERAV_RF
IRAV_RF
IRMX_RF
IRMN_RF
ERAV_RF
AIMX
AIAV
BI

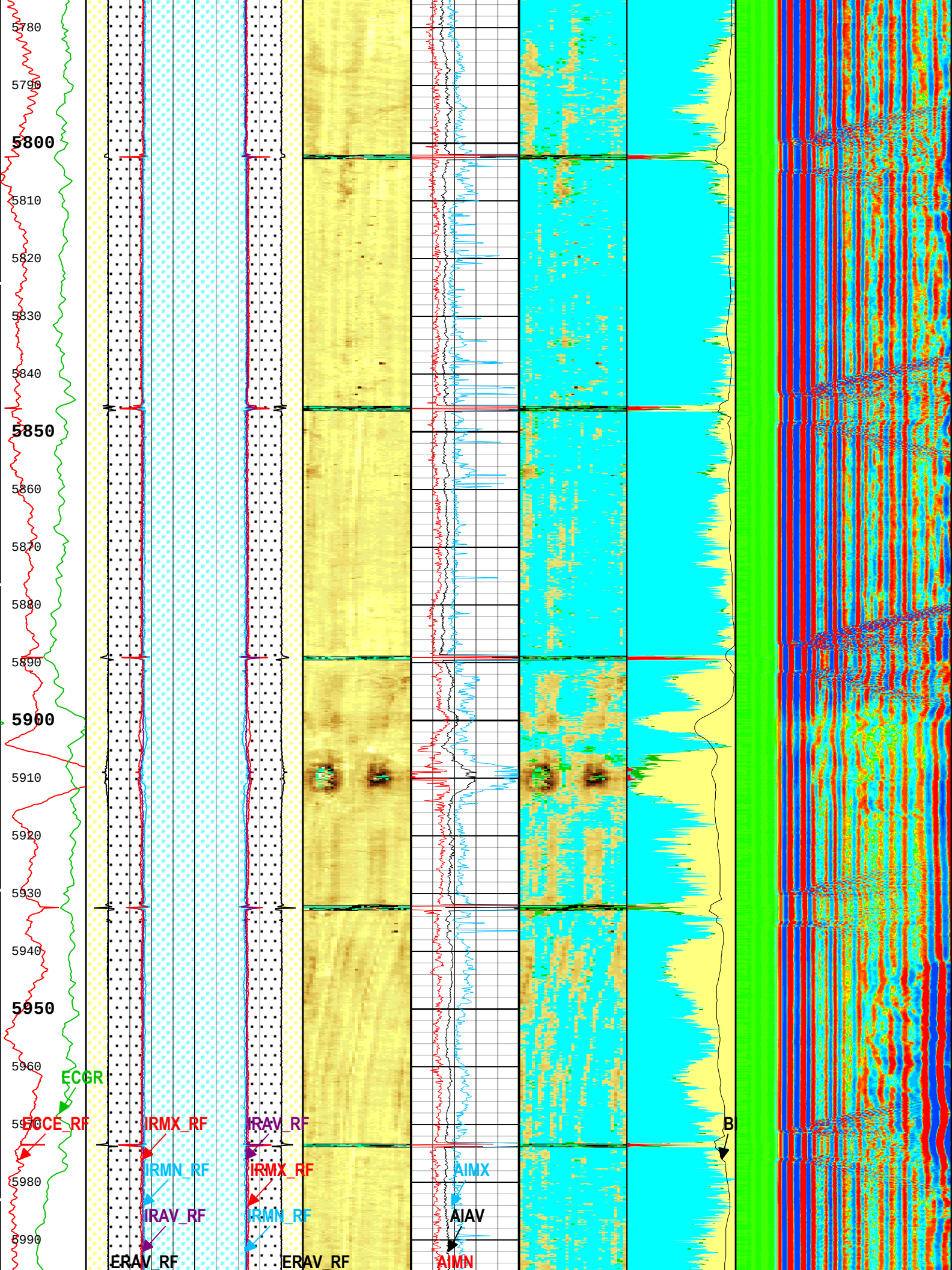
5780
5790
5800
5810
5820
5830
5840
5850
5860
5870
5880
5890
5900
5910
5920
5930
5940
5950
5960
5970
5980
5990
ECGR
ECCE_RF
IRMX_RF
IRAV_RF
IRMN_RF
IRMX_RF
IRAV_RF
IRMN_RF
ERAV_RF
ERAV_RF
AIMX
AIAV
AIMN
B

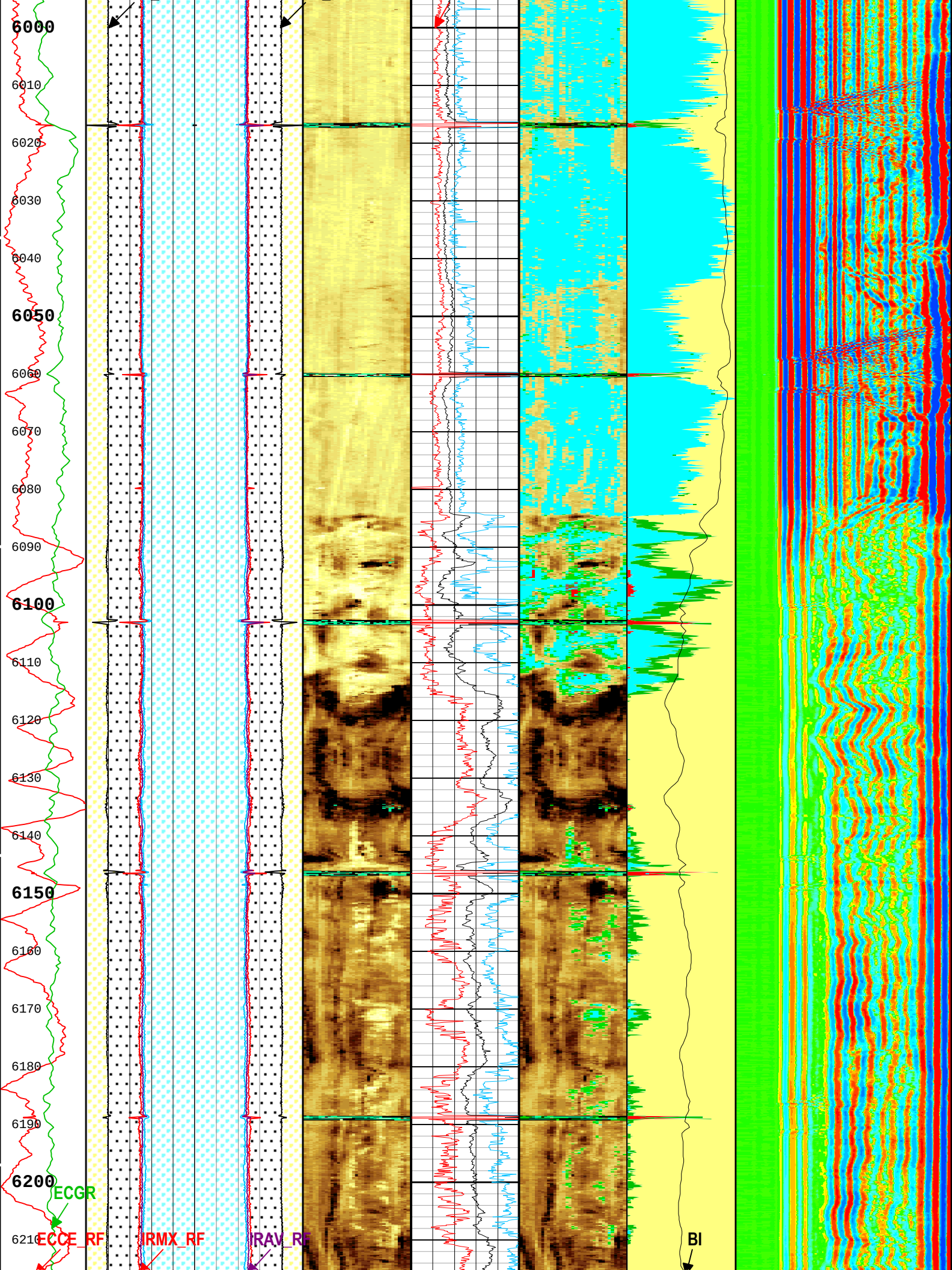
6000
6010
6020
6030
6040
6050
6060
6070
6080
6090
6100
6110
6120
6130
6140
6150
6160
6170
6180
6190
6200
6210
ECGR
ECCE_RF
IRMX_RF
IRAV_RF
BI

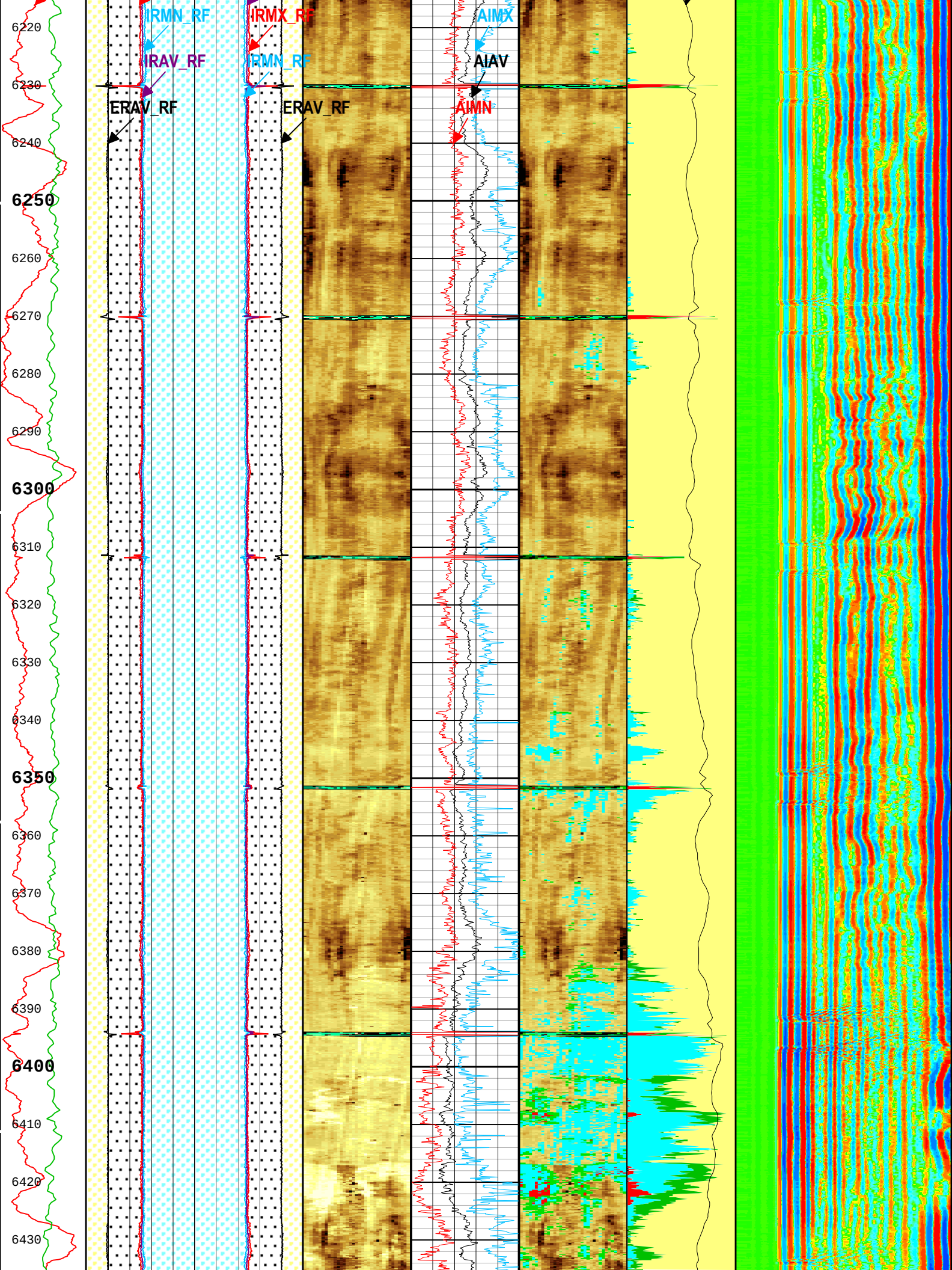
IRMN_RF
IRMX_RF
AIMX
IRAV_RF
IRMN_RF
AIAV
ERAV_RF
ERAV_RF
AIMN
6220
6230
6240
6250
6260
6270
6280
6290
6300
6310
6320
6330
6340
6350
6360
6370
6380
6390
6400
6410
6420
6430

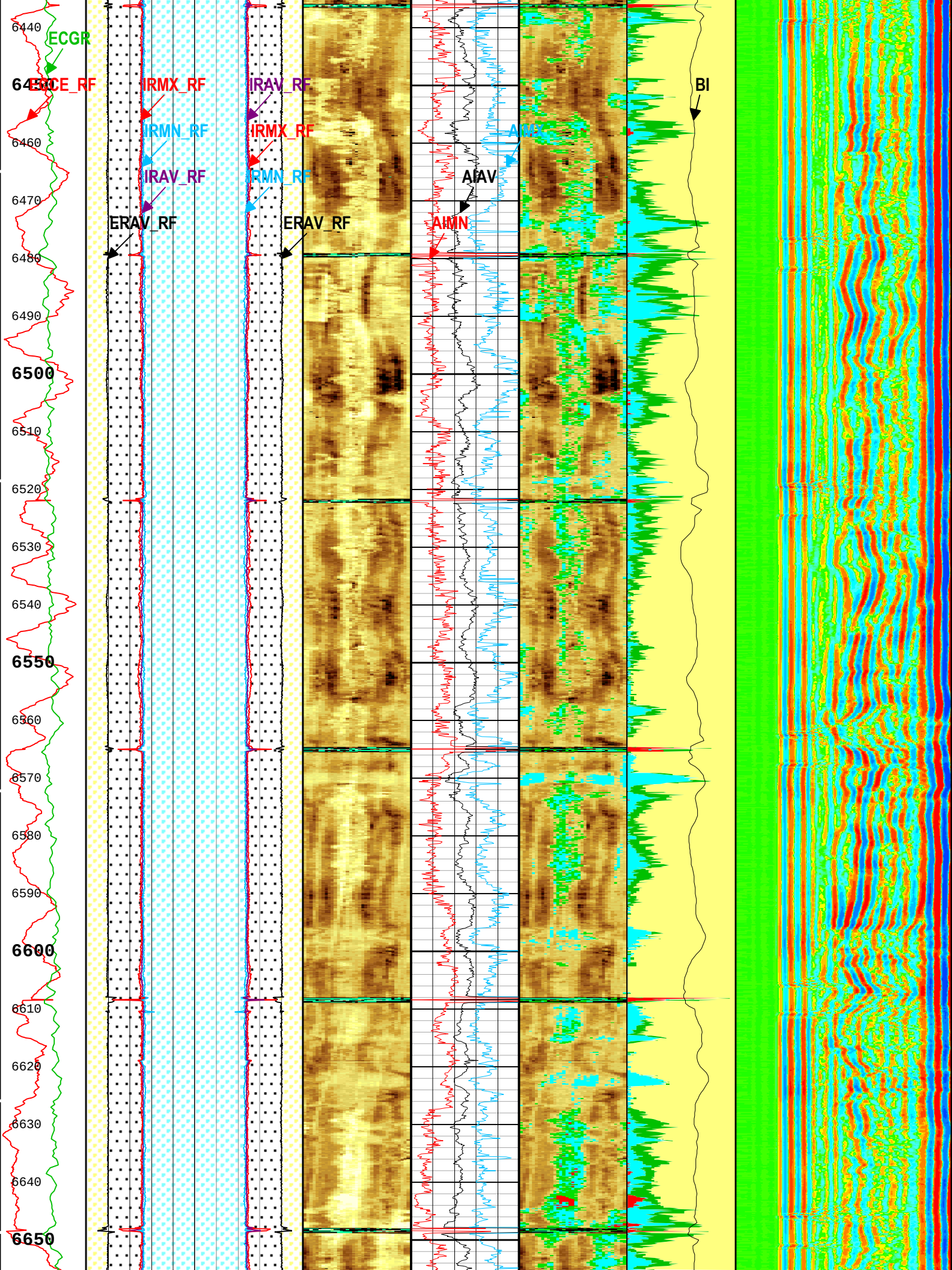
ECGR
CE_RF
IRMX_RF
IRMN_RF
IRAV_RF
ERAV_RF
IRAV_RF
IRMX_RF
IRMN_RF
ERAV_RF
AIAV
AIMN
BI
6440
6450
6460
6470
6480
6490
6500
6510
6520
6530
6540
6550
6560
6570
6580
6590
6600
6610
6620
6630
6640
6650

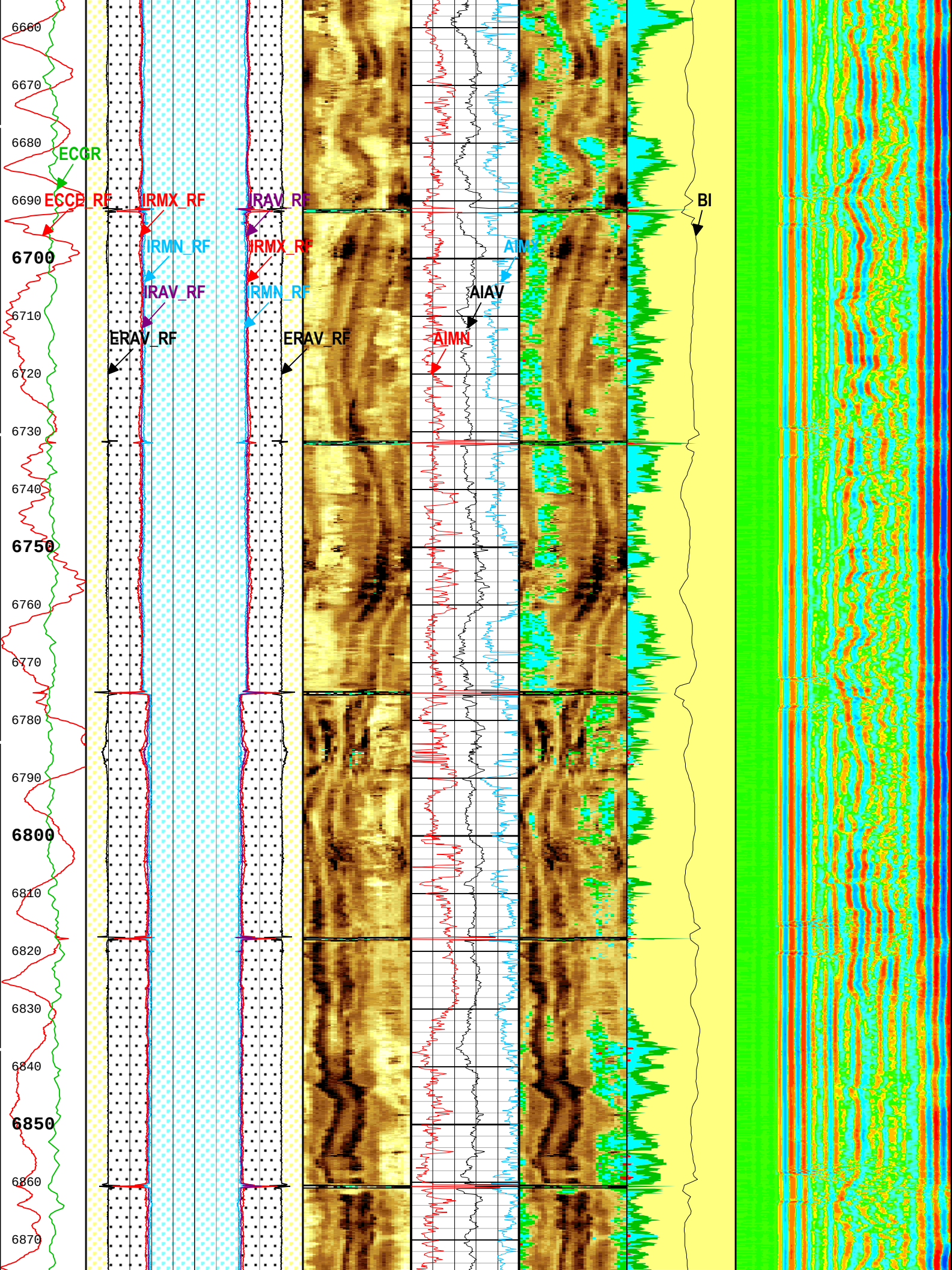
6660
6670
6680
ECGR
6690
ECCB_RF
IRMX_RF
IRAV_RF
IRAV_RF
IRMX_RF
BI
6700
IRMN_RF
IRMX_RF
AIMX
IRAV_RF
IRMN_RF
AIAV
6710
ERAV_RF
ERAV_RF
AIMN
6720
6730
6740
6750
6760
6770
6780
6790
6800
6810
6820
6830
6840
6850
6860
6870

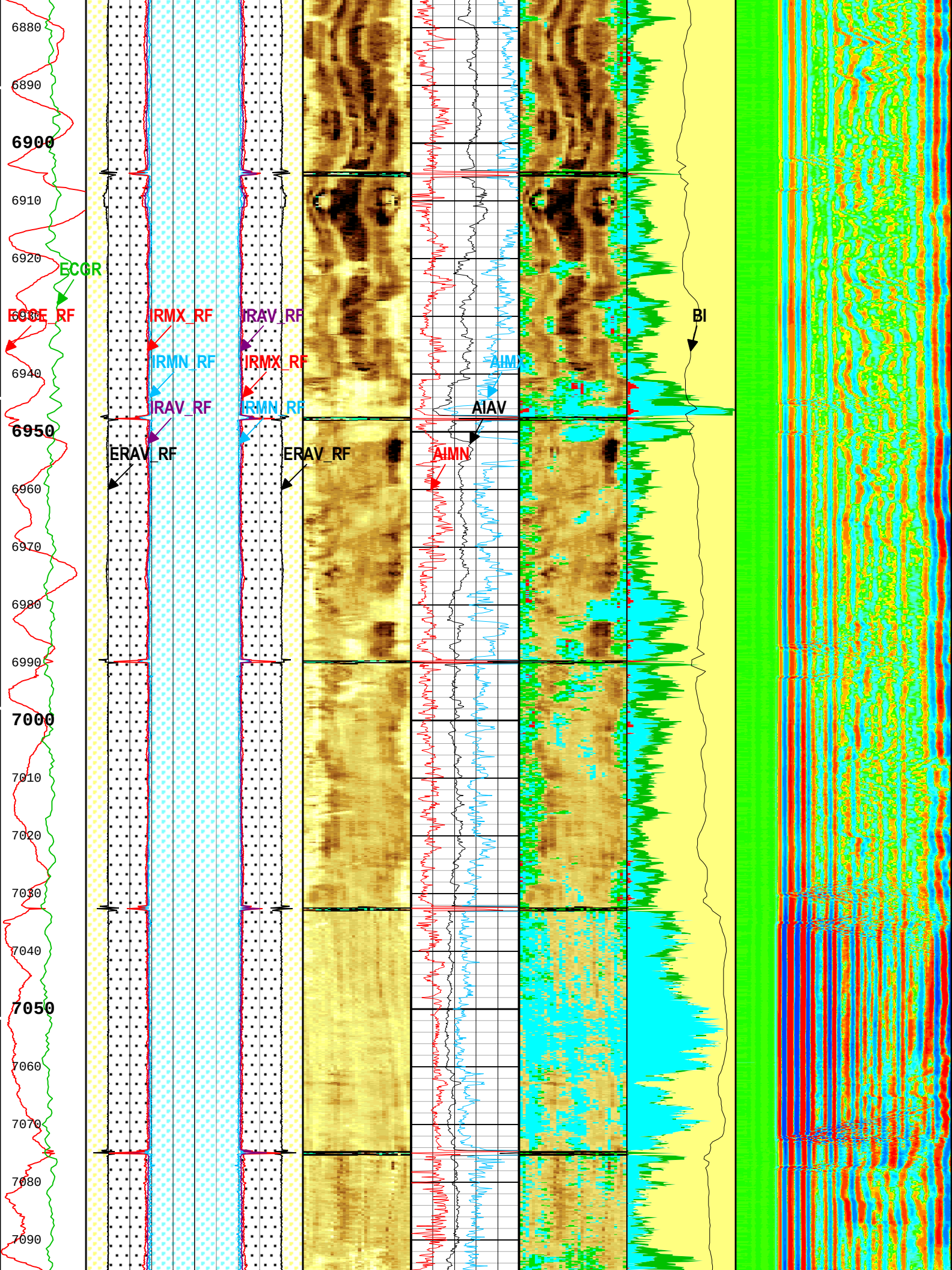
6880
6890
6900
6910
6920
6930
6940
6950
6960
6970
6980
6990
7000
7010
7020
7030
7040
7050
7060
7070
7080
7090
ECGR
ECCE_RF
IRMX_RF
IRAV_RF
IRMN_RF
IRMX_RF
IRAV_RF
IRMN_RF
ERAV_RF
ERAV_RF
AIMX
AIAV
AIMN
BI

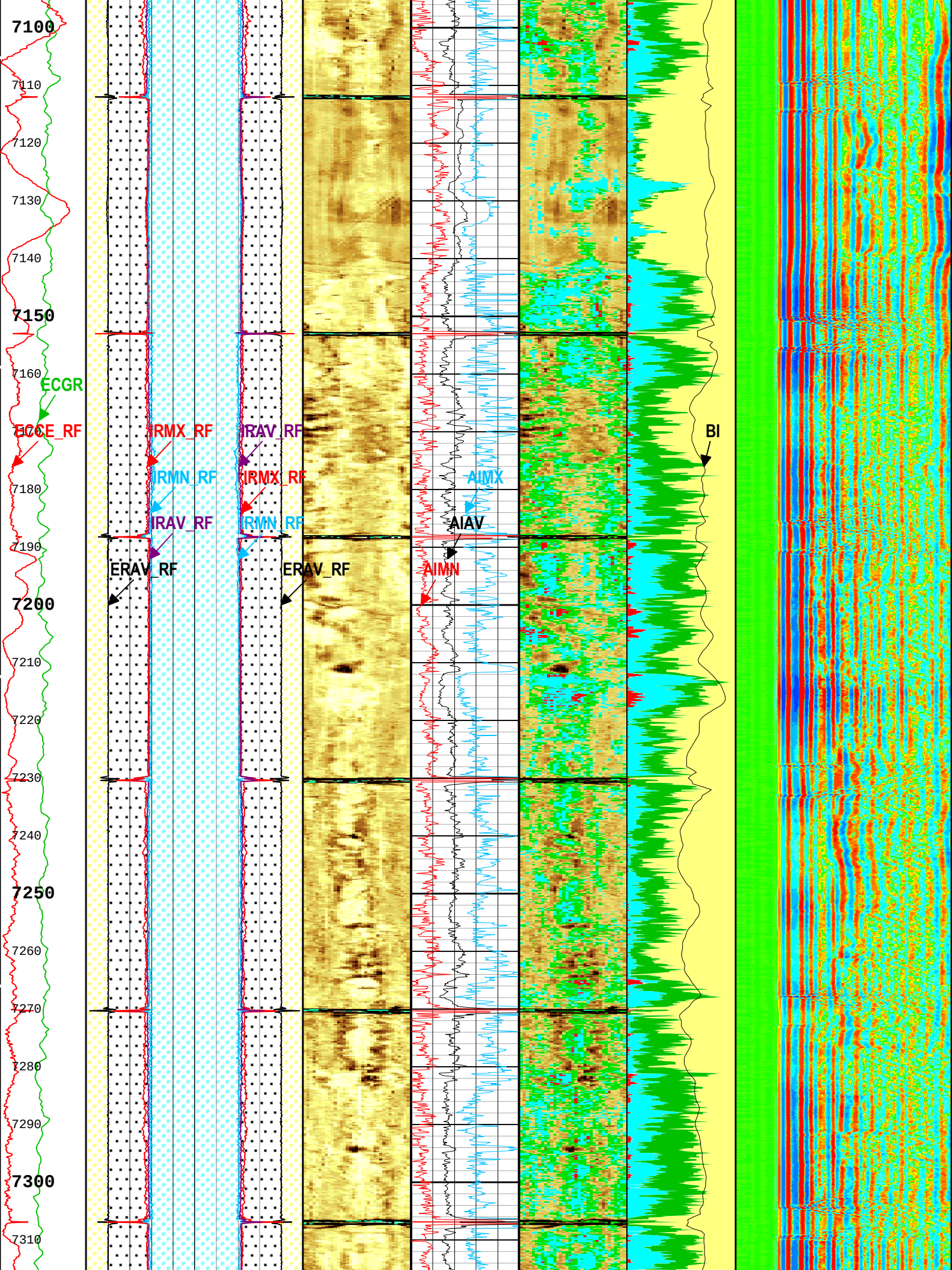
7100
7110
7120
7130
7140
7150
7160
ECGR
ECCE_RF
IRMX_RF
IRAV_RF
IRMN_RF
IRMX_RF
IRAV_RF
IRMN_RF
AIMX
AIAV
AIMN
BI
7180
7190
ERAV_RF
ERAV_RF
7200
7210
7220
7230
7240
7250
7260
7270
7280
7290
7300
7310

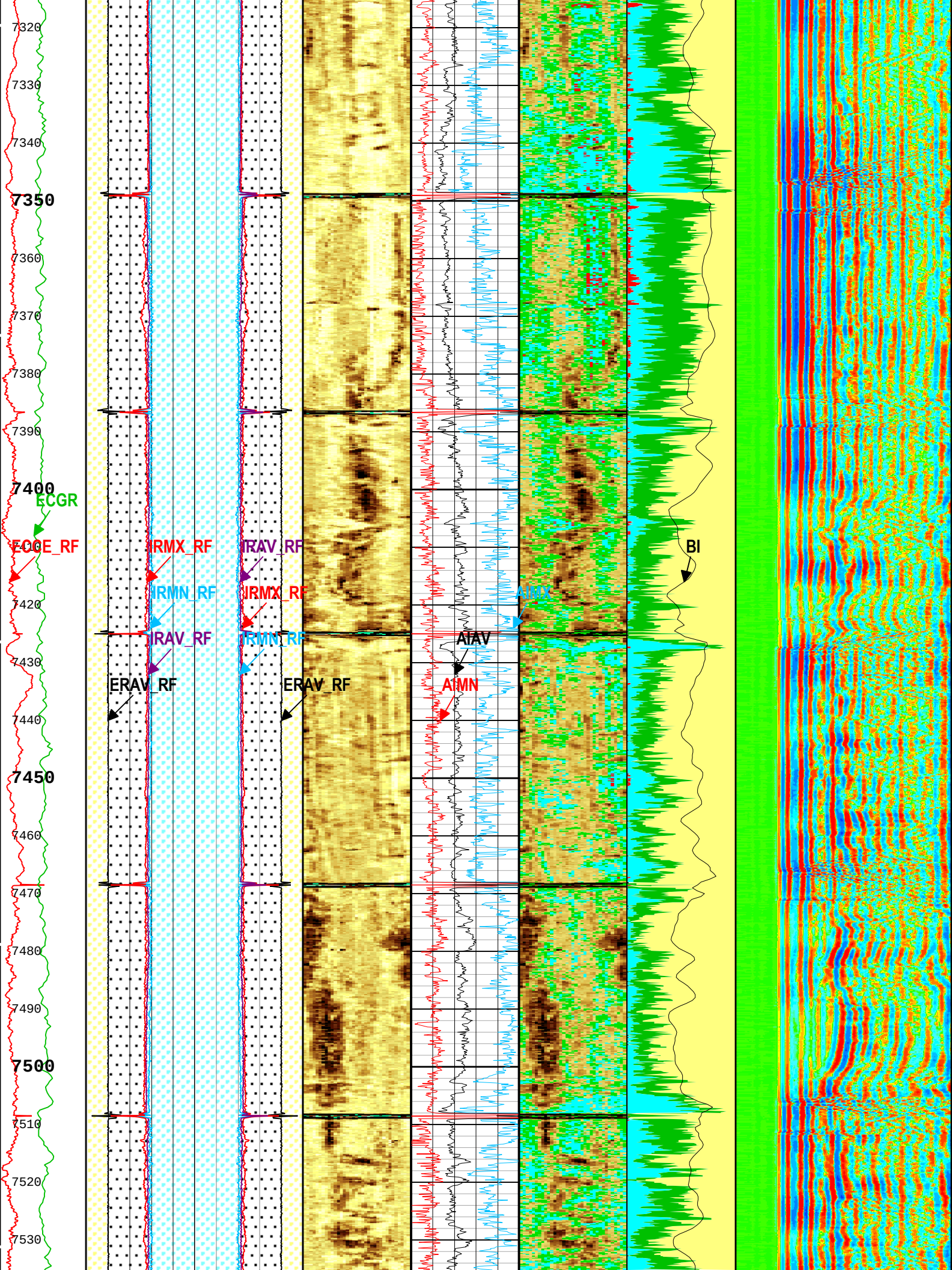
7320
7330
7340
7350
7360
7370
7380
7390
7400
ECGR
ECCE_RF
IRMX_RF
IRAV_RF
IRMN_RF
IRMX_RF
IRAV_RF
IRMN_RF
ERAV_RF
ERAV_RF
AIMX
AIAV
AIMN
BI
7420
7430
7440
7450
7460
7470
7480
7490
7500
7510
7520
7530

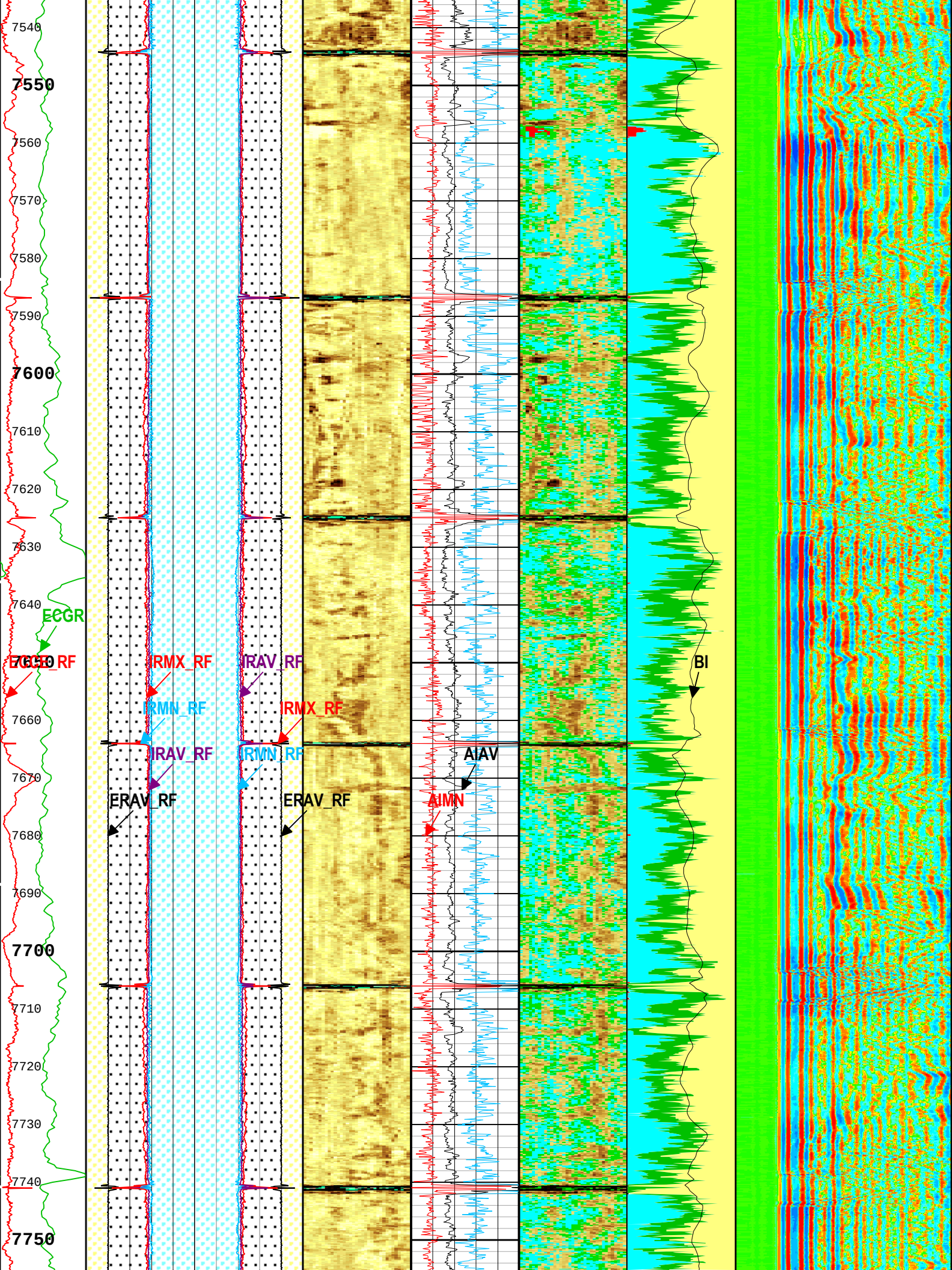
7540
7550
7560
7570
7580
7590
7600
7610
7620
7630
7640
ECGR
7650
ERMX_RF
IRMX_RF
IRAV_RF
BI
IRMN_RF
IRMX_RF
7660
IRAV_RF
IRMN_RF
AIAV
7670
ERAV_RF
ERAV_RF
AIMN
7680
7690
7700
7710
7720
7730
7740
7750

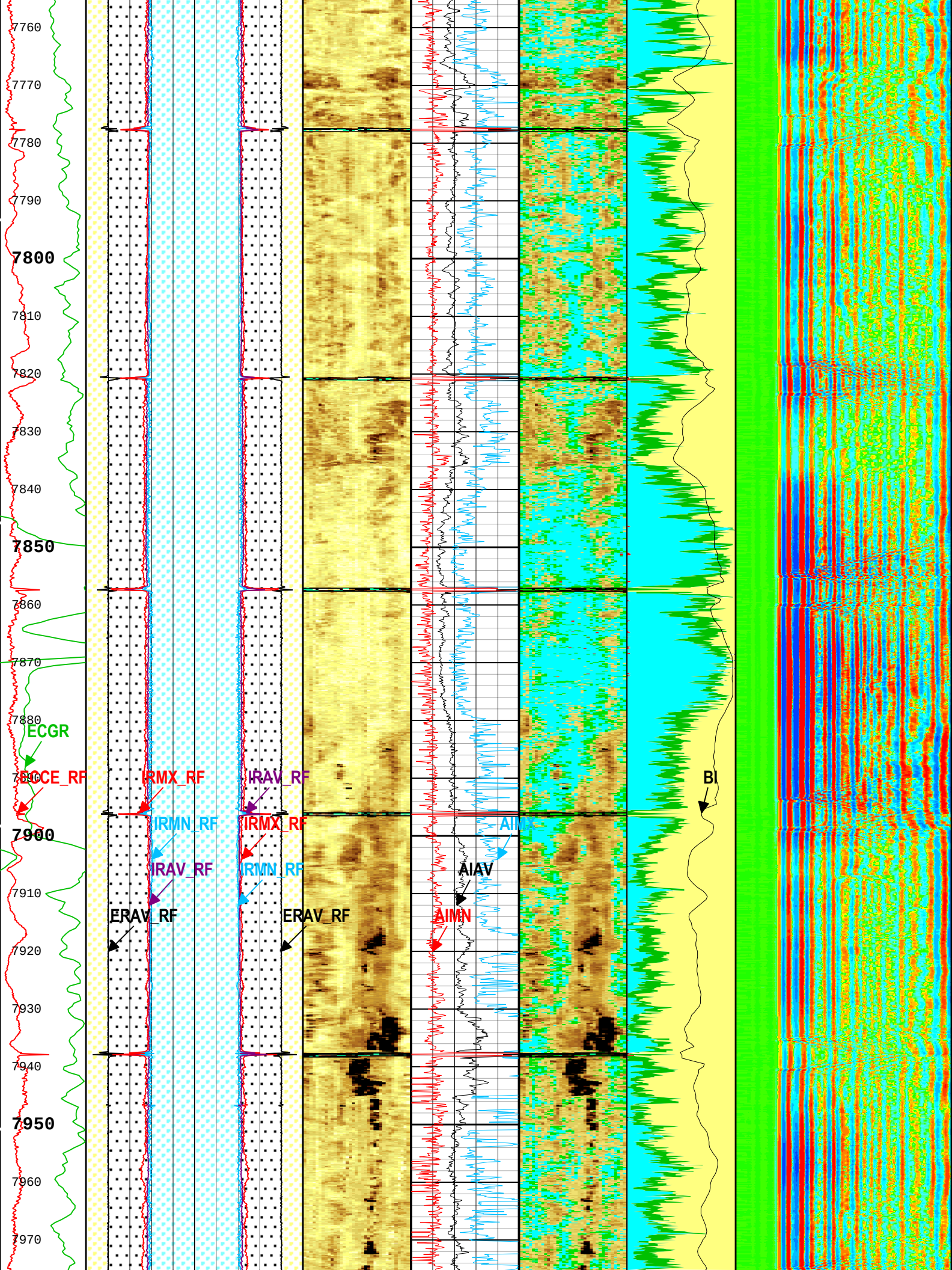
7760
7770
7780
7790
7800
7810
7820
7830
7840
7850
7860
7870
7880
7900
7910
7920
7930
7940
7950
7960
7970
ECGR
ECCE_RF
IRMX_RF
IRAV_RF
IRMN_RF
IRMX_RF
IRAV_RF
IRMN_RF
ERAV_RF
ERAV_RF
AIMX
AIAV
AIMN
BI

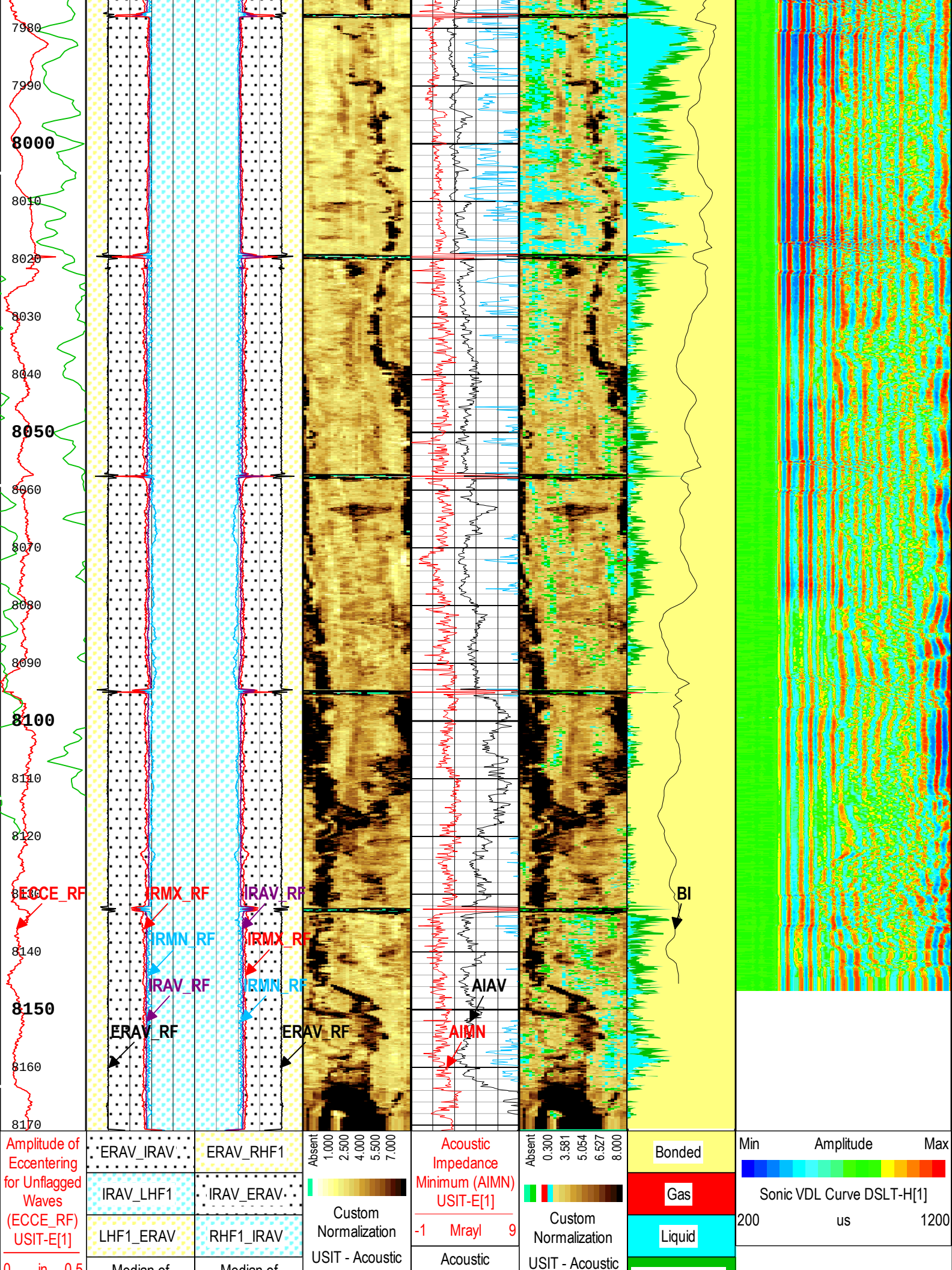
7980
7990
8000
8010
8020
8030
8040
8050
8060
8070
8080
8090
8100
8110
8120
8130
8140
8150
8160
8170
ECCE_RF
IRMX_RF
IRAV_RF
IRMN_RF
IRMX_RF
IRAV_RF
IRMN_RF
ERAV_RF
ERAV_RF
AIAV
AIMN
BI
Amplitude of Eccentering for Unflagged Waves (ECCE_RF) USIT-E[1]
0 in 0.5
ERAV_IRAV
IRAV_LHF1
LHF1_ERAV
ERAV_RHF1
IRAV_ERAV
RHF1_IRAV
Absent 1.000 2.500 4.000 5.500 7.000
Custom Normalization
USIT - Acoustic
Acoustic Impedance Minimum (AIMN) USIT-E[1]
-1 Mrayl 9
Acoustic
Absent 0.300 3.581 5.054 6.527 8.000
Custom Normalization
USIT - Acoustic
Bonded
Gas
Liquid
Min Amplitude Max
Sonic VDL Curve DSLT-H[1]
200 us 1200

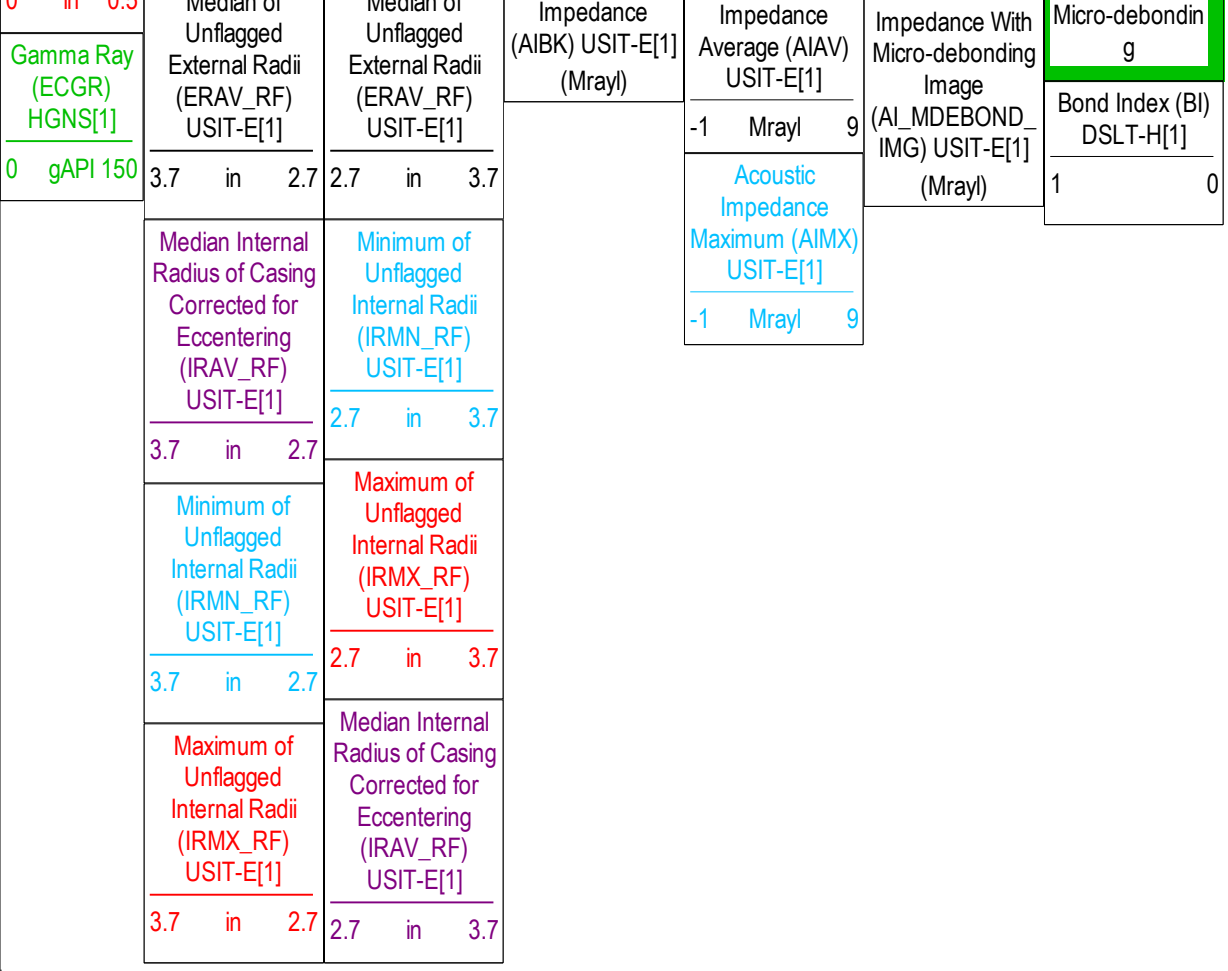

TIME_1900 - Time Marked every 60.00 (s)

Description: USI VDL Cement Format: Log (LBV1_USI-VDL (DSLT) Cement 7inch) Index Scale: 5 in per 100 ft Index Unit: ft Index Type: Measured Depth
Creation Date: 20-Oct-2016 14:28:02

Channel Processing Parameters

Two: Parameters

Parameter	Description	Tool	Value	Unit
AMSG	Auxiliary Minimum Sliding Gate	DSLT-H	140	us
ISSBAR	Barite Mud Presence Flag	Borehole	No	
BERJ	Bad Echo Rejection	USIT-E	On	
BHS	Borehole Status (Open or Cased Hole)	Borehole	Cased	
BILI	Bond Index Level for Zone Isolation	DSLT-H	0.8	
BS	Bit Size	WLSESSION	Depth Zoned	in
CASING_PRATIO	Casing Poisson Ratio	USIT-E	Standard Poisson Ratio	
CBLG	CBL Gate Width	DSLT-H	45	us
CBLO	Casing Bottom (Logger)	WLSESSION	8280	ft
CBRA	CBL LQC Reference Amplitude in Free Pipe	DSLT-H	62	mV
CDEN	Cement Density	HGNS-H	2	g/cm3
CMCF	CBL Cement Type Compensation Factor	DSLT-H	1	
CMTY(U-USIT_CEMT)	Cement Type	USIT-E	Regular Cement	
THNO	Nominal Casing Thickness - Zoned along logger depths	WLSESSION	Depth Zoned	in
DETE	Delta-T Detection	DSLT-H	E1	
DFD	Drilling Fluid Density	Borehole	9	lbm/gal
DFT	Drilling Fluid Type	Borehole	Water	
DTMD	Borehole Fluid Slowness	Borehole	206	us/ft
FCF	CBL Fluid Compensation Factor	DSLT-H	0.94	
FDII	FPM Data Interpolation Interval	USIT-E	0	ft
GCSE_DOWN_PASS	Generalized Caliper Selection for WL Log Down Passes	Borehole	BS	

GCSE_UP_PASS	Generalized Caliper Selection for WL Log Up Passes	Borehole	BS	
GOBO_CURR	Good Bond in Arbitrary Cement	DSLT-H	Depth Zoned	mV
GR_MULTIPLIER	Gamma Ray Multiplier	HGNS-H	1	
HEMA	Hematite Presence Flag	Borehole	No	
ICE_PROCESS	ICE Processing	USIT-E	Yes	
IMAR	Image Rotation	USIT-E	Off	
MAHTR	Manual High Threshold Reference for first arrival detection	DSLT-H	120	
MATT_CURR	Maximum Attenuation in Arbitrary Cement	DSLT-H	Depth Zoned	dB/ft
MCI	Minimum Cemented Interval for Isolation	DSLT-H	Depth Zoned	ft
MEAS_WLEN	Tcube Processing Window Length in Measurement Mode	USIT-E	Depth Zoned	us
MNHTR	Minimum High Threshold Reference for first arrival detection	DSLT-H	100	
MSA	Minimum Sonic Amplitude	DSLT-H	Depth Zoned	mV
MSA_CURR	Minimum Sonic Amplitude in Arbitrary Cement	DSLT-H	Depth Zoned	mV
MUD_N_FRP	Free Pipe Mud Normalization Factor	USIT-E	1.1	
MUD_N_THE	Theoretical Mud Normalization Factor	USIT-E	1	
NMSG	Near Minimum Sliding Gate	DSLT-H	285	us
NMXG	Near Maximum Sliding Gate	DSLT-H	950	us
NUMP	Number of Detection Passes	DSLT-H	2	
OPLEV	USIT Remove Flagged Data Level	USIT-E	OPT2	
RCOD	Reference Calibrator Outer Diameter	USIT-E	7	in
RCSO	Reference Calibrator Standoff	USIT-E	1.181	in
RCTH	Reference Calibrator Thickness	USIT-E	0.295	in
SDNV	Number of Vertical Samples used for Micro-debonding Computation	USIT-E	5	
SDTHOR	Acoustic Impedance STD Horizontal Threshold for Micro-debonding	USIT-E	0.5	Mrayl
SDTVER	Acoustic Impedance STD Vertical Threshold for Micro-debonding	USIT-E	0.3	Mrayl
SFAF	Sonic Formation Attenuation Factor	DSLT-H	3.25	dB/ft
SGAD	Sliding Gate Status	DSLT-H	Off	
SGCL	Sliding Gate Closing Delta-T	DSLT-H	130	us/ft
SGCW	Sliding Gate Closing Width	DSLT-H	25	us
SGDT	Sliding Gate Delta-T	DSLT-H	57	us/ft
SGW	Sliding Gate Width	DSLT-H	110	us
SLEV	Signal Level for AGC	DSLT-H	5000	mV
SOCN	Standoff Distance	HGNS-H	0.125	in
SOCO	Standoff Correction Option	HGNS-H	No	
TCUB	T^3 Processing Level	USIT-E	Loop	
THDH	Maximum Search Thickness (percentage of nominal)	USIT-E	Time Zoned	%
THDL	Minimum Search Thickness (percentage of nominal)	USIT-E	Time Zoned	%
HISC	Tool Position: Centered or Eccentered	HGNS-H	Eccentered	
U-USIT_DFSZ	Drilling Fluid Specific Acoustic Impedance	USIT-E	0.1	Mrayl
UFGDE	Fiberglass Density	USIT-E	1.95	g/cm3
UFGPS	Fiberglass Processing Selection	USIT-E	No	
UFGVL	Fiberglass Velocity	USIT-E	9678.48	ft/s
USI_FSOD	USIT USI Fluid Slowness Fits Casing Outer Diameter	USIT-E	0_OFF	
USI_FVEL_SEL	USI Fluid Velocity Selection	USIT-E	Automatic	
USI_ZMUD_SEL	USI Mud Impedance Selection	USIT-E	FreePipe Norm.	
THDP	Thickness Detection Policy	USIT-E	Fundamental	
VCAS	Ultrasonic Transversal Velocity in Casing	USIT-E	51.4	us/ft
VDLG	VDL Manual Gain	DSLT-H	5	
ZCAS	Acoustic Impedance of Casing	USIT-E	46.25	Mrayl

ZCMT	Acoustic Impedance of Cement	DSLT-H	6.8	Mrayl
ZCMT_NEAT	Acoustic Impedance of Cement in Neat Cement	DSLT-H	6.8	Mrayl
ZINI	Initial Estimate of Cement Impedance	USIT-E	-1	Mrayl
ZMUD	Acoustic Impedance of Mud	Borehole	1.48	Mrayl
ZTCM	Acoustic Impedance Threshold for Cement	USIT-E	2.6	Mrayl
ZTGS	Acoustic Impedance Threshold for Gas	USIT-E	0.3	Mrayl

TwoDepth Zoned Parameters

Parameter	Value	Start (ft)	Stop (ft)
BS	17.5	0	770
BS	12.25	770	6187
BS	11.75	6187	7421
BS	11	7421	8171
THNO	0.362	0	179
THNO	0.317	179	6774
THNO	0.362	6774	8171
GOBO_CURR	2.87	0	179
GOBO_CURR	1.87	179	6774
GOBO_CURR	2.87	6774	8171
MATT_CURR	11.82	0	179
MATT_CURR	13.39	179	6774
MATT_CURR	11.82	6774	8171
MCI	21.68	0	770
MCI	10	770	8171
MEAS_WLEN	22.5	0	179
MEAS_WLEN	19.62	179	6774
MEAS_WLEN	22.5	6774	8171
MSA	1.33	0	179
MSA	0.78	179	6774
MSA	1.33	6774	8171
MSA_CURR	1.33	0	179
MSA_CURR	0.78	179	6774
MSA_CURR	1.33	6774	8171

All depth are actual.

TwoTime Zoned Parameters

Pass Log[9]:Up

Parameter	Value	Start Time	Stop Time	Start Depth (ft)	Stop Depth (ft)
THDH	125	20-Oct-2016 09:51:44	20-Oct-2016 10:20:40	8171.38	6648.71
THDL	60	20-Oct-2016 09:51:44	20-Oct-2016 10:20:40	8171.38	6648.71

Pass Log[11]:Up

THDH	125	20-Oct-2016 10:26:34	20-Oct-2016 12:34:00	6648.71	113.27
THDL	60	20-Oct-2016 10:24:53	20-Oct-2016 12:00:23	6648.71	1633.75
THDL	70	20-Oct-2016 12:00:23	20-Oct-2016 12:34:00	1633.75	113.27

Pass Log[14]:Up

THDH	130	20-Oct-2016 12:53:24	20-Oct-2016 12:58:23	155.15	5.56
THDL	70	20-Oct-2016 12:53:24	20-Oct-2016 12:58:23	155.15	5.56

All depth are at tool zero.

Tool Control Parameters

Tool Control Parameters

Two: Parameters

Parameter	Description	Tool	Value	Unit
AGMN	Minimum Gain of Cartridge	USIT-E	-12	dB
AGMX	Maximum Gain of Cartridge	USIT-E	18	dB
DDEL	Digitizing Delay	DSLT-H	0	us
U-USIT_DDT5	USIC Downhole Decimation for T5 only	USIT-E	0_NONE	
DOT(DOS)	Distance between Opposite Transducer Faces	USIT-E	2.874	in
MODE	DSLT Acquisition Mode	DSLT-H	CBL	
RATE	DSLT Firing Rate	DSLT-H	15 Hz	
DTFS	DSLT Telemetry Frame Size	DSLT-H	536	
DWCO	Digitizer Word Count	DSLT-H	250	
EMXV	EMEX Voltage	USIT-E	Time Zoned	V
HRES	Horizontal Resolution	USIT-E	10 deg	
MOTOR_PROTECT	Motor Protection	USIT-E	On	
SDTH	Switch Down Threshold	DSLT-H	20000	
SGAI	Selectable Acquisition Gain	DSLT-H	x1	
SUTH	Switch Up Threshold	DSLT-H	1000	
TMUC	Type of Mud	USIT-E	BRI	
UACLV_PERM	Ultrasonic ACLV Permanent	USIT-E	No	
ULOG	Logging Objective	USIT-E	MEASUREMENT	
UMFR	Modulation Frequency	USIT-E	333333	Hz
USFR	Ultrasonic Sampling Frequency	USIT-E	500000	Hz
UPAT	USIT Emission Pattern	USIT-E	Pattern 500 KHz	
UWKM	USIT Working Mode	USIT-E	Uncompressed 10 deg at 1.5 in LF	
USIT_DEPTHLOG	Starting Depth Log for Ultrasonics	USIT-E	Time Zoned	ft
USSP	Ultrasonic Service	USIT-E	USI	
VRES	Vertical Resolution	USIT-E	1.5 in	
WINB	Window Begin Time	USIT-E	25	us
WINE	Window End Time	USIT-E	90	us
WMOD	Waveform Firing Mode	DSLT-H	Full	

TwoTime Zoned Parameters

Pass Log[9]:Up

Parameter	Value	Start Time	Stop Time	Start Depth (ft)	Stop Depth (ft)
EMXV	50	20-Oct-2016 09:51:44	20-Oct-2016 10:20:40	8171.38	6648.71

Pass Log[11]:Up

EMXV	60	20-Oct-2016 10:24:53	20-Oct-2016 11:05:14	6648.71	4600.07
EMXV	65	20-Oct-2016 11:05:14	20-Oct-2016 12:34:00	4600.07	113.27

Pass Log[14]:Up

EMXV	100	20-Oct-2016 12:53:24	20-Oct-2016 12:54:59	155.15	76.32
EMXV	110	20-Oct-2016 12:54:59	20-Oct-2016 12:57:44	76.32	16.88
EMXV	125	20-Oct-2016 12:57:44	20-Oct-2016 12:58:23	16.88	5.56

All depth are at tool zero.

Composite 1

Main Pass 5 IN = 100 FT

Composite Summary

Run Name	Pass Objective	Direction	Top	Bottom	Start	Stop	DSC Mode	Depth Shift	Include Parallel Data
Two	Log[9]:Up	Up	6640.29 ft	8171.85 ft	20-Oct-2016 9:51:39 AM	20-Oct-2016 10:20:40 AM	ON	1.47 ft	No
Two	Log[11]:Up	Up	36.69 ft	6737.51 ft	20-Oct-2016 10:24:53 AM	20-Oct-2016 12:34:00 PM	ON	1.35 ft	No
Two	Log[14]:Up	Up	5.56 ft	155.15 ft	20-Oct-2016 12:53:24 PM	20-Oct-2016 12:58:23 PM	ON	1.96 ft	No

All depths are referenced to toolstring zero

Log

Company:Southern California Gas Company Well:Frew 4

Composite 1:S008

Description: USI Composite Format: Log (LBV1_USI Composite 7inch) Index Scale: 5 in per 100 ft Index Unit: ft Index Type: Measured Depth Creation Date: 20-Oct-2016 14:28:19

TIME_1900 - Time Marked every 60.00 (s)

USIT Processing Flags (UFLG[0]) USIT-E[1]

1 - UFLG 1 Value within [0.0 - 1.5] - :
2 - UFLG 2 Value within [1.5 - 2.5] - :
3 - UFLG 3 Value within [2.5 - 3.5] - :
4 - UFLG 4 UFLG 5 UFLG 6 Value within [3.5 - 6.5] - :
5 - UFLG 7 UFLG 8 UFLG 9 Value within [6.5 - 10] - :

- UTIM Error
- Pulse Origin Not Detected
- WINLEN Error
- Casing Thickness Error
- Loop Processing Error

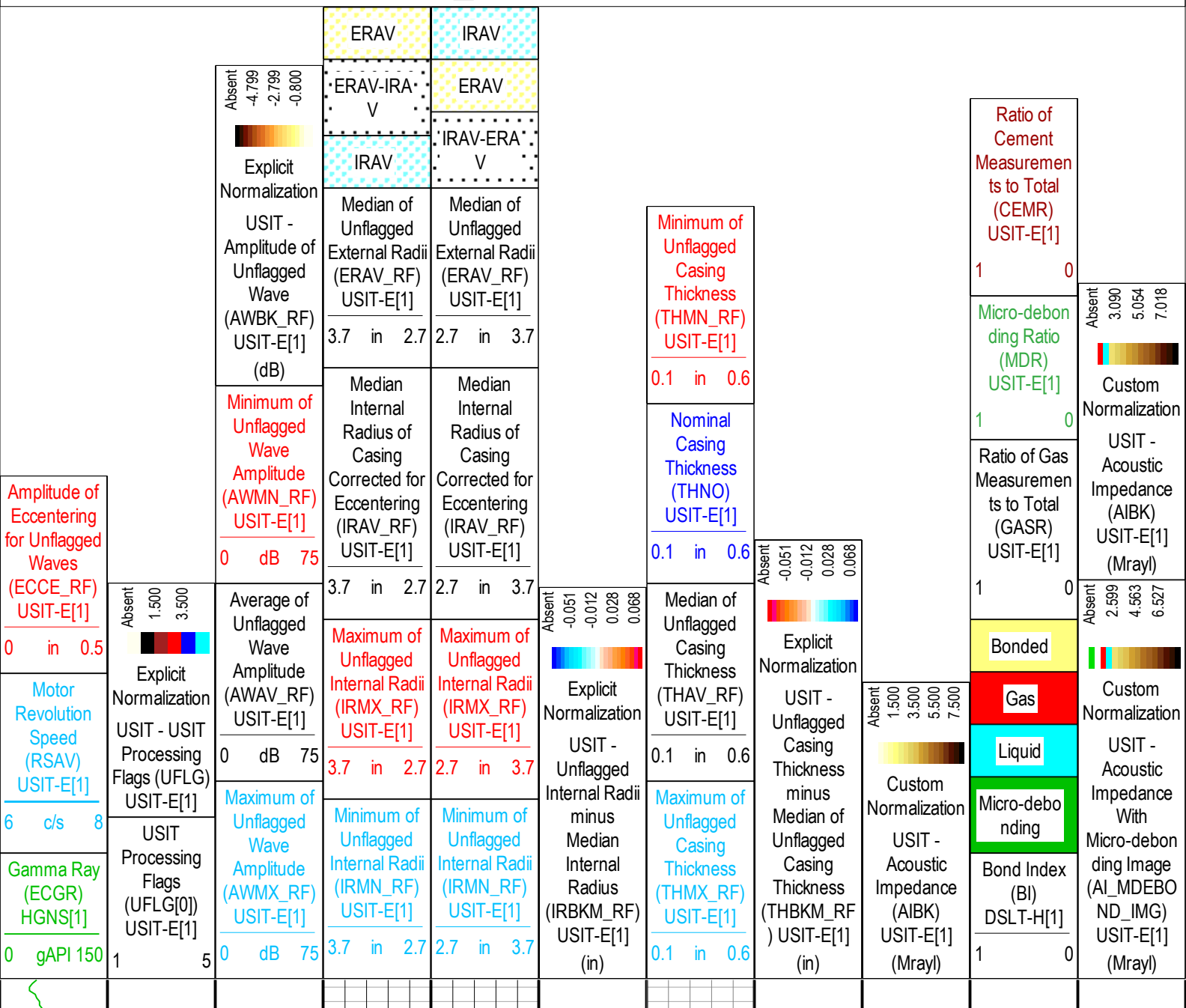

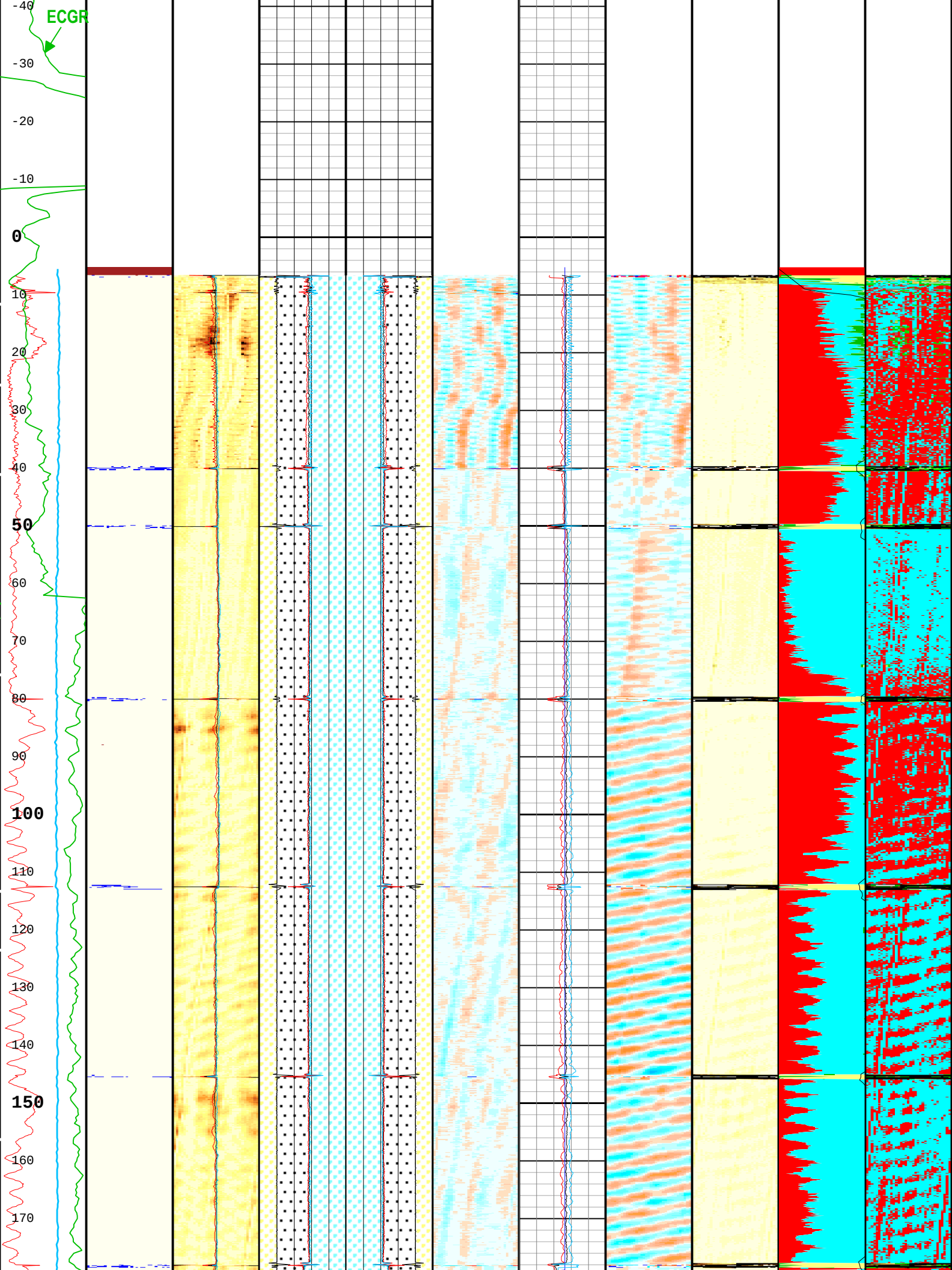
ECGR
-40
-30
-20
-10
0
10
20
30
40
50
60
70
80
90
100
110
120
130
140
150
160
170

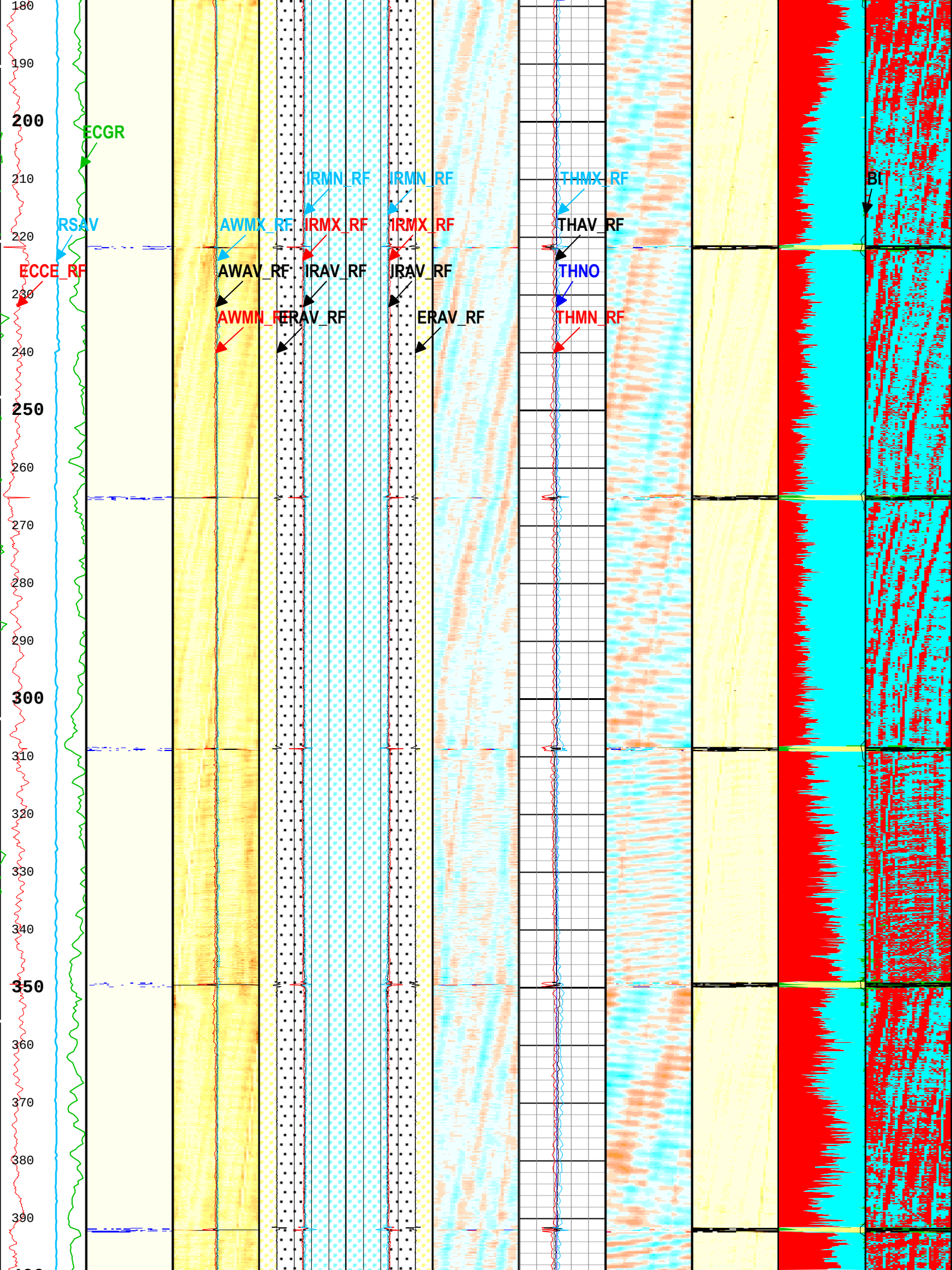
180
190
200
210
220
230
240
250
260
270
280
290
300
310
320
330
340
350
360
370
380
390
ECGR
RSAV
ECCE_RF
AWMX_RF
AWAV_RF
AWMN_RF
IRMN_RF
IRMX_RF
IRAV_RF
ERAV_RF
IRMN_RF
IRMX_RF
IRAV_RF
ERAV_RF
THMX_RF
THAV_RF
THNO
THMN_RF
BI

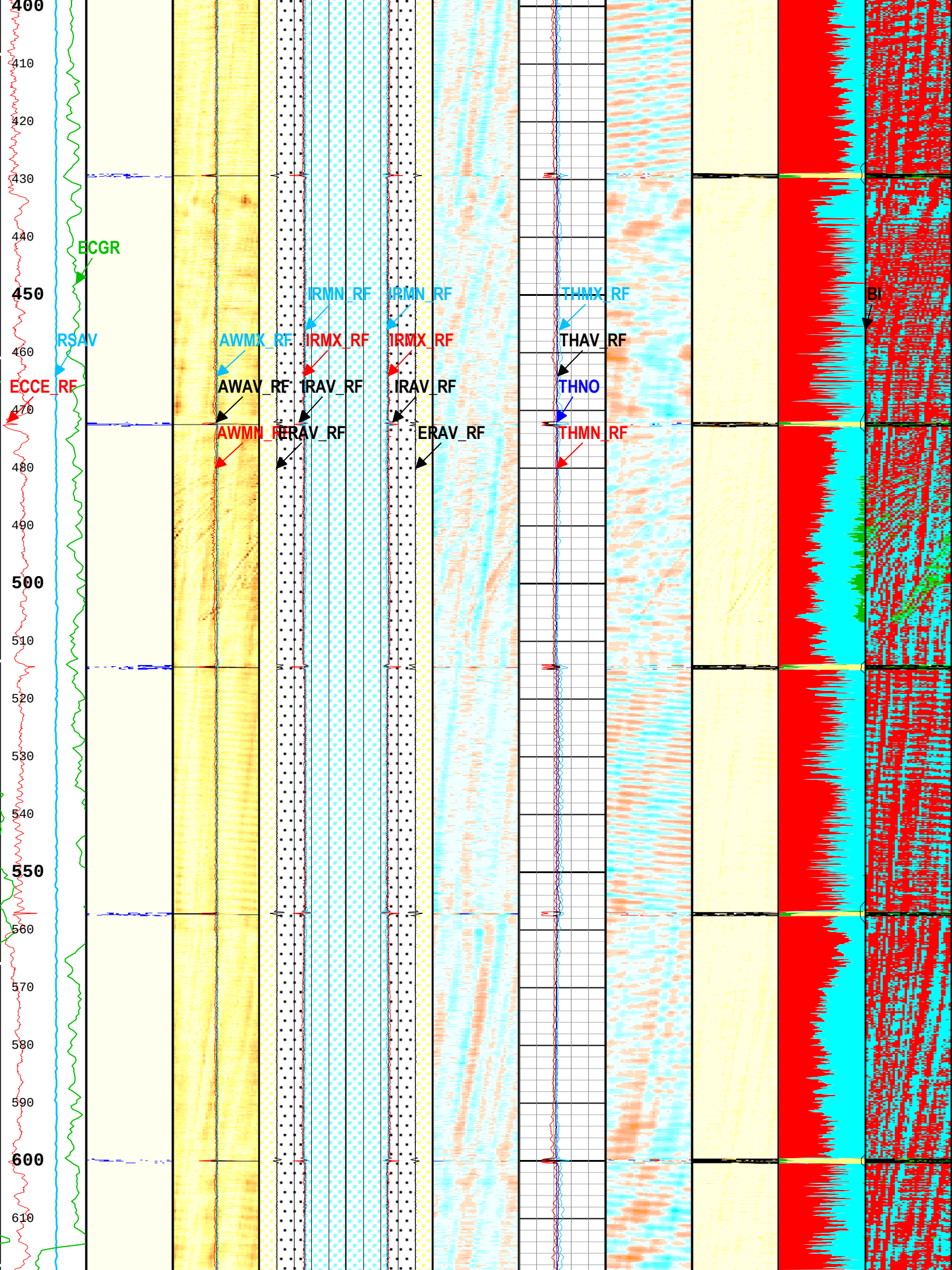
400
410
420
430
440
450
460
470
480
490
500
510
520
530
540
550
560
570
580
590
600
610
ECGR
RSAV
ECCE_RF
IRMN_RF
IRMN_RF
AWMX_RF
IRMX_RF
IRMX_RF
AWAV_RF
IRAV_RF
IRAV_RF
AWMN_RF
ERAV_RF
ERAV_RF
THMX_RF
THAV_RF
THNO
THMN_RF
BI

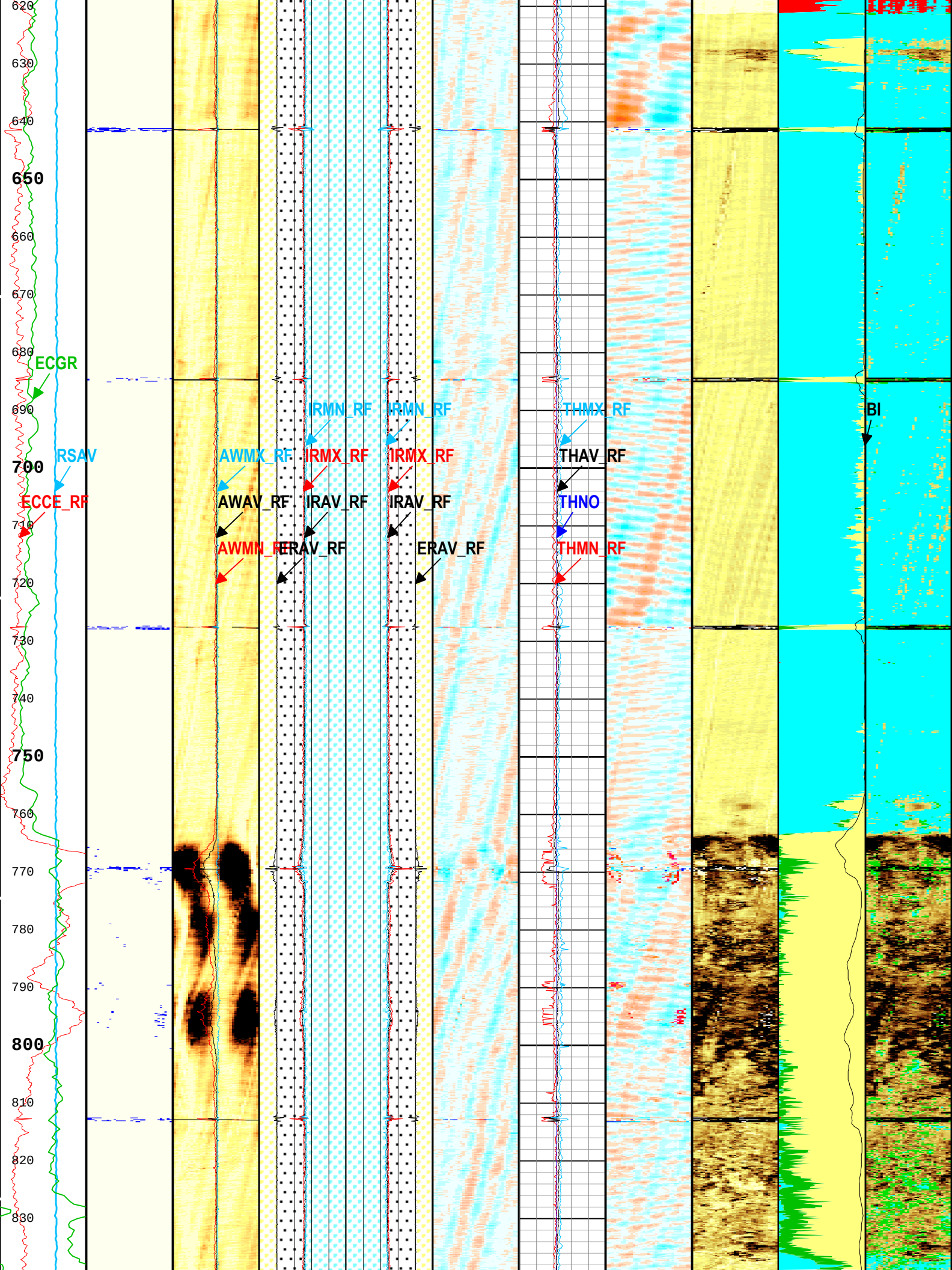
620
630
640
650
660
670
680
690
700
710
720
730
740
750
760
770
780
790
800
810
820
830
ECGR
RSAV
ECCE_RF
IRMN_RF
IRMN_RF
AWMX_RF
IRMX_RF
IRMX_RF
AWAV_RF
IRAV_RF
IRAV_RF
AWMN_RF
ERAV_RF
ERAV_RF
THMX_RF
THAV_RF
THNO
THMN_RF
BI

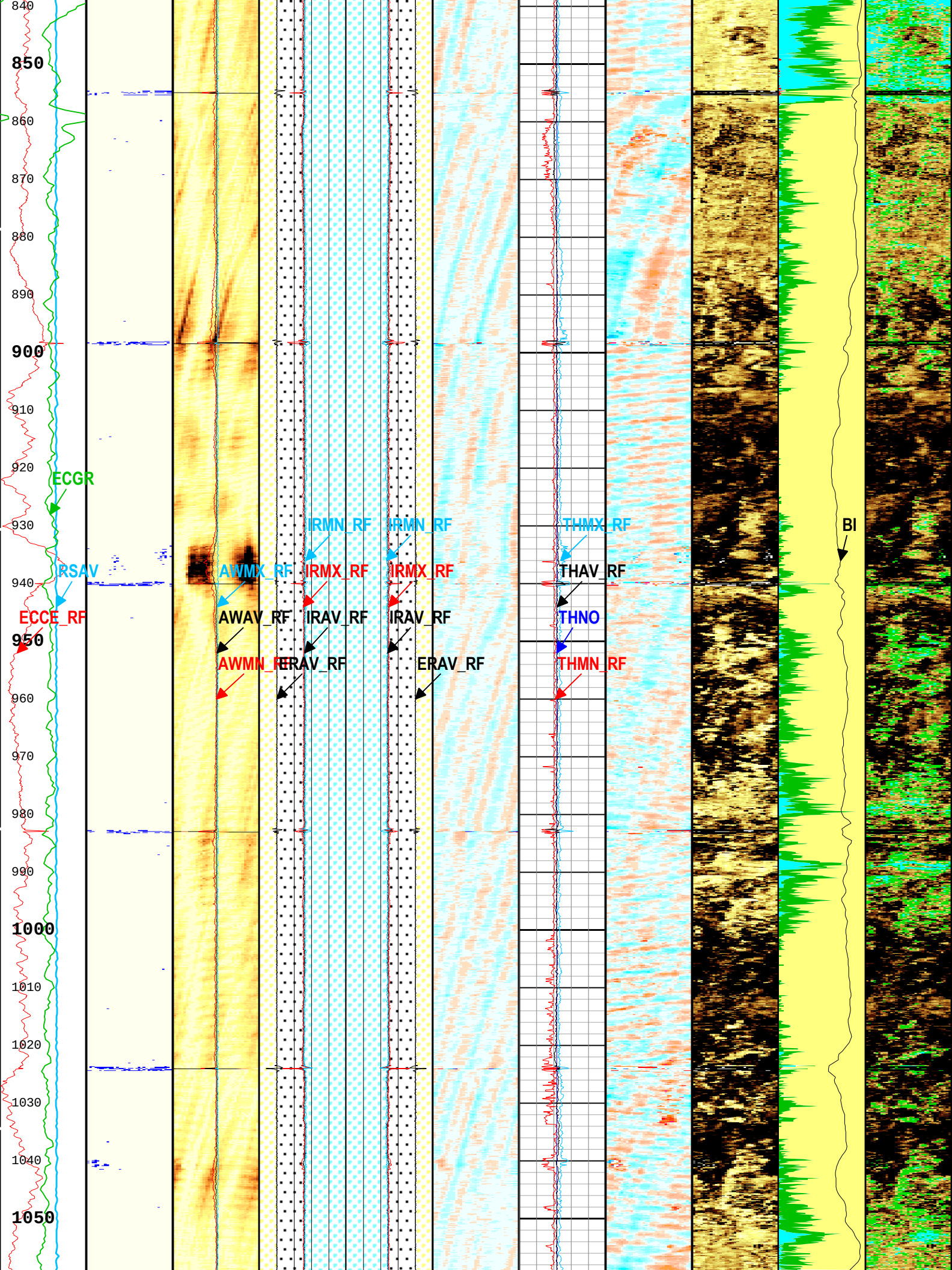
840
850
860
870
880
890
900
910
920
930
940
950
960
970
980
990
1000
1010
1020
1030
1040
1050
ECGR
RSAV
ECCE_RF
IRMN_RF
IRMN_RF
AWMX_RF
IRMX_RF
IRMX_RF
AWAV_RF
IRAV_RF
IRAV_RF
AWMN_RF
ERAV_RF
ERAV_RF
THMX_RF
THAV_RF
THNO
THMN_RF
BI

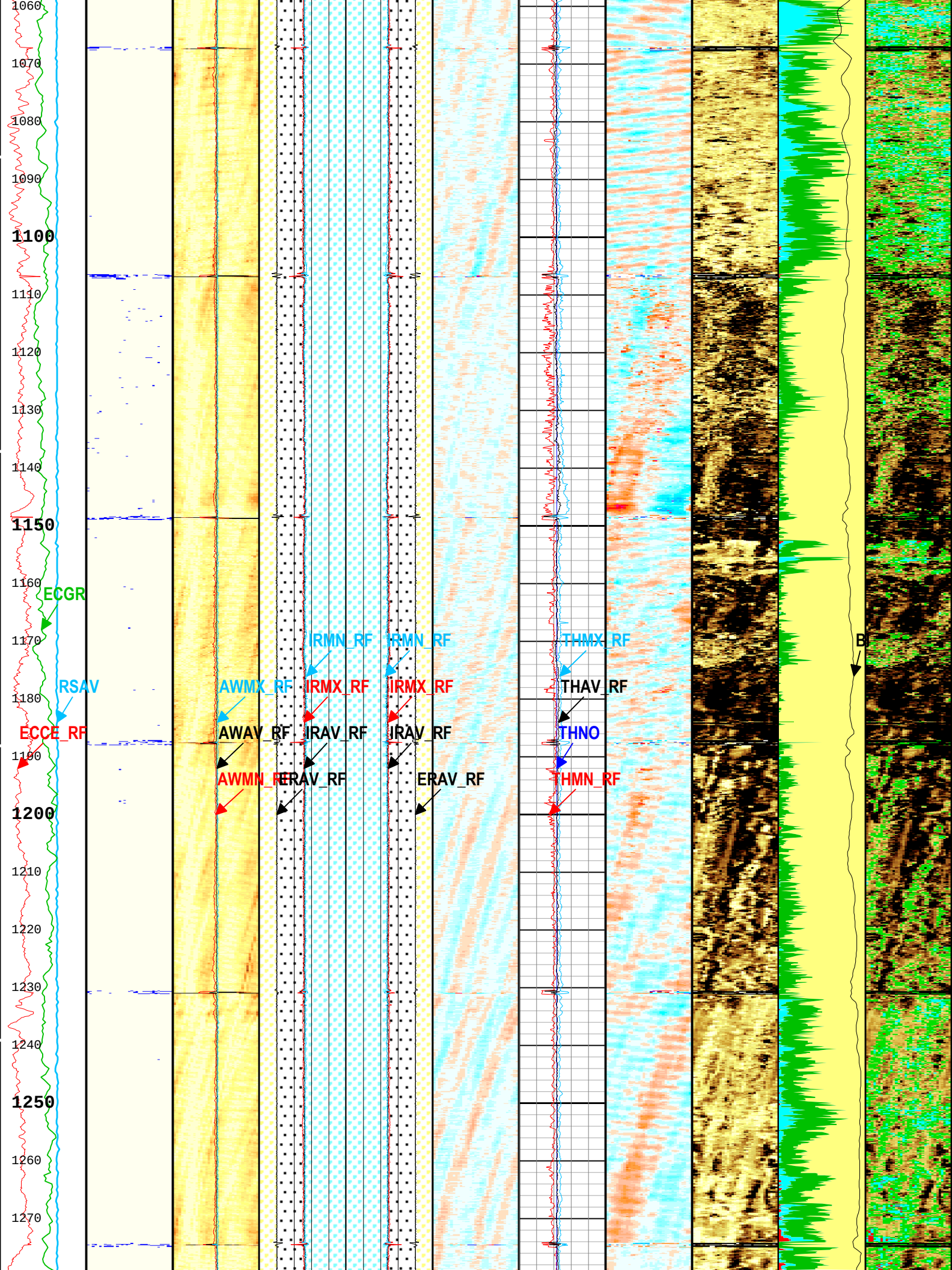
1060
1070
1080
1090
1100
1110
1120
1130
1140
1150
1160
1170
1180
1190
1200
1210
1220
1230
1240
1250
1260
1270
ECGR
RSAV
ECCE_RF
IRMN_RF
IRMN_RF
AWMX_RF
IRMX_RF
IRMX_RF
AWAV_RF
IRAV_RF
IRAV_RF
AWMN_RF
ERAV_RF
ERAV_RF
THMX_RF
THAV_RF
THNO
THMN_RF
B

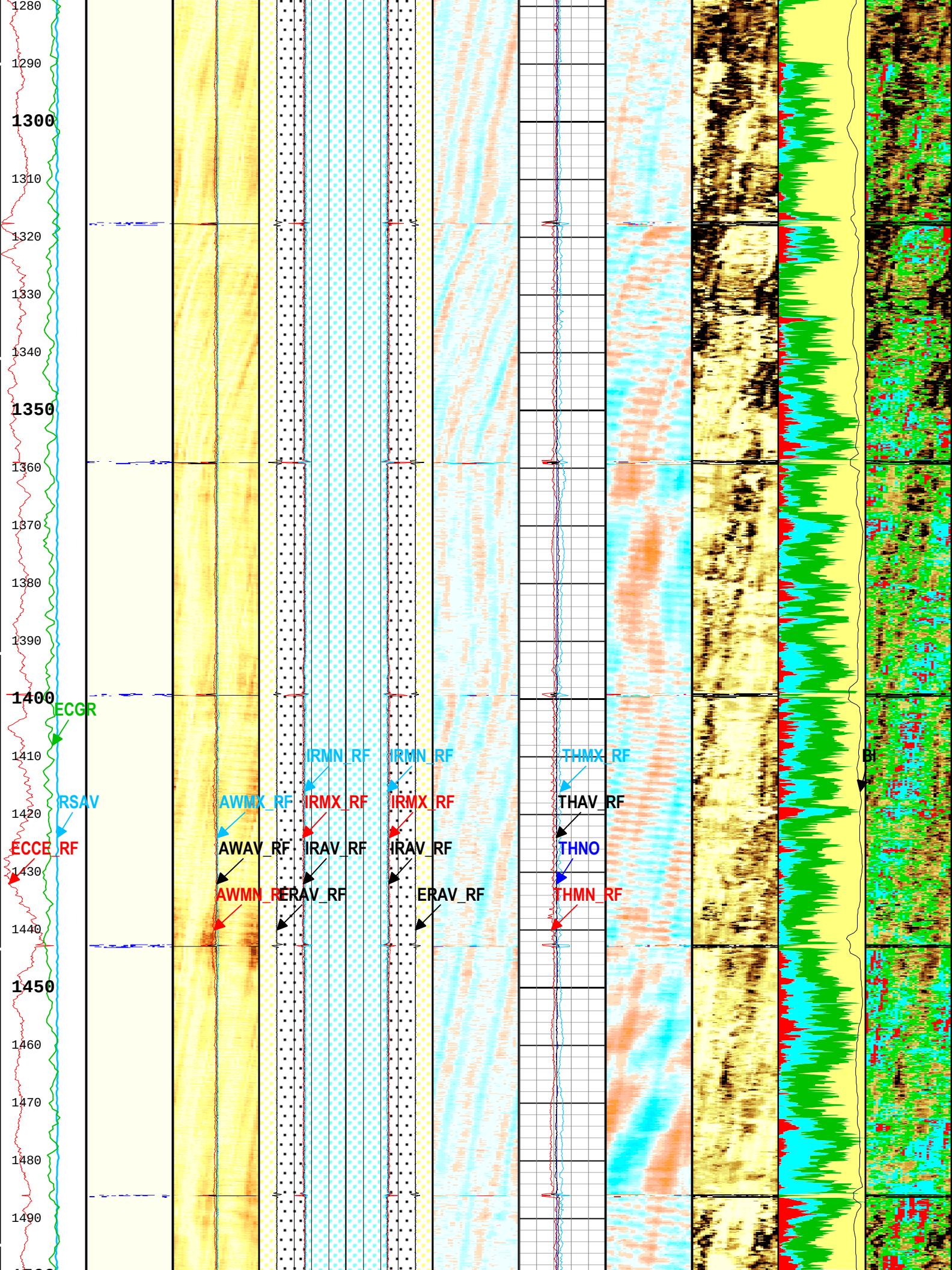
1280
1290
1300
1310
1320
1330
1340
1350
1360
1370
1380
1390
1400
1410
1420
1430
1440
1450
1460
1470
1480
1490
ECGR
RSAV
ECCE_RF
AWMX_RF
AWAV_RF
AWMN_RF
IRMN_RF
IRMX_RF
IRAV_RF
ERAV_RF
IRMN_RF
IRMX_RF
IRAV_RF
ERAV_RF
THMX_RF
THAV_RF
THNO
THMN_RF
BI

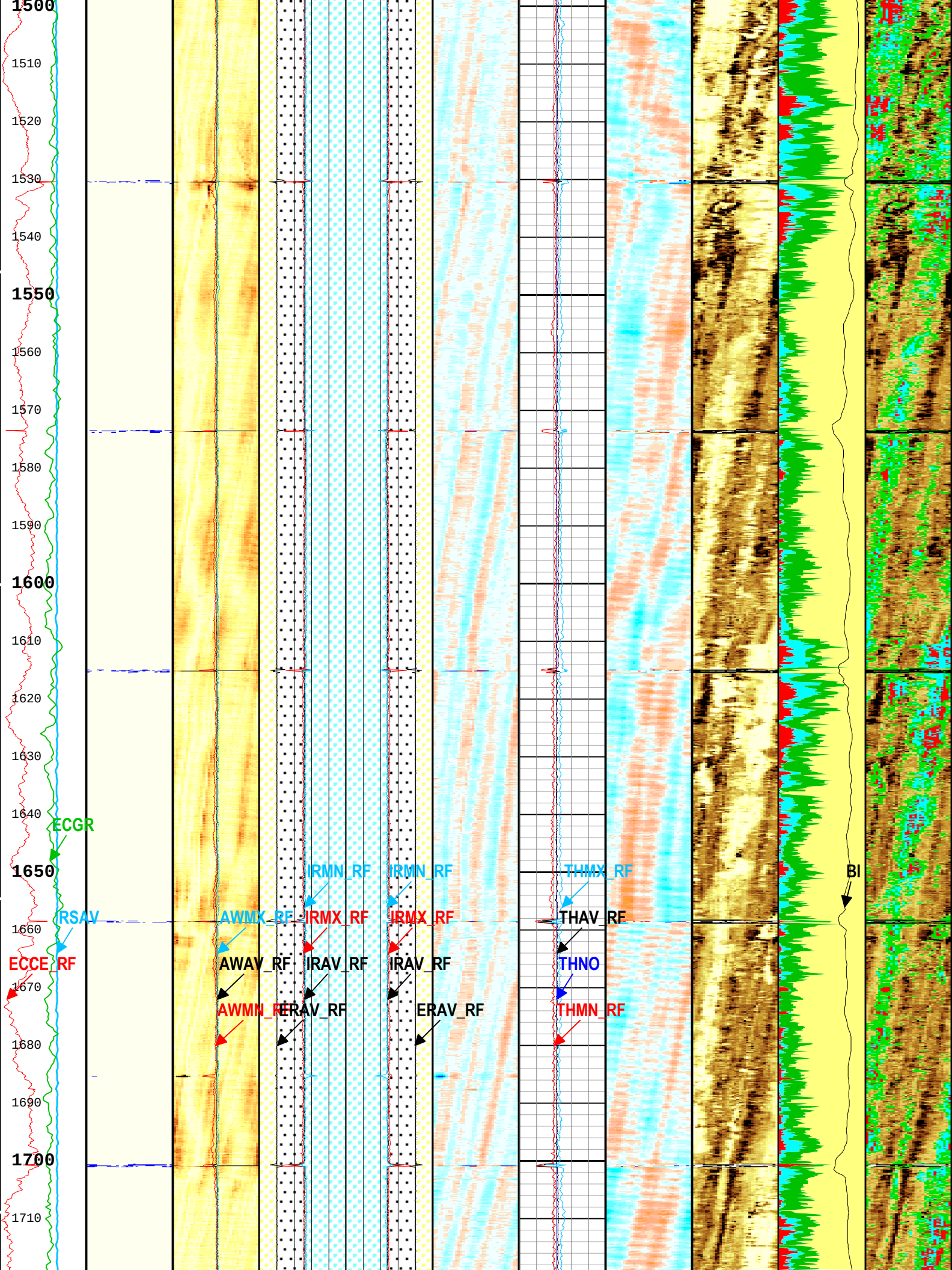
1500
1510
1520
1530
1540
1550
1560
1570
1580
1590
1600
1610
1620
1630
1640
1650
1660
1670
1680
1690
1700
1710
ECGR
RSAV
ECCE_RF
AWMX_RF
AWAV_RF
AWMN_RF
IRMN_RF
IRMX_RF
IRAV_RF
ERAV_RF
IRMN_RF
IRMX_RF
IRAV_RF
ERAV_RF
THMX_RF
THAV_RF
THNO
THMN_RF
BI

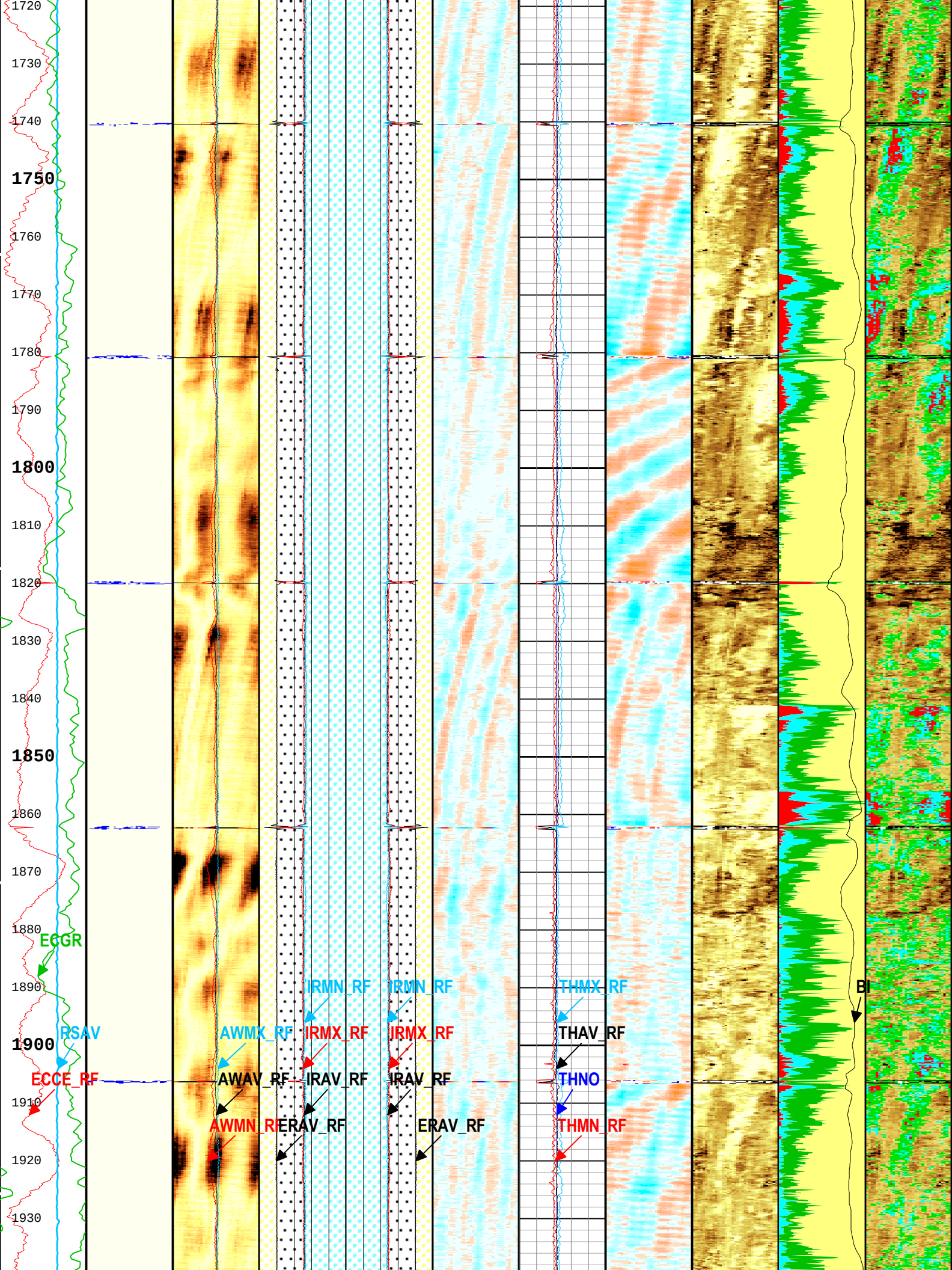
1720
1730
1740
1750
1760
1770
1780
1790
1800
1810
1820
1830
1840
1850
1860
1870
1880
1890
1900
1910
1920
1930
ECGR
RSAV
ECCE_RF
AWAV_RF
AWMX_RF
AWMN_RF
IRMN_RF
IRMX_RF
IRAV_RF
ERAV_RF
IRMN_RF
IRMX_RF
IRAV_RF
ERAV_RF
THMX_RF
THAV_RF
THNO
THMN_RF
BI

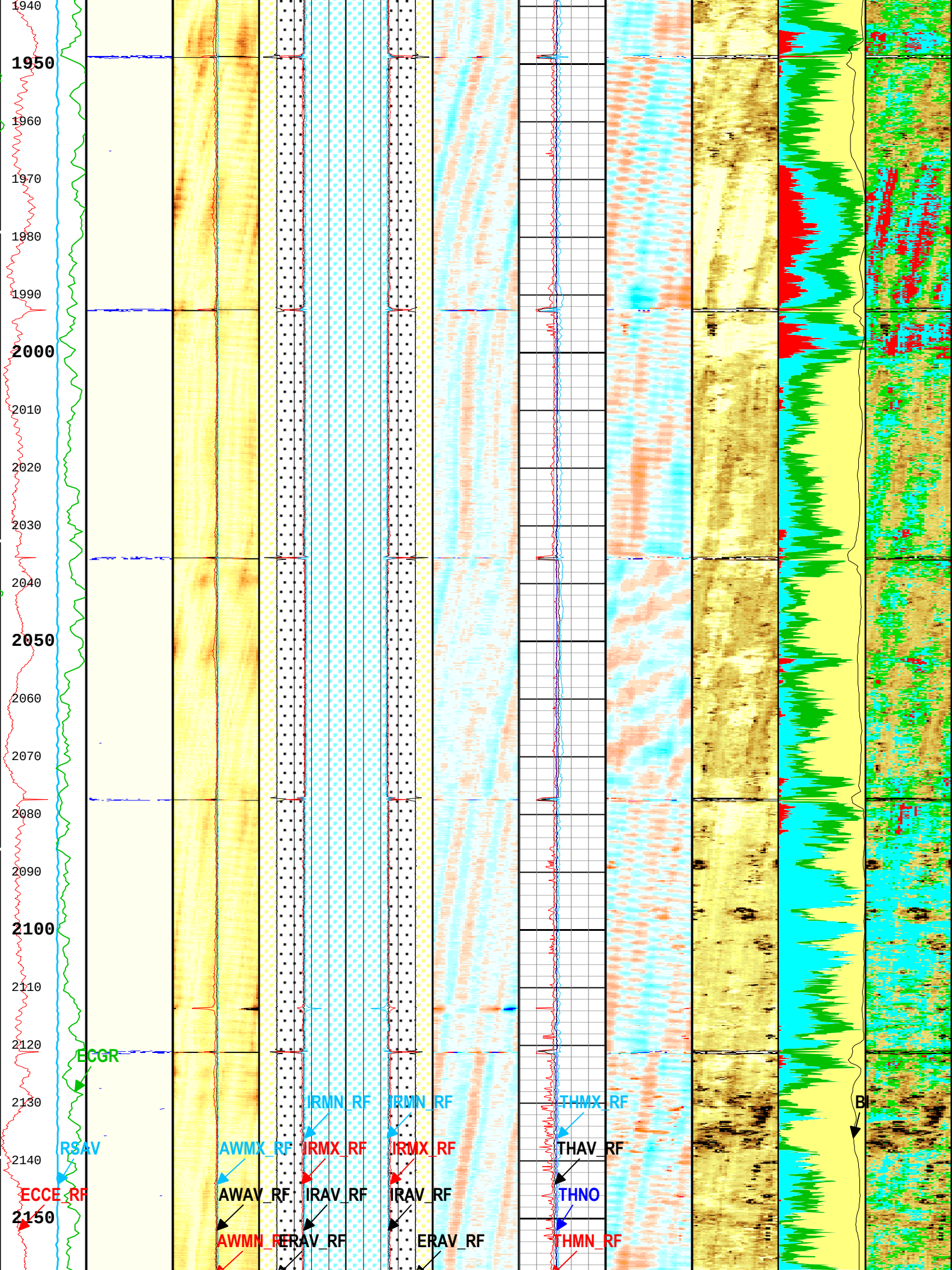
1940
1950
1960
1970
1980
1990
2000
2010
2020
2030
2040
2050
2060
2070
2080
2090
2100
2110
2120
2130
2140
2150
ECGR
RSAV
ECCE_RF
IRMN_RF
AWMX_RF
IRMX_RF
AWAV_RF
IRAV_RF
AWMN_RF
ERAV_RF
IRMN_RF
IRMX_RF
IRAV_RF
ERAV_RF
THMX_RF
THAV_RF
THNO
THMN_RF
BI

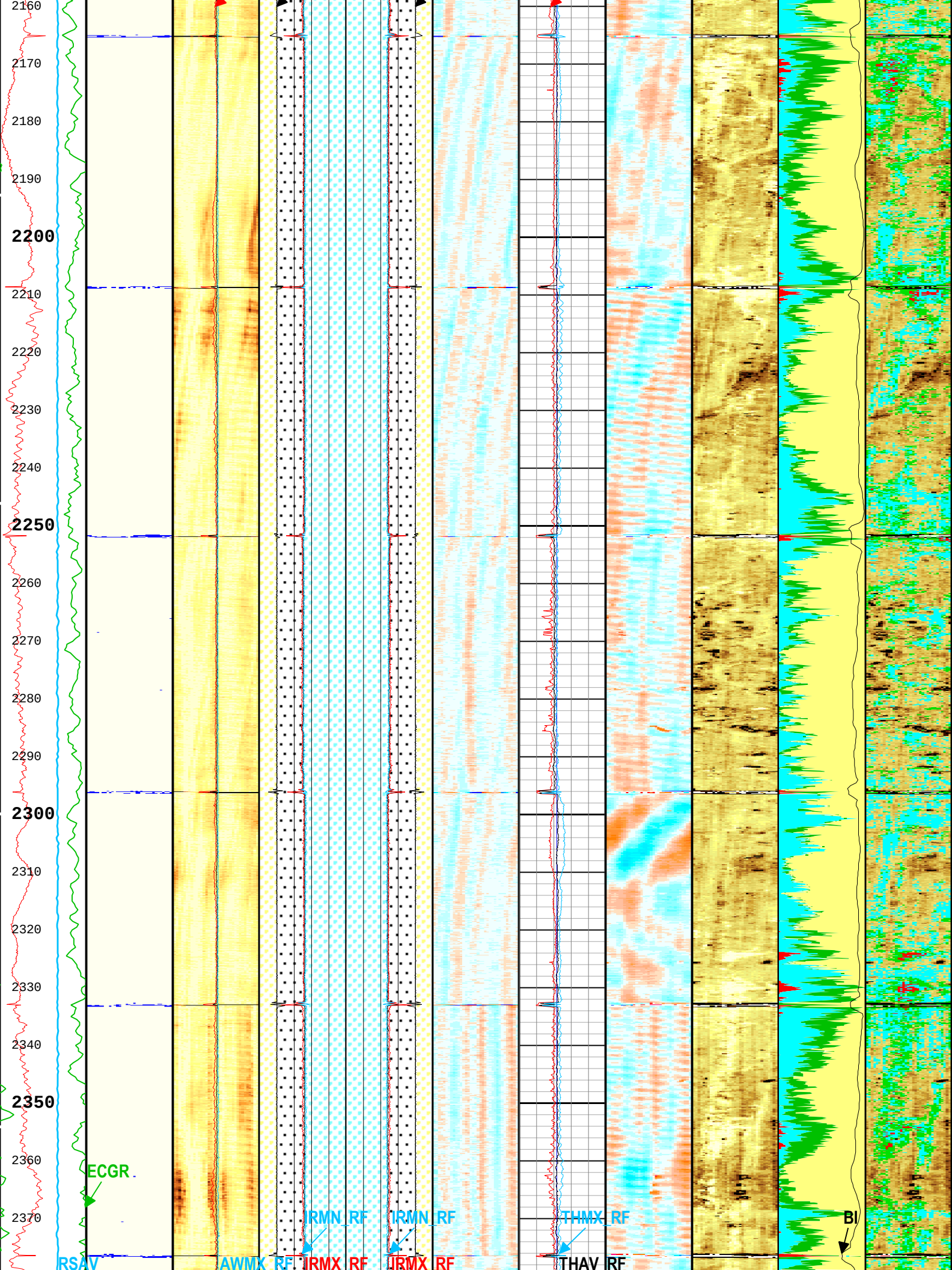
2160
2170
2180
2190
2200
2210
2220
2230
2240
2250
2260
2270
2280
2290
2300
2310
2320
2330
2340
2350
2360
2370
ECGR
RSAV
AWMX_RF
IRMN_RF
IRMX_RF
IRMN_RF
IRMX_RF
THMX_RF
THAV_RF
BI

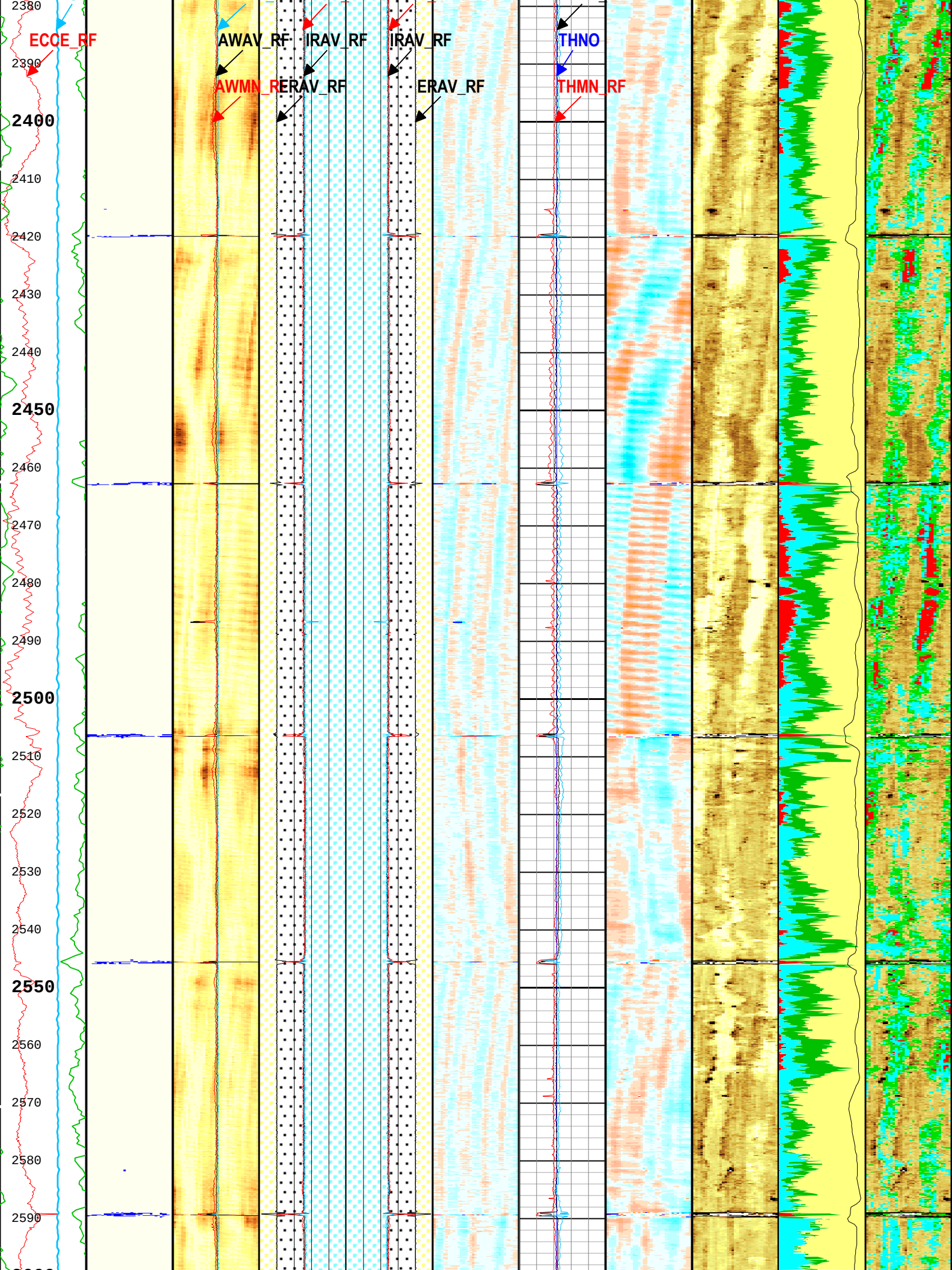
ECCE_RF
AWAV_RF
IRAV_RF
IRAV_RF
THNO
AWMN_RF
ERAV_RF
ERAV_RF
THMN_RF
2380
2390
2400
2410
2420
2430
2440
2450
2460
2470
2480
2490
2500
2510
2520
2530
2540
2550
2560
2570
2580
2590

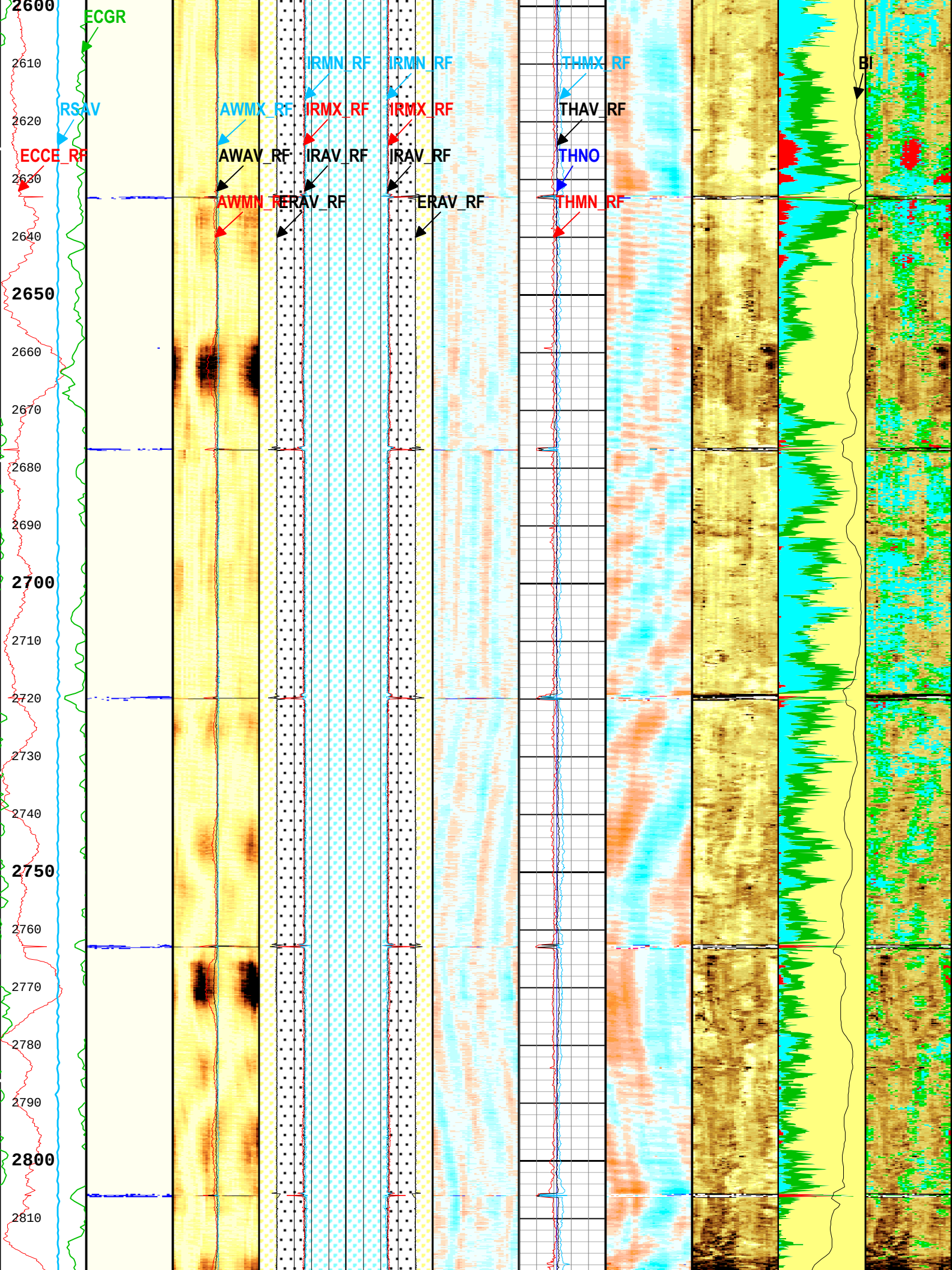
ECGR
RSAV
ECCE_RF
AWMX_RF
AWAV_RF
AWMN_RF
IRMN_RF
IRMX_RF
IRAV_RF
ERAV_RF
IRMN_RF
IRMX_RF
IRAV_RF
ERAV_RF
THMX_RF
THAV_RF
THNO
THMN_RF
BI
2600
2610
2620
2630
2640
2650
2660
2670
2680
2690
2700
2710
2720
2730
2740
2750
2760
2770
2780
2790
2800
2810

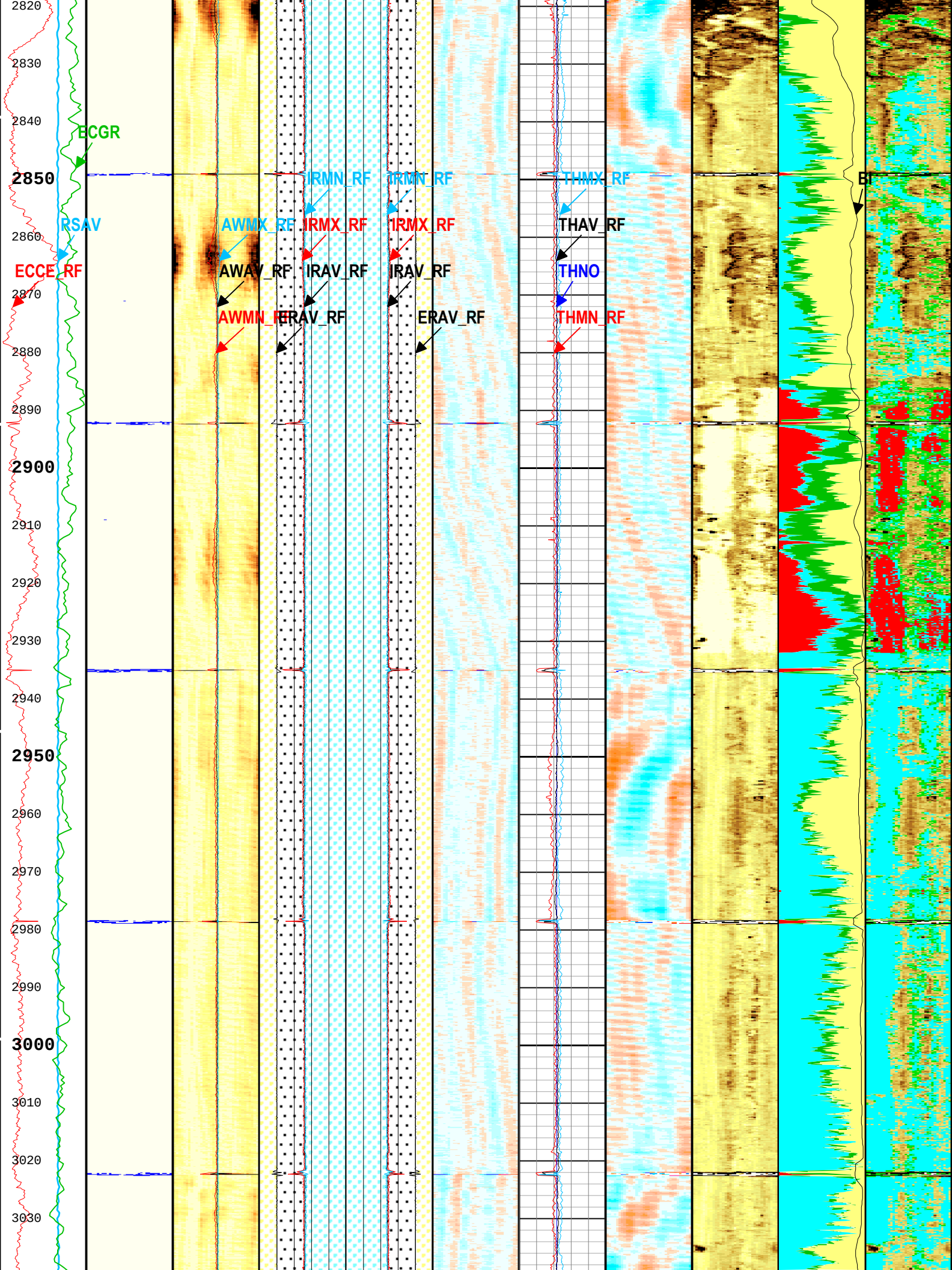
2820
2830
2840
2850
2860
2870
2880
2890
2900
2910
2920
2930
2940
2950
2960
2970
2980
2990
3000
3010
3020
3030
ECGR
RSAV
ECCE_RF
AWMX_RF
AWAV_RF
AWMN_RF
IRMN_RF
IRMX_RF
IRAV_RF
ERAV_RF
IRMN_RF
IRMX_RF
IRAV_RF
ERAV_RF
THMX_RF
THAV_RF
THNO
THMN_RF
BI

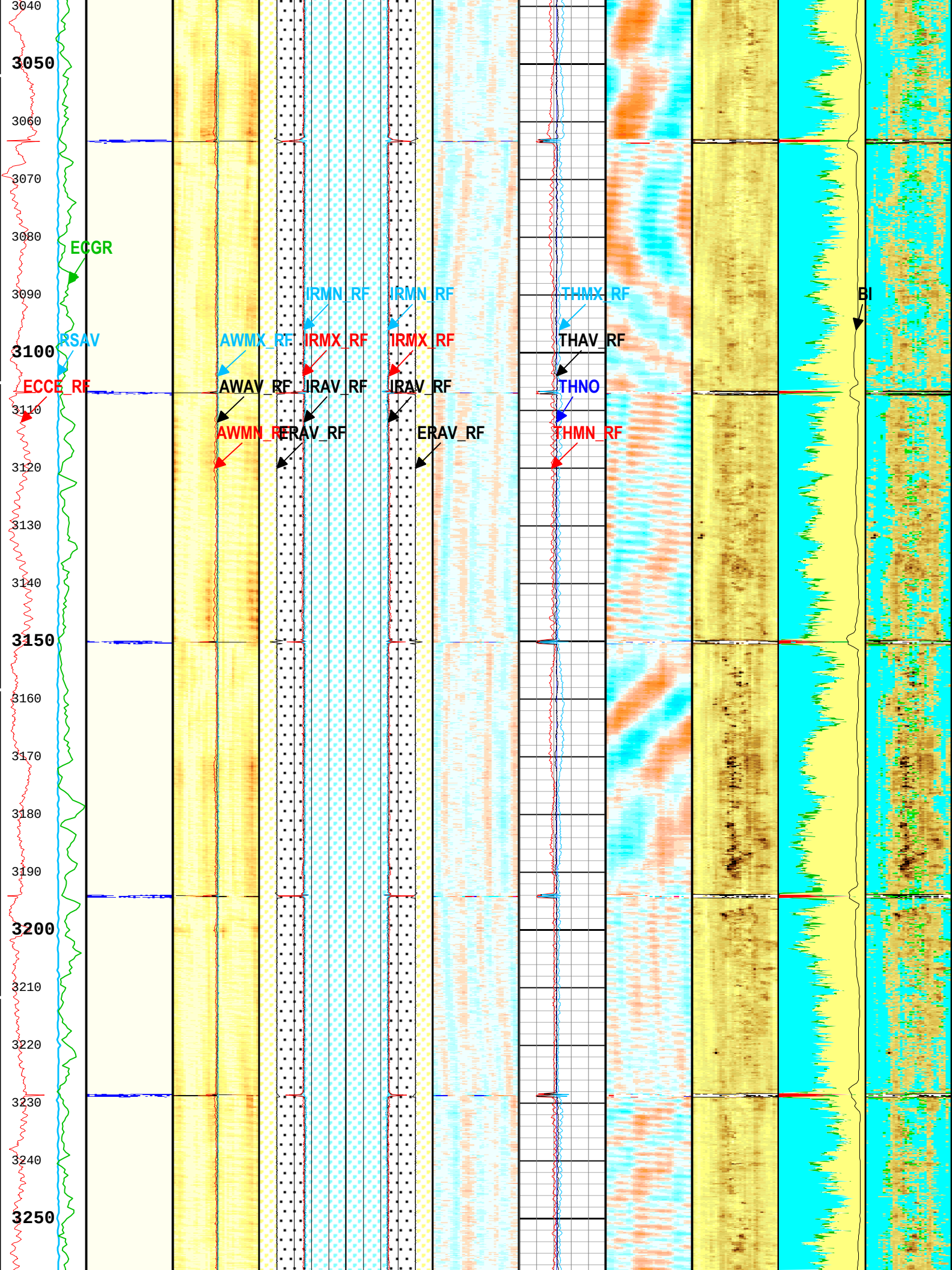
3040
3050
3060
3070
3080
3090
3100
3110
3120
3130
3140
3150
3160
3170
3180
3190
3200
3210
3220
3230
3240
3250
ECGR
RSAV
ECCE_RF
AWMX_RF
AWAV_RF
AWMN_RF
IRMN_RF
IRMX_RF
IRAV_RF
ERAV_RF
IRMN_RF
IRMX_RF
IRAV_RF
ERAV_RF
THMX_RF
THAV_RF
THNO
THMN_RF
BI

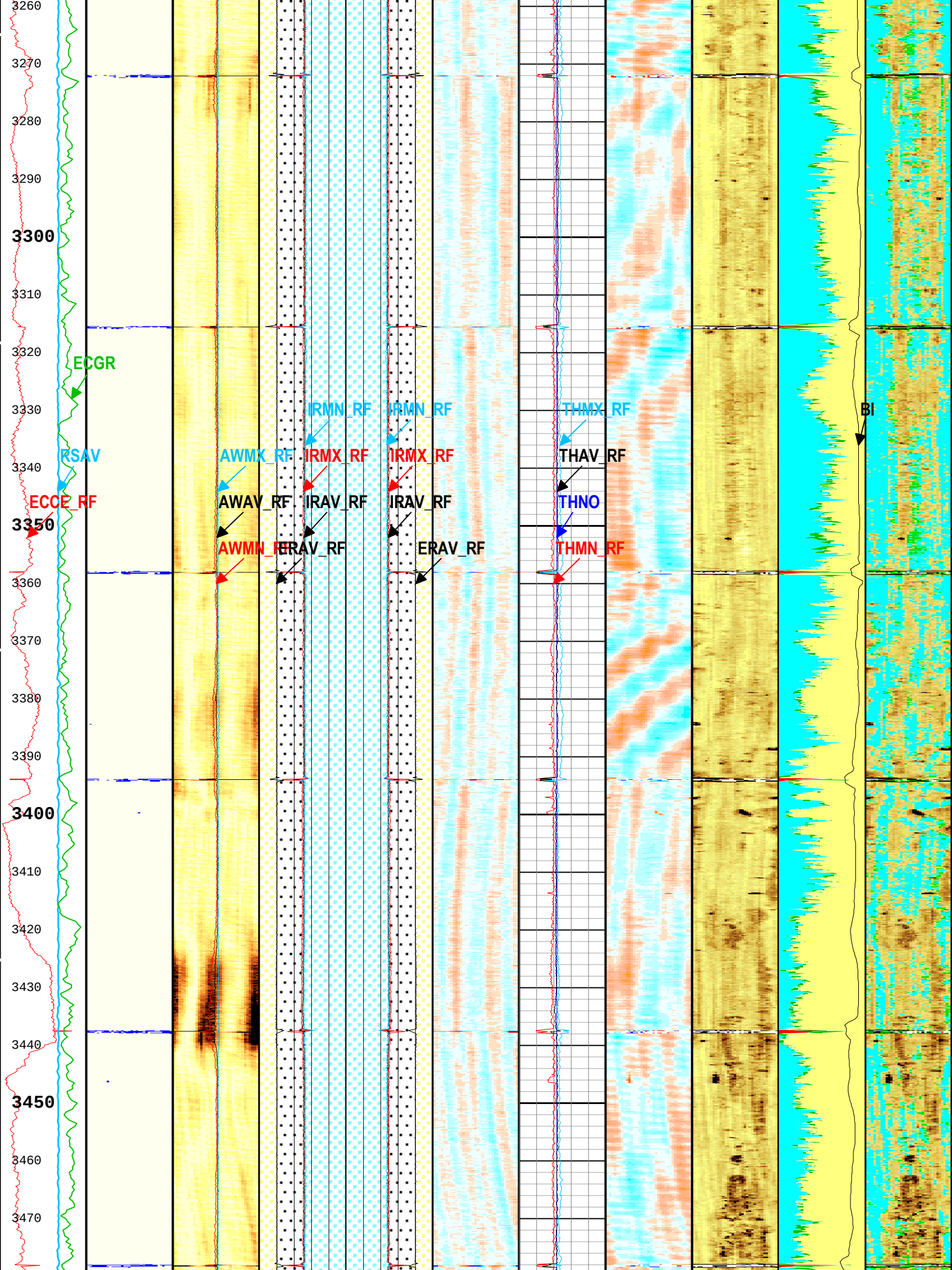
3260
3270
3280
3290
3300
3310
3320
3330
3340
3350
3360
3370
3380
3390
3400
3410
3420
3430
3440
3450
3460
3470
ECGR
RSAV
ECCE_RF
AWMX_RF
AWAV_RF
AWMN_RF
IRMN_RF
IRMX_RF
IRAV_RF
ERAV_RF
IRMN_RF
IRMX_RF
IRAV_RF
ERAV_RF
THMX_RF
THAV_RF
THNO
THMN_RF
BI

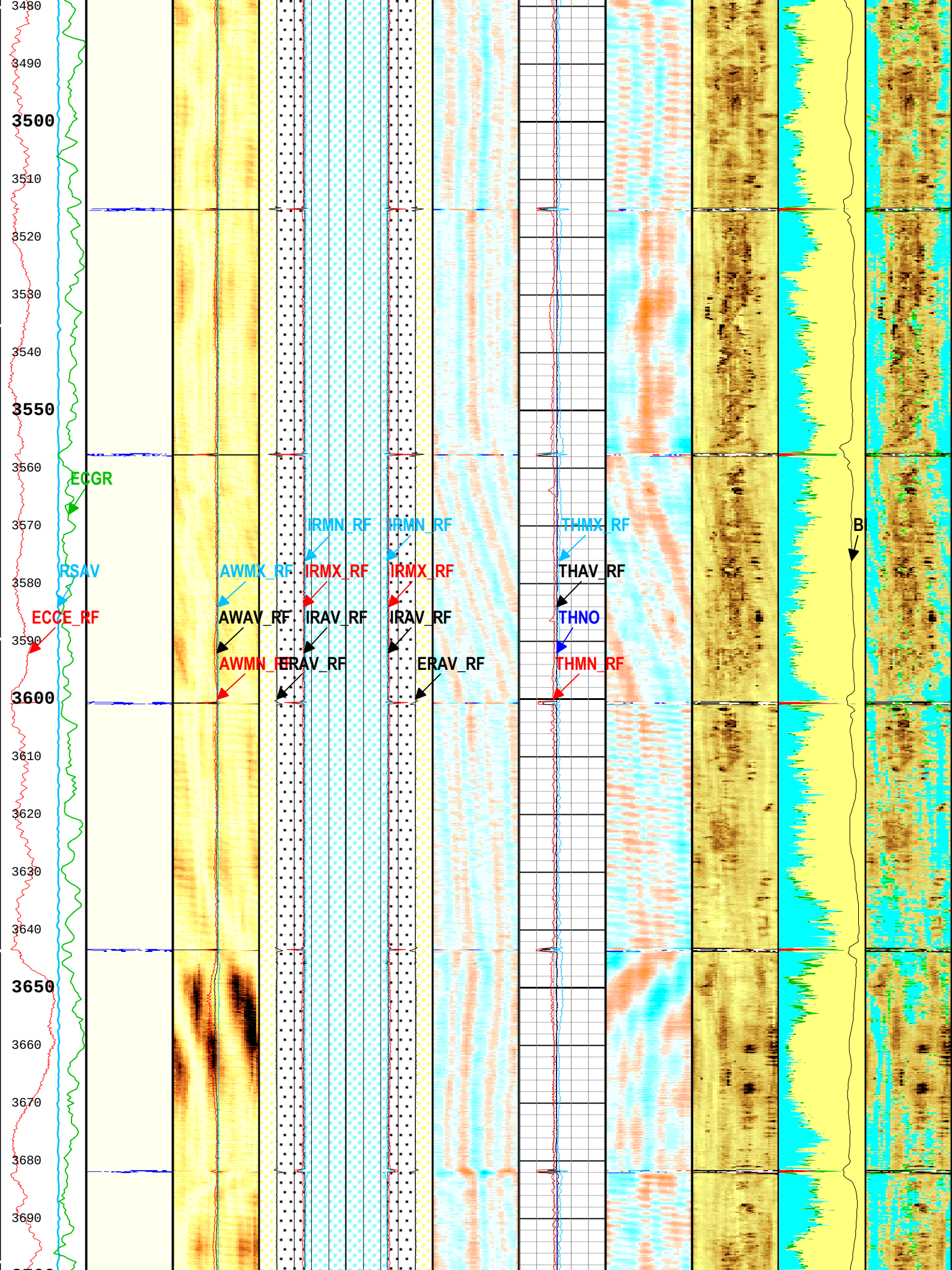
3480
3490
3500
3510
3520
3530
3540
3550
3560
3570
3580
3590
3600
3610
3620
3630
3640
3650
3660
3670
3680
3690
ECGR
RSAV
ECCE_RF
AWMX_RF
AWAV_RF
AWMN_RF
IRMN_RF
IRMX_RF
IRAV_RF
ERAV_RF
IRMN_RF
IRMX_RF
IRAV_RF
ERAV_RF
THMX_RF
THAV_RF
THNO
THMN_RF
B

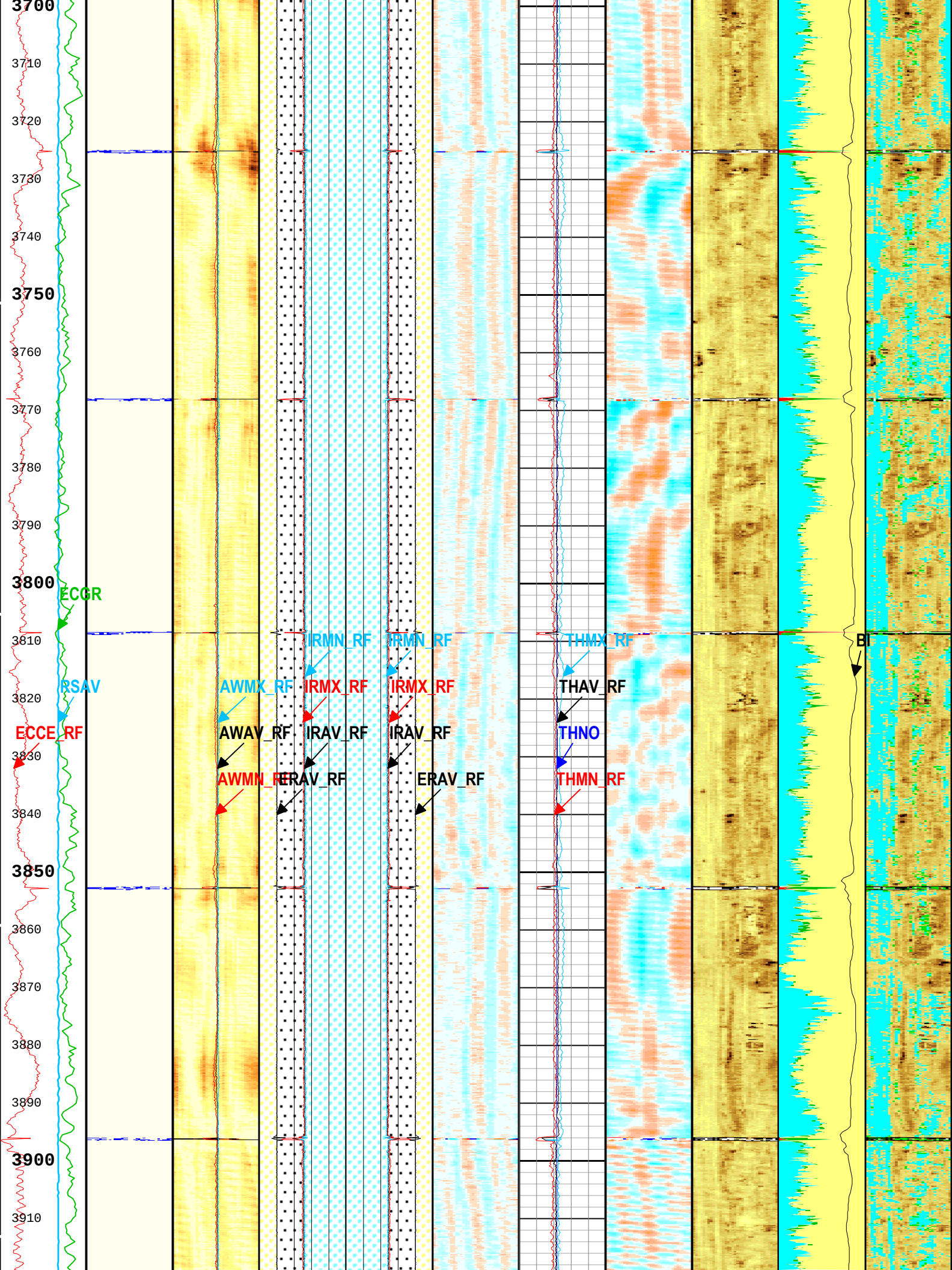
3700
3710
3720
3730
3740
3750
3760
3770
3780
3790
3800
3810
3820
3830
3840
3850
3860
3870
3880
3890
3900
3910
ECGR
RSAV
ECCE_RF
IRMN_RF
IRMN_RF
THMX_RF
AWMX_RF
IRMX_RF
IRMX_RF
THAV_RF
AWAV_RF
IRAV_RF
IRAV_RF
THNO
AWMN_RF
ERAV_RF
ERAV_RF
THMN_RF
BI

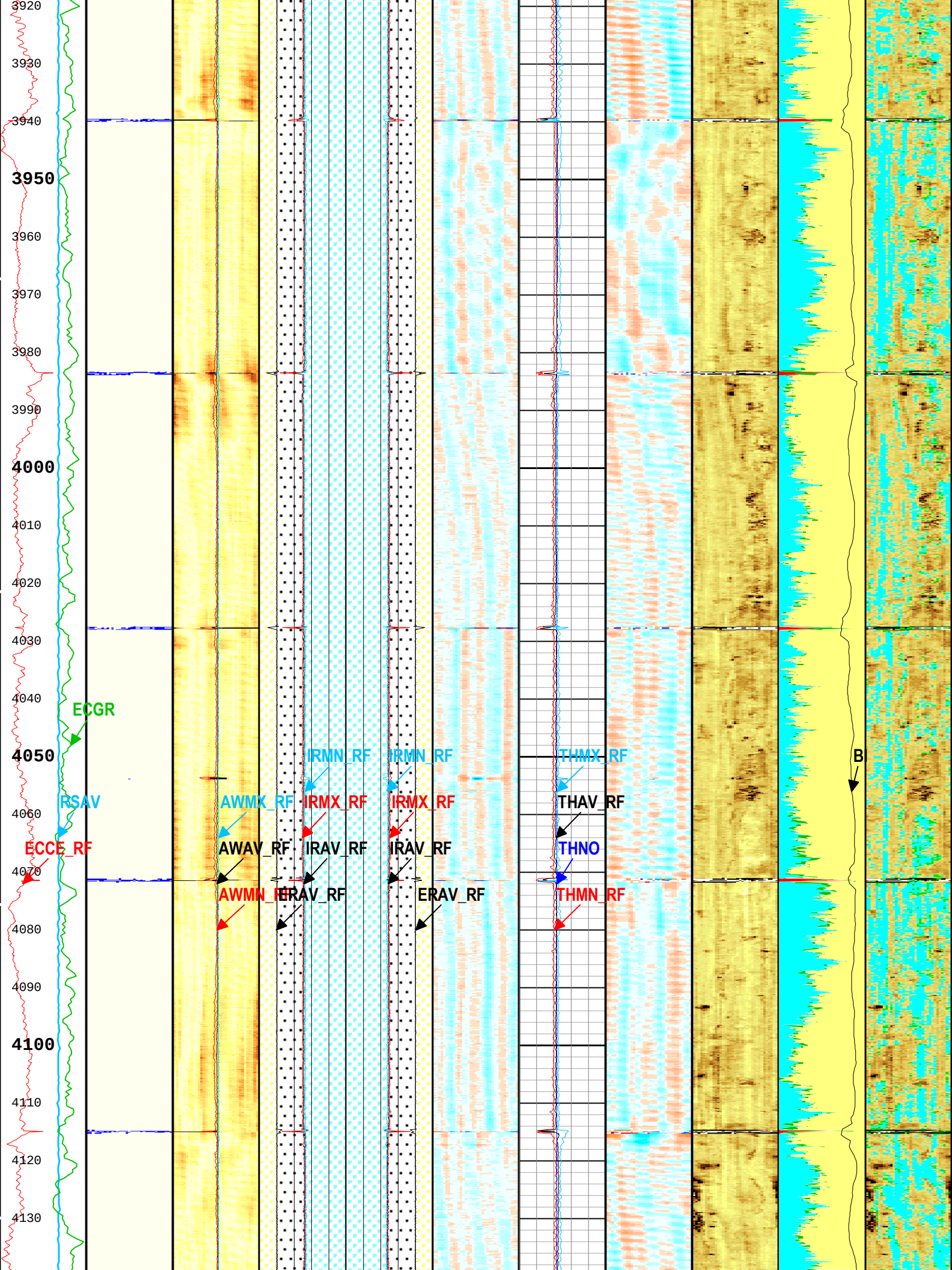
3920
3930
3940
3950
3960
3970
3980
3990
4000
4010
4020
4030
4040
4050
4060
4070
4080
4090
4100
4110
4120
4130
ECGR
RSAV
ECCE_RF
IRMN_RF
IRMN_RF
THMX_RF
B
AWMX_RF
IRMX_RF
IRMX_RF
THAV_RF
AWAV_RF
IRAV_RF
IRAV_RF
THNO
AWMN_RF
ERAV_RF
ERAV_RF
THMN_RF

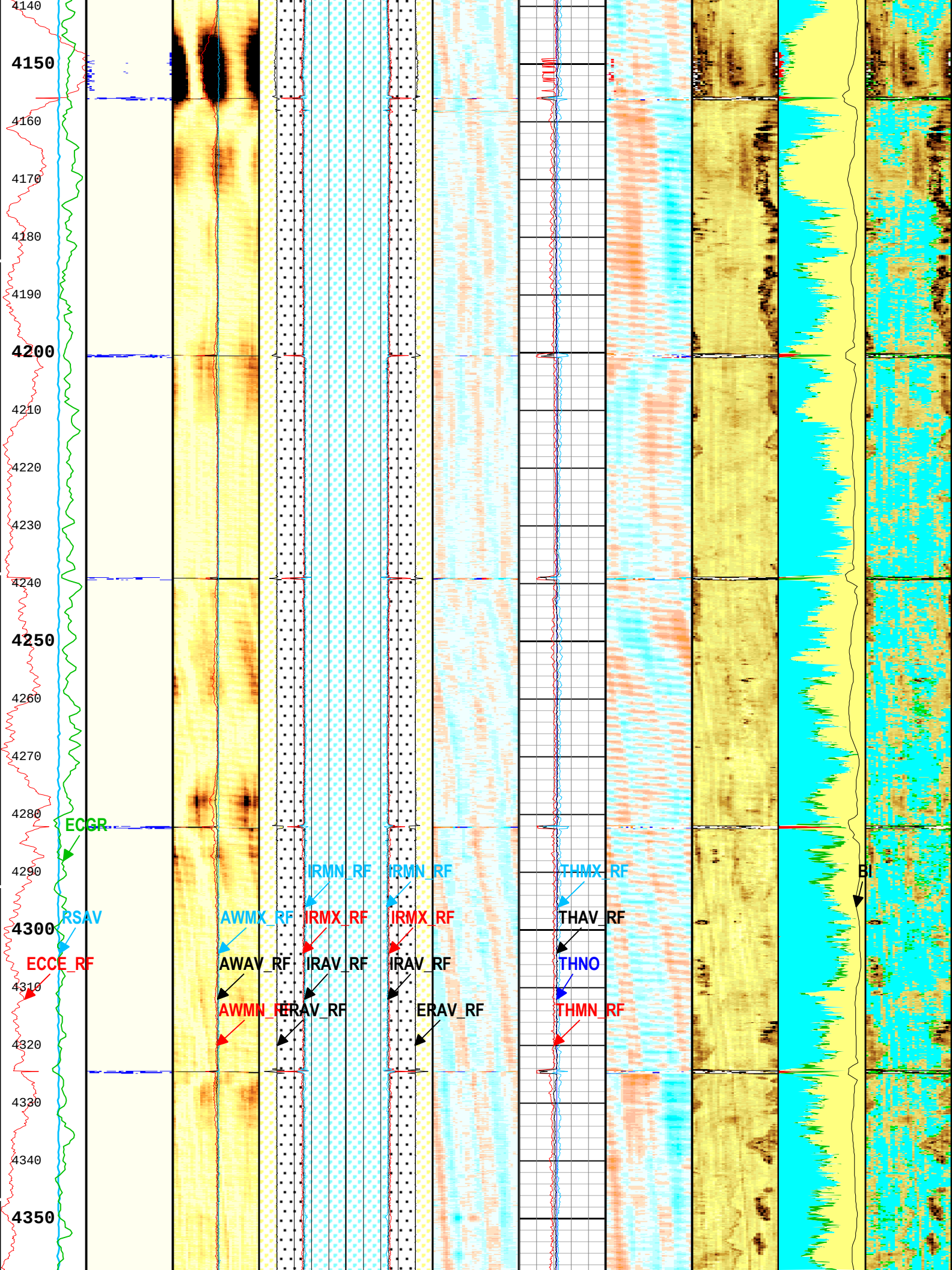
4140
4150
4160
4170
4180
4190
4200
4210
4220
4230
4240
4250
4260
4270
4280
4290
4300
4310
4320
4330
4340
4350
ECGR
RSAV
ECCE_RF
AWMX_RF
AWAV_RF
AWMN_RF
IRMN_RF
IRMX_RF
IRAV_RF
ERAV_RF
IRMN_RF
IRMX_RF
IRAV_RF
ERAV_RF
THMX_RF
THAV_RF
THNO
THMN_RF
BI

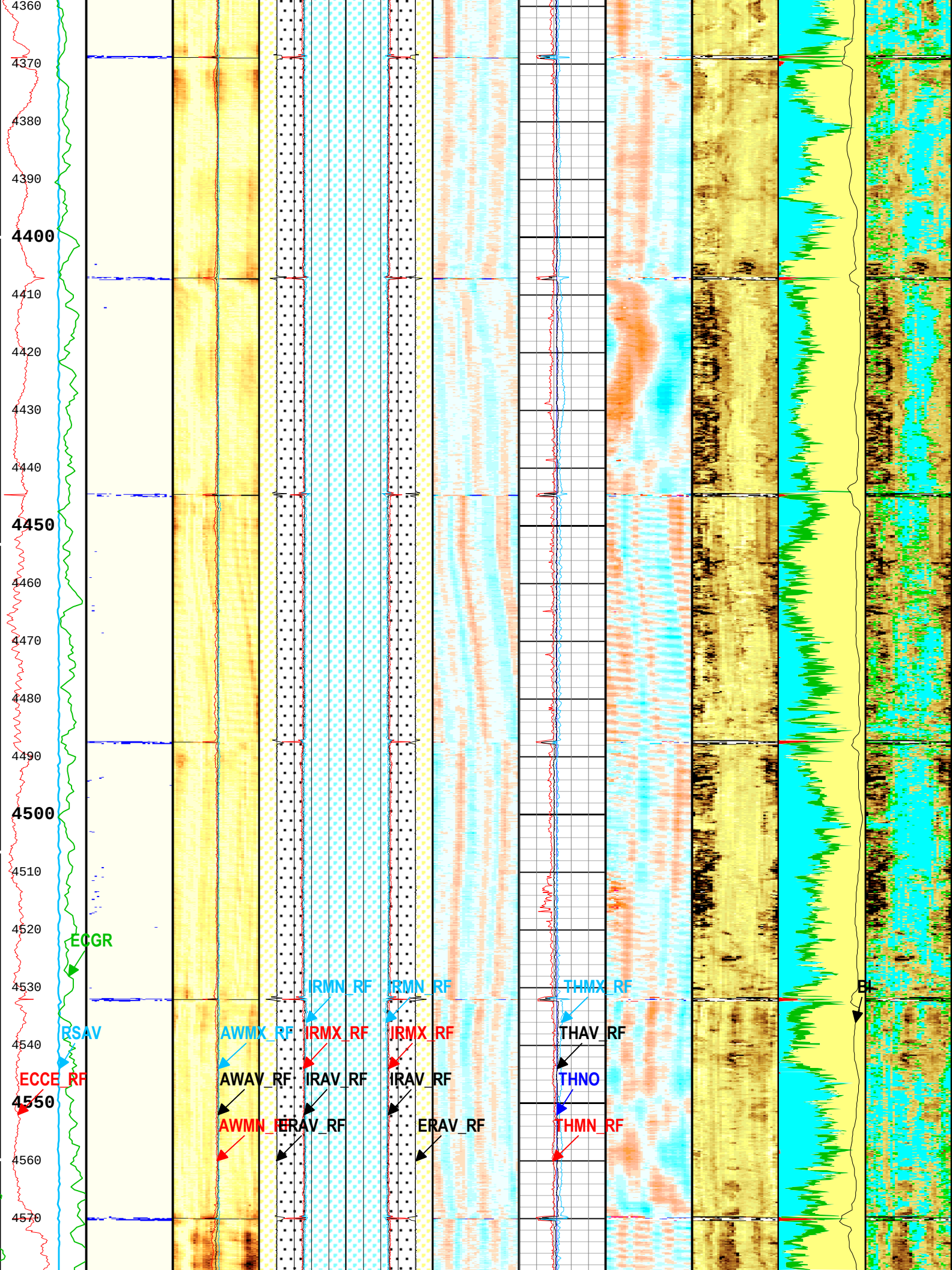
4360
4370
4380
4390
4400
4410
4420
4430
4440
4450
4460
4470
4480
4490
4500
4510
4520
4530
4540
4550
4560
4570
ECGR
RSAV
ECCE_RF
IRMN_RF
IRMN_RF
THMX_RF
AWMX_RF
IRMX_RF
IRMX_RF
THAV_RF
AWAV_RF
IRAV_RF
IRAV_RF
THNO
AWMN_RF
ERAV_RF
ERAV_RF
THMN_RF
BI

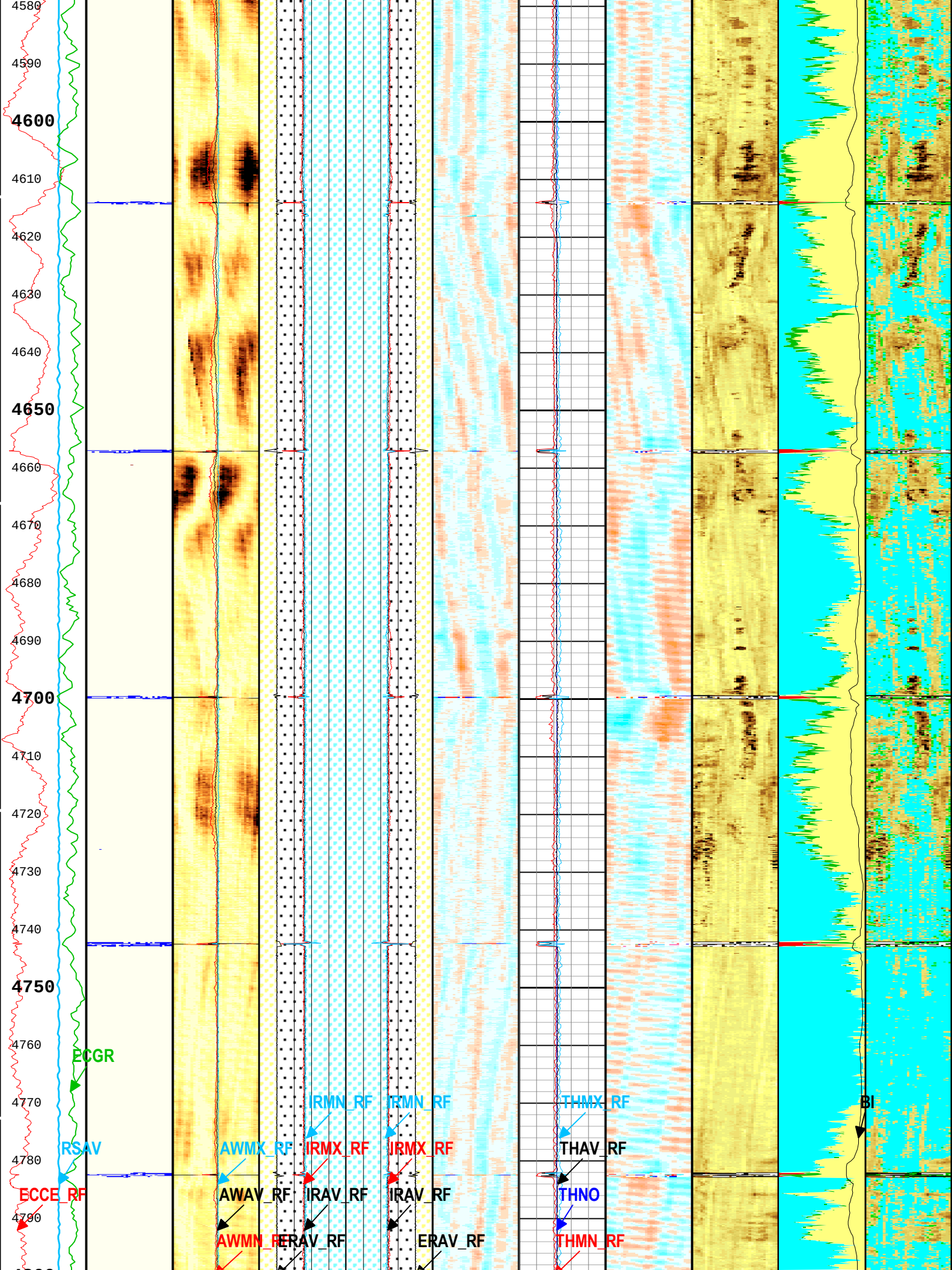
4580
4590
4600
4610
4620
4630
4640
4650
4660
4670
4680
4690
4700
4710
4720
4730
4740
4750
4760
4770
4780
4790
ECGR
RSAV
ECCE_RF
IRMN_RF
IRMN_RF
AWMX_RF
IRMX_RF
IRMX_RF
AWAV_RF
IRAV_RF
IRAV_RF
AWMN_RF
ERAV_RF
ERAV_RF
THMX_RF
THAV_RF
THNO
THMN_RF
BI

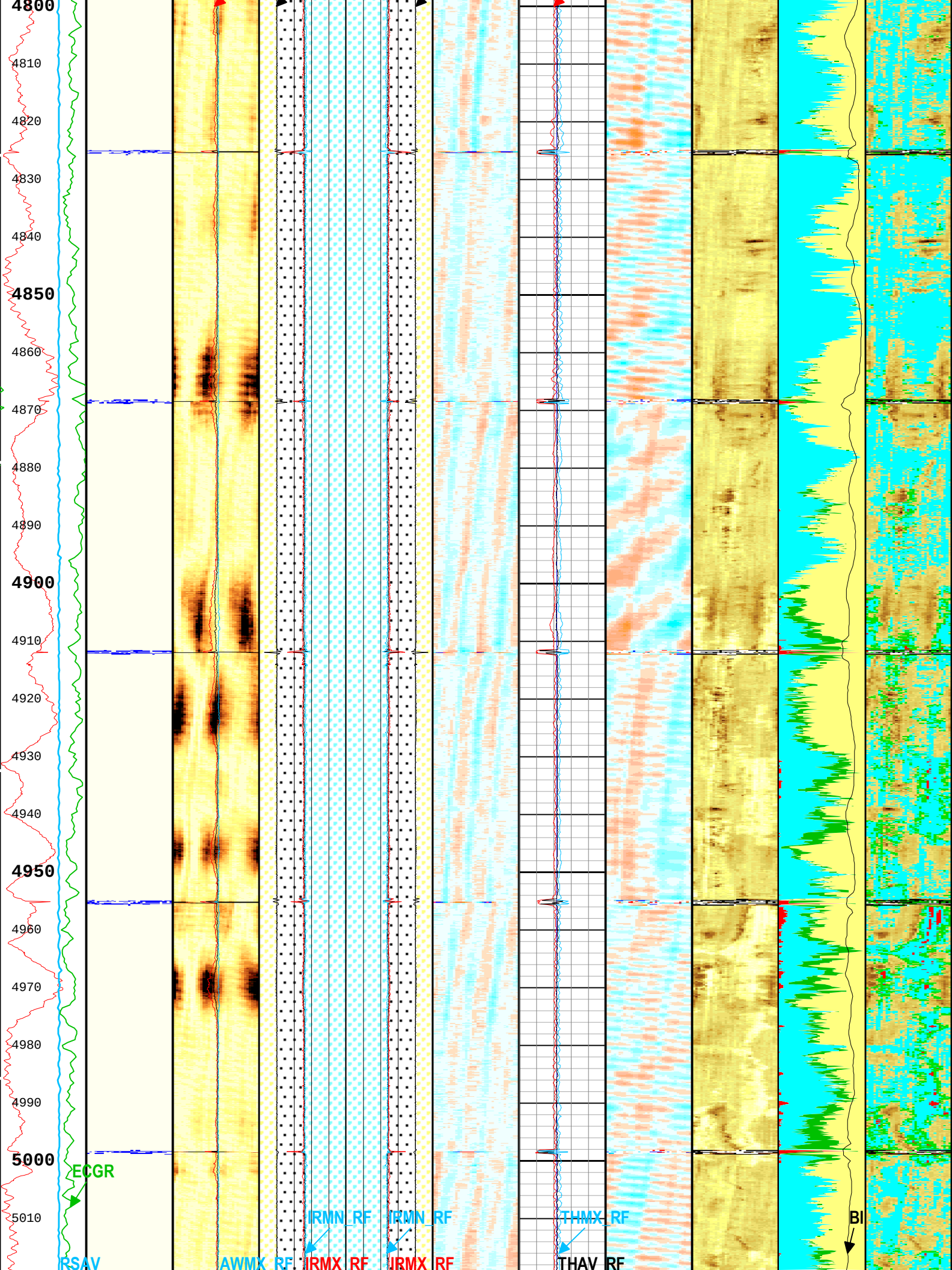
4800
4810
4820
4830
4840
4850
4860
4870
4880
4890
4900
4910
4920
4930
4940
4950
4960
4970
4980
4990
5000
5010
ECGR
RSAV
AWMX_RF
IRMN_RF
IRMX_RF
IRMN_RF
IRMX_RF
THMX_RF
THAV_RF
BI

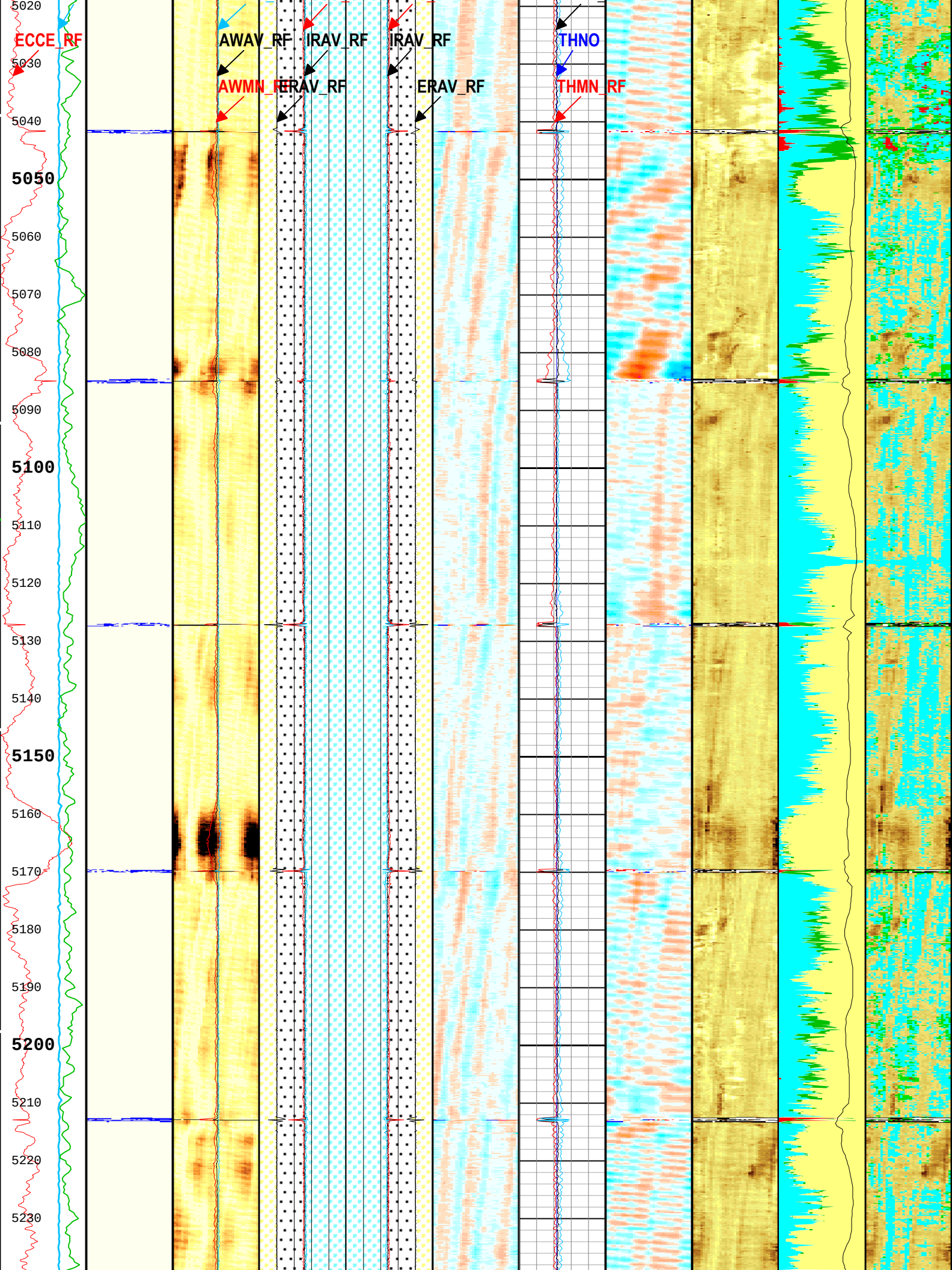
ECCE_RF
AWAV_RF
IRAV_RF
IRAV_RF
THNO
AWMN_RF
ERAV_RF
ERAV_RF
THMN_RF
5020
5030
5040
5050
5060
5070
5080
5090
5100
5110
5120
5130
5140
5150
5160
5170
5180
5190
5200
5210
5220
5230

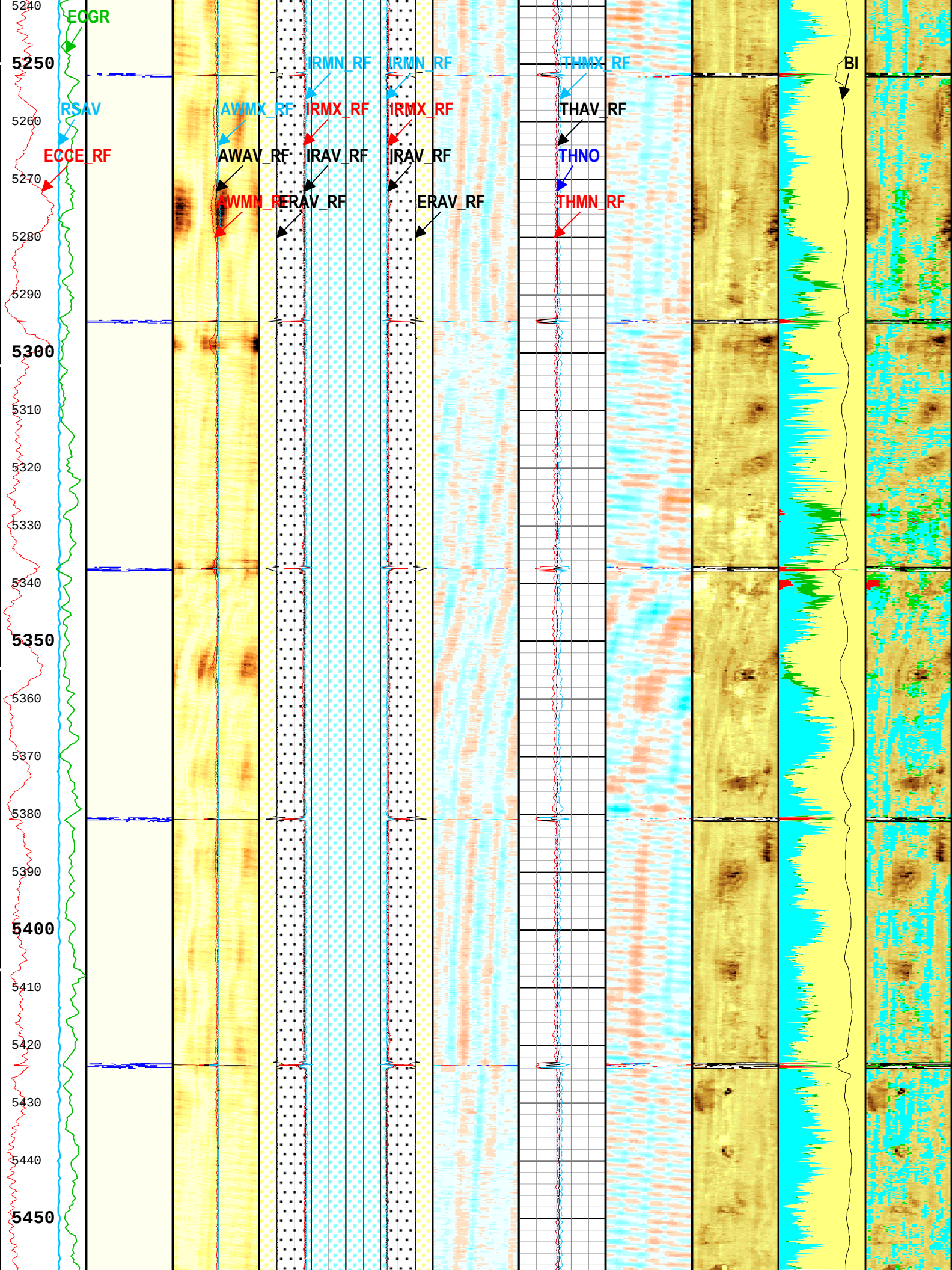
ECGR
RSAV
ECCE_RF
AWMX_RF
AWAV_RF
AWMN_RF
IRMN_RF
IRMX_RF
IRAV_RF
ERAV_RF
IRMN_RF
IRMX_RF
IRAV_RF
ERAV_RF
THMX_RF
THAV_RF
THNO
THMN_RF
BI
5240
5250
5260
5270
5280
5290
5300
5310
5320
5330
5340
5350
5360
5370
5380
5390
5400
5410
5420
5430
5440
5450

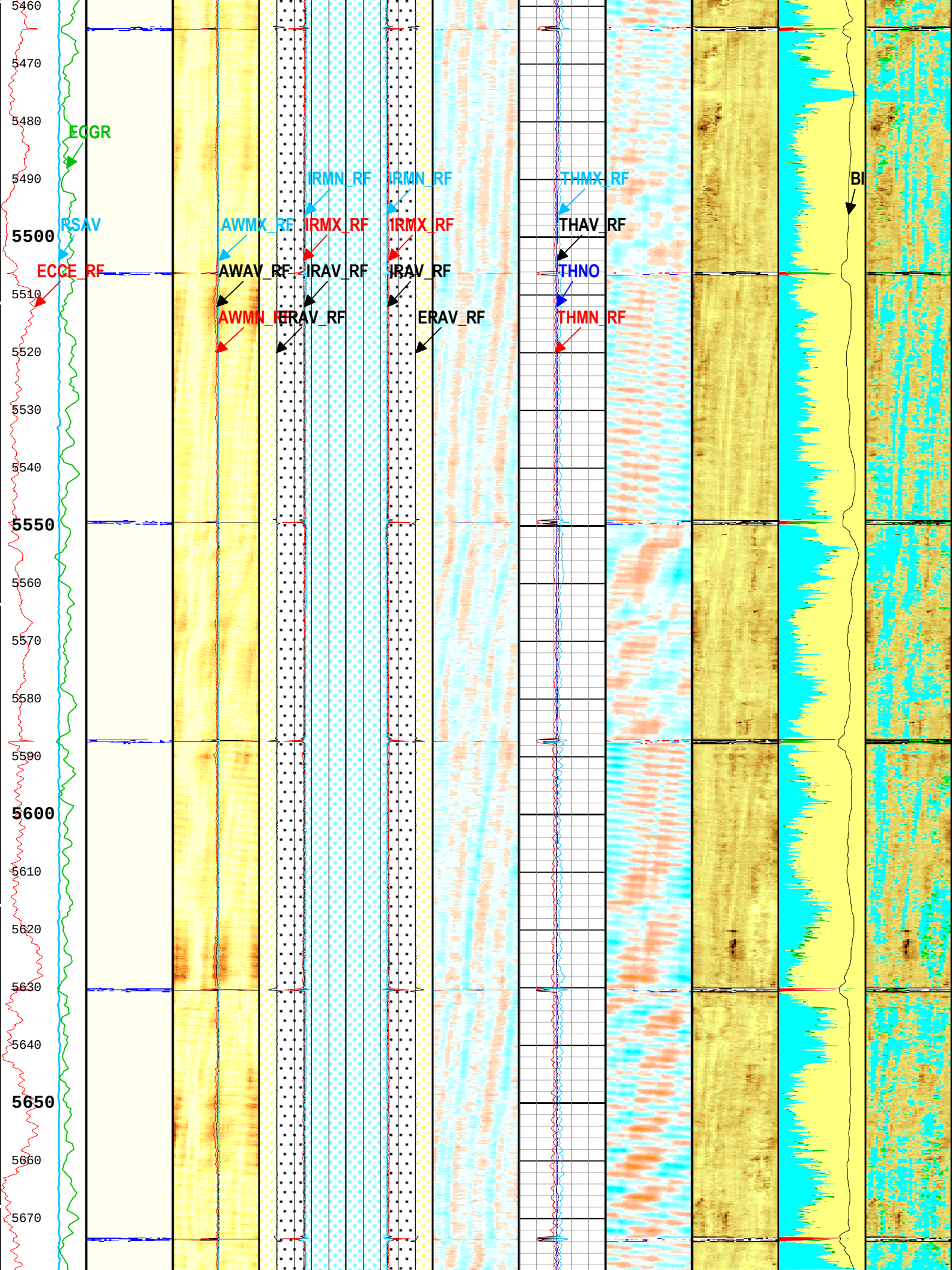
5460
5470
5480
5490
5500
5510
5520
5530
5540
5550
5560
5570
5580
5590
5600
5610
5620
5630
5640
5650
5660
5670
ECGR
RSAV
ECCE_RF
IRMN_RF
IRMN_RF
THMX_RF
AWMX_RF
IRMX_RF
IRMX_RF
THAV_RF
AWAV_RF
IRAV_RF
IRAV_RF
THNO
AWMN_RF
ERAV_RF
ERAV_RF
THMN_RF
BI

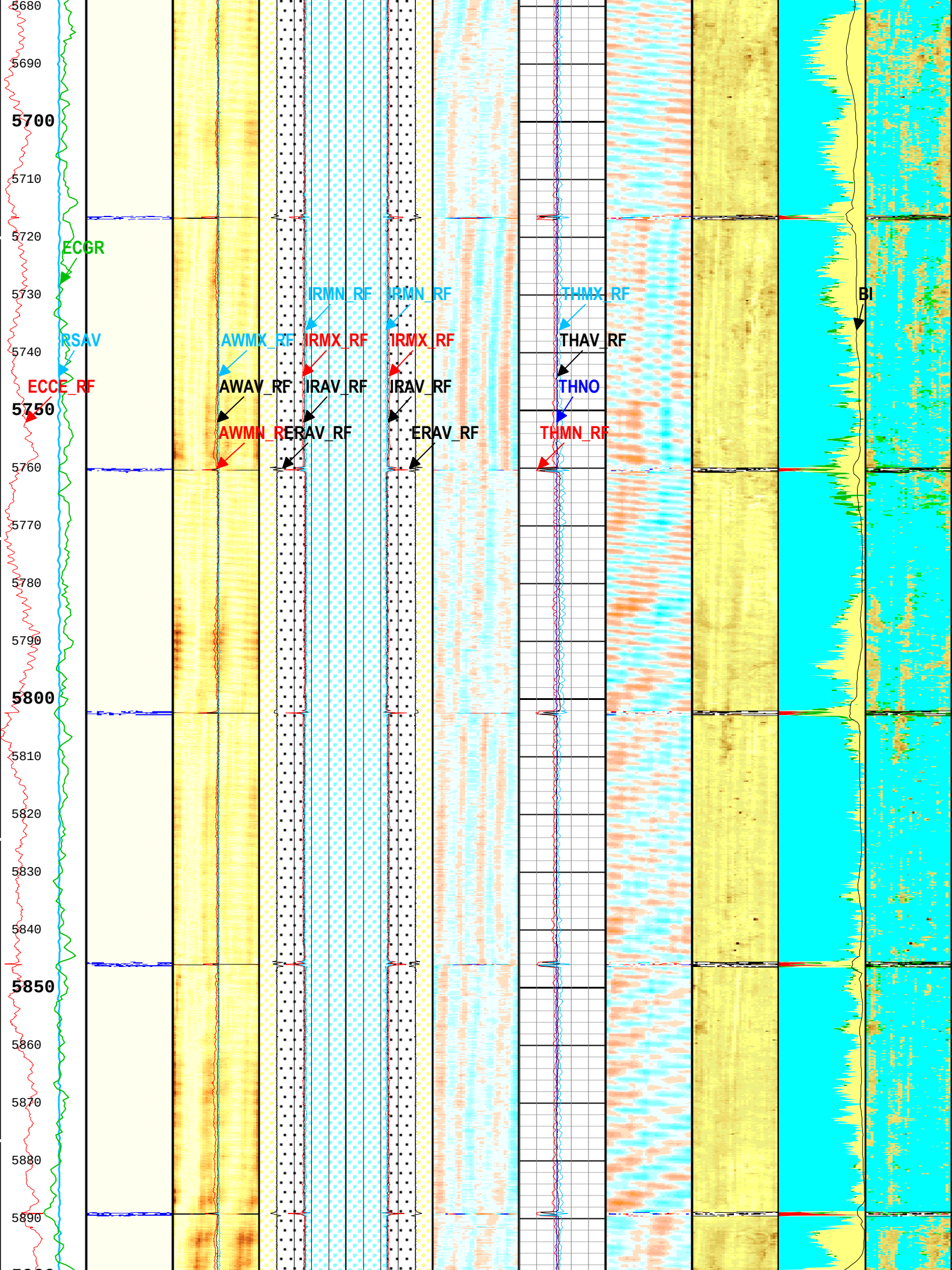
5680
5690
5700
5710
5720
5730
5740
5750
5760
5770
5780
5790
5800
5810
5820
5830
5840
5850
5860
5870
5880
5890
ECGR
RSAV
ECCE_RF
AWMX_RF
AWAV_RF
AWMN_RF
IRMN_RF
IRMX_RF
IRAV_RF
ERAV_RF
IRMN_RF
IRMX_RF
IRAV_RF
ERAV_RF
THMX_RF
THAV_RF
THNO
THMN_RF
BI

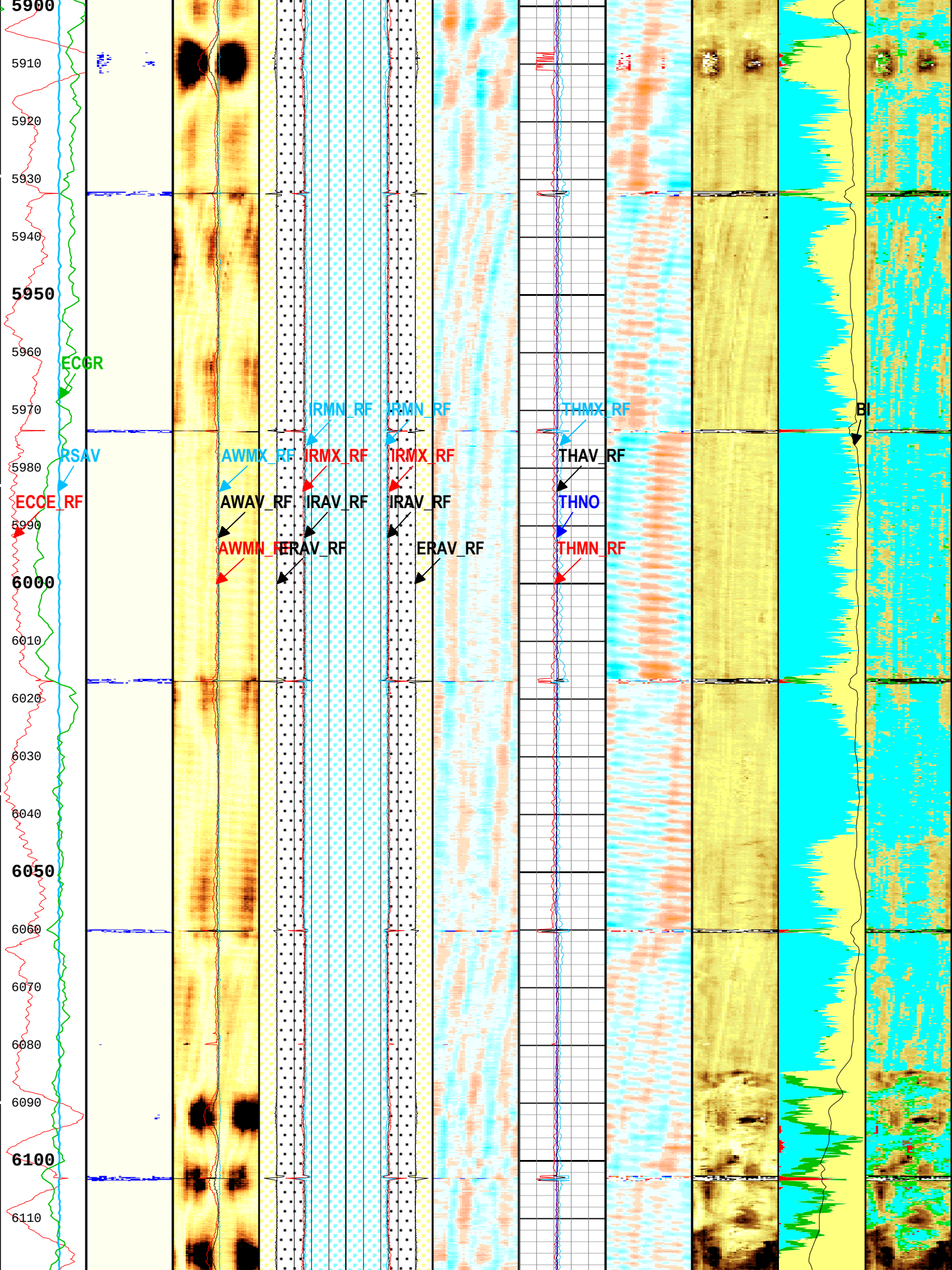
5900
5910
5920
5930
5940
5950
5960
5970
5980
5990
6000
6010
6020
6030
6040
6050
6060
6070
6080
6090
6100
6110
ECGR
RSAV
ECCE_RF
IRMN_RF
IRMN_RF
THMX_RF
BI
AWMX_RF
IRMX_RF
IRMX_RF
THAV_RF
AWAV_RF
IRAV_RF
IRAV_RF
THNO
AWMN_RF
ERAV_RF
ERAV_RF
THMN_RF

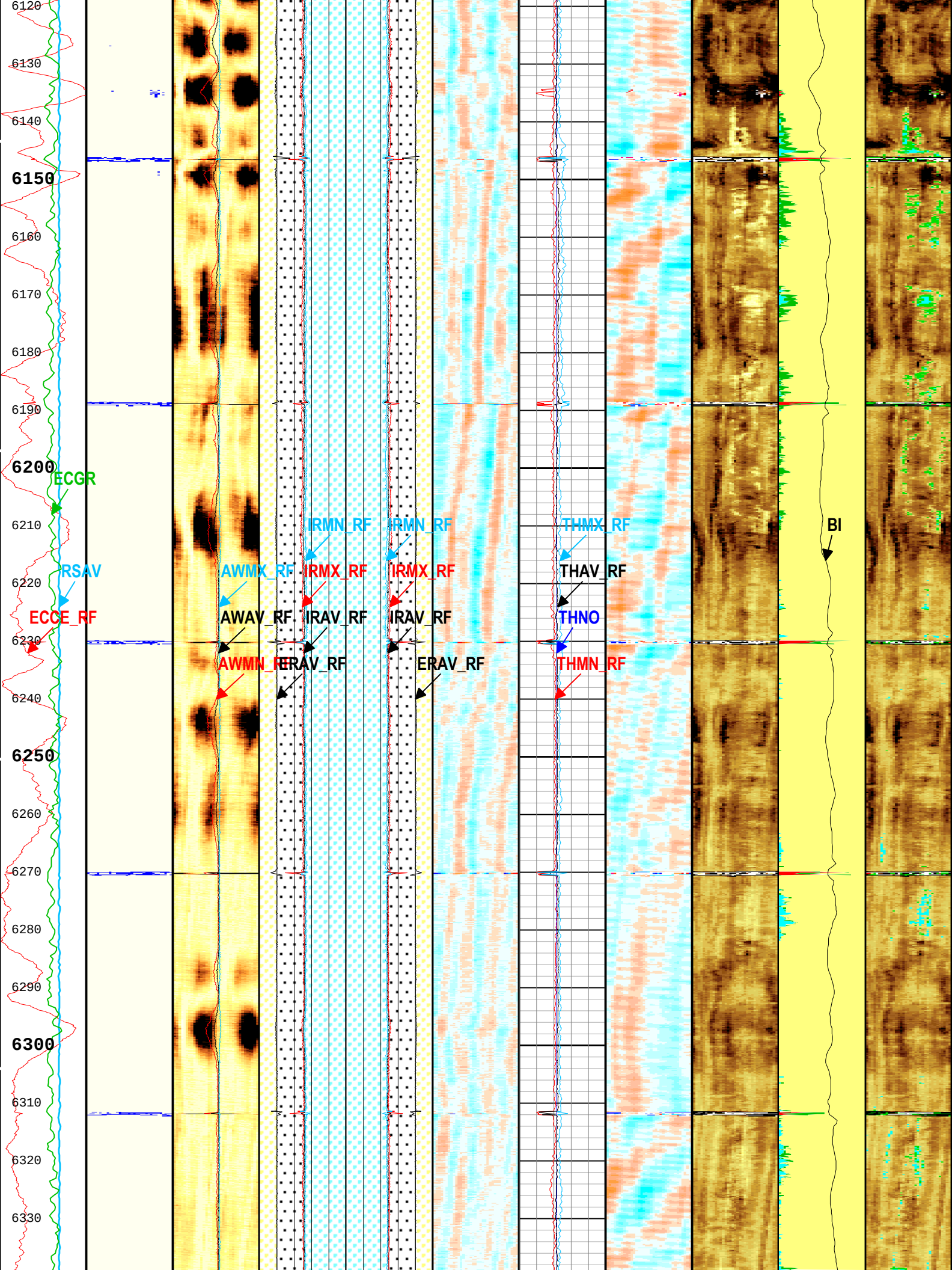
6120
6130
6140
6150
6160
6170
6180
6190
6200
6210
6220
6230
6240
6250
6260
6270
6280
6290
6300
6310
6320
6330
ECGR
RSAV
ECCE_RF
IRMN_RF
AWMX_RF
IRMX_RF
AWAV_RF
IRAV_RF
AWMN_RF
ERAV_RF
IRMN_RF
IRMX_RF
IRAV_RF
ERAV_RF
THMX_RF
THAV_RF
THNO
THMN_RF
BI

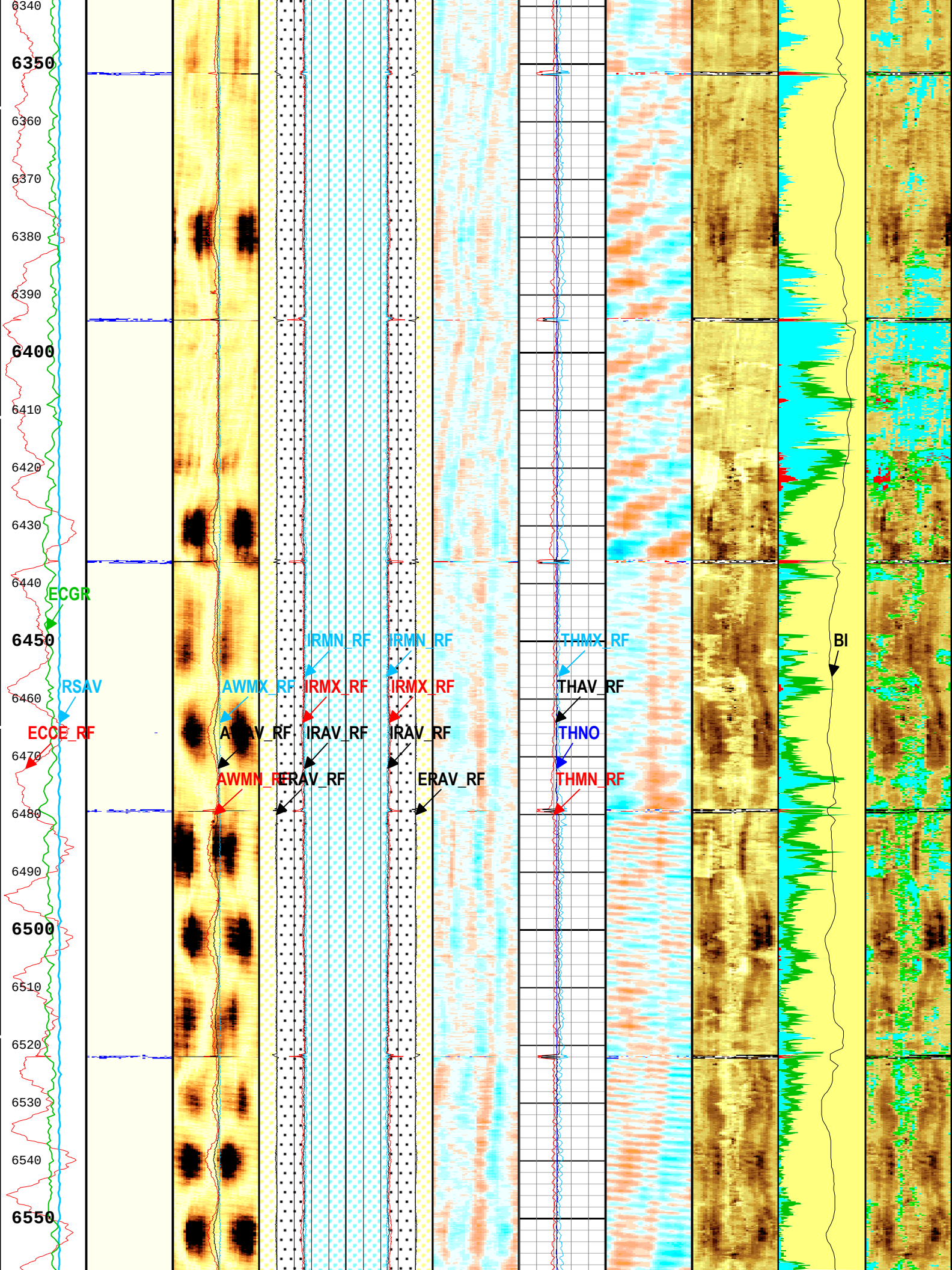
6340
6350
6360
6370
6380
6390
6400
6410
6420
6430
6440
6450
6460
6470
6480
6490
6500
6510
6520
6530
6540
6550
ECGR
RSAV
ECCE_RF
IRMN_RF
IRMN_RF
AWMX_RF
IRMX_RF
IRMX_RF
IRAV_RF
IRAV_RF
IRAV_RF
AWMN_RF
ERAV_RF
ERAV_RF
THMX_RF
THAV_RF
THNO
THMN_RF
BI

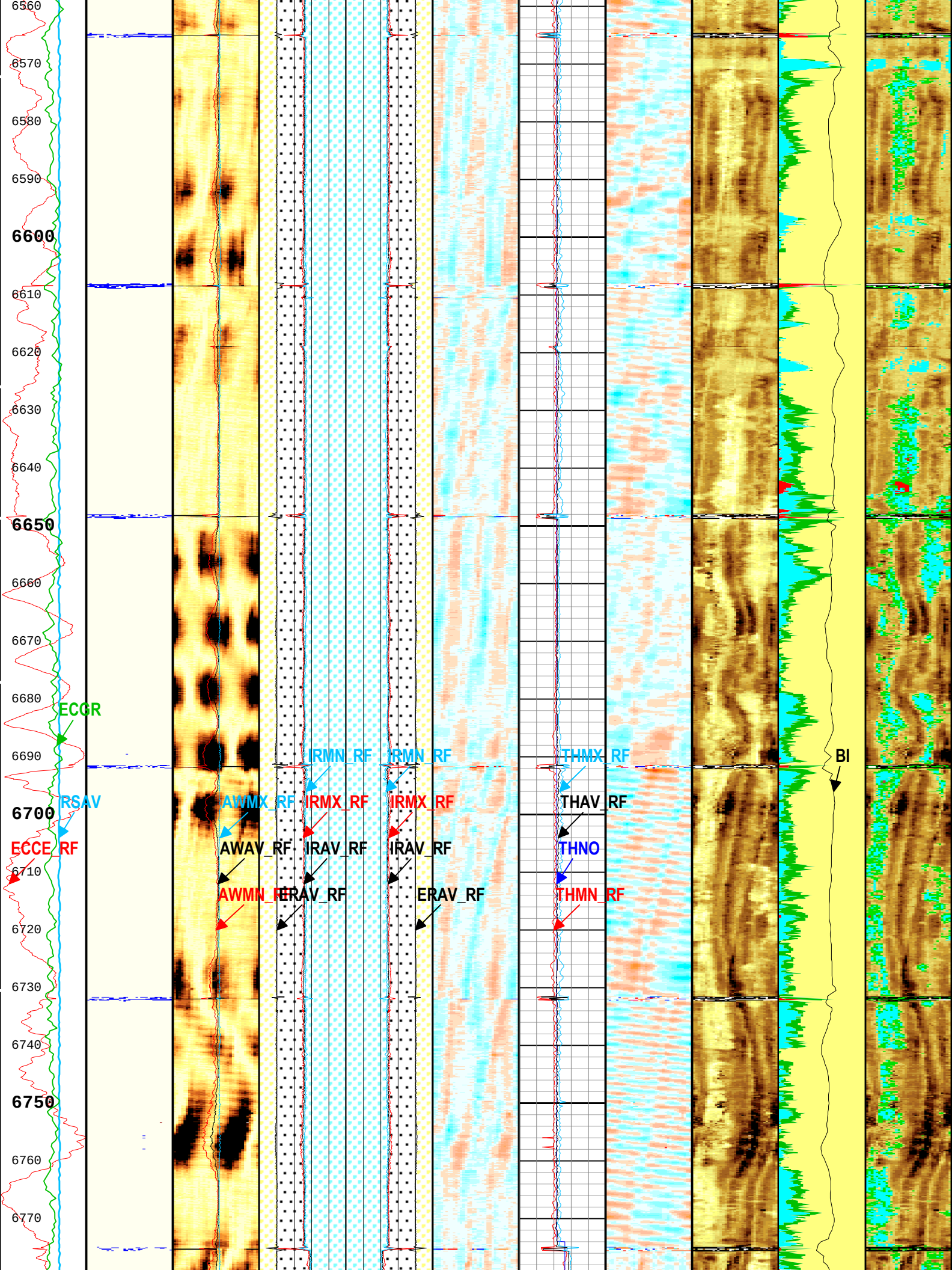
6560
6570
6580
6590
6600
6610
6620
6630
6640
6650
6660
6670
6680
6690
6700
6710
6720
6730
6740
6750
6760
6770
ECGR
RSAV
ECCE_RF
IRMN_RF
IRMN_RF
THMX_RF
AWMX_RF
IRMX_RF
IRMX_RF
THAV_RF
AWAV_RF
IRAV_RF
IRAV_RF
THNO
AWMN_RF
ERAV_RF
ERAV_RF
THMN_RF
BI

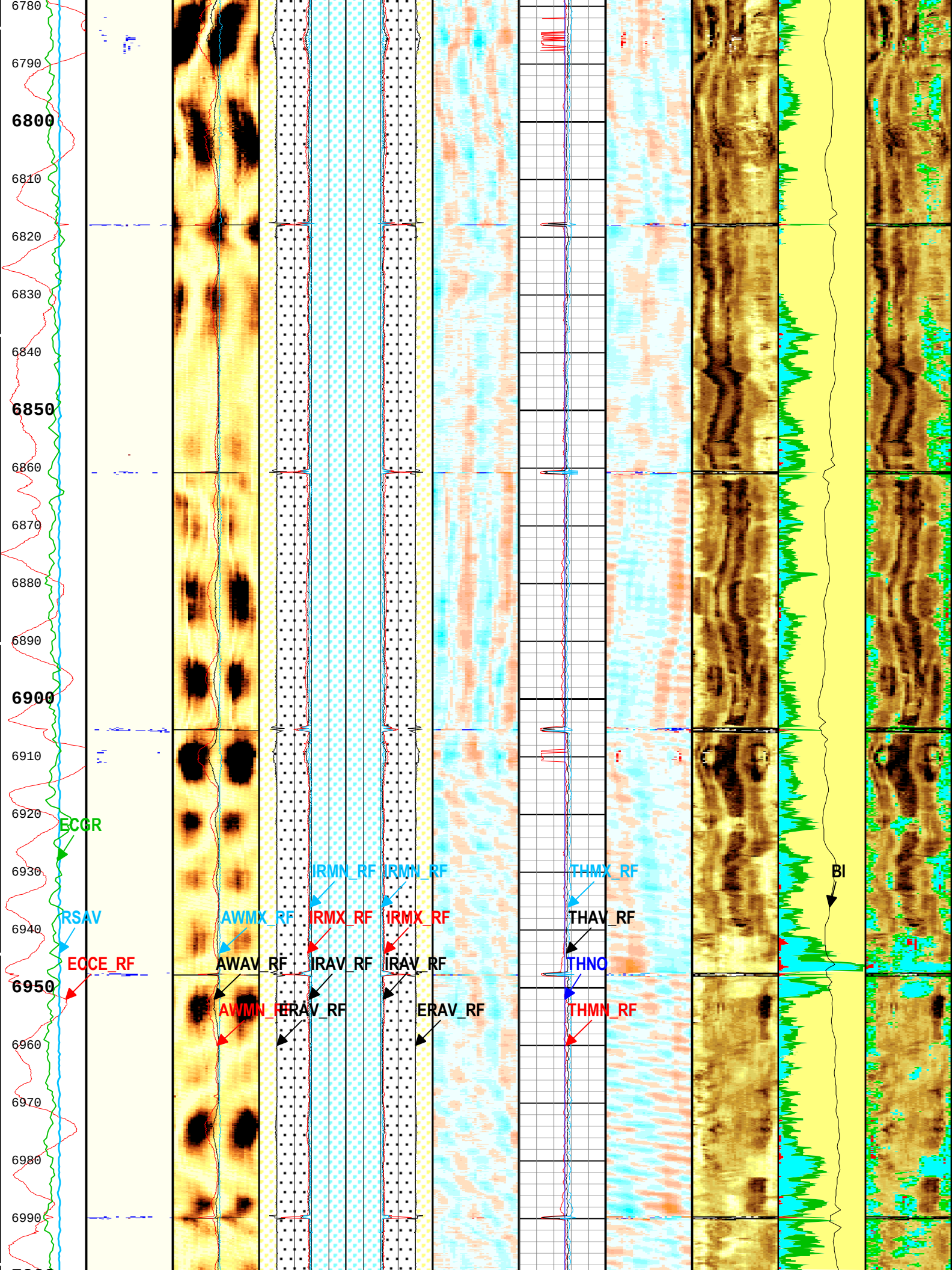
6780
6790
6800
6810
6820
6830
6840
6850
6860
6870
6880
6890
6900
6910
6920
6930
6940
6950
6960
6970
6980
6990
ECGR
RSAV
ECCE_RF
AWAV_RF
AWMX_RF
AWMN_RF
IRMN_RF
IRMX_RF
IRAV_RF
ERAV_RF
IRMN_RF
IRMX_RF
IRAV_RF
ERAV_RF
THMX_RF
THAV_RF
THNO
THMN_RF
BI

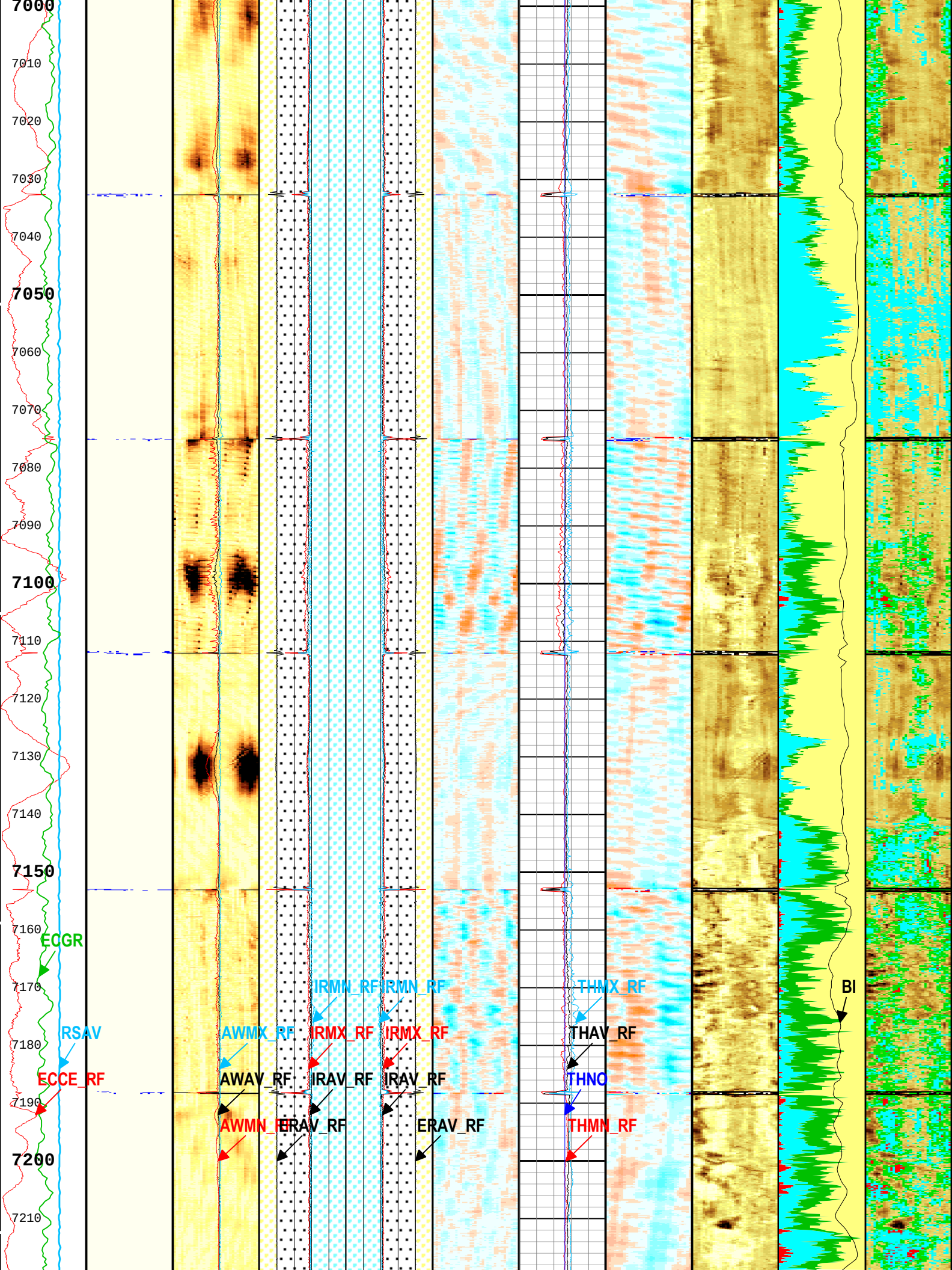
7000
7010
7020
7030
7040
7050
7060
7070
7080
7090
7100
7110
7120
7130
7140
7150
7160
7170
7180
7190
7200
7210
ECGR
RSAV
ECCE_RF
AWMX_RF
AWAV_RF
AWMN_RF
IRMN_RF
IRMX_RF
IRAV_RF
ERAV_RF
IRMN_RF
IRMX_RF
IRAV_RF
ERAV_RF
THMX_RF
THAV_RF
THNO
THMN_RF
BI

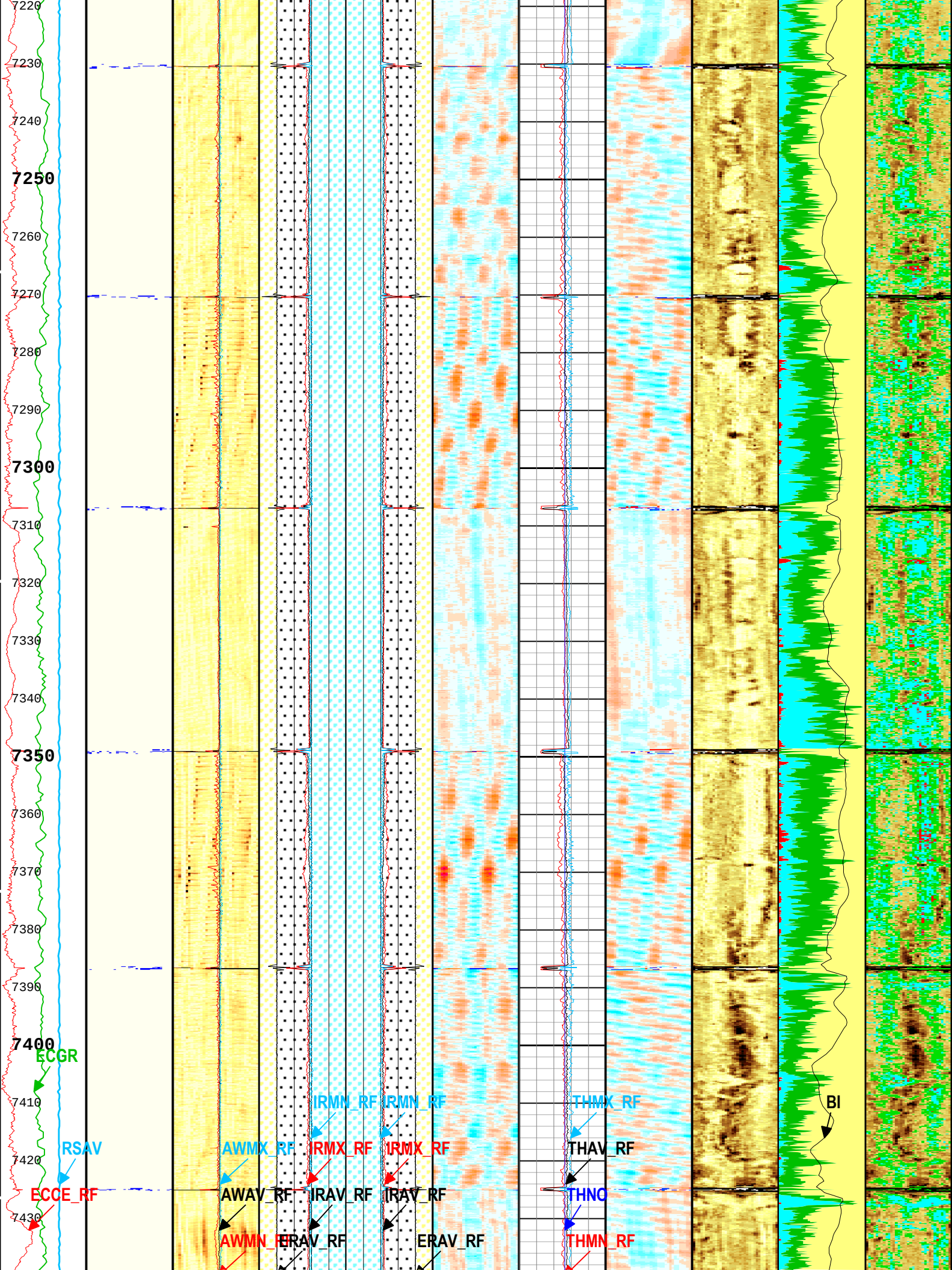
7220
7230
7240
7250
7260
7270
7280
7290
7300
7310
7320
7330
7340
7350
7360
7370
7380
7390
7400
7410
7420
7430
ECGR
RSAV
ECCE_RF
IRMN_RF
IRMN_RF
AWMX_RF
IRMX_RF
IRMX_RF
AWAV_RF
IRAV_RF
IRAV_RF
AWMN_RF
ERAV_RF
ERAV_RF
THMX_RF
THAV_RF
THNO
THMN_RF
BI

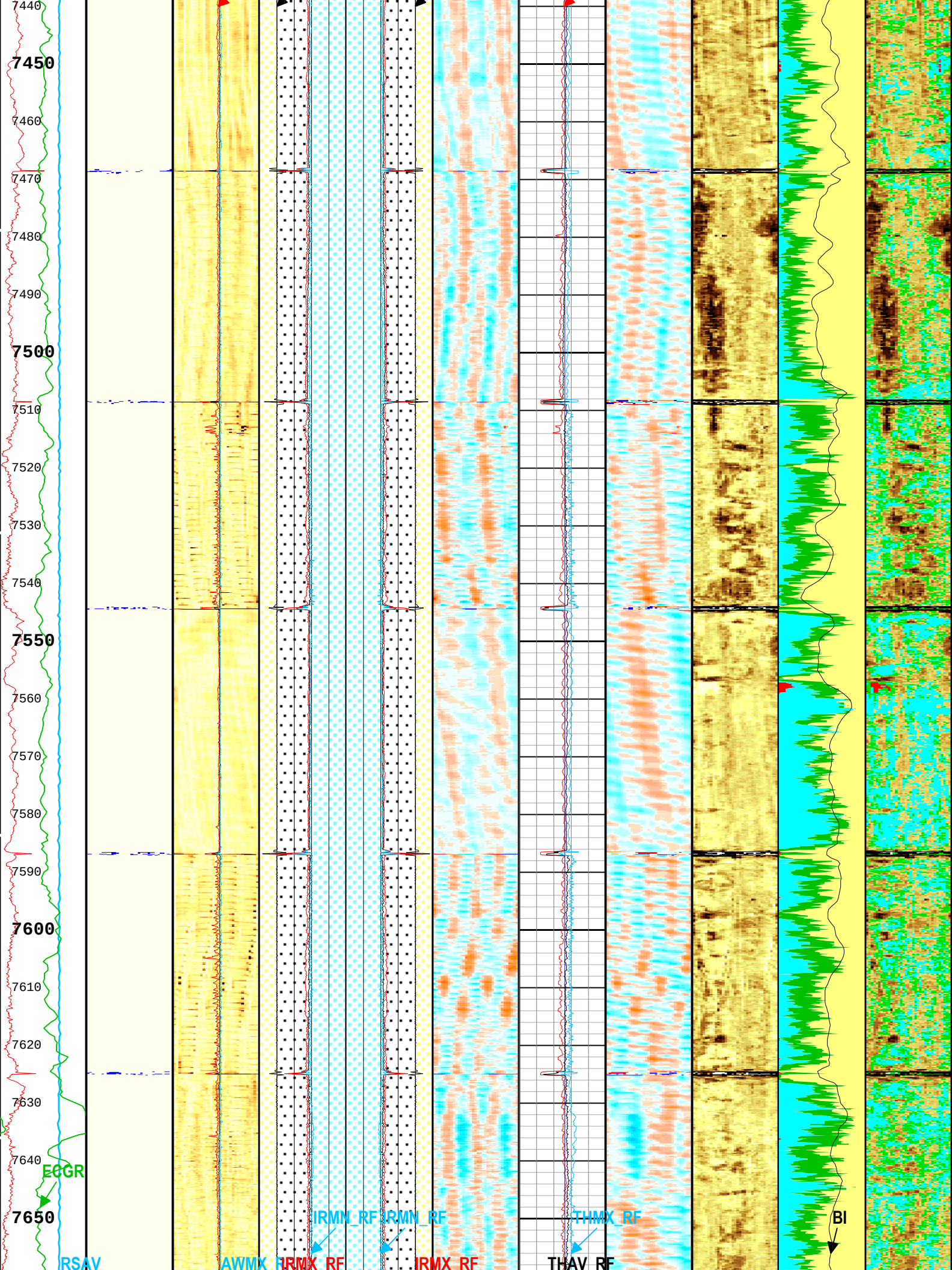
7440
7450
7460
7470
7480
7490
7500
7510
7520
7530
7540
7550
7560
7570
7580
7590
7600
7610
7620
7630
7640
7650
ECGR
RSAV
AWMX
IRMX_RF
IRMN_RF
IRMN_RF
IRMX_RF
THMX_RF
THAV_RF
BI

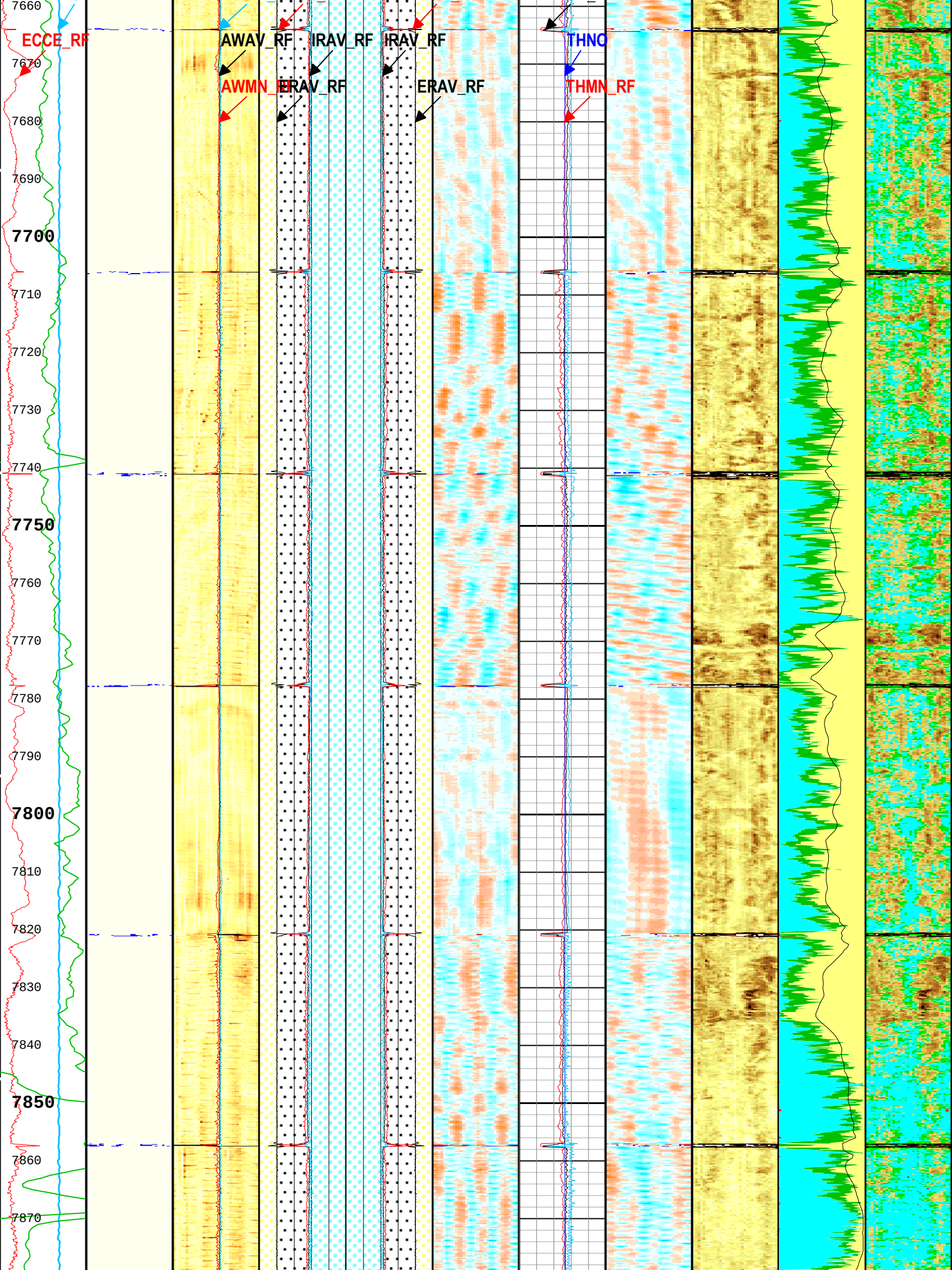
ECCE_RF
AWAV_RF
IRAV_RF
IRAV_RF
THNO
AWMN_RF
ERAV_RF
ERAV_RF
THMN_RF
7660
7670
7680
7690
7700
7710
7720
7730
7740
7750
7760
7770
7780
7790
7800
7810
7820
7830
7840
7850
7860
7870

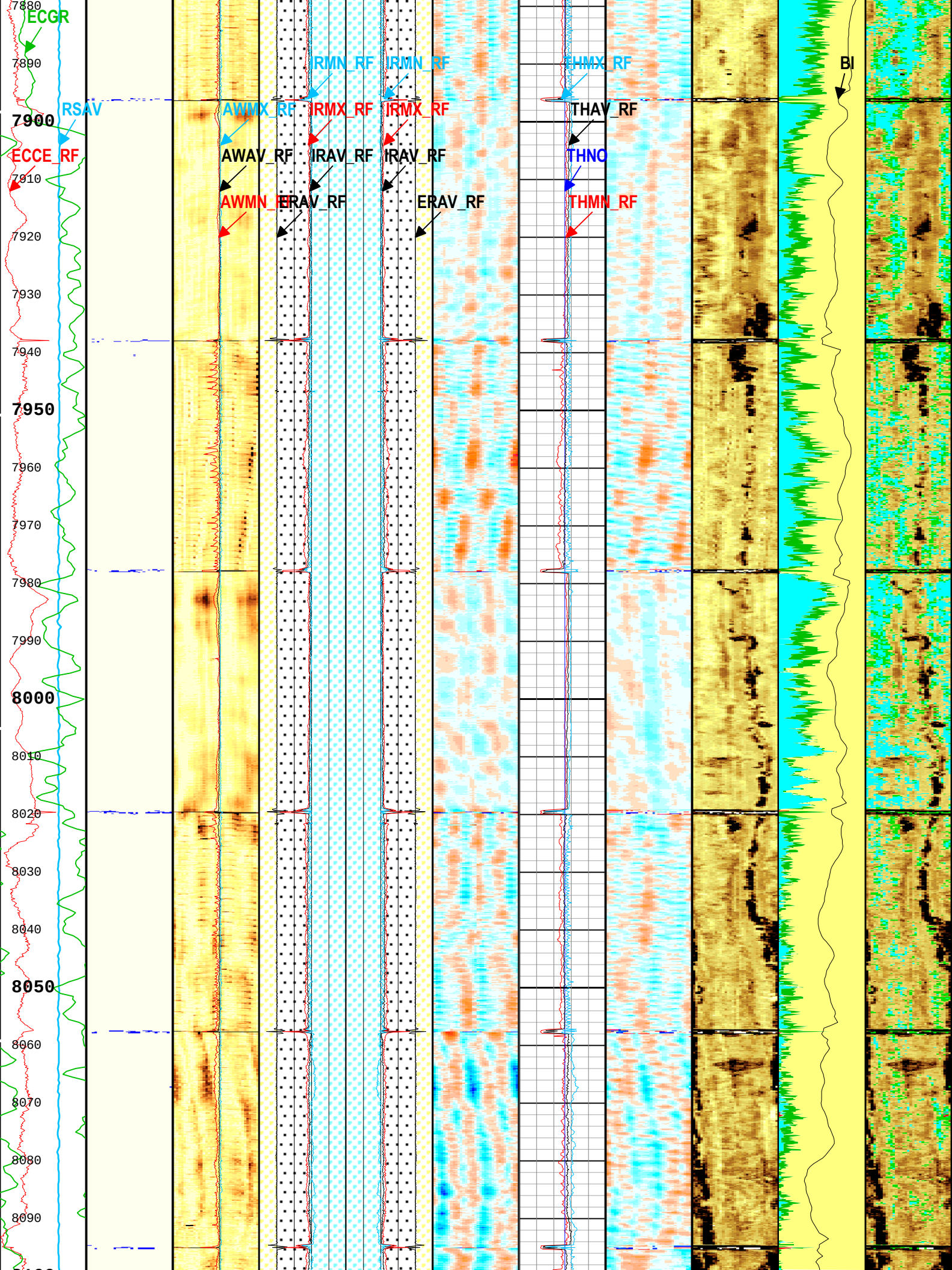
ECGR
RSAV
ECCE_RF
AWMX_RF
AWAV_RF
AWMN_RF
IRMN_RF
IRMX_RF
IRAV_RF
ERAV_RF
IRMN_RF
IRMX_RF
IRAV_RF
ERAV_RF
THMX_RF
THAV_RF
THNO
THMN_RF
BI
7880
7890
7900
7910
7920
7930
7940
7950
7960
7970
7980
7990
8000
8010
8020
8030
8040
8050
8060
8070
8080
8090

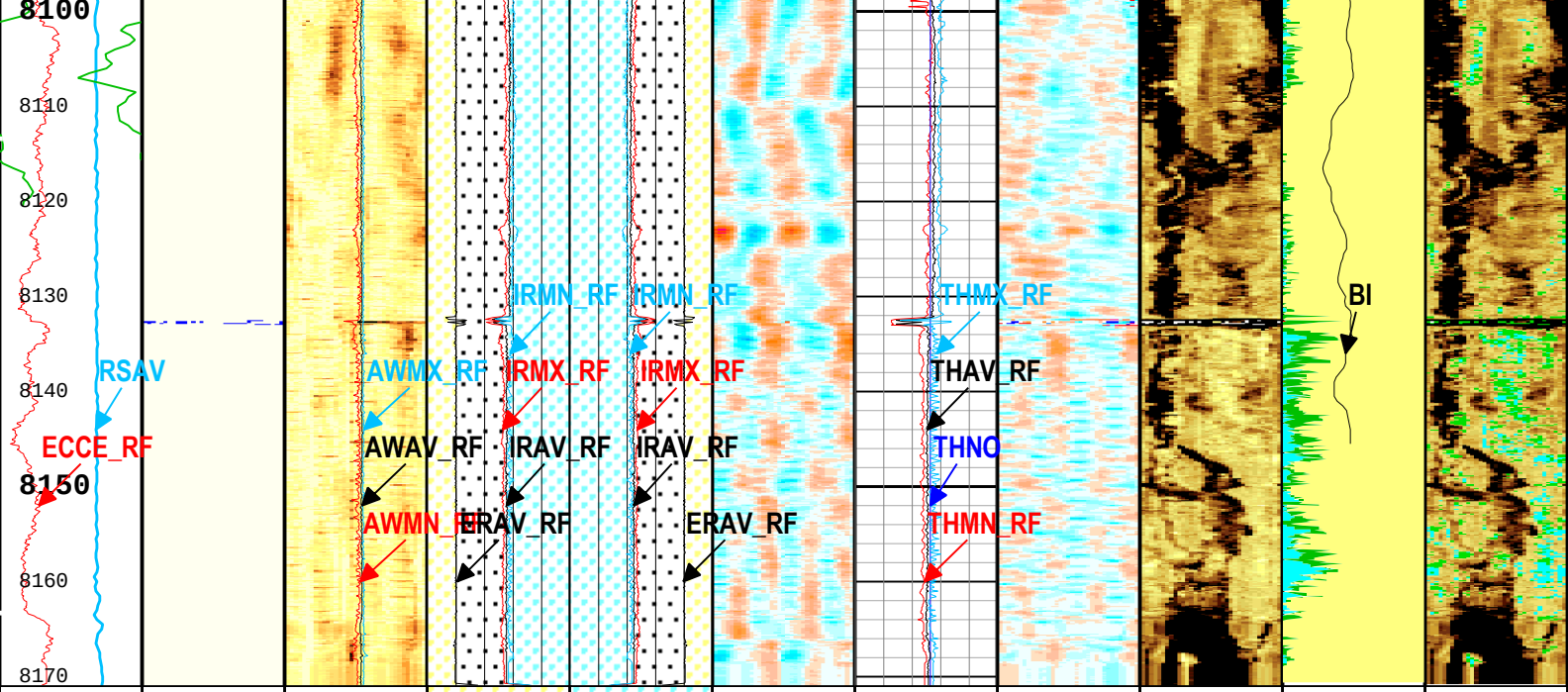

Amplitude of Eccentering for Unflagged Waves (ECCE_RF) USIT-E[1]
0 in 0.5

Motor Revolution Speed (RSAV) USIT-E[1]
6 c/s 8

Gamma Ray (ECGR) HGNS[1]
0 gAPI 150

Absent 1.500 3.500
Explicit Normalization
USIT - USIT Processing Flags (UFLG) USIT-E[1]

USIT Processing Flags (UFLG[0]) USIT-E[1]
1 5

Absent -4.799 -2.799 -0.800
Explicit Normalization
USIT - Amplitude of Unflagged Wave (AWBK_RF) USIT-E[1] (dB)

Minimum of Unflagged Wave Amplitude (AWMN_RF) USIT-E[1]
0 dB 75

Average of Unflagged Wave Amplitude (AWAV_RF) USIT-E[1]
0 dB 75

Maximum of Unflagged Wave Amplitude (AWMX_RF) USIT-E[1]
0 dB 75

ERAV
ERAV-IRAV
IRAV

Median of Unflagged External Radii (ERAV_RF) USIT-E[1]
3.7 in 2.7

Median Internal Radius of Casing Corrected for Eccentering (IRAV_RF) USIT-E[1]
3.7 in 2.7

Maximum of Unflagged Internal Radii (IRMX_RF) USIT-E[1]
3.7 in 2.7

Minimum of Unflagged Internal Radii (IRMN_RF) USIT-E[1]
3.7 in 2.7

IRAV
ERAV
IRAV-ERAV

Median of Unflagged External Radii (ERAV_RF) USIT-E[1]
2.7 in 3.7

Median Internal Radius of Casing Corrected for Eccentering (IRAV_RF) USIT-E[1]
2.7 in 3.7

Maximum of Unflagged Internal Radii (IRMX_RF) USIT-E[1]
2.7 in 3.7

Minimum of Unflagged Internal Radii (IRMN_RF) USIT-E[1]
2.7 in 3.7

Absent -0.051 -0.012 0.028 0.068
Explicit Normalization
USIT - Unflagged Internal Radii minus Median Internal Radius (IRBKM_RF) USIT-E[1] (in)

Minimum of Unflagged Casing Thickness (THMN_RF) USIT-E[1]
0.1 in 0.6

Nominal Casing Thickness (THNO) USIT-E[1]
0.1 in 0.6

Median of Unflagged Casing Thickness (THAV_RF) USIT-E[1]
0.1 in 0.6

Maximum of Unflagged Casing Thickness (THMX_RF) USIT-E[1]
0.1 in 0.6

Absent -0.051 -0.012 0.028 0.068
Explicit Normalization
USIT - Unflagged Casing Thickness minus Median of Unflagged Casing Thickness (THBKM_RF) USIT-E[1] (in)

Absent 1.500 3.500 5.500 7.500
Custom Normalization
USIT - Acoustic Impedance (AIBK) USIT-E[1] (Mrayl)

Ratio of Cement Measurements to Total (CEMR) USIT-E[1]
1 0

Micro-debonding Ratio (MDR) USIT-E[1]
1 0

Ratio of Gas Measurements to Total (GASR) USIT-E[1]
1 0

Bonded
Gas
Liquid
Micro-debonding

Bond Index (BI) DSLT-H[1]
1 0

Absent 3.090 5.054 7.018
Custom Normalization
USIT - Acoustic Impedance (AIBK) USIT-E[1] (Mrayl)

Absent 2.599 4.563 6.527
Custom Normalization
USIT - Acoustic Impedance With Micro-debonding Image (AI_MDEBOND_IMG) USIT-E[1] (Mrayl)

USIT Processing Flags (UFLG[0]) USIT-E[1]

1 - UFLG 1 Value within [0.0 - 1.5] - :

2 - UFLG 2 Value within [1.5 - 2.5] - :

UTIM Error

Pulse Origin Not Detected

3 - UFLG 3 Value within [2.5 - 3.5] - :
4 - UFLG 4 UFLG 5 UFLG 6 Value within [3.5 - 6.5] - :
5 - UFLG 7 UFLG 8 UFLG 9 Value within [6.5 - 10] - :

WINLEN Error
Casing Thickness Error
Loop Processing Error

TIME_1900 - Time Marked every 60.00 (s)

Description: USI Composite Format: Log (LBV1_USI Composite 7inch) Index Scale: 5 in per 100 ft Index Unit: ft Index Type: Measured Depth Creation Date: 20-Oct-2016 14:28:19

Two

Cement Log 2 IN = 100 FT

Pass Summary

Run Name	Pass Objective	Direction	Top	Bottom	Start	Stop	DSC Mode	Depth Shift	Include Parallel Data
Two	Log[6]:Up	Up	6845.38 ft	8162.42 ft	19-Oct-2016 2:46:42 PM	19-Oct-2016 3:11:08 PM	ON	2.05 ft	No

All depths are referenced to toolstring zero

Log

Company:Southern California Gas Company Well:Frew 4

Two: Log[6]:Up:S008

Description: USI Cement Format: Log (LBV1_USI Cement 7inch) Index Scale: 2 in per 100 ft Index Unit: ft Index Type: Measured Depth Creation Date: 20-Oct-2016 14:28:43

TIME_1900 - Time Marked every 60.00 (s)

ERAV_IRAV | ERAV_RHF1
IRAV_LHF1 | IRAV_ERAV
LHF1_ERAV | RHF1_IRAV

Median of Unflagged External Radii (ERAV_RF) USIT-E
3.7 in 2.7

Median of Unflagged External Radii (ERAV_RF) USIT-E
2.7 in 3.7

Median Internal Radius of Casing Corrected for Eccentering (IRAV_RF) USIT-E
3.7 in 2.7

Median Internal Radius of Casing Corrected for Eccentering (IRAV_RF) USIT-E
2.7 in 3.7

Minimum of Unflagged Internal Radii (IRMN_RF) USIT-E
3.7 in 2.7

Minimum of Unflagged Internal Radii (IRMN_RF) USIT-E
2.7 in 3.7

Gamma Ray (ECGR) HGNS-H
0 gAPI 150

Amplitude of Eccentering for Unflagged Waves (ECCE_RF) USIT-E
0 in 0.5

Maximum of Unflagged Internal Radii (IRMX_RF) USIT-E
3.7 in 2.7

Maximum of Unflagged Internal Radii (IRMX_RF) USIT-E
2.7 in 3.7

Absent 0.500 1.500 2.500 3.500 4.500 5.500 6.500 7.500
Custom Normalization
USIT - Acoustic Impedance (AIBK) USIT-E (Mrayl)

Acoustic Impedance Minimum (AIMN) USIT-E
-1 Mrayl 9

Acoustic Impedance Average (AIAV) USIT-E
-1 Mrayl 9

Acoustic Impedance Maximum (AIMX) USIT-E
-1 Mrayl 9

Bonded
Gas
Liquid
Micro-debonding

Absent -500.000 2.599 3.581 4.563 5.545 6.527 7.509
Custom Normalization
USIT - Acoustic Impedance With Micro-debonding Image (AI_MDEBOND_IMG) USIT-E (Mrayl)

6800

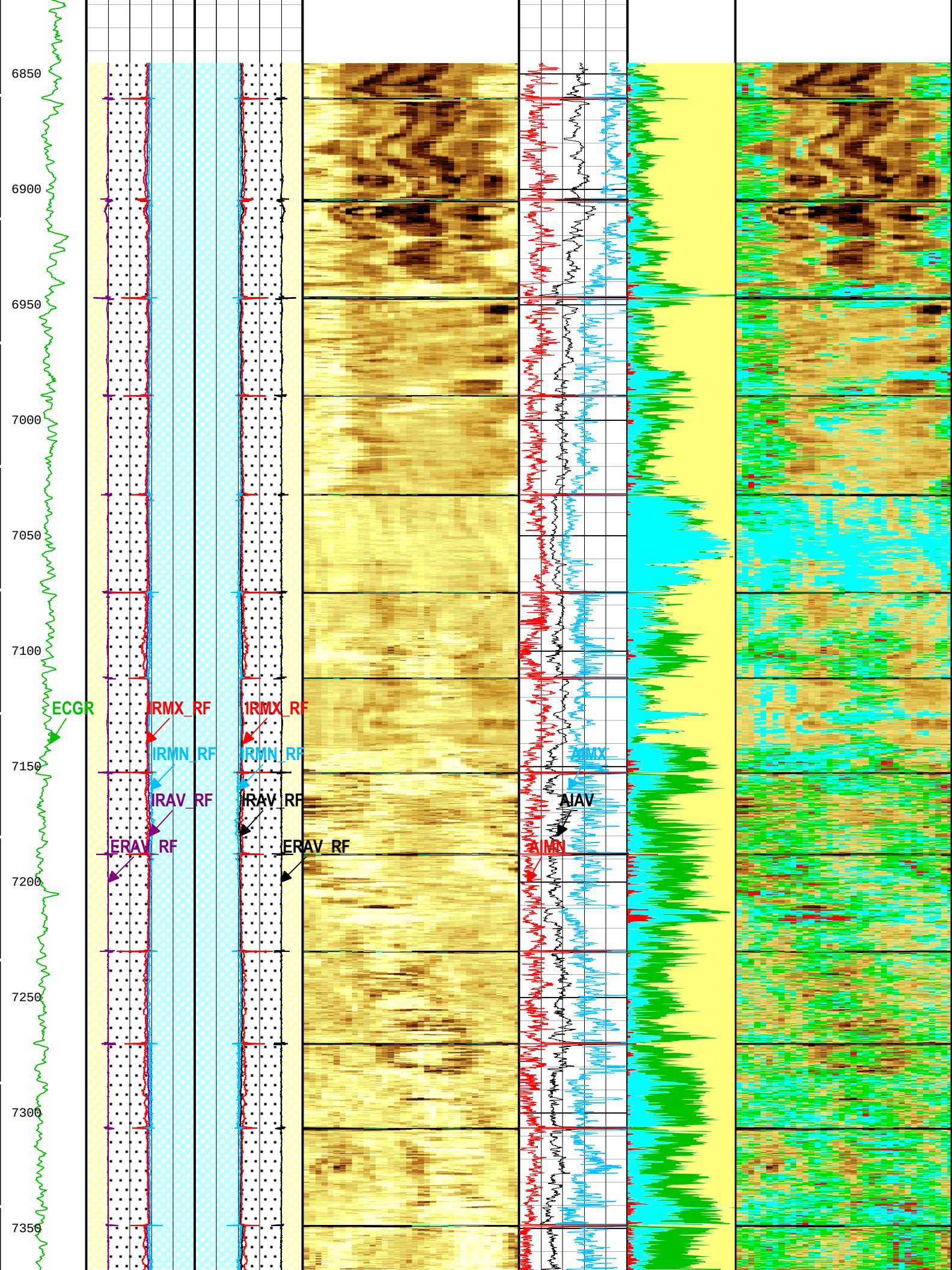
6850
6900
6950
7000
7050
7100
7150
7200
7250
7300
7350
ECGR
IRMX_RF
IRMN_RF
IRAV_RF
ERAV_RF
1RMX_RF
1RMN_RF
1RAV_RF
ERAV_RF
AIMX
AIAV
AIMN

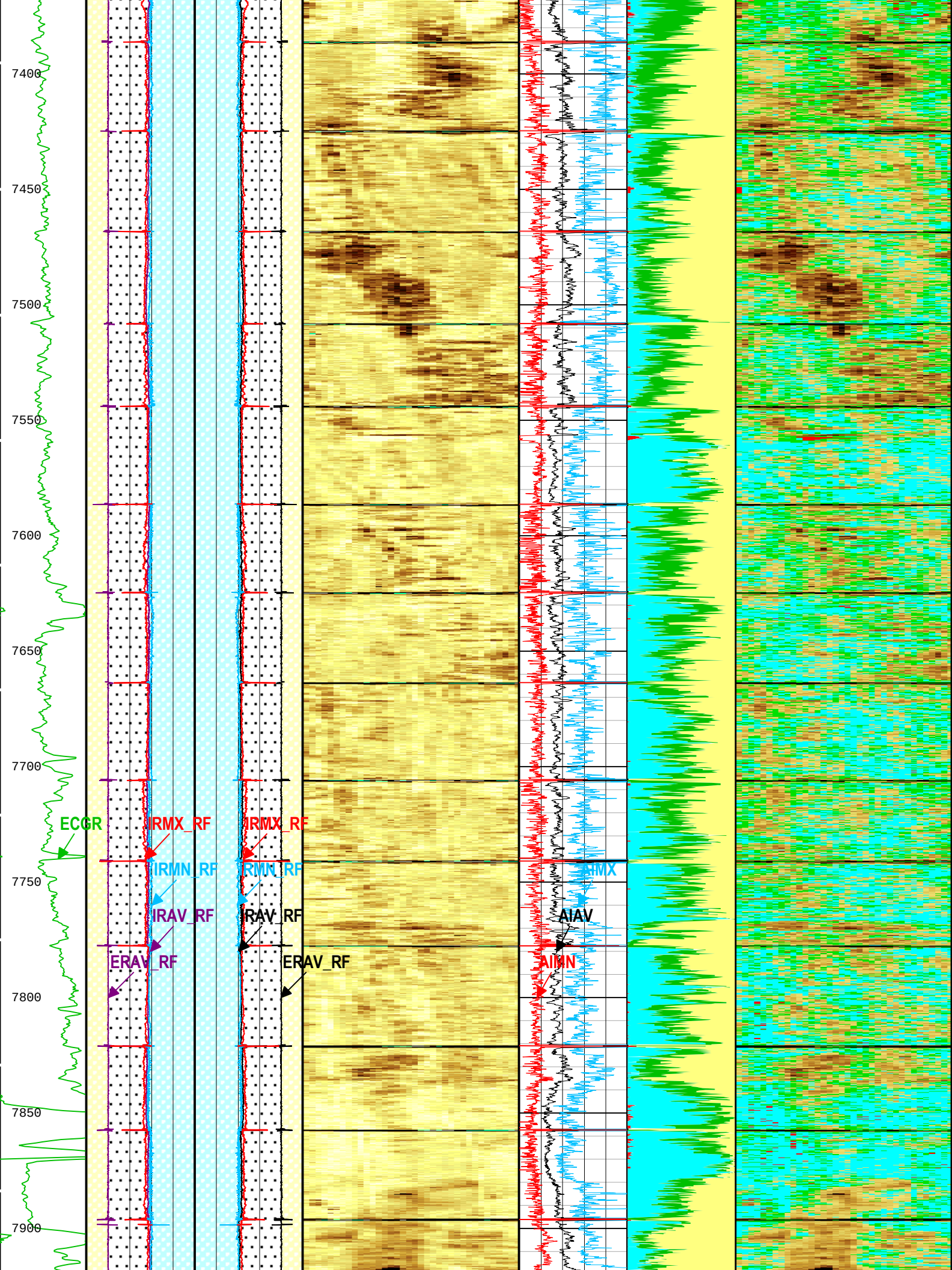
7400
7450
7500
7550
7600
7650
7700
7750
7800
7850
7900
ECGR
IRMX_RF
IRMX_RF
IRMN_RF
IRMN_RF
IRAV_RF
IRAV_RF
ERAV_RF
ERAV_RF
AIMX
AIAV
AIMN

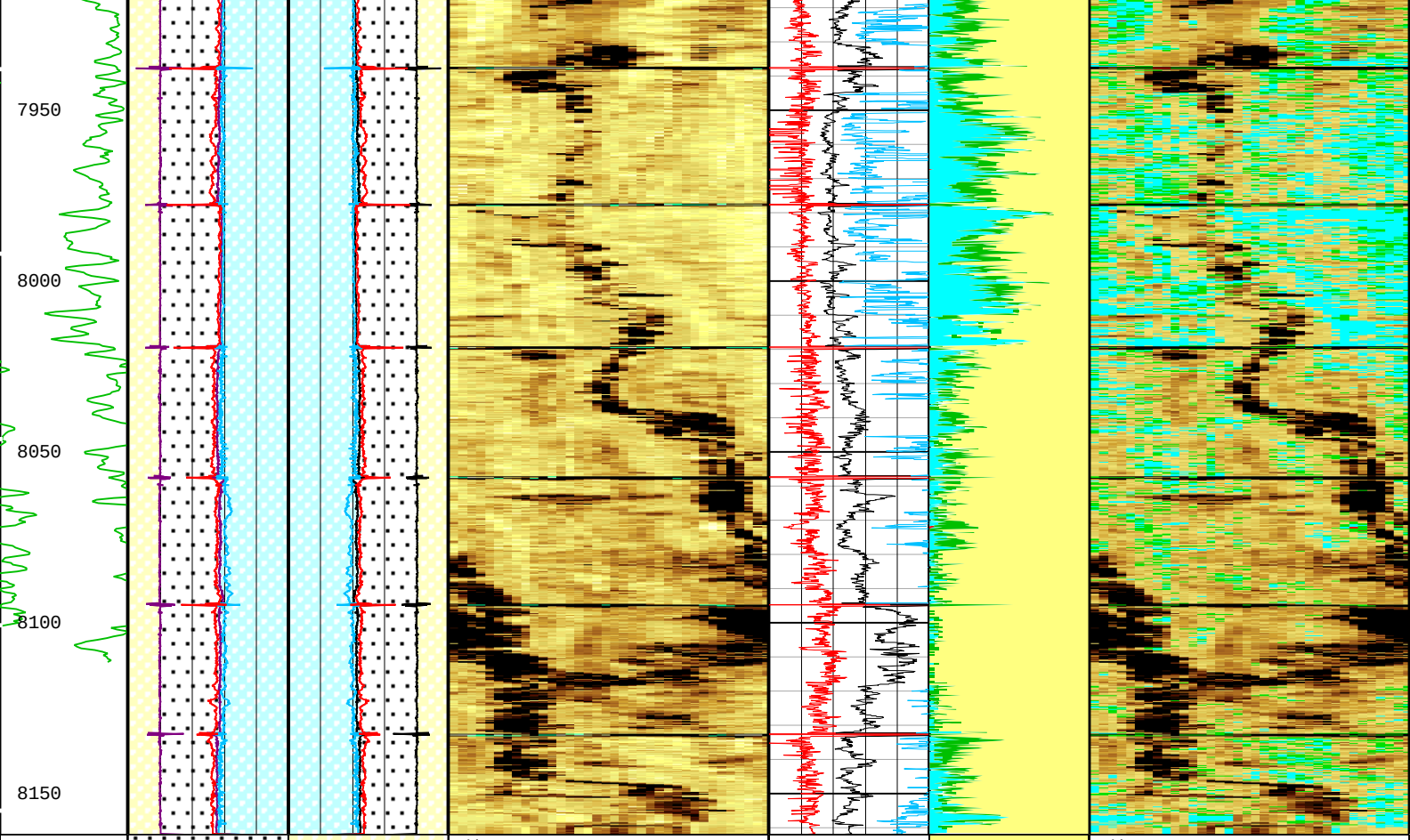

Gamma Ray (ECGR) HGNS-H
0 gAPI 150

Amplitude of Eccentering for Unflagged Waves (ECCE_RF) USIT-E
0 in 0.5

ERAV_IRAV

IRAV_LHF1

LHF1_ERAV

Median of Unflagged External Radii (ERAV_RF) USIT-E
3.7 in 2.7

Median Internal Radius of Casing Corrected for Eccentering (IRAV_RF) USIT-E
3.7 in 2.7

Minimum of Unflagged Internal Radii (IRMN_RF) USIT-E
3.7 in 2.7

Maximum of Unflagged Internal Radii (IRMX_RF) USIT-E
3.7 in 2.7

ERAV_RHF1

IRAV_ERAV

RHF1_IRAV

Median of Unflagged External Radii (ERAV_RF) USIT-E
2.7 in 3.7

Median Internal Radius of Casing Corrected for Eccentering (IRAV_RF) USIT-E
2.7 in 3.7

Minimum of Unflagged Internal Radii (IRMN_RF) USIT-E
2.7 in 3.7

Maximum of Unflagged Internal Radii (IRMX_RF) USIT-E
2.7 in 3.7

Custom Normalization
USIT - Acoustic Impedance (AIBK) USIT-E (Mrayl)

Acoustic Impedance Minimum (AIMN) USIT-E
-1 Mrayl 9

Acoustic Impedance Average (AIAV) USIT-E
-1 Mrayl 9

Acoustic Impedance Maximum (AIMX) USIT-E
-1 Mrayl 9

Bonded

Gas

Liquid

Micro-debonding

Custom Normalization
USIT - Acoustic Impedance With Micro-debonding Image (AI_MDEBOND_IMG) USIT-E (Mrayl)

TIME_1900 - Time Marked every 60.00 (s)

Description: USI Cement Format: Log (LBV1_USI Cement 7inch) Index Scale: 2 in per 100 ft Index Unit: ft Index Type: Measured Depth Creation Date: 20-Oct-2016 14:28:43

Composite 1

Corrosion 5 in = 100 ft

Composite Summary

Run Name	Pass Objective	Direction	Top	Bottom	Start	Stop	DSC Mode	Depth Shift	Include Parallel Data
Two	Log[9]:Up	Up	6640.29 ft	8171.85 ft	20-Oct-2016 9:51:39 AM	20-Oct-2016 10:20:40 AM	ON	1.47 ft	No
Two	Log[11]:Up	Up	36.69 ft	6737.51 ft	20-Oct-2016 10:24:53 AM	20-Oct-2016 12:34:00 PM	ON	1.35 ft	No
Two	Log[14]:Up	Up	5.56 ft	155.15 ft	20-Oct-2016 12:53:24 PM	20-Oct-2016 12:58:23 PM	ON	1.96 ft	No

All depths are referenced to toolstring zero

Log

Company:Southern California Gas Company Well:Frew 4

Composite 1:S008

Description: USI Composite Format: Log (LBV1_USI Corrosion 7inch) Index Scale: 5 in per 100 ft Index Unit: ft Index Type: Measured Depth Creation Date: 20-Oct-2016 14:28:48

TIME_1900 - Time Marked every 60.00 (s)

USIT Processing Flags (UFLG[0]) USIT-E[1]

1 - UFLG 1 Value within [0.0 - 1.5] - :
2 - UFLG 2 Value within [1.5 - 2.5] - :
3 - UFLG 3 Value within [2.5 - 3.5] - :
4 - UFLG 4 UFLG 5 UFLG 6 Value within [3.5 - 6.5] - :
5 - UFLG 7 UFLG 8 UFLG 9 Value within [6.5 - 10] - :

UTIM Error
Pulse Origin Not Detected
WINLEN Error
Casing Thickness Error
Loop Processing Error

Amplitude of Eccentering for Unflagged Waves (ECCE_RF) USIT-E[1]
0 in 0.5

Motor Revolution Speed (RSAV) USIT-E[1]

Absent 1.500 3.500
Explicit Normalization
USIT - USIT Processing Flags (UFLG) USIT-E[1]

Absent -5.200 -3.600 -2.000 -0.400
Explicit Normalization
USIT - Amplitude of Unflagged Wave (AWBK_RF) USIT-E[1] (dB)

Minimum of Unflagged Wave Amplitude (AWMN_RF) USIT-E[1]
0 dB 75

Average of Unflagged Wave Amplitude (AWAV_RF) USIT-E[1]
0 dB 75

Maximum of

Absent -0.059 -0.028 0.004 0.035 0.068
Explicit Normalization
USIT - Unflagged

Internal Radius Averaged Value (IRAV) USIT-E[1]
2.7 in 3.7

Internal Radius Maximum Value (IRMX) USIT-E[1]
2.7 in 3.7

ERAV | IRAV
ERAV-IRAV | ERAV
IRAV | IRAV-ERAV

Median of Unflagged External Radii (ERAV_RF) USIT-E[1]
3.7 in 2.7

Median of Unflagged External Radii (ERAV_RF) USIT-E[1]
2.7 in 3.7

Median Internal Radius of Casing Corrected for Eccentering (IRAV_RF) USIT-E[1]
3.7 in 2.7

Median Internal Radius of Casing Corrected for Eccentering (IRAV_RF) USIT-E[1]
2.7 in 3.7

Maximum of Unflagged Internal Radii (IRMX_RF) USIT-E[1]
3.7 in 2.7

Maximum of Unflagged Internal Radii (IRMX_RF) USIT-E[1]
2.7 in 3.7

Minimum of

Minimum of

Absent -0.059 -0.028 0.004 0.035 0.068
Explicit Normalization
USIT - Unflagged Casing Thickness minus Median of

Minimum of Unflagged Casing Thickness (THMN_RF) USIT-E[1]
0.1 in 0.6

Nominal Casing Thickness (THNO) USIT-E[1]
0.1 in 0.6

Median of Unflagged Casing Thickness (THAV_RF) USIT-E[1]
0.1 in 0.6

Maximum of Unflagged

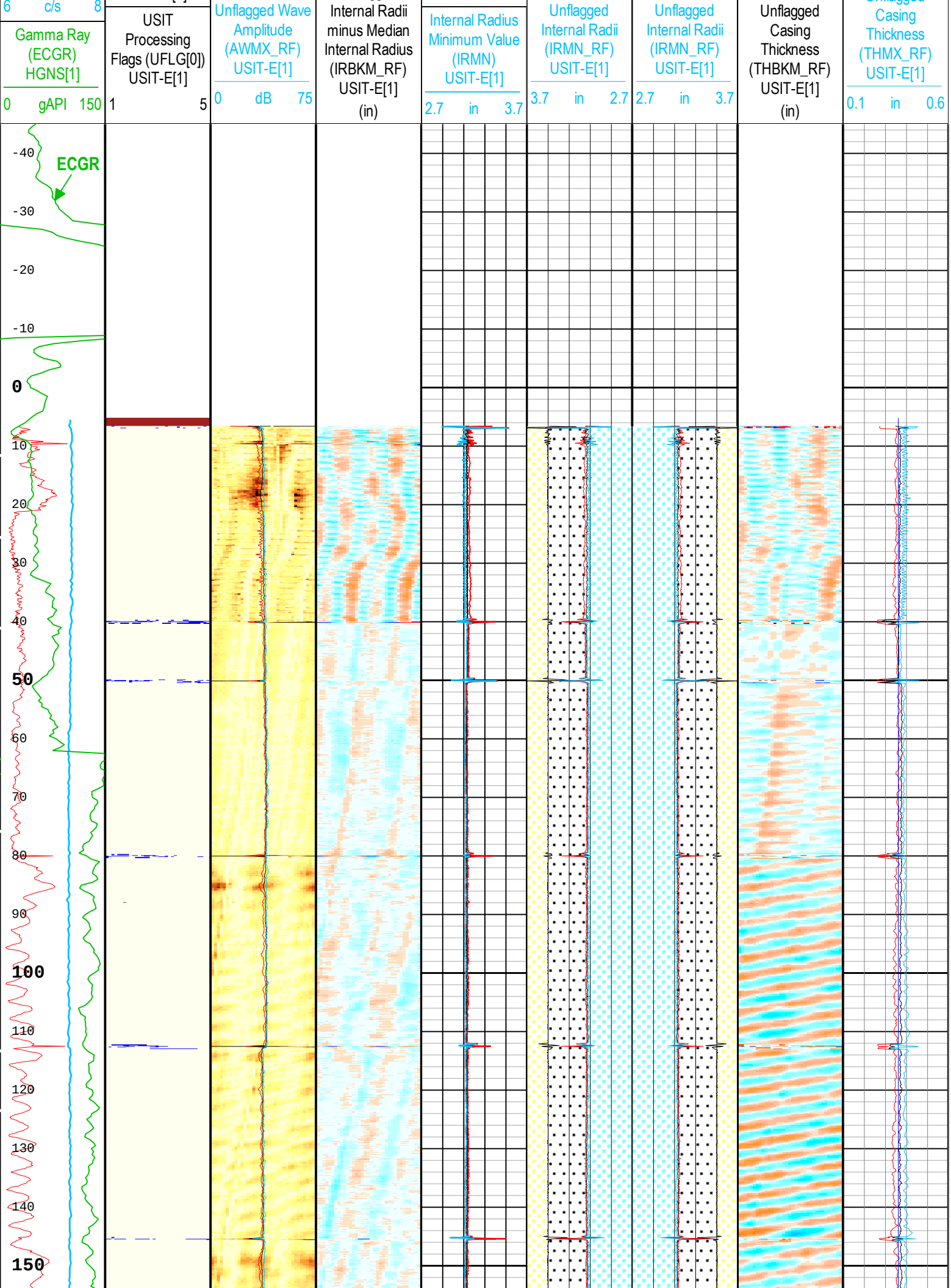
6 c/s 8
Gamma Ray (ECGR) HGNS[1]
0 gAPI 150
USIT Processing Flags (UFLG[0]) USIT-E[1]
1 5
Unflagged Wave Amplitude (AWMX_RF) USIT-E[1]
0 dB 75
Internal Radii minus Median Internal Radius (IRBKM_RF) USIT-E[1] (in)
Internal Radius Minimum Value (IRMN) USIT-E[1]
2.7 in 3.7
Unflagged Internal Radii (IRMN_RF) USIT-E[1]
3.7 in 2.7
Unflagged Internal Radii (IRMN_RF) USIT-E[1]
2.7 in 3.7
Unflagged Casing Thickness (THBKM_RF) USIT-E[1] (in)
Unflagged Casing Thickness (THMX_RF) USIT-E[1]
0.1 in 0.6
ECGR
-40
-30
-20
-10
0
10
20
30
40
50
60
70
80
90
100
110
120
130
140
150

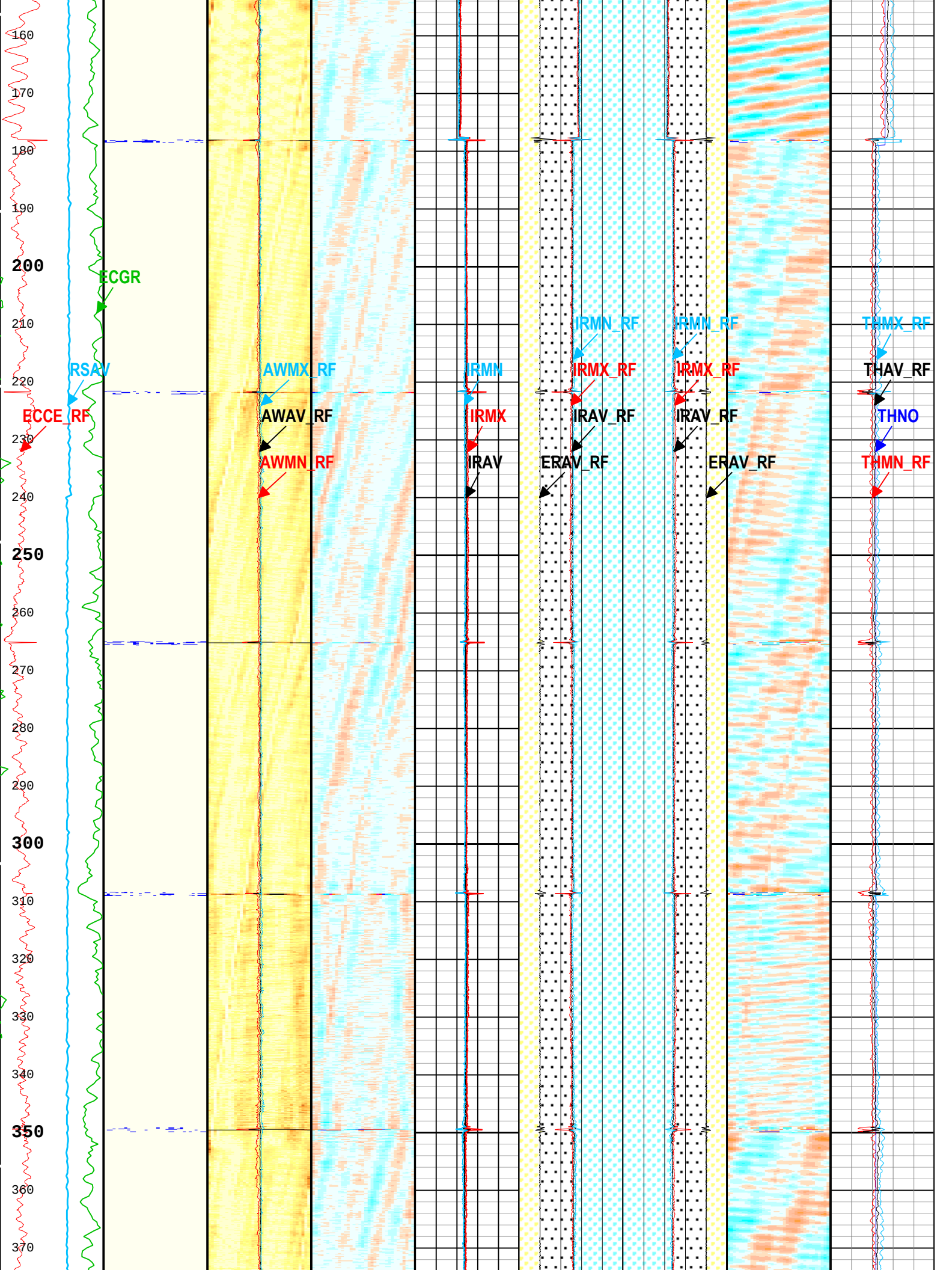
160
170
180
190
200
210
220
230
240
250
260
270
280
290
300
310
320
330
340
350
360
370
ECGR
RSAV
ECCE_RF
AWMX_RF
AWAV_RF
AWMN_RF
IRMN
IRMX
IRAV
IRMN_RF
IRMX_RF
IRAV_RF
ERAV_RF
IRMN_RF
IRMX_RF
IRAV_RF
ERAV_RF
THMX_RF
THAV_RF
THNO
THMN_RF

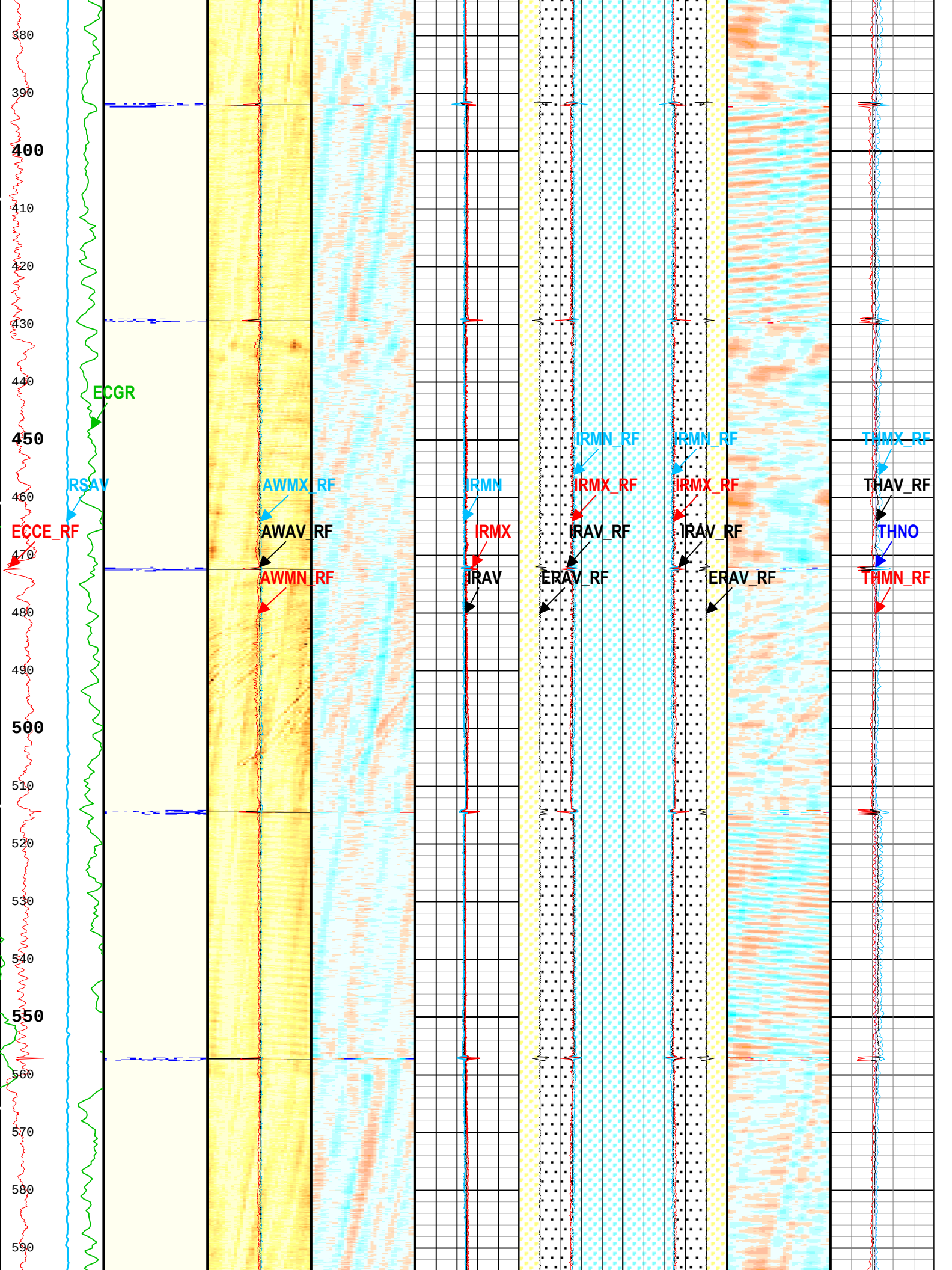
380
390
400
410
420
430
440
450
460
470
480
490
500
510
520
530
540
550
560
570
580
590
ECGR
RSAV
ECCE_RF
AWMX_RF
AWAV_RF
AWMN_RF
IRMN
IRMX
IRAV
IRMN_RF
IRMX_RF
IRAV_RF
ERAV_RF
IRMN_RF
IRMX_RF
IRAV_RF
ERAV_RF
THMX_RF
THAV_RF
THNO
THMN_RF

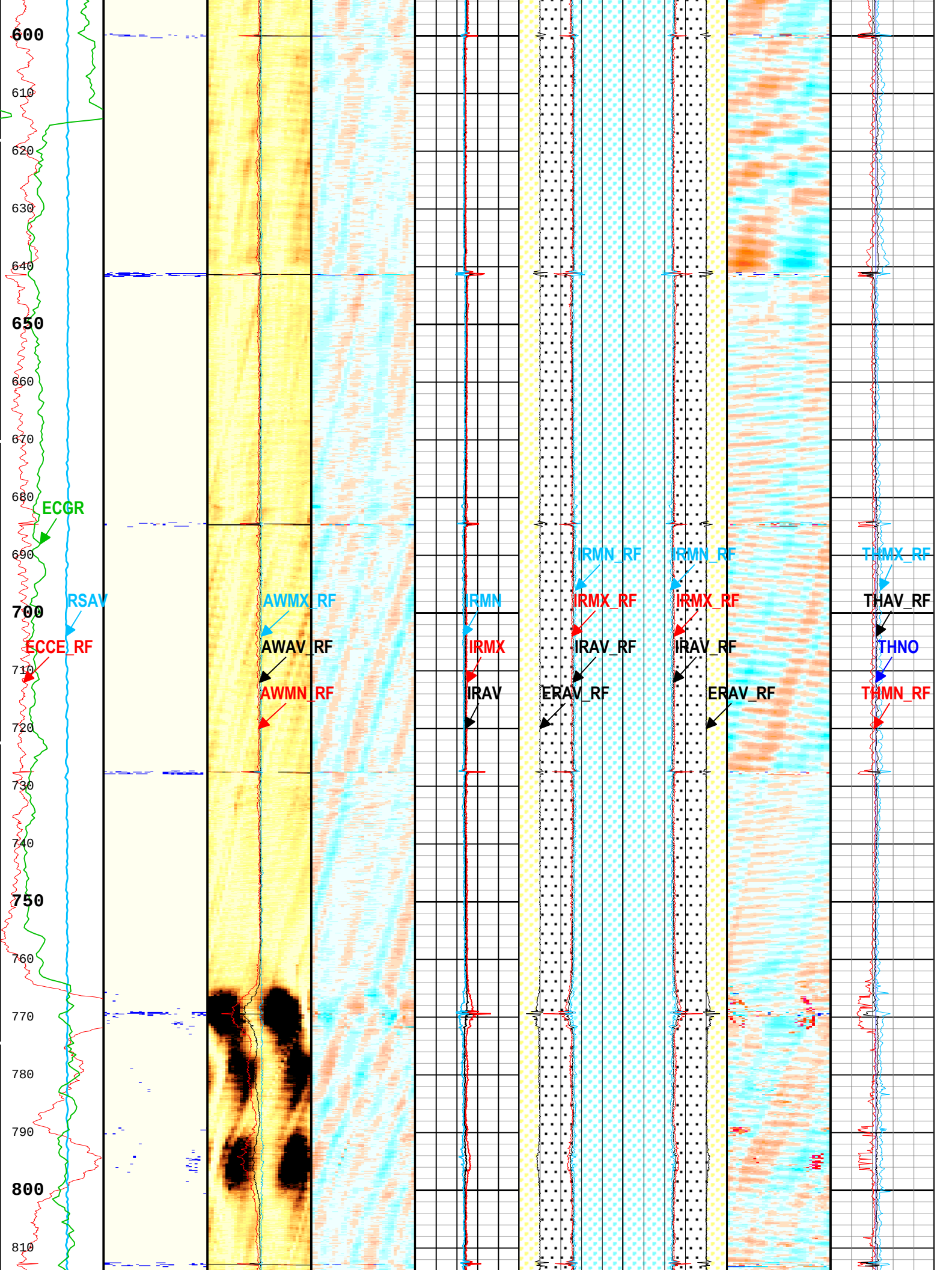
600
610
620
630
640
650
660
670
680
690
700
710
720
730
740
750
760
770
780
790
800
810
ECGR
RSAV
ECCE_RF
AWMX_RF
AWAV_RF
AWMN_RF
IRMN
IRMX
IRAV
IRMN_RF
IRMX_RF
IRAV_RF
ERAV_RF
IRMN_RF
IRMX_RF
IRAV_RF
ERAV_RF
THMX_RF
THAV_RF
THNO
THMN_RF

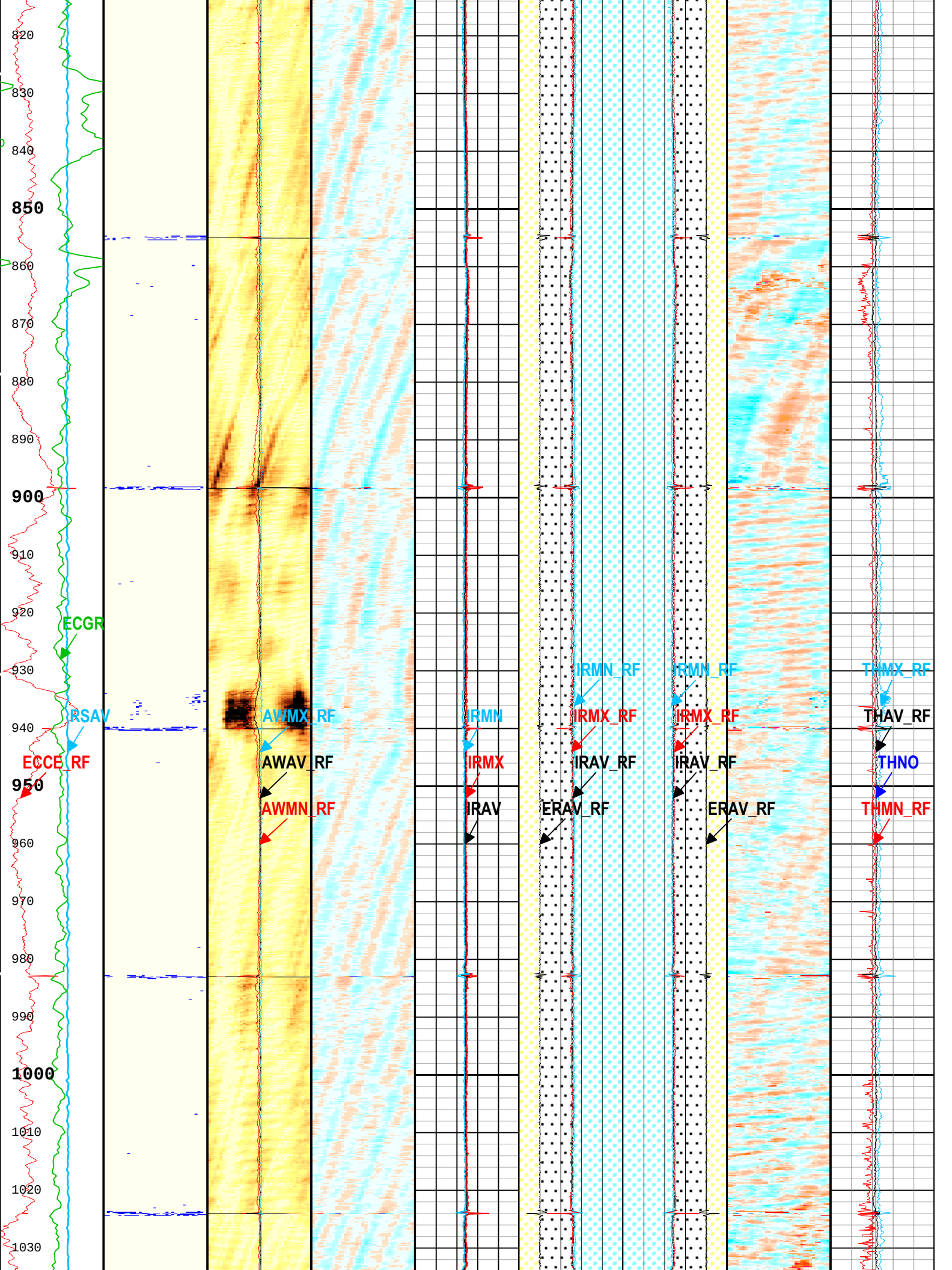
820
830
840
850
860
870
880
890
900
910
920
930
940
950
960
970
980
990
1000
1010
1020
1030
ECGR
RSAV
ECCE_RF
AWMX_RF
AWAV_RF
AWMN_RF
IRMN
IRMX
IRAV
IRMN_RF
IRMX_RF
IRAV_RF
ERAV_RF
IRMN_RF
IRMX_RF
IRAV_RF
ERAV_RF
THMX_RF
THAV_RF
THNO
THMN_RF

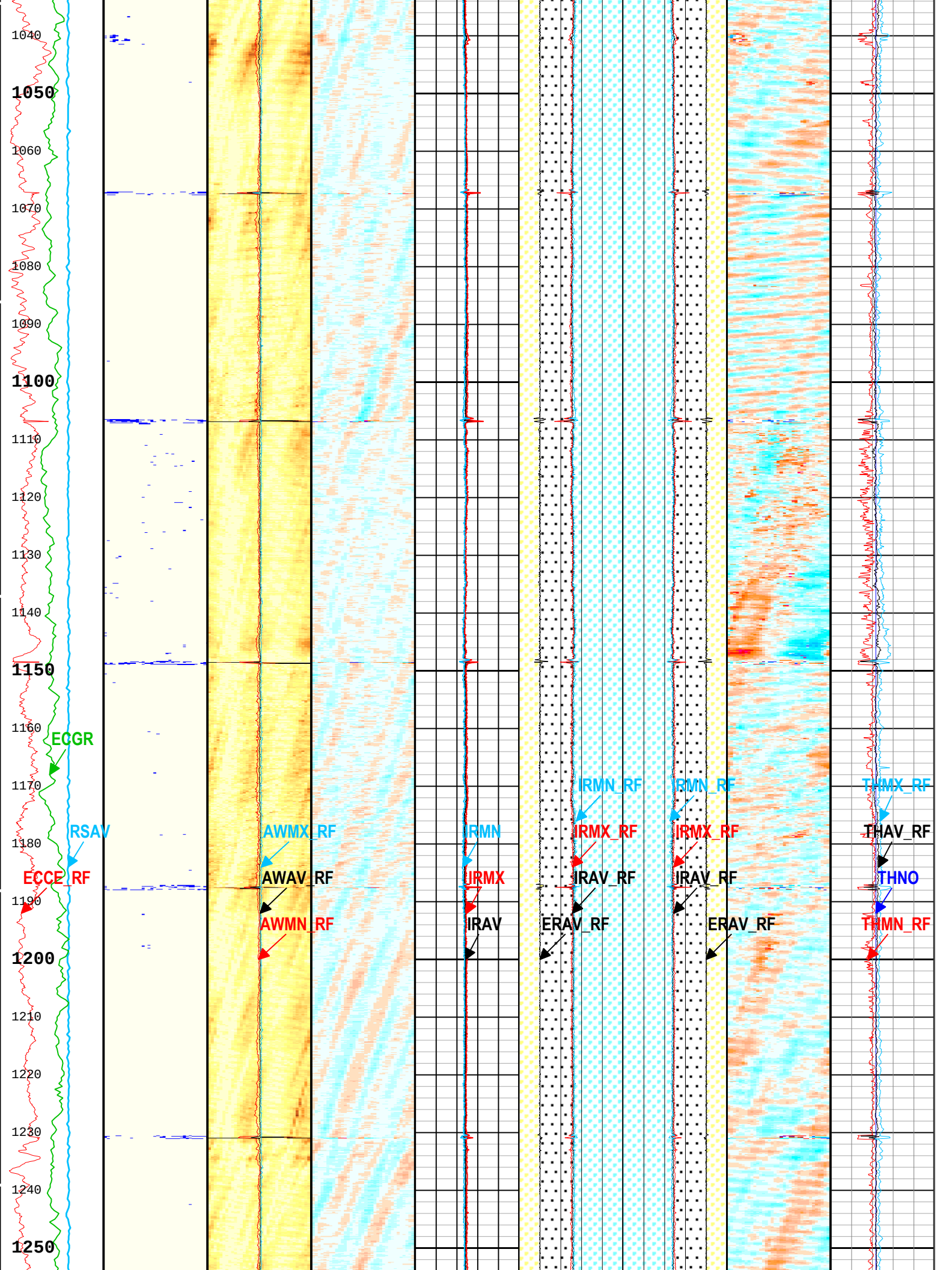
1040
1050
1060
1070
1080
1090
1100
1110
1120
1130
1140
1150
1160
1170
1180
1190
1200
1210
1220
1230
1240
1250
ECGR
RSAV
ECCE_RF
AWMX_RF
AWAV_RF
AWMN_RF
IRMN
IRMX
IRAV
IRMN_RF
IRMX_RF
IRAV_RF
ERAV_RF
IRMN_RF
IRMX_RF
IRAV_RF
ERAV_RF
THMX_RF
THAV_RF
THNO
THMN_RF

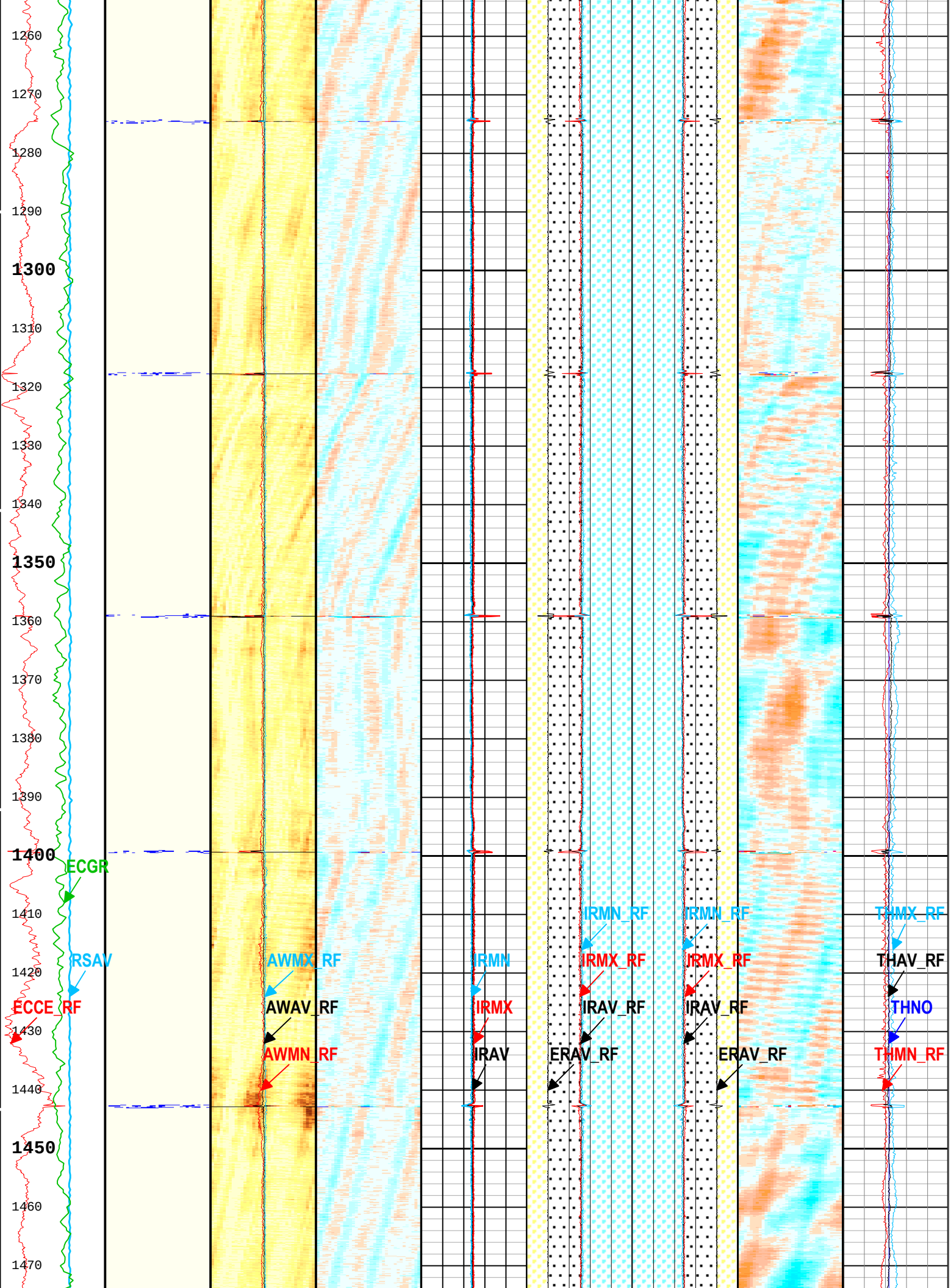
1260
1270
1280
1290
1300
1310
1320
1330
1340
1350
1360
1370
1380
1390
1400
1410
1420
1430
1440
1450
1460
1470
ECGR
RSAV
ECCE_RF
AWMX_RF
AWAV_RF
AWMN_RF
IRMN
IRMX
IRAV
IRMN_RF
IRMX_RF
IRAV_RF
ERAV_RF
IRMN_RF
IRMX_RF
IRAV_RF
ERAV_RF
THMX_RF
THAV_RF
THNO
THMN_RF

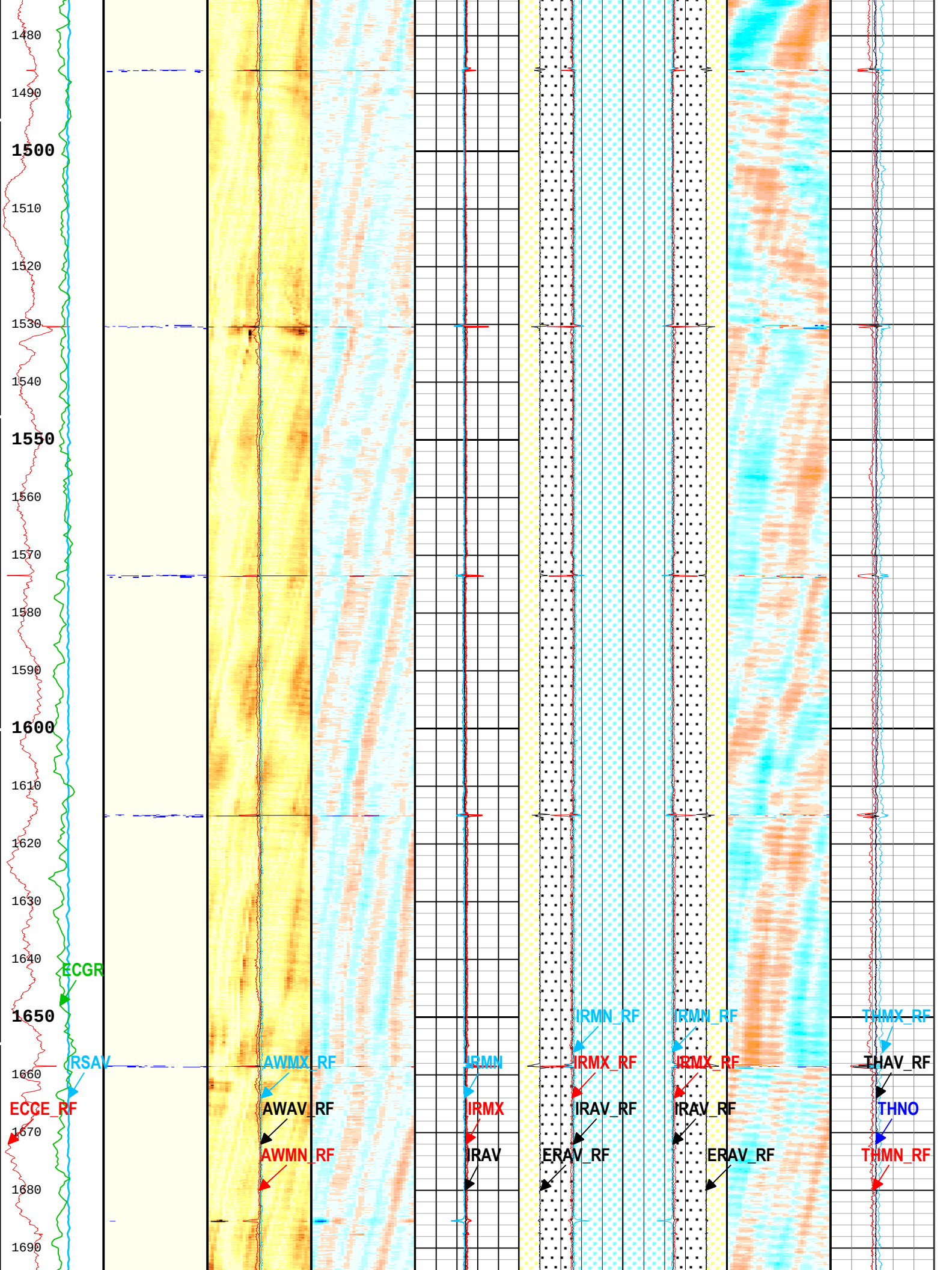
1480
1490
1500
1510
1520
1530
1540
1550
1560
1570
1580
1590
1600
1610
1620
1630
1640
1650
1660
1670
1680
1690
ECGR
RSAV
ECCE_RF
AWMX_RF
AWAV_RF
AWMN_RF
IRMN
IRMX
IRAV
IRMN_RF
IRMX_RF
IRAV_RF
ERAV_RF
IRMN_RF
IRMX_RF
IRAV_RF
ERAV_RF
THMX_RF
THAV_RF
THNO
THMN_RF

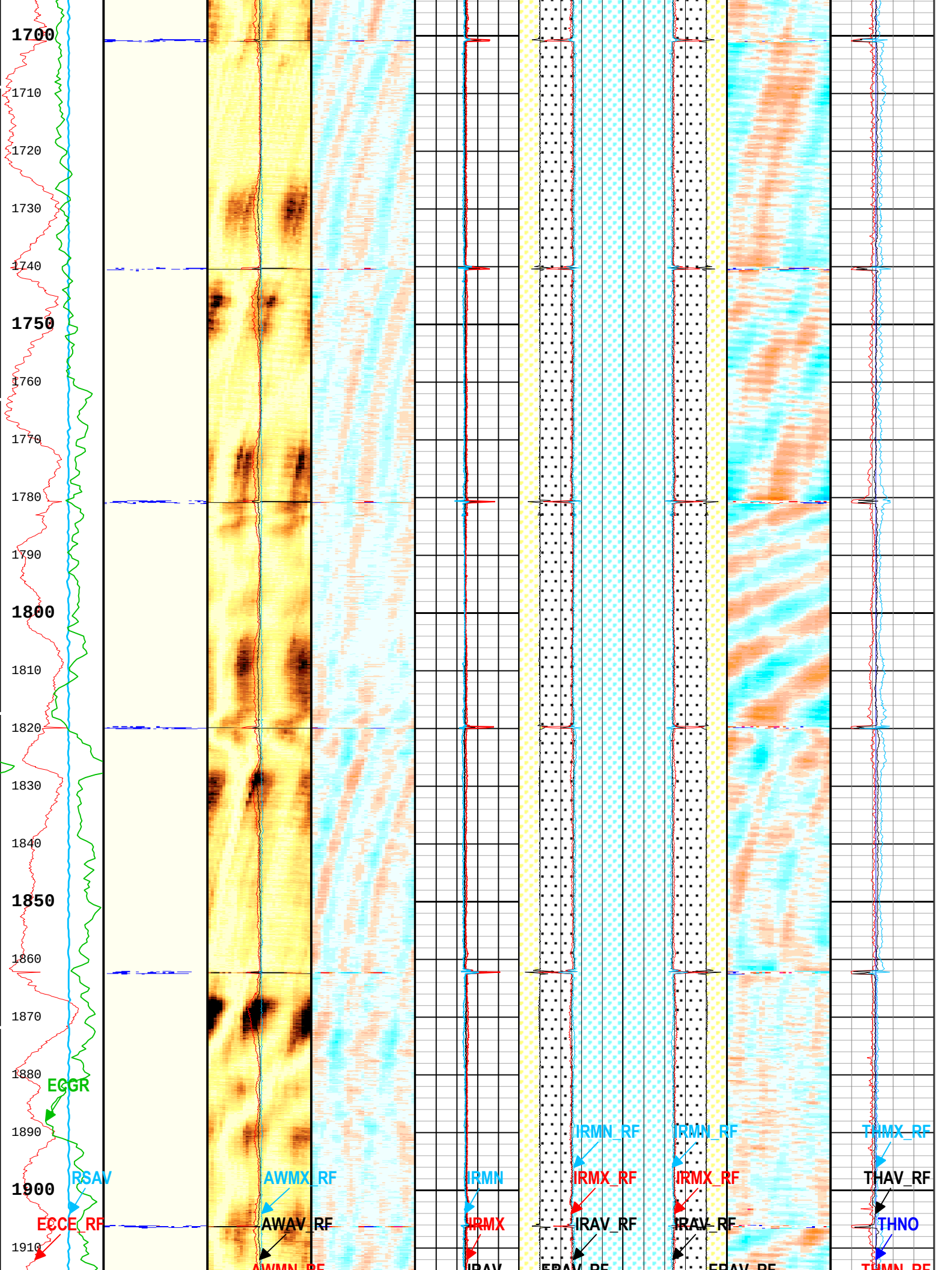
1700
1710
1720
1730
1740
1750
1760
1770
1780
1790
1800
1810
1820
1830
1840
1850
1860
1870
1880
1890
1900
1910
ECGR
RSAV
ECCE_RF
AWMX_RF
AWAV_RF
AWMN_RF
IRMN
IRMX
IRAV
IRMN_RF
IRMX_RF
IRAV_RF
IRMN_RF
IRMX_RF
IRAV_RF
THMX_RF
THAV_RF
THNO
THMN_RF

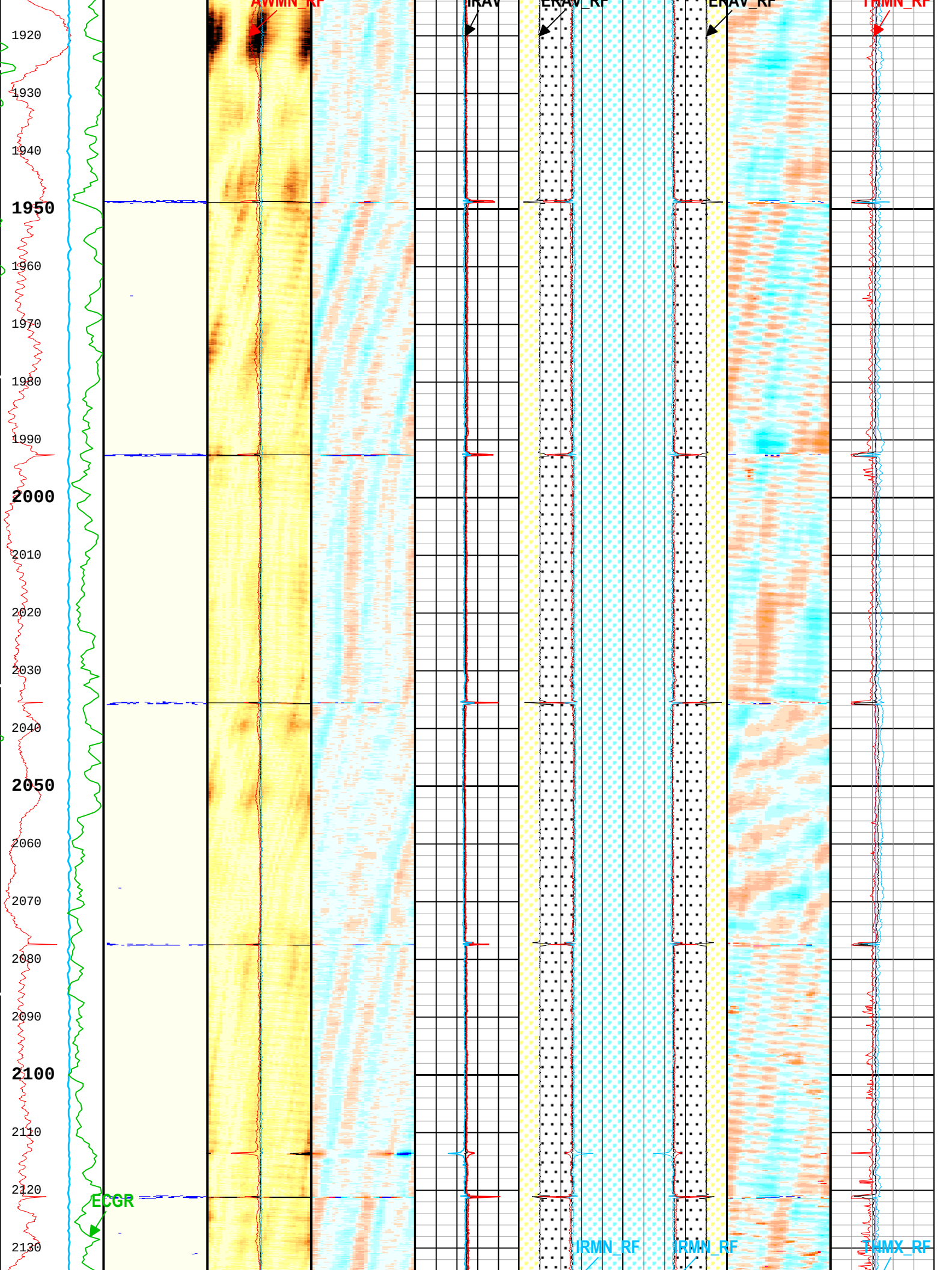
AWMN_RF
IRAV
ERAV_RF
ERAV_RF
THMN_RF
1920
1930
1940
1950
1960
1970
1980
1990
2000
2010
2020
2030
2040
2050
2060
2070
2080
2090
2100
2110
2120
2130
ECGR
IRMN_RF
IRMN_RF
THMX_RF

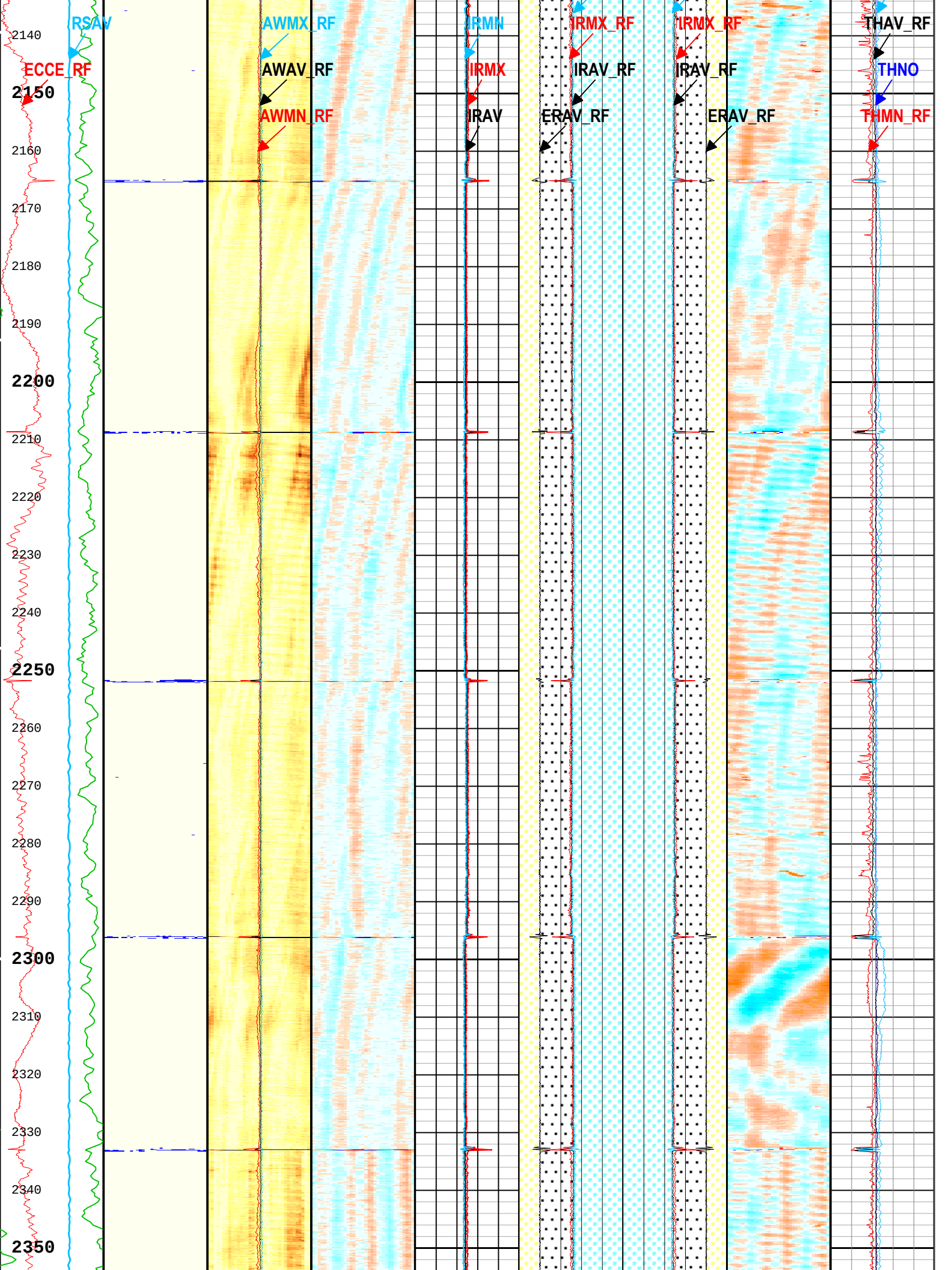
RSAV
ECCE_RF
AWMX_RF
AWAV_RF
AWMN_RF
IRMN
IRMX
IRAV
IRMX_RF
IRAV_RF
ERAV_RF
IRMX_RF
IRAV_RF
ERAV_RF
THAV_RF
THNO
THMN_RF
2140
2150
2160
2170
2180
2190
2200
2210
2220
2230
2240
2250
2260
2270
2280
2290
2300
2310
2320
2330
2340
2350

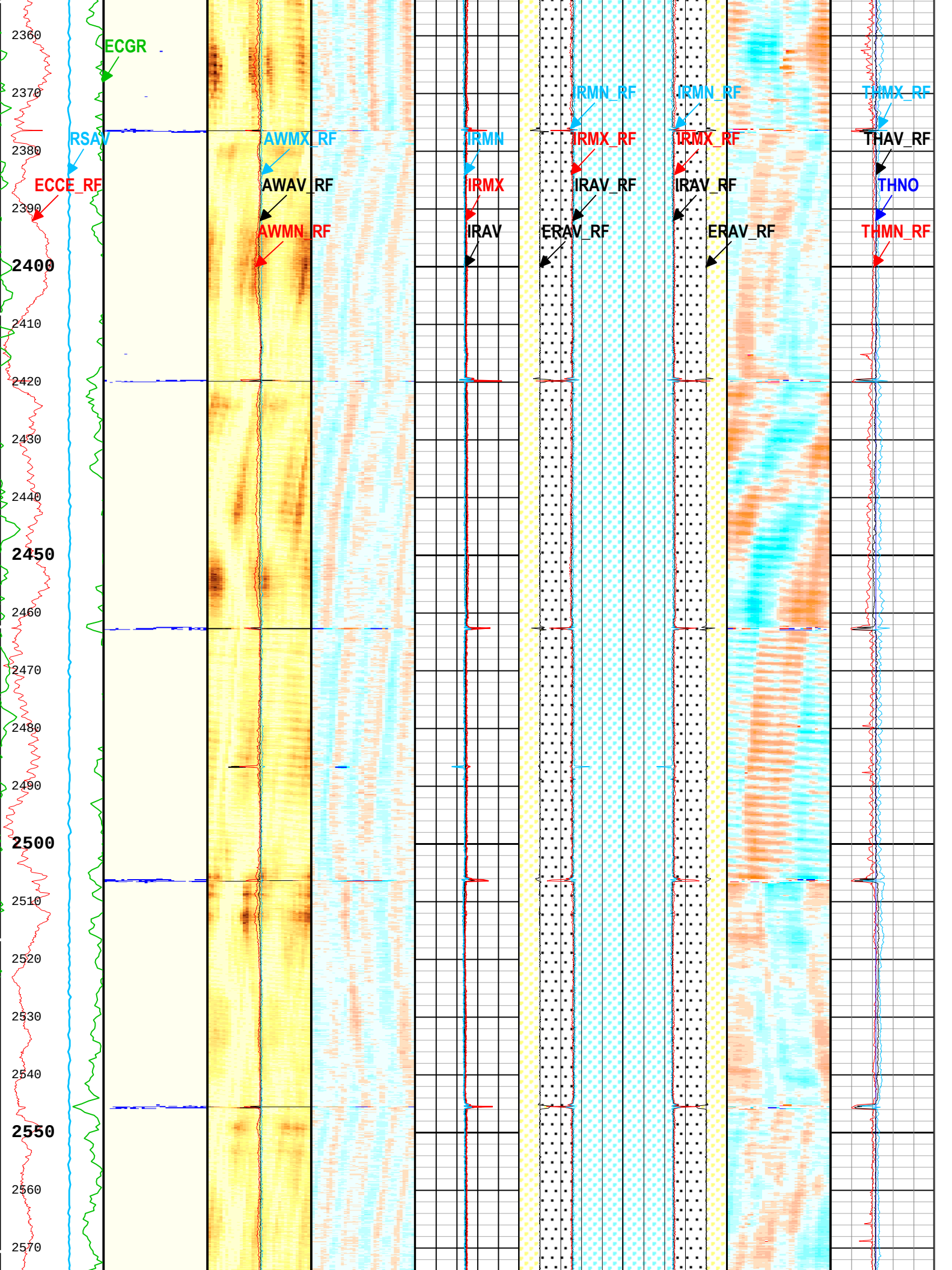
ECGR
RSAV
ECCE_RF
AWMX_RF
AWAV_RF
AWMN_RF
IRMN
IRMX
IRAV
IRMN_RF
IRMX_RF
IRAV_RF
ERAV_RF
IRMN_RF
IRMX_RF
IRAV_RF
ERAV_RF
THMX_RF
THAV_RF
THNO
THMN_RF
2360
2370
2380
2390
2400
2410
2420
2430
2440
2450
2460
2470
2480
2490
2500
2510
2520
2530
2540
2550
2560
2570

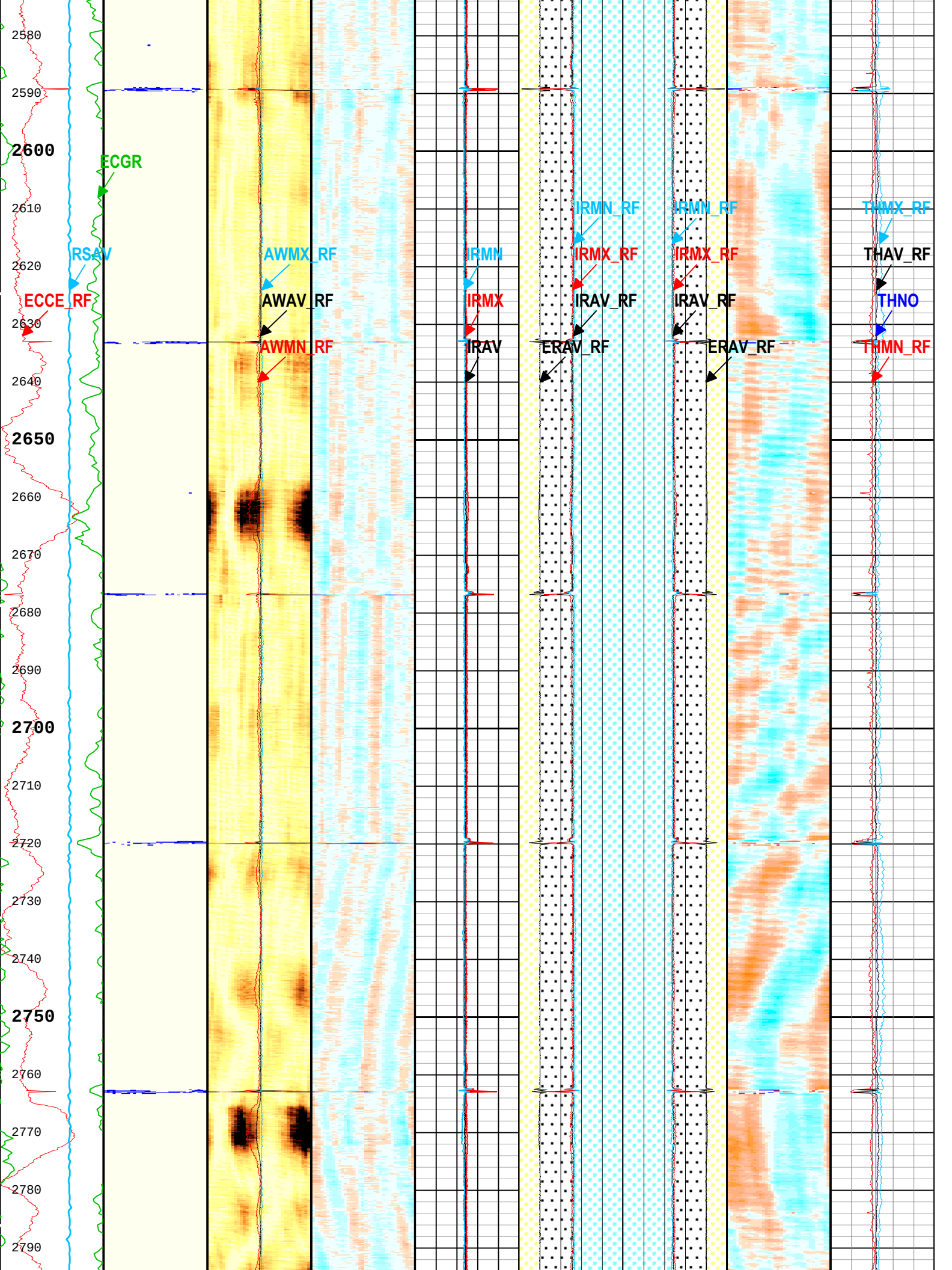
2580
2590
2600
2610
2620
2630
2640
2650
2660
2670
2680
2690
2700
2710
2720
2730
2740
2750
2760
2770
2780
2790
ECGR
RSAV
ECCE_RF
AWMX_RF
AWAV_RF
AWMN_RF
IRMN
IRMX
IRAV
IRMN_RF
IRMX_RF
IRAV_RF
ERAV_RF
IRMN_RF
IRMX_RF
IRAV_RF
ERAV_RF
THMX_RF
THAV_RF
THNO
THMN_RF

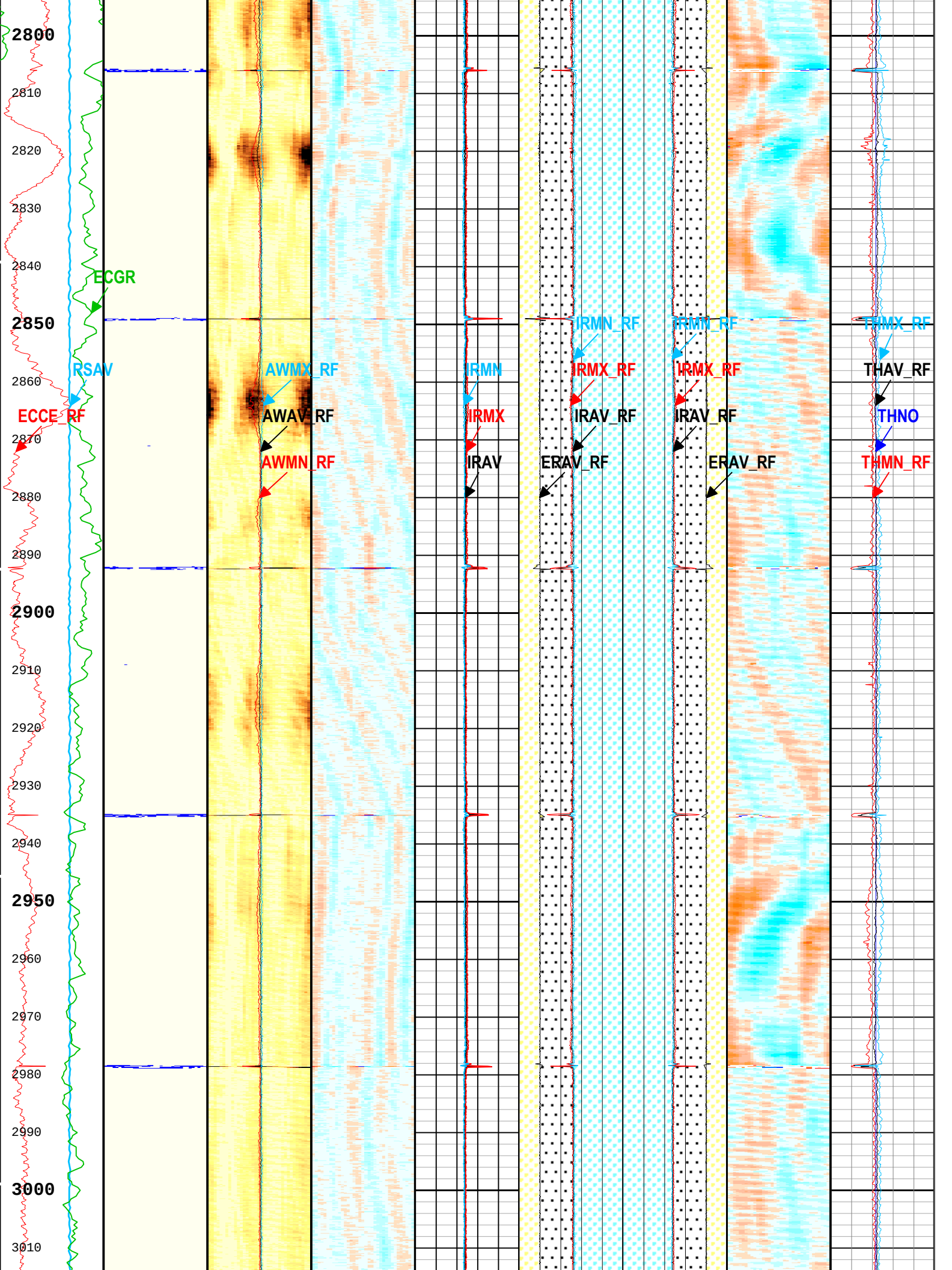
2800
2810
2820
2830
2840
2850
2860
2870
2880
2890
2900
2910
2920
2930
2940
2950
2960
2970
2980
2990
3000
3010
ECGR
RSAV
ECCE_RF
AWMX_RF
AWAV_RF
AWMN_RF
IRMN
IRMX
IRAV
IRMN_RF
IRMX_RF
IRAV_RF
ERAV_RF
IRMN_RF
IRMX_RF
IRAV_RF
ERAV_RF
THMX_RF
THAV_RF
THNO
THMN_RF

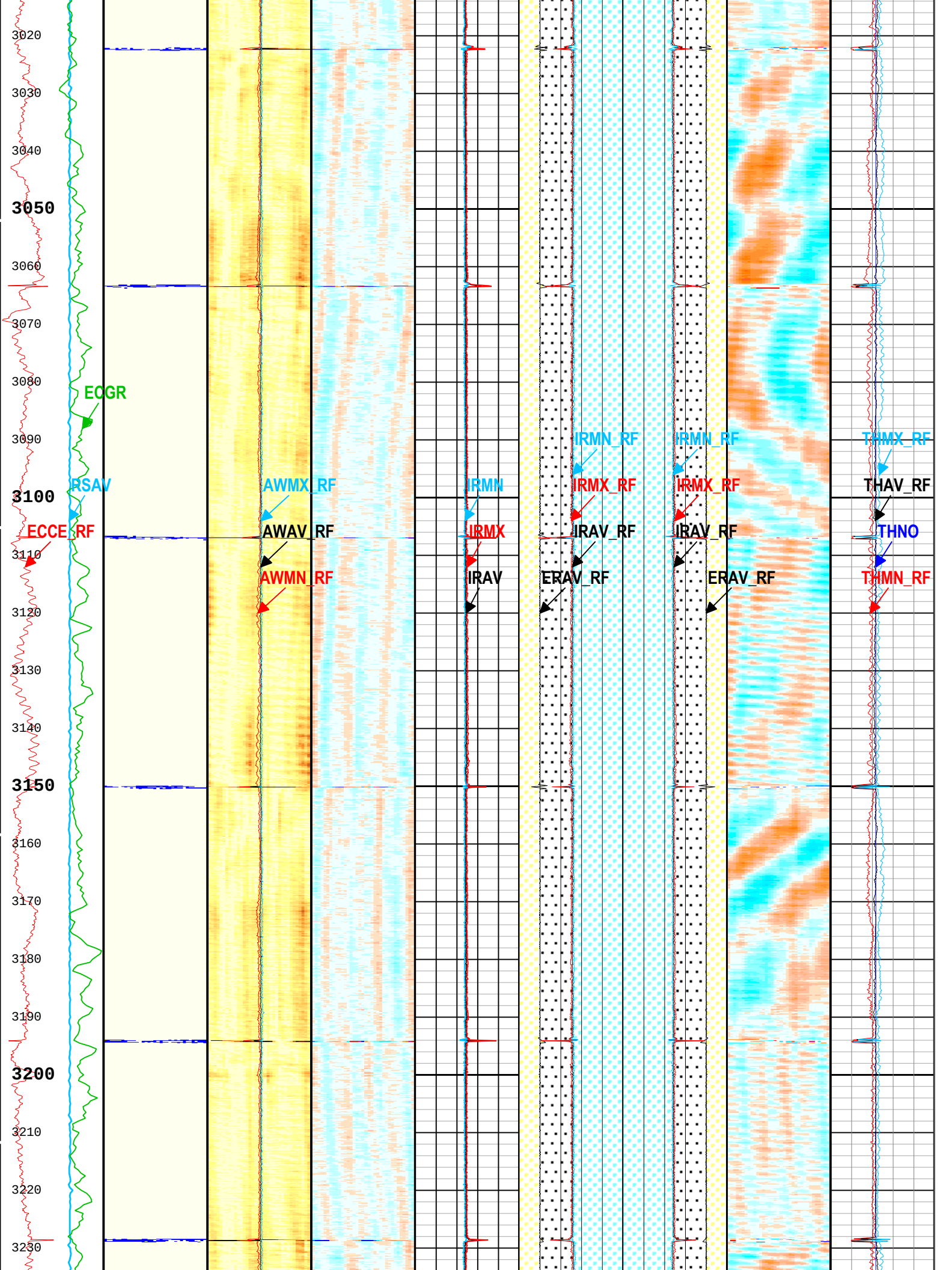
3020
3030
3040
3050
3060
3070
3080
3090
3100
3110
3120
3130
3140
3150
3160
3170
3180
3190
3200
3210
3220
3230
ECGR
RSAV
ECCE_RF
AWMX_RF
AWAV_RF
AWMN_RF
IRMN
IRMX
IRAV
IRMN_RF
IRMX_RF
IRAV_RF
ERAV_RF
IRMN_RF
IRMX_RF
IRAV_RF
ERAV_RF
THMX_RF
THAV_RF
THNO
THMN_RF

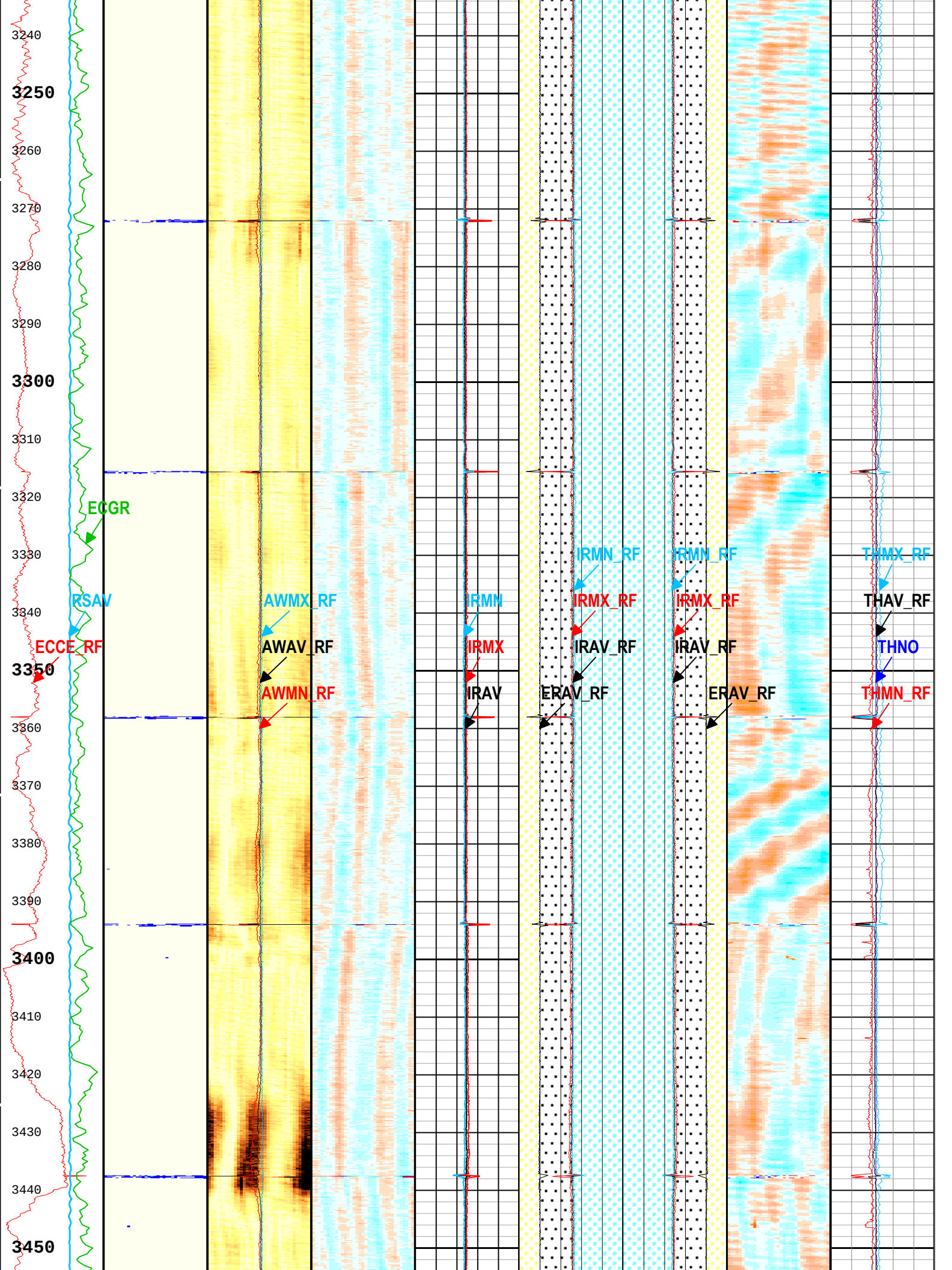
3240
3250
3260
3270
3280
3290
3300
3310
3320
3330
3340
3350
3360
3370
3380
3390
3400
3410
3420
3430
3440
3450
ECGR
RSAV
ECCE_RF
AWMX_RF
AWAV_RF
AWMN_RF
IRMN
IRMX
IRAV
IRMN_RF
IRMX_RF
IRAV_RF
ERAV_RF
IRMN_RF
IRMX_RF
IRAV_RF
ERAV_RF
THMX_RF
THAV_RF
THNO
THMN_RF

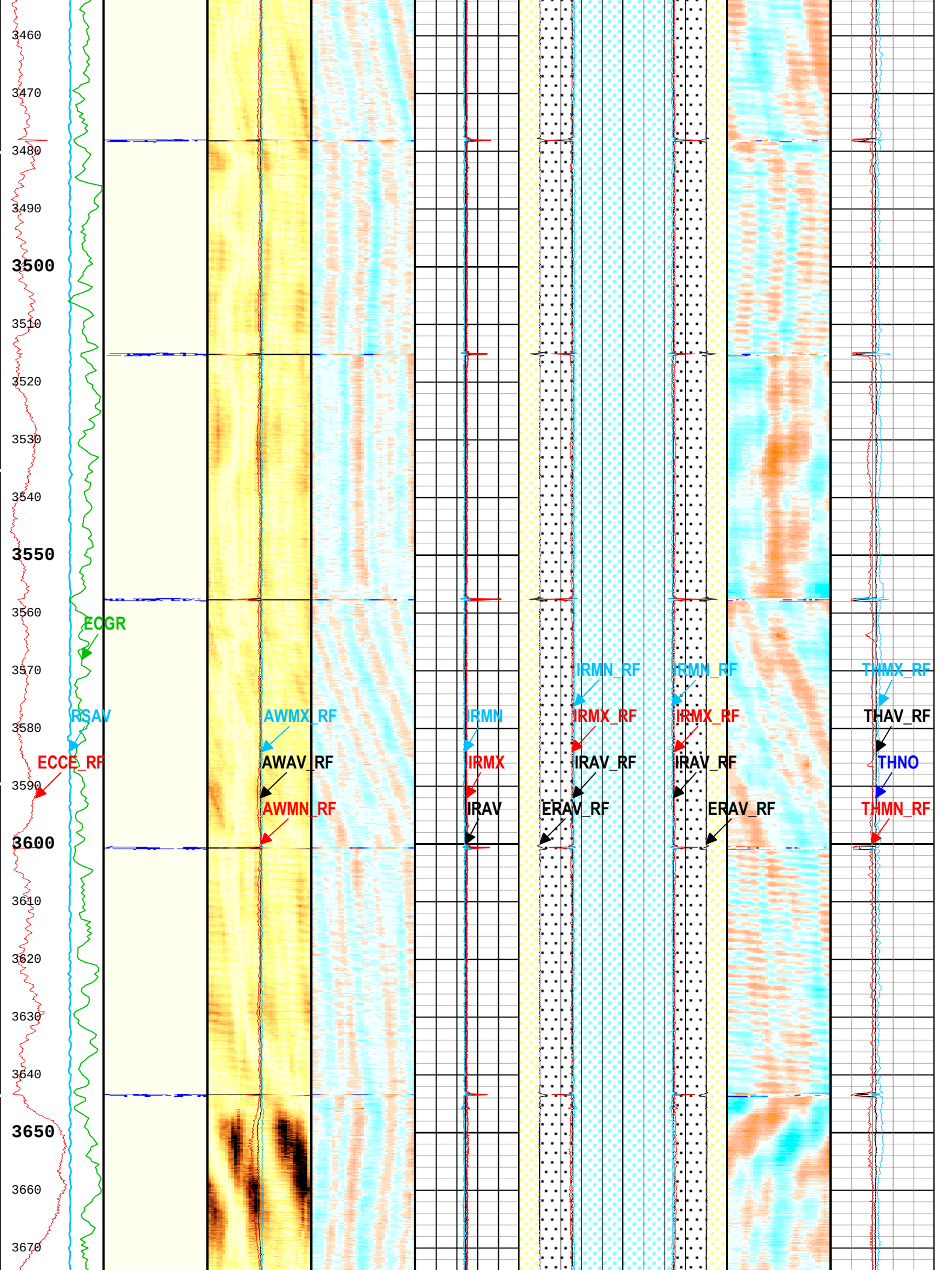
3460
3470
3480
3490
3500
3510
3520
3530
3540
3550
3560
3570
3580
3590
3600
3610
3620
3630
3640
3650
3660
3670
ECGR
RSAV
ECCE_RF
AWMX_RF
AWAV_RF
AWMN_RF
IRMN
IRMX
IRAV
IRMN_RF
IRMX_RF
IRAV_RF
ERAV_RF
IRMN_RF
IRMX_RF
IRAV_RF
ERAV_RF
THMX_RF
THAV_RF
THNO
THMN_RF

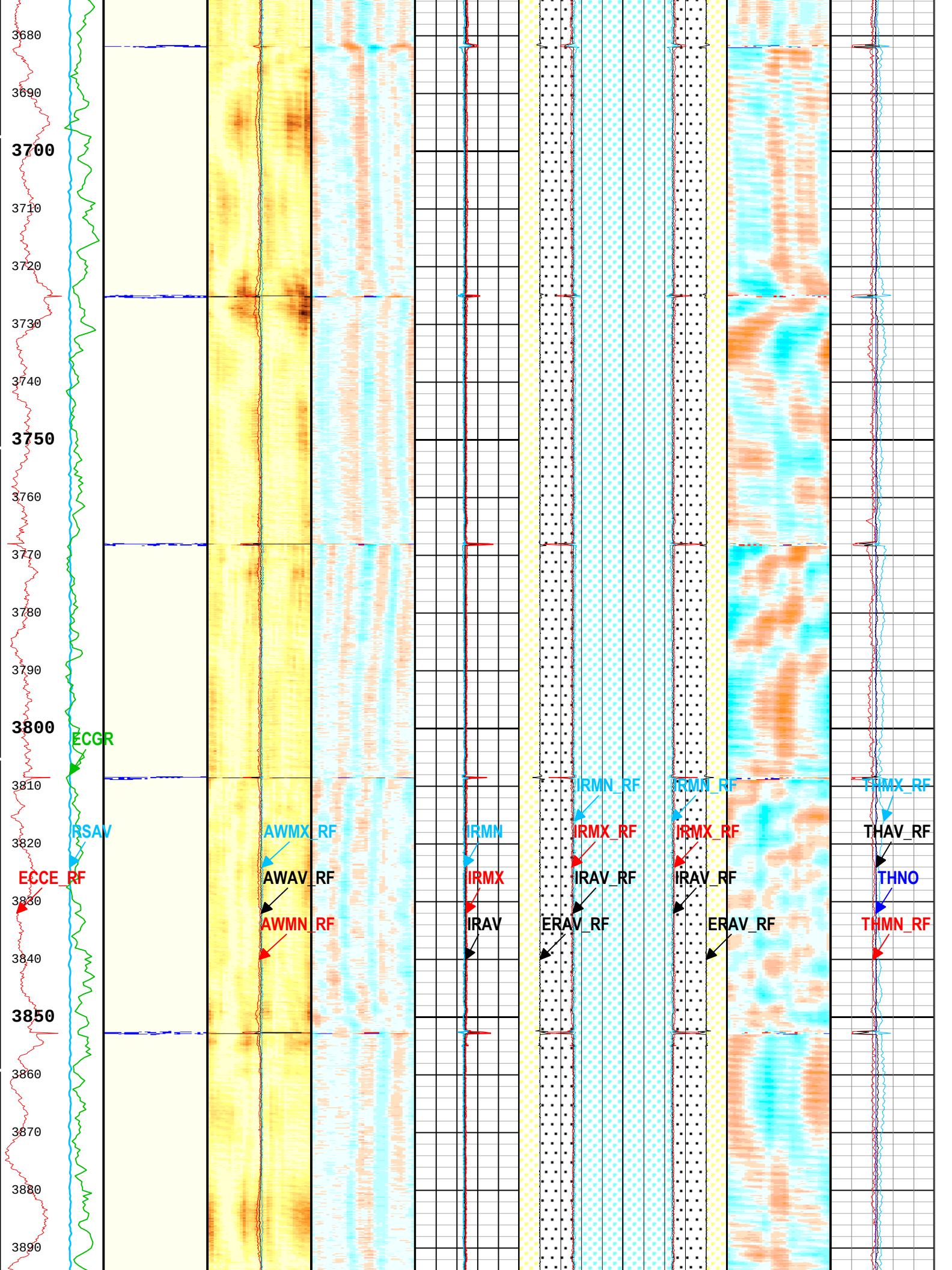
3680
3690
3700
3710
3720
3730
3740
3750
3760
3770
3780
3790
3800
3810
3820
3830
3840
3850
3860
3870
3880
3890
ECGR
RSAV
ECCE_RF
AWMX_RF
AWAV_RF
AWMN_RF
IRMN
IRMX
IRAV
IRMN_RF
IRMX_RF
IRAV_RF
ERAV_RF
IRMN_RF
IRMX_RF
IRAV_RF
ERAV_RF
THMX_RF
THAV_RF
THNO
THMN_RF

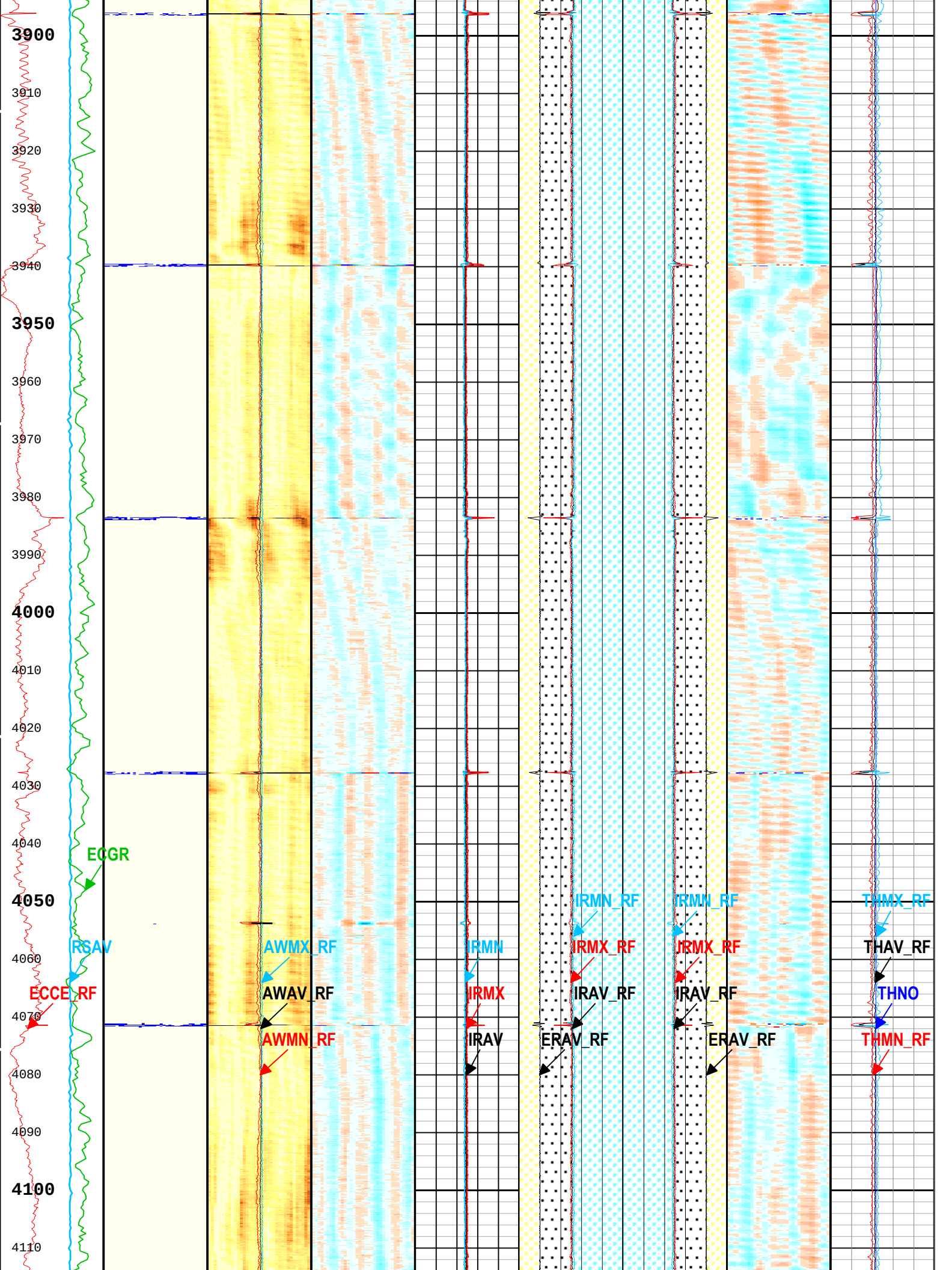
3900
3910
3920
3930
3940
3950
3960
3970
3980
3990
4000
4010
4020
4030
4040
4050
4060
4070
4080
4090
4100
4110
ECGR
RSAV
ECCE_RF
AWMX_RF
AWAV_RF
AWMN_RF
IRMN
IRMX
IRAV
IRMN_RF
IRMX_RF
IRAV_RF
ERAV_RF
IRMN_RF
IRMX_RF
IRAV_RF
ERAV_RF
THMX_RF
THAV_RF
THNO
THMN_RF

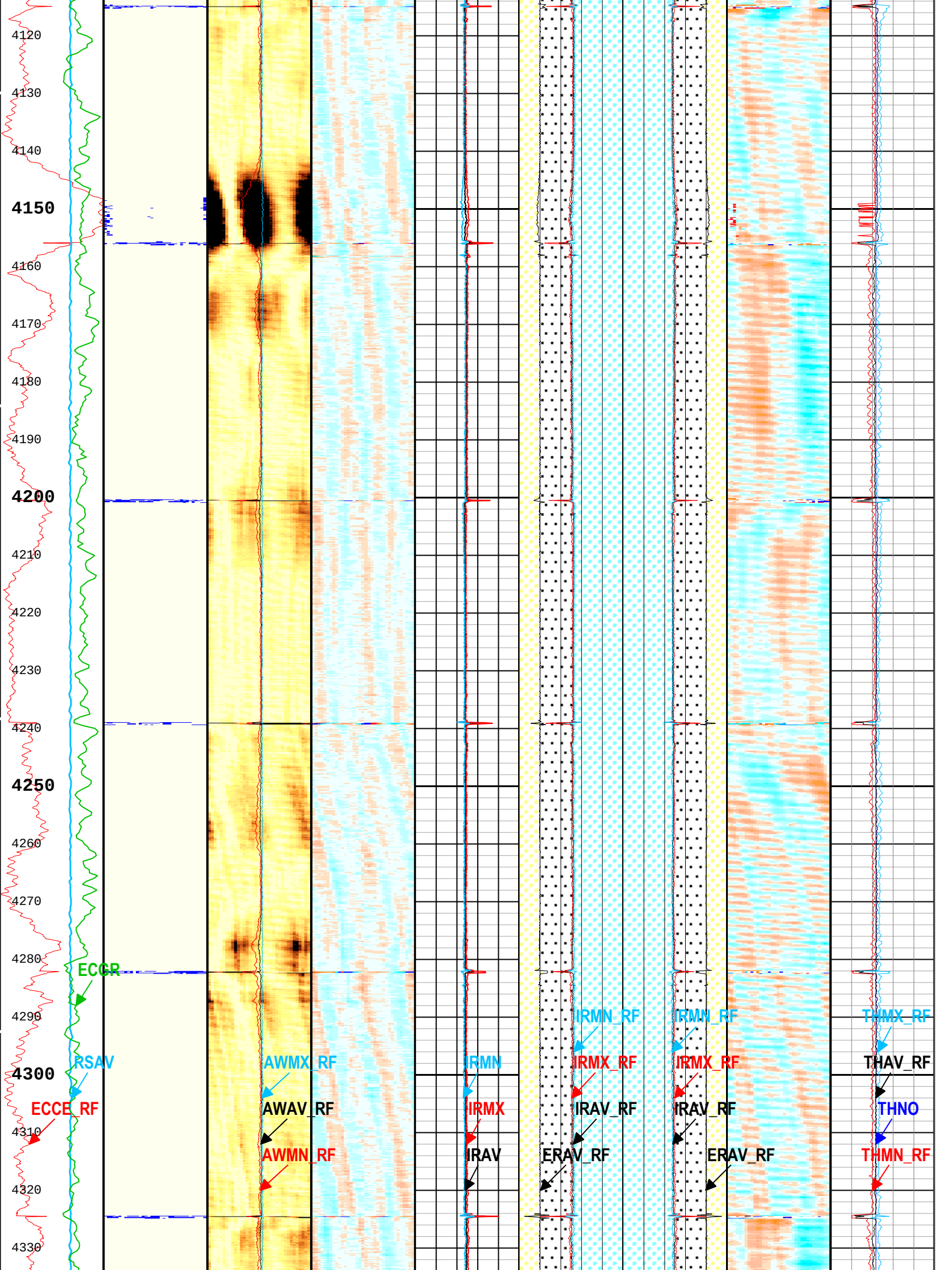
4120
4130
4140
4150
4160
4170
4180
4190
4200
4210
4220
4230
4240
4250
4260
4270
4280
4290
4300
4310
4320
4330
ECCR
RSAV
ECCE_RF
AWMX_RF
AWAV_RF
AWMN_RF
IRMN
IRMX
IRAV
IRMN_RF
IRMX_RF
IRAV_RF
ERAV_RF
IRMN_RF
IRMX_RF
IRAV_RF
ERAV_RF
THMX_RF
THAV_RF
THNO
THMN_RF

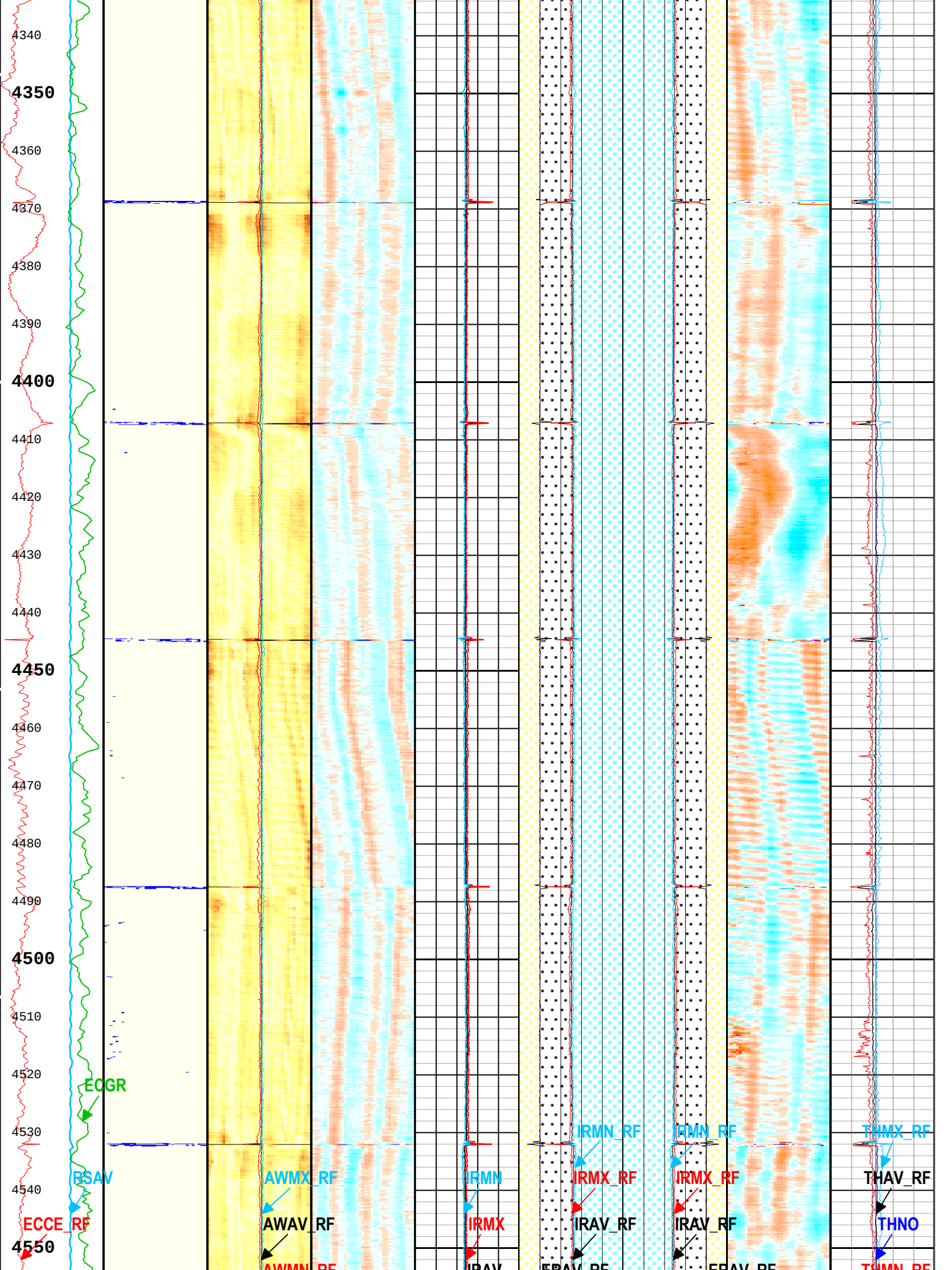
4340
4350
4360
4370
4380
4390
4400
4410
4420
4430
4440
4450
4460
4470
4480
4490
4500
4510
4520
4530
4540
4550
ECGR
RSAV
ECCE_RF
AWMX_RF
AWAV_RF
AWMN_RF
IRMN
IRMX
IRAV
IRMN_RF
IRMX_RF
IRAV_RF
IRMN_RF
IRMX_RF
IRAV_RF
THMX_RF
THAV_RF
THNO
THMN_RF

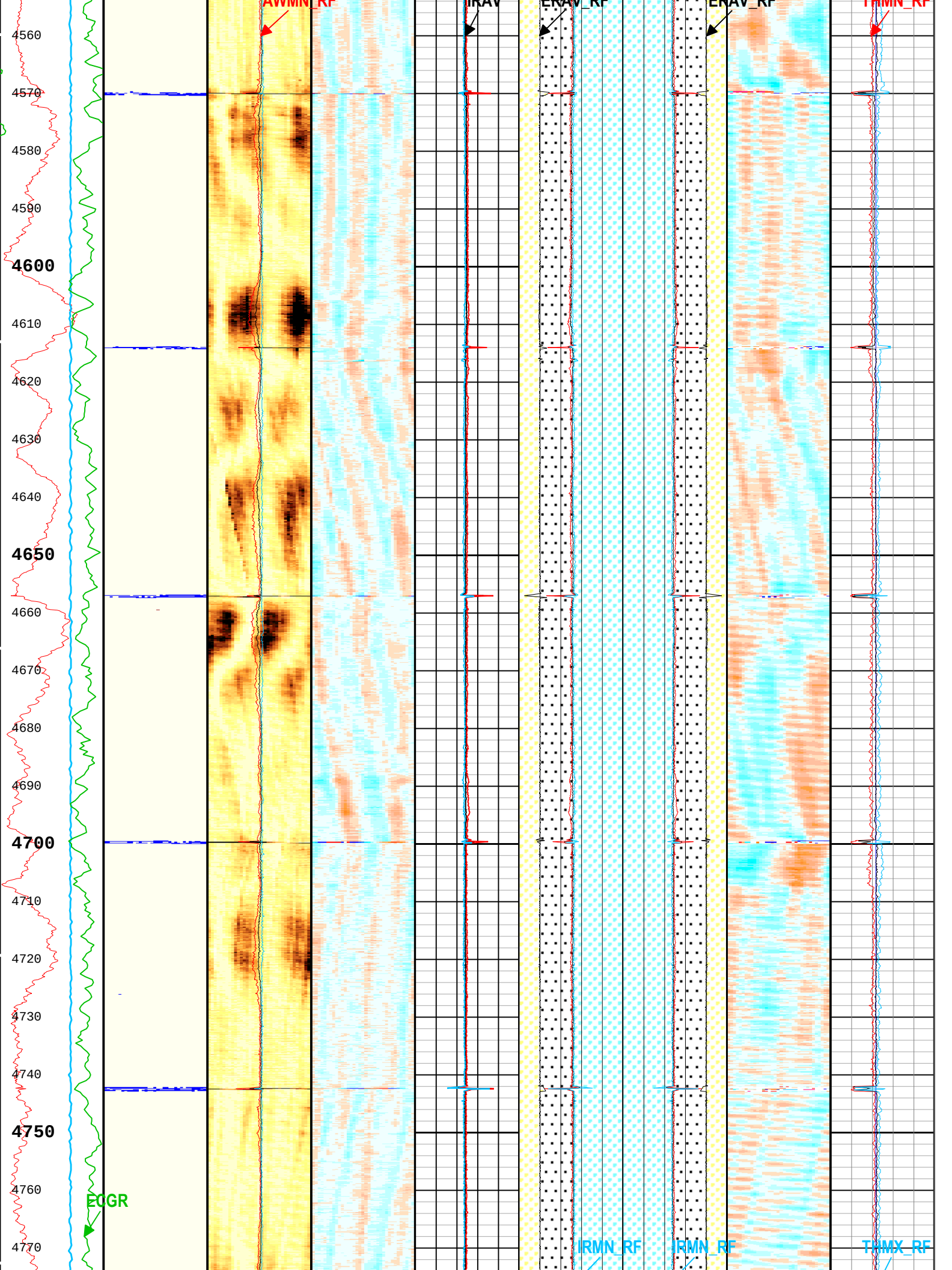
AWMN_RF
IRAV
ERAV_RF
ERAV_RF
TRMN_RF
4560
4570
4580
4590
4600
4610
4620
4630
4640
4650
4660
4670
4680
4690
4700
4710
4720
4730
4740
4750
4760
4770
ECGR
IRMN_RF
RMN_RF
TRMX_RF

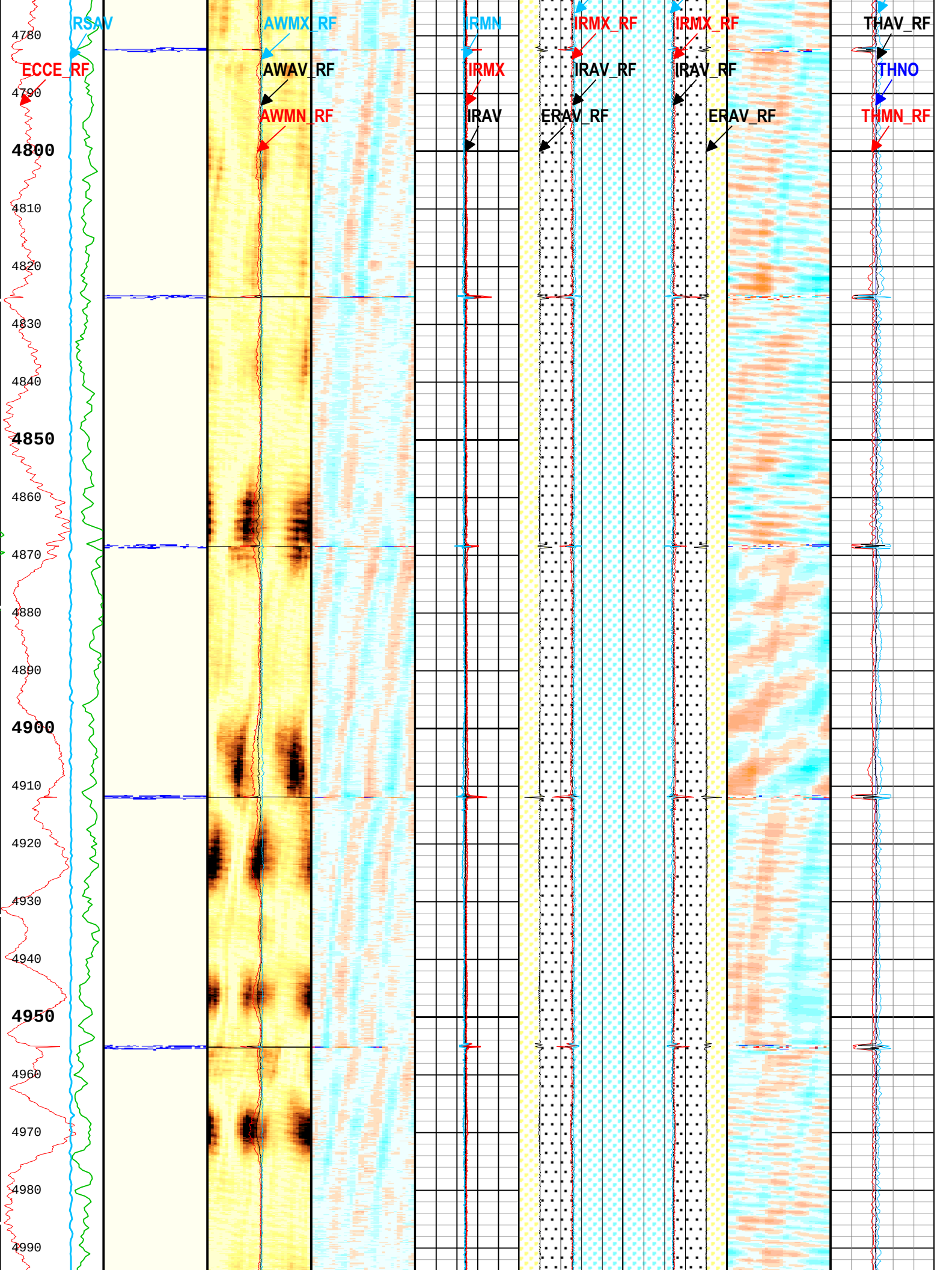
RSAV
ECCE_RF
AWMX_RF
AWAV_RF
AWMN_RF
IRMN
IRMX
IRAV
IRMX_RF
IRAV_RF
ERAV_RF
IRMX_RF
IRAV_RF
ERAV_RF
THAV_RF
THNO
THMN_RF
4780
4790
4800
4810
4820
4830
4840
4850
4860
4870
4880
4890
4900
4910
4920
4930
4940
4950
4960
4970
4980
4990

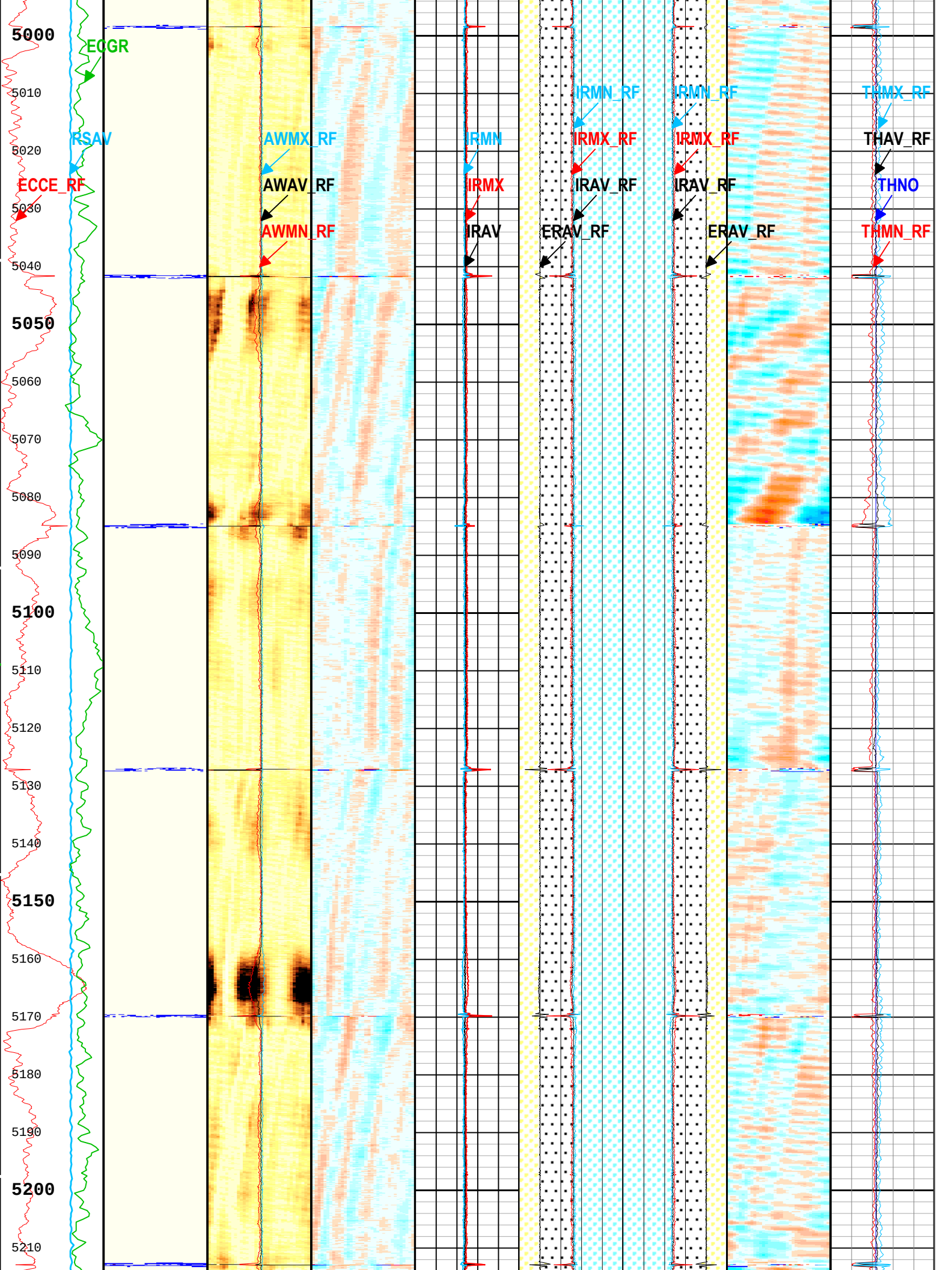
5000
5010
5020
5030
5040
5050
5060
5070
5080
5090
5100
5110
5120
5130
5140
5150
5160
5170
5180
5190
5200
5210
ECGR
RSAV
ECCE_RF
AWMX_RF
AWAV_RF
AWMN_RF
IRMN
IRMX
IRAV
IRMN_RF
IRMX_RF
IRAV_RF
ERAV_RF
IRMN_RF
IRMX_RF
IRAV_RF
ERAV_RF
THMX_RF
THAV_RF
THNO
THMN_RF

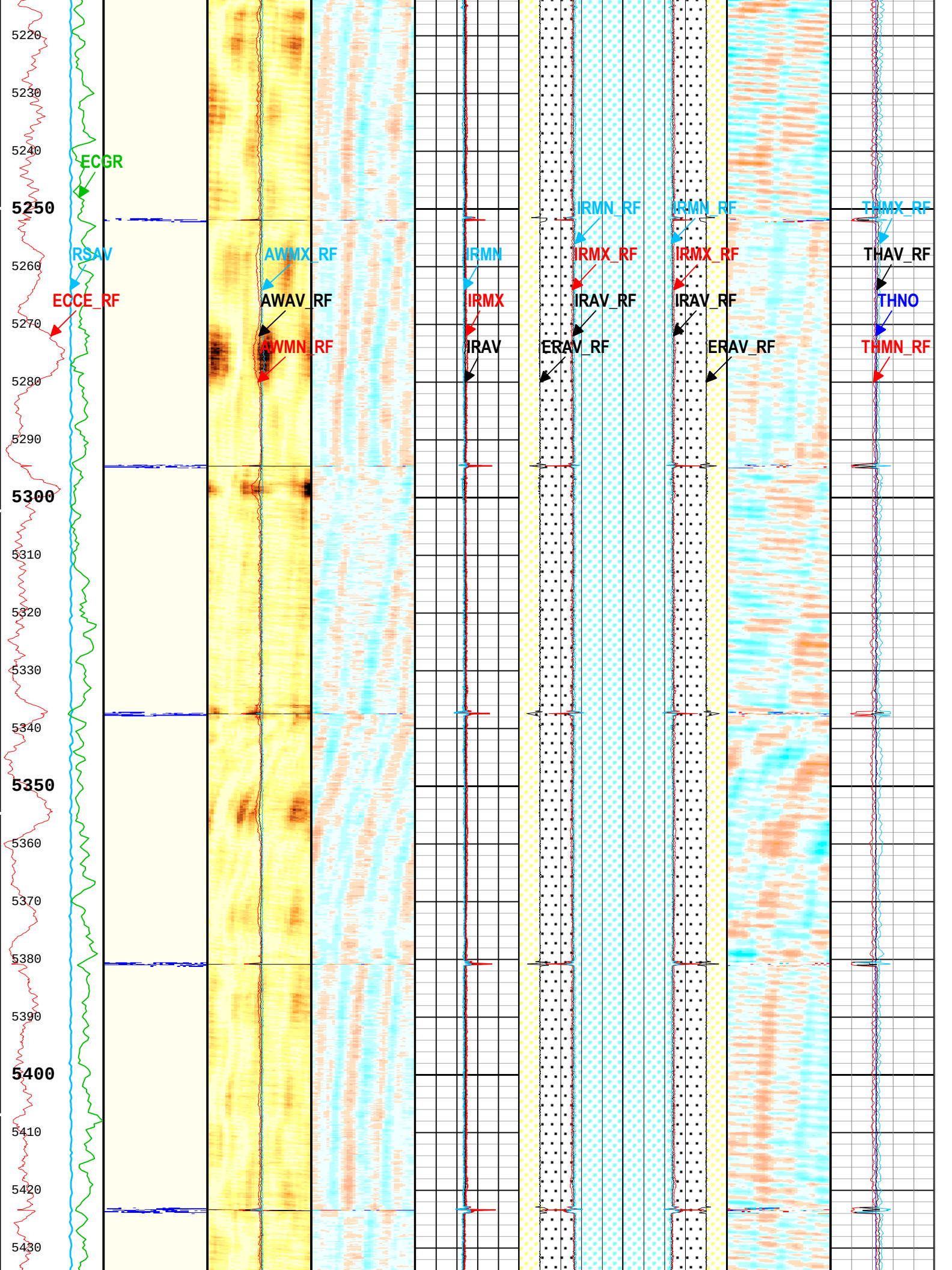
5220
5230
5240
5250
5260
5270
5280
5290
5300
5310
5320
5330
5340
5350
5360
5370
5380
5390
5400
5410
5420
5430
ECGR
RSAV
ECCE_RF
AWMX_RF
AWAV_RF
AWMN_RF
IRMN
IRMX
IRAV
IRMN_RF
IRMX_RF
IRAV_RF
ERAV_RF
IRMN_RF
IRMX_RF
IRAV_RF
ERAV_RF
THMX_RF
THAV_RF
THNO
THMN_RF

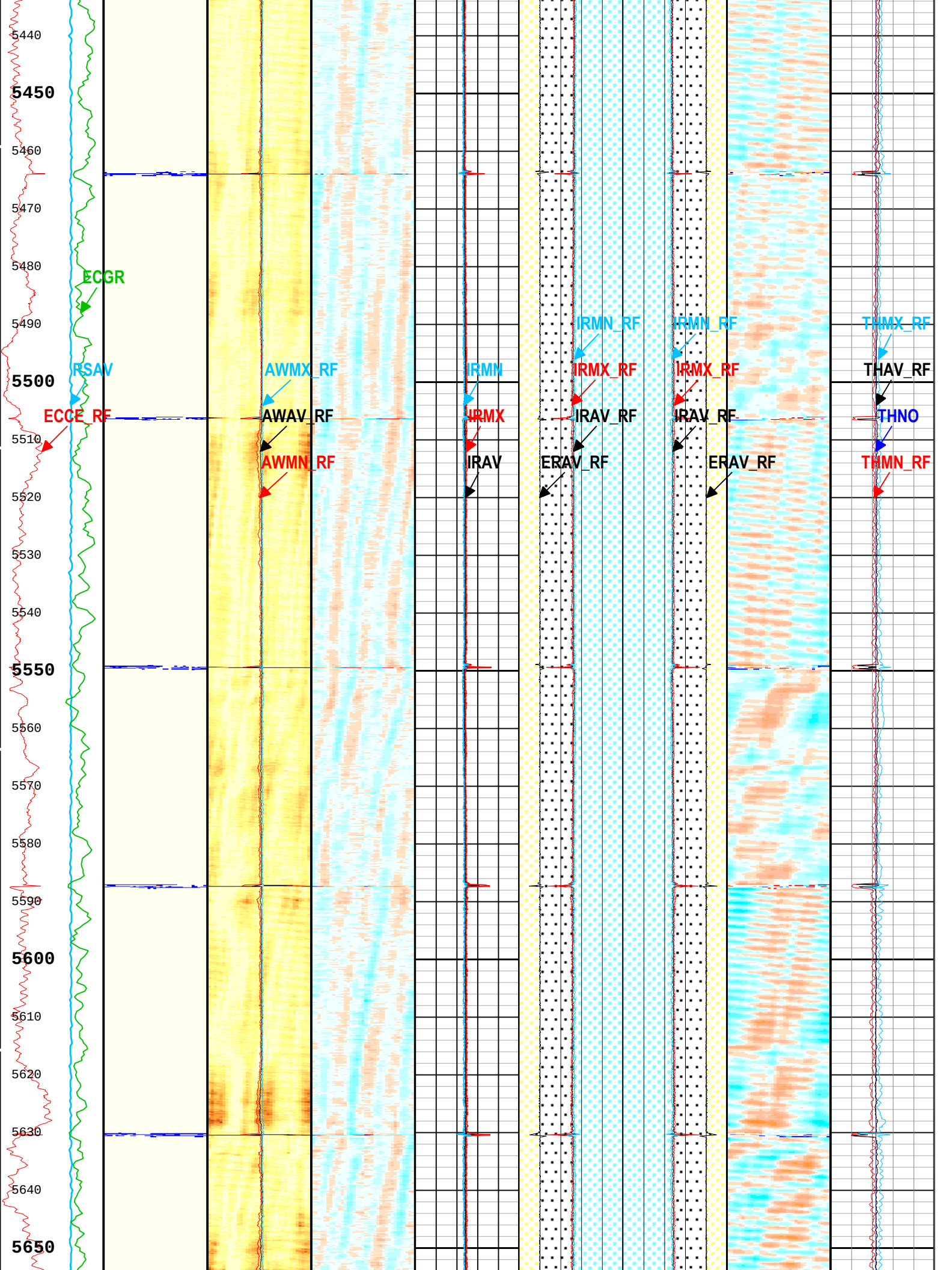
5440
5450
5460
5470
5480
5490
5500
5510
5520
5530
5540
5550
5560
5570
5580
5590
5600
5610
5620
5630
5640
5650
ECGR
RSAV
ECCE_RF
AWMX_RF
AWAV_RF
AWMN_RF
IRMN
IRMX
IRAV
IRMN_RF
IRMX_RF
IRAV_RF
ERAV_RF
IRMN_RF
IRMX_RF
IRAV_RF
ERAV_RF
THMX_RF
THAV_RF
THNO
THMN_RF

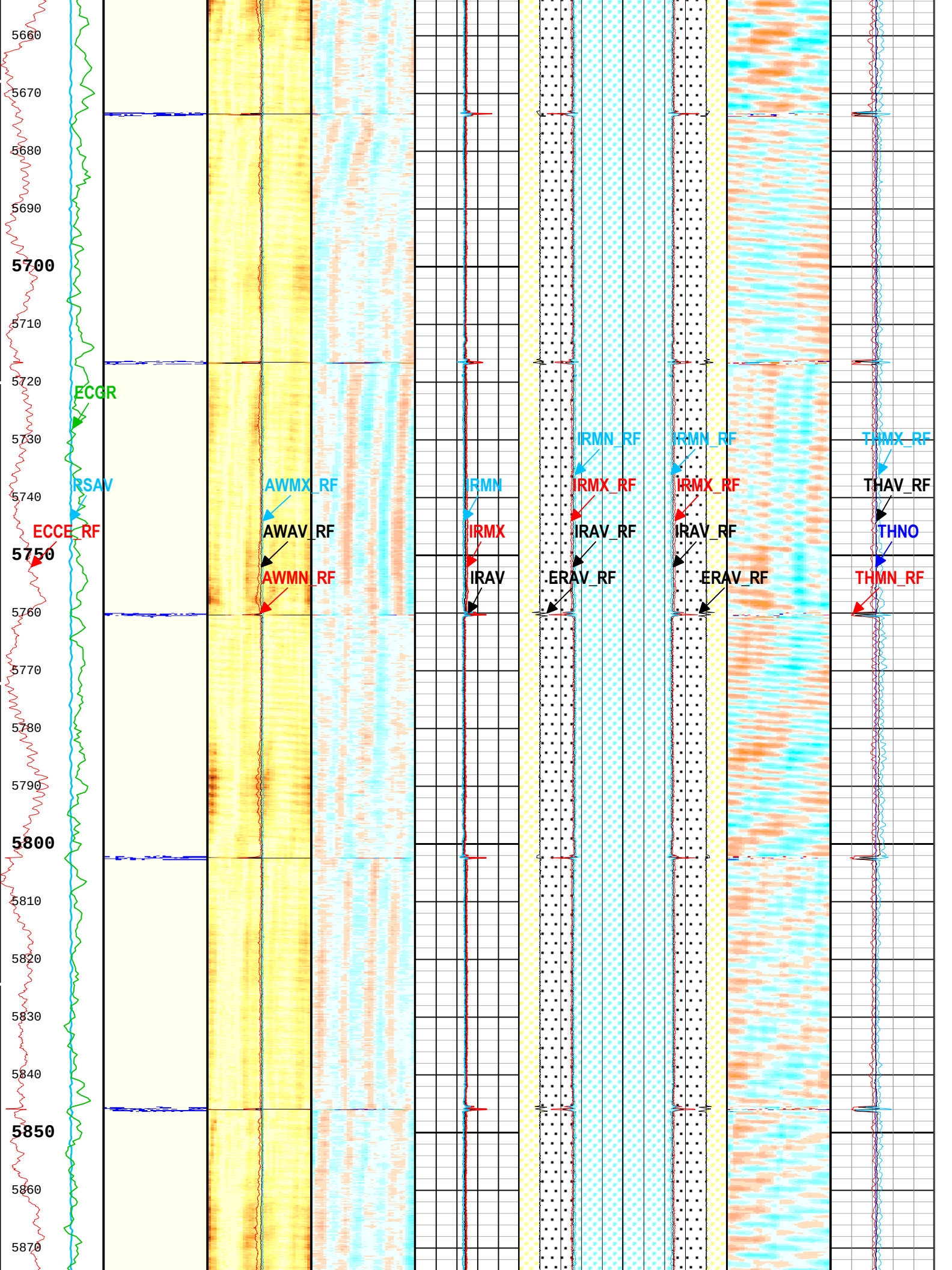
5660
5670
5680
5690
5700
5710
5720
5730
5740
5750
5760
5770
5780
5790
5800
5810
5820
5830
5840
5850
5860
5870
ECGR
RSAV
ECCE_RF
AWMX_RF
AWAV_RF
AWMN_RF
IRMN
IRMX
IRAV
IRMN_RF
IRMX_RF
IRAV_RF
ERAV_RF
IRMN_RF
IRMX_RF
IRAV_RF
ERAV_RF
THMX_RF
THAV_RF
THNO
THMN_RF

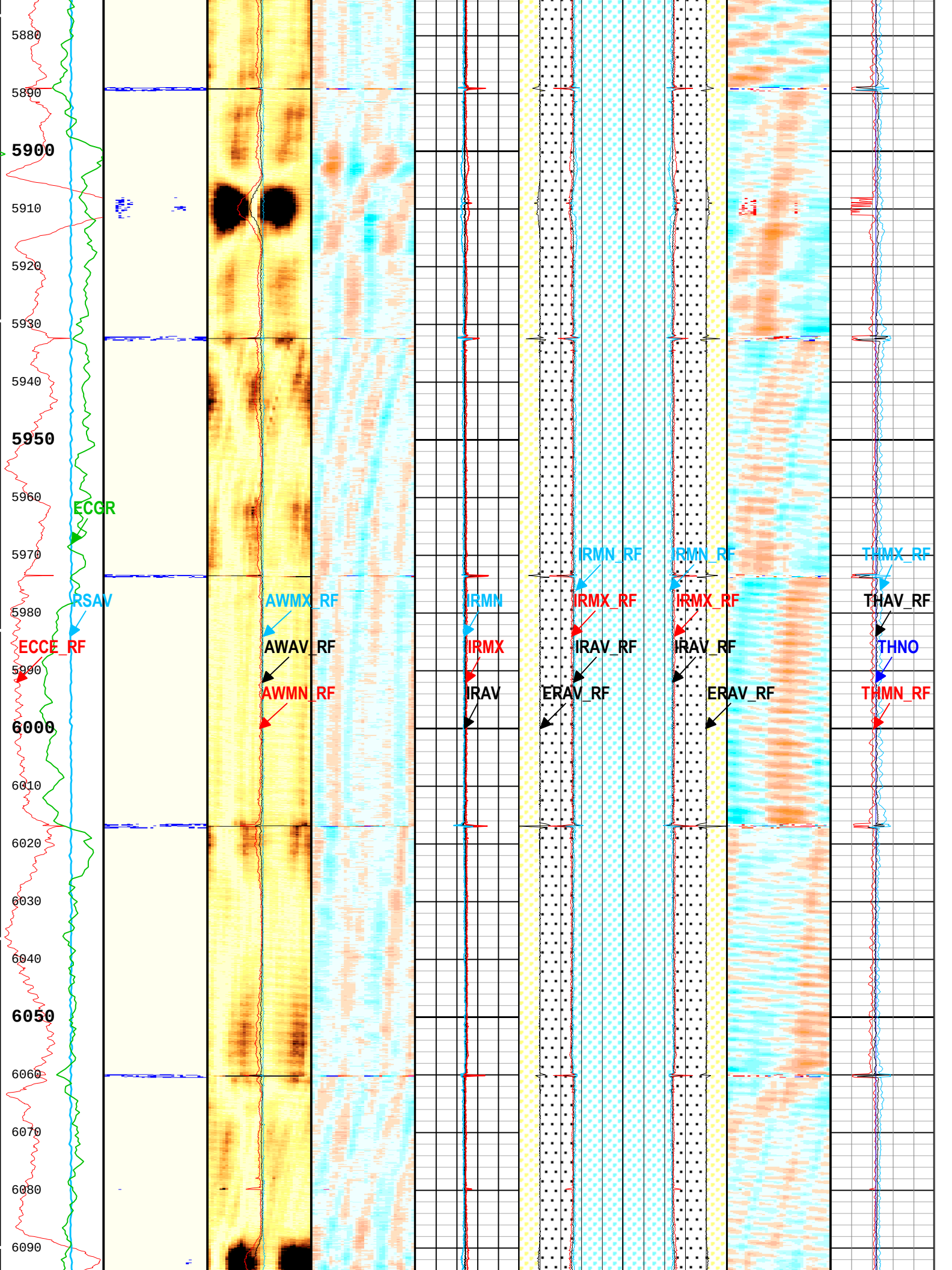
5880
5890
5900
5910
5920
5930
5940
5950
5960
5970
5980
5990
6000
6010
6020
6030
6040
6050
6060
6070
6080
6090
ECGR
RSAV
ECCE_RF
AWMX_RF
AWAV_RF
AWMN_RF
IRMN
IRMX
IRAV
IRMN_RF
IRMX_RF
IRAV_RF
ERAV_RF
IRMN_RF
IRMX_RF
IRAV_RF
ERAV_RF
THMX_RF
THAV_RF
THNO
THMN_RF

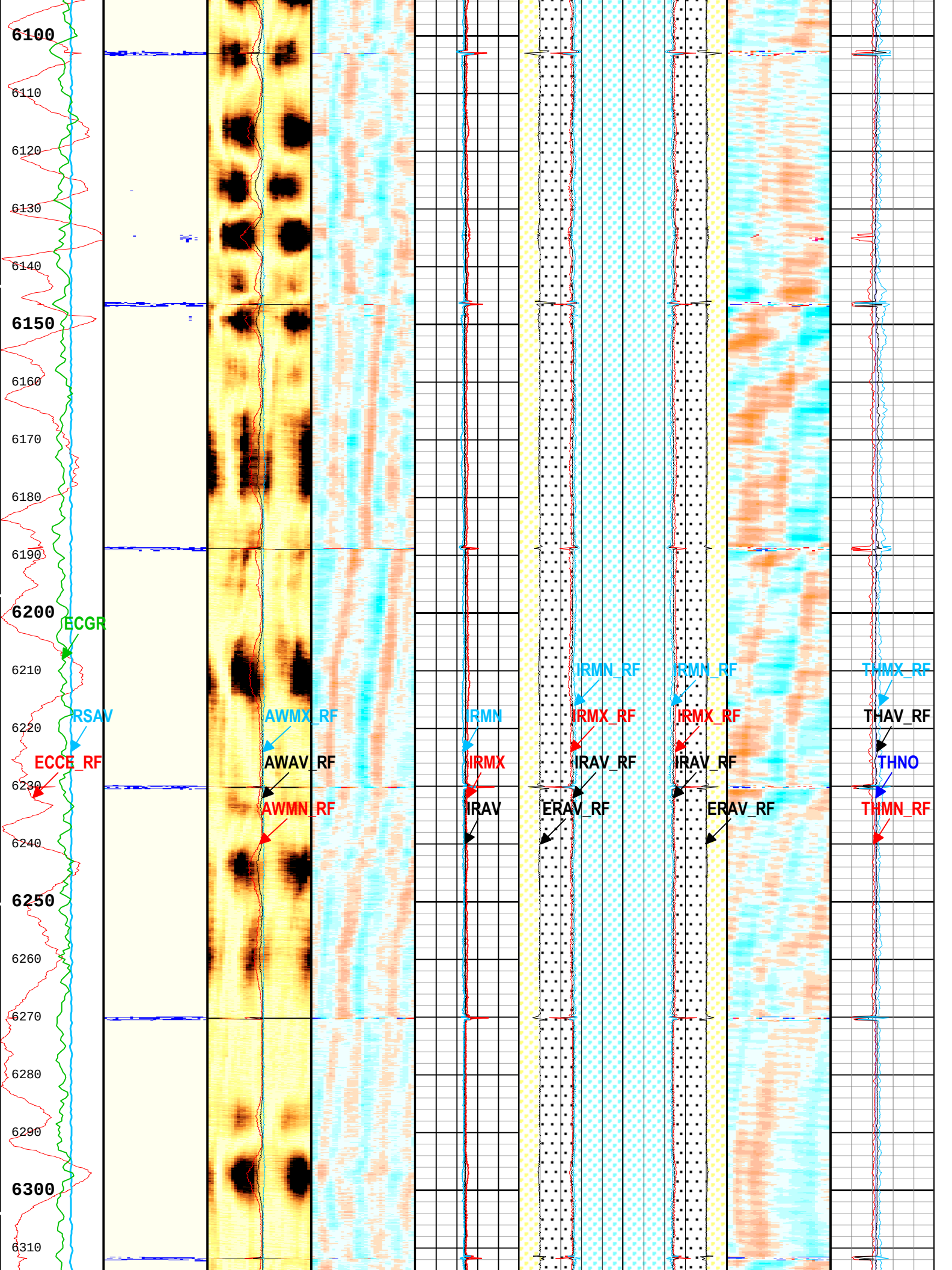
6100
6110
6120
6130
6140
6150
6160
6170
6180
6190
6200
6210
6220
6230
6240
6250
6260
6270
6280
6290
6300
6310
ECGR
RSAV
ECCE_RF
AWMX_RF
AWAV_RF
AWMN_RF
IRMN
IRMX
IRAV
IRMN_RF
IRMX_RF
IRAV_RF
ERAV_RF
IRMN_RF
IRMX_RF
IRAV_RF
ERAV_RF
THMX_RF
THAV_RF
THNO
THMN_RF

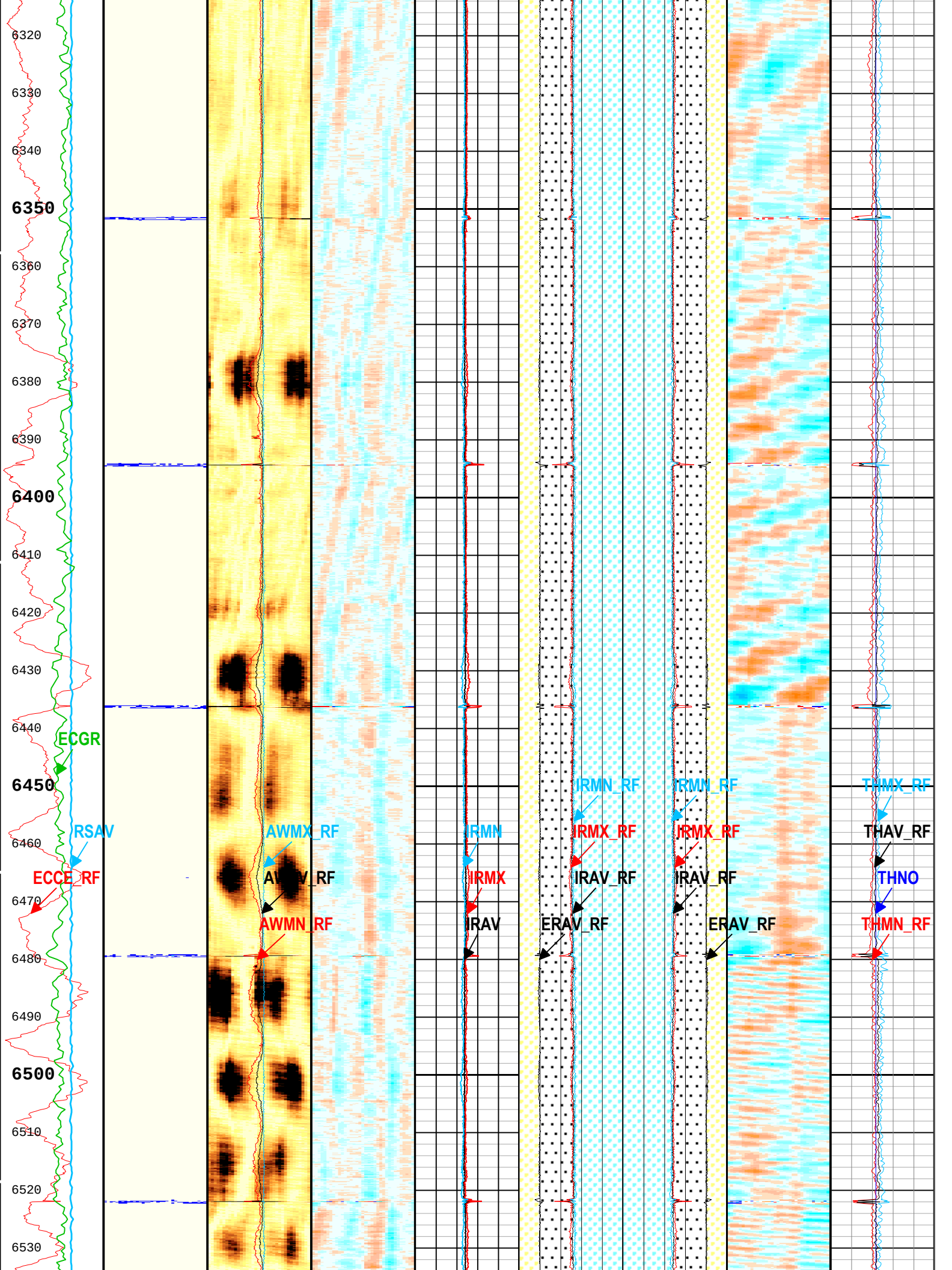
6320
6330
6340
6350
6360
6370
6380
6390
6400
6410
6420
6430
6440
6450
6460
6470
6480
6490
6500
6510
6520
6530
ECGR
RSAV
ECCE_RF
AWMX_RF
AWMN_RF
IRMN
IRMX
IRAV
IRMN_RF
IRMX_RF
IRAV_RF
ERAV_RF
IRMN_RF
IRMX_RF
IRAV_RF
ERAV_RF
THMX_RF
THAV_RF
THNO
THMN_RF

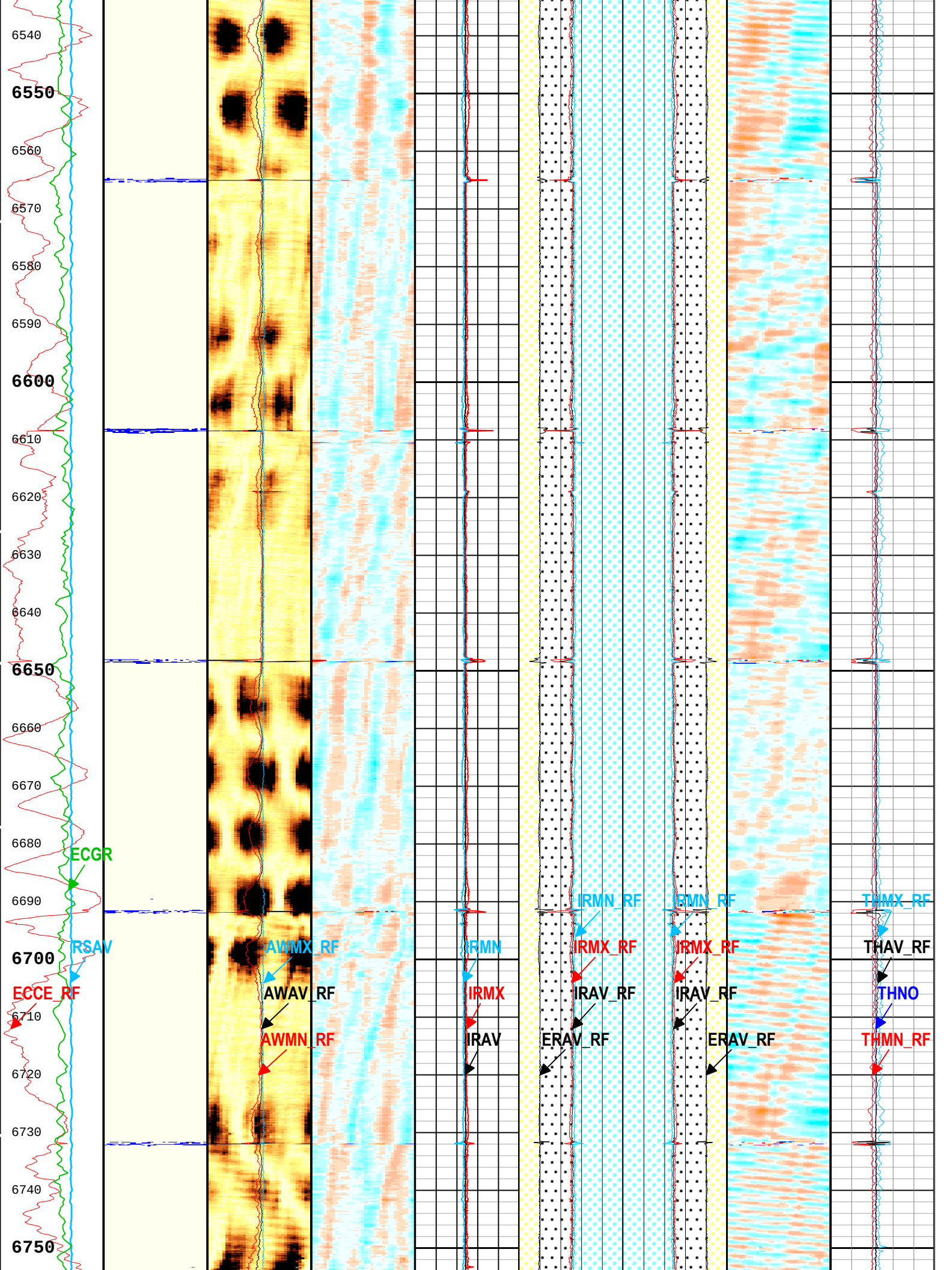
6540
6550
6560
6570
6580
6590
6600
6610
6620
6630
6640
6650
6660
6670
6680
6690
6700
6710
6720
6730
6740
6750
ECGR
RSAV
ECCE_RF
AWMX_RF
AWAV_RF
AWMN_RF
IRMN
IRMX
IRAV
IRMN_RF
IRMX_RF
IRAV_RF
ERAV_RF
IRMX_RF
IRAV_RF
ERAV_RF
THMX_RF
THAV_RF
THNO
THMN_RF

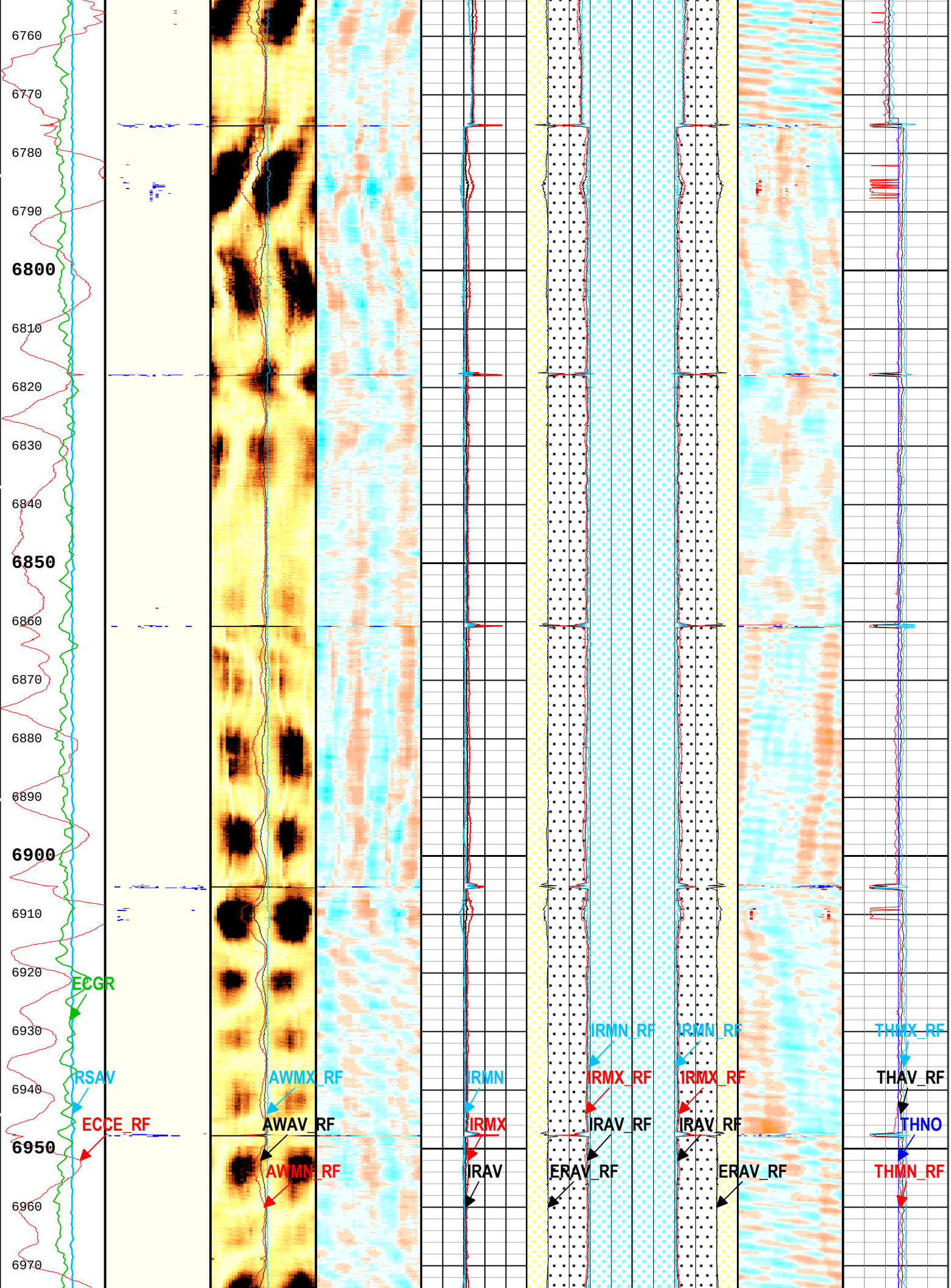
6760
6770
6780
6790
6800
6810
6820
6830
6840
6850
6860
6870
6880
6890
6900
6910
6920
6930
6940
6950
6960
6970
ECGR
RSAV
ECCE_RF
AWMX_RF
AWAV_RF
AWMN_RF
IRMN
IRMX
IRAV
IRMN_RF
IRMX_RF
IRAV_RF
ERAV_RF
IRMN_RF
IRMX_RF
IRAV_RF
ERAV_RF
THMX_RF
THAV_RF
THNO
THMN_RF

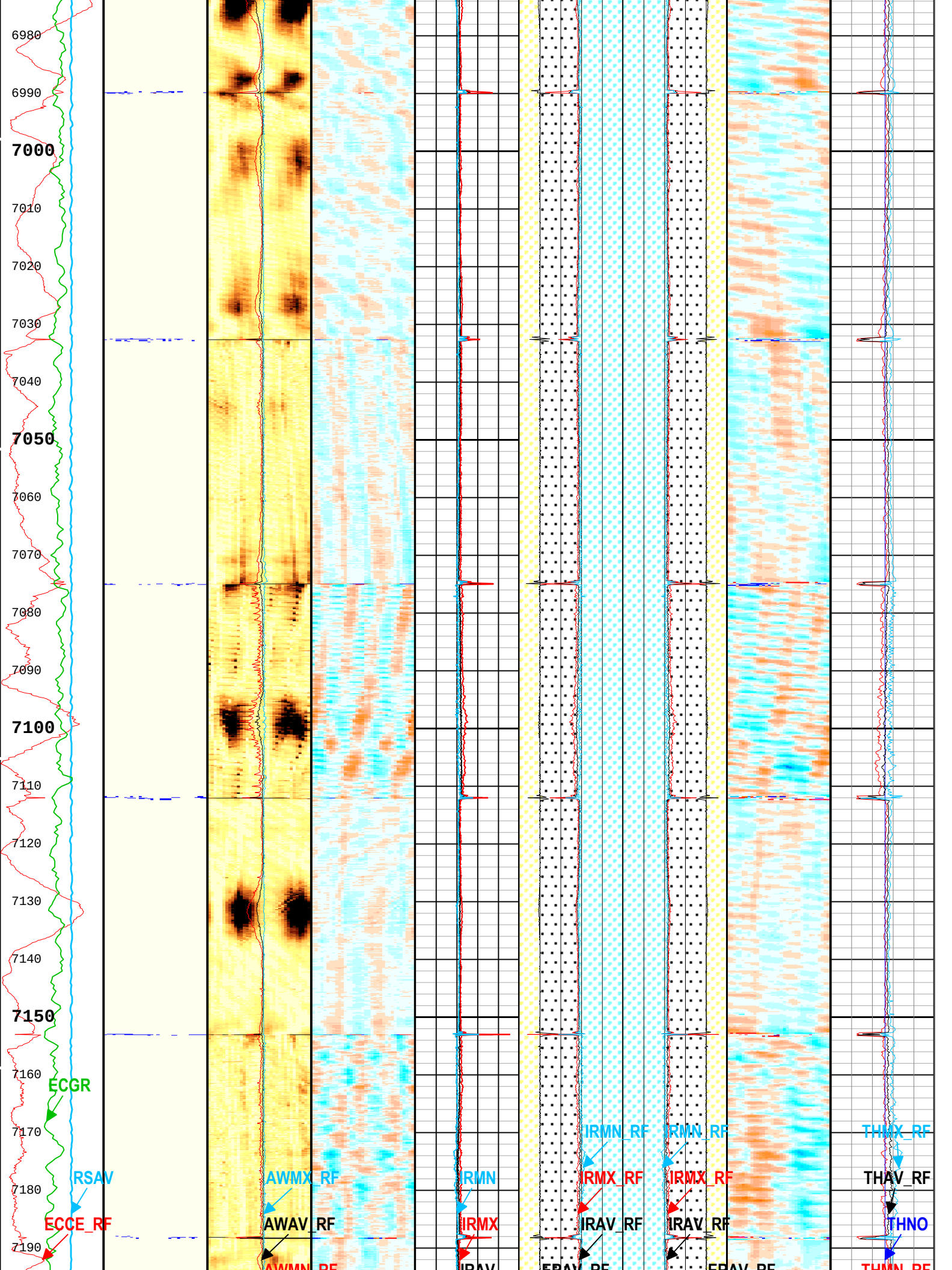
6980
6990
7000
7010
7020
7030
7040
7050
7060
7070
7080
7090
7100
7110
7120
7130
7140
7150
7160
7170
7180
7190
ECGR
RSAV
ECCE_RF
AWMX_RF
AWAV_RF
AWMN_RF
IRMN
IRMX
IRAV
IRMN_RF
IRMX_RF
IRAV_RF
IRMN_RF
IRMX_RF
IRAV_RF
THMX_RF
THAV_RF
THNO
THMN_RF

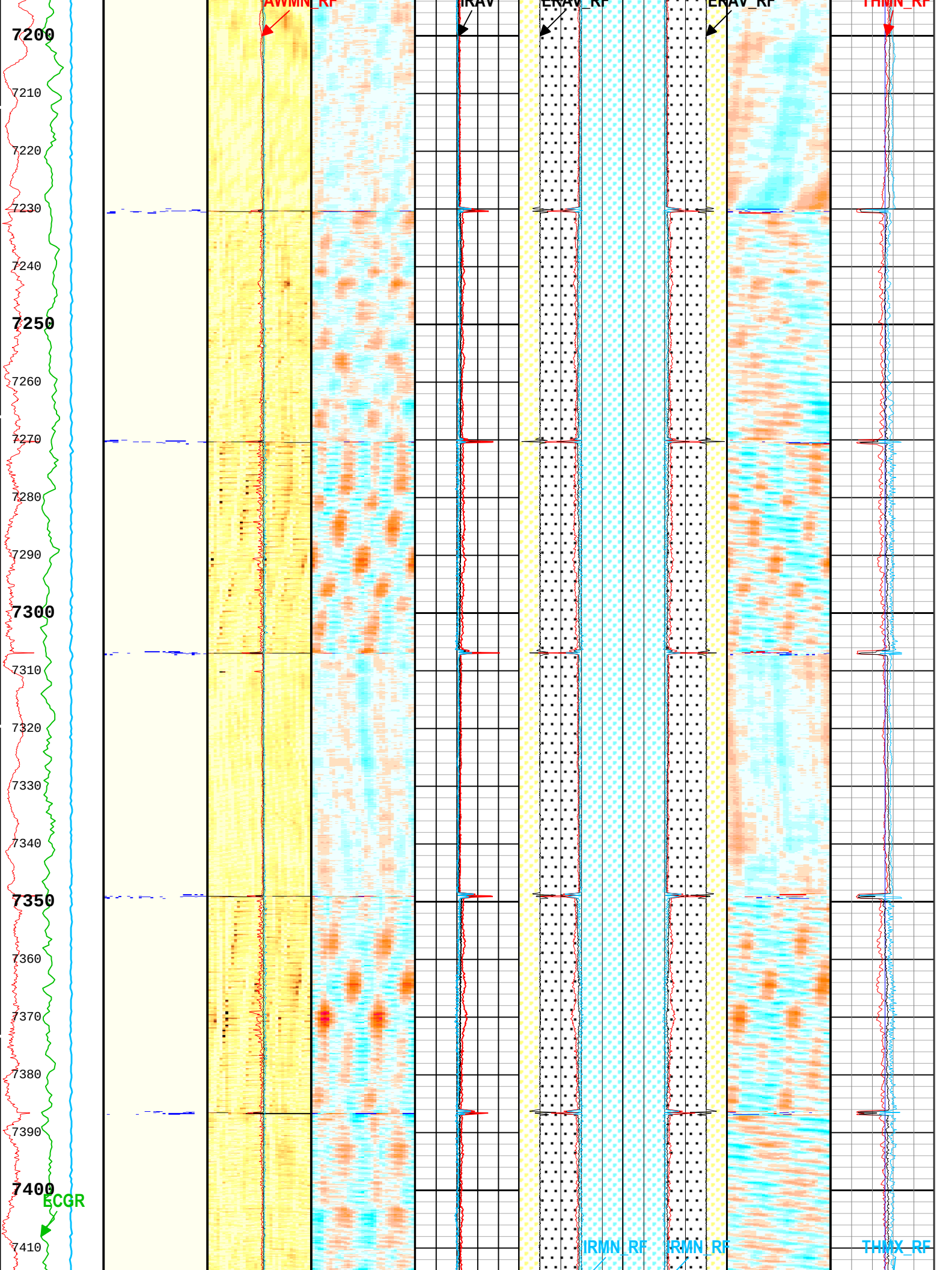
AWMN_RF
IRAV
ERAV_RF
ERAV_RF
THMN_RF
7200
7210
7220
7230
7240
7250
7260
7270
7280
7290
7300
7310
7320
7330
7340
7350
7360
7370
7380
7390
7400
ECGR
7410
IRMN_RF
IRMN_RF
THMX_RF

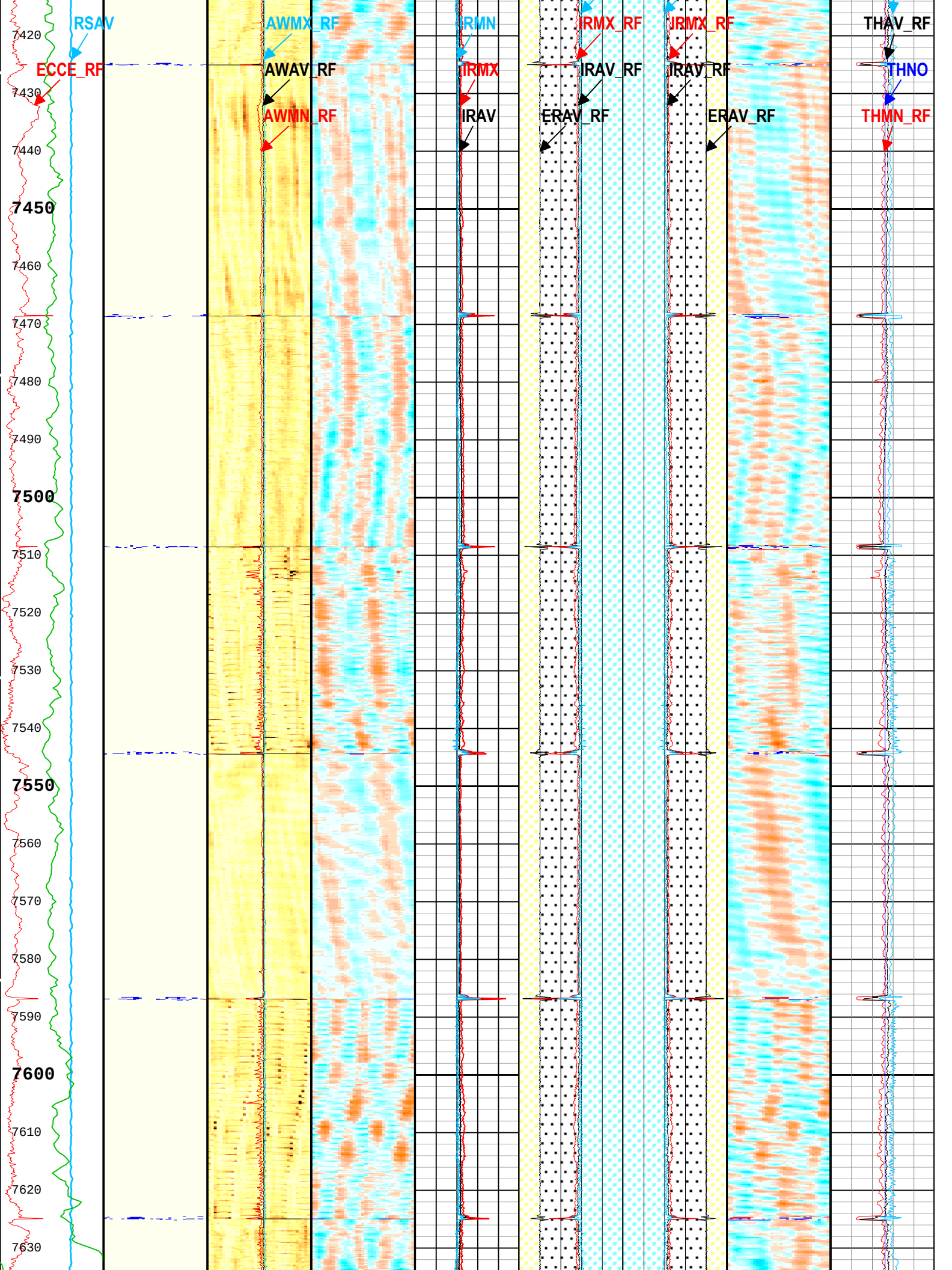
RSAV
ECCE_RF
AWMX_RF
AWAV_RF
AWMN_RF
IRMN
IRMX
IRAV
IRMX_RF
IRAV_RF
ERAV_RF
IRMX_RF
IRAV_RF
ERAV_RF
THAV_RF
THNO
THMN_RF
7420
7430
7440
7450
7460
7470
7480
7490
7500
7510
7520
7530
7540
7550
7560
7570
7580
7590
7600
7610
7620
7630

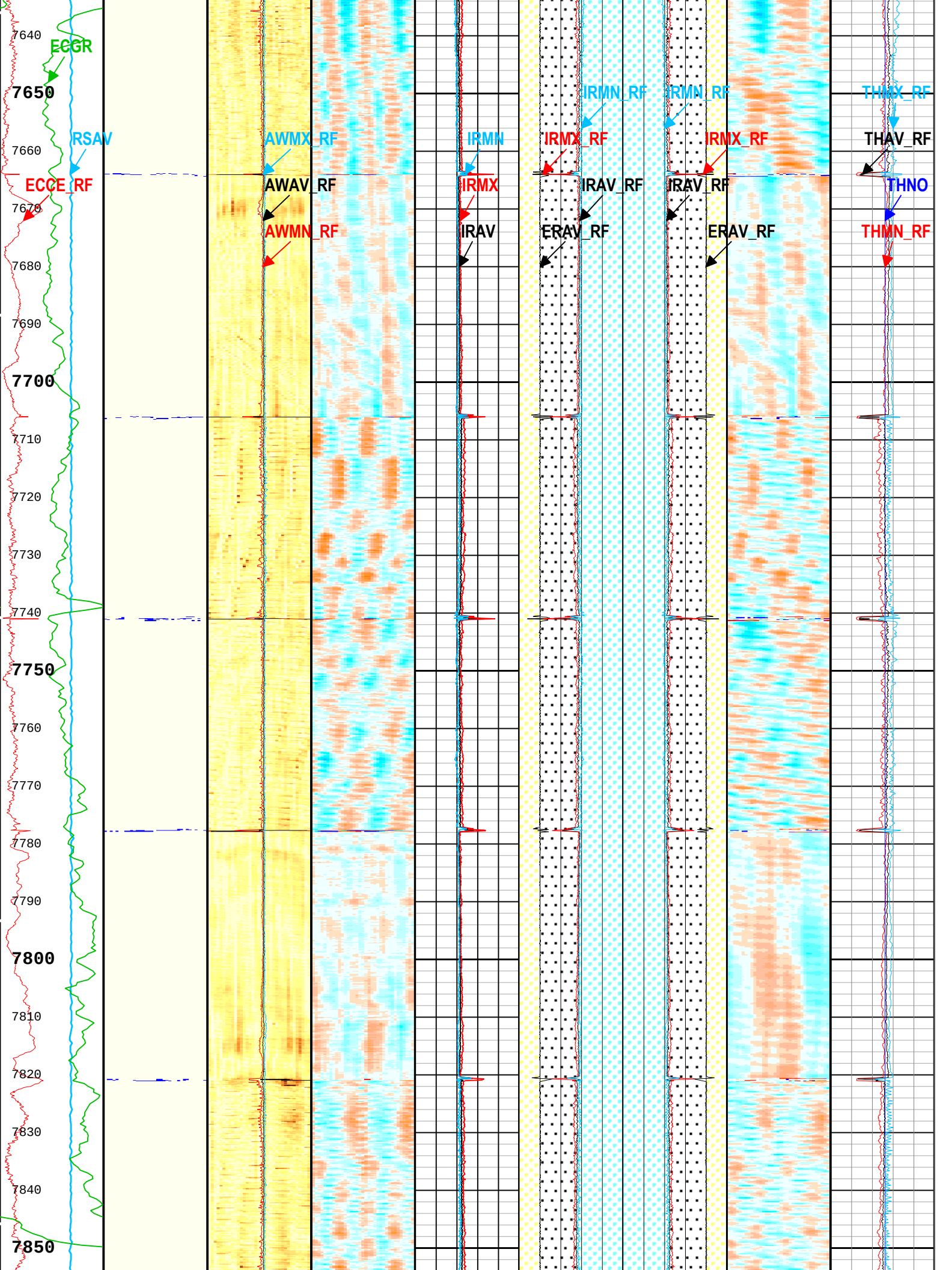
ECGR
RSAV
ECCE_RF
AWMX_RF
AWAV_RF
AWMN_RF
IRMN
IRMX
IRAV
IRMN_RF
IRMX_RF
IRAV_RF
ERAV_RF
IRMN_RF
IRMX_RF
IRAV_RF
ERAV_RF
THMX_RF
THAV_RF
THNO
THMN_RF
7640
7650
7660
7670
7680
7690
7700
7710
7720
7730
7740
7750
7760
7770
7780
7790
7800
7810
7820
7830
7840
7850

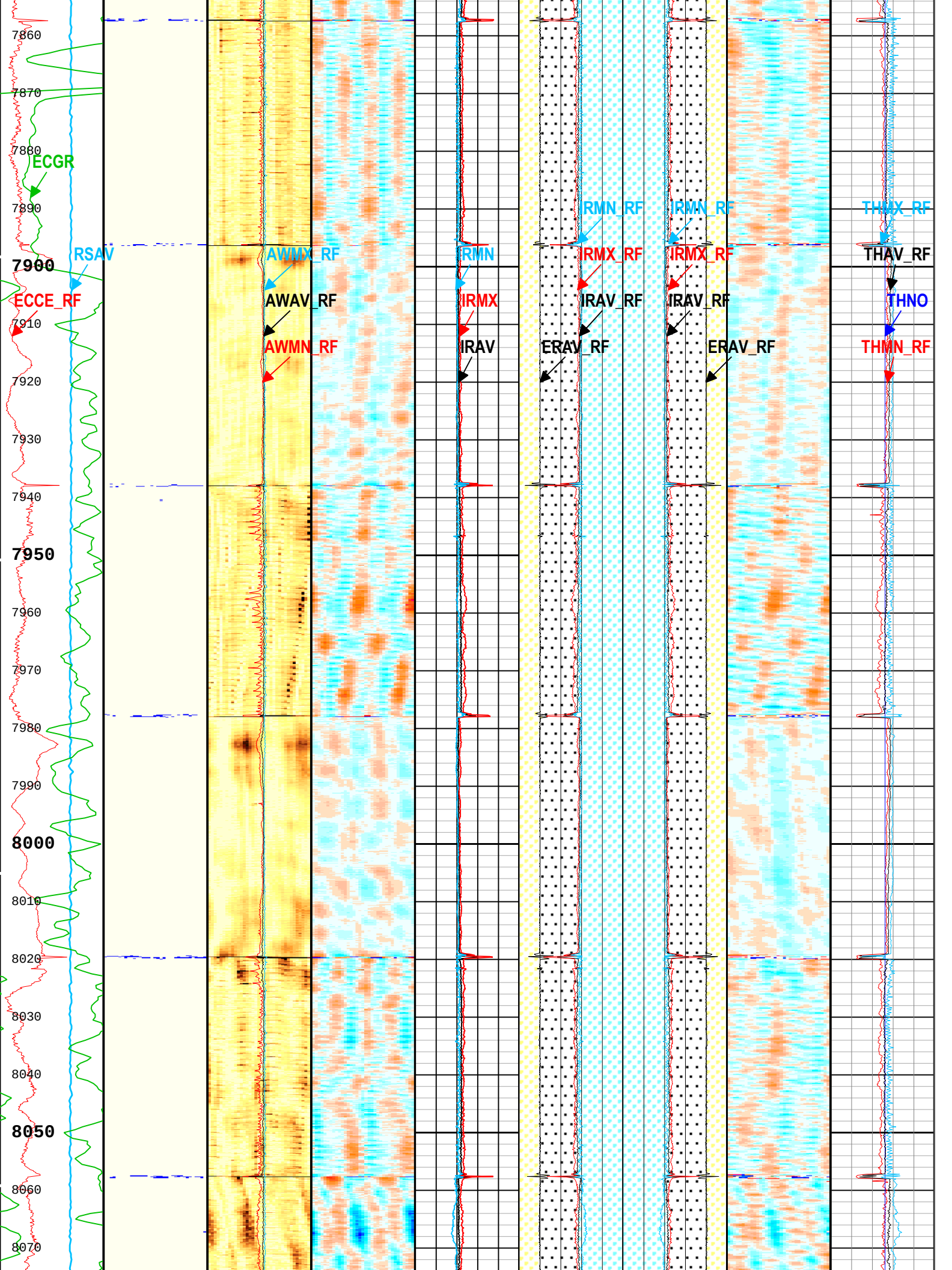
7860
7870
7880
7890
7900
7910
7920
7930
7940
7950
7960
7970
7980
7990
8000
8010
8020
8030
8040
8050
8060
8070
ECGR
RSAV
ECCE_RF
AWMX_RF
AWAV_RF
AWMN_RF
IRMN
IRMX
IRAV
IRMN_RF
IRMX_RF
IRAV_RF
ERAV_RF
IRMN_RF
IRMX_RF
IRAV_RF
ERAV_RF
THMX_RF
THAV_RF
THNO
THMN_RF

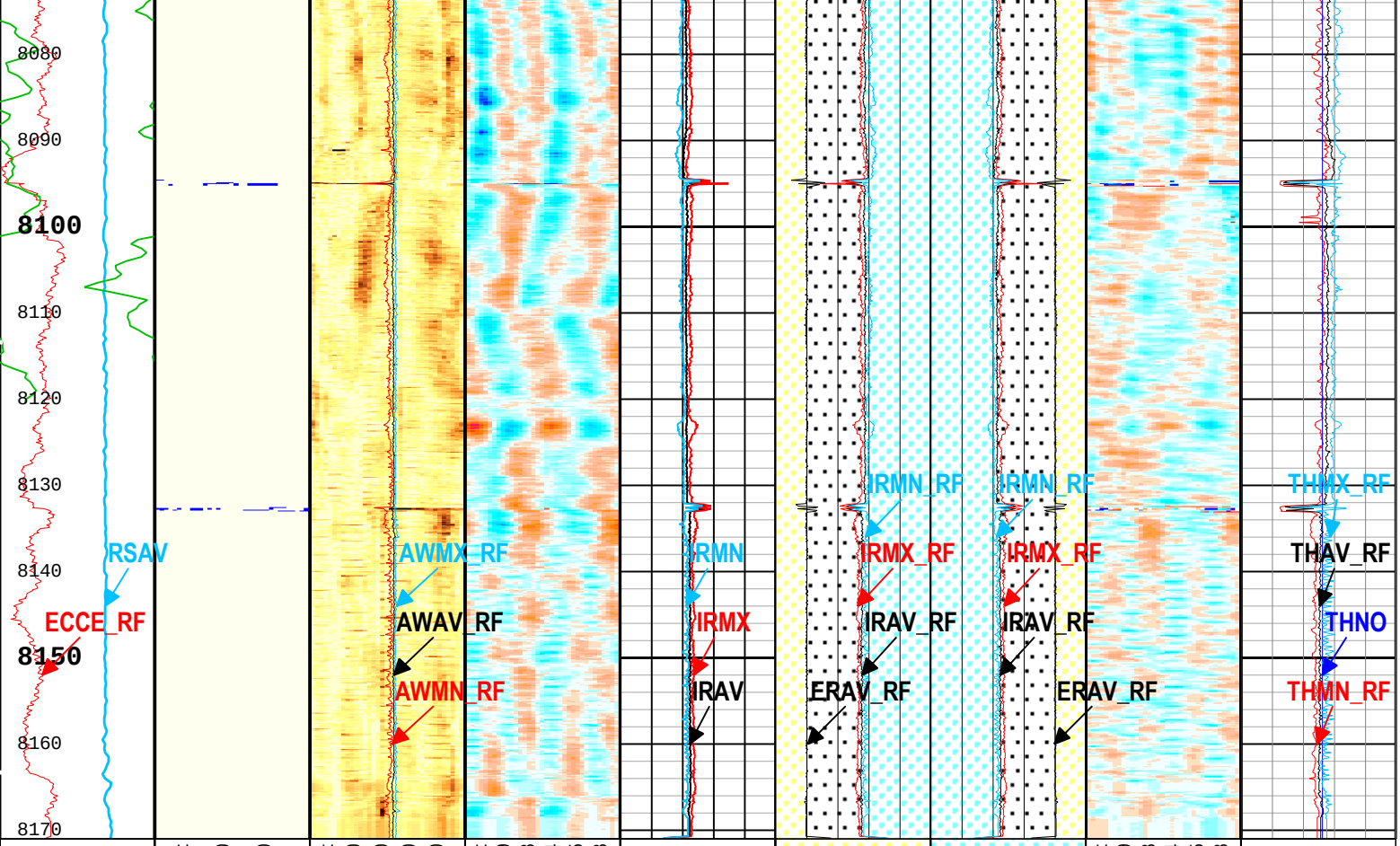

Amplitude of Eccentering for Unflagged Waves (ECCE_RF) USIT-E[1]
0 in 0.5

Motor Revolution Speed (RSAV) USIT-E[1]
6 c/s 8

Gamma Ray (ECGR) HGNS[1]
0 gAPI 150

Absent 1.500 3.500
Explicit Normalization
USIT - USIT Processing Flags (UFLG) USIT-E[1]

USIT Processing Flags (UFLG[0]) USIT-E[1]
1 5

Absent -5.200 -3.600 -2.000 -0.400
Explicit Normalization
USIT - Amplitude of Unflagged Wave (AWBK_RF) USIT-E[1] (dB)

Minimum of Unflagged Wave Amplitude (AWMN_RF) USIT-E[1]
0 dB 75

Average of Unflagged Wave Amplitude (AWAV_RF) USIT-E[1]
0 dB 75

Maximum of Unflagged Wave Amplitude (AWMX_RF) USIT-E[1]
0 dB 75

Absent -0.059 -0.028 0.004 0.035 0.068
Explicit Normalization
USIT - Unflagged Internal Radii minus Median Internal Radius (IRBKM_RF) USIT-E[1] (in)

Internal Radius Averaged Value (IRAV) USIT-E[1]
2.7 in 3.7

Internal Radius Maximum Value (IRMX) USIT-E[1]
2.7 in 3.7

Internal Radius Minimum Value (IRMN) USIT-E[1]
2.7 in 3.7

ERAV | IRAV
ERAV-IRAV | ERAV
IRAV | IRAV-ERAV

Median of Unflagged External Radii (ERAV_RF) USIT-E[1]
3.7 in 2.7

Median of Unflagged External Radii (ERAV_RF) USIT-E[1]
2.7 in 3.7

Median Internal Radius of Casing Corrected for Eccentering (IRAV_RF) USIT-E[1]
3.7 in 2.7

Median Internal Radius of Casing Corrected for Eccentering (IRAV_RF) USIT-E[1]
2.7 in 3.7

Maximum of Unflagged Internal Radii (IRMX_RF) USIT-E[1]
3.7 in 2.7

Maximum of Unflagged Internal Radii (IRMX_RF) USIT-E[1]
2.7 in 3.7

Minimum of Unflagged Internal Radii (IRMN_RF) USIT-E[1]
3.7 in 2.7

Minimum of Unflagged Internal Radii (IRMN_RF) USIT-E[1]
2.7 in 3.7

Absent -0.059 -0.028 0.004 0.035 0.068
Explicit Normalization
USIT - Unflagged Casing Thickness minus Median of Unflagged Casing Thickness (THBKM_RF) USIT-E[1] (in)

Minimum of Unflagged Casing Thickness (THMN_RF) USIT-E[1]
0.1 in 0.6

Nominal Casing Thickness (THNO) USIT-E[1]
0.1 in 0.6

Median of Unflagged Casing Thickness (THAV_RF) USIT-E[1]
0.1 in 0.6

Maximum of Unflagged Casing Thickness (THMX_RF) USIT-E[1]
0.1 in 0.6

5.7 in 2.7 | 2.7 in 5.7

USIT Processing Flags (UFLG[0]) USIT-E[1]

1 - UFLG 1 Value within [0.0 - 1.5] - :	UTIM Error
2 - UFLG 2 Value within [1.5 - 2.5] - :	Pulse Origin Not Detected
3 - UFLG 3 Value within [2.5 - 3.5] - :	WINLEN Error
4 - UFLG 4 UFLG 5 UFLG 6 Value within [3.5 - 6.5] - :	Casing Thickness Error
5 - UFLG 7 UFLG 8 UFLG 9 Value within [6.5 - 10] - :	Loop Processing Error

TIME_1900 - Time Marked every 60.00 (s)

Description: USI Composite Format: Log (LBV1_USI Corrosion 7inch) Index Scale: 5 in per 100 ft Index Unit: ft Index Type: Measured Depth Creation Date: 20-Oct-2016 14:28:48

Composite 1

USI Compressed Goodwin

Composite Summary

Run Name	Pass Objective	Direction	Top	Bottom	Start	Stop	DSC Mode	Depth Shift	Include Parallel Data
Two	Log[9]:Up	Up	6640.29 ft	8171.85 ft	20-Oct-2016 9:51:39 AM	20-Oct-2016 10:20:40 AM	ON	1.47 ft	No
Two	Log[11]:Up	Up	36.69 ft	6737.51 ft	20-Oct-2016 10:24:53 AM	20-Oct-2016 12:34:00 PM	ON	1.35 ft	No
Two	Log[14]:Up	Up	5.56 ft	155.15 ft	20-Oct-2016 12:53:24 PM	20-Oct-2016 12:58:23 PM	ON	1.96 ft	No

All depths are referenced to toolstring zero

Log

Company:Southern California Gas Company Well:Frew 4

Composite 1:S008

Description: USI Goodwin Format: Log (Import of USI Goodwin) Index Scale: 0.1 in per 100 ft Index Unit: ft Index Type: Measured Depth Creation Date: 20-Oct-2016 14:29:06

TIME_1900 - Time Marked every 60.00 (s)

Minimum Acoustic Impedance 1 (MIN_AI1) USIT-E[1]	Minimum Acoustic Impedance 3 (MIN_AI3) USIT-E[1]	Minimum Acoustic Impedance 5 (MIN_AI5) USIT-E[1]	Minimum Acoustic Impedance 7 (MIN_AI7) USIT-E[1]
0 Mrayl 10	0 Mrayl 10	0 Mrayl 10	0 Mrayl 10
Maximum Acoustic Impedance 1 (MAX_AI1) USIT-E[1]	Maximum Acoustic Impedance 3 (MAX_AI3) USIT-E[1]	Maximum Acoustic Impedance 5 (MAX_AI5) USIT-E[1]	Maximum Acoustic Impedance 7 (MAX_AI7) USIT-E[1]
0 Mrayl 10	0 Mrayl 10	0 Mrayl 10	0 Mrayl 10
Average Acoustic Impedance 1 (AV_AI1) USIT-E[1]	Average Acoustic Impedance 3 (AV_AI3) USIT-E[1]	Average Acoustic Impedance 5 (AV_AI5) USIT-E[1]	Average Acoustic Impedance 7 (AV_AI7) USIT-E[1]
0 Mrayl 10	0 Mrayl 10	0 Mrayl 10	0 Mrayl 10

Minimum Acoustic Impedance 2 (MIN_AI2) USIT-E[1]	Minimum Acoustic Impedance 4 (MIN_AI4) USIT-E[1]	Minimum Acoustic Impedance 6 (MIN_AI6) USIT-E[1]	Minimum Acoustic Impedance 8 (MIN_AI8) USIT-E[1]	Minimum Acoustic Impedance 9 (MIN_AI9) USIT-E[1]	Acoustic Impedance Minimum (AIMN) USIT-E[1]
0 Mrayl 10	0 Mrayl 10	0 Mrayl 10	0 Mrayl 10	0 Mrayl 10	-1 Mrayl 9
Maximum	Maximum	Maximum	Maximum	Maximum	Acoustic

GR

0 gAPI 150

-1000.000 3.090 5.054 7.018

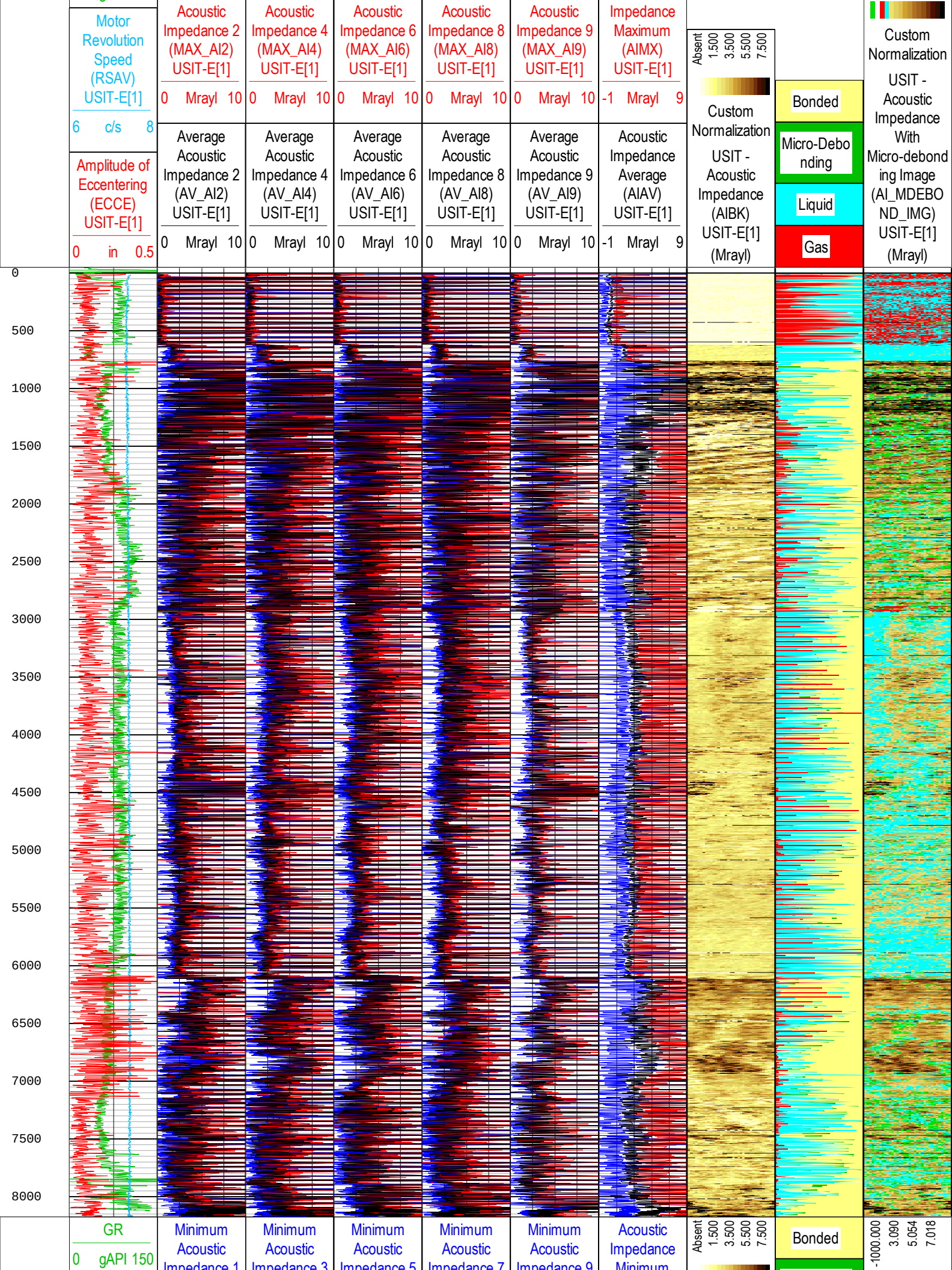
Motor Revolution Speed (RSAV) USIT-E[1]
6 c/s 8
Amplitude of Eccentering (ECCE) USIT-E[1]
0 in 0.5
Acoustic Impedance 2 (MAX_AI2) USIT-E[1]
0 Mrayl 10
Acoustic Impedance 4 (MAX_AI4) USIT-E[1]
0 Mrayl 10
Acoustic Impedance 6 (MAX_AI6) USIT-E[1]
0 Mrayl 10
Acoustic Impedance 8 (MAX_AI8) USIT-E[1]
0 Mrayl 10
Acoustic Impedance 9 (MAX_AI9) USIT-E[1]
0 Mrayl 10
Impedance Maximum (AIMX) USIT-E[1]
-1 Mrayl 9
Average Acoustic Impedance 2 (AV_AI2) USIT-E[1]
0 Mrayl 10
Average Acoustic Impedance 4 (AV_AI4) USIT-E[1]
0 Mrayl 10
Average Acoustic Impedance 6 (AV_AI6) USIT-E[1]
0 Mrayl 10
Average Acoustic Impedance 8 (AV_AI8) USIT-E[1]
0 Mrayl 10
Average Acoustic Impedance 9 (AV_AI9) USIT-E[1]
0 Mrayl 10
Acoustic Impedance Average (AIAV) USIT-E[1]
-1 Mrayl 9
Absent 1.500 3.500 5.500 7.500
Custom Normalization
USIT - Acoustic Impedance (AIBK) USIT-E[1] (Mrayl)
Bonded
Micro-Debonding
Liquid
Gas
Custom Normalization
USIT - Acoustic Impedance With Micro-debonding Image (AI_MDEBOND_IMG) USIT-E[1] (Mrayl)
0
500
1000
1500
2000
2500
3000
3500
4000
4500
5000
5500
6000
6500
7000
7500
8000
GR
0 gAPI 150
Minimum Acoustic Impedance 1
Minimum Acoustic Impedance 3
Minimum Acoustic Impedance 5
Minimum Acoustic Impedance 7
Minimum Acoustic Impedance 9
Acoustic Impedance Minimum
Absent 1.500 3.500 5.500 7.500
Bonded
-1000.000 3.090 5.054 7.018

Motor Revolution Speed (RSAV) USIT-E[1] 6 c/s 8	Impedance 1 (MIN_AI1) USIT-E[1] 0 Mrayl 10	Impedance 3 (MIN_AI3) USIT-E[1] 0 Mrayl 10	Impedance 5 (MIN_AI5) USIT-E[1] 0 Mrayl 10	Impedance 7 (MIN_AI7) USIT-E[1] 0 Mrayl 10	Impedance 9 (MIN_AI9) USIT-E[1] 0 Mrayl 10	Minimum (AIMN) USIT-E[1] -1 Mrayl 9
Amplitude of Eccentering (ECCE) USIT-E[1] 0 in 0.5	Maximum Acoustic Impedance 1 (MAX_AI1) USIT-E[1] 0 Mrayl 10	Maximum Acoustic Impedance 3 (MAX_AI3) USIT-E[1] 0 Mrayl 10	Maximum Acoustic Impedance 5 (MAX_AI5) USIT-E[1] 0 Mrayl 10	Maximum Acoustic Impedance 7 (MAX_AI7) USIT-E[1] 0 Mrayl 10	Maximum Acoustic Impedance 9 (MAX_AI9) USIT-E[1] 0 Mrayl 10	Acoustic Impedance Maximum (AIMX) USIT-E[1] -1 Mrayl 9
	Average Acoustic Impedance 1 (AV_AI1) USIT-E[1] 0 Mrayl 10	Average Acoustic Impedance 3 (AV_AI3) USIT-E[1] 0 Mrayl 10	Average Acoustic Impedance 5 (AV_AI5) USIT-E[1] 0 Mrayl 10	Average Acoustic Impedance 7 (AV_AI7) USIT-E[1] 0 Mrayl 10	Average Acoustic Impedance 9 (AV_AI9) USIT-E[1] 0 Mrayl 10	Acoustic Impedance Average (AIAV) USIT-E[1] -1 Mrayl 9
	Minimum Acoustic Impedance 2 (MIN_AI2) USIT-E[1] 0 Mrayl 10	Minimum Acoustic Impedance 4 (MIN_AI4) USIT-E[1] 0 Mrayl 10	Minimum Acoustic Impedance 6 (MIN_AI6) USIT-E[1] 0 Mrayl 10	Minimum Acoustic Impedance 8 (MIN_AI8) USIT-E[1] 0 Mrayl 10		
	Maximum Acoustic Impedance 2 (MAX_AI2) USIT-E[1] 0 Mrayl 10	Maximum Acoustic Impedance 4 (MAX_AI4) USIT-E[1] 0 Mrayl 10	Maximum Acoustic Impedance 6 (MAX_AI6) USIT-E[1] 0 Mrayl 10	Maximum Acoustic Impedance 8 (MAX_AI8) USIT-E[1] 0 Mrayl 10		
	Average Acoustic Impedance 2 (AV_AI2) USIT-E[1] 0 Mrayl 10	Average Acoustic Impedance 4 (AV_AI4) USIT-E[1] 0 Mrayl 10	Average Acoustic Impedance 6 (AV_AI6) USIT-E[1] 0 Mrayl 10	Average Acoustic Impedance 8 (AV_AI8) USIT-E[1] 0 Mrayl 10		

Custom Normalization USIT - Acoustic Impedance (AIBK) USIT-E[1] (Mrayl)

Micro-Debonding

Liquid

Gas

Custom Normalization USIT - Acoustic Impedance With Micro-debonding Image (AI_MDEBOND_IMG) USIT-E[1] (Mrayl)

TIME_1900 - Time Marked every 60.00 (s)

Description: USI Goodwin Format: Log (Import of USI Goodwin) Index Scale: 0.1 in per 100 ft Index Unit: ft Index Type: Measured Depth Creation Date: 20-Oct-2016 14:29:06

XYZ

Company:Southern California Gas Company Well:Frew 4
Composite 1:S008

Fluid Acoustic Slowness vs Depth

2D Cross Plot

Index Range: From 5.25 to 8171.50 ft

DEPTH-U-USIT_DFSL — — - DEPTH-CFVL
— — - DEPTH-FVEM (FVEM : Data Not Found)

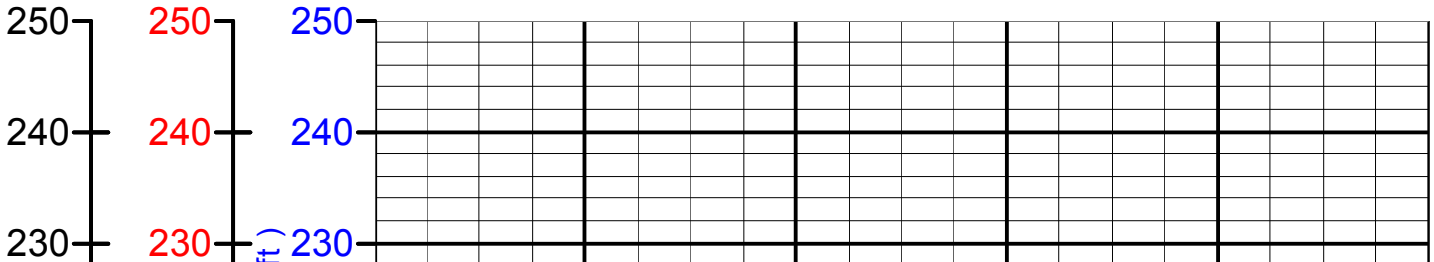

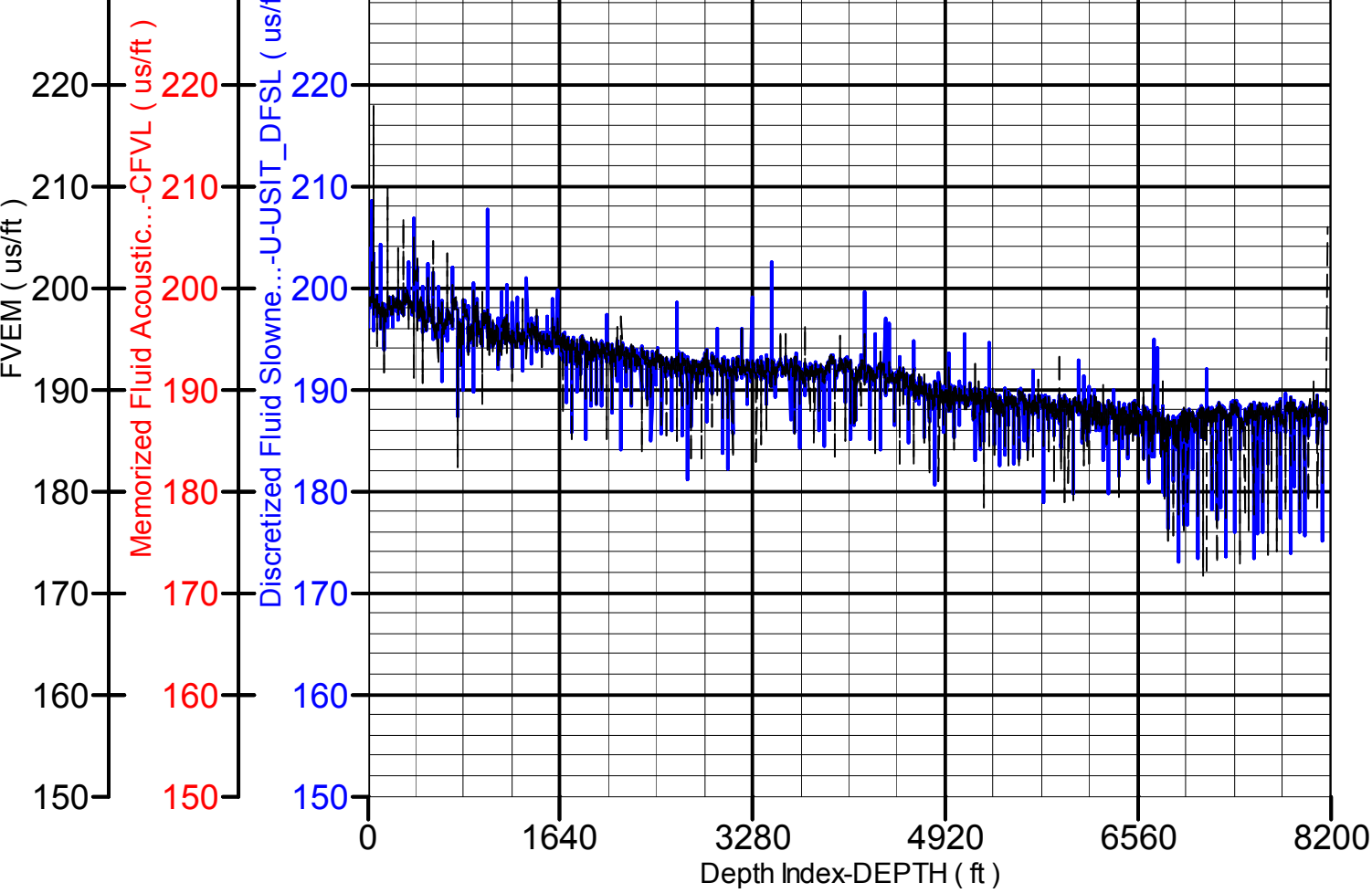

XYZ

Company:Southern California Gas Company Well:Frew 4
Composite 1:S008

Theoretical Acoustic Impedance of Mud vs Depth

2D Cross Plot

Index Range: From 5.25 to 8171.50 ft

DEPTH-CZMD
DEPTH-AIBH (AIBH : Data Not Found)
DEPTH-AIBL (AIBL : Data Not Found)
DEPTH-AIBM (AIBM : Data Not Found)

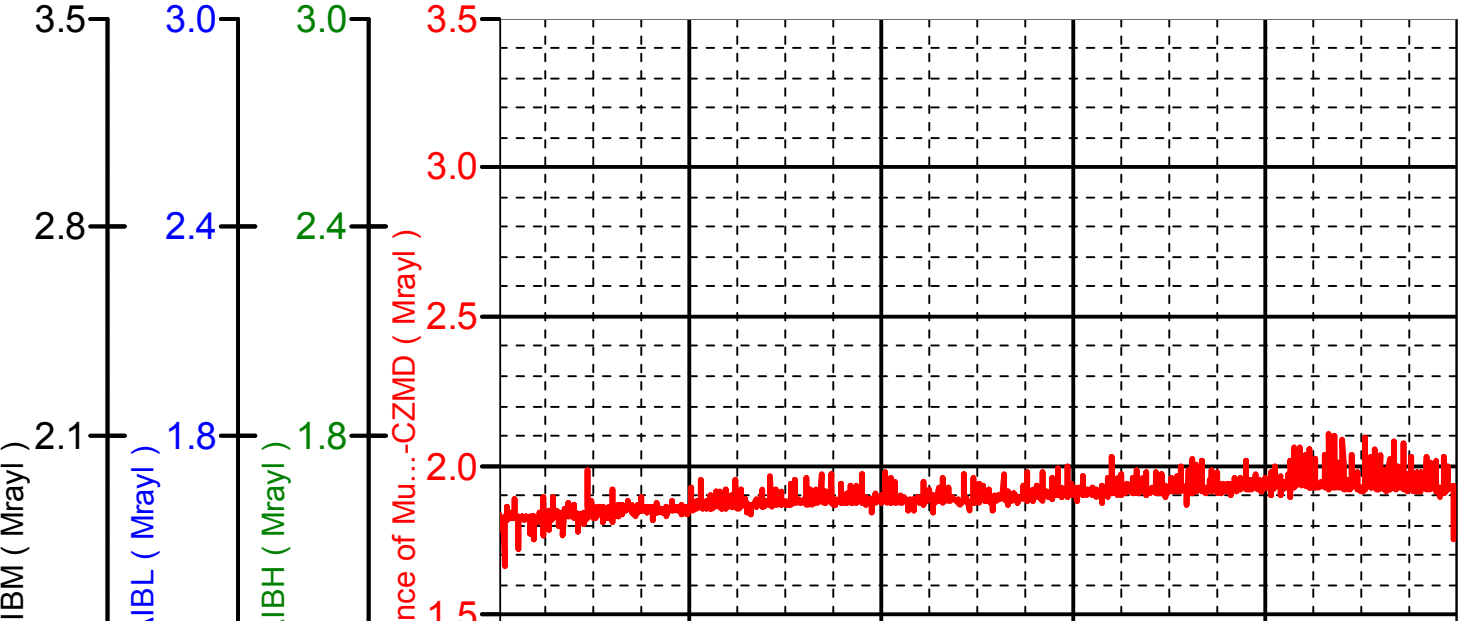

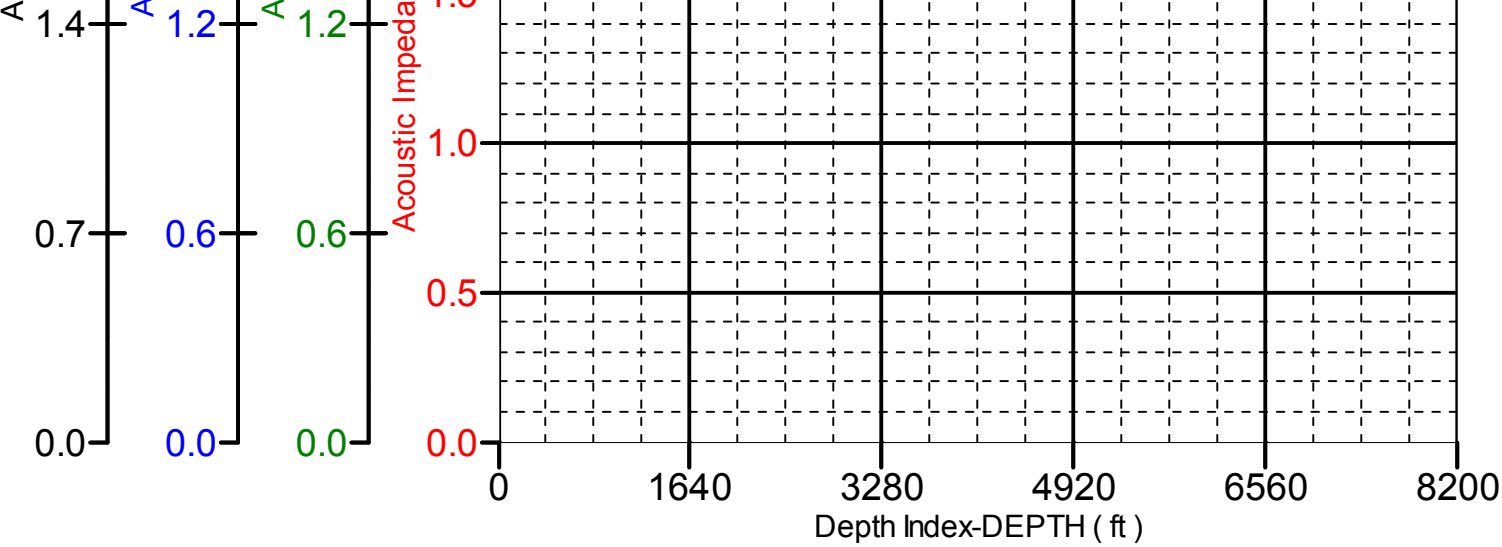

Company:	Southern California Gas Company
Well:	Frew 4
Field:	Aliso Canyon
County:	Los Angeles
State:	California

Schlumberger

Ultrasonic Imager

Ultrasonic Imager

Gamma Ray - CCL

7" casing

Ex. II - 23

Due to the large file size, please view document DOGGR_03700667_Vertilog_9-6-1988 at the below publicly available website. The native file of this document is available upon request.

(https://secure.conservation.ca.gov/WellRecord/037/03700667/03700667%20Vertilog_9-6-88.pdf) (accessed March 20, 2020)

VERTILOG®

Dresser Atlas DRESSER

CUSTOMER	SOUTHERN CALIFORNIA GAS COMPANY	DATE	9-6-88
WELL	FREW No. 4	SERVICE ORDER NO.	124201
FIELD	ALISO CANYON	COUNTY LOS ANGELES	STATE CALIFORNIA
CASING SIZE	7"	WEIGHT(S) 23#, 26#	GRADE N-80, J-55 NOMINAL WALL THICKNESS
TOTAL FOOTAGE INSPECTED	8180'	FROM SURFACE	TO 8180' DEPTH

SUBSURFACE CASING INSPECTION REPORT

SUMMARY

172	LENGTHS WERE FOUND TO SHOW NO EVIDENCE OF CORROSION EXCEEDING PERCENT OF THE NOMINAL BODY WALL.	20 CLASS 1
12	LENGTHS WERE FOUND TO SHOW EVIDENCE OF CORROSION EXCEEDING PERCENT BUT LESS THAN 41 PERCENT OF THE NOMINAL BODY WALL.	20 CLASS 2
12	LENGTHS WERE FOUND TO SHOW EVIDENCE OF CORROSION EXCEEDING PERCENT BUT LESS THAN 61 PERCENT OF THE NOMINAL BODY WALL.	40 CLASS 3
2	LENGTHS WERE FOUND TO SHOW EVIDENCE OF CORROSION EXCEEDING PERCENT OF THE NOMINAL BODY WALL.	60 CLASS 4
198	TOTAL LENGTHS	
8180'	TOTAL FOOTAGE	

REFERENCE FOR FOOTAGE MEASURE: GROUND LEVEL + 8.25'

LENGTHS ARE NUMBERED FROM: SURFACE

COMMENTS

CHART # 7N20E
CHART # 7N1E
CHART # 7J6E

SERVICED BY

DA-1363-C (08/82)

VERTILOG®

Western Atlas International
A Litton/Dresser Company

PAGE_____ OF_____

CUSTOMER	SOUTHERN CALIFORNIA GAS COMPANY	WORK ORDER NO.	124201	DATE	9-6-88
LEASE/WELL NO.	FREW No. 4	CUSTOMER ORDER NO.			
FIELD	ALISO CANYON	COUNTY	LOS ANGELES	STATE	CALIFORNIA
CASING O.D.	7"	WEIGHT(S)	23#, 26#	NOMINAL WALL THICKNESS	GRADE N-80, J-55
TOTAL FOOTAGE INSPECTED	8180'	FROM	SURFACE	TO	8180' DEPTH

SUBSURFACE CASING DEFECT REPORT

LENGTH NO.	TYPE DEFECT	PENETRATION
INSIDE 13-3/8" CASING		
7	OD IP	21 - 40
13	OD IP	21 - 40
20	OD IP	41 - 60
21	OD IP	41 - 60
OUTSIDE 13-3/8" CASING		
23	OD IP	41 - 60
25	OD IP	21 - 40
26	OD IP	21 - 40
27	OD IP	41 - 60
28	OD IP	41 - 60
29	OD GC	21 - 40
30	OD IP	21 - 40
31	OD IP	21 - 40
32	OD IP	41 - 60
47	OD IP	21 - 40
49	OD IP	21 - 40
56	OD IP	21 - 40
61	OD IP	21 - 40
72	OD IP	61 - 80
83	OD IP	21 - 40
106	OD IP	41 - 60
107	OD IP	41 - 60
108	OD IP	41 - 60
109	OD IP	61 - 80
111	OD IP	41 - 60
113	OD IP	41 - 60
114	OD IP	41 - 60

ABBREVIATIONS:

O.D. – OUTSIDE DIAMETER
I.D. – INSIDE DIAMETER
I.S. – INSIDE SURFACE PIPE
T.L. – THROUGHOUT LENGTH
I.P. – ISOLATED PITTING
C.C. – CIRCUMFERENTIAL CORROSION
G.C.-GENERAL CORROSION

WA-1364-C (10/87)

Ex. II - 24

Schlumberger

Company: Southern California Gas Company

Well: Frew 4

Field: Aliso Canyon

County: Los Angeles State: California

Ultrasonic Imager

Gamma Ray - CCL

7" casing

County:	Los Angeles
Field:	Aliso Canyon
Location:	
Well:	Frew 4
Company:	Southern California Gas Company

Location:

		Elev.: K.B.	2428.00 ft
		G.L.	2419.75 ft
		D.F.	
Permanent Datum:	Ground Level	Elev.:	2419.75 f
Log Measured From:	Kelly Bushing	8.25 ft	above Perm.Datum
Drilling Measured From:	Kelly Bushing		

API Serial No.	Section:	Township:	Range:
04-037-00667-00	29	3N	16W

Logging Date		19-Oct-2016	
Run Number		Two	
Depth Driller		8176.00 ft	
Schlumberger Depth		8176.00 ft	
Bottom Log Interval		8168.00 ft	
Top Log Interval		7.00 ft	
Casing Fluid Type		KCl Brine with Polymer	
Salinity			
Density		9 lbm/gal	
Fluid Level		8.00 ft	
BIT/CASING/TUBING STRING			
Bit Size		11.00 in	
From		7421.00 ft	
To		8300.00 ft	
Casing/Tubing Size		7 in	
Weight		26 lbm/ft	
Grade		N80	
From		6774.00 ft	
To		8280.00 ft	
Max Recorded Temperatures			
Logger on Bottom	Time	20-Oct-2016 09:51:00	
Unit Number	Location:	3189 Ventura	
Recorded By		I. Kartawidjaja	
Witnessed By		Mr. Tom McMahon	

Disclaimer

THE USE OF AND RELIANCE UPON THIS RECORDED-DATA BY THE HEREIN NAMED COMPANY (AND ANY OF ITS AFFILIATES, PARTNERS, REPRESENTATIVES, AGENTS, CONSULTANTS AND EMPLOYEES) IS SUBJECT TO THE TERMS AND CONDITIONS AGREED UPON BETWEEN SCHLUMBERGER AND THE COMPANY, INCLUDING: (a) RESTRICTIONS ON USE OF THE RECORDED-DATA; (b) DISCLAIMERS AND WAIVERS OF WARRANTIES AND REPRESENTATIONS REGARDING COMPANY'S USE AND RELIANCE UPON THE RECORDED-DATA; AND (c) CUSTOMER'S FULL AND SOLE RESPONSIBILITY FOR ANY INFERENCE DRAWN OR DECISION MADE IN CONNECTION WITH THE USE OF THIS RECORDED-DATA.

Contents

1. Header
2. Disclaimer
3. Contents
4. Well Sketch
5. Borehole Size/Casing/Tubing Record
6. Remarks and Equipment Summary
7. Job Event Summary
8. USI Fluid Properties Measurement
9. Composite 1 Main Pass 5 in = 100 ft
   9.1 Integration Summary
   9.2 Software Version
   9.3 Composite Summary
   9.4 Log (LBV1_USI-VDL (DSLT) Cement 7inch)
   9.5 Parameter Listing
10. Composite 1 Main Pass 5 IN = 100 FT
   10.1 Integration Summary
   10.2 Composite Summary
   12.2 Composite Summary
   12.3 Log (LBV1_USI Corrosion 7inch)
13. Composite 1 USI Compressed Goodwin
   13.1 Integration Summary
   13.2 Composite Summary
   13.3 Log (Import of USI Goodwin)
14. XYZ (USI Fluid Acoustic Slowness vs Depth)
15. XYZ (USI Theoretical Acoustic impedance of mud vs Depth)
16. Tail

10.3 Log (LBV1_USI Composite 7inch)
11. Two Cement Log 2 IN = 100 FT
11.1 Integration Summary
11.2 Composite Summary
11.3 Log (LBV1_USI Cement 7inch)
12. Composite 1 Corrosion 5 in = 100 ft
12.1 Integration Summary

Well Sketch

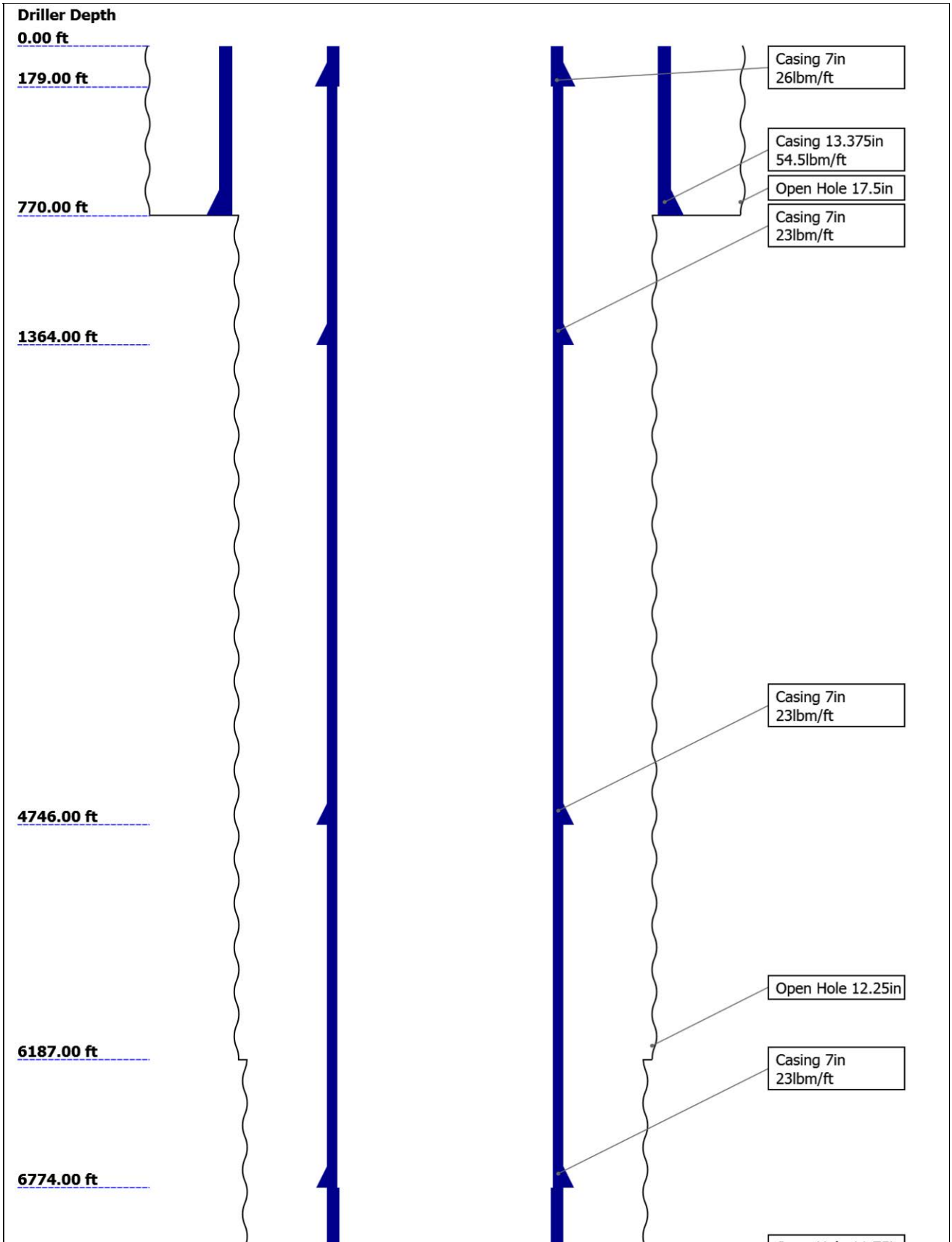

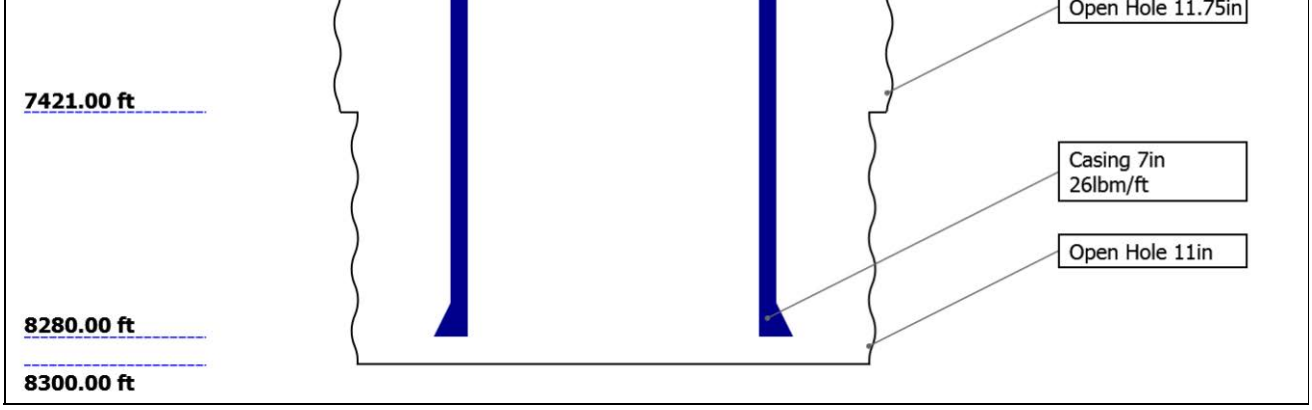

Borehole Size/Casing/Tubing Record

Bit						
Bit Size (in)	17.5	12.25	11.75	11		
Top Driller (ft)	0	770	6187	7421		
Top Logger (ft)	0	770	6187	7421		
Bottom Driller (ft)	770	6187	7421	8300		
Bottom Logger (ft)	770	6187	7421	8300		
Casing						
Size (in)	13.375	7	7	7	7	7
Weight (lbm/ft)	54.5	26	23	23	23	26
Inner Diameter (in)	12.615	6.276	6.366	6.366	6.366	6.276
Grade	J55	N80	N80	J55	N80	N80
Top Driller (ft)	0	0	179	1364	4746	6774
Top Logger (ft)	0	0	179	1364	4746	6774
Bottom Driller (ft)	770	179	1364	4746	6774	8280
Bottom Logger (ft)	770	179	1364	4746	6774	8280

Remarks and Equipment Summary

Two: Toolstring

Equip name	Length	MP name	Offset
LEH-QT:2867 LEH-QT:2867	**57.51**	Red	
DTC-H ECH-KC DTC-H	**54.59**	**CTEM** **HV** **TelStatus** **ToolStatus**	**53.69** **0.00** **51.59** **51.59**
HGNS-H:3923 HGNH:4819 NPV-N NSR-F:1303 HMCA-H HGNS-H:3923 HACCZ-H:4177	**51.59**	**Temperature** **GR** **CNL Porosity** **HGNS** **HMCA** **Accelerometer**	**51.57** **50.85** **44.52** **42.18** **42.18** **0.00**
AH-184[	**42.18**		

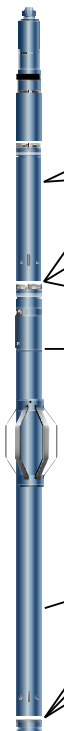

Two: Remarks

Depth correlated to Neutron Lifetime Log dated 4-19-74. Tied-in to Neutron curves between 7700-8100 ft

USIT logged at 10 deg 1.5 inch, speed 3200 fph. No hi-res repeat recorded as requested by client.

Main pass recorded with 0 psi surface pressure. Repeat pass recorded with 1000 psi from TD to ~6900 ft.

Logged from above top of sand at ~8168 ft to surface.

Rig: Ensign 334

Toolstring ran as per toolsketch.

Two centralizers on USIS and two CME-Y used to centralize ultrasonic tool.

Thank you for choosing Schlumberger!

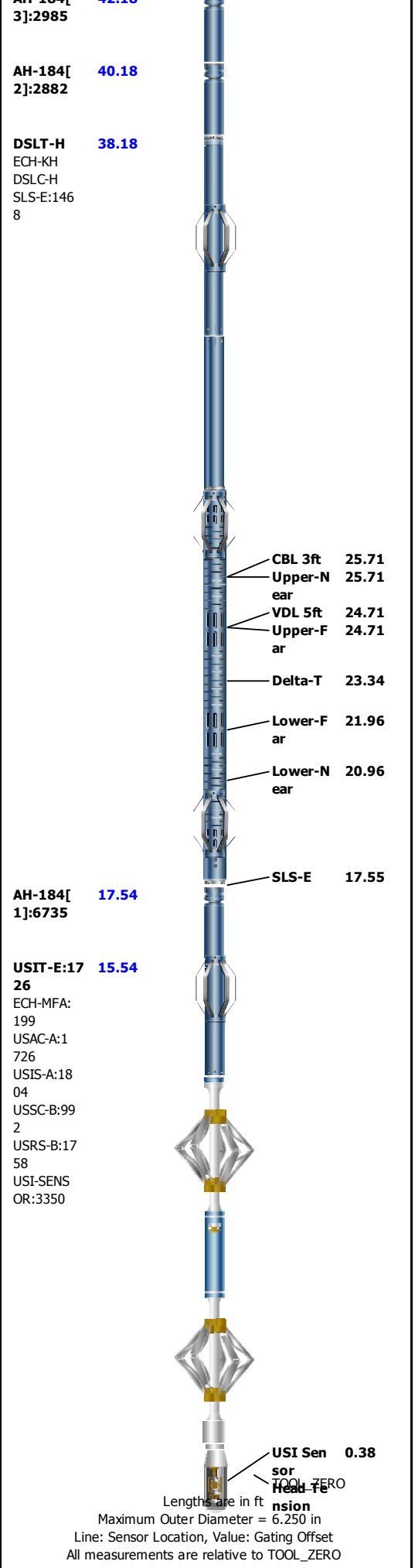

Job Event Summary

Event	Time	Duration	Interval	Remark

Event	Time	Duration	Interval	Remark
Log[1]:Down	Oct-19-2016 13:19	01:54:44	185.28 - 8127.82 ft	Fluid Properties Measurement
Log[6]:Up	Oct-19-2016 14:46	00:24:25	8162.42 - 6845.38 ft	Repeat Pass 1000 PSI
Log[9]:Up	Oct-20-2016 09:51	00:29:01	8170.38 - 6638.82 ft	Main Pass #1 0 PSI
Log[11]:Up	Oct-20-2016 10:24	02:09:06	6736.16 - 35.34 ft	Main Pass #2 0 PSI
Log[14]:Up	Oct-20-2016 12:53	00:04:58	153.18 - 3.59 ft	Main Pass #3 0 PSI

USIT - Fluid Properties Measurement

Run Name	Pass Name	Start Depth(ft)	Stop Depth(ft)
Run 1	Log[11]:Up	6737.51	36.69

Fluid Velocity = "Automatic".
CFVL equals DFSL channel

Start Depth(ft)	Stop Depth(ft)	Start Value(us/ft)	End Value(us/ft)

Mud Impedance = "FreePipe Norm.".
Free Pipe normalization zone is : 120.75m(396.17ft) to 129.39m(424.50ft)
MUD_N_FRP = 1.10
DFD = 1.08g/cm3(9.00lbm/gal)
CZMD median computed in free pipe normalization interval = 1.80 MRayl

Start Depth(ft)	Stop Depth(ft)	Start Value(Mrayl)	End Value(Mrayl)

Composite 1

Main Pass 5 in = 100 ft

Software Version

Acquisition System	Version
Maxwell 2016 SP1	6.1.58882.3100
Application Patch	Wireline_Hotfix-Perfo-2016SP1_6.1.63773

Computation	Description	Version
CEVAL	Sonic Cement Evaluation Computation Ensemble provides common Parameters and Channels	6.1.58882.3100
Cementation	Cementation Computation Application	6.1.58882.3100

SoftwareVersion_Tool	SoftwareVersion_Run Version	SoftwareVersion_Build Version
WAFE-SEC	Synergy SV451EC version 9.10	Synergy SV451EC version 9.10
WAFE-FEC	Synergy SV451EC version 9.10	Synergy SV451EC version 9.10
WAFE-TMDI	Synergy SV451EC version 46.19	Synergy SV451EC version 46.19

Tool Elements	Description	Software Version	Firmware Version
HGNS-H	HILT Gamma-Ray and Neutron Sonde, 150 degC	6.1.58882.3100	2.0
SLS-E	Sonic Logging Sonde E supports 3'-5'BHC DT and CBL/VDL	6.1.58882.3100	4.0
USI-SENSOR	USIT Transducer Element	6.1.58882.3100	DSP: v1.82

Composite Summary

Run Name	Pass Objective	Direction	Top	Bottom	Start	Stop	DSC Mode	Depth Shift	Include Parallel Data
Two	Log[9]:Up	Up	6640.29 ft	8171.85 ft	20-Oct-2016 9:51:39 AM	20-Oct-2016 10:20:40 AM	ON	1.47 ft	No
Two	Log[11]:Up	Up	36.69 ft	6737.51 ft	20-Oct-2016 10:24:53 AM	20-Oct-2016 12:34:00 PM	ON	1.35 ft	No
Two	Log[14]:Up	Up	5.56 ft	155.15 ft	20-Oct-2016 12:53:24 PM	20-Oct-2016 12:58:23 PM	ON	1.96 ft	No

All depths are referenced to toolstring zero

Log

Company:Southern California Gas Company Well:Frew 4
Composite 1:S008

Description: USI VDL Cement Format: Log (LBV1_USI-VDL (DSLT) Cement 7inch) Index Scale: 5 in per 100 ft Index Unit: ft Index Type: Measured Depth
Creation Date: 20-Oct-2016 14:28:02

TIME_1900 - Time Marked every 60.00 (s)

ERAV_IRAV ERAV_RHF1

IRAV_LHF1

IRAV_ERAV

LHF1_ERAV

RHF1_IRAV

Median of Unflagged External Radii (ERAV_RF) USIT-E[1]

3.7 in 2.7

Median of Unflagged External Radii (ERAV_RF) USIT-E[1]

2.7 in 3.7

Median Internal Radius of Casing Corrected for Eccentering (IRAV_RF) USIT-E[1]

3.7 in 2.7

Minimum of Unflagged Internal Radii (IRMN_RF) USIT-E[1]

2.7 in 3.7

Minimum of Unflagged Internal Radii (IRMN_RF) USIT-E[1]

3.7 in 2.7

Maximum of Unflagged Internal Radii (IRMX_RF) USIT-E[1]

2.7 in 3.7

Amplitude of Eccentering for Unflagged Waves (ECCE_RF) USIT-E[1]

0 in 0.5

Maximum of Unflagged Internal Radii (IRMX_RF) USIT-E[1]

3.7 in 2.7

Median Internal Radius of Casing Corrected for Eccentering (IRAV_RF) USIT-E[1]

2.7 in 3.7

Absent 1.000 2.500 4.000 5.500 7.000

Custom Normalization

USIT - Acoustic Impedance (AIBK) USIT-E[1] (Mrayl)

Acoustic Impedance Minimum (AIMN) USIT-E[1]

-1 Mrayl 9

Acoustic Impedance Average (AIAV) USIT-E[1]

-1 Mrayl 9

Acoustic Impedance Maximum (AIMX) USIT-E[1]

-1 Mrayl 9

Absent 0.300 3.581 5.054 6.527 8.000

Custom Normalization

USIT - Acoustic Impedance With Micro-debonding Image (AI_MDEBOND_IMG) USIT-E[1] (Mrayl)

Bonded

Gas

Liquid

Micro-debonding

Bond Index (BI) DSLT-H[1]

1 0

Min Amplitude Max

Sonic VDL Curve DSLT-H[1]

200 us 1200

Gamma Ray (ECGR) HGNS[1]

0 gAPI 150

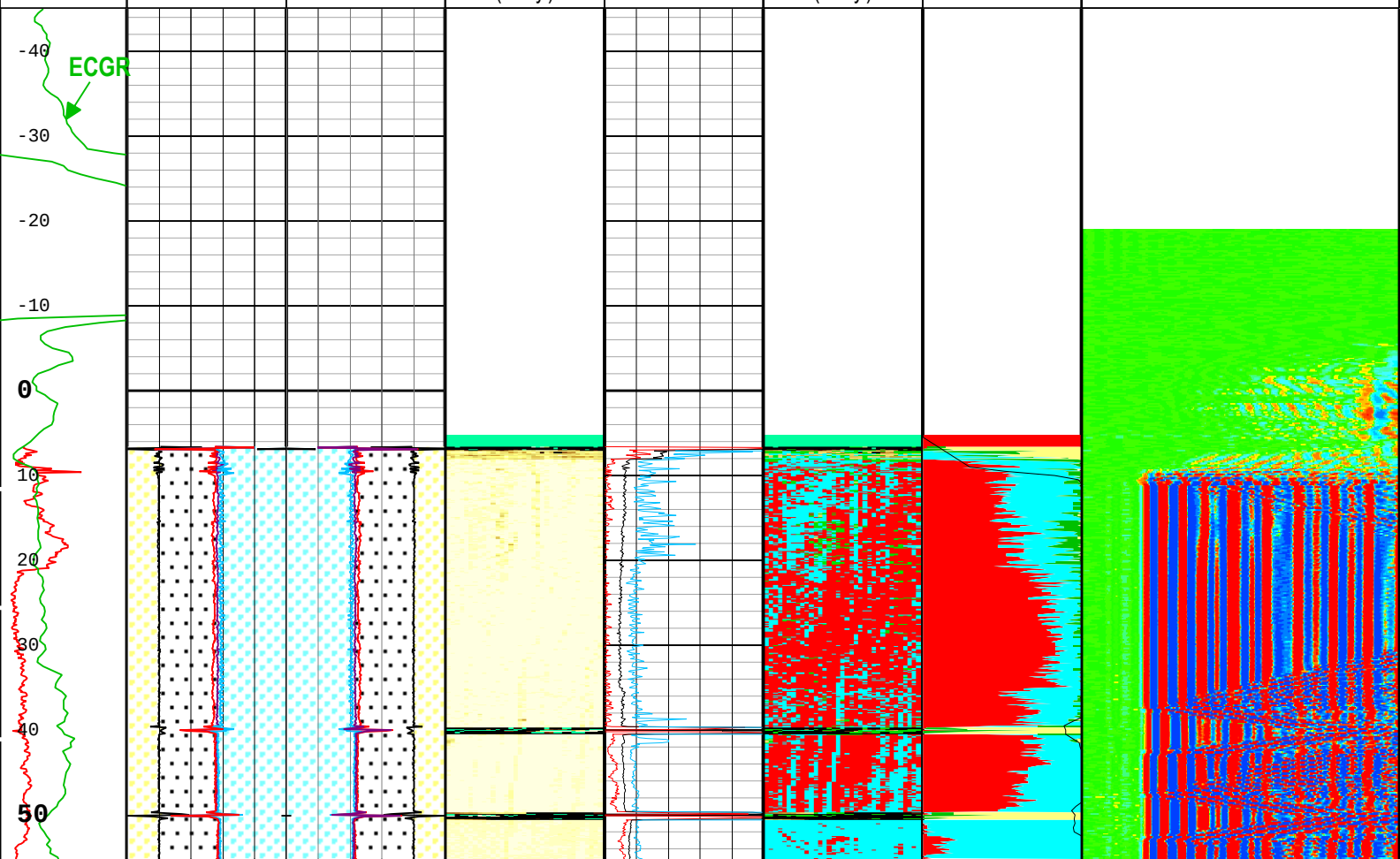

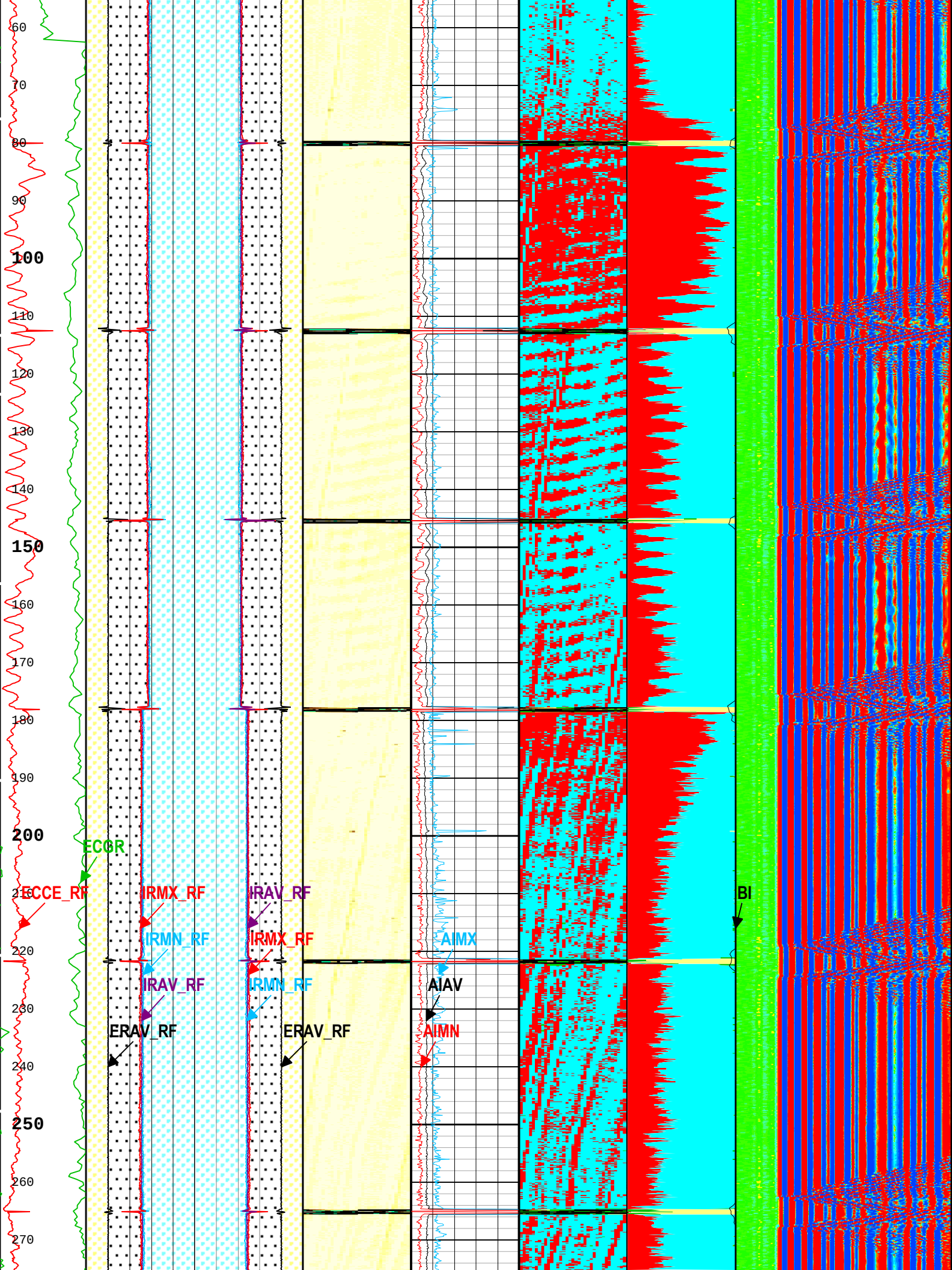
60
70
80
90
100
110
120
130
140
150
160
170
180
190
200
210
220
230
240
250
260
270
ECGR
ECCE_RF
IRMX_RF
IRAV_RF
IRMN_RF
IRMX_RF
IRAV_RF
IRMN_RF
ERAV_RF
ERAV_RF
AIMX
AIAV
AIMN
BI

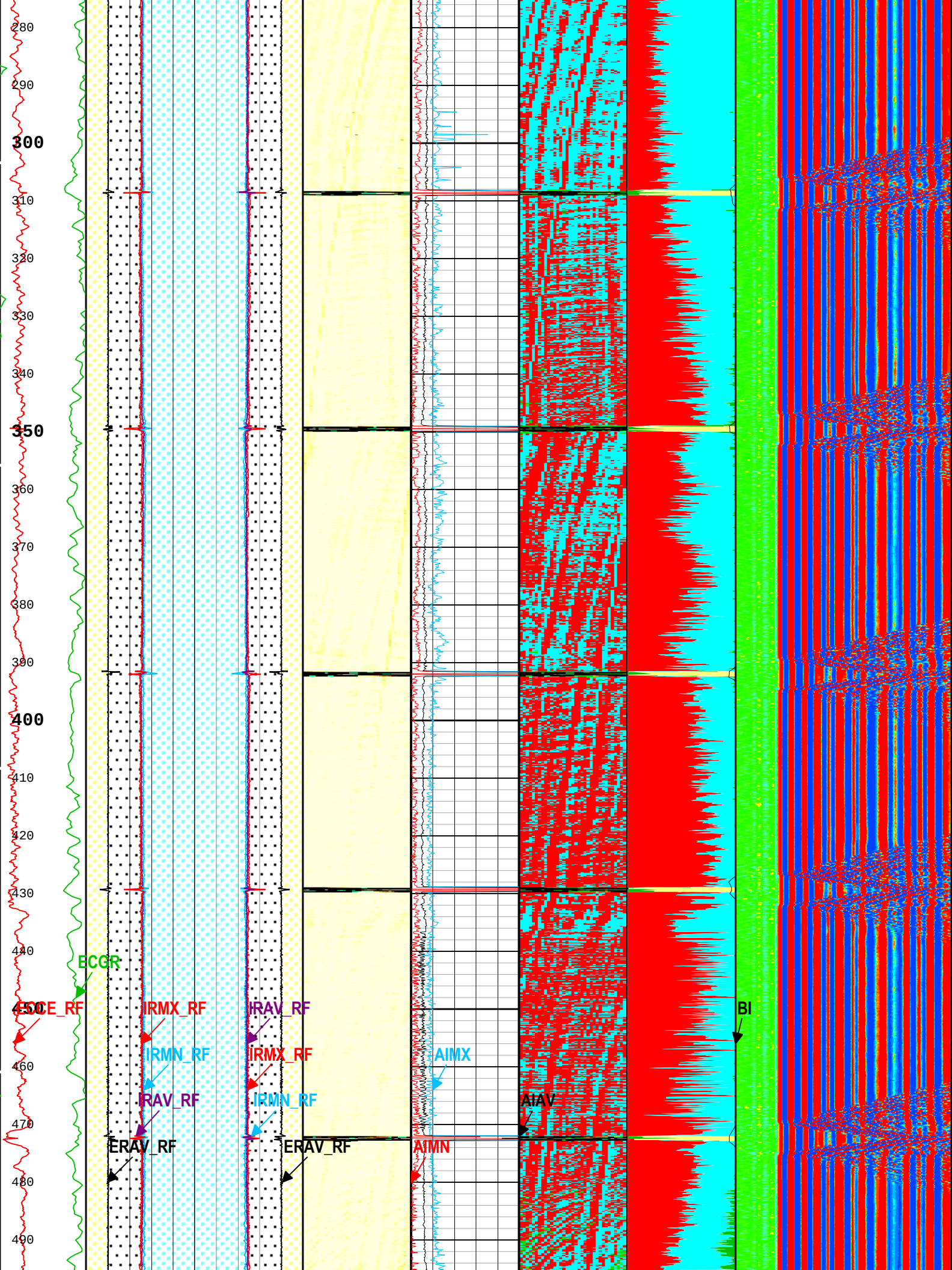
280
290
300
310
320
330
340
350
360
370
380
390
400
410
420
430
440
450
460
470
480
490
ECGR
ECCE_RF
IRMX_RF
IRAV_RF
IRMN_RF
IRMX_RF
IRAV_RF
IRMN_RF
ERAV_RF
ERAV_RF
AIMX
AIMN
AIAV
BI

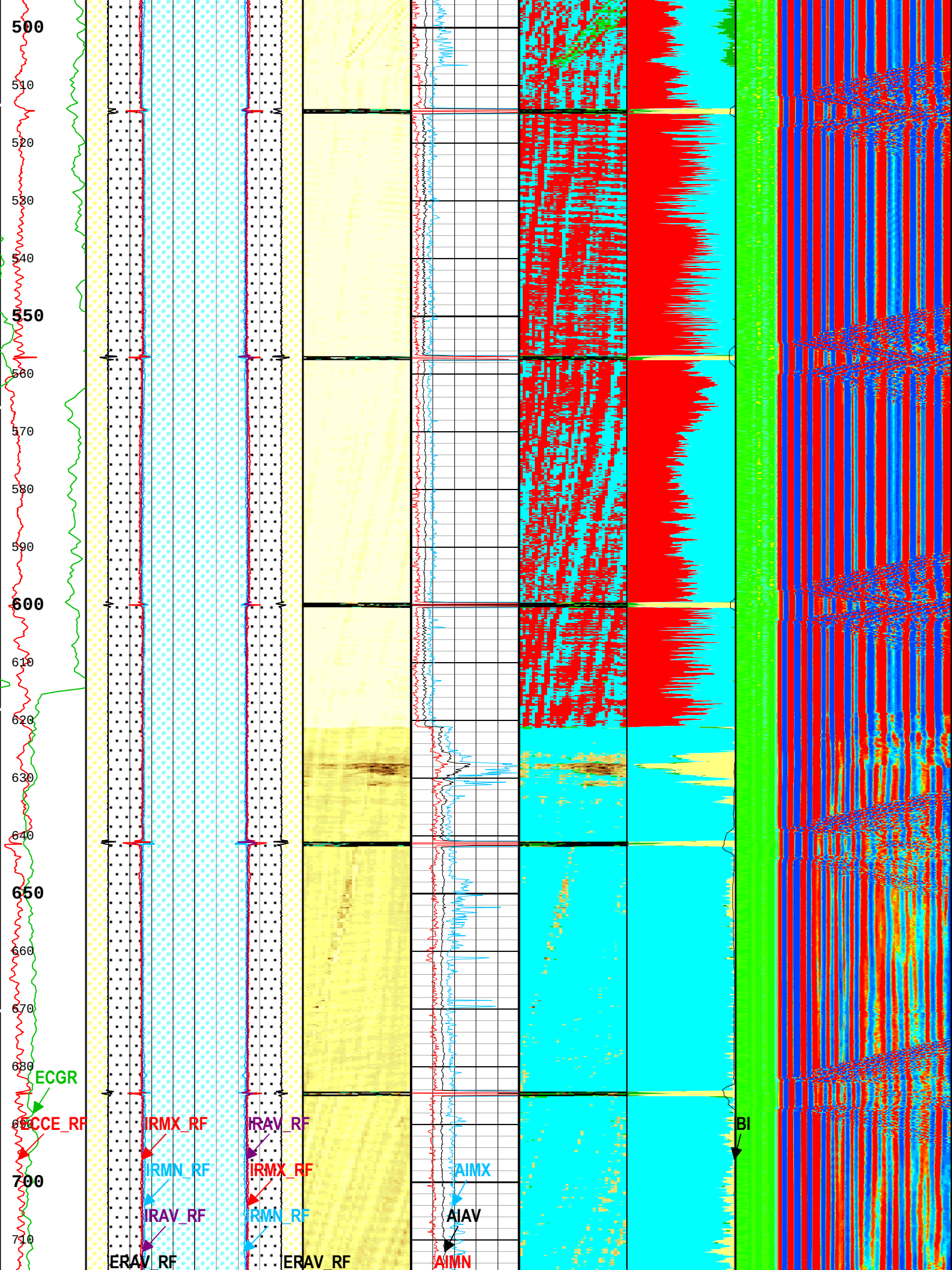
500
510
520
530
540
550
560
570
580
590
600
610
620
630
640
650
660
670
680
690
700
710
ECGR
CCE_RF
IRMX_RF
IRMN_RF
IRAV_RF
ERAV_RF
IRAV_RF
IRMX_RF
IRMN_RF
ERAV_RF
AIMX
AIAV
AIMN
BI

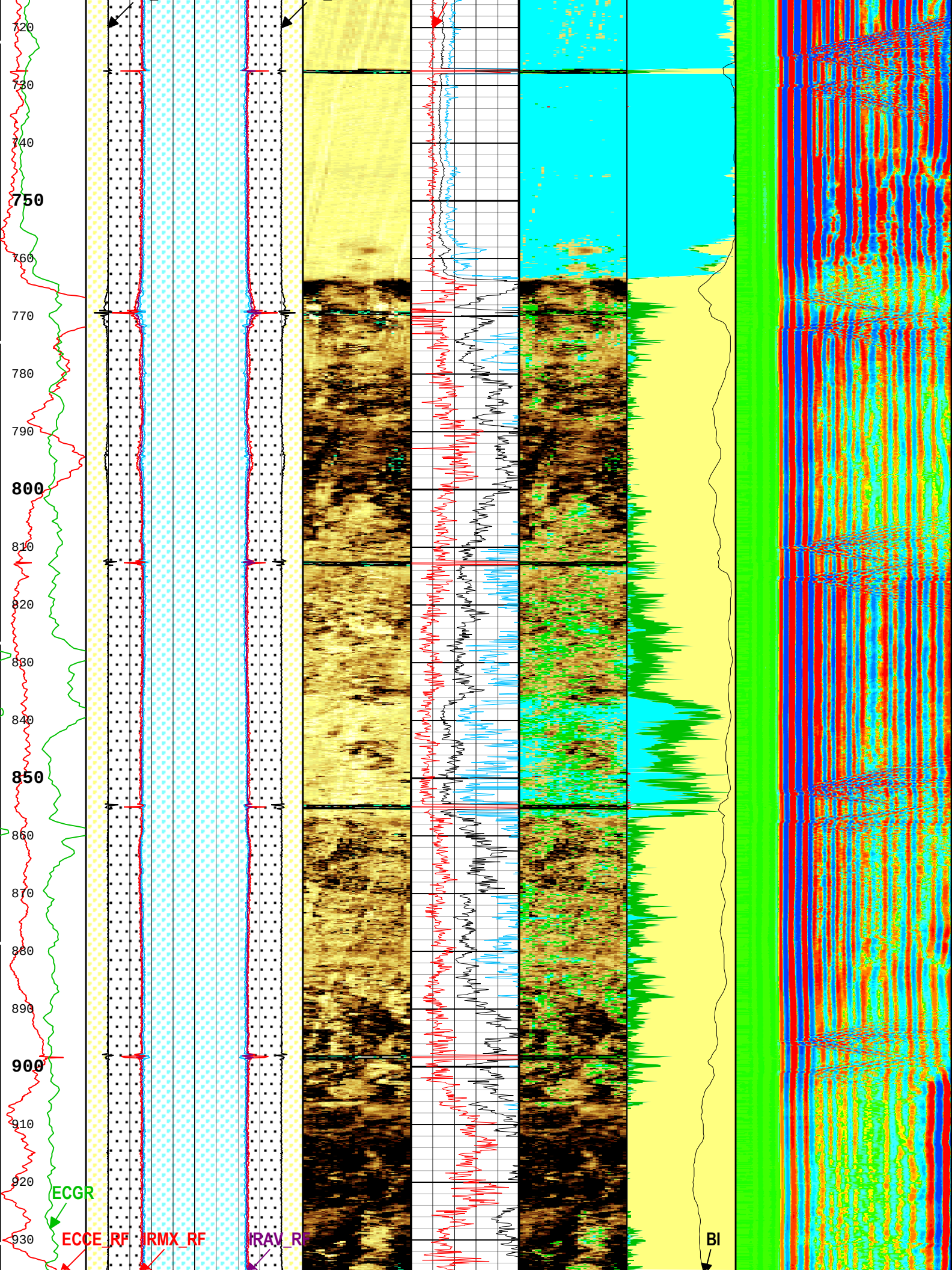
720
730
740
750
760
770
780
790
800
810
820
830
840
850
860
870
880
890
900
910
920
930
ECGR
ECCE_RF
IRMX_RF
IRAV_RF
BI

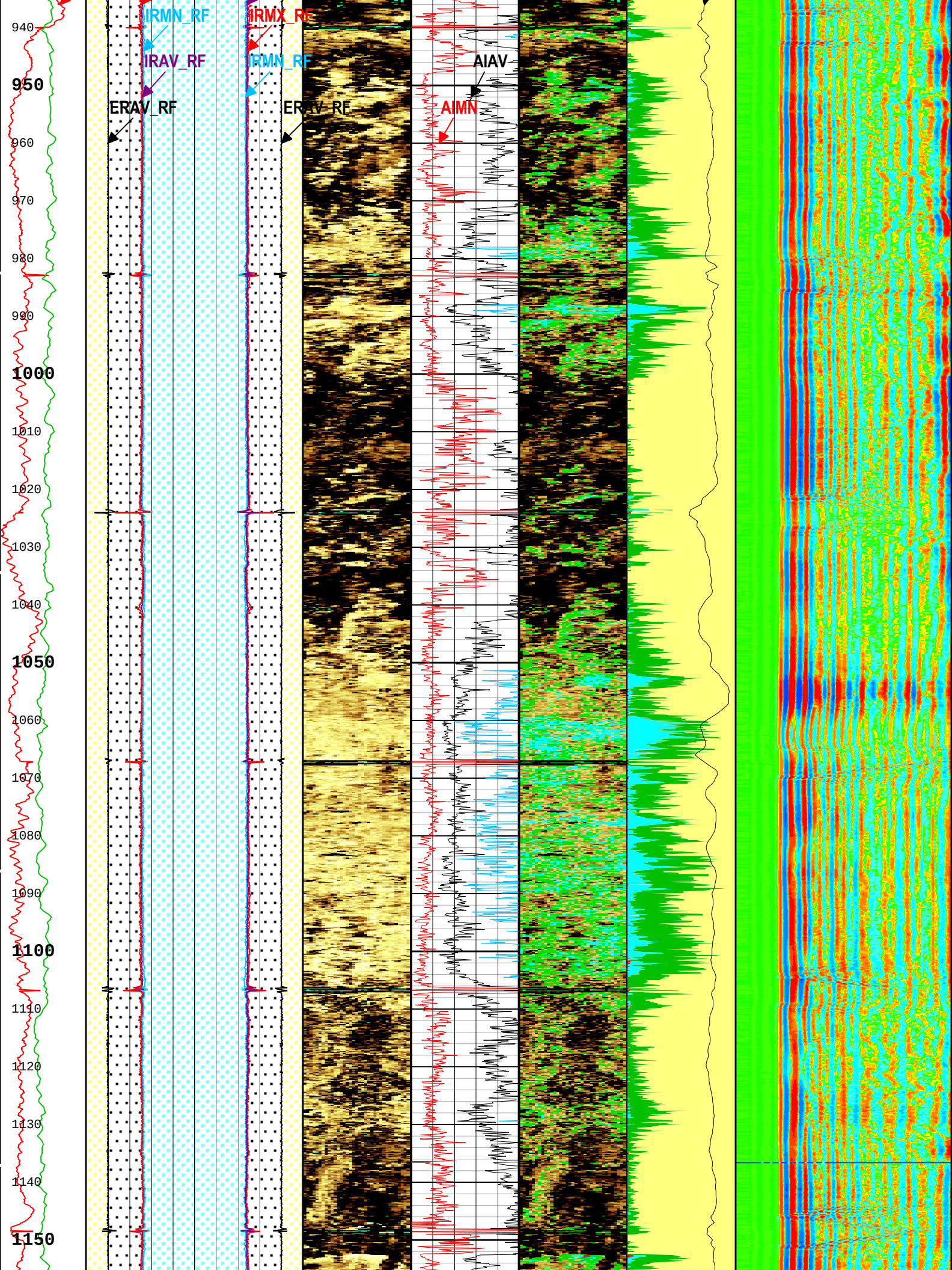
IRMN_RF
IRMX_RF
IRAV_RF
IRMN_RF
AIAV
ERAV_RF
ERAV_RF
AIMN
940
950
960
970
980
990
1000
1010
1020
1030
1040
1050
1060
1070
1080
1090
1100
1110
1120
1130
1140
1150

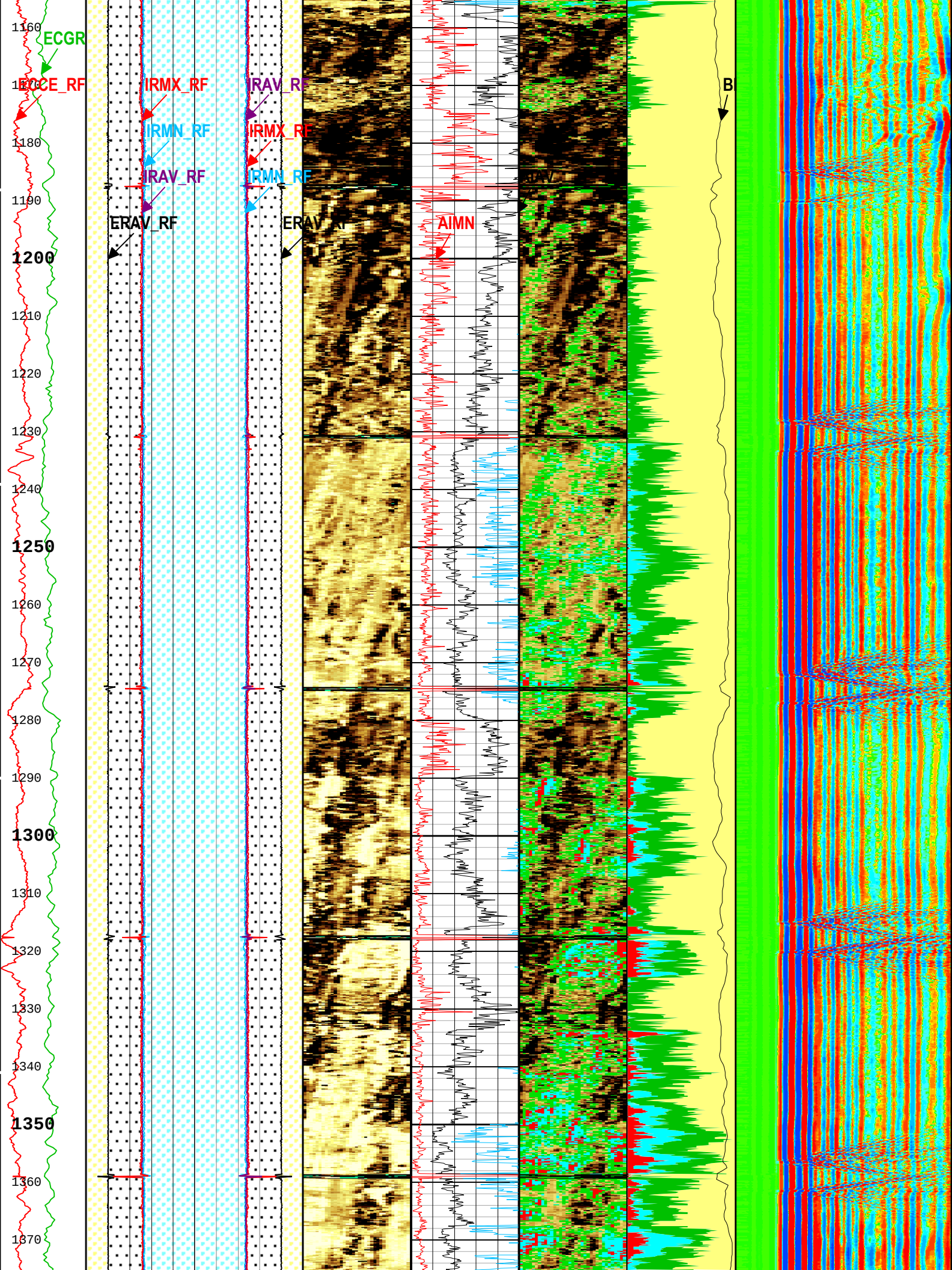
ECGR
ECCE_RF
IRMX_RF
IRAV_RF
IRMN_RF
IRMX_RF
IRAV_RF
IRMN_RF
ERAV_RF
ERAV_RF
AIMN
B
1160
1180
1200
1210
1220
1230
1240
1250
1260
1270
1280
1290
1300
1310
1320
1330
1340
1350
1360
1370

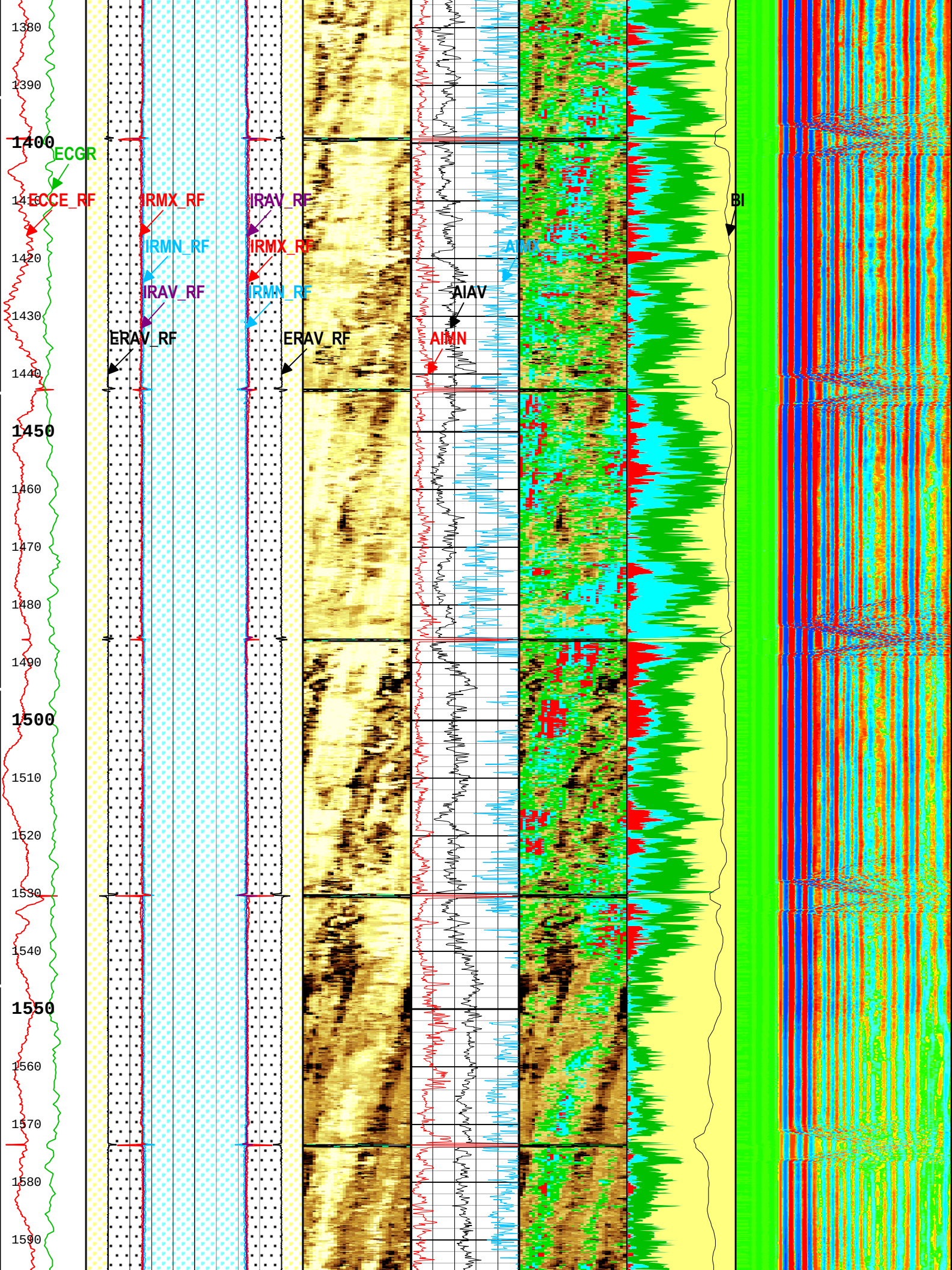
1380
1390
1400
ECGR
ECCE_RF
IRMX_RF
IRAV_RF
IRMN_RF
IRMX_RF
IRAV_RF
IRMN_RF
AIMN
AIAV
AIMN
ERAV_RF
ERAV_RF
BI
1420
1430
1440
1450
1460
1470
1480
1490
1500
1510
1520
1530
1540
1550
1560
1570
1580
1590

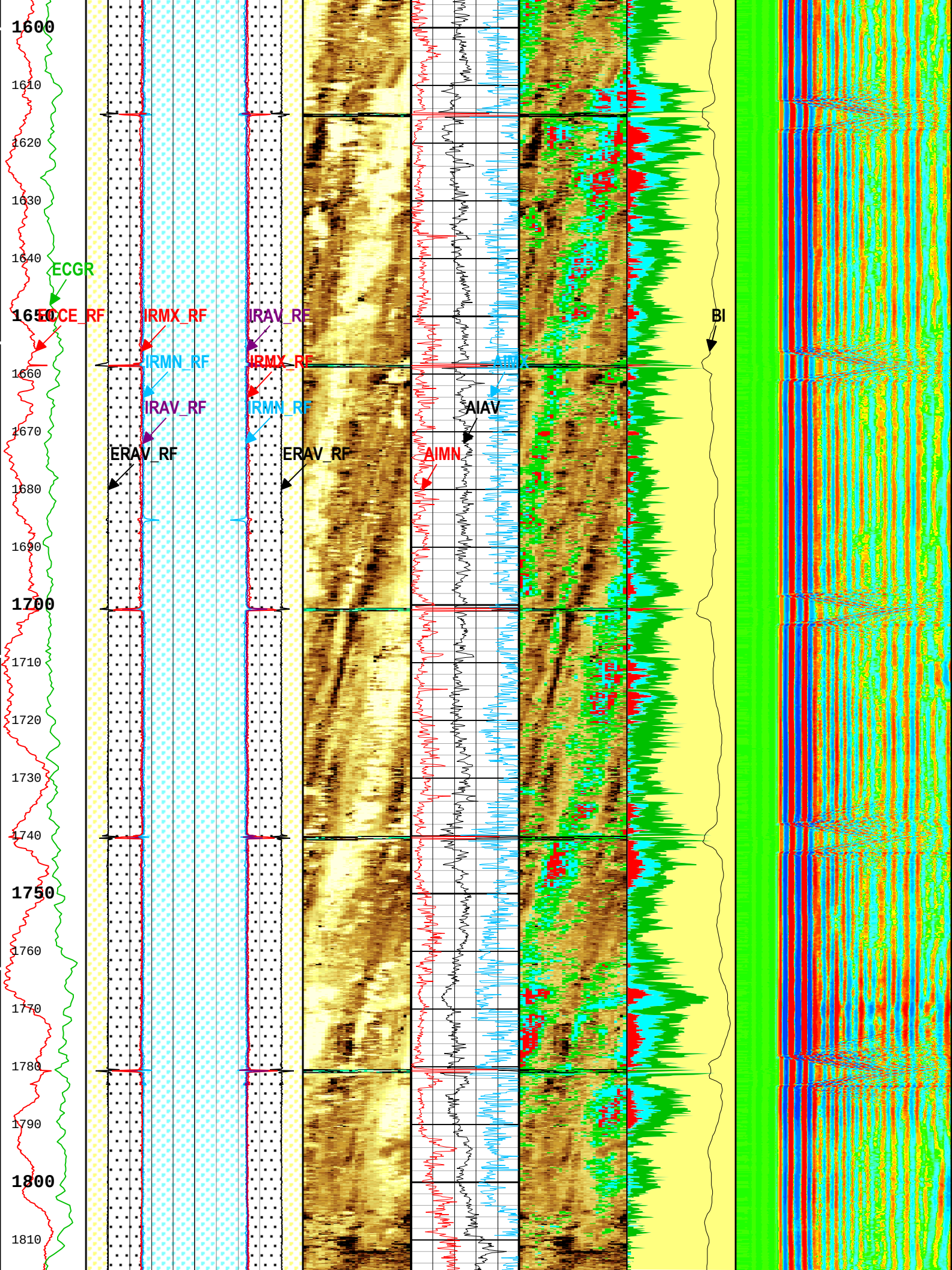
1600
1610
1620
1630
1640
1650
1660
1670
1680
1690
1700
1710
1720
1730
1740
1750
1760
1770
1780
1790
1800
1810
ECGR
CE_RF
IRMX_RF
IRAV_RF
IRMN_RF
IRMX_RF
IRAV_RF
IRMN_RF
ERAV_RF
ERAV_RF
AIMX
AIAV
AIMN
BI

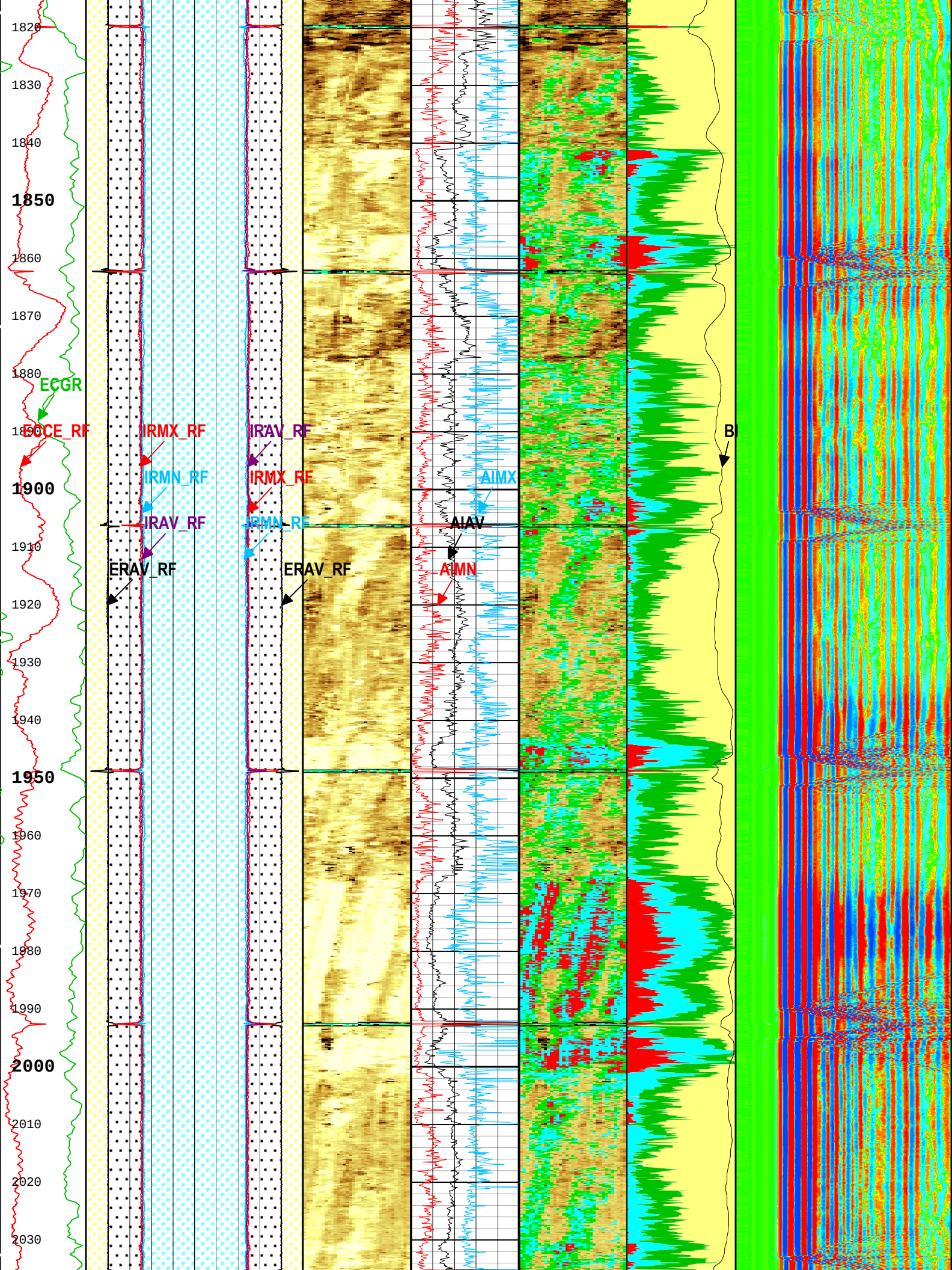
1820
1830
1840
1850
1860
1870
1880
1890
1900
1910
1920
1930
1940
1950
1960
1970
1980
1990
2000
2010
2020
2030
ECGR
ECCE_RF
IRMX_RF
IRMN_RF
IRAV_RF
ERAV_RF
IRAV_RF
IRMX_RF
IRMN_RF
ERAV_RF
AIMX
AIAV
AIMN
B

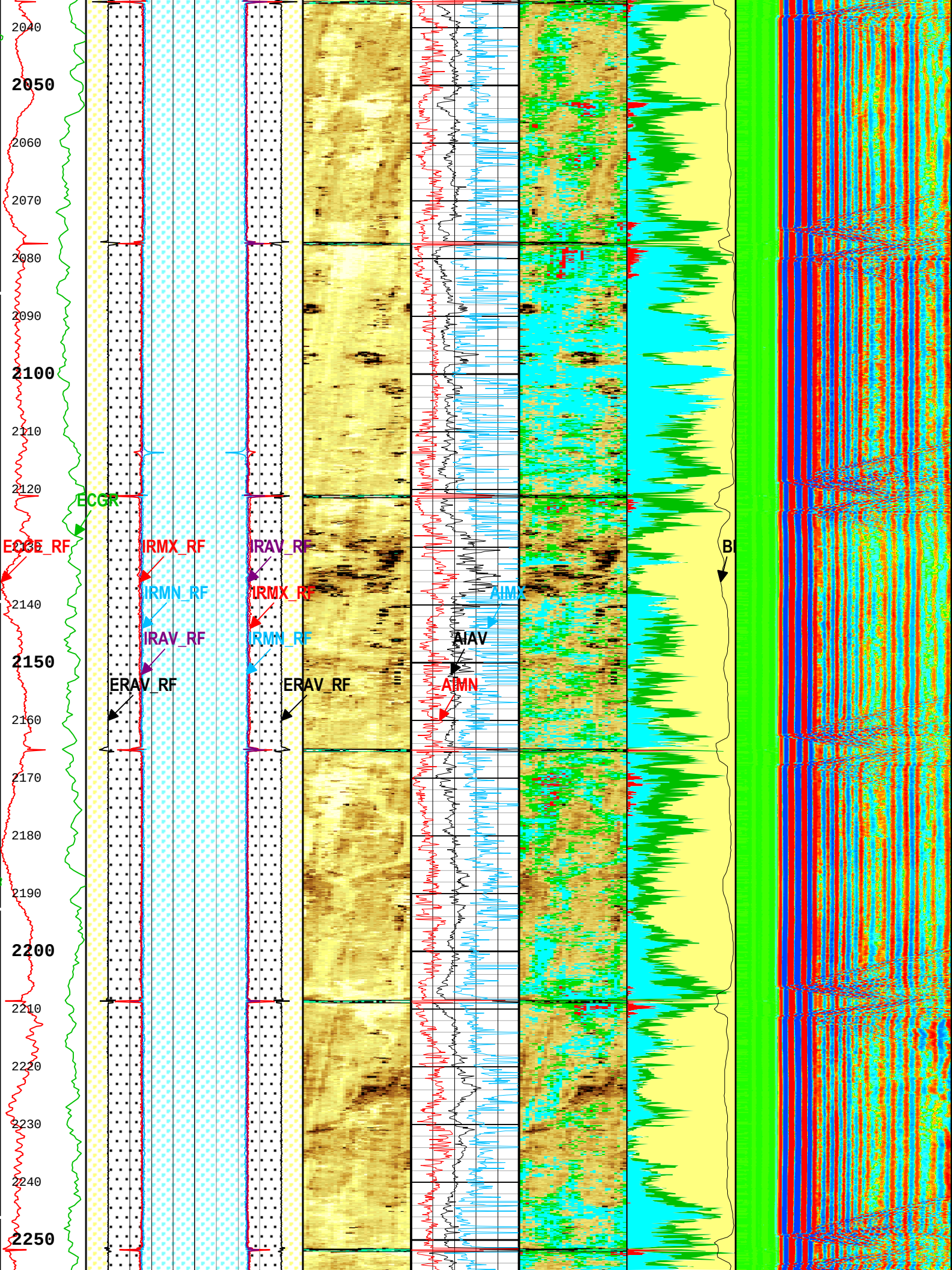
2040
2050
2060
2070
2080
2090
2100
2110
2120
2140
2150
2160
2170
2180
2190
2200
2210
2220
2230
2240
2250
ECGR
ECGE_RF
IRMX_RF
IRMN_RF
IRAV_RF
ERAV_RF
IRAV_RF
IRMX_RF
IRMN_RF
ERAV_RF
AIMX
AIAV
AIMN
BI

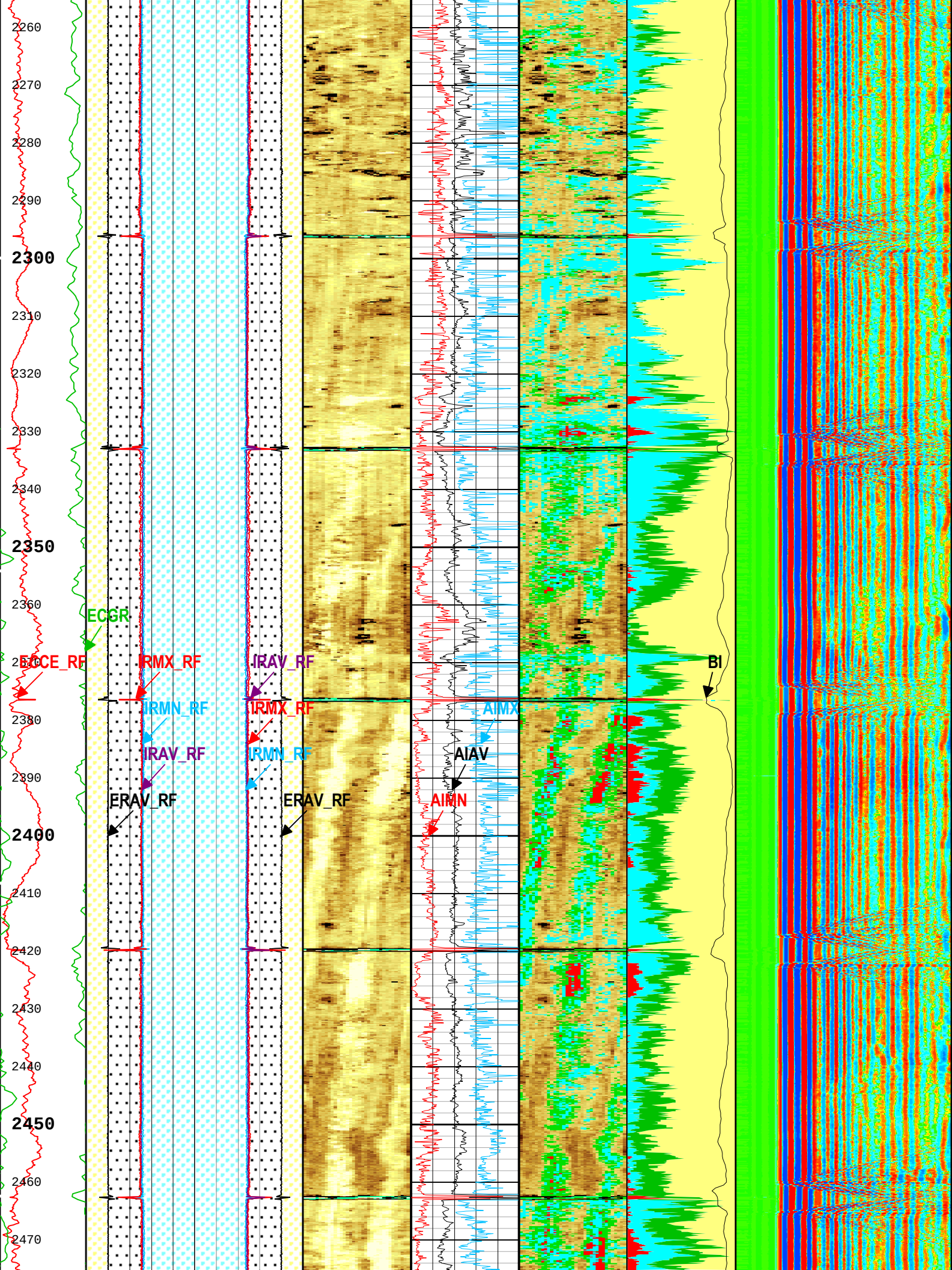
2260
2270
2280
2290
2300
2310
2320
2330
2340
2350
2360
2370
2380
2390
2400
2410
2420
2430
2440
2450
2460
2470
ECGR
ECCE_RF
IRMX_RF
IRAV_RF
IRMN_RF
IRAV_RF
ERAV_RF
IRAV_RF
IRMX_RF
IRMN_RF
ERAV_RF
AIMX
AIAV
AIMN
BI

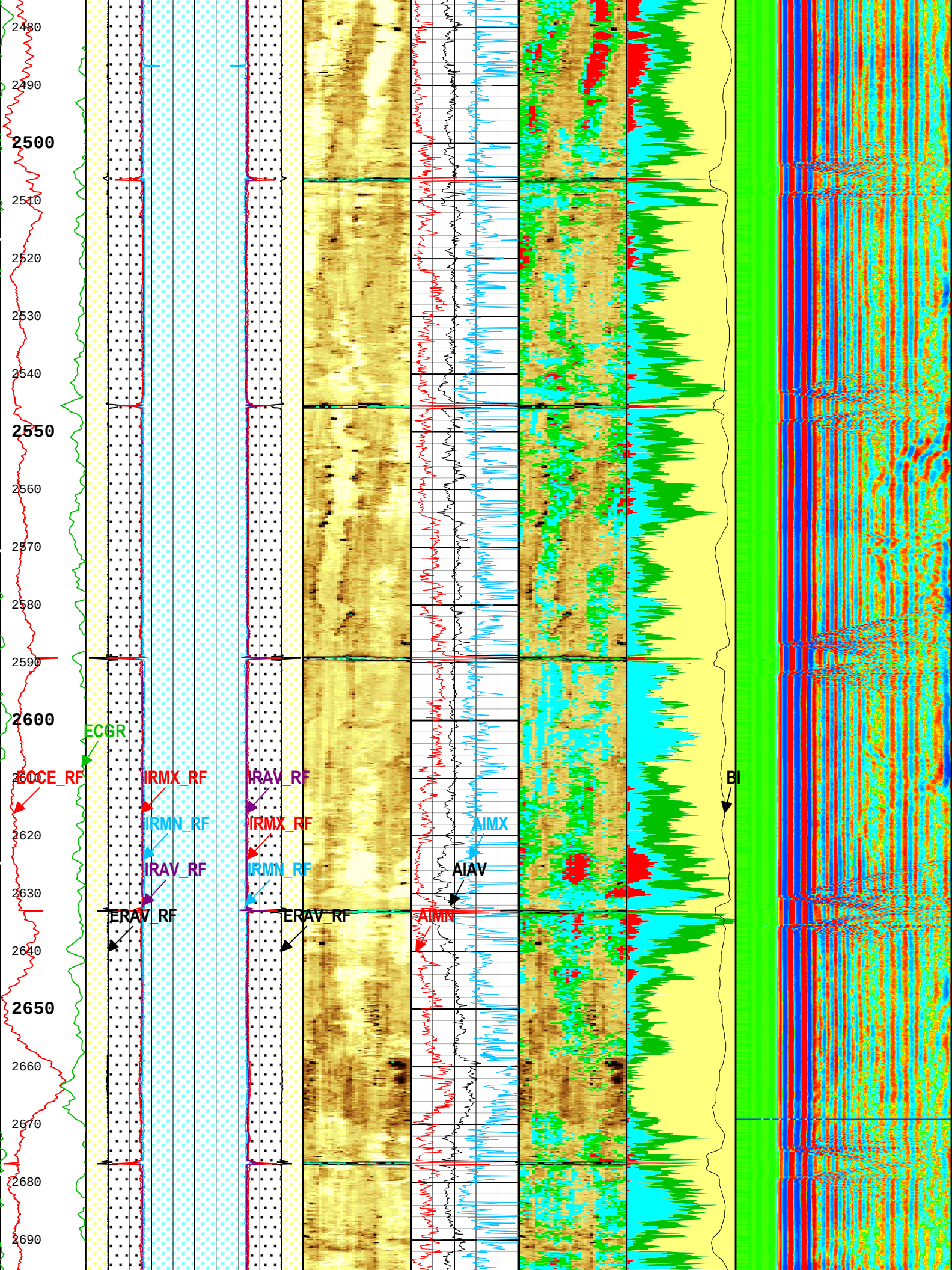
2480
2490
2500
2510
2520
2530
2540
2550
2560
2570
2580
2590
2600
2610
2620
2630
2640
2650
2660
2670
2680
2690
ECGR
ECCE_RF
IRMX_RF
IRMN_RF
IRAV_RF
ERAV_RF
IRAV_RF
IRMX_RF
IRMN_RF
ERAV_RF
AIMX
AIAV
AIMN
BI

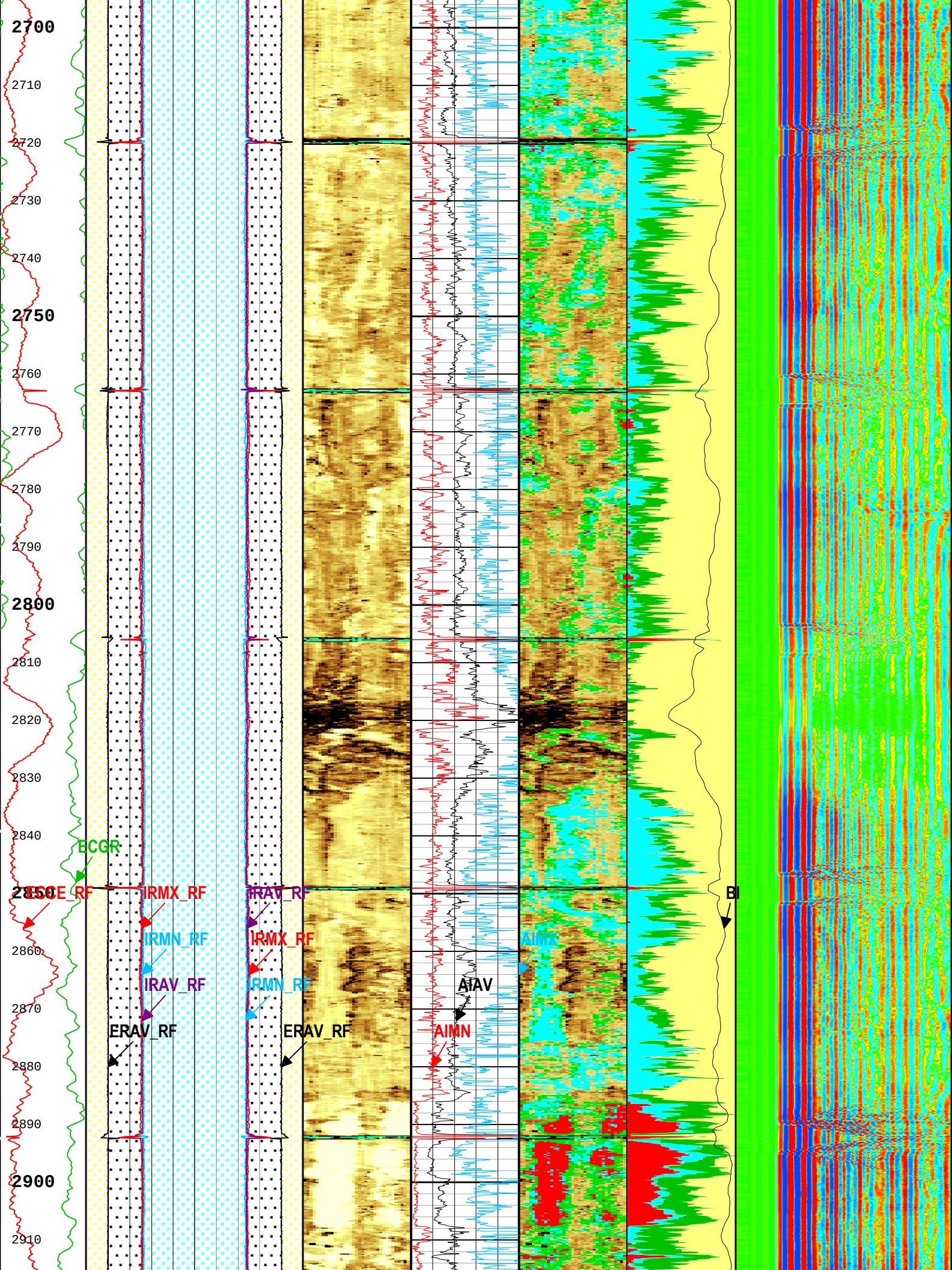
2700
2710
2720
2730
2740
2750
2760
2770
2780
2790
2800
2810
2820
2830
2840
2850
2860
2870
2880
2890
2900
2910
ECGR
IRMX_RF
IRMN_RF
IRAV_RF
ERAV_RF
IRAV_RF
IRMX_RF
IRMN_RF
ERAV_RF
AIMX
AIAV
AIMN
BI

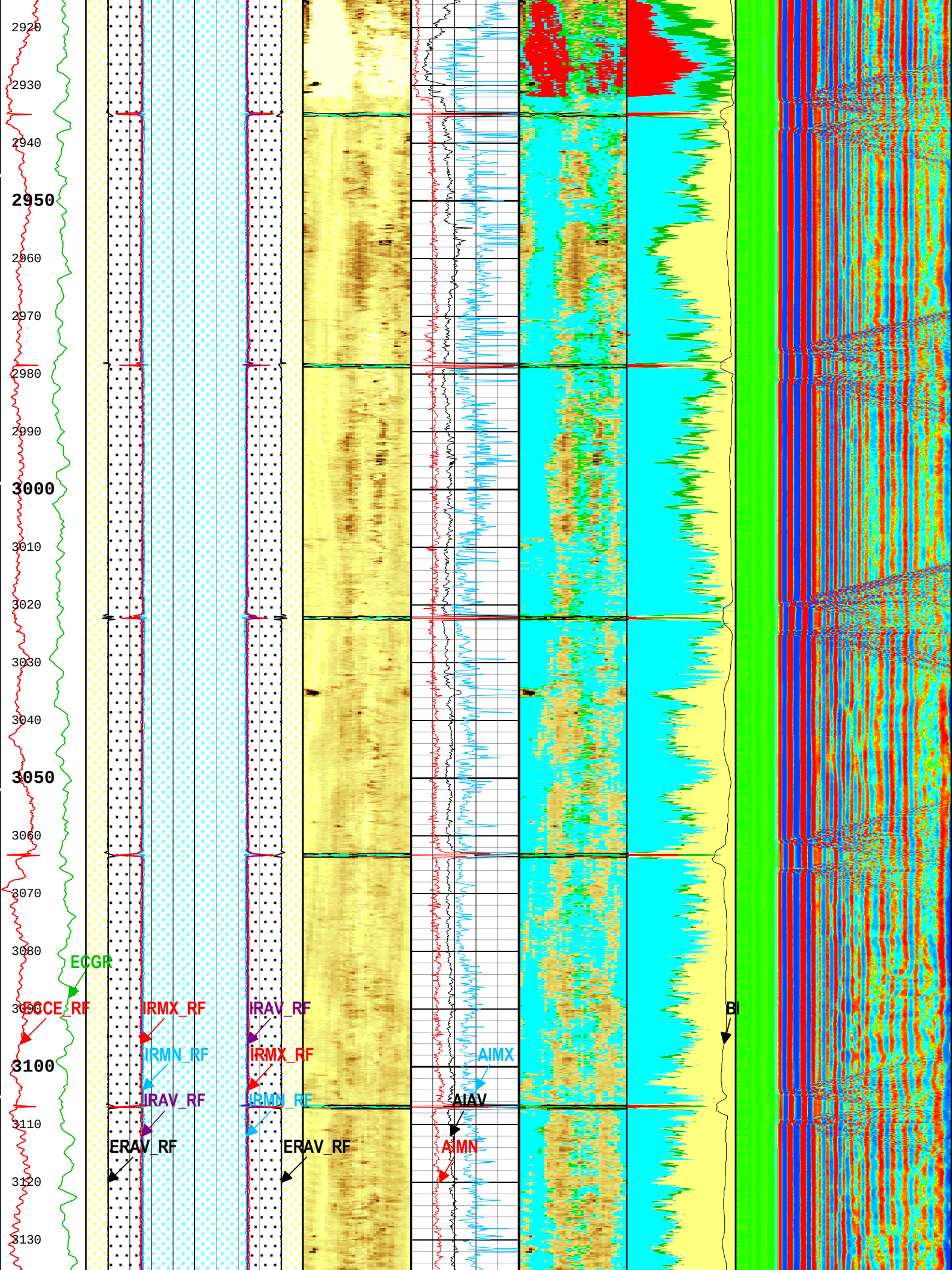
2920
2930
2940
2950
2960
2970
2980
2990
3000
3010
3020
3030
3040
3050
3060
3070
3080
3090
3100
3110
3120
3130
ECGR
ECCE_RF
IRMX_RF
IRMN_RF
IRAV_RF
ERAV_RF
IRAV_RF
IRMX_RF
IRMN_RF
ERAV_RF
AIMX
AIAV
AIMN
BI

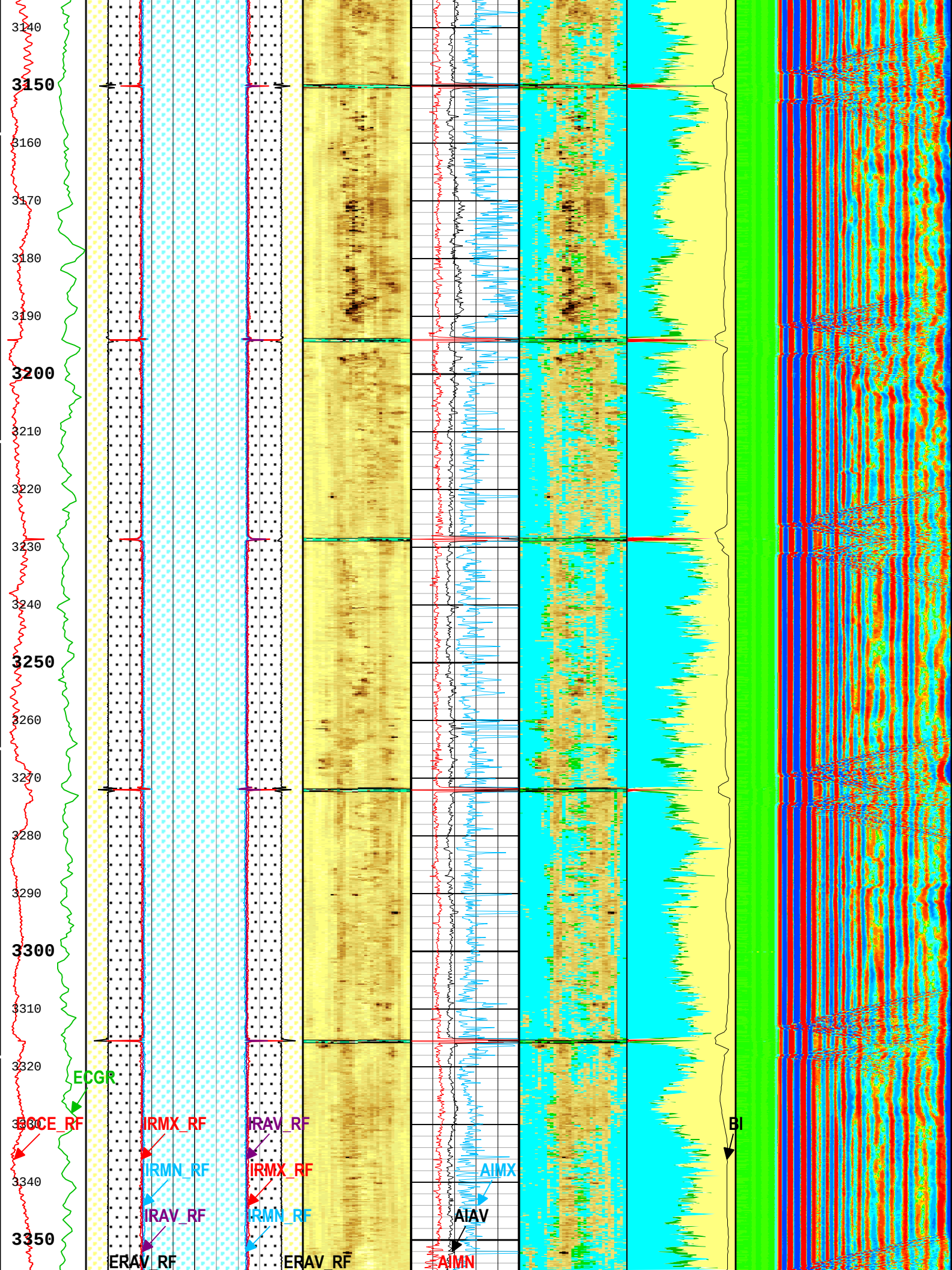
3140
3150
3160
3170
3180
3190
3200
3210
3220
3230
3240
3250
3260
3270
3280
3290
3300
3310
3320
3330
3340
3350
ECGR
CCE_RF
IRMX_RF
IRMN_RF
IRAV_RF
ERAV_RF
IRAV_RF
IRMX_RF
IRMN_RF
ERAV_RF
AIMX
AIAV
AIMN
BI

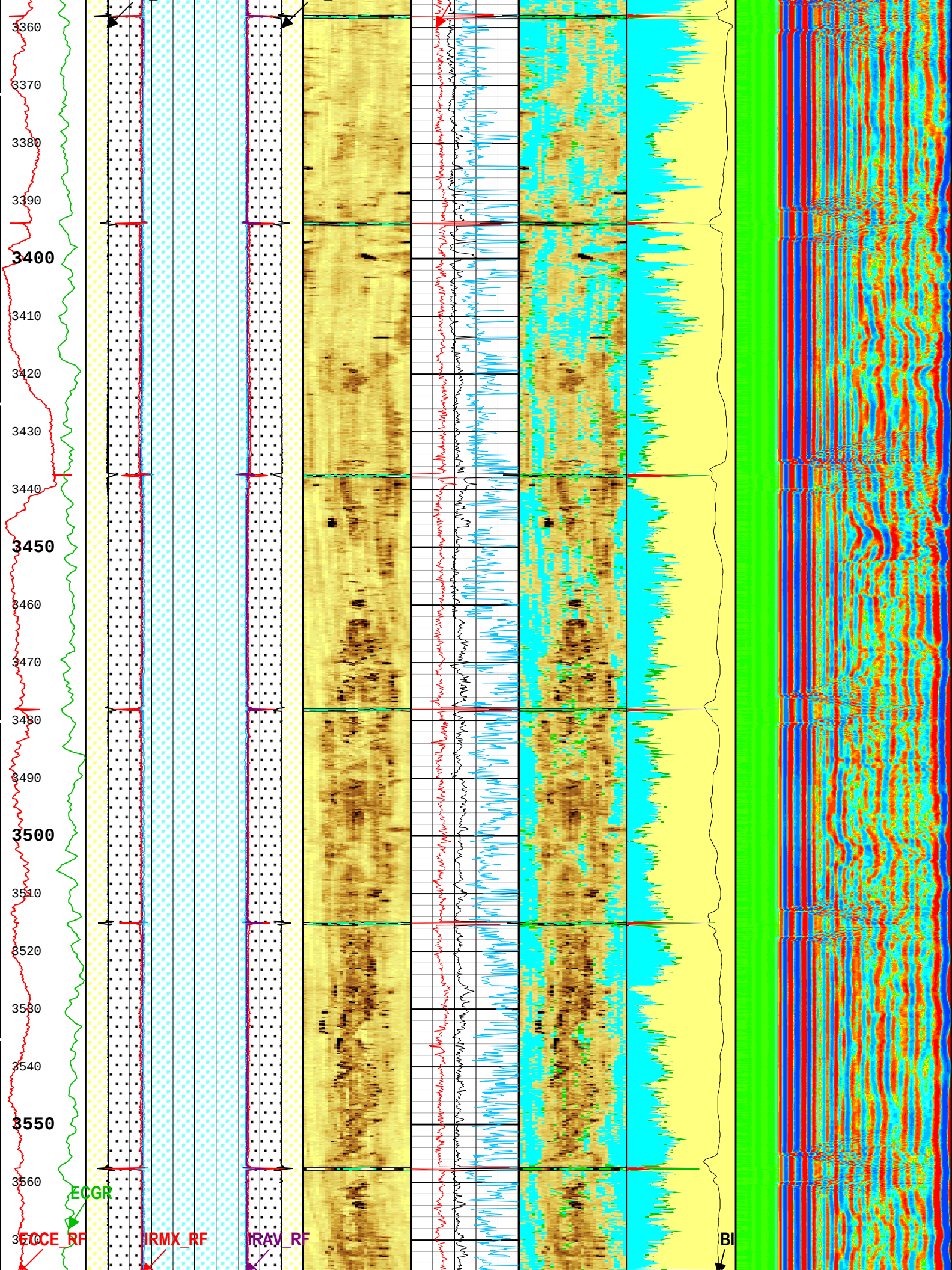
3360
3370
3380
3390
3400
3410
3420
3430
3440
3450
3460
3470
3480
3490
3500
3510
3520
3530
3540
3550
3560
ECGR
ECCE_RF
IRMX_RF
IRAV_RF
BI

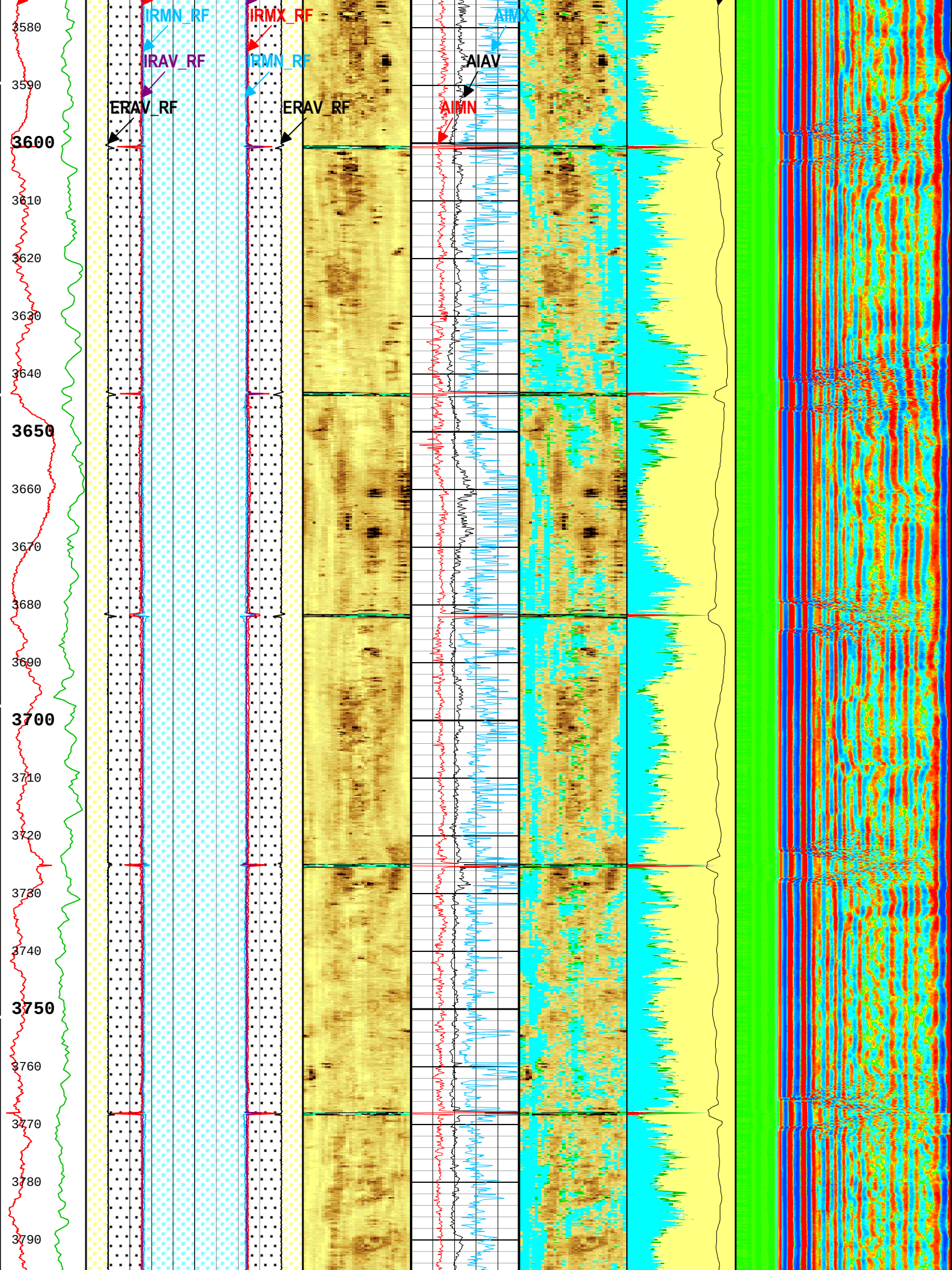
IRMN_RF
IRMX_RF
AIMX
IRAV_RF
IRMN_RF
AIAV
ERAV_RF
ERAV_RF
AIMN
3580
3590
3600
3610
3620
3630
3640
3650
3660
3670
3680
3690
3700
3710
3720
3730
3740
3750
3760
3770
3780
3790

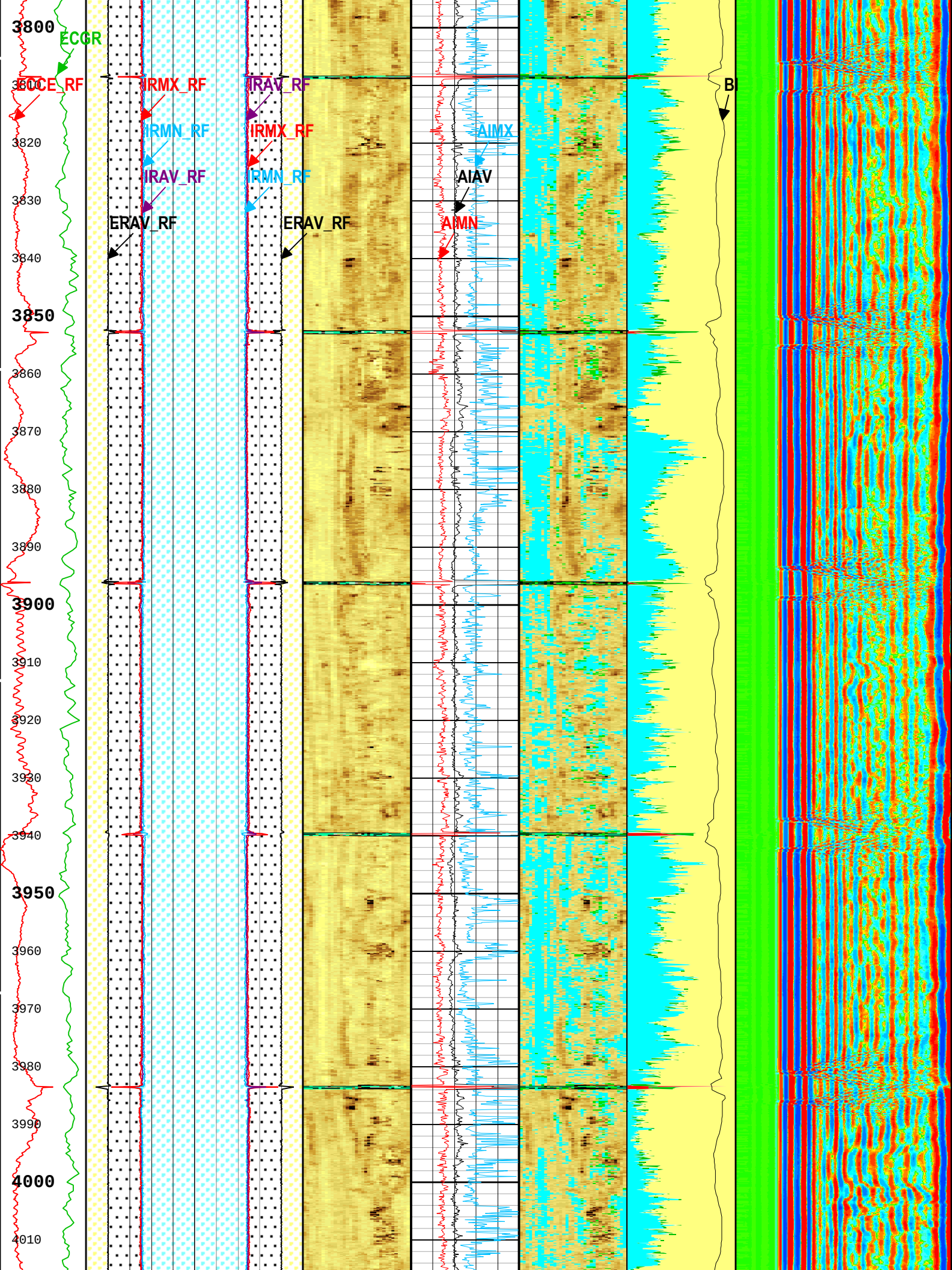
3800
ECGR
ECCE_RF
IRMX_RF
IRAV_RF
IRMN_RF
IRMX_RF
IRAV_RF
IRMN_RF
AIMX
AIAV
AIMN
ERAV_RF
ERAV_RF
B
3820
3830
3840
3850
3860
3870
3880
3890
3900
3910
3920
3930
3940
3950
3960
3970
3980
3990
4000
4010

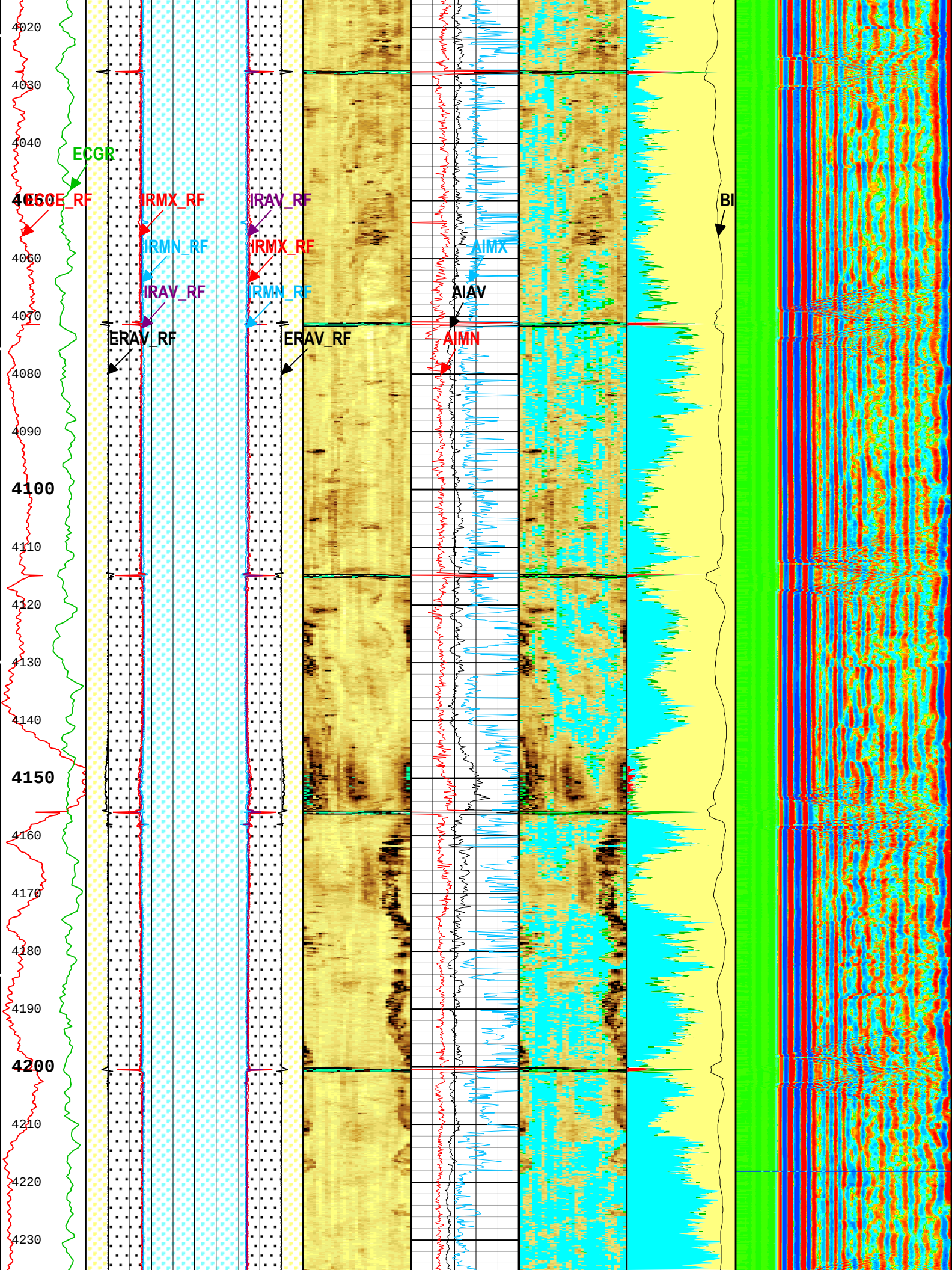
4020
4030
4040
ECGR
4050
ECDE_RF
IRMX_RF
IRAV_RF
IRMN_RF
IRMX_RF
IRAV_RF
IRMN_RF
AIMX
AIAV
AIMN
BI
4060
4070
ERAV_RF
ERAV_RF
4080
4090
4100
4110
4120
4130
4140
4150
4160
4170
4180
4190
4200
4210
4220
4230

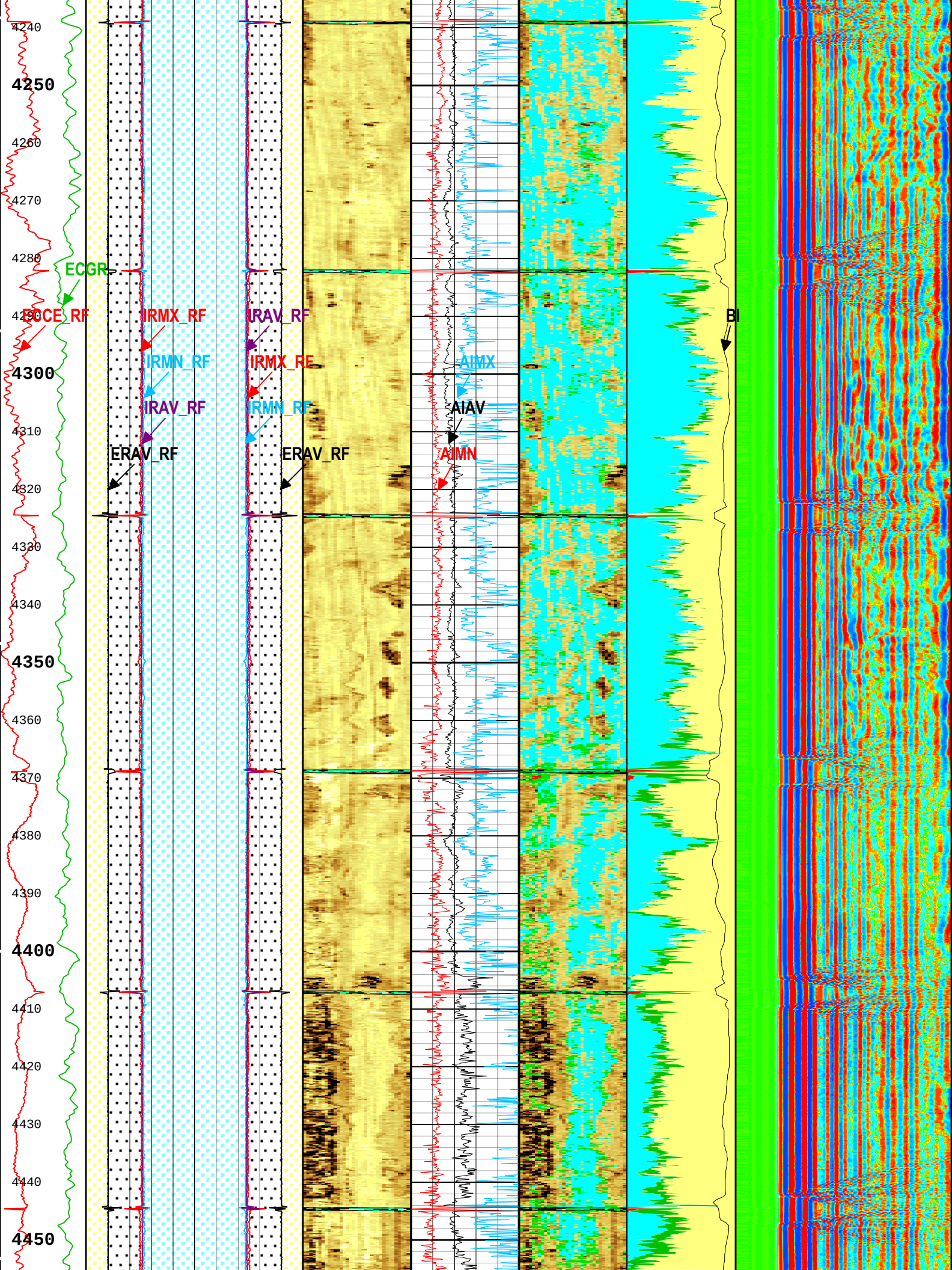
4240
4250
4260
4270
4280
4290
4300
4310
4320
4330
4340
4350
4360
4370
4380
4390
4400
4410
4420
4430
4440
4450
ECGR
ECE_RF
IRMX_RF
IRMN_RF
IRAV_RF
ERAV_RF
IRAV_RF
IRMX_RF
IRMN_RF
ERAV_RF
AIMX
AIAV
AIMN
BI

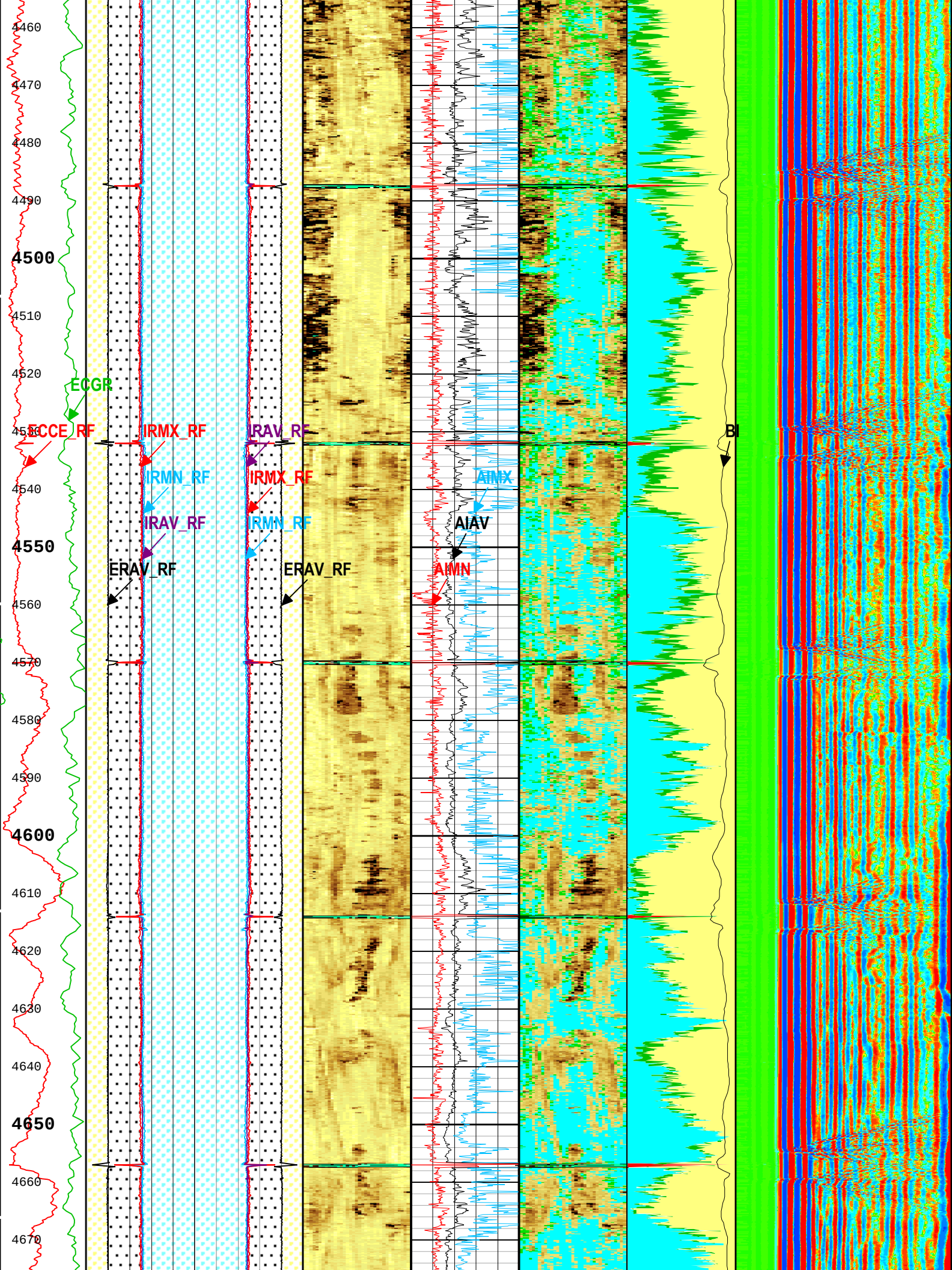
4460
4470
4480
4490
4500
4510
4520
4530
4540
4550
4560
4570
4580
4590
4600
4610
4620
4630
4640
4650
4660
4670
ECGR
ECCE_RF
IRMX_RF
IRAV_RF
IRMN_RF
IRMX_RF
IRAV_RF
IRMN_RF
ERAV_RF
ERAV_RF
AIMX
AIAV
AIMN
BI

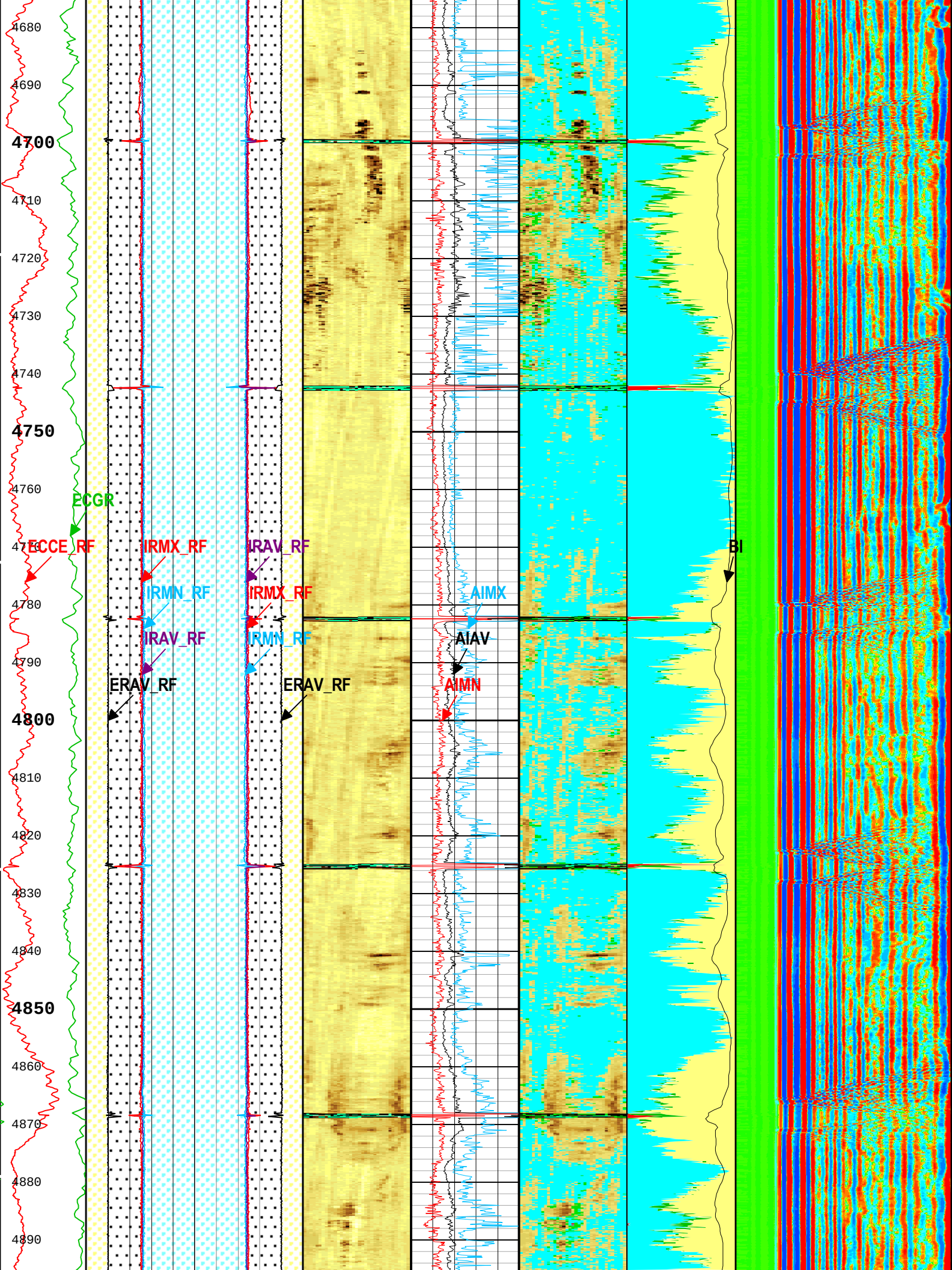
4680
4690
4700
4710
4720
4730
4740
4750
4760
4770
4780
4790
4800
4810
4820
4830
4840
4850
4860
4870
4880
4890
ECGR
ECCE_RF
IRMX_RF
IRAV_RF
IRMN_RF
IRMX_RF
IRAV_RF
IRMN_RF
ERAV_RF
ERAV_RF
AIMX
AIAV
AIMN
BI

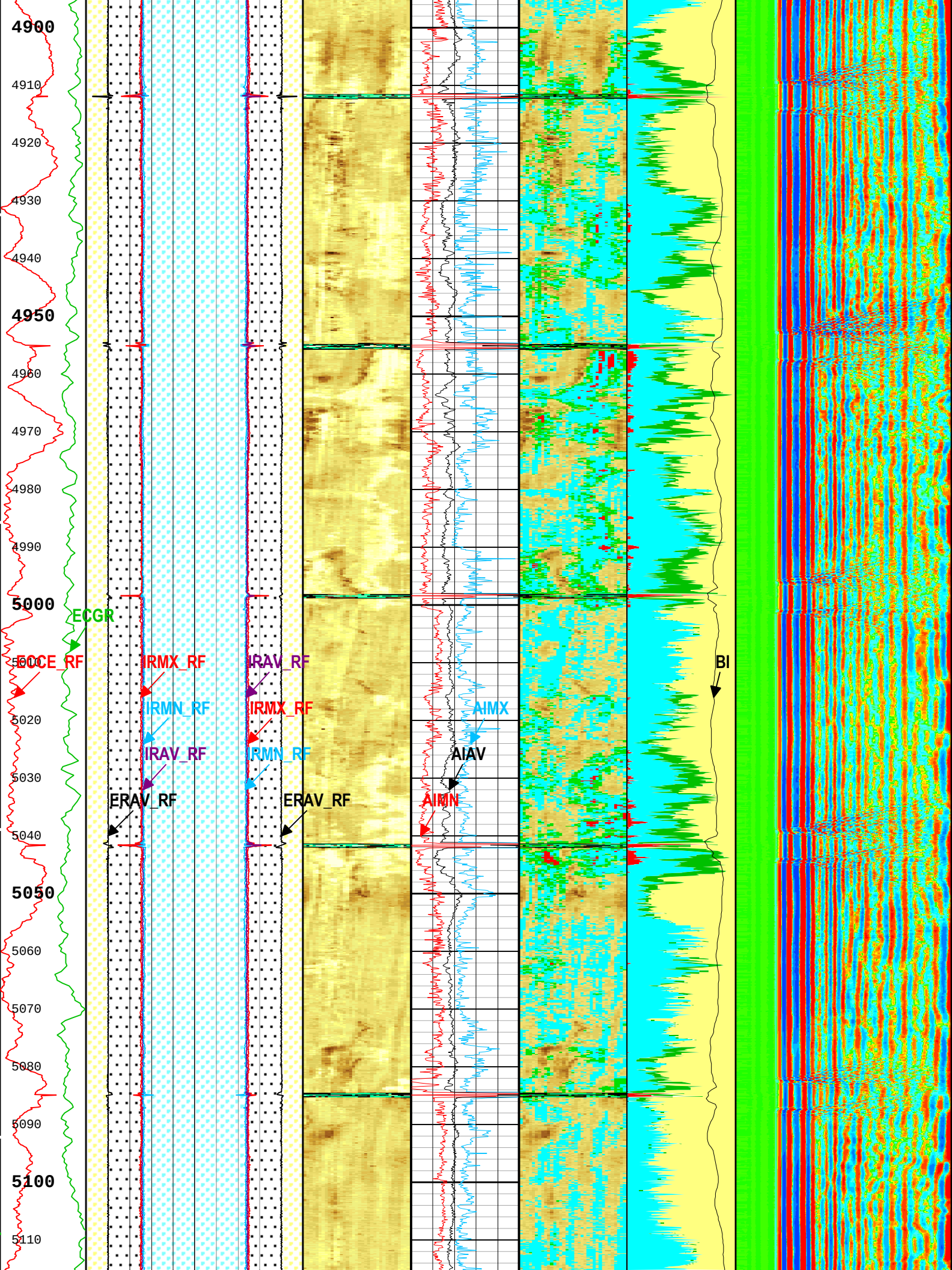
4900
4910
4920
4930
4940
4950
4960
4970
4980
4990
5000
5010
5020
5030
5040
5050
5060
5070
5080
5090
5100
5110
ECGR
ECCE_RF
IRMX_RF
IRAV_RF
IRMN_RF
IRMX_RF
IRAV_RF
IRMN_RF
ERAV_RF
ERAV_RF
AIMX
AIAV
AIMN
BI

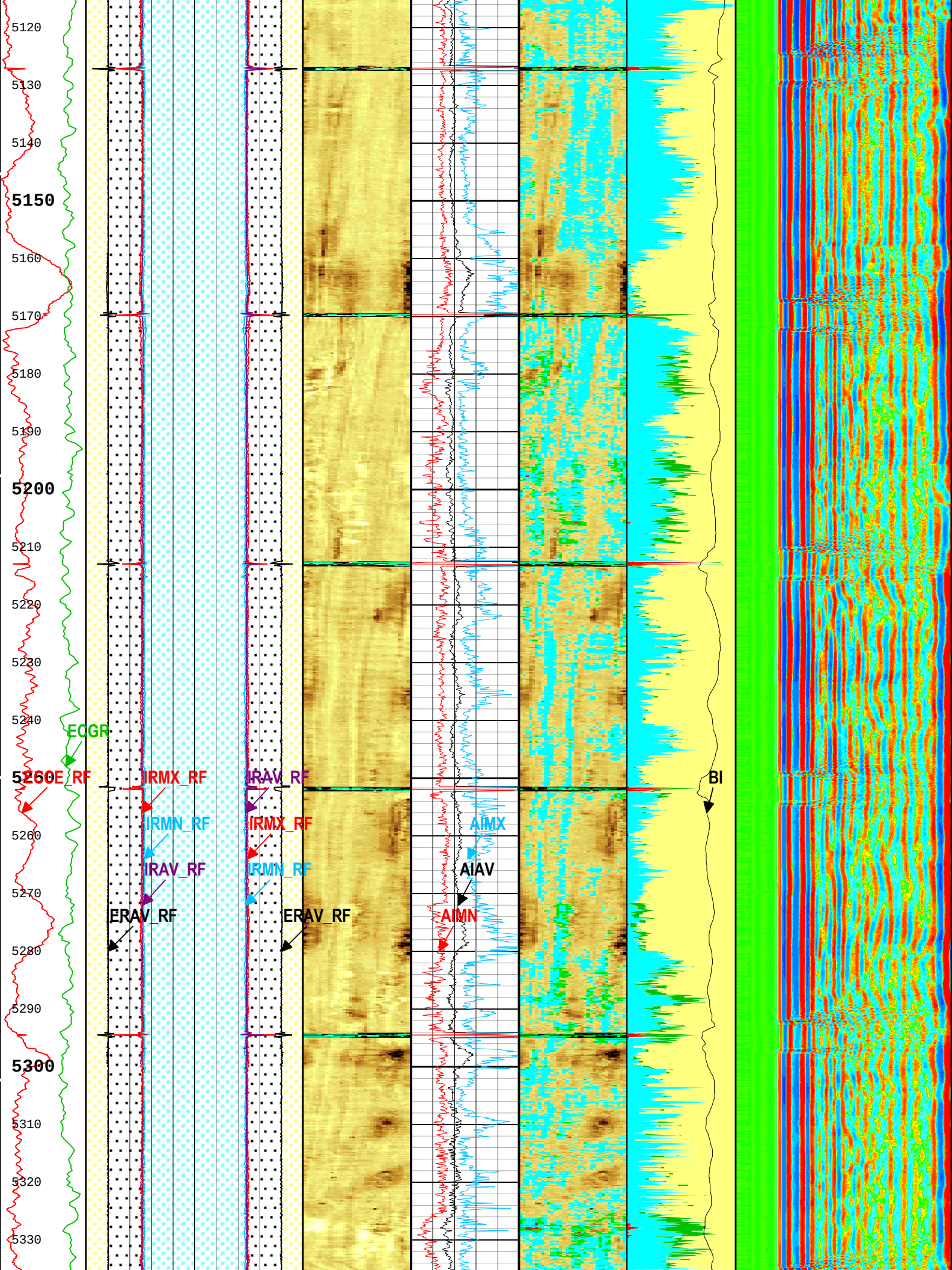
5120
5130
5140
5150
5160
5170
5180
5190
5200
5210
5220
5230
5240
5250
5260
5270
5280
5290
5300
5310
5320
5330
ECGR
ERAV_RF
IRMX_RF
IRMN_RF
IRAV_RF
ERAV_RF
IRAV_RF
IRMX_RF
IRMN_RF
ERAV_RF
AIMX
AIAV
AIMN
BI

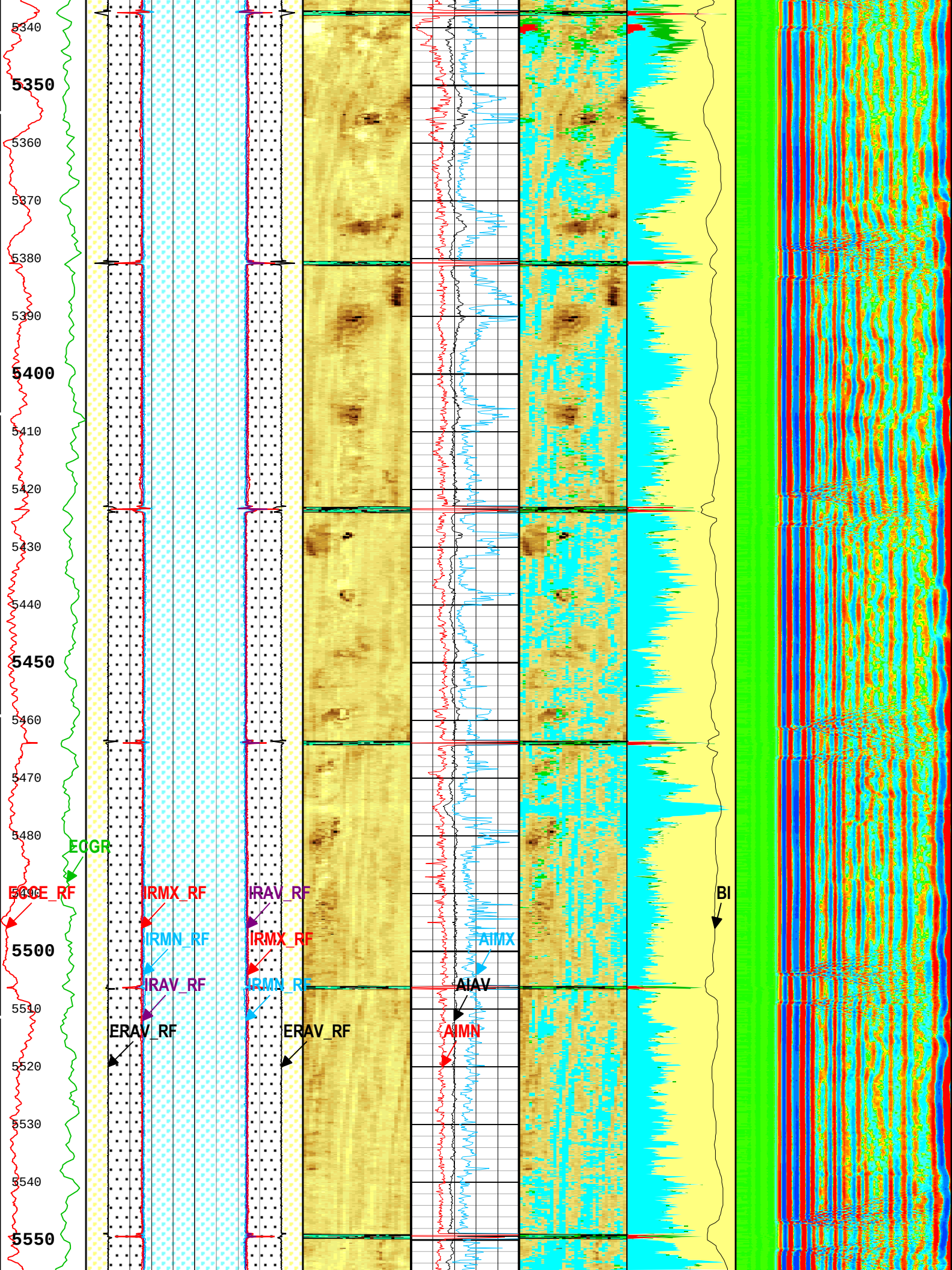
5340
5350
5360
5370
5380
5390
5400
5410
5420
5430
5440
5450
5460
5470
5480
5500
5510
5520
5530
5540
5550
ECGR
ECCE_RF
IRMX_RF
IRAV_RF
IRMN_RF
IRMX_RF
IRAV_RF
IRMN_RF
ERAV_RF
ERAV_RF
AIMX
AIAV
AIMN
BI

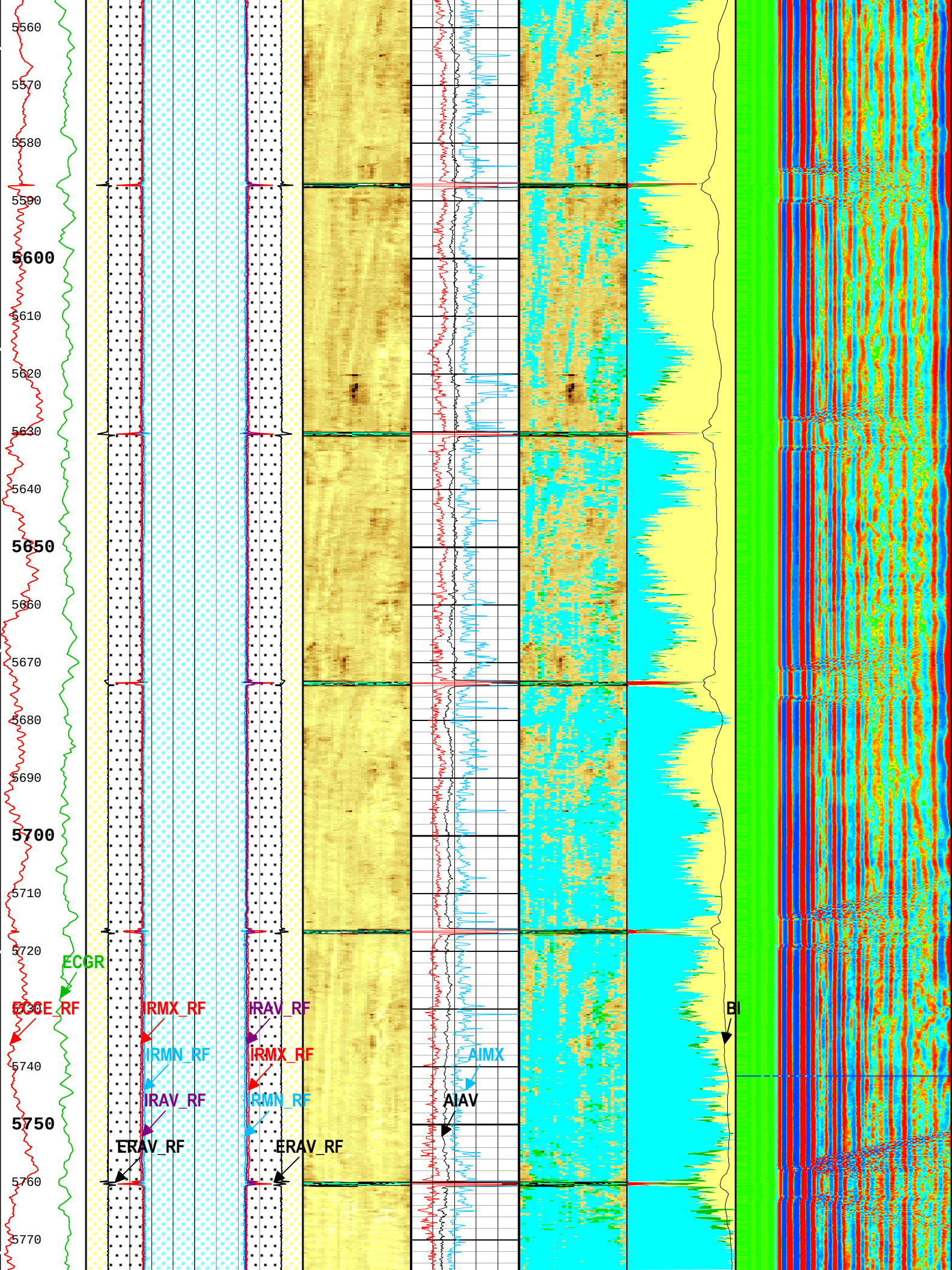
5560
5570
5580
5590
5600
5610
5620
5630
5640
5650
5660
5670
5680
5690
5700
5710
5720
5730
5740
5750
5760
5770
ECGR
ECCE_RF
IRMX_RF
IRMN_RF
IRAV_RF
ERAV_RF
IRAV_RF
IRMX_RF
IRMN_RF
ERAV_RF
AIMX
AIAV
BI

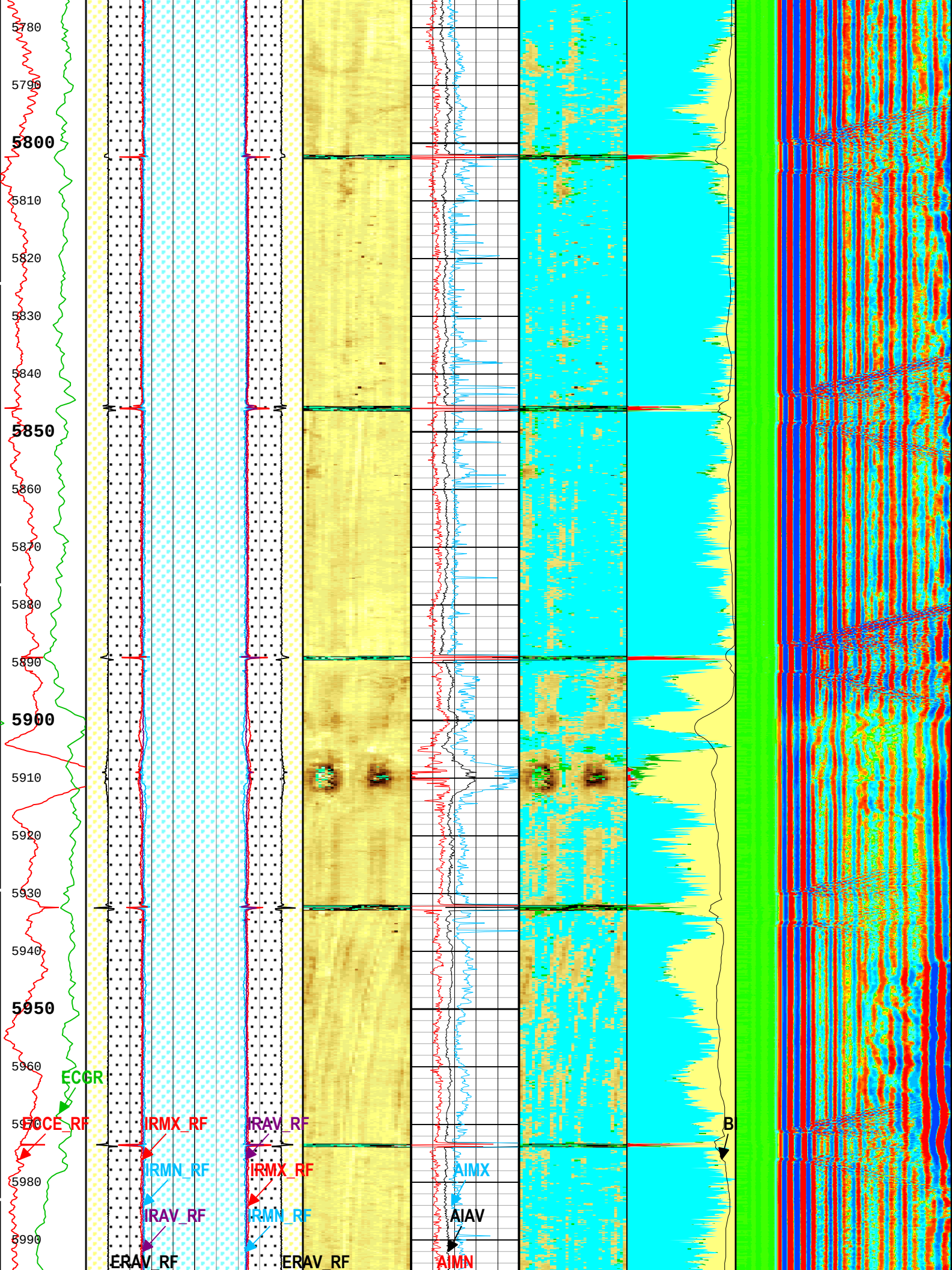
5780
5790
5800
5810
5820
5830
5840
5850
5860
5870
5880
5890
5900
5910
5920
5930
5940
5950
5960
5970
5980
5990
ECGR
ECCE_RF
IRMX_RF
IRAV_RF
IRMN_RF
IRMX_RF
IRAV_RF
IRMN_RF
ERAV_RF
ERAV_RF
AIMX
AIAV
AIMN
B

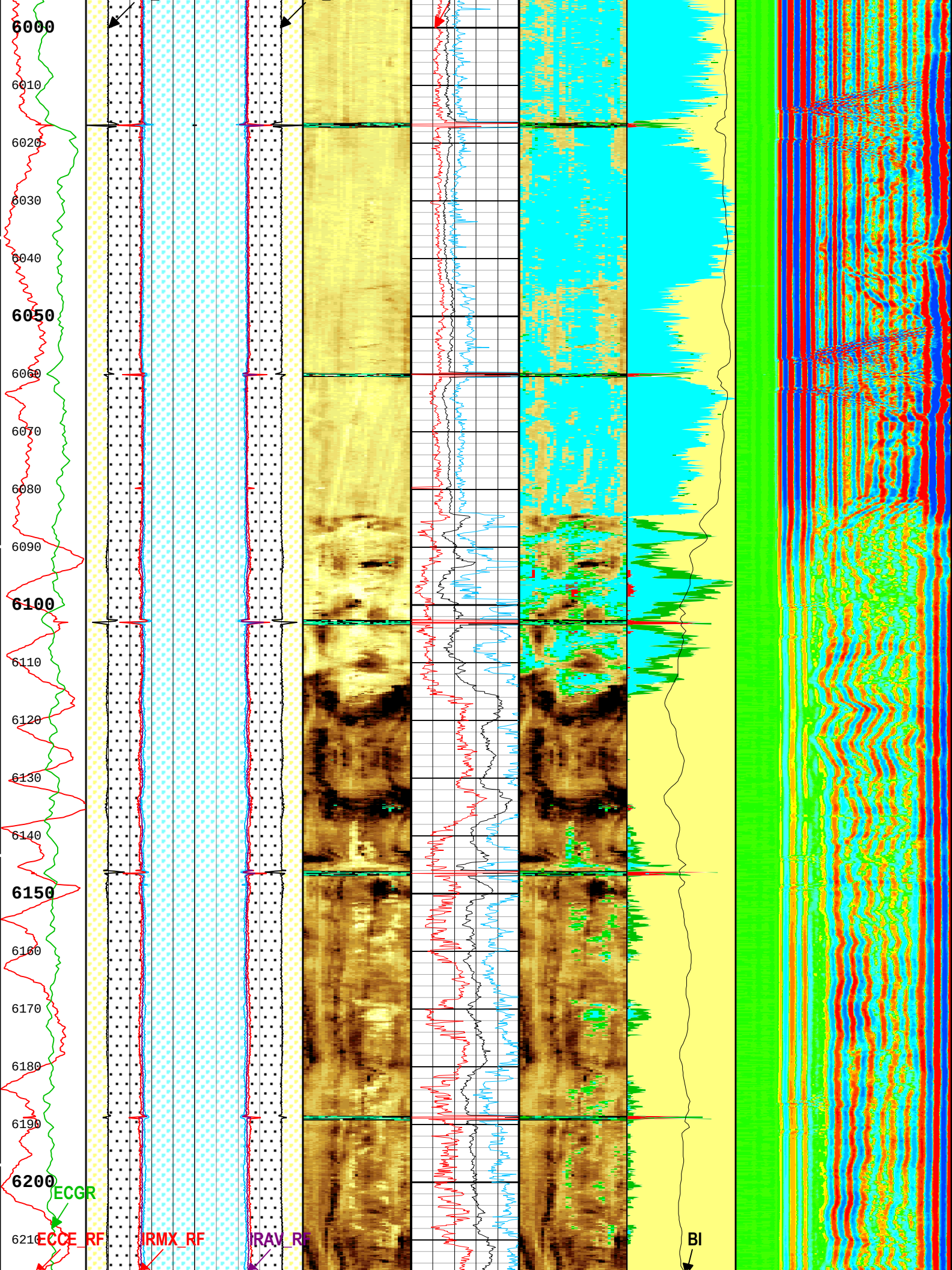
6000
6010
6020
6030
6040
6050
6060
6070
6080
6090
6100
6110
6120
6130
6140
6150
6160
6170
6180
6190
6200
6210
ECGR
ECCE_RF
IRMX_RF
IRAV_RF
BI

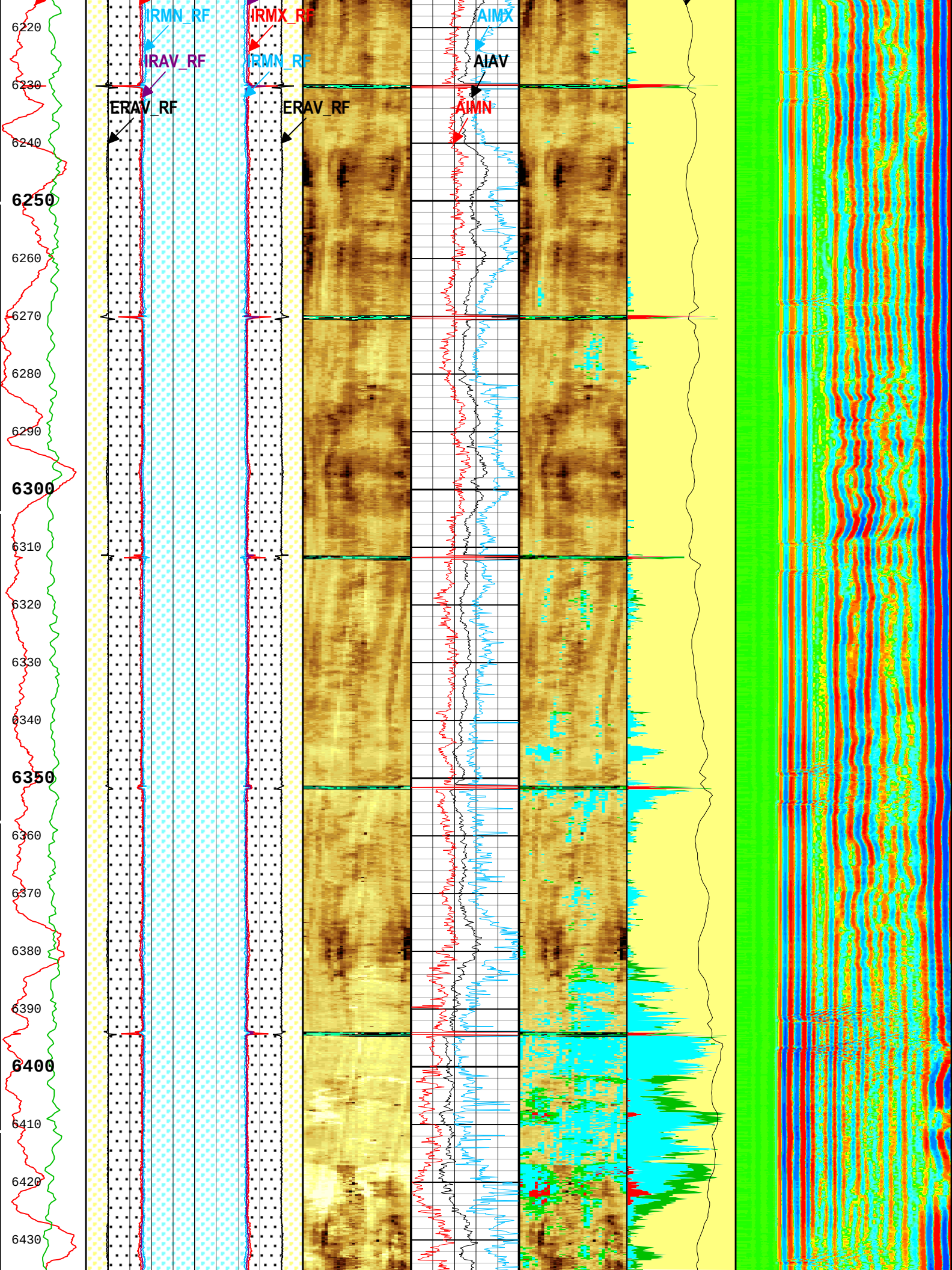
IRMN_RF
IRMX_RF
AIMX
IRAV_RF
IRMN_RF
AIAV
ERAV_RF
ERAV_RF
AIMN
6220
6230
6240
6250
6260
6270
6280
6290
6300
6310
6320
6330
6340
6350
6360
6370
6380
6390
6400
6410
6420
6430

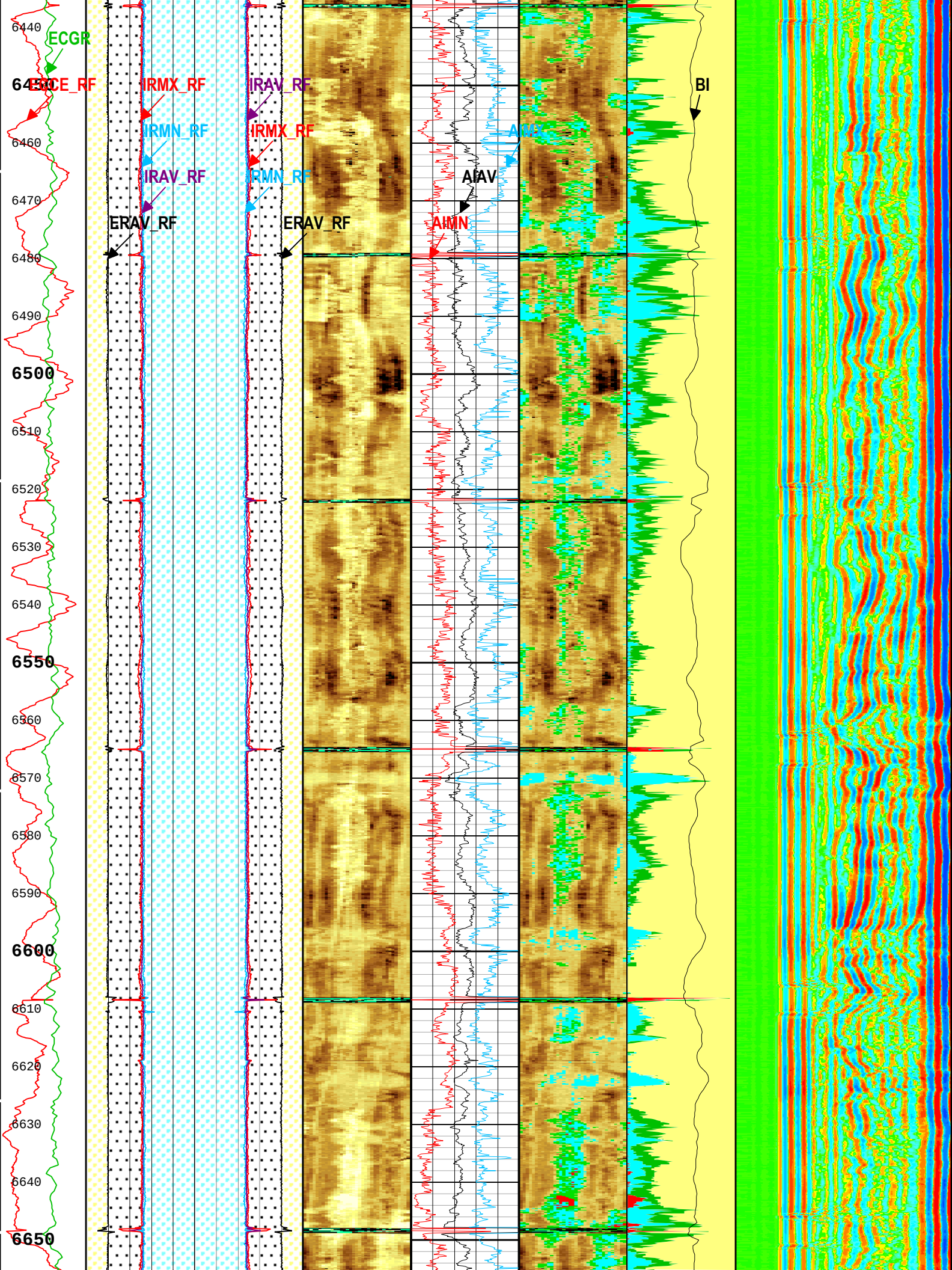
ECGR
CE_RF
IRMX_RF
IRMN_RF
IRAV_RF
ERAV_RF
IRAV_RF
IRMX_RF
IRMN_RF
ERAV_RF
AIAV
AIMN
BI
6440
6450
6460
6470
6480
6490
6500
6510
6520
6530
6540
6550
6560
6570
6580
6590
6600
6610
6620
6630
6640
6650

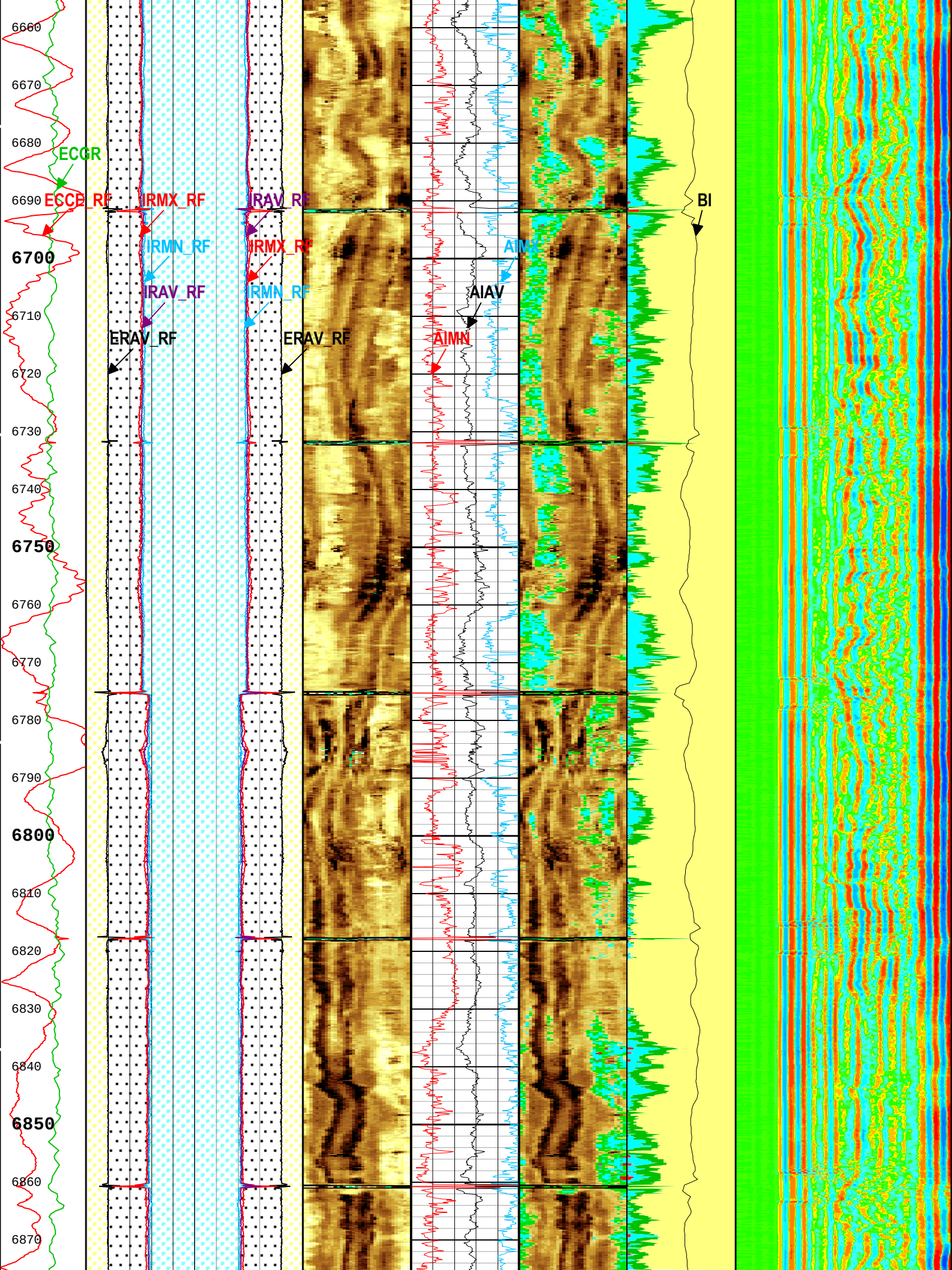
6660
6670
6680
ECGR
6690
ECCB_RF
IRMX_RF
IRAV_RF
IRAV_RF
IRMX_RF
BI
6700
IRMN_RF
IRMX_RF
AIMX
IRAV_RF
IRMN_RF
AIAV
6710
ERAV_RF
ERAV_RF
AIMN
6720
6730
6740
6750
6760
6770
6780
6790
6800
6810
6820
6830
6840
6850
6860
6870

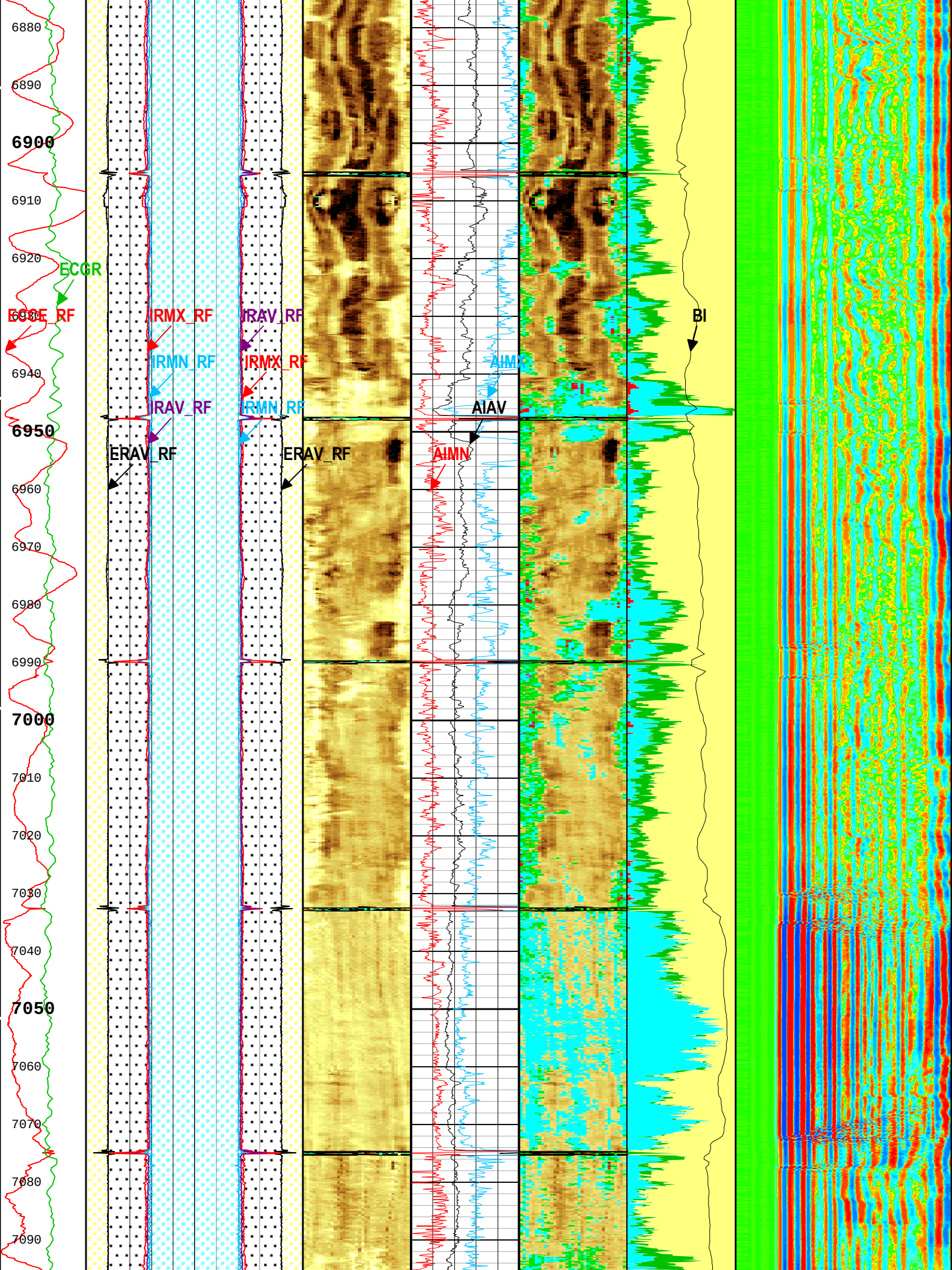
6880
6890
6900
6910
6920
6930
6940
6950
6960
6970
6980
6990
7000
7010
7020
7030
7040
7050
7060
7070
7080
7090
ECGR
ECCE_RF
IRMX_RF
IRAV_RF
IRMN_RF
IRMX_RF
IRAV_RF
IRMN_RF
ERAV_RF
ERAV_RF
AIMX
AIAV
AIMN
BI

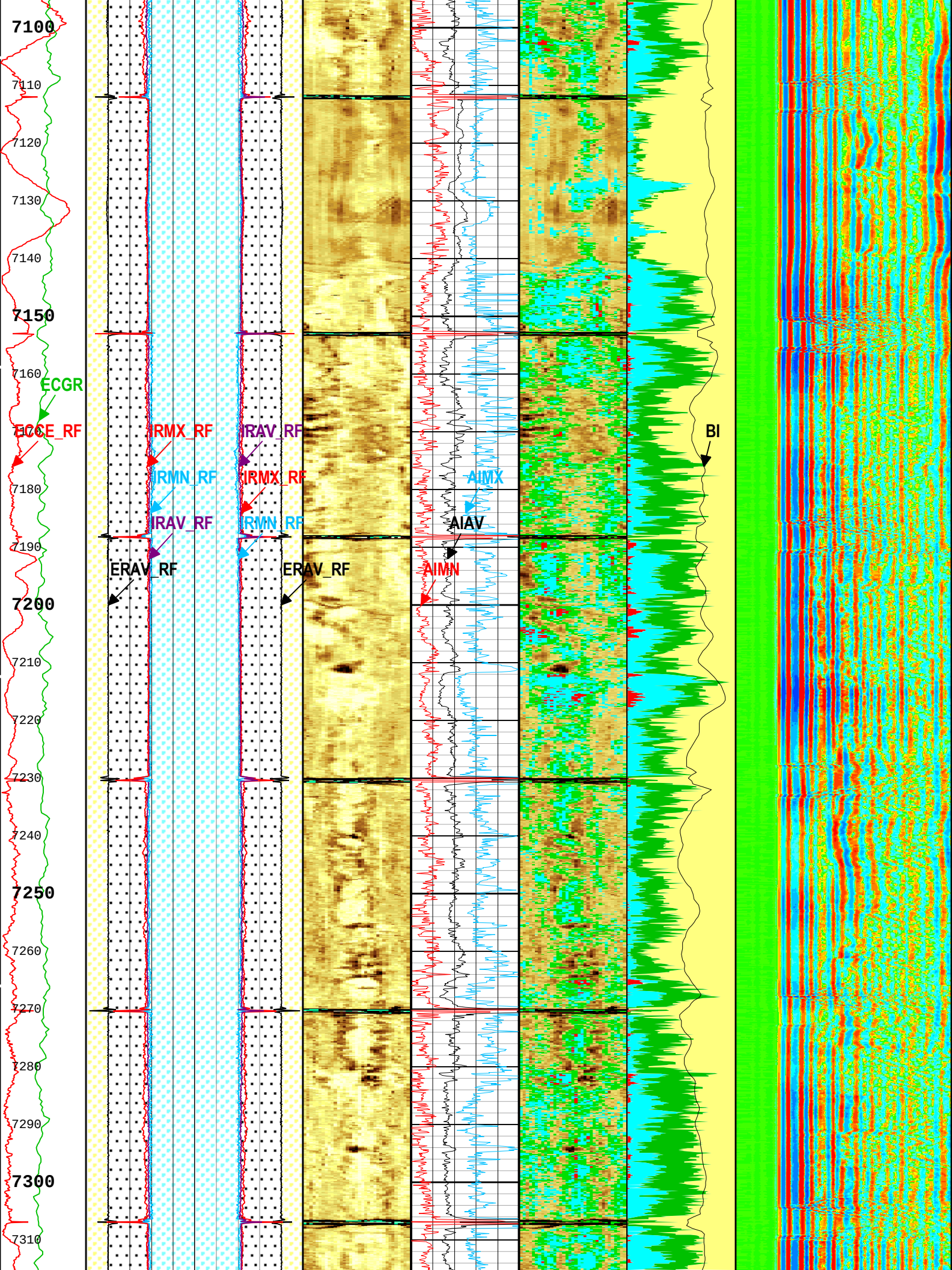
7100
7110
7120
7130
7140
7150
7160
ECGR
ECCE_RF
IRMX_RF
IRAV_RF
IRMN_RF
IRMX_RF
IRAV_RF
IRMN_RF
AIMX
AIAV
AIMN
BI
7180
7190
ERAV_RF
ERAV_RF
7200
7210
7220
7230
7240
7250
7260
7270
7280
7290
7300
7310

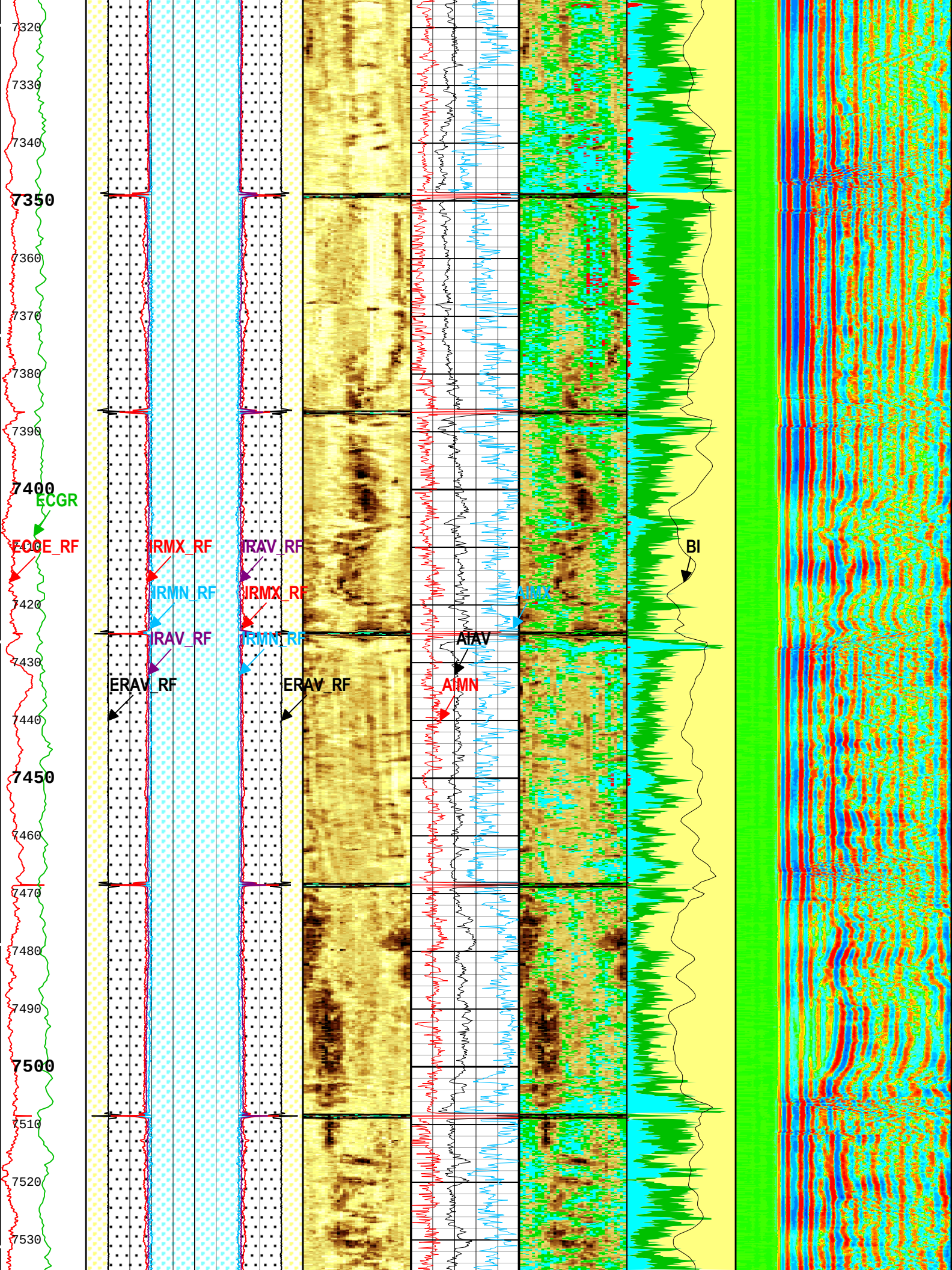
7320
7330
7340
7350
7360
7370
7380
7390
7400
ECGR
ECCE_RF
IRMX_RF
IRAV_RF
IRMN_RF
IRMX_RF
IRAV_RF
IRMN_RF
ERAV_RF
ERAV_RF
AIMX
AIAV
AIMN
BI
7420
7430
7440
7450
7460
7470
7480
7490
7500
7510
7520
7530

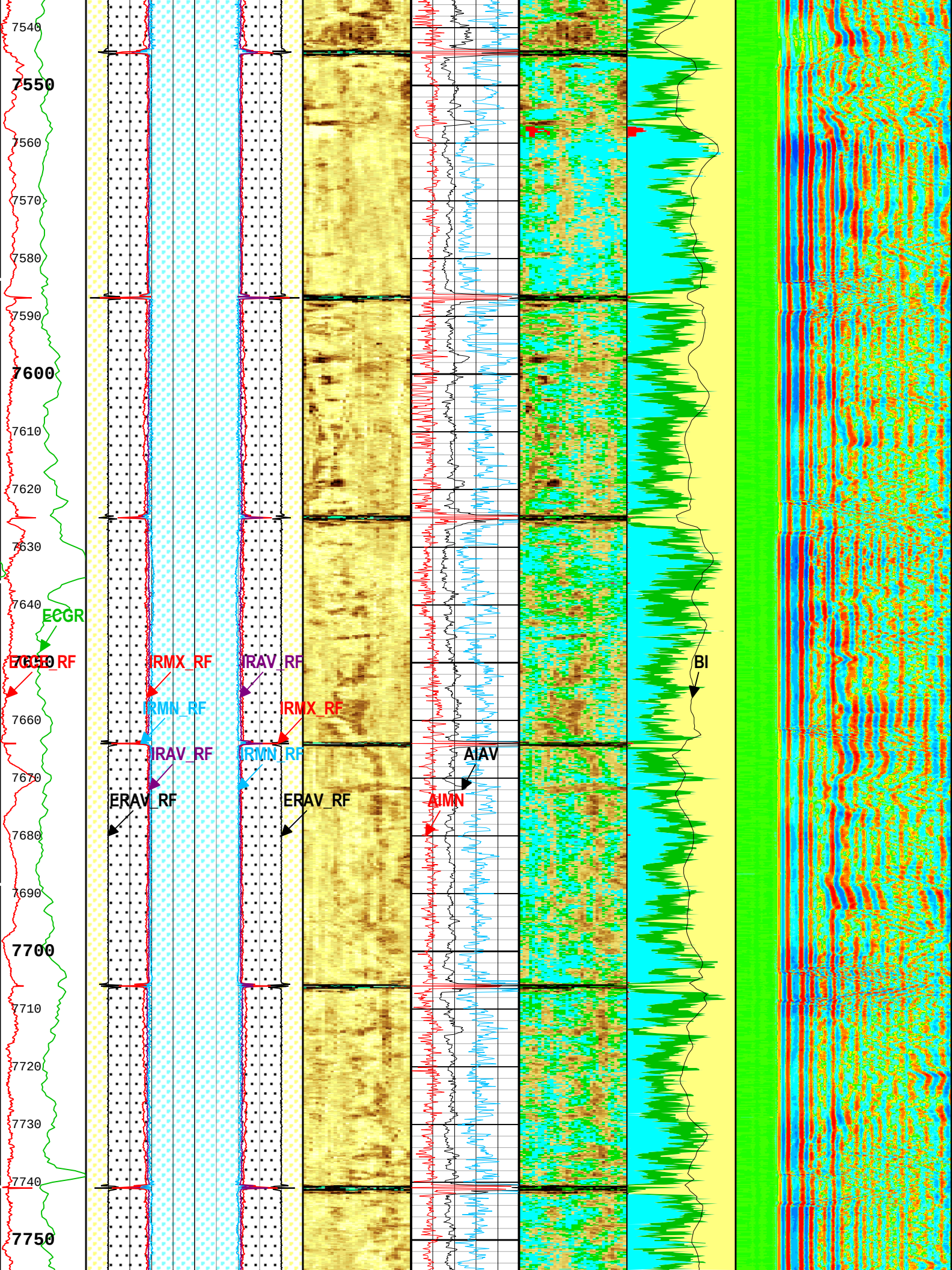
7540
7550
7560
7570
7580
7590
7600
7610
7620
7630
7640
ECGR
7650
ERMX_RF
IRMX_RF
IRAV_RF
BI
IRMN_RF
IRMX_RF
7660
IRAV_RF
IRMN_RF
AIAV
7670
ERAV_RF
ERAV_RF
AIMN
7680
7690
7700
7710
7720
7730
7740
7750

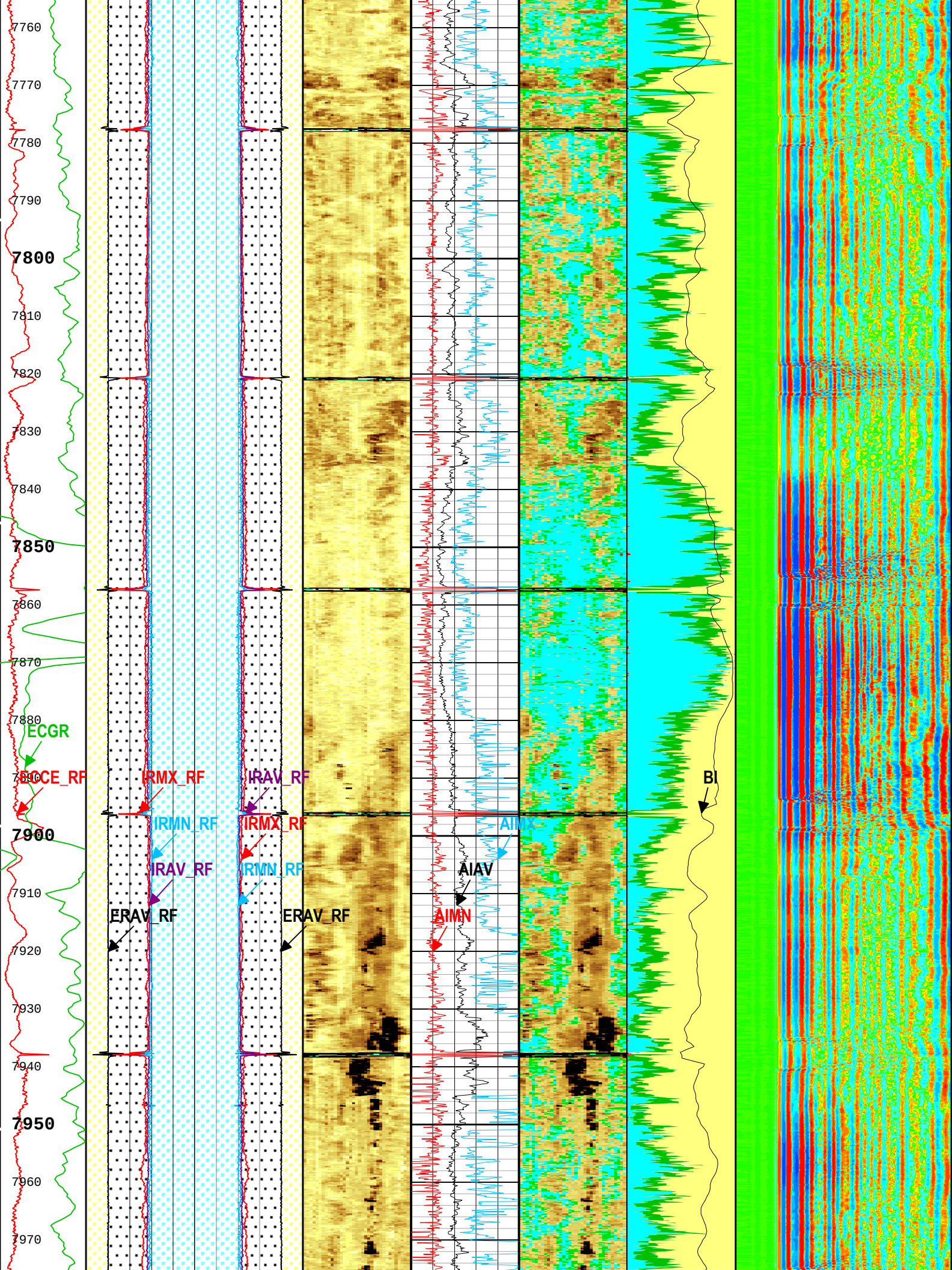
7760
7770
7780
7790
7800
7810
7820
7830
7840
7850
7860
7870
7880
7900
7910
7920
7930
7940
7950
7960
7970
ECGR
ECCE_RF
IRMX_RF
IRAV_RF
IRMN_RF
IRMX_RF
IRAV_RF
IRMN_RF
ERAV_RF
ERAV_RF
AIMX
AIAV
AIMN
BI

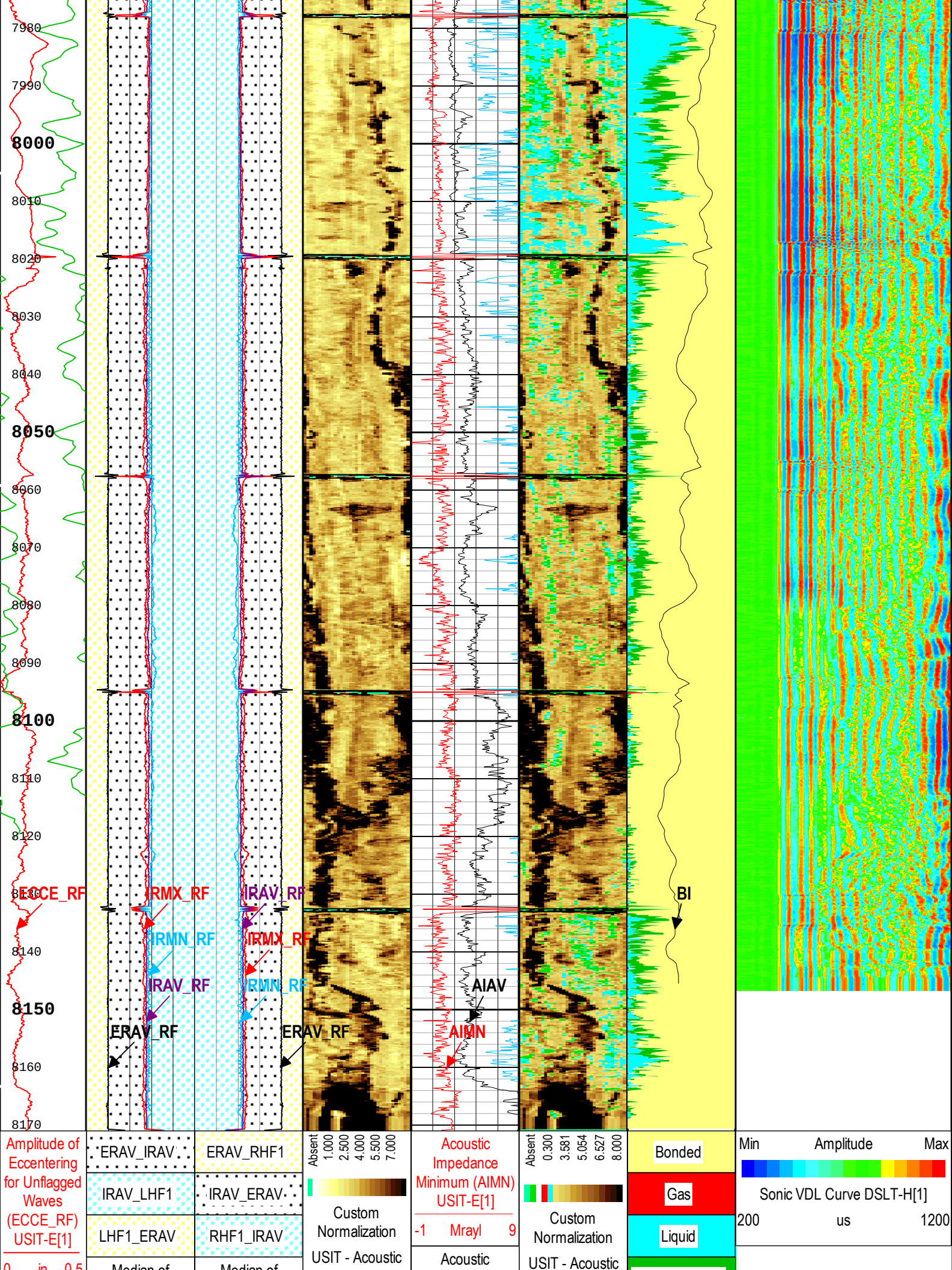
7980
7990
8000
8010
8020
8030
8040
8050
8060
8070
8080
8090
8100
8110
8120
8130
8140
8150
8160
8170
ECCE_RF
IRMX_RF
IRAV_RF
IRMN_RF
IRMX_RF
IRAV_RF
IRMN_RF
ERAV_RF
ERAV_RF
AIAV
AIMN
BI
Amplitude of Eccentering for Unflagged Waves (ECCE_RF) USIT-E[1]
0 in 0.5
ERAV_IRAV
IRAV_LHF1
LHF1_ERAV
ERAV_RHF1
IRAV_ERAV
RHF1_IRAV
Absent 1.000 2.500 4.000 5.500 7.000
Custom Normalization
USIT - Acoustic
Acoustic Impedance Minimum (AIMN) USIT-E[1]
-1 Mrayl 9
Acoustic
Absent 0.300 3.581 5.054 6.527 8.000
Custom Normalization
USIT - Acoustic
Bonded
Gas
Liquid
Min Amplitude Max
Sonic VDL Curve DSLT-H[1]
200 us 1200

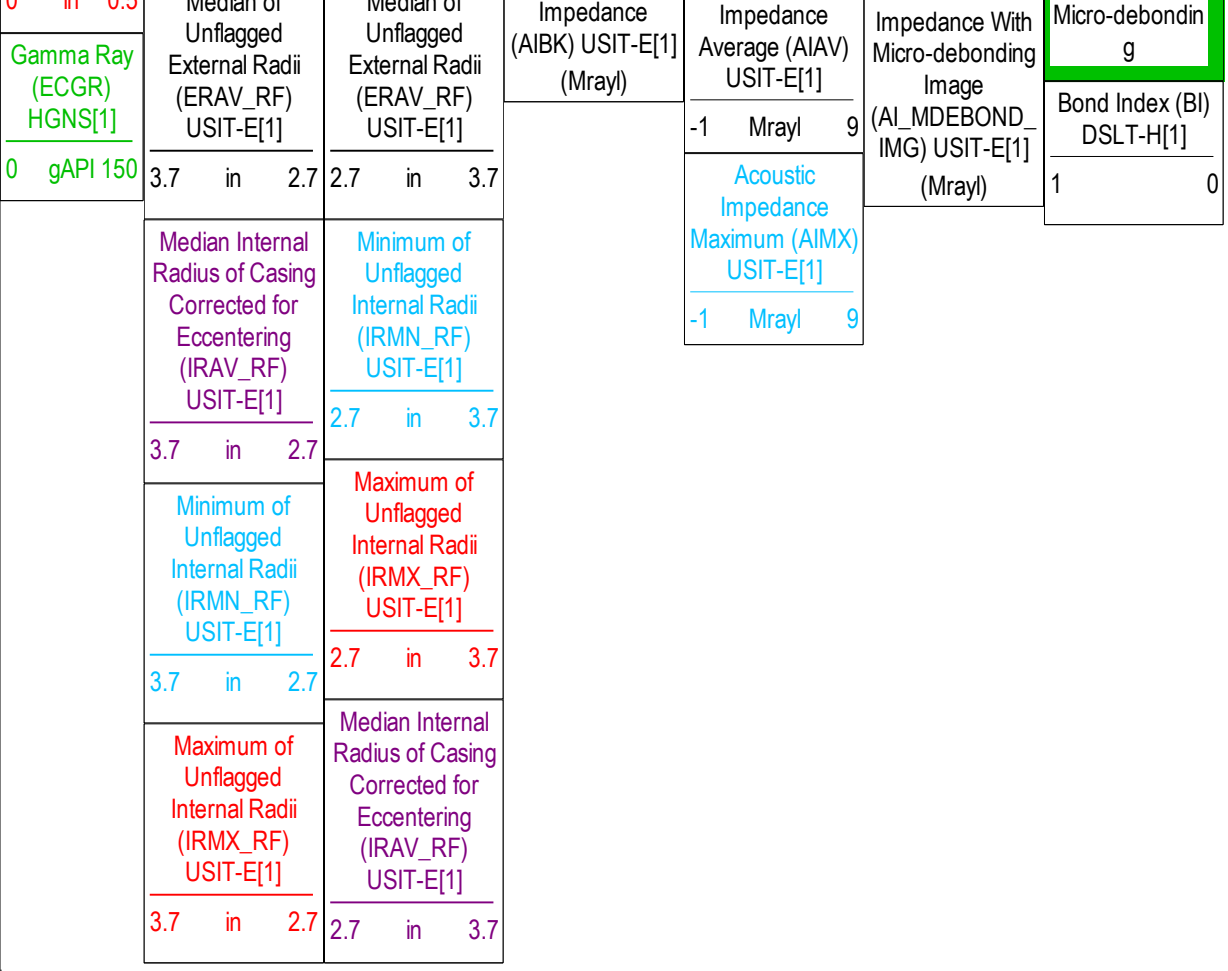

TIME_1900 - Time Marked every 60.00 (s)

Description: USI VDL Cement Format: Log (LBV1_USI-VDL (DSLT) Cement 7inch) Index Scale: 5 in per 100 ft Index Unit: ft Index Type: Measured Depth
Creation Date: 20-Oct-2016 14:28:02

Channel Processing Parameters

Two: Parameters

Parameter	Description	Tool	Value	Unit
AMSG	Auxiliary Minimum Sliding Gate	DSLT-H	140	us
ISSBAR	Barite Mud Presence Flag	Borehole	No	
BERJ	Bad Echo Rejection	USIT-E	On	
BHS	Borehole Status (Open or Cased Hole)	Borehole	Cased	
BILI	Bond Index Level for Zone Isolation	DSLT-H	0.8	
BS	Bit Size	WLSESSION	Depth Zoned	in
CASING_PRATIO	Casing Poisson Ratio	USIT-E	Standard Poisson Ratio	
CBLG	CBL Gate Width	DSLT-H	45	us
CBLO	Casing Bottom (Logger)	WLSESSION	8280	ft
CBRA	CBL LQC Reference Amplitude in Free Pipe	DSLT-H	62	mV
CDEN	Cement Density	HGNS-H	2	g/cm3
CMCF	CBL Cement Type Compensation Factor	DSLT-H	1	
CMTY(U-USIT_CEMT)	Cement Type	USIT-E	Regular Cement	
THNO	Nominal Casing Thickness - Zoned along logger depths	WLSESSION	Depth Zoned	in
DETE	Delta-T Detection	DSLT-H	E1	
DFD	Drilling Fluid Density	Borehole	9	lbm/gal
DFT	Drilling Fluid Type	Borehole	Water	
DTMD	Borehole Fluid Slowness	Borehole	206	us/ft
FCF	CBL Fluid Compensation Factor	DSLT-H	0.94	
FDII	FPM Data Interpolation Interval	USIT-E	0	ft
GCSE_DOWN_PASS	Generalized Caliper Selection for WL Log Down Passes	Borehole	BS	

GCSE_UP_PASS	Generalized Caliper Selection for WL Log Up Passes	Borehole	BS	
GOBO_CURR	Good Bond in Arbitrary Cement	DSLT-H	Depth Zoned	mV
GR_MULTIPLIER	Gamma Ray Multiplier	HGNS-H	1	
HEMA	Hematite Presence Flag	Borehole	No	
ICE_PROCESS	ICE Processing	USIT-E	Yes	
IMAR	Image Rotation	USIT-E	Off	
MAHTR	Manual High Threshold Reference for first arrival detection	DSLT-H	120	
MATT_CURR	Maximum Attenuation in Arbitrary Cement	DSLT-H	Depth Zoned	dB/ft
MCI	Minimum Cemented Interval for Isolation	DSLT-H	Depth Zoned	ft
MEAS_WLEN	Tcube Processing Window Length in Measurement Mode	USIT-E	Depth Zoned	us
MNHTR	Minimum High Threshold Reference for first arrival detection	DSLT-H	100	
MSA	Minimum Sonic Amplitude	DSLT-H	Depth Zoned	mV
MSA_CURR	Minimum Sonic Amplitude in Arbitrary Cement	DSLT-H	Depth Zoned	mV
MUD_N_FRP	Free Pipe Mud Normalization Factor	USIT-E	1.1	
MUD_N_THE	Theoretical Mud Normalization Factor	USIT-E	1	
NMSG	Near Minimum Sliding Gate	DSLT-H	285	us
NMXG	Near Maximum Sliding Gate	DSLT-H	950	us
NUMP	Number of Detection Passes	DSLT-H	2	
OPLEV	USIT Remove Flagged Data Level	USIT-E	OPT2	
RCOD	Reference Calibrator Outer Diameter	USIT-E	7	in
RCSO	Reference Calibrator Standoff	USIT-E	1.181	in
RCTH	Reference Calibrator Thickness	USIT-E	0.295	in
SDNV	Number of Vertical Samples used for Micro-debonding Computation	USIT-E	5	
SDTHOR	Acoustic Impedance STD Horizontal Threshold for Micro-debonding	USIT-E	0.5	Mrayl
SDTVER	Acoustic Impedance STD Vertical Threshold for Micro-debonding	USIT-E	0.3	Mrayl
SFAF	Sonic Formation Attenuation Factor	DSLT-H	3.25	dB/ft
SGAD	Sliding Gate Status	DSLT-H	Off	
SGCL	Sliding Gate Closing Delta-T	DSLT-H	130	us/ft
SGCW	Sliding Gate Closing Width	DSLT-H	25	us
SGDT	Sliding Gate Delta-T	DSLT-H	57	us/ft
SGW	Sliding Gate Width	DSLT-H	110	us
SLEV	Signal Level for AGC	DSLT-H	5000	mV
SOCN	Standoff Distance	HGNS-H	0.125	in
SOCO	Standoff Correction Option	HGNS-H	No	
TCUB	T^3 Processing Level	USIT-E	Loop	
THDH	Maximum Search Thickness (percentage of nominal)	USIT-E	Time Zoned	%
THDL	Minimum Search Thickness (percentage of nominal)	USIT-E	Time Zoned	%
HISC	Tool Position: Centered or Eccentered	HGNS-H	Eccentered	
U-USIT_DFSZ	Drilling Fluid Specific Acoustic Impedance	USIT-E	0.1	Mrayl
UFGDE	Fiberglass Density	USIT-E	1.95	g/cm3
UFGPS	Fiberglass Processing Selection	USIT-E	No	
UFGVL	Fiberglass Velocity	USIT-E	9678.48	ft/s
USI_FSOD	USIT USI Fluid Slowness Fits Casing Outer Diameter	USIT-E	0_OFF	
USI_FVEL_SEL	USI Fluid Velocity Selection	USIT-E	Automatic	
USI_ZMUD_SEL	USI Mud Impedance Selection	USIT-E	FreePipe Norm.	
THDP	Thickness Detection Policy	USIT-E	Fundamental	
VCAS	Ultrasonic Transversal Velocity in Casing	USIT-E	51.4	us/ft
VDLG	VDL Manual Gain	DSLT-H	5	
ZCAS	Acoustic Impedance of Casing	USIT-E	46.25	Mrayl

ZCMT	Acoustic Impedance of Cement	DSLT-H	6.8	Mrayl
ZCMT_NEAT	Acoustic Impedance of Cement in Neat Cement	DSLT-H	6.8	Mrayl
ZINI	Initial Estimate of Cement Impedance	USIT-E	-1	Mrayl
ZMUD	Acoustic Impedance of Mud	Borehole	1.48	Mrayl
ZTCM	Acoustic Impedance Threshold for Cement	USIT-E	2.6	Mrayl
ZTGS	Acoustic Impedance Threshold for Gas	USIT-E	0.3	Mrayl

TwoDepth Zoned Parameters

Parameter	Value	Start (ft)	Stop (ft)
BS	17.5	0	770
BS	12.25	770	6187
BS	11.75	6187	7421
BS	11	7421	8171
THNO	0.362	0	179
THNO	0.317	179	6774
THNO	0.362	6774	8171
GOBO_CURR	2.87	0	179
GOBO_CURR	1.87	179	6774
GOBO_CURR	2.87	6774	8171
MATT_CURR	11.82	0	179
MATT_CURR	13.39	179	6774
MATT_CURR	11.82	6774	8171
MCI	21.68	0	770
MCI	10	770	8171
MEAS_WLEN	22.5	0	179
MEAS_WLEN	19.62	179	6774
MEAS_WLEN	22.5	6774	8171
MSA	1.33	0	179
MSA	0.78	179	6774
MSA	1.33	6774	8171
MSA_CURR	1.33	0	179
MSA_CURR	0.78	179	6774
MSA_CURR	1.33	6774	8171

All depth are actual.

TwoTime Zoned Parameters

Pass Log[9]:Up

Parameter	Value	Start Time	Stop Time	Start Depth (ft)	Stop Depth (ft)
THDH	125	20-Oct-2016 09:51:44	20-Oct-2016 10:20:40	8171.38	6648.71
THDL	60	20-Oct-2016 09:51:44	20-Oct-2016 10:20:40	8171.38	6648.71

Pass Log[11]:Up

THDH	125	20-Oct-2016 10:26:34	20-Oct-2016 12:34:00	6648.71	113.27
THDL	60	20-Oct-2016 10:24:53	20-Oct-2016 12:00:23	6648.71	1633.75
THDL	70	20-Oct-2016 12:00:23	20-Oct-2016 12:34:00	1633.75	113.27

Pass Log[14]:Up

THDH	130	20-Oct-2016 12:53:24	20-Oct-2016 12:58:23	155.15	5.56
THDL	70	20-Oct-2016 12:53:24	20-Oct-2016 12:58:23	155.15	5.56

All depth are at tool zero.

Tool Control Parameters

Tool Control Parameters

Two: Parameters

Parameter	Description	Tool	Value	Unit
AGMN	Minimum Gain of Cartridge	USIT-E	-12	dB
AGMX	Maximum Gain of Cartridge	USIT-E	18	dB
DDEL	Digitizing Delay	DSLT-H	0	us
U-USIT_DDT5	USIC Downhole Decimation for T5 only	USIT-E	0_NONE	
DOT(DOS)	Distance between Opposite Transducer Faces	USIT-E	2.874	in
MODE	DSLT Acquisition Mode	DSLT-H	CBL	
RATE	DSLT Firing Rate	DSLT-H	15 Hz	
DTFS	DSLT Telemetry Frame Size	DSLT-H	536	
DWCO	Digitizer Word Count	DSLT-H	250	
EMXV	EMEX Voltage	USIT-E	Time Zoned	V
HRES	Horizontal Resolution	USIT-E	10 deg	
MOTOR_PROTECT	Motor Protection	USIT-E	On	
SDTH	Switch Down Threshold	DSLT-H	20000	
SGAI	Selectable Acquisition Gain	DSLT-H	x1	
SUTH	Switch Up Threshold	DSLT-H	1000	
TMUC	Type of Mud	USIT-E	BRI	
UACLV_PERM	Ultrasonic ACLV Permanent	USIT-E	No	
ULOG	Logging Objective	USIT-E	MEASUREMENT	
UMFR	Modulation Frequency	USIT-E	333333	Hz
USFR	Ultrasonic Sampling Frequency	USIT-E	500000	Hz
UPAT	USIT Emission Pattern	USIT-E	Pattern 500 KHz	
UWKM	USIT Working Mode	USIT-E	Uncompressed 10 deg at 1.5 in LF	
USIT_DEPTHLOG	Starting Depth Log for Ultrasonics	USIT-E	Time Zoned	ft
USSP	Ultrasonic Service	USIT-E	USI	
VRES	Vertical Resolution	USIT-E	1.5 in	
WINB	Window Begin Time	USIT-E	25	us
WINE	Window End Time	USIT-E	90	us
WMOD	Waveform Firing Mode	DSLT-H	Full	

TwoTime Zoned Parameters

Pass Log[9]:Up

Parameter	Value	Start Time	Stop Time	Start Depth (ft)	Stop Depth (ft)
EMXV	50	20-Oct-2016 09:51:44	20-Oct-2016 10:20:40	8171.38	6648.71

Pass Log[11]:Up

EMXV	60	20-Oct-2016 10:24:53	20-Oct-2016 11:05:14	6648.71	4600.07
EMXV	65	20-Oct-2016 11:05:14	20-Oct-2016 12:34:00	4600.07	113.27

Pass Log[14]:Up

EMXV	100	20-Oct-2016 12:53:24	20-Oct-2016 12:54:59	155.15	76.32
EMXV	110	20-Oct-2016 12:54:59	20-Oct-2016 12:57:44	76.32	16.88
EMXV	125	20-Oct-2016 12:57:44	20-Oct-2016 12:58:23	16.88	5.56

All depth are at tool zero.

Composite 1

Main Pass 5 IN = 100 FT

Composite Summary

Run Name	Pass Objective	Direction	Top	Bottom	Start	Stop	DSC Mode	Depth Shift	Include Parallel Data
Two	Log[9]:Up	Up	6640.29 ft	8171.85 ft	20-Oct-2016 9:51:39 AM	20-Oct-2016 10:20:40 AM	ON	1.47 ft	No
Two	Log[11]:Up	Up	36.69 ft	6737.51 ft	20-Oct-2016 10:24:53 AM	20-Oct-2016 12:34:00 PM	ON	1.35 ft	No
Two	Log[14]:Up	Up	5.56 ft	155.15 ft	20-Oct-2016 12:53:24 PM	20-Oct-2016 12:58:23 PM	ON	1.96 ft	No

All depths are referenced to toolstring zero

Log

Company:Southern California Gas Company Well:Frew 4

Composite 1:S008

Description: USI Composite Format: Log (LBV1_USI Composite 7inch) Index Scale: 5 in per 100 ft Index Unit: ft Index Type: Measured Depth Creation Date: 20-Oct-2016 14:28:19

TIME_1900 - Time Marked every 60.00 (s)

USIT Processing Flags (UFLG[0]) USIT-E[1]

1 - UFLG 1 Value within [0.0 - 1.5] - :
2 - UFLG 2 Value within [1.5 - 2.5] - :
3 - UFLG 3 Value within [2.5 - 3.5] - :
4 - UFLG 4 UFLG 5 UFLG 6 Value within [3.5 - 6.5] - :
5 - UFLG 7 UFLG 8 UFLG 9 Value within [6.5 - 10] - :

- UTIM Error
- Pulse Origin Not Detected
- WINLEN Error
- Casing Thickness Error
- Loop Processing Error

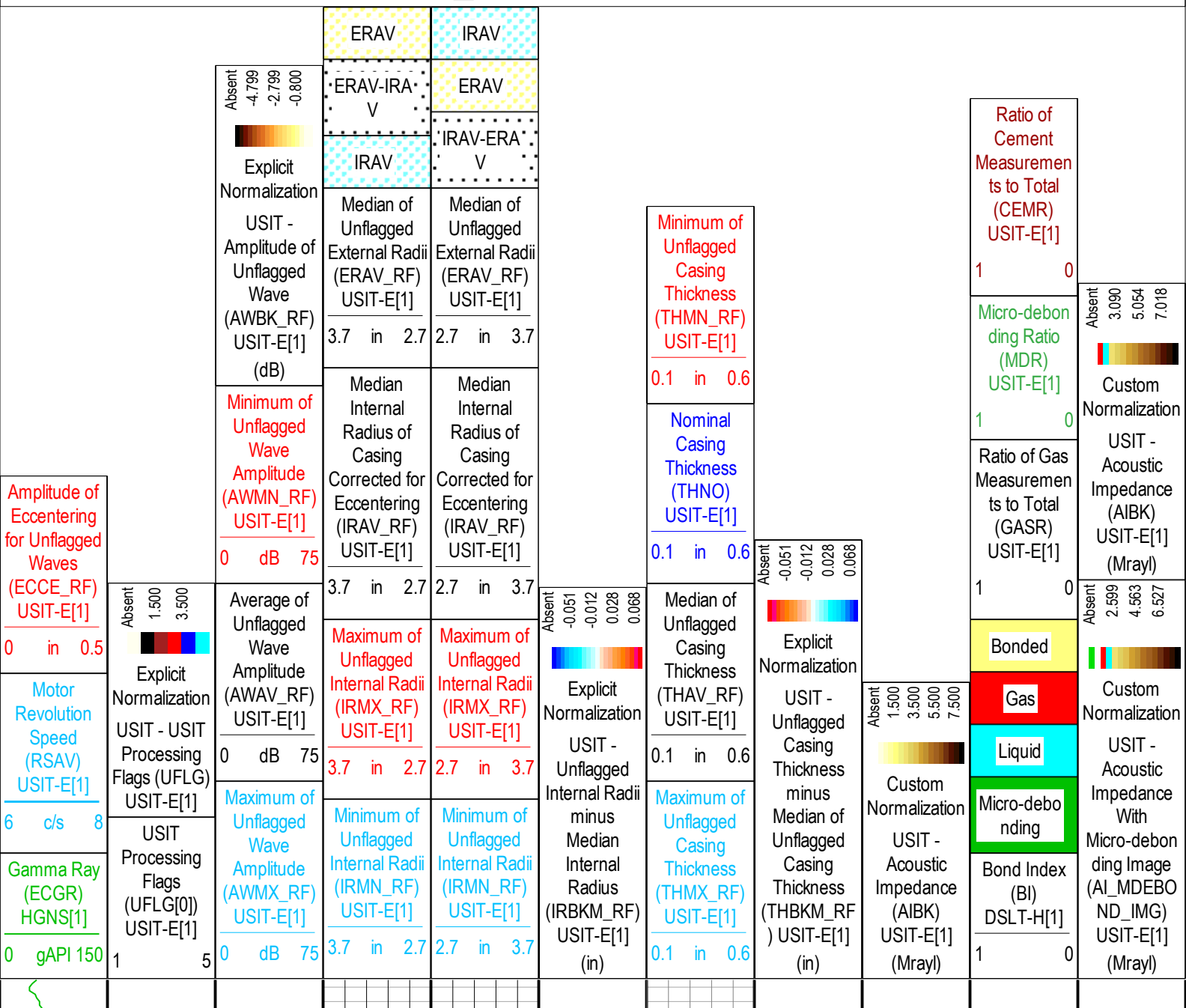

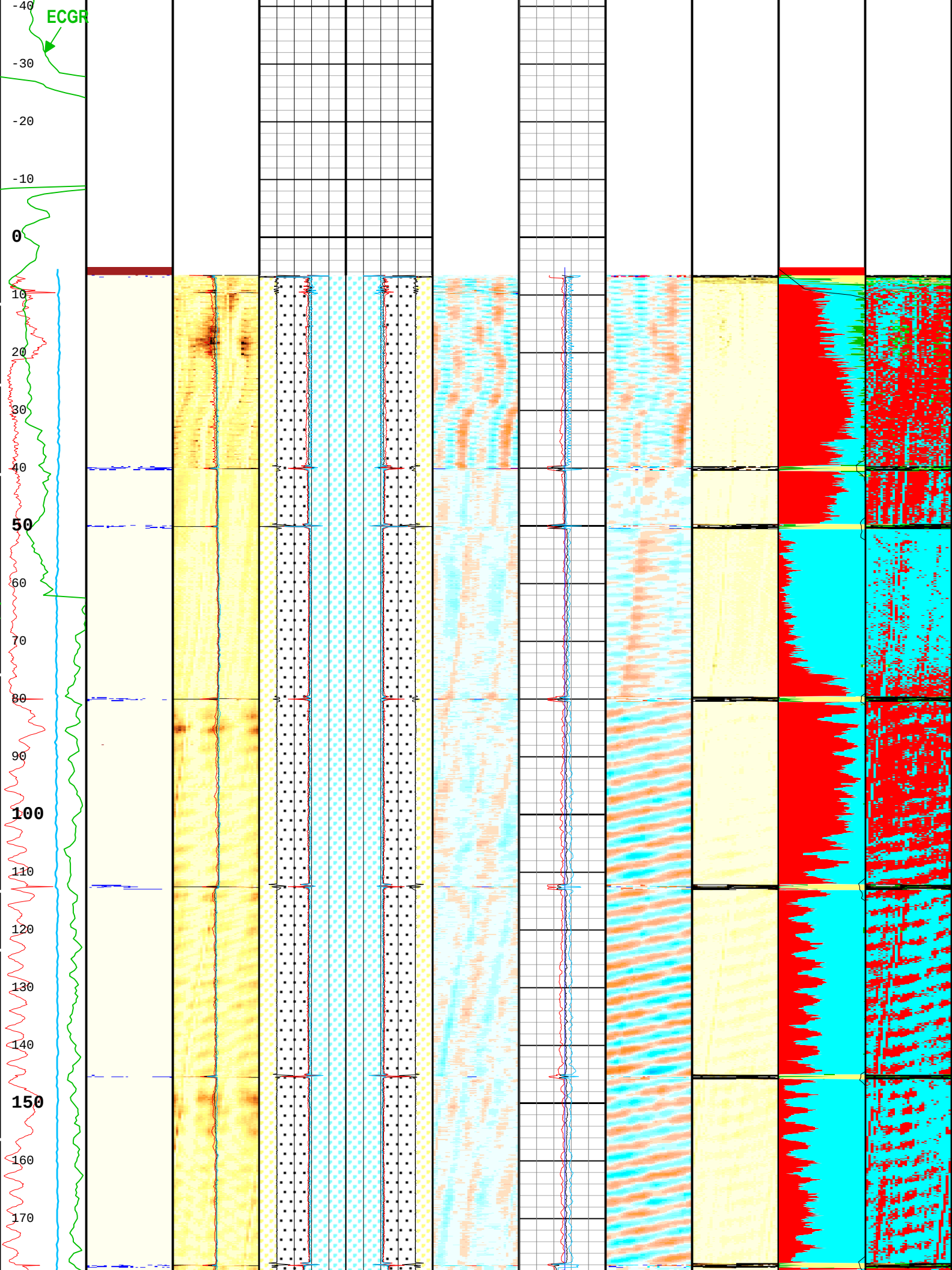
ECGR
-40
-30
-20
-10
0
10
20
30
40
50
60
70
80
90
100
110
120
130
140
150
160
170

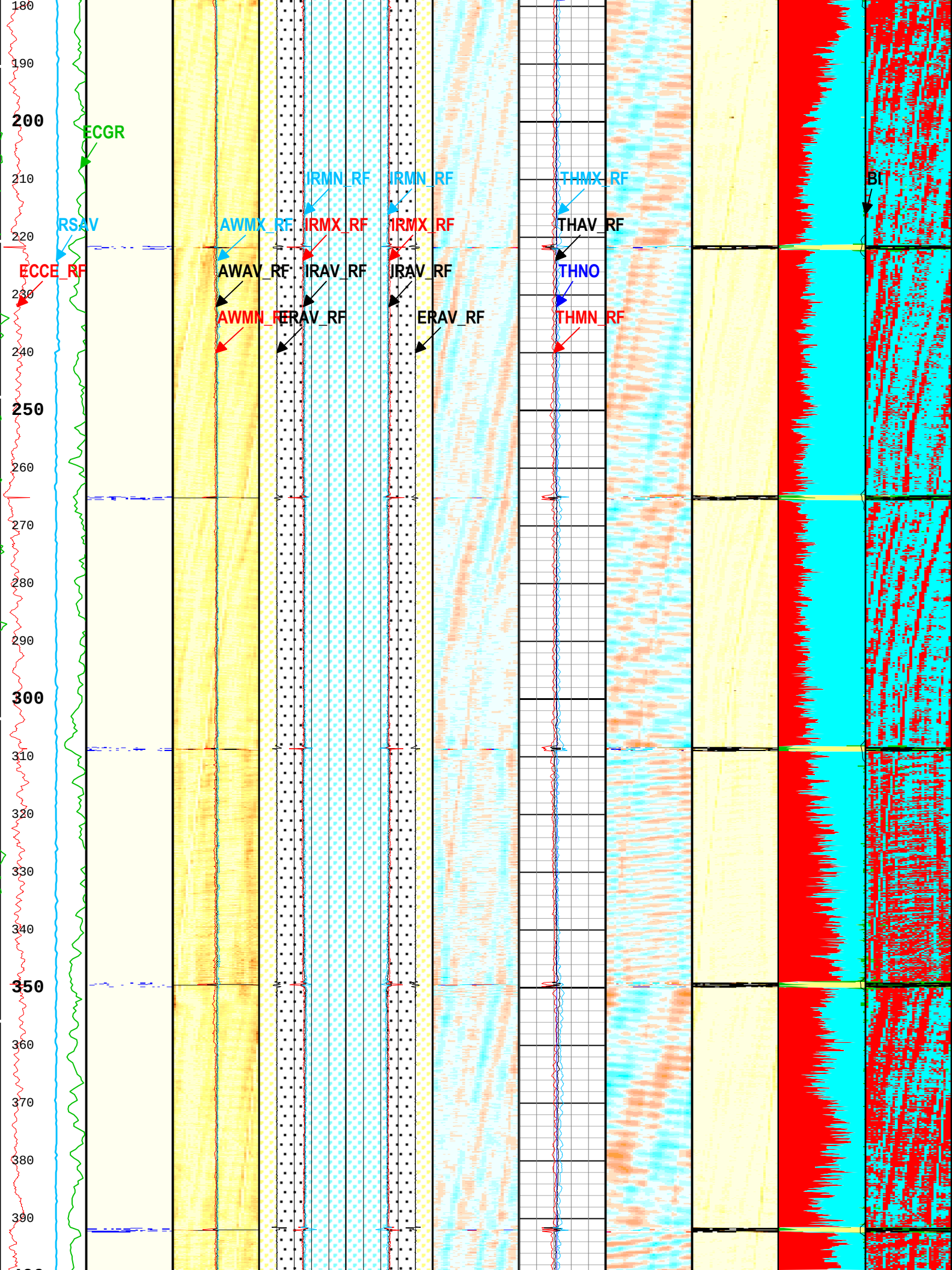
180
190
200
210
220
230
240
250
260
270
280
290
300
310
320
330
340
350
360
370
380
390
ECGR
RSAV
ECCE_RF
AWMX_RF
AWAV_RF
AWMN_RF
IRMN_RF
IRMX_RF
IRAV_RF
ERAV_RF
IRMN_RF
IRMX_RF
IRAV_RF
ERAV_RF
THMX_RF
THAV_RF
THNO
THMN_RF
BI

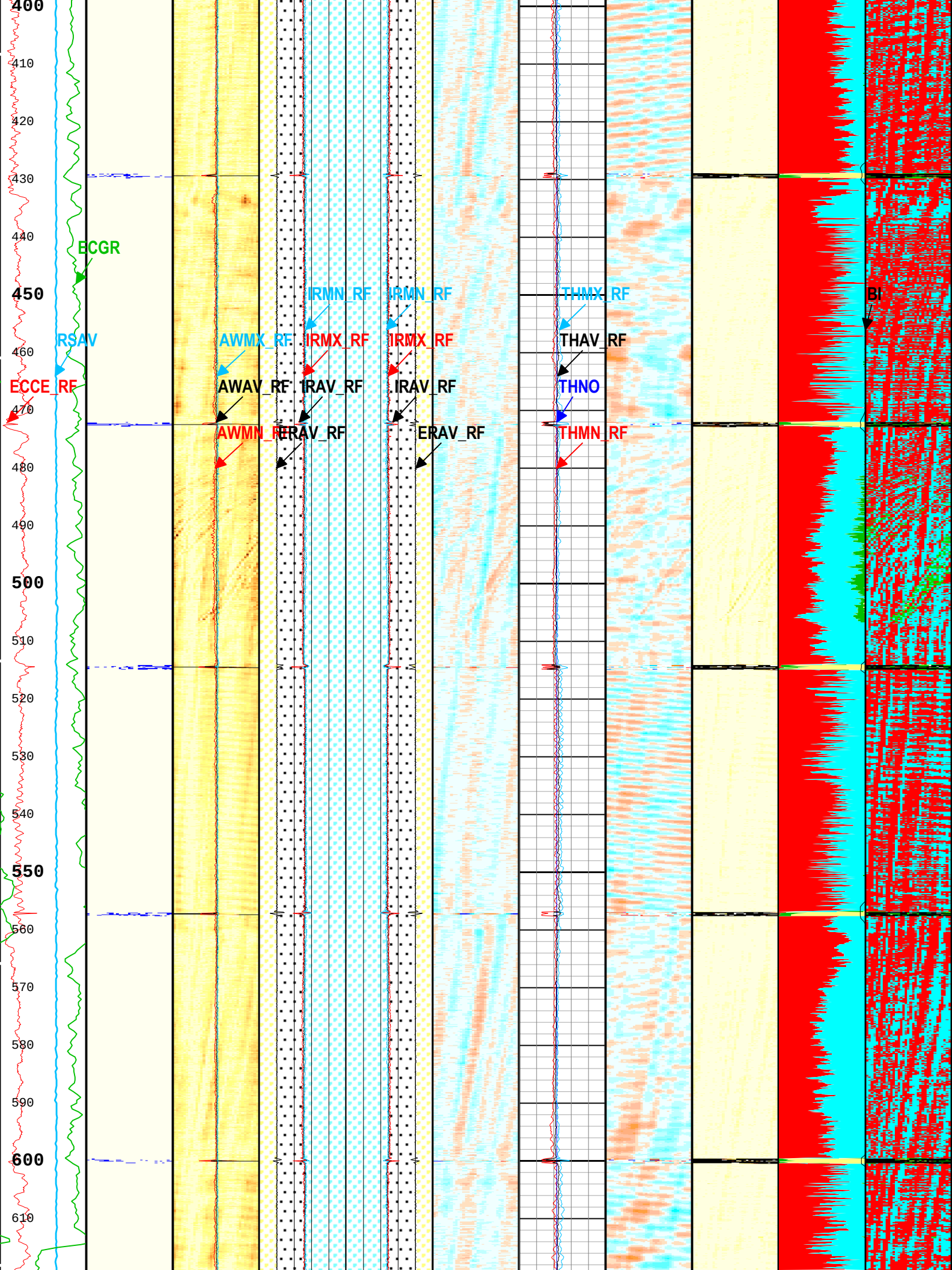
400
410
420
430
440
450
460
470
480
490
500
510
520
530
540
550
560
570
580
590
600
610
ECGR
RSAV
ECCE_RF
IRMN_RF
IRMN_RF
AWMX_RF
IRMX_RF
IRMX_RF
AWAV_RF
IRAV_RF
IRAV_RF
AWMN_RF
ERAV_RF
ERAV_RF
THMX_RF
THAV_RF
THNO
THMN_RF
BI

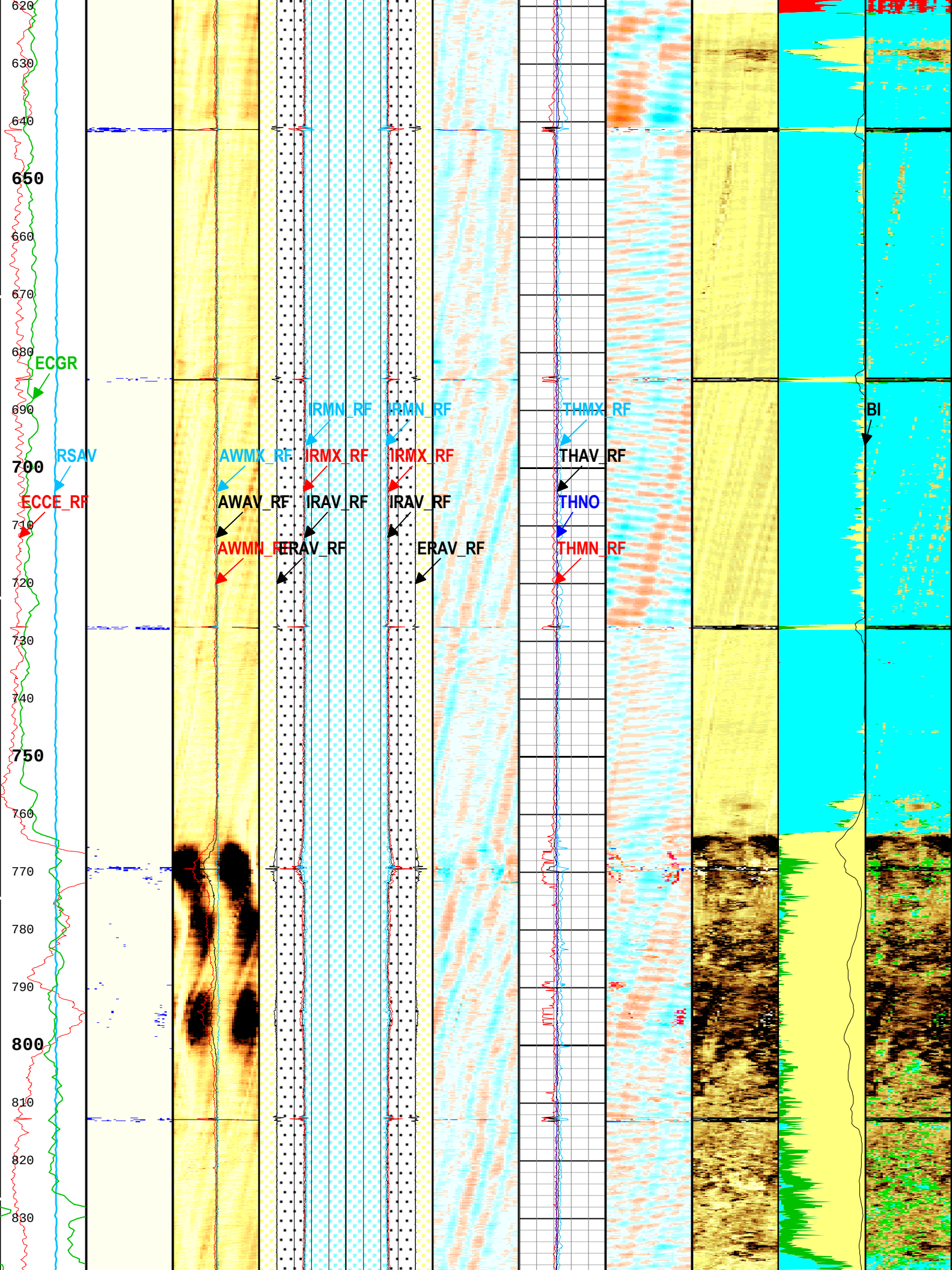
620
630
640
650
660
670
680
690
700
710
720
730
740
750
760
770
780
790
800
810
820
830
ECGR
RSAV
ECCE_RF
IRMN_RF
IRMN_RF
AWMX_RF
IRMX_RF
IRMX_RF
AWAV_RF
IRAV_RF
IRAV_RF
AWMN_RF
ERAV_RF
ERAV_RF
THMX_RF
THAV_RF
THNO
THMN_RF
BI

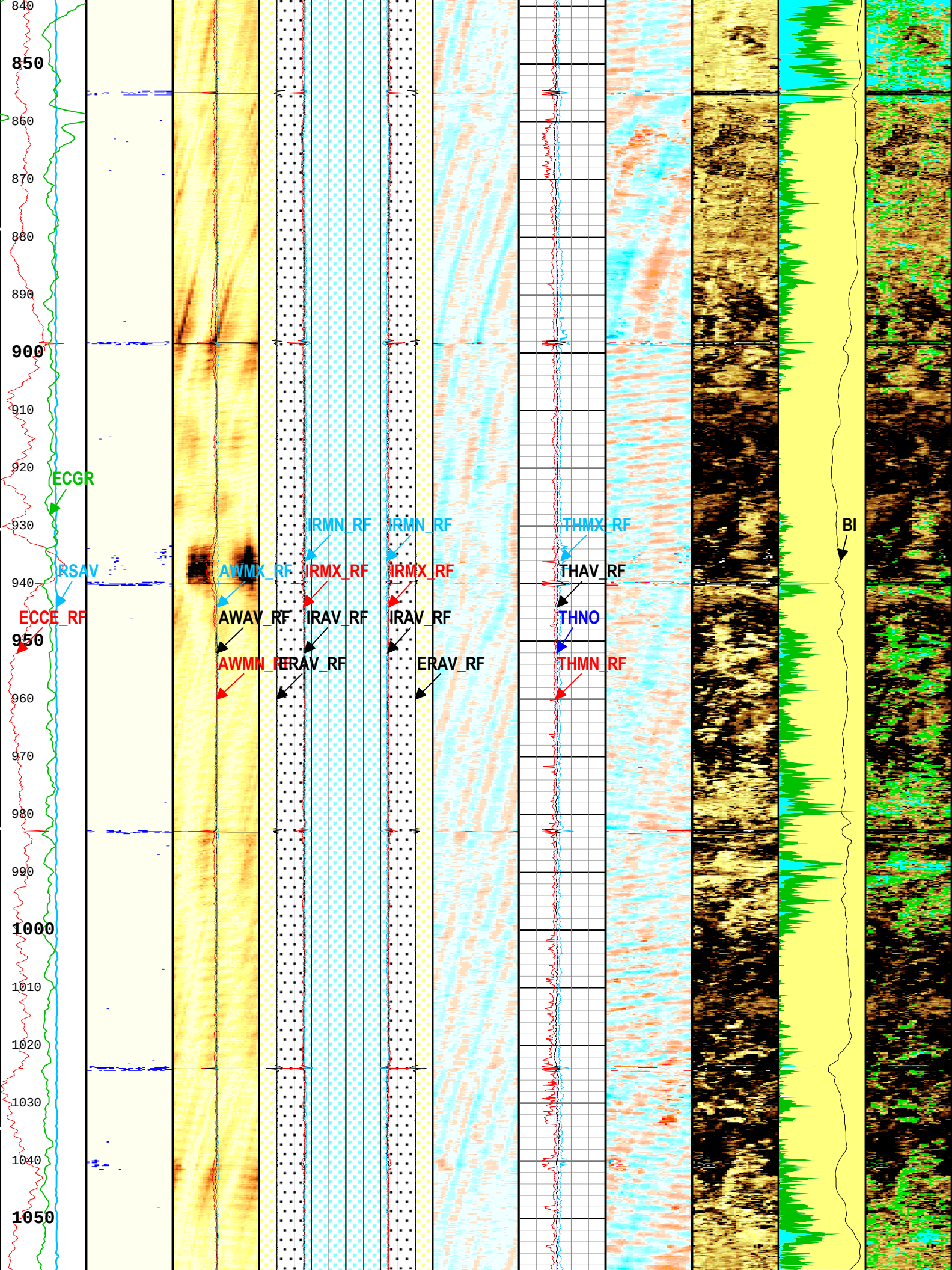
840
850
860
870
880
890
900
910
920
930
940
950
960
970
980
990
1000
1010
1020
1030
1040
1050
ECGR
RSAV
ECCE_RF
IRMN_RF
IRMN_RF
AWMX_RF
IRMX_RF
IRMX_RF
AWAV_RF
IRAV_RF
IRAV_RF
AWMN_RF
ERAV_RF
ERAV_RF
THMX_RF
THAV_RF
THNO
THMN_RF
BI

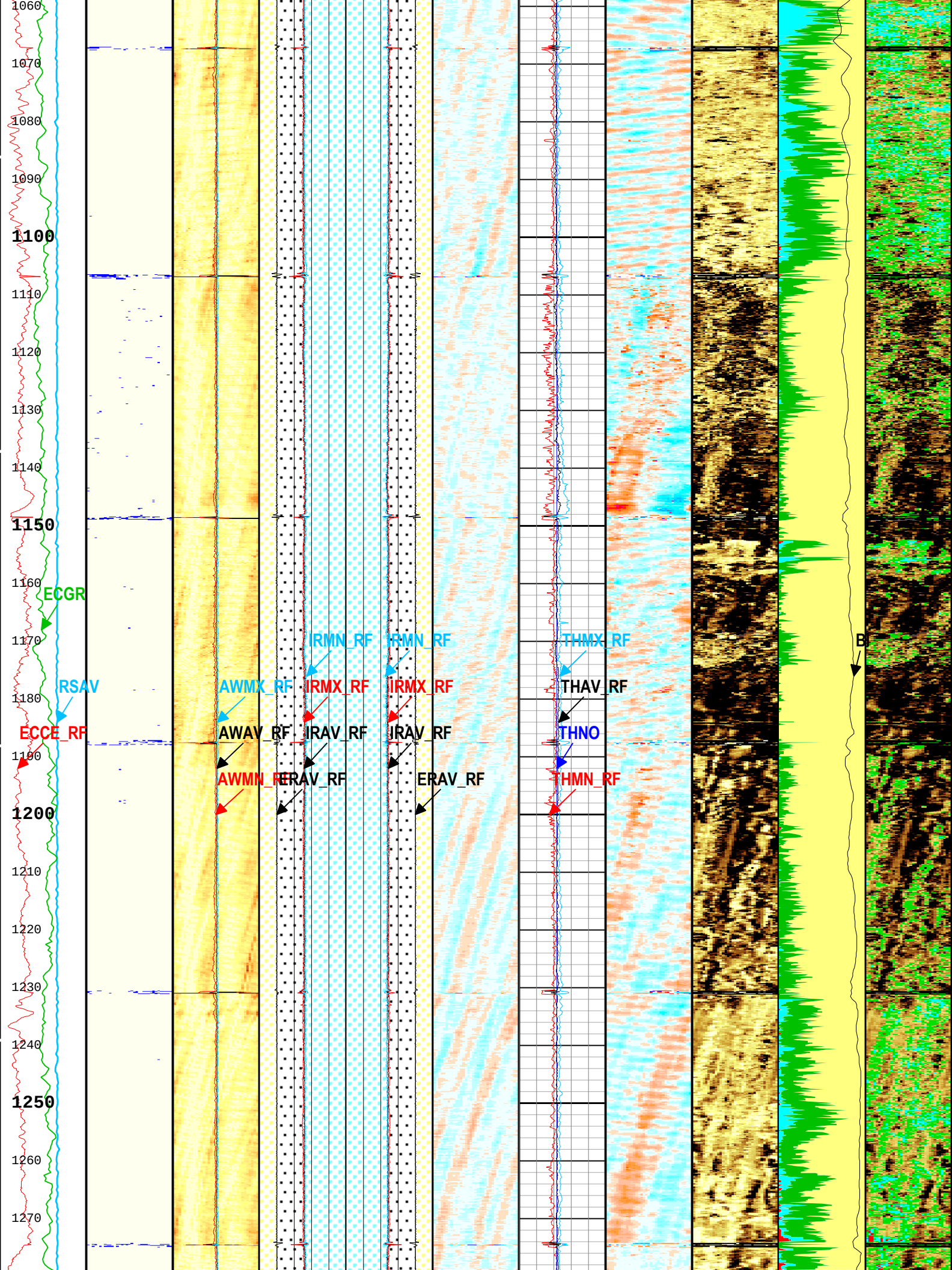
1060
1070
1080
1090
1100
1110
1120
1130
1140
1150
1160
1170
1180
1190
1200
1210
1220
1230
1240
1250
1260
1270
ECGR
RSAV
ECCE_RF
IRMN_RF
IRMN_RF
AWMX_RF
IRMX_RF
IRMX_RF
AWAV_RF
IRAV_RF
IRAV_RF
AWMN_RF
ERAV_RF
ERAV_RF
THMX_RF
THAV_RF
THNO
THMN_RF
B

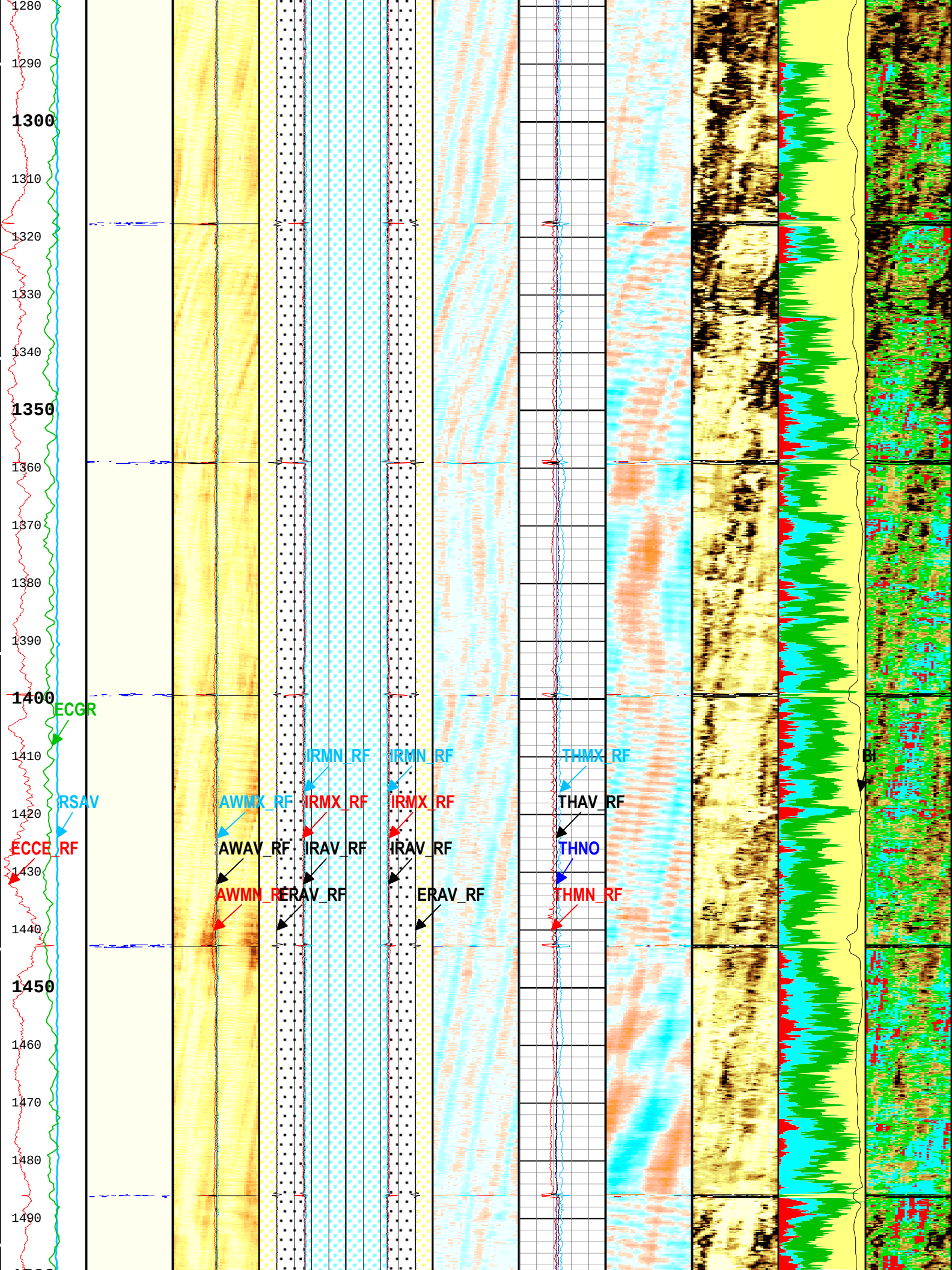
1280
1290
1300
1310
1320
1330
1340
1350
1360
1370
1380
1390
1400
1410
1420
1430
1440
1450
1460
1470
1480
1490
ECGR
RSAV
ECCE_RF
AWMX_RF
AWAV_RF
AWMN_RF
IRMN_RF
IRMX_RF
IRAV_RF
ERAV_RF
IRMN_RF
IRMX_RF
IRAV_RF
ERAV_RF
THMX_RF
THAV_RF
THNO
THMN_RF
BI

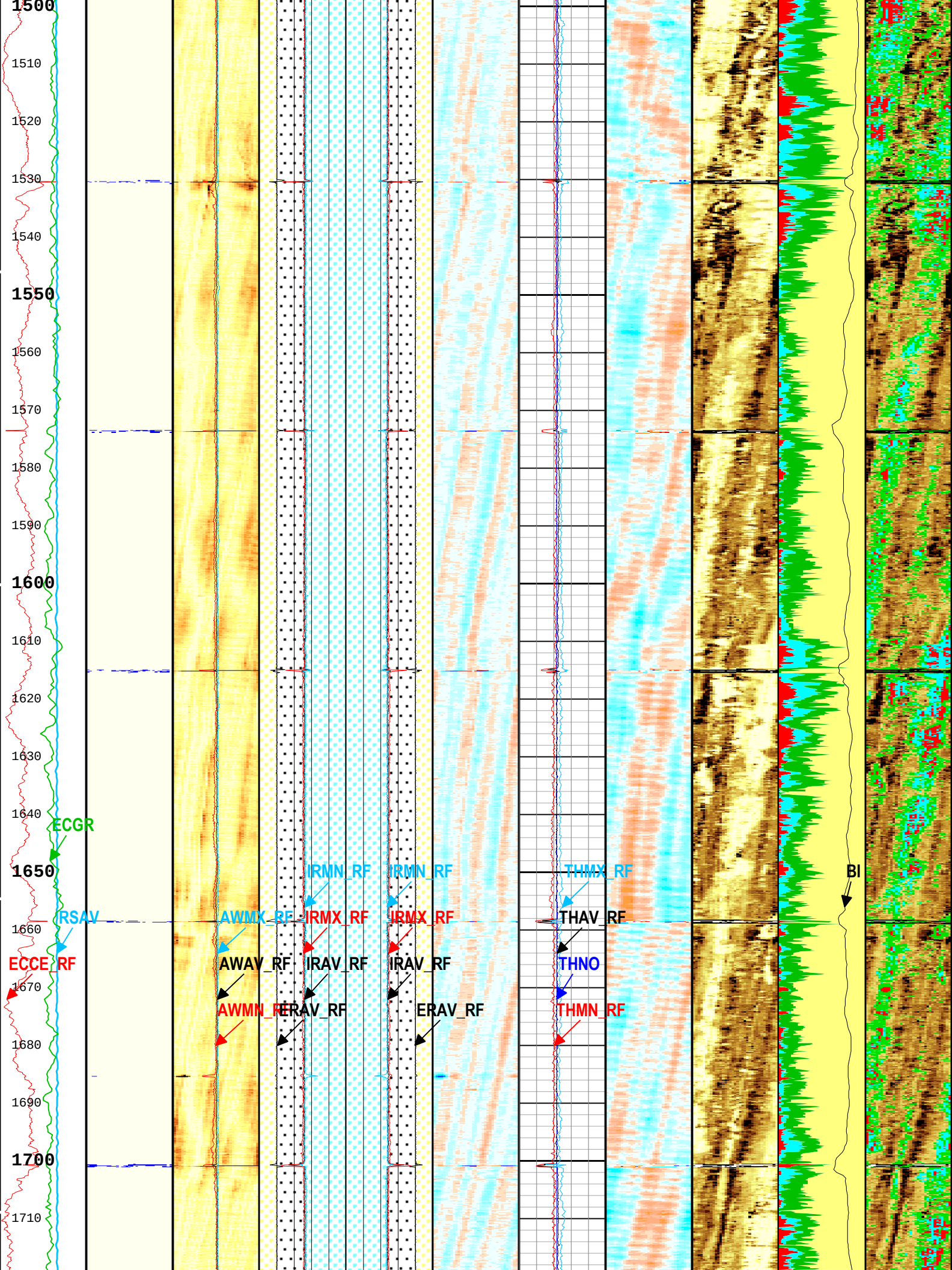
1500
1510
1520
1530
1540
1550
1560
1570
1580
1590
1600
1610
1620
1630
1640
1650
1660
1670
1680
1690
1700
1710
ECGR
RSAV
ECCE_RF
AWMX_RF
AWAV_RF
AWMN_RF
IRMN_RF
IRMX_RF
IRAV_RF
ERAV_RF
IRMN_RF
IRMX_RF
IRAV_RF
ERAV_RF
THMX_RF
THAV_RF
THNO
THMN_RF
BI

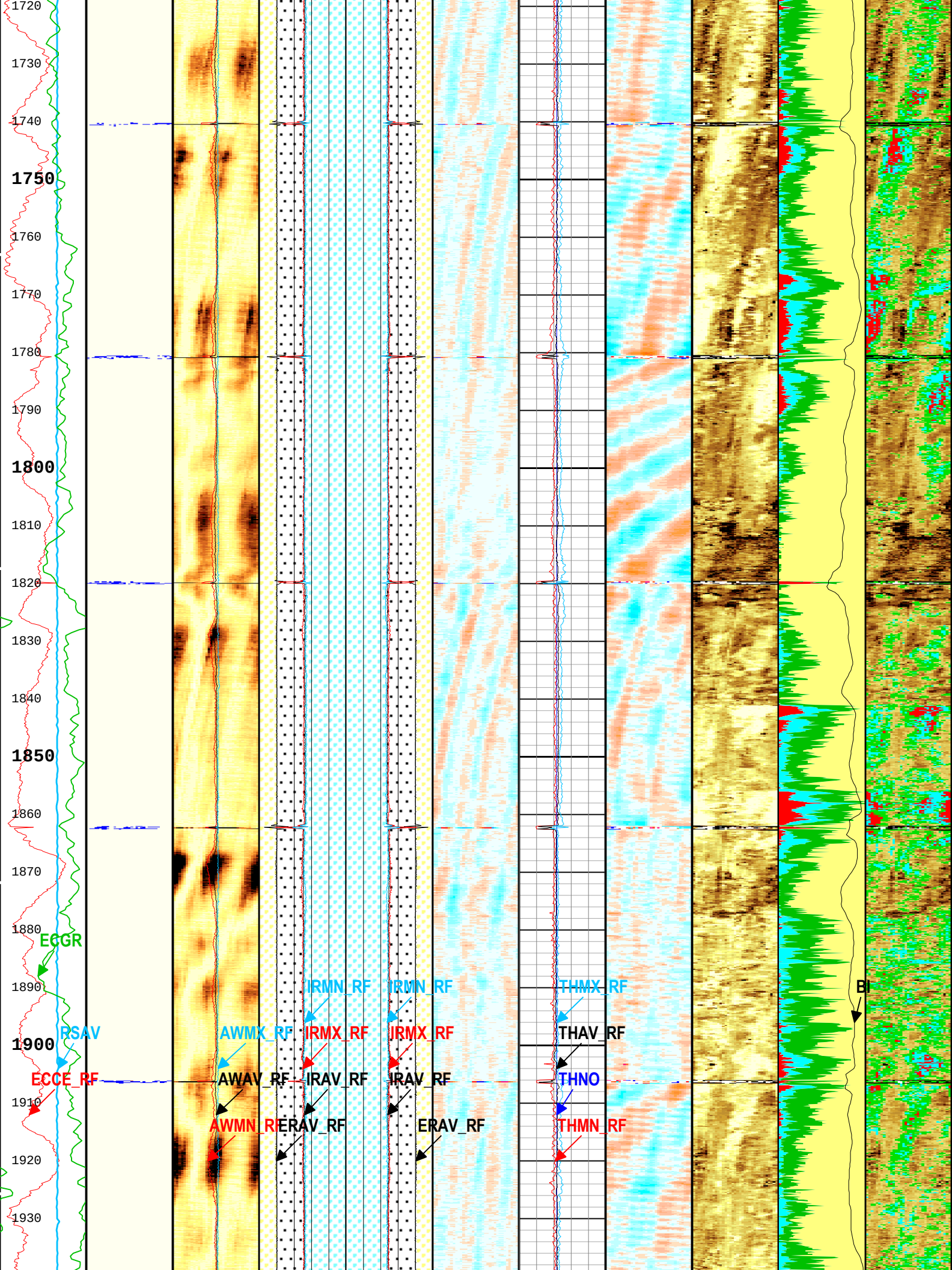
1720
1730
1740
1750
1760
1770
1780
1790
1800
1810
1820
1830
1840
1850
1860
1870
1880
1890
1900
1910
1920
1930
ECGR
RSAV
ECCE_RF
AWAV_RF
AWMX_RF
AWMN_RF
IRMN_RF
IRMX_RF
IRAV_RF
ERAV_RF
IRMN_RF
IRMX_RF
IRAV_RF
ERAV_RF
THMX_RF
THAV_RF
THNO
THMN_RF
BI

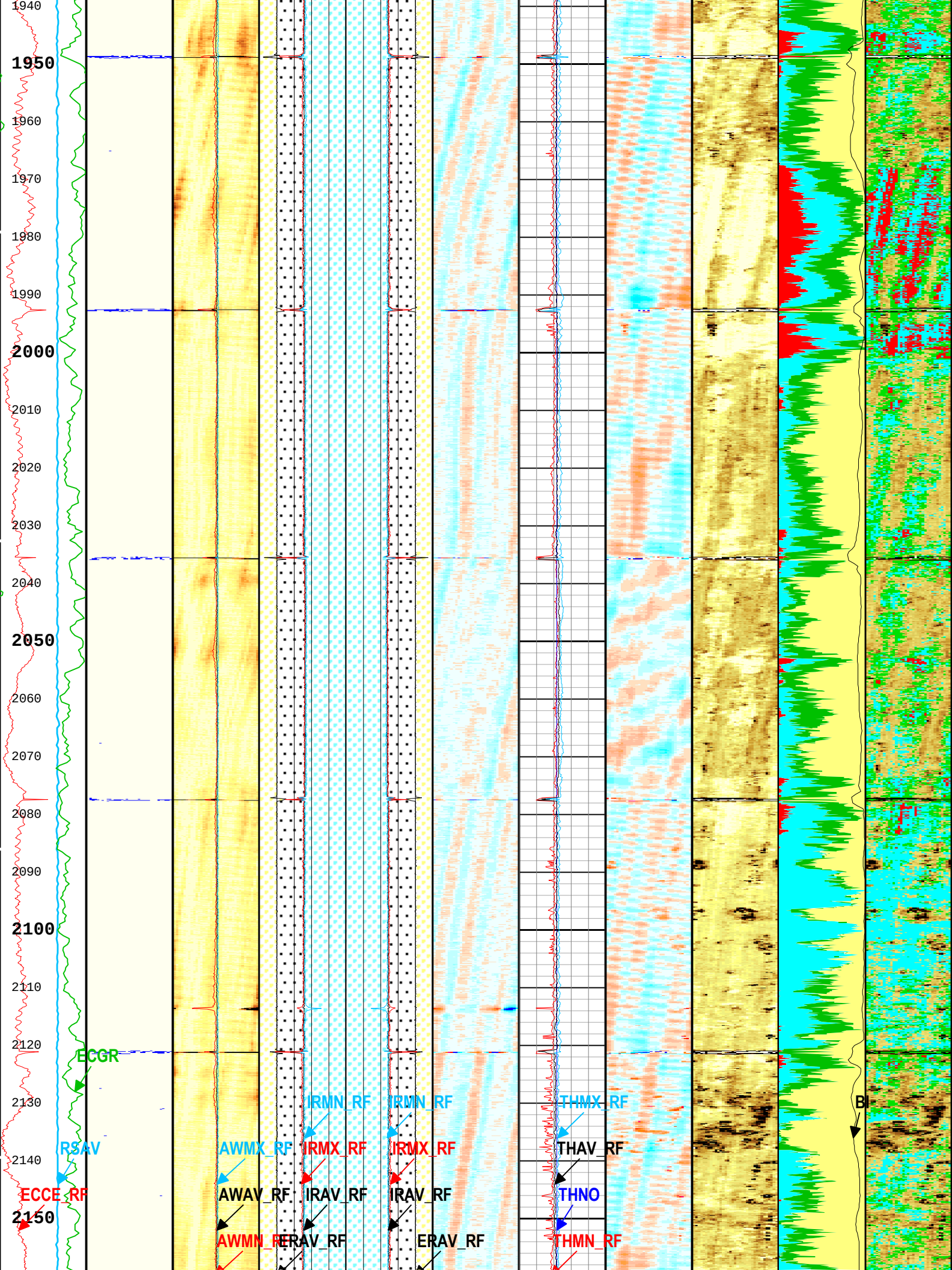
1940
1950
1960
1970
1980
1990
2000
2010
2020
2030
2040
2050
2060
2070
2080
2090
2100
2110
2120
2130
2140
2150
ECGR
RSAV
ECCE_RF
IRMN_RF
AWMX_RF
IRMX_RF
AWAV_RF
IRAV_RF
AWMN_RF
ERAV_RF
IRMN_RF
IRMX_RF
IRAV_RF
ERAV_RF
THMX_RF
THAV_RF
THNO
THMN_RF
BI

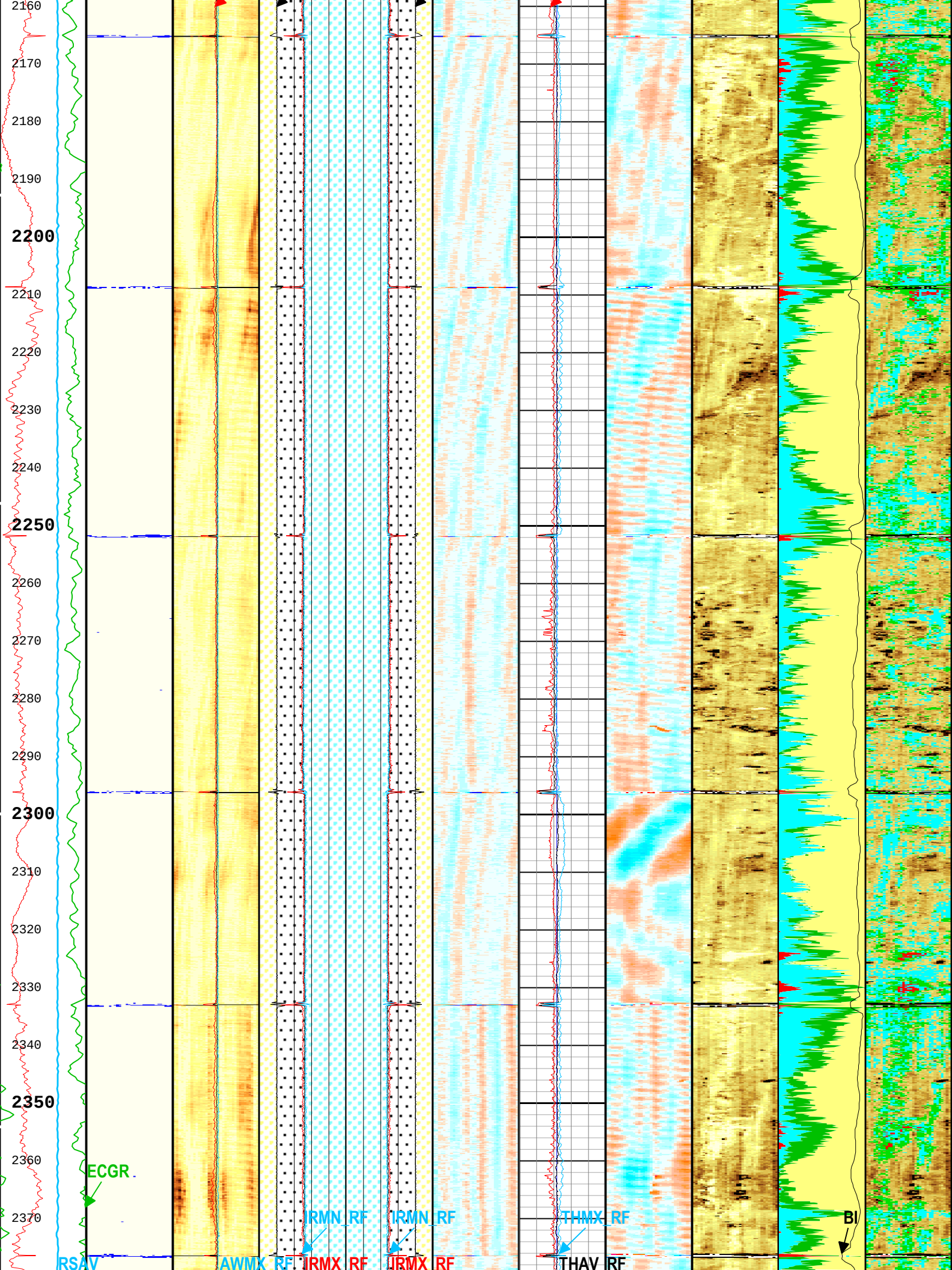
2160
2170
2180
2190
2200
2210
2220
2230
2240
2250
2260
2270
2280
2290
2300
2310
2320
2330
2340
2350
2360
2370
ECGR
RSAV
AWMX_RF
IRMN_RF
IRMX_RF
IRMN_RF
IRMX_RF
THMX_RF
THAV_RF
BI

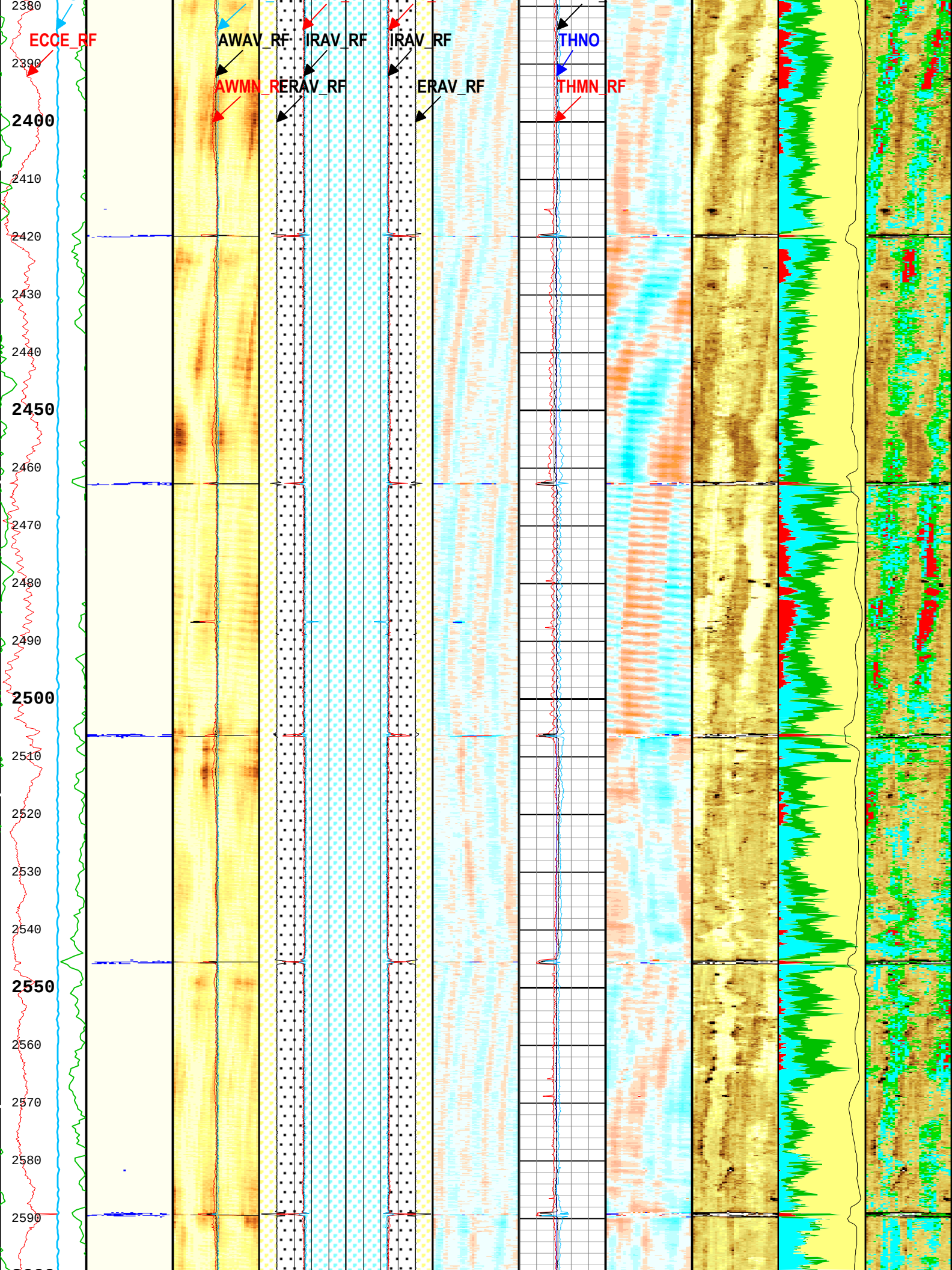
ECCE_RF
AWAV_RF
IRAV_RF
IRAV_RF
THNO
AWMN_RF
ERAV_RF
ERAV_RF
THMN_RF
2380
2390
2400
2410
2420
2430
2440
2450
2460
2470
2480
2490
2500
2510
2520
2530
2540
2550
2560
2570
2580
2590

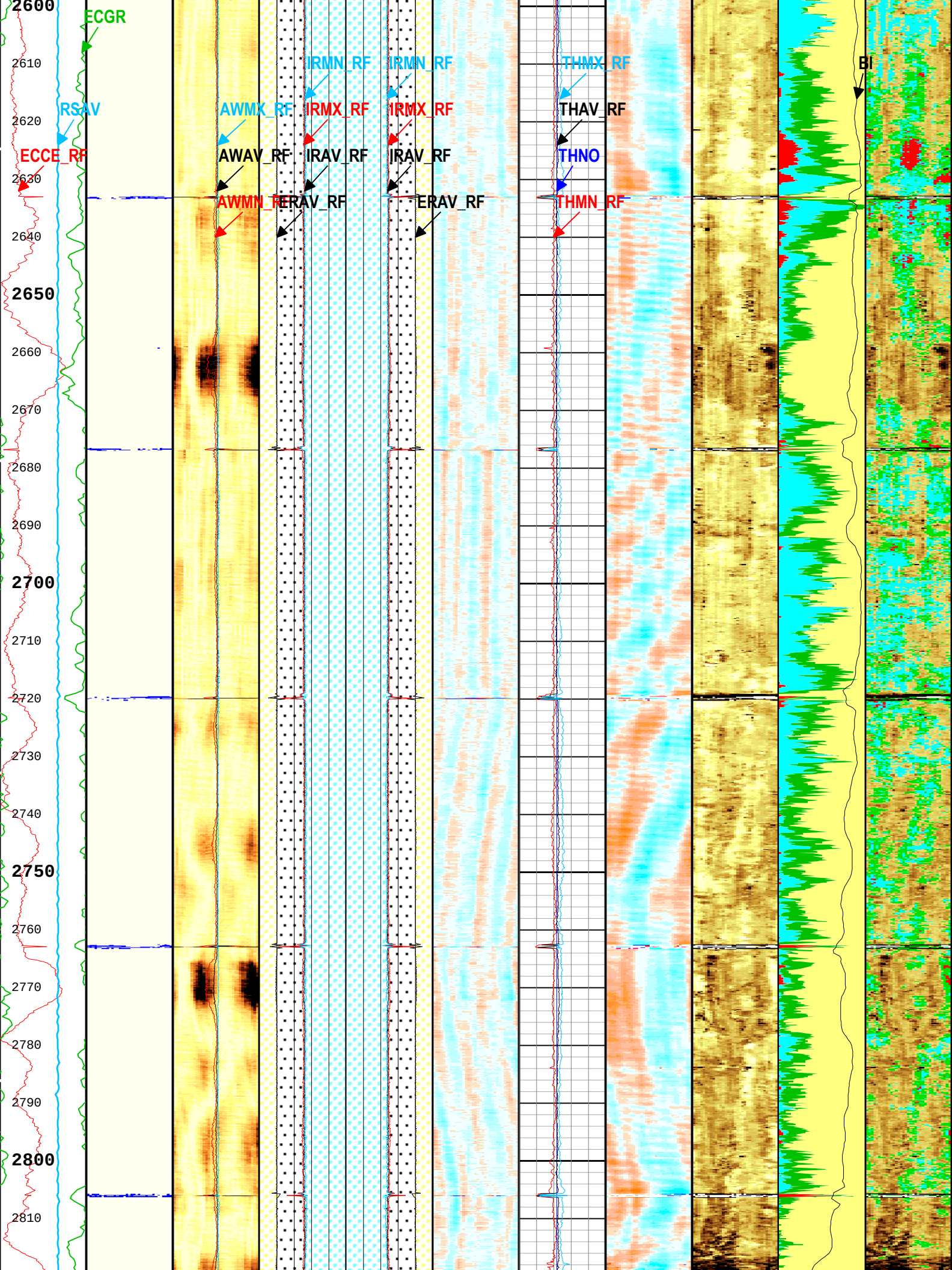
ECGR
RSAV
ECCE_RF
AWMX_RF
AWAV_RF
AWMN_RF
IRMN_RF
IRMX_RF
IRAV_RF
ERAV_RF
IRMN_RF
IRMX_RF
IRAV_RF
ERAV_RF
THMX_RF
THAV_RF
THNO
THMN_RF
BI
2600
2610
2620
2630
2640
2650
2660
2670
2680
2690
2700
2710
2720
2730
2740
2750
2760
2770
2780
2790
2800
2810

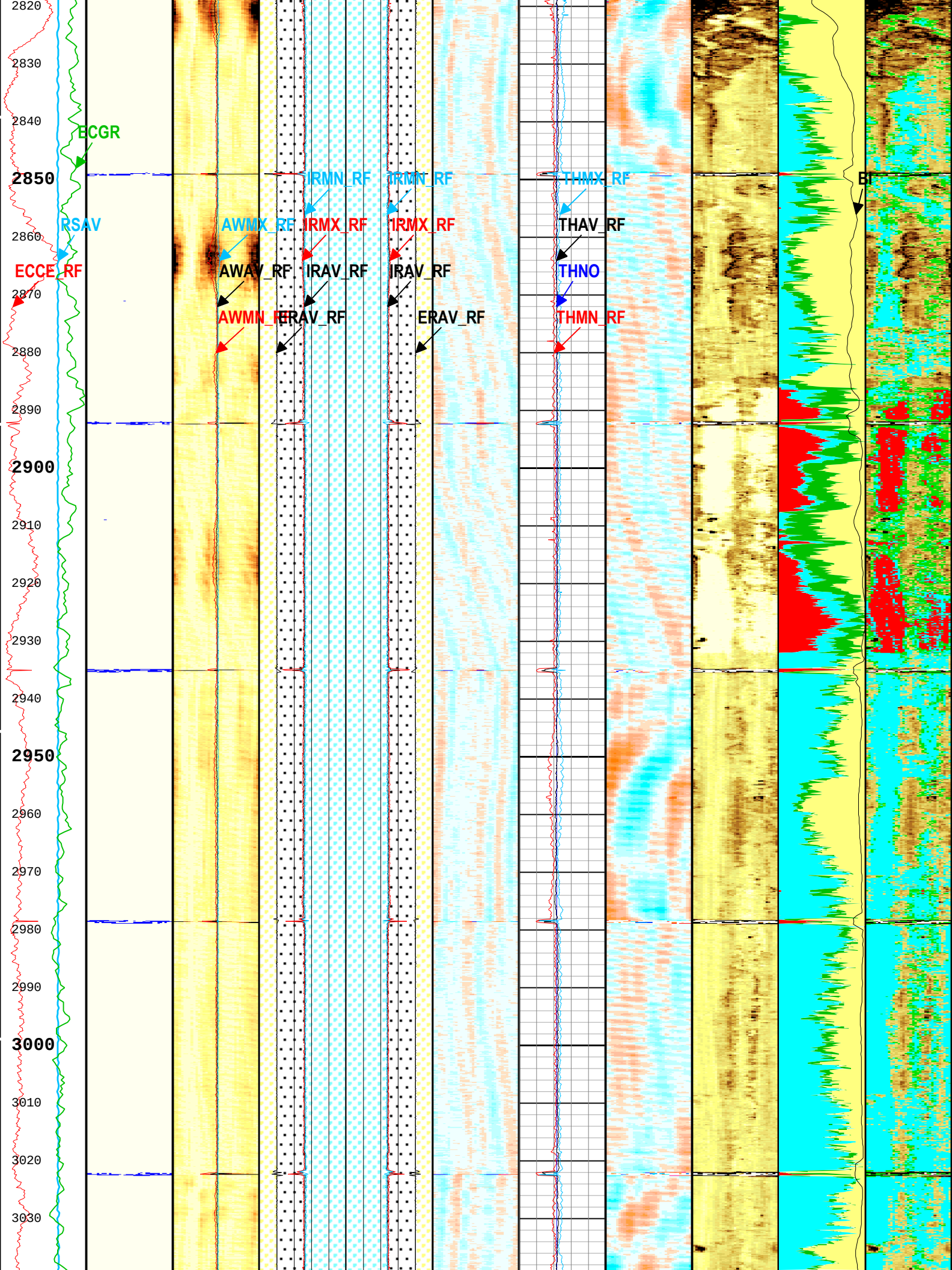
2820
2830
2840
2850
2860
2870
2880
2890
2900
2910
2920
2930
2940
2950
2960
2970
2980
2990
3000
3010
3020
3030
ECGR
RSAV
ECCE_RF
AWMX_RF
AWAV_RF
AWMN_RF
IRMN_RF
IRMX_RF
IRAV_RF
ERAV_RF
IRMN_RF
IRMX_RF
IRAV_RF
ERAV_RF
THMX_RF
THAV_RF
THNO
THMN_RF
BI

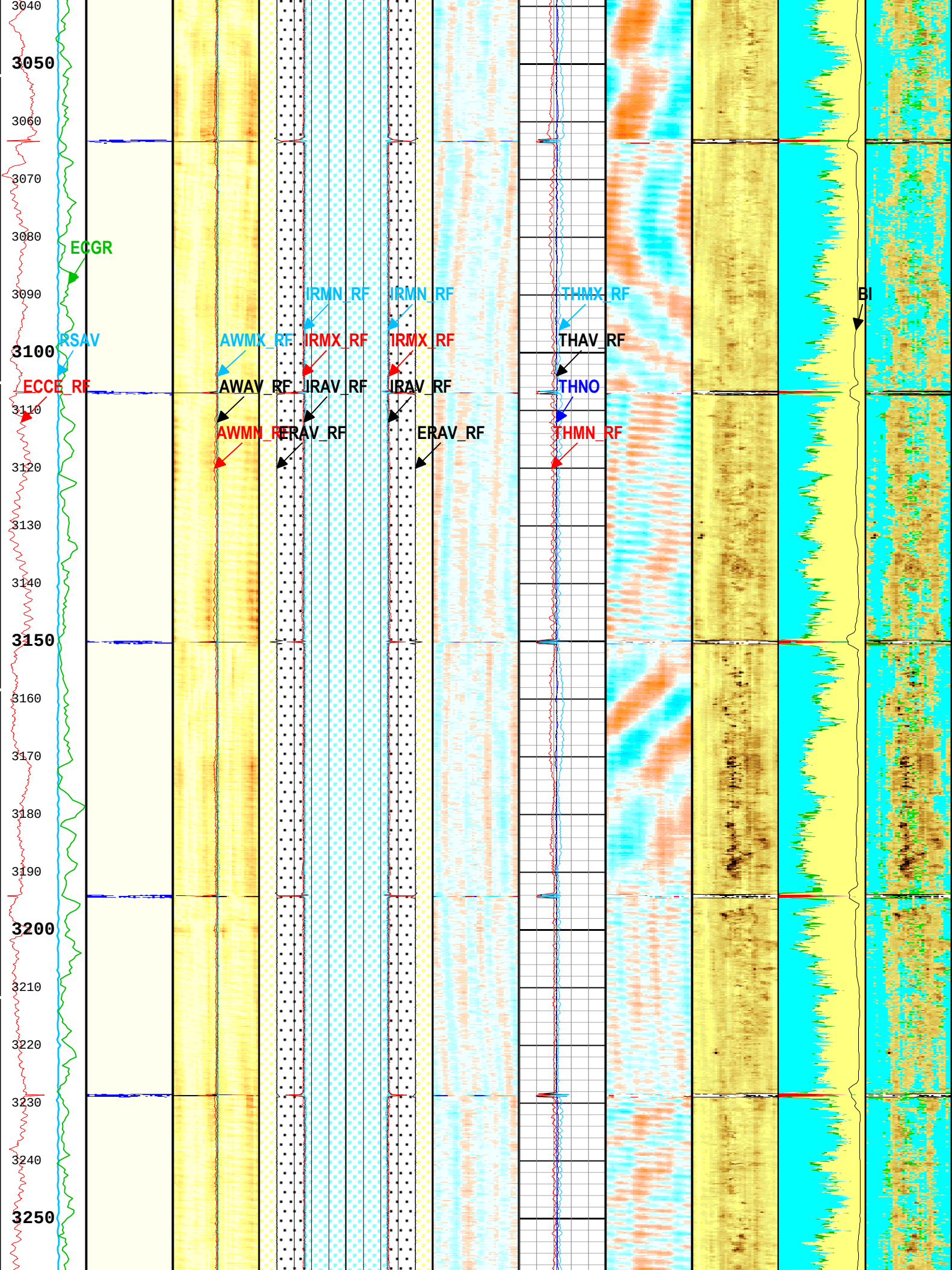
3040
3050
3060
3070
3080
3090
3100
3110
3120
3130
3140
3150
3160
3170
3180
3190
3200
3210
3220
3230
3240
3250
ECGR
RSAV
ECCE_RF
AWMX_RF
AWAV_RF
AWMN_RF
IRMN_RF
IRMX_RF
IRAV_RF
ERAV_RF
IRMN_RF
IRMX_RF
IRAV_RF
ERAV_RF
THMX_RF
THAV_RF
THNO
THMN_RF
BI

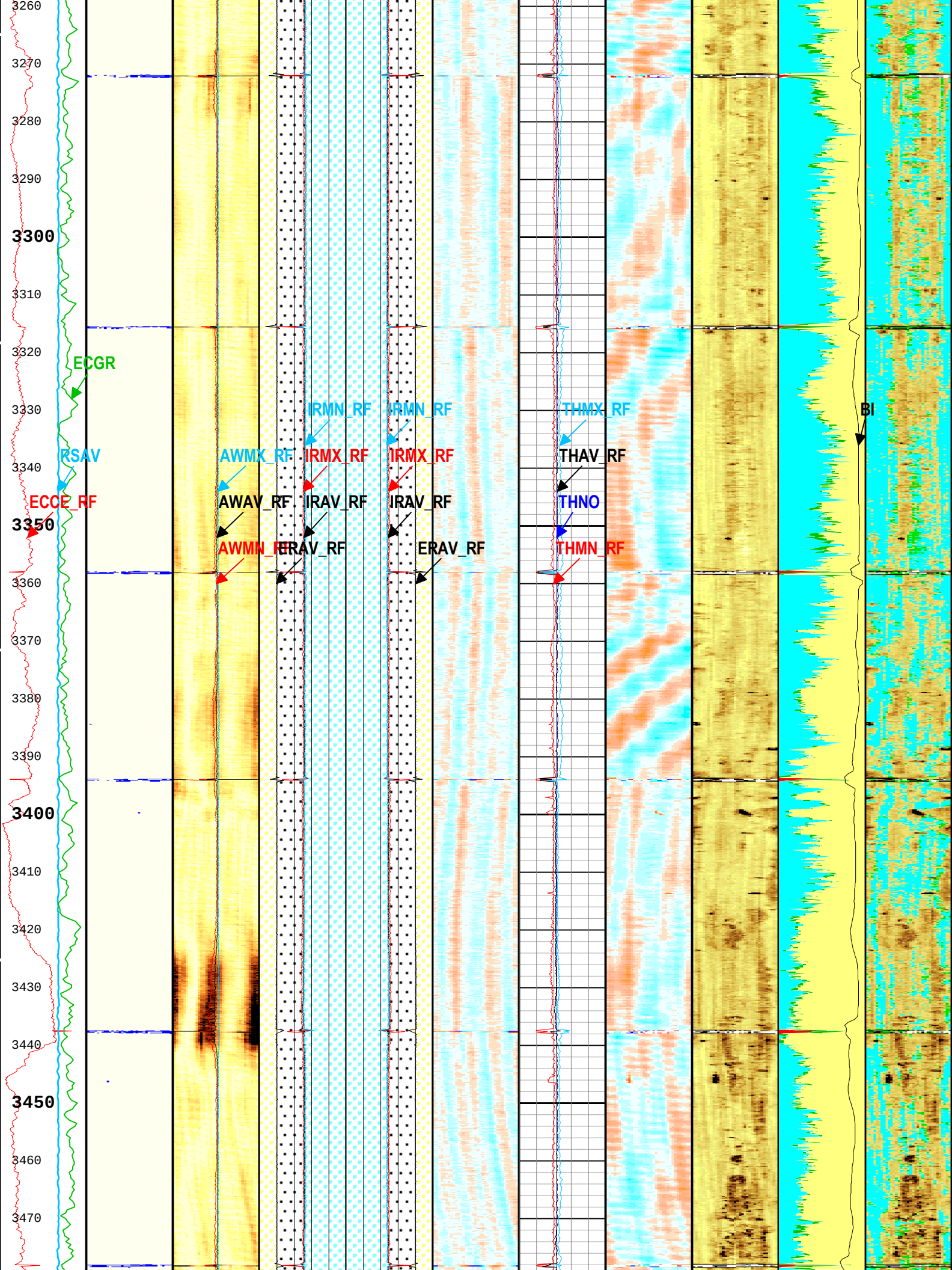
3260
3270
3280
3290
3300
3310
3320
3330
3340
3350
3360
3370
3380
3390
3400
3410
3420
3430
3440
3450
3460
3470
ECGR
RSAV
ECCE_RF
AWMX_RF
AWAV_RF
AWMN_RF
IRMN_RF
IRMX_RF
IRAV_RF
ERAV_RF
IRMN_RF
IRMX_RF
IRAV_RF
ERAV_RF
THMX_RF
THAV_RF
THNO
THMN_RF
BI

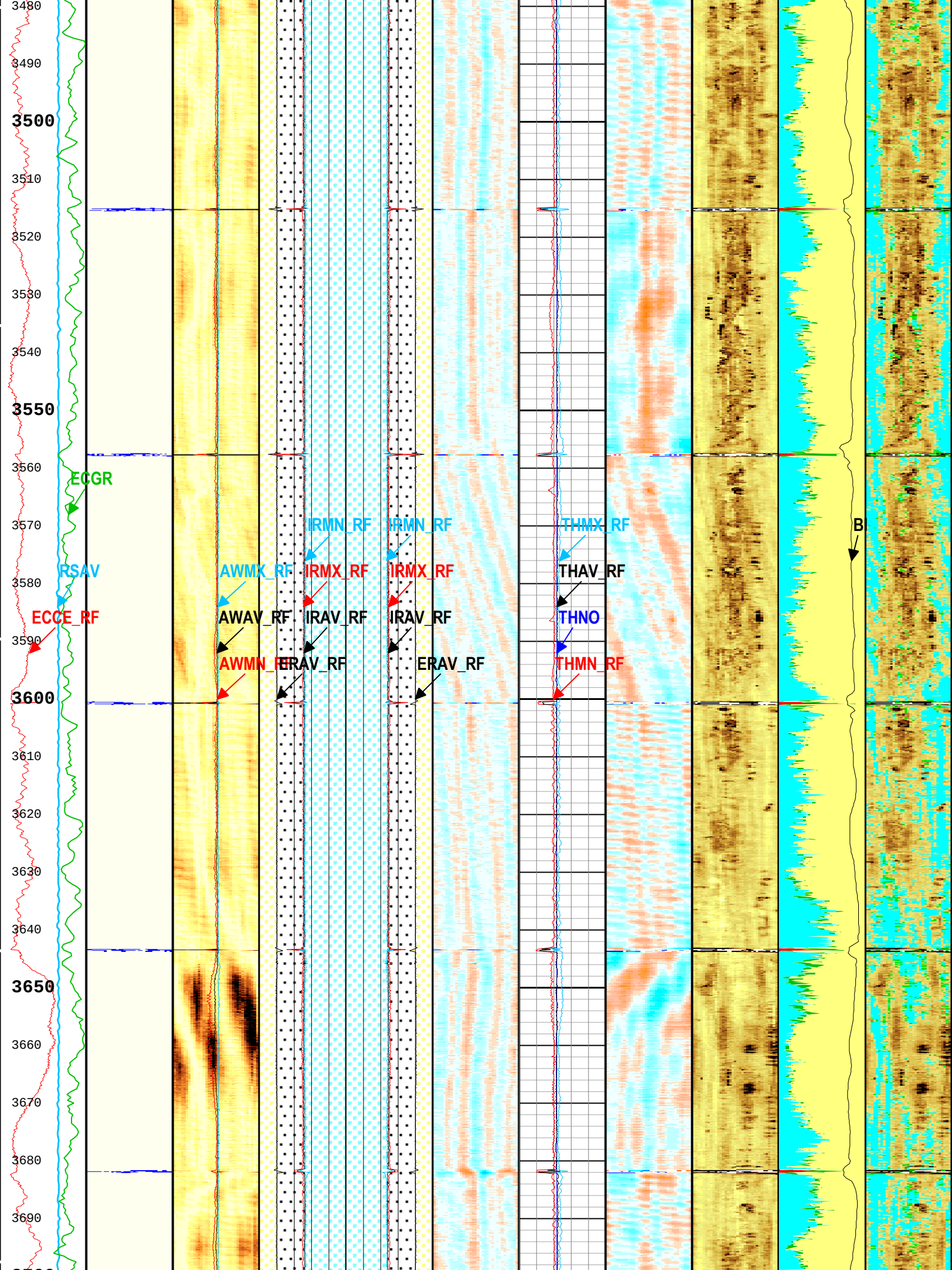
3480
3490
3500
3510
3520
3530
3540
3550
3560
3570
3580
3590
3600
3610
3620
3630
3640
3650
3660
3670
3680
3690
ECGR
RSAV
ECCE_RF
AWMX_RF
AWAV_RF
AWMN_RF
IRMN_RF
IRMX_RF
IRAV_RF
ERAV_RF
IRMN_RF
IRMX_RF
IRAV_RF
ERAV_RF
THMX_RF
THAV_RF
THNO
THMN_RF
B

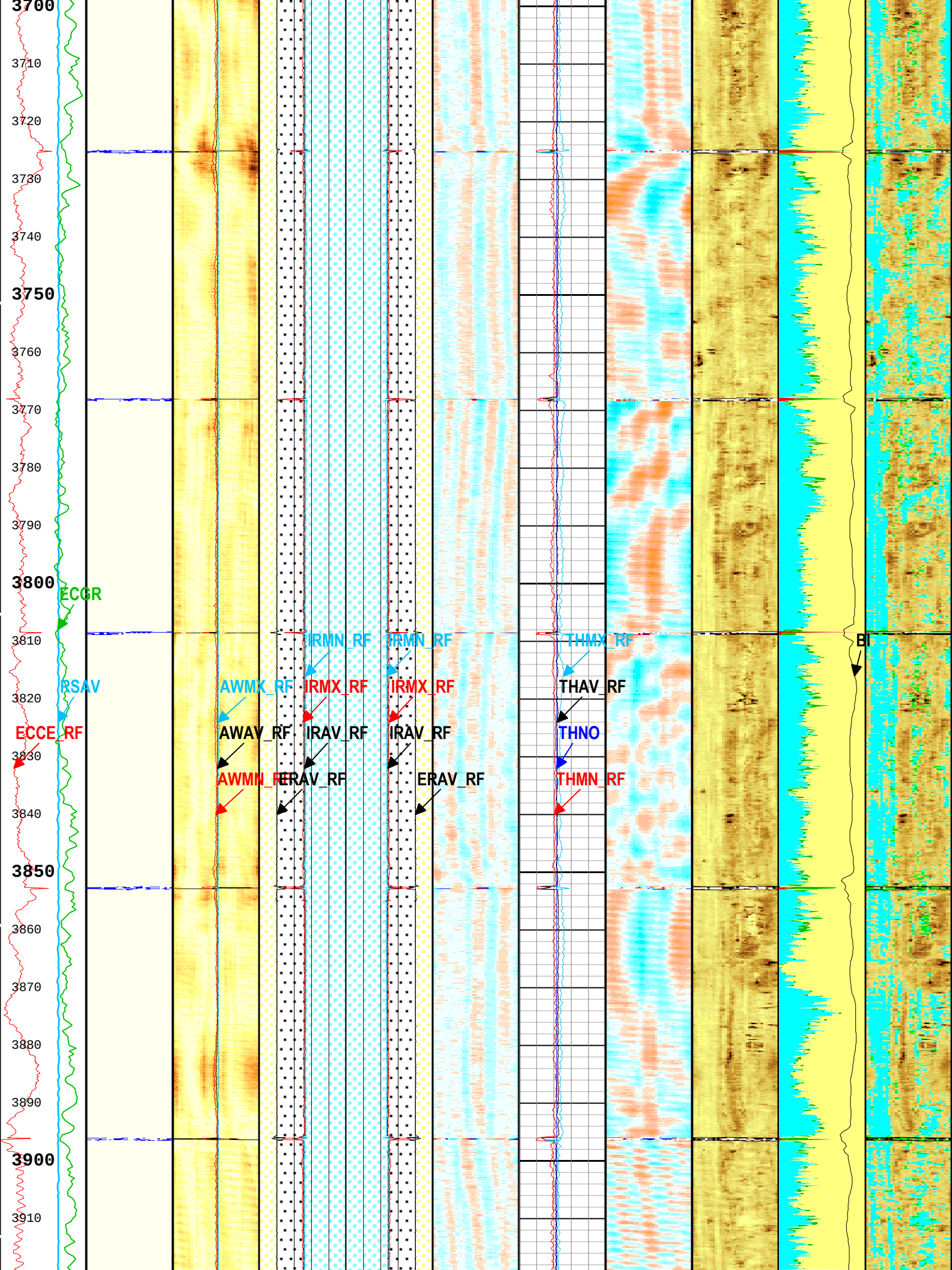
3700
3710
3720
3730
3740
3750
3760
3770
3780
3790
3800
3810
3820
3830
3840
3850
3860
3870
3880
3890
3900
3910
ECGR
RSAV
ECCE_RF
IRMN_RF
IRMN_RF
THMX_RF
AWMX_RF
IRMX_RF
IRMX_RF
THAV_RF
AWAV_RF
IRAV_RF
IRAV_RF
THNO
AWMN_RF
ERAV_RF
ERAV_RF
THMN_RF
BI

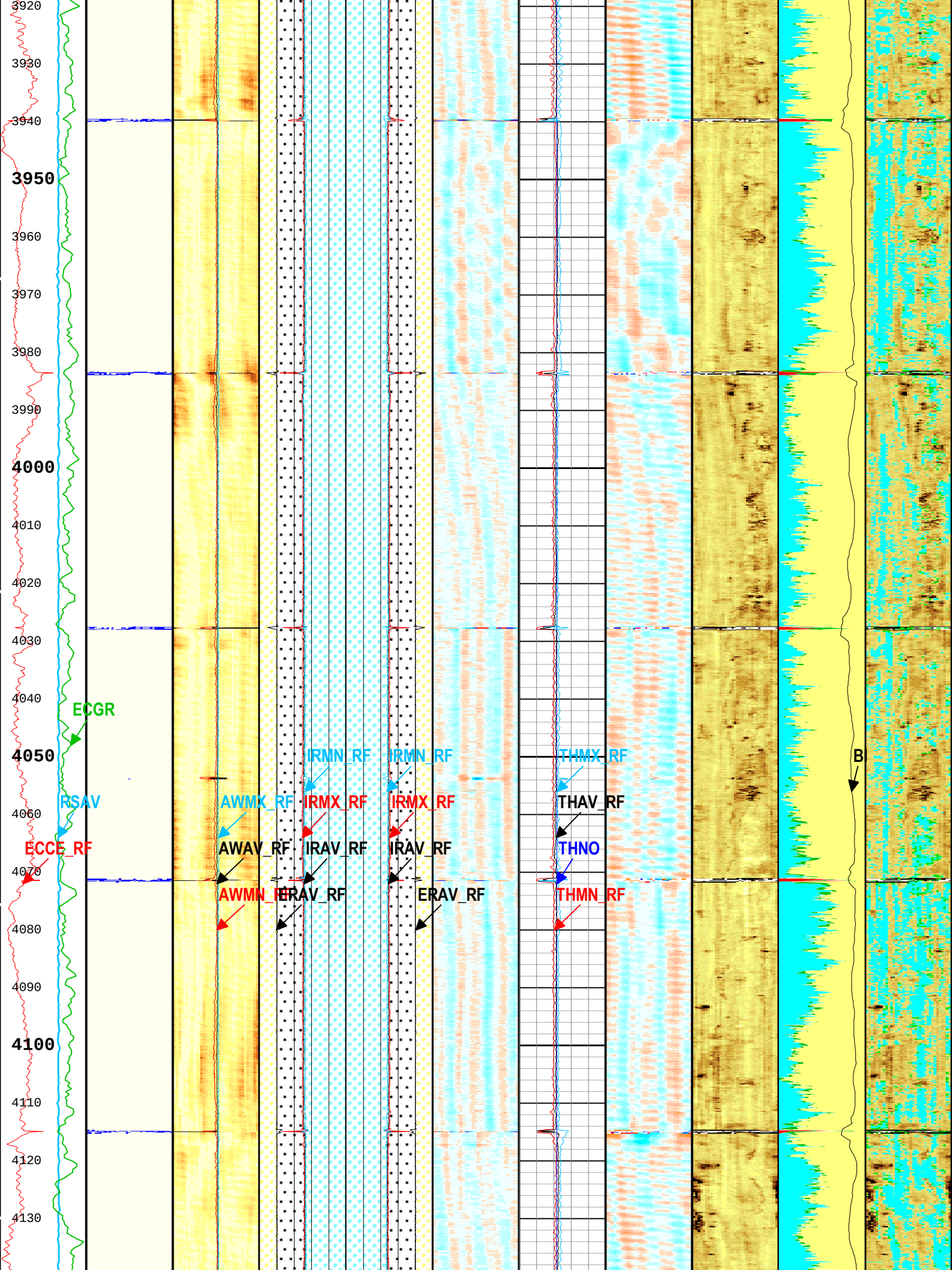
3920
3930
3940
3950
3960
3970
3980
3990
4000
4010
4020
4030
4040
4050
4060
4070
4080
4090
4100
4110
4120
4130
ECGR
RSAV
ECCE_RF
IRMN_RF
IRMN_RF
THMX_RF
B
AWMX_RF
IRMX_RF
IRMX_RF
THAV_RF
AWAV_RF
IRAV_RF
IRAV_RF
THNO
AWMN_RF
ERAV_RF
ERAV_RF
THMN_RF

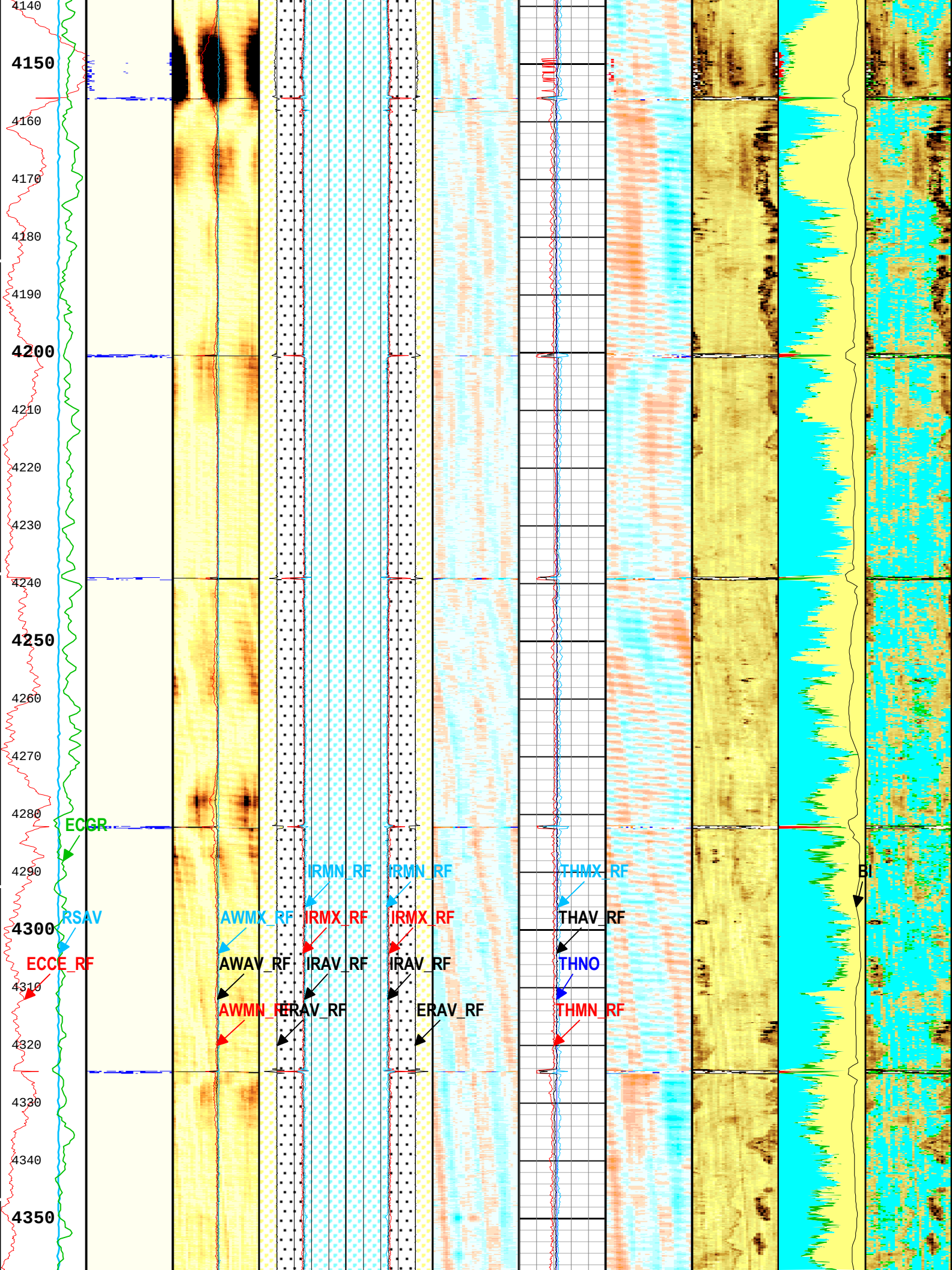
4140
4150
4160
4170
4180
4190
4200
4210
4220
4230
4240
4250
4260
4270
4280
4290
4300
4310
4320
4330
4340
4350
ECGR
RSAV
ECCE_RF
AWMX_RF
AWAV_RF
AWMN_RF
IRMN_RF
IRMX_RF
IRAV_RF
ERAV_RF
IRMN_RF
IRMX_RF
IRAV_RF
ERAV_RF
THMX_RF
THAV_RF
THNO
THMN_RF
BI

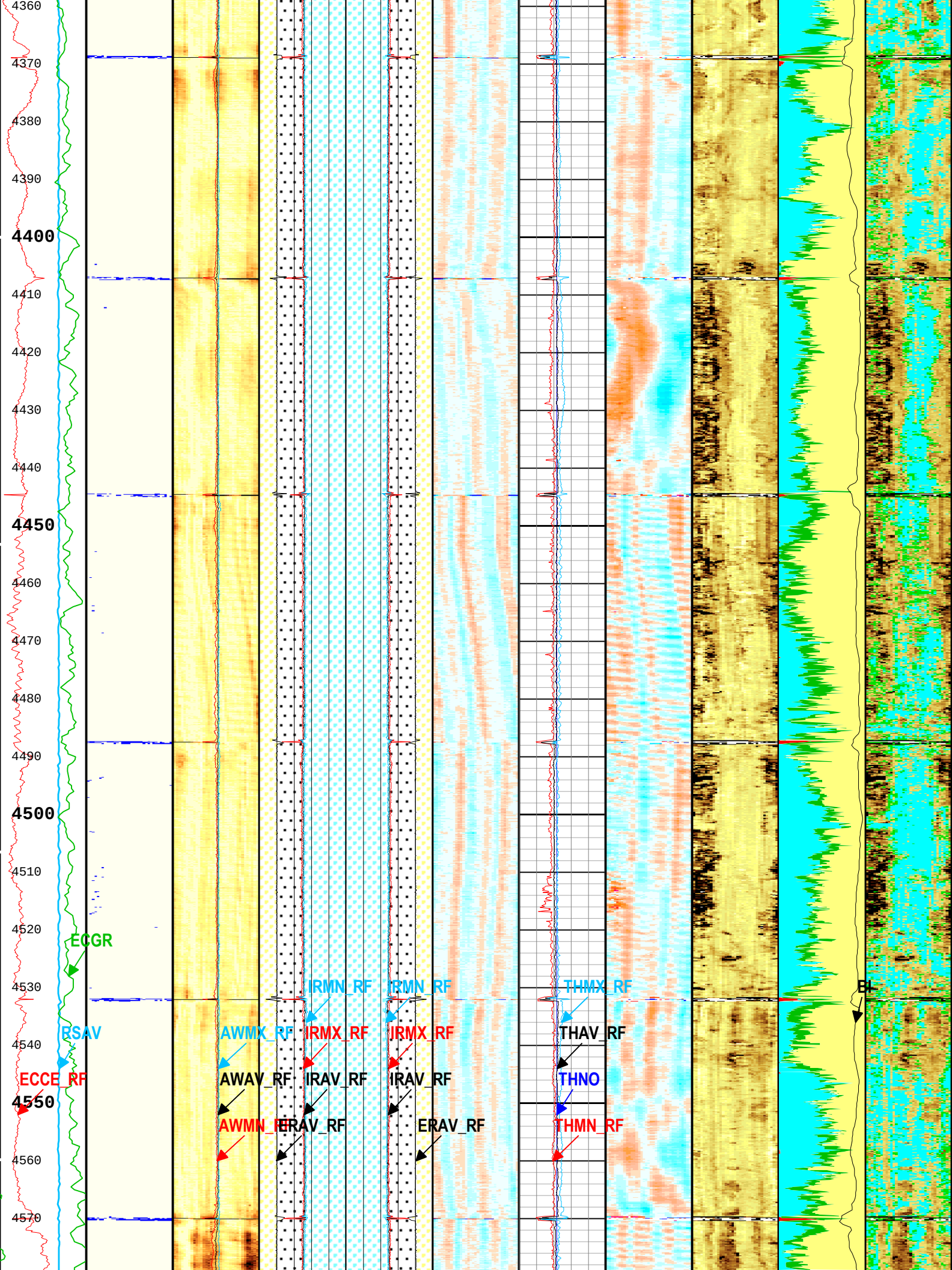
4360
4370
4380
4390
4400
4410
4420
4430
4440
4450
4460
4470
4480
4490
4500
4510
4520
4530
4540
4550
4560
4570
ECGR
RSAV
ECCE_RF
IRMN_RF
IRMN_RF
THMX_RF
AWMX_RF
IRMX_RF
IRMX_RF
THAV_RF
AWAV_RF
IRAV_RF
IRAV_RF
THNO
AWMN_RF
ERAV_RF
ERAV_RF
THMN_RF
BI

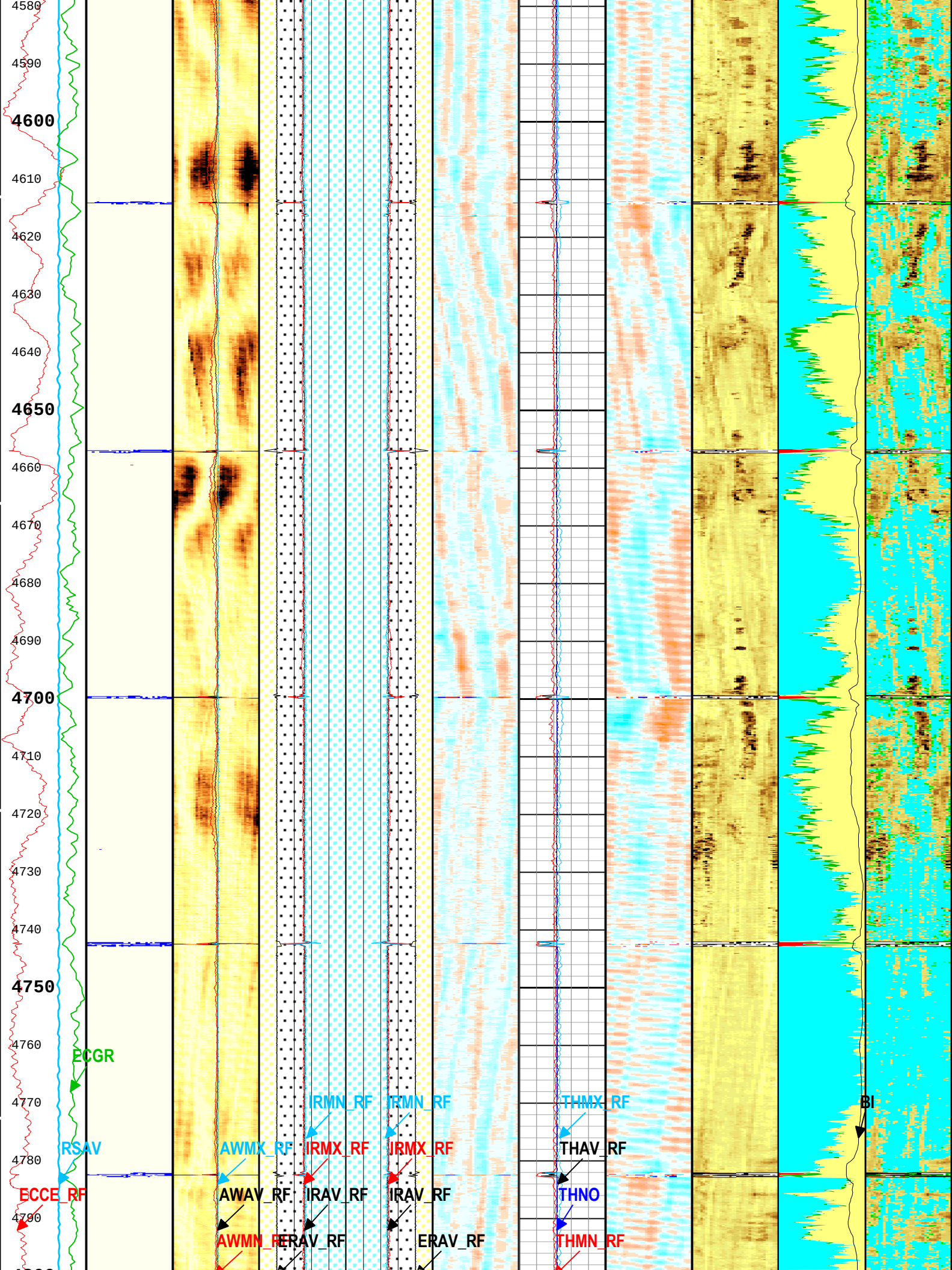
4580
4590
4600
4610
4620
4630
4640
4650
4660
4670
4680
4690
4700
4710
4720
4730
4740
4750
4760
4770
4780
4790
ECGR
RSAV
ECCE_RF
IRMN_RF
IRMN_RF
AWMX_RF
IRMX_RF
IRMX_RF
AWAV_RF
IRAV_RF
IRAV_RF
AWMN_RF
ERAV_RF
ERAV_RF
THMX_RF
THAV_RF
THNO
THMN_RF
BI

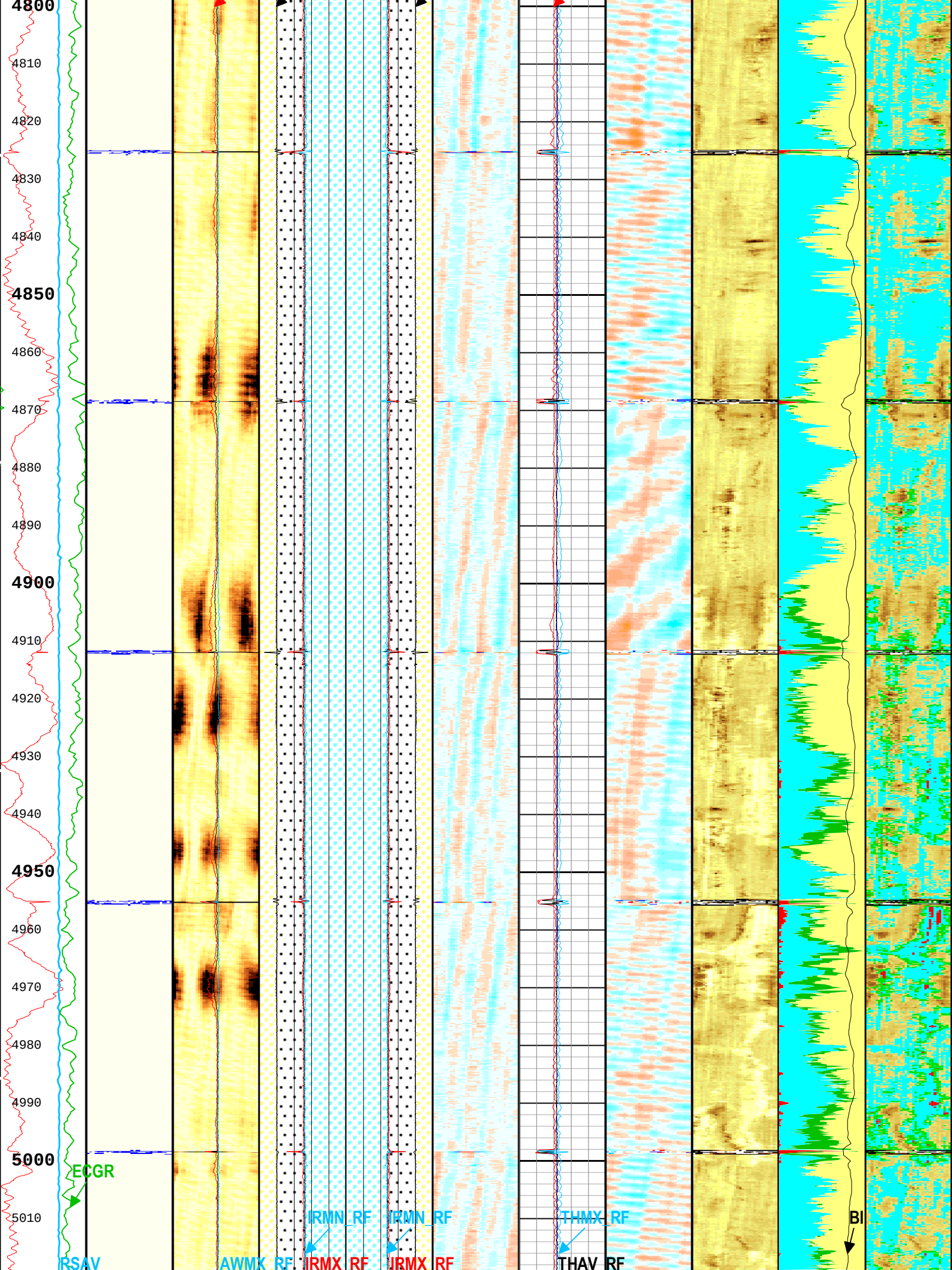
4800
4810
4820
4830
4840
4850
4860
4870
4880
4890
4900
4910
4920
4930
4940
4950
4960
4970
4980
4990
5000
5010
ECGR
RSAV
AWMX_RF
IRMN_RF
IRMX_RF
IRMN_RF
IRMX_RF
THMX_RF
THAV_RF
BI

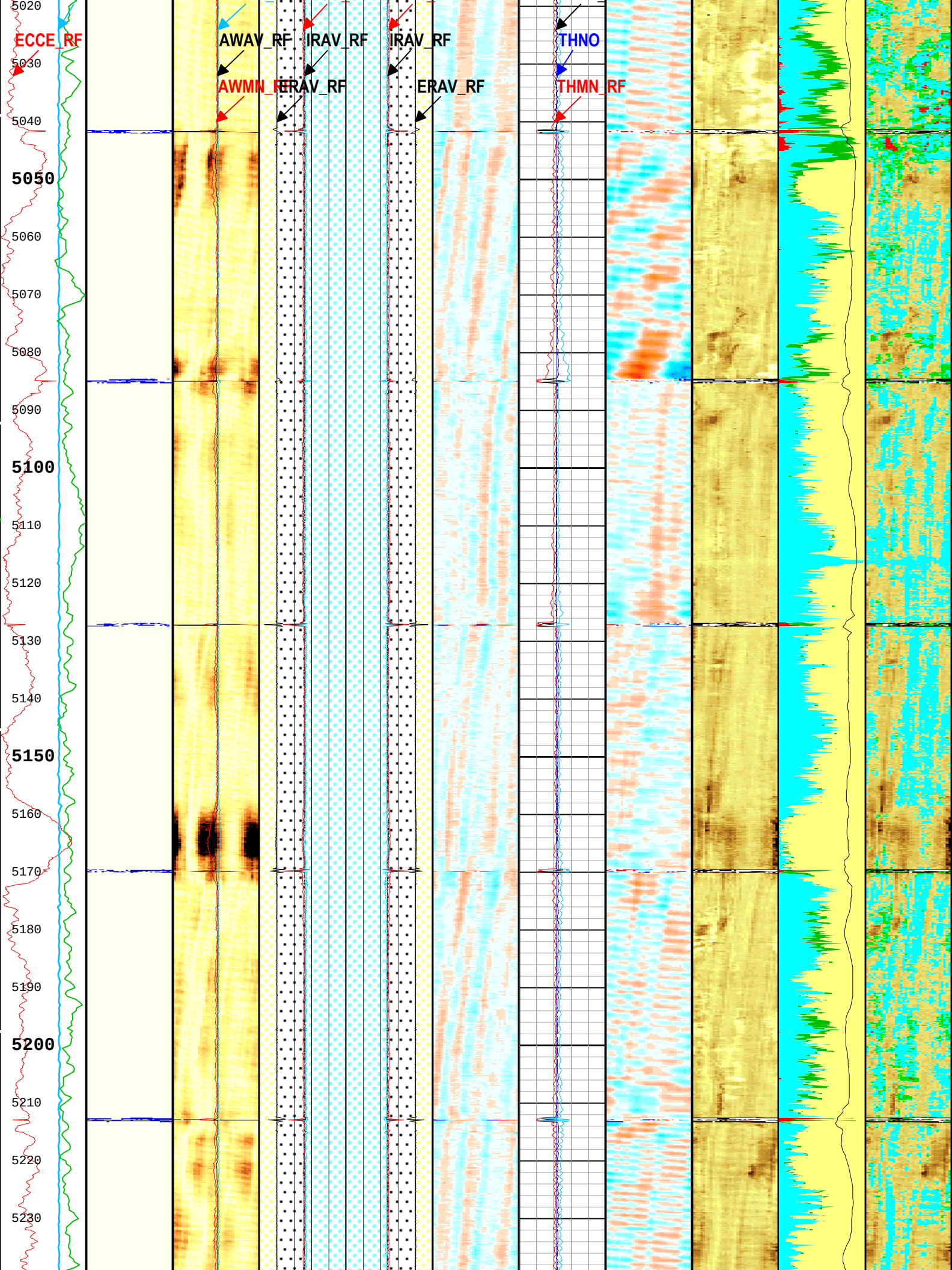
ECCE_RF
AWAV_RF
IRAV_RF
IRAV_RF
THNO
AWMN_RF
ERAV_RF
ERAV_RF
THMN_RF
5020
5030
5040
5050
5060
5070
5080
5090
5100
5110
5120
5130
5140
5150
5160
5170
5180
5190
5200
5210
5220
5230

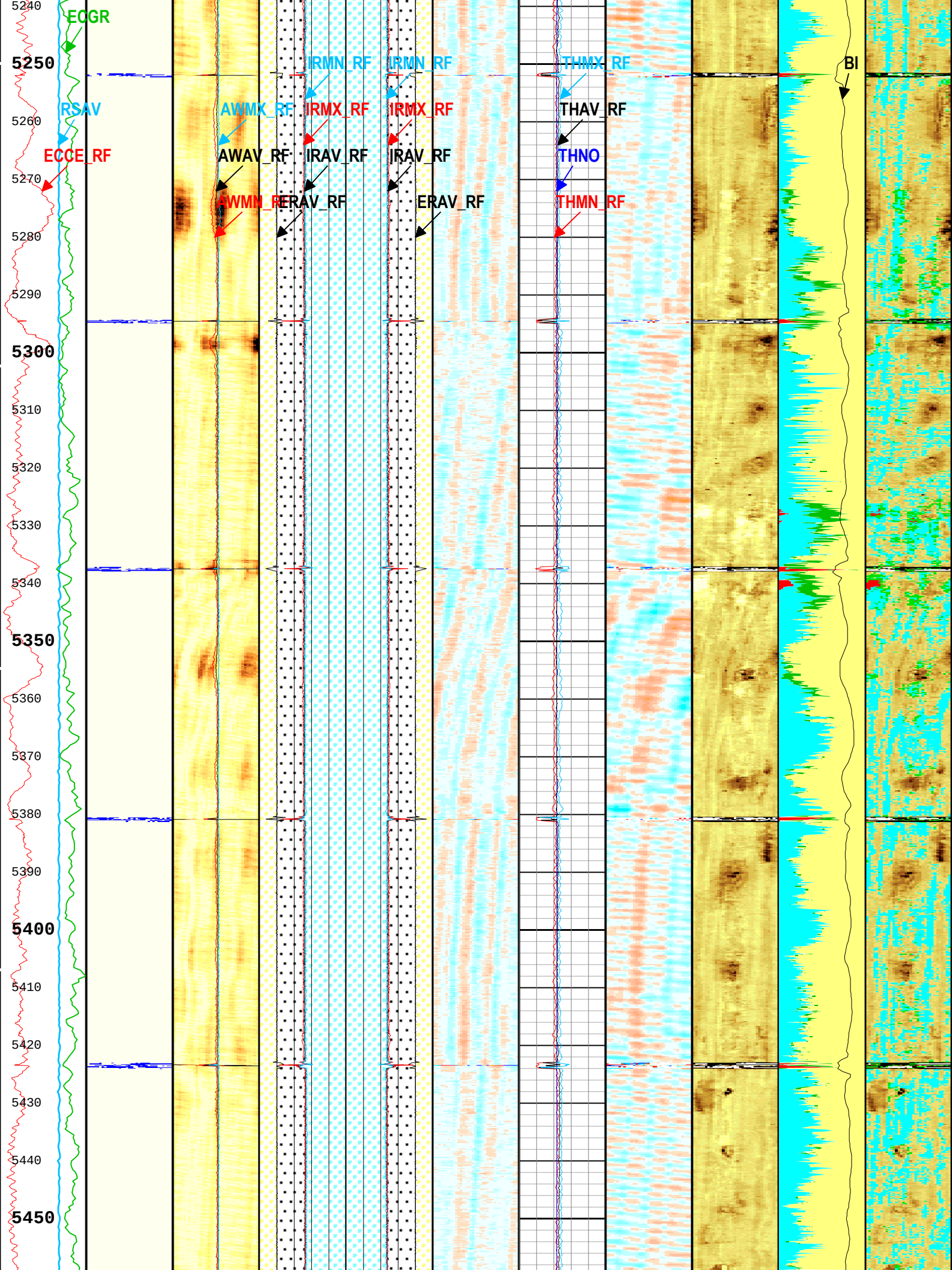
ECGR
RSAV
ECCE_RF
AWMX_RF
AWAV_RF
AWMN_RF
IRMN_RF
IRMX_RF
IRAV_RF
ERAV_RF
IRMN_RF
IRMX_RF
IRAV_RF
ERAV_RF
THMX_RF
THAV_RF
THNO
THMN_RF
BI
5240
5250
5260
5270
5280
5290
5300
5310
5320
5330
5340
5350
5360
5370
5380
5390
5400
5410
5420
5430
5440
5450

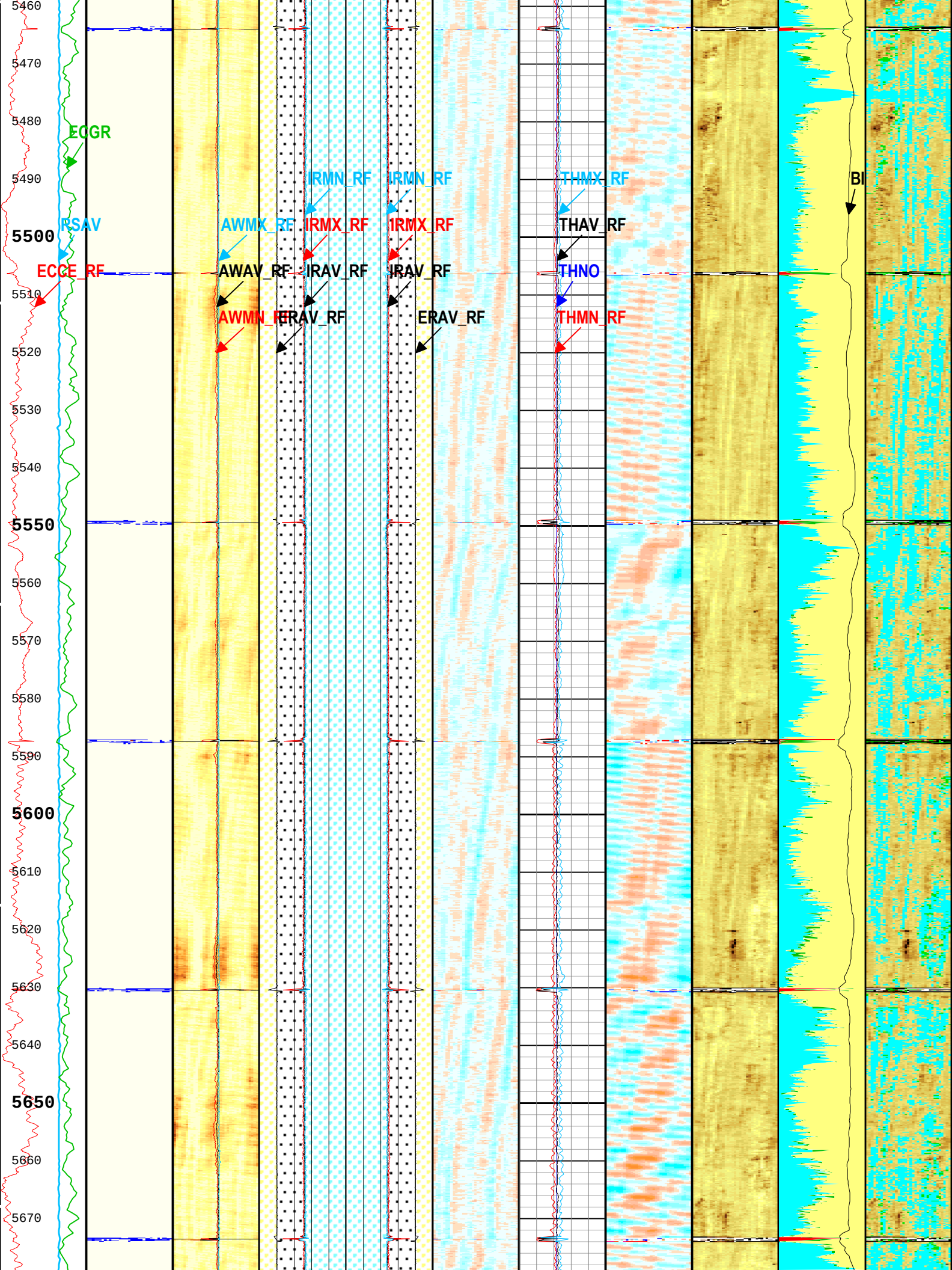
5460
5470
5480
5490
5500
5510
5520
5530
5540
5550
5560
5570
5580
5590
5600
5610
5620
5630
5640
5650
5660
5670
ECGR
RSAV
ECCE_RF
IRMN_RF
IRMN_RF
THMX_RF
AWMX_RF
IRMX_RF
IRMX_RF
THAV_RF
AWAV_RF
IRAV_RF
IRAV_RF
THNO
AWMN_RF
ERAV_RF
ERAV_RF
THMN_RF
BI

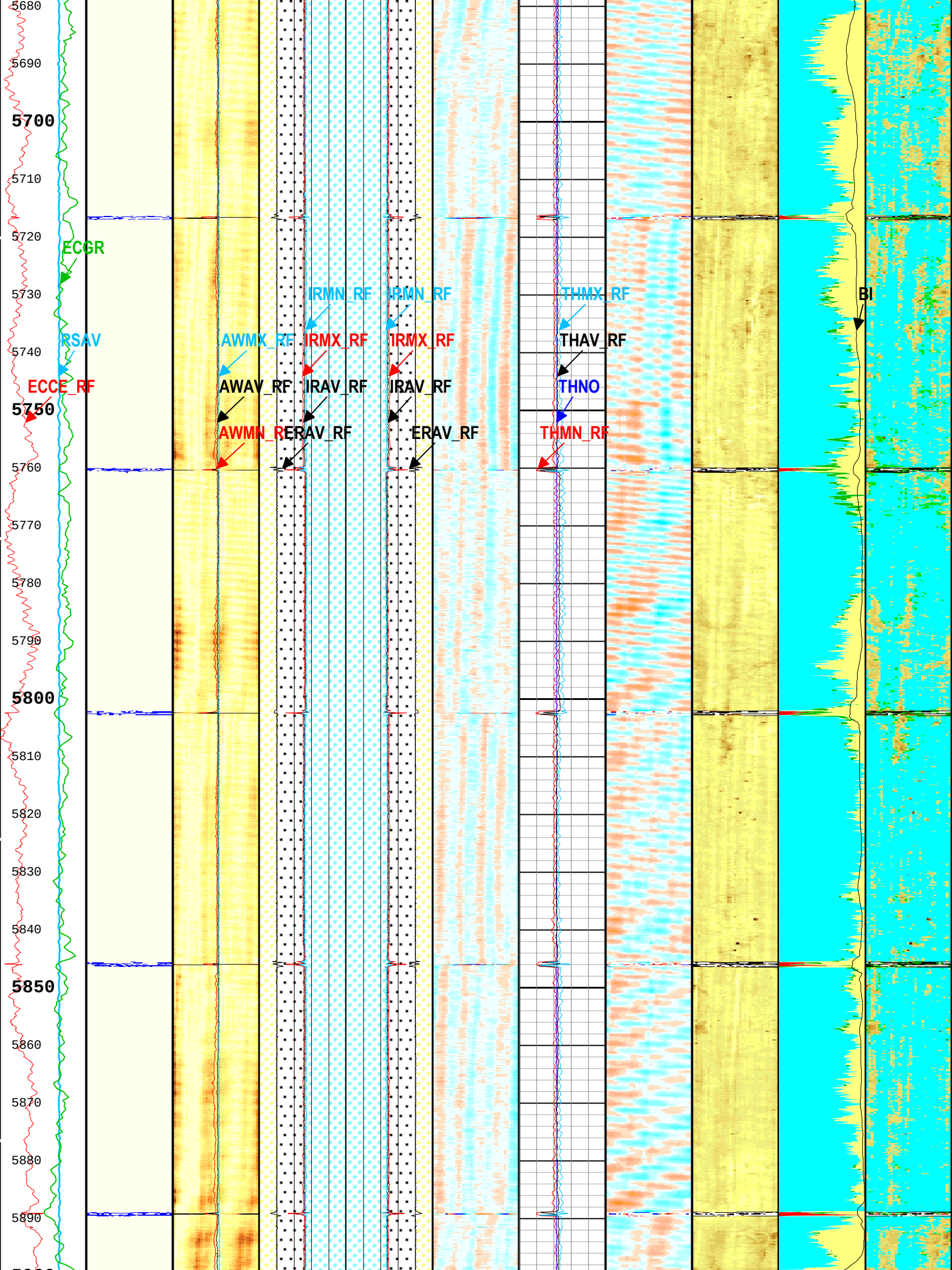
5680
5690
5700
5710
5720
5730
5740
5750
5760
5770
5780
5790
5800
5810
5820
5830
5840
5850
5860
5870
5880
5890
ECGR
RSAV
ECCE_RF
AWMX_RF
AWAV_RF
AWMN_RF
IRMN_RF
IRMX_RF
IRAV_RF
ERAV_RF
IRMN_RF
IRMX_RF
IRAV_RF
ERAV_RF
THMX_RF
THAV_RF
THNO
THMN_RF
BI

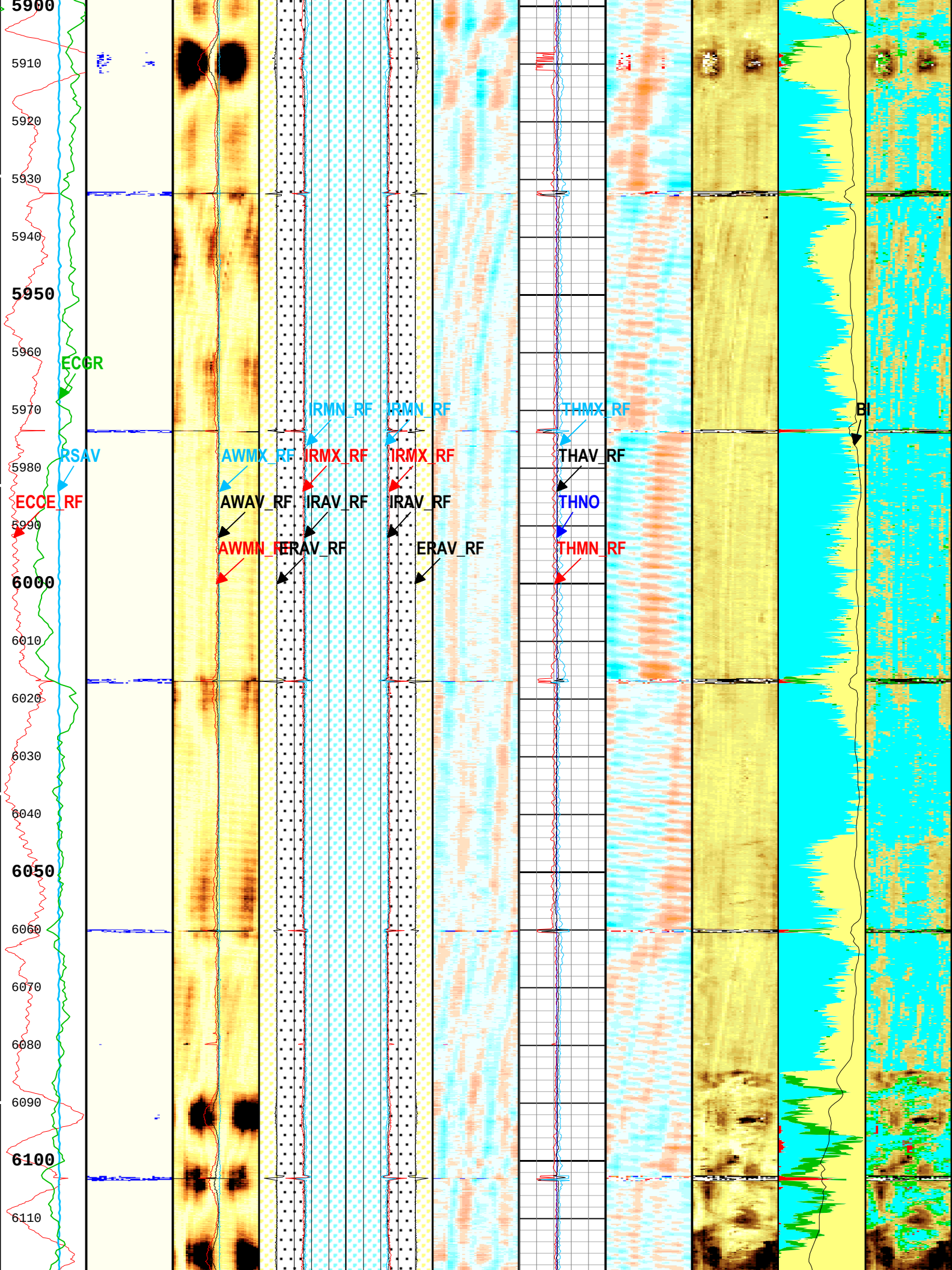
5900
5910
5920
5930
5940
5950
5960
5970
5980
5990
6000
6010
6020
6030
6040
6050
6060
6070
6080
6090
6100
6110
ECGR
RSAV
ECCE_RF
IRMN_RF
IRMN_RF
THMX_RF
BI
AWMX_RF
IRMX_RF
IRMX_RF
THAV_RF
AWAV_RF
IRAV_RF
IRAV_RF
THNO
AWMN_RF
ERAV_RF
ERAV_RF
THMN_RF

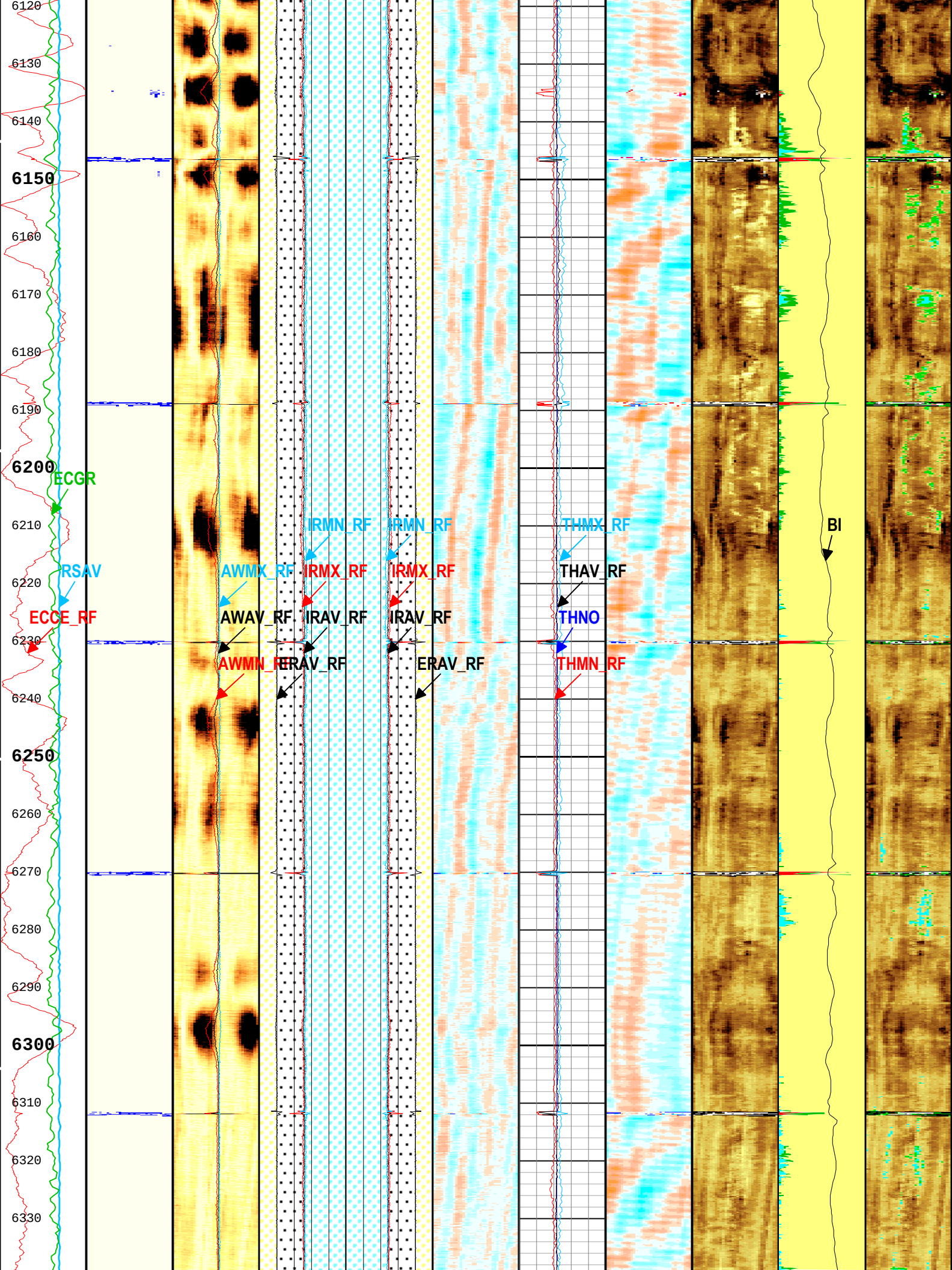
6120
6130
6140
6150
6160
6170
6180
6190
6200
6210
6220
6230
6240
6250
6260
6270
6280
6290
6300
6310
6320
6330
ECGR
RSAV
ECCE_RF
IRMN_RF
AWMX_RF
IRMX_RF
AWAV_RF
IRAV_RF
AWMN_RF
ERAV_RF
IRMN_RF
IRMX_RF
IRAV_RF
ERAV_RF
THMX_RF
THAV_RF
THNO
THMN_RF
BI

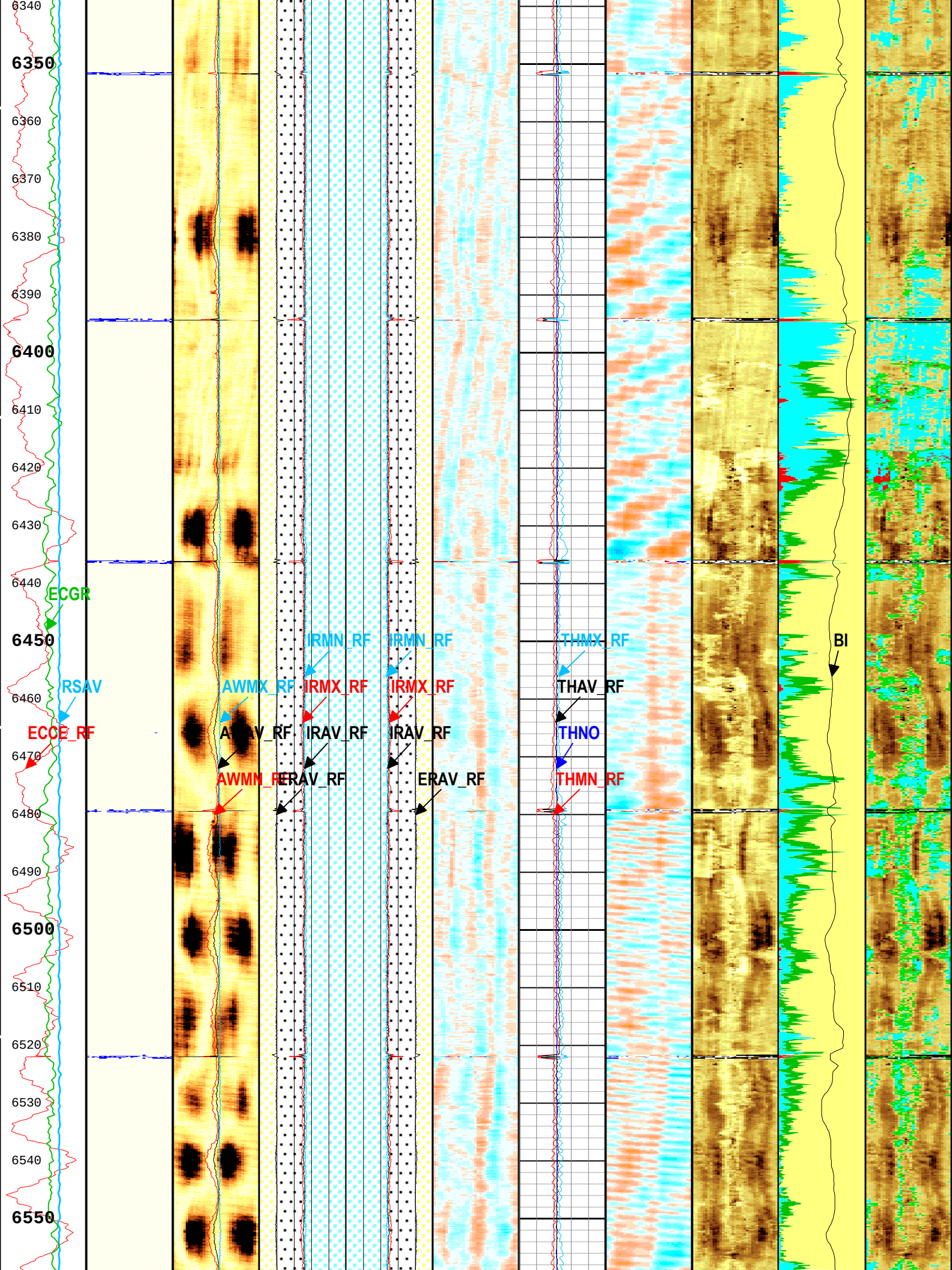
6340
6350
6360
6370
6380
6390
6400
6410
6420
6430
6440
6450
6460
6470
6480
6490
6500
6510
6520
6530
6540
6550
ECGR
RSAV
ECCE_RF
IRMN_RF
IRMN_RF
AWMX_RF
IRMX_RF
IRMX_RF
IRAV_RF
IRAV_RF
IRAV_RF
AWMN_RF
ERAV_RF
ERAV_RF
THMX_RF
THAV_RF
THNO
THMN_RF
BI

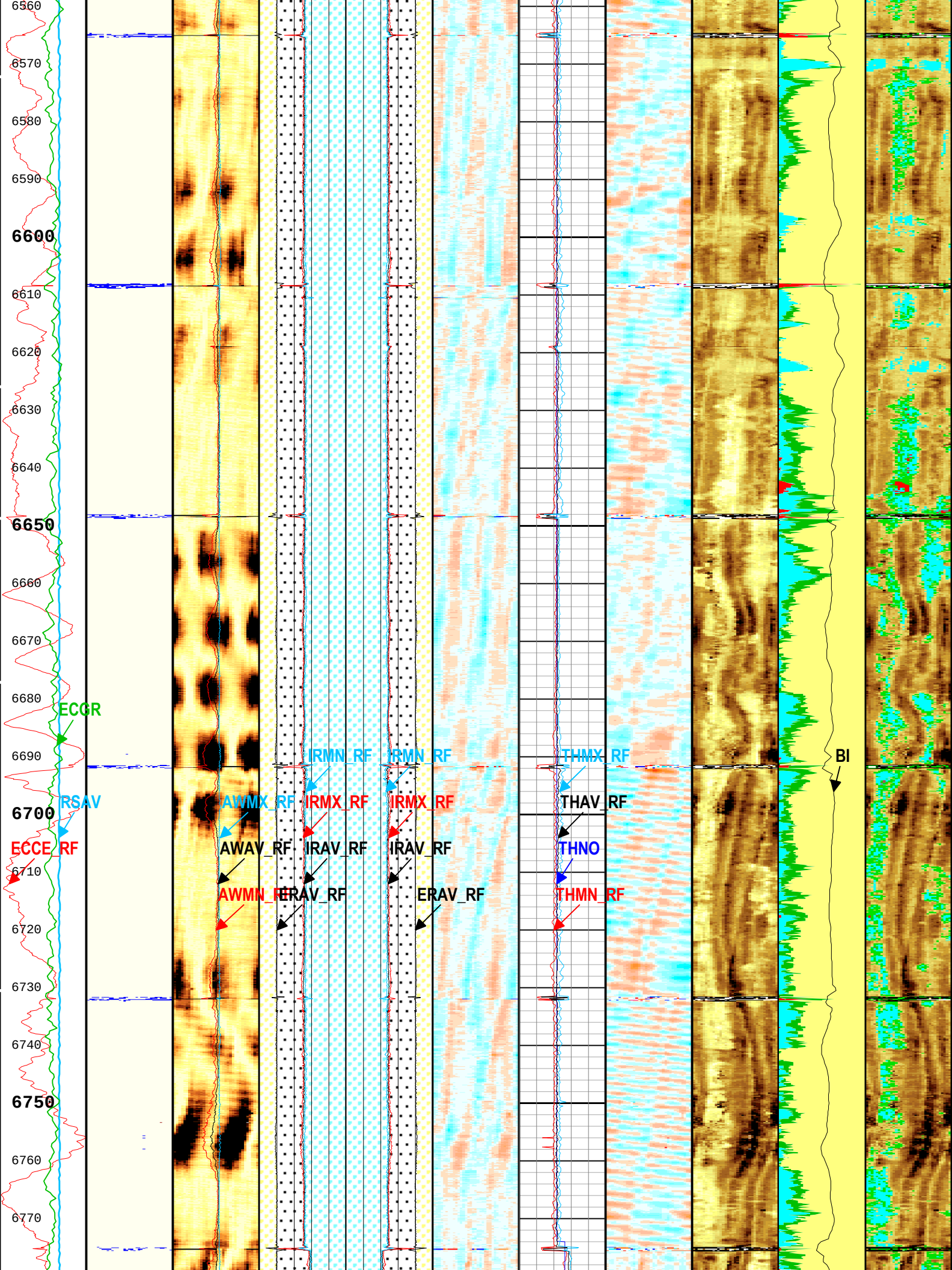
6560
6570
6580
6590
6600
6610
6620
6630
6640
6650
6660
6670
6680
6690
6700
6710
6720
6730
6740
6750
6760
6770
ECGR
RSAV
ECCE_RF
IRMN_RF
IRMN_RF
THMX_RF
AWMX_RF
IRMX_RF
IRMX_RF
THAV_RF
AWAV_RF
IRAV_RF
IRAV_RF
THNO
AWMN_RF
ERAV_RF
ERAV_RF
THMN_RF
BI

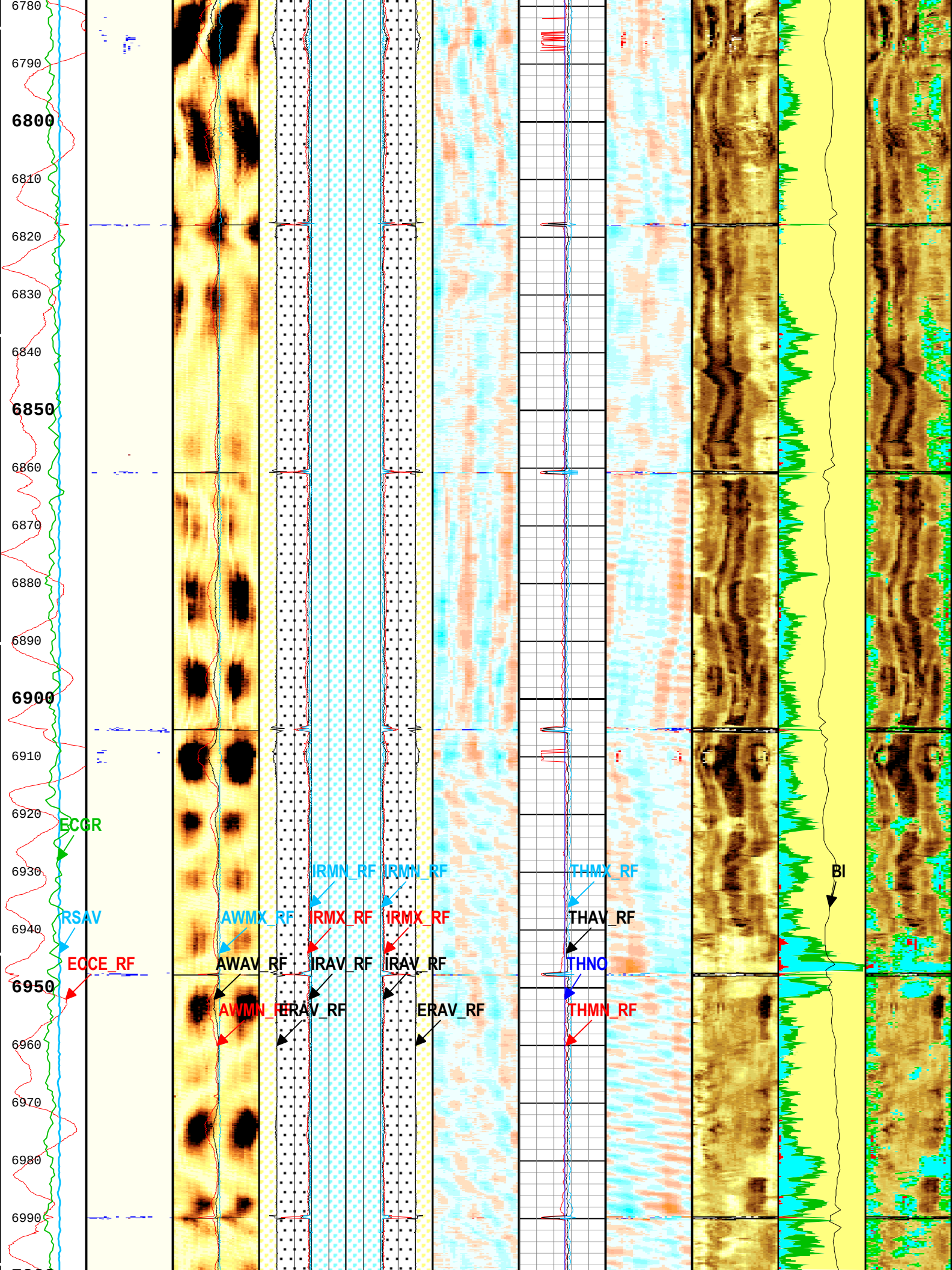
6780
6790
6800
6810
6820
6830
6840
6850
6860
6870
6880
6890
6900
6910
6920
6930
6940
6950
6960
6970
6980
6990
ECGR
RSAV
ECCE_RF
AWAV_RF
AWMX_RF
AWMN_RF
IRMN_RF
IRMX_RF
IRAV_RF
ERAV_RF
IRMN_RF
IRMX_RF
IRAV_RF
ERAV_RF
THMX_RF
THAV_RF
THNO
THMN_RF
BI

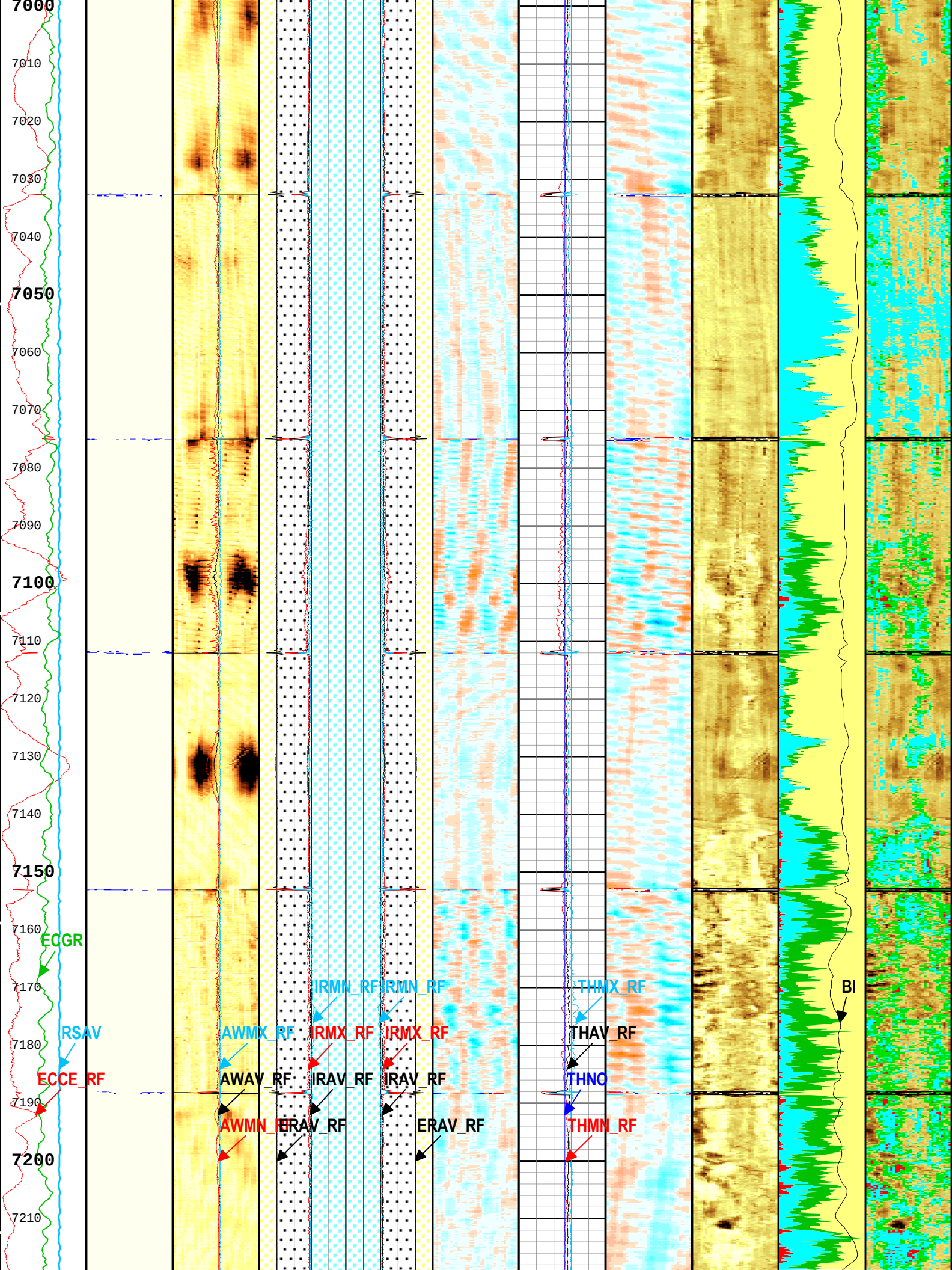
7000
7010
7020
7030
7040
7050
7060
7070
7080
7090
7100
7110
7120
7130
7140
7150
7160
7170
7180
7190
7200
7210
ECGR
RSAV
ECCE_RF
AWMX_RF
AWAV_RF
AWMN_RF
IRMN_RF
IRMX_RF
IRAV_RF
ERAV_RF
IRMN_RF
IRMX_RF
IRAV_RF
ERAV_RF
THMX_RF
THAV_RF
THNO
THMN_RF
BI

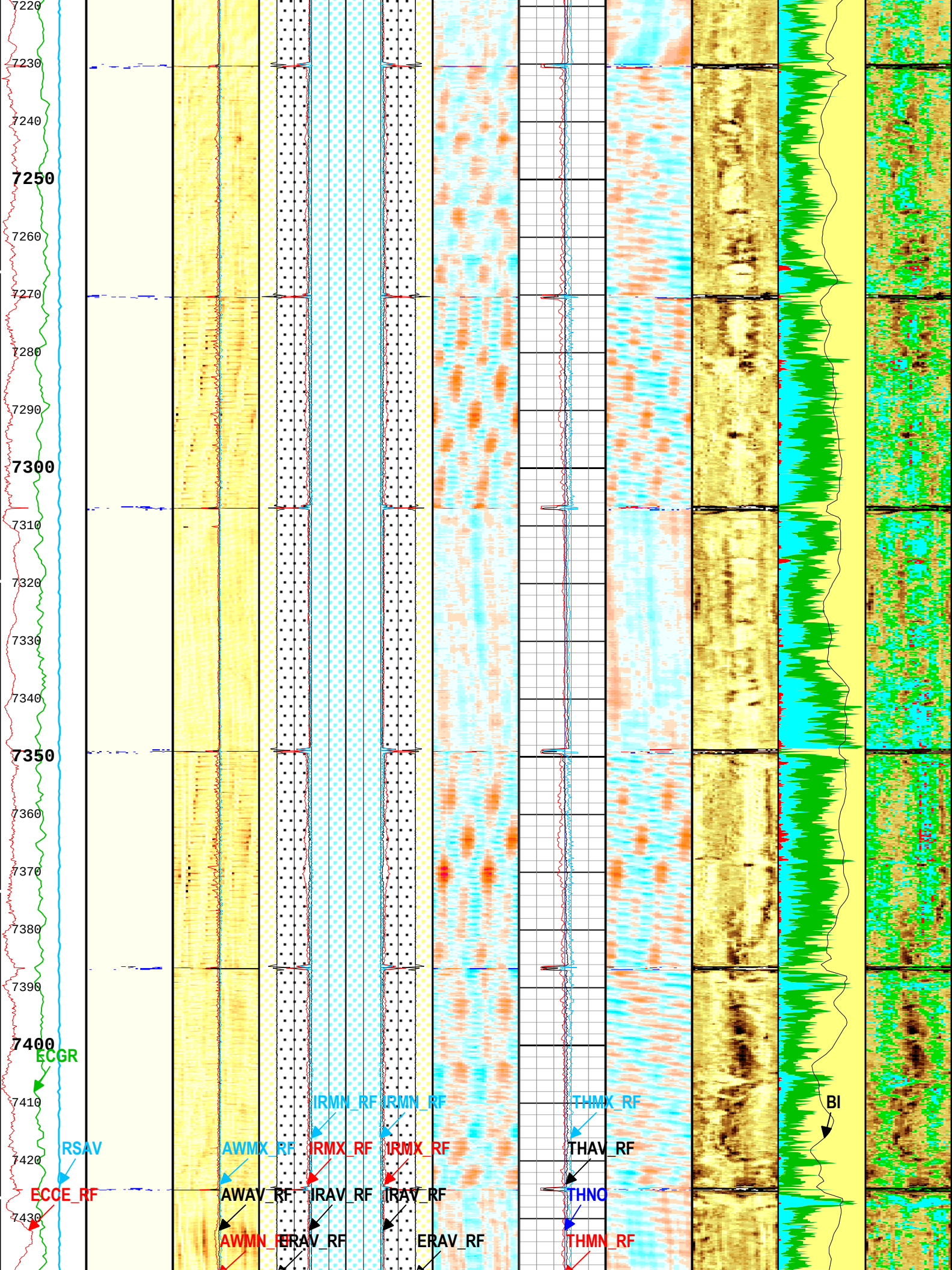
7220
7230
7240
7250
7260
7270
7280
7290
7300
7310
7320
7330
7340
7350
7360
7370
7380
7390
7400
7410
7420
7430
ECGR
RSAV
ECCE_RF
IRMN_RF
IRMN_RF
AWMX_RF
IRMX_RF
IRMX_RF
AWAV_RF
IRAV_RF
IRAV_RF
AWMN_RF
ERAV_RF
ERAV_RF
THMX_RF
THAV_RF
THNO
THMN_RF
BI

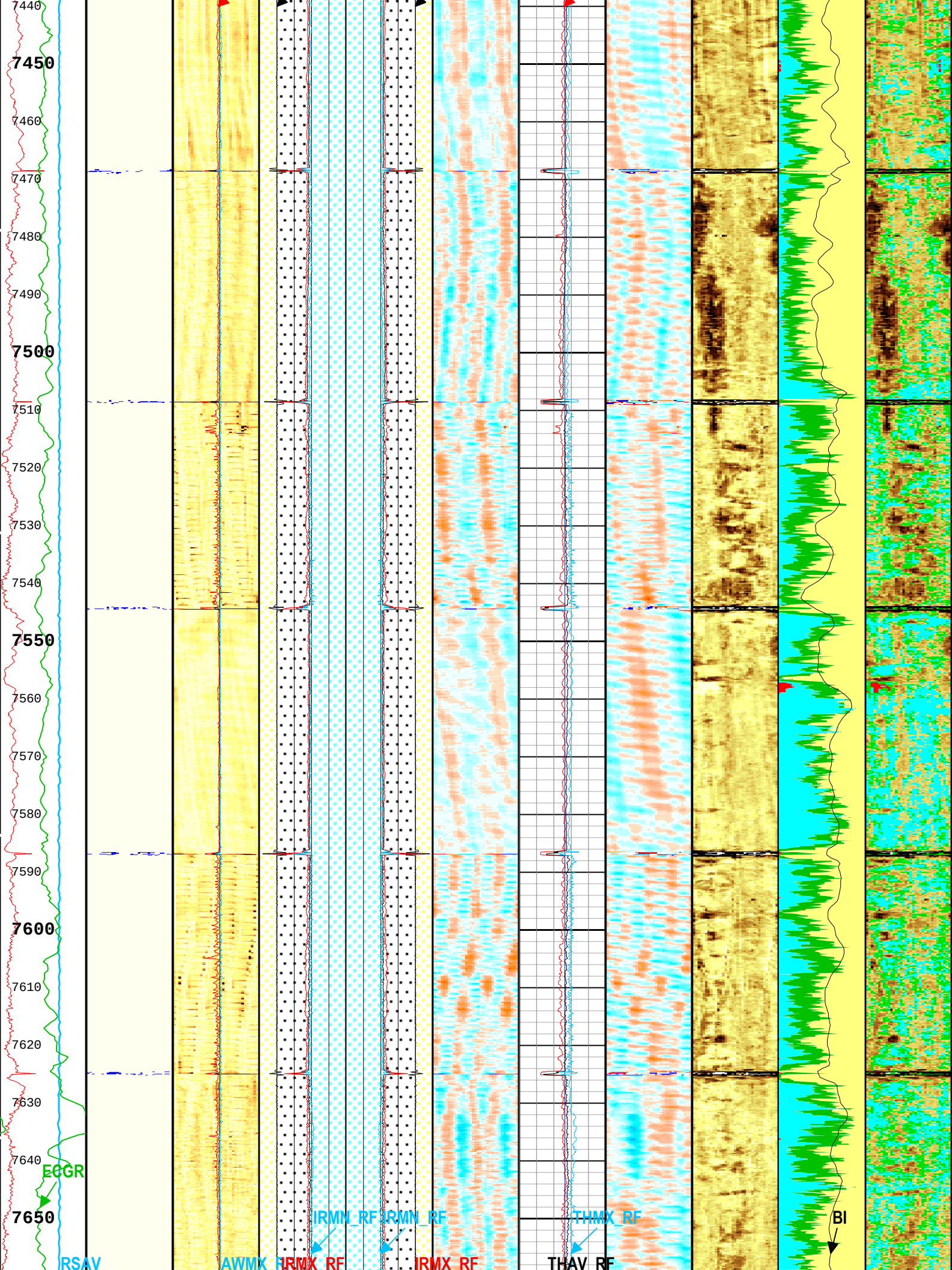
7440
7450
7460
7470
7480
7490
7500
7510
7520
7530
7540
7550
7560
7570
7580
7590
7600
7610
7620
7630
7640
7650
ECGR
RSAV
AWMX
IRMX_RF
IRMN_RF
IRMN_RF
IRMX_RF
THMX_RF
THAV_RF
BI

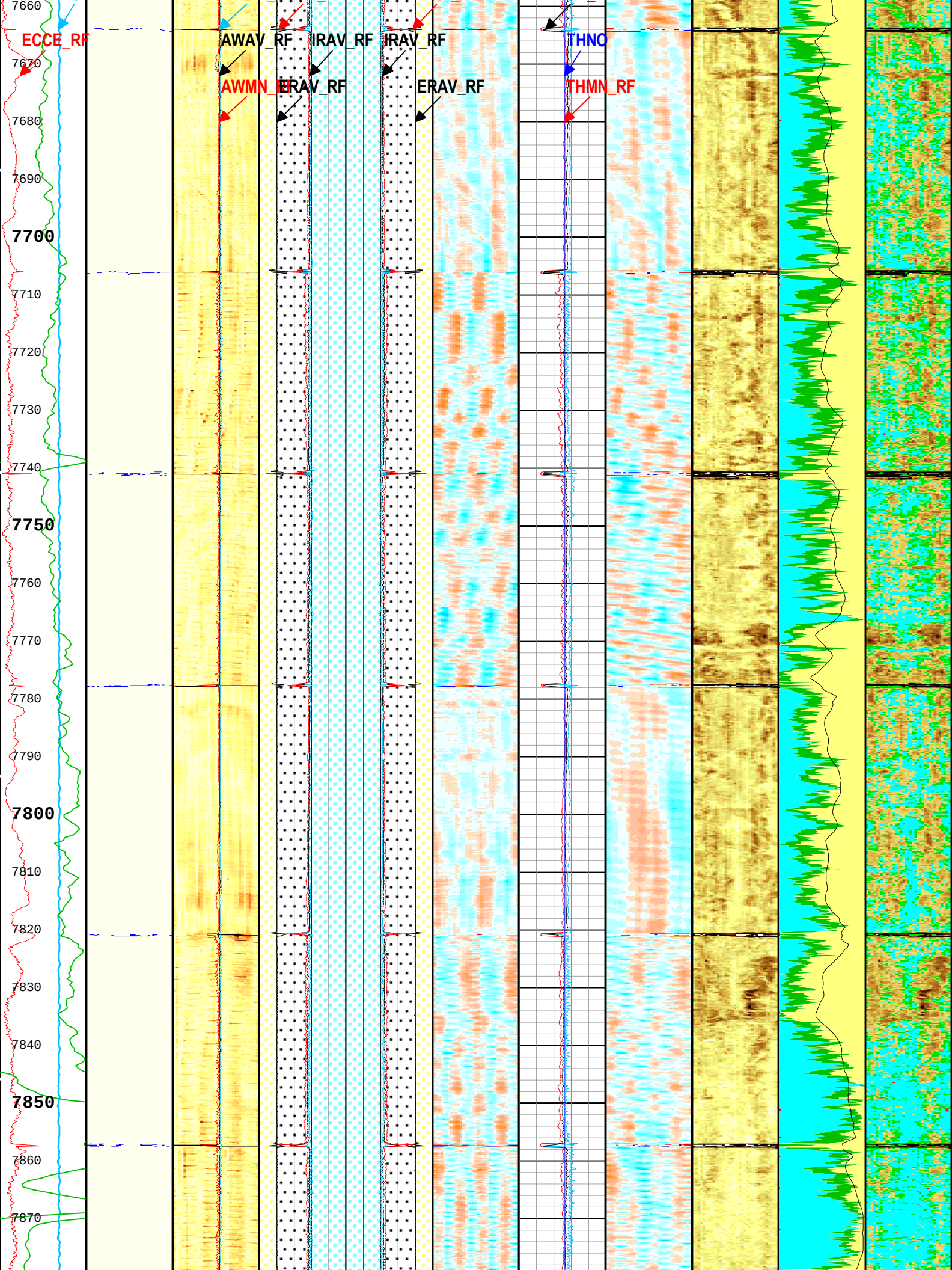
ECCE_RF
AWAV_RF
IRAV_RF
IRAV_RF
THNO
AWMN_RF
ERAV_RF
ERAV_RF
THMN_RF
7660
7670
7680
7690
7700
7710
7720
7730
7740
7750
7760
7770
7780
7790
7800
7810
7820
7830
7840
7850
7860
7870

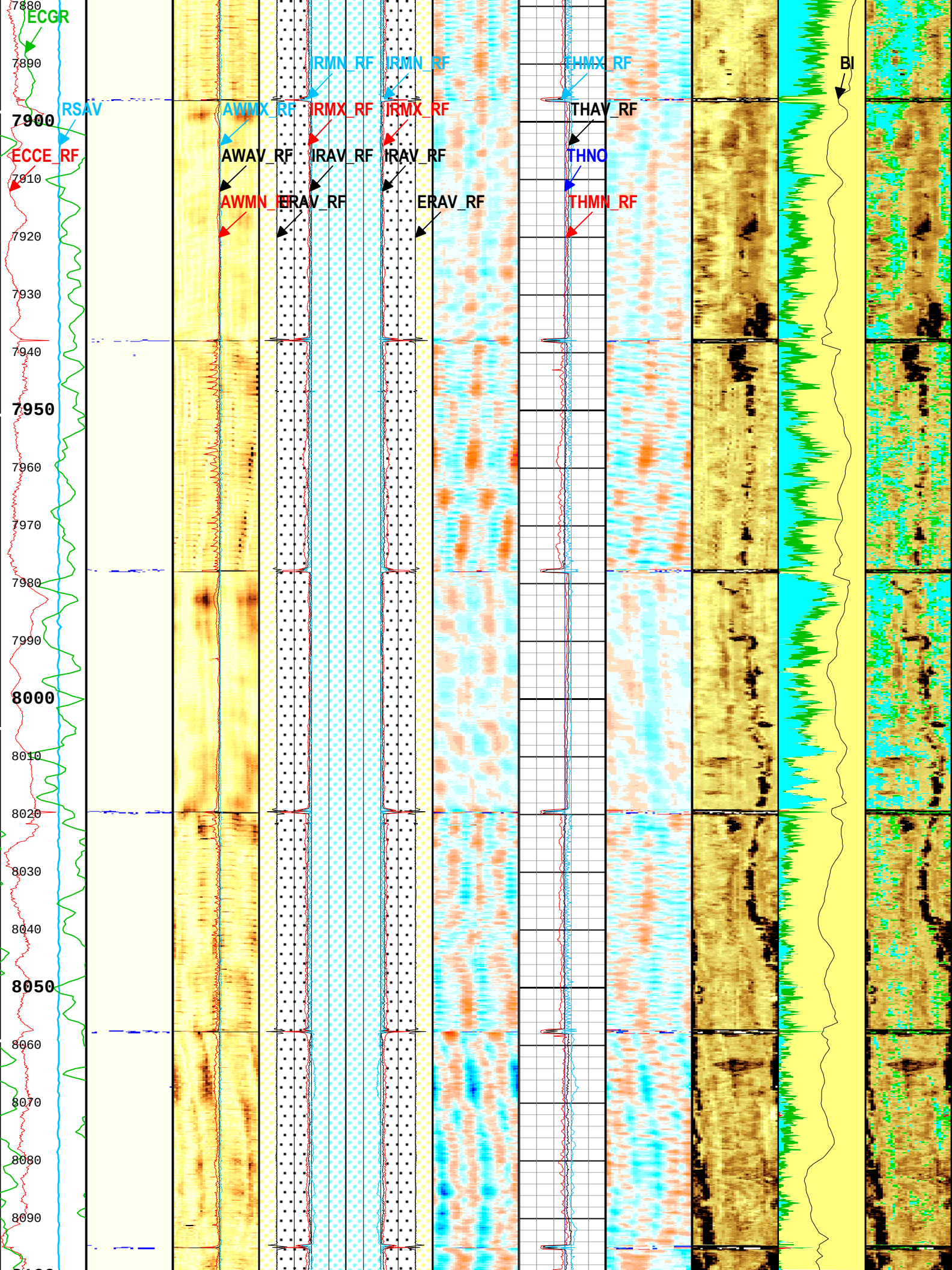
ECGR
RSAV
ECCE_RF
AWMX_RF
AWAV_RF
AWMN_RF
IRMN_RF
IRMX_RF
IRAV_RF
ERAV_RF
IRMN_RF
IRMX_RF
IRAV_RF
ERAV_RF
THMX_RF
THAV_RF
THNO
THMN_RF
BI
7880
7890
7900
7910
7920
7930
7940
7950
7960
7970
7980
7990
8000
8010
8020
8030
8040
8050
8060
8070
8080
8090

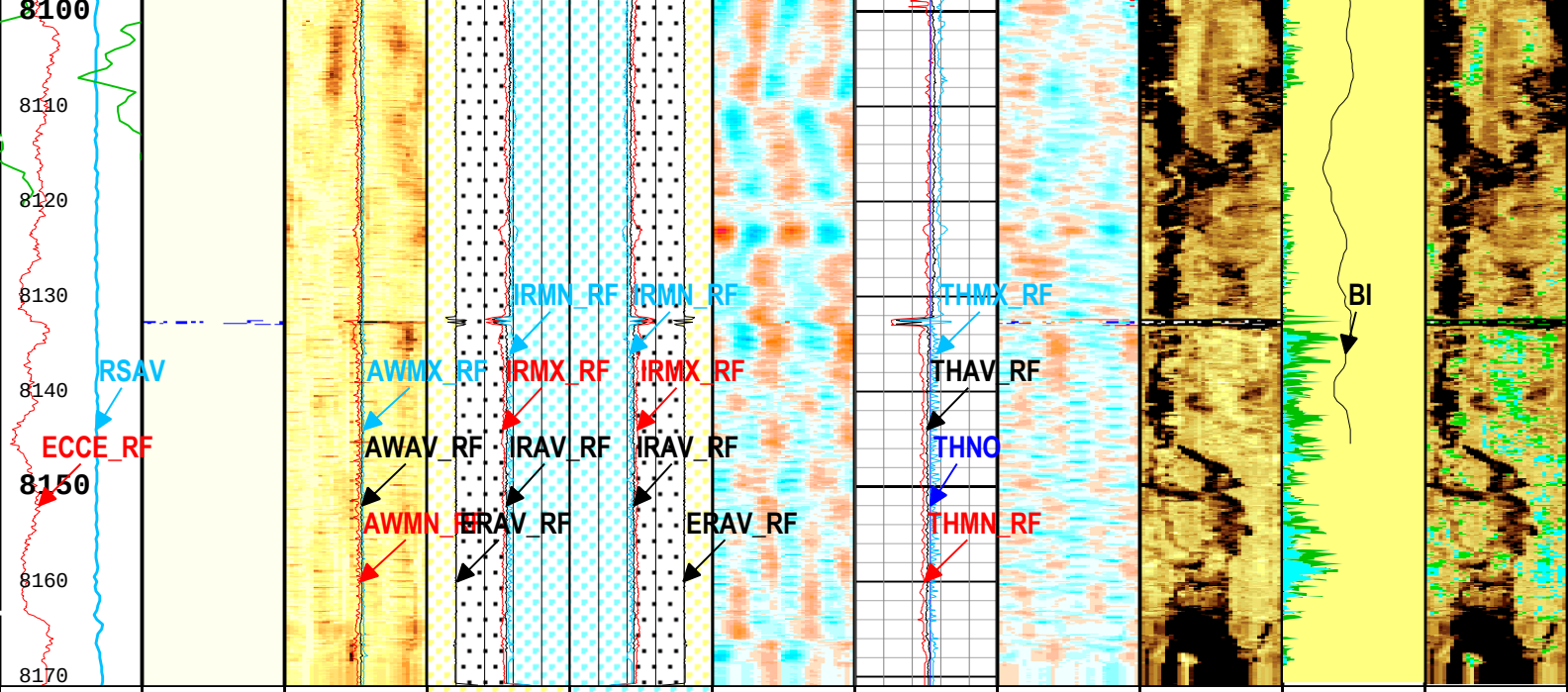

Amplitude of Eccentering for Unflagged Waves (ECCE_RF) USIT-E[1]
0 in 0.5

Motor Revolution Speed (RSAV) USIT-E[1]
6 c/s 8

Gamma Ray (ECGR) HGNS[1]
0 gAPI 150

Absent 1.500 3.500
Explicit Normalization
USIT - USIT Processing Flags (UFLG) USIT-E[1]

USIT Processing Flags (UFLG[0]) USIT-E[1]
1 5

Absent -4.799 -2.799 -0.800
Explicit Normalization
USIT - Amplitude of Unflagged Wave (AWBK_RF) USIT-E[1] (dB)

Minimum of Unflagged Wave Amplitude (AWMN_RF) USIT-E[1]
0 dB 75

Average of Unflagged Wave Amplitude (AWAV_RF) USIT-E[1]
0 dB 75

Maximum of Unflagged Wave Amplitude (AWMX_RF) USIT-E[1]
0 dB 75

ERAV
ERAV-IRAV
IRAV

Median of Unflagged External Radii (ERAV_RF) USIT-E[1]
3.7 in 2.7

Median Internal Radius of Casing Corrected for Eccentering (IRAV_RF) USIT-E[1]
3.7 in 2.7

Maximum of Unflagged Internal Radii (IRMX_RF) USIT-E[1]
3.7 in 2.7

Minimum of Unflagged Internal Radii (IRMN_RF) USIT-E[1]
3.7 in 2.7

IRAV
ERAV
IRAV-ERAV

Median of Unflagged External Radii (ERAV_RF) USIT-E[1]
2.7 in 3.7

Median Internal Radius of Casing Corrected for Eccentering (IRAV_RF) USIT-E[1]
2.7 in 3.7

Maximum of Unflagged Internal Radii (IRMX_RF) USIT-E[1]
2.7 in 3.7

Minimum of Unflagged Internal Radii (IRMN_RF) USIT-E[1]
2.7 in 3.7

Absent -0.051 -0.012 0.028 0.068
Explicit Normalization
USIT - Unflagged Internal Radii minus Median Internal Radius (IRBKM_RF) USIT-E[1] (in)

Minimum of Unflagged Casing Thickness (THMN_RF) USIT-E[1]
0.1 in 0.6

Nominal Casing Thickness (THNO) USIT-E[1]
0.1 in 0.6

Median of Unflagged Casing Thickness (THAV_RF) USIT-E[1]
0.1 in 0.6

Maximum of Unflagged Casing Thickness (THMX_RF) USIT-E[1]
0.1 in 0.6

Absent -0.051 -0.012 0.028 0.068
Explicit Normalization
USIT - Unflagged Casing Thickness minus Median of Unflagged Casing Thickness (THBKM_RF) USIT-E[1] (in)

Absent 1.500 3.500 5.500 7.500
Custom Normalization
USIT - Acoustic Impedance (AIBK) USIT-E[1] (Mrayl)

Ratio of Cement Measurements to Total (CEMR) USIT-E[1]
1 0

Micro-debonding Ratio (MDR) USIT-E[1]
1 0

Ratio of Gas Measurements to Total (GASR) USIT-E[1]
1 0

Bonded
Gas
Liquid
Micro-debonding

Bond Index (BI) DSLT-H[1]
1 0

Absent 3.090 5.054 7.018
Custom Normalization
USIT - Acoustic Impedance (AIBK) USIT-E[1] (Mrayl)

Absent 2.599 4.563 6.527
Custom Normalization
USIT - Acoustic Impedance With Micro-debonding Image (AI_MDEBOND_IMG) USIT-E[1] (Mrayl)

USIT Processing Flags (UFLG[0]) USIT-E[1]

1 - UFLG 1 Value within [0.0 - 1.5] - :

2 - UFLG 2 Value within [1.5 - 2.5] - :

UTIM Error

Pulse Origin Not Detected

3 - UFLG 3 Value within [2.5 - 3.5] - :
4 - UFLG 4 UFLG 5 UFLG 6 Value within [3.5 - 6.5] - :
5 - UFLG 7 UFLG 8 UFLG 9 Value within [6.5 - 10] - :

WINLEN Error
Casing Thickness Error
Loop Processing Error

TIME_1900 - Time Marked every 60.00 (s)

Description: USI Composite Format: Log (LBV1_USI Composite 7inch) Index Scale: 5 in per 100 ft Index Unit: ft Index Type: Measured Depth Creation Date: 20-Oct-2016 14:28:19

Two

Cement Log 2 IN = 100 FT

Pass Summary

Run Name	Pass Objective	Direction	Top	Bottom	Start	Stop	DSC Mode	Depth Shift	Include Parallel Data
Two	Log[6]:Up	Up	6845.38 ft	8162.42 ft	19-Oct-2016 2:46:42 PM	19-Oct-2016 3:11:08 PM	ON	2.05 ft	No

All depths are referenced to toolstring zero

Log

Company:Southern California Gas Company Well:Frew 4

Two: Log[6]:Up:S008

Description: USI Cement Format: Log (LBV1_USI Cement 7inch) Index Scale: 2 in per 100 ft Index Unit: ft Index Type: Measured Depth Creation Date: 20-Oct-2016 14:28:43

TIME_1900 - Time Marked every 60.00 (s)

ERAV_IRAV | ERAV_RHF1
IRAV_LHF1 | IRAV_ERAV
LHF1_ERAV | RHF1_IRAV

Median of Unflagged External Radii (ERAV_RF) USIT-E
3.7 in 2.7

Median of Unflagged External Radii (ERAV_RF) USIT-E
2.7 in 3.7

Median Internal Radius of Casing Corrected for Eccentering (IRAV_RF) USIT-E
3.7 in 2.7

Median Internal Radius of Casing Corrected for Eccentering (IRAV_RF) USIT-E
2.7 in 3.7

Minimum of Unflagged Internal Radii (IRMN_RF) USIT-E
3.7 in 2.7

Minimum of Unflagged Internal Radii (IRMN_RF) USIT-E
2.7 in 3.7

Gamma Ray (ECGR) HGNS-H
0 gAPI 150

Amplitude of Eccentering for Unflagged Waves (ECCE_RF) USIT-E
0 in 0.5

Maximum of Unflagged Internal Radii (IRMX_RF) USIT-E
3.7 in 2.7

Maximum of Unflagged Internal Radii (IRMX_RF) USIT-E
2.7 in 3.7

Absent 0.500 1.500 2.500 3.500 4.500 5.500 6.500 7.500
Custom Normalization
USIT - Acoustic Impedance (AIBK) USIT-E (Mrayl)

Acoustic Impedance Minimum (AIMN) USIT-E
-1 Mrayl 9

Acoustic Impedance Average (AIAV) USIT-E
-1 Mrayl 9

Acoustic Impedance Maximum (AIMX) USIT-E
-1 Mrayl 9

Bonded
Gas
Liquid
Micro-debonding

Absent -500.000 2.599 3.581 4.563 5.545 6.527 7.509
Custom Normalization
USIT - Acoustic Impedance With Micro-debonding Image (AI_MDEBOND_IMG) USIT-E (Mrayl)

6800

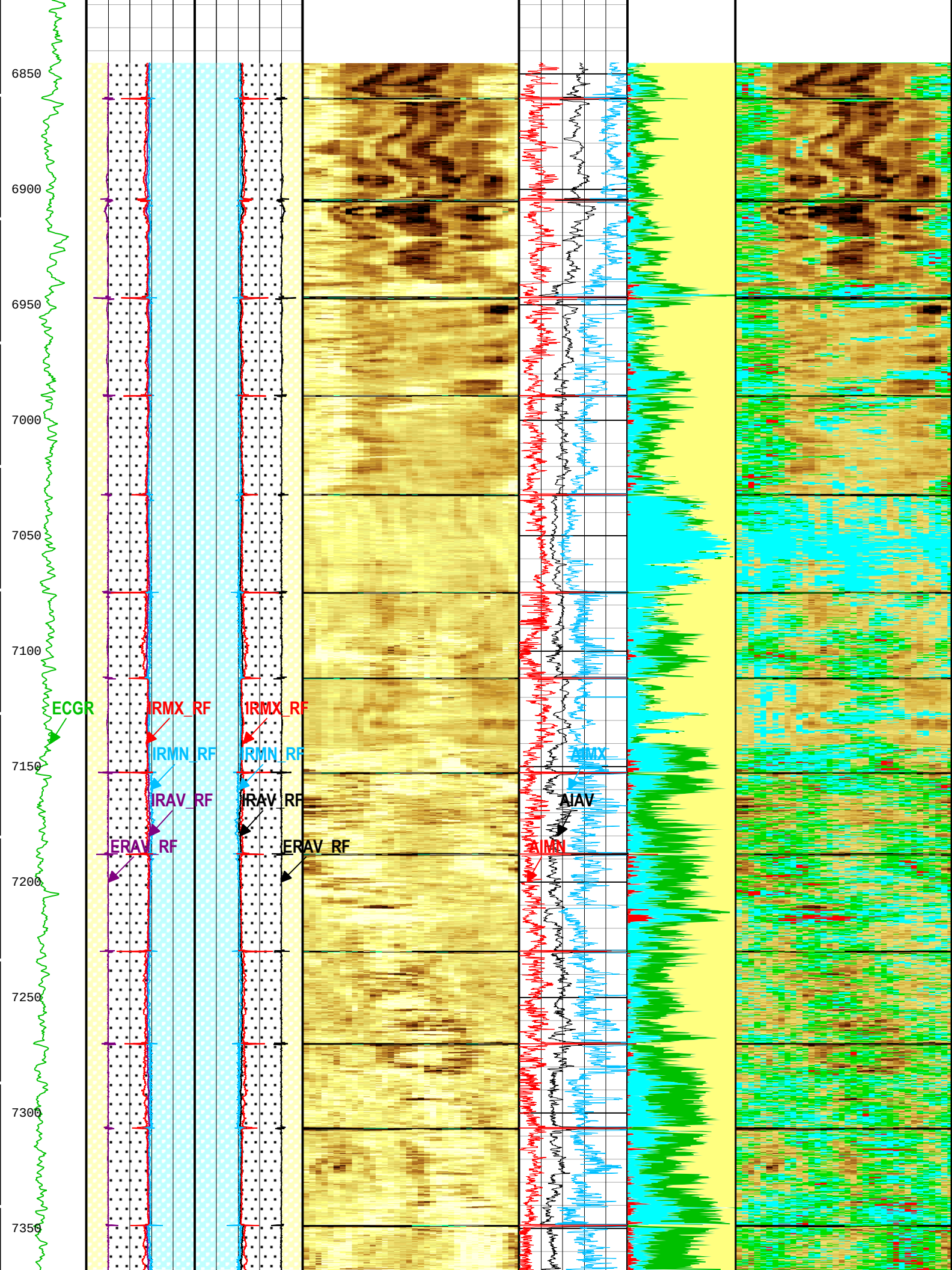
6850
6900
6950
7000
7050
7100
7150
7200
7250
7300
7350
ECGR
IRMX_RF
IRMN_RF
IRAV_RF
ERAV_RF
1RMX_RF
1RMN_RF
1RAV_RF
ERAV_RF
AIMX
AIAV
AIMN

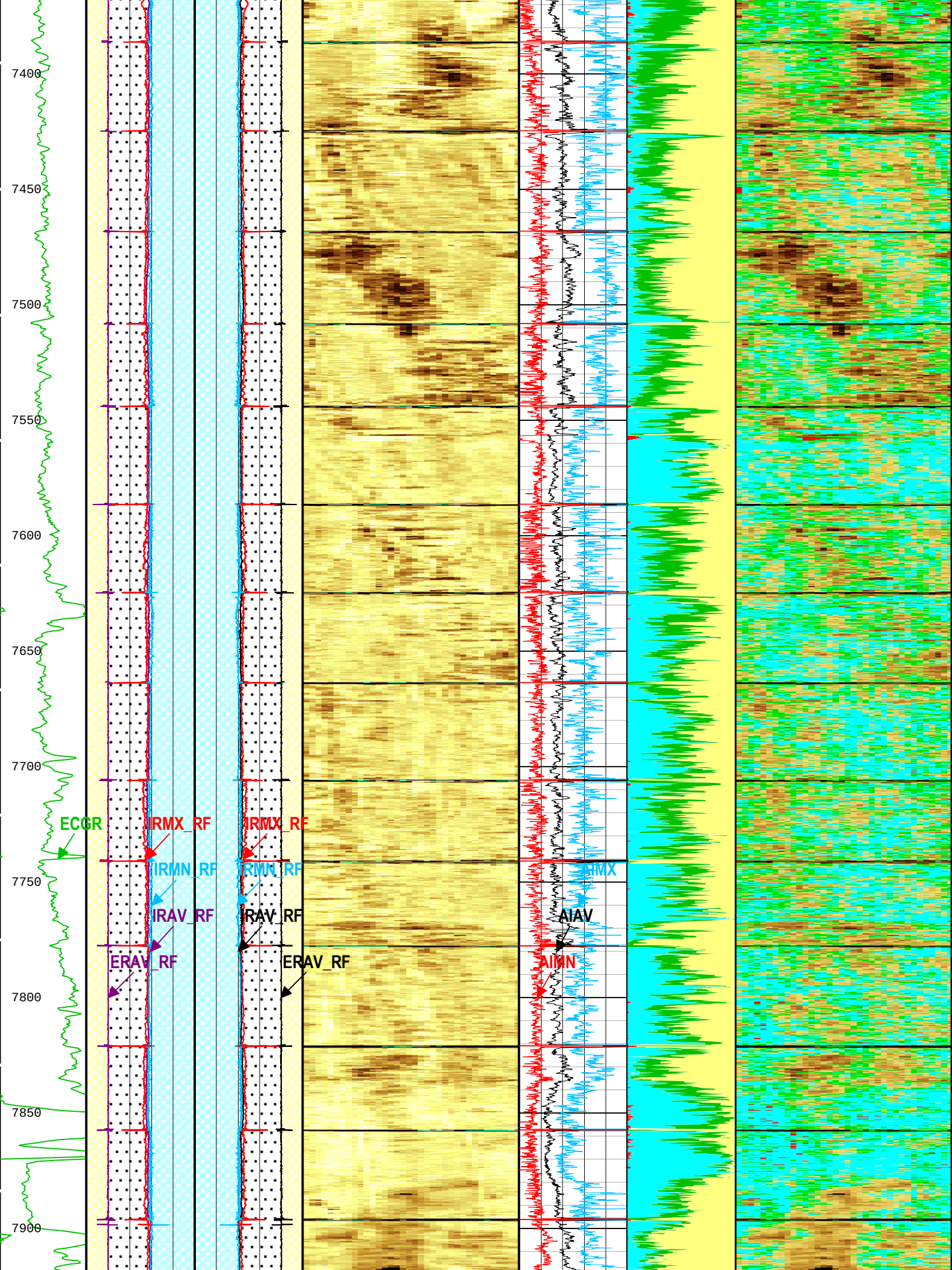
7400
7450
7500
7550
7600
7650
7700
7750
7800
7850
7900
ECGR
IRMX_RF
IRMX_RF
IRMN_RF
IRMN_RF
IRAV_RF
IRAV_RF
ERAV_RF
ERAV_RF
AIMX
AIAV
AIMN

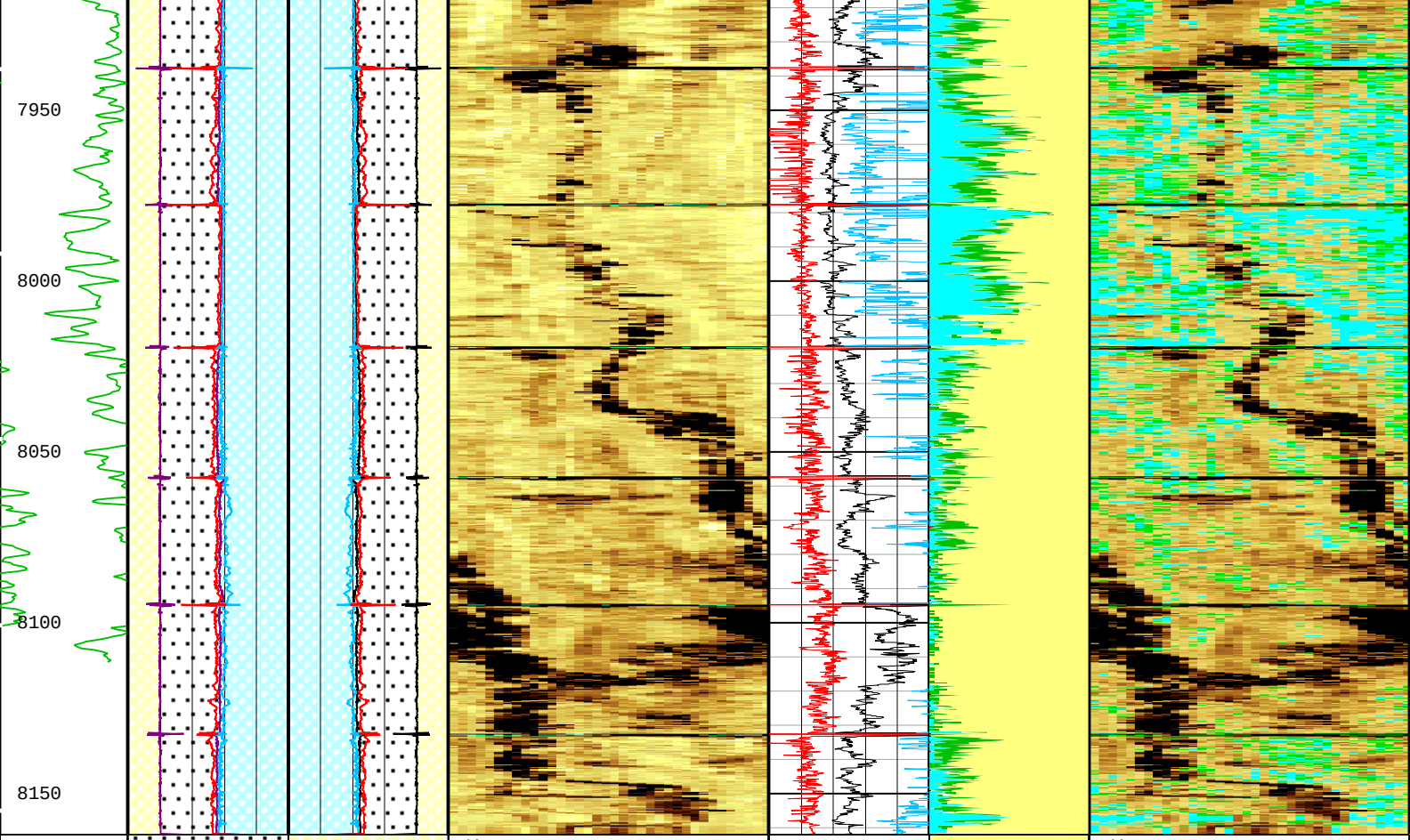

Gamma Ray (ECGR) HGNS-H
0 gAPI 150

Amplitude of Eccentering for Unflagged Waves (ECCE_RF) USIT-E
0 in 0.5

ERAV_IRAV

IRAV_LHF1

LHF1_ERAV

Median of Unflagged External Radii (ERAV_RF) USIT-E
3.7 in 2.7

Median Internal Radius of Casing Corrected for Eccentering (IRAV_RF) USIT-E
3.7 in 2.7

Minimum of Unflagged Internal Radii (IRMN_RF) USIT-E
3.7 in 2.7

Maximum of Unflagged Internal Radii (IRMX_RF) USIT-E
3.7 in 2.7

ERAV_RHF1

IRAV_ERAV

RHF1_IRAV

Median of Unflagged External Radii (ERAV_RF) USIT-E
2.7 in 3.7

Median Internal Radius of Casing Corrected for Eccentering (IRAV_RF) USIT-E
2.7 in 3.7

Minimum of Unflagged Internal Radii (IRMN_RF) USIT-E
2.7 in 3.7

Maximum of Unflagged Internal Radii (IRMX_RF) USIT-E
2.7 in 3.7

Custom Normalization
USIT - Acoustic Impedance (AIBK) USIT-E (Mrayl)

Acoustic Impedance Minimum (AIMN) USIT-E
-1 Mrayl 9

Acoustic Impedance Average (AIAV) USIT-E
-1 Mrayl 9

Acoustic Impedance Maximum (AIMX) USIT-E
-1 Mrayl 9

Bonded

Gas

Liquid

Micro-debonding

Custom Normalization
USIT - Acoustic Impedance With Micro-debonding Image (AI_MDEBOND_IMG) USIT-E (Mrayl)

TIME_1900 - Time Marked every 60.00 (s)

Description: USI Cement Format: Log (LBV1_USI Cement 7inch) Index Scale: 2 in per 100 ft Index Unit: ft Index Type: Measured Depth Creation Date: 20-Oct-2016 14:28:43

Composite 1

Corrosion 5 in = 100 ft

Composite Summary

Run Name	Pass Objective	Direction	Top	Bottom	Start	Stop	DSC Mode	Depth Shift	Include Parallel Data
Two	Log[9]:Up	Up	6640.29 ft	8171.85 ft	20-Oct-2016 9:51:39 AM	20-Oct-2016 10:20:40 AM	ON	1.47 ft	No
Two	Log[11]:Up	Up	36.69 ft	6737.51 ft	20-Oct-2016 10:24:53 AM	20-Oct-2016 12:34:00 PM	ON	1.35 ft	No
Two	Log[14]:Up	Up	5.56 ft	155.15 ft	20-Oct-2016 12:53:24 PM	20-Oct-2016 12:58:23 PM	ON	1.96 ft	No

All depths are referenced to toolstring zero

Log

Company:Southern California Gas Company Well:Frew 4

Composite 1:S008

Description: USI Composite Format: Log (LBV1_USI Corrosion 7inch) Index Scale: 5 in per 100 ft Index Unit: ft Index Type: Measured Depth Creation Date: 20-Oct-2016 14:28:48

TIME_1900 - Time Marked every 60.00 (s)

USIT Processing Flags (UFLG[0]) USIT-E[1]

1 - UFLG 1 Value within [0.0 - 1.5] - :
2 - UFLG 2 Value within [1.5 - 2.5] - :
3 - UFLG 3 Value within [2.5 - 3.5] - :
4 - UFLG 4 UFLG 5 UFLG 6 Value within [3.5 - 6.5] - :
5 - UFLG 7 UFLG 8 UFLG 9 Value within [6.5 - 10] - :

UTIM Error
Pulse Origin Not Detected
WINLEN Error
Casing Thickness Error
Loop Processing Error

Amplitude of Eccentering for Unflagged Waves (ECCE_RF) USIT-E[1]
0 in 0.5

Motor Revolution Speed (RSAV) USIT-E[1]

Absent 1.500 3.500
Explicit Normalization
USIT - USIT Processing Flags (UFLG) USIT-E[1]

Absent -5.200 -3.600 -2.000 -0.400
Explicit Normalization
USIT - Amplitude of Unflagged Wave (AWBK_RF) USIT-E[1] (dB)

Minimum of Unflagged Wave Amplitude (AWMN_RF) USIT-E[1]
0 dB 75

Average of Unflagged Wave Amplitude (AWAV_RF) USIT-E[1]
0 dB 75

Maximum of

Absent -0.059 -0.028 0.004 0.035 0.068
Explicit Normalization
USIT - Unflagged

Internal Radius Averaged Value (IRAV) USIT-E[1]
2.7 in 3.7

Internal Radius Maximum Value (IRMX) USIT-E[1]
2.7 in 3.7

ERAV | IRAV
ERAV-IRAV | ERAV
IRAV | IRAV-ERAV

Median of Unflagged External Radii (ERAV_RF) USIT-E[1]
3.7 in 2.7

Median of Unflagged External Radii (ERAV_RF) USIT-E[1]
2.7 in 3.7

Median Internal Radius of Casing Corrected for Eccentering (IRAV_RF) USIT-E[1]
3.7 in 2.7

Median Internal Radius of Casing Corrected for Eccentering (IRAV_RF) USIT-E[1]
2.7 in 3.7

Maximum of Unflagged Internal Radii (IRMX_RF) USIT-E[1]
3.7 in 2.7

Maximum of Unflagged Internal Radii (IRMX_RF) USIT-E[1]
2.7 in 3.7

Minimum of

Minimum of

Absent -0.059 -0.028 0.004 0.035 0.068
Explicit Normalization
USIT - Unflagged Casing Thickness minus Median of

Minimum of Unflagged Casing Thickness (THMN_RF) USIT-E[1]
0.1 in 0.6

Nominal Casing Thickness (THNO) USIT-E[1]
0.1 in 0.6

Median of Unflagged Casing Thickness (THAV_RF) USIT-E[1]
0.1 in 0.6

Maximum of Unflagged

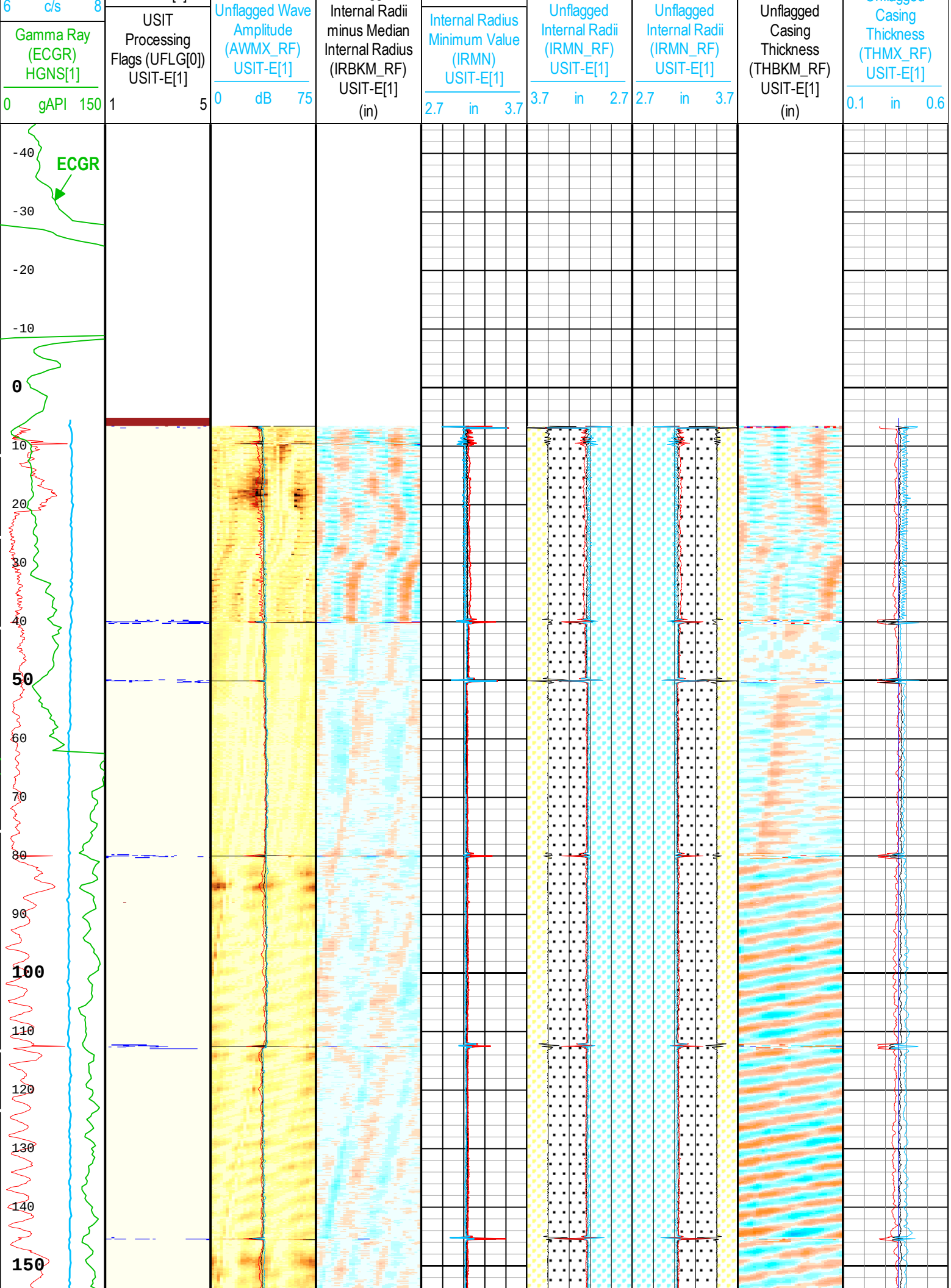
6 c/s 8
Gamma Ray (ECGR) HGNS[1]
0 gAPI 150
USIT Processing Flags (UFLG[0]) USIT-E[1]
1 5
Unflagged Wave Amplitude (AWMX_RF) USIT-E[1]
0 dB 75
Internal Radii minus Median Internal Radius (IRBKM_RF) USIT-E[1] (in)
Internal Radius Minimum Value (IRMN) USIT-E[1]
2.7 in 3.7
Unflagged Internal Radii (IRMN_RF) USIT-E[1]
3.7 in 2.7
Unflagged Internal Radii (IRMN_RF) USIT-E[1]
2.7 in 3.7
Unflagged Casing Thickness (THBKM_RF) USIT-E[1] (in)
Unflagged Casing Thickness (THMX_RF) USIT-E[1]
0.1 in 0.6
ECGR
-40
-30
-20
-10
0
10
20
30
40
50
60
70
80
90
100
110
120
130
140
150

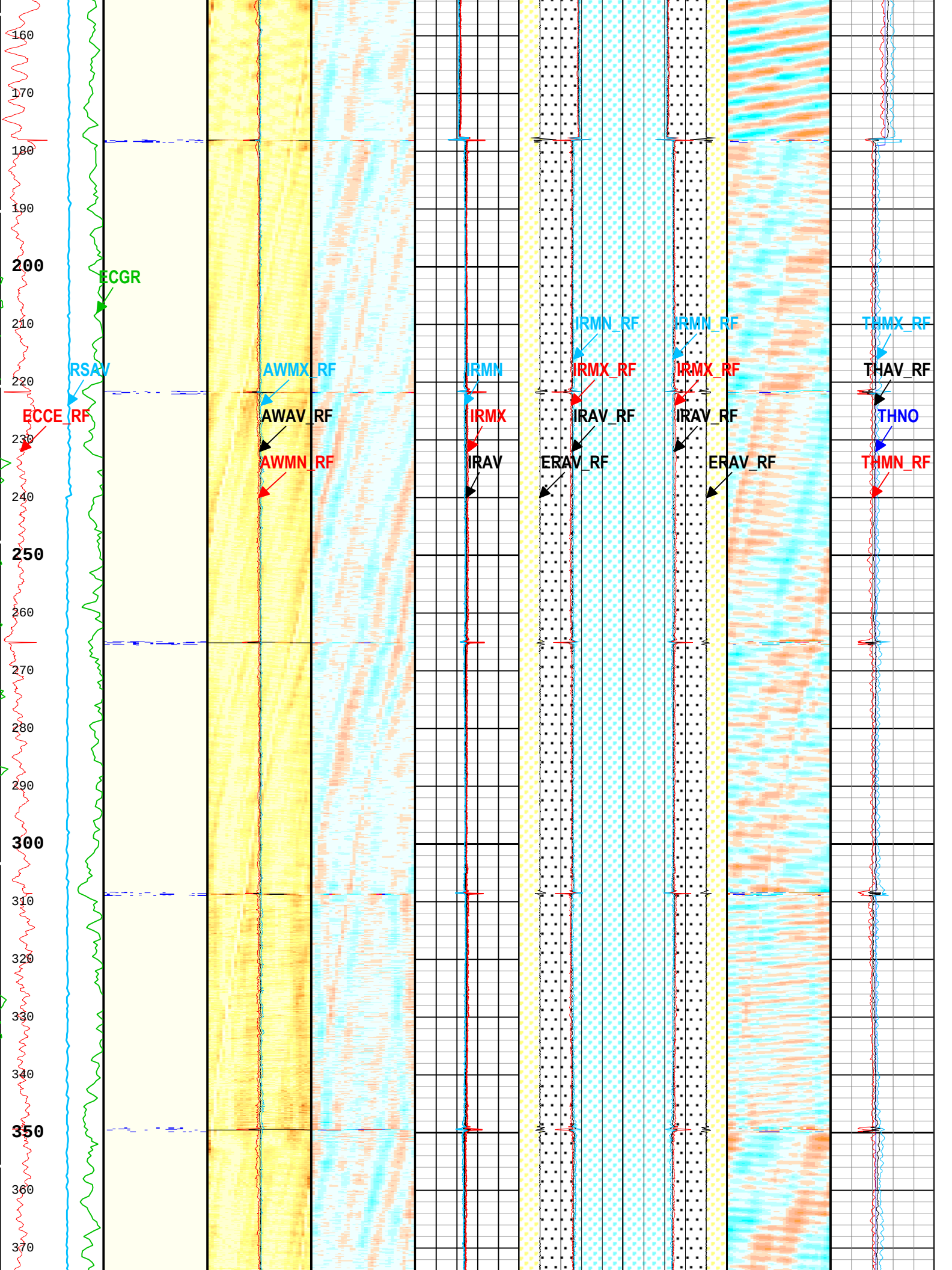
160
170
180
190
200
210
220
230
240
250
260
270
280
290
300
310
320
330
340
350
360
370
ECGR
RSAV
ECCE_RF
AWMX_RF
AWAV_RF
AWMN_RF
IRMN
IRMX
IRAV
IRMN_RF
IRMX_RF
IRAV_RF
ERAV_RF
IRMN_RF
IRMX_RF
IRAV_RF
ERAV_RF
THMX_RF
THAV_RF
THNO
THMN_RF

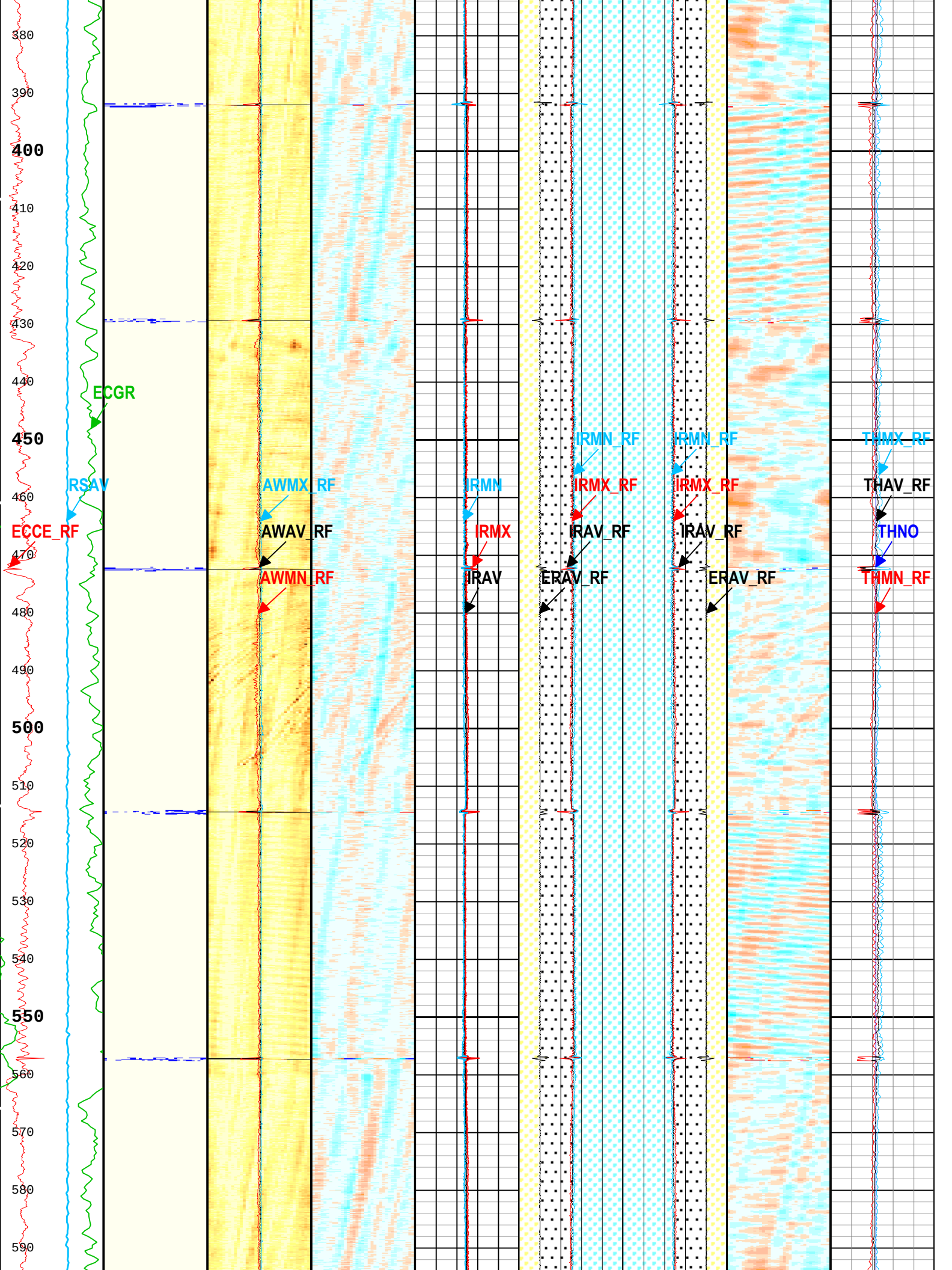
380
390
400
410
420
430
440
450
460
470
480
490
500
510
520
530
540
550
560
570
580
590
ECGR
RSAV
ECCE_RF
AWMX_RF
AWAV_RF
AWMN_RF
IRMN
IRMX
IRAV
IRMN_RF
IRMX_RF
IRAV_RF
ERAV_RF
IRMN_RF
IRMX_RF
IRAV_RF
ERAV_RF
THMX_RF
THAV_RF
THNO
THMN_RF

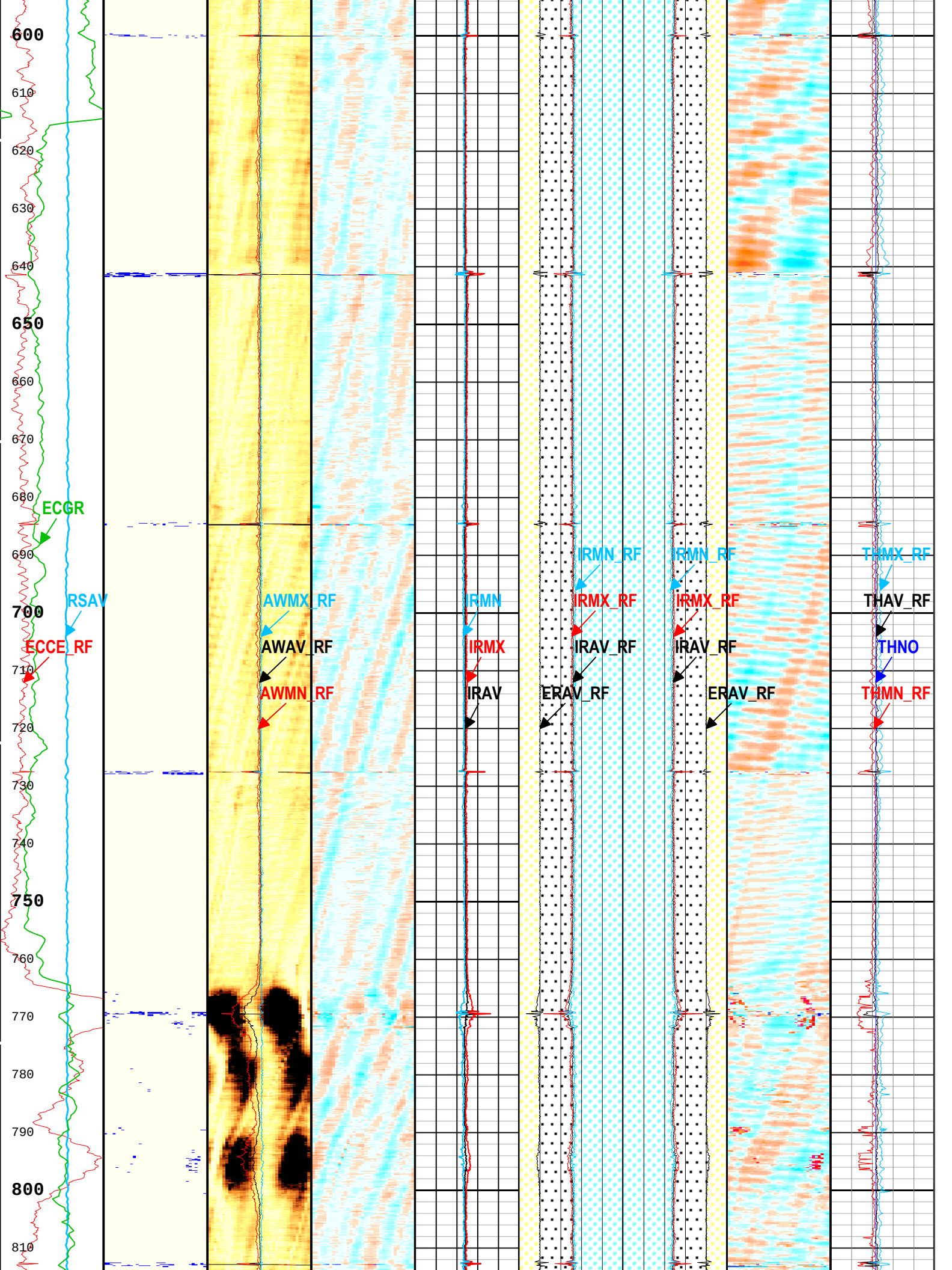
600
610
620
630
640
650
660
670
680
690
700
710
720
730
740
750
760
770
780
790
800
810
ECGR
RSAV
ECCE_RF
AWMX_RF
AWAV_RF
AWMN_RF
IRMN
IRMX
IRAV
IRMN_RF
IRMX_RF
IRAV_RF
ERAV_RF
IRMN_RF
IRMX_RF
IRAV_RF
ERAV_RF
THMX_RF
THAV_RF
THNO
THMN_RF

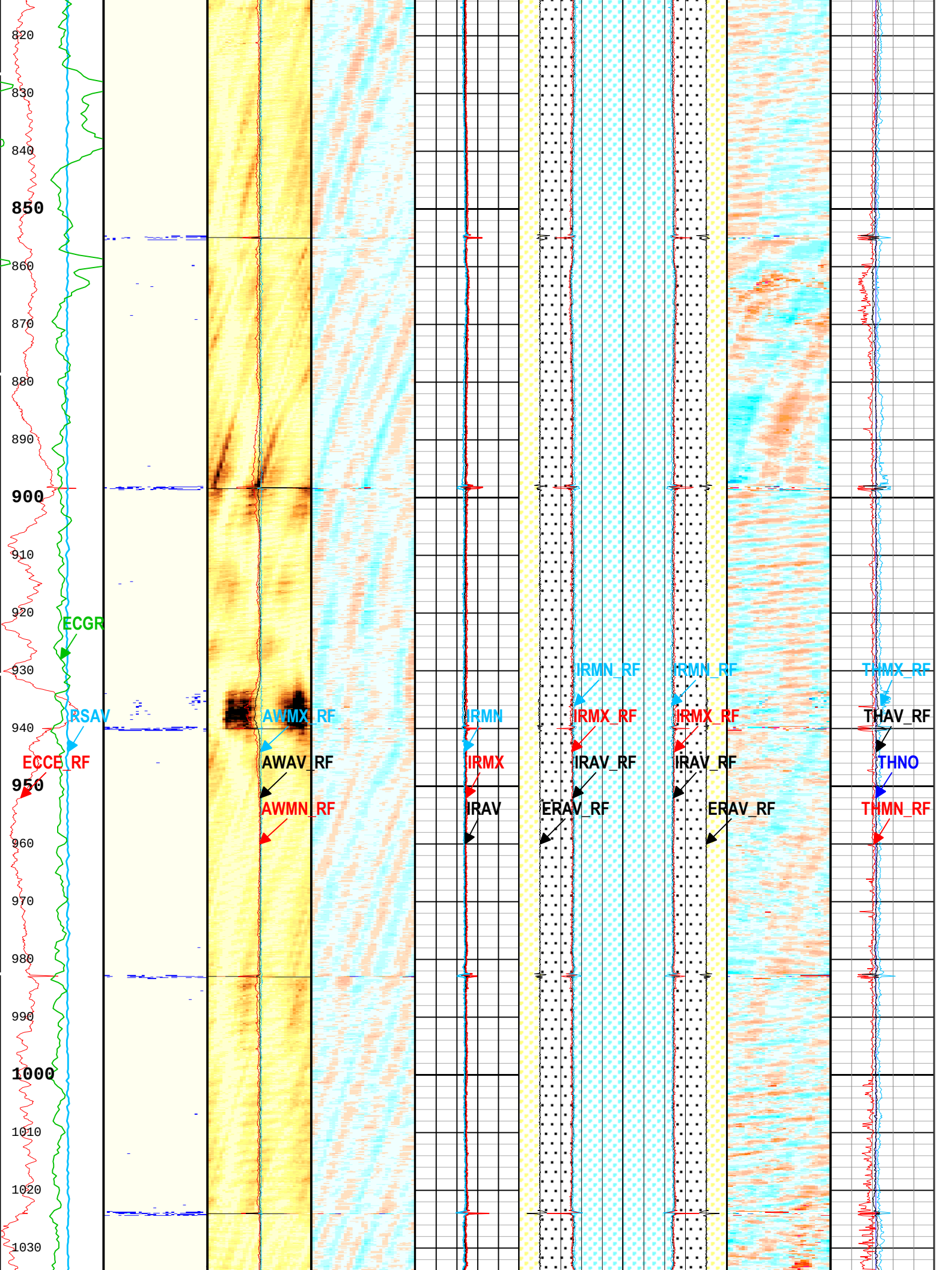
820
830
840
850
860
870
880
890
900
910
920
930
940
950
960
970
980
990
1000
1010
1020
1030
ECGR
RSAV
ECCE_RF
AWMX_RF
AWAV_RF
AWMN_RF
IRMN
IRMX
IRAV
IRMN_RF
IRMX_RF
IRAV_RF
ERAV_RF
IRMN_RF
IRMX_RF
IRAV_RF
ERAV_RF
THMX_RF
THAV_RF
THNO
THMN_RF

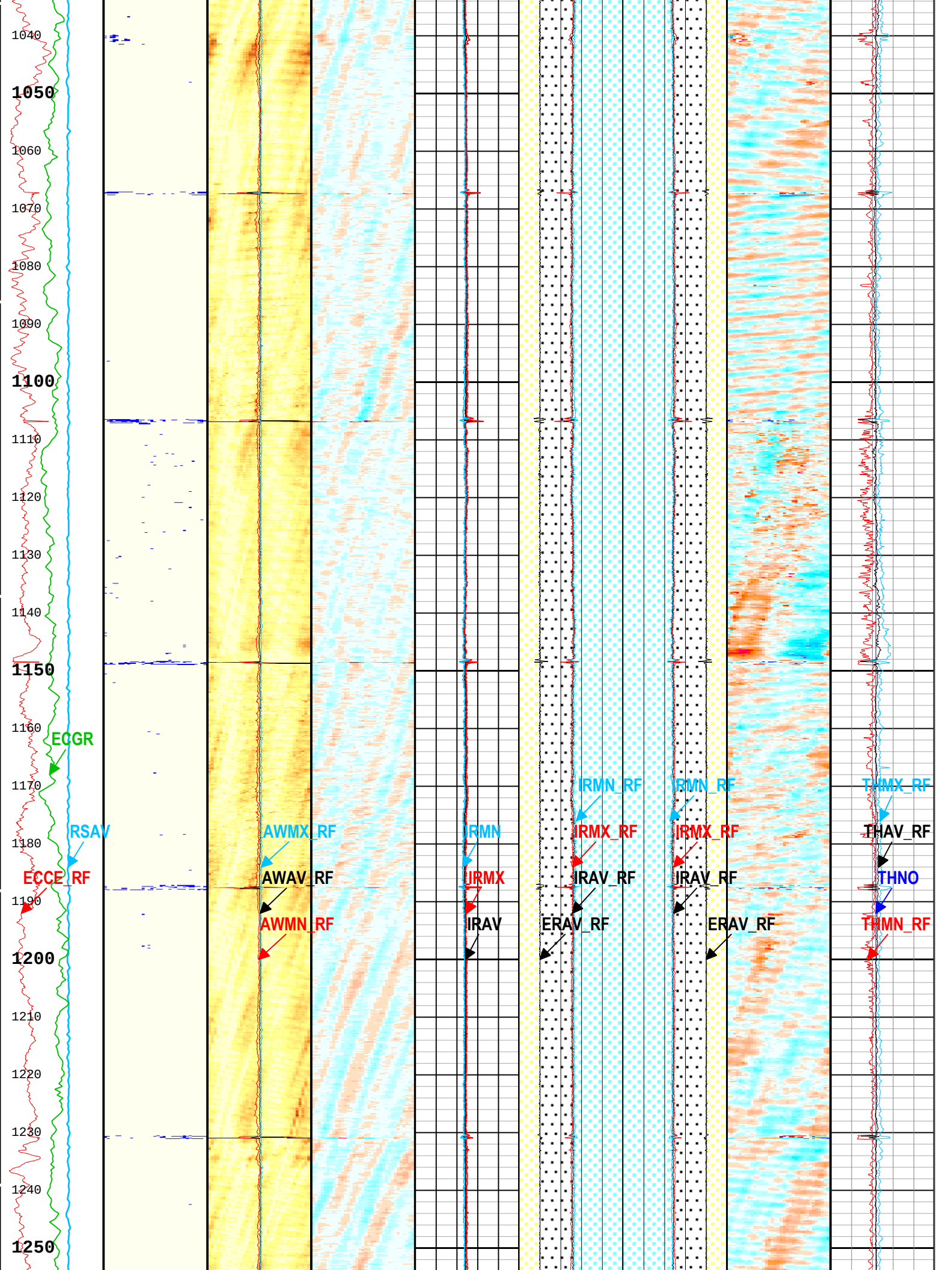
1040
1050
1060
1070
1080
1090
1100
1110
1120
1130
1140
1150
1160
1170
1180
1190
1200
1210
1220
1230
1240
1250
ECGR
RSAV
ECCE_RF
AWMX_RF
AWAV_RF
AWMN_RF
IRMN
IRMX
IRAV
IRMN_RF
IRMX_RF
IRAV_RF
ERAV_RF
IRMN_RF
IRMX_RF
IRAV_RF
ERAV_RF
THMX_RF
THAV_RF
THNO
THMN_RF

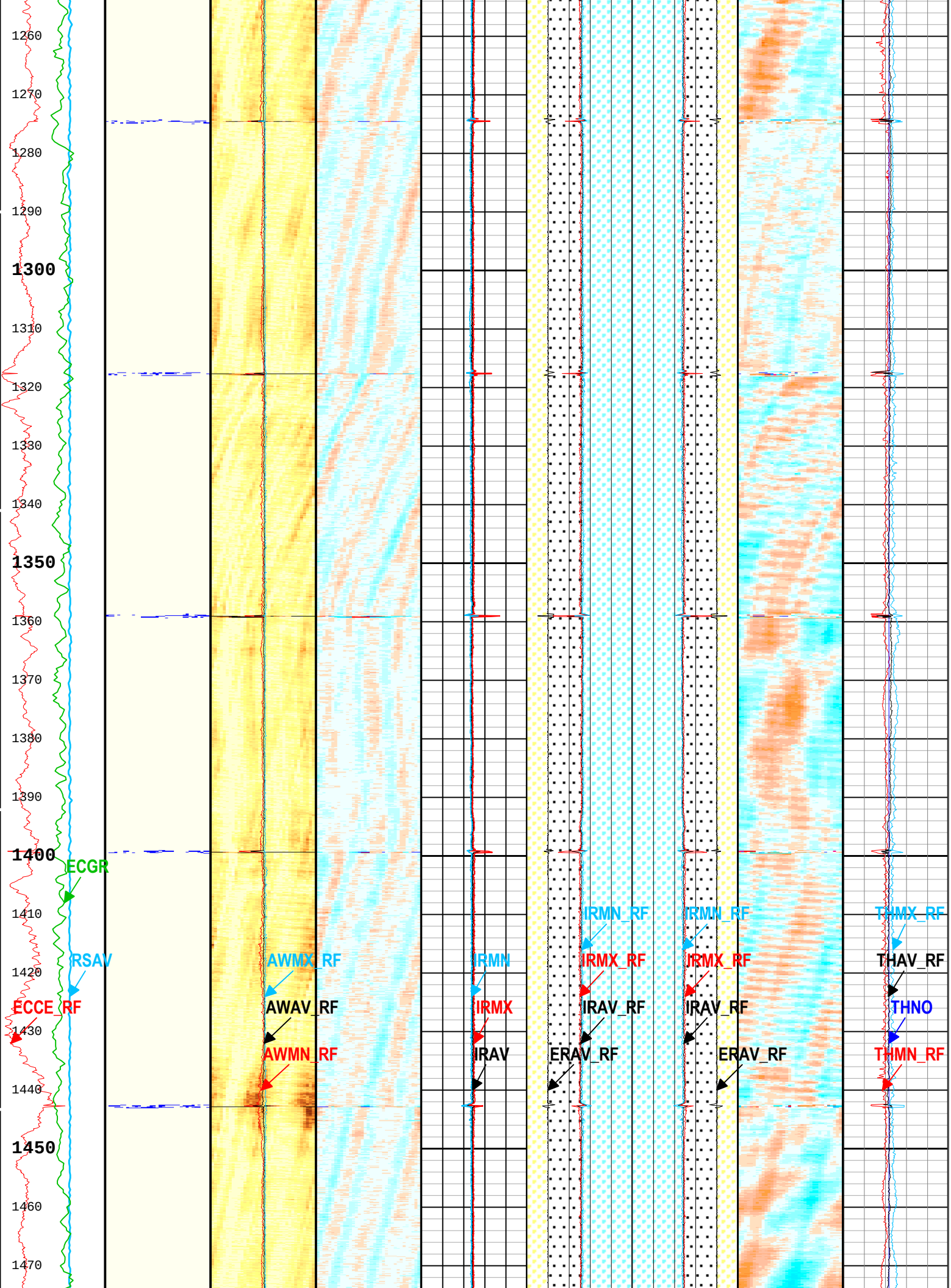
1260
1270
1280
1290
1300
1310
1320
1330
1340
1350
1360
1370
1380
1390
1400
1410
1420
1430
1440
1450
1460
1470
ECGR
RSAV
ECCE_RF
AWMX_RF
AWAV_RF
AWMN_RF
IRMN
IRMX
IRAV
IRMN_RF
IRMX_RF
IRAV_RF
ERAV_RF
IRMN_RF
IRMX_RF
IRAV_RF
ERAV_RF
THMX_RF
THAV_RF
THNO
THMN_RF

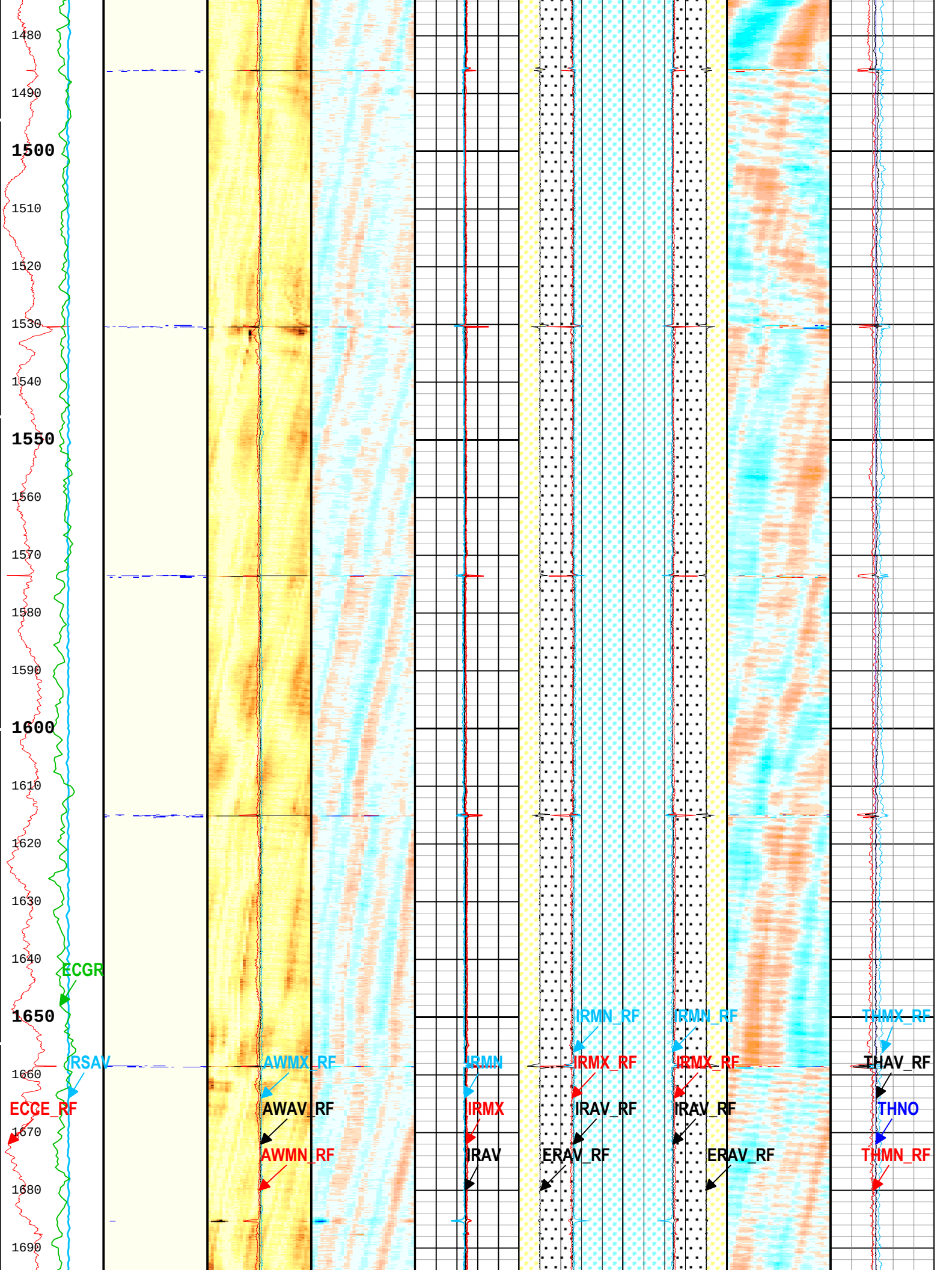
1480
1490
1500
1510
1520
1530
1540
1550
1560
1570
1580
1590
1600
1610
1620
1630
1640
1650
1660
1670
1680
1690
ECGR
RSAV
ECCE_RF
AWMX_RF
AWAV_RF
AWMN_RF
IRMN
IRMX
IRAV
IRMN_RF
IRMX_RF
IRAV_RF
ERAV_RF
IRMN_RF
IRMX_RF
IRAV_RF
ERAV_RF
THMX_RF
THAV_RF
THNO
THMN_RF

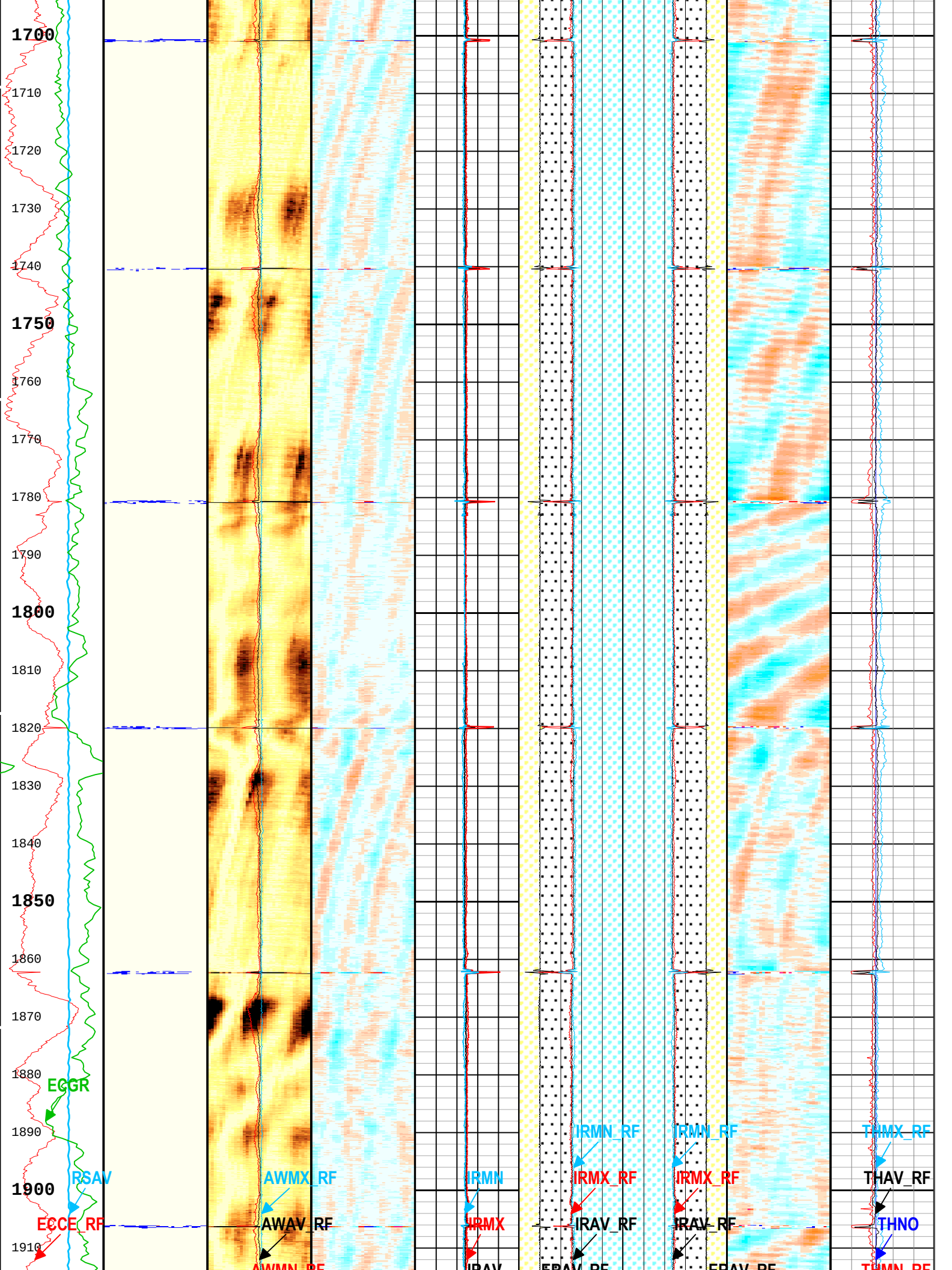
1700
1710
1720
1730
1740
1750
1760
1770
1780
1790
1800
1810
1820
1830
1840
1850
1860
1870
1880
1890
1900
1910
ECGR
RSAV
ECCE_RF
AWMX_RF
AWAV_RF
AWMN_RF
IRMN
IRMX
IRAV
IRMN_RF
IRMX_RF
IRAV_RF
IRMN_RF
IRMX_RF
IRAV_RF
THMX_RF
THAV_RF
THNO
THMN_RF

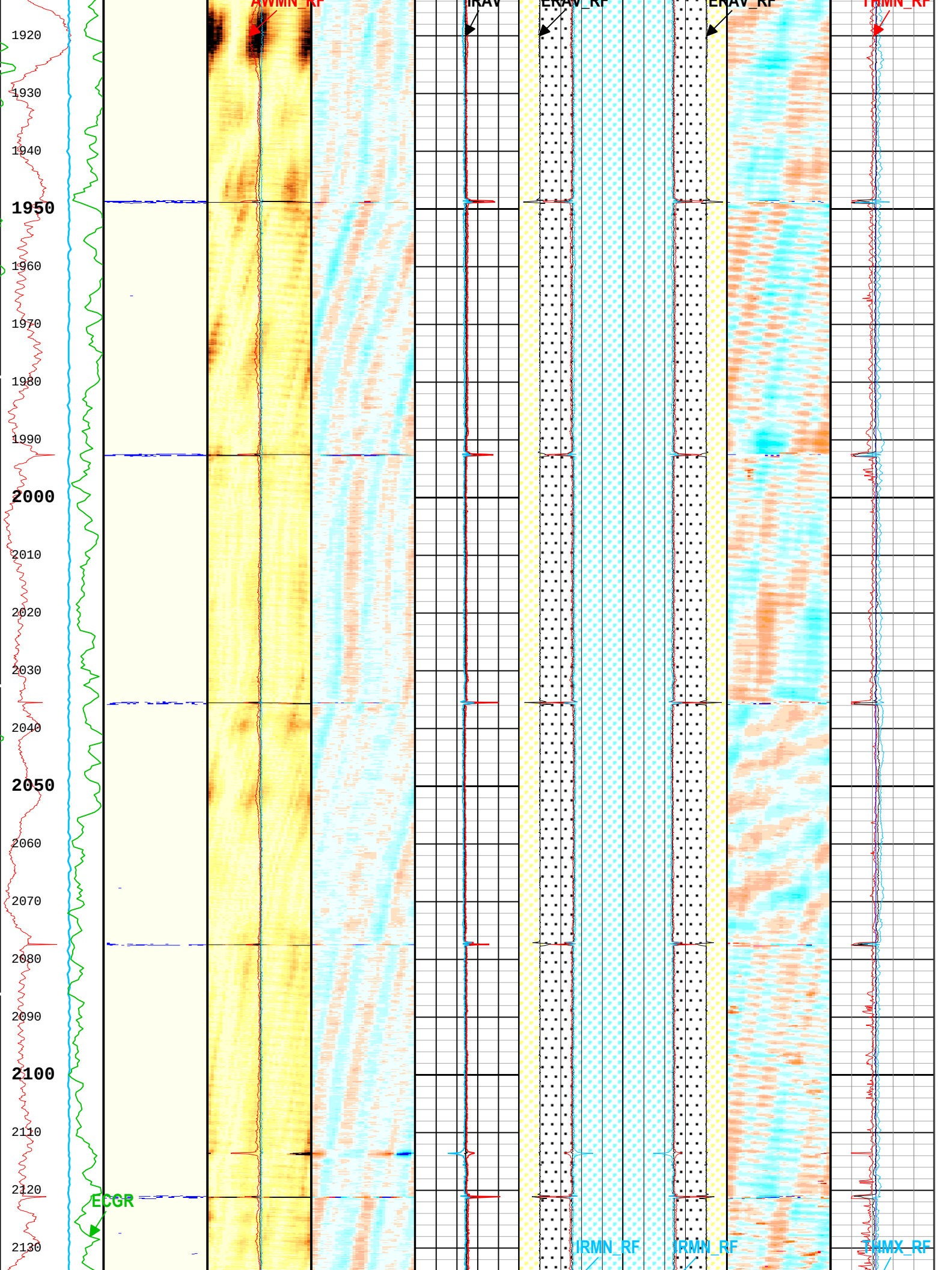
AWMN_RF
IRAV
ERAV_RF
ERAV_RF
THMN_RF
1920
1930
1940
1950
1960
1970
1980
1990
2000
2010
2020
2030
2040
2050
2060
2070
2080
2090
2100
2110
2120
2130
ECGR
IRMN_RF
IRMN_RF
THMX_RF

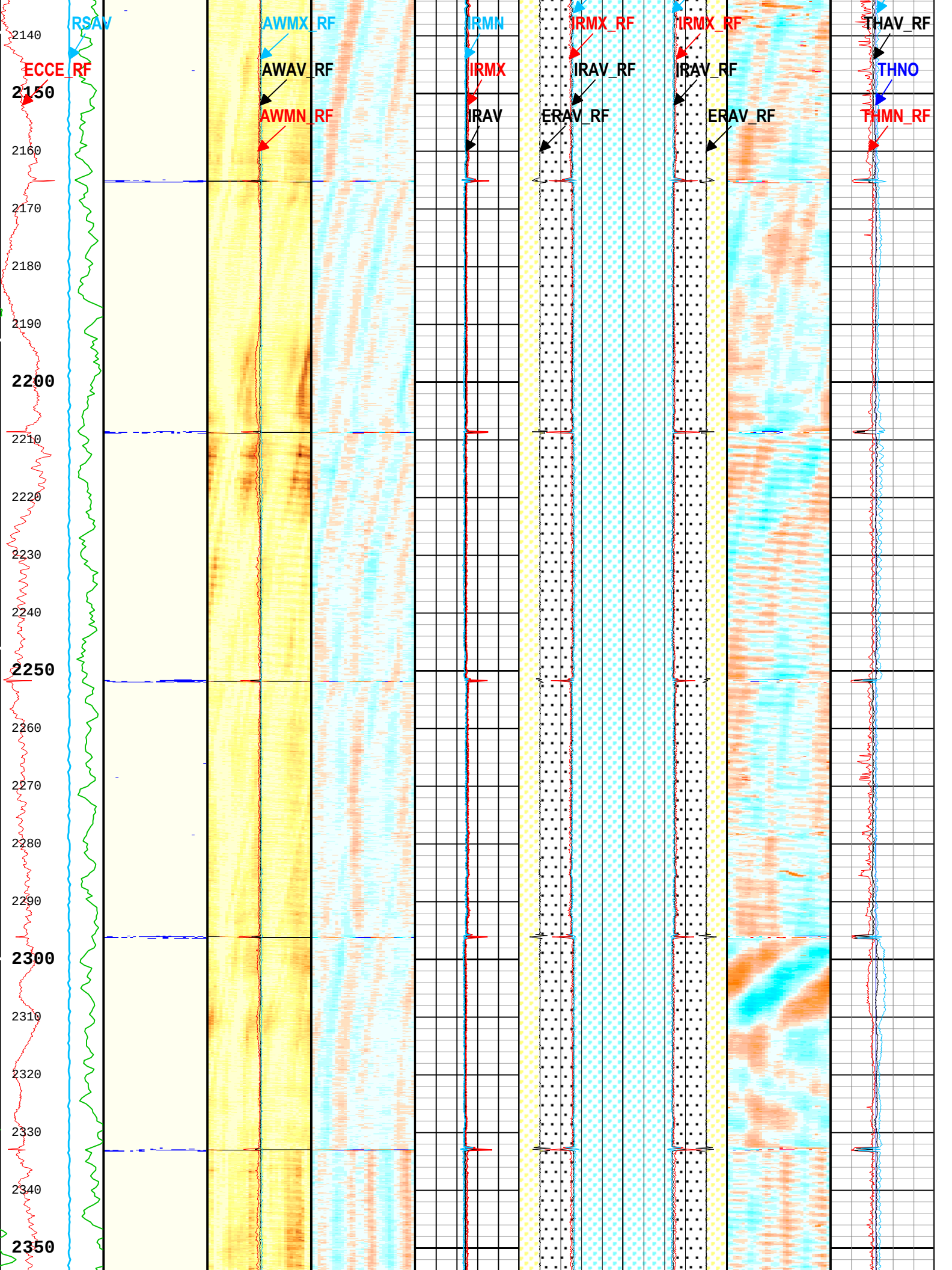
RSAV
ECCE_RF
AWMX_RF
AWAV_RF
AWMN_RF
IRMN
IRMX
IRAV
IRMX_RF
IRAV_RF
ERAV_RF
IRMX_RF
IRAV_RF
ERAV_RF
THAV_RF
THNO
THMN_RF
2140
2150
2160
2170
2180
2190
2200
2210
2220
2230
2240
2250
2260
2270
2280
2290
2300
2310
2320
2330
2340
2350

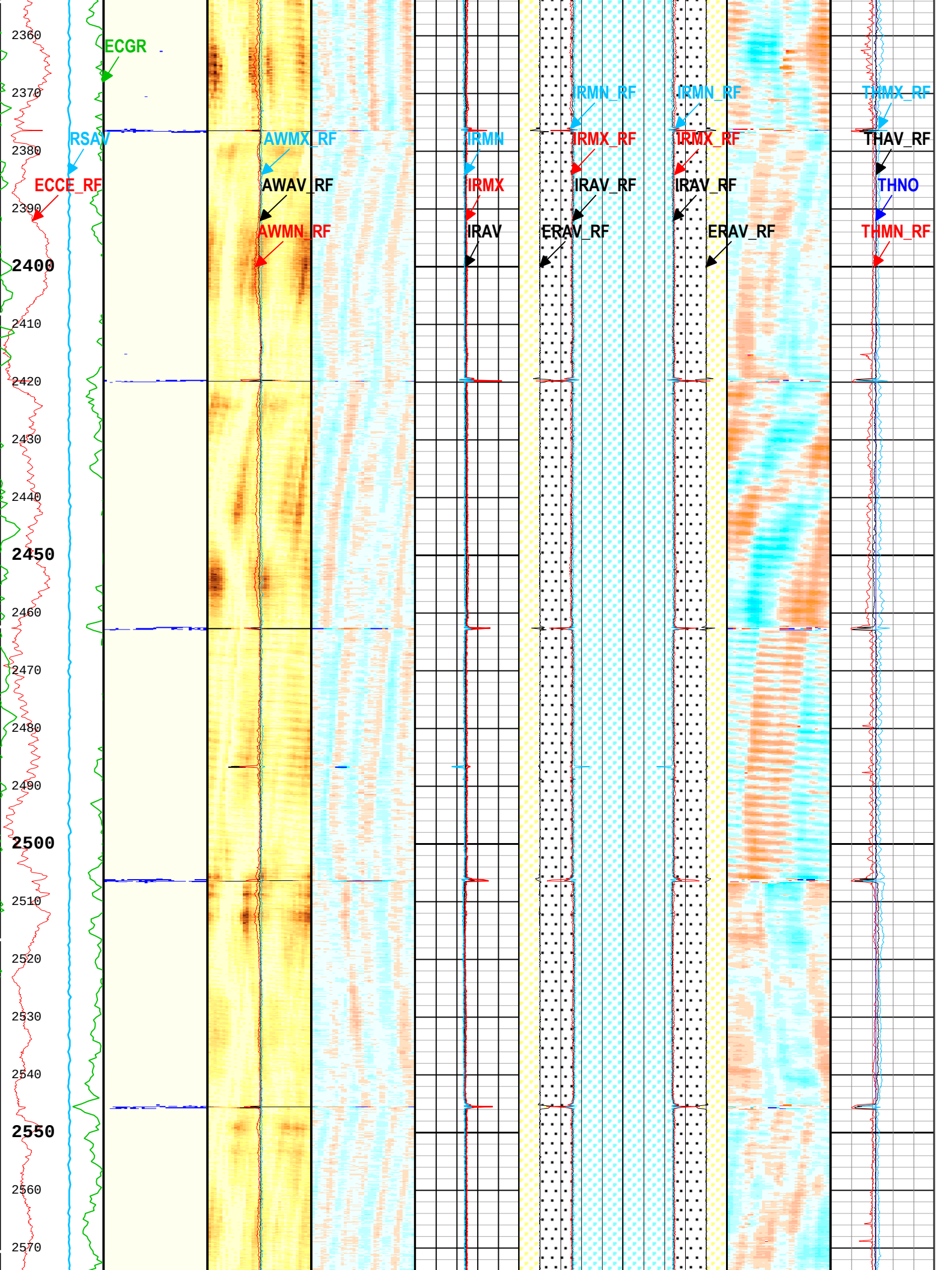
ECGR
RSAV
ECCE_RF
AWMX_RF
AWAV_RF
AWMN_RF
IRMN
IRMX
IRAV
IRMN_RF
IRMX_RF
IRAV_RF
ERAV_RF
IRMN_RF
IRMX_RF
IRAV_RF
ERAV_RF
THMX_RF
THAV_RF
THNO
THMN_RF
2360
2370
2380
2390
2400
2410
2420
2430
2440
2450
2460
2470
2480
2490
2500
2510
2520
2530
2540
2550
2560
2570

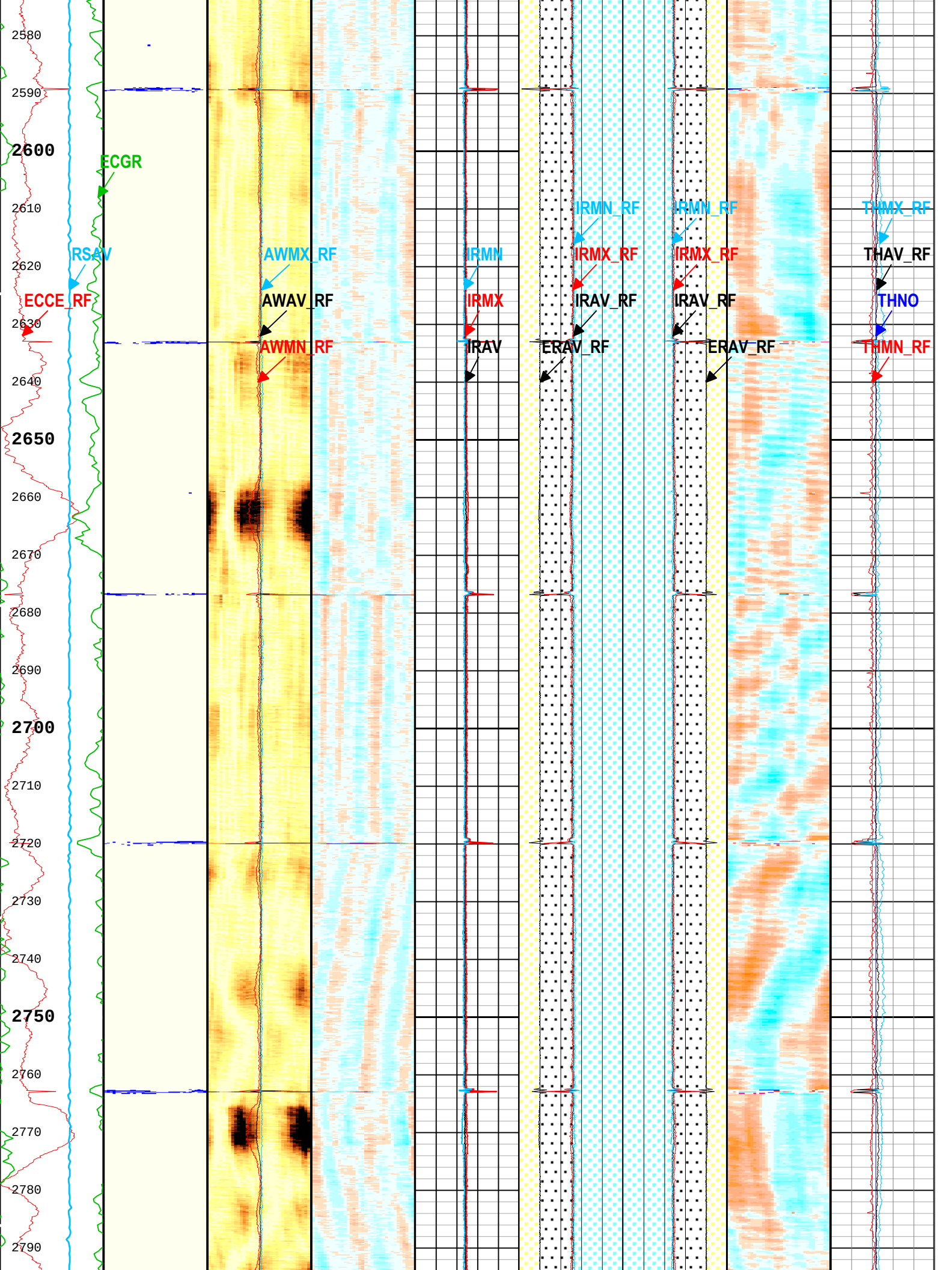
2580
2590
2600
2610
2620
2630
2640
2650
2660
2670
2680
2690
2700
2710
2720
2730
2740
2750
2760
2770
2780
2790
ECGR
RSAV
ECCE_RF
AWMX_RF
AWAV_RF
AWMN_RF
IRMN
IRMX
IRAV
IRMN_RF
IRMX_RF
IRAV_RF
ERAV_RF
IRMN_RF
IRMX_RF
IRAV_RF
ERAV_RF
THMX_RF
THAV_RF
THNO
THMN_RF

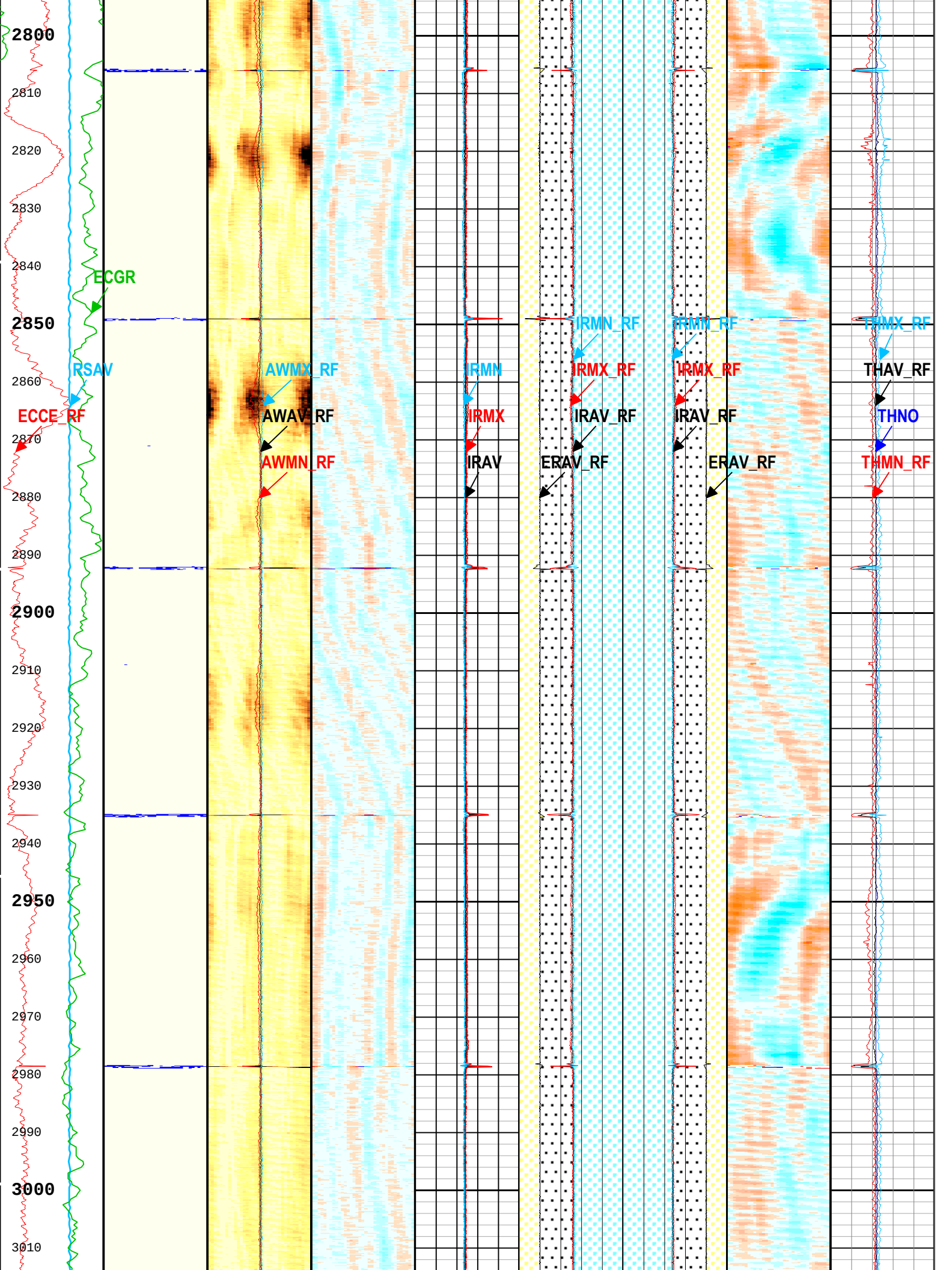
2800
2810
2820
2830
2840
2850
2860
2870
2880
2890
2900
2910
2920
2930
2940
2950
2960
2970
2980
2990
3000
3010
ECGR
RSAV
ECCE_RF
AWMX_RF
AWAV_RF
AWMN_RF
IRMN
IRMX
IRAV
IRMN_RF
IRMX_RF
IRAV_RF
ERAV_RF
IRMN_RF
IRMX_RF
IRAV_RF
ERAV_RF
THMX_RF
THAV_RF
THNO
THMN_RF

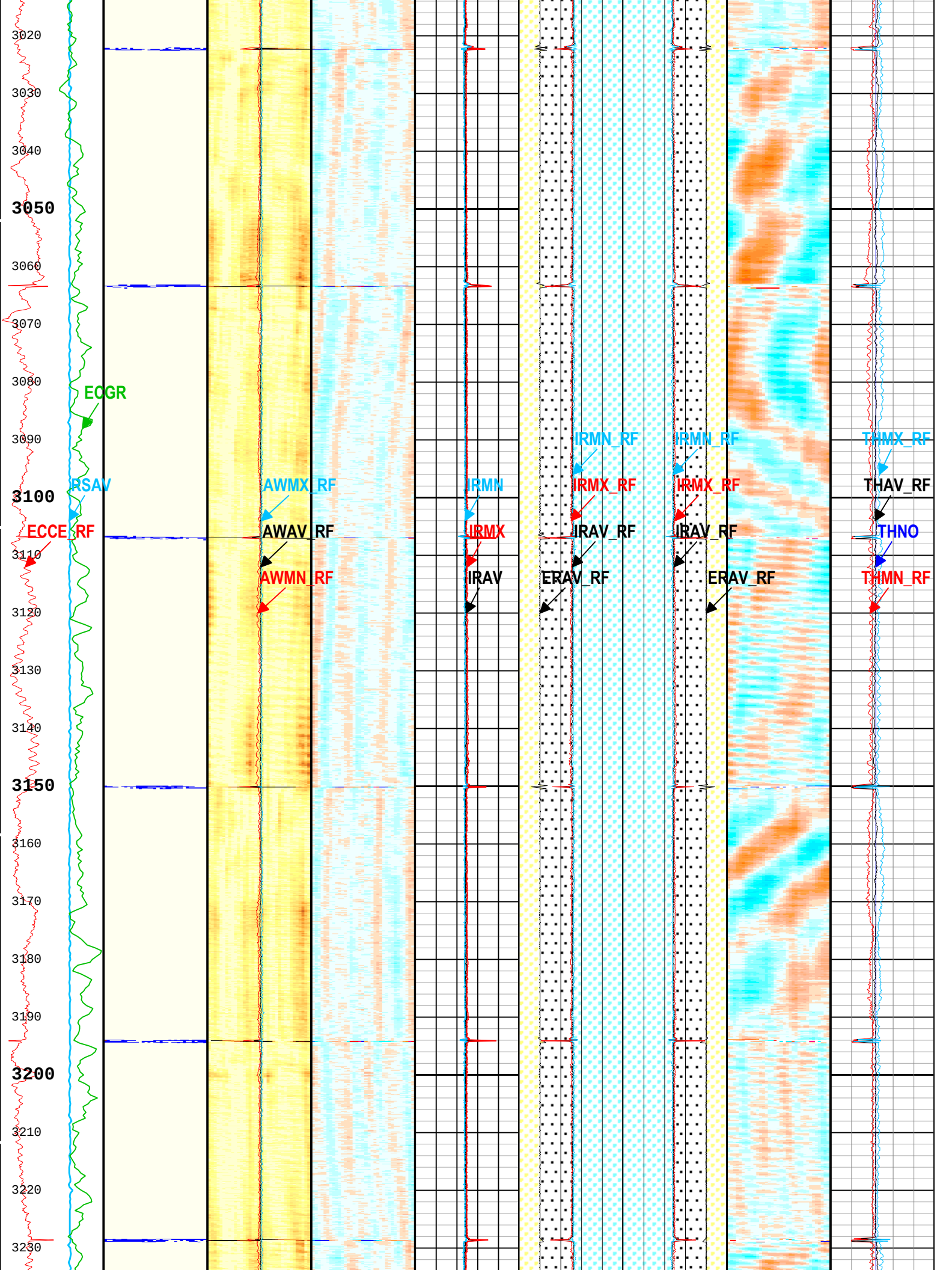
3020
3030
3040
3050
3060
3070
3080
3090
3100
3110
3120
3130
3140
3150
3160
3170
3180
3190
3200
3210
3220
3230
ECGR
RSAV
ECCE_RF
AWMX_RF
AWAV_RF
AWMN_RF
IRMN
IRMX
IRAV
IRMN_RF
IRMX_RF
IRAV_RF
ERAV_RF
IRMN_RF
IRMX_RF
IRAV_RF
ERAV_RF
THMX_RF
THAV_RF
THNO
THMN_RF

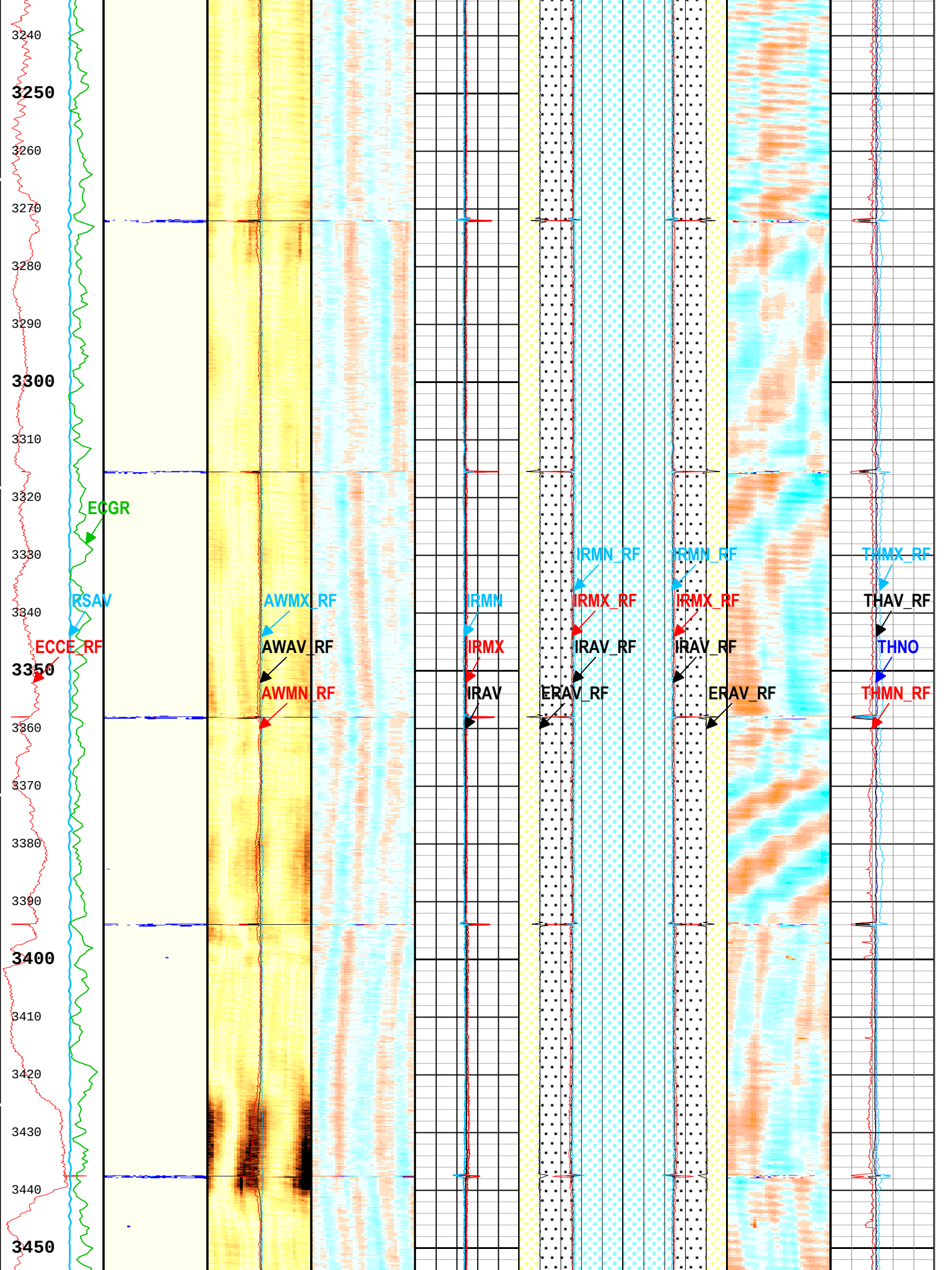
3240
3250
3260
3270
3280
3290
3300
3310
3320
3330
3340
3350
3360
3370
3380
3390
3400
3410
3420
3430
3440
3450
ECGR
RSAV
ECCE_RF
AWMX_RF
AWAV_RF
AWMN_RF
IRMN
IRMX
IRAV
IRMN_RF
IRMX_RF
IRAV_RF
ERAV_RF
IRMN_RF
IRMX_RF
IRAV_RF
ERAV_RF
THMX_RF
THAV_RF
THNO
THMN_RF

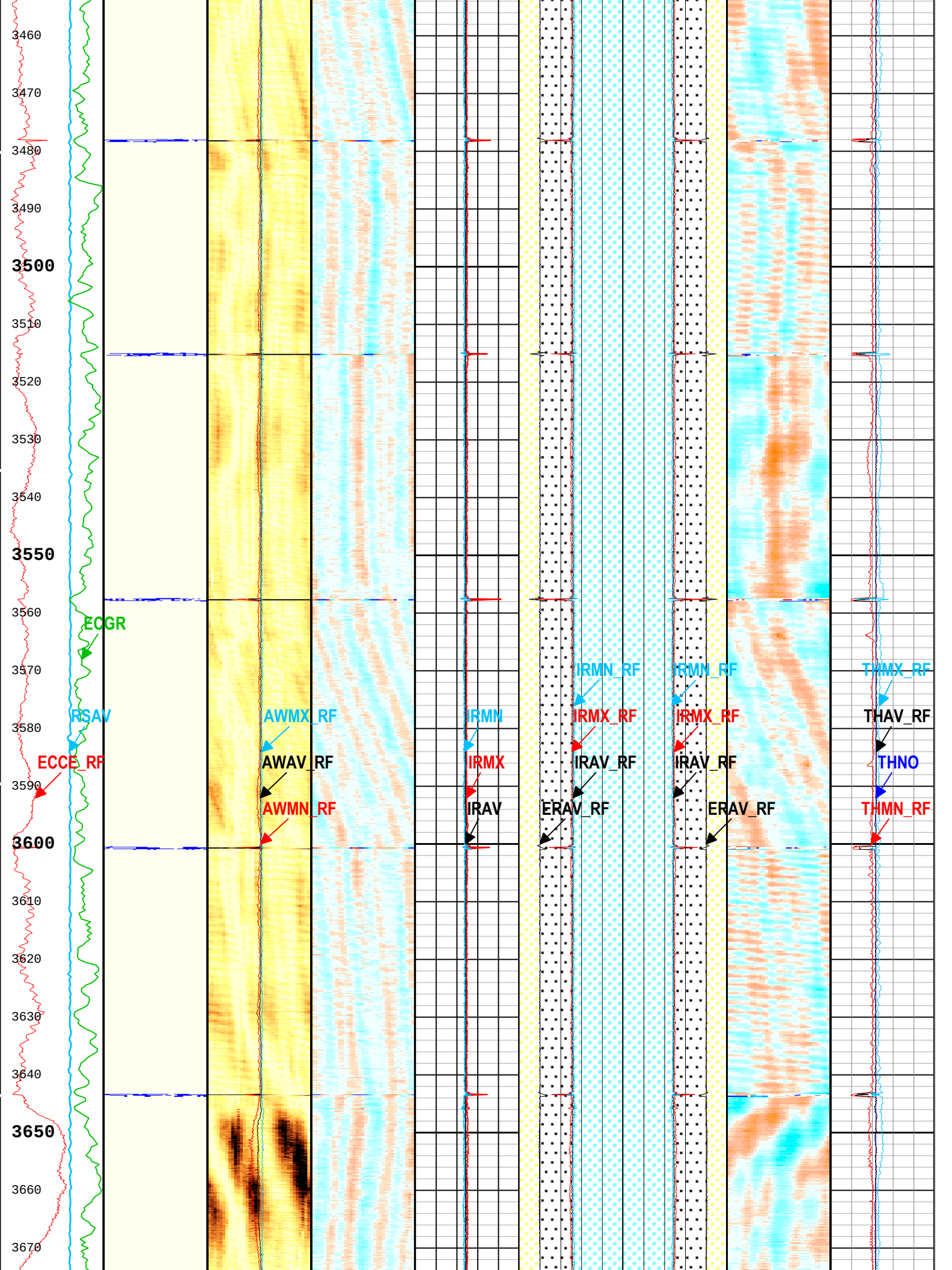
3460
3470
3480
3490
3500
3510
3520
3530
3540
3550
3560
3570
3580
3590
3600
3610
3620
3630
3640
3650
3660
3670
ECGR
RSAV
ECCE_RF
AWMX_RF
AWAV_RF
AWMN_RF
IRMN
IRMX
IRAV
IRMN_RF
IRMX_RF
IRAV_RF
ERAV_RF
IRMN_RF
IRMX_RF
IRAV_RF
ERAV_RF
THMX_RF
THAV_RF
THNO
THMN_RF

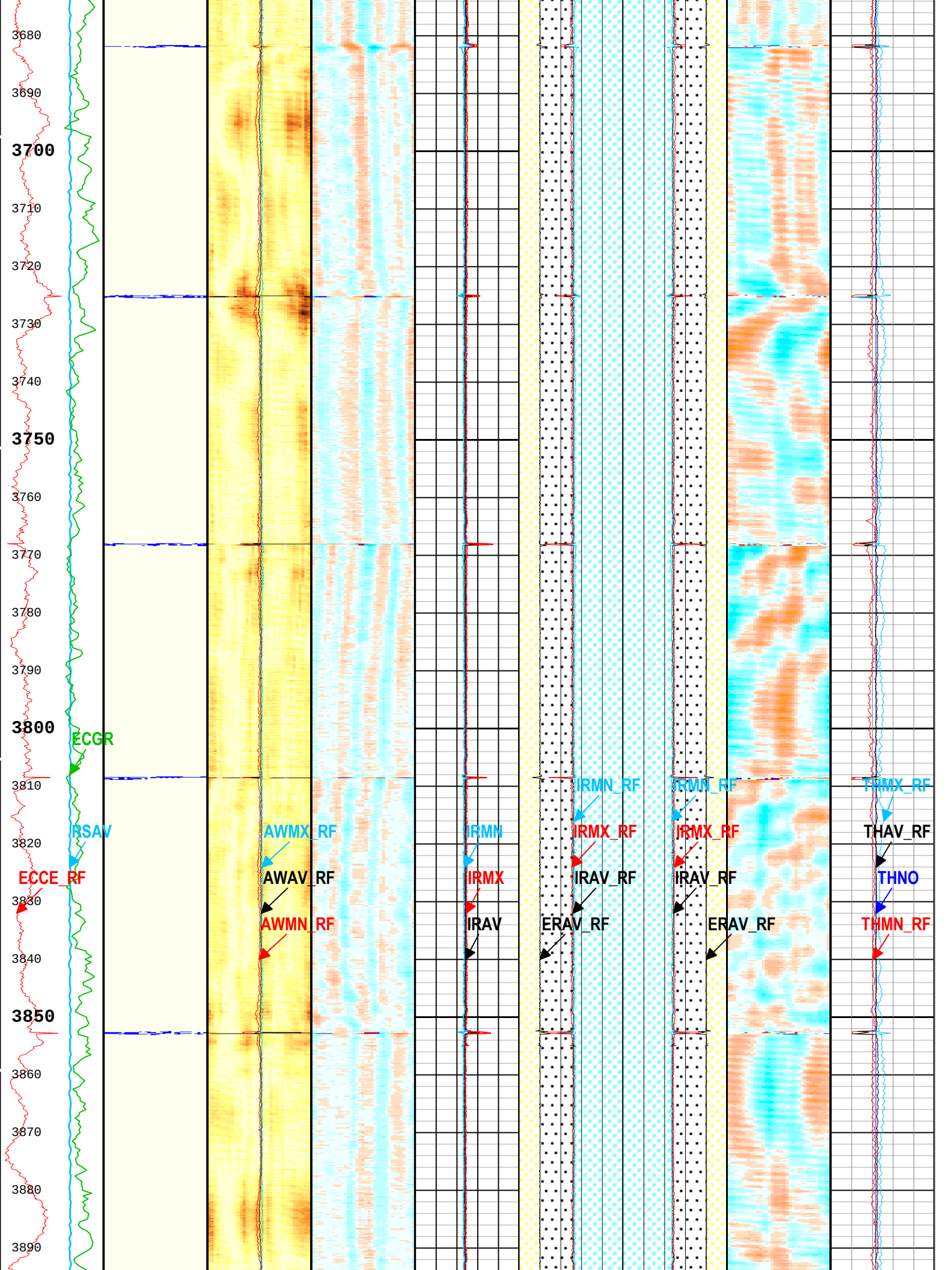
3680
3690
3700
3710
3720
3730
3740
3750
3760
3770
3780
3790
3800
3810
3820
3830
3840
3850
3860
3870
3880
3890
ECGR
RSAV
ECCE_RF
AWMX_RF
AWAV_RF
AWMN_RF
IRMN
IRMX
IRAV
IRMN_RF
IRMX_RF
IRAV_RF
ERAV_RF
IRMN_RF
IRMX_RF
IRAV_RF
ERAV_RF
THMX_RF
THAV_RF
THNO
THMN_RF

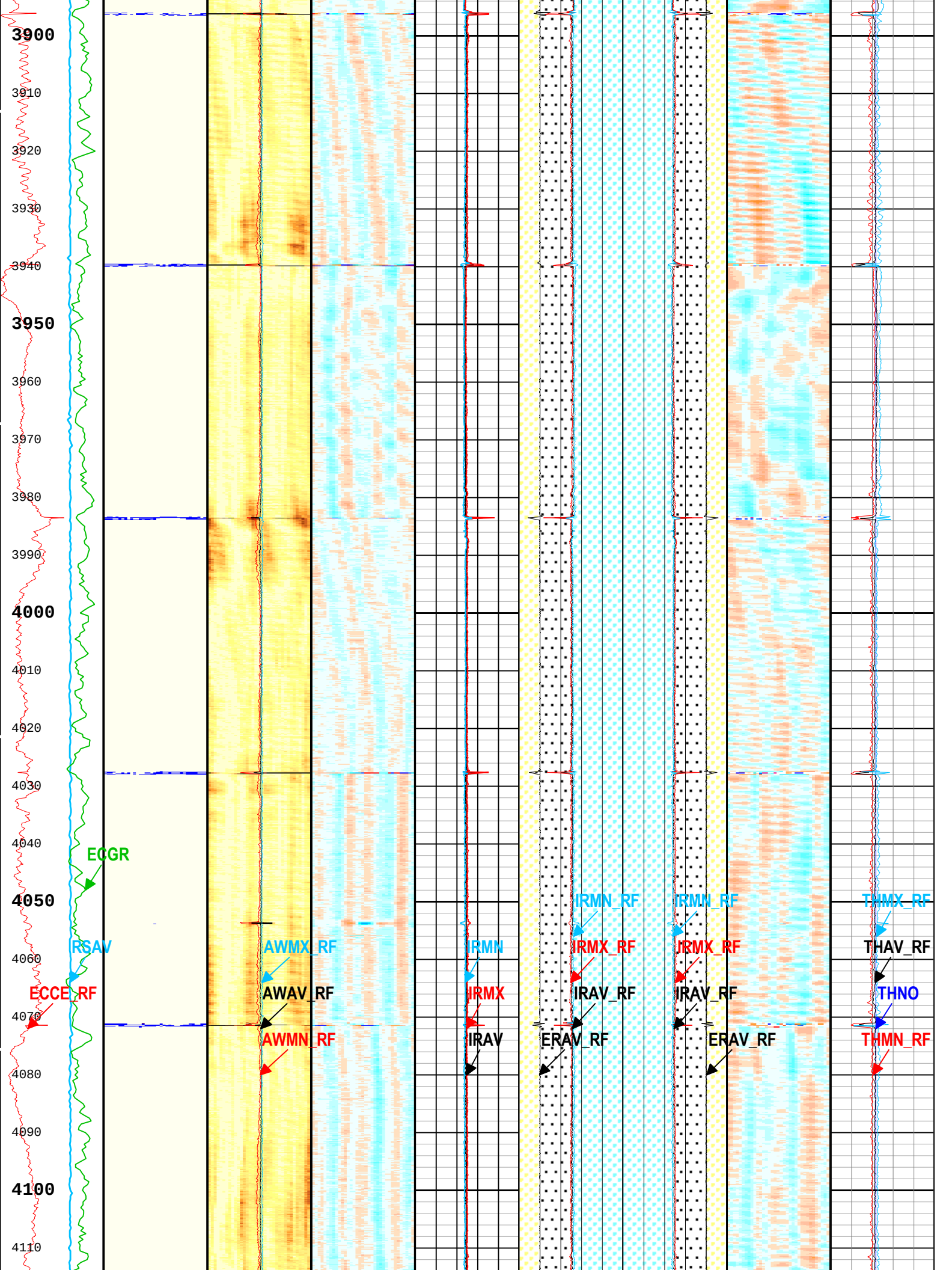
3900
3910
3920
3930
3940
3950
3960
3970
3980
3990
4000
4010
4020
4030
4040
4050
4060
4070
4080
4090
4100
4110
ECGR
RSAV
ECCE_RF
AWMX_RF
AWAV_RF
AWMN_RF
IRMN
IRMX
IRAV
IRMN_RF
IRMX_RF
IRAV_RF
ERAV_RF
IRMN_RF
IRMX_RF
IRAV_RF
ERAV_RF
THMX_RF
THAV_RF
THNO
THMN_RF

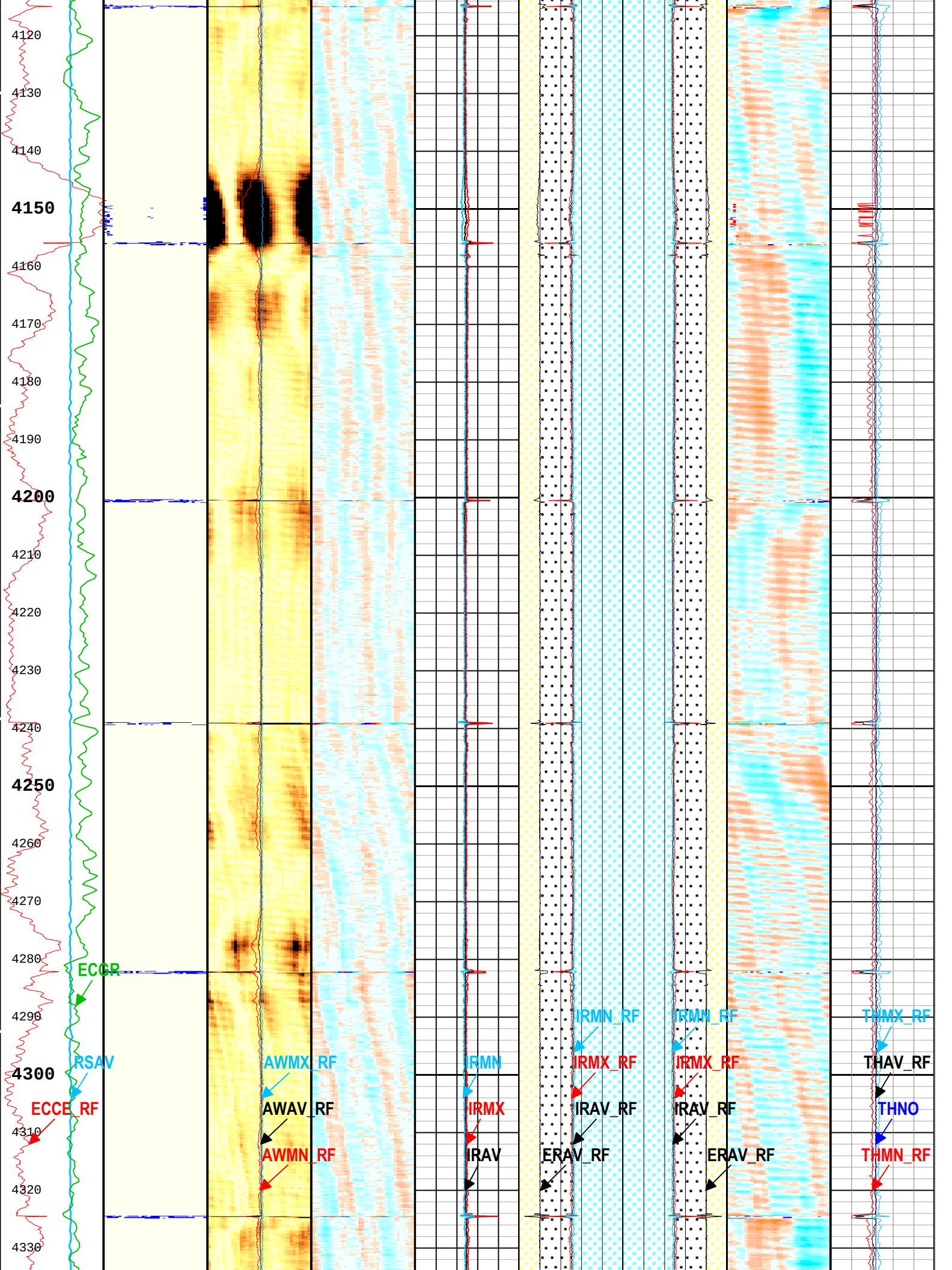
4120
4130
4140
4150
4160
4170
4180
4190
4200
4210
4220
4230
4240
4250
4260
4270
4280
4290
4300
4310
4320
4330
ECCR
RSAV
ECCE_RF
AWMX_RF
AWAV_RF
AWMN_RF
IRMN
IRMX
IRAV
IRMN_RF
IRMX_RF
IRAV_RF
ERAV_RF
IRMN_RF
IRMX_RF
IRAV_RF
ERAV_RF
THMX_RF
THAV_RF
THNO
THMN_RF

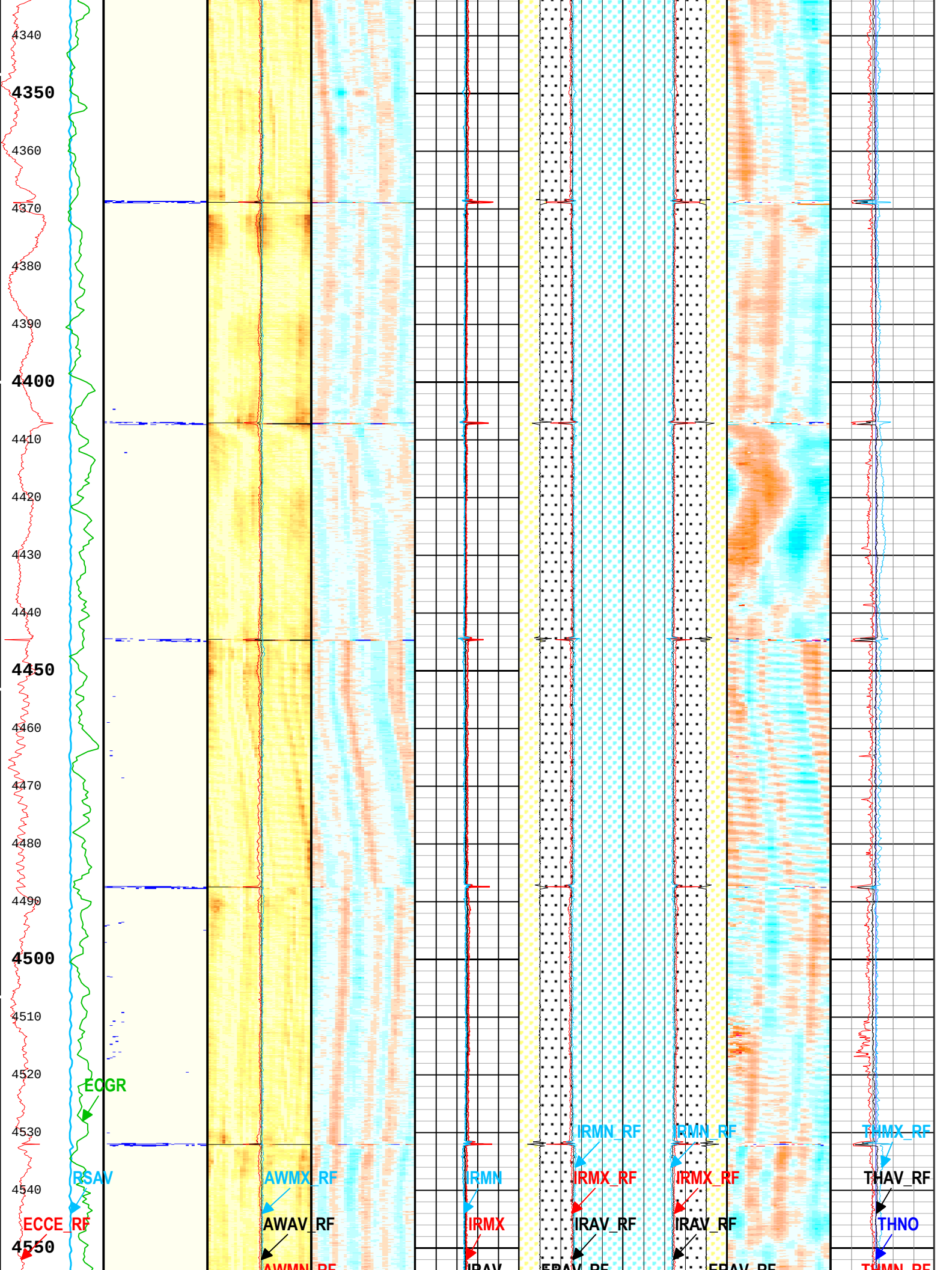
4340
4350
4360
4370
4380
4390
4400
4410
4420
4430
4440
4450
4460
4470
4480
4490
4500
4510
4520
4530
4540
4550
ECGR
RSAV
ECCE_RF
AWMX_RF
AWAV_RF
AWMN_RF
IRMN
IRMX
IRAV
IRMN_RF
IRMX_RF
IRAV_RF
IRMN_RF
IRMX_RF
IRAV_RF
THMX_RF
THAV_RF
THNO
THMN_RF

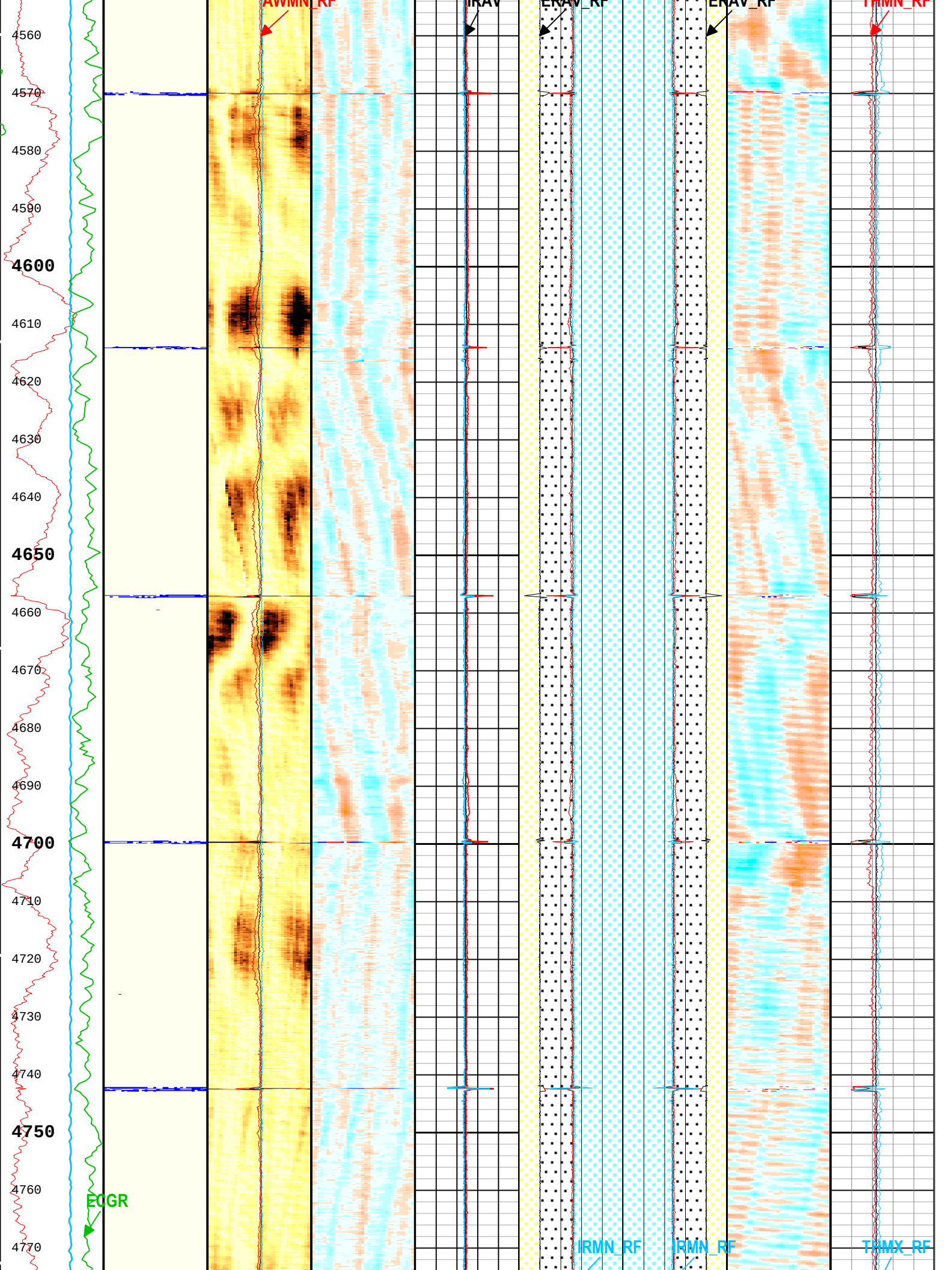
AWMN_RF
IRAV
ERAV_RF
ERAV_RF
TRMN_RF
4560
4570
4580
4590
4600
4610
4620
4630
4640
4650
4660
4670
4680
4690
4700
4710
4720
4730
4740
4750
4760
4770
ECGR
IRMN_RF
RMN_RF
TRMX_RF

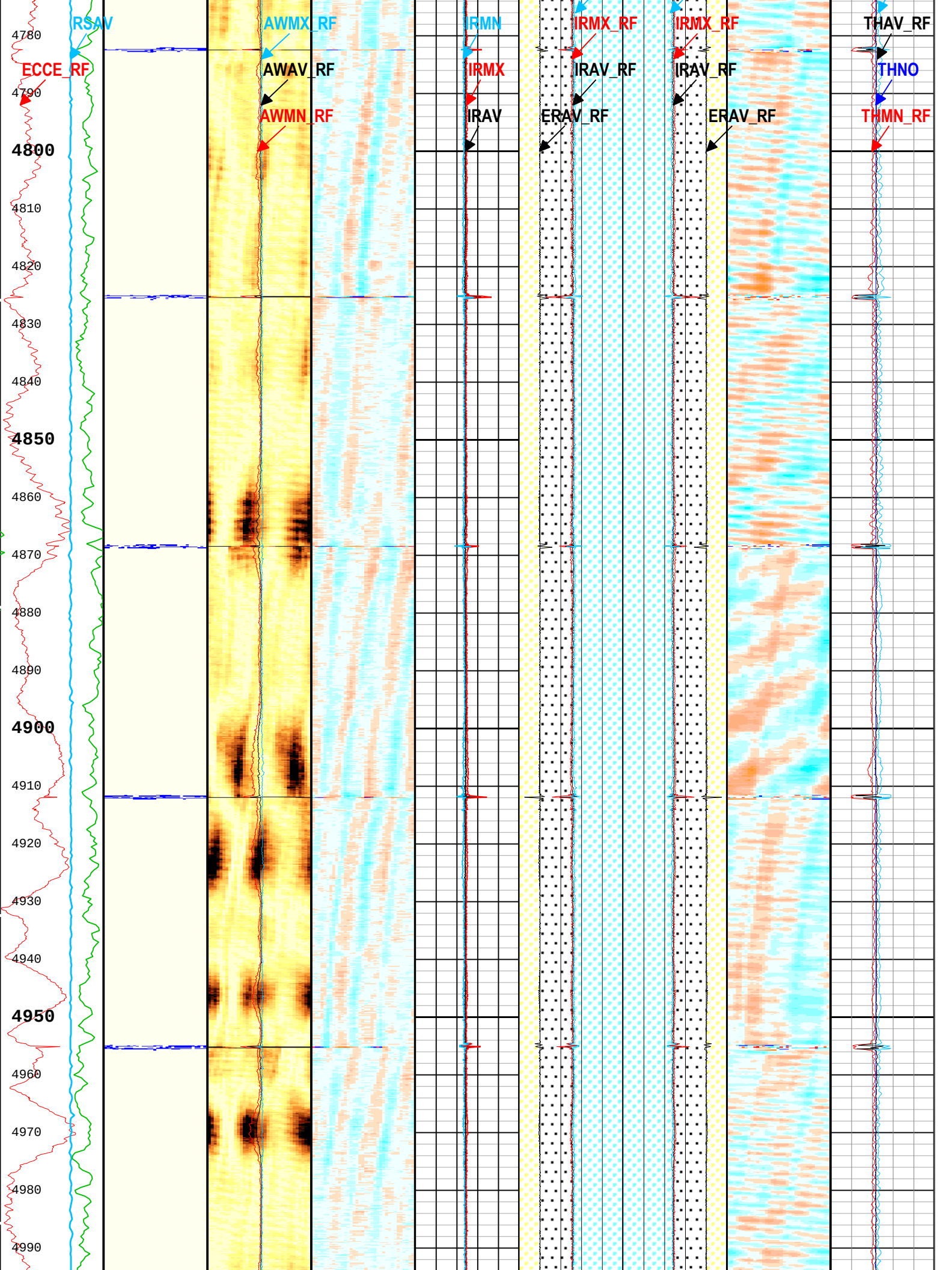
RSAV
ECCE_RF
AWMX_RF
AWAV_RF
AWMN_RF
IRMN
IRMX
IRAV
IRMX_RF
IRAV_RF
ERAV_RF
IRMX_RF
IRAV_RF
ERAV_RF
THAV_RF
THNO
THMN_RF
4780
4790
4800
4810
4820
4830
4840
4850
4860
4870
4880
4890
4900
4910
4920
4930
4940
4950
4960
4970
4980
4990

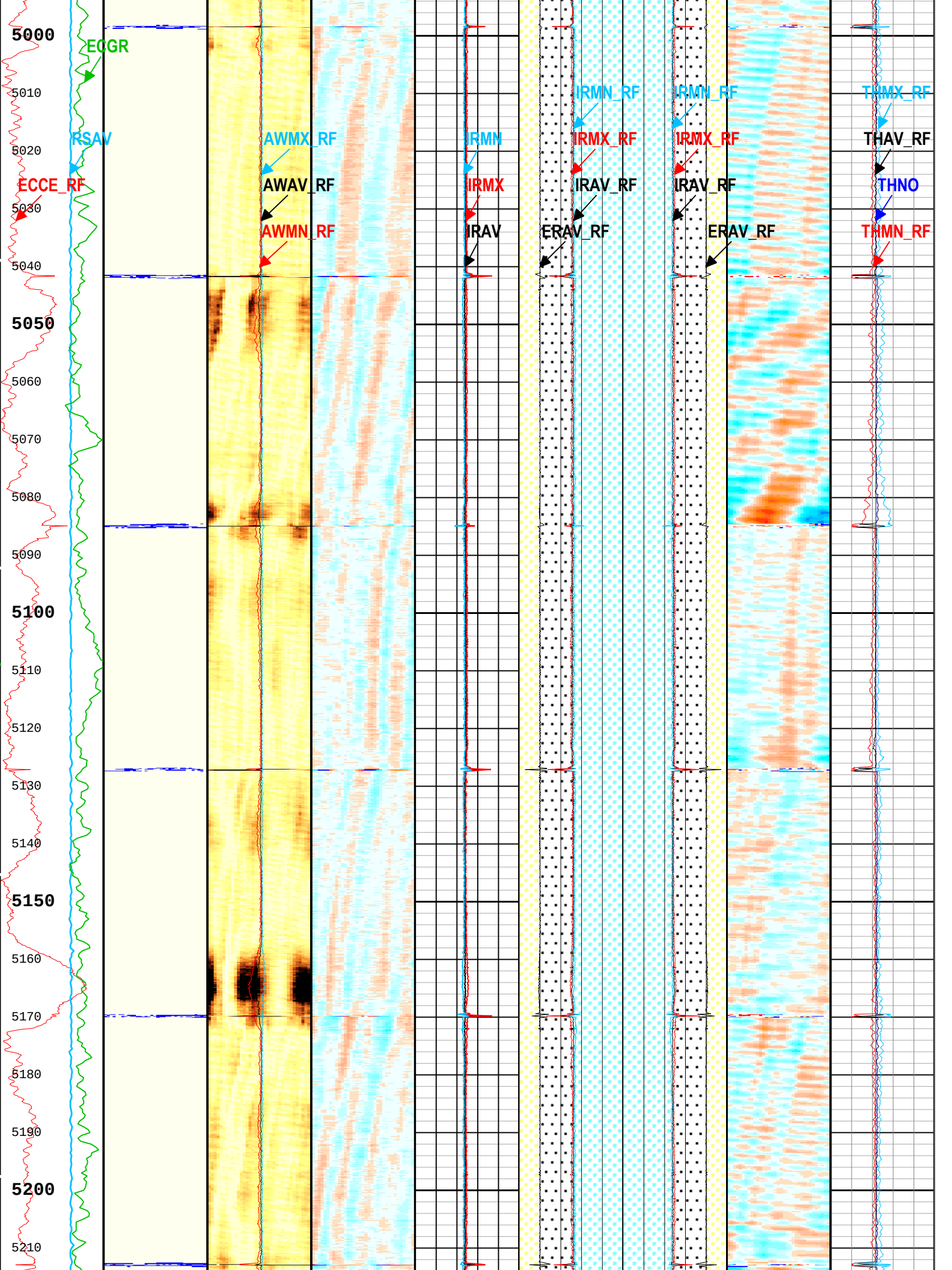
5000
5010
5020
5030
5040
5050
5060
5070
5080
5090
5100
5110
5120
5130
5140
5150
5160
5170
5180
5190
5200
5210
ECGR
RSAV
ECCE_RF
AWMX_RF
AWAV_RF
AWMN_RF
IRMN
IRMX
IRAV
IRMN_RF
IRMX_RF
IRAV_RF
ERAV_RF
IRMN_RF
IRMX_RF
IRAV_RF
ERAV_RF
THMX_RF
THAV_RF
THNO
THMN_RF

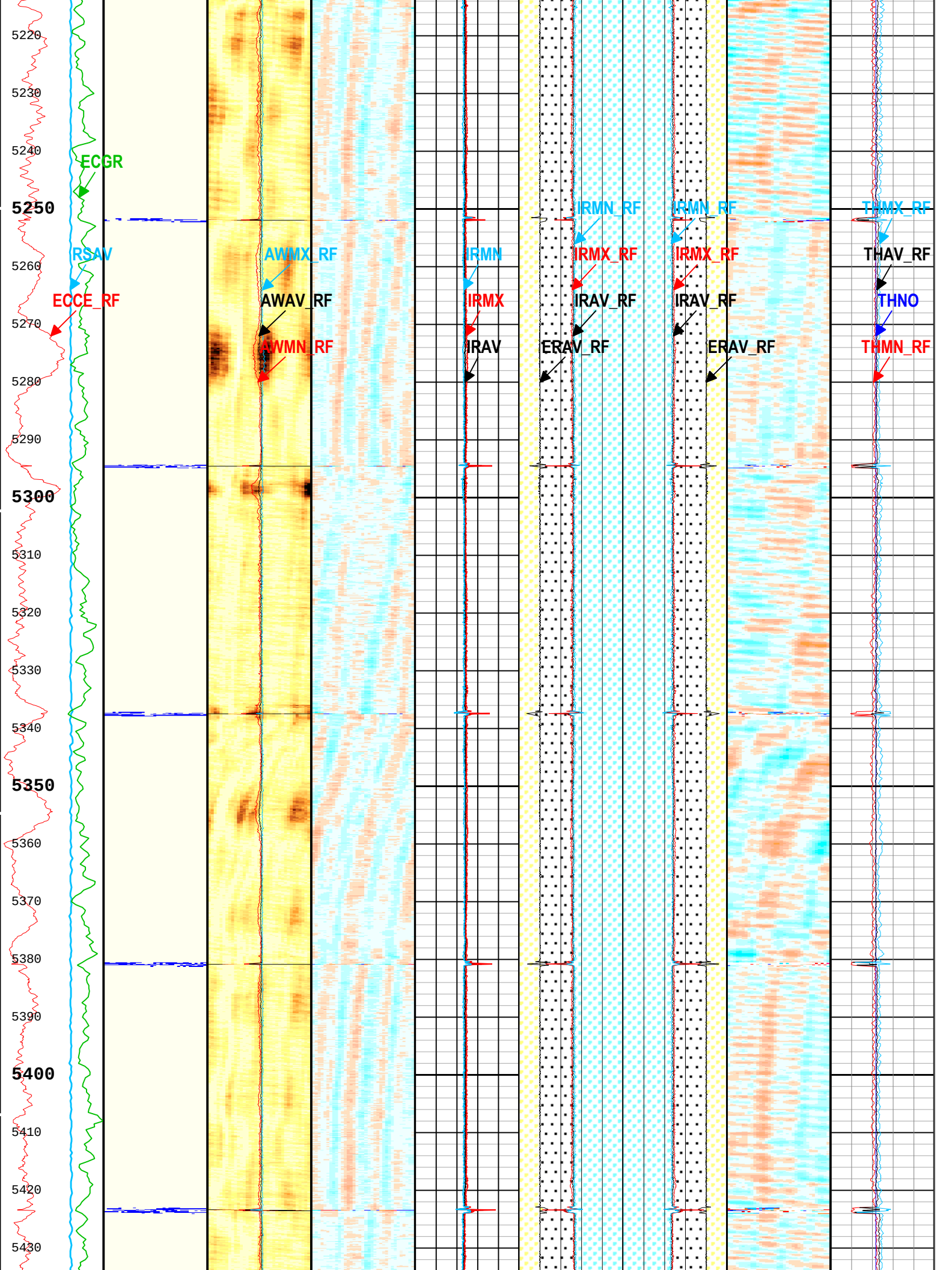
5220
5230
5240
5250
5260
5270
5280
5290
5300
5310
5320
5330
5340
5350
5360
5370
5380
5390
5400
5410
5420
5430
ECGR
RSAV
ECCE_RF
AWMX_RF
AWAV_RF
AWMN_RF
IRMN
IRMX
IRAV
IRMN_RF
IRMX_RF
IRAV_RF
ERAV_RF
IRMN_RF
IRMX_RF
IRAV_RF
ERAV_RF
THMX_RF
THAV_RF
THNO
THMN_RF

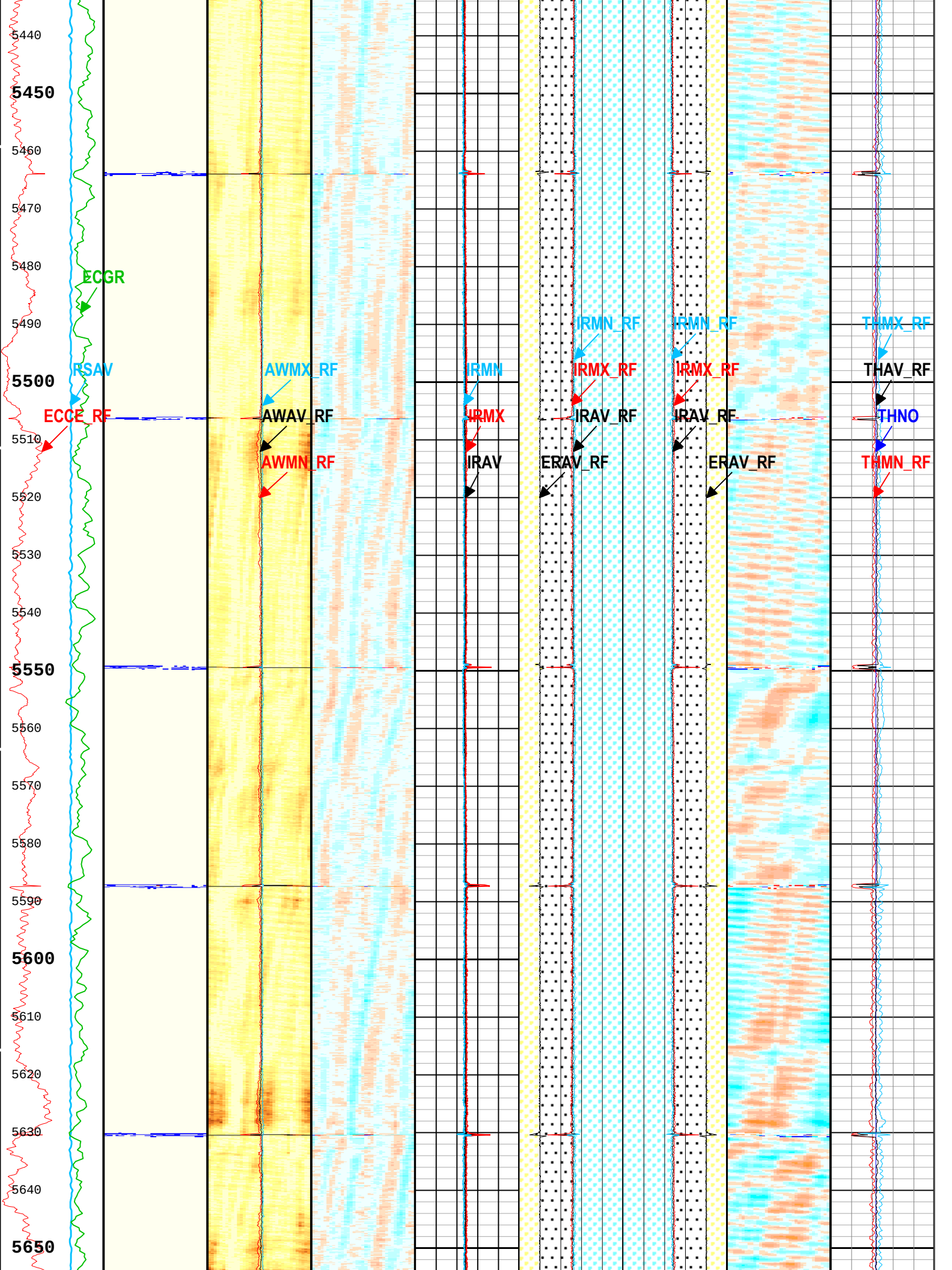
5440
5450
5460
5470
5480
5490
5500
5510
5520
5530
5540
5550
5560
5570
5580
5590
5600
5610
5620
5630
5640
5650
ECGR
RSAV
ECCE_RF
AWMX_RF
AWAV_RF
AWMN_RF
IRMN
IRMX
IRAV
IRMN_RF
IRMX_RF
IRAV_RF
ERAV_RF
IRMN_RF
IRMX_RF
IRAV_RF
ERAV_RF
THMX_RF
THAV_RF
THNO
THMN_RF

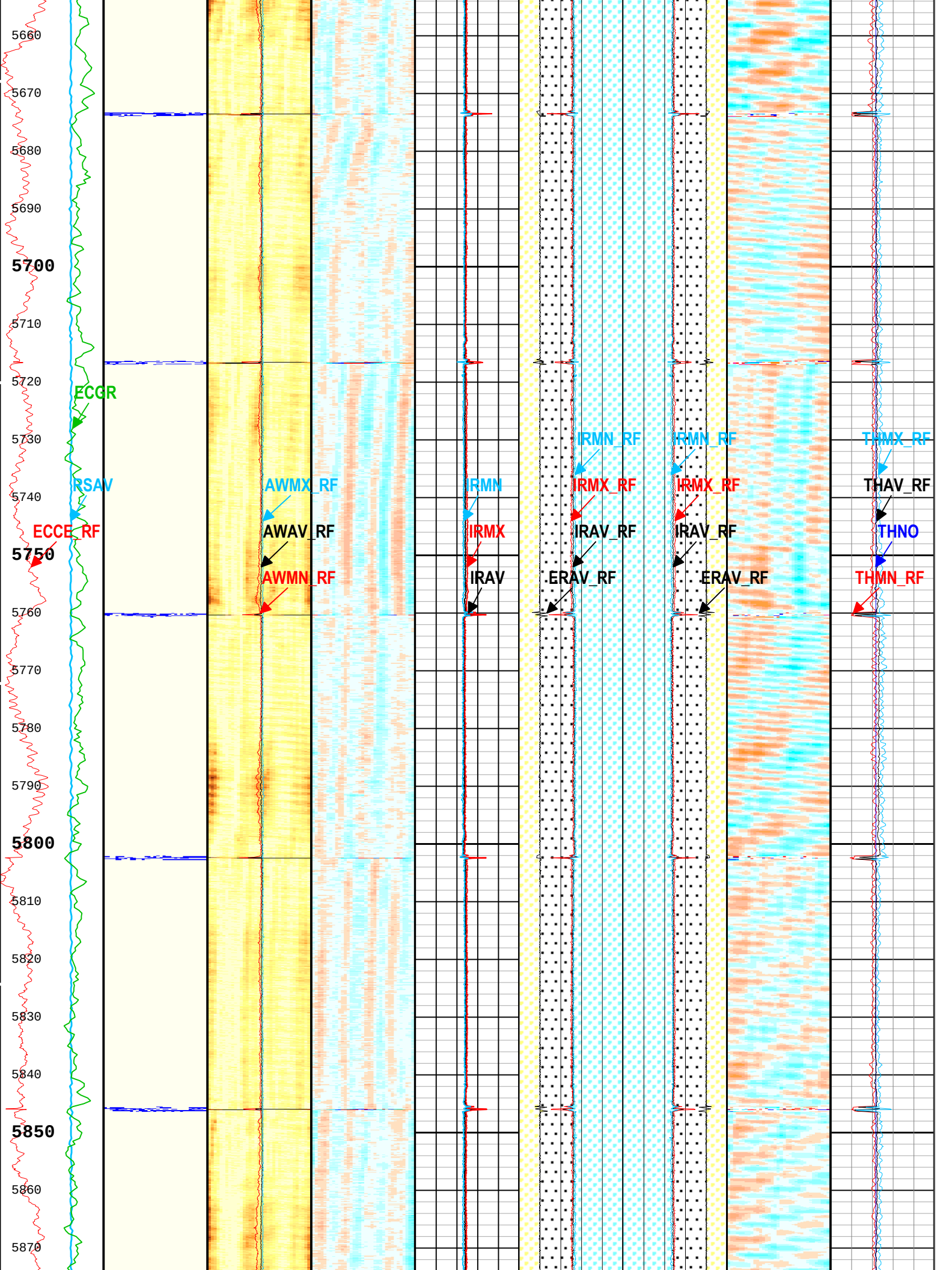
5660
5670
5680
5690
5700
5710
5720
5730
5740
5750
5760
5770
5780
5790
5800
5810
5820
5830
5840
5850
5860
5870
ECGR
RSAV
ECCE_RF
AWMX_RF
AWAV_RF
AWMN_RF
IRMN
IRMX
IRAV
IRMN_RF
IRMX_RF
IRAV_RF
ERAV_RF
IRMN_RF
IRMX_RF
IRAV_RF
ERAV_RF
THMX_RF
THAV_RF
THNO
THMN_RF

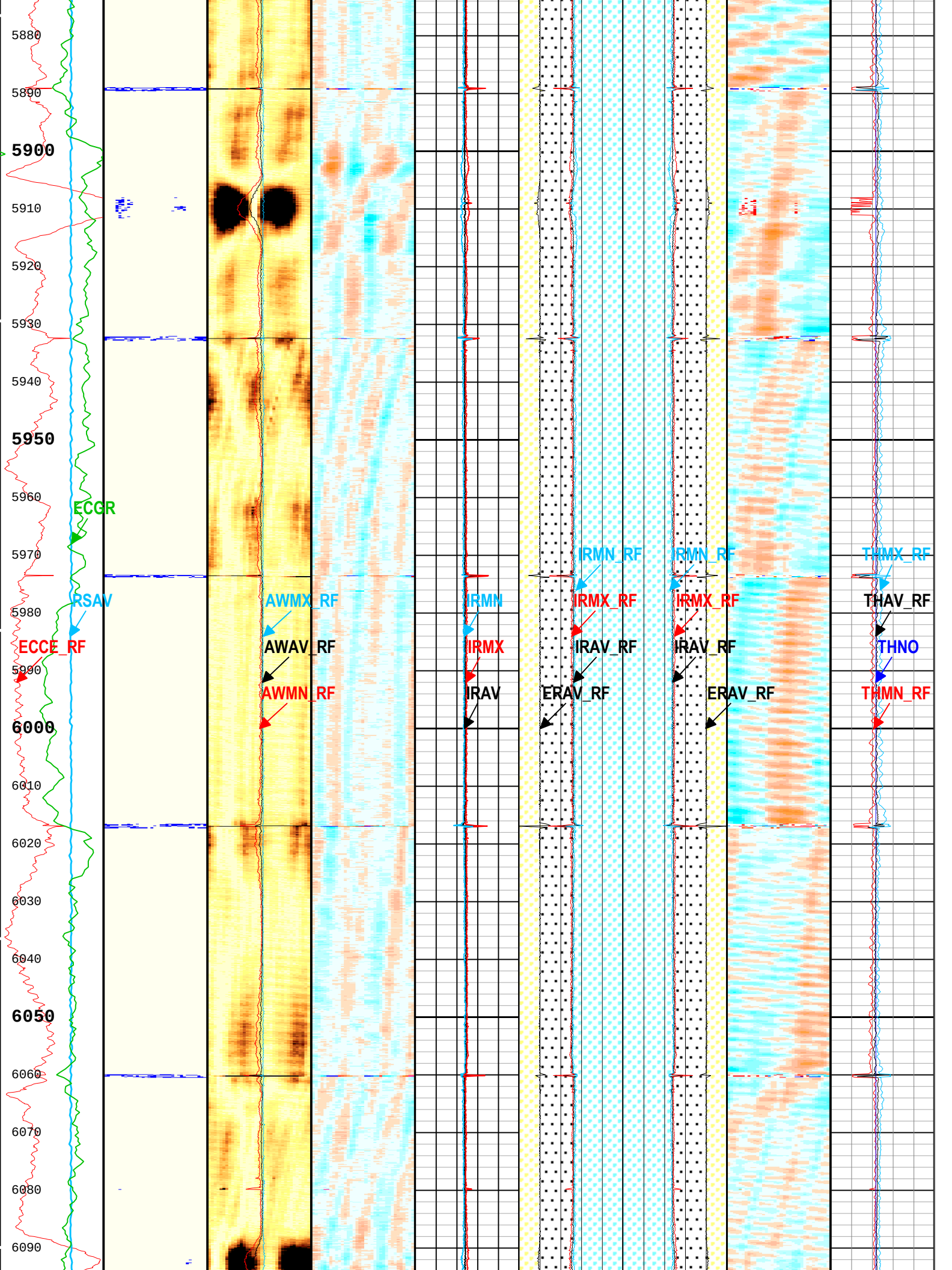
5880
5890
5900
5910
5920
5930
5940
5950
5960
5970
5980
5990
6000
6010
6020
6030
6040
6050
6060
6070
6080
6090
ECGR
RSAV
ECCE_RF
AWMX_RF
AWAV_RF
AWMN_RF
IRMN
IRMX
IRAV
IRMN_RF
IRMX_RF
IRAV_RF
ERAV_RF
IRMN_RF
IRMX_RF
IRAV_RF
ERAV_RF
THMX_RF
THAV_RF
THNO
THMN_RF

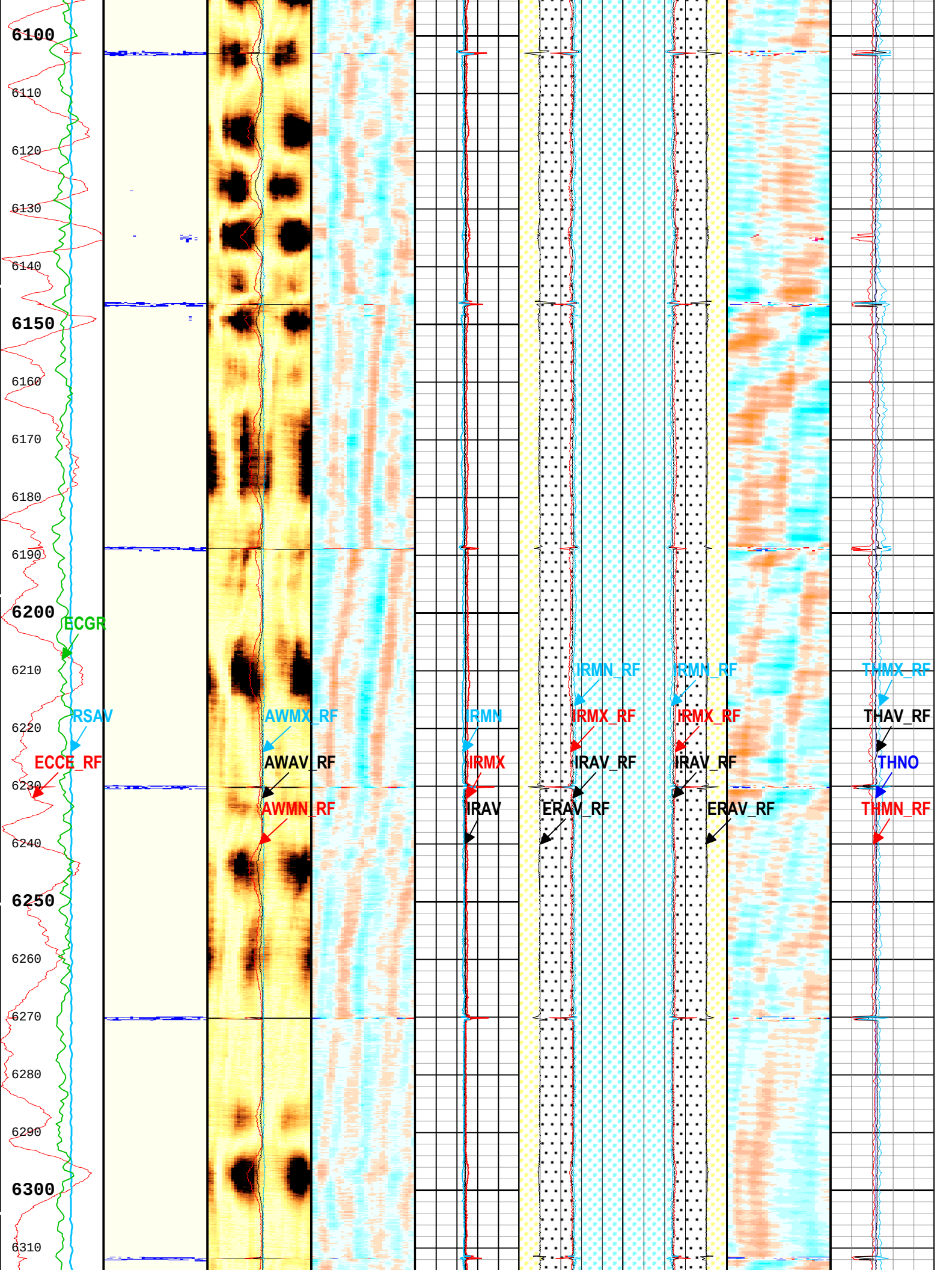
6100
6110
6120
6130
6140
6150
6160
6170
6180
6190
6200
6210
6220
6230
6240
6250
6260
6270
6280
6290
6300
6310
ECGR
RSAV
ECCE_RF
AWMX_RF
AWAV_RF
AWMN_RF
IRMN
IRMX
IRAV
IRMN_RF
IRMX_RF
IRAV_RF
ERAV_RF
IRMN_RF
IRMX_RF
IRAV_RF
ERAV_RF
THMX_RF
THAV_RF
THNO
THMN_RF

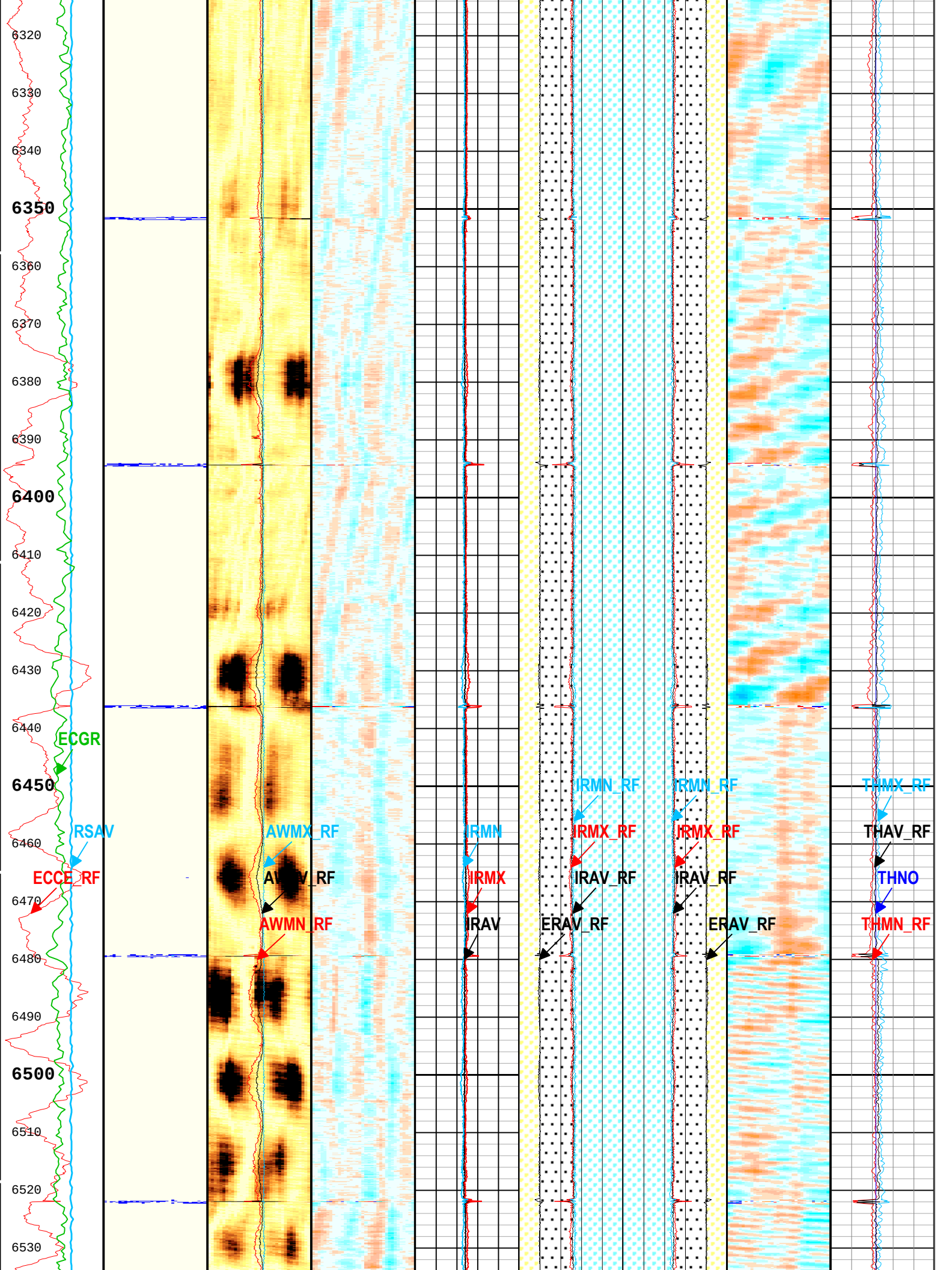
6320
6330
6340
6350
6360
6370
6380
6390
6400
6410
6420
6430
6440
6450
6460
6470
6480
6490
6500
6510
6520
6530
ECGR
RSAV
ECCE_RF
AWMX_RF
AWMN_RF
IRMN
IRMX
IRAV
IRMN_RF
IRMX_RF
IRAV_RF
ERAV_RF
IRMN_RF
IRMX_RF
IRAV_RF
ERAV_RF
THMX_RF
THAV_RF
THNO
THMN_RF

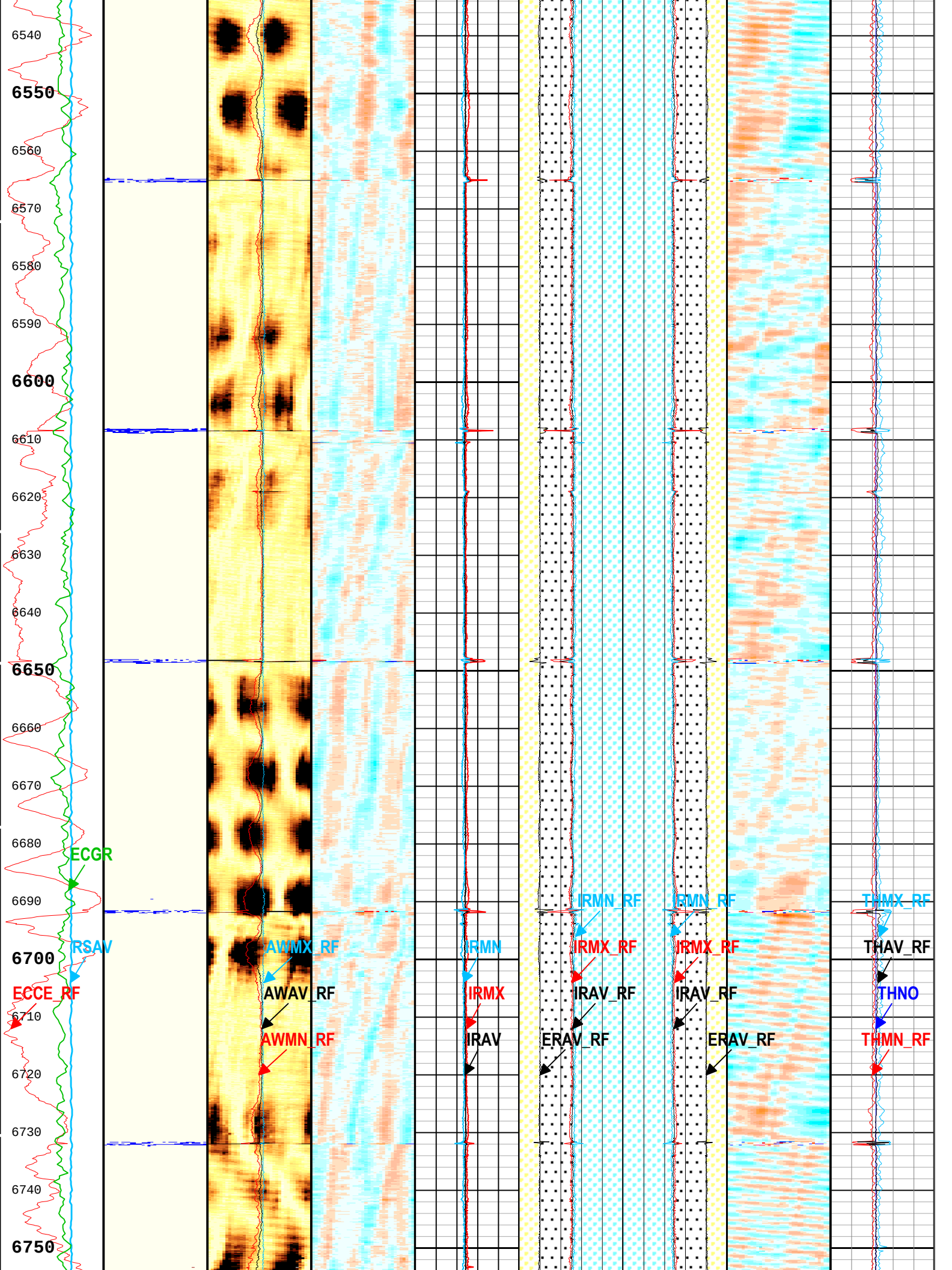
6540
6550
6560
6570
6580
6590
6600
6610
6620
6630
6640
6650
6660
6670
6680
6690
6700
6710
6720
6730
6740
6750
ECGR
RSAV
ECCE_RF
AWMX_RF
AWAV_RF
AWMN_RF
IRMN
IRMX
IRAV
IRMN_RF
IRMX_RF
IRAV_RF
ERAV_RF
IRMX_RF
IRAV_RF
ERAV_RF
THMX_RF
THAV_RF
THNO
THMN_RF

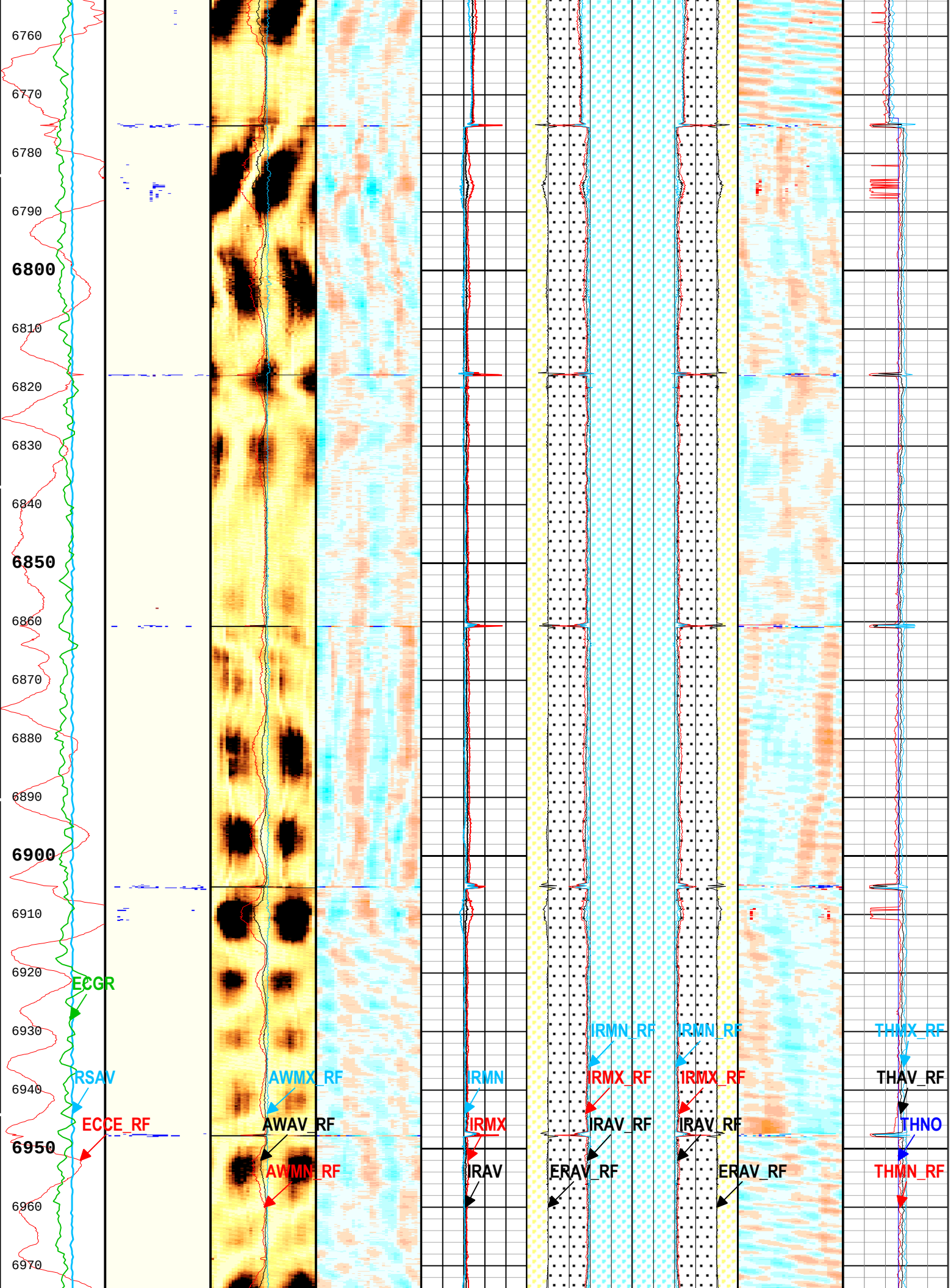
6760
6770
6780
6790
6800
6810
6820
6830
6840
6850
6860
6870
6880
6890
6900
6910
6920
6930
6940
6950
6960
6970
ECGR
RSAV
ECCE_RF
AWMX_RF
AWAV_RF
AWMN_RF
IRMN
IRMX
IRAV
IRMN_RF
IRMX_RF
IRAV_RF
ERAV_RF
IRMN_RF
IRMX_RF
IRAV_RF
ERAV_RF
THMX_RF
THAV_RF
THNO
THMN_RF

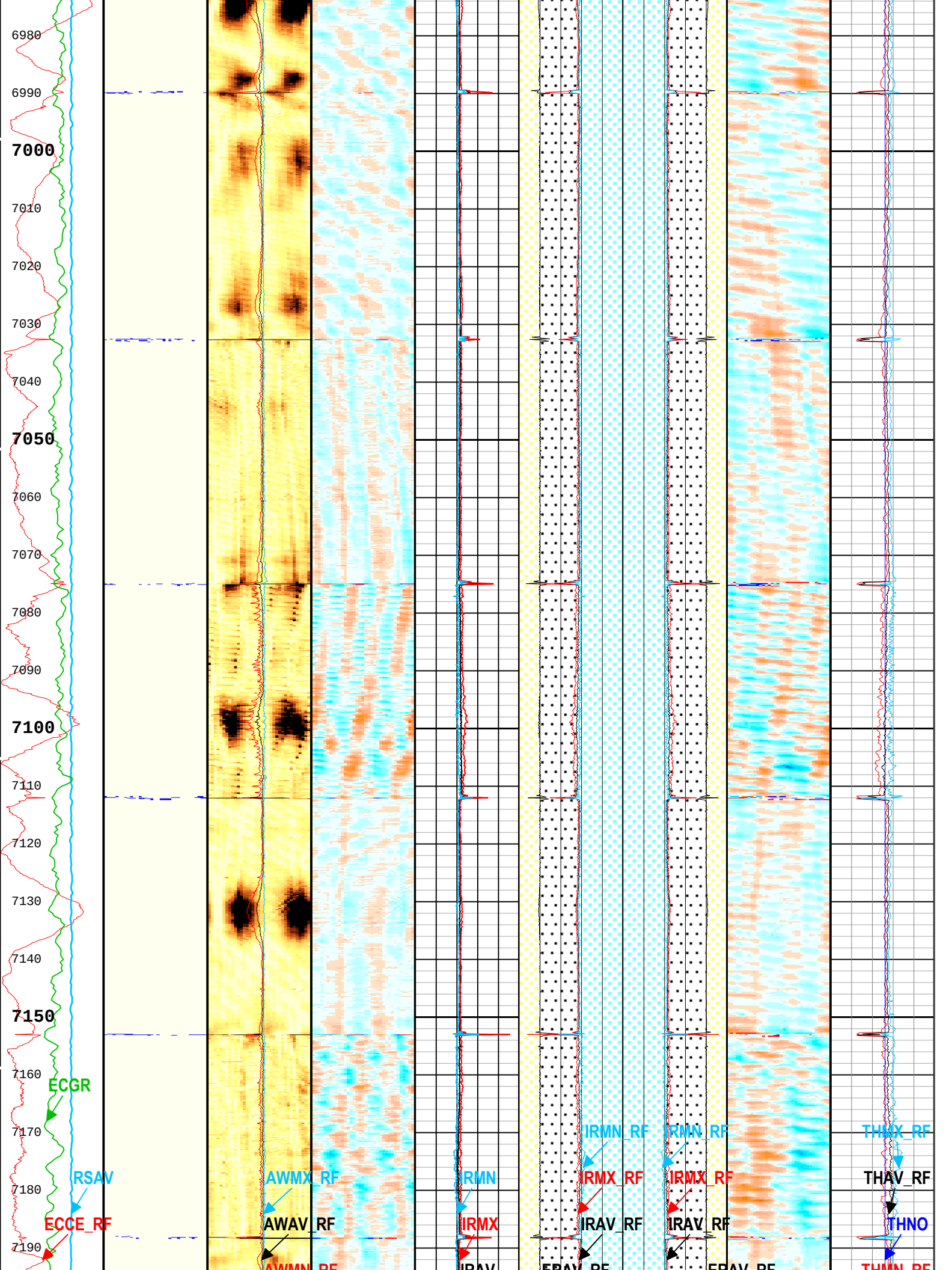
6980
6990
7000
7010
7020
7030
7040
7050
7060
7070
7080
7090
7100
7110
7120
7130
7140
7150
7160
7170
7180
7190
ECGR
RSAV
ECCE_RF
AWMX_RF
AWAV_RF
AWMN_RF
IRMN
IRMX
IRAV
IRMN_RF
IRMX_RF
IRAV_RF
IRMN_RF
IRMX_RF
IRAV_RF
THMX_RF
THAV_RF
THNO
THMN_RF

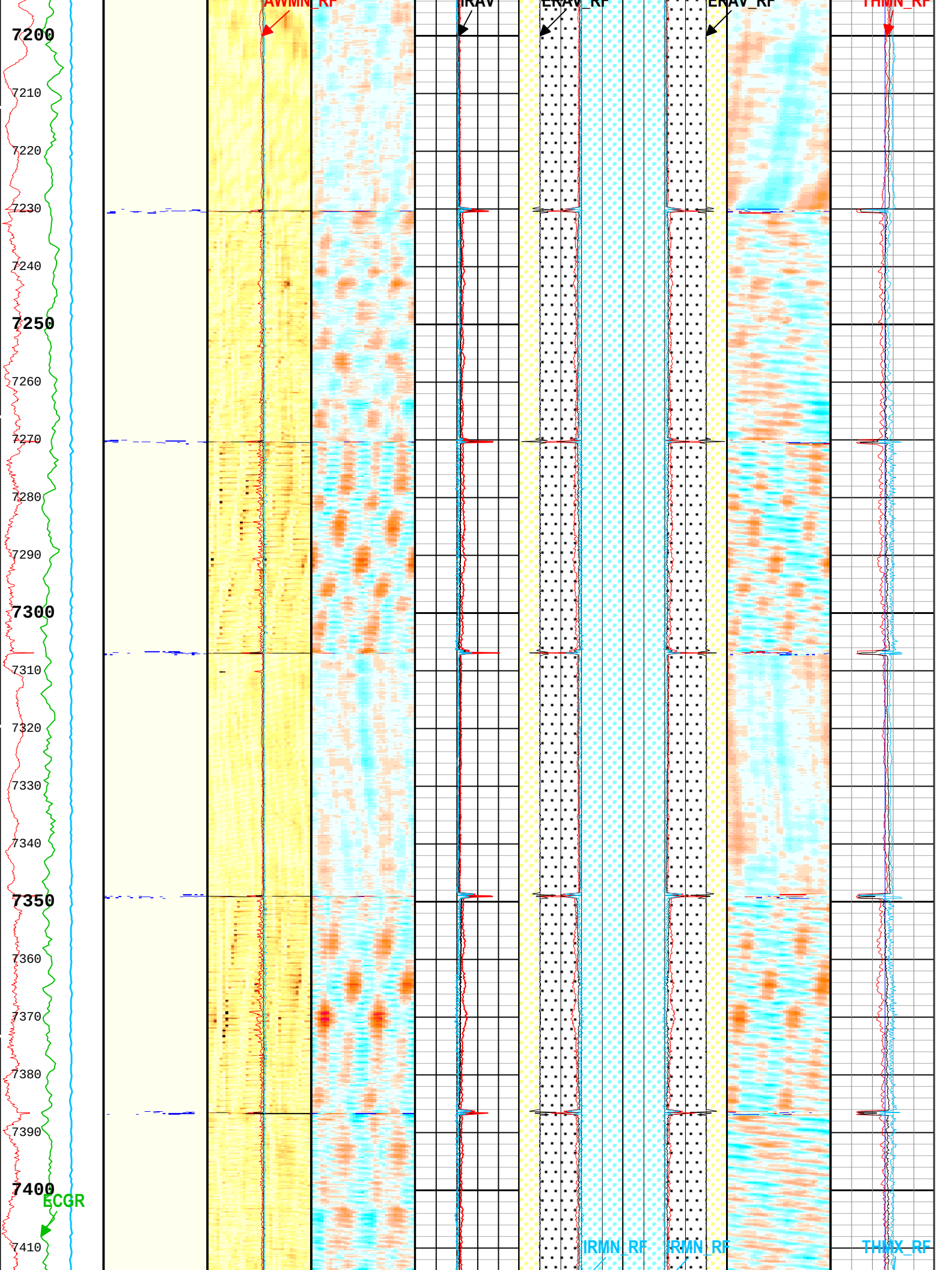
AWMN_RF
IRAV
ERAV_RF
ERAV_RF
THMN_RF
7200
7210
7220
7230
7240
7250
7260
7270
7280
7290
7300
7310
7320
7330
7340
7350
7360
7370
7380
7390
7400
ECGR
7410
IRMN_RF
IRMN_RF
THMX_RF

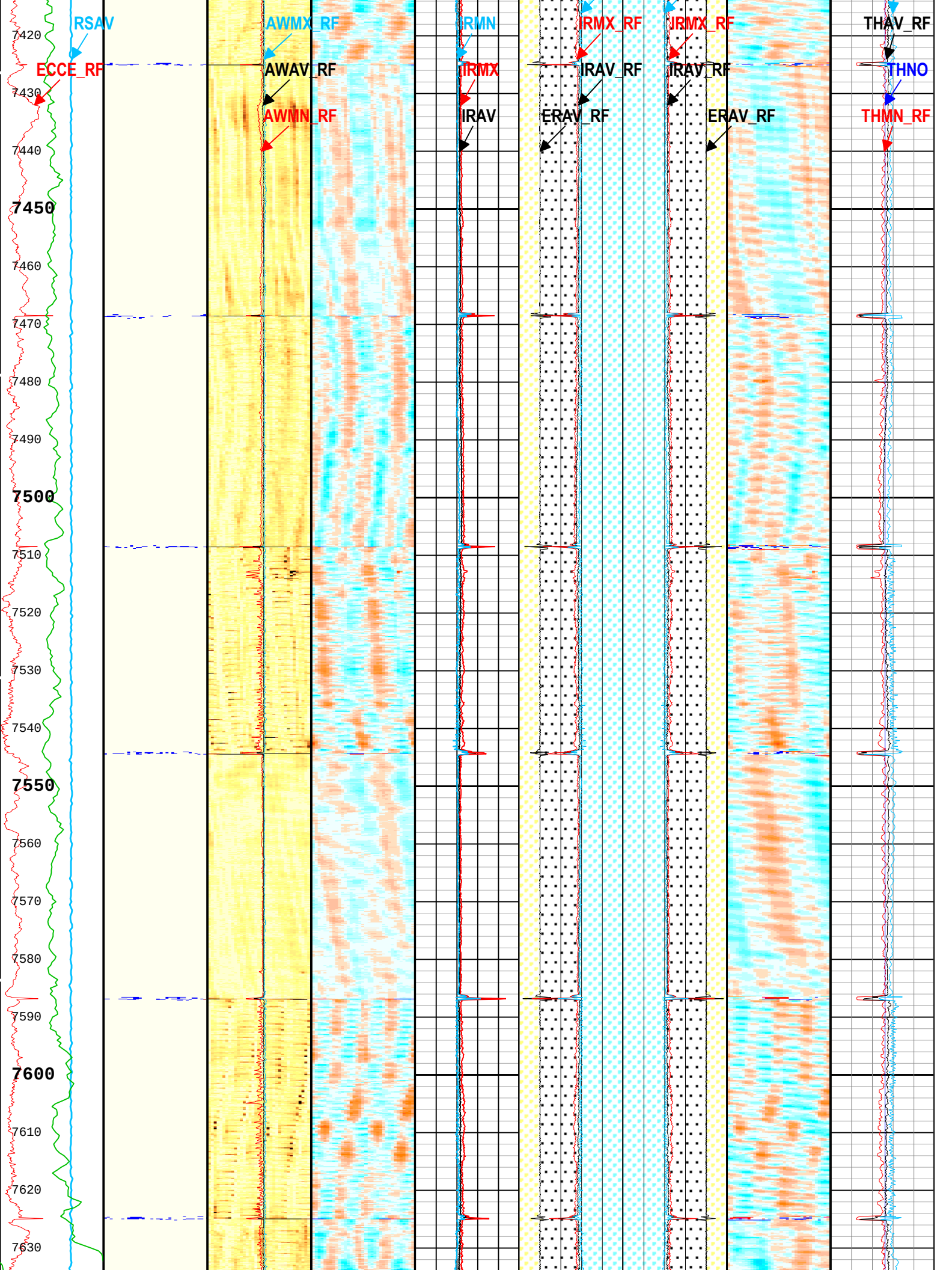
RSAV
ECCE_RF
AWMX_RF
AWAV_RF
AWMN_RF
IRMN
IRMX
IRAV
IRMX_RF
IRAV_RF
ERAV_RF
IRMX_RF
IRAV_RF
ERAV_RF
THAV_RF
THNO
THMN_RF
7420
7430
7440
7450
7460
7470
7480
7490
7500
7510
7520
7530
7540
7550
7560
7570
7580
7590
7600
7610
7620
7630

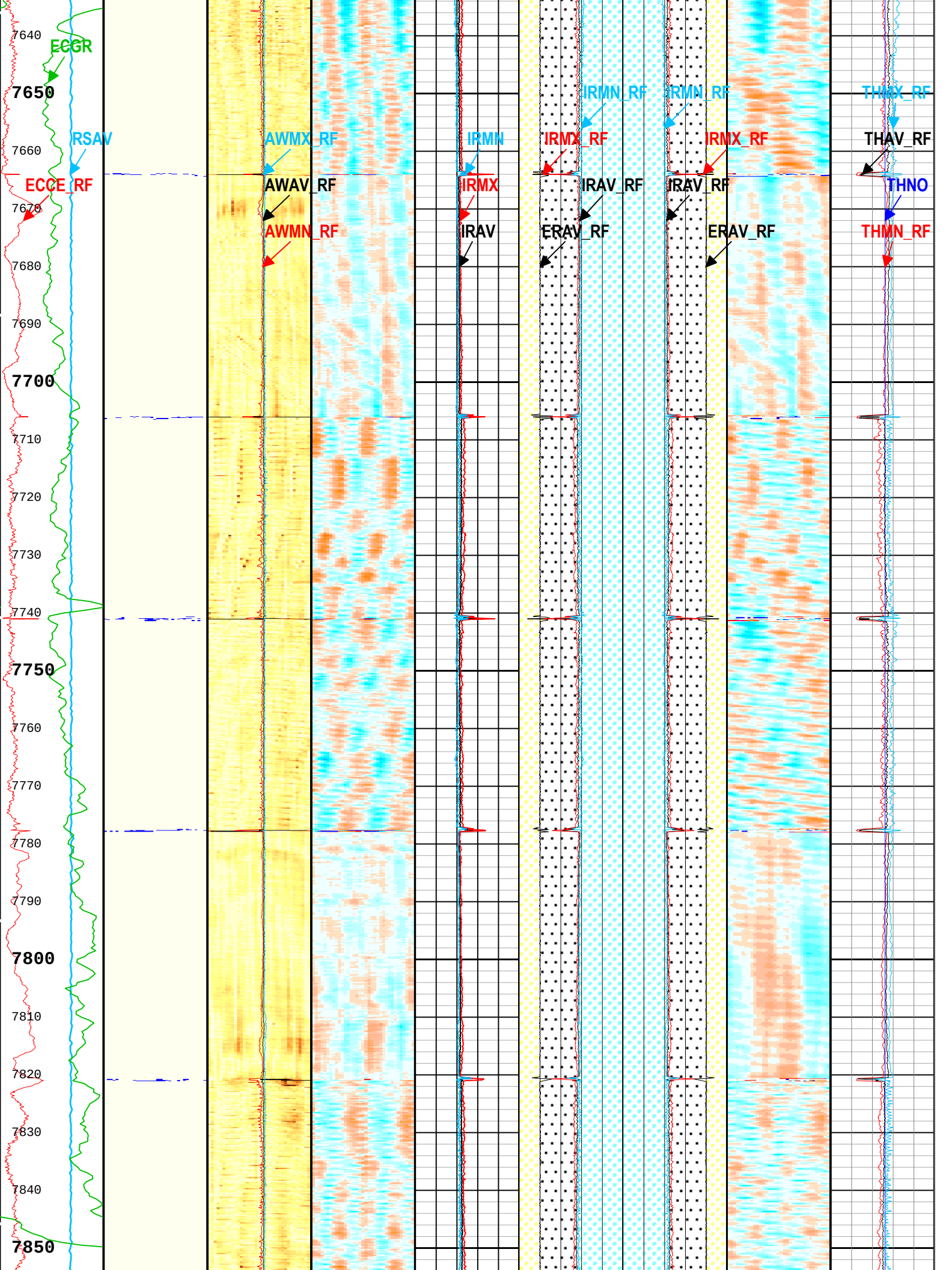
ECGR
RSAV
ECCE_RF
AWMX_RF
AWAV_RF
AWMN_RF
IRMN
IRMX
IRAV
IRMN_RF
IRMX_RF
IRAV_RF
ERAV_RF
IRMN_RF
IRMX_RF
IRAV_RF
ERAV_RF
THMX_RF
THAV_RF
THNO
THMN_RF
7640
7650
7660
7670
7680
7690
7700
7710
7720
7730
7740
7750
7760
7770
7780
7790
7800
7810
7820
7830
7840
7850

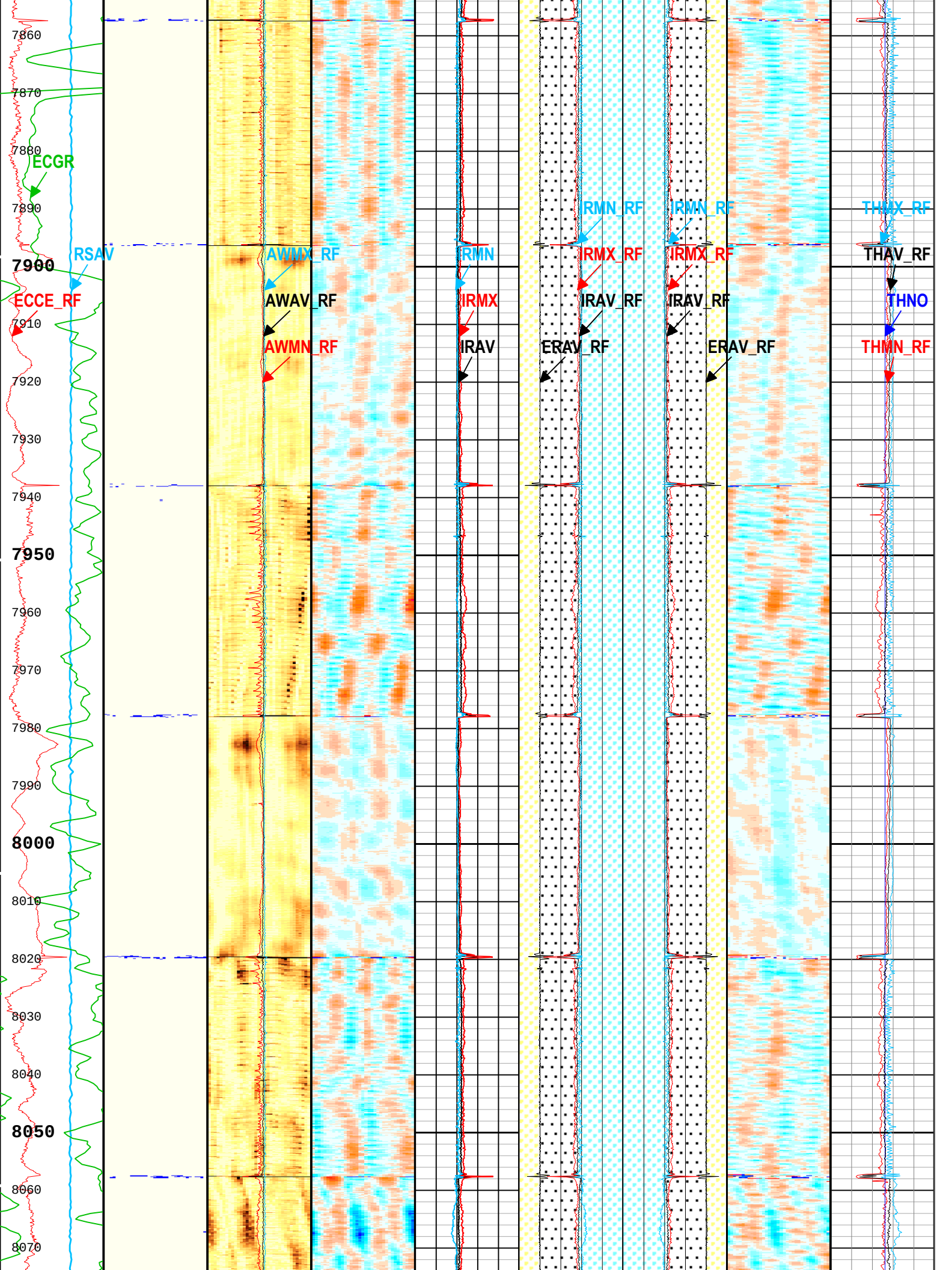
7860
7870
7880
7890
7900
7910
7920
7930
7940
7950
7960
7970
7980
7990
8000
8010
8020
8030
8040
8050
8060
8070
ECGR
RSAV
ECCE_RF
AWMX_RF
AWAV_RF
AWMN_RF
IRMN
IRMX
IRAV
IRMN_RF
IRMX_RF
IRAV_RF
ERAV_RF
IRMN_RF
IRMX_RF
IRAV_RF
ERAV_RF
THMX_RF
THAV_RF
THNO
THMN_RF

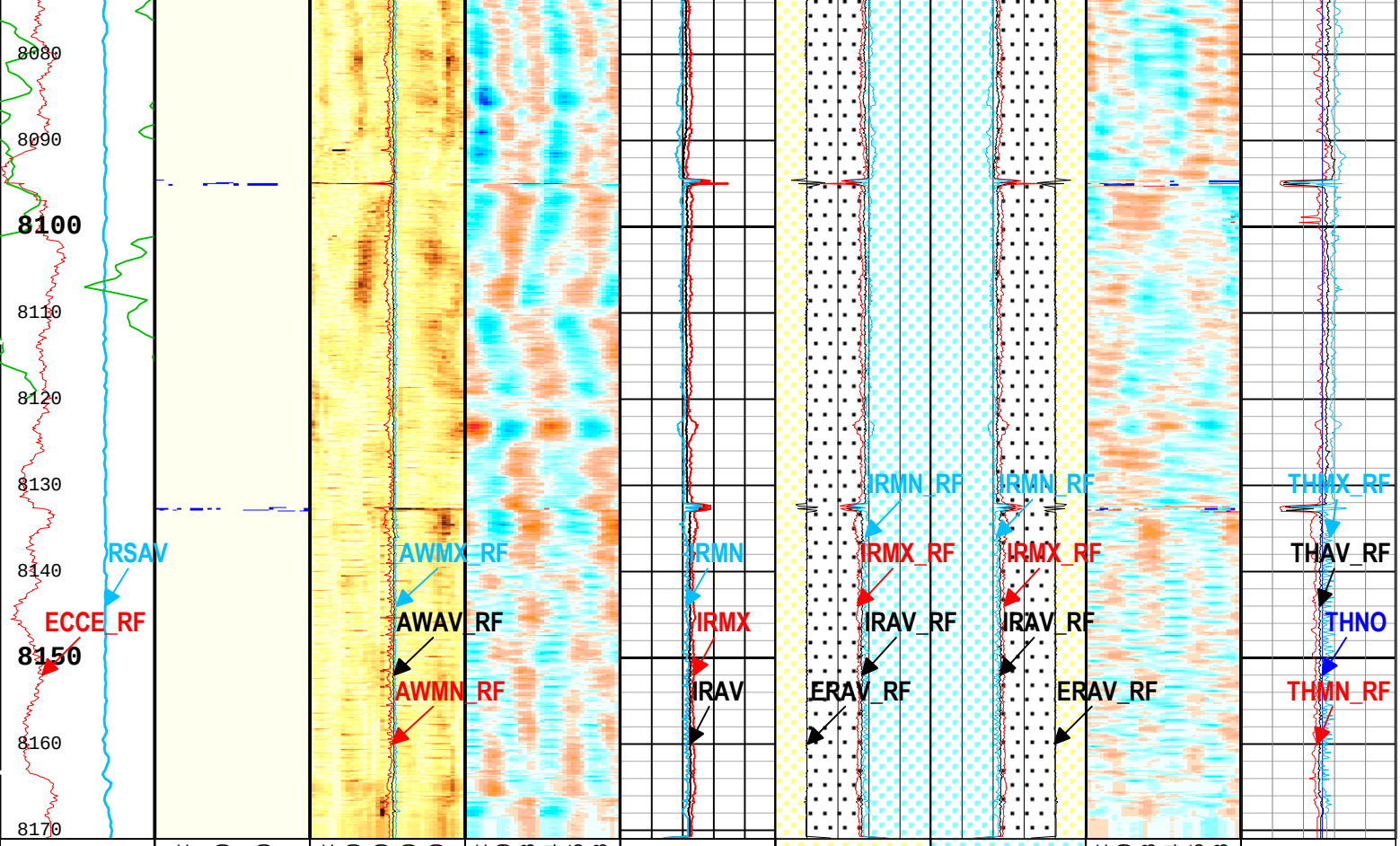

Amplitude of Eccentering for Unflagged Waves (ECCE_RF) USIT-E[1]
0 in 0.5

Motor Revolution Speed (RSAV) USIT-E[1]
6 c/s 8

Gamma Ray (ECGR) HGNS[1]
0 gAPI 150

Absent 1.500 3.500
Explicit Normalization
USIT - USIT Processing Flags (UFLG) USIT-E[1]

USIT Processing Flags (UFLG[0]) USIT-E[1]
1 5

Absent -5.200 -3.600 -2.000 -0.400
Explicit Normalization
USIT - Amplitude of Unflagged Wave (AWBK_RF) USIT-E[1] (dB)

Minimum of Unflagged Wave Amplitude (AWMN_RF) USIT-E[1]
0 dB 75

Average of Unflagged Wave Amplitude (AWAV_RF) USIT-E[1]
0 dB 75

Maximum of Unflagged Wave Amplitude (AWMX_RF) USIT-E[1]
0 dB 75

Absent -0.059 -0.028 0.004 0.035 0.068
Explicit Normalization
USIT - Unflagged Internal Radii minus Median Internal Radius (IRBKM_RF) USIT-E[1] (in)

Internal Radius Averaged Value (IRAV) USIT-E[1]
2.7 in 3.7

Internal Radius Maximum Value (IRMX) USIT-E[1]
2.7 in 3.7

Internal Radius Minimum Value (IRMN) USIT-E[1]
2.7 in 3.7

ERAV | IRAV
ERAV-IRAV | ERAV
IRAV | IRAV-ERAV

Median of Unflagged External Radii (ERAV_RF) USIT-E[1]
3.7 in 2.7

Median of Unflagged External Radii (ERAV_RF) USIT-E[1]
2.7 in 3.7

Median Internal Radius of Casing Corrected for Eccentering (IRAV_RF) USIT-E[1]
3.7 in 2.7

Median Internal Radius of Casing Corrected for Eccentering (IRAV_RF) USIT-E[1]
2.7 in 3.7

Maximum of Unflagged Internal Radii (IRMX_RF) USIT-E[1]
3.7 in 2.7

Maximum of Unflagged Internal Radii (IRMX_RF) USIT-E[1]
2.7 in 3.7

Minimum of Unflagged Internal Radii (IRMN_RF) USIT-E[1]
3.7 in 2.7

Minimum of Unflagged Internal Radii (IRMN_RF) USIT-E[1]
2.7 in 3.7

Absent -0.059 -0.028 0.004 0.035 0.068
Explicit Normalization
USIT - Unflagged Casing Thickness minus Median of Unflagged Casing Thickness (THBKM_RF) USIT-E[1] (in)

Minimum of Unflagged Casing Thickness (THMN_RF) USIT-E[1]
0.1 in 0.6

Nominal Casing Thickness (THNO) USIT-E[1]
0.1 in 0.6

Median of Unflagged Casing Thickness (THAV_RF) USIT-E[1]
0.1 in 0.6

Maximum of Unflagged Casing Thickness (THMX_RF) USIT-E[1]
0.1 in 0.6

5.7 in 2.7 | 2.7 in 5.7

USIT Processing Flags (UFLG[0]) USIT-E[1]

1 - UFLG 1 Value within [0.0 - 1.5] - :	UTIM Error
2 - UFLG 2 Value within [1.5 - 2.5] - :	Pulse Origin Not Detected
3 - UFLG 3 Value within [2.5 - 3.5] - :	WINLEN Error
4 - UFLG 4 UFLG 5 UFLG 6 Value within [3.5 - 6.5] - :	Casing Thickness Error
5 - UFLG 7 UFLG 8 UFLG 9 Value within [6.5 - 10] - :	Loop Processing Error

TIME_1900 - Time Marked every 60.00 (s)

Description: USI Composite Format: Log (LBV1_USI Corrosion 7inch) Index Scale: 5 in per 100 ft Index Unit: ft Index Type: Measured Depth Creation Date: 20-Oct-2016 14:28:48

Composite 1

USI Compressed Goodwin

Composite Summary

Run Name	Pass Objective	Direction	Top	Bottom	Start	Stop	DSC Mode	Depth Shift	Include Parallel Data
Two	Log[9]:Up	Up	6640.29 ft	8171.85 ft	20-Oct-2016 9:51:39 AM	20-Oct-2016 10:20:40 AM	ON	1.47 ft	No
Two	Log[11]:Up	Up	36.69 ft	6737.51 ft	20-Oct-2016 10:24:53 AM	20-Oct-2016 12:34:00 PM	ON	1.35 ft	No
Two	Log[14]:Up	Up	5.56 ft	155.15 ft	20-Oct-2016 12:53:24 PM	20-Oct-2016 12:58:23 PM	ON	1.96 ft	No

All depths are referenced to toolstring zero

Log

Company:Southern California Gas Company Well:Frew 4

Composite 1:S008

Description: USI Goodwin Format: Log (Import of USI Goodwin) Index Scale: 0.1 in per 100 ft Index Unit: ft Index Type: Measured Depth Creation Date: 20-Oct-2016 14:29:06

TIME_1900 - Time Marked every 60.00 (s)

Minimum Acoustic Impedance 1 (MIN_AI1) USIT-E[1]	Minimum Acoustic Impedance 3 (MIN_AI3) USIT-E[1]	Minimum Acoustic Impedance 5 (MIN_AI5) USIT-E[1]	Minimum Acoustic Impedance 7 (MIN_AI7) USIT-E[1]
0 Mrayl 10	0 Mrayl 10	0 Mrayl 10	0 Mrayl 10
Maximum Acoustic Impedance 1 (MAX_AI1) USIT-E[1]	Maximum Acoustic Impedance 3 (MAX_AI3) USIT-E[1]	Maximum Acoustic Impedance 5 (MAX_AI5) USIT-E[1]	Maximum Acoustic Impedance 7 (MAX_AI7) USIT-E[1]
0 Mrayl 10	0 Mrayl 10	0 Mrayl 10	0 Mrayl 10
Average Acoustic Impedance 1 (AV_AI1) USIT-E[1]	Average Acoustic Impedance 3 (AV_AI3) USIT-E[1]	Average Acoustic Impedance 5 (AV_AI5) USIT-E[1]	Average Acoustic Impedance 7 (AV_AI7) USIT-E[1]
0 Mrayl 10	0 Mrayl 10	0 Mrayl 10	0 Mrayl 10

Minimum Acoustic Impedance 2 (MIN_AI2) USIT-E[1]	Minimum Acoustic Impedance 4 (MIN_AI4) USIT-E[1]	Minimum Acoustic Impedance 6 (MIN_AI6) USIT-E[1]	Minimum Acoustic Impedance 8 (MIN_AI8) USIT-E[1]	Minimum Acoustic Impedance 9 (MIN_AI9) USIT-E[1]	Acoustic Impedance Minimum (AIMN) USIT-E[1]
0 Mrayl 10	0 Mrayl 10	0 Mrayl 10	0 Mrayl 10	0 Mrayl 10	-1 Mrayl 9
Maximum	Maximum	Maximum	Maximum	Maximum	Acoustic

GR

0 gAPI 150

-1000.000 3.090 5.054 7.018

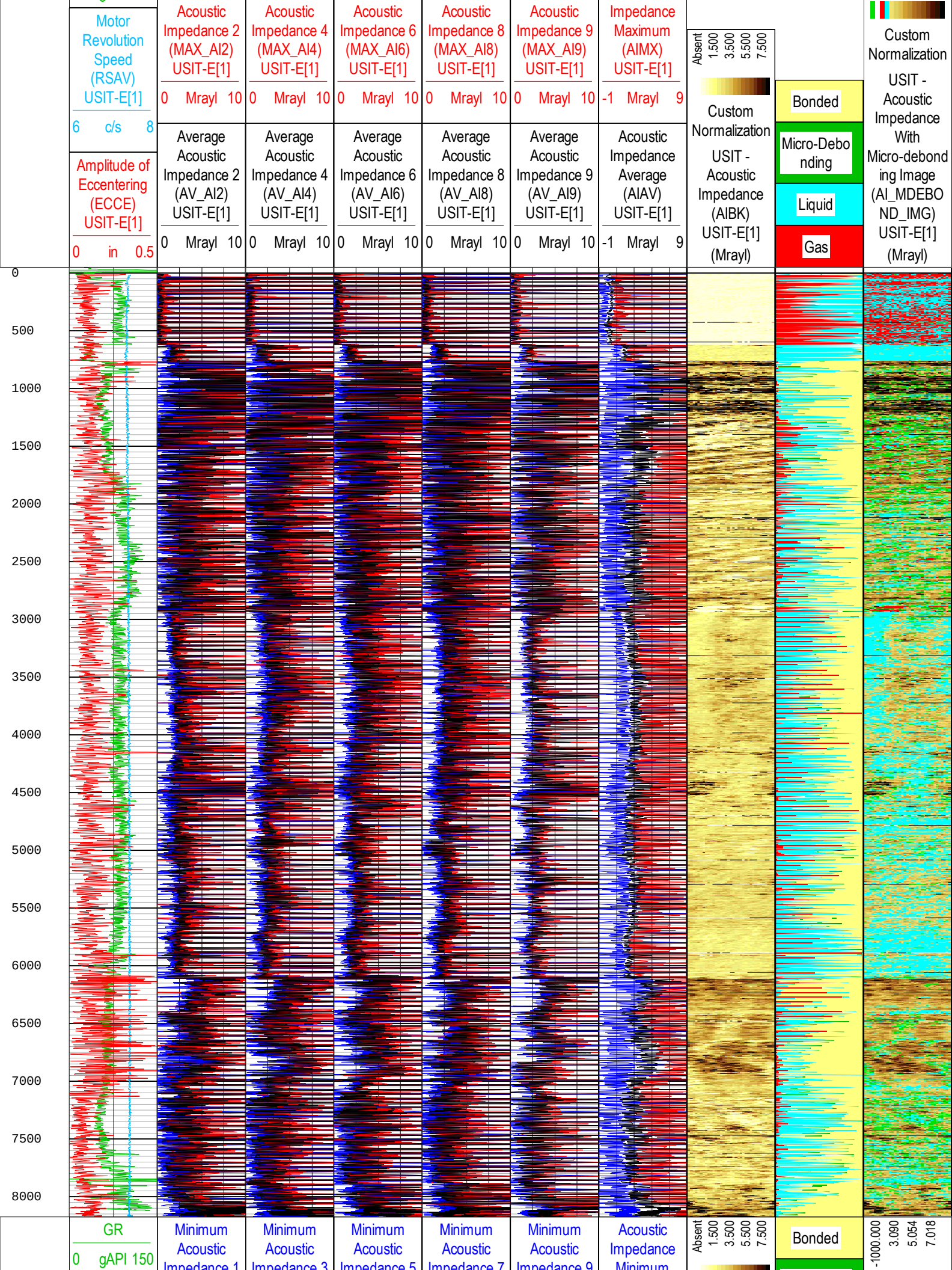
Motor Revolution Speed (RSAV) USIT-E[1]
6 c/s 8
Amplitude of Eccentering (ECCE) USIT-E[1]
0 in 0.5
Acoustic Impedance 2 (MAX_AI2) USIT-E[1]
0 Mrayl 10
Acoustic Impedance 4 (MAX_AI4) USIT-E[1]
0 Mrayl 10
Acoustic Impedance 6 (MAX_AI6) USIT-E[1]
0 Mrayl 10
Acoustic Impedance 8 (MAX_AI8) USIT-E[1]
0 Mrayl 10
Acoustic Impedance 9 (MAX_AI9) USIT-E[1]
0 Mrayl 10
Impedance Maximum (AIMX) USIT-E[1]
-1 Mrayl 9
Average Acoustic Impedance 2 (AV_AI2) USIT-E[1]
0 Mrayl 10
Average Acoustic Impedance 4 (AV_AI4) USIT-E[1]
0 Mrayl 10
Average Acoustic Impedance 6 (AV_AI6) USIT-E[1]
0 Mrayl 10
Average Acoustic Impedance 8 (AV_AI8) USIT-E[1]
0 Mrayl 10
Average Acoustic Impedance 9 (AV_AI9) USIT-E[1]
0 Mrayl 10
Acoustic Impedance Average (AIAV) USIT-E[1]
-1 Mrayl 9
Absent 1.500 3.500 5.500 7.500
Custom Normalization
USIT - Acoustic Impedance (AIBK) USIT-E[1] (Mrayl)
Bonded
Micro-Debonding
Liquid
Gas
Custom Normalization
USIT - Acoustic Impedance With Micro-debonding Image (AI_MDEBOND_IMG) USIT-E[1] (Mrayl)
0
500
1000
1500
2000
2500
3000
3500
4000
4500
5000
5500
6000
6500
7000
7500
8000
GR
0 gAPI 150
Minimum Acoustic Impedance 1
Minimum Acoustic Impedance 3
Minimum Acoustic Impedance 5
Minimum Acoustic Impedance 7
Minimum Acoustic Impedance 9
Acoustic Impedance Minimum
Absent 1.500 3.500 5.500 7.500
Bonded
-1000.000 3.090 5.054 7.018

Motor Revolution Speed (RSAV) USIT-E[1] 6 c/s 8	Impedance 1 (MIN_AI1) USIT-E[1] 0 Mrayl 10	Impedance 3 (MIN_AI3) USIT-E[1] 0 Mrayl 10	Impedance 5 (MIN_AI5) USIT-E[1] 0 Mrayl 10	Impedance 7 (MIN_AI7) USIT-E[1] 0 Mrayl 10	Impedance 9 (MIN_AI9) USIT-E[1] 0 Mrayl 10	Minimum (AIMN) USIT-E[1] -1 Mrayl 9
Amplitude of Eccentering (ECCE) USIT-E[1] 0 in 0.5	Maximum Acoustic Impedance 1 (MAX_AI1) USIT-E[1] 0 Mrayl 10	Maximum Acoustic Impedance 3 (MAX_AI3) USIT-E[1] 0 Mrayl 10	Maximum Acoustic Impedance 5 (MAX_AI5) USIT-E[1] 0 Mrayl 10	Maximum Acoustic Impedance 7 (MAX_AI7) USIT-E[1] 0 Mrayl 10	Maximum Acoustic Impedance 9 (MAX_AI9) USIT-E[1] 0 Mrayl 10	Acoustic Impedance Maximum (AIMX) USIT-E[1] -1 Mrayl 9
	Average Acoustic Impedance 1 (AV_AI1) USIT-E[1] 0 Mrayl 10	Average Acoustic Impedance 3 (AV_AI3) USIT-E[1] 0 Mrayl 10	Average Acoustic Impedance 5 (AV_AI5) USIT-E[1] 0 Mrayl 10	Average Acoustic Impedance 7 (AV_AI7) USIT-E[1] 0 Mrayl 10	Average Acoustic Impedance 9 (AV_AI9) USIT-E[1] 0 Mrayl 10	Acoustic Impedance Average (AIAV) USIT-E[1] -1 Mrayl 9
	Minimum Acoustic Impedance 2 (MIN_AI2) USIT-E[1] 0 Mrayl 10	Minimum Acoustic Impedance 4 (MIN_AI4) USIT-E[1] 0 Mrayl 10	Minimum Acoustic Impedance 6 (MIN_AI6) USIT-E[1] 0 Mrayl 10	Minimum Acoustic Impedance 8 (MIN_AI8) USIT-E[1] 0 Mrayl 10		
	Maximum Acoustic Impedance 2 (MAX_AI2) USIT-E[1] 0 Mrayl 10	Maximum Acoustic Impedance 4 (MAX_AI4) USIT-E[1] 0 Mrayl 10	Maximum Acoustic Impedance 6 (MAX_AI6) USIT-E[1] 0 Mrayl 10	Maximum Acoustic Impedance 8 (MAX_AI8) USIT-E[1] 0 Mrayl 10		
	Average Acoustic Impedance 2 (AV_AI2) USIT-E[1] 0 Mrayl 10	Average Acoustic Impedance 4 (AV_AI4) USIT-E[1] 0 Mrayl 10	Average Acoustic Impedance 6 (AV_AI6) USIT-E[1] 0 Mrayl 10	Average Acoustic Impedance 8 (AV_AI8) USIT-E[1] 0 Mrayl 10		

Custom Normalization USIT - Acoustic Impedance (AIBK) USIT-E[1] (Mrayl)

Micro-Debonding

Liquid

Gas

Custom Normalization USIT - Acoustic Impedance With Micro-debonding Image (AI_MDEBOND_IMG) USIT-E[1] (Mrayl)

TIME_1900 - Time Marked every 60.00 (s)

Description: USI Goodwin Format: Log (Import of USI Goodwin) Index Scale: 0.1 in per 100 ft Index Unit: ft Index Type: Measured Depth Creation Date: 20-Oct-2016 14:29:06

XYZ

Company:Southern California Gas Company Well:Frew 4
Composite 1:S008

Fluid Acoustic Slowness vs Depth

2D Cross Plot

Index Range: From 5.25 to 8171.50 ft

DEPTH-U-USIT_DFSL — — - DEPTH-CFVL
— — - DEPTH-FVEM (FVEM : Data Not Found)

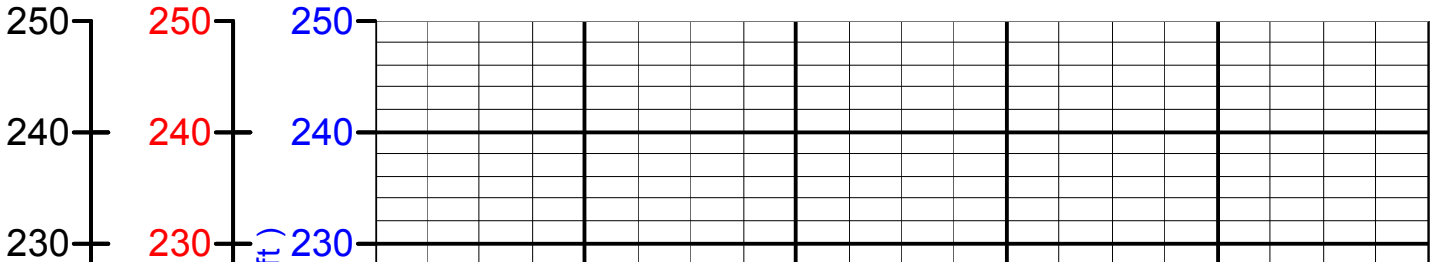

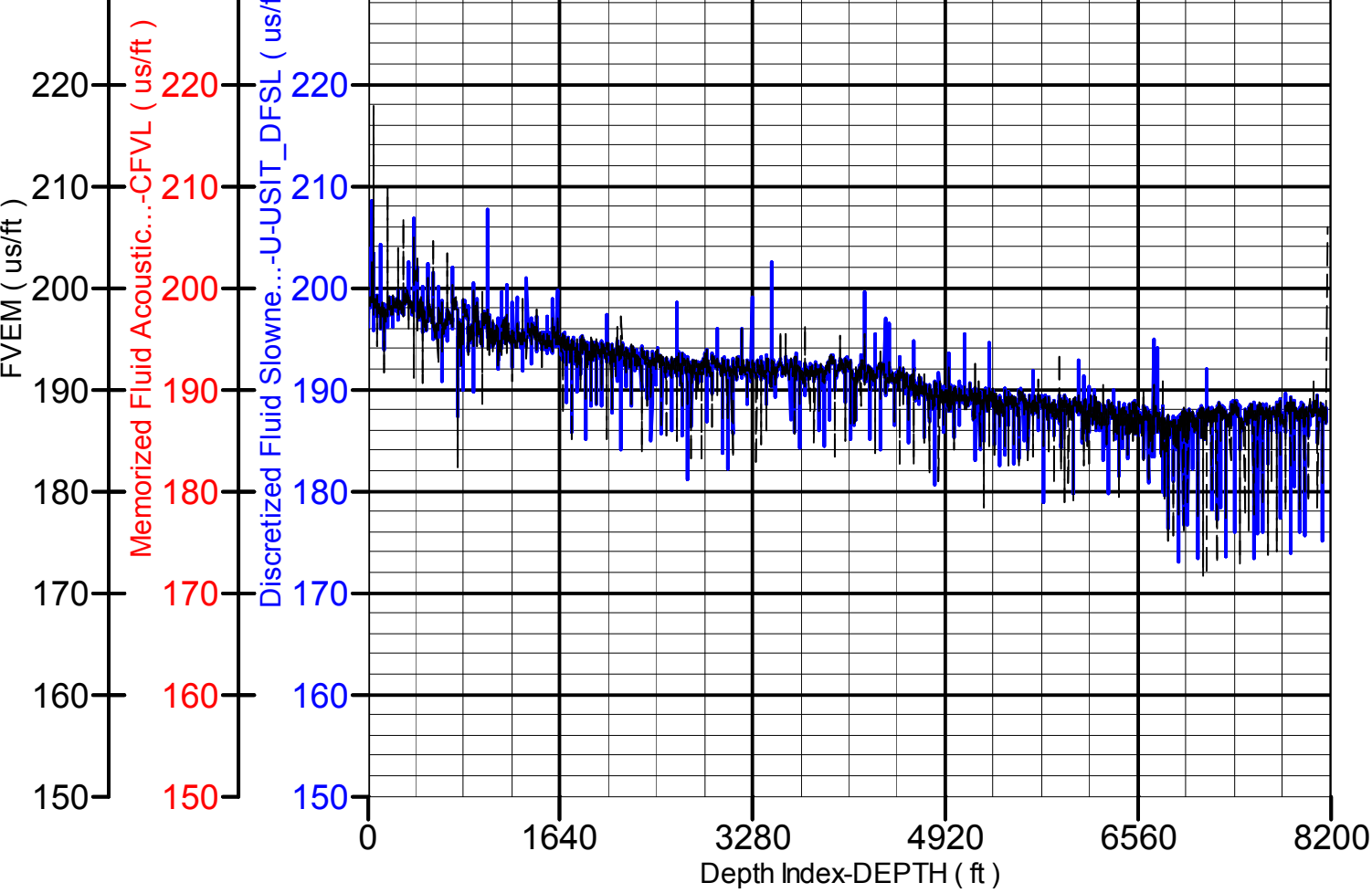

XYZ

Company:Southern California Gas Company Well:Frew 4
Composite 1:S008

Theoretical Acoustic Impedance of Mud vs Depth

2D Cross Plot

Index Range: From 5.25 to 8171.50 ft

DEPTH-CZMD
DEPTH-AIBH (AIBH : Data Not Found)
DEPTH-AIBL (AIBL : Data Not Found)
DEPTH-AIBM (AIBM : Data Not Found)

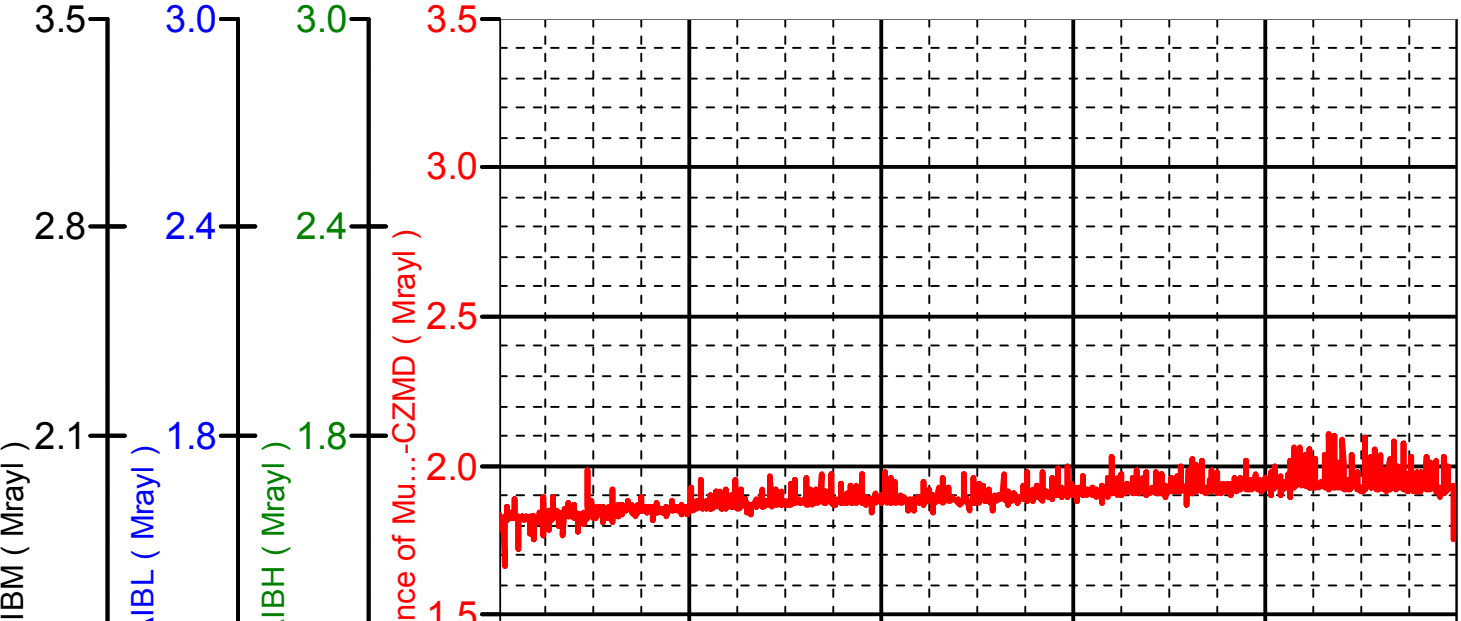

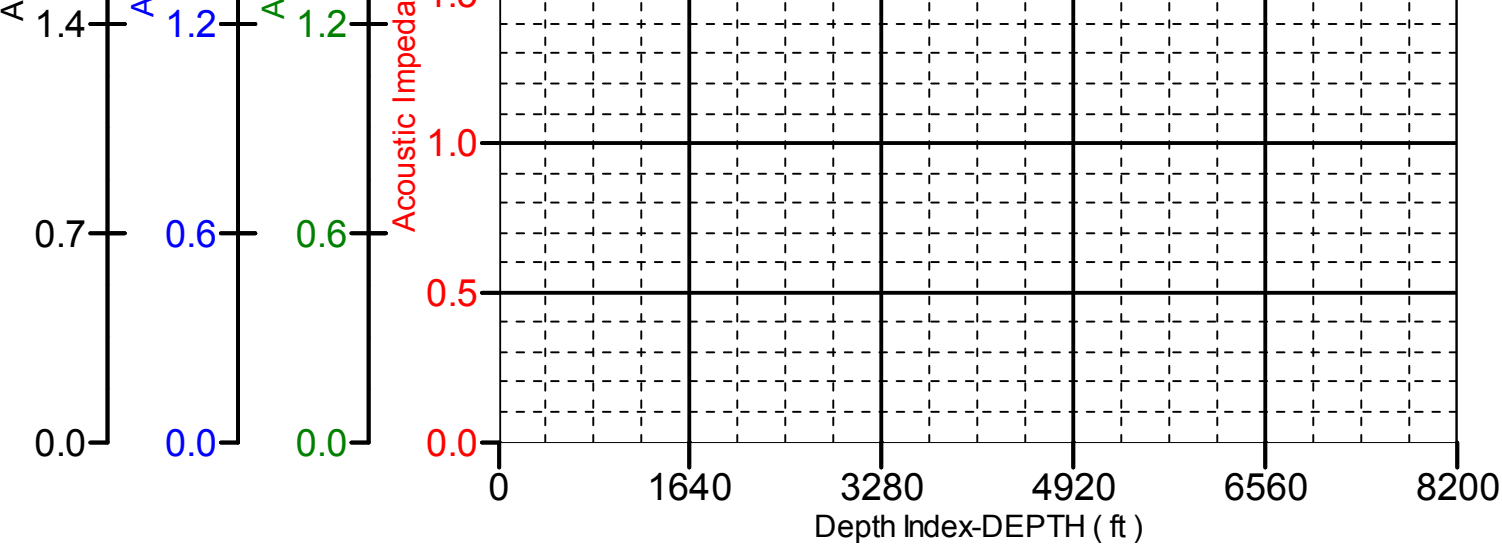

Company:	Southern California Gas Company
Well:	Frew 4
Field:	Aliso Canyon
County:	Los Angeles
State:	California

Schlumberger

Ultrasonic Imager

Ultrasonic Imager

Gamma Ray - CCL

7" casing

Ex. II - 25

Ex. II - 26

Due to the large file size, please view document DOGGR_03700761_Vertilog_1-17-1989 at the below publicly available website. The native file of this document is available upon request.

(https://secure.conservation.ca.gov/WellRecord/037/03700761/tifs/03700761_Vertilog_1-17-1989.tif) (accessed March 20, 2020)

file

SOUTHERN CALIFORNIA gas COMPANY

INTEROFFICE CORRESPONDENCE

R M Hijazi

TO M. E. Melton FROM R. M. Hijazi DATE Jan. 23, 1989

SUBJECT Casing Inspection Log and Pressure Test Results
SS-8 and SS-9, Aliso Canyon

Casing inspection logs (Vertilogs), recently run by Atlas Wireline Services, show three main areas of casing corrosion in Standard Sesnon 8 and no significant corrosion in Standard Sesnon 9.

There appears to be approximately 48% isolated metal loss in the casing in SS-8 at a depth of 3253' and approximately 45% metal loss at depths of 3314' and 3321'. Recent temperature surveys do not indicate anomalies at these depths. Both SS-8 and SS-9 were pressure tested to 1900 psi at the surface using 63 #/ft3 fluid in the hole. Neither of the two wells leaked.

RMH:hr

64-F

Ex. II - 27

MICROBIOLOGICALLY INFLUENCED CORROSION (MIC):

Methods of Detection in the Field

GRI Field Guide 1990

Microbiologically Influenced Corrosion (MIC):

Methods of Detection in the Field

GRI Report No. ~~88/0113~~ 90/0299 [revised 1991]

Gas Research Institute
Chicago, Illinois

GRI FIELD GUIDE 1991

Legal Notice

This document was prepared by Bioindustrial Technologies, Inc. (BTI), Siebert Materials Engineering, Inc. (SMEI), Midwest Research Institute (MRI), and Radian Corporation as an account of work sponsored by the Gas Research Institute (GRI). Neither GRI, members of GRI, nor any person acting on behalf of them:

a. Makes any warranty or representation, expressed or implied, with respect to accuracy, completeness, or usefulness of the information, method or process disclosed in this report may not infringe privately owned rights; or

b. Assumes any liability with respect to the use of, or for damages resulting from the use of, any information, apparatus, method, or process disclosed in this report;

c. References to trade names or specific commercial products, commodities, or services do not represent or constitute an endorsement, recommendation, or favoring by GRI, SMEI, MRI, or Radian of specific commercial product, commodity, or service.

Acknowledgments

This field guide has been prepared under the direction of the Gas Research Institute. A preliminary version of this guide was prepared under GRI Contract 5086-271-1208 in June 1988 as GRI Report 88/0113 and field tested by several gas pipeline companies. The field guide was compiled by Bioindustrial Technologies, Inc., Siebert Materials Engineering, Inc., and Midwest Research Institute. The 1990 version was produced under GRI Contract 5088-260-1747, under the direction of Mr. James R. Frank. The 1991 update was produced as part of GRI Contract 5088-260-1747 with Radian Corporation under the direction of GRI Project Manager Daniel Werner.

Table of Contents

Purpose of This Guide 1
Background Information 2
External Corrosion Site Samples 3
Internal Corrosion Site Samples 3
How To Use This Guide 4
Materials Needed 6
Procedure for Determining MIC at Suspected Corrosion Sites 7
Mechanical Removal 9
Additional Mechanical Cleaning 9
Final Mechanical Cleaning 10
Scoring Samples Other Than Corrosion Product 12
Site Information Form
Summary Data Sheet

Figure 1 - Localized External Corrosion with Deposits, Pits, Craters and Some General Attack 13

Figure 2 - Disbonded Pipeline Coating Associated with Localized External Corrosion 14

Figure 3 - Example of a Biological Test Kit (Shows MICKIT™ III-C) 15

Figure 4 - Media Reactions for SRB, APB, and Uninoculated 16

Figure 5 - Media Reactions for APB, SRB, Anaerobes and Aerobes 17

(Continued)

Figure 6 - Condition of Pipe After Brush-Blast Sandblasting 18

Figure 7 - Close-up of Sandblasted Surface Showing MIC Pattern 19

Figure 8 - Cup-Type Scooped Out Hemispherical Pits on Flat Surfaces with Craters in Pits 20

Figure 9 - Corrosion Pits with Striations 21

Figure 10 - Corrosion Pits with Striations 22

Figure 11 - Surface Pit Showing Corrosion Product in Pit 23

Figure 12 - Same Pit After Corrosion Product is Scraped Out 24

Figure 13 - Same Pit After Cleaning with Nylon Brush (Note Cup-Like Pits Inside Large Pit) 25

Figure 14 - Cross-Section of Pit Showing Tunnels (20X Magnification) 26

Figure 15 - Close-up View of Tunnels (100X Magnification) 27

Purpose of This Guide

This guide is designed to help gas industry personnel determine whether or not the corrosion occurring at a particular site is microbiologically influenced corrosion (MIC) and to provide data useful to GRI's ongoing research program. It is useful for determining whether bacteria potentially capable of causing MIC are present in large numbers in fluid samples. Additionally, the data collected by users of this field guide are important in identifying the types of sites most susceptible to MIC and the effects of environmental factors and materials on MIC processes.

This version of the field guide primarily addresses external pipe corrosion and readily accessible internal corrosion sites and is the result of research funded by the Gas Research Institute and the collaboration of interested gas pipeline companies. Future guides will address monitoring of fluids, on-line monitoring methods, cathodic protection, and coatings. Continuing research by GRI will continue to focus on the development of practical and cost-effective methods of mitigating MIC in the gas industry.

Background Information

Microbiologically influenced corrosion is seldom attributed to the action of just one type of microorganism, but more often to the activities of several different organisms which form a community. Because microbial communities are common inhabitants in the environment, MIC is a problem in many industries.

A common type of MIC results in localized attack of carbon steels in the form of pitting, although some general attack takes place as well (see Figure 1). Some cases of severe pitting found under nodules formed at holidays in coatings have been attributed to MIC. Intact coatings may provide some protection against MIC; however, when holidays occur, corrosion often exists under the adjacent disbonded coating (see Figure 2).

Three types of evidence are used to estimate whether MIC is likely at a particular site: metallurgical, chemical, and biological. The GRI program has discovered that the presence of the metallurgical fingerprint is fairly definitive. Chemical and biological data are supportive, and are useful for estimating whether a potential for MIC exists in cases where only fluid samples are available or where corrosion has not progressed so that a metallurgical fingerprint is clearly defined.

The MIC of carbon steels usually has been attributed to sulfate-reducing bacteria (SRB). Recent evidence suggests that many other microorganisms, principally anaerobic and facultatively anaerobic bacteria, are also involved in the corrosion of carbon steel in part due to their ability to produce organic acids.

External Corrosion Site Samples

External samples are usually portions of the corrosion products on the outer surface of excavated pipe and include nodules, pit contents, and scale. Samples of soil or water on, or adjacent to, the pipe can also be tested for MIC-related organisms. However, bacteria are frequently found in soil whether or not corrosion is present. Therefore, a positive soil test for MIC-related microorganisms is not confirmation of MIC, but it is an indicator of the potential for MIC at that site.

Internal Corrosion Site Samples

Internal samples are usually water or other liquids obtained from inside pipes, separators, drips, or water dumps. Analysis of liquid samples does not always give an accurate assessment of MIC activities occurring at the pipe surface; rather, they are an indication of the potential for MIC and the effectiveness of treatments being applied. Refer to "Scoring Samples Other Than Corrosion Product" for procedures to be used with these samples. Installation of sidestream test loops is the best way to monitor sessile bacteria, internal corrosion, and treatment methods. In the event

thata pipe is opened, samples of nodules, scale, pit contents, or biofilm material can be collected for analysis. These samples can be used in the following procedures.

How To Use This Guide

This guide is to be used by corrosion technicians during examination of a corrosion site. Data sheets are included for recording information and observations at the corrosion site. Corrosion characteristics and test results are assigned numerical values and then used to determine the probability that the corrosion is MIC.

For biological and chemical analyses, any brand of test kit capable of estimating numbers of SRB and acid-producing bacteria (APB) and chemical parameters is suitable. For purposes of providing GRI with a standarized data set, consistent with data previously collected for GRI, the use of MICKIT™ III-C and IV is encouraged but not essential. A set of detailed instructions is included in these test kits.

Read the entire guide and have materials ready before you begin sampling. Once the site is exposed, pit material or corrosion product should be collected and processed immediately.

Key Contacts

Address questions regarding the GRI program to:

Mr. Daniel Werner
Pipeline Operations Research
Gas Research Institute
8600 West Bryn Mawr Avenue
Chicago, IL 60631
(312)399-8306

Address additional questions and MICKIT requests to:

Dr. Dan Pope
Bioindustrial Technologies, Inc.
40200 Industrial Park Circle
Georgetown, TX 78626
(512)869-0580

To order additional Field Manuals, blank data forms, MIC videotape, or 1989 Annual Report contact:

Ms. Jane Wessels
Radian Corporation
8501 N. Mo-Pac Blvd.
P.O. Box 201088
Austin, TX 78720-1088
(512)454-4797

Other sources of information on MIC:

National Association of Corrosion Engineers
1440 South Creek Drive
Houston, TX 77084-4906
(713)492-0535

Materials Needed

These materials can be purchased separately or in kit form. As indicated earlier, GRI's data base has been developed using MICKIT™ III C test kit for acid-producing bacteria (APB) and sulfate-reducing bacteria (SRB) and MICKIT™ IV test kit for chemical analysis.

To test for APB and SRB

Depending upon the test kit used, it may include the following:

- media for detection of APB and SRB
- any standard SRB media (for detection of SRB)
- ADS sample collection bottle
- two 3-cc syringes with 21-gauge needles
- alcohol spongette
- 1 sterile wooden sampling stick
- 1 cotton swab (for sampling biofilms)
- styrofoam tray to hold and protect bottles

To test for chemical composition of corrosion product

Test kits should include:

- 3 normal HCl
- sulfide indicator strips
- Fe^{2+} indicator strips
- Fe^{3+} indicator strips
- sodium acetate
- potassium oxalate
- pH paper
- deionized water
- disposable sample cuvettes

Notes: These items can be purchased separately.
MICKIT III C and IV are trademarks of Bioindustrial Technologies, Inc.

Other equipment

Hand lens/field microscope (5X-60X)
Metal cleaning equipment
  spatula/pocket knife
  nylon brush (toothbrush)
  brass wire brush
  pit depth gauge
  sandblasting equipment (if available)
35-mm camera

When possible, take color photographs of the involved area (e.g., pit, nodule, debris, etc.) **before** and **after** sampling and cleaning.

Procedure for Determining MIC at Suspected Corrosion Sites

Prior to excavation, have kit in hand. Also measure pipe-to-soil potential before excavation.

The pipe should be excavated carefully to avoid disturbing the surface conditions at the sampling site. The coating around the suspected area of corrosion should be carefully removed using a knife or similar instrument. Sample contamination must be kept to a minimum; therefore, avoid touching the corrosion product or soil to be sampled with hands or tools other than those to be used in sample collection.

Once the site is exposed, pit material or corrosion product should be collected and processed immediately.

Fill out the Site Information Form as the required information becomes available. All of the information requested may not be available. Please provide as much as possible since this information will become part of the GRI MIC research program data base. The information provided will be coded and considered confidential and will not be reproduced with reference to company name or geographic location.

Three types of evidence are used to estimate whether MIC is likely at a particular site:

- metallurgical fingerprint (fairly definitive)
- biological (supportive), and
- chemical (supportive).

Determine whether nodules (discrete "buildup" of deposits) or aggregates of these are present at the corrosion site (see Figures 1, 2, and 11 for examples from field sites). If so, record the information on the GRI Summary Data Sheet (question no. 1). The Site Information Form and the Summary Data Sheet are shown on pages 28 and 29 of this handbook. A supply of these forms accompanies a copy of the field guide. Extra forms are available from Radian Corporation (c/o Jane Wessels), P.O. Box 201088, Austin, Texas 78720-1088 (512/454-4797).

After the proper incubation period, interpret the media reactions according to kit directions (see Figures 4 and 5). Record the number of bottles showing positive results for each type media on the Summary Data Sheet (question no. 2). For example, if four turbid MC media bottles and three black SRB media bottles were observed, you would record 4 and 3 on the Summary Data Sheet.

Observe metal and pit contents under the deposits. Record the results on the Summary Data Sheet (question no. 3).

An area that was scraped shiny should not be recorded as shiny metal.

Using the test kit for chemical analysis, determine the presence of carbonate, sulfide, calcium, iron and pH. Follow the directions included with the kit. Record the results on the Summary Data Sheet (question no. 4).

Any deposit remaining over or in the corrosion site should be carefully removed so as not to damage the metal surface. Follow the procedure below for cleaning the pipe surface.

Mechanical Removal

Start by removing the deposit using a clean spatula or pocket knife, being careful not to dig into the metal. After removing as much deposit as possible without damaging the metal, continue cleaning with a dry stiff brush (e.g., a nylon toothbrush).

Do not use a metal brush since it can damage the metallurgical pattern. If the dry brush does not completely remove the material, the deposit should be wetted and brushed again. Dry the area with a blast of compressed air or rub the area with the alcohol swab.

Additional Mechanical Cleaning

If the surface is not yet clean, a brass wire brush may be used. To limit the damage to the metallurgical picture, brush only in the direction of the length of the pipe.

Final Mechanical Cleaning

If the surface is not yet clean, use a light/blast type sandblast at low air pressure (75-125 psi). The sand used by GRI investigations for this purpose is:

Ottawa Industrial Sand
Designation: F125 Mesh: AFS grain fineness 126; average mesh size 183.126
Density: 103.5 lb/cu ft (compacted); 87.0 lb/cu ft (uncompacted)

Refer to Figure 6 for an example of typical surface deposit condition as excavated and after sandblasting.

The clean corrosion site should be examined first with the unaided eye and then using a low power (e.g., 5X to 60X) magnifying lens or microscope. Low-power hand microscopes can be obtained from Cole-Parmer, Radio Shack, and other distributors.

Compare the observed surface with those in Figures 7 to 13, which are examples of MIC. Record the results on the Summary Data Sheet (question no. 5).

1. Look for cup-type, scooped-out hemispherical pits on the flat surface of the pipe and craters up to 2 to 3 inches across. Sometimes the cup-type pits occur on the inside surface of the craters, as in Figures 7, 8, 11, 12, and 13. If present, record this on the Summary Data Sheet.

2. Look for the striation lines (contour lines) that run parallel to the length of the pipe, as in Figures 7, 9, and 10. If present, record the results on the Summary Data Sheet.

3. Look very carefully at the surface of the craters. Look for tunnels on the upstream and downstream surfaces of the craters. They should also run parallel to the length of the pipe, as in Figures 7 and 11 to 15. If present, record this on the Summary Data Sheet.

4. Are the tunnels in the direction that is parallel to the rolling direction of the pipe? If so, record this on the Summary Data Sheet.

Tally the results on the Summary Data Sheet (question no. 6), and use the scoring guide on the sheet to determine the probability that the corrosion is microbially related.

Scoring Samples Other Than Corrosion Product

Test results on samples of soils on or adjacent to the pipe and liquids (produced or process waters, hydrocarbons, etc.) should be viewed as indicators of the potential of MIC, since these samples are in contact with pipe surfaces. The only way to score the sample for the probability of MIC is by using bacterial culture and sulfide results. In general, positive results will occur for the presence of bacteria; however, the more bacteria present, the greater the potential exists for the development of MIC if the pipe is not properly coated, cathodically protected, or maintained. Record the data on the Summary Data Sheet in the section noted for samples other than corrosion product (question no. 7). Use the scoring system for samples other than corrosion product to help determine the potential for MIC. Subsequent field guides will address these samples in more detail.

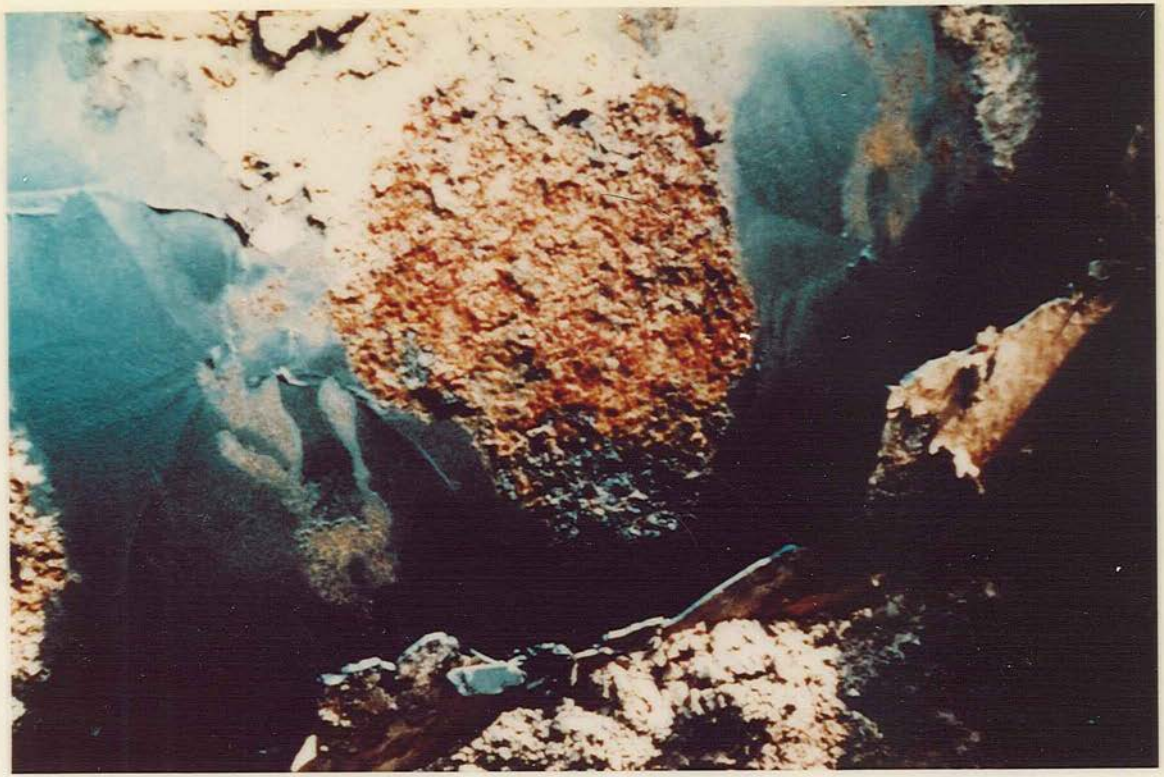

Figure 1. Localized External Corrosion with Deposits, Pits, Craters and Some General Attack

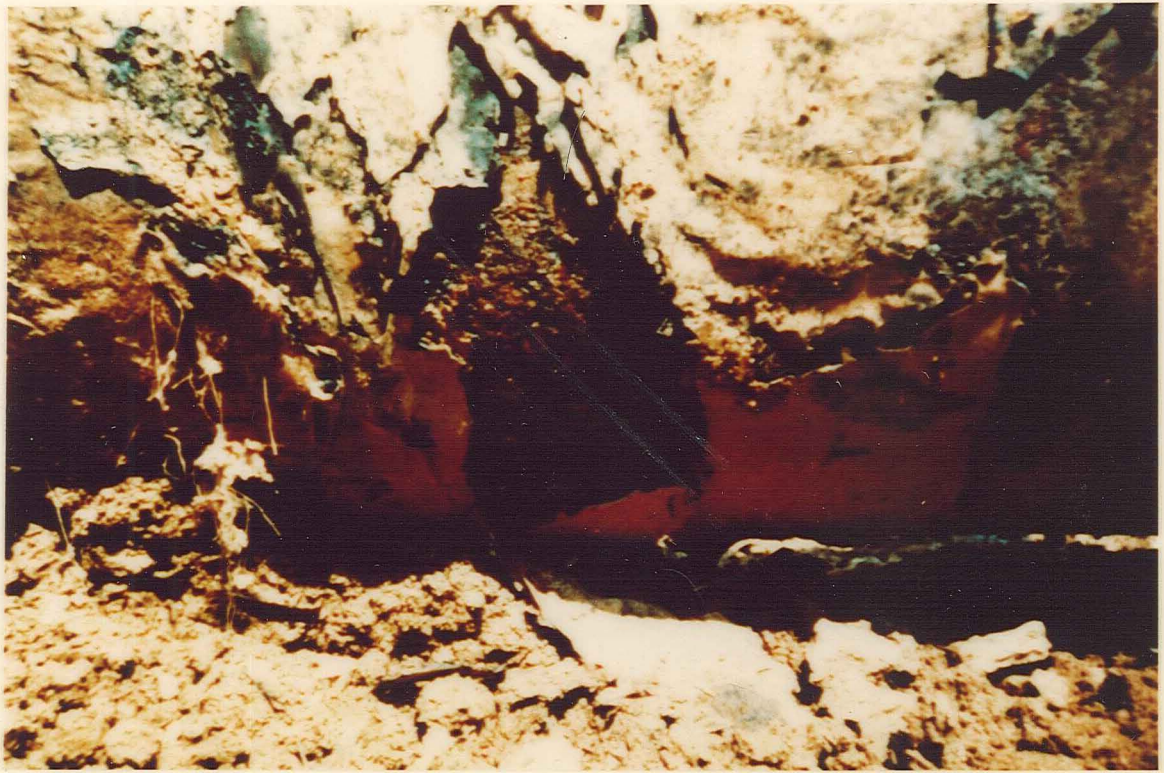

Figure 2. Disbonded Pipeline Coating Associated with Localized External Corrosion

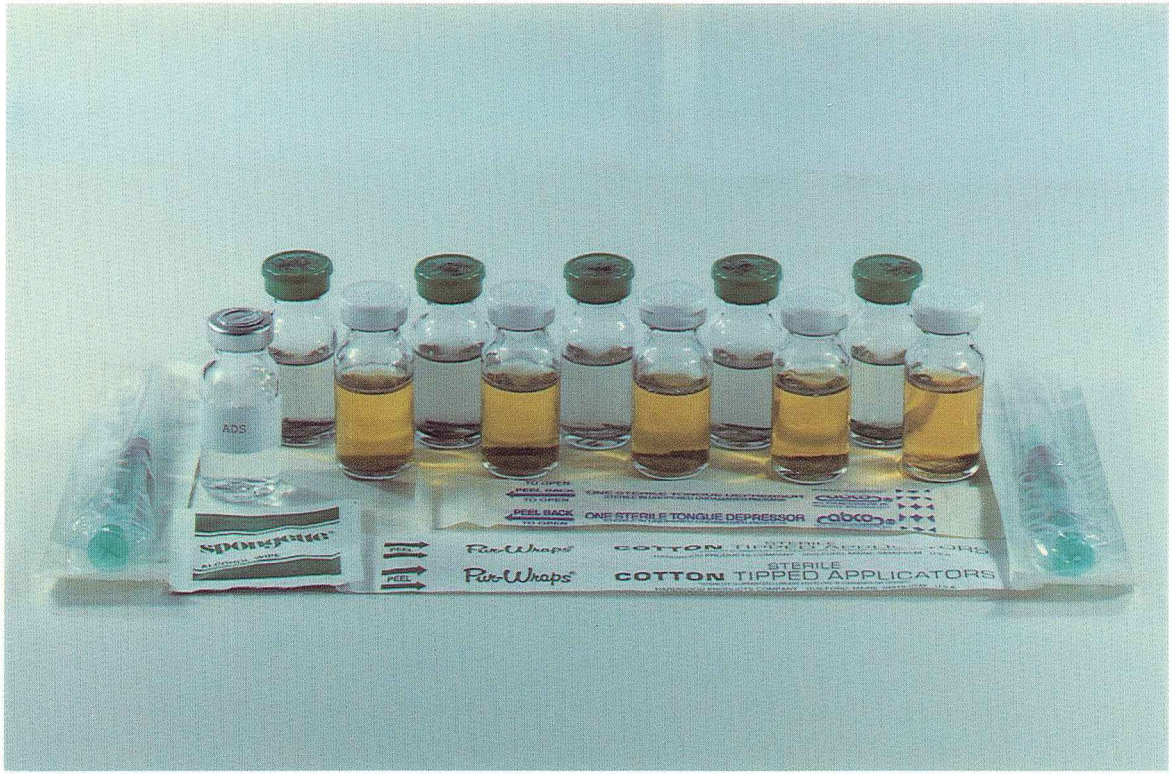

Figure 3. Example of a Biological Test Kit (shows MICKIT™ III C)

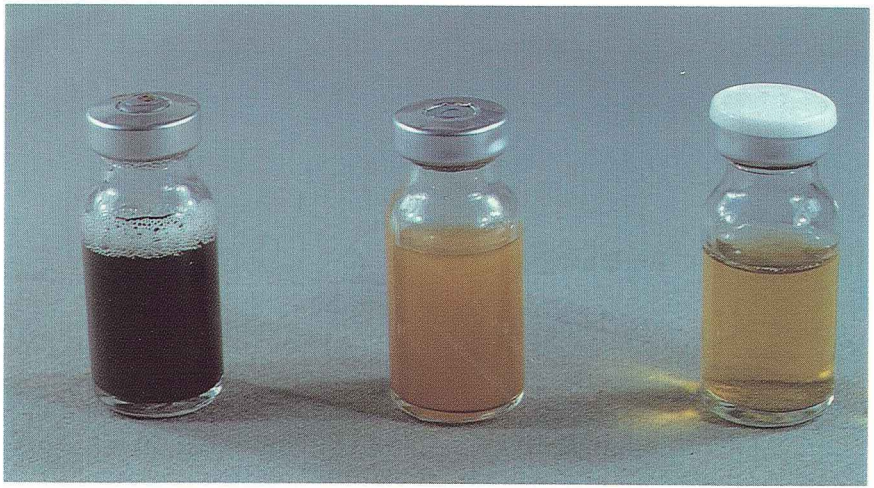

BLACK
Positive
for SRB

TURBID
Positive
for APB

UNINOCULATED

Figure 4. BTI-MC Media Reactions for SRB, APB, and Uninoculated

NEGATIVE	YELLOW Positive for APB	NEGATIVE	BLACK Positive for SRB	NEGATIVE	TURBID Positive for ANAEROBES	NEGATIVE	TURBID Positive for AEROBES

Figure 5. Media Reactions for APB, SRB, Anaerobes and Aerobes

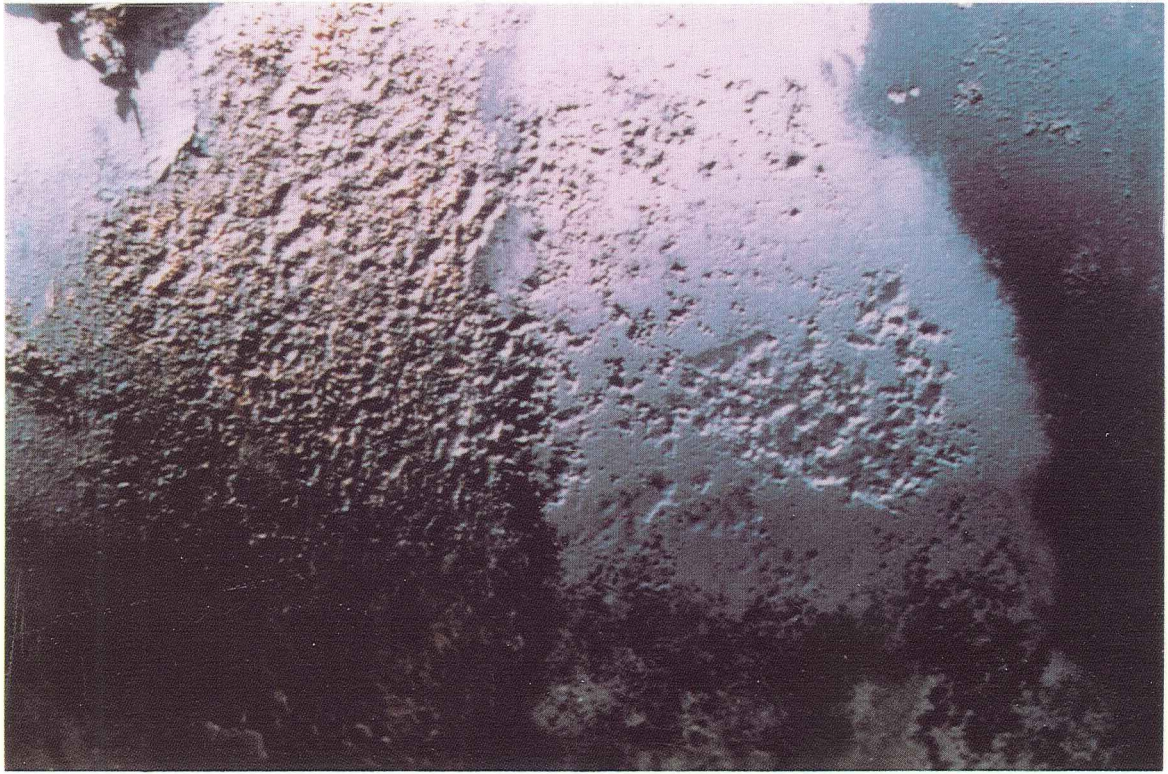

Figure 6. Condition of Pipe After Brush-blast Sandblasting

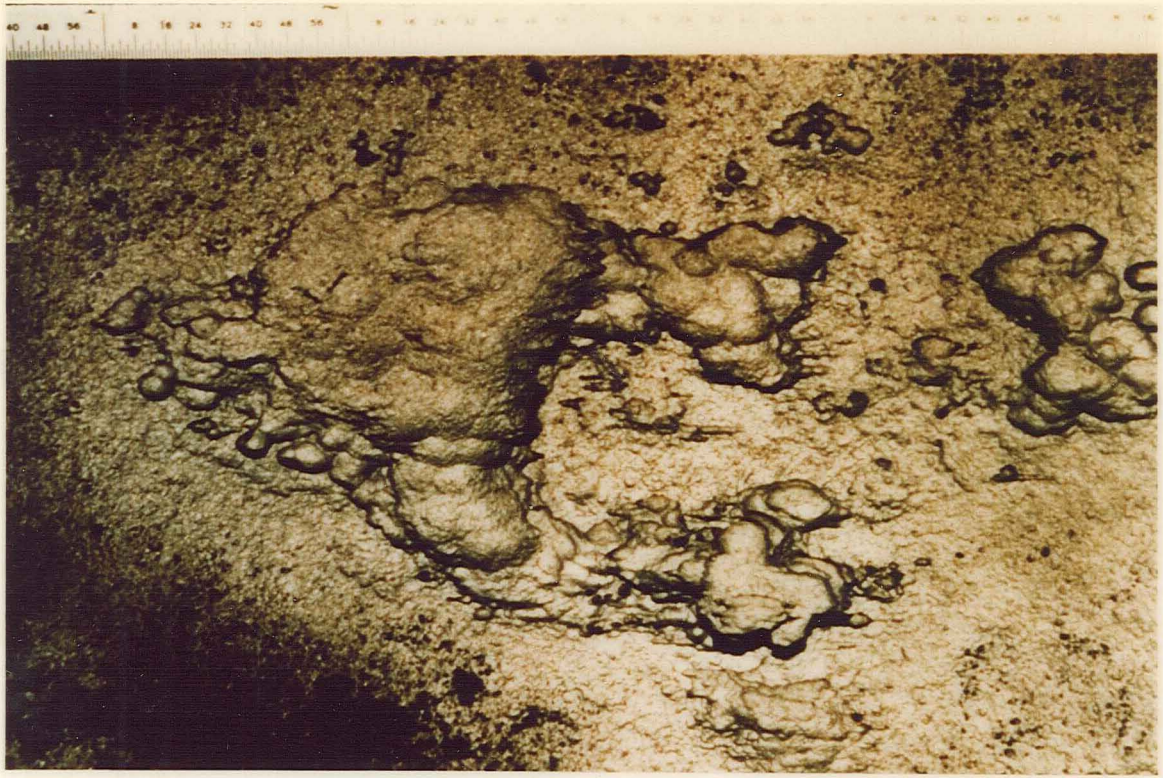

Figure 7. Close-up of Sandblasted Surface Showing MIC Pattern

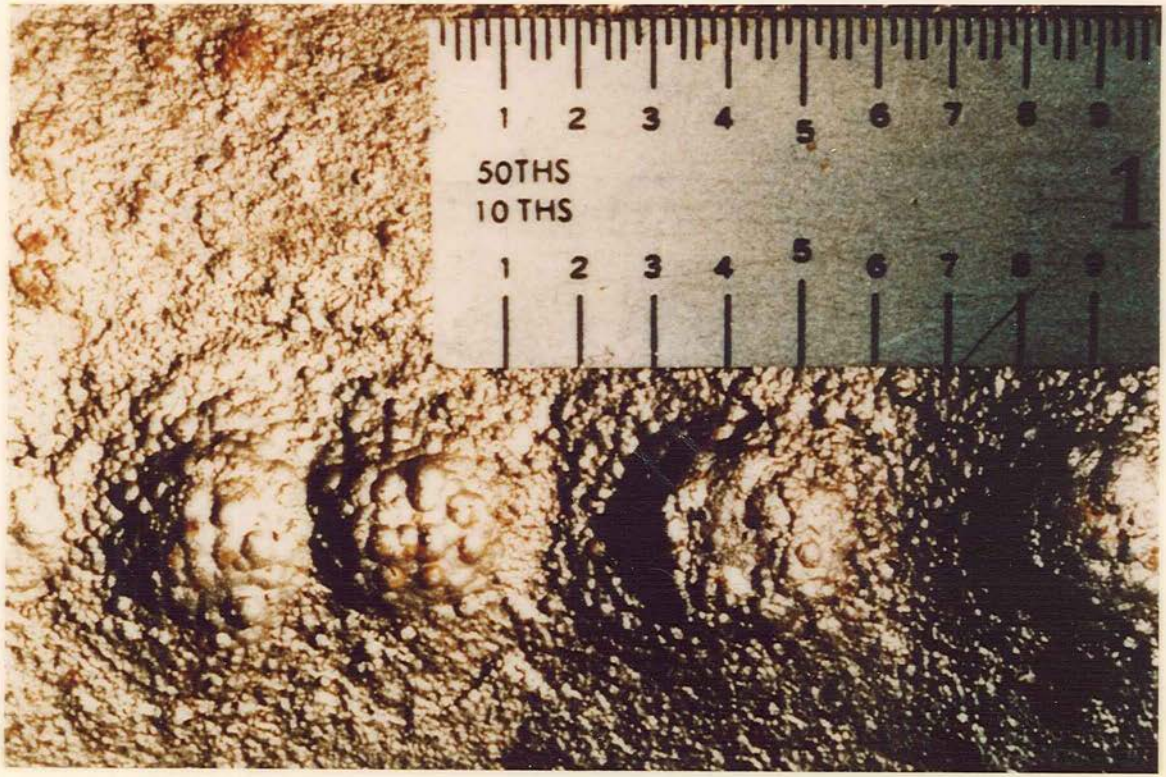

Figure 8. Cup-type Scooped Out Hemispherical Pits on Flat Surfaces with Craters in Pits

Figure 9. Corrosion Pits with Striations

Figure 10. Corrosion Pits with Striations

Figure 11. Surface Pit Showing Corrosion Product in Pit

Figure 12. Same Pit After Corrosion Product is Scraped Out

Figure 13. Same Pit After Cleaning with Nylon Brush (Note Cup-like Pits Inside Large Pit)

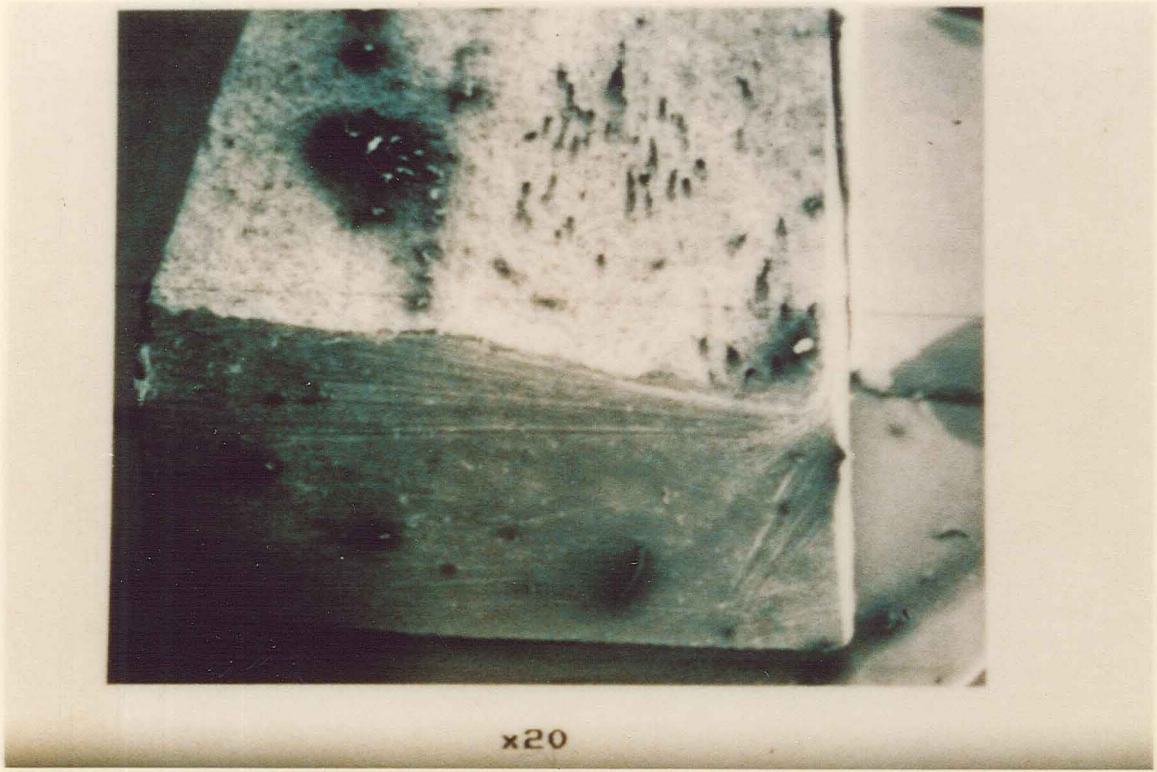

Figure 14. Cross-section of Pit Showing Tunnels (20X Magnification)

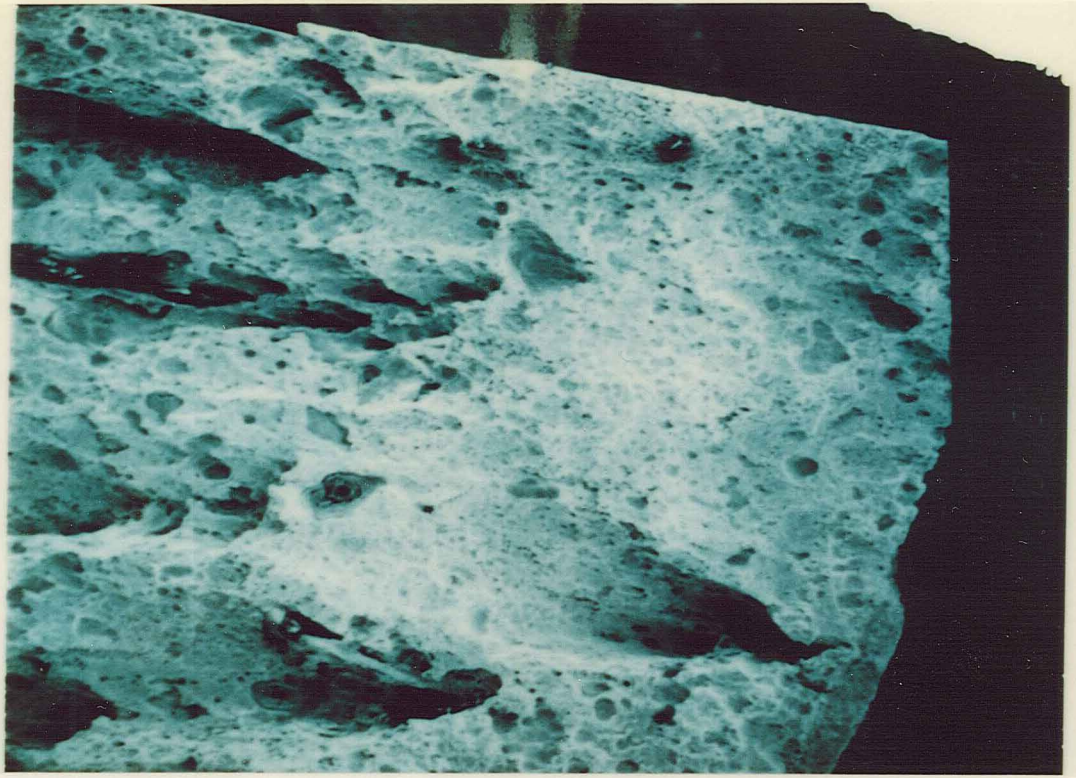

Figure 15. Close-up View of Tunnels (100X Magnification)

GRI SITE INFORMATION FORM

Provide as much information as possible.

Information Regarding Location and Company

Pipeline Company _____ Date inspected _____

Pipe location _____ Pipeline No. _____

State/County _____ Pipeline section No. _____

Information Regarding Pipe

Manufacturer _____ Wall thickness _____

Age of pipe _____ Pipe grade _____

Leak history _____ Specifications _____
(SML5, ERW, DSAW)

Information Regarding Coating

Manufacturer _____ Condition _____

Type coating _____ Bond to pipe _____

Type recoating _____ Water under coating? _____

Information Regarding Soil and Site

Type terrain _____ Pipe depth _____

Type soil _____ Odor at site? _____

Soil resistivity _____ Moisture at pipe? _____

Soil pH _____ Other _____

Information Regarding Corrosion Site and Products

Pipe thickness _____ Length of pit family _____

Color of sample _____, Maximum pit depth _____

Information Regarding Storage and Production Sites

Formation _____ pH of liquids _____

Iron in liquid _____ Manganese in liquid _____

Other chem. info. _____ Other chem. info. _____

Biocide used _____ Corrosion inhibitor _____

Other chemicals _____ Other information _____

History of chemicals in use, if known _____

Additional comments _____

Send completed forms and request blank forms from:

Radian Corp.
8501 Mo-Pac Blvd.
P. O. Box 202088
Attn: Ms. Jane Wessels
(512) 454-4797

GRI SUMMARY DATA SHEET
Scoring Corrosion Samples

What media type did you use? (Results may differ between commerical types.)

Media Type	Formula Used	Company
MC	_____	_____
APB	_____	_____
SRB	_____	_____

Question No.	Points	Score
1. Are deposits present? _____	Yes = 1	_____
Approximate number _____		
Approximate size _____		
2. Number of positive (turbid) bottles of MC media	_____	
Number of positive (black) bottles of SRB or MC media	_____	
Record the higher number of positive bottles above (0-5) (MC or SRB, not both)		_____
3. Are pit contents grey or black?	Yes = 1	_____
Is metal surface under the deposit shiny or black?	Yes = 1	_____
4. Calcium carbonate present? or	Yes = 0	_____
Iron carbonate present? or	Yes = 2	_____
Calcium and iron carbonate? and	Yes = 1	_____
Sulfide present?	Yes = 1	_____
5. Are cup-type pits present?	Yes = 1	_____
Are striation lines present?	Yes = 1	_____
Are tunnels present?	Yes = 5	_____
Are tunnels rolling direction?	Yes = 1	_____

Probability of MIC: **Total Score**

6. ≤6 Very unlikely 7-10 Likely ≥11 Very likely

Scoring Samples Other Than Corrosion Products

7. A positive sulfide reaction?	Yes = 1	_____
Highest number of positive bottles in MIC or SRB media (not both!)		_____
	Total Score	_____

Probability of MIC:

<3 points
low probability

>3 points
high probability

Ex. II - 28

© 2002 ASM International. All Rights Reserved.© 2002 ASM International. All Rights Reserved. www.asminternational.org
ASM Handbook Volume 11: Failure Analysis and Prevention (#06072G)

Biological Corrosion Failures

Thomas R. Jack, NOVA Chemicals Ltd.

MICROORGANISMS can directly or indirectly affect the integrity of many materials used in industrial systems. Most metals, including iron, copper, nickel, aluminum, and their alloys, are more or less susceptible to damage (Ref 1–3). Only titanium and its alloys appear to be generally resistant (Ref 4). This review focuses initially on the mechanisms of microbially induced or influenced corrosion (MIC) of metallic materials as an introduction to the recognition, management, and prevention of microbiological corrosion failures in piping, tanks, heat exchangers, cooling towers, and so on. Numerous reviews of MIC have appeared over the last decade (Ref 2, 5–12). Two recent publications (Ref 13, 14) present broader discussions of MIC, including a useful introduction to microbial problems seen with nonmetallic materials such as polymers, composites, concrete, glass, wood, and stone.

Viable microorganisms can be found over a surprisingly wide range of temperature, pressure, salinity, and pH (Ref 1). In the 1950s, pioneering work by Zobell isolated sulfate-reducing bacteria (SRB) that grew at 104 °C (219 °F) and pressures of 1000 bar from oil-bearing geological formations deep underground (Ref 15). Microbial communities exist in environments as diverse as subzero snowfields to deep ocean thermal vents. Halophiles evolved to live at extreme salinities turn pink the evaporation pans used to win salt from seawater. Sulfur-oxidizing bacteria create very acidic conditions (pH < 1) by producing sulfuric acid as an end product of their metabolism, while other microorganisms survive the opposite end of the pH scale. Given these examples, it should not be surprising that microorganisms have been implicated in the accelerated corrosion and cracking of a correspondingly wide range of industrial systems. For example, the involvement of thermophilic SRB in the severe intergranular pitting of 304L stainless steel condenser tubes in a geothermal electrical power plant operating at >100 °C (> 210 °F) has been reported (Ref 16). In another example, microbiological activity and chloride concentrated under scale deposits were blamed for the wormhole pitting of carbon steel piping used to transport a slurry of magnesium hydroxide and alumina at pH 10.5 (Ref 17).

Whatever the environmental conditions, microorganisms need water, a source of energy to drive their metabolism, and nutrients to provide essential building materials (carbon, nitrogen, phosphorus, trace metals, etc.) for cell renewal and growth. An understanding of these factors can sometimes help in failure investigations. Energy may be derived from sunlight through photosynthesis or from chemical reactions. The importance of photosynthetic metabolism is limited in the context of this article to above-ground facilities or submerged structures that receive sunlight. For closed systems and buried facilities, microbial metabolism is based on energy derived from oxidation reduction (redox) reactions. Under aerobic conditions, reduction of oxygen to water complements the metabolic oxidation of organic nutrients to carbon dioxide. Under anaerobic conditions, electron acceptors other than oxygen can be used. Figure 1 illustrates the range of pH and redox potential where anaerobic forms of microbial metabolism tend to be found (Ref 18).

Whatever the metabolism, electrochemical reactions catalyzed by enzymes provide energy for cell growth. Many of these reactions are not important under abiotic conditions, because they are kinetically slow in the absence of organisms. By promoting these reactions, microbes produce metabolites and conditions not found under abiotic conditions. In some cases, electrons released by the oxidation of metals are used directly in microbial metabolism. In other cases, it is the chemicals and conditions created by microbial activity that promote MIC. Secondary effects can also be important. These include such things as the biodegradation of lubricants and protective coatings designed to prevent wear or corrosion in an operating system, or the alteration of flow regimes and heat-transfer coefficients due to the biological fouling of metal surfaces.

Given the potential impact of MIC on a wide range of industrial operations, it is not surprising that microbiological effects are of significant concern in failure analysis and prevention. Microbially induced corrosion problems afflict water-handling operations and manufacturing processes in oil and gas production, pipelining, refining, petrochemical synthesis, power production, fermentation, waste water treatment, drinking water supply, pulp and paper making, and other industrial sectors. Microbially induced corrosion is also a concern whenever metals are exposed directly to the environment in applications including marine or buried piping, storage tanks, ships, nuclear waste containers, pilings, marine platforms, and so on.

Microbial Involvement in Corrosion

Corrosion involves the oxidation of metal atoms, *M*, in an anodic region with a loss of electrons to a complementary reduction reaction in a cathodic region elsewhere on the metal surface (Fig. 2). In the reduction reaction, an electron acceptor, *X*, receives the electrons given up by the oxidation process. The driving force for corro-

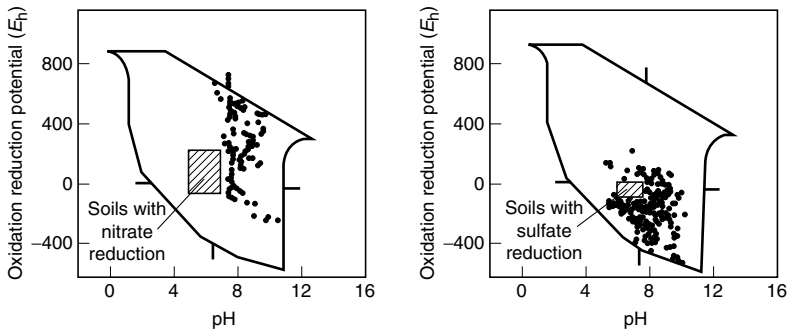

Fig. 1 The pH and oxidation reduction potential for growth of anaerobic bacteria able to reduce nitrate or sulfate (dots in plots) and for soils dominated by the microbial metabolism (boxes). Aerobic bacteria grow over a wide range of pH at $E_h > 300$ mV (normal hydrogen electrode). Source: Ref 19

© 2002 ASM International. All Rights Reserved.© 2002 ASM International. All Rights Reserved. www.asminternational.org

sion is the free energy released by the overall chemical reaction resulting from combined cathodic and anodic half-reactions:

Anodic reaction	$M \rightarrow M^{n+} + n$ electrons
Cathodic reaction	$mX + n$ electrons $\rightarrow mX^{n/m-}$
Overall corrosion reaction	$M + mX \rightarrow M^{n+} + mX^{n/m-}$

(Eq 1)

where n, p, and m are integer values chosen to charge balance the equations based on the number of electrons given up by the metal being oxidized or taken up by the electron acceptor being reduced.

Because metals are good electrical conductors, the cathodic and anodic processes can occur at different locations on a metal surface exposed to a common electrolyte. Where anodes and cathodes frequently change location, general corrosion is seen, but when the anode becomes focused in one location, pitting results. In pitting, the rate of penetration is, to a large measure, a function of the relative size of the cathodic and anodic areas involved in the corrosion cell and is usually much higher than that seen for general corrosion.

The rate of metal loss is determined by the slowest, or rate-determining, step in the corrosion process. For example, where the availability of electron acceptor X is limiting, the corrosion rate depends on the transport kinetics for the arrival of X at the metal surface from the surrounding solution (Fig. 2). Where the availability of X is not a constraint, other processes may be rate limiting. For example, a buildup of primary reaction products such as M^{n+} on the anodic surface can polarize the anode, stifle the rate of metal oxidation, and limit the overall rate of corrosion by anodic polarization. Similarly, a buildup of primary cathodic reaction products, $X^{n/m-}$, can slow the overall process through cathodic polarization. A common example of this occurs under anaerobic conditions, where $X = H^+$. In this case, reduction of protons from the electrolyte leads to formation of atomic hydrogen on the metal surface. To escape the surface, atoms of hydrogen must combine to form molecular hydrogen that can then be lost to solution or enter the steel matrix, as shown in Fig. 3.

Byproducts of the various reactions involved may limit the corrosion process by altering the environment at the metal surface (Eq 2–6). For example, reduction of protons at the metal surface (Eq 3) raises the local pH. This can lead to the formation of insoluble deposits. The formation of ferrous carbonate on a steel surface by the sequence of events shown in Eq 2 to 6 provides one example. Precipitation of calcium or magnesium ions from the electrolyte as insoluble carbonates that can passivate a metal surface is another:

$$Fe \rightarrow Fe^{2+} + 2 \text{ electrons} \quad \text{(Eq 2)}$$

$$2H^+ + 2 \text{ electrons} \rightarrow 2H\cdot \text{ (cathodic hydrogen)} \quad \text{(Eq 3)}$$

$$H_2O \leftrightarrow H^+ + OH^- \quad \text{(Eq 4)}$$

$$OH^- + HCO_3^- \rightarrow CO_3^{2-} \quad \text{(Eq 5)}$$

$$CO_3^{2-} + Fe^{2+} \rightarrow FeCO_3 \quad \text{(Eq 6)}$$

Microorganisms accelerate corrosion by changing the nature or kinetics of the rate-controlling reaction or process. They can be directly involved in the electron transfer processes in the electrochemical cell represented by Eq 1 or be less directly involved through a number of mechanisms, including depolarization of the anode or cathode, disruption of passivating films, or rapid regeneration or provision of the electron acceptor, X.

Direct Involvement in the Corrosion Process

Corrosion Mechanisms Involving SRB. Perhaps the best-known mechanism of MIC involves corrosion cells generated and sustained on steel surfaces by the action of anaerobic SRB. These organisms reduce sulfate to sulfide in their metabolism and are commonly found in mixed microbial communities present in soils and natural waters. In industrial systems, biodegradable materials, such as some of the hydrocarbons found in oil and gas operations (Ref 20) or susceptible components of coating materials (Ref 21, 22), can provide a source of nutrients for microbial growth. Cathodic hydrogen formed on a metal surface (Eq 3) by active corrosion or by cathodic protection (CP) can specifically promote growth of organisms, including SRB that are able to use hydrogen in their metabolism (Ref 23). Severe corrosion cells develop as sulfide, produced by the microbial reduction of sulfate, combines with ferrous ions, released by the corrosion process, to produce insoluble black iron sulfides:

$$4Fe + SO_4^{2-} + 8H^+ \rightarrow FeS + 3Fe^{2+} + 4H_2O \quad \text{(Eq 7)}$$

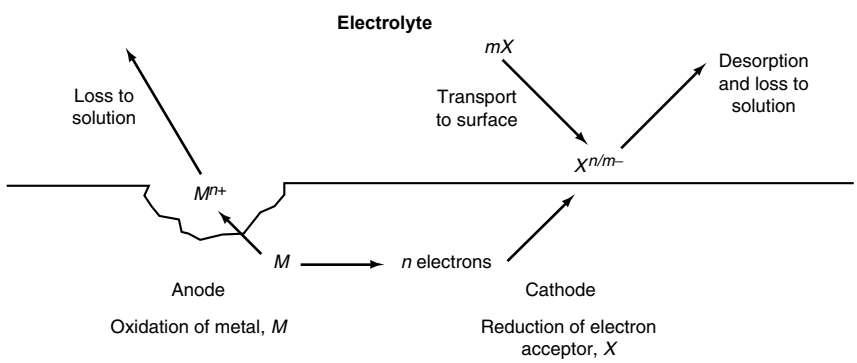

Fig. 2 Schematic diagram of a generic corrosion cell showing anodic oxidation of the metal (M) complemented by cathodic reduction of an electron acceptor (X). The corrosion rate can be controlled by the rate of arrival of X at the cathodic surface, a buildup of metal ions, M^+, at the anode, or a buildup of reduced oxidant, $X^{n/m-}$, at the cathode.

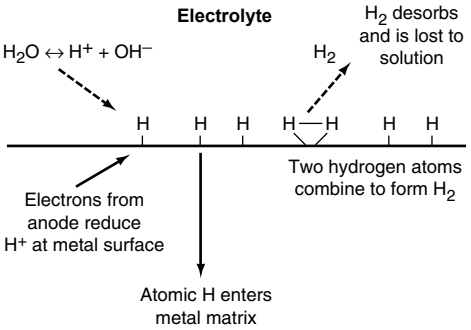

Fig. 3 Schematic diagram of the cathodic surface of an anaerobic corrosion cell in which H^+ is reduced to H on metal surface. The atomic hydrogen formed escapes the cathodic surface by combining to form molecular hydrogen, $2H \rightarrow H_2$, that desorbs from the surface or by entry as atomic hydrogen into the metal matrix.

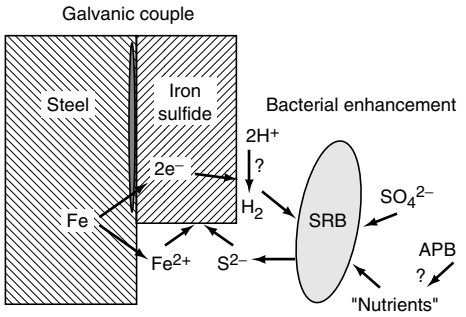

Fig. 4 Schematic diagram of the mechanism in an FeS corrosion cell created by the action of SRB. Iron sulfide sets up a galvanic couple with steel, sustained and extended by the further action of SRB. The bacteria use electrons from the corrosion process, possibly in the form of cathodic hydrogen, to reduce soluble sulfate. Enzyme assays for sulfate reductase and for hydrogenase have been developed as commercially available kits for assessing SRB activity in corrosion sites. The presence of specific iron sulfides is also used to identify this form of MIC. Acid-producing bacteria (APB) may have a role in providing nutrients to SRB, as suggested, and are often found in association.

© 2002 ASM International. All Rights Reserved.© 2002 ASM International. All Rights Reserved. www.asminternational.org
ASM Handbook Volume 11: Failure Analysis and Prevention (#06072G)

Various versions of this MIC mechanism have been suggested (Ref 9). Figure 4 illustrates a plausible mechanism base on a galvanic couple formed between iron and iron sulfide sustained and extended by the active involvement of SRB. The way in which electrons are transferred from iron sulfide to the SRB, for example, is not well resolved. It may occur directly or via formation of cathodic hydrogen, as shown in Fig. 4, or by another reaction involving reduction of H_2S (Ref 6):

$$H_2S + \text{electron} \rightarrow HS^- + H\cdot \quad \text{(Eq 8)}$$

Typical rates of metal loss for unprotected line pipe steel in an SRB/FeS corrosion scenario are 0.2 mm/year (0.008 in./year) for general corrosion and 0.7 mm/year (0.028 in./year) for pitting corrosion (Ref 24), but the corrosion rate observed depends on the concentration of FeS involved (Fig. 5). Consistent with the importance of this corrosion process in industrial facilities, commercial test kits have been developed for enumerating or assessing the activity of SRB in operating systems (Ref 25).

Formation of MIC corrosion cells involving iron sulfide need not be limited to the SRB. Reference 26 describes the corrosive action of bacteria isolated from oil production facilities that are able to reduce thiosulfate to sulfide. These organic-acid-producing organisms could generate a corrosion cell based on iron sulfide but would not show up in SRB assays based on sulfate reduction.

Corrosion by Microbially Produced Manganese (IV). Recent work has shown that microbially produced MnO_2 can corrode (Eq 9) steel, provided that contact is made with the metal surface (Ref 27):

$$Fe + MnO_2 + 4H^+ \rightarrow Fe^{2+} + Mn^{2+} + 2H_2O \quad \text{(Eq 9)}$$

Although the scenario is somewhat more complex than suggested by Eq 9 and 10 there is evidence that marine biofilms help to sustain the corrosion process by the rapid regeneration of MnO_2 (Eq 10) (Ref 28). Manganese-oxidizing organisms have been implicated in the MIC of 304L stainless steel welds (Ref 29). Formation of manganic oxide ennobles the potential of stainless steel in natural waters (Ref 30). Ennoblement shifts the potential above the repassivation potential to the pitting potential for stainless steel and furnishes the increased cathodic current density needed to propagate nucleated corrosion sites:

$$O_2 + Mn^{2+} \xrightarrow[\text{microbial catalysis}]{} MnO_2 \quad \text{(Eq 10)}$$

Other electron acceptors involved in microbial metabolism include oxygen, nitrate, iron (III), and carbon dioxide. All of these species could theoretically be involved as the electron acceptor, *X*, in the corrosion of metals (Eq 1) but evidence for direct MIC based on other electron acceptors is limited. A more general discussion of possible links between electrochemical reactions mediated in microbial metabolism and corrosion is provided in Ref 18.

Indirect Involvement in the Corrosion Process

Microorganisms can influence the corrosion process by a number of less direct mechanisms.

Depolarization Mechanisms. As previously noted, a buildup of hydrogen on the cathodic surface can stifle the corrosion process through cathodic polarization (Fig. 3). Microorganisms with hydrogenase enzymes are able to use hydrogen and have been widely cited as accelerating anaerobic corrosion through cathodic depolarization. Even though this concept has been challenged (Ref 6), commercial kits for hydrogenase activity are available for assessing MIC in practical applications (Ref 25).

Metabolites, such as organic acids produced by acid-producing bacteria (APB), may alleviate anodic polarization. Organic acids can form soluble chemical complexes with metal ions released by the corrosion process, reducing the buildup of M^{n+} on anodic surfaces. Figure 6 illustrates the damaging effect of trace levels of acetate (the conjugate base of the organic acid acetic acid) in the corrosion of steel exposed to carbon-dioxide-saturated brine. Acid-producing bacteria and organic acids at the levels shown in Fig. 6 have been identified in external corrosion sites in an extensive Gas Research Institute (GRI) program on pipeline MIC. Commercial kits and guides were produced for enumerating APB in field samples and for identifying related MIC sites (Ref 32, 33). Fungal production of organic acids has been implicated in the corrosion of posttensioned cables used in construction (Ref 34).

Production of Corrosive Metabolites. Other microbial metabolites have been recognized as agents of MIC. The many scenarios involving various sulfur species that are produced and consumed by microorganisms have been reviewed (Ref 35), and as-yet poorly described microbially produced phosphorus compounds in MIC have been implicated (Ref 11). It has been suggested that hydrogen peroxide produced in biofilms plays a role in the crevice corrosion of 304 and 316L stainless steel (Ref 36).

Alteration of Surface Environments to Create Concentration Cells. In many industrial water systems, colonization of metal surfaces by sessile microorganisms creates a new environment on the surface that may favor corrosion. During the colonization process, microbes from the aqueous phase quickly adhere to exposed steel surfaces and proceed to generate a slime made up of excreted extracellular polysaccharides (EPS). The slime envelops the organisms and creates a unique milieu for further development of microbial communities and possible MIC. The slime holds water, collects nutrients, and recruits other microbes as well as particulates and other debris from the liquid phase. Organisms in the biofilm are protected from direct exposure to biocides at dosages that would readily kill planktonic organisms freely suspended in the water phase. The metal surface is similarly shielded from doses of corrosion inhibitors added to the system.

Corrosion commonly occurs due to concentration cells established under the biofilm, where

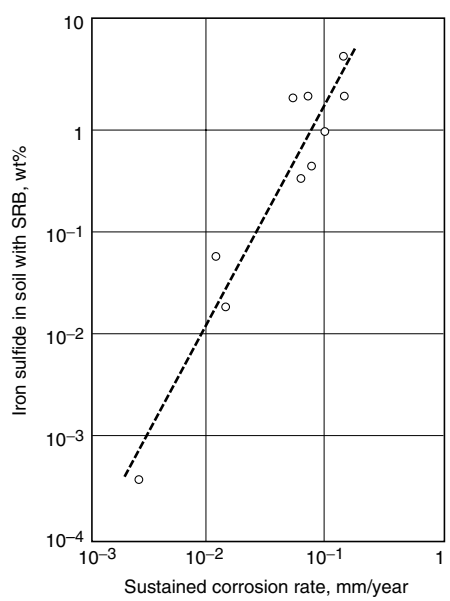

Fig. 5 Rate of corrosion of unprotected steel in biologically active soil as a function of iron sulfide present

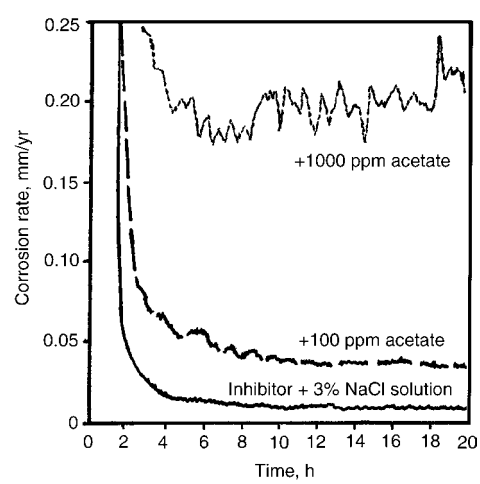

Fig. 6 Initial corrosion rates for steel exposed to carbonated 3% NaCl solution with 0, 100, and 1000 ppm acetate of 4, 9, and 18 mm/year (0.2, 0.4, and 0.7 in./year), respectively. This order is sustained after addition of 25 ppm of a corrosion inhibitor, despite a significant reduction in the corrosion rate in all cases. Source: Ref 31, reproduced with permission of National Association of Corrosion Engineers International

© 2002 ASM International. All Rights Reserved.© 2002 ASM International. All Rights Reserved. www.asminternational.org

oxygen levels are depleted and metabolite (e.g., organic acid) concentrations may be high. Slime-forming organisms are a recommended target of monitoring programs for cooling water systems (Ref 37) as are iron- and manganese-oxidizing bacteria capable of laying down deposits of metal oxides on affected surfaces. Mobile anions such as chloride are attracted to the corroding surface under a biofilm and associated deposits by the release of positively charged metal ions. Concentration of chloride can accelerate the corrosion process further, especially in systems that rely on a passivating film on the metal surface to protect the underlying metal matrix from corrosion.

Alteration of Passivating Layers. Some metals are protected from corrosion by the formation of a passivating film of metal oxide or other insoluble deposits. It has been suggested that microbial acceleration of corrosion on copper is the result of incorporation of EPS into the copper oxide on the metal surface (Ref 38). This disrupts the passivating film and is accompanied by a reduction in pH due to metabolic activity. In a more complex example, 316L stainless steel exposed to a flowing microbial culture of *Citrobacter freundii* in the laboratory was selectively colonized at grain boundaries (Ref 39, 40). This led to the local depletion of chromium and iron content relative to nickel in the subsurface region of the superficial oxide. A coculture of *C. freundii* and the SRB, *Desulfovibrio gigas,* similarly selectively colonized grain-boundary regions and enhanced the local depletion of iron and the accumulation of sulfur. The authors of the study suggested that these changes weakened the oxide layer, predisposing the metal to a higher frequency of pitting due to attack by chloride. It has been noted that microorganisms can also produce organic acids and create conditions for formation of HCl or metal chlorides, including $FeCl_3$, under biofilms (Ref 2). These agents cause the passivating layer on stainless steel to fail, allowing pitting and crevice corrosion to proceed.

Massive failures due to pitting in water system components, such as utility condensers made of stainless steel, were identified as an MIC problem in the 1970s (Ref 6). Corrosion damage was ascribed to metastable sulfur oxyanions produced by SRB in the reduction of sulfate or formed in the oxidation of biogenic iron sulfide to elemental sulfur in oxygenated water (Ref 41). Sulfur oxyanions, such as thiosulfate and tetrathionate, have been shown to reduce the pitting potential of stainless steel and promote the localized corrosion of both stainless steels and nickel-base alloys (e.g., Inconels) with or without the presence of chloride (Ref 6, 41). One proposed mechanism involves the release of elemental sulfur by the disproportionation or reduction of thiosulfate anions at the metal surface. The elemental sulfur enhances the anodic dissolution process and accelerates pitting. Active SRB help to inhibit repassivation of the metal surface where chloride is present as a pitting agent.

Microbial Involvement in Environmentally Assisted Cracking

Environmentally assisted cracking (EAC) of susceptible materials under stress can be exacerbated by microbial activity. Potentially affected forms of EAC include sulfide-stress cracking (SSC), hydrogen-induced cracking (HIC), stress-oriented hydrogen-induced cracking (SOHIC), near-neutral pH stress-corrosion cracking (SCC), and corrosion fatigue. Accelerated corrosion and enhanced hydrogen uptake can increase the probability of cracking as well as subsequent crack growth rates.

Microorganisms can influence hydrogen uptake by a metal directly through the microbial production of hydrogen. Alternately, microbial activity can promote entry of cathodic hydrogen into the metal matrix through production of recombination poisons that prevent the formation and escape of molecular hydrogen from the metal surface (Fig. 3). Inside the steel, hydrogen concentrates in areas of stress, such as the plastic zone at the tip of a growing crack, or in areas of imperfection in the metal matrix, such as inclusions or grain boundaries. In the former location, hydrogen causes embrittlement of the metal and facilitates the cracking process in, for example, SCC (Ref 42). At imperfections, formation of molecular hydrogen can force voids to form in a metal matrix through a buildup of gas pressure. This can lead to macroscopic blistering and cracking within the steel matrix in the form of HIC or SOHIC. In general, these effects are of greater concern in higher-strength steels (Ref 43).

Only a modest amount of work has been done on the involvement of microorganisms in EAC relative to the potential importance of this topic. The HIC of high-tensile-strength hard-drawn steel wire used for prestressing concrete pipe on exposure to laboratory cultures of the hydrogen-producing anaerobe, *Clostridium acetobutylicum,* has been demonstrated (Ref 44). While this simple experiment demonstrates a principle, the real-world situation is likely to be more complicated due to competing effects, such as passivation of the metal surface and consumption of hydrogen by the mixed microbial population likely to be present.

Metabolites, such as hydrogen sulfide or thiosulfate, can act as poisons for the hydrogen recombination reaction and drive cathodic hydrogen into steel (Fig. 3). Sulfide can accelerate crack growth rates even at trace concentrations. Corrosion fatigue crack growth rates (per stress cycle) in RQT 701 steel exposed to seawater have been shown to increase with increasing levels of sulfide exposure in either biotic or abiotic environments (Ref 45). It has also been noted that hydrogen permeation through steel under CP in artificial seawater was greater for a mixed culture of bacteria producing 160 ppm of sulfide than it was for the same concentration of sulfide without bacteria. Attempts to demonstrate these effects more generally led to the conclusion that the microbial scenarios may involve inhibition of hydrogen permeation and crack growth as well as enhancement. Complex lab results have been reported on the enhanced permeation of hydrogen through carbon steel exposed to cultures of SRB isolated from oilfield waters (Ref 46). It was suggested that an initial enhancement in hydrogen flux caused by the bacteria was stifled for a time by formation of a protective iron sulfide (mackinawite) on the steel surface. Accelerated hydrogen permeation was later reestablished, an effect that the researchers attributed to production of additional sulfide and organic acids by the organisms disrupting the protective film.

In addition to corrosion and hydrogen effects, the buildup of certain microbial metabolites in an environment may also foster crack growth by EAC. One example is the production of high levels of CO_2 needed to sustain near-neutral pH SCC (Ref 42). This CO_2 may arise in SCC sites on buried pipelines through biological activity in the surrounding environment or be formed more directly by biodegradation of susceptible components in protective coatings or other materials used in construction of a facility (Ref 21).

Metabolic intermediates in the microbial oxidation and reduction of sulfur can also cause trouble (Ref 35). Metastable sulfur oxyanions (e.g., thiosulfate and tetrathionate) can promote severe intergranular stress-corrosion cracking (IGSCC) of sensitized austenitic stainless steels and nickel-base Inconel alloys at very low concentrations in acidic to slightly acidic solution (Ref 41). As noted previously, metastable sulfur oxyanions can be produced by microbial activity or by secondary oxidation of biogenically produced iron sulfides. One suggested mechanism for their role in IGSCC involves disproportionation of the oxyanion to release elemental sulfur in the acidified crack tip. This would enhance anodic dissolution of chromium-depleted grain boundaries, enabling accelerated cracking. In this case, promotion of crack growth results from enhanced corrosion at the crack tip rather than a hydrogen embrittlement effect.

General souring of an operating environment through the biological formation of hydrogen sulfide is a serious concern in the oil and gas sector. Significant concentrations of hydrogen sulfide require production facilities to be constructed for "sour service" to avoid integrity problems. Souring of oil and gas reservoirs during prolonged production or of gas storage caverns over time can threaten production infrastructure designed to handle "sweet" sulfide-free crude oil or gas. Consequently, control of in situ souring has attracted considerable effort (Ref 47).

Degradation of Protective Systems

Microbiological influence on the integrity of metal systems need not involve direct mediation of corrosion or cracking processes. In some situations, microbiological activity predisposes metals to integrity problems through degradation

© 2002 ASM International. All Rights Reserved.© 2002 ASM International. All Rights Reserved. www.asminternational.org
ASM Handbook Volume 11: Failure Analysis and Prevention (#06072G)

of protective systems, including corrosion inhibitors, coatings, CP, or lubricants.

Corrosion inhibitors are chemicals introduced into industrial systems to reduce the rate of metal loss. In some cases, these chemicals act as nutrients for MIC problems and are destroyed through biodegradation. In a long-term audit of water recycle systems in a large oilfield, failure costs were found to be inversely related to the residual concentrations of treatment chemicals used to control corrosion, as one would hope. The chemical treatment package included a filming amine corrosion inhibitor and ammonium bisulfite as an oxygen scavenger. Closer inspection of the data, however, showed that the residual concentrations of the oxygen scavenger correlated with measured corrosion rates, indicating that the ammonium bisulfite was actually being used as a nutrient by the SRB responsible for the corrosion observed. The microbial population had to be independently controlled by targeted biocide addition (Ref 48). This problem of conflicting effects by different additives is a common issue in the design of cost-effective chemical treatment programs.

As environmental concerns push treatment chemical suppliers to less toxic, biodegradable materials (see Ref 49 for an example), competition between biocides intended to reduce microbial populations and corrosion inhibitors that may feed them will become more common.

Protective Coatings. Buried structures and interior surfaces of tanks and piping are often protected by the application of protective coatings. While these coatings have improved over the years, many older coatings were susceptible to biodegradation in service. Microbial attack can be seen, for example, in some polyvinyl chloride (PVC) coatings. While the polymer itself remains relatively inert due to its large molecular size, biological degradation of plasticizers used to make the material flexible can occur (Ref 50). Loss of plasticizer in older PVC tape coatings on pipelines has led to embrittlement and coating failure in service. In a related example, the adhesive used to affix polyethylene tape coatings to line pipe has been found to be a source of nutrients for microbial sulfate reduction in external corrosion sites (Ref 21). Biodegradation of adhesive may contribute to the loss of adhesion seen when these coatings are exposed to biologically active soils (Ref 51). Coating failures of this sort block CP and have led to corrosion and SCC problems on operating pipeline systems (Ref 22, 42).

The modern trend to more environmentally friendly, safer materials also affects the formulation of paints and coatings used to protect industrial systems. This has raised concern that these changes will coincidentally result in a loss of resistance to microbial degradation for products in service (Ref 52). A conflicting strategy of adding more biocides to new formulations has been proposed.

Cathodic Protection. Buried or submerged structures and some interior surfaces in processing facilities are protected by imposition of an electrical potential that prevents oxidation of metal. This can be achieved through the use of sacrificial anodes or by an impressed current system. In either case, maintenance of a protective potential requires the provision of an adequate current density. Production of iron sulfides by active SRB can compromise CP potentials by draining current from exposed steel surfaces. Figure 7 shows the increase in current demand in a laboratory soil box with time as SRB active in the soil produce increasing quantities of electrically conducting iron sulfides around steel coupons at a fixed potential. An increased current demand has also been seen for stainless steel surfaces when a steady-state biofilm is present (Ref 53) and in lab experiments involving an anaerobic slime-forming APB (*Vibrio natriegens*) in pure culture (Ref 54). In the latter case, production of organic acids and exopolymers by *V. natriegens* affected the formation of calcerous scales that would normally seal the cathodically protected surface, reducing current demand. In locations where increased current demand cannot be met, the protective potential is lost. In the field, affected locations may show up as a local dip in close-interval-potential surveys.

Lubricants protect metal components from corrosion and wear in service. In some cases, these lubricants contain biodegradable hydrocarbons that support microbial growth where water is available and other conditions permit. Microbial growth is, in turn, often accompanied by the production of surfactants that stabilize water/oil emulsions. These extend the interface available for microbial activity and can be quite stubborn to break. The combined effect of biodegradation and emulsification can compromise the performance of lubricants, leading to failure of metal components (Ref 55). A case study involving the failure of bearings in a marine engine is given in Ref 56. Commercial kits are available to track microbial growth in lubricants and identify impending problems in large marine engines as well as other applications.

Failure Analysis

Although MIC is acknowledged to occur on a wide range of metals, most reported failure analyses have focused on iron, copper, aluminum, and their alloys. This is not surprising, given the importance of these metals in industrial applications.

Steel and Iron

Industry Experience. Failure analysis for steel and iron can begin with an assessment of the susceptibility of an operating system to MIC, based on industry experience. It appears that almost any system with free water present can host microbial activity, provided there is a source of nutrients and an absence of toxic material. In processing facilities, an increase in pressure drop or loss of flow through piping systems (Fig. 8) or a marked decline in the efficiency of heat exchangers are indicators of possible biological fouling. A history of failures due to unexpectedly high corrosion penetration rates may indicate MIC. Favored locations for failures include low spots where water can collect in piping, dead-end or shut-in piping, tank bottoms at the interface between liquid hydrocarbons and underlying water, or areas heavily fouled with surface deposits (Fig. 9). Microbially induced corrosion problems are found in refineries, cooling water systems, sprinkler water systems, oilfield water-handling systems, oil pipelines, and pulp and paper mills but are not recognized as a major issue in steam systems (Ref 57).

For external corrosion, past experience of susceptible metal surfaces exposed to a wide range of natural environments has led to a general understanding of where corrosive conditions, including MIC, can be expected to occur (Ref 58, 59).

For soils, corrosion rates for steel and iron have been correlated with the pH, oxidation reduction potential, resistivity, and water content of the soil as well as with the type of soil. Very dry soils that lack the electrolyte needed to support active corrosion cells are benign. Moist, aerobic soils, where oxygen can readily reach exposed steel, show corrosion rates typically in the range of 0.04 to 0.2 mm/year (0.002 to 0.008 in./year). Anaerobic soil environments, where oxygen is absent and where SRB have not precipitated extensive iron sulfide deposits, show intermediate corrosion rates of 0.002 to 0.01 mm/year (0.00008 to 0.0004 in./year). Where the focused action of SRB has exposed unprotected steel to extensive iron sulfide deposits, very high corrosion rates, >0.2 mm/year (>0.008 in./year), can be seen.

Attempts have been made to identify factors in soil environments that favor MIC by SRB for

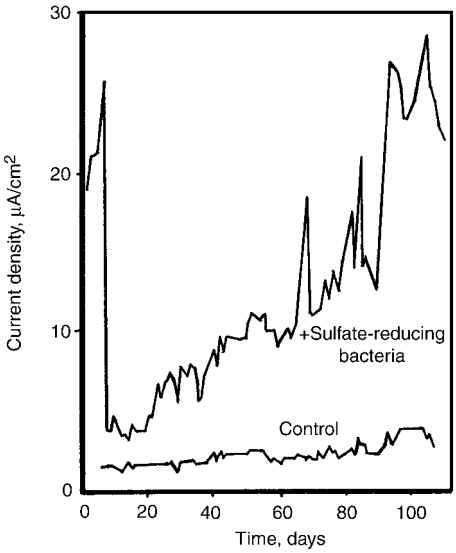

Fig. 7 Current demand needed to sustain a set CP potential increases with time for steel in soil as SRB produce increasing quantities of iron sulfide.

© 2002 ASM International. All Rights Reserved.© 2002 ASM International. All Rights Reserved. www.asminternational.org

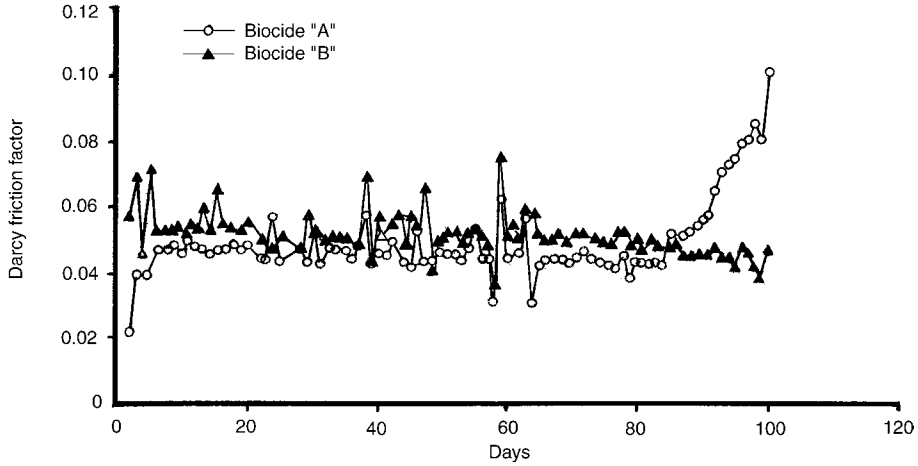

Fig. 8 Friction factors for flow through instrumented sidestreams under biocide treatment in an oilfield-produced water system can indicate biofouling. In this case, biocide "A" loses control of microbial fouling after 80 days, relative to biocide "B," in a comparison carried out in a field performance evaluation facility equipped with parallel test lines (see Fig. 14).

buried pipe (Ref 60, 61). Table 1 summarizes conditions that correlate with elevated SRB populations. Based on correlations of this sort, predictive models have been developed to prioritize maintenance activities in particular areas.

Anaerobic sediments in freshwater or marine environments generally host anaerobic microbial populations, including SRB that can create MIC problems. Guides have been developed at the University of Manchester Institute of Science and Technology to assess the potential risk of MIC due to SRB for sheet piling in sediments in ports and harbors and for design of CP systems on subsea pipelines (Ref 62).

Identification of MIC Sites. Possible MIC sites are often tentatively identified by the rapidity, severity, and localized nature of the corrosion. Confirmation is based on analysis of metallurgical damage, microorganisms, corrosion products, deposits, and environmental factors. There is no single approach to this problem, but a number of guides have been published (Ref 5, 7, 32, 33, 37, 63).

Guides for identification of internal and external MIC were developed through a major GRI program for natural gas pipelines. The guides provide a scorecard for the identification of MIC sites on mild steel, based on three types of evidence (Ref 32, 33):

- *Metallurgical:* appearance of the corrosion damage
- *Biological:* cell counts for SRB, APB, and general bacterial population
- *Chemical:* identification of corrosion products and other deposits

The metallurgical evidence is given the heaviest weighting, sufficient to pronounce MIC as being "very likely" in the absence of any other evidence from biological or chemical tests. Key features of the metallurgical fingerprint ascribed to MIC include corrosion pits composed of several smaller pits with hemispherical or cuplike appearance, striations in the direction of rolling in the steel pit bottom, and tunneling into the sides of the corrosion pit (Fig. 10). The guides provide appropriate photographs and methods for identification of these features. Biological analyses assess the number of viable SRB, APB, and anaerobic bacteria present. Chemical analysis of corrosion products has limited application in the scorecard and is more fully addressed later. Commercial kits have been developed for the analysis of the biological and chemical criteria used in the guides. Use of these tools is not confined to pipeline applications or soil environments. They are generally useful wherever the corrosion of carbon steel is observed (Ref 64).

A complementary approach to use of an MIC scorecard is based on the analysis of corrosion products and other deposits found on the corroded surface (Ref 20). This approach was developed for pipeline facilities suffering external corrosion (Ref 22). Qualitative chemical analysis can be done in the field to identify the presence of iron (II), iron (III), calcium, sulfide, and carbonate. Addition of acid to a sample can detect carbonate (by extensive bubble formation) and sulfide (by the odor of hydrogen sulfide or by its reaction with a color indicator such as lead acetate). Iron (II) and (III) can be detected in the resulting acid solution using standard ferricyanide and thiocyanate tests. Addition of a solution of oxalate to the test solution after buffering with excess sodium acetate yields a white precipitate if calcium is present. These qualitative chemical assays have been made available commercially in the form of a test kit through the GRI program noted previously. X-ray diffraction (XRD) analysis of crystalline material in corrosion products and associated deposits can provide more detailed insight (Ref 24). A summary of corrosion products indicating different corrosion scenarios is given in Table 2.

The presence of a hard, white, calcium carbonate scale is good evidence that effective CP potentials were achieved on metal surfaces where it is found. Identification of the very severe corrosion scenario due to iron sulfide corrosion cells developed by SRB can be made

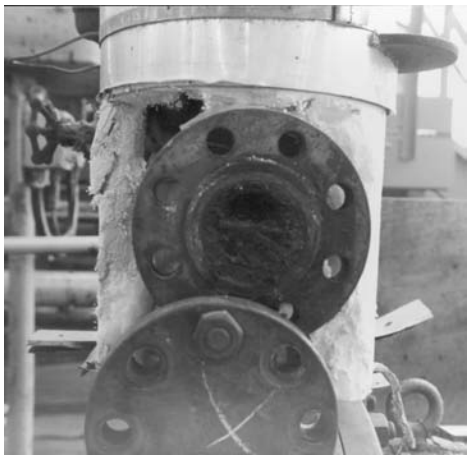

Fig. 9 Dead-end piping reveals extensive black deposits through an open flange in refinery piping.

Fig. 10 Microbially induced corrosion showing striations in the bottom and tunneling into the walls of overlapping pits, as described in Ref 32

Table 1 Factors correlating with sulfate-reducing bacteria (SRB) numbers for buried pipeline sites

Factor	Correlation coefficient	Range
Bacterial numbers (acid-producing bacteria)	0.829	$10^3 - 10^8$ cells/g wet soil
Total organic carbon in groundwater	0.645	0.05–1.2%
Soil resistivity	−0.642	500–30,000 Ω · cm
Soil water content	0.626	5–36%
Soil oxidation reduction potential	−0.545	−316 to 384 mV (CSE)
Sulfate in groundwater	0.455	0.3–200 mg/g wet soil
Clay	0.407	N/A

Note: CSE, copper-copper sulfate electrode. Source: Ref 60

© 2002 ASM International. All Rights Reserved.© 2002 ASM International. All Rights Reserved. www.asminternational.org
ASM Handbook Volume 11: Failure Analysis and Prevention (#06072G)

based on analysis of corrosion products, as noted in Table 2. The observation of iron (II) sulfide in association with severe pitting or areas of significant metal loss in contact with dense, black corrosion products is definitive for this scenario. In some failure sites, extensive iron (II) sulfide present as a finely divided, black solid causes the general blackening of soil and corrosion deposits (Fig. 11). The additional presence of iron (III) suggests secondary oxidation has occurred, with potentially very serious corrosion consequences (Table 2) (Ref 24). In extreme cases, overlapping corrosion pits can lead to extensive areas of metal loss sufficient to cause pressurized piping or vessels to fail through rupture. This type of failure presents an inherently greater risk than formation of a leak due to perforation of the steel by isolated pitting.

Table 2 does not include corrosion scenarios due to APB. This possibility can be assessed using the methods described in the MIC field guides described previously or by analysis of deposits for organic acids.

A cryptic guide to the identification of corrosion in oil and gas operations offers two MIC scenarios (Ref 65). One, based on SRB, is identified by:

- Slope-walled pits within pits
- Attached SRB
- A source of sulfate

A second scenario, based on APB, is identified by:

- Steep-sided, sharp-edged, "fibery"-bottomed pits
- Attached APB
- Trace organic materials (presumably organic acids)

Reference 37 describes a wider range of tests and considerations for cooling water systems, and active and passive MIC scenarios are considered. In active scenarios, the organisms participate directly in corrosion processes. Microorganisms involved include SRB and acid producers. In this case, sulfur-oxidizing aerobic bacteria, such as *Thiobacilli,* that produce very acidic conditions and denitrifiers capable of reducing the pH to 3 are considered as well as the organic APB. Consideration of aerobic organisms is consistent with highly oxygenated environments found in cooling water circuits. Passive corrosion scenarios include underdeposit attack due to concentration cells set up under biofilms by slime-forming microbes or iron- and manganese-oxidizing bacteria (referred to as "metal depositors" by the researchers). Other organisms considered include algae that produce dense, thick mats of biomass on sunlit surfaces in cooling towers. These can foster underdeposit attack due to concentration cells and produce high levels of oxygen as well as nutrients for other organisms. In one case, ammonia released by the decay of algal biomass was blamed for SCC in a brass condenser.

The following four factors in the identification of corrosion as MIC were looked for (Ref 37):

- Presence of microorganisms or their byproducts
- Microbiologically unique corrosion morphology
- Specific corrosion products and deposits
- Compatible environmental conditions

The use of these factors for diagnosis of MIC scenarios in cooling water systems is addressed in Table 3.

Corrosion-Resistant Alloys of Steel

Microbially induced corrosion on stainless steel leads mostly to pitting or crevice corrosion failures. Statistical analysis of corrosion failures seen in once-through cooling systems on the Rhine River show that a disproportionate number occur in stainless steel systems relative to carbon steel. Estimates of MIC as a percent of total corrosion failures for stainless steel systems may be as high as 20% but are probably <10% (Ref 66).

Weldments in Stainless Steel. Most failures are associated with welds, because areas of joining tend to be inherently more susceptible to corrosive attack than the base material. Studies have shown that heat-tinted zones are especially vulnerable. These zones are created in a welding process where material above the scaling temperature is contacted by air. The result is a mi-

Table 2 Indicator minerals found as corrosion products in various corrosion scenarios seen in pipeline excavations and laboratory soil box tests

Corrosion scenario	Corrosion products (color, chemistry, mineral form)	Corrosion rate, mm/year
Simple corrosion processes		
Abiotic aerobic corrosion (O_2 is the electron acceptor, *X*, in cathodic reaction, Eq 2)	Yellow/orange/brown/black iron (III) oxides, including lepidocrosite, goethite, magnetite, maghemite, hematite	0.04–0.2
Abiotic anaerobic corrosion (H^+ as *X* in cathodic reaction, Eq 2)	Pasty or dispersed white iron (II) carbonate (siderite)	0.002–0.01
Anaerobic MIC (SRB with biotic iron sulfide as *X*, Eq 2)	Black, finely divided iron (II) sulfides, including amorphous iron sulfide, mackinawite, greigite	0.2 general 0.7 pitting
Secondary transformations involving MIC		
Aerobic → anaerobic MIC (SRB/"FeS")	Iron (II) sulfides, including marcasite and pyrite	. . .
Anaerobic MIC (SRB/"FeS") → aerobic	Elemental sulfur, iron (III) oxides + residual anaerobic corrosion products	2–5(a)

(a) This very high corrosion rate may not be sustained beyond the period of secondary oxidation of the anaerobic site.

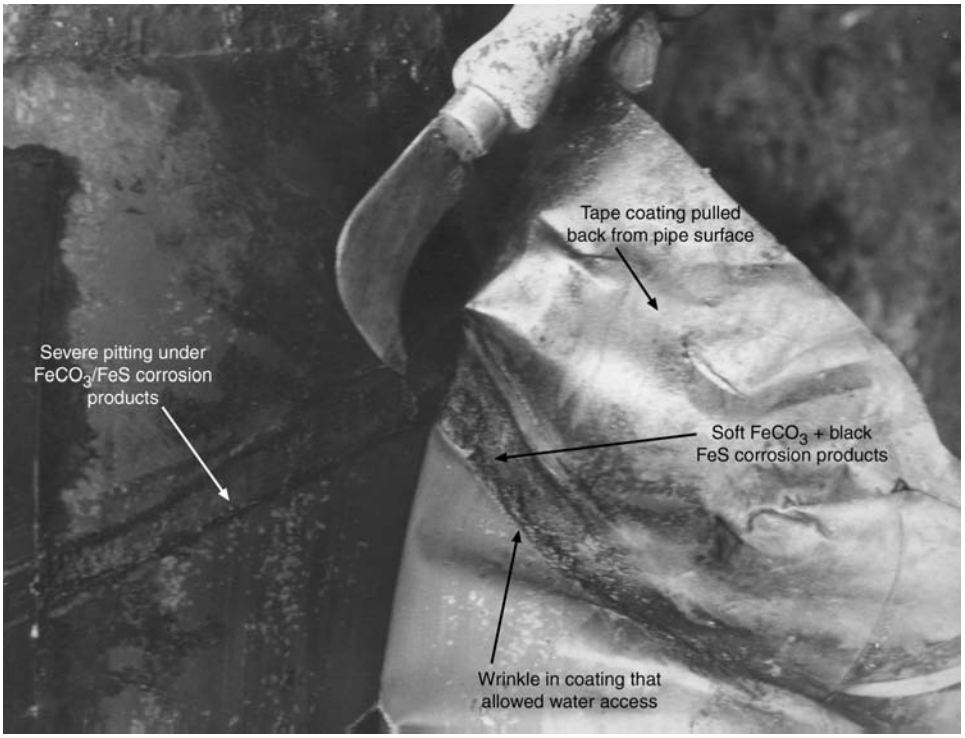

Fig. 11 FeS/SRB corrosion under disbonded polyolefin tape coating on a buried pipeline in a wet anaerobic location shows soft, black corrosion products rich in iron sulfides overlying severe pitting

© 2002 ASM International. All Rights Reserved.© 2002 ASM International. All Rights Reserved. www.asminternational.org

gration of chromium into the surface scale, leaving underlying material depleted and susceptible to corrosion. Removing the heat-tinted scale and underlying surface by pickling, electrochemical cleaning, or mechanical grinding prevents corrosion damage with or without bacteria (Ref 67, 68) for 304L, 308L, or 316L material. It has been suggested that pickling is the most effective approach (Ref 69). Heat tinting can be avoided by use of an effective inert gas blanket in the welding procedure.

Microbially induced corrosion is perhaps the only mechanism that can perforate stainless steel piping in neutral aqueous service, such as river water cooling, in a matter of months (Ref 70). It is suggested that this may be due to the ratio of cathodic to anodic areas, where a single phase, for example, ferrite, is preferentially attacked relative to a large area of less susceptible material. Penetration rates of 17 mm/year (0.7 in./year) in United Numbering System (UNS) 30800 welds have been reported. Perforation of 316L stainless steel weldments in piping with 5.5 mm (0.2 in.) wall thickness in industrial water systems under intermittent flow in four months has been described (Ref 70).

Preferential attack of some sort is a common feature of MIC case studies (Ref 63, 70–73). Corrosion is often focused on the weld material or at the fusion line for the weld (Fig. 12a). Pit surfaces are often described as dendritic, consistent with preferential corrosion (Ref 63, 71–73), but the preferential attack of a single phase need not be a feature of MIC. From detailed study of UNS 30800 weld specimens, it has been concluded that either ferrite or austenite can be preferentially attacked, or they may corrode together, depending on a number of possible conditions (Ref 70). Abiotic attack by $FeCl_3$ solutions has been found to give similar effects to MIC, based on comparison of chemically degraded specimens with samples from identified MIC sites (Ref 70, 74). Preferential attack can also occur in a single phase, due to cold work effects on microstructure (Ref 70, 74).

As previously noted, microbially induced intergranular pitting and IGSCC can occur in sensitized stainless steels, where low chromium content at grain boundaries allows preferential dissolution (Ref 41). However, it has been found that transgranular pitting due to MIC in the heat-affected zone in socket-welded specimens of 304 stainless steel exposed to flowing lakewater (500 to 600 ppm chloride) over 6 to 18 months was not focused in sensitized areas (Ref 74). Instead, pitting occurred along deformation lines left by cold working of the metal during manufacturing. Annealing the material at 1150 °C (2100 °F) was suggested as a way to remove these features and increase resistance of the material to MIC. No pitting was seen in the base metal for either furnace-sensitized or girth-welded specimens of 304 or 316 stainless steel after similar exposure (Ref 74).

A number of trends seem apparent, based on past failure analyses:

- Microbially induced corrosion is often associated with stagnant, untreated water being left in piping over extended periods (Ref 63–72). It has been suggested that intermittent flow or low flow rates are most damaging (Ref 75).
- Damage often occurs at many welds in an affected section of piping. In one power plant cooling system using lake water, radiography indicated that 50% of the welds in 316L piping showed indications of deep MIC pitting (Ref 72).
- Pitting seems more prevalent in the bottom third of the pipe (Ref 63).
- Low pH or high chloride concentrations in the pit environment enhance attack (Ref 76).

It has been noted that higher alloying in weld combinations seems to improve resistance to MIC (Ref 76). This observation is supported by a systematic laboratory study of stainless steel (304, 316L, and 317L) and Ni-Cr-Mo (alloy 625) alloy weldments cleaned of surface thermal oxides (Ref 77); however, later work on as-received welds showed that thermal oxides produced during the welding process can obscure this dependence. In all cases, exposure of specimens to lake water augmented by active SRB reduced the polarization resistance of the alloys relative to sterile controls. This was true even for alloys with 9% Mo content; however, no documented corrosion failures due to MIC in alloys with 6% Mo or more could be found to support the idea

Table 3 Factors for the diagnosis of MIC scenarios in cooling water systems

Microorganism (metabolite)	Corrosion morphology	Specific corrosion products and deposits
Active MIC		
Sulfate-reducing bacteria (sulfide)	Clustered hemispherical pits on stainless steel, Carpenter 20, aluminum, carbon steel. Rare on titanium. Copper poorly defined Very irregular pit surface in less noble metals	Metal sulfides present Voluminous, brown, friable tubercles of iron (III) oxides over pit
Acid producers (lower-pH organic acids for acid-producing bacteria)(a)	Corrosion is localized, moderate Striations in steel under tubercles, as for preferential acid dissolution of microstructure in rolling direction	None stated
Passive MIC		
Slimers (gelatinous mass with high microbial numbers)	General corrosive attack under slime Pitting if SRB present	Rusting may color surfaces brown

(a) Acid producers are often associated with SRB but outnumber them in this case. Organisms such as *Clostridia, Thiobacillus,* and *Nitrobacter* are cited as potential acid producers. Source: Ref 37

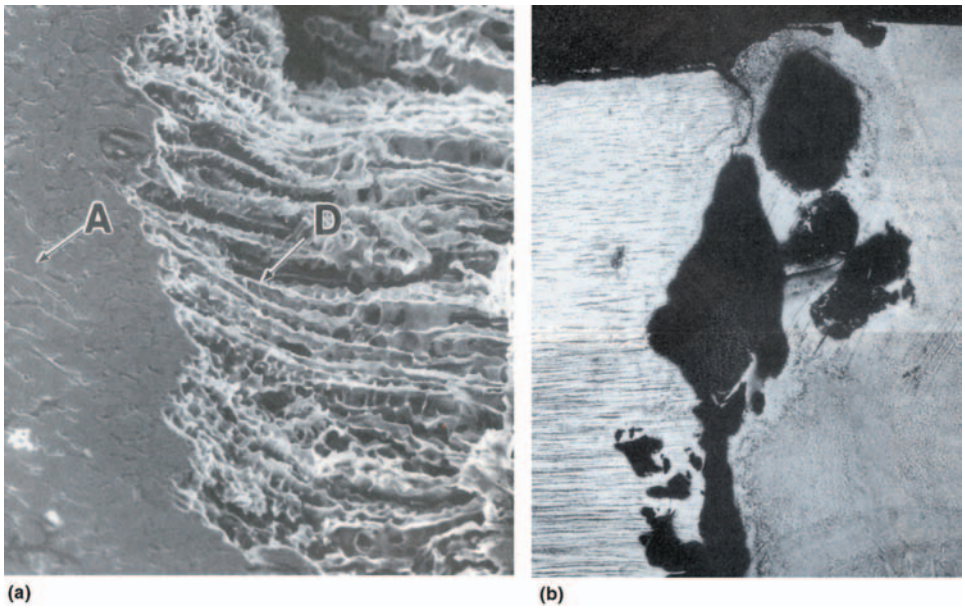

Fig. 12 MIC of stainless steel weldments. (a) MIC showing a surface view of interdendritic attack at the fusion line of a stainless steel weldment. "A," nondentritite; "D," dendrite. (b) Cross section of MIC at a stainless steel weldment showing extensive corrosion of weld metal and fusion line, with a relatively small opening at the bold surface. Source: Ref 71. Reproduced with permission of National Association of Corrosion Engineers International

© 2002 ASM International. All Rights Reserved.© 2002 ASM International. All Rights Reserved. www.asminternational.org
ASM Handbook Volume 11: Failure Analysis and Prevention (#06072G)

that elevated molybdenum content can provide added resistance to corrosion damage (Ref 2).

It was recommended that failure analysis for stainless steel cooling systems include biological analysis of associated water and deposits, chemical analysis of water, and radiography of welds (Ref 63). Microbially induced corrosion in pitting at weldments in stainless steel was identified by (Ref 74):

- The combination of bacteria present and morphology of pits
- Corrosion features with small surface openings leading to bulbous cavities in the steel matrix at welds
- The absence of other agents that could account for the attack

While SRB in mixed populations are a favorite for laboratory studies, and sulfides are often found in associated deposits on affected metal surfaces in the field, the microbiology found in case studies tends to be complex. A wide range of organisms can be present, especially in cooling systems drawing on natural waters. All sorts of bacteria were found to be present in once-through cooling systems using untreated river water, including sulfur oxidizers, iron oxidizers, iron reducers, SRB, nitrogen oxidizers, and denitrifiers (Ref 66). Aerobes, anaerobes, SRB, and APB were reported to be present in slimes and nodules on the metal surface (Ref 74). The presence of iron oxidizers and slimers for MIC problems in UNS S30800 stainless steel welds has been cited (Ref 69), while *Gallionella* in characteristic MIC pits has been specifically identified (Ref 63). Enhanced numbers of manganese-oxidizing bacteria have been noted in deposits formed on corroded welds in 304L stainless steel specimens exposed to Lake of Constance water in lab studies (Ref 29).

Surface deposits in nine case studies (Ref 63, 66–68, 72) contained iron, silicon, and sulfur in >75% of the samples analyzed (Fig. 13). Manganese, chromium, and aluminum were also frequently found (>50% of samples), but more soluble ions, such as chloride and potassium, were detected in less than half the samples.

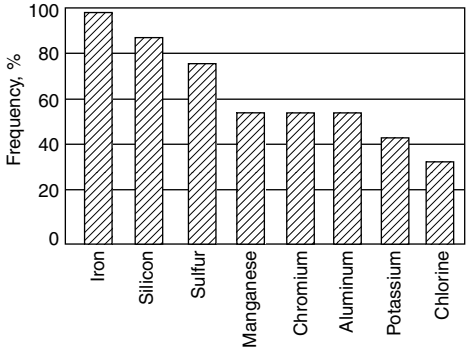

Fig. 13 Most commonly found elements in nine deposits from MIC sites in stainless steel cooling water systems (expressed as percent of deposits showing element). Source: Ref 63, 66, 71

At least two sorts of surface deposits were reported. Most of the surface of service water piping receiving lake water was covered by a tightly packed, black, slimy deposit that had a high content of manganese and iron, with trace sulfide, silicon, and aluminum present (Ref 72). No corrosion was reported under these deposits. Rust-colored deposits found in a small area (6.5 cm^2) at the weld were rich in chromium and iron, with sulfur, chlorine, aluminum, and silicon in smaller concentrations. This rust-colored deposit covered the opening of an extensive corrosion cavity in the underlying metal (Fig. 12b). This is a unique form of pitting associated with MIC in weldments in stainless steel. The cavity openings are often associated with rust-colored stains on the surface metal or with rust-colored deposits rich in iron and manganese (Ref 63, 66).

Radiography or destructive testing of field specimens reveals the large cavities to be a series of pits branching off one another to give a bulbous and irregular void volume sometimes associated with tunneling in the direction of rolling along stringers of ferrite or austenite (Ref 63, 74). This form of pitting is focused on weld metal or the fusion line, with wall perforation occurring through a second small opening on the opposite metal surface. The frequent observation of sulfide in associated surface deposits (Fig. 13) implies that SRB are commonly involved at some stage, but iron-oxidizing bacteria, particularly *Gallionella,* found in the pits have come to be associated with this corrosion morphology. *Gallionella* oxidize Fe^{2+} to Fe^{3+} in their metabolism, leading to the formation of characteristic rust-colored deposits. The acidity of the hydrated ferric ion produced decreases the pH of the local environment. Whether *Gallionella* initiate pitting or are attracted to the anodic area by the release of ferrous ions through a previously existing anaerobic corrosion process is not clear. The latter seems more likely. Once iron-oxidizing organisms are established, reduction in the pH of the corrosion pit and concentration cells established by the buildup of iron (III) oxide deposits help to drive the corrosion process.

Literature reports identify several possible MIC scenarios on stainless steel weldments. Table 4 summarizes the organisms and features that may be useful in failure analysis.

Stainless Steels. Corrosion-resistant alloys can suffer MIC failures in the body of the material not associated with welds. Numerous reports of pitting and crevice corrosion due to MIC have been noted for austenitic (304, 304L, and 316L) stainless steels (Ref 2).

Microbially induced corrosion has been described in underdeposit corrosion in heat exchangers cooled with lake water in tubes made of American Iron and Steel Institute (AISI) type 304L stainless steel and nickel alloys (UNS N08800, N08025, and N08028) (Ref 78). Pitting was found under calcite (calcium carbonate) deposits after one year for N08800 and 304L, while deep pits were found after three years for molybdenum-containing alloys N08025 and N08028. Failure analysis found that microorganisms played a key role in the degradation process. Anaerobic methanogens promoted deposition of calcium carbonate, setting the stage for crevice corrosion. Oxygen introduced with flow on startup then oxidized biogenic sulfides produced by SRB during periods of stagnation, when anaerobic conditions prevailed. Formation of thiosulfate through oxidation stabilized metastable pitting in the affected alloys, promoting corrosion even at low chloride levels. It has been suggested that the same mechanism was responsible for perforation of 316 stainless steel weldments (Ref 71).

Elemental mapping of deposits in and around the pits that formed under the calcite deposits showed:

- High levels of nickel, iron, and sulfur around the pit
- Chromium as the major metal component in the pit
- Chlorine at low levels or not at all

The calcite scale overlying corrosion stains on the metal surface was etched and contained enhanced levels of iron, nickel, and chromium derived from the corrosion process (Ref 78).

An example of MIC in martensitic stainless steel under severe service conditions has been described (Ref 79). Rapid corrosion under a thick, slimy, jellylike deposit on stainless steel (UNS S40300) drive chain systems in clarifiers in a wastewater treatment plant led to 40% metal loss in the first year of operation. The steel had

Table 4 MIC scenarios that may play a role in the corrosion of weldments in stainless steel

MIC by	Mechanism	Indicators	Ref
Manganese oxidizers	Ennoblement of stainless steel potential due to MnO_2	Elevated manganese-oxidizing organisms, manganese, and possibly chloride in deposits	29, 30
SRB primary	Sulfides, SRB facilitate chloride attack in anaerobic systems	Dark-colored corrosion products, with iron sulfide, chloride, and a high ratio of Fe^{2+}/Fe^{3+}; near-neutral pH	71
SRB secondary oxidation	Pitting stabilized by thiosulfate formed by oxidation of sulfides	Cyclic anaerobic, aerobic conditions; surface of corrosion products in pit oxidized red, orange, or brown	71
Iron-oxidizing bacteria	Decrease of pH by oxidation of Fe^{2+} to Fe^{3+} in pits	Red/orange corrosion products rich in Fe^{3+}; iron-oxidizing organisms such as *Gallionella;* pH acidic	63

SRB, sulfate-reducing bacteria

© 2002 ASM International. All Rights Reserved.© 2002 ASM International. All Rights Reserved. www.asminternational.org

been tempered for wear resistance at the cost of reduced corrosion resistance. Components made of 304L substituted into service in the unit corroded at half the rate of 403 but were subject to unacceptable levels of wear. The gray outer layer of the slime was rich in silicon and oxygen, with carbon, sulfur, and chlorine present in decreasing amounts. The dark-black inner layer showed major amounts of sulfur, chromium, and oxygen. Sulfate-reducing bacteria, APB, slime formers, and pseudomonads were all identified in samples of water and slime. High levels of biogenic hydrogen sulfide were generally present in the water phase, but the atmosphere over the fluid in the clarifiers was aerobic. This led to proliferation of sulfide- and sulfur-oxidizing organisms (*Thiothrix* and *Beggiatoa*) at the interface, producing very acidic local conditions for exposed components of the chain system. The high chloride content of the wastewater (up to 200 ppm) was also an issue. Given the extreme operating environment created, in part, by microbial activity, finding materials able to offer a reasonable service life at an acceptable cost remains a challenge.

Copper and Its Alloys

Copper is widely used in a variety of applications, because it is relatively low-cost, strong, and corrosion resistant. In addition, it conducts heat and electricity well and is readily formed, machined, and joined. Copper and brasses (copper and zinc alloys) are used, for example, in electrical wiring, water piping, architectural applications, heat exchangers, condensers, bearings, and valves, while bronzes (silicon, tin, and aluminum-amended copper) are used in bearings, impellers, pumps, screens, and special-purpose tubing. Cupronickel alloys are used in heat exchanger tubing and ships.

Copper is more-or-less susceptible to MIC in all its forms; however, copper-base alloys do show significant resistance to biofouling (Ref 80). Copper-nickel alloys, in particular, are used in marine applications, because of their resistance to both fouling and corrosion. Resistance to biofouling appears to be based on the slow release of toxic copper ions.

Elevated production of slime by microbial biofilms that develop on copper and its alloys suggests that EPS acts as a binding agent for copper ions that would otherwise inhibit microbial growth (Ref 81). The EPS exopolymers tend to be acidic and contain functional groups that bind metal ions. This capability has been linked to the formation of copper concentration cells under biofilms, the transport of metal ions away from the corroding surface, and variations in potential on the underlying surface (Ref 82). Incorporation of EPS in the oxide surface film that normally protects copper and its alloys from corrosive attack is a key reason for the occurrence of MIC in potable water systems (Ref 38). While EPS may bind the metal ions released by corrosion, it also allows an influx of mobile anions to balance the buildup of positive charge at the corroding surface. Chloride and other aggressive anions can be concentrated under biofilms, leading to disruption of passive films that would otherwise protect the metal surface.

Concentration cells set up under biofilms and production of corrosive metabolites, such as reduced pH, organic acids, and anaerobic sulfide, can lead to corrosion of copper and copper alloys. Copper is susceptible to pitting, especially in acidic media where oxidants are present. In alkaline media, production of ammonia or ammonium salts can promote SCC.

Sulfide production by SRB is one of the most potent MIC scenarios. Sulfate-reducing bacteria can become established during long periods of stagnation or in periods of intermittent flow in water systems (Ref 75). Copper sulfides deposited in the protective film by bacterial activity are rapidly oxidized when a flow of oxygenated water is introduced into the system, resulting in exposure and corrosion of the underlying metal. Failure analysis can be based on identification of specific copper sulfides formed as corrosion products. These include digenite (Cu_9S_5), spionkopite ($Cu_{39}S_{28}$), chalcocite (Cu_2S), and covellite (CuS). It is thought that digenite, formed initially, undergoes subsequent transformation to chalcocite, the most characteristic corrosion product for sulfate-reducing bacteria MIC scenarios (Ref 80). Djurleite ($Cu_{1.96}S$) formed in a SRB scenario may deposit as a passivating film, but this is likely to lack the mechanical stability needed to provide lasting protection to the metal surface in most industrial situations (Ref 2). The biogenic origin of the sulfide in MIC scenarios on copper has been supported by stable isotope analysis showing enrichment of ^{32}S in the corrosion products relative to the sulfate present in solution (Ref 35).

Pitting morphology can also provide a key to the identification of MIC in failure analysis. Two forms of pitting have been identified with MIC in potable water systems (Ref 80). One of these has been dubbed "pepper-pot pitting." In this form of damage, a conical cap of gray corrosion products (copper sulfate and cupric oxide) overlies a cluster of pits. Sulfides are present in some pits, and biofilms rich in EPS are invariably seen. In the second morphology identified with MIC, hemispherical pits are filled with crystalline cuprous oxide, with chloride often present at the metal surface. A tubercle over these pits is composed of pale-green basic copper sulfate carbonate ($Cu(OH)_x(SO4)_y$) and blue $Cu(OH)_2 \cdot CaCO_3$. Tubercles are covered by an outer layer of black cupric oxide, in some cases. Biofilm materials are seen associated with the original metal surface and with the tubercle.

Example 1: MIC of Brass Piping. A failure of buried brass (92% Cu, 8% Zn) piping used to carry drinking water in wet clay soil after less than two years service was attributed to MIC (Ref 83). Excavation showed the presence of soil blackened by deposition of sulfides and high numbers of SRB around the pipe. The external pipe surface showed a loss of zinc consistent with selective leaching of this metal from the alloy, and the groundwater contained appreciable levels of chloride that may have assisted in the breakdown of the passivating film protecting the metal surface.

A comparison was done of the corrosion failure of power station condenser tubing cooled by seawater for two copper alloys, an aluminum brass alloyed with arsenic (UNS C68700, ASTM B111, or CuZn20Al Deutsche Industrie-Normen (DIN) 17660), and a cupronickel 70-30 alloy with iron added (C71500, ASTM B111, or CuNi30Fe DIN17665) (Ref 84). Both kinds of tube had identical dimensions and had seen similar service, with failure occurring by perforation from internal pitting under sediment deposits. The presence of $Cu_{2-x}S$ in the corrosion products implicated MIC by SRB as the cause of failure, but this occurred more rapidly in the cupronickel alloy. The copper sulfide was close to stoichiometric Cu_2S on the aluminum brass but enriched in sulfur on the cupronickel tube. In the latter, large spherical pits were seen, with perforation taking the form of large, round holes. In the aluminum brass, big elliptic pits were seen, with small holes perforating the tube wall. These differences were attributed to differences in the pitting mechanism for the two alloys.

Alloy Cu-10%Ni (UNS C70600) is used extensively for condenser tubing in seawater applications, because it offers good corrosion resistance at reasonable cost. In polluted, brackish waters, however, severe localized corrosion has led to failures within three years of service. An investigation of MIC in these systems used online monitoring techniques and found elevated numbers of SRB in both the water phase (10^7 cells mL^{-1}) and in a surface biofilm (10^5 cells mL^{-1}) (Ref 85). A chlorination treatment intended to control the microbial problem destabilized the protective oxide film on the metal surface and made matters worse.

Example 2: SCC of Admiralty Brass Condenser Tubes. Microbes initiated SCC failures in admiralty brass condenser tubes in a nuclear plant cooled by freshwater (Ref 86). About 2500 tubes had to be replaced over a span of six years' operation. Analyses were carried out for microorganisms, water chemistry (for both intake and outfall), and corrosion products in the operating system and on test coupons exposed to the operating environment. Nitrate-reducing bacteria from the lakewater used in cooling were found to produce high levels of ammonia (5.8 mg/L) when established in biofilms. Ammonia levels at the metal surface were 300 times higher than background levels in the lake water. Copper amine complexes were identified in the surface deposits, and nitrate and oxygen in the incoming water were considered as accelerating factors for the cracking process.

Aluminum and Its Alloys

Aluminum is the third most abundant metal in the crust of the earth and second only to iron in

ASM International is the society for materials engineers and scientists, a worldwide network dedicated to advancing industry, technology, and applications of metals and materials.

ASM International, Materials Park, Ohio, USA
www.asminternational.org

This publication is copyright © ASM International®. All rights reserved.

Publication title	Product code
ASM Handbook Volume 11: Failure Analysis and Prevention	06072G

To order products from ASM International:

Online Visit www.asminternational.org/bookstore

Telephone 1-800-336-5152 (US) or 1-440-338-5151 (Outside US)

Fax 1-440-338-4634

Mail Customer Service, ASM International
9639 Kinsman Rd, Materials Park, Ohio 44073-0002, USA

Email CustomerService@asminternational.org

In Europe American Technical Publishers Ltd.
27-29 Knowl Piece, Wilbury Way, Hitchin Hertfordshire SG4 0SX, United Kingdom
Telephone: 01462 437933 (account holders), 01462 431525 (credit card)
www.ameritech.co.uk

In Japan Neutrino Inc.
Takahashi Bldg., 44-3 Fuda 1-chome, Chofu-Shi, Tokyo 182 Japan
Telephone: 81 (0) 424 84 5550

Terms of Use. This publication is being made available in PDF format as a benefit to members and customers of ASM International. You may download and print a copy of this publication for your personal use only. Other use and distribution is prohibited without the express written permission of ASM International.

No warranties, express or implied, including, without limitation, warranties of merchantability or fitness for a particular purpose, are given in connection with this publication. Although this information is believed to be accurate by ASM, ASM cannot guarantee that favorable results will be obtained from the use of this publication alone. This publication is intended for use by persons having technical skill, at their sole discretion and risk. Since the conditions of product or material use are outside of ASM's control, ASM assumes no liability or obligation in connection with any use of this information. As with any material, evaluation of the material under end-use conditions prior to specification is essential. Therefore, specific testing under actual conditions is recommended.

Nothing contained in this publication shall be construed as a grant of any right of manufacture, sale, use, or reproduction, in connection with any method, process, apparatus, product, composition, or system, whether or not covered by letters patent, copyright, or trademark, and nothing contained in this publication shall be construed as a defense against any alleged infringement of letters patent, copyright, or trademark, or as a defense against liability for such infringement.

Ex. II - 29

Become a Member | Sign In

MATERIALS PERFORMANCE

Search...

Subscribe

HOME MAGAZINE NEWS TOPICS RESOURCES ADVERTISE
SUBMIT MANUSCRIPT

Home / A Closer Look at Microbiologically Influenced Corrosion

Materials Selection & Design Chemical Treatment

A Closer Look at Microbiologically Influenced Corrosion

By *Kathy Riggs Larsen* on 7/29/2015 2:11 PM

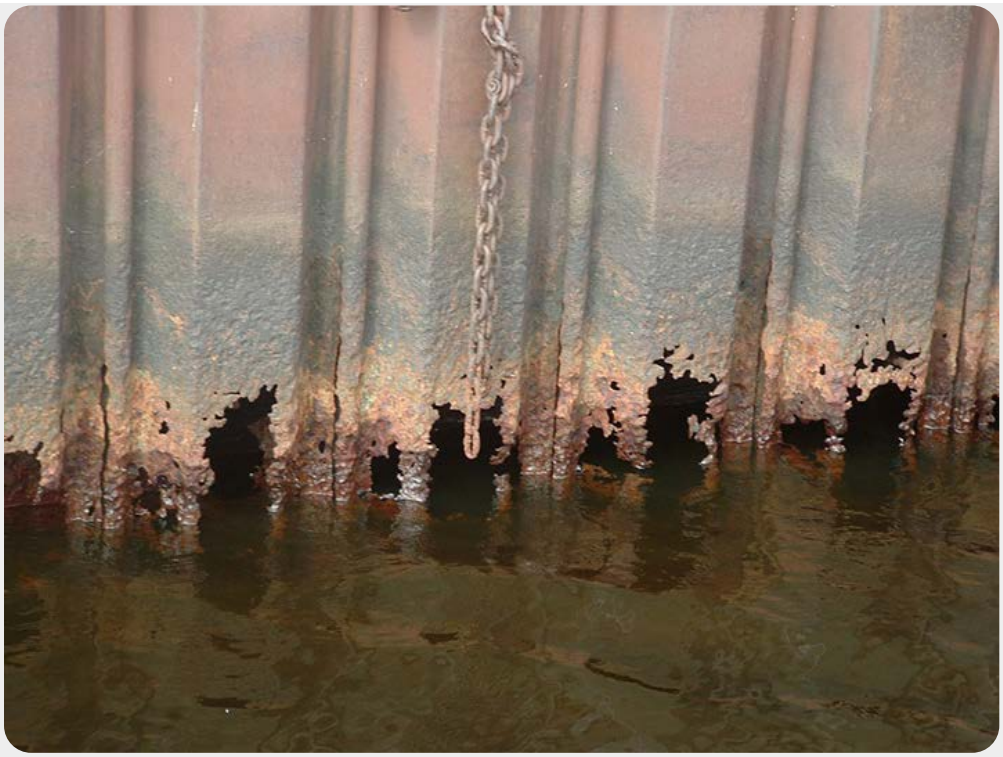

MIC of pilings in the Duluth Superior Harbor in Duluth, Minnesota. Photo courtesy of Gene Clark, University of Wisconsin Sea Grant Institute.

FACEBOOK TWITTER LINKEDIN EMAIL

Microbiologically influenced corrosion (MIC) refers to corrosion caused by the presence and activities of microorganisms—microalgae, bacteria, and fungi. While microorganisms do not produce unique types of corrosion, they can accelerate corrosion reactions or shift corrosion mechanisms. Microbial action has been identified as a contributor to rapid corrosion of metals and alloys exposed to soils; seawater, distilled water, and freshwater; crude oil, hydrocarbon fuels, and process chemicals; and sewage. Many industries and infrastructure are affected by MIC, including oil production, power generation, transportation, and water and waste water.[1]

To better understand MIC and the corrosion threats it poses to pipelines, vessels, and structures, *Materials Performance* asked several NACE International members and others from industry, government, and academia to comment on the impact of MIC and challenges faced when identifying and mitigating MIC. Panelists are Richard Eckert and Torben Lund Skovhus with Det Norske Veritas (DNV); Gary Jenneman with ConocoPhillips; Sylvie Le Borgne with the Metropolitan Autonomous University at Mexico City; and Jason S. Lee and Brenda J. Little, FNACE, with the U.S. Naval Research Laboratory. (See their biographies in the sidebar, “Meet the Panelists.”)

MP: How does MIC impact structures, vessels, and pipelines?

Le Borgne: The first reports of MIC are from the nineteenth century. Most of the studies have been in relation to metallic materials. However, other materials such as concrete, plastics, and new materials or coatings increasingly used nowadays should be included. MIC affects a variety of structures, vessels, and pipelines by directly or indirectly influencing the overall corrosion process, and is usually estimated to account for 20% of the total cost of corrosion. Due to the complexity of systems involving microorganisms, it is generally difficult to precisely quantify the influence of MIC to the overall corrosion process.

Microbial ecology studies have clearly demonstrated that microbes can survive and be active in a wide variety of environments including many man-made structures and environments. Systems where MIC is especially important include hydrocarbon and fuel (gas and liquid) transmission and storage systems, as well as hazardous materials transport and storage structures. These systems provide adequate environmental conditions and substrates for microbial development, and the participation of microorganisms in corrosion has been clearly demonstrated and MIC failures documented. Utilities such as drinking water and sewer systems also provide adequate conditions for MIC development. However in such systems, MIC has often been underestimated, as has been corrosion in general.

Eckert and Skovhus: MIC typically manifests itself as localized (i.e., pitting) corrosion—with wide variation in rate, including rapid metal loss rates—both internally and externally on pipelines, vessels, tanks, and other fluid handling equipment. Despite advances in the understanding of MIC, it remains difficult to accurately predict where MIC will occur and estimate the rate of degradation. MIC can occur as an independent corrosion mechanism or in conjunction with other corrosion mechanisms. These characteristics present challenges to implementing effective corrosion management of engineered systems in which MIC is an applicable threat.

Jenneman: Although the techniques to identify MIC are nonstandard and subject to interpretation, the places where we suspect MIC to occur experience rapid pitting, usually at interfaces where solids such as scale, wax, and or other solids can settle out or precipitate. Areas downstream of welds, where cleaning pigs have difficulty removing deposits, as well as dead legs, low-velocity areas, and tank bottoms where solids and bacteria/biofilms can accumulate, are particularly susceptible to attack. Often this pitting is very isolated, with one hole surrounded by a number of shallower pits. Pitting rates range from a few mpy to >250 mpy.

Lee: MIC in itself is not a unique corrosion mechanism; rather it produces conditions that increase the susceptibility of materials to corrosion processes such as pitting, embrittlement, and under deposit corrosion (UDC). MIC can result in orders of magnitude increases in corrosion rates. The most devastating issue regarding MIC is its general lack of predictability—both spatially and temporally.

Little: In almost all cases MIC produces localized attack that reduces strength and/or results in loss of containment.

MP: What are the current techniques used to identify MIC?

Le Borgne: Current techniques to identify MIC after it has occurred or when it is suspected are based on detecting and identifying the (causative/present) microorganisms; examining the damaged material (pit morphologies), and analyzing the corrosion products in search of biogenic structures. Concerning the detection and identification of microorganisms, the traditionally used techniques generally involve culture techniques with already prepared media tests kits to detect the growth of specific microorganisms known to participate in MIC in specific environments, such as sulfate-reducing bacteria (SRB), acid-producing bacteria, nitrate-reducing bacteria, or iron-reducing bacteria.

These kits are relatively easy to use although they need some basic laboratory expertise; the samples are inoculated directly in the field immediately after the sample has been collected. These kits also have the advantage of detecting only active bacteria, even in very low numbers. However, these kits can be rather unspecific and allow the growth of other types of microorganisms. Some years ago, genetic techniques had been proposed to allow a better detection and identification of microorganisms in MIC. These techniques need

special expertise. Careful sampling is needed to avoid contaminations as these techniques are extremely sensitive and the samples must be transported and stored under special conditions to avoid degradation of the nucleic acids.

Following total DNA extraction from the samples, the total content and identity of virtually all the microorganisms present can be determined by different methods, from genetic fingerprints to pyrosequencing. When DNA is the starting material for these analyses, all the microorganisms, whether dead or alive, are detected. It cannot be determined which microorganisms were metabolically active when the sample was taken. RNA extraction from environmental samples is very challenging and is not a routine technique.

Lee: Advancements in molecular microbiology provide numerous methods to determine which ones are there, how many there are, and what they are doing. Metallurgical sectioning and microscopy provide information about material composition, corrosion morphology, and spatial relationships between microorganisms and sites of corrosion. Multiple techniques are used to determine the electrochemical properties of materials exposed to biologically active media. Surface science and crystallography provide the chemical and structural identity of corrosion products.

Jenneman: It is recommended when trying to justify MIC as a contributing or root cause of corrosion that the following lines of evidence be examined:

1. Biological: In this case we will chemically characterize the water for essential microbiological nutrients (e.g., organics, nitrogen, phosphorus) and perform microbiological testing, if possible, to determine if the environment can support growth and activity. We will use culture-based and molecular methods to determine the types/numbers of microorganism present if good samples are available. Other physical properties (temperature, pH, ionic strength) of the environment will also be checked and evaluated.

2. Chemical: In this case we work with corrosion engineers who will look at water chemistry, gas analyses, corrosion models, etc. to determine if abiotic mechanisms such as carbon dioxide (CO_2) corrosion can explain the corrosion.

3. Metallurgical: In this case both microbiologists and corrosion engineers will examine corrosion products (using x-ray fluorescence [XRF] and x-ray diffraction [XRD]) and pit locations/morphology, as well as determine maximum pit depth using surface profilometry to determine if parameters are consistent with MIC and/or other mechanisms

4. Operational: Many operational conditions and changes can influence the likelihood for MIC, e.g., low-velocity/stagnant conditions, pigging frequency, types of pigs, biocide usage, rapid failures, changes in temperature, introduction of oxygen, and upward trending of bacteria. All of these available lines of evidence and facts are then weighed to determine if MIC is the root cause or a contributing factor.

Eckert and Skovhus: MIC is identified by evaluating the physical conditions, chemical composition, microbiology, and metallurgy of the susceptible component or system. The integration of this data is what ultimately determines the extent to which MIC may be contributing to the observed corrosion. Therefore, the techniques used to identify MIC are varied and cross-disciplinary and require expertise in materials, corrosion, microbiology, chemical treatment, and asset operations. Although microbiological conditions are only one piece of the MIC puzzle, the counting of viable bacteria has historically received the most emphasis. Serial dilution using liquid culture media, despite its limitations, has been the predominant method used to identify viable bacteria.

The type (formulation) of the culture medium and incubation temperature determines the numbers and types of microorganisms that will grow. Since no culture medium can approximate the complexity of a natural environment, liquid culture provides favorable growth conditions for only about 1 to 10% of the natural microbiological population under ideal circumstances. Further, some microorganisms are incapable of growth in typical liquid media (e.g. some Archaea). While these factors bias culture-based results, serial dilution results are still useful for monitoring general trends of growth in some systems.

Molecular microbiological methods (MMM), long used in health care and forensics, have gained popularity in the analysis of microbiological corrosion and are now included in a number of NACE standards and publications, including TM0194-2004,[2] 3T199, [3] TM0212-2012, [4] and the forthcoming revision of TM0106-2006.[5] MMM require only a small amount of sample (liquid, biofilm, solid) with or without live microorganisms. After genetic materials are extracted from the sample, assays are specific and render a more accurate quantification of various types of microorganisms than culture tests. Molecular techniques that are finding increased use include quantitative polymerase chain reaction (qPCR), denaturing gradient gel electrophoresis (DGGE), and fluorescent in situ hybridization (FISH).

Little: Despite the limitations of liquid/solid culture techniques, it is my opinion that most industries use some form of culture to establish a most probable number (MPN) of viable organisms. Relating MPN to the likelihood of MIC is a questionable practice that can only be reliable in limited applications. NACE TM0212-2012 describes microscopic analyses, chemical assays, and molecular methods for evaluating MIC. Most of the research in MIC testing is related to molecular techniques that identify and quantify microorganisms. It is not clear that molecular techniques have provided a more accurate tool for predicting the likelihood of MIC. These techniques may provide a tool for assessing mitigation strategies. Microorganisms do produce mineralogical fingerprints that can be used to identify MIC. In many cases, MIC is assumed when there is no obvious cause of corrosion.

MP: What are the challenges faced when establishing MIC as the probable cause of corrosion?

Eckert and Skovhus: Since microorganisms are ubiquitous, and some are capable of life in even the most extreme environments, the greatest challenge is determining the degree to which MIC contributes to corrosion in conjunction with other relevant corrosion mechanisms. For example, biofilms that increase MIC susceptibility in pipelines often occur where the fluid velocity is continuously low enough to promote water accumulation and solid particle deposition. Deposit or sediment buildup may also allow UDC mechanisms, such as concentration cells, to occur.

Distinguishing the relative contributions of the biofilm and concentration cells, for example, may be difficult depending on the information available to the investigator. The second challenge is effectively collecting and integrating corrosion, microbiological, chemical, operational, design, mitigation, and metallurgical data to determine the predominant corrosion mechanisms that are present. Corrosion threat assessment for MIC should be conducted in view of all other applicable corrosion mechanisms for the asset. Identifying the predominant corrosion mechanisms supports the establishment of mitigation measures that are likely to have the greatest benefit.

Finally, establishing MIC as the probable cause of corrosion in a failed component may be particularly difficult since the failure event itself is likely to have altered the conditions that caused the corrosion damage. Careful sample preservation and field sample collection from representative undamaged areas can aid in forensic corrosion investigations. The identification of MIC as a damage mechanism should not be based solely on the

presence, number, or type of microorganisms on a corroded component.

Lee: MIC is a very subtle study. Rarely can a case of suspected MIC be confirmed without evidence from multiple analysis techniques and sciences. The presence of microbes alone does not prove the existence of MIC. Microorganisms exist throughout the environment. The greatest challenge is proving that microorganisms actually influenced the electrochemical properties of the system. In addition, higher numbers of microorganisms does not necessarily mean increased likelihood of MIC. Molecular techniques are required to detect the individual activities of each microbe species. A system baseline of normal operating conditions, where predictable corrosion occurs (e.g. uniform corrosion of carbon steel [CS] in freshwater), is required for comparison with suspected MIC cases.

Jenneman: There are really no definitive tests or accepted standardized methodologies that can be applied to directly implicate MIC as the probable cause. It is often determined through a process of deduction of the facts and elimination of other mechanisms. Therefore a challenge is to develop standardized tests and approaches that can be widely accepted by the industry. However, MIC is a complex problem involving various aspects of materials science, electrochemistry, and microbiology that necessitates the involvement of scientists and engineers from various disciplines to take on this challenge. Also, the potentially large number of microbial types and activities involved challenges us to develop better mechanistic understandings of how these microorganisms and activities influence corrosion processes.

Little: MIC does not produce a unique corrosion morphology, making it impossible to identify MIC without specific testing.

Le Borgne: Challenges include the nature of the collected samples and whether they are from biofilms or bulk water. Only microorganisms in biofilms influence the corrosion process, although these microorganisms proceed from the surrounding bulk liquid phase. The number of corrosive or potentially corrosive microorganisms detected in the bulk water is not related to the intensity of the attack. Live microorganisms may not be detected in the samples, but dead organisms that participated in the attack or influenced the corrosion process are present on the surface of the material and in the corrosion products.

The microorganisms may act as consortia and not as isolated organisms, which may complicate the diagnosis and interpretation of the data. Different techniques are available for studying and diagnosing MIC. These analyses are generally performed in parallel and a multidisciplinary approach is necessary and might not always be easy to manage. There must be a link between the microbiological studies, the pit morphologies, and the composition of the corrosion products in order to clearly establish MIC as a corrosion mechanism, which may contribute from 0 to 100% in a corrosion process.

MP: Are current identification technologies adequate or is additional research necessary to develop more effective methods to identify MIC?

Little: The identification tools that can be used to determine that MIC has taken place appear to be adequate. There are recent refinements in sample preparation and fixation for more accurate molecular analyses. However, there are few tools/technologies for predicting MIC before it occurs.

Eckert and Skovhus: Current technologies, when used in combination with each other, can usually provide adequate information to assess and characterize MIC. Since MIC must typically be diagnosed using a combination of data (chemical, microbiological, metallurgical, operational, etc.), no single technology or tool can reliably identify MIC in all cases. Many operators have used extended coupon analysis to collect chemical, microbiological, and corrosion data from one sample point with much success.

The integration of results from MMM with other corrosion information is one area where additional research is needed to take advantage of the vast amount of information provided by genetic technologies. Researchers and asset owners are both continuing to find new insights resulting from collaboration between corrosion/materials professionals and microbiologists. Distinguishing the effect of MIC in combination with other abiotic external corrosion mechanisms on buried metallic structures and the influence of cathodic protection (CP) potentials more negative than -850 mV are other areas that deserve further attention and additional research—the pipeline industry would benefit from additional engineering guidance in this area.

Lee: Additional research is needed in development of a link between biological activity and corrosion rate. Real-time monitoring of corrosion rate and microbiology currently is not available. Lab-on-chip devices being developed are promising for use in microbiological monitoring programs, but academic disagreements still exist on which microbial markers are most important. Corrosion sensors have also become more sophisticated, but still lack the ability to be used in prediction of long-term corrosion susceptibility.

Le Borgne: Many identification technologies are available to provide a complete description of systems where MIC might have occurred. Some of these techniques require specific expertise and do not give an immediate response. However, more research is required in order to develop portable devices or online/remote sensors to detect MIC. The development of international standards and actualized protocols and programs that take the peculiarities of each system into account and allow the determination of risk factors is also needed to prevent MIC before it occurs in different facilities.

Jenneman: Better methods are definitely required to identify MIC. The traditional culture testing is very slow and does not give a very complete picture of the microbial communities involved in the corrosion. The newer molecular methods (e.g., DGGE, qPCR, and metagenomic sequencing) are gaining more widespread use and may eventually replace culture testing as costs decrease and availability of these technologies to oilfield end users increases. They do have the advantage of providing a faster and more complete picture of the microbial communities, but they currently require highly skilled professionals to perform the testing and interpret the results.

There are currently no accepted standards by which these tests are performed and no accepted models to help the end user interpret the results. These tests are typically outsourced to specialized laboratories and require the end user to understand the potential pitfalls of sampling, preservation, procedural nuances, and interpretation of results. There are currently industry-sponsored programs aimed at applying genomic technologies to better understand and identify MIC.

MP: When MIC is established as the corrosion mechanism, what are the mitigation and monitoring strategies typically used? Are these strategies effective?

Eckert and Skovhus: Common strategies for internal MIC mitigation in oil and gas pipelines include maintenance pigging and chemical treatment. Depending upon the pigging frequency and pig design, maintenance pigging can be effective in removing deposits/biofilm that promote MIC. A further benefit of removing deposits is increasing the effectiveness of chemical treatment by allowing the chemical to reach the exposed metal surface. Chemical treatment is typically performed using corrosion inhibitors (some with the added benefit of a biocidal tendency), biocides, and combinations of these chemicals. External MIC on buried structures and pipelines is more challenging to diagnose and mitigate properly, since nearly all soils are naturally rich with microbiological activity.

Furthermore, CP and an external coating are essentially the only mitigation options for external corrosion (including MIC) on direct buried pipe. Pipeline industry guidelines often call for applied potentials more negative than -850 mV when MIC is suspected; however, additional research is needed in this area to validate the effectiveness of more negative potentials in consideration of other parameters that influence external corrosion of buried structures. Regardless of the type of system, monitoring the effectiveness of MIC mitigation measures must include corrosion monitoring in addition to any microbiological monitoring that is performed, since ultimately the goal of mitigation is to control corrosion. Often MIC mitigation programs are focused on measuring microbial numbers, types or activity, which can be helpful in optimizing mitigation but is not a replacement for corrosion monitoring.

Little: Accelerated low water corrosion (ALWC) of CS in saline waters is a form of MIC most often attributed to microorganisms in the sulfur cycle (i.e., SRB and sulfur-oxidizing bacteria). Both CP and coatings have been effective in preventing ALWC.

Jenneman: Biocides are still the chemicals of choice when mitigating MIC; however, biocides usually need to be combined with a mechanical or chemical cleaning program to enhance their effectiveness, especially if the biofilms and corrosion are already firmly established. Biocides are comprised of both oxidizing and non-oxidizing chemicals. Both can be effective, but the environment and metallurgy will often dictate the choice. Other strategies are possible, including the injection of biostats or inhibitors. We have found that some low-toxicity film-forming corrosion inhibitors can inhibit MIC development in model laboratory flow cells.

Other tactics include developing new chemicals and surfaces (e.g., nanomaterials) that will not allow bacteria to attach and form biofilms, or destroy microorganisms on contact. In addition, application of natural chemicals can interfere with the quorum sensing capacity that microbial communities rely on to form mature biofilms, potentially rendering them less corrosive. Unfortunately, much of the testing to evaluate these techniques is targeted at controlling the microbes themselves and not the corrosion.

Testing that simply addresses the reduction of microbial populations without addressing the changes in corrosiveness is insufficient. To determine the effectiveness of these strategies, it is necessary to have effective monitoring and inspection strategies. Monitoring can be used to examine effectiveness of the mitigation strategy to deliver the chemicals, control microbiological growth, and reduce corrosiveness of the environment; however, monitoring is only as good as the locations selected and samples collected, as well as the analyses performed.

Le Borgne: The main problem associated with the use of chemicals is the adaptation capacity of microorganisms that allow them to develop resistance mechanisms and, in some cases, the ability to biodegrade these products. Constant injection of chemical products is necessary. Recently, the injection of nitrate in oilfields has been described as an effective technique to control MIC by SRB; however, the long-term effects of this manipulation of the environment have not been evaluated. Strategies based on the use of bacteriophage to control specific bacterial populations have also been proposed. These strategies, as well as their long-term effects, have to be tested.

MP: When selecting materials for new construction and/or predicting material lifetime, is MIC a consideration?

Lee: In my experience, often times MIC is not a consideration in materials selection. Certain materials have been shown to not be susceptible to MIC (e.g. titanium and high Ni-Cr alloys), but these alloys are often cost prohibitive. In the last 20 years, MIC has gained traction in industrial, commercial, and military sectors. The result of unexpected failures due to MIC has increased the attention of MIC and its consideration in material

selection. While many sectors are hiring corrosion scientists and engineers to deal with increased failure concerns, MIC still lags behind in consideration in the field of corrosion.

Le Borgne: To my knowledge, it is rarely considered, at least in the systems I have been involved in. MIC is not usually taken into account until it occurs and few reports deal with prevention and the assessment of risk factors associated with MIC. If such information could be systematized and proper documentation of MIC failures cases organized, then MIC could be taken into account in materials selection. Standardized protocols and test methods are also needed to test for MIC of materials under laboratory conditions and norms must be established.

Jenneman: Yes. In some cases, particularly where the risks (e.g., dead legs and low-velocity sections) and consequences are high (e.g. oil and gas lines), we have changed from CS to corrosion resistant alloys (typically duplex stainless steels [SS]) as a means to mitigate the impact of MIC. I cannot say this will be effective in all cases, but we have seen good results in some instances thus far. Also, the application of fusion-bonded epoxies to tank bottoms and the use of non-metals (e.g., glass-reinforced epoxy [GRE] or high-density polyethylene [HDPE]) for low-pressure water lines can be effective strategies to combat MIC.

More research is needed on the effect of MIC in non-austenitic, high-alloyed SS and non-metallic coatings to qualify them for use in various MIC environments. Unfortunately, to my knowledge, there are currently no reliable mechanistic MIC models that can be used to predict material lifetimes in CS or SS.

Little: Certainly, reports of ALWC as a global problem in saline waters has forced design engineers and insurers to question the probability of MIC in specific locations and to plan accordingly.

Eckert and Skovhus: The threat of MIC needs to be considered in the design of new projects to enable monitoring and mitigation for managing MIC during the operational stage of the asset. More importantly, designing to reduce the potential for conditions that would promote MIC (e.g. dead legs, low velocity) should be part of the development process. Materials selection should be based upon the anticipated operating conditions through the life of the asset and the intended design life.

Few metallic materials commonly used for engineered structures exhibit complete resistance to MIC, therefore material selection is usually based primarily on other engineering requirements for the project. While a number of models have been proposed to rank the susceptibility of a system to MIC, widely accepted models for reliable prediction of MIC corrosion rates have yet to be developed, and in fact may remain elusive due to the vast range of conditions under which MIC can occur.

MP: Recent research has demonstrated new MIC-based corrosion mechanisms. Has this new information changed the approach to managing MIC?

Lee: The traditional understanding of MIC involves the formation of a biofilm that provides a niche for corrosive microorganisms to proliferate. Recent research has demonstrated that metal surfaces alone can produce redox, oxygen, and nutrient gradients without an established biofilm. Many mitigation and monitoring strategies operate under the assumption of a substantial biofilm presence and treat accordingly.

Little: The list of microorganisms that can influence corrosion and the causative mechanisms is constantly growing. Recent research has, in general, demonstrated the metabolic flexibility of causative organisms. Most recently it has been demonstrated that some bacteria can accept electrons for iron (iron is the electron donor). However, it is not clear that increased understanding has translated into increased predictability.

Eckert and Skovhus: Research continues to confirm that MIC does not occur by any single, exclusive mechanism, and that various microbial consortia in different environments have established novel ways to use the energy sources available to them. The increased knowledge of microorganisms in industrial systems brought about by application of genetic methods has resulted in new understanding, and at the same time raised new questions about how the activities of specific microorganisms contribute to corrosion. Increased knowledge of the ways in which microorganisms influence corrosion through both biotic and abiotic processes will ultimately lead to improved mitigation and monitoring strategies and technologies. However, even with improved understanding of MIC mechanisms, development and implementation of innovative MIC management technologies will take time.

Jenneman: The recent revelations of the ability of certain SRB and methanogens to directly use electrons from metallic iron prior to the formation of molecular hydrogen is indeed opening our eyes to the different ways in which microorganisms can influence corrosion and to the need to expand our approaches and methods when looking for these causative agents of MIC. We need to better understand how these microorganisms accomplish this and how to detect their presence and control their activity. Their presence and potential activity can also impact how we currently manage and formulate the risks to our pipelines and facilities.

Le Borgne: To my knowledge it has not changed the approach yet, at least in the systems I have been involved in. It will probably take some time until this new knowledge is incorporated and taken into account in the field.

References

1 B.J. Little, J.S. Lee, *Microbiologically Influenced Corrosion* (Hoboken, NJ: John Wiley & Sons, 2007).
2 NACE Standard TM0194-2004, “Field Monitoring of Bacterial Growth in Oilfield Systems” (Houston, TX: NACE International, 2004).
3 NACE Publication 3T199, “Techniques for Monitoring Corrosion and Related Parameters in Field Applications” (Houston, TX: NACE, 2013).
4 NACE Standard TM0212-2012, “Detection, Testing, and Evaluation of Microbiologically Influenced Corrosion on Internal Surfaces of Pipelines” (Houston, TX: NACE, 2012).
5 NACE Standard TM0106-2006, “Detection, Testing, and Evaluation of Microbiologically Influenced Corrosion (MIC) on External Surfaces of Buried Pipelines” (Houston, TX: NACE, 2006).

Bibliography

A Practical Evaluation of 21st Century Microbiological Techniques for the Upstream Oil and Gas Industry. 1st ed. London, U.K.: Energy Institute, 2012.

Borenstein, S.W. *Microbiologically Influenced Corrosion Handbook.* Cambridge, U.K.: Woodhead Publishing Ltd, 1994.

Videla, H.A. *Manual of Biocorrosion.* Boca Raton, FL: CRC Press, 1996.

MEET THE PANELISTS:

Richard Eckert

Richard Eckert is a principal engineer—corrosion management at Det Norske Veritas (U.S.A.), Inc., in Dublin, Ohio. He has been involved with pipeline corrosion/failure investigation and forensic corrosion engineering for over 30 years. A NACE member for more than 20 years, Eckert has a B.S. degree in engineering metallurgy from Western Michigan University, is a NACE-certified Senior Internal

Corrosion Technologist, and currently serves as chair of the NACE Books Committee, vice chair of the NACE Publications Committee, and is a member of the NACE Institute Certification Commission. He is chair of NACE Task Group (TG) 254. Eckert received the NACE Presidential Achievement Award in 2004.

Gary Jenneman

Gary Jenneman is a principal scientist within the Global Production Excellence group of ConocoPhillips in Bartlesville, Oklahoma, where he has worked for the past 26 years. Jenneman has held various technical and supervisory positions in the areas of corrosion and oilfield microbiology. He holds a Ph.D. in microbiology from the University of Oklahoma and has 12 U.S. patents and numerous publications in the areas of microbiologically enhanced oil recovery, MIC, reservoir souring, and biodesulfurization. As a NACE member, he has served on various NACE technical committees and panels over the past 15 years.

Sylvie Le Borgne

Sylvie Le Borgne is a professor researcher in the Department of Process and Technology at the Metropolitan Autonomous University at Mexico City, Mexico. Some of her research interests are in environmental microbiology, biocorrosion, and biodeterioration, as well as other topics in the area of biotechnology. She has been directly involved in petroleum biotechnology from 1999 to 2005. She was a recipient of the Carlos Casas Campillo prize in 2004, given by the Mexican Society of Biotechnology and Bioengineering to young researchers under 36 years old.

Jason S. Lee

Jason S. Lee has worked as a materials engineer since 2001 at the U.S. Naval Research Laboratory, Stennis Space Center, Mississippi. A NACE member since 1999, Lee has chaired numerous MIC technical symposia and is currently vice chair of Technology Exchange Group (TEG) 187X. His research for the Navy focuses on the basic science aspects of MIC, computational corrosion modeling, improved fundamental understanding of the localized corrosion, and electrochemistry of metals and alloys exposed to marine environments. Lee received his B.S. degree in chemistry and cellular/molecular biology from the University of Michigan, and his M.S. and his Ph.D. degrees in materials science and engineering from the University of Virginia.

Brenda J. Little, FNACE

Brenda J. Little, is a senior scientist for marine molecular processes at the Naval Research Laboratory (NRL), Stennis Space Center, Mississippi. At NRL, she has worked on MIC projects for the Department of Transportation and the U.S. Army

Corps of Engineers, and has served as a consultant to NASA. In addition to her accomplishments in basic research, Little also works on U.S. Navy assets to identify and control MIC. Her research has been used to determine the cause of corrosion failures in weapons systems, seawater piping systems, storage tanks, and other U.S. Navy equipment.

Torben Lund Skovhus

Torben Lund Skovhus is project manager at Det Norske Veritas (DNV GL) in the Corrosion Management & Technical Advisory Group in Bergen, Norway. For almost 10 years he has been working with DTI Oil & Gas as a consultant and oil field microbiologist for oil and gas operators and chemical vendors worldwide. He is an author of more than 30 technical and scientific articles related to molecular biology, oil field microbiology, corrosion management, reservoir souring, and MIC. He is the editor of three books and the founder of the International Symposium on Applied Microbiology and Molecular Biology in Oil Systems (ISMOS). He has a M.S. degree in biology and a Ph.D. from the Microbiology Department at University of Aarhus, Denmark. A NACE member, he is the chair of NACE TEG 286X. "mod A?BR g

Related Articles

- The Fine Art of Predicting Failures Just Before They Occur
- Review of Applicable Indices for Evaluation of Water Quality
- Lead Contamination of Condensed Water
- Corrosion of Old Whaling Station Processing Equipment in Antarctica
- SCC Failure of a Super Duplex Separator Vessel in an Ammonium Nitrate Plant
- Failure Analysis of Pyrolysis Furnace Transfer Line Tubes

MORE ARTICLES

- Coatings & Linings
- Cathodic Protection
- Chemical Treatment
- Materials Selection & Design
- Phorgotten Phenomena
- Failure Analyses
- Case Histories

- Corrosion Basics

WHITE PAPERS

- Galvanic Corrosion Protection: Those Old Galvanic Potential Tables Are Finally Being Replaced

View All >>

WEBINARS

- Industrial Applications: ProRox® vs. Calcium Silicate

View All >>

Materials Performance
15835 Park Ten Pl., Houston, TX 77084
Tel: +1 281-228-6200
© Copyright 2017 *Materials Performance* Magazine | Privacy Policy | Terms of Use

NACE INTERNATIONAL
The Worldwide Corrosion Authority®

Ex. II - 30

Public Advocates Office
California Public Utilities Commission

505 Van Ness Avenue
San Francisco, California 94102
Tel: 415-703-2381
Fax: (415) 703-2057

http://publicadvocates.cpuc.ca.gov

PUBLIC ADVOCATES OFFICE RESPONSES TO SOUTHERN CALIFORNIA GAS COMPANY'S FIRST SET OF DATA REQUESTS

Order Instituting Investigation into SoCalGas' Practices and Operations of the Aliso Canyon Storage Facility and the Uncontrolled Release of Natural Gas, I.19-06-016

Data Request No: SoCalGas-CalAdvocates-01

Date of This Request: January 9, 2020

Response Date: January 24, 2020

GENERAL OBJECTIONS

The Public Advocates Office provides the following Responses (Responses) to Southern California Gas Company's (SoCalGas) First Set of Data Requests to the Public Advocates Office dated January 9, 2020 (SoCalGas DR 1). Questions from SoCalGas DR 1 are reproduced below, followed by Public Advocates Office Responses, solely for ease of reference. The Public Advocates Office does not adopt or admit any question or any portion of any question as correct or true. The Public Advocates Office reserves the right to supplement, clarify, revise, or correct any or all of the Responses and objections herein, and to assert additional objections or privileges, in one or more subsequent supplemental response(s). Responses pertaining to questions of law or legal conclusions have been prepared with the assistance of counsel.

The Public Advocates Office objects to each data request to the extent it mischaracterizes Public Advocates Office Opening Testimony.

The Public Advocates Office objects to each data request to the extent it is overly broad, unduly burdensome, or not reasonably calculated to lead to the discovery of admissible evidence.

The Public Advocates Office objects to each instruction, definition, and data request to the extent that it seeks information or documents protected from disclosure by the attorney-client privilege, attorney work product doctrine, or any other applicable privilege.

The Public Advocates Office objects to each instruction, definition, and data request as overbroad and unduly burdensome to the extent it seeks documents or information that are readily or more accessible to SoCalGas from SoCalGas's own files, from documents or information in SoCalGas's possession, or from documents or information that SoCalGas previously produced to the Public Advocates Office. Responding to such requests would be oppressive, unduly burdensome, and unnecessarily expensive, and the burden of responding to

Public Advocates Office
California Public Utilities Commission

505 Van Ness Avenue
San Francisco, California 94102
Tel: 415-703-2381
Fax: (415) 703-2057

http://publicadvocates.cpuc.ca.gov

such requests is substantially the same or less for SoCalGas as for the Public Advocates Office. All such documents and information will not be produced.

The Public Advocates Office incorporates by reference every general objection set forth above into each specific response set forth below. A specific response may repeat a general objection for emphasis or some other reason. The failure to include any general objection in any specific response does not waive any general objection to that request.

DATA REQUESTS AND RESPONSES

YOU allege on page 5 of YOUR PREPARED TESTIMONY that had "SoCalGas management acted in accordance with recommendation from its staff, corrosion issues for SS-25 could have been identified, monitored, and remediated decades prior to the Leak." YOU further allege on page 9 of YOUR PREPARED TESTIMONY that had "SoCalGas' management properly administered the program, the corrosion issues on SS-25 would have been timely identified." With these references in mind, please answer the following:

Question 1

Please identify the earliest date that YOU contend SoCalGas could have identified "corrosion issues" in SS-25.

Response to Question 1

The Public Advocates Office objects to this question on the ground that SoCalGas attempts to shift the burden of investigation of its wells contrary to Public Utilities (PU) Code Section 451. The Public Advocates Office further objects to the question on the grounds that this question is unduly burdensome in that it requires the Public Advocates Office to gather and analyze all the information that is or was in SoCalGas's sole possession and control. The Public Advocates Office further objects that information responsive to this question is in SoCalGas's sole possession and control.

Subject to and without waiver of the foregoing objections, the Public Advocates Office responds as follows:

Please see Public Advocates Office Opening Testimony (Opening Testimony), pages 3-5, which states:

> In 1988, SoCalGas began a program to perform casing integrity logs (known as Vertilog) and hydrostatic pressure testing on 20 candidate wells, including SS-25….
>
> Vertilog logging inspections were [ultimately] performed on only seven of the 20 wells, which did not include SS-25. Moreover, only five of the seven logged wells have surviving records. Of the five wells with surviving records, each included corrosion indications of at least 20 percent loss in wall thickness, with one well having an indication of over 60 percent loss in wall thickness….

Public Advocates Office
California Public Utilities Commission

505 Van Ness Avenue
San Francisco, California 94102
Tel: 415-703-2381
Fax: (415) 703-2057

http://publicadvocates.cpuc.ca.gov

> … Given the condition of the inspected wells (as indicated by the 20 percent or greater corrosion rate and the subsequent remediation), a prudent manager would have inspected the remaining 13 candidate wells to ensure the absence of similar integrity issues. SoCalGas' management, however, failed to undertake a timely inspection of these wells, including SS-25, and consequently failed to identify and address corrosion issues. (Footnotes omitted)

Please also see Blade Report Root Cause Analysis of the Uncontrolled Hydrocarbon Release from Aliso Canyon (Blade Report), Volume 4, at page 2, which states: "There is no way to know what an inspection of the SS-25 casing would have shown in 1988, but it is possible that corrosion was present and detectable, and steps could have been taken to avoid the leak in 2015."

The Public Advocates Office contends that corrosion issues in SS-25 could have been identified as early as 1988 if SoCalGas had fully implemented its proposed 1988 Vertilog and hydrostatic pressure testing program.

Question 2

Please identify all tools available in or around 1988 that were capable of detecting corrosion on the outer diameter of casings in gas storage wells.

Response to Question 2

The Public Advocates Office objects to this question as vague and ambiguous, particularly as to the phrase "tools." The Public Advocates Office also objects to this question on the ground that SoCalGas attempts to shift the burden of investigation of its wells contrary to PU Code Section 451. The Public Advocates Office further objects to the question on the grounds that this question is unduly burdensome in that it requires the Public Advocates Office to gather and analyze all the information that is or was in SoCalGas's sole possession and control. The Public Advocates Office further objects that information responsive to this question is in SoCalGas's sole possession and control.

Subject to and without waiver of the foregoing objections, the Public Advocates Office responds as follows:

Pressure testing was an available method of identifying the integrity of casings in gas storage wells in 1988. (*See* Blade Report, page 197, Section 4.6.1: "Section 1724.10(j)(1): MIT Part 1. Prior to commencing injection operations, each injection well must pass a pressure test of the casing-tubing annulus to determine the absence of leaks." SS-25 was pressure tested in 1973, 1976, and 1979.) Please also see Opening Testimony, page 6, which states: "…SoCalGas could have proceeded with testing the integrity of the 13 remaining wells through pressure testing, as originally proposed in the 1988 Interoffice Memo. While SoCalGas may have originally planned for the pressure testing to identify leaks at casing collars, pressure testing would also have assessed the mechanical integrity of the wells." (Footnotes omitted).

Public Advocates Office
California Public Utilities Commission

505 Van Ness Avenue
San Francisco, California 94102
Tel: 415-703-2381
Fax: (415) 703-2057

http://publicadvocates.cpuc.ca.gov

Question 3

Please identify the minimum amount of corrosion or metal loss that YOU contend would necessitate remediation.

Response to Question 3

The Public Advocates Office objects to this question as vague and ambiguous, particularly as to the phrase "necessitate remediation." The Public Advocates Office also objects to this question on the ground that SoCalGas attempts to shift the burden of investigation of its wells contrary to PU Code Section 451. The Public Advocates Office further objects to the question on the grounds that this question is unduly burdensome in that it requires the Public Advocates Office to gather and analyze all the information that is or was in SoCalGas's sole possession and control. The Public Advocates Office further objects that information responsive to this question is in SoCalGas's sole possession and control.

Subject to and without waiver of the foregoing objections, the Public Advocates Office responds as follows:

There is no minimum amount of corrosion or metal loss that should necessitate remediation; instead, once the wellbore is proven to be found in a corrosive environment, such a finding would "necessitate immediate remediation." Thus, once SoCalGas found that its wells had come in contact with the corrosive environment, SoCalGas should have taken action to remediate any corrosion issues. As to SS-25 specifically, despite knowledge that its wells existed in a corrosive environment, SoCalGas performed no wall thickness inspections or any other corrosion remediation measures from the time when Vertilog results in similar wells showed corrosion issues in 1988 until the leak occurred on October 23, 2015.

Question 4

Please identify all LAWS in effect as of 1988 that required gas storage operators to perform Vertilog testing of casings in gas storage wells.

Response to Question 4

The Public Advocates Office objects to this question on the ground that information responsive to this question is equally available and is known, or should be known, to SoCalGas. The Public Advocates Office further objects that this question calls for a legal conclusion. As this question pertains to questions of law or legal conclusions, it has been prepared with the assistance of counsel.

Subject to and without waiver of the foregoing objections, the Public Advocates Office responds as follows:

PU Code Section 451 states: "Every public shall furnish and maintain such adequate, efficient, just, and reasonable service, instrumentalities, equipment, and facilities … as are necessary to promote the safety, health, comfort, and convenience of its patrons, employees, and the public."

Public Advocates Office
California Public Utilities Commission

505 Van Ness Avenue
San Francisco, California 94102
Tel: 415-703-2381
Fax: (415) 703-2057

http://publicadvocates.cpuc.ca.gov

YOU allege on pages 8-9 of YOUR PREPARED TESTIMONY that:

> Using an assumption that the production casings of each well would have had 0 percent Outer Diameter (OD) penetration (wall thickness loss) at the time they were installed and the percentage of OD Penetration found by the Vertilog results in 1988, it is possible to estimate a localized linear corrosion rate in units MPY. From the results in Table 1, the wells given Vertilog inspections had a corrosion rate from 1.4 to 4.6 MPY.39 Given the almost 5 MPY corrosion rate and an existing wall thickness loss exceeding 60 percent, the wall thickness would be reduced to 80 percent in as few as 14 years, or by 2002. [Footnote 40 omitted] … SoCalGas failed to perform this basic corrosion rate calculation with the 1988 Vertilog results, leaving SoCalGas' management uninformed and unable to assess the risk of casing failure events.

Footnote 39 provides the following citation:

> In an open water system, a corrosion rate of around 1 MPY is normal. Having corrosion rate of around 10 [MPY], you should take action. Corrosion rates of 20 MPY and above, you should be concerned, as the corrosion is "eating" the metal rather fast. Merus Oil and Gas, https://www.merusonline.com/mpy-milsper-year/.

With this reference in mind, please answer the following:

Question 5

Please describe YOUR basis, including any supporting literature or analysis, for assuming a "linear" rate of corrosion to estimate the rate of metal loss.

Response to Question 5

There are several assumptions that can be made for the corrosion rate of Aliso Canyon's production casings (i.e., linear, exponential, logarithmic). The assumption of a linear rate of corrosion is the most conservative estimate for this corrosion rate assessment that still fits the data presented by the Blade Report. Please see Blade Report, pages 123-124:

> The failure occurred through a patch of corrosion. This patch of corrosion was characterized by striated grooves, and the ends of the groove had a sharp 'V' shape. Further, these grooves consisted of grooves within, almost fractal in nature. Examination of the ends of the grooves revealed tunnels that began at the emds pf the groove and that penetrated parallel to the groove into the metal. One sample revealed the formation of multiple parallel tunnels that aligned and developed into grooves.
>
> … Many of these descriptions of corrosion deposits have been identified in literature as caused by MIC. The literature data were generated from controlled experiments with deliberate exposure to microbes.

Public Advocates Office
California Public Utilities Commission

505 Van Ness Avenue
San Francisco, California 94102
Tel: 415-703-2381
Fax: (415) 703-2057

http://publicadvocates.cpuc.ca.gov

> …
>
> The SS-25 well was originally constructed as an oil well with the 7 in. production casing. The top of the cement on the 7 in. casing was around 7,000 ft and above the cement was drilling fluid. Based on the available data, this fluid would have had a pH ranging from 10.5 to 12.5 at the time of well construction.… The drilling fluid either leaked off or was displaced with ground water over time.
>
> … The microbiological organisms grew in population and caused physio-chemical reactions that likely caused the corrosion process to occur. The corrosion rates would have been quite low, on an average of 5 to 10 mpy. This is expected because, as corrosion occurs, a scale is formed on steel surface and there is no mechanism of removal of this scale. Any further corrosion requires mass transfer through the scale. The corrosion rates are anticipated to be low in a relatively stagnant environment.…

A logarithmic corrosion rate would best fit an environment where most of the corrosion occurs immediately after the production casing comes in contact with the corrosive environment. The Blade Report finds that a period of time must have passed while the high pH drilling fluid was displaced before microbes could begin corroding the casing. A logarithmic assumption, therefore, does not match the data put forth by the Blade Report, so it was rejected.

An exponential corrosion rate may have been a reasonable fit for the corrosion occurring on the production casing. Corrosion as a process is a function of the surface area of the production casing in contact with the corrosive aqueous environment. As more of the surface of the casing is corroded and more "grooves and tunnels" appear, more surface area of the production casing comes in contact with the corrosive environment. This leads to more corrosion, which in turn increases the surface area by creating more grooves and tunnels. This corrosion of the outer diameter of the production casing therefore fits an exponential corrosion rate.

However, an issue with assuming an exponential corrosion rate is that in order to accurately document the nature of the corrosion, at least three data points are needed to fit the curve. Since SoCalGas has provided proof of only one wall thickness examination on its wellbores in their more than 60-year lifespan (Vertilog testing in 1988), there is not enough data to accurately estimate the exponential nature of the corrosion. Had SoCalGas performed other regular wall thickness measurement inspections, those data points may have better fit an exponential rate of corrosion to the wellbores.

As a result, the only available assumption is a linear local approximation of corrosion, which is a conservative estimate given the lack of data taken by SoCalGas. With the one wall thickness measurement in 1988 (for 7 of the 20 prioritized wells), and an assumption that the production casing was placed into the ground with a 0% Wall Thickness loss, it is possible to approximate a constant rate of corrosion while the casing was in the ground. This linear assumption balances the exponential growth of surface area in contact with the corrosive environment with Blade

Public Advocates Office
California Public Utilities Commission

505 Van Ness Avenue
San Francisco, California 94102
Tel: 415-703-2381
Fax: (415) 703-2057

http://publicadvocates.cpuc.ca.gov

Report's explanation of "scale formation" on the steel, which could have slowed corrosion of previously exposed casing.

It is important to note that this assumption would overestimate corrosion early in the lifespan of the production casing and underestimate the corrosion late in the corrosion's lifespan. However, by the time 60% Wall Thickness loss had been identified by Vertilog testing of similar casings, linear approximation would have been the conservative estimate. As time went on, actual corrosion rate would likely be a much larger MPY ("Mils Per Year") corrosion rate than the available linear assumption. The Blade Report accounts for this issue when it estimates the corrosion rate as "an average of 5 to 10 mpy."

Question 6

Please state all facts supporting YOUR assumption that the corrosion of SS-25 occurred in a linear fashion.

Response to Question 6

Please see Public Advocates Office's response to Question 5.

Question 7

Assuming the accuracy and reliability of YOUR corrosion rate calculation for Porter 37 (4.5 MPY as of 1988), what remedial action(s), if any, do YOU contend SoCalGas should have taken in or around 1988 respecting well Porter 37?

Response to Question 7

The Public Advocates Office objects to this question on the ground that SoCalGas attempts to shift the burden of investigation and maintenance of its wells contrary to PU Code Section 451. The Public Advocates Office further objects to the question on the grounds that this question is unduly burdensome in that it requires the Public Advocates Office to gather and analyze all the information that is or was in SoCalGas's sole possession and control. The Public Advocates Office further objects that information responsive to this question is in SoCalGas's sole possession and control.

Subject to and without waiver of the foregoing objections, the Public Advocates Office responds as follows:

Please see Opening Testimony, page 9, which states: "Given the poor condition of the inspected wells, it would have been prudent for SoCalGas management to confirm that the remaining 13 wells did not also have compromised integrity. SoCalGas management failed to do so. Instead it claimed that continued Vertilog inspections would not have achieved SoCalGas' intended purposes of the 1988 program. Even if this claim is correct, SoCalGas' management could still

Public Advocates Office
California Public Utilities Commission

505 Van Ness Avenue
San Francisco, California 94102
Tel: 415-703-2381
Fax: (415) 703-2057

http://publicadvocates.cpuc.ca.gov

have confirmed the integrity of the remaining 13 wells through other measures, such as pressure testing, as SoCalGas had originally proposed."

Please also see the Blade Report, page 219:

> When a failure of some component in a system occurs, it is not uncommon to conduct a failure analysis depending on the severity of the failure and its consequences. The purpose of the failure analysis is to determine why it happened, how to prevent its recurrence, and, of equal importance, determine if it was because of an isolated problem or if it was a potentially systemic problem. If the problem appears to be systemic, then a risk assessment is commonly done to determine the likelihood of the failure occurring elsewhere, what the potential consequences might be, and how tolerable the risk is. With this understanding of the nature of the problem and potential risks, existing procedures can then be changed or new ones developed to monitor and mitigate the risks.
>
> … Blade's review of the Aliso Canyon well files shows that 40% of the wells had casing failures (leaks, tight spots, parted casing) with an average of 2 failures per well (99 failures in 49 wells).
>
> … Despite this, there is no evidence that SoCalGas conducted a formal failure analysis or follow-up risk assessment on any of the casing failures to determine why they occurred. Nor was there an investigation of the reasons for, and the potential consequences of, the corrosion.

Question 8

Assuming the accuracy and reliability of YOUR corrosion rate calculations for Porter 46 (1.4 MPY as of 1988), what remedial action(s), if any, do YOU contend SoCalGas should have taken in or around 1988 respecting well Porter 46?

Response to Question 8

The Public Advocates Office objects to this question on the ground that SoCalGas attempts to shift the burden of investigation and maintenance of its wells contrary to PU Code Section 451. The Public Advocates Office further objects to the question on the grounds that this question is unduly burdensome in that it requires the Public Advocates Office to gather and analyze all the information that is or was in SoCalGas's sole possession and control. The Public Advocates Office further objects that information responsive to this question is in SoCalGas's sole possession and control.

Subject to and without waiver of the foregoing objections, the Public Advocates Office responds as follows:

Please see Public Advocates Office's response to Question 7.

Public Advocates Office
California Public Utilities Commission

505 Van Ness Avenue
San Francisco, California 94102
Tel: 415-703-2381
Fax: (415) 703-2057

http://publicadvocates.cpuc.ca.gov

Question 9

Assuming the accuracy and reliability of YOUR corrosion rate calculations for Standard Sesnon 8 (3.0 MPY as of 1988), what remedial action(s), if any, do YOU contend SoCalGas should have taken in or around 1988 respecting well Standard Sesnon 8?

Response to Question 9

The Public Advocates Office objects to this question on the ground that SoCalGas attempts to shift the burden of investigation and maintenance of its wells contrary to PU Code Section 451. The Public Advocates Office further objects to the question on the grounds that this question is unduly burdensome in that it requires the Public Advocates Office to gather and analyze all the information that is or was in SoCalGas's sole possession and control. The Public Advocates Office further objects that information responsive to this question is in SoCalGas's sole possession and control.

Subject to and without waiver of the foregoing objections, the Public Advocates Office responds as follows:

Please see Public Advocates Office's response to Question 7.

Question 10

Assuming the accuracy and reliability of YOUR corrosion rate calculations for Standard Sesnon 9 (1.5 MPY as of 1988), what remedial action(s), if any, do YOU contend SoCalGas should have taken in or around 1988 respecting well Standard Sesnon 9?

Response to Question 10

The Public Advocates Office objects to this question on the ground that SoCalGas attempts to shift the burden of investigation and maintenance of its wells contrary to PU Code Section 451. The Public Advocates Office further objects to the question on the grounds that this question is unduly burdensome in that it requires the Public Advocates Office to gather and analyze all the information that is or was in SoCalGas's sole possession and control. The Public Advocates Office further objects that information responsive to this question is in SoCalGas's sole possession and control.

Subject to and without waiver of the foregoing objections, the Public Advocates Office responds as follows:

Please see Public Advocates Office's response to Question 7.

Public Advocates Office
California Public Utilities Commission

505 Van Ness Avenue
San Francisco, California 94102
Tel: 415-703-2381
Fax: (415) 703-2057

http://publicadvocates.cpuc.ca.gov

Question 11

Assuming the accuracy and reliability of YOUR corrosion rate calculations for Frew 4 (4.6 MPY as of 1988), what remedial action(s), if any, do YOU contend SoCalGas should have taken in or around 1988 respecting well Frew 4?

Response to Question 11

The Public Advocates Office objects to this question on the ground that SoCalGas attempts to shift the burden of investigation and maintenance of its wells contrary to PU Code Section 451. The Public Advocates Office further objects to the question on the grounds that this question is unduly burdensome in that it requires the Public Advocates Office to gather and analyze all the information that is or was in SoCalGas's sole possession and control. The Public Advocates Office further objects that information responsive to this question is in SoCalGas's sole possession and control.

Subject to and without waiver of the foregoing objections, the Public Advocates Office responds as follows:

Please see Public Advocates Office's response to Question 7.

Question 12

Assuming that as of 1988 SS-25 had a "normal" corrosion rate of "around 1 MPY," as cited in footnote 39 of YOUR PREPARED TESTIMONY, what remedial action(s), if any, do YOU contend SoCalGas should take taken?

Response to Question 12

The Public Advocates Office objects to this question as it mischaracterizes the Opening Testimony. The Public Advocates Office further objects to this question on the ground that SoCalGas attempts to shift the burden of investigation and maintenance of its wells contrary to PU Code Section 451. The Public Advocates Office further objects to the question on the grounds that this question is unduly burdensome in that it requires the Public Advocates Office to gather and analyze all the information that is or was in SoCalGas's sole possession and control. The Public Advocates Office further objects that information responsive to this question is in SoCalGas's sole possession and control.

Subject to and without waiver of the foregoing objections, the Public Advocates Office responds as follows:

Question 12 mischaracterizes the findings of the Blade Report, which determined the corrosion rates to have been 'an average of 5 to 10 mpy." (Blade Report, page 124.) Further, please see Public Advocates Office's response to Question 7.

Public Advocates Office
California Public Utilities Commission

505 Van Ness Avenue
San Francisco, California 94102
Tel: 415-703-2381
Fax: (415) 703-2057

http://publicadvocates.cpuc.ca.gov

Question 13

Please identify all LAWS in effect as of 1988 that required gas storage operators to perform corrosion rate calculations for gas storage wells.

Response to Question 13

The Public Advocates Office objects to this question on the ground that information responsive to this question is equally available and is known, or should be known, to SoCalGas. The Public Advocates Office further objects that this question calls for a legal conclusion. As this question pertains to questions of law or legal conclusions, it has been prepared with the assistance of counsel.

Subject to and without waiver of the foregoing objections, the Public Advocates Office responds as follows:

PU Code Section 451 states: "Every public shall furnish and maintain such adequate, efficient, just, and reasonable service, instrumentalities, equipment, and facilities … as are necessary to promote the safety, health, comfort, and convenience of its patrons, employees, and the public."

YOU allege on page 11 of YOUR PREPARED TESTIMONY that: "[t]he fact that SS-25 was not cathodically protected, replaced, or taken out of service prior to the Leak meant that the corrosion was unmitigated." With this reference in mind, please answer the following:

Question 14

Do YOU contend that SoCalGas should have applied cathodic protection to SS-25?

Response to Question 14

The Public Advocates Office objects to this question as it mischaracterizes the Opening Testimony. The Public Advocates Office further objects to this question on the ground that SoCalGas attempts to shift the burden of investigation and maintenance of its wells contrary to PU Code Section 451. The Public Advocates Office further objects to the question on the grounds that this question is unduly burdensome in that it requires the Public Advocates Office to gather and analyze all the information that is or was in SoCalGas's sole possession and control. The Public Advocates Office further objects that information responsive to this question is in SoCalGas's sole possession and control.

Subject to and without waiver of the foregoing objections, the Public Advocates Office responds as follows:

If cathodic protection were applied to SS-25 prior to the invasion of groundwater, the resulting corrosion would not have occurred. Please also see the Blade Report, page 215: "For the 7 in. casing to have corroded, it must have been in direct contact with an environment that allowed the corrosion mechanism to exist, and a corrosion protection mechanism must have been absent. Cathodic protection systems, for example, are commonly used to protect pipelines from

Public Advocates Office
California Public Utilities Commission

505 Van Ness Avenue
San Francisco, California 94102
Tel: 415-703-2381
Fax: (415) 703-2057

http://publicadvocates.cpuc.ca.gov

corrosion and are sometimes used on surface casing strings. While a cathodic protection system would have provided corrosion protection to the 11 3/4 in. casing, it would not have protected the 7 in. casing inside the 11 3/4 in. casing"

Question 15

Do YOU contend that cathodic protection would have prevented the SS-25 LEAK?

Response to Question 15

The Public Advocates Office objects to this question as it mischaracterizes the Opening Testimony. The Public Advocates Office further objects to this question on the ground that SoCalGas attempts to shift the burden of investigation and maintenance of its wells contrary to PU Code Section 451. The Public Advocates Office further objects to the question on the grounds that this question is unduly burdensome in that it requires the Public Advocates Office to gather and analyze all the information that is or was in SoCalGas's sole possession and control. The Public Advocates Office further objects that information responsive to this question is in SoCalGas's sole possession and control.

Subject to and without waiver of the foregoing objections, the Public Advocates Office responds as follows:

Please see Public Advocates Office's response to Question 14.

YOU allege on page 11 of YOUR PREPARED TESTIMONY that:

> PU Code Section 451 mandates SoCalGas to operate its wells in a manner that promotes the safety and health of the public. This may include, for example, taking proactive actions to prevent a gas leak by carrying out technical analyses, inspecting of testing the wells (e.g., for well corrosion, for the strength of the well casing to withstand high pressure, etc.). Had SoCalGas taken such preventative measures in due time, it may have been able to prevent the SS-25 failure, which resulted in negative consequences to the health and safety of the public. However, SoCalGas failed to do so.

(Internal footnotes omitted). With this reference in mind, please answer the following:

Question 16

Please identify all LAWS in effect at the time of the LEAK that required gas storage operators to carry out "technical analyses" as used in the above passage from YOUR PREPARED TESTIMONY.

Public Advocates Office
California Public Utilities Commission

505 Van Ness Avenue
San Francisco, California 94102
Tel: 415-703-2381
Fax: (415) 703-2057

http://publicadvocates.cpuc.ca.gov

Response to Question 16

The Public Advocates Office objects to this question on the ground that information responsive to this question is equally available and is known, or should be known, to SoCalGas. The Public Advocates Office further objects that this question calls for a legal conclusion. As this question pertains to questions of law or legal conclusions, it has been prepared with the assistance of counsel.

Subject to and without waiver of the foregoing objections, the Public Advocates Office responds as follows:

PU Code Section 451 states: "Every public shall furnish and maintain such adequate, efficient, just, and reasonable service, instrumentalities, equipment, and facilities … as are necessary to promote the safety, health, comfort, and convenience of its patrons, employees, and the public."

Question 17

Please identify all LAWS in effect at the time of LEAK that required gas storage operators to "inspect[] or test[] the wells (e.g., for well corrosion, for the strength of the well casing to withstand high pressure, etc.)" as used in the above passage from YOUR PREPARED TESTIMONY.

Response to Question 17

The Public Advocates Office objects to this question on the ground that information responsive to this question is equally available and is known, or should be known, to SoCalGas. The Public Advocates Office further objects that this question calls for a legal conclusion. As this question pertains to questions of law or legal conclusions, it has been prepared with the assistance of counsel.

Subject to and without waiver of the foregoing objections, the Public Advocates Office responds as follows:

PU Code Section 451 states: "Every public shall furnish and maintain such adequate, efficient, just, and reasonable service, instrumentalities, equipment, and facilities … as are necessary to promote the safety, health, comfort, and convenience of its patrons, employees, and the public."

Question 18

Do YOU contend that Public Utilities Code section 451 imposes a STRICT LIABILITY standard of liability?

Response to Question 18

The Public Advocates Office objects to this question on the ground that information responsive to this question is equally available and is known, or should be known, to SoCalGas. The Public

Public Advocates Office
California Public Utilities Commission

505 Van Ness Avenue
San Francisco, California 94102
Tel: 415-703-2381
Fax: (415) 703-2057

http://publicadvocates.cpuc.ca.gov

Advocates Office further objects that this question calls for a legal conclusion. As this question pertains to questions of law or legal conclusions, it has been prepared with the assistance of counsel.

Subject to and without waiver of the foregoing objections, the Public Advocates Office responds as follows:

The language of PU Code Section 451 speaks for itself.

YOU allege on pages 15-16 of YOUR PREPARED TESTIMONY "seven incidents involving missed compliance actions on surveys and inspections done for SS-25." The dates of these seven alleged "missed compliance actions range from the year 2000 through 2013." With this reference in mind, please answer the following:

Question 19

Did any of the seven surveys or inspections for SS-25 document any anomalies regarding the condition of SS-25?

Response to Question 19

The Public Advocates Office objects to this question as vague and ambiguous, particularly as to the phrase "anomalies regarding the condition of SS-25." The Public Advocates Office also objects to this question as it mischaracterizes the Opening Testimony. The Public Advocates Office further objects to this question on the ground that SoCalGas attempts to shift the burden of investigation and maintenance of its wells contrary to PU Code Section 451. The Public Advocates Office further objects to the question on the grounds that this question is unduly burdensome in that it requires the Public Advocates Office to gather and analyze all the information that is or was in SoCalGas's sole possession and control. The Public Advocates Office further objects that information responsive to this question is in SoCalGas's sole possession and control.

Subject to and without waiver of the foregoing objections, the Public Advocates Office responds as follows:

The information available from the seven incidents involving missed compliance by SoCalGas is insufficient to make any conclusion regarding the actual condition of SS-25. Only two of the seven surveys or inspections are specific to SS-25. The remaining five surveys or inspections pertain to a group of wells, which include, but do not speak specifically to, SS-25.

END OF DATA REQUESTS AND RESPONSES

Ex. II - 31

ASME B31G-2012
(Revision of ASME B31G-2009)

Manual for Determining the Remaining Strength of Corroded Pipelines

Supplement to ASME B31 Code for Pressure Piping

AN AMERICAN NATIONAL STANDARD

The American Society of Mechanical Engineers

Copyright ASME International
Provided by IHS under license with ASME
No reproduction or networking permitted without license from IHS

INTENTIONALLY LEFT BLANK

Copyright ASME International
Provided by IHS under license with ASME
No reproduction or networking permitted without license from IHS

ASME B31G-2012
(Revision of ASME B31G-2009)

Manual for Determining the Remaining Strength of Corroded Pipelines

Supplement to ASME B31 Code for Pressure Piping

AN AMERICAN NATIONAL STANDARD

The American Society of Mechanical Engineers
Three Park Avenue • New York, NY • 10016 USA

Copyright ASME International
Provided by IHS under license with ASME
No reproduction or networking permitted without license from IHS

Date of Issuance: October 24, 2012

The next edition of this Manual is scheduled for publication in 2015.

ASME issues written replies to inquiries concerning interpretations of technical aspects of this Manual. Periodically certain actions of the ASME B31 Committee may be published as Code Cases. Code Cases and interpretations are published on the ASME Web site under the Committee Pages at http://cstools.asme.org/ as they are issued.

Errata to codes and standards may be posted on the ASME Web site under the Committee Pages to provide corrections to incorrectly published items, or to correct typographical or grammatical errors in codes and standards. Such errata shall be used on the date posted.

The Committee Pages can be found at http://cstools.asme.org/. There is an option available to automatically receive an e-mail notification when errata are posted to a particular code or standard. This option can be found on the appropriate Committee Page after selecting "Errata" in the "Publication Information" section.

ASME is the registered trademark of The American Society of Mechanical Engineers.

This Manual was developed under procedures accredited as meeting the criteria for American National Standards. The Standards Committee that approved the Manual was balanced to assure that individuals from competent and concerned interests have had an opportunity to participate. The proposed Manual was made available for public review and comment that provides an opportunity for additional public input from industry, academia, regulatory agencies, and the public-at-large.

ASME does not "approve," "rate," or "endorse" any item, construction, proprietary device, or activity.

ASME does not take any position with respect to the validity of any patent rights asserted in connection with any items mentioned in this document, and does not undertake to insure anyone utilizing a standard against liability for infringement of any applicable letters patent, nor assumes any such liability. Users of a code or standard are expressly advised that determination of the validity of any such patent rights, and the risk of infringement of such rights, is entirely their own responsibility.

Participation by federal agency representative(s) or person(s) affiliated with industry is not to be interpreted as government or industry endorsement of this code or standard.

ASME accepts responsibility for only those interpretations of this document issued in accordance with the established ASME procedures and policies, which precludes the issuance of interpretations by individuals.

No part of this document may be reproduced in any form,
in an electronic retrieval system or otherwise,
without the prior written permission of the publisher.

The American Society of Mechanical Engineers
Three Park Avenue, New York, NY 10016-5990

Copyright © 2012 by
THE AMERICAN SOCIETY OF MECHANICAL ENGINEERS
All rights reserved
Printed in U.S.A.

Copyright ASME International
Provided by IHS under license with ASME
No reproduction or networking permitted without license from IHS

CONTENTS

Foreword iv
Committee Roster v
Correspondence With the B31 Committee vi
Summary of Changes vii

1 Introduction 1

2 Evaluation Methods 6

3 Tables of Allowable Length of Corrosion 8

Figures
1.12-1 Corrosion Pit Interaction Distances 5
1.13-1 Helically Oriented Corrosion Pattern 5
2.1-1 Corrosion Parameters Used in Analysis 7

Tables
3-1 Values of *L* for Pipe Sizes ≥ NPS 2 and < NPS 6 9
3-1M Values of *L* for Pipe Sizes ≥ 60 mm and < 168 mm O.D. 9
3-2 Values of *L* for Pipe Sizes ≥ NPS 6 and < NPS 10 10
3-2M Values of *L* for Pipe Sizes ≥ 168 mm and < 273 mm O.D. 11
3-3 Values of *L* for Pipe Sizes ≥ NPS 10 and < NPS 16 12
3-3M Values of *L* for Pipe Sizes ≥ 273 mm and < 406 mm O.D. 13
3-4 Values of *L* for Pipe Sizes ≥ NPS 16 and < NPS 20 14
3-4M Values of *L* for Pipe Sizes ≥ 406 mm and < 508 mm O.D. 15
3-5 Values of *L* for Pipe Sizes ≥ NPS 20 and < NPS 24 16
3-5M Values of *L* for Pipe Sizes ≥ 508 mm and < 610 mm O.D. 17
3-6 Values of *L* for Pipe Sizes ≥ NPS 24 and < NPS 30 18
3-6M Values of *L* for Pipe Sizes ≥ 610 mm and < 762 mm O.D. 19
3-7 Values of *L* for Pipe Sizes ≥ NPS 30 and < NPS 36 20
3-7M Values of *L* for Pipe Sizes ≥ 762 mm and < 914 mm O.D. 21
3-8 Values of *L* for Pipe Sizes ≥ NPS 36 and < NPS 42 22
3-8M Values of *L* for Pipe Sizes ≥ 914 mm and < 1 066 mm O.D. 23
3-9 Values of *L* for Pipe Sizes ≥ NPS 42 and < NPS 48 24
3-9M Values of *L* for Pipe Sizes ≥ 1 066 mm and < 1 219 mm O.D. 27
3-10 Values of *L* for Pipe Sizes ≥ NPS 48 and < NPS 52 30
3-10M Values of *L* for Pipe Sizes ≥ 1 219 mm and < 1 320 mm O.D. 33
3-11 Values of *L* for Pipe Sizes ≥ NPS 52 and < NPS 56 36
3-11M Values of *L* for Pipe Sizes ≥ 1 320 mm and < 1 422 mm O.D. 39
3-12 Values of *L* for Pipe Sizes ≥ NPS 56 Through NPS 60 42
3-12M Values of *L* for Pipe Sizes ≥ 1 422 mm Through 1 524 mm O.D. 45

Copyright ASME International
Provided by IHS under license with ASME
No reproduction or networking permitted without license from IHS

FOREWORD

It has been recognized within the pipeline industry that some sections of high-pressure pipelines, particularly those with long service histories, may experience corrosion. It has also been recognized, through theoretical analysis, scientific research and testing, and industry operating experience, that some amount of metal loss due to corrosion can be tolerated without impairing the ability of the pipeline to operate safely. In 1984, ASME published the first edition of the B31G Manual for Determining the Remaining Strength of Corroded Pipelines. The B31G document provided pipeline operators with a simplified evaluation method based on the results of analysis and tests. The application of B31G has enabled pipeline operators to reliably determine safe operating pressure levels for pipe affected by corrosion, and to determine whether repairs are necessary in order to continue operating safely.

B31G continued to be reissued by ASME with only minor revisions over time, although other corrosion evaluation methods had evolved since B31G's initial publication. A majority of these other methods are based on the same theoretical model from which the original B31G method was derived, but may offer some refinement in accuracy. Subsequently, an effort was undertaken to update the B31G document to recognize certain other corrosion evaluation methods that have proven sound and that have seen successful use in the pipeline industry. Incorporation of these other methods into a recognized Code document provides the pipeline operator or other user with a formalized framework within which to use such methodologies, as well as a wider range of codified technical options with which to make an evaluation. The 2009 revision of B31G reflected those objectives.

The 2012 edition of B31G was approved by the American National Standards Institute (ANSI) on September 20, 2012.

Copyright ASME International
Provided by IHS under license with ASME
No reproduction or networking permitted without license from IHS

ASME B31 COMMITTEE
Code for Pressure Piping

(The following is the roster of the Committee at the time of approval of this Standard.)

STANDARDS COMMITTEE OFFICERS

M. L. Nayyar, *Chair*
J. E. MeYER, *Vice Chair*
N. Lobo, *Secretary*

STANDARDS COMMITTEE PERSONNEL

R. J. T. Appleby, ExxonMobil Development Co.
C. Becht IV, Becht Engineering Co.
A. E. Beyer, Fluor Enterprises, Inc.
K. C. Bodenhamer, Enterprise Products Co.
C. J. Campbell, Air Liquide
J. S. Chin, TransCanada Pipeline U.S.
D. D. Christian, Victaulic
D. L. Coym, Intertek Moody
C. J. Melo, *Alternate,* S & B Engineers and Constructors, Ltd.
R. P. Deubler, Fronek Power Systems, LLC
P. D. Flenner, Flenner Engineering Services
J. W. Frey, Stress Engineering Service, Inc.
D. R. Frikken, Becht Engineering Co.
R. A. Grichuk, Fluor Enterprises, Inc.
R. W. Haupt, Pressure Piping Engineering Associates, Inc.
B. P. Holbrook, Babcock Power, Inc.
G. A. Jolly, Vogt Valves/Flowserve Corp.
N. Lobo, The American Society of Mechanical Engineers
W. J. Mauro, American Electric Power
J. E. Meyer, Louis Perry & Associates, Inc.
M. L. Nayyar, Consultant
R. G. Payne, Alstom Power, Inc.
G. R. Petru, EPCO Inc.
E. H. Rinaca, Dominion Resources, Inc.
M. J. Rosenfeld, Kiefner/Applus — RTD
R. J. Silvia, Process Engineers and Constructors, Inc.
W. J. Sperko, Sperko Engineering Services, Inc.
F. W. Tatar, FM Global
K. A. Vilminot, Black & Veatch
A. Soni, *Delegate,* Engineers India Ltd.
L. E. Hayden Jr., *Ex-Officio,* Consultant
W. J. Koves, *Ex-Officio,* Pi Engineering Software, Inc.
A. P. Rangus, *Ex-Officio,* Bechtel
J. T. Schmitz, *Ex-Officio,* Southwest Gas Corp.
R. A. Appleton, *Contributing Member,* Refrigeration Systems Co.

B31 MECHANICAL DESIGN TECHNICAL COMMITTEE

W. J. Koves, *Chair,* Pi Engineering Software, Inc.
G. A. Antaki, *Vice Chair,* Becht Engineering Co.
C. E. O'Brien, *Secretary,* The American Society of Mechanical Engineers
C. Becht IV, Becht Engineering Co.
J. P. Breen, Becht Engineering Co.
N. F. Consumo Sr., GE Energy (IGCC) NPI
J. P. Ellenberger
D. J. Fetzner, BP Exploration Alaska, Inc.
J. A. Graziano, Consultant
R. W. Haupt, Pressure Piping Engineering Associates, Inc.
B. P. Holbrook, Babcock Power, Inc.
R. A. Leishear, Savannah River National Laboratory
G. D. Mayers, Alion Science & Technology
T. Q. McCawley, TQM Engineering, PC
R. J. Medvick, Consultant
J. C. Minichiello, Bechtel National, Inc.
A. W. Paulin, Paulin Research Group
R. A. Robleto, KBR
M. J. Rosenfeld, Kiefner/Applus — RTD
T. Sato, Japan Power Engineering and Inspection Corp.
G. Stevick, Berkeley Engineering & Research, Inc.
H. Kosasayama, *Delegate,* JGC Corp.
P. Cakir-Kavcar, *Contributing Member,* Bechtel Corp.
E. C. Rodabaugh, *Honorary Member,* Consultant

Copyright ASME International
Provided by IHS under license with ASME
No reproduction or networking permitted without license from IHS

CORRESPONDENCE WITH THE B31 COMMITTEE

General. ASME Standards are developed and maintained with the intent to represent the consensus of concerned interests. As such, users of this Standard may interact with the Committee by requesting interpretations, proposing revisions, and attending Committee meetings. Correspondence should be addressed to:

Secretary, B31 Standards Committee
The American Society of Mechanical Engineers
Three Park Avenue
New York, NY 10016-5990

Proposing Revisions. Revisions are made periodically to the Standard to incorporate changes that appear necessary or desirable, as demonstrated by the experience gained from the application of the Standard. Approved revisions will be published periodically.

The Committee welcomes proposals for revisions to this Standard. Such proposals should be as specific as possible, citing the paragraph number(s), the proposed wording, and a detailed description of the reasons for the proposal, including any pertinent documentation.

Proposing a Case. Cases may be issued for the purpose of providing alternative rules when justified, to permit early implementation of an approved revision when the need is urgent, or to provide rules not covered by existing provisions. Cases are effective immediately upon ASME approval and shall be posted on the ASME Committee Web page.

Requests for Cases shall provide a Statement of Need and Background Information. The request should identify the standard, the paragraph, figure or table number(s), and be written as a Question and Reply in the same format as existing Cases. Requests for Cases should also indicate the applicable edition(s) of the standard to which the proposed Case applies.

Interpretations. Upon request, the B31 Standards Committee will render an interpretation of any requirement of the Standard. Interpretations can only be rendered in response to a written request sent to the Secretary of the B31 Standards Committee.

The request for an interpretation should be clear and unambiguous. It is further recommended that the inquirer submit his/her request in the following format:

Subject:	Cite the applicable paragraph number(s) and the topic of the inquiry.
Edition:	Cite the applicable edition of the Standard for which the interpretation is being requested.
Question:	Phrase the question as a request for an interpretation of a specific requirement suitable for general understanding and use, not as a request for an approval of a proprietary design or situation. The inquirer may also include any plans or drawings that are necessary to explain the question; however, they should not contain proprietary names or information.

Requests that are not in this format may be rewritten in the appropriate format by the Committee prior to being answered, which may inadvertently change the intent of the original request.

ASME procedures provide for reconsideration of any interpretation when or if additional information that might affect an interpretation is available. Further, persons aggrieved by an interpretation may appeal to the cognizant ASME Committee or Subcommittee. ASME does not "approve," "certify," "rate," or "endorse" any item, construction, proprietary device, or activity.

Attending Committee Meetings. The B31 Standards Committee regularly holds meetings, which are open to the public. Persons wishing to attend any meeting should contact the Secretary of the B31 Standards Committee.

Copyright ASME International
Provided by IHS under license with ASME
No reproduction or networking permitted without license from IHS

ASME B31G-2012
SUMMARY OF CHANGES

Following approval by the B31 Committee and ASME, and after public review, ASME B31G-2012 was approved by the American National Standards Institute on September 20, 2012.

Changes given below are identified on the pages by a margin note, **(12),** placed next to the affected area.

Page	*Location*	*Change*
2	1.5	In the nomenclature, definition of P_F revised
7	2.3	First sentence revised
9	Table 3-1	In eighth column, second entry revised
	Table 3-1M	In eighth column, second entry revised
10	Table 3-2	In fifth column, second entry revised
11	Table 3-2M	In fifth column, second entry revised
14	Table 3-4	In second column, first entry revised
15	Table 3-4M	In second column, first entry revised
22	Table 3-8	In third column, first entry revised
23	Table 3-8M	In third column, first entry revised

SPECIAL NOTES:

The interpretations to ASME B31G are included in this edition as a separate section for the user's convenience.

Copyright ASME International
Provided by IHS under license with ASME
No reproduction or networking permitted without license from IHS

INTENTIONALLY LEFT BLANK

Copyright ASME International
Provided by IHS under license with ASME
No reproduction or networking permitted without license from IHS

MANUAL FOR DETERMINING THE REMAINING STRENGTH OF CORRODED PIPELINES

1 INTRODUCTION

1.1 Scope

This document is intended solely for the purpose of providing guidance in the evaluation of metal loss in pressurized pipelines and piping systems. It is applicable to all pipelines and piping systems within the scope of the transportation pipeline codes that are part of ASME B31 Code for Pressure Piping, namely: ASME B31.4, Pipeline Transportation Systems for Liquid Hydrocarbons and Other Liquids; ASME B31.8, Gas Transmission and Distribution Piping Systems; ASME B31.11, Slurry Transportation Piping Systems; and ASME B31.12, Hydrogen Piping and Pipelines, Part PL. Where the term *pipeline* is used, it may also be read to apply to piping or pipe conforming to the acceptable applications and within the technical limitations discussed below.

1.2 Acceptable Applications

The application of this document is limited to the evaluation of wall loss in metal pipe within the following limitations:

(a) metal loss in pipelines located belowground, aboveground, or offshore

(b) metal loss due to external or internal corrosion

(c) metal loss produced by grinding where used to completely remove mechanical damage, cracks, arc burns, manufacturing defects, or other defects from the pipe surface

(d) metal loss in field bends, induction bends, and elbows

(e) metal loss that incidentally affects longitudinal or helical electric seam welds or circumferential electric welds of sound quality and having ductile characteristics, provided workmanship flaws are not present in sufficiently close proximity to interact with the metal loss

(f) metal loss of any depth with respect to the pipe wall, except that due consideration shall be given to the accuracy of measurements and effective corrosion rates when the depth of metal loss exceeds 80% of the actual pipe wall dimension

(g) metal loss in new pipe where allowed by the applicable code of construction

(h) metal loss in pipe material having ductile fracture initiation characteristics [see paras. 1.7(e) and (f)] unless using a Level 3 assessment in accordance with paras. 2.2(b) and 2.4

(i) metal loss in pipe operating at temperatures above ambient within the range of operating temperature recognized by the governing standard, and provided material strength properties at temperature are considered

(j) metal loss in pipe operating at any level of allowable design hoop stress [see paras. 1.4(a) and (b) for additional considerations]

(k) metal loss in pipe where internal pressure is the primary loading [see paras. 1.4(c) and (d) for additional considerations]

1.3 Exclusions

This document does not apply to the following:

(a) crack-like defects or mechanical surface damage not completely removed to a smooth contour by grinding

(b) metal loss in indentations or buckles resulting in radial distortion of the pipe wall larger than 6% of the pipe outside diameter, unless a Level 3 assessment is performed in accordance with para. 2.4

(c) grooving corrosion, selective corrosion, or preferential corrosion affecting pipe seams or girth welds

(d) metal loss in fittings other than bends or elbows

(e) metal loss affecting material having brittle fracture initiation characteristics [see paras. 1.7(e) and (f)] unless a Level 3 assessment is performed in accordance with para. 2.4

(f) pipe operating at temperatures outside the range of operating temperature recognized by the governing standard or operating at temperatures in the creep range

1.4 Additional Considerations

The user is cautioned that additional considerations may apply in certain situations, described below.

(a) Pipe operating at low hoop stress levels due to internal pressure (e.g., less than 25% of SMYS) may be perforated by corrosion without inducing structural material failure. The methods and criteria provided herein do not address failure by perforation.

(b) Pipe affected by general corrosion of the pipe wall (i.e., corrosion-caused wall loss over the entire pipe surface) effectively operates at a greater hoop stress than

Copyright ASME International
Provided by IHS under license with ASME
No reproduction or networking permitted without license from IHS

the nominal hoop stress based on the original wall dimension. Evaluation of individual deep pits within a generally corroded area should account for the effect of wall loss due to general corrosion.

(c) Under conditions normally encountered in buried pipelines, the hoop stress due to internal pressure is the largest stress and will govern the mode of failure. High longitudinal stresses in tension acting on metal loss having a significant circumferential extent, in unrestrained piping, could change the failure mode from longitudinal to circumferential. The methods and criteria provided herein do not address circumferential failure due to high longitudinal tensile stresses. For such situations, the user should refer to a more comprehensive fitness-for-purpose guidance document, such as API 579-1/ASME FFS-1–2007, Fitness-for-Service.

(d) Metal loss having a significant circumferential extent and acted on by high longitudinal stresses in compression could be susceptible to wrinkling or buckling. Also, the combination of hoop stress due to internal pressure and longitudinal compression could interact to lower the failure pressure in the metal loss area. The methods and criteria provided herein do not address buckling or wrinkling, or interaction of hoop stress with longitudinal compressive stresses. For such situations, the user should refer to a more comprehensive fitness-for-purpose guidance document, such as API 579-1/ASME FFS-1.

(12) **1.5 Nomenclature**

A = local area of metal loss in the longitudinal plane
A_C = cross-sectional area of Charpy impact specimen
A_0 = local original metal area = Lt
C_V = Charpy V-notched impact absorbed energy
D = specified outside diameter of the pipe
d = depth of the metal loss
E = elastic modulus of steel
L = length of the metal loss
L_e = effective length = $L(\pi/4)$
M = bulging stress magnification factor
$MAOP$ = maximum allowable operating pressure
MOP = maximum operating pressure
P_F = estimated failure pressure = $2S_Ft/D$
P_O = operating pressure, may equal MAOP or MOP
P_S = safe operating pressure = P_F/SF
S_F = estimated failure stress level
S_{flow} = flow stress, defined in para. 1.7(b)
S_O = hoop stress at the operating pressure, calculated as $P_OD/2t$
S_{UT} = specified ultimate tensile strength at temperature, may equal SMTS
S_{YT} = specified yield strength at temperature, may equal SMYS
SF = safety factor
$SMTS$ = specified minimum tensile strength at ambient conditions
$SMYS$ = specified minimum yield strength at ambient conditions
t = pipe wall thickness
z = L^2/Dt
z_e = L_e^2/Dt

1.6 Analysis Level

The user may choose to conduct a Level 0, Level 1, Level 2, or Level 3 analysis, depending on the quantity and quality of data available with which to perform an evaluation, and on the desired degree of refinement of the analysis.

(a) A Level 0 evaluation is one that relies on the tables of allowable defect length and depth found in section 3. These tables are carried over without change from earlier editions of ASME B31G and have been supplemented by the addition of tables in metric units. It is intended that a Level 0 evaluation be conducted in the field without the need for performing detailed calculations.

(b) A Level 1 evaluation is a simple calculation that relies on single measurements of the maximum depth and axial extent of metal loss. It is intended that a Level 1 evaluation be conducted in the field by an engineer, corrosion technician, coating inspector, or other individual having appropriate training. A Level 1 evaluation is also suitable for use in prioritizing metal-loss anomalies identified by inline inspection.

(c) A Level 2 evaluation is one that incorporates a greater level of detail than a Level 1 evaluation in order to produce a more accurate estimate of the failure pressure. It typically relies on detailed measurements of the corroded surface profile, accounting for the actual distribution of metal loss, and involves repetitive computations that may be facilitated by the use of computer software or spreadsheets. It is intended that a Level 2 evaluation be conducted by an engineer or technician having appropriate training. A Level 2 evaluation may be suitable for use in prioritizing metal-loss anomalies identified by high-resolution inline inspection.

(d) A Level 3 evaluation is a detailed analysis of a specific flaw in accordance with a user-defined methodology, with full justification for loadings, boundary conditions, material properties, and failure criteria. It is intended that a Level 3 evaluation be conducted by a technical specialist having appropriate expertise in the subject of fitness-for-service assessment.

1.7 Material Properties and Other Data

(a) Specified minimum material properties shall be used when conducting Level 0, Level 1, or Level 2 evaluations for the purpose of determining the need for a repair. Actual material properties from mill test reports (MTRs) or laboratory testing, if known with sufficient

Copyright ASME International
Provided by IHS under license with ASME
No reproduction or networking permitted without license from IHS

confidence to warrant their usage, may be used with Level 3 evaluations. Statistical representations of material properties may be used with Levels 1, 2, or 3 for purpose of establishing a probability of failure; however, the details of such analyses are outside the scope of this document.

(b) Flow stress is a concept relevant to fracture mechanics and is used in the Level 1, Level 2, and Level 3 evaluations. It is not a property specified in a material grade or finished product standard. Research indicates that it may be defined variously as given below.

(1) S_{flow} for plain carbon steel operating at temperatures below 250°F (120°C) may be defined by $S_{\text{flow}} = 1.1 \times \text{SMYS}$. S_{flow} shall not exceed SMTS.

(2) S_{flow} for plain carbon and low-alloy steel having SMYS not in excess of 70 ksi (483 MPa) and operating at temperatures below 250°F (120°C) may be defined by $S_{\text{flow}} = \text{SMYS} + 10$ ksi (69 MPa). S_{flow} shall not exceed SMTS.

(3) S_{flow} for plain carbon and low-alloy steel having SMYS not in excess of 80 ksi (551 MPa) may be defined by $S_{\text{flow}} = (S_{YT} + S_{UT})/2$, where S_{YT} and S_{UT} are specified at the operating temperature in accordance with the ASME Boiler and Pressure Vessel Code, Section II, Part D; applicable pipe product specification; or room temperature strength multiplied by the temperature derating factor specified by the applicable construction code. Linear interpolation of strength values is allowed between listed temperatures.

(c) This document does not prescribe which definition for flow stress should be used where more than one definition applies. Where more than one definition applies, the various definitions produce acceptable though not necessarily identical results when used with any given evaluation method. It is noted that S_{flow} was defined as $1.1 \times \text{SMYS}$ in previous editions of B31G. This definition remains an inherent element of the Level 0 assessment and is recommended with the Level 1 assessment performed in accordance with para. 2.2(a).

(d) Only the specified nominal wall thickness shall be used for the uncorroded wall thickness when conducting a Level 0 evaluation. If known with confidence, the actual uncorroded wall thickness may be used with a Level 1, Level 2, or Level 3 evaluation, with a suitable adjustment of the hoop stress due to internal pressure.

(e) Pipe body material may be considered to have adequate ductile fracture initiation properties for purposes of this Standard if the material operates at a temperature no colder than 100°F (55°C) below the temperature at which 85% shear appearance is observed in a Charpy V-notched impact test.

(f) Electric resistance welded (ERW) seams that have been subjected to a normalizing heat treatment, single and double submerged arc welded seams, and girth welds made using the shielded metal arc, gas metal arc, flux cored arc, and submerged arc processes (manual or automated, and in any combination) are considered to have adequate ductile fracture initiation properties for purposes of this Standard. Other seam and weld types shall be investigated to establish fracture properties before applying methods described herein to metal loss affecting such welds. Consideration shall be given to the disposition of workmanship flaws or manufacturing flaws within a weld or seam that could interact with metal loss due to corrosion.

(g) Some operating conditions, such as low-temperature service, or long-term exposure to sour environments or to very high temperatures, could adversely affect the ductility and fracture toughness properties of some materials. It is the user's responsibility to consider such conditions where necessary before applying methods described herein.

1.8 Evaluation Procedure

Evaluations shall be carried out in accordance with the procedures described in section 2. In addition, the following considerations apply:

(a) Units may be in any self-consistent system. It is the responsibility of the user to determine unitary conversion factors as may be required.

(b) This document makes no recommendation as to which evaluation level and evaluation method to select. All methods described herein have been demonstrated to provide reliable and conservative results when they are applied correctly and within stated limitations. Not all methods give identical numerical results or consistent degrees of conservatism. It is the pipeline operator's responsibility to select an evaluation method, based on experience and judgment, that is consistent with its operating procedures.

(c) Original source reference documents for each methodology are cited. Further references may be found in other documents available in the public domain. While each method can be applied as presented, source documents may provide additional information to the user. The user should consider referring to applicable sources as necessary in order to best implement a given method.

(d) Other evaluation methods may evolve or come into use which were not contemplated by this document. It is not the intention of this document to prohibit their use, but the user of such methods shall be able to demonstrate that the objective of a safe and reliable assessment of metal loss can be achieved.

1.9 Safety Factors and the Meaning of Acceptance

A flaw or anomaly is considered acceptable where the computed failure stress is equal to or greater than the hoop stress at the operating pressure multiplied by a suitable safety factor. There is no single safety factor that is suitable for all types of pipeline construction, for all modes of pipeline operation, or for all types of flaws or anomalies.

Copyright ASME International
Provided by IHS under license with ASME
No reproduction or networking permitted without license from IHS

This document recommends a minimum safety factor equal to the ratio of the minimum hydrostatic test pressure required for the given type of pipeline construction to the MAOP or MOP, but usually not less than 1.25. Larger factors of safety may be appropriate in some cases, e.g., in locations of greater risk to the public or the environment. Lesser factors of safety may be justified in some circumstances, e.g., for limited periods of time, or where additional procedures are in place to limit modes of operation, or in a remote location having reduced consequences of failure. In establishing the safety factor for a given pipeline segment, the pipeline operator shall give consideration to the accuracy of corrosion depth and length measurements, rates of corrosion growth, the characteristics of the pipe, the reliability of surge control or excess pressure limiting methods, and the presence of external factors that affect risk.

When evaluating anomalies identified by inline inspection, use of larger factors of safety will result in smaller flaws being left in service following field investigation and pipeline repairs. This can increase the reassessment interval to the next inline inspection.

1.10 Software

The use of commercial or proprietary computer software packages, as well as purpose-written programs or spreadsheets, can greatly facilitate Level 1 evaluations, and is practically a necessity for conducting thorough Level 2 and Level 3 evaluations. It is the user's responsibility to verify the accuracy and reliability of all software and spreadsheets, and to train personnel in their correct usage.

Validation of software should include documented evidence that correct results are obtained over the full range of parameters that could reasonably be expected to occur when making evaluations. The following document summarizes the results of burst tests and service failures of line pipe affected by corrosion or artificial metal loss, and which have previously been used for the purpose of validating the evaluation methods presented herein: Kiefner, J. F., Vieth, P. H., and Roytman, I., "Continued Validation of RSTRENG," PRCI Catalog No. L51749, Contract PR 218-9304, Dec. 20, 1996.

Validation may be demonstrated by comparison of calculated results against published benchmark test data such as that found in the above reference, or against results produced by another recognized evaluation method that have been calculated in accordance with this Standard.

Validation of third-party software should also demonstrate that adequate checks or warnings are produced when parameters fall outside ranges that will ensure correct results.

1.11 Accuracy

Consideration should be given to the accuracy of recorded flaw sizes, particularly where indirect methods are used to locate and size the flaws. Methods accounting for uncertainty in indirectly sized flaws include increasing the flaw dimension in order to account for detection tool error, or statistical analysis of the probable flaw sizes or risk of failure.

Metal-loss corrosion anomalies indicated by inline inspection may be evaluated by a Level 1 or Level 2 evaluation method. The user is cautioned against overstating the precision of evaluations applied with flaw dimensions indicated by inline inspection without adequate calibration or verification of actual flaw sizes by investigations carried out in the field.

1.12 Flaw Interaction

The methods described herein are suitable for evaluating isolated areas of metal loss. Corrosion may occur such that multiple areas of metal loss are closely spaced longitudinally or transversely. If spaced sufficiently closely, the metal loss areas may interact so as to result in failure at a lower pressure than would be expected based on an analysis of the separate flaws. The following guideline is suggested with reference to Fig. 1.12-1, based on limited testing and analysis:

(a) Flaws are considered interacting if they are spaced longitudinally or circumferentially from each other within a distance of 3 times the wall thickness ($3t$). Interacting flaws should be evaluated as a single flaw combined from all interacting flaws.

(b) Flaws are considered noninteracting if spaced outside of the above dimensions. Noninteracting flaws should be evaluated as separate flaws.

Care should be exercised when grouping or clustering anomalies indicated by inline inspection for purposes of evaluating interaction during the prioritization process. Consideration should be given to minimum thresholds of metal loss for reliable detection and sizing, minimum thresholds for reporting, and the expected mode of coating failure (e.g., localized failure versus disbondment over large areas). Methods employed for clustering of inline inspection anomalies should be validated by field verification of actual flaw dimensions and spacing.

1.13 Flaw Orientation

Corrosion caused by disbondment of continuous wrapped coatings may exhibit a helical pattern. If the helical pattern lies at an angle less than 45 deg to the pipe axis, the overall length of the corroded area indicated as L_1 in Fig. 1.13-1 shall be considered in the evaluation. If the helical pattern lies at an angle of 45 deg or greater to the pipe axis, it is sufficient to consider the most severe longitudinal section through the corroded area having a length L_2 in Fig. 1.13-1.

Corrosion may occur with a circumferential orientation, e.g., adjacent to a girth weld. It shall be evaluated for safe operating pressure as with corrosion having a helical angle greater than 45 deg to the pipe axis. Evaluation of the circumferential extent of corrosion subject

Copyright ASME International
Provided by IHS under license with ASME
No reproduction or networking permitted without license from IHS

Fig. 1.12-1 Corrosion Pit Interaction Distances

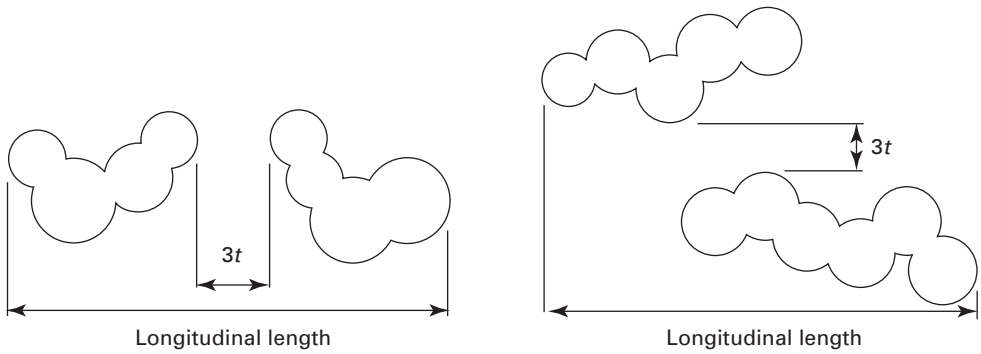

Fig. 1.13-1 Helically Oriented Corrosion Pattern

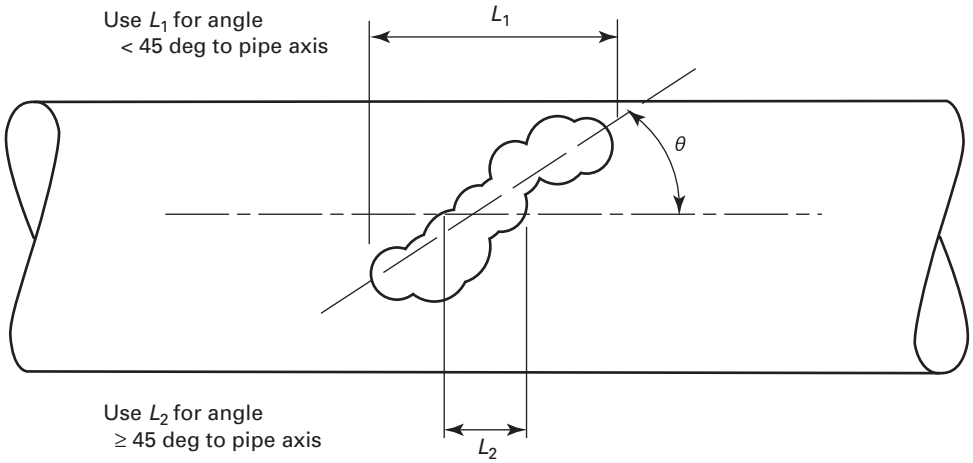

Copyright ASME International
Provided by IHS under license with ASME
No reproduction or networking permitted without license from IHS

to high axial pipe stresses is outside the scope of this document. For such situations, the user should refer to a more comprehensive fitness-for-purpose guidance document, such as API 579-1/ASME FFS-1.

2 EVALUATION METHODS

2.1 Level 0 Evaluation

Tables of allowable length of corrosion are found in section 3. The tables are carried over without change from previous editions of B31G and have been supplemented by the addition of tables in metric units. They were calculated from the equations for a Level 1 evaluation in accordance with the original B31G methodology. They provide a ready reference of maximum corrosion lengths for a range of pipe sizes and depths of corrosion. The tables may be used to determine the maximum allowable longitudinal extent of a contiguous area of corrosion or an interacting cluster of metal loss areas.

Evaluations shall be carried out consistent with the procedure described in the following steps:

Step 1. Determine pipe diameter and nominal wall thickness from appropriate records or direct measurement of the pipe.

Step 2. Determine applicable pipe material properties from appropriate records.

Step 3. Clean the corroded pipe surface to bare metal. Care should be taken when cleaning corroded areas of a pressurized pipe.

Step 4. Measure the maximum depth of the corroded area, d, and longitudinal extent of the corroded area, L, as shown in Fig. 2.1-1.

Step 5. Locate the table corresponding to the size of the pipe, D.

Step 6. In the table, locate the row showing a depth equal to the measured maximum depth of the corroded area. If the exact measured value is not listed, choose the row showing the next greater depth.

Step 7. Read across to the column showing the wall thickness of the pipe. If the nominal wall thickness is not listed, use the column for the next thinner wall. The value, L, found at the intersection of the wall thickness column and the depth row is the maximum allowable longitudinal extent of such a corroded area.

Step 8. The metal loss area on the pipe is acceptable if its measured length, L, does not exceed the value of L given in the table.

The tables produce results that may be more conservative than those obtained by performing a Level 1, Level 2, or Level 3 analysis, particularly for operating hoop stress levels less than 72% of SMYS, and also for very long corroded areas. Therefore, the tables may show that a given corroded area is unsuitable for the current operating pressure, while the use of equations given below may show that it is acceptable.

The tables were designed to provide a minimum factor of safety of 1.39 for pipelines operating with a hoop stress of 72% of SMYS. Application of the tables to the evaluation of corrosion in pipelines operating at hoop stress levels greater than 72% of SMYS will result in a factor of safety that is proportionately less.

2.2 Level 1 Evaluation

Level 1 evaluations shall be carried out consistent with the procedure described in the following steps:

Step 1. Determine pipe diameter and nominal wall thickness from appropriate records or direct measurement of the pipe.

Step 2. Clean the corroded pipe surface to bare metal. Care should be taken when cleaning corroded areas of a pressurized pipe.

Step 3. Measure the maximum depth of the corroded area, d, and longitudinal extent of the corroded area, L, as shown in Fig. 2.1-1.

Step 4. Determine applicable pipe material properties from appropriate records.

Step 5. Select an evaluation method and calculate the estimated failure stress, S_F.

Step 6. Define an acceptable safety factor, SF.

Step 7. Compare S_F to $SF \times S_O$.

Step 8. The flaw is acceptable where S_F is equal to or greater than $SF \times S_O$, or where P_F is equal to or greater than $SF \times P_O$.

If the flaw is unacceptable based on Step 8 above, the pressure can be reduced such that it is less than P_F/SF.

(a) Original B31G

$$M = (1 + 0.8z)^{1/2}$$

For $z \leq 20$,

$$S_F = S_{\text{flow}} \left[\frac{1 - \frac{2}{3}(d/t)}{1 - \frac{2}{3}(d/t)/M} \right]$$

For $z > 20$,

$$S_F = S_{\text{flow}}(1 - d/t)$$

Note that previous editions of B31G incorporated a definition for flow stress of $S_{\text{flow}} = 1.1 \times \text{SMYS}$. For consistency in comparison to results obtained from evaluations performed to an earlier edition, use of the same definition for flow stress is recommended.

Copyright ASME International
Provided by IHS under license with ASME
No reproduction or networking permitted without license from IHS

Fig. 2.1-1 Corrosion Parameters Used in Analysis

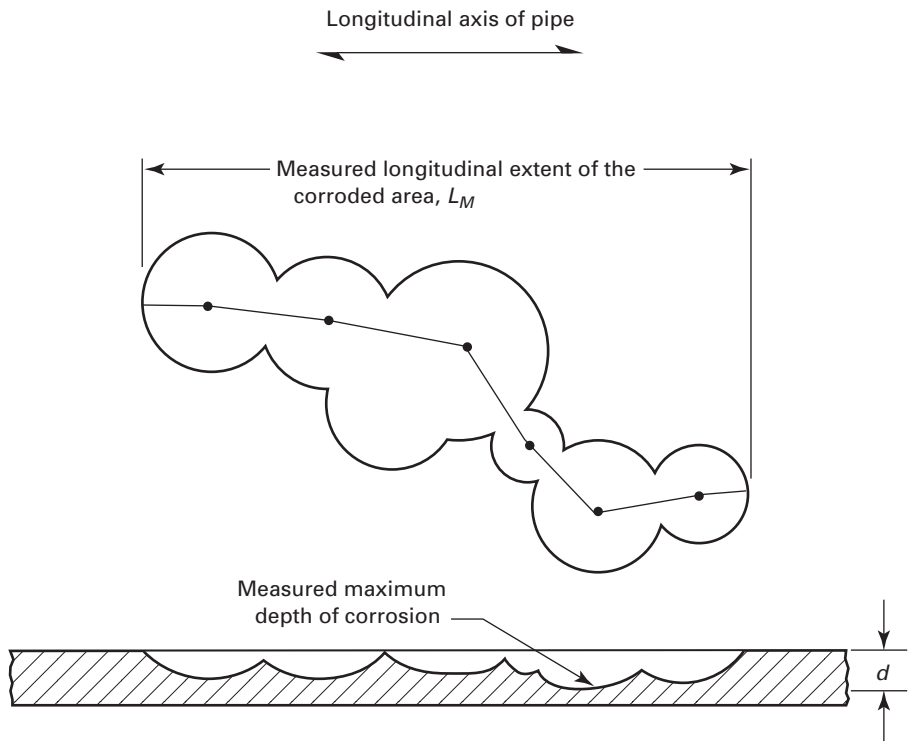

[References: ANSI/ASME B31G-1984 and ASME B31G-1991.]

(b) Modified B31G. For $z \leq 50$,

$$M = (1 + 0.6275z - 0.003375z^2)^{1/2}$$

For $z > 50$,

$$M = 0.032z + 3.3$$

$$S_F = S_{\text{flow}} \left[\frac{1 - 0.85(d/t)}{1 - 0.85(d/t)/M} \right]$$

[References: (1) Kiefner, J. F., and Vieth, P. H., "Project PR3-805: A Modified Criterion for Evaluating the Remaining Strength of Corroded Pipe," AGA Catalog No. L51609, Dec. 22, 1989; (2) Kiefner, J. F., and Vieth, P. H., "New Method Corrects Criterion for Evaluating Corroded Pipe," Oil & Gas Journal, Aug. 6 and Aug. 20, 1990.]

(c) API 579 Level 1. The "API 579 Level 1" assessment, when reduced to its simplest form, is of a similar format to the other Level 1 methods presented herein, and therefore qualifies as a Level 1 assessment for purposes of meeting the requirements of this document.

(12) 2.3 Level 2 Evaluation

Level 2 evaluations are performed using what is known as the Effective Area Method. Level 2 evaluations shall be carried out using a procedure similar to the ten steps described for Level 1, except that the Effective Area Method generally requires several measurements of the depth of corrosion or remaining wall thickness throughout the corroded area. The Effective Area Method is expressed as follows:

$$S_F = S_{\text{flow}} \left[\frac{1 - A/A_0}{1 - (A/A_0)/M} \right]$$

The Effective Area Method evaluates, by iteration, all possible combinations of local metal loss, A, with respect to original material, A_0. It requires for input a detailed longitudinal distribution or profile of metal loss. The detailed profile is established by obtaining several measurements of metal loss or remaining wall thickness throughout the metal loss area. Such measurements may be arranged in a grid pattern, or may follow a "river bottom" path through the deepest areas of metal loss. Increments of measurement need not be uniform, subject to limitations of application software. If using a grid pattern, the analysis must be repeated along each meridian to establish the governing solution. For a corroded profile defined by n measurements of depth of corrosion including the end points at nominally full wall thickness, $n!/2(n - 2)!$ iterations are required to examine all possible combinations of local metal loss with respect to surrounding remaining material. The local solution resulting in the lowest calculated failure stress shall govern.

Copyright ASME International
Provided by IHS under license with ASME
No reproduction or networking permitted without license from IHS

Owing to its iterative nature, it is a practical necessity to use a computer program or other algorithmic approach (e.g., a spreadsheet) in order to carry out an evaluation using the Effective Area Method.

The "API 579 Level 2" assessment, when reduced to its simplest form, is equivalent to the Effective Area Method presented herein, and therefore qualifies as a Level 2 assessment for purposes of meeting the requirements of this document. Refer to API 579-1/ASME FFS-1 for detailed instructions.

[References: Same as in para. 2.2(b).]

2.4 Level 3 Evaluation

A Level 3 evaluation typically involves a detailed analysis, such as a finite element analysis of the corroded region. The analysis should accurately consider or account for all factors that could affect the accuracy of results, including loadings including internal pressure and external forces; boundary conditions and constraints; ovality, deformations, misalignments, and discontinuities; material stress–strain characteristics; and effects of the flaw on the overall distribution of loads and stresses. A failure criterion should be developed that considers the strain capacity or fracture resistance characteristics of the material. Similar issues should be considered in developing a suitable safety factor as were described for a Level 1 or Level 2 analysis.

3 TABLES OF ALLOWABLE LENGTH OF CORROSION

The following are applicable to Tables 3-1 through 3-12M:

(a) Metal loss having a maximum depth of 10% of the nominal pipe wall thickness or less is not limited as to allowable length.

(b) Metal loss having a maximum depth exceeding 80% of the nominal pipe wall thickness shall not be evaluated using the tables of allowable length.

Copyright ASME International
Provided by IHS under license with ASME
No reproduction or networking permitted without license from IHS

Table 3-1 Values of *L* for Pipe Sizes ≥ NPS 2 and < NPS 6 (12)

Depth, *d*, in.	Wall Thickness, *t*, in.							
	0.083	0.109	0.125	0.141	0.154	0.172	0.188	0.218
0.01	1.99	No limit	No limit	No limit	No limit	No limit	No limit	No limit
0.02	0.92	1.94	2.44	2.59	2.71	2.86	2.99	No limit
0.03	0.53	0.85	1.13	1.51	1.94	2.86	2.99	3.22
0.04	0.39	0.60	0.75	0.93	1.11	1.40	1.74	2.74
0.05	0.31	0.47	0.58	0.70	0.82	1.00	1.18	1.62
0.06	0.25	0.39	0.48	0.58	0.66	0.79	0.92	1.21
0.07	. . .	0.33	0.41	0.49	0.56	0.67	0.77	0.99
0.08	. . .	0.28	0.35	0.43	0.49	0.58	0.67	0.84
0.09	. . .	. . .	0.31	0.38	0.43	0.51	0.59	0.74
0.10	. . .	. . .	0.27	0.33	0.39	0.46	0.53	0.66
0.11	. . .	. . .	. . .	0.30	0.35	0.41	0.48	0.60
0.12	. . .	. . .	. . .	. . .	0.31	0.38	0.43	0.55
0.13	. . .	. . .	. . .	. . .	. . .	0.34	0.40	0.50
0.14	. . .	. . .	. . .	. . .	. . .	. . .	0.37	0.46
0.15	. . .	. . .	. . .	. . .	. . .	. . .	0.34	0.43
0.16	. . .	. . .	. . .	. . .	. . .	. . .	. . .	0.40
0.17	. . .	. . .	. . .	. . .	. . .	. . .	. . .	0.37

Table 3-1M Values of *L* for Pipe Sizes ≥ 60 mm and < 168 mm O.D. (12)

Depth, *d*, mm	Wall Thickness, *t*, mm							
	2.1	2.8	3.2	3.6	3.9	4.4	4.8	5.5
0.3	50.5	No limit	No limit	No limit	No limit	No limit	No limit	No limit
0.5	23.2	49.1	62.0	65.8	68.8	72.7	76.0	No limit
0.8	13.4	21.7	28.7	38.3	49.2	72.7	76.0	81.9
1.0	9.8	15.1	19.0	23.7	28.1	35.6	44.2	69.5
1.3	7.8	11.9	14.7	17.9	20.8	25.3	29.9	41.1
1.5	6.4	9.8	12.1	14.6	16.8	20.1	23.4	30.7
1.8	. . .	8.3	10.3	12.4	14.3	17.0	19.5	25.0
2.0	. . .	7.2	9.0	10.8	12.4	14.7	16.9	21.4
2.3	. . .	. . .	7.9	9.5	11.0	13.0	14.9	18.8
2.5	. . .	. . .	6.9	8.5	9.8	11.6	13.4	16.8
2.8	. . .	. . .	. . .	7.6	8.8	10.5	12.1	15.2
3.0	. . .	. . .	. . .	. . .	8.0	9.6	11.0	13.9
3.3	. . .	. . .	. . .	. . .	. . .	8.7	10.1	12.8
3.6	. . .	. . .	. . .	. . .	. . .	. . .	9.3	11.8
3.8	. . .	. . .	. . .	. . .	. . .	. . .	8.5	10.9
4.1	. . .	. . .	. . .	. . .	. . .	. . .	. . .	10.2
4.3	. . .	. . .	. . .	. . .	. . .	. . .	. . .	9.5

Copyright ASME International
Provided by IHS under license with ASME
No reproduction or networking permitted without license from IHS

(12) **Table 3-2 Values of *L* for Pipe Sizes ≥ NPS 6 and < NPS 10**

Depth, *d*, in.	Wall Thickness, *t*, in.							
	0.083	0.125	0.156	0.188	0.203	0.219	0.250	0.312
0.01	3.32	No limit	No limit	No limit	No limit	No limit	No limit	No limit
0.02	1.53	4.08	4.55	5.00	No limit	No limit	No limit	No limit
0.03	0.88	1.89	3.37	5.00	5.20	5.40	5.77	No limit
0.04	0.65	1.25	1.90	2.91	3.61	4.65	5.77	6.44
0.05	0.51	0.97	1.40	1.97	2.30	2.73	3.86	6.44
0.06	0.42	0.80	1.13	1.54	1.77	2.04	2.67	4.77
0.07	. . .	0.68	0.96	1.29	1.46	1.66	2.11	3.37
0.08	. . .	0.59	0.83	1.11	1.25	1.42	1.77	2.68
0.09	. . .	0.52	0.74	0.98	1.10	1.24	1.54	2.26
0.10	. . .	0.46	0.66	0.88	0.99	1.11	1.37	1.97
0.11	. . .	. . .	0.59	0.80	0.90	1.01	1.24	1.76
0.12	. . .	. . .	0.54	0.73	0.82	0.92	1.13	1.60
0.13	. . .	. . .	. . .	0.66	0.75	0.85	1.04	1.46
0.14	. . .	. . .	. . .	0.61	0.69	0.78	0.96	1.35
0.15	. . .	. . .	. . .	0.56	0.64	0.72	0.89	1.26
0.16	. . .	. . .	. . .	. . .	0.59	0.67	0.83	1.18
0.17	. . .	. . .	. . .	. . .	. . .	0.63	0.78	1.10
0.18	. . .	. . .	. . .	. . .	. . .	. . .	0.73	1.04
0.19	. . .	. . .	. . .	. . .	. . .	. . .	0.69	0.98
0.20	. . .	. . .	. . .	. . .	. . .	. . .	0.65	0.93
0.21	. . .	. . .	. . .	. . .	. . .	. . .	. . .	0.88
0.22	. . .	. . .	. . .	. . .	. . .	. . .	. . .	0.84
0.23	. . .	. . .	. . .	. . .	. . .	. . .	. . .	0.80
0.24	. . .	. . .	. . .	. . .	. . .	. . .	. . .	0.76

Copyright ASME International
Provided by IHS under license with ASME
No reproduction or networking permitted without license from IHS

Table 3-2M Values of *L* for Pipe Sizes ≥ 168 mm and < 273 mm O.D. (12)

Depth, *d*, mm	Wall Thickness, *t*, mm							
	2.1	3.2	4.0	4.8	5.2	5.6	6.4	7.9
0.3	84.4	No limit	No limit	No limit	No limit	No limit	No limit	No limit
0.5	38.8	103.6	115.7	127.0	No limit	No limit	No limit	No limit
0.8	22.4	48.0	85.6	127.0	132.0	137.1	146.4	No limit
1.0	16.4	31.8	48.1	73.8	91.6	118.1	146.4	163.6
1.3	13.0	24.6	35.5	50.0	58.5	69.3	98.0	163.6
1.5	10.7	20.3	28.7	39.1	44.9	51.7	67.8	121.1
1.8	. . .	17.3	24.3	32.6	37.1	42.2	53.6	85.5
2.0	. . .	15.0	21.1	28.2	31.9	36.0	45.0	68.1
2.3	. . .	13.1	18.7	24.9	28.1	31.6	39.1	57.4
2.5	. . .	11.6	16.7	22.3	25.1	28.3	34.8	50.2
2.8	. . .	. . .	15.0	20.2	22.8	25.6	31.4	44.8
3.0	. . .	. . .	13.6	18.4	20.8	23.4	28.7	40.6
3.3	. . .	. . .	. . .	16.9	19.1	21.5	26.4	37.2
3.6	. . .	. . .	. . .	15.5	17.6	19.8	24.4	34.4
3.8	. . .	. . .	. . .	14.3	16.3	18.4	22.7	32.0
4.1	. . .	. . .	. . .	. . .	15.1	17.1	21.2	29.9
4.3	. . .	. . .	. . .	. . .	. . .	15.9	19.8	28.0
4.6	. . .	. . .	. . .	. . .	. . .	. . .	18.6	26.4
4.8	. . .	. . .	. . .	. . .	. . .	. . .	17.5	25.0
5.1	. . .	. . .	. . .	. . .	. . .	. . .	16.4	23.6
5.3	. . .	. . .	. . .	. . .	. . .	. . .	. . .	22.4
5.6	. . .	. . .	. . .	. . .	. . .	. . .	. . .	21.3
5.8	. . .	. . .	. . .	. . .	. . .	. . .	. . .	20.2
6.1	. . .	. . .	. . .	. . .	. . .	. . .	. . .	19.2

Copyright ASME International
Provided by IHS under license with ASME
No reproduction or networking permitted without license from IHS

Table 3-3 Values of *L* for Pipe Sizes ≥ NPS 10 and < NPS 16

Depth, *d*, in.	Wall Thickness, *t*, in.							
	0.156	0.219	0.250	0.307	0.344	0.365	0.438	0.500
0.02	5.80	No limit	No limit	No limit	No limit	No limit	No limit	No limit
0.03	4.29	6.87	7.34	No limit	No limit	No limit	No limit	No limit
0.04	2.41	5.92	7.34	8.14	8.62	8.87	No limit	No limit
0.05	1.78	3.48	4.91	8.14	8.62	8.87	9.72	10.39
0.06	1.44	2.59	3.40	5.77	8.62	8.87	9.72	10.39
0.07	1.22	2.11	2.69	4.13	5.53	6.62	9.72	10.39
0.08	1.06	1.81	2.26	3.30	4.22	4.85	8.37	10.39
0.09	0.94	1.59	1.96	2.80	3.48	3.93	6.10	9.38
0.10	0.84	1.42	1.74	2.45	2.99	3.35	4.92	6.95
0.11	0.75	1.28	1.57	2.19	2.65	2.94	4.18	5.64
0.12	0.68	1.17	1.44	1.98	2.39	2.64	3.67	4.81
0.13	. . .	1.08	1.32	1.82	2.18	2.40	3.29	4.23
0.14	. . .	1.00	1.22	1.68	2.01	2.21	2.99	3.80
0.15	. . .	0.92	1.14	1.56	1.86	2.05	2.75	3.46
0.16	. . .	0.86	1.06	1.46	1.74	1.91	2.55	3.19
0.17	. . .	0.80	0.99	1.37	1.64	1.79	2.39	2.97
0.18	. . .	. . .	0.93	1.29	1.54	1.69	2.24	2.77
0.19	. . .	. . .	0.88	1.22	1.46	1.60	2.12	2.61
0.20	. . .	. . .	0.82	1.15	1.38	1.51	2.00	2.47
0.21	. . .	. . .	. . .	1.09	1.31	1.44	1.90	2.34
0.22	. . .	. . .	. . .	1.04	1.25	1.37	1.81	2.23
0.23	. . .	. . .	. . .	0.99	1.19	1.30	1.73	2.12
0.24	. . .	. . .	. . .	0.94	1.13	1.25	1.66	2.03
0.25	. . .	. . .	. . .	. . .	1.08	1.19	1.59	1.95
0.26	. . .	. . .	. . .	. . .	1.03	1.14	1.52	1.87
0.27	. . .	. . .	. . .	. . .	0.99	1.09	1.46	1.80
0.28	. . .	. . .	. . .	. . .	. . .	1.05	1.41	1.73
0.29	. . .	. . .	. . .	. . .	. . .	1.00	1.35	1.67
0.30	. . .	. . .	. . .	. . .	. . .	. . .	1.31	1.61
0.31	. . .	. . .	. . .	. . .	. . .	. . .	1.26	1.55
0.32	. . .	. . .	. . .	. . .	. . .	. . .	1.21	1.50
0.33	. . .	. . .	. . .	. . .	. . .	. . .	1.17	1.45
0.34	. . .	. . .	. . .	. . .	. . .	. . .	1.13	1.41
0.35	. . .	. . .	. . .	. . .	. . .	. . .	1.09	1.36
0.36	. . .	. . .	. . .	. . .	. . .	. . .	. . .	1.32
0.37	. . .	. . .	. . .	. . .	. . .	. . .	. . .	1.28
0.38	. . .	. . .	. . .	. . .	. . .	. . .	. . .	1.24
0.39	. . .	. . .	. . .	. . .	. . .	. . .	. . .	1.20
0.40	. . .	. . .	. . .	. . .	. . .	. . .	. . .	1.16

Copyright ASME International
Provided by IHS under license with ASME
No reproduction or networking permitted without license from IHS

Table 3-3M Values of *L* for Pipe Sizes ≥ 273 mm and < 406 mm O.D.

Depth, *d*, mm	Wall Thickness, *t*, mm							
	4.0	5.6	6.4	7.8	8.7	9.3	11.1	12.7
0.5	147.4	No limit	No limit	No limit	No limit	No limit	No limit	No limit
0.8	109.1	174.6	186.5	No limit	No limit	No limit	No limit	No limit
1.0	61.3	150.4	186.5	206.7	218.8	225.4	No limit	No limit
1.3	45.2	88.3	124.8	206.7	218.8	225.4	246.9	263.8
1.5	36.5	65.9	86.4	146.6	218.8	225.4	246.9	263.8
1.8	30.9	53.7	68.2	104.8	140.5	168.1	246.9	263.8
2.0	26.9	45.9	57.3	83.9	107.1	123.3	212.7	263.8
2.3	23.8	40.3	49.8	71.0	88.3	99.8	155.0	238.4
2.5	21.3	36.0	44.3	62.1	76.0	85.0	124.9	176.5
2.8	19.2	32.6	40.0	55.5	67.3	74.7	106.1	143.3
3.0	17.3	29.8	36.5	50.4	60.6	67.0	93.1	122.2
3.3	. . .	27.4	33.6	46.2	55.3	61.0	83.5	107.5
3.6	. . .	25.3	31.1	42.7	51.0	56.1	76.0	96.5
3.8	. . .	23.4	28.9	39.7	47.4	52.0	69.9	87.9
4.1	. . .	21.8	27.0	37.1	44.2	48.5	64.9	81.0
4.3	. . .	20.3	25.2	34.8	41.5	45.5	60.6	75.3
4.6	. . .	. . .	23.7	32.8	39.1	42.9	56.9	70.5
4.8	. . .	. . .	22.2	31.0	37.0	40.5	53.7	66.3
5.1	. . .	. . .	20.9	29.3	35.1	38.4	50.9	62.7
5.3	. . .	. . .	. . .	27.8	33.3	36.5	48.4	59.4
5.6	. . .	. . .	. . .	26.4	31.7	34.8	46.1	56.6
5.8	. . .	. . .	. . .	25.1	30.2	33.1	44.0	54.0
6.1	. . .	. . .	. . .	23.8	28.8	31.7	42.1	51.6
6.4	. . .	. . .	. . .	. . .	27.5	30.3	40.3	49.5
6.6	. . .	. . .	. . .	. . .	26.3	29.0	38.7	47.5
6.9	. . .	. . .	. . .	. . .	25.1	27.7	37.2	45.7
7.1	. . .	. . .	. . .	. . .	. . .	26.6	35.7	44.0
7.4	. . .	. . .	. . .	. . .	. . .	25.5	34.4	42.4
7.6	. . .	. . .	. . .	. . .	. . .	. . .	33.2	40.9
7.9	. . .	. . .	. . .	. . .	. . .	. . .	32.0	39.5
8.1	. . .	. . .	. . .	. . .	. . .	. . .	30.8	38.1
8.4	. . .	. . .	. . .	. . .	. . .	. . .	29.7	36.9
8.6	. . .	. . .	. . .	. . .	. . .	. . .	28.7	35.7
8.9	. . .	. . .	. . .	. . .	. . .	. . .	27.7	34.6
9.1	. . .	. . .	. . .	. . .	. . .	. . .	. . .	33.5
9.4	. . .	. . .	. . .	. . .	. . .	. . .	. . .	32.4
9.7	. . .	. . .	. . .	. . .	. . .	. . .	. . .	31.4
9.9	. . .	. . .	. . .	. . .	. . .	. . .	. . .	30.5
10.2	. . .	. . .	. . .	. . .	. . .	. . .	. . .	29.6

Copyright ASME International
Provided by IHS under license with ASME
No reproduction or networking permitted without license from IHS

(12) **Table 3-4 Values of *L* for Pipe Sizes ≥ NPS 16 and < NPS 20**

Depth, *d*, in.	Wall Thickness, *t*, in.							
	0.188	0.250	0.312	0.344	0.375	0.438	0.500	0.625
0.02	7.77	No limit	No limit	No limit	No limit	No limit	No limit	No limit
0.03	7.77	8.96	No limit	No limit	No limit	No limit	No limit	No limit
0.04	4.52	8.96	10.01	10.51	10.97	No limit	No limit	No limit
0.05	3.06	6.00	10.01	10.51	10.97	11.86	12.67	No limit
0.06	2.39	4.15	7.41	10.51	10.97	11.86	12.67	No limit
0.07	2.00	3.28	5.23	6.75	8.84	11.86	12.67	14.17
0.08	1.73	2.75	4.17	5.14	6.34	10.21	12.67	14.17
0.09	1.52	2.39	3.51	4.24	5.08	7.44	11.45	14.17
0.10	1.37	2.13	3.07	3.65	4.30	6.00	8.48	14.17
0.11	1.24	1.92	2.74	3.23	3.77	5.10	6.88	13.85
0.12	1.13	1.75	2.48	2.91	3.37	4.47	5.87	10.53
0.13	1.03	1.61	2.27	2.66	3.06	4.01	5.16	8.65
0.14	0.95	1.49	2.10	2.45	2.81	3.65	4.63	7.43
0.15	0.87	1.39	1.96	2.28	2.61	3.36	4.22	6.56
0.16	. . .	1.30	1.83	2.13	2.43	3.12	3.89	5.91
0.17	. . .	1.21	1.72	1.99	2.28	2.91	3.62	5.40
0.18	. . .	1.14	1.62	1.88	2.15	2.74	3.38	4.99
0.19	. . .	1.07	1.53	1.78	2.03	2.58	3.18	4.64
0.20	. . .	1.00	1.44	1.68	1.92	2.45	3.01	4.35
0.21	. . .	. . .	1.37	1.60	1.83	2.32	2.85	4.10
0.22	. . .	. . .	1.30	1.52	1.74	2.21	2.72	3.88
0.23	. . .	. . .	1.24	1.45	1.66	2.11	2.59	3.69
0.24	. . .	. . .	1.18	1.38	1.59	2.02	2.48	3.52
0.25	. . .	. . .	. . .	1.32	1.52	1.94	2.38	3.36
0.26	. . .	. . .	. . .	1.26	1.45	1.86	2.28	3.22
0.27	. . .	. . .	. . .	1.21	1.39	1.79	2.19	3.10
0.28	. . .	. . .	. . .	. . .	1.34	1.72	2.11	2.98
0.29	. . .	. . .	. . .	. . .	1.28	1.65	2.03	2.87
0.30	. . .	. . .	. . .	. . .	1.23	1.59	1.96	2.77
0.31	. . .	. . .	. . .	. . .	. . .	1.53	1.90	2.68
0.32	. . .	. . .	. . .	. . .	. . .	1.48	1.83	2.59
0.33	. . .	. . .	. . .	. . .	. . .	1.43	1.77	2.51
0.34	. . .	. . .	. . .	. . .	. . .	1.38	1.71	2.43
0.35	. . .	. . .	. . .	. . .	. . .	1.33	1.66	2.36
0.36	. . .	. . .	. . .	. . .	. . .	. . .	1.61	2.29
0.37	. . .	. . .	. . .	. . .	. . .	. . .	1.56	2.23
0.38	. . .	. . .	. . .	. . .	. . .	. . .	1.51	2.16
0.39	. . .	. . .	. . .	. . .	. . .	. . .	1.46	2.11
0.40	. . .	. . .	. . .	. . .	. . .	. . .	1.42	2.05
0.41	. . .	. . .	. . .	. . .	. . .	. . .	. . .	1.99
0.42	. . .	. . .	. . .	. . .	. . .	. . .	. . .	1.94
0.43	. . .	. . .	. . .	. . .	. . .	. . .	. . .	1.89
0.44	. . .	. . .	. . .	. . .	. . .	. . .	. . .	1.84
0.45	. . .	. . .	. . .	. . .	. . .	. . .	. . .	1.80
0.46	. . .	. . .	. . .	. . .	. . .	. . .	. . .	1.75
0.47	. . .	. . .	. . .	. . .	. . .	. . .	. . .	1.71
0.48	. . .	. . .	. . .	. . .	. . .	. . .	. . .	1.67
0.49	. . .	. . .	. . .	. . .	. . .	. . .	. . .	1.63
0.50	. . .	. . .	. . .	. . .	. . .	. . .	. . .	1.59

Copyright ASME International
Provided by IHS under license with ASME
No reproduction or networking permitted without license from IHS

Table 3-4M Values of *L* for Pipe Sizes ≥ 406 mm and < 508 mm O.D. (12)

Depth, *d*, mm	Wall Thickness, *t*, mm							
	4.8	6.4	7.9	8.7	9.5	11.1	12.7	15.9
0.5	197.4	No limit	No limit	No limit	No limit	No limit	No limit	No limit
0.8	197.4	227.6	No limit	No limit	No limit	No limit	No limit	No limit
1.0	114.8	227.6	254.2	267.0	278.7	No limit	No limit	No limit
1.3	77.7	152.3	254.2	267.0	278.7	301.2	321.9	No limit
1.5	60.8	105.4	188.2	267.0	278.7	301.2	321.9	No limit
1.8	50.7	83.2	132.9	171.4	224.5	301.2	321.9	359.8
2.0	43.8	69.9	105.8	130.6	161.2	259.5	321.9	359.8
2.3	38.7	60.8	89.3	107.7	129.1	189.1	290.8	359.8
2.5	34.7	54.1	77.9	92.8	109.3	152.4	215.4	359.8
2.8	31.4	48.8	69.6	82.1	95.7	129.5	174.8	351.8
3.0	28.6	44.5	63.0	73.9	85.6	113.6	149.1	267.5
3.3	26.2	41.0	57.8	67.5	77.8	101.8	131.1	219.8
3.6	24.1	37.9	53.4	62.2	71.4	92.7	117.7	188.7
3.8	22.2	35.3	49.7	57.8	66.2	85.3	107.3	166.7
4.1	. . .	32.9	46.4	54.0	61.7	79.1	98.9	150.1
4.3	. . .	30.8	43.6	50.7	57.9	73.9	91.9	137.1
4.6	. . .	28.9	41.1	47.7	54.5	69.5	86.0	126.6
4.8	. . .	27.1	38.8	45.1	51.5	65.6	80.9	117.9
5.1	. . .	25.5	36.7	42.8	48.9	62.1	76.4	110.5
5.3	. . .	. . .	34.8	40.6	46.4	59.0	72.5	104.2
5.6	. . .	. . .	33.0	38.6	44.2	56.2	69.0	98.6
5.8	. . .	. . .	31.4	36.8	42.2	53.7	65.8	93.7
6.1	. . .	. . .	29.9	35.1	40.3	51.3	63.0	89.4
6.4	. . .	. . .	. . .	33.5	38.6	49.2	60.3	85.5
6.6	. . .	. . .	. . .	32.0	36.9	47.2	57.9	81.9
6.9	. . .	. . .	. . .	30.6	35.4	45.4	55.7	78.7
7.1	. . .	. . .	. . .	. . .	33.9	43.6	53.6	75.7
7.4	. . .	. . .	. . .	. . .	32.5	42.0	51.7	72.9
7.6	. . .	. . .	. . .	. . .	31.2	40.4	49.9	70.4
7.9	. . .	. . .	. . .	. . .	. . .	39.0	48.2	68.0
8.1	. . .	. . .	. . .	. . .	. . .	37.6	46.5	65.8
8.4	. . .	. . .	. . .	. . .	. . .	36.3	45.0	63.7
8.6	. . .	. . .	. . .	. . .	. . .	35.0	43.6	61.8
8.9	. . .	. . .	. . .	. . .	. . .	33.8	42.2	60.0
9.1	. . .	. . .	. . .	. . .	. . .	. . .	40.9	58.2
9.4	. . .	. . .	. . .	. . .	. . .	. . .	39.6	56.6
9.7	. . .	. . .	. . .	. . .	. . .	. . .	38.4	55.0
9.9	. . .	. . .	. . .	. . .	. . .	. . .	37.2	53.5
10.2	. . .	. . .	. . .	. . .	. . .	. . .	36.1	52.0
10.4	. . .	. . .	. . .	. . .	. . .	. . .	. . .	50.7
10.7	. . .	. . .	. . .	. . .	. . .	. . .	. . .	49.3
10.9	. . .	. . .	. . .	. . .	. . .	. . .	. . .	48.1
11.2	. . .	. . .	. . .	. . .	. . .	. . .	. . .	46.9
11.4	. . .	. . .	. . .	. . .	. . .	. . .	. . .	45.7
11.7	. . .	. . .	. . .	. . .	. . .	. . .	. . .	44.5
11.9	. . .	. . .	. . .	. . .	. . .	. . .	. . .	43.4
12.2	. . .	. . .	. . .	. . .	. . .	. . .	. . .	42.4
12.4	. . .	. . .	. . .	. . .	. . .	. . .	. . .	41.3
12.7	. . .	. . .	. . .	. . .	. . .	. . .	. . .	40.3

Copyright ASME International
Provided by IHS under license with ASME
No reproduction or networking permitted without license from IHS

Table 3-5 Values of *L* for Pipe Sizes ≥ NPS 20 and < NPS 24

Depth, *d*, in.	Wall Thickness, *t*, in.							
	0.219	0.250	0.344	0.406	0.469	0.500	0.562	0.625
0.03	9.38	10.02	No limit	No limit	No limit	No limit	No limit	No limit
0.04	8.08	10.02	11.75	No limit	No limit	No limit	No limit	No limit
0.05	4.74	6.70	11.75	12.77	13.72	14.17	No limit	No limit
0.06	3.54	4.64	11.75	12.77	13.72	14.17	15.02	No limit
0.07	2.88	3.66	7.54	12.77	13.72	14.17	15.02	15.84
0.08	2.46	3.08	5.75	8.86	13.72	14.17	15.02	15.84
0.09	2.16	2.68	4.74	6.83	10.21	12.80	15.02	15.84
0.10	1.93	2.38	4.08	5.66	7.94	9.48	14.12	15.84
0.11	1.75	2.15	3.61	4.89	6.61	7.69	10.61	15.49
0.12	1.60	1.96	3.26	4.34	5.73	6.56	8.67	11.77
0.13	1.47	1.80	2.97	3.92	5.09	5.77	7.42	9.67
0.14	1.36	1.67	2.74	3.58	4.60	5.18	6.54	8.31
0.15	1.26	1.55	2.54	3.31	4.22	4.72	5.88	7.34
0.16	1.17	1.45	2.38	3.08	3.90	4.35	5.37	6.61
0.17	1.09	1.36	2.23	2.89	3.64	4.04	4.95	6.04
0.18	. . .	1.27	2.10	2.72	3.41	3.78	4.61	5.57
0.19	. . .	1.19	1.99	2.56	3.21	3.56	4.32	5.19
0.20	. . .	1.12	1.88	2.43	3.04	3.36	4.07	4.87
0.21	. . .	. . .	1.79	2.31	2.89	3.19	3.85	4.59
0.22	. . .	. . .	1.70	2.20	2.75	3.04	3.65	4.34
0.23	. . .	. . .	1.62	2.10	2.63	2.90	3.48	4.13
0.24	. . .	. . .	1.55	2.01	2.51	2.77	3.32	3.93
0.25	. . .	. . .	1.48	1.92	2.41	2.66	3.18	3.76
0.26	. . .	. . .	1.41	1.84	2.31	2.55	3.05	3.61
0.27	. . .	. . .	1.35	1.77	2.22	2.45	2.94	3.46
0.28	. . .	. . .	. . .	1.70	2.14	2.36	2.83	3.33
0.29	. . .	. . .	. . .	1.64	2.06	2.27	2.73	3.21
0.30	. . .	. . .	. . .	1.57	1.99	2.19	2.63	3.10
0.31	. . .	. . .	. . .	1.51	1.92	2.12	2.54	2.99
0.32	. . .	. . .	. . .	1.46	1.85	2.05	2.46	2.90
0.33	. . .	. . .	. . .	. . .	1.79	1.98	2.38	2.81
0.34	. . .	. . .	. . .	. . .	1.73	1.92	2.31	2.72
0.35	. . .	. . .	. . .	. . .	1.67	1.86	2.24	2.64
0.36	. . .	. . .	. . .	. . .	1.62	1.80	2.17	2.56
0.37	. . .	. . .	. . .	. . .	1.56	1.74	2.11	2.49
0.38	. . .	. . .	. . .	. . .	. . .	1.69	2.05	2.42
0.39	. . .	. . .	. . .	. . .	. . .	1.64	1.99	2.35
0.40	. . .	. . .	. . .	. . .	. . .	1.59	1.93	2.29
0.41	. . .	. . .	. . .	. . .	. . .	. . .	1.88	2.23
0.42	. . .	. . .	. . .	. . .	. . .	. . .	1.83	2.17
0.43	. . .	. . .	. . .	. . .	. . .	. . .	1.78	2.12
0.44	. . .	. . .	. . .	. . .	. . .	. . .	1.73	2.06
0.45	. . .	. . .	. . .	. . .	. . .	. . .	. . .	2.01
0.46	. . .	. . .	. . .	. . .	. . .	. . .	. . .	1.96
0.47	. . .	. . .	. . .	. . .	. . .	. . .	. . .	1.91
0.48	. . .	. . .	. . .	. . .	. . .	. . .	. . .	1.86
0.49	. . .	. . .	. . .	. . .	. . .	. . .	. . .	1.82
0.50	. . .	. . .	. . .	. . .	. . .	. . .	. . .	1.78

Copyright ASME International
Provided by IHS under license with ASME
No reproduction or networking permitted without license from IHS

Table 3-5M Values of *L* for Pipe Sizes ≥ 508 mm and < 610 mm O.D.

Depth, *d*, mm	Wall Thickness, *t*, mm							
	5.6	6.4	8.7	10.3	11.9	12.7	14.3	15.9
0.8	238.1	254.4	No limit	No limit	No limit	No limit	No limit	No limit
1.0	205.1	254.4	298.5	No limit	No limit	No limit	No limit	No limit
1.3	120.5	170.3	298.5	324.3	348.5	359.8	No limit	No limit
1.5	89.8	117.8	298.5	324.3	348.5	359.8	381.5	No limit
1.8	73.3	93.1	191.6	324.3	348.5	359.8	381.5	402.3
2.0	62.6	78.2	146.0	225.2	348.5	359.8	381.5	402.3
2.3	54.9	68.0	120.4	173.5	259.5	325.1	381.5	402.3
2.5	49.1	60.4	103.7	143.8	201.7	240.8	358.6	402.3
2.8	44.4	54.6	91.8	124.3	168.0	195.4	269.5	393.4
3.0	40.6	49.8	82.7	110.2	145.5	166.7	220.2	299.1
3.3	37.3	45.8	75.5	99.5	129.3	146.6	188.5	245.7
3.6	34.5	42.4	69.6	91.0	116.9	131.6	166.1	211.0
3.8	32.0	39.4	64.6	84.1	107.1	119.9	149.4	186.3
4.1	29.7	36.8	60.4	78.3	99.1	110.5	136.4	167.8
4.3	27.7	34.4	56.6	73.3	92.4	102.7	125.8	153.3
4.6	. . .	32.3	53.4	69.0	86.6	96.1	117.1	141.6
4.8	. . .	30.3	50.5	65.1	81.6	90.4	109.6	131.8
5.1	. . .	28.5	47.8	61.7	77.2	85.5	103.3	123.6
5.3	. . .	. . .	45.4	58.7	73.3	81.1	97.7	116.5
5.6	. . .	. . .	43.2	55.9	69.8	77.1	92.8	110.3
5.8	. . .	. . .	41.2	53.4	66.7	73.6	88.4	104.8
6.1	. . .	. . .	39.3	51.0	63.8	70.4	84.4	99.9
6.4	. . .	. . .	37.5	48.9	61.1	67.5	80.9	95.5
6.6	. . .	. . .	35.8	46.9	58.7	64.8	77.6	91.6
6.9	. . .	. . .	34.2	45.0	56.4	62.3	74.6	88.0
7.1	. . .	. . .	. . .	43.2	54.3	60.0	71.8	84.6
7.4	. . .	. . .	. . .	41.5	52.3	57.8	69.2	81.6
7.6	. . .	. . .	. . .	39.9	50.4	55.8	66.8	78.7
7.9	. . .	. . .	. . .	38.4	48.7	53.8	64.6	76.1
8.1	. . .	. . .	. . .	37.0	47.0	52.0	62.5	73.6
8.4	. . .	. . .	. . .	. . .	45.4	50.3	60.5	71.3
8.6	. . .	. . .	. . .	. . .	43.9	48.7	58.6	69.1
8.9	. . .	. . .	. . .	. . .	42.4	47.2	56.8	67.0
9.1	. . .	. . .	. . .	. . .	41.1	45.7	55.1	65.1
9.4	. . .	. . .	. . .	. . .	39.7	44.3	53.5	63.2
9.7	. . .	. . .	. . .	. . .	. . .	42.9	52.0	61.5
9.9	. . .	. . .	. . .	. . .	. . .	41.6	50.5	59.8
10.2	. . .	. . .	. . .	. . .	. . .	40.3	49.1	58.2
10.4	. . .	. . .	. . .	. . .	. . .	. . .	47.7	56.6
10.7	. . .	. . .	. . .	. . .	. . .	. . .	46.4	55.2
10.9	. . .	. . .	. . .	. . .	. . .	. . .	45.1	53.7
11.2	. . .	. . .	. . .	. . .	. . .	. . .	43.9	52.4
11.4	. . .	. . .	. . .	. . .	. . .	. . .	. . .	51.1
11.7	. . .	. . .	. . .	. . .	. . .	. . .	. . .	49.8
11.9	. . .	. . .	. . .	. . .	. . .	. . .	. . .	48.6
12.2	. . .	. . .	. . .	. . .	. . .	. . .	. . .	47.4
12.4	. . .	. . .	. . .	. . .	. . .	. . .	. . .	46.2
12.7	. . .	. . .	. . .	. . .	. . .	. . .	. . .	45.1

Copyright ASME International
Provided by IHS under license with ASME
No reproduction or networking permitted without license from IHS

Table 3-6 Values of *L* for Pipe Sizes ≥ NPS 24 and < NPS 30

Depth, *d*, in.	Wall Thickness, *t*, in.							
	0.250	0.312	0.375	0.438	0.469	0.500	0.562	0.625
0.03	10.97	No limit	No limit	No limit	No limit	No limit	No limit	No limit
0.04	10.97	12.26	13.44	No limit	No limit	No limit	No limit	No limit
0.05	7.34	12.26	13.44	14.53	15.03	15.52	No limit	No limit
0.06	5.08	9.07	13.44	14.53	15.03	15.52	16.45	No limit
0.07	4.01	6.41	10.83	14.53	15.03	15.52	16.45	17.35
0.08	3.37	5.10	7.77	12.51	15.03	15.52	16.45	17.35
0.09	2.93	4.30	6.22	9.12	11.19	14.02	16.45	17.35
0.10	2.61	3.76	5.27	7.35	8.70	10.38	15.47	17.35
0.11	2.35	3.35	4.61	6.24	7.24	8.43	11.62	16.96
0.12	2.15	3.04	4.13	5.48	6.28	7.19	9.50	12.90
0.13	1.98	2.79	3.75	4.91	5.58	6.32	8.13	10.60
0.14	1.83	2.57	3.45	4.47	5.04	5.68	7.17	9.10
0.15	1.70	2.39	3.19	4.11	4.62	5.17	6.44	8.04
0.16	1.59	2.24	2.98	3.82	4.27	4.77	5.88	7.24
0.17	1.49	2.10	2.79	3.57	3.98	4.43	5.43	6.61
0.18	1.39	1.98	2.63	3.35	3.74	4.15	5.05	6.11
0.19	1.31	1.87	2.49	3.16	3.52	3.90	4.73	5.69
0.20	1.23	1.77	2.36	2.99	3.33	3.69	4.45	5.33
0.21	. . .	1.68	2.24	2.85	3.16	3.50	4.21	5.02
0.22	. . .	1.59	2.13	2.71	3.01	3.33	4.00	4.76
0.23	. . .	1.51	2.03	2.59	2.88	3.17	3.81	4.52
0.24	. . .	1.44	1.94	2.48	2.75	3.04	3.64	4.31
0.25	. . .	. . .	1.86	2.37	2.64	2.91	3.49	4.12
0.26	. . .	. . .	1.78	2.28	2.53	2.79	3.35	3.95
0.27	. . .	. . .	1.71	2.19	2.43	2.69	3.22	3.79
0.28	. . .	. . .	1.64	2.10	2.34	2.59	3.10	3.65
0.29	. . .	. . .	1.57	2.02	2.26	2.49	2.99	3.52
0.30	. . .	. . .	1.51	1.95	2.17	2.40	2.88	3.39
0.31	. . .	. . .	. . .	1.88	2.10	2.32	2.78	3.28
0.32	. . .	. . .	. . .	1.81	2.03	2.24	2.69	3.17
0.33	. . .	. . .	. . .	1.75	1.96	2.17	2.61	3.07
0.34	. . .	. . .	. . .	1.69	1.89	2.10	2.53	2.98
0.35	. . .	. . .	. . .	1.63	1.83	2.03	2.45	2.89
0.36	. . .	. . .	. . .	. . .	1.77	1.97	2.38	2.81
0.37	. . .	. . .	. . .	. . .	1.71	1.91	2.31	2.73
0.38	. . .	. . .	. . .	. . .	. . .	1.85	2.24	2.65
0.39	. . .	. . .	. . .	. . .	. . .	1.79	2.18	2.58
0.40	. . .	. . .	. . .	. . .	. . .	1.74	2.12	2.51
0.41	. . .	. . .	. . .	. . .	. . .	. . .	2.06	2.44
0.42	. . .	. . .	. . .	. . .	. . .	. . .	2.00	2.38
0.43	. . .	. . .	. . .	. . .	. . .	. . .	1.95	2.32
0.44	. . .	. . .	. . .	. . .	. . .	. . .	1.89	2.26
0.45	. . .	. . .	. . .	. . .	. . .	. . .	. . .	2.20
0.46	. . .	. . .	. . .	. . .	. . .	. . .	. . .	2.15
0.47	. . .	. . .	. . .	. . .	. . .	. . .	. . .	2.09
0.48	. . .	. . .	. . .	. . .	. . .	. . .	. . .	2.04
0.49	. . .	. . .	. . .	. . .	. . .	. . .	. . .	1.99
0.50	. . .	. . .	. . .	. . .	. . .	. . .	. . .	1.94

Copyright ASME International
Provided by IHS under license with ASME
No reproduction or networking permitted without license from IHS

Table 3-6M Values of *L* for Pipe Sizes ≥ 610 mm and < 762 mm O.D.

Depth, *d*, mm	Wall Thickness, *t*, mm							
	6.4	7.9	9.5	11.1	11.9	12.7	14.3	15.9
0.8	278.7	No limit	No limit	No limit	No limit	No limit	No limit	No limit
1.0	278.7	311.4	341.4	No limit	No limit	No limit	No limit	No limit
1.3	186.5	311.4	341.4	368.9	381.8	394.2	No limit	No limit
1.5	129.1	230.5	341.4	368.9	381.8	394.2	417.9	No limit
1.8	102.0	162.8	275.0	368.9	381.8	394.2	417.9	440.7
2.0	85.6	129.6	197.4	317.8	381.8	394.2	417.9	440.7
2.3	74.5	109.3	158.1	231.6	284.2	356.2	417.9	440.7
2.5	66.2	95.5	133.9	186.7	221.0	263.8	392.9	440.7
2.8	59.8	85.2	117.2	158.6	184.0	214.1	295.2	430.9
3.0	54.5	77.2	104.9	139.1	159.4	182.6	241.2	327.6
3.3	50.2	70.8	95.3	124.7	141.6	160.6	206.5	269.1
3.6	46.4	65.4	87.5	113.5	128.1	144.2	182.0	231.1
3.8	43.2	60.8	81.1	104.4	117.3	131.4	163.7	204.1
4.1	40.3	56.9	75.6	96.9	108.5	121.1	149.4	183.8
4.3	37.7	53.4	70.9	90.6	101.2	112.5	137.8	167.9
4.6	35.4	50.3	66.8	85.1	94.9	105.3	128.2	155.1
4.8	33.2	47.5	63.1	80.3	89.4	99.1	120.1	144.4
5.1	31.2	44.9	59.8	76.1	84.6	93.6	113.1	135.4
5.3	. . .	42.6	56.9	72.3	80.4	88.8	107.0	127.6
5.6	. . .	40.5	54.2	68.8	76.5	84.5	101.6	120.8
5.8	. . .	38.5	51.7	65.7	73.0	80.6	96.8	114.8
6.1	. . .	36.6	49.4	62.9	69.9	77.1	92.5	109.5
6.4	. . .	. . .	47.2	60.3	67.0	73.9	88.6	104.7
6.6	. . .	. . .	45.2	57.8	64.3	71.0	85.0	100.3
6.9	. . .	. . .	43.3	55.5	61.8	68.2	81.7	96.3
7.1	. . .	. . .	41.5	53.4	59.5	65.7	78.7	92.7
7.4	. . .	. . .	39.9	51.4	57.3	63.3	75.8	89.3
7.6	. . .	. . .	38.3	49.5	55.2	61.1	73.2	86.2
7.9	. . .	. . .	. . .	47.7	53.3	59.0	70.7	83.3
8.1	. . .	. . .	. . .	46.1	51.5	57.0	68.4	80.6
8.4	. . .	. . .	. . .	44.4	49.7	55.1	66.2	78.1
8.6	. . .	. . .	. . .	42.9	48.1	53.3	64.2	75.7
8.9	. . .	. . .	. . .	41.4	46.5	51.7	62.2	73.4
9.1	. . .	. . .	. . .	. . .	45.0	50.0	60.4	71.3
9.4	. . .	. . .	. . .	. . .	43.5	48.5	58.6	69.3
9.7	. . .	. . .	. . .	. . .	. . .	47.0	56.9	67.3
9.9	. . .	. . .	. . .	. . .	. . .	45.6	55.3	65.5
10.2	. . .	. . .	. . .	. . .	. . .	44.2	53.7	63.7
10.4	. . .	. . .	. . .	. . .	. . .	. . .	52.2	62.0
10.7	. . .	. . .	. . .	. . .	. . .	. . .	50.8	60.4
10.9	. . .	. . .	. . .	. . .	. . .	. . .	49.4	58.9
11.2	. . .	. . .	. . .	. . .	. . .	. . .	48.1	57.4
11.4	. . .	. . .	. . .	. . .	. . .	. . .	. . .	55.9
11.7	. . .	. . .	. . .	. . .	. . .	. . .	. . .	54.5
11.9	. . .	. . .	. . .	. . .	. . .	. . .	. . .	53.2
12.2	. . .	. . .	. . .	. . .	. . .	. . .	. . .	51.9
12.4	. . .	. . .	. . .	. . .	. . .	. . .	. . .	50.6
12.7	. . .	. . .	. . .	. . .	. . .	. . .	. . .	49.4

Copyright ASME International
Provided by IHS under license with ASME
No reproduction or networking permitted without license from IHS

Table 3-7 Values of *L* for Pipe Sizes ≥ NPS 30 and < NPS 36

Depth, *d*, in.	Wall Thickness, *t*, in.						
	0.250	0.312	0.375	0.438	0.500	0.625	0.688
0.03	12.27	No limit	No limit	No limit	No limit	No limit	No limit
0.04	12.27	13.71	15.03	No limit	No limit	No limit	No limit
0.05	8.21	13.71	15.03	16.24	17.35	No limit	No limit
0.06	5.68	10.14	15.03	16.24	17.35	No limit	No limit
0.07	4.49	7.17	12.10	16.24	17.35	19.40	20.35
0.08	3.77	5.70	8.69	13.99	17.35	19.40	20.35
0.09	3.28	4.81	6.96	10.19	15.68	19.40	20.35
0.10	2.91	4.20	5.89	8.22	11.61	19.40	20.35
0.11	2.63	3.75	5.16	6.98	9.42	18.97	20.35
0.12	2.40	3.40	4.62	6.12	8.04	14.42	20.35
0.13	2.21	3.11	4.19	5.49	7.07	11.85	15.82
0.14	2.04	2.88	3.85	5.00	6.35	10.17	13.07
0.15	1.90	2.68	3.57	4.60	5.78	8.98	11.25
0.16	1.77	2.50	3.33	4.27	5.33	8.09	9.96
0.17	1.66	2.35	3.12	3.99	4.95	7.39	8.98
0.18	1.56	2.21	2.94	3.75	4.63	6.83	8.21
0.19	1.46	2.09	2.78	3.53	4.36	6.36	7.59
0.20	1.38	1.98	2.63	3.35	4.12	5.96	7.07
0.21	. . .	1.88	2.50	3.18	3.91	5.62	6.63
0.22	. . .	1.78	2.38	3.03	3.72	5.32	6.26
0.23	. . .	1.69	2.27	2.89	3.55	5.05	5.93
0.24	. . .	1.61	2.17	2.77	3.39	4.82	5.64
0.25	. . .	. . .	2.08	2.65	3.25	4.61	5.38
0.26	. . .	. . .	1.99	2.54	3.12	4.42	5.15
0.27	. . .	. . .	1.91	2.44	3.00	4.24	4.94
0.28	. . .	. . .	1.83	2.35	2.89	4.08	4.74
0.29	. . .	. . .	1.75	2.26	2.79	3.93	4.57
0.30	. . .	. . .	1.68	2.18	2.69	3.80	4.41
0.31	. . .	. . .	. . .	2.10	2.60	3.67	4.26
0.32	. . .	. . .	. . .	2.03	2.51	3.55	4.12
0.33	. . .	. . .	. . .	1.96	2.43	3.44	3.99
0.34	. . .	. . .	. . .	1.89	2.35	3.33	3.86
0.35	. . .	. . .	. . .	1.82	2.27	3.23	3.75
0.36	. . .	. . .	. . .	. . .	2.20	3.14	3.64
0.37	. . .	. . .	. . .	. . .	2.13	3.05	3.54
0.38	. . .	. . .	. . .	. . .	2.07	2.96	3.44
0.39	. . .	. . .	. . .	. . .	2.01	2.88	3.35
0.40	. . .	. . .	. . .	. . .	1.94	2.81	3.26
0.41	. . .	. . .	. . .	. . .	. . .	2.73	3.18
0.42	. . .	. . .	. . .	. . .	. . .	2.66	3.10
0.43	. . .	. . .	. . .	. . .	. . .	2.59	3.02
0.44	. . .	. . .	. . .	. . .	. . .	2.53	2.95
0.45	. . .	. . .	. . .	. . .	. . .	2.46	2.87
0.46	. . .	. . .	. . .	. . .	. . .	2.40	2.81
0.47	. . .	. . .	. . .	. . .	. . .	2.34	2.74
0.48	. . .	. . .	. . .	. . .	. . .	2.28	2.68
0.49	. . .	. . .	. . .	. . .	. . .	2.23	2.62
0.50	. . .	. . .	. . .	. . .	. . .	2.17	2.56
0.51	. . .	. . .	. . .	. . .	. . .	. . .	2.50
0.52	. . .	. . .	. . .	. . .	. . .	. . .	2.44
0.53	. . .	. . .	. . .	. . .	. . .	. . .	2.39
0.54	. . .	. . .	. . .	. . .	. . .	. . .	2.33
0.55	. . .	. . .	. . .	. . .	. . .	. . .	2.28

Copyright ASME International
Provided by IHS under license with ASME
No reproduction or networking permitted without license from IHS

Table 3-7M Values of *L* for Pipe Sizes ≥ 762 mm and < 914 mm O.D.

Depth, *d*, mm	Wall Thickness, *t*, mm						
	6.4	7.9	9.5	11.1	12.7	15.9	17.5
0.8	311.6	No limit	No limit	No limit	No limit	No limit	No limit
1.0	311.6	348.1	381.7	No limit	No limit	No limit	No limit
1.3	208.5	348.1	381.7	412.5	440.7	No limit	No limit
1.5	144.3	257.7	381.7	412.5	440.7	No limit	No limit
1.8	114.0	182.0	307.4	412.5	440.7	492.7	517.0
2.0	95.7	144.9	220.7	355.3	440.7	492.7	517.0
2.3	83.2	122.2	176.8	258.9	398.2	492.7	517.0
2.5	74.0	106.7	149.7	208.7	294.9	492.7	517.0
2.8	66.8	95.3	131.0	177.3	239.3	481.8	517.0
3.0	61.0	86.3	117.2	155.6	204.1	366.3	517.0
3.3	56.1	79.1	106.5	139.4	179.5	300.9	401.9
3.6	51.9	73.1	97.8	126.9	161.2	258.4	331.9
3.8	48.3	68.0	90.6	116.8	146.9	228.2	285.8
4.1	45.1	63.6	84.6	108.4	135.4	205.5	252.9
4.3	42.2	59.7	79.3	101.3	125.8	187.8	228.1
4.6	39.6	56.2	74.7	95.1	117.7	173.4	208.6
4.8	37.1	53.1	70.6	89.8	110.8	161.5	192.8
5.1	34.9	50.3	66.9	85.0	104.7	151.3	179.6
5.3	. . .	47.7	63.6	80.8	99.3	142.7	168.5
5.6	. . .	45.2	60.6	77.0	94.5	135.1	158.9
5.8	. . .	43.0	57.8	73.5	90.2	128.4	150.6
6.1	. . .	40.9	55.2	70.3	86.2	122.4	143.2
6.4	. . .	. . .	52.8	67.4	82.6	117.0	136.6
6.6	. . .	. . .	50.6	64.6	79.3	112.2	130.7
6.9	. . .	. . .	48.4	62.1	76.3	107.7	125.4
7.1	. . .	. . .	46.5	59.7	73.4	103.6	120.5
7.4	. . .	. . .	44.6	57.5	70.8	99.9	116.0
7.6	. . .	. . .	42.8	55.4	68.3	96.4	111.9
7.9	. . .	. . .	. . .	53.4	65.9	93.2	108.1
8.1	. . .	. . .	. . .	51.5	63.7	90.1	104.5
8.4	. . .	. . .	. . .	49.7	61.6	87.3	101.2
8.6	. . .	. . .	. . .	48.0	59.6	84.6	98.1
8.9	. . .	. . .	. . .	46.3	57.7	82.1	95.2
9.1	. . .	. . .	. . .	. . .	55.9	79.7	92.5
9.4	. . .	. . .	. . .	. . .	54.2	77.4	89.8
9.7	. . .	. . .	. . .	. . .	52.5	75.3	87.4
9.9	. . .	. . .	. . .	. . .	50.9	73.2	85.0
10.2	. . .	. . .	. . .	. . .	49.4	71.3	82.8
10.4	. . .	. . .	. . .	. . .	. . .	69.4	80.7
10.7	. . .	. . .	. . .	. . .	. . .	67.6	78.6
10.9	. . .	. . .	. . .	. . .	. . .	65.8	76.7
11.2	. . .	. . .	. . .	. . .	. . .	64.2	74.8
11.4	. . .	. . .	. . .	. . .	. . .	62.5	73.0
11.7	. . .	. . .	. . .	. . .	. . .	61.0	71.3
11.9	. . .	. . .	. . .	. . .	. . .	59.5	69.6
12.2	. . .	. . .	. . .	. . .	. . .	58.0	68.0
12.4	. . .	. . .	. . .	. . .	. . .	56.6	66.4
12.7	. . .	. . .	. . .	. . .	. . .	55.2	64.9
13.0	. . .	. . .	. . .	. . .	. . .	. . .	63.5
13.2	. . .	. . .	. . .	. . .	. . .	. . .	62.0
13.5	. . .	. . .	. . .	. . .	. . .	. . .	60.6
13.7	. . .	. . .	. . .	. . .	. . .	. . .	59.3
14.0	. . .	. . .	. . .	. . .	. . .	. . .	58.0

Copyright ASME International
Provided by IHS under license with ASME
No reproduction or networking permitted without license from IHS

(12) **Table 3-8 Values of *L* for Pipe Sizes ≥ NPS 36 and < NPS 42**

Depth, *d*, in.	Wall Thickness, *t*, in.							
	0.250	0.281	0.312	0.375	0.406	0.469	0.562	0.688
0.03	13.44	14.25	No limit	No limit	No limit	No limit	No limit	No limit
0.04	13.44	14.25	15.01	16.46	No limit	No limit	No limit	No limit
0.05	8.99	13.40	15.01	16.46	17.13	18.41	No limit	No limit
0.06	6.22	8.22	11.11	16.46	17.13	18.41	20.15	No limit
0.07	4.92	6.21	7.85	13.26	17.13	18.41	20.15	22.30
0.08	4.13	5.09	6.25	9.52	11.89	18.41	20.15	22.30
0.09	3.59	4.37	5.27	7.62	9.16	13.70	20.15	22.30
0.10	3.19	3.86	4.60	6.46	7.60	10.66	18.94	22.30
0.11	2.88	3.47	4.11	5.65	6.56	8.87	14.23	22.30
0.12	2.63	3.15	3.72	5.06	5.82	7.69	11.63	22.30
0.13	2.42	2.90	3.41	4.59	5.26	6.83	9.95	17.33
0.14	2.24	2.68	3.15	4.22	4.81	6.18	8.78	14.31
0.15	2.08	2.50	2.93	3.91	4.44	5.66	7.89	12.33
0.16	1.94	2.33	2.74	3.65	4.13	5.23	7.20	10.91
0.17	1.82	2.19	2.57	3.42	3.87	4.88	6.65	9.84
0.18	1.71	2.06	2.42	3.22	3.64	4.58	6.18	9.00
0.19	1.60	1.94	2.29	3.04	3.44	4.31	5.79	8.31
0.20	1.51	1.83	2.17	2.89	3.26	4.08	5.45	7.75
0.21	. . .	1.73	2.06	2.74	3.10	3.87	5.16	7.27
0.22	. . .	1.64	1.95	2.61	2.95	3.69	4.90	6.85
0.23	. . .	. . .	1.85	2.49	2.82	3.52	4.67	6.49
0.24	. . .	. . .	1.76	2.38	2.70	3.37	4.46	6.18
0.25	. . .	. . .	. . .	2.28	2.58	3.23	4.27	5.89
0.26	. . .	. . .	. . .	2.18	2.48	3.10	4.10	5.64
0.27	. . .	. . .	. . .	2.09	2.38	2.98	3.94	5.41
0.28	. . .	. . .	. . .	2.00	2.28	2.87	3.79	5.20
0.29	. . .	. . .	. . .	1.92	2.19	2.76	3.66	5.00
0.30	. . .	. . .	. . .	1.84	2.11	2.66	3.53	4.83
0.31	. . .	. . .	. . .	. . .	2.03	2.57	3.41	4.66
0.32	. . .	. . .	. . .	. . .	1.95	2.48	3.30	4.51
0.33	. . .	. . .	. . .	. . .	. . .	2.40	3.19	4.37
0.34	. . .	. . .	. . .	. . .	. . .	2.32	3.09	4.23
0.35	. . .	. . .	. . .	. . .	. . .	2.24	3.00	4.11
0.36	. . .	. . .	. . .	. . .	. . .	2.17	2.91	3.99
0.37	. . .	. . .	. . .	. . .	. . .	2.10	2.83	3.87
0.38	. . .	. . .	. . .	. . .	. . .	. . .	2.74	3.77
0.39	. . .	. . .	. . .	. . .	. . .	. . .	2.67	3.67
0.40	. . .	. . .	. . .	. . .	. . .	. . .	2.59	3.57
0.41	. . .	. . .	. . .	. . .	. . .	. . .	2.52	3.48
0.42	. . .	. . .	. . .	. . .	. . .	. . .	2.45	3.39
0.43	. . .	. . .	. . .	. . .	. . .	. . .	2.38	3.31
0.44	. . .	. . .	. . .	. . .	. . .	. . .	2.32	3.23
0.45	. . .	. . .	. . .	. . .	. . .	. . .	. . .	3.15
0.46	. . .	. . .	. . .	. . .	. . .	. . .	. . .	3.07
0.47	. . .	. . .	. . .	. . .	. . .	. . .	. . .	3.00
0.48	. . .	. . .	. . .	. . .	. . .	. . .	. . .	2.93
0.49	. . .	. . .	. . .	. . .	. . .	. . .	. . .	2.87
0.50	. . .	. . .	. . .	. . .	. . .	. . .	. . .	2.80
0.51	. . .	. . .	. . .	. . .	. . .	. . .	. . .	2.74
0.52	. . .	. . .	. . .	. . .	. . .	. . .	. . .	2.68
0.53	. . .	. . .	. . .	. . .	. . .	. . .	. . .	2.62
0.54	. . .	. . .	. . .	. . .	. . .	. . .	. . .	2.56
0.55	. . .	. . .	. . .	. . .	. . .	. . .	. . .	2.50

Copyright ASME International
Provided by IHS under license with ASME
No reproduction or networking permitted without license from IHS

Table 3-8M Values of *L* for Pipe Sizes ≥ 914 mm and < 1 066 mm O.D. (12)

Depth, *d*, mm	Wall Thickness, *t*, mm							
	6.4	7.1	7.9	9.5	10.3	11.9	14.3	17.5
0.8	341.4	361.9	No limit	No limit	No limit	No limit	No limit	No limit
1.0	341.4	361.9	381.4	418.1	No limit	No limit	No limit	No limit
1.3	228.4	340.2	381.4	418.1	435.0	467.6	No limit	No limit
1.5	158.1	208.9	282.3	418.1	435.0	467.6	511.8	No limit
1.8	124.9	157.6	199.4	336.8	435.0	467.6	511.8	566.3
2.0	104.9	129.4	158.7	241.7	302.1	467.6	511.8	566.3
2.3	91.2	111.0	133.9	193.6	232.8	348.1	511.8	566.3
2.5	81.1	98.0	116.9	164.0	193.0	270.6	481.2	566.3
2.8	73.2	88.0	104.3	143.5	166.7	225.4	361.6	566.3
3.0	66.8	80.1	94.6	128.4	147.9	195.2	295.4	566.3
3.3	61.4	73.6	86.7	116.7	133.5	173.5	252.9	440.2
3.6	56.9	68.1	80.1	107.2	122.1	156.9	222.9	363.6
3.8	52.9	63.4	74.5	99.3	112.8	143.7	200.5	313.1
4.1	49.4	59.3	69.6	92.6	105.0	132.9	183.0	277.1
4.3	46.2	55.6	65.4	86.9	98.3	123.9	168.8	249.9
4.6	43.3	52.3	61.6	81.8	92.5	116.2	157.0	228.5
4.8	40.7	49.3	58.2	77.3	87.4	109.5	147.1	211.2
5.1	38.3	46.5	55.1	73.3	82.8	103.6	138.5	196.8
5.3	...	44.0	52.2	69.7	78.7	98.4	131.1	184.6
5.6	...	41.6	49.6	66.3	75.0	93.7	124.5	174.1
5.8	...	...	47.1	63.3	71.6	89.5	118.6	164.9
6.1	...	...	44.8	60.5	68.5	85.6	113.3	156.9
6.4	...	...	...	57.8	65.6	82.0	108.5	149.7
6.6	...	...	...	55.4	62.9	78.7	104.1	143.2
6.9	...	...	...	53.1	60.3	75.7	100.1	137.3
7.1	...	...	...	50.9	58.0	72.8	96.3	132.0
7.4	...	...	...	48.8	55.7	70.2	92.9	127.1
7.6	...	...	...	46.9	53.6	67.7	89.6	122.6
7.9	...	...	...	...	51.6	65.3	86.6	118.4
8.1	...	...	...	...	49.7	63.0	83.8	114.5
8.4	...	...	...	...	...	60.9	81.1	110.9
8.6	...	...	...	...	...	58.9	78.6	107.5
8.9	...	...	...	...	...	56.9	76.2	104.3
9.1	...	...	...	...	...	55.1	73.9	101.3
9.4	...	...	...	...	...	53.3	71.8	98.4
9.7	...	...	...	...	...	...	69.7	95.7
9.9	...	...	...	...	...	...	67.7	93.2
10.2	...	...	...	...	...	...	65.8	90.7
10.4	...	...	...	...	...	...	64.0	88.4
10.7	...	...	...	...	...	...	62.2	86.1
10.9	...	...	...	...	...	...	60.5	84.0
11.2	...	...	...	...	...	...	58.9	82.0
11.4	...	...	...	...	...	...	...	80.0
11.7	...	...	...	...	...	...	...	78.1
11.9	...	...	...	...	...	...	...	76.3
12.2	...	...	...	...	...	...	...	74.5
12.4	...	...	...	...	...	...	...	72.8
12.7	...	...	...	...	...	...	...	71.1
13.0	...	...	...	...	...	...	...	69.5
13.2	...	...	...	...	...	...	...	68.0
13.5	...	...	...	...	...	...	...	66.4
13.7	...	...	...	...	...	...	...	65.0
14.0	...	...	...	...	...	...	...	63.5

Copyright ASME International
Provided by IHS under license with ASME
No reproduction or networking permitted without license from IHS

Table 3-9 Values of *L* for Pipe Sizes ≥ NPS 42 and < NPS 48

Depth, *d*, in.	Wall Thickness, *t*, in.																
	0.344	0.406	0.438	0.469	0.500	0.562	0.625	0.688	0.750	0.812	0.875	0.938	1.000	1.062	1.125	1.188	1.250
0.03	No limit	No limit	No limit	No limit	No limit	No limit	No limit	No limit	No limit	No limit	No limit	No limit	No limit	No limit	No limit	No limit	No limit
0.04	17.03	No limit	No limit	No limit	No limit	No limit	No limit	No limit	No limit	No limit	No limit	No limit	No limit	No limit	No limit	No limit	No limit
0.05	17.03	18.50	19.21	19.88	20.53	No limit	No limit	No limit	No limit	No limit	No limit	No limit	No limit	No limit	No limit	No limit	No limit
0.06	17.03	18.50	19.21	19.88	20.53	21.77	No limit	No limit	No limit	No limit	No limit	No limit	No limit	No limit	No limit	No limit	No limit
0.07	10.93	18.50	19.21	19.88	20.53	21.77	22.95	24.08	No limit	No limit	No limit	No limit	No limit	No limit	No limit	No limit	No limit
0.08	8.33	12.85	16.55	19.88	20.53	21.77	22.95	24.08	25.14	No limit	No limit	No limit	No limit	No limit	No limit	No limit	No limit
0.09	6.87	9.90	12.06	14.80	18.55	21.77	22.95	24.08	25.14	26.16	27.16	No limit	No limit	No limit	No limit	No limit	No limit
0.10	5.92	8.21	9.72	11.51	13.74	20.46	22.95	24.08	25.14	26.16	27.16	28.12	29.03	No limit	No limit	No limit	No limit
0.11	5.24	7.09	8.26	9.58	11.15	15.37	22.44	24.08	25.14	26.16	27.16	28.12	29.03	29.92	No limit	No limit	No limit
0.12	4.72	6.29	7.25	8.30	9.51	12.56	17.06	24.08	25.14	26.16	27.16	28.12	29.03	29.92	30.79	31.65	No limit
0.13	4.31	5.68	6.50	7.38	8.36	10.75	14.02	18.72	25.14	26.16	27.16	28.12	29.03	29.92	30.79	31.65	32.46
0.14	3.97	5.19	5.91	6.67	7.51	9.48	12.04	15.46	20.25	26.16	27.16	28.12	29.03	29.92	30.79	31.65	32.46
0.15	3.69	4.80	5.44	6.11	6.84	8.53	10.63	13.32	16.82	21.75	27.16	28.12	29.03	29.92	30.79	31.65	32.46
0.16	3.44	4.47	5.05	5.65	6.31	7.78	9.57	11.78	14.54	18.17	23.31	28.12	29.03	29.92	30.79	31.65	32.46
0.17	3.23	4.18	4.72	5.27	5.86	7.18	8.75	10.63	12.89	15.75	19.56	24.84	29.03	29.92	30.79	31.65	32.46
0.18	3.05	3.93	4.43	4.94	5.48	6.68	8.08	9.72	11.65	14.00	17.00	20.93	26.23	29.92	30.79	31.65	32.46
0.19	2.88	3.72	4.18	4.66	5.16	6.26	7.52	8.98	10.66	12.66	15.14	18.25	22.22	27.60	30.79	31.65	32.46
0.20	2.73	3.52	3.96	4.41	4.88	5.89	7.05	8.37	9.86	11.60	13.71	16.28	19.43	23.48	29.04	31.65	32.46
0.21	2.59	3.35	3.76	4.18	4.63	5.57	6.65	7.85	9.20	10.74	12.58	14.76	17.36	20.59	24.80	30.45	32.46
0.22	2.46	3.19	3.59	3.99	4.40	5.29	6.29	7.40	8.63	10.03	11.65	13.55	15.77	18.44	21.80	26.11	31.74
0.23	2.35	3.05	3.42	3.80	4.20	5.04	5.98	7.01	8.15	9.42	10.88	12.56	14.49	16.77	19.56	23.00	27.32
0.24	2.24	2.91	3.27	3.64	4.02	4.82	5.70	6.67	7.72	8.89	10.23	11.74	13.45	15.43	17.81	20.67	24.13
0.25	2.14	2.79	3.14	3.49	3.85	4.61	5.45	6.36	7.35	8.43	9.66	11.04	12.57	14.33	16.40	18.84	21.72
0.26	2.04	2.67	3.01	3.35	3.70	4.43	5.22	6.09	7.02	8.03	9.17	10.43	11.83	13.40	15.24	17.36	19.82
0.27	1.95	2.57	2.89	3.22	3.55	4.25	5.02	5.84	6.72	7.67	8.73	9.90	11.18	12.62	14.26	16.15	18.29
0.28	. . .	2.46	2.78	3.10	3.42	4.10	4.83	5.61	6.45	7.35	8.34	9.43	10.62	11.93	13.43	15.12	17.02
0.29	. . .	2.37	2.68	2.98	3.30	3.95	4.65	5.40	6.20	7.05	7.99	9.02	10.12	11.34	12.71	14.25	15.95
0.30	. . .	2.28	2.58	2.88	3.18	3.81	4.49	5.21	5.97	6.79	7.68	8.64	9.68	10.81	12.08	13.49	15.03
0.31	. . .	2.19	2.49	2.78	3.07	3.68	4.34	5.04	5.76	6.54	7.39	8.30	9.28	10.34	11.52	12.82	14.24
0.32	. . .	2.11	2.40	2.68	2.97	3.56	4.20	4.87	5.57	6.32	7.13	8.00	8.92	9.92	11.02	12.23	13.54
0.33	. . .	. . .	2.31	2.59	2.87	3.45	4.07	4.72	5.39	6.11	6.88	7.71	8.59	9.53	10.57	11.70	12.92
0.34	. . .	. . .	2.23	2.50	2.78	3.34	3.94	4.57	5.22	5.91	6.66	7.45	8.29	9.18	10.17	11.23	12.37
0.35	. . .	. . .	2.16	2.42	2.69	3.24	3.82	4.43	5.07	5.73	6.45	7.21	8.01	8.87	9.80	10.80	11.87
0.36	. . .	. . .	. . .	2.34	2.61	3.14	3.71	4.31	4.92	5.56	6.26	6.99	7.76	8.57	9.46	10.41	11.42
0.37	. . .	. . .	. . .	2.27	2.52	3.05	3.61	4.19	4.78	5.41	6.07	6.78	7.52	8.30	9.15	10.05	11.01
0.38	. . .	. . .	. . .	. . .	2.45	2.96	3.51	4.07	4.65	5.26	5.90	6.59	7.30	8.05	8.86	9.73	10.64
0.39	. . .	. . .	. . .	. . .	2.37	2.88	3.41	3.96	4.53	5.12	5.74	6.40	7.09	7.81	8.59	9.42	10.29
0.40	. . .	. . .	. . .	. . .	2.30	2.80	3.32	3.86	4.41	4.98	5.59	6.23	6.90	7.59	8.34	9.14	9.97

Copyright ASME International
Provided by IHS under license with ASME
No reproduction or networking permitted without license from IHS

Table 3-9 Values of *L* for Pipe Sizes ≥ NPS 42 and < NPS 48 (Cont'd)

Depth, *d*, in.	Wall Thickness, *t*, in.																
	0.344	0.406	0.438	0.469	0.500	0.562	0.625	0.688	0.750	0.812	0.875	0.938	1.000	1.062	1.125	1.188	1.250
0.41	...	...	...	...	...	2.72	3.23	3.76	4.30	4.86	5.45	6.07	6.71	7.39	8.11	8.88	9.67
0.42	...	...	...	...	...	2.65	3.15	3.66	4.19	4.74	5.31	5.92	6.54	7.19	7.89	8.63	9.40
0.43	...	...	...	...	...	2.57	3.07	3.57	4.09	4.62	5.18	5.77	6.38	7.01	7.69	8.40	9.14
0.44	...	...	...	...	...	2.50	2.99	3.49	3.99	4.51	5.06	5.64	6.22	6.84	7.50	8.18	8.90
0.45	...	...	...	...	...	...	2.91	3.40	3.90	4.41	4.95	5.50	6.08	6.68	7.31	7.98	8.67
0.46	...	...	...	...	...	...	2.84	3.32	3.81	4.31	4.83	5.38	5.94	6.52	7.14	7.79	8.46
0.47	...	...	...	...	...	...	2.77	3.24	3.72	4.21	4.73	5.26	5.81	6.38	6.98	7.61	8.25
0.48	...	...	...	...	...	...	2.70	3.17	3.64	4.12	4.62	5.15	5.68	6.24	6.82	7.43	8.06
0.49	...	...	...	...	...	...	2.64	3.09	3.56	4.03	4.52	5.04	5.56	6.10	6.67	7.27	7.88
0.50	...	...	...	...	...	...	2.57	3.02	3.48	3.94	4.43	4.93	5.44	5.97	6.53	7.11	7.71
0.51	...	...	...	...	...	...	...	2.96	3.40	3.86	4.34	4.83	5.33	5.85	6.40	6.96	7.55
0.52	...	...	...	...	...	...	...	2.89	3.33	3.78	4.25	4.73	5.23	5.73	6.27	6.82	7.39
0.53	...	...	...	...	...	...	...	2.83	3.26	3.70	4.17	4.64	5.12	5.62	6.14	6.69	7.24
0.54	...	...	...	...	...	...	...	2.76	3.19	3.63	4.08	4.55	5.02	5.51	6.03	6.56	7.10
0.55	...	...	...	...	...	...	...	2.70	3.12	3.56	4.00	4.46	4.93	5.41	5.91	6.43	6.96
0.56	...	...	...	...	...	...	...	...	3.06	3.49	3.93	4.38	4.84	5.31	5.80	6.31	6.83
0.57	...	...	...	...	...	...	...	...	3.00	3.42	3.85	4.30	4.75	5.21	5.69	6.19	6.70
0.58	...	...	...	...	...	...	...	...	2.94	3.35	3.78	4.22	4.66	5.12	5.59	6.08	6.58
0.59	...	...	...	...	...	...	...	...	2.88	3.29	3.71	4.14	4.58	5.03	5.49	5.98	6.46
0.60	...	...	...	...	...	...	...	...	2.82	3.22	3.64	4.07	4.50	4.94	5.40	5.87	6.35
0.61	...	...	...	...	...	...	...	...	...	3.16	3.58	4.00	4.42	4.85	5.31	5.77	6.24
0.62	...	...	...	...	...	...	...	...	...	3.10	3.51	3.93	4.34	4.77	5.22	5.67	6.14
0.63	...	...	...	...	...	...	...	...	...	3.04	3.45	3.86	4.27	4.69	5.13	5.58	6.04
0.64	...	...	...	...	...	...	...	...	...	2.99	3.39	3.79	4.20	4.61	5.05	5.49	5.94
0.65	...	...	...	...	...	...	...	...	...	...	3.33	3.73	4.13	4.54	4.97	5.40	5.84
0.66	...	...	...	...	...	...	...	...	...	...	3.27	3.66	4.06	4.47	4.89	5.32	5.75
0.67	...	...	...	...	...	...	...	...	...	...	3.21	3.60	3.99	4.39	4.81	5.23	5.66
0.68	...	...	...	...	...	...	...	...	...	...	3.15	3.54	3.93	4.32	4.73	5.15	5.57
0.69	...	...	...	...	...	...	...	...	...	...	3.10	3.48	3.87	4.26	4.66	5.07	5.49
0.70	...	...	...	...	...	...	...	...	...	...	3.04	3.42	3.80	4.19	4.59	5.00	5.41
0.71	...	...	...	...	...	...	...	...	...	...	...	3.37	3.74	4.13	4.52	4.92	5.33
0.72	...	...	...	...	...	...	...	...	...	...	...	3.31	3.69	4.06	4.45	4.85	5.25
0.73	...	...	...	...	...	...	...	...	...	...	...	3.26	3.63	4.00	4.39	4.78	5.18
0.74	...	...	...	...	...	...	...	...	...	...	...	3.21	3.57	3.94	4.32	4.71	5.10
0.75	...	...	...	...	...	...	...	...	...	...	...	3.15	3.52	3.88	4.26	4.64	5.03
0.76	...	...	...	...	...	...	...	...	...	...	...	...	3.46	3.82	4.20	4.58	4.96

Copyright ASME International
Provided by IHS under license with ASME
No reproduction or networking permitted without license from IHS

Table 3-9 Values of *L* for Pipe Sizes ≥ NPS 42 and < NPS 48 (Cont'd)

Depth, *d*, in.	Wall Thickness, *t*, in.																
	0.344	0.406	0.438	0.469	0.500	0.562	0.625	0.688	0.750	0.812	0.875	0.938	1.000	1.062	1.125	1.188	1.250
0.77	...	...	...	...	...	...	...	...	...	...	...	...	3.41	3.77	4.14	4.51	4.89
0.78	...	...	...	...	...	...	...	...	...	...	...	...	3.36	3.71	4.08	4.45	4.82
0.79	...	...	...	...	...	...	...	...	...	...	...	...	3.30	3.66	4.02	4.39	4.76
0.80	...	...	...	...	...	...	...	...	...	...	...	...	3.25	3.60	3.96	4.33	4.69
0.81	...	...	...	...	...	...	...	...	...	...	...	...	...	3.55	3.91	4.27	4.63
0.82	...	...	...	...	...	...	...	...	...	...	...	...	...	3.50	3.85	4.21	4.57
0.83	...	...	...	...	...	...	...	...	...	...	...	...	...	3.45	3.80	4.16	4.51
0.84	...	...	...	...	...	...	...	...	...	...	...	...	...	3.40	3.75	4.10	4.45
0.85	...	...	...	...	...	...	...	...	...	...	...	...	...	...	3.70	4.05	4.39
0.86	...	...	...	...	...	...	...	...	...	...	...	...	...	...	3.65	3.99	4.34
0.87	...	...	...	...	...	...	...	...	...	...	...	...	...	...	3.60	3.94	4.28
0.88	...	...	...	...	...	...	...	...	...	...	...	...	...	...	3.55	3.89	4.23
0.89	...	...	...	...	...	...	...	...	...	...	...	...	...	...	3.50	3.84	4.17
0.90	...	...	...	...	...	...	...	...	...	...	...	...	...	...	3.45	3.79	4.12
0.91	...	...	...	...	...	...	...	...	...	...	...	...	...	...	...	3.74	4.07
0.92	...	...	...	...	...	...	...	...	...	...	...	...	...	...	...	3.69	4.02
0.93	...	...	...	...	...	...	...	...	...	...	...	...	...	...	...	3.64	3.97
0.94	...	...	...	...	...	...	...	...	...	...	...	...	...	...	...	3.59	3.92
0.95	...	...	...	...	...	...	...	...	...	...	...	...	...	...	...	3.55	3.87
0.96	...	...	...	...	...	...	...	...	...	...	...	...	...	...	...	...	3.82
0.97	...	...	...	...	...	...	...	...	...	...	...	...	...	...	...	...	3.77
0.98	...	...	...	...	...	...	...	...	...	...	...	...	...	...	...	...	3.73
0.99	...	...	...	...	...	...	...	...	...	...	...	...	...	...	...	...	3.68
1.00	...	...	...	...	...	...	...	...	...	...	...	...	...	...	...	...	3.64

Copyright ASME International
Provided by IHS under license with ASME
No reproduction or networking permitted without license from IHS

Table 3-9M Values of *L* for Pipe Sizes ≥ 1 066 mm and < 1 219 mm O.D.

Depth, *d*, mm	Wall Thickness, *t*, mm																
	8.7	10.3	11.1	11.9	12.7	14.3	15.9	17.5	19.1	20.6	22.2	23.8	25.4	27.0	28.6	30.2	31.8
0.8	No limit	No limit	No limit	No limit	No limit	No limit	No limit	No limit	No limit	No limit	No limit	No limit	No limit	No limit	No limit	No limit	No limit
1.0	432.5	No limit	No limit	No limit	No limit	No limit	No limit	No limit	No limit	No limit	No limit	No limit	No limit	No limit	No limit	No limit	No limit
1.3	432.5	469.9	488.1	505.0	521.5	No limit	No limit	No limit	No limit	No limit	No limit	No limit	No limit	No limit	No limit	No limit	No limit
1.5	432.5	469.9	488.1	505.0	521.5	552.8	No limit	No limit	No limit	No limit	No limit	No limit	No limit	No limit	No limit	No limit	No limit
1.8	277.7	469.9	488.1	505.0	521.5	552.8	583.0	611.7	No limit	No limit	No limit	No limit	No limit	No limit	No limit	No limit	No limit
2.0	211.6	326.3	420.4	505.0	521.5	552.8	583.0	611.7	638.7	No limit	No limit	No limit	No limit	No limit	No limit	No limit	No limit
2.3	174.5	251.4	306.4	376.0	471.2	552.8	583.0	611.7	638.7	664.5	689.8	No limit	No limit	No limit	No limit	No limit	No limit
2.5	150.3	208.4	246.9	292.3	348.9	519.7	583.0	611.7	638.7	664.5	689.8	714.2	737.5	No limit	No limit	No limit	No limit
2.8	133.0	180.1	209.8	243.4	283.2	390.5	570.0	611.7	638.7	664.5	689.8	714.2	737.5	760.0	No limit	No limit	No limit
3.0	119.8	159.7	184.1	210.8	241.5	319.1	433.4	611.7	638.7	664.5	689.8	714.2	737.5	760.0	782.2	803.8	No limit
3.3	109.4	144.2	165.0	187.4	212.4	273.1	356.1	475.5	638.7	664.5	689.8	714.2	737.5	760.0	782.2	803.8	824.5
3.6	100.8	131.9	150.1	169.4	190.7	240.8	305.7	392.7	514.4	664.5	689.8	714.2	737.5	760.0	782.2	803.8	824.5
3.8	93.6	121.9	138.1	155.2	173.8	216.6	270.0	338.2	427.3	552.4	689.8	714.2	737.5	760.0	782.2	803.8	824.5
4.1	87.5	113.4	128.2	143.6	160.2	197.6	243.2	299.3	369.3	461.4	592.0	714.2	737.5	760.0	782.2	803.8	824.5
4.3	82.1	106.2	119.8	133.9	148.9	182.3	222.2	269.9	327.5	400.0	496.8	630.8	737.5	760.0	782.2	803.8	824.5
4.6	77.3	99.9	112.6	125.5	139.3	169.6	205.2	246.8	295.8	355.5	431.9	531.7	666.3	760.0	782.2	803.8	824.5
4.8	73.1	94.4	106.2	118.3	131.0	158.9	191.0	228.1	270.8	321.6	384.5	463.5	564.4	701.0	782.2	803.8	824.5
5.1	69.3	89.5	100.6	111.9	123.8	149.6	179.1	212.6	250.5	294.8	348.3	413.4	493.4	596.5	737.6	803.8	824.5
5.3	65.8	85.0	95.6	106.3	117.5	141.6	168.8	199.4	233.6	272.9	319.5	374.9	441.0	523.0	630.0	773.6	824.5
5.6	62.6	81.0	91.1	101.2	111.8	134.4	159.8	188.1	219.3	254.7	296.0	344.2	400.5	468.4	553.8	663.1	806.1
5.8	59.6	77.3	87.0	96.6	106.7	128.1	151.9	178.2	206.9	239.2	276.4	319.1	368.1	425.9	496.7	584.3	693.8
6.1	56.9	74.0	83.2	92.4	102.0	122.4	144.8	169.4	196.2	225.9	259.7	298.2	341.6	391.9	452.3	524.9	612.9
6.4	54.3	70.8	79.7	88.6	97.8	117.2	138.5	161.7	186.7	214.2	245.4	280.4	319.3	363.9	416.5	478.5	551.7
6.6	51.9	67.9	76.5	85.0	93.9	112.4	132.7	154.7	178.2	204.0	232.8	265.0	300.4	340.5	387.0	441.0	503.5
6.9	49.6	65.2	73.5	81.7	90.2	108.1	127.5	148.3	170.6	194.8	221.8	251.5	284.0	320.4	362.3	410.1	464.6
7.1	. . .	62.6	70.7	78.7	86.9	104.0	122.6	142.6	163.7	186.6	211.9	239.6	269.7	303.1	341.1	384.1	432.3
7.4	. . .	60.2	68.0	75.8	83.7	100.3	118.2	137.3	157.4	179.1	203.0	229.0	257.1	288.0	322.8	361.8	405.2
7.6	. . .	57.9	65.5	73.1	80.8	96.8	114.1	132.4	151.7	172.4	195.0	219.5	245.8	274.6	306.8	342.5	381.9
7.9	. . .	55.7	63.2	70.5	78.0	93.6	110.2	127.9	146.4	166.1	187.7	210.9	235.7	262.6	292.6	325.6	361.7
8.1	. . .	53.6	60.9	68.1	75.4	90.5	106.6	123.7	141.5	160.4	181.0	203.1	226.5	251.9	279.9	310.7	343.9
8.4	. . .	. . .	58.8	65.8	72.9	87.6	103.3	119.8	136.9	155.1	174.8	195.9	218.2	242.2	268.6	297.3	328.2
8.6	. . .	. . .	56.7	63.6	70.6	84.9	100.1	116.1	132.7	150.2	169.1	189.3	210.5	233.3	258.2	285.3	314.2
8.9	. . .	. . .	54.8	61.5	68.3	82.3	97.1	112.6	128.7	145.6	163.8	183.2	203.5	225.2	248.9	274.4	301.6
9.1	. . .	. . .	. . .	59.5	66.2	79.9	94.3	109.4	125.0	141.3	158.9	177.5	197.0	217.7	240.3	264.5	290.1
9.4	. . .	. . .	. . .	57.6	64.1	77.5	91.6	106.3	121.4	137.3	154.3	172.2	190.9	210.8	232.3	255.4	279.7
9.7	. . .	. . .	. . .	. . .	62.2	75.3	89.1	103.4	118.1	133.5	150.0	167.3	185.3	204.4	225.0	247.0	270.2
9.9	. . .	. . .	. . .	. . .	60.3	73.1	86.6	100.6	115.0	129.9	145.9	162.7	180.1	198.5	218.3	239.3	261.4
10.2	. . .	. . .	. . .	. . .	58.4	71.1	84.3	98.0	112.0	126.5	142.0	158.3	175.1	192.9	211.9	232.1	253.3

Copyright ASME International
Provided by IHS under license with ASME
No reproduction or networking permitted without license from IHS

Table 3-9M Values of *L* for Pipe Sizes ≥ 1 066 mm and < 1 219 mm O.D. (Cont'd)

Depth, *d*, mm	Wall Thickness, *t*, mm																
	8.7	10.3	11.1	11.9	12.7	14.3	15.9	17.5	19.1	20.6	22.2	23.8	25.4	27.0	28.6	30.2	31.8
10.4	...	...	...	...	...	69.1	82.1	95.5	109.1	123.3	138.4	154.2	170.5	187.7	206.0	225.5	245.7
10.7	...	...	...	...	...	67.2	79.9	93.0	106.4	120.3	135.0	150.3	166.1	182.7	200.5	219.2	238.7
10.9	...	...	...	...	...	65.4	77.9	90.7	103.8	117.4	131.7	146.6	162.0	178.1	195.3	213.4	232.1
11.2	...	...	...	...	...	63.6	75.9	88.5	101.3	114.6	128.6	143.1	158.1	173.7	190.4	207.9	226.0
11.4	...	...	...	...	...	...	74.0	86.4	99.0	111.9	125.6	139.8	154.4	169.6	185.8	202.7	220.2
11.7	...	...	...	...	...	...	72.2	84.3	96.7	109.4	122.8	136.6	150.9	165.7	181.4	197.8	214.8
11.9	...	...	...	...	...	...	70.4	82.4	94.5	106.9	120.0	133.6	147.5	161.9	177.2	193.2	209.7
12.2	...	...	...	...	...	...	68.6	80.5	92.4	104.6	117.4	130.7	144.3	158.4	173.3	188.8	204.8
12.4	...	...	...	...	...	...	67.0	78.6	90.3	102.3	114.9	127.9	141.2	155.0	169.5	184.7	200.2
12.7	...	...	...	...	...	...	65.3	76.8	88.3	100.2	112.5	125.3	138.3	151.7	165.9	180.7	195.8
13.0	...	...	...	...	...	...	...	75.1	86.4	98.1	110.2	122.7	135.5	148.6	162.5	176.9	191.7
13.2	...	...	...	...	...	...	...	73.4	84.6	96.0	108.0	120.3	132.7	145.6	159.2	173.3	187.7
13.5	...	...	...	...	...	...	...	71.8	82.8	94.1	105.8	117.9	130.1	142.8	156.1	169.8	183.9
13.7	...	...	...	...	...	...	...	70.2	81.1	92.2	103.7	115.6	127.6	140.0	153.0	166.5	180.2
14.0	...	...	...	...	...	...	...	68.6	79.4	90.3	101.7	113.4	125.2	137.4	150.1	163.3	176.8
14.2	...	...	...	...	...	...	...	...	77.7	88.5	99.8	111.2	122.9	134.8	147.3	160.3	173.4
14.5	...	...	...	...	...	...	...	...	76.1	86.8	97.9	109.2	120.6	132.4	144.7	157.3	170.2
14.7	...	...	...	...	...	...	...	...	74.6	85.1	96.0	107.2	118.4	130.0	142.1	154.5	167.1
15.0	...	...	...	...	...	...	...	...	73.1	83.5	94.2	105.2	116.3	127.7	139.6	151.8	164.2
15.2	...	...	...	...	...	...	...	...	71.6	81.9	92.5	103.3	114.3	125.4	137.1	149.1	161.3
15.5	...	...	...	...	...	...	...	...	...	80.3	90.8	101.5	112.3	123.3	134.8	146.6	158.6
15.7	...	...	...	...	...	...	...	...	...	78.8	89.2	99.7	110.3	121.2	132.5	144.1	155.9
16.0	...	...	...	...	...	...	...	...	...	77.3	87.6	98.0	108.5	119.2	130.3	141.8	153.3
16.3	...	...	...	...	...	...	...	...	...	75.8	86.0	96.3	106.6	117.2	128.2	139.4	150.8
16.5	...	...	...	...	...	...	...	...	...	...	84.5	94.7	104.9	115.3	126.1	137.2	148.4
16.8	...	...	...	...	...	...	...	...	...	...	83.0	93.0	103.1	113.4	124.1	135.0	146.1
17.0	...	...	...	...	...	...	...	...	...	...	81.5	91.5	101.4	111.6	122.1	132.9	143.8
17.3	...	...	...	...	...	...	...	...	...	...	80.1	89.9	99.8	109.8	120.2	130.9	141.6
17.5	...	...	...	...	...	...	...	...	...	...	78.7	88.4	98.2	108.1	118.4	128.9	139.4
17.8	...	...	...	...	...	...	...	...	...	...	77.3	87.0	96.6	106.4	116.6	126.9	137.4
18.0	...	...	...	...	...	...	...	...	...	...	...	85.6	95.1	104.8	114.8	125.1	135.3
18.3	...	...	...	...	...	...	...	...	...	...	...	84.1	93.6	103.2	113.1	123.2	133.4
18.5	...	...	...	...	...	...	...	...	...	...	...	82.8	92.1	101.6	111.4	121.4	131.4
18.8	...	...	...	...	...	...	...	...	...	...	...	81.4	90.7	100.1	109.8	119.7	129.6
19.1	...	...	...	...	...	...	...	...	...	...	...	80.1	89.3	98.6	108.2	118.0	127.7
19.3	...	...	...	...	...	...	...	...	...	...	...	...	87.9	97.1	106.6	116.3	126.0

Copyright ASME International
Provided by IHS under license with ASME
No reproduction or networking permitted without license from IHS

Table 3-9M Values of *L* for Pipe Sizes ≥ 1 066 mm and < 1 219 mm O.D. (Cont'd)

Depth, *d*, mm	Wall Thickness, *t*, mm																
	8.7	10.3	11.1	11.9	12.7	14.3	15.9	17.5	19.1	20.6	22.2	23.8	25.4	27.0	28.6	30.2	31.8
19.6	...	...	...	...	...	...	...	...	...	...	...	...	86.6	95.7	105.1	114.7	124.2
19.8	...	...	...	...	...	...	...	...	...	...	...	...	85.2	94.3	103.6	113.1	122.5
20.1	...	...	...	...	...	...	...	...	...	...	...	...	83.9	92.9	102.1	111.5	120.9
20.3	...	...	...	...	...	...	...	...	...	...	...	...	82.7	91.5	100.7	110.0	119.2
20.6	...	...	...	...	...	...	...	...	...	...	...	...	...	90.2	99.3	108.5	117.6
20.8	...	...	...	...	...	...	...	...	...	...	...	...	...	88.9	97.9	107.0	116.1
21.1	...	...	...	...	...	...	...	...	...	...	...	...	...	87.6	96.5	105.6	114.5
21.3	...	...	...	...	...	...	...	...	...	...	...	...	...	86.4	95.2	104.1	113.1
21.6	...	...	...	...	...	...	...	...	...	...	...	...	...	...	93.9	102.8	111.6
21.8	...	...	...	...	...	...	...	...	...	...	...	...	...	...	92.6	101.4	110.1
22.1	...	...	...	...	...	...	...	...	...	...	...	...	...	...	91.3	100.1	108.7
22.4	...	...	...	...	...	...	...	...	...	...	...	...	...	...	90.1	98.7	107.3
22.6	...	...	...	...	...	...	...	...	...	...	...	...	...	...	88.9	97.5	106.0
22.9	...	...	...	...	...	...	...	...	...	...	...	...	...	...	87.7	96.2	104.6
23.1	...	...	...	...	...	...	...	...	...	...	...	...	...	...	...	94.9	103.3
23.4	...	...	...	...	...	...	...	...	...	...	...	...	...	...	...	93.7	102.0
23.6	...	...	...	...	...	...	...	...	...	...	...	...	...	...	...	92.5	100.8
23.9	...	...	...	...	...	...	...	...	...	...	...	...	...	...	...	91.3	99.5
24.1	...	...	...	...	...	...	...	...	...	...	...	...	...	...	...	90.1	98.3
24.4	...	...	...	...	...	...	...	...	...	...	...	...	...	...	...	...	97.1
24.6	...	...	...	...	...	...	...	...	...	...	...	...	...	...	...	...	95.9
24.9	...	...	...	...	...	...	...	...	...	...	...	...	...	...	...	...	94.7
25.1	...	...	...	...	...	...	...	...	...	...	...	...	...	...	...	...	93.5
25.4	...	...	...	...	...	...	...	...	...	...	...	...	...	...	...	...	92.4

Copyright ASME International
Provided by IHS under license with ASME
No reproduction or networking permitted without license from IHS

Table 3-10 Values of L for Pipe Sizes ≥ NPS 48 and < NPS 52

Depth, d, in.	Wall Thickness, t, in.																
	0.344	0.406	0.438	0.469	0.500	0.562	0.625	0.688	0.750	0.812	0.875	0.938	1.000	1.062	1.125	1.188	1.250
0.03	No limit	No limit	No limit	No limit	No limit	No limit	No limit	No limit	No limit	No limit	No limit	No limit	No limit	No limit	No limit	No limit	No limit
0.04	18.20	No limit	No limit	No limit	No limit	No limit	No limit	No limit	No limit	No limit	No limit	No limit	No limit	No limit	No limit	No limit	No limit
0.05	18.20	19.78	20.54	21.26	21.95	No limit	No limit	No limit	No limit	No limit	No limit	No limit	No limit	No limit	No limit	No limit	No limit
0.06	18.20	19.78	20.54	21.26	21.95	23.27	No limit	No limit	No limit	No limit	No limit	No limit	No limit	No limit	No limit	No limit	No limit
0.07	11.69	19.78	20.54	21.26	21.95	23.27	24.54	25.74	No limit	No limit	No limit	No limit	No limit	No limit	No limit	No limit	No limit
0.08	8.91	13.73	17.69	21.26	21.95	23.27	24.54	25.74	26.88	No limit	No limit	No limit	No limit	No limit	No limit	No limit	No limit
0.09	7.35	10.58	12.89	15.82	19.83	23.27	24.54	25.74	26.88	27.97	29.03	No limit	No limit	No limit	No limit	No limit	No limit
0.10	6.33	8.77	10.39	12.30	14.69	21.87	24.54	25.74	26.88	27.97	29.03	30.06	31.04	No limit	No limit	No limit	No limit
0.11	5.60	7.58	8.83	10.24	11.92	16.44	23.99	25.74	26.88	27.97	29.03	30.06	31.04	31.99	No limit	No limit	No limit
0.12	5.04	6.72	7.75	8.87	10.16	13.43	18.24	25.74	26.88	27.97	29.03	30.06	31.04	31.99	32.92	33.83	No limit
0.13	4.60	6.07	6.94	7.89	8.94	11.49	14.99	20.01	26.88	27.97	29.03	30.06	31.04	31.99	32.92	33.83	34.70
0.14	4.24	5.55	6.32	7.13	8.03	10.13	12.87	16.53	21.65	27.97	29.03	30.06	31.04	31.99	32.92	33.83	34.70
0.15	3.94	5.13	5.81	6.53	7.32	9.11	11.36	14.23	17.99	23.25	29.03	30.06	31.04	31.99	32.92	33.83	34.70
0.16	3.68	4.77	5.40	6.04	6.74	8.32	10.24	12.60	15.54	19.42	24.92	30.06	31.04	31.99	32.92	33.83	34.70
0.17	3.46	4.47	5.04	5.63	6.27	7.67	9.35	11.36	13.78	16.84	20.91	26.55	31.04	31.99	32.92	33.83	34.70
0.18	3.26	4.21	4.74	5.28	5.86	7.14	8.63	10.39	12.45	14.96	18.18	22.38	28.04	31.99	32.92	33.83	34.70
0.19	3.08	3.97	4.47	4.98	5.52	6.69	8.04	9.60	11.40	13.54	16.18	19.51	23.75	29.51	32.92	33.83	34.70
0.20	2.92	3.77	4.24	4.71	5.21	6.30	7.54	8.95	10.54	12.41	14.66	17.40	20.77	25.10	31.05	33.83	34.70
0.21	2.77	3.58	4.02	4.47	4.94	5.96	7.10	8.39	9.83	11.49	13.45	15.78	18.56	22.01	26.52	32.56	34.70
0.22	2.63	3.41	3.83	4.26	4.71	5.66	6.73	7.91	9.23	10.72	12.46	14.49	16.86	19.71	23.31	27.91	33.93
0.23	2.51	3.26	3.66	4.07	4.49	5.39	6.39	7.50	8.71	10.07	11.63	13.43	15.49	17.93	20.91	24.59	29.20
0.24	2.39	3.11	3.50	3.89	4.29	5.15	6.10	7.13	8.26	9.51	10.93	12.55	14.38	16.49	19.03	22.09	25.80
0.25	2.29	2.98	3.35	3.73	4.12	4.93	5.83	6.80	7.86	9.02	10.33	11.80	13.44	15.32	17.53	20.14	23.22
0.26	2.18	2.86	3.22	3.58	3.95	4.73	5.59	6.51	7.50	8.58	9.80	11.15	12.64	14.33	16.29	18.56	21.19
0.27	2.09	2.74	3.09	3.44	3.80	4.55	5.36	6.24	7.18	8.20	9.33	10.59	11.95	13.49	15.25	17.26	19.55
0.28	. . .	2.63	2.97	3.31	3.66	4.38	5.16	6.00	6.89	7.85	8.92	10.09	11.35	12.76	14.36	16.17	18.20
0.29	. . .	2.53	2.86	3.19	3.52	4.22	4.97	5.78	6.63	7.54	8.54	9.64	10.82	12.12	13.59	15.23	17.05
0.30	. . .	2.44	2.76	3.08	3.40	4.08	4.80	5.57	6.38	7.25	8.21	9.24	10.35	11.56	12.91	14.42	16.07
0.31	. . .	2.34	2.66	2.97	3.28	3.94	4.64	5.38	6.16	6.99	7.90	8.88	9.92	11.05	12.32	13.71	15.22
0.32	. . .	2.26	2.56	2.87	3.17	3.81	4.49	5.21	5.95	6.75	7.62	8.55	9.53	10.60	11.78	13.08	14.48
0.33	. . .	. . .	2.47	2.77	3.07	3.69	4.35	5.04	5.76	6.53	7.36	8.25	9.18	10.19	11.30	12.51	13.81
0.34	. . .	. . .	2.39	2.68	2.97	3.57	4.21	4.89	5.58	6.32	7.12	7.97	8.86	9.82	10.87	12.01	13.22
0.35	. . .	. . .	2.31	2.59	2.88	3.46	4.09	4.74	5.42	6.13	6.90	7.71	8.56	9.48	10.47	11.55	12.69
0.36	. . .	. . .	. . .	2.50	2.79	3.36	3.97	4.60	5.26	5.95	6.69	7.47	8.29	9.16	10.11	11.13	12.21

Copyright ASME International
Provided by IHS under license with ASME
No reproduction or networking permitted without license from IHS

Table 3-10 Values of *L* for Pipe Sizes ≥ NPS 48 and < NPS 52 (Cont'd)

Depth, *d*, in.	Wall Thickness, *t*, in.																
	0.344	0.406	0.438	0.469	0.500	0.562	0.625	0.688	0.750	0.812	0.875	0.938	1.000	1.062	1.125	1.188	1.250
0.37	...	...	...	2.42	2.70	3.26	3.86	4.47	5.11	5.78	6.49	7.25	8.04	8.87	9.78	10.75	11.77
0.38	...	...	...	...	2.62	3.17	3.75	4.35	4.97	5.62	6.31	7.04	7.80	8.60	9.47	10.40	11.37
0.39	...	...	...	...	2.54	3.08	3.65	4.23	4.84	5.47	6.14	6.85	7.58	8.35	9.19	10.07	11.00
0.40	...	...	...	...	2.46	2.99	3.55	4.12	4.71	5.33	5.98	6.66	7.37	8.12	8.92	9.77	10.66
0.41	...	...	...	...	...	2.91	3.45	4.02	4.59	5.19	5.83	6.49	7.18	7.90	8.67	9.49	10.34
0.42	...	...	...	...	...	2.83	3.36	3.92	4.48	5.06	5.68	6.33	6.99	7.69	8.44	9.23	10.05
0.43	...	...	...	...	...	2.75	3.28	3.82	4.37	4.94	5.54	6.17	6.82	7.50	8.22	8.98	9.77
0.44	...	...	...	...	...	2.68	3.19	3.73	4.26	4.82	5.41	6.02	6.65	7.31	8.01	8.75	9.51
0.45	...	...	...	...	...	...	3.11	3.64	4.16	4.71	5.29	5.88	6.50	7.14	7.82	8.53	9.27
0.46	...	...	...	...	...	...	3.04	3.55	4.07	4.60	5.17	5.75	6.35	6.97	7.63	8.33	9.04
0.47	...	...	...	...	...	...	2.96	3.47	3.98	4.50	5.05	5.62	6.21	6.82	7.46	8.13	8.82
0.48	...	...	...	...	...	...	2.89	3.39	3.89	4.40	4.94	5.50	6.07	6.67	7.29	7.95	8.62
0.49	...	...	...	...	...	...	2.82	3.31	3.80	4.31	4.84	5.39	5.94	6.52	7.13	7.77	8.43
0.50	...	...	...	...	...	...	2.75	3.23	3.72	4.22	4.74	5.27	5.82	6.39	6.98	7.60	8.24
0.51	...	...	...	...	...	...	...	3.16	3.64	4.13	4.64	5.17	5.70	6.26	6.84	7.45	8.07
0.52	...	...	...	...	...	...	...	3.09	3.56	4.04	4.54	5.06	5.59	6.13	6.70	7.29	7.90
0.53	...	...	...	...	...	...	...	3.02	3.48	3.96	4.45	4.96	5.48	6.01	6.57	7.15	7.74
0.54	...	...	...	...	...	...	...	2.95	3.41	3.88	4.37	4.87	5.37	5.89	6.44	7.01	7.59
0.55	...	...	...	...	...	...	...	2.89	3.34	3.80	4.28	4.77	5.27	5.78	6.32	6.87	7.44
0.56	...	...	...	...	...	...	...	...	3.27	3.73	4.20	4.68	5.17	5.67	6.20	6.75	7.30
0.57	...	...	...	...	...	...	...	...	3.20	3.65	4.12	4.60	5.08	5.57	6.09	6.62	7.16
0.58	...	...	...	...	...	...	...	...	3.14	3.58	4.04	4.51	4.98	5.47	5.98	6.50	7.03
0.59	...	...	...	...	...	...	...	...	3.07	3.51	3.97	4.43	4.90	5.37	5.87	6.39	6.91
0.60	...	...	...	...	...	...	...	...	3.01	3.45	3.89	4.35	4.81	5.28	5.77	6.28	6.79
0.61	...	...	...	...	...	...	...	...	...	3.38	3.82	4.27	4.73	5.19	5.67	6.17	6.67
0.62	...	...	...	...	...	...	...	...	...	3.32	3.75	4.20	4.64	5.10	5.58	6.07	6.56
0.63	...	...	...	...	...	...	...	...	...	3.25	3.69	4.12	4.57	5.02	5.48	5.97	6.45
0.64	...	...	...	...	...	...	...	...	...	3.19	3.62	4.05	4.49	4.93	5.40	5.87	6.35
0.65	...	...	...	...	...	...	...	...	...	...	3.55	3.98	4.41	4.85	5.31	5.77	6.25
0.66	...	...	...	...	...	...	...	...	...	...	3.49	3.92	4.34	4.77	5.22	5.68	6.15

Copyright ASME International
Provided by IHS under license with ASME
No reproduction or networking permitted without license from IHS

Table 3-10 Values of *L* for Pipe Sizes ≥ NPS 48 and < NPS 52 (Cont'd)

Depth, *d*, in.	Wall Thickness, *t*, in.																
	0.344	0.406	0.438	0.469	0.500	0.562	0.625	0.688	0.750	0.812	0.875	0.938	1.000	1.062	1.125	1.188	1.250
0.67	...	...	...	...	...	...	...	...	...	...	3.43	3.85	4.27	4.70	5.14	5.59	6.05
0.68	...	...	...	...	...	...	...	...	...	...	3.37	3.79	4.20	4.62	5.06	5.51	5.96
0.69	...	...	...	...	...	...	...	...	...	...	3.31	3.72	4.13	4.55	4.98	5.42	5.87
0.70	...	...	...	...	...	...	...	...	...	...	3.25	3.66	4.07	4.48	4.91	5.34	5.78
0.71	...	...	...	...	...	...	...	...	...	...	...	3.60	4.00	4.41	4.83	5.26	5.70
0.72	...	...	...	...	...	...	...	...	...	...	...	3.54	3.94	4.34	4.76	5.19	5.61
0.73	...	...	...	...	...	...	...	...	...	...	...	3.48	3.88	4.28	4.69	5.11	5.53
0.74	...	...	...	...	...	...	...	...	...	...	...	3.43	3.82	4.21	4.62	5.04	5.45
0.75	...	...	...	...	...	...	...	...	...	...	...	3.37	3.76	4.15	4.55	4.96	5.38
0.76	...	...	...	...	...	...	...	...	...	...	...	...	3.70	4.09	4.49	4.89	5.30
0.77	...	...	...	...	...	...	...	...	...	...	...	...	3.64	4.03	4.42	4.83	5.23
0.78	...	...	...	...	...	...	...	...	...	...	...	...	3.59	3.97	4.36	4.76	5.16
0.79	...	...	...	...	...	...	...	...	...	...	...	...	3.53	3.91	4.30	4.69	5.09
0.80	...	...	...	...	...	...	...	...	...	...	...	...	3.48	3.85	4.24	4.63	5.02
0.81	...	...	...	...	...	...	...	...	...	...	...	...	...	3.80	4.18	4.56	4.95
0.82	...	...	...	...	...	...	...	...	...	...	...	...	...	3.74	4.12	4.50	4.89
0.83	...	...	...	...	...	...	...	...	...	...	...	...	...	3.69	4.06	4.44	4.82
0.84	...	...	...	...	...	...	...	...	...	...	...	...	...	3.63	4.01	4.38	4.76
0.85	...	...	...	...	...	...	...	...	...	...	...	...	...	...	3.95	4.32	4.70
0.86	...	...	...	...	...	...	...	...	...	...	...	...	...	...	3.90	4.27	4.64
0.87	...	...	...	...	...	...	...	...	...	...	...	...	...	...	3.84	4.21	4.58
0.88	...	...	...	...	...	...	...	...	...	...	...	...	...	...	3.79	4.16	4.52
0.89	...	...	...	...	...	...	...	...	...	...	...	...	...	...	3.74	4.10	4.46
0.90	...	...	...	...	...	...	...	...	...	...	...	...	...	...	3.69	4.05	4.40

Copyright ASME International
Provided by IHS under license with ASME
No reproduction or networking permitted without license from IHS

Table 3-10M Values of L for Pipe Sizes ≥ 1 219 mm and < 1 320 mm O.D.

Depth, d, mm	Wall Thickness, t, mm																
	8.7	10.3	11.1	11.9	12.7	14.3	15.9	17.5	19.1	20.6	22.2	23.8	25.4	27.0	28.6	30.2	31.8
0.8	No limit	No limit	No limit	No limit	No limit	No limit	No limit	No limit	No limit	No limit	No limit	No limit	No limit	No limit	No limit	No limit	No limit
1.0	462.4	No limit	No limit	No limit	No limit	No limit	No limit	No limit	No limit	No limit	No limit	No limit	No limit	No limit	No limit	No limit	No limit
1.3	462.4	502.3	521.8	539.9	557.5	No limit	No limit	No limit	No limit	No limit	No limit	No limit	No limit	No limit	No limit	No limit	No limit
1.5	462.4	502.3	521.8	539.9	557.5	591.0	No limit	No limit	No limit	No limit	No limit	No limit	No limit	No limit	No limit	No limit	No limit
1.8	296.9	502.3	521.8	539.9	557.5	591.0	623.3	653.9	No limit	No limit	No limit	No limit	No limit	No limit	No limit	No limit	No limit
2.0	226.2	348.8	449.4	539.9	557.5	591.0	623.3	653.9	682.8	No limit	No limit	No limit	No limit	No limit	No limit	No limit	No limit
2.3	186.6	268.8	327.5	402.0	503.7	591.0	623.3	653.9	682.8	710.4	737.5	No limit	No limit	No limit	No limit	No limit	No limit
2.5	160.7	222.8	264.0	312.5	373.0	555.6	623.3	653.9	682.8	710.4	737.5	763.5	788.4	No limit	No limit	No limit	No limit
2.8	142.2	192.5	224.3	260.2	302.7	417.5	609.4	653.9	682.8	710.4	737.5	763.5	788.4	812.4	No limit	No limit	No limit
3.0	128.1	170.7	196.8	225.4	258.2	341.1	463.3	653.9	682.8	710.4	737.5	763.5	788.4	812.4	836.2	859.3	No limit
3.3	116.9	154.2	176.4	200.3	227.1	292.0	380.6	508.3	682.8	710.4	737.5	763.5	788.4	812.4	836.2	859.3	881.4
3.6	107.8	141.0	160.5	181.1	203.9	257.4	326.8	419.8	549.9	710.4	737.5	763.5	788.4	812.4	836.2	859.3	881.4
3.8	100.1	130.3	147.7	165.9	185.8	231.5	288.7	361.6	456.8	590.5	737.5	763.5	788.4	812.4	836.2	859.3	881.4
4.1	93.5	121.3	137.1	153.5	171.2	211.3	260.0	320.0	394.8	493.3	632.9	763.5	788.4	812.4	836.2	859.3	881.4
4.3	87.8	113.5	128.1	143.1	159.1	194.9	237.5	288.6	350.1	427.7	531.1	674.4	788.4	812.4	836.2	859.3	881.4
4.6	82.7	106.8	120.3	134.2	148.9	181.3	219.3	263.9	316.2	380.1	461.7	568.4	712.3	812.4	836.2	859.3	881.4
4.8	78.2	100.9	113.6	126.5	140.1	169.9	204.2	243.9	289.5	343.8	411.1	495.5	603.3	749.4	836.2	859.3	881.4
5.1	74.1	95.7	107.6	119.7	132.4	160.0	191.4	227.2	267.8	315.1	372.3	442.0	527.5	637.7	788.6	859.3	881.4
5.3	70.3	90.9	102.2	113.6	125.6	151.3	180.4	213.2	249.7	291.7	341.6	400.8	471.4	559.1	673.5	827.0	881.4
5.6	66.9	86.6	97.4	108.2	119.5	143.7	170.8	201.0	234.4	272.3	316.4	368.0	428.1	500.7	592.0	708.9	861.8
5.8	63.8	82.7	93.0	103.3	114.0	136.9	162.4	190.5	221.2	255.7	295.5	341.2	393.5	455.3	531.0	624.6	741.7
6.1	60.8	79.1	88.9	98.8	109.1	130.8	154.8	181.1	209.7	241.5	277.7	318.8	365.1	418.9	483.5	561.2	655.3
6.4	58.1	75.7	85.2	94.7	104.5	125.3	148.0	172.8	199.6	229.0	262.3	299.7	341.4	389.0	445.2	511.5	589.8
6.6	55.5	72.6	81.8	90.9	100.3	120.2	141.9	165.3	190.5	218.0	248.9	283.3	321.1	364.0	413.8	471.5	538.3
6.9	53.0	69.7	78.5	87.4	96.5	115.5	136.3	158.6	182.4	208.3	237.1	268.9	303.7	342.6	387.3	438.4	496.7
7.1	. . .	66.9	75.5	84.1	92.9	111.2	131.1	152.4	175.0	199.5	226.5	256.2	288.4	324.1	364.7	410.6	462.2
7.4	. . .	64.3	72.7	81.0	89.5	107.2	126.4	146.8	168.3	191.5	217.0	244.9	274.8	307.9	345.1	386.8	433.1
7.6	. . .	61.9	70.0	78.1	86.4	103.5	121.9	141.5	162.2	184.3	208.5	234.7	262.8	293.5	328.0	366.2	408.2
7.9	. . .	59.6	67.5	75.4	83.4	100.0	117.8	136.7	156.5	177.6	200.6	225.5	252.0	280.8	312.8	348.1	386.6
8.1	. . .	57.3	65.1	72.8	80.6	96.8	114.0	132.2	151.3	171.5	193.5	217.1	242.2	269.3	299.3	332.1	367.7
8.4	. . .	. . .	62.8	70.3	78.0	93.7	110.4	128.0	146.4	165.8	186.9	209.4	233.2	258.9	287.1	317.8	350.9
8.6	. . .	. . .	60.7	68.0	75.4	90.8	107.0	124.1	141.8	160.6	180.8	202.4	225.1	249.4	276.1	305.0	335.9
8.9	. . .	. . .	58.6	65.8	73.0	88.0	103.8	120.4	137.6	155.7	175.1	195.8	217.5	240.7	266.0	293.3	322.4
9.1	. . .	. . .	. . .	63.6	70.8	85.4	100.8	116.9	133.6	151.1	169.9	189.8	210.6	232.8	256.8	282.7	310.2

Copyright ASME International
Provided by IHS under license with ASME
No reproduction or networking permitted without license from IHS

Table 3-10M Values of *L* for Pipe Sizes ≥ 1 219 mm and < 1 320 mm O.D. (Cont'd)

Depth, *d*, mm	Wall Thickness, *t*, mm																
	8.7	10.3	11.1	11.9	12.7	14.3	15.9	17.5	19.1	20.6	22.2	23.8	25.4	27.0	28.6	30.2	31.8
9.4	...	...	...	61.6	68.6	82.9	97.9	113.7	129.8	146.8	164.9	184.1	204.1	225.4	248.4	273.0	299.0
9.7	...	...	...	...	66.5	80.5	95.2	110.5	126.3	142.7	160.3	178.9	198.1	218.5	240.6	264.1	288.8
9.9	...	...	...	...	64.4	78.2	92.6	107.6	122.9	138.9	156.0	173.9	192.5	212.2	233.3	255.8	279.4
10.2	...	...	...	...	62.5	76.0	90.1	104.7	119.7	135.3	151.9	169.2	187.2	206.2	226.6	248.2	270.7
10.4	...	...	...	...	...	73.9	87.7	102.0	116.7	131.8	148.0	164.9	182.3	200.6	220.3	241.0	262.7
10.7	...	...	...	...	...	71.9	85.5	99.5	113.8	128.6	144.3	160.7	177.6	195.4	214.3	234.4	255.2
10.9	...	...	...	...	...	69.9	83.3	97.0	111.0	125.5	140.8	156.8	173.2	190.4	208.8	228.1	248.2
11.2	...	...	...	...	...	68.0	81.1	94.6	108.3	122.5	137.5	153.0	169.0	185.7	203.5	222.2	241.6
11.4	...	...	...	...	...	...	79.1	92.4	105.8	119.7	134.3	149.5	165.1	181.3	198.6	216.7	235.4
11.7	...	...	...	...	...	...	77.1	90.2	103.3	116.9	131.2	146.1	161.3	177.1	193.9	211.5	229.6
11.9	...	...	...	...	...	...	75.2	88.0	101.0	114.3	128.3	142.8	157.7	173.1	189.5	206.5	224.1
12.2	...	...	...	...	...	...	73.4	86.0	98.7	111.8	125.5	139.7	154.2	169.3	185.2	201.9	218.9
12.4	...	...	...	...	...	...	71.6	84.0	96.5	109.4	122.9	136.8	151.0	165.7	181.2	197.4	214.0
12.7	...	...	...	...	...	...	69.9	82.1	94.4	107.1	120.3	133.9	147.8	162.2	177.4	193.2	209.3
13.0	...	...	...	...	...	...	...	80.3	92.4	104.8	117.8	131.2	144.8	158.9	173.7	189.1	204.9
13.2	...	...	...	...	...	...	...	78.5	90.4	102.7	115.4	128.6	141.9	155.7	170.2	185.3	200.6
13.5	...	...	...	...	...	...	...	76.7	88.5	100.6	113.1	126.0	139.1	152.6	166.8	181.6	196.6
13.7	...	...	...	...	...	...	...	75.0	86.7	98.5	110.9	123.6	136.4	149.7	163.6	178.0	192.7
14.0	...	...	...	...	...	...	...	73.4	84.9	96.6	108.7	121.2	133.8	146.9	160.5	174.6	189.0
14.2	...	...	...	...	...	...	...	...	83.1	94.7	106.6	118.9	131.3	144.1	157.5	171.3	185.4
14.5	...	...	...	...	...	...	...	...	81.4	92.8	104.6	116.7	128.9	141.5	154.6	168.2	182.0
14.7	...	...	...	...	...	...	...	...	79.7	91.0	102.6	114.6	126.6	139.0	151.9	165.2	178.7
15.0	...	...	...	...	...	...	...	...	78.1	89.2	100.7	112.5	124.3	136.5	149.2	162.3	175.5
15.2	...	...	...	...	...	...	...	...	76.5	87.5	98.9	110.5	122.1	134.1	146.6	159.4	172.5
15.5	...	...	...	...	...	...	...	...	...	85.9	97.1	108.5	120.0	131.8	144.1	156.7	169.5
15.7	...	...	...	...	...	...	...	...	...	84.2	95.3	106.6	118.0	129.6	141.7	154.1	166.7
16.0	...	...	...	...	...	...	...	...	...	82.6	93.6	104.8	116.0	127.4	139.3	151.5	163.9
16.3	...	...	...	...	...	...	...	...	...	81.1	91.9	102.9	114.0	125.3	137.0	149.1	161.2
16.5	...	...	...	...	...	...	...	...	...	...	90.3	101.2	112.1	123.2	134.8	146.7	158.7
16.8	...	...	...	...	...	...	...	...	...	...	88.7	99.5	110.3	121.3	132.7	144.4	156.2

Copyright ASME International
Provided by IHS under license with ASME
No reproduction or networking permitted without license from IHS

Table 3-10M Values of *L* for Pipe Sizes ≥ 1 219 mm and < 1 320 mm O.D. (Cont'd)

Depth, *d*, mm	Wall Thickness, *t*, mm																
	8.7	10.3	11.1	11.9	12.7	14.3	15.9	17.5	19.1	20.6	22.2	23.8	25.4	27.0	28.6	30.2	31.8
17.0	...	...	...	...	...	...	...	...	...	...	87.1	97.8	108.5	119.3	130.6	142.1	153.7
17.3	...	...	...	...	...	...	...	...	...	...	85.6	96.2	106.7	117.4	128.5	139.9	151.4
17.5	...	...	...	...	...	...	...	...	...	...	84.1	94.6	105.0	115.6	126.6	137.8	149.1
17.8	...	...	...	...	...	...	...	...	...	...	82.7	93.0	103.3	113.8	124.6	135.7	146.9
18.0	...	...	...	...	...	...	...	...	...	...	...	91.5	101.7	112.0	122.8	133.7	144.7
18.3	...	...	...	...	...	...	...	...	...	...	...	90.0	100.1	110.3	120.9	131.7	142.6
18.5	...	...	...	...	...	...	...	...	...	...	...	88.5	98.5	108.6	119.1	129.8	140.5
18.8	...	...	...	...	...	...	...	...	...	...	...	87.0	97.0	107.0	117.4	127.9	138.5
19.1	...	...	...	...	...	...	...	...	...	...	...	85.6	95.5	105.4	115.7	126.1	136.6
19.3	...	...	...	...	...	...	...	...	...	...	...	...	94.0	103.8	114.0	124.3	134.7
19.6	...	...	...	...	...	...	...	...	...	...	...	...	92.5	102.3	112.4	122.6	132.8
19.8	...	...	...	...	...	...	...	...	...	...	...	...	91.1	100.8	110.7	120.9	131.0
20.1	...	...	...	...	...	...	...	...	...	...	...	...	89.7	99.3	109.2	119.2	129.2
20.3	...	...	...	...	...	...	...	...	...	...	...	...	88.4	97.9	107.6	117.6	127.5
20.6	...	...	...	...	...	...	...	...	...	...	...	...	...	96.4	106.1	115.9	125.8
20.8	...	...	...	...	...	...	...	...	...	...	...	...	...	95.0	104.7	114.4	124.1
21.1	...	...	...	...	...	...	...	...	...	...	...	...	...	93.7	103.2	112.8	122.5
21.3	...	...	...	...	...	...	...	...	...	...	...	...	...	92.3	101.8	111.3	120.9
21.6	...	...	...	...	...	...	...	...	...	...	...	...	...	...	100.4	109.8	119.3
21.8	...	...	...	...	...	...	...	...	...	...	...	...	...	...	99.0	108.4	117.8
22.1	...	...	...	...	...	...	...	...	...	...	...	...	...	...	97.6	107.0	116.2
22.4	...	...	...	...	...	...	...	...	...	...	...	...	...	...	96.3	105.6	114.8
22.6	...	...	...	...	...	...	...	...	...	...	...	...	...	...	95.0	104.2	113.3
22.9	...	...	...	...	...	...	...	...	...	...	...	...	...	...	93.7	102.8	111.9

Copyright ASME International
Provided by IHS under license with ASME
No reproduction or networking permitted without license from IHS

Table 3-11 Values of L for Pipe Sizes ≥ NPS 52 and < NPS 56

Depth, d, in.	Wall Thickness, t, in.															
	0.406	0.438	0.469	0.500	0.562	0.625	0.688	0.750	0.812	0.875	0.938	1.000	1.062	1.125	1.188	1.250
0.04	No limit	No limit	No limit	No limit	No limit	No limit	No limit	No limit	No limit	No limit	No limit	No limit	No limit	No limit	No limit	No limit
0.05	20.58	21.38	22.12	22.84	No limit	No limit	No limit	No limit	No limit	No limit	No limit	No limit	No limit	No limit	No limit	No limit
0.06	20.58	21.38	22.12	22.84	24.22	No limit	No limit	No limit	No limit	No limit	No limit	No limit	No limit	No limit	No limit	No limit
0.07	20.58	21.38	22.12	22.84	24.22	25.54	26.80	No limit	No limit	No limit	No limit	No limit	No limit	No limit	No limit	No limit
0.08	14.29	18.42	22.12	22.84	24.22	25.54	26.80	27.98	No limit	No limit	No limit	No limit	No limit	No limit	No limit	No limit
0.09	11.01	13.42	16.47	20.64	24.22	25.54	26.80	27.98	29.11	30.22	No limit	No limit	No limit	No limit	No limit	No limit
0.10	9.13	10.82	12.81	15.28	22.77	25.54	26.80	27.98	29.11	30.22	31.29	29.55	No limit	No limit	No limit	No limit
0.11	7.89	9.19	10.66	12.41	17.11	24.97	26.80	27.98	29.11	30.22	31.29	29.55	33.29	No limit	No limit	No limit
0.12	7.00	8.06	9.24	10.58	13.98	18.99	26.80	27.98	29.11	30.22	31.29	32.31	33.29	34.27	35.21	No limit
0.13	6.32	7.23	8.21	9.31	11.96	15.60	20.83	27.98	29.11	30.22	31.29	32.31	33.29	34.27	35.21	36.12
0.14	5.78	6.58	7.42	8.36	10.55	13.39	17.20	22.54	29.11	30.22	31.29	32.31	33.29	34.27	35.21	36.12
0.15	5.34	6.05	6.80	7.61	9.49	11.83	14.82	18.72	24.20	30.22	31.29	32.31	33.29	34.27	35.21	36.12
0.16	4.97	5.62	6.29	7.02	8.66	10.65	13.11	16.18	20.21	25.93	31.29	32.31	33.29	34.27	35.21	36.12
0.17	4.65	5.25	5.86	6.52	7.99	9.73	11.82	14.35	17.52	21.76	27.63	32.31	33.29	34.27	35.21	36.12
0.18	4.38	4.93	5.50	6.10	7.43	8.99	10.81	12.96	15.58	18.92	23.29	29.19	33.29	34.27	35.21	36.12
0.19	4.14	4.65	5.18	5.74	6.96	8.37	9.99	11.86	14.09	16.85	20.31	24.72	30.71	34.27	35.21	36.12
0.20	3.92	4.41	4.90	5.43	6.56	7.84	9.31	10.97	12.91	15.26	18.11	21.62	26.13	32.31	35.21	36.12
0.21	3.73	4.19	4.66	5.15	6.20	7.39	8.73	10.23	11.95	14.00	16.42	19.32	22.91	27.60	33.89	36.12
0.22	3.55	3.99	4.43	4.90	5.89	7.00	8.24	9.61	11.16	12.97	15.08	17.54	20.52	24.26	29.05	35.31
0.23	3.39	3.81	4.23	4.67	5.61	6.65	7.80	9.07	10.48	12.11	13.98	16.13	18.66	21.76	25.60	30.39
0.24	3.24	3.64	4.05	4.47	5.36	6.34	7.42	8.59	9.89	11.38	13.06	14.96	17.17	19.81	23.00	26.85
0.25	3.10	3.49	3.88	4.28	5.13	6.07	7.08	8.18	9.39	10.75	12.28	13.99	15.94	18.25	20.96	24.17
0.26	2.97	3.35	3.73	4.11	4.92	5.81	6.78	7.81	8.93	10.20	11.61	13.16	14.91	16.95	19.32	22.06
0.27	2.85	3.22	3.58	3.95	4.73	5.58	6.50	7.47	8.53	9.71	11.02	12.44	14.04	15.87	17.97	20.35
0.28	2.74	3.10	3.45	3.81	4.56	5.37	6.25	7.17	8.17	9.28	10.50	11.82	13.28	14.94	16.83	18.94
0.29	2.64	2.98	3.32	3.67	4.39	5.18	6.01	6.90	7.85	8.89	10.03	11.26	12.62	14.14	15.85	17.75
0.30	2.54	2.87	3.20	3.54	4.24	5.00	5.80	6.64	7.55	8.54	9.62	10.77	12.03	13.44	15.01	16.73
0.31	2.44	2.77	3.09	3.42	4.10	4.83	5.60	6.41	7.28	8.22	9.24	10.32	11.51	12.82	14.26	15.84
0.32	2.35	2.67	2.98	3.30	3.97	4.67	5.42	6.20	7.03	7.93	8.90	9.92	11.03	12.26	13.61	15.07
0.33	. . .	2.57	2.88	3.19	3.84	4.52	5.25	6.00	6.80	7.66	8.58	9.56	10.61	11.76	13.02	14.38
0.34	. . .	2.49	2.79	3.09	3.72	4.39	5.09	5.81	6.58	7.41	8.29	9.22	10.22	11.31	12.50	13.76

Copyright ASME International
Provided by IHS under license with ASME
No reproduction or networking permitted without license from IHS

Table 3-11 Values of *L* for Pipe Sizes ≥ NPS 52 and < NPS 56 (Cont'd)

Depth, *d*, in.	Wall Thickness, *t*, in.															
	0.406	0.438	0.469	0.500	0.562	0.625	0.688	0.750	0.812	0.875	0.938	1.000	1.062	1.125	1.188	1.250
0.35	...	2.40	2.69	2.99	3.61	4.26	4.93	5.64	6.38	7.18	8.02	8.91	9.86	10.90	12.02	13.21
0.36	...	...	2.61	2.90	3.50	4.13	4.79	5.47	6.19	6.96	7.78	8.63	9.54	10.52	11.59	12.71
0.37	...	...	2.52	2.81	3.40	4.01	4.66	5.32	6.01	6.76	7.55	8.36	9.24	10.18	11.19	12.25
0.38	...	...	...	2.72	3.30	3.90	4.53	5.17	5.85	6.57	7.33	8.12	8.95	9.86	10.82	11.83
0.39	...	...	...	2.64	3.20	3.80	4.41	5.04	5.69	6.39	7.13	7.89	8.69	9.56	10.48	11.45
0.40	...	...	...	2.56	3.11	3.69	4.29	4.90	5.54	6.22	6.94	7.67	8.45	9.28	10.17	11.09
0.41	...	...	...	...	3.03	3.60	4.18	4.78	5.40	6.06	6.76	7.47	8.22	9.03	9.88	10.76
0.42	...	...	...	...	2.94	3.50	4.08	4.66	5.27	5.91	6.59	7.28	8.01	8.78	9.60	10.46
0.43	...	...	...	...	2.86	3.41	3.97	4.55	5.14	5.77	6.42	7.10	7.80	8.56	9.35	10.17
0.44	...	...	...	...	2.79	3.33	3.88	4.44	5.02	5.63	6.27	6.93	7.61	8.34	9.11	9.90
0.45	...	...	...	...	...	3.24	3.78	4.33	4.90	5.50	6.13	6.76	7.43	8.14	8.88	9.65
0.46	...	...	...	...	...	3.16	3.69	4.23	4.79	5.38	5.99	6.61	7.26	7.95	8.67	9.41
0.47	...	...	...	...	...	3.08	3.61	4.14	4.68	5.26	5.85	6.46	7.09	7.76	8.46	9.18
0.48	...	...	...	...	...	3.01	3.52	4.05	4.58	5.14	5.73	6.32	6.94	7.59	8.27	8.97
0.49	...	...	...	...	...	2.93	3.44	3.96	4.48	5.03	5.60	6.19	6.79	7.43	8.09	8.77
0.50	...	...	...	...	...	2.86	3.37	3.87	4.39	4.93	5.49	6.06	6.65	7.27	7.92	8.58
0.51	...	...	...	...	...	...	3.29	3.79	4.30	4.83	5.38	5.93	6.51	7.12	7.75	8.40
0.52	...	...	...	...	...	...	3.22	3.71	4.21	4.73	5.27	5.81	6.38	6.97	7.59	8.22
0.53	...	...	...	...	...	...	3.14	3.63	4.12	4.64	5.16	5.70	6.25	6.84	7.44	8.06
0.54	...	...	...	...	...	...	3.07	3.55	4.04	4.54	5.06	5.59	6.13	6.70	7.29	7.90
0.55	...	...	...	...	...	...	3.01	3.48	3.96	4.46	4.97	5.48	6.02	6.58	7.16	7.74
0.56	...	...	...	...	...	...	...	3.41	3.88	4.37	4.87	5.38	5.91	6.45	7.02	7.60
0.57	...	...	...	...	...	...	...	3.34	3.80	4.29	4.78	5.28	5.80	6.34	6.89	7.46
0.58	...	...	...	...	...	...	...	3.27	3.73	4.21	4.69	5.19	5.69	6.22	6.77	7.32
0.59	...	...	...	...	...	...	...	3.20	3.66	4.13	4.61	5.10	5.59	6.11	6.65	7.19
0.60	...	...	...	...	...	...	...	3.14	3.59	4.05	4.53	5.01	5.50	6.01	6.53	7.07
0.61	...	...	...	...	...	...	...	...	3.52	3.98	4.45	4.92	5.40	5.90	6.42	6.95
0.62	...	...	...	...	...	...	...	...	3.45	3.91	4.37	4.83	5.31	5.81	6.31	6.83
0.63	...	...	...	...	...	...	...	...	3.39	3.84	4.29	4.75	5.22	5.71	6.21	6.72
0.64	...	...	...	...	...	...	...	...	3.32	3.77	4.22	4.67	5.13	5.62	6.11	6.61
0.65	...	...	...	...	...	...	...	...	...	3.70	4.15	4.59	5.05	5.52	6.01	6.50
0.66	...	...	...	...	...	...	...	...	...	3.63	4.08	4.52	4.97	5.44	5.92	6.40
0.67	...	...	...	...	...	...	...	...	...	3.57	4.01	4.44	4.89	5.35	5.82	6.30
0.68	...	...	...	...	...	...	...	...	...	3.51	3.94	4.37	4.81	5.27	5.73	6.20
0.69	...	...	...	...	...	...	...	...	...	3.45	3.87	4.30	4.74	5.19	5.65	6.11
0.70	...	...	...	...	...	...	...	...	...	3.39	3.81	4.23	4.66	5.11	5.56	6.02

Copyright ASME International
Provided by IHS under license with ASME
No reproduction or networking permitted without license from IHS

Table 3-11 Values of *L* for Pipe Sizes ≥ NPS 52 and < NPS 56 (Cont'd)

Depth, *d*, in.	Wall Thickness, *t*, in.															
	0.406	0.438	0.469	0.500	0.562	0.625	0.688	0.750	0.812	0.875	0.938	1.000	1.062	1.125	1.188	1.250
0.71	...	...	...	...	...	...	...	...	...	...	3.75	4.17	4.59	5.03	5.48	5.93
0.72	...	...	...	...	...	...	...	...	...	...	3.69	4.10	4.52	4.95	5.40	5.84
0.73	...	...	...	...	...	...	...	...	...	...	3.63	4.04	4.45	4.88	5.32	5.76
0.74	...	...	...	...	...	...	...	...	...	...	3.57	3.97	4.38	4.81	5.24	5.68
0.75	...	...	...	...	...	...	...	...	...	...	3.51	3.91	4.32	4.74	5.17	5.60
0.76	...	...	...	...	...	...	...	...	...	...	...	3.85	4.25	4.67	5.09	5.52
0.77	...	...	...	...	...	...	...	...	...	...	...	3.79	4.19	4.60	5.02	5.44
0.78	...	...	...	...	...	...	...	...	...	...	...	3.73	4.13	4.54	4.95	5.37
0.79	...	...	...	...	...	...	...	...	...	...	...	3.68	4.07	4.47	4.88	5.29
0.80	...	...	...	...	...	...	...	...	...	...	...	3.62	4.01	4.41	4.82	5.22
0.81	...	...	...	...	...	...	...	...	...	...	...	...	3.95	4.35	4.75	5.15
0.82	...	...	...	...	...	...	...	...	...	...	...	...	3.89	4.29	4.69	5.08
0.83	...	...	...	...	...	...	...	...	...	...	...	...	3.84	4.23	4.62	5.02
0.84	...	...	...	...	...	...	...	...	...	...	...	...	3.78	4.17	4.56	4.95
0.85	...	...	...	...	...	...	...	...	...	...	...	...	...	4.11	4.50	4.89
0.86	...	...	...	...	...	...	...	...	...	...	...	...	...	4.06	4.44	4.83
0.87	...	...	...	...	...	...	...	...	...	...	...	...	...	4.00	4.38	4.76
0.88	...	...	...	...	...	...	...	...	...	...	...	...	...	3.95	4.33	4.70
0.89	...	...	...	...	...	...	...	...	...	...	...	...	...	3.89	4.27	4.64
0.90	...	...	...	...	...	...	...	...	...	...	...	...	...	3.84	4.21	4.58
0.91	...	...	...	...	...	...	...	...	...	...	...	...	...	...	4.16	4.53
0.92	...	...	...	...	...	...	...	...	...	...	...	...	...	...	4.10	4.47
0.93	...	...	...	...	...	...	...	...	...	...	...	...	...	...	4.05	4.41
0.94	...	...	...	...	...	...	...	...	...	...	...	...	...	...	4.00	4.36
0.95	...	...	...	...	...	...	...	...	...	...	...	...	...	...	3.95	4.31
0.96	...	...	...	...	...	...	...	...	...	...	...	...	...	...	...	4.25
0.97	...	...	...	...	...	...	...	...	...	...	...	...	...	...	...	4.20
0.98	...	...	...	...	...	...	...	...	...	...	...	...	...	...	...	4.15
0.99	...	...	...	...	...	...	...	...	...	...	...	...	...	...	...	4.10
1.00	...	...	...	...	...	...	...	...	...	...	...	...	...	...	...	4.05

Copyright ASME International
Provided by IHS under license with ASME
No reproduction or networking permitted without license from IHS

Table 3-11M Values of *L* for Pipe Sizes ≥ 1 320 mm and < 1 422 mm O.D.

Depth, *d*, mm	Wall Thickness, *t*, mm															
	10.3	11.1	11.9	12.7	14.3	15.9	17.5	19.1	20.6	22.2	23.8	25.4	27.0	28.6	30.2	31.8
1.0	No limit	No limit	No limit	No limit	No limit	No limit	No limit	No limit	No limit	No limit	No limit	No limit	No limit	No limit	No limit	No limit
1.3	522.8	543.1	562.0	580.2	No limit	No limit	No limit	No limit	No limit	No limit	No limit	No limit	No limit	No limit	No limit	No limit
1.5	522.8	543.1	562.0	580.2	615.2	No limit	No limit	No limit	No limit	No limit	No limit	No limit	No limit	No limit	No limit	No limit
1.8	522.8	543.1	562.0	580.2	615.2	648.7	680.6	No limit	No limit	No limit	No limit	No limit	No limit	No limit	No limit	No limit
2.0	363.1	467.7	562.0	580.2	615.2	648.7	680.6	710.6	No limit	No limit	No limit	No limit	No limit	No limit	No limit	No limit
2.3	279.7	340.9	418.4	524.3	615.2	648.7	680.6	710.6	739.4	767.6	No limit	No limit	No limit	No limit	No limit	No limit
2.5	231.9	274.8	325.3	388.2	578.3	648.7	680.6	710.6	739.4	767.6	794.7	750.6	No limit	No limit	No limit	No limit
2.8	200.4	233.5	270.8	315.1	434.5	634.3	680.6	710.6	739.4	767.6	794.7	750.6	845.6	No limit	No limit	No limit
3.0	177.7	204.8	234.6	268.7	355.0	482.3	680.6	710.6	739.4	767.6	794.7	820.6	845.6	870.3	894.4	No limit
3.3	160.5	183.6	208.5	236.4	303.9	396.2	529.1	710.6	739.4	767.6	794.7	820.6	845.6	870.3	894.4	917.4
3.6	146.8	167.0	188.5	212.2	267.9	340.2	437.0	572.4	739.4	767.6	794.7	820.6	845.6	870.3	894.4	917.4
3.8	135.6	153.7	172.7	193.4	241.0	300.5	376.3	475.5	614.7	767.6	794.7	820.6	845.6	870.3	894.4	917.4
4.1	126.2	142.7	159.8	178.2	219.9	270.6	333.0	410.9	513.4	658.7	794.7	820.6	845.6	870.3	894.4	917.4
4.3	118.2	133.3	148.9	165.6	202.9	247.2	300.3	364.4	445.1	552.8	701.9	820.6	845.6	870.3	894.4	917.4
4.6	111.2	125.2	139.7	155.0	188.7	228.3	274.6	329.1	395.6	480.6	591.7	741.4	845.6	870.3	894.4	917.4
4.8	105.0	118.2	131.6	145.8	176.8	212.6	253.8	301.3	357.9	427.9	515.8	628.0	780.0	870.3	894.4	917.4
5.1	99.6	112.0	124.6	137.8	166.5	199.3	236.5	278.7	328.0	387.5	460.0	549.0	663.7	820.8	894.4	917.4
5.3	94.6	106.4	118.3	130.7	157.5	187.8	221.9	259.9	303.6	355.5	417.1	490.7	582.0	701.0	860.7	917.4
5.6	90.2	101.3	112.6	124.4	149.6	177.8	209.2	244.0	283.4	329.4	383.0	445.6	521.1	616.2	737.9	897.0
5.8	86.1	96.8	107.5	118.7	142.5	169.0	198.2	230.3	266.2	307.6	355.1	409.6	473.9	552.7	650.1	772.0
6.1	82.3	92.6	102.9	113.5	136.1	161.1	188.5	218.3	251.3	289.0	331.8	380.0	436.1	503.2	584.1	682.0
6.4	78.8	88.7	98.6	108.8	130.4	154.1	179.9	207.7	238.4	273.0	311.9	355.3	404.9	463.4	532.4	613.9
6.6	75.6	85.1	94.6	104.4	125.1	147.7	172.1	198.3	226.9	259.1	294.8	334.3	378.8	430.6	490.7	560.3
6.9	72.5	81.8	91.0	100.4	120.2	141.8	165.1	189.8	216.8	246.8	279.9	316.1	356.6	403.1	456.3	516.9
7.1	69.7	78.6	87.5	96.7	115.8	136.5	158.6	182.2	207.6	235.8	266.6	300.1	337.3	379.6	427.4	481.1
7.4	67.0	75.7	84.3	93.2	111.6	131.5	152.8	175.2	199.3	225.9	254.9	286.1	320.4	359.2	402.6	450.8
7.6	64.4	72.9	81.3	89.9	107.7	126.9	147.3	168.8	191.8	217.0	244.3	273.5	305.5	341.4	381.1	424.9
7.9	62.0	70.3	78.5	86.8	104.1	122.7	142.3	162.9	184.9	208.8	234.7	262.2	292.2	325.6	362.3	402.4
8.1	59.7	67.8	75.8	83.9	100.7	118.7	137.6	157.4	178.5	201.4	226.0	252.0	280.3	311.5	345.7	382.7
8.4	. . .	65.4	73.2	81.1	97.5	114.9	133.3	152.4	172.6	194.5	218.0	242.8	269.4	298.8	330.8	365.2
8.6	. . .	63.1	70.8	78.5	94.5	111.4	129.2	147.6	167.1	188.2	210.6	234.2	259.6	287.3	317.4	349.6

Copyright ASME International
Provided by IHS under license with ASME
No reproduction or networking permitted without license from IHS

Table 3-11M Values of *L* for Pipe Sizes ≥ 1 320 mm and < 1 422 mm O.D. (Cont'd)

Depth, *d*, mm	Wall Thickness, *t*, mm															
	10.3	11.1	11.9	12.7	14.3	15.9	17.5	19.1	20.6	22.2	23.8	25.4	27.0	28.6	30.2	31.8
8.9	...	60.9	68.4	76.0	91.6	108.1	125.3	143.2	162.0	182.3	203.8	226.4	250.6	276.9	305.3	335.6
9.1	...	...	66.2	73.6	88.9	104.9	121.7	139.0	157.3	176.8	197.5	219.2	242.3	267.3	294.3	322.8
9.4	...	...	64.1	71.4	86.3	101.9	118.3	135.1	152.8	171.7	191.6	212.5	234.6	258.5	284.2	311.2
9.7	...	...	...	69.2	83.8	99.1	115.0	131.4	148.6	166.9	186.2	206.2	227.5	250.4	274.9	300.6
9.9	...	...	...	67.1	81.4	96.4	112.0	127.9	144.6	162.3	181.0	200.4	220.8	242.8	266.3	290.8
10.2	...	...	...	65.0	79.1	93.8	109.0	124.6	140.8	158.1	176.2	194.9	214.6	235.8	258.3	281.8
10.4	...	...	...	...	76.9	91.3	106.2	121.4	137.2	154.0	171.6	189.7	208.8	229.2	250.9	273.4
10.7	...	...	...	...	74.8	88.9	103.5	118.4	133.8	150.2	167.3	184.9	203.3	223.1	243.9	265.6
10.9	...	...	...	...	72.8	86.7	101.0	115.5	130.6	146.5	163.2	180.3	198.2	217.3	237.4	258.3
11.2	...	...	...	...	70.8	84.5	98.5	112.7	127.5	143.1	159.3	175.9	193.3	211.9	231.3	251.5
11.4	...	...	...	...	...	82.3	96.1	110.1	124.5	139.8	155.6	171.8	188.7	206.7	225.6	245.1
11.7	...	...	...	...	...	80.3	93.8	107.6	121.7	136.6	152.0	167.9	184.3	201.8	220.1	239.0
11.9	...	...	...	...	...	78.3	91.6	105.1	119.0	133.6	148.7	164.1	180.2	197.2	215.0	233.3
12.2	...	...	...	...	...	76.4	89.5	102.8	116.4	130.7	145.5	160.5	176.2	192.8	210.1	227.9
12.4	...	...	...	...	...	74.5	87.5	100.5	113.9	127.9	142.4	157.1	172.4	188.6	205.5	222.8
12.7	...	...	...	...	...	72.7	85.5	98.3	111.4	125.2	139.4	153.9	168.8	184.6	201.1	217.9
13.0	...	...	...	...	...	...	83.5	96.2	109.1	122.6	136.6	150.7	165.4	180.8	196.8	213.2
13.2	...	...	...	...	...	...	81.7	94.1	106.9	120.1	133.8	147.7	162.1	177.2	192.8	208.8
13.5	...	...	...	...	...	...	79.8	92.1	104.7	117.7	131.2	144.8	158.9	173.6	189.0	204.6
13.7	...	...	...	...	...	...	78.1	90.2	102.6	115.4	128.6	142.0	155.8	170.3	185.3	200.6
14.0	...	...	...	...	...	...	76.3	88.3	100.5	113.2	126.2	139.3	152.9	167.1	181.7	196.7
14.2	...	...	...	...	...	...	...	86.5	98.5	111.0	123.8	136.7	150.0	163.9	178.3	193.0
14.5	...	...	...	...	...	...	...	84.7	96.6	108.9	121.5	134.2	147.3	161.0	175.1	189.4
14.7	...	...	...	...	...	...	...	83.0	94.7	106.8	119.2	131.8	144.6	158.1	171.9	186.0
15.0	...	...	...	...	...	...	...	81.3	92.9	104.9	117.1	129.4	142.1	155.3	168.9	182.7
15.2	...	...	...	...	...	...	...	79.6	91.1	102.9	115.0	127.1	139.6	152.6	165.9	179.5
15.5	...	...	...	...	...	...	...	...	89.4	101.0	112.9	124.9	137.2	150.0	163.1	176.4
15.7	...	...	...	...	...	...	...	...	87.7	99.2	111.0	122.8	134.9	147.5	160.4	173.5
16.0	...	...	...	...	...	...	...	...	86.0	97.4	109.0	120.7	132.6	145.0	157.7	170.6
16.3	...	...	...	...	...	...	...	...	84.4	95.7	107.2	118.7	130.4	142.6	155.2	167.8
16.5	...	...	...	...	...	...	...	...	...	94.0	105.3	116.7	128.3	140.3	152.7	165.1
16.8	...	...	...	...	...	...	...	...	...	92.3	103.5	114.8	126.2	138.1	150.3	162.5
17.0	...	...	...	...	...	...	...	...	...	90.7	101.8	112.9	124.2	135.9	147.9	160.0
17.3	...	...	...	...	...	...	...	...	...	89.1	100.1	111.1	122.2	133.8	145.6	157.5
17.5	...	...	...	...	...	...	...	...	...	87.6	98.4	109.3	120.3	131.7	143.4	155.2
17.8	...	...	...	...	...	...	...	...	...	86.0	96.8	107.5	118.4	129.7	141.3	152.8

Copyright ASME International
Provided by IHS under license with ASME
No reproduction or networking permitted without license from IHS

Table 3-11M Values of L for Pipe Sizes ≥ 1 320 mm and < 1 422 mm O.D. (Cont'd)

Depth, d, mm	Wall Thickness, t, mm															
	10.3	11.1	11.9	12.7	14.3	15.9	17.5	19.1	20.6	22.2	23.8	25.4	27.0	28.6	30.2	31.8
18.0	...	...	...	...	...	...	...	...	...	...	95.2	105.8	116.6	127.8	139.2	150.6
18.3	...	...	...	...	...	...	...	...	...	...	93.6	104.1	114.8	125.9	137.1	148.4
18.5	...	...	...	...	...	...	...	...	...	...	92.1	102.5	113.1	124.0	135.1	146.3
18.8	...	...	...	...	...	...	...	...	...	...	90.6	100.9	111.4	122.2	133.2	144.2
19.1	...	...	...	...	...	...	...	...	...	...	89.1	99.4	109.7	120.4	131.2	142.1
19.3	...	...	...	...	...	...	...	...	...	...	...	97.8	108.1	118.6	129.4	140.2
19.6	...	...	...	...	...	...	...	...	...	...	...	96.3	106.5	116.9	127.6	138.2
19.8	...	...	...	...	...	...	...	...	...	...	...	94.8	104.9	115.3	125.8	136.3
20.1	...	...	...	...	...	...	...	...	...	...	...	93.4	103.4	113.6	124.1	134.5
20.3	...	...	...	...	...	...	...	...	...	...	...	92.0	101.9	112.0	122.4	132.7
20.6	...	...	...	...	...	...	...	...	...	...	...	...	100.4	110.5	120.7	130.9
20.8	...	...	...	...	...	...	...	...	...	...	...	...	98.9	108.9	119.0	129.2
21.1	...	...	...	...	...	...	...	...	...	...	...	...	97.5	107.4	117.4	127.5
21.3	...	...	...	...	...	...	...	...	...	...	...	...	96.1	105.9	115.9	125.8
21.6	...	...	...	...	...	...	...	...	...	...	...	...	...	104.5	114.3	124.2
21.8	...	...	...	...	...	...	...	...	...	...	...	...	...	103.0	112.8	122.6
22.1	...	...	...	...	...	...	...	...	...	...	...	...	...	101.6	111.3	121.0
22.4	...	...	...	...	...	...	...	...	...	...	...	...	...	100.2	109.9	119.4
22.6	...	...	...	...	...	...	...	...	...	...	...	...	...	98.9	108.4	117.9
22.9	...	...	...	...	...	...	...	...	...	...	...	...	...	97.5	107.0	116.4
23.1	...	...	...	...	...	...	...	...	...	...	...	...	...	...	105.6	115.0
23.4	...	...	...	...	...	...	...	...	...	...	...	...	...	...	104.3	113.5
23.6	...	...	...	...	...	...	...	...	...	...	...	...	...	...	102.9	112.1
23.9	...	...	...	...	...	...	...	...	...	...	...	...	...	...	101.6	110.7
24.1	...	...	...	...	...	...	...	...	...	...	...	...	...	...	100.3	109.4
24.4	...	...	...	...	...	...	...	...	...	...	...	...	...	...	...	108.0
24.6	...	...	...	...	...	...	...	...	...	...	...	...	...	...	...	106.7
24.9	...	...	...	...	...	...	...	...	...	...	...	...	...	...	...	105.4
25.1	...	...	...	...	...	...	...	...	...	...	...	...	...	...	...	104.1
25.4	...	...	...	...	...	...	...	...	...	...	...	...	...	...	...	102.8

Copyright ASME International
Provided by IHS under license with ASME
No reproduction or networking permitted without license from IHS

Table 3-12 Values of L for Pipe Sizes ≥ NPS 56 Through NPS 60

Depth, d, in.	Wall Thickness, t, in.															
	0.406	0.438	0.469	0.500	0.562	0.625	0.688	0.750	0.812	0.875	0.938	1.000	1.062	1.125	1.188	1.250
0.04	No limit	No limit	No limit	No limit	No limit	No limit	No limit	No limit	No limit	No limit	No limit	No limit	No limit	No limit	No limit	No limit
0.05	21.36	22.19	22.96	23.71	No limit	No limit	No limit	No limit	No limit	No limit	No limit	No limit	No limit	No limit	No limit	No limit
0.06	21.36	22.19	22.96	23.71	25.13	No limit	No limit	No limit	No limit	No limit	No limit	No limit	No limit	No limit	No limit	No limit
0.07	21.36	22.19	22.96	23.71	25.13	26.50	27.81	No limit	No limit	No limit	No limit	No limit	No limit	No limit	No limit	No limit
0.08	14.83	19.11	22.96	23.71	25.13	26.50	27.81	29.03	No limit	No limit	No limit	No limit	No limit	No limit	No limit	No limit
0.09	11.43	13.93	17.09	21.42	25.13	26.50	27.81	29.03	30.21	31.36	No limit	No limit	No limit	No limit	No limit	No limit
0.10	9.48	11.23	13.29	15.86	23.63	26.50	27.81	29.03	30.21	31.36	32.47	33.53	No limit	No limit	No limit	No limit
0.11	8.19	9.54	11.07	12.87	17.75	25.91	27.81	29.03	30.21	31.36	32.47	33.53	34.55	No limit	No limit	No limit
0.12	7.26	8.37	9.59	10.98	14.50	19.70	27.81	29.03	30.21	31.36	32.47	33.53	34.55	35.56	36.54	No limit
0.13	6.56	7.50	8.52	9.66	12.42	16.19	21.62	29.03	30.21	31.36	32.47	33.53	34.55	35.56	36.54	37.48
0.14	6.00	6.82	7.70	8.67	10.95	13.90	17.85	23.39	30.21	31.36	32.47	33.53	34.55	35.56	36.54	37.48
0.15	5.54	6.28	7.06	7.90	9.84	12.28	15.37	19.43	25.11	31.36	32.47	33.53	34.55	35.56	36.54	37.48
0.16	5.16	5.83	6.53	7.28	8.98	11.06	13.61	16.79	20.98	26.91	32.47	33.53	34.55	35.56	36.54	37.48
0.17	4.83	5.45	6.08	6.77	8.29	10.10	12.27	14.89	18.19	22.58	28.68	33.53	34.55	35.56	36.54	37.48
0.18	4.54	5.12	5.71	6.33	7.71	9.33	11.22	13.45	16.16	19.63	24.17	30.29	34.55	35.56	36.54	37.48
0.19	4.29	4.83	5.38	5.96	7.22	8.68	10.37	12.31	14.62	17.48	21.07	25.66	31.87	35.56	36.54	37.48
0.20	4.07	4.57	5.09	5.63	6.80	8.14	9.66	11.39	13.40	15.83	18.79	22.43	27.12	33.53	36.54	37.48
0.21	3.87	4.35	4.83	5.34	6.44	7.67	9.06	10.62	12.41	14.52	17.04	20.05	23.78	28.64	35.17	37.48
0.22	3.68	4.14	4.60	5.08	6.11	7.27	8.55	9.97	11.58	13.46	15.65	18.21	21.29	25.18	30.15	36.65
0.23	3.52	3.95	4.39	4.85	5.82	6.90	8.10	9.41	10.87	12.57	14.51	16.73	19.36	22.58	26.56	31.54
0.24	3.36	3.78	4.20	4.64	5.56	6.58	7.70	8.92	10.27	11.81	13.56	15.53	17.82	20.56	23.86	27.86
0.25	3.22	3.62	4.03	4.44	5.33	6.29	7.35	8.49	9.74	11.16	12.74	14.52	16.54	18.93	21.75	25.08
0.26	3.09	3.48	3.87	4.27	5.11	6.03	7.03	8.10	9.27	10.58	12.05	13.66	15.48	17.59	20.05	22.89
0.27	2.96	3.34	3.72	4.10	4.91	5.79	6.74	7.76	8.86	10.08	11.43	12.91	14.57	16.47	18.64	21.12
0.28	2.85	3.21	3.58	3.95	4.73	5.58	6.48	7.44	8.48	9.63	10.89	12.26	13.78	15.51	17.46	19.65
0.29	2.74	3.09	3.45	3.81	4.56	5.37	6.24	7.16	8.14	9.23	10.41	11.69	13.09	14.68	16.45	18.42
0.30	2.63	2.98	3.32	3.67	4.40	5.19	6.02	6.90	7.84	8.86	9.98	11.18	12.48	13.95	15.57	17.36
0.31	2.53	2.87	3.21	3.55	4.25	5.01	5.81	6.65	7.55	8.53	9.59	10.71	11.94	13.30	14.80	16.44
0.32	2.44	2.77	3.10	3.43	4.11	4.85	5.62	6.43	7.29	8.23	9.23	10.30	11.45	12.73	14.12	15.64
0.33	. . .	2.67	2.99	3.32	3.98	4.70	5.44	6.22	7.05	7.95	8.91	9.92	11.01	12.21	13.52	14.92
0.34	. . .	2.58	2.89	3.21	3.86	4.55	5.28	6.03	6.83	7.69	8.61	9.57	10.61	11.74	12.97	14.28

Copyright ASME International
Provided by IHS under license with ASME
No reproduction or networking permitted without license from IHS

Table 3-12 Values of *L* for Pipe Sizes ≥ NPS 56 Through NPS 60 (Cont'd)

Depth, *d*, in.	Wall Thickness, *t*, in.															
	0.406	0.438	0.469	0.500	0.562	0.625	0.688	0.750	0.812	0.875	0.938	1.000	1.062	1.125	1.188	1.250
0.35	...	2.49	2.80	3.11	3.74	4.42	5.12	5.85	6.62	7.45	8.33	9.25	10.24	11.31	12.47	13.71
0.36	...	...	2.70	3.01	3.63	4.29	4.97	5.68	6.43	7.22	8.07	8.96	9.90	10.92	12.02	13.19
0.37	...	...	2.62	2.92	3.52	4.17	4.83	5.52	6.24	7.01	7.83	8.68	9.58	10.56	11.61	12.72
0.38	...	...	...	2.83	3.42	4.05	4.70	5.37	6.07	6.82	7.61	8.43	9.29	10.23	11.23	12.28
0.39	...	...	...	2.74	3.33	3.94	4.57	5.23	5.91	6.63	7.40	8.19	9.02	9.92	10.88	11.88
0.40	...	...	...	2.66	3.23	3.83	4.45	5.09	5.75	6.46	7.20	7.96	8.77	9.63	10.55	11.51
0.41	...	...	...	...	3.14	3.73	4.34	4.96	5.61	6.29	7.01	7.75	8.53	9.37	10.25	11.17
0.42	...	...	...	...	3.06	3.63	4.23	4.84	5.47	6.14	6.83	7.55	8.31	9.11	9.97	10.85
0.43	...	...	...	...	2.97	3.54	4.13	4.72	5.34	5.99	6.67	7.37	8.10	8.88	9.70	10.55
0.44	...	...	...	...	2.89	3.45	4.02	4.61	5.21	5.85	6.51	7.19	7.90	8.66	9.45	10.27
0.45	...	...	...	...	...	3.36	3.93	4.50	5.09	5.71	6.36	7.02	7.71	8.45	9.22	10.01
0.46	...	...	...	...	...	3.28	3.83	4.39	4.97	5.58	6.21	6.86	7.53	8.25	8.99	9.76
0.47	...	...	...	...	...	3.20	3.74	4.29	4.86	5.46	6.07	6.71	7.36	8.06	8.78	9.53
0.48	...	...	...	...	...	3.12	3.66	4.20	4.75	5.34	5.94	6.56	7.20	7.88	8.58	9.31
0.49	...	...	...	...	...	3.04	3.57	4.11	4.65	5.22	5.82	6.42	7.05	7.71	8.39	9.10
0.50	...	...	...	...	...	2.97	3.49	4.02	4.55	5.12	5.70	6.29	6.90	7.54	8.21	8.90
0.51	...	...	...	...	...	...	3.41	3.93	4.46	5.01	5.58	6.16	6.76	7.39	8.04	8.71
0.52	...	...	...	...	...	...	3.34	3.85	4.37	4.91	5.47	6.03	6.62	7.24	7.88	8.53
0.53	...	...	...	...	...	...	3.26	3.76	4.28	4.81	5.36	5.92	6.49	7.09	7.72	8.36
0.54	...	...	...	...	...	...	3.19	3.69	4.19	4.72	5.26	5.80	6.37	6.96	7.57	8.19
0.55	...	...	...	...	...	...	3.12	3.61	4.11	4.62	5.15	5.69	6.25	6.83	7.43	8.04
0.56	...	...	...	...	...	...	...	3.53	4.02	4.53	5.06	5.59	6.13	6.70	7.29	7.88
0.57	...	...	...	...	...	...	...	3.46	3.95	4.45	4.96	5.48	6.02	6.58	7.15	7.74
0.58	...	...	...	...	...	...	...	3.39	3.87	4.37	4.87	5.38	5.91	6.46	7.02	7.60
0.59	...	...	...	...	...	...	...	3.32	3.79	4.28	4.78	5.29	5.80	6.34	6.90	7.46
0.60	...	...	...	...	...	...	...	3.25	3.72	4.20	4.70	5.19	5.70	6.23	6.78	7.33
0.61	...	...	...	...	...	...	...	...	3.65	4.13	4.61	5.10	5.60	6.13	6.66	7.21
0.62	...	...	...	...	...	...	...	...	3.58	4.05	4.53	5.02	5.51	6.02	6.55	7.09
0.63	...	...	...	...	...	...	...	...	3.51	3.98	4.45	4.93	5.42	5.92	6.44	6.97
0.64	...	...	...	...	...	...	...	...	3.45	3.91	4.38	4.85	5.33	5.83	6.34	6.86
0.65	...	...	...	...	...	...	...	...	...	3.84	4.30	4.77	5.24	5.73	6.24	6.75
0.66	...	...	...	...	...	...	...	...	...	3.77	4.23	4.69	5.16	5.64	6.14	6.64
0.67	...	...	...	...	...	...	...	...	...	3.71	4.16	4.61	5.07	5.55	6.04	6.54
0.68	...	...	...	...	...	...	...	...	...	3.64	4.09	4.54	4.99	5.47	5.95	6.44
0.69	...	...	...	...	...	...	...	...	...	3.58	4.02	4.46	4.92	5.38	5.86	6.34
0.70	...	...	...	...	...	...	...	...	...	3.51	3.95	4.39	4.84	5.30	5.77	6.24

Copyright ASME International
Provided by IHS under license with ASME
No reproduction or networking permitted without license from IHS

Table 3-12 Values of *L* for Pipe Sizes ≥ NPS 56 Through NPS 60 (Cont'd)

Depth, *d*, in.	Wall Thickness, *t*, in.															
	0.406	0.438	0.469	0.500	0.562	0.625	0.688	0.750	0.812	0.875	0.938	1.000	1.062	1.125	1.188	1.250
0.71	...	...	...	...	...	...	...	...	...	...	3.89	4.32	4.76	5.22	5.69	6.15
0.72	...	...	...	...	...	...	...	...	...	...	3.83	4.26	4.69	5.14	5.60	6.06
0.73	...	...	...	...	...	...	...	...	...	...	3.76	4.19	4.62	5.07	5.52	5.98
0.74	...	...	...	...	...	...	...	...	...	...	3.70	4.12	4.55	4.99	5.44	5.89
0.75	...	...	...	...	...	...	...	...	...	...	3.64	4.06	4.48	4.92	5.36	5.81
0.76	...	...	...	...	...	...	...	...	...	...	...	4.00	4.42	4.85	5.29	5.73
0.77	...	...	...	...	...	...	...	...	...	...	...	3.94	4.35	4.78	5.21	5.65
0.78	...	...	...	...	...	...	...	...	...	...	...	3.87	4.29	4.71	5.14	5.57
0.79	...	...	...	...	...	...	...	...	...	...	...	3.82	4.22	4.64	5.07	5.49
0.80	...	...	...	...	...	...	...	...	...	...	...	3.76	4.16	4.58	5.00	5.42
0.81	...	...	...	...	...	...	...	...	...	...	...	...	4.10	4.51	4.93	5.35
0.82	...	...	...	...	...	...	...	...	...	...	...	...	4.04	4.45	4.86	5.28
0.83	...	...	...	...	...	...	...	...	...	...	...	...	3.98	4.39	4.80	5.21
0.84	...	...	...	...	...	...	...	...	...	...	...	...	3.93	4.33	4.73	5.14
0.85	...	...	...	...	...	...	...	...	...	...	...	...	...	4.27	4.67	5.07
0.86	...	...	...	...	...	...	...	...	...	...	...	...	...	4.21	4.61	5.01
0.87	...	...	...	...	...	...	...	...	...	...	...	...	...	4.15	4.55	4.94
0.88	...	...	...	...	...	...	...	...	...	...	...	...	...	4.10	4.49	4.88
0.89	...	...	...	...	...	...	...	...	...	...	...	...	...	4.04	4.43	4.82
0.90	...	...	...	...	...	...	...	...	...	...	...	...	...	3.99	4.37	4.76
0.91	...	...	...	...	...	...	...	...	...	...	...	...	...	...	4.32	4.70
0.92	...	...	...	...	...	...	...	...	...	...	...	...	...	...	4.26	4.64
0.93	...	...	...	...	...	...	...	...	...	...	...	...	...	...	4.20	4.58
0.94	...	...	...	...	...	...	...	...	...	...	...	...	...	...	4.15	4.52
0.95	...	...	...	...	...	...	...	...	...	...	...	...	...	...	4.10	4.47
0.96	...	...	...	...	...	...	...	...	...	...	...	...	...	...	...	4.41
0.97	...	...	...	...	...	...	...	...	...	...	...	...	...	...	...	4.36
0.98	...	...	...	...	...	...	...	...	...	...	...	...	...	...	...	4.31
0.99	...	...	...	...	...	...	...	...	...	...	...	...	...	...	...	4.25
1.00	...	...	...	...	...	...	...	...	...	...	...	...	...	...	...	4.20

Copyright ASME International
Provided by IHS under license with ASME
No reproduction or networking permitted without license from IHS

Table 3-12M Values of *L* for Pipe Sizes ≥ 1 422 mm Through 1 524 mm O.D.

Depth, *d*, mm	Wall Thickness, *t*, mm															
	10.3	11.1	11.9	12.7	14.3	15.9	17.5	19.1	20.6	22.2	23.8	25.4	27.0	28.6	30.2	31.8
1.0	No limit	No limit	No limit	No limit	No limit	No limit	No limit	No limit	No limit	No limit	No limit	No limit	No limit	No limit	No limit	No limit
1.3	542.6	563.6	583.2	602.1	No limit	No limit	No limit	No limit	No limit	No limit	No limit	No limit	No limit	No limit	No limit	No limit
1.5	542.6	563.6	583.2	602.1	638.4	No limit	No limit	No limit	No limit	No limit	No limit	No limit	No limit	No limit	No limit	No limit
1.8	542.6	563.6	583.2	602.1	638.4	673.2	706.3	No limit	No limit	No limit	No limit	No limit	No limit	No limit	No limit	No limit
2.0	376.8	485.4	583.2	602.1	638.4	673.2	706.3	737.5	No limit	No limit	No limit	No limit	No limit	No limit	No limit	No limit
2.3	290.3	353.8	434.2	544.1	638.4	673.2	706.3	737.5	767.3	796.5	No limit	No limit	No limit	No limit	No limit	No limit
2.5	240.7	285.1	337.6	402.9	600.1	673.2	706.3	737.5	767.3	796.5	824.7	851.5	No limit	No limit	No limit	No limit
2.8	207.9	242.3	281.1	327.0	450.9	658.2	706.3	737.5	767.3	796.5	824.7	851.5	877.5	No limit	No limit	No limit
3.0	184.4	212.6	243.5	278.9	368.4	500.5	706.3	737.5	767.3	796.5	824.7	851.5	877.5	903.2	928.1	No limit
3.3	166.5	190.5	216.3	245.3	315.4	411.1	549.1	737.5	767.3	796.5	824.7	851.5	877.5	903.2	928.1	952.1
3.6	152.3	173.3	195.7	220.2	278.0	353.0	453.5	594.0	767.3	796.5	824.7	851.5	877.5	903.2	928.1	952.1
3.8	140.7	159.5	179.2	200.7	250.1	311.8	390.5	493.4	637.9	796.5	824.7	851.5	877.5	903.2	928.1	952.1
4.1	131.0	148.1	165.8	185.0	228.2	280.8	345.6	426.4	532.8	683.6	824.7	851.5	877.5	903.2	928.1	952.1
4.3	122.6	138.3	154.6	171.9	210.5	256.5	311.7	378.1	461.9	573.6	728.4	851.5	877.5	903.2	928.1	952.1
4.6	115.4	130.0	144.9	160.8	195.9	236.9	285.0	341.6	410.5	498.7	614.0	769.4	877.5	903.2	928.1	952.1
4.8	109.0	122.7	136.6	151.3	183.5	220.6	263.4	312.7	371.4	444.0	535.2	651.7	809.5	903.2	928.1	952.1
5.1	103.3	116.2	129.3	143.0	172.8	206.8	245.4	289.2	340.4	402.2	477.4	569.8	688.8	851.7	928.1	952.1
5.3	98.2	110.4	122.7	135.7	163.5	194.9	230.2	269.7	315.1	368.9	432.9	509.2	603.9	727.5	893.2	952.1
5.6	93.6	105.2	116.9	129.1	155.2	184.5	217.1	253.2	294.1	341.8	397.5	462.4	540.8	639.5	765.7	930.8
5.8	89.3	100.4	111.6	123.2	147.9	175.4	205.7	238.9	276.2	319.2	368.5	425.0	491.8	573.6	674.7	801.2
6.1	85.4	96.1	106.7	117.8	141.3	167.2	195.7	226.5	260.8	299.9	344.3	394.4	452.5	522.2	606.2	707.8
6.4	81.8	92.0	102.3	112.9	135.3	159.9	186.7	215.5	247.4	283.3	323.7	368.7	420.2	480.9	552.5	637.0
6.6	78.4	88.3	98.2	108.4	129.8	153.2	178.6	205.8	235.5	268.9	306.0	346.9	393.1	446.9	509.3	581.4
6.9	75.3	84.8	94.4	104.2	124.8	147.2	171.3	197.0	224.9	256.1	290.4	328.0	370.0	418.3	473.6	536.5
7.1	72.3	81.6	90.8	100.3	120.1	141.6	164.6	189.0	215.4	244.7	276.7	311.5	350.0	393.9	443.5	499.2
7.4	69.5	78.5	87.5	96.7	115.8	136.5	158.5	181.8	206.8	234.4	264.5	296.9	332.5	372.8	417.8	467.8
7.6	66.8	75.7	84.4	93.3	111.8	131.7	152.9	175.1	199.0	225.2	253.5	283.8	317.1	354.2	395.5	440.9
7.9	64.3	72.9	81.4	90.1	108.1	127.3	147.7	169.0	191.8	216.7	243.5	272.1	303.3	337.9	376.0	417.6
8.1	61.9	70.3	78.6	87.1	104.5	123.1	142.8	163.4	185.2	209.0	234.5	261.6	290.9	323.2	358.7	397.1
8.4	. . .	67.9	76.0	84.2	101.2	119.3	138.3	158.1	179.1	201.9	226.2	251.9	279.6	310.1	343.3	379.0
8.6	. . .	65.5	73.4	81.5	98.0	115.6	134.1	153.2	173.4	195.3	218.6	243.1	269.4	298.2	329.4	362.8

Copyright ASME International
Provided by IHS under license with ASME
No reproduction or networking permitted without license from IHS

Table 3-12M Values of *L* for Pipe Sizes ≥ 1 422 mm Through 1 524 mm O.D. (Cont'd)

Depth, *d*, mm	Wall Thickness, *t*, mm															
	10.3	11.1	11.9	12.7	14.3	15.9	17.5	19.1	20.6	22.2	23.8	25.4	27.0	28.6	30.2	31.8
8.9	...	63.3	71.0	78.9	95.1	112.2	130.1	148.6	168.2	189.2	211.5	235.0	260.0	287.4	316.8	348.2
9.1	...	...	68.7	76.4	92.2	108.9	126.3	144.3	163.2	183.5	205.0	227.5	251.4	277.4	305.4	335.0
9.4	...	...	66.5	74.1	89.5	105.8	122.8	140.2	158.5	178.2	198.9	220.5	243.4	268.3	294.9	323.0
9.7	...	...	...	71.8	86.9	102.8	119.4	136.4	154.2	173.2	193.2	214.0	236.0	259.8	285.2	312.0
9.9	...	...	...	69.6	84.5	100.0	116.2	132.7	150.0	168.5	187.8	207.9	229.2	252.0	276.3	301.8
10.2	...	...	...	67.5	82.1	97.3	113.1	129.3	146.1	164.0	182.8	202.2	222.7	244.7	268.0	292.4
10.4	...	...	...	...	79.8	94.8	110.2	126.0	142.4	159.8	178.1	196.9	216.7	237.9	260.3	283.7
10.7	...	...	...	...	77.6	92.3	107.4	122.9	138.9	155.8	173.6	191.8	211.0	231.5	253.1	275.6
10.9	...	...	...	...	75.5	89.9	104.8	119.9	135.5	152.1	169.3	187.1	205.7	225.5	246.4	268.1
11.2	...	...	...	...	73.5	87.6	102.2	117.0	132.3	148.5	165.3	182.6	200.6	219.9	240.1	261.0
11.4	...	...	...	...	...	85.4	99.8	114.3	129.2	145.0	161.5	178.3	195.8	214.5	234.1	254.3
11.7	...	...	...	...	...	83.3	97.4	111.6	126.3	141.8	157.8	174.2	191.3	209.4	228.4	248.0
11.9	...	...	...	...	...	81.3	95.1	109.1	123.5	138.6	154.3	170.3	187.0	204.6	223.1	242.1
12.2	...	...	...	...	...	79.3	92.9	106.6	120.8	135.6	150.9	166.6	182.9	200.1	218.0	236.5
12.4	...	...	...	...	...	77.3	90.8	104.3	118.2	132.7	147.7	163.1	179.0	195.7	213.2	231.2
12.7	...	...	...	...	...	75.4	88.7	102.0	115.7	129.9	144.7	159.7	175.2	191.6	208.6	226.1
13.0	...	...	...	...	...	...	86.7	99.8	113.2	127.3	141.7	156.4	171.6	187.6	204.3	221.3
13.2	...	...	...	...	...	...	84.8	97.7	110.9	124.7	138.9	153.3	168.2	183.8	200.1	216.7
13.5	...	...	...	...	...	...	82.9	95.6	108.6	122.2	136.1	150.3	164.9	180.2	196.1	212.3
13.7	...	...	...	...	...	...	81.0	93.6	106.4	119.8	133.5	147.4	161.7	176.7	192.3	208.1
14.0	...	...	...	...	...	...	79.2	91.7	104.3	117.4	130.9	144.6	158.6	173.4	188.6	204.1
14.2	...	...	...	...	...	...	...	89.8	102.2	115.2	128.5	141.9	155.7	170.1	185.1	200.3
14.5	...	...	...	...	...	...	...	87.9	100.2	113.0	126.1	139.3	152.8	167.0	181.7	196.6
14.7	...	...	...	...	...	...	...	86.1	98.3	110.9	123.8	136.7	150.1	164.0	178.4	193.0
15.0	...	...	...	...	...	...	...	84.4	96.4	108.8	121.5	134.3	147.4	161.1	175.3	189.6
15.2	...	...	...	...	...	...	...	82.7	94.5	106.8	119.3	131.9	144.9	158.3	172.2	186.3
15.5	...	...	...	...	...	...	...	...	92.7	104.9	117.2	129.6	142.4	155.6	169.3	183.1
15.7	...	...	...	...	...	...	...	...	91.0	103.0	115.2	127.4	140.0	153.0	166.4	180.0
16.0	...	...	...	...	...	...	...	...	89.3	101.1	113.1	125.2	137.6	150.5	163.7	177.0
16.3	...	...	...	...	...	...	...	...	87.6	99.3	111.2	123.1	135.3	148.0	161.0	174.2
16.5	...	...	...	...	...	...	...	...	...	97.5	109.3	121.1	133.1	145.6	158.4	171.4
16.8	...	...	...	...	...	...	...	...	...	95.8	107.4	119.1	131.0	143.3	155.9	168.7
17.0	...	...	...	...	...	...	...	...	...	94.1	105.6	117.1	128.9	141.0	153.5	166.0
17.3	...	...	...	...	...	...	...	...	...	92.5	103.9	115.2	126.8	138.8	151.1	163.5
17.5	...	...	...	...	...	...	...	...	...	90.9	102.1	113.4	124.8	136.7	148.8	161.0
17.8	...	...	...	...	...	...	...	...	...	89.3	100.4	111.6	122.9	134.6	146.6	158.6

Copyright ASME International
Provided by IHS under license with ASME
No reproduction or networking permitted without license from IHS

Table 3-12M Values of *L* for Pipe Sizes ≥ 1 422 mm Through 1 524 mm O.D. (Cont'd)

Depth, *d*, mm	Wall Thickness, *t*, mm															
	10.3	11.1	11.9	12.7	14.3	15.9	17.5	19.1	20.6	22.2	23.8	25.4	27.0	28.6	30.2	31.8
18.0	...	...	...	...	...	...	...	...	...	...	98.8	109.8	121.0	132.6	144.4	156.3
18.3	...	...	...	...	...	...	...	...	...	...	97.2	108.1	119.2	130.6	142.3	154.0
18.5	...	...	...	...	...	...	...	...	...	...	95.6	106.4	117.3	128.7	140.2	151.8
18.8	...	...	...	...	...	...	...	...	...	...	94.0	104.7	115.6	126.8	138.2	149.6
19.1	...	...	...	...	...	...	...	...	...	...	92.5	103.1	113.8	124.9	136.2	147.5
19.3	...	...	...	...	...	...	...	...	...	...	...	101.5	112.2	123.1	134.3	145.4
19.6	...	...	...	...	...	...	...	...	...	...	...	100.0	110.5	121.4	132.4	143.4
19.8	...	...	...	...	...	...	...	...	...	...	...	98.4	108.9	119.6	130.5	141.5
20.1	...	...	...	...	...	...	...	...	...	...	...	96.9	107.3	117.9	128.7	139.6
20.3	...	...	...	...	...	...	...	...	...	...	...	95.4	105.7	116.3	127.0	137.7
20.6	...	...	...	...	...	...	...	...	...	...	...	...	104.2	114.6	125.2	135.8
20.8	...	...	...	...	...	...	...	...	...	...	...	...	102.7	113.0	123.5	134.0
21.1	...	...	...	...	...	...	...	...	...	...	...	...	101.2	111.5	121.9	132.3
21.3	...	...	...	...	...	...	...	...	...	...	...	...	99.7	109.9	120.2	130.5
21.6	...	...	...	...	...	...	...	...	...	...	...	...	...	108.4	118.6	128.8
21.8	...	...	...	...	...	...	...	...	...	...	...	...	...	106.9	117.1	127.2
22.1	...	...	...	...	...	...	...	...	...	...	...	...	...	105.5	115.5	125.6
22.4	...	...	...	...	...	...	...	...	...	...	...	...	...	104.0	114.0	124.0
22.6	...	...	...	...	...	...	...	...	...	...	...	...	...	102.6	112.5	122.4
22.9	...	...	...	...	...	...	...	...	...	...	...	...	...	101.2	111.1	120.8
23.1	...	...	...	...	...	...	...	...	...	...	...	...	...	...	109.6	119.3
23.4	...	...	...	...	...	...	...	...	...	...	...	...	...	...	108.2	117.8
23.6	...	...	...	...	...	...	...	...	...	...	...	...	...	...	106.8	116.4
23.9	...	...	...	...	...	...	...	...	...	...	...	...	...	...	105.4	114.9
24.1	...	...	...	...	...	...	...	...	...	...	...	...	...	...	104.1	113.5
24.4	...	...	...	...	...	...	...	...	...	...	...	...	...	...	...	112.1
24.6	...	...	...	...	...	...	...	...	...	...	...	...	...	...	...	110.7
24.9	...	...	...	...	...	...	...	...	...	...	...	...	...	...	...	109.4
25.1	...	...	...	...	...	...	...	...	...	...	...	...	...	...	...	108.0
25.4	...	...	...	...	...	...	...	...	...	...	...	...	...	...	...	106.7

Copyright ASME International
Provided by IHS under license with ASME
No reproduction or networking permitted without license from IHS

INTENTIONALLY LEFT BLANK

Copyright ASME International
Provided by IHS under license with ASME
No reproduction or networking permitted without license from IHS

ASME B31G INTERPRETATIONS VOLUME 1

Replies to Technical Inquiries October 30, 2009 through April 30, 2012

FOREWORD

It has been agreed to publish interpretations issued by the B31 Committee concerning B31G as part of the update service to the Manual. The interpretations have been assigned numbers in chronological order. Each interpretation applies either to the latest Edition at the time of issuance of the interpretation or the Edition stated in the reply. Subsequent revisions to the Manual may have superseded the reply.

These replies are taken verbatim from the original letters, except for a few typographical and editorial corrections made for the purpose of improved clarity. In some instances, a review of the interpretation revealed a need for corrections of a technical nature. In these cases, a revised reply bearing the original interpretation number with the suffix R is presented. In the case where an interpretation is corrected by errata, the original interpretation number with the suffix E is used.

ASME procedures provide for reconsideration of these interpretations when or if additional information is available which the inquirer believes might affect the interpretation. Further, persons aggrieved by an interpretation may appeal to the cognizant ASME committee or subcommittee. As stated in the Statement of Policy in the Code documents, ASME does not "approve," "certify," "rate," or "endorse" any item, construction, proprietary device, or activity.

For detailed instructions on preparation of technical inquiries to the B31 Committee, refer to "Correspondence With the B31 Committee" in the front matter.

Copyright ASME International
Provided by IHS under license with ASME
No reproduction or networking permitted without license from IHS

Interpretation: G-1-01

Subject: ASME B31G-2009

Date Issued: September 29, 2011

File: 11-1259

Question (1): When calculating the term $z = L^2/Dt$, is t in this case the corroded pipe wall thickness?

Reply (1): No. Dimension t is the uncorroded pipe wall thickness.

Question (2): When calculating the failure stress (S_F), is t the corroded pipe wall thickness?

Reply (2): Yes.

Question (3): When calculating the hoop stress (S_O or S_h), is t in this case the corroded pipe wall thickness?

Reply (3): No. Dimension t is the uncorroded pipe wall thickness.

Question (4): Does t represent the uncorrroded pipe wall thickness?

Reply (4): Yes.

Copyright ASME International
Provided by IHS under license with ASME
No reproduction or networking permitted without license from IHS

ASME CODE FOR PRESSURE PIPING, B31

Power Piping B31.1-2012
Process Piping B31.3-2010
Tuberías de Proceso B31.3-2010
Pipeline Transportation Systems for Liquids and Slurries. B31.4-2012
Refrigeration Piping and Heat Transfer Components B31.5-2010
Gas Transmission and Distribution Piping Systems B31.8-2010
Managing System Integrity of Gas Pipelines B31.8S-2010
Gestión de Integridad de Sistemas de Gasoductos B31.8S-2010
Building Services Piping B31.9-2011
Slurry Transportation Piping Systems. B31.11-2002
Hydrogen Piping and Pipelines. B31.12-2011
Standard for the Seismic Design and Retrofit of Above-Ground Piping Systems B31E-2008
Manual for Determining the Remaining Strength of Corroded Pipelines: Supplement to ASME B31 Code for Pressure Piping. B31G-2012
Standard Test Method for Determining Stress Intensification Factors (*i*-Factors) for Metallic Piping Components B31J-2008
Pipeline Personnel Qualification. B31Q-2010
Calificación del Personal de Líneas de Tuberías B31Q-2010
Standard Toughness Requirements for Piping B31T-2010

The ASME Publications Catalog shows a complete list of all the Standards published by the Society. For a complimentary catalog, or the latest information about our publications, call 1-800-THE-ASME (1-800-843-2763).

Copyright ASME International
Provided by IHS under license with ASME
No reproduction or networking permitted without license from IHS

ASME Services

ASME is committed to developing and delivering technical information. At ASME's Customer Care, we make every effort to answer your questions and expedite your orders. Our representatives are ready to assist you in the following areas:

ASME Press
Codes & Standards
Credit Card Orders
IMechE Publications
Meetings & Conferences
Member Dues Status
Member Services & Benefits
Other ASME Programs
Payment Inquiries
Professional Development
  Short Courses
Publications
Public Information
Self-Study Courses
Shipping Information
Subscriptions/Journals/Magazines
Symposia Volumes
Technical Papers

How can you reach us? It's easier than ever!

There are four options for making inquiries* or placing orders. Simply mail, phone, fax, or E-mail us and a Customer Care representative will handle your request.

Mail
ASME
22 Law Drive, Box 2900
Fairfield, New Jersey
07007-2900

Call Toll Free
US & Canada: 800-THE-ASME
(800-843-2763)
Mexico: 95-800-THE-ASME
(95-800-843-2763)
Universal: 973-882-1167

Fax—24 hours
973-882-1717
973-882-5155

E-Mail—24 hours
customercare@asme.org

* Customer Care staff are not permitted to answer inquiries about the technical content of this code or standard. Information as to whether or not technical inquiries are issued to this code or standard is shown on the copyright page. All technical inquiries must be submitted in writing to the staff secretary. Additional procedures for inquiries may be listed within.

Copyright ASME International
Provided by IHS under license with ASME
No reproduction or networking permitted without license from IHS

INTENTIONALLY LEFT BLANK

Copyright ASME International
Provided by IHS under license with ASME
No reproduction or networking permitted without license from IHS

ASME B31G-2012

ISBN 978-0-7918-3448-0

A12112

Copyright ASME International
Provided by IHS under license with ASME
No reproduction or networking permitted without license from IHS

Ex. II - 32

Cathodic Protection
(Second Edition)

John Morgan

National Association of Corrosion Engineers

Occasionally insulating units are placed in pits or above ground. When they are it is sensible to cover the actual joint, particularly a flanged joint, with a resin glass fiber cover so that it cannot accidentally be short-circuited, say by a metal spanner; on breaking such a bond an incendive spark could easily occur. The problems of interference and other reasons for longitudinal separation of pipelines are given in the chapter of electrolysis and interference.

Modern long distance pipelines are protected over long distances and in many cases there is a limited number of points where power is available. Usually at the end of the pipeline, at a terminal or storage depot, power supplies are available. The pipe is isolated at this point so that cathodic protection can be applied separately and at different levels to the depot itself and to the pipeline. The pipeline potential at the impressed current station will probably have a potential of -1.5 V to copper sulfate to achieve the maximum spread. It would be uneconomical and, in fact, difficult to protect the remainder of the depot to this level. The isolating coupling or, indeed, in many cases two or three isolating couplings, are used to enable these different levels of protection to be used.

Vertical Pipes

Well Casings

Most well casings are constructed of steel tubes joined together to be in good electrical contact. The tubes are coated prior to installation though this coating cannot be relied upon to prevent their corrosion as it will be damaged during installation. At the top of the well one or two larger diameter pipes may be placed concentrically over the well tube and may enclose 10 per cent to 20 per cent of the total depth, the system being shown schematically in Fig. 132. Cathodic protection can be applied to the well casing tubes though only to the outer one where there are a multiplicity of concentric tubes. Because cathodic protection will cause a change in potential between these tubes, the space between them should be grouted with concrete or filled with clean inhibited sand if grouting is impossible.

It is difficult to measure the potential of the well casing though in some cases a half cell could be lowered so as to be outside the bottom of the casing and a potential measurement made relative to this half cell. The potential gradients in the tube metal may be measured by lowering a series of devices which will make metallic contact to the tubes down the well and from these measurements the current flowing in the tubes can be determined. Fig. 133 shows the type of potential variations that would be obtained by such a survey, the practical values varying with the geological strata and with the pipe resistance. A modification of the zero current ammeter similar to that used in pipe surveys could be employed to determine this current directly.

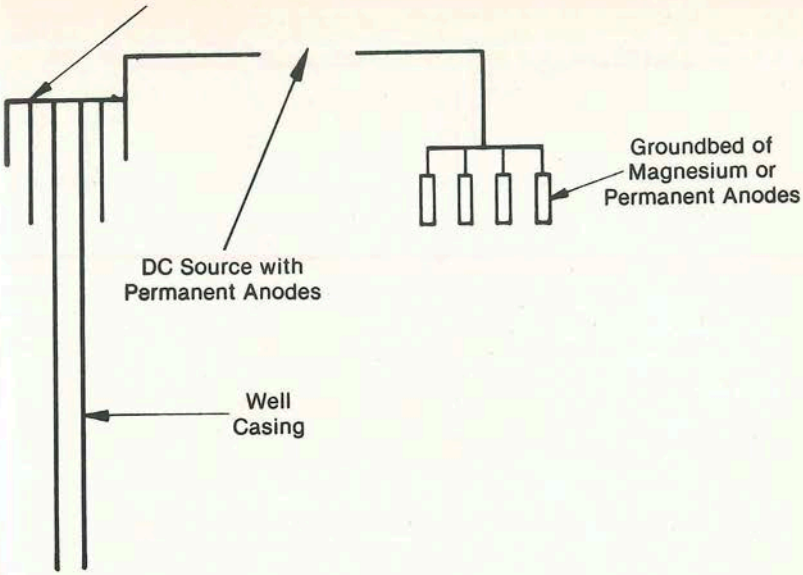

FIGURE 132 - Well casing with cathodic protection anodes.

The well casing will be protected when the metal potential curve indicates that the flow of current in the casing is increasing towards the top of the well as this means that the well must be receiving current and so is cathodic throughout its length. This is used as the criterion of protection.

Alternatively, a plot may be made of the potential against the log of current. There will be a break in the curve and it has been shown that where the curved section becomes a straight line as described earlier the casing will be adequately protected. This technique was developed by Haycock and has proved to be effective in a number of oil fields.

The spread of protection will be governed by the same parameters that affected the spread in a normal pipeline. The lengths of the casing will not be great, a spread of full protection of more than 10,000 ft. will rarely be needed and the current required for protection will usually be less than 15 amp, generally only 2 to 3 amp being sufficient. For isolated wells magnesium can be used, a typical anode installation may be a group of five or six high potential packaged anodes.

There will be an increase in potential at the top of the well, just as there is at the drainage point on the pipeline. In many cases this will detract from the driving potential of low voltage anodes so their use will not generally be possible.

Often the well is connected to a small pipeline or several wells may ex-

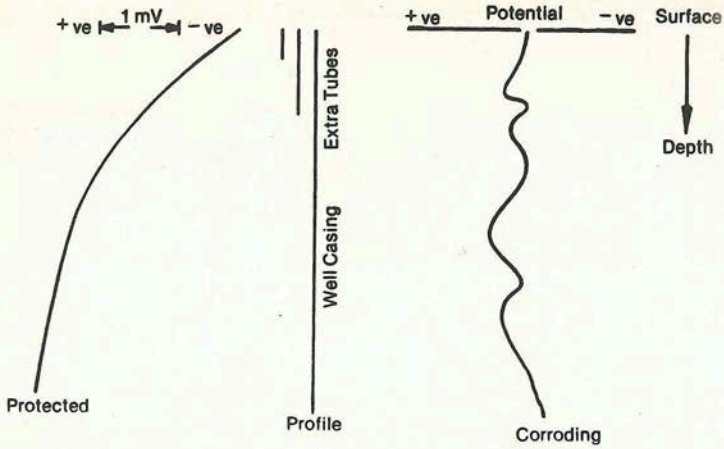

FIGURE 133 - Potentials along well casing.

ist in a group or small field, in which case, providing power is available, an impressed current installation would be preferable. The overprotection at the well head will mean that magnesium anodes, if used to protect a large group of inter-connecting well head piping, will be unattractive. Even with the use of impressed current it might well be that isolation of the wells will prove to be worthwhile. When a gathering line is connected to a well head then both may require an increased protection in order to achieve a spread. Where there are several wells there is unlikely to be any shielding of one well by another as their diameter is very small in comparison with their length.

Some wells have screens at their bottom end and these can be protected by the general system if the screen is in water or a conducting strata as it would be in an artesian well. The inside of the casing or pumps at the lower end will not receive protection by these techniques. Red water, which is often caused by the prolonged contact of the well and pumps, can be prevented by complete cathodic protection of the lower end of the well though this is not achieved from the outside.

Piles

Many buildings nowadays are constructed on steel piles driven some considerable depth into the ground. Often these are used solely to allow a concrete pile to be formed within them and their corrosion is of little consequence. When their corrosion is to be avoided the outside of the piles can be protected cathodically. The piles must be electrically continuous one with another or if not they must be bonded together. It is essential that the bond-

Ex. II - 33

NACE Standard TM0106-2016
Item No. 21248

Reaffirmation 2016-03-20
Revised 2015-02-01
Approved 2006-06-23

Detection, Testing, and Evaluation of Microbiologically Influenced Corrosion (MIC) on External Surfaces of Buried Pipelines

This NACE International standard represents a consensus of those individual members who have reviewed this document, its scope, and provisions. Its acceptance does not in any respect preclude anyone, whether he or she has adopted the standard or not, from manufacturing, marketing, purchasing, or using products, processes, or procedures not in conformance with this standard. Nothing contained in this NACE International standard is to be construed as granting any right, by implication or otherwise, to manufacture, sell, or use in connection with any method, apparatus, or product covered by Letters Patent, or as indemnifying or protecting anyone against liability for infringement of Letters Patent. This standard represents minimum requirements and should in no way be interpreted as a restriction on the use of better procedures or materials. Neither is this standard intended to apply in all cases relating to the subject. Unpredictable circumstances may negate the usefulness of this standard in specific instances. NACE International assumes no responsibility for the interpretation or use of this standard by other parties and accepts responsibility for only those official NACE International interpretations issued by NACE International in accordance with its governing procedures and policies which preclude the issuance of interpretations by individual volunteers.

Users of this NACE International standard are responsible for reviewing appropriate health, safety, environmental, and regulatory documents and for determining their applicability in relation to this standard prior to its use. This NACE International standard may not necessarily address all potential health and safety problems or environmental hazards associated with the use of materials, equipment, and/or operations detailed or referred to within this standard. Users of this NACE International standard are also responsible for establishing appropriate health, safety, and environmental protection practices, in consultation with appropriate regulatory authorities if necessary, to achieve compliance with any existing applicable regulatory requirements prior to the use of this standard.

CAUTIONARY NOTICE: NACE International standards are subject to periodic review, and may be revised or withdrawn at any time. NACE International requires that action be taken to reaffirm, revise, or withdraw this standard no later than five years from the date of initial publication. The user is cautioned to obtain the latest edition. Purchasers of NACE International standards may receive current information on all standards and other NACE International publications by contacting the NACE International Membership Services Department, 15835 Park Ten Place, Houston, Texas 77084 (telephone +1 [281] 228-6200).

ABSTRACT

This standard describes types of microorganisms, mechanisms by which MIC occurs, methods of testing for the presence of bacteria, research results, and interpretation of testing results for external surfaces of buried, ferrous-based metal pipelines and related components. Appendixes are included for media specifications (nonmandatory Appendix A), dilution procedures (nonmandatory Appendix B), and site inspection and testing (nonmandatory Appendix C). This standard is maintained Task Group 237.

KEYWORDS

MIC, microorganisms, sampling, MMM, biofilm, bacteria, Archaea

ISBN 1-57590-206-0
©2016, NACE International
Robert Carnahan - Invoice 144726 downloaded on 2/14/2020 7:33:38 PM Single-user licence only, copying/networking prohibited

Foreword

In NACE standards, the terms shall, must, should, and may are used in accordance with the definitions of these terms in the NACE Publications Style Manual, 4th ed., Paragraph 7.4.1.9. Shall and must are used to state mandatory requirements. The term should is used to state something considered good and is recommended but is not mandatory. The term may is used to state something considered optional.

Microbiologically influenced corrosion (MIC) is corrosion caused by the presence or activity (or both) of microorganisms in biofilms on the surface of the corroding material. Many materials, including most metals and some nonmetals, can be degraded in this manner. Microbiologically mediated reactions can alter both rates and types of electrochemical reactions in a corrosion cell. These reactions influence pitting, crevice corrosion, differential aeration cells, concentration cells, dealloying, and galvanic corrosion. Therefore, MIC investigations require microbiological, chemical, and metallurgical testing for proper diagnosis. The conclusion that MIC has taken place should be based on the preponderance of circumstantial evidence. Microorganisms are often resistant to many control methods and can be a serious external corrosion threat to pipelines.

This NACE standard test method applies to the external surfaces of ferrous-based metal pipeline facilities and describes types of microorganisms, mechanisms by which MIC occurs, methods for sampling, and testing for the presence of microorganisms, research results, and interpretation of testing results. Sections 1 through 4 of this standard discuss the technical aspects of MIC. Sections 5 through 7 discuss field equipment and testing procedures.

This standard is intended for use by pipeline operators, pipeline service providers, government agencies, and any other persons or companies involved in planning or managing pipeline integrity. Portions of Sections 3 and 4 of this standard are excerpted from Peabody's Control of Pipeline Corrosion, Chapter 14—"Microbiologically Influenced Corrosion,"[1] and enclosed in quotation marks.

This standard was prepared by Task Group (TG) 237, "Microbiologically Influenced Corrosion on External Surfaces of Buried Pipelines: Detection, Testing, and Evaluation—Standard." It was revised in 2015 by TG 237. TG 237 is administered by Specific Technology Group (STG) 35, "Pipelines, Tanks, and Well Casings," and is sponsored by STG 60, "Corrosion Mechanisms." This standard is issued by NACE International under the auspices of STG 35.

Robert Carnahan - Invoice 144726 downloaded on 2/14/2020 7:33:38 PM Single-user licence only, copying/networking prohibited

Detection, Testing, and Evaluation of Microbiologically Influenced Corrosion (MIC) on External Surfaces of Buried Pipelines

1. General 4
2. Definitions 4
3. Introduction 8
4. External MIC of Pipelines 12
5. Sampling Equipment 14
6. Sampling and Testing Procedures 15
7. Testing Guidelines 17
8. Application of Test Methods to Pipelines and Interpretation of Data 25
References 27
Bibliography 29
Appendix A (Nonmandatory) Site Inspection and Testing 31

Figures

Figure 1: Examples of Various Pit Morphologies as Viewed in Cross Section ...15
Figure 2: (Live, Inactive, and Dead) Typically Present in Samples from the Oil Industry that are Enumerated Using Various MMMs as Compared to the MPN (Culturing) Method 21
Table 1: Comparisons of MMMs 21

Robert Carnahan - Invoice 144726 downloaded on 2/14/2020 7:33:38 PM Single-user licence only, copying/networking prohibited

Section 1: General

1.1 While the evaluation, monitoring, and mitigation of MIC cannot be prescribed in one particular manner for any given pipeline, this standard describes methodologies by which the appropriate tools and techniques may be selected and practically applied to external surfaces of buried, ferrous-based metal pipelines and related components. The methods presented in this standard represent the general consensus of industry experts in pipeline corrosion and microbiology at the time this standard was published.

1.2 Appendix A (Nonmandatory) provides a site inspection and testing checklist.

1.3 All applicable safety and environmental codes, rules, and regulations must be followed when using this standard.

1.4 The term “pipeline” as used in this standard generally refers to any pipe or component of a pipeline system for which the mechanism of external MIC is of interest to the user of this standard.

Section 2: Definitions

Abiotic: The absence of living organisms, their biological components, or the metabolic activities of living organisms.

Acid-producing bacteria (APB): Aerobic or anaerobic bacteria that produce organic acids as an end product of their metabolism. A few organisms (e.g., Thiobacillus) are also capable of producing mineral acids (typically under aerobic conditions).

Aeration: (1) Exposing to the action of air. (2) Causing air to bubble through. (3) Introducing air into a solution by spraying, stirring, or similar method. (4) Supplying or infusing with air, as in sand or soil. (5) The introduction of air into the pulp in a flotation cell to form air bubbles.

Aerobic: Containing air or free molecular oxygen.

Aerobic microorganism (aerobe): A microorganism that uses oxygen as the final electron acceptor in metabolism.

Anaerobic microorganism (anaerobe) bacteria: A microorganism that does not require oxygen for metabolism.

Archaea: Unicellular microorganisms that are genetically distinct from bacteria and eukaryotes, which often inhabit extreme environmental conditions. *Archaea* include halophiles (microorganisms that may inhabit extremely salty environments), methanogens (microorganisms that produce methane), and thermophiles (microorganisms that can thrive in extremely hot environments). *Archaeoglobus* is a common *Archaea*.

Archaeoglobus: Microorganisms that grow at high temperatures between 60 and 95 °C (140 and 203 °F), with optimal growth at 83 °C (181°F) (ssp. *A. fulgidus* VC-16).2 They are sulfate-reducing *archaea*, coupling the reduction of sulfate to sulfide with the oxidation of many different organic carbon sources, including complex polymers. *Archaeoglobus*spe - cies have been isolated from oil reservoirs and production systems; however, this group of microorganisms is normally not measured with current culturing techniques.

Autoclave: A pressurized, steam-heated vessel used for sterilization.

Robert Carnahan - Invoice 144726 downloaded on 2/14/2020 7:33:38 PM Single-user licence only, copying/networking prohibited

Basal: The minimal level for, or essential for maintenance of vital activities of an organism, such as basal metabolism.

Biofilm: Microbial growth at an interface in which individual cells are bound within a matrix of extracellular polymeric materials.

Biotic: Involving the presence or metabolic activities of living organisms.

Carbohydrate: Any of the group of organic compounds composed of carbon, hydrogen, and oxygen, including sugars, starches, and celluloses.

Cathodic protection (CP): A technique to reduce the corrosion rate of a metal surface by making that surface the cathode of an electrochemical cell.

Coating: (1) A liquid, liquefiable, or mastic composition that, after application to a surface, is converted into a solid protective, decorative, or functional adherent film. (2) (In a more general sense) a thin layer of solid material on a surface that provides improved protective, decorative, or functional properties.

Coating system: The complete number and types of coats applied to a substrate in a predetermined order. (When used in a broader sense, surface preparation, pretreatments, dry film thickness, and manner of application are included.)

Culture medium: A sterile solution or other substrate that is formulated to promote the growth of a particular type or group of microorganisms. (Also called growth medium.)

4-,6-diamidino-2-phenylindole (DAPI): A stain for optical microscopy that targets the Deoxyribonucleic acid (DNA) in all (i.e., living and inactive) microbial cells.

Denaturing gradient gel electrophoresis (DGGE): A molecular microbiological method used to profile the most abundant microbial groups in a sample.

Dielectric coating: A coating that does not conduct electricity. For the purposes of this standard, it also inhibits the passage of an electric current relative to the coating's dielectric strength.

Disbondment: The loss of adhesion between a coating and the substrate.

Dissimilatory: Metabolic reactions in which a reductant is used as an electron acceptor and not incorporated into the cell (e.g., dissimilatory sulfate or nitrate reduction); metabolic changes that convert complex molecules into simple ones.

Eukaryotes: Cells having a true nucleus, bound by a double membrane. Prokaryotic cells have no nucleus.

Facultative: Capable of growing either with or without the presence of a specific environmental factor, e.g., oxygen.

Fluorescence in situ hybridization (FISH): A molecular microbiological method used for enumeration of microorganisms. The method is based on gene probes targeting ribosomal Ribonucleic acid (RNA) (16S or 23S rRNA) in microbial cells. Only living and active cells contain sufficient ribosomes that can be detected by FISH. Gene probes consist of two parts: (1) an artificial DNA strand complementary to the ribosomal RNA in the target cell; and (2) a fluorescing molecule covalently attached to the probe that enables observation of the target microorganism in the microscope.

Fungi: Nucleated, usually filamentous, spore-bearing parasitic organisms devoid of chlorophyll, including molds, mildews, smuts, mushrooms, yeast, and others.

Robert Carnahan - Invoice 144726 downloaded on 2/14/2020 7:33:38 PM Single-user licence only, copying/networking prohibited

Growth: Increase in the quantity of metabolically active protoplasm, accompanied by an increase in cell number, cell size, or both.

Growth medium: See Culture medium.

Heterotrophic: An organism that obtains nourishment from the ingestion and breakdown of organic matter.

Holiday: A discontinuity in a protective coating that exposes unprotected surface to the environment.

Inoculum: A small quantity of microorganisms used to start a new culture.

Inorganic acid: A compound composed of hydrogen and a nonmetal element or radical. They can range from acids of great strength (e.g., hydrochloric acid [HCl] and sulfuric acid [H_2SO_4] to those that are very weak (e.g., boric acid). A substance that yields hydrogen ions (which can act as a proton donor) and the conjugate base ions when dissolved in water. (Also called a mineral acid.)

Isotonic: Having uniform tension of a solution; having the same osmotic pressure as the fluid phase of a cell or tissue.

Metal-oxidizing bacteria: Bacteria (most notably iron and manganese oxidizing bacteria) that derive their energy from oxidizing one oxidation state of a metal to another.

Metal-reducing bacteria (MRB): Bacteria that when in direct contact with solid iron (Fe^{+3}) and manganese (Mn+4) oxides them and produces soluble ions (Fe^{+2} and Mn^{+2}), resulting in dissolution of surface oxides and localized corrosion.[1]

Methanogens: Microorganisms that produce methane as a metabolic byproduct in anoxic (i.e., oxygen-free) conditions. They are classified as *Archaea*, a group quite distinct from bacteria. Some are extremophiles and found in environments such as oil field systems, hot springs, and submarine hydrothermal vents, as well as in the "solid" rock of the Earth's crust, kilometers below the surface. Methanogens are common *Archaea* in oil production systems; however, they are normally not measured with current culturing techniques. Methanogens are involved in MIC by consuming hydrogen at the metal surface and thereby creating a depolarization.

Microaerophilic: Pertaining to those microorganisms requiring free oxygen, but in very low concentration for optimum growth.

Microbiologically influenced corrosion (MIC): Corrosion affected by the presence or activity, or both, of microorganisms. (Note: The microorganisms that are responsible for MIC are typically found in biofilms on the surface of the corroding material. Many materials, including most metals and some nonmetals, can be degraded in this manner.)

Microbe: See *microorganism.*

Microorganism: An organism of microscopic or ultramicroscopic size. Bacteria, *Archaea,* and fungi are microorganisms. Bacteria and *Archaea* are combined and called prokaryotes. Fungi belong to eukaryotes (*Eukarya*).

Mineral acid: See inorganic acid.

Monosaccharide: A carbohydrate that cannot be hydrolyzed to a simpler carbohydrate.

Morphology: A branch of biology that deals with structure and form of an organism at any stage of its life history.

Robert Carnahan - Invoice 144726 downloaded on 2/14/2020 7:33:38 PM Single-user licence only, copying/networking prohibited

Most probable number method (MPN): A technique that does not rely on quantitative assessment of individual cells; instead, it relies on specific qualitative attributes of the microorganism being counted. The important aspect of MPN methodology is the ability to estimate a microbial population size based on a process-related attribute. The MPN technique estimates microbial population sizes in a liquid substrate. The methodology for the MPN technique is dilution and incubation of replicated cultures across several serial dilution steps.

Motile: Exhibiting or capable of movement.

Organic acid: Weak acid that contains carbon (correctly classified as carboxylic acids because they contain a carboxyl group, -COOH). Organic acids (e.g., formic, acetic, lactic) are the end product of metabolism by a variety of microorganisms. (Also called *short-chain fatty acids.*)

Organism: A complex structure of interdependent and subordinate elements whose relations and properties are largely determined by their function as a whole. (Also see *microorganism.*)

Oxidation-reduction potential: The potential of a reversible oxidation-reduction reaction in a given electrolyte reported on the standard hydrogen electrode scale. (also called *redox potential*)

Permeation: The migration of water from the soil through the coating to the pipe surface by diffusion.

Phosphate buffer: Solution made of dibasic potassium phosphate (K_2HPO_4) and sodium phosphate (Na_2HPO_4).

Pipe-to-soil potential: See *structure-to-electrolyte potential.*

Polymerase chain reaction (PCR): A molecular technique which allows the production of large quantities of a specific DNA from a DNA template using a simple enzymatic reaction without a living organism. A quantitative version of PCR is called quantitative polymerase chain reaction (qPCR).

Polysaccharide: A carbohydrate composed of many monosaccharides.

Prokaryotes: The prokaryotes are divided into two domains: the bacteria and the *Archaea*. *Archaea* were originally thought to live only in inhospitable conditions such as extremes of temperature, pH, and radiation, but have been found in all types of habitats. Sulfate-reducing prokaryotes (SRP) consist of both sulfate-reducing bacteria and sulfate-reducing *Archaea*.

Quantitative polymerase chain reaction (qPCR): A molecular microbiological method used to quantify the total number of microorganisms or a specific genus/species of microorganisms in nearly any type of sample. qPCR can be used for both fluid and solid samples, as well as microorganisms collected via membrane filtration. This method does not underestimate microorganisms that do not grow in culture. This method uses synthetic DNA (called primers) tagged with a fluorescent molecule or synthetic DNA mixed with a DNA intercalating agent (dye) to quantify microorganisms using a modified version of polymerase chain reaction (PCR).

Redox potential (E_h): See *oxidation-reduction potential.*

Ringers solution: An aqueous solution of chlorides that is isotonic to animal tissues.

Sterile: (1) Free of any living microorganisms. (2) Not introducing microorganisms that are foreign to the host body or subject under study.

Robert Carnahan - Invoice 144726 downloaded on 2/14/2020 7:33:38 PM Single-user licence only, copying/networking prohibited

Structure-to-electrolyte potential: The potential difference between the surface of a buried or submerged metallic structure and the electrolyte that is measured with reference to an electrode in contact with the electrolyte.

Substratum: A solid surface; often refers to a surface colonized by microorganisms.

Sulfate-reducing *Archaea*(SRA): A group of anaerobic *Archaea* that perform dissimilatory reduction of sulfate, resulting in sulfide formation. They are most likely to grow at reservoir conditions (60 to 95 °C [140 to 203 °F]).

Sulfate-reducing bacteria (SRB): A group of anaerobic bacteria that perform dissimilatory reduction of sulfate, resulting in sulfide formation. They grow at a broad range of temperatures.

Sulfate-reducing prokaryotes (SRP): A group of microorganisms that consists of both sulfate-reducing bacteria (SRB) and sulfate-reducing *Archaea*(SRA).

Tenting: A tent-shaped void formed along the girth weld or longitudinal seam-weld reinforcement in a pipe when the external coating is not in continuous intimate contact with the pipe and weld surfaces.

Water leaching: The removal of soluble constituents from a coating by water.

Section 3: Introduction

3.1 MIC is corrosion affected by the presence or activity (or both) of microorganisms in biofilms on the surface of the corroding material. Many materials, including most metals and some nonmetals, can be degraded in this manner. MIC can result from the activities of microorganisms, including bacteria, Archaea, and fungi[1] in biofilms or in the local environment directly in contact with the corroding material.[2] This standard is primarily focused on the effects of bacteria and Archaea. In one survey, Jack et al.[3] reported that MIC was responsible for 27% of the corrosion deposits on the exterior of line pipe. Pope and Morris[4] reported that almost all cases of MIC on external surfaces of coated pipes were associated with disbonded or damaged coatings. The following general statements are commonly accepted regarding microorganisms.[1]

3.1.1 Individual microorganisms are usually small in size (they typically are from 0.2 to 10 µm (8 to 400 µin) in length by up to 2 or 3 µm [80 to 120 µin] in width)—a quality that allows them to penetrate crevices and other areas. Colonies of microorganisms can grow to macroscopic proportions.[1]

3.1.2 Microorganisms may be motile, capable of migrating to more favorable conditions or away from less favorable conditions (e.g., toward food sources or away from toxic materials).

3.1.4 Certain microorganisms can withstand a wide range of temperatures (at least -10 to 99 °C [14 to 210 °F]), pH levels, and oxygen concentrations.[1]

3.1.5 Microorganisms grow in colonies and form biofilms, making survival more likely under adverse conditions.

3.1.6 Under favorable conditions, microorganisms can reproduce very quickly (generation times of 18 min have been reported).[1]

3.1.7 Individual microbial cells can be widely and quickly dispersed by water or other modes, thus the potential for some cells in the population to reach more favorable environments is good.

Robert Carnahan - Invoice 144726 downloaded on 2/14/2020 7:33:38 PM Single-user licence only, copying/networking prohibited

3.1.8 Many microorganisms can quickly adapt to use a wide variety of different nutrient sources. For example, Pseudomonas fluorescens can use more than 100 different compounds as sole sources of carbon and energy, including sugars, lipids, alcohols, phenols, and organic acids.[1]

3.1.9 Many microorganisms form extracellular polysaccharide materials (capsules or slime layers). The resulting slimes are sticky and trap organisms and debris (food), resist penetration of toxicants, (e.g., biocides or corrosion inhibitors), and hold the cells between the source of the nutrients (the bulk fluid) and the surface.[1]

3.1.10 Many bacteria and fungi produce spores that are resistant to temperature, acids, alcohols, disinfectants, drying, freezing, and other adverse conditions. Spores may remain viable for hundreds of years and germinate on finding favorable conditions. In the natural environment, there is a difference between survival and growth. Microorganisms can withstand long periods of starvation and desiccation. If conditions are alternating wet and dry, microbes may survive dry periods and grow only during the wet periods.

3.1.11 Microorganisms may be resistant to many chemicals (antibiotics, disinfectants, and others) by virtue of their ability to degrade these chemicals or by being impenetrable (because of slime, cell wall, or cell membrane characteristics). Resistance may be easily acquired by mutation or acquisition of a plasmid (essentially by naturally occurring genetic exchange between cells, i.e., genetic engineering in the wild).

3.2 Mechanisms for MIC

MIC typically takes place in the presence of microbial consortia that are comprised of more than one physiological type of microorganism. Depending on the environment, these microbes may include metal-oxidizing bacteria, sulfate-reducing prokaryotes (SRP), acid-producing bacteria (APB), metal-reducing bacteria (MRB), and methanogens that interact in complex ways within the structure of biofilms.[5,6] MIC does not produce a unique form or morphology of corrosion. Instead, MIC can result in pitting, crevice corrosion, underdeposit corrosion (UDC), and dealloying, in addition to galvanic corrosion.

Simply by their presence on a metal surface, microorganisms may set up the proper conditions for pitting or crevice corrosion. Once localized corrosion has been initiated, microbial reactions can maintain suitable conditions (e.g., low oxygen concentration) for continued pit/crevice growth. Under anaerobic reducing conditions, MIC may be observed when there is some mechanism for the removal or transformation of corrosion products (e.g., a transition from stagnation to flow) or the introduction of oxygen to a previously anaerobic environment. The following discussion about individual MIC mechanisms is directly related to carbon steel.[1]

3.2.1 Sulfate Reduction

Sulfate-reducing bacteria (SRB) are a diverse group of anaerobic microorganisms that can be isolated from a variety of subsurface environments. If the aerobic respiration rate within a biofilm is greater than the oxygen diffusion rate during biofilm formation, the metal/biofilm interface can become anaerobic and provide a niche for sulfide production by SRB. The critical thickness of the biofilm required to produce anaerobic conditions depends on the availability of oxygen and the rate of respiration. SRB concentrations may be proportional to sulfate concentrations. The distribution of favorable pH ranges from 6 to 12, although SRB can adapt to other less optimum conditions. SRB grow in soil, fresh water, or salt water under anaerobic conditions.

Robert Carnahan - Invoice 144726 downloaded on 2/14/2020 7:33:38 PM Single-user licence only, copying/networking prohibited

Many species of SRB have been identified, differing in morphology and in the organic substances that they can metabolize. They have in common the ability to oxidize certain organic substances to organic acids or carbon dioxide by reduction of inorganic sulfate to sulfide. In the absence of oxygen, the metabolic activity of SRB causes accumulation of hydrogen sulfide near metal surfaces. This is particularly evident when metal surfaces are covered with biofilms. The concentration of sulfide is highest near the metal surface.

Iron sulfide forms quickly on carbon steels and covers the surface if both ferrous and sulfide ions are available. Formation of iron sulfide minerals stimulates the cathodic reaction. Once electrical contact is established, a galvanic couple develops with the mild steel surface as an anode, and electron transfer occurs through the iron sulfide. Under conditions such as low ferrous ion concentrations, adherent and temporarily protective films of iron sulfides are formed on the steel surface, with a consequent reduction in corrosion rate.[7,8]

Although SRB are anaerobic in their metabolism, studies by Hardy and Brown demonstrated that the availability of oxygen can increase corrosion in the presence of SRB.[9] They found that the corrosion rates of mild steel in anaerobic cultures of SRB were low (6.74 µm/y [0.265 mpy]), while subsequent exposure to air caused higher corrosion rates (610 µm/y [24 mpy]).

The most prevalent mechanism for the observed corrosion in a study reported by Jack et al.[10] was the formation of a galvanic couple between steel and microbiologically produced iron sulfides. The couple is normally short-lived because the iron sulfide matrix becomes saturated with electrons derived from the corrosion process. In the presence of SRB, however, the corrosion process is perpetuated because SRB removes electrons (in the corrosion process) from the iron sulfide surface. This process may involve the formation of cathodic hydrogen on the iron sulfide or the direct transfer of electrons from the iron sulfide matrix to redox proteins in the bacterial cell wall. Corrosion rates associated with this mechanism were proportional to the amount of iron sulfide in the corrosion cell.

Sulfate-reducing *Archaea* (SRA) are like SRB, obtaining their energy by oxidizing organic compounds or molecular hydrogen (H_2) while reducing sulfates to sulfides, especially to hydrogen sulfide.[11] SRA consist of the genera *Archaeoglobus*. *Archaeoglobus* grow at temperatures in the range of 60 to 95 °C (140 to 203 °F), with optimal growth at 83 °C (181 °F) (ssp. A. fulgidus VC-16).[2] Previously, *Archaeoglobus* species have been isolated from oil reservoirs and oil production systems; however, this group of microorganisms is normally not measured with current culturing techniques. SRA are known to cause the corrosion of iron and steel in oil and gas processing systems by producing iron sulfide.

The formation of H_2S by SRA activity can have profound effects in terms of reservoir souring, health/safety/environmental threats, and materials degradation.

3.2.2 Acid Production

Organic acids are produced by both bacteria and fungi. This process is anaerobic for some microorganisms or aerobic for other microorganisms and fungi. Most final products of APB are short-chained fatty acids (e.g., acetic, formic, and lactic acids). The role of APB in MIC is controversial. Pope et al.[12] proposed that APB produce biogenic organic acids that are directly responsible for corrosion in the absence of SRB. Jack et al.[13] reported that the main role of APB is to provide the environment and nutrients for SRB growth. Other bacterial species can produce aggressive inorganic acids, such as sulfuric acid (H_2SO_4), in aerobic environments. Microorganisms in the soil as well as other environments can locally generate high concentrations of carbon dioxide. The carbon dioxide dissolves in the water, producing carbonic acid. Carbon-

Robert Carnahan - Invoice 144726 downloaded on 2/14/2020 7:33:38 PM Single-user licence only, copying/networking prohibited

ic acid solution is corrosive to pipeline steels and can lead to general attack, pitting attack, and stress corrosion cracking.[1]

3.2.3 Metal Deposition

3.2.3.1 Microorganisms can also affect corrosion by creating differential aeration cells on the surface of the metal and fixing the location of anodic sites beneath colonies of microorganisms. The organisms most often cited as causing differential aeration cells are those organisms capable of depositing iron and manganese oxides.

3.2.3.2 Iron-oxidizing bacteria produce orange-red tubercles of iron oxides and hydroxides by oxidizing ferrous ions from the bulk medium or the substratum. Iron-depositing bacteria are microaerophilic and may require synergistic associations with other bacteria to maintain low oxygen conditions in their immediate environment. Deposits of cells and metal ions create oxygen concentration cells that effectively exclude oxygen from the area immediately under the deposit and initiate a series of events that individually or collectively are very corrosive.

In an oxygenated environment, the area immediately under individual deposits becomes deprived of oxygen. That area becomes a relatively small anode compared to the large surrounding oxygenated cathode. Cathodic reduction of oxygen can result in an increase in pH of the solution in the vicinity of the metal. The metal forms metal cations at anodic sites. If the metal hydroxide is the thermodynamically stable phase in the solution, the metal ions are hydrolyzed by water, forming hydrogen (H^+) ions. If cathodic and anodic sites are separated from one another, the pH at the anode decreases and that at the cathode increases.

The pH at the anode depends on specific hydrolysis reactions. In addition, chloride (Cl^-) ions from the electrolyte migrate to the anode to neutralize any buildup of charge, forming heavy metal chlorides that are extremely corrosive. Under these circumstances, pitting involves the conventional features of differential aeration, a large cathode-to-anode surface area, and the development of acidity and metallic chlorides. Pit initiation depends on mineral deposition by microorganisms.

3.2.3.3 Manganese oxidation and deposition is coupled to cell growth and metabolism of organic carbon. The reduced form of manganese (Mn^{+2}) is soluble and the oxidized forms (Mn_2O_3, MnOOH, Mn_3O_4, and MnO_2) are insoluble. As a result of microbial action, manganese oxide deposits are formed on buried or submerged materials including metal, stone, glass, and plastic, and can occur in natural waters that have manganese concentrations as low as 10 to 20 ppb. For mild steel corrosion under anodic control, manganese oxides can elevate corrosion current. The current can be significant for biomineralized oxides that provide large mineral surface areas. Given sufficient conductivity, manganese oxide can sometimes serve as a cathode to support corrosion at an oxygen-depleted anode within the deposit.

3.2.4 Metal Reduction

Dissimilatory iron and/or manganese reduction occurs in several microorganisms, including anaerobic and facultative aerobic bacteria. Inhibitor and competition experiments suggest that iron (Fe^{+3}) and manganese (Mn^{+4}) are efficient electron acceptors that are similar to nitrate in redox ability and are capable of out-competing electron acceptors of lower potential, such as sulfate or carbon dioxide.[14]

Robert Carnahan - Invoice 144726 downloaded on 2/14/2020 7:33:38 PM Single-user licence only, copying/networking prohibited

MRB in direct contact with solid Fe^{+3} and Mn^{+4} oxides produce soluble ions (Fe^{+2} and Mn^{+2}). The result is dissolution of surface oxides and localized corrosion.[1]

3.2.5 Methanogens

Methanogens produce methane as a metabolic by-product in anoxic conditions. They are classified as *Archaea*, a group quite distinct from bacteria.

Methanogens typically thrive in environments in which all electron acceptors other than CO_2 (such as oxygen, nitrate, sulfate, and trivalent iron) have been depleted. They are common in wetlands, where they are responsible for marsh gas, and in the guts of animals such as ruminants and humans. Others are extremophiles, found in environments such as oilfield systems, hot springs, and submarine hydrothermal vents, as well as in the "solid" rock kilometers below the surface of the Earth's crust. Methanogens are common *Archaea* in oil production systems; however, they are normally not measured with current culturing techniques.[15,16]

Methanogens are known to promote MIC in steel and other metal structures by consuming hydrogen formed at the corrosion cathode.[17]

Section 4: External MIC of Pipelines

4.1 Environment

The potential for MIC of buried pipelines is controlled by the availability of nutrients, water, and electron acceptors. Peabody reported data from Harris[18] that indicated soil moisture content and bacterial cell counts were greater in backfill material than in undisturbed earth adjacent to a pipeline. Trench backfill is not as consolidated and allows greater penetration of moisture and increased oxygen diffusion. Anaerobic bacteria thrive in waterlogged, dense soil. Alternating moisture and oxygen concentrations influence the growth of bacterial populations. Despite the numerous mechanisms that one would predict for MIC of buried pipelines, most failures have been attributed to the presence and activities of SRB and APB. In general, sandy soils favor APB; high-clay soils support populations of both kinds of organisms. To protect against all forms of external corrosion and cracking, several coating materials have been used, including coal tar derivatives, asphalts, polyolefin tapes, and fusion-bonded epoxies (FBE). Line pipe has been further protected by CP. Although these are sound measures, MIC can occur in the presence of these preventative measures, if one or both break down or are not properly maintained.[1]

4.2 Coatings

4.2.1 Differing environmental conditions (e.g., soil moisture, microflora, nutrients) in both field surveys and laboratory experiments make it difficult to interpret coatings performance and draw comparisons. Comparisons between field surveys and laboratory experiments must not exceed stated condition limitations. Tenting of coatings along irregularities on the pipe surface, especially at long seam or girth welds, can create gaps between the coating and the pipe surface that fill with groundwater and introduce microorganisms that may create corrosion cells under the disbonded coating. Tape coatings are particularly susceptible to tenting while liquid- or powder-applied coatings are more resistant to this type of failure mechanism. Tenting has been most prevalent in wet high-clay soils on unstable, geologically active slopes that are subject to high service temperatures. The high service temperatures promote coating disbondment. Not all coating materials are affected by soil bacteria under all conditions. Coatings derived from both coal (tars) and petroleum (asphalts) pass some exposure tests and fail oth-

Robert Carnahan - Invoice 144726 downloaded on 2/14/2020 7:33:38 PM Single-user licence only, copying/networking prohibited

ers. Materials that, by themselves, show resistance to attack by microorganisms fail when combined or reinforced with other materials.[1]

4.2.2 Jack et al.[10] demonstrated that certain coatings disbond more readily after being exposed to soils containing SRB and APB. Polyethylene (PE) coating damage proceeded linearly with time. PE tape coatings supported higher bacterial counts than extruded PE or FBE, presumably because of the presence of biodegradable adhesive/primer components in the coating system. Susceptibility to disbonding was high with FBE, higher with extruded PE, and highest with PE tape. Two types of coating damage were reported: 1) damage caused by water leaching and 2) damage caused by permeation. Both mechanisms affect intact coatings and coatings around holidays. At existing holidays, damaged FBE coatings experience an increased susceptibility to coating disbondment.

4.2.3 Peabody reported that coal tars, coal-tar epoxies, and coal-tar enamels were immune to disbonding because of activities of microorganisms, which would likely lessen the chances of corrosion, including MIC. Early coatings based on asphalt were subject to oxidation and loss of low-molecular-weight components through biodegradation and biodeterioration, resulting in a permeable, embrittled coating.[3] Pendrys[19] demonstrated that, with time, asphalt could be degraded by microorganisms selected from soil. Harris[18] demonstrated that bacteria commonly found in pipeline soils can degrade asphalt, tape adhesives, kraft paper (expendable once the pipeline is in place), as well as the binders and fillers used in felt pipeline wrappers. The next-generation coatings were based on polyvinyl chloride (PVC) or PE. The PVC tape was unstable in service. Plasticizers constitute up to 50 wt% of a PVC product and can be effectively lost through biodeterioration and water dissolution. PE coatings rely on adhesives to attach the polyolefin layer to the primed steel surface.[1]

4.3 Cathodic Protection

For CP levels more negative than –850 mV (–880 mV to –1,000 mV) polarized vs. a saturated copper/copper sulfate ($Cu/CuSO_4$) reference electrode, it has been demonstrated that bacteria levels, including SRB, can increase in saturated soils, seawater, and marine sediments[1,20-22] so that if the CP is intermittent, MIC can occur at a higher rate than if CP were not previously present.[23] MIC has at least three effects on CP of pipelines.

4.3.1 When microbial activity is present and the coating is compromised, the potential level required to mitigate corrosion is a more negative value. Pope and Morris[4] found that pipeline failures were often in contact with wet clays with little scaling potential, creating a situation in which the demand for CP continues at a high level over long periods of time and in which CP may not be distributed equally over the surface of coating holidays and surrounding disbondments. Microorganisms colonize and initiate corrosion at such sites. Research by Barlo and Berry[24] determined that the current criteria specified in NACE SP0169[25] for CP of buried pipelines (0.85 V versus $Cu/CuSO_4$) were generally valid in concept. However, the critical values for the criteria varied with the environment. Elevated temperature (60 °C [140 °F]), mill scale, and anaerobic bacteria affect CP requirements—100 to 200 mV more cathodic (negative) change in protection potential is required compared to the condition absent those factors.[1]

4.3.2 MIC can increase the kinetics of corrosion reactions, increasing the CP current necessary to achieve a given level of polarization.

4.3.3 Microorganisms can attack certain pipeline coatings, increasing exposed metal surface area and further increasing the CP current used to achieve a given level of polarization. Water intrusion at breaks in the coating may cause corrosion

Robert Carnahan - Invoice 144726 downloaded on 2/14/2020 7:33:38 PM Single-user licence only, copying/networking prohibited

where the remaining dielectric coating may block CP. It should be noted, however, that when sufficient CP levels exist, corrosion is mitigated even in the presence of increased levels of bacteria. The difficulty is determining what is adequate for providing protection in each situation without adversely affecting the coating.[1]

Section 5: Sampling Equipment

5.1 Certain procedures may be used to collect samples.

5.1.1 Typical equipment and supplies should include some or all of the following:

(a) Sterile plastic or glass containers (10 to 125 mL [0.33 to 4.20 oz]).
(b) Sterile plastic sample collection bags.
(c) Sterile metal scalpels.
(d) Sterile cotton or polyester-fiberfill swabs.
(e) Sterile wooden spatulas (tongue depressors).
(f) Sterile 1 to 5 mL (0.03 to 0.1 oz) syringes.
(g) Sterile disposable plastic pipettes.
(h) Sterile latex gloves.
(i) Ice chest with refrigerant.
(j) Digital or film camera.
(k) Magnifying lens (5 to 60x).
(l) Marking pens (for wet surfaces).
(m) Nylon bristle brushes.
(n) Mechanical pit depth gauge.
(o) Labels.
(p) pH paper or meter.
(q) Culture media.
(r) Ultrasonic thickness (UT) meter to measure metal thickness.
(s) Sterile vials of phosphate-buffer solution.
(t) Formaldehyde (36.5%) for fixation on site (for use with DAPI method) or 2% glutaraldehyde as a general fixative.

5.2 Sterile containers must not contain any chemical that inhibits microbial survival. Collection containers may contain sterile phosphate buffer, Ringers solution, or other holding medium for suspension of solid samples. If samples are to be analyzed for chemical composition, they must be maintained separately from samples transferred to a holding medium. Most sampling containers are glass or plastic.

5.2.1 Glass containers should have screw-down caps and must have been sterilized using a combination of pressure and temperature over time (100 kPa [14.5 psig] steam at approximately 121 °C [250 °F] for a minimum of 20 min). Glass containers may be reused many times after cleaning and sterilization.

5.2.2 Plastic containers are usually disposable; however, some can be cleaned and autoclaved. In most cases, plastic sampling containers have rigid walls, but polyethylene flexible-walled containers with closure ties can be used.

5.2.3 Sterile plastic bags provide a lightweight sample container. Plastic bags designed for domestic use are not sterile and must not be used for sample collection.

5.2.4 Sterile, individually wrapped supplies can be purchased from most pharmacies and all scientific supply stores. Sterile bags and tubes are usually ordered in bulk, and the interiors remain sterile until opened.

Robert Carnahan - Invoice 144726 downloaded on 2/14/2020 7:33:38 PM Single-user licence only, copying/networking prohibited

Section 6: Sampling and Testing Procedures

6.1 Site Inspection

6.1.1 Before excavation of the pipeline, the topography and soil type of the area surrounding the dig should be noted. The site should be photographed both close up and from a distance. The photos should complement one another so that they can be aligned and compared. A ruler should be included in photographs to indicate relative dimensions.

6.1.2 The following measurements provide useful information:

6.1.2.1 Soil resistivity using ASTM[1] G5726 Wenner 4 point or similar method.

6.1.2.2 Pipe-to-soil potential.

6.1.2.3 Redox potential (E_h) as the potential of a platinum electrode using a saturated copper copper-sulfate reference electrode.

6.1.2.4 Soil pH to compare with under-coating pH measurements to determine effectiveness of CP.

6.1.3 Exposure of the pipe should be slow and careful to avoid damage to the pipe and areas of sampling. Soil should be removed from the pipe surface carefully to expose the coating surface. In most cases, products adhering to the coating surface shall not be removed until they are at a laboratory or other suitable location where analyses can be performed. Color photographs of corroded areas and their relationship to the pipe surface should be taken.

6.1.4 The following should be noted and recorded (see checklist in Appendix A):

6.1.4.1 Coating type (e.g., coal tar, asphalt, bitumen, tape, FBE), type of damage (e.g., disbonding, holidays, blistering, seam tenting, cracking, wrinkling, or none), extent of damage (percentage of exposed area), and location (circumferential and longitudinal position on the pipe in relation to weld seams and coating seam, if present).

6.1.4.2 Characteristics of soil: moist, dry, or wet; silt, sand, gravel, rock, or clay; odor; discoloration associated with a buried object; local chemical composition, e.g., presence of salts, cations, anions, such as chlorides, sulfates, carbonates, etc.

6.1.4.3 Relationship of corroded area within overall system: depth, light, engineering design (welds, seams), etc.

6.2 Description of Corrosion Products

6.2.1 Corrosion products: color (brown, black, white, or gray), shape (deposit, nodule, or films), texture, and odor.

6.2.2 The form of any visible corrosion: shapes, sizes, and depths of pits; crevice corrosion; UDC should be noted (See Figure 1).

6.2.3 Any visible biological accumulations in corroded areas: form, color, texture, or odor (e.g., none, earth, rotten eggs, etc.).

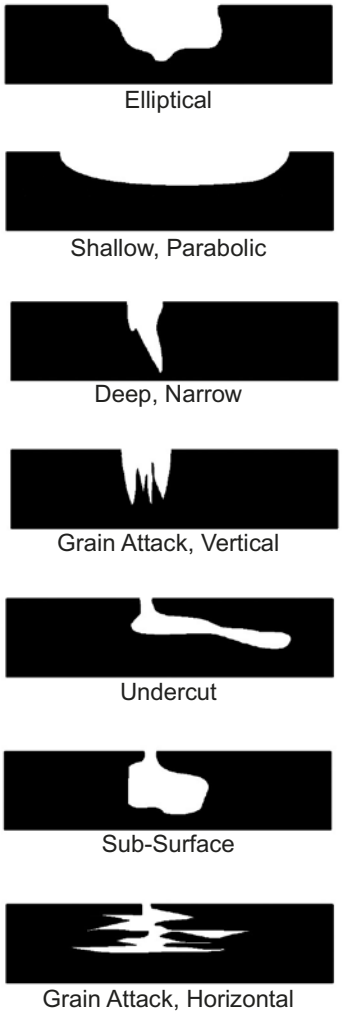

FIGURE 1: Examples of Various Pit Morphologies as Viewed in Cross Section.[27]

[1] ASTM International (ASTM), 100 Barr Harbor Drive, PO Box C700, West Conshohocken, PA 19428.
[2] European Federation of Corrosion (EFC), 1 Carlton House Terrace, London, SW 1Y 5DB, UK.

Robert Carnahan - Invoice 144726 downloaded on 2/14/2020 7:33:38 PM Single-user licence only, copying/networking prohibited

6.2.4 Chemical testing for sulfides and carbonates.

6.3 Coating Inspection

6.3.1 Once the pipe is exposed, the soil, water, and deposits must be sampled immediately and stored or tested. The coating surrounding the suspected area of corrosion should be carefully removed using a knife or similar instrument. Sample contamination of corrosion with soil or water must be kept to a minimum. Contact with the soil, corrosion product, or film with hands or tools other than sterile implements must be avoided.

6.3.2 Coating inspection for MIC testing purposes must precede any other coating evaluation. Likely areas of active corrosion or MIC should be identified using ILI tools or visual inspection. Damaged coatings should be carefully removed using a sterile scalpel to expose the steel.

6.4 Sample Collection

6.4.1 Whenever possible, a clean working surface should be used, because if proper precautions are not taken, dust or dirt on the working surface or general area can potentially contaminate the inside of sample containers when a sterile sample bottle is uncapped. Ideally, the containers should be handled by gripping the lower part of the bottle, and skin contact with the upper part of the container must be avoided.

6.4.2 If a small volume of liquid is present under the coating, a sample should be taken using a sterile syringe or polyester-fiberfill swab. Both the liquid in the syringe and on the swab may be used for the enumeration of microorganisms as described later. The swab must be stored in a sterile plastic tube until tested.

6.4.3 The pH of any liquid found under the coating should be tested using pH (1 to 14) paper or a meter with a microsensor electrode. The coating should be carefully sliced to a length to allow the test paper to be slipped behind the coating. The coating should be pressed against the pH paper for a few seconds and then lifted. The pH paper may then be removed. The color of the paper in relation to the chart provided with the paper should be noted and recorded. A syringe or pipette should be used to extract a small amount of liquid to measure pH by putting a drop or two of liquid on the microsensor. If possible, the pH of any available groundwater (typically at pipe level) away from the pipe should be determined for reference.

6.4.4 If surface deposits or corrosion products are fragile, they should be scraped from the pipe. Corrosion products must be collected by scraping the area with a sterile scalpel, or swabbing with a sterile polyester-fiberfill swab.

6.4.5 Multiple samples, when present, are typically taken from one or more of the following locations:

6.4.5.1 Undisturbed soil immediately next to the exposed pipe-steel surface or at an area of coating damage.

6.4.5.2 Deposits associated with visual evidence of pipe corrosion, especially those pit contents underneath nodules or tubercules that have been removed and are more likely to be uncontaminated with soil or groundwater. (Note: it should be identified when corrosion samples are known or suspected to be contaminated from outside sources).

6.4.5.3 Scale or biofilm on the steel surface or the backside of the coating.

Robert Carnahan - Invoice 144726 downloaded on 2/14/2020 7:33:38 PM Single-user licence only, copying/networking prohibited

6.4.5.4 Liquid trapped behind the coating.

6.4.5.5 Fresh, undisturbed soil at pipe depth at least 1 m (3 ft) transverse to the pipe. This location, such as the ditch wall, acts as a reference from which to determine whether the microbial population near the pipe is elevated.

6.4.5.6 Additional samples should be taken from other locations where bacterial activity is suspected and tested.

6.4.5.7 Solid and liquid samples must be placed in clean, sterile, sealed, and carefully labeled containers. The containers should be filled to no more than 60% maximum volume. The bag or tube must be sealed tightly, and the whole bagged sample sealed again within a second plastic bag to reduce the risk of leakage.

6.4.5.8 Sample containers should be labeled with the location of the dig site, sample origin, date, sampling time, and the tests that have been performed on the sample. Extraneous dust, dirt, and debris shall not be introduced into the sample at the time of collection. The interior surfaces of sample containers or any other parts likely to be in direct contact with the sample must not have been directly handled.

6.5 Sample Transport

6.5.1 Changes in detectable numbers and types of microorganisms can occur rapidly after removal of samples from the environment. One should arrive at the corrosion site with all solutions, media, and other necessary materials. If that is not possible, liquids and solids can also be transported to a laboratory or other facility for processing and testing. The major concern in transporting samples for microbiological evaluation is to ensure that microorganisms remain alive and active without multiplication. Sample collection may expose microorganisms to abrupt changes in pressure, temperature, atmosphere, and light, causing redistribution in numbers and types of microorganisms in the original sample.

6.5.2 After collection, samples should be stored in the dark away from temperature extremes. When transit times are less than 6 h, liquid samples can be maintained at the original collection temperature by storing in an insulated container. If the sample has been collected from sources above 30 °C (86 °F), intrinsic heat can maintain the microbial population without significant changes. If the transit time is longer than 6 h, the sample temperature should be lowered to less than 10 °C (50 °F) to restrict growth and competition. A standard method used to control post-sampling shifts in microflora has been to provide a cold-temperature shock by packing ice packs around sample containers to bring the temperature down to within the range of 1 to 4 °C (34 to 39 °F), which reduces microbial activity to a basic survival metabolic mode. Prolonged storage for periods of longer than a few days can cause changes in the microflora and should be avoided.

Section 7: Testing Guidelines

7.1 Field vs. Laboratory Testing

7.1.1 Bacteria, being living organisms, are highly sensitive to changes in their environment (e.g., temperature, salinity, and dissolved gases). Additionally, many chemical species associated with microbial metabolism, such as organic acids or sulfide compounds, can be rapidly oxidized or degraded. Thus, to obtain results that accurately represent pipeline conditions, certain tests relevant to MIC inves-

Robert Carnahan - Invoice 144726 downloaded on 2/14/2020 7:33:38 PM Single-user licence only, copying/networking prohibited

tigation or monitoring must be performed within minutes or hours of sample collection. Historically, this has been one of the factors that resulted in the lack of meaningful data for use in MIC assessment of pipelines because the analytical results may be misleading. Therefore, collecting samples for microbiological analysis should be avoided when pipe and coating have been extensively handled, exposed to atmosphere or sunlight for extended periods of time, or otherwise exposed to conditions where dehydration, extreme temperature changes, or contamination could occur. If such samples are analyzed, the compromising conditions should be documented so they may be taken into consideration when a final evaluation of the data at that site is performed.

7.1.2 As technology has improved, more types of tests and more sophisticated analyses have been made available for use in the field (i.e., near the point where samples are collected). Because indicators of the environmental conditions under which MIC may occur are readily degraded or lost after removal of a sample from the pipeline, a general rule for improving the quality of data is to perform testing on location whenever practical. Proper sample preservation and handling procedures must be followed diligently and consistently in cases in which testing cannot be performed in the field.

7.1.3 Results from both corrosion and microbiological tests should be integrated when evaluating the threat, likelihood, or presence of MIC. Information on both types of tests is provided in Section 7. Many of the test procedures described here are equally useful for evaluating external MIC.

7.2 Microbiological Culture Testing

7.2.1 Although MIC is often attributed to a single type of microorganism, more often the corrosion is caused by the activities of several different organisms that form a community. Microbiological testing of buried pipelines has generally included testing for SRB, APB, general aerobic organisms, general anaerobic organisms, and in some cases, iron-depositing and iron-reducing bacteria. It should be noted that iron-depositing and iron-reducing bacteria are very difficult to grow in culture, and microscopic analysis is more commonly used for detection of these bacteria.

7.2.2 The objective of the microbiological culture techniques described in this standard is to approximate the size of the viable bacterial population in a solid or liquid sample using semi-quantitative estimates, or preferably, the most probable number (MPN) method when sample replication is employed.[28,29] Such estimates are based on the assumption that bacteria are normally distributed in liquids or solids. Microorganisms in solid and liquid environmental samples are usually enmeshed in particulates. Typically, a suspension of solid samples is made in a Ringers solution or phosphate buffer. Particles should be dispersed so that colony forming units are separated to maximize the accuracy of the estimate. Water samples should be mixed by shaking or stirring for 10 to 60 sec just prior to dilution.

7.2.3 To culture microorganisms, a small amount of liquid or a suspension of a solid is added to a solution or solid that contains nutrients. The small sample is called an inoculum, and the nutrient is called the culture or growth medium. There are normally three considerations when growing microorganisms: type of culture medium, incubation temperature, and length of incubation.

7.2.4 The type of medium used to culture microorganisms determines to a large extent the numbers and types of microorganisms that grow. No growth medium can approximate the complexity of a natural environment. Under ideal circumstances, liquid culture provides favorable growth conditions for 1 to 10% of the natural population.[30] Typically, the presence of specific types of organisms is

Robert Carnahan - Invoice 144726 downloaded on 2/14/2020 7:33:38 PM Single-user licence only, copying/networking prohibited

established, and a standard methodology is used so that comparisons can be made. There are no “correct” culture media. A convenient method is to purchase prepared, pre-measured, pre-sterilized media. Test kits also generally include syringes, swabs, and marking pens. Several culture media formulations for various groups of microorganisms are included in NACE Standard TM0194.28

7.2.5 Highly colored samples may sometimes interfere with culture interpretations.

7.3 Microscopy Methods—General

7.3.1 Microscopy is most commonly used to examine liquid or solid samples directly to determine the overall numbers of microorganisms present without regard to their viability or species. The procedure involves placing a few µL of sample on a glass slide, preparing the slide for examination using various staining techniques, and examining the slide with a light microscope at magnifications from approximately 500x to 1,500x. Depending on the method of sample preparation, the detection limit for all microorganisms present in a liquid sample, including viable, nonviable, and dead cells, is approximately 102 to 103 cells per mL. Levels of microorganisms in coastal seawaters are typically > 106 cells per mL. This procedure is typically performed in the laboratory.

7.3.2 Microorganisms structurally consist of lipids and proteins that degrade and break down once the cell dies if the sample is not preserved after collection. Samples collected for microscopy are often preserved (fixed) using a formaldehyde or glutaraldehyde phosphate buffer solution. This type of preservation kills the microorganisms but preserves or fixes the structure of the cell. Fixative solution vials are commercially available. Typically only a few mL of the liquid or solid sample are preserved in the fixative.

7.3.3 One advantage of microscopy is that only a minute amount of sample is required for examination. A surface swab can provide adequate sample material (e.g., when no bulk liquid or solid is present).

7.4 Epifluorescent Microscopy

7.4.1 Epifluorescent microscopy involves treating the sample with a stain that fluoresces when viewed under a specific wavelength of ultraviolet light. This technique helps distinguish microorganisms from debris, or may be used to examine specific cellular structures of microorganisms. Hydrocarbons and some organic materials may interfere with epifluorescent microscopy as they give auto-fluorescence and obscure the signal from the biological material. This procedure is typically performed in the laboratory.

7.4.2 Biological stains such as acridine orange (N,N,N’,N’-tetramethylacridine-3,6-diamine), fluorescein isothiocyanate (FITC), and DAPI are used for epifluorescent microscopy. A variety of microbiological test kits are commercially available. Acridine orange is a common nucleic acid stain that permeates cells to interact with DNA and RNA.

7.4.3 Fluorescent probes have been developed to “label” specific groups of microorganisms, or to distinguish live vs. dead cells in a sample. Fluorescent in situ hybridization (FISH) probes are used to identify and quantify certain species and groups of microorganisms. Because FISH labels only microorganisms with a certain content of ribosomal RNA, it is only active cells or cells that have recently been active that are enumerated. Quantitative use of FISH probes is discussed in Paragraph 7.8.2.

7.4.4 The DAPI method quantifies all intact microorganisms containing DNA

Robert Carnahan - Invoice 144726 downloaded on 2/14/2020 7:33:38 PM Single-user licence only, copying/networking prohibited

(both living and inactive cells) in almost any type of liquid sample.[31,32] DAPI is often used in combination with FISH analysis to help distinguish the total cell count from the number of cells that are labeled using the FISH probes. The full DAPI method may be completed in less than half a day in a laboratory. The liquid sample is filtered whereby microorganisms (cells of bacteria, *Archaea*, and fungi) are collected on a filter. These are subsequently stained with a fluorescent dye that binds to the DNA in the cells and then washed to remove excess dye. Cells are manually counted using an epifluorescence microscope. Fluid samples should be fixed in the field with formaldehyde (36%) to a final concentration of 2% in the sample. Adequate sample amounts for this type of testing are 50 to 100 mL (1.6 to 3.40 oz) of fluid depending on the cell density.

7.4.5 Microscopy and biochemical methods have been used for many years, and genetic methods are now becoming available for the detection, quantification, and in some cases identification of microorganisms present at corrosionsites. [33-35]

7.5 Adenosine Triphosphate Photometry (ATP)

7.5.1 ATP, related to energy production and consumption, is present in all living cells. When cells die, however, ATP rapidly degrades. Consequently, the quantity of ATP in field samples is approximately proportional to the number of living microorganisms in that sample. ATP may give an indication of the viable biomass present in living organisms, and may be measured using an enzymatic reaction that generates light when ATP is present. The intensity of the light is measured in a photomultiplier, the output being proportional to the amount of ATP.

7.5.2 Several commercial field test kits are available for ATP quantification. Quantification of ATP typically relies on photometers that measure the amount of light emitted when the ATP within the sample is allowed to react with a particular enzyme. Before the reaction, the sample to be quantified is filtered and treated with gold buffers. These buffers assist in releasing the ATP from the organism so they can react with the enzyme. Finally, the sample and enzyme are combined and analyzed. Advantages of ATP measurement include speed to results (less than 10 min per sample), no underestimation of unculturable organisms, and use in any sample type including produced fluids, oil/emulsions, and solids. ATP measures should be backed up with at least one additional method for more specific quantification of the microorganism (e.g., SRB).

7.6 Hydrogenase Measurements

7.6.1 Hydrogenase is an enzyme produced by bacteria that use hydrogen as an energy source. Testing for the presence of the hydrogenase is one method used to enumerate bacteria populations in corrosion deposits and water samples in the field.

7.6.2 Quantification of bacteria populations using this method first involves extraction of the hydrogenase enzyme from the sample. The extracted enzyme is preserved in a solution that maintains enzyme activity and then placed within a reaction chamber where hydrogen is introduced. The hydrogen is oxidized and a redox indicator color change reveals the presence of the hydrogenase enzyme (refer to NACE Standard TM0194). The reaction typically is not rapid; it can take anywhere from 30 min to 4 h. The reaction time and developed color intensity together are used to measure the relative activity of the enzyme.

7.7 Adenosine Phosphosulfate Reductase (APS)

7.7.1 APS reductase is an enzyme specifically associated with SRB. Measurement of the APS reductase present in a bacterial sample provides an indication of the active SRB concentration. Detection and measurement are based on immunological methods and may be performed using a field kit.

Robert Carnahan - Invoice 144726 downloaded on 2/14/2020 7:33:38 PM Single-user licence only, copying/networking prohibited

7.7.2 The test involves exposure of the sample to small particles containing antibodies. These particles specifically capture the APS reductase enzyme. The particles, now mixed with APS reductase, are subsequently isolated on a porous membrane and exposed to specific indicator chemicals. Reaction between the particles and chemicals results in a color change that is proportional to the concentration of the APS reductase in the sample.

7.8 Molecular Microbiological Methods (MMM)

7.8.1 MMM, also referred to as genetic methods, are culture-independent approaches that provide direct analysis of samples without the bias introduced by the growth process used during culturing. Because no prior growth of microorganisms is required, MMMs accept very small amounts of any type of sample (liquid, biofilm, solid) with or without live bacteria. After genetic materials are extracted from the sample, assays that are very specific and render a more precise quantification of various types of bacteria than culture tests are performed in the laboratory.[36,37] A comparison of MMMs is shown in Table 1 and Figure 2.

Table 1
Comparison of MMMs[31]

MMM	Method Based On	Living Cells Counted?	Dead Cells Counted?	Quantitative Method?	Information Yielded
DAPI	Microscopy	Yes	Yes	Yes	Total cell counts (live and dead)
FISH	Microscopy	Yes	No	Yes	Total numbers of live bacteria Total numbers of live Archaea Total numbers of live SRB Total numbers of live SRA
DGGE	PCR	Yes	Yes	No	Comparison of populations Identification of abundant microorganisms
qPCR	PCR	Yes	Yes	Yes	Numbers of total bacteria Numbers of total Archaea Numbers of SRB Numbers of SRA Numbers of three groups of methanogens2

7.8.2 Quantitative FISH—quantitative FISH is a MMM in which only living and active cells are stained with a fluorescent dye visible during epifluorescence microscopy. Unlike the DAPI method, FISH probes may be designed to attach only to selected groups of microorganisms (e.g., specific types of SRB or SRA). Therefore, only the specific target microorganisms are visible and may be enumerated during subsequent microscopy. The quantitative FISH method does not underestimate organisms that do not grow in culture. FISH is a microscopy method that uses synthetic oligonucleotides (synthetic DNA) tagged with a fluorescent molecule (dye). Together, the synthetic DNA and the fluorescent molecule are referred to as a probe. The probe is mixed with the bacteria in a fluid sample and the numbers of bacteria (or *Archaea*) that take up the probe and have it hybridize to their rRNA are counted. The quantitative FISH method differentiates active/alive microorganisms from dead microorganisms. A probe may be designed to detect a general population (e.g., total bacteria or total *Archaea*) or a specific genus or species (e.g., *Desulfovibrio desulfuricans*). A given sample is analyzed using several different probes to understand the prokaryotic diversity in a sample, and which types/species of microorganisms are most abundant. The preparation steps for the quantitative FISH method are different from the DAPI method. However, cells stained for the quantitative FISH method are counted in the same manner as in direct bacterial counts (for the DAPI method) in the laboratory. Adequate sample amounts for this type of testing are in the range of 50 to 100 mL (1.6 to 3.40 oz) of fluid depending on the cell density. Samples are filtered onto 0.2 µm

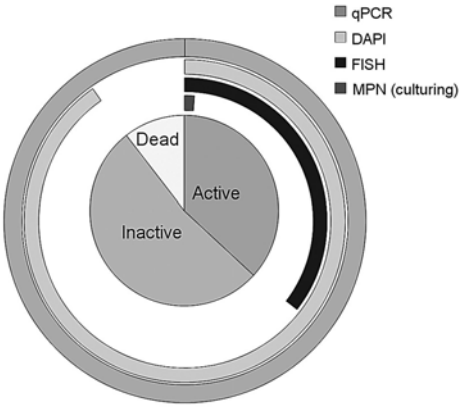

FIGURE 2: An Illustration of the Portions of the Different Pools of Microorganisms (Live, Inactive, and Dead) Typically Present in Samples from the Oil Industry that are Enumerated Using Various MMMs as Compared to the MPN (Culturing) Method. Each of the Methods Indicated is Discussed Further in the Text.[37]

Robert Carnahan - Invoice 144726 downloaded on 2/14/2020 7:33:38 PM Single-user licence only, copying/networking prohibited

filters. FISH probes are selected to target total bacteria and *Archaea*, as well as specific groups of relevance (e.g., SRB). The samples are inspected by epifluorescence microscopy at 1,000x magnification. The cells stained with each probe are counted and related to the overall number of cells obtained by the DAPI method (see Paragraph 7.4.4).

7.8.3 qPCR—PCR and qPCR is a MMM to amplify a single or few copies of a piece of DNA across several orders of magnitude, generating millions of copies of a particular DNA sequence. The qPCR is an emerging method for enumerating microorganisms in complex environmental samples, particularly in solid samples where epifluorescence microscopy (used for the DAPI method and FISH method) may be difficult to perform because of background interference. The qPCR method enumerates genes rather than individual cells by applying a modified polymerase chain reaction (PCR) method. Like the quantitative FISH method, the qPCR method may be applied to count total cells or specific groups of microorganisms (e.g., SRP or methanogenic *Archaea*).[9,15,38,39] Because qPCR targets the DNA in all prokaryotes, the qPCR method measures living, inactive, and dead microorganisms. qPCR may be used to quantify the total number of microorganisms or a specific genus/species of microorganisms in nearly any type of sample, including produced fluids, oil/emulsion, and solids. The qPCR method does not underestimate organisms that do not grow in culture. qPCR may be done on both fluid and solid samples as well as microorganisms collected via membrane filtration. qPCR uses synthetic DNA (called primers) tagged with a fluorescent molecule or synthetic DNA mixed with a DNA intercalating agent (dye) to quantify organisms using a modified version of the PCR method. Briefly, total prokaryotic DNA is extracted and amplified using primers that target to a conserved region of the bacterial DNA. The region used may make the assay very general (meaning counting total bacteria or *Archaea*), or very specific (meaning counting a single genus or species). Similar to quantitative FISH, the qPCR method may be used to enumerate a very general group of bacteria (i.e., total bacteria or *Archaea*) or very specific organism (e.g., *Desulfovibrio desulfuricans*). Adequate sample amounts for this type of testing are 50 mL (1.7 oz) of fluid, 2.0 to 5 g (0.07 to 0.1 oz) of solid, or a 0.2 or 0.45 µm filter with a minimum of 10 mL (0.30 oz) of fluid passed through it.

7.8.4 DGGE—MMM method based on the PCR method that is used for comparing microbial communities across a number of different samples. During DGGE, genetic material in individual samples is amplified by PCR and subsequently compared by electrophoresis. DGGE is used for identifying dominant groups of microorganisms in individual samples and for evaluating how the microorganisms are distributed between samples.[41-43] DGGE may be performed on any fluid or solid sample, as well as bacteria collected via membrane filtration. Adequate sample amounts for this type of testing are 50 mL (1.7 oz) of fluid, 2 to 5 g (0.07 to 0.1 oz) of solid, or a 0.2 or 0.45 µm filter with a minimum of 10 mL (0.30 oz) of fluid passed through it.

7.9 Organic Acids

Organic acids such as butyric, pyruvic, propionic, and acetic acid are by-products or intermediary species of microbial metabolism. Gas chromatography-mass spectrometry (GC-MS) or high-pressure liquid chromatography (HPLC) are used in the laboratory to identify and quantify organic acid species in properly preserved samples. Organic acids quickly degrade; therefore, samples are preserved by filtration into nitrogen-purged vials and maintained at 4 °C (40 °F) until analysis is performed.

7.10 Chemical Analysis

7.10.1 Corrosion products should be taken from the steel surface, coating, or optimally, from the pit contents underneath a deposit that has been removed. The color

Robert Carnahan - Invoice 144726 downloaded on 2/14/2020 7:33:38 PM Single-user licence only, copying/networking prohibited

and type of sample collected should be noted in each case. Although liquid or corrosion product samples are often limited in volume, when sampled from externally corroded pipe, on-site tests should be performed because significant chemical changes can occur over a short period of time. Additionally, compositional analyses, i.e., anions, cations/metals, and organic acids should be performed in the laboratory.

7.10.2 Field tests on liquids should include pH, total alkalinity, and dissolved hydrogen sulfide. Field tests on solids and corrosion products should include pH and a qualitative analysis for the presence of sulfides and carbonates. Carbonates are present if noticeable bubbling occurs when a drop of dilute hydrochloric acid is placed on a small portion of the corrosion product. Sulfides can be detected by the characteristic odor of rotten eggs or by exposing the acid-treated corrosion product to lead-acetate test paper. A white-to-brown color change occurs in the presence of sulfides. Follow-up testing in the laboratory with more sophisticated analytical equipment (e.g., energy dispersive spectroscopy [EDS], x-ray diffraction [XRD], etc.) to determine the elemental and mineral phases present should be performed to verify field tests. When collecting corrosion product samples from steel surfaces, coating, or pit contents for laboratory analysis, a large enough sample should be taken to enable testing by various methods. Avoid reusing the material from one test method for another test method if multiple tests are performed.

7.11 Pipeline Examination

7.11.1 When examining external surfaces of the exposed pipeline, disbonded coating, corrosion products, soil, and other materials should be removed from the pipe wall using a clean spatula or knife, with care taken not to scratch the metal. Any remaining material should be removed with a clean, dry, stiff brush, e.g., nylon bristle brush. A brush with metal bristles obscures the pit features. In cases when all of the product cannot be removed with this method, a brass bristle brush may be used in the longitudinal direction. The area may subsequently be cleaned with an air blast or an alcohol swab. A shiny metallic surface in the pit suggests the possibility of active corrosion. However, judgment should be used to differentiate this condition from one created by scraping the steel surface with a metallic object, such as the knife or spatula used to clean the surface or to obtain the sample product.

7.11.2 The steel surface shall be inspected for corrosion, and any damage shall be carefully documented. When possible, gauges should be used to measure the pit depths. Also, the length of the corroded area in relation to the circumferential and longitudinal position should be determined. The newly cleaned corroded area should first be examined without magnification. Then, a low-power magnifying lens at 5 to 50x power should be used to examine the detail of the corrosion pits. An example checklist is in Appendix A.

7.12 Analysis of Pipeline Samples

7.12.1 Careful analysis of pipeline samples (pipe sections or components that have been removed from service) may provide useful information regarding internal corrosion mechanisms.

7.12.2 Precautions should be taken to avoid contamination of the external surfaces of the pipeline before, during, and after the pipe section or component is removed from service. If inadvertent alteration of the external surface of the pipeline sample occurs, the nature of the alteration should be noted to aid in correct interpretation of subsequent testing results.

7.12.3 Alteration of pipeline samples can occur as a result of removal efforts, exposing the surface deposits to oxygen, soil, foreign matter, temperature changes, and contamination from handling.

Robert Carnahan - Invoice 144726 downloaded on 2/14/2020 7:33:38 PM Single-user licence only, copying/networking prohibited

7.12.4 Samples should be collected immediately after the pipe section or component is removed from service (i.e., within minutes when possible). Corrosion products and biofilms can change profoundly on exposure to air, affecting test results.

7.12.5 When samples cannot be collected immediately after a pipe section or component is removed, the external surfaces and deposits may be covered temporarily with new, clean, plastic sheeting to minimize exposure to air until samples are collected. This practice may compromise the condition of the surface samples to an unknown extent, and should be used only when samples cannot be collected immediately.

7.12.6 Culture tests of samples from pipe that has been exposed to air, dehydration, and potential contamination for extended periods of time (i.e., days) should not be relied on for providing useful data.

7.12.7 The internal condition of pipeline samples at the time of removal should be carefully and thoroughly documented; these data are important in the interpretation of both field and laboratory tests. An example checklist is provided in Appendix A.

7.12.8 Field and laboratory tests of pipeline samples for external corrosion analysis should be directed toward characterization of the biological, chemical, and metallurgical conditions present in the pipeline. In particular, distinction should be made between samples collected in corroded areas vs. areas where no corrosion is present.

7.12.9 Corrosion features on the pipeline sample should be protected from further corrosion after removal of the pipeline sample. Microscopic features of corrosion damage are easily lost because of oxidation or improper handling.

7.12.10 Optical microscopy and scanning electron microscopy (SEM) of internal corrosion features may provide useful information regarding the origin and growth of localized corrosion.

7.12.11 Metallographic examination of corroded areas removed from pipeline samples may provide information about the nature of the corrosion relative to the microstructure of the pipeline. Particularly, selective or preferential corrosion of microstructural features may be determined from metallographic examination.

7.12.12 Chemical analysis of microscopic corrosion features using EDS or other microanalytical techniques may provide useful data regarding localized corrosion initiation mechanisms.

7.12.13 Preservation methods, such as in situ histological embedment of biofilms and corrosion products, may yield samples suitable for microscopic examination using fluorescent staining techniques, phase contrast examination of thin sections, and transmission electron microscopy (TEM).

7.12.14 Interpretation of data collected from pipeline samples should be performed as described in Section 8.

7.13 Data and Records Management

All data and information, e.g., sample collection method used, should be documented on field data sheets or in logbooks with permanent ink.

7.14 Inspection Techniques

7.14.1 Inspection data are used to detect and monitor corrosion-related dam-

Robert Carnahan - Invoice 144726 downloaded on 2/14/2020 7:33:38 PM Single-user licence only, copying/networking prohibited

age. Techniques include visual inspection, ultrasonic testing (UT), radiographic testing (RT), and magnetic flux methods. Inspection may be used for establishing the orientation, distribution, density, size, shape, and extent of external corrosion damage; however, inspection results alone do not establish the presence of MIC. Inspection data should be integrated with other information about the internal environment of the pipeline.

7.14.2 The results of ILI may provide information about the location and severity of external corrosion relative to operating parameters, design, elevation, and other considerations.

7.14.3 An external corrosion direct assessment (ECDA) standard has been published for pipelines in ANSI/NACE SP0502.[43] As for ILI data, ECDA methods provide information about the location and severity of external corrosion relative to pipeline design and operating conditions.

Section 8: Application of Test Methods to Pipelines and Interpretation of Data

8.1 Data Interpretation

8.1.1 Because microorganisms are ubiquitous, the presence of bacteria or other microorganisms does not necessarily indicate a causal relationship with external corrosion observed on a pipeline. In fact, microorganisms can nearly always be cultured from natural environments. Therefore, merely detecting viable bacteria in liquid or solid samples associated with external corrosion does not necessarily prove that MIC has occurred.

8.1.2 To determine the cause of external corrosion, all chemical, microbiological, metallurgical, and operational data about the pipeline site must be examined, integrated, and analyzed. Analytical results from samples obtained in the corroded area should be compared with the results from reference samples taken outside the corroded area.

8.1.3 To determine the presence of external MIC on a pipeline, microbiological, operational, and chemical data must be integrated. Analysis of the data should demonstrate that microorganisms and their activities have provided the predominant influence over the corrosion mechanism present on the pipeline, as opposed to abiotic mechanisms.

8.1.4 Pipeline operators may collect data in support of internal MIC analysis in conjunction with other routine sampling, maintenance, integrity assessment, inspection, and environmental and regulatory compliance activities.

8.1.5 Interpretation of data relative to the assessment or determination of MIC on a pipeline should consider a number of factors that can influence both corrosion and microorganism growth, including: soil type, soil composition, groundwater composition (if present), temperature, coating condition, and cathodicprotection.

8.1.6 Interpretation of data related to bulk phase (macro scale) conditions must be done in consideration of the fact that microorganisms can exist and flourish in microniches. For example, pipelines may experience little or no corrosion damage as a result of a wide range of conditions throughout the majority of the pipeline, yet be affected by MIC in a small area of a specific section of the pipeline because of the unique environment present only at that location.

Robert Carnahan - Invoice 144726 downloaded on 2/14/2020 7:33:38 PM Single-user licence only, copying/networking prohibited

8.1.7 Because MIC is a complex mechanism that involves electrochemistry, microbiology, corrosion control, pipeline operation and design, as well as engineering and integrity assessment, plans to evaluate MIC of pipelines and analyze data should include input from those with expertise in the respective fields. Pipeline operators should seek input from a multidisciplinary team whenever possible, so as not to emphasize one aspect of science or technology over another.

8.2 Corrosion Damage Investigation

8.2.1 MIC is suggested by increased levels of viable microorganisms associated with pit areas that were uncontaminated by adjacent groundwater or soil, or by microscopic determination of iron and manganese bacteria in corrosion deposits. These are often good indicators of microbial involvement.

8.2.2 To validate MIC as the cause of internal corrosion, the following three conditions must be met:

8.2.2.1 Condition 1—Assuming there is no known or suspected contamination from outside sources, demonstration of increased levels of specific types of viable microorganisms (bacteria or fungi) associated with the corrosion, relative to samples taken outside the corroded area.

8.2.2.2 Condition 2—Chemical indicators that support the microbiological evidence (e.g., elevated levels of sulfide or sulfur in pit deposits from SRB and SRA, or organic acids from APB) are identified in the corroded area.

8.2.2.3 Condition 3—Biotic factors (the presence or activities of living organisms) are identified as the primary contributor to the corrosion damage. The objective of this verification step is to establish that the presence of specific biotic conditions was the predominant contributor to the corrosion observed. The influence of abiotic factors (chemical or physical conditions unrelated to living organisms) on the corrosion mechanism also must be considered in all cases. The nature of the corrosion damage to the pipeline system should be consistent with the nature of the identified microorganism(s) and their by-products, or their physical influence on the formation of corrosion cells. For example, if viable APB or methanogens are concentrated at the corrosion damage relative to the environment, and evidence of their metabolic activity (organic acids) is determined to be associated with the corrosion, the nature of the corrosion damage should be consistent with these observations (e.g., accelerated corrosion damage or pitting beneath biofilms or deposits). This is an important step in the final diagnosis because it is often difficult to discern between the relative contributions of various factors (biotic and abiotic) affecting localized corrosion.

8.3 Corrosion Mitigation

8.3.1 The methods described in this standard may be used to determine the need for, and effectiveness of, mitigation measures for controlling MIC. Specific procedures for mitigating external MIC of pipelines are beyond the scope of this standard.

8.3.2 NACE SP0169 provides general information about methods for controlling external MIC by design, operation, and specific measures, such as coatings and cathodic protection.

8.3.3 The mitigation measures used to control external corrosion of pipelines may be effective for both biotic and abiotic corrosion mechanisms.

Robert Carnahan - Invoice 144726 downloaded on 2/14/2020 7:33:38 PM Single-user licence only, copying/networking prohibited

References

1. A.W. Peabody, R.L. Bianchetti, ed., *Peabody's Control of Pipeline Corrosion*, 2nd ed., (Houston, TX: NACE, 2001).

2. H.P. Klenk, et al, "The Complete Genome Sequence of the Hyperthermophilic, Sulfate-Reducing Archaeon *Archaeoglobus Fulgidus*," *Nature* 390 (November 1997): p. 364.

3. T.R. Jack, M.J. Wilmott, R.L. Sutherby, R.G. Worthingham, "External Corrosion of Line Pipe—A Summary of Research Activities," *MP* 35, 3 (1996): p. 18.

4. D.H. Pope, E.A. Morris III, "Some Experiences With Microbiologically Influenced Corrosion of Pipelines," *MP* 34, 5 (1995): p. 23.

5. B.J. Little, et al, "Impact of Biofilms on the Electrochemical Behavior of Stainless Steels in Natural Seawater," *J. Biofouling* 3, 45 (1991).

6. T.L. Skovhus, K.B. Sørensen, J. Larsen, K. Rasmusssen, M. Jensen, "Rapid Determination of MIC in Oil Production Facilities with a DNA-based Diagnostic Kit," SPE International Conference on Oilfield Corrosion, paper no. SPE 130744 (Richardson, TX: SPE, 2010).

7. S. Papavinasam, A. Doiron, R.W. Revie, "Effect of Surface Layers on the Initiation of Internal Pitting Corrosion in Oil and Gas Pipelines," *CORROSION* 65, 10 (Houston, TX: NACE, 2009): p. 663.

8. S. Demoz, Papavinasam, O. Omotoso, K. Michaelian, R.W. Revie, "Effect of Field Operational Variables on the Propagation of Internal Pitting Corrosion of Oil and Gas Pipelines," *CORROSION* 65, 11 (Houston, TX: NACE, 2009): p. 741.

9. J.A. Hardy, J.L. Brown, "The Corrosion of Mild Steel by Biogenic Sulfide Films Exposed to Air," *CORROSION* 40, 12 (1984): p. 650.

10. T.R. Jack, G. Van Boven, M. Wilmott, R. Worthingham, "Evaluating Performance of Coatings Exposed to Biologically Active Soils," *MP* 35, 3 (1996): p. 39.

11. J. Larsen, K.B. Sørensen, B. Højris, T.L. Skovhus, "Significance of Troublesome Sulfate-Reducing Prokaryotes (SRP) in Oilfield Systems," CORROSION 2009, paper no. 09389 (Houston, TX: NACE, 2009).

12. D.H. Pope, T.P. Zintel, A.K. Kuruvilla, O.W. Siebert, "Organic Acid Corrosion of Carbon Steel: A Mechanism of Microbiologically Influenced Corrosion," CORROSION/88, paper no. 88007 (Houston, TX: NACE, 1988).

13. K.R. Kearns, B.J. Little, Microbiologically Influenced Corrosion Testing, (West Conshohocken, PA: ASTM, 1994), p. 108.

14. C. Myers, K.H. Nealson, "Bacterial Manganese Reduction and Growth with Manganese Oxide as the Sole Electron Acceptor," *Science* 240, 4857 (1988): p. 1319.

15. J. Larsen, K. Rasmussen, H. Pedersen, K. Sørensen, T. Lundgaard, T.L. Skovhus, "Consortia of MIC Bacteria and Archaea Causing Pitting Corrosion in Top Side Oil Production Facilities," CORROSION 2010, paper no. 10252 (Houston, TX: NACE, 2010).

16. M. Davies, P.J.B. Scott, *Oilfield Water Technology* (Houston, TX: NACE, 2006), p. 213.

17. I.B. Beech, J. Sunner, "Biocorrosion: Towards Understanding Interactions Between Biofilms and Metals," *Current Opinion in Biotechnology* 15, 3 (2004): p. 181.

18. J.O. Harris, "Bacterial Activity at the Bottom of Back-Filled Pipeline Ditches," *CORROSION* 16, 3 (1960): p. 441.

19. J.P. Pendrys, "Biodegradation of Asphalt Cement-20 by Aerobic Bacteria," *Application and Environmental Technology* 55, 6 (1989): p. 1357.

20. N.J. Dowling, M.W. Mittleman, J.C. Danko, eds., *Microbially Influenced Corrosion and Biodeterioration* (Knoxville, TN: University of Tennessee, 1991), p. 61.

21. J. Guezennec, "Influence of Cathodic Protection of Mild Steel on the Growth of Sulfate-Reducing Bacteria at 35 °C in Marine Sediments," *Biofouling* 3, 4 (1991): p. 339.

Robert Carnahan - Invoice 144726 downloaded on 2/14/2020 7:33:38 PM Single-user licence only, copying/networking prohibited

22. J. Guezennec, M. Therene, “A Study of the Influence of Cathodic Protection on the Growth of SRB and Corrosion in Marine Sediments by Electrochemical Techniques,” 1st European Federation of Corrosion Workshop on Microbiological Corrosion, held March 7-9, 1988 (London, U.K.: EFC[2]1988), p. 93.

23. P.E. Sanders, S. Maxwell, “Microfouling, Macrofouling, and Corrosion of Metal Test Specimens in Seawater,” in Proc. of the International Conference Sponsored by the National Physical Laboratory and the Metals Society (Teddington, U.K.: Metals Society,[3] 1983), p. 74.

24. T.J. Barlo, W.E. Berry, “An Assessment of the Current Criteria for Cathodic Protection of Buried Steel Pipelines,” *MP* 23, 9 (1984): p. 9.

25. NACE SP0169 (latest revision), “Control of External Corrosion on Underground or Submerged Metallic Piping Systems” (Houston, TX: NACE).

26. ASTM G57 (latest revision), “Standard Test Method for Field Measurement of Soil Resistivity Using the Wenner Four-Electrode Method” (West Conshohocken, PA: ASTM).

27. R.B. Eckert, *Field Guide for Investigating Internal Corrosion of Pipelines* (Houston, TX: NACE, 2003).

28. NACE Standard TM0194 (latest revision), “Field Monitoring of Bacterial Growth in Oilfield Systems” (Houston, TX: NACE).

29. *Standard Methods for the Examination of Water and Wastewater* (Washington, DC: APHA,(4) Denver, CO: AWWA,(5) and Alexandria, VA: WEF,(6) 2006).

30. P.J.B. Scott, “Expert Consensus on MIC: Prevention and Monitoring—Part 1,” *MP* 43, 3 (2004): p. 50.

31. J. Larsen, T.L. Skovhus, M. Agerbæk, T.R. Thomsen, P.H. Nielsen, “Bacterial Diversity Study Applying Novel Molecular Methods on Halfdan Produced Waters,” CORROSION 2006, paper no. 06668 (Houston, TX: NACE, 2006).

32. J. Larsen, S. Zwolle, B.V. Kjellerup, B. Frølund, J.L. Nielsen, P.H. Nielsen, “Identification of Bacteria Causing Souring and Biocorrosion in the Halfdan Field by Application of New Molecular Techniques,” CORROSION 2005, paper no. 05629 (Houston, TX: NACE, 2005).

33. D.H. Pope, T.P. Zintel, “Methods for the Investigation of Under-Deposit Microbiologically Influenced Corrosion.” CORROSION/88, paper no. 88249 (Houston, TX: NACE, 1988).

34. X. Zhu, J. Lubeck, K. Lowe, A. Daram, J.J. Kilbane II, “Improved Method for Monitoring Microbial Communities in Gas Pipelines,” CORROSION 2004, paper no. 04592 (Houston, TX: NACE, 2004).

35. T.L. Skovhus, B. Højris, A.M. Saunders, T.R. Thomsen, M. Agerbæk, J. Larsen, “Practical Use of New Microbiology Tools in Oil Production,” SPE Offshore Europe Conference 2007, paper no. SPE 109104 (Richardson, TX: SPE, 2007).

36. X.Y. Zhu, A. Ayala, H. Modi, J.J. Kilbane II, “Applications of Quantitative, Real-Time PCR in Monitoring Microbiologically Influenced Corrosion (MIC) in Gas Pipelines,” CORROSION 2005, paper no. 05493 (Houston, TX: NACE, 2005).

37. C. Whitby, T.L. Skovhus, eds., *Applied Microbiology and Molecular Biology in Oilfield Systems* (New York, NY: Springer, 2011).

38. K. Takai, K. Horikoshi, “Rapid Detection and Quantification of Members of the Archaeal Community by Quantitative PCR Using Fluorogenic Probes,” *Applied and Environmental Microbiology* 66, 11 (2000): p. 5066.

39. T.L. Skovhus, N.B. Ramsing, C. Holmstrom, S. Kjelleberg, I. Dahllof, “Real-Time Quantitative PCR for Assessment of Abundance of *Pseudoalteromonas* Species in Marine Samples,” *AEM* 70, 4 (2004): p. 2373.

[2] European Federation of Corrosion (EFC), 1 Carlton House Terrace, London, SW 1Y 5DB, UK.
[3] The Metals Society, 1 Carlton House Terrace, London, SW1Y 5DB.
[4] American Public Health Association (APHA), 800 I St. NW, Washington, DC 20001.
[5] American Water Works Association (AWWA), 6666 W. Quincy Ave., Denver, CO 80235.
[6] Water Environment Federation (WEF), 601 Wythe Street, Alexandria, VA 22314-1994.

Robert Carnahan - Invoice 144726 downloaded on 2/14/2020 7:33:38 PM Single-user licence only, copying/networking prohibited

40. R. Sooknah, S. Papavinasam, R. W. Revie, "Validation of a Predictive Model for Microbiologically Influenced Corrosion," CORROSION 2008, paper no. 08503 (Houston, TX: NACE).

41. J. Larsen, T.L. Skovhus, A.M. Saunders, B. Højris, M. Agerbæk, "Molecular Identification of MIC Bacteria from Scale and Produced Water: Similarities and Differences," CORROSION 2008, paper no. 08652 (Houston, TX: NACE, 2008).

42. V.V. Keasler, et al, "Identification and Analysis of Biocides Effective Against Sessile Organisms," SPE International Symposium on Oilfield Chemistry 2009, paper no. SPE 121082 (Richardson, TX: SPE, 2009).

43. ANSI/NACE Standard SP0502 (latest revision), "Pipeline External Corrosion Direct Assessment Methodology" (Houston, TX: NACE).

Bibliography

T.J. Barlo, W.E. Berry, "An Assessment of the Current Criteria for Cathodic Protection of Buried Steel Pipelines," *MP* 23, 9 (1984): p. 9.

NACE SP0169 (latest revision), "Control of External Corrosion on Underground or Submerged Metallic Piping Systems" (Houston, TX: NACE).

ASTM G57 (latest revision), "Standard Test Method for Field Measurement of Soil Resistivity Using the Wenner Four-Electrode Method" (West Conshohocken, PA: ASTM).

R.B. Eckert, *Field Guide for Investigating Internal Corrosion of Pipelines* (Houston, TX: NACE, 2003).

NACE Standard TM0194 (latest revision), "Field Monitoring of Bacterial Growth in Oilfield Systems" (Houston, TX: NACE).

Standard Methods for the Examination of Water and Wastewater (Washington, DC: APHA,(4) Denver, CO: AWWA,(5) and Alexandria, VA: WEF,(6) 2006).

P.J.B. Scott, "Expert Consensus on MIC: Prevention and Monitoring—Part 1," *MP* 43, 3 (2004): p. 50.

J. Larsen, T.L. Skovhus, M. Agerbæk, T.R. Thomsen, P.H. Nielsen, "Bacterial Diversity Study Applying Novel Molecular Methods on Halfdan Produced Waters," CORROSION 2006, paper no. 06668 (Houston, TX: NACE, 2006).

J. Larsen, S. Zwolle, B.V. Kjellerup, B. Frølund, J.L. Nielsen, P.H. Nielsen, "Identification of Bacteria Causing Souring and Biocorrosion in the Halfdan Field by Application of New Molecular Techniques," CORROSION 2005, paper no. 05629 (Houston, TX: NACE, 2005).

D.H. Pope, T.P. Zintel, "Methods for the Investigation of Under-Deposit Microbiologically Influenced Corrosion." CORROSION/88, paper no. 88249 (Houston, TX: NACE, 1988).

X. Zhu, J. Lubeck, K. Lowe, A. Daram, J.J. Kilbane II, "Improved Method for Monitoring Microbial Communities in Gas Pipelines," CORROSION 2004, paper no. 04592 (Houston, TX: NACE, 2004).

T.L. Skovhus, B. Højris, A.M. Saunders, T.R. Thomsen, M. Agerbæk, J. Larsen, "Practical Use of New Microbiology Tools in Oil Production," SPE Offshore Europe Conference 2007, paper no. SPE 109104 (Richardson, TX: SPE, 2007).

X.Y. Zhu, A. Ayala, H. Modi, J.J. Kilbane II, "Applications of Quantitative, Real-Time PCR in Monitoring Microbiologically Influenced Corrosion (MIC) in Gas Pipelines," CORROSION 2005, paper no. 05493 (Houston, TX: NACE, 2005).

C. Whitby, T.L. Skovhus, eds., *Applied Microbiology and Molecular Biology in Oilfield Systems* (New York, NY: Springer, 2011).

K. Takai, K. Horikoshi, "Rapid Detection and Quantification of Members of the Archaeal Community by Quantitative PCR Using Fluorogenic Probes," *Applied and Environmental Microbiology* 66, 11 (2000): p. 5066.

Robert Carnahan - Invoice 144726 downloaded on 2/14/2020 7:33:38 PM Single-user licence only, copying/networking prohibited

T.L. Skovhus, N.B. Ramsing, C. Holmstrom, S. Kjelleberg, I. Dahllof, "Real-Time Quantitative PCR for Assessment of Abundance of *Pseudoalteromonas* Species in Marine Samples," *AEM* 70, 4 (2004): p. 2373.

R. Sooknah, S. Papavinasam, R. W. Revie, "Validation of a Predictive Model for Microbiologically Influenced Corrosion," CORROSION 2008, paper no. 08503 (Houston, TX: NACE).

J. Larsen, T.L. Skovhus, A.M. Saunders, B. Højris, M. Agerbæk, "Molecular Identification of MIC Bacteria from Scale and Produced Water: Similarities and Differences," CORROSION 2008, paper no. 08652 (Houston, TX: NACE, 2008).

V.V. Keasler, et al, "Identification and Analysis of Biocides Effective Against Sessile Organisms," SPE International Symposium on Oilfield Chemistry 2009, paper no. SPE 121082 (Richardson, TX: SPE, 2009).

ANSI/NACE Standard SP0502 (latest revision), "Pipeline External Corrosion Direct Assessment Methodology" (Houston, TX: NACE).

[7] Gas Technology Institute (GTI), formerly Gas Research Institute (GRI), 1700 S. Mount Prospect Road, Des Plaines, IL 60018-1804.

Robert Carnahan - Invoice 144726 downloaded on 2/14/2020 7:33:38 PM Single-user licence only, copying/networking prohibited

Appendix A
(Nonmandatory)
Site Inspection and Testing

A1.1 A sample checklist used for site inspection and testing is provided in Table A1:

Table A1
Site Inspection and Testing Checklist

Paragraph No.	Inspection Point	Observations
6.1.1	**Observations prior to excavation**	
	General topography of site	
	Soil type	
6.1.2	**Measurements prior to excavation**	
	Soil resistivity	
	Pipe-to-soil potential	
	Close interval survey	
	Current mapping	
	Redox potential	
	Other	
6.1.3	**Observations during excavation**	
	Method of excavation	
	Coating damaged while digging?	
	Soil depth to top of pipe	
	Special features (bend, fitting, etc.)	
	Previous repair area?	
	Observations after excavation	
6.1.4.1	Coating type (coal tar, asphalt, bitumen, tape, wax, epoxy)	
	Nature of coating damage (disbonding, blistering, tenting, cracking, wrinkling)	
	Extent of coating damage (length, circumference, area of pipe exposed)	
	Location of coating damage relative to pipe girth and seam welds, and coating seam if applicable	
	Typical location of coating damage (top, bottom, sides, random)	
	Coating repairs	
	Age of coating	
	Plant or field application	
6.1.4.2	**Soil moisture level**	
	Soil type (silt, sand, gravel, rock, clay, peat, other)	
	Discoloration near pipeline	
	Soil strata depths	
	Running water (spring)	
	Seasonal effects at location	
	Soil or groundwater pH	
	Soil pH around pipeline	
	Note soil samples collected for analysis	

Robert Carnahan - Invoice 144726 downloaded on 2/14/2020 7:33:38 PM Single-user licence only, copying/networking prohibited

6.1.4.3	**Relationship of corrosion to:**	
	Distance from nearest compressor station	
	Inlets, outlets, taps, fittings	
	Heat sources or temperature change	
	Construction/material changes	
	Recent repairs or damage	
	Power lines	
	Other pipelines or underground facilities	
6.2.1	**Corrosion products/deposits color**	
	Nature of deposits (scale, nodule, film)	
	Deposit texture (hard, soft, friable)	
	Deposit odor	
	Deposit strata (note changes in layers if they exist)	
	Note visual differences between general deposits and localized deposits associated with corrosion	
	Relationship between coating and deposits (e.g., beneath coating, on top of coating, etc.)	
	Calcareous deposits present?	
	Chemical spot testing results	
	Note deposit samples collected for analysis	
	Visible biological accumulations in deposits or on pipe	
	Liquid present beneath coating?	
6.2.2	**Observations of corrosion damage**	
	Nature of corrosion damage	
	Isolated pitting	
	Isolated pitting within areas of general corrosion	
	Linked pitting within areas of general corrosion	
	General metal loss with few deeper pits	
	Etching or general metal loss with no pitting	
	Selective attack at welds	
	Crevice corrosion (at flange joints, mechanical joints)	
	Pit morphology (elliptical, parabolic, narrow, grain attack, subsurface). See Figure 1.	
	Pit features (striations, tunnels, cup shape, pits within pits, undercutting, strata levels, grooves, shiny, dull)	
	Other observations	
	Severity of corrosion:	
	Longitudinal extent	
	Circumferential extent	
	Maximum wall loss	
	Profile of wall loss	
	Maximum/average pit depth	
	Maximum/average pit diameter	
	Pit length vs. pit width	
	Depth/diameter ratio	
	Where is corrosion the most severe?	

Robert Carnahan - Invoice 144726 downloaded on 2/14/2020 7:33:38 PM Single-user licence only, copying/networking prohibited

6.4	**Samples collected for microbial and chemical analysis**	***Note whether sample was collected and exact location of sample.***
	Soil samples	
	a. Undisturbed soil next to pipe	
	b. Undisturbed soil, bottom of ditch	
	c. Undisturbed soil, ditch wall, pipe elevation	
	d. Soil in contact with coating damage or corrosion	
	Coating/deposit samples	
	a. Disbonded or damaged coating	
	b. Deposits at corrosion sites	
	c. Deposits where no corrosion occurred	
	d. Scale, biofilm, liquids from under coating	
	Corrosion samples	
	a. Corrosion products or nodules	
	b. Material from beneath nodules	
	c. Surface swab of pit contents	
	d. Pipe sample cut-out	
	General information and history	
	Year of installation	
	Pipe diameter and wall thickness	
	Pipe grade and manufacturer	
	Year of CP installation	
	Type of CP system	

Robert Carnahan - Invoice 144726 downloaded on 2/14/2020 7:33:38 PM Single-user licence only, copying/networking prohibited

Robert Carnahan - Invoice 144726 downloaded on 2/14/2020 7:33:38 PM Single-user licence only, copying/networking prohibited

Robert Carnahan - Invoice 144726 downloaded on 2/14/2020 7:33:38 PM Single-user licence only, copying/networking prohibited

NACE Standard TM0106-2016
Item #00000

ISBN 1-57590-000-0
NACE International

Robert Carnahan - Invoice 144726 downloaded on 2/14/2020 7:33:38 PM Single-user licence only, copying/networking prohibited

Ex. II - 34

Paper No.
9452

Cathodic Protection and MIC - Effects of Local Electrochemistry

Stefan Jansen
Deltares
Princetonlaan 6
3584 CB Utrecht
The Netherlands

Jan Gerritse
Deltares
Princetonlaan 6
3584 CB Utrecht
The Netherlands

Mirjam van Burgel
DNV GL Oil and Gas
Energieweg 17
9743 AN Groningen
The Netherlands

Markus Büchler
Swiss Society for Corrosion Protection (SGK)
Technoparkstrasse 1
CH-8005 Zürich
Switzerland

ABSTRACT

Uncertainties are present about the mechanisms of cathodic protection (CP) and its effectiveness to limit or completely stop Microbiologically Influenced Corrosion (MIC). The goal of this research was to improve the understanding of the mechanisms of CP by determining the interactions between corrosion and local chemical parameters, such as pH, under varying CP conditions, both in the absence and presence of MIC.

Electrical resistance (ER) probes, covered with a biofilm of sulphate-reducing microorganisms, were subjected to a series of CP potentials. In some cases MIC could not be stopped by CP, even at very negative potentials. The application of CP potentials resulted in an increase of the pH near the steel surface. In the absence of a biofilm CP could raise the pH above 13, whereas the pH remained below 8 in the presence of an active MIC biofilm. These findings show that MIC biofilms can reduce the effectiveness of CP by maintaining a mild pH, supporting their activity.

Once biofilms have established, it may be very hard or even impossible to stop MIC with CP, irrespective of the potential applied. This suggests that CP strategies should be aimed at preventing MIC biofilms to develop from the start.

Key words: MIC, electrical resistance probe, cathodic protection, biofilm, sulphate-reducers, microsensors, pH, electrochemistry.

©2017 by NACE International.
Requests for permission to publish this manuscript in any form, in part or in whole, must be in writing to
NACE International, Publications Division, 15835 Park Ten Place, Houston, Texas 77084.
The material presented and the views expressed in this paper are solely those of the author(s) and are not necessarily endorsed by the Association.

INTRODUCTION

Microbiologically influenced corrosion (MIC) has been identified as one of the major causes of failures of underground steel infrastructure. Uncertainties are present about the mechanisms of cathodic protection (CP) and its effectiveness to limit or completely stop MIC. Several different mechanisms for the effect of CP on MIC have been proposed, including formation of alkalinity and electrostatic effects at the metal surface.[1]

To prevent or mitigate corrosion using cathodic protection (CP), the right potential should be applied. A criterion of -0.95 V (vs. Cu-$CuSO_4$) is widely used, but its robustness has been questioned by several authors.[1,2] A crucial factor is the role of environmental conditions and the ensuing electrochemical and microbiological reactions following the application of CP.

Recently, a model was developed which is able to explain mechanisms of cathodic protection and limitations of the current threshold values.[2] In spite of the successful description of corrosion phenomena by this model, some input parameters still remain unclear. The spread resistance is one uncertain parameter. It is determined by soil microstructure and local soil electrolyte chemistry. The latter strongly depends on the applied potential and the resulting electrochemical reaction occurring at the steel surface at a given rate as well as on the coupled mass transport. The combined effects of applied protection current, mass transport and microbial activity in the soil adjacent to a defect are currently not well understood. Especially the role of sulphate-reducing bacteria is unclear: the presence of these bacteria can influence the local environment by affecting pH (most likely by acidification), but also by affecting levels of Fe^{2+} concentration due to formation of precipitates such as iron sulphides. A better understanding of these processes is necessary to understand the occurrence of MIC and the effectiveness of CP.

The goal of this research was to answer the following questions:

- How effective is CP in the absence and presence of Microbiologically Influenced Corrosion (MIC)?
- What factors explain the effectiveness of CP in the absence and presence of MIC?
- What does this mean for CP protection criteria?

In order to answer these questions, we determined the interactions between corrosion and local chemical parameters such as pH under varying CP conditions, in the absence and presence of MIC.

EXPERIMENTAL PROCEDURE

1. Relation between CP and local pH in synthetic solutions

In a first series of experiments the effect of the current density on the pH near a steel surface with a hemispherical shape was investigated in simulated soils. The pH-value at the steel surface was measured with sensors previously described.[3] All experiments were performed in quartz sand. To determine the relation between applied potential and local pH, a probe was used consisting of a platinum wire. The probe's geometry was based on a hemisphere with 1 cm diameter that was subjected to a galvanostatic current (Figure 1). The pH and spread resistance were measured over time until steady state was achieved.

©2017 by NACE International.
Requests for permission to publish this manuscript in any form, in part or in whole, must be in writing to
NACE International, Publications Division, 15835 Park Ten Place, Houston, Texas 77084.
The material presented and the views expressed in this paper are solely those of the author(s) and are not necessarily endorsed by the Association.

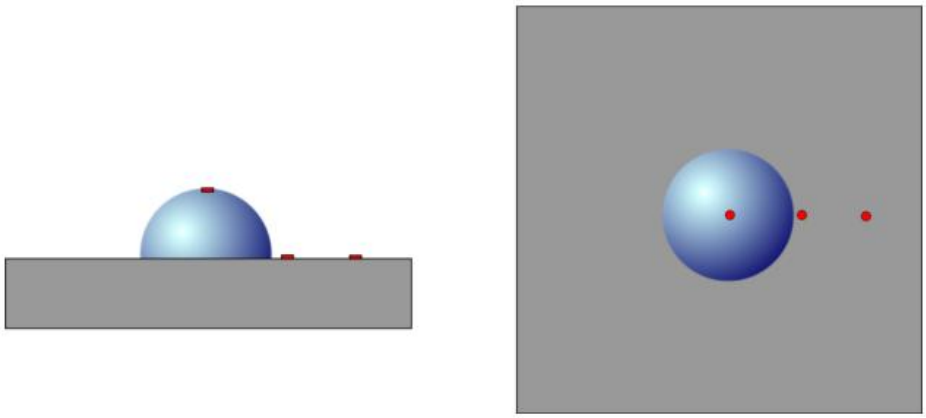

Figure 1: Experimental set-up for measuring the spread resistance and pH as a function of soil condition and current density over time. A steel hemisphere was used as cathode. The locations of pH-sensors are schematically indicated by red dots.

2. Abiotic corrosion and Microbiologically Influenced Corrosion (MIC) in groundwater (laboratory experiments)

To study abiotic corrosion and Microbiologically Influenced Corrosion, a setup was used consisting of and ER probe exposed to groundwater (Figure 2). The ER probes used in these experiments were obtained from Metricorr. These sensors consist of a steel surface which can be exposed to a chosen environment, and a reference steel surface which is not exposed. By measuring electrical resistance the thickness of the steel can be determined over time. Electrical parameters such as DC and AC currents and potentials were measured with a Metricorr† logger.

A biofilm of MIC-causing sulphate-reducing microorganisms was grown on the steel surface of an ER probe placed in an anaerobic reactor. For this purpose, a flow of groundwater containing sulphate reducing microorganisms was pumped along the steel surface of the ER probe. Growth of a MIC biofilm was initiated by adding 5 mM Na_2SO_4 to the groundwater reservoir and intermittent doses of 12 mM sodium-D,L-lactate to the reactor. Formation of a MIC biofilm representative of those present in the field is ensured by using groundwater from a location in the North of the Netherlands, where MIC on underground pipelines was reported to occur frequently. Details on the experimental approach and setup were described before.[4]

† Trade Name

©2017 by NACE International.
Requests for permission to publish this manuscript in any form, in part or in whole, must be in writing to
NACE International, Publications Division, 15835 Park Ten Place, Houston, Texas 77084.
The material presented and the views expressed in this paper are solely those of the author(s) and are not necessarily endorsed by the Association.

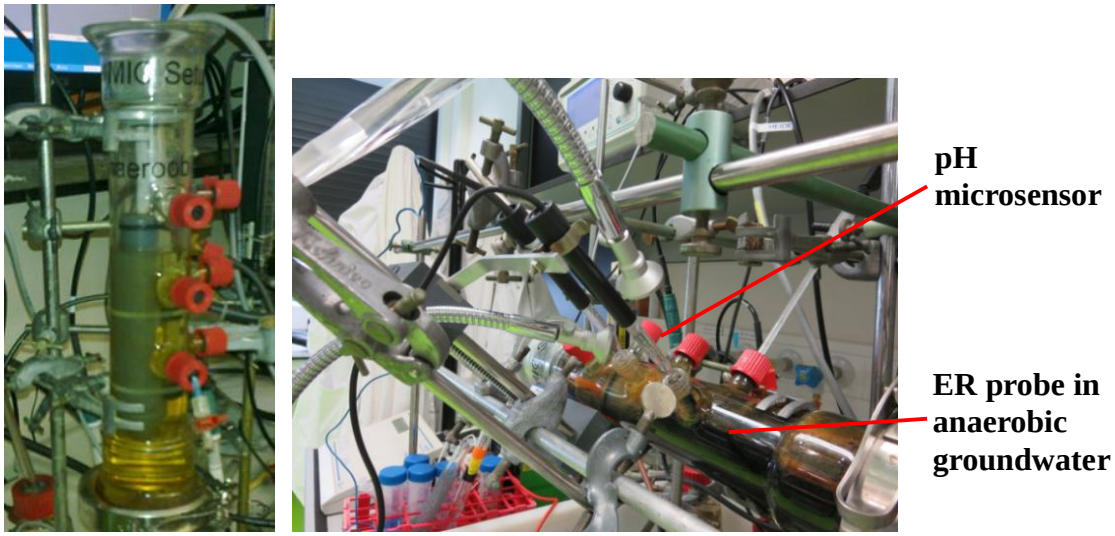

Figure 2: Left: ER probe in anaerobic reactor containing groundwater; right: close-up of setup for measurement for gradients using microsensors.

With the ER-probe, corrosion rates were measured under various chosen CP values and groundwater conditions, in combination with measurement of electrical DC and AC parameters. In all experiments with CP, the applied potential (imposed voltage) was adjusted with a potentiostat. The corrosion potential on the steel surface of the probe (EDC) was measured with respect to an Ag/AgCl reference electrode. Small scale gradients of pH and redox potential in the biofilm at the steel surface were measured using mini-pH sensors or microsensors mounted in a micromanipulator.

Microsensor measurements

Microsensors were used to measure gradients of pH and redox potential in a MIC biofilm on a micrometer scale, and to determine the effect of CP and groundwater flow on these profiles. For these measurements, either a mini pH sensor was used, or microsensors. The minisensors were from the type WTW SenTix MIC D. The microsensors were obtained from Unisense[†]. The microsensors for redox potential and pH had a tip size of 25 µm.

3. Microbiologically Influenced Corrosion (MIC) in groundwater (field experiments)

Field experiments were performed at a location in the north of the Netherlands. This location was chosen because it is located in an area where external MIC has been discovered on several spots on underground pipelines. The soil parameters of this area are largely determined by the presence of peat. The top layer of a few decimeters consists of humus rich soil and, largely excavated, peat. Underneath is yellow sand. The groundwater level ranges throughout the year from 0,5 to 1,3 meters below ground level.

On the field site 25 groundwater monitoring wells were installed. These consisted of PVC tubes with an external diameter of Ø75 mm and had depths ranging from 1.6 to 3.2 meters below surface level. The deepest of the PVC tubes was provided with a well screen consisting of vertical slits (20 cm x 0.5 mm) to allow the groundwater to flow from the relevant depth into the well. A filter wick was covering the slotted part of the tube. Thus, by inserting the ER (bio)probes in the monitoring wells, it was possible to carry out measurements in the groundwater at a controlled depth and location.

[†]Trade Name

©2017 by NACE International.
Requests for permission to publish this manuscript in any form, in part or in whole, must be in writing to
NACE International, Publications Division, 15835 Park Ten Place, Houston, Texas 77084.
The material presented and the views expressed in this paper are solely those of the author(s) and are not necessarily endorsed by the Association.

The effect of cathodic protection (CP) on (microbiological) corrosion on the ER probes was studied with the set-up depicted in Figure 3. With a rectifier (Delta ES030-5) a cathodic protection potential was applied between the probe and its environment. A steel anode was located in a nearby ditch. The applied CP potential was measured with an Ag/AgCl reference electrode which was located in the monitoring well adjacent to the probe. A Metricorr logger measured the thickness of the probe, electric potential with respect to the reference cell and current density (DC and AC). Details on the field setup and experimental approach were described before.[4]

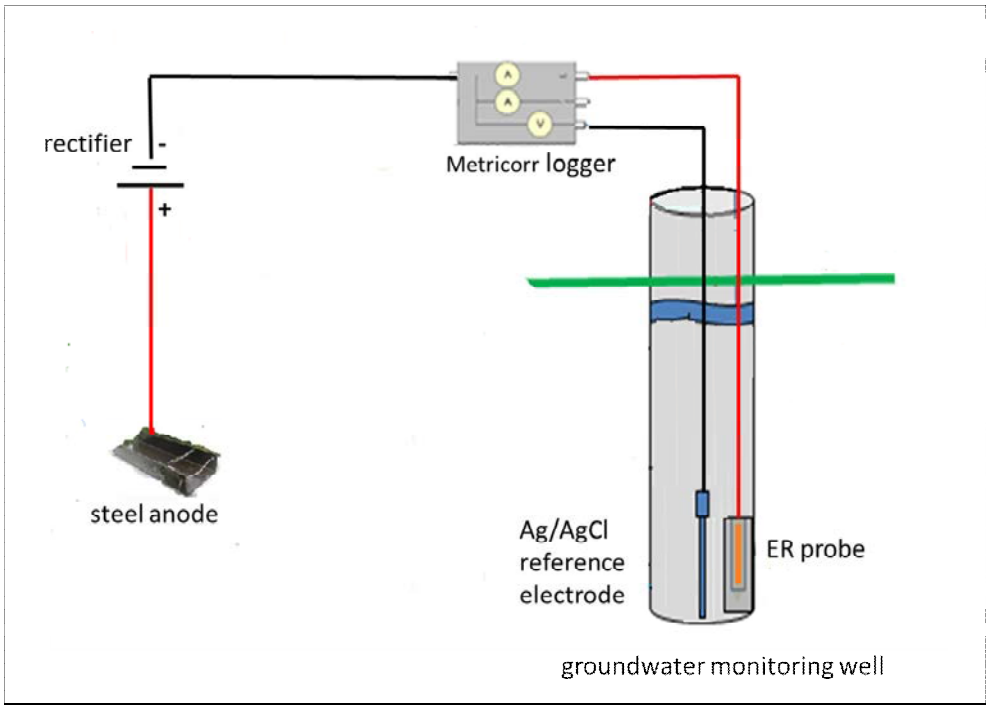

Figure 3: Experimental set-up to measure interaction between CP and corrosion in the field.

RESULTS

1. Effects of pH and cathodic protection in well-defined abiotic laboratory media

The results of the measurements of the pH distribution in synthetic soil are shown in Figure 4. After applying the current the pH reached a steady state value within a few hours. After one week, the pH gradient reached several centimeters into soil. At the steel surface the pH-value was in the range of 12.5 or above for current densities of 1 A/m^2 or 10 A/m^2, respectively. Corresponding values of the pH are typical for steel in concrete and are associated with the formation of a stable passive film on the steel surface. This finding is in line with calcareous deposits that are commonly found at coating defects. These deposits often have diameters in the range of several tens of centimeters. Since their formation is controlled by the increase of the pH and the precipitation of calcium carbonate they can be considered as a qualitative measure of the dimension of the increased pH and its extent into the surrounding soil.

©2017 by NACE International.
Requests for permission to publish this manuscript in any form, in part or in whole, must be in writing to
NACE International, Publications Division, 15835 Park Ten Place, Houston, Texas 77084.
The material presented and the views expressed in this paper are solely those of the author(s) and are not necessarily endorsed by the Association.

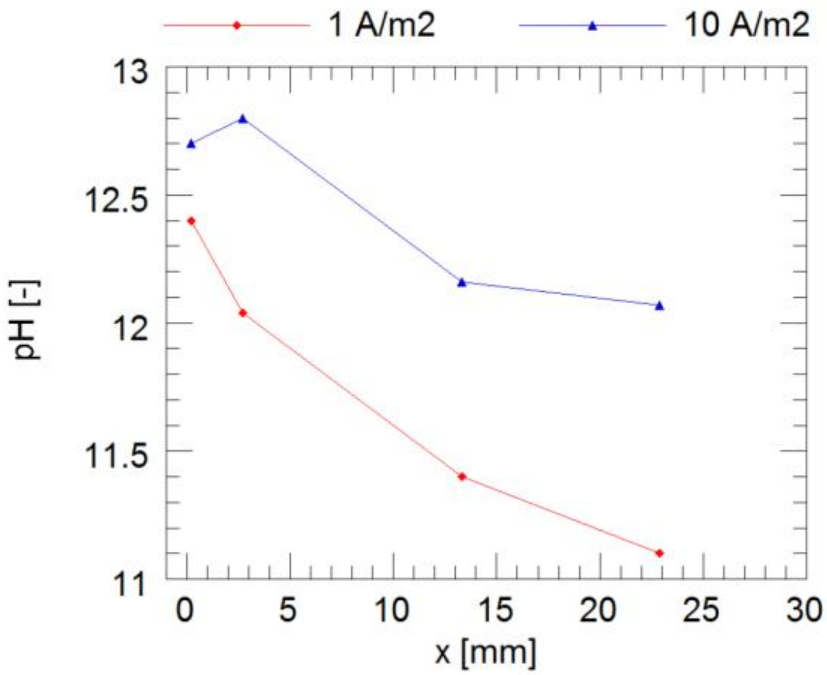

Figure 4: Distribution of the pH into soil after one week of cathodic protection.

2. Cathodic protection, pH and corrosion in groundwater (laboratory experiments)

Effects of CP on abiotic corrosion

Cathodic protection is reported to have a large effect on pH gradients.[5,6] We measured the effect of cathodic protection on pH at the steel surface of ER probes using a pH mini-electrode. The results can be found in Figure 5. A clear effect of imposed voltage on the pH can be seen: with a more negative CP potential, the pH strongly increases (up to pH 14 at -2000 mV). This effect is in accordance with the effects reported in literature.[5,6]

To rule out the potential disturbance of the signal by direct electrical contact between steel surface and pH sensor, the pH minisensor was positioned at a slight distance from the steel surface. The pH value hardly changed by this, indicating that the curves reflect actual pH values. Another test confirming this conclusion was performed by applying the pH indicator phenolphtalein in the medium. This indicator showed a pink colour upon CP. Phenolphtalein is colourless at neutral pH and turns purple in the pH range from 8 to 12, and turns colourless above pH 13. The indicator showed a pink colour upon applying CP. This gives further proof for the pH effects reported in Figure 5. It is also remarkable that the indicator mainly turns pink at the edges of the steel surface, whereas no colour is visible at the centre of the steel surface. This indicates that the pH at the center of the steel surface is higher than 13, which is in line with the measurements in Figure 5.

©2017 by NACE International.
Requests for permission to publish this manuscript in any form, in part or in whole, must be in writing to
NACE International, Publications Division, 15835 Park Ten Place, Houston, Texas 77084.
The material presented and the views expressed in this paper are solely those of the author(s) and are not necessarily endorsed by the Association.

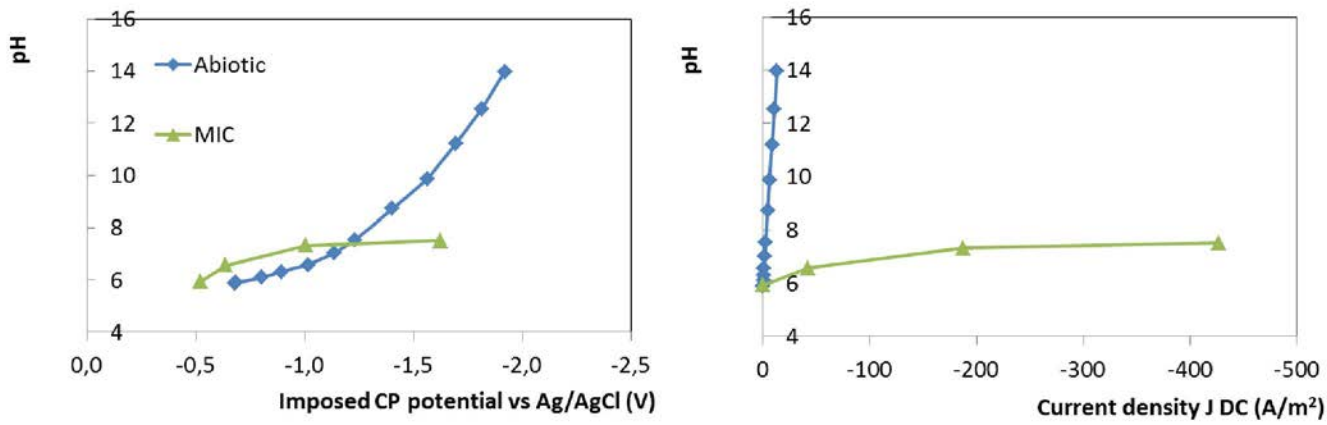

Figure 5: pH upon application of various levels of CP versus applied potential (versus Ag/AgCl) (left) and current density J DC (right) of abiotic ER probe (blue) and MIC ER probe (green).

Effects of CP on Microbiologically Influenced Corrosion (MIC)

The effect of the applied potential of Cathodic Protection (CP) on the MIC rates is presented for two cases (Figure 6 and 7).

In Figure 6, the relative MIC rate is presented compared to the maximally measured MIC rate for this MIC ER probe (in %) as a function of applied CP potential. For this MIC biofilm, the MIC rate gradually decreases with increasing CP potential.

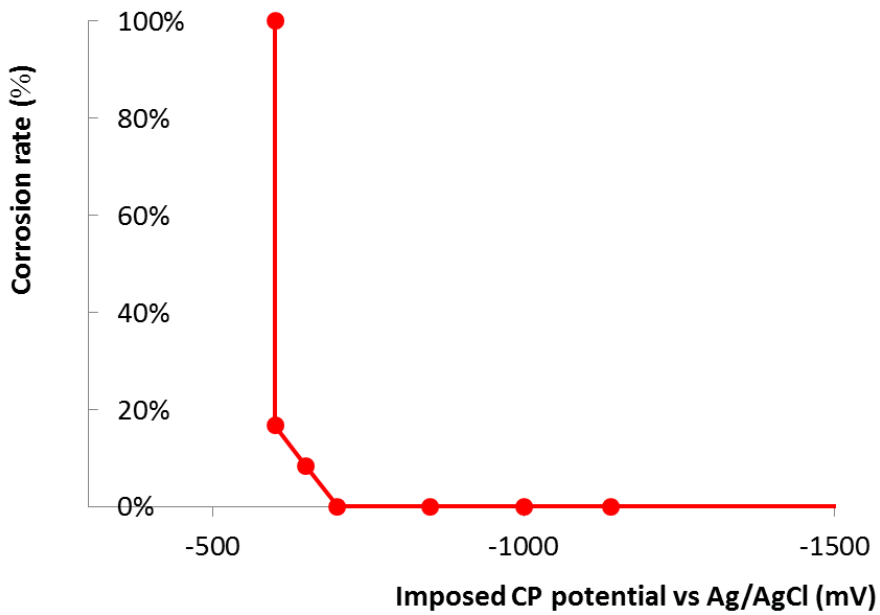

Figure 6: Effect of imposed CP potential on corrosion rate measures using an MIC ER probe, expressed as % compared to the maximal corrosion rate.

For another biofilm however, a different situation was observed (Figure 7). First, the MIC could be stopped completely. However at a later moment, MIC could not be stopped, even at CP potentials as high as -1000 mV vs. Ag/AgCl.

©2017 by NACE International.
Requests for permission to publish this manuscript in any form, in part or in whole, must be in writing to
NACE International, Publications Division, 15835 Park Ten Place, Houston, Texas 77084.
The material presented and the views expressed in this paper are solely those of the author(s) and are not necessarily endorsed by the Association.

The local pH was measured in the biofilms that could not be stopped corroding by CP (Figure 5). In comparison to abiotic corrosion, a striking difference is visible. Inside the MIC biofilm the pH remained below 7.5, in spite of increasing the CP potential to -1700 mV (Figure 5). Another important observation was that the presence of a biofilm, the current densities are 40 to 100 times higher than current densities in the absence of MIC.

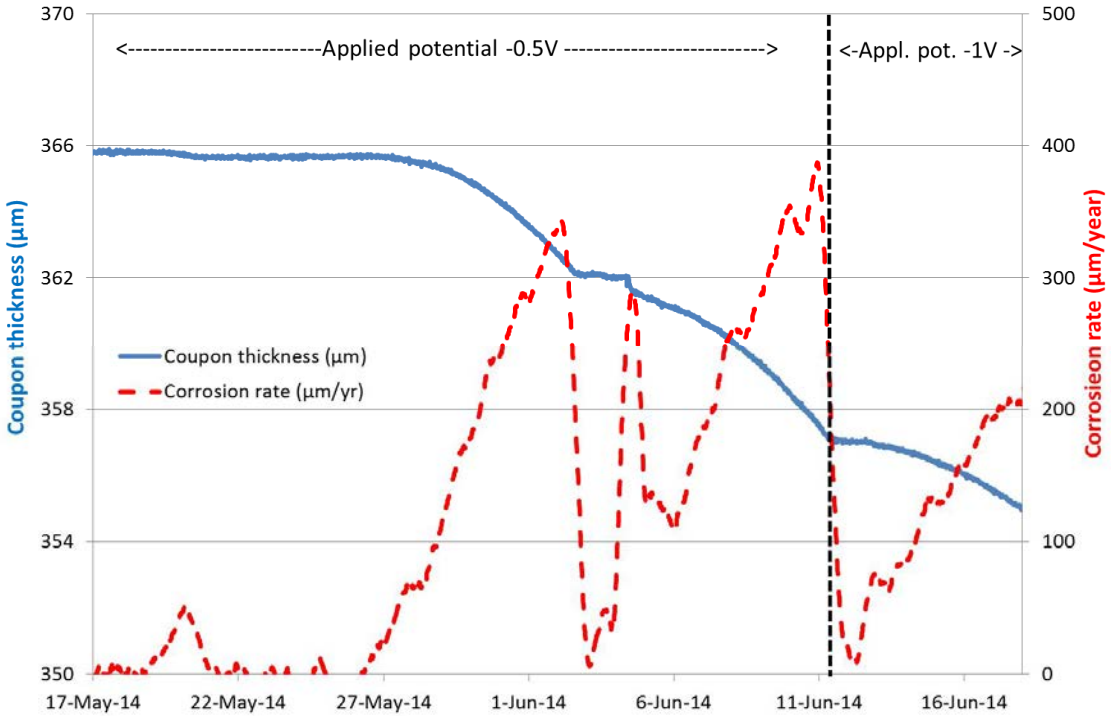

Figure 7: Coupon thickness and corrosion rate measured with fast corroding MIC ER probe.

©2017 by NACE International.
Requests for permission to publish this manuscript in any form, in part or in whole, must be in writing to
NACE International, Publications Division, 15835 Park Ten Place, Houston, Texas 77084.
The material presented and the views expressed in this paper are solely those of the author(s) and are not necessarily endorsed by the Association.

3. Field experiments

To test the effectiveness of CP in the field, ER bioprobes preloaded with a MIC biofilm in the laboratory were transferred to the field and, after an adaptation time, exposed to a series of CP potentials (Figure 8).

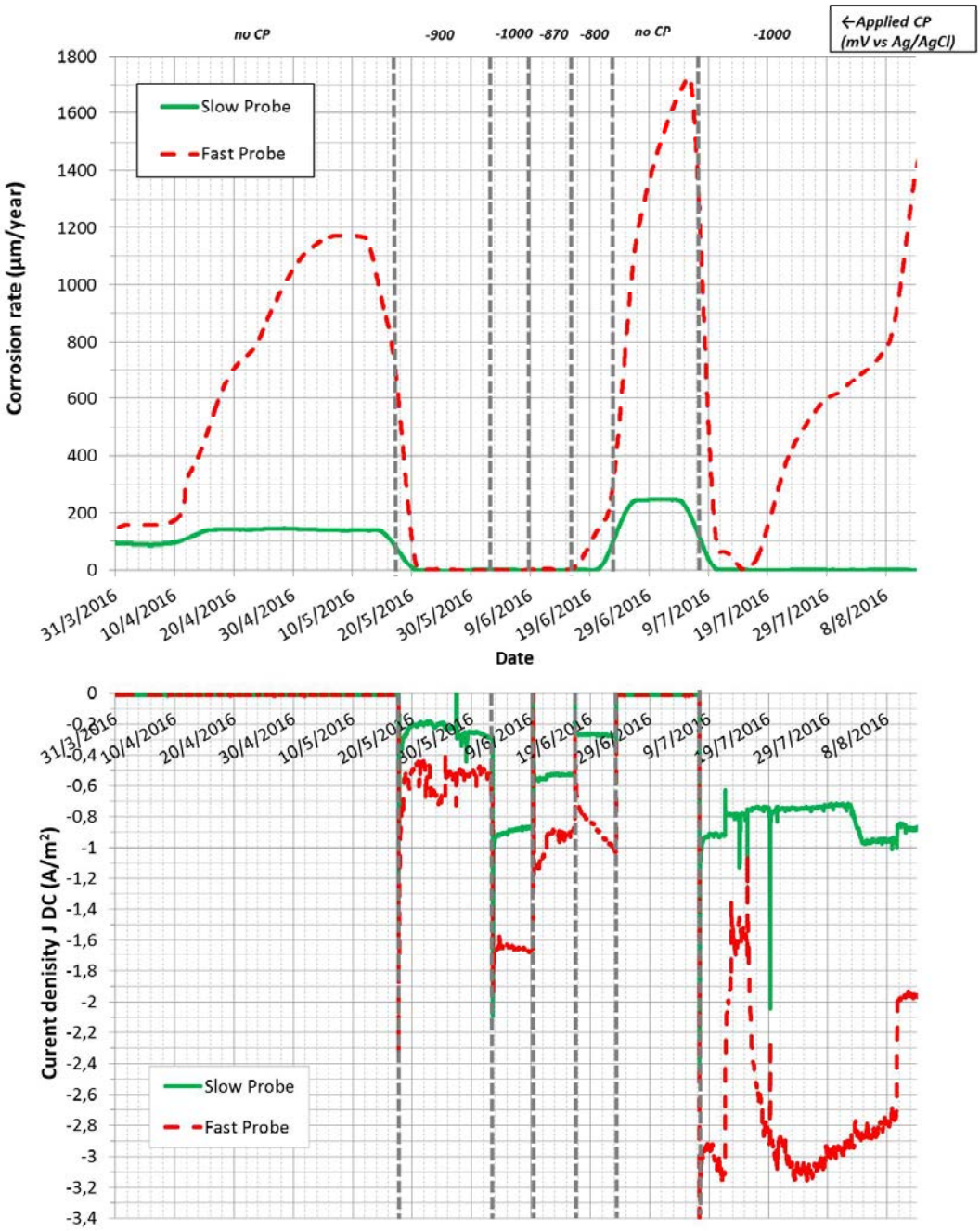

Figure 8: Corrosion rate (top) and current density (bottom) measured for MIC bioprobes in the field over time. Applied CP potentials (vs. Ag/AgCl) indicated at the top of the figure.

On two probes with different grades of microbiological corrosion, different levels of CP were applied, in two series over time. In between the series, no CP was applied. In the first CP series, for both probes the MIC could be stopped completely. The stronger corroding probe needed higher applied values to stop MIC completely (-1000 mV versus -870 mV vs Ag/AgCl). Remarkable is that for both probes,

©2017 by NACE International.
Requests for permission to publish this manuscript in any form, in part or in whole, must be in writing to
NACE International, Publications Division, 15835 Park Ten Place, Houston, Texas 77084.
The material presented and the views expressed in this paper are solely those of the author(s) and are not necessarily endorsed by the Association.

corrosion rates increased after the application of CP, indicating that despite the fact that corrosion stops during the application of CP, the biofilm is becoming more active. In the second CP series, MIC could not be stopped on the fastest corroding probe (red line in Figure 8), even at CP potentials as high as -1000 mV vs. Ag/AgCl. The slower corroding probe (green line), immediately stopped corroding at this applied CP potential. For the faster corroding probe which cannot be stopped with CP, the current densities were about two times higher than those for the slow corroding probe (Figure 8).

CONCLUSIONS

Cathodic Protection (CP) appears to work at least partly via a pH mechanism. In the absence of microorganisms, a clear elevation of the pH near the steel surface is observed. In the presence of MIC, three interesting phenomena were observed:

- MIC can in some cases not be stopped by CP, even in case of very negative applied potentials;
- Within a MIC biofilm, the increase of pH upon CP can be significantly less than in the absence of a MIC biofilm;
- In the presence of a MIC biofilm the DC current upon CP is much higher than in the absence of a biofilm (40-100x).

The exact mechanisms determining this pH-control inside the biofilm remain to be resolved. Some hypotheses are:
1. The microorganisms are able to couple sulphate-reduction to the oxidation of hydrogen (H_2) to protons (H^+). By doing so, the protons taken up from the groundwater to form H_2 at the steel surface exposed to CP are recycled, and thus a potential pH increase is counteracted (Figure 9);
2. The biofilm has a strong chemical pH-buffering capacity, for example related to the presence of iron-sulphide and siderite precipitates, and organic molecules.

One of the most important findings is the suggestion that CP can feed MIC microorganisms at the steel surface by providing them with energy via electrons and/or hydrogen. There are strong indications that, once certain biofilms have established, it is very hard or even impossible to stop them with CP, irrespective of the potential applied. Instead of stopping an already established biofilm, CP strategies should therefore be aimed at preventing MIC biofilms to develop from the start.

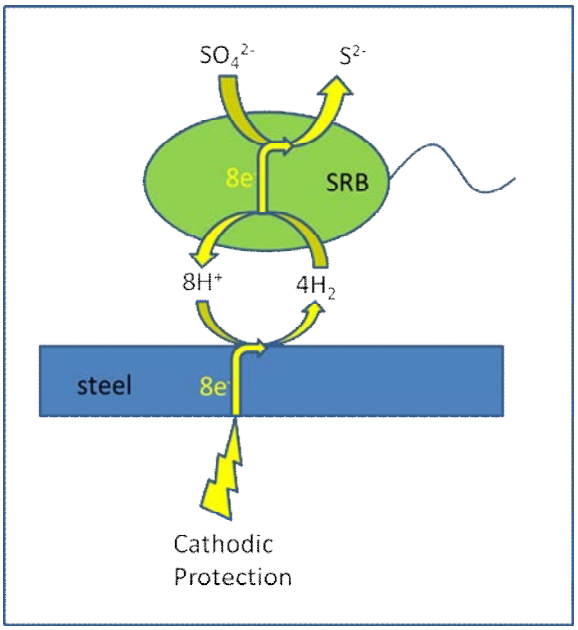

Figure 9: Schematic depiction of potential mechanism of electron coupling of MIC at the steel surface.

©2017 by NACE International.
Requests for permission to publish this manuscript in any form, in part or in whole, must be in writing to
NACE International, Publications Division, 15835 Park Ten Place, Houston, Texas 77084.
The material presented and the views expressed in this paper are solely those of the author(s) and are not necessarily endorsed by the Association.

ACKNOWLEDGEMENTS

We thank Andre Cinjée, Berthil Slim and David Joos for practical assistance.

REFERENCES

1. R. Javaherdashti, "*Microbiologically Influenced Corrosion; An engineering insight*," 2nd ed. (Switzerland: Springer, 2017), p. 171.

2. M. Büchler, "A new perspective on cathodic protection criteria promotes discussion," *Material Performance* 54, 1 (2015): p. 44.

3. M. Büchler, H.-G. Schöneich, "Investigation of Alternating Current Corrosion of Cathodically Protected Pipelines: Development of a Detection Method, Mitigation Measures, and a Model for the Mechanism", *Corrosion* 65 (2009): p. 578.

4. S. Jansen, M. van Burgel, B. Slim, J. Geritse, "Effects of environmental conditions on external Microbiologically Influenced Corrosion (MIC) of underground pipelines: a laboratory and field study using Electrical Resistance (ER) bioprobes," In: T.L. Skovhus, D. Enning, J.S. Lee, "*Microbiologically Influenced Corrosion in the Upstream Oil and Gas Industry*", (New York, USA: CRC Press, 2017), p. 413-434.

5. K. Miyanaga, R. Terashi, H. Kawai, H. Unno, Y. Tanji, "Biocidal effect of cathodic protection on bacterial viability in biofilm attached to carbon steel," *Biotechnology and Bioengineering* 97 (2007): p. 850.

6. N.G. Thompson, T.J. Barlo, "Fundamental Process of Cathodically Protecting Steel Pipelines," *International Gas Research Conference* (1983) p. 274.

©2017 by NACE International.
Requests for permission to publish this manuscript in any form, in part or in whole, must be in writing to
NACE International, Publications Division, 15835 Park Ten Place, Houston, Texas 77084.
The material presented and the views expressed in this paper are solely those of the author(s) and are not necessarily endorsed by the Association.

View publication stats

Ex. II - 35

ASM Handbook, Volume 13C: Corrosion: Environments and Industries
S.D. Cramer, B.S. Covino, Jr., editors, p97-106
DOI: 10.1361/asmhba0004114

Copyright © 2006 ASM International ®
All rights reserved.
www.asminternational.org

Well Casing External Corrosion and Cathodic Protection

W. Brian Holtsbaum, CC Technologies Canada Ltd.

THE PORTION OF THE WELL OF CONCERN is that portion of the casing in contact with the formation either directly or through a cement barrier. It must be noted that where multiple casing strings are used, only that portion of each casing string in contact with the formation applies to this discussion.

Well Casing Corrosion

The corrosion mechanism will vary depending on the depth and the conditions at various parts of the casing. Gordon et al. (Ref 1) reported corrosion on well casings above a depth of 60 m (200 ft) that was due to oxygen enhanced by chlorides and sulfates in the soil while below that depth corrosion was caused by carbon-dioxide-rich formation water. These conclusions were based on scale analyses, sidewall core analyses, and soil analyses. In addition to these mechanisms, galvanic corrosion (especially if the casing is connected to surface facilities), anaerobic bacteria supported by drilling mud, and stray-current electrolysis are other possible causes of corrosion (Ref 2). Cementing the casing in place helps reduce the corrosion rate but does not eliminate it (Ref 3).

The procedure for predicting the probability and/or rate of corrosion is given in NACE RP0186 (Ref 4) and can be summarized:

1. Study the corrosion history of the well or other wells in the area (Ref 5).
2. Study the downhole environment, including the resistivity logs, different strata, drilling mud, and cement zones.
3. Inspect any casing that has been pulled (Ref 1).
4. Review the results of pressure tests.
5. Review the results of downhole wall thickness tests (Ref 1).
6. Review the results of casing potential profiles (CPP).
7. Review the oil/gas/water well maintenance records.

In a given area, after the first leak has occurred, the subsequent accumulated number of casing leaks often follows a straight-line relationship with time when presented on a semilog plot, that is, the log of the leaks versus time (Ref 5–7). This in effect means that the leak rate is increasing tenfold over equal periods of time. Repairs to the casing will alter this relationship as a repair often replaces several potential leaks; however, the leak rate will not be reduced to a tolerable level until cathodic protection is applied.

As part of many drilling programs it is common practice to pump cement into the annular space between the well borehole and the casing, usually to a point above the producing formation (sometimes from surface to producing formation depth and other times only portions of the casing strings are cemented) to achieve a seal. The cement in newer wells is often brought to the surface. However, in older wells, the cement was only sufficient to achieve a seal from the oil- and/or gas-bearing formation and therefore was brought from the bottom to a specific point along the casing. It should be noted that sections of casing pressed into the formation before cement injection will not necessarily have a cover of cement, or at the most, a very thin layer that is inadequate for corrosion control. Furthermore sections of casing not in the cement will continue to be exposed to the remains of the drilling mud.

The formation of corrosion cells can be:

- Local or pitting
- Between the cement and noncement sections of casing
- Between differential temperature zones
- Between brine formations and relatively inert rock
- Between the well casing and the surface facilities if there is a metallic connection

In addition, corrosive gases from a formation, such as carbon dioxide (CO_2) and hydrogen sulfide (H_2S) in an aqueous environment, can cause more aggressive attack.

Direct-current (dc) stray-current interference is another possible source of external corrosion. These may come from other cathodic protection systems, surface welding, or dc operated equipment. Alternating-current (ac) stray current in high current densities can also be a source of corrosion (Ref 8). Stray current accelerates corrosion on the casing if it discharges into the formation when returning to its source.

Detection of Corrosion

The two principal methods for detecting well casing corrosion include metal-loss (corrosion-monitoring) tools and casing current measurement. Both are described in this section.

Metal-Loss Tools

Casing monitoring tools for corrosion consist of three basic types: mechanical tools, electromagnetic tools, and ultrasonic tools (Ref 9).

The mechanical caliper tool is the oldest method where many "fingers" are spaced around a tool mandrel. When the tool is pulled past an anomaly, these fingers either extend into a defect or are pushed in by scale, a dent, or a buckle in the casing.

Electromagnetic tools consist of:

- High-resolution magnetic flux leakage and eddy-current devices
- An "electromagnetic thickness, caliper, and properties measurement" device

The source of magnetic flux comes from the electromagnet (or permanent magnet) in the tool. As the tool moves along the casing, the magnetic flux through the casing wall is constant until it is distorted by a change in the pipe wall thickness. The flux leakage induces current in sensing coils that is related to the penetration of the defect in the casing wall. A uniform thinning of the casing wall may be detected only as a defect at the beginning and end as there may be little change in flux leakage in between. Strictly, a magnetic flux tool cannot discriminate between a defect in the inside or the outside of the casing.

However, by adding a high-frequency eddy current that can be generated in the same tool, which induces a circulating current through the inner skin of the casing wall, discrimination

between internal and external defects can be achieved. Sensing coils on the tool then detect the high-frequency field. A metal flaw or loss in the inside of the casing impedes the formation of circulating currents, and the change in this current is a measure of the surface quality and approximate vertical height of the defect. By comparing the defects from the electromagnetic to those obtained from the eddy-current signals in the tool, the external defects can be defined by a process of elimination.

The ultrasonic tool has transducers around the tool that act as both transmitters and receivers of an acoustic signal. The reflected signal is then analyzed for casing thickness, internal diameter, casing wall roughness, and defects. In addition, a cement evaluation can be included.

Tool Limitations. Since each tool has limitations, it may be necessary to run more than one tool depending on the type of flaw expected. In spite of the limitations, these tools can provide a reasonably accurate assessment of the casing metal loss; unfortunately, they can only detect corrosion damage after it has occurred.

Casing Current Measurement

According to Faraday's law (Eq 1), the metal loss due to corrosion is proportional to the dc current and the length of time that it leaves the metal and enters the electrolyte:

$$W = \frac{MtI}{nF} \qquad \text{(Eq 1)}$$

where W is weight loss in grams (g); M is the atomic weight in grams (g); t is the time in seconds (s); I is the current in amperes (A); n is the number of electrons transferred per atom of metal consumed in the corrosion reaction; and F is Faraday's constant (96,500 coulombs per gram equivalent weight).

For steel, this equates to a metal loss of 9.1 kg/A-yr (20.1 lb/A-yr). If the current can be measured then the metal loss, as a measure of weight, for a given period of time can be calculated.

An axial current at any point in the casing can be calculated from Ohm's law (Eq 2) by measuring a voltage (microvolt, μV) drop across a known length of casing resistance:

$$I_p = \frac{V_2}{R_p} \qquad \text{(Eq 2)}$$

where I_p is the axial current in casing (μA); V_2 is the axial voltage drop between two contact points along the casing pipe (μV); and R_p is the casing pipe wall resistance between the two contact points (Ω).

This voltage measurement is commonly called a casing potential profile (CPP), but the intent is to assess the axial and radial current profile in the casing. By determining an axial current value and direction between consecutive points in the casing, a radial current pickup or discharge can then be predicted in accordance with Kirchoff's current law, which states "the sum of the current at any junction must equal zero." Figure 1 illustrates three possible current measurement scenarios (A, B, and C); in all cases, the junction in Kirchoff's current law is at the center of each scenario.

The anodic or corroding sections of a casing are at the sections of current discharge, while the current pickup areas are cathodic and are not corroding. Scenario A of Fig. 1 shows the axial current increasing from 1.5 to 2.0 A; therefore, there must have been a 0.5 A pickup in between, indicating that this section is cathodic. The current of 2.0 A coming up the casing in scenario B is greater than the 1.5 A that continues up the casing; thus, 0.5 A must have discharged from the section in between the two points, causing this to be anodic or corroding. The current of 1.0 A that is coming downhole at the top of scenario C is in the reverse direction from the 1.5 A coming uphole; therefore, the current coming into the casing section from both ends must discharge from the pipe section somewhere in between. This section is therefore anodic and would be corroding.

By measuring the axial current at regular intervals along the casing, a complete current map along the casing can be obtained as shown in Fig. 2. Such a test is called a casing potential profile (CPP), and the plot in Fig. 2 is called an axial current profile. Both the amount and the direction of current have to be determined to predict a current pickup or discharge. An increasing slope coming uphole (equal to a negative change in depth per change in current going downhole) in Fig. 2 indicates a current pickup (cathodic section), while the reverse slope indicates a current discharge (anodic section). The amount of metal loss can be predicted for a given period of time on the assumption that the relative current will remain the same.

Determination of the amount of current pickup and discharge along the casing in Fig. 2 results in the radial current profile shown in Fig. 3. Referring to Fig. 2, the direction of net current flow at about "85% of depth" is in the downhole direction as it crosses the zero (0) current axis, while the current below that depth is coming uphole. This causes a current discharge centering

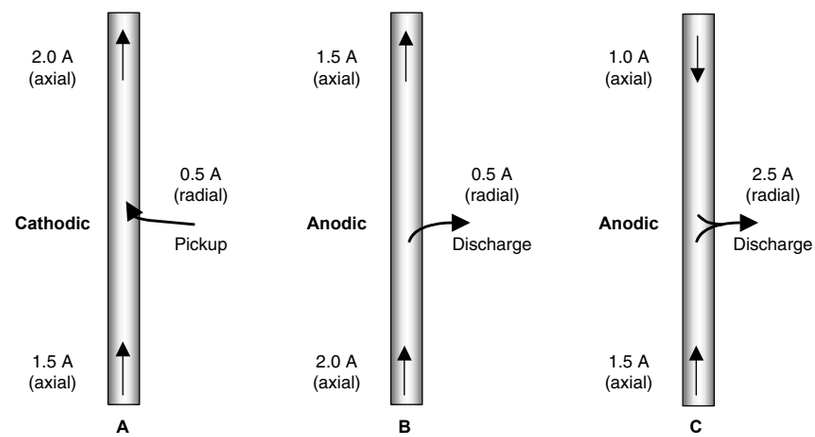

Fig. 1 Example of radial current pickup or discharge from axial current. Refer to the text for a discussion of scenarios A, B, and C.

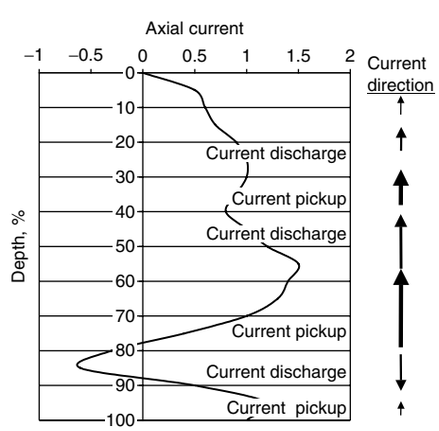

Fig. 2 Example of axial current profile in casing without cathodic protection

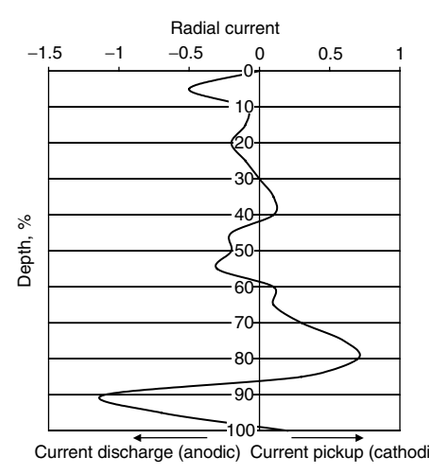

Fig. 3 Calculation of radial current profile from Fig. 2

at about 90% of depth as shown in Fig. 3. This is the same as scenario C in Fig. 1. In a similar fashion, the current at a depth between 0 and 25% and also 40 and 55% of depth is less than the current below, although in the same direction, which is the same as scenario B in Fig. 1. This also indicates a current discharge (anodic) area. The remainder of the casing in this example is picking up current and is cathodic, which fits the condition illustrated by scenario A in Fig. 1.

Limitations and Advantages of Casing Current Measurements. Casing current measurements, are only sensitive enough to measure long-line currents and do not detect local corrosion cells that exist between the spacing of the two contacts.

The advantage of this test is that macrocorrosion can be predicted before it occurs. However, the assumption that the current magnitude and location will stay the same can create a large error. The existence of local corrosion pits will be missed, and these can represent a large amount of the corrosion taking place (Ref 9, 10).

Cathodic Protection of Well Casings

At one time there was a concern that cathodic protection current applied at the surface would not reach the bottom of deeper well casings. Blount and Bolmer (Ref 11) conducted polarization tests with a reference electrode located at the top and the bottom of well casings and concluded that cathodic protection is feasible to a depth of at least 1000 m (3300 ft). Subsequent tests have shown that it is feasible to depths up to at least 3960 m (13,000 ft).

Two methods of determining the amount of cathodic protection current required are described in this section: a casing polarization (E log I) test and a CPP test. The first test attempts to predict when the casing becomes a polarized electrode, while the second test confirms if an adequate amount of cathodic protection current is being discharged from the anode bed(s) to ensure current is being picked up along the length of the casing being tested.

E log I Test (Tafel Potential)

The E log I test is a measurement of the polarized casing-to-soil (electrolyte) potential (E) compared to the logarithm of different increments of applied current (I). The casing-to-soil potential is measured with respect to a remote reference electrode, often a copper/copper-sulfate reference electrode (CSE). "Remote" in this case is a point where the electrical voltage gradient is zero. Polarization is considered to take place at the intersection of the two straight lines as shown at point "A" in Fig. 4. At the intersection of the upper straight line (point "B"), the curve becomes a hydrogen overvoltage curve and obeys the Tafel equation.

In the early years, the point where the two straight lines intersected (Fig. 4, point A) was taken as the current required for the protection of the well casing. This not only gave widely varying results depending on the relative slope of the two lines, but also provided current requirements that were found to be too low to protect the casings. The laboratory and field research of Blount and Bolmer (Ref 11) confirmed that the intersection of the upper portion of the Tafel slope with the curve was the point of corrosion control and proved to yield more consistent results (Fig. 4, point B). This point is normally used to establish a cathodic protection criterion for the casing.

A schematic of a typical E log I test is shown in Fig. 5. The test is conducted by impressing an increment of current for period of time and then measuring the "instant off" potential when the applied current is briefly interrupted. This process is repeated at increasing increments of current to a point beyond where the Tafel break in a plot between the instant off potential (E) and the logarithm of the current (log I) occurs (point B in Fig. 4). There has been extensive experimentation both in the laboratory and the field (Ref 11–13) comparing the current increments and the length of time at each increment to allow polarization to occur. The conclusion was that the best results occur when the increments of current and the time intervals between current increases are constant. A sufficient time interval must be established that ensures polarization will be complete before proceeding to the next current value. Although the current increment and time needs to be established for each E log I test, current increments of 0.5 A and time intervals of 10 min is often a practical combination. The time interval has been reduced to 5 min under certain circumstances where the well polarizes more quickly. It must be noted that too short of time intervals can yield an inaccurate higher current requirement as polarization may not be complete at given current values before the test current is increased incrementally.

Equipment (Fig. 6) can be set to automatically interrupt the current and record casing-to-electrolyte potentials continuously during the current interruption. In this way, the existence of a "spike" can be seen and the appropriate instant off casing-to-soil potential selected for each current interval. Furthermore, the current output

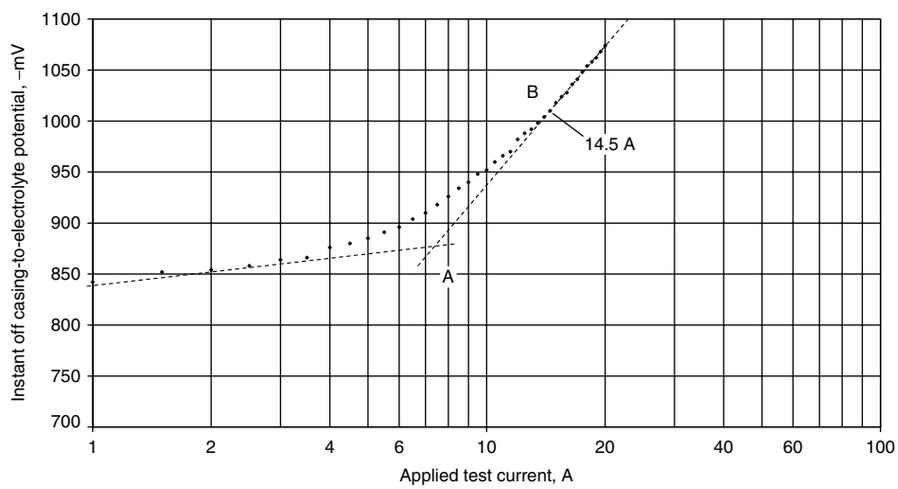

Fig. 4 An example of an E log I plot. Refer to text for a discussion of points A and B.

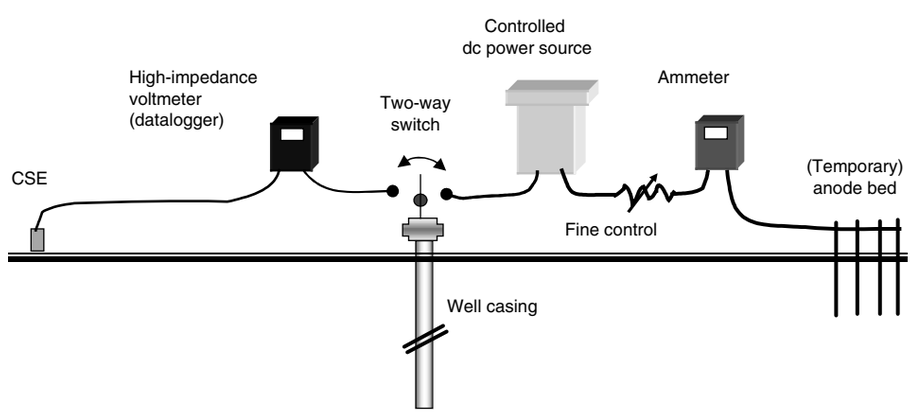

Fig. 5 Basic E log I test. CSE, copper/copper-sulfate reference electrode; dc, direct current.

can be controlled using silicon-controlled rectifiers (SCRs) to ensure that it remains constant during the test interval and that the desired fine incremental output control can be achieved.

Often a premature ending of the test occurs because the *E* log *I* profile was interpreted incorrectly as having straightened out. This variance is likely due to reactions that are taking place at different times or at different points as the test proceeds. To protect against stopping the test prematurely, a linear plot of *E* versus *I* should be made as the test proceeds to ensure that the test has left a straight-line relationship indicating that polarization is occurring. Often there is an early straight-line segment or the profile starts to leave the linear straight-line relationship only to return to the same slope. These early deviations are false indications as shown by the data from Fig. 4 plotted on a linear profile in Fig. 7. The Tafel break of interest in the *E* log *I* plot is beyond that determined by the linear plot (12.5 A) and becomes the criterion for protection for that well casing, as shown by point B in Fig. 4.

Subsequent *E* log *I* analysis by this method has compared favorably to the current requirement determined by CPP test results provided that the break (Fig. 4, point B) was selected after the straight-line relationship has ended on a linear plot. When this method is not used, an erroneous analysis of the *E* log *I* test can be expected (Ref 14).

Advantages and Limitations. An advantage of the *E* log *I* test is that it can be performed while the well is still in production. However, the casing still should be electrically isolated from all other structures for this test, or at least one must be able to measure the portion of the test current returning from the casing by perhaps using a clamp-on ammeter that can either fit around the wellhead or individually around all of the lines, instrument tubing, and conduit that connects to the well.

One disadvantage of the *E* log *I* test is the concern as to whether the test "sees" the lower part of the casing.

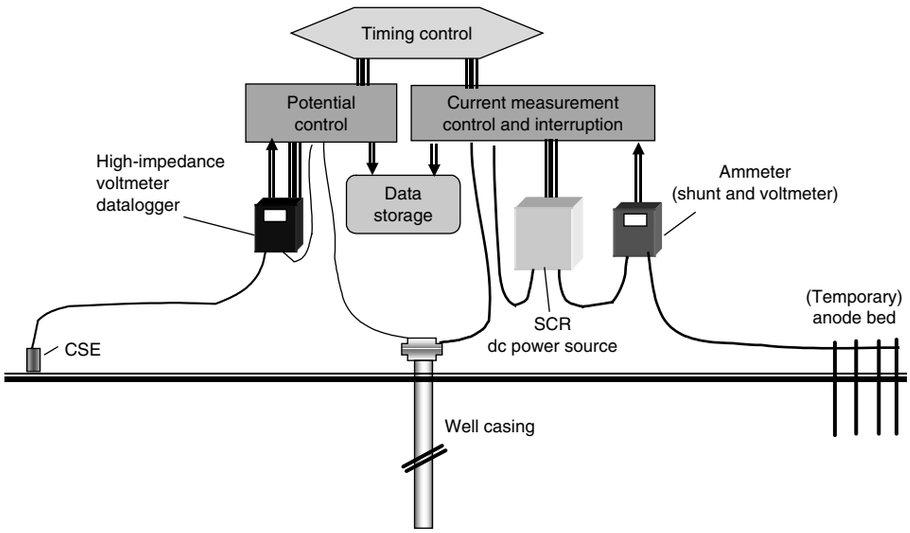

Fig. 6 Automatically controlled *E* log *I* test. CSE, copper/copper-sulfate reference electrode; dc, direct current; SCR, silicon-controlled rectifier

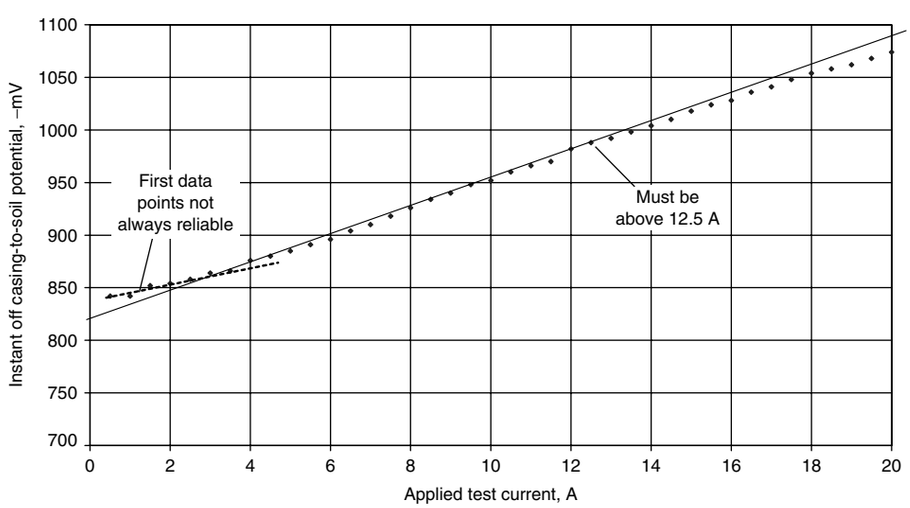

Fig. 7 Linear plot showing where the curve leaves a linear relationship. Tafel point on *E* log *I* must be at a higher current than the point that deviated from a linear straight line in this figure. Data generated from Fig. 4

Casing Potential Profile

The CPP test for cathodic protection is similar to that described previously for predicting corrosion from casing current measurements except that now a current pickup is desired at all locations similar to that illustrated in Fig. 1 (scenario A). The casing has to be electrically isolated from all surface structures and the service rig during this test, otherwise the current returning at the wellhead must be measured.

The original CPP tool had two contacts that were 3 m (10 ft) to 7.6 m (25 ft) apart. The tool was stopped at regular intervals for microvolt (μV) measurements. Davies and Sasaki (Ref 13) describe a newer CPP tool (the CPET corrosion-protection evaluation tool) that has four rows of knife contacts that are 0.6 m (2 ft) apart between rows (Fig. 8). Measurements taken between the different rows of contacts include the pipe resistance, a voltage drop (μV_2) between the inner 0.6 m (2 ft) contacts, and another voltage drop (μV_6) across the outer contacts 1.8 m (6 ft) apart.

Pipe (Casing) Resistance Determination. Using a conventional four-pin resistance test (the same test is often used in conjunction with a resistivity measurement), the instrument

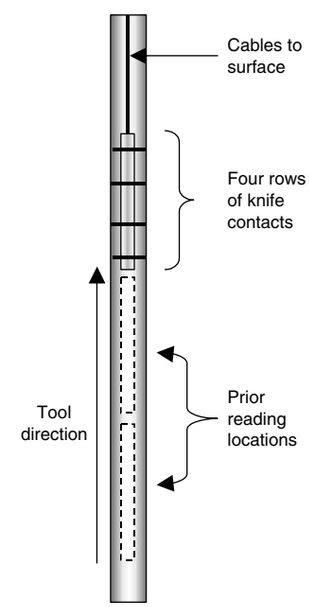

Fig. 8 CPET casing potential profile tool. CPET, corrosion protection evaluation tool

impresses a known current (I_{test}) between the outer contacts and measures the resulting voltage (V_2) across the inner 0.6 m (2 ft) contacts. This then allows the casing resistance between these 0.6 m (2 ft) contacts (R_2) to be calculated by using Ohm's law ($R_2 = V_2/I_{test}$).

Casing Axial Current Determination. Once the pipe resistance for the test point has been determined the axial current can then be calculated by $I_2 = V_2/R_2$. Identical measurements and calculations are made across all other sets of contacts and the results averaged. Normally, the results across the 0.6 m (2 ft) and 1.8 m (6 ft) rows are reported ($I_2 = V_2/R_2$ and $I_6 = V_6/R_6$). The radial current is then calculated between consecutive current measurements noting current direction.

It must be understood that the current in the casing when measured at any given point is the accumulation of all of the current pickup less any discharge on the casing below that point. Also the cathodic protection current direction has to be toward the top of the casing in order to return to the dc power source. Therefore, only when cathodic protection has been successfully applied does a plot of the axial casing current continually increase from the bottom to the top of the casing, thus indicating a continuous current pickup.

Figure 9 illustrates two cathodic protection trials with current applied. From the plots it can be seen that trial 1 did not eliminate all of the anodic areas. Thus, the applied current was increased until the anodic areas were eliminated as indicated by the axial current increasing continuously from the casing bottom to top, trial 2.

Trial 1 in Fig. 9 shows an axial current pickup at all but two sections. One current discharge is at approximately 55% of depth and the other at approximately 85% of depth; both of which are identified by "downward" slopes on the profile. The axial current at 85% of depth is in the downhole direction as it crosses the zero (0) current axis, while the current below is coming uphole. While the axial current at 55% of depth is in the same downward direction, the current above is less than that below, which also indicates a current discharge or an anodic section.

Since this was unsatisfactory, the current was increased for trial 2 (it must be noted that during an actual test, time must be given to ensure a steady state has been achieved after ampere adjustments before another log is run to obtain reliable results). Here, continuous axial current pickup occurred from bottom to top as shown by the positive slope in the accumulated current profile. The total current value established by this test now becomes the criterion for cathodic protection. It should be noted that errors can occur in this measurement due to poor contacts. However, this is the best technology available at the present time to determine the amount of cathodic protection current required to protect a well casing, or a portion of a well casing.

A partial CPET plot is shown in Fig. 10 that illustrates the axial current, radial current, and the casing thickness. The casing thickness is an estimate based on Faraday's law (Eq 1) and the assumption that the radial current discharge has remained the same over time. As a result, the casing thickness estimate may not be a true measure of the wall thickness remaining. Experience has shown that there is often quite a discrepancy between corrosion-prediction losses by this method when compared to actual metal-loss measurements.

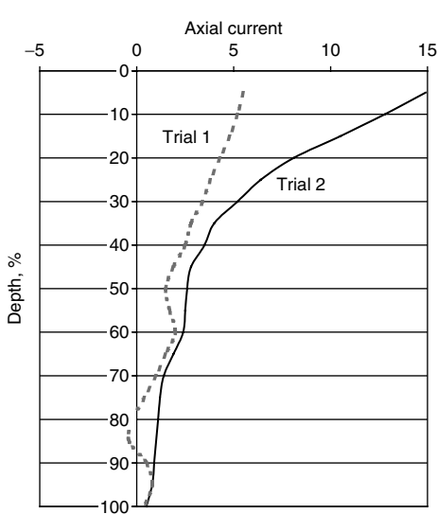

Fig. 9 Sample casing potential profile axial current profile

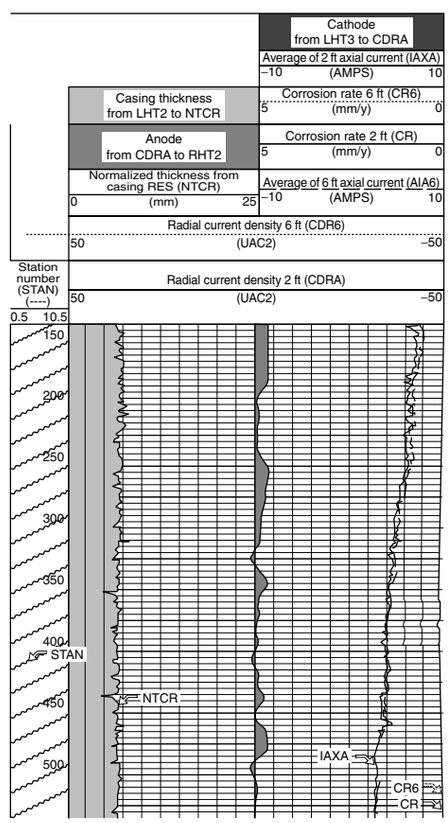

Fig. 10 CPET axial and radial current plot with a conventional rectifier and casing thickness. Total current is 15.3 A.

Factors Influencing the use of CPP Tests. Even though CPP is probably the best means now available to establish the current required for a well casing, it is not often used. The main reasons are associated with the cost of running the tool, both direct and indirect costs. Some of the reasons include:

- In order to run the tool the well has to be taken out of service. This in itself limits the number of potential candidates unless there is a very urgent need to take a well out of service.
- Depending on the fluid in the well bores, many wells will have to be "killed" before the tool can be run.
- In order for the tool to make good contact with the casing, any scale or product buildup on the inside of the casing will have to be cleaned off before the tool is run.
- There are not many CPET tools available worldwide, and the older CPP tool is not available. Coordinating the work is therefore vital to ensure the well and the tool are available at the same time.
- A cathodic protection system: anodes, rectifier (or some other suitable dc power source), cabling, and so forth, must be constructed and operating in advance of the downhole log if the test is to verify a current requirement target.
- If the testing is to determine cathodic protection current requirements, then weeks or even months between runs might be necessary in order to allow a steady state to be achieved between output adjustments.
- Since completion practices for wells in the same producing area can vary significantly, multiple tests on multiple wells may be necessary to arrive at current return criteria that meet all of the well completion variations.

Mathematical Modeling of Total Current Requirement for Well Casing Cathodic Protection

Several mathematical models (Ref 15–19) have been developed to estimate the total current required to protect a well casing by cathodic protection that can be summarized:

- Current density
- An attenuation equation
- A modified attenuation equation
- A computerized equivalent circuit using formation resistivity, nonlinear polarization characteristics, and well casing information

The current density model applies an empirical current density to the surface area of other well casings of similar characteristics to the source of the empirical data to estimate the total current requirement of each well casing. The

variations in well depth and completion such as the amount of the casing that was cemented between it and the formation and the quality of the cement can make this approach quite inaccurate. Verification by field tests on typical well casings in a given geographical area is advised.

Attenuation calculations modified from those used on pipelines were applied initially to casings to estimate a potential at a given depth based on the potential change at the surface. The relationship developed by Schremp and Newton (Ref 16) is given by Eq 3 to calculate the potential change at any given depth in the casing with the applied current source being interrupted:

$$e_x = e_o \exp\left[\frac{-1.648.7(r_1)(x_1)(I_1)\exp(-x_1/L_1)}{e_o}\right] \quad \text{(Eq 3)}$$

where e_o is the potential change at wellhead when applied current is momentarily interrupted (mV); e_x is the potential change at depth x_1 from the wellhead (mV); r_1 is the unit resistance of the innermost casing (Ω/m or Ω/ft); x_1 is the distance from wellhead (m or ft); I_1 is the current in the innermost casing (A); and L_1 is the length of innermost casing (m or ft).

A more sophisticated mathematical model was developed by Dabkowski (Ref 17), and a spreadsheet version was developed by Smith et al. (Ref 18).

Casing-to-Anode Separation

The spacing of the anode to the casing can also change the current required for a particular casing as illustrated by data from Blount and Bolmer (Ref 11) plotted in Fig. 11. The current requirement to protect the casing increases if the anode is brought too close to the casing. There is an optimum distance beyond which a further increase in distance is of no benefit. Hamberg et al. (Ref 7) also demonstrated a similar result in offshore well casings.

A comparison of the distribution of current in two similar casings that were 2600 m (8530 ft) (well casing "A") and 2475 m (8120 ft) (well casing "B") deep in the same area but with different casing-to-anode separations is shown in Fig. 12. The excess current being impressed onto the casing near the surface helps provide an understanding of this change in current requirement due to the casing-to-anode separation (Ref 14).

Blount and Bolmer (Ref 11) found that the anode bed should be at least 30 m (100 ft) from casings that were on the order of 1220 m (4000 ft) deep. This distance should be increased for deeper wells for optimum performance. The anode bed in either the E log I or the CPP test should therefore be located at a distance from the well casing similar to where the permanent anode bed will be installed.

Coated Casings

Coatings are available that are durable enough to withstand many of the rigors of a casing installation. Although significant coating damage is expected, Orton et al. (Ref 20) reported that the current requirement of a coated casing with bare couplings and no effort to repair coating damage can be reduced to less than 10% of that of a similar bare casing. A further benefit is that a reduction in the current requirement will also reduce the interference effects on nearby structures and casings as discussed below.

Cathodic Protection Systems

The cathodic protection system for a well casing requires the same consideration as that for a pipeline. There are two types of cathodic protection systems used for well casings and pipelines: sacrificial anode systems and impressed-current systems (see the article "cathodic protection" in Volume 13A for additional information).

Sacrificial Anode Systems. In the early years, a sacrificial anode system was often used for wells where a low current requirement was predicted. Sacrificial anode systems are still appropriate for more shallow wells with a low current requirement.

An impressed-current cathodic protection system is the most common type for well casings due to the amount of current typically required for protection. A separate installation (Fig. 13) is common at each well. If two or more wellheads are in close proximity, interference can result (Ref 21–23).

Power Sources. Where ac power is available, it is likely that a standard or pulse-type rectifier will be used as a dc power source. Otherwise, thermoelectric generators, solar, wind-powered generators, and engine-driven generators are all possible candidates for the dc power source.

Thermoelectric generators (TEG) have a limited power availability; therefore, the anode bed resistance should be kept low to obtain the required current. The available power from a TEG usually peaks at around 0.6 to 1.2 Ω and reduces as the circuit resistance increases. The manufacturer's technical information must be consulted. A clean regulated fuel source such as natural gas or propane is required.

Both solar- and wind-generated power need batteries as a backup power source to provide cathodic protection current when there is either no sun or wind, respectively. The use of solar is

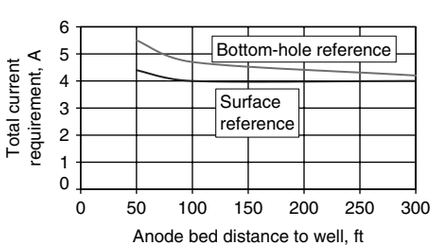

Fig. 11 An example of the change in current requirements with anode to well spacing. Source: Ref 11

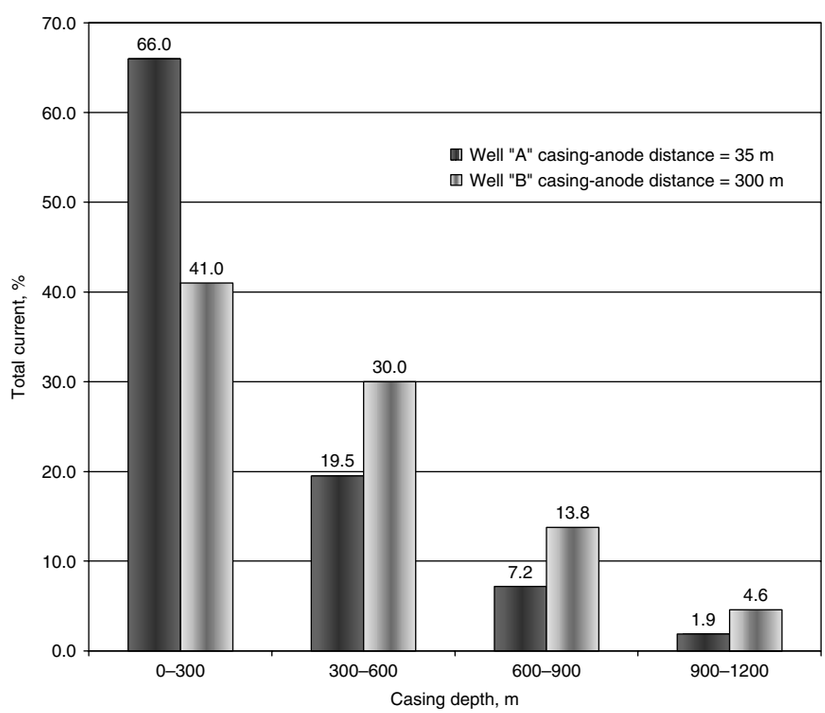

Fig. 12 An actual example of current distribution in similar casings but with different casing-to-anode distances. Source: Ref 18

less popular in the northern regions where there is a lack of sunlight in the winter, and wind power is not appropriate unless the area is historically windy.

Engine-generator systems are best used with an ac generator feeding a rectifier for dc output and control. Maintenance on dc generators has proved to be high in the past, resulting in many outages during the year. Although to a lesser degree than the dc generator, the ac generator also requires maintenance and regular inspections.

Pulse rectifiers provide a high-voltage dc pulse of short duration. The frequency of the pulse may be from 1000 to 5000 Hz, but the duty cycle is normally set in the range of 10 to 15%. Bich and Bauman (Ref 24) reported that total current requirements can be reduced to 50% or less using a pulse rectifier instead of a conventional rectifier, and more current will reach the lower portions of the casing. The improved performance is attributed to the waveform. However, Dabkowski (Ref 25) showed mathematically that the pulse from the rectifiers would attenuate to 0 at 500 to 1000 m (1640 to 3280 ft) from the casing top, suggesting that any improved performance is not due to the pulse. It has been the author's experience that cathodic protection with pulse rectifiers can be achieved down to 80% of the comparable current to a conventional rectifier, but not the significant reduction suggested by Bick and Bauman. Further work needs to be completed to validate any of these claims. The digital instrumentation measuring the pulse rectifier output is another factor in this comparison, as errors can be realized depending on the sampling rate. A major disadvantage of pulse rectifiers is noise interference, especially on communication equipment that may be servicing the well. This can be reduced by locating the pulse rectifier away from the electrical/communication building, not paralleling electrical cables, and using deep anodes.

Regardless of the power source, one negative cable must be connected to the well casing while a second negative cable is often run to the isolated surface facilities to assist in interference mitigation.

The anode bed design and location is largely dictated by the soil layer resistivity and the location of surface facilities and pipelines. If uniform low-resistivity soil conditions exist at a surface location that is sufficiently remote from the casing and other structures, a shallow anode type of anode bed can be used. Where high-resistivity conditions exist at the surface but more suitable strata exist underneath, a deep anode bed would be preferred. The latter anode bed will also tend to reduce interference with surface facilities, as the major portion of the anode gradient exists below pipeline and foundation depth. It must be noted that the same spacing between the casing and anode must be maintained whichever type of anode bed is used, as going deeper does not change the distance between the structures.

The anode bed should be located at an equal or greater distance than the temporary anode bed to the casing that was used during the current requirement test. However, a minimum spacing of 30 m (100 ft) from the well for shallow wells but preferably greater than 50 m (165 ft) should be maintained. The separation between anodes and structures not receiving current will vary depending on the voltage gradients in the soil but should be 100 m (300 ft) or more. Otherwise, provision for interference control discussed below must be considered.

Direct-Current Stray-Current Interference

Stray current can be defined as current in an unintended path. Many sources of current use the earth as part of their electrical circuit. Conductors in the earth such as well casings and pipelines provide opportune parallel paths for current intended for another purpose.

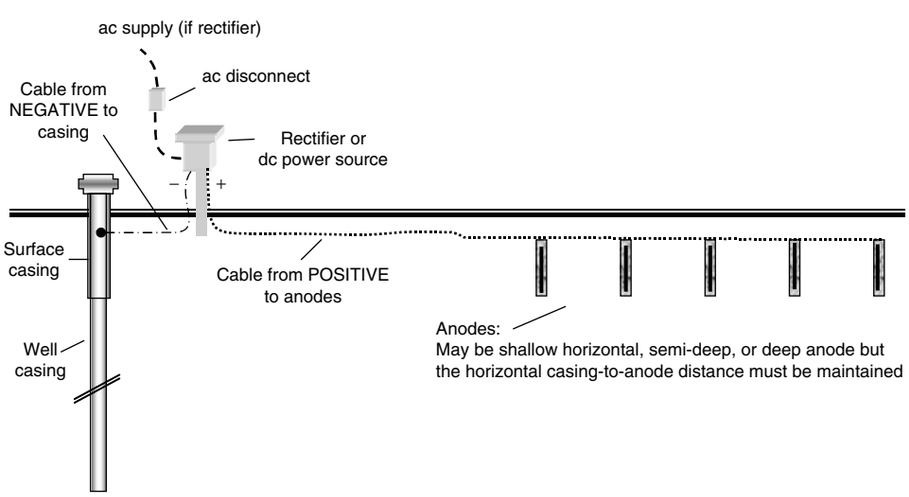

Fig. 13 Typical cathodic protection installation

The area of stray-current pickup is similar to cathodic protection and not of concern. However, the manner by which that current returns to its original source is of concern. Should that current *leave* the casing to enter the soil, the casing in that location is anodic and accelerated corrosion occurs.

Stray-Current Pickup. A stray current may be picked up at the surface, in which case the current must discharge into the soil downhole to return to its source. Alternately, a current discharge near the surface to either facilities near the wellhead or to the surface casing may occur, in which case there will have to be a current pickup downhole. Both cases (Fig. 14) are a cause for concern as there is a current discharge occurring at some point along the casing.

Since an electronegative shift in casing-to-soil potentials occurs with the application of cathodic protection, a stray-current pickup at a lower depth with a discharge near the surface can be detected by an electropositive shift in casing-to-electrolyte potentials, with the reference electrode located near the wellhead, when the foreign dc power source (s) is energized. Conversely, a current pickup at the surface will be detected by an electronegative shift in potentials when the foreign current source comes on. The area of current discharge will then be at a point lower on the casing, and its location would have to be defined by a CPP log, or similar.

Stray-current pickup on pipeline systems away from the well casing can result in a stray-current discharge from the well casing if the two structures are continuous. In these cases, a current pickup is normally close to the anode bed while the discharge is near the wellhead. However, it is conceivable that the current pickup and discharge points can develop at other points, especially if varying coating qualities or vastly differing resistivities exist along the pipeline or casing.

Stray-Current Sources. The stray current may come from a relatively steady-state source such as another cathodic protection system (Ref 21–23) or a high-voltage dc power line ground, or it may come from a dynamic source such as a transit system, welding machines, dc mine equipment or, finally, from telluric current that is a natural source of stray current (Ref 26).

Interference Control. Interference can be controlled by:

- Providing a metallic return path for the stray current
- Moving the offending anode bed or ground
- Adjusting the current distribution in the foreign system
- Installing and/or adjusting a cathodic protection system on the well casing to counter the stray-current effects
- Using common cathodic protection systems (Ref 21)
- Balancing wellhead potentials

A well casing cathodic protection system can also cause interference on surface facilities or

pipelines. In this case, a second negative circuit is often provided in the rectifier to both control interference and assist with the protection of the surface facilities or pipelines.

Orton et al. (Ref 20) reported that a coated casing reduced the cathodic protection current requirement to 10% of a bare well casing. This in turn will reduce the tendency for mutual interference of nearby casings.

Isolation of Well Casings

The purpose of isolating a well casing from surface facilities is twofold: (a) it eliminates a macrocorrosion cell between the casing and the surface facilities, and (b) it allows the cathodic protection current distribution to be controlled between the well casing and the surface facilities.

In addition, an isolating feature allows the current impressed on the well casing to be directly measured in the connecting cable. If not isolated, a means of measuring the current return from the casing itself must be established, such as a clamp-on ammeter around the wellhead at the surface, to confirm that the "current" criterion is being met.

From a cathodic protection standpoint, the preferred location for this isolation is at the wellhead. However, some operators locate it a distance away in the event of a fire at the well so that the isolating material does not melt and complicate firefighting procedures. All tubing conduits and pipe supports must also be isolated if they are bypassing the isolating feature.

If the product from the well contains a large amount of brine, there is a risk of "internal" interference. This occurs where current picked up on the opposite side of the isolation uses the brine as a path around the isolation. In such a case, corrosion is seen only on one side of the isolating feature (Fig. 15A).

A "long-path" isolation, which consists of an isolating feature and an internally coated or lined section of pipe (Fig. 15B), can be used to reduce the internal interference. If this is not effective in controlling internal interference, the isolating feature should be omitted.

Commissioning and Monitoring

Inspection. A cathodic protection system must operate continuously to be effective. Regular inspection of the dc power supply to ensure that the required current is being provided in all circuits is necessary throughout the year. A more detailed inspection should be conducted annually. A description of the cathodic protection system operation and the records is given in NACE RP0186 (Ref 4).

Inspections of the dc power source should only be made by persons who are trained and qualified to work on electrical equipment. The use of strict safety practices including lockout/tagout procedures is especially necessary when working

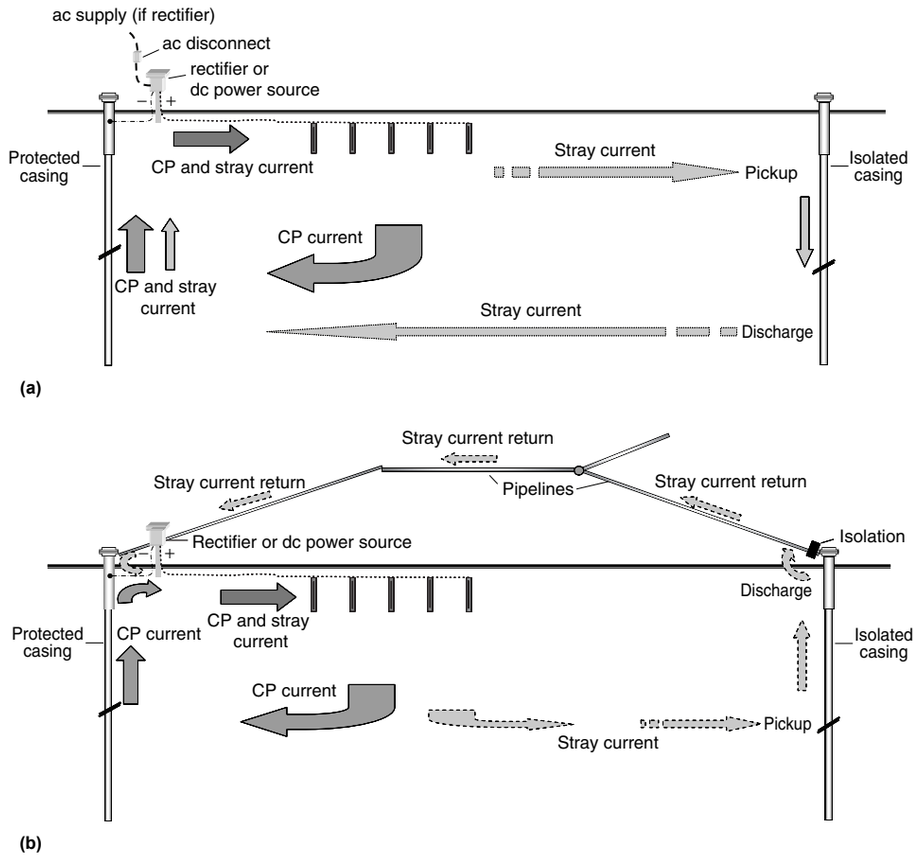

Fig. 14 Direct-current stray-current interference. (a) Stray-current pickup near top with discharge downhole. (b) Stray-current pickup downhole with discharge near top. CP, cathodic protection

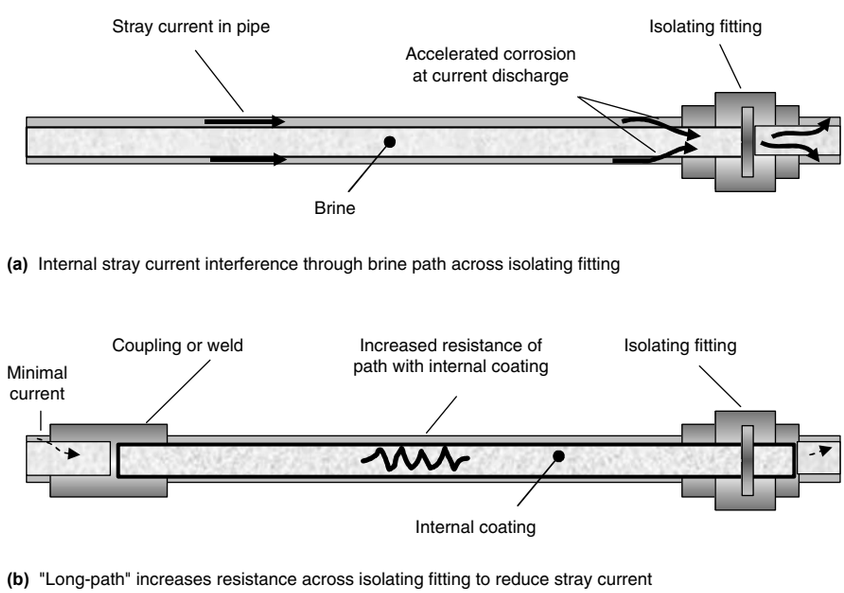

Fig. 15 (a) Internal interference across an isolating feature and (b) reduced by a long-path isolating feature

on the rectifiers. The routine readings should include these measurements:

- dc power source current output
- dc power source voltage output
- dc power source adjustment setting (tap setting if applicable)
- dc current in secondary circuits
- dc interference control devices
- Power meter or fuel supply where applicable

The annual inspection should include:

- Completion inspection of the dc power source
  (a) Calibration of the dc power source current output
  (b) Calibration of the dc power source voltage output
  (c) Direct-current power source adjustment setting (tap setting if applicable)
  (d) Calibration of the dc in secondary circuits
- Measurement of the well-to-electrolyte potential
- Measurement of the surface facility structure-to-electrolyte potentials
- Testing the effectiveness of wellhead isolation, if applicable
- Measurement of the current returning from the casing at the wellhead with a clamp-on ammeter, if there is no isolation
- Confirmation that dc interference control devices are providing the necessary control
- Specialty tests applicable to the specific cathodic protection installation

Corrosion-control records are of paramount importance in an effective corrosion-control program. They will be used to establish a need for enhancements of the corrosion-control program and to ensure that the existing corrosion-control equipment is operating. The records should include but not be limited to:

Historical:

- Well completion data including casing sizes and lengths, cementing information and well total depth
- Corrosion leaks identifying well, depth, internal or external, date of failure compared to date of drilling and/or workover (s)
- Inspections of casing failures and corrosion products
- Electrical well logs (wall thickness, CPP identifying corrosion, and resistivity)
- Coating type and thickness, if applicable
- Drawing of well casing strings and lease equipment and piping
- System map of the field
- Location and type of electrical isolation

Cathodic Protection:

- Current requirement tests (CPP log(s), E log I test(s), and soil resistivity in layers near the surface)
- Design and drawings of cathodic protection installation detailing:
  (a) Well location
  (b) Piping and lease facilities
  (c) dc power source type, rating and location
  (d) Description of energy supply for dc power source
  (e) Cable type(s) and location
  (f) Cable to wellhead and piping connections
  (g) Anode beds type and location
  (h) Anode material type, spacing and depth
  (i) Backfill type and amount
  (j) Junction box and test station details

Interference Control:

- Records of all tests pertaining to interference on the well from other systems and on other systems from the well cathodic protection system
- List of owners and contacts involved in the interference control program
- Description of the method of interference mitigation, including control devices and target values of current and potential
- If bonds or directional devices are used, the location, type, resistance value, current, and current direction

All records must show the date, the name of the inspector or tester and, if different, the names of those who make recommendations. Any changes in current output must be correlated with other measurements taken.

Cathodic Protection Summary

For new wells, the use of an abrasion-resistant underground coating on those portions of the casing exposed to the strata should be considered as part of a corrosion-control program, as this will greatly reduce the amount of cathodic protection current required for protection. If coating is used, though, a cathodic protection system must be planned and implemented immediately, as a coating alone will concentrate corrosion at the coating holidays.

Prior to applying cathodic protection, a review of the existing well historical data should be made to assess the possibility of corrosion that will cause premature and costly failure repairs. Electrical logging tools, which are reasonably accurate, are available to assess the metal loss that has occurred and to predict the possibility of future corrosion.

Provided the proper amount of current is applied and maintained, cathodic protection of well casings has proved to be an effective means of minimizing corrosion on the casing. The cathodic protection current can be determined by various means; however, two of the more reliable results have to date been with CPP type of testing and polarization tests (E log I). The former test is difficult to perform in that the well has to be taken out of service, which usually results in few candidate wells in an older field. Also it may be necessary to perform multiple tests, with time provided between tests to allow for steady-state conditions to be achieved, which adds to the cost of the test. The E log I test must be correctly analyzed to identify the Tafel point on the profile; otherwise, a current less than that necessary may be defined as the criterion. Another option is to use a mathematical model; however, the validity of this option should be confirmed by tests at the start of the cathodic protection program.

Another factor in designing well casing cathodic protection systems is to remember that the amount of cathodic protection current required is also dependent on the spacing between the casing and the anodes, up to a certain distance, and that distance must be defined for each well. If the anodes are placed within that distance, the current requirement increases. Once a cathodic protection current requirement is established for a temporary anode bed, the same distance or greater should be used in the final cathodic protection design.

Isolation of the casing from other facilities is another important cathodic protection system design consideration. Isolating the well casing from surface facilities is preferred to eliminate the macrocorrosion cell between the casing and these structures without cathodic protection and to provide a means for controlling and measuring the cathodic protection current to the casing. However, if the product inside the isolation contains a large quantity of brine, either a "long-path" isolating fitting should be used to minimize internal interference, or in some cases the isolator may have to be removed entirely.

Generally, cathodic protection systems using conventional rectifiers are designed and installed for the protection of the casings, although pulse rectifiers have also been used. Particular attention has to be placed on the size and the location of the anode bed in order to achieve the required current output for the desired life of the anode bed.

Stray current must also be considered during the cathodic protection system design. Stray-current interference from other dc power sources will accelerate corrosion on the casing if it encourages a current discharge into the formation. A common source is from other cathodic protection systems in the same oil/gas field, but can also come from other sources not related to the oil/gas field. Several methods have been outlined to either avoid or minimize these interference effects. Any stray-current control device must be continuously inspected and maintained.

Detailed records must be kept on the history of the well, electrical logs, casing repairs, and on the operation of the corrosion-control equipment. These records must be able to stand up to future legal scrutiny.

REFERENCES

1. B.A. Gordon, W.D. Grimes, and R.S. Treseder, Casing Corrosion in the South Belridge Field, *Mater. Perform.,* March 1984, p 9
2. W.R. Lambert and G.G. Campbell, Cathodic Protection of Casings in the Gas Storage Wells, *Appalachian Underground Short Course,* Fourth Annual proceedings, West Virginia University, p 502

3. C. Brelsford, C.A. Kuiper, and C. Rounding, "Well Casing Cathodic Protection Evaluation Program in the Spraberry (Trend Area) Field," paper 03201, Corrosion 2003, NACE International
4. "Application of Cathodic Protection for Well Casings," RP0186, NACE International
5. W.F. Gast, A 20-Year Review of the Use of Cathodic Protection for Well Casings, *Mater. Perform.,* Jan 1986, p 23
6. W.C. Koger, Casing Corrosion in the Hugoton Gas Field, *Corrosion,* Oct 1956
7. A. Hamberg, M.D. Orton, and S.N. Smith, "Offshore Well Casing Cathodic Protection," paper 64, Corrosion/87, National Association of Corrosion Engineers. Reprinted from *Mater. Perform.,* March 1988, p 26
8. R.G. Wakelin, R.A. Gummow, and S.M. Seagall, "AC Corrosion—Case Histories, Test Procedures and Mitigation," paper 565, Corrosion/98, NACE International
9. B. Dennis, "Casing Corrosion Evaluations using Wireline Techniques," Schlumberger of Canada, Calgary, Alberta, Canada
10. B. Husock, Methods for Determining Current Requirements for Cathodic Protection of Well Casings—Review, *Mater. Perform.,* Jan 1984, p 39
11. F.E. Blount and P.W. Bolmer, Feasibility Studies on Cathodic Protection of Deep Well External Casing Surfaces, *Mater. Protect.,* Aug 1962, p 10
12. E.W. Haycock, Current Requirement for Cathodic Protection of Oil Well Casing, *Corrosion,* Nov 1957, p 767t
13. D.H. Davies and K. Sasaki, Advances in Well Casing Cathodic Protection Evaluation, *Mater. Perform.,* Aug 1989, p 17
14. W.B. Holtsbaum, "External Protection of Well Casings Using Cathodic Protection," Canadian Region Western Conference, National Association of Corrosion Engineers, Feb 20, 1989
15. J.K. Ballou and F.W. Schremp, Cathodic Protection of Oil Well Casings at Kettleman Hills, California, *Corrosion,* Vol 13 (No. 8), 1957, p 507
16. F.W. Schremp and L.E. Newton, paper 63, Corrosion/79, National Association of Corrosion Engineers
17. J. Dabkowski, "Assessing the Cathodic Protection Levels of Well Casings," American Gas Association, Jan 1983
18. S.N. Smith, A. Hamberg, and M.D. Orton, "Modified Well Casing Cathodic Protection Attenuation Calculation," paper 65, Corrosion 87, National Association of Corrosion Engineers
19. M.A. Riordan and R.P. Sterk, Well Casing as an Electrochemical Network in Cathodic Protection Design, *Mater. Protect.,* July 1963, p 58
20. M.D. Orton, A. Hamberg, and S.N. Smith, "Cathodic Protection of Coated Well Casing," paper 66, Corrosion/87, National Association of Corrosion Engineers
21. W.F. Gast, Well Casing Interference and Potential Equalization Investigation, *Mater. Protect.,* May 1974, p 31
22. G.R. Robertson, Effects of Mutual Interference Oil Well Casing Cathodic Protection Systems, *Mater. Protect.,* March 1967, p 36
23. R.F. Weeter and R.J. Chandler, Mutual Interference between Well Casings with Cathodic Protection, *Mater. Perform.,* Jan 1974, p 26
24. N.N. Bich and J. Bauman, Pulsed Current Cathodic Protection of Well Casings, *Mater. Perform.,* April 1995, p 17
25. J. Dabkowski, Pulsed Rectifier Limitations for Well Casing Cathodic Protection, *Mater. Perform.,* Oct 1995, p 25
26. D. Warnke and W.B. Holtsbaum, "Impact of Thin Film Coatings on Cathodic Protection," paper IPC 02-27325, ASME International Pipeline Conference, 2002

SELECTED REFERENCES

- "Application of Cathodic Protection for Well Casings," RP0186, NACE International
- W. von Baeckmann, W. Schwenk, and W. Prinz, Ed., *Cathodic Corrosion Protection,* Gulf Publishing, 1997, p 415–426

Ex. II - 36

NACE SP0186-2007
(formerly RP0186-2001)
Item No. 21031

Standard Practice

Application of Cathodic Protection for External Surfaces of Steel Well Casings

This NACE International standard represents a consensus of those individual members who have reviewed this document, its scope, and provisions. Its acceptance does not in any respect preclude anyone, whether he or she has adopted the standard or not, from manufacturing, marketing, purchasing, or using products, processes, or procedures not in conformance with this standard. Nothing contained in this NACE International standard is to be construed as granting any right, by implication or otherwise, to manufacture, sell, or use in connection with any method, apparatus, or product covered by Letters Patent, or as indemnifying or protecting anyone against liability for infringement of Letters Patent. This standard represents minimum requirements and should in no way be interpreted as a restriction on the use of better procedures or materials. Neither is this standard intended to apply in all cases relating to the subject. Unpredictable circumstances may negate the usefulness of this standard in specific instances. NACE International assumes no responsibility for the interpretation or use of this standard by other parties and accepts responsibility for only those official NACE International interpretations issued by NACE International in accordance with its governing procedures and policies which preclude the issuance of interpretations by individual volunteers.

Users of this NACE International standard are responsible for reviewing appropriate health, safety, environmental, and regulatory documents and for determining their applicability in relation to this standard prior to its use. This NACE International standard may not necessarily address all potential health and safety problems or environmental hazards associated with the use of materials, equipment, and/or operations detailed or referred to within this standard. Users of this NACE International standard are also responsible for establishing appropriate health, safety, and environmental protection practices, in consultation with appropriate regulatory authorities if necessary, to achieve compliance with any existing applicable regulatory requirements prior to the use of this standard.

CAUTIONARY NOTICE: NACE International standards are subject to periodic review, and may be revised or withdrawn at any time in accordance with NACE technical committee procedures. NACE International requires that action be taken to reaffirm, revise, or withdraw this standard no later than five years from the date of initial publication and subsequently from the date of each reaffirmation or revision. The user is cautioned to obtain the latest edition. Purchasers of NACE International standards may receive current information on all standards and other NACE International publications by contacting the NACE International FirstService Department, 1440 South Creek Dr., Houston, Texas 77084-4906 (telephone +1 281/228-6200).

Reaffirmed 2007-03-10
Reaffirmed 2001-09-20
Reaffirmed September 1984
Approved March 1986
NACE International
1440 South Creek Drive
Houston, TX 77084-4906
+1 281/228-6200

ISBN:1-57590-134-X
©2007, NACE International

Foreword

Oil and gas wells represent a large capital investment. It is imperative that corrosion of well casings be controlled to prevent loss of oil and gas, environmental damage, and personnel hazards, and in order to ensure economical depletion of oil and gas reserves.

This NACE International standard practice identifies procedures to determine the need for cathodic protection (CP) and the current requirements to achieve CP of well casings associated with oil and gas production and gas storage. It also outlines practices for the design and installation of CP systems and for their operation and maintenance. The purpose of this standard is to ensure more effective prevention of corrosion of well casings by making available reliable information about CP as it relates to well casings. This standard is intended for use by corrosion engineers in oil and gas production, especially those concerned with the CP of steel well casings.

This standard was originally prepared in 1986 by Unit Committee T-1E on Cathodic Protection and Task Group (TG) T-1J-2, a component of Unit Committee T-1J on Storage Wells. It was reaffirmed in 1994 by Unit Committee T-1E, and in 2001 and 2007 by Specific Technology Group (STG) 35 on Pipelines, Tanks, and Well Casings. The STG membership consists of representatives from oil and gas producing and storage companies, equipment manufacturers, consulting firms, and CP service companies. Included in the membership are persons involved in design, consulting, research, construction, maintenance, and manufacturing and supply of materials, all of whom are concerned with the establishment and maintenance of cathodic protection systems used with well casings. This standard is issued by NACE under the auspices of STG 35.

In NACE standards, the terms *shall, must, should,* and *may* are used in accordance with the definitions of these terms in the *NACE Publications Style Manual*, 4th ed., Paragraph 7.4.1.9. *Shall* and *must* are used to state mandatory requirements. The term *should* is used to state something considered good and is recommended but is not mandatory. The term *may* is used to state something considered optional.

NACE International

Standard Practice

Application of Cathodic Protection for External Surfaces of Steel Well Casings

Contents

1. General 1
2. Definitions 1
3. Determination of Need for CP 4
4. Criterion for CP and Current Requirements 5
Bibliography for Section 4 6
5. Design of CP Systems for Well Casings 7
Bibliography for Section 5 9
6. Installation of CP Systems 10
7. Control of Interference Currents 11
Bibliography for Section 7 13
8. Operation and Maintenance of CP Systems 13
9. Corrosion Control Records 14
References 16
Appendix A: Casting Potential Profile (Nonmandatory) 16
Appendix B: E- Log I Test (Nonmandatory) 19
Appendix C: Electromagnetic Casing Inspection Instruments (Nonmandatory) 21
Appendix D: Well Completion Design and Other Factors Associated with CP (Nonmandatory) 23
TABLES
Table C.1—Instrument Effectiveness 22
FIGURES
Figure A1—Casing Potential Profile Tool 17
Figure A2—Typical Casing Potential Profile Plot 18
Figure B1—Equipment Set-Up for E-Log-I Test 20
Figure B2—Sample E-Log-I Plot 21

Section 1: General

1.1 This standard presents acknowledged procedures for the control of external corrosion of steel well casings by applying CP. This standard is intended to be a guide for establishing minimum requirements for corrosion control when CP is practical and cost-effective.

1.2 This standard does not designate practices for specific situations. The complexity of some casing spacing, subsurface proximity to other casings, and environmental conditions preclude standardizing the application of CP. Deviation from this standard may be warranted in specific situations, provided those in responsible charge can demonstrate that the objectives expressed in this standard have been achieved.

1.3 This standard does not include corrosion control methods based on chemical control of the environment.

1.4 This standard applies only to well casing exteriors and not to internal corrosion, or to corrosion of other surface or downhole equipment.

1.5 The provisions of this standard should be applied under the direction of competent persons knowledgeable in the physical sciences, principles of engineering, and mathematics. They may have acquired knowledge by professional education and related practical experience and should be qualified to practice corrosion control for well casings by the use of CP. Such persons may be registered professional engineers recognized as being qualified as corrosion specialists in the appropriate fields of corrosion control by NACE International. Their professional activities should include suitable experience in well casing corrosion control practices.

Section 2: Definitions[1]

Alternating Current (AC): Current whose direction changes with time.

Ampere: Unit of current that is one coulomb per second.

Anode: The electrode of an electrochemical cell at which oxidation occurs. Electrons flow away from the anode in the external circuit. Corrosion usually occurs and metal ions enter the solution at the anode.

Backfill: Material placed in a hole to fill the space around the anodes, vent pipe, and buried components of a cathodic protection system.

Casing Potential Profile: Voltage (IR) drop and current direction versus casing depth is plotted. Amount of current is determined from the IR drop and casing resistance. (See nonmandatory Appendix A.)

Casing-to-Electrolyte: See *Structure-to-Electrolyte Potential.*

Casing-to-Reference Electrode: See *Structure-to-Electrolyte Potential.*

Cathode: The electrode of an electrochemical cell at which reduction is the principal reaction. Electrons flow toward the cathode in the external circuit.

Cathodic Protection: A technique to reduce the corrosion of a metal surface by making that surface the cathode of an electrochemical cell.

Cement: Cement slurry fills the space between the casing and the sides of the wellbore to a predetermined height above the bottom of the well.

Continuity Bond: A connection, usually metallic, that provides electrical continuity between structures that can conduct electricity.

Corrosion: The deterioration of a material, usually a metal, that results from a reaction with its environment.

Counterpoise: A conductor or system of conductors arranged beneath a power line, located on, above, or most frequently, below the surface of the earth and connected to the footings of the towers or poles supporting the power line.

Coupling (or Collar): Well casing joint connector.

Current Density: The current to or from a unit area of an electrode surface.

[1] Definitions in this section are those presented in the *NACE Glossary of Corrosion-Related Terms* and those that reflect the common usage among practicing corrosion control personnel. In many cases, in the interest of brevity and practicality, the strict scientific definitions are abbreviated or paraphrased.

Deep Groundbed: One or more anodes installed vertically at a nominal depth of 15 m (50 ft) or more below the earth's surface in a drilled hole for the purpose of supplying cathodic protection.

Dielectric Coating: A coating that does not conduct electricity.

Direct Current (DC): Current whose direction does not change with time.

Drainage: Conduction of electric current from an underground or submerged metallic structure by means of a metallic conductor.

E-log-I: A test that indicates the cathodic protection current required by a slope change on the cathodic polarization diagram. (Refer to nonmandatory Appendix B.)

Electrical Isolation: The condition of being electrically separated from other metallic structures or the environment.

Electric Log: A survey taken in the open borehole of a well to determine the lateral formation resistivity.

Electrolyte: A chemical substance containing ions that migrate in an electric field. For the purposes of this standard, electrolyte refers to the soil or liquid adjacent to and in contact with a buried or submerged metallic structure, including the moisture and other chemicals contained therein.

Electroosmotic Effect: The effects of the movements in an electric field of liquid with respect to colloidal particles immobilized in a porous diaphragm or a single capillary tube.

Fault Current: A current that flows from one conductor to ground or to another conductor due to an abnormal connection (including an arc) between the two. A fault current flowing to the ground may be called a ground fault current.

Field: A group of wells in close physical proximity, usually considered a unit when applying cathodic protection. It may be an oil or natural gas production field or a natural gas storage field.

Foreign Structure: Any metallic structure that is not intended as a part of a system under cathodic protection.

Galvanic Anode: A metal that provides sacrificial protection to another metal that is more noble when electrically coupled in an electrolyte. This type of anode is the electron source in one type of cathodic protection.

Gamma Ray Neutron Log: Gamma ray is a measurement of the natural radioactivity of a formation. Neutron log is used for delineation of porous formations. Data are used to identify the formations in the earth.

Groundbed: One or more anodes installed below the earth's surface for the purpose of supplying cathodic protection.

Impressed Current: An electric current supplied by a device employing a power source that is external to the electrode system. (An example is direct current for cathodic protection.)

Instant-Off Potential: The polarized half-cell potential of an electrode taken immediately after the cathodic protection current is stopped, which closely approximates the potential without IR drop (i.e., the polarized potential) when the current was on.

Interference Bond: An intentional metallic connection, between metallic systems in contact with a common electrolyte, designed to control electrical current interchange between the systems.

Intermediate Casing: A string of casing set to protect a section of hole and to allow drilling to continue to a greater depth. Also called protection casing string.

IR Drop: The voltage across a resistance in accordance with Ohm's law.

Isolation: See *Electrical Isolation*.

Lithology: Rock formations traversed by well casing.

Long-Line Current: Current through the earth between an anodic and a cathodic area that returns along an underground metallic structure.

Mutual Interference: An electrical DC interference on a well originating from within the cathodic protection system of several wells and structures, such as several DC power sources for a group of wells.

Native State Potential: The potential with zero groundbed current.

Negative Return: A point of connection between the cathodic protection negative cable and the protected structure.

Ohm: A resistance that passes one ampere of current when a one-volt potential is applied.

Packaged Anode: An anode that, when supplied, is already surrounded by a selected conductive backfill material.

Photovoltaic: Generation of an electromotive force when radiant energy falls on the boundary between two dissimilar materials.

Pipe-to-Soil Potential: See *Structure-to-Electrolyte Potential*.

Polarization: The change from the open-circuit potential as a result of current across the electrode/electrolyte interface. In this standard, polarization is considered to be the change of potential of a metal surface resulting from current to or from an electrolyte.

Potential Profile Log: See *Casing Potential Profile*.

Production Casing: Casing that extends through the surface and intermediate casings, sometimes only to the tip of the zone but almost always through the producing or storing zone.

Rectifier: A device to convert AC power to DC power.

Reference Electrode: An electrode whose open-circuit potential is constant under similar conditions of measurement, which is used for measuring the relative potentials of other electrodes.

Resistivity: (1) The resistance per unit length of a substance with uniform cross section. (2) A measure of the ability of an electrolyte (e.g., soil) to resist the flow of electric charge (e.g., cathodic protection current). Resistivity data are used to design a groundbed for a cathodic protection system.

Right-of-Way: Right of passage, as over another's property.

Self-Interference: See *Mutual Interference*.

Shunt: A precise resistor with known resistance in an electrical circuit used to measure a voltage (IR) drop, which is used to calculate the amount of current in amperes.

Soil Resistivity: A measure of the ability of a soil or formation to conduct electricity expressed in units of ohm-centimeters or ohm-meters. Data are used to design a groundbed for a cathodic protection system.

Structure-to-Electrolyte Potential: The potential difference between the surface of a buried or submerged metallic structure and the electrolyte that is measured with reference to an electrode in contact with the electrolyte.

Structure-to-Structure Potential: The potential difference between metallic structures, or sections of the same structure, in a common electrolyte.

Surface Casing: A casing string extending from the surface to a depth great enough to keep surface waters and loose earth from entering the well.

Surface Groundbed: One or more anodes installed below the earth's surface for the purpose of supplying cathodic protection less than 15 m (50 ft) in depth for the anodes.

Tafel Plot, Tafel Diagram, Tafel Line: A plot of the relationship between the change in potential (E) and the logarithm of the current density (log *i*) of an electrode when it is polarized in both the anodic and cathodic directions from its open-circuit potential.

Tafel Segment: That portion of the Tafel plot that appears as a straight line when current is plotted on the logarithmic scale and potential change is plotted on the linear scale. The beginning of the Tafel segment is that point on the curve at which the current-potential relationship follows the straight line with increasing current increments and deviates from the straight line with decreasing current increments.

Tafel Slope: The slope of the straight-line portion of the E log *i* curve on a Tafel plot. (The straight-line portion usually occurs at more than 50 mV from the open-circuit potential.)

Test Wire: An insulated wire attached to a structure (usually buried) such as a pipeline and brought to a terminal convenient for making electrical tests to evaluate cathodic protection.

Tubing: A pipe inside the production casing through which oil is pumped, or liquid is removed from the natural gas storage zone.

Union (Isolating): See *Electrical Isolation*.

Voltage: An electromotive force, or a difference in electrode potentials expressed in volts.

Well: A steel-cased hole associated with the production and storage of oil or gas.

Wellbore *(also called bore hole)*: A hole drilled into the earth for the installation of a deep groundbed system.

Wellhead: Valves and other aboveground fittings electrically connected to the production, surface, and intermediate casings. May be called a "christmas tree" when referring to oil and natural gas production and storage wells.

Well Casing: See *Production Casing*, *Intermediate Casing*, and *Surface Casing*.

Section 3: Determination of Need for CP

3.1 Introduction

3.1.1 The purpose of this section is to indicate those factors that should be considered in determining whether a well casing requires CP.

3.1.2 Metallic structures in contact with soil or submerged under water are subject to corrosion. Adequate procedures should be adopted to ensure that corrosion is not affecting safe and economical operation of well casings.

3.2 The decisions governing the need for CP of well casings shall be based on data obtained from corrosion surveys, operating records, prior tests with similar systems in similar environments, and on a study of design specifications and engineering, operating, and economic requirements.

3.2.1 The usual procedures for predicting the probability and rate of corrosion of a particular metallic casing system are as follows:

(a) The corrosion history of the well casing in question or of other systems of the same material in the same general area or in similar environments should be studied. The history should include cumulative leak frequency and downhole data obtained from workover (reconditioning) records.

(b) The environment surrounding a well casing should be studied. Once the nature of the environment has been determined, the probable corrosiveness can be estimated by referring to actual corrosion experience on similar well casings in similar environmental conditions. It should be remembered that formation water changes caused by production or injection methods may be contributing factors. One source of environmental data is the formation resistivity logs run on wells being investigated and on surrounding wells.

(c) The casing should be mechanically or electrically inspected for evidence of corrosion. The condition of the casing system should be carefully determined and recorded. (See nonmandatory Appendix C.)

(d) The casing should be inspected to determine whether there are any anodic areas. A well casing potential profile tool is commonly used for these investigations. (See nonmandatory Appendix A.)

(e) Maintenance records detailing leak locations and wall thickness surveys, which can be used as a guide for locating areas of maximum corrosion, should be reviewed.

(f) Statistical treatments of available leak data should be considered.

(g) The results of pressure testing should be reviewed; under certain conditions, this may help determine whether corrosion has occurred.

(h) When the well casing is pulled, it should be visually inspected.

(i) Close communication should be maintained with those responsible for the workover of a well.

3.2.2 Environmental and physical factors governing the need for CP are as follows:

3.2.2.1 The nature or constituents of the product being produced or stored.

3.2.2.2 Location of the well casing system in a sparsely or densely populated area and the frequency of visits by personnel.

3.2.2.3 Location of the well casing system as related to other facilities.

3.2.2.4 Influence of DC sources foreign to the system.

3.2.2.5 The introduction of secondary or tertiary recovery systems, which can sometimes increase corrosion rates on the backside of a well casing.

3.2.3 Economic factors

3.2.3.1 Costs of maintaining the well casing in service for its expected life may include repairing corrosion leaks, reconditioning, or replacing all or portions of the system.

3.2.3.2 In addition to the direct costs that result from corrosion, contingent costs may be incurred. The more common types of contingent costs are:

(a) Public liability claims.

(b) Property damage claims.

(c) Damage to natural facilities, such as municipal or irrigation water supplies, forests, parks, and scenic areas.

(d) Cost of cleanup of product lost to surroundings.

(e) Cost of individual casing workover(s) as related to corrosion leak(s).

(f) Plant shutdown and start-up costs.

(g) Loss of deliverability because of possible permanent formation damage caused by casing leak(s).

(h) Cost of lost product.

(i) Loss of revenue through interruption of service.

(j) Loss of contracts or good will through interruption of service.

(k) Loss of reclamation or salvage value of well casing.

(l) Loss of well casing, rendering well unusable for production or injection purposes.

3.2.3.3 The usual costs for protecting well casings are the costs of installing and operating CP. Other corrosion control costs may include:

(a) Inhibitors and bactericides used in drilling fluids.

(b) Corrosion-resistant materials.

(c) Cement for zones known to be corrosive.

(d) Electrical isolation to limit possible foreign current discharge from casings and to ensure that CP currents are applied to the well casing.

(e) Dielectric coating on the outer surface of casing.

Section 4: Criterion for CP and Current Requirements

4.1 Introduction

4.1.1 The determination of design current requirements depends, in part, on prior experience with similar structures or environments in which the method has been used successfully. The first-time user is strongly urged to consult a person experienced in well casing CP before finalizing a design.

4.1.2 Certain methods have been developed through laboratory experiment, or have been derived empirically by evaluating data from successful CP systems. These methods are presented in Paragraph 4.3 and can be used to assist with the design process; they are not intended to be a comprehensive or limiting list.

4.2 Criterion for CP

4.2.1 The CP current applied to the well casing shall be considered adequate when measurements indicate that a net flow of current to the casing has eliminated all anodic areas.

4.3 Methods of Determining Design Current Requirements

4.3.1 A profile tool is a device used to measure a voltage (IR) drop across a portion of well casing in service by electrically isolating two sets of contacts from each other. The voltage readings are used to indicate the magnitude and direction of the current flow in the casing. Details of the test method and interpretation of the data are given in Appendix A.

4.3.2 Average current density (mA/m^2) may be used to calculate the quantity of CP current required to prevent external corrosion. The current density used should be dictated by the downhole completion practice and formations (e.g., cementing practices, formation resistivities, water salinity, etc.) encountered in a given well. Current densities usually vary from 10 to 200 mA/m^2.

4.3.3 Mathematical modeling may also be used to determine design current requirements. The effect of applied CP current downhole can be calculated from electrical measurements at the wellhead. The applied voltage and current distribution can be calculated as a function of well depth. Usually, a downhole potential criterion is established as the accepted indication of protection. Several calculation methods are available, and others are being developed.

4.3.3.1 One method of mathematical modeling uses a modified attenuation equation. The native state potential is measured and recorded. It also requires well casing data and current drain measurements made after polarization of the well.

4.3.3.2 Another method uses formation resistivity data to establish a potential attenuation curve for a casing to which CP has been applied.

4.3.3.3 A third method models the well casing by a computerized equivalent electrical circuit incorporating resistivity profiles, nonlinear polarization characteristics, and the well casing data.

4.3.4 E-log-I method

4.3.4.1 The principle behind the E-log-I method is that when current is impressed through the earth onto a metallic well casing, the potential between the well casing and reference electrode is shifted.

The potential shift for a given current level depends on the following factors:

(a) The length of time the current is applied.

(b) Current density, which is affected by factors such as well depth, casing sizes, and cement.

(c) Properties of the electrolyte.

4.3.4.2 As increasing levels of current are impressed, polarization begins on the surface of the casing. The E-log-I data are plotted to enable selection of a current level at which polarization begins. (Details of the test method and interpretation of the data are given in Appendix B.)

4.4 Methods of Evaluating Effectiveness

4.4.1 A combination of procedures is always advised for evaluating the effectiveness of CP.

Bibliography for Section 4

Ballou, J.K., F.W. Schremp. "Cathodic Protection of Oil Well Casings at Kettleman Hills, California." Corrosion 13, 8 (1957): pp. 507-514.

Bates, R.D., B.W. Bradley. "Cathodic Protection of Oil Well Casings." Materials Protection 5, 7 (1966): pp. 33-35.

Battle, J.L. "Corrosion of Casing in Oil and Gas Wells." Corrosion 9, 9 (1953): pp. 313-320.

Blount, F.E., P.W. Bolmer. "Feasibility Studies of Cathodic Protection of Deep Well External Casing Surfaces." Materials Protection 1, 8 (1962): pp. 10-23.

Dabkowski, J. "Assessing the Cathodic Protection Levels of Well Casings." Final Report PRCI Project, 1983, pp. 106-151.

Dabkowski, J. "Monitoring Cathodic Protection of Well Casings." American Gas Association Conference Proceedings, Operating Section, held May 5-7, 1980. Salt Lake City, UT: AGA, 1980, p. T-411.

Doremus, E.P., F.B. Thorn. "Cathodic Protection Stops Casing Corrosion in Fullerton Field." Oil & Gas Journal 67, 31 (1969): pp. 123-124, 127-128.

Hamlin, A.W. "Cathodic Protection of Gas Storage Wells." West Virginia University Technical Bulletin No. 11-1, 1979, pp. 157-161.

Haycock, E.W. "Current Requirement for Cathodic Protection of Well Casing." Corrosion 13, 11 (1957): pp. 767-773.

Heinrichs, H.J., W.O. Ingram, B.G. Schellenberger. "Cathodic Protection Requirements for Well Casings." Journal of Canadian Petroleum Technology 17, 3 (1978): pp. 54-61.

Hodge, R.E. "Cathodic Protection of Natural Gas Storage Wells." Gas 44, 3 (1968): pp. 63-66.

Husock, B. "Methods for Determining Current Requirements for Cathodic Protection of Well Casings—A Review." Materials Performance 23, 1 (1984): pp. 39-44.

Ingram W.O., B.G. Schellenberger. "Deep Well Casing Cathodic Protection Requirements." Journal of Canadian Petroleum Technology 18, 2 (1979): pp. 39-43.

Kirklen, C.A. "Effectiveness of Well Casing Cathodic Protection." Journal of Petroleum Technology 28 (1974): pp. 724-730.

Pace, F.A., S.E. Krupick. "Reduction of Leaks by Using Cathodic Protection—East Texas Field." Journal of Petroleum Technology 34, 7 (1982): pp. 1437-1442.

Paver, E.C. "Cathodic Protection of Storage Well Casings." Gas Age 32, 12 (1965): pp. 22-27.

Phillips, C.S. "External Protection of Well Casings." West Virginia University Technical Bulletin No. 113, 1974, pp. 581-588.

Riordan, M.A., R.P. Steck. "Well Casing as an Electrochemical Network in Cathodic Protection Design." Materials Protection 2, 7 (1963): p. 58.

Roberson, G.R., F.W. Schremp. "Optimizing the Distribution of Cathodic Protection Current." Journal of Petroleum Technology 22, 7 (1970): pp. 812-816.

Schremp, F.W. "Cathodic Protection of Well Casings Offshore." Journal of Petroleum Technology 34, 8 (1982): p. 1863.

Schremp, F.W., L.E. Newton. "Use of Wellhead Electrical Measurements to Calculate Bottomhole Cathodic Protection of Well Casings." CORROSION/79, paper No. 63. Houston, TX: NACE International, 1979.

Titterington, Y.W. "Cathodic Protection of Well Casing." West Virginia University Technical Bulletin No. 48, 1957, pp. 302-312.

Toncre, A.C. "Cathodic Protection of Well Casings in Saudi Arabia." Metallic Corrosion 7 (1981): pp. 6-11.

Unz, M. "Cathodic Protection of Borehole Casing." Materials Performance 14, 10 (1975): pp. 40-47.

Section 5: Design of CP Systems for Well Casings

5.1 Introduction

5.1.1 This section presents recommended procedures for designing CP systems that effectively control corrosion of well casings in contact with the earth. The design should satisfy the criterion in Section 4 and be reliable for the intended operating life of the system.

5.1.2 CP for pipelines is considered separately from well protection when applicable.

5.2 Objectives of CP System Design

5.2.1 Enable application of sufficient protective current to the well casings to meet the criterion for CP.

5.2.2 Minimize the stray current to foreign underground structures. (See Section 7.)

5.2.3 Design a groundbed with a lifetime that is commensurate with the required life of the protected structure.

5.2.4 Provide for periodic maintenance of the groundbed.

5.2.5 Provide a power source and groundbed with sufficient capacity to include connecting pipelines and other structures as required.

5.3 Considerations in the Design of CP Systems

5.3.1 CP applied to the well casings and the connecting pipelines and structures may be a source of mutual interference. (Refer to Section 7.)

5.3.2 Electrical grounding procedure requirements should be considered in the CP design.

5.3.3 In designing a CP system for well casings, the following should be considered:

5.3.3.1 Availability of AC power should be determined.

5.3.3.2 The proposed installation site should be investigated for any hazardous conditions.

5.3.3.3 The AC power source for the CP rectifier should be a suitable distance from the well structure to ensure a safe working area.

5.3.3.4 Materials and installation practices that conform to applicable codes (e.g., National Electrical Manufacturers Association [NEMA][(2)] Standards, National Electrical Code [NEC],[(3)] and practices of NACE International) should be specified.

5.3.3.5 The CP system should be selected and designed for optimum economies of installation, maintenance, and operation.

5.3.3.6 Materials and installation practices that ensure safe and dependable operation throughout the intended service life of the CP system should be specified.

5.3.3.7 A system for optimum currents should be selected. Excessive current can be detrimental to buried or submerged metallic structures.

5.3.3.8 The current requirement data for pipelines connected to wells should be studied so that the groundbeds may be placed in the proper locations. This allows appropriate distribution of current to wells and pipelines.

5.3.3.9 Electrical interference from foreign sources should be investigated and the results included as a design consideration. (See Section 7.)

5.4 Considerations Influencing Location of Anodes

5.4.1 The anode that will be closest to a well should be placed at a distance determined by testing or accepted empirical means.

5.4.2 Plans for long- and short-term additions or changes in buried physical structures.

5.4.3 Location of pipelines connected to wells.

(2) National Electrical Manufacturers Association (NEMA), 1300 North 17th Street, Suite 1847, Rosslyn, VA 22209.
(3) National Electrical Code (NEC), National Fire Protection Association, 1 Batterymarch Park, Quincy, MA 02269.

5.4.4 Pipelines used as a negative return and those electrically isolated.

5.4.5 Soil resistivity.

5.4.6 Use of surface or deep vertical type of groundbed.

5.4.7 Location of foreign structures.

5.4.8 Placement where likelihood of physical disturbance or damage is minimal.

5.5 Types of CP Systems for Well Casings

5.5.1 Impressed current system

5.5.1.1 Surface groundbed

5.5.1.2 Deep groundbed

5.5.2 Galvanic anode system

5.6 Considerations in the Selection of the Type of CP System

5.6.1 Current requirements

5.6.1.1 The total casing surface area to receive CP, including surface casings and that portion of intermediate and production casing that is to receive protection.

5.6.2 Soil resistivity

5.6.2.1 Resistivity and installation space availability influence the choice of a surface or deep groundbed installation. High-resistivity formations that restrict the flow of current to the casing may necessitate placement of anodes below such formations.

5.6.2.1.1 Resistivity to a 15-m (50-ft) depth for a surface groundbed may be determined by surface measurements or experience.

5.6.2.1.2 Resistivity for depths greater than 15 m (50 ft) for a deep groundbed may be determined by surface measurement, formation resistivity log, or experience.

5.6.3 Future drilling of wells in the area of CP influence.

5.6.4 Future development of the right-of-way area and extensions to the pipeline system connected to wells jointly protected by the same power source and groundbed.

5.6.5 The cost of installation, operation, and maintenance.

5.6.6 Physical space available and condition of land surface for ease of facility installation, ingress, and egress.

5.6.7 Proximity of foreign structures.

5.6.8 Ability to procure easement.

5.6.9 Interference effect.

5.6.10 Power source availability.

5.7 Factors Determining Anode Current Output, Operating Life, and Efficiency

5.7.1 Various anode materials have different rates of deterioration when discharging a given current density from the anode surface in a specific environment. For a given current output, the anode life depends on the anode and backfill materials and the number of anodes in the CP system. Anode performance data may be used to calculate the probable deterioration rate.

5.7.2 The resistance to electrolyte of the anode system may be calculated from available data. Formulas and graphs relating to these factors are available.

5.7.3 The use of a special backfill material with impressed current anodes lengthens their useful life and reduces the effective anode-to-earth electrical resistance. The most common backfill materials are metallurgical coke, calcined petroleum coke, and natural or manufactured graphite.

5.7.4 Entrapment of gas generated by the anodic reaction can impair the ability of the impressed current groundbed to deliver the required current. Suitable provision should be made for venting the anodes, particularly in a deep groundbed. Increasing the number of anodes may reduce gas blockage by reducing current discharge from each anode.

5.7.5 Electroosmotic effects could impair the ability of the impressed current groundbed to deliver the required current. Suitable provisions should be made to ensure adequate moisture around the anodes. Increasing the number of impressed current anodes may reduce electroosmotic effects.

5.7.6 Special applications such as deep groundbeds require careful selection of cables and wires. Refer to NACE SP0572.[1]

5.8 Impressed Current System Design Considerations

5.8.1 Groundbed location and total current required should be determined.

5.8.2 A deep groundbed may be used when lithology prevents equitable distribution of current to the total depth of the well casing. Placing anodes in relatively

low-resistivity shallow formations compared with deeper formations may concentrate excessive current on upper portions of the well casing and deprive the deeper portions of sufficient current. Refer to NACE SP0572.

5.8.3 Placement of groundbeds too close to a well casing may prevent flow of sufficient current to a lower depth. Increasing total current may create interference with other wells and structures.

5.8.4 The performance of vertically or horizontally placed anodes can be affected by their spacing. In a soil of a given resistivity, the output of an impressed current groundbed may be improved by increasing the space between anodes, assuming the additional cable resistance is considered.

5.8.5 DC power sources that can be used:

5.8.5.1 Rectifier units to convert AC to DC power.

5.8.5.2 Thermoelectric generators.

5.8.5.3 Photovoltaic power systems.

5.8.5.4 Wind- or power-driven generators or alternators with rectification.

5.9 Galvanic Anode System Design Considerations

5.9.1 Galvanic anodes have limited use for CP of well casings.

5.10 Design Factors in Applying CP to More than One Well

5.10.1 Several wells may be cathodically protected as a group. When applying CP, the wells should be treated as a unit, along with associated pipelines or structures, using one or more power sources and groundbeds. Care must be taken to ensure adequate current distribution throughout the length of each well.

5.10.1.1 Well casings in a group may vary in length.

5.10.1.2 Well spacing may vary.

5.10.1.3 Intermediate casings may vary in length.

5.10.1.4 Wells with identical completion procedures and equal lengths of casing may have different current requirements.

5.10.2 The current requirements and electrical resistances of any connecting pipeline, when used as a negative return to a rectifier, can limit the amount of current reaching the well casings.

5.10.3 If detrimental electrical interference is encountered, each CP system must be designed to counteract the effects.

5.10.4 CP design varies regarding the physical field parameters. The most effective design considers:

5.10.4.1 Total amount of current required for casings and other structures.

5.10.4.2 Soil resistivity for installation of anodes.

5.10.4.3 Location of well casing with respect to pipelines and other structures.

5.10.4.4 The individual current demand of each well.

5.10.5 Typical CP design options

5.10.5.1 One DC power source and one groundbed for one or several wells.

5.10.5.2 One DC power source and more than one groundbed for several wells.

5.10.5.3 More than one DC power source and one groundbed for several wells.

5.10.6 Perimeter or isolated wells may require a separate CP system.

Bibliography for Section 5

Diffenderfer, R.B. "Cathodic Protection System Design." West Virginia University Technical Bulletin No. 4-1, 1976, pp. 593-603.

Doniquian, T.M. "Pulse Rectifier." Oil & Gas Journal (July 1982): pp. 221-229.

Dwight, H.B. "Calculations of Resistance to Ground." Electrical Engineering 55 (1936): pp. 1319-1328. Also in Materials Performance 22, 4 (1983): pp. 23-33.

NACE Publication 2B160. "Use of High Silicon Cast Iron for Anodes." Houston, TX: NACE International, 1960.

NACE Publication TPC 5. Corrosion Control in Petroleum Production. Houston, TX: NACE International, 1979, pp. 53-65.

Parker, M.E., E.G. Peatlie. Pipeline Corrosion and Cathodic Protection—A Field Manual. Houston, TX: Gulf Publishing Company, 1984, pp. 59-77.

Peabody, A.W. Control of Pipeline Corrosion. Houston, TX: NACE International, 1967, pp. 94-104, 116-119.

Tefankjian, D.A. "Application of Cathodic Protection." West Virginia University Technical Bulletin No. 6-3, 1975, pp. 131-147.

Section 6: Installation of CP Systems

6.1 Introduction

6.1.1 This section presents recommended procedures for installation of CP systems that achieve protection of the well casing structures when design considerations recommended in Section 5 and Appendix D have been followed.

6.2 Construction Specifications

6.2.1 All construction work performed on CP systems shall be done in accordance with construction drawings and specifications. The construction specifications shall be in accordance with recommended practices in Section 5 and nonmandatory Appendix D.

6.3 Construction Supervision

6.3.1 All construction work performed on CP systems shall be under the supervision of a trained and qualified inspector. It shall be the inspector's function to verify that the installation is made in strict accordance with the drawings and specifications, or that exceptions are made only with the express consent of qualified personnel, when it can be demonstrated that the effectiveness of the system is not impaired. It should also be the inspector's function to verify that construction methods and techniques are in accordance with good practices.

6.3.2 All deviations from construction specifications shall be noted on as-built drawings.

6.4 Galvanic Anodes

6.4.1 Inspection and handling

6.4.1.1 Packaged anodes shall be inspected and steps taken to ensure that the backfill material completely surrounds the anode. The individual container for the backfill material and anode should be intact. If individually packed anodes are supplied in waterproof containers, the containers should be removed before installation. Packaged anodes should be kept dry during storage.

6.4.1.2 The lead wire must be securely connected to the anode. The lead wire should be inspected to ensure that it is not damaged. Care should be taken to avoid damage to insulation and kinking of the lead wire.

6.5 Impressed Current Systems

6.5.1 Inspection and handling

6.5.1.1 The rectifier or other power source shall be inspected to ensure that internal connections are mechanically secure and that no damage is apparent. Rating of the direct current source output should comply with construction specifications. Care should be exercised in handling and installation.

6.5.1.2 Impressed current anodes shall be inspected for conformity to specified anode material and size and length of lead wire, and to ensure that the cap, if used, is secure. Care should be exercised to avoid cracking or damaging anodes during handling and installation.

6.5.1.3 The lead wire shall be inspected carefully for defects in insulation (e.g., cracks, abrasions, or excessive thinning below specified thickness). Care should be taken to avoid damage to insulation in the wire. Defects in the lead wire must be repaired or the anode/wire unit must be rejected.

6.5.1.4 Anode backfill material shall conform to specifications.

6.5.2 Installation provisions

6.5.2.1 The rectifier or other power source should be installed so that the possibility of damage or vandalism is minimized.

6.5.2.2 Wiring to rectifiers shall comply with all local and national electrical codes and requirements of the utility supplying power. An external disconnect switch on AC wiring shall be provided. The rectifier case shall be grounded adequately.

6.5.2.3 Impressed current power supplies should be designed to prevent reverse current flow when the unit is not operational.

6.5.2.4 Impressed current anodes should be installed vertically, horizontally, or in deep holes as indicated in the construction specifications. Backfill material, when specified, should be packed around the anodes, eliminating voids. Care shall be taken to avoid damage to the anode,

wire, and wire connection to the anode during installation.

6.5.2.5 The conductor (negative lead wire) to the structure shall be connected as indicated in the specifications. Conductor connections to the power source must be mechanically secure and electrically conductive. Before the power source is energized, it must be verified that the negative conductor is connected to the structure and the positive conductor is connected to the anodes and to the power source output terminals. After the power source is energized, suitable electrical measurements shall be made to verify that these connections are correct.

6.5.2.6 Underground negative lead wire shall be effectively insulated. Bare or ineffectively insulated wire may require a substantial amount of the total protective current.

6.5.2.7 Underground splices on the positive lead cable to anodes shall be kept to a minimum. Connections between cable and conductor from each anode shall be mechanically secure and electrically conductive. If buried or submerged, these connections must be sealed to prevent moisture penetration so that electrical isolation is ensured. If the insulation integrity on the buried or submerged positive lead cable, including splices, is damaged, the cable may corrode and fail prematurely.

6.5.2.8 When specifications call for burial of the anode cable, care must be taken to avoid damage to the insulation. Sufficient slack shall be left in the cable to avoid strain on connections and anode leads caused by settling. Backfill materials used around cables should be free of rocks and foreign materials that might damage the wire insulation when installed in the trench. Cables may be installed by plowing if proper precautions are taken.

6.6 Corrosion Control Test Stations and Bonds

6.6.1 Refer to Section D.5 of Appendix D for design of corrosion control test stations and bonds.

6.7 Isolating the Wellhead from Pipelines and Other Structures

6.7.1 Refer to Section D.2 of Appendix D for design of electrical isolation.

Section 7: Control of Interference Currents

7.1 Introduction

7.1.1 This section presents recommended practices for the detection and mitigation of interference currents.The mechanisms and detrimental effects of interference currents are described.

7.2 Mechanism of Interference Current

7.2.1 Interference current corrosion on a well casing differs from electrochemical corrosion caused by other conditions. The source of the corrosion current is foreign or separate from the affected well. The foreign structure may be electrically bonded to or isolated from the affected well. Interfering currents may enter or leave the casing at several locations along the well casing. The damage from an interference current occurs in the area where the current leaves the well casing and enters the electrolyte.

7.2.2 The severity of interference resulting from stray electrical current depends on several factors:

7.2.2.1 Distance between wells.

7.2.2.2 Location of pipelines with respect to wells.

7.2.2.3 Location of interfering current source.

7.2.2.4 Depth of well casing.

7.2.2.5 Location of highly conductive earth formations.

7.2.2.6 Magnitude of potential gradient in the earth that the affected well penetrates. These gradients are created by current flowing to other structures.

7.2.2.7 Location of electric power line grounding system.

7.2.2.8 Quality and extent of the cementing program on the well casing.

7.2.3 Sources of interference currents:

7.2.3.1 Constant current—Sources that have essentially constant DC output are CP rectifiers, thermoelectric generators, photovoltaic and windmill battery units, etc.

7.2.3.2 Fluctuating current—Typical sources are DC electrified railway systems, mine hauling systems, pumps, welding machines, DC power systems, etc.

7.2.3.3 An interference current may originate in a foreign CP system on nearby wells or pipelines that are electrically isolated from the affected well.

7.2.3.4 Mutual interference current can result from CP applied to other wells in a metallically connected system that includes the affected well.

7.3 Detection of Interference Currents

7.3.1 During well casing CP surveys, personnel should look for electrical changes and facilities that may be a source of interference current.

7.3.1.1 A change in casing-to-electrolyte potential when foreign electrical sources are switched off and on is cause to investigate for downhole well casing interference.

7.3.1.2 Well casing current measurement and downhole well casing potential profiles should be used to assess the presence and magnitude of interference current.

7.3.1.3 The presence of external corrosion and perforation of well casing may be determined by using an electromagnetic thickness measurement tool to find changes in wall thickness.

7.3.2 When interference current is suspected, appropriate tests should be conducted to determine its presence and magnitude. All affected parties shall be notified before tests are performed. (Notification should be channeled through an Underground Corrosion Control Coordinating Committee, where one exists).[4] Any one or a combination of the following procedures can be used to determine the existence or extent of interference:

7.3.2.1 Casing potential changes shall, where practical, be measured with respect to a remote reference electrode. The reference electrode shall be placed beyond the earth gradient field of interfering current. The foreign direct current source should be turned on and off during the test.

7.3.2.2 Change in the magnitude of well casing current should be measured, and the direction of flow should be determined while performing a well casing potential profile. The foreign direct current source should be turned off and on during the test.

7.3.2.3 The variation in current output of the suspected source of interference current should be determined and compared with measurements obtained in Paragraphs 7.3.2.1 and 7.3.2.2. This may require correlation of data with time.

7.4 Methods for Resolving Interference Corrosion Problems

7.4.1 Each interference problem is unique and the solution should be mutually satisfactory to all parties involved.

7.4.2 Mutual interference between well casings may be minimized when wellheads within the electrically connected system are adjusted to equal potential with respect to a remote reference electrode.

7.4.3 The interfering current source should be removed or relocated.

7.4.4 The effect of interference current may be counteracted by adding CP to the affected well.

7.4.5 Mutual interference between wells in a common CP system may be reduced by providing an interference bond, with a current drain regulating device, from the wells to the rectifier.

7.4.5.1 An interference bond of proper resistance should be designed and installed.

7.4.5.2 A current regulating device should be installed in the rectifier cable connected to the wellhead.

7.4.5.3 The current discharge from interfering cathodic rectifiers should be adjusted to eliminate or decrease interference.

7.4.6 The CP groundbed should be relocated.

7.4.7 The design of the CP system should be modified when connecting pipelines (used as negative returns) require a high percentage of the total current for protecting the wells.

[4] Information on Underground Corrosion Control Coordinating Committees may be available from the Technical Activities Division, 1440 South Creek Drive, Houston, TX 77084-4906 (telephone: +1 281/228-6200). Underground Corrosion Control Coordinating Committees are asked to keep NACE International Headquarters informed of their activities, but records are more current on some of the groups than on others.

7.4.7.1 Rectifiers and groundbed with reduced current output per unit should be added.

7.4.7.2 The dielectric coating of connecting pipelines should be improved to reduce the total required current.

7.5 Methods to Indicate Resolution of Interference

7.5.1 A satisfactory downhole well casing potential profile log indicating current that is adequate to eliminate anodic areas on affected casing should be obtained.

7.5.2 Sufficient CP currents, interpreted from surface test data or empirical calculation, should be applied to affected well casing.

7.5.3 Interference current discharges should be neutralized as determined by applicable criteria.

Bibliography for Section 7

Gast, W.F. "Well Casing Interference and Potential Equalization Investigation." *Materials Performance* 13, 5 (1974): pp. 31-36.

Kilpatrick, J.M., L.V. Collings. "Use of Casing Potential Profile Test for Well Casing Interference Studies." API Production Division Southwestern District Spring Meeting, Reprint No. 906-12-L. Washington, DC: American Petroleum Institute (API), March 1967, p. 15.

Roberson, G.R. "Effect of Mutual Interference." *Materials Protection* 6, 3 (1967): p. 36.

Weeter, R.F., R.J. Chandler. "Mutual Interference Between Well Casings with Cathodic Protection." *Materials Performance* 13, 1 (1974): pp. 26-30.

Section 8: Operation and Maintenance of CP Systems

8.1 Introduction

8.1.1 The purpose of this section is to designate procedures and practices for energizing and maintaining continuous, effective, and efficient operation of CP systems.

8.1.1.1 Electrical measurements and inspections are necessary to determine that protection has been established according to the applicable criterion and that each part of the CP system is operating properly. Conditions that affect protection may change with time, however, and corresponding changes are required in the CP system to maintain protection. Periodic measurements and inspections shall be made to detect changes in the conditions that affect the CP system. Local conditions may exist in which operating experience indicates that surveys and inspections should be made more frequently than recommended herein.

8.1.1.2 Care should be exercised in selecting the location, number, and type of electrical measurements used to determine the adequacy of CP.

8.2 Tests shall be conducted after each CP system is energized to determine whether the system is satisfying the applicable criterion and is operating efficiently. Tests shall include one or more of the following types of measurements and must relate to the criterion established by this standard.

8.2.1 Casing-to-reference-electrode potential, as applicable.

8.2.2 Calculation technique to estimate CP effectiveness (refer to Paragraph 4.3.3).

8.2.3 Structure-to-structure potential.

8.2.4 Current flow.

8.2.5 Well casing potential profile (refer to Paragraph 4.3.1 and Appendix A).

8.3 Periodic tests are suggested to ensure the continuity of CP; the electrical measurements used in the tests may include one or more of the measurements listed in Paragraph 8.2.

8.4 Inspection and tests of CP facilities should be conducted as follows to ensure their proper operation and maintenance:

8.4.1 All sources of impressed current shall be checked at intervals not to exceed two months. Evidence of proper functioning may include the current output, normal power consumption, a visual or audible signal indicating normal operation, or the satisfactory electrical state of the protected casing.

8.4.2 All impressed current protective facilities should be inspected annually as part of a preventive maintenance program to minimize in-service failure. Inspections may include a check for electrical shorts, ground connections, meter accuracy, efficiency, and circuit resistance.

8.4.3 Reverse current switches, diodes, and inteference bonds, whose failure would jeopardize structure protection, shall be inspected for proper functioning at intervals not to exceed two months.

8.4.4 The effectiveness of electrical isolation fittings and continuity bonds shall be evaluated during periodic testing. This may be accomplished by on-site inspection or by evaluating corrosion test data.

8.5 The test equipment used for obtaining each electrical value shall be of an appropriate type. Instruments and related equipment shall be maintained in good operating condition and checked annually for accuracy.

8.6 Remedial measures shall be taken when periodic tests and inspections indicate that protection is no longer adequate according to applicable criteria. These measures may include:

8.6.1 Repair, replacement, or adjustment of components of CP systems.

8.6.2 Providing supplementary facilities when additional CP is necessary.

8.6.3 Repair, replacement, or adjustment of continuity and interference bonds.

8.6.4 Removal of accidental metallic contacts.

8.6.5 Repair of defective electrical isolation devices.

Section 9: Corrosion Control Records

9.1 Introduction

9.1.1 The purpose of this section is to describe corrosion control records that document in a clear, concise, workable manner the data pertinent to the design, installation, maintenance, and effectiveness of corrosion control measures for well casings.

9.2 Relative to determination of the need for corrosion control, the following should be recorded when applicable:

9.2.1 Information on corrosion leaks (e.g., date, well identity, location).

9.2.2 Electromagnetic casing thickness measurements.

9.2.3 Casing potential profile data.

9.2.4 Coating type applied to external surfaces of casings.

9.3 Relative to structure design, the following should be recorded:

9.3.1 Location and design of wellhead and associated electrical isolation devices.

9.3.2 Design and procedure for isolating or bonding any associated electrical power source grounding system.

9.3.3 Design and location of test leads, bond cables, and other test facilities.

9.3.4 Details of any other corrosion control measures taken.

.

9.4 Relative to the design of corrosion control facilities, the following should be recorded:

9.4.1 Results of current requirement tests and how the tests were performed.

9.4.2 Results of soil resistivity surveys at groundbed locations, and where the surveys were made with respect to other wells, pipelines, and structures.

9.4.3 Interference tests and design of interference bonds and drainage switch installations, including:

9.4.3.1 Location of interference source relative to location of wells and other structures.

9.4.3.2 Scheduling of interference tests, correspondence with coordinating committees, coordinating committee minutes, and direct communication with the concerned companies.

9.4.3.3 Record of interference tests conducted, including location of tests, name of company involved, and results.

9.5 Relative to the installation of corrosion control facilities, the following should be recorded:

9.5.1 Installation of CP facilities

9.5.1.1 Impressed current systems

(a) Location and date placed in service.

(b) Type, size, depth, backfill, and spacing of anodes.

(c) Number of anodes.

(d) Location of groundbed anodes with respect to wells, pipelines, and other structures.

(e) Specifications of rectifier or other energy source.

(f) Type(s) and size(s) of buried cable.

9.5.1.2 Galvanic anode systems

(a) Location and date placed in service.

(b) Type, size, backfill, and spacing of anodes.

(c) Number of anodes.

9.5.2 Installation of interference bonds and drainage switches

9.5.2.1 Details of interference bond installation

(a) Locations and names of companies involved.

(b) Resistance value or other pertinent information.

(c) Magnitude and polarity of drainage current.

9.5.2.2 Details of drainage switch installation

(a) Locations and names of companies involved.

(b) Type of switch or equivalent device.

(c) Data showing effective operating adjustment.

9.5.2.3 Details of other remedial measures

9.6 Records of surveys, inspections, and tests set forth in Sections 4, 5, 7, and 8 should be maintained to demonstrate that applicable criteria for interference control and CP have been satisfied.

9.6.1 Current drained from the well casing should be recorded at intervals consistent with company requirements.

9.6.2 Other electrical measurements should be recorded as required to monitor the CP for each well and to satisfy the criterion for CP of the wells.

9.7 Relative to the maintenance of corrosion control facilities, the following information should be recorded:

9.7.1 Maintenance of CP facilities

9.7.1.1 Repair of rectifiers or other DC energy sources.

9.7.1.2 Repair or replacement of anodes, connections, and cable.

9.7.2 Maintenance of interference bonds and drainage switches

9.7.2.1 Repair of interference bonds.

9.7.2.2 Repair of drainage switches or equivalent devices.

9.7.3 Maintenance, repair, and replacement of electrical isolation devices, test leads, and other test facilities.

9.8 Records sufficient to demonstrate the evaluation of the need for and the effectiveness of corrosion control measures should be retained as long as the facility involved remains in service. Other related corrosion control records should be retained for a period that satisfies individual company needs.

References

1. NACE SP0572 (latest revision), "Design, Installation, Operation, and Maintenance of Impressed Current Deep Anode Beds" (Houston, TX: NACE).

2. F.W. Anney, "Electrical Resistivity of Oil-Country Tubular Steels," U.S. Steel Technical Report, March 31, 1971.

3. NACE SP0177 (latest revision), "Mitigation of Alternating Current and Lightning Effects on Metallic Structures and Corrosion Control Systems" (Houston, TX: NACE).

4. ANSI/ASME B31.8 (latest revision), "Gas Transmission and Distribution Piping Systems" (New York, NY: ANSI, and New York, NY: ASME).

5. NACE SP0169 (latest revision), "Control of External Corrosion on Underground or Submerged Metallic Piping Systems" (Houston, TX: NACE).

Appendix A—Casing Potential Profile (Nonmandatory)

A.1 Introduction

A.1.1 This appendix describes a typical potential profile tool, its function, and use. Procedures for interpreting data are covered. This appendix supplements Paragraph 4.3.1 of this standard.

A.1.2 The name "casing potential profile" has been widely accepted. The measurement is actually a potential difference, and the plotted data represent a casing potential difference profile. The tool measures a potential difference between two points on the casing as opposed to the potential of a pipe as measured in a pipe-to-soil potential in evaluating pipeline corrosion. The term *potential difference* is used interchangeably with voltage (IR) drop.

A.1.3 A casing potential profile should be performed under the direction of a person qualified by knowledge and experience in this particular endeavor.

A.2 Types of Casing Potential Profile Tools

A.2.1 A typical casing potential profile tool consists of two contacts positioned 3 to 8 m (10 to 26 ft) apart on tubing and separated by an electrical insulator. A wire is attached to each contact and brought to the surface to a voltmeter. The tool is moved along the inside of the casing to take voltage drop measurements as needed. (Refer to Figure A1.)

A.2.2 Some of the contact devices are:

A.2.2.1 Spring-loaded knives that continuously contact the casing while moving up or down. Tension is increased against the casing wall by manipulating the position of knives.

A.2.2.2 "Pipe cutter" wheels permanently tensioned on spreader arms. Wheels continuously ride the casing wall at constant pressure.

A.2.2.3 Spreader arms with contactors that are opened and closed by an electric motor or mechanical means from the ground level. Pressure against the casing wall is adjustable.

A.3 Effect of Electrical Resistance on Data

A.3.1 Variable circuit resistance affects voltage (IR) drop readings. Because the electrical resistance of steel casing is extremely low (in the μ-ohm per m range), the equipment design and procedure used to measure voltage are critical. For example, the voltage measured across approximately 6 m (20 ft) of casing can be in the range of 1 to 5,000 μV. The resistance portion of the electrical circuit consists of the following:

A.3.1.1 The well casing between the profile tool's upper and lower contacts.

A.3.1.2 Other permanent tool fittings and cable and connectors.

A.3.1.3 Contact of the knives to the casing wall at each setting.

A.3.2 Resistance tables for the various casing grades are available.[2] The resistance of the casing for a given API[(5)] grade changes as downhole temperature increases.

[(5)] American Petroleum Institute (API), 1220 L St. NW, Washington, DC 20005.

The resistance of the casing can be measured prior to installation.

A.3.3 A voltage (IR) drop measured across a given length of casing and total resistance can be used to calculate the current flow. The resistance value should be corrected for changes caused by temperature and grade of steel.

A.4 Other Influences on the Measured Voltage (IR) Drop

A.4.1 Thermal voltage differences between upper and lower contacts, casing wall, and knives. This is caused by the contacts riding continuously on the casing wall.

A.4.2 Resistance between contacts and casing wall. Foreign material on the casing wall can increase the total resistance and give an erroneous voltage (IR)

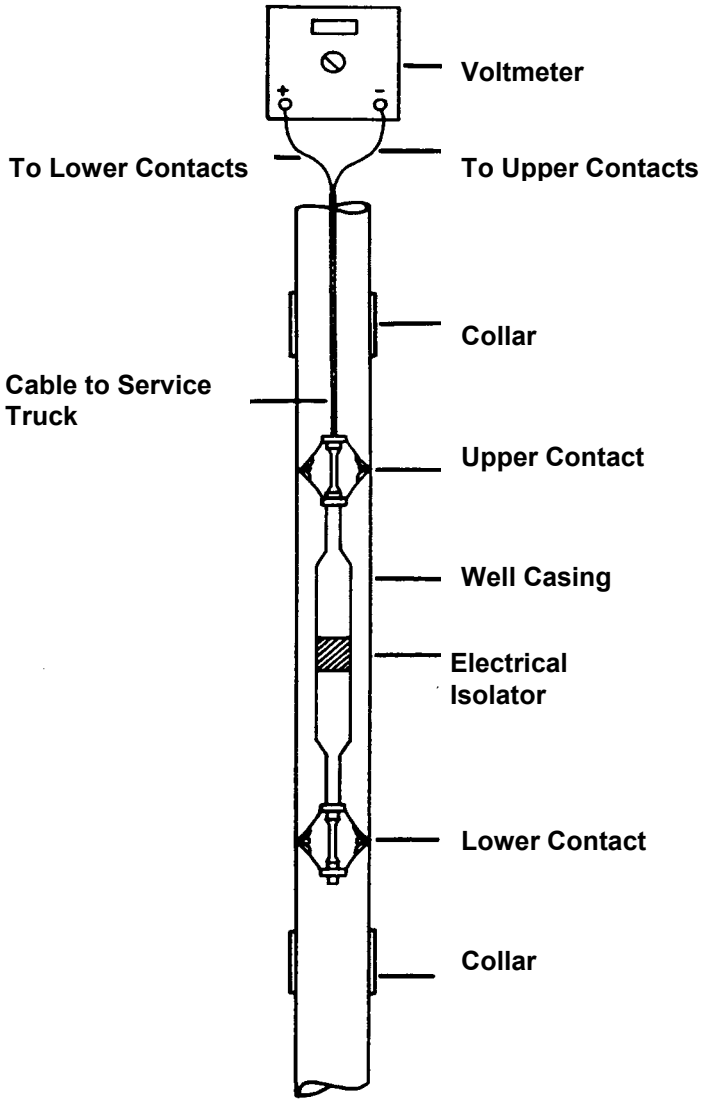

FIGURE A1—Casing Potential Profile Tool

drop reading. Some foreign materials commonly encountered are corrosion products, scale, petroleum deposits, corrosion inhibitors, and moisture.

A.4.3 Ineffective electrical insulation between upper and lower contacts.

A.4.4 Electrically conductive fluid in the casing and in contact with the tool.

A.5 Use of Instruments

A.5.1 Voltmeters with a high impedance and resolution of 1 μV and a short response time are required. They should also have AC rejection and be temperature compensated. Instruments should be calibrated annually.

A.5.2 The accepted procedure is to connect the positive (+) terminal of the voltmeter to the lower contact of the potential tool. A positive reading indicates current flowing up the casing (from positive to negative), and a negative reading indicates current flowing down the casing.

A.5.3 The tool is stopped at a given location in the well casing, and the IR drop readings are repeated, if required, until an acceptable one is obtained. An acceptable reading is one that is consistent with the log and other available data.

A.6 Data Use and Interpretation

A.6.1 A typical example of a casing potential profile plot is shown in Figure A2.

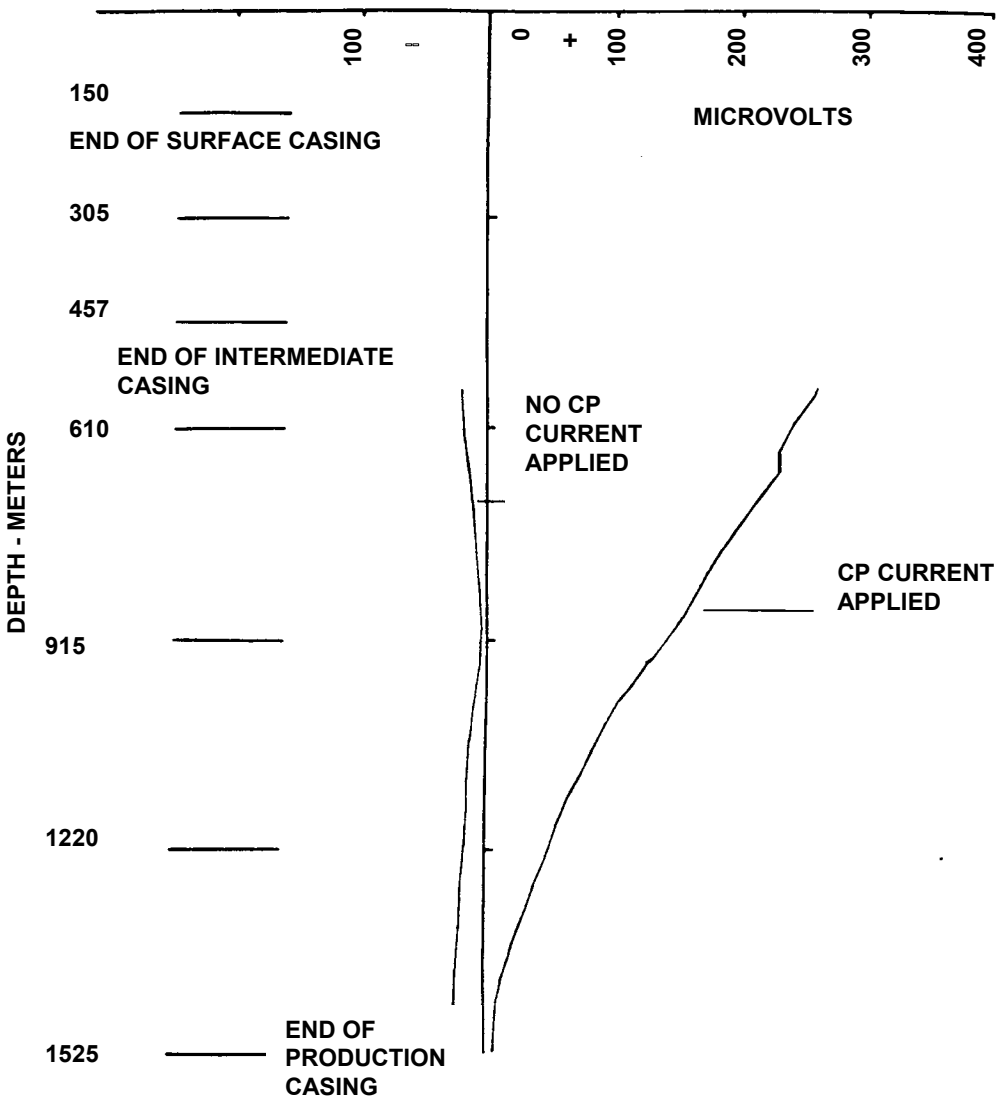

FIGURE A2—Typical Casing Potential Profile Plot

A.6.2 Considerations in interpreting casing potential profile data:

A.6.2.1 Abrupt or inconsistent changes in single readings may indicate poor contact of the tool with the casing wall.

A.6.2.2 Data taken from a production casing shielded by other casing in the well are not necessarily indicative of current gain or discharge from the production casing to the formation.

A.6.2.3 A positive slope of the plotted voltage (IR) drop versus depth normally indicates an increase in the amount of current being picked up by the casing.

A.6.2.4 A negative slope of the voltage (IR) drop normally indicates a discharge of current from the casing.

A.6.2.5 Changes in slope are caused by a change in current or resistance. Resistance changes can be caused by:

(a) Change of wall thickness (e.g., corrosion, manufacturer's tolerance).

(b) Change of API pipe grade.

(c) The bridging of collars by the contacts of the tool.

A.6.2.6 Each voltage (IR) drop reading taken on a section of the casing (typically several meters) measures the long-line current. The local anodic cells are not detectable within the span of the tool. Current pickup is not necessarily uniform along the casing between tool contacts. Therefore, the current density at a given area on the casing may be greater or less than that indicated.

A.6.2.7 Casing potential profile data give a reasonable indication of the amount of current flowing and indicate a direction of current flow. The data cannot be interpreted to determine whether sufficient current is being applied to cancel all corrosion cells.

A.7 Well data for each well can assist in interpreting potential profile readings. These data may include the following:

A.7.1 API grade, diameter, length, and weight of casing joint and its location in the well.

A.7.2 Collar locator, used to facilitate positioning of a casing potential profile tool between collars.

A.7.3 Electromagnetic logs, which help determine changes in wall thickness and grade of casing, and allow evaluation of the inner wall surface condition.

A.7.4 Formation resistivity logs that identify strata that may alter current distribution.

A.7.5 Leak history and repair methods.

A.7.6 Other types of logs for a given well can aid in interpreting casing potential profile data. Refer to Paragraph D.7.4 of Appendix D.

A.8 Interference Testing with the Casing Potential Profile Tool

A.8.1 The casing potential profile tool is valuable when used to determine electrical DC interference. Data obtained pertain only to the conditions prevailing at the time of the test.

Appendix B—E-Log-I Test
(Nonmandatory)

B.1 Introduction

B.1.1 The purpose of this appendix is to outline the procedure for performing an E-log-I test and to give guidelines for interpretation of data. This appendix supplements Paragraph 4.3.4 of this standard.

B.2 General

B.2.1 An E-log-I test should be performed under the direction of a person qualified by knowledge of and experience in this particular endeavor.

B.3 Prerequisites to Performing an E-log-I Test

B.3.1 All buried metallic structures must be electrically isolated from the casing.

B.3.2 The temporary groundbed should be located at a sufficient distance from the well to give optimum current distribution along the well casing. When feasible, it should be placed where permanent bed location is anticipated.

B.3.3 Other buried metallic structures should be located.

B.3.4 Foreign rectifiers or other DC sources that could influence the test should be located.

B.3.5 The locations of high-resistivity strata that make it difficult to force current through underlying formations should be determined.

B.3.6 Placement of the reference electrode should be based on well depth, well spacing, and distance to foreign structures, and it should be beyond the influence of the test groundbed.

B.4 Test Procedure

B.4.1 After the equipment is set up (see Figure B1), the test should be conducted according to the following steps.

B.4.1.1 The "native state" potential, i.e., the potential with zero groundbed current, should be measured and recorded.

B.4.1.2 The test should then be begun by impressing current through the groundbed onto the well casing at the predetermined level (typically 0.1 A, as in Figure B2, for the selected time, typically two or three minutes).

B.4.1.3 At the end of the selected time, the current flow should be interrupted and the potential should be observed. Within a fraction of a second, the potential will drop abruptly. It will then begin a gradual "decay." The potential of interest is that just prior to the start of the decay. This is frequently referred to as the instant-off potential.

B.4.1.4 The current interruption should last no more than two seconds. A higher current should then be applied to the casing at the next predetermined current level. Typically, increments from 0.1 to 2.0 A are used.

B.4.1.5 The current increments should be selected to meet the requirements of individual conditions and to ensure the proper interpretation of the E-log-I test.

B.4.1.6 Time intervals should be consistent throughout the test.

B.5 Interpretation of Test Results

B.5.1 Figure B2 is an example of an E-log-I curve. Casing-electrolyte potentials and current applied are plotted on semilogarithmic scales. The interpretation of the curve is dependent on the experience of the operator. The current required is usually taken at the intersection, point A, or the first point lying on the Tafel segment, point B.

B.5.2 If the E-log-I results have not been verified for a given group of wells, additional testing such as the casing potential profile log should be conducted.

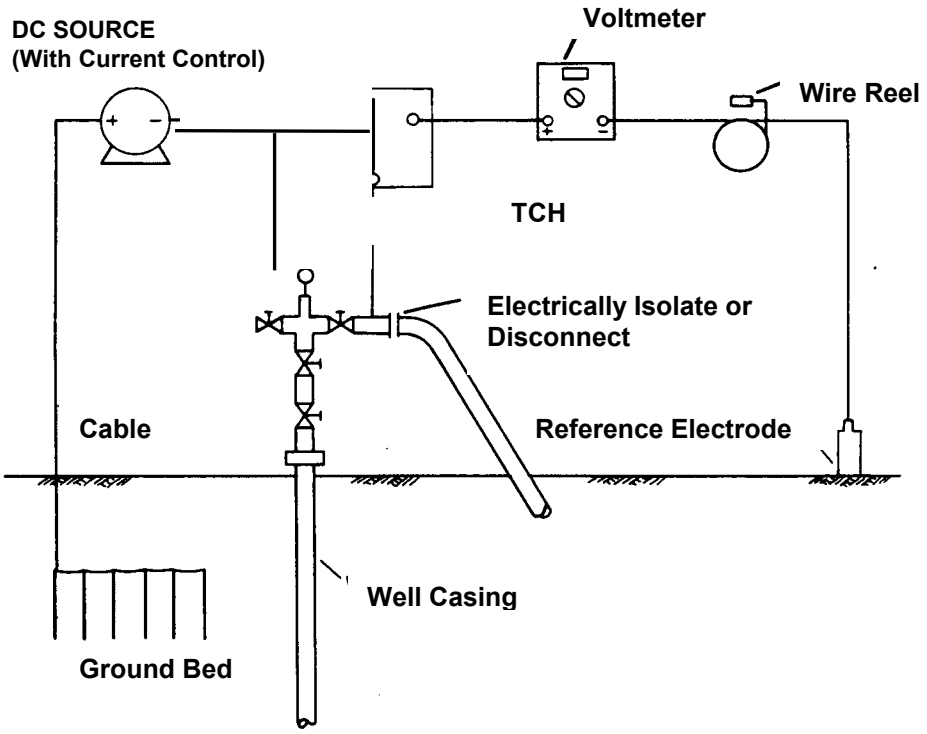

FIGURE B1—Equipment Set-Up for E-Log-I Test

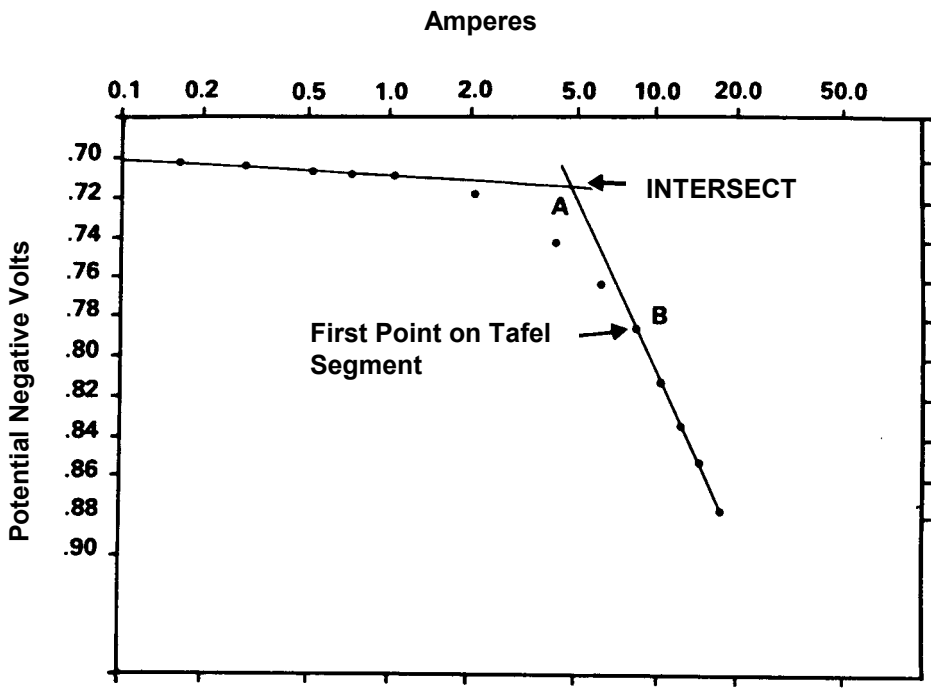

FIGURE B2—Sample E-Log-I Plot

Appendix C—Electromagnetic Casing Inspection Instruments (Nonmandatory)

C.1 Introduction

C.1.1 Subsurface electromagnetic inspection instruments are used to inspect the casing wall for defects. The inspection helps in determining a need to install a CP system or in determining its effectiveness after installation. These instruments fall into two broad categories; one induces an AC electromagnetic field into the casing wall and the other, a DC electromagnetic field into the casing wall. A comparison of these electromagnetic inspection instruments points out the differences in the methods of measurement and the significance of these differences.

C.2 Corrosion Inspection Instruments

C.2.1 The AC inspection instrument derives its signal by detecting the amount of phase shift measured between the low-frequency transmitter coil and the receiver coil. The transmitter coil is energized with a low-frequency AC current, causing an electromagnetic field to be induced into the casing. The field is detected by the receiver coil, usually located 300 to 600 mm (12 to 24 in.) away.

C.2.1.1 The amount of phase shift of the received signal from the transmitter is related to the properties of the casing. These properties are:

(a) Casing weight.

(b) Casing size.

(c) Casing grade, including permeability and conductivity.

(d) Metallic influence outside casing, if inspected casing is inside another casing (e.g., scratchers, centralizers).

C.2.1.2 The predominant response is a result of the change in the casing weight. Because there is an “averaging” effect between the transmitter and receiver coil, there must be significant metal loss (e.g., by corrosion) with respect to normal casing weight to cause a meaningful change in the phase shift.

C.2.1.3 The accuracy is such that a change from one API casing weight to another of the same size

casing is detectable. It is responsive to the change in the amount of metal, whether the change is internal or external.

C.2.1.4 Supplementally, a noncontact electronic caliper is usually available for added internal information, and some instruments are also equipped with a set of closely spaced coils to provide uncalibrated indications of small defects.

C.2.2 The DC inspection instrument derives its casing defect signal by detecting a disturbance in an otherwise stable magnetic field within and surrounding the casing wall. The stable magnetic field is induced into the casing wall. A defect such as a corrosion pit causes a field irregularity or "flux leakage" at that point on both sides of the casing wall, whether the defect itself is on the inside or the outside wall of the casing. This disturbance can be created by a single pit, an isolated defect, or by a group of closely located pits, i.e., general corrosion. The instrument sensors detecting the field disturbances are small and are in contact (as close as possible) with the internal circumferential surface of the casing.

C.2.2.1 Signals emitted by these sensors are caused by changes in the field disturbances, which vary because of:

(a) The strength of the induced DC magnetic field.

(b) Defect depth.

(c) Defect shape.

(d) Metallic influence outside casing (e.g., scratchers, centralizers, another casing).

(e) Casing wall thickness.

(f) Casing size.

(g) Casing grade, including permeability and conductivity.

(h) The speed with which the sensor passes the defect.

C.2.2.2 Techniques currently in use utilize the amplitude of the sensor signal. Although casing wall thickness affects the signal amplitude, the sensor does not discern that thickness; the amplitude response is usually calibrated to indicate depth of defect penetration in percent of the total casing wall thickness.

C.2.2.3 Instrument sensitivity is normally limited to defect depths greater than 20% of the casing wall and defect areas greater than 32 mm (1.3 in.) in diameter. Accuracy of the corrosion defect measurement is approximately ±15% of defect depth in ideal single-string conditions when the casing information is known (e.g., weight, grade, etc.)

C.3 The information presented in Table C.1 may be used to determine which instrument is the most effective for certain situations.

C.3.1 Normally, operating conditions for both instruments are for temperatures up to 177°C (351°F), pressures of 100 MPa (14,500 psi), and casing sizes from 110- to 250-mm (4.3- to 9.8-in.) outside diameters. Some instruments can operate in conditions beyond these limits. The performance of either instrument is degraded when run in a multistring casing; however, the DC instrument's operation is less affected.

C.3.2 The running of base logs as soon as possible is recommended for better evaluation of future data.

C.3.3 Clean casing walls result in more reliable inspections.

TABLE C.1—Instrument Effectiveness

Type of Instrument	Detects Casing Collars	Detects Small Defects and Defect Depths	Detects Large Holes in Casing	Detects Casing Weight Change	Detection of Outer Casing String	Detects Parted Casing String	Detects Drill Pipe Wear
AC	Yes	No	Yes	Yes	Yes	Yes	Yes
DC	Yes	Yes	Yes	No	No	Yes	No

Appendix D—Well Completion Design and Other Factors Associated with CP (Nonmandatory)

D.1 Introduction

D.1.1 The purpose of this appendix is to provide accepted corrosion control practices for the design of CP systems for oil production, natural gas production, and natural gas storage wells and associated aboveground facilities. A person qualified to practice corrosion control should be consulted during all phases of well design and installation (see Paragraph 1.5.) These recommendations should not be construed as taking precedence over recognized electrical safety practices. Electrical grounding procedures at the well surface must conform to local, state, and national codes.

D.2 Electrical Isolation

D.2.1 Isolating devices consisting of flange assemblies, prefabricated insulating joints, unions, and couplings should be installed to isolate the well production casing electrically from other wells, associated pipelines, gauge lines, and structures when required to facilitate the application of corrosion control. These devices should be properly rated for temperature, pressure, and dielectric strength. Installation of isolating devices should be avoided in enclosed areas where combustible atmospheres are likely to be present. Typical locations at which electrical insulating devices may be considered are as follows:

D.2.1.1 Where facilities change ownership, e.g., the wellhead.

D.2.1.2 At the junction of bare well casing and associated pipelines and facilities.

D.2.1.3 At the junction of dissimilar metals (to prevent galvanic corrosion).

D.2.2 Isolating devices

D.2.2.1 Inspection and electrical measurements should be performed to ensure that electrical isolation is adequate.

D.2.2.2 Buried isolating devices should be suitably coated or wrapped with insulating material to prevent electrical current transfer through the surrounding soil.

D.2.2.3 Additional or special isolating devices may be needed on pipelines containing conductive fluids.

D.2.3 The need for lightning and fault current protection at isolating devices should be considered. Cable connections from isolating devices to arrestors should be short, direct, and of a size suitable for short-term, high current loading.

D.2.4 When electrical contact would adversely affect CP, well casings should be electrically isolated from supporting pipe stanchions and structures.

D.2.5 When an isolating device is required, proper pressure-rated materials manufactured to perform this function should be used and installed according to manufacturer's recommendations.

D.2.6 As much distance as is practical should separate well casings, associated pipelines, and other facilities from electric transmission tower footings, ground cables, and counterpoise. Regardless of separation, consideration should always be given to lightning and fault current protection of well casings and safety of personnel. (See NACE SP0177.[3])

D.2.7 Plastic fittings used in chemical pump lines must meet electrical and physical requirements.

D.2.8 Isolation of high-temperature natural gas discharge and oil lines requires special design considerations for use of materials.

D.2.9 Nonmetallic isolators should meet specifications for use in buried and aboveground applications, as required.

D.3 Electrical Continuity

D.3.1 Consideration should be given to the electrical properties of screwed casing couplings. To ensure electrical continuity, low-electrical-resistance thread compounds should be used.

D.4 Coatings

D.4.1 A dielectric coating used on a well casing requires a surface that provides a good physical bond between it and the formation or cement to ensure a sealed environment. NOTE: Coatings used on well casings require special dielectric, physical, and chemical qualities, which are beyond the scope of this standard.

D.5 Corrosion Control Test Stations and Bonds

D.5.1 Test stations for potential and current measurements should be provided at the well to

facilitate CP testing. Such use may include, but not be limited to, the following:

D.5.1.1 Well production casing.

D.5.1.2 Well surface and intermediate casings.

D.5.1.3 Dehydration, oil pumping, natural gas compressor, and other similar facilities.

D.5.1.4 Foreign metallic pipelines or facilities near the well.

D.5.1.5 Gauge lines.

D.5.2 Test leads should be color coded or otherwise permanently identified. Wire should be installed with slack. Damage to wire insulation should be avoided. Test leads should not be exposed to excessive sunlight. Aboveground test stations are preferred. If test stations are flush with the ground, adequate conductor slack should be provided within the test station to facilitate test connections.

D.5.3 An isolating device can be accommodated by attaching an appropriate test wire and low-resistance current-carrying cable to each side of the device. These cables and wires should be appropriately color coded or labeled and terminated at a convenient location for bonding when needed. Shunts may be used to measure current.

D.5.4 The test station may accommodate current-carrying cable when a pipeline is utilized as the negative return. Current-carrying cable or wire should not be used as a contact for taking casing-to-reference-electrode potentials.

D.5.5 Attachment of test leads and cables to steel well casings and equipment

D.5.5.1 Test leads are usually attached to an aboveground fitting, which is directly connected to the well casing. Soldering or thermit welding may be used to attach wire or cable when heating requirements do not exceed the temperature limit for casing and fittings. NOTE: Care should be taken to ensure that specified temperature limits are not exceeded during thermit welding to prevent damage to the pipe by copper penetration. Consult ANSI[(6)]/ASME[(7)] B31.8[4],Paragraph 862.115 on Electrical Connections and Monitoring Points, for additional guidelines on thermit welding. Mechanical connections to flanges and other fittings can be used if they remain secure and maintain low resistance. Refer to NACE SP0169.[5]

D.5.5.2 Attaching test wires directly to the production casing below ground level is beyond the scope of this standard. Special consideration must be given to requirements for cementing and completion procedures.

D.5.6 Coating of test wire attachments

D.5.6.1 All test lead wire and cable should be coated with a direct burial type of electrical isolating material. Attachments to fittings or casings should be coated with a dielectric material. The coating should be compatible with the existing coating on the fitting or casing.

D.6 CP

D.6.1 Refer to Sections 5 and 6 of this standard for the design and installation of CP.

D.7 Information Useful for the Design and Monitoring of a CP System

D.7.1 Well piping system specifications and practices.

D.7.1.1 Total length, size, weight, API grade, and location of each casing string in the well.

D.7.1.2 Electrical resistance of steel casing. Tables are available for various grades and temperatures. [(8)]

D.7.1.3 Coatings (dielectric)—well casings and connecting pipelines.

D.7.1.4 Cement types and grades, and locations of cemented intervals.

D.7.1.5 Drilling mud—type, inhibitor.

D.7.1.6 Additives to cement or mud.

D.7.1.7 Completion data regarding backfill around casing and the location of cement or other material.

D.7.1.8 Surface well fittings such as valves for access to casing.

D.7.1.9 Locations of metallic scratchers and centralizers.

D.7.1.10 Locations of metallic stress rings.

---

(6) American National Standards Institute (ANSI), 1819 L St., NW, Washington, DC 20036.
(7) ASME International (ASME), Three Park Avenue, New York, NY 10016-5990.
(8) Casing resistance data tables available from Manager, Casing Inspection Services, Dresser Atlas, Box 1407, Houston, TX 77251. Tables were based in part on data found in a U.S. Steel Technical Report.[2]

D.7.1.11 Acidizing procedures.

D.7.2 Well and associated pipeline site environments

D.7.2.1 Existing and proposed CP systems.

D.7.2.2 Possible interference sources (see Section 7 of this standard).

D.7.2.3 Surface environmental conditions.

D.7.2.4 Foreign buried metallic structures (including location, ownership, and corrosion control practices).

D.7.2.5 Site accessibility.

D.7.2.6 AC power availability.

D.7.2.7 Status of well's electrical isolation from foreign structures.

D.7.3 Field survey, corrosion test data, and operating experience

D.7.3.1 Electrical resistivity of the electrolyte (soil).

D.7.3.2 Electrical continuity (low resistance is required across well casing threaded couplings).

D.7.3.3 Cumulative leak history.

D.7.3.4 Interference current data.

D.7.4 Well logs used to supplement other test data utilized for design

D.7.4.1 Electromagnetic alternating current and direct current logs (thickness gauge).

D.7.4.2 Electric log—formation resistivity normally available from well completion data.

D.7.4.3 Gamma ray neutron log—determines relative lithology for location of high-resistivity formations.

D.7.4.4 Collar locator log—facilitates other logs such as casing potential profile.

D.7.4.5 Cement bond log or temperature log—indicates where cement is located between well casing and formation.

D.7.4.6 Optical inspection inside casing.

D.7.4.7 Caliper log (mechanical feelers) to determine internal wall thickness change or defects such as corrosion pits.

D.7.4.8 Dual induction resistivity log.

Ex. II - 37

Symposium on Casing Cathodic Protection Theory†

PREFACE

JOHN W. STOUT*

The protection of oil-well casing from outside corrosion is of prime importance to the oil industry. Cathodic protection is one method that is being applied on a large scale in several California oil fields to reduce or control outside casing corrosion. This symposium was conceived to briefly describe the theory of casing cathodic protection and to give the industry the benefit of the case histories of four current major casing cathodic protection projects in California

PART 1
FUNDAMENTALS OF CATHODIC PROTECTION AS APPLIED TO OIL-WELL CASING

F. W. SCHREMP‡

ABSTRACT

This paper presents a review of the processes of corrosion and cathodic protection of oil-well casing Various criteria used for the determination of cathodic current requirements are discussed A comparison also is made of the advantages and limitations of each criterion.

INTRODUCTION

This paper is concerned with the processes of corrosion and cathodic protection of iron in an earth-electrolyte environment. A review of corrosion processes is presented before discussion of cathodic protection because the concepts of cathodic protection are intimately associated with the processes of corrosion Electron flow is used as the convention of current flow throughout the paper Electron flow is opposite to the direction of positive current flow.

Corrosion

Corrosion in an electrolyte is an electrochemical process. Metal goes into solution at anode areas, and a current of electrons flows through the metal and is discharged at cathode areas The amount of current flowing is controlled by the relative areas of anodes and cathodes as well as the potential differences existing between the anodes and cathodes. Potential differences may be caused by surface defects in the metal and/or differential environmental conditions such as variations in electrolyte concentration, pH, and dissolved oxygen content, to name a few.

The corrosion of iron involves the solution of iron at anodic areas and deposition of hydrogen at the cathodic areas. The process goes on in such a way that the electrolyte remains electrically neutral; i.e., an equivalent number of positive ions are displaced from the electrolyte for every iron atom dissolved into the electrolyte. Typical iron corrosion reactions are shown in Fig 1.

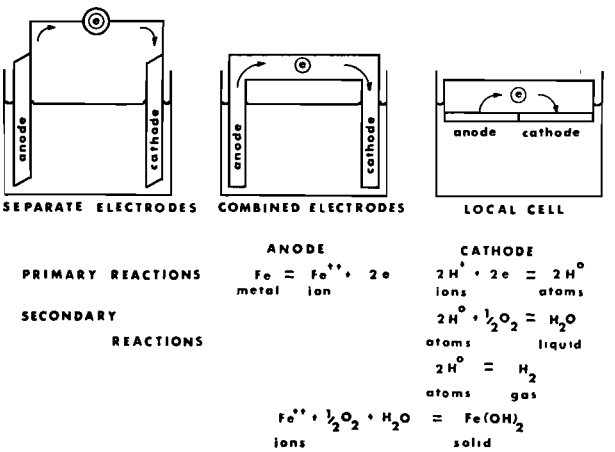

Fig. 1 (Schremp)—Corrosion Reactions of Iron in an Electrolyte

*Standard Oil Co of California, Taft, Calif
†Presented at the spring meeting of the Pacific Coast District, Division of Production, Los Angeles, Calif, April 30 and May 1, 1959
‡California Research Corp, La Habra, Calif.

Hydrogen film formation is the primary cathode reaction and tends to limit the corrosion process in two ways *1*, by insulating the iron surface from the electrolyte, and *2*, by increasing the tendency for hydrogen to re-enter solution and thus oppose the tendency for iron to dissolve. Formation of a hydrogen film is called "polarization" and removal is called "depolarization."

A hydrogen film usually is not sufficient to stop corrosion completely because the film may be damaged by the formation and release of hydrogen-gas bubbles or combination of hydrogen with dissolved oxygen. In either case, removal of the hydrogen film permits the corrosion process to continue. In acid solutions, the hydrogen film is destroyed mainly by the formation and release of hydrogen gas In alkaline solutions, the hydrogen combines with dissolved oxygen.

Dissolved iron usually is precipitated as iron hydroxide. If the precipitate falls on the metal surface, it may slow the corrosion process by acting like a protective coating Iron hydroxide also will react with dissolved oxygen to form ferric hydroxide and may reduce the corrosion rate if the supply of dissolved oxygen is limited.

It is apparent from this discussion that corrosion may be controlled if the cathode areas are maintained in a polarized condition and if hydroxide and insoluble reaction products are deposited on the cathode areas Perhaps the most effective way to achieve a polarized condition is to apply a counter current between the metal and the electrolyte sufficient to neutralize the corrosion current and thus prevent the metal from going into solution Application of a counter current is called cathodic protection. Subsequent sections of this paper will be devoted to the discussion of cathodic protection and the criteria that have been developed to implement its use.

Cathodic Protection

Use of a counter current has been called cathodic protection because the corroding metal surface is made the cathode in a cell reaction involving the metal and a sacrificial anode. Such a system is illustrated in Fig. 2

Electrochemically, magnesium is more inclined to dissolve than iron, and as a result electrons are released at the magnesium anode and flow through the external circuit to the steel casing, thereby offsetting the tendency for iron to dissolve. Of course, the fact that a metal is more electronegative than iron; i e., shows a greater tendency to dissolve, does not mean that the metal can be used effectively as a sacrificial anode to prevent the corrosion of iron. Sufficient electrons must be supplied by the anode to satisfy the demands of all the cathode areas on the steel surface High ground resistance and too small a potential difference between the anode and the casing will prevent most metals that are electronegative to iron from being useful as sacrificial anodes.

One way of circumventing the problem of too small a potential difference is to use a rectifier system that can

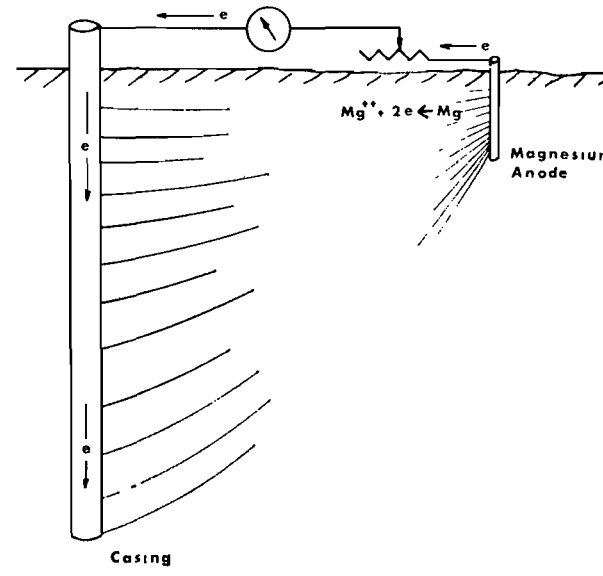

Fig. 2 (Schremp)—Cathodic Protection Using A Sacrificial Anode

supply large amounts of current and an anode bed made from scrap iron, carbon rods, or Duriron. The rectifier system can then be adjusted to supply the desired amount of current to the casing.

Determination of cathodic current requirements for oil-well casings is difficult because direct measurement of corrosion currents is impractical Instead, a number of criteria have been developed that are useful in estimating current requirements Several of the more widely used criteria are discussed in the following section.

Criteria for Current Requirements

Three of the criteria for cathodic current requirements are illustrated by the use of a polarization-potential diagram The diagram of a single anode and cathode cell is shown in Fig 3. Lines E_c-S' and E_a-S are the polarization curves for the cathode and anode, respectively. The point E_c represents the open circuit potential of the cathode area and E_a, the open circuit

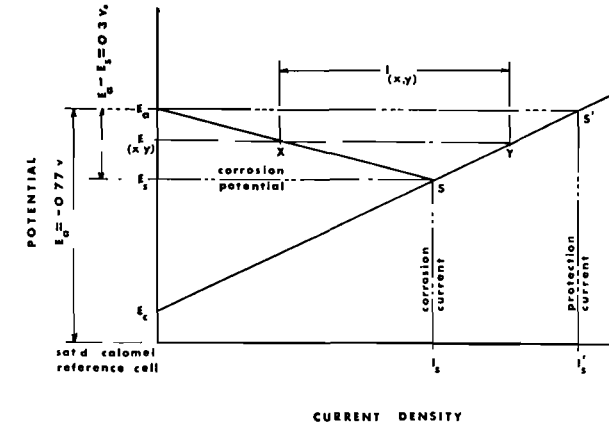

Fig. 3 (Schremp)—Polarization Diagram of a Single Corrosion Cell Illustrating Various Criteria for Cathodic Protection

potential of the anode area Both potentials refer to a saturated calomel half cell Point S defines the corrosion potential E_S and current I_S of the combined cell.

Cathodic-protection theory requires that the cathode potential shift along S-S' toward Y and the anode potential along S-E_a toward X when a counter current is applied to the cell Theory also states that when X reaches E_a, i e, when the polarized potential $E_{(x,y)}$ of the cell equals the open circuit potential E_a of the anode, the anode current is zero and corrosion ceases. Point S', therefore, defines the external current I_S' required to stop corrosion.

Following is a brief discussion of the more widely used criteria.

1. Pipe-to-soil potential. According to this criterion, corrosion will stop when the pipe-to-soil potential is equal to the open circuit potential of the anode areas Laboratory work shows that the open circuit anode potential depends upon the activity of ferrous ions in the corrosive environment. Pure iron in equilibrium with a solution of ferrous ions, $Fe(OH)_2$ at pH = 8 3, has a potential of —0.77 volts referred to a saturated calomel half cell, —0 85 volts referred to Cu; $CuSO_4$ Hence, if the pipe-to-soil potential of the casing can be raised to a value of —0.77 volts referred to saturated calomel, corrosion will stop Schweidtfeger and McDorman[1] verified this behavior in a series of experiments involving the corrosion of steel in various soils. Of course, field conditions may affect the potential at which corrosion stops, but the result is to lower the potential requirement The potential criterion of —0 77 volts may, therefore, err on the conservative side Ballou and Schremp[2] have attempted to extend the usefulness of this criterion to oil-well casing by proposing a relationship between down-hole pipe-to-soil behavior and surface measurements Their work indicates that down-hole polarization may be estimated from surface measurements alone

2. Potential shift. Field experience has shown that the corrosion potential of steel seldom is more than 0 2 to 0 3 volts below the open circuit potential of the anodic areas This is true because polarization of buried steel is largely under cathodic control Reference to Fig. 3 shows that the first and second criteria are similar because they both depend upon raising the casing potential to the open circuit potential of the anode areas.

3. Current density This criterion is based almost entirely upon field experience Pipeline engineers have found that current densities ranging from 0.5 to 20 milliamperes per square foot of exposed pipe surface will prevent corrosion in surroundings ranging from high-resistivity soil to sea water. Current densities in the range of 1½ to 3 milliamperes per square foot appear to be satisfactory for the prevention of casing corrosion.

4. Break in the polarization potential, log-current curve. This criterion was first reported by Britton[3] in 1931 and is best explained by the use of polarization diagrams. Polarization under cathodic control is shown in Fig. 4a, and polarization under mixed control, in 4b. Associated with each curve is a plot of the polarization potential-vs -log applied current

Reference to Fig 4a shows that under cathodic control the cell potential is virtually the same as the open circuit potential of the anode area. Application of counter-current to such a system causes no change in the cell potential until a certain minimum current, I_S is exceeded. Application of currents greater than I_S causes the potential to increase. The increase in potential with applied current now obeys the Tafel equation for hydrogen overvoltage. Protective current is indicated by I_S' and corresponds to the break in the *E-vs.-log I* curve

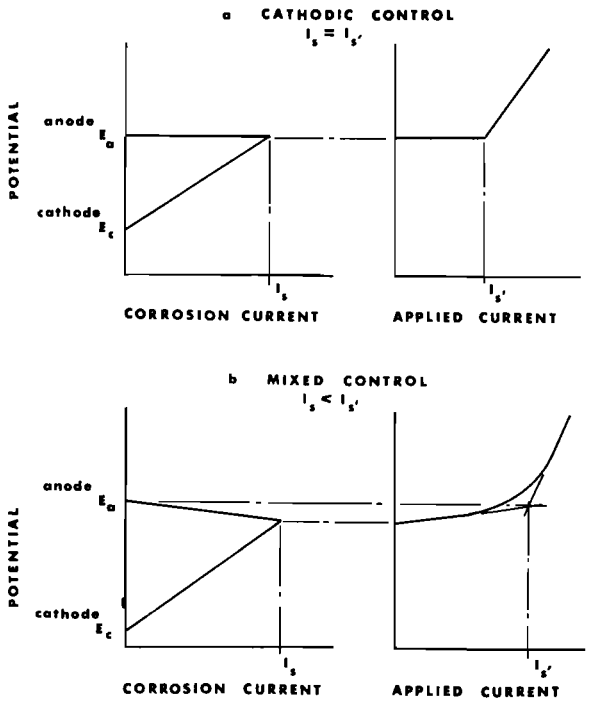

Fig. 4 (Schremp)—Effect of Polarization on Current Requirements

Fig 4b shows that the corrosion current I_S is less than the required protective current I_S'. Polarization behavior under mixed control is different from the behavior under cathodic control because the anode and cathode polarization potentials are not identical functions of the applied current. For low values of applied current, the composite polarization potential increases slightly At higher values of applied current, the slope of the *E-vs.-log I* curve continues to increase Ultimately, values of current are reached that cause the polarization potential to obey the Tafel equation. Mixed control makes difficult the determination of the current required to prevent corrosion One way to determine current from the *E-vs.-log I* curve is to extend the straight-line portions of the curve and use the point of intersection to indicate the proper current.

[1]References are at the end of Part 1

Eldredge and Haycock[4] studied current requirements under mixed control behavior and found that for oil-well casings a more accurate indication of current is given by the point at which the *E-vs.-log I* curve straightens out and begins to obey the Tafel equation Both the intersection and Eldredge-Haycock criteria are illustrated in Fig 5.

A fifth and final criterion involves the measurement of IR drops along the casing The plot of IR drops vs. well depth is called a potential profile. Inasmuch as the IR drops are a function of the corrosion current flowing in the casing, changes in the slope of the potential profile indicate regions where current is either being picked up or discharged from the casing. Corrosive intervals are indicated by negative slopes on the potential profile. Erasure of negative slopes by the use of counter-current is believed to indicate cessation of corrosion

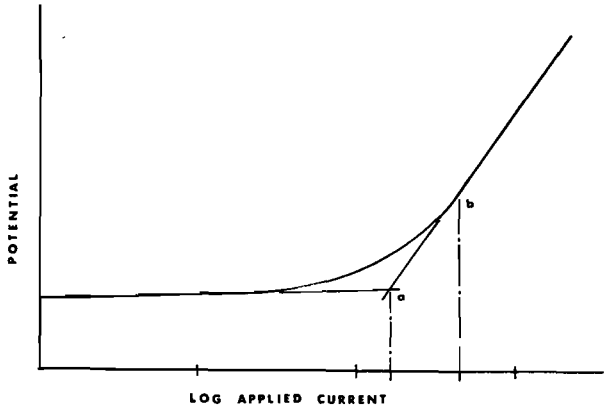

Fig. 5 (Schremp)—Current-potential Curve Showing Two Ways of Estimating Current Requirements

The measurement of potential profiles has been described in detail elsewhere.[5,6,7] For purposes of this paper, the potential-profile logging setup is shown schematically in Fig. 6. An explanatory profile is shown in Fig 7.

Reference to Fig. 7 shows that in region *A*, electrons are flowing from the casing and the slope of the potential profile is positive This indicates a cathodic region. In region *B* the slope is vertical, indicating that current is not entering or leaving the casing Such behavior might result if the casing were cemented through the interval Region *C*, which is anodic, shows a negative slope on the potential profile Electrons are entering the casing and metal is being dissolved. Region *D* is another cathodic area. No mention is made of the direction current flowing in the casing because it has no bearing on the interpretation of the potential profile. The slope of the profile through various intervals is important because it indicates the rate at which electrons enter or leave the casing. Severity of corrosion increases as the negative slope approaches the horizontal.

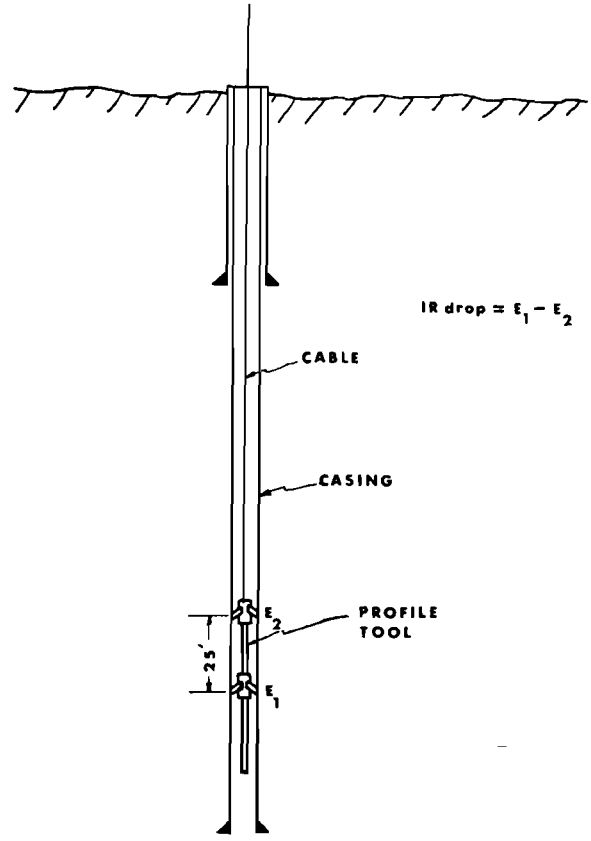

Fig. 6 (Schremp)—Casing-potential Profile Logging Setup

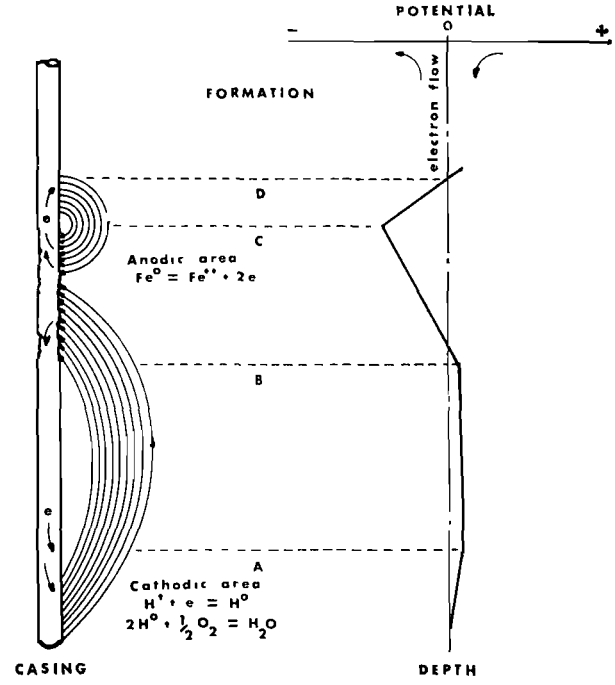

Fig. 7 (Schremp)—Casing-potential Profile

Table 1 (Schremp)

Advantages and Limitations of the Various Criteria Used to Estimate Cathodic Protection Current Requirements

Criterion	Advantages	Limitations
1. Pipe-to-soil potential of —0 85 volts (Cu; $CuSO_4$ reference)	Inexpensive measurement to make If used properly, will give a conservative estimate of current required.	Potential should be measured at the bottom of the casing. Usefulness of Ballou, Schremp-type surface measurements not completely evaluated.
2 Potential shift	Same as *1*.	Depends upon the assumption that the average corrosion potential of steel is 0.2-0 3 volts more cathodic than the open circuit anode potential. Potential shift also should be measured down hole.
3. Current density	Useful in making preliminary estimates of current requirements.	This is only a secondary criterion. Knowledge of cathodic-protection requirements for a given area must be available if reliable estimates are to be made.
4 "Break" in *E-log I* curve	Does not depend upon the open circuit anode potential to arrive at an estimate of current required. Gives a reasonably accurate estimate of current requirements. Relatively inexpensive to use.	Break in *E-log I* curve must be quite distinct if reliable estimates of current requirements are to be made Also, this method will not indicate the amount of current needed to prevent severe local cell action.
5 Potential profile	Indicates the probable location of gross anodic areas. Gives a qualitative picture of gross corrosion on the casing.	Erasure of negative slopes usually results in too low an estimate of cathodic current required. Profile cannot identify local cell action, hence erasure of negative slopes cannot indicate complete protection. Measurements are expensive to make.

SUMMARY

Cathodic protection involves the application of sufficient counter-current to neutralize the corrosion current and prevent iron from going into solution. Five criteria for estimating current requirements were discussed. Perhaps the most widely used criterion is the "break" in the *E-log I* curve Popularity of this criterion probably results from the relative simplicity of measurement. all measurements can be made above ground.

The relative usefulness of each criterion previously discussed is indicated in Table 1

REFERENCES

[1]Schwerdtfeger, W. J and McDorman, O N. *J. Research,* National Bureau of Standards, **47**, 104 (1951).

[2]Ballou, J. K. and Schremp, F. W. *Corrosion,* **13** [8] 35 (1957)

[3]Evans, U. R, Bannister, L. C; and Britton, S. C: *Proc. Royal Soc. A.,* **131**, 367 (1931).

[4]Haycock, E W: *Corrosion,* **13** [11] 89 (1957).

[5]Ewing, S. P and Bayhi, J. F: *Corrosion,* **4** [6] 264 (1948).

[6]Sudbury, J. D; Landers, J. E; and Shock, D. A· *J. Petr. Tech.,* **7** [6] 92, (1955).

[7]Barrett, J. P and Gould, E. D.· *World Oil,* **142** [3] 149 (1956).

BIBLIOGRAPHY

Speller, F. N· *Corrosion, Causes and Prevention,* McGraw Hill, New York, 1951

Cathodic Protection, A Symposium, by the Electrochemical Society and the National Association of Corrosion Engineers, published by NACE, 1949.

Contributions of J. M. Pearson to *Mitigation of Underground Corrosion,* published by NACE, 1956.

PART 2
CASING CATHODIC PROTECTION — SAN MIGUELITO FIELD

JACK A. BIREN*

ABSTRACT

Cathodic protection of oil-well casings in the San Miguelito Field has been effective in reducing oil-well casing failures Ten amperes of protective current as determined empirically with potential-profile techniques were recommended to provide protection from "normal" corrosion and from interference from surrounding cathodically protected wells Separate rectifier control and anode beds which serve from 1 to 4 wells are used in the 160 well installations Anode-to-soil resistance has prevented the use of recommended amperage at many wells Most failures have occurred in the first 10 years of well life, indicating a polarizing effect Evaluation cannot be completed until the 10-amp current is applied to all wells However, some protection is afforded at present current levels.

INTRODUCTION

A cathodic-protection installation believed to be the first to include all well casings in an entire oil field was put in operation during February 1956 at Continental's Grubb Lease, Ventura County, California Casing failures which have been attributed to external corrosion began in 1940 and increased logarithmically with time until a total of 29 such failures had occurred prior to completion of the cathodic-protection installation In addition to the loss of two wells and the resultant redrilling of another, the repair costs ranged from $7,557 to $70,956 and averaged $33,200 per well. In five instances where production could be continued by flowing or gas lifting through macaroni inside the tubing, the casings were not repaired These are marginal wells where it has been established that the cost of wash-over work to recover the tubing and packers from the casing is excessive in relation to the indicated reserves.

The record of known and probable failure depths in relation to the top of cement outside the casing as determined by temperature surveys or calculations indicates that in 21 of the 29 wells where casings failed, the holes were found where the casing was *not* cemented In only 4 wells were the holes indicated to be in cemented pipe Holes located partly in cemented pipe and partly in uncemented pipe were found in 2 wells whereas the failure depths have not been pin-pointed in relation to the cement top in the remaining 2 wells. These data, of course, are not an attempt to evaluate the completeness of the cement sheath nor its actual effective top, but do tend to support the theory that a cement coating does give some protection against external casing corrosion.

*Continental Oil Co , Los Angeles, Calif

Determination of Current Requirements

Empirical methods were used to determine the amount of current to be applied to the wells at San Miguelito. In June 1954 a series of potential profiles were run in 4 Grubb Lease wells Three of these wells are situated on one well site with the casing heads less than 20 ft apart.

To determine the interference effect of adjacent wells, a current of 12 amp was applied to one of these wells while a profile was run on another — the two wells being in electric contact only through the ground A definite anodic slope was developed above 1,500 ft but none below that depth This effect was eliminated when all wells in the group were electrically connected at the surface.

A sharp anodic slope was noted in the potential profiles at the base of the surface pipe, which was cause for concern. To minimize the possible corrosion of the casing at this point, it was recommended that a casing centralizer be placed here in all new wells to assure metallic contact at this point.

In all 4 wells surveyed the potential surveys showed a tendency for external corrosion to occur over large areas of the casing These corrosive areas as defined by the profiles corresponded to the location of known failures in two of the surveyed wells No failures had been noted in the other two wells at that time, yet failure did occur in both prior to completion of the cathodic-protection installation.

The application of 3 to 5 amp of protection current was sufficient to remove all the anodic slopes from the profiles of the 4 wells tested. A trial run using 5 amp of impressed current was immediately started on one of the test wells and continued for a period of 6 months. At the end of this period the 7-in. casing was washed over and recovered from 5,200 ft The inspection and tests of the primary solids deposits revealed the following evidences of the effectiveness of the cathodic protection.

1 The corroded areas of the Grubb 61 casing were as predicted by the potential-profile survey.

2. A thin calcareous deposit was found in scattered areas over most of the pipe recovered indicating that cathodic protection was being effective to the depth of casing recovered.

3. The surface pipe effect was not sufficiently severe to prevent the use of cathodic protection

The recovered casing was replaced with a new casing string which was landed with a lead-seal casing bowl set over the stub of the old pipe at 5,200 ft. The new pipe was not cemented. Immediately after landing the

new pipe, a potential profile was run. In contrast to the smooth anodic areas found in the profile of the old pipe, a very erratic series of breaks in the curve was found in this same hole with new pipe and new mud Time is apparently a factor in the establishment of equilibrium conditions within the hole.

Five amperes of impressed current on the new pipe were effective in smoothing out the erratic potential profile. It was concluded at that time that the application of 5 amp should be sufficient to protect each well in the San Miguelito Field. Subsequent interference tests have indicated 10 amp are needed

Application of Cathodic Protection

The cathodic-protection installations for Continental Oil Company's 160 Grubb Lease wells use separate rectifier control and 3 anodes for each well. The selenium rectifiers used at 1 and 2 well installations are rated at 20 volts and 15 amp per well, whereas those for 3 and 4 well installations are rated at 40 volts and 15 amp per well Voltmeters are installed on each rectifier, and ammeters are provided to indicate the current to each well on multiple and single well units alike. All rectifiers are pole mounted.

Each rectifier is connected to an anode bed which has 3 anodes for each well served by the rectifier, i.e., the anode bed for a 3-well installation has 9 anodes Graphite anodes 3 in × 60 in are set 1 ft off bottom inside a 12-in. augered hole back-filled with coke breeze to 1 ft above the anode, then 1 ft of gravel caps the coke breeze and the hole is filled to the surface with dirt. Anode beds are placed at least 150 ft from the wells involved. Care was taken to avoid adjacent wells, pipelines, and other surface structures which might adversely effect the casing-to-earth potentials at depth.

Operational tests include the periodic readings of the voltmeter and ammeters at the rectifiers. Differences and variances in the readings are considered to be indicative of the anode-bed effectiveness and operational problems. It has been noted that in the moist shale areas the recommended current flow is attained at less than rectifier-capacity voltage. However, the sandy soils in other areas afford resistances which have prevented the minimum recommended current from being applied at capacity voltages Relocation of anode beds to areas where they may be wetted and the addition of anodes in some areas are being effected to reduce anode-to-soil resistance. Evidence of rodent damage to the insulating sheath of the buried cathodic-protection cables has been found. The extent of this problem has not been determined to date

Interference tests were run in a well situated on the easterly side of the lease in an area of dense well spacing. Potential profiles were run to a depth of 5,800 ft with several variations of current applications on the test wells and offsetting wells. Eight amperes were sufficient current to remove the anodic slopes from the potential-profile curve with current applied to the surrounding wells An *E-log I* curve run at the time substantiated the 8-amp requirement. It was concluded that an interference or stray-current problem does exist between wells under cathodic protection and those wells in a field either with insufficient protection or with no protection. It was therefore recommended that a minimum of 10 amp should be applied to each well in the field and that necessary revisions be made in the anode beds to achieve the 10 amp per well.

Results of Three Years of Cathodic Protection

In February 1959, the cathodic-protection system at Continental Oil Company's San Miguelito operations completed three years of operation A deflection in the logarithmic-failure curve (Fig 1) at the time cathodic protection was applied would indicate a reduction in the rate of increasing casing failures. The 13 failures which have occurred since application of the protective current include second failures in 3 of the wells while 9 of the troubled wells had less than the recommended protective 10-amp current applied because of operational problems Extrapolation of the failure rate prior to the application of cathodic protection would indicate that 15 additional casing failures might have occurred

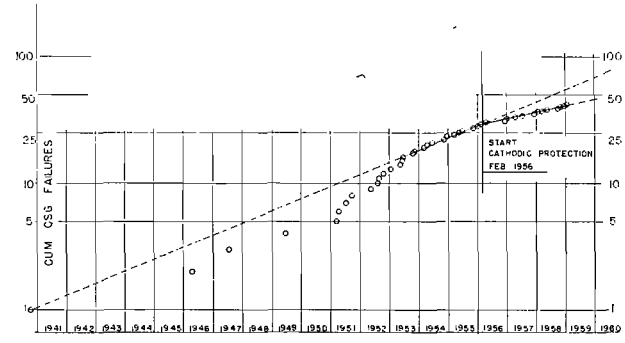

Fig. 1 (Biren)—Casing Failures Vs. Time
Continental Oil Co. — Grubb Lease — Ventura County, Calif.

during these past three years had the current not been applied It is realized, however, that other factors may have been involved in effecting this change. These factors include the following.

1. High well-completion rate during the 10-year period just before starting cathodic protection.
2. Condition and grade of the casing when run.
3. Nature of the drilling fluid.
4. Effect of polarization of the steel-casing surface.
5. Interference or stray currents from the cathodic-protection system itself.

The number of well failures which have occurred in each year of well service is indicated graphically in Fig. 2. It is noted that very few failures have occurred after 9 years of service. This is believed to be the effect of polarization The single failures in the extreme positions, 1st and 12th years, are perhaps indicative of the effect of the grade of casing used. The early failure was in cold-worked S-95 steel while the 12th-year failure was in H-40 steel. Inasmuch as both of the 19th-year failures occurred in wells with lower than

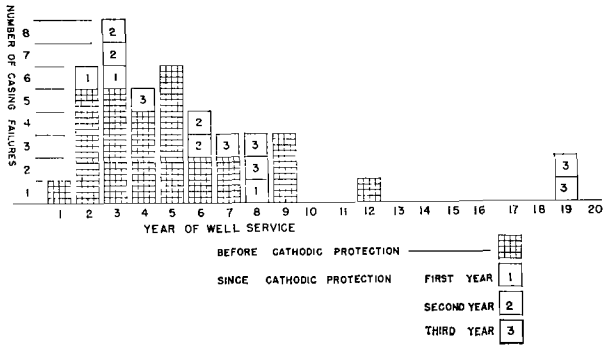

Fig. 2 (Biren)—Casing Failures Vs. Year of Well Service
Continental Oil Co — Grubb Lease — Ventura County, Calif.

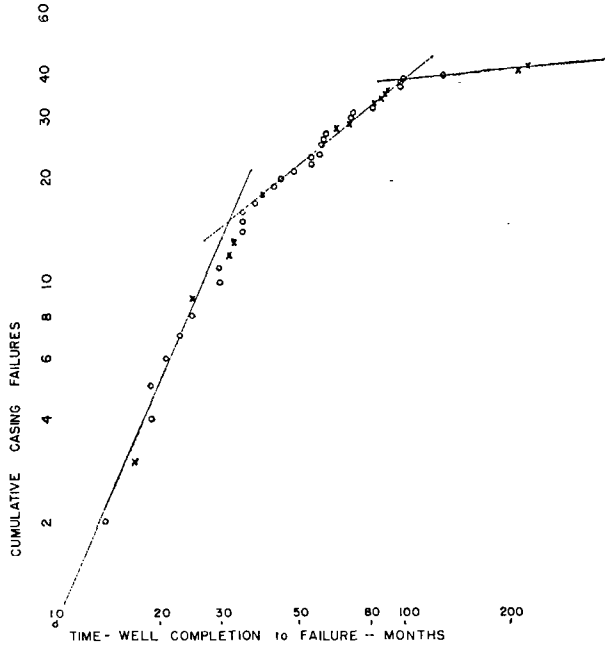

Fig. 3 (Biren)—Casing Failures Vs. Time in Hole
Continental Oil Co. — Grubb Lease — Ventura County, Calif.

recommended protective current, it is suspected that interference may be responsible.

The log-log plot of cumulative well failures vs. time from well completion to failure (Fig. 3) would indicate three phases in the process of failures It is believed that the middle slope between 32 and 102 months is perhaps the norm, whereas the failures earlier than 32 months occurred either before polarization or because of some pipe defect. The latter failures after 102 months (9 years) are accounted for by the grade of pipe, H-40, which is apparently more resistive to corrosion and failures caused by insufficient protective current or interference.

CONCLUSIONS

A reduction in the rate of increasing oil-well casing failures in the San Miguelito Field has been effected by the application of a cathodic-protection current during the past three years This reduction has been accomplished despite lower than recommended applied amperages on many wells. In fact, most failures which have occurred since application of the protective current have been in areas where anode-to-soil resistivity has restricted the use of recommended minimum amperages

Casing polarization or stabilization of electropotential conditions within the casing well-bore annulus has been effective in confining the critical period for external casing corrosion to the first 9 years of well life Field tests have shown that an interference or stray current problem does exist between wells under cathodic protection and those wells in a field either with insufficient protection or with no protection. The solution of the problem of applying the 10-amp current to those wells in resistive soil areas is necessary before evaluation of the San Miguelito oil-well casing cathodic protection system can be completed

ACKNOWLEDGMENT

It is the writer's desire to thank the Continental Oil Company for permission to publish this paper and to acknowledge the planning and field work done by J. D. Lung, J W. Wolfe, Jr., and H. F. Gerckens.

Appreciation is extended also for the use of the unpublished reports on this project by W. D. Greathouse, J. D. Sudbury, and J. E. Landers of Continental Oil Company's Research and Development Department, which were essential to the preparation of this paper.

PART 3
TWO YEARS OF CATHODIC-PROTECTION EXPERIENCE IN THE VENTURA FIELD

B. W. BRADLEY*

ABSTRACT

Cathodic protection was applied to approximately 500 of Shell Oil Company's Ventura oil-well casings in January 1957. Before that time Shell was experiencing in Ventura about 12 casing-corrosion failures per year, and the trend was increasing at about one additional failure per year During 1957, with cathodic protection applied to approximately 500 wells, only 9 casing-corrosion failures occurred. This was in line with anticipated results. However, continuing study of the problem during that year indicated certain features of the

*Shell Oil Co , Ventura, Calif.

Ventura cathodic-protection system could cause stray current interference between wells on a given drilling island The conditions found most troublesome included *1*, grouping of anode beds in low-resistance soil near one well on multiwell drilling islands; *2*, location of anode beds near surface lines; *3*, shorted insulated unions; and *4*, abandoned surface lines Casing-potential surveys in three wells, which experienced corrosion failures in rapid succession during early 1958, confirmed the need to correct these causes of stray current Accordingly, all cathodic-protection units were turned off after approximately 18 months of operation as a precautionary measure while the problem was evaluated and corrected The nine 1957 casing-corrosion failures and 11 in 1958 were below the past failure trend and indicated that some degree of protection was obtained in spite of stray currents during these 18 months of protection and lack of protection during the last 7 months

By the end of 1958 cathodic-protection equipment in a test block of 46 wells was revised for stray-current control. Casing-potential surveys in 2 wells within the block revealed that cathodic protection can be applied to densely drilled wells without adverse effects of stray currents to that number of wells.

INTRODUCTION

Starting in 1949 efforts were made to control oil-well casing-corrosion failures in the Ventura Field The various schemes, which included full-string cementing, high pH drilling mud, bactericide in high pH mud, and oil-base mud, were either ineffective or too expensive. During this time the annual number of failures was increasing and it appeared that cathodic protection might be an effective and profitable way to reduce the failure rate Accordingly, investigations into the use of cathodic protection were begun in early 1955 The results of this work and the method of applying cathodic protection to the Ventura well casings were reported by Kerr[1] in 1957. As stated by Kerr the current potential-curve criterion, plus economic considerations, was used as the basis for selecting current requirements of 27 amp per well.

Kerr's work indicated cathodic protection could be applied satisfactorily to deep oil-well casings, and a test block of 27 wells was placed under protection. However, the casing-failure rate took a decided increase in 1955, as shown in Fig. 1, which indicated an increasing number of failures might be experienced in the coming years. Therefore, Shell undertook a field-wide installation of cathodic protection shortly after completing the test-block work, and before the results could be studied and evaluated. The installation of equipment was completed by January 1957, when 475 well casings were placed under cathodic protection New wells drilled in 1957 brought the total well casings under protection to about 500 by January 1958.

[1] Reference is at the end of Part 3

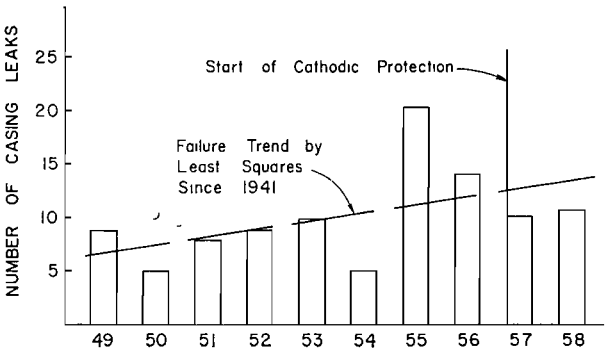

Fig. 1 (Bradley)—Annual Casing Failures — Ventura Field

Ventura Field Topography and Oil-production Facilities

Before discussing the main subject of this report, cathodic-protection stray currents, it is important to first visualize the characteristics of the field. This field is widely known as one of the nation's prolific oil producers due partly to 22 producing reservoirs. To develop these reserves, wells have been drilled into each sand on a given spacing. In localities where two or more sands overlie one another the spacing patterns often result in wells being drilled very near one another, say as close as 50 ft

The problem of close well spacings is further complicated by the rugged terrain of the area with elevation changes of as much as 300 ft occurring within a horizontal distance as short as 600 ft. Because of the rugged nature of the land, all semi-flat areas are at a premium. Thus, the high density of wells is further squeezed together on drilling islands cut from the hills.

Each of these drilling islands is served by pipelines supplying mud, fuel gas, and water Additional pipelines for the wells located on each island are flow lines, gas-lift lines, hydraulic-lift oil lines, and in some instances fuel gas and water lines for pumping equipment or well servicing These lines are buried where they cross the drilling island or lease roads, but are laid on the surface or pipe racks elsewhere. As the result of inevitable changes and continued development, some lines are abandoned in place or covered by many feet of fill dirt.

In summary, on the Shell leases in the Ventura Field, comprising about 1,860 acres, approximately 620 wells have been drilled This is equivalent to 1 well every 3 acres, which are grouped even closer together on the surface because of the rugged topography of the area.

Indications of Stray Currents

On completion of the installation work, field studies were undertaken in 1957 to check the circuits and to determine the degree of protection being obtained. Several anomalies were observed, but not understood at that time. The first well re-entered to study a wellhead-to-soil potential anomaly (Taylor 430) gave the casing-potential profile shown in Fig. 2 with all wells on the drilling island under protection. (For test

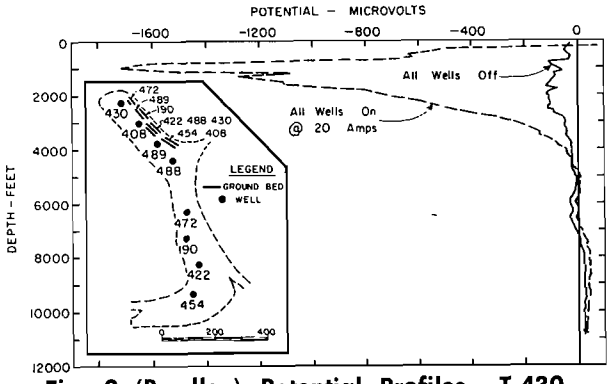

Fig. 2 (Bradley)—Potential Profiles — T-430 Original Anodes

purposes 20-amp protective current was used for all casing-potential surveys.) With Taylor 430 on protection alone a normal profile indicating protection was obtained. Taylor 430 was 1 well on an 8-well island, and as shown in the insert, the anode beds for all wells had been bunched in low-resistant soil near Taylor 430

Grouping of anode beds in this manner had been based on a study of ground-bed sites which revealed that soil type was the predominant factor controlling circuit resistance. Shale outcrops throughout the field provided circuit resistances much smaller than other soils, and had been selected as anode-bed sites in order to save power costs. It was reasoned that because all wells would be under protection, the current would seek out the well casing it was to protect without interfering with protection to other wells The profiles in Taylor 430 showed this was not the case.

It was hypothesized that the bunched anode beds were the major cause of interference Accordingly, the beds were revised to place each bed closer to the well it protected than any other casing, and repeat surveys were conducted. The results of this work are shown in Fig. 3. With all wells on the potential profile indicates a protected profile with somewhat less protection than if Taylor 430 was on protection alone With all wells on the drilling island off, a corroding condition was observed This condition was thought caused by stray current from anode beds protecting wells on adjacent drilling islands, but was of little consequence inasmuch

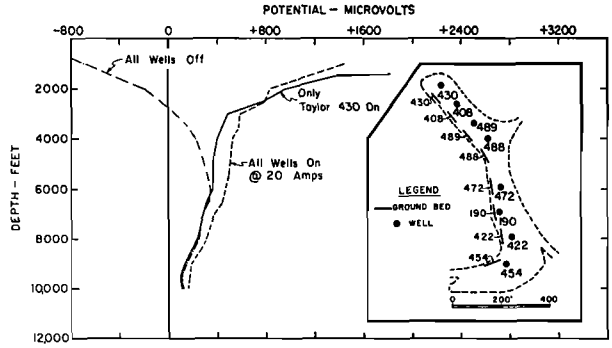

Fig. 3 (Bradley)—Potential Profiles — T-430 Revised Anodes

as all cathodic-protection units were to be on all the time.

1957 Activities

Throughout 1957 this problem was studied in the field, and although other situations of poorly located anode beds were found to be causing adverse conditions, none were as severe by wellhead-to-remote soil potential measurements as found at Taylor 430. Each of these cases was corrected as soon as the opportunity presented itself.

During 1957 Shell Oil Company experienced only 9 casing failures attributable to corrosion As shown in Fig. 1, this was 3 failures below the average for the last 4 years, and also 3 failures below the trend line established since 1941. Thus, in spite of the known interference problems, which were being corrected, the failure frequency was down somewhat.

Casing Failures in Early 1958

During the first 4 months of 1958, potential-profile surveys were made in 3 wells while they were being worked over to repair casing leaks. The results of these surveys are discussed individually following

Taylor 397

The potential profile obtained in this well, along with the anode wellhead arrangement on this island, is shown in Fig. 4. Wellhead-to-remote soil potentials taken before re-entering the well indicated what was interpreted as a questionable degree of protection. The flow of current to Taylor 398 could easily have been straying on to and off of Taylor 397 casing as suggested by the potential profile. It was thought at the time that the interfering stray currents were one or a combination of the following

1. Stray current from anode beds on this island
2. Surface-line stray currents from other anode beds; and possibly
3. Stray current from anode beds on nearby drilling islands.

However, with Taylor 397 protected alone (no interfering stray currents from this island or to surrounding islands) protection was still not attained Inasmuch as

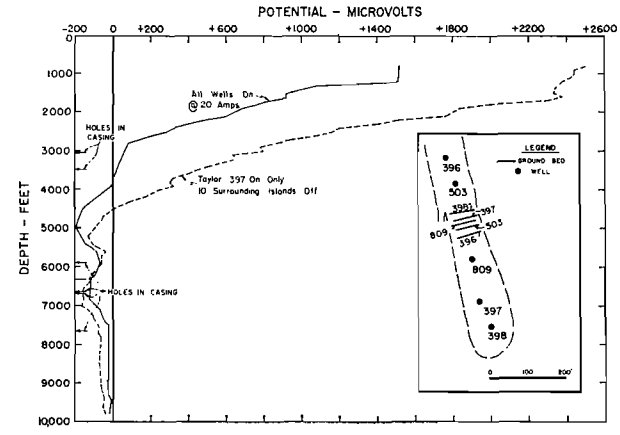

Fig. 4 (Bradley)—Potential Profiles — T-397 Original Anodes

the "on alone" profile was made with practically no chance of interfering stray current, it was assumed that proper protection for some time would be required to overcome the damage. At the time this explanation did not seem too logical, but was the only explanation possible.

Although six holes and a split were found in the casing, the well gave indications of a failure before installation of cathodic protection. Nevertheless, the conditions caused by the arrangement of these beds could contribute corrosion damage to this well casing After revising the anodes on this island, a survey was run in Taylor 809, a neighboring well, which indicated adequate protection was possible with proper anode placement as described later.

Taylor 462

A potential profile was run in this well during a workover to repair a casing leak. Based on the knowledge obtained from the Taylor 430 and Taylor 397 anode and well arrangements, it was suspected that Taylor 462 was being damaged by stray currents created by the situation shown in Fig. 5 Therefore, a few days before re-entering the well a new bed was installed on the Taylor 462 island (see Fig. 6) which should have corrected the situation. However, the profile revealed a condition which apparently was the result of surface-line stray currents and/or the residual effects of damage by the poorly placed anodes. Support for the latter theory was gained when another "on alone" profile, run after leaving the well protected by 35 amp for 15 min, was shifted a marked amount in the protected direction. The influence of stray current from *1*, anodes on surrounding drilling islands and/or *2*, surface-line stray currents is shown by the "both wells off" curve.

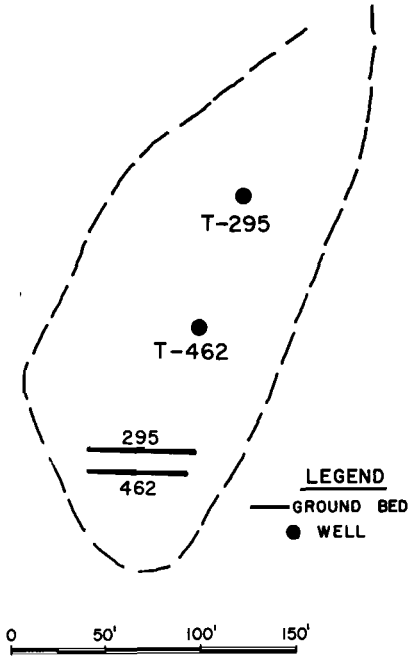

Fig. 5 (Bradley)—Old Position of Ground Beds and Wells — T-462

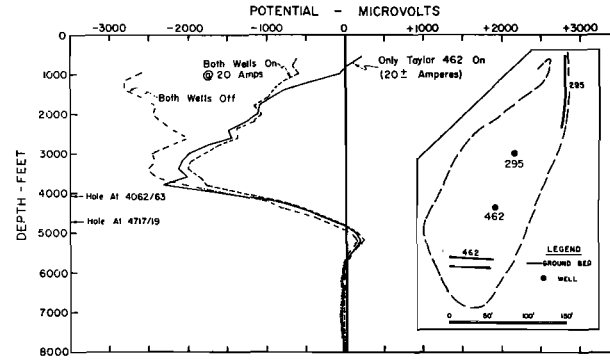

Fig. 6 (Bradley)—Potential Profiles — T-462 New Anodes

Taylor 453

The next casing-potential survey was run in Taylor 453 during a casing-repair workover. Wellhead-to-remote soil potentials on this well gave values thought indicative of protection Although the anodes were poorly located on this island, as shown in Fig 7 insert, there should have been no stray current from this island interfering with protection to Taylor 453. However, two anodic intervals, see Fig. 7, were revealed by the casing-potential profile. When protection to the casings of all wells on Taylor 453 island was turned off, the presence of stray current became evident.

Tests in 46-well Block

These experiences all apparently involved some manifestation of stray current which was neither thoroughly understood nor controlled. In addition to the stray current from poorly placed anodes, it was known that considerable stray current existed on surface lines at this time inasmuch as the work to control these had just begun. Furthermore, there was possibly some stray current flowing directly to these wells from anodes on nearby islands. However, the amount of stray current from each source was unknown.

In view of these conditions it was possible that damage might be occurring to an unknown number of well casings Therefore, it was decided to turn off

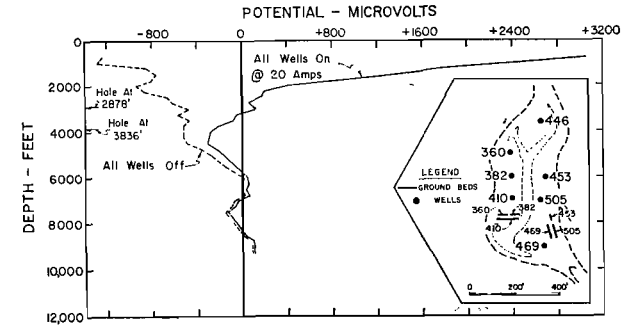

Fig. 7 (Bradley)—Potential Profiles — T-453 Original Anodes

Fig. 8 (Bradley)—Test Block, Shell Wells and Leases

protection to all casings, and to thoroughly evaluate the problem in a selected block of wells. The block selected, see Fig. 8, contained many multi-well islands, large concentrations of surface lines, and two wells in which previous potential surveys had been made.

17-well Test

The first step consisted of revising the equipment to properly protect 17 wells in a group of 5 drilling islands located within the 46-well test block. New anodes were installed so each bed would be nearer the casing it protected than any other casing. The old anodes were left in place for comparative tests. Cables were installed to drain stray current from all surface lines back to the offending rectifiers. The current drained back was measured by permanent shunts, and could be adjusted by changing resistors as shown in Fig. 9 and explained later.

After completing this work a potential survey was run in Taylor 809, a well centrally located on a 5-well island with only the 17 wells under protection. It was also located next to Taylor 397 which was previously reported to have been subjected to stray currents. The first potential profile was made under the original conditions, i.e., old anode beds and no control of surface-line

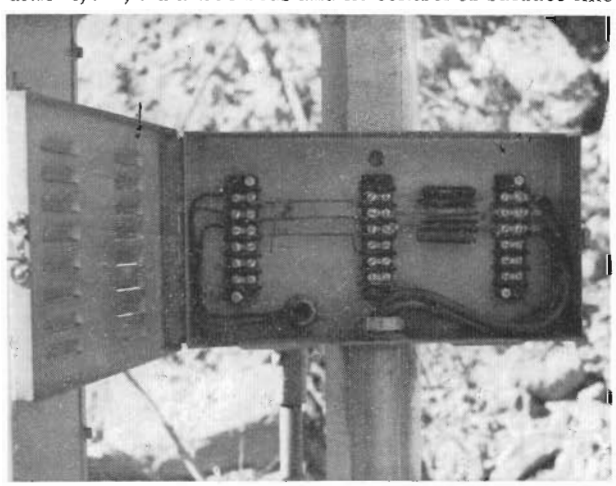

Fig. 9 (Bradley)—Drain Resistors and Shunts — Three-well Island

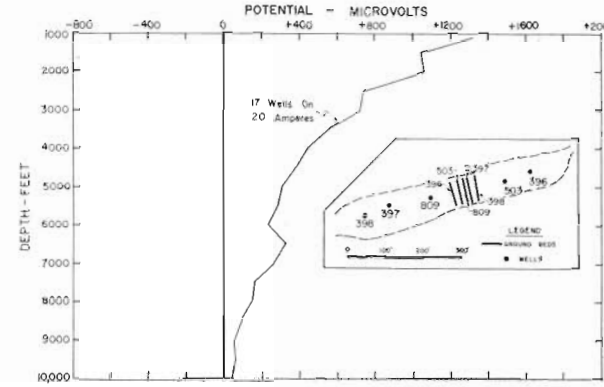

Fig. 10 (Bradley)—Potential Profiles T-809 Old Anodes

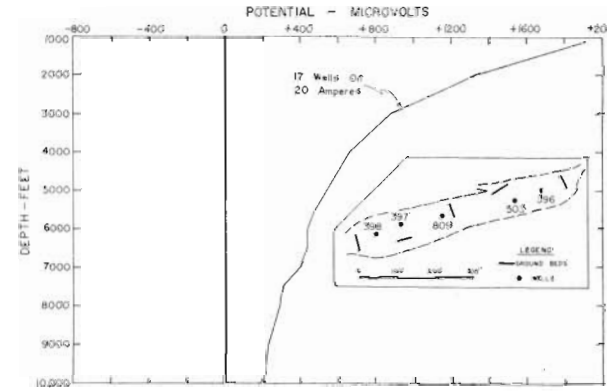

Fig. 11 (Bradley)—Potential Profiles T-809 New Anodes

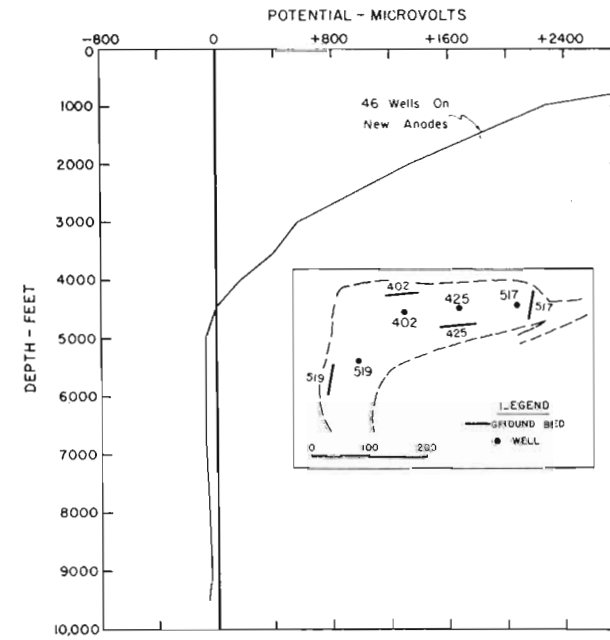

Fig. 12 (Bradley)—Potential Profiles — T-402 New Anodes

stray currents as shown in Fig. 10. Although the apparent anodic interval at 1,500 to 2,000 ft could have been caused by a change in casing weight, the corroding condition at 6,000 to 6,500 ft was caused by stray currents.

All wells were then protected with the new anode beds and no surface-line stray currents. A potential profile indicating satisfactory protection is shown in Fig. 11.

46-well Test

The next step consisted of revising equipment for the remaining wells in the 46-well test block in the manner described previously, and making similar casing potential surveys in a well (Taylor 402) centrally located in the block (see Fig. 8).

Considering the experience in Taylor 809 the first profile was made with all 46 wells protected by new anode beds and surface-line stray current controlled. The surprising results, which revealed the casing to be unprotected below 4,500 ft, are shown in Fig. 12. In the ensuing investigation it was found that this well had been damaged at some time by stray current flowing through a shorted flow-line insulating union. Because the well had never been protected by properly placed anodes, the results of damage had never been overcome. In an attempt to overcome the theorized residual damage (protection had been turned off 5 months at the time) the well was protected overnight by 50 amp. On the following morning a repeat potential survey with all wells under ideal protection at 20 amp gave the results in Fig. 13.

To determine if the indicated protection shown in Fig. 13 resulted from the overnight protection at 50 amp, a repeat profile was made two days later. The results were the same as shown in Fig. 13. During the intervening two days the well was subjected to miscellaneous currents and ideally protected overnight by 20 amp as were all 46 wells.

Observations During Test-block Work

During the revision work in the 46-well test block several significant problems were encountered. These problems and other pertinent observations are summarized following.

1. Surface-line Stray Currents

Theoretically, to control stray currents on surface lines it is necessary to *1*, elevate lines near anodes on wooden blocks; *2*, move anode beds or pipelines when they are located too near each other; and *3*, establish a current-drain connection from each pipeline back to the offending rectifier. However, from a practical viewpoint all pipelines lying together in one group can be treated as one line by electrically bonding them together and providing one drain cable back to the rectifier. It was found in a few instances that some pipelines act like individuals and require separate drain cables for proper stray-current control. On multi-well islands several current-drain cables were usually required to drain

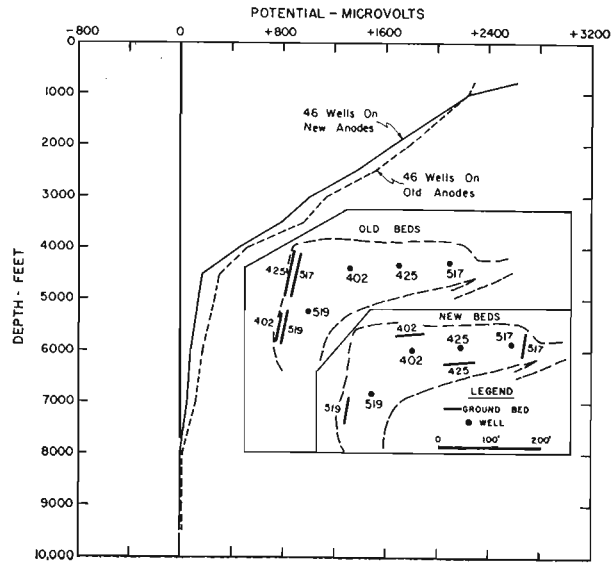

Fig. 13 (Bradley)—Potential Profiles — T-402 Old and New Anodes

current back to each rectifier. Fig. 9 illustrates the rather simple circuits on a 3-well island with a minimum of pipelines to pick up stray current. Fig. 14 illustrates the multiple circuits existing on an 8-well island crossed by numerous pipelines. To arrive at the proper drain current the stray current in each line (or group of lines) was measured under conditions of no-current and full-current output. The resistors were then inserted

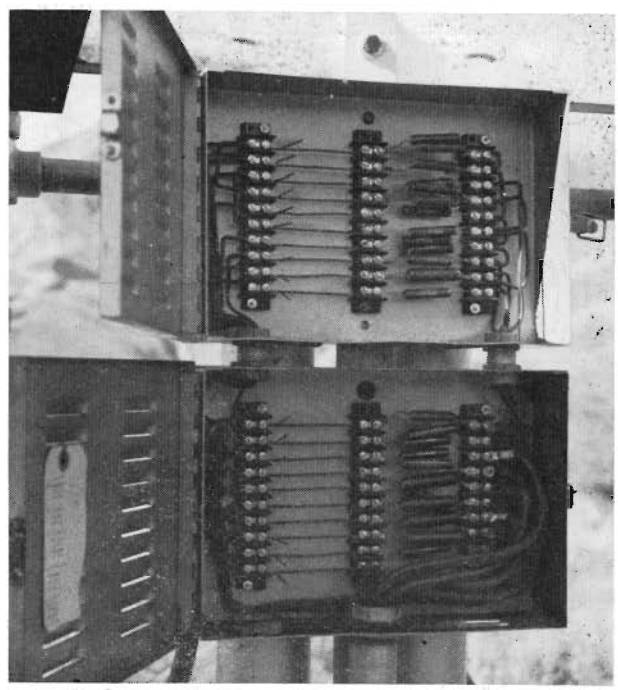

Fig. 14 (Bradley)—Drain Resistors and Shunts — Eight-well Island

Table 1 (Bradley)
Surface-line Stray Currents on Pipelines Leaving 46-well Test Block

Condition	Total Current Leaving Block, Amperes
1. No cathodic protection.	4
2. 45 old anodes on (no control of surface-line stray currents).	157
3. 46 new anodes on (with surface-line stray-current control)	0.8*

*Current entering block

on a trial and error basis until there was less than 0.1 amp of stray current on every line leaving the island.

To obtain some idea of the amount of surface-line stray current that existed under the original and revised conditions, an envelope was drawn around the 46-well area on a map, and the current flowing in the 198 lines that crossed the envelope was measured. The results, which are shown in Table 1, illustrate the severity of the surface-line stray current without control measures.

Fig. 15 illustrates how surface-line stray currents can cause interfering stray currents on well casings In the assumed case the surface-line stray current corrodes both the surface line and a nearby foreign well casing. However, the surface-line stray current can be controlled by draining the current back to the offending rectifier as previously described. Although this still leaves some stray current to flow directly through the soil to the nearby foreign well, even that can be overcome by placing the foreign well under protection as shown by the protected profiles of Fig. 11 and 13. Although Fig. 15 shows 2 amp of stray current flowing through the soil to the neighboring well and 2 amp of

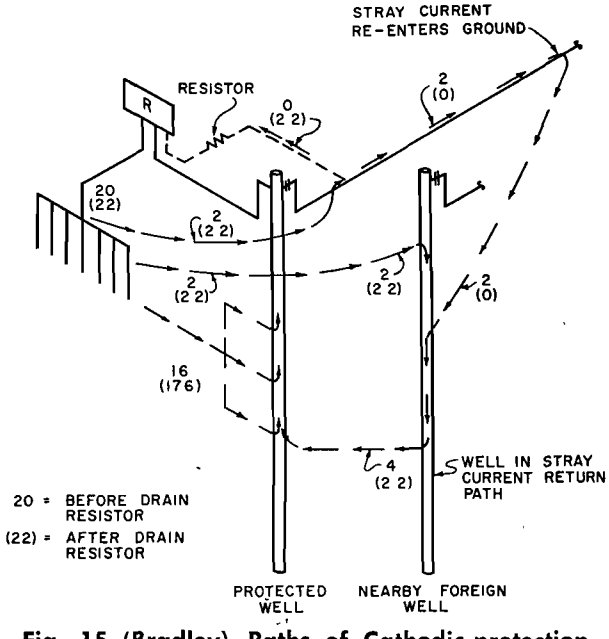

Fig. 15 (Bradley)—Paths of Cathodic-protection Stray Currents

stray current on the flow line, tests have shown that on multi-well islands the surface-line stray current is by far the largest and most significant stray current. For instance, detailed tests on a 5-well island indicate that stray current flowing directly through the soil was about 1 25 amp per anode bed while as much as 5 8 amp per anode bed were leaving the island via the surface pipelines

To control the surface-line stray currents, illustrated in Fig 15, and still obtain about 20-amp protection to the casing, it is necessary to increase rectifier output by approximately the amount of current drained from the surface lines. In Fig. 15, it is 2-amp drain or 22-amp rectifier output This 10-percent increase in current divides itself proportionately to the various parallel circuits Thus, 16 amp current flowing directly to the well casing is increased 10 percent to 17.6 amp and 2 amp stray current to the nearby well is increased 10 percent to 2 2 amp Nevertheless, control of the surface-line stray currents reduces the total stray currents attempting to flow onto nearby well casings. An analysis of these circuits is presented in Table 2.

Table 2 (Bradley)
Cathodic-protection Circuit Currents

	Without Drain Resistor	With Drain Resistor
Protected-well Circuit		
Current direct to protected well	16	17 6
Current via stray routes to protected well	4	2.2
Total current protecting well	20	19.8
Current returned by drain resistor from flow line	0	2.2
Rectifier output	20	22 0
Flow-line Circuit		
Corroding stray current	2	0
Foreign-well Circuit		
Corroding current directly through soil	2	2.2
Corroding current from flow lines	2	.0
Total corroding stray currents	4	2.2

2. Abandoned-line Stray Currents

In several instances during the revision work it was impossible to control the surface-line stray current in spite of direct electrical short circuits back to the rectifier from a certain pipeline. This was found to result from pipelines abandoned in place years ago and now located unknown very near the anode beds Old maps and the memories of old timers were helpful in locating abandoned lines when stray-current conditions typical of such conditions were encountered. These lines were removed to control stray currents

3. Shorted Insulated Unions

In several cases in which it was initially impossible to control surface-line stray currents by drain resistors, it was discovered that the troublesome lines were flow or gas lines connected to a well without an insulated union or through a shorted union. In such cases the current would flow directly to the well inasmuch as shorted unions provide a very low-resistant path to the well casing which provides an exceptional anode.

CONCLUSIONS

In view of the foregoing tests and analyses it appears that the 46 wells in the test block can be placed under proper cathodic protection. Similar techniques should apply to large groups of densely located wells, although other conditions now unknown might become apparent It has been shown that proper application of cathodic protection to well casings can only be accomplished by *1*, proper location of the anode beds; and *2*, control of the surface-line stray currents, which often requires *a*, removal of abandoned lines, *b*, adequate insulation of wells from connecting lines; *c*, elevation of lines when near anode beds, and *d*, occasionally moving either the anode bed or pipelines.

ACKNOWLEDGMENT

The author wishes to thank Shell Oil Company for permission to publish this report, and to acknowledge the assistance of F E. Field in planning and executing the test work, and the tireless efforts of W. W Salisbury, J A Trapasso, and J J Walker in gathering the large amount of data required to analyze these problems In addition, appreciation is extended to L B Nelson, Shell Pipe Line Corporation; E. W Wallace, Shell Oil Company; E W Haycock and W J Warren, Shell Development Company, for their helpful suggestions concerning the test work.

REFERENCE

[1]Kerr, A. W. Cathodic Protection of Casing, Ventura Field, Paper No 801-33-G, presented at the spring meeting of the Pacific Coast District, Division of Production, American Petroleum Institute, Los Angeles, Calif, May 16 and 17, 1957.

PART 4
CASING CATHODIC PROTECTION EXPERIENCE AT KETTLEMAN HILLS

FRED L. SMALL*

ABSTRACT

Forty-five installations for cathodic protection of well casing have been made at Kettleman Hills since June 1956. This report covers the results of operation, with special emphasis on the correlation of *E-log I* test (determination of wellhead potential vs. the logarithm of the drained current) to indicate current-drain demand with the actual current drain established by usage Theory and manipulation of the test have been covered in other papers and will not be discussed herein [1,2,3]

BACKGROUND HISTORY

General

The wells being protected are generally the most valuable wells They represent a good cross-section of all wells at Kettleman Hills and are scattered throughout the field. The wells have completion dates from 1930 to the present, and represent all producing zones.

There has been no casing failure reported in any of the 45 wells under cathodic protection Based on experience prior to cathodic protection, two casing failures should have occurred in this group if no cathodic protection had been applied

Anode Beds

All installations are graphite anode beds with air-cooled rectifiers. Both selenium and silicon-diode rectifiers have been installed; neither appears superior to the other at this time. Each installation was originally designed to serve one well only. However, inasmuch as usage has shown that surplus capacity was available

*Standard Oil Co of California, Western Operations, Inc, Avenal, Calif

[1]References are at the end of Part 4

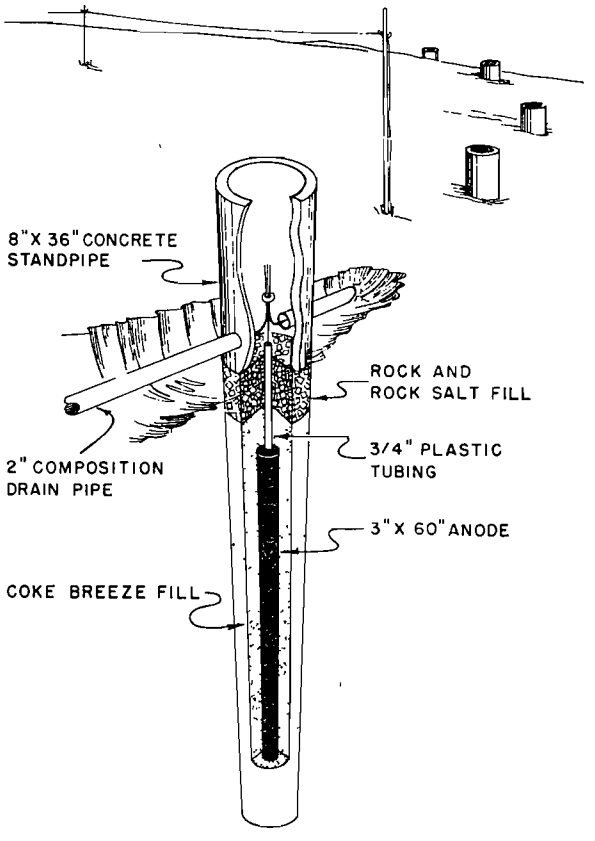

Fig. 1 (Small)—Vertical Anode-bed Installation

at some installations, adjacent wells have been tied in to utilize this excess capacity for partial protection Four such dual installations are now in use, and more will probably be made

The first installations made were with anodes in series, laid in a trench. Much trouble has been experienced with rodents eating the insulation off the buried cable, necessitating many costly repair jobs. All later installations have utilized 3 in. by 60 in graphite anodes installed vertically, in 12-in. diameter by 10-ft deep drilled holes, and packed with coke breeze. The anodes are hooked up in parallel to a header cable protected by 2-in. composition drain pipe. No trouble has been encountered at these installations with rodents Fig 1 shows the general layout of later installations.

Where possible, the anode beds have been located near waste-water sumps or drainage ditches to keep loop resistance down. All other anode beds are watered periodically. Where watering is necessary, salt is added to the water.

PREDICTING CURRENT REQUIRED FOR PROTECTION

Surface-casing to Half-cell Potential

On the basis of a limited number of tests (3), (5), it has been determined that a surface-casing to half-cell potential of —1 00 to —1 02 volts will give a casing to half-cell potential at the bottom of the hole of —0 85 volts or more. Variations undoubtedly occur, but it is believed there are more overprotected wells than underprotected wells in the field

E-log I Curve

The *E-log I* curve of this paper is the "Wellhead Current Potential Curve" of Kerr,[1] "Log Current Potential Curve" of Haycock,[2] and "Null Potential Curve" of Ballou and Schremp[3] Half cell refers to the copper-copper sulfate half cell in common pipeline-protection use.

E-log I tests were made on 33 of the wells. All of the *E-log I* tests were run using a surface or wellhead connection and a half cell located approximately 300 ft from the well. All of the tests were made using the anode bed installed for actual protection A truck-mounted welding generator was used as the power source. Control of the generator output at low amperages is difficult, and a variable rheostat was used in most recent tests

A few pointers on actual testing, picked up by experience, are worthy of mention.

1. Apparatus should be checked out by running a test on a pipeline or unimportant well before being used for critical well testing A final check at the well site, using a water or gas line as the cathode before hooking up to the well, will prevent many poor tests.

2. Approximate amperage desired for each drain point should be predetermined, and the setting marked if possible.

3. An overdrain of current, even of short duration, nullifies the results. If an overdrain occurs during the first part of the test before the curve is reached, the test is probably of no value If an overdrain occurs, the test should be stopped and the well allowed to come back to its original state before the test is made This might take a few hours or several days.

4. Timing is quite important The actual duration of the drain period does not seem to be as important as having each drain period the same. A 4-min. drain period, with 1 min to read and reset, was considered optimum for the work at Kettleman Hills.

5. The "off" potential decays rapidly and must be obtained within a second or two to be of value. Plotting results as they are obtained will enable the operator to preset, approximately, the potentiometer or voltmeter and get more consistent readings

Table 1 gives the *E-log I* predicted drain compared with the actual drain established by use Summarizing this table, there appear to be:

11 tests — good correlation with actual
11 tests — fair correlation with actual.
11 tests — poor correlation with actual

This summary does not look favorable for the *E-log I* prediction However, other factors investigated change the picture considerably.

SOURCES OF ERROR

Insulating Flanges

All insulating flanges of wells to be protected were checked and repaired, where necessary, before running *E-log I* tests or applying protection Toward the latter stages of the survey, an improved method of testing insulating flanges was used (4) This new method and equipment indicated several flanges previously thought to be effective were actually defective

Repairing the defective insulating flanges has lowered the current drain dramatically in some cases. At other wells there has not been much improvement.

Well 8-21J is an example of the benefits obtained by repairing a defective insulating flange. This well had a good *E-log I* curve, with an indicated drain of 18 amp However, after putting it under cathodic protection, a surface casing potential of —1 00 volts could be attained only part of the time with 50-amp drain. The old method of testing insulating flanges showed all to be good With the new instrument, a 3-in. flange showed defective and was replaced in December 1958. The surface-casing potential immediately went to —1 07 volts. Since then, the current drain has been reduced to 35 amp and will probably be cut back more.

There is no way of knowing if defective flanges were shorted at the time of the *E-log I* test or became shorted later.

Effect of Overdrain of Current

The effect of overdrain of current of the *E-log I* test was noted at well 323-21J, where drain of 20 amp for about 1 min was inadvertently made at the start of the first drain period. The drain was stopped and the well allowed to rest about 15 min; then the test was started

Table 1 (Small)
E-Log I Vs. Actual Current Demand

Well No.	Date Installed	*E-Log I* Indicated Demand, Amperes	Actual Current Demand, Amperes	Difference in Amperes, Base-actual	*E-Log I* as Percent of Actual	Correlation[1]	Remarks
First Group							
87-20J	6-56	19	25	— 6	76	Fair	
344-20J	6-56	11	15	— 4	70	Fair	DIF, 12-58[2]
8-21J	6-56	18	35	—17	51	Poor	DIF, 12-58[3]
27-21J	6-56	23	35	—12	66	Poor	
324-35J	6-56	22	30	— 8	73	Poor	DIF, 12-58
32-2P	7-56	30	25	+ 5	120	Fair	DIF, 3-57[4]
36-2P	7-56	17	23	— 6	74	Fair	
343-3P	7-56	21	30	— 9	70	Poor	DIF, 12-58
341-12P	7-56	20	22	— 2	91	Good	
631-12P	7-56	28	25	+ 3	112	Good	
634-12P	7-56	14	15	— 1	93	Good	
642-12P	7-56	15	12	+ 3	125	Good	
E27-7Q	8-56	21	30	— 9	70	Poor	
8-8Q	9-56	25	25	—	100	Good	
36-17Q	9-56	9	13	— 4	66	Fair	DIF — not repaired
E67-17Q	9-56	32	30	+ 2	107	Good	DIF — not repaired
87-17Q	9-56	33	22	+11	150	Poor	
333-18Q	9-56	31	10	+21	210	Poor	
341-18Q	8-56	31	25	+ 6	124	Fair	DIF, 2-57
61-20Q	8-56	34	30	+ 4	113	Fair	
44-21Q	8-56	21	34	—13	62	Poor	DIF[5]
32-27Q	8-56	53	44	+11	121	Fair	DIF, 3-57
Second Group							
36-20J	5-58	45	25	+20	180	Poor	
47-20J	3-58	28	25	+ 3	112	Good	
331-20J	7-58	25	30	— 5	83	Fair	
332-20J	7-58	15	15	—	100	Good	
323-21J[6]	7-58	26	17	+ 9	153	Poor	
343-28J	4-58	36	40	— 4	90	Good	
65-30J[7]	4-58	21	45	—24	47	Poor	
27-34J	3-58	31	25	+ 6	124	Fair	
38-34J	3-58	15	20	— 5	75	Fair	
V32-7Q	3-58	39	40	— 1	97	Good	
632-7Q	12-58	27	27	—	100	Good	DIF, 12-58

Correlation first group	good.	6	fair	8	poor . . . 8
Correlation second group	good	5	fair.	3	poor 3
Correlation all wells	good . .	11 tested	fair . .	11	poor . . 11

[1]Good — difference less than 4 amp unless actual demand over 35 amp, then difference 10 percent or less.
Fair — difference 4 to 7 amp incl. unless actual demand over 35 amp, then difference 11 to 20 percent.
Poor — difference over 7 amp
[2]DIF = defective insulating flange — month and year repaired.
[3]8-21J — before repairing insulating flange, 50 amp would not keep current potential up to —1 00 volt Since repairing, current cut back to 35 amp
[4]32-3P — required 45 amp before repairing insulating flange.
[5]44-21Q — repaired insulating flange June 1957 40 amp brought current potential up to —1 00 volt Repaired December 1958, cut to 34 amp, probably will go lower
[6]323-21J — overdrain of 20 amp at start of test. Discard
[7]765-30J — loop resistance too high, could not get around bend of curve Probably has defective 6-in. insulating flange. Discard test

again The original casing to half-cell potential was —0.725 volts. At the start of the test the second time it was —0 764 volts The curve obtained was ragged, and the current drain indicated was 53 percent greater than that determined by operation Fig 2 gives a plot of the curve, along with a curve obtained from a similar well that checked very well with the actual.

There is a good possibility that the other three wells with "poor" correlation and excessively high *E-log I* indicated drain were also subjected to an overdrain during testing

This test points out the importance of avoiding an overdrain of current, especially at the lower amperage readings.

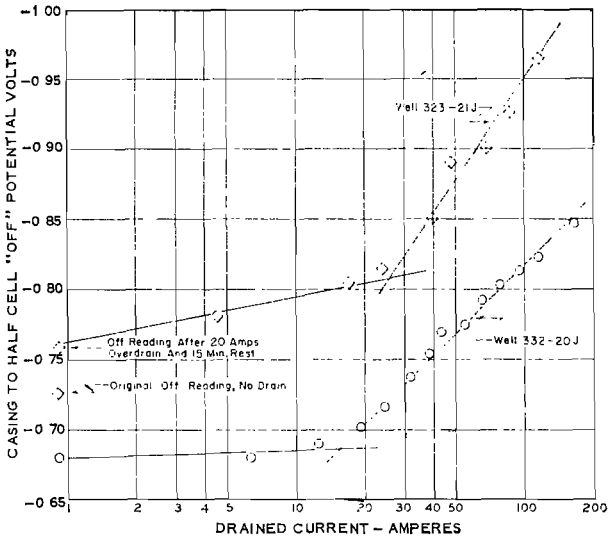

Fig. 2 (Small)—*E-Log I* Curves—Kettleman North Dome Unit

Disregarding the tests made on wells with faulty insulating flanges and the four tests suspected of overdrain, it is possible to come up with a different picture from Table 1.

Well No.	Predicted	Actual	Difference, Amperes	Correlation
87-20J	19	25	— 6	Fair
47-20J	28	25	+ 3	Good
331-20J	25	30	— 5	Fair
332-20J	15	15	—	Good
27-21J	23	35	—12	Poor
343-28J	36	40	— 4	Good
27-34J	31	25	+ 6	Fair
38-34J	15	20	— 5	Fair
36-2P	17	23	— 6	Fair
341-12P	20	22	— 2	Good
631-12P	28	25	+ 3	Good
634-12P	14	15	— 1	Good
642-12P	15	12	+ 3	Good
E27-7Q	21	30	— 9	Poor
V32-7Q	39	40	— 1	Good
8-8Q	25	25	—	Good
61-20Q	34	30	+ 4	Fair

9 — Good correlation = 53 percent } 88 percent
6 — Fair correlation = 35 percent
2 — Poor correlation = 12 percent
Total 17 100 percent

It is believed that with improved technique the accuracy and reliability of the test will be further improved.

Costs of *E-Log I* Tests

With the equipment we have used, two men are necessary to run the test and a third man to operate the welding generator. The actual test time is about 1 hour, 15 min, with another 45 min to set up and move. In addition, about 2 hours or more engineering time are needed to plan the program and interpret results.

The cost (equipment and manpower) of the foregoing test is approximately $50. As mentioned earlier, we have used permanent beds, already installed, for the anode. If it is necessary to install temporary anode beds for the test, the cost will be much higher.

Current Density

Table 2 gives the current drain necessary to give a surface-casing to half-cell potential of —1.00 to —1.02 volts, and the current density in milliamperes per square foot (ma per sq ft) of the exposed casing area which is defined for our purposes as all casing not behind other casing; that is, all casing exposed to formation including that behind cement.

The current density varies from a low of 0 5 ma per sq ft to a high of 2.1 ma per sq ft The average is 1 3 ma per sq ft.

The bare casing area, defined as the exposed area not behind cement, has also been calculated for a few of the newer wells. The current density based on bare casing area varied from 1 3 to 2.5 ma per sq ft.

Casing area would probably have merit in sizing installations if all variable and influencing factors were known However, it is currently not considered a reliable method to size installations at Kettleman Hills

CONCLUSIONS

1. Cathodic protection at Kettleman Hills has reduced the casing-failure rate.

2 The *E-log I* test to indicate current drain from a casing is only 70 percent accurate on the basis of tests tabulated. However, it is believed this rather low accuracy is probably the result of errors of technique and faulty insulation flanges, rather than to a fundamental fault in the test itself. With improved technique, it is believed the test should indicate the actual drain demanded within 10 percent.

3. The test should be a valuable aid in engineering studies aimed at determining the economy of protecting a field or a group of wells.

4. The usefulness of the test in sizing individual installations is something that would depend to some degree on individual circumstances, but to a large degree on the care and preparation devoted to each test.

The Future

Because of the good experience in reducing forecasted casing failures in 45 wells at Kettleman Hills, 100 more wells in this field are being considered for cathodic protection.

The economics of continued use of the *E-log I* method of predicting future cathodic-protection requirements has been carefully considered Because this method is subject to errors, and experience has permitted development of an average requirement, it has been decided to install future anodes and rectifiers of slightly greater capacity than the average current demand found necessary in the present 45 wells being protected cathodically. This plan will save the costs of *E-log I* tests, and will permit any excess capacity to be used to partially protect less economic wells that otherwise would not be protected. If more capacity is needed, additional anodes will be added and the rectifier changed.

Table 2 (Small)
Current Density on Protected Wells

Well No.	Depth, Feet	Current Drain Required, Amperes	Exposed Casing Area, Square Feet	Milliamperes per Square Foot	Bare Casing Area, Square Feet	Milliamperes per Square Foot	Date Insulating Flange Repaired
287-19J	8,060	20	18,689	1.1			
8-20J	8,895	22	23,226	1.0			
36-20J	11,175	25	27,176	0.9			
47-20J	8,105	25	21,120	1.2			
87-20J	8,167	25	21,254	1.2			
331-20J	11,640	30	20,979	1.4	12,181	2.5	
332-20J	11,660	15	21,734	0.7	10,592	1.4	
344-20J	11,386	15	20,117	0.8	10,193	1.3	12-58
8-21J	8,217	35	22,011	1.6			12-58
27-21J	11,450	35	26,738	1.3			
343-28J	11,683	17	21,765	0.8	7,601	2.2	
H-6	10,624	40	21,878	1.8			
65-30J	9,143	40	22,995	1.7			
341-30J	8,265	45	21,980	2.0			
323-21J	10,910	40	22,499	1.8			
83-32J	8,290	35	20,825	1.7			
E72-33J	10,060	30	23,408	1.3			
27-34J	8,043	25	22,736	1.1			
38-34J	8,819	20	24,825	0.8			
324-35J	10,441	30	24,204	1.2			12-58
V45-1P	8,795	40	22,160	1.8			
E32-2P	10,035	25	20,342	1.2			10-57
E36-2P	9,775	23	19,784	1.2			
81-3P	8,032	25	17,928	1.4			
87-3P	7,981	25	26,595	0.9			
343-3P	10,173	30	23,329	1.3			12-58
341-12P	10,300	22	17,790	1.2			
631-12P	8,150	25	17,617	1.4			
634-12P	7,932	15	15,590	1.0			
642-12P	7,997	12	17,414	0.7			
E27-7Q	9,852	30	23,693	1.3			
V32-7Q	9,225	40	27,578	1.5			
V42-7Q	9,250	32	20,265	1.6			12-58
611-7Q	8,941	25	21,700	1.2			
632-7Q	9,170	27	20,525	1.3			12-58
8-8Q	7,992	25	23,162	1.1			
36-17Q	7,725	13	19,329	0.7			not repaired
E67-17Q	10,126	30	24,822	1.2			not repaired
87-17Q	7,925	22	22,042	1.0			
333-18Q	10,940	10	21,735	0.5			
341-18Q	10,010	25	22,809	1.1			2-57
61-20Q	7,095	30	23,250	1.3			
44-21Q	7,519	34	17,239	2.0			6-57 and 12-58
32-27Q	7,795	44	21,013	2.1			3-57
72-27Q	8,040	35	21,678	1.6			12-58

REFERENCES

[1]Kerr, A W Cathodic Protection of Casing, Ventura Field, Paper No 801-33-G, presented at the spring meeting of the Pacific Coast District, Division of Production, American Petroleum Institute, Los Angeles, Calif., May 16 and 17, 1957.

[2]Haycock, E W: Current Requirement for Cathodic Protection of Oil Well Casing, presented at the 13th Annual Conference, National Association of Corrosion Engineers, St. Louis, Mo, March 11-15, 1957.

[3]Ballou, J. K and Schremp, F. W: Cathodic Protection of Oil Well Casing, presented at National Association of Corrosion Engineers Convention, New York, N Y, March 1956.

[4]Sneddon, Thomas: A Method to Find Shorts in a Distribution System, *Gas*, March (1958)

[5]Unpublished Kettleman North Dome Unit reports.

PART 5
CASING CATHODIC PROTECTION — COALINGA NOSE UNIT PROJECT

C. E. HEDBORG*

ABSTRACT

The pipeline criterion of maintaining a minimum pipe-to-soil potential of —850 millivolts relative to a copper-sulfate reference electrode has been used in providing cathodic protection for well casings at the Coalinga Nose Unit A polarization period of 2,000 hours is required for wellhead potentials to reach equilibrium with a 25-amp current. However, short-term test data can be used to predict long-term polarization levels. Down-hole measurement indicates that protection extends to total depth of a 7,000-ft casing. Casing potentials were observed to decline 30 millivolts per 1,000 ft of depth after 42 days drainage time. At 300 days drainage time the decline had decreased to 10 5 millivolts per 1,000 ft.

Criteria for Protection

The pipeline criterion of maintaining a minimum pipe-to-soil potential of —850 millivolts with respect to a saturated copper-sulfate reference electrode has been used in determining well-casing cathodic-protection current requirements at the Coalinga Nose Unit (CNU), Fresno County, California

Current Requirement Tests

Tests to determine the cathodic-protection current requirements were conducted on 10 wells which were selected as being representative of all wells in the field These tests were divided into two parts: a short-term test period of 10 to 24 hours duration followed by a long-term test period of about 6 months duration.

The data obtained from the short-term tests were used as a basis for designing permanent, impressed-current cathodic-protection installations for the 10 test wells. These permanent installations were then operated and observed for about 6 months, following which a program of installing protection installations on all wells of economic value to the unit was started. There are at present 130 wells under protection at the CNU.

During the short-term tests, casing-to-soil potentials were measured only at the well head. Based on work conducted by other companies[1], it was assumed that the casing-to-soil potentials would decrease by 20 millivolts for each 1,000 ft of depth A 7,000-ft well, which is average for the CNU, would therefore require a wellhead potential of —990 millivolts in order to have an indicated potential of —850 millivolts at total depth. Fig 1 shows a schematic diagram of the equipment and circuits used during the tests The anode bed was located from 250 to 300 ft from the well. The reference electrode was placed on the surface of the ground, 300 ft from the well head and in a direction opposite from the anode bed

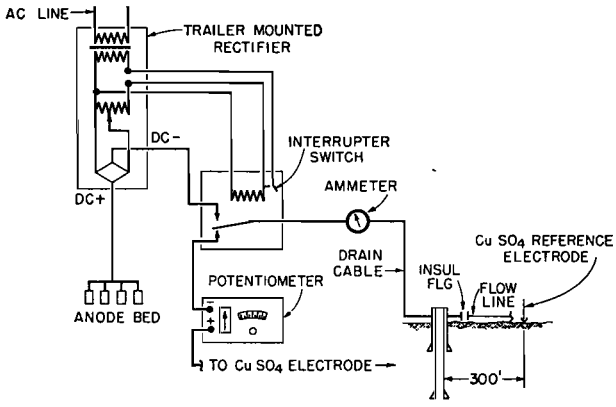

Fig. 1 (Hedborg)—Test Equipment

In order to eliminate the inclusion of ohmic (i e, IR drop) potentials, all casing-potential measurements were taken with the current momentarily interrupted. The circuit shown in Fig. 1 makes possible the measurement of power-off potentials with a minimum drain-current interruption time The results of the short-term tests are shown on Fig 2 In these tests we were trying to determine the current required to produce a power-off potential of —850 millivolts at total depth. As stated earlier, this would require a wellhead potential of —990 millivolts.

As indicated by Fig 2, the casings take an appreciable period of time to respond to electrical drainage.

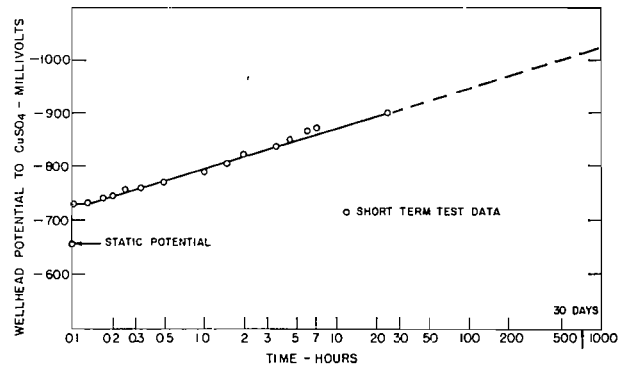

Fig. 2 (Hedborg)—*E-log* Time Curve — 25-amp Drain Potentials are measured with respect to a remote saturated Cu SO_4 reference electrode. All potential measurements made with power momentarily interrupted. All adjacent rectifiers within 2,000 ft shut down during these tests.

*Union Oil Co of California, Brea, Calif
[1] References are at the end of Part 5

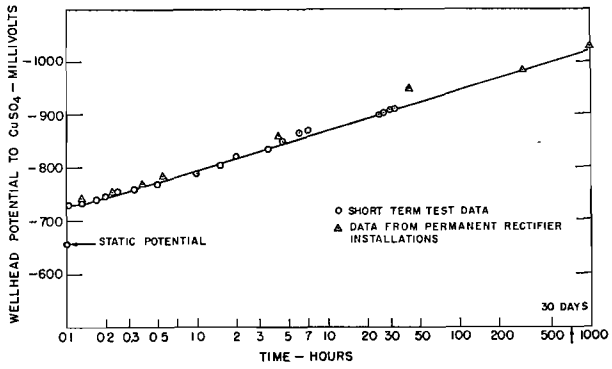

Fig. 3 (Hedborg)—*E-log* Time Curve — 25-amp Drain Potentials are measured with respect to a remote saturated Cu SO_4 reference electrode. All potential measurements made with power momentarily interrupted. All adjacent rectifiers within 2,000 ft shut down during these tests.

However, by plotting the short-term test data as potential vs. the logarithm of the drainage time and by extrapolating the resulting curve, it appeared reasonable to assume that a 25-amp drain current would produce the desired wellhead potential in about 30-days time The curve shown on Fig. 2 is typical of all of the wells tested Based on these short-term tests, permanent-rectifier installations having direct-current capacities of 30 amp and 50 volts were installed at the 10 test wells.

Fig 3 shows the *E-log* time curve for the same well shown on Fig. 2 after 1,000 hours at 24 amp It can be seen that the points fell on the curve indicated by the short-term tests. Although not shown on this curve, the wellhead potentials stabilized at about 1,060 millivolts after 2,000 hours drainage time at 24 amp.

A down-hole potential survey was conducted on one of the test wells after it had been on protection for 42 days. This survey consisted of lowering a single-point contacting tool inside the casing and measuring power-off potential differences, for various depth positions, between the casing and a surface reference electrode. The results of this work are shown on Fig. 4. The same type of survey was conducted on another well in the field after it had been under protection for 300 days. The results of this survey are also shown on Fig. 4.

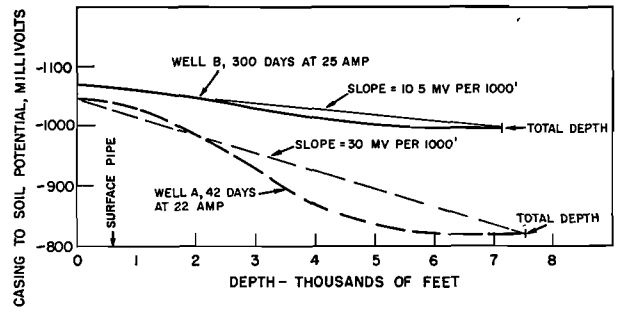

Fig. 4 (Hedborg)—Casing-to-soil Potential Vs. Depth Potentials are measured with respect to a remote saturated Cu SO_4 reference electrode. All potential measurements made with power momentarily interrupted. All adjacent rectifiers within 2,000 ft shut down during these tests.

These two curves show that there has been a considerable reduction in the slope of the attenuation curve The average slope for Well A after 42 days drainage was 30 millivolts per 1,000 ft The slope for Well B after 300 days drainage time was 10 5 millivolts per 1,000 ft The reduced slope of the attenuation curve is, it is believed, the result of a gradual accumulation of calcareous coatings on the casing. The relatively flat slope for Well B probably indicates that an equilibrium condition has been reached The 30-millivolt attenuation figure obtained on Well A indicated that a wellhead potential of —1,060 millivolts was required for the protection of 7,000 ft of casing. A rectifier output of about 25 amp was required to maintain this potential. Up to December 1958, all the rectifiers in the field were operated at this current value. At this time, however, the down-hole survey on Well B indicated that the wells were being overprotected. Gradual reductions in rectifier output are therefore being made so as to yield wellhead potentials that are commensurate with the 10.5-millivolt attenuation figure. At the present writing the amount of current reduction possible has not been accurately established

Results to Date

In order to minimize interference, all anode beds were kept a minimum distance of 200 ft from the nearest surface facility As an additional safeguard, the surface facilities are given partial protection by the application of a 1-amp drain at each protected well. This current is applied by installing a bypass resistor around the flow-line insulating flange. To date, no interference damage has been evidenced

Some failures of silicon-diode rectifier elements have occurred as a result of lightning storms. Most of these failures took place during a storm which the local power company classed as unusually severe. Our present opinion is that these lightning failures do not constitute a serious problem The costs to place a damaged rectifier back in service have averaged $25. This includes material and labor The benefits of the silicon diodes are: *1*, higher conversion efficiency; and *2*, greater resistance to high ambient temperatures Under the conditions prevailing at Coalinga it is believed that these advantages justify the continued use of silicon rectifier elements.

The anode beds are of the graphite-rod type with each rod being installed in a 14-in. diameter, 20-ft. deep hole. The annular space surrounding the 4-in diameter rods was filled with calcined petroleum coke. The installations at Coalinga are all of the single-well type: that is, a separate anode bed and rectifier is installed for each well Anode beds of from 5 to 8 rods were installed at a distance of from 250 to 300 ft from the well head At a few sites it has been necessary

to provide facilities for wetting the anode beds in order to reduce contact resistance.

Experience has indicated that there are many ways in which an insulating joint can become inoperative For example, it has been found that the insulation material in certain types of fittings is easily damaged As a result of this, we consider it desirable to make periodic routine checks on all insulating joints in the field. These routine checks have led us to the conclusion that the flange-type insulation joint is the most reliable. A uniform color coding has proved a valuable aid in preventing the accidental bypassing of insulating joints by copper tubing fittings such as on pressure gages, flow meters, etc

CONCLUSIONS

There have been but two casing failures at the CNU during its life. One of these was attributable to external corrosion; this failure occurred on a 14-year-old well. The fact that no additional failures have occurred since protection was first applied in April 1957 is not sufficient evidence to permit drawing of conclusions as to the efficacy of cathodic protection. However, based on theoretical considerations, favorable pipeline experiences, and published data[2] on the results of full-scale field-evaluation tests, we believe cathodic protection to be an effective method of preventing external casing corrosion.

REFERENCES

[1]Ballou, J. K. and Schremp, F. W: Cathodic Protection of Oil Well Casings at Kettleman Hills, California, *Corrosion* **13** [8] 35, Aug (1957)

[2]Greathouse, W D, Lehman, J J; Landers, J. E; and Sudbury, J D: Field Evaluation of Cathodic Protection of Casing, AIME Paper No 1127-G, presented at Houston, Texas, Oct. 1958; *J. Petr. Tech.*, **11** [12] 354, Dec (1959)

Ex. II - 38

Understanding How Components Fail

Donald J. Wulpi

AMERICAN SOCIETY FOR METALS
Metals Park, Ohio 44073

Copyright © 1985
by the
AMERICAN SOCIETY FOR METALS
All rights reserved

No part of this book may be reproduced, stored in a retrieval system, or transmitted, in any form or by any means, electronic, mechanical, photocopying, recording, or otherwise, without the prior written permission of the publisher.

Nothing contained in this book is to be construed as a grant of any right of manufacture, sale, or use in connection with any method, process, apparatus, product, or composition, whether or not covered by letters patent or registered trademark, nor as a defense against liability for the infringement of letters patent or registered trademark.

In writing this book, the author has drawn upon both his personal experience and the available literature. As the text itself makes clear, there is often no single or simple remedy for component failure. The author makes no representation or warranty as to the appropriateness or success of any method or procedure herein suggested.

The terms "fail" and "failure" as used in this book are intended to mean cessation of function or usefulness, and carry no implication of negligence or malfeasance.

Library of Congress Catalog Card Number: 84-73304
ISBN: 0-87170-189-8
SAN: 204-7586

PRINTED IN THE UNITED STATES OF AMERICA

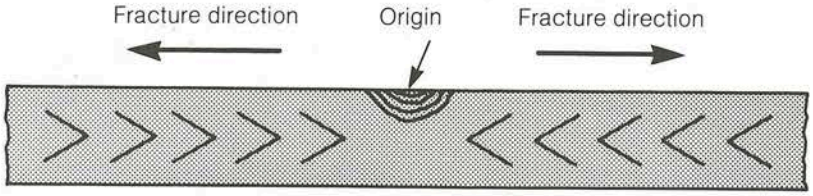

Note the classic chevron or herringbone marks that point toward the origin of the fracture, where there usually is some type of stress concentration, such as a welding defect, fatigue crack, or stress-corrosion crack. The plane of the fracture is always perpendicular to the principal tensile stress that caused the fracture at that location.

Fig. 2. Sketch of pattern of brittle fracture of a normally ductile steel plate, sheet, or flat bar.

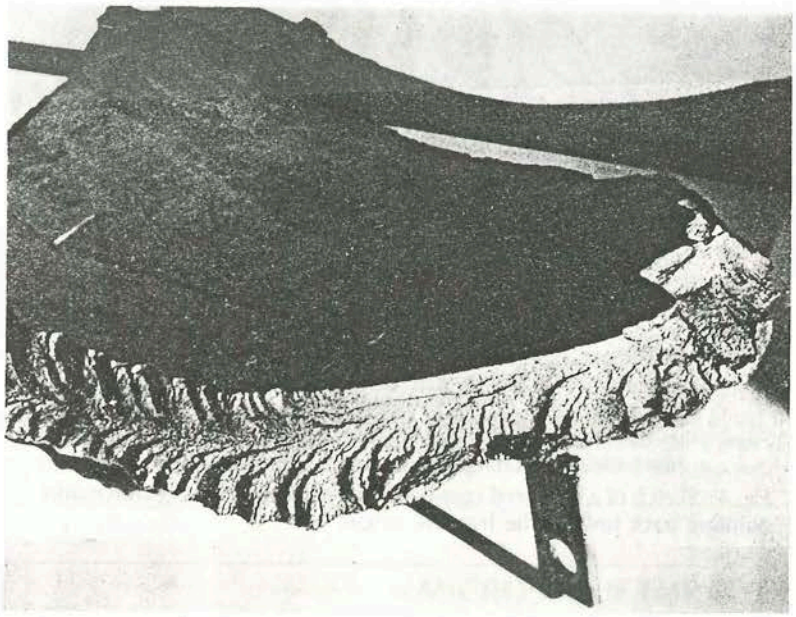

Fig. 3. Fragment of a thick-walled fractured drum. The fracture, which started at the right side of the photo, ran rapidly to the left, resulting in a well-defined chevron pattern. (Ref 10)

sitioned so that it just grazes the projections of the surface texture. See Fig. 2 through 8 for illustrations of these marks.

Brittle fractures of some parts may have a pattern of radial lines, or ridges, emanating from the origin in a fan-like pattern. Again, it may be difficult to perceive the texture of the fracture surface unless the light is carefully controlled. See Fig. 9 through 11.

Brittle fractures of extremely hard, fine-grain metals usually

Ex. II - 39

Interpretation of Temperature Logs in Water- and Gas-injection Wells and Gas-producing Wells†

JAMES M. BIRD*

ABSTRACT

The movement of fluids in a bore hole is a problem of interest to petroleum engineers. There are several tools available to detect and record the direction and extent of this movement. The use of temperature surveys for this purpose is the subject of this paper. The general shape of temperature logs in water-injection wells is discussed in the light of the principles of heat transfer involved. The mathematics is evolved to express this relationship, followed by empirical data substantiating the assumptions on which the mathematics is based. The importance of correct field techniques in running this type of survey is emphasized. The reversibility of the concepts developed are demonstrated in analyzing temperature curves in a well flowing water and oil. An analysis of field data is shown. The similarity and differences between a flowing water and oil well and a gas-producing well are demonstrated, with suggestions as to a method of interpreting temperature logs of the latter type.

Temperature Surveys in Water-injection Wells

It is acknowledged that important factors affecting the profitable operation of a water flood are the number of feet of sand being flooded and the rate at which each foot is taking water. Further, it is helpful to know that the intake well is operating mechanically as intended. Such things as ineffective plug-backs, packers, cement jobs, and leaky pipe can be detrimental to the profit-making ability of a water drive. It is hoped that it can be demonstrated here that temperature logs of active intake wells can be an aid to answering questions such as these.

Referring to Fig. 1, let us assume a geothermal gradient defined by Curve 1. If the surface lines are buried and if the water-intake well is a reasonable distance from the pressure plant, we can assume that water enters the well at surface temperature. Imagining that there is an infinite amount of water moving down the pipe, it is evident that a temperature survey run under these conditions would show no change in temperature down to a depth where something less than an infinite amount of water is flowing. Further, it is evident that when a depth is reached where no fluid is moving, the temperature curve must increase to the indigenous subsurface temperature for that particular depth. A hypothetical curve illustrating a temperature log of a well taking an infinite amount of water is illustrated by the dashed curve to the left of Fig. 1. The water must leave the hole in the area of the wall between a point slightly above where the curve leaves the input temperature and where it arrives at the geothermal gradient temperature. Referring to Fig. 1, the water must leave the hole between the depths *A* and *B*. Considering the case of a temperature log of this intake well when it is taking something less than an infinite amount, it is apparent that the resultant curve must lie in the area between the infinite volume curve just discussed and the geothermal gradient or zero volume curve. This area is cross-hatched on Fig. 1. As this finite quantity of water moves down the hole, it tends to increase in temperature as it comes into the presence of a progressively hotter environment as defined by Curve 1. The factors governing the quantity of heat q that is driven into the water can be related by the expression:

$$q = \frac{2\pi k\,(T_E - T_W)\,dh}{\ln \dfrac{R_e}{R_w}} \qquad (1)$$

wherein:

T_E = the temperature of the earth at the depth in question.

T_W = the temperature of the water.

k = the coefficient of heat conduction.

dh = the differential thickness.

R_e = radius from the center of the bore hole to where T_E exists.

R_w = the well radius.

*Bird Well Surveys, Bradford, Pa.

†Presented at the spring meeting of the Eastern District, Division of Production, White Sulphur Springs, W.Va., June 1954.

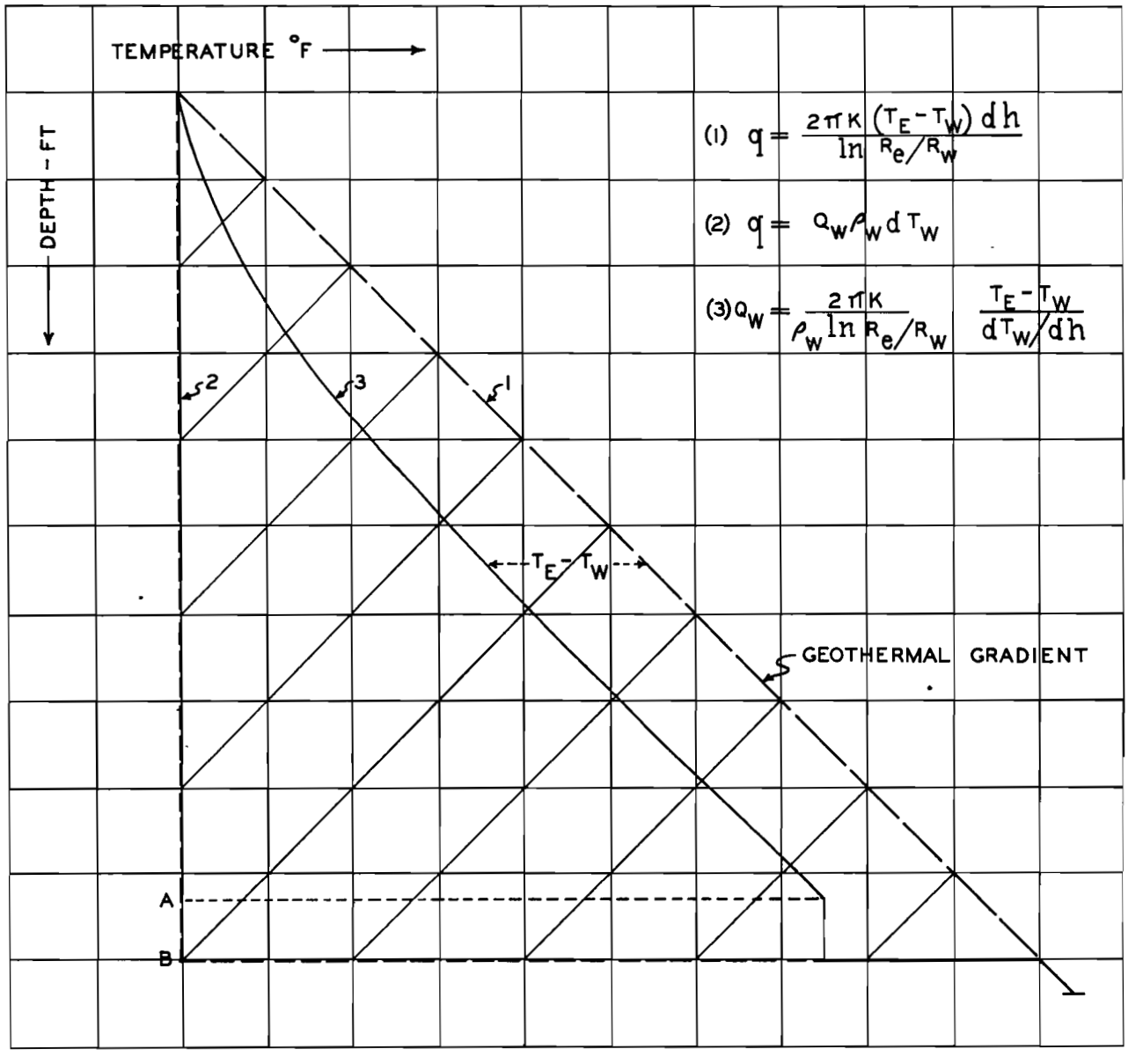

Fig. 1—Theoretical Water-injection Wells

This is true assuming *a*, the heat flow in the angular direction is zero; and *b*, the heat flow in the vertical direction is steady, i.e., as much heat enters below as leaves above in a unit of time. Postulating that everything on the right-hand side of this expression remains constant as the water moves down the hole, it is evident that the value of q depends largely upon the value of $T_E - T_W$. As the water moves down the well, $T_E - T_W$ will increase as the water temperature departs from the geothermal gradient. This greater difference in temperature causes more heat to be driven into the water. The effect of this heat being absorbed by the water is expressed by this relationship:

$$q = Q_W \rho_W dT_W \tag{2}$$

wherein:

Q_W = barrels of water per day.

ρ_W = density of water.

The resultant shape of the curve is the product of these two effects. The farther the water temperature departs from the temperature of the earth, the more Btu's are driven into the water. So long as the quan-

Table 1
Application of Equations to Published Data and Temperature Surveys

	State	Well-bore Condition	$T_E - T_W$, Deg F.	dt/dh, Deg F. per Ft	Δ	H_2O Volume, Bbl per Day
1	Pa.	H_2O outside 2-in.—2 packers	7.07	0.0131	540	97
2			5.00	0.0170	294	49.5
3			9.2	0.0130	708	108
4	W. Va.	5-in. cemented	13.2	0.0090	1,360	318
5			13.7	0.0080	1,710	275
6			13.2	0.0092	1,435	274
7			11.1	0.0092	1,210	210
8			7.6	0.0081	940	149
9	Pa.	6¼-in. open hole	5.49	0.0110	499	75
10	Pa.	H_2O outside 2-in.	7.5	0.0040	1,875	432
11	N.Y.	H_2O outside 2-in.	6.7	0.172	390	49
12			7.9	0.0140	565	45
13			5.7	0.0190	300	24
14	Ill.	4-in. cemented	11.2	0.0157	714	144
15	Pa.	H_2O outside 2-in. with tail pipe	0.84	0.0130	64	9
16			3.5	0.0085	412	72
17	Pa.	H_2O outside 2-in.	2.48	0.0037	790	128
18			4.6	0.00116	3,960	585
19	Calif.	7-in. cemented—perforated	82.0	0.0015	5,460	900
20			52.0	0.0013	4,020	750
21	Ky.	4-in. cemented	3.91	0.0323	121	24
22	Pa.	H_2O outside 2-in.	9.2	0.0115	800	130
23			8.4	0.0077	1,090	125
24	W. Va.	5-in. cemented	4.5	0.0105	428	45
25			5.6	0.0105	534	88
26			9.8	0.0100	980	250

tity of the water moving down into the well is constant, the absorption of this increased amount of Btu's causes the temperature of the water to increase proportionately. A change in the slope of the temperature curve results from this increased absorption of Btu's. This change in slope is in the direction that brings T_W closer to T_E. Thus the departure of the water temperature from the earth's temperature is self-limiting; and after sufficient depth is reached, the slope of the curve will approach parallelism with the geothermal gradient. One of a family of curves of this type is illustrated by Curve 3, Fig. 1.

Equation (1) relates factors that cause Btu's to be forced into the fluid, and equation (2) shows the effect on the water temperature of the absorption of these Btu's. Equating the two and solving for Q_W we obtain:

$$Q_W = \frac{2\pi k}{\rho_W \ln \frac{R_e}{R_w}} \; \frac{T_E - T_W}{\frac{dT_W}{dh}} \qquad (3)$$

For constant values of heat conductivity, water density, well-bore radius, and external heat radius, Q_W should plot as a straight line vs. $T_E - T_W/(dT_W/dh)$, which we will call Δ.

To test the practical usefulness of these equations, they were applied to the published work of Sayre and Wertman[1] and T. J. Nowak[2] as well as

[1] References are at the end of the paper.

temperature profiles run by Bird Well Surveys. Table 1 lists the results and Fig. 2 is the plot of these figures. Points 22 and 23 were taken from Sayre and Wertman, points 19 and 20 from data of T. J. Nowak. It is interesting to note the wide range in intake rates, the variety of pipe sizes, and the geographical distribution. The grouping of the points about a straight line substantiates the hypothesis that k remains fairly constant and that when dealing with water-injection wells corrections for $ln\ R_e/R_w$ are not critically necessary. It should be pointed out that the annular space between the pipe and the wall of the earth must be filled with something other than air or gas for proper heat conduction. However, in most cases this space is filled with mud, water, or cement, and this does not present a problem. In all cases these surveys were run in wells that had been

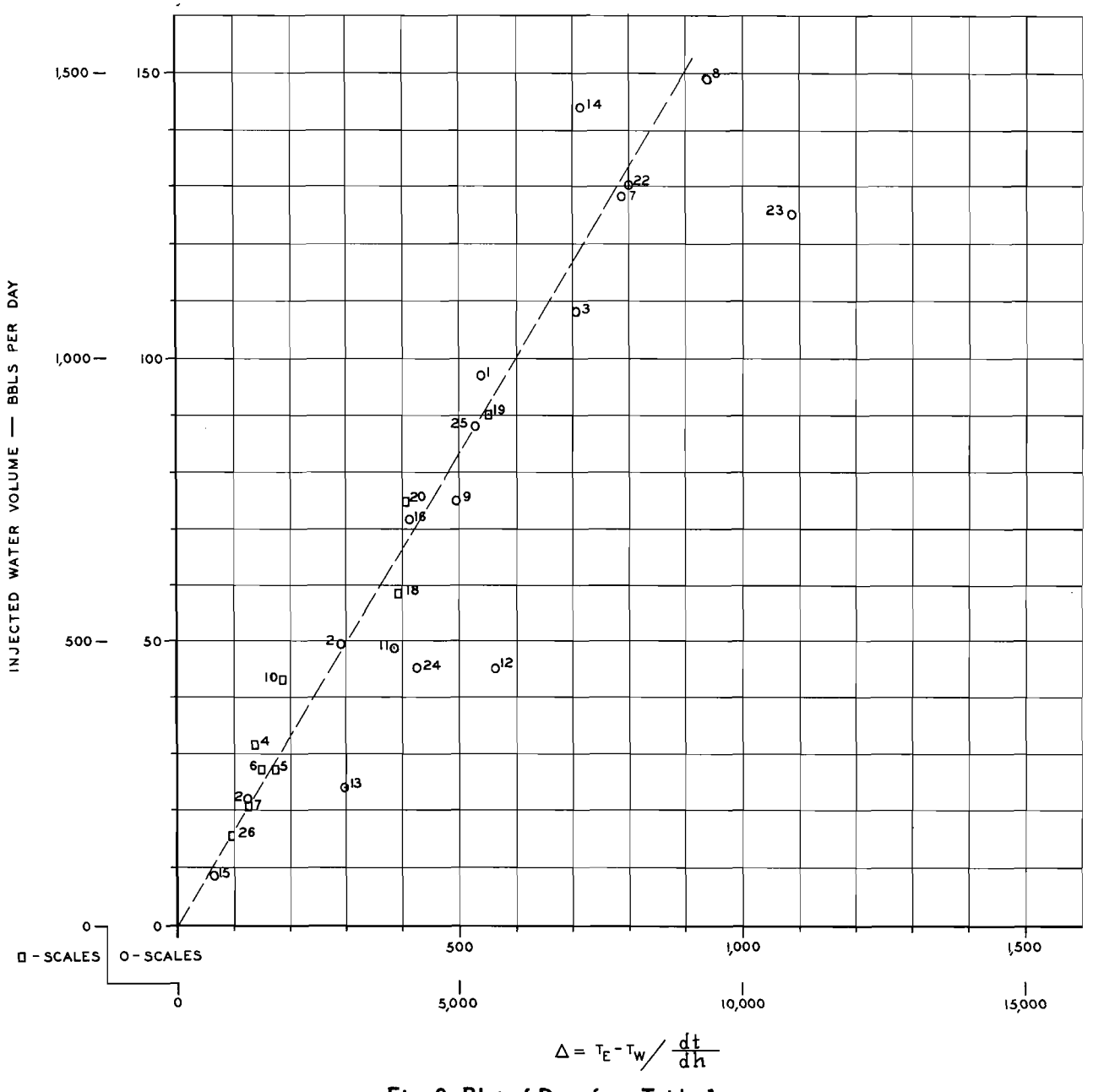

Fig. 2–Plot of Data from Table 1

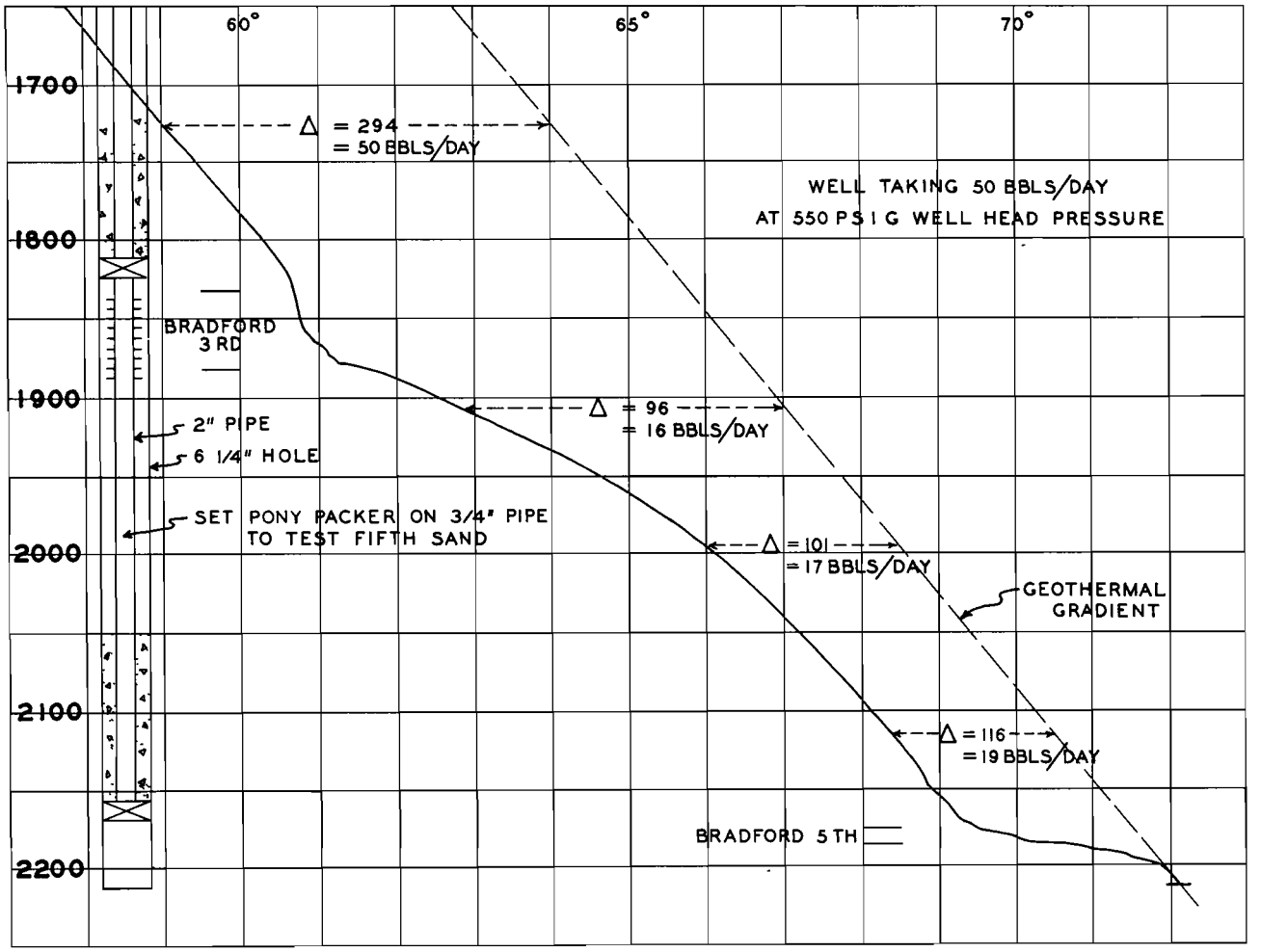

Fig. 3—Water-injection Well

taking a specific quantity of water without interruption for a considerable time prior to making the temperature measurements. Further, these stabilized conditions were not disturbed in making the temperature measurements. Fig. 2 demonstrates that a factor of six to one yields good results in converting Δ into barrels per day.

Going back to Curve 2 of Fig. 1, let us follow the water down the well and see what happens when the water comes to the top of the first zone of permeability. The sand matrix immediately takes on the temperature of the permeating water, and a cold front is formed, which moves back into the sand. Bulletin No. 60 of the Penn State College Mineral Industries Experiment Station, of Greenstein and Preston[3] demonstrates how this wave front is formed and moves through the sand increasing R_e. Therefore, the water that passes on down the hole will not change in temperature in traversing this zone of permeability because this portion of the wall has taken on the temperature of the water itself. At the bottom of the first permeable section less water is flowing down the well, but $T_E - T_W$ is, if anything, slightly larger than it was at the top of the permeability where more water was flowing. This slightly increased amount of heat flowing into less water in unit time causes the slope of the temperature log to become more horizontal. The water temperature rises quickly as it moves down the hole until a new equilibrium is established or until the slope again approximates the geothermal gradient at a new value of $T_E - T_W$. It should be pointed out that it is not necessary for this new equilibrium to be established before taking a new value for Δ. In theory, neglecting changes in R_e, Δ should remain constant at all points along this curve. Any changes in the value of Δ with depth must be in descending order and must reflect the movement of a smaller quantity of water. One other

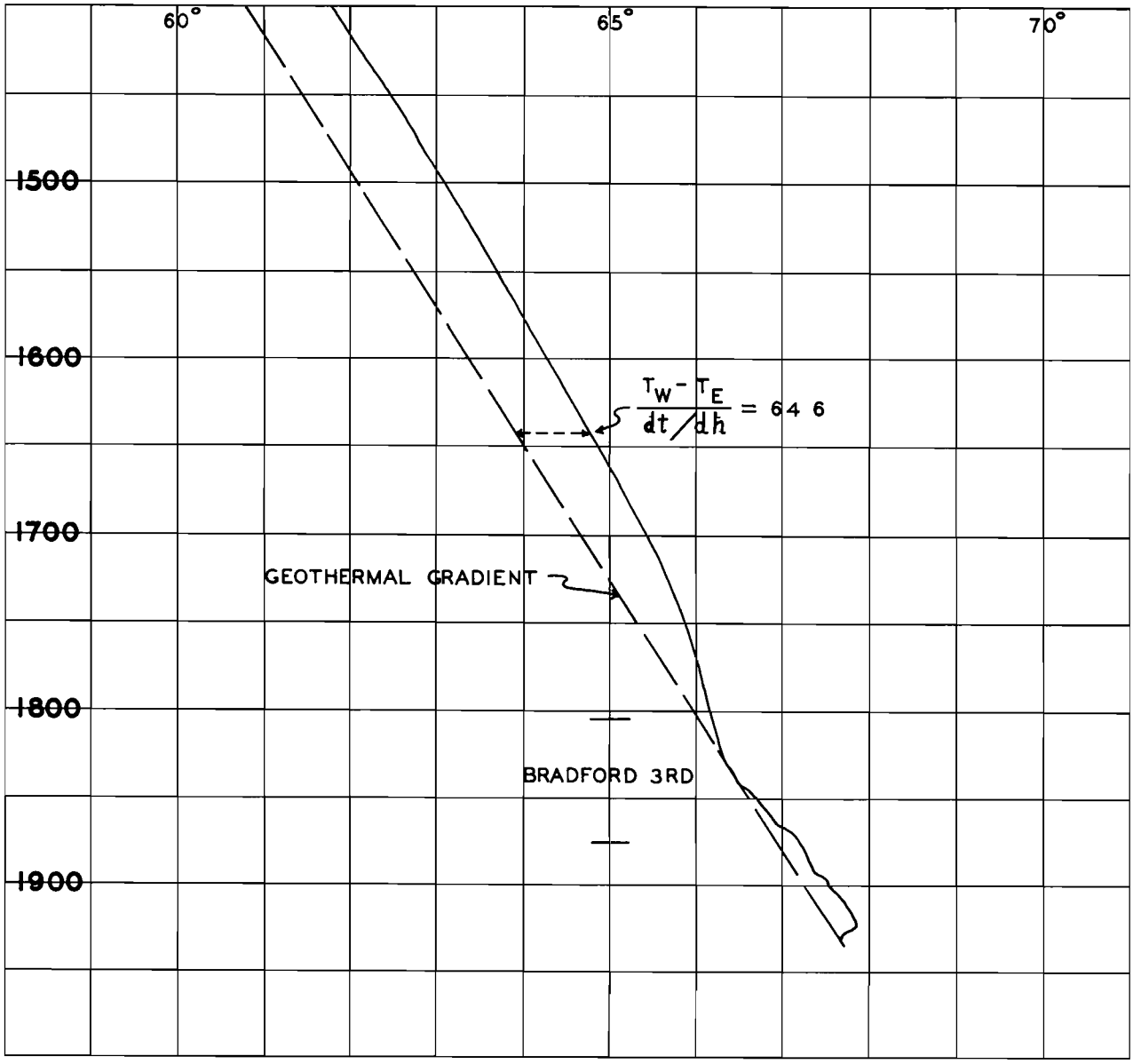

Fig. 4—Flowing Water-flood Well (Open-hole)

aspect of this phenomenon that should be noted is that changes in the diameter of the hole or pipe affect the velocity of the water but do not affect the quantity moving in unit time. From this it would seem that this method is insensitive to variations in the hole diameter. This conclusion is borne out by Table 1.

Fig. 3 is an actual temperature log of an intake well in operation illustrating this reaction. The indigenous earth-temperature curve is obtained by projecting the pocket temperature back up the hole.

There are several methods available for picking the proper slope to use in projecting this gradient if no shut-in temperature log is available. If the well is deep enough for the opposing forces governing Δ to reach equilibrium, the slope of the injection temperature curve itself can be used. In lieu of this, a mean surface temperature can be estimated and a constant-slope indigenous earth-temperature curve computed, using the pocket temperature. Assuming this gradient, Δ was computed at various points along the constant injection-temperature curve between the two zones of permeability; Δ changes very little over this depth, and the values correspond to the maximum and minimum intake rates of 19 and 16 bbl per day. Months after completing this survey

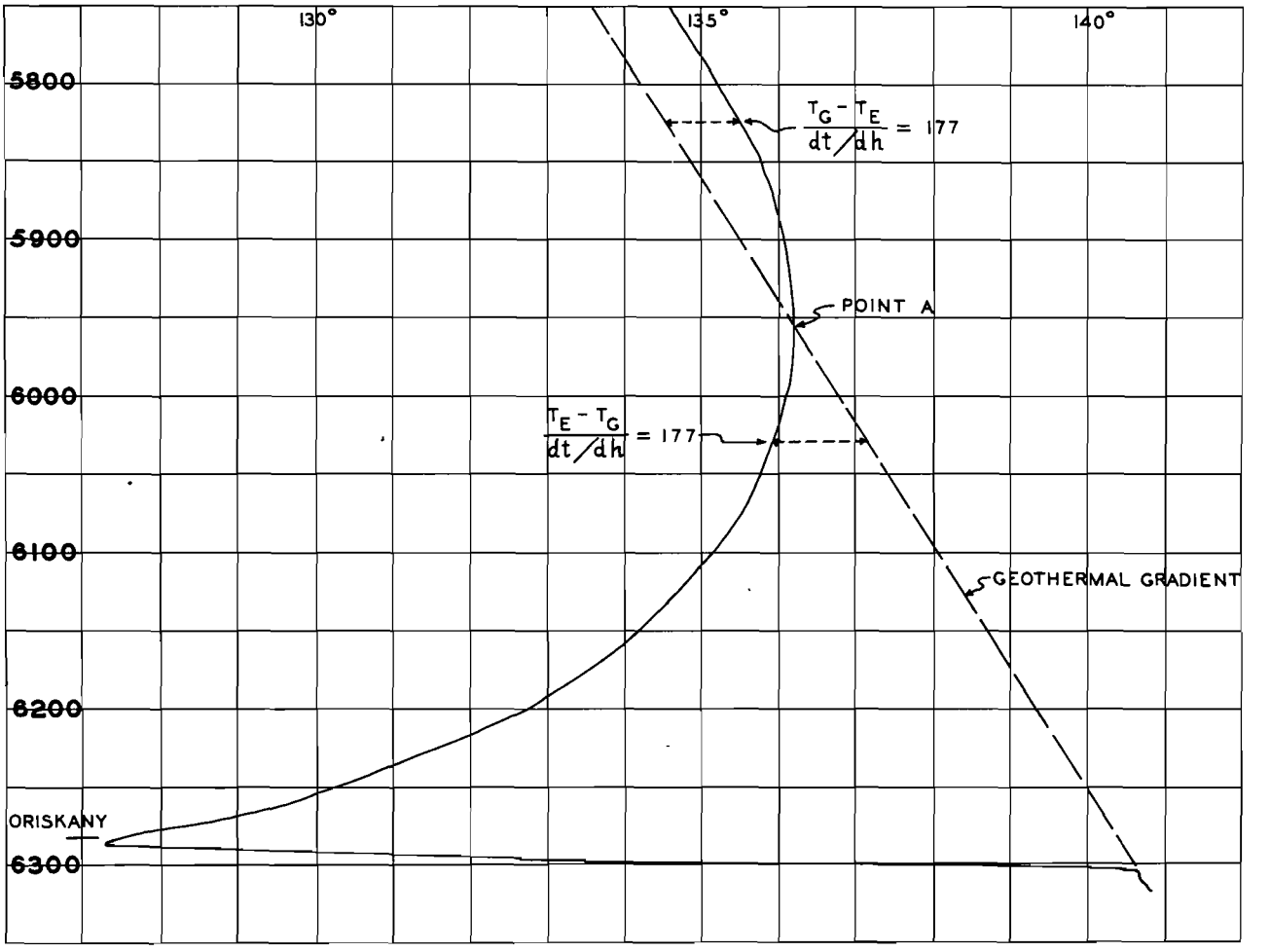

Fig. 5—Producing Gas Well

a small string of pipe with a "pony" packer was run into the well and set in the interval between the two sands; and the lower sand was found to be taking 16 bbl of water a day at the same wellhead pressure that had been established in making the original survey.

Temperature Surveys in a Well Flowing Water and Oil

Let us now consider the case of a flowing well. Presumably, the fluid enters the bore hole at the indigenous formation temperature. This might not be the case in a secondary-recovery project (see reference 1). However, if the distance between intake and outlet wells is great, the fluid temperature will differ only slightly from the indigenous temperature. As the fluid moves up the hole over impervious formations, there will be a tendency for it to be cooled, because of the fact that it is passing progressively cooler formations. The temperature of the water departs from the indigenous temperature, but in doing so causes $T_W - T_E$ to become greater. The larger this differential temperature becomes, the greater the rate of cooling becomes. The same self-limiting phenomenon takes place as was discussed in the case of an injection well, only the process is reversed. After moving up the hole a sufficient distance, the slope of the curve approaches parallelism with the indigenous-temperature curve. Fig. 4 illustrates such a temperature curve. Here again it is necessary that a stabilized flowing condition be established. Points 15 and 16 on Fig. 2 show how points taken from two of this type well fall in line with similar computation taken from an injection well.

Temperature Curve of a Well Flowing Gas

Much effort in the past directed toward interpreting temperature logs of gas-producing wells has revolved around the magnitude of the temperature kick. Attempts to allocate the total volume of gas to two or more gas-producing horizons by using the degree of

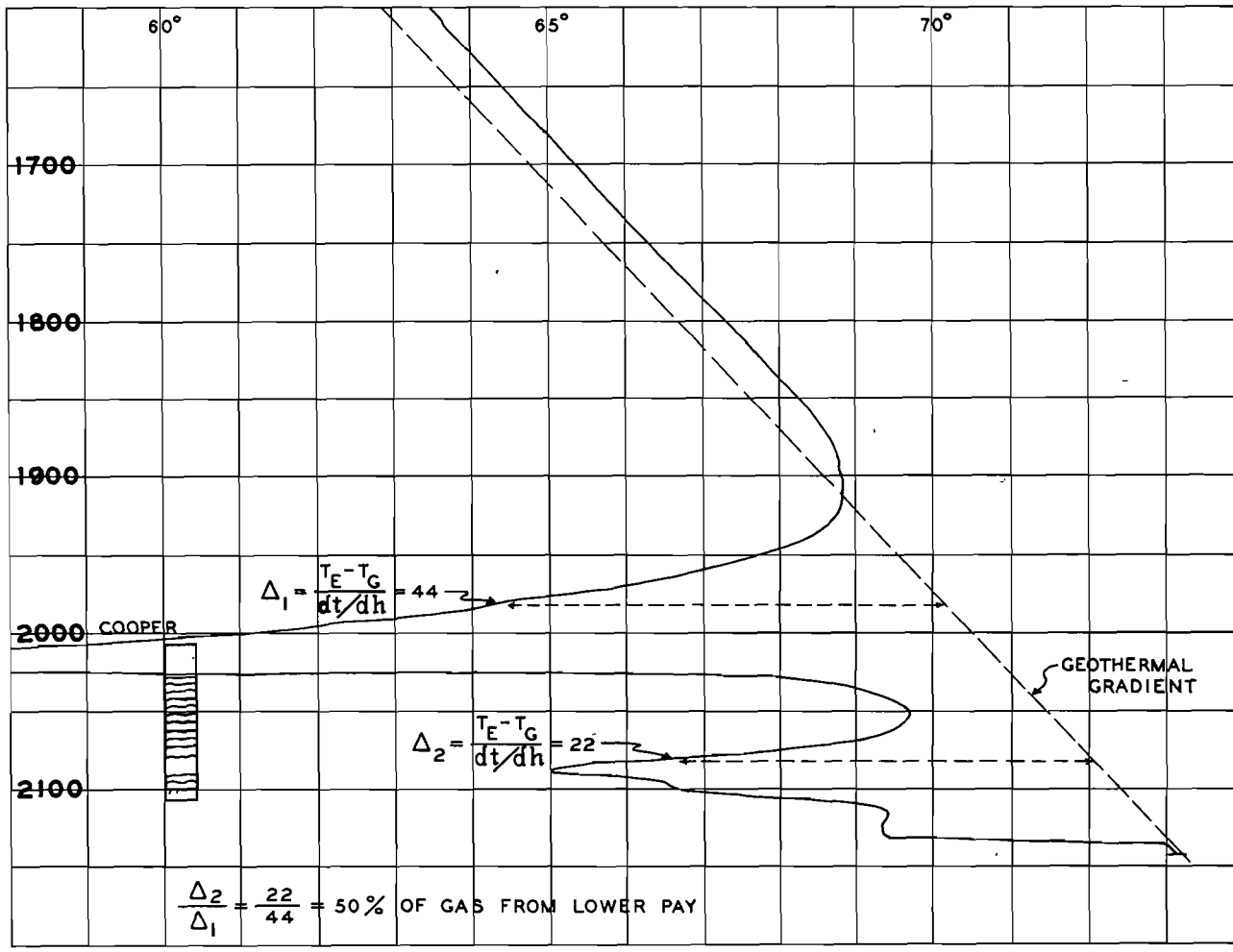

Fig. 6—Producing Gas Well

cooling of the gas in entering the bore hole have generally met with failure because of the nature of this cooling phenomenon. The degree of cooling is dependent upon the pressure drop and upon the type of porosity and its distribution, as well as the volume of gas that is expanding. Applying appropriate values to these variables in order to compute the volume of gas is usually impossible. In an effort to overcome these difficulties the technique discussed previously was applied to a producing gas well.

The gas, in moving into the bore hole, must expand and arrives at a temperature that is less than the indigenous temperature for that depth. In moving up the hole it will warm up. The amount of heat moving into the gas is expressed again by an equation similar to (1), where corrections are made for the efficiency with which heat can be transferred through the gas to itself. The effect of this heat on the temperature of the gas can be expressed by an equation similar to (2), except that a different factor is used for the density and specific heat of the gas depending upon the constituents that make up the gas and the pressure and temperatures involved. The quantity of gas can, nevertheless, be equated with Δ. It is believed that this will be fairly independent of the temperature at which the gas arrived in the hole. As the gas moves up the hole, two things happen. The gas warms up and the indigenous temperature of the earth gets less. Finally there is a point reached where no temperature change takes place. This is marked point A on Fig. 5. It is the place where the temperature curve of the flowing gas crosses the geothermal gradient curve. The temperature curve of the flowing gas must be vertical at point A. I suggest that temperature curves run where this does not seem to be the case are faulty curves

caused usually by improper logging speeds or improper conditioning of the well. Above point A the curve is analogous to that of the flowing water well discussed. Fig. 5 illustrates how a projection of the indigenous gradient taken in the pocket of the well passes through point A. It also illustrates that similar values of Δ will be computed on either the heating or cooling side of point A.

Fig. 6 illustrates the application of this method applied to a well with two pays. Δ_2 is computed above the lower pay and Δ_1 above the upper. Δ_1 can be equated with the total production, and Δ_2/Δ_1 will give that proportion being produced by the lower sand. Sufficient empirical data are not available to publish a conversion factor from Δ to cubic feet per day.

CONCLUSIONS

Information as to the direction and amount of fluid that is moving in a bore hole can be derived from a study of a temperature profile of this moving fluid. Knowledge of the indigenous earth temperature is necessary. Success in this interpretation depends further upon making the temperature measurements under steady-state flow conditions. Care must be taken that the temperature measurements recorded are representative of the temperature of the fluid.

ACKNOWLEDGEMENT

Acknowledgement is made of the help of Dr. John Calhoun and Robert Newman of Penn State University. It was their insight into the nature of the basic concepts presented in this paper that made it possible. Further, thanks are extended to all the people of Bird Well Surveys who helped gather this data.

REFERENCES

[1] Sayre, A. T. and Wertman, W. T: Effects of Water Flooding on Reservoir Temperatures in the Bradford, Pa. Oil Field, *Producers Monthly,* Jan. (1952).

[2] Nowak, T.J: The Estimation of Water-injection Profiles from Temperature Surveys, presented at Fall Meeting, Petroleum Branch, AIME, Oct. 23-24, 1952, Los Angeles, Calif.

[3] Greenstein, R. I. and Preston, F: *Bulletin No. 60,* Mineral Industries Experiment Station, The Pennsylvania State College, 1952.

Ex. II – 40

SOCIETY OF PETROLEUM ENGINEERS OF AIME
6200 North Central Expressway
Dallas, Texas 75206

PAPER NUMBER SPE 2965

THIS IS A PREPRINT—SUBJECT TO CORRECTION

EVALUATION OF GAS STORAGE WELL COMPLETIONS WITH WELL LOGS

By

B. A. Smith, Member AIME, and M. R. Neal, Member AIME,
Schlumberger Well Services, Houston, Texas

© Copyright 1970
American Institute of Mining, Metallurgical, and Petroleum Engineers, Inc.

This paper was prepared for the 45th Annual Fall Meeting of the Society of Petroleum Engineers of AIME, to be held in Houston, Tex., Oct. 4-7, 1970. Permission to copy is restricted to an abstract of not more than 300 words. Illustrations may not be copied. The abstract should contain conspicuous acknowledgment of where and by whom the paper is presented. Publication elsewhere after publication in the JOURNAL OF PETROLEUM TECHNOLOGY or the SOCIETY OF PETROLEUM ENGINEERS JOURNAL is usually granted upon request to the Editor of the appropriate journal provided agreement to give proper credit is made.

Discussion of this paper is invited. Three copies of any discussion should be sent to the Society of Petroleum Engineers office. Such discussion may be presented at the above meeting and, with the paper, may be considered for publication in one of the two SPE magazines.

ABSTRACT

Many of the problems connected with the underground storage of natural gas, in both aquifer and depleted reservoirs, can be solved by the proper application of modern wireline logging tools.

Well logs are useful in gas storage wells for the location and inventory of gas-bearing zones, determination of levels where gas enters or is produced from the formation, determining well deliverability, and the location of casing leaks as well as points where the pipe is defective due to corrosion. Logs run after the well is completed can help to evaluate the effectiveness of a stimulation process or the mechanical integrity of the completion. Logs run at intervals, as the storage well is produced, can define changes in gas saturation, movement of fluid contacts, and growth of the gas bubble, thus permitting a periodic inventory.

Major changes in injection patterns and withdrawal rates are usually symptoms of problems. Suitable logging programs can help define these problems and indicate the remedial action necessary to bring the field back to maximum efficiency.

The open-hole logs and the logs run immediately after completion provide valuable background information for the interpretation of logs run later in the life of the well. In existing storage fields, where background information is not available, data must be gathered in order to help define the existing problems. A thorough evaluation of the existing subsurface hardware must also be made.

Small-diameter tools and pressure-control systems are available with which most logging operations may be made in either tubing or casing without interrupting the well operation.

Field examples from gas storage projects in several different areas are used to illustrate the interpretation techniques.

EVALUATION OF GAS STORAGE WELL COMPLETIONS WITH WELL LOGS

By

B. A. Smith, and M. R. Neal

INTRODUCTION

The steadily increasing demand for natural gas has created a need for more facilities for storing gas that is produced during the warm season for use during the cold season. A common type of storage facility now in use is the underground gas storage reservoir.

The sizes of the underground storage reservoirs range from relatively small, with only a few wells, to huge reservoirs, with hundreds of wells. Their uses vary from meeting peak demand for a few hours a day in the coldest weather to furnishing most of the gas used in the area during the winter season.

Gas storage reservoirs are of two main types: ***depleted storage reservoirs*** which once contained gas or oil and water, or a combination of all three, and ***aquifer storage reservoirs*** which originally contained only water.

Besides problems common to all wells, there are many which are peculiar to gas storage wells and reservoirs. The problems encountered, and the method of evaluation used, will depend on the type of reservoir. Some of these problems are:

1. Location of zones where gas is stored.
2. Determining where withdrawal gas is coming from or where injected gas is entering the formation.
3. Determining deliverability and ways to improve deliverability.
4. Location of leaks in the casing.
5. Locating corrosion, or zones of weakness in the casing, which may lead to future leaks.
6. Tracing and finding gas lost through leaks.
7. Inventory — or determination of amount of gas in storage.
8. Evaluating stimulation methods and locating zones affected by stimulation.

EVALUATION OF NEW WELL COMPLETIONS

When new gas storage fields are being developed a complete evaluation can eliminate or simplify many of the problems described above. This includes both open-hole formation evaluation before casing is set and cased-hole evaluation of well performance and hardware integrity.

The open-hole programs are necessary for complete interpretation of most subsequent cased-hole logs. A complete open-hole suite might include the Density, Neutron, and Sonic logs for porosity and lithology information, Induction log for saturation, and Microlog for indication of the permeable zones.[1]

The objectives of the initial cased-hole logs should be considered in two groups; evaluation before perforating, and evaluation after perforating.

BEFORE PERFORATING

The cased-hole program before perforating should be designed to furnish:

1. Base Neutron logs for future use in inventory calculations or diagnosis of well problems.
2. Evaluation of cement bonding and zone isolation.
3. Evaluation of integrity of the casing.
4. Depth control.

The base Neutron log and the open-hole logs furnish background information useful in computing the gas inventory from subsequent Neutron logs run later in the life of the well.[2] The base Neutron log is also useful for tying in to formation depths and for locating gas, behind the casing or in thief zones, which has escaped from the storage zone or leaked through the casing.

Base Neutron logs should be run with water in the casing and also with gas or air in the casing. Both are necessary because in a storage well the liquid level in the casing will vary with the injection-withdrawal cycle. In future inventory calculations the "wet" Neutron will be used as a reference below the liquid level and the "dry" Neutron as a reference above.

The base "wet" Neutron log and Cement Bond log should both be run before perforating in order to have the casing full of water to the surface. The base "dry" Neutron log is run after the water has been removed from the casing in preparation for perforating. The well must be evaluated from total depth to surface since casing leaks or thief zones may occur at any level.

[1]References are at end of paper.

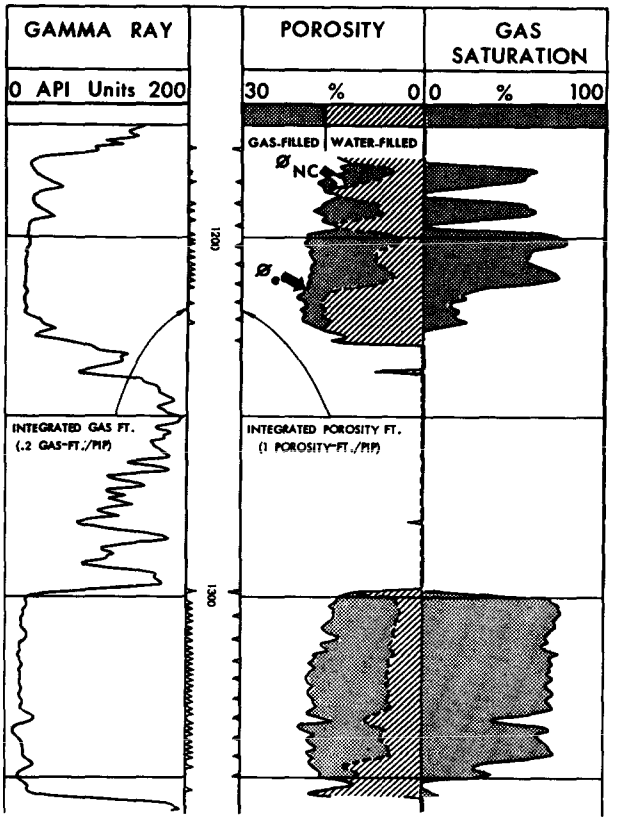

Fig. 1 — Computed log comparing porosity, ϕ_e, from open-hole logs, with porosity, ϕ_{NC}, from the cased-hole Neutron (center), and showing computed gas saturation curve (right).

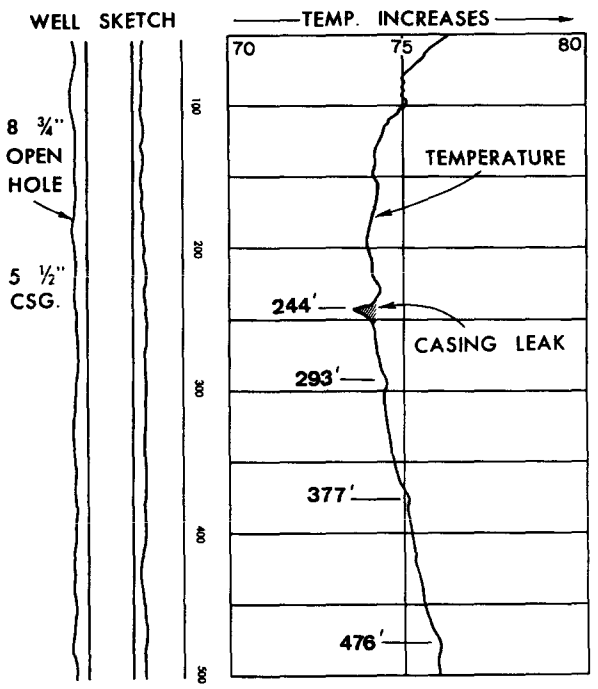

Fig. 2 — Temperature log showing a small casing leak.

Fig. 1 is a presentation of the results which may be derived from the open-hole and cased-hole logs. The Gamma Ray log on the left-hand side (Track 1) shows upper and lower non-shaly zones and a shale bed in between. In Track 2 (center), the fluid-filled porosity, computed from open-hole logs, is the solid curve, and the porosity computed from the cased-hole Neutron log is the dashed curve. The porosity response for the cased-hole Neutron was derived by cross-plotting open-hole porosity data with base Neutron logs run prior to gas injection. Gas saturation, computed from the difference between the two porosities, is presented in Track 3 (right). Integrated porosity-feet is given by the pips on the right side of the depth track, and integrated hydrocarbon-feet by the pips on the left side.

Evaluation of the quality of cement bonding to casing and of zone isolation is done with the Cement Bond Log, an acoustic device.[3] The usefulness of the Cement Bond Log is greatly enhanced by the addition of a VDL log (acoustic wave train log in variable density presentation)[4], which confirms the indications of the Cement Bond Log and reveals the quality of bonding between the cement and formation.

If the pressure test of the casing, made before perforating, indicates casing leaks these may be located with the Temperature log.

Temperature logs can locate gas leaks. They may also be used to detect fluid movements behind casing, thus providing a check on zone isolation. Fig. 2 shows a Temperature log which was used to locate a small leak in a gas storage well before final completion. The anomaly at 244 ft clearly shows the gas leak. Calculations indicated the rate of loss through this leak to be 900 SCF of gas per day at 1000 psig. A casing patch was set over this interval. Further pressure testing indicated the leak was sealed, and the well was completed.

An interesting feature of this log is the presence of heating anomalies shown at 293, 377, and 476 ft. When correlated with open-hole logs, each of these anomalies corresponds to a caved zone. They are probably caused by heat of hydration in the annular cement. This heat is still evident on the log even though the well had been cemented for 65 days.

A Casing Collar log provides convenient depth references for use on subsequent logging or perforating operations in the well. Casing-collar depths may be tied in to formation depths by comparing them with features on cased-hole Gamma Ray or Neutron logs. (For example of Casing Collar log, see Fig. 8.)

AFTER PERFORATING

The cased-hole program after perforating should be designed to:

1. Investigate the effect of perforation and stimulation.

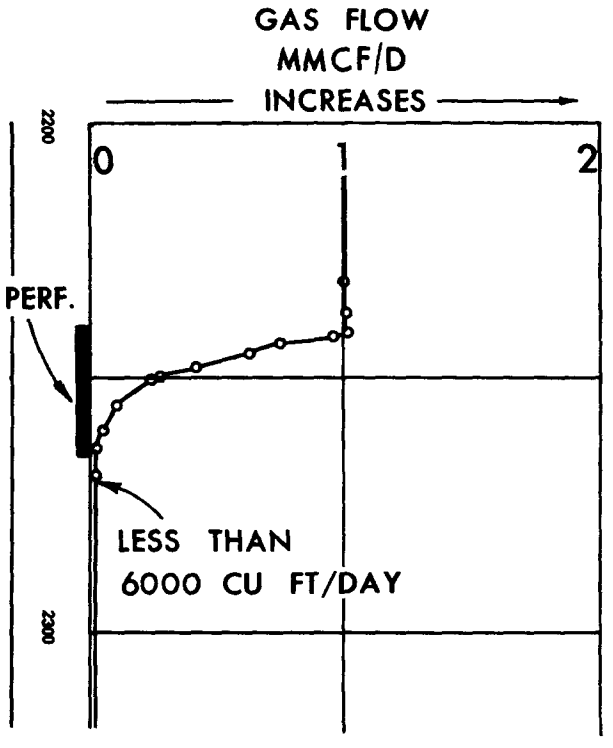

Fig. 3a — Packer Flowmeter log showing gas-injection profile.

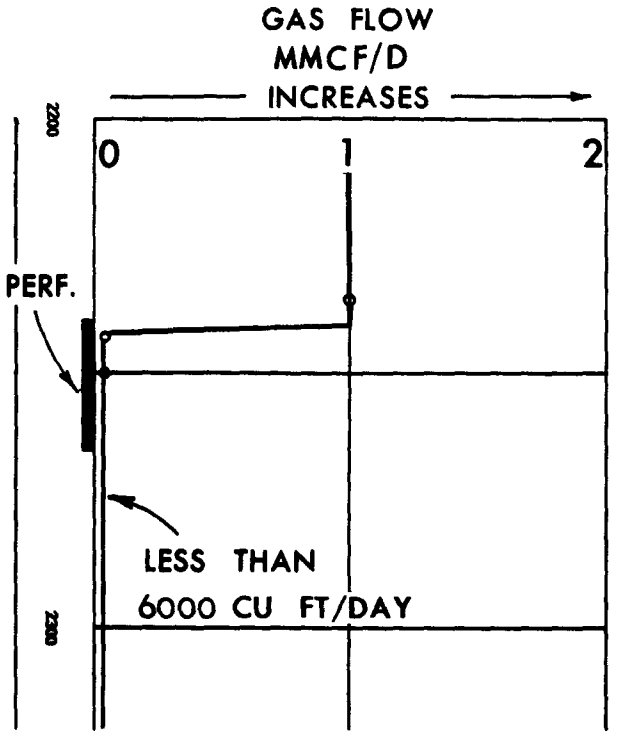

Fig. 3b — Packer Flowmeter log showing most of injected gas is entering through the top two feet of perforations.

2. Assure that the completion is performing as designed.
3. Furnish a reference set of logs for use in studying any future production problems.

A typical set of after-completion logs includes Flowmeter, Gradiomanometer[5], Temperature log, and Pipe Inspection logs. Normally this program will fulfill the three requirements given above.

Perforations, stimulation, and well performance can be evaluated in several ways. Figs. 3a and 3b show profiles of flow rates measured versus depth on Packer Flowmeter surveys run in two offset wells. In Fig. 3a the smooth decrease of flow rate shows distribution of gas injection over the bed, but with most of the gas entering the upper part of the bed. However, Fig. 3b shows that practically all of the injected gas in the adjacent well is entering through the top two feet of the perforations. This could indicate any one of a variety of problems such as ineffective perforations or stimulation, permeable streaks in the formation, skin damage, etc. Further investigation of this zone proved the problem was caused by insufficient injection pressure. Increasing the injection pressure resulted in acceptance of injected gas throughout the perforated interval.

Fig. 4 shows a Continuous Flowmeter log run in a well which had been completed using the "limited-entry" technique. Injection was through the tubing-casing annulus. The log indicates that 55% of the injected gas was entering the formation through the bottom two perforations, although

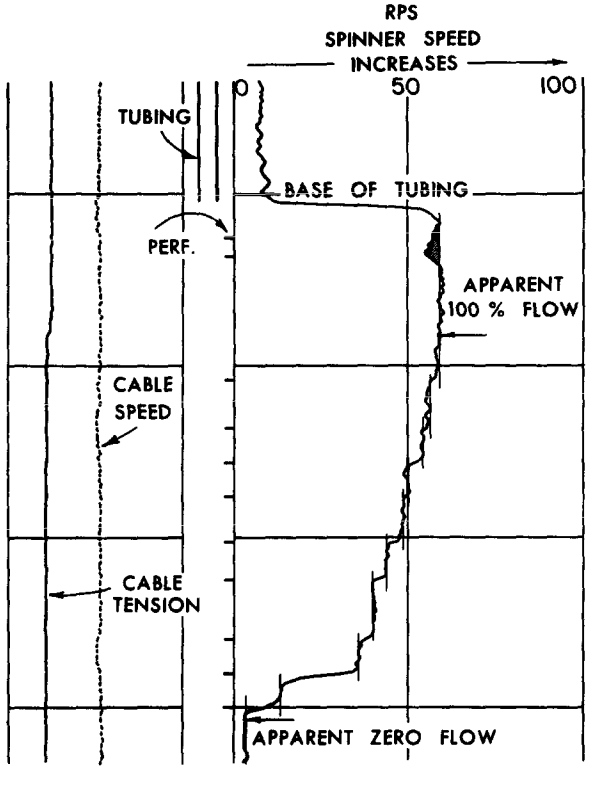

Fig. 4 — Continuous Flowmeter log showing that 55% of injected gas is entering the formation through bottom two perforations.

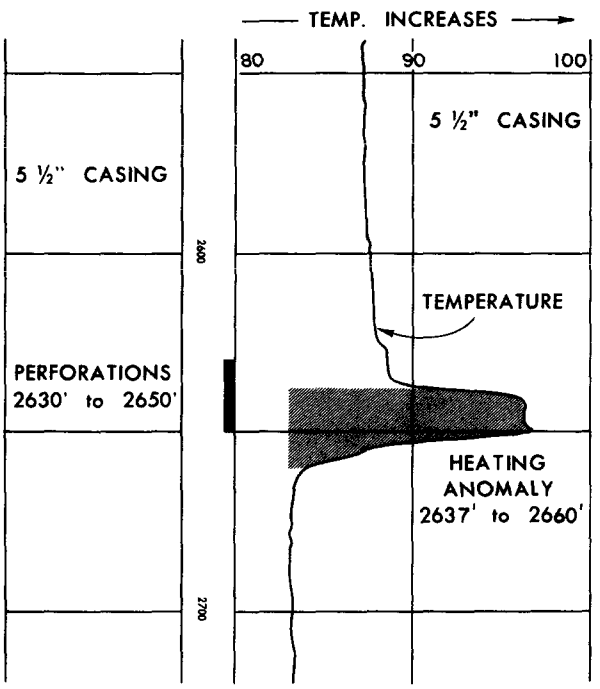

Fig. 5 — Large heating anomaly on Temperature log shows where acid has reacted in formation.

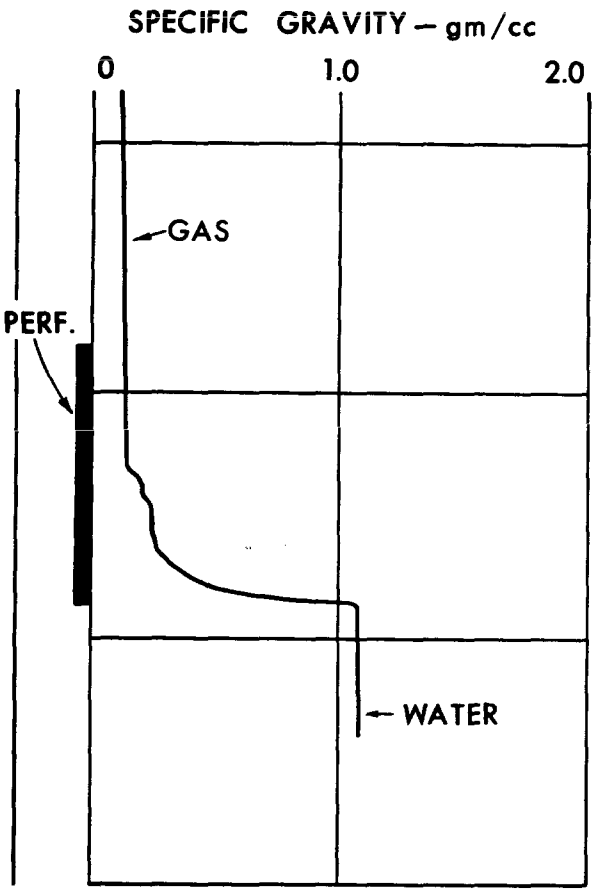

Fig. 6 — A typical Gradiomanometer log.

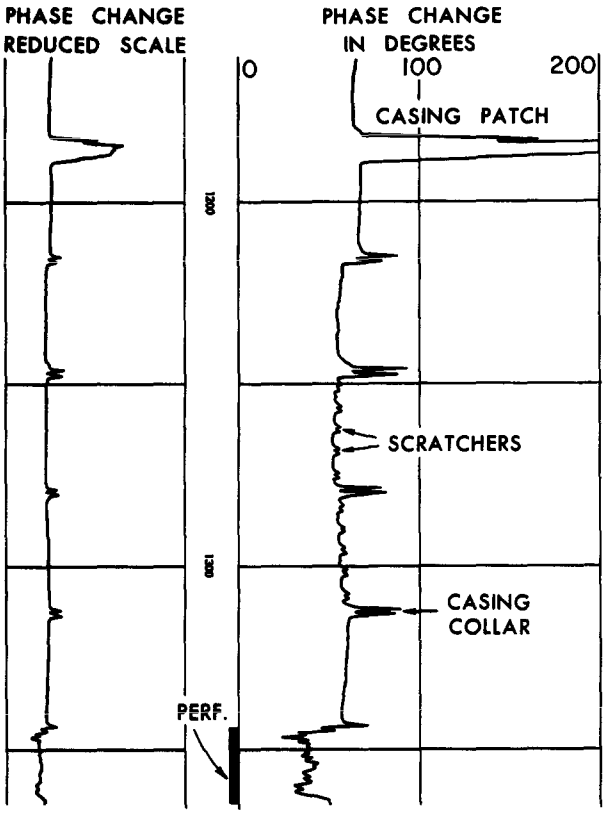

Fig. 7 — Scratchers, casing patch, casing collars, and perforations are apparent on Pipe Inspection log.

some gas is entering each of the other perforations except the top two.

Both Fig. 3b and Fig. 4 are cases of ***new wells*** that did not perform as designed. Both wells required remedial action for efficient operation.

The effects of stimulation may be checked with a Temperature log. Fig. 5 shows a Temperature log run to check the effect of acidizing a carbonate reservoir. The large heating anomaly shows clearly where the acid has reacted in the formation. A similar procedure may be used to detect zones where hydraulic fracturing fluids have entered the formation.[6]

The Temperature and Flowmeter logs supply complementary information. The Flowmeter shows where fluids or stimulation agents enter or leave the casing and the Temperature log shows where these same fluids enter or leave the formation. Both items of information are necessary to evaluate well performance and design remedial action if necessary.

A typical Gradiomanometer log[5] is shown in Fig. 6. This log of hole-fluid density is valuable for indicating the lowest point of gas injection or withdrawal from a formation. This information is necessary when trying to shut off water on the withdrawal cycle and when making studies of water encroachment or water coning.

The final log necessary for the well completion package is the Pipe Inspection log. This log responds to average casing thickness. A typical Pipe Inspection log run in a new well is shown in Fig. 7. Note how clearly casing collars, scratchers, casing patches, perforations, and other variations in the casing makeup are indicated.

The Pipe Inspection log may be run either before or after perforating since the wellbore fluid has no effect on the log. The tool works equally well in gas, air, water or oil.

The primary purpose of the Pipe Inspection log in a new well is to provide a reference for future logs. With a base log for comparison, corrosion can be detected when as little as 3 to 5% of the original casing thickness has been affected. With this early detection it is generally possible to take timely remedial action before any gas is lost.

EVALUATION OF DEPLETED-RESERVOIR STORAGE FIELDS

Many of the fields presently used for, or being converted to, gas storage originally contained gas or oil. These depleted fields make ideal gas storage reservoirs since the two requisites, 1) a porous, permeable formation, and 2) an impermeable cap rock, are already known to exist. Some of the wells in these fields were drilled before the advent of well logging. Records on these old wells (some as old as the 1800's) are meager, and in many cases complete casing records are not available. Depleted fields with few or no records present a different problem than new completions, and a different approach must be used.

Before problems can be defined or remedial action designed, as much information as possible must be gathered on each well. Basically the following questions should be answered:

1. Where are the original casing strings located?
2. Where are the storage zones located?
3. Is there a mechanical problem in the well such as leaks, corrosion, incipient failure of a casing string, etc.?
4. Are there any zones of gas accumulation other than the storage zones?
5. Where is gas entering and leaving the formation?
6. In a water-drive reservoir, where is the fluid level in the wellbore and in the formation at different periods during the injection-withdrawal cycle?

Many of these questions can be answered by running appropriate logs.

A typical logging program for a gas expansion reservoir would include Gamma Ray-Neutron, Cement Top Locator, Temperature, Flowmeter, Caliper, Cement Bond log, and Pipe Inspection log. For a water drive reservoir the Gradiomanometer and possibly a Thermal Neutron Decay Time log should be added.[7, 8]

The Gamma Ray log is used for correlation and definition of formation boundaries. It may also be used to delineate water flows, which exist or have occurred behind casing, by detecting deposits of radioactive scale.[9]

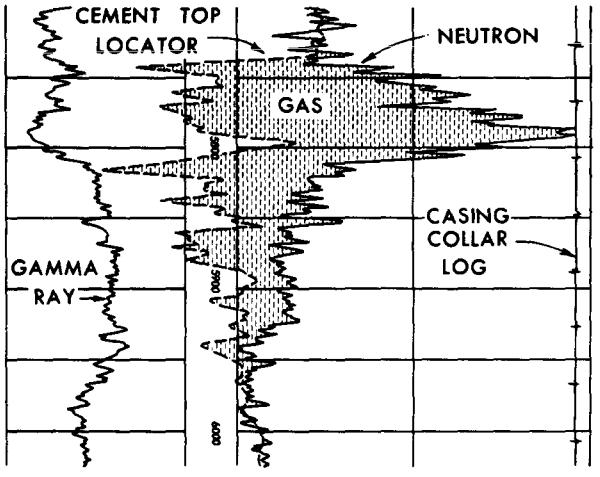

Fig. 8 — Separation between Cement Top Locator log and Neutron log indicates presence of gas.

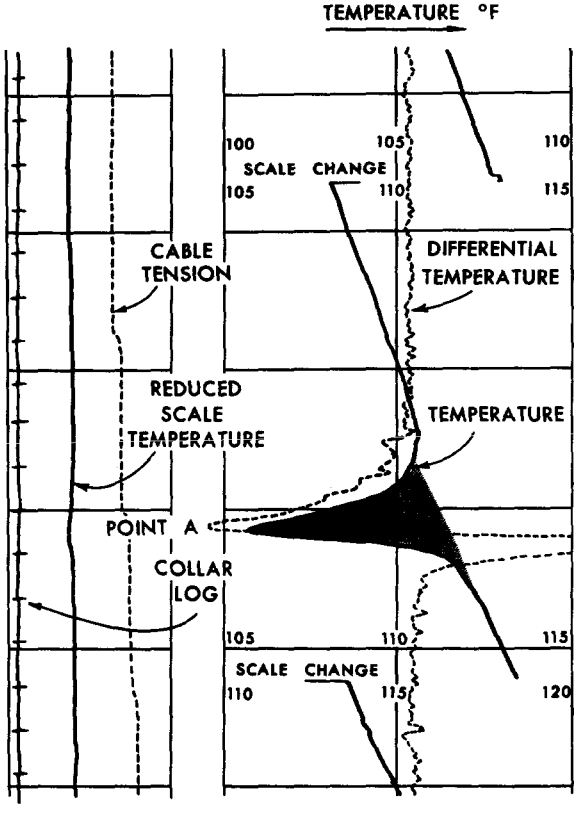

Fig. 9 — Temperature log showing a casing leak at Point A.

The Neutron and Cement Top Locator may be compared to find gas either in open hole or behind casing. In this application, the Cement Top Locator serves as a qualitative cased-hole density log. (Note the indication of gas by separation of curves in Fig. 8.) Without porosity data it is difficult to determine the presence of gas behind casing with only one of these logs. However, a comparison of the two gives positive identification of gas.

The Temperature log is run with the well flowing and rerun at periodic shut-in intervals. Location of zones which have taken injected gas or produced gas are more easily identified from the shut-in runs. These zones will retain their temperature anomaly while the surrounding formations will return to their normal geothermal temperatures. Much information about the well's mechanical condition and the gas-producing zones can be derived from these logs.

Fig. 9, run 48 hours after shut-in, shows a casing leak where 36,000 cu ft/day of gas is escaping. A study of the temperature gradients indicates the gas is coming up the casing to Point A, leaving the wellbore, and continuing up the hole in the casing-formation annulus. Exact points of entry of gas into the formation could not be determined since the original geothermal gradient for this well was not available. However, no gas accumulation zones were noted above Point A, so the lost gas apparently migrates away from the well.

Fig. 10 is a Temperature log which shows a casing leak located several thousand feet above the intended storage formation. Analysis of this log and companion logs indicated

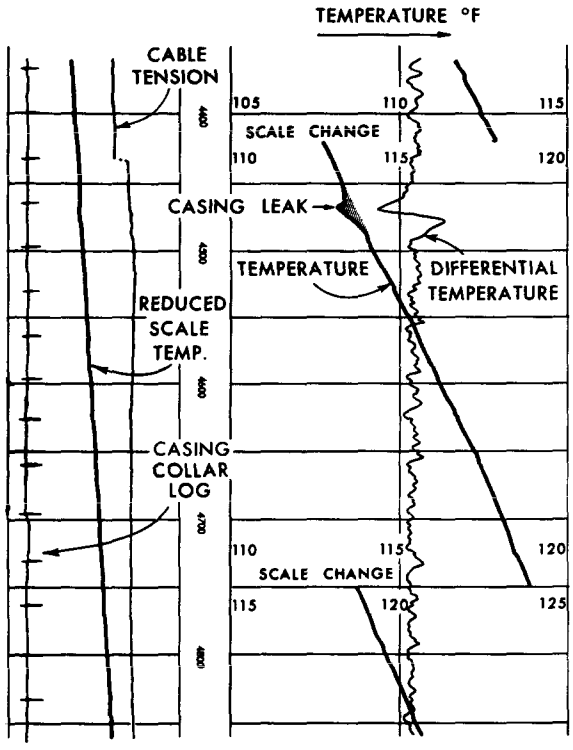

Fig. 10 — A casing leak several thousand feet above the intended storage zone is indicated by Temperature log.

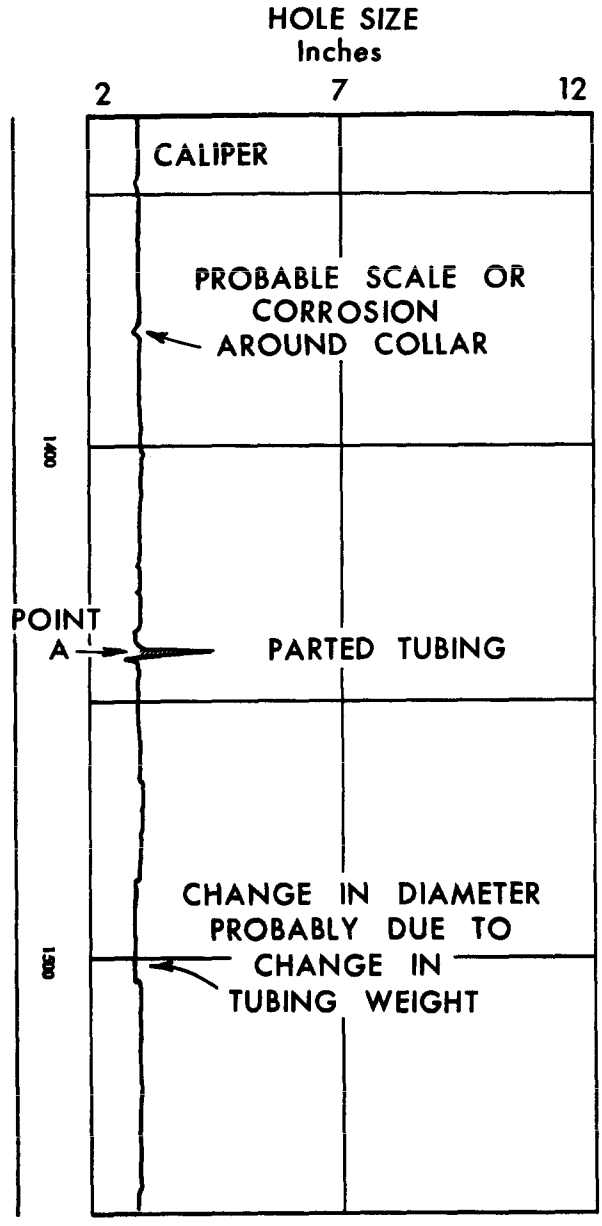

Fig. 11 — Caliper log showing parted tubing at Point A.

this to be a gas accumulation zone which produced gas back into the wellbore during low pressure cycles.

Flowmeter logs are run to determine how much gas is flowing and where the gas is entering the borehole. In open-hole completions a Caliper log must be run in order to convert the velocity information from the Continuous Flowmeter to the desired volumetric flow rate information.

In old wells where the records are very poor it is sometimes necessary to run the Caliper even in the casing and tubing to completely analyze well performance. Fig. 11 shows a Caliper which indicates parted tubing at Point A.

The Pipe Inspection log is run to find zones of incipient failure in the casing string. Corrosion, perforations, and

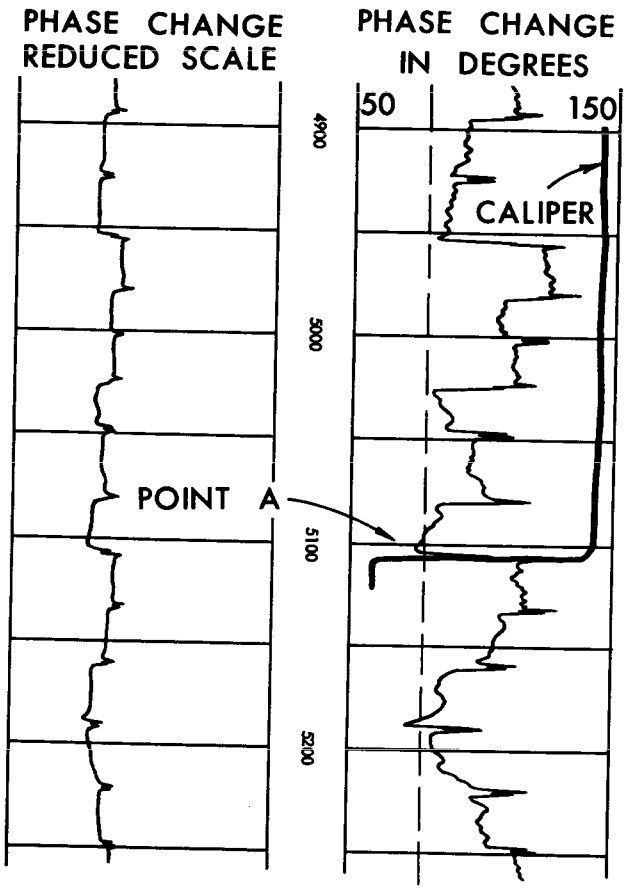

other hardware characteristics are pinpointed. For instance, Fig. 12 also indicates excessively thin casing in several sections. One such section is located at Point A. On the basis of this log and the anticipated future casing pressures it was decided to plug and abandon this well. During the plugging operations the casing collapsed. A Caliper log run in the collapsed casing is superimposed over the Pipe Inspection log of Fig. 12. The Caliper indicates the casing to be collapsed at Point A.

The correct program for gathering information on a well is not necessarily limited to the logs described. It should be tailored to the particular well and field conditions being investigated. The reservoir drive system, completion method, casing program, and many other factors must be studied before deciding on a program. One system is to log a few wells and analyze the results. If the desired information is not clear, alter the program and try again. In this manner an optimum program can be established for any set of conditions.

When the information on the well has been secured it is analyzed, and any rework programs are then defined. The well in Fig. 13 has several defects which should be rectified.

Fig. 12 — Pipe Inspection log shows the casing to be excessively thin at Point A. Subsequent Caliper log shows casing collapsed at that point.

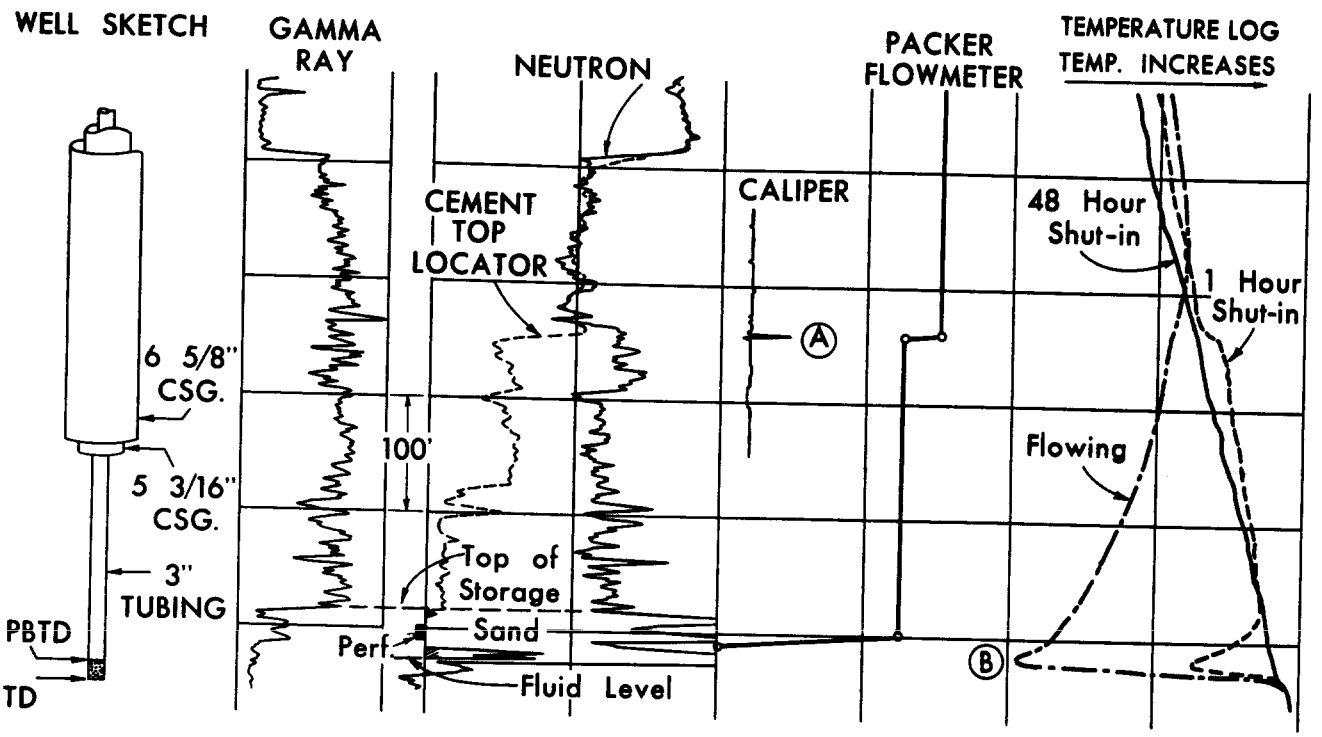

Fig. 13 — Several problems in this well were defined by logs. Caliper and Packer Flowmeter indicate the tubing to be parted at Point A. Temperature log (Point B) indicates gas is being produced from formation below perforated interval.

The parted tubing, indicated by the Caliper and Packer Flowmeter at A, should be replaced. The tubing should be reset and perforated opposite the zone of gas production as indicated by B on the Temperature Log. Because extensive rework would have been necessary for this well it was considered more economical to plug it and drill an offset well.

After necessary rework programs are completed, the same set of after-completion logs described in evaluation of new well completions should be run. These will serve two purposes:

1. To check the effectiveness of reconditioning.
2. To furnish a reference set of logs for analyzing future difficulties.

EVALUATION OF PRODUCTION PROBLEMS

When production problems occur, the logging program must be selected in a different manner than in new-well or depleted-reservoir cases previously discussed. There is no standard logging program which will solve all production problems. Instead, a deliberate step-by-step analysis of the problem must be completed.

The first step is to study all available history on the well such as the drilling and completion records, the open- and cased-hole logs, and the injection-withdrawal records over the life of the well, etc. This information, together with the recent history of problems, will lead to many questions concerning downhole dynamics of the well.

When the study is complete and the questions have been listed, the next step is to decide what log is most likely to answer the important questions. This log should be run and the data again analyzed with the additional information available. If the answers are now clear the remedial work can be planned. If the problem is still not well defined the log to run next must be selected. This process of logging and analysis should be repeated until the production problem is defined.

The following is an example of a production problem which occurred in a new, aquifer storage field. Approximately 40 wells had been completed and gas injection had started. After several short-term tests had been successfully completed, it was decided to make a full-scale withdrawal test.

During the test the gas production from several wells virtually stopped. Since less than 50% of the theoretically available gas had been produced, a solution had to be found.

Four of the wells, which were still producing gas and some water, were chosen to analyze the problem. A well sketch typical of these completions is shown in Fig. 14a.

It was decided to run a Neutron log to determine if there was still gas in the storage zone. Comparison of this log (solid curve of Fig. 14b) with the base Neutron log (not shown) indicated that much gas was still present in the

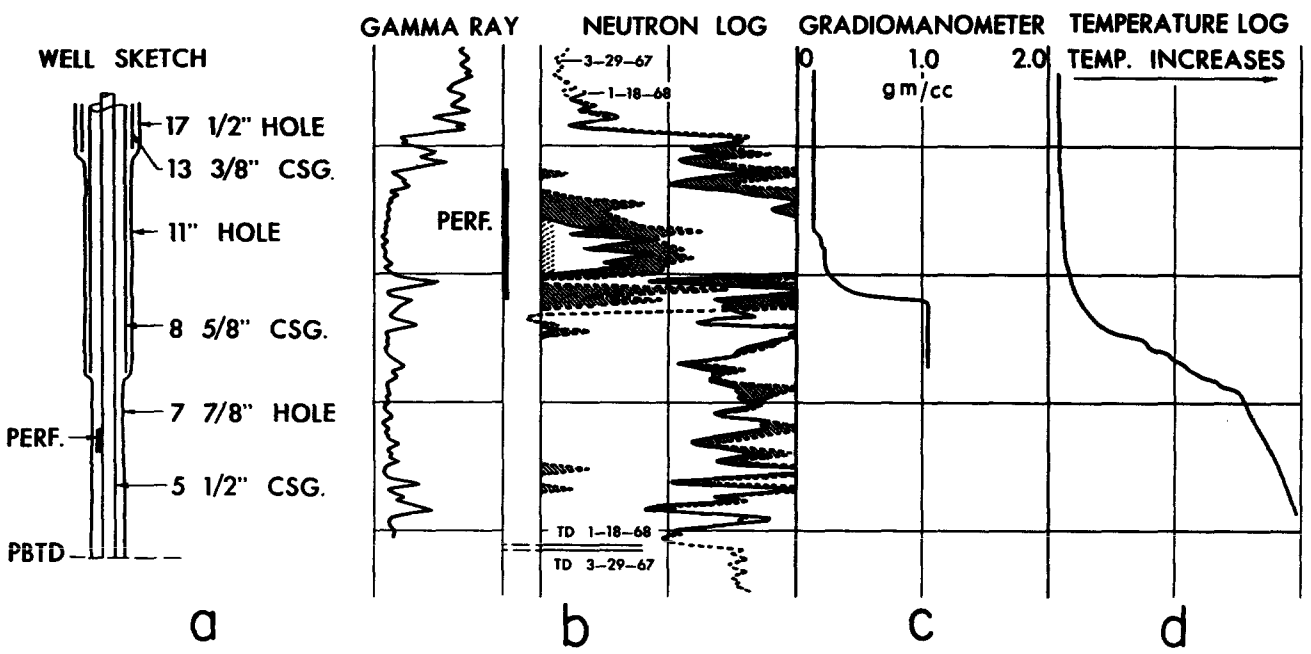

Fig. 14 — Logs run in a storage field that was experiencing production problems. Neutron log indicates gas still present in storage zone. Gradiomanometer shows that some water was being produced from perforations. Temperature log indicates gas production was coming from formations below the perforations.

storage zone, but did show a reduction from the previous Neutron log (dotted curve) run after gas injection. It also indicated that some gas had been produced from zones below the perforated zone.

After this, a Flowmeter and Gradiomanometer were run to determine if all the production was coming from the perforations. The Gradiomanometer, shown in Fig. 14c, showed that the casing was full of water below the bottom of the perforations, and contained gas from there on up. The Flowmeter confirmed this. The original Cement Bond log on this well had indicated good zone isolation.

A Temperature log was run while the well was producing to try to find out why gas production had dropped in the other wells. The log, shown in Fig. 14d, indicated that the formation was being cooled below the perforated zone. This implies a movement of gas from the formation below the perforated zone, and one can conclude that the aquifer below the perforated zone is a much better reservoir for gas storage than the one perforated. With this information, the original permeability information was restudied. It showed the upper 50 feet of the storage formation to have relatively low permeability and porosity. The results of the same logging program performed on all four wells showed the same characteristics. It was therefore defined as a field problem rather than a problem in one or a few wells.

From the data now available it appeared that gas was preferentially flowing from the more permeable sand lower in the formation. The flow was restricted by the low permeability opposite the perforations. Since there was poor communication between the porous, permeable zone and the perforations, there was a rapid decline in pressure, hence in the production, as gas previously injected into the upper zone was produced.

To test this theory two wells were perforated over a 20 foot section below the original perforations and in the more permeable zone. These were not the wells logged, but the wells that were virtually dead in the same field. The results were:

1. Both wells came back on gas naturally without swabbing.
2. Both wells, when they had cleaned up and stabilized, were several hundred percent better than on original tests.

On the basis of these tests the other wells in the field were reperforated with much the same results.

It is important to complete the study of a production problem while the well is still dynamic (producing normally). If the problem continues and finally kills the well, usually little or no information about the cause of the problem can be obtained. There are exceptions, but in general the well must be dynamic to define a production problem.

A case in which the problem was defined after a well had gone to water and died occurred in a small 11-well field. Sev-

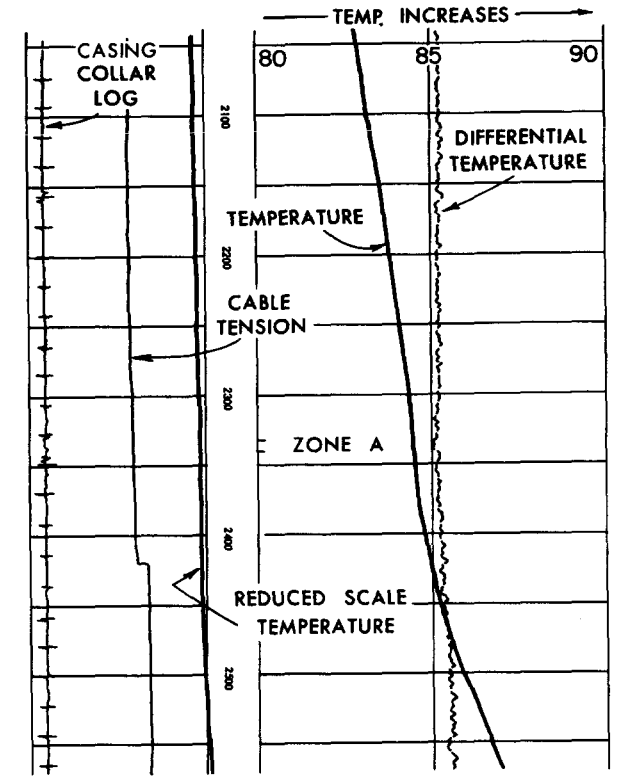

Fig. 15 — Temperature log shows water production from Zone A flowing down to the bottom of the casing and into the wellbore.

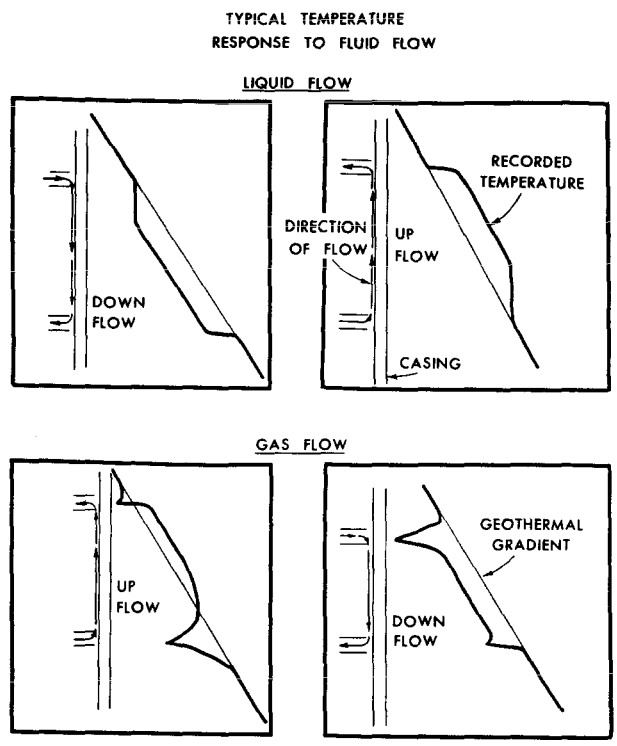

Fig. 16 — Theoretical sketch of Temperature log responses to liquid and gas flow.

eral wells in this field had already been abandoned due to water production.

Consideration was being given to abandoning the field. It was decided to make a final effort to determine if the water was coming from the storage sand or was channeling from a water zone. A decision was made to log one of the dead wells in an attempt to solve the problem.

The water was swabbed to several hundred feet below the static fluid level. While the well was filling again to the static level several Temperature logs were run. One of these logs is shown in Fig. 15.

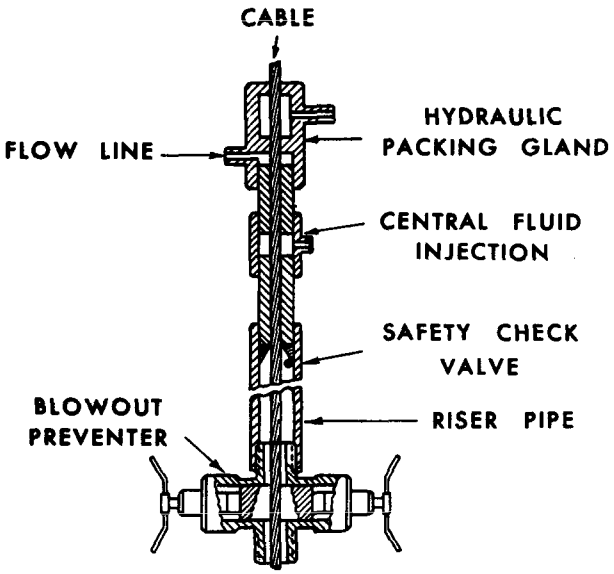

Fig. 17 — High-pressure wellhead control assembly (schematic).

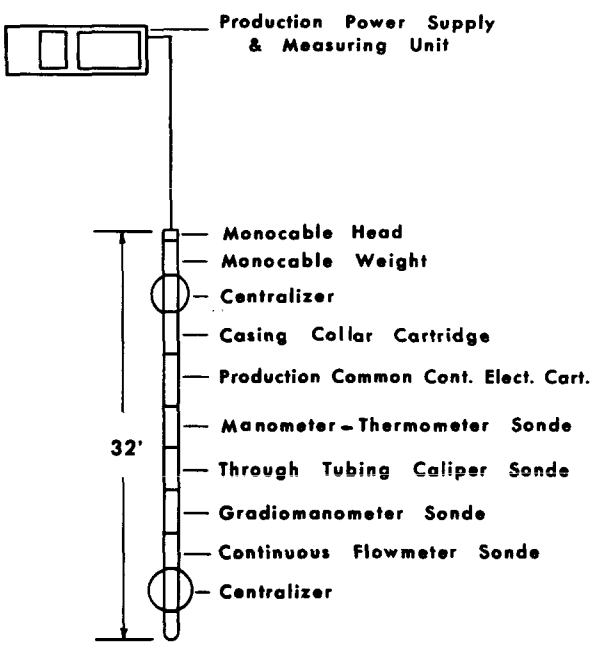

Fig. 18 — Production Combination Tool.

Close examination of the Temperature log reveals the differential curve goes to zero at Zone A. This indicates the temperature gradient was zero at this level. When the flowing fluid is liquid, the temperature curve will be vertical only where fluid leaves the formation.[10] (Compare the theoretical temperature curves for liquid and gas production shown in Fig. 16.) Therefore, water is being produced from Zone A and flowing around the bottom of the casing to the wellbore.

On the basis of this analysis the well was perforated and squeezed between the storage zone and Zone A. The well was then swabbed and put back on the line. It cleaned up, and no more water problems occurred. On the basis of these results, a second well was also squeezed and put back on production with similar success.

DESCRIPTION OF TOOLS AVAILABLE FOR DYNAMIC WELL STUDIES

Ten years ago results such as have been described were impossible for two reasons:

1. Wellhead control equipment had not been developed which could handle even relatively low pressure gas without freezing off at the control head. Even if freeze-off had not been a problem the large amounts of gas escaping made the operation costly and dangerous, and the results questionable.
2. Tools had not been developed for making meaningful dynamic studies of well conditions.

In the last decade these problems have been overcome. Dynamic well control is now possible by use of high pressure

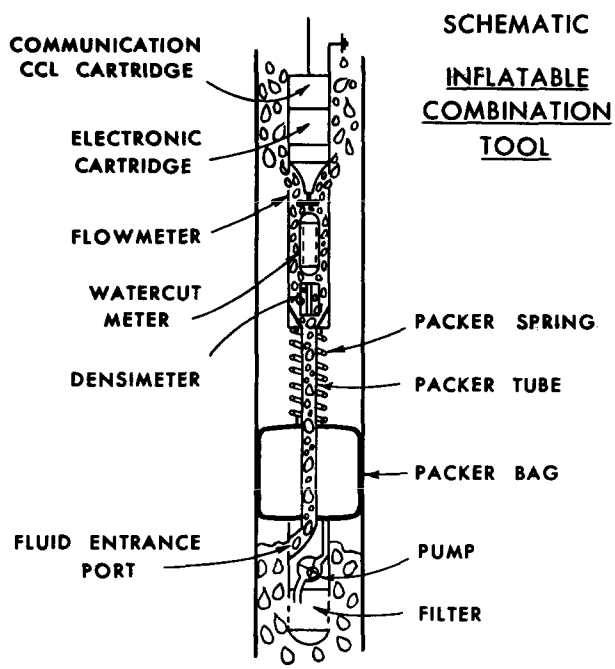

Fig. 19 — Inflatable Combination Tool (schematic).

wellhead control assemblies (Fig. 17). Wellhead control equipment is available which can safely control up to 15,000 psi of wellhead pressure without loss of gas. Since gas loss does not occur, freeze-off is not a problem; there is no danger of fire or explosion, and the results obtained truly represent the dynamics of the well.

The second problem has become overcome by development of tools designed to be used in wells under dynamic conditions. In addition, many of the more familiar services have been redesigned and improved for thru-tubing work.

Two new tools applicable to dynamic studies are the Production Combination Tool[11], and the Inflatable Combination Tool.

The Production Combination Tool (Fig. 18) is designed to make, sequentially, five individual measurements on one trip in the well. These five measurements, each recorded continuously versus depth, are: temperature, pressure, flow rate, hole size, and fluid density. A Casing Collar Log is recorded along with each of the five measurements for positive depth control.

The advantages of running five services on one trip in the hole are many. Probably the most important is the ability to take all measurements under the same well conditions, and in a shorter time.

The Inflatable Combination Tool[5] (Fig. 19) makes level-by-level measurements of flow rate, fluid density, and water cut index. It provides data for the analysis of low-volume multiphase flow. That is, oil, gas and water can be

TABLE I

Tools Available for Evaluation of Well Completions

Tool	Function	Tool Diameter in inches	Minimum Pipe Size (Internal Diameter)
Gamma Ray-Neutron Log	Determine: gas inventory, formation depth and thickness, gas-liquid contacts, lithology, porosity index	1 11/16 3 5/8	2-inch tubing
Cement Bond Log	Determine: zone isolation, cement top	1 11/16 3.9	2-inch tubing
Thermal Decay Time Log	Locate hydrocarbons behind pipe Evaluate fluid saturations	1 11/16 3 5/8	2-inch tubing
Pipe Inspection Log	Locate corrosion damage, Evaluate economic life remaining in casing	3 1/4 5	3 3/4-inch I.D.
Packer Flowmeter	Determine: contribution of each zone to total production or injection, Indicate changes of flow pattern (low flow rates)	1 11/16 2	2-inch tubing
Continuous Flowmeter	Determine: contribution of each zone to total production or injection. Indicate changes of flow pattern (high flow rates)	1 11/16 2	2-inch tubing
Production Combination Tool	Includes: Continuous Flowmeter, High Resolution Thermometer, Collar Locator, Manometer, and Gradiomanometer	1 11/16	2-inch tubing
Inflatable Combination Tool	Determine production or injection profiles and identify fluids	1 11/16 2 1/8	2-inch tubing
Gradiomanometer	Determine: gas entries, fluid contacts	1 11/16	2-inch tubing
High Resolution Thermometer	Determine: fluid entries, lowest depth of production or injection. Locate: fluid flow behind pipes, gas leaks. Determine geothermal gradients	1 11/16	2-inch tubing
Radioactive Tracer	Locate flow of injected fluids behind casing, Determine travel paths of injected fluids	1 3/8	1 3/4-inch tubing
Fluid Sampler	Recover a representative volume of wellbore fluids for PVT work	1 11/16	2-inch tubing
Thru-Tubing Caliper	Determine hole size	1 11/16	2-inch tubing
Cement Top Locator	Determine apparent density of casing-formation annulus and/or formation	1 11/16 3 5/8	2-inch tubing
Casing-Collar Locator	Locate casing collars for depth reference	1 11/16 3 5/8	2-inch tubing

differentiated at each depth or station in the hole at flow rates as low as approximately 10 barrels per day. The source of water or oil problems in gas storage wells may therefore be isolated and treated.

Other wireline operations applicable to dynamic well studies are: Gamma Ray-Neutron Log, Cement Top Location Log, Cement Bond Log, Radioactive Tracer Log, Thermal Neutron Decay Time Log, Fluid Sampler, and Pipe Inspection Log.

Most of these tools are available in 1 11/16-inch diameter for thru-tubing work. Table I lists available tools, their uses, and sizes.

CONCLUSIONS

Comprehensive evaluation of gas storage completions requires a coordinated information package. For maximum value, this package must be planned prior to drilling the well and must be tailored to the unique problems associated with gas storage wells.

In depleted gas storage reservoirs such coordinated information packages are usually not available. However, using a well planned data gathering program as a base, many of the problems associated with renovating old depleted fields may be avoided. Those problems which cannot be avoided may be treated before they become disastrous.

When problems with the normal production cycle of the storage well do occur, these problems can usually be isolated and often treated without interrupting well operation.

REFERENCES

1. Schmidt, A. W., Tinch, D. H., Carpenter, B. N., and Hoyle, W. R.: "Computerized Log Analysis for Efficiently Evaluating Gas Wells and Gas Storage Reservoirs," *J. Pet Tech.* (Sept., 1968), **20**(9), 959-970.
2. Lovan, T. E. Jr.: "Logging Observation Wells in Gas Storage," *J. Pet Tech.* (July, 1964), **16**(7), 745-750.
3. Pardue, G. H., Morris, R. L., Gollwitzer, L. H., and Moran, J. H.: "Cement Bond Log — A Study of Cement and Casing Variables," *Trans.*, AIME (1963), **228**, 545-555.
4. Brown, H. D., Grijalva, V. E., and Raymer, L. L.: "New Developments in Sonic Wave Train Display and Analysis in Cased Holes," *Trans.*, SPWLA 11th Annual Logging Symposium (May, 1970), Paper F.
5. Wade, R. T., and Cantrell, R. C.: "Production Logging: The Key to Optimum Well Performance," *J. Pet. Tech.* (Feb. 1965), **17**(2), 137-144.
6. Agnew, B. G.: "Evaluation of Fracture Treatments with Temperature Surveys," *Trans.*, AIME (1966), **237**, 892-898.
7. Wahl, J. S., Nelligan, W. B., Frentrop, A. H., Johnstone, C. W., and Schwartz, R. J.: "The Thermal Decay Time Log," SPE of AIME Fall Meeting, Houston, Sept. 29-Oct. 2, 1968, Paper SPE 2252.
8. Clavier, C., Hoyle, W. R., and Meunier, D.: "Quantitative Interpretation of Thermal Neutron Decay Time Logs," SPE of AIME Fall Meeting, Denver, Sept. 28-Oct. 1, 1969, Paper SPE 2658.
9. Killion, H. W.: "Fluid Migration Behind Casing Revealed by Gamma Ray Logs," *The Log Analyst,* (Jan.-Mar., 1966), **6**(5), 46-49.
10. Loeb, J. and Poupon, A.: "Temperature Logs in Production and Injection Wells," Presented at 27th Meeting of the European Association of Exploration Geophysicists (1965).
11. Meunier, D., Tixier, M. P., and Bonnet, J. L.: "The Production Combination Tool — A New System for Production Monitoring," SPE of AIME Fall Meeting, Houston, Oct. 4-7, 1970, Paper SPE 2957.

ACKNOWLEDGMENT

The authors wish to express their appreciation to the oil companies for releasing the logs used in the examples.

Ex. II – 41

EPA/600/
R-94/124

United States
Environmental Protection
Agency

Office of Research and
Development
Washington DC 20460

EPA/600/R-94/124
July 1994

PA

Temperature, Radioactive Tracer, and Noise Logging for Injection Well Integrity

EPA/600/R-94/124
July 1994

Temperature, Radioactive Tracer, and Noise Logging for Injection Well Integrity

by

R. M. McKinley
Exxon Production Research

Cooperative Agreement No. CR-818926

Project Officer

Jerry T. Thornhill
Extramural Activities and Assistance Division
Robert S. Kerr Environmental Research Laboratory
Ada, Oklahoma 74820

ROBERT S. KERR ENVIRONMENTAL RESEARCH LABORATORY
OFFICE OF RESEARCH AND DEVELOPMENT
U.S. ENVIRONMENTAL PROTECTION AGENCY
ADA, OKLAHOMA 74820

Printed on Recycled Paper

DISCLAIMER

Although the information in this document has been developed in cooperation with the United States Environmental Protection Agency, it does not necessarily reflect the views of the Agency and no official endorsement should be inferred.

All research projects making conclusions or recommendations based on environmentally related measurements associated with the Environmental Protection Agency are required to participate in the Agency Quality Assurance Program. This project was conducted under an approved Quality Assurance Project Plan. The procedures specified in this plan were used without exception. Information on the plan and documentation of the quality assurance activities and results are available from the Project Officer.

FOREWORD

EPA is charged by Congress to protect the nation's land, air and water systems. Under a mandate of national environmental laws focused on air and water quality, solid waste management and the control of toxic substances, pesticides, noise and radiation, the Agency strives to formulate and implement actions which lead to a compatible balance between human activities and the ability of natural systems to support and nurture life.

The Robert S. Kerr Environmental Research Laboratory is the Agency's center of expertise for investigation of the soil and subsurface environment. Personnel at the Laboratory are responsible for management of research programs to: (a) determine the fate, transport and transformation rates of pollutants in the soil, the unsaturated and saturated zones of the subsurface environment; (b) define the processes to be used in characterizing the soil and subsurface environment as a receptor of pollutants; (c) develop techniques for predicting the effect of pollutants on ground water, soil, and indigenous organisms; and (d) define and demonstrate the applicability and limitations of using natural processes, indigenous to the soil and subsurface environment, for the protection of this resource.

This report presents a discussion of three tools that can be used for determining the mechanical integrity of injection wells. Each tool is unique in its own right and can be applied to specific problems encountered in injection well mechanical integrity determinations. The ability to understand the application of each tool will help to assure that the use of injection wells for disposal of waste will not endanger underground sources of drinking water.

Clinton W. Hall
Director
Robert S. Kerr Environmental Research Laboratory

ABSTRACT

Regulations of the Environmental Protection Agency require that an injection well exhibit both internal and external mechanical integrity. The external mechanical integrity consideration is that there is no significant fluid movement into an underground source of drinking water through vertical channels adjacent to the injection well bore.

Mechanical integrity problems both related and not-related to injection can be investigated using the three logging tools: radioactive tracer, noise and temperature.

The operational principles of each tool are discussed, followed by the principles by which the tools detect flow and examples of the tool being used in such application. Finally, general operational guidelines are outlined to assist the reader in the application of each tool.

CONTENTS

	Page No.
Foreword	iii
Abstract	iv
Figures	vii
Tables	xi
Acknowledgements	xii
Introduction	1
Temperature Surveys	2
Continuous Recording Thermometers	2
Tool Specifications	5
Logging Procedures	5
Static Temperature Gradients	5
Non-Static Temperature Gradients	7
Temperature Behavior in Deep Injection Wells	12
Temperature Behavior in Shallow Injection Wells	35
Temperature Signatures for Non-Related, Behind-Pipe Flow	40
Logging for Lithology Influence	44
Radioactive Tracer Surveys	46
Modern Radioactive Tracer Tools	47
Tool Resolution	49
Tool Specifications	49
Logging Procedures	50
Injection Profile from Slug Tracking	56
Slug Timing	56
Slug Area	59
Injection Profiles from Velocity Shots	62
Comparison of Tracer Profile with Temperature Profile	65
Velocity Shots with Overlapping Intervals	67
Quality Control in Profile Surveys	71
Logging for Casing Leaks with Well Shut-In	80
Logging for Injection Confinement	81
Slug Tracking Procedure for Behind-Pipe Flow	81
Velocity Shot Procedure for Behind-Pipe Flow	92
Quality Control Revisited	108
Noise (Sound Surveys)	112
Noise Logging Tools	113
Surface Processing of Microphone Output	114
Tool Sensitivity	116
Noise Log Format	117
Cable Attenuation	119

Tool Specifications 121
Logging Procedures 121
Noise Log Characteristics 123
Loudness 123
Character 126
Pitch 129
Sound Level-Flow Rate Relation 132
Water Flow Behind Casing 132
Water Flow Past Tool 136
Gas Flow Through Liquid 139
Vertical Resolution on Noise Logs 140
Noise Surveys for Injection Confinement 143
Noise Surveys for Non-Related Flow Behind Pipe 150
Attenuation by Gas Dispersed in Water 154
Quality Control Revisited 156
Summary of Procedures for Temperature, Radioactive Tracer and Noise Surveying 159

FIGURES

Figure No.		*Page No.*
1.	A surface recording, continuous thermometer	3
2.	A section of a temperature survey from a well flowing mainly water at 1800 BPD	4
3.	Temperature logs from same thermometer in gas well but with processing by two different surface panels	5
4.	Static temperature gradients in the Texas-Louisiana area	6
5.	Static temperature gradient variations in a sand-shale sequence	8
6.	Static temperature survey from a well penetrating a salt dome	8
7.	Hypothetical influence of lithology on wellbore temperature warming with time to static conditions	10
8.	Wellbore influence on temperature surveys	11
9.	Computed injection temperature profiles for a deep, saltwater disposal well	12
10.	Relationship between temperature profile and rate for an injection well	13
11.	Computed injection profile at 1,000 BPD with equal amounts injected at each of 10 locations	14
12.	Injection temperature survey on a well that had been hydraulically fractured three weeks earlier	16
13.	Slopes, dT/dz, and displacements, ΔT, necessary for rate estimations	17
14.	Temperature profile around a well with $R_w = 0.54$ ft. on injection at a wellbore temperature of 123°F and at 500 BPD rate	19
15.	Temperature recovery with time of fluid in wellbore of well in Figure 14	20
16.	Injecting and subsequent shut-in surveys on a well that was hydraulically fractured three weeks prior	21
17.	Temperature surveys computed for a well on injection at 500 BPD with varying amounts of loss behind pipe to thief zone located 200 feet above	24
18.	Temperature survey from well on injection at 990 BPD salt water	25
19.	6-hr shut-in temperature surveys past the thief zone depicted on Figure 17	26
20.	Injecting and shut-in temperature surveys from well on continuous injection at about 500 BPD for almost one year	27
21.	Temperature surveys from a well on 600 BPD injection at a water temperature 2°F warmer than average from long-term injection	30
22.	Temperature surveys from a well on injection at 960 BPD with flow behind pipe even on shut-in status	31
23.	Shut-in temperature surveys across a thief zone at 500-510 feet charged by flow behind casing from injection interval at 5,600 feet	33
24.	Temperature surveys from deep injector with shallow tubing leak at A and casing leak at B	34
25.	Computed temperature surveys injecting (—) and shut-in (---) from a well receiving 500 BPD water with various leaks behind pipe from injection perforations up to a shallower thief zone	35

26. Shut-in temperature surveys for wells injecting near surface temperature 36
27. Shut-in temperature surveys for wells injecting hot water 37
28. Loss in survey resolution due to "stairstepping" and to logging upward 38
29. Surveys from an old injection well taking 1,800 BPD water 39
30. Temperature surveys from an old production well with water flow behind casing from depth A to depth B 42
31. Behind-casing water flow into depleted hydrocarbon sands penetrated by wells with deeper injection zones 42
32. Behind-casing crossflow of liquid (oil) in a new well still slightly cooler than static temperature 44
33. Temperature logging a new injection well for lithology signatures 45
34. Schematic of a radioactive tracer tool for injection logging 48
35. A radioactive slug tracking record from a well on injection at about 600 BPD water 50
36. Slug tracking below the perforations of Figure 35 well 51
37. Velocity shot record above the perforations of the Figure 35 well on 600 BPD water injection 52
38. Five methods for timing the travel of a stationary velocity shot 53
39. Location of five timing points on the records of Figure 37 54
40. Profile for slug tracking surveys from Figure 35 58
41. Injection profiling by slug "area" from a tracked slug survey 61
42. Tracer placement in the annular volume between a 1.5-inch tool and a 6-inch plexiglass pipe 64
43. Tracer tool for ejecting slug at centerline of pipe 65
44. Injecting temperature survey from well with tracer survey shown on Figure 35 66
45. Tracer and temperature surveys from an injection well that has been fractured inadvertently. 67
46. Control of vertical resolution by overlapping 1-ft stations with a tool having normal detector spacing 68
47. Good quality tracked slug survey in well on injection at 150 BPD 72
48. Injection profile for tracked slug survey of Figure 47 with injection rate of 152 BPD 73
49. Velocity shots at two locations in the well giving the slug survey of Figure 47 75
50. Velocity shot #4 with rounded (concave) leading edge typical of well-mixed shot in laminar flow 75
51. Temperature surveys from well on water injection at 152 BPD 78
52. Crossflow check after three hours of shut-in time following water injection at 152 BPD 79
53. Drags on five successive days through a radioactive slug ejected at 7,270 feet in a shut-in injection well 80
54. Tracer slug tracking surveys for behind-pipe loss to zones above perforations; rate = 70 BPD 83-84
55. Surveys before (base) and after tracer dump followed by ten minutes of injection at 70 BPD 85

56. Five flow-profiling drags in a well on injection at a nominal 500 BPD 86
57. Behind-pipe flow detection by slug tracking in well in injection at a nominal 500 BPD 88
58. Packer leak check by the slug tracking method in well on injection at 720 BPD 89
59. Corrected run #1 with spurious base activity subtracted 90
60. Crossflow check after one hour shut-in period on 900 BPD injection well 91
61. Stationary velocity-shot check for packer leak for well of Figure 60 while on injection at a nominal rate of 900 BPD 93
62. A properly scaled, stationary velocity shot test for packer integrity with an annular velocity resolution of 0.35 ft/min leak rate 94
63. Hypothetical velocity shot response to stagnant slug caught under packer on Figure 58 95
64. Channel checks on well of Figure 32 with well on brine injection at 400 BPD 96
65. Channel check by velocity shot method below perforations at 5,820-25 feet with well on injection at 600 BPD 97
66. Slug tracking survey from same well as velocity shot of Figure 65 with same injection rate of 600 BPD 99
67. Temperature surveys from a well after 536 barrels of water injected and well shut-in 100
68. Channel check, velocity-shot survey with well injecting 2 BBL/min. 101
69. Shut-in temperature survey on a new well 103
70. Temperature surveys before and after 40 BBLs of mud pumped down tubing 103
71. Three velocity shots in well of Figure 70 104
72. Collar log run after velocity shots on Figure 71 105
73. Velocity shots above tubing leak @ 1 BPM rate 106-107
74. Slug tracking survey from well on injection at 950 BPD 109
75. Temperature surveys from well of Figure 74 110
76. Shut-in crossflow check on well of Figure 74 111
77. Noise (sound) logging sonde with piezoelectric detection elements shown separately 114
78. Noise log format illustrating typical ambient or dead well levels 117
79. Noise log format with a 20-BPD water flow behind pipe into a gas zone depleted by 250 PSI 118
80. Logging cable attenuation factors for two wireline sizes 120
81. Sound carry-away from a source in water 122
82. Noise log from a shut-in oil well with 815 PSIG tubing pressure 124
83. Noise log from mud-filled open hole in the vicinity of well blowing out of control 125
84. Noise log character as related to flow path 126
85. Noise log from a 500-BPD flow of high pressure water behind 9 5/8 inch casing in a well being drilled 127
86. Noise log from shut-in well with water flow behind-pipe at an estimated rate of 5,000 BPD 128

87. Temperature surveys on well of Figure 86 before and after a workover to eliminate behind-pipe flow from deep aquifer into shallow aquifers 129
88. Noise log from well with a very weak gas flow from annulus 130
89. Frequency content (pitch) at a noise peak produced by two different types of flow behind pipe 130
90. Sound level-rate correlation for water flow behind the pipe in which sonde is located 133
91. Noise log from well on water injection at 26,800 BPD and 1,300 PSI in 7" casing 136
92. Comparison of noise log and spinner survey injection profile for a rate of 25,000 BPD 139
93. 2,000-Hz noise "cut" for two independent sound sources of equal magnitude but different distances apart inside casing 141
94. Submergence of weaker source beneath the residual from a stronger one ten feet away 142
95. Noise log with 4 and 6-kHz cuts for improved vertical resolution from a gravel-packed gas well flowing three million std. ft^3/day 142
96. Noise survey with well on injection at 10,800 BPD and 1,400 PSI 144
97. Noise survey from well of Figure 96 with injection rate reduced to 5,000 BPD 145
98. Shut-in noise survey on Figure 97 well with 135 PSI excess pressure on injection zones 146
99. Surveys on a one-year old injection well with a current injection rate of 5,000 BPD 147
100. Noise log from well on water injection at 3,500 BPD with a flow of about 350 BPD behind casing from top perfs to the zone at middle perfs through an acid frac 148
101. A shut-in noise survey on an injection well with leak in hanger assembly of wellhead 150
102. Noise log with water flow at surface of ~400 BPD from 5 1/2 x 8 5/8 annulus under 70 PSI differential 151
103. Temperature surveys run one day apart, first with annulus shut-in at 70 PSIG and then with annulus on flow at 340-520 BPD water 153
104. Noise logs, flowing and shut-in, from a watered out-gas zone produced to hold back water 155
105. Temperature and noise surveys from a shut-in well with an 800-BPD water flow behind 4 1/2 inch casing from 4,360 feet to the surface 156
106. Noise logs from long string, H, of shut-in gas well with pressure on annulus 157

TABLES

Table No.		*Page No.*
1.	How lithology affects static thermal gradients	7
2.	How lithology affects dynamic thermal equilibrium	9
3.	Minimum shut-in periods necessary to detect leaks behind pipe into zones above the injection interval	28
4.	Suggested gamma recording sensitivity for radioactive tracer tools with 5 μc total charge of iodine-131 in water	55
5.	Slug tracking data from surveys on Figure 35	57
6.	Slug "area" data from Figure 41 slug tracking survey	60
7.	Velocity shot data for well of Figure 47	76
8.	Cross-sectional area for noise logging tools	138
9.	Logging procedures for temperature, radioactive tracer, and noise surveying	159

ACKNOWLEDGEMENTS

This report is based on a training session prepared for the United States Environmental Protection Agency and East Central University by Dr. R. M. McKinney (Exxon Production Research–Retired). Many thanks to Pat Powell, Dynamac Corporation, and Carol House, CDSI, for their untiring efforts in putting the manuscript in final form.

Temperature, Radioactive Tracer, and Noise Logging for Injection Well Integrity

Introduction

This report describes the application of the above logging tools to injection well operation in order to infer the answer to two questions:

(1) Is the injected water entering intervals other than the interval approved for disposal?

(2) Does the presence of the borehole allow crossflow from saltier water formations into underground sources of drinking water?

The problems associated with positive answers to these questions are referred to as related and nonrelated injection well problems, respectively. In actuality, noninjection related problems in one borehole can generally be traced to long standing related problems in other wellbores. For this reason, injection related problems are the first discussed as consideration is given to how each of the three logging tools tells if injected fluid is being confined to the approved interval. This discussion will necessarily entail consideration of proper use of each tool as well as a detailed look at what the survey results mean. The entire field of production logging is somewhat unique in that how one does things is usually more important than what one does.

Once the problem of confinement, or the lack of such, is dealt with, then the use of the tools for noninjection related flows from abnormally pressured into normally pressured zones or from normally pressured into depleted zones will be discussed. The operational procedures and the interpretational guidelines for these situations are not the same as those for demonstrating confinement. In general, the radioactive tracer tool must be replaced by neutron activation tools that create a tracer behind pipe as well as inside pipe. These latter tools are a specialty in their own right and are not discussed in these notes.

The tools are introduced in the same order as listed in the title: Temperature, Radioactive Tracer, and Noise. This ordering recognizes both general utility and level of expertise necessary for effective utilization. A temperature survey has unique features unmatched by any of the other logging tools. Furthermore, it is the least likely to mislead the interpreter provided one is thoroughly trained in its use. To the uninitiated, a temperature survey can, however, be rather perplexing.

As each tool is introduced, its operational principles are discussed briefly. Next, those principles by which the tool detects flow are given in some detail. This understanding is necessary if the log analyst is to "know what to expect" on the log. This development is then followed by

numerous examples in the form of illustrations. Finally, general operational guidelines are attempted now that the reader has a basis to not only appreciate the significance of such but also to recognize their specific limitations.

Temperature Surveys

The temperature logging tool is the oldest of the production surveying instruments. Records of its use to indicate downhole flow dates back into the middle 1930's. These early thermometers were run on "slick" line and recorded downhole, usually on oxide-coated metal charts of the same sort as those found in downhole pressure "bombs." The sensing element in these earliest thermometers was a column of mercury whose expansion or contraction positioned a floating piston to which was attached the "scribing" pen. In time, these sensors were replaced by vapor-pressure type detectors, that is, by bulbs partially filled by a volatile liquid whose vapor pressure increased with temperature. This pressure, in turn, was measured by a bourdon type element already in use in pressure gauges. This latter type of thermometer has survived to the present time and is still in use, mainly for bottomhole temperature measurements. As surveying tools they are cumbersome to use. Not only do they require careful shop calibration but, also, their slow response requires the operator to make stops of 5 to 15 minutes' duration each at those stations selected for temperature measurement. By way of contrast, modern electric wireline thermometers not only have better resolution, but also have sufficiently rapid response time that, at logging speeds of 30 feet per minute, a continuous record can be obtained that parallels true borehole fluid temperature variation with depth and that lags by no more than about one degree Fahrenheit. These are the tools described in this document.

Continuously Recording Thermometers: A schematic of a modern, electric wireline thermometer appears on frame A of Figure 1. A cage, open to wellbore fluid, is located at the bottom of the tool. Contained in this cage is a thermistor that senses the surrounding fluid temperature. The preferred sensor is a platinum element of some sort, either a tiny coil of platinum wire or a platinum-film resistor. Platinum is an ideal temperature sensor because its resistivity is stable and increases linearly with temperature over a wide range. Thus, the tool makes a continuous measurement of the resistance of the thermistor, which, by shop calibration, is directly related to the temperature of the sensor's environment. In actual construction, the thermistor is either one branch of a bridge circuit or has a constant current passed through it. In either case, the voltage drop across the sensor is directly proportional to its resistance. This voltage is used to control the frequency output of a voltage-controlled oscillator, the "spikes" from which are transmitted up the logging cable to be counted at the surface. So long as the pulses (spikes) are of high enough voltage to be detectable at the surface, the tool output is independent of the length (resistance) of logging cable between the tool and the surface recorders.

On analog recording trucks, the transmitted counts per minute are converted to a voltage by a counting circuit and recorded on a pen-and-ink strip-chart recorder as a temperature, or gradient, trace. This is trace 1 on Figure 2, a section of temperature log from a flowing well that produces 1,800 barrels per day (BPD) of liquids most of which is water. The scale in degrees Fahrenheit at the bottom of the log goes with this trace. As frame (A), Figure 1, shows, an amplified trace

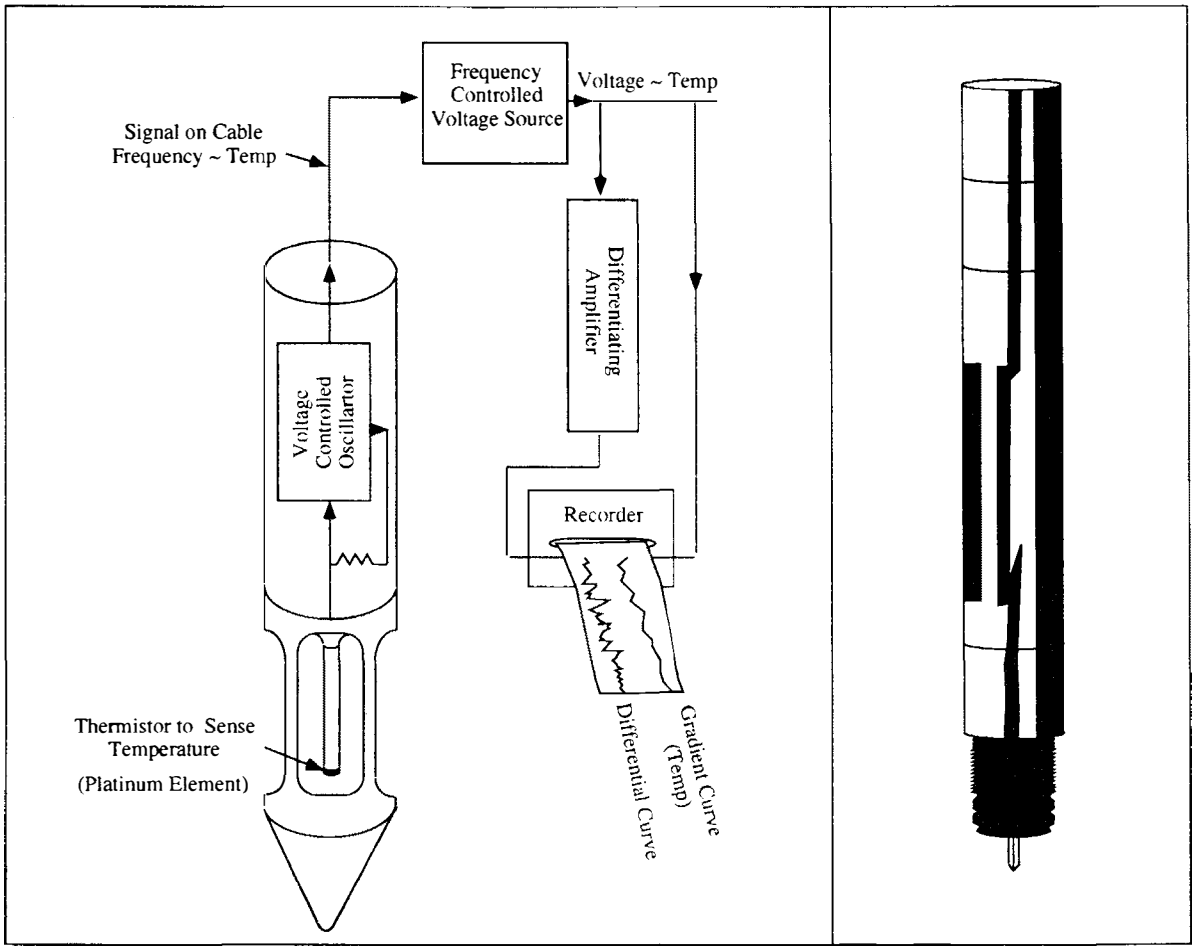

(A) Schematic of Tool (B) Actual Tool

Figure 1. A surface recording, continuous thermometer.

of temperature changes can be generated by the output of a differentiating amplifier whose input is the same voltage that gives the temperature record. The resulting "differential" trace magnifies the changes in slope on the temperature curve and, as is evident from curve 2 on Figure 2, is well worth the additional charge even though no absolute scale is associated with the trace.

When used in the manner illustrated in Figure 2, a temperature survey becomes a high-precision flow survey that has the best vertical resolution of all logging tools. For example, the increase in slope recorded at depth A on the differential trace 2 fixes the bottommost point of production more precisely than the depth scale itself can be established. Depth A can be shifted by no more than the width of the pen mark, ± 1/2 foot. Furthermore, the tool will resolve temperature changes as small as 0.05°F. An excursion of about this size is caused by the small entry at depth C on the log of Figure 2. This is the only flow meter that would detect such a small entry. The large entry at depth B is, of course, quite evident as is the lack of entries from anywhere in the middle set of perforations. The accuracy of the absolute temperature values on Figure 2 depends completely on when and how carefully the tool was last calibrated.

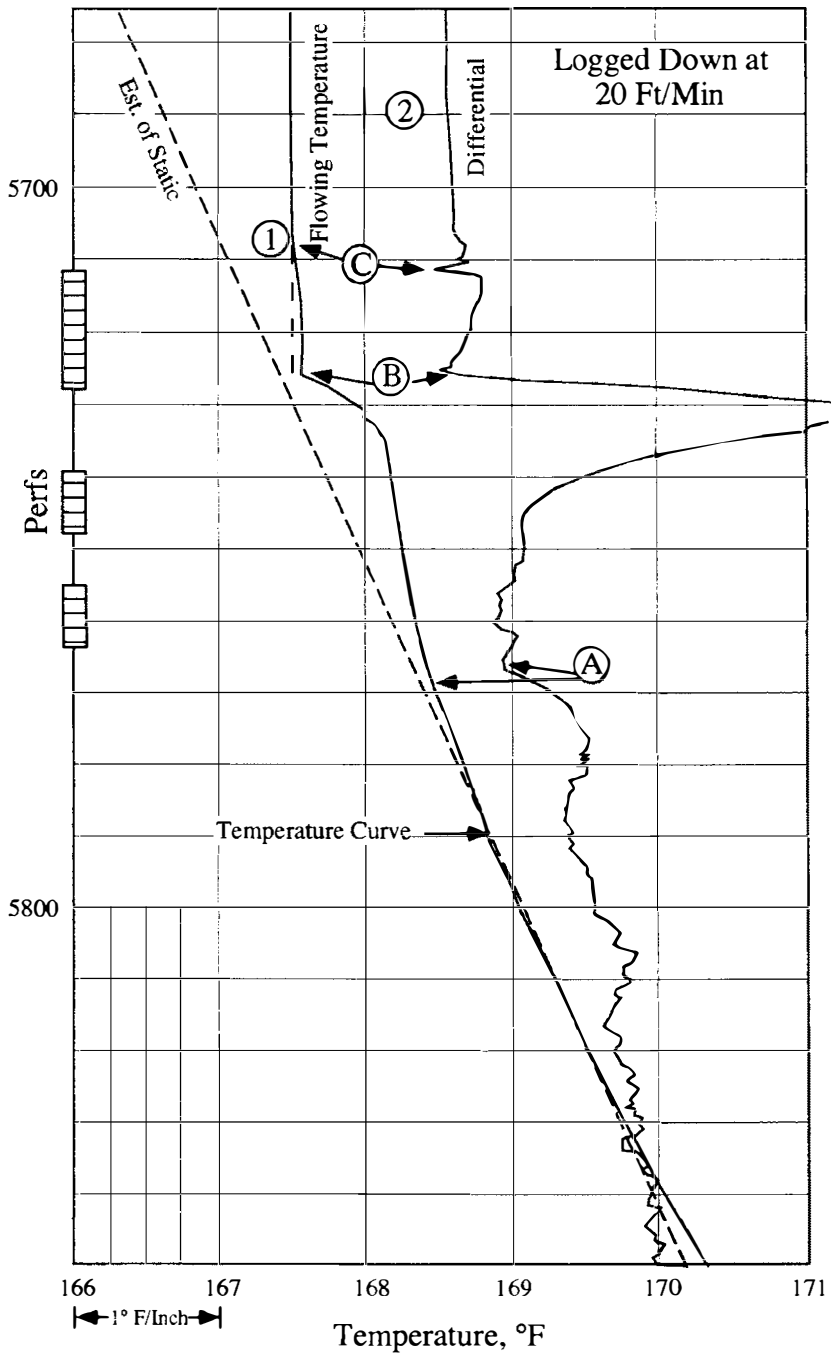

Figure 2. A section of a temperature survey from a well flowing mainly water at 1800 BPD.

On digital logging trucks, the pulses transmitted up the logging cable are processed for tape storage by a binary coded digit unit (BCD). This is essentially a counting device with its own separate clock that is not synchronized with the downhole "clock" or tool. The conversion from pulses per minute to binary coded digits therefore introduces a sampling error that is considerable relative to the resolution of the downhole tool. Before display, this noise is filtered from the record with "suppressor" filters. The resulting degradation in signal quality is evident from a comparison of frames A and B of Figure 3 which show the results of processing the same temperature log by analog and digital panels, respectively.

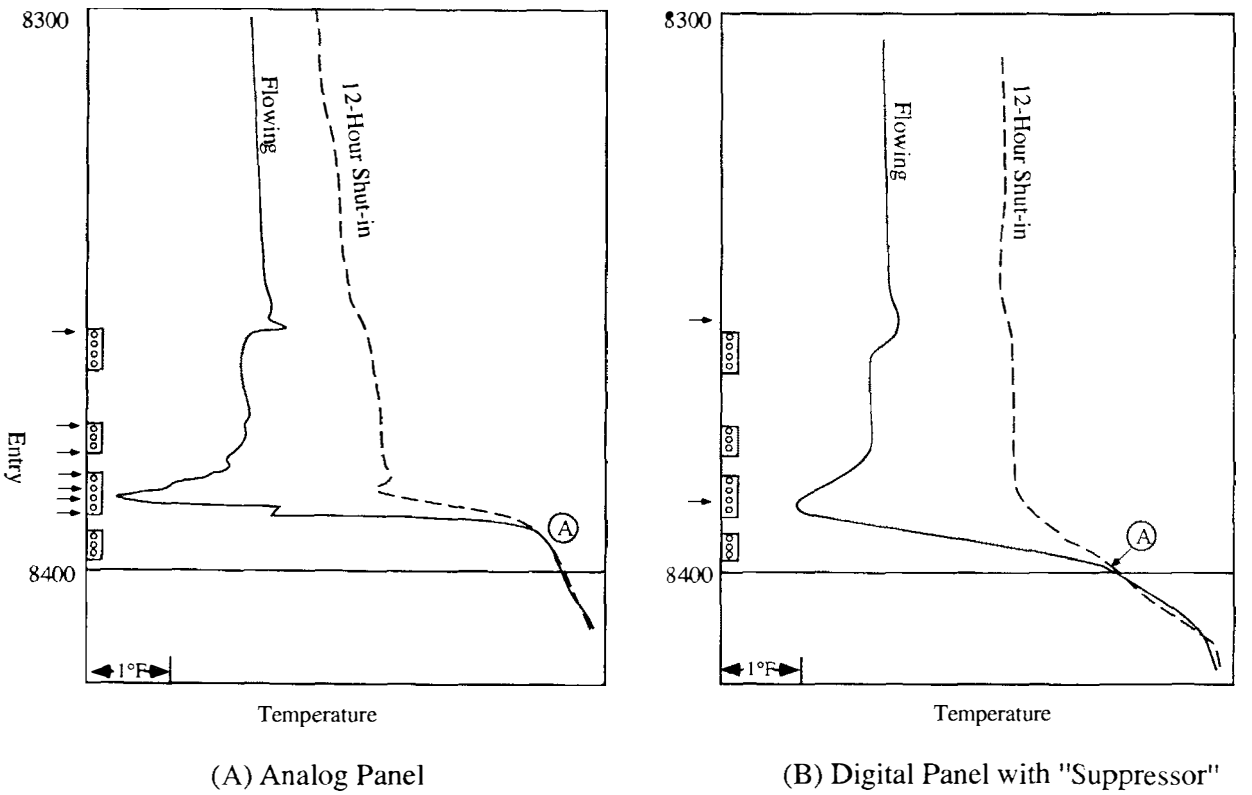

(A) Analog Panel

(B) Digital Panel with "Suppressor"

Figure 3. Temperature logs from same thermometer in gas well but with processing by two different surface panels.

Tool Specifications: Modern temperature survey tools are designed to function at pressures up to 20,000 PSIG and at temperatures of 350° to 400°F. Special high-temperature tools are also available which extend the operating range up to about 550°F. The combined length of the cage containing the sensor and the barrel containing the electronics is no more than about 4 feet. This short length allows the tool to be run in combination with other surveying instruments. The diameter of commercial tools range from a minimum of 7/8-inch to a maximum of 1 11/16-inch. The small 7/8-inch version is used extensively to survey down the annulus of wells on rod pumps. They are also useful for passing through tight spots in old injection wells. A 1 3/8-inch diameter instrument is the preferred choice for use in 2-inch tubing that contains nipples of various types.

Logging Procedures: Temperature surveys are best run going into the hole with the temperature sensor located as near as possible to the bottom end of the tool string. This allows the sensor to contact fluid that has not been mixed vertically by the passage of the tool and wireline. The tool need not be run with centralizers and the logging speed should not exceed 40 ft/min with 20 to 30 ft/min being preferable. The survey should start at least 100 feet above the zone of interest to allow time for the moving tool to stabilize.

Static Temperature Gradients: The static temperature in a wellbore increases gradually with depth into the well. In most areas of the North American continent, this increase will occur at a rate between 0.5 and 2.5 degrees Fahrenheit for each 100-foot increase in depth, with a value of

1.7°F/100 ft (3°C/100 M) being typical. The major portion of this static gradient results from heat production in the earth's crust by radioactive decay of minerals; consequently, local gradients reflect primarily the relative richness in shale of the subsurface. Typical static gradients in Texas and Louisiana are illustrated on Figure 4. These are all measured in wells that have never undergone injection or production and that have been shut-in for at least one year after completion.

The detailed variations in static gradients are determined by variations in the effective thermal conductivity, k, of the combined rock and pore fluids. Typical values for k in BTU/Hr-ft^2-(°F/ft) for various earth materials as well as for water, oil and gas are listed in Table 1. As the size of k decreases, the size of the static gradient increases, that is, the rate at which temperature increases with depth becomes larger. From this table, one can infer that it is the water content mainly that

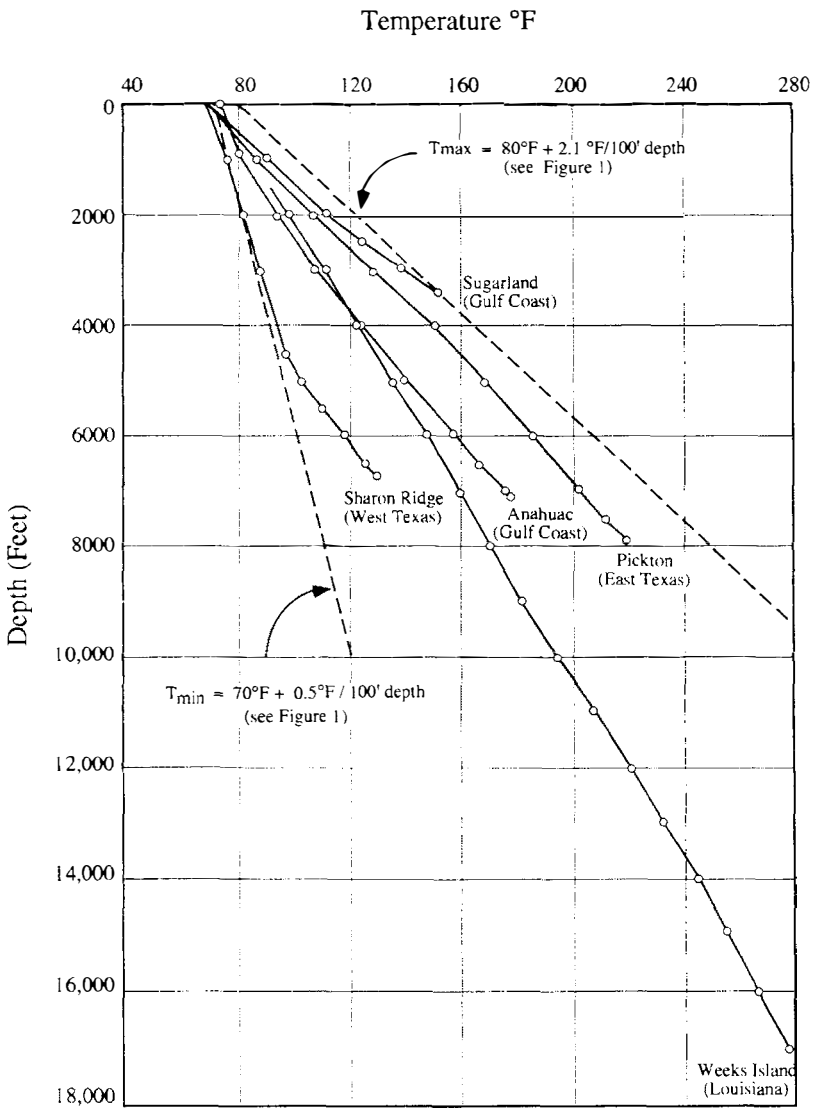

Figure 4. Static temperature gradients in the Texas-Louisiana area.

TABLE 1. HOW LITHOLOGY AFFECTS STATIC THERMAL GRADIENTS (POROUS MATERIALS ARE WATER SATURATED)

Material	Thermal Conductivity, k BTU/hr-ft^2 - (°F/ft)	Increasing Geothermal Gradient
Quartzite	13	
Salt	13	
Anhydrite	13	↓
Dolomite	2.5	
Limestone	1.5	
Sandstone	1.5	
Shale	0.9	
Gypsum	0.8	
Cement	0.4	
Water	0.4	
Oil	0.085	
Gas	0.040	

Thermal Conductivity, k = Heat Flux/Temperature Gradient

determines the location of a particular lithotype in this ordering. Thus, a shale section, which has high water content, would show a static gradient that is $1.5/0.9 \simeq 1.7$ times larger than that in a clean sand section. Figure 5 shows that this magnitude of variation does indeed show up provided the strata in the sequence are sufficiently thick. The numbers in Table 1 show that non-porous lithologies will exhibit the smallest static gradients. This effect is illustrated on Figure 6, which is a static temperature survey from a well drilled into a salt dome near Sugarland, Texas. The gradient of 2.6°F/100 ft. in the shale above the salt is abnormally high because of the large heat flux upward through the salt "chimney" of high thermal conductivity. The shale gradient is, thus, influenced by factors other than its conductivity and radioactive mineral content.

Non-Static Temperature Gradients: Whenever an injection well is shut-in for logging, the wellbore fluid temperature begins its change towards static conditions. The time required to reach static conditions is generally, however, longer than what can be devoted to logging operations. Consequently, the logging operations will usually take place with the wellbore in a thermally dynamic state, that is, with the wellbore temperature displaced from static temperature. In such a state, the thermal conductivity alone does not control the rate at which a given lithology returns to static temperature. Rather, it is the thermal diffusivity that determines the dynamic rate of change with time in the wellbore. This physical property has the dimensions of length^2/time and is the ratio formed by division of the thermal conductivity, k, by the product of density,

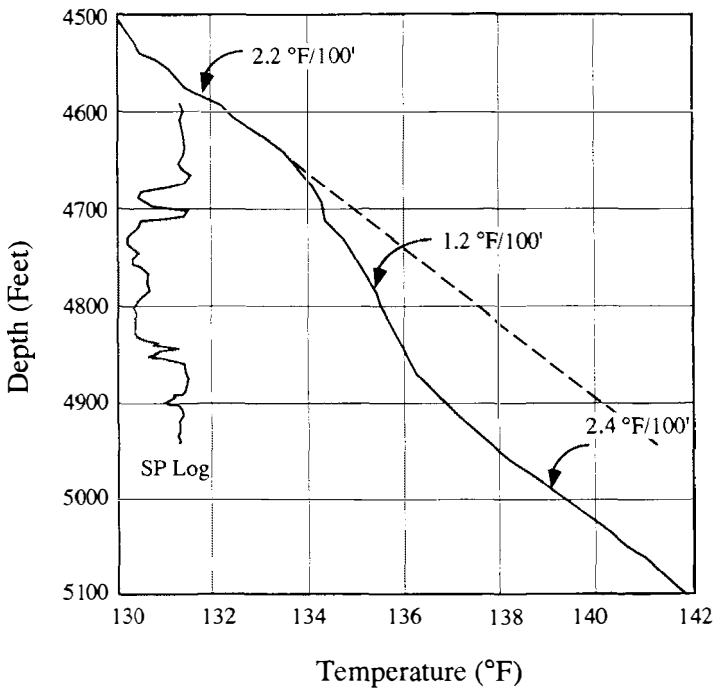

Figure 5. Static temperature gradient variations in a sand-shale sequence.

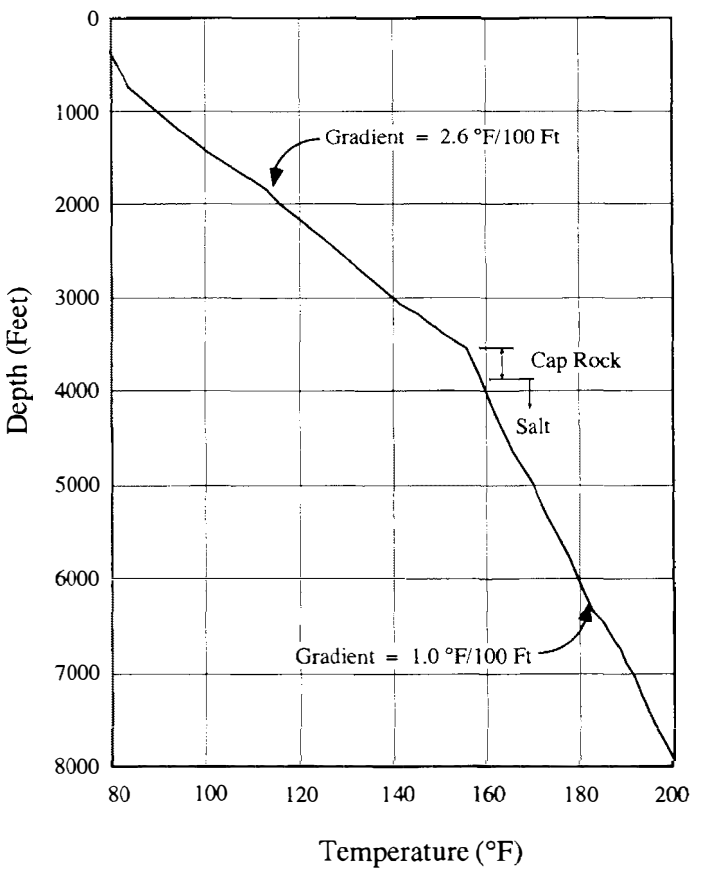

Figure 6. Static temperature survey from a well penetrating a salt dome.

ρ, and specific heat, Cp. The larger the value of thermal diffusivity, the more rapidly will a material return to static temperature once disturbed. Typical values of thermal diffusivity for various lithotypes appear in Table 2. A pattern can be seen generally similar to that evident from Table 1. Namely, shales lag behind other lithotypes in their recovery to static temperature. This, again, is a consequence of the high water content of shales. Conversely, the non-porous, non-hydrated materials recover most rapidly. Figure 7 is a "cartoon" illustrating the influence lithology can exert on temperature surveys run in a well that is returning to static temperature from the cold side. The hardest material, the siltstone, leads all other lithologies in the return to static temperature thereby appearing as a "hot" spot on the surveys. Likewise, the shales lag everything else and appear as "cold" spots. Had the return been from the hot side of static, then the "direction" of anomalies would be the reverse, the siltstone would be the "cold" spot whereas the shales would appear as warmer areas. The main point of Figure 7 is that lithology can add significant character to shut-in temperature surveys from a well that is still considerably disturbed from static conditions. This character will, however, become progressively less severe as shut-in time increases and the wellbore temperature approaches static. This behavior is in contrast to that of a true injection anomaly whose influence will persist even on otherwise static surveys.

TABLE 2. HOW LITHOLOGY AFFECTS DYNAMIC THERMAL EQUILIBRIUM (POROUS MATERIALS ARE WATER SATURATED)

Material	Thermal Diffusivity $\alpha = k/\rho c_p$ ft²/hr	Increasing Lag Time
Quartzite	0.14	
Salt	0.11	
Anhydrite	0.06	↓
Dolomite	0.07	
Limestone	0.05	
Sandstone	0.05	
Shale	0.03	
Gypsum	0.02	
Cement	0.01	
Gas	0.008	
Water	0.006	
Oil	0.003	

Thermal Diffusivity, α (ft²/hr), α = Conductivity / Density x Specific Heat

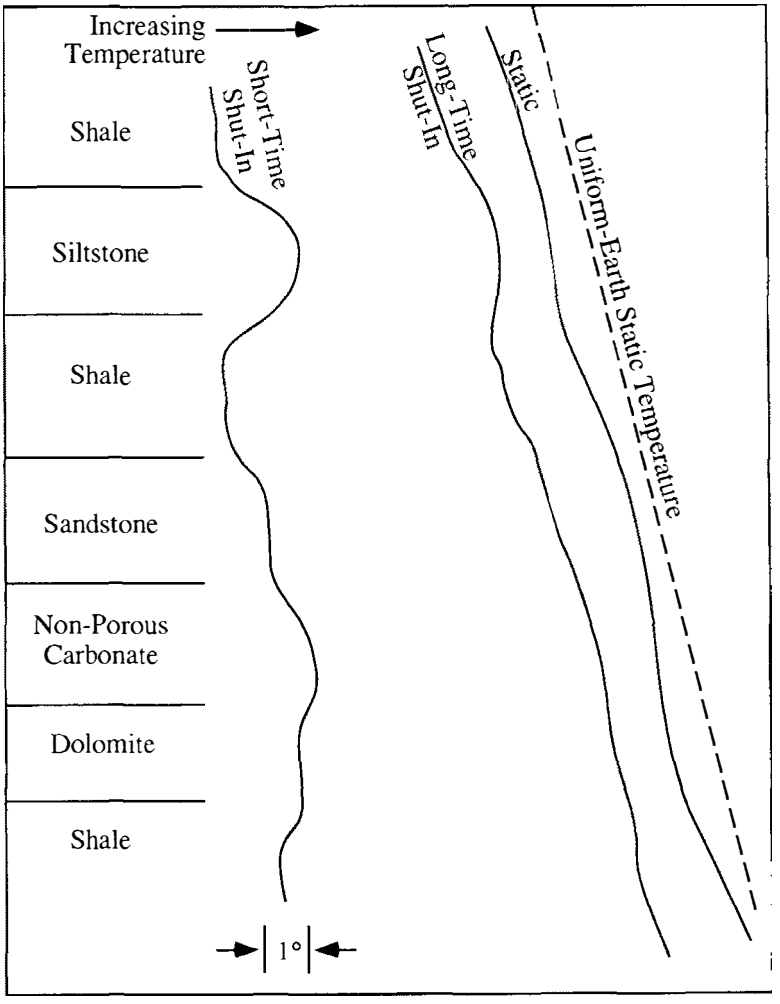

Figure 7. Hypothetical influence of lithology on wellbore temperature warming with time to static conditions.

Frame A of Figure 8 shows that details of a well's completion also add character to any shut-in survey made in a non-static wellbore. Usually, those parts of the wellbore that are more insulated will lead the lesser insulated portions in the return to static temperature. This behavior is a consequence of the fact that the formation behind the better insulated parts is less disturbed than is that behind the lesser insulated portions. For example, the behavior of the temperature at the casing shoe on frame A at 8,000 feet is the type usually seen on shut-in surveys. In actuality, the reverse behavior is sometimes seen on very short shut-in surveys on which the better insulation is still preserving the wellbore fluid temperature at values closer to that existing at shut-in. This apparently contradictory behavior is, in fact, the consequence of an exceedingly useful and unique feature of temperature surveys; namely, the "distance into the formation" that is examined can be varied by simply varying the shut-in time.

Like lithology influence, completion influences also die out as the wellbore temperature approaches static. Furthermore, completion effects serve as excellent quality control checks on both the operation of the tool and the sensitivity selected for display.

Frame B of Figure 8 shows an additional feature common to shut-in surveys from shut-in wells that were on injection. This feature is the sudden "catch up" in temperature that occurs when a thermometer first enters a liquid column from gas and is thereby in better thermal contact with its environment. Since the water level is typically within a few hundred feet of the surface in an injection well that "goes on vacuum" when shut-in, the direction that catch-up takes depends on whether ambient air temperature is hotter or cooler than the wellbore liquid. Frame B of Figure 8 illustrates the case of cooler air.

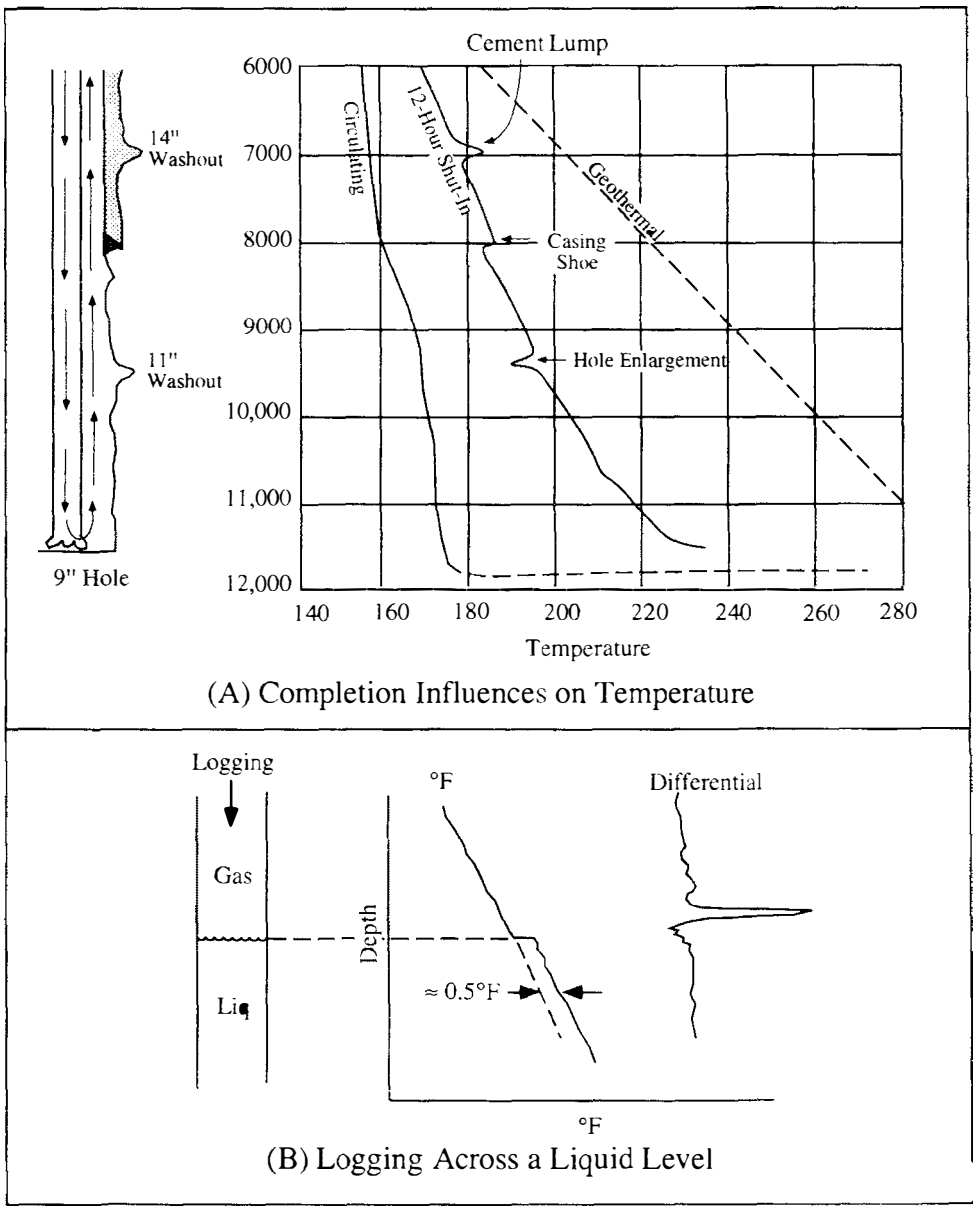

Figure 8. Wellbore influence on temperature surveys.

Temperature Behavior in Deep Injection Wells: Most saltwater disposal wells inject into zones at least 2,000 feet deep whose static temperature generally exceeds 115°F. The injection therefore cools the wellbore in the vicinity of the injection zone. Once injection is started, the flowing temperatures in the injection "string" quickly settle to a stable value. In fact, by the time that the tubular volume has been displaced three times, the temperature has made 90% of the necessary adjustment to reach its stable value. This rapid stabilization occurs because the heat transfer from the earth through the tubulars and into the moving stream is at a quite low rate, typically in the range of 50 to 200 BTU/hr per foot of wellbore. In the familiar terminology of "air conditioning," this rate of heat exchange is less than 0.02 tons of "conditioning." Consequently, the injected fluid quite literally carries its temperature down with it.

Figure 9 contains three temperature surveys computed for a well on injection at two different rates, 500 and 5,000 BPD. The earth is uniform with a linear gradient of 1.65°F per 100 feet of depth. One-half of the total volumetric rate is injected into porosity at two depths, 6,500 and 7,000 feet, depths B and C respectively. Two inch tubing is set at 5,500 feet, depth A, on a packer in 5 1\2 inch casing. Surveys 1 and 2 compare the profiles for injection at the rate of 500 BPD but with water at two different surface temperatures, 110°F and 80°F, respectively. The

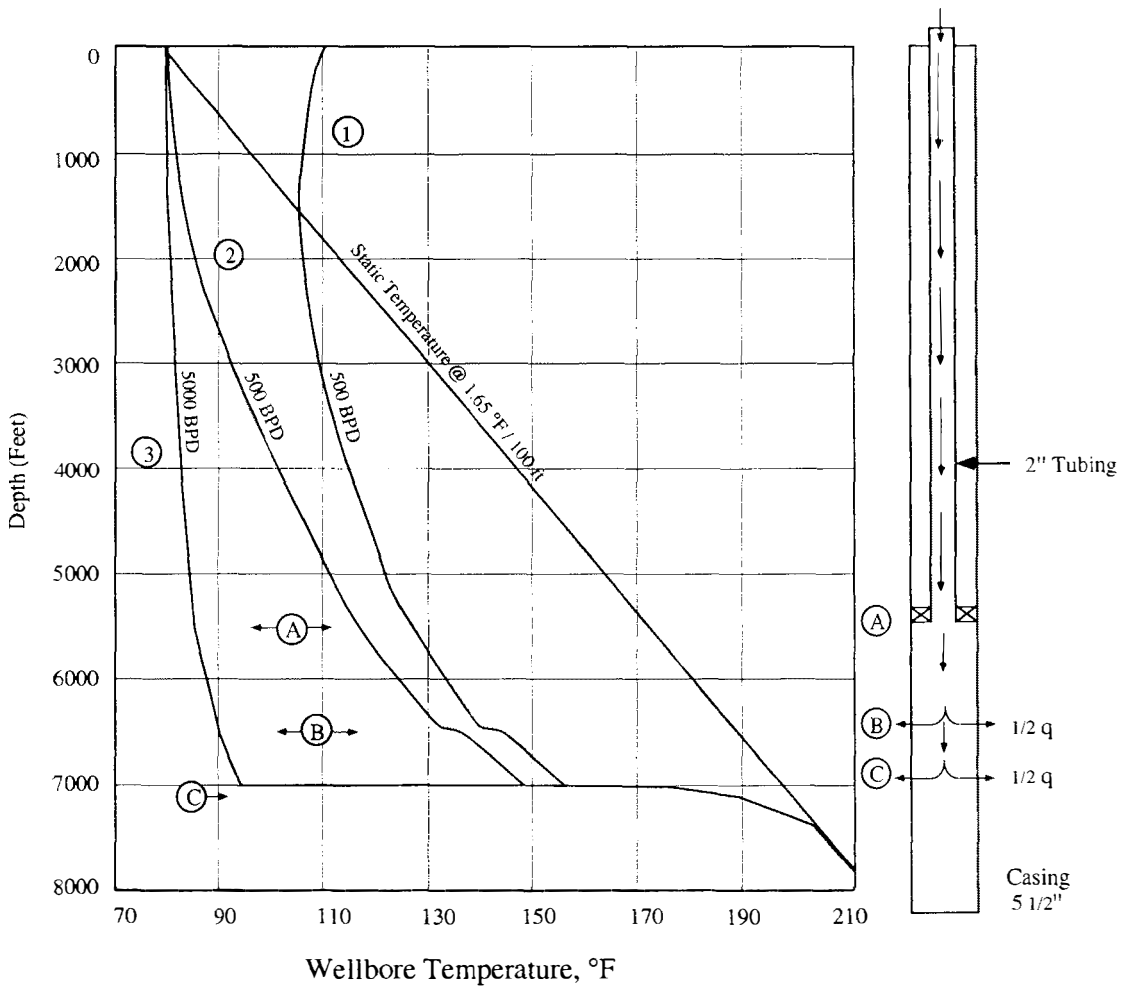

Figure 9. Computed injection temperature profiles for a deep, saltwater disposal well.

latter is static temperature at the surface. If survey 2 is shifted vertically to 1,550 feet, the depth at which survey 1 crosses the static gradient, then the two surveys would overlay each other. Furthermore, surface temperature is seen to have little influence on the profiles at the injection depths. Below the static temperature crossing depth, each profile drops nearly vertically before beginning to bend back towards static. A comparison of surveys 2 and 3 shows that the higher the rate, the more nearly vertical the profile remains. The injection gradient, dt/dz, the rate of temperature change with depth, is therefore inversely related to injection rate. If the injection zones are sufficiently deep, or the injection rate is sufficiently small, each injection profile will become parallel to the static temperature line and be displaced to the cold side by an amount, $\Delta T = T_{static} - T$, that is constant and directly proportional to the injection rate. In fact, if one makes an energy balance on a small length, ΔZ, of wellbore, the following expression for volumetric rate at any depth, Z is obtained:

$$q = \frac{A}{\rho c_p} \times \frac{\Delta T}{\frac{dT}{dZ}}, \qquad (1)$$

$$\Delta T = T_{static} - T_{wellbore},$$

This relationship is illustrated graphically on Figure 10 and is the expression needed for flow profiling. The constant A in Eq.(1) depends upon the size and completion details of the wellbore as well as the relevant thermal properties. At two locations with similar completions in a wellbore, the respective rate/ratio is thus

$$\frac{q_2}{q_1} = \frac{\Delta T_2}{\Delta T_1} \cdot \frac{\left(\frac{dt}{dz}\right)_1}{\left(\frac{dt}{dz}\right)_2} \qquad (2)$$

This expression is very useful. On the computed surveys of Figure 9, the injecting temperature gradients increase slightly below the end of the tubing string at 5,500 feet, depth A. This increased gradient is the result of the increased heat transfer to a unit of fluid at the slower velocity and more intimate contact with the casing. On the more common depth scales of 1-5

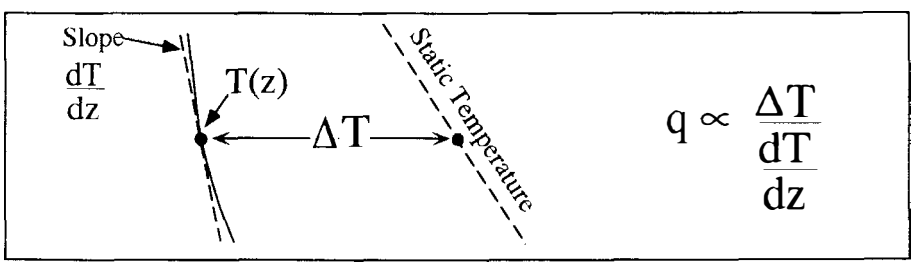

Figure 10. Relationship between temperature profile and rate for an injection well.

inches per 100 feet, this increase is difficult to recognize. As already illustrated on frame A of Figure 8, the completion has more influence on the shut-in surveys.

What is more apparent on the three injecting surveys of Figure 9 is the "catch-up" behavior in temperature that occurs immediately below the topmost loss of fluid into porosity at depth B, 6,500 feet. This sudden increase in slope makes it easy to recognize the location of each injection interval. The "catch-up," of course, results from the decreased amount of mass flow leaving depth B in the wellbore relative to that arriving at B from above. According to equation (1), a decrease in rate q mandates a decrease in the ratio $\Delta T/(dT/dz)$, which below depth B is affected by a small decrease in ΔT and a larger increase in dT/dz. In fact, between depths B and C the rate of temperature increase with depth stabilizes at a value about twice as large as is the value immediately above depth B, only one-half the volumetric injection rate survives the first loss. The final loss from the well is into porosity at 7,000 feet, depth C. Below this deepest point of injection, the temperature begins its final return to static, a process occurring over some 500 feet below C on Figure 9. The exact distance required for this return depends on several things, the amount of temperature displacement from static, the response time of the thermometer, the logging speed, and the length of time the well has been on injection.

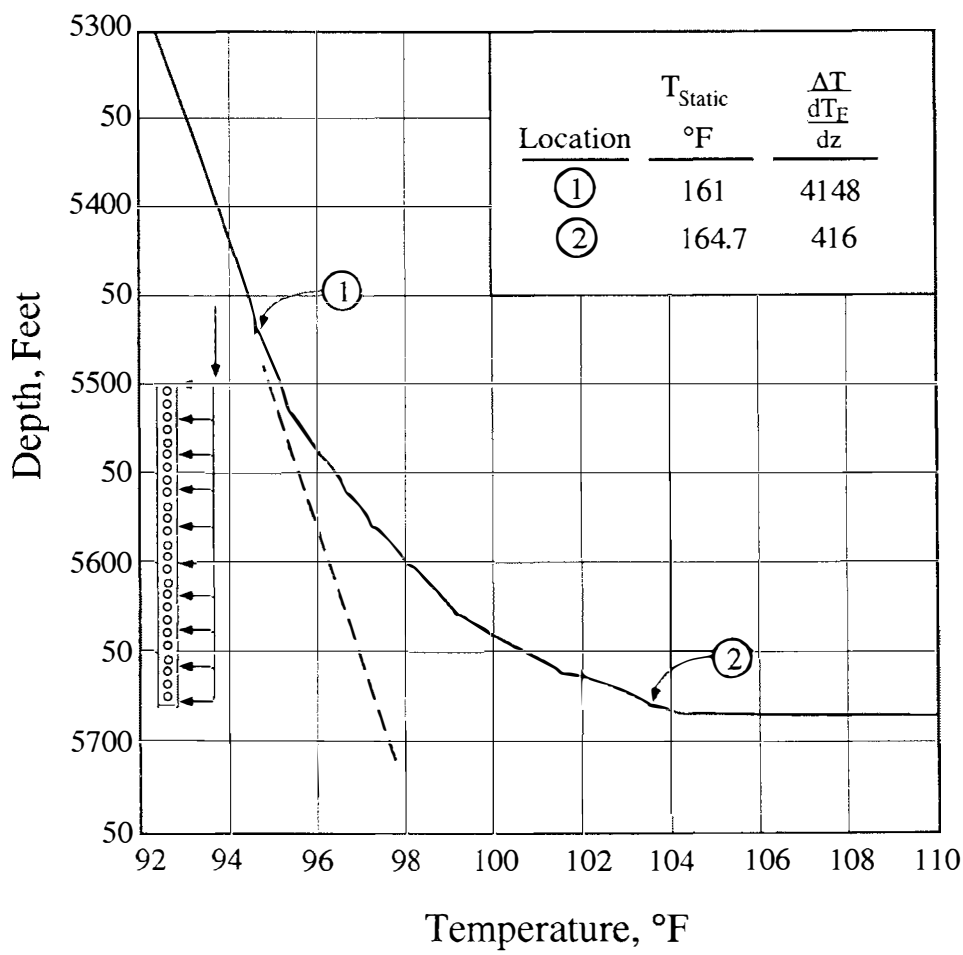

Figure 11. Computed injection profile at 1,000 BPD with equal amounts injected at each of 10 locations.

The injection zones of Figure 9 are mathematical points devoid of interval thickness. On actual logs it is possible to find, within a given interval, the discrete points of injection with much better vertical resolution than is possible with other flowmeters. This idea is illustrated, again by computed example, on Figure 11 that shows an injection zone 175 feet thick that accepts a total volumetric rate of 1,000 BPD with injection occurring in ten equal increments of 100 BPD each at ten, equally-spaced locations. The discrete increases in slope identify the points of injection. This figure also illustrates the application of flow profiling relation expressed by equation (2). The total injection rate is represented by the ratio

$$\frac{\Delta T}{\frac{dT}{dz}} = 4148$$

as calculated at location 1. The injection that survives to the bottom of the perforated interval is represented by the corresponding value of 416, computed for the stable slope at depth 2. This latter value is accordingly only 10% of the former. In theory, similar calculations can be made for each of the ten injection points, but, in fact, some "adjustment" distance is required between exit points for the profiling technique to be valid.

The reader may be puzzled by the fact that on Figure 11 the injection temperature at the deepest exit, the bottom of the perforated interval, is only slightly warmer than that at the topmost exit even though only 10% of the injection reaches the bottom exit. The displacement from static at the top of the perforations is 66°F whereas that at the bottom is ~ 61°F. This seems paradoxical, but actually is not. The total injection rate brings the cold to 5,500 feet at the interval top. Even a small fraction of this rate can travel the remaining 175 feet to the bottom of the interval quickly enough to avoid much warming. It is slope increases that identify losses.

Figure 11 also allows one to perceive the injection profile that would result from that hypothetical situation of uniform injectivity per unit length. This would produce, over the injection interval, a temperature profile that with increasing depth is <u>concave</u> towards static. This behavior is opposite the <u>convex</u> recovery associated with the isolated injection locations depicted on Figure 9. It is this latter type of behavior that will almost without exception be observed on actual temperature surveys.

The above concepts can be applied to the injection profile given on Figure 12. The surveys on this figure come from a well that had been shut-in since the time that a sand-propped, hydraulic fracturing operation had been carried out three weeks earlier. Fracture proppant still filled the wellbore below the bottom of the perforated interval. A base log, survey 1 on Figure 12, was run before the well was further disturbed in any way. This log is regarded as the "static" reference survey even though the cooling residual from the pumping done during fracturing is still evident in the perforated interval three weeks after the fact. After the base log was completed, the thermometer was pulled back up to 8,400 feet and water injection started at a rate of 5,800 BPD. Two hours later the injection logging, survey 2, was started. By the time this run was completed, the well had been on injection for 2 1/2 hours at the 5,800 BPD rate. Approximately 600 barrels of water was pumped during this time, a volume about 530 barrels in excess of the tubular

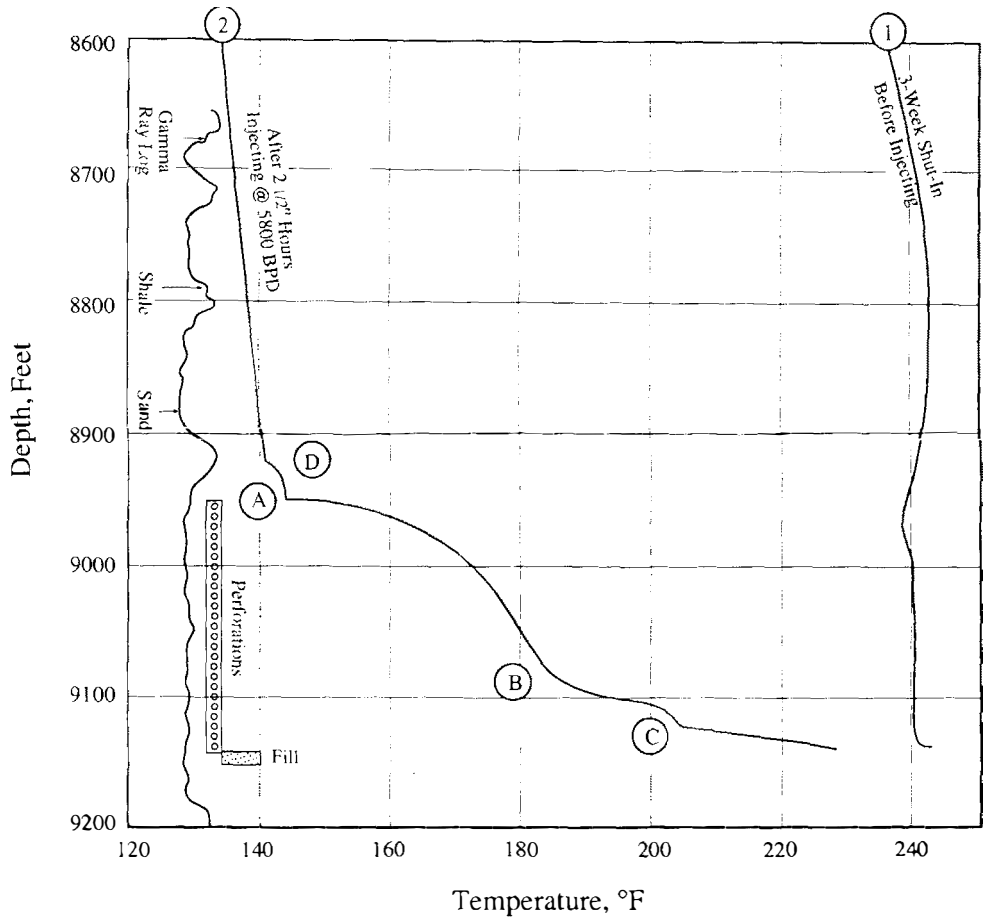

Figure 12. Injection temperature survey on a well that had been hydraulically fractured three weeks earlier.

volume of the well. For the 185-foot perforated interval this is an "overflush" of 530/185 $\simeq$ 3 BBLs/ft. Generally, a minimum overflush of 2 BBLs/ft is required to insure that subsequent shut-in surveys reveal the porosity that took the injected water. In this case, however, the injectivity was far from uniform over the 240-foot sand interval that had been fractured. Within the perforated interval, one can identify at most three depths at which fluid is lost from the wellbore into porosity. These are depths A at the top of perforations and depths B and C near the bottom. The sudden change in slope at two of these locations, A and C, identify very localized exits of the type displayed previously on Figure 9. The third, more gradual change in slope at depth B may reflect a twenty or so foot thick interval of relatively uniform injectivity of the sort illustrated on Figure 11. One can also see immediately that the majority of the injected fluid leaves the wellbore at the top of the perforations, depth A. The injecting gradient below this depth stabilizes at a value much larger than that associated with total injection rate, the profile above 8900 feet.

The slope and displacement values necessary for use in equation (2) for flow profiling are set up graphically on Figure 13. Values for the full injection stream are calculated at 8,750 feet, although other locations could have been used on the stable profile. The determination of the

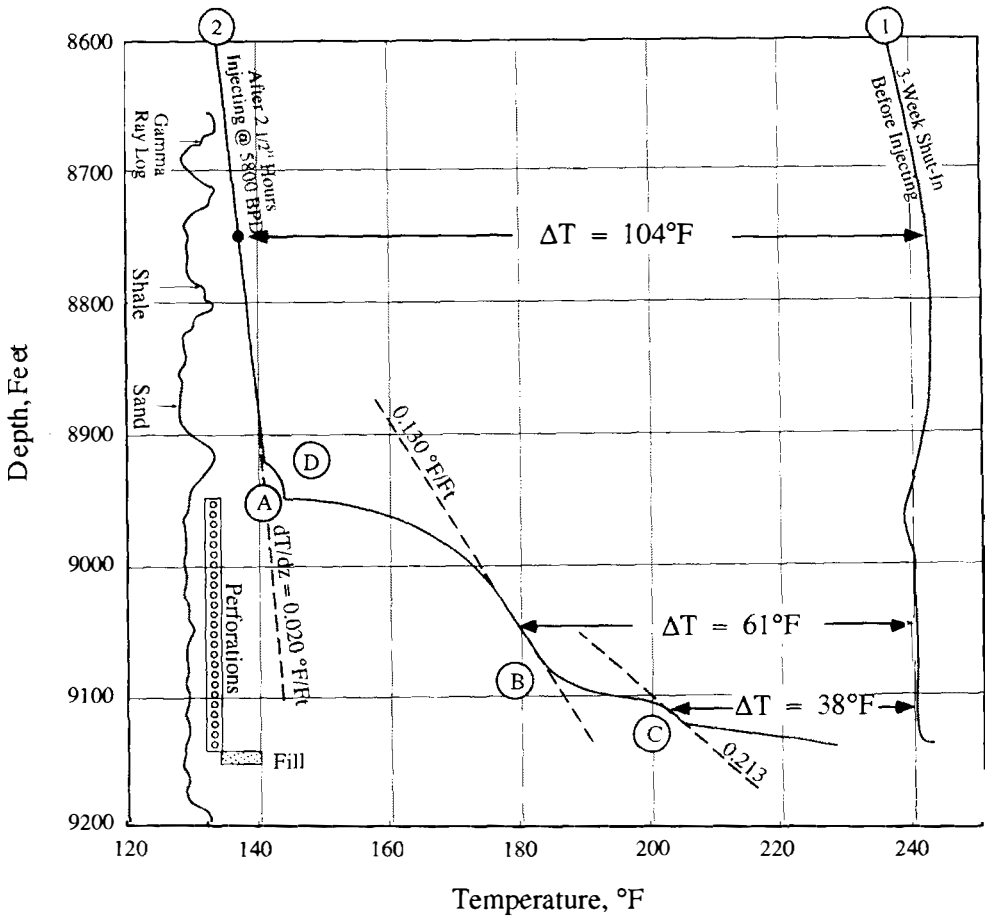

Figure 13. Slopes, dt/dz, and displacements, ΔT, necessary for rate estimations.

displacement ΔT = 104 °F is illustrated on Figure 13 . The slope of the tangent at this depth, the dotted line labeled dT/dz = 0.020 °F/ft, is determined as follows: From 8,600 to 9,100 feet the temperature along the line warms from 133° to 143°F. Thus dT = 143 - 133 = 10 °F over a distance dz = 9,100 - 8,600 = 500 feet, so that

$$\frac{dT}{dz} = \frac{10}{500} = 0.020 \text{ °F/ft.}$$

To estimate the amount of the injection that survives the loss at depth A, a stable section of slope at depth of 9,050 feet is selected. In the section of very rapid change immediately below the loss at A, the slope is influenced by the logging speed and the response characteristics of the tool as well as by the actual rate of temperature change with depth. For this reason, this section is avoided when estimating slopes. Above the deepest loss, depth C, there is insufficient record to provide a slope with much reliability. The value shown on Figure 13 is therefore only a rough estimation.

If the rate of injection into porosity at each of the three depths A, B and C are designated by the symbols q_A, q_B, and q_C, respectively, then the slope and displacement on Figure 13 at 8,750 feet is the result of the total rate, $q_A + q_B + q_C$. Likewise, those at 9,050 feet result from the sum $q_B + q_C$. Finally, the numbers at 9,110 represent q_C alone. These facts are summarized below.

Depth, Feet	Total Flow in Wellbore	Displacement from Static, °F	Injection Gradient, °F/ft
8,750	$q_A + q_B + q_C$	104	0.020
9,050	$q_B + q_C$	61	0.130
9,110	q_C	38	0.213

According to equation (2)

$$\frac{q_B + q_c}{q_A + q_B + q_c} = \frac{61}{104} \times \frac{0.020}{0.130} = 0.09$$

Consequently, only 9% of the total injection survives the first loss at depth A. Some 91% is therefore injected at this depth. Likewise, at depth C,

$$\frac{q_C}{q_A + q_B + q_C} = \frac{38}{104} \times \frac{0.020}{0.213} = 0.03$$

which leaves

$$\frac{q_B}{q_A + q_B + q_C} = 0.09 - 0.03 = 0.06$$

The injectivity profile, thus, is even more non-uniform than one might suspect by a simple visual inspection of Figure 12 alone. Such insight, not precise flow profiles, is the value of the procedure outlined in the above calculations.

A discussion of the apparent loss at 8,920 feet, depth D on Figure 12, is deferred for a subsequent section where behind-pipe flow is introduced. According to the gamma-ray log on the figure, this "loss" is still at the top of the completed zone and, as such, cannot be a loss to sands above.

The injection survey of Figure 12 will be discussed further, but for now additional materials need to be developed. Therefore, focus again on the computed profiles of Figure 9, in particular, survey 2 for injected water at surface temperature. This figure shows only the temperature in the wellbore itself, which at 6,000 feet is, for example, 123 °F. This location is 500 feet above the topmost injection zone. The solid curves on Figure 14 show what happens to the temperature in the formation away from the wellbore as a function of the length of time that the well has been on injection. The recovery from a wellbore temperature of 123 °F to a static value of 179 °F is logarithmic in distance, R, away from the well over most of the disturbed region of the formation. If the well has been on injection for only 2 hours, then most of the recovery to static

temperature occurs within 1.5 feet of the wellbore. At a distance of 2.5 feet, the temperature is undisturbed from its static value. Even after 10 years of continuous injection, the resulting temperature disturbance extends for only 350 feet away from the wellbore. This distance, L, away from the wellbore that is disturbed can be estimated from the relation

$$L\ (\text{ft}) = 3.5\ \sqrt{\alpha t_I}$$

α = Thermal diffusivity, $(\text{ft})^2$ / hr
t_I = Injection time, hours

For example, Figure 14 was computed for $\alpha = 0.05$, a value that according to Table 2 is typical for porous sands or carbonates; consequently, for t_I=10 years = 87,600 hrs:

$$L = 3.5\ \sqrt{0.05 \times 87{,}600} = 3.5 \times 66 = 230\ \text{ft.}$$

By this distance the temperature on Figure 14 is within 2 °F of static, i.e., over 95 % of the recovery has occurred. The lesson of significance illustrated by the solid curves on Figure 14 is that conduction of heat in the earth is an exceedingly slow process. Energy transport by flow, i.e., by convection, easily outdistances the spread by conduction. This point is illustrated by the dash curves on Figure 14. These show the temperature profiles that would exist if an injection

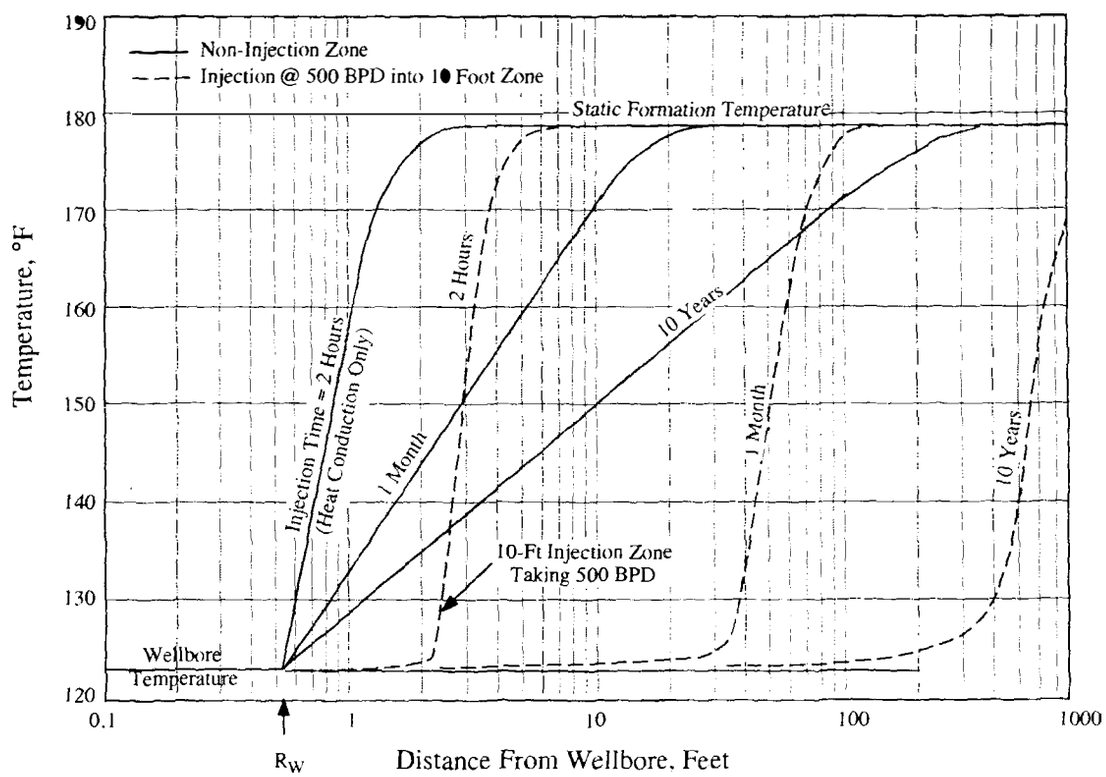

Figure 14. Temperature profile around a well with R_w = 0.54 ft. on injection at a wellbore temperature of 123°F and at 500 BPD rate. Earth is uniform with static temperature of 179°F and with diffusivity of α = 0.05 ft²/hr.

zone 10 feet thick at this location received 500 barrels of water per day. After only 2-hours' injection, the injection zone has been cooled almost to the injection water temperature for some two feet away from the wellbore, a distance beyond which conduction would have hardly made any disturbance to static temperature. The contrast between the two processes increases with injection time. A very significant consequence of this difference is the attendant difference in rate of temperature recovery in the wellbore with time once an injection well is shut off. Those areas of the wellbore opposite porosity that have received injected fluid will not return to static nearly as quickly as will those areas that have not. In deep injection wells, zones taking water will remain cooler than surrounding areas. This different rate of warm up is illustrated on Figure 15 for the situation described on Figure 14. If, for example, the well is shut-in after 2 hours of continuous injection, then 3 hours later the wellbore fluid temperature opposite a zone free of injection has warmed up to 163 °F from an injection value of 123 °F . This change represents 71% of the total recovery to the static 179 °F. By contrast, the center temperature in the injection zone has just started to warm up. Even after 10 years of injection, a 24-hour shut-in survey will show a 7 °F difference between injection and non-injection locations. The point is: Shut-in temperature surveys are excellent for detection of those porous regions that have stored injected water. The well whose injectivity survey was given in Figure 12 will illustrate this idea.

Figure 16 reproduces those logs already given on Figure 12 and adds five shut-in surveys that were run 1, 3, 6, 12, and 24 hours after the 2 1/2-hour period of injection at 5,800 BPD. The 1-hour shut-in survey is dominated by a phenomenon often seen on wells that have been fractured, intentionally or otherwise. The warm "nose" on the survey between depths A and G is the result

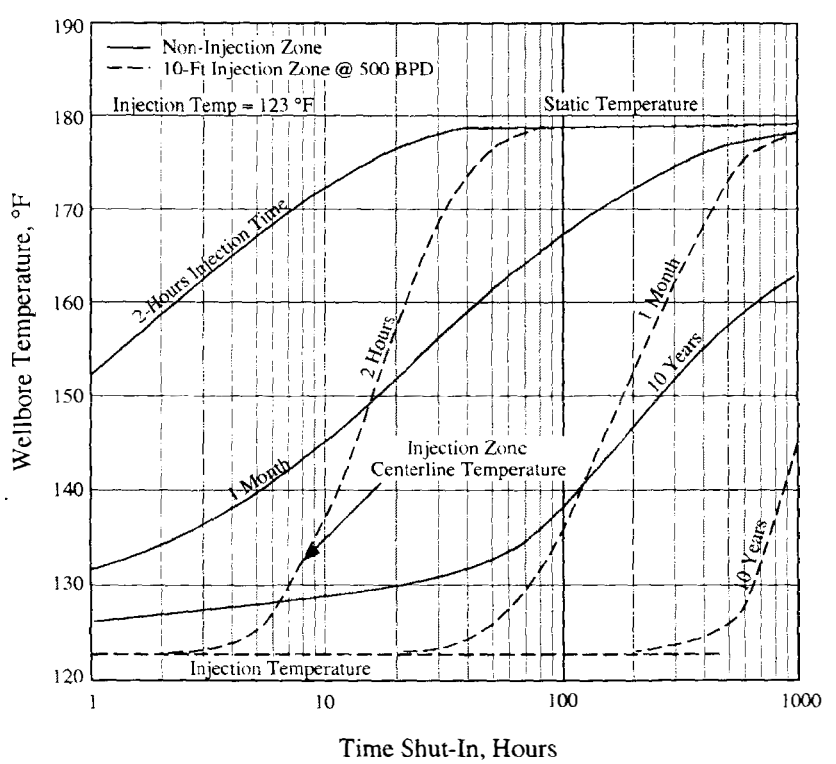

Figure 15. Temperature recovery with time of fluid in wellbore of well in Figure 14.

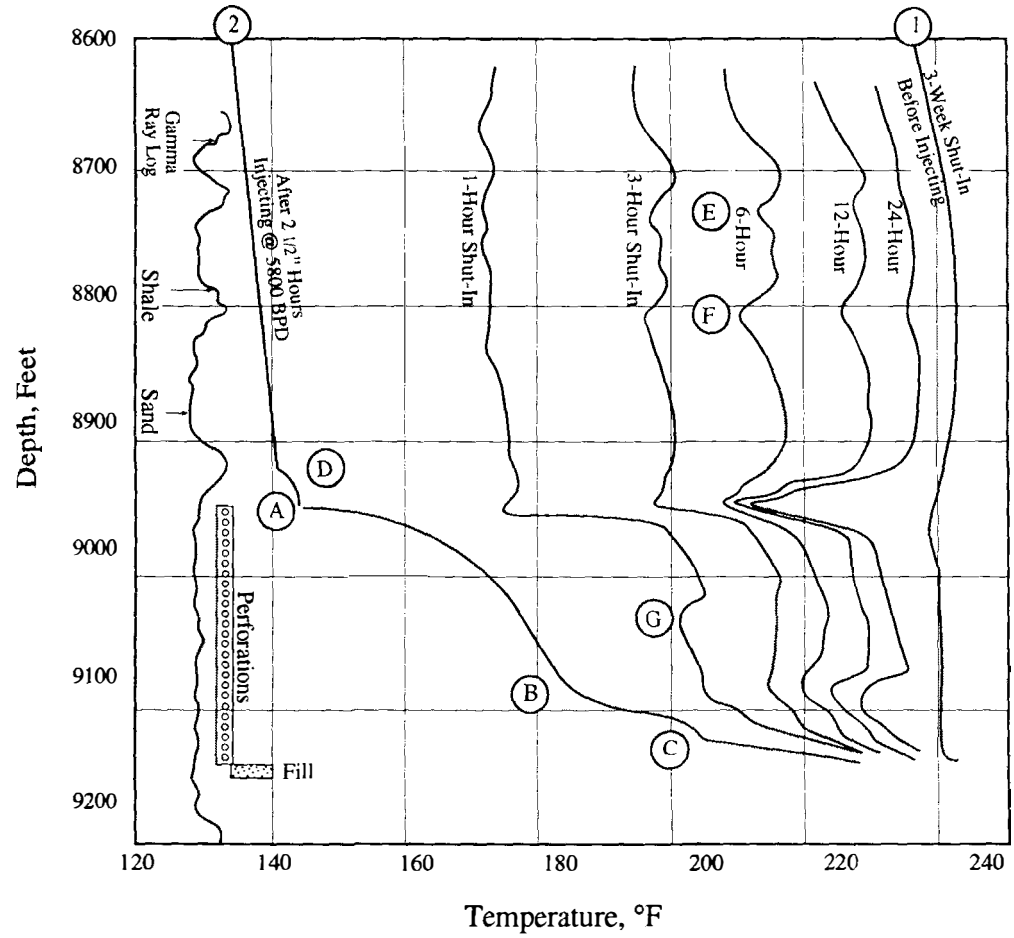

Figure 16. Injecting and subsequent shut-in surveys on a well that was hydraulically fractured three weeks prior.

of flow from one wing of the fracture through the wellbore and into the other wing of the fracture. Injection opens these wings somewhat. The crossflow is then set up by different rates of closure in the two wings. This effect has displaced to the warmer side all the surveys through the perforated interval. However, the 6, 12 and 24-hour records show the same qualitative behavior that was described in the discussion relative to Figures 14 and 15. Namely, cold spots show up at the porous intervals at the depths where fluid was lost from the wellbore, depths A, B, and C. The storage at depth C is hardly noticeable on the 24-hour shut-in survey. This location received only some 3% or 18 barrels of the 604 barrels injected in the 2 1/2 hours, according to the profile from the injecting survey. The behavior at depths B and C on the shut-in runs indicate that the 3% amount may have been an overestimation and that most of the 9% or 54 barrels surviving the first loss at depth A was injected into porosity at depth B. In contrast, the temperature at depth A, the location of porosity that took 550 barrels of the 604 barrels injected, hardly changes in the time elapsed from the 6-hour to the 24-hour surveys. This comparison is proof of the previous assertion that the depth "seen" into the formation increases with time of shut-in. The injected fluid spread farther away from the wellbore at depth A than at the other two depths.

To determine if any of the injected water was lost to sands above the perforated zone, look on the shut-in surveys for cold spots above the "disposal zone." The 3, 6 and 12-hour surveys show definite cooler locations at depths E and F, 8,725 and 8,810 feet, respectively. However, the gamma ray log shows that shales, not sands, are located at these depths. Because of their very low permeability, shales would not take injection in preference to sands. In addition, Figure 7 shows that because of the influence of lithology, shales should show up as cooler regions on shut-in surveys to the cold side of static temperature. One can conclude that no fluid storage areas are seen above the interval of sand that was perforated, thus injection was confined to the proper interval. This conclusion was arrived at in two steps:

(1) The injecting survey showed losses from the wellbore only in the designated interval,

(2) At least two sequential shut-in surveys showed fluid storage only in porosity within the same interval.

The presence of lithology influence on shut-in surveys is obviously time dependent. On Figure 16 the influence is not yet developed on the 1-hour shut-in survey and has almost disappeared on the 24-hour run. However, when present this influence is the most sensitive indicator we have to the absence of flow behind pipe. Some flow will inevitably persist after shut-in by virtue of either pressure in the injection zone or falling liquid level in the wellbore itself. Almost any flow at all will overcome the influence of lithology. This fact can be demonstrated in the following fashion. In the time interval from 1 to 6 hours the wellbore fluid temperature at 8,880 feet, the location of a sand, warms 41°F from 176 °F to 217 °F at an average rate of 41/5 = 8.2 °F/hr. During this same time the shale at 8,810 only warms by 37°F, an average rate of 7.4 °F/hr. The difference in rate of 0.8 °F/hr amounts to a rate of heat transfer to the water contained in 1 foot of 5 1/2-inch wellbore of

$$\dot{q}_H = (\rho C_p V_{5.5}) \times 0.8 \text{ °F/hr}$$

$$q_H = 62.5 \times 1 \times 0.1305 \times 0.8 = 6.5 \text{ BTU/hr-ft}$$

Any leakage behind pipe that will absorb this amount of energy with negligible rise in temperature will therefore obliterate the lithology influence. The annular volume between 5 1/2-inch casing and 8-inch hole is 0.184 ft^3/ft. If this volume is displaced N times in one hour, then the corresponding volumetric rate is;

$$q = 0.184 \text{ N ft}^3\text{/hr} = 0.786 \text{ N BPD}$$

If this flow changes temperatures by no more than, say, 0.1°F over the one-foot length, then the shale excursion at depth F, a change of about 1°F/ft., would be subdued by a factor of ten and thus rendered insignificant. This 0.1 °F/ft would result from a heat transfer rate of

$$q_H \text{ (flow)} = \rho C_p q \times 0.1$$

$$q_H \text{ (flow)} = 62.5 \times 1 \times 0.184N \times 0.1 = 1.15 \text{ N } \frac{\text{BTU}}{\text{hr-ft}}$$

This energy transfer should equal the amount $q_h = 6.5 \frac{BTU}{Hr\text{-}Ft}$ resulting from lithology influence. Thus

$$1.15\,N = 6.5,$$

or

$$N = 5.6,$$

which corresponds to a leak rate q = 0.786 N = 4.4 BPD. No other logging tool has a rate resolution this low.

The preceding discussion has demonstrated how confined injection shows up on temperature surveys. In fact, some behind-pipe flow also shows up on Figure 13. The apparent small loss from the wellbore at depth D on the injecting survey results from flow exiting at the top of the perforations and then flowing up behind pipe to the top of the fracture which was stopped by the plastic shale at 8,920 feet . In the crossflow interval AD, the net flow downward is less than it is above D; consequently, the survey records a "loss" at depth D.

This "loss" type of behavior is illustrated on Figure 17 at a thief zone located at 5,600 feet, some 200 feet above the injection zone at 5,800 feet. The curves on this figure were computed for a well on injection at 500 BPD with varying amounts of loss from 0 to 500 BPD by flow behind casing from the perforations upward to the thief zone. A 100% loss shifts the survey back towards static by about one-fifth of the total displacement associated with no loss. From the figure, one can see that the flowing survey itself will show the influence of a loss to a shallower thief zone whenever this loss amounts to at least 20% of the flow inside the pipe.

The injecting survey of Figure 18 illustrates a behind-pipe loss to a higher injection zone whose perforations had been cemented by a "squeeze." At the time the survey was run, the well had been on injection for 4 hours at a rate of 990 BPD. Three apparent losses to porosity are evident on the log at depths 1, 2 and 3. The bottom loss, depth 3, is at the presently completed injection zone; however, the other two losses are located at supposedly squeezed perforations. The most obvious conclusion is that these perforations have "broken down" and are taking part of the injection intended for location 3. On the left side of Figure 18 appear stationary flowmeter readings made with a diverting type flowmeter, a "basket" spinner tool, at four locations A, B, C, and D. The readings at locations A and B are the same; thus, there is no fluid loss from the wellbore at depth 1. The temperature log must therefore be responding to behind-pipe flow. Now, between depths C and D, the spinner does show a loss from the wellbore of an amount of fluid equal to

$$100\left(1 - \frac{7.1}{11.6}\right) = 39\%$$

of the total injection rate. This fluid obviously exits the wellbore at location 2 on the temperature survey. Therefore, the squeezed perforations at ~5,910 feet have broken down. Of the water leaving the wellbore here, part or all then flows behind pipe up to the topmost zone just below 5,800 feet.

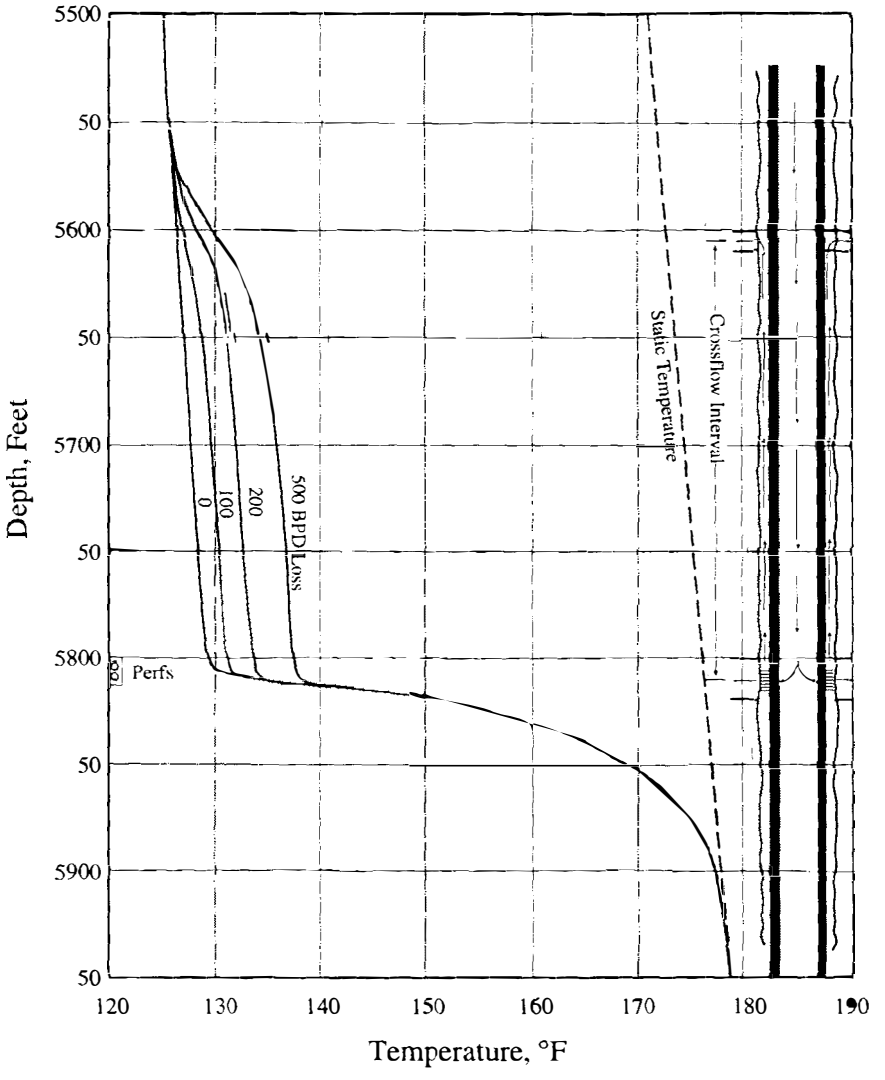

Figure 17. Temperature surveys computed for a well on injection at 500 BPD with varying amounts of loss behind pipe to thief zone located 200 feet above.

As might be expected, the shut-in temperature surveys are most sensitive to small losses from injection zones. A leakage rate of one barrel per day into porosity will eventually show up if it persists for a long enough time. Figure 19 shows computed shut-in surveys for the thief zone situation depicted on Figure 17. Each solid curve on Figure 19 is a 6-hour shut-in survey across the thief zone at 5,600 to 5,610 feet and the rates are the behind-pipe losses from the primary injection zone at 5,800 feet. The leak is assumed to have existed at the indicated rate for one month prior to logging. If injection into the well had also been going on for only one month, then the figure shows that a shut-in period of 6-hours would begin to reveal quite small leaks into

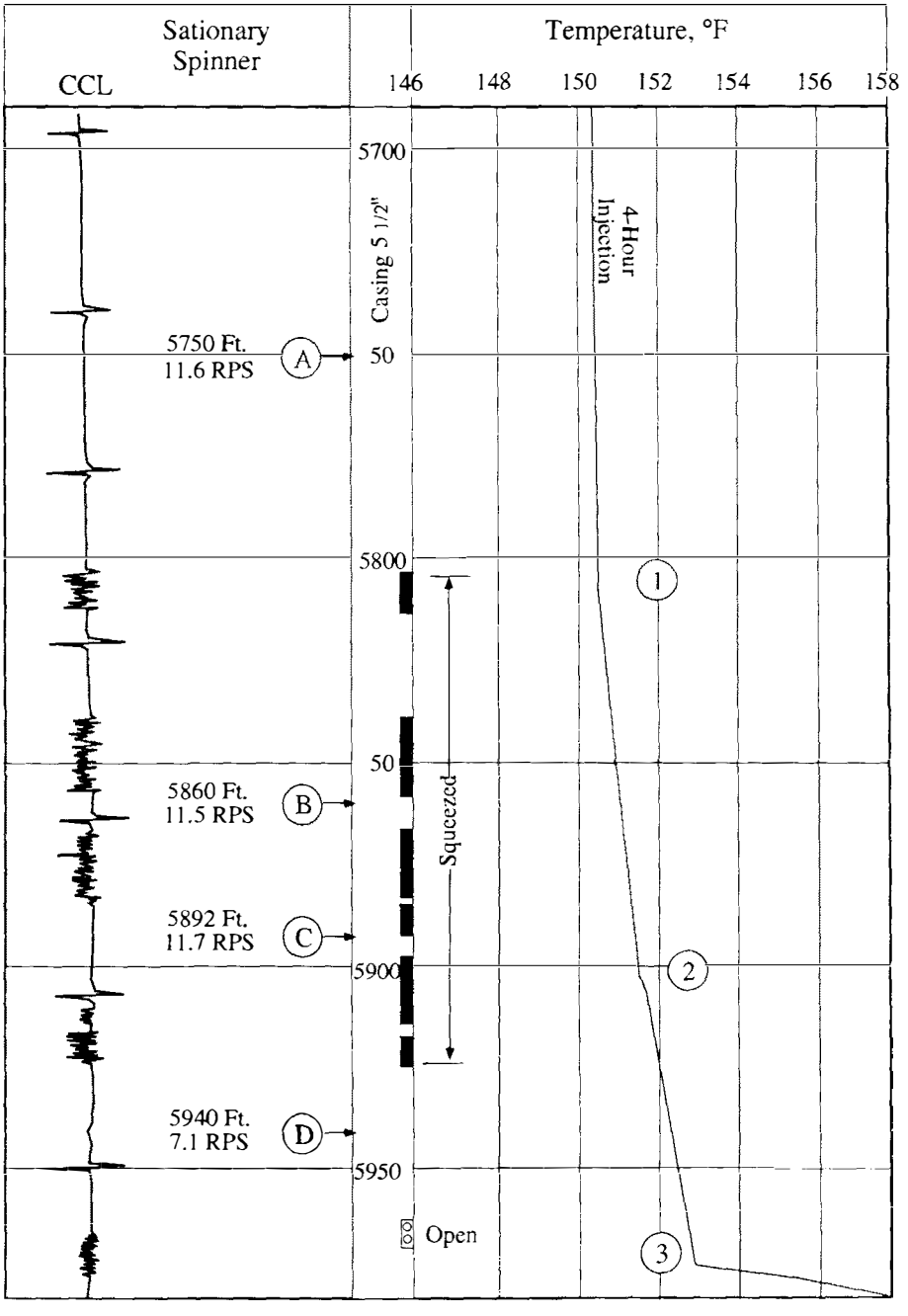

Figure 18. Temperature survey from well on injection at 990 BPD salt water.

storage porosity at 5,600 feet . However, had the well been on injection for a year prior to the development of the leak, then even a 500 BPD leak would have been hidden by the residual conductive cooling from the long period of the flow of cold water past this location in the wellbore. Consequently, in planning the shut-in surveys that are to follow the injecting survey, one must obviously take into account the length of time that a well has been on continuous injection. The shut-in times listed in Table 3 can serve as planning guide provided at least two shut-in surveys are run, one at the beginning of the listed interval and one at the end of the

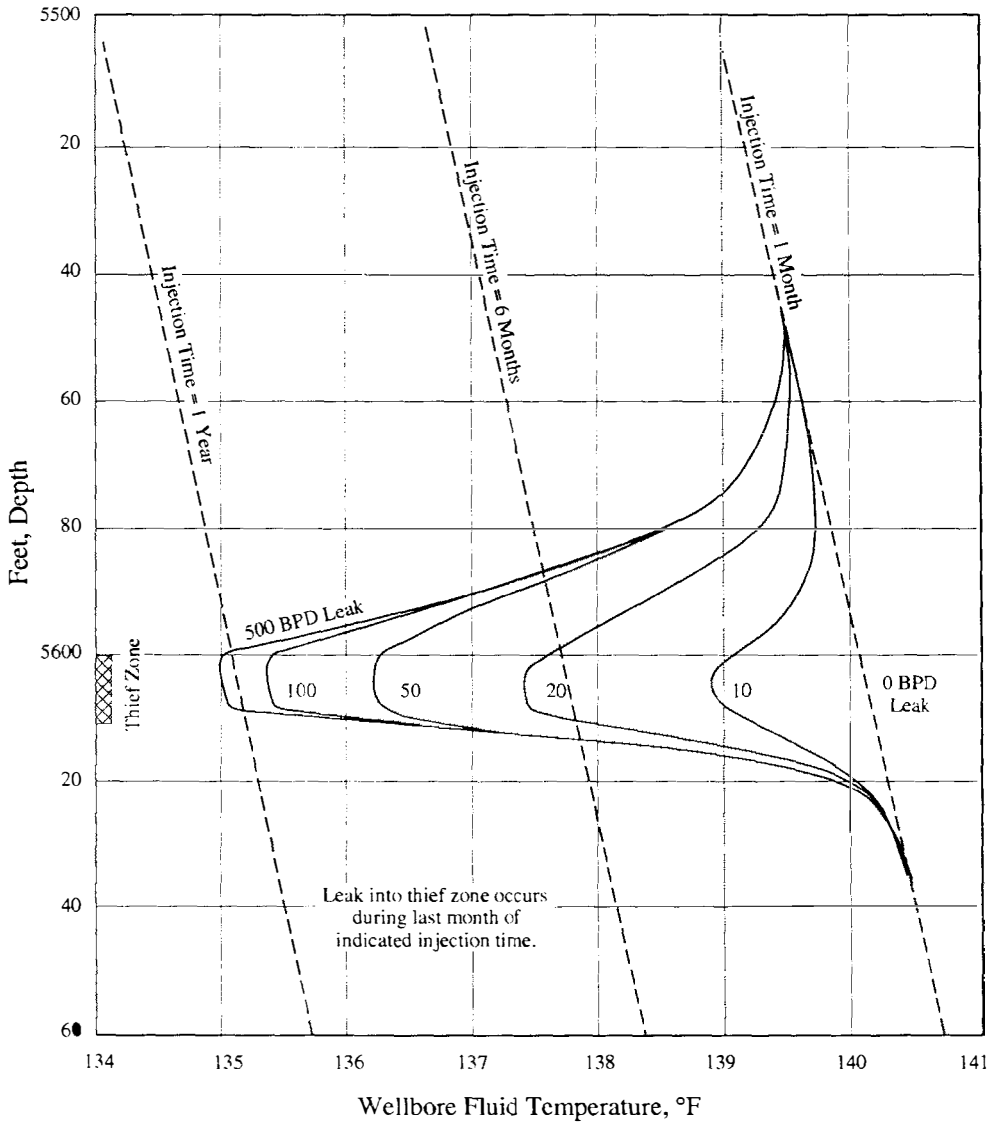

Figure 19. 6-hr shut-in temperature surveys past the thief zone depicted on Figure 17. Computed for a one-month old leak.

interval. For example, if a well has been on injection for 10 years prior to shut-in, then Figure 15 shows that after 96-hours of shut-in, a section of wellbore opposite a non-injection zone would have warmed from 123°F to 138°F. At this temperature, Figure 19 indicates that a 20 BPD leak would just begin to show up. Consequently, this survey along with one at 192-hours shut-in should not miss the storage porosity. When used according to the guidelines of Table 3, temperature surveys can detect leaks that all the other tools will miss. The use of proper timing of surveys is illustrated by the runs reproduced on Figure 20. These surveys include an injecting run followed by shut-in surveys after 1, 3, 12 and 24 hours, respectively. The well had been on injection at about 500 BPD for nearly one year. All the porous zones indicated on the neutron porosity log are dolomitic developments in limestone. The perforations are into the bottom

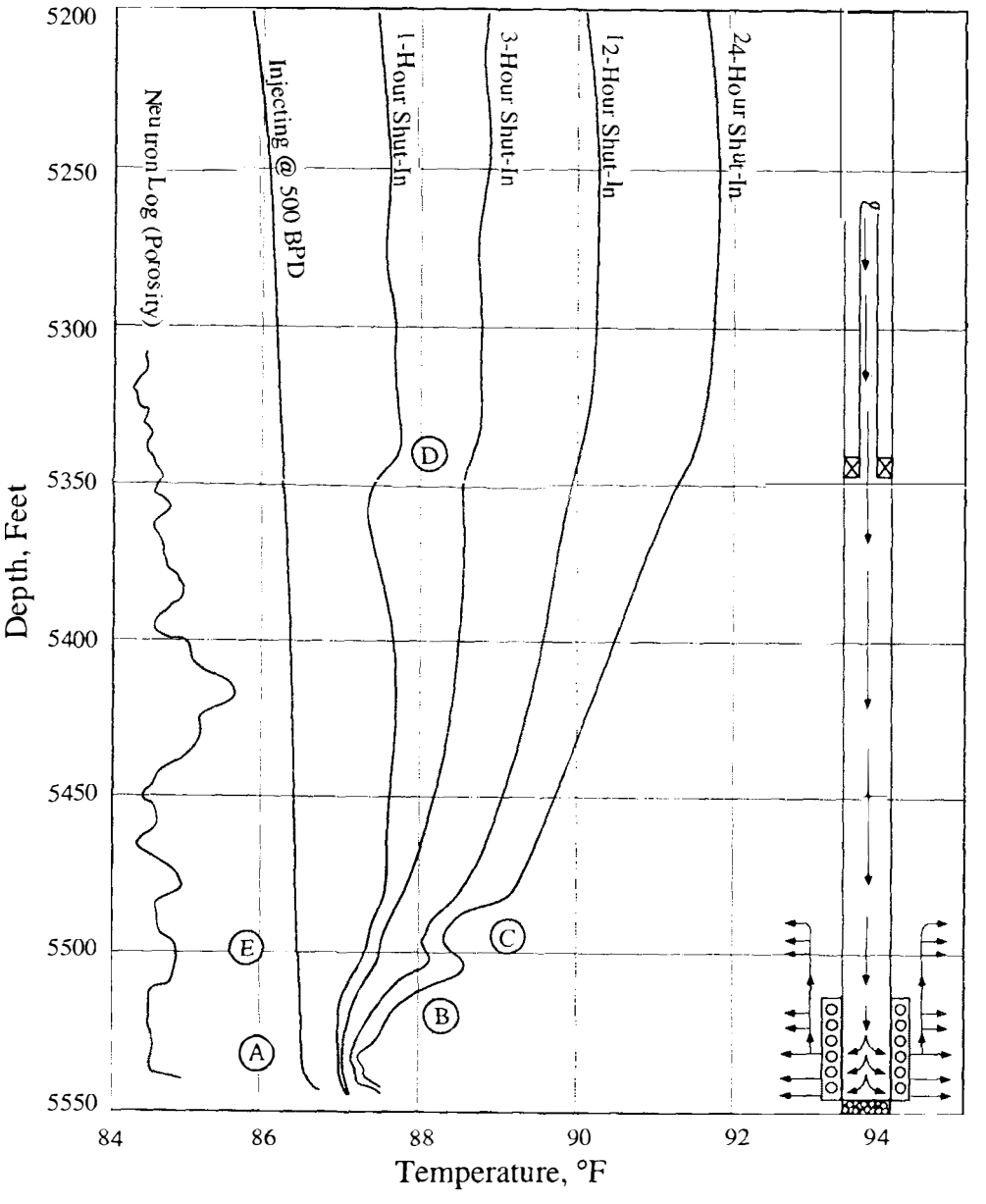

Figure 20. **Injecting and shut-in temperature surveys from well on continuous injection at about 500 BPD for almost one year.**

member of a lithological unit of lime that extends upwards to 5,150 feet. The injecting survey shows that almost all the currently injected water is leaving the wellbore below depth A at 5,530 feet, which is the bottom 15 feet of the 33-foot perforated interval. There is a slight indication of a "loss" at depth E in the porous member immediately above the disposal zone; however, it is so slight that one would not call it significant. The 1 and 3-hour shut-in surveys show that fluid

storage is occurring over much of the porous interval, at least two-thirds of the net pay. This conclusion is supported by the 12 and 24 hour shut-in runs that show injection into porosity below depth B at 5,516 feet. The slowly recovering temperature below depth A, 5,530 feet, is the result of the vast majority of the injected fluid entering porosity below this depth. The bottom ten feet of net pay is the location at which long term injection has taken place. The 12 and 24-hour shut-in surveys reveal conditions that were hidden by conduction cooling on the 1 and 3-hour runs; namely, fluid storage signatures appear at depth C, which is located in the porous interval immediately above the injection interval. The small indicated "loss" at depth E on the injecting survey may, indeed, be of significance and some injection is now taking place at this interval due either to a casing leak at this depth or to a loss behind pipe from the injection zone below. Subsequently, examination of a radioactive tracer survey will suggest that this flow occurs behind pipe.

TABLE 3. MINIMUM SHUT-IN PERIODS NECESSARY TO DETECT LEAKS BEHIND PIPE INTO ZONES ABOVE THE INJECTION INTERVAL

Prior Length of Continuous Injection	Minimum Shut-In Time to Detect Leaks of Several Weeks Standing
1 Month	6 - 12 Hours
6 Months	12 - 24 Hours
1 Year	24 - 48 Hours
5 Years	48 - 96 Hours
10 Years	96 - 192 Hours

Figure 7 (page 10) illustrates that lithology influence is such that porous dolomitic intervals will tend to lag non-porous intervals; so how would one differentiate what is seen at depth C on Figure 20 as being the result of injection at this depth rather than the influence of lithology? Two aspects of behavior rule against lithology. First is the "growth" of the signature with time on the 12 and 24-hour surveys. This is backwards to both the time progression indicated on the hypothetical Figure 7 and the actual behavior seen on Figure 16 at depths E and F. The second, and stronger, negative aspect is the shut-in behavior above the suspect depth C, Figure 20. Above 5,470 feet are located much thicker porous and non-porous intervals. Furthermore, the 1-hour shut-in survey shows a muted influence of this lithology on the slight "lead" in recovery evident in the tight section between 5,400 and 5,450 feet. Thus, lithology cannot account for the signature at depth C.

Nevertheless, uncertainty about lithology has made it a common practice to add a radioactive tracer survey to the temperature surveys when checking for confined injection. The tracer tool has incredible sensitivity to flow behind pipe, a feature not present in the injecting temperature survey when flow is upwards behind pipe. This practice, however, has caused the loss from industry of the original philosophy behind running surveys of the type shown on Figure 20. If

one intends to run the tracer tool anyway, then why run anything beyond the 1 and 3-hour shut-in surveys? The reason is contained in the discussion that follows.

Figure 20 is the first example of non-confined injection into a deep disposal zone. It also illustrates how problems typically develop. Quite likely, only the bottom fifteen feet of the perforations "broke" down to injection when the well was initially completed. The pressure increase associated with continued injection into a limited interval has caused the hard rock to fracture up into the next porous interval capable of relieving the pressure. These fractures may leave the wellbore with sufficient rapidity that they intersect the next porosity at a distance from the well that exceeds the range of all tools used for the injecting survey, temperature, radioactive tracer, and neutron activation survey. Only the long shut-in temperature surveys reveal this placement of fluid in porosity away from the well.

On Figure 20, the 1 and 3-hour shut-in surveys depict the influence of completion at depth D, 5,345 feet, in the same fashion as Figure 8 (page 11), frame A, at the casing shoe. On both figures, the extra insulation above the indicated depths causes a more rapid return to static. On Figure 20, this influence is already attenuated on the 3-hour survey and is practically absent from the 12 and 24-hour runs.

Finally, the astute reader may have noticed a "peculiar" behavior to the shut-in logs below depth A on Figure 20. The temperature warms during the first hour more than it does during the next 24 hours. This behavior merely means that the water currently injected is slightly cooler than the long-time "average" injection temperature. This particular set of logs were run in mid December in West Texas. Quite obviously, the temperature of water injected into a formation at any particular time may also be warmer than average zonal temperature in an old injection well. This was the situation when the temperature surveys in Figure 21 were recorded. During injection, water arrived at the disposal perforations about 2°F warmer than the average temperature of the injection zone which has received water for many years. The injecting survey shows losses at only two depths, A and B, inferring that most of remaining perforations are plugged. The "catch-up" shifts below each of these depths is to the cooler side because, as the shut-in surveys show, the "static" condition for current injection is a cooled formation, not one at normal temperature for this depth. Above 5,425 feet , the recovery is in the normal direction, i.e., from the cool side. The shut-in surveys all show the "warmed" storage porosity receiving current injection. The continued "growth" of these injection signatures for 12-hours of shut-in proves that the "current" injection profile has existed for some time and is not something that happened just recently. On Figure 21 is the relic, at depth C, of an earlier period of disposal into the zone immediately below the current completion.

The surveys in Figure 21 also refute the old saw, still being played, that an injecting temperature survey from an old injector "don't show you nothing." This is an outgrowth of the old, all too common procedure that tolerates a recording sensitivity of more like 10 °F/inch rather than the 1°F/inch employed for surveys of Figure 21. The figure further shows, on the 12-hour shut-in survey, that injection has taken place into the porosity over the entire interval during times past.

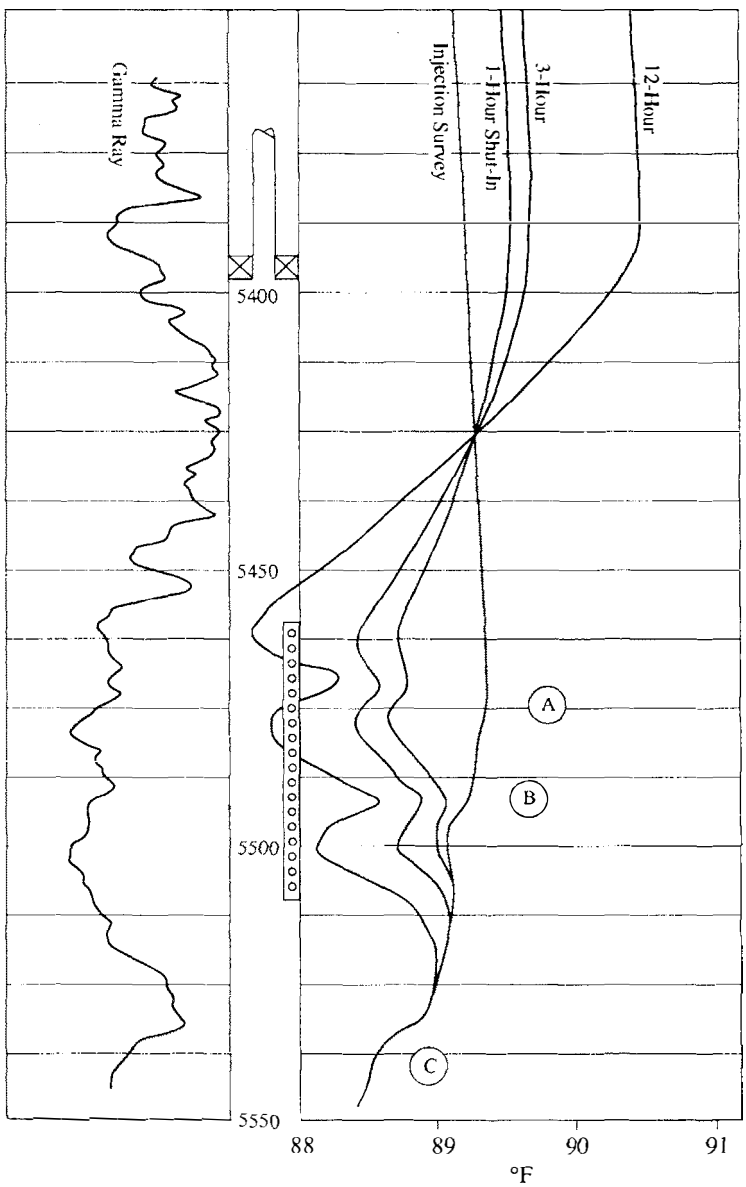

Figure 21. **Temperature surveys from a well on 600 BPD injection at a water temperature 2°F warmer than average from long-term injection.**

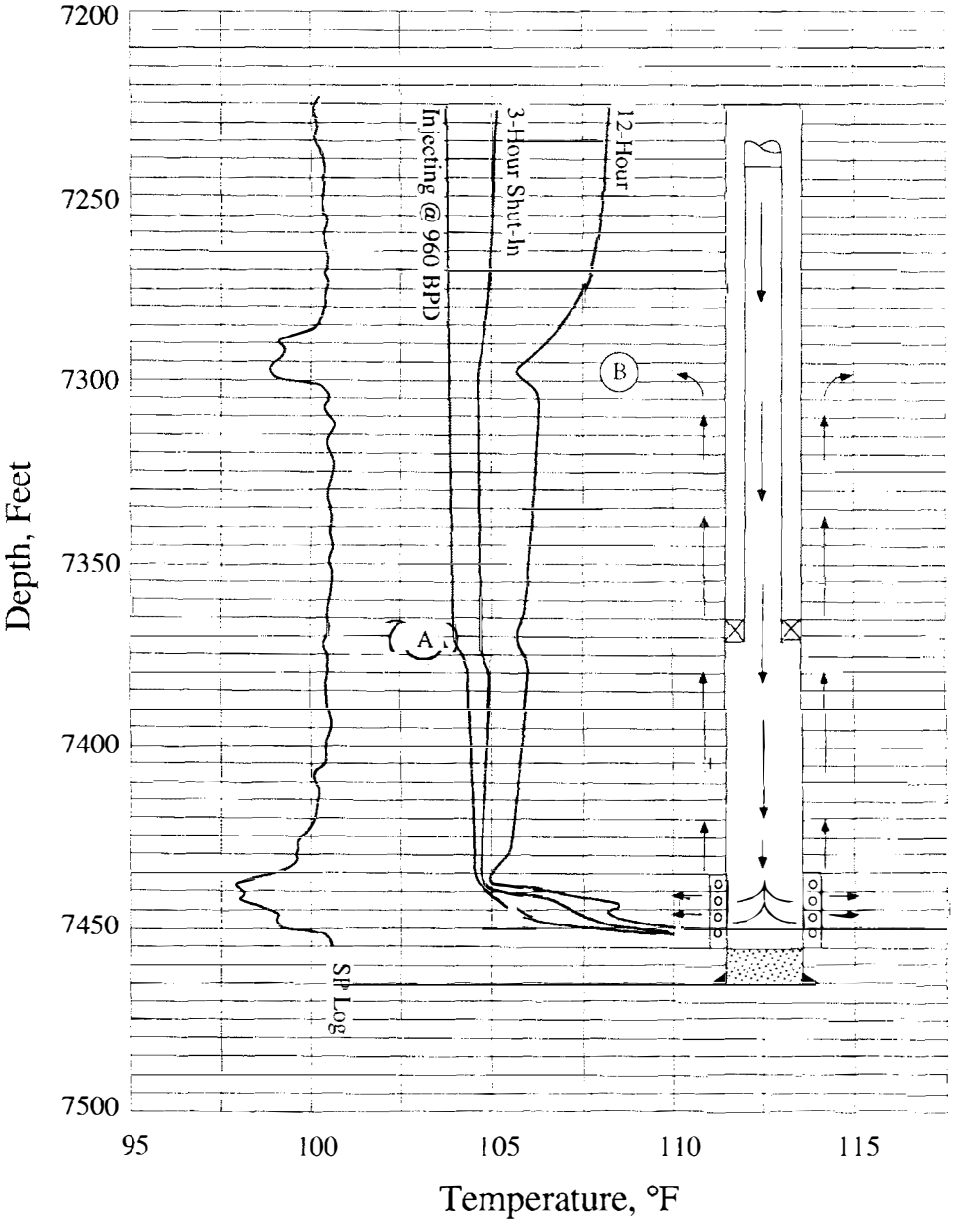

Figure 22. **Temperature surveys from a well on injection at 960 BPD with flow behind pipe even on shut-in status.**

Finally, the shut-in surveys show that over the lifetime of this well, the completion has prevented any injection into the thin porous interval located only three feet above the designated injection interval and only seven feet above the top of the perforations.

The following comments are best understood by reference to Figure 9 (page 12) that contains three computed injection surveys. The insulation offered by the stagnant annular fluid effectively hides from the thermometer during injection any flow that occurs behind pipe above the packer, i.e., above depth A on Figure 9. Consequently, the most one should expect to see on an injection survey is the type of change at the depth of the packer that is evident on Figure 17 (page 24) at the thief zone. The "loss" would appear to occur at a depth that corresponds to the end of the tubing string. This type of behavior is evident on the injecting survey of Figure 22 where the first "loss" appears at depth A, the end of the tubing. The 12-hour shut-in survey, however, clearly shows the storage porosity located at depth B, some seventy-five feet above depth A. This same survey also shows flow from the injection interval up to depth B as continuing after the well is shut off injection. Actually, the warm up on the injecting survey of Figure 22 is located some ten feet below the end of tubing. The thermometer hangs free usually until the entire tool clears the tubing, thus thermal contact with the casing wall typically does not occur for some 10 - 20 feet below the end of the tubing.

The same insulation that shields the thermometer in the tubing string also protects any behind-pipe flow from the injected stream flowing in the tubing. Once the leaking fluid goes above depth A on Figure 9, then it tends to carry its temperature upward with the flow in the same manner that injection inside the tubing carries its temperature downward. Thus, if one turns Figure 9 upside down and locates the tubing packer at zero depth, then survey 1 can be viewed as the temperature in a stream flowing behind casing upward into two shallow zones at depths B and C, respectively. This is not, however, the temperature profile that the thermometer in the tubing string will measure while the well is on injection. The influence of the behind-pipe flow will show up primarily as storage signatures on the shut-in surveys. Suppose that the leak charged zones on Figure 9 at 500 feet . The shut-in residual at this depth depends on the surface temperature of the injected water. Consequently, the storage signature on the shut-in surveys is dependent on injected fluid temperature. This fact is illustrated by the two frames of Figure 23, each computed for a month old injection well that has a behind-pipe leak from an injection interval at 5,600 feet up to a shallow zone at 500 feet. Injection rate into the well is 500 BPD while the leak rate is the value listed for each of the eleven shut-in surveys on the figure. Each frame is for a particular surface temperature for the injected water. The leak crossflow ceases when the well is shut in.

Frame A shows surveys run after a 6-hour shut-in following one month of injection of water at the surface temperature of 80°F. The 250 and 500 BPD leaks arrive at 500 feet at a temperature that is hotter than static at that depth. The 100 BPD leak, however, has cooled to nearly static temperature at 500 feet. It is evident on the survey simply because the 6-hour shut-in temperature on either side of 500 feet is still to the cool side of static. The leak would be hidden on a single, long-time shut-in survey. Leak rates less than 100 BPD are cooled by the injection and arrive at 500 feet colder than static temperature.

The behavior of the 12-hour shut-in surveys of frame B, Figure 23, after injection of water at 110°F is unusual at first glance. The variation, of course, is the result of a hot residual left from the hot water injection. At the 500-foot thief zone, this residual keeps the wellbore temperature at about 98°F after 12 hours of shut-in. The 500 BPD leak arrives at the thief zone about 2°F hotter than this residual and thus appears as a hotter signature on the survey. The 250 BPD leak, however, reaches the thief zone cooler than the 98°F residual. Thus, the wellbore temperature is reduced at the thief zone, the location where the cooler leak fluid is stored in porosity surrounding the wellbore and extending laterally away from it. The 100 BPD leak arrives at about static temperature. Lesser rates of leakage are warmed by the injection of hot water prior to shut-in. For this reason, the 20 and 10 BPD leaks give surveys on frame B of Figure 23 that progress to the hot residual as the rate decreases.

The lesson of Figure 23 is that one does not know exactly what to expect as a result of behind-pipe leakage from a deep disposal zone to shallow strata. It is therefore a wise procedure to run at least two shut-in surveys to ascertain any portions of the shallow wellbore that appear to be "locked" at a relatively unchanging temperature as a result of injection. Furthermore, the surveys on frame B of Figure 23 suggest that the appropriate shut-in times are at the tail end of the intervals of times listed in Table 3.

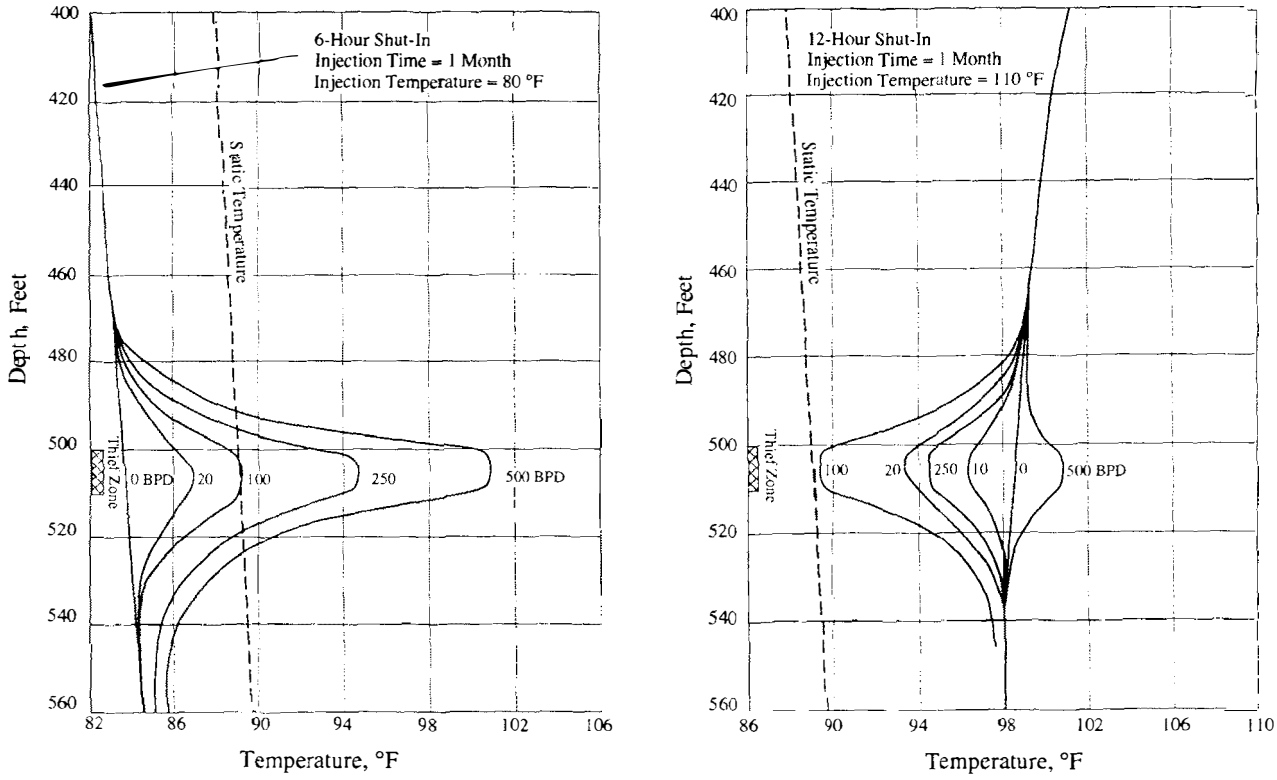

(A) Injection Water Temperature of 80°F

(B) Injection Water Temperature of 110°F

Figure 23. Shut-in temperature surveys across a thief zone at 500-510 feet charged by flow behind casing from injection interval at 5,600 feet.

In reality, deep disposal zones hardly ever leak into shallow strata as a result of flow behind pipe. Deep injectors pollute at shallow depths mainly as a result of tubing, packer and casing leaks. External corrosion can reduce casing wall thickness to the point that annular pressure from a tubing or packer leak will cause the casing to rupture. Subsidence and fault instability are common causes of casing failure in parts of the USA. Tubing and casing leaks are easy to detect on both injection and shut-in surveys as Figure 24 illustrates. The injecting survey shows a slope change at depth A but very little "catch-up" because the loss from the tubing continues downward in the casing. The typical "loss" signature occurs at depth B where the leak exits the casing. The 12-hour shut-in survey places the storage porosity at the same depth as the casing leak. From the relative positions of the static temperature and the injection survey, one can tell how the storage areas should appear on the shut-in runs. The loss at depth B on Figure 24 should cool any porosity in the neighborhood of the leak. This situation can be contrasted with the computed injection survey 1 on Figure 9 (page 12), where any casing leaks above 1,500 feet would add fluid that is warmer than the static temperature of receptor porosity. The storage signature on shut-in surveys would then appear as a "hot spot." The variability evident on Figure 23 for leaks behind pipe is thus removed for casing leaks.

Temperature Behavior in Shallow Injection Wells: These are the type of disposal wells most likely to pollute fresh water sands by loss from the injection zone. The temperature behavior in these wells is no different from the theory and examples that have already been examined for deep injection wells. Therefore, the reader should once again refer to the computed injection

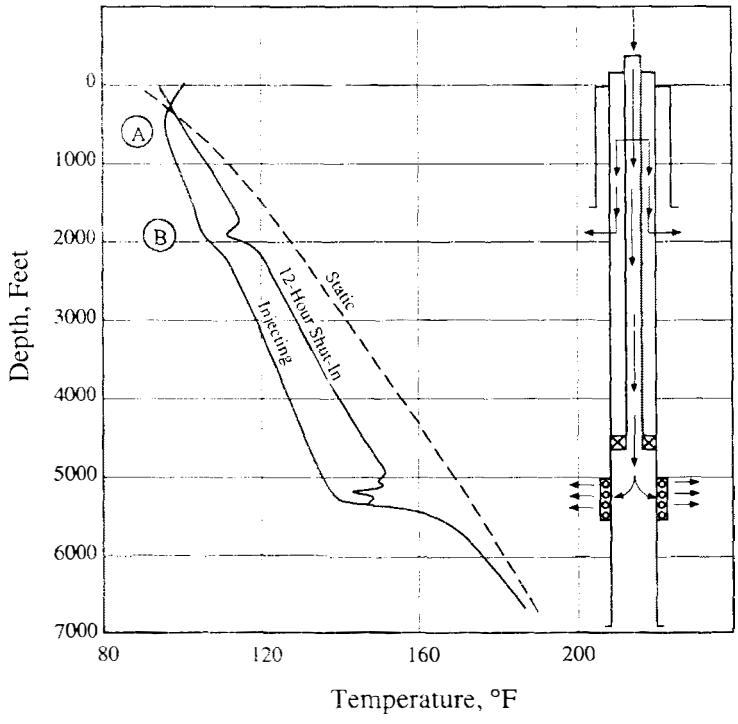

Figure 24. Temperature surveys from deep injector with shallow tubing leak at A and casing leak at B.

profiles on Figure 9, and, this time, imagine that the injection zone is located at 1,000 feet rather than at the deeper locations of the figure. Two things are then evident: First, the contrast in temperature between the injected water and the static wellbore is reduced. Temperature surveys must now be recorded at high sensitivity as a matter of course. Second, the type of storage signatures that one can expect depends entirely on the surface temperature of the injected water. These two facts are illustrated by the computed injecting and shut-in surveys appearing on frames A and B of Figure 25. In each frame, the well has been on injection for one month at a rate of 500 BPD into perforations opposite a 25-foot thick disposal zone at 975 to 1,000 feet. During this same month water has leaked from the perforated interval behind pipe up to a 10-foot thief zone located at 800 feet on frame A and at 825 feet on frame B, respectively. The two frames are computed for different water temperatures at the surface, frame A for water at the surface temperature of 80°F and frame B for 110°F water which is 30°F hotter than surface temperature. Each frame contains, as solid lines, two surveys with the well on injection at 500 BPD. One survey is for no leakage from the injection interval, 0 BPD leak, whereas the other allocates all 100% of injection, 500 BPD leak, to the flow behind pipe. Each frame also contains four surveys taken 12 hours after both injection and flow behind pipe has ceased. These surveys, shown as dashed lines, are for leak rates of 0, 10, 50, and 500 BPD.

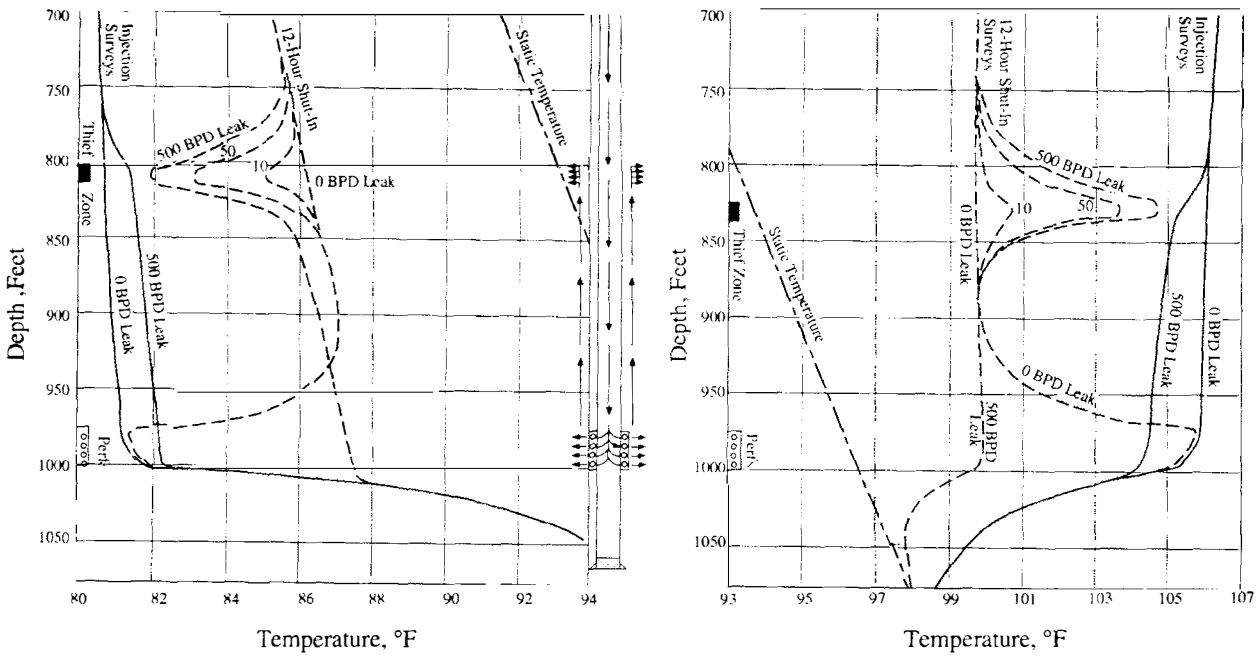

(A) Injection at 80°F Surface Temperature

(B) Injection at 110°F Surface Temperature

Figure 25. Computed temperature surveys injecting (—) and shut-in (---) from a well receiving 500 BPD water with various leaks behind pipe from injection perforations up to a shallower thief zone.

The length of the crossflow interval on Figure 25 is the same 200 feet, approximately, as that on Figure 19 (page 26) for loss from a deep injection zone. Furthermore, the rate of charge per foot of thief zone thickness is the same for the two figures. Yet twice the shut-in time is required on Figure 25 to produce storage roughly the same size as those of Figure 19. This additional time is a direct consequence of the decreased contrast between injected water temperature and static temperature. The second feature, dependence on surface temperature of injected water, is responsible for the cooler storage signatures on frame A and the warmer ones on frame B.

Shut-in temperature surveys for the two situations are given on Figures 26 and 27. Injecting surveys were not run for the four situations depicted on these figures. At the sensitivity used for the surveys, 1°F/inch or 2°F/inch, the injection surveys would be off scale anyway. In each figure the two frames contrast profiles for confined injection, frame A, with profiles for behind pipe leakage into porous intervals immediately above the injection zone, frame B. On the surveys of Figure 26, the injected water is at or near surface temperature. The resulting storage signatures are therefore cooler than the non-storage areas. The only new feature to these logs is the "nose" evident on frame B, Figure 26, at 2,180 feet, the top of the topmost injection zone. This "nose" is a signature of confinement of injection to depths below its location and is not an uncommon feature in clastic environments. It arises because of the interaction of two conditions: the decreased thermal conductivity of shale rich sediments and the change in direction of heat

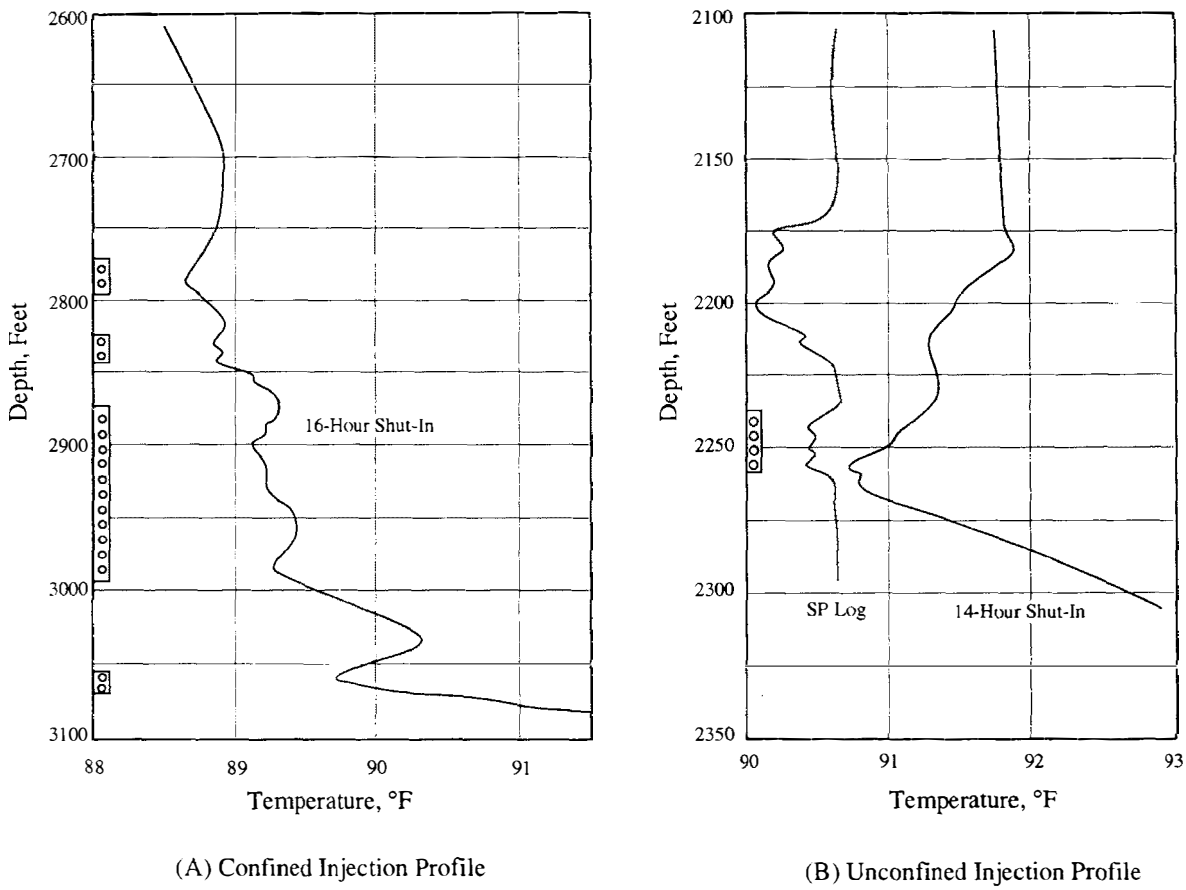

Figure 26. Shut-in temperature surveys for wells injecting near surface temperature.

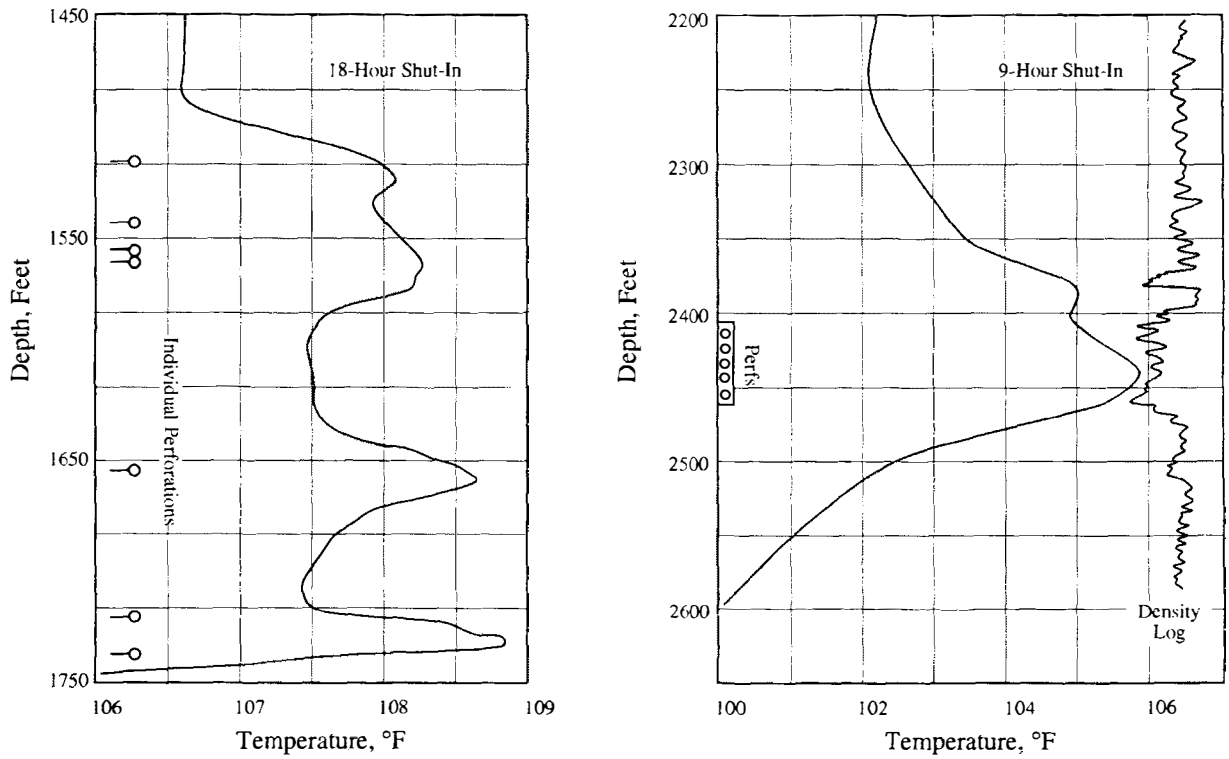

(A) Confined Injection Profile

(B) Unconfined Injection Profile

Figure 27. Shut-in temperature surveys for wells injecting hot water.

flux with vertical depth. Above an injection zone, heat flows to the well bore in a nearly lateral direction whereas this flow acquires a large vertical component at the top of an injection zone. Thus, the vertical temperature gradient must increase accordingly. The rapid change in thermal properties with depth restricts the variation to relatively small vertical intervals, thereby making the "nose" more noticeable in clastics. Like the signatures of lithology and completion, the presence of this "nose" is a matter of proper timing and is not necessarily present on any particular survey. As has already been noted, a "nose" could also be caused by the presence of a fracture, but for different reasons.

The storage signatures on Figure 27 are warm "spots" as the result of water injection at a temperature above surface temperature. These signatures are similar to those already observed on Figure 21, for a deep injector. The warm spots on Figure 27 are smeared more by vertical heat conduction due to longer injection times.

Before leaving related injection well problems, there is a need to discuss two additional reasons for loss in survey resolution besides the digitizing noise illustrated in Figure 3 (page 5). These additional reasons are excessive inertia in the recording system and the practice of logging upward rather than downward. Both are trademarks of the novice operator who does not know how to run a temperature survey, and accordingly, should not be a problem. That these problems

do exist, however, is evident from the surveys on frames A and B of Figure 28, two sets of surveys from the same injection well. Frame A shows an injecting survey at 700 BPD and a 9-hour shut-in survey after injection is stopped. Although both surveys were logged in the correct direction, downward, both show the "stairstepping" characteristic of excessive recording inertia. On an older analog panel this inertia is usually the result of failure to properly set the driving circuit that just overcomes recording pen friction. On a digital truck the stairstepping results from a sampling interval that is too long relative to the logging speed, or, in trade jargon, too large a time constant for the logging speed. Stairstepping can also occur if the display sensitivity exceeds the resolution of the tool. This is clearly not the case for the survey of frame A, Figure 28 because the steps amount to nearly 1/2 degree Fahrenheit! As a consequence of the inertia, the first loss on the injecting survey that can be called "real" is the major loss at depth A, located about midway down the perforated interval. Higher exits are lost in the inertial threshold.

In frame B of Figure 28, the thermometer is jerked off bottom and then moved upward at a constant speed. In this particular situation, such a procedure compounds all errors, those due to stabilization time necessary for the tool to track borehole fluid temperature and those due to mixing of borehole fluid ahead of the sensor. The result is a total loss of injection detail across the perforated interval.

The best of procedures can still produce the kind of temperature log appearing on Figure 29 to the right of the wellbore sketch for an old injection well. These surveys are of the seemingly

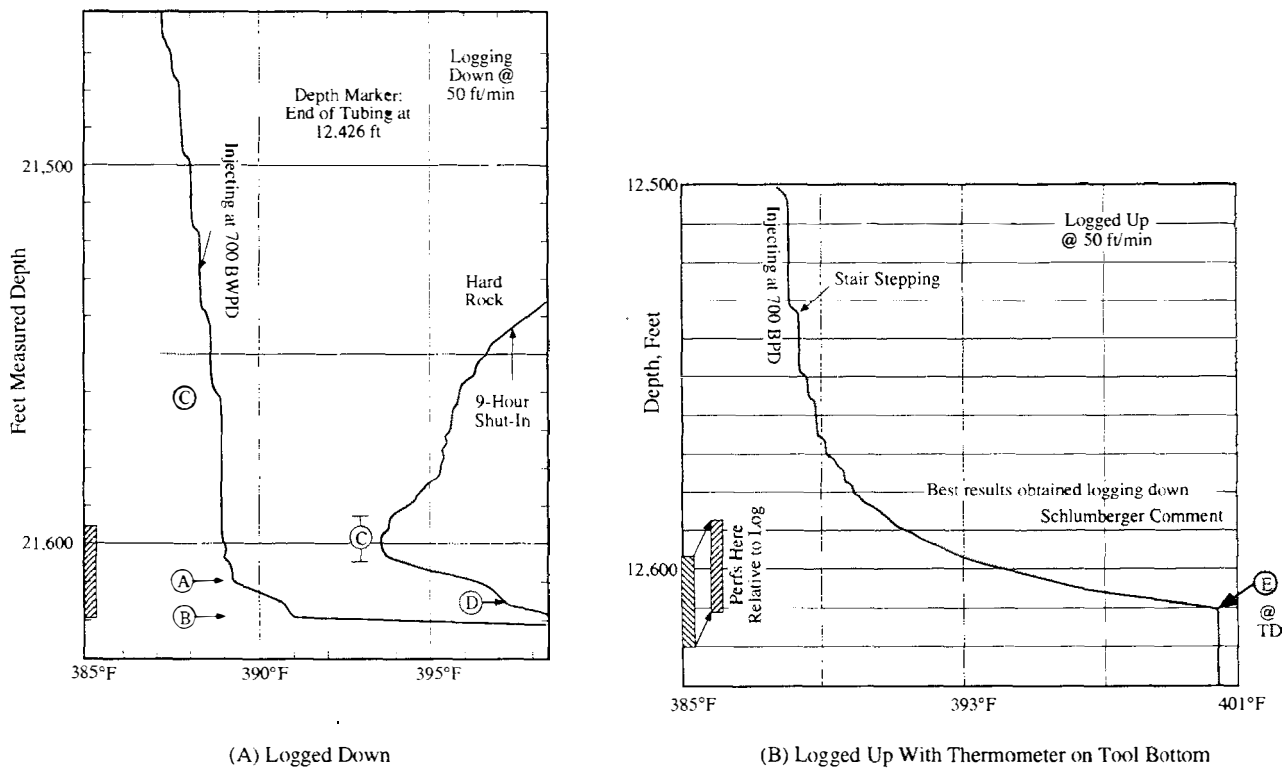

(A) Logged Down

(B) Logged Up With Thermometer on Tool Bottom

Figure 28. Loss in survey resolution due to "stairstepping" (excessive recording inertia) and to logging upward.

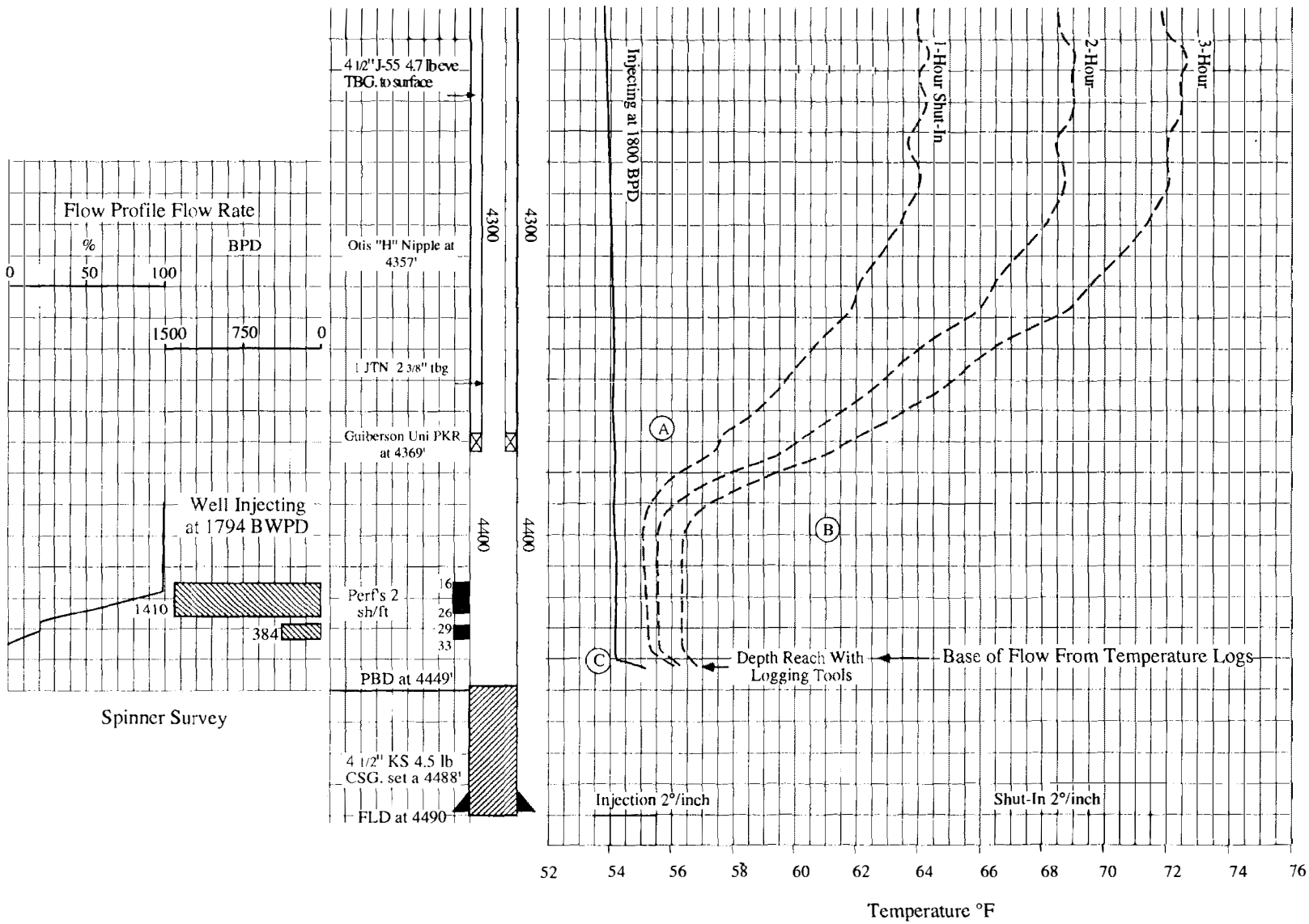

Figure 29. Surveys from an old injection well taking 1,800 BPD water.

"don't tell us nothing" variety. Actually, this is not the case. At depth A, the 1-hour shut-in survey shows the correct response to the completion. Furthermore, this response attenuates with time as it should. With these quality control checks as assurance, we should ask what sort of well conditions can produce the type of surveys we see. First, the injecting survey shows that the majority of the injected fluid reaches depth C, which is seven feet below the deepest perforation. The spinner survey, to the left on the wellbore on Figure 29, shows that 79% of the injected water leaves the wellbore at the top perforated interval. Finally, the shut-in temperature surveys show injection cooling up to depth B, a location some fifteen feet above the topmost perforation. This indicates a fractured wellbore situation, although probably not an intentional condition. The timing of the shut-in surveys is such that the influential storage is in the fracture, not the formation. One would expect a more or less uniform storage in the fracture, which is what the surveys show. The deficiency, thus, lies with the user, not with the tool.

Temperature Signatures For Noninjection Related, Behind-Pipe Flow: An effective cementing operation is more difficult if the wellbore passes through either very depleted or abnormally pressured zones. Cement opposite a depleted zone tends to dewater by filtrate loss to the low pressure zone. The cement then shrinks badly upon setting or fails to set at all in the sense of developing any strength to speak of.

Abnormally high-pressured zones tend to flow into the wellbore in regions where there is premature setting of cement above and below the zone. In this manner, crossflow behind-pipe can be set up before the cement has ever cured. If the cement is weighted too much, then one runs the equally bad risk of fracturing a formation and not being able to even pump cement to the desired height behind pipe. There are well known areas in the U.S. where primary cementing is nearly impossible across certain zones.

Depletion in water zones typically occurs at shallow depths, 1,000 feet or less, as a result of production for municipal, agricultural, or industrial usage. Their locations are generally known before a new well is drilled. Consequently, it is usually the old wells that were not completed so as to cover these zones that pose the major threat to these zones. Even worse, many of these old wells were abandoned years ago!

The mountainous areas of the U.S. are the only locations that have artesian, naturally over pressured water zones at shallow depths. A much more extensive problem is the charging of shallow strata by wells that blow out of control during drilling or by casing leaks in both production wells and injection wells. The first indication of these formations is usually an unpleasant surprise for the driller. Shallow disposal zones, of course, may become significantly over-pressured as a result of years of injection.

Temperature surveys are the most sensitive of the various production logging methods for locating noninjection related crossflow behind pipe in shut-in injection wells or in recently completed wells that are no more than a couple of months old. This sensitivity arises from the fact that these types of wellbores are not at static temperature. Flow into the wellbore region, however, brings its temperature along with it. If this flow is not at true geothermal, it will at least be at a temperature that is different from that caused by injection down the well. Thus,

even during injection, the non-related flow will "clamp" the back side of the casing at a temperature that is constant and different from values elsewhere. This is particularly the case at the source where the flow completely surrounds the wellbore. During injection, the heat transfer at shallow depths from the earth into the water flowing inside tubing that is inside casing typically amounts to only 15 btu/hr per foot of wellbore length. If the noninjection related flow rate per foot of wellbore is designated as q', then the temperature change caused by the 15 btu/hr - ft heat transfer is

$$\Delta T = \frac{15}{\rho c_p q'}, \text{ with q' in cu.ft./hr,}$$

$$\Delta T = \frac{15 \times 24}{62.5 \times 1 \times 5.615} \frac{1}{q'}, \text{ with q' in BPD,}$$

$$\Delta T = \frac{1.03}{q'}$$

A 5 BPD flow from a 10 foot zone, q' = 0.5, will thus only change temperature by about 2°F. Furthermore, this flow will continue once the well is shut-in. After about six hours, the fluid temperature in the tubing string will have almost equilibrated with the temperature of the source zone. Once an injection well that has noninjection related flow behind casing is shut-in, then the wellbore temperature will quickly change to a value reflecting the source temperature at the source depth. It will then change very slowly, if at all, at this location. This behavior, unlike injection related problems, is relatively insensitive to the length of time the well has been on injection. The only planning necessary is to allow sufficient shut-in time for the tubing fluid temperature to reflect conditions on the back side of the casing. Generally, surveys after about 6 hours shut-in will accomplish this.

These ideas are illustrated by the shut-in surveys of Figure 30 that are from a middle eastern oil production well. A shallow, artesian aquifer at depth A is flowing behind pipe down to a lower pressured water zone at depth B. The wellbore temperature at the source depth is at a nearly static value already on the 3-day shut-in and remains at this value. The true perspective of the "injection" from A to B is only evident on the 30-day shut-in survey. This perspective, however, is not necessary to comprehend the nature of the problem.

Frames A and B on Figure 31 show noninjection related flow signatures on single-pass temperature surveys after relatively short periods of shut-in time. Injection zones are below the deepest log depth on the figures so that static temperature lies off scale to the warmer side. In each frame, the shifts toward static are the result of water flow upward behind casing into hydrocarbon formations badly depleted by years of production.

Newly drilled or worked over wells show the same type of noninjection related flow signatures as those from deep injection wells. If no flow occurs in a new well, then three to six months after a well is completed the wellbore fluid is still a degree or so removed from static temperature. The bottom two-thirds of the wellbore is cooler than static whereas the top third is generally warmer.

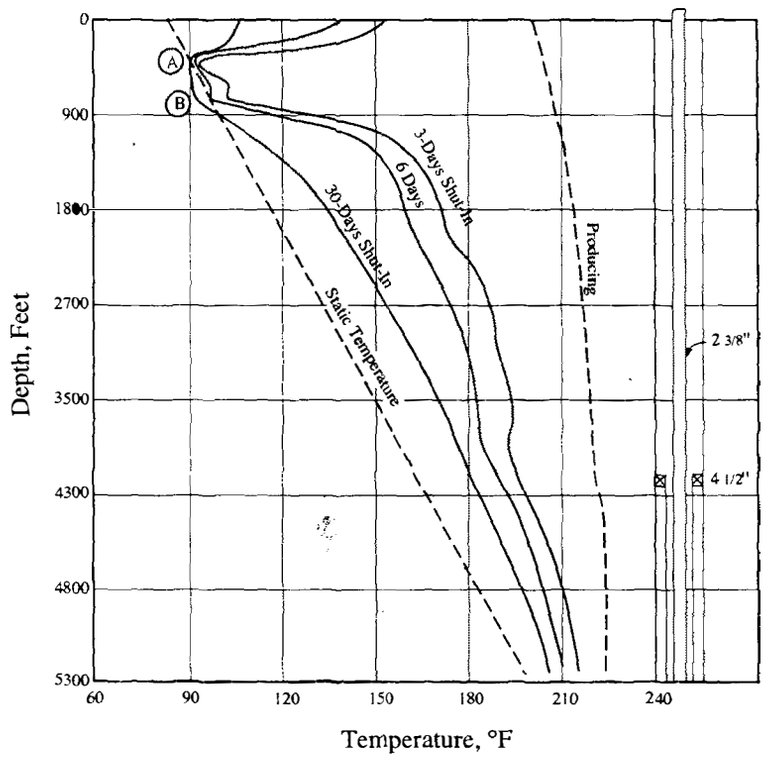

Figure 30. Temperature surveys from an old production well with water flow behind casing from Depth A to Depth B.

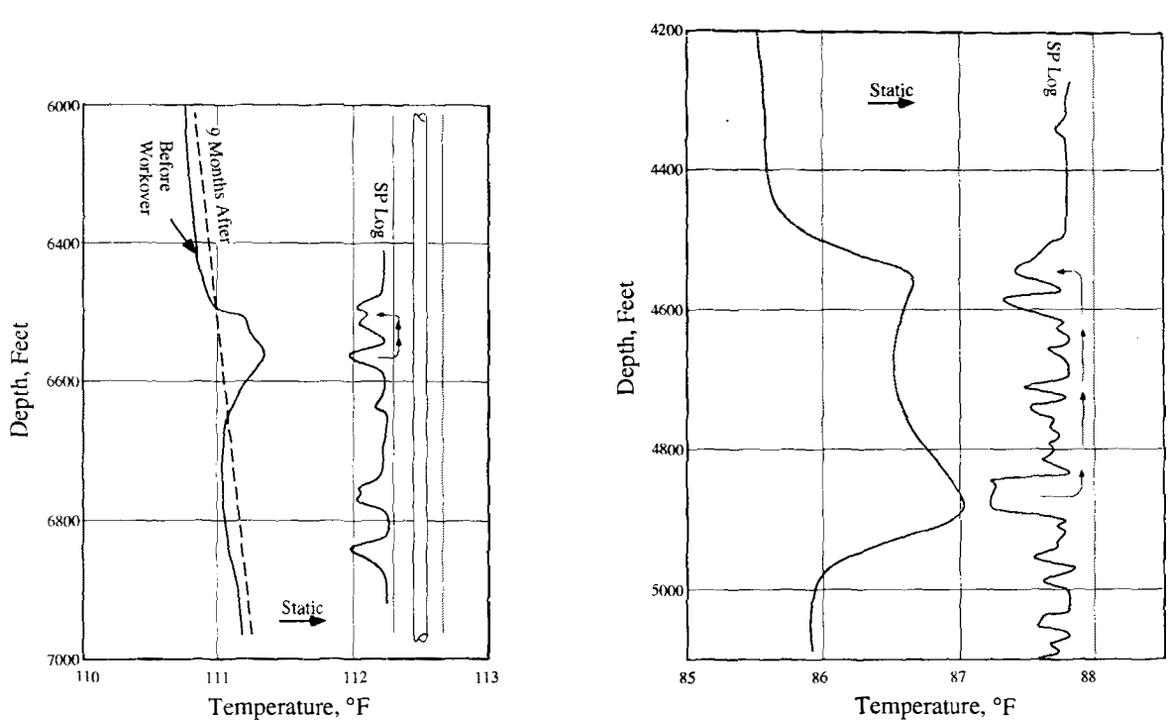

(A) Six-Hour Shut-In Surveys Before and After Workover

(B) 12-Hour Shut-In Survey

Figure 31. Behind-casing water flow into depleted hydrocarbon sands penetrated by wells with deeper injection zones.

This profile is the residual from the relatively long period of mud circulation during the drilling operation. Any flow to the wellbore counters this residual and shifts the wellbore temperature towards static conditions.

This type of behavior is shown on the temperature surveys of Figure 32. Frame A on this figure contains a curve labeled curve-1 that is a survey at a sensitivity of 2°F/inch from a one-month old well that has not yet been perforated for production in the formation whose top shows on the gamma ray log at 8,140 feet. Oil flow into the vicinity of the wellbore is clearly evident on the log by the warming behavior at depth A, 8,150 feet. Furthermore, the log shows that this oil flows upward behind pipe to depth F, 7,976 feet. Numerous losses, presumably to fractured zones known to exist in the 174-foot crossflow interval, are indicated by labels B through E. The validity of these signatures can be judged by the noise-free character of the survey on either side of the crossflow interval. The heating over the entire interval is a result of the wellbore still being cooler than static temperature in those areas free of flow to the wellbore. A six-foot interval was perforated on either side of 8,150 feet and the zone was tested. Wide open, it would only flow 94 BPD of oil. The leak rate recorded on frame A of Figure 32 can then be no more than 10 to 15 BPD based on the maximum pressure drop available over a 174 foot column of oil replacing water.

Once the completion tested oil, the well was killed in preparation for a workover. One day after the kill, another logging company ran the temperature survey appearing on frame B of Figure 32, this time at a sensitivity of only 4°F/inch. Moreover, stairstepping is evident in the trace for temperature at the locations marked by arrows. The quality of the record is so poor that only the gross crossflow interval from depth A, 8,152 feet, to depth C, 7,959 feet, is evident along with the one major loss at depth B, 7,991 feet. The intermediate losses evident on frame A, cannot even be detected on the differential trace of frame B. The response of the differential trace at the source depth A, 8,152 feet is also of interest. The temperature curve shows that this response is due to a rapid <u>two degree</u> Fahrenheit decrease in temperature below depth A. A comparison of this differential response with that on Figure 2 (page 4) at depth B, the location of rapid <u>one-half degree</u> temperature increase, shows how easily quality control is lost if diligent control is not maintained.

The preceding examples show that the only new feature in the use of temperature surveys to detect noninjection related flow behind pipe is the reliance on shut-in surveys alone. It is wise to have at least two run at shut-in times in the range of 12 to 36 hours. Use of such a timed sequence makes it possible to detect leaks that amount to only a few barrels a day. As we have pointed out, this sensitivity is a consequence of the well not being at static conditions when logged.

In regard to this sensitivity, the influence of lithology is usually greater at shallow depths due to increased variation in thermal properties. Furthermore, shallow sands that are on production near a given well often flow past the well at a drift velocity sufficient to add their signature to a shut-in temperature survey from the well. Consequently, it is a good practice to log a well in a given area purely for background data.

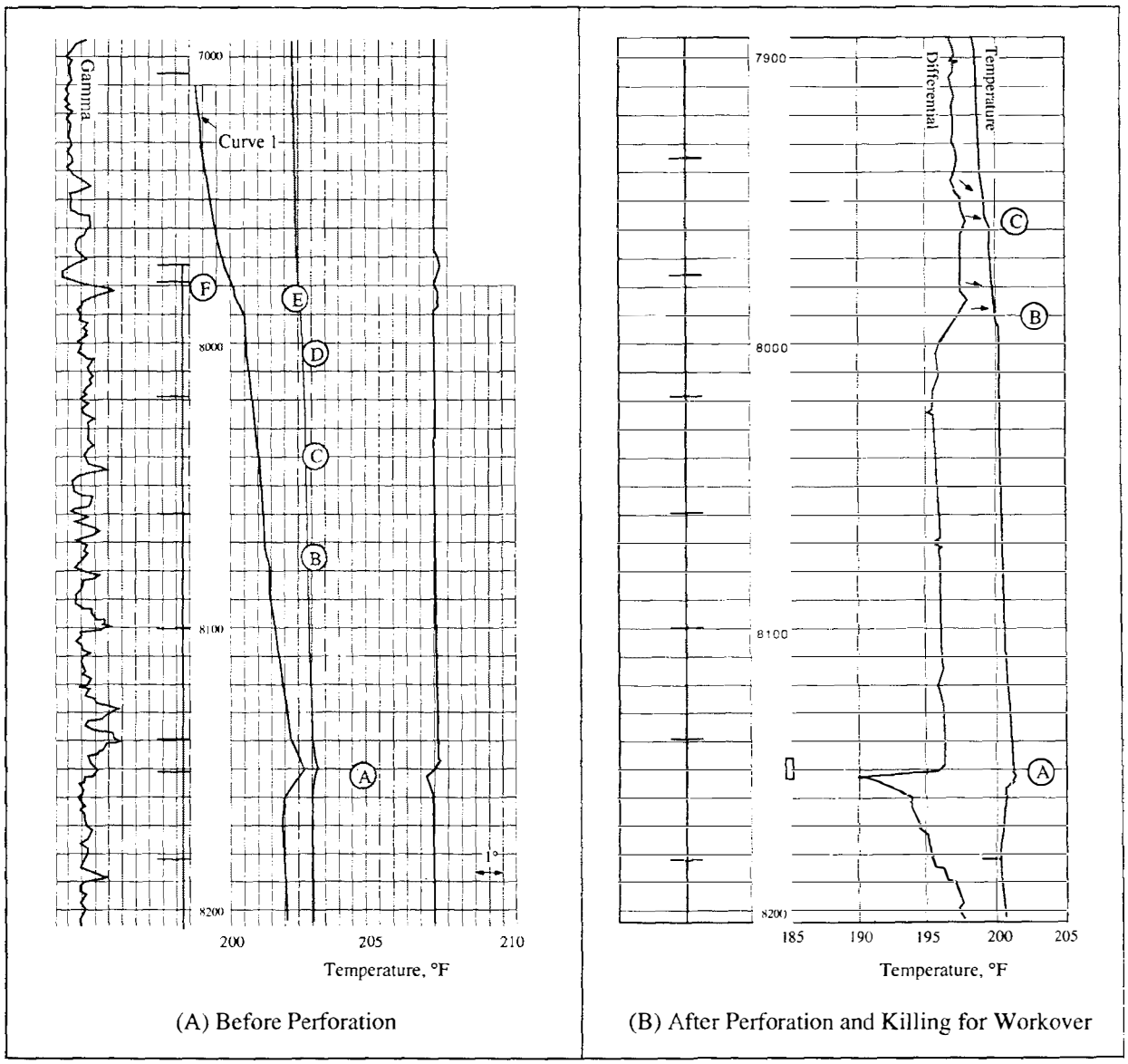

Figure 32. Behind-casing crossflow of liquid (oil) in a new well still slightly cooler than static temperature.

Logging for Lithology Influence: The next sequence of temperature surveys illustrate a logging sequence that was run during the first day of operation of a new injection well at a low enough injection pressure to insure water entry only into the depleted zone that had been perforated for water flooding. The logs were run as a reference for the influence of lithology because the well penetrated a potpourri, as evidenced by the lithotype labels appearing on the left-hand side of Figure 33. This mix clearly influences the short shut-in time surveys shown on the right of the figure. From the top, there is the tendency of the shale above A to lag the sand at B in recovery. The sand, in turn, lags the siltstone in the interval below C. Further, the carbonate section between D and E has a temperature survey reflecting the porous and non-porous pattern of the SP and gamma ray logs. The completion influence is seen at depth F. Finally, the carbonate

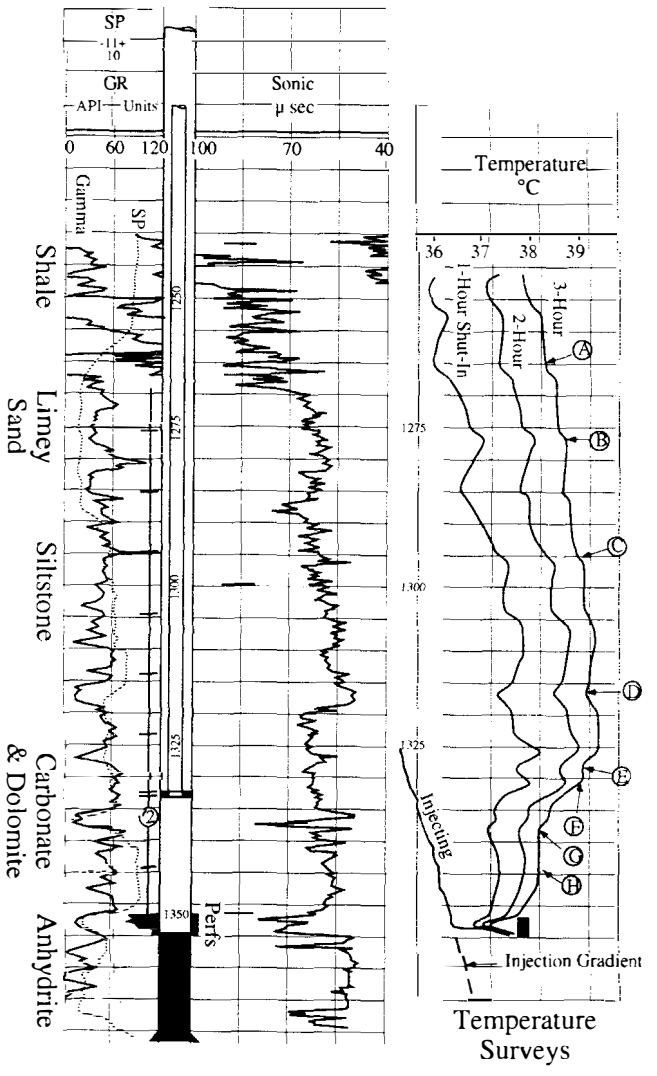

Figure 33. Temperature logging a new injection well for lithology signatures.

porosity is again reflected in the interval GH below the tubing packer. Because of limited daylight in the winter, the three shut-in runs are about one day's work in themselves. Consequently, the base information continued in Figure 33 is essential to any interpretation of injection confinement on future surveys. In particular, the next zone up, zone 2 on Figure 33, had already been charged by leaks in older injection wells in other parts of this field.

This last example ends the discussion, formally at least, of temperature logging and leads to the second tool, the radioactive tracer logger. This tool is the most sensitive instrument for the detection of fluid movement inside and immediately outside of pipe. Fractional barrels per day of movement can be detected outside pipe provided it can be tagged and then pumped behind the casing. Fortunately, the significance of a radioactive tracer survey is generally easier to

comprehend than that for a temperature survey. Consequently, the associated discussion will be much briefer. Ease of interpretation, however, should not be confused with "correctness" of interpretation. The tracer tool has its own peculiarities and limitations that must be appreciated to use it effectively.

Radioactive Tracer Surveys

The radioactive tracer tool is a direct consequence of the widespread availability of radioactive isotopes that accompanied the growth in atomic physics research in the United States. An enormous surge in the application of tracers to tag materials occurred in the late forties and throughout the fifties as the operation of particle accelerators produced these materials in quantity. The high resolution provided by "radio-assay" was, of course, already well known at this time. The advantage of the gamma ray as a non-destructive tag that could be detected external to the host was also clearly established. Furthermore, the increased usage of the natural gamma ray logging tool for formation evaluation soon showed that the underground environment was also not excessively radioactive.

Most of the activity underground results from the decay of natural isotopes of potassium and thorium with some support added by uranium. Shales, where these materials concentrate, typically register about 100 API units on a gamma ray log. This activity amounts to about 6 microcuries per ton of material, an exceedingly low concentration in view of the fact that most radio assaying methods employed this amount of activity in grams of material.

The earliest use of the radioactive tracer method was to tag water so as to follow the injection of this water into open-hole completions. The tagging material was added to the water at the surface and a gamma ray logging tool, i.e, a Geiger-Muller ionization tube, was used to track the movement downhole. By the early fifties, the self-contained tool that carried its own source of tagging material had evolved.

The most widely used tagging material for water is an aqueous solution of sodium iodide, NaI, containing the isotope of iodine I-131. The decay of this isotope produces, in addition to beta particles, gamma radiation 80% of whose energy is in the 0.3 - 0.4 million electron volt range. The half-life is ideal at 8.05 days. Furthermore, in solution the iodine is a negative ion, I^-. As such, the material is not absorbed on rock surfaces which tend to be electronegative. It, thus, can be pumped into porosity and away from the wellbore out of range of the tool.

The fact that 90% of the gammas registered by a tracer tool originate from within a foot of the detector is also one of the limitations on the method. It, like all nuclear logging tools, has limited depth of investigation.

On the positive side, the tracer tool is the highest resolution flowmeter available. With this tool, vertical speeds as low as 2 feet per week can be detected. Moreover, it is the only absolute flowmeter available. The British hydrodynamist, G. I. Taylor, showed in 1954 that if a slug of tagged water is mixed uniformly over the cross section of a pipe, then the centroid of the material subsequently moves with the average or superficial velocity of the stream, $\hat{v}$. Timing the

movement of a tracer slug produces a number for $\hat{V}$ which can be converted to the volumetric rate by multiplication by the cross-sectional area of the pipe, A:

$$q = A\hat{V}$$

No calibration factor is involved for either laminar or turbulent flow. Tracer determined velocities are typically measured in units of feet per minute so that the above equation gives cubic feet per minute with A expressed in square feet. In terms of barrels per day, the expression becomes

$$q\ (BPD) = 256\ A\hat{V} \qquad (3)$$

A = Cross-sectional area, ft^2

$\hat{V}$ = Average velocity, ft/min

Before further comments, the features of the modern tracer tool must be examined.

Modern Radioactive Tracer Tools: The schematic of a 1 3/8 -inch diameter tracer tool is shown in Figure 34. The assembly consists of two tools, a reservoir and pump section at the top and a detector section at the bottom made up of two gamma sensors and the associated circuity necessary to amplify and transmit the detector counts. In the figure, a casing collar locator, CCL, is placed between the two detectors. The resulting five-foot spacing between the detectors is fairly typical in domestic use. It is also not unusual to find a temperature sensor of the type described on page 2 at the bottom of the tool. In fact, all companies can run the thermometer with the tracer tool.

The reservoir section contains tagged field brine that is ejected in discrete volumes into the wellbore by a positive displaced piston driven by the electric motor shown on the figure. The amount displaced into the wellbore on a given "shot" depends on how long the operator activates the electric motor. A normal shot displaces about 1/100 of the reservoir volume, but the operator can displace the entire reservoir in one step if he so chooses. A particular tool may have one, two or four ejection orifices spaced around the tool barrel at the top of the reservoir. The orifices are plugs that can be removed for loading the reservoir at the surface. The more ejection ports the better the mixing of each shot with wellbore fluid.

At the surface, a concentrated aqueous solution of sodium iodide containing about 5 microcuries of I-131 is diluted with about one pint or 500 CC's of field brine in a metal syringe, the discharge end of which can be threaded into a hole in the tracer tool that normally contains an ejection orifice. Although sanitary, this method of loading traps air in the reservoir. This air is purged in the bottom of the hole prior to any logging operations.

A normal "shot" from a 100-shot tool will typically contain about 0.05 microcuries of I-131. In the immediate vicinity of a detector capable of such a response, this concentration would correspond to some 150,000 API units of activity which is 1,500 times background, even in

shales. It is therefore no surprise that the tool can detect even minute flows behind pipe so long as the tagged fluid is in the near vicinity of the well.

Two detectors are present on the tool of Figure 34. This is done in order to minimize timing errors whenever the tool is used for stationary measurements of fluid velocity. If the slug is timed as it goes past each detector, then the exact time of ejection from the reservoir is not required for a velocity determination.

Early versions of the tracer tool invariably used Geiger counters as gamma ray detectors. The modern trend, however, is to the use of scintillation crystals due to their higher sensitivity to gamma radiation and to their ability to measure radiation intensity as well as the number of incident gammas per unit time. These tools are likely to have only one detector.

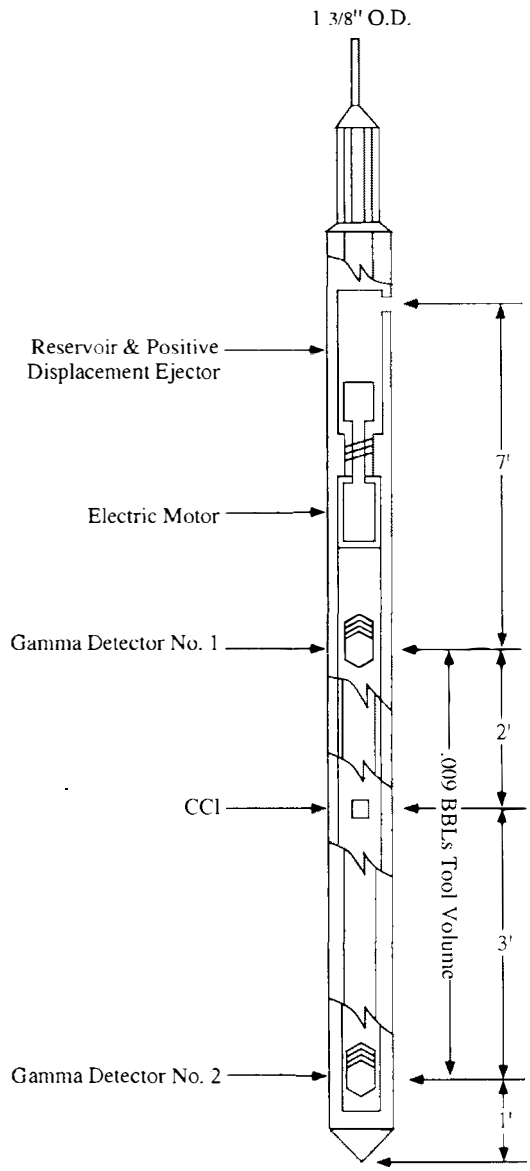

Figure 34. Schematic of a radioactive tracer tool for injection logging.

Tool Resolution: The proficiency of a gamma detector is important at both high and low count rates. A scintillation crystal is superior to a Geiger counter on both ends of the scale for gamma detection. A Geiger counter is basically a particle detection device. The passage of, say, an alpha particle through the low pressured gas in the tube ionizes the gas so a pulse of current can pass between electrodes. Gamma rays, however, being devoid of mass, are inefficient ionizers. This inefficiency establishes the low count rate threshold. Once the tube pulses, then time is required for the ions to neutralize before the next pulse can occur. If this "down time" is denoted by t seconds/count, then the count rate, C_i, registered in response to a true rate C_t is:

$$C_i = C_t - C_t \times C_i t$$

$$\text{or} \qquad C_i = C_t (1 - C_i t) \qquad (4)$$

The "down time" for an ionization tube is of the order of one-third of millisecond, i.e., $t \approx 3 \times 10^{-4}$ seconds; thus, at a true count rate of $C_t = 500$ cps, equation (4) gives an indicated count $C_i =$ 435 cps, a 13% error. Consequently, the tubes are usually employed in bundles of several tubes so that at least one tube can be active at any given time.

As already mentioned, a normal shot contains about 0.05 μc (microcuries) of I-131 in about 5 grams of diluent. One curie, by definition, gives 3.7×10^{10} disintegrations per second; therefore, an unmixed shot can generate a count of $C_t = 3.7 \times 10^{10} \times 0.05 \times 10^{-6} = 1{,}850$ cps. Given dilution on ejection and counter inefficiency, the actual value is closer to 1,000 cps. The previous calculations by equation (4) showed that this is an excessive count rate for a single Geiger tube.

A scintillation crystal, on the other hand, has no such rate limitation because its "down time" is essentially zero. Furthermore, even a very low energy gamma incident upon the crystal will excite the emission of a pulse of light whose intensity is directly proportional to the energy level of the gamma. The light pulses are amplified in number by photomultiplier tubes to give an extremely sensitive detector. A crystal, however, is far more delicate and "temperamental" than an ionization tube. Consequently, Geiger counters remain in widespread usage on tracer tools.

In summary, a tool that records satisfactorily its own gamma ray log at a sensitivity of 40 API units per inch has plenty of resolution for radioactive tracer work. Geiger tube devices may be non-linear at high count rates, however.

Tool Specifications: The dimensions appearing on Figure 34 clearly illustrate a tool much longer than the temperature logger. The entire assembly typically runs about 15 feet in length with collar locator and temperature probe. If the tool is to pass into a liner, then centralizers must also be attached. This adds another 5 feet of tool. The tool diameter may therefore become the critical factor in the use of the tool. Fortunately, the same diameters are available for this tool as those listed for the thermometer, as small as 7/8-inch and as large as 1 11/16-inches. This range includes devices with scintillation detectors as well as with Geiger counters. As with the thermometer, a popular size is the 1 3/8-inch tool shown in Figure 34.

Temperature and pressure ratings are also comparable to those for the thermometer. The main difference is in the increased length of tool before sinker bar addition. The use of a single detector tool will reduce the length by 5 to 6 feet.

Logging Procedures: Logging with the radioactive tracer tool is done in two ways, both of which may be used on any given job. One way is to eject a "shot" of tracer into the injection stream and then record the location of the slug with time by successive gamma ray intensity surveys, or "drags," of the wellbore. This depth-mode logging is usually called a slug tracking procedure. It affords one a quick and easily understood picture of where the injected water is going. This fact is illustrated by the surveys on Figure 35 for a well on injection at about 600 BPD brine into a single set of perforations. For this record, a slug of tagged brine was ejected at 9,510 feet with the well on injection; then eleven successive surveys of gamma ray intensity, records A through K, along the wellbore were recorded, in this case, by the bottom detector. Each record or drag was made by the operator quickly dropping the tool until the detector passed

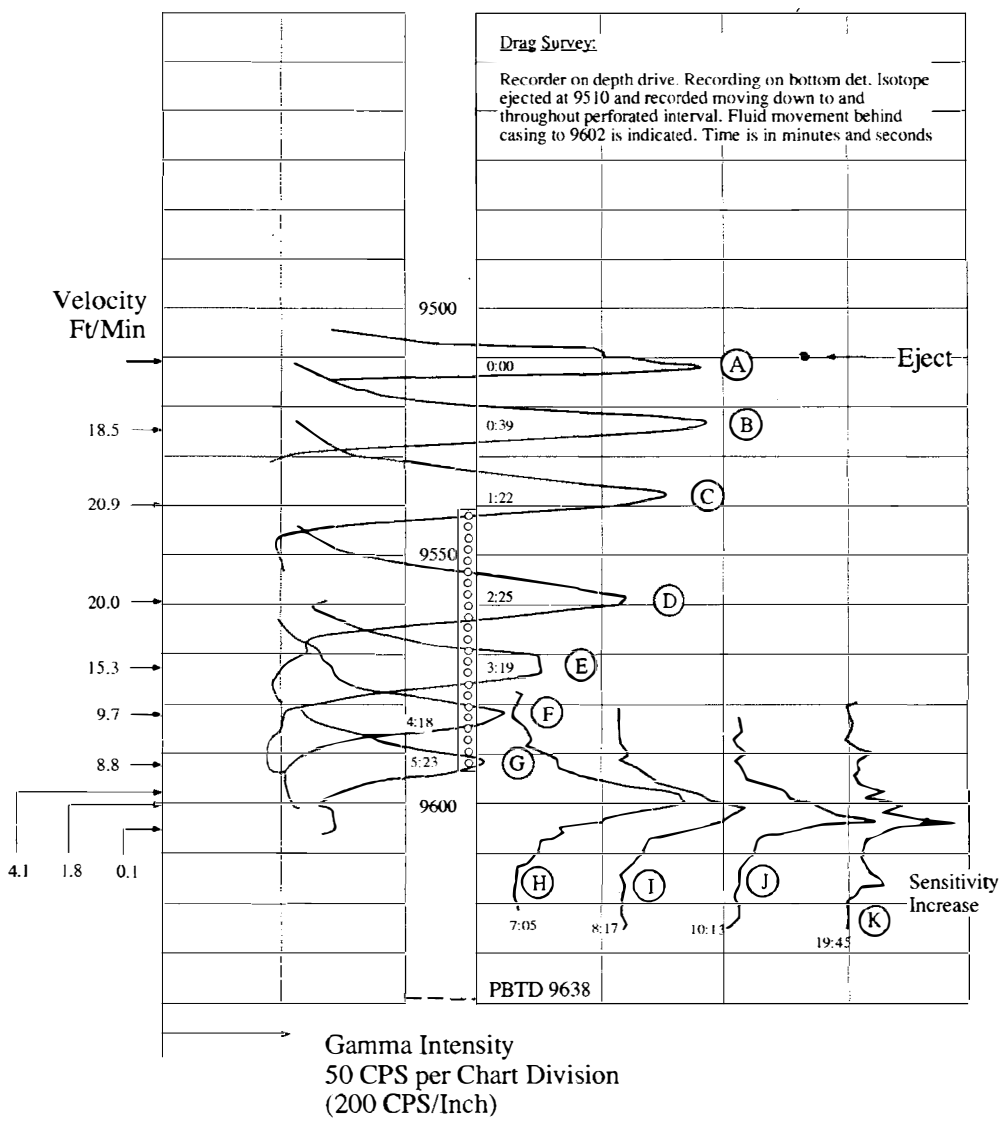

Figure 35. A radioactive slug tracking record from a well on injection at about 600 BPD water.

through the slug and then logging back upward at constant speed with the recorder on depth drive. As the detector records through the maximum or peak activity, the operator notes the corresponding time. These times are listed on the figure as minutes:seconds at the depth of maximum activity. The numbers start at 0:00 at the peak for drag A, and increase to 19:45 for drag K. The operator adjusts his logging speeds so as to "catch" the slug at 10-20 foot intervals in the full flow stream above the perforations. As the slug moves down the wellbore, even before reaching the perforations, it spreads vertically and drops in peak amplitude accordingly as a result of mixing by flow turbulence and by the movement of the logging tool through the slug two times for each drag. A visual inspection of the slug "size" alone is enough to show that practically all the injected fluid makes it to depth D, 9,560 feet, before leaving the wellbore. All the injection thus occurs over the bottom half of the perforated interval. The final survey, K, shows that some of the water has flowed all the way down to 9,605 feet, some twelve feet below the bottom perforation. In order to place the location of this flow, inside or outside pipe, the operator ejected another slug at 9,604 feet. The two logging runs on Figure 36 overlay, showing that this slug remains at the ejection depth. Therefore, the flow revealed on drags H through K is behind casing.

The slug tracking technique offers a clear picture of what is going on in and immediately around the wellbore. But, as a flow profiling technique, it obviously has poor vertical resolution. The second method of tool use overcomes this deficiency. First, however, it should be mentioned that operators are historically negligent in recording the detector sensitivity employed in surveying. The log heading stated that the drags on Figure 35 were recorded at a gamma sensitivity of 200 counts/sec per inch of chart, yet the operator apparently increased the sensitivity for the last survey, drag K. The activity of the storage spike in the perforation at 9,590 feet has increased from the previous survey even through 9 1/2 minutes of injection ensued! In fact, the operator may have increased sensitivity from survey I through K.

The second way the tracer tool is used entails stationary measurements of travel times between two detectors. To conduct such a velocity shot, the operator positions the tool so as to place the detectors at chosen locations, turns his recorder to time drive at a speed of anywhere from 1/2 inch of log per minute to 10 inches/min, and turns on both gamma detectors; hopefully, both at the same sensitivity. He then ejects a slug of tagged brine into the moving stream and continues the record until the slug passes both detectors. The resulting travel time between detectors of known spacing is an inverse velocity measurement that is free of lag error between the "firing" at the surface and actual ejection downhole.

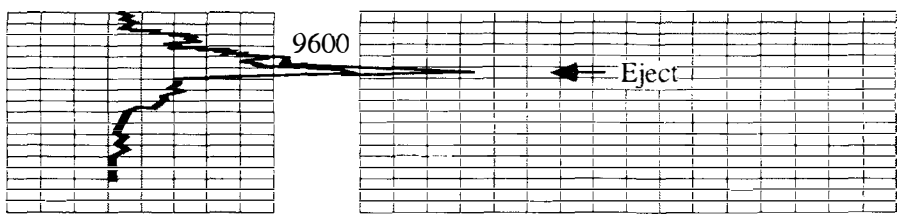

Figure 36. Slug tracking (2 surveys) below the perforations of Figure 35 well.

Figure 37 shows a velocity shot taken above the perforations in the well of Figure 35, a well on injection at some 600 BPD. The two detectors on this particular tool are spaced 5.5 feet apart. The left-hand trace is the output of the bottom detector, positioned at 9,505.0 feet, whereas the right-hand trace is from the top detector at 9,499.5 feet. The recorder is on time drive at a nominal speed of 1 inch/minute. With 10 vertical log divisions per inch, the nominal vertical scale is 60/10 or 6 seconds per chart division. A calibration, however, gave 23.5 chart divisions in two minutes of time. The vertical time scale is therefore 120/23.5 = 5.1 seconds per chart division. The ejected slug arrives first at the top detector, the maximum activity, point A, appearing some 3.5 chart divisions after the ejection marker. The maximum intensity at the bottom detector, point B, arrives later after some 6.2 chart divisions following the eject mark. The difference between arrivals A and B can be measured directly at 2.7 chart divisions without reference to the ejection marker. This, of course, is the advantage of the dual detector tool. This difference represents a nominal travel time Δt = 2.7 cd x 6 sec/cd or Δt = 16.2 seconds over 5.5 feet. In view of the calibration, the actual travel time is Δt = 2.7 x 5.1 = 13.8 seconds, a value some 14 % lower than nominal. This travel time is representative of the full flow stream and is customarily used only as a reference for subsequent shots within the perforated interval. Consequently, the speed calibration of the chart drive is often omitted and only the nominal speed, 1 inch/minute in this case, is listed. Actually, this speed is too slow in the case of Figure 37. A drive speed of 5 inches/minute would have been more appropriate as this would have separated points A and B by some 14 chart divisions and would have allowed a more accurate evaluation of travel time.

The timing of the difference in peak values illustrated in Figure 37 is the most commonly used of five different ways that have been proposed. All five are illustrated on Figure 38. On this figure,

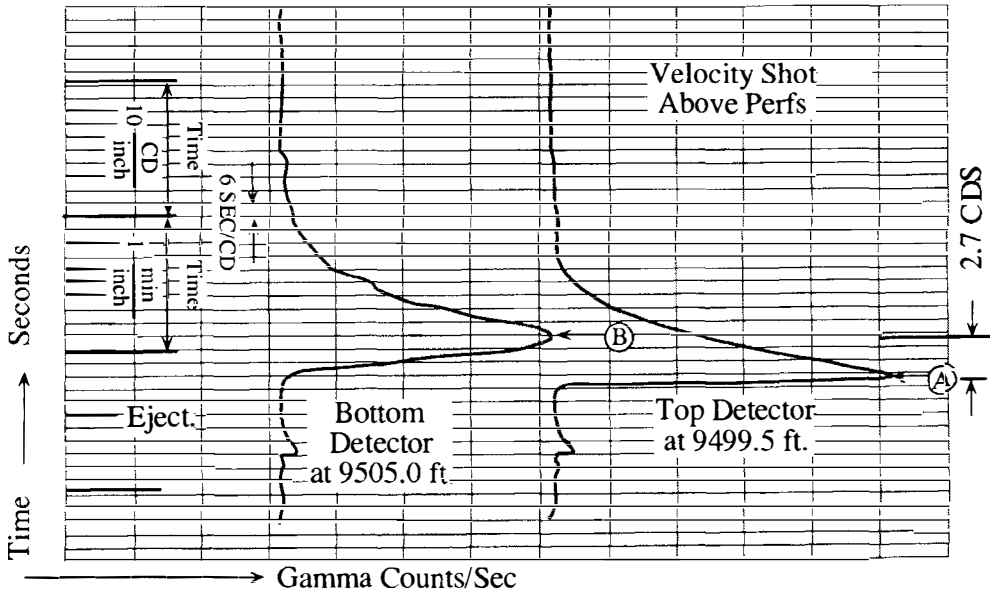

Figure 37. Velocity shot record above the perforations of the Figure 35 well on 600 BPD water injection.

the peak time is designated by point 2 and as method #2. The obvious ambiguity in the location of this point on Figure 38 is eliminated by the peak "shaping" procedure that locates point 3 by the intersection of the dashed lines on the figure. These lines are the tangents at the inflection points to the leading and the trailing edges of the pulse in activity. The remaining three methods of timing utilize "first arrivals" which are, necessarily, faster than peak travel times. If the leading-edge tangent line is continued to its intersection with the base line, then the resulting point 1 defines a "first arrival" that is independent of tool sensitivity. This is obviously not the case when one tries to locate point 5 as the "first" point at which the gamma ray activity exceeds the base line activity. Whenever the leading edge of the pulse is very sharp, as at the top detector in Figure 37, points 1 and 5 will coincide. Finally, there is a so-called "half-peak" arrival time that is determined by the intersection with the leading edge of the pulse of a line parallel to the base line and passing through a point at one-half the maximum or peak amplitude. This procedure gives point 4 on Figure 38. The intersection with the leading edge occurs near the inflection point, as Figure 38 demonstrates.

The five timing points are marked in Figure 39 on each of the pulses from Figure 37 and the corresponding travel times in chart divisions are tabulated. As the table shows, the "eyeballed" or estimated first arrival are usually the least reliable whenever the sensitivity is such that the pulses do not "peg" the recorder.

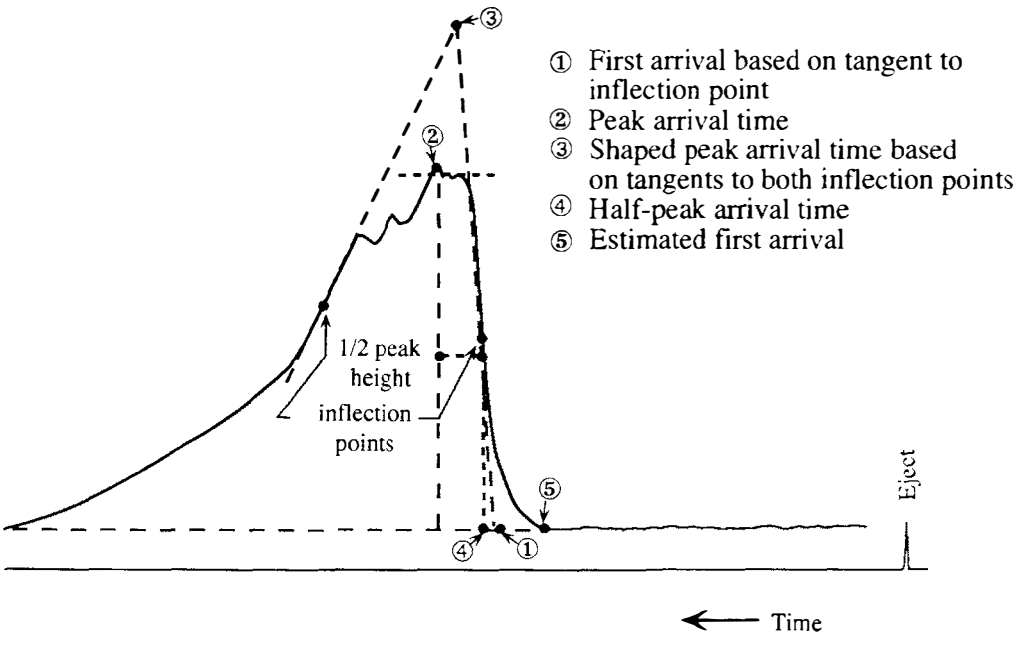

Figure 38. Five methods for timing the travel of a stationary velocity shot.

TRAVEL TIMES, Δt CHART DIVISIONS, FOR Figure 39 POINTS

Point	*Method*	*Δt*
2	Peak Arrival	2.7
3	Shaped-Peak Arrival	2.5
1	Inflection First Arrival	1.0
4	Half-Peak Arrival	1.0
5	"Eyeball" First Arrival	0.5

For pulses of the quality of those on Figure 39, nothing more complicated than peak travel times is necessary. As the pulses become more dispersed, one can usually get by with the peak shaping approach. Once the pulses have become very "strung out", at very low rates for example, then about the only consistent approach is the half-peak technique. The same method should, of course, be used for all velocity shots on a given survey.

However timed, the stationary, velocity-shot technique allows the vertical resolution to be controlled by the amount the tool is moved in the well between "shots." This is the only way that one can survey sets of perforations that are spaced twenty or less feet apart and retain any quantitative vitality. Likewise, the method is required when detailing within a short perforated interval.

The velocity shot is, however, an instantaneous sample of, typically, 30 seconds or less duration. As such, the resulting travel times are much more sensitive to rate fluctuations than are the tracked slug surveys of the type shown on Figure 35. Because the latter method samples more wellbore in a given time interval, various drags are more likely to share a common rate of injection. In the velocity shot method, it is good practice to replicate near the end of the survey some of the shots done early in the survey.

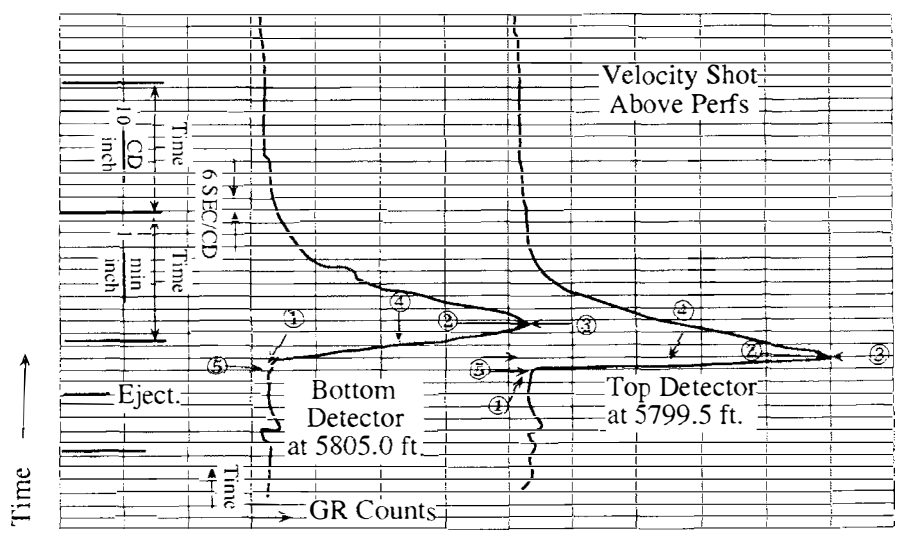

Figure 39. Location of five timing points on the records of Figure 37.

Figures 35 and 37 are demonstrations of the observation that both slug tracking and velocity shot procedures are usually employed on any given job. A lot of record is collected; consequently, it is very helpful to have a section of the log devoted to listing where and at what time each ejection occurred, the size of the shot, and the sensitivity at which it was recorded. Because this is seldom done, one has to assume that the sequence of operations proceeded from the bottom of log to the top in order of shot number.

Finally, recommended recording sensitivities are listed in Table 4. The scale common to all service companies is the API units/inch since the actual counts/second per inch will vary from company to company. Thus, the values in the table are keyed to normal gamma ray log sensitivity of 40 API units/inch.

TABLE 4. SUGGESTED GAMMA RECORDING SENSITIVITY FOR RADIOACTIVE TRACER TOOLS WITH 5 μC TOTAL CHARGE OF IODINE-131 IN WATER

Purpose of Record	API Units/Inch
Gamma Ray Log for Depth Control	40
Detection of Behind-Pipe Flow	200
Flow Profiling Inside Pipe	1000

This table states that the response to shots ejected to detect flow behind casing should be recorded at about one-fifth the sensitivity used for gamma ray logging. This choice keeps in perspective that small amount of tracer that can be squeezed behind pipe in almost any well. Likewise, the response to shots ejected to track flow inside pipe can be recorded at about one twenty-fifth normal API sensitivity. This level allows the slug to be recorded without "pegging."

The remaining "sensitivity" is the chart speed used when a stationary velocity shot is recorded. As the shot on Figure 37 illustrates, it is easy to lose precision in timing if the chart drive is too slow. The recording speed, S, should be adjusted according to fluid velocity so as to space the peaks from the two detectors about 5 - 10 chart divisions apart. If the spacing between detectors is L feet, then the number of chart divisions is approximately given by:

$$\text{No. CD's} = 10\,\frac{SL}{\hat{V}} \qquad (5)$$

$$\text{No. CD's} = 5 - 10$$

If 10 chart divisions are chosen, then Equation 5 gives the necessary chart drive as:

$$S = \frac{\hat{V}}{L} \qquad (6)$$

S = Time-drive speed, in/min
$\hat{V}$ = Fluid velocity, ft/min
L = Detector spacing, ft

For example, the water velocity associated with the shots on Figure 37 is about 20 ft/min and the detector spacing is 5.5 feet so that equation 6 gives

$$S = \frac{20}{5.5} = 3.6 \text{ in/min}$$

With available speeds of 1/2, 1, 2,5, 10 inches/min, one would therefore select a speed S = 5 in/min rather than the 1 in/min actually used on Figure 37.

With these procedural details out of the way, a more detailed look at what the surveys mean is in order.

Injection Profile from Slug Tracking: Please refer to the slug tracking survey contained on Figure 35. This survey showed that most of the injection left the wellbore over the bottom half of the 52-ft long perforated interval. The injection will now be profiled in more detail.

There are two ways that slug tracking surveys are used to profile flow. Both ways assume that the slug of tracers is uniformly mixed over the cross sectional area of the casing when ejected so that equation 3 relates the volumetric rate to the apparent slug movement. Some operators, immediately after ejecting a shot, will work the tool through the slug a few times before starting the logging operation. Others do not bother, as was the case with the operator who ran the survey of Figure 35 (page 50). The bifurcated shape of the slug recorded on drag A shows that it was not well mixed over the cross section. Furthermore, the "size" of the slug recorded on drag A is less than that recorded on the next pass, drag B. When drag A passed through the slug, most of the tracer material was on a side of the pipe away from the tool. The operator is depending on fluid turbulence and subsequent logging runs to mix the slug.

Slug Timing: The more common of the two profiling methods makes use of the peak location-time data on Figure 35 to calculate velocities for each drag after the first. Slug A is located at 9,512 feet when the clock was started. On drag B the peak had moved to 9,524 feet and 39 seconds of time had elapsed on the clock. Thus, the apparent velocity between these depths is

$$\hat{V} = \frac{(9524 - 9512)}{39} \times 60 = 18.5 \text{ ft/min}$$

In a like fashion, the velocities of slugs C through I are determined in the table below and listed on the left-hand side of Figure 35. Incomplete mixing has only minimal influence on the timing

of slugs over a twelve-foot interval. Consequently, the average velocity for slugs B, C, and D can be taken as representative of the full flow stream, i.e., for 100% injection rate the velocity is

$$\hat{V}_{100\%} = \frac{1}{3}(18.5 + 20.9 + 20.0) = 19.5 \text{ ft/min}$$

The variation in these numbers can be the result of either timing errors or actual rate fluctuations. Common practice assigns the percent flow for a particular drag to the midpoint depth of the interval between it and the preceding drag. Thus, the 100% point for drag B is assigned to a depth of :

$$9{,}512.0 + 12/2 = 9{,}518 \text{ feet}$$

This is an arbitrary practice that would be in error even if the only loss in the interval occurred at exactly the midpoint depth!

TABLE 5. SLUG TRACKING DATA FROM SURVEYS ON FIGURE 35

Drag	Peak Location	ΔL Ft.	Δt Sec.	$\hat{V}$ Ft./Min.		% Flow in Well	Interval Mid-Point
A	9512.0	---	---	---		100	---
B	9524.0	12.0	39	18.5		100	9518
C	9538.3	14.3	43	20.9	19.5	100	9531
D	9559.2	20.9	63	20.0		100	9549
E	9573.0	13.8	54	15.3		78	9566
F	9582.5	9.5	59	9.7		50	9578
G	9592.0	9.5	65	8.8		45	9587
H	9599.0	7.0	102	4.1		0	9593*
I	9601.2	2.2	72	1.8		0	

* Base of Perforations

The numbers in the above table are graphed on Figure 40 and indicate the initial impression that most of the flow is lost from the bottom half of the perforated interval was correct.

The above survey came from a section of wellbore with a constant casing size. If the cross-sectional area changes from one drag to the next, then the velocities must be corrected to a common area by multiplication by the ratio of the actual area to the reference area.

To appreciate the extent to which any discrete timing procedure can smear a flow profile, consider the following hypothetical situation. Suppose four drags, A, B, C, and D, are measured and the peaks are spaced exactly 10 feet apart. The entire stream flows over the interval from A to B

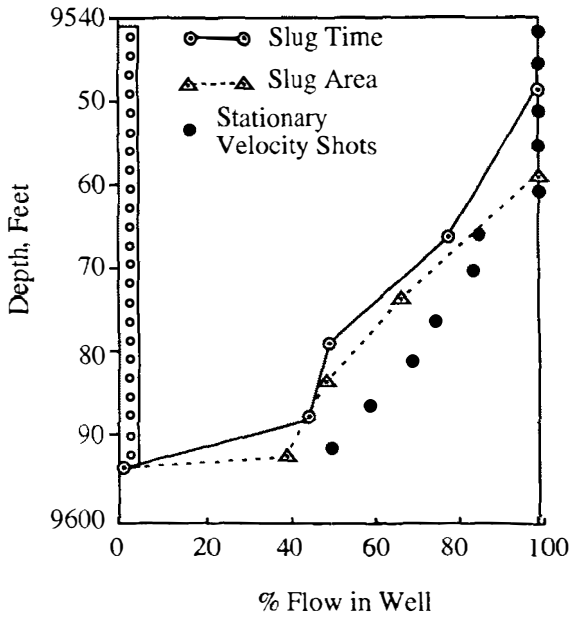

Figure 40. Profile for slug tracking surveys from Figure 35.

requiring 10 seconds for the transit. Thus, a velocity of 1 ft/sec., associated with 100% of flow as listed in the table below, is assigned to the midpoint of interval AB.

Drag	ΔL Ft.	Δt Sec.	$\hat{V}$ Ft./Sec	% Flow
A	10	10	1.00	100
B	10	10	1.00	100
C	10	15	0.67	67
D	10	20	0.50	50

Now, at the midpoint of interval BC, exactly 50% of the flow exits the wellbore and the remaining 50% continues on to C and D. The travel from B to C will thus be half the way at a speed of 1.0 ft/sec and the remaining half at only 0.5 ft/sec. Thus the travel time will be

$$\Delta t_{bc} = \frac{5\ \text{ft}}{1.0\ \frac{\text{ft}}{\text{sec}}} + \frac{5\ \text{ft}}{0.5\ \frac{\text{ft}}{\text{sec}}} = 15\ \text{sec}$$

as shown in the table. The apparent velocity is then 10/15 = 0.67 ft/sec. The travel time from C to D will be 20 seconds. As the table shows, the resulting "profile" allocates a 33% loss, rather than 50%, to the mid-point of interval BC and carries a 17% loss over to the mid-point of interval CD where no loss actually occurred. This behavior is characteristic of any interval velocity technique. The loss from the first interval is underestimated and a little final loss is carried one interval beyond the actual.

Before looking at the second method of profiling, which avoids the dispersion inherent to timing, it should be pointed out that the velocities on Figure 35 and in the tabulated results of page 57 are the superficial velocities that are related to volumetric rates by equation 3, which is

$$q\ (\text{BPD}) = 256\ A\hat{V} \qquad (3)$$

The survey on Figure 35 is in 5 1/2-inch, 17 lb/ft casing with a cross-sectional area A = 0.1305 sq. ft. At 100% flow, the timed slug velocity is $\hat{V}$ = 19.5 ft/min. Therefore, the injection rate, q, is

$$q = 256 \times 0.1305 \times 19.5 = 651 \text{ BPD.}$$

As was pointed out in the introduction, this type of survey is the only one that gives a velocity that requires no adjustment to superficial velocity. Most pipe tables also list the pipe capacity, C, in bbls/ft directly so that the rate can be obtained by

$$q = 1440\ c\hat{V} \qquad (3A)$$

where c = Pipe capacity, bbls/ft

$\hat{V}$ = Superficial velocity, ft/min

Slug Area: The second method of flow profiling from slug tracking data makes use of the area under the recorded intensity curve for a given drag. If the gamma intensity is assumed to be proportional to the concentration of tracer, then the area under the curve is proportional to the total amount of tracer in the wellbore at a given drag location. This area would then decrease in proportion to the fluid loss from the wellbore. The assumption of direct proportionality between intensity and concentration is strictly valid only whenever a detector is surrounded by a tracer concentration that is uniform not only across the pipe cross-section but also in the vertical direction. In such a situation, loss in peak height alone would be sufficient for flow profiling. Drags A, B, and C on Figure 35 show that peak intensity alone is insufficient because this value decreases as the slug spreads vertically.

Furthermore, a gamma ray originating at a particular location can be counted from about a foot away from its origin. Thus the area under a drag curve accumulates multiple counts due to "carry-away." This influence can be minimized by use of a number proportional to the area that is obtained by multiplication of the peak height by the width of the pulse at one-half peak height.

For example, drag A on Figure 41 has a peak height of 70 millimeters as shown. At half this height, the pulse width is 5.2 mm, so the product 70 x 5.2 = 364 $(mm)^2$ is the number to be assigned as an area. In a similar fashion, the other drags through G can be measured to give the numbers in Table 6. The "growth" in slug area through drag C is the result of poor mixing after ejection. The tracer material went to the pipe wall when it squirted from the tool orifice. If not intentionally mixed upon ejection, then about three drags through the slug is needed to achieve cross-sectional mixing. Fortunately, drags C and D can be averaged to give a reference area of 490 mm^2 for the full flow stream, the 100% point.

The percentages in Table 6 are based on this reference. These percentages are graphed as dashed lines for comparison on Figure 40. They show even more of the injection leaving the wellbore over the bottom half of the perforated interval than does the timed slug profile. Note in the table that the slug area is assigned to the location of peak intensity for the drag as this measurement is instantaneous at this depth. The apparent loss of 34% between drags D and E is, of course, smeared over the 14-foot interval separating the peak location.

Table 6. Slug "Area" Data from Figure 41 Slug Tracking Survey

Drag	Location Ft.	Height mm	Weight mm	Product Area, mm^2		% Flow in Well
A	9512	70.0	5.2	364		100
B	9524	71.4	5.5	393		100
C	9538	64.0	7.6	486	490	100
D	9559	58.0	8.5	493		100
E	9573	43.1	7.5	323		66*
F	9582	37.2	6.5	242		49
G	9592	33.8	5.7	193		39

* Relative to 490 mm^2

The method does, however, confine the loss to the interval over which it actually occurs. No fluid loss is carried over to the next interval as with the timed slug method. Moreover, the method is unaffected by variations in injection rate or by changes in cross-sectional area so long as fluid jets are avoided.

The recording sensitivity and the logging speed should be kept constant for the drags that are to be used for profiling, drags A through G in the case of figures 35 and 41. Each of the drags on Figure 41 was run with the tool moving upwards as the tracer slug moves down to meet the tool. Consequently, the apparent width of a given peak will be shorter on the record than it actually is by the amount that the slug moves down while the tool passes through it. Let W denote the

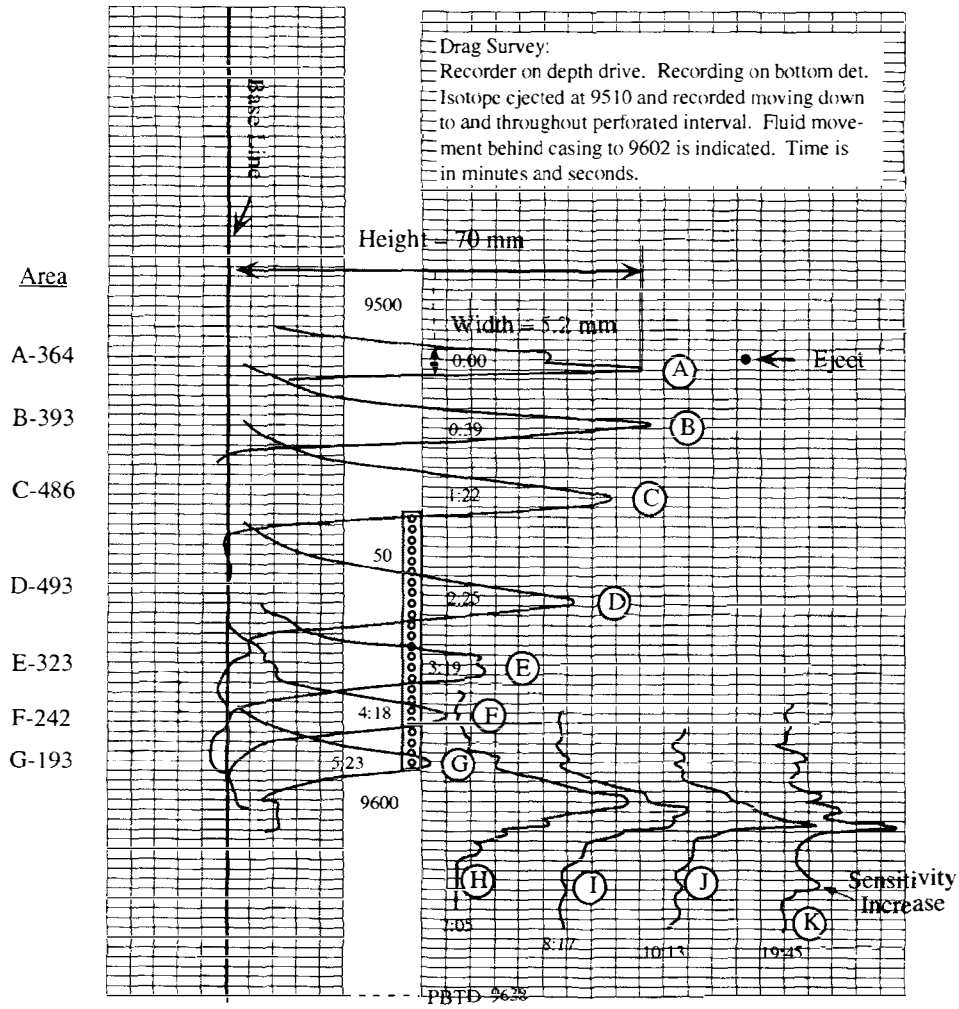

"Area" = (Pulse Height) x (Width @ Half-Height)

Figure 41. Injection profiling by slug "area" from a tracked slug survey.

actual slug width, W_{app} the width on the record, and δ the distance traveled by the slug as the tool passes through. Then

$$W_{app} = W - \delta$$

If V_L is the line or logging speed upward, then the time required for the tool to pass through the slug is

$$\Delta t = \frac{W_{app}}{V_L} = \frac{1}{V_L}(W - \delta).$$

During this time the slug moves a distance δ given by

$$\delta = \hat{V}\Delta t .$$

From these two equations one obtains the following expression for δ:

$$\delta = W \frac{\hat{V}}{V_L + \hat{V}}$$

from which

$$W_{App} = \frac{W}{1 + \frac{\hat{V}}{V_L}},$$

or

$$W = W_{app} (1 + \hat{V}/V_L)$$

At the logging speeds typically used for drag surveys, 200 ft/minute or higher, the correction to the apparent width as taken from the record is generally insignificant.

In spite of its approximate nature, the slug area method of profiling shown on Figure 41 gives a slightly better answer than does the times slug method of Figure 35. This is shown on Figure 40 where the two methods may be compared to the profile given by eleven velocity shots made over the perforated interval.

Injection Profiles from Velocity Shots: The increased vertical resolution afforded by stationary velocity shots is apparent from the comparison already made on Figure 40. This increased resolution is purchased with increased logging time. Consequently, the chance of including errors due to rate variations also increases. For example, the total 20 shots associated with the testing that gave the data for the velocity shots on Figure 40 were spaced over nearly half an hour. By contrast, the logging for drags A through G on Figure 41 occupied less than six minutes of time. The common procedure is to make the velocity shots in a single progression, top to bottom or vice versa, without doubling back to check on previous shots. If this check is to be done, specific instructions must be given to this effect.

The various methods for travel-time selection have already been illustrated on the velocity shot of Figure 39 taken in the 100% flow stream. The travel time of 13.8 seconds quoted for this shot was the peak travel time. This time is assigned to the depth at the mid-point of the detectors, i.e., to 5,802 feet in Figure 39. The velocity shot data are tabulated as shot number, mid-point depth, and travel time in exactly the same fashion as was the timed slug data in the table on page 57. The travel times are commonly referred to as "reaction time." Since the detector spacing is the same for all shots, the percentage profile is done with reciprocal travel time without conversion to a velocity. Thus, in the well of Figure 39, a travel time of 20 seconds, relative to 13.8 seconds for full flow, would correspond to (13.8/20) x 100 = 69% of the total rate. This is the point graphed as a solid dot on Figure 40 at a mid-point depth of 9,581 feet.

A question that usually arises is the meaning that one attaches to the velocity associated with the 13.8 second travel time for the velocity shot of Figure 39; namely how is the number

$$V = \frac{5.5 \text{ ft}}{13.8 \text{ sec}} \times 60 \frac{\text{sec}}{\text{min}} = 24 \frac{\text{ft}}{\text{min}}$$

related to the volumetric injection rate? It is obviously bigger than the superficial velocity $\hat{V}$ = 19.5 ft/min determined from the timed slug data in the table on page 57. This is not unexpected since the cross-sectional area determining V is the annular area between the tool and the casing wall. For the velocity shot in question, the tool was a 1 3/8 inch diameter instrument with a cross-sectional area of 0.0103 square feet inside casing with an area of 0.1305 square feet. An area correction on the value for V thus gives

$$V_c = \frac{0.1305 - 0.0103}{0.1305} \times 24 = 22.1 \text{ ft/min},$$

a number that is still larger than $\hat{V}$ = 19.5 ft/min. Theoretical relations between V_c and $\hat{V}$ exists but the assumptions are so restrictive that they are of little practical utility. Consequently, the rate equation for velocity shot data is usually simply

$$q = \frac{C}{\Delta t},$$

where Δt = velocity shot travel time, seconds,
C = calibration constant, BPD-sec.

The calibration constant is determined from a surface measured injection rate and a downhole travel time in the full flow stream. For example, suppose q = 650 BPD (the rate calculated from the timed slug) and that Δt = 13.8 seconds as measured by the velocity shot in the 100% flow stream, then C = 650 x 13.8 = 8,970. The velocity shot is therefore not an absolute measure of volumetric rate as is the timed slug. The reason for this is the incomplete mixing that accompanies ejection from a stationary tool followed by only about five feet of travel prior to gamma intensity measurement. If one is desperate for an estimated rate, one can assume that

$$\hat{V} = \alpha V_c,$$

where α = 0.7 - 0.9,

for the "sharp" pulses of the type shown on Figure 39 (page 54). Because of the poor mixing, the apparent travel time of the shot slug depends almost entirely on how the material is distributed by the ejection jet into the annular volume between tool and casing. Figure 42 shows two extremes of tracer placement by a tool centralized in a low velocity stream. In frame A, a high velocity jet from a single ejection port plasters the material against the wall of the pipe. The subsequent rebound, just beginning on the figure, is the only mixing the material gets. In fact, in viscous polymer water, the slug may not rebound at all! The resulting pulse that such a shot gives can

range from satisfactory to a very smeared-out, low-intensity signature with ill defined travel time. The tool on frame B of Figure 42 has four ejection ports and can place large shots at lower velocity to give much better mixing in the pipe along with a sharper pulse whose peak is clearly defined. Tracer tools are available that avoid the placement problem by virtue of slug ejection downward into the center of pipe. Such a tool is pictured on Figure 43. The decentralizing "elbow" on this instrument positions the ejector at the centerline of whatever size pipe is involved. Because this places the tracer material in the higher velocity part of the pipe, the resulting gamma intensity pulse has sharp leading and trailing edges with well-defined travel time. It is the preferred tool for profiling flows of viscous water.

Considering the work that went into the preparation of the injection profile on Figure 40 (page 58), one must also determine how representative it is of the actual injectivity. This is done in the next section.

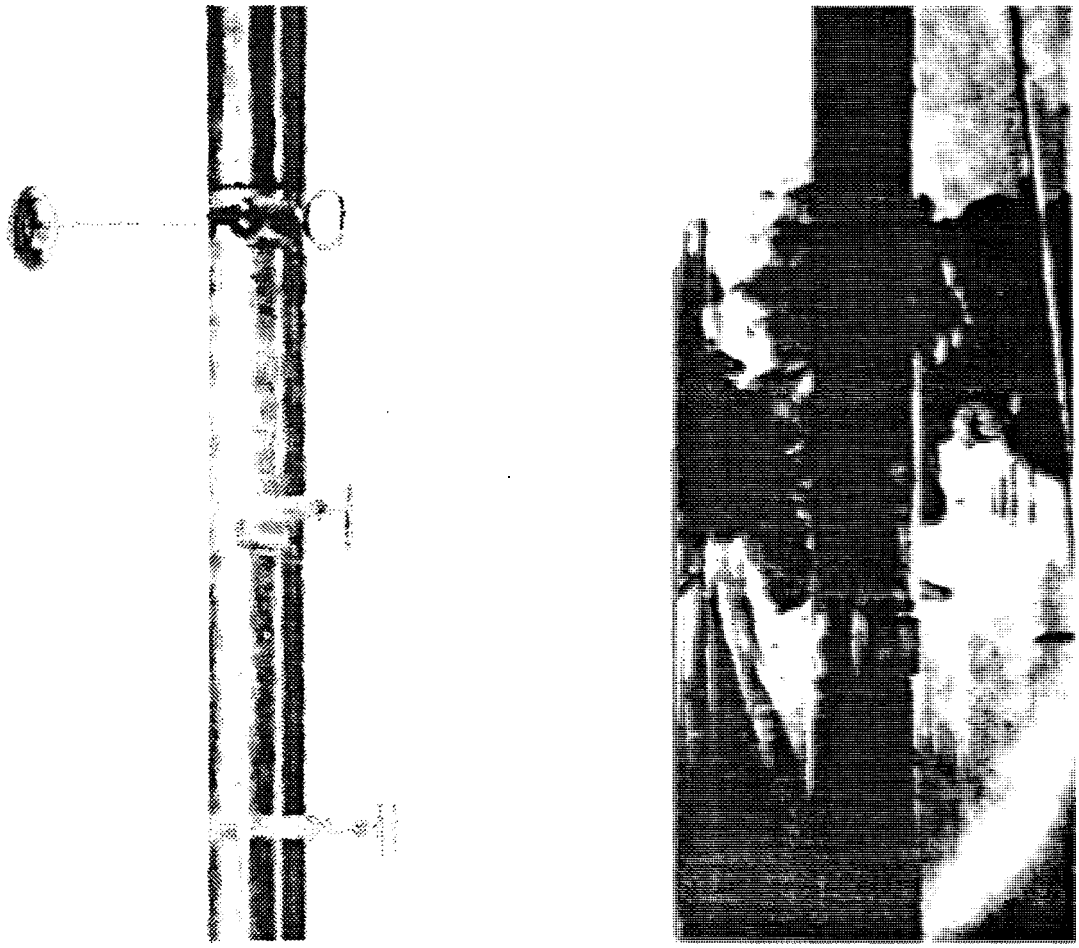

Figure 42. Tracer placement in the annular volume between a 1.5-inch tool and a 6-inch plexiglass pipe (courtesy Atlas Wireline).

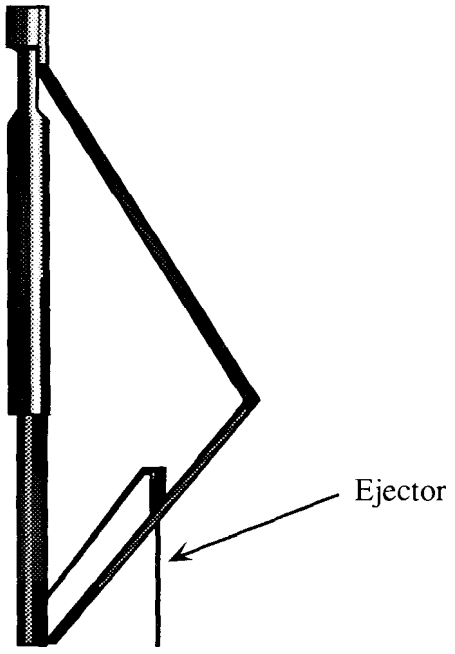

Figure 43. Tracer tool for ejecting slug at centerline of pipe (courtesy of Atlas Wireline).

Comparison of Tracer Profile with Temperature Profile: The initial drag surveys on Figures 35 (page 50) and 36 established that at least some of the injected water goes behind the pipe into porosity at 9,605 feet. The most detailed flow profile, the velocity shot data on Figure 40, places 50% of the flow exiting at the very bottom of the perforated interval. This is, presumably, the amount lost behind pipe to lower porosity. Therefore, one would conclude that only 50% of injected water is entering into the completed-interval porosity. This hypothesis can be checked. The injecting temperature survey given on Figure 44 indicates that the hypothesis is in fact, wrong! Every bit of the injected fluid is going into the porosity at 9,605 feet because the temperature survey shows no losses above this depth. Apparently, the formation has fractured downward from intended porosity into that below the completion. The tracer tool is correctly recording those depths where the water leaves the wellbore region in the fracture. The decreasing vertical velocities associated with the tracer drags on Figure 35 reflect increasing lateral velocities in the fracture itself so as to conduct the same mass rate in a form of a "spill" into the fracture. This comparison illustrates emphatically the necessity of corroborating surveys in production logging. No logging tool is an absolute, stand-alone device in all situations. Yet the belief is so strong that the "more easily interpreted" tracer data is the "right" answer that common practice is to allocate 50% injection to the completed interval even though the temperature survey is available for comparison. At least, in this example, the tagged water stayed close enough to the wellbore to be evident on the drags of Figure 35 even below the perforated interval.

But this is not always the case. Frame A on Figure 45 shows seven drags through shot #2 ejected at 5,400 feet in a well on water injection. Drag 4 already shows significant loss at the top of the

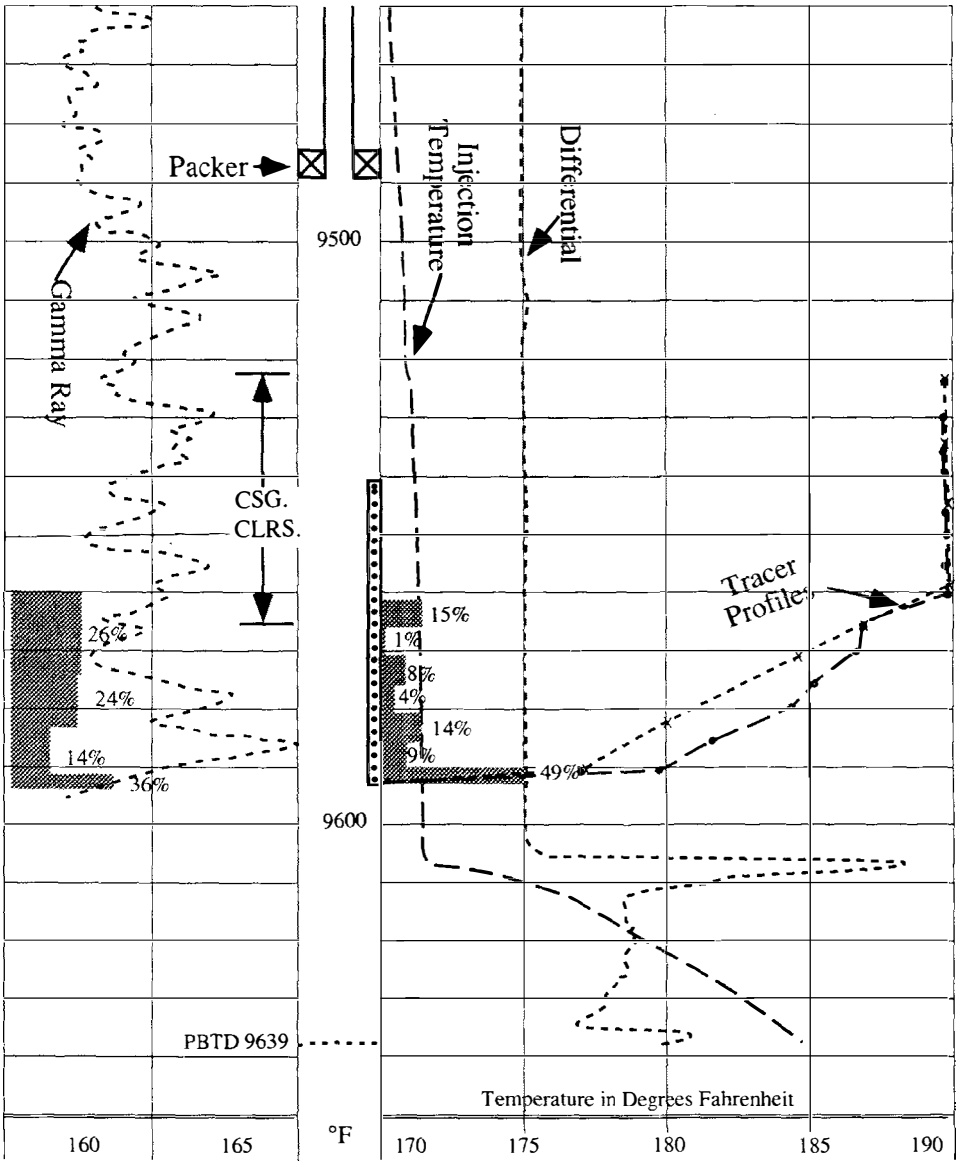

Figure 44. Injecting temperature survey from well with tracer survey shown on Figure 35.

short perforated interval at depth A on frame A. Drags 6 and 7 reveal that the vertical travel of the slug peak ceases at the bottom of the same perforations. The slug is pumped away at this location. Compare this behavior with that below the perforations in Figure 35. The velocity shot survey also showed no flow below a depth of 5,427 feet, as indicated on frame A of Figure 45. The slug travel to the bottom of the porosity of zone A at 5,431 feet apparently occurs behind pipe. As a result of the tracer survey, the entire injection was allocated to zone A. Yet the injecting temperature survey on frame B of Figure 45 shows no loss at all across this zone, depth 1 on frame B. The first loss is at depth A, the top of the thick zone of porosity evident on the

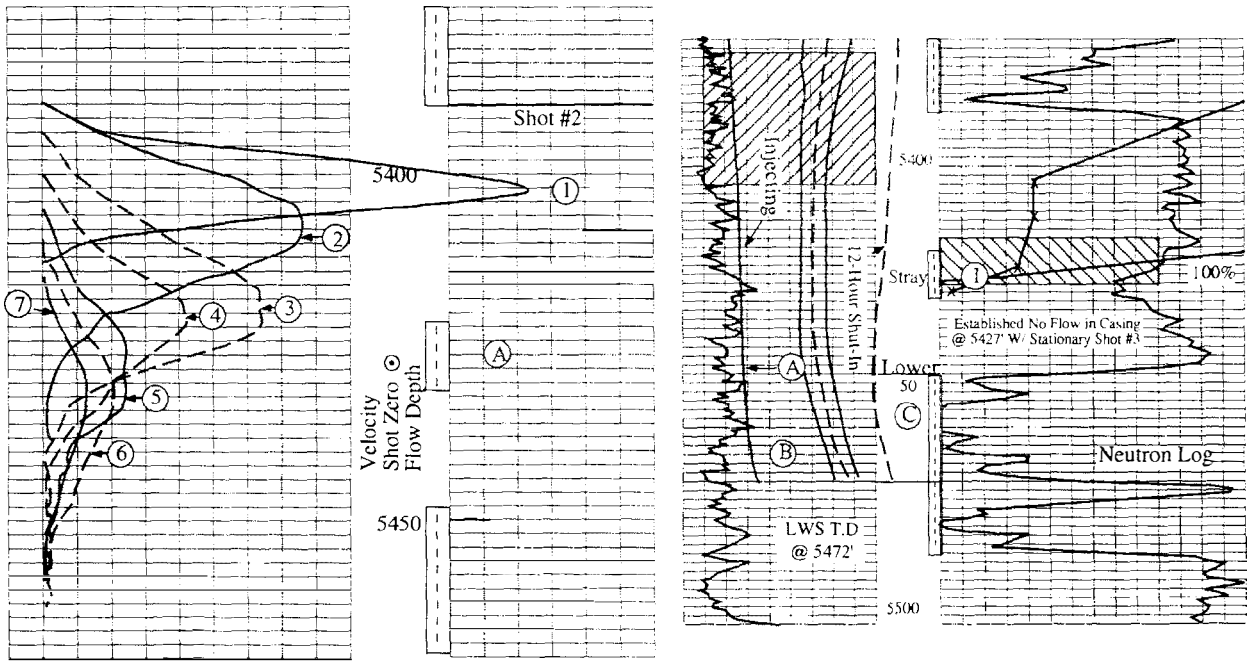

(A) Tracer Survey With Well On Injection

(B) Temperature Surveys From Same Well

Figure 45. Tracer and temperature surveys from an injection well that has been fractured inadvertently.

neutron log of frame B. The next loss is at depth B, a location in the same thick zone. Furthermore, the 12-hour shut-in temperature survey on frame B of Figure 45 shows absolutely no storage at the porosity indicated at depth 1. The only storage signature is at depth C, the top portion of the thick zone. The entire stream is actually injected into this zone not the one indicated by the tracer loss surveys on frame A. Perforations into the thick zone have plugged with continued injection, the formation has fractured from the thin zone down into the better permeability in the thick interval, and the injected stream is presently exiting the wellbore into the fracture through the thin-zone perforations. As this stream "spills" away from the wellbore, it is quickly lost to the tracer tool.

Special procedures are needed if the tracer tool is employed to demonstrate injection confinement. This is the subject of the final topic in the discussion of the radioactive tracer method. Some additional comments on the vertical resolution of the velocity shot method of surveying should be made at this time. The resolution of the shot data on Figure 40 was set by the 5.5 foot separation between the two detectors. This spacing, however, is not a restriction on the vertical resolution that can be achieved. This fact is demonstrated in the next section. The technique also allows one to limit the smearing effect already described for timed slugs to small distances.

Velocity Shots with Overlapping Intervals: Suppose the two detectors are spaced five feet apart. The tool can, of course, only measure five-foot travel times directly. If, however, the tool is only

moved by a distance of one foot after each shot, then any shot relogs four feet of the previous 5-foot interval and picks up one foot of new travel time. In this fashion, one-foot travel times, $\Delta t'$, can be calculated from five-foot times, Δt. Consider the 8.5-foot perforated interval shown on frame A of Figure 46. Suppose that injection is occurring only in the top four feet of the interval in a uniform fashion so that equal amounts are lost in each foot of interval. If 50% of the total stream is injected into the 4-foot interval and 50% continues to other sets of perforations deeper, then the true injection profile appears on frame A of Figure 46 in the form of a bar graph showing the 12.5% of the total injection that exits over each foot of the 4-foot interval. If the survey is made with the actual spacing of detectors as the interval between shots, then two shots will span the entire perforations. The resulting smearing will then be so bad that roughly 25% of the injection appears to exit over the top half of the perforations and 25% over the bottom half, i.e., the injection appears to be uniform over the entire perforated interval. This is clearly unacceptable. So, instead, velocity shots will be taken at 1-foot intervals starting with the tool positioned so that the bottom detector is just above the top perforation at location 1 on frame A of Figure 46.

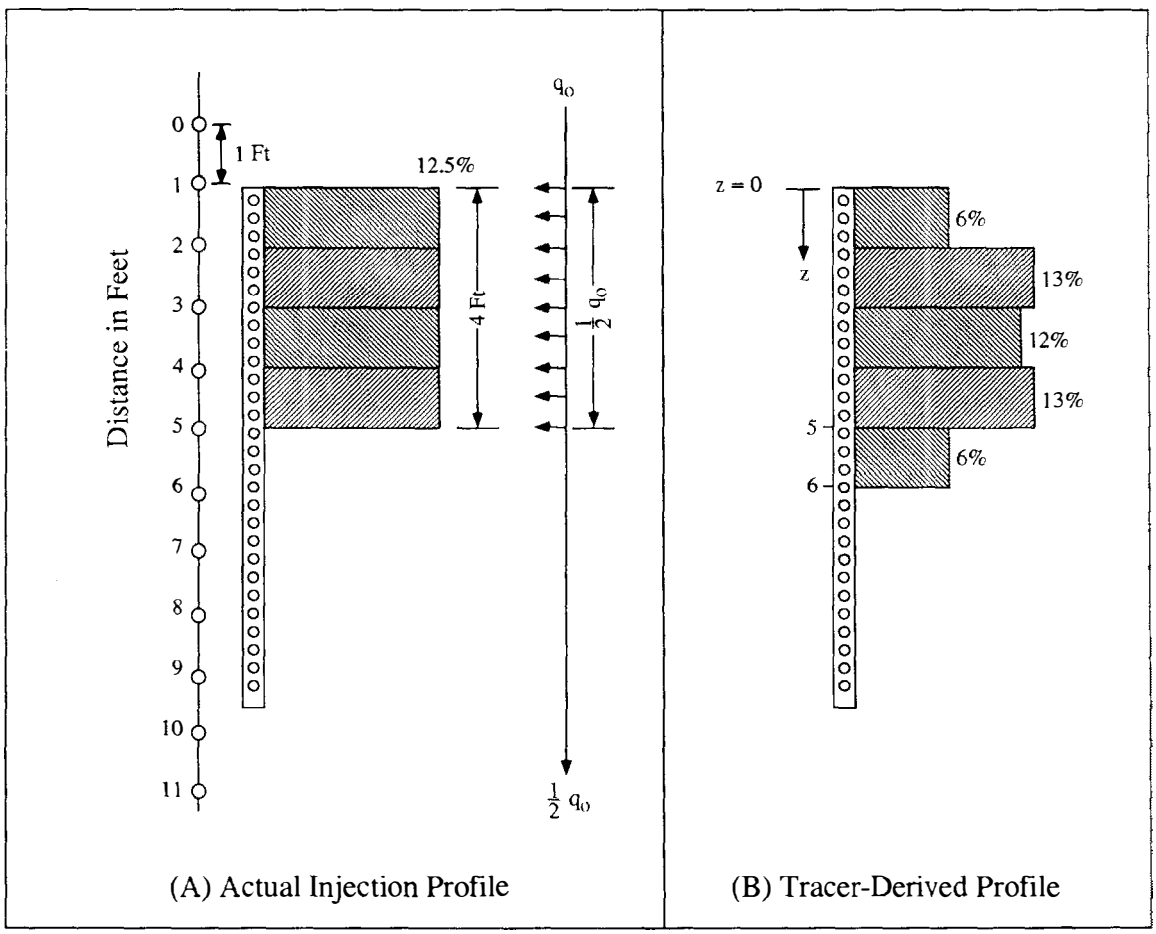

Figure 46. Control of vertical resolution by overlapping 1-ft stations with a tool having normal detector spacing.

The top detector is 5 feet above location 1. Both detectors are in the full flow stream, q_o. The first measured travel is thus the reference for 100% flow:

$$\Delta t_o = 5\Delta t_o'$$

where Δt_o is the 5-foot reference time and $\Delta t_o'$ is the 1-foot reference time for 100% flow. Therefore

$$\Delta t_o' = \frac{1}{5}\Delta t_o \text{ (at location 1)}$$

The tool is now moved so that the bottom detector is one foot deeper at location 2 on frame A, Figure 46. The resulting travel time, Δt_1, measured over five feet is

$$\Delta t_1 = \Delta t_1' + 4\Delta t_0'$$

$$\Delta t_1 = \Delta t_1' + \frac{4}{5}\Delta t_0$$

or

$$\Delta t_1' = \Delta t_1 - \frac{4}{5}\Delta t_0 \text{ (at location 2),}$$

This is the travel time for the first 1-foot increment into the perforated interval. This result can also be written as

$$\Delta t_1' = \Delta t_1 - \Delta t_0 + \Delta t_0' .$$

In this form it has an obvious geometric significance. When the tool is lowered by one foot to a current location from a previous location, the movement of the bottom detector adds an increment of one foot length. Likewise, the movement of the top detector leaves behind an increment of equal length. The last expression, stated in words rather than symbols, is:

> "The travel time for the added increment is equal to the difference in 5-foot travel times in the current and in the previous location plus the incremental travel time for the increment left behind."

In the above form the statement is perfectly general. For example, for shot #5, five feet into the perforations, the bottom detector moves from location 5 to location 6 on frame A of Figure 46. Likewise, the top detector moves from location 0 to location 1 leaving behind an increment with a travel time of $\Delta t_o'$. Thus

$$\Delta t_5' = \Delta t_5 - \Delta t_4 + \Delta t_0' .$$

For shot #6, the bottom detector moves from location 6 to location 7 whereas the top detector moves 1 foot into the perforated interval leaving an increment with a travel time of $\Delta t_1'$.

Consequently,

$$\Delta t_6' = \Delta t_6 - \Delta t_5 + \Delta t_1' ,$$

or, in general

$$\Delta t_N' = \Delta t_N - \Delta t_{N-1} + \Delta t_{N-5}' ,$$

where the N-5 arises from the 5-foot spacing between detectors. Shot #6, six feet into the perforations and two feet beyond the injection interval in frame A of Figure 46, is required in order for the survey to register zero injectivity in the added increment. The corresponding apparent profile is shown on frame B of Figure 46. Here we see that half the true injection is lost from the first increment of the perforated interval and is allocated instead to the increment just beyond the last increment to actually receive injection.

The profile in frame B of Figure 46 is quite simple to calculate. If a distance parameter z is measured from the top of the perforations downward as shown on frame B, Figure 46, then the velocity in the perforated interval is given by

$$V(z) = V_o \left(1 - \frac{z}{8}\right); \quad 0 \le z \le 4 \text{ ft}$$

$$V(z) = \frac{1}{2} V_o \qquad ; \quad z > 4 \text{ ft}$$

where V_o is the full stream velocity. The travel time over an increment extending from z_i to z_j is thus

$$\Delta t_{ij} = \int_{z_i}^{z_j} \frac{dz}{V(z)} = \frac{1}{V_o} \int_{z_i}^{z_j} \frac{dz}{\left(1 - \frac{z}{8}\right)}$$

recognizing that $\Delta t_0' = \frac{1}{V_0}$ minutes, we obtain after integration

$$\Delta t_{ij} = 8\, \Delta t_0' \ln\left(\frac{8 - z_i}{8 - z_j}\right); \quad z_j \le 4 \text{ ft},$$

for the interval travel time. For example, $z_i = 0$ and $z_j = 1$ for the first foot into the perforations, interval 1-2 on frame A, Figure 46. Thus

$$\Delta t_{12} = 8\, \Delta t_0' \ln\left(\frac{8}{7}\right) = 1.068\, \Delta t_0'$$

For the fifth foot, interval 5-6, $z_i = 4$ and $z_j = 5$, so that $V(z) = 1/2\, V_o$ and $\Delta t_{56} = \frac{2}{V_0} = 2\Delta t_0'$. In this fashion, the following numbers are obtained.

Shot	Frame A Interval	$\Delta t'$	% Flow in Well	% Loss to Interval
0	0-1	$\Delta t'_o$	100	
1	1-2	$1.068\ \Delta t'_o$	94	6
2	2-3	$1.233\ \Delta t'_o$	81	13
3	3-4	$1.459\ \Delta t'_o$	69	12
4	4-5	$1.785\ \Delta t'_o$	56	13
5	5-6	$2\ \Delta t'_o$	50	6
6	6-7	$2\ \Delta t'_o$	50	0

The numbers in the last column are graphed on frame B of Figure 46.

The technique of overlapping intervals must be initiated with a shot in a location where the fluid velocity is constant over the spacing between detectors. One can, of course, log upward as well as downward. The general rule stated on page 69 is independent of direction.

Quality Control in Profile Surveys: Numerous comments have been made about the tracked slug survey of Figure 35 (page 50), and the stationary velocity shot of Figure 37 (page 52). In reality, the survey quality is not all that good. The slug tracked on Figure 35 was not mixed when first ejected and a common baseline was not employed for all subsequent drags through the perforated interval. On the velocity shot in Figure 37, the time drive of 1 inch per minute is much too slow for the slug velocity.

The following example is a higher quality survey. The example comes from a well on a quite low rate of injection of some 150 BPD into two perforated intervals. The completion is 5 1/2-inch, 17 lb/ft casing. A 12-drag tracked slug survey is given on Figure 47. Tool motion was used to mix the tracer slug immediately after ejection. The baseline indicated by the double line serves as a reference for all the drags. This survey was conducted in a manner so as to insure quality from both slug area analysis and slug timing.

The peak times are not shown on the log of Figure 47. Instead, they were tabulated on a section of the log. A visual inspection of the surveys on Figure 47 shows most of the injected water is still in the wellbore on drag #7, whereas drag #8 shows considerable loss. From the relative location of the respective peaks on these drags it will not be possible to tell if this loss occurs right at the bottom of the top set of perforations or right at the top of the bottom set. The velocity shots will have to decide the issue. The data from the tracked slug survey is tabulated below. The "area" listed in column 3 of the tabulation is the product of the peak height and half-height width as illustrated on drag 1 of Figure 47.

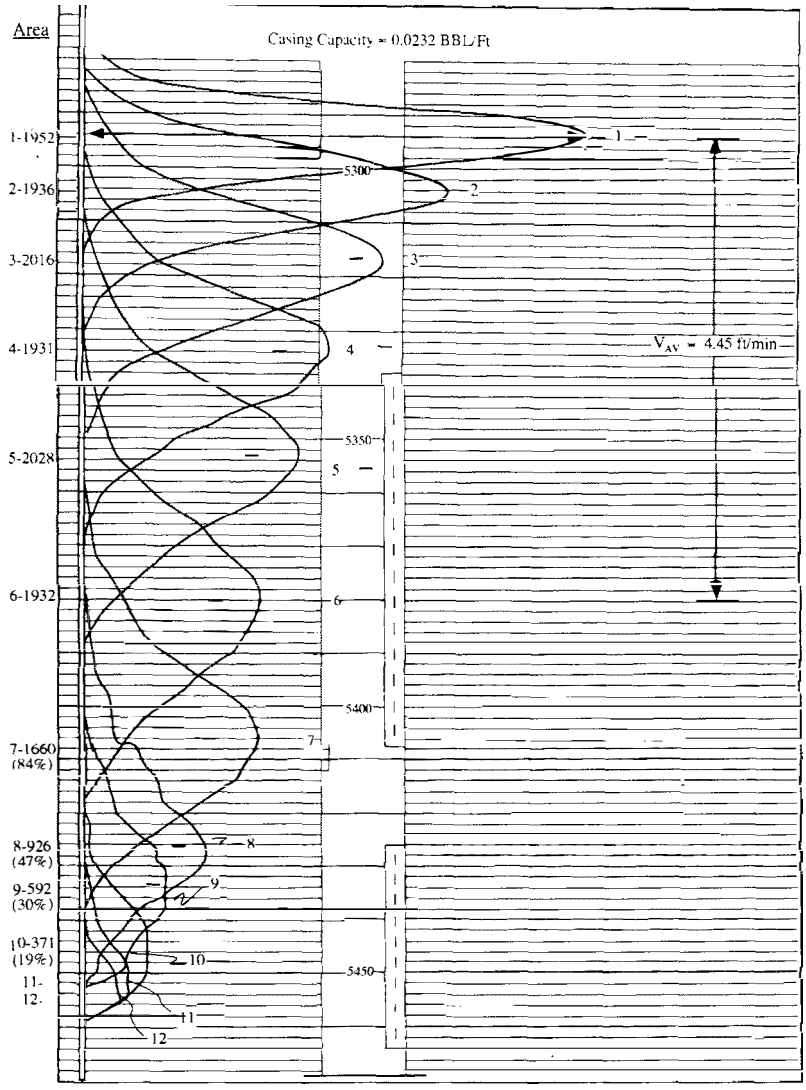

Figure 47. Good quality tracked slug survey in well on injection at 150 BPD.

Drag No.	Peak Location	"Area" mm²	% Flow	Travel Interval	Time Secs	$\hat{V}$ Ft/Min	% Flow	Depth @ Mid-Point
1	5294	1952	100		0			
2	5304	1936	100	10	132	4.55	100	5299
3	5316	2016	100	12	161	4.50	100	5310
4	5334	1931	100	18	237	4.56	100	5325
5	5353	2028	100	19	270	4.22	100	5343
6	5380	1932	100	27	367	4.42	100	5366
7	5406	1660	84	26	405	3.85	87	5393
8	5426	926	47	20	496	2.42	54	5416
9	5433	592	30	7	255	1.65	37	5430
10	5446	371	19	13	626	1.25	28	5440
11	5452	176	9	6	781	0.49	11	5449
12	5453	96	5	1	755	0.08	2	5452.5

1966 (Drags 1–6)

4.45 (Drags 2–6)

The values for this area, as a result of the mixing after ejection, are free of the initial "growth" that distorted the survey of Figure 35. The individual values for drags 1 - 6 are all within 4% of the average.

The corresponding average velocity of $\hat{V}$ = 4.45 ft/min along with a pipe capacity of C = 0.0232 bbls/foot gives by equation (3A), page 59:

$$q = 1440 \times 0.0232 \times 4.45 = 149 \text{ BPD}$$

for the injection rate. This is the same as the metered rate of 152 BPD. The injection profile data tabulated above are plotted on Figure 48. The only difference arises from the assignment of the timed slug data to the midpoint location. Had these values been assigned to the peak location instead, the two approaches would have given the same profile.

Both profiles show apparent loss between perforations which actually occurred at the perforations. As already stated, a velocity shot between the two sets of perforations is needed for correct allocation.

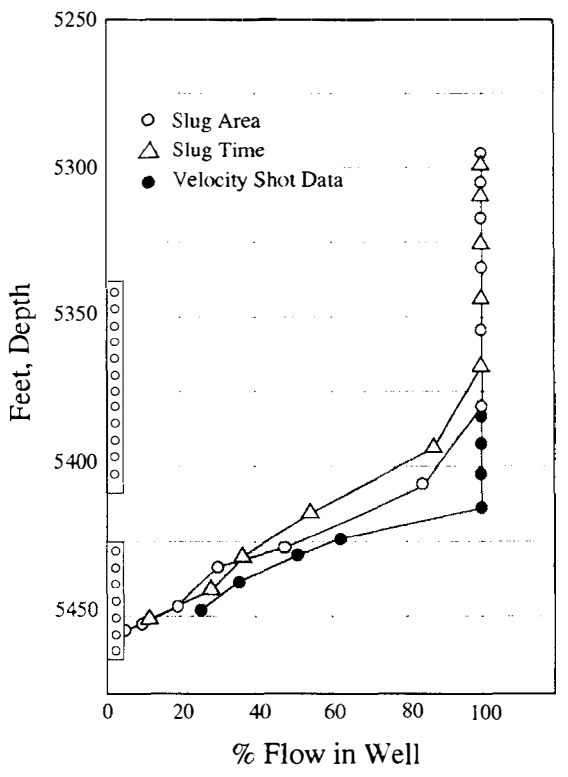

Figure 48. Injection profile for tracked slug survey of Figure 47 with injection rate of 152 BPD.

The detectors for velocity shots are spaced 5 feet apart. For the average velocity V = 4.45 ft/min given in the tabulation on page 72 for the full flow stream, the chart drive speed, according to equation (6), page 56, should be no slower than

$$S = \frac{\hat{V}}{L} = \frac{4.45}{5} \approx 1 \text{ in/min},$$

a speed that would give 10 chart divisions, roughly, between peak locations at 6 seconds per chart division. The actual time drive employed was 2 in/min for a nominal 3 seconds per chart division. A calibration, however, gave 25 chart divisions of travel in 123 seconds of time, or 123/25 = 4.92 seconds per chart division. This is the scale for all subsequent stationary shots. A total of 17 shots were made for flow profiling purposes. Two of these are illustrated on Figure 49. Frame A is a shot in the full flow stream with the top and bottom detectors at 5,300 and 5,305 feet, respectively. The pulses are turned around relative to each other so that gamma intensity on the record from the bottom detector, the left-hand trace on frame A, increases from left to right. On the other trace from the top detector, however, intensity increases in the opposite direction, right to left. For some reason, this procedure is thought to facilitate analysis and, as such, is a harmless quirk favored by many logging operators. On frame A, peaks are marked by arrows. The locations should be at the mid-point of the pulse width about the peak. Otherwise, pulse-shaping, method 3 on Figure 38, should be used to fix a peak location. On frame A, the peaks are separated by 12.4 chart divisions or 12.4 x 4.92 = 61.0 seconds. This corresponds to an apparent velocity of (5/61) x 60 = 4.92 ft/min. As things happened, 13 out of the 17 shots were in the 100% flow stream. From these an average velocity of 5.48 ft/min was determined. The tool diameter and casing size in this example are both the same as those for the velocity shot of Figure 37. Consequently, the area correction is the same as that carried out on page 32, or V_c = 0.921 x 5.48 = 5.05 ft/min. This value is again larger than the superficial velocity $\hat{V}$ = 4.45 ft/min associated with the drag surveys of Figure 47.

Frame B on Figure 49 is the velocity shot taken with both detectors located between the two sets of perforations. On this frame the peak travel time is 16 chart divisions which is longer than the 12.4 cd's associated with the 100% shot of frame A. Nominally only 12.4/16 = 0.78 of the flow passes the top set of perforations.

Actually, at the low rates involved in this example, the peak shape and apparent travel time becomes quite dependent upon the ejected tracer distribution. In such situations, those travel times that are associated with the first arrivals, methods 1, 4, and 5 on Figure 38, are much less sensitive to tracer distribution than are the peak travel times. For this reason, the half-peak points have been marked on the leading edge of all four pulses appearing on Figure 49. The travel time associated with these points on frame A is 11.0 chart divisions whereas on frame B they are separated by 10.0 chart divisions. Likewise, the travel times for the "first arrivals" are the same. No measurable injection loss occurs in the top set of perforations! The loss that appears to occur between the perforations on the profile of Figure 48 in conjunction with the tracked slug is thus associated with the top of the bottom set of perforations.

Figure 50, for velocity shot #4, shows how strung out the pulses become. For this shot, the top and bottom detectors were at 5,435 and 5,440 feet, respectively. In contrast to the pulses on

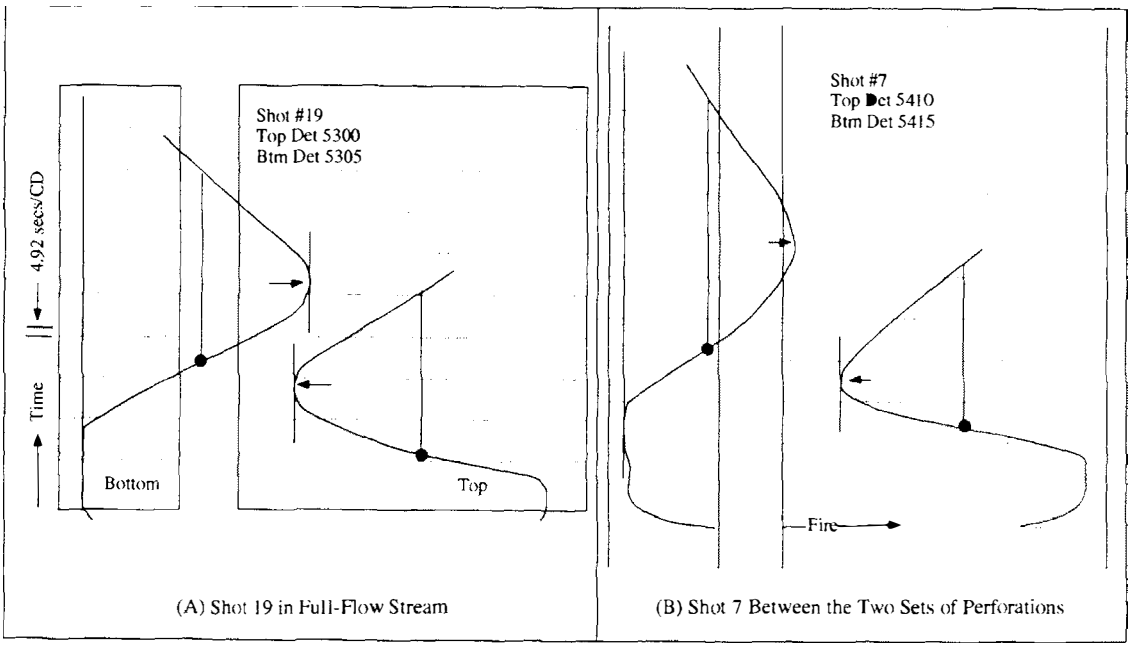

Figure 49. Velocity shots at two locations in the well giving the slug survey of Figure 47. Injection rate is 152 BPD in 5 1/2-inch, 17 lb/ft casing. Perforations at 5338-5408 and 5426-5464.

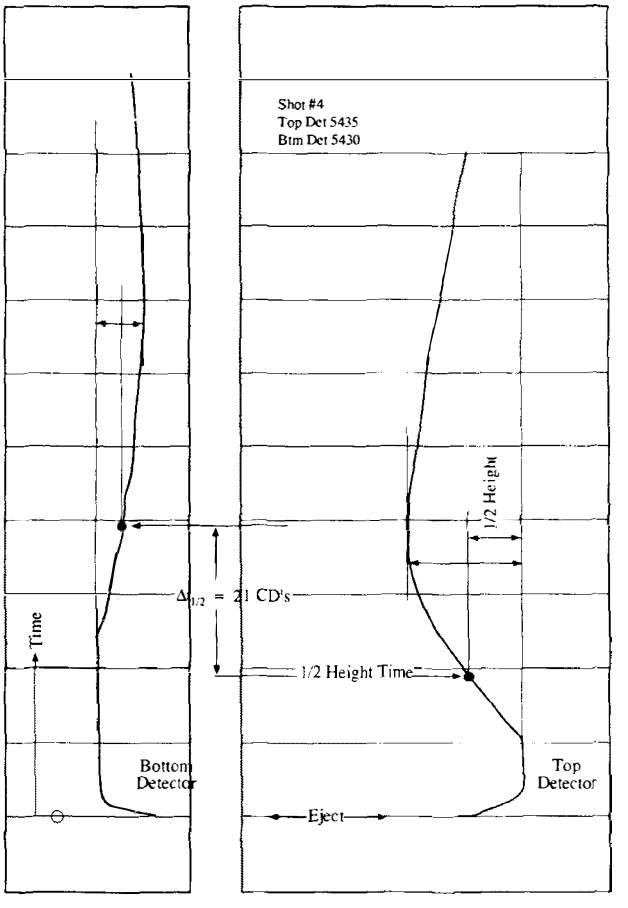

Figure 50. Velocity shot #4 with rounded (concave) leading edge typical of well-mixed shot in laminar flow.

Figure 49, the ones on Figure 50 have leading edges that are rounded over (concave) without inflection points. This shape is characteristic of a well-mixed slug in a laminar flow stream. For a velocity shot under these conditions, theory predicts that both the peak and leading edge travels at a velocity that is twice the superficial, i.e., $V_c = 2\hat{V}$. It has already been seen that for previous velocity shots in turbulent flows $V_c \approx \hat{V} / 0.8 = 1.25\hat{V}$. Consequently, one should in theory increase the travel times measured in laminar flow before comparison with those measured in portions of the well where flow is turbulent. From the above figures, the laminar peak travel times should be increased by a factor of 2/1.25 = 1.60 for comparison with turbulent peak times. In theory, the factor for leading edge travel time is 1.32.

One might then speculate that, instead of the 21 chart divisions associated with the half-peak travel time shown on Figure 50, one should use a value in the range of 28 - 34 chart divisions for comparison to the 100% value of 9.88 chart divisions listed in Table 6. Actually, the full-flow velocity of 4.45 ft/min is just in the turbulent range so that the first loss drops the stream into the laminar regime.

TABLE 7. VELOCITY SHOT DATA FOR WELL OF FIGURE 47

Shot #	Top Detector	Bottom Detector	Half-Peak Separation, CD		% Flow in Well
20	5285	5290	10.0		100
19	5300	5305	11.0		100
18	5315	5320	10.0		100
17	5325	5330	10.0		100
16	5333	5338	8.0		100
15	5338	5443	10.0		100
13	5350	5355	10.0	9.88	100
12	5360	5365	7.5		100
11	5370	5375	10.8		100
10	5380	5385	11.0		100
9	5390	5395	10.0		100
8	5400	5405	10.1		100
7	5410	5415	10.0		100
6	5421	5426	12.2		61*
5	5426	5431	14.0		53
4	5435	5440	21.0		36
3	5445	5450	29.0		26

* Relative to 9.88/1.32 = 7.48 cd's for 100% flow where 1.32 is laminar correction factor

These facts follow from the value of Reynold's number for the full flow stream. This number, N_{Re}, is defined as

$$N_{Re} = 129 \frac{\rho \hat{V}(D_p - D_t)}{\mu} \qquad (7)$$

where ρ = Density, gm/cc
D_p = Pipe inside diameter, inches
D_t = Tool diameter, inches
$\hat{V}$ = Average velocity of fluid, ft/min
μ = Fluid viscosity, centipoises

for the flow to be laminar $N_{re} \leq 2{,}000$: consequently,

$$\hat{V}_{Lam} \leq \frac{2000}{129} \frac{\mu}{\rho(D_p - D_t)} \qquad (8)$$

For D_p = 4.9 inches, D_t = 1.375 inches, μ = 0.82 cp, and ρ = 1.06 gm/cc, equation (8) gives for the onset of laminar flow

$$\hat{V}_{Lam} \leq 15.50 \times \frac{0.82}{1.06 \times (4.9 - 1.375)},$$

$$\hat{V}_{Lam} \leq 3.40 \text{ ft/min}.$$

Consequently, the large loss "between" perforations shown on the drag profile of Figure 48 will drop the flow into the laminar region because 3.40/4.45 = 0.76. It is therefore simpler to correct the 100% flow value of 9.88 chart divisions than it is to correct all readings below shot #7 in the tabular results above. This single correction is made by 9.88/1.32 = 7.48 CD's as the reference for 100% flow in the table. For example, shot #6 gives for the percent flow in the well:

$$\% \text{ Flow} = 100 \times \frac{7.48}{12.2} = 61,$$

and, likewise for the remaining shots. The velocity shot profile is shown as solid circles on Figure 48. The location for a given shot is taken at the mid-point depth between the two detectors. The velocity shot data do not show the 15%, or so, loss over the bottom half of the top set of perforations that the drag surveys indicate. This injection may be of a sporadic nature or it may not be within the ability of the velocity shot to detect a loss of this size. The tabulated half-peak travel times show variations of this magnitude. Both survey methods place the majority of the injection as exiting over the top half of the bottom set of perforations.

The injecting temperature survey of Figure 51 also does not show a loss over the top set of perforations. The first "exit" shows up at a depth A some 6 feet above the top of the bottom set of perforations. This most likely is the result of flow behind pipe upward from the top of the lower perforations. The short-time shut-in surveys indicate that such a crossflow takes place.

The injecting temperature survey also shows flow to the base of the interval at depth B. Given the large exit over the top half of the bottom set of perforations evident on the tracer survey, the flow to the base of the unit is also probably behind pipe in a fracture. The 12-hour shut-in temperature survey shows the major storage at 5,450 feet, location C, in the lower perforated interval.

However, there is a storage signature at depth D in the bottom part of the upper set of perforations. The storage in the top part of this interval around 5,350 feet is a relic of "injections past."

In summary, this example presented a good quality tracer survey with tracked slug data that was quite easy to interpret, its main disadvantage being that of insufficient vertical resolution. The velocity shots, although quite well run, then required for their interpretation a laminar correction whose validity is uncertain. So, whereas the problem of vertical resolution was eliminated, additional concerns were added. Finally, the temperature surveys revealed more details of the injection pattern.

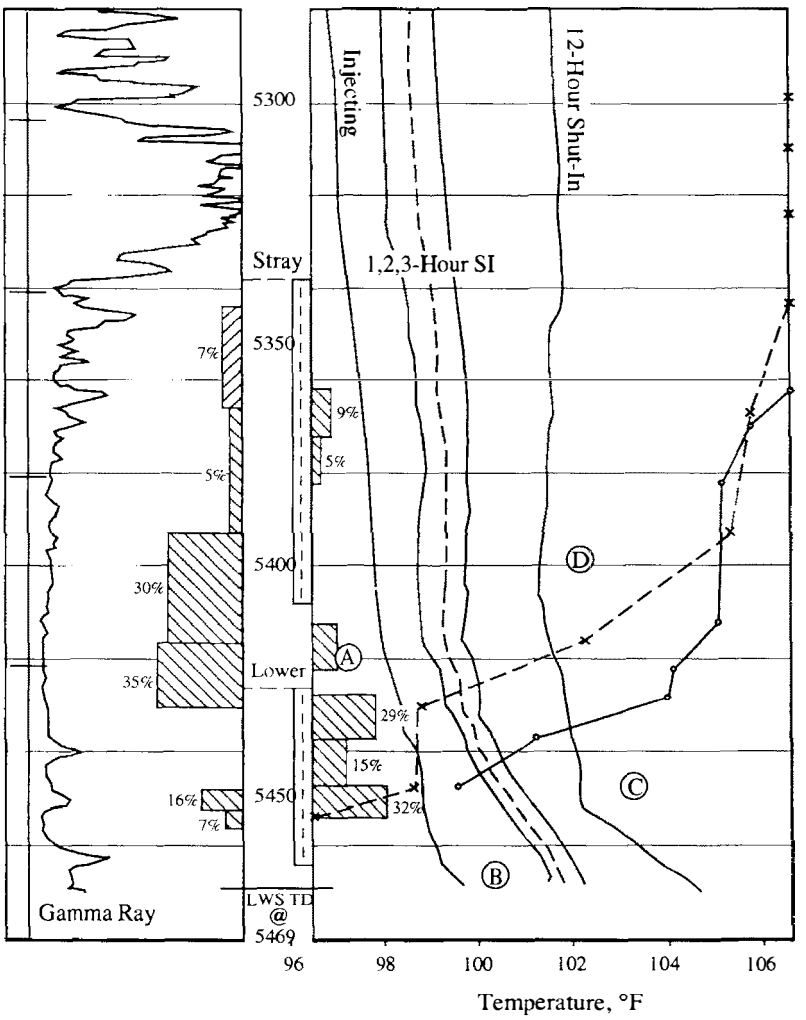

Figure 51. Temperature surveys from well on water injection at 152 BPD.

It should be added that once the well is shut off injection, a crossflow check should also be run with the tracer tool. Very small interzonal flows can be detected in the wellbore in this manner. A crossflow check on the well under discussion after three hours of shut in is given in Figure 52. Four shots of tracer were ejected as the tool was lowered past four selected locations then a logging run was made back up the well. This gave the solid line survey on Figure 52. The tool was then again lowered to the bottom of the well and, after 5 minutes of elapsed time, a second drag was made through the 4 slugs. This drag is the dashed curve on Figure 52. Note that, at the time each drag is recorded, the same number of passes upward through the slug have been made as were made downward. This procedure keeps the dispersion from tool movement symmetric about the peak. Thus, the peak, or more properly, the centroid, of the control slug #1 has not moved in the five minutes between drags. The remaining slugs have each moved upward during this same time with slug #2 travelling some 4 feet while the other two covered only 3 feet during the same time. The crossflow pattern is then mainly from the bottom set of perforations upward into the top of the top set of perforations with a little contribution from the lower portion of the top set. This pattern is shown on the left of Figure 52. The 4 and 3-foot travels in 5 minutes represent velocities of 0.80 and 0.60 ft/min, respectively. With a casing capacity of C = 0.0232 bbls/ft, equation (3A) gives for these velocities volumetric rates of 27 and 20 BPD, respectively, values shown on the left of Figure 52. The crossflow pattern is supportive of the injection profile in the sense that those zones taking injection become the source zones for shut-in crossflow.

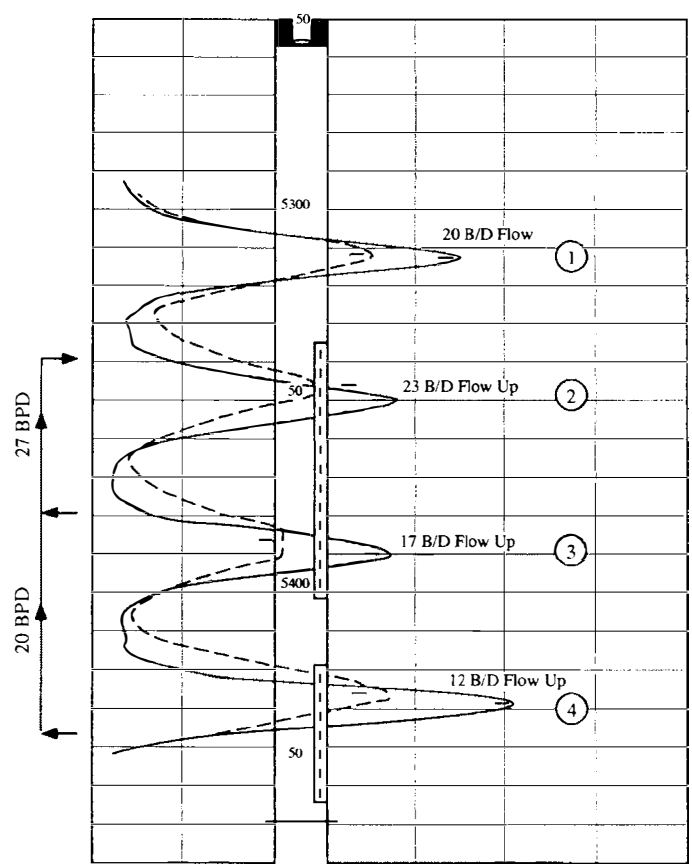

Figure 52. Crossflow check after three hours of shut-in time following water injection at 152 BPD. Drags are five minutes apart.

Logging for Casing Leaks with Well Shut-In: If an injection well has positive wellhead pressure when shut-in, then the above crossflow check procedure is the most sensitive method available for the detection of casing leaks anyplace in the wellbore. With the well shut-in, at least overnight, a slug of tracer is placed in the casing above the topmost perforations. If the pressured injection zones backflow to casing leaks, then the tracer slug will accordingly move upward in the wellbore. With proper procedure, incredibly small leaks can be detected in this fashion. Figure 53 presents five drags run on five successive days after placement of a tracer shot twenty feet above an injection zone in a shut-in well. The logging tool, of course, was left downhole during the sequence. Removal of 7,300 feet of 5/16-inch cable would allow at least an equal volume, 0.7 bbls, of inflow from injection zones below. In the 7- inch, 23 lb/ft casing, this would have displaced the slug upward by some 18 feet! Also, careful depth control is necessary, preferably by the presence of a cable "flag" placed on the line at the surface at a given depth prior to slug placement. Furthermore, the recorder should be checked for record "stretch" after each logging run.

Even the service company doing the logging did not believe the precision illustrated on Figure 53 was possible, although this was common knowledge in the early days of the tracer instrument. During the elapsed 4 days the centroid of the slug has drifted upward by at most 1 foot; consequently, any leak has a velocity no greater than 1 foot per 4 days, or

$$\hat{V} \leq 1.736 \times 10^{-4} \text{ ft/min},$$

from which

$$q \leq 9.82 \times 10^{-3} \text{ BPD},$$

a value that is about 1 cc per minute! This is in spite of the fact that a crossflow of some 50 BPD was in progress between the injection zones themselves during the logging operation.

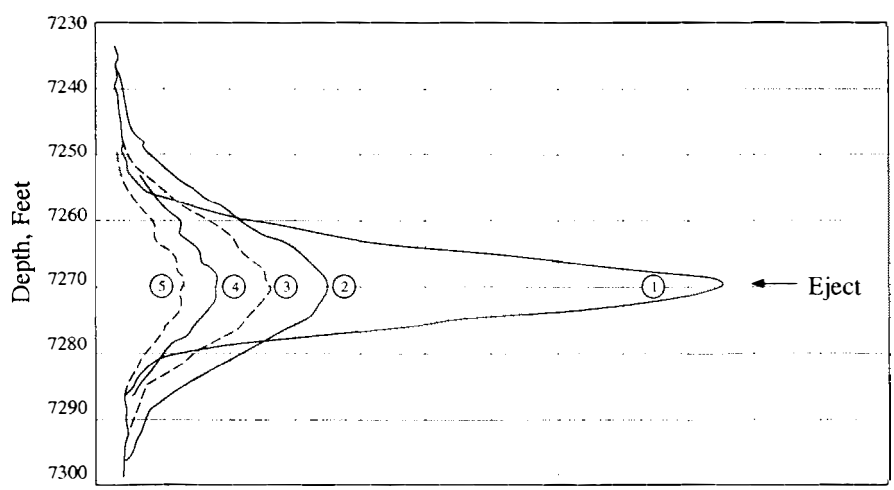

Figure 53. Drags on five successive days through a radioactive slug ejected at 7,270 feet in a shut-in injection well. Logging tool left in well between drags!

This is, therefore, the preferred method of testing tubular integrity in injection wells with positive wellhead pressure. Otherwise, the procedures described in the following section should be used.

Logging for Injection Confinement: With proper use, the radioactive tracer technique is the most sensitive method available for the detection of loss from an injection zone due to flow behind pipe. Proper use entails a realization that the tools sensitivity can be either underutilized or abused. For this reason, Table 4 (page 55) includes a recommended recording sensitivity of about one-fifth that used for a gamma ray log, namely, a sensitivity of 200 API units/inch is a good compromise for behind-pipe flow detection. At full gamma log sensitivity, even a "whiff" of tracer squeezed between the pipe and cement leaves a significant signature on the record. Any repair attempted on the basis of such a signature will cause far more damage than that which it is attempting to cure.

The limited depth of investigation of the gamma tool is another factor to keep in mind. The consequence of the exponential decrease of gamma ray intensity with distance has already been demonstrated by examples. At the recommended recording sensitivity, any gamma ray originating more than 15 inches away will appear as a statistical event lost in the overall background.

The same two techniques used for flow profiling are also employed in logging for flow behind pipe, that is, both slug tracking and stationary velocity shots are in use. The principal difference that one encounters in the case of logging for leaks is that operators who routinely use both methods while profiling will use only the stationary procedure in doing "channel checks" and "packer checks" for behind-pipe and casing leak, respectively. Yet this method is the least suited of the two for this application, as will be explained below. Consequently, the logging operator should be given specific directions as to the logging procedure to use for leak detection.

Slug Tracking Procedure for Behind-Pipe Flow: As in the procedure for profiling, this method involves the ejection of a normal shot of tracer followed by subsequent logging drags over the wellbore with the recorder on depth drive. As already mentioned, this procedure gives a very graphic, overall picture of the flow pattern in the wellbore. As such, the method allows one to distinguish true behind-pipe flow due to poor completion from tracer spreading due to vertical permeability close to the wellbore. Likewise, tracer spreading in fluid eddies often found at the base of the bottom perforated interval or immediately below a tubing string terminated by a packer can be recognized for what it actually is. These situations are all too often classified as poor mechanical integrity conditions by operators who rely exclusively on velocity shot techniques.

The operational procedure for slug tracking, however, requires some modifications to that used for flow profiling. Prior to any tracer ejection for flow profiling, a check should be made for loss behind pipe from the topmost perforations. This is done in the following way. First, a base gamma ray log is run at 200 API units per inch recording sensitivity. At this time the well is pristine relative to tracer contamination; consequently, the base log should show small excursions that correlate to the normal gamma log, sands should be recognizable from shales.

After the base log is completed, a normal shot of tracer is ejected within 20 feet above the top perforation. The slug is not intentionally mixed by tool movement so as to minimize dispersion upward. Successive logging runs are then made, at the same sensitivity as the base run, to tell if the slug, after reaching the perforations, splits with a portion returning upward behind pipe. This is all done, of course, with the well on normal injection. At the recommended recording sensitivity, the intensity will "peg" as the tool goes through the slug while it is still in the wellbore. Also, that tracer "plastered" against the casing wall at the point of ejection will be in evidence on many of the subsequent drags. Any significant amount of tracer that moves upward behind pipe will be recognizable easily from a comparison of any subsequent drag to the base survey.

The above procedure is illustrated for the injection well whose temperature surveys appeared on Figure 33 on page 45. As explained at that point, the well was new and was logged for the purpose of control on normal lithology signatures. The temperature logs showed the injection confined to the top half of the injection interval. This is now corroborated with the tracer tool. Frame A on Figure 54 repeats the completion and logging details given previously on Figure 33. The gamma ray log on this frame is an open-hole log recorded at a sensitivity of 48 API units per inch or 12 API units per chart division. Frame B of Figure 54 shows the base gamma log at 240 API units/inch that was run just prior to tracer ejection. Not only is the completed interval lithology evident on this log, but the zone of concern at depth 2 is also evident as well. This logging was conducted downward because part of the record is in the tubing set just above depth 2.

Frame C on Figure 54 shows the first two drags made after a normal shot was ejected 5 meters above the perforations. The ejection depth, 1,347 meters, is marked by an arrow. On each drag, the base log is reproduced as the solid curve whereas the current survey appears as a shaded area between curves. Above the slug, the two curves are indistinguishable as they should be. In the one minute of elapsed time represented by the two surveys, the slug has not been pumped down to the perforations.

It has, however, reached its deepest injection depth on the final five drags appearing on frame D of Figure 54. Still there is no distinction above the ejection depth between the base log and the current drag, the dotted curve. All that is shown over the 17-minute interval is that the slug is pumped away into the top half of the perforated section. This is exactly what the temperature log, Figure 33, revealed! Figure 54 illustrates a well run confinement test as far as the perforated interval is concerned.

In an older well, one would next run a "packer leak check" by ejecting a slug of tracer immediately below the end of tubing and repeating the same type of logging sequence. This procedure is illustrated in a subsequent example.

Once the leak check surveys are completed, the recording sensitivity can be reduced and any desired profile in surveys conducted. At the reduced sensitivity, any minor behind-pipe contamination is of no importance.

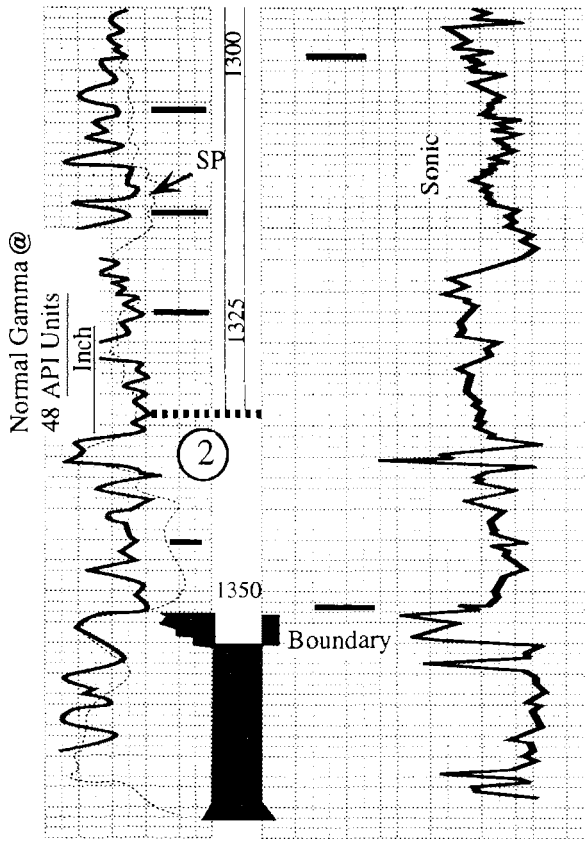

A) Completion details with gamma @ 48 API units/inch

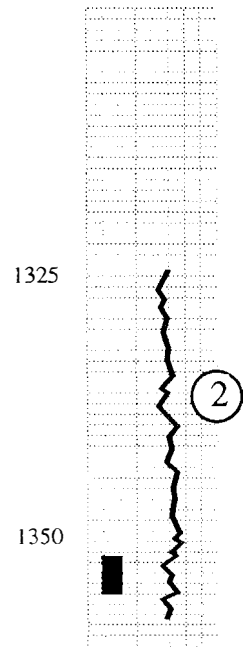

B) Base gamma @ 240 API/inch prior to ejection of tracer

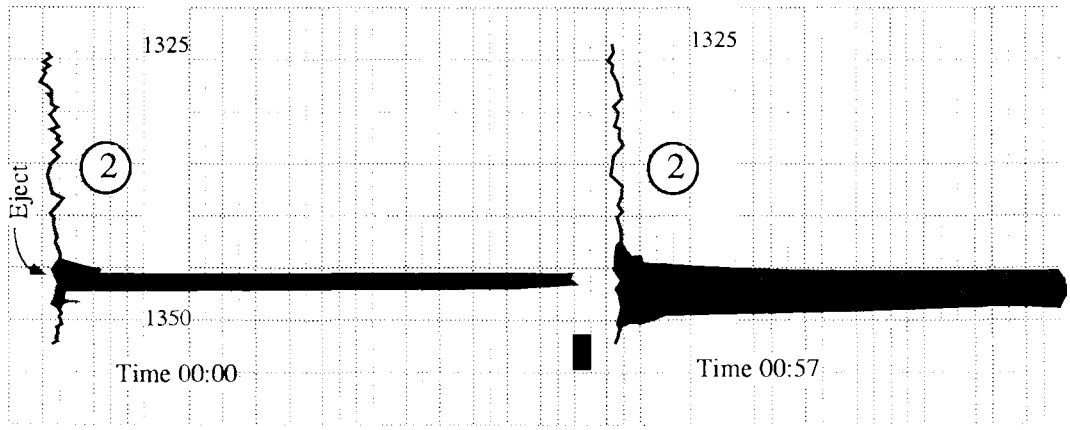

C) First two drags after shot ejection at depth of 1347 meters without mixing. Time in min:secs

Figure 54. Tracer slug tracking surveys for behind-pipe loss to zones above perforations; rate = 70 BPD.

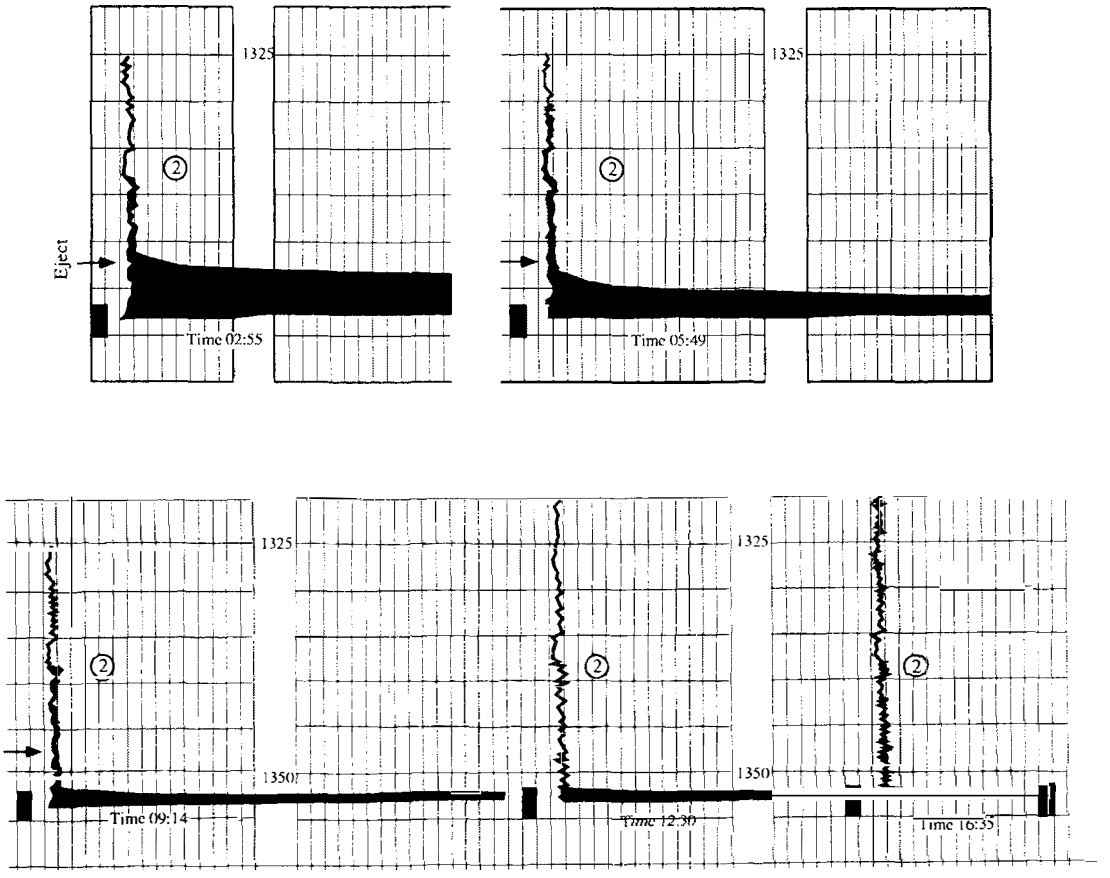

(D) Final Five Drags Through Slug After Ejection at 1347 Meters

Figure 54 (cont). Tracer slug tracking surveys for behind-pipe loss to zones above perforations; rate = 70 BPD.

After the tracer work is completed, it is a good idea to rerun the gamma ray log at normal sensitivity as a quality control check on instrumentation. The unused tracer is also dumped to prevent bringing it back to the surface. Often the two operations are combined into one final leak test. This was done in the present example. After the gamma log was rerun at 48 API units/ inch, the contents of the tracer tool was dumped by one long shot at 1,347 meters, injection was continued for an additional 10 minutes, the well was then shut-in and gamma ray log run once more. The resulting logs appear on Figure 55 where the solid curve, labeled base, is the gamma log run prior to the tracer dump and the dotted curve, labeled background, is the final gamma log run after the dump. The two logs fail to track over about four meters at depth 1 on the figure with the "prior" log being more active at this depth. The obvious question, of course, is whether this is the result of tracer put behind pipe during the confinement test but not picked up at the lower recording sensitivity. In this example, the dump test proves that this is not what happened. Equally often, however, the tracer will be dumped in the bottom of the well to decay naturally. This would leave the task of explaining why the log labeled "base" on Figure 55 is more active at depth 1 than is the original open hole log on frame A of Figure 54. Regardless of the reason for its occurrence, the anomaly that is at depth 1 on the logs of Figure 55 can be placed in perspective relative to the recommended procedure on Figure 54. Below the tubing on Figure

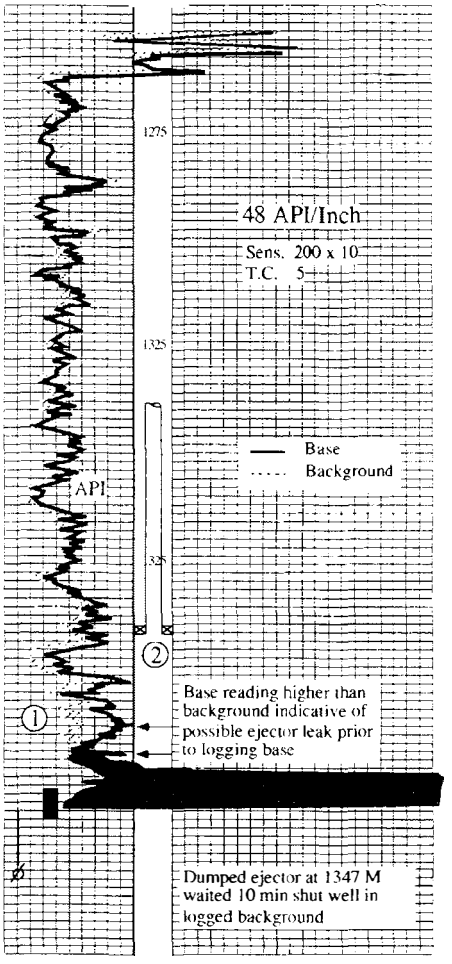

Figure 55. Surveys before (base) and after tracer dump followed by ten minutes of injection at 70 BPD.

55, the dotted trace is displaced about one chart division to the left side of the solid trace. This separation increases to about two chart divisions over the 5-meter interval at depth 1. The discrepancy is, therefore, one chart division over a 5-meter interval. Relative to the sensitivity used for the two drags on frame C of Figure 54, the discrepancy is 1 x 48/240 = 0.2 chart divisions over a 5-meter interval. This area can be compared to the "area" for the drag in frame C at 00:57 seconds as the slug appears to have been mixed to some degree at this time. The "width" of this peak is about the same 5 meters of that of the anomaly. Yet, the "pegged" amplitude alone is 28 chart divisions; consequently, the true amplitude would exceed this value by at least one-half again. The reference area would then have an amplitude of some 50 or so chart divisions. The discrepancy could thus represent a flow of at most 70 BPD x (0.2/50) = 0.3 BPD or 1/2 CC per second! Even if real, such a leak could not be squeezed with any degree of success. The 0.2 chart divisions is about the width of the line on the base log of frame B on Figure 54. The five drags on frame D, Figure 54, show numerous locations where the dotted-line survey departs from the base log by this amount due to normal statistical variation alone. The point to be made is that the sensitivity employed for normal gamma ray logs is too high for general use in confinement tests. Anything that can be dealt with will already be apparent at the sensitivity displayed on Figure 54.

This fact is illustrated by the next example. The temperature surveys on Figure 20 (page 27) revealed a loss to a zone immediately above a disposal zone that could result from either a casing leak or behind-pipe flow. The tracer survey considered next shows that the problem is the result of a leak behind casing. That this is the case is already apparent on the flow-profiling drags appearing on Figure 56. Contrary to the recommended procedure, the flow profiling was done before any channel checks or packer checks. This is an acceptable way of doing the surveys provided one can allow about one-half hour of injection between the profiling surveys and the leak check shots. The drags on Figure 56 show that most injection is leaving the wellbore over the bottom half of the perforations which is what the injecting temperature survey on Figure 20, also revealed. However, drag 4 further reveals that some tracer has split off and moved back uphole behind pipe to permeability in sand C immediately above the injection zone. This fact is even more evident on drag 5 of Figure 56. The two drags together show two permeability spikes marked by arrows on Figure 56.

Whenever a tracer material leaves the wellbore and enters pore space, some tagged material is absorbed on the rock surface and is thus held at this location for a time that depends on the strength of absorption. For the anionic iodine, I-, this absorption is a weak process.

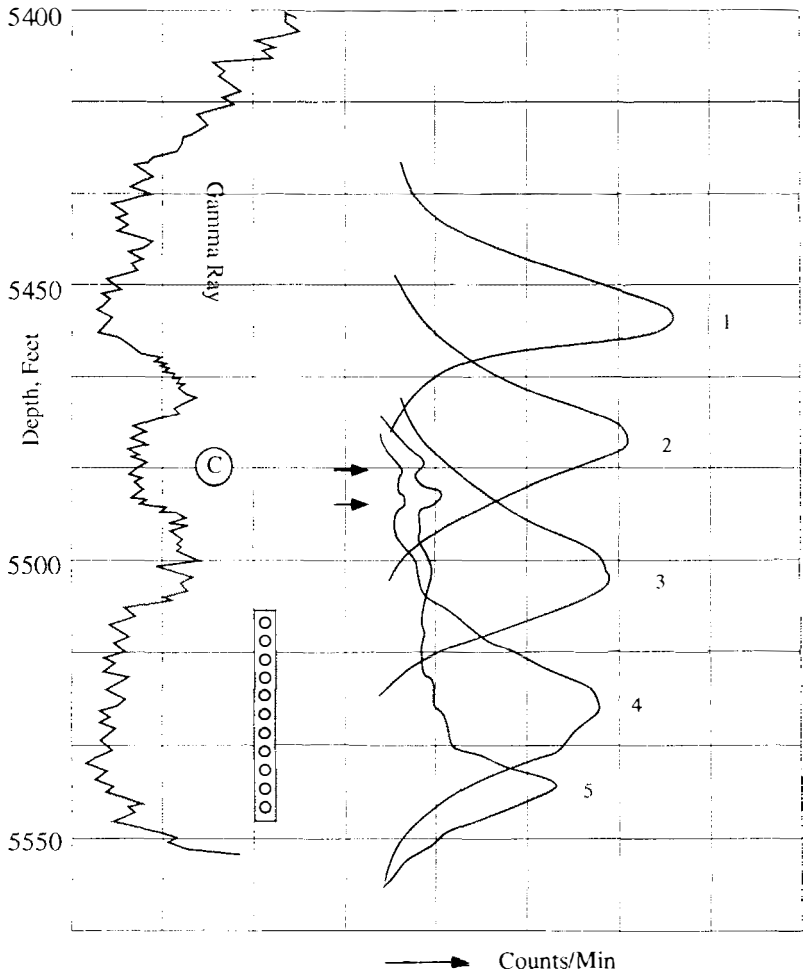

Figure 56. Five flow-profiling drags in a well on injection at a nominal 500 BPD.

Consequently, continued injection washes the surface clean and displaces the tracer into the formation. By contrast, tagged metal ions, cations, lock to the rock so tightly that they are still evident on the injection points even after a week of continuous injection.

It is the creation of the injection spikes that enables the slug tracking procedure to distinguish behind-pipe flow of tracer to porosity from spread to tracer due to vertical permeability around the well. In the latter case, tracer is already in the formation so that no discreet "exit" spikes develop on the drags. Instead, the tracer just seems to drift away from the slug like the edge of a bank of fog. An example of this behavior will be given subsequently.

In the example at hand, injection was continued for one hour after the drag survey of Figure 56 was completed before a "channel check" or confinement survey was initiated. After this time, with the well still on injection, a base log was run at 200 API units/inch with the result shown by the leftmost trace on Figure 57. At this sensitivity, the sand at C is free of tracer pollution. Consequently, a normal shot was ejected at a specified depth of 5,515 feet at the top of the perforated interval although subsequent drags showed that the material actually ejected at a depth closer to 5,520 feet. Five of the nine drags through the slug are depicted on Figure 57. The first survey through the slug, labeled 0:00, was actually made somewhat over a minute after ejection. By this time the slug has mixed and traveled nearly to the bottom of the perforations. By the time of the drag labeled 1:17, some of the tracer has split off and gone upward behind pipe and into the first of the two permeability exits already observed on Figure 56. The drags on the bottom row of Figure 57 exhibit both the permeability spikes. In fact, by 10:08 (minutes:seconds) most of the tracer had been displaced into the formations at both the perforated interval and at zone C. There remains on the record three "permeability" spikes in the bottom half of the completed zone, a residual at the depth of ejection and two "permeability" spikes in zone C.

The massive tracer dump test was not run because the behind-pipe flow appeared on all the tracer surveys. A closure gamma ray was not run for the same reasons.

The drags of Figure 57 exhibit the true signature of tracer flow behind pipe. The only feature missing is a drag before the tracer reaches exit porosity. If, on the drag of 1:17 at the right top of the figure, the permeability spike at sand C is leveled to the height behind it, then the picture is that of a slug not yet at an exit depth. The slug front is sharply defined with tracer simply stretched out behind this front. This behavior contrasts with the hypothetical figures typically presented in discussions on tracer logging. These show tracer slugs moving behind pipe with the same bell-shaped signatures as those on Figure 56 for the slug moving inside the casing. The area open to flow behind pipe is so constricted and tortuous that the bell shape is not preserved. Only in relatively large, uniform annular areas does this type of signature appear.

Because the permeability "spikes' are a significant feature, the reader is asked to go back to the tracked slug survey that started the tracer discussion, Figure 35, and examine the last drag, K, in the sequence. The four spikes at 9,605, 9,601, 9,598, and 9,590 feet are all "permeability spikes." The development of these spikes is evident on the surveys H, I, and J. These features also serve as quality control checks on procedure.

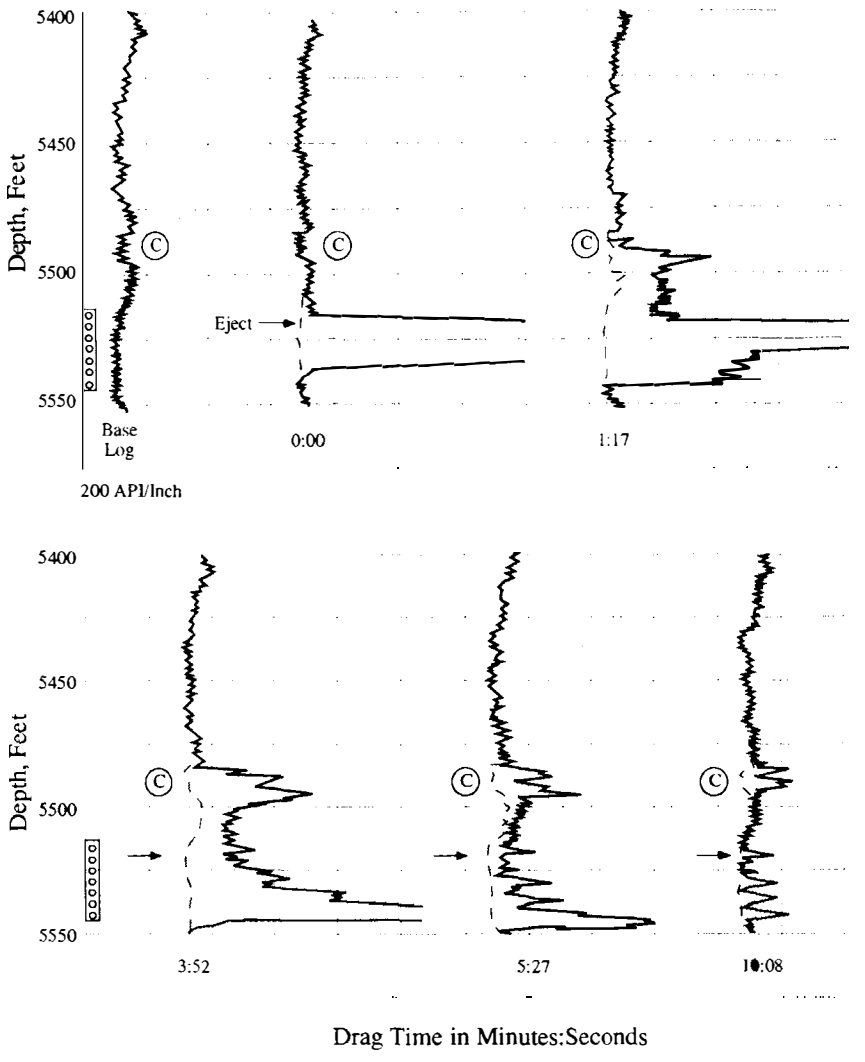

Figure 57. Behind-pipe flow detection by slug tracking in well in injection at a nominal 500 BPD.

The slug tracking method is also the preferred way to check for leaks past the packer and into the tubing-casing annulus. For this purpose, a normal slug is ejected in the tubing above its end and successive drags at a sensitivity of 200 API units per inch run to track the slug's progression. The logging is done downward so as to successfully navigate the end of tubing. An example of this type of survey is on Figure 58. The left-most trace is a gamma-ray log, labeled "correlation gamma-ray," run at 80 API units/inch because of the "hot spot" at depth 1 on the figure. This region of high intensity results from a cobalt-60 tagged cement slug behind pipe at this depth. The base gamma ray log, labeled as such, was run before any tracer ejection at 400 API units/ inch. This is not sufficient sensitivity to show any of the lithology character evident on the correlation gamma, but was again a compromise to avoid domination by the tagged cement. With the injection rate steady at 720 BPD a normal shot of tracer was ejected in the tubing at depth 2, 4,250 feet, a location 28 feet above the end of tubing. Seven consecutive surveys were then run from 4,200 feet to total depth. The times listed below each drag are the times that the logging started at 4,200 feet. The first survey, run #1, was started at 3:30 pm very quickly after the slug was ejected. Full stream velocity in the tubing is 129 ft/min; in the casing 22 ft/min; and

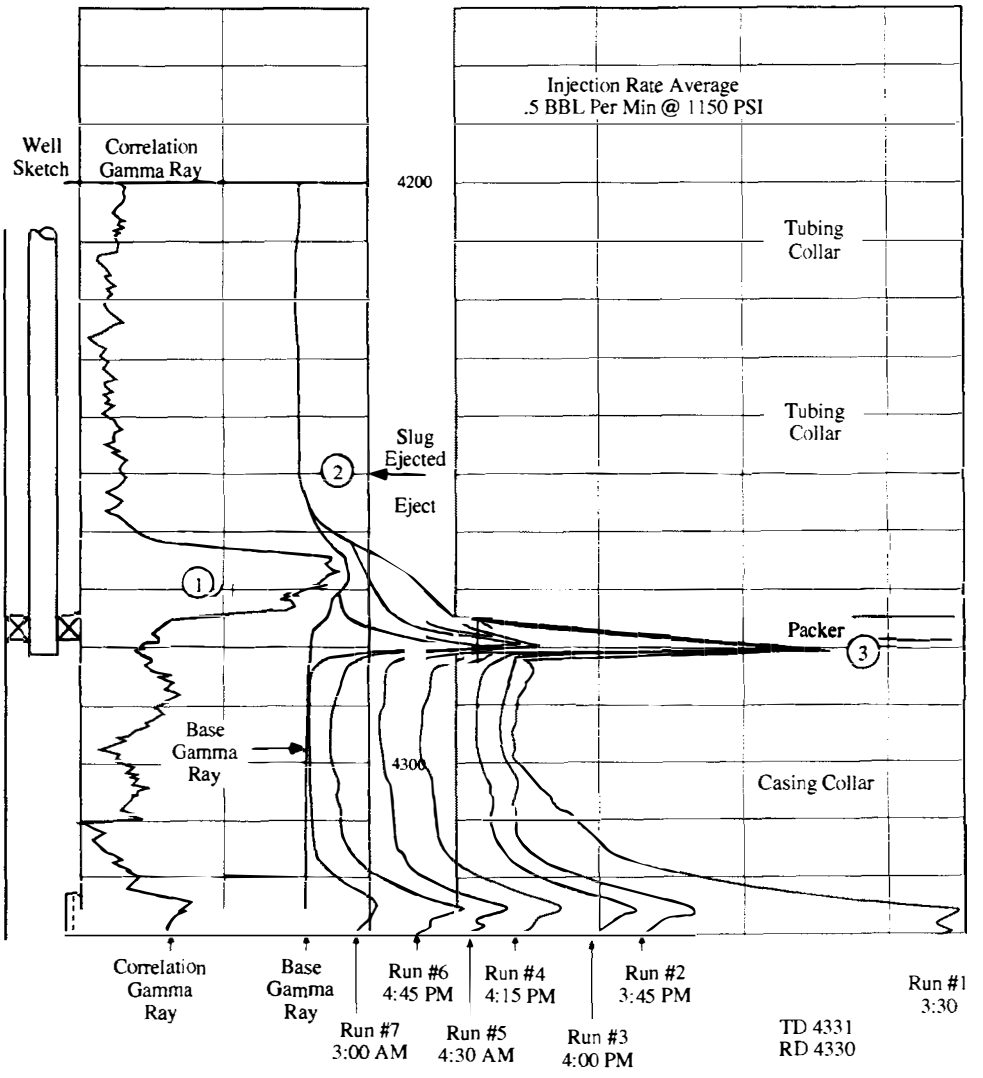

Figure 58. Packer leak check by the slug tracking method in well on injection at 720 BPD.

in the annulus 28 ft/min. In the 3+ minutes required to log from 4,200 feet to 4,330 feet at 40 ft/min, the main part of the slug has reached the perforated interval at 4,321-4,330 feet and two permeability spikes are developing. Two things should be noted about drag #1. First, the activity due to tagged cement adds to the tracer activity thereby distorting the shape of the intensity curve across region 1. In fact, without the prior gamma logs, run #1 alone would suggest flow up the backside of the tubing to about 4,260 feet, a depth nearly eighteen feet above the packer! The second feature to note on run #1 is the large slug of tracer at depth 3, a location immediately below the collar signature of the end of tubing. Subsequent drags, on fifteen minute intervals, show that the slug is stationary at this location. Furthermore, the concentration of tracer at depth 3 remains nearly unchanged through run #4, a drag started 45 minutes after ejection.

Actually, there is a third feature to drag or run #1 that is easily overlooked. The intensity below the slug at depth 3 decreases to a value much larger than the background level on the base log.

In fact, run #6, one hour and 15 minutes later, is still above base line activity from depth 3 all the way to the perforations, where injection spikes persist at high levels.

Here is what has happened. As the tracer slug exited the end of the tubing, a large portion was trapped in a turbulent eddy circulating under the packer. This material was then slowly, but continuously, washed out of the eddy and carried down to the perforations by the continued injection.

The skeptical reader can accept the above argument and still ask how one can be confident that the eddy did not also slowly drain upward into region 1 as well. The additive nature of gamma emissions from independent sources allows us to correct the drags after ejection for the distortion from the cement emissions. The increased activity due to cement that is evident on the base log is subtracted from the activity recorded for the drag under correction. The result of this correction to run #1 is given on Figure 59. Here, the peak asymmetry is clearly downward, not upward.

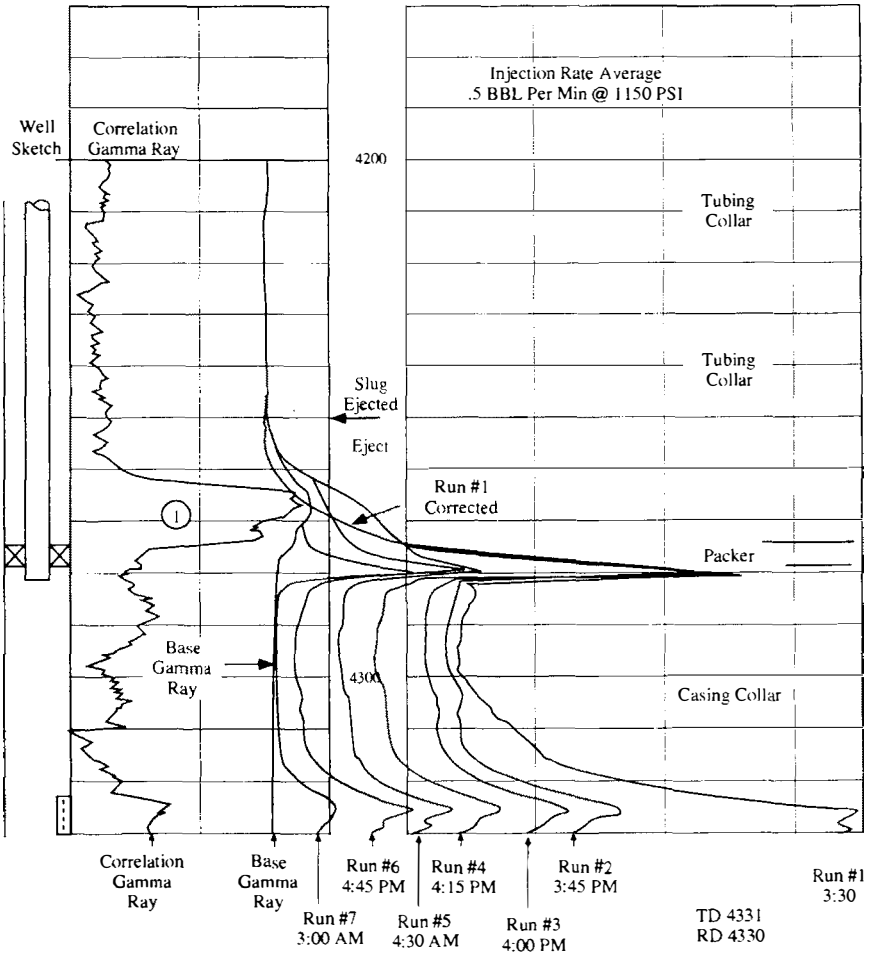

Figure 59. Corrected run #1 with spurious base activity subtracted.

Figure 58 thus demonstrates a case of a perfectly valid verification of packer integrity by a test that, thanks to the quirks of completion and flow pattern, is easily misconstrued. In fact, the figure is a testimonial to the ability of the slug tracking method to reveal the "big picture." Had only a stationary, velocity shot packer check been made, the eddy would have been incorrectly identified as a "slow " packer leak.

A shut-in crossflow check that reveals movement past the end of a tubing string is given on Figure 60, where three drags run on 15 minute intervals are depicted. Four slugs of tracer were injected, the first slug being placed immediately under the packer and the remaining three spotted over the interval of open perforations. Slug 1 was intended to be a control shot; however, its behavior was interpreted as evidence of a leak past the tubing packer at 4,347 feet into the squeezed perforations in the casing above the packer. There is, certainly, movement inside the casing. During the 30 minute period slug #2 moves upward 27 feet with an irregular velocity averaging 0.9 ft/min. For a casing capacity C = 0.0232 bbls/ft, the corresponding volumetric rate is q = 1440 x 0.0232 x 0.9 = 30 BPD. The three surveys through slug #1 show two things:

1) The slug is in a stagnant location because its peak is stationary, but tracer material is being washed out of the slug because its peak is rapidly dropping in intensity.

2) The presence of slugs 1' and 1" show that this washed material is carried upward; presumably, by the flow from the perforations that moves slugs 2 and 3.

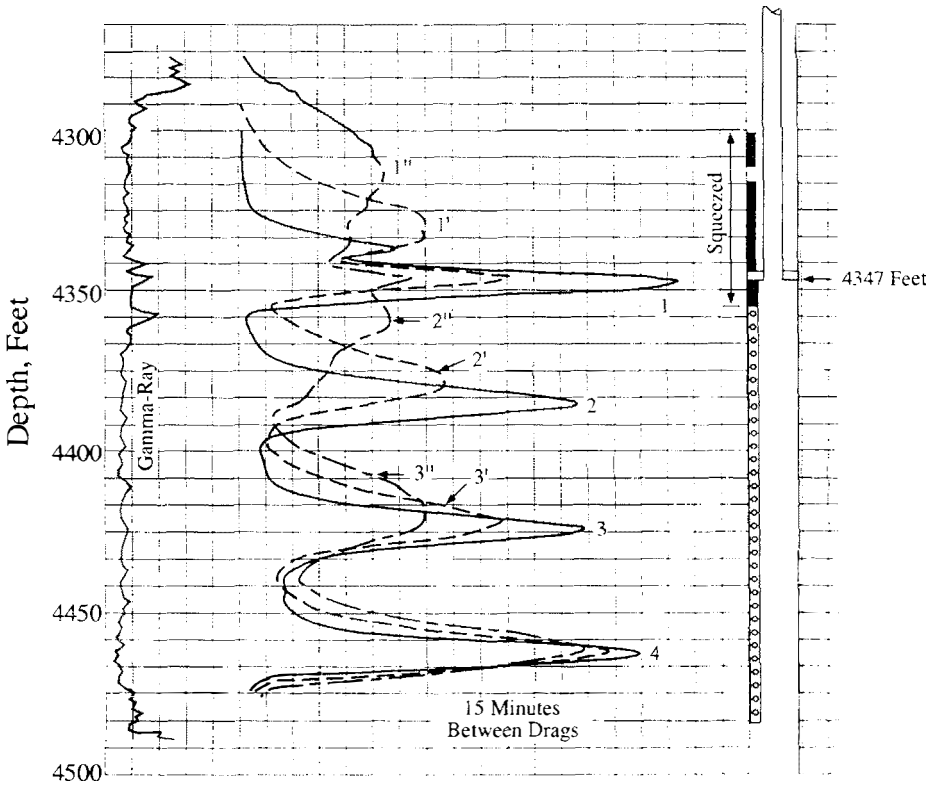

Figure 60. Crossflow check after one hour shut-in period on 900 BPD injection well.

The shape of drags 1' and 1" has the same bell-type signature as the ejected slug; consequently, the flow is inside pipe somewhere, the question is where! The location that would immediately come to mind is the annular space between the tubing and casing with flow into the squeezed intervals shown on Figure 60. There are, however, three features to the surveys that rule out this type of crossflow:

- First, drags 1' and 1" show no injection spikes even though tracer covers the entire squeezed interval;
- Second, the tracer drag 1" shows no slowing down that is necessary for it to accommodate the lithology on the gamma-ray log that shows a porosity limit at 4288 feet;
- Third, and most important, a flow past the packer would not leave the stagnant pocket of tracer at location 1.

The flow depicted is therefore into the tubing string and upward, not behind tubing. The well does have positive pressure. Hence, the behavior could signify a tubing-to-casing-to-environment leak at shallower depths.

Figure 60 illustrates one of the problems most common to unsupervised tracer surveying; namely, the failure to carry through on an observed situation to the point that one knows what one is seeing. The behavior may be the result of nothing more than failure to seal around the logging cable at the surface or failure of the wing valve to completely shut-off backflow from the well. Lack of annular pressure when the well is on pump certainly suggests this is the case. Furthermore, had the logging operator run two more drags, he would have established that slug 1 did not stop at the top of the unit containing the squeezed perforations. A "procedure" called for three drags, and three drags were run, no more nor less!

The point of Figure 60 is that tracer transport that does not require the flow to squeeze past or around obstacles maintains a simple slug shape as a characteristic signature. This shape is not maintained, for example, on Figure 57, once the tracer starts to move behind pipe.

In combination, Figures 59 and 60 illustrate another point. One often hears or reads statements to the effect that tracer surveys, either radioactive or activation type, give results that "are easy to interpret." The correct statement should be worded differently: The surveys give the most graphic and most easily comprehended picture available. The reasons for what is seen on the survey, however, can be just as obscure as on any other logging procedure. This point is generally not emphasized sufficiently in most discussions on production logging.

For the above reasons, the next method of leak check, the stationary velocity shot procedure, is the least preferred way of confinement demonstration.

<u>Velocity Shot Procedure for Behind-Pipe Flow:</u> The stationary or velocity shot method of leak checks is by far the more popular technique among logging engineers simply because it is easier to perform than is the slug tracking technique. One stops the tool, say, just above the top

perforation, and, with the well on injection, ejects a slug of tracer into the moving stream. With the recorder on time drive, the operator can observe the slug go past the two stationary detectors on its way to the perforations. This far, we have a standard velocity shot. However, for the leak check, the recording is continued sufficiently long to insure that no tracer doubles back behind pipe and, again, passes the detectors on its way up. With one detector close to the perforation, the record length can be held to a minute or so duration without fear of failure to detect leaks.

A sensitivity of 200 API units/inch is again recommended for the stationary record. Because two detectors are available, common practice uses the higher sensitivity on only one detector record. This allows the other one to record the slug shape inside the casing without pegging.

A similar procedure is employed to check packer integrity while the well is on injection. This technique is illustrated on Figure 61 for the same well that appeared on the shut-in test of Figure 60. The tool is stopped with the ejector port located at 4,238 feet as shown on frame A of Figure 61. The top detector was located four feet deeper at 4,342 feet whereas the bottom detector was at 4,347 feet at the end of the tubing string. The top detector output was recorded on an insensitive scale on the right-hand side of frame B, that provides very little information other than the fact that the slug passed the detector within 1 chart division, or 1.18 seconds, after

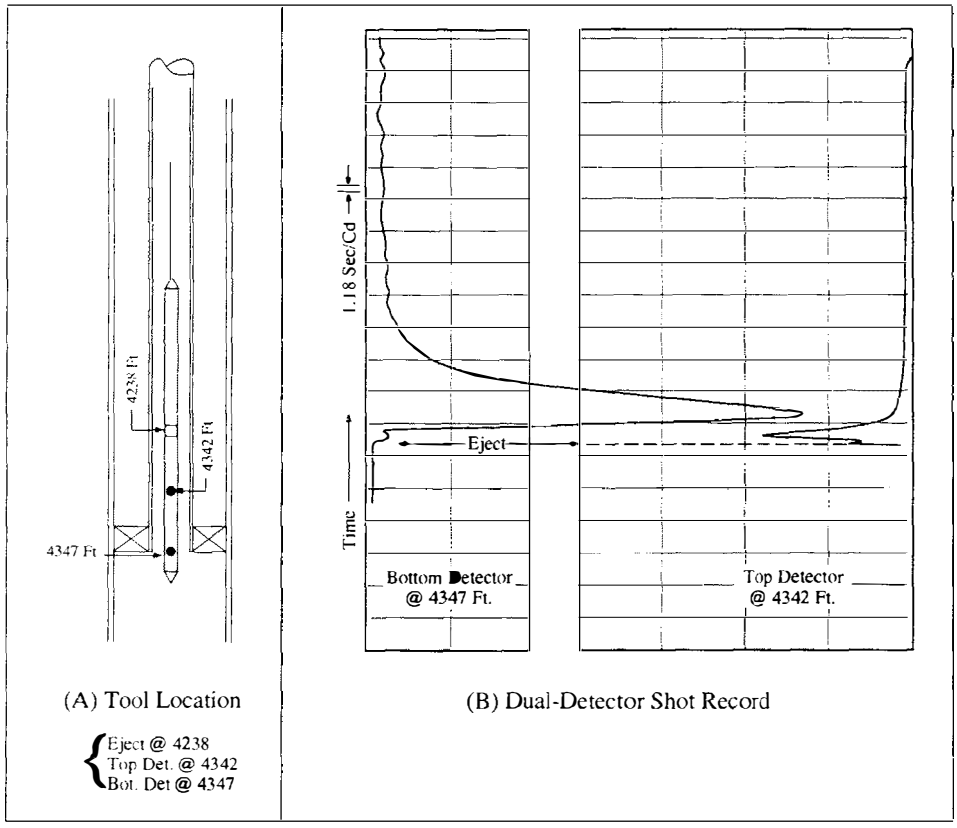

Figure 61. Stationary velocity-shot check for packer leak for well of Figure 60 while on injection at a nominal rate of 900 BPD.

ejection. The record from the bottom trace is at higher sensitivity although still not at the 200 API units/inch appropriate to behind-pipe logging. With the bottom detector at the end of the tubing, any doubling back at the packer would have added to and distorted the primary record from the passing slug. As no such distortion is in evidence, we must conclude that the packer is sealing. The record was continued for 57 chart divisions, or 68 seconds, after the slug passed the bottom detector. Had this detector been located, say, five feet above the end of tubing, then the record length would have been too short. The packer check alone does not eliminate the possibility of leaks higher in the tubing. Consequently, it is puzzling that the logging operator did not pursue the shut-in flow detected on Figure 60 for this well. All that the results of the packer check proves is that a leaking packer is not responsible for this flow.

A somewhat better technique of stationary packer check is illustrated on Figure 62 for the same well that was the subject of the behind-pipe tests of Figures 56 and 57. The end of tubing in this well is located at a collar log depth of 4,341 feet. For a quick packer test, the operator stopped the tracer tool with the bottom detector at 4,340 feet, a location 1 foot above the end of tubing. The output of this one detector was then recorded at a sensitivity of 200 API units/inch for some

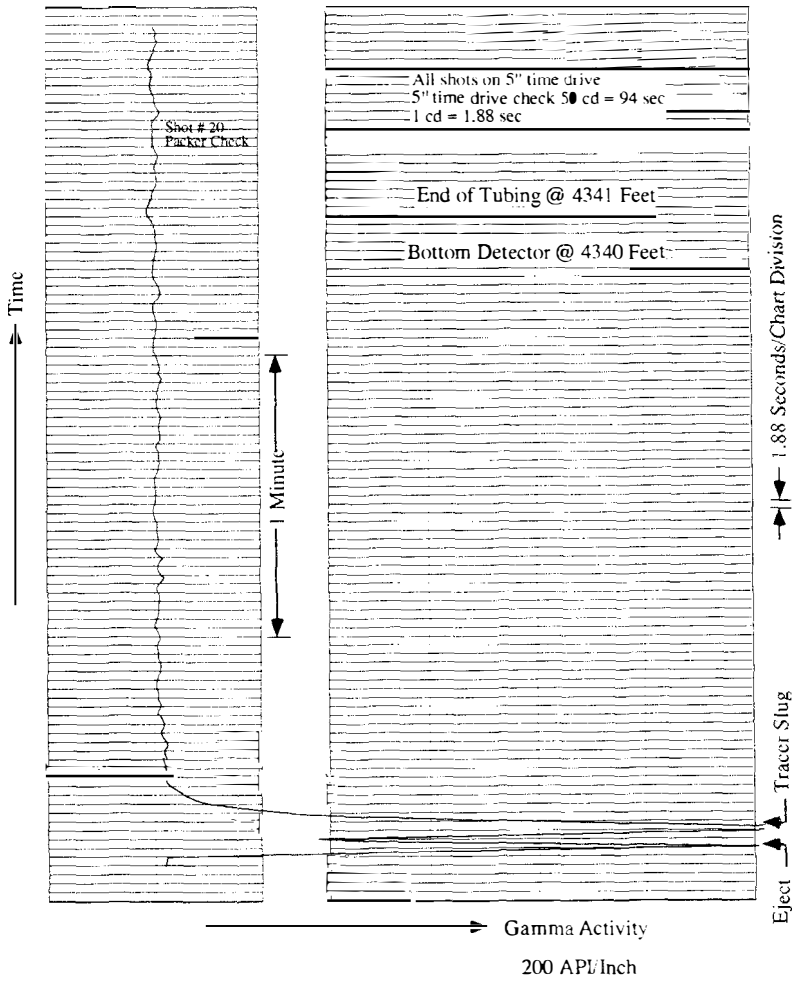

Figure 62. A properly scaled, stationary v 'ocity shot test for packer integrity with an annular velocity resolution of 0.35 ft/min leak rate.

three minutes after a shot ejection in the tubing above the detector. During this procedure, the well remained on injection at 500 BPD nominally. The record shows no return past the detector for the 92 chart divisions or 2.88 minutes after-shot duration. Any packer leak is then at a velocity of less than 1/2.88 = 0.35 ft/min. For an annular capacity of C = 0.0178 bbls/ft, any leak rate is therefore less than 9 BPD. This resolution is typical for operators who are not given specific directions on how long to record on a stationary leak check test.

As long as the stationary packer checks are benign, they are a fast, simple way of surveying. If "leaks" are indicated, however, one is wise to switch over to the tracked slug procedure to chase down the reason for the behavior. For example, we can draw a hypothetical velocity shot for the packer check that was done on Figure 58, by the slug tracking method. Suppose a single detector tool was positioned with the detector located one-foot above the tubing end and a shot of tracer ejected above the detector. From what is seen on Figure 58, the expected gamma response at the detector would be as shown on Figure 63. The high level of activity caught below the packer in the eddy would give a reading at the detector that would make one suspect a "slow" leak through the packer. At this point one would run drag surveys to establish that the activity originated in the "stagnant" eddy as was done on Figure 58.

Stationary velocity shots are also commonly used as so called "channel checks" for flow behind pipe above and below perforations. The procedure is illustrated on frames B and C of Figure 64.

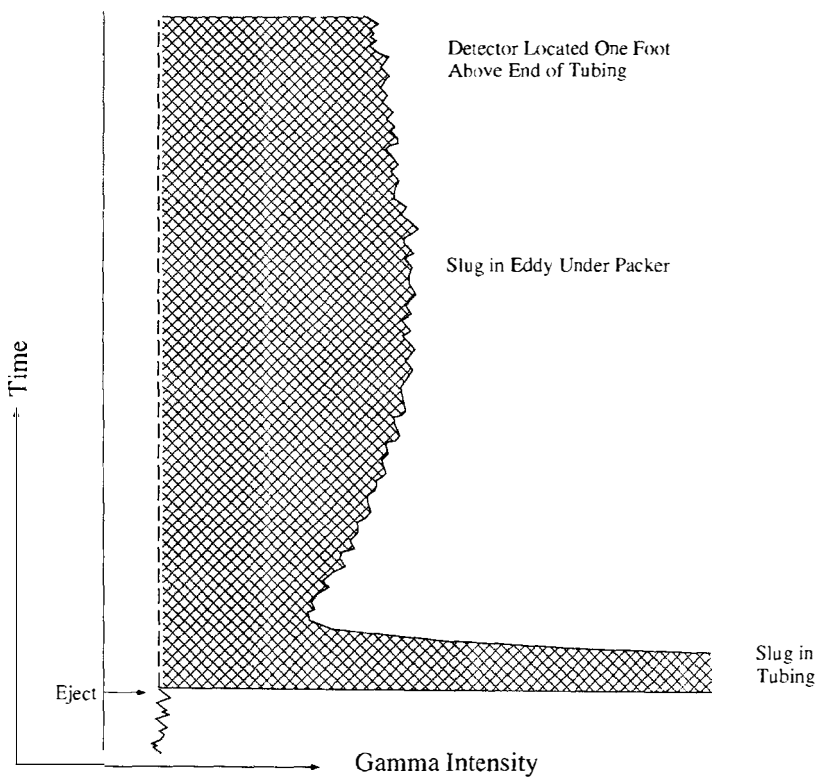

Figure 63. Hypothetical velocity shot response to stagnant slug caught under packer on Figure 58.

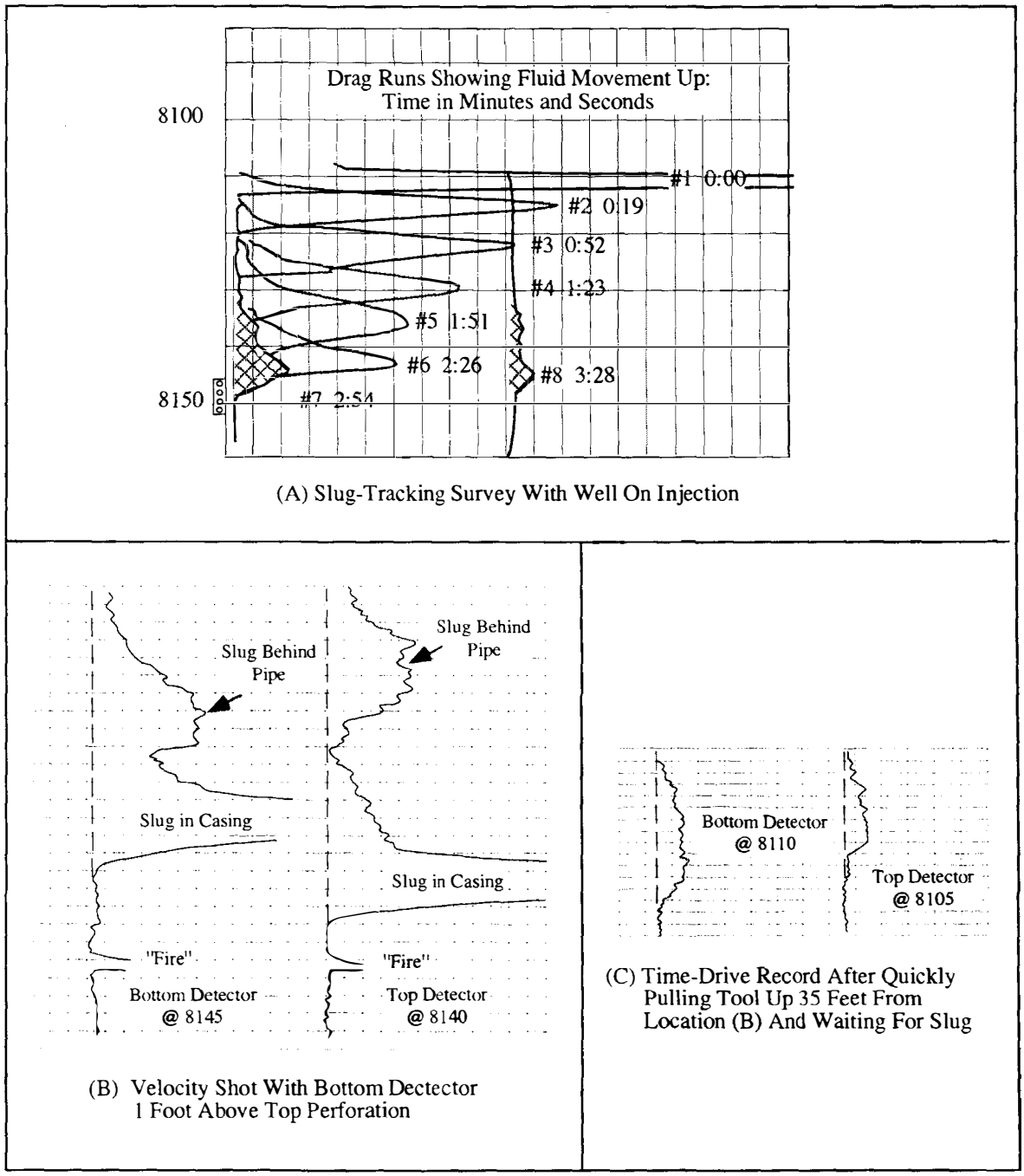

Figure 64. Channel checks on well of Figure 32 with well on brine injection at 400 BPD.

These surveys come from the same well whose temperature surveys, Figure 32 (page 44), showed crossflow behind casing from an oil zone perforated at 8,146-52 feet. The well was killed in preparation for workover and a pump-in tracer test was run to corroborate the temperature surveys. Frame A on Figure 64 shows a slug-tracking survey done initially for

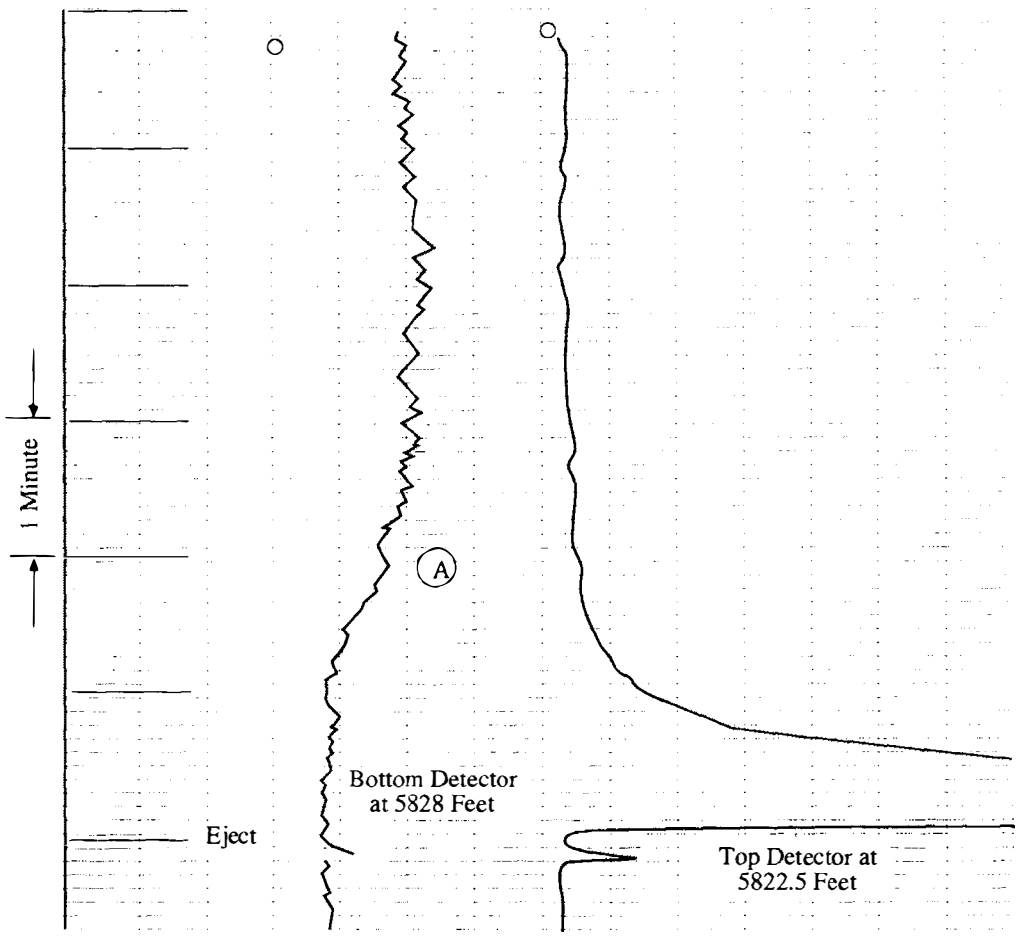

Figure 65. Channel check by velocity shot method below perforations at 5,820 - 25 feet with well on injection at 600 BPD.

injection rate estimation. By the time of drag 6, tracer has reached the perforations. Drags 7 and 8 show this material spreading upward behind pipe. After the drag survey was completed, injection at 400 BPD was continued another half hour to flush the tracer behind pipe. Then, with injection maintained, the tool was positioned with the bottom detector one foot above the top of perforations and the velocity shot of frame B, was carried out. The output of both detectors were recorded at high sensitivity. On the journey downward inside the casing, the ejected slug passes the top detector first. An additional travel time of 18 seconds is required for the tracer slug to pass the bottom detector. Very shortly after passage of this sensor, the tracer doubles back over the 1-foot distance from the top perforation to reappear at the bottom detector. In 13 seconds more the tracer passes the top detector. Once this happened, the logging operator quickly pulled the tool upward stopping with the lower detector at 8,110 feet. With the recorder on time drive, he then waited for the tracer to arrive as shown on frame C.

From the condition of the slugs on frame C, a location 40 feet above the perforations, it is apparent that they cannot be tracked much farther up the wellbore. To do this, the tool contents should be dumped just above the perforations and slug-tracking surveys initiated. In this fashion, a large shot can be followed behind pipe for some 2,000 feet before it is too dispersed for accurate detection.

Frame B also illustrates the fact that, in passing a fixed location, the tracer behind the pipe exhibits the same type of "shape" as that inside pipe. This presentation mode is the source of the misconception, previously mentioned, that this is the "shape" over distance of the tracer distribution behind the casing. Frame A shows, of course, that this is not correct.

The velocity shot channel check, while fast and easy to run, suffers from the same limited "scope of vision" as does the packer check by the same procedure. The velocity shot of Figure 65 was made at the base of perforations in a well on injection at about 600 BPD. The shot serves as a "channel check" at the base of the bottom set of perforations located at 5,820 - 25 feet. The top sensor was positioned at the midpoint of the interval at 5,822.5 feet. This allowed the bottom detector, 5.5 feet deeper, to be positioned at 5,828 feet, three feet below the bottom perforations for a channel check. Accordingly, its output was recorded at a greater sensitivity than was the output from the top detector. The traces show that the leading edge of the tracer arrived at the top detector some 1.5 chart divisions or 1.5 x 6 = 9 seconds after ejection. Likewise, a small concentration of tracer "arrives" at the bottom detector some 15 chart divisions or 90 seconds after ejection, time A. If the differential time of 81 seconds is allocated to the travel over the three foot distance from the bottom perforation to the detector, then the associated velocity is 2.2 ft/min. Consequently, if the tool is dropped another five feet down the hole, the tracer should get to the bottom detector by 2.5 minutes after relocating. Unfortunately, the logging operator was content to say that the signature was due to a small channel and "close shop."

The signature on Figure 65 from the bottom detector has the same slowly dispersing behavior shown of Figure 63 for the tracer ensnared by the eddy current beneath a packer. In fact, the signature is the result of the same type of phenomenon. Figure 66, an 11-drag slug-tracking survey from the same well, helps to understand what is happening. Drags 1 through 5 show that practically all injected water reaches the bottom set of perforations before exiting the wellbore. This rapid change in flow direction over a five-foot long interval sets up turbulence in the form of eddies that can scour the wellbore for a significant distance below the perforations. Drags 7 through 11 show that the slug peak slows down to a stop at the bottom perforations. However, a comparison of the leading edges of these same drags with that for drag 6 reveals that at the same time the slug starts to slow down its leading edge starts to disperse below the base of the perforations. By the time of drag 11, this dispersion has carried tracer some 14 feet below the base. Some of this spread is obviously the result of logging repeatedly through the tracer slug; however, the situation is clearly more severe than that of previous examples, say, for instance, that shown by drag 8 on frame A of Figure 64. After viewing Figure 66, the reader should not be surprised to see the appearance of tracer on Figure 65 at a detector situated only three feet below the base of perforations. This would probably not have happened if a good portion of the injected water exited the wellbore at the top set of perforations. The condition is a result of the particular state of flow in the well.

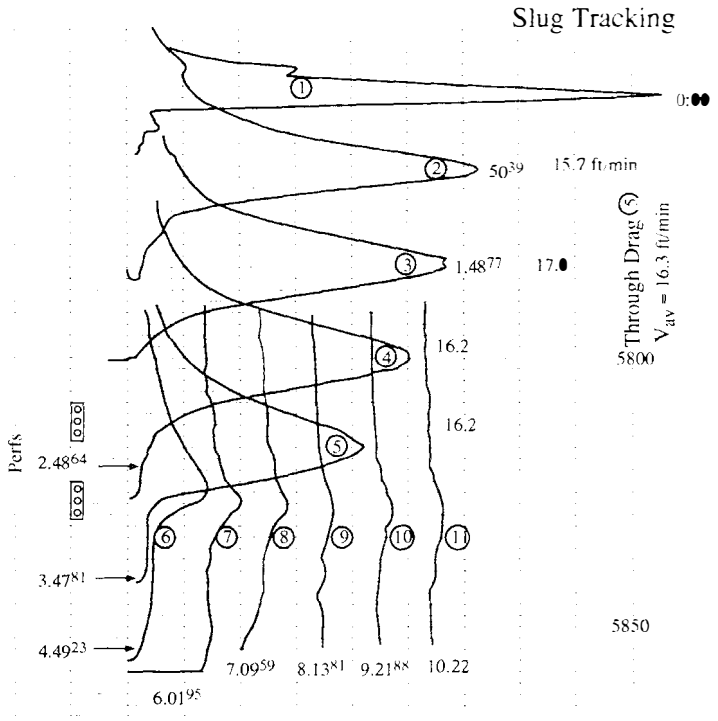

Figure 66. Slug tracking survey from same well as velocity shot of Figure 65 with same injection rate of 600 BPD.

The same slowly dispersive behavior shown on the trace from the bottom detector on Figure 65 is also characteristic of the signature produced by velocity shot "channel checks" in formations with good vertical permeability. If the tracer can spread through porosity either upward or downward from the perforations, then this movement will be detected provided the flow is within about one foot of the wellbore. On a stationary, velocity-shot channel check, this situation is very difficult to distinguish from that due to a small, behind casing leak. Failure by the logging operator to follow such flow has resulted in many unnecessary workover attempts. The "leak" will only extend to the top or bottom of the porous interval if it is the result of vertical permeability. Consequently, one should always provide open-hole or cased-hole lithology logs to the operator if there is the possibility of tracer spread by vertical flow in a formation.

For example, the gamma-ray log on the left-hand side of Figure 67 shows that the top set of perforations are located at the bottom of a lithological unit that extends upward from the shale at 11,611 feet to a second shale "break" at 11,464 feet at the top of the log. Furthermore, this unit is known to have good vertical permeability. The temperature surveys on the right-hand track confirm the presence of vertical permeability. These surveys were run after 536 barrels of water had been injected into a previously static well at about 2 bbl/min rate. An injecting log was not run; however, the shut-in surveys show that some injected water reached the total depth of 11,653 feet. Likewise the surveys show that most of 536 barrels stayed in porosity in the interval identified as BE on the temperature surveys. This interval is seen to be a subunit on the gamma-ray log. The topmost perforations are into the bottom of this subunit. The surveys further show

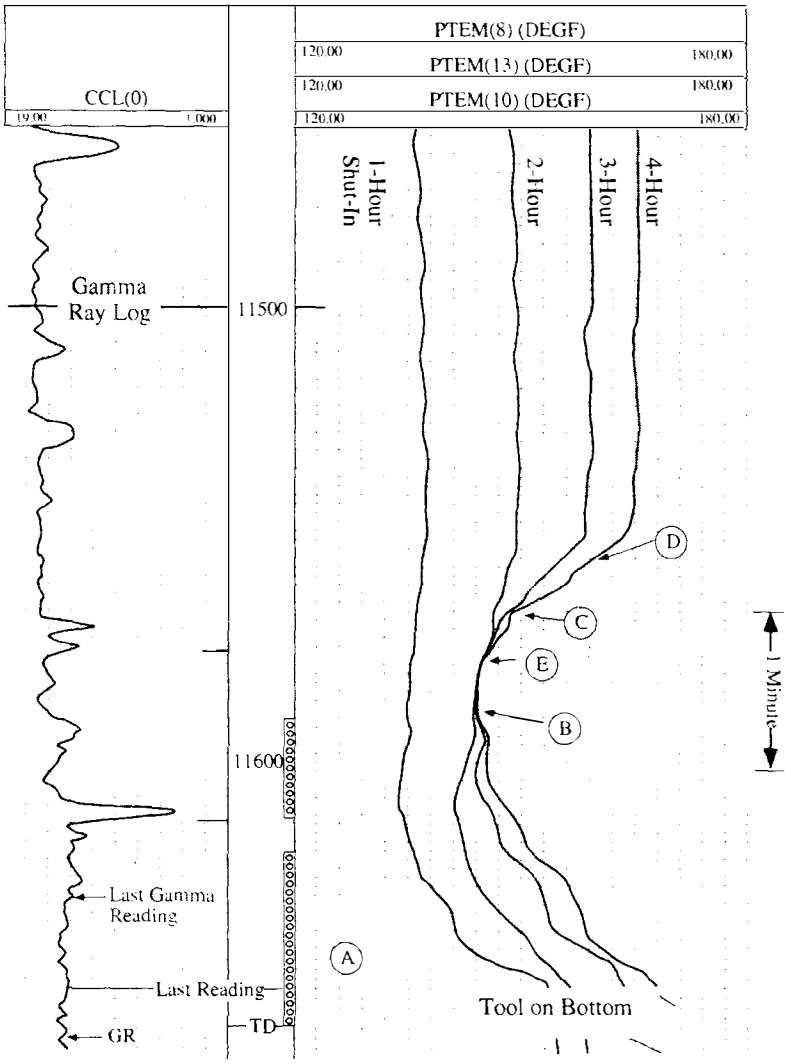

Figure 67. Temperature surveys from a well after 536 barrels of water injected and well shut-in.

some injection up to depth C, 11,566 feet, and the possibility of the injected water reaching as far up as depth D at 11,555 feet. Because the well had been static prior to injection, the relative behavior of the shut-in surveys also reveal that the water reached interval BE by vertical flow through the formation, not by flow directly behind pipe. Had the latter been the case, the injection "cold" would have been in direct contact with the wellbore and would have been in clear evidence on the 1 and 2 hour shut-in surveys. The small amount of storage at the bottom of the top set of perforations does appear on these traces.

The third of three velocity shots made as "channel checks" while injecting into the well is illustrated on Figure 68. The logging tool makeup and its location for this shot is shown on frame A of the figure. Three detectors, one above the ejector and two below, are identified by the numbers 1,2, and 3 on frame A. The output from each of these sensors is labeled correspondingly on frame B. The output for detector 1 is recorded at normal gamma log sensitivity of 40 API units per inch whereas a sensitivity of 100 API units per inch is employed

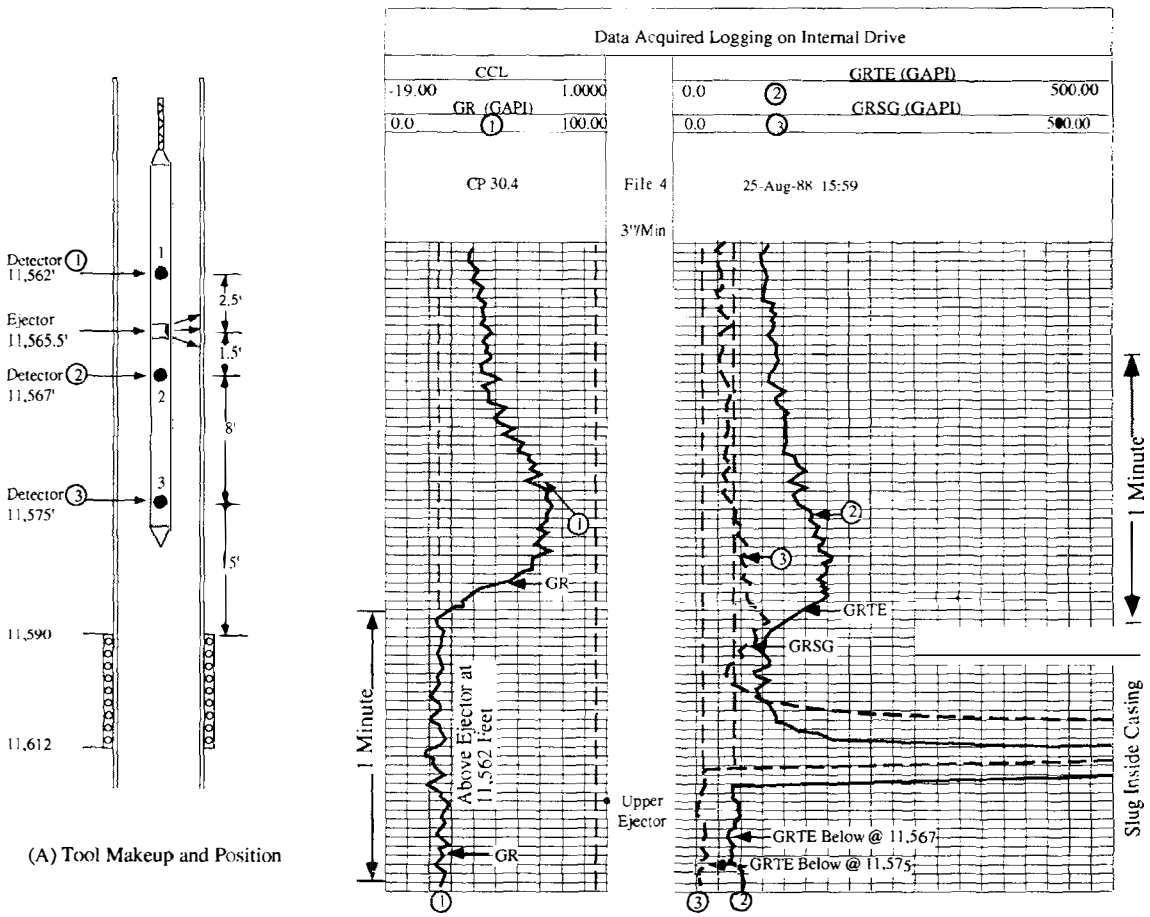

Figure 68. Channel check, velocity-shot survey with well injecting 2 BBL/min.

for the other two detectors. All three record sensitivities therefore exceed the recommended 200 API units per inch and, accordingly, each will respond to quite small tracer concentrations. The ejected tracer slug, of course, "pegs" the output of detectors 2 and 3 as it moves down past these sensors inside the pipe. The leading edge of the slug moves over the eight-foot spacing between the two detectors in about 2 chart divisions or 2 x 2 = 4 seconds of time. The peaks require 3 x 2 = 6 seconds for an apparent velocity of 80 ft/min. The downward traveling slug does not appear on the record from detector 1 because it is ejected below this detector. Tracer, however does double back and reappear on all three records in the order 3-2-1 as an upward-traveling slug. The leading edge arrives back at detector 3 about 12 chart divisions, or 24 seconds, after it passes going down inside the casing. For this slug to reach the perforations while inside casing required 4 sec x (15/8) = 7.5 seconds. The return then used 24 - 7.5 = 16.5 seconds. This corresponds to a frontal velocity of (15/16.5) x 60 = 55 ft/min. Likewise, the 4 foot progression from detector 2 to detector 1 required at most 1.5 chart divisions, or 3 seconds, thus averaging 80 ft/min. The low level of intensity of the return tracer on all detectors means that, for the flow to be directly behind pipe, only a small part of the original slug broke away to move upward. At the frontal velocities estimated above, we would anticipate that the tracer would simply move on past as it did on frames B and C of Figure 64, with a frontal velocity of only 20-30 ft/min. Instead, the tracer "tails" out more like the behavior of the captive slug on Figure 65.

Two additional velocity shots at locations below that on frame B of Figure 68 showed the same type of behavior; namely, return slugs of low amplitude, high frontal velocity, and slowly dispersed trailing edges. Of these three characteristics, the "strung-out" trailing edge would, therefore, seem to also be the velocity-shot signature of tracer spread by virtue of vertical permeability around the wellbore.

With only the results of frame B, Figure 68 known, an analyst could not tell what the "picture" meant for sure. Poor completion integrity would certainly be a possibility. Of course, what the logging operator should have done was dump the remaining tracer just above the top set of perforations and then track the slug going upward to see if it stopped at the unit top, i.e., at about 11,470 feet on the gamma-ray log of Figure 67.

From the tenor of the last three examples, the reader may have guessed already that sloppy procedure is a problem in the application of the tracer tool for behind-pipe flow detection. The problem arises inadvertently. The tool produces such a graphic "picture," the tendency is to jump to the most obvious conclusion of what the picture means. Work is thereby terminated before alternate conclusions can be discredited. In a very real sense, the tool is "too good." The closing section will discuss this problem further.

The next sequence of logs will illustrate the combined use of the temperature and tracer logs to diagnose a complex combination of tubing and casing failure. The temperature log on Figure 69 is from a new well that had undergone only brief periods of injection but still should have a wellbore temperature colder than static. This is clearly not the case below a zone at depth C that had served as a mud disposal zone at the time the well was drilled. In fact, the temperature log shows crossflow from depth B in the open-hole section up to the disposal zone at depth C. The most obvious interpretation of the log is that shown by the dashed line on the wellbore sketch, namely flow from depth B in the open-hole completion past the packer and up the tubing-casing annulus to a casing failure at depth A. Because this depth is above the cement top behind the casing, the flow can then continue unimpeded to the disposal zone at depth C. This interpretation, however, was not supported by a temperature survey run after 40 barrels of mud were pumped down the tubing. This log, shown on Figure 70, revealed a tubing failure at a collar at 12,900 feet, depth A on the figure. During the survey, the logging tool encountered an obstacle it could not pass at 13,170 feet.

In view of these additional complexities, the entire length of the tubing was then checked with the tracer tool. Velocity shots were taken every 1,000 feet. The tool was positioned and the mud pumps started. When the rate was up to 0.5 bbls/min a slug of tagged water was ejected and the travel time to a single detector 4 feet below was recorded. This sequence of operations could be run quickly without a lot of mud loss. The tracer survey showed tubing integrity from surface down to the failure seen on the temperature survey of Figure 70 at 12,900 feet. Three of the velocity shots are reproduced on Figure 71. The records on frames A and B were obtained with the detector above the suspect collar. The tracer slug on both records traverses the 4-foot spacing between injector and detector in one chart division or in about 3 seconds. However, when the detector is located at 12,900 feet, a travel time of 10 cd's or 60 seconds is required for the same journey. Most of the mud, obviously, exited the tubing between the depths associated

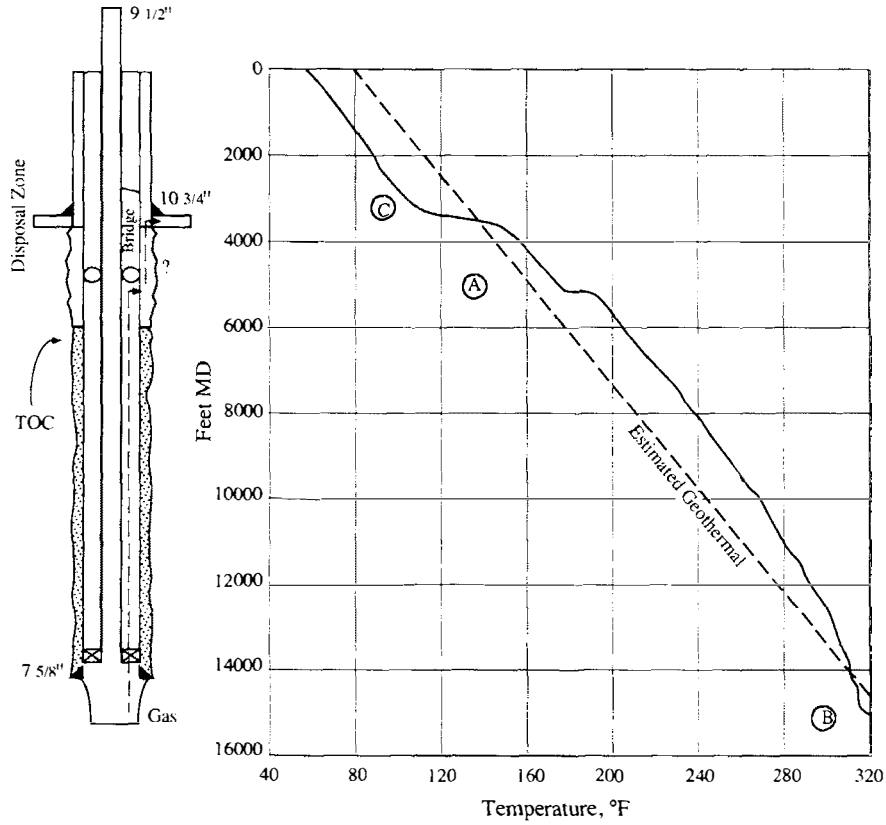

Figure 69. Shut-in temperature survey on a new well.

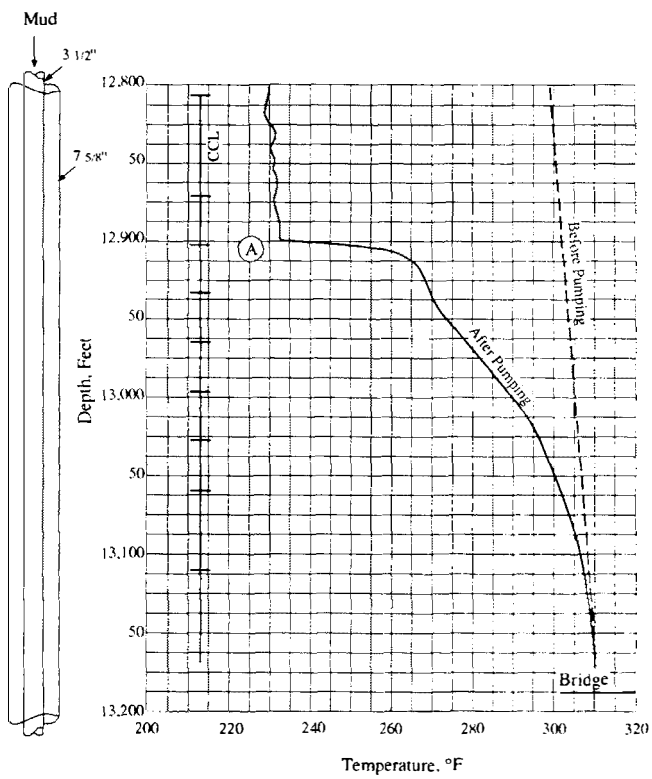

Figure 70 Temperature surveys before and after 40 BBLs of mud pumped down tubing.

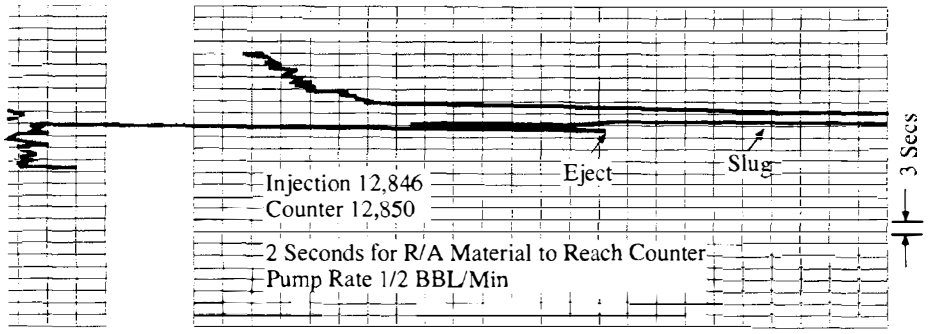

(A) Detector at 12,850 Feet and Time Drive at 2 Inches/Minute

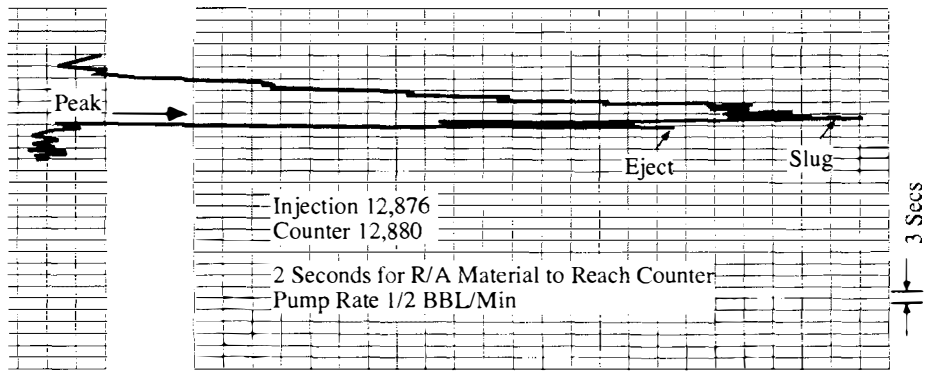

(B) Detector at 12,880 Feet and Time Drive at 2 Inches/Minute

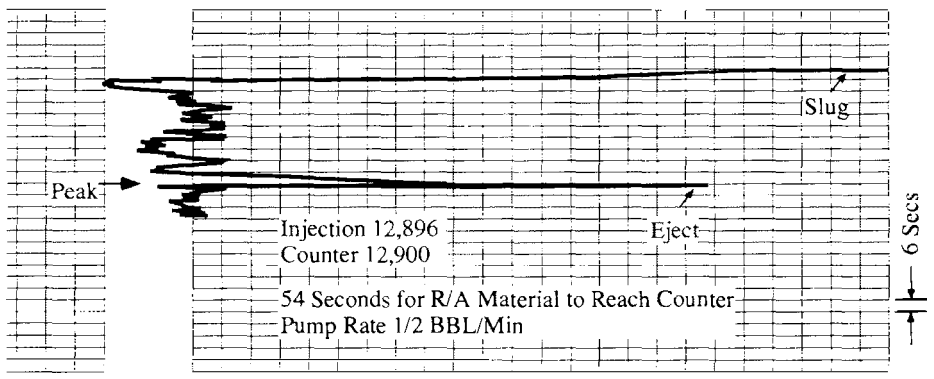

(C) Detector at 12,900 Feet and Time Drive at 1 Inch/Minute

Figure 71. Three velocity shots in well of Figure 70.

with frames B and C, i.e., between 12,880 feet and 12,900 feet. The recorder was put back on depth drive and a short collar log record obtained. This log appears on Figure 72. The leaking collar is at depth A, 12,888 feet. Note that this depth is 4 feet shallower than the location shown for the same collar on the CCL record of Figure 70, the temperature survey. The tracer tool, in essence, has been employed for depth control. Consequently, a marker was put on the logging cable with the detector located at the bad collar. This marker is the reference for subsequent logging work.

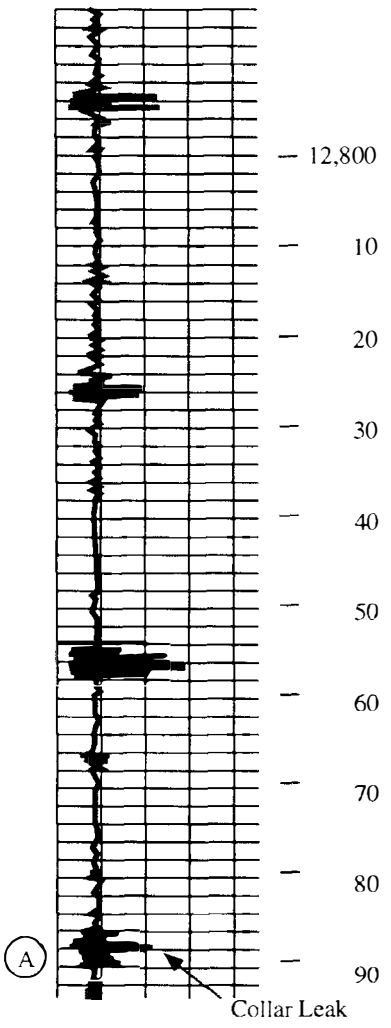

Figure 72. Collar log run after velocity shots on Figure 71.

The next sequence of operations involved the use of the tracer tool to find out where the mud goes once it exits the tubing. One would expect the mud to go upward, from what is seen on the temperature log of Figure 70. To check this expectation, the tracer tool was positioned with the detector at 12,800 feet, a location 88 feet above the bad collar. Injection rate was brought up to 1 bbl/min and a shot of tracer "fired." Frame A on Figure 73 shows the result. At the 6 sec/chart division record speed, the ejection mark on frame A is indistinguishable from the activity caused by the passage of the slug moving down inside the tubing. The reappearance of the slug moving upward in the annulus between the 3 1/2" tubing and 7 5/8" casing is evident as a well defined slug with relatively high amplitude on frame A. The centroid of the slug passes the detector some 22 chart divisions after its initial appearance on the way down. This is a travel time of 6 x 22 = 132 seconds for the double back over the 88-foot distance from the detector to the collar. The transit time inside the tubing can be determined from the velocity shot data of Figure 71

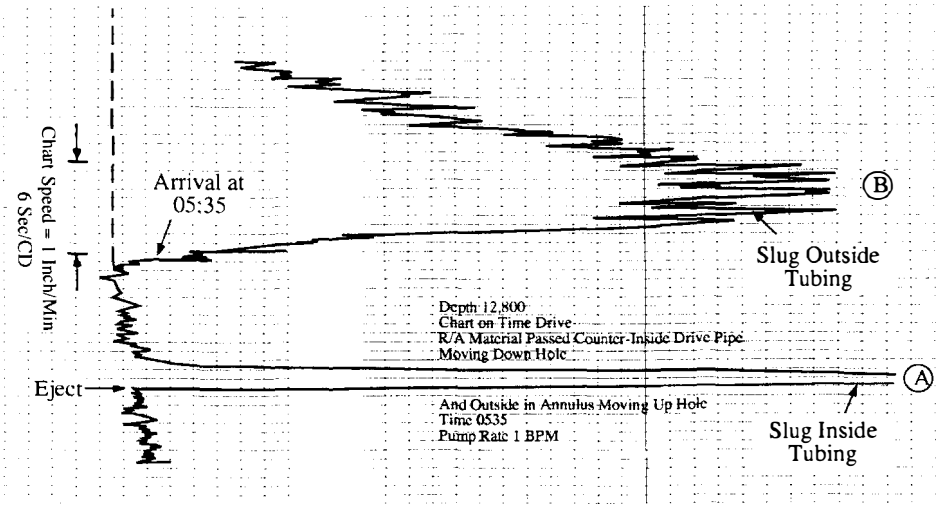

(A) Detector at 12,800 Feet (88 Feet Above Bad Collar) With a Time Drive of 1 Inch/Min.

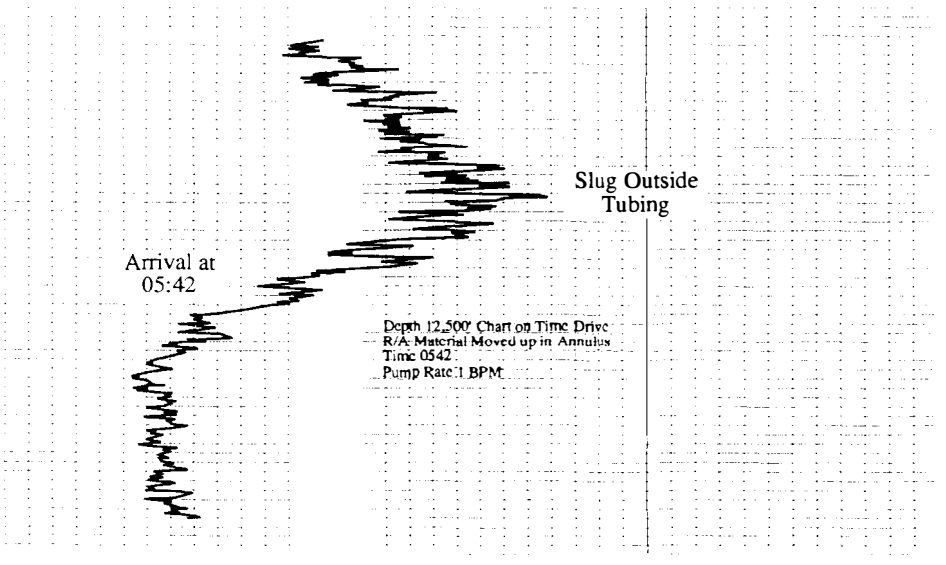

(B) Detector Quickly Moved to 12,500 Feet Depth, Time Drive at 1 Inch/Min.

Figure 73. Velocity shots above tubing leak @ 1 BPM rate.

taken at a rate of 0.5 BPM. At this rate, the slug went the four feet from ejector to detector in 3 seconds. Thus, the 88-foot travel at twice the rate would require a time

$$\Delta t_{in} = \frac{88}{4} \times \frac{0.5}{1} \times 3 = 33 \text{ seconds.}$$

This leaves for the outside, annular travel a transit time

$$\Delta t_{out} = 132 - 33 = 99 \text{ seconds,}$$

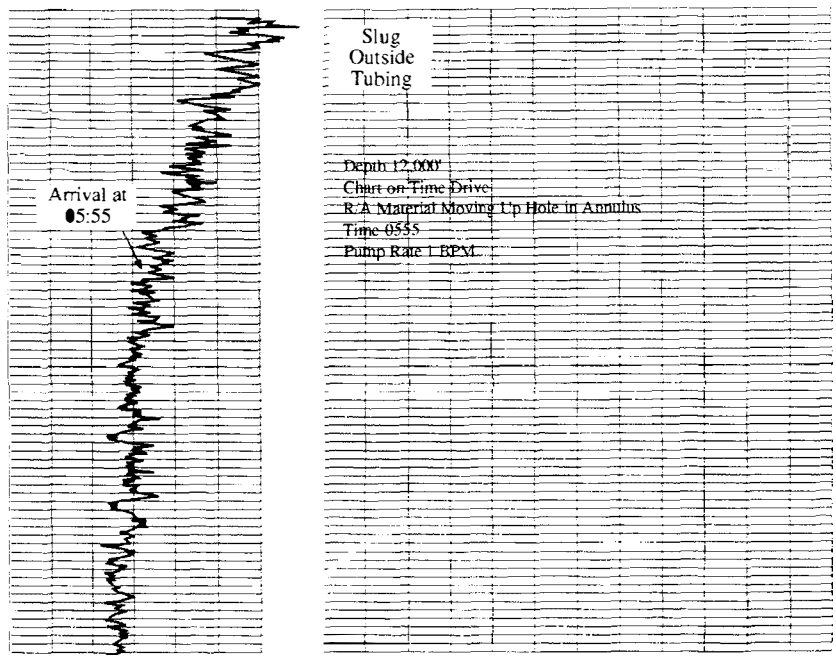

(C) Tool Pulled to 12,000 Feet and Detector Put on Time Drive at 1 Inch/Min.

Figure 73 (continued). Velocity shots above tubing leak @ 1 BPM rate.

or

$$V_c = \frac{88}{99} \times 60 = 53 \text{ ft/min}$$

for the apparent fluid velocity associated with the annular area between tubing and casing. According to the results of page 63

$$\hat{V} \approx 0.8\ V_c = 0.8 \times 53 = 42.4 \text{ ft/min.}$$

The annular capacity is 0.0307 bbl/ft from pipe tables. Consequently, the volumetric rate associated with the upward traveling slug is

$$q = 0.0307 \text{ x } 42.4 = 1.3 \text{ bpm}$$

Because the nominal pump rate was 1 bpm, one can conclude that, once out of the tubing, all the injected mud goes upward behind the tubing. The record on frame B of Figure 73 was obtained with the detector quickly repositioned 300 feet farther up the well at 12,500 feet. The slug arrives some 7 minutes after it was detected at 12,800 feet. It still has a cohesive appearance and a relatively high amplitude even after traveling some 388 feet in the annular space. The apparent velocity between the two positions is 300/7 = 42.9 ft/min, the same as previously estimated after correction. The slug is well-mixed at this juncture. Frame C is a similar record with the detector

at 12,000 feet. The leading edge of the slug has dispersed considerably over the 833-foot journey. The trailing edge, which was not recorded, would be even more spread out. The thirteen minutes travel time between the stations on frames B and C represents a velocity of 500/13 = 38.5 ft/min, a value representing a volumetric rate of 1.2 bpm.

After the tracer work was completed, an impression block was run to determine the nature of the "obstacle" that was encountered on the logging run of Figure 70 but not on the run of Figure 69 one day earlier. The "obstruction" was only a tight spot due to a kink, or "dogleg," in the tubing.

In a turn-about of sorts, the tracer tool has been used to help decide what the original temperature survey of Figure 69 revealed. The flow exits the tubing at 12,900 feet at the bad collar, then continues up the annular space between tubing and casing to a failure in the casing at depth A on Figure 69. From here flow goes upward behind the casing to the disposal zone at depth C.

In this example, you will also note a philosophy at work which is directed towards use of the tools in a fashion that illuminates the overall problem piece by piece. Each speculation is verified before adding the next one. In complex situations, this approach will generally lead to a resolution quicker than will an attempt to do everything in a single survey. This example is also well suited to the slug tracking tracer procedure; however, application of the velocity shot method minimized the amount of mud usage.

Quality Control Revisited: Figure 60 (page 91) presented a drag survey that possibly missed a tubing-casing leak because the survey was not properly carried to a conclusion. Likewise, the velocity shots for the two examples depicted on Figures 65 and 68 both suffer from the same lapse in procedure. This is the most common type of error in quality control and is easily prevented by proper supervision. Basic errors can, however, creep into the most unlikely situations as the final example will illustrate.

Figure 74 shows a slug tracking survey consisting of 13 drags in a well on injection at a rate of 950 BPD. A comparison of drags 5 and 6 shows that most of the water exits the wellbore at the top set of perforations. An injection spike appears about the middle of these perforations at depth A on drags 6 and 7. The 100 % superficial velocity from drags 3 and 4 is 41.3 ft/min, whereas the value from drags 5 and 6 is 13.6 ft/min. Consequently, at least 100 (1-13.6/41.3) = 67% of the injection exits over the top perforations. Drags 7 through 13 clearly show the centroid of the tracer distribution stopping at depth B, 4,478 feet. In fact, a close inspection of drag 6 shows that it has split into two parts. One peak is at 4,452 feet whereas the second is already at depth B with the remaining drags. This latter peak has thus moved faster than the slug peaks in the full-flow stream. The accumulation at depth B must then include tracer that flows behind the casing. Yet no injection spikes develop on any of the drags below depth B. Furthermore, all drags from 6 on show tracer dispersing downward below depth B, again without the development of injection spikes. This vertical spread continues to depth C, 4,525 feet, and the logging operator has chosen to "channel" it on down to depth D at 4,576 feet.

Yet the injecting temperature survey on Figure 75 shows that the bulk of the water got to and no deeper than depth A, 4,500 feet. Furthermore, the 4 hr. shut-in log reveals that the porosity that

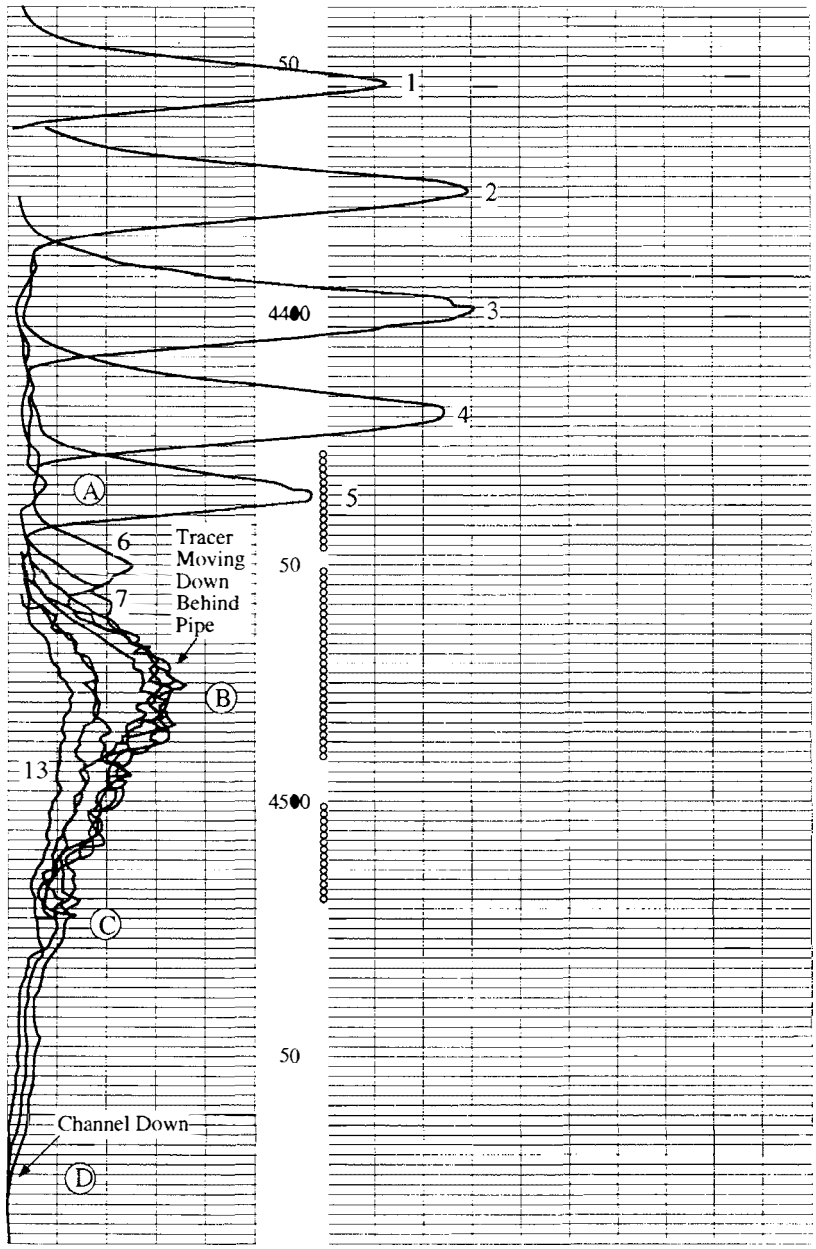

Figure 74 Slug tracking survey from well on injection at 950 BPD.

stores present or past injected water is confined to the interval from depth B, 4,440 feet, down to depth A, 4,500 feet. The operator is so biased by the tracer survey, however, that he has labeled a "channel" down to depth C, 4,614 feet. This is an incorrect interpretation.

The two different surveys indicate that the well is fractured from the differences in apparent depths at which water is "lost" from the wellbore. There is also no difficulty in the continuation

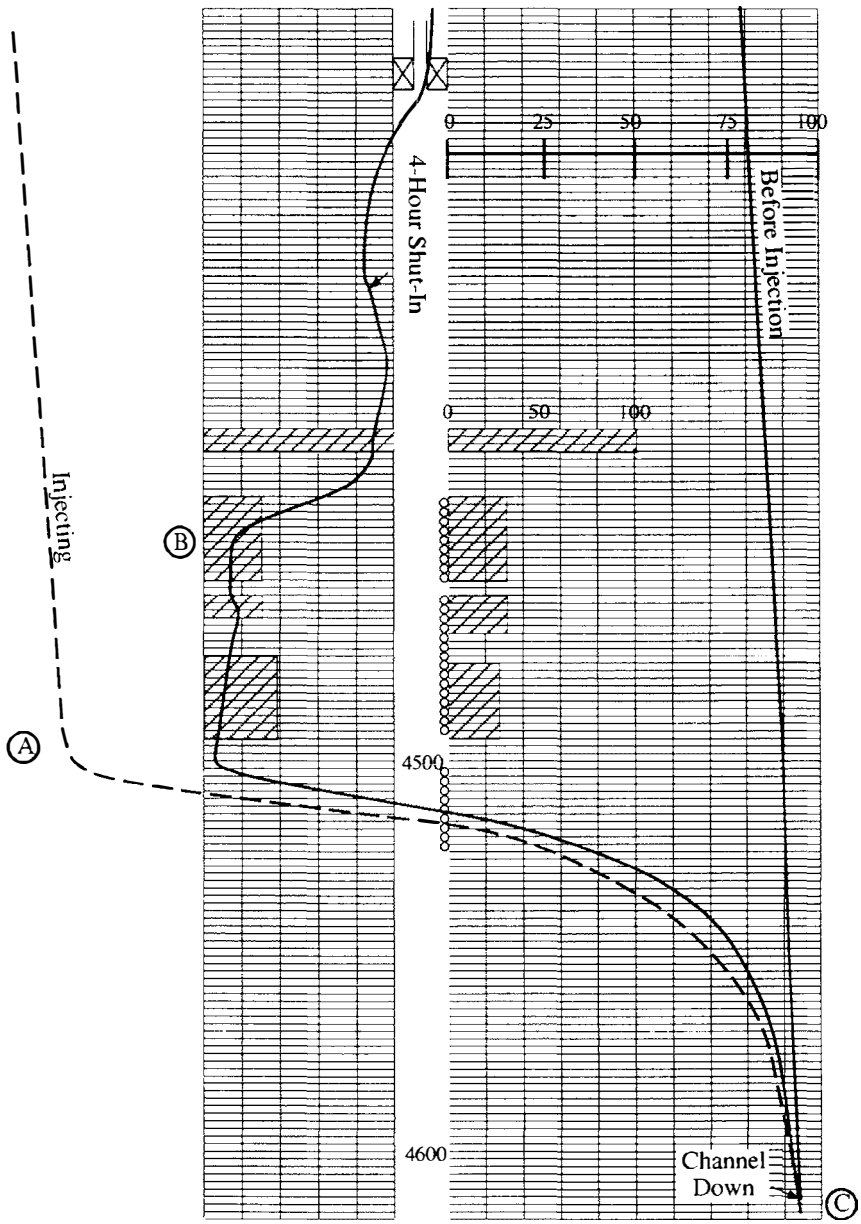

Figure 75. Temperature surveys from well of Figure 74 (recorded @ 2F/inch).

of behind-pipe flow down to 4,500 feet on the tracer survey of Figure 74 so as to agree with what the temperature surveys of Figure 75 show. The difficulty arises in the attempt to explain the dispersion of tracer at least 30 feet below 4,500 feet. This spread is uncorroborated on the temperature surveys.

A crossflow check with the well shut-in, as discussed previously, is also an excellent quality control indicator. It offers the key to what is going on in this particular example.

Figure 76 shows the location of two slugs, 2 and 3, ejected at 4,470 feet and at 4,542 feet, respectively, with the well shut off injection. Three drags were run through the bottom slug 3 at

the elapsed time in minutes as listed. Seven drags were made through the top slug 2 in a sequence that was incomprehensible to the individual subsequently redrafting the log in final form as only four times are listed. Two things are clear: first, both slugs are stationary. This is no surprise because it had been decided from the injecting survey of Figure 74 that most movement below 4,450 feet was occurring behind casing. The second feature on Figure 76 is the surprise. In dropping the tool downward so as to log upward, the operator has smeared tracer out over the entire interval to be logged. He has apparently done the same thing in the stagnant area of the wellbore below depth B on Figure 74. The vertical resolution of the survey is thereby destroyed. This problem would have been difficult to pin down, however, without control slug 3 on Figure 76.

In fact, the dispersion of tracer below depth B on Figure 74 closely resembles the signature produced on slug tracking surveys by tracer spread through vertical permeability around the wellbore. The only distinction is the large amplitudes.

A final feature evident on the drag surveys of Figure 74 is the paucity of "permeability," or injection, spikes. This is characteristic of fractured wellbores. Most of the tracer moves away from the wellbore region in the fracture before entering formation porosity.

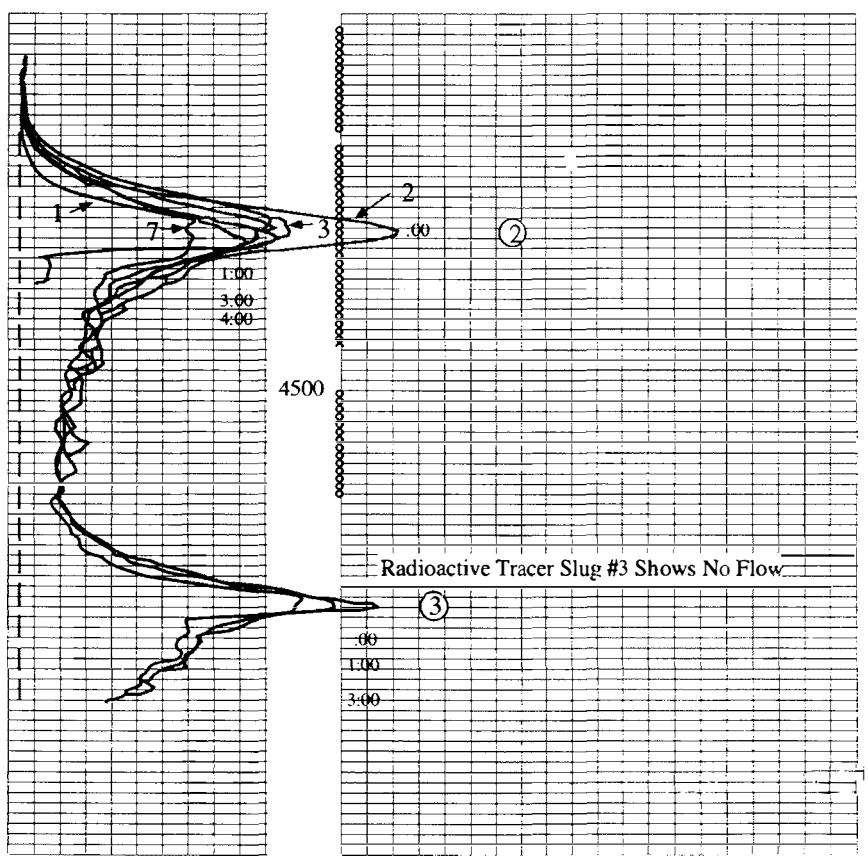

Figure 76. Shut-in crossflow check on well of Figure 74.

This final example concludes the discussion of radioactive tracer surveying of injection wells. The limited scope prohibited a general discussion of the wide selection of tracers available that can be made water, oil, or mutually soluble. Gaseous tracers are also commonplace. All these variations evolved for application to either producing wells or gas injection wells rather than to water disposal wells. There has been no discussion of the use of multiple tracers that emit gamma rays of different energy levels and, accordingly, can be identified by spectral logging techniques. The application of this technology is still limited primarily to the evaluation of staged, well stimulation treatments.

At this point, attention is directed to the final surveying tool, the noise logging tool, that utilizes the sound created by fluid turbulence as a "tag" to follow flow downhole.

Noise (Sound) Surveys

The sounds of moving fluids are so commonplace in everyday life to go almost unnoticed. Only when the movement influences our well being do we tend to bring these sounds to the conscious forefront. Who, for example, cannot recall being lulled by the soothing gurgle of a shallow stream of water on its way along an irregular path. In contrast, the sharp clap of thunder following a nearby bolt of lightening is startling in the extreme. The same sound, when heard from a distance, is little more than an ominous rumble, the higher pitches having been attenuated by the intervening air. Likewise, the intense scream of a jet plane's exhaust is quite painful in proximity but quickly resides to more of a bothersome roar with distance from an airport. These emotions are but a few of the myriad elicited by a single source, fluid turbulence.

It is therefore not surprising that this turbulence can be used to detect flow; particularly, flow behind-pipe where the cramped space and numerous constrictions give the high velocities and sudden expansions necessary for significant levels of turbulence. Actually, noise surveys first came into widespread application for a particular type of problem, the bubbling of a small amount of gas upward through liquid. The need to detect such flows was an unwelcome side effect of deep drilling that started in earnest domestically in the early sixties. The operation of cementing from great depths to surface proved difficult. All too often gas pressure appeared on the annuli of intermediate casing "strings" before the drilling itself was even completed. At this point, the resulting small gas flow was more of a nuisance to be dealt with than a threat to the well integrity. Nonetheless, the location of the source of gas was a challenge that led to the evolution of the noise logging tool.

Because of this mode of evolution, a stigma has been attached to the noise logging tool to the effect "that it is no good for anything except gas." As with most myths, there is some truth to this contention. The correct statement would be that the tool has its greatest sensitivity to the flow of gas upward through liquid, an application for which its resolution is typically about 10 cu. ft/day or 3 cc/sec volumetric rate. For the detection of single-phase flow, gas, water, oil, or whatever, the tool relies on the turbulence created as the fluid is forced across a constriction or past an obstacle. The acceleration of the flow across a localized pressure drop is an effective source of turbulent sound. The intensity of this sound, however, depends on both the volumetric rate and the pressure differential that accelerates this rate. Thus the tool resolution becomes

dependent on pressure differences as well as on rate and a unique lowest rate alone cannot be specified. This feature will be described in detail under a section devoted to tool resolution. The material in this section will allow an estimation of the rate resolution for each particular situation.

The noise tool does have two advantageous features for water flow that are lacking in the case of the tracer instruments. The first of these is the greater depth of investigation offered by the sound source. The frequency range of the tool is such that practically all the sound attenuation is the result of geometric spreading of sound intensity away from the source. Thus, the squared amplitude attenuates as the reciprocal of squared distance. The amplitude drops, accordingly, as the reciprocal of distance, a much lower attenuation rate than the exponential rate associated with gamma rays. Therefore, the tool can "hear better at a distance." More strings of casing can intervene between tool and sound source.

The second advantage enjoyed by the noise tool is the fact that the flow of water past the tool inside casing or inside the annular space between tubing and casing does not create much turbulent noise. In fact, with a 1 11/16 - inch tool in 5 1/2 - inch casing, an injection rate of 850 BPD with a velocity $\hat{V} = 25$ ft/min past the tool is required to raise the sound level above the normal ambient level typical of commercial tools in "dead" wells. This low level of sound is characteristic of any single-phase flow in straight conduits with constant cross-sectional area. The tool can, therefore, easily distinguish flow behind pipe from flow inside pipe. Furthermore, behind-pipe flow, either up or down, can be detected with the well on injection, provided the injection pumps themselves are not so noisy that logging is impossible.

The above comment raises the issue of the complicating influence of extraneous sources of noise, especially that due to surface machinery, on the quality of a noise survey. The failure to recognize such sources is characteristic of an inexperienced logging engineer. Otherwise, the interpretation of a noise log is just as straightforward as a tracer survey. The underlying physical principles are even simpler.

Noise Logging Tools: A commercial noise logging sonde is nothing more than a microphone that is constructed in a way that will withstand the abuse to which a logging tool is subjected. A schematic of the instrument appears on frame A of Figure 77. The piezoelectric crystals convert the oscillating pressure associated with sound transmission within the wellbore to an oscillating voltage that is input directly to an amplifier - cable driver combination. The latter sends the oscillating voltage up the logging cable to surface recorders. The sonde is therefore quite simple in construction and, consequently, is very reliable.

The piezoelectric transducers, pictured individually on frame B, are hollow cylinders made up of ceramic matrix containing a small amount of a highly polar compound, typically, lead zirconate. When the crystals are deformed by a force on their surface, the bound charges on the lead zirconate are separated and the surface becomes charged. A radial compression, for example, causes the inner surface of the crystals of frame B to become electropositive relative to the outside surface, thus, the crystals convert sound to voltage.

Frame C shows six crystals assembled for encapsulation in an epoxy, cast cylinder that gives the strength necessary to withstand wellbore pressure. As shown, the crystals are wired in parallel for purposes of electrical redundancy. So long as one crystal remains intact, the package will function normally. The more sophisticated tools utilize a pressure balanced housing for the crystals. A bellows transmits wellbore pressure to silicone fluid that completely surrounds the individual transducers. All tools have a covering over the microphone section in the form of a thin metal sheath or a teflon sleeve as protection against wellbore fluid.

Frame A shows that at the surface the microphone output goes to a speaker, or more typically to a set of headphones, that allows the logging operator to listen to the acoustical environment downhole. The human ear remains one of the most "diagnostic" of all sonic instruments! This also allows the operator to hear any tool creep that continues after the tool is supposedly stopped to take a sound level measurement.

Surface Processing of Microphone Output: At each location, stationary sound level measurements are made in a way that reveals the pitch content or frequency structure of the transmitted signal. As illustrated on frame A of Figure 77, the signal is input to at least four high-pass filters simultaneously. Each of these filters reject those oscillating voltages with frequencies below its cut-off setting and output those with higher or equal frequencies. The

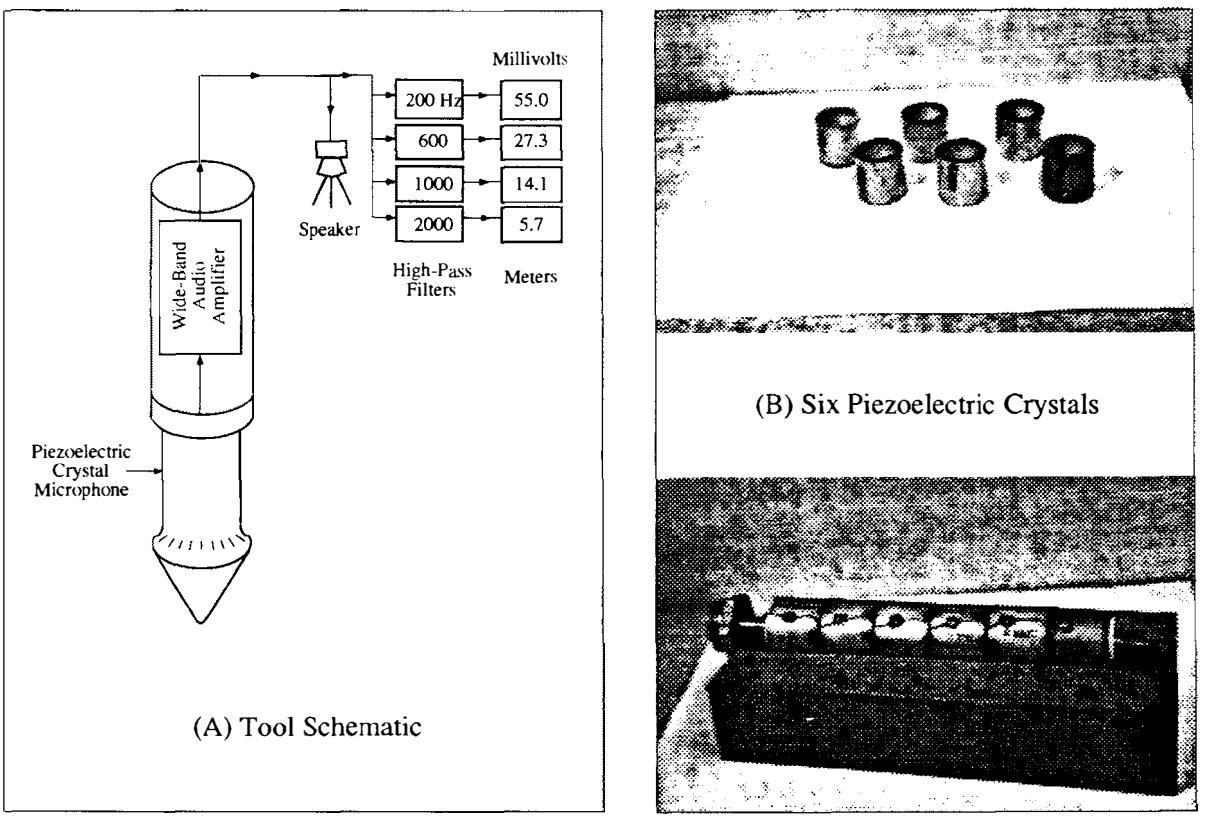

Figure 77. Noise (sound) logging sonde with piezoelectric detection elements shown separately.

settings shown on frame A, Figure 77, are standard for most companies, the lowest cut-off being 200 Hz. The remaining filters reject below 600, 1,000, and 2,000 Hz, respectively. In this sequence, the filters progressively remove from the low end of the audible sound range up to about the start of what would correspond to the soprano range in music. The amplitude of the output from the filters must then decrease in the same progression from 200 to 2,000 Hz as shown by the figures labeled "millivolts" on frame A.

The output of each filter, typically, serves as the input to its own millivolt meter, which, in turn, has a visual display of the light-emitting diode digits form. Once the meters have settled down after the tool is stopped, the operator activates the recording system that averages the output amplitude from each filter for a fixed period of time and then stores this average. The manner in which numbers are retained varies from pad and pencil, to paper tape, to magnetic tape depending on the particular company doing the logging. All the companies preserve at least the four frequency cuts illustrated on Figure 77, frame A, at each stop along with a depth reading.

The frequencies associated with the filters depicted on frame A are not arbitrarily chosen. The lowest setting, 200 Hz, eliminates most of the logging truck vibrations, for example, that are transmitted down the taut logging cable but is still low enough to detect the action of gas moving upward through liquid. The other settings are based on experimental data as to how best to distinguish the gas-through-liquid situation from the single-phase situation. More comments on this topic appear in a subsequent section on frequency content of sound from flow behind pipe.

Narrow band filters are not used generally to provide numbers for a noise log. The broad band readings tend to mute the influence of the resonant peaks that are inevitably present in the sound amplitudes.

One service company uses a digital processing scheme that divides the microphone output into ten frequency bands, corrects each band for cable attenuation, then recombines the bands required to represent the high-pass readings on frame A. These numbers are tabulated as "cable corrected" values along with the uncorrected measurements; however, it is usually the latter values that appear on the actual log.

Another company uses a software processing package with their noise tool that requires a sequence of band pass readings at four different high cut-off frequency settings but at the same low frequency cut-off of 100 hertz. Their "window" W6 band passes amplitudes from 100 Hz to 10,000 Hz and is a number analogous to the 200 Hz high-pass amplitude shown in connection with frame A. In fact this number is relabeled as WIH, window-1 high pass, on their log presentation. Their windows W3, W2 and W1 are bandpass amplitudes at 100-2,000 Hz, 100-1,000-Hz, and 100-600 Hz, respectively. These readings are used to generate the remaining three high-pass values shown on Figure 77. Thus, on their logs, the following four numbers replace the 200,600, 1,000 and 2,000-Hz readings of Figure 77:

$$W1H = W6, \qquad (100 - 10k\ Hz)$$

$$W2H = \sqrt{(W6)^2 - (W1)^2}, \qquad (600 - 10\ kHz)$$

$$W3H = \sqrt{(W6)^2 - (W2)^2}, \quad (1{,}000 - 10\ \text{kHz})$$

$$W4H = \sqrt{(W6)^2 - (W3)^2}, \quad (2{,}000 - 10\ \text{kHz})$$

Tabulated values on these noise logs contain numbers for two additional bandpass measurements, windows W4 and W5, which span the ranges 100-4,000 Hz and 100-8,000 Hz, respectively. Two additional high-pass values are computed from these and tabulated as W5H, a 4-kHz high-pass value, and W6H, an 8-kHz cut. Because logging cables severely attenuate signals with frequency components as high or higher than 10 kHz, the above scheme would appear, at first glance, to be the same as the simpler method of Figure 77. But there is a big difference in the results! The lower frequency components of the sound, whatever their origin, have amplitudes that are usually more variable with time than are the amplitudes at higher frequencies. Furthermore, extraneous noise sources are more intense at the lower frequencies. Each measurement in the above scheme is "polluted" by these frequencies. Consequently, the "noise" level in the noise itself can be unacceptably high. A higher frequency "cut" can exceed in value a lower frequency "cut," a clearly impossible situation for the instantaneous "cuts" of frame A on Figure 77. Tool resolution is compromised by the surface processing of tool output, a situation all too similar to that described in the notes for digitally recorded temperature logs.

Tool Sensitivity: This topic would normally appear under tool specifications but it is important enough to consider separately. Whatever the manner of signal processing, there is a standard unit of reference for the noise logging system. In this standard system, the logging tool is immersed in water along with a sound source. A sinusoidal pressure oscillation in the water with an amplitude of 1×10^{-6} PSI (root mean square) and a frequency anyplace in the range 200-2,000 Hz will produce a reading of 1 millivolt on the appropriate meter. In the past, companies have attempted to maintain their tools at this standard level within $\pm$ 3 decibels. Thus:

$$1 \times 10^{-6}\ \text{PSI} \Leftrightarrow 1 \times (10)^{\pm 3/20} = 0.7077 - 1.414\ \text{Millivolts (RMS)}.$$

With the hard economic times, companies have become sloppy in their attention to quality control. At this time, only one manufacturer supplies a calibration certificate with each tool. The actual calibration is done at Naval Facilities in San Diego, California. Relative to the usual specification units, the above standard millivolt system output is equivalent to a sensitivity of – 134 decibels relative to 1 volt per micro pascal.

The proliferation of digital processing programs has also degraded standardization. These programs are generally written to process sinusoidal signals at unit net gain and are seldom tested with actual flow noise. Consequently, the most that can be said at present is that companies supposedly record at sensitivities of 1/2 to 1 times standard units. Because of the wide range of signal levels to which the tool must respond, most companies have a provision to decrease tool sensitivity by a fixed factor of 10.

Tool sensitivity is important because it determines the output level to be expected for a tool in a shut-in well that is totally free of any flow. This is the so-called "dead well" or "ambient"

output. All quality control checks for extraneous noise must, or course, be referenced to this level.

Finally, it should be mentioned that one company measures the tool output in decibel units with 1 millivolt representing 70 decibel units. In this system, an output of X decibels is therefore the following number of millivolts:

$$\text{Millivolts} = 10^{Y}$$

$$Y = 1/20\,(X - 70)$$

$$X = \text{No. of decibels}$$

These decibel values are then presented on a linear log format rather than on the logarithmic format that is typical for the noise log.

Noise Log Format: A Typical noise log format displays four numbers for the four high-pass readings on frame A of Figure 77 in millivolts for each stationary measurement. These numbers are usually given on a logarithmic scale as illustrated by the frames on Figure 78. The records on both these logs come from "dead" wells and illustrate ambient behavior under two completely different conditions. Frame A on Figure 78 is a portion of a log from an injection well that has been shut in for 24 hours. The ambient level is, accordingly, low-ranging from 1 to about 2

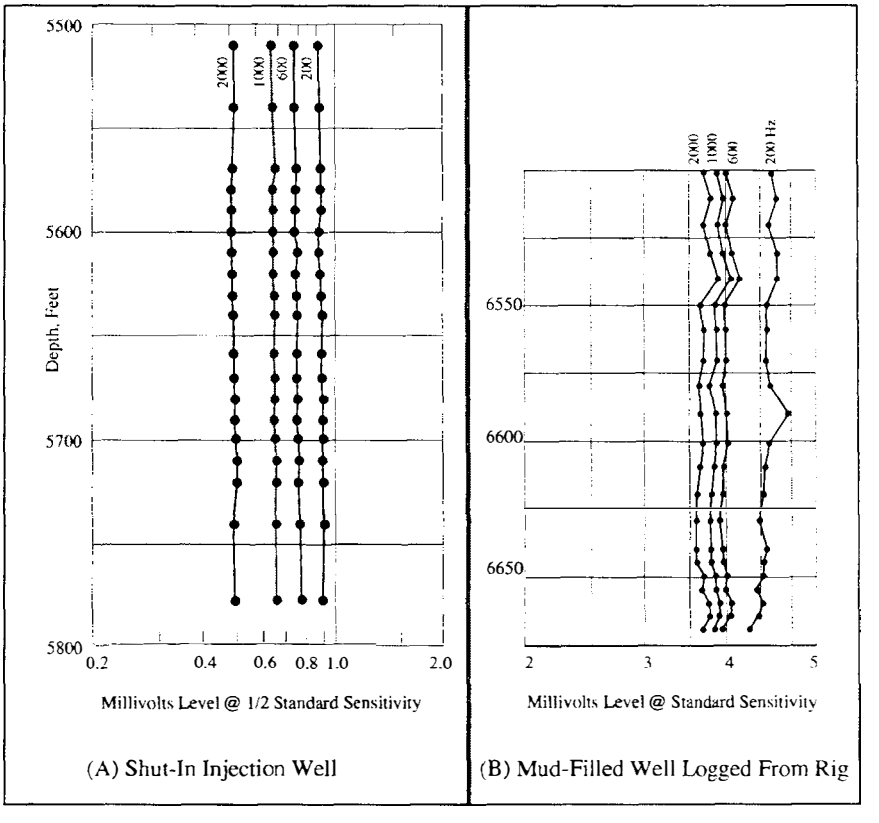

Figure 78. Noise log format illustrating typical ambient or dead well levels.

standard units. In contrast, the record on frame B is from a noisier environment, namely, an open-hole section beneath a drilling rig. Here, the ambient levels are in the range of 4 to 5 standard millivolts. Note also that the variation in noise level from station to station is greatest on the lowest frequency curve, the 200-Hz trace. This fact was claimed without any demonstration in the previous discussion on data processing. The high-pass method employed restricts this variation to the frequency cut to which it actually belongs.

For comparison, Figure 79 shows a noise log from a shut-in well that has a behind-pipe crossflow of water upward into a gas zone that was pressure depleted from production. Only at the top of this log, above the water level, are the noise levels on all cuts at about dead-well values. At the bottom of the log, a location over 1,000 feet away from the noise source at depth A, only the 2,000-Hz cut has decayed to ambient level. The lowest frequency cut, the 200-Hz curve, still has an amplitude that is 36% of the peak value at depth A. This is an illustration of the already mentioned ability of the tool to "detect from a distance."

The log also shows that most of the 250 PSI pressure differential between the sands is dissipated at one constriction located at depth A. This is an unusual situation for flow behind pipe. Also, the behavior of the four high-pass readings at the peak, depth A, shows that the sound amplitude drops very little from the 200-Hz reading through the 1,000-Hz reading. Yet the 2,000-Hz values is only about 1/3 of the 1,000-Hz value. This behavior means the most intense components in the sound occur at a pitch, or frequency, near 1,000 Hz. The spectrum peaks at

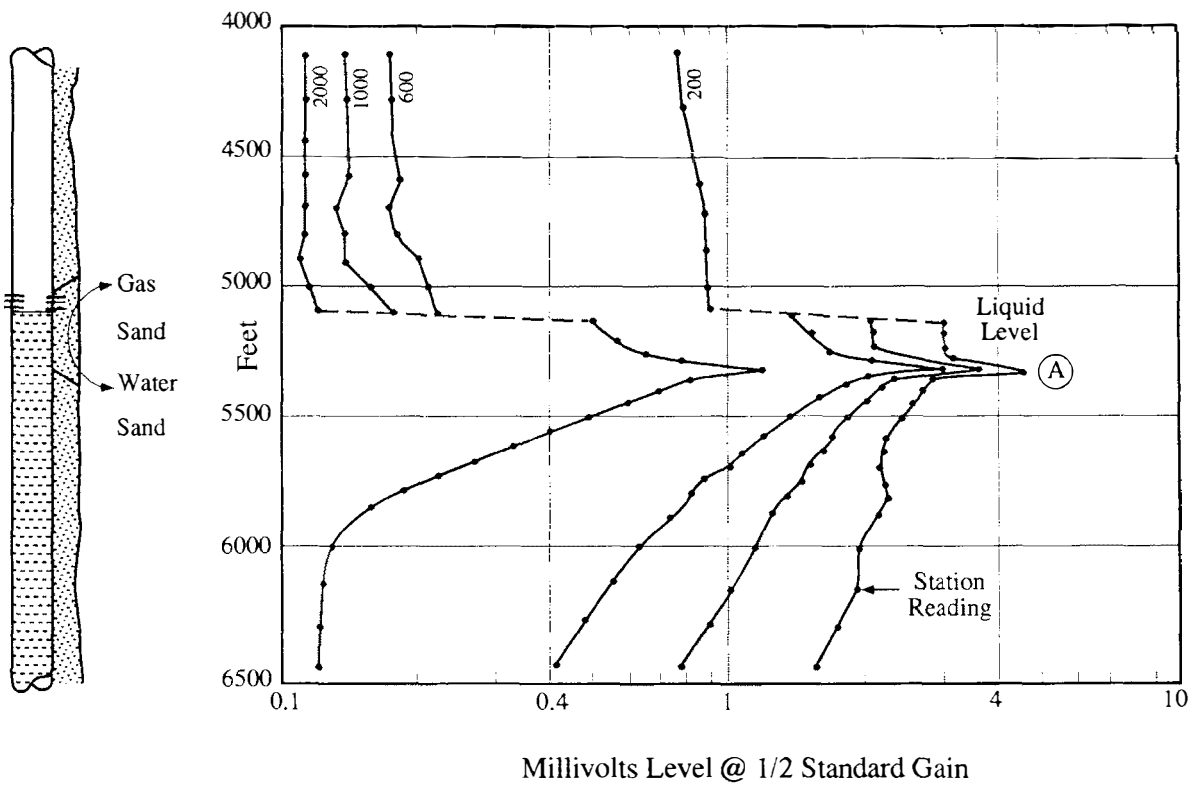

Figure 79. Noise log format with a 20-BPD water flow behind pipe into a gas zone depleted by 250 PSI.

ncy. Most single-phase flows produce dominant pitches of 100 Hz or higher when
ıg over a constriction. We have, therefore, partially justified the filter setting depicted
ʌ of Figure 77, the tool schematic.

level exerts an enormous influence on the log character on Figure 79. The loss in
l that occurs when the detector leaves the water column is the result of two factors.
the sound in water, a pressure wave exerts a force on the sound much greater than an
city oscillation in gas would produce because of the larger water density. The "so-
ıpling is better with water around the microphone. Second, the water surface itself
through interfacial tension any oscillations that attempt to cross. This noise log
t an interface is brought up because it is not unusual to have a water level in an
'ell.

ambient noise levels on all three logs are slightly to either the high or low side of 1
illivolt level. This is typical for dead-well levels free of extraneous noise.
tly, this level serves as a quality control check on noise logging procedure. Every log
e locations with levels already ambient or decaying towards ambient. Exact values
t also depend on the length of logging cable on the reel and on its size. This is why
t values at the top of the log on Figure 79 are somewhat smaller than those on frame
78 even though both logs were recorded at one-half standard sensitivity. Corrections
ngth are discussed in the next subsection.

<u>ıuation:</u> The tool schematic on frame A, Figure 77, shows that the amplified voltage
ıe microphone is transmitted directly up the logging cable of the surface unit.
the wide range of signal level over which the tool must operate, no attempt is made to
tage levels to spikes as was done with the thermometer. Consequently, the logging
acts as filter attenuating the higher frequency components of the tool output more
an the lower frequency ones. AC current is lost from the cable primarily by
storage in the insulating material that separates the conductor from the outside wire
example, a logging cable 7/32-inch in diameter and 24,000 feet long has over 1
capacitance in this insulating material. The insulation acts like a capacitor that shunts
n the conductor to ground, i.e., to the outside sheath. Also, the "resistance" that a
fers to an AC current is inversely proportional to the signal frequency.

ırrect way to account for cable filtering is to divide the signal into narrow-band
orrect the amplitude of each segment according to its center frequency, and then
he segments. This is a tedious operation because the recombination must account for
ıift also due to cable capacitance. Fortunately, it is not necessary to go to this degree
ecause the cable correction is generally small, it is usually not even made. When it is
ıuch simpler procedure can be used that is perfectly satisfactory.

numbers measured at each station, one can correct only that value whose high-pass
uency is closest to the dominant frequency. For example, on the log of Figure 79, the
h A has a dominant frequency not much larger than 1,000-Hz. This cut, whose
2 x 3 = 6 standard millivolts, would be the one corrected for cable attenuation by a

factor appropriate to 1,000-Hz frequency. Such factors, labeled F_L, appear on Figure 80 fc common sizes of production logging cable, 7/32-inch diameter for the left-hand figure and inch on the right-hand figure. The cable length, L, on the abscissa of each figure is expres thousands of feet. A line is present on each figure not only for the four high-pass filter set in general use, but also for two higher frequency settings, 4 and 6 kHz, that are present on company panels in case they are needed for better vertical resolution.

Use of the correction factors is straightforward. The log on Figure 79, for example, was recorded on a truck that had 23,600 feet of 7/32-inch cable on its reel. For this length, the hand figure on Figure 80 gives, from the 1,000-Hz line, F_L = 1.65, thus, the corrected nois associated with the peak at depth A on Figure 79 is

$$N_{1,000} = 3x2 \text{ x } 1.65 = 9.9 \text{ std. mv},$$

A value that will be of use in the section on rate resolution. A correction on any other of t three remaining numbers measured at depth A on the log of Figure 79 with the factors fro Figure 80 is inappropriate. For example, at 200-HZ, F_L =1.20, whereas the log peak value millivolts. Thus

$$N_{200} = 4.5 \text{ x } 2 \text{ x } 1.2 = 10.8$$

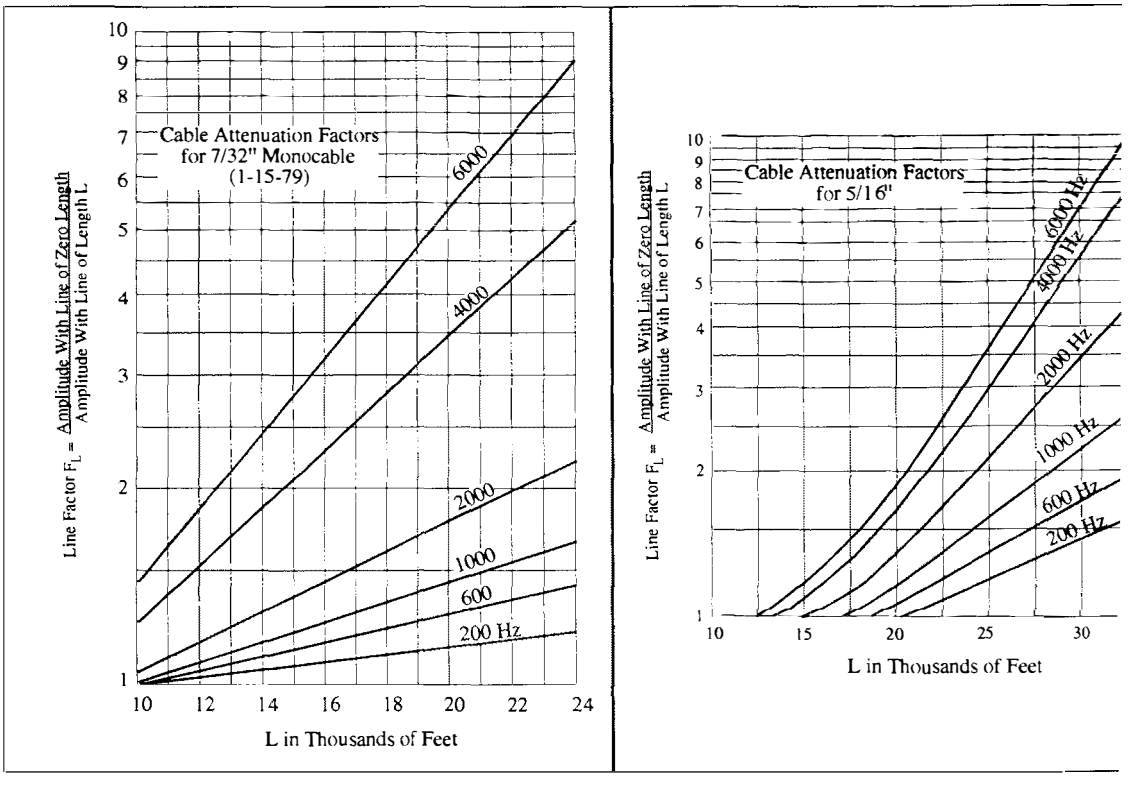

Figure 80. Logging cable attenuation factors for two wireline sizes.

Although seemingly valid, this number has no meaning because the dominant pitch contributing most of the amplitude to this measurement is closer to 1,000 Hz.

In the past, noise logging tools were manufactured with so-called "line-compensating" features. These tools contained signal generators that, when activated, would produce a constant voltage tone at each of the four frequencies, 200, 600, 1,000 and 2,000 Hz. In the surface panel, gains were adjusted to give the same output from each filter. This approach, however, allows the logging operator too much flexibility in "knob turning."

At the present time, variations from company to company in tool sensitivity are generally greater than variations due to cable filtering. The corrections may, therefore, not be sufficient to bring two companies logs into agreement.

Tool Specifications: The most important of the tool's specifications, its fixed sensitivity, has been discussed in some detail already. Suffice it to say that the ± 3 decibel tolerance quoted allows, in the extreme, the output in millivolts of two tools to differ by a factor of 2. Most companies exert better control than this in-house, but it is not uncommon to see this level of variation from company to company.

Noise logging instruments are available in diameters that range from as large as 1 11/16 inches (1.69 inches) to as small as 1 inch. The 1 3/8-inch diameter is also popular for this tool. The microphone section itself is generally less than 8-inches in length so that even in the usual combination with a thermometer, one still has a very compact instrument, generally less than 5-feet long.

The better noise logging sondes are rated for operation at 400 °F and 20,000 PSIG. A more common temperature rating is in the range of 300° to 350 °F, a rating that will accommodate practically all injection wells but may be too low for deep production wells, especially gas wells.

Logging Procedures: The noise logging tool does not need to be run with centralizers. Furthermore, direction of logging is of no consequence to the taking of stationary readings. The most obvious procedural question is related to the proper spacing between readings. In general, spacing is not all that critical a factor because of the long-distance carry away that is already evident on the log of Figure 79. A coarse grid of stops can be selected so as to accommodate the total interval to be logged and then additional time can be dedicated to more detail at crucial locations such as cement tops, casing shoes, perforations, zones of interest or around noise peaks.

A single station measurement will typically require from 3 to 4 minutes from time of arrival to completion. Add to this about 1 minute for tool relocation and you have a logging rate of about 15 stations per hour. A four hour long logging run would thus accommodate 60 measurements. Suppose we have 3,000 feet to survey. A coarse grid of stations 100 feet apart would use 30 of these 60 and leave 30 stops for detailing, which is usually sufficient. At this density, no noise peak could be located more than 50 feet from a measuring station. It is obvious from the log behavior on Figure 79 that very little would be inadvertently skipped over by such a spacing. The lines on Figure 81 allow a more specific answer as to what might be missed. This figure

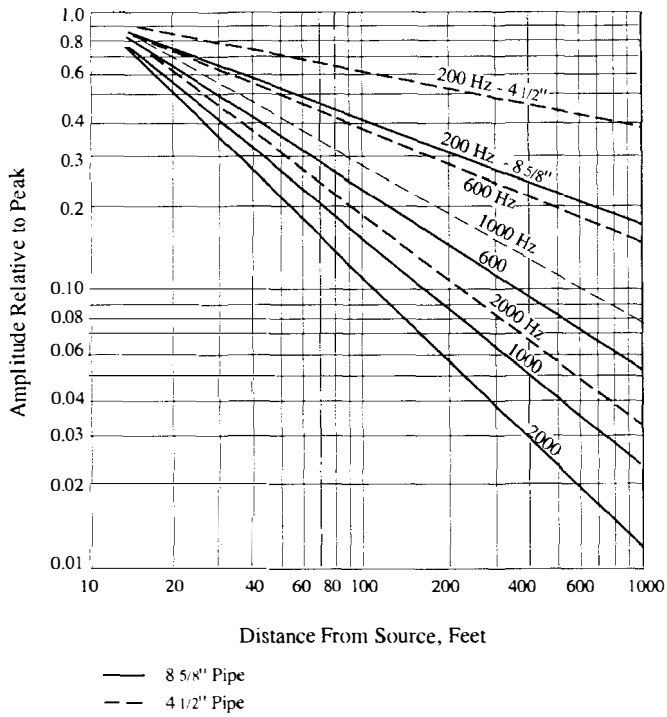

Figure 81. Sound carry-away from a source in water.

shows, for two casing sizes, the amount of sound carry-away with distance as a fraction of the peak value at the source. For each pipe size, four lines are present, one for each frequency on the noise log. The figure shows, for example, that in 8 5/8-inch casing the 1,000-Hz sound level fifty feet from a source is still 0.26 of the peak value. Suppose the ambient 1,000-Hz level is the 0.14 millivolt reading associated with the log on Figure 79. Then for a peak to be lost in this background, its amplitude could be no greater than $0.14/0.26 \approx 0.6$ millivolts. In such a fashion, the sample spacing and its consequences can be determined prior to the actual logging operation.

The use of a fine station spacing embedded in a coarser grid is illustrated on the log in frame A of Figure 78. This survey was actually run to determine if any non-related crossflow was occurring between sands located at 5,600 and 5,700 feet. A 30-foot station spacing is used in the approach to the sands, both from above and from below. Twenty feet above a sand, the station spacing is reduced to 10 feet and retained at this value through the zone and for 20 feet below it. This procedure was repeated at each of the two sands with one 20-foot spacing between the two. In frame B of Figure 78, the location of interest is at the bottom of the log. A 10-foot sample interval is used in the approach to this depth with a reduction to 5-foot intervals over the last thirty feet of log.

The log on Figure 79 shows four different stations spacings. A 250-foot interval appears on the approach to the perforation from above. This interval is reduced to 100 feet with the tool still 400 feet from the perforations. A further reduction of 50-foot intervals is made when the noise level increased as the tool enters the water column. This spacing is carried on for 400 feet below the peak at depth A. At this point, the 2,000-Hz level is almost back to ambient value so the operator increases the sample interval to 150 feet over the bottom part of the log. The immediate

symmetry about the peak value at depth A means that the actual peak is located very near the station stop depth. Its location appears to be a bit off the regular 50-foot spacing; consequently, the logging operator most likely searched for this location. Had he measured only at the stations on either side of the peak, then the largest amplitude would have been 0.8 millivolts on the 2,000-Hz curve rather than the 1.2 millivolts measured at depth A. The apparent peak would be 67% of its actual value. At a regular 50-foot spacing, a peak would be within 25 feet of a measurement. The 2,000-Hz line on Figure 80 for 4-1/2-inch pipe shows that the apparent amplitude is about 50% of true value.

The logs on figures 78 and 79 were recorded with the well shut in. This is the correct way to log for non-related, behind-pipe flow. If an injection well has positive wellhead pressure, it is also a good way to log for injection confinement. A packer check can easily be run in such a situation. For an injection confinement test, the well should also be logged on injection . A "channel check" is possible with the tool in the casing; however, the flow velocity past the tool in the tubing will generally create too much noise for a valid packer check while on injection. The logs on figures 78 and 79 utilize a range of station spacing that is typical, 5 to 250 feet. The particulars in spacing arrangement are worked out relative to the situation at hand.

Noise Log Characteristics: There are three features to every noise log that are pertinent to what the log means. These are: (1) sound levels on all four cuts, (2) variation in level on a particular cut from station to station, and (3) the frequency content of the sound at a peak in level. These three features can be referred to succinctly as loudness, character, and pitch, respectively. Loudness relates to the severity of the problem, character to how flow is taking place, and pitch to the type of flow-single phase or gas through liquid. Each of these features is discussed in some detail because, in combination, they form the basis for noise log interpretation.

Loudness: The measured sound levels on a noise log are significant for two reasons. In the first place, the level increase above ambient is obviously related to the severity of the problem. For example, at depth A on the log of Figure 79, there is a peak in noise level to values from 1.2 to 4.5 millivolts for the four cuts. These are considerably higher levels than ambient, for which the same four cuts range from 0.12 to 0.8 millivolts. Although one cannot associate a degree of severity with the increase at this point in development, one would agree that if another run six months down the road gave levels at depth A that were three times higher, this would signify an increase in the flow rate. The actual relation to rate is given in subsequent sections devoted to specific flow situations, but for now it is the low end of the loudness range that will be discussed.

In the second place, the level of sound on a noise log is the best quality control index available. Ambient levels under proper logging conditions have been demonstrated to fall just on either side of the 1 millivolt level, depending on environment and logging cable. If this level does not appear anywhere on the log with the well shut in, then there usually will be an extraneous noise source that has gone unrecognized. The log will either be useless, or worse, will lead the interpreter to incorrect conclusions.

The log on Figure 82 is from an oil well that is shut-in with a tubing pressure of 815 PSIG. Only at the deepest station do the values of noise level appear to be settling down to ambient values.

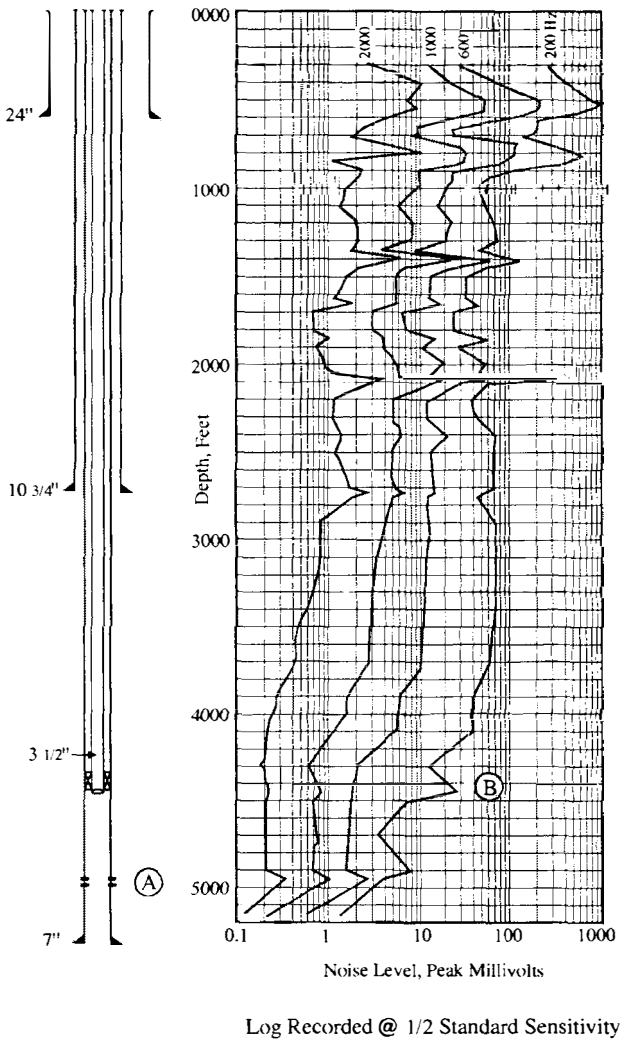

Figure 82. Noise log from a shut-in oil well with 815 PSIG tubing pressure.

Even the perforations at depth A are producing. The sustained levels above the end of the tubing, depth B, indicate that this flow is entering the tubing and flowing through the narrow space between tubing and logging tool. From what is seen at shallower depths, this flow reaches all the way to the surface. Finally, the flow appears to go in surges as witnessed by the many peaks. Steady flow up the tubing would not exhibit this character. In short, what this log shows is the result of a lubricator seal at the surface leaking sporadically. More specifically, one sees on the log the extreme sensitivity that the tool has to the movement of gas through liquid. A slight loss of seal pressure allows carbon dioxide and nitrogen to flash from the oil and bubble upward. Each time this happens the flow surges. All this confusion is the result of attempting to log a high pressure well without the use of a grease-injection controlhead. Sloppy procedure!

The term "peak millivolts" that appears on the abscissa of this log is a common way to designate a tool with one-half the standard sensitivity. Likewise"peak-to-peak" is sometimes used to designate standard sensitivity.

The log on Figure 82 is also typical of what can happen in a shut-in injection well that has positive tubing pressure. A loss in seal pressure will allow dissolved air to flash.

Compare the noise level on Figure 82 with that on Figure 83. The lower part of the log on Figure 83 was shown on frame B on Figure 78. The levels on Figure 83 are 10 to 25 times lower than the values on Figure 82. At the worst, location 3, the levels on Figure 83 rise only about 25% above ambient values. Yet the control demonstrated above and below locations 1-4 is sufficiently good that significance can be attached to the peaks at these locations. As a check, a second pass was made over the interval 6,325-6,475 feet to insure that the peaks repeated. The four peaks are, in fact, at depths of closest approach to a well blowing out of control nearby, with the closest approach being at location 3.

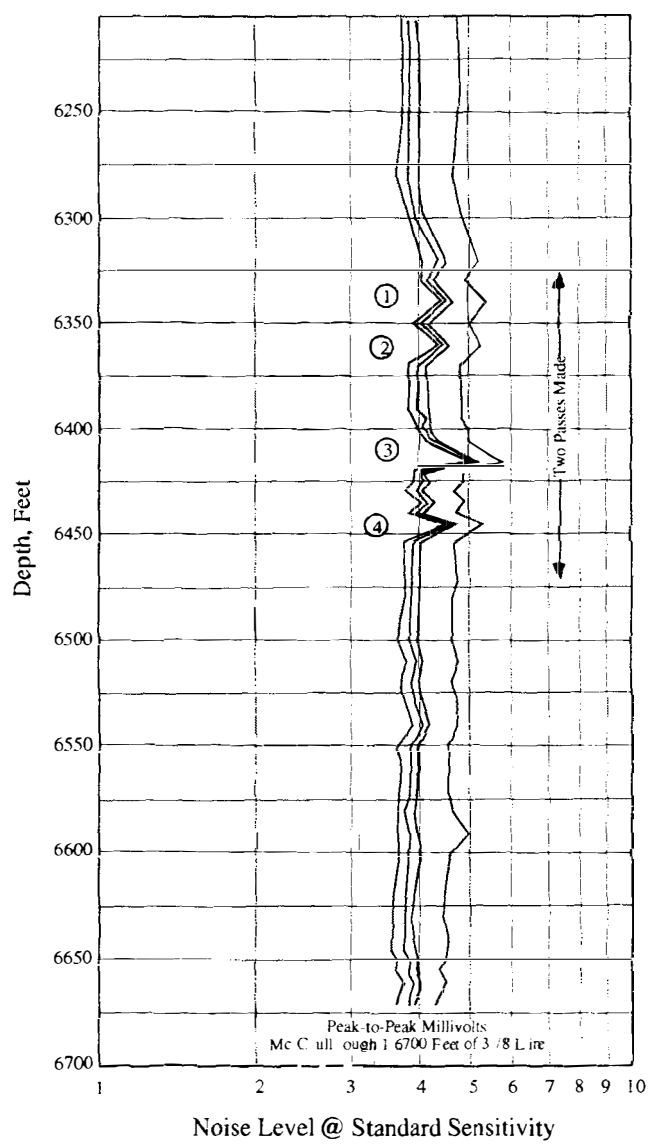

Figure 83. Noise log from mud-filled open hole in the vicinity of well blowing out of control.

The significance attached to loudness on a noise log is therefore relative to not only problem severity but also to procedural quality control.

Character: It has already been indicated that the variation in level of sound on a particular "cut" from station to station is related to the path followed by a steadily flowing stream. This fact is incorporated into the hypothetical situation of behind-pipe flow illustrated on Figure 84. A crossflow is depicted from zone A to zone C past a single constriction at location B. An acceleration occurs across a pressure drop at each of these locations, on entry to the wellbore region behind pipe at depth A, on passage through the tight spot at depth B, and on exit from wellbore at depth C. Accordingly, a peak in the sound level occurs at each of these locations, the magnitude of which is directly proportional to the pressure drop at that location. Most of the pressure difference between zones A and C is dissipated at these three locations. Had the flow occurred inside the casing, then the peak in sound level at depth B would not be present. Also, an actual situation may be such that the pressure drop at either the entry, depth A, or the exit, depth C, or at both may be so small that the associated peak is not recognizable above the residual sound carry-away from the peak at depth B.

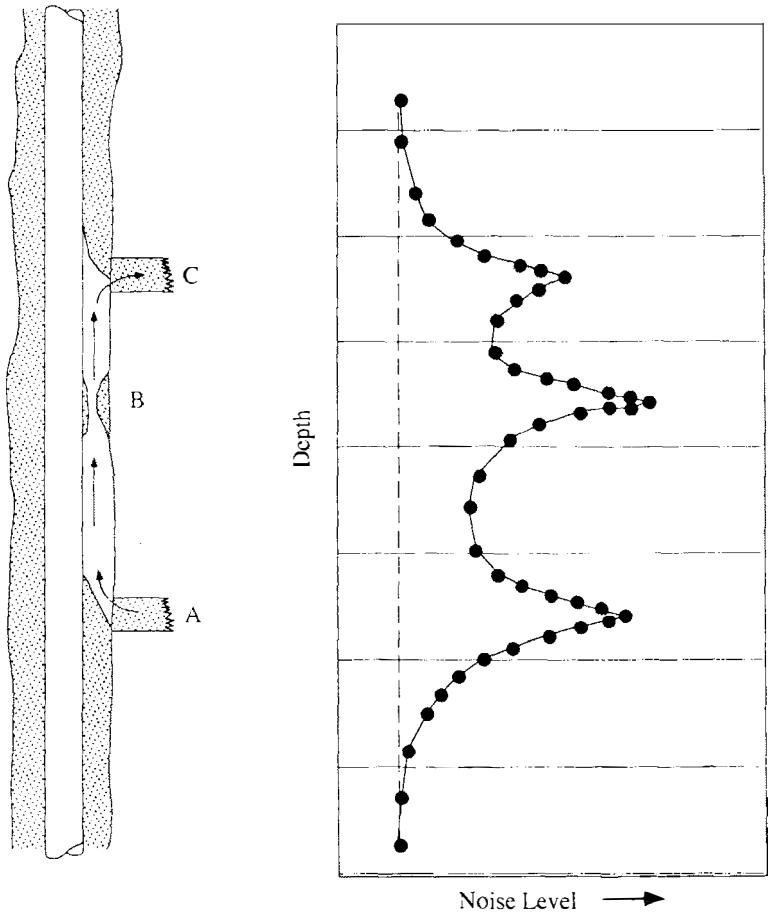

Figure 84. Noise log character as related to flow path.

The type of information available from record character is demonstrated by the next two examples, both of which involve the flow of water behind casing.

Figure 85 shows a noise log from a well experiencing an underground blowout that commenced when the drill bit penetrated an abnormally pressured water zone at the bottom of the open hole section. This water is charging porosity in a normally pressured zone at depth A. Above this location, sound levels decay to ambient levels slightly to the high side of the 1 millivolt value. Within the crossflow interval below depth A, the number of peaks in any one curve is limited only by the station spacing in use, not by the actual number of constrictions which apparently are numerous indeed. The flow is therefore behind the intermediate string of 9 5/8-inch casing shown at 17,000 feet. It is the cement and not the casing itself that has failed. The crossflow rate of 500 BPD was estimated from a rate measured when the water flow was diverted to the surface.

Compare the character on the log of Figure 85 with that appearing on Figure 86, another example of water crossflow behind pipe at a much higher estimated rate of 5,000 BPD. The cut on Figure 86 with the best vertical resolution, the highest frequency curve at 2,000-Hz shows on two locations, D and E, in nearly 4,000 feet of interval at which peaks in noise level occur. As will be seen shortly, the single peak at depth D is associated with an entry from a source aquifer located at this depth whereas the double-peak structure at depth E results from two exits into porosity at two locations in the same shallow aquifer. Not a single tight spot is evident in

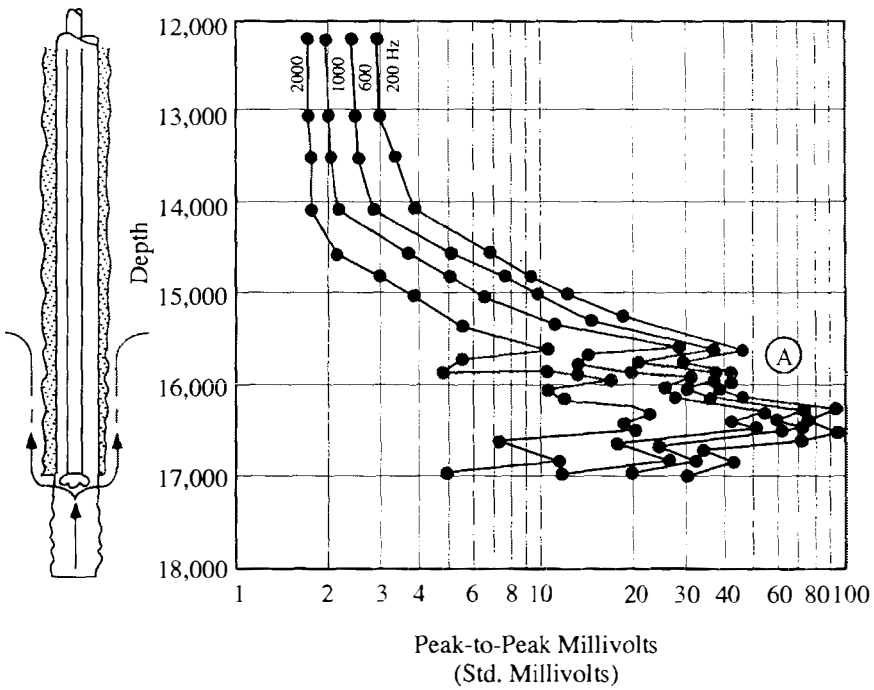

Figure 85. Noise log from a 500-BPD flow of high pressure water behind 9 5/8-inch casing in a well being drilled.

between! The flow is obviously taking a path of nearly constant cross-sectional area. The well completion sketch on the left-hand side of Figure 86, unfortunately, shows several possible routes satisfying this requirement.

Two temperatures surveys from this well appear on Figure 87. The log on frame A was run 1.4 months after the well was shut off production, the same time at which the noise log of Figure 86 was recorded. The survey shows the water flow as originating at depth D and progressing to depth E with a minor loss at depth F. The noise log of Figure 86 shows that there is very little pressure differential left at the location of minor loss, depth F. Most of the charging has apparently already happened!

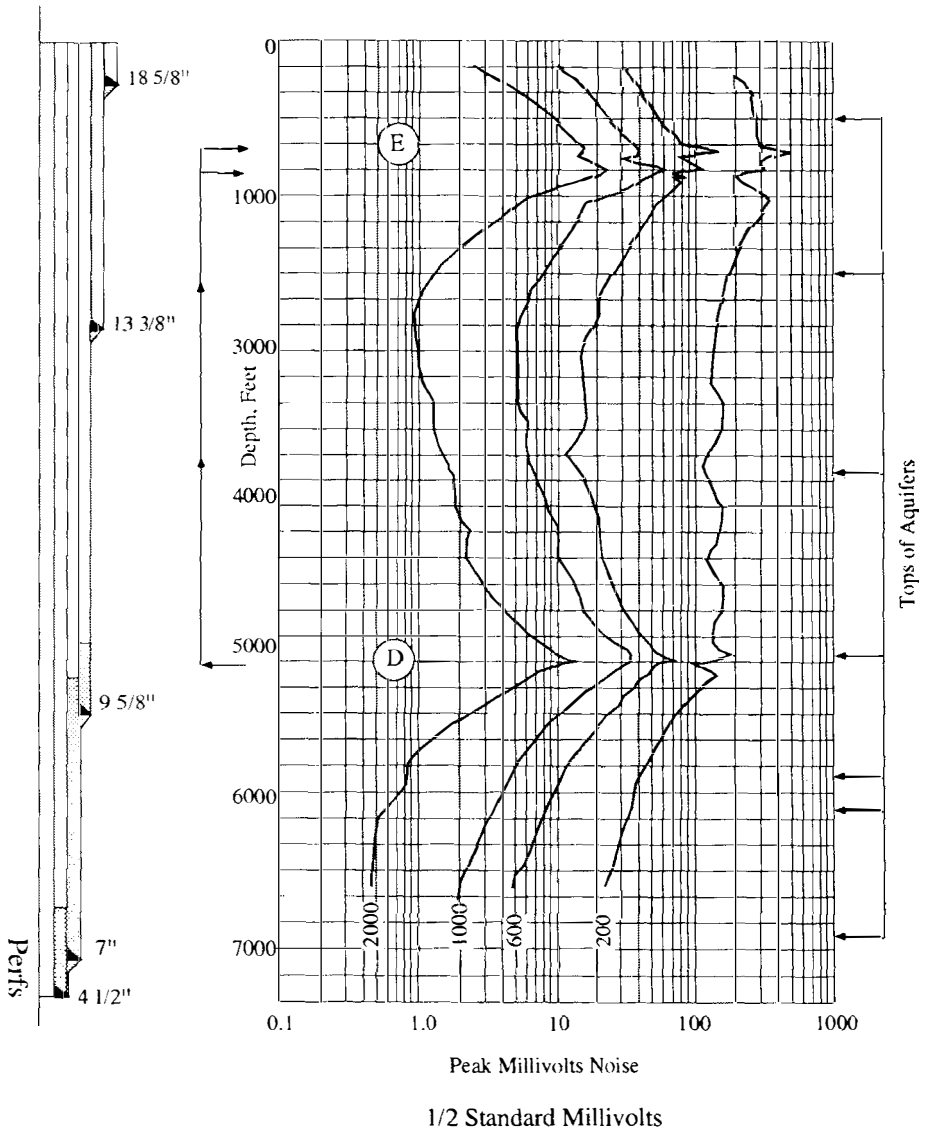

Figure 86. Noise log from shut-in well with water flow behind-pipe at an estimated rate of 5,000 BPD.

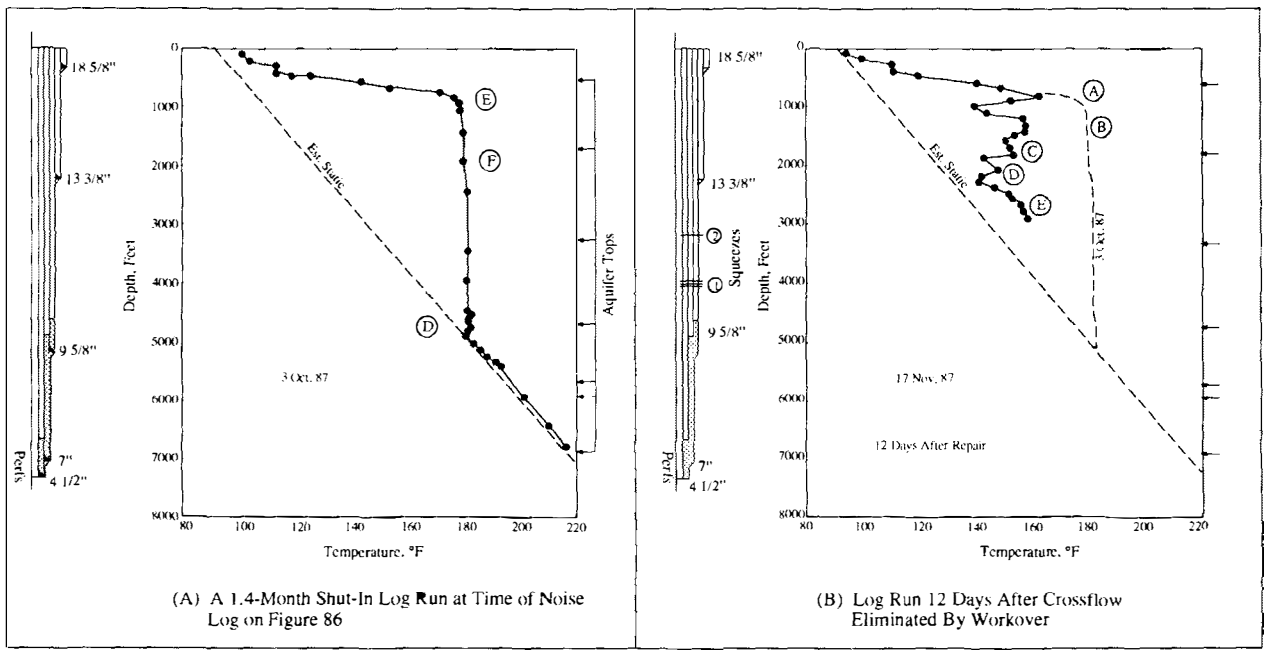

Figure 87. Temperature surveys on well of Figure 86 before and after a workover to eliminate behind-pipe flow from deep aquifer into shallow aquifers.

After a workover, the well was left shut-in for 12 days so that the survey shown on frame B of Figure 87 could be run. Storage signatures associated with porosity taking water are marked on the log. Locations A and B on this figure correspond to the peak locations on the noise log of Figure 86.

Finally, the log on Figure 88 allows one to compare on the same log the character in noise levels to flow along a tortuous path to that along a smooth path. The log was run with a small annular gas flow in progress. The lack of character to levels above the cement top, located at depth A, relative to those below the cement top is very evident.

As the log on Figure 82 demonstrated, character can also be introduced by extraneous noise sources that are intermittent in nature. Common sources of this type will be covered in a final section on quality control.

Pitch: The third feature to a noise log that is essential to interpretation is the pitch or frequency content at a particular peak in noise level. Whenever the flow is occurring behind pipe, frequency content is an excellent indicator of single-phase flow as opposed to the flow of gas upward through liquid. This fact is illustrated by the experimental data appearing on Figure 89. These data are from an experimental assembly consisting of a joint of casing with a flow channel in the cement behind the joint. A string of 2-inch tubing is inside the casing and the logging sonde is inside the tubing. The entire assembly is filled with water.

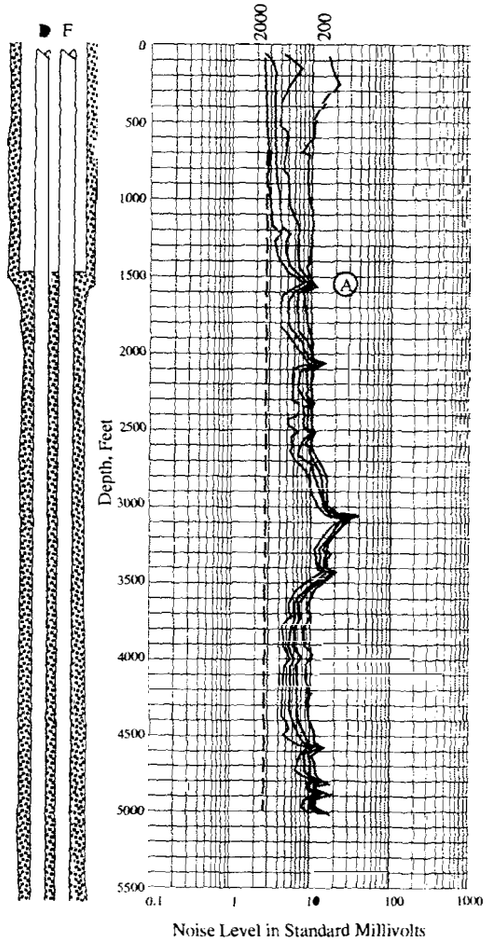

Figure 88. Noise log from well with a very weak gas blow from annulus (D-string logged).

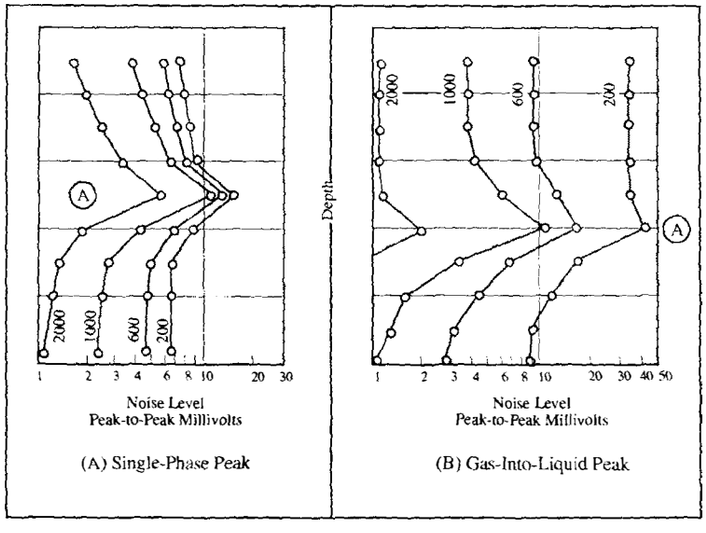

Figure 89. Frequency content (pitch) at a noise peak produced by two different types of flow behind pipe.

The record on frame A of Figure 89 resulted from water acceleration into the channel from a porous plug located at depth A. The first three measurements at 200, 600, and 1,000-Hz are "bunched together" in the 10-16 standard millivolt range whereas the 2,000-Hz cut has dropped to 5.5 standard millivolts. Thus, the dominant frequency of the sound is near 1,000 Hz. This type of behavior is typical of the turbulent sound generated by high velocity, single-phase flow behind pipe. At least three "cuts" through 1,000-Hz will be bunched together and all four may be if the dominant frequency moves up into the 2,000-Hz range. Lower velocity flow of water inside casing generates much lower frequency sounds until the rates become quite high.

A comparison of the frequency behavior at the peak at depth A on Figure 79, with the 20 BPD water flow, frame A of Figure 89, indicates that the behavior is the same. Likewise, at any of the peaks on Figure 85, the 500 BPD water flow, the first three readings are bunched together in the same fashion as are those on frame A of Figure 89. For the gas flow behind pipe shown on the log of Figure 88 all four "cuts" are crowded together at most of the peaks. Thus, the dominant frequency is closer to 2,000-Hz for this case. This is not a distinction between single-phase gas as opposed to water alone, because water can also generate peaks with frequencies this high or higher. Higher velocities are, of course, required for water because of the higher viscous attenuation in water.

The frequency behavior exhibited on frame B of Figure 89 resulted from a small rate of gas bubbling from the porous plug into a water-filled channel. In contrast to those on frame A, the levels at the peak on frame B are spread out over a range from 2 to 42 standard millivolts. There is obviously quite a bit of sound at the lower frequencies. In fact, the level in the band from 200 to 600-Hz alone

$$N_{200} - N_{600} = 42 - 17,$$

$$\Delta N = 25 \text{ std. millivolts},$$

exceeds the level associated with all frequencies above 1,000-Hz, i.e.

$$\Delta N > N_{1,000} = 11 \text{ std. millivolts}.$$

This strong component of lower frequency sound is generated by the collapse of liquid upon itself during the cycle of uplift and fallback of water associated with entry and subsequent rise of each discrete bubble or slug of gas. This process accompanies a particular slug of gas as it rises through the water; consequently, the level on the 200-Hz curve remains at a high value even above the entry depth A on frame B of Figure 89.

The frequency behavior exhibited on this frame is a characteristic of a gas-liquid system and will be manifest for flow either inside or outside casing. As gas velocity increases, the churning action in the liquid also increases to the point that the liquid begins to foam or froth. From this point, the frequency character starts a transition from that of frame B back to that of frame A. Rapidly decreasing sound levels also accompany this transition back to single-phase type

behavior. Most behind-pipe flows of gas through liquid exhibit frame B type frequency behavior until the gas simply lifts the liquid out of the flow path.

The third noise log with water flow behind pipe examined, Figure 86, had an estimated crossflow rate of 5,000 BPD. Yet the peak frequency structure at both the source depth D and the exit depth E is of the "spread out" type of frame B on Figure 89, for gas moving through liquid. Note also that the 200-Hz level is practically constant from the source throughout the 4,000-foot interval to the exit peaks. The noise logging tool is responding to the dissolution of gas, nitrogen and carbon dioxide, at the entry depth D, and the subsequent travel of gas upward. Evidence of gas cooling at the source is evident on the temperature log on frame A of Figure 87, at depth D.

The type of frequency character exhibited on Figure 86, is not that unusual in connection with behind-pipe flow of ground water. Gas flow through liquid is such a strong sound source that a little gas evolution will dominate the noise log levels. This actually increases the sensitivity of the tool above that which it has for single-phase flow alone, provided the gas does not stay dispersed as very tiny bubbles that move with the water.

The example logs considered so far are sufficient to show that, in combination, the three features, loudness, character, and pitch determine what a noise log means from a qualitative standpoint. But one must relate the loudness to flow rate for the tool to be effective.

Sound Level-Flow Rate Relation: Compare once again the sound level at the peak, depth A, on Figure 79 with the levels at the peaks on the log of Figure 85, all of which have a dominant pitch of about 1,000 Hz, the same as that of peak on Figure 79 (page 118). On the latter figure, the level is only $N_{1,000} = 6$ standard millivolts even though the sound source is directly behind the casing in which the tool is located. This value is considerably less than the level at 1,000-Hz of any of the five peaks appearing on Figure 85, which from depth A downward reads 30, 31, 54, 51, and 27 standard millivolts, respectively, and this with the tool removed by two strings of pipe from the sources located behind the casing. Intuition would therefore attribute more behind-pipe flow to the situation on Figure 85 than to that producing the log on Figure 79. However, the pressure drops associated with the peaks are quite different. The single peak on Figure 79 accounts for 250 PSI pressure difference whereas the five peaks on Figure 85 combined dissipate some 2,000 PSI of abnormal pressure. Consequently, the levels cannot be related to rate alone. The necessary relationships are given in the following subsections.

Water Flow Behind Casing: The turbulence created by the acceleration of a single-phase fluid past a constriction is directly proportional in intensity to the power expended to achieve the acceleration. This is simply a statement of energy conservation because all the power is lost to fluid frictional dissipation. Thus, the level of sound at a peak is proportional to the rate of pump work creating the peak, that is, to the product $\Delta p \times q$, where Δp is the pressure drop across the constriction and q is the volumetric rate. The constant of proportionality between sound level, N, and pump power, Δpq, is determined experimentally with apparatus of the type that was described in connection with Figure 89. If the 1,000-Hz cut is chosen as the calibration level, then the relationship takes the specific form

$$\Delta p \times q = 1{,}100\ Np \times (N_{1,000} - 6), \qquad (9a)$$

where

Δ_p	=	pressure drop across, peak, psi
q	=	volumetric rate, BPD
N_p	=	number of pipe strings between tool and noise source
$N_{1,000}$	=	level at peak on 1000-Hz cut, standard millivolts

The experimental basis for the above relationship is given by the correlation on Figure 90 for $N_p = 1$, i.e., for the water flow behind the same casing in which the tool is located. Equation 9a represents the straight line shown on the figure for noise levels greater than 7 standard millivolts on the 1000-Hz cut. For example, at $N_{1,000} = 15$ the line shows $\Delta p \times q = 10 \times 10^3 = 10{,}000$ whereas equation 9a gives $\Delta p \times q = 1{,}100 \times 1 \times (15\text{-}6) = 9{,}900$. The scatter of data on Figure 90 arises from the presence of values for many different types of geometric configurations to the flow path behind pipe. This causes an uncertainty in rate of about a factor of 2 within the value given by equation 9a; however, geometry behind cemented pipe is never known with any degree of confidence.

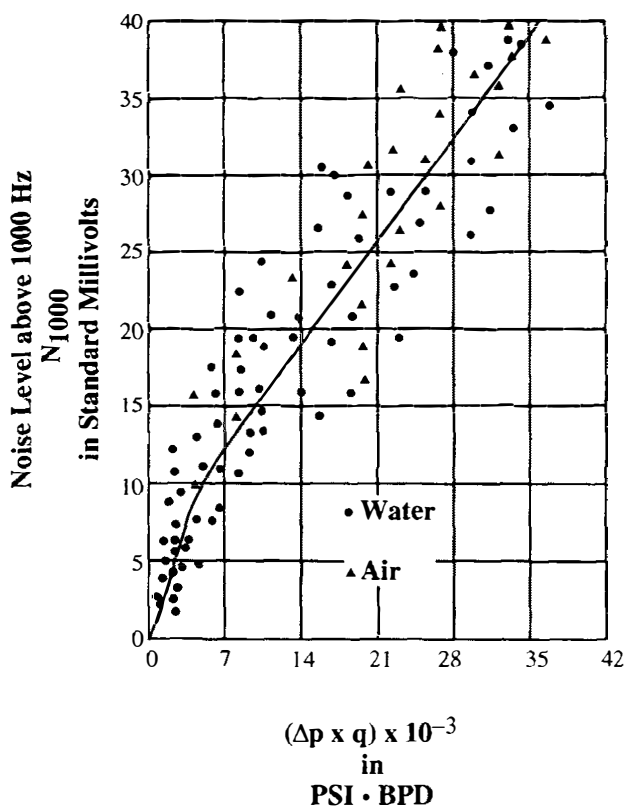

Figure 90. Sound level-rate correlation for water flow behind the pipe in which sonde is located (N_p =1).

The relation expressed by equation 9a can be applied directly to the peak at depth A on the log of Figure 79. After cable correction, the value for $N_{1,000}$ was:

$$N_{1,000} = 3 \times 2 \times 1.65 = 9.9 \text{ std mv.}$$

It had also been noted that this peak had dissipated the known 250-PSI pressure deferential between zones so that $\Delta p = 250$ PSI for the peak, with $N_p = 1$, equation 9a gives

$$250\ q = 1{,}100 \times 1 \times (9.9 - 6),$$

$$q = 17 \text{ BPD.}$$

A value that, fortuitously, is close to the estimated rate of 20 BPD. From the scatter on Figure 90, one could expect $\Delta p \times q$ to be in the range of 1,800 to 7,000 with corresponding rates of 7-28 BPD.

Refer now to the log on Figure 85. If one attempts to apply equation 9a to a particular peak, the appropriate value for Δp is unknown because all that is known is the total pressure difference of 2,000 PSI over all the peaks. This total pressure drop, however, is the sum of the individual drops at each peak. From the form of equation 9a, if Δp_{TOT}, the total drop, is used, then the corresponding noise level is the sum for the individual levels, i.e.,

$$\Delta p_{TOT} \times q = N_p \sum_{i=1}^{5} (N_{1000_i} - 6),$$

where the $N_{1,000_i}$, are the individual 1,000-Hz cuts at the five peaks on Figure 85. This particular log was run on 25,100 feet of 7/32 inch logging cable. The corresponding attenuation correction factor from Figure 80, is $F_L \simeq 1.75$ at the dominant frequency of 1,000 Hz. Thus, the corrected peak values of the 1,000-Hz cut are, in order from Depth A on Figure 85, downward:

$$\sum_{i=1}^{5} (N_{1000_i} - 6) = (30 \times 1.75 - 6) + (31 \times 1.75 - 6) + (54 \times 1.75 - 6) + (51 \times 1.75 - 6) + (27 \times 1.75 - 6)$$

$$\sum_{i=1}^{5} (N_{1000_i} - 6) = 308 \text{ std. mv.}$$

With 2 strings of pipe between the sonde and the leak, $N_p = 2$, and we have

$$\Delta p_{TOT} \times q = 1{,}100 \times 2 \times 308 = 677{,}600.$$

For an estimated Δp_{TOT} = 2,000 PSI, the corresponding rate is

$$q = \frac{677{,}600}{2000} = 339 \text{ BPD},$$

a value to the low side of the estimated 500 BPD rate.

It should be noted that the use of the 1,000-Hz cut on Figure 90 and in equation 9a is simply a matter of choice. There are data points on the figure for peaks with dominant frequencies in the 2,000-Hz range similar to the peaks appearing on the log of Figure 88. Consequently, the cable correction factor by which the $N_{1,000}$ levels are multiplied should be that appropriate to the dominant frequency. In the case of Figure 88, the cable factor at 2,000 Hz is the proper one.

At noise levels below about 8 standard millivolts, the correlation on Figure 90 is represented by

$$\Delta p \times q = 350\, N_p \times N_{1,000} \qquad (9b)$$

$$\text{for} \quad N_{1000} \leq 8 \text{ std. mv.},$$

which gives a convenient expression for the resolution that a noise log from a shut-in well has to water flow behind pipe. If it is considered that, for recognition $N_{1,000} \geq 2\, N_{1,000}$ (BKG), i.e., a peak must exceed twice background level, then the previous expression gives

$$q \geq 700\, \frac{N_p \times N_{1000}(\text{BKG})}{\Delta p} \qquad (10)$$

where q = minimum detectable rate, BPD

N_p = number of pipe strings between logging tool and leak

$N_{1,000}$ (BKG) = background noise level above 1,000-Hz, std. mv.

Δp = pressure difference available for behind-pipe flow

This expression allows the tool resolution for any particular situation to be estimated in advance. It also shows that the tool efficacy is completely dependent upon the pressure difference available to drive flow. As Δp becomes small, the detectable rate increases rapidly.

At a background level of 1 standard millivolts and a driving differential Δp = 100 PSI, equation 10 gives $q \geq 7\, N_p$, a condition that makes the noise logger comparable to temperature and tracer tools. If, however, the pressure difference drops to Δp = 10 PSI, then $q \geq 70\, N_p$ and the tool is no longer comparable to the other two.

Water Flow Past Tool: If the noise log is run while the well is on injection, then the noise generated by flow past the tool may determine the appropriate background level whenever the tool is above the perforations. Likewise, carry-away from this source may dominate the background below the perforations.

For example, the noise log on Figure 91 came from a water flood well on injection at a rate of 26,800 BPD at 1,300 PSI tubing pressure. This rate produces, in the 7-inch casing, a velocity of 508 ft/min past the logging tool. This velocity is sufficient to produce a dominant frequency at the same 1,000 Hz previously observed for behind-pipe flow. Furthermore, the level of sound is quite high, 1,300 millivolts at 0.1 standard sensitivity. In terms of the previous logs, $N_{1,000}$ = 13,000 standard millivolts!

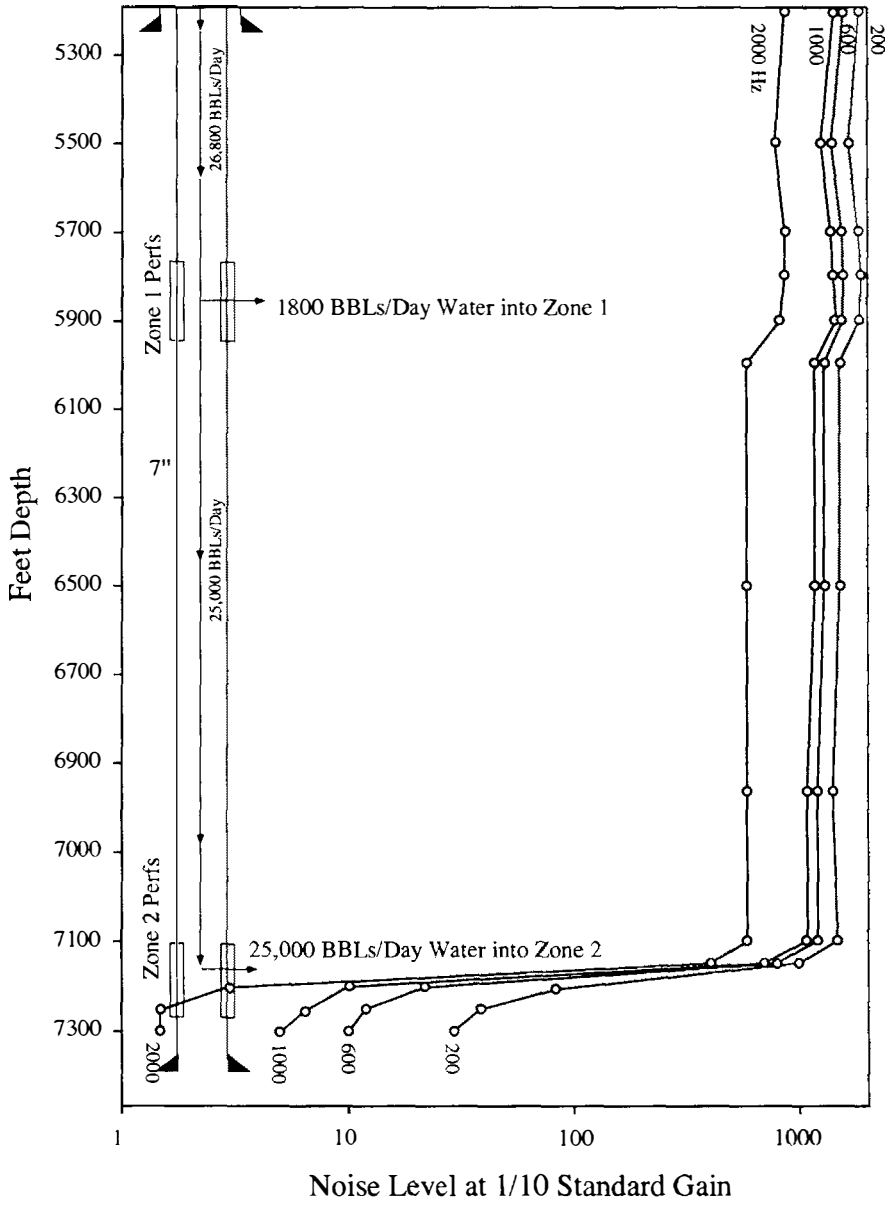

Figure 91. Noise log from well on water injection at 26,800 BPD and 1,300 PSI in 7" casing.

At this injection rate, the log gives an excellent injection profile. A small amount of water is lost to the perforations and into zone 1, but the vast majority of the injected water leaves over about the top one third of the perforated interval in zone 2. Above zone 2 the injection noise is still $N_{1,000}$ = 11,000 std. mv.

According to equation 9a, this level could hide any flow doubling back upward outside the casing whose rate did not exceed

$$q = 1100 \times \frac{1100 \text{ std. mv.}}{1750 \text{ psi}} = 7{,}000 \text{ BPD}$$

where 1,750 PSI is the total injection head. This rate resolution is about the same as the 20% of flow that the temperature log can detect during injection.

If, however, the injection rate to the bottom perforations was only 10,000 BPD, then the noise due to flow past the tool would drop to 700 standard millivolts. At the same injection pressure, the resolution would be $q \geq 440$ BPD or 4.4% of injection rate. At 5,000 BPD, the resolution for behind-pipe flow would further increase to 2% of the injection rate.

The above statements make use of the relationship for noise level due to water flow past the tool that will now be developed. In a smooth geometry, the turbulent pressure drop, Δp, in equation 9a can be expressed in terms of a friction factor, f, per foot of pipe as

$$\Delta p = f \rho V^2 = f \rho \left(\frac{q}{A}\right)^2,$$

where ρ is the fluid density and A is the area between the tool and the casing. Thus, equation 9a is of the form

$$N_{1000} = B\rho \frac{q^3}{A^2}$$

where B is a calibration constant. For a water density of 62.5 lb/ft^3, the combined value ρB as experimentally determined gives the following relationship for the noise level caused by flow past the tool:

$$N_{1,000} = 3.3 \times 10^{-11} (q^3/A^2) \qquad (11)$$

where
- $N_{1,000}$ = 1,000-hz cut in std. millivolts
- q = volumetric rate, BPD
- A = cross-sectional area between tool and pipe.

For a given volumetric rate, tool size, and casing size, equation 11 can be used to estimate the sound level resulting from water flow past the tool. As an aid to the use of this expression, the cross-sectional areas for common tool sizes are listed in Table 8:

TABLE 8. CROSS-SECTIONAL AREA FOR NOISE LOGGING TOOLS

Tool Diameter Inches	Cross-Sectional Area
1	0.0054
1 3/8	0.0103
1 1/2	0.0123
1 5/8	0.0144
1 11/16	0.0155

These values can be subtracted from pipe areas given in commonly available tables. For example, the 7-inch, 23 lb/ft casing on Figure 91 has an area of 0.221 sq. ft. A 1 11/16-inch tool was used to log the well. Therefore, in equation 11

$$A = 0.221 - 0.0155 = 0.2055.$$

For a rate q = 25,000 BPD, the level from equation 11 is

$$N_{1000} = 3.3. \times 10^{-11} \times \frac{(25{,}000)^3}{(0.2055)^2}$$

$$N_{1000} = 12{,}200 \text{ std. millivolts}$$

This value is as close to the measured level of 1100 x 10 = 11,000 standard millivolts as can be expected without specific tool calibration.

Equation 11 provides the relation needed to convert the noise levels through, say, the bottom set of perforations in zone 2 into a flow profile. Because $q \propto \sqrt[3]{\text{level}}$ by equation 11, it is simple to construct the injection profile shown on Figure 92. For this profile, the 2,000-Hz cut has been used as the one with the best vertical resolution. Zero flow has been assigned to $N_{2,000} = 1.5$ millivolts as Figure 91 indicates. Still, Figure 92 indicates that, relative to the spinner survey, sound carry-away has "smeared' the profile downward somewhat. Nevertheless, the noise log profile is quite acceptable. Equation 11 also shows that more typical injection rates like 2,000 BPD will not raise the noise level in the wellbore by very much. For example, 5 1/2-inch, 17 lb/ft casing has an area of 0.1305 sq. ft, so that with a 1 11/16-inch logging tool A = 0.1305 - 0.0155 = 0.115. At q = 2,000 BPD, equation 11 gives $N_{1,000} = 20$ std. millivolts. Consequently, the tool, even above the perforations, has a resolution for behind-pipe flow that by equation 9a is :

$$\Delta p \times q = 15{,}400 \text{ PSI} \bullet \text{BPD},$$

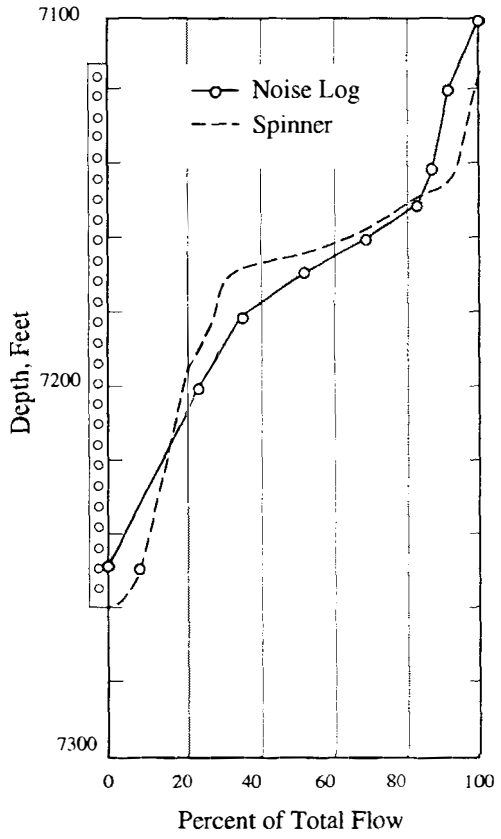

Figure 92. Comparison of noise log and spinner survey injection profile for a rate of 25,000 BPD.

while the well is on injection. For a 500 PSI injection head, this is equivalent to a 31 BPD rate behind casing, a value plenty low enough for surveillance purposes. This is obviously not the case when the tool is located in the tubing. Suppose a 1 11/16-inch tool is in 2 3/8-inch tubing. Then A = 0.02171 - 0.0155 = 0.00621 sq.ft. For a 2,000 BPD rate, equation 11 gives $N_{1,000}$ = 6,850 std mv. A packer check is, therefore, not possible with the well on injection. Most injection zones, however, will be over pressured at an injection well itself. Consequently, a packer check can be made during shut-in.

The influence that the dissolution of a small amount of gas that coalesces into rising bubbles or slugs can have on the noise levels associated with water flow outside pipe has already been seen on at least one noise log, Figure 86. Likewise, the log on Figure 82 showed what an even smaller amount of gas flow upward through oil inside the casing could do to the levels. This influence is put on a quantitative basis in the next sub-section.

Gas Flow Through Liquid: The discussion associated with Figure 89 established that gas movement upward through liquid produced a large component of sound in the band $\Delta = N_{200} - N_{600}$ between the lowest two frequency cuts. In fact, for gas rates below about 1,000 ft^3/day at flow conditions, the gas rate is directly proportional to the sound level in this band. The appropriate relationships are:

$$q_{gas} = \frac{N_p \Delta}{2}; \text{ flow behind casing} \qquad (12A)$$

$$q_{gas} = \frac{\Delta}{15}; \text{ flow inside casing} \qquad (12\ B)$$

where q_{gas} = gas rate, cu. ft./day, at downhole temperature and pressure
Δ = N_{200} - N_{600}, std. millivolts, noise level between 200 and 600-Hz cuts
N_p = number of pipe strings between tool and flow

These expressions are based on measurements from the same type of apparatus described in connection with Figure 89, and are approximate in nature.

On Figure 86, at the source depth D, 4,800 feet,

$$\Delta = 2 \times (170\text{-}70) = 200 \text{ std mv}$$

The source is at least 2 pipe strings removed from the tool so that

$$N_p \simeq 2$$

From equation 12A $\qquad q_{gas} = 2 \times 200/2 = 200$ cu. ft./day

at a depth of 4,800 feet and a temperature of 180 °F (Figure 87). At standard conditions, this rate would be about 150 times larger, i.e.,

$$q_{gas} = 30{,}000 \text{ scf/d},$$

or about 6 scf/bbl of water, which is not an unreasonable value for flashed carbon dioxide.

The log on Figure 82 is the result of a small surface leak through the tubing. At depth in the tubing $\Delta \simeq 2 \times (70\text{-}10) = 120$ std mv. From equation 12 B, $q_{gas} = 120/15 = 8$ ft^3/day. This figure may make the leak hypotheses a bit more palatable.

<u>Vertical Resolution On Noise Logs:</u> Any event may be lost in the background sound or in the carry-away from a nearby peak. No explanation of why this happens was given because the concept is widespread in everyday life. Everyone is familiar with the bedside units that generate synthetic sounds that supposedly mimic pleasing natural sounds such as surf or rainfall, the intent being for these to "drown out" disturbing background noise. Because sound amplitude is oscillatory, the only way that the level from two separate sources could be the sum of the individual levels is for the two sources to be in phase with each other. Otherwise, some destructive interference results from the combinations.

This property of sound creates no problem in the vertical resolution of sources having comparable amplitudes. This fact is demonstrated on Figure 93 that shows the 2,000-Hz cut alone as the tool passes two sound sources of equal magnitude but spaced at different distances apart. Even at the closest spacing shown, 2 feet apart, the two peaks are clearly resolved at a 1-foot sample interval. The resolution would be even better with a sample interval of 0.5 feet.

The problem comes with peaks of unequal magnitude, a situation in which the presence of a small amplitude source is not evident above the residual from another much higher amplitude source. A progression to this condition is apparent at the top peak on Figure 94, which is located ten feet away from a second peak whose amplitude is the larger of the two. In frame B, the top peak at 12 millivolts amplitude is barely evident above the residual from the 56 millivolt peak ten feet away. On frame C, the 5 millivolt peak at the top location is unrecognizable above the 9 millivolt residual from the deeper peak.

The attenuation with distance shown by the sound levels on both Figures 93 and 94 is more rapid than that indicated on Figure 81 (page 122), for sound carry-away because the sources are in the casing with the logging tool and, thus, "blow" directly upon the microphone as it passes.

In order to obtain better vertical resolution, most companies have two more high-pass filters in addition to the normal four. These two pass at frequencies above 4,000 Hz and 6,000 Hz, respectively, and can be switched to two of the voltmeters normally used for the regular four cuts. These two values can, therefore, be added to the normal four numbers at any station. This procedure is illustrated on the flowing noise log of Figure 95. The log was run to profile the

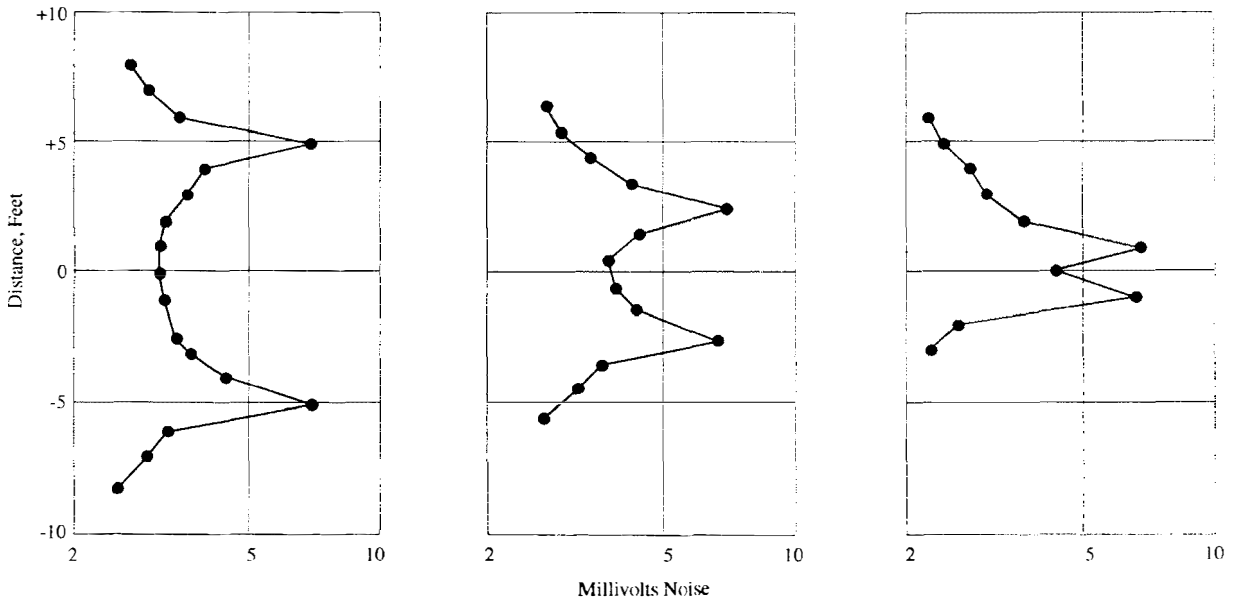

(A) 10-Foot Spacing (B) 5-Foot Spacing (C) 2-Foot Spacing

Figure 93. 2000-Hz noise "cut" for two independent sound sources of equal magnitude but different distances apart inside casing.

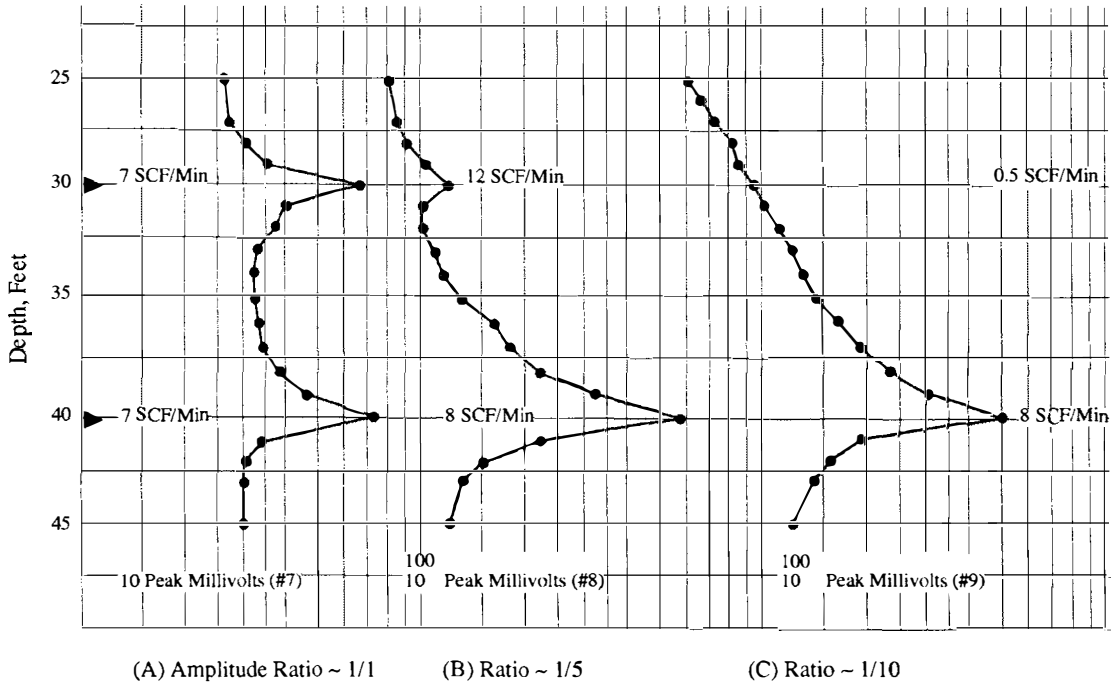

Figure 94. Submergence of weaker source beneath the residual from a stronger one ten feet away. Both sources are inside casing.

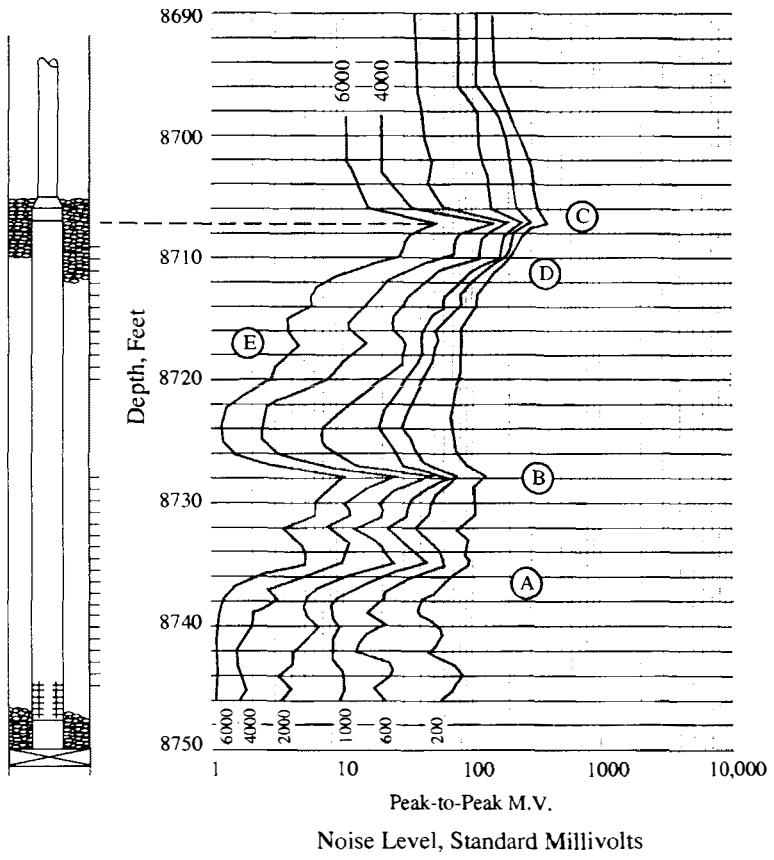

Figure 95. Noise log with 4 and 6-kHz cuts for improved vertical resolution from a gravel-packed gas well flowing three million std. ft³/day.

production of gas from a gravel-packed completion in casing with two intervals perforated. The perforations were logged with 1 foot station intervals at a dry gas rate of 3 million SCF/day. The 4 and 6-kHz values were added to the normal four from 8,698 feet down. None of the six cuts resolve individual peaks very well in the highest productivity interval, AB, over the top half of the bottom set of perforations. However, at depth E, a peak that is just beginning to be ill defined by the 2,000-Hz cut is well defined on the 4,000 and 6,000 cuts. On the latter, a second peak appears just above depth E that is not evident on any of the lower frequency cuts. The entry into the screen at depth C is above the topmost perforations in the casing. This suggests that both the screen and the perforations in the top set may be nearly plugged by fines.

All the material presented so far has been in preparation for the next two sections that deal with the use of the noise survey to demonstrate either injection confinement or the lack of non-related crossflow behind casing. Whereas the radioactive tracer tool is the preferred complement to the thermometer for injection confinement surveys, there are situations where the injection occurs behind the string of pipe in which logging tools must be run. Dual completions, for example, fall in this category. Here, the noise log becomes of use as an inexpensive way of surveying with a tool that does not have to be either "fished" out or cemented in place in the event it is lost downhole.

Noise Surveys For Injection Confinement: Most injection zones are over pressured to some degree. This can be true for wells that do not stand full during injection, that is, for wells that inject on "vacuum." Salt water with a gradient of 0.50 PSI/ft. over-pressures a formation about 40 PSI for each 1,000 feet of water column. Thus, a zone at 3,000 feet will have 80 PSI excess pressure even though the brine level in the wellbore stands 1,000 feet below the surface. Consequently, a noise survey on the injection well shut off of injection will have a higher sensitivity to loss behind pipe to zones above the target interval than will a survey run while injection is in progress. This supposes that the injection rate exceeds about 2,000 BPD. At rates no larger than 2,000 BPD, an injecting survey will be more sensitive. As with all generalizations, these can be wrong. They are given to justify to the reader that, like the other tools discussed, noise surveys should also include both injection and shut-in surveys if the tool is used to evaluate confinement. Unlike temperature surveys, shut-in noise logs can be run as soon as injection ceases.

The best way to proceed from here is to simply examine cases of both confined injection and unconfined injection.

The noise survey of Figure 96 was run with a well on injection at a rate of 10,800 BPD and 1,400 PSI tubing pressure. Two intervals are targeted for injection as indicated on the figure. The survey shows all the injection entering the top portion of the top set of perforations. Within the tool resolution, there is no indication of flow upward behind pipe from the perforations. The signature is thus one of confinement to the top zone. Above the perforations, the noise level is N1,000 $\simeq$ 1,200 std mv whereas the net injection head at the 1,400 PSI tubing pressure is about 1,250 PSI. Equation 9A indicates a rate resolution behind pipe of:

$$q \geq 1100 \times \frac{1200}{1250} \approx 1100 \text{ BPD},$$

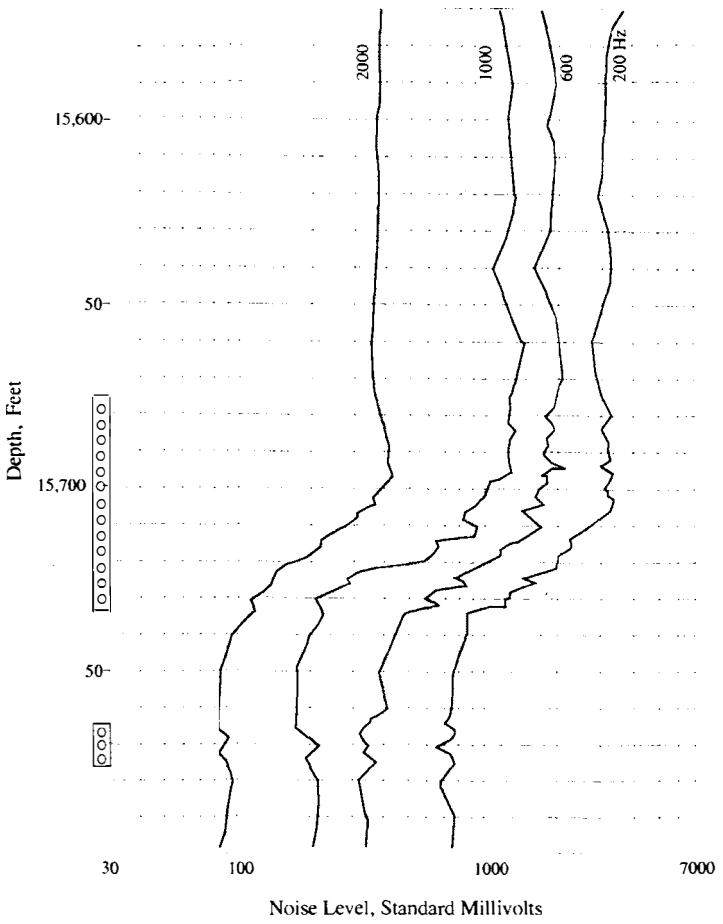

Figure 96. Noise survey with well on injection at 10,800 BPD and 1,400 PSI. Casing is 7-inch, 29 lb/ft and tool is 1 1/2-inch.

or about 10% of total rate. The behavior of the 2,000-Hz curve indicates that this may be a conservative estimate, however. The speed up of exiting water is evident by the increased level over the entire top half of the upper set of perforations. This suggests that by adding the 4,000 and 6,000-Hz cuts, we could obtain excellent sensitivity to behind-pipe flow even while injecting at this high rate.

The cross-sectional area of the 7-inch, 29 lb/ft. casing is 0.2085 ft^2 whereas the tool cross-section is 0.0123 ft^2. Thus, in equation 11, A = 0.2085 - 0.0123 = 0.1962 ft^2. Therefore,

$$N_{1000} = 3.3 \times 10^{-11} \times \frac{(10{,}800)^3}{(0.1962)^2}$$

$$N_{1,000} = 1{,}080 \text{ std. mv.}$$

as compared to the measured value $N_{1,000}$ = 1,200 std. mv. Note also that this value is only about 1/3 the value of the 200-Hz cut. The dominant frequency is in the 600-1,000 Hz range for the inside casing flow. As a result, the four cuts are more spread out relative to each other.

The four cuts are even more spread out on Figure 97, a noise survey with the rate reduced to 5,000 BPD. The dominant frequency at this rate is near 600 Hz. The injection is again seen to be confined to the upper portion of the top set of perforations with no indication of loss behind pipe from the top interval. The movement behind pipe within the upper half of the top perforations is even more evident on the 2,000-Hz curve of Figure 97. Also, some fluid acceleration in this same location is now evident on the 200-Hz curve. Obviously, the sensitivity to flow behind pipe is greater at this lower rate. Above the perforations, $N_{1,000}$ = 150 std. mv. whereas the injection head has dropped to 575 PSI; consequently, equation 9A predicts

$$q \geq 1100 \times \frac{(150 - 6)}{575} = 280 \text{ BPD},$$

as compared to 1,100 BPD at 10,800 BPD. Again, this figure is conservative given the behind-pipe noise evident within the perforations. Still, it is only 5.6% of the injection rate.

The flow noise from 5,000 BPD inside the casing is given by equation 11 as $N_{1,000}$ = 110 std. mv. as compared to the measured value of 150 std. mv.

On both figures 96 and 97, the sound levels below the perforations do not decay very rapidly. The levels reduce to about 20%-30% of the peak values at a distance of about 50 feet and then

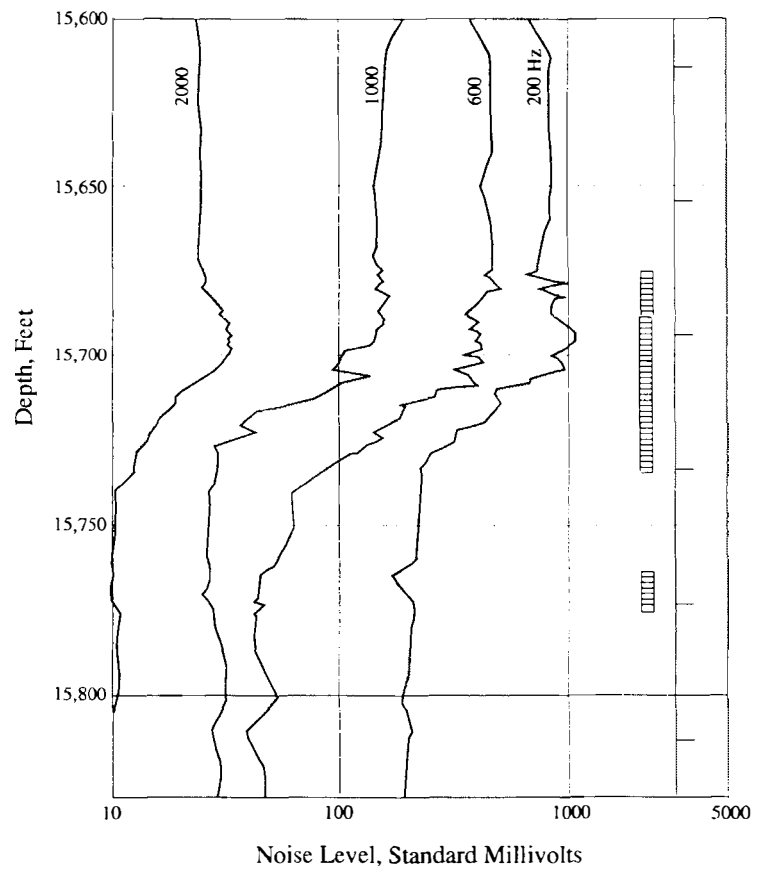

Figure 97. Noise survey from well of Figure 96 with injection rate reduced to 5,000 BPD.

settle down at relatively constant levels. This behavior is not in accordance with the carry-away pattern depicted on Figure 81 for behind-pipe sources. In fact, the residual levels on figures 96 and 97 are the result of waveguide transmission away from the flow noise source inside the casing above the perforations. A level at about 20% of full flow noise is typical of the mode of transmission in water.

When the injection well was shut in, the water level in the 3 1/2 inch tubing dropped to a stable level that placed 135 PSI excess pressure at the injection zones. The noise survey of Figure 98 was then run. This survey included a "packer check" as well as a "channel check." At a background noise level $N_{1,000}$ = 1.5 std. mv., equation 10 establishes a leak rate resolution of

$$q \geq 700 \times \frac{1 \times 1.5}{135} = 8 \text{ BPD},$$

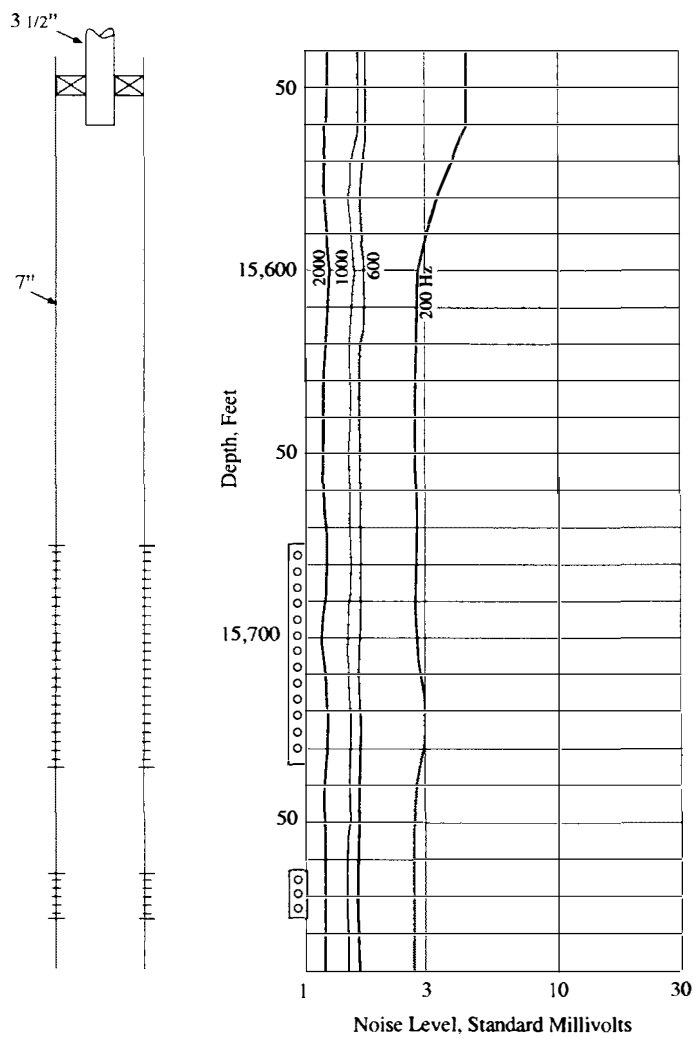

Figure 98. Shut-in noise survey on Figure 97 well with 135 PSI excess pressure on injection zones.

a value that shows the advantage of having charged the zone above normal pressure. Had this not been the case, the injection rate could have been further reduced to about 1,000 BPD and the well surveyed while on injection. At this rate, the flow noise at 1,000-Hz would be about at the 1.5 std. mv. background level.

The next example involves an injection well that is about one year old. Current injection rate is 5,000 BPD at some 200 PSI net injection head. This particular well had been acid fractured in an attempt to insure that injection reached all three zones perforated, either inside or outside the 7-inch, 32 lb/ft casing. Flowmeter and temperature surveys appear on Figure 99. Note that the temperature surveys include both injection and shut-in passes and the shut-in times include both short and long times. The latter, at 28 hours, is in the recommended range listed in Table 3 for a 1 year old injection well. The spinner survey on frame A of Figure 99 shows that all the injection leaves the wellbore over the upper half of the top perforated interval with nothing,

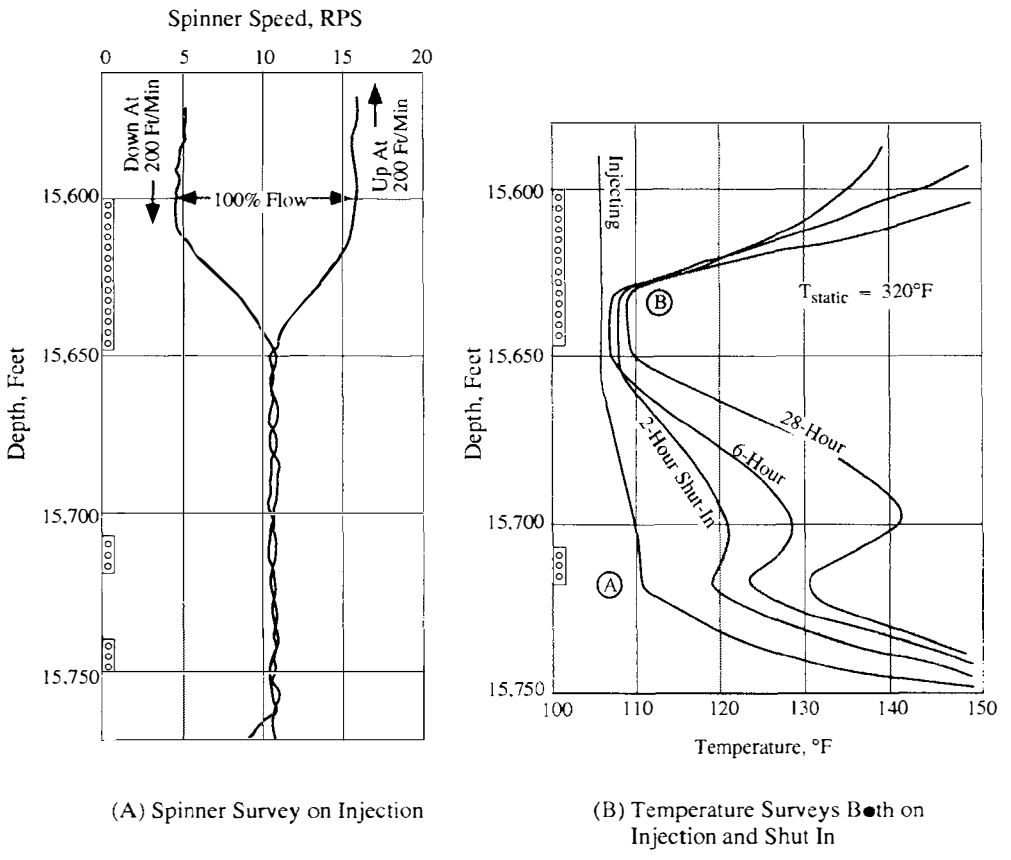

(A) Spinner Survey on Injection

(B) Temperature Surveys Both on Injection and Shut In

Figure 99. Surveys on a one-year old injection well with a current injection rate of 5,000 BPD.

within tool resolution, reaching the lower two intervals.

The temperature surveys on frame B of Figure 99 show that, although most of the injection stays in porosity located in the lower part of the top perforated zone, some of the injected water reaches the perforated interval just below 15,700 ft. Slopes on the injection temperature survey correspond to about 10% of the total rate, or 500 BPD, flowing to this depth. As this amount is within spinner resolution, we would conclude that this flow occurs in an acid fracture outside the 7-inch casing.

This outside-of-casing flow is confirmed by the noise survey of Figure 100, run with the well on injection at about 3,500 BPD. The behind-casing flow is clearly evident on all cuts at levels above the noise created by the flow inside casing. The level created on the 2,000-Hz cut by the flow outside is at some locations nearly 3 times the level from flow inside even though only about 10% of the total gets behind the casing.

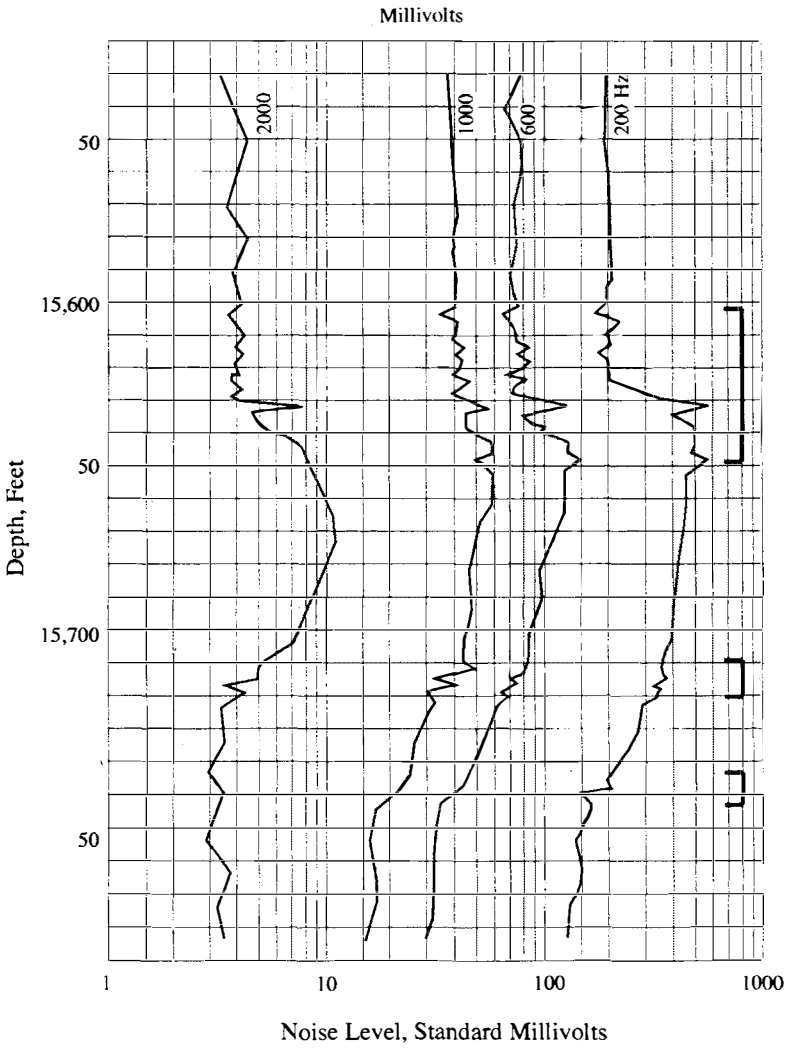

Figure 100. Noise log from well on water injection at 3,500 BPD with a flow of about 350 BPD behind casing from top perfs to the zone at middle perfs through an acid frac.

The curve with the best vertical resolution, the 2,000-Hz cut, shows that the behind-pipe flow stops at the middle set of perforations. Someone looking at the lower frequency cuts might be tempted to carry on to the bottom perforations, yet the levels on all cuts at this location are close to the expected carry-away levels from the chart on Figure 81 for large pipe and a 30 ft distance between the 15,700 ft. location and the bottom interval.

Another feature evident on the noise log of Figure 100 is the way statistical variations in flow sound take on an "air" of importance whenever the sample density increases. This is dramatically illustrated by the apparent activity on all cuts in the record over the top 20 feet of the upper perforations relative to the activity above, where stations are more widely spaced. Within the 20 feet, the same variance is being sampled more often than above, yet it "looks" more significant. The spinner survey on frame A of Figure 99 clearly shows that very little flow is lost from the wellbore over the top 20 feet of perforations, however. This is verified on the noise log by the fact that the average level on any cut within the top 20 feet of perforations is no different from the level above.

An example of a casing leak appears on the noise log of Figure 101, which was run in a shut-in injection well completed as shown with a 9 5/8 inch injection "string." The well had the same 840 PSI shut-in pressure on both the 9 5/8 inch "tubing" head and the 9 5/8 x 13 3/8 inch annulus. The purpose of the logging was to find the location of the leak in the 9 5/8 inch injection string. The noise tool was dropped to a depth of 4,000 feet and a reading taken with the annulus pressure undisturbed. As the points on left-hand side of the log show, the sound level was at ambient value. The actual readings ranged from 0.22 to 1.5 millivolts at one-fifth of standard sensitivity, or from 1.1 to 7.5 standard millivolts. The annulus was then opened sufficiently to flow 300 BPD water with a small amount of gas. The noise level at 4,000 feet increased to the values shown on the right-hand side of the log on Figure 101. These high levels are quite obviously not the result of a 300 BPD water flow past the tool. At 4,000 feet, the noise band

$$\Delta = N_{200} - N_{600} = 450 - 100 = 350 \text{ mv}$$

has more amplitude than everything above $N_{1,000} = 50$ mv. This, of course, is the signature of gas moving upward through liquid. The high noise levels are thus the result of gas dissolution from the water. In terms of standard units:

$$\Delta = 350 \times 5 = 1{,}750 \text{ std mv}$$

According to equation 12B

$$q_{gas} = 1{,}750/15 = 117 \text{ ft}^3/\text{day}$$

at the pressure and temperature existing at 4,000 feet. This would correspond to about 16,000 std. cu. ft./day, which is not much gas.

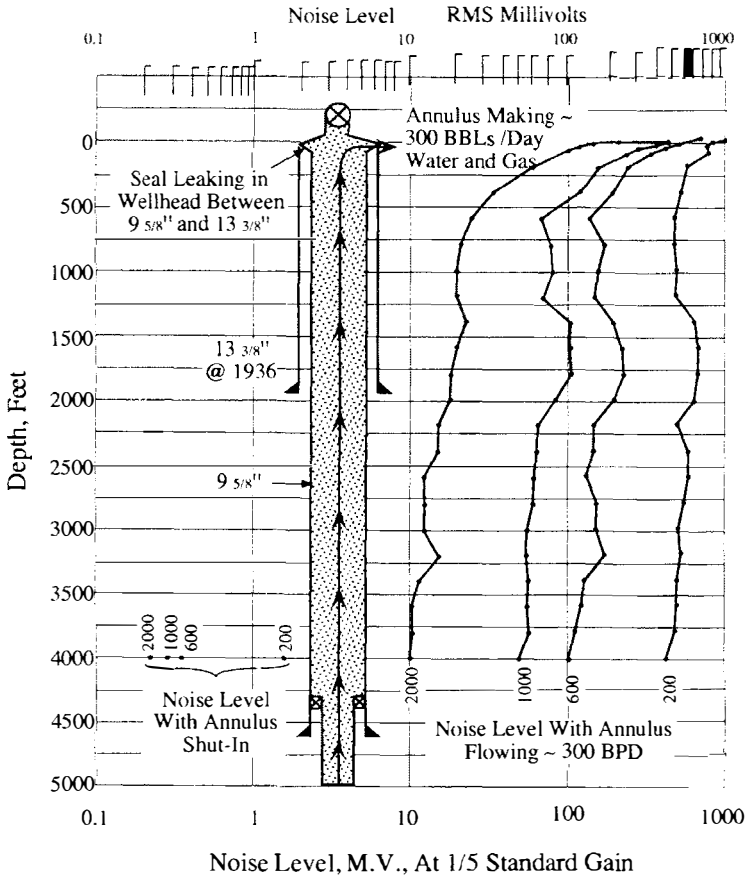

Figure 101. A shut-in noise survey on an injection well with leak in hanger assembly of wellhead.

With the annulus on flow, the well was logged upward from 4,000 feet on 200-foot station intervals without any decrease in levels all the way to the surface. The leak is therefore in the seal assembly of the wellhead itself.

Noise Surveys For Noninjection Related Flow Behind Pipe: Logging for noninjection related crossflow behind pipe is done with the well-shut-in. Under these conditions, some portions of the wellbore should be at ambient or dead-well levels on every log. Thus, a quality control check is available on the log itself. One has the background level for use in the rate resolution estimation available from equation 10. Suppose, for example, that the background is $N_{1,000} = 3.8$ std. mv. and that the polluting zone is 70 PSI higher in pressure than the depleted zone into which it crossflows. Then $\Delta p = 70$ PSI in equation 10 and the tool would have a resolution of :

$$q \geq 700 \times 3.8/70 = 38 \text{ BPD}$$

for flow immediately behind the casing string containing the sonde, i.e., for $N_p = 1$. If the tool is located in tubing which is inside casing with the leak outside the casing, then $N_p = 2$ and the resolution is only 76 BPD. The background level would have to be further reduced if the resolution is to be improved. This may not be possible in some situations; consequently, at pressure differences below 100 PSI, the noise tool resolution will generally not be as good as that available from the temperature tool.

Example noise logs from shut-in wells with water flow behind pipe at rates from 20 BPD up to 5,000 BPD have already been examined on figures 79, 85, and 86. Consequently, only one more example of non-related flow is considered.

This example involves a well that had been sitting closed in for some 6 months after drilling and cementing of production casing had been completed. During this time, 70 PSIG of water pressure built up on the annulus between 5 1/2 inch production casing and 8 5/8 inch surface casing. With the annulus open and the pressure at 0 PSIG, the well would flow water at approximately 400 BPD. The source of this flow was to be identified before a workover was undertaken. For this purpose, a combined temperature-noise survey was conducted. Static surveys were run one day, then the well was relogged the next day with the annulus flowing. The program called for the entire 4,500 feet of wellbore to be logged. Stations 100 feet apart were used for the course noise log grid. This was to be reduced to 20 foot stations for 100 feet on either side of the calculated top of cement at 2,500 feet behind the 5 1/2 inch production casing. This would leave at least five station stops for detailing across the 8 5/8 inch shoe at 300 feet or wherever necessary. The shut-in noise log showed only dead-well levels, the four cuts "straddling" the 1 mv. level. The log run with the annulus on flow at rates from 340 to 520 BPD is shown on Figure 102. At the bottom of the well, the 1,000-Hz and 2,000-Hz levels have settled down to values close to the ambient levels from the previous day. The two lower frequency cuts at 600 Hz and 200 Hz are still decaying from higher levels above.

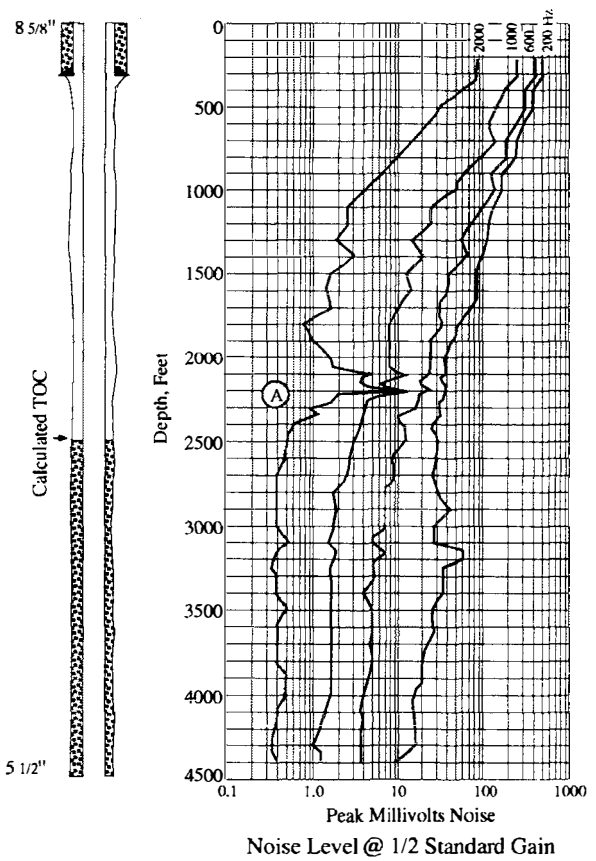

Figure 102. Noise log with water flow at surface of ~ 400 BPD from 5 1/2 x 8 5/8 annulus under 70 PSI differential.

The source of flow was detected before the cement top was reached and the detailed logging was done at depths of 2,000-2,300 feet. The 2,000-Hz curve shows two peaks in this interval, one at 2,100 feet and the other at 2,200 feet. Above 2,100 feet the 2,000-Hz curve does not decay back to ambient value before it becomes influenced by carry-away from the largest sound source, which is the flow through the annulus valve at the surface.

From the relative positions of the 1,000 and 2,000-Hz readings at 2,200 feet, depth A of Figure 102, the dominant frequency of the source is 2,000-Hz or higher. Likewise, the peak at 2,100 feet depth shows a dominant frequency closer to 1,000 Hz. Consequently, there is a single-phase flow of water alone, according to the discussion related to Figure 89. Note, however, that these two peaks do not show on the 200 and 600- Hz curves. The carry-away from the source at the surface is concealing the peaks on these two cuts! The shallowest measurements on the log are at 200 feet. The levels at 1,200 feet are generally in agreement with the 1000-ft. residuals as predicted by the lines on Figure 81, for 4 1/2 inch pipe.

The values on Figure 102 were recorded at one/half standard sensitivity on a truck whose reel contained 17,100 feet of 7/32-inch logging cable. For this cable length, Figure 80 gives the following correction factors:

$$F_L = 1.30 \text{ at } 1{,}000\text{-Hz},$$

$$F_L = 1.55 \text{ at } 2{,}000\text{-Hz}.$$

The corrected readings at the two peaks on Figure 102 are therefore:

$$\text{at } 2{,}100 \text{ ft.} : N_{1000} = 12 \times 2 \times 1.30 = 31 \text{ std. mv.}$$

$$\text{at } 2{,}200 \text{ ft.}: N_{1000} = 13 \times 2 \times 1.55 = 40 \text{ std. mv.}$$

These are the values needed in equation 9A along with $N_p = 1$, $\Delta p = 70$ PSI, to give

$$q = 1{,}100/70 \times [(31-6) + (40-6)] ,$$

$$q = 927 \text{ BPD} ,$$

whereas the actual rate was closer to 500 BPD. As was mentioned in connection with equation 9A, a factor of 2 is not unusual.

A rate resolution can also be estimated from the log on Figure 102. The 2,000-Hz cut could drop to 0.5 mv. on the log before being lost in background. Thus, the peak value of 9 mv. at depth A, 2,200 ft., could drop by a factor 9/0.5 = 18. For the same pressure differential of 70 PSI, the rate resolution is:

$$q \geq 500/18 = 28 \text{ BPD} ,$$

a value not too different from the 38 BPD previously estimated.

Temperature surveys from the well appear on Figure 103. The log taken with flow from the annulus shows production that commences at a depth of 2,250 feet. This location is at the bottom of a water sand according to the open-hole logs from the well. Likewise, the noise log spike at 2,200 feet is already at the top of this sand. The sound sources are apparently at locations where the borehole wall has collapsed around the casing.

The character on the flowing survey of Figure 103 is the result of the unsteady rate as noted on the curve. A comparison of the shut-in and flowing surveys shows no flow from below depth B, 2250 feet. Although the surveys are separated by about 3 °F, they track each other perfectly below depth B. The separation is most likely an operator inconsistency in "log scaling," that is, in setting up the log scale relative to the temperature measurement with the tool stationary at the top of the well. Alternately, the difference may be the result of the need to "manually shift" the recording pen several times to accommodate the 70+ degree range. Each time the trace starts off scale to the right-hand side of the chart, it is shifted back to the left-hand side of the chart. On "analog" trucks this process is accomplished by hand, so if the trace wanders a bit off-scale before the operator notices, then absolute error can creep into the record. This is of no consequence so far as interpretation is concerned.

The important point is that the "anomalies" need not be at the same location on the temperature and the noise surveys whenever the flow is behind casing.

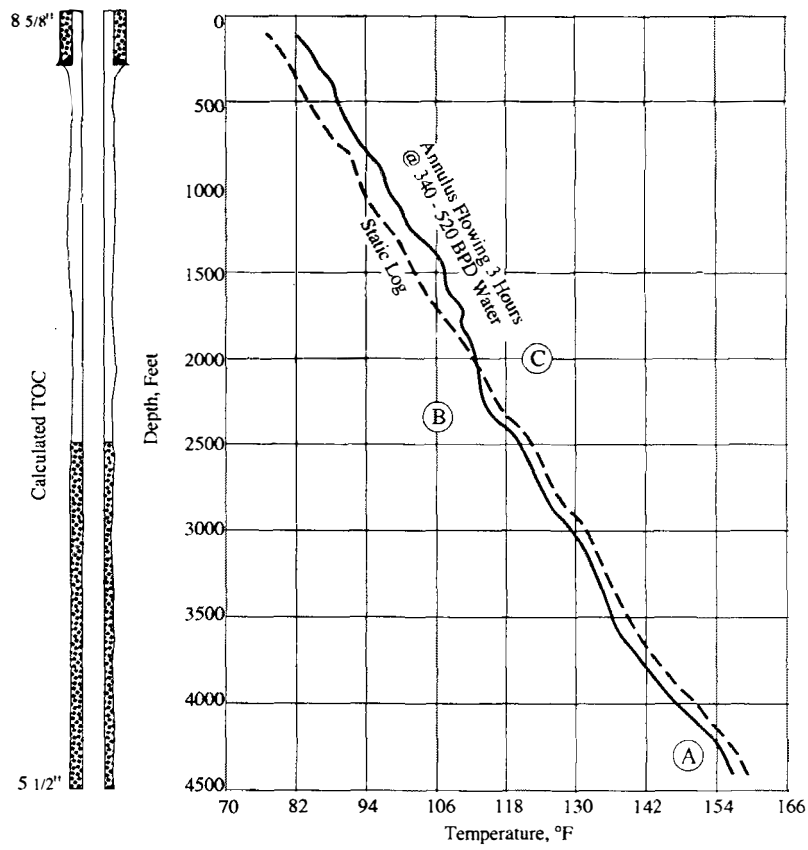

Figure 103. Temperature surveys run one day apart, first with annulus shut-in at 70 PSIG and then with annulus on flow at 340-520 BPD water.

The temperature survey would have been even more influenced by the non-related flow had it been run when pressure first appeared on the annulus. At this time the well was less than one month old and was still disturbed from static. The movement of water to pressure the annulus would have returned the temperature to static at depth B, 2,200 ft., even on a shut-in log.

In the U.S., normal water sands in an area with hydrocarbon production can become overpressured because of blowouts on wells being drilled and as a result of leaks from oil or gas wells already in existence. Noise logs showed gas-in-water flow signatures that conformed to the pattern shown at the peak in frame B of Figure 89. There is an exception to this signature that is described in the next section.

Attenuation by Gas Dispersed in Water: The signature demonstrated on frame B of Figure 89 and on the actual logs of Figures 86, and 101, is the result of the buoyant movement of gas through water. If there is no relative movement, then the source of noise is not present. This can happen when gas that comes out of solution in water remains dispersed as small bubbles in the water and moves with the water. Even worse, a dispersion of this type is "dead" acoustically in that it attenuates severely the frequencies employed in noise logging. This phenomenon is easily demonstrated by means of a glass of water, a spoon, and an "alka-seltzer" tablet (a chemical source of carbon dioxide). First, tap on the side of the glass with the spoon to hear a clear ring in the form of a bell-like "ding, ding, ...ding." Now drop the "alka-seltzer" tablet into the glass of water, at the same time continuing to tap the side with the spoon. The tablet hardly drops below the water's surface before all the "ding" is gone and your tapping produces only a hollow sounding "thunk, thunk,...thunk."

The noise log on the top, frame A of Figure 104, illustrates the deadening influence above the water entry into the wellbore at depth B. When the watered-out well is on production at 3,830 BPD water, gas that comes out of solution is swept along with the high velocity water and remains dispersed as small bubbles in the water. This fact is evident from the relative attenuation on either side of the peak due to entry at depth B on frame A. Below this depth, the log shows normal carry away from the peak. In contrast, the sound levels above depth B quickly attenuate to low levels that are less than those caused by water alone at 3,800 BPD.

All the frequency behavior on frame A is that of single-phase flow. However, with the well shut-in, the entry appears on frame B at depth A as a normal gas in-liquid signature. At a reduced water velocity, the gas bubbles have time to coalesce and move relative to the water. In this example, we have a situation in which a lower rate of water flow could create more noise than would a higher rate.

The same type of behavior can occur at the source of non-related water flow behind pipe. This is illustrated by the next example. The problem is water pressure on the 4 1/2" x 8 5/8 " annulus of a new well that has no production tubing. When opened, the annulus flows brine at rates approaching 1,000 BPD. A disposal zone located at about 4,500 feet was suspected as the brine source. A flowing temperature log was provided in frame A of Figure 105. The rate of flow from the annulus at the surface was 823 BPD average with ± 100 BPD fluctuations. The temperature survey shows at depth A, 4,360 feet, the warming that is caused by water flowing to

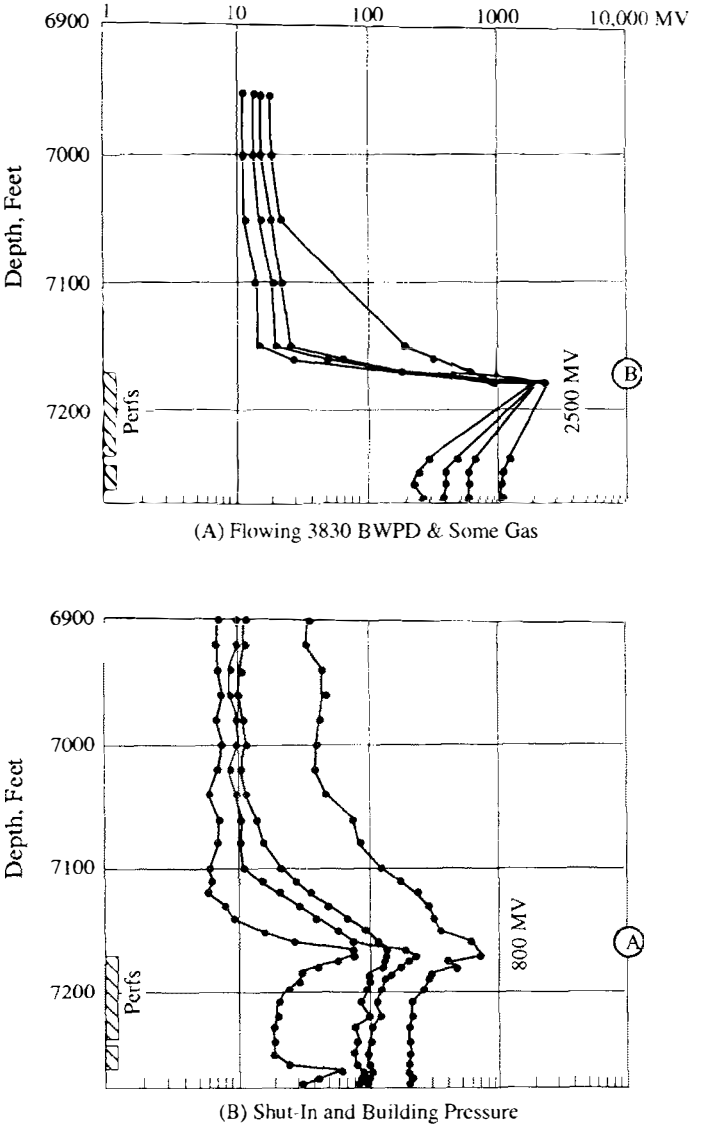

Figure 104. Noise logs, flowing and shut-in, from a watered out-gas zone produced to hold back water.

the wellbore of a new well that is still to the cool side of static. This source is nearly 200 feet above the disposal zone, but the latter was still "suspect" because it was the "only pressured zone around." The noise log on frame B shows what the actual situation is. A compact depth scale is used on the noise log to better show the rapid attenuation above the source, depth A, relative to that below this depth. Note also the low signal levels. The noise log signature is that of gas dispersed in water. The zone at 4,360 feet has been over pressured as a result of having been charged with gas at some other location, presumably from a blowout on a well being drilled. This is another situation in which lower rates of flow would give higher noise levels. At 800 BPD rate, the brine made it all the way up to 1,000 feet before enough gas had coalesced to give a gas-in-liquid signature on the noise log.

In closing the treatment of the noise logging tool, the topic of quality control must be discussed so as to "rehash" comments already made and to add some new ideas not yet introduced.

Quality Control Revisited: Quality control in noise logging is perhaps more subtle in some ways than it is for the temperature and radioactive tracer tools. Poor quality can occur in spite of the best of intentions. For example, compare again the logs on Figures 105 and 88. The latter looks like the better quality of the two, but it actually is not. The station sampling interval of 100-foot stops on the log of Figure 105 was designed to accommodate the 4,500 feet of wellbore with at least 15 stations on closer spacing about the cement top or the 8 5/8" shoe as needed. As things developed, the close spacing was actually used on either side of the source depth A. The procedure, thus, adapted to the situation. On the other hand, the well on Figure 88 (page 130) is surveyed on a constant interval density of one measurement every 50 feet. With over 7,500 feet of wellbore to potentially survey, a total of 150 measurements would be needed, which is more than can be done in a normal day. Consequently, the operator ran out of time before he ran out of hole! He never got to the source of the gas blow at the surface. A better quality sampling scheme would use a coarse density with 200 foot intervals to within about 200 feet of the estimated top of cement. Then the interval could be reduced to 50 feet across the cement top and past the 8 5/8-inch shoe. This would have shown that the source was below the cement top. The interval could have been increased again to 200 feet to total depth with a second fine density where the deepest peak appeared. Detail can always be added at locations where it is needed.

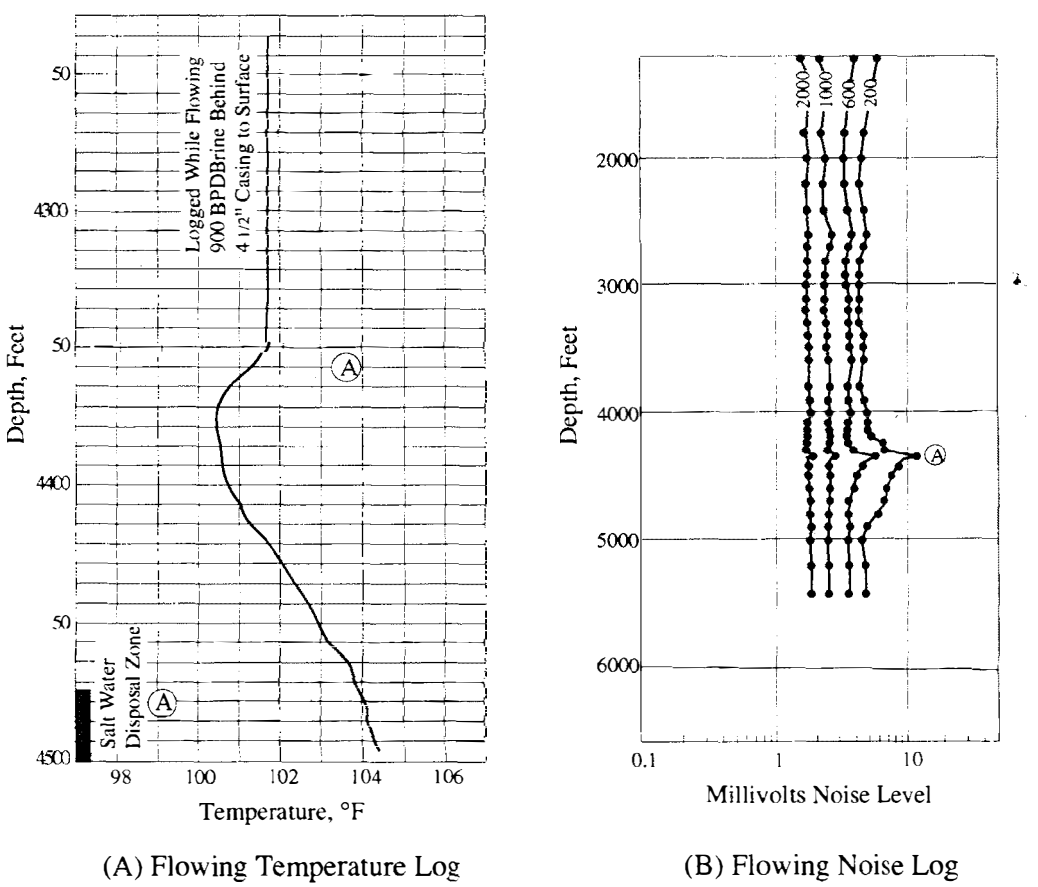

(A) Flowing Temperature Log

(B) Flowing Noise Log

Figure 105. Temperature and noise surveys from a shut-in well with an 800-BPD water flow behind 4 1/2-inch casing from 4,360 feet to the surface.

Another example of poor quality spacing appears on the two logs of Figure 106. These logs are from a dual tubingless, gas well that has pressure on the annulus. Both production strings were shut off production overnight before the logging, which was done in the longer of the two, string H. The liquid level in the annulus is evident on both logs, at depth A on the log of frame A and at depth B on frame B. This means that there is flow in the annulus in both cases although the annulus was shut-in for the log on frame A. The completion picture on the left-hand side of Figure 106 shows three locations that require logging on close station spacing: the shoe at 1,500 feet, the estimated top of cement at 3,000 feet, and the F-string perforations at 4,160 feet. If 30 measurements were devoted to these locations, then about 30 more would be left for a coarser density. With a potential 6,000 feet to survey, the latter density would require station intervals of 200 feet spacing each. The resulting seven measurements in interval from the top of the well to the 1,500-foot shoe would have given plenty of detail over a location where no sound sources are expected anyway. Instead, the operator expended 25 of his stops in this part of the well. The rest of the well will, of course, be inadequately covered. He zips across the cement top on a 500-

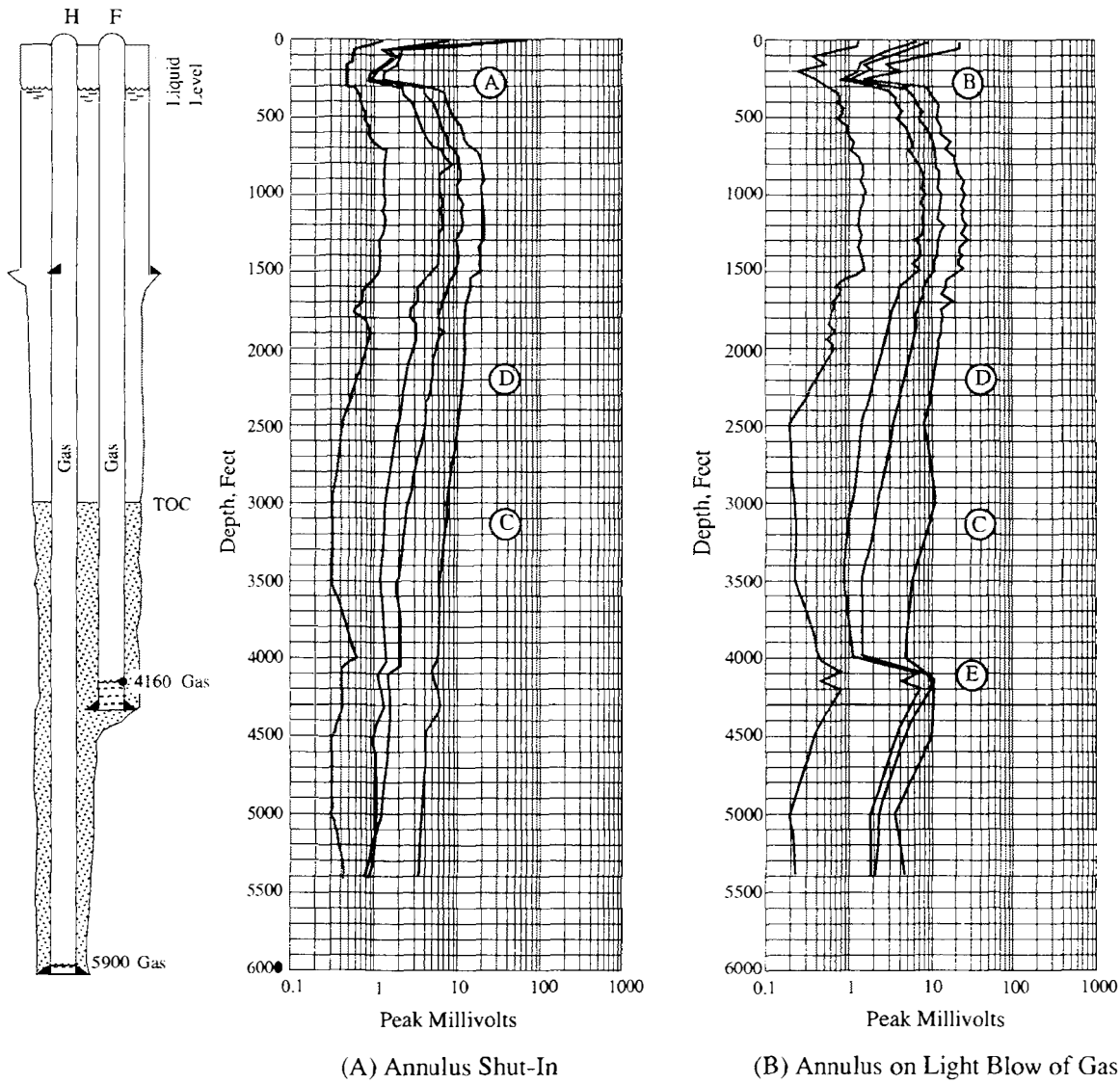

Figure 106. Noise logs from long string, H, of shut-in gas well with pressure on annulus.

foot interval. The behavior at the two stations at 2,000 and 2,500 feet "cries out" for more detail over the interval. The 2,000-Hz cut shows that the stations straddle a source. This is most likely a charged zone that is maintaining the annulus pressure.

A comparison of frames A and B shows that the operation of venting the annulus starts a small amount of gas moving at the liquid level at the perforations in the short string, depth E of frame B. Again, the definition is poor at this location because of the widely spaced measurements, but this behavior means that there is probably a small tubing leak someplace above the cement top. This may be the source of noise missed at depth D. Overall, the logging leaves us not quite sure why there is annular pressure on the well.

The above losses in quality resulted from poor planning before actually logging. Other losses can occur during actual logging. It has already been seen what leaks in the lubricator can do to the quality of a noise log. Flow line leaks can do the same thing.

Tool movement during measurement is another common type of noise pollution, particularly for operators who allow computers to do the logging and never actually listen to what they are recording. A little reel creep can generate a lot of noise. Wind gusts at the surface can also cause the lubricator to sway and move the tool. When a well is logged from the floor of a drilling rig, the top sheave, or wireline pulley, is customarily attached to the travelling block and pulled up about 20 feet above the rig floor. This creates a long pendulum, from the travelling block to the crown block, to "swing in the breeze" from wind action on the surface of the travelling block. If a noise log is to be run, it is a good idea to pull the travelling block with sheave to the top of the derrick near the crown so that the pendulum swing is reduced to a minimum.

Some noise sources cannot be eliminated. The situation leading to the log of Figure 102 is one such case. The variance on this log is higher than desirable on all the cuts. This is particularly evident on the log at 3,000 ft. and is the result of flow instability induced variance in the large sound source created by the surface venting operation. The unstable flow is, unfortunately, a fact that cannot be changed.

Likewise, the motion of a fixed platform offshore causes the drilling template on bottom to grind against the casing of wells completed through the holes in the template. On a calm day, this level is low enough for logging to be done. By a depth of 1,500 feet or so, the background will have decayed to the normal ambient levels of about 1 millivolt. In rough weather, this noise will carry down many thousands of feet, however.

If the logging is done from a floating vessel, such as a drillship or a semi-submersible rig, the only thing that can be done is to take measurements at the trough and crest of each heave when the tool is momentarily stationary.

The sound of the grease injection pump that pressures the leak control held on top of the lubricator will carry down several hundred feet. Consequently, the top portion of a well is logged when the pump is not running.

Good operators quickly learn about the things discussed above, but one cannot depend on having experienced people anymore, no matter what company is used. In fact, the customer himself must assume responsibility for the quality of any production survey he runs, not just for noise surveys.

Summary of Procedures for Temperature, Radioactive Tracer and Noise Surveying

The procedures listed in Table 9 are intended to serve both the well operators need for injectivity information and the regulatory agency's need for integrity information. Any particular situation may, therefore, require only a certain part of a given procedure. The appropriate part can be identified from the column in the table that tells what the corresponding logging operation is supposed to show.

The procedures represent the minimum logging operations required to accomplish the stated goals. Each listed procedure can be enriched by additional logging in almost every specific situation. Likewise, a procedure may need to be modified slightly for special circumstances. However, failure to collect the type of logs that give the stated information will generally result in uncertainty in the question of confinement and integrity because these features are the most sensitive to procedure.

TABLE 9. LOGGING PROCEDURES FOR TEMPERATURE, RADIOACTIVE TRACER, AND NOISE SURVEYING

Reason for Logging: Demonstrate injection confinement and allocate injected water to various zones.

Tool Combination: Temperature and Radioactive Tracer

LOGGING PROCEDURE	WHAT LOGS SHOULD SHOW
(1) Leave well on injection while rigging up. Shut-in only long enough to hang tools in top of well,	
(2) Inject 1/2 hour before logging,	
(3) Run injecting temperature log going in hole at 20-40 ft/min. Record at 1 degree F/inch sensitivity	(3) Where injection is leaving wellbore from surface to total depth.
(4) Run depth correlation logs,	(4) True depth of surveys.
(5) Run radioactive tracer channel check above perforations with slug tracking method at a sensitivity of 1/5 normal gamma ,	(5) Behind-pipe flow above perforations.

(6) Run velocity shot packer check at same sensitivity with 5-minute record,	(6) Packer or tubing leaks.
(7) Do flow profiling work and bottom channel check,	(7) Injection profile among various zones
(8) Shut well off injection and run 2-hr shut-in temperature survey from 200 feet above perforations down to total depth as per step (3),	(8) Porosity taking current injection.
(9) Run shut-in tracer crossflow check by slug tracking method,	(9) Quality control and casing leaks.
(10) Run two longer time shut-in temperature surveys as in step (8) but at times according to the intervals in Table 3,	(10) Porosity taking injection outside perforated interval and long-time injection locations inside perfs.
(11) If confinement uncertainty still exists, return well to injection and run tracer dump test,	(11) Corroboration of previous surveys.

Tool Combination: Temperature and Noise

LOGGING PROCEDURE	WHAT LOGS SHOULD SHOW
(1) Run injecting temperature survey as per steps (1)-(3) above,	(1) Where injection is leaving wellbore.
(2) Run injecting noise survey from total depth to end of tubing. Allow 20 measurements on a coarse station interval and 15 measurements on finer grid just above top perforations and within perforations,	(2) Where injection is leaving casing below tubing. Check behind-pipe resolution by Eq. 9A or 9B.
(3) Shut well off injection and run 2-hr shut-in temperature survey as per step 8 above,	(3) Porosity taking current injection.
(4) Run shut-in noise survey at same spacing density as in step (2) of this procedure, but add four fine grid points past packer location in tubing,	(4) Behind-pipe loss from injection zone and packer leak. Check rate resolution with Eq. (10).
(5) Run two long-time shut-in temperature surveys per step (10) in the previous procedure,	(5) All porosity taking injected water.

Reason for Logging: Detection of non-related flow behind pipe in an existing injection well

Tool Combination: *Temperature and Noise*

LOGGING PROCEDURE	WHAT LOG SHOULD SHOW
(1) Shut well in overnight before logging,	
(2) Run shut-in temperature logging down at 30-50 ft/min depending on suspect interval to be logged. Start 200 feet above top of interval of interest and carry 200 feet below,	(2) Regions returning to static more rapidly than normal.
(3) Run shut-in noise log over same interval. Plan stations to give 40 measurements on coarse grid and 20 on finer grid at critical points like suspect formations, cement tops, casing shoes, etc,	(3) Pressure-driven flow behind pipe. Check tool rate resolution with Eq. (10).
(4) Keep well shut-in for additional 12 to 24 hours and run second temperature survey per step (2) in this procedure,	(4) Cross-flow behind pipe when used in conjunction with log from step (2).

Reason for Logging: Detection of non-related flow on new well.

Tool Combination: *Temperature and Noise*

LOGGING PROCEDURE	WHAT LOG SHOULD SHOW
(1) Log well within two weeks of completion or circulate prior to logging,	(1) A non-static wellbore.
(2) Proceed from step (2) in above procedure,	(2) Any crossflow behind pipe.

☆U.S. GOVERNMENT PRINTING OFFICE: 1994-550-001/00166

Ex. II – 42

Specialized Applications of Noise Logging

R.M. McKinley, SPE-AIME, Exxon Production Research Co.
F.M. Bower, Exxon Production Research Co.

Introduction

A 1973 paper[1] described how the noise logger can detect flow through poor-quality cement behind pipe. This idea is illustrated in Fig. 1. Turbulence generated by fluid moving from Sand A to Sand C creates within the tubing a sound field whose intensity is greater than the ambient noise level in the wellbore. The logging sonde, which is simply a microphone, transmits this sound level to the surface, where it is decomposed into frequencies characteristic of the type of flow. A depth record of noise level will reveal peaks at those locations where the fluid rapidly changes velocity. For example, see entry point (A), constriction (B), and exit point (C) in Fig. 1.

For this type of application, the noise log complements the temperature log very well. But this tool has other uses, too. We have found that the noise log is a valuable aid to logging methods that track fluid movement in the wellbore. The purpose of this paper, therefore, is to extend noise logging technology into the general area of flow inside casing. Specifically, we discuss how to calibrate the sonde for use in the following situations: (1) axial flow past the sonde, (2) flow from perforations, (3) liquid production from gas perforations, (4) sand production from perforations. For each case, the particular calibration coefficients refer to the standard detector sensitivity and load described by McKinley *et al.*[1]

0149-2136/79/0011-6784$00.25
©1979 Society of Petroleum Engineers of AIME

Noise From Axial Flow Past Sonde

Single-Phase Flow

Suppose that the logging sonde is hanging in a wellbore down which water is being injected. The velocity increase acquired by the water while flowing past the sonde will generate turbulence. This can be detected as noise. Recall the familiar hiss from overhead pipes in steam-heated buildings. We can expect a similar sound from flow past the logging tool. The experiments described in Ref. 1 show that a single-phase fluid accelerating across a constriction radiates a noise intensity directly proportional to the pump work required to move the fluid. The same concept applies here. If Δp is the pressure differential required to flow a volumetric rate, q, past the sonde, then the resulting noise level should be proportional to the product Δpq.

This is, in fact, the case, as Fig. 2 shows. Data in Fig. 2 were measured in a flow loop with a vertical test section whose diameter varied over the range indicated. Flow rates varied from 0.1 to 30 Mcf/D. From the data correlation, we have $N^*_{600} = A \times \Delta pq$, where A is a constant and N^*_{600} is the noise level (at standard sensitivity) above 600 Hz. For turbulent flow, $\Delta p = B\rho(q/A_s)^2$, where B is a drag coefficient, ρ is the fluid density, and A_s is the cross-sectional area for flow between the pipe wall and sonde.

This paper describes the use of the noise logging technique to monitor flow inside casing. Calibrations for the following flow situations are shown: axial flow past the sonde, flow from perforations, liquid production from gas-zone perforations, and sand production from perforations. The forms of the correlating equations are independent of specific tool design.

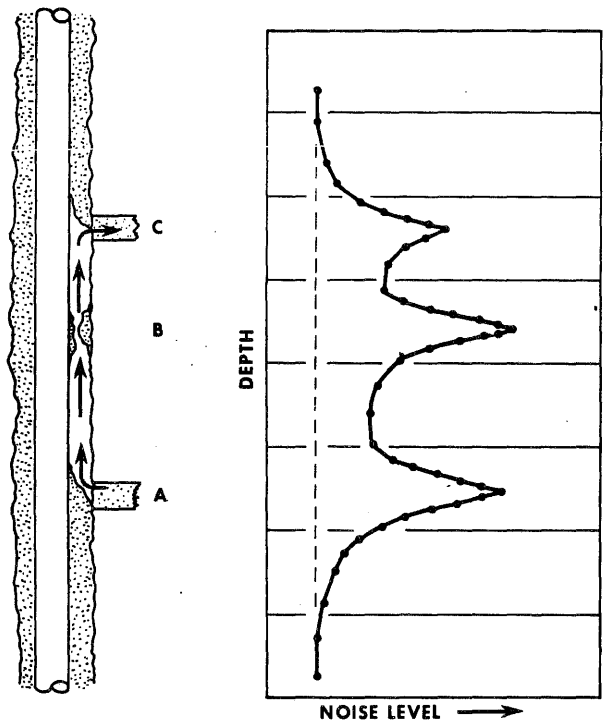

Fig. 1 – How crossflow behind tubing affects the noise level inside tubing.

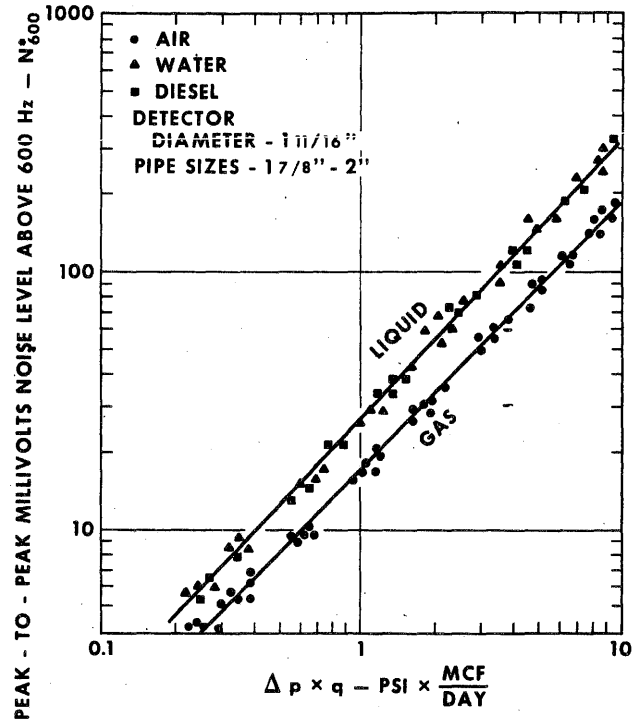

Fig. 2 – Noise level generated by flow past a detector.

Combining these two relationships gives

$$N^*_{600} = C\frac{\rho q^3}{A_s^2}, \quad \ldots\ldots (1)$$

where C is a constant analogous to a drag coefficient. As happens to the latter, the value of C decreases with increasing Reynold's number until the flow becomes turbulent. For Reynold's number greater than 6,000, we find that for gas or liquid, $C=(4\pm1.5)\times10^{-6}$. Thus,

$$N^*_{600} = 4\times10^{-6}\frac{\rho q^3}{A_s^2}. \quad \ldots\ldots (2)$$

Inverting this,

$$q = 63\left(\frac{A_s^2 N^*_{600}}{\rho}\right)^{1/3}, \quad \ldots\ldots (3)$$

where q is in units of thousand cubic feet per day at flowing temperature and pressure, ρ is in pounds per cubic foot, A_s is in square feet, and the noise level above 600 Hz is in standardized peak-to-peak (p-p) millivolts. For the SI metric system of units, the numerical coefficient of Eq. 3 becomes 0.25.

These are the calibrating equations. Significantly, they show that noise level is a function of flow rate or velocity cubed. This is the advantage the tool has over linear meters. The noise level will be a sensitive indicator of small changes in an otherwise high flow-rate situation, as illustrated in Fig. 3.

The 600-Hz noise level measurements were obtained from a well on injection at 25,000 B/D water. A spinner survey had shown that a lower perforated interval (below 8,900 ft) was taking most of the water, while only about 1,000 B/D appeared to be entering the perforations shown in Fig. 3. This 1,000 B/D is 4% of the total flow, which is at the resolution of the spinner. On the other hand, the change in noise level across the interval is 19%. Furthermore, the noise level indicates water is going into the top half of the perforated interval. To ascertain the amount of injection, we apply Eq. 3 to the noise levels above and below the interval. Above the interval, $N_{600}=1{,}610$ RMS mV. Before this value can be used in Eq. 3, it first must be converted from RMS millivolts to peak-to-peak millivolts. This entails multiplying the value by 2.83. Next, the value must be corrected for attenuation caused by the logging cable and for the specific gain of the particular logging sonde. These factors (available from each logging company offering the service) are 1.6 and 2.0, respectively. The total correction factor is 9.06. Therefore, $N^*_{600}=14{,}490$ p-p mV, while below the interval, $N_{600}=1{,}310$ and $N^*_{600}=11{,}773$.

The 7-in. wellbore pipe has a 6.37-in. ID while the OD of the tool is 1.69 in. Therefore,

$$A_s = \frac{\pi}{4}\,\frac{(6.37+1.69)(6.37-1.69)}{144}$$
$$= 0.206 \text{ sq ft } (0.0191\text{m}^2),$$

and

$$A_s^2 = 0.0424 \text{ (ft)}^4 \ (3.65\times10^{-4}\text{m}^4).$$

At the injection temperature, $\rho=61$ lbm/cu ft (977 kg/m^3). Substituting these values into Eq. 3, we obtain a flow rate above the perforations of

$$q = \left(63\,\frac{0.0424\times14{,}490}{61}\right)^{1/3}$$
$$= 136 \text{ Mcf/D} = 24{,}230 \text{ B/D } (0.044 \text{ m}^3/\text{s}),$$

which compares closely with the spinner total injection of 25,000 B/D. Below the perforated interval, the flow rate is

$$q = 24{,}230 \times \left(\frac{11{,}773}{14{,}490}\right)^{1/3}$$

$$= 22{,}610 \text{ B/D } (0.042 \text{ m}^3/\text{s}).$$

The net injection into the interval, therefore, is $\Delta q = 24{,}230 - 22{,}610 = 1{,}620$ B/D (0.003 m^3/s), which illustrates the tool resolution for this type of application.

However, the same cubic relationship that ensures this type of sensitivity also means that the tool will not detect low flow rates. At 600 Hz, the ambient noise level in a typical well is $N^*_{600} = 2$ p-p mV, which means that for 7-in. casing, the minimum detectable rate is

$$q = 63\left(\frac{0.0424 \times 2}{61}\right)^{1/3}$$

$$= 7.03 \text{ Mcf/D} = 1{,}250 \text{ B/D } (0.0023 \text{ m}^3/\text{s}).$$

This situation could be improved by adding turbulence generators to the tool body.

In the above example, the agreement between the spinner rate and that estimated from the noise log is closer than is usually the case. For water injection rates down to 5,000 B/D in 7-in. casing, the noise-log derived rates have been within 25% of the flowmeter rates, provided, of course, that the injection equipment itself is not the dominant noise source. Nearby injection pumps can create mechanical vibrations that carry to total depth in a well. Furthermore, at low flow rates, the noise level at a particular depth may be the result of carry-away from noise sources located at other depths within the well. This is the situation, for example, on the log in Fig. 4 from a flowing oil well. The noise levels above the topmost perforations are much too large to result from the 1,400-B/D flow past the sonde. This high residual noise results from the high values at the perforations.

Finally, here are a few comments on the use of the 600-Hz level. A complete spectrum for this type of axial flow would show a peak amplitude at about 600 Hz for the lower flow rates; consequently, this cut will pick up these lower rates better than a higher frequency cut. Moreover, this frequency is sufficiently low so that for liquids the numerical value for the coefficient C should be independent of pipe size. Our field data verify this. For gases, however, some dependence of the coefficient C on pipe size occurs. The value given seems to be correct for tubing up to 2⅞ in., which is the limit of our field data.

Gas/Liquid Flow

We also have calibrated the sonde for gas/liquid two-phase axial flow, but the results are not very useful.

NOISE LOGGER SENSITIVE TO SMALL RATE CHANGES

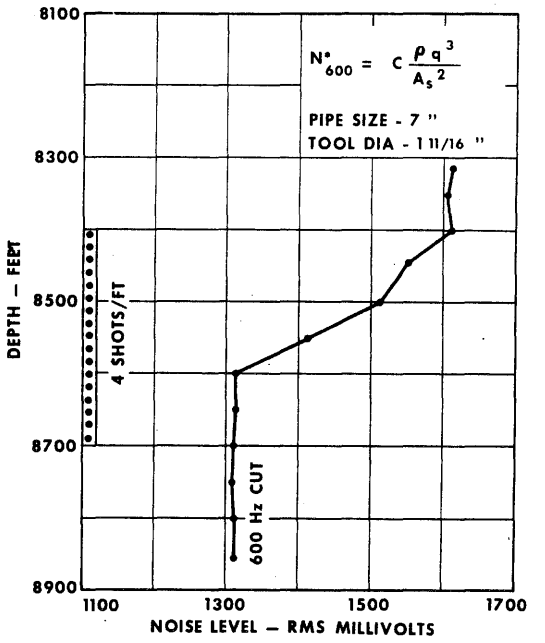

Fig. 3 – Noise profile across a perforated interval, taking 4% of total injection.

NOISE LOGGING FOR PERFORATION FLOW

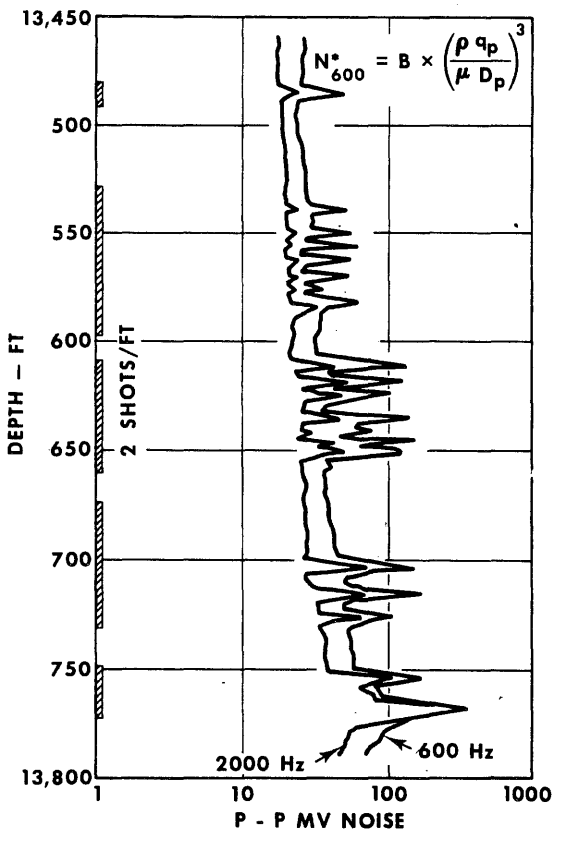

Fig. 4 – Noise log from an oil well flowing 1,400 B/D.

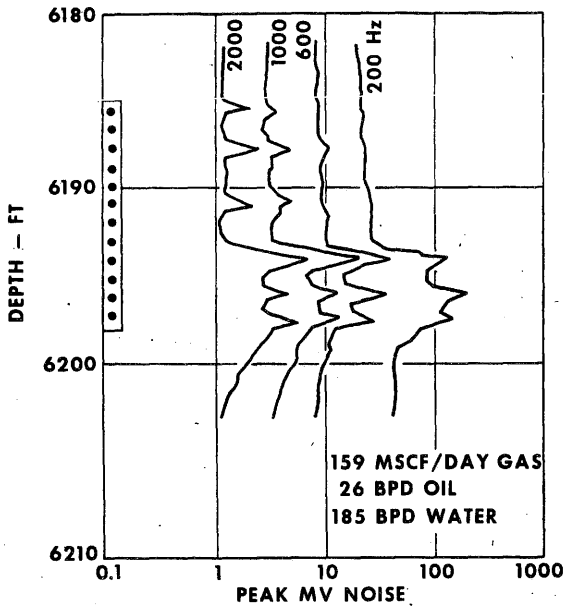

Fig. 5 – Noise log from a well flowing gas and liquid at 2,160 psi and 180°F bottomhole conditions.

More often than not, the state of the gas/liquid mixture is determined by the tangential fluid velocity at the perforations rather than by axial velocity in the tubing. The log in Fig. 5, taken over the perforated interval of a well producing considerable gas and water with a lesser amount of oil, illustrates the influence of the perforations. The loss in noise level above 6,194 ft results from foam generation at this point with the subsequent decoupling of sonde from fluid. The lower frequency cuts lose character. This foam persisted all the way up the wellbore until the pressure dropped to a point where expansion broke the foam. This is not uncommon. Consequently, we will not pursue the flow-loop correlations. Rather, we proceed to the topic of flow from perforations.

Flow From Perforations

Single-Phase Flow

Consider a perforation at least 6 in. deep and 0.5 in. in diameter. Even at formation porosities as low as 5%, the porous surface area of the perforation tunnel is still several times greater than the cross-sectional area. This means that the velocity of fluid entering the perforation tunnel is less than that of the fluid leaving the hole in the casing. Because maximum velocity determines noise level, the hole in the casing wall acts as an isolated noise source, just as any orifice does. This hole is acoustically independent of the formation. Thus, we again may write $N^*_{600} = A' \times (\Delta pq)$, where A' is a constant of proportionality. For an orifice with coefficient B':

$$\Delta p = B' \rho \frac{q^2}{A_p^2} = \frac{16B'}{\pi^2} \frac{\rho q^2}{D_p^4},$$

so

$$N^*_{600} = C' \frac{\rho q^3}{D_p^4}, \quad \ldots\ldots\ldots\ldots\ldots\ldots\ldots (4)$$

where D_p is the perforation diameter and C' is an acoustical orifice coefficient. A jet stream from a perforation actually transports the turbulent field to the sonde, a process whose effectiveness depends on the jet cohesiveness. The latter in turn is inversely proportional to the kinematic viscosity, μ/ρ, of the fluid in the pipe. Hence, we need $\rho q/\mu$ rather than q in Eq. 4. This substitution gives

$$N^*_{600} = C'' \left(\frac{\rho^4 q^3}{\mu^3 D_p^4} \right), \quad \ldots\ldots\ldots\ldots\ldots\ldots (5)$$

or

$$N^*_{600} = C'' \left(\frac{\rho^{1.33} q}{\mu D_p^{1.33}} \right). \quad \ldots\ldots\ldots\ldots\ldots\ldots (6)$$

To test this relationship, we constructed a core holder similar to those used in standard perforation evaluation[2], with the exception that the holder could be fastened to and could admit flow into a section of casing. Perforations were drilled into the core sections along with equal-sized holes in the casing wall. In this fashion, we ran flow tests on cores whose permeabilities ranged from 1 to 3,000 md, with perforations of diameter ranging from 1/16 to ½ in. and depths from 1 to 10 in. The size dependency given by Eq. 6 is needed to correlate the resulting data in its entirety. But in a field situation, one hardly ever will know the perforation diameter, D_p, with any degree of precision. For gases, the same is true for the density, ρ, at bottomhole conditions. We therefore simplify Eq. 6 to

$$N^*_{600} = C'' X_p^3, \quad \ldots\ldots\ldots\ldots\ldots\ldots\ldots (7)$$

where $X_p = \rho q_p / \mu D_p$.

This accomplishes two things. First, it removes some of the pretentiousness from estimating the influence of perforation diameter. But more important, the need for estimating downhole density of gases is eliminated because $\rho q = (\rho q)_{sc}$. Use of density at standard conditions gives the volumetric flow rate at these same conditions. An expression like Eq. 7 is satisfactory for perforation with diameters in the range of ¼ to ½ in., as Fig. 6 demonstrates. The composite data are represented by Eq. 8:

$$N^*_{600} = 3.84 \times 10^{-5} X_p^{2.86}, \quad \ldots\ldots\ldots\ldots\ldots (8)$$

which inverts to

$$\begin{cases} X_p = 35 (N^*_{600})^{0.35} \\ \quad = \dfrac{\rho q_p}{\mu D_p}, \end{cases} \quad \ldots\ldots\ldots\ldots\ldots\ldots\ldots (9)$$

where q_p (Mcf/D) is the volumetric flow rate from the perforation, ρ (lb/cu ft) is the fluid density, μ (cp) is the fluid viscosity, and D_p (in.) is the perforation diameter. For the SI metric system of units, the coefficient in Eq. 9 becomes 7234 instead of 35. The flow rates appearing in Fig. 6 range from 0.1 to 20 Mcf/D. Once more, the nearly cubic dependence of

noise level on flow rate assures that the most prolific perforations will stand out.

An excellent illustration of this is given by Robinson[3] in his Fig. 15. Robinson shows a log from a flowing gas well producing 5.9 MMscf/D dry gas. The perforations are 12 single shots spaced sufficiently far apart so that each one is recognizable on the log. Noise levels at the perforations are given in our Table 1. Four perforations near the middle are flowing a high percentage of total gas. Some of the noise levels are more than 10 times higher than our data in Fig. 6. Therefore, we are extrapolating in these instances with Eq. 9 for values of X_p.

To obtain the total production from the summed X's, we use the following values:

$$\rho_{sc} = 0.045 \text{ lbm/cu ft } (0.721 \text{ kg/m}^3),$$
$$\mu = 0.024 \text{ cp } (0.000\,024 \text{ Pa}\cdot\text{s})$$
$$D_p = 0.45 \text{ in. } (11.4 \text{ mm})$$

Then,

$$q_{sc} = \frac{\mu D_p}{\rho_{sc}} \Sigma X_p$$
$$= \frac{0.024 \times 0.45 \times 18{,}762}{0.045}$$
$$= 4.5 \text{ MMscf/D } (1.47 \text{ m}^3/\text{s}).$$

The 25% error is within the accuracy of Eq. 9. Such close agreement generally will not be obtained because of the tool's inability to resolve noise peaks associated with closely spaced perforations. The important point is illustrated by the magnitude variation of the noise levels in Table 1. Four centrally located perforations are producing almost 50% of the gas.

For a second application of Eq. 9, we refer to the log shown in Fig. 4 from an oil well flowing at 1,400 B/D. Since this well has thick-walled casing perforated with a through-tubing gun, we would expect the spotty production evident in the figure. There are about 20 points of major productivity with the second and third intervals being the biggest contributors. Furthermore, the bottom peak appears to result from a plugged perforation. The sound pitch at this point is considerably higher than elsewhere, as the 2000-Hz curve illustrates. Discounting this last peak for the moment, we find for the remaining 19 peaks that $\Sigma X_p = 5{,}609$ (1.6×10^6), which, with the values $\rho = 51$ lbm/cu ft (817 kg/m^3), $\mu = 0.6$ cp $(6 \times 10^{-4}$ Pa·s), and $D_p = 0.2$ in. (5.08 mm) gives an oil rate of

$$q = \frac{0.6 \times 0.2 \times 5{,}609}{51}$$
$$= 13 \text{ Mcf/D} = 2{,}350 \text{ RB/D } (4.33 \times 10^{-3} \text{ m}^3/\text{s}),$$

whereas the actual rate was

$$q = 1{,}400 \times 1.25 = 1{,}750 \text{ RB/D}.$$

TABLE 1 – NOISE LEVELS AT 12 PERFORATIONS IN A GAS WELL FLOWING 5.9 Mscf/D (Ref. 3)

N^*_{600}	X_p(Eq. 9)
7,150	782
13,325	972
18,850	1,097
113,000	2,054
139,000	2,208
188,000	2,455
188,000	2,455
58,500	1,630
42,250	1,456
52,000	1,566
45,500	1,494
3,250	593
Total	18,762 (3.88×10^6)

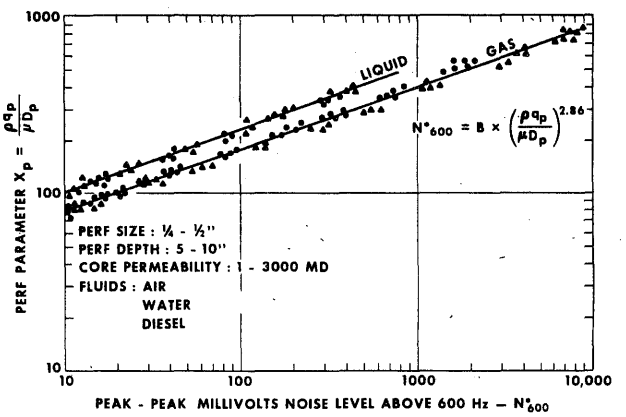

Fig. 6 – Noise level generated by single-phase flow from a deep perforation.

Single-Phase Flow from Plugged Perforations

When flowing, a gas well perforation 6 in. deep would emit an "organ tone" with a pitch of

$$f = \frac{c}{4\ell} \approx \frac{1{,}000}{4 \times 0.5} = 500 \text{ Hz}.$$

This tone would not be emitted by a plugged or very shallow perforation. We illustrate this difference with the noise spectra in Fig. 7, where the tone at 450 Hz is evident on Spectrum A, the unplugged perforation. Therefore, we can learn to recognize plugged perforations in gas wells from their flowing spectra. But even a loose pack in a perforation will eliminate the organ tone without adding much incremental pressure drop along the perforation. The important question is: How much flowing pressure loss results from the plug? To help answer this question, we have prepared the correlation in Fig. 8, which shows the incremental pressure loss per unit rate in 6-in.-deep perforations as a function of the 4000-Hz noise cut at the perforation. The form of the correlation occurs as follows:

$$N^*_{4000} = A \times (\Delta p q_p),$$

thus,

$$\frac{\Delta p}{q_p} = A' \frac{4{,}000}{q_p^2},$$

TABLE 2 – ESTIMATES OF PERFORATION PRESSURE LOSS FROM PLUGGING FOR THE OIL WELL IN FIG. 4

Depth (ft)	N^*_{4000}	N^*_{4000}/q_p^2	$\Delta p/q_p$ (Fig. 8)	Δp (psi)
13,486	15.4	64	0	0
13,585	22.0	91	3	0
13,620	36.3	150	18	9
13,762	60.0	249	70	34
13,754	72.0	298	100	49
13,770	203.0	841	260	127

$$q_p = \frac{1750 \times 5.615}{20 \times 1000} = 0.49 \text{ Mcf/D/perf}$$

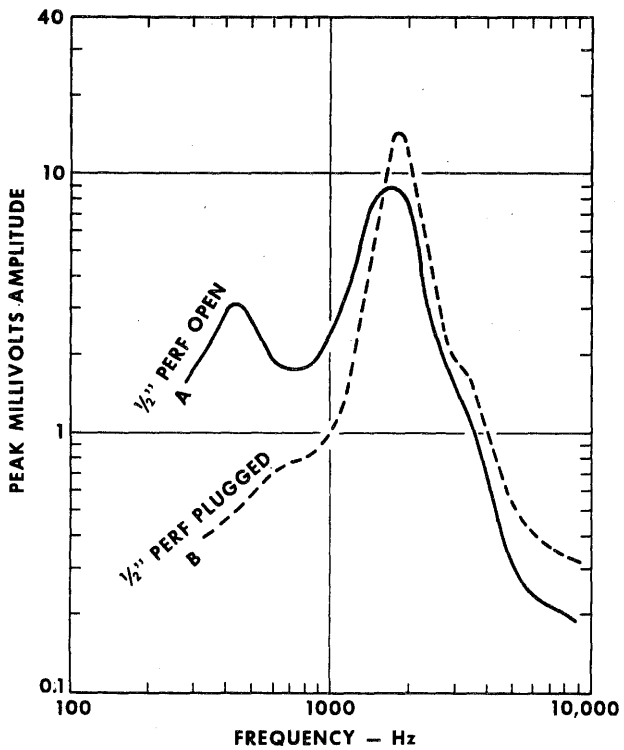

Fig. 7 – Flowing noise spectra for open and plugged perforations.

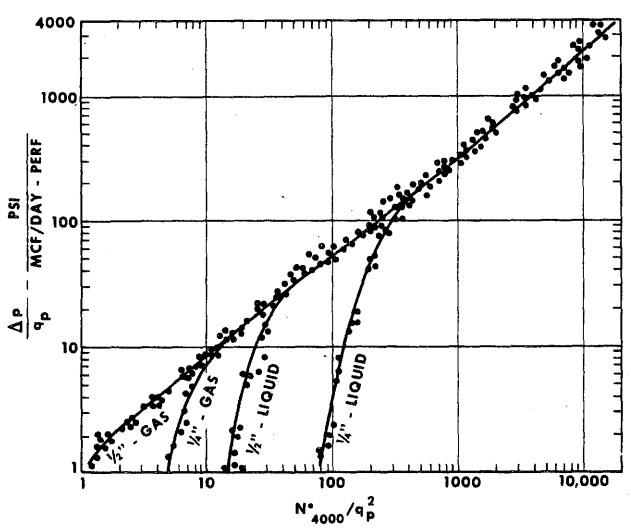

Fig. 8 – Correlation of 4000-Hz noise level with incremental pressure drop caused by perforation plugging.

where Δp (psi) and q_p (Mcf/D) are at bottomhole conditions. We return now to the oil well in Fig. 4. Table 2 summarizes values for N^*_{4000} at selected depths along with the incremental values of Δp obtained from Fig. 8 (¼-in. liquid curve). The estimated pressure loss across the plugged perforation at 13,770 ft is 127 psi. This represents nearly one-half the total flowing drawdown for this particular well. Thus, the perforation is flowing at only about one-half its potential rate.

Liquid Production From Perforations in Gas Zone

In some wells, a perforation flowing gas and liquid produces the liquid as discrete droplets that are carried away. In other wells, the liquid may be produced into a foamy environment. In either situation, the liquid incident on the sonde enriches the noise with higher frequency components, giving a log similar to that opposite the plugged perforation in Fig. 4. We have found that for an open perforation flowing dry gas,

$$\frac{N^*_{2000}}{X_p^3} \leq 3 \times 10^{-5}; (3 \times 10^{-12})(\text{dry gas}), \quad \ldots . (10)$$

where $X_p = (\rho q_p / \mu D_p)$ gas. As one would expect, increasing values above the Eq.-10 threshold reflect increasing concentrations of water in the jet stream. Our data give a relationship approximated by

$$q_{\text{liq}} = 1.5 D_p \frac{N^*_{2000}}{\sqrt{X_p}}, \quad \ldots\ldots\ldots\ldots\ldots\ldots . (11)$$

where q_{liq} is the liquid flow rate in barrels per day and D_p is in inches. For the SI metric system of units, the constant becomes 1.56×10^{-3}, rather than 1.5.

For example, a log from a gas well flowing 1 MMscf/D showed that 20 perforations produced most of the gas. The well also was producing 200 B/D salt water. We estimate that

$$\left(\frac{\rho q_p}{\mu}\right)\text{gas} = \frac{0.054 \times 1{,}000}{0.018 \times 20} = 150,$$

$$X_p = \frac{150}{0.45} = 333(6.88 \times 10^4).$$

At all entry points except one,

$$\frac{N^*_{2000}}{X_p^3} \leq 1 \times 10^{-5}(1 \times 10^{-12}),$$

while at this one perforation the ratio increased to 19×10^{-5}. At this location, $N^*_{2000} = 7{,}050$ p-p mV. These values, when substituted into Eq. 11 with $D_p = 0.45$ in., give

$$q_{\text{liq}} = \frac{1.5 \times 0.45 \times 7{,}050}{\sqrt{333}}$$

$$= 261 \text{ B/D } (4.80 \times 10^{-4} \text{ m}^3/\text{s}).$$

Consequently, this perforation probably was producing most of the water. A workover verified this.

Gas-Liquid Flow From Perforations

Whenever liquid is the continuous phase in the wellbore, a perforation jet stream with gas creates such a high level of noise inside the casing that the condition of the perforation itself is of minor consequence. However, the noise contains information about the jet stream. As McKinley *et al.*[1] explained, the noise in 200- to 600-Hz band is proportional to gas rate, while Eq. 11 shows that liquid content of the jet is related to the higher frequency noise. The correlation in Fig. 9 uses these ideas. This figure, on which the actual data points are omitted, shows percent by volume, y_{gas}, of gas in the jet stream as a function of the ratio of noise levels, $\Delta^*/\sqrt{N^*_{2000}}$, *where* $\Delta^* = N^*_{200} - N^*_{600}$ is the noise level in the 200- to 600-Hz frequency band. The gas percentage could not be correlated totally independent of liquid production rate. This is the reason for the parametric values shown on the curves. Also, note the gas rate restriction ($q_{gas} \leq 0.6$ Mcf/D/perf) that results from the tendency of the fluids to become foamy.

Fig. 9 helps us to diagnose what is happening in the well illustrated in Fig. 5. We also have a density log and a spinner survey from this well. The former showed gas production from the entire perforated interval. This production and the resulting wellbore turbulence complicates the spinner interpretation.

Looking at the noise log in Fig. 5, we see the gas flow from the lower perforations. This flow is evident from the separation between the 200- and 600-Hz curves. Energy in this band is greater than everything above 1000 Hz. We have mentioned already the foam production at 6,194 ft, which suggests this depth is the point of oil entry. Altogether, there are six major entry points. We then may estimate the liquid rate per entry point as

$$q_{liq} = \frac{185 + 26}{6} = 35 \text{ B/D/perf.}$$

From the water curves in Fig. 9, we find the jet-stream gas concentration shown in Col. 4 of Table 3.

Ignore for the moment the last two columns in Table 3. The estimated gas percentages, y_{gas}, show relatively lower gas concentrations at the bottom of the interval (6,198 ft) and at 6,194 ft. This further suggests that these depths may be the water and oil entry points, respectively. To confirm this, we will need flow rates from these locations. The noise log will help estimate these rates.

Figs. 10A and 10B show correlations of gas flow rates at downhole conditions as a function of Δ^* and N^*_{2000}, respectively, with liquid rates as parameters. These charts are for gas/water flow from perforations with the indicated diameter range. We have similar charts for smaller perforations as well as for gas/oil flow. These are not needed here because the liquid in our example is almost all water.

From Fig. 10A, we see that the relationship between Δ^* and q_{gas} is not very sensitive to liquid rate. This rate is reflected more strongly in the N^*_{2000} values in Fig. 10B. This figure then is sufficient to establish values for both q_{gas} and q_{liq}. The charts are

TABLE 3 – ANALYSIS OF RESULTS FROM THE NOISE LOG IN FIG. 5

	Depth (ft)	Δ^*	N^*_{2000}	y_{gas} (Fig. 9) (%)	q_{gas} (Mcf/D)	q_{liq} (B/D)
	6,198	365	84	22	0.10	100
	6,196	633	70	40	0.15	35
	6,194	378	126	20	0.10	100
Totals					0.35	235

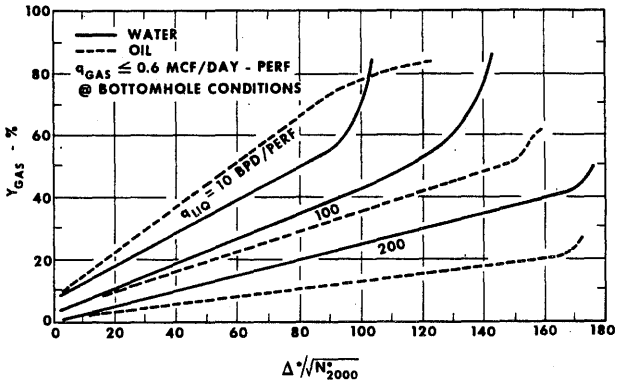

Fig. 9 – Volume percent of gas in perforation jet stream vs noise ratio.

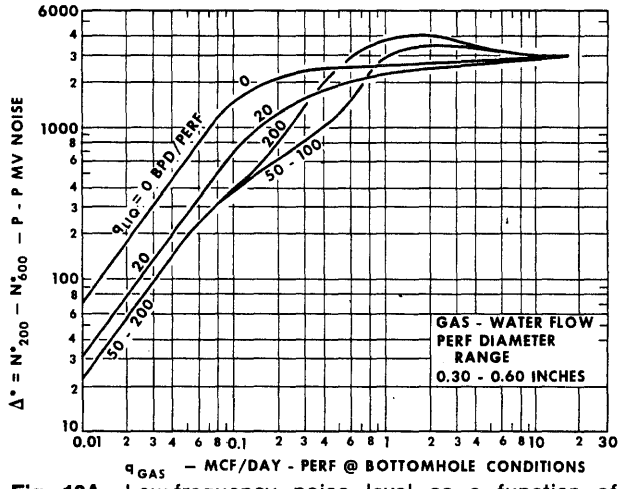

Fig. 10A – Low-frequency noise level as a function of gas/water flow rate from perforations.

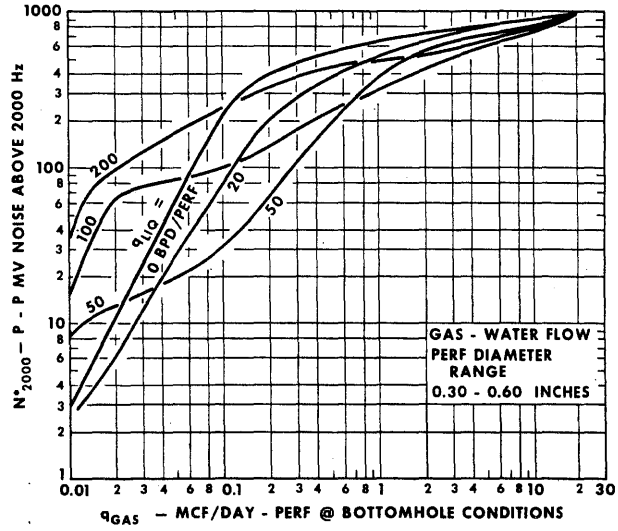

Fig. 10B – High-frequency noise level as a function of gas/water flow rate from perforations.

used in the following manner: All possible solutions consistent with the measured value of Δ^* first are read by projecting this value horizontally across Fig. 10A. These values of q_{gas} and q_{liq} then are transferred to Fig. 10B to give a set of predicted values for N^*_{2000}. The correct solution is the one with N^*_{2000} nearest the measured value. For example, we see from Table 3 that at 6,198 ft, $\Delta^* = 365$ p-p mV, and $N^*_{2000} = 84$ p-p mV. Entering the first of the values onto Fig. 10A gives the possible solutions shown in Cols. 1 and 2 below.

q_{liq}	q_{gas} (Fig. 10A)	N^*_{2000} (Fig. 10B)
0	0.034	31
20	0.060	36
50	0.10	32
100	0.10	100
200	0.094	230

If these values now are transferred to Fig. 10B, we find the numbers for N^*_{2000} in the last column above. Comparing these numbers with the measured value, $N^*_{2000} = 84$, gives the solution at 6,198 ft of

$$\begin{cases} q_{gas} = 0.10 \text{ Mcf/D} \\ q_{liq} = 100 \text{ B/D} \end{cases}$$

In a like manner, we establish the other two entries in the last two columns in Table 3. At 6,196 ft, a liquid rate of either 20 B/D or 50 B/D is consistent; thus, the average is listed. We observe from Table 3 that comparable amounts of liquid are produced at both 6,198 and 6,194 ft. Therefore, the 6,198-ft depth is not the only point of water entry. A squeeze and reperforate workover was tried without success.

Table 3 shows the deepest three entry points producing the observed total liquid (211 B/D) along with an amount of gas equal at standard conditions to

$$q = 0.35 \times 130 = 45.5 \text{ Mscf/D } (0.015 \text{ m}^3/\text{s}).$$

Much of the gas must, therefore, enter at the top three peaks. Dry-gas jetting into a foamy environment is similar to single-phase flow. Our data show that for dry-gas flow into foam, the gas jet-stream group is related to noise level by

$$X_p = 47 \times (N^*_{1000})^{0.35}, \quad \ldots\ldots\ldots\ldots\ldots\ldots (12)$$

where the 1000-Hz cut is used rather than the 600-Hz cut. For the SI metric system, the constant 47 in Eq. 12 should be replaced by 9714. Using Eq. 12 at the top three entries, we find $\Sigma X_p = 670$ (1.38×10^5).

This, in turn, gives

$$q_{sc} = \frac{0.018 \times 0.45 \times 670}{0.054},$$

$$= 100 \text{ Mscf/D } (0.033 \text{ m}^3/\text{s}).$$

This amount added to that produced from the lower perforations accounts for the observed gas rate of 159 Mscf/D.

The individual rate estimates as above can be considerably in error for several reasons. First, the individual perforations may be resolved poorly because of (1) either the distance between stops during the logging operation or (2) the interference from adjacent perforations. Secondly, at higher flow rates, noise level becomes only a weak function of flow rate, as shown in Figs. 10A and 10B. This is the result of foam production in the wellbore. We have, therefore, found that the estimated rates are more useful in the relative sense, illustrated by the previous example.

Sand Production From Perforations

Above 4000 Hz, noise created by fluid movement – even water droplets impacting on the tool – decays very rapidly as frequency rises. This results from fluid viscosity. Such is not the case when sand grains hit the sonde or the casing wall. These impacts produce a very broadband noise spectrum whose major peaks are the result of tool resonances. The rate at which noise level decreases with frequency is, therefore, a good indicator of sand in a perforation jet stream. If we define a decay ratio as

$$R = \frac{N^*_{4000}}{N^*_{4000} - N^*_{6000}}, \quad \ldots\ldots\ldots\ldots\ldots\ldots (13)$$

then a jet stream with entrained sand has the following threshold values in our experimental chamber.

Single-Phase Flow

$$R > 2.5. \quad \ldots\ldots\ldots\ldots\ldots\ldots (14)$$

Gas/Liquid Flow

$$R > \begin{cases} 3.5; X_p < 100(2.0 \times 10^4) \\ 2 \log X_p - 0.5; X_p \geq 100, \end{cases} \quad \ldots\ldots\ldots\ldots (15)$$

where

$$X_p = X_{p_{liq}} + X_{p_{gas}}.$$

These relationships, which assume a jet noise level at least four times ambient values, provide criteria for detecting sand production.

We also can relate noise level to sand concentration in the jet stream:

$$C_{sand} = B\left[\frac{N^*_{4000}}{X_p^3} - 1 \times 10^{-5}\right], \quad \ldots\ldots\ldots\ldots (16)$$

where

$$C_{sand} = \frac{\text{lbm/D sand}}{\left(\frac{\rho q_p}{\mu}\right)_{\text{fluid}}}. \quad \ldots\ldots\ldots\ldots\ldots\ldots (17)$$

The coefficient B, which equals 3.5×10^4 for 16-20 mesh sand, varies inversely with mesh size. In the SI metric system, the coefficient B equals 3.1×10^8, while the threshold value 1×10^{-5} becomes $1 \times$

10^{-12}. The sand rate then is in kilograms per second rather than pounds per day. All the above correlations come from laboratory data and have not been field tested.

Conclusions

We have illustrated how the noise log can be calibrated for flow inside casing. The forms of the calibration equations are more important than the particular numerical coefficients which will change as the tools evolve. In general, for single-phase flow, noise level increases as the cube of the volumetric flow rate and decreases as the square of the cross-sectional area normal to flow. Gas/liquid flows are more complex.

Specifically, we show how to use noise levels to estimate (1) axial flow rate past the sonde for single-phase flow, (2) flow rate from perforations for single-phase or gas/liquid flow, (3) pressure drop across a plugged perforation, (4) liquid flow rate from perforations in a gas well, and (5) sand production rate from perforations.

Those correlations using jet-stream noise at perforations are especially useful when standard methods fail to give a clear diagnosis. We do not wish, however, to leave the impression that the noise log is a substitute for standard flowmeter surveys. Instead, this device should be viewed as a relatively inexpensive complement that provides estimates of flow rates. The accuracy of these estimates will depend on how well a particular tool is calibrated for a particular problem.

Nomenclature

A_s = cross-sectional area, normal to flow, sq ft (m^2)
C_{sand} = sand concentration defined by Eq. 17
D_p = perforation diameter, in. (m)
f = frequency, Hz
N_f^* = noise level, peak-to-peak millivolts, above frequency f at standardized sensitivity
p = pressure, psi (Pa)
Δp = pressure difference, psi (Pa)
q = volumetric flow rate, at flowing temperature and pressure, Mcf/D (m^3/s)
q_{liq} = liquid flow rate, B/D (m^3/s)
q_p = volumetric flow rate, from a single perforation, Mcf/D/perf (m^3/s)
q_{sc} = volumetric flow rate, at standard conditions, Mscf/D (m^3/s)
X_p = jet-stream group defined by Eq. 9 (dimensionless in consistent units)
y_{gas} = percent gas, by volume, in perforation jet stream
$\Delta^* = N_{200}^* - N_{600}^*$ = noise level in 200- to 600-Hz band
μ = fluid viscosity at bottomhole conditions, cp (Pa·s)
ρ = fluid density at bottomhole conditions, lbm/cu ft (kg/m^3)

References

1. McKinley, R.M., Bower, F.M., and Rumble, R.C.: "The Structure and Interpretation of Noise From Flow Behind Cemented Casing," *J. Pet. Tech.* (March 1973) 329-338.
2. *API Recommended Procedure 43,* 2nd ed., American Petroleum Inst., Dallas (Nov. 1971).
3. Robinson, W.S.: "Field Results from the Noise Logging Technique," *J. Pet. Tech.* (Nov. 1976) 1370-1376.

SI Metric Conversion Factors

B/D	× 1.589 873	E−01	=	m^3/d
cp	× 1.000*	E−03	=	Pa·s
cycles/sec	× 1.000*	E+00	=	Hz
°F	(°F−32)/1.8		=	°C
ft	× 3.048*	E−01	=	m
in.	× 2.540*	E−02	=	m
lbm/cu ft	× 1.601 846	E−02	=	kg/m^3
Mcf/D	× 2.863 640	E−02	=	$10^3 m^3/s$
psi	× 6.894 757	E+00	=	kPa
scf/D	× 2.863 640	E−02	=	std m^3/s
sq ft	× 9.290 304	E−02	=	m^2

*Conversion factor is exact.

JPT

Original manuscript received in Society of Petroleum Engineers office Sept. 15, 1977. Paper accepted for publication April 21, 1978. Revised manuscript received Aug. 24, 1979. Paper (SPE 6784) first presented at the SPE-AIME 52nd Annual Fall Technical Conference and Exhibition, held in Denver, Oct. 9-12, 1977.

Ex. II - 43

Exponent®
Engineering & Scientific Consulting

Robert A. Carnahan, P.E.

Principal Engineer | Materials & Corrosion Engineering
5401 McConnell Avenue | Los Angeles, CA 90066
(310) 754-2715 tel | robcarn@exponent.com

Professional Profile

Mr. Carnahan specializes in failure analysis of engineering components and systems by combining expertise in metallurgical engineering, corrosion, materials science, and mechanical engineering.

Mr. Carnahan has performed failure analysis of a wide variety of machinery and equipment related to aerospace, automotive, construction, maritime, pipeline, power generation, and petrochemical industries. Mr. Carnahan has investigated failures of petrochemical plant equipment including heat exchangers, pressure vessels, and HF storage hardware, and has investigated failures of oil and natural gas pipelines and oil and gas well casings. Mr. Carnahan has performed failure analysis of various gas turbine components. He has investigated failures of various types of water and sewage piping, including cast iron, PVC, and asbestos cement. Mr. Carnahan has investigated failures of fire protection system components including sprinklers, piping (steel and CPVC), and couplings. He has also analyzed a multitude of plumbing product failures.

Mr. Carnahan's skills include fractography, microscopy, microstructural analysis, welding and joining, mechanical testing, and stress analysis. Mr. Carnahan also has experience with laboratory evaluation of microbiologically influenced corrosion (MIC) and has worked on a number of MIC related projects, including oil pipelines, sanitary sewer piping, and heat exchangers.

Prior to joining Exponent, Mr. Carnahan performed metallurgical failure analysis and corrosion investigations of nuclear power plant components for the General Electric Company.

Academic Credentials & Professional Honors

M.S., Metallurgical Engineering, University of Michigan, Ann Arbor, 1980

B.S., Materials and Metallurgical Engineering, University of Michigan, Ann Arbor, summa cum laude, 1979

General Electric Honors Cooperative Program

Tau Beta Pi

Clarence A. Siebert Scholarship, University of Michigan

Licenses and Certifications

Licensed Professional Mechanical Engineer, California, #M31519

Licensed Professional Mechanical Engineer, Arizona, #62030

Licensed Professional Mechanical Engineer, Nevada, #024746

Licensed Professional Mechanical Engineer, Texas, #132350

Licensed Professional Engineer, Utah # 9855287-2202

Licensed Professional Engineer, Michigan # 6201068806

Certified Corrosion and Materials Professional (API 571), American Petroleum Institute

Prior Experience

Senior Engineer, General Electric Company, Nuclear Energy Division, 1980-1986

Senior Engineer, General Electric Company, Aerospace Division, 1987-1988

Professional Affiliations

ASM International (formerly American Society for Metals) (member)

National Association of Corrosion Engineers (member)

American Society of Mechanical Engineers (member)

Society of Plastics Engineers (member)

Publications

McDonald B, Ross B, Carnahan RA. The Bellevue crane disaster. Engineering Failure Analysis 2011 Oct; 18(7):1621-1636

Dracup B, Reza A, Carnahan RA, Christiansen E, Ross B. A case study of two shiploader fires in a coal and pet coke facility. 11th International Conference, Fire and Materials, January 2007.

Kadlec R, Westmann R, Carnahan RA, Haghi M, Deyerl E. Failure analysis of heavy truck trailer axle tubes. Experimental Model Research and Testing of Thin Walled Structures, 1997.

Andrew S, Carnahan RA. Fitness-for-service of chloride ton containers. NACE Corrosion '96, Paper No. 650, 1996.

Foulds J, Carnahan RA. Examination of Sabine 2 hot reheat pipe seam weld cracking. Electric Power Research Institute, RP2253-17, Final Report, June 1994.

Carnahan RA. Alternative alloys for BWR pipe applications. Appendix J, Electric Power Research Institute Report NP-2671-LD, October 1982.

Presentations

Carnahan RA. Tribological coating development for SP-100 sliding interfaces. 5th Symposium on Space Nuclear Power Systems, Albuquerque, NM, 1988.

Carnahan RA. Field piping sensitization surveillance. International Workshop on Low Temperature

Sensitization, Electric Power Research Institute, Palo Alto, CA, 1982.

Selected Reports

Moore D, Rau C, Carnahan RA. Triumph air repair / World Airways arbitration. Exponent FaAA Report, February 2006.

Carnahan RA. Whiting motorcycle headlight examination. Exponent FaAA Report to the United States Department of Justice, May 2005 (Rule 26B Report).

Hertzberg J, Reza A, Carnahan RA. Robertshaw TS-11 and 7000 series gas valve investigation. Exponent FaAA Report, October 2004.

Carnahan RA. Investigation of the whitefly screen damage at Houweling's Nursery. Exponent FaAA Report, March 2004.

Carnahan RA. Investigation of the August 2003 skeg cracking on the M/V St. Lucia. Exponent FaAA Report, March 2004.

Carnahan RA. Monrovia Villas copper pipe failure investigation. Exponent FaAA Report, November 2003.

Carnahan RA. Investigation of Disney Concert Hall exterior panel staining. Exponent FaAA Report, September 2003.

Carnahan RA. Steam turbine blade failure investigation. Exponent FaAA Report, July 2003.

Colwell J, Carnahan RA. Conveyor belt fires at the Wilmington Calciner — Preliminary Report. Exponent FaAA Report, May 2003.

Carnahan RA, Shekerlian S, Saraf V. Investigation of the Cedar Point Insane Tower collapse. Exponent FaAA Report, June 2002.

Rau C, Carnahan RA. Evaluation of the JT8D-200 compressor blade failures. Exponent FaAA Report, March 2002.

Carnahan RA, Moore D. Evalution of the potassium carbonate contactor (V501) failure at the Nuevo Energy Rincon Onshore Facility. Exponent FaAA Report, October 2001.

Carnahan RA. Investigation of La Prensa Grafica printing press bearer damage. Exponent Failure Analysis Associates Report, April 1998.

Carnahan RA, MacNab A. Low NOx burner performance, Boiler No. 3, Century City. Failure Analysis Associates, Inc. Report, August 1994.

Foulds J, Carnahan RA. Examination of failed expansion joint bellows from Craig Station, Unit 2. Failure Analysis Associates, Inc. Report, December 1993.

Carnahan RA. The effect of copper based fungicides on pitting corrosion behavior of aluminum piping. Failure Analysis Associates, Inc. Report, March 1993.

Carnahan RA. Analysis of the couch roll bearing failure at Gaylord Container Corporation. Failure Analysis Associates, Inc. Report, July 1992.

Ross B, Carnahan RA. Examination of Durham Grange fuel storage tanks. Failure Analysis Associates, Inc. Report, September 1989.

Ross B, Carnahan RA. Evaluation of Accupac (hex pump) character toothpaste dispenser failures. Failure Analysis Associates, Inc. Report, August 1989.

Carnahan RA. Examination of a cracked jet pump beam from Peach Bottom 3. General Electric Company Report, July 1983.

MF Aleskey, Carnahan RA. Improvements in jet pump hold-down beam service life. General Electric Company Report, December 1981.

Carnahan RA, Cutt JC. Millstone Point 1 isolation condenser and shutdown cooling system piping cracks. General Electric Company Report, May 1981.